

Introduction to Biology

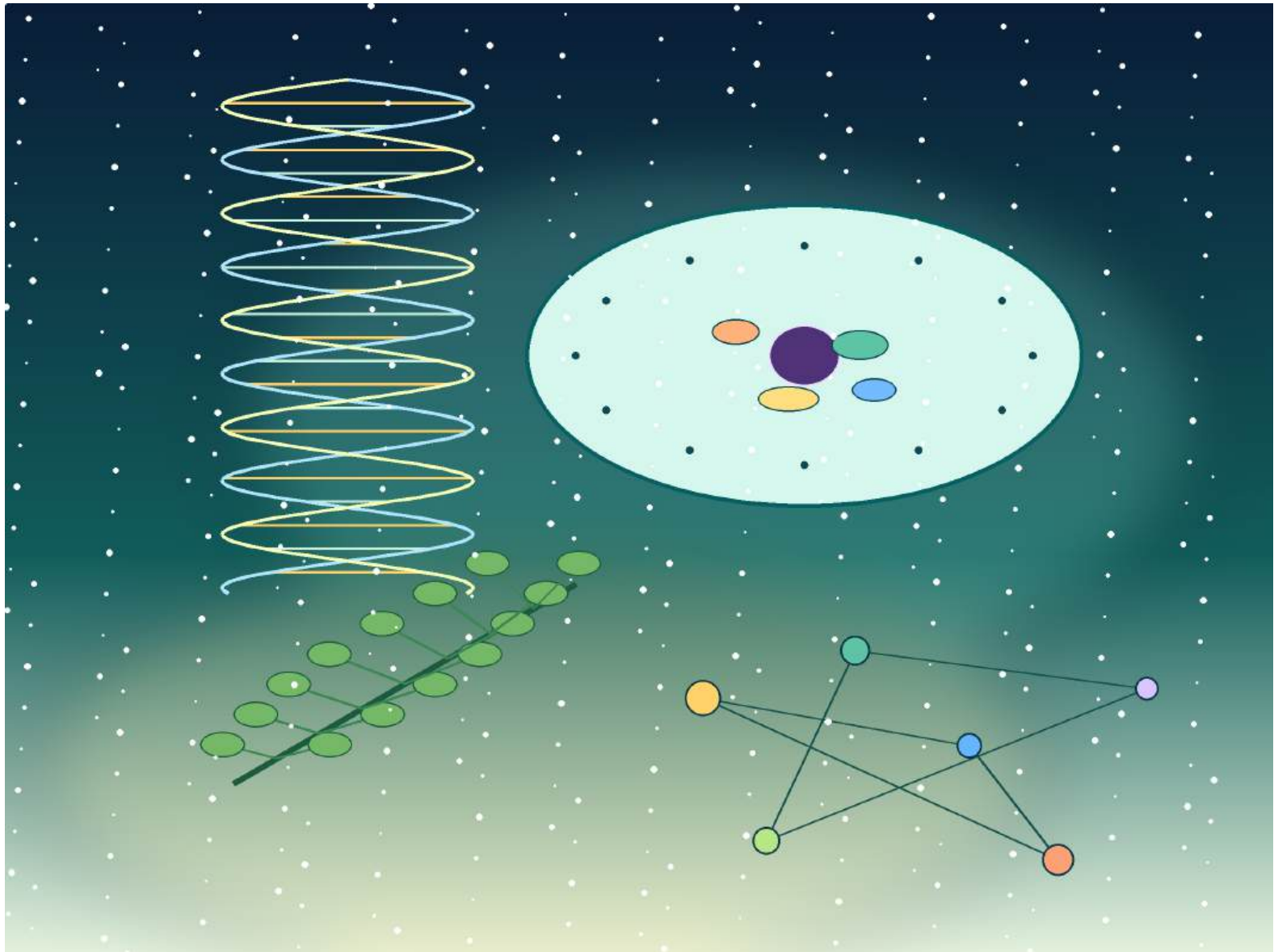
A Generative Approach

Daniel Ari Friedman

Active Inference Institute

daniel@activeinference.institute

ORCID: [0000-0001-6232-9096](https://orcid.org/0000-0001-6232-9096)



Publishing Information

Introduction to Biology
A Generative Approach

Daniel Ari Friedman

Active Inference Institute
daniel@activeinference.institute
ORCID: 0000-0001-6232-9096

Edition 1.0 – 2026

Text license: CC BY 4.0
Source-code license: Apache-2.0
DOI: 10.5281/zenodo.20286478
Source repository: https://github.com/docxology/biology_textbook

“The tree which moves some to tears of joy is in the eyes of others only a green thing that stands in the way. Some see nature all ridicule and deformity... and some scarce see nature at all. But to the eyes of the man of imagination, nature is imagination itself.”

— William Blake

Acknowledgements

This open textbook is built from a living chain of public scholarship, open-source tools, tested computational models, and classroom-facing biological explanation. The author thanks the students, educators, research communities, open-science maintainers, and standards bodies whose work makes a reproducible, adaptable biology text possible.

Suggested citation: Friedman, D. A. (2026). *Introduction to Biology: A Generative Approach* (Edition 1.0). Active Inference Institute. https://github.com/docxology/biology_textbook. <https://doi.org/10.5281/zenodo.20286478>.

This open textbook is generated from version-controlled Markdown, tested Python modules, programmatic figures, and rendered Mermaid diagrams. Corrections and improvements may be submitted via the source repository linked above.

Accessibility note: the compact PDF is optimized for dense print. Reader-profile builds, HTML output, and source Markdown can be generated from the same manuscript materials.

Contents

Front Matter	69
Dedication	69
Acknowledgements	70
About This Textbook	71
Computational Philosophy	71
What Makes This Textbook Different	71
How to Navigate This Book	71
Suggested reading paths	72
Notation and conventions	72
Scholarship and source practice	72
Textbook Concept Map	73
Accessing source materials	73
Course Planning Grid	74
Preface	75
A Textbook Built With Code	75
Five Big Ideas in Biology	75
Evolution: the unifying theory of life	75
Structure and function are inseparable	75
Information — storage, transfer, expression	75
Emergent properties: the whole exceeds the parts	76
Cells: the universal unit of life	76
How Science Actually Works	76
How to Use the Unit Introductions	76
Scope and Organization	76
Reading paths by goal	77
How to Use This Book	77
Computational Infrastructure	78
Pedagogical Standards	78
Open Science Commitment	78
Acknowledgements	78
Unit 0 — Systems Science for Biology: Introduction	79
Why This Unit Matters	79
Landmark Discoveries	79
Key Concepts and Connections	79
Current Evidence Thread	80
Chapter Roadmap	80
Connections Across the Textbook	80
Computational Toolbox — Unit 0	81
Cross-Unit Integration	81
0.1 Systems Science and Emergence	82
0.1.1 Learning Objectives	82
0.1.1.1 Study Blueprint	82
0.1.2 Opening Vignette: The Birth of Systems Thinking	83
0.1.3 What Is a System?	83
0.1.3.1 Isolated, Closed, and Open Systems	83
0.1.3.2 Equifinality and Multifinality	83
0.1.4 Feedback: The Grammar of Self-Regulation	83
0.1.4.1 Negative (Stabilizing) Feedback	84

0.1.4.2	A Linear Negative-Feedback Worked Example	84
0.1.4.3	Positive (Amplifying) Feedback	85
0.1.4.4	Feedback With Delay: Period and Damping	85
0.1.4.5	Feed-Forward and Anticipatory Control	85
0.1.5	Emergence Across Biological Levels	86
0.1.5.1	Levels of Biological Emergence	86
0.1.5.2	Strong and Weak Emergence	86
0.1.6	Hierarchy and Scale	86
0.1.6.1	Cross-Scale Constraints	87
0.1.6.2	Modular Organization and Evolvable Interfaces	87
0.1.7	Nonlinearity and Thresholds	88
0.1.7.1	A Simple Nonlinear Equation: The Hill Function	88
0.1.7.2	Worked Example: Calculating Cooperative Binding	88
0.1.7.3	Bistability and the Toggle Switch	89
0.1.8	Nonlinear Dynamics: Bifurcations, Limit Cycles, and Chaos	89
0.1.8.1	Phase Space and Trajectories	89
0.1.8.2	Bifurcations and Qualitative State Changes	89
0.1.8.3	Limit Cycles and Biological Oscillators	89
0.1.8.4	Chaos and the Lorenz Attractor	89
0.1.9	Biological Oscillators: From Genes to Heartbeats	90
0.1.9.1	The Circadian Clock	90
0.1.9.2	The Cardiac Pacemaker	90
0.1.9.3	The Cell Cycle	90
0.1.9.4	Shared Feedback Architecture of Biological Oscillators	90
0.1.10	Scale-Free Networks in Biology	91
0.1.10.1	Mechanisms Generating Scale-Free Biological Networks	91
0.1.10.2	Functional Consequences of Hub-Dominated Networks	91
0.1.11	Information, Entropy, and Self-organization	91
0.1.11.1	Shannon Information and Biological Signal Content	92
0.1.11.2	Mutual Information and Signaling Fidelity	92
0.1.12	Systems Thinking in Biology: Practical Implications	92
0.1.12.1	From Hill kinetics to a computational switch	92
0.1.12.2	Feed-forward and feedback motifs in gene networks	93
0.1.12.3	Why systems biology is not “fancy reductionism”	93
0.1.13	Current Evidence and Frontier Biology: Systems Science and Emergence	93
0.1.14	Unit 0 Integration: Using Systems Science Without Overclaiming	93
0.1.14.1	Failure Modes of Systems Explanations	94
0.1.15	Summary	94
0.1.16	Key Terms	94
0.1.17	Discussion Questions	94
0.1.18	Review Questions	95
0.1.19	Further Reading and Source Notes: Systems Science and Emergence	95
0.1.20	Companion Source Module: Systems Science and Emergence	96
0.2	Complex Adaptive Systems	97
0.2.1	Learning Objectives	97
0.2.1.1	Study Blueprint	97
0.2.2	Opening Vignette: From Sandpiles to the Santa Fe Institute	98
0.2.3	What Is a Complex Adaptive System?	98
0.2.4	Agents and Agent Rules	98
0.2.4.1	Boids and Flocking	98
0.2.4.2	Ant-Colony Optimization and Stigmergy	99

0.2.4.3	Immune Surveillance as Distributed Adaptation	99
0.2.5	Self-organization in Biology	99
0.2.5.1	Slime Moulds: A Class Example	99
0.2.5.2	Termite Mounds as Collective Construction	99
0.2.5.3	Embryonic Development as Coordinated Self-organization	99
0.2.5.4	Turing Patterns and Reaction–Diffusion	100
0.2.6	Attractors and Phase Space	100
0.2.6.1	Basins of Attraction and Landscape Geometry	100
0.2.7	Phase Transitions and Criticality	100
0.2.7.1	The Ising Picture of Cell-Fate Switching	101
0.2.7.2	Power Laws and Scale-Free Behavior	101
0.2.7.3	Worked Example: Scaling in Power-Law Distributions	101
0.2.8	Adaptation and Evolution as CAS Processes	102
0.2.8.1	Fitness Landscapes and Adaptive Walks	102
0.2.8.2	Worked Example: Escape From a Fitness Valley	103
0.2.8.3	Genetic Algorithms: Evolution in a Computer	103
0.2.8.4	Quorum sensing: a molecular vote without a mayor	104
0.2.8.5	Trophic cascades: top-down reshaping of food webs	104
0.2.8.6	The Immune System as CAS	104
0.2.9	Noise, Stochasticity, and Bifurcation	104
0.2.9.1	Noise in Genetic Switches	104
0.2.9.2	Fold Bifurcations and Hysteresis: Lake Eutrophication	105
0.2.9.3	The Logistic Map: A Worked Bifurcation Diagram	105
0.2.10	Robustness and Fragility	105
0.2.11	CAS Across Biological Scales	106
0.2.11.1	Agent-Based Models Across Biological Scales	106
0.2.12	Synthesis and Practical Implications	107
0.2.13	Current Evidence and Frontier Biology: Complex Adaptive Systems	107
0.2.14	Unit 0 Integration: From Systems to Adaptive Agents	108
0.2.14.1	Diagnostic Workflow for CAS Explanations	108
0.2.15	Summary	108
0.2.16	Key Terms	108
0.2.17	Discussion Questions	108
0.2.18	Review Questions	109
0.2.19	Further Reading and Source Notes: Complex Adaptive Systems	110
0.2.20	Companion Source Module: Complex Adaptive Systems	110
0.3	Active Inference and Free Energy	111
0.3.1	Learning Objectives	111
0.3.1.1	Study Blueprint	111
0.3.2	Opening Vignette: Helmholtz and the Unconscious Inference	112
0.3.3	Maintaining Viable States Under Uncertainty	112
0.3.4	Markov Blankets: The Mathematical Skin of an Agent	112
0.3.4.1	Markov Blanket Definition	112
0.3.4.2	Why Markov Blankets Matter	113
0.3.5	The Free Energy Principle	113
0.3.6	Predictive Processing and the Bayesian Brain Hypothesis	114
0.3.6.1	Hierarchical Predictive Coding	114
0.3.6.2	The Canonical Microcircuit	114
0.3.6.3	Precision and Attention	114
0.3.6.4	Worked Example: Bayesian Updating and Prediction Error	115
0.3.7	Active Inference as a Perception-Action Loop	115

0.3.7.1	Homeostasis vs. Allostasis	116
0.3.7.2	Worked Example — Free Energy Minimization via Action	116
0.3.7.3	Expected Free Energy and Policy Selection	116
0.3.7.4	Epistemic vs. Instrumental Value (worked numerical example)	117
0.3.8	Embodied Active Inference	117
0.3.9	Active Inference and Evolution	117
0.3.9.1	Free Energy Minimization Beyond Brains	118
0.3.10	Computational Psychiatry and Precision-Weighting Disorders	118
0.3.10.1	Anxiety and Interoceptive Hyper-precision	118
0.3.10.2	Depression and the Dark-Room Problem	118
0.3.10.3	Schizophrenia and Aberrant Salience	118
0.3.10.4	Autism-Spectrum Predictive Differences	118
0.3.11	Active Inference Applications Beyond Neuroscience	119
0.3.11.1	Immune Recognition as Population-Level Inference	119
0.3.11.2	Developmental Patterning as Hierarchical Inference	119
0.3.11.3	Evolutionary Active Inference	119
0.3.11.4	Ecology and Collective Behavior	119
0.3.12	Connections to Other Units	119
0.3.12.1	Interoceptive active inference and psychiatry (conceptual)	120
0.3.13	The Free Energy Principle in Context	120
0.3.14	Current Evidence and Frontier Biology: Active Inference and Free Energy	120
0.3.15	Unit 0 Integration: When Active Inference Is the Right Tool	121
0.3.15.1	Bridge to history and philosophy	121
0.3.16	Summary	121
0.3.17	Key Terms	121
0.3.18	Discussion Questions	122
0.3.19	Review Questions	122
0.3.20	Further Reading and Source Notes: Active Inference and Free Energy	123
0.3.21	Companion Source Module: Active Inference and Free Energy	123
0.4	History and Philosophy of Biology	124
0.4.1	Learning Objectives	124
0.4.1.1	Study Blueprint	124
0.4.2	Opening Vignette: Darwin, Wallace, and Evidence Before an Audience	125
0.4.3	Why History and Philosophy Belong in Introductory Biology	125
0.4.4	Biology as Practice: Instruments, Organisms, and Arguments	126
0.4.5	Ancient and Global Knowledge Traditions in Biology and Medicine	126
0.4.6	Natural History, Classification, and Empire	126
0.4.7	Experiment, Mechanism, and the Laboratory	126
0.4.8	Darwin, Wallace, and Historical Causation	127
0.4.9	Genetics, Molecular Biology, and the Modern Synthesis	127
0.4.10	Mechanism, Function, and Teleology	127
0.4.10.1	Tinbergen’s Four Questions	127
0.4.11	Species, Individuals, and the Boundaries of Life	128
0.4.12	Development, Nature-Nurture, and Inheritance	129
0.4.13	Microbiology, Disease, Symbiosis, and Self	129
0.4.14	Models, Evidence, and Explanation	129
0.4.15	Levels of Explanation and Causal Pluralism	129
0.4.16	First-Principles Claim Audit	130
0.4.16.1	Claim Audit in Practice	130
0.4.17	Current Evidence and Frontier Biology: History and Philosophy of Biology	131
0.4.18	Ethics, Values, and Public Biology	132

0.4.19	Synthesis: A Checklist for Biological Claims	132
0.4.20	Summary	132
0.4.21	Key Terms	132
0.4.22	Discussion Questions	133
0.4.23	Review Questions	133
0.4.24	Further Reading and Source Notes: History and Philosophy of Biology	133
0.4.25	Companion Source Module: History and Philosophy of Biology	133
Unit I	Chemistry of Life: Introduction	135
	Why This Unit Matters	135
	Landmark Discoveries	135
	Key Concepts and Connections	136
	Current Evidence Thread	136
	Chapter Roadmap	136
	Connections Across the Textbook	136
	Computational Toolbox — Unit I	137
	Cross-Unit Integration	137
1	Atoms, Molecules, and Chemical Bonds	138
1.1	Learning Objectives	138
1.1.1	Study Blueprint	139
1.1.2	Subatomic Particles and Atomic Identity	139
1.1.3	Isotopes and Their Biological Applications	140
1.1.4	Electron Shells, Orbitals, and Valence	140
1.1.5	Orbital Hybridization in Biological Molecules	141
1.1.6	Lewis Structures and Formal Charge	141
1.1.7	Electronegativity Drives Polarity in Biology	141
1.2	Chemical Bonds as Biological Forces	142
1.2.1	Covalent Bonds and Molecular Stability	142
1.2.2	Ionic Interactions in Biological Solutes	143
1.2.3	Hydrogen Bonds in Water, Proteins, and Nucleic Acids	143
1.2.4	Van der Waals Forces and Lipid Packing	144
1.3	Functional Groups and Biomolecular Reactivity	145
1.4	Resonance Structures and Delocalized Electrons	146
1.4.1	The Peptide Bond as a Resonance Hybrid	146
1.4.2	Resonance in Carboxylate Ions	146
1.4.3	Aromatic Systems in Biology	146
1.5	Chirality and Stereochemistry	146
1.5.1	Enantiomers and Biological Specificity	146
1.5.2	R/S Configuration	146
1.5.3	Geometric Isomerism in Fatty Acids	147
1.6	Redox Reactions in Biology	147
1.6.1	Oxidation and Reduction	147
1.6.2	Reduction Potentials and Electron Transfer	147
1.6.3	Biological Electron Carriers	148
1.7	The Mole Concept and Molarity	148
1.8	pH and Buffers	149
1.8.1	The pH Scale	149
1.8.2	Henderson-Hasselbalch Equation	149
1.8.3	Buffer Capacity in Physiological Fluids	149
1.8.4	Comparison of Biological pH Buffering Systems	150
1.8.5	Titration Curves and pKa Estimation	151

1.9	Worked Examples: Buffers, Redox, and Physiological pH	151
1.10	Key Comparison: Bond Types in Biology	152
1.11	Computational Bridge	152
1.12	Current Evidence and Frontier Biology: Atoms, Molecules, and Chemical Bonds	153
1.13	Summary	153
1.14	Key Terms	153
1.15	Review Questions	154
1.16	Further Reading and Source Notes: Atoms, Molecules, and Chemical Bonds	154
1.17	Companion Source Module: Atoms, Molecules, and Chemical Bonds	154
2	Water — The Molecule of Life	156
2.1	Learning Objectives	156
2.1.1	Study Blueprint	156
2.2	Molecular Structure and Polarity	157
2.2.1	The Hydrogen Bond Network in Detail	157
2.3	Physical Properties Explained by Hydrogen Bonding	158
2.3.1	High Heat Capacity ($C_p = 4.18 \text{ J g}^{-1} \text{ K}^{-1}$)	158
2.3.2	High Heat of Vaporisation ($\Delta_{\text{vap}}H = 44 \text{ kJ/mol}$ at 37 degrees C)	158
2.3.3	High Surface Tension ($\gamma = 72.8 \text{ mN/m}$ at 20 degrees C)	158
2.3.4	Density Anomaly — Ice Floats	159
2.4	Water as a Solvent	159
2.4.1	Hydrophilic Interactions and the Hydration Shell	159
2.4.2	The Dielectric Constant and Electrostatic Screening	159
2.4.3	Hydrophobic Effect and Entropy-Driven Assembly	160
2.4.4	Amphipathic Molecules and Self-Assembly	160
2.5	Osmotic Pressure — The van ’t Hoff Equation	161
2.5.1	Derivation of the van ’t Hoff Equation	161
2.5.2	Worked Examples: Osmotic Pressure and Isotonic Fluids	161
2.5.3	Tonicity and Cell Behavior	163
2.6	Diffusion — Fick’s First Law	164
2.6.1	The Stokes-Einstein Equation	164
2.6.2	Mean Diffusion Distance and Biological Design	165
2.6.3	Biological Applications of Fick’s Law	165
2.6.4	Solubility Rules and the Thermodynamics of Dissolution	165
2.6.5	The Hydrophobic Effect Quantified	166
2.6.6	Colligative Property: Osmotic Pressure (van ’t Hoff)	167
2.6.7	Water Activity and Biological Processes	167
2.6.8	Proton Hopping — The Grotthuss Mechanism	167
2.6.9	Ice Nucleation and Cryopreservation	168
2.7	Aquaporins — Molecular Water Channels	168
2.7.1	Discovery and Structure	168
2.7.2	Aquaporin Family and Functions	168
2.7.3	Aquaporins in Disease	168
2.8	Colligative Properties and Freezing/Boiling Shifts	169
2.8.1	Boiling Point Elevation and Freezing Point Depression	169
2.8.2	Antifreeze Proteins and Cryoprotective Adaptations	169
2.9	Water Activity and Microbial Growth	170
2.9.1	Definition of Water Activity	170
2.9.2	Water Activity and Food Preservation	170
2.10	Water and Adaptation	170
2.11	Current Evidence and Frontier Biology: Water — The Molecule of Life	171
2.12	Quantitative Summary of Water’s Physical Properties	171

2.12.1	Extremophiles and Water	171
2.13	Computational Bridge	171
2.14	Summary	172
2.15	Key Terms	172
2.16	Review Questions	172
2.17	Further Reading and Source Notes: Water — The Molecule of Life	173
2.18	Companion Source Module: Water — The Molecule of Life	173
3	Biological Macromolecules	174
3.1	Learning Objectives	174
3.1.1	Study Blueprint	175
3.1.2	Condensation and Hydrolysis	175
3.1.3	Worked Example: The Thermodynamics of Polymerization	176
3.2	Carbohydrates as Energy Stores and Structural Polymers	177
3.2.1	Monosaccharides and Ring Chemistry	177
3.2.2	Disaccharides and Polysaccharides	177
3.2.3	The Glycosidic Bond: α vs. β	178
3.2.4	Branching, Linkages, and Polymer Diversity	179
3.2.5	Glycoproteins and Proteoglycans	179
3.3	Lipids, Membranes, and Energy Storage	180
3.3.1	Fatty Acids and Membrane Fluidity	180
3.3.2	Glycerophospholipids and Bilayer Architecture	180
3.3.3	Quantitative Properties of the Lipid Bilayer	181
3.3.4	Sphingolipids in Membranes and Signaling	182
3.3.5	Sterols and Steroid Hormones	182
3.3.6	Waxes and Other Lipids	182
3.4	Proteins as Folded Catalytic and Structural Polymers	183
3.4.1	Amino Acid Chemistry and Side-Chain Diversity	183
3.4.2	The Peptide Bond	183
3.4.3	Ramachandran Plots and Backbone Dihedral Angles	183
3.4.4	Levels of Protein Structure	184
3.4.5	Thermodynamics of Protein Folding	185
3.4.6	Intrinsically Disordered Proteins (IDPs)	186
3.4.7	Post-Translational Modifications (PTMs)	187
3.5	Nucleic Acids as Information Polymers	188
3.5.1	Nucleotide Monomers and Phosphodiester Linkages	188
3.5.2	DNA Structure, Base Pairing, and Helical Geometry	188
3.5.3	Worked Example: DNA Melting Temperature from %GC	189
3.5.4	RNA Structure and Diversity	190
3.5.5	Ribozymes: Catalytic RNA	191
3.6	Key Comparisons Among Macromolecule Classes	191
3.6.1	The Four Macromolecule Classes Compared	191
3.6.2	Storage vs. Structural Polysaccharides	192
3.7	Computational Bridge	192
3.8	Current Evidence and Frontier Biology: Biological Macromolecules	192
3.8.1	Current Evidence Map: AI Structure Claims Need Validation	193
3.9	Summary	193
3.10	Key Terms	193
3.11	Review Questions	194
3.12	Further Reading and Source Notes: Biological Macromolecules	194
3.13	Companion Source Module: Biological Macromolecules	194

4	Enzymes and the Kinetics of Catalysis	196
4.1	Learning Objectives	196
4.1.1	Study Blueprint	196
4.1.2	Transition State Theory	197
4.1.3	Active Site Architecture	197
4.2	Enzyme Classification (EC Numbers)	198
4.3	The Michaelis-Menten Equation	199
4.3.1	Deriving the Michaelis-Menten Equation	199
4.3.2	Interpretation of Kinetic Parameters	200
4.3.3	Lineweaver-Burk Analysis	200
4.4	Enzyme Inhibition and Kinetic Signatures	202
4.4.1	Competitive Inhibition and Apparent Km	202
4.4.2	Uncompetitive Inhibition and Coupled Km/Vmax Shifts	203
4.4.3	Mixed (Noncompetitive) Inhibition	203
4.4.4	Irreversible Inhibition and Covalent Inactivation	203
4.4.5	Lineweaver-Burk Patterns Summary	204
4.5	Multi-substrate Kinetics: Bi-Bi Mechanisms	204
4.5.1	Sequential (Ternary Complex) Mechanisms	205
4.5.2	Ping-Pong (Double-Displacement) Mechanism	205
4.6	Allosteric Regulation and Cooperativity	205
4.6.1	The Hill Equation	205
4.6.2	Concerted (MWC) and Sequential Models	206
4.6.3	Aspartate Transcarbamoylase (ATCase) — A Model Allosteric Enzyme	206
4.6.4	Why Cooperativity Improves Pathway Control	207
4.7	Environmental Factors Affecting Enzyme Activity	207
4.7.1	Temperature Effects on Enzyme Rate and Stability	207
4.7.2	pH Effects on Active-Site Chemistry	208
4.7.3	Cofactors and Coenzymes	208
4.8	Industrial and Biotechnological Enzymes	209
4.8.1	CRISPR-Cas9 as a Nuclease Enzyme	209
4.8.2	Industrial and Therapeutic Enzyme Applications	209
4.8.3	Enzyme Engineering Approaches	210
4.8.4	Quantitative Metrics for Engineered Enzymes	210
4.9	Worked Examples: Rates, Inhibition, and Catalytic Efficiency	210
4.10	Computational Bridge	211
4.11	Bridge to Systems: From Enzyme Kinetics to Metabolic Flux	211
4.11.1	Pathway Flux is Set by Multiple Enzymes, Not One	211
4.11.2	Enzyme Saturation Modes Determine Pathway Behavior	212
4.11.3	Branching Points and Connectivity	212
4.12	Current Evidence and Frontier Biology: Enzymes and the Kinetics of Catalysis	212
4.12.1	Current Evidence Map: Enzyme Engineering Evidence Chain	213
4.13	Summary	213
4.14	Key Terms	213
4.15	Review Questions	213
4.16	Further Reading and Source Notes: Enzymes and the Kinetics of Catalysis	214
4.17	Companion Source Module: Enzymes and the Kinetics of Catalysis	214
Unit II — The Cell: Introduction		215
Why This Unit Matters		215
Landmark Discoveries		215
Key Concepts and Connections		215
Current Evidence Thread		215

	Chapter Roadmap	216
	Connections Across the Textbook	216
	Computational Toolbox — Unit II	216
	Cross-Unit Integration	217
5	Cell Theory and Cell Types	218
5.1	Learning Objectives	218
5.1.1	Study Blueprint	218
5.2	The Cell as the Fundamental Unit of Life	218
5.2.1	Historical Development of Cell Theory	218
5.2.2	The Three Original Postulates	219
5.2.3	Modern Additions to Cell Theory	219
5.3	Size, Scale, and the Surface-to-Volume Constraint	219
5.3.1	Orders of Magnitude in Biology	219
5.3.2	The Mathematics of Cell Size	220
5.4	Worked Example: Surface-to-Volume Calculation	220
5.4.1	Diffusion Time and Cell Size	221
5.4.2	Exceptions to Small Cell Size	221
5.4.3	The Cube Law and Why Giant Cells Are Impossible	221
5.4.4	Quantitative Comparison: Prokaryote vs. Eukaryote	222
5.5	Microscopy: Seeing the Cell	222
5.5.1	Light Microscopy, Contrast, and Resolution	223
5.5.2	Electron Microscopy and Ultrastructure	223
5.5.3	Super-Resolution Microscopy	223
5.6	Prokaryotic Cells and Cellular Economy	224
5.6.1	Prokaryotic Cell Features and Constraints	224
5.6.2	Prokaryotic Cell Structure	224
5.6.3	The Prokaryotic Cytoskeleton — A Recent Revolution	225
5.6.4	Detailed Comparison: Bacteria vs. Archaea	226
5.7	Eukaryotic Cells and Compartmentalization	227
5.7.1	Eukaryotic Organelle Inventory	227
5.7.2	Compartmentalization: The Eukaryotic Advantage	228
5.8	Endosymbiotic Theory and Organelle Origins	228
5.8.1	Evidence for Endosymbiosis	228
5.8.2	Primary and Secondary Endosymbiosis	228
5.8.3	LUCA: The Last Universal Common Ancestor	229
5.8.4	Viral Replication: Lytic vs. Lysogenic Cycles	229
5.9	The Minimal Cell: JCVI-syn3.0	230
5.10	Extremophile Cells and Environmental Limits	230
5.10.1	Extremophile Cell Strategies	230
5.10.2	Implications for Astrobiology	230
5.11	Cell Type Classification	231
5.11.1	Nutritional Classification by Carbon and Energy Source	231
5.11.2	Oxygen Requirements and Aerotolerance	231
5.12	Computational Bridge	231
5.13	Current Evidence and Frontier Biology: Cell Theory and Cell Types	231
5.14	Summary	232
5.15	Review Questions	232
5.16	Discussion Questions	233
5.17	Further Reading and Source Notes: Cell Theory and Cell Types	233
5.18	Key Terms	233
5.19	Companion Source Module: Cell Theory and Cell Types	234

6	Cell Structure and Organelles	235
6.1	Learning Objectives	235
6.1.1	Study Blueprint	235
6.2	Quantitative Organelle Inventory	236
6.3	The Nucleus — The Information Center	237
6.3.1	Nuclear Envelope, Pores, and Lamina	237
6.3.2	Protein Targeting and Sorting	237
6.3.3	Chromatin and Nucleosomes	239
6.3.4	Nucleolus and Ribosome Biogenesis	239
6.4	Mitochondria — Power Plants of the Cell	240
6.4.1	Mitochondrial Structural Organization and Cristae	240
6.4.2	Mitochondrial DNA (mtDNA)	240
6.4.3	Mitochondrial Dynamics: Fusion and Fission	240
6.5	The Endomembrane System and Secretory Pathway	241
6.5.1	Endoplasmic Reticulum Structure and Protein/Lipid Processing	241
6.5.2	Golgi Apparatus and Vesicular Sorting	243
6.5.3	Lysosomes and Acid Hydrolase Compartments	244
6.6	Cytoskeletal Filaments and Cellular Mechanics	244
6.6.1	Actin Microfilaments and Cortical Force Generation	244
6.6.2	Tubulin Microtubules and Intracellular Transport	245
6.6.3	Worked Example: Motor Protein Kinematics and Energetics	245
6.6.4	Intermediate Filaments and Tensile Strength	246
6.7	Centrosomes, Centrioles, and Cilia	247
6.7.1	Centrosome/MTOC as the Microtubule Organizing Center	247
6.7.2	Cilia and Flagella	247
6.8	Peroxisomes and Single-Membrane Oxidative Compartments	247
6.8.1	Peroxisome Metabolism, Detoxification, and Biosynthesis	248
6.8.2	Peroxisome Biogenesis and Protein Import	248
6.9	Cell Adhesion and Junctions	248
6.9.1	Cell Adhesion Molecules	248
6.9.2	Cell Junctions and Tissue Barrier Architecture	249
6.10	The Proteasome — Protein Quality Control	249
6.10.1	The 26S Proteasome	249
6.10.2	Ubiquitination — The Degradation Signal	249
6.11	CRISPR Applications in Organelle Biology	250
6.12	Computational Bridge	250
6.12.1	Mitochondrial Base Editors Without Double-Strand Breaks	250
6.13	Current Evidence and Frontier Biology: Cell Structure and Organelles	250
6.13.1	Current Evidence Map: Membrane-Bound and Condensate Organization	251
6.14	Summary	251
6.15	Review Questions	251
6.16	Further Reading and Source Notes: Cell Structure and Organelles	252
6.17	Key Terms	252
6.18	Companion Source Module: Cell Structure and Organelles	253
7	Membrane Structure and Transport	254
7.1	Learning Objectives	254
7.1.1	Study Blueprint	254
7.1.2	Membrane Lipid Composition	254
7.1.3	Lipid Rafts and Membrane Microdomains	256
7.1.4	Updates to the Fluid Mosaic Model	256
7.2	Membrane Proteins as Transporters, Receptors, and Anchors	256

7.2.1	Functions of Membrane Proteins	257
7.3	Passive Transport Down Electrochemical Gradients	257
7.3.1	Simple Diffusion Through the Lipid Bilayer	257
7.3.2	Osmosis and the van't Hoff Equation	258
7.3.3	Facilitated Diffusion via Channels	259
7.3.4	Ion Channel Gating Kinetics	260
7.3.5	Electroneutral vs. Electrogenic Transport	260
7.3.6	Facilitated Diffusion via Carriers (Uniporters)	261
7.4	Worked Example: GLUT Transporter Kinetics	261
7.5	Active Transport Coupled to Energy Input	262
7.5.1	Primary Active Transport — Pumps	262
7.5.2	ABC Transporters and ATP-Powered Pumping	263
7.5.3	Secondary Active Transport	263
7.6	The Nernst Equation and Membrane Potential	263
7.6.1	Electrochemical Potential and Ion Driving Force	263
7.6.2	Derivation of the Nernst Equation	263
7.7	Worked Example: Nernst Potential	264
7.7.1	Goldman-Hodgkin-Katz Equation	265
7.8	Worked Example: Goldman Equation	265
7.9	Membrane Potential and the Action Potential	266
7.9.1	Phases of the Action Potential	266
7.9.2	Hodgkin-Huxley Model	267
7.9.3	Saltatory Conduction Along Myelinated Axons	267
7.10	Bulk Transport: Endocytosis and Exocytosis	267
7.10.1	Exocytosis and SNARE-Mediated Membrane Fusion	267
7.10.2	SNARE Mechanism in Detail	268
7.10.3	Vesicle Coat Proteins in Detail	268
7.10.4	Endocytosis and Cargo Internalization	269
7.11	Computational Bridge	269
7.11.1	Predicted Transporter Structures and Experimental Tests	270
7.12	Current Evidence and Frontier Biology: Membrane Structure and Transport	270
7.12.1	Current Evidence Map: Transporter Structure to Function	270
7.13	Summary	270
7.14	Review Questions	271
7.15	Further Reading and Source Notes: Membrane Structure and Transport	271
7.16	Key Terms	272
7.17	Companion Source Module: Membrane Structure and Transport	272
8	Cell Signaling and Communication	273
8.1	Learning Objectives	273
8.1.1	Study Blueprint	273
8.1.2	Types of Cell Signaling by Distance	273
8.1.3	Signal Transduction Logic	274
8.1.4	Signal Amplification Cascades — A Quantitative Treatment	274
8.1.5	Quantitative Foundations of Signal Transduction	276
8.1.6	Worked Example: Receptor Fractional Occupancy	276
8.1.7	Worked Example: Signal Amplification Through a Kinase Cascade	277
8.2	Cell-Surface Receptors and Signal Initiation	277
8.2.1	G Protein-Coupled Receptors (GPCRs)	277
8.2.2	The G-Protein Cycle in Detail	278
8.2.3	GPCR Desensitisation and β -Arrestin	279
8.2.4	Second Messenger Kinetics	279

8.2.5	Receptor Tyrosine Kinases (RTKs)	280
8.2.6	Receptor Tyrosine Kinase Activation in Detail	281
8.2.7	The MAP Kinase Cascade — Three-Tier Hierarchy	282
8.2.8	Ligand-Gated Ion Channels	283
8.3	Intracellular Receptors for Lipid-Soluble Signals	283
8.4	Developmental, Cytokine, and Termination Pathways	284
8.4.1	Wnt/Beta-Catenin Pathway	284
8.4.2	JAK-STAT Pathway	284
8.4.3	Notch Pathway and Contact-Dependent Cell Fate	284
8.4.4	Signal Termination Mechanisms	284
8.5	Crosstalk and Signal Integration	285
8.5.1	Convergence and Divergence	285
8.5.2	Scaffold Proteins and Signaling Specificity	285
8.5.3	Positive and Negative Feedback Loops	285
8.5.4	Computational Approaches to Signaling Networks	286
8.6	The Cell Cycle — Control Through CDK-Cyclin Complexes	286
8.6.1	Cell-Cycle Phases and CDK-Cyclin Control	286
8.6.2	Tumor Suppressors and Checkpoint Control	287
8.7	Apoptosis — Programmed Cell Death	287
8.7.1	Intrinsic (Mitochondrial) Pathway	287
8.7.2	Extrinsic (Death Receptor) Pathway	287
8.7.3	Other Forms of Regulated Cell Death	288
8.8	Cancer as Dysregulated Signaling	288
8.8.1	Oncogenes and Their Normal Counterparts	288
8.8.2	Targeted Cancer Therapies	288
8.8.3	Clinical Pharmacology of Cell Signaling	289
8.8.4	Crosstalk and Signal Integration — How Cells Process Multiple Signals	290
8.9	Computational Bridge	290
8.9.1	Spatial Transcriptomics: Signaling in Tissue Context	290
8.10	Current Evidence and Frontier Biology: Cell Signaling and Communication	291
8.10.1	Current Evidence Map: Spatial Single-Cell Signaling Evidence	291
8.11	Summary	291
8.12	Review Questions	292
8.13	Further Reading and Source Notes: Cell Signaling and Communication	292
8.14	Key Terms	292
8.15	Companion Source Module: Cell Signaling and Communication	293
Unit III — Energy and Metabolism: Introduction		294
Why This Unit Matters		294
Landmark Discoveries		294
Key Concepts and Connections		294
Current Evidence Thread		294
Chapter Roadmap		295
Connections Across the Textbook		295
Computational Toolbox — Unit III		296
Cross-Unit Integration		296
9	Bioenergetics and Cellular Respiration	297
9.1	Learning Objectives	297
9.1.1	Study Blueprint	297
9.2	Thermodynamics of Life	299
9.2.1	First and Second Laws	299

9.2.2	Gibbs Free Energy: A Derivation From First Principles	299
9.2.3	Standard Free Energy and Actual Free Energy	299
9.2.4	Worked Example: Free Energy and Equilibrium	301
9.2.5	Worked Example: Complete Glucose Oxidation	301
9.2.6	ATP as Energy Currency	301
9.3	Glycolysis as Cytosolic Glucose Oxidation	302
9.3.1	Ten Enzymatic Steps	302
9.3.2	Regulation of Glycolysis	303
9.3.3	ATP and Reducing-Equivalent Accounting	303
9.4	Gluconeogenesis: Reverse But Not the Reverse	304
9.4.1	The Four Bypass Reactions	304
9.4.2	The Four Bypass Enzymes in Detail	304
9.4.3	Reciprocal Regulation of Glycolysis and Gluconeogenesis	305
9.5	The Cori Cycle and the Glucose-Alanine Cycle	305
9.5.1	The Cori Cycle (Lactate Shuttle)	305
9.5.2	The Glucose-Alanine Cycle	305
9.6	Pyruvate Oxidation and the Citric Acid Cycle	306
9.6.1	Pyruvate Dehydrogenase Complex (PDC)	306
9.6.2	TCA Cycle (Krebs Cycle / Citric Acid Cycle)	307
9.6.3	Anaplerotic and Cataplerotic Reactions	308
9.7	Oxidative Phosphorylation and Proton-Motive Force	309
9.7.1	Electron Transport Chain (ETC)	309
9.7.2	Reactive Oxygen Species and Antioxidant Defense	309
9.7.3	ATP Synthase — the Rotary Nanomotor	311
9.7.4	How the “30–32 ATP” Number Is Calculated: P/O Ratios	312
9.7.5	Worked Example: Total ATP Yield	312
9.8	Substrate-Level vs. Oxidative Phosphorylation: A Quantitative Comparison	313
9.9	Fermentation and NAD ⁺ Regeneration	314
9.10	Uncoupling Proteins and Brown Adipose Thermogenesis	314
9.10.1	UCP1: The Brown Adipose Thermogenin	314
9.10.2	Physiological Roles of Lactate	315
9.11	Metabolic Poisons and Inhibitors	315
9.11.1	Electron-Transport Chain Inhibitors	315
9.11.2	Uncouplers and Proton Leak	316
9.11.3	ATP Synthase Inhibitors	316
9.12	Computational Bridge	316
9.13	Current Evidence and Frontier Biology: Bioenergetics and Cellular Respiration	316
9.13.1	Current Evidence Map: Respiration Evidence Accounting	317
9.14	Summary	317
9.15	Review Questions	317
9.16	Further Reading and Source Notes: Bioenergetics and Cellular Respiration	318
9.17	Key Terms	318
9.18	Companion Source Module: Bioenergetics and Cellular Respiration	319
10	Photosynthesis	320
10.1	Learning Objectives	320
10.1.1	Study Blueprint	320
10.2	Photosynthesis as Light-Driven Carbon Fixation	320
10.2.1	Chloroplast Structure and Thylakoid Compartments	321
10.3	Light Absorption and Energy Transfer	321
10.3.1	Photosynthetic Pigments and Light Absorption	321
10.3.2	Photon Energy and Quantum Efficiency	321

10.3.3	Antenna Complexes and Light-Harvesting Architecture	322
10.3.4	Energy Transfer Mechanisms	322
10.4	Light-Dependent Reactions	323
10.4.1	Photosystem II (PS II)	323
10.4.2	Cytochrome b ₆ f Complex	323
10.4.3	Photosystem I (PS I)	324
10.4.4	The Z-Scheme: Standard Electrode Potentials	324
10.4.5	Linear vs. Cyclic Electron Flow	325
10.4.6	Chemiosmotic ATP Synthesis (Chloroplast)	325
10.4.7	Worked Example: Energy Requirements for Carbon Fixation	325
10.4.8	Worked Example: Calvin Cycle Stoichiometry	326
10.5	The Calvin Cycle (Light-Independent Reactions)	326
10.5.1	RuBisCO: Structure and Catalytic Mechanism	327
10.5.2	Carboxylation (Carbon Fixation)	328
10.5.3	Calvin-Cycle Reduction of 3-PGA	328
10.5.4	Regeneration of RuBP	328
10.5.5	Photosynthetic Stoichiometry and Energy Balance	328
10.5.6	Worked Example: Energy Efficiency of Photosynthesis	328
10.6	Photorespiration and Rubisco Oxygenase Activity	329
10.7	C3, C4, and CAM Photosynthesis	329
10.7.1	Why CO ₂ -Concentrating Mechanisms Evolved	329
10.7.2	C3 Photosynthesis (First stable product: 3-PGA)	330
10.7.3	C4 Photosynthesis (First stable product: oxaloacetate, 4C)	330
10.7.4	CAM Photosynthesis (Temporal separation)	330
10.7.5	Water-Use Efficiency	330
10.7.6	Comparing C3, C4, and CAM Photosynthesis	331
10.8	Regulation of the Calvin Cycle	331
10.8.1	The Thioredoxin/Ferredoxin Redox Regulation System	331
10.8.2	CO ₂ Concentration Effects	332
10.8.3	Stromal pH and Mg ²⁺ in the Light	333
10.8.4	CP12 Regulation of Calvin-Cycle Enzymes	333
10.9	Photoprotection: Non-Photochemical Quenching	333
10.9.1	The Three Components of NPQ	333
10.9.2	qE: The Xanthophyll Cycle in Detail	333
10.9.3	Carotenoid Quenching of Triplet States	334
10.9.4	State Transitions (qT)	334
10.9.5	Other Photoprotective Mechanisms	334
10.10	Evolutionary Origins of Photosynthesis	334
10.11	Artificial Photosynthesis and Solar Fuels	335
10.11.1	Comparison: Natural vs. Artificial Light Conversion	335
10.11.2	Why Plants Lag PV (and Why It May Not Matter)	335
10.11.3	Key Research Directions	336
10.12	Computational Bridge	336
10.12.1	Synthetic Photosynthesis and Rubisco Engineering	336
10.13	Current Evidence and Frontier Biology: Photosynthesis	338
10.13.1	Current Evidence Map: Photosynthesis Under Stress	338
10.14	Summary	339
10.15	Review Questions	339
10.16	Further Reading and Source Notes: Photosynthesis	340
10.17	Key Terms	340
10.18	Companion Source Module: Photosynthesis	340

11	Metabolic Integration and Regulation	342
11.1	Learning Objectives	342
11.1.1	Study Blueprint	342
11.2	Metabolic Pathways as Coupled Flux Networks	343
11.2.1	Fasting Physiology: Fuel Switch Timeline	344
11.3	Insulin Signaling: The PI3K/Akt/mTOR Pathway	344
11.4	Glucagon Signaling: cAMP/PKA Pathway	345
11.4.1	The Phosphorylase Kinase Cascade — A Signal Amplifier	345
11.5	Gluconeogenesis and Fasting Glucose Supply	347
11.6	Glycogen Metabolism and Rapid Glucose Storage	347
11.6.1	Glycogen Branching and Granule Architecture	347
11.6.2	Glycogen Synthase and Glycogen Phosphorylase Regulation	347
11.7	Fatty Acid Oxidation (Beta-Oxidation)	348
11.7.1	Activation and Transport	348
11.7.2	Beta-Oxidation Steps (Each Cycle)	348
11.7.3	ATP Yield from Palmitoyl-CoA (C16:0)	348
11.8	Fatty Acid Synthesis	349
11.9	Ketone Body Metabolism	349
11.10	AMPK — The Cellular Energy Gauge	349
11.10.1	AMPK Activation: LKB1 vs CaMKK β	350
11.10.2	Adenylate Energy Charge and Metabolic State	351
11.11	Worked Example: Energy Charge	351
11.12	Worked Example: Flux Control Coefficient	352
11.13	mTORC1 — The Growth Integrator and Nutrient Sensor	353
11.13.1	Amino Acid Sensing: The Ragulator Complex and Lysosome	353
11.13.2	Rapamycin: Mechanism of Action	353
11.14	The Randle Cycle (Glucose-Fatty Acid Cycle)	354
11.14.1	Metabolic Flexibility Across Feeding and Fasting	354
11.15	Hormonal Coordination at the Whole-Organism Level	354
11.16	Substrate (Futile) Cycles	355
11.17	Obesity and Metabolic Syndrome	355
11.17.1	Visceral Fat as an Endocrine Organ	355
11.18	Metabolic Control Analysis	357
11.18.1	Metabolomics: Measuring the Metabolic State	357
11.19	Computational Bridge	358
11.20	Current Evidence and Frontier Biology: Metabolic Integration and Regulation	358
11.21	Summary	358
11.22	Review Questions	359
11.23	Further Reading and Source Notes: Metabolic Integration and Regulation	360
11.24	Key Terms	360
11.25	Companion Source Module: Metabolic Integration and Regulation	360
Unit IV — Molecular Genetics: Introduction		362
Why This Unit Matters		362
Landmark Discoveries		362
Key Concepts and Connections		362
Current Evidence Thread		362
Chapter Roadmap		363
Connections Across the Textbook		363
Computational Toolbox — Unit IV		364
Cross-Unit Integration		364

12	DNA Replication and the Cell Cycle	365
12.1	Learning Objectives	365
12.1.1	Study Blueprint	365
12.2	DNA as the Genetic Material	366
12.2.1	DNA Double Helix Structure	366
12.3	DNA Replication and Genome Copying Fidelity	366
12.3.1	Origins of Replication and Licensing	367
12.3.2	The Replication Fork Machinery	368
12.3.3	Replication Fork Enzymes and Their Roles	368
12.3.4	mRNA Vaccines: A Modern Application of Nucleic Acid Technology	369
12.3.5	Leading and Lagging Strands	371
12.3.6	PCNA Sliding Clamp – The Processivity Engine	372
12.3.7	DNA Proofreading and Fidelity	372
12.3.8	Telomeres and Telomerase	372
12.4	The Cell Cycle	374
12.4.1	Cell Cycle Phases	374
12.4.2	Cyclin-CDK Complexes: The Cell Cycle Engine	375
12.4.3	Specific Checkpoint Failures in Cancer	376
12.4.4	Cell Cycle Checkpoints	377
12.4.5	The DNA Damage Response: ATM/ATR and p53	377
12.4.6	Cancer and the Cell Cycle	378
12.5	Mitosis: Molecular Events at Each Stage	379
12.6	Meiosis: Generating Genetic Diversity	380
12.6.1	Meiosis I (Reductive Division)	380
12.6.2	Meiosis II (Equational Division)	380
12.6.3	Sources of Genetic Diversity	380
12.7	DNA Damage and Repair	380
12.7.1	Types of DNA Damage	380
12.7.2	DNA Repair Pathways and Cell-Cycle Context	381
12.8	Worked Example: Telomere Shortening and the Hayflick Limit	381
12.9	Worked Example: Replication Fork Dynamics	382
12.10	Computational Bridge	382
12.11	Current Evidence and Frontier Biology: DNA Replication and the Cell Cycle	382
12.12	Summary	383
12.13	Review Questions	383
12.14	Further Reading and Source Notes: DNA Replication and the Cell Cycle	383
12.15	Key Terms	384
12.16	Companion Source Module: DNA Replication and the Cell Cycle	384
13	Gene Expression	385
13.1	Learning Objectives	385
13.1.1	Study Blueprint	386
13.2	Transcription as RNA Synthesis from DNA	386
13.2.1	Central Dogma and Information Flow in Gene Expression	386
13.2.2	Prokaryotic Transcription and Sigma-Factor Promoters	386
13.2.3	Eukaryotic Transcription and RNA Polymerase Specialization	387
13.2.4	Eukaryotic Promoter Elements	387
13.2.5	The Pre-Initiation Complex (PIC) Assembly	387
13.3	RNA Processing in Eukaryotes	389
13.3.1	5' Capping and mRNA Stability	389
13.3.2	3' Polyadenylation and Transcript Lifetime	389
13.3.3	Pre-mRNA Splicing: The Spliceosome	389

13.3.4	Alternative Splicing and Transcript Diversity	390
13.3.5	Nonsense-Mediated Decay (NMD)	390
13.4	Translation and Ribosome-Mediated Protein Synthesis	391
13.4.1	The Genetic Code	391
13.4.2	Ribosome Structure and Catalytic RNA	391
13.4.3	Translation Initiation, Elongation, and Termination	392
13.4.4	IRES Elements — Cap-Independent Translation Initiation	393
13.4.5	Ribosome Profiling — A Window Into Translation Dynamics	394
13.4.6	Nonsense-Mediated Decay (NMD) — Mechanism in Mechanistic Detail	394
13.4.7	Translation Fidelity — Mechanism and Error Rate	395
13.5	Post-Translational Modifications and Protein Degradation	396
13.5.1	Post-Translational Modifications (PTMs)	396
13.5.2	The Ubiquitin-Proteasome System	397
13.6	Gene Regulation Across DNA, RNA, and Chromatin	397
13.6.1	Prokaryotic Gene Regulation: The Lac Operon	397
13.6.2	The Trp Operon (Repressible System)	398
13.6.3	Eukaryotic Gene Regulation: Multiple Levels	398
13.6.4	RNA-Based Regulation	399
13.6.5	Epigenetic Regulation of Transcriptional State	400
13.6.6	Gene Regulation in Development: Hox Genes	400
13.7	Worked Example: Reading Frame and Protein Prediction	400
13.8	Computational Bridge	401
13.9	Current Evidence and Frontier Biology: Gene Expression	401
13.10	Summary	402
13.11	Review Questions	402
13.12	Further Reading and Source Notes: Gene Expression	402
13.13	Key Terms	403
13.14	Companion Source Module: Gene Expression	403
14	Mutations, CRISPR, and Genomics	404
14.1	Learning Objectives	404
14.1.1	Study Blueprint	404
14.2	Types of Mutations	405
14.2.1	Mutation Rates: A Quantitative Framework	405
14.2.2	Nucleotide-Level (Point) Mutations	405
14.2.3	Insertions, Deletions, and Frameshifts	406
14.2.4	Copy Number Variants and Structural Mutations	406
14.2.5	Trinucleotide Repeat Expansion Disorders	406
14.3	Mutagenic Agents and DNA-Damage Mechanisms	407
14.3.1	Physical Mutagens: Radiation and Replication Stress	407
14.3.2	Chemical Mutagens and Base-Altering Reactions	407
14.3.3	The Ames Test	408
14.4	DNA Damage and Repair	408
14.4.1	DNA Damage — Quantitative Background	408
14.4.2	DNA Repair Pathway Specificity and Disease Consequences	409
14.4.3	Base Excision Repair (BER) — Mechanism in Detail	410
14.4.4	Comparing NER and MMR — A Side-by-Side Table	411
14.4.5	HR vs NHEJ — Pathway Choice Mechanism	412
14.5	CRISPR-Cas9: Mechanism and Applications	413
14.5.1	Natural CRISPR Immunity	413
14.5.2	Engineered CRISPR-Cas9	413
14.5.3	Beyond Cas9: Expanded Toolkit	413

14.5.4	Therapeutic Applications (2024-2025)	414
14.6	Genomics: The Human Genome	414
14.6.1	Human Genome Composition	415
14.6.2	Transposable Elements — Mechanism and Genomic Impact	415
14.6.3	Structural Variants — Inversions, CNVs, and Disease	416
14.6.4	Genomic Variation Across SNVs, Structural Variants, and Haplotypes	417
14.6.5	The ENCODE Project	417
14.7	Next-Generation Sequencing Technologies	417
14.7.1	Pangenome Graph Reasoning	418
14.8	Genome-Wide Association Studies (GWAS)	418
14.9	Comparative Genomics and Molecular Evolution	419
14.9.1	Mutation Rates — Spontaneous vs Induced	419
14.10	Personal Genomics and Ethical Issues	421
14.10.1	Pharmacogenomics and Evidence-Governed Prescribing	421
14.10.2	Ethical Considerations in Personal and Clinical Genomics	421
14.11	Worked Example: Per-Gene De Novo Mutation Probability	422
14.12	Worked Example: Mutation Analysis	422
14.13	Computational Bridge	423
14.13.1	Post-Approval CRISPR Therapeutics: Casgevy and the Safety Frontier	423
14.13.2	The Telomere-to-Telomere (T2T) Consortium: A Truly Complete Human Genome	423
14.14	Current Evidence and Frontier Biology: Mutations, CRISPR, and Genomics	424
14.14.1	Current Evidence Map: Genome Editing From Variant to Follow-Up	424
14.15	Summary	424
14.16	Review Questions	425
14.17	Further Reading and Source Notes: Mutations, CRISPR, and Genomics	425
14.18	Key Terms	425
14.19	Companion Source Module: Mutations, CRISPR, and Genomics	426
15	Chromatin and Epigenetic Mechanisms	427
15.1	Learning Objectives	427
15.1.1	Study Blueprint	427
15.2	Chromatin Structure and Nucleosome Organization	429
15.2.1	The Nucleosome as the Fundamental Chromatin Unit	429
15.2.2	Higher-Order Chromatin Compaction	429
15.2.3	Topologically Associating Domains (TADs)	430
15.2.4	A/B Compartments	430
15.3	Histone Modifications — The Histone Code	431
15.3.1	Histone-Code Reference Table	431
15.3.2	Histone Acetylation and Open Chromatin	433
15.3.3	Histone Methylation and Context-Dependent Silencing or Activation	434
15.3.4	Phosphorylation and Ubiquitination	434
15.4	Polycomb and Trithorax — Cellular Memory Systems	435
15.4.1	Polycomb Repressive Complexes — Structural Detail	435
15.4.2	Trithorax Group (TrxG) — Antagonising Polycomb	435
15.5	DNA Methylation and Stable Transcriptional Repression	437
15.5.1	CpG Methylation Mechanism	437
15.5.2	The DNA Methylation Machinery — In Depth	437
15.5.3	CpG Islands and Gene Regulation	438
15.5.4	Quantitative Maintenance Through Replication	438
15.6	Genomic Imprinting — Mechanisms and Reciprocal Phenotypes	440
15.6.1	Imprint Control Regions (ICRs) — The Master Switch	440
15.6.2	The IGF2/H19 Locus — Insulator-based Imprinting (Detailed Mechanism)	440

15.6.3	The 15q11–q13 Locus — Prader–Willi / Angelman Mechanism	441
15.6.4	Beckwith–Wiedemann and Silver–Russell — Reciprocal Disorders	441
15.7	X-Chromosome Inactivation (Lyonization) — In Depth	441
15.8	Chromatin Remodeling Complexes — Mechanism in Detail	443
15.8.1	The Four Major Remodeller Families	443
15.8.2	SWI/SNF Specifically — The Cancer-Most-Mutated Remodeller	444
15.8.3	Targeted Epigenome Editing with dCas9 Fusions	444
15.9	Current Evidence and Frontier Biology: Chromatin and Epigenetic Mechanisms	445
15.9.1	Current Evidence Map: Epigenetic Causality Ladder	446
15.10	Summary	446
15.11	Further Reading and Source Notes: Chromatin and Epigenetic Mechanisms	446
15.12	Companion Source Module: Chromatin and Epigenetic Mechanisms	446
16	Epigenetic Inheritance and Disease	448
16.1	Learning Objectives	448
16.2	Three-Dimensional Genome Organization and Phase Separation	448
16.2.1	TADs, Loops, and Compartments — Spatial Layers	448
16.2.2	Biomolecular Condensates and Phase Separation	448
16.2.3	Study Blueprint	450
16.3	Non-Coding RNAs in Gene Regulation	450
16.3.1	MicroRNAs (miRNAs) and Post-Transcriptional Repression	450
16.3.2	Long Non-Coding RNAs (lncRNAs)	451
16.3.3	Small Interfering RNAs (siRNAs) and piRNAs	451
16.4	Epigenetic Reprogramming and Inheritance	451
16.4.1	Mitotic Heritability of Epigenetic Marks — Detailed Mechanism	451
16.4.2	Germline Reprogramming and Epigenetic Resetting	452
16.4.3	Evidence for Transgenerational Epigenetic Inheritance in Humans	452
16.5	Cancer Epigenetics and Clinical Translation	453
16.5.1	The Cancer Epigenome — Two Concurrent Patterns	453
16.5.2	Approved and Investigational Epigenetic Drugs	453
16.5.3	Clinical Trial Vignettes — Three Paradigm Therapies	454
16.5.4	A Checklist for Interpreting Cancer Epigenomes	455
16.6	Computational Bridge	456
16.7	Current Evidence and Frontier Biology: Epigenetic Inheritance and Disease	457
16.7.1	Current Evidence Map: Epigenetic Causality Ladder	457
16.8	Summary	458
16.9	Review Questions	458
16.10	Further Reading and Source Notes: Epigenetic Inheritance and Disease	459
16.11	Key Terms	459
16.12	Discussion Questions	460
16.13	Companion Source Module: Epigenetic Inheritance and Disease	461
Unit V — Classical Genetics and Heredity: Introduction		462
Why This Unit Matters		462
Landmark Discoveries		462
Key Concepts and Connections		462
Current Evidence Thread		462
Chapter Roadmap		463
Connections Across the Textbook		463
Computational Toolbox — Unit V		463
Cross-Unit Integration		464
17	Mendelian Principles and Probability	465

17.1	Learning Objectives	465
17.1.1	Study Blueprint	465
17.2	Mendel’s Experiments: Historical Context	465
17.3	Mendel’s Laws of Segregation and Independent Assortment	467
17.3.1	Law of Segregation (Mendel’s First Law)	467
17.3.2	The Molecular Basis of Mendel’s Laws: From Bivalents to Binomials	467
17.3.3	Law of Independent Assortment (Mendel’s Second Law)	468
17.4	Monohybrid Crosses and Single-Gene Segregation	468
17.4.1	The Standard Monohybrid Cross	468
17.4.2	The Testcross as a Genotype-Revealing Cross	469
17.4.3	Probability Rules for Independent Genetic Events	469
17.5	Worked Example: Probability Rules in a Monohybrid Cross	469
17.6	Dihybrid and Trihybrid Crosses	470
17.6.1	The Dihybrid Cross	470
17.6.2	The Forked-Line (Branch Diagram) Method	470
17.7	Worked Example: Trihybrid Cross Probabilities	470
17.8	Current Evidence and Frontier Biology: Mendelian Principles and Probability	471
17.9	Summary	471
17.10	Further Reading and Source Notes: Mendelian Principles and Probability	471
17.11	Companion Source Module: Mendelian Principles and Probability	471
18	Mendelian Extensions and Human Genetics	473
18.1	Learning Objectives	473
18.2	Extensions to Mendelian Genetics	473
18.2.1	Incomplete Dominance and Dosage-Sensitive Phenotypes	473
18.2.2	Codominance and Joint Allelic Expression	473
18.2.3	Multiple Alleles and Population-Level Variation	473
18.2.4	Pleiotropy and Multi-Trait Gene Effects	474
18.2.5	Epistasis: When One Gene Masks Another	474
18.2.6	Polygenic Inheritance and Quantitative Traits	476
18.2.7	Penetrance and Expressivity	477
18.2.8	Genomic Imprinting and Parent-of-Origin Effects	478
18.2.9	Maternal Effect Genes	478
18.2.10	Study Blueprint	478
18.3	Human Genetic Disorders: Mechanism Meets Mendel	479
18.3.1	Autosomal Dominant Disorders: Huntington’s Disease and CAG Repeat Expansion	479
18.3.2	Autosomal Recessive Disorders: PKU and the Logic of Newborn Screening	479
18.3.3	Other key autosomal disorders	480
18.3.4	Achondroplasia and Marfan as Autosomal Dominant Models	481
18.3.5	X-linked disorders: the molecular basis of male susceptibility	481
18.4	GWAS: Mendel Meets the Genome	483
18.4.1	How GWAS works	483
18.4.2	What GWAS has revealed	484
18.4.3	Polygenic risk scores (PRS)	484
18.4.4	GWAS as the modern face of Mendel’s program	485
18.4.5	The Manhattan Plot and Genome-Wide Significance	485
18.4.6	Polygenic Risk Scores: Detailed Example	485
18.4.7	Clinical Interpretation and Governance Checkpoint	485
18.5	The Chi-Squared (χ^2) Test	486
18.5.1	Formula and Procedure	486
18.5.2	Worked Example: Chi-Squared Test for a 3:1 Ratio	486
18.5.3	Worked Example: Dihybrid Chi-Squared Test	487

18.6	Pedigree Analysis and Inheritance-Pattern Inference	487
18.6.1	Pedigree Symbols and Conventions	487
18.6.2	Inheritance Pattern Recognition	487
18.6.3	Worked Pedigree Problem	488
18.7	Worked Example: Conditional Probability in Pedigrees	488
18.8	Worked Example: Complex Multi-Locus Genetics	488
18.9	Computational Bridge	489
18.10	Current Evidence and Frontier Biology: Mendelian Extensions and Human Genetics	490
18.11	Summary	490
18.12	Review Questions	490
18.13	Further Reading and Source Notes: Mendelian Extensions and Human Genetics	491
18.14	Key Terms	491
18.15	Companion Source Module: Mendelian Extensions and Human Genetics	492
19	Chromosomal Inheritance and Linkage	493
19.1	Learning Objectives	493
19.1.1	Study Blueprint	493
19.2	The Chromosome Theory of Heredity	493
19.3	Chromosome Architecture: The Hardware of Heredity	494
19.3.1	Centromeres and Kinetochore Attachment	494
19.3.2	Telomeres and Chromosome-End Protection	494
19.3.3	Euchromatin and Heterochromatin	494
19.4	Meiosis vs. Mitosis: Two Cell-Division Programs	495
19.4.1	Molecular details of meiotic recombination	495
19.5	Sex Chromosomes and Sex Determination	497
19.5.1	Mammalian Sex Determination (XX/XY)	497
19.5.2	Non-Mammalian Sex Determination	498
19.6	X-Inactivation and Dosage Compensation	498
19.6.1	Lyon Hypothesis and X-Inactivation	498
19.6.2	Molecular Mechanism of X-Inactivation	498
19.6.3	Dosage Compensation Across Species and Beyond Sex Chromosomes	498
19.7	X-Linked Inheritance	500
19.7.1	X-Linked Recessive Inheritance	500
19.8	Worked Example: X-Linked Recessive Inheritance	500
19.9	Linkage and Recombination	501
19.9.1	Morgan’s Experiments	501
19.9.2	Map Distance and Recombination Frequency	501
19.9.3	Three-Point Test Cross	502
19.10	Worked Example: Three-Point Test Cross in <i>Drosophila</i>	502
19.10.1	Mapping Functions and Recombination Interference	503
19.10.2	LOD Score Analysis	503
19.10.3	Recombination Hotspots and Sex Differences in Map Length	503
19.11	Chromosomal Abnormalities and Dosage Imbalance	504
19.11.1	Aneuploidy: Non-Disjunction in Meiosis I vs. Meiosis II	504
19.11.2	Structural Chromosomal Rearrangements: Detailed Survey	506
19.12	Genomic Imprinting and Uniparental Disomy	510
19.12.1	The principle of imprinting	510
19.12.2	Canonical imprinted regions	510
19.12.3	Mechanisms causing imprinting disorders	510
19.12.4	Connection to chromosome behavior	511
19.13	Recombination Mapping: Physical vs. Genetic Distance	511
19.14	Inbreeding and the Inbreeding Coefficient	511

19.14.1	The Inbreeding Coefficient (F)	511
19.14.2	Consequences of Inbreeding	512
19.15	Worked Example: Linkage Analysis	512
19.16	Computational Bridge	513
19.17	Current Evidence and Frontier Biology: Chromosomal Inheritance and Linkage	513
19.18	Summary	513
19.19	Review Questions	514
19.20	Further Reading and Source Notes: Chromosomal Inheritance and Linkage	514
19.21	Key Terms	514
19.22	Companion Source Module: Chromosomal Inheritance and Linkage	515
20	Population Genetics	516
20.1	Learning Objectives	516
20.1.1	Study Blueprint	516
20.1.2	Chapter Roadmap for Population-Genetic Forces	517
20.2	The Gene Pool as Population-Level Genetic Variation	517
20.2.1	Allele and Genotype Frequencies	517
20.3	Worked Example: Allele Frequencies from Genotype Counts	518
20.4	Hardy-Weinberg Equilibrium	518
20.4.1	Deriving Hardy-Weinberg Genotype Frequencies	518
20.4.2	Testing for Hardy-Weinberg Equilibrium	519
20.4.3	HWE as a Clinical Tool	520
20.5	Worked Example: Cystic Fibrosis Carrier Frequency	520
20.6	Natural Selection and Allele-Frequency Change	521
20.6.1	Fitness and Selection	521
20.6.2	Change in Allele Frequency Under Selection	521
20.7	Worked Example: Recessive Deleterious Allele	521
20.7.1	Types of Selection	522
20.7.2	Heterozygote Advantage (Balancing Selection)	522
20.8	Genetic Drift in Finite Populations	523
20.8.1	Wright-Fisher Model	523
20.8.2	Effective Population Size (N_e)	523
20.8.3	Bottleneck and Founder Effects	525
20.9	Gene Flow (Migration)	525
20.9.1	One-Island Model	525
20.9.2	Measuring Population Differentiation: F_{ST}	526
20.9.3	Interpreting F_{ST} in Human Populations	526
20.10	Mutation-Selection Balance and New Variation	527
20.10.1	Mutation-Selection Balance	527
20.11	Worked Example: Mutation-Selection Balance	527
20.12	Molecular Evolution and Sequence Substitution	528
20.12.1	Neutral Theory [Kimura, 1968]	528
20.12.2	The Nearly Neutral Theory	528
20.12.3	Ka/Ks (dN/dS) Ratio	528
20.13	Population Structure and Ancestry Inference	528
20.13.1	Wright's F-Statistics	528
20.13.2	Population Structure Inference with STRUCTURE	528
20.14	Coalescent Theory and Genealogy Backward in Time	529
20.14.1	The Coalescent Framework	529
20.14.2	Molecular Clocks in Population Genetics	529
20.15	Worked Example: Molecular Clock Estimate	529
20.16	Worked Example: Combined Population-Genetics Calculations	530

20.17	Computational Bridge	530
20.18	Current Evidence and Frontier Biology: Population Genetics	531
20.18.1	Current Evidence Map: Ancestry-Aware Variant Interpretation	531
20.19	Summary	531
20.20	Review Questions	531
20.21	Further Reading and Source Notes: Population Genetics	532
20.22	Key Terms	532
20.23	Companion Source Module: Population Genetics	532
Unit VI — Evolution: Introduction		534
Why This Unit Matters		534
Landmark Discoveries		534
Key Concepts and Connections		534
Current Evidence Thread		534
Chapter Roadmap		535
Connections Across the Textbook		535
Computational Toolbox — Unit VI		536
Cross-Unit Integration		536
21	Natural Selection and Adaptation	537
21.1	Learning Objectives	537
21.1.1	Study Blueprint	537
21.2	Historical Context of Evolutionary Thought	537
21.2.1	Pre-Darwinian Ideas	537
21.2.2	Darwin’s Voyage on HMS Beagle (1831–1836)	538
21.2.3	Wallace’s Independent Discovery	538
21.2.4	The Three Conditions for Natural Selection	538
21.2.5	The Modern Synthesis and Beyond	538
21.3	Evidence for Evolution Across Fossils, Genomes, and Development	539
21.3.1	Fossil Record and Temporal Sequence Evidence	539
21.3.2	Comparative Anatomy and Homology	539
21.3.3	Embryology and Developmental Homology	539
21.3.4	Biogeography and Historical Dispersal	540
21.3.5	Molecular Evidence from Sequence Similarity and Shared Variants	540
21.4	Mechanisms of Natural Selection	541
21.4.1	Fitness as Reproductive Success in Context	541
21.4.2	Directional Selection and Trait-Mean Shifts	542
21.4.3	Worked Example: Estimating the Selection Coefficient	543
21.4.4	Stabilizing Selection and Intermediate Optima	543
21.4.5	Disruptive (Diversifying) Selection	543
21.4.6	Worked Example: Selection Coefficient and Allele Frequency Dynamics	544
21.4.7	Sexual Selection and Mating Success	544
21.4.8	Kin Selection and Inclusive Fitness	546
21.4.9	Evolutionary Game Theory: Hawk–Dove and the ESS	546
21.4.10	The Breeder’s Equation	547
21.4.11	Worked Example: Response to Selection Over Multiple Generations	548
21.4.12	Evolvability, Modularity, and Developmental Constraints	549
21.4.13	Frequency-Dependent Selection	549
21.4.14	Balancing Selection and Maintained Polymorphism	550
21.5	Adaptation and Its Limits	551
21.5.1	Adaptation and Exaptation	551
21.5.2	Phylogenetic Constraints on Adaptive Pathways	551

21.5.3	Developmental Constraints on Phenotypic Variation	551
21.5.4	Evolutionary Trade-Offs and Constraint Surfaces	551
21.5.5	Coevolution and Reciprocal Selection	552
21.6	Macroevolution and Evolutionary Rates	552
21.6.1	Microevolution and Macroevolution	552
21.6.2	Punctuated Equilibrium and Tempo of Change	552
21.6.3	Evolutionary Novelties and Key Innovations	553
21.6.4	Mass Extinctions and Selective Regime Shifts	553
21.6.5	The Modern Extended Evolutionary Synthesis	554
21.7	Evolution Observed in Real Time	555
21.7.1	Laboratory Evolution as Experimental Selection	555
21.7.2	Natural Experiments in Contemporary Evolution	556
21.7.3	Punctuated Equilibrium versus Phyletic Gradualism: Empirical Signatures	556
21.7.4	Species Selection: Macroevolution as a Higher-Level Process	556
21.8	Computational Bridge	557
21.8.1	Evolution in the Synthetic Age: CRISPR Gain-of-Function Research and Evolutionary Ethics	557
21.9	Current Evidence and Frontier Biology: Natural Selection and Adaptation	558
21.10	Summary	558
21.11	Key Terms	558
21.12	Review Questions	559
21.13	Companion Source Module: Natural Selection and Adaptation	560
22	Genetic Drift, Gene Flow, and Speciation	561
22.1	Learning Objectives	561
22.1.1	Study Blueprint	562
22.2	Genetic Drift as Random Allele-Frequency Change	562
22.2.1	Genetic Drift as Sampling Error in Finite Populations	562
22.2.2	Wright-Fisher Sampling Mathematics	562
22.2.3	Effective Population Size	563
22.2.4	Worked Example: Effective Population Size	564
22.2.5	The Neutral Theory and Nearly Neutral Theory	564
22.2.6	Bottleneck Effect and Loss of Variation	564
22.2.7	Founder Effect and Colonization History	565
22.2.8	Worked Example: Effective Population Size with Unequal Sex Ratio	566
22.3	Gene Flow and Mutation	567
22.3.1	Gene Flow as Migration-Mediated Allele Exchange	567
22.3.2	Measuring Population Differentiation: F_{ST}	567
22.3.3	Isolation by Distance	567
22.3.4	Secondary Contact and Hybrid Zones	567
22.3.5	Coalescent Theory and the TMRCA	568
22.3.6	Mutation as the Ultimate Source of Variation	569
22.3.7	Mutation-Selection Balance	570
22.4	Species Concepts and the Boundaries of Lineages	570
22.4.1	Biological Species Concept (BSC)	570
22.4.2	Morphological/Typological Species Concept	570
22.4.3	Phylogenetic Species Concept (PSC)	571
22.4.4	Ecological Species Concept	571
22.4.5	Cohesion Species Concept	571
22.4.6	Ring Species and Gradual Reproductive Isolation	571
22.5	Speciation Mechanisms Across Geography and Gene Flow	571
22.5.1	Allopatric Speciation by Geographic Isolation	571
22.5.2	Peripatric Speciation in Small Peripheral Populations	572

22.5.3	Parapatric Speciation Along Environmental Gradients	572
22.5.4	Sympatric Speciation Without Geographic Separation	572
22.6	Reproductive Isolation Before and After Fertilization	574
22.6.1	Haldane’s Rule	574
22.6.2	Prezygotic Barriers to Mating or Fertilization	574
22.6.3	Postzygotic Barriers to Hybrid Fitness	575
22.6.4	Reinforcement by Selection Against Hybrids	575
22.6.5	Hybridization and Introgression	575
22.7	Adaptive Radiation and Ecological Opportunity	576
22.7.1	Hawaiian Honeycreepers as Island Adaptive Radiation	576
22.7.2	Cichlid Fish in African Great Lakes	576
22.7.3	Galapagos Finches and Beak-Trait Diversification	577
22.7.4	Mammalian Radiation After K-Pg Extinction	577
22.8	Computational Bridge	577
22.8.1	Worked Example: Kimura’s Neutral Fixation Probability	578
22.9	Current Evidence and Frontier Biology: Genetic Drift, Gene Flow, and Speciation	578
22.10	Summary	578
22.11	Key Terms	579
22.12	Review Questions	579
22.13	Companion Source Module: Genetic Drift, Gene Flow, and Speciation	580
23	Phylogenetics and the Tree of Life	581
23.1	Learning Objectives	581
23.1.1	Study Blueprint	581
23.2	What Phylogenetics Reveals About Shared History	581
23.2.1	Applications Beyond Systematics	583
23.2.2	Phylogenetic Diversity and the EDGE Framework	583
23.3	Tree Terminology and Reading Phylogenies	583
23.3.1	Fundamental Tree Components	583
23.3.2	Paraphyletic and Polyphyletic Groups	584
23.3.3	Character Types and Phylogenetic Signal	584
23.3.4	Rooting Trees with Outgroups and Clocks	585
23.3.5	Reading Trees Correctly	585
23.3.6	Eusociality as a Character on a Tree	586
23.4	Phylogenetic Reconstruction Methods	586
23.4.1	Distance-Based Tree Reconstruction: UPGMA and Neighbor-Joining	586
23.4.2	Worked Example: One UPGMA Clustering Step from a Distance Matrix	586
23.4.3	Maximum Parsimony and Minimum-Change Trees	587
23.4.4	Worked Example: Computing a Parsimony Score for a Small Character Matrix	587
23.4.5	Maximum Likelihood (ML)	588
23.4.6	Bayesian Inference and Posterior Tree Distributions	589
23.4.7	Bootstrap Analysis and Branch-Support Uncertainty	589
23.4.8	Gene Tree versus Species Tree Discordance	590
23.4.9	Worked Example: Molecular Clock Calibration — Cytochrome b in Mammals	591
23.5	Molecular Clocks and Divergence-Time Estimation	592
23.5.1	The Molecular Clock Hypothesis	592
23.5.2	Clock Calculations from Sequence Divergence	592
23.5.3	Worked Example: Estimating Divergence Time using Jukes-Cantor	592
23.5.4	Rate Calibration with Fossils and Tip Dates	593
23.5.5	Strict vs. Relaxed Clocks	593
23.5.6	Molecular Clock Limitations: Rate Heterogeneity, Generation Time, and Saturation	593
23.5.7	Tip Dating and Bayesian Skyline Plots	593

23.5.8	A timeline of major events in life’s phylogeny	593
23.5.9	Ancestral Sequence Reconstruction (ASR)	595
23.5.10	Domain Bacteria and Prokaryotic Phylogenetic Diversity	596
23.5.11	Domain Archaea and the Eukaryote Connection	596
23.5.12	Domain Eukarya and Endosymbiotic Origins	597
23.5.13	Endosymbiotic Theory in Tree-of-Life Reconstruction	597
23.5.14	Horizontal Gene Transfer and the Web of Life	597
23.6	Human Phylogeny and Hominin Evolution	598
23.6.1	Great Apes and Molecular Phylogeny	598
23.6.2	Fossil Hominins and Mosaic Human Evolution	599
23.6.3	Out of Africa	599
23.6.4	Archaic Introgression from Neanderthals and Denisovans	599
23.7	Computational Bridge	600
23.7.1	Long-Read Sequencing and Deep-Divergence Phylogenetics	600
23.8	Current Evidence and Frontier Biology: Phylogenetics and the Tree of Life	601
23.9	Summary	601
23.10	Key Terms	601
23.11	Review Questions	602
23.12	Companion Source Module: Phylogenetics and the Tree of Life	603
	Unit VII — Microbiology: Introduction	604
	Why This Unit Matters	604
	Landmark Discoveries	604
	Key Concepts and Connections	604
	Current Evidence Thread	604
	Chapter Roadmap	605
	Connections Across the Textbook	605
	Computational Toolbox — Unit VII	605
	Cross-Unit Integration	606
24	Bacteria, Archaea, and Viruses	607
24.1	Learning Objectives	607
24.1.1	Study Blueprint	607
24.2	Bacteria – Domain Overview and Cell Structure	607
24.2.1	The Three Domains of Life	607
24.2.2	Prokaryotic Cell Features	609
24.2.3	Bacterial Cell Wall: Peptidoglycan	609
24.2.4	Peptidoglycan Biosynthesis: A Step-by-Step Antibiotic Atlas	609
24.2.5	Gram Staining: The Foundational Diagnostic Test	611
24.3	Bacterial Morphology and Metabolic Diversity	612
24.3.1	Morphology and Arrangement	612
24.3.2	Metabolic Diversity and Energy Harvesting	612
24.3.3	Major Pathogenic Groups	613
24.4	Bacterial Genetics, Signaling and Sociality	613
24.4.1	Binary Fission and Exponential Growth	613
24.4.2	Worked Example: Calculating Bacterial Growth	614
24.4.3	Worked Example: Inferring Generation Time from an OD Growth Curve	614
24.4.4	Horizontal Gene Transfer	615
24.4.5	Plasmids and Mobile Genetic Elements	615
24.4.6	Two-Component Signal Transduction	616
24.4.7	Biofilms and Quorum Sensing	617
24.4.8	Endospores and Dormancy Under Stress	618

24.5	Archaea and Extremophile Cell Biology	618
24.5.1	Distinguishing Archaeal Features	618
24.5.2	Archaeal Lipid Biochemistry: Why Hot Vents Don't Melt Membranes	618
24.5.3	Major Archaeal Groups	619
24.5.4	Asgard Archaea: The Closest Living Relatives of Eukaryotes	619
24.5.5	Archaeal Biotechnology and Thermostable Enzymes	620
24.6	Viruses as Genome-Delivery Replicators	621
24.6.1	Viral General Features and Host Dependence	621
24.6.2	Baltimore Classification by Genome Type and Replication Strategy	621
24.6.3	Bacteriophage Life Cycles	621
24.6.4	Animal Virus Replication	623
24.6.5	The HIV Life Cycle	623
24.6.6	Prions and Protein-Based Infectious States	623
24.6.7	Phage Therapy: A Pre-Antibiotic Idea Returns to the Clinic	624
24.7	Antibiotic Mechanisms and Resistance	625
24.7.1	Antibiotic Classes by Mechanism	625
24.7.2	Selective Toxicity and Therapeutic Index	626
24.7.3	Resistance Mechanisms in Detail	626
24.7.4	WHO Priority Pathogens (ESKAPE)	626
24.8	CRISPR-Cas: Bacterial Adaptive Immunity	627
24.8.1	Stage 1 — Spacer Acquisition (Adaptation)	627
24.8.2	Stage 2 — crRNA Biogenesis	627
24.8.3	Stage 3 — Interference (Targeting)	628
24.8.4	Anti-CRISPR Proteins	628
24.8.5	Worked Example: Designing a CRISPR-Cas9 Guide RNA for Targeted Cleavage	629
24.9	Computational Bridge	630
24.9.1	SARS-CoV-2 Variant Evolution: Real-Time Darwin in a Global Population	630
24.10	Current Evidence and Frontier Biology: Bacteria, Archaea, and Viruses	630
24.10.1	Current Evidence Map: AMR Movement Across One Health	631
24.11	Summary	631
24.12	Key Terms	631
24.13	Review Questions	633
24.14	Further Reading and Source Notes: Bacteria, Archaea, and Viruses	634
24.15	Companion Source Module: Bacteria, Archaea, and Viruses	634
25	Microbial Ecology and the Microbiome	635
25.1	Learning Objectives	635
25.1.1	Study Blueprint	636
25.2	Measuring Microbial Communities Across Scales	636
25.2.1	The Great Plate Count Anomaly	636
25.2.2	Culture-Independent Methods	636
25.2.3	The 16S rRNA Amplicon Pipeline: From Sample to ASV Table	637
25.2.4	OTU vs ASV: A Decade-Long Methodological Shift	638
25.2.5	Other Omics Layers	638
25.2.6	Diversity Metrics for Microbial Communities	639
25.2.7	Worked Example: Estimating Species Richness using Chao1	640
25.2.8	Worked Example: Species-Area Relationship for Marine Microbial Communities	641
25.3	The Human Microbiome	642
25.3.1	Human Microbiome Scale, Body-Site Ecology, and Gene Content	642
25.3.2	Gut Microbiome Gradients and Functional Guilds	642
25.3.3	Core vs Variable Microbiome and the F/B Ratio	642
25.3.4	Oral Microbiome and Biofilm Niches	643

25.3.5	Skin Microbiome Across Moist, Dry, and Sebaceous Sites	643
25.3.6	Vaginal Microbiome and Lactobacillus-Dominated Protection	643
25.4	Microbiome Functions and Host Interactions	643
25.4.1	Microbiome–Host Molecular Communication	643
25.4.2	Metabolic Functions of Microbial Communities	644
25.4.3	Immune Development Shaped by Early Microbial Exposure	645
25.4.4	Gut-Brain Axis	645
25.4.5	Colonization Resistance Against Pathogen Invasion	646
25.5	Dysbiosis and Disease	646
25.6	Environmental Microbiology Across Soil, Ocean, and Biofilms	647
25.6.1	Soil Microbiology and Rhizosphere Processes	647
25.6.2	Termite Guts as Lignocellulose Bioreactors	647
25.6.3	Marine and Environmental Microbiome Diversity	647
25.6.4	Microbial Biogeochemistry in Carbon, Nitrogen, and Sulfur Cycles	648
25.6.5	Phage–Host Dynamics: Kill-the-Winner	649
25.6.6	Biofilms as Structured Microbial Communities	649
25.6.7	Quorum Sensing and Density-Dependent Gene Regulation	650
25.6.8	Bioremediation and Engineered Microbial Metabolism	650
25.7	Microbial Biotechnology for Production and Environmental Engineering	651
25.7.1	Industrial Fermentation and Metabolic Control	651
25.7.2	Recombinant Protein Production	652
25.7.3	Environmental Biotechnology and Waste-Stream Remediation	652
25.8	Computational Bridge	652
25.9	Current Evidence and Frontier Biology: Microbial Ecology and the Microbiome	653
25.9.1	Current Evidence Map: Microbiome Causality Ladder	653
25.10	Summary	653
25.11	Key Terms	654
25.12	Review Questions	655
25.13	Further Reading and Source Notes: Microbial Ecology and the Microbiome	656
25.14	Companion Source Module: Microbial Ecology and the Microbiome	656
26	Host Immunity and Vaccines	657
26.1	Learning Objectives	657
26.1.1	Study Blueprint	657
26.2	Host-Pathogen Relationships and Virulence	657
26.2.1	Koch’s Postulates	657
26.2.2	Molecular Koch’s Postulates	659
26.2.3	The Infection Continuum	659
26.2.4	Virulence Factors and Host-Tissue Damage	659
26.2.5	Toxins and Molecular Mechanisms of Pathogenesis	660
26.3	Innate Immunity and Rapid Pattern Recognition	660
26.3.1	Physical and Chemical Barriers	660
26.3.2	Pattern Recognition Receptors (PRRs)	661
26.3.3	The Complement System: Three Pathways, One Cascade	661
26.3.4	Phagocytosis and Cellular Effectors	663
26.3.5	Worked Example: Quantifying the Neutrophil Oxidative Burst	663
26.3.6	Inflammation and Vascular Recruitment of Immune Cells	664
26.4	Adaptive Immunity: Antigen Presentation, T Cells, and Clonal Specificity	665
26.4.1	MHC Molecules and Antigen Presentation	665
26.4.2	T Cell Activation and Differentiation	665
26.5	B Cells and Antibodies	666
26.5.1	B Cell Activation	666

26.5.2	Germinal Center Reaction	666
26.5.3	Antibody Structure and Function	666
26.5.4	Antibody Classes and Effector Functions	667
26.6	Vaccines and Immunological Memory	668
26.6.1	Vaccine Platforms: Eight Strategies for Inducing Memory	668
26.6.2	Antigenic Variation: How Pathogens Outpace Antibody Responses	669
26.6.3	Herd Immunity and Population-Level Protection	670
26.6.4	Worked Example: Calculating Herd Immunity Threshold (Three Pathogens)	671
26.6.5	R_0 Comparison: Why Pathogens Differ	671
26.6.6	Adjuvants and Innate Immune Activation	672
26.7	Current Evidence and Frontier Biology: Host Immunity and Vaccines	673
26.7.1	Current Evidence Map: Intervention Choice Across Pathogens	673
26.8	Summary	673
26.9	Further Reading and Source Notes: Host Immunity and Vaccines	674
26.10	Companion Source Module: Host Immunity and Vaccines	674
27	Antimicrobial Resistance and Epidemiology	675
27.1	Learning Objectives	675
27.2	Antibiotic Resistance Mechanisms in Multidrug-Resistant Pathogens	675
27.2.1	Mechanism 1: Enzymatic Inactivation	675
27.2.2	Mechanism 2: Target Modification	676
27.2.3	Mechanism 3: Efflux Pumps	677
27.2.4	Mechanism 4: Reduced Permeability	677
27.2.5	Mechanism 5: Bypass / Target Overproduction	677
27.2.6	Resistance in Action: A Pan-Resistant <i>Klebsiella pneumoniae</i>	677
27.2.7	Study Blueprint	678
27.3	Epidemiology of antimicrobial resistance and epidemiology	678
27.3.1	Key Epidemiological Metrics	678
27.3.2	Worked Example: Estimating R_0 from an Epidemic Curve	679
27.3.3	Worked Example: Herd Immunity Threshold and Required Vaccination Coverage	679
27.3.4	Major antimicrobial resistance and epidemiologys	680
27.3.5	One Health and Emerging Pathogens	682
27.4	Computational Bridge	684
27.4.1	mRNA Vaccine Platforms: From Lab Curiosity to Global Deployment	684
27.4.2	cGAS–STING: Innate Cytosolic DNA Sensing and Anti-Tumor Immunity	684
27.5	Current Evidence and Frontier Biology: Antimicrobial Resistance and Epidemiology	684
27.5.1	Current Evidence Map: Intervention Choice Across Pathogens	685
27.6	Summary	685
27.7	Review Questions	686
27.8	Further Reading and Source Notes: Antimicrobial Resistance and Epidemiology	687
27.9	Key Terms	687
27.10	Companion Source Module: Antimicrobial Resistance and Epidemiology	688
Unit VIII — Botany — Plant Biology: Introduction		689
Why This Unit Matters		689
Landmark Discoveries		689
Key Concepts and Connections		689
Current Evidence Thread		689
Chapter Roadmap		690
Connections Across the Textbook		690
Computational Toolbox — Unit VIII		691
Cross-Unit Integration		691

28	Plant Structure and Water Relations	692
28.1	Learning Objectives	692
28.1.1	Study Blueprint	692
28.2	The Plant Body Plan	692
28.2.1	Root System Architecture and Soil Exploration	692
28.2.2	Plant Architecture: Phytomers and Plastochrons	694
28.2.3	Shoot System Architecture and Light Capture	694
28.2.4	Leaf Anatomy for Gas Exchange and Photosynthesis	694
28.3	Plant Tissue Systems	695
28.3.1	Dermal Tissue System	695
28.3.2	Ground Tissue System	695
28.3.3	Vascular Tissue System – Xylem in Detail	695
28.4	Water Relations – Water Potential	697
28.4.1	Worked Example: Calculating Water Potential	697
28.4.2	Worked Example: A Leaf Cell at Dawn vs Midday	697
28.4.3	Quantitative Turgor Relations and Plasmolysis	698
28.5	Water Transport Pathways	699
28.5.1	Apoplast vs Symplast Pathways	699
28.5.2	Root Anatomy in Depth — The Endodermis as Filter	699
28.6	Transpiration and the Cohesion-Tension Mechanism	700
28.6.1	Historical Context: The Birth of Cohesion-Tension Theory [Dixon and Joly, 1894]	700
28.6.2	Detailed TACT Mechanism	700
28.6.3	Cohesion-Tension Theory: Embolism Evidence and Synchrotron Imaging	700
28.6.4	Xylem Transport Parameters	702
28.6.5	Cavitation and Embolism	702
28.6.6	Worked Example: Water Potential in the Transpiration Stream	702
28.7	Stomatal Regulation of Water Loss and CO2 Uptake	703
28.7.1	Stomatal Opening — Guard Cell Ion Fluxes	703
28.7.2	Stomatal Closure – ABA Signaling Cascade in Detail	703
28.7.3	Other Factors Affecting Stomata	704
28.7.4	Water-Use Efficiency	704
28.8	Phloem Transport – The Münch Pressure-Flow Model	705
28.8.1	Phloem Loading — Apoplastic vs Symplastic Pathways	705
28.8.2	The Münch Pressure-Flow Hypothesis [Münch, 1930]	706
28.9	Nutrient Uptake and Mineral Nutrition	707
28.9.1	Essential Mineral Nutrients and Deficiency Logic	707
28.9.2	Nitrogen Fixation Symbiosis	708
28.9.3	Mycorrhizal Associations and Nutrient Exchange	708
28.10	Adaptations for Water and Nutrient Acquisition	709
28.10.1	Xerophyte Adaptations to Water Deficit	709
28.10.2	Hydrophyte Adaptations to Flooded Environments	709
28.10.3	Carnivorous Plants and Nutrient Acquisition	709
28.11	Computational Bridge	709
28.12	Current Evidence and Frontier Biology: Plant Structure and Water Relations	710
28.12.1	Current Evidence Map: Hydraulic Safety Tradeoff	710
28.13	Summary	710
28.14	Key Terms	711
28.15	Review Questions	711
28.16	Further Reading and Source Notes: Plant Structure and Water Relations	712
28.17	Companion Source Module: Plant Structure and Water Relations	712
29	Plant Reproduction and Development	714

29.1	Learning Objectives	714
29.1.1	Study Blueprint	714
29.2	Alternation of Generations	715
29.2.1	Worked Example: Tracking Ploidy Through the Angiosperm Life Cycle	716
29.3	Plant Group Reproductive Strategies	716
29.3.1	Non-Vascular Plants (Bryophytes)	716
29.3.2	Seedless Vascular Plants (Ferns and Allies)	717
29.3.3	Gymnosperms and Naked-Seed Reproduction	717
29.3.4	Angiosperms (Flowering Plants)	717
29.4	Angiosperm Flower Structure and the ABCDE Model	717
29.4.1	Flower Architecture and Reproductive Organ Identity	717
29.4.2	The ABCDE Model and MADS-Box Floral Quartets [Coen and Meyerowitz, 1991]	718
29.5	Gametophyte Generation – Cellular Architecture	719
29.5.1	Male Gametophyte: Microsporogenesis and Pollen Grain Architecture	719
29.5.2	Female Gametophyte: Megasporogenesis and the Polygonum-Type Embryo Sac	720
29.6	Pollination, Pollen-Pistil Interactions, and Double Fertilization	721
29.6.1	Pollination Systems and Pollen Transfer Strategies	721
29.6.2	Pollen-Pistil Interactions: Self-Incompatibility (SI) Systems	721
29.6.3	Polyploidy and Speciation in Plants	722
29.6.4	Double Fertilization [Nawaschin, 1898]	723
29.6.5	Worked Example: Endosperm Ploidy and Parental Genome Dosage	724
29.7	Endosperm Development and Seed Biology	725
29.7.1	Endosperm Development: Free-Nuclear, Cellular, Helobial	725
29.7.2	Seed Dormancy: Five Classes and Triggers	725
29.7.3	Germination Physiology — Molecular Framework	726
29.8	Embryogenesis and Meristem Organization	727
29.8.1	Early Embryogenesis and Body-Axis Formation	727
29.8.2	Shoot Apical Meristem (SAM) – Stem Cell Niche	728
29.8.3	Worked Example: Calculating the Golden Angle in Phyllotaxis	728
29.8.4	Root Apical Meristem (RAM)	729
29.9	Fruit Development, Vegetative Reproduction, and Apomixis	729
29.9.1	Fruit Development: Hormonal Regulation, Parthenocarpy, and Climacteric Ripening	729
29.9.2	Fruit Types and Dispersal	730
29.9.3	Vegetative Reproduction: Mechanisms and Practical Applications	731
29.9.4	Apomixis: Sporophytic and Gametophytic Pathways	731
29.9.5	Plant Biotechnology in Reproduction and Crop Improvement	732
29.10	Current Evidence and Frontier Biology: Plant Reproduction and Development	733
29.11	Key Terms	733
29.12	Review Questions	734
29.13	Further Reading and Source Notes: Plant Reproduction and Development	735
29.14	Computational Bridge	735
29.15	Summary	735
29.16	Companion Source Module: Plant Reproduction and Development	736
30	Plant Responses to the Environment	737
30.1	Learning Objectives	737
30.1.1	Study Blueprint	737
30.2	Plant Hormone Networks and Growth Decisions	737
30.2.1	Auxin (Indole-3-Acetic Acid, IAA)	737
30.2.2	Gibberellins (GAs) and Stem Elongation	739
30.2.3	Cytokinins and Cell Division Signals	739
30.2.4	Abscisic Acid (ABA)	740

30.2.5	Ethylene and Gaseous Stress/Ripening Signals	740
30.2.6	Jasmonates (JA) and Wound Defense	740
30.2.7	Salicylic Acid (SA)	741
30.2.8	Strigolactones and Branching/Mycorrhizal Signals	741
30.3	Phototropism and Auxin-Driven Bending	741
30.3.1	Worked Example: Phototropic Curvature from a Lateral Auxin Gradient	741
30.3.2	Worked Example: Auxin Redistribution Predicts Curvature Rate	742
30.4	Gravitropism and Gravity-Sensing Root Architecture	742
30.5	Photomorphogenesis: Phytochromes and Cryptochromes	743
30.5.1	Phytochrome Biochemistry and Red/Far-Red Switching	743
30.5.2	Cryptochrome Signaling — Blue Light and FAD	744
30.6	The Plant Circadian Clock — Molecular Architecture	744
30.6.1	Morning Loop: CCA1/LHY Repressors and TOC1 Activator	744
30.6.2	Evening Loop: PRR9 → PRR7 → PRR5 → TOC1	745
30.6.3	Evening Complex: ELF3-ELF4-LUX	745
30.6.4	Temperature Compensation in Plant Circadian Clocks	745
30.6.5	Clock Outputs for Growth, Metabolism, and Flowering	745
30.7	Photoperiodism, Flowering Time, and Vernalisation	745
30.7.1	Photoperiodic Categories and Flowering Responses	745
30.7.2	Night-Length Measurement and Circadian Gating	745
30.7.3	The CONSTANS-FT (Florigen) Pathway	745
30.7.4	Vernalisation: Epigenetic Silencing of FLC	746
30.8	Touch Responses and Additional Tropisms	747
30.8.1	Gravitropism — Statolith and PIN Asymmetry (deep dive)	747
30.8.2	Touch Responses (Thigmomorphogenesis)	747
30.8.3	Hydrotropism, Thigmotropism, and Heliotropism	748
30.9	Abiotic Stress Responses	748
30.9.1	Drought – ABA Signaling Cascade	748
30.9.2	Worked Example: Calculating Water Use Efficiency (WUE)	748
30.9.3	Cold Stress – CBF-COR Pathway	749
30.9.4	Heat Stress – HSP Response	749
30.9.5	Salt Stress and Ion Homeostasis	749
30.9.6	Flooding Response and Low-Oxygen Signaling	749
30.10	Plant Immunity — A Two-Layer Defense System	749
30.10.1	Layer 1: PAMP-Triggered Immunity (PTI)	749
30.10.2	Layer 2: Effector-Triggered Immunity (ETI)	750
30.10.3	Systemic Acquired Resistance (SAR)	750
30.10.4	JA/SA Antagonism	750
30.11	Herbivory and Wound Defense – Jasmonate Signaling	751
30.12	Shade Avoidance Syndrome	751
30.13	Epigenetic Stress Memory in Plants	751
30.14	Agricultural Applications of Plant Hormone Biology	752
30.14.1	Ethylene Inhibitors — Postharvest Storage	752
30.14.2	Gibberellin Biology — The Green Revolution	752
30.14.3	Auxin Herbicides and Synthetic Growth-Regulator Toxicity	752
30.14.4	Other Hormone-Based Technologies	752
30.15	Current Evidence and Frontier Biology: Plant Responses to the Environment	753
30.15.1	Current Evidence Map: Plant Stress Response Decision	753
30.16	Key Terms	753
30.17	Review Questions	754
30.18	Further Reading and Source Notes: Plant Responses to the Environment	755
30.19	Computational Bridge	755

30.20	Summary	755
30.21	Companion Source Module: Plant Responses to the Environment	756
Unit IX — Zoology and Systems Physiology: Introduction		757
	Why This Unit Matters	757
	Landmark Discoveries	757
	Key Concepts and Connections	757
	Current Evidence Thread	758
	Chapter Roadmap	758
	Connections Across the Textbook	758
	Computational Toolbox — Unit IX	759
	Cross-Unit Integration	759
31	Circulation and Respiration	760
31.1	Learning Objectives	760
31.1.1	Study Blueprint	760
31.2	Evolution of Cardiovascular Systems	760
31.3	Heart Anatomy and the Cardiac Cycle	762
31.3.1	Cardiac Conduction System	762
31.3.2	The Cardiac Cycle	762
31.4	Cardiac Output and Blood Pressure	763
31.4.1	Cardiac Output as Heart Rate Times Stroke Volume	763
31.4.2	Blood Pressure and Vascular Resistance	763
31.4.3	Blood Flow – Poiseuille’s Law	764
31.4.4	Worked Example: Cardiac Reserve	764
31.4.5	Baroreceptor Reflex — Beat-to-Beat Blood Pressure Control	764
31.4.6	RAAS Cascade — Long-term Blood Pressure and Volume Control	765
31.5	Digestive, Nutritional, Renal, and Excretory Integration	766
31.6	Capillary Fluid Exchange and the Lymphatic System	766
31.6.1	Starling Forces in Capillary Exchange	766
31.6.2	The Lymphatic System	767
31.7	Worked Example: Hypoalbuminaemia and Net Filtration Pressure	767
31.8	Oxygen Transport by Hemoglobin	767
31.8.1	Hemoglobin Structure and Cooperative Binding	767
31.8.2	O ₂ -Hb Dissociation Curve and the Hill Equation	767
31.9	Worked Example: Bohr Effect and 2,3-BPG in Exercise	769
31.9.1	CO ₂ Transport	770
31.10	Respiratory System and Ventilation	770
31.10.1	Respiratory Tract Anatomy and Alveolar Architecture	770
31.10.2	Lung Mechanics and Pressure Gradients	770
31.10.3	Pulmonary Surfactant — Laplace’s Law and Alveolar Stability	771
31.10.4	Lung Volumes and Spirometry	771
31.11	Gas Exchange Across the Alveolar-Capillary Barrier	772
31.12	Worked Example: Alveolar Oxygen Diffusion	772
31.12.1	Respiratory Control by Chemoreceptors and Brainstem Circuits	773
31.12.2	Worked Example: Fick’s Law of Diffusion and O ₂ Delivery Matched by Cardiac Output	773
31.13	Exercise Physiology — Integrated Cardiovascular and Respiratory Adjustments	774
31.13.1	Cardiovascular Adjustments During Exercise	774
31.13.2	Respiratory Adjustments During Exercise	775
31.14	Homeostatic Control of Temperature, Fluids, and Electrolytes	775
31.14.1	Principles of Feedback, Set Points, and Allostasis	775
31.14.2	Temperature Regulation by Heat Balance	775

31.14.3	Countercurrent Heat Exchange	776
31.14.4	Hibernation, Torpor, and Heterothermy	776
31.14.5	Fluid and Electrolyte Homeostasis	776
31.15	Worked Example: Cardiac Output During Exercise	777
31.16	Computational Bridge	777
31.17	Current Evidence and Frontier Biology: Circulation and Respiration	778
31.18	Summary	778
31.19	Key Terms	778
31.20	Review Questions	779
31.21	Further Reading and Source Notes: Circulation and Respiration	779
31.22	Companion Source Module: Circulation and Respiration	780
32	Nervous System and Neural Signaling	781
32.1	Learning Objectives	781
32.1.1	Study Blueprint	781
32.2	Nervous System Organization Across Cells, Circuits, and Regions	781
32.3	Neuron Types and Structure	782
32.3.1	Neuron Classification by Function and Morphology	782
32.3.2	Neuron Structure from Dendrites to Axon Terminals	782
32.4	Glial Cells and Neural Support Functions	782
32.4.1	Astrocytes — More Than Glue	783
32.4.2	Oligodendrocytes and Myelin	783
32.4.3	Microglia — Resident Macrophages of the CNS	783
32.4.4	Blood-Brain Barrier — Molecular Architecture	784
32.5	Resting Membrane Potential	784
32.5.1	Ion Distribution and the Nernst Equation	784
32.5.2	Goldman-Hodgkin-Katz (GHK) Equation	786
32.6	Cable Properties and Passive Signal Spread	786
32.6.1	Length Constant (λ) and Spatial Attenuation	786
32.6.2	Time Constant (τ_m)	786
32.7	Worked Example: Dendritic Length Constant	787
32.7.1	Worked Example: EPSP Attenuation from Distal vs Proximal Synapses	787
32.8	Graded Potentials and Synaptic Integration	788
32.8.1	Graded Potentials and Local Voltage Changes	788
32.8.2	Summation at the Axon Hillock	788
32.9	Autonomic Nervous System	789
32.9.1	Sympathetic Division (“Fight or Flight”)	789
32.9.2	Parasympathetic Division (“Rest and Digest”)	789
32.9.3	Enteric Nervous System	789
32.10	Brain Anatomy and Function	790
32.10.1	Cerebral Cortex and Distributed Processing	790
32.10.2	Basal Ganglia and Action Selection	790
32.10.3	Cerebellum, Hippocampus, Hypothalamus, and Spinal Cord	791
32.11	Sensory Systems and Neural Coding	791
32.11.1	Somatosensation and Mechanoreceptor Pathways	791
32.11.2	Visual Pathway from Retina to Cortex	791
32.11.3	Proprioception and Body-Position Feedback	792
32.11.4	Musculoskeletal Control and Behavior	792
32.12	Brain Imaging — Reading Activity Through Indirect Signals	792
32.12.1	fMRI and the BOLD signal	792
32.12.2	EEG and oscillation bands	792
32.12.3	Connectivity, MEG, NIRS, PET	793

32.12.4	Neural Prosthetics and Brain-Computer Interfaces	793
32.13	Pain Pathways and Nociceptive Processing	793
32.13.1	Nociceptors and transduction	793
32.13.2	Ascending pathway — the spinothalamic tract	793
32.13.3	Descending Modulation of Pain Signals	793
32.14	Sleep — Two-Process Model	794
32.14.1	Sleep Architecture Across NREM and REM Stages	794
32.14.2	The two-process model (Borbély, 1982)	794
32.14.3	Functions of sleep	794
32.15	Neural Plasticity and Activity-Dependent Change	795
32.16	Worked Example: Potassium Equilibrium Potential	795
32.17	Worked Example: Resting Potential from the Goldman-Hodgkin-Katz Equation	795
32.18	Current Evidence and Frontier Biology: Nervous System and Neural Signaling	796
32.19	Key Terms	796
32.20	Review Questions	797
32.21	Further Reading and Source Notes: Nervous System and Neural Signaling	798
32.22	Computational Bridge	798
32.22.1	Optogenetics: Light-Gated Ion Channels as Tools for Mapping Neural Circuits	798
32.23	Summary	798
32.24	Companion Source Module: Nervous System and Neural Signaling	799
33	Action Potentials and Synaptic Transmission	800
33.1	Learning Objectives	800
33.1.1	Study Blueprint	800
33.2	The Hodgkin-Huxley Model	800
33.2.1	Hodgkin-Huxley Gating Variables	802
33.2.2	Biophysical Interpretation of the Action Potential	802
33.2.3	Channel Pharmacology and Excitability	803
33.3	Refractory Periods and Directional Propagation	803
33.4	Myelination and Conduction Velocity	803
33.4.1	Unmyelinated Conduction and Cable Spread	803
33.4.2	Myelinated Axons – Saltatory Conduction	803
33.4.3	Worked Example: Myelination Gain — Saltatory vs Continuous Conduction	804
33.4.4	Multiple Sclerosis and Demyelinating Conduction Failure	804
33.5	Chemical Synaptic Transmission	805
33.5.1	Synapse Types and Functional Polarity	805
33.5.2	Presynaptic Machinery for Vesicle Fusion	805
33.5.3	Synaptic Vesicle Pools	805
33.5.4	Short-term plasticity — facilitation and depression	806
33.5.5	Tsodyks-Markram model	806
33.5.6	Worked Example: Quantal Analysis at the Neuromuscular Junction	807
33.5.7	Postsynaptic Receptors and Ionotropic/Metabotropic Signaling	807
33.6	Neurotransmitter Systems and Receptor Families	808
33.6.1	Glutamate as the Major Excitatory Transmitter	808
33.6.2	GABA as the Major Inhibitory Transmitter	809
33.6.3	Acetylcholine at Neuromuscular and Autonomic Synapses	809
33.6.4	Dopamine in Reward, Movement, and Precision Signals	809
33.6.5	Serotonin (5-HT)	809
33.6.6	Norepinephrine in Arousal and Autonomic Modulation	809
33.7	Computational Neuroscience and AI Models	809
33.7.1	Computational Neuroscience Models	809
33.7.2	Machine Learning for Neural Data Analysis	810

33.7.3	AI for Drug Discovery in Neurology	811
33.7.4	Brain-Computer Interfaces (BCIs)	811
33.7.5	Ethical Considerations in AI and Neurotechnology	811
33.7.6	Neuropeptides and Slow Modulatory Signaling	812
33.8	Synaptic Plasticity and Memory	813
33.8.1	Long-Term Potentiation (LTP)	813
33.8.2	Long-Term Depression (LTD)	813
33.9	Neuropharmacology: Synaptic and Ion-Channel Drug Mechanisms	813
33.10	Worked Example: Quantal Release at the Neuromuscular Junction	815
33.11	Current Evidence and Frontier Biology: Action Potentials and Synaptic Transmission	815
33.12	Key Terms	816
33.13	Review Questions	816
33.14	Further Reading and Source Notes: Action Potentials and Synaptic Transmission	817
33.15	Computational Bridge	817
33.16	Summary	817
33.17	Companion Source Module: Action Potentials and Synaptic Transmission	818
34	Endocrine Signaling and Homeostasis	819
34.1	Learning Objectives	819
34.1.1	Study Blueprint	819
34.2	Endocrine System Overview	819
34.2.1	Endocrine vs Nervous System	819
34.2.2	Hormone Classes — Synthesis, Transport, and Mechanism	820
34.2.3	Quantitative Endocrinology	822
34.3	Hypothalamic-Pituitary Axes	823
34.3.1	HPA Axis (Hypothalamic-Pituitary-Adrenal) — Detailed Cortisol Physiology	823
34.3.2	HPT Axis (Hypothalamic-Pituitary-Thyroid) — Detailed Mechanism	825
34.3.3	Worked Example: Thyroid Hormone Negative Feedback and TSH Compensatory Rise	826
34.3.4	HPG Axis and Reproductive Hormones	828
34.4	Pancreatic Hormones, Glucose Homeostasis, and Energy Balance	828
34.4.1	Insulin signaling — molecular detail	828
34.4.2	Worked Example: Postprandial Glucose Clearance and Insulin Dose Scaling	829
34.4.3	Diabetes Mellitus	830
34.4.4	Adrenal Gland — Zonal Architecture	831
34.4.5	Growth Hormone Axis and IGF-1	831
34.5	Prostaglandins and Eicosanoids	832
34.5.1	Synthesis from arachidonic acid	832
34.5.2	COX-1 vs COX-2 — distinct physiology	832
34.5.3	Pharmacological targets	833
34.6	Endocrine Disruption	833
34.6.1	Mechanisms of disruption	834
34.6.2	Bisphenol A (BPA) and other xenoestrogens	834
34.6.3	Phthalates, PFAS, and other major EDCs	834
34.6.4	Vulnerability of development	835
34.7	Current Evidence and Frontier Biology: Endocrine Signaling and Homeostasis	836
34.7.1	Current Evidence Map: Allostasis and Immune-Endocrine Coupling	836
34.8	Summary	836
34.9	Further Reading and Source Notes: Endocrine Signaling and Homeostasis	836
34.10	Companion Source Module: Endocrine Signaling and Homeostasis	836
35	Immune System Architecture	838
35.1	Learning Objectives	838

35.2	Immune System Architecture and Effector Logic	838
35.2.1	Innate Immunity	838
35.2.2	Pattern Recognition Receptors (PRRs)	839
35.2.3	Complement System Overview	841
35.2.4	Adaptive Immunity Overview	842
35.2.5	T Cell Development and Selection	843
35.2.6	B Cell Activation and Antibody Diversification	844
35.2.7	Cytokine Network Reference	845
35.2.8	Immunological Memory — Why Memory Cells Respond Faster	846
35.2.9	Tolerance and Autoimmunity	847
35.2.10	Hypersensitivity Reactions (Gell-Coombs Classification)	848
35.2.11	Immunotherapy	849
35.2.12	Study Blueprint	852
35.3	Worked Example: Innate Recognition to Effector Response	852
35.4	Worked Example: Clonal Expansion	853
35.5	Computational Bridge	853
35.6	Current Evidence and Frontier Biology: Immune System Architecture	853
35.6.1	Current Evidence Map: From Pattern Recognition to Protective Memory	854
35.7	Summary	854
35.8	Connections: See section 11 for insulin/glucagon integration, section 26 for PAMP recognition, and section 31 for stress axes.	855
35.9	Review Questions	855
35.10	Further Reading and Source Notes: Immune System Architecture	856
35.11	Key Terms	856
35.12	Companion Source Module: Immune System Architecture	857
Unit X — Ecology: Introduction		858
Why This Unit Matters		858
Landmark Discoveries		858
Key Concepts and Connections		858
Current Evidence Thread		858
Chapter Roadmap		859
Connections Across the Textbook		859
Computational Toolbox — Unit X		859
Cross-Unit Integration		860
36	Population Ecology and Growth Models	861
36.1	Learning Objectives	861
36.1.1	Study Blueprint	861
36.1.2	Chapter Roadmap for Population Models and Conservation Decisions	862
36.2	Populations as Bounded, Measurable Units	862
36.2.1	Population Attributes: Size, Density, and Age Structure	862
36.2.2	Dispersion Patterns Across Space	863
36.3	Life Tables and Survivorship Curves	863
36.3.1	Survivorship Curves and Age-Specific Mortality	864
36.3.2	Reproductive Value and Future Genetic Contribution	864
36.4	Exponential Growth Under Unlimited Resources	865
36.4.1	Real-World Examples of Near-Exponential Growth	865
36.5	Logistic Growth and Density Dependence	865
36.5.1	Density-Dependent Factors	866
36.5.2	Density-Independent Factors	867
36.5.3	Maximum Sustainable Yield (MSY)	867
36.5.4	Extensions of the Logistic Model	867

36.6	The Allee Effect	868
36.6.1	Strong vs. Weak Allee Effects	868
36.6.2	Mechanisms of Allee Effects	868
36.7	Lotka-Volterra Competition and Predator-Prey	870
36.7.1	Interspecific Competition and Niche Overlap	870
36.7.2	Lotka-Volterra Predator-Prey	871
36.7.3	Lynx-Hare Cycle: A Case Study	872
36.8	r vs. K Selection and Life History Theory	872
36.8.1	Beyond r-K: Modern Life History Theory	872
36.9	Age-Structured Population Models and the Leslie Matrix	873
36.9.1	Leslie Matrix Construction	873
36.9.2	Sensitivity and Elasticity Analysis	874
36.9.3	Stage-Structured Generalisations	874
36.10	Individual-Based Population Models and Stochastic Simulation	875
36.11	Population Viability Analysis and Extinction-Risk Forecasting	875
36.11.1	Inputs to a PVA	875
36.11.2	Outputs and Decision Rules	876
36.11.3	Worked Example — California Condor PVA	876
36.11.4	Limitations and Honest Use	876
36.12	Metapopulation Dynamics Across Habitat Patches	876
36.12.1	The Levins Model	877
36.12.2	Source-Sink Dynamics [Pulliam, 1988]	877
36.12.3	Rescue Effect and Connectivity	877
36.12.4	Visualizing Metapopulation and Source-Sink Dynamics	877
36.13	Estimating Population Size	877
36.13.1	Mark-Recapture Methods	877
36.13.2	Distance Sampling and Detection Probability	878
36.14	Human Population Demographics	878
36.14.1	Age Structure and Population Pyramids	878
36.14.2	Total Fertility Rate (TFR) and Replacement Level	879
36.15	Worked Examples: Leslie Matrices and Population Growth	879
36.15.1	Worked Example: Leslie Matrix Projection	879
36.15.2	Worked Example: Mark-Recapture Estimation	879
36.15.3	Worked Example: Logistic Projection and r/K Strategist Vulnerability	880
36.15.4	Concept Check (Analyze) — Allee Effects and Minimum Viable Population	880
36.15.5	Concept Check (Evaluate) — Leslie Matrix Sensitivity and Where to Manage	881
36.16	Current Evidence and Frontier Biology: Population Ecology and Growth Models	881
36.17	Key Terms	881
36.18	Review Questions	882
36.19	Further Reading and Source Notes: Population Ecology and Growth Models	883
36.20	Computational Bridge	883
36.21	Summary	883
36.22	Companion Source Module: Population Ecology and Growth Models	884
37	Community Interactions and Succession	885
37.1	Learning Objectives	885
37.1.1	Study Blueprint	885
37.1.2	Chapter Roadmap for Interaction Networks and Biodiversity Metrics	885
37.2	Community Structure, Interaction Strength, and Scale	887
37.2.1	Emergent Properties of Communities	887
37.2.2	Rank-Abundance Models	887
37.2.3	Types of Biotic Interactions	887

37.3	Competition Theory and Coexistence Mechanisms	889
37.3.1	Lotka-Volterra Interspecific Competition	889
37.3.2	Competitive Exclusion Principle (Gause’s Law)	889
37.3.3	Hutchinson’s Niche Concept	889
37.3.4	Modern Coexistence Theory [Chesson, 2000]	889
37.4	Predation, Keystone Species, and Trophic Cascades	890
37.4.1	Predator-Prey Arms Races	890
37.4.2	Hare-Lynx Cycle	891
37.4.3	Keystone Species and Disproportionate Community Effects	891
37.4.4	Trophic Cascades Across Food-Web Levels	891
37.5	Mutualism, Parasitism, and Facilitation	892
37.5.1	Mutualism and Reciprocal Fitness Benefits	892
37.5.2	Pollination, Myrmecochory, and Ant-Plant Mutualisms	892
37.5.3	Parasitism and Disease Ecology	892
37.5.4	Facilitation and Positive Species Interactions	893
37.6	Ecological Succession and Community Assembly Over Time	893
37.6.1	Mechanisms of Succession	893
37.6.2	Climax Community Concept	894
37.6.3	Intermediate Disturbance Hypothesis (IDH)	894
37.6.4	Alternative Stable States and Regime Shifts	895
37.7	Measuring Biodiversity Across Alpha, Beta, and Gamma Scales	895
37.7.1	Alpha, Beta, and Gamma Diversity	895
37.7.2	Shannon-Wiener Diversity Index (H')	896
37.7.3	Simpson Diversity Index ($1 - D$)	896
37.7.4	Pielou’s Evenness (J')	896
37.7.5	Worked Example: Shannon Diversity and Evenness	896
37.7.6	Beta Diversity: Measuring Turnover	896
37.8	Current Evidence and Frontier Biology: Community Interactions and Succession	897
37.9	Summary	897
37.10	Further Reading and Source Notes: Community Interactions and Succession	897
37.11	Companion Source Module: Community Interactions and Succession	898
38	Biodiversity and Food Webs	899
38.1	Learning Objectives	899
38.2	Island Biogeography Theory	899
38.2.1	MacArthur-Wilson Equilibrium Model	899
38.2.2	Visualizing Food Web Connectance and Modularity	899
38.2.3	Species-Area Relationship	900
38.2.4	Empirical Tests of Island Biogeography	900
38.2.5	SLOSS Debate in Reserve Design	900
38.2.6	Extinction Debt After Habitat Loss	900
38.2.7	Metapopulation Dynamics (Levins, 1969; Hanski, 1994)	901
38.2.8	Study Blueprint	901
38.3	Food Web Structure and Network Ecology	902
38.3.1	Food Web Topology	902
38.3.2	Cascade Effects and Robustness	902
38.3.3	Complexity-Stability Debate	903
38.4	Neutral Theory of Biodiversity	903
38.4.1	The Neutral Assumption	903
38.4.2	Predictions and Empirical Successes	903
38.4.3	Limits and Synthesis	903
38.5	Trait-Based biodiversity and food webs	904

38.5.1	Grime’s CSR Triangle	904
38.5.2	The Leaf Economics Spectrum	904
38.5.3	Functional Diversity and Community Assembly	905
38.6	Biological Control and Ecological Risk Management	905
38.6.1	Three Classical Strategies	905
38.6.2	Classical Successes and Failures	905
38.6.3	Risk Assessment and Modern Practice	906
38.7	Worked Example: Shannon Diversity in a Forest Patch	906
38.7.1	Worked Example: Intermediate Disturbance Hypothesis Quantified	906
38.7.2	Concept Check (Analyze) — Trophic Cascades, Efficiency, and Eutrophication	907
38.7.3	Concept Check (Evaluate) — Biotic Resistance and Invasive Species	907
38.8	Current Evidence and Frontier Biology: Biodiversity and Food Webs	908
38.9	Summary	908
38.10	Review Questions	909
38.11	Further Reading and Source Notes: Biodiversity and Food Webs	910
38.12	Computational Bridge	910
38.13	Key Terms	910
38.14	Companion Source Module: Biodiversity and Food Webs	911
39	Ecosystem Ecology	912
39.1	Learning Objectives	912
39.1.1	Study Blueprint	912
39.2	Ecosystem Concepts and System Boundaries	913
39.2.1	The Two Fundamental Processes	913
39.2.2	Ecosystem Services and Human Well-Being	913
39.3	Trophic Structure and Energy Flow	914
39.3.1	Ecological Efficiency Across Trophic Transfers	914
39.3.2	Production Efficiency by Organism Group	915
39.4	Primary Productivity and Carbon Fixation	916
39.4.1	The Productivity Hierarchy	916
39.4.2	Global Primary Production	916
39.4.3	Factors Limiting GPP	917
39.4.4	Measuring Net Primary Productivity	917
39.4.5	ANPP, BNPP, and Their Ratio	918
39.5	The Carbon Cycle and Climate Change	918
39.5.1	Carbon Reservoirs Across Atmosphere, Ocean, Land, and Rock	918
39.5.2	Annual Carbon Fluxes (2020s)	919
39.5.3	The Biological Pump	919
39.5.4	Key Climate Feedbacks	919
39.6	The Nitrogen Cycle	920
39.6.1	Key Nitrogen Transformations	920
39.6.2	Biological Nitrogen Fixation	921
39.6.3	Anthropogenic Nitrogen Disruption	921
39.7	The Phosphorus Cycle	922
39.7.1	Phosphorus Reservoirs and Fluxes	922
39.7.2	P Limitation in Ecosystems	922
39.7.3	The Redfield Ratio	922
39.7.4	Phosphorus Crisis in Food Systems	923
39.8	The Sulfur Cycle	923
39.8.1	Key Sulfur Transformations	923
39.8.2	The CLAW Hypothesis	923
39.8.3	Acid Rain and Sulfur/Nitrogen Deposition	923

39.9	Nutrient Cycling Models: Open and Closed Ecosystem Budgets	924
39.9.1	Hubbard Brook: The Watershed That Defined the Field	924
39.10	Marine Ecosystem Ecology and the Biological Pump	925
39.10.1	Productivity Zones of the Ocean	925
39.10.2	Biological Pump and Its Efficiency	925
39.11	Soil Formation, Pedogenesis, and Soil-Carbon Feedbacks	926
39.11.1	Five State Factors (Jenny 1941)	926
39.11.2	Soil Horizons and Vertical Differentiation	926
39.11.3	Three Stages of Pedogenesis	926
39.11.4	Social Insects as Soil Engineers	927
39.11.5	Soil Carbon and Climate Feedback	927
39.12	Coupled Biogeochemical Cycles and Ecological Stoichiometry	927
39.12.1	The Redfield Ratio Revisited	927
39.12.2	Stoichiometric Coupling of C, N, P, Fe, and S	927
39.12.3	Planetary Boundaries and Biogeochemical Overshoot	927
39.13	Quantifying Ecosystem Services in Earth-System Science	928
39.13.1	Quantifying and Valuing Services	928
39.13.2	The Gaia Hypothesis: Critical Evaluation	928
39.14	The Water Cycle (Hydrological Cycle)	929
39.14.1	Key Hydrological Fluxes	929
39.15	Ecosystem Services and Conservation Economics	929
39.15.1	Biodiversity-Ecosystem Functioning (BEF)	929
39.15.2	Payment for Ecosystem Services (PES)	929
39.16	Worked Example: Net Primary Productivity and Trophic Transfer	930
39.17	Worked Example: Nutrient Pool Mass Balance and Residence Time	930
39.17.1	Worked Example — Carbon Budget, NEP, and the Sink-to-Source Tipping Point	931
39.17.2	Concept Check (Analyze) — Redfield Stoichiometry, Liebig’s Law, and Coastal Hypoxia	932
39.17.3	Concept Check (Evaluate) — Ecosystem Service Valuation	932
39.18	Current Evidence and Frontier Biology: Ecosystem Ecology	932
39.18.1	Current Evidence Map: Agroecology as Coupled Fluxes	933
39.19	Key Terms	933
39.20	Review Questions	934
39.21	Further Reading and Source Notes: Ecosystem Ecology	935
39.22	Computational Bridge	935
39.23	Summary	935
39.24	Companion Source Module: Ecosystem Ecology	936
40	Biomes and Conservation Biology	937
40.1	Learning Objectives	937
40.1.1	Study Blueprint	937
40.2	Biomes as Climate-Filtered Ecological Regions	937
40.2.1	Climate as the Master Variable	937
40.2.2	The Nine Major Terrestrial Biomes	939
40.2.3	Five Major Aquatic Biome Types	939
40.2.4	Lake Stratification and Turnover	940
40.2.5	Coral Reef Bleaching	940
40.3	Climate Change and Biome Boundary Shifts	942
40.3.1	Key Findings (2023-2025)	942
40.3.2	Biome Suitability Modeling	942
40.3.3	Climate Velocity and Dispersal Limits	942
40.4	Conservation Biology Fundamentals	943
40.4.1	IPBES Global Assessment: The Quantified Crisis	943

40.4.2	Quantified Drivers (IPBES 2019)	943
40.4.3	The Sixth Mass Extinction	944
40.4.4	IUCN Red List Categories (2025 Update)	944
40.5	Population Viability and the 50/500 Rule	945
40.5.1	Minimum Viable Population (MVP)	945
40.5.2	Franklin’s 50/500 Rule	945
40.5.3	Population Viability Analysis (PVA)	946
40.6	Extinction Debt and Its Conservation Implications	946
40.6.1	Mathematical Framework for Extinction Debt	946
40.6.2	Relaxation Time After Habitat Loss	946
40.6.3	Case Studies of Delayed Extinction	946
40.7	Reserve Design for Area, Connectivity, and Edge Effects	947
40.7.1	Island Biogeography Applied to Conservation	947
40.7.2	SLOSS Debate Resolution	948
40.7.3	Diamond’s Design Principles (1975, updated)	948
40.7.4	Edge Effects and Fragment Microclimates	948
40.7.5	Habitat Corridors and Connectivity Trade-Offs	949
40.8	Emerging Conservation Strategies	949
40.8.1	Rewilding and Trophic Restoration	949
40.8.2	Conservation Genomics for Diversity and Management	950
40.8.3	Assisted Gene Flow and Assisted Migration	950
40.8.4	Climate-Adaptive Management	951
40.8.5	Visualizing Reserve Design Principles	951
40.9	Climate Velocity, Refugia, and Species Range Shifts	952
40.9.1	Refugia and Their Identification	952
40.10	Ecosystem-Based Adaptation and Climate-Resilience Planning	952
40.10.1	Major EbA Strategies	953
40.10.2	Quantified Performance of Ecosystem-Based Adaptation	953
40.10.3	Limits of EbA	953
40.11	International Conservation Frameworks	954
40.11.1	Conservation Agreements: CITES, CBD, GBF, and Paris Agreement	954
40.11.2	The 30x30 Target	954
40.11.3	Payments for Ecosystem Services	954
40.12	Worked Example: Species-Area Prediction for Island Birds	954
40.13	Worked Example: Effective Population Size and the 50/500 Rule	955
40.13.1	Minimum Viable Population and Genetic Rescue: Case Studies from Conservation Biology	955
40.13.2	Worked Example — Island Biogeography and Species-Area Loss	956
40.13.3	Concept Check (Analyze) — Metapopulation Dynamics and Corridor Effects	957
40.13.4	Concept Check (Evaluate) — Climate Velocity and the Boreal-Tundra Tipping Point	957
40.14	Current Evidence and Frontier Biology: Biomes and Conservation Biology	957
40.14.1	Current Evidence Map: Conservation Decision Evidence Chain	958
40.15	Key Terms	958
40.16	Review Questions	959
40.17	Further Reading and Source Notes: Biomes and Conservation Biology	960
40.18	Computational Bridge	960
40.19	Summary	961
40.20	Companion Source Module: Biomes and Conservation Biology	961
Lab A — Systems Science and Emergence		962
Learning Objectives		962
Alignment and Rubric Map		962
Lab Context: Systems Science and Emergence		962

Pre-Lab (to complete before class)	962
Paper-Based Materials	962
Paper-Based Investigation	963
Part 1 — Identifying Systems	963
Part 2 — Feedback Loop Diagrams	963
Part 3 — Hill Curve by Hand	963
Part 4 — Complicated vs. Complex	963
Data Tables	964
Evidence and Reproducibility Checklist	964
Paper-Based Evidence Upgrade	964
Source-Governance Checkpoint	965
Worked Example: Stock-and-flow projection of a small mammal population	965
Analysis Questions	965
Post-Lab Synthesis	966
Discussion Questions	966
Safety and Ethics Notes	966
Lab B — Complex Adaptive Systems	967
Learning Objectives	967
Alignment and Rubric Map	967
Lab Context: Complex Adaptive Systems	967
Pre-Lab (to complete before class)	967
Paper-Based Materials	967
Paper-Based Investigation	968
Part 1 — The Logistic Map by Hand	968
Part 2 — Attractor Landscape and Tipping Points	968
Part 3 — Robustness Versus Redundancy	968
Data Tables	968
Evidence and Reproducibility Checklist	969
Paper-Based Evidence Upgrade	969
Source-Governance Checkpoint	969
Worked Example: Logistic-Map Period Doubling	969
Analysis Questions	970
Post-Lab Synthesis	970
Discussion Questions	970
Safety and Ethics Notes	970
Lab C — Active Inference and Free Energy	971
Learning Objectives	971
Alignment and Rubric Map	971
Lab Context: Active Inference and Free Energy	971
Pre-Lab (to complete before class)	971
Paper-Based Materials	972
Paper-Based Investigation	972
Part 1 — Hand-computed Bayesian Update	972
Part 2 — Perceptual vs. Active Inference	972
Part 3 — Behavior Scenario Classification	972
Data Tables	972
Evidence and Reproducibility Checklist	973
Paper-Based Evidence Upgrade	973
Source-Governance Checkpoint	973
Worked Example: Bayesian update of a discrete food-location belief	973

Analysis Questions	974
Post-Lab Synthesis	974
Discussion Questions	974
Safety and Ethics Notes	974
Lab D — History and Philosophy of Biology	975
Learning Objectives	975
Alignment and Rubric Map	975
Pre-Lab Concept Questions	975
Paper-Based Materials	975
Paper-Based Investigation	976
Part 1 — Sort the Source Cards	976
Part 2 — Build an Evidence Map	976
Part 3 — Compare Two Explanations	976
Part 4 — Check the Explanation Level	976
Part 5 — Modern Transfer Case	977
Data Tables	977
Part 6 — Prelude Capstone Matrix	977
Paper-Based Evidence Upgrade	977
Evidence and Reproducibility Checklist	977
Source-Governance Checkpoint	977
Analysis Questions	978
Safety and Ethics Notes	978
Debrief and Reflection	978
Lab — Atoms, Molecules, and Chemical Bonds	979
Learning Objectives	979
Alignment and Rubric Map	979
Lab Context: Atoms, Molecules, and Chemical Bonds	979
Paper-Based Materials	979
Paper-Based Investigation	980
Data Recording	980
Evidence and Reproducibility Checklist	980
Paper-Based Evidence Upgrade	980
Worked Example: Polarity of O–H versus C–H and solubility prediction	981
Source-Governance Checkpoint	981
Analysis Questions	981
Post-Lab Synthesis	981
Optional Hands-On Extension	982
Safety and Ethics Notes	982
Debrief and Reflection	982
Further Reading (Lab)	982
Lab — Water — The Molecule of Life	983
Learning Objectives	983
Alignment and Rubric Map	983
Lab Context: Water — The Molecule of Life	983
Paper-Based Materials	983
Paper-Based Investigation	984
Data Recording	984
Evidence and Reproducibility Checklist	984
Paper-Based Evidence Upgrade	984
Worked Example: Temperature rise of a desert organism using $q = m c \Delta T$	985

Source-Governance Checkpoint	985
Analysis Questions	985
Post-Lab Synthesis	986
Optional Hands-On Extension	986
Safety and Ethics Notes	986
Debrief and Reflection	986
Further Reading (Lab)	986
Lab — Biological Macromolecules	987
Learning Objectives	987
Alignment and Rubric Map	987
Pre-Lab (to complete before class)	987
Lab Context: Biological Macromolecules	987
Paper-Based Materials	987
Paper-Based Investigation	988
Part D — Enzyme Hydrolysis Data	988
Part E — Sucrose Hydrolysis Model	988
Part F — AI Structure Evidence Check	988
Data Recording	988
Evidence and Reproducibility Checklist	989
Paper-Based Evidence Upgrade	989
Worked Example: Estimating protein concentration from a standard curve	989
Source-Governance Checkpoint	990
Analysis Questions	990
Post-Lab Synthesis	990
Extension Analysis Questions	990
Optional Wet-Lab Extension	991
Safety and Ethics Notes	991
Debrief and Reflection	991
Further Reading (Lab)	991
Lab — Enzymes and the Kinetics of Catalysis	992
Learning Objectives	992
Alignment and Rubric Map	992
Lab Context: Enzymes and the Kinetics of Catalysis	992
Paper-Based Materials	992
Paper-Based Investigation	993
Data Recording	993
Evidence and Reproducibility Checklist	993
Paper-Based Evidence Upgrade	993
Worked Example: Michaelis–Menten rate at two substrate levels	994
Source-Governance Checkpoint	994
Analysis Questions	994
Post-Lab Synthesis	994
Optional Wet-Lab Extension	995
Safety and Ethics Notes	995
Debrief and Reflection	995
Further Reading (Lab)	995
Lab — Cell Theory and Cell Types	996
Learning Objectives	996
Alignment and Rubric Map	996
Pre-Lab (to complete before class)	996

Lab Context: Cell Theory and Cell Types	996
Paper-Based Materials	996
Paper-Based Investigation	997
Extension — Microbial Diversity Image Packet	997
Part E — Scale Bar Arithmetic	997
Data Recording	997
Evidence and Reproducibility Checklist	997
Paper-Based Evidence Upgrade	998
Worked Example: Diffusion Time Across a 15 micrometre Cell	998
Source-Governance Checkpoint	998
Analysis Questions	998
Post-Lab Synthesis	999
Extension Analysis Questions	999
Optional Microscopy Extension	999
Safety and Ethics Notes	999
Debrief and Reflection	999
Further Reading (Lab)	999
Lab — Cell Structure and Organelles	1001
Learning Objectives	1001
Alignment and Rubric Map	1001
Pre-Lab (to complete before class)	1001
Lab Context: Cell Structure and Organelles	1001
Paper-Based Materials	1001
Paper-Based Investigation	1002
Extension — Cell-Type Organelle Profile	1002
Part E — Scale-Bar Arithmetic in Action	1002
Data Recording	1002
Evidence and Reproducibility Checklist	1003
Paper-Based Evidence Upgrade	1003
Worked Example: Surface-to-Volume Ratio of a 20 μm Cell vs a 2 μm Bacterium	1003
Source-Governance Checkpoint	1004
Analysis Questions	1004
Post-Lab Synthesis	1004
Extension Analysis Questions	1004
Optional Microscopy Extension	1004
Safety and Ethics Notes	1004
Debrief and Reflection	1004
Further Reading (Lab)	1005
Lab — Membrane Structure and Transport	1006
Learning Objectives	1006
Alignment and Rubric Map	1006
Lab Context: Membrane Structure and Transport	1006
Paper-Based Materials	1006
Paper-Based Investigation	1007
Data Recording	1007
Evidence and Reproducibility Checklist	1007
Paper-Based Evidence Upgrade	1007
Worked Example: Predicting Water Movement from Water-Potential Components	1008
Source-Governance Checkpoint	1008
Analysis Questions	1008

Post-Lab Synthesis	1009
Optional Wet-Lab Extension	1009
Safety and Ethics Notes	1009
Debrief and Reflection	1009
Further Reading (Lab)	1009
Lab — Cell Signaling and Communication	1010
Learning Objectives	1010
Alignment and Rubric Map	1010
Lab Context: Cell Signaling and Communication	1010
Paper-Based Materials	1010
Paper-Based Investigation	1011
Data Recording	1011
Evidence and Reproducibility Checklist	1011
Paper-Based Evidence Upgrade	1011
Worked Example: Signal Amplification in a Four-Step Kinase Cascade	1012
Source-Governance Checkpoint	1012
Analysis Questions	1012
Post-Lab Synthesis	1013
Safety and Ethics Notes	1013
Debrief and Reflection	1013
Further Reading (Lab)	1013
Lab — Bioenergetics and Cellular Respiration	1014
Learning Objectives	1014
Alignment and Rubric Map	1014
Lab Context: Bioenergetics and Cellular Respiration	1014
Paper-Based Materials	1014
Paper-Based Investigation	1014
Data Recording	1015
Evidence and Reproducibility Checklist	1015
Paper-Based Evidence Upgrade	1015
Worked Example: ATP Yield and Gas-Exchange Proxies	1015
Source-Governance Checkpoint	1016
Analysis Questions	1016
Post-Lab Synthesis	1016
Optional Demonstration Extension	1016
Safety and Ethics Notes	1017
Debrief and Reflection	1017
Further Reading (Lab)	1017
Lab — Photosynthesis	1018
Learning Objectives	1018
Alignment and Rubric Map	1018
Pre-Lab Inquiry Questions	1018
Lab Context: Photosynthesis	1018
Paper-Based Materials	1018
Paper-Based Investigation	1019
Part 1: Experimental Design and Hypothesis Testing	1019
Part 2: Computational Biology Exercise — Data Analysis with Python	1019
Part 3: Light Intensity and Inverse-Square Law	1020
Part 4: CAM vs C3 Comparison (Extended Investigation)	1020
Data Recording	1020

Evidence and Reproducibility Checklist	1020
Paper-Based Evidence Upgrade	1020
Worked Example: Net O2 Evolution Above the Light Compensation Point	1021
Source-Governance Checkpoint	1021
Analysis Questions	1021
Post-Lab Synthesis	1022
Extension Analysis Questions	1022
Group Project Extension (Multi-Session)	1022
Real-World Problem Solving: Climate Change and Photosynthesis	1022
Optional Wet-Lab Extension	1023
Safety and Ethics Notes	1023
Debrief and Reflection	1023
Further Reading (Lab)	1023
Lab — Metabolic Integration and Regulation	1024
Learning Objectives	1024
Alignment and Rubric Map	1024
Pre-Lab Inquiry Questions	1024
Lab Context: Metabolic Integration and Regulation	1024
Paper-Based Materials	1024
Paper-Based Investigation	1025
Part 1: Glucose Tolerance Test Analysis	1025
Part 2: Computational Biology Exercise — Statistical Analysis with Python	1025
Part 3: Allosteric Regulation Modeling	1026
Data Recording	1026
Evidence and Reproducibility Checklist	1026
Paper-Based Evidence Upgrade	1026
Worked Example: How Long Would Liver Glycogen Alone Last in a Fast?	1027
Source-Governance Checkpoint	1027
Analysis Questions	1027
Post-Lab Synthesis	1027
Extension Analysis Questions	1028
Group Project Extension (Multi-Session)	1028
Real-World Problem Solving: Metabolic Diseases	1028
Safety and Ethics Notes	1028
Debrief and Reflection	1028
Further Reading (Lab)	1029
Lab — DNA Replication and the Cell Cycle	1030
Learning Objectives	1030
Alignment and Rubric Map	1030
Pre-Lab Inquiry Questions	1030
Lab Context: DNA Replication and the Cell Cycle	1030
Paper-Based Materials	1030
Paper-Based Investigation	1031
Part 1: Mitotic Index Determination from Image Cards	1031
Part 2: Computational Biology Exercise — Cell Cycle Modeling with Python	1031
Part 3: Semiconservative Replication Analysis	1032
Data Recording	1032
Evidence and Reproducibility Checklist	1032
Paper-Based Evidence Upgrade	1032
Worked Example: Replicon Size and S-Phase Timing in Humans	1033

Source-Governance Checkpoint	1033
Analysis Questions	1033
Post-Lab Synthesis	1033
Extension Analysis Questions	1033
Group Project Extension (Multi-Session)	1034
Real-World Problem Solving: Cancer Diagnostics	1034
Safety and Ethics Notes	1034
Debrief and Reflection	1034
Further Reading (Lab)	1034
Lab — Gene Expression	1035
Learning Objectives	1035
Alignment and Rubric Map	1035
Lab Context: Gene Expression	1035
Paper-Based Materials	1035
Paper-Based Investigation	1036
Data Recording	1036
Evidence and Reproducibility Checklist	1036
Paper-Based Evidence Upgrade	1036
Worked Example: Steady-State mRNA Levels Under Promoter Repression	1037
Source-Governance Checkpoint	1037
Analysis Questions	1037
Post-Lab Synthesis	1037
Safety and Ethics Notes	1038
Debrief and Reflection	1038
Further Reading (Lab)	1038
Lab — Mutations, CRISPR, and Genomics	1039
Learning Objectives	1039
Alignment and Rubric Map	1039
Pre-Lab Inquiry Questions	1039
Lab Context: Mutations, CRISPR, and Genomics	1039
Paper-Based Materials	1039
Paper-Based Investigation	1040
Part 1: Mutation Classification and Analysis	1040
Part 2: Computational Biology Exercise — CRISPR gRNA Design and Efficiency Analysis	1041
Part 3: Gel Electrophoresis Interpretation	1041
Part 4: Pangenome, Database, and Prime-Editing Decision Cards	1041
Data Recording	1041
Evidence and Reproducibility Checklist	1042
Paper-Based Evidence Upgrade	1042
Worked Example: KRAS Codon 12 GGT to GTT in Human Cancer	1042
Source-Governance Checkpoint	1042
Analysis Questions	1043
Post-Lab Synthesis	1043
Extension Analysis Questions	1043
Group Project Extension (Multi-Session)	1043
Real-World Problem Solving: Genome Editing Ethics	1044
Safety and Ethics Notes	1044
Debrief and Reflection	1044
Further Reading (Lab)	1044
Lab — Chromatin and Epigenetic Mechanisms	1045

Learning Objectives	1045
Alignment and Rubric Map	1045
Pre-Lab Inquiry Questions	1045
Lab Context: Chromatin and Epigenetic Mechanisms	1045
Paper-Based Materials	1045
Paper-Based Investigation	1046
Part 1: Epigenetic Data Analysis	1046
Part 2: Computational Biology Exercise — Epigenetic Age Prediction with Python	1046
Source-Governance Checkpoint	1047
Evidence and Reproducibility Checklist	1047
Paper-Based Evidence Upgrade	1047
Lab — Epigenetic Inheritance and Disease	1048
Alignment and Rubric Map	1048
Lab Context: Epigenetic Inheritance and Disease	1048
Paper-Based Materials	1048
Paper-Based Investigation	1048
Data Recording	1048
Evidence and Reproducibility Checklist	1049
Paper-Based Evidence Upgrade	1049
Worked Example: Estimating Methylated CpG Sites in Cancer vs Normal	1049
Analysis Questions	1049
Post-Lab Synthesis	1050
Extension Analysis Questions	1050
Group Project Extension (Multi-Session)	1050
Real-World Problem Solving: Epigenetic Ethics	1050
Safety and Ethics Notes	1051
Source-Governance Checkpoint	1051
Debrief and Reflection	1051
Further Reading (Lab)	1051
Lab — Mendelian Principles and Probability	1052
Learning Objectives	1052
Alignment and Rubric Map	1052
Pre-Lab Inquiry Questions	1052
Lab Context: Mendelian Principles and Probability	1052
Example Pedigree — Autosomal Recessive Trait (Cystic Fibrosis)	1053
Paper-Based Materials	1053
Paper-Based Investigation	1053
Part 1: Punnett Square Analysis	1053
Part 2: Computational Biology Exercise — Statistical Analysis with Python	1053
Source-Governance Checkpoint	1054
Evidence and Reproducibility Checklist	1054
Paper-Based Evidence Upgrade	1054
Lab — Mendelian Extensions and Human Genetics	1055
Alignment and Rubric Map	1055
Lab Context: Mendelian Extensions and Human Genetics	1055
Paper-Based Materials	1055
Paper-Based Investigation	1055
Data Recording	1055
Evidence and Reproducibility Checklist	1056
Paper-Based Evidence Upgrade	1056

Worked Example: Chi-Squared Test on a Dihybrid Cross	1056
Analysis Questions	1056
Extension Analysis Questions	1057
Group Project Extension (Multi-Session)	1057
Real-World Problem Solving: Genetic Counseling	1057
Post-Lab Synthesis	1057
Safety and Ethics Notes	1058
Source-Governance Checkpoint	1058
Debrief and Reflection	1058
Further Reading (Lab)	1058
Lab — Chromosomal Inheritance and Linkage	1059
Learning Objectives	1059
Alignment and Rubric Map	1059
Pre-Lab Inquiry Questions	1059
Lab Context: Chromosomal Inheritance and Linkage	1059
Paper-Based Materials	1059
Paper-Based Investigation	1060
Part 1: Genetic Linkage Mapping	1060
Part 2: Computational Biology Exercise — Linkage Analysis with Python	1060
Part 3: Karyotype Analysis	1061
Data Recording	1061
Evidence and Reproducibility Checklist	1061
Paper-Based Evidence Upgrade	1061
Worked Example: X-linked Hemophilia A Carrier Cross	1062
Source-Governance Checkpoint	1062
Analysis Questions	1062
Extension Analysis Questions	1063
Group Project Extension (Multi-Session)	1063
Real-World Problem Solving: Genetic Counseling	1063
Post-Lab Synthesis	1063
Safety and Ethics Notes	1063
Debrief and Reflection	1063
Further Reading (Lab)	1064
Lab — Population Genetics	1065
Learning Objectives	1065
Alignment and Rubric Map	1065
Lab Context: Population Genetics	1065
Paper-Based Materials	1065
Paper-Based Investigation	1065
Data Recording	1066
Evidence and Reproducibility Checklist	1066
Paper-Based Evidence Upgrade	1067
Worked Example: Hardy-Weinberg Allele Frequency Estimation	1067
Source-Governance Checkpoint	1067
Analysis Questions	1067
Post-Lab Synthesis	1068
Safety and Ethics Notes	1068
Debrief and Reflection	1068
Further Reading (Lab)	1068
Lab — Natural Selection and Adaptation	1069

Learning Objectives	1069
Alignment and Rubric Map	1069
Pre-Lab Inquiry Questions	1069
Lab Context: Natural Selection and Adaptation	1069
Paper-Based Materials	1070
Paper-Based Investigation	1070
Part 1: Predator-Prey Selection Simulation	1070
Part 2: Computational Biology Exercise — Selection Coefficient Analysis with Python	1070
Part 3: Finch Beak Analysis	1071
Data Recording	1071
Evidence and Reproducibility Checklist	1071
Paper-Based Evidence Upgrade	1071
Worked Example: Allele Frequency Change Under Selection	1072
Source-Governance Checkpoint	1072
Analysis Questions	1072
Extension Analysis Questions	1073
Group Project Extension (Multi-Session)	1073
Real-World Problem Solving: Evolution and Medicine	1073
Post-Lab Synthesis	1073
Safety and Ethics Notes	1074
Debrief and Reflection	1074
Further Reading (Lab)	1074
Lab — Genetic Drift, Gene Flow, and Speciation	1075
Learning Objectives	1075
Alignment and Rubric Map	1075
Pre-Lab Inquiry Questions	1075
Lab Context: Genetic Drift, Gene Flow, and Speciation	1075
Paper-Based Materials	1076
Paper-Based Investigation	1076
Part 1: Founder Effect Simulation	1076
Part 2: Computational Biology Exercise — Population Genetics Analysis with Python	1076
Part 3: Morphological Divergence Analysis	1077
Data Recording	1077
Evidence and Reproducibility Checklist	1077
Paper-Based Evidence Upgrade	1077
Worked Example: Effective Population Size with Unequal Sex Ratio	1078
Source-Governance Checkpoint	1078
Analysis Questions	1078
Extension Analysis Questions	1079
Group Project Extension (Multi-Session)	1079
Real-World Problem Solving: Conservation Genetics	1079
Post-Lab Synthesis	1079
Safety and Ethics Notes	1079
Debrief and Reflection	1080
Further Reading (Lab)	1080
Lab — Phylogenetics and the Tree of Life	1081
Learning Objectives	1081
Alignment and Rubric Map	1081
Lab Context: Phylogenetics and the Tree of Life	1081
Paper-Based Materials	1081

Paper-Based Investigation	1081
Data Recording	1082
Evidence and Reproducibility Checklist	1082
Paper-Based Evidence Upgrade	1082
Worked Example: UPGMA Tree from a Pairwise Distance Matrix	1083
Source-Governance Checkpoint	1083
Analysis Questions	1083
Post-Lab Synthesis	1083
Safety and Ethics Notes	1084
Debrief and Reflection	1084
Further Reading (Lab)	1084
Lab — Bacteria, Archaea, and Viruses	1085
Learning Objectives	1085
Alignment and Rubric Map	1085
Pre-Lab Inquiry Questions	1085
Lab Context: Bacteria, Archaea, and Viruses	1085
Paper-Based Materials	1085
Paper-Based Investigation	1086
Part 1: Gram-Stain Image Classification	1086
Part 2: Computational Biology Exercise — Bacterial Growth Analysis with Python	1086
Part 3: Serial Dilution and Colony Counting from Plate Images	1087
Part 4: AMR Network and Fungal Triage Cards	1087
Data Recording	1087
Evidence and Reproducibility Checklist	1087
Paper-Based Evidence Upgrade	1088
Worked Example: Exponential growth of an E. coli culture	1088
Source-Governance Checkpoint	1088
Analysis Questions	1088
Extension Analysis Questions	1089
Group Project Extension (Multi-Session)	1089
Real-World Problem Solving: Microbial Ethics	1089
Post-Lab Synthesis	1089
Safety and Ethics Notes	1089
Debrief and Reflection	1089
Further Reading (Lab)	1090
Lab — Microbial Ecology and the Microbiome	1091
Learning Objectives	1091
Alignment and Rubric Map	1091
Pre-Lab Inquiry Questions	1091
Lab Context: Microbial Ecology and the Microbiome	1091
Paper-Based Materials	1091
Paper-Based Investigation	1092
Part 1: Community Diversity from Case Packets	1092
Part 2: Computational Biology Exercise — Diversity Analysis with Python	1092
Part 3: Microbial Interaction Network Analysis	1093
Data Recording	1093
Evidence and Reproducibility Checklist	1093
Paper-Based Evidence Upgrade	1093
Worked Example: Shannon Diversity Index for a Microbial Community	1094
Source-Governance Checkpoint	1094

Analysis Questions	1094
Extension Analysis Questions	1095
Group Project Extension (Multi-Session)	1095
Real-World Problem Solving: Microbial Ethics	1095
Post-Lab Synthesis	1095
Safety and Ethics Notes	1095
Debrief and Reflection	1095
Further Reading (Lab)	1096
Lab — Host Immunity and Vaccines	1097
Learning Objectives	1097
Alignment and Rubric Map	1097
Pre-Lab Inquiry Questions	1097
Lab Context: Host Immunity and Vaccines	1097
Paper-Based Materials	1097
Paper-Based Investigation	1098
Part 1: Epidemic Curve Analysis	1098
Source-Governance Checkpoint	1099
Evidence and Reproducibility Checklist	1099
Paper-Based Evidence Upgrade	1099
Lab — Antimicrobial Resistance and Epidemiology	1100
Alignment and Rubric Map	1100
Lab Context: Antimicrobial Resistance and Epidemiology	1100
Paper-Based Materials	1100
Paper-Based Investigation	1100
Part 3: Herd Immunity Calculation	1100
Part 4: Current Intervention Decision Matrices	1100
Data Recording	1101
Evidence and Reproducibility Checklist	1101
Paper-Based Evidence Upgrade	1101
Worked Example: Herd Immunity Threshold from R-zero	1102
Analysis Questions	1102
Extension Analysis Questions	1102
Group Project Extension (Multi-Session)	1102
Real-World Problem Solving: Epidemic Ethics	1103
Post-Lab Synthesis	1103
Safety and Ethics Notes	1103
Source-Governance Checkpoint	1103
Debrief and Reflection	1103
Further Reading (Lab)	1104
Lab — Plant Structure and Water Relations	1105
Learning Objectives	1105
Alignment and Rubric Map	1105
Pre-Lab Inquiry Questions	1105
Lab Context: Plant Structure and Water Relations	1105
Paper-Based Materials	1105
Paper-Based Investigation	1106
Part 1: Anatomical Diagram and Tissue Identification	1106
Part 2: Computational Biology Exercise — Transpiration Analysis with Python	1106
Part 3: Transpiration Dataset and Model Check	1107
Data Recording	1107

Evidence and Reproducibility Checklist	1107
Paper-Based Evidence Upgrade	1108
Worked Example: Water Potential and Osmotic Equilibrium	1108
Source-Governance Checkpoint	1108
Analysis Questions	1108
Extension Analysis Questions	1109
Group Project Extension (Multi-Session)	1109
Real-World Problem Solving: Plant Water Relations and Agriculture	1109
Post-Lab Synthesis	1109
Optional Wet-Lab Demonstration	1109
Safety and Ethics Notes	1109
Debrief and Reflection	1109
Further Reading (Lab)	1110
Lab — Plant Reproduction and Development	1111
Learning Objectives	1111
Alignment and Rubric Map	1111
Pre-Lab Inquiry Questions	1111
Lab Context: Plant Reproduction and Development	1111
Paper-Based Materials	1111
Paper-Based Investigation	1112
Part 1: Flower Anatomy and Pollination Strategy Cards	1112
Part 2: Computational Biology Exercise — Pollen Tube Growth Analysis with Python	1112
Part 3: Pollen Germination Dataset	1113
Data Recording	1113
Evidence and Reproducibility Checklist	1114
Paper-Based Evidence Upgrade	1114
Worked Example: Reproductive Success and Seed Survival	1114
Source-Governance Checkpoint	1114
Analysis Questions	1114
Extension Analysis Questions	1115
Group Project Extension (Multi-Session)	1115
Real-World Problem Solving: Plant Reproduction and Agriculture	1115
Post-Lab Synthesis	1115
Optional Wet-Lab Demonstration	1116
Safety and Ethics Notes	1116
Debrief and Reflection	1116
Further Reading (Lab)	1116
Lab — Plant Responses to the Environment	1117
Learning Objectives	1117
Alignment and Rubric Map	1117
Lab Context: Plant Responses to the Environment	1117
Paper-Based Materials	1117
Paper-Based Investigation	1118
Data Recording	1118
Evidence and Reproducibility Checklist	1119
Paper-Based Evidence Upgrade	1119
Worked Example: Photoperiodism and Night Length	1119
Source-Governance Checkpoint	1119
Analysis Questions	1119
Post-Lab Synthesis	1120

Safety and Ethics Notes	1120
Debrief and Reflection	1120
Further Reading (Lab)	1120
Lab — Circulation and Respiration	1121
Learning Objectives	1121
Alignment and Rubric Map	1121
Lab Context: Circulation and Respiration	1121
Paper-Based Materials	1121
Paper-Based Investigation	1122
Data Recording	1122
Evidence and Reproducibility Checklist	1122
Paper-Based Evidence Upgrade	1123
Worked Example: Cardiac Output and Fick Calculation in Exercise	1123
Source-Governance Checkpoint	1123
Analysis Questions	1123
Post-Lab Synthesis	1124
Safety and Ethics Notes	1124
Debrief and Reflection	1124
Further Reading (Lab)	1124
Lab — Nervous System and Neural Signaling	1125
Learning Objectives	1125
Alignment and Rubric Map	1125
Lab Context: Nervous System and Neural Signaling	1125
Paper-Based Materials	1125
Paper-Based Investigation	1126
Data Recording	1126
Evidence and Reproducibility Checklist	1127
Paper-Based Evidence Upgrade	1127
Worked Example: Median Nerve Conduction Velocity	1127
Source-Governance Checkpoint	1127
Analysis Questions	1127
Post-Lab Synthesis	1128
Safety and Ethics Notes	1128
Debrief and Reflection	1128
Further Reading (Lab)	1128
Lab — Action Potentials and Synaptic Transmission	1129
Learning Objectives	1129
Alignment and Rubric Map	1129
Lab Context: Action Potentials and Synaptic Transmission	1129
Paper-Based Materials	1129
Paper-Based Investigation	1130
Data Recording	1130
Evidence and Reproducibility Checklist	1130
Paper-Based Evidence Upgrade	1131
Worked Example: Nernst Potential for Na ⁺ at 37 C	1131
Source-Governance Checkpoint	1131
Analysis Questions	1131
Post-Lab Synthesis	1132
Safety and Ethics Notes	1132
Debrief and Reflection	1132

Further Reading (Lab)	1132
Lab — Endocrine Signaling and Homeostasis	1133
Learning Objectives	1133
Alignment and Rubric Map	1133
Lab Context: Endocrine Signaling and Homeostasis	1133
Paper-Based Materials	1133
Paper-Based Investigation	1134
Source-Governance Checkpoint	1134
Evidence and Reproducibility Checklist	1134
Paper-Based Evidence Upgrade	1134
Lab — Immune System Architecture	1135
Alignment and Rubric Map	1135
Lab Context: Immune System Architecture	1135
Paper-Based Materials	1135
Paper-Based Investigation	1135
Data Recording	1135
Evidence and Reproducibility Checklist	1136
Paper-Based Evidence Upgrade	1136
Worked Example: Interpreting an Abnormal Thyroid Panel	1136
Analysis Questions	1137
Post-Lab Synthesis	1137
Safety and Ethics Notes	1137
Source-Governance Checkpoint	1137
Debrief and Reflection	1137
Further Reading (Lab)	1138
Lab — Population Ecology and Growth Models	1139
Learning Objectives	1139
Alignment and Rubric Map	1139
Lab Context: Population Ecology and Growth Models	1139
Paper-Based Materials	1139
Paper-Based Investigation	1140
Data Recording	1140
Evidence and Reproducibility Checklist	1140
Paper-Based Evidence Upgrade	1141
Worked Example: Logistic Growth Rate Below Carrying Capacity	1141
Source-Governance Checkpoint	1141
Analysis Questions	1141
Post-Lab Synthesis	1142
Safety and Ethics Notes	1142
Debrief and Reflection	1142
Further Reading (Lab)	1142
Lab — Community Interactions and Succession	1143
Learning Objectives	1143
Alignment and Rubric Map	1143
Lab Context: Community Interactions and Succession	1143
Paper-Based Materials	1143
Paper-Based Investigation	1144
Source-Governance Checkpoint	1144
Evidence and Reproducibility Checklist	1144

Paper-Based Evidence Upgrade	1144
Lab — Biodiversity and Food Webs	1145
Alignment and Rubric Map	1145
Lab Context: Biodiversity and Food Webs	1145
Paper-Based Materials	1145
Paper-Based Investigation	1145
Data Recording	1145
Evidence and Reproducibility Checklist	1146
Paper-Based Evidence Upgrade	1146
Worked Example: Shannon Diversity and Evenness in Two Communities	1146
Analysis Questions	1147
Post-Lab Synthesis	1147
Safety and Ethics Notes	1147
Source-Governance Checkpoint	1147
Debrief and Reflection	1147
Further Reading (Lab)	1147
Lab — Ecosystem Ecology	1149
Learning Objectives	1149
Alignment and Rubric Map	1149
Lab Context: Ecosystem Ecology	1149
Paper-Based Materials	1149
Paper-Based Investigation	1150
Data Recording	1150
Evidence and Reproducibility Checklist	1151
Paper-Based Evidence Upgrade	1151
Worked Example: Trophic Efficiencies in a Grassland Ecosystem	1151
Source-Governance Checkpoint	1151
Analysis Questions	1151
Post-Lab Synthesis	1152
Safety and Ethics Notes	1152
Debrief and Reflection	1152
Further Reading (Lab)	1152
Lab — Biomes and Conservation Biology	1153
Learning Objectives	1153
Alignment and Rubric Map	1153
Lab Context: Biomes and Conservation Biology	1153
Paper-Based Materials	1153
Paper-Based Investigation	1154
Data Recording	1154
Evidence and Reproducibility Checklist	1155
Paper-Based Evidence Upgrade	1155
Worked Example: Heterozygosity Loss in a Small Tiger Population	1155
Source-Governance Checkpoint	1156
Analysis Questions	1156
Post-Lab Synthesis	1156
Safety and Ethics Notes	1156
Debrief and Reflection	1156
Further Reading (Lab)	1157
Questions — Systems Science and Emergence	1158

Questions 1–10: Recall and Comprehension	1158
Recall Questions (1 mark each)	1158
Instructor Use and Coverage Notes	1158
Application Questions (2 marks each)	1158
Synthesis Questions (4 marks each)	1159
Questions 11–20: Application and Analysis	1159
Data and Model Interpretation Questions (3 marks each)	1159
Questions 21–30: Synthesis and Evaluation	1160
Evaluation and Design Questions (4 marks each)	1161
Questions — Complex Adaptive Systems	1162
Questions 1–10: Recall and Comprehension	1162
Recall Questions (1 mark each)	1162
Instructor Use and Coverage Notes	1162
Application Questions (2 marks each)	1162
Synthesis Questions (4 marks each)	1163
Questions 11–20: Application and Analysis	1163
Data and Model Interpretation Questions (3 marks each)	1163
Questions 21–30: Synthesis and Evaluation	1164
Evaluation and Design Questions (4 marks each)	1164
Questions — Active Inference and Free Energy	1166
Questions 1–10: Recall and Comprehension	1166
Recall Questions (1 mark each)	1166
Instructor Use and Coverage Notes	1166
Application Questions (2 marks each)	1166
Synthesis Questions (4 marks each)	1167
Questions 11–20: Application and Analysis	1167
Data and Model Interpretation Questions (3 marks each)	1167
Questions 21–30: Synthesis and Evaluation	1168
Evaluation and Design Questions (4 marks each)	1168
Questions — History and Philosophy of Biology	1170
Recall Questions (1 mark each)	1170
Instructor Use and Coverage Notes	1170
Questions 1–10: Recall and Comprehension	1170
Application Questions (2 marks each)	1171
Questions 11–20: Application and Analysis	1171
Synthesis Questions (4 marks each)	1171
Questions 21–30: Synthesis and Evaluation	1171
Questions — Atoms, Molecules, and Chemical Bonds	1173
Instructor Use and Coverage Notes	1173
Questions 1–10: Recall and Comprehension	1173
Questions 11–20: Application and Analysis	1174
Questions 21–30: Synthesis and Evaluation	1175
Questions — Water — The Molecule of Life	1178
Instructor Use and Coverage Notes	1178
Questions 1–10: Recall and Comprehension	1178
Questions 11–20: Application and Analysis	1179
Questions 21–30: Synthesis and Evaluation	1181
Questions — Biological Macromolecules	1184

Instructor Use and Coverage Notes	1184
Questions 1–10: Recall and Comprehension	1184
Questions 11–20: Application and Analysis	1185
Questions 21–30: Synthesis and Evaluation	1187
Questions — Enzymes and the Kinetics of Catalysis	1190
Instructor Use and Coverage Notes	1190
Questions 1–10: Recall and Comprehension	1190
Questions 11–20: Application and Analysis	1191
Questions 21–30: Synthesis and Evaluation	1193
Questions — Cell Theory and Cell Types	1196
Instructor Use and Coverage Notes	1196
Questions 1–10: Recall and Comprehension	1196
Questions 11–20: Application and Analysis	1197
Questions 21–30: Synthesis and Evaluation	1199
Questions — Cell Structure and Organelles	1202
Instructor Use and Coverage Notes	1202
Questions 1–10: Recall and Comprehension	1202
Questions 11–20: Application and Analysis	1203
Questions 21–30: Synthesis and Evaluation	1205
Questions — Membrane Structure and Transport	1208
Instructor Use and Coverage Notes	1208
Questions 1–10: Recall and Comprehension	1208
Questions 11–20: Application and Analysis	1209
Questions 21–30: Synthesis and Evaluation	1210
Questions — Cell Signaling and Communication	1213
Instructor Use and Coverage Notes	1213
Questions 1–10: Recall and Comprehension	1213
Questions 11–20: Application and Analysis	1214
Questions 21–30: Synthesis and Evaluation	1215
Questions — Bioenergetics and Cellular Respiration	1218
Instructor Use and Coverage Notes	1218
Questions 1–10: Recall and Comprehension	1218
Questions 11–20: Application and Analysis	1219
Questions 21–30: Synthesis and Evaluation	1220
Questions — Photosynthesis	1222
Instructor Use and Coverage Notes	1222
Questions 1–10: Recall and Comprehension	1222
Questions 11–20: Application and Analysis	1223
Questions 21–30: Synthesis and Evaluation	1224
Questions — Metabolic Integration and Regulation	1227
Instructor Use and Coverage Notes	1227
Questions 1–10: Recall and Comprehension	1227
Questions 11–20: Application and Analysis	1228
Questions 21–30: Synthesis and Evaluation	1229
Questions — DNA Replication and the Cell Cycle	1232
Instructor Use and Coverage Notes	1232

Questions 1–10: Recall and Comprehension	1232
Questions 11–20: Application and Analysis	1233
Questions 21–30: Synthesis and Evaluation	1234
Questions — Gene Expression	1236
Instructor Use and Coverage Notes	1236
Questions 1–10: Recall and Comprehension	1236
Questions 11–20: Application and Analysis	1237
Questions 21–30: Synthesis and Evaluation	1239
Questions — Mutations, CRISPR, and Genomics	1242
Instructor Use and Coverage Notes	1242
Questions 1–10: Recall and Comprehension	1242
Questions 11–20: Application and Analysis	1243
Questions 21–30: Synthesis and Evaluation	1245
Questions — Chromatin and Epigenetic Mechanisms	1248
Instructor Use and Coverage Notes	1248
Questions 1–10: Recall and Comprehension	1248
Questions 11–20: Application and Analysis	1249
Questions 21–30: Synthesis and Evaluation	1251
Questions — Epigenetic Inheritance and Disease	1253
Instructor Use and Coverage Notes	1253
Questions 1–10: Recall and Comprehension	1253
Questions 11–20: Application and Analysis	1255
Questions 21–30: Synthesis and Evaluation	1256
Questions — Mendelian Principles and Probability	1258
Instructor Use and Coverage Notes	1258
Questions 1–10: Recall and Comprehension	1258
Questions 11–20: Application and Analysis	1259
Questions 21–30: Synthesis and Evaluation	1260
Questions — Mendelian Extensions and Human Genetics	1263
Instructor Use and Coverage Notes	1263
Questions 1–10: Recall and Comprehension	1263
Questions 11–20: Application and Analysis	1264
Questions 21–30: Synthesis and Evaluation	1266
Questions — Chromosomal Inheritance and Linkage	1268
Instructor Use and Coverage Notes	1268
Questions 1–10: Recall and Comprehension	1268
Questions 11–20: Application and Analysis	1269
Questions 21–30: Synthesis and Evaluation	1270
Questions — Population Genetics	1273
Instructor Use and Coverage Notes	1273
Questions 1–10: Recall and Comprehension	1273
Questions 11–20: Application and Analysis	1274
Questions 21–30: Synthesis and Evaluation	1275
Questions — Natural Selection and Adaptation	1278
Instructor Use and Coverage Notes	1278
Questions 1–10: Recall and Comprehension	1278

Questions 11–20: Application and Analysis	1278
Questions 21–30: Synthesis and Evaluation	1280
Questions — Genetic Drift, Gene Flow, and Speciation	1282
Instructor Use and Coverage Notes	1282
Questions 1–10: Recall and Comprehension	1282
Questions 11–20: Application and Analysis	1283
Questions 21–30: Synthesis and Evaluation	1284
Questions — Phylogenetics and the Tree of Life	1286
Instructor Use and Coverage Notes	1286
Questions 1–10: Recall and Comprehension	1286
Questions 11–20: Application and Analysis	1286
Questions 21–30: Synthesis and Evaluation	1288
Questions — Bacteria, Archaea, and Viruses	1290
Instructor Use and Coverage Notes	1290
Questions 1–10: Recall and Comprehension	1290
Questions 11–20: Application and Analysis	1291
Questions 21–30: Synthesis and Evaluation	1292
Questions — Microbial Ecology and the Microbiome	1295
Instructor Use and Coverage Notes	1295
Questions 1–10: Recall and Comprehension	1295
Questions 11–20: Application and Analysis	1296
Questions 21–30: Synthesis and Evaluation	1298
Questions — Host Immunity and Vaccines	1300
Instructor Use and Coverage Notes	1300
Questions 1–10: Recall and Comprehension	1300
Questions 11–20: Application and Analysis	1301
Questions 21–30: Synthesis and Evaluation	1303
Questions — Antimicrobial Resistance and Epidemiology	1306
Instructor Use and Coverage Notes	1306
Questions 1–10: Recall and Comprehension	1306
Questions 11–20: Application and Analysis	1308
Questions 21–30: Synthesis and Evaluation	1309
Questions — Plant Structure and Water Relations	1312
Instructor Use and Coverage Notes	1312
Questions 1–10: Recall and Comprehension	1312
Questions 11–20: Application and Analysis	1313
Questions 21–30: Synthesis and Evaluation	1314
Questions — Plant Reproduction and Development	1317
Instructor Use and Coverage Notes	1317
Questions 1–10: Recall and Comprehension	1317
Questions 11–20: Application and Analysis	1318
Questions 21–30: Synthesis and Evaluation	1320
Questions — Plant Responses to the Environment	1323
Instructor Use and Coverage Notes	1323
Questions 1–10: Recall and Comprehension	1323
Questions 11–20: Application and Analysis	1324

Questions 21–30: Synthesis and Evaluation	1326
Questions — Circulation and Respiration	1329
Instructor Use and Coverage Notes	1329
Questions 1–10: Recall and Comprehension	1329
Questions 11–20: Application and Analysis	1330
Questions 21–30: Synthesis and Evaluation	1331
Questions — Nervous System and Neural Signaling	1334
Instructor Use and Coverage Notes	1334
Questions 1–10: Recall and Comprehension	1334
Questions 11–20: Application and Analysis	1335
Questions 21–30: Synthesis and Evaluation	1336
Questions — Action Potentials and Synaptic Transmission	1339
Instructor Use and Coverage Notes	1339
Questions 1–10: Recall and Comprehension	1339
Questions 11–20: Application and Analysis	1340
Questions 21–30: Synthesis and Evaluation	1342
Questions — Endocrine Signaling and Homeostasis	1346
Instructor Use and Coverage Notes	1346
Questions 1–10: Recall and Comprehension	1346
Questions 11–20: Application and Analysis	1347
Questions 21–30: Synthesis and Evaluation	1349
Questions — Immune System Architecture	1352
Instructor Use and Coverage Notes	1352
Questions 1–10: Recall and Comprehension	1352
Questions 11–20: Application and Analysis	1354
Questions 21–30: Synthesis and Evaluation	1355
Questions — Population Ecology and Growth Models	1358
Instructor Use and Coverage Notes	1358
Questions 1–10: Recall and Comprehension	1358
Questions 11–20: Application and Analysis	1359
Questions 21–30: Synthesis and Evaluation	1360
Questions — Community Interactions and Succession	1363
Instructor Use and Coverage Notes	1363
Questions 1–10: Recall and Comprehension	1363
Questions 11–20: Application and Analysis	1364
Questions 21–30: Synthesis and Evaluation	1366
Questions — Biodiversity and Food Webs	1368
Instructor Use and Coverage Notes	1368
Questions 1–10: Recall and Comprehension	1368
Questions 11–20: Application and Analysis	1370
Questions 21–30: Synthesis and Evaluation	1371
Questions — Ecosystem Ecology	1373
Instructor Use and Coverage Notes	1373
Questions 1–10: Recall and Comprehension	1373
Questions 11–20: Application and Analysis	1374
Questions 21–30: Synthesis and Evaluation	1375

Questions — Biomes and Conservation Biology	1378
Instructor Use and Coverage Notes	1378
Questions 1–10: Recall and Comprehension	1378
Questions 11–20: Application and Analysis	1379
Questions 21–30: Synthesis and Evaluation	1381
Appendix A — Curriculum Map	1384
Unit 0	1384
— Systems Science and Emergence	1384
— Complex Adaptive Systems	1384
— Active Inference and Free Energy	1384
— History and Philosophy of Biology	1384
Unit I	1385
— Atoms, Molecules, and Chemical Bonds	1385
— Water — The Molecule of Life	1385
— Biological Macromolecules	1385
— Enzymes and the Kinetics of Catalysis	1386
Unit II	1386
— Cell Theory and Cell Types	1386
— Cell Structure and Organelles	1386
— Membrane Structure and Transport	1386
— Cell Signaling and Communication	1387
Unit III	1387
— Bioenergetics and Cellular Respiration	1387
— Photosynthesis	1387
— Metabolic Integration and Regulation	1388
Unit IV	1388
— DNA Replication and the Cell Cycle	1388
— Gene Expression	1388
— Mutations, CRISPR, and Genomics	1388
— Chromatin and Epigenetic Mechanisms	1389
— Epigenetic Inheritance and Disease	1389
Unit V	1389
— Mendelian Principles and Probability	1389
— Mendelian Extensions and Human Genetics	1389
— Chromosomal Inheritance and Linkage	1390
— Population Genetics	1390
Unit VI	1390
— Natural Selection and Adaptation	1390
— Genetic Drift, Gene Flow, and Speciation	1390
— Phylogenetics and the Tree of Life	1391
Unit VII	1391
— Bacteria, Archaea, and Viruses	1391
— Microbial Ecology and the Microbiome	1391
— Host Immunity and Vaccines	1392
— Antimicrobial Resistance and Epidemiology	1392
Unit VIII	1392
— Plant Structure and Water Relations	1392
— Plant Reproduction and Development	1392
— Plant Responses to the Environment	1393
Unit IX	1393
— Circulation and Respiration	1393

— Nervous System and Neural Signaling	1393
— Action Potentials and Synaptic Transmission	1393
— Endocrine Signaling and Homeostasis	1394
— Immune System Architecture	1394
Unit X	1394
— Population Ecology and Growth Models	1394
— Community Interactions and Succession	1395
— Biodiversity and Food Webs	1395
— Ecosystem Ecology	1395
— Biomes and Conservation Biology	1395
Appendix B — Instructor Orchestration Guide	1397
Reusable Teaching Loop	1397
Chapter Orchestration Matrix	1397
Unit 0	1397
Unit I	1398
Unit II	1399
Unit III	1399
Unit IV	1400
Unit V	1401
Unit VI	1402
Unit VII	1403
Unit VIII	1404
Unit IX	1404
Unit X	1406
Appendix C — Mathematical Review for Biology	1408
C.1 Logarithms and the Natural Log	1408
Definition	1408
Key identities	1408
Worked example — doubling time	1408
C.2 Differential and Integral Calculus	1408
Derivatives as rates	1408
Integration as accumulation	1408
First-order ODE: exponential growth and decay	1409
Logistic growth (nonlinear)	1409
C.3 Basic Probability	1409
Independent events	1409
Conditional probability and Bayes’ theorem	1409
Binomial distribution	1409
Poisson distribution	1409
C.4 Dimensional Analysis	1410
Example — diffusion distance	1410
Standard SI units used in this book	1410
Non-SI units common in biology	1410
C.5 Linear Algebra Miniature	1410
Matrices as transitions	1410
Eigenvalues and equilibrium	1410
C.6 Common Pitfalls in Biological Math	1411
C.7 Key Equations Quick Reference	1411
Michaelis-Menten equation	1411
Hill equation (cooperative binding)	1411

Nernst equation	1411
Goldman-Hodgkin-Katz equation	1411
Henderson-Hasselbalch equation	1412
Water potential	1412
Further Reading and Source Notes	1412
Appendix D — Units, Physical Constants, and Biological Ranges	1413
D.1 SI Base and Derived Units	1413
Metric prefixes	1413
D.2 Universal Physical Constants	1413
D.3 Energy Conversions	1414
ATP hydrolysis benchmarks	1414
D.4 Pressure Conversions	1414
D.5 Concentration Conversions	1414
D.6 Biological Magnitudes — Quick Reference	1415
Time scales	1415
Length scales	1415
Energy scales	1415
Organismal physiology reference scales	1416
D.7 Fundamental Biological Constants	1416
Appendix E — A Periodic Table for Biology	1417
E.1 The Six Bulk Elements (CHNOPS)	1417
E.2 Essential Macro-Minerals (Electrolytes + Osteogenics)	1417
E.3 Trace Elements (Enzyme Cofactors)	1418
E.4 Ultra-Trace and Context-Dependent Elements	1419
E.5 Life Without an Expected Element	1419
E.6 Quick Lookup: Which Chapter Covers Each Element?	1419
Appendix F — Master Glossary of Biological Terms	1421
A	1421
B	1422
C	1422
D	1423
E	1423
F	1424
G	1424
H	1425
I	1426
K	1426
L	1426
M	1427
N	1427
O	1427
P	1428
R	1428
S	1429
T	1429
V	1429
W	1430
X	1430
Z	1430
Additional Terms	1430

C (continued)	1430
D (continued)	1430
E (continued)	1430
F (continued)	1431
G (continued)	1431
H (continued)	1431
I (continued)	1431
K (continued)	1432
L (continued)	1432
M (continued)	1432
N (continued)	1432
O (continued)	1432
P (continued)	1432
R (continued)	1433
S (continued)	1433
T (continued)	1434
V (continued)	1434
W (continued)	1434
Appendix G — Index of Key Terms	1435
	1435
A	1435
B	1435
C	1435
D	1435
E	1435
F	1436
G	1436
H	1436
I	1436
K	1436
L	1436
M	1436
N	1436
O	1436
P	1436
R	1437
S	1437
T	1437
V	1437
W	1437
X	1437
Z	1437

Front Matter

Dedication

*To the active minds who encounter biology not as a collection of facts,
but as a living, computable, immersive, and mathematically rich discipline —
and to those who show them the way.*

Acknowledgements

The author gratefully acknowledges many contributions, learnings, and sources of inspiration.

Scientific foundations. This textbook builds on foundational scholarship in molecular biology, biochemistry, physiology, ecology, and evolution—including the textbooks of Alberts et al. (*Molecular Biology of the Cell*), Campbell & Reece (*Biology*), Stryer (*Biochemistry*), Lehninger (*Principles of Biochemistry*), the primary literature cited throughout each chapter, and the open curriculum [OpenStax Biology 2e](#). We cite specific experimental results at point of use with full author credit and pause in gratitude to the researchers whose work makes this synthesis possible.

Open science. This textbook is open source and open access. The source code is licensed under the Apache-2.0 license, and the text is licensed under the Creative Commons Attribution 4.0 International license. Sources, figures, tests, and rendered outputs are maintained in the [biology textbook repository](#). The work builds on, and contributes to, the open-science community whose code, data, lifeways, and scholarship have made this work freely available, computationally grounded, and broadly accessible.

Open educational resources. Open textbook adoption in U.S. and Canadian higher education has grown from roughly 1-in-400 classes in 2013 to about 1-in-80 by 2023, measured from syllabus-assigned titles rather than download counts [[Open Syllabus Project, 2023](#)]. At the University of Georgia, courses that switched to OpenStax materials—including introductory biology—showed improved grade distributions and lower D/F/W rates compared with prior commercial-textbook terms [[Colvard et al., 2018](#)]. This book treats [OpenStax Biology 2e](#) as conceptual inspiration and a public reference point, not as a derivative work.

Biology education. This textbook supports introductory through upper-division biology courses—survey, majors, pre-health, and computation-first reading paths—with active learning, companion labs, and question banks aligned to each chapter. Suggested reading paths in the navigation section below map units to common course designs.

Research project template. The build pipeline, testing infrastructure, and multi-project architecture are based on the author’s [Research Project Template](#). The template provides version control, testing, documentation, and publication tooling used to build this textbook.

About This Textbook

Computational Philosophy

This *Introduction to Biology: A Generative Approach* integrates biological narrative explanation and conceptual elaboration, with formalisms, models, computational connections, and empirical studies. When a chapter introduces a model (enzyme kinetics, predator–prey dynamics, action potentials), the corresponding computation is implemented in the accompanying Python modules and used to generate figures where appropriate. Every aspect of this textbook is designed to help students move between mechanisms, measurements, and models: what a system does, how we know, and what a simple quantitative model can predict (and where it breaks).

What Makes This Textbook Different

Feature	This Textbook	Traditional Textbook
Figures	Generated from mathematical models; reproducible	Static graphics
Equations	Derived and numerically validated	Stated without derivation
Code	Python modules for every major model	Absent
Diagrams	Mermaid process diagrams; automatically rendered	Hand-drawn
Opening vignettes	Landmark experiment narrative opening each chapter	Absent
Curriculum map	Generated chapter/lab/question/standards alignment	Usually external
Master glossary	225 terms with etymology and chapter cross-references	Chapter-end lists
Instructor edition	Question-bank model answers rendered as blockquotes (exp ort.include_solutions: true)	Student edition hides solutions
Open access	CC BY 4.0; fully open source	Copyright restricted
Citations	Inline, with year and journal	Often chapter-end primarily

How to Navigate This Book

The textbook is organized from systems-level orientation through molecular, cellular, organismal, evolutionary, and ecological scales. The entries below are generated from `manuscript/config.yaml` so navigation stays aligned with the rendered table of contents.

- **Unit 0 — Systems Science for Biology:** Systems Science and Emergence; Complex Adaptive Systems; Active Inference and Free Energy; History and Philosophy of Biology.
- **Unit I — Chemistry of Life:** Atoms, Molecules, and Chemical Bonds; Water — The Molecule of Life; Biological Macromolecules; Enzymes and the Kinetics of Catalysis.
- **Unit II — The Cell:** Cell Theory and Cell Types; Cell Structure and Organelles; Membrane Structure and Transport; Cell Signaling and Communication.
- **Unit III — Energy and Metabolism:** Bioenergetics and Cellular Respiration; Photosynthesis; Metabolic Integration and Regulation.
- **Unit IV — Molecular Genetics:** DNA Replication and the Cell Cycle; Gene Expression; Mutations, CRISPR, and Genomics; Chromatin and Epigenetic Mechanisms; Epigenetic Inheritance and Disease.
- **Unit V — Classical Genetics and Heredity:** Mendelian Principles and Probability; Mendelian Extensions and Human Genetics; Chromosomal Inheritance and Linkage; Population Genetics.
- **Unit VI — Evolution:** Natural Selection and Adaptation; Genetic Drift, Gene Flow, and Speciation; Phylogenetics and the Tree of Life.
- **Unit VII — Microbiology:** Bacteria, Archaea, and Viruses; Microbial Ecology and the Microbiome; Host Immunity and Vaccines; Antimicrobial Resistance and Epidemiology.
- **Unit VIII — Botany — Plant Biology:** Plant Structure and Water Relations; Plant Reproduction and Development; Plant Responses to the Environment.
- **Unit IX — Zoology and Systems Physiology:** Circulation and Respiration; Nervous System and Neural Signaling; Action Potentials and Synaptic Transmission; Endocrine Signaling and Homeostasis; Immune System Architecture.
- **Unit X — Ecology:** Population Ecology and Growth Models; Community Interactions and Succession; Biodiversity and Food Webs; Ecosystem Ecology; Biomes and Conservation Biology.
- **Laboratory activities:** one companion lab follows each chapter in the same canonical order.
- **Question banks:** one 30-item question bank follows each chapter in the same canonical order.
- **Appendix A — Curriculum Map:** reference material generated or ordered from the same manifest.

- **Appendix B — Instructor Orchestration Guide:** reference material generated or ordered from the same manifest.
- **Appendix C — Mathematical Review for Biology:** reference material generated or ordered from the same manifest.
- **Appendix D — Units, Physical Constants, and Biological Ranges:** reference material generated or ordered from the same manifest.
- **Appendix E — A Periodic Table for Biology:** reference material generated or ordered from the same manifest.
- **Appendix F — Master Glossary of Biological Terms:** reference material generated or ordered from the same manifest.
- **Appendix G — Index of Key Terms:** reference material generated or ordered from the same manifest.
- Source modules: `src/biology/<domain>/` contains the tested Python implementations for the quantitative models used throughout the book.

Suggested reading paths

Path	Emphasis	Notes
AP / first-year survey	Unit I — Chemistry of Life: Introduction; Unit II — The Cell: Introduction; Unit III — Energy and Metabolism: Introduction; selected genetics/evolution chapters; Unit X — Ecology: Introduction	Skim the systems orientation; prioritize metabolism and genetics core narratives.
Pre-health / majors	Unit I — Chemistry of Life: Introduction through Unit IX — Zoology and Systems Physiology: Introduction; Unit X — Ecology: Introduction; systems orientation as setup	Add labs for quantitative skills; pair each physiology chapter with its Python bridge.
Ecology / environmental focus	Unit I — Chemistry of Life: Introduction and Unit II — The Cell: Introduction as review; Photosynthesis; Unit VI — Evolution: Introduction; Unit VII — Microbiology: Introduction; Unit X — Ecology: Introduction	Emphasize population models, biogeochemistry, conservation metrics in <code>ecology.py</code> .
Computation-first	Unit 0 — Systems Science for Biology: Introduction plus any later unit	Read “Bridge to computation” blocks first, then narrative; run <code>scripts/generate_figures.py</code> .

Notation and conventions

- Logarithms: \ln = natural log; \log_{10} used where orders of magnitude matter (pH, viral titre, doubling time).
- Concentrations: square brackets $[X]$ denote molarity unless a chapter states otherwise.
- Genetics: italic gene symbols (*lacZ*); protein products often Roman with capital initial (LacZ) where conventional.
- Units: SI base units; physiology at 37 °C, pH 7.4, sea level unless noted.
- Glossary and cross-link numbering in the glossary and cross-links match the PDF table of contents (sequential numbering from `config.yaml`, including Unit 0 — Systems Science for Biology: Introduction when present).

Scholarship and source practice

Biology changes because methods change: better microscopes, longer reads, larger cohorts, improved models, and more inclusive sampling can most revise a claim that once looked settled. When reading this book, treat every important statement as part of a source chain:

Source type	Best use	Question to ask
Primary research article	Evidence for a specific method, dataset, result, or mechanism	What exactly was measured, and in which organism, cell type, population, or environment?
Review or textbook synthesis	Orientation across a field or controversy	Which primary findings does the synthesis depend on, and are any newer results likely to change it?
Public dataset or database	Reusable evidence for comparison, reanalysis, and reproducibility	How were samples selected, processed, filtered, and annotated?
Institutional report or guideline	Current public-health, clinical, biodiversity, or policy status	What date, jurisdiction, and decision context does the guidance assume?
Model or simulation	A testable simplification of a mechanism	Which assumptions, parameters, or boundary conditions would change the conclusion?

For recent or numeric claims, prefer the source closest to the measurement and write one sentence naming what would change your confidence. For example, a claim about antimicrobial resistance should identify the organism-resistance pair, surveillance population, and selection pressure; a claim about biodiversity loss should separate population trends, extinction risk, land-use drivers, and value judgments. This is why chapter answer keys ask for both a core response and a scholarship check.

Textbook Concept Map

The instructional blocks form an interdependent architecture. The diagram below shows primary dependency paths and integrative threads.

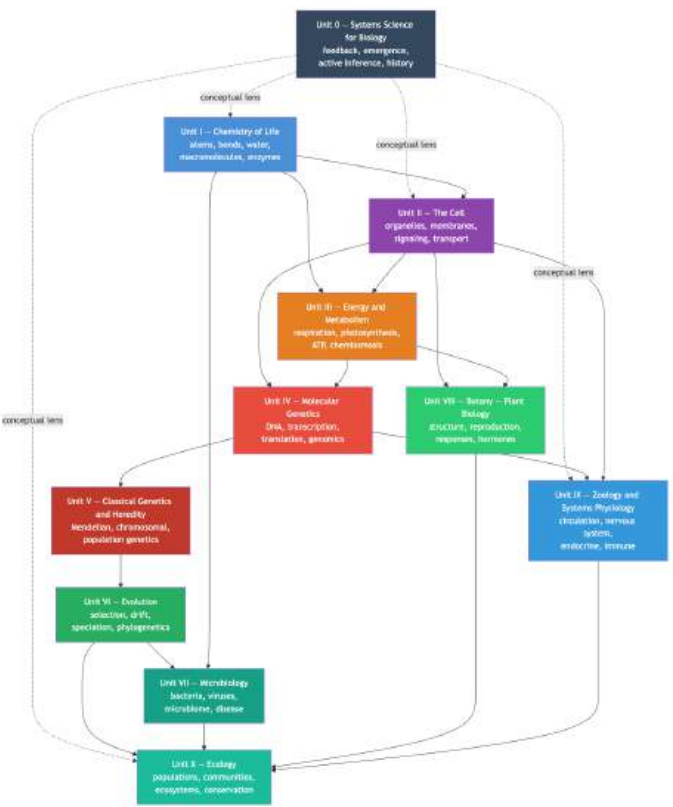


Figure 1. Generated dependency map derived from manuscript/config.yaml: dashed links show the systems orientation as a conceptual lens, and solid arrows show dependencies through the canonical unit sequence.

Accessing source materials

Resource	Location
Living source (Git)	biology textbook source repository — manuscript Markdown, <code>src/biology/</code> modules, maintenance scripts, and tests
Archival citation (DOI)	Zenodo archival DOI record — cite this record for a fixed edition snapshot
Combined PDF / HTML	Build from the repository with <code>uv run python scripts/03_render_pdf.py --project biology_textbook</code> (from the template root) or the project's <code>biology_analysis.py</code> workflow
Figures and diagrams	<code>scripts/generate_figures.py</code> (matplotlib) and <code>scripts/generate_diagrams.py</code> (registered Mermaid); inline Mermaid in chapters renders during PDF preprocessing
Corrections and extensions	Open an issue or pull request on the book repository; substantive edits should keep <code>chapter \cref</code> labels and <code>config.yaml</code> ordering in sync

The table below provides a per-chapter difficulty rating (Level 1/3 to Level 3/3), an estimated student reading time, and a suggested lecture allotment. Unit and chapter cells list canonical titles from `manuscript/config.yaml` as clickable `\hyperref` links to each section. The grid is auto-generated by `scripts/insert_chapter_metadata.py` from the canonical table of contents in `manuscript/config.yaml` plus `src/biology/chapter_metadata.py` — edit those sources and re-run the script to refresh this grid.

74

Preface

A Textbook Built With Code

Welcome to *Introduction to Biology: A Generative Approach* — Instructor Edition with visible model answers in the question-bank appendices — an open-source textbook covering introductory biology across Unit 0 — Systems Science for Biology: Introduction, the thematic sequence from Unit I — Chemistry of Life: Introduction through Unit X — Ecology: Introduction, and 44 core chapters, plus optional laboratories and question banks in the appendices. Where this text uses quantitative models, the corresponding computations are implemented as tested Python modules.

Whether we examine Michaelis–Menten enzyme kinetics, Lotka–Volterra predator–prey dynamics, or Hodgkin–Huxley action potentials, the underlying mathematical model exists as a working module in the accompanying codebase. Many figures are generated programmatically. Process diagrams are expressed using Mermaid where it improves clarity. For instructors and independent learners, this supports inspection, extension, and reproducible re-generation of results.

The philosophy is: understand biology by computing biology.

How to read this book digitally: The reference build is a compact PDF with LaTeX typesetting. Not all screen readers handle mathematical notation the same way in PDF; the same sources also produce HTML for some workflows. The [biology textbook source repository](#) contains the manuscript, figures, tests, and code; the [Zenodo archival DOI record](#) identifies a fixed edition snapshot. If you need larger type or margins, a reader typography profile is documented (paired edits to `manuscript/config.yaml` and `manuscript/preamble.md` — see `docs/accessibility.md` in the project tree). The book does not re-express every formula in natural language; where precision matters, work through the worked examples and the linked `src/biology` modules.

Accessible formats: The compact PDF is optimized for print density, not for every reader. For screen-reader review, HTML/MathJax workflows usually preserve reading order and mathematical navigation better than a dense PDF. Figures and Mermaid diagrams include alt text plus captions, and the large-type reader profile increases margins, font size, and line spacing without changing chapter order or cross-reference IDs.

Five Big Ideas in Biology

Biology is a vast and diverse science, but a small set of orienting themes recurs across its subdisciplines. This book groups them as Five Big Ideas (Evolution; Information; Structure and function; Systems and emergence; Cells). They map pedagogically to the five core concepts in AAAS *Vision and Change in Undergraduate Biology Education* [[vis](#), [2011](#)]; that report also defines six core competencies (quantitative reasoning, modeling, data interpretation, and related practice skills), which this text addresses through labs, models, and inquiry—not as a sixth numbered “big idea” heading. Unit 0 — Systems Science for Biology: Introduction adds an optional systems orientation: active inference and the free energy principle are graduate-depth lenses for connecting feedback, prediction, and behavior [[Friston, 2017](#), [Parr et al., 2022](#)], not part of the introductory-biology canon that Vision & Change defines for the core undergraduate sequence. The themes below recur across the units that follow.

Evolution: the unifying theory of life

“Nothing in biology makes sense except in the light of evolution.” — Theodosius [Dobzhansky](#) [[1973](#)]

Evolution by natural selection explains the origin of species, the genetic code being nearly universal, the homology between a human arm and a bat wing, and why influenza vaccines must be redesigned every year. Unit VI — Evolution: Introduction, Unit V — Classical Genetics and Heredity: Introduction, and Unit IV — Molecular Genetics: Introduction develop this idea from population genetics algorithms to phylogenetic tree reconstruction.

Structure and function are inseparable

A phospholipid bilayer is 7 nm thick and amphipathic — and those two structural facts explain every property of biological membranes (Unit I — Chemistry of Life: Introduction and Unit II — The Cell: Introduction). The α -helix of hemoglobin’s subunits explains its cooperativity and the Bohr effect (Unit I — Chemistry of Life: Introduction and Unit IX — Zoology and Systems Physiology: Introduction). The T-shaped architecture of the mitochondrial ATP synthase explains rotary catalysis (Unit III — Energy and Metabolism: Introduction). In biology, whenever you ask *how*, the answer is typically embedded in *shape*.

Information — storage, transfer, expression

DNA is not merely a chemical; it is a code. An alphabet of four nucleotides encodes a program of 20 amino acids, creating an effectively unlimited diversity of proteins. Unit IV — Molecular Genetics: Introduction (Molecular Genetics) examines the molecular machinery that reads this code — from DNA helicases to ribosomes — and how errors in the code drive disease and evolution. Unit V — Classical Genetics and Heredity: Introduction (Classical Genetics) examines how the code is transmitted between generations. Unit VII — Microbiology: Introduction (Microbiology) shows how viruses inject their own code into host cells.

Emergent properties: the whole exceeds the parts

A single neuron can fire or remain silent. A brain can think. A single predator can collapse an entire intertidal community (Unit X — Ecology: Introduction). A slight imbalance in NAD⁺/NADH ratio shunts metabolism from aerobic to anaerobic (Unit III — Energy and Metabolism: Introduction). Emergence — complex behavior arising from simple rules — is everywhere in biology, and understanding it requires systems thinking: tracking flows, feedback loops, and nonlinear dynamics, not just cataloguing parts.

Cells: the universal unit of life

Every living organism is composed of one or more cells, sharing a common molecular toolkit: phospholipid membranes, DNA, ribosomes, ATP. Unit II — The Cell: Introduction examines the cell as a physical and computational system. Unit VII — Microbiology: Introduction through Unit IX — Zoology and Systems Physiology: Introduction extend this to specialized cells: bacteria, plant cells, neurons, immune cells. Understanding the cell is not a module to be completed — it is a perspective to carry through every subsequent chapter.

How Science Actually Works

This textbook presents science not as a collection of established facts but as a dynamic, self-correcting process of inquiry. Understanding how scientific knowledge is generated, tested, and revised is as important as knowing what is currently accepted.

The hypothetico-deductive method. A hypothesis is a testable, falsifiable prediction. Barry Marshall and Robin Warren’s hypothesis that bacteria cause peptic ulcers (not stress) was so contrary to medical consensus that Marshall famously drank a *Helicobacter pylori* culture to demonstrate the relationship [Marshall et al., 1985]. Their Nobel Prize-winning work illustrates how a single decisive experiment can overturn decades of received wisdom.

Models and computation as scientific tools. Modern biology is inseparable from mathematical modeling. The Michaelis-Menten equation (1913) is a model. The Hardy-Weinberg principle is a model. The Hodgkin-Huxley equations (1952) were Nobel Prize-winning models. A model is not a simplification that sacrifices truth; it is a commitment to precision — stating *exactly* what you are and are not claiming. The Python modules in this textbook implement these models so that you can inspect their assumptions, vary their parameters, and see where they break.

Primary literature vs. textbook synthesis. This textbook cites primary papers at point of use. When you see “(Author et al., Year, *Journal*)” inline, that citation points to the experiment or calculation that established the claim. Science journalism, textbooks, and Wikipedia involve more layers of interpretation. Primary papers are the ultimate authority — and learning to read them is a core competency this textbook aims to develop.

Revision is not failure. Every chapter in this book contains examples of ideas revised or overturned: the flat earth was replaced by a spherical one; Lamarckian inheritance was replaced by Darwinian selection; the DNA double helix replaced protein as the genetic material; the “lock-and-key” enzyme model was replaced by “induced fit”. A willingness to revise beliefs on evidence is not weakness — it is the engine of scientific progress.

How to Use the Unit Introductions

Each unit begins with a `unit_intro.md` page containing:

- A narrative hook explaining why this area of biology matters and what surprises it holds
- A landmark discoveries table citing the experiments that established the field
- A concept map (Mermaid diagram) showing how the chapters connect to each other and to other units
- A chapter roadmap mapping each chapter to its core question and key equation

Use these pages as advance organisers — read them before starting the unit and return to them when you feel you have lost the conceptual thread. The best moment to understand how a jigsaw piece fits is before you lose sight of the box.

Scope and Organization

The textbook proceeds from atoms to ecosystems, following the standard introductory course arc. The table below is generated from `manuscript/config.yaml`; unit and chapter titles are plain TOC titles from the canonical manifest.

Instructional block	Core chapters
Unit 0 — Systems Science for Biology: Introduction	Systems Science and Emergence; Complex Adaptive Systems; Active Inference and Free Energy; History and Philosophy of Biology
Unit I — Chemistry of Life: Introduction	Atoms, Molecules, and Chemical Bonds; Water — The Molecule of Life; Biological Macromolecules; Enzymes and the Kinetics of Catalysis
Unit II — The Cell: Introduction	Cell Theory and Cell Types; Cell Structure and Organelles; Membrane Structure and Transport; Cell Signaling and Communication
Unit III — Energy and Metabolism: Introduction	Bioenergetics and Cellular Respiration; Photosynthesis; Metabolic Integration and Regulation
Unit IV — Molecular Genetics: Introduction	DNA Replication and the Cell Cycle; Gene Expression; Mutations, CRISPR, and Genomics; Chromatin and Epigenetic Mechanisms; Epigenetic Inheritance and Disease
Unit V — Classical Genetics and Heredity: Introduction	Mendelian Principles and Probability; Mendelian Extensions and Human Genetics; Chromosomal Inheritance and Linkage; Population Genetics
Unit VI — Evolution: Introduction	Natural Selection and Adaptation; Genetic Drift, Gene Flow, and Speciation; Phylogenetics and the Tree of Life
Unit VII — Microbiology: Introduction	Bacteria, Archaea, and Viruses; Microbial Ecology and the Microbiome; Host Immunity and Vaccines; Antimicrobial Resistance and Epidemiology
Unit VIII — Botany — Plant Biology: Introduction	Plant Structure and Water Relations; Plant Reproduction and Development; Plant Responses to the Environment
Unit IX — Zoology and Systems Physiology: Introduction	Circulation and Respiration; Nervous System and Neural Signaling; Action Potentials and Synaptic Transmission; Endocrine Signaling and Homeostasis; Immune System Architecture
Unit X — Ecology: Introduction	Population Ecology and Growth Models; Community Interactions and Succession; Biodiversity and Food Webs; Ecosystem Ecology; Biomes and Conservation Biology

Reading paths by goal

Goal	Where to start	How to use the code
Exam / course survey	Unit intros + chapter summaries + the companion question bank that follows each chapter	Answer odd-numbered questions first; check module footers for <code>bio.py.*</code> imports.
Wet-lab or clinical bridge	Unit II — The Cell: Introduction, Unit IV — Molecular Genetics: Introduction, Unit VII — Microbiology: Introduction, and Unit IX — Zoology and Systems Physiology: Introduction	Read boxed clinical / systems notes; pair with labs in the same unit.
Modeling / CS	Unit 0 — Systems Science for Biology: Introduction, then any unit’s “Bridge to computation”	Run examples with <code>uv run python</code> from the project root; regenerate figures with <code>scripts/generate_figures.py</code> .
Ecology / field biology	Unit VI — Evolution: Introduction and Unit X — Ecology: Introduction, plus Photosynthesis	Focus on <code>ecology.py</code> functions cited in chapter footers; work Lotka–Volterra and logistic examples by hand then in Python.

How to Use This Book

Each chapter is designed for introductory biology learners and can be read in two modes:

1. Concept-first: Read the narrative, work the examples, and do the questions.
2. Model-first: Run the companion modules and treat the text as interpretation of model behavior.

For each concept, the integrated approach is:

1. Conceptual narrative — the biological story and mechanism in plain language with precise vocabulary.
2. Quantitative framework — equations, derivations, and worked numerical examples.
3. Primary citations — key papers (author, year, journal) supporting mechanisms; citations are included where used.
4. Python source — model code in the project’s biology modules (importable and runnable).

5. Figures — generated by `src/visualization/plots.py` (`ALL_FIGURE_GENERATORS`) and `src/mermaid/biology_diagrams.py`.

6. Clinical connections — boxed examples connecting molecular mechanisms to human disease, therapy, and public health.

7. Review and discussion questions — a 30-item companion question bank per chapter, plus end-of-chapter review questions, from calculation to synthesis (Unit 0 — Systems Science for Biology: Introduction uses discussion prompts; other units mix numeric and conceptual items).
-

Computational Infrastructure

The project’s biology code is organized by domain:

```
src/biology/
├─ biochemistry/    - Enzyme kinetics, macromolecule analysis
├─ cell/            - Membrane biophysics, signaling, organelles
├─ genetics/        - Mendelian ratios, Hardy-Weinberg, linkage mapping
├─ physiology/      - Homeostasis, hemoglobin, cardiac models
├─ ecology/         - Population dynamics, community models
├─ evolution/       - Drift simulation, fitness landscapes
├─ microbiology/    - Growth curves, MIC, viral cycles
├─ botany/          - Water potential, transpiration, photosynthesis pathways
└─ neuroscience/   - Action potentials, synapse models
```

Diagram generation:

```
src/mermaid/biology_diagrams.py - diagram factories registered in ALL_BIOLOGY_DIAGRAMS
src/visualization/plots.py      - matplotlib figure generators (ALL_FIGURE_GENERATORS)
```

Most code conforms to the project’s no-mocks policy: tests use real computations.

Pedagogical Standards

What this book assumes: basic chemistry (atomic structure, covalent bonds, pH), basic algebra, and optional access to Python. No prior biology is required.

Mathematical notation is standard across most chapters:

- Concentrations in mol/L (M) or mmol/L (mM) as context requires
- Reaction rates in $\text{M}\cdot\text{s}^{-1}$ or $\mu\text{mol}\cdot\text{min}^{-1}\cdot\text{mg protein}^{-1}$
- Genetic distances in centimorgans (cM)
- Most physiological parameters indexed to standard conditions (37 °C, pH 7.4, sea level) unless stated

Primary citations follow the format Author (year), *Journal*, and are embedded inline. They are selective: landmark results and a small number of current references where they materially clarify the consensus.

Open Science Commitment

This book is released under the Creative Commons Attribution 4.0 International Licence (CC BY 4.0): you may freely use, adapt, and redistribute it with attribution. Most accompanying source code is released under the Apache-2.0 Licence.

The entire textbook — source markdown files, Python modules, figure scripts, and the build pipeline — is publicly available. The intent is for this resource to be a living, improvable document rather than a static product. Pull requests are welcome.

Acknowledgements

This textbook was developed as part of the Research Project Template infrastructure for open, reproducible science education. Gratitude to the open-source communities behind [Pandoc](#), [LaTeX](#), [Mermaid](#), and [matplotlib](#).

Unit 0 — Systems Science for Biology: Introduction

Unit 0 — Systems Science for Biology: Introduction · Introduction

Why This Unit Matters

The modern study of biology began by reducing living phenomena to their smallest parts — cells, molecules, genes. This reductionist strategy yielded extraordinary insight. Yet the more we learned about individual components, the clearer it became that biology cannot be explained by parts alone: a neuron firing is not a thought, a gene is not a behavior, a metabolic pathway is not a cell. What emerges from the *interaction* of parts — properties no single component possesses in isolation — is the subject of systems science.

Unit 0 — Systems Science for Biology: Introduction introduces four interlocking frameworks that recur in every subsequent unit:

1. Systems science — the general theory of organized complexity: how hierarchical systems form, how feedback governs their behavior, how new properties emerge.
2. Complex adaptive systems — how populations of agents with local rules give rise to robust, evolvable, collective behavior.
3. Active inference and the free energy principle — a mathematically grounded account of how living agents maintain themselves by predicting and acting on their environments.
4. History and philosophy of biology — the source-critical practice of asking where biological concepts came from, what they assume, and how evidence and values revise them.

Reading Unit 0 — Systems Science for Biology: Introduction is optional but recommended: it supplies the vocabulary of emergence, attractors, bifurcations, allostasis, and precision that makes Unit I — Chemistry of Life: Introduction through Unit X — Ecology: Introduction fit together as a single coherent theory of living organization.

Landmark Discoveries

Year	Contribution	Significance
1867	Hermann von Helmholtz — [Helmholtz, 1867]	First framing of perception as unconscious inference
1932	Walter Cannon — [Cannon, 1932]	Coined <i>homeostasis</i> ; proposed regulated internal milieu
1948	Norbert Wiener — [Wiener, 1948]	Formalised feedback control; bridged engineering and biology
1968	Ludwig von Bertalanffy — [von Bertalanffy, 1968]	Articulated open systems and hierarchy across disciplines
1977	Ilya Prigogine and Grégoire Nicolis — [Prigogine and Nicolis, 1977]	Dissipative structures and non-equilibrium self-organization
1987	Per Bak, Tang & Wiesenfeld — [Bak et al., 1987]	Self-organized criticality and power-law scaling in CAS
1992	John Holland — [Holland, 1992]	Genetic algorithms; formal CAS framework
2010	Karl Friston — [Friston, 2010]	Free energy principle as a unified theory of brain function
2015	Peter Sterling — [Sterling, 2012]	Predictive allostasis, contrasting error-correction homeostasis

Key Concepts and Connections

- System — a set of interacting components forming an integrated whole; open systems exchange matter and energy with their environment.
- Emergence — properties of a system that cannot be explained solely by properties of its components (e.g., consciousness emerges from neural circuits; life emerges from biochemistry).
- Feedback — output fed back as input, shaping future behavior; negative feedback stabilizes, positive feedback amplifies.
- Attractor — a region of phase space toward which trajectories converge; phase transitions move a system between attractors.
- Complex adaptive system (CAS) — a system of adaptive agents whose collective behavior self-organizes without central control.
- Free energy — a variational upper bound on surprise; minimizing it unifies perception, action, and learning.
- Homeostasis vs. allostasis — passive correction to a fixed set-point vs. predictive adjustment of set-points based on context.

These ideas are deliberately general: every subsequent unit of the textbook re-encounters them. Feedback appears in enzyme regulation (Unit I — Chemistry of Life: Introduction), in signaling cascades (Unit II — The Cell: Introduction), in metabolic flux (Unit III — Energy and Metabolism: Introduction), in population

dynamics ([Unit X — Ecology: Introduction](#)), and in neural control ([Unit IX — Zoology and Systems Physiology: Introduction](#)). Attractors describe cell-fate decisions ([Unit II — The Cell: Introduction](#)), bistable genetic switches ([Unit IV — Molecular Genetics: Introduction](#)), and ecosystem stable states ([Unit X — Ecology: Introduction](#)). Active inference recurs as the unifying framework for physiology ([Unit IX — Zoology and Systems Physiology: Introduction](#)) and behavior.

Current Evidence Thread

Systems-science and complexity claims are not evidenced the way a single-gene knockout is; the evidence is whether a model’s assumptions survive contact with data. A claim earns confidence when its generative model exposes the parameters and boundary that matter, when a perturbation or time-series test could have falsified it but did not, and when an explicit null or alternative model fails where it succeeds. Across this unit — emergence, adaptive agents, active inference, and the history/philosophy of biological concepts — read each idea as such a model and ask what observation would move you. As you move through the chapters, keep a two-column note: claim on the left, evidence that would change my confidence on the right. By the end of the unit, each major idea should be tied to a measurement, model, citation, or paper-based lab decision.

Chapter Roadmap

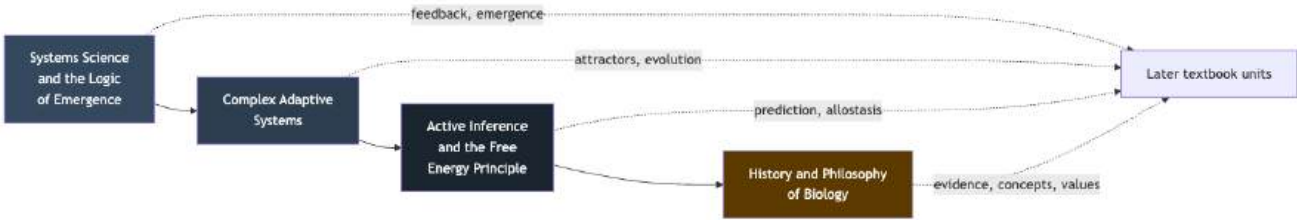


Figure 2. Opening-unit roadmap: systems science introduces feedback and emergence, complex adaptive systems adds attractors and evolution, active inference connects prediction and allostasis, and history/philosophy connects evidence, concepts, and values to later units.

Chapter	Core question	Key tools
0.1 Systems Science	<i>How does organization arise from interaction?</i>	Feedback, hierarchy, Hill equation, delay oscillation
0.2 Complex Adaptive Systems	<i>How do simple local rules produce robust global behavior?</i>	Phase space, bifurcation, fitness landscape, power laws
0.3 Active Inference	<i>How do living agents maintain themselves against disorder?</i>	Bayesian inference, free energy, precision, allostasis
0.4 History and Philosophy of Biology	<i>How did biology’s concepts, evidence practices, and values become what they are?</i>	Source analysis, mechanism/function, individuality, model critique

Connections Across the Textbook

- [Unit I — Chemistry of Life: Introduction](#) — Chemistry of Life: thermodynamic gradients (section 0.1) explain why proteins fold spontaneously; catalysis is a feedback-regulated modular system.
- [Unit II — The Cell: Introduction](#) — The Cell: organelles are modules; the fluid-mosaic membrane is a self-organized phase; signaling cascades are hierarchical feedback loops.
- [Unit III — Energy and Metabolism: Introduction](#) — Energy and Metabolism: glycolysis and the TCA cycle are classic examples of allosteric feedback and feed-forward control.
- [Unit IV — Molecular Genetics: Introduction–V](#) — Genetics: regulatory networks, bistable switches, and epigenetic memory are CAS par excellence.
- [Unit VI — Evolution: Introduction](#) — Evolution: fitness landscapes from section 0.2 are the formal substrate of selection.
- [Unit VII — Microbiology: Introduction](#) — Microbiology: biological-self questions from section 0.4 clarify microbiomes, symbiosis, pathogens, and host boundaries.
- [Unit IX — Zoology and Systems Physiology: Introduction](#) — Physiology and Neuroscience: allostasis from section 0.3 and predictive coding replace simple fixed-set-point homeostasis as the model of central control.
- [Unit X — Ecology: Introduction](#) — Ecology: phase transitions, alternative stable states, and tipping points apply the mathematics of section 0.2 directly.

Computational Toolbox — Unit 0

The four **Unit 0 — Systems Science for Biology: Introduction** chapters are conceptual rather than algorithmic, but they motivate every piece of code and evidence check used later:

- Hill cooperative binding: cell-biology helpers, especially `hill_equation()`.
- Receptor occupancy: cell-signaling helpers for ligand binding and response.
- Logistic dynamics: ecology helpers for growth under carrying capacity.
- Lotka–Volterra oscillation: ecology helpers for predator–prey cycles.
- Bayesian update: neuroscience-style posterior inference, illustrated in section **0.3**.
- Source and citation closure: table-of-contents, bibliography, cross-reference, and curriculum helpers that keep claims traceable across chapters, labs, and question banks.

Each concrete chapter later in the textbook either uses one of these helpers or gives the reader a chance to write the next one.

Source modules: `src/biology/` (general framework across most domains). Figures: `src/mermaid/biology_diagrams.py` — systems-level diagrams reused throughout the book.

Cross-Unit Integration

Unit 0 — Systems Science for Biology: Introduction closes by foreshadowing the chemistry to come. The thermodynamic gradients, feedback regulation, and emergent-property arguments you just met are not abstract — they will reappear in **Unit I — Chemistry of Life: Introduction** as the physical reason why proteins fold spontaneously, why enzymes shift activation-energy landscapes without changing equilibria, and why membrane lipids self-assemble into bilayers without any genetic “instruction.” The free-energy minimization framework that organized this unit’s discussion of active inference is the same Gibbs free energy that determines whether a covalent bond forms or hydrolyzes. When you encounter **Unit I — Chemistry of Life: Introduction**’s chemistry, read it not as a separate vocabulary but as the molecular substrate where the systems principles of **Unit 0 — Systems Science for Biology: Introduction** are first realized in matter.

% Unit 0 chapters render as 0.1, 0.2, ... without shifting Unit I.

0.1 Systems Science and Emergence

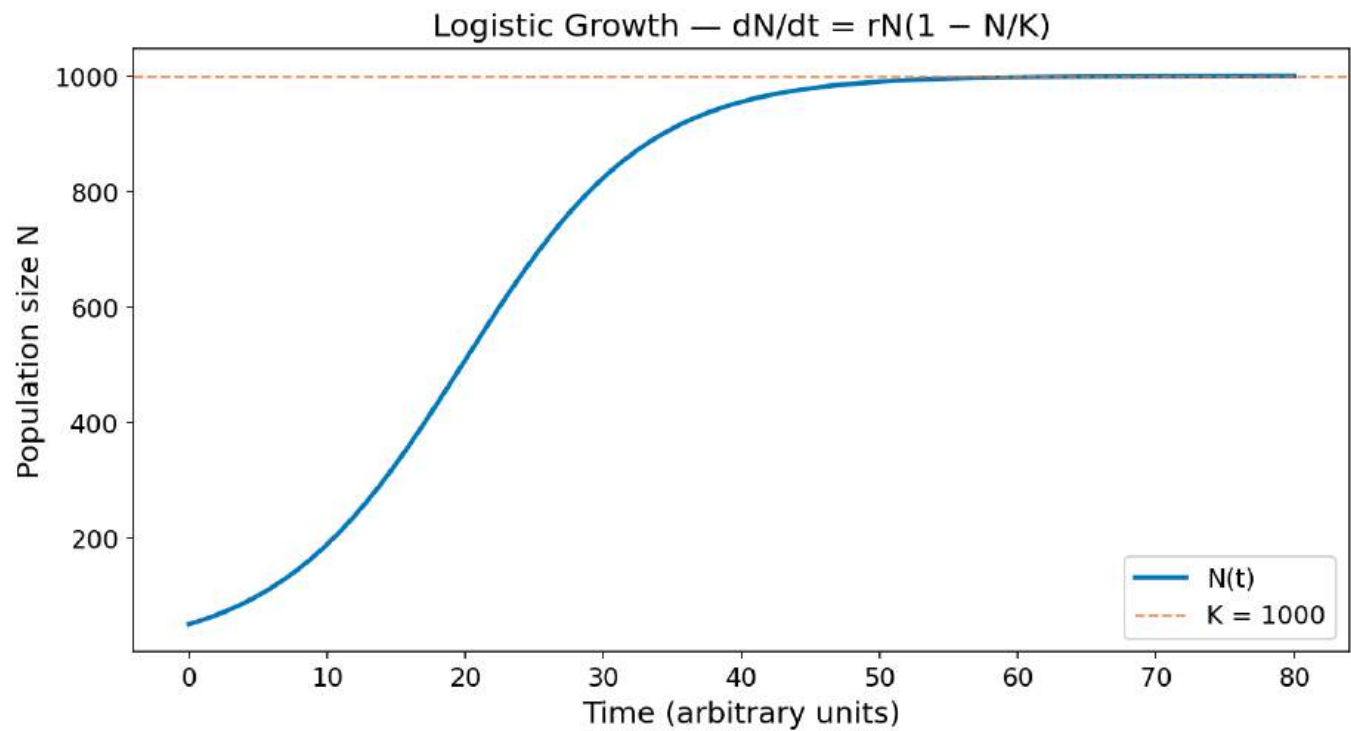


Figure 3. Logistic population growth as a canonical nonlinear systems-science exemplar. The S-shaped curve is generated by a single difference equation in which a positive birth process is balanced by a density-dependent self-limiting term that turns on as the population approaches carrying capacity K .

Level 2/3 · 35 min read · 50 min lecture · Prerequisites: none

0.1.1 Learning Objectives

By the end of this chapter, students will be able to:

1. Define *system* and identify boundary, components, environment, and relationships in biological examples.
2. Describe positive and negative feedback loops and give biological examples of each.
3. Explain what emergence is and why it cannot be predicted from component-level analysis alone.
4. Apply the concepts of hierarchy, modularity, and scale to cellular and organismal biology.
5. Distinguish between linear and nonlinear system behavior.
6. Analyze delayed feedback loops and predict whether they will damp, oscillate, or destabilise.
7. Recognize hub-heavy network structure in biological data, test scale-free claims cautiously, and explain functional implications.
8. Apply the Hill equation, the chemostat equations, and simple oscillator models to quantitative problems.

0.1.1.1 Study Blueprint

- Big idea: Biological explanation improves when parts, interactions, feedback, and scale are kept in view together.
- Core concepts: systems boundaries, feedback, emergence, state variables.
- Framework alignment: Vision & Change: Systems, Structure and function; AP Biology: Systems Interactions; NGSS-style topics: Structure and Function, Interdependent Relationships in Ecosystems.
- Model or quantitative lens: Box-and-arrow causal models with explicit inputs, outputs, and feedback signs.
- Data skill: Translate a verbal biological system into variables, links, and testable predictions.
- Practice cadence: Questions and Methods, Representing and Describing Data, Argumentation.
- Common misconception to repair: A system is not just a list of parts; the interactions are part of the explanation.
- Primary lab: Lab A — Systems Science and Emergence.

- Question bank: [Questions — Systems Science and Emergence](#).
- Transfer task: Apply the same feedback map to a cell, organism, and ecosystem, then name what changes at each scale.
- Bridge to computation: `biology.crossref_validator.validate`.

0.1.2 Opening Vignette: The Birth of Systems Thinking

In 1948, Norbert Wiener published *Cybernetics: or Control and Communication in the Animal and the Machine*, arguing that the same mathematical principles of feedback and self-regulation govern thermostats, servomechanisms, and the human nervous system. Two decades later, Ludwig von Bertalanffy’s *General System Theory* (1968) [[von Bertalanffy, 1968](#)] proposed that most complex phenomena — from a cell to a city — share general organizational laws: openness, hierarchy, equifinality, and emergent order.

Their insight was radical: biology cannot be understood by dissecting organisms into parts and studying each in isolation. Instead, one must study *relationships* — the flows of matter, energy, and information that connect components and give rise to behavior no component possesses alone. When Walter Cannon coined [homeostasis](#) in 1932 [[Cannon, 1932](#)], he was describing a systems-level property: the blood glucose concentration of 5 mM is not a property of any single cell but an emergent steady-state of millions of feedback interactions between pancreatic β -cells, hepatocytes, skeletal myocytes, and adipocytes.

This chapter introduces the core vocabulary and conceptual toolkit of systems science — the intellectual scaffolding that unifies every subsequent chapter in this textbook. We will move from definitions (what is a system?) through dynamics (feedback, delay, oscillation, chaos) to architecture (hierarchy, modularity, hub-heavy networks), then close with information, entropy, and the practical implications of a systems perspective for biomedicine.

0.1.3 What Is a System?

A system is a set of components that interact to produce collective behavior. Three elements define any system:

- Components — the identifiable parts (atoms, molecules, cells, organisms, species).
- Relationships — the interactions and constraints between components (chemical bonds, metabolic pathways, predator–prey links).
- Boundary — the interface that separates the system from its environment, through which matter and energy may flow.

0.1.3.1 Isolated, Closed, and Open Systems

Table 1. Isolated, Closed, and Open Systems: Type and Energy exchange.

Type	Energy exchange	Matter exchange	Biological occurrence
Isolated	None	None	Idealised primarily — not found in nature
Closed	Yes	No	Rare; some thermal models
Open	Yes	Yes	Most living systems

Most living systems are open systems. They import free energy and matter (food, sunlight), perform work, and export entropy (heat, excreta). This continuous throughput is what allows them to maintain internal order — a thermodynamic feat that distinguishes the living from the non-living.

0.1.3.2 Equifinality and Multifinality

Bertalanffy emphasized that open systems often display equifinality: the same final state can be reached from different starting conditions and along different trajectories. A vertebrate embryo robustly produces the species-typical body plan despite considerable variation in initial cell positions, ploidy, or even surgical perturbation. Conversely, multifinality describes the same starting condition giving rise to different outcomes — identical twins acquiring distinct microbiomes, for example. Both properties contradict naive linear cause-and-effect intuition and motivate the systems-level vocabulary that follows.

Concept Check 1: A surgeon removes part of an early sea-urchin embryo. The remaining cells reorganise to produce a smaller but otherwise normal larva. Identify which open-system property (equifinality, multifinality, or neither) this illustrates, and explain why a watch — a non-living complicated system — would not behave this way.

0.1.4 Feedback: The Grammar of Self-Regulation

Feedback occurs when a fraction of a system’s output is returned as input, altering subsequent behavior. Biological regulation is almost entirely feedback-based.

0.1.4.1 Negative (Stabilizing) Feedback

Negative feedback opposes deviations from a set point. It is the mechanistic basis of homeostasis.

Examples:

- Body temperature regulation — warming activates sweating and vasodilation, cooling activates shivering and vasoconstriction.
- Blood glucose — rising glucose triggers insulin secretion, promoting uptake; falling glucose triggers glucagon, promoting glycogenolysis.
- **Gene** expression — product inhibition of the first **enzyme** in a biosynthetic pathway (end-product inhibition).
- Baroreceptor reflex — a fall in arterial pressure unloads stretch receptors in the carotid sinus, increasing sympathetic tone within seconds.
- Renin–angiotensin–aldosterone system — falling renal perfusion pressure activates a hormonal cascade that retains sodium and water on a slower (minutes-to-hours) timescale.

Connection (clinical) — glucose, insulin, and type 2 diabetes Fasting plasma glucose near 5 mM is maintained by a negative-feedback loop: β -cells release insulin when glucose rises; insulin increases **GLUT4**-mediated uptake in muscle and adipose and restrains hepatic glucose output; glucagon opposes insulin when glucose falls. In type 2 diabetes mellitus, insulin resistance shifts the loop: the same insulin concentration produces less effect, so higher glucose is “needed” to clear a meal; β -cells compensate until they fail. Drugs target *nodes* in this network — metformin (hepatic gluconeogenesis), GLP-1 agonists (incretin axis), SGLT2 inhibitors (renal glucose excretion) — illustrating how systems biology informs combination therapy rather than single-molecule “magic bullets.”

0.1.4.2 A Linear Negative-Feedback Worked Example

Consider a regulator with set point $x^* = 5$ mM, current state x , and proportional response

$$\frac{dx}{dt} = -k(x - x^*) + d(t)$$

(1)

where $k > 0$ is the gain and $d(t)$ is a disturbance. With $k = 0.5 \text{ min}^{-1}$, an injection that lifts x to 8 mM at $t = 0$ produces an exponential return $x(t) - x^* = 3 e^{-0.5t}$ mM. The deviation halves every $\ln 2/k \approx 1.4$ minutes. Doubling the gain to $k = 1 \text{ min}^{-1}$ halves the half-time to 0.7 minutes. Higher gain returns the system faster, but delayed feedback can turn excessive gain into oscillation or instability. This trade-off — speed versus stability — is the central design problem of every physiological control system.

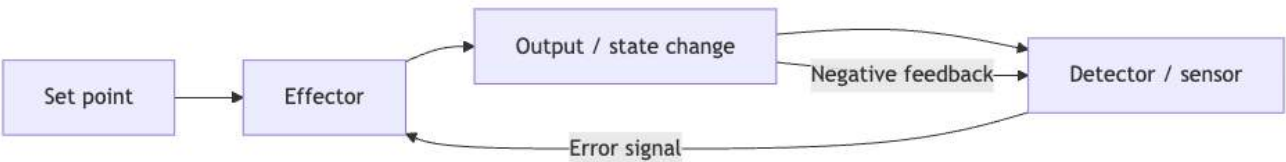


Figure 4. Canonical negative-feedback control loop: set point to effector to output, with the detector returning an error signal that opposes deviation.

Concept Check (Analysis): A negative-feedback loop controlling blood glucose has a time delay τ of 15 minutes between insulin secretion and glucose uptake. Using the Barkhausen criterion for oscillation (gain \times phase shift ≥ 1 at some frequency), explain why this delay could produce insulin oscillations of approximately 2τ period. What pharmacological intervention would damp the oscillations without eliminating glucose regulation?

Concept Check (Evaluation): A bistable genetic switch (lac operon) shows hysteresis: it requires inducer concentration $I > 0.8$ mM to switch ON, but once ON, remains ON until $I < 0.2$ mM. (a) Sketch the bifurcation diagram (steady-state vs. I). (b) Explain why hysteresis is adaptive for the cell: what would happen if the switch were monostable? (c) Identify one molecular mechanism that could eliminate hysteresis, and one that could widen the hysteresis loop.

Worked Example — Steady-State Analysis of a Negative-Feedback Loop: Consider a simple model of cortisol regulation: cortisol C is produced at rate α , cleared at rate βC , and inhibits its own production with Hill coefficient $n = 2$ and half-saturation K . The steady state satisfies $\alpha/(1 + (C/K)^2) = \beta C$. With $\alpha = 100 \text{ nM/h}$, $\beta = 0.5 \text{ h}^{-1}$, $K = 50 \text{ nM}$, solve for the steady-state cortisol concentration, then predict how a stress event that doubles α transiently shifts the steady state and how negative feedback returns it. *Solution:* Setting $100/(1 + (C/50)^2) = 0.5C$ and letting $x = C/50$ gives $100/(1 + x^2) = 25x \Rightarrow 4 = x(1 + x^2) \Rightarrow x \approx 1.28 \Rightarrow C \approx 64 \text{ nM}$. After stress doubles α to 200 nM/h , the new steady state satisfies $200/(1 + x^2) = 25x \Rightarrow 8 = x(1 + x^2) \Rightarrow x \approx 1.65 \Rightarrow C \approx 82 \text{ nM}$ — a 28% increase despite a 100% increase in production. Negative feedback strongly attenuates the stress response because the Hill-2 self-inhibition concentrates around K .

0.1.4.3 Positive (Amplifying) Feedback

Positive feedback amplifies deviations. It underlies rapid, switch-like biological transitions.

Examples:

- **Action potential** initiation — sodium influx depolarizes membrane, opening more Na⁺ channels (Hodgkin cycle).
- Childbirth contraction — oxytocin stimulates contractions, which stimulate more oxytocin release.
- **Apoptosis** — executioner **caspases** activate upstream caspases, accelerating cell death.
- Blood-clotting cascade — thrombin generates more thrombin via factor V and factor VIII activation, producing exponential burst once a threshold is crossed.
- LH surge — rising oestradiol switches from negative to positive feedback on the hypothalamic-pituitary axis, triggering ovulation.

Positive feedback systems are inherently unstable unless ultimately bounded by a negative feedback or a hard limit (refractory period, resource exhaustion, anatomical constraint).

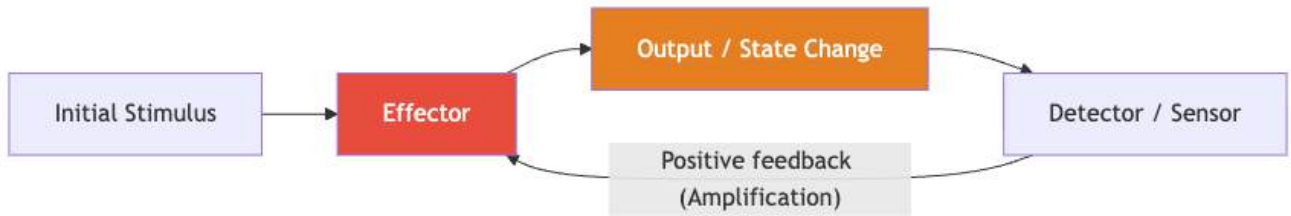


Figure 5. Positive-feedback loop in which detector output amplifies the effector, driving rapid state change until a limit or refractory bound applies.

Concept Check 2: Childbirth and the action potential are both positive-feedback processes, yet neither runs away forever. Identify the *bounding* mechanism in each case (anatomical, refractory, or chemical) and explain why pure positive feedback without an explicit bound would be lethal.

0.1.4.4 Feedback With Delay: Period and Damping

Real biology is rarely instantaneous. Gene expression requires **transcription** and **translation** (minutes to hours); vascular responses require perfusion (seconds); neural reflexes require axonal conduction (milliseconds). A delay τ between detecting a perturbation and responding to it fundamentally changes feedback behavior:

$$\frac{dx}{dt} = -k x(t - \tau)$$

(2)

- When $k\tau \ll 1$: the system returns smoothly to equilibrium (overdamped).
- When $k\tau \approx 1/2$: damped oscillations appear — the system overshoots, undershoots, and asymptotes over several cycles.
- When $k\tau > \pi/2$: the damping turns negative and the system breaks into sustained oscillations with angular frequency $\omega \approx \sqrt{k/\tau}$.

This last regime is where biological clocks live. Circadian oscillators (PER/CRY feedback, about 24 h), cardiac pacemakers (HCN channel gating, about 1 s), and cell-cycle oscillators (cyclin–CDK, about 24 h) most exploit delayed negative feedback to generate rhythms. The period is approximately twice the transcriptional and translational delay plus degradation lag.

Worked Example — Circadian period from delay. Suppose mammalian *PER* transcription takes 45 min, mRNA export and translation 30 min, and *PER* **protein** degradation has half-life 6 h. The total negative-feedback delay is $\tau \approx 7.5$ h, and because oscillation period $\approx 2\pi\tau/\sqrt{k\tau}$ the characteristic rhythm lands near 24 h for plausible rate constants. **Mutations** that shorten *PER* stability (e.g. familial advanced sleep-phase syndrome, *PER2* S662G) empirically shorten the period to about 20 h — consistent with reducing τ . This is why “biological clocks” are as much about delays as about reaction rates.

0.1.4.5 Feed-Forward and Anticipatory Control

Purely reactive feedback can primarily correct an error after it has developed. Many biological systems add a feed-forward pathway that uses an upstream signal to predict and pre-empt the disturbance. Examples:

- The cephalic phase of digestion releases insulin before glucose enters the bloodstream, smoothing post-prandial spikes.
- Sensory cortex anticipates expected stimuli and subtracts prediction from input, improving signal-to-noise.
- Cerebellar internal models generate predicted motor outcomes before execution, allowing correction mid-movement.

Feed-forward without feedback is brittle — any mis-prediction persists uncorrected — so real biology layers the two. This is the formal bridge to allostasis (section 0.3): predictive control of internal state with dynamic set-points, anticipating rather than merely correcting.

Connection (clinical) — diabetic insulin pumps. Hybrid closed-loop pumps combine continuous glucose monitoring (feedback) with announcements of meals or exercise (feed-forward). Pumps that respond purely to measured glucose chronically lag behind meals because gut absorption dynamics are faster than subcutaneous insulin uptake; adding a feed-forward “meal bolus” reduces post-prandial excursions by 30–50% without raising hypoglycaemia rates. The engineering principle is identical to the cephalic phase the body evolved millions of years ago.

0.1.5 Emergence Across Biological Levels

Emergence refers to properties of a system that cannot be explained solely by properties of its components. Emergent properties are *relational* — they arise from the pattern of interaction, not from any single part.

“The whole is more than the sum of its parts.” — Aristotle, *Metaphysics* (paraphrase)

0.1.5.1 Levels of Biological Emergence

Table 2. Levels of Biological Emergence: Level and Emergent properties.

Level	Emergent properties	Components
Molecular	Enzyme catalysis, membrane fluidity	Atoms and bonds
Cellular	Metabolism, replication, signaling	Organelles and molecules
Tissue	Contractility, conductance, secretion	Cells
Organism	Consciousness, immunity, homeostasis	Tissues and organs
Colony / social group	Task allocation, swarm choice, nest climate regulation	Related or interacting organisms plus signals and modified habitat
Population	Heredity, selection, drift	Individual organisms
Ecosystem	Nutrient cycling, energy flow	Populations and abiotic factors

Social-insect colonies are useful boundary cases for this table because they sit between organism-level physiology and population-level ecology. A honeybee swarm choosing a nest site, an ant colony allocating workers to foraging trails, or a termite colony regulating mound airflow has colony-level properties that no worker possesses in isolation [Seeley, 2010, Dorigo and Stützle, 2004, Ocko et al., 2017]. Calling such a colony a *superorganism* is an analogy with limits, but it can be a productive systems model when the analysis names the boundary, the colony-level regulated variable, and the worker-level interactions that generate it [Bourke, 2011].

0.1.5.2 Strong and Weak Emergence

Philosophers distinguish:

- Weak emergence — properties are novel relative to component-level description but *in principle* derivable from it (e.g., liquidity from molecular interactions).
- Strong emergence — properties that cannot, even in principle, be reduced to component interaction (consciousness remains a contested candidate).

For practical biology, the key insight is that *explaining components is not the same as explaining the system*. A complete molecular catalog of a neuron does not explain perception; a complete genome does not specify the body plan without the cytoplasmic and developmental context that interprets it.

Concept Check 3: Liquidity is often given as a paradigm of weak emergence: it is not a property of any single H₂O molecule but is in principle derivable from the molecular interaction Hamiltonian. Identify *one* biological property that is plausibly weakly emergent and *one* that is contested as possibly strongly emergent. What would it take to upgrade the contested property from “we cannot yet derive it” to “it is in principle underivable”?

0.1.6 Hierarchy and Scale

Biological organization is hierarchical. Each level exhibits emergent properties relative to the level below, and is *nested* within levels above.

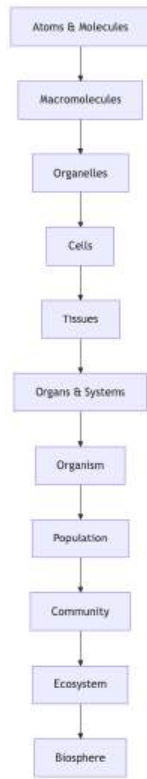


Figure 6. Nested hierarchy of biological organization, from atoms and molecules up through cells and organisms to the biosphere, each level emergent from the one below.

0.1.6.1 Cross-Scale Constraints

Higher-level organization *constrains* lower-level behavior (downward causation), while lower-level mechanisms *generate* higher-level properties (upward causation). For example:

- A cell’s membrane potential (tissue-level context) constrains which genes are expressed.
- A mutation (molecular level) can alter the organismal **phenotype** and hence population fitness.
- Tissue architecture constrains diffusion gradients that, in turn, pattern gene expression (developmental biology’s central feedback).

0.1.6.2 Modular Organization and Evolvable Interfaces

Living systems are modular — composed of semi-independent subsystems with defined interfaces. Modularity confers:

- Robustness: a failure in one module need not propagate to others.
- Evolvability: modules can be rewired or duplicated with limited pleiotropic effects.
- Decomposability: scientists can study modules in isolation (the logic underlying reductionism’s power).

Concept Check 4: The MAPK cascade (Ras → Raf → MEK → ERK) is often described as a module with a well-defined input (Ras activation) and output (ERK phosphorylation). List two biological consequences of this modularity — one that is *evolutionarily* useful (robust to rewiring) and one that is *clinically* worrisome (a single drug target that blocks many cell types).

Applied Systems / Clinical Connection — multimorbidity as boundary choice. A patient with heart failure, chronic kidney disease, and type 2 diabetes is poorly represented as three isolated “organ problems.” Diuretics improve pulmonary congestion but change renal perfusion and electrolyte balance; SGLT2 inhibitors alter renal glucose handling and intravascular volume; beta-blockers reshape autonomic feedback. A systems map makes the first modeling decision explicit: where is the boundary? A cardiology-focused boundary may optimize ejection fraction while missing renal compensation; a whole-patient boundary treats drug choice as intervention on coupled feedback loops. This is the practical clinical meaning of emergence, hierarchy, and allostatic regulation [Cannon, 1932, Sterling, 2012].

0.1.7 Nonlinearity and Thresholds

Simple systems obey *linear* relationships: double the input, double the output. Most biological systems are nonlinear — small changes can produce large effects, or large changes may produce negligible effects. Population growth illustrates bounded nonlinearity: density-dependent feedback bends exponential rise toward a carrying capacity (figure 3; same equation re-derived in ecological context at figure 215 with full treatment in Population Ecology and Growth Models).

Key nonlinear phenomena in biology:

Table 3. Modular Organization and Evolvable Interfaces: Phenomenon and Description.

Phenomenon	Description	Example
Threshold effects	Response absent below a critical input, present above	Action potential firing threshold (about −55 mV)
Bistability	System flips between two stable states	Lac operon switch; cell-cycle entry
Hysteresis	History-dependent state	Epigenetic gene silencing
Oscillations	Sustained rhythmic output	Circadian clocks; cardiac pacemakers
Chaos	Aperiodic but deterministic dynamics	Some cardiac arrhythmias; population cycles

0.1.7.1 A Simple Nonlinear Equation: The Hill Function

Cooperative binding (e.g., hemoglobin–oxygen, transcription factors) follows the Hill equation:

$$\theta = \frac{[L]^n}{K_d^n + [L]^n}$$

(3)

where θ is fractional occupancy, $[L]$ is ligand concentration, K_d is the dissociation constant, and n is the Hill coefficient. For $n > 1$, binding is cooperative, producing a sigmoidal (switch-like) response. The slope at half-occupancy scales with n , so a Hill coefficient of $n = 4$ produces a transition that is roughly four times sharper than a $n = 1$ saturable response.

0.1.7.2 Worked Example: Calculating Cooperative Binding

Problem: A dimeric transcription factor binds to DNA cooperatively with a Hill coefficient of $n = 2$. The dissociation constant K_d for the DNA binding site is 5 nM. What fraction of target promoters (θ) will be bound by the transcription factor when its intracellular concentration is 10 nM? What would the occupancy be if binding were non-cooperative ($n = 1$)?

Solution:

1. Calculate occupancy for cooperative binding ($n = 2$):

Using the Hill equation:

$$\theta = \frac{[L]^n}{K_d^n + [L]^n}$$

Substitute $[L] = 10$ and $K_d = 5$:

$$\theta = \frac{10^2}{5^2 + 10^2} = \frac{100}{25 + 100} = \frac{100}{125} = 0.80$$

The transcription factor occupies 80% of the promoters.

2. Calculate occupancy for non-cooperative binding ($n = 1$):

$$\theta = \frac{10^1}{5^1 + 10^1} = \frac{10}{5 + 10} = \frac{10}{15} \approx 0.67$$

Without cooperativity, primarily 67% of promoters are bound.

This calculation demonstrates how positive cooperativity steepens the dose-response curve, allowing a system to switch from off (unbound) to on (bound) over a narrower range of ligand concentrations, underpinning nonlinear threshold effects in biology.

0.1.7.3 Bistability and the Toggle Switch

Combine two mutually inhibiting genes and you obtain a toggle switch with two stable attractors and an unstable separator. Mathematically the rate equations look like

$$\frac{du}{dt} = \frac{\alpha_1}{1 + v^n} - u, \quad \frac{dv}{dt} = \frac{\alpha_2}{1 + u^n} - v \tag{4}$$

For $n > 1$ and balanced production rates $\alpha_1 \approx \alpha_2$, the system has three fixed points: $(u_{\text{high}}, v_{\text{low}})$, $(u_{\text{low}}, v_{\text{high}})$, and an unstable saddle in between. Each cell commits to one of the two outcomes as a function of initial conditions and noise — the molecular embodiment of cell-fate decision-making. Variations on this motif underlie phage λ lysis-vs-lysogeny, the lac operon’s bistable response to lactose, and embryonic stem-cell differentiation.

Concept Check 5: A biotechnology company engineers a synthetic toggle switch into *E. coli* and observes that, when both inducer ligands are equal, roughly half the population sits in state A and half in state B. Why does the population split rather than every cell choosing the same state? Sketch the relevant phase portrait and identify the role of stochastic gene expression noise.

0.1.8 Nonlinear Dynamics: Bifurcations, Limit Cycles, and Chaos

The earlier feedback and bistability examples hinted at oscillations and alternative stable states. Nonlinear dynamics [Strogatz, 2018] provides the formal vocabulary for these and other behaviors.

0.1.8.1 Phase Space and Trajectories

The phase space of a system is the space of possible internal states. A two-variable system (e.g. predator–prey densities, or a gene’s mRNA and protein abundance) has a 2-D phase plane in which each system trajectory is a curve. Fixed points are states where the derivatives vanish; limit cycles are closed trajectories that nearby trajectories spiral towards or away from.

0.1.8.2 Bifurcations and Qualitative State Changes

A bifurcation is a qualitative change in the structure of phase space as a control parameter varies. Three biologically important kinds:

- Saddle-node (fold) bifurcation — two fixed points (one stable, one unstable) collide and annihilate. Underlies catastrophic transitions in lake eutrophication and ecological regime shifts.
- Hopf bifurcation — a stable fixed point loses stability and is replaced by a small-amplitude limit cycle. Underlies the *birth* of biological oscillations (cardiac pacing, circadian rhythm onset in development).
- Pitchfork bifurcation — one fixed point splits into three, generating bistability. Underlies cell-fate commitment and morphogenetic symmetry breaking.

0.1.8.3 Limit Cycles and Biological Oscillators

A limit cycle is a closed trajectory toward which neighboring trajectories converge. Biological oscillators that are robustly limit-cycle:

- Circadian clocks (about 24 h period) — TTFLs (transcription–translation feedback loops) involving *CLOCK/BMAL1* and *PER/CRY* in mammals; *KaiABC* in cyanobacteria — the latter operates without transcription, demonstrating that a phosphorylation cycle alone can implement a biological clock.
- Cardiac pacemaker (about 1 s) — sino-atrial node cells use HCN (“funny”) current and Ca^{2+} cycling; their limit cycle is robust to $\pm 20\%$ perturbations of any single ionic conductance.
- Cell-cycle oscillator (about 24 h) — cyclin synthesis and APC-mediated cyclin destruction; phosphorylation of CDK targets reaches threshold, triggers mitosis, then resets the loop.
- Glycolytic oscillations in yeast (about 30 s–10 min) — feedback between phosphofructokinase and downstream metabolites.

0.1.8.4 Chaos and the Lorenz Attractor

When a deterministic nonlinear system has at least three dynamical variables, sustained motion can be chaotic — bounded, aperiodic, and exquisitely sensitive to initial conditions. The Lorenz system

$$\dot{x} = \sigma(y - x), \quad \dot{y} = x(\rho - z) - y, \quad \dot{z} = xy - \beta z \tag{5}$$

was originally derived as a toy model of atmospheric convection but applies (with reinterpreted variables) to laser dynamics, glycolysis, and population ecology. Trajectories are confined to a butterfly-shaped strange attractor with non-integer (fractal) dimension. Two trajectories that start within 10^{-6} of each other diverge until they separate by order unity within a finite time set by the system’s leading Lyapunov exponent λ : the separation grows like $\delta(t) \approx \delta_0 e^{\lambda t}$.

Biological chaos is documented (with varying confidence) in:

- Polymorphic ventricular tachycardia (“torsades de pointes” exhibits chaotic cardiac dynamics).
- Some EEG dynamics in seizure transitions.
- Population cycles of the Canadian lynx and Soay sheep, modulated by weather and density-dependent disease.
- Single-neuron interspike intervals in some cortical recordings.

Connection (clinical) — defibrillation as state-space reset. Ventricular fibrillation can be modeled as the heart’s pacemaker leaving its limit cycle and entering a chaotic regime in which thousands of small re-entrant circuits prevent coordinated contraction. A defibrillator delivers a brief, high-energy shock that depolarizes essentially every myocyte simultaneously, “resetting” the system to the basin of attraction of the normal sinus-rhythm limit cycle. The intervention is a phase-space *kick*, not a chemical correction — pure dynamical-systems medicine.

Concept Check 6: A phase-plane portrait shows a stable spiral that, as a parameter μ is increased past a critical value μ_c , becomes encircled by a small closed orbit. (a) Name the bifurcation. (b) Predict whether the resulting oscillation amplitude depends linearly or quadratically on $\mu - \mu_c$ near the bifurcation. (c) Name one cardiac or circadian disorder consistent with a Hopf bifurcation gone wrong.

0.1.9 Biological Oscillators: From Genes to Heartbeats

Biological oscillators are textbook applications of delayed negative feedback (equation (2)) and limit-cycle dynamics.

0.1.9.1 The Circadian Clock

The mammalian circadian clock is a transcription–translation feedback loop (TTFL). CLOCK and BMAL1 heterodimerise and activate transcription of *Per1*, *Per2*, *Cry1*, and *Cry2*. PER and CRY proteins accumulate, translocate to the nucleus, and inhibit CLOCK/BMAL1, closing a negative-feedback loop with a delay set by transcription, translation, dimerization, and post-translational modification (notably casein-kinase-1 ϵ phosphorylation of PER). Mutations that alter CK1 ϵ or PER2 phosphorylation sites shift the clock’s period from the wild-type about 24 h to as little as 20 h or as much as 28 h, providing molecular evidence for the delay-period relationship of equation (2).

0.1.9.2 The Cardiac Pacemaker

Sino-atrial node cells lack a true resting potential. Instead, their membrane potential oscillates between roughly -60 mV (maximum diastolic potential) and 0 mV (peak of action potential). Three ionic currents — funny current I_f , T-type Ca^{2+} current $I_{Ca,T}$, and L-type Ca^{2+} current $I_{Ca,L}$ — operate on different timescales to generate the pacemaker limit cycle, which is robust to $\pm 20\%$ changes in any one conductance.

0.1.9.3 The Cell Cycle

In rapidly dividing cells the cyclin–CDK system is the master oscillator. M-cyclin accumulates linearly during interphase; once a threshold is reached, M-CDK activity is amplified by a positive-feedback bistable switch (Wee1 inactivation, Cdc25 activation), driving entry into mitosis. APC/C-mediated cyclin destruction collapses M-CDK activity, the bistable switch flips back, and the cycle resets. This is a relaxation oscillator: a slow build-up followed by a fast release, mathematically distinct from the harmonic oscillation of the circadian clock.

0.1.9.4 Shared Feedback Architecture of Biological Oscillators

Table 4. Shared Feedback Architecture of Biological Oscillators: Oscillator and Period.

Oscillator	Period	Mechanism class
Circadian (PER/CRY)	about 24 h	Delayed transcriptional negative feedback
Cardiac (SAN)	about 1 s	Coupled ionic currents, limit cycle
Cell cycle (cyclin–CDK)	hours–days	Relaxation oscillator with bistable switch
Glycolysis (yeast PFK)	seconds–minutes	Allosteric metabolic feedback
Calcium spikes	seconds	IP3R/RyR feedback with diffusion

The lesson: oscillators are not exotic; they are nature’s default solution to the problem of *temporal coordination*, and the same handful of feedback architectures appears across kingdoms and timescales.

0.1.10 Scale-Free Networks in Biology

Many biological networks are hub-heavy rather than random: a few nodes have many interactions, while most nodes have few. Some datasets are well approximated by scale-free degree distributions, $P(k) \propto k^{-\gamma}$, but the universality of strict power laws is contested and depends on sampling, curation, and statistical testing [Barabási and Albert, 1999, Barabási and Oltvai, 2004, Broido and Clauset, 2019]. The durable biological lesson is therefore not “everything is scale-free”; it is that hub structure, modularity, and heavy-tailed connectivity can change robustness, vulnerability, and controllability.

Biologically validated examples include:

- Protein–protein interaction networks of yeast, fly, and human ($\gamma \approx 2.5$).
- Metabolic networks — substrates such as ATP, NADH, and water are hubs connecting hundreds of reactions.
- Gene-regulatory networks — master regulators like *p53* or *MYC* control hundreds of downstream targets.
- Food webs — apex species with broad diets contrast with specialist links.
- Brain connectomes — cortical “rich-club” hubs disproportionately interconnect distant brain regions.

0.1.10.1 Mechanisms Generating Scale-Free Biological Networks

Two mechanisms can generate scale-free-like or hub-heavy architecture:

1. Preferential attachment — new nodes preferentially connect to already-popular nodes (Barabási-Albert model). In biology this maps onto gene duplication: a duplicated gene inherits its parent’s interaction partners, so highly-connected proteins beget more highly-connected proteins.
2. Optimization under cost-and-benefit — connections have wiring cost; a few high-degree hubs minimize total path length while limiting cost.

0.1.10.2 Functional Consequences of Hub-Dominated Networks

Table 5. Functional Consequences of Hub-Dominated Networks: Property and Random network.

Property	Random network	Scale-free network
Robustness to random failure	Fragile	Robust (random hits usually miss hubs)
Robustness to targeted attack on hubs	Robust	Fragile
Path length between random nodes	$\propto \ln N$	$\propto \ln \ln N$ (ultra-small)
Clustering coefficient	Low	High

This has direct biomedical implications. *Random* genetic perturbations (background mutation rates) usually miss hubs, so cells tolerate them. But *targeted* perturbation of hub proteins — exactly what cancer-driver mutations and many viral effectors do — can cripple the network. The same logic underlies the success of TP53, MYC, and KRAS as cancer drivers: they sit at network hubs.

Connection (medical) — antibiotic targets and the metabolic hub. Many successful antibiotics target hub enzymes in bacterial metabolism (e.g. RNA polymerase, ribosome, dihydrofolate reductase). Hubs are tempting because perturbing one node disables many downstream pathways; they are also dangerous because human homologues, where they exist, suffer comparable disruption — explaining the side-effect profiles of trimethoprim or rifampin.

0.1.11 Information, Entropy, and Self-organization

Living systems process information: they detect signals (genetic, chemical, mechanical, photonic) and use that information to generate ordered responses. From a thermodynamic perspective:

$$\Delta G = \Delta H - T\Delta S$$

(6)

Life builds local order (decreases local entropy) by doing work, and in so doing increases entropy of the surroundings. Self-organization — spontaneous formation of ordered structures — occurs when energy dissipation enables pattern formation (e.g., Bénard cells, Turing patterns in morphogenesis, the spiral waves of slime-mould aggregation).

0.1.11.1 Shannon Information and Biological Signal Content

Claude Shannon defined the information content of a discrete probability distribution as

$$H(X) = - \sum_i p_i \log_2 p_i$$

(7)

with units of bits when the logarithm is base 2. A signaling pathway that distinguishes “ligand absent” from “ligand present” carries at most one bit; a four-state developmental switch carries at most two; a transcription factor that selects among 1000 target promoters carries up to about 10 bits. Empirical studies of cytokine signaling pathways suggest mammalian cells extract on the order of 1 bit per pathway from ligand concentration — far less than the upper bound, because biological noise eats most of the channel capacity.

0.1.11.2 Mutual Information and Signaling Fidelity

The mutual information $I(X; Y) = H(Y) - H(Y \mid X)$ measures how much knowing the input X reduces uncertainty about output Y . For a noisy biological channel,

$$I(X; Y) = \frac{1}{2} \log_2 \left(1 + \frac{\sigma_{\text{signal}}^2}{\sigma_{\text{noise}}^2} \right)$$

(8)

Doubling the signal-to-noise ratio adds about half a bit. The diminishing returns of this expression explain why cells often build *parallel* signaling channels (multiple receptor tyrosine kinases, multiple cytokine receptors) rather than refining one channel indefinitely — additional channels add capacity additively, not logarithmically.

- Concept Check 7: A yeast cell at steady state maintains an intracellular K^+ concentration of 140 mM against an extracellular concentration of 5 mM. From the perspective of the second law of **thermodynamics**, is this local concentration gradient a violation of entropy increase? Identify the ultimate entropy source and the thermodynamic machinery (at least two molecular components) that sustains the gradient.
- Concept Check 8: Empirical estimates suggest a single mammalian cytokine pathway carries about 1 bit of mutual information about ligand concentration. What does this imply about the distinguishability of “low,” “medium,” and “high” concentrations from a single pathway alone, and why might inflammation cascades evolve to use multiple cytokines rather than ever-finer measurements of one?

0.1.12 Systems Thinking in Biology: Practical Implications

Table 6. Mutual Information and Signaling Fidelity: Principle and Biomedical implication.

Principle	Biomedical implication
Emergence	Drug targets must be evaluated in system context, not in isolation
Feedback	Blocking one regulatory loop often activates compensatory loops
Hierarchy	A mutation’s effect depends on its network context
Nonlinearity	Dose–response curves are rarely linear; threshold effects matter
Modularity	Synthetic biology exploits modular parts to engineer novel circuits
Scale-free	Hub targeting is potent but risks broad collateral damage

0.1.12.1 From Hill kinetics to a computational switch

The earlier nonlinear-threshold discussion introduced the Hill equation as a model of cooperative binding. The same mathematics appears when transcription factors bind clustered sites, when oxygen binds hemoglobin, and when receptors oligomerise. Running the project code makes the threshold tangible:

```
from biology.cell.cell_biology import hill_equation

kd, n = 10.0, 3.0
for L in (1.0, 5.0, 10.0, 20.0):
    theta = hill_equation(ligand_concentration=L, kd=kd, hill_coefficient=n)
    print(f"[L] = {L:5.1f} μM → fractional occupancy θ = {theta:.3f}")
```

For $n > 1$, a narrow concentration band separates “mostly off” from “mostly on” — the molecular implementation of a bistable or switch-like response that subsequent units link to gene circuits, metabolism, and neural firing.

0.1.12.2 Feed-forward and feedback motifs in gene networks

Beyond simple loops, network motifs [Alon, 2019] recur in transcriptional regulation: coherent feed-forward loops (two parallel paths to the same target, both activating or both repressing) can filter noise and enforce delays; incoherent feed-forward loops can generate pulses or adaptation. These motifs appear thousands of times in *E. coli* and yeast regulatory graphs. Recognizing them helps you predict how a drug that blocks one edge may reroute flux through another — the compensatory feedback that often limits single-target therapy. Tyson, Chen and Novak [Tyson et al., 2003] catalog the recurring “sniffers, buzzers, toggles and blinkers” of cell biology, each of which corresponds to a small network motif with a stereotyped temporal signature.

0.1.12.3 Why systems biology is not “fancy reductionism”

A naive reading of systems biology is that it builds bigger models of more parts. The deeper claim is methodological: certain *questions* (will the loop oscillate? Is the basin deep enough to resist noise? Does the network tolerate hub deletion?) cannot be answered by any amount of better single-component data. They require *system-level* metrics — gain, delay, basin depth, Lyapunov exponent, mutual information — which primarily acquire meaning at the level of the assembled system. Reductionism delivers parts; systems biology delivers grammars.

0.1.13 Current Evidence and Frontier Biology: Systems Science and Emergence

For Systems Science and the Logic of Emergence, frontier biology belongs inside the evidence logic of the chapter. Systems models are useful when they expose assumptions, uncertainty, and failure modes rather than merely producing elegant diagrams. The core reading question is this: system boundary choice, feedback sign, and scale determine whether a model explains or hides the biology.

- What to verify: identify the observation, model, assay, or dataset that would make the claim stronger or weaker.
- What to qualify: state the scale, organism, cell type, environmental condition, or population where the claim is expected to hold.
- What to compare: test at least one alternative explanation, baseline, or null model before treating the pattern as causal.
- What to cite: distinguish primary evidence, review synthesis, public dataset, and institutional guidance; for recent or numeric claims, prefer the source closest to the measurement and state what has changed since it was published.

For systems claims, identify the regulated variable, feedback sign, sensor, comparator, effector, and delay before naming a loop or emergent property.

Single-cell and spatial technologies now sharpen that source practice: a modern systems-biology claim should ask which scale was actually measured, whether the tissue context was preserved, and how perturbation closes the loop between discovery and mechanism [Fischer et al., 2025]. A beautiful network inferred from snapshots is a hypothesis until perturbation, time-series, or independent validation tests its causal edges.

Source practice: Use control, network, perturbation, or measurement sources that expose system boundaries and feedback evidence rather than treating a diagram as proof.

0.1.14 Unit 0 Integration: Using Systems Science Without Overclaiming

Systems language is powerful because it travels across scales, but that portability can become vagueness. Before calling something a system, write down four commitments:

1. Boundary: what is inside, what is outside, and what crosses the boundary?
2. State variables: what quantities describe the system well enough to answer the question?
3. Interactions: which edges are causal, which are correlations, and which are unknown?
4. Timescale: what changes fast, what changes slowly, and what has already been assumed constant?

This checklist connects the rest of this opening unit. **Complex Adaptive Systems** asks what happens when many bounded systems act as agents. **Active Inference and Free Energy** asks when the boundary can be formalised as a Markov blanket with sensory and active states. **History and Philosophy of Biology** asks how boundaries, variables, and mechanisms became accepted scientific categories in the first place.

0.1.14.1 Failure Modes of Systems Explanations

A systems explanation is weak when it merely renames complexity. “Everything is connected” is not a model. A usable systems claim should predict what happens when one connection is cut, one delay is shortened, one module is isolated, or one boundary is redrawn. If none of those perturbations would change the explanation, the diagram is decorative rather than explanatory.

0.1.15 Summary

- A system is defined by components, relationships, and boundary; equifinality and multifinality distinguish living open systems from contrived isolated ones.
- Most living systems are open systems that import free energy and export entropy.
- Negative feedback achieves homeostasis; positive feedback generates rapid transitions; delay turns stabilizing loops into oscillators.
- Emergent properties arise from patterns of interaction and cannot be reduced to component properties alone.
- Emergence also appears at colony scale: social-insect colonies can regulate nest climate, food discovery, or collective choice through worker interactions and environmental signals.
- Biological organization is hierarchical, modular, predominantly nonlinear, and often hub-heavy; strict scale-free claims require explicit statistical tests.
- Bifurcations classify how qualitative dynamical behavior changes — saddle-node (catastrophes), Hopf (oscillation onset), pitchfork (symmetry-breaking commitment).
- Biological oscillators (circadian, cardiac, cell-cycle) realize delayed-feedback limit cycles; chaos appears in some cardiac and population dynamics.
- Hill-type cooperativity implements sharp molecular thresholds; the toggle switch implements bistable cell-fate decisions; network motifs (feed-forward loops) shape dynamics and compensation under perturbation.
- Information theory bounds how much a noisy biological channel can convey, motivating parallel rather than refined signaling architecture.

0.1.16 Key Terms

system · emergence · negative feedback · positive feedback · homeostasis · allostasis · hierarchy · modularity · nonlinearity · bistability · bifurcation · limit cycle · chaos · Lyapunov exponent · scale-free network · hub · self-organization · superorganism · Hill equation · toggle switch · open system · network motif · feed-forward loop · mutual information · equifinality

0.1.17 Discussion Questions

1. Name a biological process at each of three hierarchical levels (molecular, cellular, organismal). For each, identify what would be lost by studying primarily the level below it.
2. Describe a biological example of hysteresis — a system where the current state depends on history, not just the present inputs. How might hysteresis contribute to cell identity or memory?
3. The bacterium *E. coli* regulates the *lac* operon with a bistable switch: cells either fully express or fully repress the operon, with very few in intermediate states. Why might bistability be advantageous compared to a graded (linear) response? Under what physiological contexts might a graded response be preferred?
4. A patient takes a drug that blocks a key kinase in an oncogenic signaling pathway. Initial tumor regression is observed, but within months the tumor re-grows. Propose at least two systems-level mechanisms (feedback compensation, alternative pathway activation, or selection) that could explain this relapse. How would systems science inform rational combination therapy?
5. Turing patterns — periodic spatial self-organization arising from reaction–diffusion kinetics — have been proposed to explain animal coat markings, digit spacing, and hair follicle arrangement. What does the existence of Turing patterns in biology suggest about the relationship between physics, chemistry, and life?
6. Sketch the glucose–insulin–glucagon feedback graph. Annotate where metformin, GLP-1 receptor agonists, and SGLT2 inhibitors act. Why might adding a second drug class outperform doubling the dose of one class?

7. Using the Hill equation with $n = 4$ and $K_d = 8 \mu\text{M}$, estimate θ at $[L] = 4 \mu\text{M}$ and at $[L] = 16 \mu\text{M}$. How does cooperativity sharpen the transition compared with $n = 1$?
8. Explain how a delay τ in a negative-feedback loop with gain k can convert a stable equilibrium into a sustained oscillation. Use the conditions $k\tau \ll 1$, $k\tau \approx 1/2$, and $k\tau > \pi/2$ to predict three qualitatively different behaviors and give a biological example of each.
9. Protein–protein interaction networks often contain hubs, even when a strict scale-free law is not established. Why can hub-heavy architecture make cells robust to many random gene losses yet vulnerable to perturbations that target hub proteins (e.g., adenovirus E1B targeting p53)? How would you design an antiviral that exploits this asymmetry without overclaiming the network model?
10. The cardiac pacemaker is extraordinarily robust to $\pm 20\%$ perturbation of any single ionic conductance. Why might this robustness be a general property of well-designed limit-cycle oscillators, and what does it predict about the genetic redundancy you would expect to find in clock genes?

0.1.18 Review Questions

1. State the three elements that define any system (components, relationships, boundary) and classify isolated, closed, and open systems by their matter and energy exchange. Why are most living systems necessarily open?
2. Define equifinality and multifinality and give a biological example of each. Explain why a surgically reduced sea-urchin embryo producing a normal small larva illustrates equifinality, whereas a damaged watch does not behave this way.
3. Contrast negative and positive feedback by sign and biological role. For one positive-feedback process (action potential, childbirth, or the clotting cascade), identify the explicit bounding mechanism and explain why unbounded positive feedback would be lethal.
4. Using the delayed-feedback equation $dx/dt = -k x(t - \tau)$, predict the qualitative behavior for $k\tau \ll 1$, $k\tau \approx 1/2$, and $k\tau > \pi/2$. Explain why biological clocks (circadian, cardiac, cell-cycle) live in the last regime and how shortening PER stability shortens the circadian period.
5. Using the Hill equation with $K_d = 5 \text{ nM}$ and a dimeric ($n = 2$) transcription factor at $[L] = 10 \text{ nM}$, compute fractional occupancy, then recompute for $n = 1$. Explain quantitatively how cooperativity sharpens a dose–response curve into a switch.
6. Distinguish weak from strong emergence. Give one biological property that is plausibly weakly emergent and one that is contested as possibly strongly emergent, and state what evidence would upgrade the contested case from “not yet derivable” to “in principle underivable.”
7. Compare saddle-node, Hopf, and pitchfork bifurcations by what happens to fixed points and which biological transition each underlies (catastrophic regime shift, oscillation onset, cell-fate commitment). For a stable spiral that gains a small limit cycle as a parameter crosses μ_c , name the bifurcation and a disorder consistent with it failing.
8. Explain why hub-heavy protein-interaction networks can be robust to random gene loss but fragile to targeted hub attack. Use this asymmetry to explain why TP53, MYC, and KRAS are potent cancer drivers and to propose the logic of a hub-exploiting antiviral.
9. Evaluate, using the mutual-information expression $I = \frac{1}{2} \log_2(1 + \sigma_{\text{signal}}^2/\sigma_{\text{noise}}^2)$, why a single cytokine pathway conveying about 1 bit cannot reliably distinguish “low/medium/high” concentrations, and why evolution favors parallel signaling channels over ever-finer measurement of one channel.
10. Synthesis: the chapter argues systems biology is “not fancy reductionism.” Defend or challenge this claim by identifying at least three system-level metrics (e.g. gain, delay, basin depth, Lyapunov exponent, mutual information) that acquire meaning primarily at the assembled-system level, and give a concrete question that no amount of better single-component data could answer.

0.1.19 Further Reading and Source Notes: Systems Science and Emergence

- Bertalanffy, L. von (1968). *General System Theory* [von Bertalanffy, 1968]. Braziller.
- Strogatz, S. H. (2018). *Nonlinear Dynamics and Chaos* (2nd ed.) [Strogatz, 2018]. Westview Press.
- Tyson, J. J., Chen, K. C., & Novak, B. (2003). Sniffers, buzzers, toggles and blinkers: dynamics of regulatory and signaling pathways in the cell [Tyson et al., 2003]. *Current Opinion in Cell Biology*, 15(2), 221–231.
- Alon, U. (2019). *An Introduction to Systems Biology: Design Principles of Biological Circuits* (2nd ed.) [Alon, 2019]. CRC Press.
- Cannon, W. B. (1932). *The Wisdom of the Body* [Cannon, 1932]. W. W. Norton.
- Mitchell, P. (1961). Coupling of phosphorylation to electron and hydrogen transfer by a chemi-osmotic type of mechanism [Mitchell, 1961]. *Nature*, 191, 144–148. (A worked example of a feedback motif powering metabolism.)

0.1.20 Companion Source Module: Systems Science and Emergence

Systems Science and Emergence should leave a reproducible trail from a biological claim to the code, figure, diagram, or paper-based activity that can test it. Use the surfaces below to inspect the chapter’s assumptions, rerun the relevant model, or compare the manuscript explanation with companion labs and figures.

Table 7. Companion source surfaces for Systems Science and Emergence.

Surface	Use it for
<code>src/biology/cell/cell_biology.py</code> (<code>hill_equation</code> , <code>receptor_occupancy</code> , <code>signal_amplification</code>)	Turn feedback, thresholds, and signaling gain into inspectable calculations.
<code>src/biology/ecology/ecology.py</code> (<code>logistic_growth</code>)	Compare linear intuition with bounded growth and carrying-capacity dynamics.
<code>src/biology/biochemistry/biochemistry.py</code> (<code>reaction_free_energy</code>)	Connect system directionality to thermodynamic constraints.
<code>src/visualization/plots.py</code> (<code>plot_logistic_growth</code>) and <code>src/mermaid/biology_diagrams.py</code> (<code>population_growth_stages_diagram</code>)	Check whether graphical summaries preserve the same model assumptions.

Reproducibility check: change one parameter at a time, record the sign of the response, and explain whether the result reflects feedback, saturation, or an arbitrary boundary choice. Cross-reference: pair this with section 0.2, section 9, and section 36.

0.2 Complex Adaptive Systems

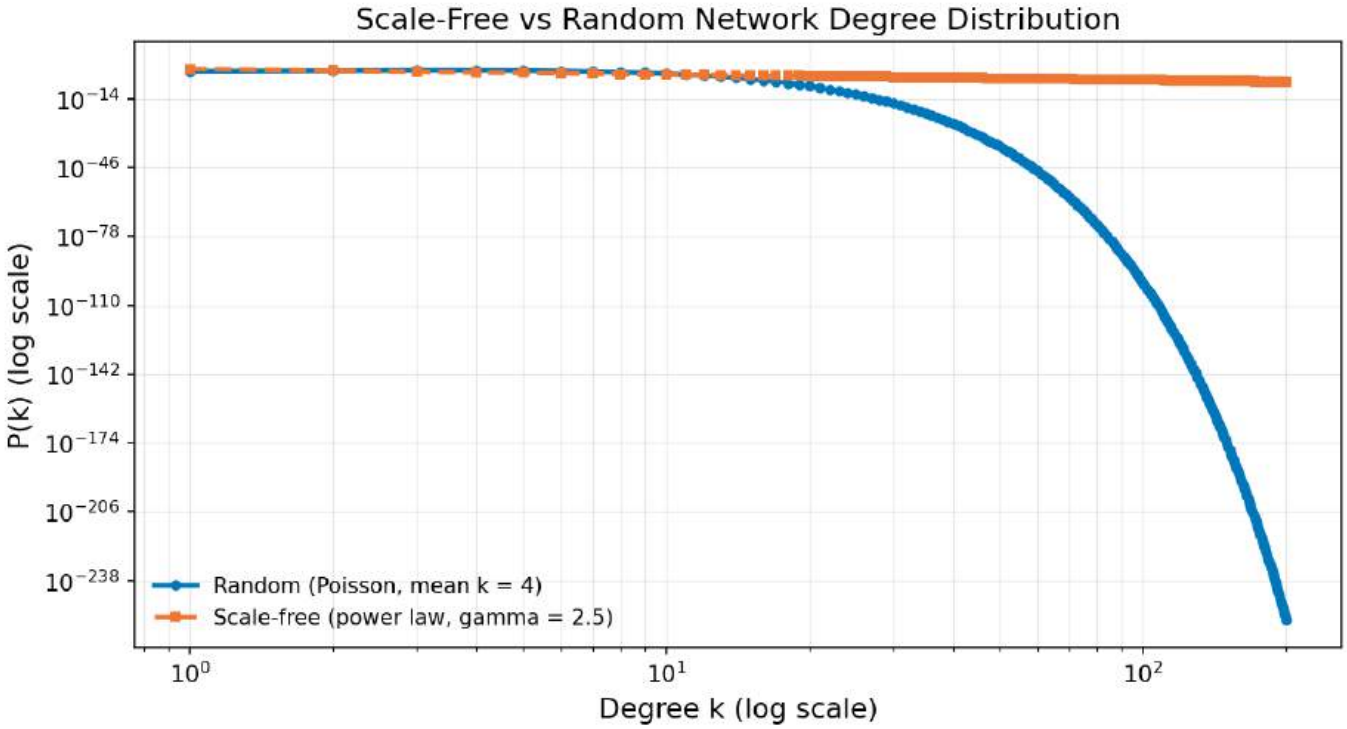


Figure 7. Scale-free versus random network degree distributions on log–log axes. The Poisson curve from a random (Erdős–Rényi) network falls off sharply past its mean degree, while the power-law curve $P(k) \propto k^{-\text{gamma}}$ from a scale-free network keeps a fat tail of hubs at high degrees. Biological networks of regulatory, metabolic, and protein-interaction data often resemble the latter pattern.

Level 2/3 · 35 min read · 50 min lecture · Prerequisites: section 0.1

0.2.1 Learning Objectives

By the end of this chapter, students will be able to:

1. Define a complex adaptive system and identify its distinguishing characteristics.
2. Describe how local rules among agents give rise to global order without a central controller.
3. Explain the roles of selection, variation, and adaptation in biological CAS.
4. Identify phase transitions and attractors in biological systems.
5. Recognize CAS dynamics at cellular, organismal, population, and ecosystem levels.
6. Analyze fitness landscapes using the NK model and predict the consequences of ruggedness.
7. Apply the logistic map to demonstrate how a single nonlinear equation can generate fixed points, oscillations, and chaos.
8. Connect biological CAS to engineered analogs such as genetic algorithms, neural networks, and ant-colony optimization.

0.2.1.1 Study Blueprint

- Big idea: Local rules can generate population-level patterns without a central controller.
- Core concepts: nonlinearity, self-organization, attractors, power laws.
- Framework alignment: Vision & Change: Systems, Structure and function; AP Biology: Systems Interactions; NGSS-style topics: Structure and Function, Interdependent Relationships in Ecosystems.
- Model or quantitative lens: Agent-rule and scaling arguments for emergent biological patterns.
- Data skill: Distinguish deterministic trends from stochastic variation in repeated simulations.
- Practice cadence: Questions and Methods, Representing and Describing Data, Argumentation.
- Common misconception to repair: Emergence is not mysterious; it is a reproducible consequence of interactions plus constraints.
- Primary lab: Lab B — Complex Adaptive Systems.
- Question bank: Questions — Complex Adaptive Systems.

- Transfer task: Compare flocking, immune activation, and microbial biofilms as adaptive systems.
 - Bridge to computation: `biology.ecology.ecology.logistic_growth`.
-

0.2.2 Opening Vignette: From Sandpiles to the Santa Fe Institute

In 1987, physicist Per Bak placed grains of sand one-by-one onto a pile and discovered a startling regularity: the pile spontaneously organized itself to a “critical” state where avalanches across a wide size range obeyed a power law — many small, few large, with no characteristic scale. He called this self-organized criticality [Bak et al., 1987] and argued it was a signature of complex adaptive systems throughout nature, from earthquakes to extinction cascades to neural firing patterns (*Physical Review Letters*, 1987).

That same year, the Santa Fe Institute was founded in New Mexico with an audacious charter: to study complex systems across disciplinary boundaries. Economists (W. Brian Arthur), biologists (Stuart Kauffman [Kauffman, 1993]), computer scientists (John Holland [Holland, 1992]), and physicists (Murray Gell-Mann) worked shoulder-to-shoulder, discovering that the same mathematics — agent-based models, fitness landscapes, power-law distributions — described stock markets, immune systems, and ecosystems alike.

The central biological insight: the immune system does not have a commander. The brain does not have a central processor. An ant colony does not have a foreman. In each case, simple agents following local rules generate intelligent collective behavior — emergence without design. This chapter explores how that principle operates from the molecular to the planetary scale, equipping you with tools (fitness landscapes, attractor analysis, power-law diagnostics, agent-based simulation, bifurcation theory) you will use throughout the rest of the textbook.

0.2.3 What Is a Complex Adaptive System?

A complex adaptive system (CAS) is a network of many interacting agents that:

1. Adapt — agents alter their behavior based on experience or selection.
2. Self-organize — ordered collective behavior emerges from local interactions without central control.
3. Co-evolve — the environment of each agent is partly constituted by the other agents; most adapt together.
4. Exhibit nonlinear dynamics — small perturbations can cascade into large effects (or large inputs may have minimal impact).

The central insight of CAS theory is that complexity is endogenous: it is generated by the interaction rules themselves, not imposed from outside.

CAS theory unifies vocabulary that previously belonged to separate disciplines. The “selection pressure” of an evolutionary biologist, the “energy landscape” of a chemist, the “objective function” of a computer scientist, and the “potential well” of a physicist are different names for the same mathematical object: a real-valued function over agent state that rules drive the system to extremise.

0.2.4 Agents and Agent Rules

In a CAS, the fundamental unit is the agent — an entity with internal state, sensors, and action capabilities. Agents follow local rules based on local information. No agent knows the global state.

0.2.4.1 Boids and Flocking

Computer scientist Craig Reynolds [1987] demonstrated that three simple rules produce realistic flocking behavior in simulated birds (“boids”):

1. Cohesion — steer towards the average position of nearby boids.
2. Alignment — steer toward the average heading of nearby boids.
3. Separation — avoid crowding; steer away from nearby boids.

No boid knows the global shape of the flock. The flock emerges from purely local interaction.

This principle recurs throughout biology:

- Quorum sensing in bacteria produces **biofilm** formation.
- Cytokine gradients direct immune cell recruitment.
- **Action potential** propagation in cardiac muscle coordinates the heartbeat.
- Schooling fish escape predators by aligning with neighbors faster than the predator can re-target.

0.2.4.2 Ant-Colony Optimization and Stigmergy

Ant foraging is a paradigmatic CAS. An ant deposits a pheromone trail as it returns from a food source; subsequent ants probabilistically follow stronger trails and reinforce them. Shorter trails are reinforced faster (more round-trips per unit time), while pheromone evaporation weakens abandoned routes. The colony therefore converges on near-optimal paths through local reinforcement and decay, not through any ant holding a map.

This **stigmergic** mechanism — communication through environmental modification — was named from termite nest-building work and then abstracted into ant-colony-optimization algorithms for routing, scheduling, and search problems [Grassé, 1959, Dorigo and Stützle, 2004]. The lesson is precise: a single ant is noisy and limited, but the colony can act as a distributed solver because the environment stores partial information.

Social insects also make the boundary between organism and collective negotiable. A honeybee swarm deciding where to nest integrates waggle dances, quorum-like thresholds, and inhibitory signals; field tracking confirms that dance-recruited bees fly toward advertised locations rather than merely becoming more active [Riley et al., 2005, Seeley, 2010]. The colony behaves like a **superorganism** as an analogy grounded in task allocation, communication, and colony-level reproduction, not as a claim that the group has a literal brain.

0.2.4.3 Immune Surveillance as Distributed Adaptation

Each lymphocyte carries a single antigen receptor specificity. The immune system as a whole performs continuous surveillance not because any cell is “smart” but because billions of differently-specific cells circulate, sample, and clonally expand on contact with cognate antigen. Negative selection in the thymus removes self-reactive clones; affinity maturation in the germinal center runs micro-evolution within the lymph node. The system has no commander; collective decision emerges from local rules.

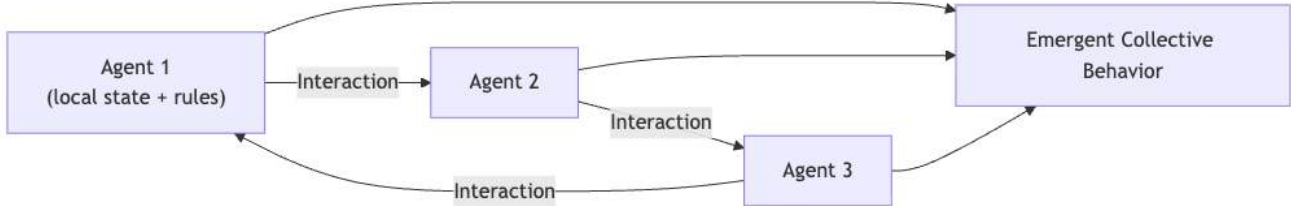


Figure 8. Three locally interacting agents exchange signals in a ring; their combined dynamics produce emergent collective behavior not visible in any single agent.

Concept Check 1: A swarm-intelligence start-up wants to control a fleet of drones using boid rules but discovers that during certain wind conditions the flock fragments. Hypothesize which of the three rules (cohesion, alignment, separation) most likely needs reweighting and explain how a change in radius of “nearby” might restore coherence.

0.2.5 Self-organization in Biology

0.2.5.1 Slime Moulds: A Class Example

Dictyostelium discoideum (slime mould) spends most of its life as independent amoebae. When starved, individual cells begin secreting cyclic AMP (cAMP), triggering a collective aggregation into a multicellular slug and eventually a fruiting body. No single cell plans the fruiting body; the entire developmental program is orchestrated by local cAMP gradients — a spectacular example of biological self-organization.

0.2.5.2 Termite Mounds as Collective Construction

Termites build elaborate mounds by following primarily local construction rules (place, remove, or reinforce soil pellets where cues indicate work). The architecture emerges from millions of local decisions, not from a blueprint read by any individual termite. Modern mound-physics work shows that the structure can couple wind, solar heating, and internal porosity to gas exchange, so “air conditioning” is an emergent physical consequence of collective construction rather than a designed appliance [Ocko et al., 2017]. Termite mounds are therefore a clean bridge between behavior, architecture, and physiology: local building rules alter the abiotic environment, and that altered environment feeds back on colony survival.

0.2.5.3 Embryonic Development as Coordinated Self-organization

The body plan of a vertebrate emerges from a single fertilized cell through cell division, migration, and differentiation guided by local chemical gradients (morphogens). The French flag model of positional information — cells adopt different fates depending on the local concentration of a morphogen — captures the CAS logic of development.

0.2.5.4 Turing Patterns and Reaction–Diffusion

Alan Turing’s 1952 paper on morphogenesis showed that two interacting chemicals — a local activator and a long-range inhibitor — can spontaneously break spatial symmetry to produce stripes, spots, or hexagonal patterns. The minimal model is

$$\frac{\partial u}{\partial t} = D_u \nabla^2 u + f(u, v), \quad \frac{\partial v}{\partial t} = D_v \nabla^2 v + g(u, v)$$

(9)

with $D_v \gg D_u$ (the inhibitor diffuses faster than the activator). Empirical examples include zebrafish stripe patterning, mouse hair-follicle spacing, and digit number in tetrapod limbs. Turing’s logic is the cleanest example of order-from-instability: the homogeneous state is unstable to spatial perturbations precisely because the inhibitor outruns the activator.

0.2.6 Attractors and Phase Space

The concept of an attractor is central to understanding CAS dynamics. An attractor is a set of states toward which a system tends to evolve over time.

Table 8. Turing Patterns and Reaction–Diffusion: Attractor type and Description.

Attractor type	Description	Biological example
Fixed point	System converges to a single stable state	Biochemical equilibrium; homeostatic set point
Limit cycle	System oscillates periodically	Circadian rhythm; cell cycle; cardiac pacemaker
Torus	System oscillates quasi-periodically	Coupled biological clocks
Strange attractor	Deterministic chaos; sensitive initial conditions	Some ECG arrhythmias; neuronal population dynamics

Phase space is the abstract space in which most possible system states are points. Attractors are embedded in phase space; trajectories flow toward them. Understanding biological regulation means understanding the attractor landscape of the relevant phase space.

0.2.6.1 Basins of Attraction and Landscape Geometry

The basin of attraction of an attractor A is the set of states from which trajectories flow to A . Basins are separated by separatrices — codimension-one manifolds across which a small perturbation flips the system between attractors. In Waddington’s classical metaphor for development, the embryo rolls down a “landscape” whose valleys (basins) correspond to differentiated cell types and whose ridges (separatrices) correspond to bistable cell-fate decisions. Modern single-cell RNA-seq data can be used to reconstruct an empirical analog of this landscape from observed cell-state densities.

The depth of a basin (the energy barrier to escape) determines its noise robustness; the width determines the range of initial conditions that converge to it. A deep, narrow basin is robust but inflexible; a shallow, wide basin is flexible but easily perturbed. Cancer cells often inhabit basins that are *wider* than normal (higher phenotypic plasticity) and *shallower* (easier to perturb stochastically), explaining their resistance to single-target therapy.

Concept Check 2: Both cancer cells and healthy cells inhabit a gene-expression phase space with multiple attractors (proliferative, quiescent, senescent, apoptotic). Many targeted therapies try to push malignant cells out of the proliferative basin. Why does this often fail — what does the landscape analogy predict about recurrence when the basin barrier is lower than the therapy’s “kick” amplitude? Propose a CAS-aware rationale for drug combinations rather than single agents.

0.2.7 Phase Transitions and Criticality

A phase transition is a qualitative change in system behavior at a critical parameter value. In biology:

- Protein folding — a polypeptide transitions from disordered to folded at a critical temperature.
- The lac operon — bistable switch with two stable attractors (ON and OFF) separated by an unstable threshold.
- The immune system — a subclinical infection (low pathogen load) may persist or be cleared; above a threshold, an acute inflammatory response is triggered.
- Ecosystems — beyond a critical level of nutrient loading, a clear lake can collapse into a eutrophic state — an ecological phase transition.
- Cytoplasm condensation — at high macromolecular crowding the cytoplasm transitions from liquid-like to glass-like, drastically slowing diffusion. Stress granules and P-bodies are physiological liquid-liquid phase separations.

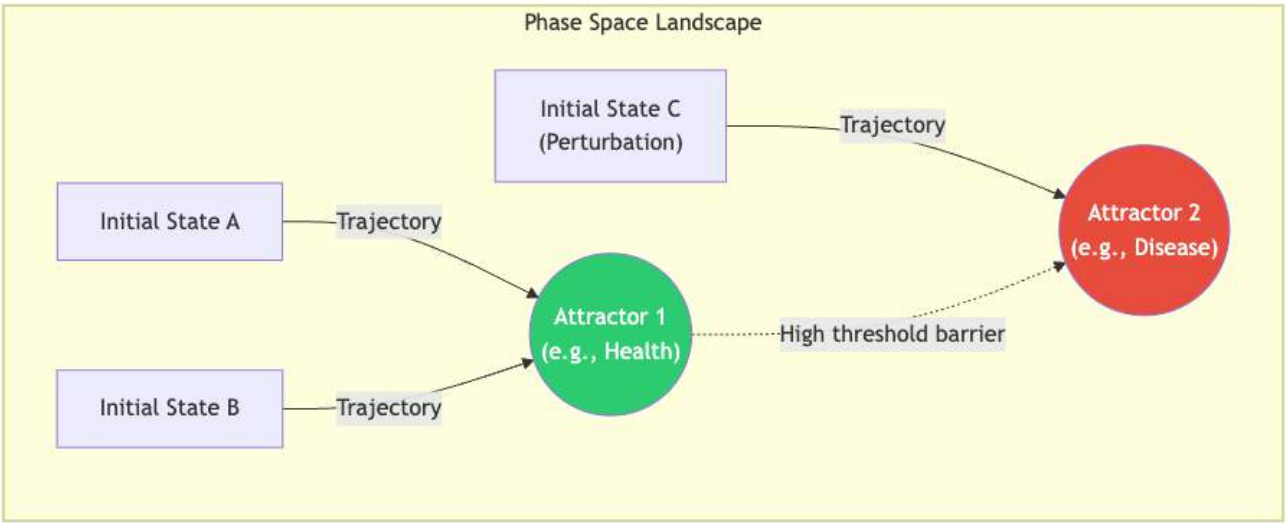


Figure 9. Phase-space landscape with separate attractor basins for health and disease states, linked by trajectories and a high barrier between basins.

0.2.7.1 The Ising Picture of Cell-Fate Switching

A toy mathematical bridge between physics and biology is the Ising model, in which spins $s_i \in \{+1, -1\}$ on a lattice interact through

$$H = -J \sum_{\langle i,j \rangle} s_i s_j - h \sum_i s_i$$

(10)

with coupling J and external field h . Below a critical temperature T_c the system spontaneously magnetises (most spins agree); above it the system is disordered. Mapping spin-up to “gene ON” and spin-down to “gene OFF” recasts cell-fate commitment as a magnetisation phase transition: at low effective “temperature” (low gene-expression noise), tightly-coupled networks lock into one of a few discrete cell types; at high temperature, expression patterns are disordered. The same mathematics describes binary opinion dynamics in social networks, illustrating how comprehensive these critical phenomena are.

0.2.7.2 Power Laws and Scale-Free Behavior

Many CAS, especially those poised near a critical phase transition (critical systems), display power-law distributions:

$$P(x) \propto x^{-\alpha}$$

(11)

where α is the scaling exponent. Power-law distributions in biology arise in:

- Protein interaction network degree distributions ($\alpha \approx 2\text{--}3$); contrast the heavy tail with the rapidly-decaying Poisson distribution expected for a random network in figure 7.
- Species abundance distributions (Preston’s lognormal-like, with power-law tail).
- Neuronal avalanche sizes [Beggs and Plenz, 2003] ($\alpha \approx 1.5$).
- Forest fire size distributions and earthquake magnitudes (Gutenberg–Richter law).
- Sizes of mass extinctions in the fossil record.
- Citations of academic papers and population sizes of cities.

The hypothesis of self-organized criticality (Bak, Tang & Wiesenfeld, 1987 [Bak et al., 1987]) proposes that many living systems automatically tune themselves to criticality, because critical systems are maximally responsive and information-transmitting. Critical neural networks have the longest correlation lengths, the highest dynamic range of stimulus encoding, and the maximum mutual information between input and output — most desirable for a brain.

0.2.7.3 Worked Example: Scaling in Power-Law Distributions

Problem: Neuronal avalanche sizes (the number of neurons firing synchronously in a cascade) in cortical slices have been empirically shown to follow a power law probability distribution $P(x) = Cx^{-\alpha}$, where the scaling exponent $\alpha \approx 1.5$. If a small avalanche involving $x = 10$ neurons occurs with a probability of 0.05

(5%), what is the probability of a massive avalanche involving $x = 100$ neurons?

Solution:

Set up the probability ratio. Because C is a constant, the ratio of probabilities for any two event sizes depends primarily on the ratio of those sizes to the negative power of α :

$$\frac{P(x_2)}{P(x_1)} = \left(\frac{x_2}{x_1}\right)^{-\alpha} \tag{12}$$

Substitute the known values ($x_1 = 10, x_2 = 100, \alpha = 1.5$):

$$\frac{P(100)}{P(10)} = \left(\frac{100}{10}\right)^{-1.5} \tag{13}$$

$$\frac{P(100)}{P(10)} = (10)^{-1.5} \tag{14}$$

$$(10)^{-1.5} = \frac{1}{\sqrt{10^3}} = \frac{1}{\sqrt{1000}} \approx \frac{1}{31.62} \approx 0.0316 \tag{15}$$

Calculate the final probability.

$$P(100) = P(10) \times 0.0316 = 0.05 \times 0.0316 \approx 0.00158 \tag{16}$$

A neuronal avalanche involving 100 neurons occurs with a probability of approximately 0.16%. Because power-law distributions possess a “fat tail” relative to Gaussian distributions, extreme outlier events (massive avalanches) remain statistically probable, illustrating how a CAS poised near criticality can periodically undergo massive, system-wide state changes.

Connection (clinical) — epileptic seizures as critical events. Cortical recordings near seizure onset show increasing mutual information between regions and rising statistical signatures of approach to a critical bifurcation. This is consistent with the brain operating just below a critical line, with seizures representing excursions across it. Closed-loop responsive neurostimulation devices (e.g. NeuroPace) detect these pre-critical signatures and deliver counter-stimulation to keep the system in the subcritical basin.

0.2.8 Adaptation and Evolution as CAS Processes

Evolution by **natural selection** is a CAS at the population level:

- Agents: individual organisms.
- Local rules: reproduction, survival, **mutation**, migration.
- Environment: partly constituted by other organisms.
- Emergent outcome: population-level adaptation, **speciation**, co-evolution.

The evolutionary process is not guided toward any particular solution. It is open-ended and path-dependent. Fitness landscapes capture the attractor structure of adaptive evolution.

0.2.8.1 Fitness Landscapes and Adaptive Walks

A fitness landscape [Kauffman, 1993] is a surface in which each point represents a possible genotype and the height represents the fitness that genotype confers. Selection drives populations “uphill” toward local peaks. The metaphor was first made concrete by Sewall Wright (1932) and later formalised by Stuart Kauffman’s NK models, which vary the number of loci N and the epistatic coupling K between them:

- $K = 0$ (no epistasis) — the landscape is a single smooth peak; evolution is a deterministic climb.
- $K = N - 1$ (maximal epistasis) — the landscape is maximally rugged, with $\sim 2^N/(N + 1)$ local peaks. Populations get trapped.
- Intermediate K — there are dozens to thousands of local peaks with valleys of mildly reduced fitness between them.

Mathematically, in an NK model with binary loci the fitness of a genotype is

$$W(x) = \frac{1}{N} \sum_{i=1}^N w_i(x_i, x_{i_1}, \dots, x_{i_K})$$

(17)

where each locus contribution w_i depends on its own state x_i and on K partner loci. For $K = 0$ each locus is independent, so the global optimum can be found one locus at a time. For $K > 0$ the contributions become entangled, generating the rugged landscape. Empirical fitness landscapes (for HIV-1 protease, the *E. coli* ribosomal protein S6, and *Aspergillus* enzymes) consistently land at intermediate K — rugged enough to trap evolution on local peaks, smooth enough that occasional valleys can be crossed.

Ruggedness predicts why evolution can take several different paths to similar fitness and why identical starting populations (as in the Lenski *E. coli* long-term evolution experiment) reach *different* adaptive solutions. In cancer, the same principle explains why single-agent targeted therapy traps tumors on a local peak; combination therapy shifts the landscape so the old peak is no longer fit, forcing movement into valleys where the tumor is more vulnerable.

Connection (clinical) — antimicrobial cycling. Hospital antibiotic stewardship sometimes deliberately *cycles* between drug classes, exploiting the fact that resistance mutations to one class may carry fitness costs on another. Each cycle reshapes the fitness landscape; resistance peaks that were locally fit under cefazolin become valleys under ciprofloxacin, evicting the population. The same logic is being explored for cancer (“evolutionary therapy” with adaptive dosing).

Applied Systems / Clinical Connection — combination therapy as landscape engineering. In a rugged disease landscape, the goal is not only to hit the current dominant clone; it is to make the next adaptive move costly. A cancer cell resistant to drug A may pay a growth-rate cost that makes it sensitive to drug B, while a bacterial mutant resistant to one antibiotic may lose the efflux or cell-wall state that protected it under another. Combination and sequence designs therefore ask a CAS question: what nearby peaks will selection reveal after the first intervention? The best regimen changes the topology of the landscape, not just the height of today’s peak [Kauffman, 1993].

0.2.8.2 Worked Example: Escape From a Fitness Valley

Problem: A bacterial population sits on a resistance peak. A double mutant would be more fit under the next drug, but the first mutation alone has a 2% fitness cost. Assume an effective population size $N_e = 10^5$ and selection coefficient against the intermediate $s = 0.02$. Is the intermediate likely to drift to appreciable frequency before being removed by selection?

Solution: A simple rule of thumb compares selection with drift using $N_e s$:

$$N_e s = 10^5 \times 0.02 = 2000$$

(18)

Because $N_e s \gg 1$, selection dominates drift. The deleterious intermediate is unlikely to persist long enough for the second mutation unless mutation supply is enormous, spatial structure protects a subpopulation, or the environment changes so the intermediate cost falls. This is why drug sequencing can work: if each step toward multidrug resistance requires crossing a valley, the treatment schedule can keep the population from climbing the next peak.

Concept Check (Analysis): A population of *E. coli* bacteria in a nutrient gradient follows a fitness landscape with two local maxima: one at [glucose] = 1 mM (metabolic optimum) and one at [glucose] = 0.1 mM (growth-rate optimum in competition). (a) Explain why natural selection alone cannot cross the fitness valley between these peaks. (b) Name two stochastic mechanisms that could move the population across the valley. (c) In which population-size regime ($N_e \ll 1/s$ or $N_e \gg 1/s$) does crossing become more likely, and why?

Concept Check (Evaluation): The sandpile model shows self-organized criticality (SOC): the distribution of avalanche sizes follows a power law $P(s) \sim s^{-\tau}$ with $\tau \approx 1.5$. Cortical neural activity in awake mammals also follows a power law with $\tau \approx 1.5$ for neuronal cascades. (a) What does this quantitative similarity suggest about the operating regime of the cortex? (b) Propose one experimental manipulation that would push the cortex below criticality (subcritical) and one that would push it above (supercritical). (c) What would be the functional cost of each deviation?

0.2.8.3 Genetic Algorithms: Evolution in a Computer

John Holland’s genetic algorithm [Holland, 1992] formalises Darwinian evolution as an optimization procedure. A population of candidate solutions (each encoded as a “chromosome”) is evaluated, the fittest are selected for reproduction, and offspring are produced by crossover (recombining parental chromosomes) and mutation. Genetic algorithms have designed:

- Antenna geometries for NASA satellites that outperform human-designed alternatives.

- Aerodynamic profiles for racing yachts.
- Schedule optimisers for hospitals.
- Trading strategies that survive market regime change.

The *biological* lesson is the inverse: just as artificial evolution solves design problems by sampling, recombining, and selecting, biological evolution discovers the metabolic and morphological inventions of life by exactly the same process — with the difference that biological “fitness functions” are themselves changing because the agents alter their environment.

0.2.8.4 Quorum sensing: a molecular vote without a mayor

Many bacteria secrete autoinducer molecules whose extracellular concentration rises with local cell density. Below a threshold, the signal is noise; above it, receptors synchronize gene expression — biofilm formation, bioluminescence (*Vibrio*), or **virulence** factor deployment (*Staphylococcus*). No cell counts its neighbors; each cell integrates a local concentration that *implicitly* encodes population size. Mathematically, positive feedback on autoinducer synthesis once a threshold is crossed is a bistable switch — a CAS motif duplicated in synthetic gene circuits. Antibiotics that fail to penetrate biofilms often select for persister subpopulations, illustrating how multicellular bacterial collectives occupy a different attractor than planktonic growth.

0.2.8.5 Trophic cascades: top-down reshaping of food webs

Removing an apex predator (wolves from Yellowstone pre-1995 [**Ripple and Beschta, 2012a**]; large sharks from coral reefs) can trigger cascading changes in herbivores, plants, and even geomorphology — not because the predator “controlled” each species, but because the network of interactions rewires. The offset prey–predator oscillations in figure 219 are the simplest mathematical caricature of such coupled dynamics. Reintroduction experiments show that restoration is not the reverse movie of removal: history and initial conditions matter (hysteresis), another CAS signature. Levin’s classic argument [**Levin, 1998**] that ecosystems and the biosphere are themselves complex adaptive systems rests on exactly this combination of nonlinear dynamics, history dependence, and multi-scale interaction.

0.2.8.6 The Immune System as CAS

The adaptive immune system is perhaps the most striking interorganismal CAS:

- B-cell clonal expansion generates antigen-specific population growth.
- Affinity maturation (somatic hypermutation + selection) is micro-evolution within the germinal center, analogous to the allele-frequency trajectories in figure 129.
- Memory is a stable population-level attractor that persists after antigen clearance.

Concept Check 3: A bacterial population is grown for 1000 generations under cycling exposure to drugs A and B. Resistance mutations to A typically reduce growth rate on B and vice versa. Sketch how the population-mean fitness on each drug evolves over time, and explain in CAS vocabulary why the drug-cycling regime keeps the population on a “treadmill” rather than letting it climb a single peak.

0.2.9 Noise, Stochasticity, and Bifurcation

Deterministic CAS models capture the *average* trajectory but miss two crucial features of real biology: noise (stochastic fluctuations in component numbers) and bifurcation (qualitative changes in system behavior at parameter boundaries).

0.2.9.1 Noise in Genetic Switches

A bistable switch such as the *lac* operon ideally sits in either a fully-repressed or fully-induced state. In individual cells, however, **transcription** factor copy numbers are low (tens to hundreds per cell), so thermal fluctuations produce stochastic transitions between the two attractors. The rate of spontaneous switching follows a Kramers-like relation:

$$k_{\text{switch}} \approx \omega_0 e^{-\Delta U/k_B T_{\text{eff}}}$$

(19)

where ΔU is the height of the barrier between attractors and T_{eff} is an effective noise temperature set by molecule copy number. This has direct clinical consequences: bacterial persister cells escape antibiotics by stochastically entering a dormant attractor; cancer cells sample a phenotypic landscape and survive chemotherapy in rare sub-states — a Darwinian process on a CAS landscape rather than on genetic variation alone.

0.2.9.2 Fold Bifurcations and Hysteresis: Lake Eutrophication

Eutrophication is the textbook ecological example of a fold bifurcation. Let P = phosphorus load and A = algal biomass. For low P the system has a single clear-water equilibrium; as P exceeds a critical value P_1 the clear state loses stability and the lake flips to a turbid, algae-dominated state. Crucially, *reducing* P below P_1 does not restore the clear state — recovery requires that P falls below a lower threshold $P_2 < P_1$. This hysteresis loop is why eutrophication management is so expensive: undoing the transition requires substantially more reduction than preventing it in the first place. The same mathematics describes coral-reef to algal-reef transitions and some epileptic-focus formation in the brain.

0.2.9.3 The Logistic Map: A Worked Bifurcation Diagram

The logistic map

$$x_{n+1} = r x_n (1 - x_n)$$

(20)

with $r \in [0, 4]$ and $x \in [0, 1]$ is one of the simplest nonlinear systems and exhibits a complete cascade from order to chaos as r increases:

Table 9. The Logistic Map: A Worked Bifurcation Diagram: Range of r and Long-term behavior.

Range of r	Long-term behavior
$0 \leq r < 1$	Population dies out: $x_n \rightarrow 0$
$1 \leq r < 3$	Single stable fixed point $x^* = 1 - 1/r$
$3 \leq r < 3.449\dots$	Period-2 limit cycle
$3.449\dots \leq r < 3.544\dots$	Period-4 limit cycle
Period-doubling cascade	Periods 8, 16, 32, ... accumulating at $r_\infty \approx 3.5699$
$r \geq r_\infty$	Chaos with periodic windows (notably period-3 near $r = 3.83$)
$r = 4$	Fully developed chaos on $[0, 1]$

The successive period-doubling thresholds approach r_∞ at a fixed ratio (the Feigenbaum constant $\delta \approx 4.6692$) that recurs in any smooth unimodal one-dimensional map and even in measurements of dripping faucets and convection rolls. This scale invariance is part of why the logistic map matters: it predicts that systems as different as insect populations and turbulent fluids will display the same quantitative route to chaos.

Worked numerical iteration ($r = 3.2, x_0 = 0.5$): $x_1 = 3.2 \cdot 0.5 \cdot 0.5 = 0.800$. $x_2 = 3.2 \cdot 0.8 \cdot 0.2 = 0.512$. $x_3 = 3.2 \cdot 0.512 \cdot 0.488 = 0.799$. $x_4 = 3.2 \cdot 0.799 \cdot 0.201 = 0.514$. The iterates settle into a period-2 oscillation between roughly 0.513 and 0.800 — a discrete-time biological oscillator from one line of code.

Connection (ecology) — boom-bust population cycles. Some insect populations (notably Australian budworm) show empirical period-doubling and chaotic dynamics that are well-modeled by logistic-like equations. Whether populations are “really chaotic” or merely noisy depends on detailed model fitting; the pedagogical point is that *no exotic mechanism* is required to generate complex temporal patterns — a single nonlinear feedback suffices.

Concept Check 4: Iterate the logistic map by hand for $r = 2.5, x_0 = 0.1$, four steps. Predict the long-term value, then iterate a few more steps to confirm. What does this tell you about the basin of attraction of the fixed point?

0.2.10 Robustness and Fragility

CAS often exhibit robustness — the ability to maintain function in the face of perturbation — paired with occasional catastrophic fragility in specific directions. Biological robustness is achieved through:

- Redundancy — multiple components performing similar functions.
- Degeneracy — structurally distinct components can perform the same function in some contexts.
- Modularity — failure in one module is localized.
- Negative feedback — deviations are automatically opposed.
- Distributed encoding — important information is represented across many components, not localized in one.

However, the same architectural features that confer robustness to typical perturbations make the system fragile to novel, coordinated, or cross-module perturbations. Antibiotic resistance evolution, autoimmunity, and cancer most reflect such fragility. This trade-off is sometimes called the robust-yet-fragile signature of CAS: highly optimized systems are *more* robust to expected perturbations and *more* fragile to unexpected ones. Carlson and Doyle named this “highly optimized tolerance” (HOT), and it explains why mature ecosystems suffer catastrophically when novel invasive species or climate regimes appear.

Concept Check 5: Consider a CAS with strong negative feedback, modular organization, and five-fold redundant sensors. Name one category of perturbation it will handle easily and one category that will nonetheless catastrophically break it. Why do the same architectural features that create robustness also create specific fragilities?

0.2.11 CAS Across Biological Scales

Table 10. The Logistic Map: A Worked Bifurcation Diagram: Scale and CAS.

Scale	CAS	Agents	Emergent collective property
Molecular	Gene regulatory network	Transcription factors, RNAs	Gene expression pattern, cell fate
Cellular	Intracellular signaling	Signal proteins, second messengers	Robust most-or-none responses
Tissue	Neural network	Neurons	Cognition, memory, perception
Organism	Immune system	B and T cells, innate cells	Adaptive immunity
Population	Evolving population	Individual organisms	Adaptation, speciation
Ecosystem	Community ecology	Species populations	Food web structure, succession
Biosphere	Gaia / planetary metabolism	Biomes, ocean basins	Atmospheric composition, climate

0.2.11.1 Agent-Based Models Across Biological Scales

Table 11. Agent-Based Models Across Biological Scales: Phenomenon and Agents.

Phenomenon	Agents	Local rules	Emergent property
Bird flocks	Boids	Cohesion, alignment, separation	Coordinated flight
Ant trails	Ants + pheromone	Deposit, follow, evaporate	Shortest path
Slime mould	<i>Dictyostelium</i>	cAMP secretion, chemotaxis	Multicellular fruiting body
Schelling segregation	Households	Move if too few neighbors of “type”	Macroscopic segregation
Game of Life	Cells on grid	Birth/death rules from neighborhood	Gliders, oscillators, computers
SIR epidemic	S, I, R classes	Contact + recovery probability	Outbreak peak, herd-immunity threshold
T-cell repertoire	Lymphocytes	Random receptor + clonal selection	Adaptive specificity

The pattern is comprehensive: the rules are absurdly simple, the global behavior is rich. This is why agent-based modeling has become a standard tool in epidemiology (COVID-19 contact networks), behavioral ecology, and synthetic biology.

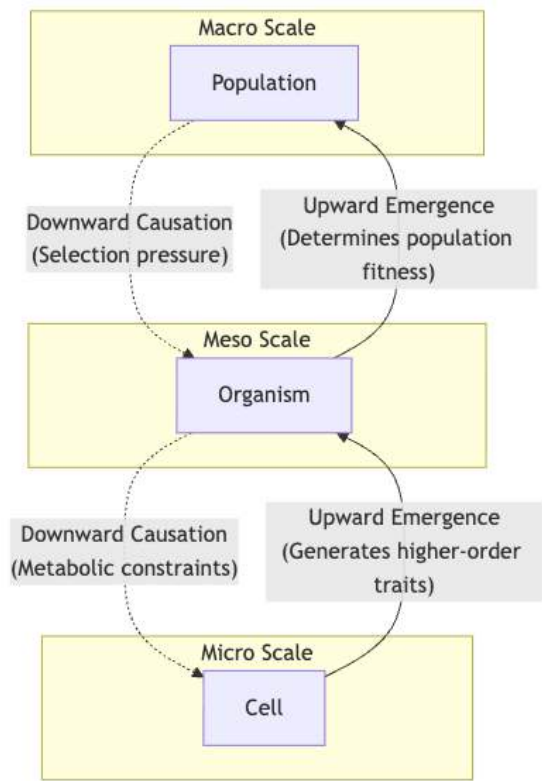


Figure 10. Cell, organ, and population levels linked by upward emergence and downward causation through selection pressure and metabolic constraints.

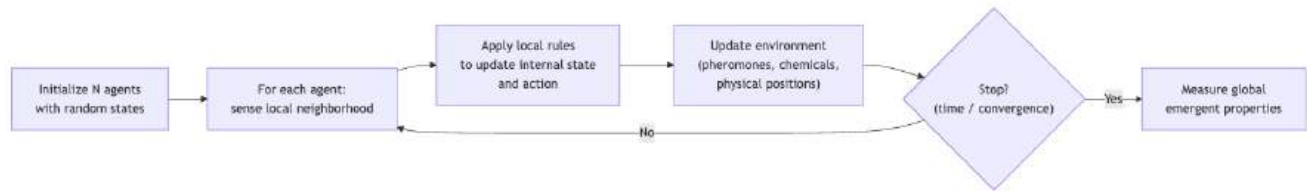


Figure 11. Agent-based modeling loop linking local rules to measured emergent behavior.

0.2.12 Synthesis and Practical Implications

CAS is not merely a metaphor; it is a *toolkit* with specific predictions:

- If you suspect a system sits at criticality, look for power-law statistics in size, duration, or wait-time distributions.
- If you suspect bistability, look for hysteresis: probe the system in both forward and reverse directions and watch for trajectory mismatch.
- If you suspect a rugged fitness landscape, look for path-dependent endpoints in replicate evolution experiments.
- If you suspect agent-based emergence, ask which global property would *not* survive removing the local rules — that is the emergent component.
- If you suspect chaos, estimate the leading Lyapunov exponent from time-series data and check for sensitive dependence on initial conditions.

These diagnostics turn CAS theory from rhetorical to actionable.

0.2.13 Current Evidence and Frontier Biology: Complex Adaptive Systems

For Complex Adaptive Systems, frontier biology belongs inside the evidence logic of the chapter. Systems models are useful when they expose assumptions, uncertainty, and failure modes rather than merely producing elegant diagrams. The core reading question is this: agent rules, heterogeneity, stochasticity, and path dependence make biological prediction conditional rather than absolute.

- What to verify: identify the observation, model, assay, or dataset that would make the claim stronger or weaker.
- What to qualify: state the scale, organism, cell type, environmental condition, or population where the claim is expected to hold.
- What to compare: test at least one alternative explanation, baseline, or null model before treating the pattern as causal.

- What to cite: distinguish primary evidence, review synthesis, public dataset, and institutional guidance; for recent or numeric claims, prefer the source closest to the measurement and state what has changed since it was published.

For complexity claims, name the interacting agents, update rule, feedback loop, and attractor or phase-space evidence before treating emergence as more than description.

Source practice: Pair simulation or network models with empirical traces of local interaction, perturbation, or time-series behavior; state what simpler linear model would miss.

0.2.14 Unit 0 Integration: From Systems to Adaptive Agents

Systems Science and Emergence defines boundaries, feedback, and dynamics. CAS reasoning adds three commitments:

1. Agents are heterogeneous. Cells, organisms, immune clones, microbial taxa, or firms in a food system do not all share the same state, history, or rule set.
2. Rules are local. Global patterns emerge from local sensing, movement, reproduction, death, learning, or signaling.
3. History matters. The same perturbation can have different outcomes after a system has crossed a threshold, acquired a mutation, changed a niche, or settled into a new attractor.

These commitments are what let CAS connect evolution, immunity, cancer, neural circuits, microbial ecology, and conservation. They also prevent a common overclaim. A system is not complex-adaptive merely because it has many parts. It becomes CAS-like when local adaptive rules, heterogeneity, and path dependence explain a global pattern better than a single representative-agent model.

0.2.14.1 Diagnostic Workflow for CAS Explanations

When you meet a later chapter case, ask:

- What are the agents?
- What local rule does each agent follow?
- What variable changes through feedback or selection?
- What global property appears after the agents interact?
- What perturbation would distinguish emergence from ordinary aggregation?

0.2.15 Summary

- A complex adaptive system is a collection of interacting agents with adaptive rules that generate emergent collective behavior.
- Self-organization arises from local interactions without central control; Turing patterns and Dictyostelium aggregation are paradigmatic examples.
- Attractors define the landscape of stable system states; phase transitions separate distinct regimes.
- Power laws and scale-free properties often signal systems poised near criticality; the Bak sandpile, neuronal avalanches, and earthquakes share statistical signatures.
- Fitness landscapes (Wright’s metaphor; Kauffman’s NK formalism) capture the structure of adaptive evolution; ruggedness predicts replicate divergence and resistance evolution.
- Genetic algorithms transplant biological evolution into computational design problems, illustrating that the search-by-variation-and-selection logic is substrate-independent.
- The logistic map demonstrates that a single nonlinear feedback can produce fixed points, period doubling, and chaos at the Feigenbaum point.
- Evolution, social-insect colonies, the immune system, neural networks, and ecosystems are major biological CAS — and so are the engineered swarm of drones, the genetic algorithm, and the social network.

0.2.16 Key Terms

complex adaptive system · agent · stigmergy · superorganism · self-organization · attractor · basin of attraction · phase space · phase transition · critical system · power law · scale-free · fitness landscape · NK model · genetic algorithm · logistic map · Feigenbaum constant · robustness · degeneracy · limit cycle · strange attractor · Turing pattern · bistable switch · hysteresis

0.2.17 Discussion Questions

1. The human gut microbiome contains about 10¹³ microbial cells from hundreds of species, interacting through metabolic cross-feeding, competition, and quorum sensing. Describe this as a CAS. What are the agents, local rules, and emergent properties? What could perturb the microbiome into a different attractor?

2. Explain why a cancer tumor is itself a CAS. What “selection pressure” drives cancer evolution? Why does targeting a single driver mutation often fail to permanently eliminate a tumor? How might CAS thinking guide combination therapies?
 3. Neural networks in the brain and artificial neural networks in deep learning both exhibit emergent computation from simple local rules. Compare and contrast the biological and artificial cases in terms of (a) learning rules, (b) architecture, (c) energy consumption, and (d) generalisation vs. overfitting.
 4. Many ecosystems exhibit hysteresis: a lake may tolerate increasing nutrient loading up to a threshold, then abruptly collapse to a eutrophic state, which cannot be reversed simply by reducing nutrient input to pre-collapse levels. What does this asymmetry imply for conservation management? How does CAS theory explain the hysteresis?
 5. The concept of “self-organized criticality” suggests that many biological networks operate near a critical point between order and disorder. What functional advantages might this confer on neural networks? What experimental evidence (e.g., neuronal avalanches [Beggs and Plenz, 2003]) supports or challenges this hypothesis?
 6. Explain quorum sensing in *Pseudomonas aeruginosa* or *Vibrio fischeri* using CAS vocabulary (agents, local rules, emergent behavior). How might blocking autoinducer synthesis differ from traditional bactericidal antibiotics in terms of resistance evolution?
 7. After wolf reintroduction in Yellowstone [Ripple and Beschta, 2012a], willow recovery along streams was attributed partly to reduced elk browsing. What other biotic or abiotic variables could confound a simple “predator → herbivore → plant” chain? How would you design a study to separate correlation from causation?
 8. The Lenski long-term evolution experiment in *E. coli* has run for >75 000 generations across 12 replicate populations on a single fitness landscape. Roughly half the populations independently evolved hypermutator phenotypes, and one acquired the ability to use citrate aerobically — but primarily after about 31 000 generations of “potentiating” mutations. What does this pattern of divergent yet partially convergent evolution reveal about fitness landscape ruggedness, contingency, and the predictability of evolutionary outcomes?
-

0.2.18 Review Questions

1. List the four defining properties of a complex adaptive system (adaptation, self-organization, co-evolution, nonlinear dynamics) and give one biological example that exhibits the complete set simultaneously.
2. Explain the chapter’s claim that “complexity is endogenous.” Using the boids model, describe how three local rules (cohesion, alignment, separation) generate a global flock that no individual agent represents.
3. Distinguish a fixed-point attractor, a limit cycle, and a strange attractor, giving one biological example of each. For the limit cycle, name the feedback feature that sustains the oscillation.
4. Apply the basin-of-attraction landscape to cancer therapy. A targeted drug delivers a “kick” that displaces malignant cells from the proliferative basin. Explain, in terms of basin depth and barrier height, why recurrence is likely when the barrier is lower than the kick amplitude, and why combination therapy reshapes rather than merely perturbs the landscape.
5. Iterate the logistic map $x_{n+1} = rx_n(1 - x_n)$ by hand for $r = 3.2$, $x_0 = 0.5$ for four steps, and classify the long-term behavior using the chapter’s r -regime table. Then explain what the Feigenbaum constant $\delta \approx 4.669$ implies about the *universality* of the route to chaos across unrelated systems.
6. Analyze self-organized criticality: identify the statistical signature (power-law size distributions) and explain, using neuronal avalanches, why a system poised near criticality maximizes dynamic range and mutual information. Why is this functionally advantageous for a brain?
7. Using Kauffman’s NK model, explain how the epistatic coupling K controls landscape ruggedness. Predict the qualitative outcome of replicate evolution experiments (e.g. the Lenski long-term *E. coli* lines) at $K = 0$, intermediate K , and $K = N - 1$, and connect ruggedness to the failure of single-agent targeted therapy.
8. Distinguish robustness, redundancy, and degeneracy. Then explain the “robust-yet-fragile” (highly-optimized-tolerance) signature: why do the same architectural features that confer robustness to expected perturbations create catastrophic fragility to novel, coordinated ones? Give one clinical or ecological example.
9. Evaluate the fold-bifurcation/hysteresis account of lake eutrophication. Why does reducing phosphorus below the original tipping point P_1 fail to restore the clear state, and what does the lower threshold P_2 imply for the cost asymmetry between prevention and remediation? Identify one other biological system governed by the same mathematics.

10. Synthesis: the chapter offers five diagnostic tests (power-law statistics, hysteresis probing, path-dependent replicate endpoints, the “remove-the-local-rules” emergence test, Lyapunov-exponent estimation). Choose a biological system of your choice, propose which two diagnostics you would run, state the falsifiable prediction each makes, and explain why a no-transition null model is essential before declaring an early-warning signal real.

0.2.19 Further Reading and Source Notes: Complex Adaptive Systems

- Holland, J. H. (1992). *Adaptation in Natural and Artificial Systems* (2nd ed.) [Holland, 1992]. MIT Press.
- Kauffman, S. A. (1993). *The Origins of Order: Self-organization and Selection in Evolution* [Kauffman, 1993]. Oxford University Press.
- Bak, P., Tang, C., & Wiesenfeld, K. (1987). Self-organized criticality [Bak et al., 1987]. *Physical Review Letters*, 59(4), 381–384.
- Levin, S. A. (1998). Ecosystems and the biosphere as complex adaptive systems [Levin, 1998]. *Ecosystems*, 1(5), 431–436.
- Beggs, J. M., & Plenz, D. (2003). Neuronal avalanches in neocortical circuits [Beggs and Plenz, 2003]. *Journal of Neuroscience*, 23(35), 11167–11177.
- Strogatz, S. H. (2018). *Nonlinear Dynamics and Chaos* (2nd ed.) [Strogatz, 2018]. Westview Press.

0.2.20 Companion Source Module: Complex Adaptive Systems

Complex Adaptive Systems should leave a reproducible trail from a biological claim to the code, figure, diagram, or paper-based activity that can test it. Use the surfaces below to inspect the chapter’s assumptions, rerun the relevant model, or compare the manuscript explanation with companion labs and figures.

Table 12. Companion source surfaces for Complex Adaptive Systems.

Surface	Use it for
src/biology/ecology/ecology.py (lotka_volterra, biodiversity_indices, logistic_growth)	Explore feedback, interaction strength, and diversity metrics as emergent summaries.
src/biology/evolution/evolution.py (simulate_selection, wright_fisher_drift, fitness_landscape_1d)	Compare selection, drift, and landscape ruggedness as agent-level rules.
src/visualization/plots.py (plot_lotka_volterra, plot_selection_simulation)	Inspect how oscillations and allele-frequency trajectories depend on starting conditions.
src/mermaid/biology_diagrams.py (food_web_diagram, population_growth_stages_diagram)	Link network structure to emergent population outcomes.

Reproducibility check: rerun or recalculate a scenario from two initial states and ask whether convergence, hysteresis, or path dependence is doing the explanatory work. Cross-reference: use section 0.1, section 20, and sections 37 and 38 as comparison cases.

0.3 Active Inference and Free Energy

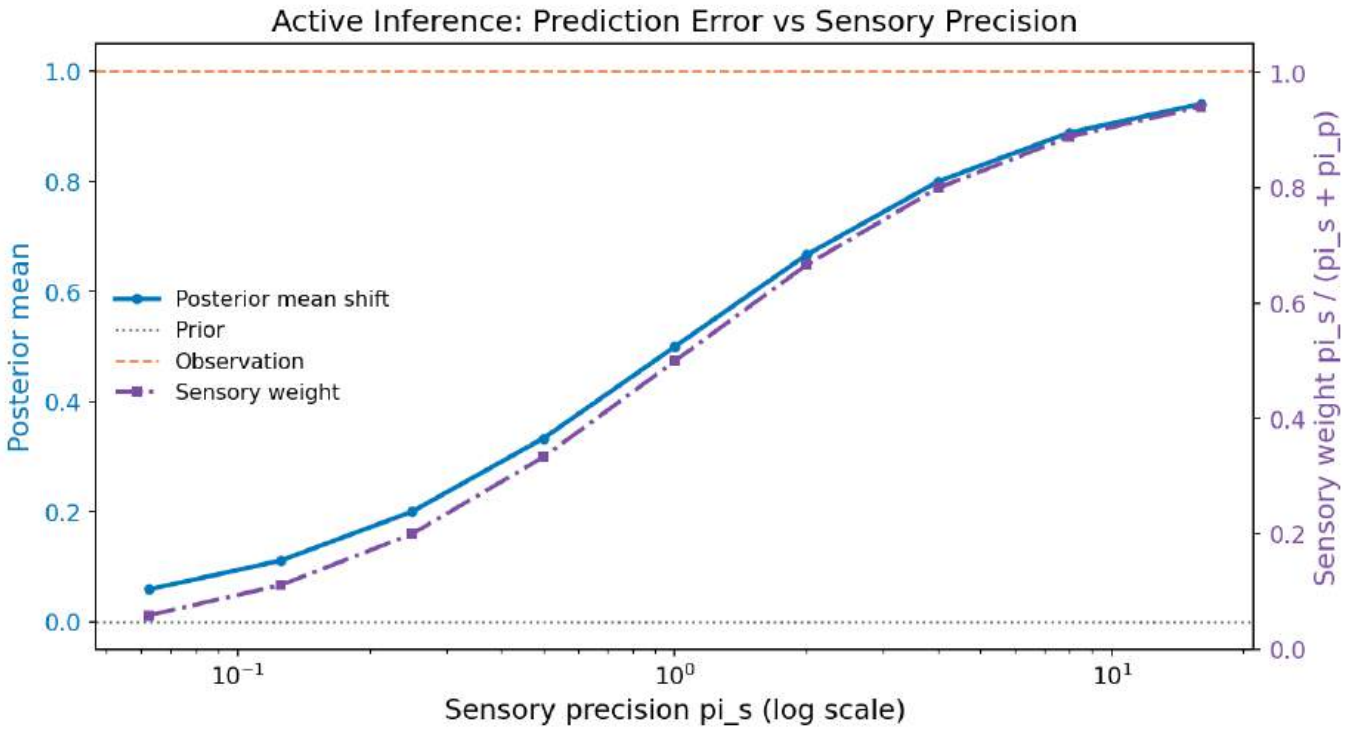


Figure 12. Posterior mean and sensory weight as functions of sensory precision π_s on a log axis. The Bayesian posterior $\mu_{\text{post}} = (\pi_p \mu_p + \pi_s y) / (\pi_p + \pi_s)$ smoothly slides from the prior toward the observation as π_s grows. The complementary sensory weight $\pi_s / (\pi_s + \pi_p)$ saturates near one, quantifying how much the observation is trusted.

Level 3/3 · 45 min read · 75 min lecture · Prerequisites: section 0.1, section 0.2

0.3.1 Learning Objectives

By the end of this chapter, students will be able to:

1. Explain what the free energy principle [Friston, 2010] states and why it is relevant to biology.
2. Describe the Bayesian brain hypothesis and how prediction-error minimization drives perception.
3. Distinguish between perceptual inference (changing beliefs to match sensory input) and active inference [Friston, 2017] (acting to fulfil predictions).
4. Connect active inference to homeostasis, allostasis [Sterling, 2012], and interoception.
5. Define a Markov blanket and identify its four state-classes (internal, external, sensory, active) in a biological system.
6. Apply expected free energy to explain how an organism balances goal-directed reward and information-gathering.
7. Describe canonical predictive-processing microcircuits in the cortex and how they implement hierarchical inference.
8. Identify connections between active inference and other frameworks in the textbook (metabolism, neural signaling, evolution, immunology, computational psychiatry).

0.3.1.1 Study Blueprint

- Big idea: Living systems reduce uncertainty by acting on the world as well as by updating internal models.
- Core concepts: prediction error, Bayesian updating, policy selection, homeostasis.
- Framework alignment: Vision & Change: Systems, Structure and function; AP Biology: Systems Interactions; NGSS-style topics: Structure and Function, Interdependent Relationships in Ecosystems.
- Model or quantitative lens: Bayesian belief updating and expected-free-energy-style policy comparison.
- Data skill: Read a small probability table and update a prediction after new evidence.
- Practice cadence: Questions and Methods, Representing and Describing Data, Argumentation.
- Common misconception to repair: Active inference is not passive prediction; action changes the sensory data that arrive next.
- Primary lab: Lab C — Active Inference and Free Energy.
- Question bank: Questions — Active Inference and Free Energy.

- Transfer task: Map prediction-error reasoning onto chemotaxis, thermoregulation, and attention.
- Bridge to computation: `biology.physiology.physiology.homeostasis_response`.

0.3.2 Opening Vignette: Helmholtz and the Unconscious Inference

In 1867, Hermann von Helmholtz proposed that perception is not passive recording but unconscious inference: the brain interprets noisy sensory signals by combining them with prior knowledge about the world. When you perceive a flat photograph as three-dimensional, your brain is making an inference — filling in depth from shadow, texture, and perspective cues that it has learned through a lifetime of experience.

For over a century, Helmholtz’s insight remained a philosophical curiosity. Then, in the early 2000s, neuroscientist Karl Friston formulated the free energy principle (FEP) — a mathematical framework that makes Helmholtz’s intuition precise. The FEP proposes that many living systems, from single cells to entire organisms, can be modeled as systems that minimize variational free energy: a tractable upper bound on the surprise (negative log-probability) of their sensory observations [Friston, 2010]. The bacterium swimming up a glucose gradient and the neuroscientist modeling the brain can, under this framework, be described with the same inferential vocabulary — inference under uncertainty.

The free energy principle does not merely explain perception. By extending inference to *action* — organisms act to make their predictions come true — it offers a broad account of sensation, movement, homeostasis, development, and evolutionary modeling [Friston, 2017, Parr et al., 2022]. This chapter introduces the framework as an optional graduate-depth systems lens and shows how it connects to major themes in this textbook while remaining one model among competing biological explanations.

0.3.3 Maintaining Viable States Under Uncertainty

Most living organisms face a fundamental challenge: they must maintain their internal organization in the face of a ceaselessly changing and uncertain environment. To survive, an organism must:

- Model its environment — build and update an internal representation of what is out there.
- Sense — gather information that reduces uncertainty about environmental states.
- Act — change the environment or its own internal state to remain within viable bounds.

This three-part loop — *model* → *sense* → *act* — is the core of what the free energy principle (FEP) formalises.

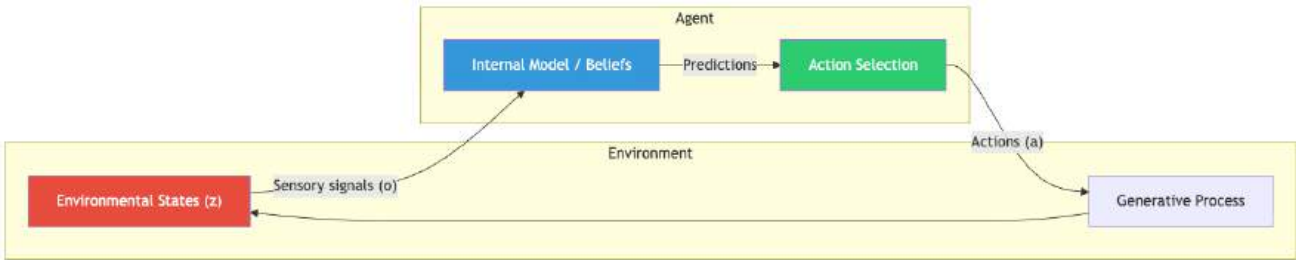


Figure 13. Active-inference loop linking environment, internal model, and action selection through sensory updates and motor output.

0.3.4 Markov Blankets: The Mathematical Skin of an Agent

Before formalising free energy, we need a way to make rigorous the boundary between an agent and its environment. The Markov blanket provides exactly this.

0.3.4.1 Markov Blanket Definition

For a set of random variables, the Markov blanket of a node is the minimal set of nodes that, once conditioned on, render the node statistically independent of every other variable in the network. For an agent that persists in time, this generalizes to a partition of states into four disjoint classes:

- External states η — the world outside the agent.
- Sensory states s — variables through which the world influences the agent (photoreceptor activations, mechanoreceptor strain, chemosensor occupancy).
- Active states a — variables through which the agent influences the world (motor neuron output, secretory activity, ciliary beating).
- Internal states μ — everything inside the agent (gene expression, membrane potentials, synaptic weights).

The blanket itself is the union $b = s \cup a$. The defining property is that internal states are conditionally independent of external states given the blanket:

$$P(\mu, \eta \mid s, a) = P(\mu \mid s, a) P(\eta \mid s, a)$$

(21)

The internal states “see” the world primarily through s and “touch” it primarily through a .

0.3.4.2 Why Markov Blankets Matter

Markov blankets give a principled definition of an agent: anything that maintains a recognisable boundary in state space *has* a Markov blanket, almost by definition. The same partition applies to a bacterium (cell membrane), a neuron (axonal/dendritic membrane), an organism (skin and sensorimotor apparatus), and a colony (collective foraging interface). Because the partition is recursive — the blanket of a blanket is a blanket — it naturally accommodates hierarchical biological organization. Here a *generative model* is the organism’s internal probabilistic model that predicts its sensory inputs from hypothesized hidden causes in the environment.

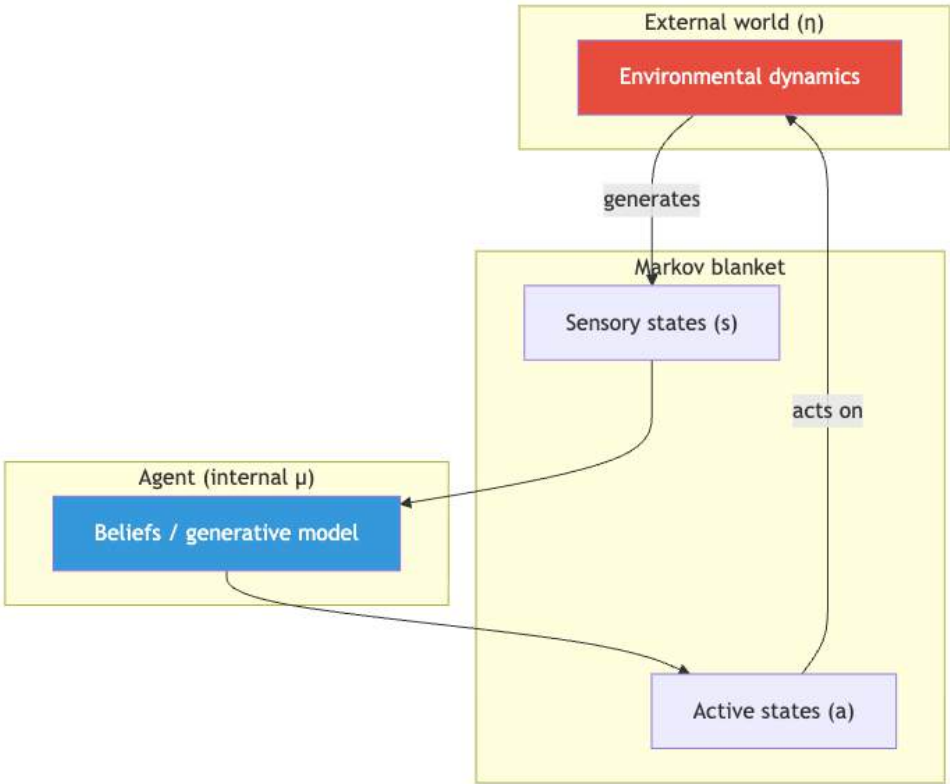


Figure 14. Markov-blanket partition: internal states couple to external states primarily through sensory and active states.

Concept Check 1: Identify sensory states, active states, internal states, and external states for (a) an *E. coli* cell performing chemotaxis, (b) a single hepatocyte, and (c) a foraging honeybee. Which states would be hardest to assign in each case, and why?

0.3.5 The Free Energy Principle

The free energy principle, developed principally by Karl Friston (UCL), proposes that many living systems can be modeled as systems that minimize variational free energy under explicit assumptions about the agent, its boundary, its observations, and its generative model.

Formally, variational free energy F provides an upper bound on surprisal (the log-probability of sensory observations under a model):

$$F = \underbrace{D_{KL}[Q(z) \parallel P(z \mid o)]}_{\text{complexity (posterior mismatch)}} - \underbrace{\ln P(o)}_{\text{surprise (negative log-evidence)}}$$

(22)

where:

- $Q(z)$ is the agent’s approximate posterior belief over hidden causes z .
- $P(z|o)$ is the true posterior.
- D_{KL} is the Kullback–Leibler divergence.
- $P(o)$ is the probability of observations o under the generative model.

Because the true posterior is generally intractable, agents minimize F as a proxy for maximizing their evidence (model fit to sensory data).

Equivalently, free energy decomposes as:

$$F = \underbrace{\mathbb{E}_Q[\ln Q(z) - \ln P(z)]}_{\text{complexity (prior mismatch)}} - \underbrace{\mathbb{E}_Q[\ln P(o | z)]}_{\text{expected log-likelihood (accuracy)}}$$

(23)

The first term penalises beliefs that deviate from priors; the second rewards beliefs that predict observations well. Minimizing F balances prior expectations against sensory evidence — exactly the logic of Bayesian inference.

Concept Check 2: An organism’s ecological **niche** can be described as the set of states its generative model treats as probable. Why does a penguin housed in a tropical aquarium experience persistent free energy, even when fed and safe? Describe two distinct strategies the penguin might use to minimize it and explain why behavioral change (return to cold water) is usually faster than belief update.

0.3.6 Predictive Processing and the Bayesian Brain Hypothesis

The Bayesian brain hypothesis (Helmholtz 1867; Friston 2005; Clark 2013) proposes that the brain is fundamentally a prediction machine: it maintains a hierarchical generative model of the world and continuously uses that model to predict incoming sensory signals.

0.3.6.1 Hierarchical Predictive Coding

In the predictive processing framework, the brain generates top-down predictions from higher cortical areas toward lower sensory areas. Lower areas compute the prediction error — the difference between what was predicted and what was received:

$$\varepsilon = o - \hat{o}$$

(24)

Prediction errors propagate upward, driving updates to the generative model. When predictions are accurate, prediction errors approach zero and neural activity is minimized — an energetically efficient coding strategy.

0.3.6.2 The Canonical Microcircuit

Anatomical and physiological evidence suggests the cortex implements predictive coding through a canonical microcircuit repeated across cortical areas. The simplified picture:

- Superficial pyramidal neurons (layers II/III) send forward signals that empirically encode prediction errors, projecting to higher cortical areas.
- Deep pyramidal neurons (layers V/VI) send backward signals that empirically encode predictions, projecting to lower areas.
- Inhibitory interneurons modulate the *gain* of error units, implementing the precision weighting described in the earlier predictive-processing discussion.

In the laminar reading of predictive coding, each cortical area is a small inference engine: it receives ascending prediction errors from below, compares them with descending predictions from above, and outputs both an updated internal state (forward) and a refined prediction (backward). The same architecture helps interpret visual cortical hierarchies ($V1 \rightarrow V2 \rightarrow V4 \rightarrow IT$), auditory streams, and somatosensory pathways, suggesting predictive coding is a broad candidate principle for cortical computation rather than a settled one-size-fits-most algorithm.

0.3.6.3 Precision and Attention

Each prediction error can be weighted by precision (inverse variance): high precision means “trust this channel.” Mathematically, a precision-weighted prediction error is

$$\xi = \pi \cdot (o - \hat{o})$$

(25)

where $\pi = 1/\sigma^2$ is the precision (figure 12 shows posterior mean and sensory weight as π_s varies on a log axis). Attention — from spatial orienting to feature selection — can be read as optimizing precision over sensory hierarchies: amplify unexpected but reliable signals, attenuate predictable ones. Sensory attenuation during self-generated movement (you tickle yourself less than others tickle you) follows because the motor command predicts somatic input, down-weighting proprioceptive precision so the tickle does not register as surprising. Disorders that mis-estimate precision (autism-spectrum hypotheses; schizophrenia-spectrum aberrant salience) reinterpret noise as meaningful structure or vice versa, producing false inference at the perceptual or interoceptive level.

0.3.6.4 Worked Example: Bayesian Updating and Prediction Error

Problem: A foraging bird maintains a prior belief about the spatial location x of a food source, modeled as a Gaussian distribution with mean $\mu_{prior} = 10$ m and variance $\sigma_{prior}^2 = 4$. The bird receives a noisy sensory observation indicating food at $o = 16$ m, with a sensory variance $\sigma_{obs}^2 = 12$. Calculate the prediction error and the new updated (posterior) belief about the food’s location.

Solution:

- 1. Calculate the prediction error:

The generative model’s prediction is the mean of the prior ($\hat{o} = 10$).

$$\varepsilon = o - \hat{o} = 16 - 10 = 6 \text{ m}$$

- 2. Calculate the optimal updating weight (Kalman gain):

In Bayesian inference with Gaussians, the weight given to the sensory evidence depends on the relative precision (inverse variance) of the prior vs the observation.

$$K = \frac{\sigma_{prior}^2}{\sigma_{prior}^2 + \sigma_{obs}^2} = \frac{4}{4 + 12} = \frac{4}{16} = 0.25$$

- 3. Calculate the posterior mean:

The new belief (μ_{post}) is the old belief plus the prediction error scaled by the optimal weight:

$$\mu_{post} = \mu_{prior} + K \cdot \varepsilon$$

$$\mu_{post} = 10 + 0.25 \cdot 6 = 10 + 1.5 = 11.5 \text{ m}$$

Due to the high uncertainty of the sensory observation compared to the prior ($\sigma_{obs}^2 = 12$ vs $\sigma_{prior}^2 = 4$), the bird primarily slightly adjusts its internal model (moving beliefs from 10 to 11.5) despite a large prediction error of 6. This formalises how sensory evidence shifts the generative model under the Free Energy Principle.

Concept Check 3: Repeat the worked example with $\sigma_{prior}^2 = 12$ and $\sigma_{obs}^2 = 4$ (i.e. a vague prior and a precise observation). Compute the new Kalman gain and the posterior mean for the same prior mean (10) and observation (16). What does the comparison reveal about how priors and likelihoods compete?

0.3.7 Active Inference as a Perception-Action Loop

Active inference extends predictive coding from perception to action. An organism can reduce prediction error in two ways:

- 1. Perceptual inference — update internal beliefs to match incoming sensory data (classic Bayesian inference).
- 2. Active inference — act on the world to make sensory data match the predictions generated by the generative model.

Under the FEP, behavior is the fulfilment of prior expectations. An organism with a prior that its body temperature will remain at 37 °C will *act* to make that prediction true when it is falsified by cold exposure (seek warmth, shiver, vasoconstrict).

This reframes homeostasis: not as the passive correction of deviations, but as the active fulfilment of generative model predictions about body state.

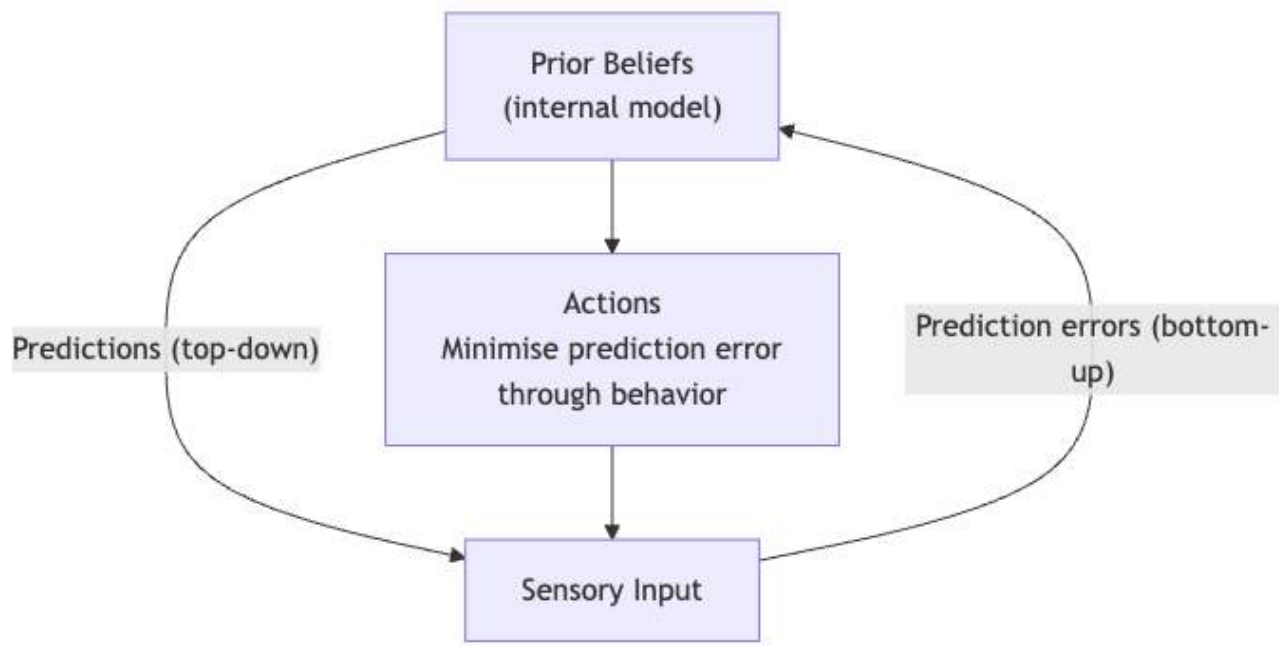


Figure 15. Predictive processing: top-down predictions, bottom-up errors, and action.

0.3.7.1 Homeostasis vs. Allostasis

Table 13. Homeostasis vs. Allostasis.

Concept	Core idea	Active inference framing
Homeostasis	Maintain a fixed set point	Precise prior over a target internal state
Allostasis	Proactively adjust the set point in anticipation of need	Updating prior expectations based on context

Allostasis — popularised by [Sterling and Eyer \[1988\]](#) — is naturally captured by active inference: the generative model changes its predictions (set points) before the perturbation arrives, explaining why the heart rate rises before exercise begins.

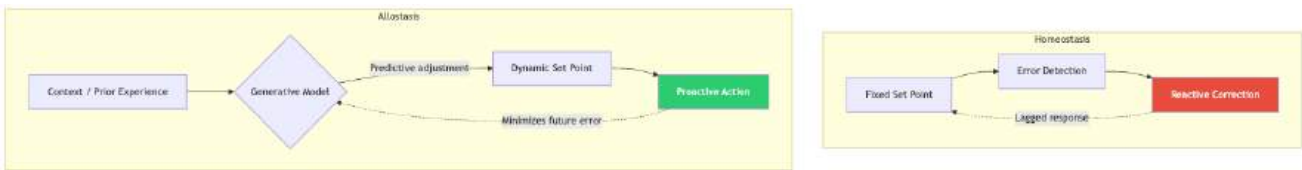


Figure 16. Reactive homeostasis corrects measured error after deviation; allostasis shifts set points proactively from a generative model.

0.3.7.2 Worked Example — Free Energy Minimization via Action

Consider an organism whose generative model encodes a prior on body temperature T :

$$P(T) = \mathcal{N}(37, 0.5^2)$$

(prior: body temperature should be 37 °C, tight precision)

(26)

Its interoceptive sensor is noisy, $P(o \mid T) = \mathcal{N}(T, 1.0^2)$. Suppose the sensor reports $o = 34$ °C (cold). The posterior belief about T is a Gaussian with mean:

$$\mu_{\text{post}} = \frac{\sigma_o^2 \cdot 37 + \sigma_{\text{prior}}^2 \cdot 34}{\sigma_o^2 + \sigma_{\text{prior}}^2} = \frac{1.0 \cdot 37 + 0.25 \cdot 34}{1.0 + 0.25} = 36.4 \text{ °C}$$

(27)

The variational free energy associated with this observation is approximately $F_{\text{before}} \approx 4.5$ nats (dominated by the log-likelihood of $o = 34$ under the prior). The agent has two ways to reduce it:

1. Perceptual inference (passive) — accept $\mu_{\text{post}} = 36.4$ °C as its new belief. F drops to about 2.1 nats.

$$G(\pi) = \underbrace{\mathbb{E}_{Q(o,z|\pi)}[\ln Q(z|\pi) - \ln Q(z|o,\pi)]}_{\text{epistemic value}} - \underbrace{\mathbb{E}_{Q(o|\pi)}[\ln P(o|C)]}_{\text{instrumental value}}$$

(28)

where C encodes the agent’s preferences (which observations are valuable). The two terms decompose action selection into:

- Epistemic (information) value — the expected reduction in uncertainty about latent causes; high for exploratory or “curious” policies.
- Instrumental (pragmatic) value — the expected log-probability of preferred outcomes; high for goal-directed policies.

Policies are selected with probability $Q(\pi) \propto e^{-G(\pi)}$: the agent prefers policies with low expected free energy. Crucially, when no information remains to be gained, the agent reduces to a reward-maximiser; when no extrinsic reward differs across policies, the agent reduces to a pure information-seeker (curiosity). This single equation thereby unifies reinforcement learning, optimal experimental design, and exploration–exploitation trade-offs that previously occupied separate literatures.

Concept Check 4: A rat in a novel maze runs in apparently random directions even when food is reliably available in one corner. Decompose this behavior into epistemic and instrumental value. What would change if the rat had explored the maze for an hour first?

Concept Check (Synthesis): During the COVID-19 pandemic, behavioral scientists documented “prediction-error fatigue” — people initially updated their beliefs rapidly about transmission risk, then stopped updating despite continued novel evidence. Using the active inference framework: (a) Model this as a precision-weighting problem — what happened to the precision assigned to new COVID-related observations over time? (b) How does this relate to the distinction between expected free energy’s epistemic and instrumental components? (c) Propose a public-health intervention that would restore appropriate precision weighting without exploiting anxiety.

0.3.7.4 Epistemic vs. Instrumental Value (worked numerical example)

Suppose an agent considers two policies, π_A and π_B , with epistemic values 1.0 and 3.0 nats and instrumental values 4.0 and 2.5 nats respectively. Then

$$G(\pi_A) = -(1.0 + 4.0) = -5.0, \quad G(\pi_B) = -(3.0 + 2.5) = -5.5$$

Both are roughly comparable, but π_B has slightly lower expected free energy because its higher information gain compensates for somewhat lower expected reward. Under softmax selection $Q(\pi_B)/Q(\pi_A) = e^{0.5} \approx 1.65$ — the agent is about 1.65× more likely to choose the more informative policy. Reducing temperature (sharpening the softmax) makes the choice nearly deterministic; raising temperature flattens it. This single mechanism can reproduce explore-exploit phenomena across species and contexts.

0.3.8 Embodied Active Inference

Active inference is inherently embodied and enactive — it requires a body that can act. The agent’s generative model must represent:

- Exteroceptive states — sensory information about the external environment.
- Interoceptive states — sensory information about the internal body (viscera, blood chemistry, proprioception).
- Action affordances — possible actions the agent can take, and their predicted sensory consequences.

The body is not merely the carrier of the brain; the brain’s generative model is shaped by bodily form, evolutionary history, and developmental experience. This 4E cognition framework — embodied, embedded, enacted, extended — is directly implied by active inference.

Concept Check 5: A patient with a pacemaker experiences “phantom palpitations” — strong sensations of irregular heart rhythm that the device rhythm itself rarely produces. Within the active-inference framework, why might long-standing tight priors about heart rhythm *create* a prediction error when the rhythm is in fact perfectly regular? What strategies — pharmacological, cognitive, or behavioral — would widen those priors?

0.3.9 Active Inference and Evolution

The free energy principle provides a formal bridge between individual-level adaptive behavior and evolutionary dynamics:

- **Natural selection** filters for organisms whose generative models minimize free energy (are accurate predictors of their ecological niche).
- The ecological niche is itself the set of environmental states that the organism’s generative model implicitly expects.

- Niche construction — organisms actively shape their environments to match their generative models — is a direct prediction of active inference applied to evolutionary time scales.

The evolutionary emergence of increasingly sophisticated generative models (from chemotaxis in bacteria to abstract planning in primates) can be framed as the phylogenetic history of free energy minimization.

0.3.9.1 Free Energy Minimization Beyond Brains

The FEP was developed in neuroscience but is not limited to it. Recent work extends active inference to:

- Single cells. A bacterium running E. coli chemotaxis can be cast as an active-inference agent whose generative model encodes a prior over “high glucose,” whose sensors read receptor occupancy, and whose actions are tumble probability and run length. Berg-and-Purcell information bounds reappear as bounds on free energy minimization.
- Immune system. B-cell affinity maturation can be read as Bayesian inference over antigen “causes,” with somatic hypermutation as a proposal distribution and selection as a posterior update. Memory cells embody high-precision priors against re-infection.
- Development. Morphogen gradients pattern tissues by reducing free energy of cell-fate “predictions”; experimentally induced perturbations are absorbed when the developmental model can re-infer position from remaining cues.
- Evolution. Natural selection itself can be framed as gradient descent on a long-timescale free energy functional, with the species’ generative model encoded in its genome and the niche acting as the sensory environment. This is the most ambitious and the most contested of the FEP’s extensions.

The unifying claim is that many systems that resist dispersion — systems modeled as maintaining a Markov blanket against thermodynamic noise — *behave as if* they minimize free energy. The “as-if” is important: the FEP is a candidate modeling description of self-organizing systems at selected timescales, not a claim that any particular molecule “computes” free energy or that Markov blankets automatically settle biological individuality.

0.3.10 Computational Psychiatry and Precision-Weighting Disorders

If the brain is a prediction machine, many psychiatric conditions admit a generative-model interpretation. The framework is provisional but increasingly testable.

0.3.10.1 Anxiety and Interoceptive Hyper-precision

If priors over “safe body state” are too tight (high precision), ordinary interoceptive fluctuations (a normal heartbeat, gut peristalsis) generate large prediction errors that the system experiences as alarming. Therapeutic interventions that improve interoceptive accuracy (mindfulness training, graded exposure, beta-blocker pharmacology) can be re-interpreted as recalibrating prior precisions and likelihood widths. Classical exposure therapy reads naturally as deliberate prediction-error minimization: the patient repeatedly experiences a feared stimulus without consequence, and Bayesian belief updating attenuates the conditioned association.

0.3.10.2 Depression and the Dark-Room Problem

Depression has been modeled as an over-precise prior on negative outcomes combined with under-weighted reward signals — the agent’s generative model “knows” that nothing it does will help, so policies with high epistemic or instrumental value are systematically discounted. Predictive-processing accounts of anhedonia explain reduced exploratory behavior as a rational response to a prior of hopelessness. The “dark-room problem” — why don’t agents simply hide in a dark room to minimize sensory surprise? — is solved by noting that prolonged darkness *itself* generates surprise relative to the organism’s evolved generative model, which expects some level of stimulation.

0.3.10.3 Schizophrenia and Aberrant Salience

Schizophrenia-spectrum hypotheses suggest a *failure* of precision regulation: prediction errors that ought to be down-weighted (because they are noise) are instead amplified, while reliable signals are attenuated. This produces “aberrant salience,” in which random noise feels meaningful and structured signals feel hollow. Some accounts link this directly to dopaminergic precision modulation in striatal circuits; clozapine and other antipsychotics may, on this reading, restore appropriate precision weighting. Hallucinations, on this view, are not failures of perception but failures of inference — top-down predictions overruling weak sensory evidence.

0.3.10.4 Autism-Spectrum Predictive Differences

A complementary account proposes that autism involves *reduced* precision on top-down priors (or *increased* precision on bottom-up sensory signals), so the world is experienced in raw sensory detail without the smoothing influence of predictions. This may explain hypersensitivity, attention to fine detail, and difficulty

with rapidly changing social cues — most of which require high-prior precision to integrate noisy data into coherent interpretations.

Connection (clinical) — limitations. These accounts are conceptually attractive but the empirical evidence for any specific computational reading is still developing. They should be read as *hypotheses* that organize current research rather than diagnostic frameworks. Patients deserve evidence-based treatments, and the FEP is a complement to — not a replacement for — careful clinical psychiatry.

Concept Check 6: A patient describes a constant feeling that “something is about to go wrong” despite no objective threat. Describe how this could arise from (a) over-precise priors on negative outcomes, (b) under-precise interoceptive likelihoods, or (c) hyperactive dopaminergic precision. What experimental measurement might distinguish the three?

0.3.11 Active Inference Applications Beyond Neuroscience

The active-inference framework has been applied — with varying degrees of empirical support — well beyond brain science.

0.3.11.1 Immune Recognition as Population-Level Inference

The adaptive immune system can be framed as a multi-agent active-inference system. Each B-cell embodies a hypothesis (its receptor specificity); the population of B-cells maintains a distribution over possible antigens; somatic hypermutation generates new hypotheses; clonal selection performs Bayesian update; and memory cells are high-precision priors that minimize future free energy of re-infection. The thymic deletion of self-reactive T-cells corresponds to clipping the prior to exclude hypotheses that would generate persistent self-reactive prediction errors.

0.3.11.2 Developmental Patterning as Hierarchical Inference

Embryonic development can be modeled as a hierarchical inference: each cell receives morphogen “observations,” combines them with priors encoded in its genome and current state, and performs an active update (differentiation, migration, division). Robustness to perturbation is then explained as *Bayesian inference over a redundant generative model*: removing one cue still leaves enough information to infer position.

0.3.11.3 Evolutionary Active Inference

If natural selection filters for free-energy-minimizing organisms, the long-time evolutionary dynamics can themselves be cast as inference over a “species-level” generative model encoded in the genome and implemented through development. Niche construction (beavers building dams, plants oxygenating the atmosphere) becomes the evolutionary analog of action: organisms reshape the world to match their inherited expectations.

0.3.11.4 Ecology and Collective Behavior

Schooling fish, foraging ants, honeybee swarms, and coordinated bacteria can be analyzed as collective active-inference systems whose Markov blankets are larger than any individual organism. The mathematical formalism predicts when collective behavior can outperform individual behavior: when individual sensory data are noisy and the environment is partially observable, a collective Bayesian posterior can be sharper than a single individual’s estimate.

Social insects make the boundary conditions unusually concrete. In ant foraging, pheromone trails are a form of **stigmergy**: each worker changes the environment, and later workers sample that changed environment as evidence for food location or trail quality [Grassé, 1959, Dorigo and Stützle, 2004]. In honeybee house-hunting and foraging, waggle-dance communication lets many scouts turn fragmentary spatial observations into a colony-level choice, while flight-track experiments show that dances can transmit usable vector information about distant resources [Riley et al., 2005, Seeley, 2010]. An active-inference reading should keep the “as-if” qualifier visible: the model is useful when observations, actions, uncertainty, and updating rules can be specified, not when collective behavior is merely renamed as inference.

0.3.12 Connections to Other Units

Table 14. Ecology and Collective Behavior: Unit and Active inference connection.

Unit	Active inference connection
Unit III — Energy and Metabolism: Introduction — Metabolism	ATP production and allostasis maintain the energetic constraints required for inference
Unit VIII — Botany — Plant Biology: Introduction — Botany	Stomatal regulation and tropisms can be modeled as active inference by plant systems
Unit IX — Zoology and Systems Physiology: Introduction — Neuroscience	Predictive coding instantiates active inference at the neural circuit level
Unit X — Ecology: Introduction — Ecology	Niche construction and habitat selection as ecosystem-level active inference

0.3.12.1 Interoceptive active inference and psychiatry (conceptual)

Interoception — the sense of the visceral body — supplies observations about heart rate, gut distension, inflammation, and temperature. If priors over “safe body state” are too tight, ordinary fluctuations may generate persistent prediction-error signals experienced as anxiety; if priors are too loose, allostatic forecasting may fail. This is not a replacement for clinical diagnosis but a generative framing that links behavior (avoidance, reassurance seeking, substance use) to error-minimization strategies. Therapies that improve interoceptive accuracy (certain mindfulness protocols, graded exposure, interoceptive training) can be understood as recalibrating precisions and priors — though the neuroscience is still being mapped experimentally.

0.3.13 The Free Energy Principle in Context

The FEP is a theoretical framework, not a claim about specific neural mechanisms. It provides a unifying mathematical language, but multiple neural implementations are consistent with it, and critics argue that broad FEP explanations must still earn discriminating predictions and clear system boundaries [Bruineberg et al., 2022, Colombo and Wright, 2017]. It should be understood alongside:

- Reinforcement learning (reward-maximizing agents). Active inference subsumes RL in the limit where epistemic value is zero (no information-seeking).
- Optimal control theory (minimum-cost action selection). Active inference subsumes OC in the limit where the generative model perfectly captures dynamics.
- Information-theoretic accounts of neural coding. Predictive coding implements rate-distortion-optimal sensory compression.
- Cybernetics (Wiener; Ashby). Cybernetic homeostasis is the special case of active inference with a fixed prior and reactive correction.

The FEP is useful as a design principle: selected living systems can be modeled as if they are minimizing free energy, just as the lens can be modeled as if it minimizes the time of light travel (Fermat’s principle). Whether neurons “really” compute KL divergences or just behave as if they do is a separate empirical question.

Concept Check 7: Reinforcement learning maximizes expected reward; optimal control minimizes expected cost; active inference minimizes expected free energy. State a biological prediction that would distinguish active inference from pure RL — i.e. a behavior that an RL agent would not produce but an active-inference agent would.

0.3.14 Current Evidence and Frontier Biology: Active Inference and Free Energy

For Active Inference and the Free Energy Principle, frontier biology belongs inside the evidence logic of the chapter. Systems models are useful when they expose assumptions, uncertainty, and failure modes rather than merely producing elegant diagrams. The core reading question is this: active-inference explanations must connect hidden states, sensory evidence, action, and measurable prediction error.

- What to verify: identify the observation, model, assay, or dataset that would make the claim stronger or weaker.
- What to qualify: state the scale, organism, cell type, environmental condition, or population where the claim is expected to hold.
- What to compare: test at least one alternative explanation, baseline, or null model before treating the pattern as causal.
- What to cite: distinguish primary evidence, review synthesis, public dataset, and institutional guidance; for recent or numeric claims, prefer the source closest to the measurement and state what has changed since it was published.

For active-inference claims, identify the agent boundary, observed state, generative-model assumption, and rival control account before calling the behavior inference.

Source practice: Cite formal FEP/active-inference work for the model, empirical physiology or behavior studies for the organism, and explicit boundary critiques when Markov blankets carry the explanation.

0.3.15 Unit 0 Integration: When Active Inference Is the Right Tool

Active inference is strongest when a biological case has these four ingredients:

1. Hidden state: something important is not directly observed, such as temperature threat, nutrient availability, body-water status, or social risk.
2. Observation: the organism receives noisy sensory evidence about that hidden state.
3. Action: the organism can change the world or its body to make future observations more expected.
4. Precision control: the system weights some errors more than others because not every signal is equally reliable or equally important.

If a case lacks action, active inference may reduce to perceptual inference or Bayesian updating. If it lacks a plausible generative model, the explanation may be little more than metaphor. If it cannot be distinguished from reinforcement learning, optimal control, or ordinary feedback, the active-inference label has not yet earned its keep.

0.3.15.1 Bridge to history and philosophy

History and Philosophy of Biology is the check on overextension. It asks whether “function”, “goal”, “model”, “self”, and “boundary” are being used as causal claims, historical claims, modeling assumptions, or value-laden descriptions. Active inference can clarify biological agency when those meanings are kept separate.

0.3.16 Summary

- The free energy principle proposes that living systems can often be modeled as minimizing variational free energy — a measure of the gap between their generative model and sensory evidence.
- Markov blankets formalise the boundary between an agent and its environment, partitioning most states into internal, sensory, active, and external classes.
- The Bayesian brain maintains hierarchical generative models that generate top-down predictions; prediction errors drive belief updating; the canonical microcircuit implements this in cortical layers.
- Active inference distinguishes perceptual inference (update beliefs) from active inference (act to fulfil predictions).
- Homeostasis and allostasis are naturally captured as prior-driven active fulfilment of body-state predictions.
- Expected free energy unifies exploration (epistemic value) and exploitation (instrumental value) in a single functional, recovering reinforcement learning and optimal experimental design as special cases.
- Active inference connects to evolution (niche construction), metabolism (energetic constraints on inference), neuroscience (predictive coding circuits), immunology, development, and computational psychiatry.
- Precision weights prediction errors; attention and sensory attenuation are interpretable as precision control; interoception links body state to psychiatric phenomenology at a systems level.
- Computational psychiatry offers FEP-grounded provisional accounts of anxiety, depression, schizophrenia, and autism — useful as research frameworks while clinical practice continues to rely on evidence-based treatment.

0.3.17 Key Terms

free energy · variational free energy · expected free energy · Markov blanket · generative model · prior belief · prediction error · predictive coding · canonical microcircuit · Bayesian brain · active inference · homeostasis · allostasis · interoception · niche construction · 4E cognition · precision · sensory attenuation · aberrant salience · epistemic value · instrumental value · policy selection

0.3.18 Discussion Questions

1. Explain the difference between perceptual inference and active inference using a concrete physiological example (e.g., cardiovascular regulation during exercise, or immune response to infection). Why does the distinction matter clinically?
2. A patient with interoceptive dysregulation has a poorly calibrated internal model of body states — they cannot accurately predict or infer their own visceral sensations. Using active inference, explain how this might manifest as anxiety, depression, or eating disorders. What therapeutic interventions might improve interoceptive precision?
3. The bacterium *E. coli* performs chemotaxis — swimming toward attractants, tumbling to reorient — guided by a two-component receptor-kinase system. Can this behavior be described in active inference terms? What would the “generative model,” “prediction error,” and “action” be for *E. coli*? Identify its Markov blanket explicitly.
4. Consider the allostatic adjustment of blood pressure in anticipation of orthostatic challenge (standing up). Compare this to the homeostatic model where blood pressure is corrected *after* it drops. Which better fits the empirical timeline of cardiovascular adjustment? How does this support an active inference account of autonomic regulation?
5. The free energy principle has been compared to Helmholtz’s observation that perception is “unconscious inference.” Is this analogy illuminating or misleading? What does the FEP add beyond classical Bayesian perception theories [Friston, 2010]? What does it risk conflating?
6. In one paragraph, explain why down-regulating somatosensory precision during a self-generated movement might prevent you from tickling yourself. How could a failure of this mechanism feel subjectively?
7. Propose an experiment (behavioral or neuroimaging) that would test whether anxious individuals assign too much precision to interoceptive prediction errors compared with controls. What would falsify your hypothesis?
8. The expected free energy functional contains both an epistemic (information-gain) term and an instrumental (reward) term. Construct a hypothetical scenario in which a pure reinforcement-learning agent and a pure active-inference agent would behave differently, and explain which behavior seems more biologically realistic.

0.3.19 Review Questions

1. Define the four state classes of a Markov blanket (η , s , a , μ) and state the conditional-independence property they enforce. Why does this partition make the boundary between an organism and its environment mathematically precise rather than merely intuitive?
2. Explain in your own words why minimizing variational free energy F is a tractable proxy for maximizing model evidence, given that the true posterior $P(z | o)$ is generally intractable. Which term of F penalises over-complex beliefs, and which rewards accurate ones?
3. Distinguish perceptual inference from active inference using the chapter’s body-temperature worked example. The agent’s free energy falls from about 4.5 nats to about 2.1 nats by belief update but approaches 0 by shivering. Explain why action reduces free energy *more completely* when the temperature prior is tight.
4. Apply the Markov-blanket partition to *E. coli* chemotaxis: assign concrete molecular identities to the sensory, active, internal, and external states, and identify which assignment is least clear-cut and why.
5. Using the expected-free-energy functional $G(\pi)$, analyze the worked policy comparison (π_A : epistemic 1.0, instrumental 4.0; π_B : epistemic 3.0, instrumental 2.5). Recompute G for each, justify why π_B is selected slightly more often, and predict how lowering the softmax temperature changes the choice.
6. The chapter reframes homeostasis and allostasis in active-inference terms. Compare the two as claims about prior precision and set-point dynamics, and explain why allostasis predicts heart rate rising *before* exercise begins whereas a purely homeostatic model does not.
7. Computational psychiatry interprets anxiety, depression, schizophrenia, and autism as different failures of precision regulation. Analyze how “over-precise priors on negative outcomes” versus “aberrant salience from amplified noise prediction errors” would produce different observable behaviors, and propose one measurement that could distinguish them.
8. Evaluate the claim that natural selection itself can be cast as gradient descent on a long-timescale free-energy functional. What does the “as-if” qualifier protect against, and what evidence would make this extension more (or less) defensible than the neuroscience applications?
9. Critically assess the FEP as a unifying framework that subsumes reinforcement learning and optimal control as limiting cases. Construct a biological prediction that an active-inference agent would make but a pure reward-maximiser would not, and explain why the difference is empirically meaningful.

10. Synthesis: the chapter argues that the current frontier is *identifiability* — very different generative models can fit the same behavior. Design a research strategy (combining out-of-sample prediction, parameter recovery, and a falsifiable neural or behavioral observable) that would let a sceptic decide whether an active-inference model genuinely explains a given dataset rather than merely curve-fitting it.

0.3.20 Further Reading and Source Notes: Active Inference and Free Energy

- Friston, K. (2010). The free-energy principle: A unified brain theory? [[Friston, 2010](#)] *Nature Reviews Neuroscience*, 11(2), 127–138.
- Friston, K., FitzGerald, T., Rigoli, F., Schwartenbeck, P., & Pezzulo, G. (2017). Active inference: A process theory [[Friston, 2017](#)]. *Neural Computation*, 29(1), 1–49.
- Sterling, P., & Laughlin, S. (2015). *Principles of Neural Design* [[Sterling and Laughlin, 2015](#)]. MIT Press.
- Sterling, P., & Eyer, J. (1988). Allostasis: A new paradigm to explain arousal pathology [[Sterling and Eyer, 1988](#)].
- Clark, A. (2016). *Surfing Uncertainty: Prediction, Action, and the Embodied Mind*. Oxford University Press.
- Parr, T., Pezzulo, G., & Friston, K. J. (2022). *Active Inference: The Free Energy Principle in Mind, Brain, and Behavior*. MIT Press.

0.3.21 Companion Source Module: Active Inference and Free Energy

Active Inference and Free Energy should leave a reproducible trail from a biological claim to the code, figure, diagram, or paper-based activity that can test it. Use the surfaces below to inspect the chapter’s assumptions, rerun the relevant model, or compare the manuscript explanation with companion labs and figures.

Table 15. Companion source surfaces for Active Inference and Free Energy.

Surface	Use it for
<code>src/biology/neuroscience/neuroscience.py</code> (<code>action_potential_hh</code> , <code>hebbian_weight_update</code>)	Connect prediction, update, and plasticity to measurable neural variables.
<code>src/biology/physiology/physiology.py</code> (<code>homeostasis_response</code>)	Compare allostatic regulation with error-correcting control.
<code>src/biology/cell/cell_biology.py</code> (<code>receptor_occupancy</code> , <code>signal_amplification</code>)	Make sensing and gain explicit rather than metaphorical.
<code>src/mermaid/biology_diagrams.py</code> (<code>nervous_system_reflex_diagram</code> , <code>hormone_signaling_diagram</code>)	Contrast reflex arcs, endocrine loops, and inference-style control diagrams.

Reproducibility check: name the hidden state, observation, action, and error term before treating a biological feedback loop as active inference. Cross-reference: compare with section [32](#), section [31](#), and section [8](#).

0.4 History and Philosophy of Biology

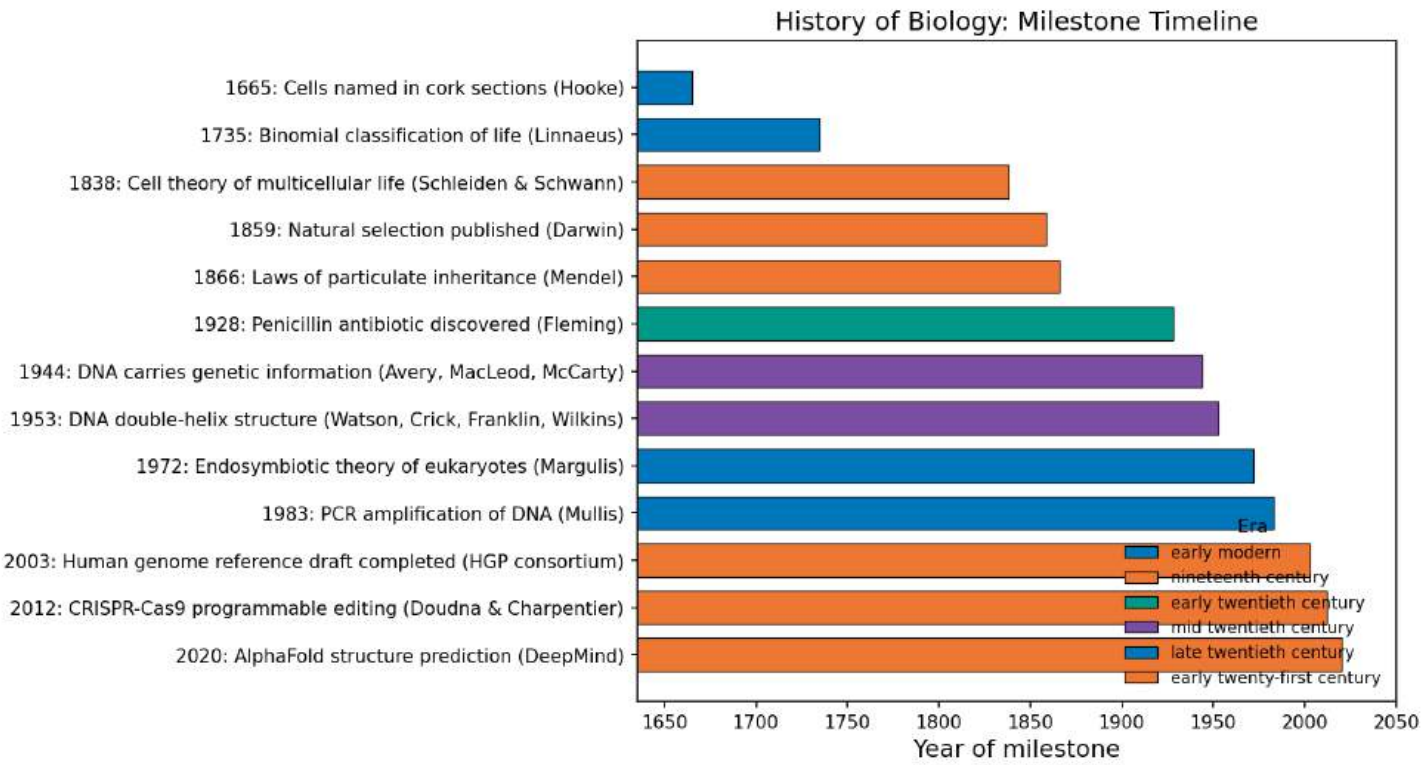


Figure 17. A chronologically ordered timeline of selected milestones in the history of biology. Bars are colored by era (microscopy, classification, cell theory, evolution, genetics, molecular biology, modern synthesis, genomics). The chart compresses several thousand years of practice into a single comparative view; the underlying milestone table is reproducible from `biology_foundations.BIOLOGY_MILESTONES`.

Level 2/3 · 80 min read · 100 min lecture · Prerequisites: section 0.1, section 0.2, section 0.3

0.4.1 Learning Objectives

By the end of this chapter, students will be able to:

1. Explain biology as a changing practice that combines observation, experiment, modeling, classification, interpretation, and ethical judgement.
2. Compare ancient and global biological traditions without reducing them to a simple prelude to modern European laboratory science.
3. Distinguish natural-history, experimental, mechanistic, mathematical, and computational styles of biological evidence.
4. Explain how Darwin, Wallace, Mendel, population genetics, and molecular biology reshaped biological explanation.
5. Compare mechanistic explanation, functional explanation, and teleological language in biological reasoning.
6. Apply Tinbergen’s four questions (mechanism, ontogeny, adaptive significance, phylogeny) to separate complementary levels of behavioral and physiological explanation.
7. Evaluate species, organisms, genes, microbiomes, and developmental systems as different candidates for biological individuality.
8. Analyze nature-nurture claims as claims about developmental systems, inheritance, environments, and evidence.
9. Identify where values enter biological research, medicine, conservation, and public communication without treating evidence as optional.

0.4.1.1 Study Blueprint

- Big idea: Biology is a changing evidence practice: its concepts of life, function, species, inheritance, and self are revised by new observations, instruments, models, and social values.
- Core concepts: biological explanation, historical evidence, function, species concepts, values in science.
- Framework alignment: Vision & Change: Systems, Structure and function; AP Biology: Systems Interactions; NGSS-style topics: Structure and Function, Interdependent Relationships in Ecosystems.
- Model or quantitative lens: Concept-map and evidence-matrix comparisons among historical claims, mechanisms, and model assumptions.
- Data skill: Classify source excerpts as observation, experiment, model, mechanism, or value-laden inference.

- Practice cadence: Questions and Methods, Representing and Describing Data, Argumentation.
- Common misconception to repair: History is not a list of dates; it explains why current biological concepts are powerful, limited, and revisable.
- Primary lab: [Lab D — History and Philosophy of Biology](#).
- Question bank: [Questions — History and Philosophy of Biology](#).
- Transfer task: Transfer source-analysis reasoning to modern debates about species, genetics, microbiomes, and biomedical ethics.
- Bridge to computation: `biology.toc.load_toc`.

0.4.2 Opening Vignette: Darwin, Wallace, and Evidence Before an Audience

On 1 July 1858, members of the Linnean Society of London heard a set of papers that neither principal author presented in person. Charles Darwin, still grieving a family death, and Alfred Russel Wallace, still in the Malay Archipelago, had independently reached the same unsettling explanation: variation, inheritance, and differential survival could make adaptation without a designing hand. Joseph Hooker and Charles Lyell arranged for extracts from Darwin’s unpublished work and Wallace’s Ternate essay to be read together [[Darwin and Wallace, 1858](#)].

The episode matters because no one placed a finch, a beetle, or a fossil on the table that evening as decisive proof. The evidence was distributed across field observations, specimens, breeding analogies, geographic patterns, correspondence, and a causal argument about populations. Darwin’s later book expanded that argument into a sustained evidential architecture: artificial selection, biogeography, homology, embryology, and the fossil record each constrained the same theory [[Darwin, 1859](#)].

This chapter asks how biology makes such claims stable enough to teach. A biological explanation is not just a fact plus a famous name. It is a practice that chooses units, draws boundaries, builds models, handles values, and states what evidence would force revision.

0.4.3 Why History and Philosophy Belong in Introductory Biology

Biology is not a finished catalog of facts. It is a changing evidence practice for asking how living systems are organized, how they persist, how they change, and how we should act when biological knowledge matters in medicine, agriculture, conservation, and public life. Systems science, complex adaptive systems, and active inference provide formal lenses; history and philosophy explain why those lenses exist, what they clarify, and where they can mislead. Mayr’s history of biological thought and Hull’s account of science as a process both emphasize that biology is deeply historical: its central objects are lineages, organisms, environments, and practices that change over time [[Mayr, 1982](#), [Hull, 1988](#)].

A first-year student often meets biology as named content: cell theory, natural selection, Mendelian inheritance, the central dogma, germ theory, ecological succession. Yet each idea came from a particular practice. Hooke’s microscopy made cells visible [[Hooke, 1665](#)]. Harvey’s circulation experiments made physiology quantitative and interventionist [[Harvey, 1628](#)]. Darwin and Wallace turned variation, biogeography, and natural history into a causal theory of adaptation [[Darwin and Wallace, 1858](#), [Darwin, 1859](#)]. Mendel’s pea crosses became a genetics framework after later researchers recognized how particulate inheritance could be combined with population thinking [[Mendel, 1866](#), [Fisher, 1930](#)]. The milestone timeline in figure 17 clusters these episodes by era so the bursts of microscopy, classification, evolution, genetics, and molecular biology are visible at a glance.

Read this chapter as a set of modules, not as a march from ignorance to truth. Each module asks: What counted as evidence? What was treated as a biological unit? Which instruments, organisms, models, and values shaped the answer?

Table 16. Study Blueprint: Module and Guiding question.

Module	Guiding question	Later cross-link
Practices and traditions	How do biological facts become stable enough to teach?	section 0.1
Natural history and experiment	What do comparison and perturbation each reveal?	section 0.2
Evolution, genes, molecules	How do historical and mechanistic causes combine?	section 21
Function, individuality, development	What counts as a unit, a purpose, or a cause?	section 25
Models, values, public biology	How should evidence guide action under uncertainty?	section 0.3

0.4.4 Biology as Practice: Instruments, Organisms, and Arguments

Scientific facts in biology travel through instruments, organisms, protocols, diagrams, model systems, databases, and arguments. A micrograph, a pedigree, a phylogenetic tree, a patch-clamp trace, a randomized clinical trial, and a genome-wide association plot are not interchangeable forms of evidence. Each filters the living world through assumptions about what counts as a unit, a cause, a measurement, and a relevant comparison.

Natural historians compare organisms across places and times. Physiologists perturb living systems and measure responses. Geneticists infer hidden inheritance rules from crosses and sequences. Evolutionary biologists use models to separate drift, selection, mutation, migration, and history. Molecular biologists connect structure to information and mechanism. Philosophers of biology ask what these practices assume when they use words such as “function”, “fitness”, “species”, “gene”, “individual”, “self”, and “cause” [Sober, 1984, Okasha, 2006].

Two lessons follow. First, biological knowledge is material: it depends on microscopes, culture media, field notebooks, model organisms, databases, and statistical tools. Second, biological knowledge is revisable: better instruments or better comparisons can change the apparent unit of explanation. Rheinberger calls experimental systems engines for producing “epistemic things”, objects that are not fully known in advance but become tractable through repeated manipulation [Rheinberger, 1997]. That idea fits the rest of this textbook: a model is useful when its assumptions, boundary conditions, and failure modes are visible.

Concept Check: A patch-clamp trace, a phylogenetic tree, and a randomized clinical trial each support different kinds of biological claims. Choose one claim each could support, then name the system boundary and the kind of evidence that would most directly weaken it.

0.4.5 Ancient and Global Knowledge Traditions in Biology and Medicine

Aristotle’s biological works treated organisms as structured wholes whose parts made sense in relation to activities such as nutrition, motion, perception, and reproduction [Aristotle, 350 BCE]. Lloyd’s comparative work on ancient Greek and Chinese science is useful here because it resists two simple mistakes: treating one tradition as the single template for rational inquiry, or treating traditions as isolated from social and institutional settings [Lloyd, 1996]. History is not a search for the first person to say a modern sentence. It is a way to understand how different communities made organisms, bodies, remedies, classification, and explanation intelligible.

Medical and biological thought also moved through Persian, Arabic, Chinese, Indian, Indigenous, and other knowledge traditions. Ibn Sina’s *Canon of Medicine* helped organize anatomy, physiology, diagnosis, and therapeutics across centuries of medical education [Ibn Sina, 1025]. Chinese materia medica and medical theory, summarized in part by Needham’s history of Chinese science, show a different way of organizing bodies, plants, illness, and intervention [Needham, 1954]. Harding’s critique of supposedly view-from-nowhere science and Haraway’s account of situated knowledge help students ask a practical question: whose organisms, whose environments, and whose risks are being made visible [Harding, 1986, Haraway, 1988]?

0.4.6 Natural History, Classification, and Empire

Natural history made biology comparative before it was laboratory-based. Linnaeus made classification portable by standardizing binomial names and arranging organisms into nested groups [Linnaeus, 1753]. Darwin’s field observations and specimens from the *Beagle* voyage became part of the evidence background for later evolutionary arguments [Darwin, 1859]. Classification did not merely name a world already sorted; it organized collections, museums, colonial routes, gardens, and commercial exchange.

That global circulation matters. Schiebinger’s work on colonial bioprospecting shows how plant knowledge moved through power relations as well as notebooks and herbarium sheets [Schiebinger, 2004]. Natural history therefore has a double legacy. It is a foundational evidence practice for biodiversity, biogeography, conservation, and evolution. It is also entangled with empire, extraction, and unequal credit. A good biological explanation should keep both facts in view.

0.4.7 Experiment, Mechanism, and the Laboratory

Natural history and experiment are complementary rather than rival practices. Hooke used microscopy to reveal a world below ordinary perception [Hooke, 1665]. Harvey used intervention and quantification to argue that blood circulates rather than being continually produced and consumed [Harvey, 1628]. Bernard’s experimental medicine made controlled perturbation a central ideal for physiology: isolate a factor, intervene, measure the response, and ask whether the result generalizes [Bernard, 1865]. Bechtel and Abrahamsen describe mechanistic explanation as an alternative to merely fitting laws: explain a phenomenon by identifying parts, operations, and organization [Bechtel and Abrahamsen, 2005].

Laboratories did not replace organisms with machines. They built controlled relationships between organisms, instruments, and questions. A frog nerve-muscle preparation, a fruit-fly cross, a bacterial plate, and a cell-free protein synthesis system each make some causal relations visible while hiding others. This is why section 0.1 insists on system boundaries: the same biological object can be a component, a system, or an environment depending on the question.

0.4.8 Darwin, Wallace, and Historical Causation

Darwin and Wallace transformed biological explanation by showing how adaptation could arise from ordinary variation, heredity, differential survival, and reproduction [Darwin and Wallace, 1858, Darwin, 1859]. The explanation of a feature could be historical rather than merely mechanical: a finch beak is explained by development, material structure, ecological function, and evolutionary history together. This is a distinctive feature of biology. The present form of an organism often carries traces of past selection, constraint, drift, migration, and contingency.

Evolution also changed the meaning of biological order. Adaptation need not imply design by intention. Population variation, local environments, and inheritance can generate fit between organism and environment without a central planner. This is one reason section 0.2 belongs before the rest of the book: natural selection is a distributed, history-sensitive process that can produce organized outcomes from local differential reproduction.

0.4.9 Genetics, Molecular Biology, and the Modern Synthesis

Mendel showed that inheritance could be particulate even when traits appear blended at the organism scale [Mendel, 1866]. Fisher’s mathematical synthesis linked relatives, variance, and natural selection [Fisher, 1930]; Haldane developed models of selection and its consequences [Haldane, 1932]; Dobzhansky, Mayr, Huxley, and others helped join genetics, systematics, paleontology, and natural selection into the Modern Synthesis [Dobzhansky, 1937, Mayr, 1942, Huxley, 1942]. The synthesis did not remove history from biology. It made history mathematically tractable through populations, allele frequencies, selection, drift, and speciation.

Molecular biology added another explanatory layer. Watson and Crick’s DNA model linked chemical structure to copying and information storage [Watson and Crick, 1953]; Franklin and Gosling’s X-ray work was part of the empirical basis for DNA structure [Franklin and Gosling, 1953]; Crick’s central-dogma framing clarified directional information transfer while leaving room for later discoveries about regulation, RNA, epigenetics, and genome architecture [Crick, 1958, 1966]. Judson’s history of molecular biology is useful because it shows discovery as a network of instruments, rival groups, model building, and interpretation rather than a single heroic moment [Judson, 1996].

The same history also warns against over-tight metaphors. “Information”, “program”, and “blueprint” can help students reason about DNA, but Keller argues that gene-centered language often overstates control when regulation is distributed across cells, organisms, and environments [Keller, 2010]. Kimura’s neutral theory and later extended-synthesis debates further show that evolutionary explanation cannot be reduced to adaptive storytelling alone [Kimura, 1983, Pigliucci and Muller, 2010, Laland et al., 2015]. Use genes as powerful explanatory units, not as the sole biological units.

0.4.10 Mechanism, Function, and Teleology

Biologists constantly use purpose-like language: hearts are “for” pumping blood, enzymes are “for” catalysing reactions, flowers are “for” attracting pollinators. The language is useful, but it is also risky. Mechanistic explanation identifies entities, activities, organization, and causal sequence [Machamer et al., 2000]. Wright’s account of function and Mayr’s distinction between teleological and teleonomic language help separate human purpose from biological function [Wright, 1973, Mayr, 1974].

0.4.10.1 Tinbergen’s Four Questions

In 1963 Nikolaas Tinbergen argued that a complete biological account of a trait or behavior must answer four complementary questions, not one [Tinbergen, 1963]. The framework remains a standard guardrail against conflating mechanism with function or development with evolutionary history [Bateson and Laland, 2013, Nesse, 2019].

Table 17. Tinbergen’s four complementary questions (mechanism, ontogeny, adaptive significance, phylogeny).

	Diachronic (historical)	Synchronic (current form)
Proximate	Ontogeny — how the trait develops across the individual lifespan	Mechanism — what biological machinery produces the trait now
Ultimate	Phylogeny — how the trait evolved across lineages	Adaptive significance — how the trait contributes to survival and reproduction today

Each cell asks a different question. Mechanism identifies stimuli, pathways, and molecular machinery (for example testosterone and song nuclei in birds, or pyrogens acting on hypothalamic thermoregulatory centers during fever). Ontogeny asks how the machinery is assembled and modified by genes, learning,

and environment (critical periods in birdsong learning; maturation of fever responses in neonates). Adaptive significance asks what fitness advantage the trait provides in its current ecological context (male song as mate attraction; fever as an anti-pathogen response despite metabolic cost). Phylogeny asks whether the trait is ancestral or derived and how comparative evidence reconstructs its history (song types clustering on oriole phylogenies; regulated hyperthermia conserved across vertebrates).

The four questions are complementary, not competing. Explaining bird song requires syrinx anatomy, developmental learning, mate-choice function, and phylogenetic comparison together. Explaining fever requires cytokine mechanisms, developmental changes in thermoregulation, selective advantage during infection, and deep evolutionary conservation together. Bateson and Laland note that modern epigenetics, plasticity, and niche construction blur sharp proximate–ultimate boundaries, but the four-question structure still disciplines inquiry by forcing researchers to state which level they are addressing [Bateson and Laland, 2013].

Concept Check: Choose fever or birdsong. For each of Tinbergen’s four questions, write one sentence that states a testable claim and one observation that would weaken it.

This distinction matters for section 0.3. Active inference can make goal-directed behavior mathematically explicit, but it should not license vague claims that every biological process “wants” something. A good functional claim states the system, the effect, the evidence that the effect matters, and whether the explanation is about current causal contribution, selected history, or a modeled preferred state.

Table 18. Translating purpose-like language into testable biological claims.

Purpose-like sentence	Defensible biological reading	Evidence needed
The heart is for pumping blood	Causal role in circulation	Pressure gradients, flow, tissue perfusion, perturbation
Flowers are for attracting pollinators	Selected-effect or current ecological role	Visitor behavior, reproductive output, phylogenetic or manipulation evidence
A cell wants glucose	Modeled preference or regulatory set point	Sensor, action, uptake response, rival metabolic explanation
A gene controls a trait	Contribution within a developmental system	Variant effect, regulatory context, environment, intervention

Recent debates over Markov blankets and explanatory pluralism make the same point from the active-inference side: a formal partition can clarify agency when the system boundary, observables, and rival models are explicit [Bruineberg et al., 2022, Colombo and Wright, 2017]. Treating every organized process as literal inference would collapse a useful modeling tool into metaphor.

Gould and Lewontin’s critique of adaptationist storytelling warns that not every trait is an optimized adaptation [Gould and Lewontin, 1979]. Some traits are by-products, constraints, historical inheritances, or consequences of developmental architecture. Function is a hypothesis to test, not a decorative label.

Concept Check: A textbook says that flowers are “for” attracting pollinators. Rewrite that claim as (a) a mechanistic claim, (b) a selected-effect functional claim, and (c) a causal-role claim, then state which version active inference could model without implying conscious purpose.

0.4.11 Species, Individuals, and the Boundaries of Life

Mayr’s biological species concept emphasized reproductive isolation [Mayr, 1942]; de Queiroz’s general lineage account treated species concepts as different operational routes to separately evolving lineages [de Queiroz, 2007]; Ghiselin and Hull argued that species can be understood as historical individuals rather than timeless classes [Ghiselin, 1974, Hull, 1978]; Okasha and Clarke show why biological individuality depends on reproduction, inheritance, cooperation, conflict, and criteria that can be multiply realized [Okasha, 2006, Clarke, 2013]. This is not a vocabulary dispute. It changes how biologists count entities, assign causes, and explain change.

Microbiomes sharpen the problem because biological identity is not exhausted by one genome or one cell lineage [The Human Microbiome Project Consortium, 2012, Sender et al., 2016]. O’Malley argues that philosophy of biology must take microbial life seriously because microbes challenge assumptions about individuality, species, sex, ecology, and evolution [O’Malley, 2014]. Gilbert, Sapp, and Tauber’s “symbiotic view of life” and Pradeu’s work on immunological selfhood both push students to treat biological boundaries as regulated, relational, and sometimes porous [Gilbert et al., 2012, Pradeu, 2012]. Margulis’s endosymbiotic theory makes the same lesson historical: some cellular parts began as organisms in relation [Sagan, 1967].

Concept Check: A lichen, a coral colony, and a human gut microbiome each blur the boundary of biological individuality. Pick one case and compare genetic, physiological, and evolutionary criteria for deciding whether it is one individual or many.

0.4.12 Development, Nature-Nurture, and Inheritance

“Nature versus nurture” is a poor frame because development is not a competition between genes and environments. Waddington’s epigenetic landscape made development visible as a canalised but perturbable process [Waddington, 1957]. Lewontin’s distinction between analysis of variance and analysis of causes explains why a statistical partition in one population does not identify a simple causal essence [Lewontin, 1974]. Oyama’s developmental-systems theory and West-Eberhard’s account of developmental plasticity show how inheritance, environment, behavior, and plasticity can jointly shape evolutionary trajectories [Oyama, 2000, West-Eberhard, 2003].

For first-year biology, the practical rule is simple: do not ask whether a trait is “genetic or environmental” until you have named the developmental process, the population, the environment, the measurement, and the intervention. The answer often changes when the system boundary changes.

0.4.13 Microbiology, Disease, Symbiosis, and Self

Microbiology changed the scale at which life was understood. Germ theory made disease transmission experimentally tractable. Molecular biology made viruses and phages central to genetics. Microbial ecology made communities, biofilms, horizontal gene transfer, and metabolic cooperation central biological phenomena. The human microbiome turned “self” from a single-genome assumption into a regulated host-microbe system [The Human Microbiome Project Consortium, 2012, O’Malley, 2014].

This module links directly to section 24 and section 25. When asking whether a microbe is part of the organism, the environment, or a disease process, name the criterion: development, metabolism, immune tolerance, ecological dependence, reproduction, or clinical outcome. Different criteria produce different boundaries, and that is a feature of the biology rather than a failure of terminology.

0.4.14 Models, Evidence, and Explanation

Models simplify. That is their strength and their danger. Levins argued that model builders trade off realism, generality, and precision, and that robust understanding often comes from comparing several imperfect models [Levins, 1966]. Wimsatt sharpened the point: false or idealised models can still help produce truer theories when their distortions are understood [Wimsatt, 1987]. Weisberg’s account of simulation and similarity gives students a useful question: similar to what, for what purpose, and under what tolerance [Weisberg, 2013]?

Historical sciences and experimental sciences use evidence differently. Cleland argues that historical sciences often work by collecting traces of past events and testing rival explanations against those traces [Cleland, 2002]. That logic is central to evolution, phylogenetics, paleontology, epidemiological reconstruction, and conservation history. Data-centric biology adds another layer: databases do not speak for themselves; Leonelli shows that data must be curated, standardized, moved, and interpreted before they become evidence [Leonelli, 2016]. Kitano’s systems-biology overview makes the same point computationally: large networks require explicit models, not just lists of parts [Kitano, 2002].

When reading a biological model, ask what unit it uses, what it leaves out, what evidence would change it, which alternatives explain the same pattern, and which decision would change if the model were wrong.

0.4.15 Levels of Explanation and Causal Pluralism

Biology often needs several explanations for the same case. A bird’s migration can be explained by neural circuits, developmental experience, ecological payoff, and evolutionary history. A fever can be explained by cytokine signaling, hypothalamic set-point change, pathogen suppression, and clinical risk. These explanations are not automatically rivals, because they answer different causal questions. The mistake is to let one level pretend to have completed the work of the relevant others.

Explanatory pluralism is not relativism. It does not say that any story is as good as any other. It says that a strong biological account names the level of organization, the causal relationship being claimed, and the test that would make that relationship fail. A molecular mechanism is incomplete if it cannot connect to phenotype; a population model is incomplete if it cannot state which organism-level processes supply its parameters; a social or ethical analysis is incomplete if it treats empirical constraints as optional.

Table 19. Tinbergen’s Four Questions: Explanation level and Typical question.

Explanation level	Typical question	Common failure mode	Stronger version
Molecular or cellular	What entities and activities produce the effect?	Treating the part as the whole explanation	State the organismal or environmental condition where the mechanism matters
Developmental	How does the trait come into being?	Treating genes and environment as separable rivals	Name the interaction, timing, and perturbation that would change the outcome
Evolutionary or historical	Why did this pattern arise in a lineage?	Turning adaptation into an untested just-so story	Compare selection with drift, constraint, phylogeny, and contingency
Ecological or social	What boundary and decision context matter?	Treating a value choice as if it were a measurement	Separate empirical constraints from risk, justice, cost, and benefit

Concept Check: A clinician says a fever is “caused by infection.” Rewrite the explanation at molecular, physiological, evolutionary, and public-health levels, then identify one observation that would weaken each level-specific claim.

0.4.16 First-Principles Claim Audit

A first-principles reading of biology starts by stripping a claim down to what cannot be wished away. The point is not to distrust every claim equally; it is to separate evidence, modeling choices, and inherited habits before reasoning from them.

Table 20. Tinbergen’s Four Questions: Claim element and First-principles question.

Claim element	First-principles question	Typical status	Example
Observation	What measurement or trace exists?	Hard constraint when reproducible	A sequence read, fossil layer, voltage trace, or field count
Boundary	Where is the system drawn?	Soft constraint	Cell, host-microbiome system, population, ecosystem
Mechanism	What entities and activities produce the phenomenon?	Hard if experimentally constrained; provisional if inferred	Enzyme active site, ion channel, pollinator behavior
Function	Is this current contribution, selected history, or modeled preference?	Often mixed	Heart pumping, flower attraction, active-inference preferred state
Model	What assumptions make prediction possible?	Assumption until tested outside the fitting case	Hardy-Weinberg equilibrium, logistic growth, Markov blanket partition
Value	Which decision, risk, or category matters?	Soft constraint that must be explicit	Disease threshold, conservation priority, research-benefit standard

The reconstructed rule is simple: keep hard constraints, mark soft constraints, and test assumptions. If a claim cannot say what would revise it, it is not yet ready to carry explanatory weight.

0.4.16.1 Claim Audit in Practice

The claim audit is a transfer tool for the rest of the book. Use it whenever a statement sounds obvious, final, or purpose-like. Start with the observation that cannot be ignored, then ask which boundary, mechanism, function, model, value, and revision test are being smuggled into the sentence.

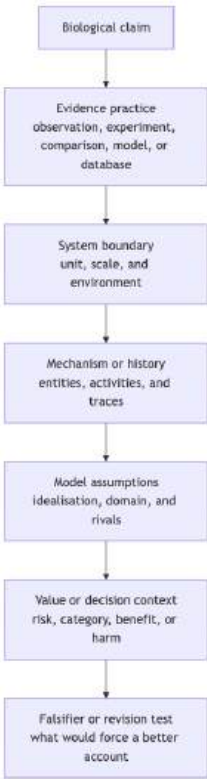


Figure 18. Claim-audit workflow: a strong biological claim states its evidence practice, boundary, mechanism or history, modeling assumptions, value context, and revision test.

Table 21. Claim Audit in Practice: Later claim and Hard constraint.

Later claim	Hard constraint	Soft constraint or assumption	Revision test
Flowers attract pollinators	Floral traits and visitor behavior can be observed and compared	“For” may mean selected effect, current causal role, or human purpose unless specified	A manipulation that changes floral traits without changing pollinator visits would weaken the functional claim
A microbiome is part of an individual	Host-microbe interactions can affect metabolism, development, immunity, and ecology	The boundary may be genetic, physiological, ecological, clinical, or evolutionary	A criterion that predicts one case but fails for lichens, corals, or gut communities needs a narrower domain
Active inference explains homeostasis	Organisms sense, act, and maintain viable internal ranges	A Markov blanket or generative model is a modeling choice, not proof that every process literally infers	A rival control or physiological model with better predictions should limit the active-inference interpretation

The point is not to slow every page into philosophy. It is to prevent category mistakes before they spread: mechanism is not the same as function, a model boundary is not a natural boundary, and a useful formalism is not automatically a general law.

0.4.17 Current Evidence and Frontier Biology: History and Philosophy of Biology

For History and Philosophy of Biology, frontier work belongs inside the evidence logic of the chapter. Historical and philosophical claims are strongest when they identify the source practice, comparison set, interpretive assumption, and possible counterevidence rather than merely listing famous names.

- What to verify: identify the primary source, scholarly synthesis, dataset, or ethical document that supports the claim.
- What to qualify: state the tradition, organism, period, population, or institutional setting where the claim applies.
- What to compare: contrast one alternative explanation, source category, or boundary choice before treating the claim as settled.

- What to cite: distinguish primary text, historical reconstruction, philosophical analysis, STS critique, and current biomedical guidance.

Treat every historical claim as a claim about practice: name who produced the evidence, what method made it visible, what unit was assumed, and what would revise the interpretation.

Source practice: Use primary sources for focal episodes and scholarly synthesis for context; avoid using chronology as a substitute for evidence.

0.4.18 Ethics, Values, and Public Biology

Values enter biology whenever researchers choose questions, define categories, enrol participants, manage risk, communicate uncertainty, or recommend interventions. Biomedical ethics often uses principles such as autonomy, beneficence, nonmaleficence, and justice [Beauchamp and Childress, 1979]. Research ethics after the Nuremberg Code and the UNESCO declaration on the human genome made consent, dignity, and human rights central constraints on biological research [Nuremberg Military Tribunal, 1947, UNESCO, 1997]. Kevles’s history of eugenics shows why biology education must distinguish evidence from ideological misuse [Kevles, 1985].

Values do not make evidence optional. They make the questions more explicit: who is affected, what harms are possible, what categories are being used, who benefits, and what uncertainty remains? Jasanoff’s STS work treats science and social order as co-produced rather than sealed off from one another [Jasanoff, 2004]. Schiebinger’s history of gender and science, Haraway’s situated knowledge, and feminist critiques such as Fausto-Sterling’s work on sex classification show that the categories used in biology can be scientifically productive, politically consequential, and revisable [Schiebinger, 1999, Haraway, 1988, Fausto-Sterling, 1993].

Douglas’s account of values in science helps distinguish epistemic values, such as explanatory power and coherence, from social and ethical values that enter when uncertainty affects policy, risk, or harm [Douglas, 2009]. A responsible biology claim should therefore say which values shaped the question and which observations still constrain the answer.

Concept Check: A conservation model ranks habitats for protection using species richness, carbon storage, and local livelihoods. Classify one hard constraint, one soft constraint, and one untested assumption in the model, then name evidence that would change the ranking.

0.4.19 Synthesis: A Checklist for Biological Claims

- Practice: What activity produced the evidence: observation, experiment, comparison, model, clinical study, or database analysis?
- Unit: What is being treated as the biological unit: gene, cell, organism, population, lineage, symbiosis, ecosystem, or patient?
- Boundary: Where does the system stop, and what changes if the boundary moves?
- Mechanism: What entities and activities are claimed to produce the phenomenon?
- Function: Is the claim about current contribution, selected history, modeled preference, or human purpose?
- History: What past events, constraints, or contingencies matter?
- Model: What assumptions make the model usable, and what do they leave out?
- Values: What decision, harm, benefit, category, or governance choice is being made?
- Revision: What evidence would force a better explanation?

0.4.20 Summary

- Biology is an evidence practice, not a finished list of names, dates, and facts.
- Natural history, experiment, mechanism, historical inference, and models answer different but compatible questions.
- Function-language is useful when causal role, selected history, modeled preference, and human purpose are kept separate.
- Species and biological individuals are boundary claims, not always sharp natural kinds.
- Developmental and microbiome examples show that genes, organisms, environments, and symbioses often share explanatory work.
- Models are tools with assumptions, domains of validity, and failure modes; they should be compared against alternatives.
- Values shape questions, categories, risks, and decisions, but evidence still constrains responsible biological action.

0.4.21 Key Terms

biological practice · natural history · experiment · classification · mechanism · function · teleology · natural selection · Modern Synthesis · neutral theory · extended synthesis · species concept · biological individual · symbiosis · biological self · developmental plasticity · developmental systems theory · model trade-

0.4.22 Discussion Questions

1. Choose one biological concept from later in the textbook and reconstruct its history as a change in evidence practice.
2. Explain why functional language is useful in biology but dangerous when treated as literal intention.
3. Compare two ways of defining species. What biological cases make each definition strong, and what cases make it break down?
4. Use a microbiome or endosymbiosis example to argue for or against the claim that organisms have clear boundaries.
5. Explain how a value can influence a biological research program without falsifying its evidence.
6. Apply Levins’s model-building trade-off to one model from ecology, genetics, physiology, or cell biology.
7. Pick one global or colonial history example and identify what knowledge moved, who received credit, and what power relation shaped the record.
8. Compare active inference, teleonomy, and ordinary functional language. Where do they overlap, and where should they be kept distinct?

0.4.23 Review Questions

1. Define biology as an evidence practice rather than a list of facts.
2. Contrast Aristotle’s teleological explanation with a modern mechanistic explanation of the same organ or behavior.
3. Explain how Harvey’s circulation work differs from Linnaean classification as a biological practice.
4. State the logic of natural selection and identify why Darwin and Wallace needed population variation.
5. Explain how Mendelian inheritance and population genetics were reconciled in the Modern Synthesis.
6. Distinguish mechanistic, functional, developmental, and evolutionary explanations using one trait.
7. Compare species as classes, species as reproductive populations, and species as historical individuals.
8. Explain why nature-nurture language can mislead when discussing development.
9. Describe one way microbiology complicates the idea of biological self.
10. Identify one place where values enter biological decision-making and state how evidence should still constrain the decision.
11. Explain why data curation is not a neutral clerical step in modern biology.
12. Use the checklist above to evaluate one claim about genes, microbes, ecosystems, or public health.

0.4.24 Further Reading and Source Notes: History and Philosophy of Biology

- Aristotle, Ibn Sina, Needham, Lloyd, Linnaeus, Schiebinger, Hooke, Harvey, Bernard, Rheinberger, Darwin, Wallace, Mendel, Fisher, Haldane, Dobzhansky, Mayr, Huxley, Watson, Crick, Franklin, Keller, Kimura, Pigliucci, and Laland anchor the chapter’s historical source spine [Aristotle, 350 BCE, Ibn Sina, 1025, Needham, 1954, Lloyd, 1996, Linnaeus, 1753, Schiebinger, 2004, Hooke, 1665, Harvey, 1628, Bernard, 1865, Rheinberger, 1997, Darwin and Wallace, 1858, Darwin, 1859, Mendel, 1866, Fisher, 1930, Haldane, 1932, Dobzhansky, 1937, Mayr, 1942, Huxley, 1942, Watson and Crick, 1953, Crick, 1958, 1966, Franklin and Gosling, 1953, Keller, 2010, Kimura, 1983, Pigliucci and Muller, 2010, Laland et al., 2015].
- Machamer, Darden, Craver, Tinbergen, Wright, Mayr, Gould, Lewontin, Sober, Hull, Ghiselin, de Queiroz, Okasha, Clarke, Bruineberg, Colombo, Douglas, Waddington, Oyama, West-Eberhard, O’Malley, Gilbert, Sapp, Tauber, Pradeu, Margulis, Levins, Wimsatt, Weisberg, Cleland, Leonelli, Kitano, Haraway, Harding, Jasanoff, Kevles, UNESCO, the Nuremberg Code, and Beauchamp and Childress anchor the philosophical, STS, modeling, and ethics spine [Machamer et al., 2000, Tinbergen, 1963, Wright, 1973, Mayr, 1974, Gould and Lewontin, 1979, Sober, 1984, Hull, 1978, Ghiselin, 1974, de Queiroz, 2007, Okasha, 2006, Clarke, 2013, Bruineberg et al., 2022, Colombo and Wright, 2017, Douglas, 2009, Waddington, 1957, Oyama, 2000, West-Eberhard, 2003, O’Malley, 2014, Gilbert et al., 2012, Pradeu, 2012, Sagan, 1967, Levins, 1966, Wimsatt, 1987, Weisberg, 2013, Cleland, 2002, Leonelli, 2016, Kitano, 2002, Haraway, 1988, Harding, 1986, Jasanoff, 2004, Kevles, 1985, UNESCO, 1997, Nuremberg Military Tribunal, 1947, Beauchamp and Childress, 1979].

0.4.25 Companion Source Module: History and Philosophy of Biology

History and Philosophy of Biology should leave a reproducible trail from a claim about biological knowledge to the evidence practice that produced it.

Table 22. Companion source surfaces for History and Philosophy of Biology.

Surface	Use it for
<code>src/biology/toc.py</code> (<code>load_toc</code>)	Inspect how chapter order, companion labels, and display numbers are derived from <code>manuscript/config.yaml</code> .
<code>src/biology/curriculum.py</code> (<code>CURRICULUM</code>)	Connect historical and philosophical concepts to lab, question-bank, misconception, and transfer records.
<code>src/biology/alignment.py</code> (<code>ALIGNMENTS</code>)	Compare biology-as-practice ideas with course standards and skills frameworks.
<code>src/biology/crossref_validator.py</code> (<code>validate</code>)	Check whether claims, labels, and references remain mechanically traceable.

Reproducibility check: before accepting a biological claim, name the evidence practice, the biological unit, the model assumption, and the value-laden decision if one is present. Cross-reference: compare this checklist with section 0.1, section 0.2, section 21, and section 25.

% Reset main chapter numbering after Unit 0.

Unit I — Chemistry of Life: Introduction

Why This Unit Matters

Every organism on Earth — a bacterium dividing in a hydrothermal vent, a redwood drawing water through 100 meters of trunk, a neuron firing in your brain right now — is made of the same about 25 elements obeying the same quantum-mechanical rules identified over the last two centuries. Chemistry is not merely a prerequisite for biology; it is biology at its most fundamental level. Understanding the electron orbitals of carbon explains why proteins fold. Understanding electronegativity explains why DNA holds its shape. Understanding pH buffers explains why a runner’s muscles do not seize in their own acid.

This unit begins with atoms and ends with molecular machines. We trace how the CHNOPS elements (carbon, hydrogen, nitrogen, oxygen, phosphorus, sulfur) combine into functional groups, how functional groups assemble into the four classes of biological macromolecules, and how enzymes — protein catalysts evolved over billions of years — accelerate reactions to the speeds that life demands. Along the way you will encounter the Pauling electronegativity scale, the Henderson-Hasselbalch equation, the Michaelis-Menten model, and the principle of chirality: the mirror-image selectivity that means L-amino acids build your proteins while D-sugars fuel your cells.

A thread connecting every chapter: water. The anomalous properties of water — its high boiling point, the cohesion-tension mechanism in plants, its role as both solvent and reactant — make Earth habitable and make most aqueous biochemistry possible. As the physical chemist Lawrence Henderson (1913) argued in *The Fitness of the Environment*, water is not an incidental solvent but the molecule around which life has been shaped by evolution.

Landmark Discoveries

Discoverer(s)	Year	Journal / Source	Discovery	Significance
Friedrich Wöhler	1828	[Wöhler, 1828]	Synthesis of urea from inorganic ammonium cyanate	Disproved vitalism; showed organic compounds obey the same chemistry as inorganic ones
Linus Pauling & Robert Corey	1951	[Pauling and Corey, 1951]	α -helix and β -sheet structures of proteins	Established that protein secondary structure is stabilized by H-bonds; first use of electronegativity to predict biological structure
James Watson & Francis Crick	1953	[Watson and Crick, 1953]	Double-helix structure of DNA	Anti-parallel, complementary base-pairing via H-bonds; immediately suggested replication mechanism
Frederic Sanger	1955	[Sanger, 1955]	Complete amino acid sequence of bovine insulin	Proved proteins are defined covalent sequences, not random polymers; introduced sequence concept
Leonor Michaelis & Maud Menten	1913	[Michaelis and Menten, 1913]	Enzyme-substrate saturation kinetics	Derived $v = V_{max}[S]/(K_m + [S])$; quantitative foundation of enzymology
Daniel Koshland	1958	[Koshland, 1958]	Induced-fit model of enzyme catalysis	Replaced lock-and-key; explained conformational changes in enzyme-substrate interaction
Jacques Monod, Jeffries Wyman & Jean-Pierre Changeux	1965	[Monod et al., 1965]	MWC model of allosteric regulation	Showed enzymes have distinct regulatory and catalytic sites; explains cooperative binding

Key Concepts and Connections

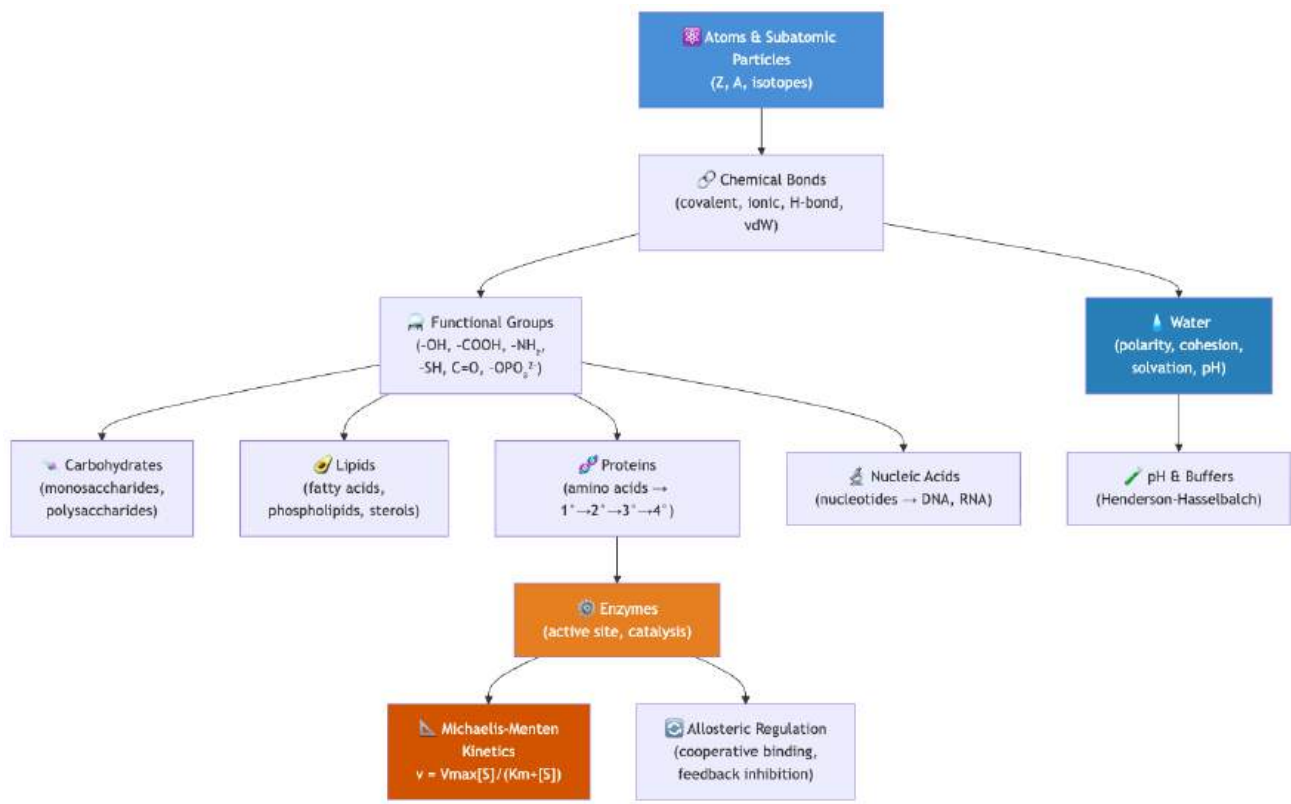


Figure 19. Chemistry-of-life concept map - arrows show conceptual dependencies; color groups: blue = atomic/molecular; orange = enzyme function.

Current Evidence Thread

Read **Unit I — Chemistry of Life: Introduction** as the point where the chemistry of life becomes measurable. Bond polarity, hydrogen bonding, and reaction thermodynamics are not abstractions here – they are quantities now read off cryo-EM maps, ultrafast spectroscopy, and kinetic assays, and structure predictions for macromolecules are accepted primarily once cryo-EM, NMR, or mutagenesis confirms them. As you move through the chapters, keep a two-column note: claim on the left, evidence that would change my confidence on the right. By the end of the unit, each major idea should be tied to a measurement, model, citation, or paper-based lab decision.

Chapter Roadmap

Chapter	Title	Core Question	Key Equation / Model
1	Atoms, Molecules, and Chemical Bonds	Why do atoms bond, and how does bond type determine biological function?	$\Delta G^{\circ'} = -nF\Delta E^{\circ'}$
2	Water — The Molecule of Life	What makes water anomalous, and why is that anomaly essential for life?	$\pi = iCRT$ (osmotic pressure)
3	Biological Macromolecules	How do four classes of polymer encode and carry out life’s functions?	Molecular weight, degree of polymerization
4	Enzymes and the Kinetics of Catalysis	How do enzymes lower activation energy, and how is their activity regulated?	$v = V_{max}[S]/(K_m + [S])$

Connections Across the Textbook

Unit I — Chemistry of Life: Introduction establishes the chemical vocabulary for the entire textbook:

- The bond energies and functional groups introduced here reappear in [Unit III — Energy and Metabolism: Introduction](#) (energy released by glucose oxidation), [Unit IV — Molecular Genetics: Introduction](#) (phosphodiester bonds of DNA), and [Unit V — Classical Genetics and Heredity: Introduction](#) (crossing-over in chromatin).
- Enzyme kinetics (section 4) reappears in [Unit III — Energy and Metabolism: Introduction](#) (PFK-1 allosteric regulation), [Unit VII — Microbiology: Introduction](#) (antibiotic targets on bacterial enzymes), and [Unit IX — Zoology and Systems Physiology: Introduction](#) (hemoglobin co-operativity).
- pH and buffers link directly to [Unit II — The Cell: Introduction](#) (lysosomal pH 4.5 vs. cytoplasmic pH 7.2), [Unit III — Energy and Metabolism: Introduction](#) (mitochondrial proton gradient), and [Unit IX — Zoology and Systems Physiology: Introduction](#) (blood acid-base balance in clinical contexts).
- Chirality of L-amino acids and D-sugars reappears in [Unit VII — Microbiology: Introduction](#) (D-amino acids in bacterial cell walls) and [Unit V — Classical Genetics and Heredity: Introduction](#) (enzyme specificity in DNA repair).

Before you begin: You should be comfortable with scientific notation, logarithms, and basic algebra. No prior chemistry or biology is assumed.

Computational Toolbox — Unit I

The following demonstrates the real `src/biology/biochemistry` functions used to generate figures and worked examples throughout [Unit I — Chemistry of Life: Introduction](#).

```
from biology.biochemistry import michaelis_menten, glycolysis_summary

# Michaelis-Menten kinetics: lactate dehydrogenase (LDH)
# Vmax = 12.0 mM/s, Km = 0.8 mM (pyruvate as substrate)
result = michaelis_menten(substrate_conc=2.0, Vmax=12.0, Km=0.8)
print(f"Reaction rate at [S]=2 mM: {result.reaction_rate:.2f} mM/s")
# Expected: Reaction rate at [S]=2 mM: 8.57 mM/s
# (= 12.0 × 2.0 / (0.8 + 2.0); Vmax/2 occurs at [S]=Km=0.8 mM)

# Glycolysis summary: net products per glucose
summary = glycolysis_summary()
print(f"Net ATP yield: {summary.net_atp} ATP per glucose")
print(f"NADH produced: {summary.net_nadh} NADH per glucose")
print(f"Steps represented: {len(summary.steps)}")
# Expected:
# Net ATP yield: 2 ATP per glucose
# NADH produced: 2 NADH per glucose
# Steps represented: 10
```

Try it yourself: Install the project environment (`uv sync`) and run `python3 -c "from biology.biochemistry import michaelis_menten; print(michaelis_menten(5, 10, 2))"`. Modify substrate concentration to trace the full saturation curve.

Source modules: `src/biology/biochemistry/biochemistry.py` — enzyme kinetics models, macromolecule analysis. Figures generated by `src/visualization/plots.py` (Michaelis-Menten plots) and `src/mermaid/biology_diagrams.py`.

Cross-Unit Integration

The chemistry of [Unit I — Chemistry of Life: Introduction](#) is the necessary prelude to the cell. Every concept introduced here — covalent and non-covalent bonds, hydrophobicity, weak interactions, protein folding driven by entropy and enthalpy — becomes operational in [Unit II — The Cell: Introduction](#)’s account of the cell membrane and the cytoskeleton. The phospholipid bilayer is a direct expression of the hydrophobic effect; membrane proteins fold so that hydrophobic side chains face the lipid interior and polar residues face the aqueous environment; ion channels exploit the same electrostatic and hydrogen-bonding logic you saw in protein structure. As you read [Unit II — The Cell: Introduction](#), return to the bonding diagrams of [Unit I — Chemistry of Life: Introduction](#) whenever a transport mechanism or membrane property feels arbitrary — it is almost always a chemistry consequence.

1 Atoms, Molecules, and Chemical Bonds

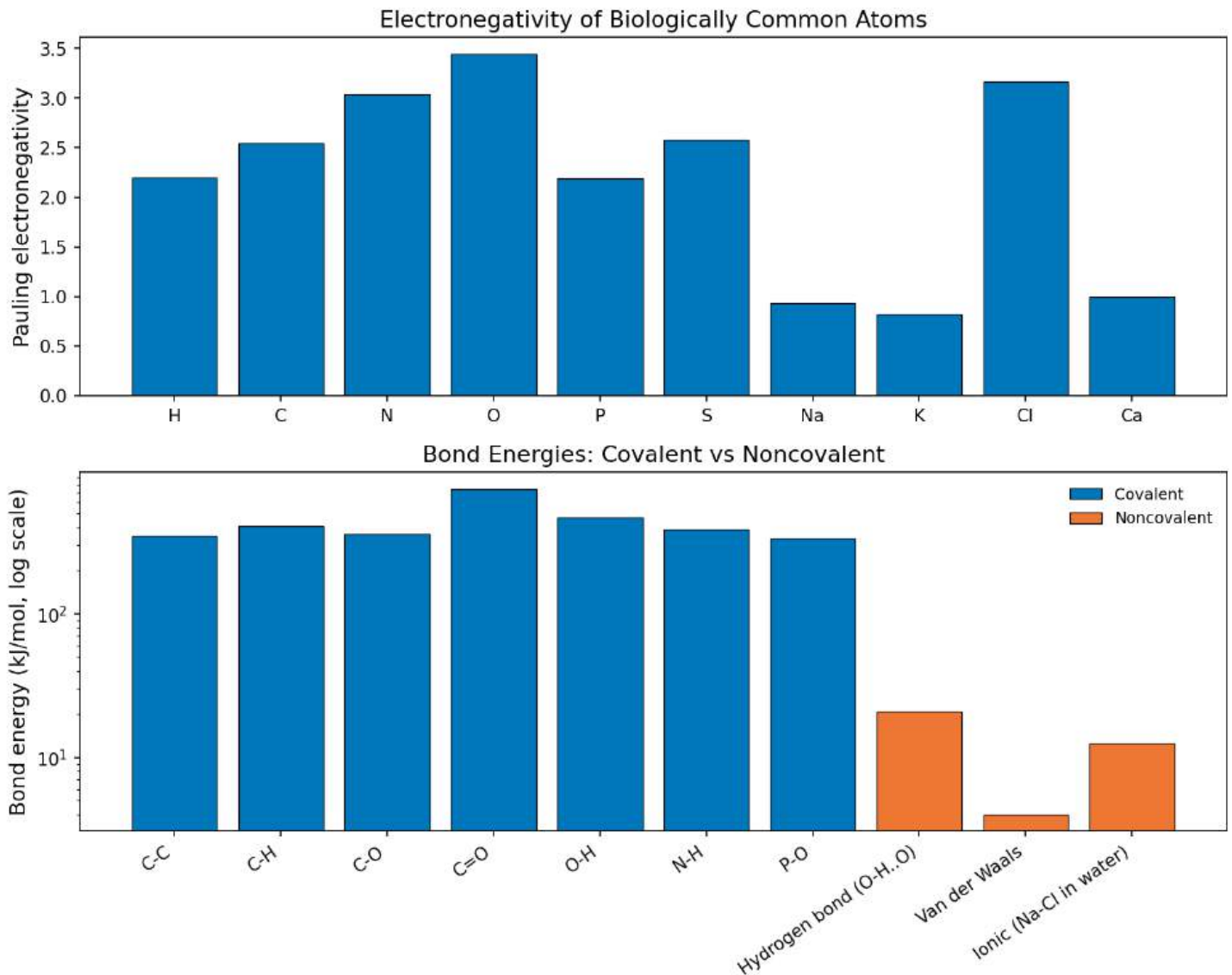


Figure 20. Quantitative chemistry behind biological molecules. The top panel shows Pauling electronegativities for the atoms most common in living matter (H, C, N, O, P, S, plus Na, K, Cl, Ca). The bottom panel shows representative bond dissociation energies on a log scale, color-coded by covalent versus noncovalent class. The order-of-magnitude separation explains why covalent backbones persist while noncovalent interactions can rearrange under physiological conditions.

Level 1/3 · 40 min read · 50 min lecture · Prerequisites: none

1.1 Learning Objectives

By the end of this chapter, you should be able to:

1. Describe the structure of an atom, including subatomic particles and their quantum mechanical behavior.
2. Explain how **electronegativity** governs covalent and ionic bond formation.
3. Distinguish between polar covalent, nonpolar covalent, and ionic bonds with biological examples.
4. Explain the roles of **hydrogen bonds** and **van der Waals forces** in biological macromolecules.
5. Interpret the concept of **pH**, **buffers**, and their physiological significance.
6. Describe **chirality** and stereoisomerism in biological molecules.
7. Explain redox reactions and their central role in bioenergetics.
8. Apply isotope chemistry to biomedical imaging and radiotherapy.

1.1.1 Study Blueprint

- Big idea: Atomic structure constrains the bonds, charges, and geometries that make biological molecules possible.
- Core concepts: valence, electronegativity, formal charge, isotopes.
- Framework alignment: Vision & Change: Structure and function, Pathways and transformations of energy and matter; AP Biology: Energetics, Systems Interactions; NGSS-style topics: Matter and Energy in Organisms and Ecosystems, Structure and Function.
- Model or quantitative lens: Formal charge and electronegativity-difference reasoning.
- Data skill: Use tabular atomic data to predict polarity, solubility, and biological reactivity.
- Practice cadence: Concept Explanation, Statistical Tests and Data Analysis, Argumentation.
- Common misconception to repair: Weak interactions are not unimportant; many weak interactions together dominate structure and specificity.
- Primary lab: Lab — Atoms, Molecules, and Chemical Bonds.
- Question bank: Questions — Atoms, Molecules, and Chemical Bonds.
- Transfer task: Use atomic reasoning to explain a medical tracer, enzyme cofactor, or membrane-solubility problem.
- Bridge to computation: biology.biochemistry.biochemistry.atp_free_energy.

Opening Vignette: The Radioactive Tracer That Exposed Cancer

In 1973, chemist Alfred Wolf and colleagues at Brookhaven National Laboratory synthesized a new molecule: fluorine-18-labeled deoxyglucose (¹⁸F-FDG). Because ¹⁸F decays with a half-life of just 109.8 minutes, emitting a positron that collides with a nearby electron to produce a pair of detectable gamma rays, the molecule could be tracked in real time inside a living body. Because FDG mimics glucose, metabolically hungry cells take it up — and cancer cells, with their vastly elevated glucose consumption (the Warburg effect, first described by Otto Warburg in 1924 [Warburg, 1924]), accumulate it at concentrations 2–10× higher than surrounding normal tissue.

Today, PET (positron emission tomography) scanning—mostly with ¹⁸F-FDG—is performed roughly two million times per year in the United States alone [Indrakanti et al., 2022, IMV Medical Information Division, 2024], guiding cancer diagnosis, staging, and treatment response assessment. None of it would be possible without understanding the atomic and subatomic physics of radioactive decay, the electronegativity that distinguishes O–H from C–H bonds, and the biochemistry of glucose transport — precisely the subjects of this chapter.

Primary sources: Warburg’s tumor-metabolism report [Warburg, 1924], the first labeled FDG chemistry [Ido et al., 1978], and human PET validation with FDG [Phelps et al., 1979].

Life is fundamentally chemistry. Every organism, from a bacterium to a blue whale, is composed of atoms obeying the same physical laws discovered in the nineteenth and twentieth centuries. Understanding life therefore begins with understanding atoms.

Of the 118 known elements, only about 25 are essential to life. Just six elements — carbon, hydrogen, nitrogen, oxygen, phosphorus, and sulfur (CHNOPS) — account for approximately 97% of the mass of a human body. Trace elements such as iron, zinc, copper, manganese, and selenium perform critical catalytic roles despite being present in minuscule quantities.

1.1.2 Subatomic Particles and Atomic Identity

An atom consists of three primary subatomic particles:

Table 23. Subatomic Particles and Atomic Identity: Particle and Charge.

Particle	Charge	Mass (Da)	Location
Proton	+1	1.007	Nucleus
Neutron	0	1.008	Nucleus
Electron	−1	0.000549	Orbital shells

The atomic number (Z) equals the number of protons, defining the element. The mass number (A) equals protons plus neutrons. Isotopes share the same atomic number but differ in neutron count.

1.1.3 Isotopes and Their Biological Applications

Isotopes are classified as stable or radioactive (radioisotopes). Radioisotopes undergo spontaneous nuclear decay, emitting alpha particles, beta particles, or gamma rays.

Table 24. Isotopes and Their Biological Applications: Isotope and Half-life.

Isotope	Half-life	Decay Type	Biological/Medical Application
¹⁴ C	5,730 years	β ⁻	Radiocarbon dating of fossils and archaeological specimens
³ H (tritium)	12.3 years	β ⁻	Tracing metabolic pathways in autoradiography
³² P	14.3 days	β ⁻	Labeling DNA/RNA in molecular biology
¹⁸ F	109.8 min	β ⁺	PET (positron emission tomography) imaging
¹³¹ I	8.0 days	β ⁻ , γ	Thyroid cancer radiotherapy
^{99m} Tc	6.0 hours	γ	SPECT imaging of bones, heart, kidneys

Clinical Connection: PET Imaging and ¹⁸F-FDG

Positron emission tomography (PET) exploits the short half-life of ¹⁸F. The glucose analog ¹⁸F-fluorodeoxyglucose (¹⁸F-FDG) is taken up by metabolically active cells. Because cancer cells have elevated glucose uptake (the Warburg effect), PET scans reveal tumors as “hot spots.” The emitted positron annihilates with a nearby electron, producing two 511 keV gamma photons detected by the scanner in coincidence.

Concept Check 1: Carbon-14 has a half-life of 5,730 years. If a fossilised bone contains 12.5% of its original ¹⁴C, approximately how old is it? (Hint: How many half-lives reduce 100% to 12.5%?)

1.1.4 Electron Shells, Orbitals, and Valence

Electrons occupy discrete energy levels called shells (principal quantum number n = 1, 2, 3, ...). Within each shell, electrons occupy orbitals — three-dimensional regions of space where the probability of finding an electron exceeds 90%.

Table 25. Electron Shells, Orbitals, and Valence: Shell (n) and Subshells.

Shell (n)	Subshells	Orbitals	Max Electrons
1	1s	1	2
2	2s, 2p	4	8
3	3s, 3p, 3d	9	18

The outermost occupied shell is the valence shell — its electron count determines chemical reactivity. Atoms are most stable when their valence shell is complete (the octet rule for second-period elements).

Key biological elements and their valences:

Table 26. Electron Shells, Orbitals, and Valence: Element and Symbol.

Element	Symbol	Atomic Number	Valence Electrons	Typical Bonds
Hydrogen	H	1	1	1
Carbon	C	6	4	4
Nitrogen	N	7	5	3
Oxygen	O	8	6	2
Phosphorus	P	15	5	5
Sulfur	S	16	6	2, 4, or 6

Carbon’s four valence electrons allow it to form four strong covalent bonds in a tetrahedral geometry (*sp*³ hybridization, bond angle 109.5 degrees), enabling virtually unlimited structural complexity — the molecular foundation of life.

1.1.5 Orbital Hybridization in Biological Molecules

Carbon’s bonding versatility arises from orbital hybridization — the linear combination of atomic *s* and *p* orbitals to form new hybrid orbitals matched to molecular geometry.

- *sp*³: One *s* + three *p* orbitals -> four equivalent hybrid orbitals pointing to the corners of a tetrahedron (109.5 degrees). Each forms a single (σ) bond. Example: methane, saturated carbons in **fatty acid** tails, the α -carbon of every amino acid.
- *sp*²: One *s* + two *p* orbitals -> three coplanar hybrid orbitals (120 degrees) plus one unhybridised *p* orbital perpendicular to the plane that overlaps with another *p* orbital to form a π -bond. Example: C=C in unsaturated fatty acids, the carbonyl carbon of every **peptide bond**, aromatic rings.
- *sp*: One *s* + one *p* orbital -> two collinear hybrid orbitals (180 degrees) plus two *p* orbitals available for two π -bonds. Example: C \equiv N in hydrogen cyanide; the C \equiv C of acetylene; rare in biology except in some natural products.

Nitrogen exhibits analogous hybridization: in primary amines (–NH₂) and the α -amino group of amino acids, nitrogen is *sp*³ with one lone pair (pyramidal geometry, bond angle about 107 degrees). In the planar peptide bond, however, the nitrogen lone pair is delocalized into the carbonyl π system; the nitrogen behaves as effectively *sp*², locking the six atoms of the peptide unit (C $_{\alpha}$ –C(=O)–N(H)–C $_{\alpha}$) into a plane.

The peptide bond between amino acids has partial double-bond character (about 40%) because of resonance between the *sp*²-hybridized C and N atoms, enforcing planarity and the *trans* configuration that constrains **protein** backbone geometry. The *cis* form is destabilised by about 8 kJ/mol relative to *trans* (except before proline, where the steric penalty is smaller and about 5% of X-Pro bonds are *cis*).

1.1.6 Lewis Structures and Formal Charge

A Lewis structure depicts every valence electron — as bonding pairs (lines) or lone pairs (dots) — making explicit which atoms share which electrons. The formal charge on an atom is what its charge would be if most bonds were nonpolar (electrons shared equally):

Formal charge = (valence electrons) – (lone-pair electrons) – $\frac{1}{2}$ (bonding electrons)

(29)

Formal charges sum to the molecular charge and help select among possible Lewis structures: the best structure minimizes formal charges and places any negative formal charge on the most electronegative atom.

Worked example — formal charge on phosphate (PO₄^{3–}): Phosphate has central P bonded to four O atoms. In the most common textbook structure, three P–O are single bonds (each O carries three lone pairs) and one P=O is a double bond (the doubly bonded O carries two lone pairs).

- *Phosphorus (group 5, 5 valence electrons)*: 0 lone-pair electrons; 5 bonds \times 2 electrons / 2 = 5 bonding electrons assigned. FC = 5 – 0 – 5 = 0.
- *Each single-bonded O (with three lone pairs)*: 6 lone-pair electrons; 1 bond \times 2 / 2 = 1 bonding electron assigned. FC = 6 – 6 – 1 = –1 (\times 3 oxygens = –3).
- *Double-bonded O (with two lone pairs)*: 4 lone-pair electrons; 2 bonds \times 2 / 2 = 2 bonding electrons. FC = 6 – 4 – 2 = 0.

Total: 0 + 3(–1) + 0 = –3, matching the overall charge. By symmetry the four oxygens are actually equivalent; resonance delocalizes the three negative charges and the double-bond character across the four P–O bonds, giving an average bond order of 1.25 and bond length 154 pm (intermediate between a P–O single bond at 163 pm and a P=O double bond at 145 pm). This delocalization explains why phosphate is such a stable leaving group — a key feature exploited by ATP, GTP, and the DNA/RNA backbone.

1.1.7 Electronegativity Drives Polarity in Biology

The Pauling electronegativity (χ) of an element predicts how strongly it pulls bonding electrons [Pauling, 1932]. Differences in χ across a bond ($\Delta\chi$) determine the partial charges that drive **hydrogen bonding**, dipole–dipole interactions, and acid-base behavior throughout biology. The chapter-opening figure 20 pairs the electronegativities for biologically common atoms with representative bond dissociation energies on a log scale.

Table 27. Electronegativity Drives Polarity in Biology: Element and χ (Pauling).

Element	χ (Pauling)	Period	Biological role
F	3.98	2	Fluorinated drugs (5-FU, FDG)
O	3.44	2	Backbone of polar bonds in water, hydroxyl, carbonyl
N	3.04	2	Amino, amide, peptide, nucleobase H-bonds
Cl	3.16	3	Cl [–] ion (electroneutrality, gastric HCl)
S	2.58	3	Disulfides, Fe–S clusters; weaker H-bonds than O

Element	χ (Pauling)	Period	Biological role
C	2.55	2	Backbone of organic chemistry
P	2.19	3	Phosphate (most polarity comes from O, not P)
H	2.20	1	H-bond donor when bonded to N/O/F
Na	0.93	3	Forms ionic Na^+ in solution
K	0.82	4	Forms ionic K^+ in solution

Three observations follow:

1. C–H bonds are nearly nonpolar ($\Delta\chi = 0.35$), which is why the saturated tails of phospholipids and the methyl groups of valine/leucine/isoleucine drive the **hydrophobic effect**.
2. O–H and N–H bonds are strongly polar ($\Delta\chi = 1.24$ and 0.84), creating the partial charges that allow water, alcohols, and amides to form **hydrogen bonds** and to dissolve in aqueous environments.
3. C=O is more polar than C–O because in the carbonyl the π electrons pile up on oxygen; this polarity makes the carbonyl carbon electrophilic — the site attacked by serine in trypsin, by water in **hydrolysis**, and by amine nucleophiles in transamination.

The peptide bond’s polarity (carbonyl O is δ^- , amide H is δ^+) is what enables the regular hydrogen bond pattern of α -helices and β -sheets. Without the electronegativity difference between O and C, there would be no protein secondary structure.

1.2 Chemical Bonds as Biological Forces

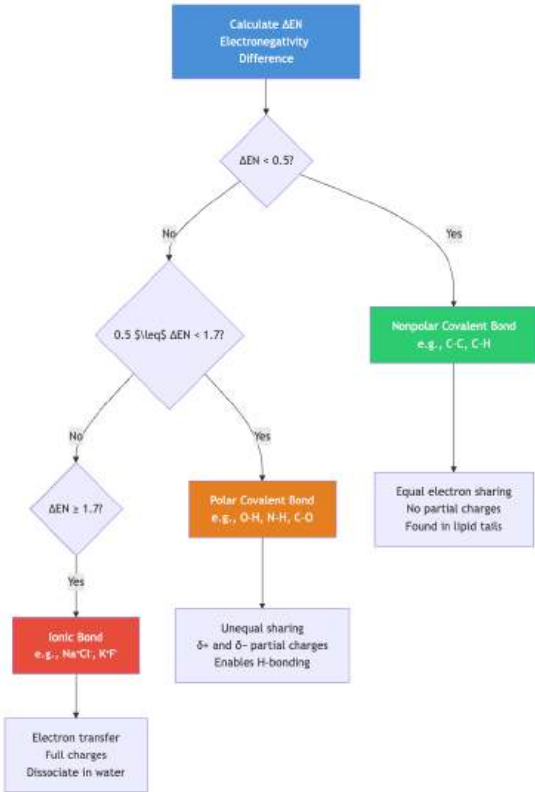


Figure 21. Electronegativity and bond type. Classification of chemical bonds by electronegativity difference (DeltaEN). The boundaries (0.5 and 1.7) are approximate; real bonds exist on a continuum.

1.2.1 Covalent Bonds and Molecular Stability

A covalent bond forms when two atoms share one or more pairs of electrons. The strength of a covalent bond is approximately 150–950 kJ/mol, far greater than thermal energy at body temperature (about 2.5 kJ/mol), making them the primary structural bonds of organic molecules.

Bond energies of biologically important bonds:

Table 28. Covalent Bonds and Molecular Stability: Bond and Energy (kJ/mol).

Bond	Energy (kJ/mol)	Bond Length (pm)	Biological Context
C–C	346	154	Hydrocarbon chains
C=C	614	134	Unsaturated fatty acids
C–H	413	109	Ubiquitous in organics
C–O	360	143	Sugars, amino acids
C=O	745	123	Peptide bonds, carboxyl groups
C–N	305	147	Amino acids
O–H	463	96	Water, hydroxyl groups
N–H	391	101	Amino groups, peptide bonds
S–S	266	205	Disulfide bridges in proteins
P–O	335	163	DNA/RNA backbone, ATP

Electronegativity is the tendency of an atom to attract electron pairs. The Pauling electronegativity scale (F = 3.98; O = 3.44; N = 3.04; C = 2.55; H = 2.20) governs bond polarity [Pauling, 1932]:

- Nonpolar covalent: $\Delta\chi < 0.5$ (e.g., C–C, C–H). Electrons shared equally. Found abundantly in lipid hydrocarbon tails.
- Polar covalent: $0.5 \leq \Delta\chi < 1.7$ (e.g., O–H, N–H, C–O). Partial charges ($\delta+$ and $\delta-$) arise. Critical for hydrogen bonding.
- Ionic: $\Delta\chi \geq 1.7$ (e.g., Na^+Cl^-). One atom effectively captures the electron(s). In solution, ionic compounds dissociate.

Worked example: Water (H₂O). Oxygen’s electronegativity (3.44) vs. hydrogen’s (2.20) gives $\Delta\chi = 1.24$ — a polar covalent bond. The two O–H bonds create a partial negative charge on oxygen ($\delta- = -0.834$ in formal charge terms) and partial positive charges on each hydrogen ($\delta+ = +0.417$ each). This polarity drives water’s exceptional biological properties (see section 2).

1.2.2 Ionic Interactions in Biological Solutes

Ionic bonds form when one atom transfers electrons to another, generating oppositely charged ions. In aqueous biological environments, ionic bonds are typically disrupted by water molecules competing for the ions. The lattice energy of NaCl is 787 kJ/mol, yet it dissolves readily because of the high dielectric constant of water ($\epsilon \approx 80$).

In proteins, ionic interactions (salt bridges) between oppositely charged residues stabilize higher-order structure. Aspartate (Asp, D, $-\text{COO}^-$) and lysine (Lys, K, $-\text{NH}_3^+$) frequently form salt bridges in **enzyme** active sites. A typical salt bridge contributes 5–20 kJ/mol to protein stability, with the strength depending on the local dielectric environment (buried salt bridges are stronger because of lower effective dielectric constant).

Concept Check 2: Why do salt bridges buried in the hydrophobic core of a protein contribute more to stability than those on the protein surface? Consider the role of the dielectric constant.

1.2.3 Hydrogen Bonds in Water, Proteins, and Nucleic Acids

A hydrogen bond forms when a hydrogen atom covalently bonded to an electronegative atom (N, O, or F) is attracted to another electronegative atom. The bond energy is 2–40 kJ/mol — weaker than covalent bonds but stronger than van der Waals forces. Hydrogen bond strengths and distances vary systematically with donor and acceptor identity:

Table 29. Hydrogen Bonds in Water, Proteins, and Nucleic Acids: H-bond type and Donor–Acceptor distance (pm).

H-bond type	Donor–Acceptor distance (pm)	Energy (kJ/mol)	Biological occurrence
F–H \cdots F [–] (low-barrier)	240	50–170	Rare in biology; fluoride enzymes
O–H \cdots O [–] (charged)	250–260	25–40	Salt bridges with carboxylates
N ⁺ –H \cdots O (charged)	260–270	15–30	Lys/Arg with Asp/Glu
O–H \cdots O (neutral)	270–280	15–25	Water, hydroxyl groups
N–H \cdots O=C (peptide)	285–310	8–20	α -helices, β -sheets

H-bond type	Donor–Acceptor distance (pm)	Energy (kJ/mol)	Biological occurrence
O–H⋯N (neutral)	280–295	10–20	Ser–His in catalytic triads
C–H⋯O (weak)	320–350	1–4	β-sheet edges, base stacking
S–H⋯O	320–360	4–10	Cys hydrogen bonds (rare)

Despite their individual weakness, hydrogen bonds collectively confer enormous structural stability:

- Water’s liquid state at room temperature (vs. the expected gas-phase at about –100 degrees C as predicted from homologous compounds H₂S, H₂Se)
- DNA double-helix stability: about 2 H-bonds per A–T base pair, about 3 H-bonds per G–C pair
- Protein secondary structure: α-helices (intrachain H-bonds every 4 residues), β-sheets (interchain H-bonds)
- Cellulose microfibrils: interchain H-bonds between glucose polymers create immense tensile strength

Geometry of hydrogen bonds:



Optimal: D–H⋯A angle about 180 degrees; H⋯A distance about 1.8–2.0 angstroms; D⋯A distance about 2.7–3.0 angstroms. Deviations from linearity weaken the bond approximately as $\cos^2 \theta$, where θ is the deviation from 180 degrees.

Types of hydrogen bonds in biology:

Table 30. Hydrogen Bonds in Water, Proteins, and Nucleic Acids: Type and Donor.

Type	Donor	Acceptor	Example
N–H⋯O	Peptide N–H	Peptide C=O	α-helix backbone
O–H⋯O	Water O–H	Carbonyl C=O	Hydration shells
N–H⋯N	Adenine N–H	Thymine N	A–T base pair
O–H⋯N	Serine O–H	Histidine N	Enzyme active sites

1.2.4 Van der Waals Forces and Lipid Packing

Van der Waals forces arise from transient dipoles induced by quantum fluctuations in electron clouds. They are extremely weak (about 0.1–10 kJ/mol) but ubiquitous. Because they scale with surface area, nonpolar molecules with large surface areas (such as cholesterol or hydrophobic protein cores) benefit significantly from van der Waals interactions.

There are three components of van der Waals forces:

1. Keesom forces (permanent dipole–permanent dipole): orientation-dependent attraction between polar molecules.
2. Debye forces (permanent dipole–induced dipole): a polar molecule induces a dipole in a nearby nonpolar molecule.
3. London dispersion forces (induced dipole–induced dipole): the main attractive forces available between nonpolar molecules; arise from instantaneous fluctuations in electron density.

The van der Waals radius defines the effective “size” of an atom. When two non-bonded atoms approach closer than the sum of their van der Waals radii, repulsive forces dominate (Pauli exclusion). This steric effect constrains the conformational space of macromolecules, as described by Ramachandran plots for proteins (see section 3).

London dispersion forces and lipid packing. The strength of dispersion forces between two nonpolar surfaces grows roughly with the polarisability and the contact area: longer alkyl chains have more electrons whose instantaneous dipoles correlate more strongly. For two parallel hydrocarbon chains, the dispersion energy of attraction is approximately 2 kJ/mol per CH₂ pair — modest individually but additive. A 16-carbon palmitic acid tail in close van der Waals contact with a neighboring tail in a phospholipid bilayer thus contributes about 30 kJ/mol of attractive interaction per chain pair, which (combined with the **hydrophobic effect**; see section 2) holds the bilayer together. Longer chains (24 carbons in sphingolipids) and saturated chains (which can pack closely) give more rigid membranes; introducing a single *cis* double bond into oleic acid kinks the chain by about 30 degrees, weakening dispersion contacts and raising membrane fluidity — the molecular reason vegetable oils are liquid while butter is solid at room temperature.

These same forces explain why geckos can walk on walls: their toe pads have millions of setae maximizing van der Waals contact with smooth surfaces, generating up to 10 N/cm² of adhesive force.

1.3 Functional Groups and Biomolecular Reactivity

Six major functional groups determine the chemical reactivity of organic molecules:

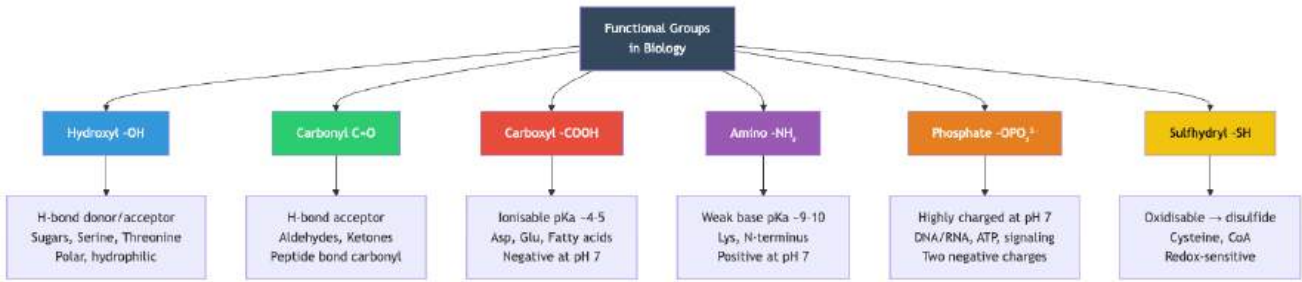


Figure 22. Major functional groups. The six major functional groups of biological chemistry, their key properties, and representative biomolecules.

Table 31. Van der Waals Forces and Lipid Packing: Functional Group and Structure.

Functional Group	Structure	Properties	Biological Role
Hydroxyl	–OH	Polar, H-bond donor/acceptor	Alcohols, sugars, serine
Carbonyl	C=O	Polar, H-bond acceptor	Ketones, aldehydes, amide bonds
Carboxyl	–COOH	Polar, ionisable (pKa about 4–5)	Amino acids, fatty acids
Amino	–NH ₂	Polar, weak base, H-bond donor	Amino acids, nucleotides, ATP
Phosphate	–OPO ₃ ^{2–}	Highly polar, charged at pH 7	DNA/RNA backbone, ATP, signaling
Sulfhydryl	–SH	Polar, oxidisable	Cysteine disulfide bridges

The phosphate group deserves special attention in biochemistry. At physiological pH, phosphate groups carry two negative charges. In ATP (adenosine triphosphate), the three sequential phosphate groups are electrostatically repulsed, storing energy that is released upon hydrolysis (about 30.5 kJ/mol under standard conditions; about 50 kJ/mol under cellular conditions; see section 9).

Additional functional groups encountered in biochemistry:

Table 32. Van der Waals Forces and Lipid Packing: Functional Group and Structure.

Functional Group	Structure	Example
Methyl	–CH ₃	DNA methylation (epigenetic silencing)
Ester	–COO–	Triacylglycerols, phospholipids
Ether	–O–	Ether lipids (plasmalogens in myelin)
Amide	–CONH–	Peptide bonds, asparagine side chain
Thioester	–COS–	Acetyl-CoA (high-energy bond)
Imine (Schiff base)	C=N	Retinal in rhodopsin, PLP-dependent enzymes

Concept Check 3: Acetyl-CoA contains a thioester bond (–COS–) with a ΔG° of hydrolysis of approximately –31.4 kJ/mol, comparable to ATP hydrolysis. Why might cells use thioester bonds as “activated” carriers of acyl groups?

1.4 Resonance Structures and Delocalized Electrons

Many biologically important molecules cannot be accurately described by a single Lewis structure. Resonance occurs when electrons (particularly π electrons and lone pairs) are delocalized across multiple atoms.

1.4.1 The Peptide Bond as a Resonance Hybrid

The peptide bond (C–N) in proteins has significant double-bond character because of resonance between two contributing structures:

Structure I: C=O with C–N single bond (nitrogen has a lone pair)

Structure II: C–O[−] with C=N⁺ double bond (lone pair delocalized into π system)

The actual bond is a resonance hybrid — the C–N bond length (132 pm) is intermediate between a single C–N (147 pm) and a double C=N (127 pm). This partial double-bond character enforces planarity and restricts rotation around the peptide bond, which is fundamental to protein backbone geometry.

1.4.2 Resonance in Carboxylate Ions

When a carboxyl group (–COOH) loses its proton at physiological pH, the resulting carboxylate (–COO[−]) has two equivalent C–O bonds (bond length 126 pm each) due to delocalization of the negative charge over both oxygen atoms. This resonance stabilization explains why carboxylate ions are weaker bases (pKa about 4–5) than alcohols (pKa about 16).

1.4.3 Aromatic Systems in Biology

The aromatic amino acids phenylalanine, tyrosine, and tryptophan contain aromatic rings with fully delocalized π electrons. These systems absorb UV light at characteristic wavelengths:

Table 33. Aromatic amino acid absorbance maxima.

Amino Acid	λ_{max} (nm)	ϵ (M ^{−1} cm ^{−1})	Application
Tryptophan	280	5,500	Protein concentration (A280)
Tyrosine	274	1,490	Protein concentration
Phenylalanine	257	200	Minor contribution

The adenine and guanine bases in nucleic acids are also aromatic heterocycles. Their π -stacking interactions contribute significantly to DNA double-helix stability (see section 3).

1.5 Chirality and Stereochemistry

1.5.1 Enantiomers and Biological Specificity

A chiral (asymmetric) carbon is bonded to four different substituents. Such a carbon exists in two mirror-image forms called enantiomers that cannot be superimposed. Life is remarkably stereospecific:

- L-amino acids are used exclusively in proteins (D-amino acids are found primarily in bacterial cell walls and some antibiotics)
- D-sugars predominate in metabolism (D-glucose, D-ribose)
- Enzymes bind a single enantiomer — the “wrong” one simply does not fit the active site

1.5.2 R/S Configuration

The Cahn-Ingold-Prelog (CIP) system assigns R (rectus) or S (sinister) designations based on the priority of substituents around the chiral center. Priority rules:

1. Higher atomic number = higher priority
2. If tied, move outward until a difference is found
3. View from opposite the lowest-priority group: clockwise = R, anticlockwise = S

For α -amino acids, the L-configuration corresponds to S in most cases (except cysteine, which is R due to sulfur’s high atomic number).

1.5.3 Geometric Isomerism in Fatty Acids

Double bonds in unsaturated fatty acids adopt either cis (Z) or trans (E) configurations:

- cis double bonds introduce a about 30-degree kink, disrupting membrane packing and increasing fluidity
- trans double bonds (produced by industrial hydrogenation) behave like saturated chains, packing tightly

Clinical Connection: Thalidomide and Chirality

The drug thalidomide was prescribed as a racemic mixture (both R and S forms) in the 1950s as a sedative for pregnant women. While the R-enantiomer is an effective sedative, the S-enantiomer is teratogenic, causing severe birth defects. This tragedy revolutionised pharmaceutical regulation, leading to requirements for enantiomeric purity testing. Tragically, even administering the pure R-form would not have prevented harm, as thalidomide racemises *in vivo*.

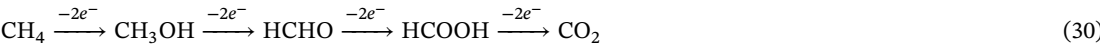
Concept Check 4: Why can’t enzymes catalyse reactions on both enantiomers of a chiral substrate with equal efficiency? Consider the three-dimensional geometry of the active site.

1.6 Redox Reactions in Biology

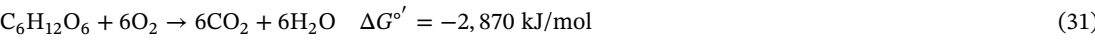
1.6.1 Oxidation and Reduction

Oxidation is the loss of electrons; reduction is the gain of electrons. The mnemonic “OIL RIG” (Oxidation Is Loss, Reduction Is Gain) applies. In biology, redox reactions frequently involve the transfer of hydrogen atoms ($H^+ + e^-$) rather than bare electrons.

Oxidation states of carbon:



Each step represents a two-electron oxidation. Carbon in methane has oxidation state -4 ; in CO_2 it is $+4$. The complete oxidation of one mole of glucose releases 2,870 kJ:



1.6.2 Reduction Potentials and Electron Transfer

The standard reduction potential ($E^{o'}$) measures the tendency of a half-reaction to gain electrons under standard biochemical conditions (pH 7, 25 degrees C, 1 M concentrations):

Table 34. Reduction potentials for selected biological half-reactions.

Half-Reaction	$E^{o'}$ (V)
$O_2 + 4H^+ + 4e^- \rightarrow 2H_2O$	+0.816
Cytochrome c (Fe^{3+}) + $e^- \rightarrow$ Cyt c (Fe^{2+})	+0.254
$NAD^+ + H^+ + 2e^- \rightarrow NADH$	−0.320
$2H^+ + 2e^- \rightarrow H_2$	−0.414

The free energy change of a redox reaction is related to the potential difference:

$$\Delta G^{o'} = -nF\Delta E^{o'} \tag{32}$$

where n = number of electrons transferred and F = Faraday constant (96,485 C/mol).

1.6.3 Biological Electron Carriers

The major electron carriers in metabolism are:

- NAD⁺/NADH: carries two electrons as a hydride ion (H[−]); central to catabolic pathways
- FAD/FADH₂: carries two electrons; tightly bound to enzymes (flavoproteins)
- NADP⁺/NADPH: carries two electrons; central to anabolic (biosynthetic) pathways
- Ubiquinone (CoQ)/Ubiquinol: lipid-soluble electron carrier in the mitochondrial inner membrane
- Cytochromes: iron-containing proteins that transfer single electrons via Fe²⁺/Fe³⁺ cycling

Concept Check 5: In the electron transport chain, electrons flow from NADH ($E^{\circ'} = -0.320\text{ V}$) to O₂ ($E^{\circ'} = +0.816\text{ V}$). Calculate $\Delta G^{\circ'}$ for the transfer of 2 electrons. Is this process thermodynamically favorable?

Concept Check (Analysis): Selenium (Se) is an essential trace element with electronegativity 2.55 (the same as carbon), but it replaces the sulfur in cysteine to form selenocysteine — the 21st amino acid, encoded by UGA (normally a stop codon). (a) Given the near-identical electronegativities of Se and S, explain what chemical property makes Se(II) a superior nucleophile for glutathione peroxidase’s catalytic mechanism. (b) Why would replacing selenocysteine with cysteine reduce catalytic efficiency by ~ 100-fold? (c) Selenium forms diselenide bonds (Se–Se) analogous to disulfide bonds but with a reduction potential of approximately -0.39 V vs -0.23 V for S–S. What does this tell you about selenoprotein redox function?

Worked Example — Radioactive Decay Kinetics in Medicine: Technetium-99m (^{99m}Tc, $t_{1/2} = 6.0\text{ h}$) is used in bone scans. A patient receives 740 MBq (20 mCi) at 8:00 AM for a scan at 11:00 AM (3 h later); biological clearance follows first-order kinetics with biological half-life $t_{\text{biol}} = 24\text{ h}$. The effective half-life is $1/t_{\text{eff}} = 1/t_{\text{phys}} + 1/t_{\text{biol}} = 1/6 + 1/24 = 5/24 \Rightarrow t_{\text{eff}} = 4.8\text{ h}$. Activity at scan time: $A = 740 \times (1/2)^{3/4.8} = 740 \times (1/2)^{0.625} = 740 \times 0.648 \approx 480\text{ MBq}$. Cumulated activity (integrating over ~ 10 effective half-lives): $\tilde{A} = A_0 \times t_{\text{eff}}/\ln 2 = 480 \times 4.8/0.693 \approx 3320\text{ MBq}\cdot\text{h}$. With a bone *S*-value of 0.0067 mGy/(MBq·h), the absorbed dose is $3320 \times 0.0067 \approx 22\text{ mGy}$ — within accepted diagnostic limits (<50 mGy) while delivering adequate image quality. This illustrates how dose planning combines physical and biological half-lives.

1.7 The Mole Concept and Molarity

The mole (mol) is the SI unit for amount of substance, equal to Avogadro’s number (N_A):

$$N_A = 6.022 \times 10^{23} \text{ mol}^{-1}$$

(33)

Molarity (M) is defined as moles of solute per liter of solution:

$$[C] = \frac{n}{V} \quad (\text{mol L}^{-1})$$

(34)

In biochemistry, cellular concentrations are typically in the millimolar (mM) to micromolar (μM) range. ATP concentration in a liver cell is approximately 3–5 mM. The dissociation constant K_d of a high-affinity antibody for its antigen might be 10^{-10} M (100 pM).

Comparison of concentration scales used in biology:

Table 35. Biological Electron Carriers: Unit and Abbreviation.

Unit	Abbreviation	Value	Typical Use
Molar	M	mol/L	Standard solutions
Millimolar	mM	10^{-3} M	Metabolite concentrations
Micromolar	μM	10^{-6} M	Enzyme concentrations
Nanomolar	nM	10^{-9} M	Hormone concentrations
Picomolar	pM	10^{-12} M	High-affinity ligand K_d

1.8 pH and Buffers

1.8.1 The pH Scale

Water autoionises:



with the equilibrium constant at 25 degrees C: $K_w = [\text{H}^+][\text{OH}^-] = 10^{-14} \text{ M}^2$.

The pH is defined as:

$$\text{pH} = -\log_{10}[\text{H}^+] \tag{36}$$

At 37 degrees C (body temperature), $K_w \approx 2.4 \times 10^{-14}$, so neutral pH is about 6.81. The slight shift is physiologically meaningful.

Key physiological pH values:

Table 36. The pH Scale: Compartment and pH.

Compartment	pH	Significance
Blood plasma	7.35–7.45	Tight regulation; acidosis/alkalosis outside this range
Lysosomes	4.5–5.0	Acid hydrolases active
Gastric juice	1.5–3.5	Pepsin active; kills pathogens
Cytoplasm (liver)	7.2	Most enzyme optima
Mitochondrial matrix	7.8–8.0	pH gradient drives ATP synthesis
Pancreatic secretions	8.0–8.5	Neutralizes gastric acid

Clinical Connection: Diabetic Ketoacidosis

In uncontrolled diabetes mellitus, insufficient insulin causes the body to rely on fatty acid oxidation, producing excess acetoacetate and β -hydroxybutyrate (ketone bodies). These are moderately strong acids (pKa about 4.7), overwhelming the bicarbonate buffer system. Blood pH can drop to 7.0–7.1, a life-threatening emergency called diabetic ketoacidosis (DKA). Treatment involves intravenous insulin, fluid replacement, and careful potassium monitoring.

1.8.2 Henderson-Hasselbalch Equation

For a weak acid HA with dissociation constant K_a :

$$\text{pH} = \text{p}K_a + \log \frac{[\text{A}^-]}{[\text{HA}]} \tag{37}$$

A buffer resists pH change when $[\text{A}^-]/[\text{HA}]$ is near 1 (i.e., pH is about $\text{p}K_a$). The effective buffer range is typically $\text{p}K_a \pm 1$. Outside this range, one component is depleted and buffer capacity drops sharply.

1.8.3 Buffer Capacity in Physiological Fluids

The buffer capacity β measures how much strong acid or base a buffer can absorb before pH shifts appreciably. Formally, β is the moles of strong base added per liter per unit pH increase:

$$\beta = \frac{dC_b}{d\text{pH}} = 2.303 \left([\text{H}^+] + [\text{OH}^-] + \frac{C_T K_a [\text{H}^+]}{(K_a + [\text{H}^+])^2} \right) \tag{38}$$

where $C_T = [\text{HA}] + [\text{A}^-]$ is the total buffer concentration. The third term peaks when $\text{H}^+ = K_a$ (i.e., $\text{pH} = \text{p}K_a$), where it reaches its maximum value of $\beta_{\text{max}} = 2.303 \cdot C_T/4 \approx 0.576 C_T$. Two practical consequences follow:

1. Buffer capacity scales linearly with total buffer concentration. A 0.1 M phosphate buffer has 10× the capacity of a 0.01 M phosphate buffer.
2. Capacity is maximal at pH = pKa and falls off rapidly outside pKa ± 1. This is why the bicarbonate buffer (pKa = 6.1) is theoretically a poor blood buffer at pH 7.4 — it is rescued primarily because the system is *open* (CO₂ is exhaled).

Worked buffer problem. A biochemist needs to prepare 1.0 L of 0.1 M Tris buffer (pKa = 8.1) at pH 7.6 for an enzyme assay, starting from solid Tris base (A[−], MW 121) and 1 M HCl. How much of each is required?

Solution: From equation (37): 7.6 = 8.1 + log $\frac{[A^-]}{[HA]}$, so log $\frac{[A^-]}{[HA]}$ = −0.5 and [A[−]]/[HA] = 10^{−0.5} = 0.316. With [HA] + [A[−]] = 0.10 M:

$$[A^-] = 0.0240\text{ M}, \quad [HA] = 0.0760\text{ M}.$$

Dissolve 0.10 mol × 121 g/mol = 12.1 g of Tris base in about 800 mL water, then titrate with 1 M HCl until pH 7.6 (requiring about 76 mL HCl, since each mole of HCl converts one mole of A[−] to HA). Bring the volume to 1.0 L. Because pH is 0.5 units below pKa, β ≈ 0.45 · 0.1 = 0.045 mol L^{−1} (pH unit)^{−1} — adding 4.5 mmol of strong acid would lower the pH by about 0.1 unit.

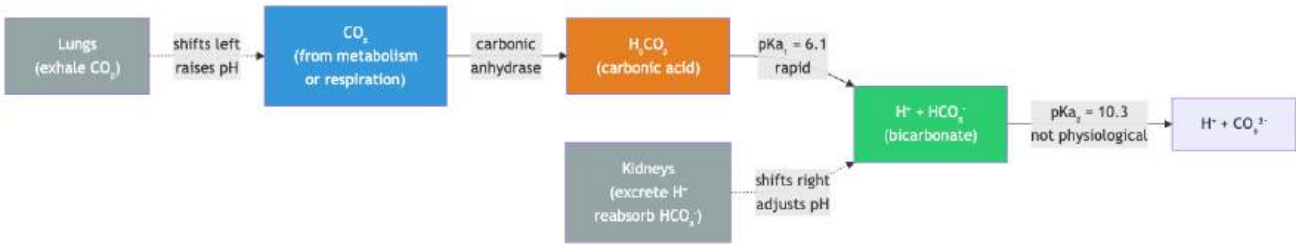


Figure 23. Bicarbonate buffer system. The bicarbonate buffer system. CO₂ produced by metabolism combines with water (catalysed by carbonic anhydrase) to form carbonic acid, which dissociates to bicarbonate and H⁺. The lungs and kidneys regulate the two ends of the equilibrium.

The bicarbonate buffer system in blood operates at pH 7.4 with:



where pKa₁ = 6.1. Despite the pH/pKa offset of about 1.3 units, the bicarbonate system is effective because CO₂ can be rapidly exhaled to shift the equilibrium (an open system). The normal ratio of [HCO₃[−]]/[CO₂] is approximately 20:1.

The phosphate buffer (H₂PO₄[−] / HPO₄^{2−}; pKa = 6.8) buffers intracellular pH and is crucial in renal pH regulation.

Protein buffers — particularly histidine residues (imidazole pKa = 6.0) — provide significant intracellular buffering. Hemoglobin alone accounts for about 60% of the buffering capacity of blood because it contains 38 histidine residues per tetramer.

1.8.4 Comparison of Biological pH Buffering Systems

Table 37. Comparison of Biological pH Buffering Systems: System and Conjugate pair.

System	Conjugate pair	pKa (37 °C)	Concentration	Compartment	Special features
Bicarbonate	H ₂ CO ₃ / HCO ₃ [−]	6.10 (apparent)	about 24 mM	Plasma, ECF	Open system: CO ₂ exhaled by lungs
Phosphate	H ₂ PO ₄ [−] / HPO ₄ ^{2−}	6.86	1–2 mM (plasma); 100 mM (cells)	ICF, urine	Major intracellular buffer
Imidazole (His)	His-H ⁺ / His	6.00	38 sites/Hb tetramer	RBC	Biggest blood buffer; Bohr effect
Ammonia	NH ₄ ⁺ / NH ₃	9.25	Variable	Renal tubule	H ⁺ excretion in acidosis
Carbonyl/amide	COOH / −COO [−]	4–5	Many sites	Proteins	Side-chain buffering
Sulfonate	−SO ₃ H / −SO ₃ [−]	< 1	Glycosaminoglycans	ECM	Typically ionized at cellular pH

The blood buffering hierarchy: bicarbonate (about 75% of capacity) > hemoglobin (about 24%) > plasma proteins/phosphate (about 1%). Despite its inferior pKa, bicarbonate dominates because (i) it is at high concentration and (ii) it is the main *open* system, with CO₂ disposal by lungs (minutes timescale) and HCO₃[−] disposal/regeneration by kidneys (hours-to-days timescale). This three-compartment design — a chemistry buffer coupled to two organ-system control loops — is the body’s solution to the problem that any closed buffer will eventually be titrated to exhaustion.

Concept Check 6: A patient is hyperventilating after a panic attack. Their pCO₂ falls from 40 mmHg to 25 mmHg while [HCO₃[−]] is briefly unchanged at 24 mM. Use equation (37) to predict the resulting blood pH. Will this be respiratory acidosis or alkalosis? Why does breathing into a paper bag help?

Concept Check 7: You are designing a buffer for an enzyme that has its optimum at pH 6.5. Two candidates are available: 100 mM MES (pKa 6.15) and 100 mM HEPES (pKa 7.55). Using equation (38), decide which provides greater buffer capacity at pH 6.5 and explain your reasoning.

1.8.5 Titration Curves and pKa Estimation

A titration curve plots pH against the volume of added base (or acid). For a monoprotic weak acid:

- At the half-equivalence point, pH = pKa (50% ionized)
- The buffer region extends from approximately pKa − 1 to pKa + 1
- At the equivalence point, most acid has been converted to conjugate base

Amino acids with ionisable side chains show multiphasic titration curves with two or three pKa values:

Table 38. Titration Curves and pKa Estimation: Amino Acid and pKa_1 (α-COOH).

Amino Acid	pKa ₁ (α-COOH)	pKa ₂ (α-NH ₃ ⁺)	pKa _R (side chain)	pI
Glycine	2.34	9.60	—	5.97
Aspartate	2.09	9.82	3.86 (−COOH)	2.77
Histidine	1.82	9.17	6.00 (imidazole)	7.59
Lysine	2.18	8.95	10.53 (−NH ₃ ⁺)	9.74

The isoelectric point (pI) is the pH at which the amino acid carries zero net charge. For amino acids without ionisable side chains, pI = (pKa₁ + pKa₂)/2.

1.9 Worked Examples: Buffers, Redox, and Physiological pH

Problem 1: A solution contains 0.05 M acetic acid (CH₃COOH, pKa = 4.76) and 0.15 M sodium acetate. What is the pH?

Solution:

$$\text{pH} = 4.76 + \log \frac{0.15}{0.05} = 4.76 + \log 3 = 4.76 + 0.477 = 5.24$$

(40)

Problem 2: What fraction of histidine’s imidazole group (pKa = 6.0) is protonated at pH 7.0?

Solution:

$$\frac{[\text{HA}]}{[\text{HA}] + [\text{A}^-]} = \frac{1}{1 + 10^{\text{pH} - \text{pK}_a}} = \frac{1}{1 + 10^{7.0 - 6.0}} = \frac{1}{11} \approx 0.091 = 9.1\%$$

(41)

Problem 3: Calculate the free energy released when 2 electrons are transferred from NADH (*E*^{o′} = −0.320 V) to O₂ (*E*^{o′} = +0.816 V).

Solution:

$$\Delta E^{\circ'} = E_{\text{acceptor}}^{\circ'} - E_{\text{donor}}^{\circ'} = +0.816 - (-0.320) = +1.136 \text{ V}$$

(42)

$$\Delta G^{\circ'} = -nF\Delta E^{\circ'} = -(2)(96,485)(1.136) = -219,213 \text{ J/mol} \approx -219.2 \text{ kJ/mol}$$

(43)

This large negative Δ*G*^{o′} drives oxidative phosphorylation, ultimately producing about 2.5 ATP per NADH (see section 9).

Problem 4: A patient’s arterial blood shows [HCO₃[−]] = 12 mM and pCO₂ = 40 mmHg. Using the Henderson-Hasselbalch equation with [CO₂] = 0.03 × pCO₂ mM and pKa = 6.1, calculate the blood pH. Is this acidosis or alkalosis?

Solution:

$$[\text{CO}_2] = 0.03 \times 40 = 1.2 \text{ mM}$$

(44)

$$\text{pH} = 6.1 + \log \frac{12}{1.2} = 6.1 + \log 10 = 6.1 + 1.0 = 7.1$$

(45)

The pH of 7.1 is below the normal range of 7.35–7.45, indicating metabolic acidosis (low bicarbonate with normal pCO₂). Normal [HCO₃[−]] is 24 mM; this patient’s value is halved.

Problem 5: The K_a of lactic acid is 1.38 × 10^{−4}. Calculate the pK_a. If a muscle cell produces lactic acid during intense exercise, what percentage is ionized at intracellular pH 6.8?

Solution:

$$\text{pK}_a = -\log(1.38 \times 10^{-4}) = 3.86$$

(46)

$$\frac{[\text{A}^-]}{[\text{HA}]} = 10^{\text{pH}-\text{pK}_a} = 10^{6.8-3.86} = 10^{2.94} = 871$$

(47)

$$\text{Fraction ionised} = \frac{871}{1 + 871} = 0.9989 = 99.9\%$$

(48)

At physiological pH, the Henderson-Hasselbalch relationship predicts that the ionized form (lactate[−]) strongly dominates over protonated lactic acid. This is why we typically refer to “lactate” rather than “lactic acid” in biological contexts.

1.10 Key Comparison: Bond Types in Biology

Table 39. Titration Curves and pK_a Estimation: Property and Covalent.

Property	Covalent	Ionic	Hydrogen Bond	Van der Waals
Strength (kJ/mol)	150–950	20–200 (in solution)	2–40	0.1–10
Distance	0.1–0.2 nm	0.2–0.3 nm	0.2–0.3 nm	0.3–0.5 nm
Directionality	Highly directional	Non-directional	Directional (about 180 degrees)	Non-directional
In water	Stable	Often disrupted	Dynamic	Very weak
Biological role	Molecular skeleton	Salt bridges, electrolytes	Structure, recognition	Packing, complementarity
Thermal disruption at 37 degrees C	No	Sometimes	Constantly breaking/reforming	Constantly fluctuating

1.11 Computational Bridge

Cellular **thermodynamics** uses the same $\Delta G = \Delta G^\circ + RT \ln Q$ form as introductory chemistry. The project implements the concentration correction explicitly:

```
from biology.biochemistry import reaction_free_energy

# ATP hydrolysis: ΔG°' ≈ -30.5 kJ/mol; equal 1 mM pools → Q = 1, so ΔG = ΔG°'
dg = reaction_free_energy(-30.5, product_conc=1e-3, reactant_conc=1e-3)
print(round(dg, 2)) # -30.5
```

Clinical / systems note: Arterial blood gas interpretation in critical care applies the same logarithmic definition of pH and buffer ratios you use with the Henderson–Hasselbalch equation; the machine-reported bicarbonate and CO₂ tension are coupled through an open buffer system analogous to the models in this chapter.

1.12 Current Evidence and Frontier Biology: Atoms, Molecules, and Chemical Bonds

For Atoms, Molecules, and Chemical Bonds, frontier biology belongs inside the evidence logic of the chapter. Chemistry-of-life claims now connect classical bonding and thermodynamics with AI-guided structure prediction and experimental validation. The core reading question is this: molecular claims need charge, polarity, geometry, concentration, and solvent context.

- What to verify: identify the observation, model, assay, or dataset that would make the claim stronger or weaker.
- What to qualify: state the scale, organism, cell type, environmental condition, or population where the claim is expected to hold.
- What to compare: test at least one alternative explanation, baseline, or null model before treating the pattern as causal.
- What to cite: distinguish primary evidence, review synthesis, public dataset, and institutional guidance; for recent or numeric claims, prefer the source closest to the measurement and state what has changed since it was published.

Treat biomolecular predictions as constrained hypotheses: compare confidence, conservation, solvent exposure, and assay evidence before claiming mechanism [Abramson et al., 2024].

Source practice: For structure and interaction claims, cite experimental structures when available and validate predictions with confidence metrics, conservation, mutagenesis, binding, or cryo-EM/X-ray/NMR evidence [Abramson et al., 2024, Bertoni et al., 2026, EMBL's European Bioinformatics Institute, 2026].

1.13 Summary

- Atoms consist of protons (nuclear charge), neutrons (nuclear mass), and electrons (chemical reactivity).
- Electronegativity differences determine bond polarity: life exploits polar O–H and N–H bonds for hydrogen bonding.
- Carbon's tetravalency and capacity for $sp^3/sp^2/sp$ hybridization is the structural basis of most organic molecules.
- Resonance delocalization stabilizes peptide bonds, carboxylate ions, and aromatic rings.
- Chirality (L-amino acids, D-sugars) is a hallmark of biological specificity.
- Redox reactions (electron transfer) drive energy metabolism; $\Delta G^{\circ'} = -nF\Delta E^{\circ'}$.
- Isotopes serve as tracers (metabolic studies) and therapeutic agents (radiotherapy, PET imaging).
- $\text{pH} = -\log[\text{H}^+]$; buffers maintain physiological pH by resisting acid/base addition through weak acid/conjugate base pairs.
- The bicarbonate buffer system is an open system regulated by lungs (CO₂) and kidneys (HCO₃[−]).
- Connections: See **Unit III — Energy and Metabolism: Introduction** (bioenergetics) for how exergonic hydrolysis of ATP couples to cellular work; **Unit IX — Zoology and Systems Physiology: Introduction** (physiology) links blood gas chemistry to ventilation and renal compensation.

1.14 Key Terms

- Atomic number (Z): Number of protons; defines the element
- Isotope: Atoms of the same element with different neutron counts
- Electronegativity: Tendency of an atom to attract bonding electrons
- Polar covalent bond: Unequal electron sharing producing partial charges
- Hydrogen bond: Weak bond between H bonded to N/O/F and another electronegative atom
- Van der Waals force: Weak attractions from transient or induced dipoles
- Functional group: Characteristic chemical group determining reactivity
- Resonance: Delocalization of electrons across multiple atoms
- Chirality: Property of a molecule with a non-superimposable mirror image
- Enantiomer: One of two mirror-image forms of a chiral molecule
- Oxidation: Loss of electrons
- Reduction: Gain of electrons
- Reduction potential ($E^{\circ'}$): Tendency of a half-reaction to gain electrons
- Molarity: Concentration in moles per liter
- pH: Negative log of hydrogen ion concentration
- Buffer: Solution that resists pH change
- Henderson-Hasselbalch equation: $\text{pH} = \text{pKa} + \log([A^-]/[HA])$
- pI (isoelectric point): pH at which a molecule has zero net charge

1.15 Review Questions

1. Draw electron-dot structures for CH₄, NH₃, and H₂O. Predict the bond angles using VSEPR theory and explain any deviations from ideal tetrahedral geometry.
2. Why does the boiling point of water (100 degrees C) far exceed that of H₂S (−60 degrees C), despite both having similar molecular masses?
3. A patient’s blood pH is measured at 7.25. Is this acidosis or alkalosis? Using the Henderson-Hasselbalch equation, calculate the [HCO₃[−]]/[CO₂] ratio this implies.
4. Explain why phosphate groups in DNA confer structural stability while also making DNA polyanionic.
5. Carbon-11 (¹¹C) has a half-life of 20.4 minutes. Why is this isotope useful for PET imaging of brain metabolism but impractical for studies lasting several hours?
6. Explain why the peptide bond is planar. Include the concept of resonance in your answer, and describe how this planarity constrains protein structure.
7. A pharmaceutical company synthesizes a chiral drug as a racemic mixture. Explain why both enantiomers might not have the same therapeutic effect, and give a historical example.
8. Using the $\Delta G^{\circ'} = -nF\Delta E^{\circ'}$ relationship, predict whether the following reaction is spontaneous: cytochrome c (reduced) donating an electron to O₂. Refer to the table of standard reduction potentials.
9. Calculate the pI of aspartate (pK_{a1} = 2.09, pK_{aR} = 3.86, pK_{a2} = 9.82). At pH 7.4, what is the net charge on aspartate?
10. A buffer is prepared with 0.1 M NaH₂PO₄ and 0.1 M Na₂HPO₄ (pK_a = 6.8). Calculate the pH. If 10 mL of 1 M HCl is added to 1 L of this buffer, what is the new pH?
11. Using reaction_free_energy with $\Delta G^{\circ'} = -30.5$ kJ/mol, compute ΔG when [ADP][Pi]/[ATP] = 0.1 vs. 2.0 (take concentrations in a consistent molar basis). Which condition better matches a working muscle fiber?
12. Compare how a closed phosphate buffer in a test tube and the open HCO₃[−]/CO₂ system in blood respond to a bolus of strong acid. Which system restores pH faster in vivo, and which organ systems do the work?
13. Using the formal-charge formula equation (29), draw a Lewis structure for the carboxylate ion −COO[−] and assign the formal charge on each atom. Explain how resonance equalises the two C–O bond lengths.
14. Sort C–C, C=C, O–H, N–H, and C–H bonds by polarity using the Pauling electronegativity table. For each bond, predict whether the H atom (where present) can serve as a hydrogen bond donor.
15. Use equation (38) to compare the buffer capacity at pH 7.4 of (a) 25 mM bicarbonate (pK_a 6.1) and (b) 25 mM phosphate (pK_a 6.8). Why does the actual buffering importance of bicarbonate in blood far exceed what this calculation predicts?

1.16 Further Reading and Source Notes: Atoms, Molecules, and Chemical Bonds

- Henderson (1913). *The Fitness of the Environment*. Macmillan.
- Pauling (1932; 1939). Electronegativity and *The Nature of the Chemical Bond* [Pauling, 1932].
- Lewis (1916). The atom and the molecule. *Journal of the American Chemical Society*, 38.
- Atkins & de Paula (latest ed.). *Atkins’ Physical Chemistry* (chapters on chemical bonding and molecular structure). Oxford University Press.
- Sanderson (1976). *Chemical Bonds and Bond Energy*. Academic Press.
- Schrödinger (1944). *What Is Life?* Cambridge University Press.

1.17 Companion Source Module: Atoms, Molecules, and Chemical Bonds

Atoms, Molecules, and Chemical Bonds should leave a reproducible trail from a biological claim to the code, figure, diagram, or paper-based activity that can test it. Use the surfaces below to inspect the chapter’s assumptions, rerun the relevant model, or compare the manuscript explanation with companion labs and figures.

Table 40. Companion source surfaces for Atoms, Molecules, and Chemical Bonds.

Surface	Use it for
src/biology/biochemistry/biochemistry.py (reaction_free_energy, atp_free_energy)	Tie bonding and reaction direction to energy accounting.
src/biology/cell/cell_biology.py (osmotic_pressure, diffusion_flux)	Connect charge, solubility, and concentration gradients to cell-scale outcomes.
src/mermaid/biology_diagrams.py (macromolecule_classification_diagram)	Place atomic and bond-level concepts inside the larger biomolecule map.

Reproducibility check: for every molecular claim, write the charge/polarity, solvent context, and unit-bearing quantity that would make the claim testable.
Cross-reference: extend the same logic in section 2, section 3, and section 7.

2 Water — The Molecule of Life

Level 1/3 · 40 min read · 50 min lecture · Prerequisites: section 1

2.1 Learning Objectives

1. Explain how water’s polarity generates its unusual physical properties.
2. Describe hydrophilic and hydrophobic interactions and their importance in cell architecture.
3. Quantify osmotic pressure using the van ’t Hoff equation and derive it from first principles.
4. Apply Fick’s First Law to describe diffusion across membranes with multiple biological applications.
5. Relate water’s properties to **homeostasis** and adaptation in living organisms.
6. Describe the structure and function of aquaporins and their clinical significance.
7. Explain colligative properties and their relevance to antifreeze organisms and cryobiology.
8. Define water activity and explain its importance for food science and microbiology.

2.1.1 Study Blueprint

- Big idea: Water’s polarity, hydrogen bonding, and ionization make cells physically possible.
- Core concepts: hydrogen bonding, cohesion, pH, buffers.
- Framework alignment: Vision & Change: Structure and function, Pathways and transformations of energy and matter; AP Biology: Energetics, Systems Interactions; NGSS-style topics: Matter and Energy in Organisms and Ecosystems, Structure and Function.
- Model or quantitative lens: Henderson-Hasselbalch and pH-scale calculations.
- Data skill: Convert between pH, hydrogen ion concentration, and buffer ratios.
- Practice cadence: Concept Explanation, Statistical Tests and Data Analysis, Argumentation.
- Common misconception to repair: Water is not an inert background; it is an active participant in structure and reaction chemistry.
- Primary lab: **Lab — Water — The Molecule of Life**.
- Question bank: **Questions — Water — The Molecule of Life**.
- Transfer task: Transfer water-property reasoning to blood buffering, plant transport, or protein folding.
- Bridge to computation: `biology.biochemistry.biochemistry.atp_free_energy`.

Opening Vignette: Life at the Boiling Point — and Below Zero

Water boils at 100 °C and freezes at 0 °C. By every prediction from homologous compounds — hydrogen sulfide (H₂S, boiling point −60 °C), hydrogen selenide (H₂Se, bp −41 °C) — water “should” be a gas at room temperature. It is not, and that deviation is why you are alive. The anomalous boiling point of water arises entirely from **hydrogen bonds**: each water molecule can donate two and accept two H-bonds, creating a dynamic, three-dimensional network that requires exceptional energy to disrupt. That high specific heat capacity (4.18 J/g·°C) **buffers** organisms against temperature swings. The high heat of vaporisation (2,260 J/g) makes sweating an efficient coolant — a marathon runner loses about 1.5 L/hour but keeps their core temperature within 1 °C.

In 2012, scientists drilling into Lake Vostok — buried 3.7 km beneath Antarctic ice under 350 atmospheres of pressure — recovered microbial DNA from supercooled water isolated from the atmosphere for 15 million years (Rogers et al., 2013, *PLOS ONE*). Life persisted in near-freezing darkness, sustained by water’s extraordinary properties. Everything in this chapter explains why.

Primary source: Rogers, S. O. et al. (2013). Physiology and phylogeny of microorganisms from Lake Vostok. PLOS ONE, 8(2), e56136.

Among known molecules on Earth, liquid water is unusually well suited as the solvent of life [Ball, 2008]. It is the most abundant molecule in living cells (about 70% of cell mass), and metabolism depends on water as solvent, reactant, product, or thermal buffer. The following properties — each a direct consequence of its molecular structure — make water biologically hard to substitute.

Water is so central to biology that astrobiologists use the mantra “follow the water” when searching for extraterrestrial life. Every known form of life requires liquid water to grow and reproduce (though anhydrobionts such as tardigrades and brine-shrimp cysts can survive years of near-total desiccation in a dormant state), and the “habitable zone” around a star is defined primarily by the temperature range permitting liquid water on a planet’s surface.

2.2 Molecular Structure and Polarity

The water molecule consists of one oxygen atom covalently bonded to two hydrogen atoms. The O–H bond length is 0.096 nm; the H–O–H bond angle is 104.5 degrees (less than the tetrahedral [Henderson, 1913] 109.5 degrees because the two lone pairs compress the bonding pairs, as predicted by VSEPR theory).

Oxygen’s high electronegativity (3.44 vs. H = 2.20) generates partial charges: δ^- on oxygen and δ^+ on each hydrogen [Pauling, 1932]. The resulting dipole moment ($\mu = 1.85$ Debye) is one of the largest for any small molecule.

Each water molecule can form up to four hydrogen bonds: two as a hydrogen-bond donor (through its two O–H hydrogens) and two as a hydrogen-bond acceptor (through its two lone pairs). This tetrahedral hydrogen bonding network gives rise to many of water’s exceptional properties.

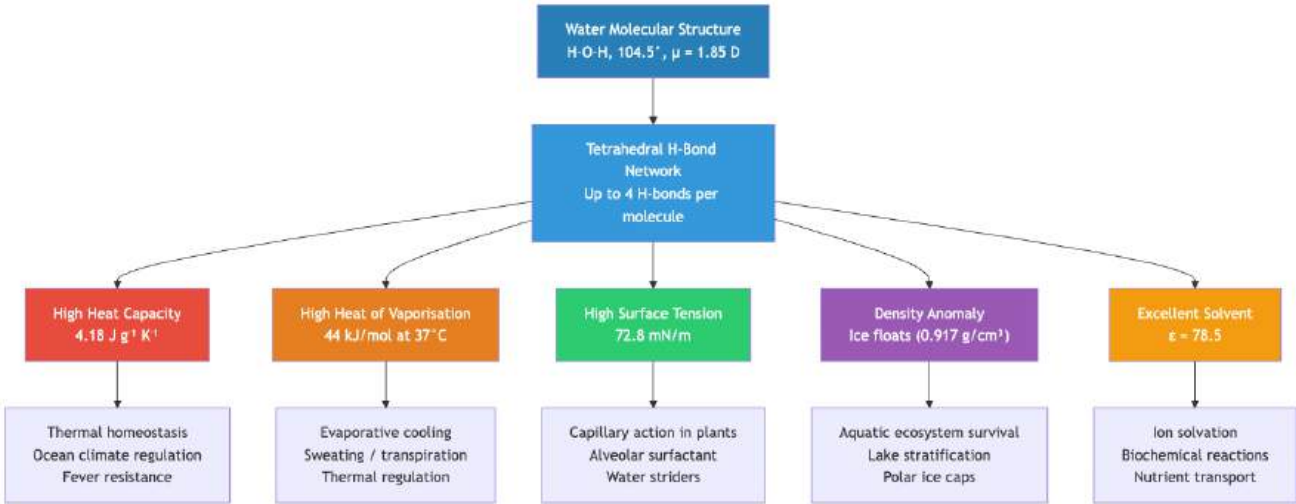


Figure 24. Water structure and hydrogen bonding. Water’s molecular structure gives rise to a tetrahedral hydrogen-bonding network, which in turn produces five extraordinary physical properties. Each property has direct biological consequences.

2.2.1 The Hydrogen Bond Network in Detail

In liquid water at 25 degrees C, each molecule forms an average of about 3.4 hydrogen bonds at any instant (out of a maximum 4) [Ball, 2008]. These bonds are dynamic, with a lifetime of approximately 1–20 picoseconds. The entire hydrogen bond network rearranges on a timescale of about 1 ps — meaning water is simultaneously highly structured and highly dynamic.

In ice, the hydrogen bond network is fully realized: every molecule forms exactly 4 hydrogen bonds in a perfect tetrahedral geometry, creating a hexagonal lattice. This explains both the lower density of ice and the hexagonal symmetry of snowflakes.

Quantitative dynamics of the H-bond network. Modern femtosecond infrared spectroscopy has measured several timescales that govern water’s behavior:

Table 41. The Hydrogen Bond Network in Detail: Process and Timescale.		
Process	Timescale	Biological relevance
O–H stretch vibration	about 10 fs	Vibrational coupling of H-bond network
Single H-bond lifetime (exchange)	1–3 ps	Faster than enzyme turnover; water “lubricates” catalysis
Translational diffusion (1 nm)	about 50 ps	Sets viscous drag on macromolecules
Hydration shell residence time at protein surface	10 ps – 1 ns	Couples to protein backbone fluctuations
Tightly bound waters (buried in protein)	μs – ms	Visible in X-ray structures; contribute to specificity
Bulk-water dielectric relaxation	about 8 ps	Determines ε at MHz/GHz

Each water molecule undergoes about 10¹² H-bond rearrangements per second — an extraordinary churn that nevertheless preserves the average network

structure. Biological molecules effectively “swim” through this fluctuating cage; their conformational dynamics are intimately coupled to the surrounding water (the “slaving” model of protein dynamics).

Concept Check 1: If each water molecule in liquid water forms an average of 3.4 hydrogen bonds and each hydrogen bond is shared between two molecules, how many hydrogen bonds exist per mole of liquid water?

2.3 Physical Properties Explained by Hydrogen Bonding

2.3.1 High Heat Capacity ($C_p = 4.18 \text{ J g}^{-1} \text{ K}^{-1}$)

Heating water requires breaking hydrogen bonds before kinetic energy of translation/rotation can increase. This buffers temperature fluctuations in organisms — an important thermal homeostasis tool. Cells with high water content resist temperature changes.

Comparison: Ethanol has $C_p = 2.44 \text{ J g}^{-1} \text{ K}^{-1}$ (barely half of water’s) despite similar molecular weight, because it has fewer H-bonds per molecule.

The high heat capacity of water has global implications: coastal climates are moderated by the ocean’s thermal inertia. The Gulf Stream carries about 1.4 petawatts ($1.4 \times 10^{15} \text{ W}$) of heat from the tropics to northern Europe, keeping Britain 5–10 degrees C warmer than equivalent latitudes in Canada.

Worked example: How much heat is required to raise the temperature of 70 kg of body water (a typical human) by 1 degree C?

$$Q = mC_p\Delta T = 70,000 \text{ g} \times 4.18 \text{ J g}^{-1} \text{ K}^{-1} \times 1 \text{ K} = 292,600 \text{ J} \approx 293 \text{ kJ}$$

(49)

This is equivalent to the energy in approximately 70 kcal of food — a substantial metabolic investment. This explains why fever is energetically costly: raising body temperature by even 2 degrees C requires about 586 kJ, roughly 20% of resting metabolic output for one hour.

2.3.2 High Heat of Vaporisation ($\Delta_{\text{vap}}H = 44 \text{ kJ/mol}$ at 37 degrees C)

Evaporating water requires breaking the hydrogen bond network. This underlies sweating as a thermoregulatory strategy: evaporating 1 g of sweat removes about 2.4 kJ of heat from the body. At metabolic rates of about 80 W, a resting person must evaporate roughly 120 mL/h at 37 degrees C to maintain steady body temperature.

Comparison with other solvents:

Table 42. Heat of vaporisation for water and comparison solvents at 37 degrees C.

Solvent	$\Delta_{\text{vap}}H$ (kJ/mol)	Boiling Point (degrees C)	Molecular Weight
Water	40.7	100	18
Ethanol	38.6	78	46
Acetone	31.3	56	58
Diethyl ether	26.5	35	74
H ₂ S	18.7	−60	34

Water has a disproportionately high heat of vaporisation relative to its molecular weight — a direct consequence of its extensive hydrogen bonding.

Thermodynamic decomposition. The high $\Delta_{\text{vap}}H$ is dominated by the enthalpic cost of breaking H-bonds. On vaporisation each molecule loses about 3.4 H-bonds; if each is worth about 10 kJ/mol on rupture, the net enthalpy is about 34 kJ/mol from H-bonds alone after correcting for double-counting of shared bonds, matched by about 7 kJ/mol from the work of expansion ($P\Delta V$) and other contributions. The corresponding entropy gain on vaporisation is $\Delta_{\text{vap}}S \approx \Delta_{\text{vap}}H/T_b \approx 109 \text{ J mol}^{-1} \text{ K}^{-1}$ (Trouton’s rule predicts about $85 \text{ J mol}^{-1} \text{ K}^{-1}$ for “normal” liquids; water’s higher value reflects the unusually structured liquid state). The enormous $\Delta_{\text{vap}}H$ is what makes evaporative cooling so efficient: each gram of sweat carries away the energy needed to disassemble its share of the H-bond network.

2.3.3 High Surface Tension ($\gamma = 72.8 \text{ mN/m}$ at 20 degrees C)

Surface molecules have fewer neighbors to form H-bonds with, creating a net inward force. Water’s surface tension is among the highest of common liquids (except mercury). This allows:

- Insects (water striders) to walk on water — their legs distribute body weight across about 2 cm^2 of surface area, resulting in pressure below the surface tension threshold
- Capillary action: water rises in narrow tubes against gravity, critical for tall plants (see section 28)
- Pulmonary alveolar **surfactant** (dipalmitoylphosphatidylcholine, DPPC) reduces surface tension to about 25 mN/m to prevent lung collapse during expiration

Clinical Connection: Neonatal Respiratory Distress Syndrome (NRDS)

Premature infants often lack sufficient pulmonary surfactant because type II pneumocytes do not mature until about 35 weeks of gestation. Without surfactant, alveolar surface tension is too high, and alveoli collapse during expiration (atelectasis). The infant must expend enormous energy to re-inflate collapsed alveoli with each breath. Treatment involves administering exogenous surfactant (e.g., beractant) directly into the trachea. The development of synthetic surfactant therapy in the 1980s dramatically reduced neonatal mortality.

2.3.4 Density Anomaly — Ice Floats

Liquid water is denser than ice because the hexagonal lattice of ice (perfect tetrahedral H-bond geometry) is less compact than the fluctuating, partially broken H-bond network of liquid water. This causes:

- Ice floats, so aquatic ecosystems are insulated below, preventing freeze-solid
- Maximum density at 4 degrees C, so lakes stratify with cold water at 4 degrees C at the bottom
- Floating sea ice reflects solar radiation (albedo effect), contributing to climate regulation

If ice were denser than water, as is the case for nearly every other substance, lakes and oceans would freeze from the bottom up, making most aquatic life unsustainable in temperate climates where water bodies freeze seasonally.

Concept Check 2: If ice sank instead of floated, how would this affect lake ecosystems during winter? Consider both the physical arrangement and biological consequences.

2.4 Water as a Solvent

2.4.1 Hydrophilic Interactions and the Hydration Shell

Hydrophilic (“water-loving”) molecules carry polar groups or charges that interact favorably with water molecules via hydrogen bonding or electrostatic attraction [Ball, 2008]. When ionic compounds dissolve in water, each ion is surrounded by a hydration shell of oriented water molecules:

- Na^+ : surrounded by about 6 water molecules (O pointing toward Na^+)
- Cl^- : surrounded by about 8 water molecules (H pointing toward Cl^-)
- Mg^{2+} : surrounded by about 6 water molecules held very tightly (residence time about $1\text{ }\mu\text{s}$ vs. about 10 ps for Na^+)

The energy cost of separating the ionic lattice is offset by the energy released from forming the hydration shell. This balance is captured by the Born equation for the free energy of ion solvation:

$$\Delta G_{\text{solv}} = -\frac{z^2 e^2 N_A}{8\pi \epsilon_0 r} \left(1 - \frac{1}{\epsilon_r}\right) \quad (50)$$

where z is the ion charge, r is the ionic radius, and ϵ_r is the dielectric constant of the solvent.

2.4.2 The Dielectric Constant and Electrostatic Screening

Water’s high dielectric constant ($\epsilon = 78.5$ at 25 degrees C) dramatically weakens electrostatic interactions between charges. Coulomb’s law in a medium:

$$F = \frac{q_1 q_2}{4\pi \epsilon_0 \epsilon_r r^2} \quad (51)$$

In water, the force between two charges is reduced by a factor of 78.5 compared to vacuum. This is why NaCl (lattice energy 787 kJ/mol) dissolves readily in water but not in hexane ($\epsilon = 1.9$).

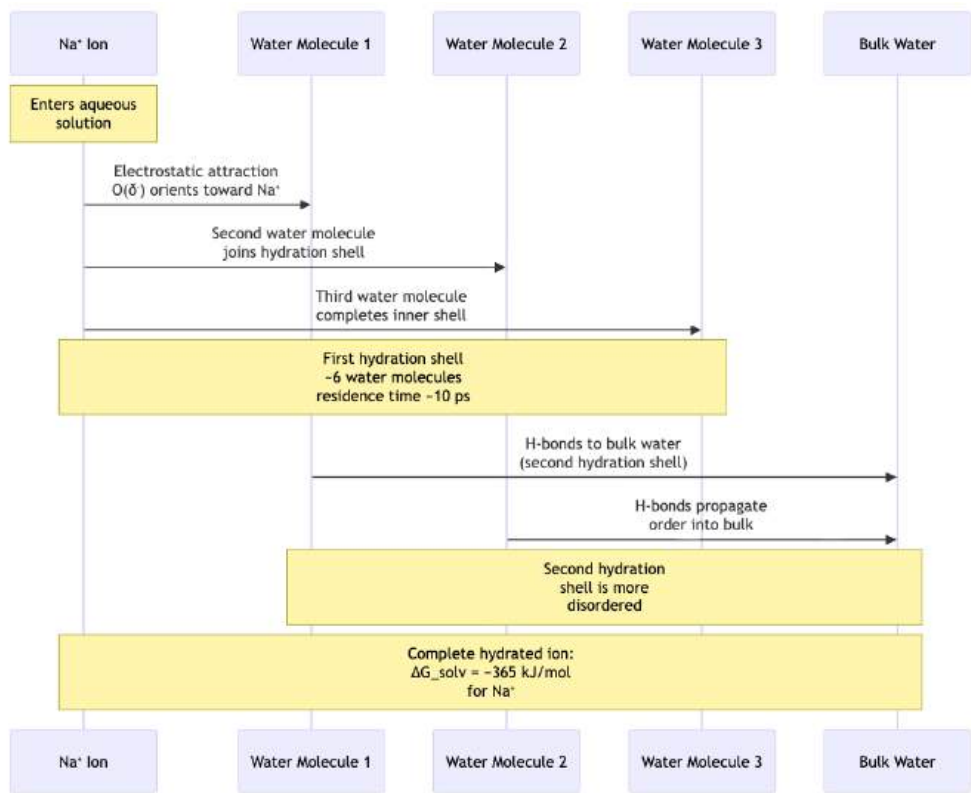


Figure 25. Hydration shells form because polar water molecules orient around ions; oxygen faces cations and hydrogens face anions, stabilizing solutes in solution.

2.4.3 Hydrophobic Effect and Entropy-Driven Assembly

Hydrophobic (“water-fearing”) molecules carry nonpolar groups (C–H, C–C) that cannot H-bond with water. When forced into aqueous solution, surrounding water molecules form a rigid, ordered cage (clathrate structure) to maintain their H-bonding network. This decreases entropy ($\Delta S < 0$).

The hydrophobic effect is therefore driven by entropy: aggregating nonpolar molecules together minimizes the clathrate-ordered water, restoring freedom to bulk water molecules (ΔS increases) [Dill, 1990]. The free energy change is:

$$\Delta G = \Delta H - T\Delta S$$

(52)

Because ΔS is positive (entropy of the system increases) and $\Delta H \approx 0$ (van der Waals interactions in the nonpolar aggregate are similar to water-water interactions), $\Delta G < 0$ — the aggregation is spontaneous.

Quantitative aspects: The transfer free energy of a hydrocarbon chain from water to a nonpolar environment is approximately -3.1 kJ/mol per CH_2 group. For a 16-carbon palmitic acid tail, the hydrophobic driving force is roughly 50 kJ/mol per chain — a substantial thermodynamic force.

The hydrophobic effect explains: - Lipid bilayer formation — phospholipid tails aggregate, forming the barrier of cell membranes (see section 7) - **Protein** folding — hydrophobic side chains buried in the core; hydrophilic on surface - Micelle formation — soap molecules orient with polar heads facing water, nonpolar tails inside - Drug partitioning — the octanol-water partition coefficient ($\log P$) predicts drug membrane permeability

Concept Check 3: Why does the hydrophobic effect become stronger at higher temperatures? Consider the $T\Delta S$ term in the Gibbs free energy equation.

2.4.4 Amphipathic Molecules and Self-Assembly

Molecules with both hydrophilic and hydrophobic regions are amphipathic (also called amphiphilic). Their self-assembly behavior depends on geometry:

Table 43. Amphipathic Molecules and Self-Assembly: Shape and Structure Formed.

Shape	Structure Formed	Example
Cone (large head, small tail)	Micelles	Bile salts, SDS
Cylinder (head and tail cross-sections similar)	Bilayers / vesicles	Phospholipids
Inverted cone (small head, large tail)	Inverted micelles	Some lipids in hexagonal phase

The critical micelle concentration (CMC) is the concentration above which amphipathic molecules spontaneously form micelles. For SDS, CMC = 8.2 mM; for bile salts, CMC = 2–12 mM depending on the species.

2.5 Osmotic Pressure — The van ’t Hoff Equation

figure 26 plots osmotic pressure versus molarity for non-electrolytes and a 1:1 electrolyte at body temperature.

When a selectively permeable membrane separates solutions of different solute concentrations, water moves from low solute (high water potential) to high solute (low water potential) by **osmosis**.

2.5.1 Derivation of the van ’t Hoff Equation

The osmotic pressure can be derived from the chemical potential of water. The chemical potential of water in a solution is:

$$\mu_{\text{water}} = \mu_{\text{water}}^{\circ} + RT \ln a_w$$

(53)

where a_w is the water activity. For dilute ideal solutions, $a_w \approx 1 - x_s$ where x_s is the mole fraction of solute. Using the approximation $\ln(1 - x) \approx -x$ for small x :

$$\mu_{\text{water}} \approx \mu_{\text{water}}^{\circ} - RTx_s$$

(54)

The osmotic pressure is the external pressure needed to restore the chemical potential to that of pure water:

$$\pi \bar{V} = RTx_s$$

(55)

For dilute solutions, $x_s \approx n_s/n_w$ and $n_w \bar{V} \approx V$, giving the van ’t Hoff equation:

$$\pi = iCRT$$

(56)

where: - i = van ’t Hoff factor (number of particles per formula unit; 2 for NaCl -> Na⁺ + Cl⁻) - C = molar solute concentration (mol L⁻¹) - R = 8.314 J mol⁻¹ K⁻¹ - T = temperature in Kelvin

2.5.2 Worked Examples: Osmotic Pressure and Isotonic Fluids

Example 1 — Blood plasma osmotic pressure: Blood plasma osmolarity is about 0.3 Osm (made up of NaCl, glucose, proteins, etc.). Using $i \cdot C_{\text{total}} = 0.3$ mol/L, T = 310 K:

$$\pi = 0.3 \times 8.314 \times 310 = 773 \text{ kPa} \approx 7.6 \text{ atm}$$

(57)

This means a 7.6 atm pressure difference would be required to completely prevent osmotic water movement — illustrating why **turgor pressure** is critical for plant cell rigidity (see section 28).

Example 2 — Sucrose solution: What osmotic pressure is generated by a 0.5 M sucrose solution at 25 degrees C? Sucrose does not dissociate, so $i = 1$:

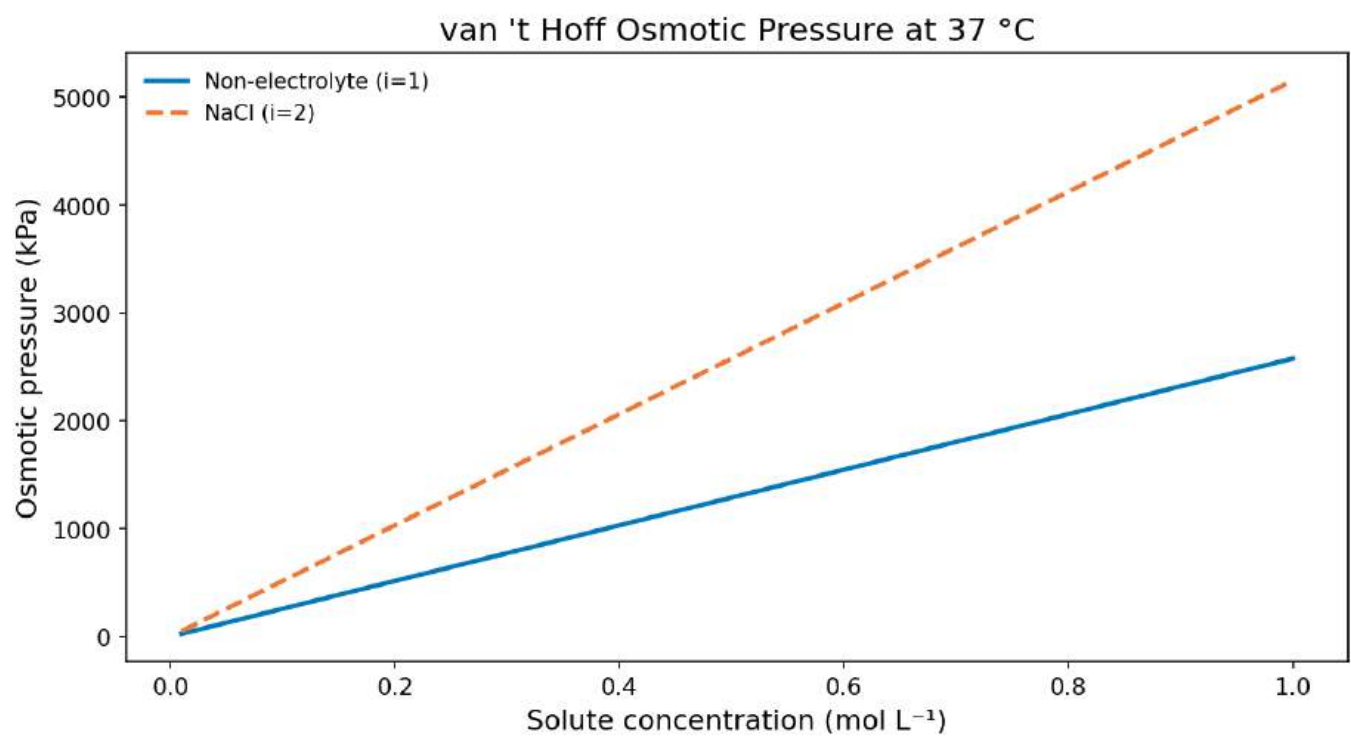


Figure 26. van 't Hoff osmotic pressure versus solute concentration at 37 °C. A non-electrolyte ($i = 1$) and a fully dissociating electrolyte ($i = 2$) produce linear rises with concentration; doubling i doubles osmotic pressure at equal molarity, explaining why saline solutions exert stronger osmotic stress than urea at the same concentration.

$$\pi = 1 \times 0.5 \times 8.314 \times 298 = 1,239 \text{ kPa} \approx 12.2 \text{ atm}$$

(58)

This is why plant cells can generate enormous turgor pressures — enough for roots to crack concrete.

Example 3 — Intravenous fluids: A nurse prepares an isotonic saline drip using NaCl. What concentration is needed? Plasma osmolarity = 0.3 Osm; NaCl *i* = 2:

$$C = \frac{0.3}{2} = 0.15 \text{ M} = 0.15 \times 58.44 = 8.77 \text{ g/L} \approx 0.9\%$$

(59)

This is the basis for “normal saline” (0.9% NaCl), almost universally used in clinical settings.

2.5.3 Tonicity and Cell Behavior

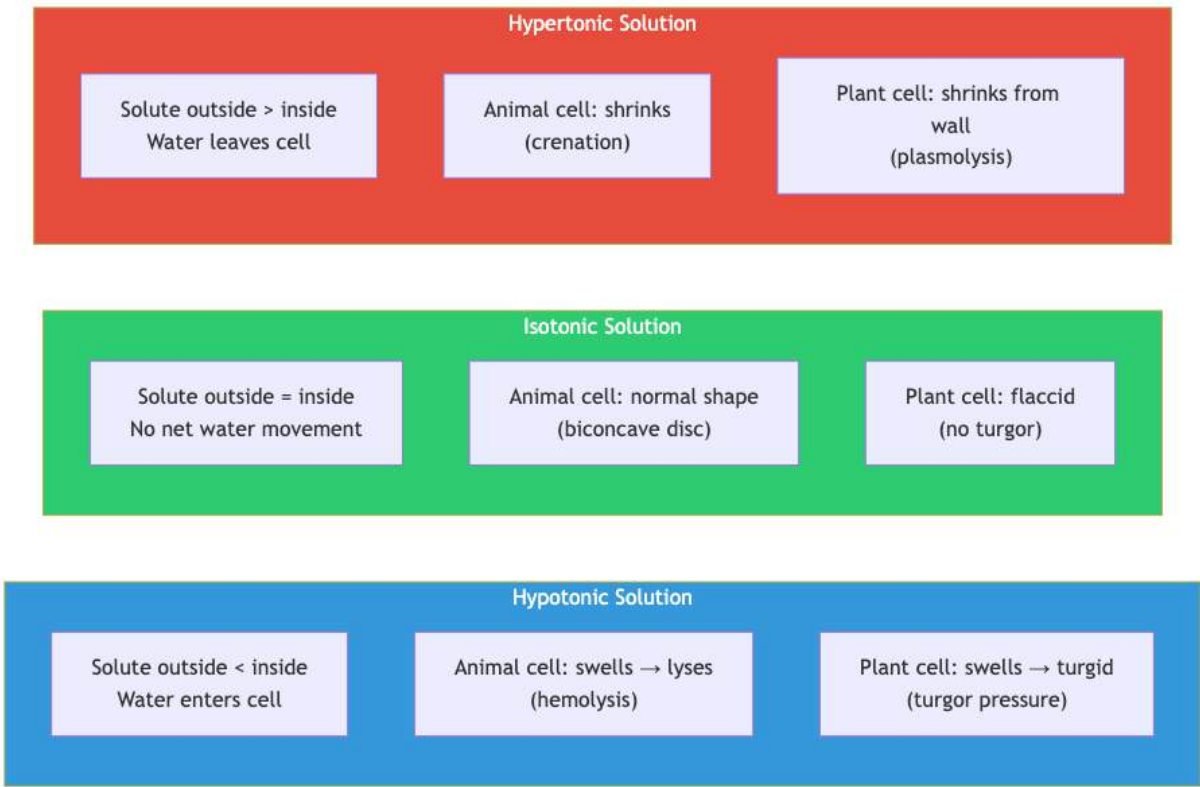


Figure 27. Tonicity and osmotic responses. Osmotic behavior of animal and plant cells in solutions of different tonicity. Plant cells are protected from lysis by their rigid cell wall, which generates turgor pressure to counterbalance osmotic influx.

Table 44. Tonicity and Cell Behavior: Condition and Relative Solute [outside].

Condition	Relative Solute [outside]	Red Blood Cell Effect	Plant Cell Effect
Isotonic (0.9% NaCl)	= inside	Normal biconcave disc	Flaccid
Hypotonic (distilled water)	< inside	Swells -> lyses (hemolysis)	Turgid (ideal for growth)
Hypertonic (2.5% NaCl)	> inside	Shrinks (crenation)	Plasmolysis

Clinical Connection: Osmotic Demyelination Syndrome

When hyponatraemia (low blood sodium, < 135 mM) is corrected too rapidly with hypertonic saline, brain cells — which had adapted to low osmolarity by losing organic osmolytes — suddenly find themselves in a hypertonic environment. Water rushes out of **neurons** and oligodendrocytes,

causing demyelination of pontine neurons. This osmotic demyelination syndrome (formerly called central pontine myelinolysis) causes devastating neurological damage including “locked-in syndrome.” The safe correction rate is less than 8 mM/24 h.

Concept Check 4: A wilted lettuce leaf placed in cold water becomes crisp again. Explain this observation using the van ’t Hoff equation and the concept of turgor pressure.

Concept Check (Analysis): The osmotic pressure equation $\pi = iMRT$ applies to dilute solutions. Red blood cells maintain $[\text{solute}]_{\text{in}} \approx 285 \text{ mOsm}$, while blood plasma is also $\approx 285 \text{ mOsm}$. (a) Calculate the osmotic pressure difference across the RBC membrane if a patient receives hypotonic saline (150 mOsm) at 310 K. (b) If the RBC can withstand a maximum transmembrane pressure of 0.5 atm before lysing, how hypotonic (in mOsm) must the solution be to cause hemolysis? (c) Mountain climbers experience altitude-related changes in blood oxygen. Would a shift in blood osmolarity affect hemoglobin’s oxygen affinity via the Bohr effect? Explain the molecular mechanism.

Worked Example — Colligative Properties and Cryoprotection: Antarctic icefish (*Chaenocephalus aceratus*) survive at -1.9 degrees C, the freezing point of seawater, through antifreeze glycoproteins (AFGPs). These molecules lower the freezing point non-colligatively by binding to nascent ice crystals. For comparison, calculate how much NaCl ($i \approx 1.9$ for partial dissociation) would be needed to lower the freezing point by 1.9 degrees C using $\Delta T_f = K_f \cdot m \cdot i$, where $K_f(\text{water}) = 1.86$ degrees C/m. Required molality: $m = 1.9/(1.86 \times 1.9) = 0.538 \text{ mol/kg}$. At 58.4 g/mol NaCl: $0.538 \times 58.4 \approx 31.4 \text{ g NaCl per kg water}$ — roughly equivalent to seawater salinity. AFGPs achieve the same protection at about 1/300 of the colligative concentration, demonstrating that their mechanism is adsorption-inhibition (blocking ice-crystal growth kinetics) rather than freezing-point depression — a qualitatively different physical mechanism.

2.6 Diffusion — Fick’s First Law

Small molecules move passively down their concentration gradients by Brownian motion — diffusion. Fick’s First Law describes the net flux J ($\text{mol m}^{-2} \text{ s}^{-1}$):

$$J = -D \frac{d[C]}{dx}$$

(60)

where: $-D$ = diffusion coefficient ($\text{m}^2 \text{ s}^{-1}$) — depends on molecule size, shape, and temperature $-d[C]/dx$ = concentration gradient (mol m^{-4})

The negative sign indicates flux is in the direction of decreasing concentration.

2.6.1 The Stokes-Einstein Equation

The diffusion coefficient is predicted by the Stokes-Einstein equation:

$$D = \frac{k_B T}{6\pi\eta r}$$

(61)

where k_B is the Boltzmann constant, T is temperature, η is solvent viscosity, and r is the hydrodynamic radius of the solute. This equation predicts that:

- Larger molecules diffuse more slowly ($D \propto 1/r$)
- Higher temperature increases diffusion ($D \propto T$)
- More viscous media slow diffusion ($D \propto 1/\eta$)

Reference diffusion coefficients at 37 degrees C:

Table 45. The Stokes-Einstein Equation: Molecule and D ($\text{m}^2 \text{ s}^{-1}$).

Molecule	D ($\text{m}^2 \text{ s}^{-1}$)	Hydrodynamic Radius (nm)
O ₂ (in water)	2.1×10^{-9}	0.16
H ₂ O (self-diffusion)	2.3×10^{-9}	0.14
Glucose	6.7×10^{-10}	0.37
ATP	3.7×10^{-10}	0.55
Hemoglobin	6.9×10^{-11}	3.1
IgG antibody	3.8×10^{-11}	5.4

Molecule	D (m ² s ^{−1})	Hydrodynamic Radius (nm)
DNA (small plasmid)	5.0 × 10 ^{−13}	about 50

2.6.2 Mean Diffusion Distance and Biological Design

Mean diffusion distance: $\bar{x} = \sqrt{2Dt}$.

For O₂ to diffuse 1 μm in water: $t = x^2/2D = (10^{-6})^2/(2 \times 2.1 \times 10^{-9}) \approx 0.24 \mu\text{s}$. For 1 mm: $t \approx 238 \text{ s} \approx 4 \text{ min}$.

This is why multicellular organisms exceeding about 1 mm require circulatory systems — diffusion alone is too slow. It also explains why:

- Mitochondria are typically < 1 μm wide (O₂ diffusion time < 1 μs)
- Capillaries are spaced no more than about 100 μm apart in metabolically active tissues
- Alveolar walls are about 0.2 μm thick (gas exchange must be nearly instantaneous)
- Neurons require active transport along axons (diffusion over 1 m would take about 16 years!)

2.6.3 Biological Applications of Fick's Law

Application 1 — Oxygen delivery to muscle fibers:

During exercise, the O₂ concentration at the capillary wall is approximately 0.13 mM, and at the center of a muscle fiber (radius 25 μm) it drops to 0.01 mM. The flux across the fiber radius:

$$J = -D \frac{\Delta C}{\Delta x} = -(2.1 \times 10^{-9}) \frac{(0.01 - 0.13) \times 10^3}{25 \times 10^{-6}} = 1.0 \times 10^{-2} \text{ mol m}^{-2} \text{ s}^{-1}$$

(62)

Application 2 — CO₂ removal from tissues:

CO₂ produced by aerobic metabolism ($D = 1.9 \times 10^{-9} \text{ m}^2/\text{s}$ in water) must diffuse from mitochondria to capillaries. Because CO₂ diffuses about 20 times faster in air than O₂ in water, gas exchange in the lungs is limited primarily by O₂ diffusion, not CO₂.

Application 3 — Neurotransmitter diffusion in the synaptic cleft:

The synaptic cleft is about 20 nm wide. For acetylcholine ($D \approx 5 \times 10^{-10} \text{ m}^2/\text{s}$):

$$t = \frac{x^2}{2D} = \frac{(20 \times 10^{-9})^2}{2 \times 5 \times 10^{-10}} = 4 \times 10^{-7} \text{ s} = 0.4 \mu\text{s}$$

(63)

This submicrosecond diffusion time ensures rapid neurotransmission, far faster than the about 0.5 ms delay of synaptic transmission (which is dominated by vesicle fusion and receptor activation).

Concept Check 5: A single-celled organism is spherical with a radius of 500 μm. Using the diffusion time equation $t = r^2/(6D)$ for three-dimensional diffusion, calculate how long it would take O₂ to diffuse from the cell surface to the center. Is this organism viable if it relies solely on diffusion for O₂ supply?

2.6.4 Solubility Rules and the Thermodynamics of Dissolution

Whether a solute dissolves in water is governed by the Gibbs free energy of solution:

$$\Delta G_{\text{soln}} = \Delta H_{\text{soln}} - T \Delta S_{\text{soln}}$$

(64)

The enthalpy term has three contributions: breaking solute-solute interactions ($\Delta H_1 > 0$), breaking solvent-solvent interactions ($\Delta H_2 > 0$), and forming solute-solvent interactions ($\Delta H_3 < 0$). The sign and magnitude of $\Delta H_{\text{soln}} = \Delta H_1 + \Delta H_2 + \Delta H_3$ depends on which set of interactions wins.

Table 46. Solubility Rules and the Thermodynamics of Dissolution: Class and Example.

Class	Example	Sign of ΔH	Sign of ΔS	Outcome
Salt with high lattice E	NaCl	small (+)	(+)	Soluble, slightly endothermic
Salt with strong hydration	CaCl ₂	(−)	(+)	Soluble, exothermic (heat packs)
Salt with weak hydration	AgCl	(+)	(+) but small	Insoluble; H wins
Polar covalent	sucrose, glucose	small	(+)	Soluble
Nonpolar in water	hexane, lipid tail	about 0	(−)	Insoluble (entropy! see hydrophobic effect)
Amphipathic	phospholipid, soap	mixed	mixed	Self-assembles into bilayers/micelles

The textbook rule “like dissolves like” is a shorthand for: when solute-solvent interactions are similar in strength to the bulk interactions they replace, $\Delta H_{\text{soln}} \approx 0$ and the (usually positive) entropy of mixing drives dissolution. When interactions differ greatly — as for ionic salts in nonpolar solvents, or alkanes in water — ΔH and/or ΔS oppose dissolution and the solute remains in its own phase.

2.6.5 The Hydrophobic Effect Quantified

The hydrophobic effect is the principal driving force for protein folding, lipid bilayer assembly, and many ligand-binding reactions. Despite its name, it is not a force; it is a thermodynamic consequence of the difficulty water has accommodating nonpolar surfaces.

When a nonpolar molecule is forced into water, the surrounding waters cannot form their full complement of H-bonds with it. They preserve their network by reorienting around the solute, sacrificing translational and rotational entropy. The free energy cost is dominated not by enthalpy but by *entropy*:

Table 47. Thermodynamic components of the hydrophobic effect.

Process	ΔH (kJ/mol)	$T\Delta S$ at 25 °C (kJ/mol)	ΔG (kJ/mol)
Transfer 1 mol benzene from oil to water	small (about 0)	−22 (entropy lost)	+22
Transfer 1 mol −CH ₂ − from water to oil	small	+3.1	−3.1 (per CH ₂)
Hydrocarbon aggregation in water (per CH ₂)	small	+3.1	−3.1

The entropic origin has a striking signature: the hydrophobic effect *strengthens* with temperature (up to about 70 °C) because the $T\Delta S$ term grows. This is why heat denatures proteins partly by *favoring* hydrophobic exposure (the cold-denaturation paradox). A 16-carbon palmitate tail, contributing about 3 kJ/mol per

–CH₂–, generates about 50 kJ/mol of effective driving force into the membrane interior — enough to make membrane partitioning essentially irreversible at biological concentrations.

2.6.6 Colligative Property: Osmotic Pressure (van 't Hoff)

The osmotic pressure of a dilute solution is given by the van 't Hoff equation:

$$\pi = i C R T \quad (65)$$

where i is the van 't Hoff factor, C is the molar solute concentration, R is the gas constant, and T is the absolute temperature. (We re-derive equation (65) from chemical potential below.)

Worked example: the osmotic pressure on a red blood cell. Plasma osmolarity is 290 mOsm at body temperature (310 K). What pressure must the cell membrane withstand if placed in pure water? Using equation (65) with $iC = 0.290 \text{ osm L}^{-1}$:

$$\pi = 0.290 \times 8.314 \text{ J mol}^{-1} \text{ K}^{-1} \times 310 \text{ K} = 747 \text{ kPa} \approx 7.4 \text{ atm}$$

This is the pressure of a vehicle tyre. The lipid bilayer cannot resist such force — placed in distilled water, a red blood cell swells and lyses (hemolysis) within seconds. Plant cells, protected by their rigid cellulose wall, can sustain similar pressures as turgor; this turgor is what keeps lettuce crisp and what allows plant roots to crack pavement.

2.6.7 Water Activity and Biological Processes

Water activity (a_w) is the effective “thermodynamic concentration” of water and is governed by the same chemical potential expression that gives osmotic pressure:

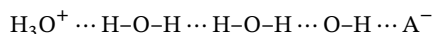
$$\mu_w = \mu_w^\circ + RT \ln a_w \quad (66)$$

Adding solutes lowers a_w below 1 (pure water), which (i) reduces the rate of water-dependent reactions including hydrolysis, (ii) inhibits microbial growth, and (iii) suppresses freezing. Most cellular processes proceed at $a_w \gtrsim 0.99$. When a_w falls below about 0.60 (e.g., honey, raisins, dried meat), microbial growth is essentially arrested — the lowest recorded growth limit, that of the xerophilic mold *Xeromyces bisporus*, is $a_w \approx 0.61$ — which is the basis of most traditional preservation methods. We will quantify this further in §8 below.

2.6.8 Proton Hopping — The Grotthuss Mechanism

Protons (H⁺, actually the hydronium ion H₃O⁺) diffuse through water roughly 7× faster than any other ion of similar size. The reason is that protons do not move as discrete particles; instead, the *charge* hops from one water molecule to the next via a chain of H-bond rearrangements — the Grotthuss mechanism (Theodor von Grotthuss, 1806).

Visualize a chain of H-bonded waters linking a proton donor to a proton acceptor:



Concerted reorientation of the O–H bonds along the chain (each requiring about 1 ps) transports a proton across many molecular diameters in a few picoseconds, *without* any individual water moving more than fractions of an angstrom. The effective diffusion coefficient of H⁺ in water ($9.3 \times 10^{-9} \text{ m}^2 \text{ s}^{-1}$) is dominated by Grotthuss hopping rather than vehicular diffusion.

Biological implications: - ATP synthase. The F_o subunit conducts protons across the mitochondrial inner membrane along a chain of buried waters and protonatable residues (Asp, Glu, Lys); rotational coupling drives ATP synthesis. The Grotthuss mechanism allows fast H⁺ flux without bulk water flow. - Cytochrome c oxidase and other proton pumps shuttle protons through “proton wires” — ordered chains of waters and titratable residues. - Aquaporin proton exclusion. Aquaporins must allow rapid H₂O passage but block proton transport (otherwise membrane potentials would collapse). They achieve this by reorienting a central water so its O–H bonds break the H-bond chain, defeating the Grotthuss mechanism while permitting “vehicular” water transport. - Photosystem II. Splits water into O₂ + 4H⁺ + 4e[−] on the lumenal side of the thylakoid; the four protons join the proton-motive force via H-bond chains in the protein.

2.6.9 Ice Nucleation and Cryopreservation

Pure liquid water can be supercooled to about −40 °C before homogeneous ice nucleation forces freezing. In real solutions, heterogeneous nucleation (initiated by surfaces, dust, or specialized proteins) usually freezes water far above −40 °C. Many bacteria (e.g., *Pseudomonas syringae*) express ice-nucleating proteins that template ice at −2 °C, weaponising frost on plant tissues so the bacteria can colonise the resulting wounds.

Cryopreservation of cells (sperm, oocytes, stem cells, organs) exploits this thermodynamics. Two strategies:

1. Slow freezing with cryoprotectants. Glycerol or DMSO at 1–3 M lowers the freezing point colligatively (equation (65)) and replaces water in hydrogen bonds at membrane surfaces, preventing the membrane damage caused by cellular dehydration. Slow cooling (0.5–1 °C/min) lets water leave cells before intracellular ice forms.
2. Vitrification. Very high cryoprotectant concentrations (50%+) plus rapid cooling (>10⁴ °C/min) glasses water before any ice nucleates. Used for human oocytes and embryos with >90% post-thaw survival.

The wood frog (*Rana sylvatica*) survives whole-body freezing for weeks using a natural variant of strategy 1: liver glycogen is rapidly converted to glucose at about 0 °C, raising blood glucose to about 250 mM (10× hyperglycaemia by mammalian standards). Glucose enters cells and lowers the freezing point intracellularly, while extracellular ice forms harmlessly.

Concept Check 6: Using equation (64), explain why ammonium nitrate (NH₄NO₃) dissolves *spontaneously* in water *despite* an endothermic enthalpy of solution. (Hint: instant cold packs use this reaction.)

2.7 Aquaporins — Molecular Water Channels

2.7.1 Discovery and Structure

While water can slowly permeate lipid bilayers by diffusion, many cell types require rapid water transport. In 1992, Peter Agre discovered aquaporins (AQPs) — integral membrane proteins that form selective water channels. Agre received the Nobel Prize in Chemistry in 2003 for this discovery.

Aquaporins are homotetramers, with each subunit forming an independent water pore. Key structural features:

- Hourglass shape: narrow constriction (2.8 angstroms diameter) allows primarily single-file water passage
- Two NPA motifs (Asn-Pro-Ala): meet at the center of the channel, creating a positive electrostatic barrier
- Aromatic/arginine (ar/R) selectivity filter: four residues at the extracellular constriction determine selectivity
- Proton exclusion mechanism: the NPA motifs reorient water molecules mid-channel, breaking the hydrogen-bond “wire” that would allow proton hopping

2.7.2 Aquaporin Family and Functions

Table 48. Aquaporin Family and Functions: Aquaporin and Primary Location.

Aquaporin	Primary Location	Function	Permeability
AQP0	Eye lens fiber cells	Lens transparency	Low water
AQP1	Red blood cells, kidney proximal tubule	Rapid water reabsorption	High water
AQP2	Kidney collecting duct	ADH-regulated water reabsorption	Regulated
AQP3	Kidney, skin	Water and glycerol transport	Aquaglyceroporin
AQP4	Brain astrocytes	Brain water homeostasis	High water
AQP5	Salivary glands, lacrimal glands	Secretory water flow	High water
AQP7	Adipocytes	Glycerol release during lipolysis	Aquaglyceroporin

A single AQP1 channel transports approximately 3 × 10⁹ water molecules per second — among the fastest known transport rates for any channel protein.

2.7.3 Aquaporins in Disease

Clinical Connection: Nephrogenic Diabetes Insipidus

Mutations in the AQP2 **gene** cause nephrogenic diabetes insipidus (NDI), a condition where the kidneys cannot concentrate urine despite adequate levels of antidiuretic **hormone** (ADH/vasopressin). Patients produce up to 20 L of dilute urine per day and must drink enormous quantities of water to avoid dehydration. The most common inherited form involves autosomal recessive mutations that cause AQP2 to misfold and be retained in the endoplasmic reticulum. Acquired NDI can result from lithium therapy (used in bipolar disorder), which downregulates AQP2 expression via mechanisms involving glycogen synthase kinase-3 β .

Clinical Connection: Cerebral Edema and AQP4

AQP4, the predominant water channel in brain astrocytes, plays a dual role in cerebral edema. In cytotoxic edema (e.g., ischemic stroke), AQP4 facilitates water influx into swelling astrocytes, worsening damage. In vasogenic edema (e.g., brain tumors), AQP4 helps clear excess extracellular water. AQP4 is also the target of autoantibodies in neuromyelitis optica (NMO/Devic’s disease), an autoimmune disorder that mimics multiple sclerosis.

2.8 Colligative Properties and Freezing/Boiling Shifts

Colligative properties depend on the number of dissolved particles, not their identity. They are direct consequences of water activity reduction by solutes.

2.8.1 Boiling Point Elevation and Freezing Point Depression

$$\Delta T_b = iK_b m \quad \text{and} \quad \Delta T_f = iK_f m$$

(67)

where $K_b = 0.512$ degrees C/m (ebullioscopic constant) and $K_f = 1.86$ degrees C/m (cryoscopic constant) for water, m is molality (mol/kg solvent), and i is the van ’t Hoff factor.

Worked example: Blood serum has an effective molality of about 0.3 m (most solutes combined). Freezing point depression:

$$\Delta T_f = 1 \times 1.86 \times 0.3 = 0.558 \text{ degrees C}$$

(68)

Clinical osmometers measure this freezing point depression to determine serum osmolality. Normal serum freezes at -0.56 degrees C, corresponding to about 290 mOsm/kg.

2.8.2 Antifreeze Proteins and Cryoprotective Adaptations

Many organisms survive sub-zero temperatures using biological antifreeze strategies:

Table 49. Antifreeze Proteins and Cryoprotective Adaptations: Organism and Strategy.

Organism	Strategy	Mechanism
Arctic fish (<i>Dissostichus</i>)	Antifreeze glycoproteins (AFGPs)	Bind ice crystal surfaces, inhibit growth
Wood frog (<i>Rana sylvatica</i>)	Freeze tolerance + glucose cryoprotectant	Allows extracellular ice; glucose prevents intracellular freezing
Antarctic midge (<i>Belgica</i>)	Dehydration + trehalose	Removes freezable water
Spruce bark beetle	Glycerol accumulation	Colligative freezing point depression to -40 degrees C
Winter rye	Antifreeze proteins + supercooling	Survives to -30 degrees C

Antifreeze proteins (AFPs) do not work by colligative effects. Instead, they bind to specific ice crystal faces via a flat, hydrophobic ice-binding surface, preventing crystal growth. This creates a difference between the melting point and the freezing point called thermal hysteresis (typically 1–5 degrees C). Fish AFPs can depress the freezing point of blood to -2.5 degrees C, matching the temperature of polar seawater.

Concept Check 7: The spruce bark beetle accumulates glycerol to about 2 M concentration in its hemolymph. Using the freezing point depression equation with $i = 1$ and $K_f = 1.86$ degrees C/m, estimate the freezing point depression. Why might the observed freezing point be lower than this calculated value?

2.9 Water Activity and Microbial Growth

2.9.1 Definition of Water Activity

Water activity (a_w) is the ratio of the vapor pressure of water in a solution to that of pure water:

$$a_w = \frac{p}{p^\circ}$$

(69)

Pure water has $a_w = 1.0$. Adding solutes lowers a_w . For an ideal dilute solution, $a_w \approx 1 - x_s$ where x_s is the mole fraction of solute.

2.9.2 Water Activity and Food Preservation

Microorganisms require a minimum a_w for growth:

Table 50. Water Activity and Food Preservation: Organism Type and Minimum a_w .

Organism Type	Minimum a_w	Example
Most bacteria	0.91	<i>Salmonella</i> , <i>E. coli</i>
Most yeasts	0.88	<i>Saccharomyces</i>
Most moulds	0.80	<i>Aspergillus</i>
Halophilic bacteria	0.75	<i>Halobacterium</i>
Xerophilic moulds	0.65	<i>Xeromyces bisporus</i>
No microbial growth	< 0.60	Honey, dried milk powder

Traditional food preservation methods most work by reducing a_w :

- Salting: NaCl reduces a_w (salted fish, cured ham)
- Sugaring: sucrose reduces a_w (jams, candied fruits, honey)
- Drying: evaporation removes water (jerky, raisins, dried herbs)
- Smoking: combines drying with antimicrobial phenols

Concept Check 8: Honey has a water activity of approximately 0.6 and an extremely high sugar content (about 80% w/w). Despite this, honey has been found in Egyptian tombs still preserved after 3,000 years. Using the concept of water activity, explain why honey is essentially immune to microbial spoilage. Why might diluted honey be more susceptible to fermentation?

Concept Check 9: Aquaporins permit water passage at $\sim 3 \times 10^9$ molecules/s yet block protons. Explain qualitatively how the channel achieves this — and why a hypothetical “leaky” aquaporin allowing Grotthuss proton hopping would be lethal to the cell.

2.10 Water and Adaptation

Because every biochemical reaction occurs in or at water, organisms in water-scarce or water-hostile environments have evolved striking adaptations to defend their hydration state. Three strategies recur across the tree of life: tolerate water loss, prevent ice formation, and economise water turnover.

Desiccation tolerance (anhydrobiosis). Tardigrades, the brine shrimp *Artemia*, many rotifers, and resurrection plants such as *Selaginella* can lose more than 95% of their body water and revive on rewetting. They replace the hydrogen bonds that normally hold macromolecules in shape with the disaccharide trehalose (together with late-embryogenesis-abundant, LEA, proteins), which vitrifies the cytoplasm into a glass that arrests molecular motion and prevents protein unfolding and membrane fusion. In this state metabolism is undetectable and survival extends by orders of magnitude.

Freeze avoidance and tolerance. Because dissolved solute depresses the freezing point primarily colligatively ($\Delta T_f = iK_fm$), small molecules alone cannot protect a fish in -1.9°C seawater. Antarctic notothenioid fish instead secrete antifreeze glycoproteins that adsorb to nascent ice crystals and arrest their growth, lowering the freezing point non-colligatively (thermal hysteresis) by roughly 1°C at millimolar concentrations. Freeze-tolerant wood frogs take the opposite route: they nucleate ice in extracellular spaces and flood cells with glucose and glycerol so that intracellular water rarely freezes.

Water economy. A kangaroo rat can survive on metabolic water alone without drinking: a nasal countercurrent exchanger recovers most respiratory water vapor, and its kidney concentrates urine roughly fivefold above plasma osmolarity. Such osmoregulatory extremes — from halophilic archaea balancing molar internal

K⁺ against a near-saturated brine exterior, to euryhaline fish reversing the direction of their gill ion pumps between fresh and salt water — show that controlling water potential and solute load (section 7) is as much a target of natural selection as any catalytic site.

2.11 Current Evidence and Frontier Biology: Water — The Molecule of Life

For Water — The Molecule of Life, frontier biology belongs inside the evidence logic of the chapter. Chemistry-of-life claims now connect classical bonding and thermodynamics with AI-guided structure prediction and experimental validation. The core reading question is this: water’s biological effects depend on hydrogen bonding, colligative context, interfaces, temperature, and solute identity.

- What to verify: identify the observation, model, assay, or dataset that would make the claim stronger or weaker.
- What to qualify: state the scale, organism, cell type, environmental condition, or population where the claim is expected to hold.
- What to compare: test at least one alternative explanation, baseline, or null model before treating the pattern as causal.
- What to cite: distinguish primary evidence, review synthesis, public dataset, and institutional guidance; for recent or numeric claims, prefer the source closest to the measurement and state what has changed since it was published.

Treat water-structure claims as context-dependent: temperature, solute identity, charge density, interfaces, and hydrogen bonding determine which interactions dominate [Abramson et al., 2024].

Source practice: Tie hydration, polarity, and colligative claims to measured potentials, solubility, spectroscopy, or thermodynamic data rather than generic molecular diagrams [Abramson et al., 2024].

2.12 Quantitative Summary of Water’s Physical Properties

Table 51. Water Activity and Food Preservation: Property and Value (25 degrees C).

Property	Value (25 degrees C)	Biological Consequence
Specific heat	4.18 J g ^{−1} K ^{−1}	Thermal buffer; clinical hypothermia therapy
Heat of vaporisation	2,442 J g ^{−1}	Evaporative cooling (sweating, transpiration)
Dielectric constant	78.5	Ion solvation; electrostatic screening
Surface tension	72.8 mN m ^{−1}	Capillary rise; alveolar function
Density at 0 degrees C	0.917 g cm ^{−3}	Ice floats; aquatic ecosystems insulated
Density at 4 degrees C	1.000 g cm ^{−3}	Maximum density drives lake stratification
Viscosity	0.89 mPa·s	Blood flow; cytoplasmic diffusion rates
Thermal conductivity	0.606 W m ^{−1} K ^{−1}	Heat distribution in tissues

2.12.1 Extremophiles and Water

Halophiles (e.g., *Halobacterium salinarum*) thrive in salt-saturated brines where water activity $a_w < 0.75$. Their protective strategy: accumulate compatible solutes (glycine betaine, ectoine) to maintain osmotic balance without disrupting enzyme function. Remarkably, halophilic enzymes have evolved surfaces rich in acidic residues (Asp, Glu) that create a hydration shell even in near-saturated salt solutions.

Xerophiles (e.g., *Artemia* brine shrimp) survive complete desiccation by replacing water with trehalose, which forms a glassy matrix. Trehalose H-bonds to membrane phospholipid head groups in place of water, preserving membrane architecture. Tardigrades (water bears) can survive in a desiccated state (tun) for decades, reviving upon rehydration.

Thermophiles face the challenge that hydrogen bonds weaken at high temperatures. *Thermus aquaticus* enzymes compensate with increased salt bridges, more compact hydrophobic cores, and proline substitutions that reduce backbone flexibility.

Psychrophiles in Antarctic ice maintain membrane fluidity by incorporating polyunsaturated fatty acids and short-chain fatty acids. Their enzymes have increased flexibility (more glycine residues, fewer prolines) to maintain activity at sub-zero temperatures — at the cost of reduced thermal stability.

2.13 Computational Bridge

The van ’t Hoff relation $\pi = iCRT$ appears throughout this chapter. The cell module implements the same expression in SI units (output in pascals):

```
from biology.cell import osmotic_pressure
```



```
# about 0.15 M NaCl, i = 2, body temperature
pi_pa = osmotic_pressure(0.15, temperature_K=310.0, solute_count=2)
print(round(pi_pa)) # about 7.7e5 Pa for about isotonic NaCl (order of several atm)
```

Clinical / systems note: Nephrogenic diabetes insipidus from AQP2 mutations illustrates how loss of selective water permeability breaks the kidney’s ability to concentrate urine despite normal vasopressin signaling — a channel-level failure of the osmotic water flux you model with π and tonicity.

2.14 Summary

- Water’s polarity and H-bonding network underlie its high heat capacity, heat of vaporisation, surface tension, and solvent properties.
- Hydrophilic/hydrophobic dichotomy drives membrane bilayer formation, protein folding, and micelle structure.
- The hydration shell stabilizes ions in solution; water’s high dielectric constant screens electrostatic interactions.
- Osmotic pressure ($\pi = iCRT$) governs water movement across semipermeable membranes with profound cellular consequences.
- Fick’s First Law ($J = -D \cdot dC/dx$) quantifies passive solute/gas diffusion; slow diffusion over mm distances necessitates circulatory systems.
- Aquaporins are selective water channels critical for renal function, brain water homeostasis, and lens transparency; mutations cause nephrogenic diabetes insipidus.
- Colligative properties (freezing point depression, boiling point elevation) are exploited by antifreeze organisms.
- Water activity determines microbial growth limits and is the basis of traditional food preservation methods.
- Connections: See [Unit II — The Cell: Introduction](#) (membrane transport and aquaporin structure), [Unit IX — Zoology and Systems Physiology: Introduction](#) (renal concentration gradients and ADH), and [Unit VIII — Botany — Plant Biology: Introduction](#) (transpiration and xylem tension).

2.15 Key Terms

- Hydrogen bond: Weak electrostatic attraction between H bonded to N/O/F and another electronegative atom
- Hydrophilic: Water-loving; molecules with polar or charged groups
- Hydrophobic effect: Entropy-driven aggregation of nonpolar molecules in water
- Clathrate: Ordered cage of water molecules around a nonpolar solute
- Amphipathic: Molecules with both hydrophilic and hydrophobic regions
- Osmosis: Net water movement across a semipermeable membrane down its concentration gradient
- Osmotic pressure (π): Pressure required to prevent osmotic water flow
- Van ’t Hoff equation: $\pi = iCRT$; relates osmotic pressure to solute concentration
- Tonicity: Relative solute concentration affecting cell volume
- Diffusion: Net movement of molecules down a concentration gradient
- Fick’s First Law: $J = -D \cdot dC/dx$; relates flux to concentration gradient
- Diffusion coefficient (D): Measure of molecular mobility in a medium
- Aquaporin: Integral membrane protein forming a selective water channel
- Colligative property: Solution property depending on particle number, not identity
- Water activity (a_w): Effective concentration of water in a solution; determines microbial growth
- Antifreeze protein: Protein that inhibits ice crystal growth via thermal hysteresis
- Dielectric constant (ϵ): Measure of a medium’s ability to screen electrostatic interactions

2.16 Review Questions

1. Draw the hydrogen bonding network around a single water molecule. How many H-bonds can one water molecule form, and why?
2. Explain why water’s heat of vaporisation is biologically important. Calculate the volume of sweat that must evaporate to remove 500 kJ of heat from the body.
3. A red blood cell is placed in a solution of 0.45% NaCl ($i = 2$, MW = 58.44). Calculate the osmolarity of this solution and predict what will happen to the cell.
4. Using Fick’s First Law, explain why alveolar walls are about 0.2 μm thick. What would happen to gas exchange efficiency if they were 10 μm thick?
5. An aquaporin channel transports 3×10^9 water molecules per second. If a red blood cell contains 200,000 AQP1 channels, how many moles of water pass through the cell membrane per second?
6. Explain the molecular mechanism by which aquaporins allow water passage but exclude protons ($\text{H}^+ / \text{H}_3\text{O}^+$).
7. A food scientist wants to reduce the water activity of a fruit jam from 0.95 to 0.80 by adding sucrose. Qualitatively, how does this protect against microbial spoilage?

8. The wood frog (*Rana sylvatica*) survives freezing by accumulating glucose in its cells. Explain, using colligative properties, how intracellular glucose prevents lethal ice crystal formation inside cells even while extracellular ice forms.
9. Compare the hydration shells of Na^+ and Mg^{2+} . Which ion has a more tightly bound hydration shell, and why? How does this affect the biological roles of each ion?
10. Derive the relationship between the mean diffusion distance and time ($\bar{x} = \sqrt{2Dt}$) starting from the concept of a random walk. Explain why this relationship makes circulatory systems necessary for organisms larger than about 1 mm.
11. Using `osmotic_pressure`, compare the osmotic pressure (Pa) of 0.30 M glucose ($i = 1$) vs. 0.15 M NaCl ($i = 2$) at 310 K. Which is closer to human plasma tonicity?
12. A child with nephrogenic diabetes insipidus excretes large volumes of dilute urine. Link this **phenotype** to aquaporin-2 trafficking in collecting ducts and the role of vasopressin (ADH) in increasing epithelial water permeability.
13. Using equation (64), predict whether n-octanol (a hydrocarbon-like alcohol) is more soluble in water at 25 °C or 60 °C. Assume $\Delta H_{\text{soln}} \approx 0$ and the dissolution is dominated by the unfavorable entropy of cage formation. How does this relate to drug partition coefficients ($\log P$)?
14. Explain how the Grotthuss mechanism allows ATP synthase to translocate about 10^4 protons per second through its F_o ring without bulk water flow. What would happen if a mutation introduced a single Pro residue that broke the proton wire?
15. Cryopreservation protocols for human embryos use vitrification (rapid cooling with high cryoprotectant concentrations) rather than slow freezing. Using your understanding of ice nucleation and water activity, explain why vitrification is preferred for delicate cells.
16. Use equation (66) to quantify the difference in chemical potential of water in pure water ($a_w = 1$) versus a 1 M sucrose solution ($a_w \approx 0.98$) at 310 K. Compare your answer to the corresponding osmotic pressure from equation (65). Are they consistent?

2.17 Further Reading and Source Notes: Water — The Molecule of Life

- Henderson (1913). *The Fitness of the Environment*. Macmillan.
- Eisenberg & Kauzmann (1969). *The Structure and Properties of Water*. Oxford University Press.
- Tanford (1980). *The Hydrophobic Effect: Formation of Micelles and Biological Membranes*. Wiley.
- Ball (2008). Water as an active constituent in cell biology. *Chemical Reviews*, 108.
- Pace (2001). The comprehensive nature of biochemistry. *Proceedings of the National Academy of Sciences*, 98.
- Franks (2000). *Water: A Matrix of Life*. Royal Society of Chemistry.

2.18 Companion Source Module: Water — The Molecule of Life

Water — The Molecule of Life should leave a reproducible trail from a biological claim to the code, figure, diagram, or paper-based activity that can test it. Use the surfaces below to inspect the chapter’s assumptions, rerun the relevant model, or compare the manuscript explanation with companion labs and figures.

Table 52. Companion source surfaces for Water — The Molecule of Life.

Surface	Use it for
<code>src/biology/cell/cell_biology.py</code> (<code>osmotic_pressure</code> , <code>diffusion_flux</code>)	Translate water potential, solute gradients, and diffusion into quantitative predictions.
<code>src/biology/botany/botany.py</code> (<code>water_potential</code> , <code>transpiration_flux</code>)	Carry water chemistry into plant transport and drought-response scenarios.
<code>src/visualization/plots.py</code> (<code>plot_light_response_curve</code>)	Use graph reading practice for environmental-response curves with clear axes and units.

Reproducibility check: state temperature, solute identity, concentration, and membrane permeability before generalizing a water-property claim. Cross-reference: connect molecular water properties to section 28 and section 7.

3 Biological Macromolecules

Polymer Hierarchy of Biological Macromolecules

	Monomer	Polymer	Assembly	Function
Proteins	Amino acid	Polypeptide	Folded protein	Catalysis, transport, structure
Nucleic acids	Nucleotide	Polynucleotide	Double helix or RNA	Information storage and transfer
Carbohydrates	Monosaccharide	Polysaccharide	Glycocalyx	Energy storage, recognition, structure
Lipids	Fatty acid	Triacylglycerol or phospholipid	Membrane bilayer	Energy, compartmentation, signaling

Figure 28. Hierarchy of biological macromolecules from monomer to polymer to assembly. Each row groups a polymer family (proteins, nucleic acids, carbohydrates, lipids) and the four columns expose the same four-step pattern: monomer, polymer, assembly, and example function. Arrows show the monomer-to-polymer-to-assembly direction; the function column anchors the chemistry to a recognisable biological role.

Level 2/3 · 55 min read · 75 min lecture · Prerequisites: section 1, section 2

3.1 Learning Objectives

- 1. Classify and compare the four classes of biological macromolecules.
- 2. Explain condensation (dehydration) and hydrolysis reactions as the basis of polymer chemistry.
- 3. Describe the structural levels of proteins and relate each level to function, including modern concepts such as intrinsically disordered proteins.
- 4. Explain nucleic acid structure, including A-form, B-form, and Z-form DNA, as well as RNA secondary structures.
- 5. Distinguish the structures and roles of carbohydrates and lipids, including glycoproteins and sphingolipids.
- 6. Describe ribozymes, their discovery, and their significance for the RNA World hypothesis.

7. Compare storage and structural roles of polysaccharides using starch, glycogen, and cellulose as examples.

3.1.1 Study Blueprint

- Big idea: Macromolecule structure links monomer chemistry to biological function and information storage.
- Core concepts: polymers, dehydration synthesis, protein structure, nucleic acids.
- Framework alignment: Vision & Change: Structure and function, Pathways and transformations of energy and matter; AP Biology: Energetics, Systems Interactions; NGSS-style topics: Matter and Energy in Organisms and Ecosystems, Structure and Function.
- Model or quantitative lens: Polymerization energetics and sequence-to-structure reasoning.
- Data skill: Classify molecules from structural evidence rather than names alone.
- Practice cadence: Concept Explanation, Statistical Tests and Data Analysis, Argumentation.
- Common misconception to repair: Structure is not decoration; small chemical changes can redirect function and recognition.
- Primary lab: Lab — Biological Macromolecules.
- Question bank: Questions — Biological Macromolecules.
- Transfer task: Explain how a mutation, lipid substitution, or glycosylation change propagates to phenotype.
- Bridge to computation: `biology.genetics.genetics.translate_mrna`.

Opening Vignette: The Protein That Won Two Nobel Prizes

In 1955, Frederick Sanger published the complete amino acid sequence of bovine insulin: 51 amino acids in two chains (A and B) linked by two disulfide bonds. It had taken him 10 years and was considered one of the most technically difficult achievements in biochemistry at the time. The revelation was not just the sequence itself, but what it implied: proteins are not random polymers — they are precisely specified sequences, encoded in **genes**, determining unique three-dimensional structures. This work earned Sanger his first Nobel Prize in Chemistry (1958).

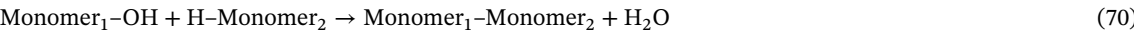
The same molecule — insulin — would later become the first human protein produced by recombinant DNA technology (1982), when the human insulin gene was inserted into *E. coli* to manufacture pharmaceutical insulin for diabetics. Before recombinant insulin, most medical insulin came from pig and cow pancreas, with shortages, immunological reactions, and ethical concerns. Today, an estimated 589 million adults aged 20–79 with diabetes worldwide [Genitsaridi et al., 2026], including those who require insulin, use a product whose existence depends on understanding the four classes of biological macromolecules this chapter explores.

Primary source: Sanger, F. & Thompson, E. O. P. (1953). The amino-acid sequence in the glycyl chain of insulin. *Biochem. J.*, 53(3), 353–374.

Biological macromolecules fall into four major classes: carbohydrates, lipids, proteins, and nucleic acids. The first three are polymers of small repeating units (monomers); lipids are an important exception — they form assemblies through noncovalent hydrophobic interactions rather than covalent polymerization. figure 28 lays out the monomer-to-polymer-to-assembly progression family by family so the same chemistry is recognizable across the four classes.

3.1.2 Condensation and Hydrolysis

Most biological polymers are built by condensation (dehydration) reactions, in which two monomers are joined with the release of one water molecule per bond:



The reverse, hydrolysis, uses water to cleave the bond. These reactions require **enzyme** catalysis (see section 4) and energy input for condensation.

Thermodynamics of bond formation:

Table 53. Hydrolysis free energies for selected biological bond types.

Bond Type	Δ <i>G</i> ^{o'} of Hydrolysis (kJ/mol)	Required Energy Source
Glycosidic	−15 to −20	UDP-glucose (activated sugar)
Peptide	−8 to −16	GTP (ribosomal translation)
Phosphodiester	−25	NTP (DNA/RNA polymerase)
Ester (lipid)	−20	Acyl-CoA (activated fatty acid)

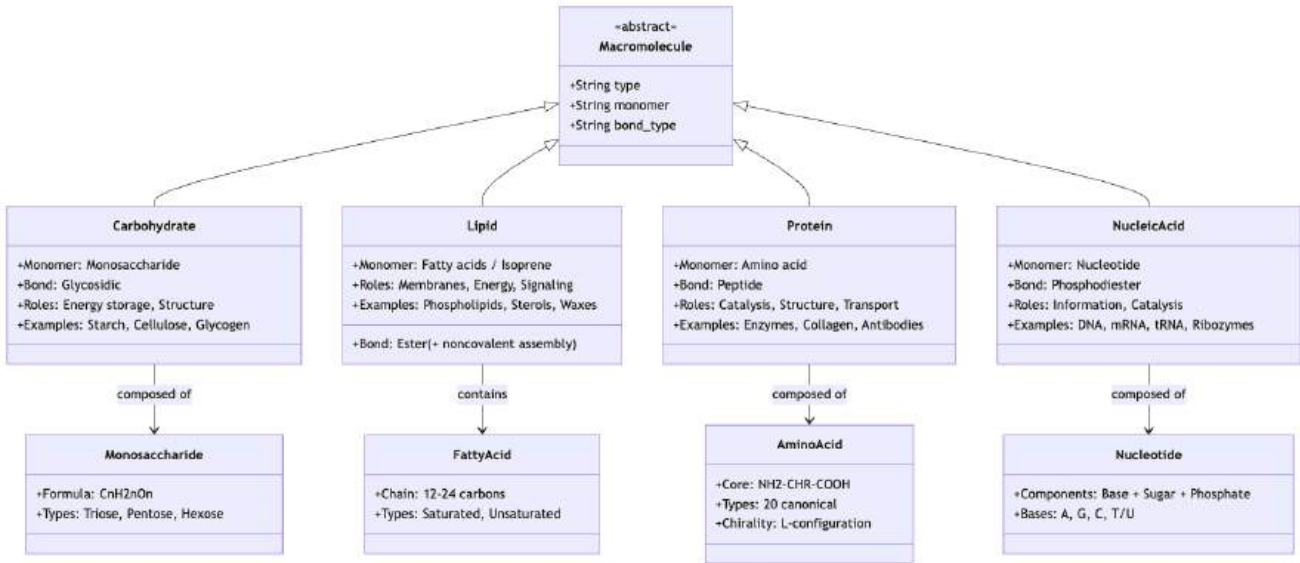


Figure 29. The four biological macromolecule families - carbohydrates, lipids, proteins, and nucleic acids - with their monomers, characteristic bonds, and cellular roles.

In each case, the monomers must first be “activated” by coupling to a high-energy carrier molecule. This coupling makes the condensation reaction thermodynamically favorable.

3.1.3 Worked Example: The Thermodynamics of Polymerization

Problem: The hydrolysis of a **peptide bond** releases approximately $\Delta G^{\circ'} = -10 \text{ kJ/mol}$. 1. What is the standard free energy change ($\Delta G^{\circ'}$) for the condensation reaction to form a single peptide bond? 2. Why does the cell require the hydrolysis of high-energy bonds (like GTP, where $\Delta G^{\circ'} \approx -30 \text{ kJ/mol}$) to drive this reaction during protein synthesis in the **ribosome**?

Solution:

1. Calculate the condensation $\Delta G^{\circ'}$: Because condensation is the exact reverse of hydrolysis, the standard free energy change has the same magnitude but the opposite sign:

$$\Delta G^{\circ'}_{\text{condensation}} = -(\Delta G^{\circ'}_{\text{hydrolysis}}) = -(-10 \text{ kJ/mol}) = +10 \text{ kJ/mol}$$

- As $\Delta G^{\circ'} > 0$, the formation of a peptide bond is thermodynamically unfavorable (endergonic) and will not occur spontaneously.
2. Calculate the coupled reaction thermodynamics: To drive an endergonic reaction forward, the cell couples it to a highly exergonic reaction. During translation elongation, the ribosome couples the formation of a peptide bond to the hydrolysis of GTP down to GDP + P_i.

Summing the free energy changes:

$$\Delta G^{\circ'}_{\text{total}} = \Delta G^{\circ'}_{\text{condensation}} + \Delta G^{\circ'}_{\text{GTP hydrolysis}}$$

$$\Delta G^{\circ'}_{\text{total}} = (+10 \text{ kJ/mol}) + (-30 \text{ kJ/mol}) = -20 \text{ kJ/mol}$$

By coupling the unfavorable peptide bond formation (+10 kJ/mol) to the favorable hydrolysis of GTP (−30 kJ/mol), the overall coupled reaction becomes highly favorable (−20 kJ/mol), driving protein synthesis forward with near-perfect unidirectionality.

Concept Check 1: Hydrolysis reactions are thermodynamically spontaneous ($\Delta G < 0$), yet polymers are kinetically stable in cells. What prevents the spontaneous hydrolysis of your DNA, proteins, and carbohydrates?

3.2 Carbohydrates as Energy Stores and Structural Polymers

3.2.1 Monosaccharides and Ring Chemistry

The simplest carbohydrates are monosaccharides with the empirical formula $(CH_2O)_n$. They are classified by: - Number of carbons: trioses (3C), tetroses (4C), pentoses (5C), hexoses (6C) - Functional group: aldoses (aldehyde) or ketoses (ketone)

Common examples:

Table 54. Monosaccharides and Ring Chemistry: Sugar and Formula.

Sugar	Formula	n	Type	Role
Glyceraldehyde	C ₃ H ₆ O ₃	3	Aldotriose	Central metabolite (glycolysis)
Dihydroxyacetone	C ₃ H ₆ O ₃	3	Ketotriose	Glycolysis intermediate
Ribose	C ₅ H ₁₀ O ₅	5	Aldopentose	RNA backbone, ATP, NAD ⁺
Deoxyribose	C ₅ H ₁₀ O ₄	5	Aldopentose	DNA backbone
Glucose	C ₆ H ₁₂ O ₆	6	Aldohexose	Primary fuel molecule
Galactose	C ₆ H ₁₂ O ₆	6	Aldohexose	Lactose component
Fructose	C ₆ H ₁₂ O ₆	6	Ketohexose	Fruit sugar, sweetest natural sugar
Mannose	C ₆ H ₁₂ O ₆	6	Aldohexose	Glycoprotein glycans

Glucose, galactose, and fructose are structural isomers — identical molecular formulas, different atom arrangements. In solution, glucose exists primarily in the ring form (pyranose, about 99%) rather than the open-chain aldehyde form. The two ring anomers, α -D-glucose and β -D-glucose, differ primarily in the orientation of the C1 hydroxyl group, but this distinction has enormous biochemical significance — enzymes discriminate exquisitely between them.

3.2.2 Disaccharides and Polysaccharides

Two monosaccharides join via a glycosidic bond to form a disaccharide:

Table 55. Disaccharides and Polysaccharides: Disaccharide and Monomers.

Disaccharide	Monomers	Bond	Biological source
Sucrose	Glucose + Fructose	$\alpha(1 \rightarrow 2)\beta$	Plants (transport sugar)
Lactose	Glucose + Galactose	$\beta(1 \rightarrow 4)$	Milk
Maltose	Glucose + Glucose	$\alpha(1 \rightarrow 4)$	Starch digestion
Trehalose	Glucose + Glucose	$\alpha(1 \rightarrow 1)\alpha$	Insect hemolymph, desiccation protectant
Cellobiose	Glucose + Glucose	$\beta(1 \rightarrow 4)$	Cellulose degradation product

Polysaccharides are long chains of monosaccharides serving structural or storage functions:

- Starch (amylose + amylopectin): $\alpha(1 \rightarrow 4)$ linkages, branching via $\alpha(1 \rightarrow 6)$ at intervals (about 25 residues for amylopectin). Storage in plants.
- Glycogen: Like amylopectin but more heavily branched (every about 10 residues). Glucose storage in animal liver (about 100 g) and muscle (about 400 g).
- Cellulose: $\beta(1 \rightarrow 4)$ glucose. Structural component of plant cell walls. Humans cannot digest it (no beta-glucosidase), but gut microbiota can; cellulose is dietary fiber.
- Chitin: $\beta(1 \rightarrow 4)$ N-acetylglucosamine. Structural component of fungal cell walls and arthropod exoskeletons — the second most abundant biopolymer on Earth after cellulose.
- Hyaluronic acid: alternating $\beta(1 \rightarrow 4)$ glucuronic acid and $\beta(1 \rightarrow 3)$ N-acetylglucosamine. Major component of extracellular matrix and synovial fluid.

The difference between starch and cellulose — both glucose polymers — lies solely in the glycosidic bond geometry (α vs. β). Yet this single difference makes cellulose rigid and indigestible versus starch flexible and readily hydrolysed.

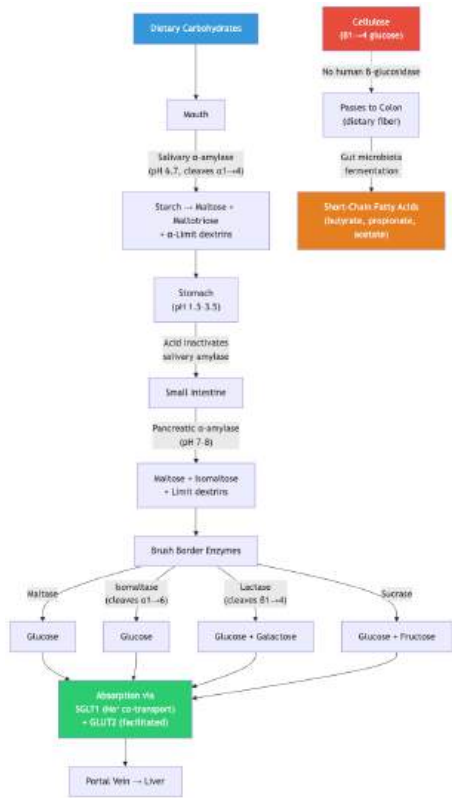


Figure 30. Digestible alpha-linked carbohydrates pass through amylase, brush-border enzymes, and portal absorption, while beta-linked cellulose bypasses human enzymes and reaches microbial fermentation in the colon.

Clinical Connection: Lactose Intolerance

Approximately 65–75% of the global adult population has reduced expression of lactase (the brush border enzyme that cleaves lactose) after weaning — the ancestral state called lactase non-persistence. Undigested lactose reaches the colon, where bacterial fermentation produces H₂, CO₂, and short-chain fatty acids, causing bloating, flatulence, and diarrhea. Lactase persistence (the ability to digest lactose as an adult) evolved independently in pastoral populations in Europe (about 7,500 years ago) and East Africa (about 3,000 years ago) due to strong selection pressure from dairy farming. This is one of the clearest examples of recent human evolution driven by cultural practices.

Concept Check 2: Glycogen is more heavily branched than amylopectin (α1->6 branch every about 10 residues vs. every about 25 residues). How does this increased branching benefit an animal that needs rapid glucose mobilization during a “fight or flight” response?

3.2.3 The Glycosidic Bond: α vs. β

The single greatest source of carbohydrate structural diversity is the glycosidic bond geometry. When a hemiacetal hydroxyl (at the anomeric carbon, C1 of the cyclic sugar) condenses with a hydroxyl of another sugar, the resulting linkage can be either α (the OH/OR on C1 points down in the standard Haworth projection, *trans* to the C6 substituent) or β (OH/OR points up, *cis* to C6).

Table 56. The Glycosidic Bond: α vs. β: Linkage and Geometry.

Linkage	Geometry	Polysaccharide example	Conformation	Digestible by humans?
α(1 → 4) (Glc–Glc)	bent	amylose, glycogen	helix	yes (amylase)
α(1 → 6)	branchpoint	amylopectin, glycogen branches	branched helix	yes (isomaltase)
β(1 → 4) (Glc–Glc)	straight	cellulose	extended ribbons	no (no β-glucosidase)
β(1 → 3)	extended	callose, paramylon (algae)	linear	no

Linkage	Geometry	Polysaccharide example	Conformation	Digestible by humans?
$\beta(1 \rightarrow 4)$ (GlcNAc–GlcNAc)	straight	chitin	extended	no
$\alpha(1 \rightarrow 2)$ (Glc–Fru)	mixed	sucrose	non-reducing	yes (sucrase)
$\beta(1 \rightarrow 4)$ (Gal–Glc)	mixed	lactose	linear	yes (lactase) until weaning

The biological consequences of this single stereochemical choice are profound: α -linked glucose polymers (starch, glycogen) form helices that pack as soft granules and are readily hydrolysed for energy storage. β -linked glucose polymers (cellulose) form extended, hydrogen-bonded sheets that pack into rigid microfibrils with tensile strength rivalling steel by weight; nature uses them as structural material (plant cell walls) precisely because they resist enzymatic attack.

3.2.4 Branching, Linkages, and Polymer Diversity

Even within the same monosaccharide and same anomeric configuration, branching frequency dramatically alters function. Glycogen (animal storage) has $\alpha(1 \rightarrow 6)$ branches every about 10 residues; amylopectin (plant storage) every about 25 residues. Heavier branching gives glycogen many more non-reducing ends per molecule — and since both glycogen synthase and glycogen phosphorylase work primarily at non-reducing ends, branching directly accelerates the rate at which glucose can be added to or removed from the polymer. During a “fight or flight” response, a hepatocyte mobilizes glucose from glycogen at about 10 mM/s; this rate would be unattainable from a linear polymer with a single non-reducing end.

3.2.5 Glycoproteins and Proteoglycans

Many proteins are covalently modified with carbohydrate chains (glycans):

Glycoproteins have relatively short, branched oligosaccharide chains attached via: - N-linked glycosylation: to asparagine (Asn) in the consensus sequence Asn-X-Ser/Thr (where X is any amino acid except Pro). Built up co-translationally on dolichol phosphate in the ER, then trimmed and modified in the Golgi. - O-linked glycosylation: to serine (Ser) or threonine (Thr); built up sequentially in the Golgi. - Other linkages: O-GlcNAc (a single GlcNAc on Ser/Thr; common cytosolic/nuclear signal), C-mannose (on Trp), GPI-anchor glycolipids (link some proteins to the membrane outer leaflet).

Table 57. Glycoproteins and Proteoglycans: Feature and N-linked.

Feature	N-linked	O-linked
Attachment residue	Asn (in Asn-X-Ser/Thr motif)	Ser, Thr
Linker sugar	GlcNAc	GalNAc (mucin-type), Gal, others
Site of attachment	ER (co-translational)	Golgi (post-translational)
Initial structure	Dolichol-P-P-GlcNAc ₂ Man ₉ Glc ₃	Single sugar at a time
Examples	Antibodies, integrins, EPO, viral spike	Mucins, blood group antigens, EGF repeats
Disease	Congenital disorders of glycosylation (CDG-I, II)	Tn syndrome (cancer marker)

Glycoproteins are ubiquitous: antibodies (IgG), blood group antigens (ABO), mucins (airway protection), and many secreted or surface proteins carry glycans. Glycosylation affects protein folding, stability, half-life, and cell-cell recognition. The SARS-CoV-2 spike protein is heavily N-glycosylated, with at least 22 sites; these glycans shield the protein from antibody neutralization, and their removal is a strategy under exploration for vaccine improvement.

Proteoglycans have very long, unbranched glycosaminoglycan (GAG) chains:

Table 58. Glycoproteins and Proteoglycans: GAG and Repeating Unit.

GAG	Repeating Unit	Location	Function
Hyaluronic acid	GlcUA-GlcNAc	Synovial fluid, vitreous humour	Lubrication, shock absorption

GAG	Repeating Unit	Location	Function
Chondroitin sulfate	GlcUA-GalNAc(SO ₄)	Cartilage, bone	Compression resistance
Heparan sulfate	GlcUA/IdoUA-GlcNAc(SO ₄)	Cell surfaces, basement membrane	Growth factor binding
Keratan sulfate	Gal-GlcNAc(SO ₄)	Cornea, cartilage	Transparency, hydration

The highly negatively charged GAGs attract enormous amounts of water (via osmotic pressure), creating a hydrated gel that resists compression — this is why cartilage can support the body’s weight.

3.3 Lipids, Membranes, and Energy Storage

Lipids are not polymers but are grouped together by their hydrophobicity — they do not form regular covalent polymers, yet their self-assembly into bilayers, vesicles, and membranes is central to cellular life [Dill, 1990].

3.3.1 Fatty Acids and Membrane Fluidity

Fatty acids are long-chain carboxylic acids. Food-relevant examples:

Table 59. Fatty Acids and Membrane Fluidity: Fatty Acid and Chain.

Fatty Acid	Chain	Double Bonds	Name	Source
CH ₃ (CH ₂) ₁₄ COOH	16:0	0	Palmitic acid (saturated)	Palm oil, meat
CH ₃ (CH ₂) ₁₆ COOH	18:0	0	Stearic acid (saturated)	Cocoa butter
C18:1 Δ ⁹	18:1	1	Oleic acid (monounsaturated)	Olive oil
C18:2 Δ ^{9,12}	18:2	2	Linoleic acid (ω-6 PUFA)	Vegetable oils
C18:3 Δ ^{9,12,15}	18:3	3	α-Linolenic acid (ω-3 PUFA)	Flaxseed, walnuts
C20:4 Δ ^{5,8,11,14}	20:4	4	Arachidonic acid (ω-6)	Meat, eggs
C20:5 Δ ^{5,8,11,14,17}	20:5	5	EPA (ω-3)	Oily fish
C22:6 Δ ^{4,7,10,13,16,19}	22:6	6	DHA (ω-3)	Fish oil, brain

Saturated fatty acids have no double bonds and pack tightly — solid at room temperature (butter, lard). Unsaturated fatty acids have *cis* double bonds introducing kinks that prevent tight packing — liquid at room temperature (olive oil). Trans fats have *trans* double bonds that pack like saturated fats — they are artificial (from industrial hydrogenation) and have adverse cardiovascular effects.

Essential fatty acids: Linoleic acid (ω-6) and α-linolenic acid (ω-3) cannot be synthesized by humans (we lack Δ12 and Δ15 desaturases) and must be obtained from the diet.

3.3.2 Glycerophospholipids and Bilayer Architecture

Glycerophospholipids (also called phosphoglycerides) are the most abundant membrane lipids. Their structure: glycerol backbone + 2 fatty acid chains at positions sn-1 and sn-2 + phosphate group at sn-3 + polar head group attached to the phosphate.

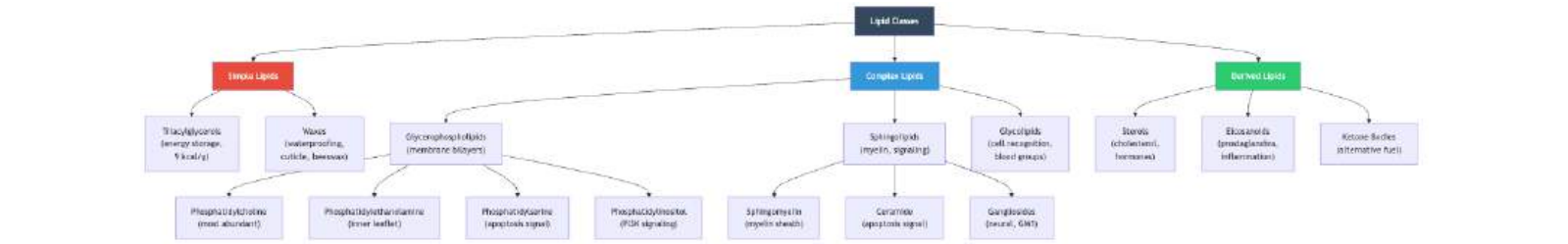


Figure 31. Lipid classes and roles. Classification of lipids. Unlike other macromolecules, lipids are classified by solubility (hydrophobicity) rather than by a common monomer structure. Note the diversity of roles: energy storage, membrane structure, signaling, and waterproofing.

Table 60. Glycerophospholipids and Bilayer Architecture: Head Group and Phospholipid.

Head Group	Phospholipid	Charge at pH 7	Location/Function
Choline	Phosphatidylcholine (PC)	Zwitterionic	Outer leaflet; most abundant
Ethanolamine	Phosphatidylethanolamine (PE)	Zwitterionic	Inner leaflet; membrane curvature
Serine	Phosphatidylserine (PS)	Net negative	Inner leaflet; flipped to outer in apoptosis
Inositol	Phosphatidylinositol (PI)	Net negative	Inner leaflet; PI3K signaling cascade

The amphipathic structure spontaneously forms bilayers in water — a thermodynamic consequence of the hydrophobic effect (see section 2).

3.3.3 Quantitative Properties of the Lipid Bilayer

The “fluid mosaic” model of Singer and Nicolson (1972) proposed that membranes are 2D fluids in which proteins and lipids diffuse laterally. Quantitative measurements — especially by fluorescence recovery after photobleaching (FRAP) and single-particle tracking — have refined this picture into a richer, multi-domain landscape.

Table 61. Quantitative Properties of the Lipid Bilayer: Property and Typical value.

Property	Typical value	Notes
Bilayer thickness	4–5 nm	Hydrophobic core about 3 nm; head-group region about 1 nm each
Area per phospholipid	60–70 Å ²	Determined by NMR, X-ray on monolayers
Lateral diffusion coefficient (<i>D</i> , lipid)	1–10 μm ² /s	A lipid traverses 1 μm in about 1 s
Lateral diffusion coefficient (<i>D</i> , integral protein)	0.01–1 μm ² /s	10–1000× slower than lipids
Rotational correlation time (lipid)	about 100 ps	Acyl chains “wag” on this timescale
Transbilayer flip-flop (phospholipid, spontaneous)	hours–days	Energy barrier from polar head moving through hydrophobic core
Transbilayer flip-flop (catalysed by flippase)	seconds	ATP-dependent; maintains lipid asymmetry
Bilayer surface tension	about 0 mN/m	Unlike air-water interface; key for vesicle stability
Bending modulus (<i>κ</i>)	10–40 <i>k_BT</i>	Resistance to curvature; depends on lipid shape, sterol content
Compressibility modulus (<i>K_A</i>)	100–300 mN/m	Resistance to area change

Property	Typical value	Notes
Permeability to water	10–100 $\mu\text{m/s}$	Surprisingly high due to small size; aquaporins boost about 10×
Permeability to Na^+	10^{-12} – 10^{-14} cm/s	Vanishingly small without channels

Lipid asymmetry. The two leaflets of the plasma membrane have very different compositions: the outer leaflet is enriched in PC, sphingomyelin, and glycolipids; the inner leaflet in PE, PS, and PI. This asymmetry is actively maintained by ATP-dependent flippases (move lipids from outer to inner) and floppases (inner to outer). When PS appears on the outer leaflet — the result of activated scramblases during apoptosis — it serves as an “eat-me” signal for macrophages. Loss of asymmetry is also a feature of activated platelets (where PS exposure on the outer leaflet provides a surface for the coagulation cascade).

Lipid rafts. Cholesterol and sphingolipids self-segregate into liquid-ordered (L_o) microdomains within a sea of liquid-disordered (L_d) phospholipids. These about 10–200 nm rafts concentrate specific signaling proteins (GPI-anchored proteins, Src-family kinases) and are now recognized as functional platforms for receptor signaling, virus budding, and immune-cell synapse assembly.

Concept Check 7: A typical phospholipid diffuses about 1 $\mu\text{m/s}$ laterally in a fluid bilayer but flips between leaflets primarily once every several hours unaided. Use the structure of a phospholipid (charged head, hydrocarbon tails) and the energetics of the hydrophobic effect to explain this 10^{12} -fold difference. Why must cells expend ATP on flippases to break this asymmetry?

3.3.4 Sphingolipids in Membranes and Signaling

Sphingolipids use sphingosine (rather than glycerol) as the backbone. Ceramide (sphingosine + fatty acid) is the core structure:

- Sphingomyelin: ceramide + phosphocholine. Major component of the myelin sheath that insulates axons; critical for nerve impulse conduction velocity.
- Cerebrosides: ceramide + single sugar (glucose or galactose). Abundant in brain.
- Gangliosides: ceramide + complex oligosaccharide containing sialic acid (Neu5Ac). GM1 is the receptor for cholera toxin.

Clinical Connection: Tay-Sachs Disease and Sphingolipid Storage

Tay-Sachs disease results from deficiency of the lysosomal enzyme hexosaminidase A, which normally degrades the ganglioside GM2. Without this enzyme, GM2 accumulates in **neurons**, causing progressive neurodegeneration. Symptoms of the classic infantile form appear at about 6 months and include cherry-red macular spots, seizures, and developmental regression; this form is invariably fatal by age 3–5. Rarer juvenile and late-onset forms, which retain partial hexosaminidase A activity, progress more slowly and are compatible with substantially longer survival. Carrier frequency is about 1/30 in Ashkenazi Jewish populations due to a **founder effect**. This is one of about 50 known lysosomal storage diseases, most caused by deficient hydrolytic enzymes.

3.3.5 Sterols and Steroid Hormones

Cholesterol has a four-ring steroid nucleus (three 6-carbon rings + one 5-carbon ring) and a hydroxyl group at C3. In membranes, cholesterol: - Inserts between phospholipids with its hydroxyl group near the head groups and its rings among the acyl chains - At high temperatures: reduces membrane fluidity by restricting phospholipid movement - At low temperatures: prevents crystallisation by disrupting ordered packing - Net effect: homeoviscous regulation that maintains consistent membrane fluidity across a temperature range

Cholesterol is the precursor to most steroid **hormones**: - Glucocorticoids (**cortisol**): stress response, anti-inflammatory - Mineralocorticoids (aldosterone): sodium/potassium balance - Androgens (testosterone): male sexual development - Oestrogens (oestradiol): female sexual development - Progestagens (progesterone): pregnancy maintenance - Vitamin D₃ (cholecalciferol): calcium absorption - Bile acids (cholic acid, chenodeoxycholic acid): fat emulsification in the duodenum

3.3.6 Waxes and Other Lipids

- Waxes: esters of long-chain fatty acids and long-chain alcohols; waterproofing (plant cuticle, bee honeycomb, whale head oil, ear wax)
- Eicosanoids: signaling lipids derived from arachidonic acid (C20:4); include prostaglandins (inflammation, fever, pain), thromboxanes (platelet aggregation), and leukotrienes (immune response)
- Isoprenoids: built from isoprene units (5C); include terpenes, carotenoids, ubiquinone (CoQ), and dolichol

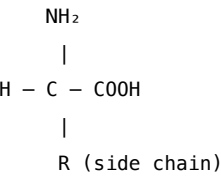
Concept Check 3: Aspirin (acetylsalicylic acid) irreversibly inhibits cyclooxygenase (COX), the enzyme that converts arachidonic acid to prostaglandins and thromboxanes. Explain why aspirin reduces both pain/inflammation and the risk of heart attacks.

3.4 Proteins as Folded Catalytic and Structural Polymers

Proteins are the most structurally and functionally diverse macromolecules. They serve as: - Structural elements (collagen, keratin, **actin**, tubulin) - Enzymes (catalysts; see section 4) - Signaling molecules (growth factors, receptors, G proteins) - Transport proteins (hemoglobin, albumin, aquaporins) - Immune molecules (antibodies) - Motor proteins (myosin, kinesin, dynein)

3.4.1 Amino Acid Chemistry and Side-Chain Diversity

The 20 canonical amino acids share a common backbone:



The α -amino group (pKa about 9.0) and α -carboxyl group (pKa about 2.0) flank the α -carbon, to which the variable R group is attached. At physiological pH 7.4, the amino group is --NH_3^+ and the carboxyl is --COO^- , forming a zwitterion.

Classification by R group character:

Table 62. Amino Acid Chemistry and Side-Chain Diversity: Class and Examples.

Class	Examples	Side chain	Properties
Nonpolar aliphatic	Ala, Val, Leu, Ile, Met, Pro	Hydrocarbon	Hydrophobic core
Aromatic	Phe, Tyr, Trp	Benzene/indole rings	UV absorption, stacking
Polar uncharged	Ser, Thr, Cys, Asn, Gln	--OH , --SH , --CONH_2	H-bonding, disulfides
Positively charged	Lys, Arg, His	--NH_3^+ , guanidinium, imidazole	Salt bridges, catalysis
Negatively charged	Asp, Glu	--COO^-	Salt bridges, metal binding

Special amino acids: - Glycine (R = H) has no stereogenic center and maximal conformational flexibility — often found in tight turns - Proline has a cyclic side chain bonded to the backbone nitrogen, restricting rotation and introducing kinks in α -helices - Cysteine can form disulfide bonds (--S--S--) with other cysteines under oxidising conditions (ER lumen, extracellular space) - Selenocysteine (the “21st amino acid”) contains selenium instead of sulfur and is encoded by UGA **codons** with a special stem-loop (SECIS element)

3.4.2 The Peptide Bond

A peptide bond forms by condensation between the carboxyl of one amino acid and the amino group of the next:



The peptide bond has partial double-bond character (about 40% double bond due to resonance), making it planar and trans (almost typically; *cis* occurs about 0.03% of the time, except before proline where *cis* occurs about 5%). This rigidity limits rotation around the $\text{C}_\alpha\text{--C}$ bond to the backbone dihedral angles φ and ψ (described on a Ramachandran plot), constraining protein conformational space.

3.4.3 Ramachandran Plots and Backbone Dihedral Angles

The polypeptide backbone has three torsional degrees of freedom per residue:

- ω (omega): rotation about the peptide C–N bond. Effectively fixed at 180° (*trans*) due to partial double-bond character; about 5% of X-Pro bonds adopt *cis* ($\omega = 0^\circ$).

- φ (phi): rotation about the N–C $_{\alpha}$ bond.
- ψ (psi): rotation about the C $_{\alpha}$ –C bond.

Because each peptide unit is rigid and planar, primarily φ and ψ can vary. The 1963 paper of G. N. Ramachandran plotted φ vs. ψ for most amino acids in known protein structures; the plot reveals dramatic clustering caused by steric clashes (Pauli repulsion between side chain, carbonyl, and amide atoms when the dihedrals approach forbidden values).

Table 63. Allowed backbone dihedral-angle regions in a Ramachandran plot.

Region	Approximate (φ , ψ)	Secondary structure
Right-handed α -helix	(-60° , -45°)	α -helix
Left-handed α -helix	($+60^{\circ}$, $+45^{\circ}$)	Rare; primarily Gly residues
β -sheet (parallel)	(-120° , $+120^{\circ}$)	Parallel β -sheet
β -sheet (antiparallel)	(-140° , $+135^{\circ}$)	Antiparallel β -sheet
Polyproline II 3_{10} -helix	(-75° , $+145^{\circ}$) (-49° , -26°)	Collagen, IDR motifs Tight helix at N/C-termini

Two amino acids escape the standard restrictions:

- Glycine has primarily an H atom for its side chain — no steric clash — and so populates the entire (φ , ψ) plane, including the disallowed regions used by left-handed helices.
- Proline’s side-chain ring fixes $\varphi \approx -65^{\circ}$, severely restricting backbone flexibility. Proline cannot occur in a regular α -helix beyond position 4 (no N–H proton available as H-bond donor) and is famous as a “helix breaker.”

Real proteins occupy the allowed regions about 98% of the time; deviations into “outlier” regions are validated indicators of either (a) genuine functional constraints (e.g., catalytic glycines in a strained conformation) or (b) modeling errors in low-resolution X-ray structures. Ramachandran statistics are now a standard quality metric for crystallographic and AlphaFold-predicted structures.

Concept Check 6: Why does Pro almost rarely occur in the middle of an α -helix, while Gly is over-represented in tight turns and loops? Frame your answer in terms of (φ , ψ) allowed regions on the Ramachandran plot.

3.4.4 Levels of Protein Structure

Primary structure: The amino acid sequence — the covalent backbone. Written conventionally from N-terminus to C-terminus. Primary structure is encoded by genes and determines most higher levels of structure (Anfinsen’s dogma).

Secondary structure: Local regular patterns of backbone H-bonds: - α -Helix: 3.6 residues/turn, rise 0.15 nm/residue, H-bond between residue i and $i + 4$. 100% right-handed in natural proteins. Helix dipole (N-terminus $\delta+$; C-terminus $\delta-$) affects function. Helix-breaking residues: Pro (kinks), Gly (too flexible). - β -Sheet: extended chains (strands) running parallel or antiparallel, H-bonded between adjacent strands. Most β -sheets are twisted. β -sheets are the structural basis of silk (fibroin) and amyloid fibrils. - 3_{10} -helix: tighter than α -helix (3 residues/turn), H-bond between i and $i + 3$. Less common; often found at helix termini. - Turns and loops: allow the polypeptide chain to reverse direction; typically on protein surface, often functionally important (e.g., CDR loops in antibodies).

Tertiary structure: The complete 3D fold, stabilized by: - Hydrophobic core packing (dominant driving force) - Disulfide bonds (Cys–S–S–Cys; formed in oxidising compartments like ER lumen) - Salt bridges (Asp/Glu with Lys/Arg) - H-bonds and van der Waals contacts

Common protein folds:

Table 64. Levels of Protein Structure: Fold and Description.

Fold	Description	Example
Globin fold	8 α -helices surrounding a haem pocket	Myoglobin, hemoglobin
TIM barrel	8 alternating $\beta\alpha$ units forming a barrel	Triosephosphate isomerase

Fold	Description	Example
β -barrel	β -sheets curved into a closed barrel	Porins, GFP
Immunoglobulin fold	Two β -sheets packed face-to-face	Antibodies, MHC
Leucine-rich repeat	Horseshoe of repeating units	Toll-like receptors

Quaternary structure: Assembly of two or more polypeptide chains (subunits). Examples: - Hemoglobin: $\alpha_2\beta_2$ tetramer; cooperative O₂ binding - Collagen: triple helix of three chains with Gly-X-Y repeats (X often Pro, Y often Hyp) - Immunoglobulin G: two heavy chains + two light chains; Y-shaped - Ribosome: RNA + >50 protein subunits

Protein denaturation: Disruption of secondary/tertiary/quaternary structure by heat, pH extremes, denaturants (urea, guanidinium), reducing agents (break disulfides). Primary structure intact; activity lost. Often irreversible (cooked egg white), but many small proteins refold spontaneously (Anfinsen’s experiment with ribonuclease A).

3.4.5 Thermodynamics of Protein Folding

Protein folding is governed by the same Gibbs equation that governs most spontaneous processes:

$$\Delta G_{\text{fold}} = \Delta H_{\text{fold}} - T \Delta S_{\text{fold}}$$

(72)

The total ΔG_{fold} for a typical small globular protein is primarily −20 to −60 kJ/mol — the difference between two enormous, partially cancelling terms.

Decomposing the folding free energy:

Table 65. Thermodynamics of Protein Folding: Contribution and Sign.

Contribution	Sign	Magnitude (typical)	Origin
Conformational entropy of backbone	$-T\Delta S < 0$ unfavorable	+500 to +1500 kJ/mol	Loss of φ/ψ freedom
Conformational entropy of side chains	unfavorable	+200 to +400 kJ/mol	Side chains lock in place
Hydrophobic effect	favorable	−300 to −1000 kJ/mol	Burial of nonpolar surface; entropy of water released
Backbone H-bonds	small	± 0 to −100 kJ/mol	Replace H-bonds to water with intramolecular ones
Van der Waals packing	favorable	−200 to −500 kJ/mol	Tight core packing
Disulfide bonds (if present)	favorable	−15 to −30 kJ/mol per S–S	Topology constraint
Net ΔG_{fold}	favorable, marginal	−20 to −60 kJ/mol	Sum of large opposing terms

The hydrophobic collapse model. The dominant driving force is the **hydrophobic effect** (see section 2) [Dill, 1990]. Folding occurs in two stages:

1. Hydrophobic collapse (microseconds): Water-exposed nonpolar side chains rapidly aggregate into a “molten globule” — a compact but loosely packed intermediate with most secondary structure formed but tertiary contacts not yet locked in.
2. Specific tertiary contact formation (milliseconds–seconds): Slow rearrangement to the unique native fold; backbone H-bonds and van der Waals packing optimize.

The marginal stability of folded proteins ($|\Delta G| \approx$ a few H-bonds’ worth) has profound consequences: small mutations can destabilise proteins enough to cause disease (e.g., a single Glu6->Val substitution causes sickle-cell hemoglobin to polymerize), and many proteins exist in a fragile balance with disordered or misfolded states.

Levinthal’s paradox and the folding funnel. A 100-residue chain with 3 backbone conformations per residue would have $3^{100} \approx 10^{47}$ possible conformations — searching them randomly at 10^{12} trials per second would take longer than the age of the universe, yet proteins fold in milliseconds. The resolution is the folding funnel: the energy landscape is biased so that energy and conformational entropy *both* decrease as the protein nears the native state. The chain rolls down the funnel via many parallel pathways rather than searching exhaustively. This conceptual breakthrough is now supported by molecular dynamics simulations and by structure-prediction systems. AlphaFold 3 extends the classroom question from “what fold does this protein adopt?” to “what complex does this protein form with DNA, RNA, ligands, ions, or modified residues?” It should be read as a powerful hypothesis generator whose confidence metrics and biochemical context still need experimental validation, especially for dynamics, alternative conformations, and low-confidence interfaces [Abramson et al., 2024].

Current evidence: AI structure models and molecular interaction claims. The AlphaFold Protein Structure Database update reported for the 2025 UniProt release improved the entry interface and structural interpretation of hundreds of millions of predicted protein models, while a 2026 EMBL-EBI/Google DeepMind/NVIDIA/SNU update began adding predicted protein complexes, starting with high-confidence homodimers [Bertoni et al., 2026, EMBL’s European Bioinformatics Institute, 2026]. For a biology student, the key habit is not “the computer solved the protein” but “the model proposes a testable molecular hypothesis.” A predicted active-site pocket, ligand pose, or interface should be checked against confidence metrics, conservation, mutagenesis, binding, kinetics, cryo-EM/X-ray/NMR evidence, and whether the biological state is static, dynamic, membrane-embedded, modified, or allosterically regulated.

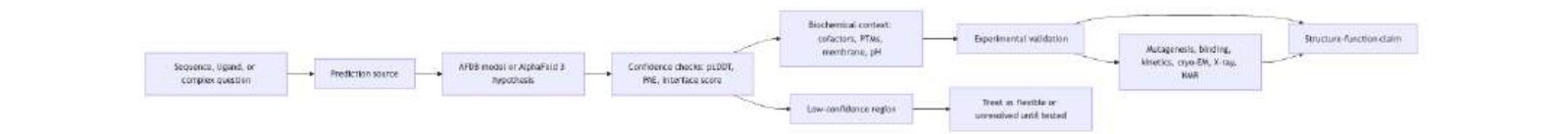


Figure 32. AI biomolecular modeling workflow. Predicted structures and complexes are evidence-generating tools; confidence metrics and independent assays determine whether a predicted contact supports a biological mechanism.

Concept Check (Evaluation): Intrinsically disordered proteins (IDPs) lack stable tertiary structure but are functionally critical — roughly 30% of human proteins are fully disordered, and 70% have disordered regions. (a) Using the hydrophobic effect and entropy arguments, explain why a protein rich in charged (Asp, Glu, Lys, Arg) and polar (Ser, Thr, Gln, Asn) residues would resist folding into a compact globule. (b) IDPs often form transient ordered structures when binding partners — propose the thermodynamic driving force for this “coupled folding and binding.” (c) Why might disorder confer an evolutionary advantage for hub proteins that interact with many partners?

Concept Check (Analysis): The amyloid fibril formed by the Alzheimer’s Aβ(1–42) peptide consists of antiparallel β-sheets stacked perpendicular to the fibril axis with ~ 4.7 angstrom inter-strand spacing and ~ 10 angstrom inter-sheet spacing. (a) Estimate the number of hydrogen bonds per meter of fibril if each strand contributes 2 backbone H-bonds and strands are 4.7 angstrom apart. (b) Why is amyloid kinetically trapped — why does a cell not simply unfold and refold the fibril? (c) Propose one molecular intervention (small molecule, antibody, or modified peptide) targeting fibril nucleation vs. one targeting fibril elongation, and explain the kinetic difference.

3.4.6 Intrinsically Disordered Proteins (IDPs)

A revolutionary modern discovery challenged the classical “structure = function” paradigm: approximately 30–50% of eukaryotic proteins contain intrinsically disordered regions (IDRs) — segments that do not adopt a fixed 3D structure under physiological conditions.

Properties of IDPs/IDRs: - Enriched in charged and polar residues (Lys, Arg, Glu, Ser, Pro, Gly); depleted in hydrophobic residues - Exist as dynamic ensembles of rapidly interconverting conformations - Often undergo coupled folding and binding — they fold upon interacting with their binding partner

Biological advantages of disorder: - Promiscuous binding: one IDR can bind multiple partners (hub proteins in signaling networks) - Large interaction surfaces: extended conformations provide large binding interfaces from a short sequence - Rapid binding kinetics: “fly-casting” mechanism allows faster association rates - Regulation by post-translational modification: many phosphorylation sites are in disordered regions

Examples: - p53 transactivation domain: disordered; folds into a helix upon binding MDM2 - Tau protein: intrinsically disordered; pathological aggregation into neurofibrillary tangles causes Alzheimer’s disease - Nucleoporin FG repeats: disordered regions form the permeability barrier of nuclear pores - α-Synuclein: disordered; aggregation into Lewy bodies is the hallmark of Parkinson’s disease

IDPs and biomolecular condensates — liquid–liquid phase separation (LLPS). A revolutionary insight of the 2010s: many cellular compartments have no membrane. The nucleolus, P-bodies, stress granules, the centrosome, heterochromatin domains, and synaptic puncta are biomolecular condensates formed by liquid–liquid phase separation. The driving force is multivalent, weak interactions between IDR-containing proteins and/or RNAs. Above a threshold concentration, the polymer-rich solution demixes into a dense droplet phase coexisting with a dilute phase, much like oil droplets in a vinaigrette.

Key features of LLPS-driven condensates: - Multivalency (multiple weak interaction modules) is required; single-site interactions give simple complexes, not phases. - Aromatic (π–π) and electrostatic (+/–) interactions between IDR residues (especially Arg, Tyr, Phe, Glu, Asp) drive demixing. - Functional consequence:

condensates concentrate biochemical reactants about 100-fold above bulk cytosol, dramatically accelerating reactions. - Disease link: ALS-causing mutations in FUS and TDP-43 transition liquid condensates into solid amyloid-like aggregates (the “liquid-to-solid” transition). Understanding LLPS is now central to neurodegeneration research.

This discovery transformed cell biology: the nucleus is not a uniform compartment but a phase-organized mosaic of dozens of distinct liquid bodies, each enriching specific molecules without membranes to maintain identity.

Clinical Connection: Amyloid Diseases and Protein Misfolding

When normally soluble proteins or IDPs misfold and aggregate into ordered, cross-β amyloid fibrils, the result can be devastating disease. Alzheimer’s disease involves amyloid-β plaques and tau tangles; Parkinson’s involves α-synuclein Lewy bodies; prion diseases (CJD, mad cow disease) involve PrP^{Sc} amyloid. Type 2 diabetes involves islet amyloid polypeptide (IAPP/amylin) deposits in pancreatic islets. Understanding protein misfolding is one of the grand challenges of molecular medicine.

Concept Check 4: If a protein with an intrinsically disordered region can bind multiple different partner proteins, what advantage does this provide to **signal transduction** networks? What are the risks?

3.4.7 Post-Translational Modifications (PTMs)

A typical eukaryotic protein is modified by a “code” of covalent chemistry layered on top of the genetic sequence. Over 400 distinct PTMs are now catalogued; the major ones are summarized below.

Table 66. Post-Translational Modifications (PTMs): PTM and Adding enzyme.				
PTM	Adding enzyme	Removing enzyme	Target residue(s)	Functional role
Phosphorylation	Kinases (518 in human)	Phosphatases	Ser, Thr, Tyr (rare on His)	Reversible “switch”; signaling, enzyme activity
Acetylation	Acetyltransferases (HATs, GCN5)	Deacetylases (HDACs, sirtuins)	Lys ε-NH ₂ , N-terminus	Chromatin opening (histones); metabolic regulation
Methylation	Methyltransferases (SET domain, PRMT)	Demethylases (KDMs, LSD1)	Lys, Arg, His; DNA at C5 of cytosine	Gene silencing/activation; epigenetic memory
Ubiquitination	E1, E2->E3 cascade	DUBs (deubiquitinases)	Lys ε-NH ₂	Protein turnover (proteasome); signaling (K63 chains)
SUMOylation	SUMO E1, E2, E3	SENPs	Lys (often in ΨKX(D/E) motif)	Nuclear transport; transcription; DNA repair
Glycosylation	Glycosyltransferases	Glycosidases	Asn (N-linked); Ser/Thr (O-linked); Trp (C-mannose)	Protein folding, half-life, recognition
O-GlcNAc	OGT	OGA	Ser, Thr (cytosolic/nuclear)	Reciprocal cross-talk with phosphorylation; nutrient sensing
Hydroxylation	Prolyl/lysyl hydroxylases	— (irreversible)	Pro, Lys (collagen, HIF-1α)	Collagen stability; oxygen sensing
Lipidation	NMTs, palmitoyltransferases	Acyl-protein thioesterases	N-terminal Gly (myristate); Cys (palmitate, prenyl)	Membrane targeting
ADP-ribosylation	PARPs	PARGs, ARH3	Glu, Asp, Arg	DNA damage signaling
Disulfide	PDI in ER	Reductants	Cys pairs	Structural; secreted protein stability
Proteolytic cleavage	Proteases	(irreversible)	Specific peptide bonds	Activation (zymogens); destruction; signal release

Phosphorylation is the most-studied PTM: about 30% of human proteins are phosphorylated on at least one residue at some point in their life cycle, controlled by 518 kinases and about 150 phosphatases. A single phosphate group adds two negative charges and about 30 kJ/mol of binding energy with phospho-recognition domains (SH2, 14-3-3, FHA), enabling switch-like regulation of activity, localization, or partnerships. Histone PTMs (acetylation of Lys, methylation of Lys/Arg,

phosphorylation of Ser/Thr) write the “histone code” that organizes chromatin into transcriptionally active and silent states (see [Unit IV — Molecular Genetics: Introduction](#)).

Ubiquitin is itself a small (76-residue) protein that is covalently attached to other proteins, usually through an isopeptide bond between its C-terminal Gly76 and a Lys ϵ -NH₂ on the substrate. Polyubiquitin chains can grow on any of ubiquitin’s seven Lys residues (or its own N-terminus), creating different chain topologies with different fates: K48 chains target proteins for proteasomal destruction; K63 chains regulate signaling and DNA repair; M1 (linear) chains regulate NF- κ B inflammation. The 2004 Nobel Prize in Chemistry recognized Aaron Ciechanover, Avram Hershko, and Irwin Rose for discovering this regulated proteolysis system.

Concept Check 8: Phosphorylation of a Ser residue adds two negative charges and about 80 Da of mass — a tiny chemical change. Yet kinase signaling cascades transmit information through millions of phosphorylation events per second across thousands of substrates. Identify two structural features of phosphate (charge, geometry, H-bond capacity) that make it an ideal “switch” molecule for biology, and contrast with why methylation (a smaller, neutral modification) is used for slower, longer-lived regulation.

3.5 Nucleic Acids as Information Polymers

3.5.1 Nucleotide Monomers and Phosphodiester Linkages

Each **nucleotide** consists of: 1. A pentose sugar (ribose in RNA; 2'-deoxyribose in DNA) 2. A nitrogenous base (purine or pyrimidine) 3. One to three phosphate groups

Bases: - Purines (two-ring): Adenine (A), Guanine (G) - Pyrimidines (one-ring): Cytosine (C), Thymine (T; DNA primarily), Uracil (U; RNA primarily)

The nucleoside is base + sugar. The nucleotide is nucleoside + phosphate(s).

Phosphodiester bond: Nucleotides are linked 3'->5' by phosphodiester bonds, forming the sugar-phosphate backbone. This backbone is highly uniform and carries a negative charge at every phosphate (one negative charge per nucleotide at physiological pH).

3.5.2 DNA Structure, Base Pairing, and Helical Geometry

DNA (deoxyribonucleic acid) is a double-stranded helix discovered by Watson and Crick in 1953, guided by X-ray diffraction data from Franklin and Wilkins and Chargaff’s rules:

- Chargaff’s rules: **A = T**; **G = C** in any double-stranded DNA
- Complementary base pairs: A–T (2 **hydrogen bonds**) and G–C (3 hydrogen bonds)
- Antiparallel strands: one runs 5'->3', its complement runs 3'->5'

Structural forms of DNA:

Table 67. DNA Structure, Base Pairing, and Helical Geometry: Feature and A-form.

Feature	A-form	B-form	Z-form
Helix direction	Right-handed	Right-handed	Left-handed
Base pairs/turn	11	10.5	12
Rise per bp	0.26 nm	0.34 nm	0.37 nm
Helix diameter	2.3 nm	2.0 nm	1.8 nm
Groove pattern	Deep narrow major, wide shallow minor	Wide major, narrow minor	Flat major, narrow deep minor
Conditions	Dehydrated, RNA-DNA hybrids	Physiological	High salt, alternating purine-pyrimidine
Biological role	dsRNA, RNA-DNA hybrids	Primary cellular form	Gene regulation (CpG islands?)

The B-form is the biologically dominant form at physiological ionic strength: - Right-handed helix; 10.5 base pairs/turn; rise 0.34 nm/bp; pitch \approx 3.6 nm; diameter 2.0 nm - Major groove (wide, about 1.2 nm) and minor groove (about 0.6 nm) — proteins bind these grooves

Base stacking: Beyond hydrogen bonding between complementary bases, the flat aromatic rings of adjacent bases stack on top of each other via π - π interactions and **van der Waals forces**. These stacking interactions contribute more to duplex stability than hydrogen bonding. This is why DNA melting temperature (T_m) increases with GC content (three H-bonds + stronger stacking) and with ionic strength (cations neutralize backbone charges).

Quantitative base-stacking energies. Nearest-neighbor stacking energies (the contribution of each adjacent base-pair *step*, not each individual base) have been calibrated from melting curves and computational chemistry:

Table 68. DNA base-stacking enthalpy for selected nearest-neighbor steps.

Step (5'->3' top strand)	Stacking ΔH (kJ/mol)	Stacking ΔS (J mol ⁻¹ K ⁻¹)	ΔG at 37 °C (kJ/mol)
AA / TT	-33.1	-92.9	-4.3
AT / AT	-30.1	-85.4	-3.6
TA / TA	-30.1	-89.1	-2.4
CA / GT	-35.6	-95.0	-6.2
GT / CA	-35.1	-93.7	-6.1
CT / GA	-32.6	-87.9	-5.4
GA / CT	-34.3	-92.9	-5.5
CG / CG	-44.4	-113.8	-9.1
GC / GC	-41.0	-102.1	-9.4
GG / CC	-33.5	-83.3	-7.7

Notice that GC steps have the strongest stacking (and therefore highest melting temperature) — this is why GC-rich regions (CpG islands, gene promoters) require greater thermal energy to denature, and why PCR primers are usually designed to be about 50% GC. The total free energy of a duplex is summed over most $n - 1$ stacking steps in an n -base-pair duplex, plus initiation/end corrections; this nearest-neighbor model (Santa Lucia, 1998) predicts T_m values within about 2 °C of measurement and is the basis of every PCR primer design tool.

A-, B-, and Z-DNA in detail. The three structural forms differ in geometry and biological occurrence:

- B-form DNA (the canonical Watson-Crick form): right-handed, 10.5 bp/turn, helical rise 0.34 nm, diameter 2.0 nm; major groove 1.2 nm wide and 0.85 nm deep; minor groove 0.6 nm wide and 0.75 nm deep. Adopted under physiological hydration. The wide, deep major groove is the principal site of sequence-specific protein binding (most transcription factors read here).
- A-form (right-handed, more compact): 11 bp/turn, rise 0.26 nm, diameter 2.3 nm; deep, narrow major groove and shallow, broad minor groove. Adopted by RNA-DNA hybrids (e.g., during transcription) and by double-stranded RNA. Forced by the 2'-OH of ribose, which sterically excludes B-geometry. The A-form transition during transcription is essential for RNA polymerase to thread its product.
- Z-form (left-handed): 12 bp/turn, rise 0.37 nm, diameter 1.8 nm; zigzag backbone (hence “Z”); flat major groove with no protein-binding pocket; narrow, deep minor groove. Adopted by sequences with alternating purine–pyrimidine patterns ((CG)_{*n*} being the canonical case) under high ionic strength or negative supercoiling. Z-DNA-binding proteins (ADAR1, ZBP1) play roles in innate immunity and CpG island regulation.

The conformational equilibrium $B \rightleftharpoons Z$ is sensitive to negative supercoiling generated behind a transcribing RNA polymerase; transient Z-DNA tracts have been observed at active promoters and are believed to participate in transcription regulation.

Human **genome**: 3.2×10^9 base pairs; if laid end-to-end, 2.2 m long but compressed into 6 μ m nucleus via **nucleosome** packaging (DNA wound around **histone** octamers in 147 bp segments).

3.5.3 Worked Example: DNA Melting Temperature from %GC

Problem: A laboratory amplifies a 100-bp segment of a CpG island whose G+C content is 50%, in a buffer of $[Na^+] = 50$ mM. Using the length-corrected empirical relation

$$T_m = 81.5 + 0.41 (\%GC) - \frac{675}{N}$$

estimate the melting temperature T_m . Then repeat for a GC-rich variant of the same length with $\%GC = 70$, and interpret the difference.

Solution:

1. Substitute the 50%-GC duplex (%GC = 50, $N = 100$, $[Na^+] = 50$ mM):

$$T_m = 81.5 + 0.41 \times 50 - \frac{675}{100} = 81.5 + 20.5 - 6.75$$

$$T_m = 95.25\text{ }^{\circ}\text{C}$$

2. Substitute the 70%-GC duplex (same $N = 100$, same $[Na^+]$):

$$T_m = 81.5 + 0.41 \times 70 - \frac{675}{100} = 81.5 + 28.7 - 6.75 = 103.45\text{ }^{\circ}\text{C}$$

The 20-percentage-point rise in G+C raises T_m by $103.45 - 95.25 = 8.20\text{ }^{\circ}\text{C}$.

Because every G–C pair contributes three hydrogen bonds and stronger base-stacking than an A–T pair, a more GC-rich duplex of the same length resists thermal denaturation more strongly — which is why GC-rich promoters and CpG islands melt last, and why PCR primers are designed around predictable T_m values.

3.5.4 RNA Structure and Diversity

RNA is single-stranded and uses uracil instead of thymine. The 2'-OH on ribose makes RNA more chemically labile than DNA (susceptible to base-catalysed hydrolysis: the 2'-OH attacks the adjacent phosphate, cleaving the backbone). This is why RNA's evolutionary niche is short-lived information (mRNA, miRNA, sRNAs) while the longer-term archive is DNA.

RNA folds on itself via intramolecular base pairing, forming complex secondary and tertiary structures. Unlike DNA's relatively uniform B-form duplex, RNA structure is wildly diverse — ribozymes, tRNAs, and ribosomal RNAs adopt 3D shapes as elaborate as folded proteins, often with deep clefts and pockets that are functional active sites.

RNA secondary structure elements:

Table 69. RNA Structure and Diversity: Element and Description.

Element	Description	Function
Stem-loop (hairpin)	Complementary bases form a stem; unpaired bases form a loop	Most common motif; regulatory elements
Internal loop	Mismatched bases within a stem	Protein binding sites
Bulge	Unpaired nucleotides on one strand of a stem	Flexibility, protein recognition
Pseudoknot	Loop base-pairs with downstream sequence	Ribosome frameshifting, telomerase
G-quadruplex	Four guanines form a planar quartet via Hoogsteen H-bonds	Telomeres, oncogene regulation
Kissing loop	Two hairpin loops interact via complementary sequences	Viral RNA dimerization

Pseudoknots illustrate the topological complexity unique to RNA. After a hairpin loop forms, *unpaired* loop bases pair with a complementary sequence located *downstream*, creating a second helix that threads through the first. The HIV-1 frameshift element is a pseudoknot that pauses the ribosome, forcing a –1 frameshift to translate the *gag-pol* polyprotein. Telomerase contains a pseudoknot in its RNA template that is essential for catalysis; mutations in this pseudoknot cause dyskeratosis congenita (a hereditary bone-marrow failure syndrome).

RNA secondary structure prediction. Whether a given RNA sequence will adopt a particular fold can be predicted computationally using thermodynamic models. The free energy of a fold is the sum of nearest-neighbor stacking energies (similar to the DNA table above) minus penalties for loops, bulges, and unpaired regions. The Zuker algorithm finds the minimum-free-energy structure in $O(n^3)$ time for a sequence of length n . Modern tools (RNAfold, ViennaRNA, NUPACK) extend this to ensembles of suboptimal structures, base-pairing probabilities, and pseudoknot prediction. Predicted folds are now routinely used to design siRNAs, mRNA vaccines (e.g., the Pfizer/Moderna COVID-19 mRNAs were sequence-optimized to favor stable secondary structures and avoid immunogenic motifs), and guide RNAs for CRISPR systems.

Ribozymes revisited — 3D structure shapes catalysis. The hammerhead ribozyme (about 40 nt, the smallest known) folds into three coaxially stacked helices that position a 2'-OH for nucleophilic attack on the adjacent phosphodiester, cleaving the backbone via an in-line mechanism. The hepatitis delta ribozyme uses a cytosine as a general acid catalyst with shifted pKa — demonstrating that RNA bases can perform acid-base chemistry analogous to enzyme side chains.

RNA types and functions:

Table 70. RNA Structure and Diversity: RNA type and Abbreviation.

RNA type	Abbreviation	Function
Messenger RNA	mRNA	Carries protein-coding sequence
Transfer RNA	tRNA	Carrier of amino acids to ribosome
Ribosomal RNA	rRNA	Structural/catalytic core of ribosome
Small nuclear RNA	snRNA	Pre-mRNA splicing (spliceosome)
MicroRNA	miRNA	Post-transcriptional gene silencing
Long non-coding RNA	lncRNA	Chromatin regulation, imprinting
Small interfering RNA	siRNA	RNA interference (gene silencing)
CRISPR RNA	crRNA	Guide for Cas nuclease (adaptive immunity)
Piwi-interacting RNA	piRNA	Transposon silencing in germ cells

3.5.5 Ribozymes: Catalytic RNA

The ribozymes — catalytically active RNAs — demonstrate that RNA was likely the primordial molecule of life in the RNA World hypothesis.

Discovery: In 1982, Thomas Cech discovered that the Group I **intron** of *Tetrahymena* rRNA catalyses its own excision (self-splicing) without any protein enzyme. Shortly after, Sidney Altman showed that the RNA component of RNase P catalyses tRNA maturation. Both received the 1989 Nobel Prize in Chemistry for demonstrating RNA catalysis.

Known ribozymes:

Table 71. Ribozymes: Catalytic RNA: Ribozyme and Reaction.

Ribozyme	Reaction	Significance
Group I intron	Phosphoester transfer (self-splicing)	First discovered ribozyme
Group II intron	Self-splicing (lariat intermediate)	Ancestor of spliceosome
RNase P	Endonuclease (tRNA 5'-end processing)	Essential in most domains of life
Hammerhead ribozyme	Self-cleavage (phosphodiester)	Smallest known ribozyme (about 40 nt)
Hepatitis delta ribozyme	Self-cleavage	Viral replication
Ribosome (23S rRNA)	Peptidyl transfer	The ribosome is a ribozyme!

The discovery that the ribosome’s peptidyl transferase activity resides in rRNA (not ribosomal proteins) was arguably the most important confirmation of the RNA World hypothesis. Thomas Steitz, Venkatraman Ramakrishnan, and Ada Yonath shared the 2009 Nobel Prize in Chemistry for elucidating ribosome structure at atomic resolution.

Clinical Connection: Ribozyme-Based Therapeutics

Engineered ribozymes (e.g., hammerhead ribozymes targeting specific mRNAs) have been explored as gene therapy tools. More practically, riboswitches — RNA elements that bind small molecules and regulate gene expression — are promising antibiotic targets. Because riboswitches are found in bacteria but not humans, drugs that interfere with riboswitch function could selectively kill pathogens. The antibiotic roseoflavin targets the FMN riboswitch in Gram-positive bacteria.

Concept Check 5: The RNA World hypothesis proposes that RNA preceded both DNA and proteins as the primordial macromolecule of life. What three properties must RNA possess to fulfil this role, and does RNA actually possess the full set?

3.6 Key Comparisons Among Macromolecule Classes

3.6.1 The Four Macromolecule Classes Compared

Table 72. The Four Macromolecule Classes Compared: Feature and Carbohydrates.

Feature	Carbohydrates	Lipids	Proteins	Nucleic Acids
Monomer	Monosaccharide	Fatty acid / isoprene	Amino acid	Nucleotide
Bond	Glycosidic	Ester / noncovalent	Peptide	Phosphodiester
Elements	C, H, O	C, H, O (+ P, N)	C, H, O, N, S	C, H, O, N, P
Energy (kcal/g)	4	9	4	—
Informational?	Somewhat (glycan code)	No	Partially (sequence)	Yes (genetic code)
Typical size	1–10 ⁶ residues	14–24C chains	50–30,000 residues	70–10 ⁹ nt
Water solubility	Most soluble	Insoluble	Variable	Soluble (highly charged)

3.6.2 Storage vs. Structural Polysaccharides

Table 73. Storage vs. Structural Polysaccharides: Feature and Starch/Glycogen (Storage).

Feature	Starch/Glycogen (Storage)	Cellulose/Chitin (Structural)
Bond type	α -glycosidic	β -glycosidic
Chain conformation	Helical (amylose) or branched	Extended, straight chains
Inter-chain interactions	Weak	Strong H-bonds between chains
Digestibility (humans)	Yes (α -amylase)	No (no β -glucosidase)
Physical properties	Granular, amorphous	Fibrous, high tensile strength

3.7 Computational Bridge

Base composition of nucleic acids feeds directly into melting temperature and PCR design. The genetics module exposes a simple GC fraction:

```
from biology.genetics import gc_content

seq = "ATGCGCGCATAA"
print(round(gc_content(seq), 3)) # 0.583
```

Clinical / systems note: Antisense oligonucleotide and siRNA therapies rely on predictable hybridization thermodynamics (GC content, length, salt) to avoid off-target binding while silencing disease alleles — the same sequence statistics you summarize with *G+C* fraction.

3.8 Current Evidence and Frontier Biology: Biological Macromolecules

For Biological Macromolecules, frontier biology belongs inside the evidence logic of the chapter. Chemistry-of-life claims now connect classical bonding and thermodynamics with AI-guided structure prediction and experimental validation. The core reading question is this: macromolecule explanations should connect sequence, structure, dynamics, modification, interaction, and assay evidence.

- What to verify: identify the observation, model, assay, or dataset that would make the claim stronger or weaker.
- What to qualify: state the scale, organism, cell type, environmental condition, or population where the claim is expected to hold.
- What to compare: test at least one alternative explanation, baseline, or null model before treating the pattern as causal.
- What to cite: distinguish primary evidence, review synthesis, public dataset, and institutional guidance; for recent or numeric claims, prefer the source closest to the measurement and state what has changed since it was published.

Use AI biomolecular models as hypotheses about folding, contact, or complex formation; compare confidence, conservation, solvent exposure, and assay evidence before treating them as structure [Abramson et al., 2024].

Protein evidence now has a provenance stack. UniProt stabilizes protein names, accessions, isoforms, sequence features, and curated functional annotations; the wwPDB archive and PDB entry pages connect atomic coordinates to deposition metadata, methods, ligands, and validation reports; EMDB supplies the density-map layer for cryo-EM structures. A defensible macromolecule claim should name the UniProt accession, PDB identifier or EMDB map when available, and whether the structural support is experimental, predicted, or an experimentally constrained model [UniProt Consortium, 2025, Worldwide Protein Data Bank, 2026, Protein Data Bank in Europe, 2026, Electron Microscopy Data Bank, 2026].

Source practice: For macromolecular structure claims, prefer experimental structures when available and validate predictions with confidence metrics, conservation, mutagenesis, binding, or cryo-EM/X-ray/NMR evidence [Abramson et al., 2024, Bertoni et al., 2026, EMBL’s European Bioinformatics Institute, 2026].

3.8.1 Current Evidence Map: AI Structure Claims Need Validation

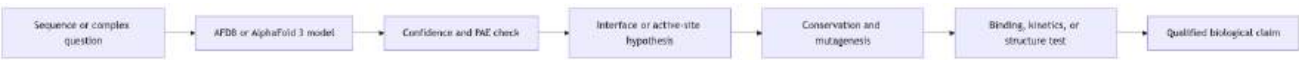


Figure 33. AI structure models are strongest when confidence, interface geometry, conservation, mutagenesis, and experimental assays converge rather than when a model is treated as final evidence \citep{abramson2024alphafold3,velankar2026alphafolddb2025,emlebi2026alphafoldcomplexes}.

3.9 Summary

- The four biological macromolecule classes (carbohydrates, lipids, proteins, nucleic acids) perform most structural and functional roles in living systems.
- Carbohydrates are linked by glycosidic bonds; proteins by peptide bonds; nucleic acids by phosphodiester bonds. Most built/broken by condensation/hydrolysis.
- Carbohydrate digestion proceeds from mouth (salivary amylase) through intestine (pancreatic amylase + brush border enzymes); cellulose passes undigested to the colon.
- Lipids are diverse: glycerophospholipids and sphingolipids form membranes; triacylglycerols store energy; sterols regulate membranes and serve as hormone precursors; eicosanoids mediate inflammation.
- Protein structure has four hierarchical levels; function depends on 3D structure, which is lost upon denaturation. Intrinsically disordered proteins challenge the classical structure-function paradigm.
- DNA exists in A, B, and Z forms; B-form dominates under physiological conditions. RNA forms complex secondary structures including pseudoknots and G-quadruplexes.
- DNA’s double helix uses complementary A–T and G–C pairing; this complementarity is the structural basis of heredity and information transfer.
- Ribozymes (catalytic RNAs) demonstrate RNA’s dual role as information carrier and catalyst, supporting the RNA World hypothesis. The ribosome itself is a ribozyme.
- Connections: See section 12 and section 13 for replication, transcription, and translation; section 17 for segregation of alleles; and section 4 for enzymes that polymerize and hydrolyse these macromolecules.

3.10 Key Terms

- Condensation reaction: Joining of monomers with loss of water
- Hydrolysis: Cleavage of a bond by addition of water
- Glycosidic bond: Covalent bond between monosaccharides
- Anomer: Stereoisomers differing at the anomeric carbon (α vs. β)
- Glycoprotein: Protein with covalently attached oligosaccharide chains
- Proteoglycan: Protein with long glycosaminoglycan chains
- Amphipathic: Having both hydrophilic and hydrophobic regions
- Sphingolipid: Lipid built on a sphingosine backbone
- Eicosanoid: Signaling lipid derived from arachidonic acid
- Peptide bond: Amide bond between amino acids; partial double-bond character
- Ramachandran plot: Map of allowed backbone dihedral angles φ and ψ
- Denaturing: Loss of higher-order protein structure
- Intrinsically disordered protein (IDP): Protein lacking fixed tertiary structure
- Amyloid fibril: Ordered cross- β aggregate of misfolded protein
- Chargaff’s rules: $A = T$ and $G = C$ in double-stranded DNA

- Base stacking: π - π interactions between adjacent bases in nucleic acids
- Ribozyme: Catalytic RNA molecule
- RNA World: Hypothesis that RNA preceded DNA and proteins in early life
- Pseudoknot: RNA structure where loop bases pair with downstream sequence

3.11 Review Questions

1. Draw the condensation reaction between two glucose molecules to form maltose. Label the glycosidic bond and identify whether it is α or β .
2. Explain why cellulose is indigestible by humans but starch is not, despite both being polymers of glucose.
3. A patient with suspected lactose intolerance undergoes a hydrogen breath test. Explain the biochemical basis of this test.
4. Compare the membrane structures formed by glycerophospholipids and sphingolipids. Why is sphingomyelin particularly abundant in the myelin sheath?
5. A protein biochemist denatures ribonuclease A with urea and β -mercaptoethanol, then slowly removes both denaturants. The enzyme regains full activity. What does this tell us about the information needed for protein folding?
6. Explain why G-C rich DNA has a higher melting temperature than A-T rich DNA. Include both hydrogen bonding and base stacking in your answer.
7. Compare the structural features of B-form and Z-form DNA. Under what conditions might Z-DNA form, and what biological significance might it have?
8. The ribosome is often called a “ribozyme.” What evidence supports this claim, and what are its implications for the RNA World hypothesis?
9. Intrinsically disordered proteins defy the classical structure-function paradigm. Describe two biological advantages of protein disorder and give a clinical example of disease caused by IDP aggregation.
10. A nutritionist claims that “a calorie from fat is more energy-dense than a calorie from carbohydrate.” Explain the biochemical basis for the statement that fats provide 9 kcal/g vs. 4 kcal/g for carbohydrates, considering the oxidation states of carbon.
11. For a 24 bp primer with $gc_content = 0.50$, explain why raising annealing temperature in PCR reduces off-target amplification. How would raising GC to 0.75 change your T_m estimate qualitatively?
12. Compare one way lipids and proteins each contribute to membrane curvature generation during vesicular trafficking. Tie your answer to amphipathic molecular architecture.
13. Use equation (72) and the table of folding contributions to estimate the change in ΔG_{fold} when a single buried Ile (about 140 \AA^2 of nonpolar surface) is mutated to Ala (about 70 \AA^2). Take $0.10 \text{ kJ mol}^{-1} \text{ \AA}^{-2}$ as the cost of exposing nonpolar surface. Predict whether the mutant will be folded at body temperature.
14. Sketch a Ramachandran plot showing the two main allowed regions (α and β) for a non-Gly, non-Pro residue. Mark where collagen’s polyproline-II helix appears and explain why α -helix is forbidden after a proline.
15. Two sequences of equal length differ in GC content: 30% vs. 70%. Using the nearest-neighbor stacking table above, predict which has the higher melting temperature and estimate the difference in ΔG (37°C) per 10 base-pair stretch.
16. Liquid-liquid phase separation forms the nucleolus, P-bodies, and stress granules. Explain why multivalent weak interactions are essential and why a protein with a single high-affinity binding site for its partner does not phase separate.
17. List three reasons why cells use post-translational modifications (PTMs) rather than relying solely on transcription/translation to regulate protein activity. Include time scales, energetic cost, and reversibility in your answer.

3.12 Further Reading and Source Notes: Biological Macromolecules

- Pauling, Corey & Branson (1951). The structure of proteins: Two hydrogen-bonded helical configurations of the polypeptide chain. *Proceedings of the National Academy of Sciences*, 37.
- Anfinsen (1973). Principles that govern the folding of protein chains. *Science*, 181.
- Watson & Crick (1953). Molecular structure of nucleic acids: A structure for deoxyribose nucleic acid. *Nature*, 171.
- Kornberg (1974). *Chromatin Structure: A Repeating Unit of Histones and DNA*. *Science*, 184.
- Fischer (1894). Einfluss der Configuration auf die Wirkung der Enzyme. *Berichte der deutschen chemischen Gesellschaft*, 27.
- Lehninger, Nelson & Cox (latest ed.). *Lehninger Principles of Biochemistry* (chapters on carbohydrates, lipids, proteins, and nucleotides). W. H. Freeman.
- Banani, Lee, Hyman & Rosen (2017). Biomolecular condensates: Organizers of cellular biochemistry. *Nature Reviews Molecular Cell Biology*, 18.

3.13 Companion Source Module: Biological Macromolecules

Biological Macromolecules should leave a reproducible trail from a biological claim to the code, figure, diagram, or paper-based activity that can test it. Use the surfaces below to inspect the chapter’s assumptions, rerun the relevant model, or compare the manuscript explanation with companion labs and figures.

Table 74. Companion source surfaces for Biological Macromolecules.

Surface	Use it for
<code>src/biology/biochemistry/biochemistry.py</code> (<code>reaction_free_energy</code> , <code>glycolysis_summary</code>)	Relate polymer chemistry and hydrolysis to energy flow.
<code>src/biology/genetics/genetics.py</code> (<code>dna_complement</code> , <code>transcribe_dna_to_mrna</code> , <code>translate_mrna</code>)	Connect nucleic-acid structure to information transfer.
<code>src/mermaid/biology_diagrams.py</code> (<code>macromolecule_classification_diagram</code> , <code>transcription_translation_diagram</code>)	Compare classification diagrams with sequence-to-function pathways.

Reproducibility check: separate sequence, three-dimensional structure, modification state, and assay evidence before claiming function. Cross-reference: use this bridge with [section 4](#), [section 13](#), and [section 14](#).

4 Enzymes and the Kinetics of Catalysis

Level 3/3 · 60 min read · 75 min lecture · Prerequisites: section 3

4.1 Learning Objectives

1. Describe how **enzymes** lower activation energy without changing the **thermodynamics** of a reaction.
2. Derive and interpret the Michaelis-Menten equation (equation (79)) and its kinetic parameters using the steady-state assumption.
3. Explain competitive, uncompetitive, mixed, and irreversible inhibition with mathematical descriptions and clinical examples.
4. Describe **allosteric** regulation and cooperativity using the Hill equation, with ATCase as a model system.
5. Explain how **pH**, temperature, and cofactors modulate enzyme activity.
6. Classify enzymes using the EC numbering system, including the seventh class (translocases).
7. Describe modern applications of enzymes in medicine and industry.

4.1.1 Study Blueprint

- Big idea: Enzymes accelerate reactions by stabilizing transition states without changing thermodynamic endpoints.
- Core concepts: activation energy, Michaelis-Menten kinetics, inhibition, allostery.
- Framework alignment: Vision & Change: Structure and function, Pathways and transformations of energy and matter; AP Biology: Energetics, Systems Interactions; NGSS-style topics: Matter and Energy in Organisms and Ecosystems, Structure and Function.
- Model or quantitative lens: Michaelis-Menten, Lineweaver-Burk, and inhibition-pattern calculations.
- Data skill: Fit or interpret enzyme-rate data and identify which parameter changed.
- Practice cadence: Concept Explanation, Statistical Tests and Data Analysis, Argumentation.
- Common misconception to repair: A catalyst changes rate, not the equilibrium constant or the sign of delta G.
- Primary lab: **Lab — Enzymes and the Kinetics of Catalysis**.
- Question bank: **Questions — Enzymes and the Kinetics of Catalysis**.
- Transfer task: Apply enzyme-kinetic reasoning to drug dosing, metabolic control, or diagnostic assays.
- Bridge to computation: `biology.biochemistry.biochemistry.michaelis_menten`.

Opening Vignette: The Enzyme That Beats Geological Time

Without the enzyme OMP decarboxylase, the spontaneous decarboxylation of orotidine 5'-monophosphate (OMP) would take approximately 78 million years at body temperature — longer than the entire duration of dinosaur dominance of land vertebrates. OMP decarboxylase accomplishes the same reaction in 25 milliseconds. That is a rate enhancement of approximately 10^{23} -fold — the largest known for any enzyme (Radzicka & Wolfenden, 1995, *Science*).

The mechanism is not conventional. OMP decarboxylase uses no metal ions, no cofactors, and performs general acid-base catalysis primarily through electrostatic destabilization of the substrate's ground state rather than direct stabilization of the transition state. Understanding how it achieves such a feat challenged enzymologists for decades and continues to inform the design of enzyme inhibitors as antifungal and antiprotazoal drugs. OMP decarboxylase is the essential enzyme in the pyrimidine biosynthesis pathway — block it, and pathogens cannot make the **nucleotides** they need to replicate.

Primary source: Radzicka, A. & Wolfenden, R. (1995). A proficient enzyme. Science, 267(5194), 90–93.

A catalyst accelerates a chemical reaction without being consumed and without altering the reaction equilibrium. Enzymes are biological catalysts — almost typically **proteins** (a few are ribozymes; see section 3) — that accelerate reaction rates by factors of 10^6 – 10^{23} compared with uncatalysed reaction rates.

The free energy change of a reaction (ΔG) dictates whether a reaction is thermodynamically spontaneous ($\Delta G < 0$) or non-spontaneous ($\Delta G > 0$). Enzymes do not alter ΔG — they alter the kinetics by providing an alternative mechanism with a lower activation energy (ΔG^\ddagger).

Remarkable rate enhancements:

Table 75. Study Blueprint: Enzyme and Uncatalysed $t_{1/2}$.

Enzyme	Uncatalysed $t_{1/2}$	Catalysed $t_{1/2}$	Rate Enhancement
OMP decarboxylase	78 million years	25 ms	10^{23}
Staphylococcal nuclease	130,000 years	about 1 ms	10^{17}
Alkaline phosphatase	7 years	about 1 ms	10^{11}
Carbonic anhydrase	5 seconds	about 1 μ s	10^7
Chorismate mutase	7.4 hours	about 1 ms	10^7

OMP decarboxylase achieves the largest known rate enhancement: without this enzyme, the spontaneous decarboxylation of orotidine 5'-monophosphate would take 78 million years — longer than the age of the dinosaurs.

4.1.2 Transition State Theory

Every reaction proceeds through a transition state (TS) — a transient, high-energy configuration that cannot be isolated. The activation energy (E_a or ΔG^\ddagger) is the energy required to reach this state from the ground state:

Rate = $A \cdot e^{-\Delta G^\ddagger/RT}$

(73)

where A is the pre-exponential factor. Lowering ΔG^\ddagger by just 17 kJ/mol increases the rate by $e^7 \approx 1,000$ -fold. Lowering it by 34 kJ/mol gives a million-fold increase.

How enzymes lower ΔG^\ddagger :

1. Proximity and orientation: Substrates are brought together in optimal geometry at the active site, with the entropic cost already paid during binding. Effective concentration of reactants in the active site can exceed 10^8 M.
2. Transition state stabilization: The enzyme active site binds the transition state *more tightly* than either substrate or product (complementarity to TS, not substrate). This is the single most important mechanism.
3. General acid-base catalysis: Amino acid side chains (His, Asp, Glu, Lys) donate/accept protons simultaneously with bond breaking/forming, stabilizing developing charges in the TS.
4. Covalent catalysis: Transient covalent enzyme-substrate intermediates (Ser proteases, Cys proteases, Lys in Schiff base enzymes). The covalent intermediate provides a lower-energy pathway.
5. Metal ion catalysis: Metal ions (Zn^{2+} , Mg^{2+} , $\text{Fe}^{2+/3+}$) stabilize negative charges, act as Lewis acids, or enable redox chemistry.
6. Electrostatic catalysis: The active site creates a microenvironment with a lower effective dielectric constant, enhancing electrostatic interactions.
7. Desolvation: Stripping water from substrate and active-site residues increases their reactivity (e.g., a “naked” carboxylate is a much stronger base than a hydrated one).

Concept Check 1: Transition state analogs — molecules that mimic the transition state geometry — are potent enzyme inhibitors. Why are they typically much tighter binders than the substrate itself? (Hint: Consider what the active site is optimized to bind.)

4.1.3 Active Site Architecture

The active site occupies roughly 1–10% of the enzyme’s total surface but accounts for most catalytic power. Key features:

- Specific geometry complementary to the transition state (more so than to the substrate)
- Hydrophobic microenvironment that enhances nucleophilicity and acid/base strength
- Flexibility: conformational changes upon substrate binding (induced fit model)
- Conserved residues: catalytic residues are highly conserved across species, even when surrounding sequences diverge

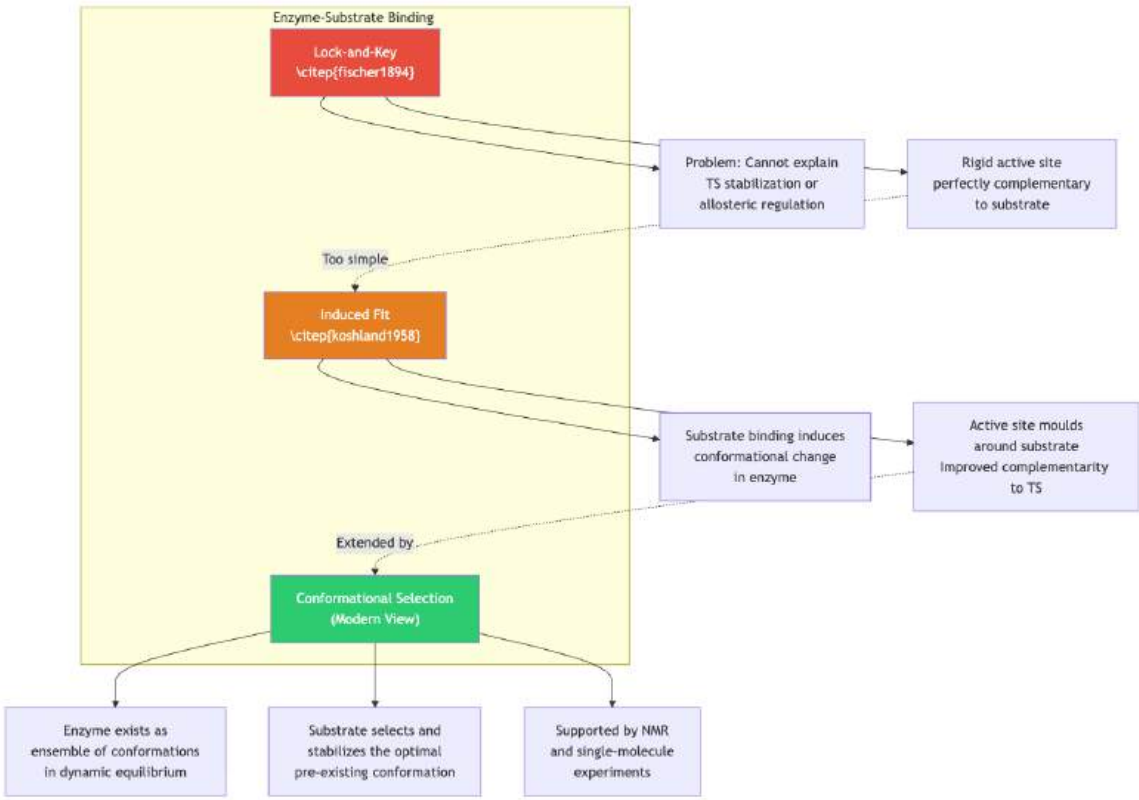


Figure 34. Models of enzyme–substrate binding. Evolution of enzyme-substrate binding models. The lock-and-key model (1894) proposed rigid complementarity. The induced-fit model (1958) introduced conformational change upon binding. The modern conformational selection model recognizes that enzymes sample multiple conformations, and substrates select the most complementary one.

The lock-and-key model [Fischer, 1894] viewed the active site as rigid. The induced-fit model [Koshland, 1958] recognized that substrate binding induces conformational changes that improve active-site complementarity — validated by crystallographic structures. The modern conformational selection model proposes that the enzyme pre-exists in an ensemble of conformations, and the substrate selects the optimal one, shifting the equilibrium.

Case study — Hexokinase: X-ray crystallography reveals that hexokinase undergoes a dramatic conformational change upon glucose binding: two lobes of the enzyme close around the substrate like a jaw, excluding water from the active site. This prevents the wasteful hydrolysis of ATP (which would occur if water could access the γ -phosphate).

4.2 Enzyme Classification (EC Numbers)

The International Union of Biochemistry and Molecular Biology (IUBMB) classifies enzymes into seven classes by reaction type, each with a four-digit EC (Enzyme Commission) number:

Table 76. Active Site Architecture: EC Class and Name.

EC Class	Name	Reaction Type	Example	EC Number
1	Oxidoreductases	Redox reactions	Lactate dehydrogenase	EC 1.1.1.27
2	Transferases	Group transfer	Hexokinase (phosphoryl)	EC 2.7.1.1
3	Hydrolases	Hydrolysis	Trypsin	EC 3.4.21.4
4	Lyases	Non-hydrolytic bond cleavage / addition to double bonds	Fumarase	EC 4.2.1.2
5	Isomerases	Isomerisation	Phosphoglucose isomerase	EC 5.3.1.9
6	Ligases	Bond formation coupled to ATP/GTP hydrolysis	DNA ligase	EC 6.5.1.1

EC Class	Name	Reaction Type	Example	EC Number
7	Translocases	Movement of ions/molecules across membranes	Na ⁺ /K ⁺ -ATPase	EC 7.2.2.6

The seventh class (translocases) was added in 2018, recognizing the catalytic nature of active transport. Enzyme names follow the pattern: Substrate(s) + reaction type + “-ase” (e.g., pyruvate kinase, lactate dehydrogenase).

Concept Check 2: The Na⁺/K⁺-ATPase pumps 3 Na⁺ out and 2 K⁺ in per ATP hydrolysed. It was traditionally classified as an ATPase (EC 3.6). Why was reclassification to translocase (EC 7) considered more appropriate?

4.3 The Michaelis-Menten Equation

Mathematical Background: The Michaelis-Menten equation uses hyperbolic functions and dimensional analysis. For a review of logarithms and rate equations, see [Appendix C — Mathematical Review for Biology](#).

4.3.1 Deriving the Michaelis-Menten Equation

In 1913, Leonor Michaelis and Maud Menten proposed a kinetic framework for enzyme-catalysed reactions. The basic mechanism:



Step 1: Write rate equations.

The rate of ES formation: $\frac{d[ES]}{dt} = k_1[E][S] - k_{-1}[ES] - k_2[ES]$

Step 2: Apply the steady-state assumption ($d[ES]/dt = 0$).

This assumes that after an initial transient, [ES] reaches a constant level because the rate of ES formation equals the rate of ES breakdown:

$$k_1[E][S] = (k_{-1} + k_2)[ES]$$

(75)

Step 3: Define the Michaelis constant.

$$K_m = \frac{k_{-1} + k_2}{k_1}$$

(76)

Step 4: Express E in terms of measurable quantities.

Total enzyme: $[E]_T = [E] + [ES]$, so $[E] = [E]_T - [ES]$

Substituting: $([E]_T - [ES])[S] = K_m[ES]$

$$[ES] = \frac{[E]_T[S]}{K_m + [S]}$$

(77)

Step 5: Calculate the initial velocity.

$$v_0 = k_2[ES] = \frac{k_2[E]_T[S]}{K_m + [S]}$$

(78)

Since $V_{max} = k_2[E]_T$ (maximum rate when most enzyme is saturated):

$$v_0 = \frac{V_{max}[S]}{K_m + [S]}$$

(79)

This is the Michaelis-Menten equation — a rectangular hyperbola (equation (79)); plotting v_0 against $[S]$ traces the saturating curve shown in figure 35, where the velocity rises steeply at low substrate and asymptotically approaches V_{max} .

4.3.2 Interpretation of Kinetic Parameters

K_m approximates the substrate affinity of the enzyme. When $S = K_m$, $v = V_{max}/2$. A low K_m means high affinity (half-saturation at low S).

Special cases: - When $k_2 \ll k_{-1}$: $K_m \approx K_d = k_{-1}/k_1$ (true dissociation constant) - When $k_2 \gg k_{-1}$: $K_m \approx k_2/k_1$ (the enzyme is so fast that ES rarely dissociates back to E + S)

V_{max} and k_{cat} : $V_{max} = k_{cat} \times [E]_T$. The catalytic constant k_{cat} (also called the turnover number) is the number of substrate molecules converted to product per enzyme molecule per second when fully saturated.

Catalytic efficiency: k_{cat}/K_m (units: $M^{-1} s^{-1}$). This is the gold standard for comparing enzyme power. The diffusion limit sets the maximum possible $k_{cat}/K_m \approx 10^8\text{--}10^9 M^{-1} s^{-1}$ (kinetically “perfect” enzymes).

Reference kinetic constants:

Table 77. Interpretation of Kinetic Parameters: Enzyme and Substrate.

Enzyme	Substrate	K_m (mM)	k_{cat} (s^{-1})	k_{cat}/K_m ($M^{-1}s^{-1}$)	Status
Carbonic anhydrase	CO ₂	12	10 ⁶	8.3×10^7	Near-perfect
Fumarase	Fumarate	0.005	800	1.6×10^8	Near-perfect
Acetylcholinesterase	Acetylcholine	0.095	1.4×10^4	1.5×10^8	Near-perfect
Catalase	H ₂ O ₂	25	4×10^7	1.6×10^9	Diffusion-limited
Lactate dehydrogenase	Pyruvate	0.047	800	1.7×10^7	Highly efficient
Hexokinase	Glucose	0.15	650	4.3×10^6	Efficient
Alcohol dehydrogenase	Ethanol	1.0	73	7.3×10^4	Moderate
Lysozyme	Hexasaccharide	0.006	0.5	8.3×10^4	Moderate

Concept Check 3: Catalase converts H₂O₂ to H₂O and O₂ with a k_{cat} of $4 \times 10^7 s^{-1}$. How many molecules of H₂O₂ does a single catalase molecule destroy per millisecond? Why is such extreme speed necessary in the cell?

4.3.3 Lineweaver-Burk Analysis

Inverting the Michaelis-Menten equation:

$$\frac{1}{v_0} = \frac{K_m}{V_{max}} \cdot \frac{1}{[S]} + \frac{1}{V_{max}}$$

(80)

The double-reciprocal (Lineweaver-Burk) plot of $1/v$ vs. $1/[S]$ is linear: - Slope = K_m/V_{max} - x-intercept = $-1/K_m$ - y-intercept = $1/V_{max}$

Worked example — Determining K_m and V_{max} :

An enzyme is assayed at five substrate concentrations:

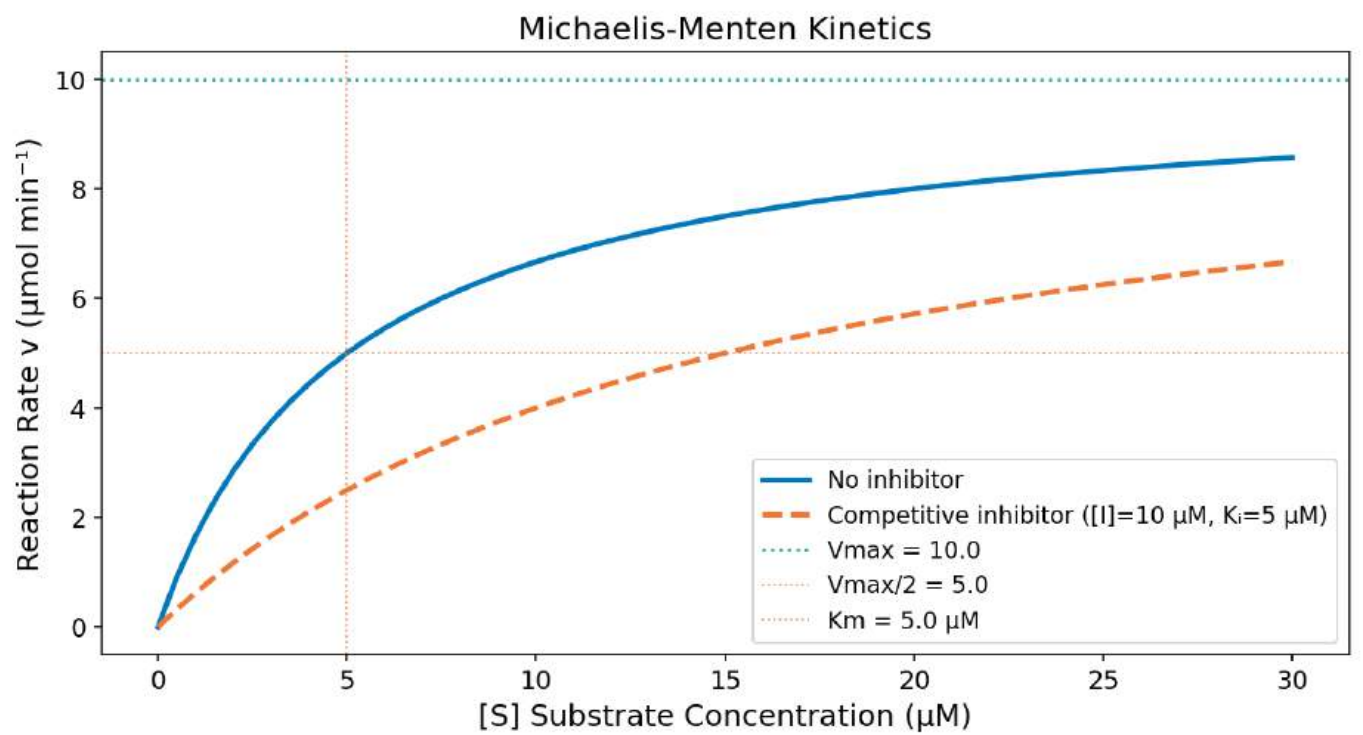


Figure 35. Michaelis–Menten kinetics: initial velocity (v_0) versus substrate concentration with an uninhibited curve, a competitive-inhibitor curve, and the V_{max} , $V_{\text{max}}/2$, and K_m reference lines annotated.

Table 78. Lineweaver-Burk Analysis: S (mM) and v₀ (μmol/min).

S (mM)	v ₀ (μmol/min)	1/S (mM ⁻¹)	1/v ₀
0.5	1.67	2.0	0.60
1.0	2.50	1.0	0.40
2.0	3.33	0.5	0.30
4.0	4.00	0.25	0.25
10.0	4.55	0.10	0.22

From the Lineweaver-Burk plot: - y-intercept = 0.20, so $V_{max} = 1/0.20 = 5.0 \mu\text{mol/min}$ - Slope = $(0.60 - 0.20)/(2.0 - 0) = 0.20$, and slope = K_m/V_{max} , so $K_m = 0.20 \times 5.0 = 1.0 \text{ mM}$

Limitations of the Lineweaver-Burk plot: It distorts experimental error at low S (high 1/S), giving those points excessive weight. Modern software uses nonlinear regression to fit the Michaelis-Menten equation directly, which is statistically superior.

4.4 Enzyme Inhibition and Kinetic Signatures

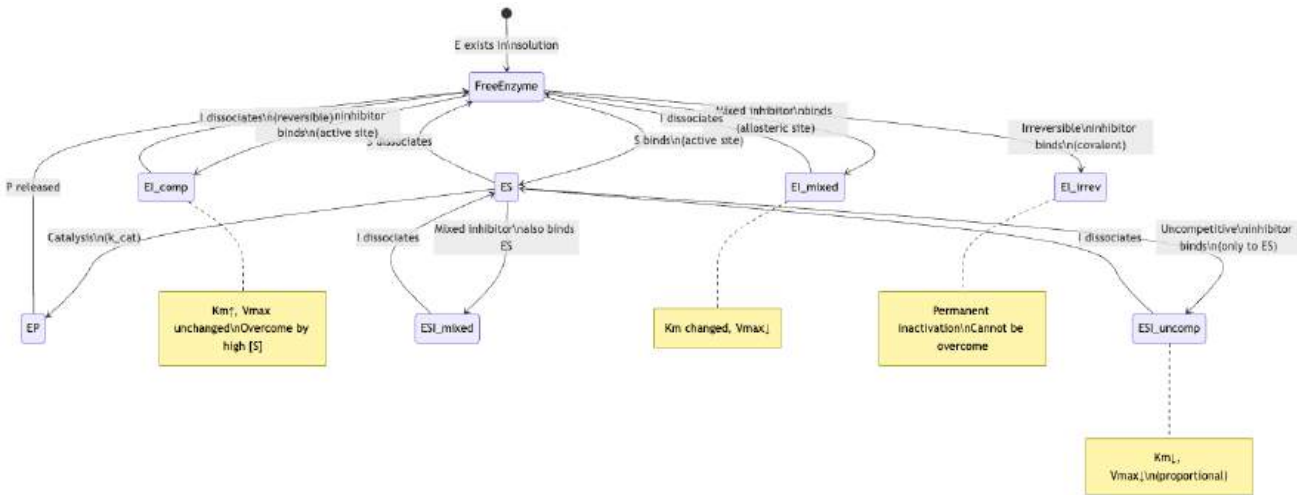


Figure 36. Enzyme inhibitors change kinetic outcomes by binding free enzyme, enzyme-substrate complex, allosteric sites, or covalent targets; the binding route determines whether K_m , V_{max} , or both change.

4.4.1 Competitive Inhibition and Apparent Km

A competitive inhibitor (I) resembles the substrate structurally and competes for the same active site. Binding of I and S are mutually exclusive:

$$E + I \rightleftharpoons EI \quad (K_i = [E][I]/[EI]) \tag{81}$$

The apparent K_m increases (less substrate affinity at fixed I) while V_{max} is unchanged (inhibition overcome by high S):

$$v_0 = \frac{V_{max}[S]}{K_m \left(1 + \frac{[I]}{K_i}\right) + [S]} \tag{82}$$

Defining $\alpha = 1 + [I]/K_i$:

$$v_0 = \frac{V_{max}[S]}{\alpha K_m + [S]} \tag{83}$$

On a Lineweaver-Burk plot: same y-intercept ($1/V_{max}$), different slopes. Lines intersect on the y-axis.

Clinical examples of **competitive inhibition**:

Table 79. Competitive Inhibition and Apparent Km: Inhibitor and Target Enzyme.

Inhibitor	Target Enzyme	Clinical Use
Methotrexate	Dihydrofolate reductase	Cancer chemotherapy
Statins (atorvastatin)	HMG-CoA reductase	Cholesterol-lowering
Sulfonamide antibiotics	Dihydropteroate synthase	Bacterial infection
Allopurinol	Xanthine oxidase	Gout
Ethanol	Alcohol dehydrogenase	Methanol/ethylene glycol poisoning

Clinical Connection: Statins and Cardiovascular Disease

Statins (e.g., atorvastatin, rosuvastatin) are competitive inhibitors of HMG-CoA reductase, the rate-limiting enzyme in cholesterol biosynthesis. By mimicking the structure of HMG-CoA, statins bind the active site with K_i values in the low nanomolar range (much lower than the K_m for HMG-CoA, about $4\text{ }\mu\text{M}$). This reduces hepatic cholesterol synthesis, upregulates LDL receptors, and lowers circulating LDL cholesterol by 30–50%. Statins are among the most widely prescribed drugs worldwide, with robust evidence for reducing cardiovascular events and mortality.

4.4.2 Uncompetitive Inhibition and Coupled Km/Vmax Shifts

An uncompetitive inhibitor binds primarily to the ES complex, not free enzyme:

$$v_0 = \frac{V_{max}[S]}{K_m + \alpha'[S]}$$

(84)

where $\alpha' = 1 + [I]/K'_i$. Both K_m and V_{max} are decreased proportionally — the ratio V_{max}/K_m ($= k_{cat}/K_m$) is unchanged. On a Lineweaver-Burk plot: parallel lines (both slope and intercepts change equally).

Uncompetitive inhibition is rare in single-substrate reactions but important in two-substrate reactions and in multi-enzyme pathways. Lithium is an uncompetitive inhibitor of inositol monophosphatase, which may contribute to its therapeutic effect in bipolar disorder.

4.4.3 Mixed (Noncompetitive) Inhibition

A mixed inhibitor binds to both free enzyme (E) and the ES complex, at a site other than the active site:

$$v_0 = \frac{V_{max}[S]}{\alpha K_m + \alpha'[S]}$$

(85)

where $\alpha = 1 + [I]/K_i$ and $\alpha' = 1 + [I]/K'_i$.

- If $\alpha = \alpha'$ ($K_i = K'_i$): pure noncompetitive inhibition. K_m unchanged, V_{max} decreased.
- If $\alpha \neq \alpha'$: mixed inhibition. Both K_m and V_{max} change.

On a Lineweaver-Burk plot: lines intersect to the left of the y-axis (not on it).

Pure noncompetitive inhibitor: Heavy metal ions (Hg^{2+} , Pb^{2+}) that bind cysteine residues distant from the active site.

4.4.4 Irreversible Inhibition and Covalent Inactivation

Irreversible inhibitors form covalent bonds with enzyme residues, permanently inactivating the enzyme. The enzyme must be replaced by new protein synthesis.

Table 80. Irreversible Inhibition and Covalent Inactivation: Inhibitor and Target.

Inhibitor	Target	Mechanism	Clinical Application
Aspirin (acetylsalicylate)	COX-1 and COX-2	Acetylates Ser530	Anti-inflammatory, antiplatelet
Penicillin / amoxicillin	Transpeptidase (DD-peptidase)	Acylates active-site Ser	Antibiotic

Inhibitor	Target	Mechanism	Clinical Application
DIPF / sarin	Acetylcholinesterase	Phosphorylates active-site Ser	Nerve agent (sarin)
Omeprazole (Prilosec)	H ⁺ /K ⁺ -ATPase	Disulfide bond with Cys813	Proton pump inhibitor (acid reflux)
Clopidogrel (Plavix)	P2Y12 receptor	Disulfide bond	Antiplatelet

Clinical Connection: Aspirin — The Oldest Irreversible Enzyme Inhibitor

Aspirin (acetylsalicylic acid) irreversibly acetylates Ser530 in cyclooxygenase (COX), preventing the conversion of arachidonic acid to prostaglandins and thromboxane A₂. Because platelets lack a nucleus and cannot synthesize new protein, a single dose of aspirin inhibits platelet COX-1 for the entire platelet lifespan (about 10 days). This is why low-dose aspirin (75–100 mg/day) is an effective antiplatelet agent for preventing heart attacks and strokes, despite its short plasma half-life of about 20 minutes.

Clinical Connection: Penicillin and Bacterial Cell Wall Synthesis

Penicillin and related β -lactam antibiotics are irreversible inhibitors of bacterial transpeptidase (also called penicillin-binding protein, PBP), the enzyme that cross-links peptidoglycan strands in the bacterial cell wall. The β -lactam ring of penicillin mimics the D-Ala–D-Ala terminus of the peptidoglycan substrate, forming a stable acyl-enzyme intermediate. Without cross-linking, the cell wall loses integrity and the bacterium lyses due to osmotic stress. Resistance arises when bacteria produce β -lactamases that hydrolyse the β -lactam ring.

4.4.5 Lineweaver-Burk Patterns Summary

Table 81. Lineweaver-Burk Patterns Summary: Inhibition Type and Apparent K_m.

Inhibition Type	Apparent K_m	Apparent V_{max}	L-B Plot Pattern
Competitive	Increases (αK_m)	Unchanged	Same y-intercept
Uncompetitive	Decreases (K_m/α')	Decreases (V_{max}/α')	Parallel lines
Pure noncompetitive	Unchanged	Decreases (V_{max}/α)	Same x-intercept
Mixed	Changes	Decreases	Intersect left of y-axis
Irreversible	N/A	Decreases (less $[E]_T$)	Same K_m , lower V_{max}

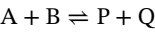
Concept Check 4: An enzyme is studied in the presence and absence of an inhibitor. In the Lineweaver-Burk plot, the two lines are parallel. What type of inhibition is this? Does the inhibitor bind the free enzyme, the ES complex, or both?

Worked Example — Competitive vs. Allosteric Inhibition Comparison: Dihydrofolate reductase (DHFR) is the target of methotrexate (MTX, competitive inhibitor, $K_i = 1\text{ nM}$) and trimethoprim (TMP, competitive inhibitor, $K_i = 1\text{ }\mu\text{M}$ for bacterial DHFR vs $100\text{ }\mu\text{M}$ for human DHFR — a 100-fold selectivity window). Given $K_m(\text{DHFR, dihydrofolate}) = 1\text{ }\mu\text{M}$, $V_{max} = 10\text{ nM/s}$, $[\text{substrate}] = 5\text{ }\mu\text{M}$, and $[\text{MTX}] = 10\text{ nM}$. *Without MTX*: $v = 10 \times 5/(1 + 5) = 8.33\text{ nM/s}$. *With MTX*: apparent $K'_m = K_m(1 + [I]/K_i) = 1(1 + 10/1) = 11\text{ }\mu\text{M}$, so $v = 10 \times 5/(11 + 5) = 3.13\text{ nM/s}$ — a 62% reduction at $[\text{MTX}]$ at just 10 \times its K_i , because the drug competes at nM while substrate is at μM . This illustrates why tight-binding competitive inhibitors can be more clinically effective than their raw K_i value suggests, especially when substrate concentration is comparable to K_m .

Concept Check (Synthesis): Allosteric enzymes like phosphofructokinase-1 (PFK-1) show sigmoidal kinetics with respect to fructose-6-phosphate (F6P). ATP at high concentrations inhibits PFK-1 allosterically (R-state stabilization by ADP/AMP; T-state stabilization by ATP). (a) Sketch the velocity vs $[\text{F6P}]$ curves for PFK-1 in the presence of 2 mM ATP, 0.2 mM ATP, and 2 mM AMP. (b) Why does sigmoidal kinetics make PFK-1 a better metabolic switch than a hyperbolic enzyme with the same V_{max} and apparent $K_{0.5}$? Quantify using the Hill equation: compare the fold-change in activity when $[\text{F6P}]$ goes from $0.5K_{0.5}$ to $2K_{0.5}$ for $n = 1$ vs $n = 4$. (c) PFK-2 produces fructose-2,6-bisphosphate (F2,6BP), a potent allosteric activator of PFK-1. Draw the control logic connecting insulin signaling, PFK-2 activity, F2,6BP levels, and glycolytic flux.

4.5 Multi-substrate Kinetics: Bi-Bi Mechanisms

The single-substrate Michaelis-Menten framework is a useful approximation, but most enzymes use *two* substrates (or one substrate plus a cofactor). Reactions of the form



are known as Bi-Bi reactions. Cleland (1963) classified them into three principal mechanisms based on the order in which substrates bind and products release.

4.5.1 Sequential (Ternary Complex) Mechanisms

- Both substrates must be bound to the enzyme *simultaneously* before any product is released. The enzyme thus passes through a ternary EAB complex.
- Ordered Bi-Bi: A binds before B; Q releases before P. Example: NAD⁺-dependent dehydrogenases such as lactate dehydrogenase, where NAD⁺ binds first and NADH leaves last.
 - Random Bi-Bi: A and B can bind in either order; products can leave in either order. Example: creatine kinase.

The general rate equation for a sequential Bi-Bi reaction (assuming rapid equilibrium and saturating second substrate) reduces to:

$$v_0 = \frac{V_{\max} [A] [B]}{K_{ia}K_b + K_b[A] + K_a[B] + [A][B]}$$

(86)

where K_a and K_b are Michaelis constants for A and B, and K_{ia} is the dissociation constant of A from the binary EA complex. Diagnostic Lineweaver-Burk pattern: plotting $1/v_0$ vs. $1/[A]$ at several fixed **B** gives a family of lines that intersect to the left of the y-axis (sequential signature).

4.5.2 Ping-Pong (Double-Displacement) Mechanism

The first substrate A binds, transfers a chemical group to the enzyme, and the first product P is released, leaving the enzyme in a covalently modified form (E). *Then B binds to E*, accepts the group, and Q is released. At no time does the enzyme contain both substrates simultaneously. Examples: aminotransferases (PLP carries the amino group between substrates), serine proteases (substrate A acylates the active-site Ser; substrate B = water deacylates), and many kinases that proceed via a phospho-enzyme intermediate.

The rate equation:

$$v_0 = \frac{V_{\max} [A] [B]}{K_b[A] + K_a[B] + [A][B]}$$

(87)

Notice the absent $K_{ia}K_b$ term in the denominator. Diagnostic Lineweaver-Burk pattern: the family of lines is parallel — a clean kinetic signature distinguishing ping-pong from sequential mechanisms.

Table 82. Ping-Pong (Double-Displacement) Mechanism: Feature and Sequential (Random or Ordered).

Feature	Sequential (Random or Ordered)	Ping-Pong
Ternary complex EAB?	Yes	No
Covalent enzyme intermediate E*?	No	Yes
Lineweaver-Burk pattern (vary A, fixed B)	Intersecting lines	Parallel lines
Examples	LDH, hexokinase, CK	AspAT, chymotrypsin, GS

Concept Check 5: A biochemist measures the rate of an enzyme reaction at varying **A** for several fixed **B** values, and obtains a family of parallel lines on a Lineweaver-Burk plot. Identify the mechanism and predict whether a covalent enzyme intermediate exists.

4.6 Allosteric Regulation and Cooperativity

Allosteric enzymes are not governed by simple **Michaelis-Menten kinetics**. They have: - Multiple subunits, typically with identical active sites - Regulatory sites distinct from active sites - Cooperative (sigmoidal) substrate binding - Modulation by effector molecules (activators or inhibitors)

4.6.1 The Hill Equation

For an enzyme with n equivalent cooperative subunits, the fraction of active sites occupied (θ) follows the Hill equation:

$$\theta = \frac{[S]^n}{K_{0.5}^n + [S]^n}$$

(88)

where n is the Hill coefficient: - $n = 1$: no cooperativity (hyperbolic, Michaelis-Menten) - $n > 1$: positive cooperativity (sigmoidal; binding one substrate increases affinity for subsequent substrates) - $n < 1$: negative cooperativity (binding decreases affinity)

Linearised Hill equation:

$$\log \frac{\theta}{1 - \theta} = n \log[S] - n \log K_{0.5}$$

(89)

A plot of $\log[\theta/(1 - \theta)]$ vs. $\log[S]$ (the Hill plot) gives a straight line with slope n and x -intercept at $\log K_{0.5}$.

Hemoglobin (see section 31) has $n \approx 2.8$ (not 4, because cooperativity is imperfect). Sigmoidal kinetics give allosteric enzymes switch-like behavior — small changes in S near $K_{0.5}$ cause large changes in activity.

Worked example: For an allosteric enzyme with $K_{0.5} = 5$ mM and $n = 3$:

At $S = 4$ mM: $\theta = \frac{4^3}{5^3 + 4^3} = \frac{64}{125 + 64} = \frac{64}{189} = 0.339$ (33.9%)

At $S = 6$ mM: $\theta = \frac{6^3}{5^3 + 6^3} = \frac{216}{125 + 216} = \frac{216}{341} = 0.634$ (63.4%)

A 50% increase in S (from 4 to 6 mM) nearly doubles the fractional saturation. This is the “switch-like” sensitivity of cooperative systems.

4.6.2 Concerted (MWC) and Sequential Models

Two models describe the molecular mechanism of cooperativity:

Monod-Wyman-Changeux (MWC) Concerted Model: - Most subunits exist in either the T-state (tense, low affinity) or R-state (relaxed, high affinity) - Most subunits transition simultaneously (concerted) - Substrate preferentially binds R-state, shifting $T \rightleftharpoons R$ equilibrium toward R - Activators stabilize R; inhibitors stabilize T

Koshland-Nemethy-Filmer (KNF) Sequential Model: - Each subunit can independently switch between T and R - Substrate binding to one subunit induces conformational changes that propagate to adjacent subunits - Explains negative cooperativity (which MWC cannot)

In reality, most allosteric systems show features of both models.

4.6.3 Aspartate Transcarbamoylase (ATCase) — A Model Allosteric Enzyme

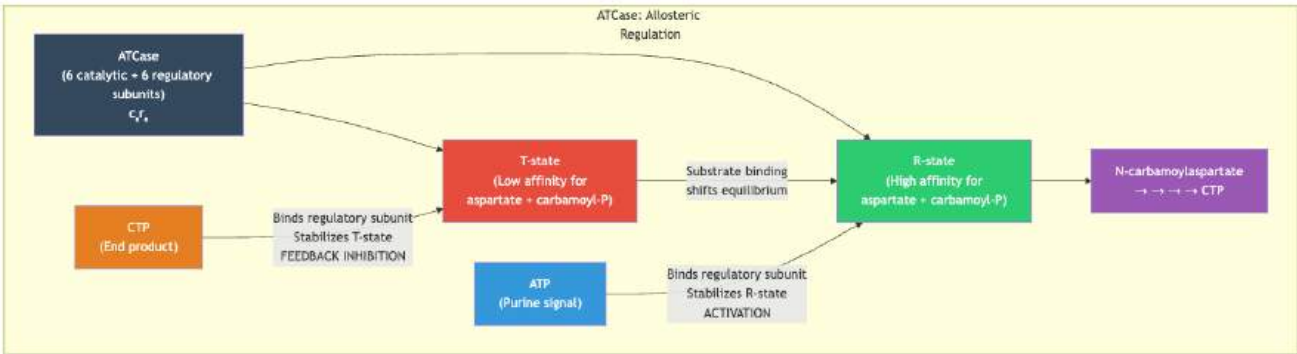


Figure 37. ATCase allostery (CTP and ATP). Allosteric regulation of ATCase. CTP (the end product of the pyrimidine pathway) is a feedback inhibitor that stabilizes the T-state. ATP (a purine nucleotide) is an activator that stabilizes the R-state, coordinating purine and pyrimidine synthesis.

ATCase (catalyses the first committed step of pyrimidine biosynthesis) is the textbook allosteric enzyme: - Structure: 6 catalytic subunits (c_3)₂ + 6 regulatory subunits (r_2)₃ = c_6r_6 (about 310 kDa) - Inhibited by CTP (end-product of the pathway — feedback inhibition) - Activated by ATP (signals adequate purine availability -> coordinate pyrimidine synthesis) - Hill coefficient $n \approx 2.5$ for N-carbamoylaspartate synthesis - T->R transition involves a 12-angstrom expansion and 10-degree rotation of catalytic trimers

This allows the cell to precisely match nucleotide biosynthesis to demand. When CTP is abundant, ATCase is inhibited; when ATP is abundant (indicating nucleotide precursors are available), ATCase is activated.

4.6.4 Why Cooperativity Improves Pathway Control

A first-glance question: why has evolution invested in elaborate allosteric machinery when simple Michaelis-Menten enzymes could in principle perform every metabolic task? The answer lies in the *control properties* of cooperative enzymes.

Compare a hyperbolic enzyme (Hill coefficient $n = 1$) and a sigmoidal enzyme ($n = 4$) in the small region around $K_{0.5}$. For a 2-fold increase in **S** near $K_{0.5}$:

Table 83. Effect of cooperativity on enzyme saturation near half-maximal substrate concentration.

Enzyme	θ at $[S] = 0.5 K_{0.5}$	θ at $[S] = 2 K_{0.5}$	Sensitivity (ratio)
Michaelis-Menten ($n = 1$)	0.33	0.67	2.0×
Cooperative ($n = 2$)	0.20	0.80	4.0×
Cooperative ($n = 4$)	0.059	0.941	16×
Cooperative ($n = 8$)	0.0039	0.9961	256×

An 8-fold increase in Hill coefficient (from $n=1$ to $n=8$) gives a 128-fold increase in switching sensitivity around $K_{0.5}$ — each doubling of n roughly squares the sensitivity ratio. This ultrasensitivity confers three regulatory advantages:

1. Steeper response to small signal changes. Glycolysis can be ramped up rapidly during exercise without requiring 10-fold changes in metabolite concentrations.
2. Sharper response thresholds. Below $K_{0.5}$ the pathway is nearly off; above $K_{0.5}$ nearly fully on. Enables clear “decision-making” at metabolic branch points.
3. Insulation from noise. Random fluctuations in **S** within the low-saturation regime cause much smaller activity changes than under MM kinetics. Stability and switch-like behavior coexist.

The same logic explains why hemoglobin’s $n \approx 2.8$ delivers about 25% of bound O_2 between arterial (pO_2 100 mmHg) and venous (40 mmHg) blood, whereas hyperbolic myoglobin would deliver about 10% of the same change. Cooperativity is biology’s tunable amplifier.

Concept Check 6: Phosphofructokinase-1 (PFK-1) is an allosteric enzyme in **glycolysis** that is activated by AMP and inhibited by ATP and citrate. Why does this regulatory pattern make metabolic sense? (Consider the energy charge of the cell.)

4.7 Environmental Factors Affecting Enzyme Activity

4.7.1 Temperature Effects on Enzyme Rate and Stability

Enzyme activity generally increases with temperature (\uparrow kinetic energy $\rightarrow \uparrow$ collision frequency $\rightarrow \uparrow$ rate) according to the Arrhenius equation:

$$k = A \cdot e^{-E_a/RT}$$

(90)

A 10 degrees C rise approximately doubles reaction rate ($Q_{10} \approx 2$). However, above the optimal temperature, denaturation of the protein occurs (tertiary and quaternary structure disrupts), sharply reducing activity. The optimal temperature for most human enzymes: about 37 degrees C.

Q_{10} calculation:

$$Q_{10} = \left(\frac{k_2}{k_1}\right)^{10/(T_2-T_1)}$$

(91)

For most enzyme reactions, $Q_{10} = 1.5\text{--}3.0$. The Q_{10} rule breaks down near the denaturation temperature.

Extremophile enzymes (extremozymes): - *Thermus aquaticus* (hot springs, 75 degrees C) Taq polymerase: thermostable DNA polymerase, the workhorse of PCR (optimal 72 degrees C). Taq achieves thermostability through increased salt bridges, compact hydrophobic core, and proline substitutions. - *Pyrococcus furiosus*

(deep-sea vent, 100 degrees C) Pfu polymerase: even more thermostable and has 3'->5' proofreading activity (higher fidelity than Taq). - *Psychrobacter* (Antarctic, -20 degrees C) enzymes: more flexible (more Gly, fewer Pro, fewer salt bridges), lower activation energy, active at sub-zero temperatures but rapidly denature at 37 degrees C.

4.7.2 pH Effects on Active-Site Chemistry

Enzyme catalysis depends on the ionization state of key active-site residues. Activity-pH curves are typically bell-shaped:

Table 84. pH Effects on Active-Site Chemistry: Enzyme and Location.

Enzyme	Location	Optimum pH	Key Catalytic Residue
Pepsin	Stomach	1.5–2.5	Asp (must be protonated)
Salivary amylase	Mouth	6.7–7.0	Glu (acid/base catalyst)
Trypsin	Intestine	7.5–8.5	His57 (must be deprotonated)
Alkaline phosphatase	Intestine/bone	8–10	Ser (phosphorylated intermediate)
Arginase	Liver	9.5–10.0	Mn ²⁺ (binuclear metal center)

The bell-shaped curve reflects the requirement for specific protonation states: the ascending limb corresponds to deprotonation of one essential residue; the descending limb to deprotonation of another.

4.7.3 Cofactors and Coenzymes

Many enzymes require non-protein cofactors for activity. The enzyme without its cofactor is the apoenzyme; the complete, active enzyme is the holoenzyme.

Table 85. Cofactors and Coenzymes: Type and Examples.

Type	Examples	Function	Dietary Source
Metal ions	Zn ²⁺ (carboxypeptidase)	Lewis acid catalysis	Red meat, shellfish
	Mg ²⁺ (kinases)	Stabilize ATP phosphate	Green vegetables
	Fe ^{2+/3+} (cytochromes)	Electron transfer	Red meat, lentils
	Cu ²⁺ (cytochrome c oxidase)	O ₂ reduction	Liver, nuts
	Mn ²⁺ (SOD, arginase)	Redox, hydrolysis	Whole grains
	Mo (xanthine oxidase)	Oxygen atom transfer	Legumes
	Se (glutathione peroxidase)	Peroxide reduction	Brazil nuts
Coenzymes	NAD ⁺ /NADH (from niacin, B3)	Hydride transfer	Meat, fish
	FAD/FADH ₂ (from riboflavin, B2)	Hydride transfer	Dairy, eggs
	Coenzyme A (from pantothenate, B5)	Acyl group transfer	Widespread
	Pyridoxal phosphate (from pyridoxine, B6)	Amino group transfer	Poultry, fish
	Thiamine pyrophosphate (from thiamine, B1)	Decarboxylation	Whole grains
	Biotin (B7)	Carboxylation	Eggs, nuts
	Tetrahydrofolate (from folate, B9)	One-carbon transfer	Leafy greens
Prosthetic groups	5'-deoxyadenosylcobalamin (from B12)	Rearrangements	Animal products
	Haem (contains Fe)	O ₂ binding, electron transfer	Synthesized endogenously
	Lipoic acid	Acyl group transfer	Synthesized endogenously

Most water-soluble vitamins (B vitamins) function as coenzyme precursors. This is why vitamin deficiencies cause enzyme dysfunction and disease:

Table 86. Cofactors and Coenzymes: Vitamin Deficiency and Coenzyme Affected.

Vitamin Deficiency	Coenzyme Affected	Disease
B1 (Thiamine)	TPP	Beriberi, Wernicke-Korsakoff syndrome
B2 (Riboflavin)	FAD	Ariboflavinosis (angular stomatitis)
B3 (Niacin)	NAD ⁺	Pellagra (dermatitis, diarrhea, dementia)
B6 (Pyridoxine)	PLP	Peripheral neuropathy
B9 (Folate)	THF	Megaloblastic anemia, neural tube defects
B12 (Cobalamin)	AdoCbl, MeCbl	Pernicious anemia, neurodegeneration

Clinical Connection: ACE Inhibitors and Zinc-Dependent Catalysis

Angiotensin-converting enzyme (ACE) is a zinc metalloprotease that converts angiotensin I to angiotensin II (a potent vasoconstrictor) and degrades bradykinin (a vasodilator). ACE inhibitors (enalapril, lisinopril, ramipril) chelate the active-site Zn²⁺, preventing catalysis. By blocking angiotensin II production and bradykinin degradation, ACE inhibitors reduce blood pressure and are first-line therapy for hypertension and heart failure. The side effect of dry cough (in about 10% of patients) is caused by bradykinin accumulation in the airways.

Concept Check 7: Most water-soluble vitamins serve as coenzyme precursors. Explain why these vitamins must be obtained from the diet (unlike fat-soluble vitamins, which can be stored). What does this imply about the recommended frequency of intake?

4.8 Industrial and Biotechnological Enzymes

Enzymes have transformed medicine and industry:

Modern enzyme biotechnology couples classical kinetics with structure-guided design, directed evolution, high-throughput screening, and increasingly AI-predicted interaction models. AlphaFold-class tools can nominate an active-site geometry or protein-complex interface, but an engineered-enzyme claim still needs measured k_{cat} , K_M , specificity, stability, expression yield, and performance under application conditions; a plausible structure is a hypothesis until kinetics and controls support it [Abramson et al., 2024, Bertoni et al., 2026].

4.8.1 CRISPR-Cas9 as a Nuclease Enzyme

The Cas9 protein from *Streptococcus pyogenes* is an RNA-guided endonuclease: - Classification: EC 3.1 (nuclease / hydrolase) - Mechanism: The guide RNA (gRNA) forms a 20-nt complementary complex with the target DNA. Cas9 unwinds the DNA and cleaves both strands using two nuclease domains: RuvC cuts the non-target strand; HNH cuts the target strand - Specificity: PAM (protospacer adjacent motif, 5'-NGG-3') is required adjacent to the target sequence - Applications: **Gene** editing, gene therapy (sickle cell disease, β -thalassaemia), diagnostics (SHERLOCK, DETECTR) - Nobel Prize 2020: Jennifer Doudna and Emmanuelle Charpentier

4.8.2 Industrial and Therapeutic Enzyme Applications

Table 87. Industrial and Therapeutic Enzyme Applications: Enzyme and Industry.

Enzyme	Industry	Application
Lipases	Biodiesel, detergents	Transesterification, stain removal
Cellulases	Biofuel	Cellulosic ethanol production
Amylases	Food, brewing	Starch liquefaction, brewing
Proteases	Detergents, leather	Protein stain removal, dehairing
Lactase	Dairy	Lactose-free milk production

Enzyme	Industry	Application
DNA polymerase (Taq)	Molecular biology	PCR amplification
Restriction enzymes	Biotechnology	Molecular cloning
Glucose isomerase	Food	High-fructose corn syrup

4.8.3 Enzyme Engineering Approaches

- Directed evolution: Random mutagenesis + screening/selection for improved properties. Frances Arnold received the 2018 Nobel Prize in Chemistry for this approach.
- Rational design: Structure-guided **mutation** of specific residues based on mechanistic understanding.
- Immobilised enzymes: Enzymes attached to solid supports for continuous-flow industrial processes. Advantages: reusability, stability, easy product separation.

4.8.4 Quantitative Metrics for Engineered Enzymes

When evaluating an engineered or evolved variant, several quantitative figures of merit are routinely compared against the wild-type enzyme:

Table 88. Quantitative Metrics for Engineered Enzymes: Metric and Definition.

Metric	Definition	What it tells you
Fold-improvement in k_{cat}	$k_{cat}^{var}/k_{cat}^{WT}$	Speed-up at saturating S
Fold-improvement in k_{cat}/K_m	$(k_{cat}/K_m)^{var}/(k_{cat}/K_m)^{WT}$	Catalytic efficiency at low S (closer to <i>in vivo</i>)
Substrate scope	# of new substrates accepted	Breadth of activity
Enantioselectivity (E-value)	$\ln[(1 - c)(1 - ee_S)]/\ln[(1 - c)(1 + ee_S)]$	Discrimination between enantiomers
Thermal stability (T_{50} , T_m)	Temp at half-activity / unfolding midpoint	Process robustness
Half-life under operating conditions	Time to lose 50% activity	Industrial economics
Specific activity	$\mu\text{mol}/\text{min}/\text{mg}$	Practical productivity
Total turnover number (TTN)	Total substrate molecules per enzyme before death	Catalyst longevity

A successful directed evolution campaign will track several of these metrics simultaneously across many rounds; the best-known successes (e.g., engineered transaminases for sitagliptin manufacture) achieved 25,000-fold rate improvements and $>10^6$ TTN over about 10 evolutionary rounds.

4.9 Worked Examples: Rates, Inhibition, and Catalytic Efficiency

Problem 1: An enzyme obeys Michaelis-Menten kinetics with $K_m = 2.0\text{ mM}$ and $V_{max} = 100\text{ }\mu\text{mol}/\text{min}$. Calculate v_0 at **S** = 0.5 mM, 2.0 mM, 10 mM, and 200 mM.

Solution:

$$v_0 = \frac{100 \times [\text{S}]}{2.0 + [\text{S}]}$$

(92)

Table 89. Quantitative Metrics for Engineered Enzymes: **S** (mM) and v_0 ($\mu\text{mol}/\text{min}$).

S (mM)	v_0 ($\mu\text{mol}/\text{min}$)	% of V_{max}
0.5	$100 \times 0.5/2.5 = 20.0$	20%
2.0	$100 \times 2.0/4.0 = 50.0$	50% (by definition, S = K_m)
10.0	$100 \times 10/12 = 83.3$	83.3%

S (mM)	v_0 ($\mu\text{mol/min}$)	% of V_{max}
200.0	$100 \times 200/202 = 99.0$	99.0% (near saturation)

Problem 2: In the presence of a competitive inhibitor at **I** = 5 mM and $K_i = 2.5$ mM, what is the new apparent K_m ? At what **S** will $v_0 = V_{\text{max}}/2$?

Solution:

$$\alpha = 1 + \frac{[I]}{K_i} = 1 + \frac{5.0}{2.5} = 3.0 \tag{93}$$
$$K_m^{\text{app}} = \alpha K_m = 3.0 \times 2.0 = 6.0 \text{ mM} \tag{94}$$

$v_0 = V_{\text{max}}/2$ when **S** = $K_m^{\text{app}} = 6.0$ mM. The inhibitor triples the substrate concentration needed for half-maximal velocity.

Problem 3: The Hill coefficient for hemoglobin is 2.8, and $K_{0.5}$ for O_2 is 26 mmHg. Calculate the fractional saturation at: (a) $\text{pO}_2 = 40$ mmHg (venous blood) (b) $\text{pO}_2 = 100$ mmHg (arterial blood)

Solution:

$$\theta = \frac{[\text{S}]^n}{K_{0.5}^n + [\text{S}]^n} \tag{95}$$

(a) $\theta = \frac{40^{2.8}}{26^{2.8} + 40^{2.8}} = \frac{40^{2.8}}{26^{2.8} + 40^{2.8}}$

$40^{2.8} = e^{2.8 \ln 40} = e^{2.8 \times 3.689} = e^{10.33} = 30,600$

$26^{2.8} = e^{2.8 \ln 26} = e^{2.8 \times 3.258} = e^{9.12} = 9,160$

$\theta = \frac{30,600}{9,160 + 30,600} = \frac{30,600}{39,760} = 0.770$ (77.0%)

(b) $100^{2.8} = e^{2.8 \times 4.605} = e^{12.89} = 396,000$

$\theta = \frac{396,000}{9,160 + 396,000} = 0.977$ (97.7%)

The difference: hemoglobin loads O_2 to 97.7% in the lungs and unloads to 77.0% in tissues, delivering about 20% of its O_2 per circuit. During exercise (venous pO_2 drops to about 20 mmHg), delivery increases substantially due to the steep part of the sigmoidal curve.

4.10 Computational Bridge

The Michaelis–Menten hyperbola is implemented directly on concentrations in μM :

```
from biology.biochemistry import michaelis_menten

res = michaelis_menten(5.0, Vmax=120.0, Km=10.0)
print(res.reaction_rate, res. efficiency) # v and v/Vmax
```

Clinical / systems note: Many drugs are mechanism-based inhibitors that shrink effective V_{max} or raise apparent K_m ; statins compete at HMG-CoA reductase’s active site, illustrating competitive themes at a clinically relevant scale.

4.11 Bridge to Systems: From Enzyme Kinetics to Metabolic Flux

A single enzyme’s K_m , V_{max} , and Hill coefficient become inputs to a higher-level question: what is the flux (J , in $\text{mol L}^{-1} \text{s}^{-1}$) through a metabolic pathway, and which enzyme limits it? This question is the bridge from this chapter to **Unit III — Energy and Metabolism: Introduction** (bioenergetics and respiration).

4.11.1 Pathway Flux is Set by Multiple Enzymes, Not One

The classical idea that a single “rate-limiting step” governs a pathway has been replaced by metabolic control analysis (MCA), developed in the 1970s by Heinrich, Rapoport, Kacser, and Burns. MCA assigns each enzyme i a flux control coefficient:

$$C_i^J = \frac{\partial \ln J}{\partial \ln [E_i]}$$

(96)

This is the fractional change in steady-state flux when the activity of enzyme i is changed by a small fraction. The summation theorem states that for any pathway:

$$\sum_i C_i^J = 1$$

(97)

Three lessons follow:

1. Control is distributed. No single enzyme has $C_i^J = 1$; instead, glycolytic flux in muscle is controlled by hexokinase ($C^J \approx 0.3$), PFK-1 ($C^J \approx 0.3$), pyruvate kinase ($C^J \approx 0.2$), and others.
2. Targeting the “rate-limiting” enzyme often disappoints. Doubling PFK-1 primarily doubles flux if $C^J = 1$, which is rarely true. This is why metabolic engineering campaigns to improve product yields often increase one enzyme tenfold for a 1.5-fold flux gain.
3. Allosteric regulation tunes the control distribution. When ATP is high, AMP is low, and ATCase or PFK-1 sit in their T-state, C^J for those enzymes rises toward 1; the cell concentrates control where it can respond quickly to demand changes.

4.11.2 Enzyme Saturation Modes Determine Pathway Behavior

The local $[S]/K_m$ ratio for each enzyme determines whether it operates near saturation or far below. Glycolytic enzymes typically operate at $[S] \approx K_m$ (around half-saturation), where the response to small $[S]$ changes is approximately linear and control coefficients are large. Enzymes whose substrates are at $\gg K_m$ (saturated) have $C^J \approx 0$ and exert no flux control. Designing a pathway thus means choosing K_m values matched to physiological metabolite concentrations — a constraint visible in the convergent evolution of glycolytic enzymes across most kingdoms of life.

4.11.3 Branching Points and Connectivity

When a metabolite sits at a branch point (e.g., glucose-6-phosphate, fed into glycolysis or the pentose phosphate pathway), the control coefficient for one branch can exceed 1, balanced by a *negative* control coefficient on the other branch. Allosteric regulation at branch points (NADPH-mediated inhibition of glucose-6-phosphate dehydrogenase; citrate inhibition of PFK-1) allows the cell to apportion flux based on demand.

Unit III — Energy and Metabolism: Introduction revisits these concepts at the level of full pathways (glycolysis, TCA cycle, electron transport) and shows how phosphorylation cascades, hormone-driven changes in enzyme abundance, and substrate cycles allow flux to vary 100-fold between rest and exercise.

Concept Check 8: Insulin treatment of a hepatocyte reduces gluconeogenic flux by about 10× within minutes, primarily by phosphorylating PFK-2/FBPase-2 to raise [fructose-2,6-bisphosphate]. Without invoking transcription, explain how this allosteric activator achieves a 10× flux reduction while individual enzyme abundances remain unchanged. Use the language of C^J and K_m .

4.12 Current Evidence and Frontier Biology: Enzymes and the Kinetics of Catalysis

For Enzymes and the Kinetics of Catalysis, frontier biology belongs inside the evidence logic of the chapter. Chemistry-of-life claims now connect classical bonding and thermodynamics with AI-guided structure prediction and experimental validation. The core reading question is this: enzyme claims should separate binding, catalysis, regulation, transport limits, and measurement conditions.

- What to verify: identify the observation, model, assay, or dataset that would make the claim stronger or weaker.
- What to qualify: state the scale, organism, cell type, environmental condition, or population where the claim is expected to hold.
- What to compare: test at least one alternative explanation, baseline, or null model before treating the pattern as causal.
- What to cite: distinguish primary evidence, review synthesis, public dataset, and institutional guidance; for recent or numeric claims, prefer the source closest to the measurement and state what has changed since it was published.

Treat biomolecular predictions as constrained hypotheses: compare confidence, conservation, solvent exposure, and assay evidence before claiming mechanism [Abramson et al., 2024].

Enzyme and pathway sources answer different parts of a mechanism. BRENDA in 2026 is the release-specific enzyme resource to cite for curated functional enzyme, ligand, kinetic, and organism-linked data; KEGG and BioCyc-style pathway databases place reactions into organism-aware pathway maps and pathway/genome databases. When a pathway diagram is used as evidence, record the EC number or reaction identifier, organism, database release or access date, and whether flux was measured experimentally or inferred from annotation [Hauenstein et al., 2026, Kanehisa Laboratories, 2026, SRI International, 2026].

Source practice: For structure and interaction claims, cite experimental structures when available and validate predictions with confidence metrics, conservation, mutagenesis, binding, or cryo-EM/X-ray/NMR evidence [Abramson et al., 2024, Bertoni et al., 2026, EMBL's European Bioinformatics Institute, 2026].

4.12.1 Current Evidence Map: Enzyme Engineering Evidence Chain



Figure 38. Enzyme-engineering claims need rate, specificity, stability, and context; a better active-site story is not enough without quantitative kinetics.

4.13 Summary

- Enzymes are protein catalysts that lower the activation energy ΔG^\ddagger without altering equilibrium.
- Rate enhancement mechanisms include proximity/orientation, transition state stabilization, acid-base catalysis, covalent catalysis, and metal ion catalysis.
- The Michaelis-Menten equation: $v_0 = V_{max}[S]/(K_m + [S])$; K_m approximates substrate affinity; k_{cat} = turnover number; k_{cat}/K_m = catalytic efficiency.
- Enzyme inhibition: competitive (increases apparent K_m), uncompetitive (decreases both K_m and V_{max}), mixed/noncompetitive (V_{max} decreases), irreversible (covalent inactivation). Each has a characteristic Lineweaver-Burk pattern.
- Allosteric enzymes exhibit sigmoidal kinetics (Hill equation); key for metabolic feedback control. ATCase is the paradigm for allosteric regulation.
- pH, temperature, and cofactor availability most modulate enzyme activity. Vitamin deficiencies impair coenzyme-dependent enzymes.
- Enzymes are classified into seven EC classes (the seventh, translocases, added in 2018).
- Modern enzyme applications include CRISPR-Cas9 gene editing, industrial biocatalysis, and directed evolution.
- Connections: See **Unit III — Energy and Metabolism: Introduction** (pathway-level flux and regulated enzymes), **Unit IV — Molecular Genetics: Introduction** (polymerases and repair enzymes), and **Unit VII — Microbiology: Introduction** (antibiotic targets in bacterial metabolism).

4.14 Key Terms

- Activation energy (ΔG^\ddagger): Energy barrier between reactants and transition state
- Active site: Region of enzyme that binds substrate and catalyses reaction
- Transition state: Highest-energy intermediate along the reaction coordinate
- Michaelis constant (K_m): Substrate concentration at half-maximal velocity
- Turnover number (k_{cat}): Maximum substrate molecules converted per enzyme per second
- Catalytic efficiency (k_{cat}/K_m): Overall measure of enzyme performance
- Competitive inhibition: Inhibitor competes with substrate for active site; overcome by high **S**
- Uncompetitive inhibition: Inhibitor binds primarily the ES complex
- Mixed inhibition: Inhibitor binds both E and ES at an allosteric site
- Irreversible inhibition: Covalent modification permanently inactivates the enzyme
- Allosteric regulation: Modulation by effector binding at a site other than the active site
- Hill coefficient (n): Measure of cooperativity; $n > 1$ = positive cooperativity
- Feedback inhibition: End product inhibits an early enzyme in its biosynthetic pathway
- Coenzyme: Organic cofactor, often derived from a water-soluble vitamin
- Prosthetic group: Tightly bound cofactor (e.g., haem, FAD)
- Holoenzyme: Complete enzyme with most cofactors bound
- Apoenzyme: Enzyme protein without its cofactor
- EC number: Four-digit enzyme classification number assigned by IUBMB
- Transition state analog: Inhibitor that mimics the transition state geometry
- Directed evolution: Laboratory technique for engineering improved enzymes

4.15 Review Questions

- Explain, using transition state theory, why an enzyme that binds the transition state 10^6 -fold more tightly than the substrate achieves a rate enhancement of approximately 10^6 -fold.
- Derive the Michaelis-Menten equation starting from the steady-state assumption. State the assumptions clearly.
- An enzyme has $K_m = 0.2$ mM and $V_{max} = 50$ μ mol/min. A competitive inhibitor ($K_i = 0.1$ mM) is added at 0.5 mM. Calculate the apparent K_m and the rate at **S** = 0.2 mM with and without inhibitor.
- On a Lineweaver-Burk plot, two lines obtained with and without an inhibitor are parallel. Identify the type of inhibition and explain what molecular event is occurring.

5. The Hill coefficient for phosphofructokinase-1 is approximately 3.8. What does this tell you about the enzyme’s response to changes in substrate concentration near $K_{0.5}$?
6. Explain how aspirin’s mechanism of action (irreversible COX inhibition) accounts for both its anti-inflammatory properties and its use as an antiplatelet drug.
7. Why do statins lower blood cholesterol more effectively than simply reducing dietary cholesterol intake? Consider the relative contributions of endogenous synthesis and dietary absorption.
8. A food scientist wants to use an immobilised enzyme in a continuous-flow reactor. What are three advantages of enzyme immobilisation over using the free enzyme in solution?
9. CRISPR-Cas9 requires a PAM sequence (5'-NGG-3') adjacent to its target. Explain why this requirement exists and how it affects the enzyme’s specificity. How does this relate to the concept of substrate recognition?
10. Pellagra (deficiency of niacin/vitamin B3) causes the “three Ds”: dermatitis, diarrhea, and dementia. Given that niacin is the precursor to NAD^+ , explain why this deficiency has such widespread systemic effects.
11. Using `michaelis_menten`, compute v at $[S] = K_m/2$, K_m , and $2K_m$ for the same V_{max} . Verify numerically that v is not linear in $[S]$ even when $[S] \ll K_m$ is often approximated as linear.
12. Explain why k_{cat}/K_m is a useful upper-bound metric for substrate discrimination under cellular subsaturating conditions, and give one evolutionary scenario where **natural selection** would increase this ratio.
13. A two-substrate enzyme is studied at varying **A** for several fixed **B**. The Lineweaver-Burk plot reveals intersecting lines that meet to the left of the y-axis. Use equation (86) and equation (87) to argue whether the mechanism is sequential or ping-pong.
14. Compare the switching sensitivity (fold-change in θ for a 2 \times change in **S** near $K_{0.5}$) of cooperative enzymes with $n = 1, 2, 4, 8$. Why do regulatory (rate-controlling) enzymes typically have $n > 2$ while housekeeping enzymes are usually hyperbolic?
15. A directed-evolution campaign improves a transaminase’s k_{cat}/K_m by 100 \times over six rounds of mutation/selection. Discuss two metrics besides k_{cat}/K_m that the campaign should monitor in parallel, and explain why k_{cat}/K_m alone is not sufficient to declare success for an industrial process.
16. Using equation (97), argue why doubling the abundance of a single “rate-limiting” glycolytic enzyme rarely doubles glycolytic flux. Suggest one cellular scenario where the flux control coefficient C^J for PFK-1 would approach 1.

4.16 Further Reading and Source Notes: Enzymes and the Kinetics of Catalysis

- Fischer (1894). Einfluss der Configuration auf die Wirkung der Enzyme. *Berichte der deutschen chemischen Gesellschaft*, 27.
- Koshland (1958). Application of a Theory of Enzyme Specificity to Protein Synthesis. *Proceedings of the National Academy of Sciences*, 44.

4.17 Companion Source Module: Enzymes and the Kinetics of Catalysis

Enzymes and the Kinetics of Catalysis should leave a reproducible trail from a biological claim to the code, figure, diagram, or paper-based activity that can test it. Use the surfaces below to inspect the chapter’s assumptions, rerun the relevant model, or compare the manuscript explanation with companion labs and figures.

Table 90. Companion source surfaces for Enzymes and the Kinetics of Catalysis.	
Surface	Use it for
<code>src/biology/biochemistry/biochemistry.py</code> (<code>michaelis_menten</code> , <code>competitive_inhibition</code> , <code>enzyme_rate_curve</code>)	Reproduce saturation curves, inhibition shifts, and parameter interpretation.
<code>src/visualization/plots.py</code> (<code>plot_michaelis_menten</code>)	Check that graph shape, axes, and units match the kinetic equation.
<code>src/mermaid/biology_diagrams.py</code> (<code>enzyme_kinetics_diagram</code>)	Keep mechanism, substrate binding, and regulation visually aligned.

Reproducibility check: report substrate range, enzyme amount, temperature, pH, and rate units before comparing kinetic parameters. Cross-reference: connect kinetics to section 11 and section 13.

Unit II — The Cell: Introduction

Why This Unit Matters

In 1665, Robert Hooke pressed a thin sliver of cork against the lens of a compound microscope he had built himself and saw, for the first time in human history, the architectural unit of life: the cell. He called them *cellulae* — small rooms — because they reminded him of monks’ chambers in a monastery. What Hooke saw in cork were dead walls. Antoni van Leeuwenhoek, a decade later, saw living cells: bacteria darting through pond water, human sperm, red blood cells coursing through capillaries. The universe had grown smaller in every direction.

Today, three and a half centuries after those first observations, the cell remains the central unit of biology — and it turns out to be far stranger and more sophisticated than Hooke could have imagined. A typical human liver cell contains about 20,000 different proteins, about 5 km of DNA, about 5,000 mitochondria, and about 10 million ribosomes, most coordinated within a volume of roughly 1,000 μm^3 . Every second, that cell performs thousands of enzymatic reactions, processes about 20 receptor signals, divides its mitochondria, degrades misfolded proteins in lysosomes at pH 4.5, and repairs about 10,000 DNA lesions in its nucleus — most simultaneously, without a central coordinator.

This unit examines the cell at three levels of resolution: the cellular (organelle inventory and function), the molecular (membrane biophysics, signal transduction), and the computational (mathematical models of cell size constraints, diffusion, and membrane potential). You will encounter the endosymbiotic theory — one of the most elegant and evidence-rich hypotheses in biology — and the minimal cell, which asks: what is the irreducible instruction set for life?

Landmark Discoveries

Discoverer(s)	Year	Journal / Source	Discovery	Significance
Robert Hooke	1665	[Hooke, 1665]	“Cells” in cork	Named and conceptualised the cellular unit; launched microscopy as a biological tool
Schleiden & Schwann	1838–39	[Schleiden, 1838, Schwann, 1839]	Cell theory (plants + animals)	First two postulates: most organisms are composed of cells
Rudolf Virchow	1855	[Virchow, 1855]	<i>Omnis cellula e cellula</i>	Third postulate: cells arise primarily from pre-existing cells; foundational to cancer biology
George Palade	1953	[Palade, 1955]	Ribosome discovery via electron microscopy	Identified the protein synthesis machinery; Nobel Prize, 1974
Peter Mitchell	1961	[Mitchell, 1961]	Chemiosmosis — proton-gradient-driven ATP synthesis	Explained mitochondrial ATP production; later became central to Unit III — Energy and Metabolism: Introduction
Lynn Margulis	1967	[Sagan, 1967]	Formal endosymbiotic theory	Proposed mitochondria and chloroplasts are descended from engulfed bacteria
J. Craig Venter et al.	2016	[Hutchison et al., 2016]	JCVI-syn3.0: minimal synthetic cell (473 genes)	Defined the lower boundary of self-replicating cellular life

Key Concepts and Connections

Current Evidence Thread

Read Unit II — The Cell: Introduction as a measurement story: cell biology is now captured as live-cell biosensor and optogenetic recordings, cryo-electron tomograms, spatial and single-cell atlases, and perturbational screens rather than static diagrams alone. As you move through the chapters, keep a two-column note: claim on the left, evidence that would change my confidence on the right. By the end of the unit, each major idea should be tied to a measurement, model, citation, or paper-based lab decision.

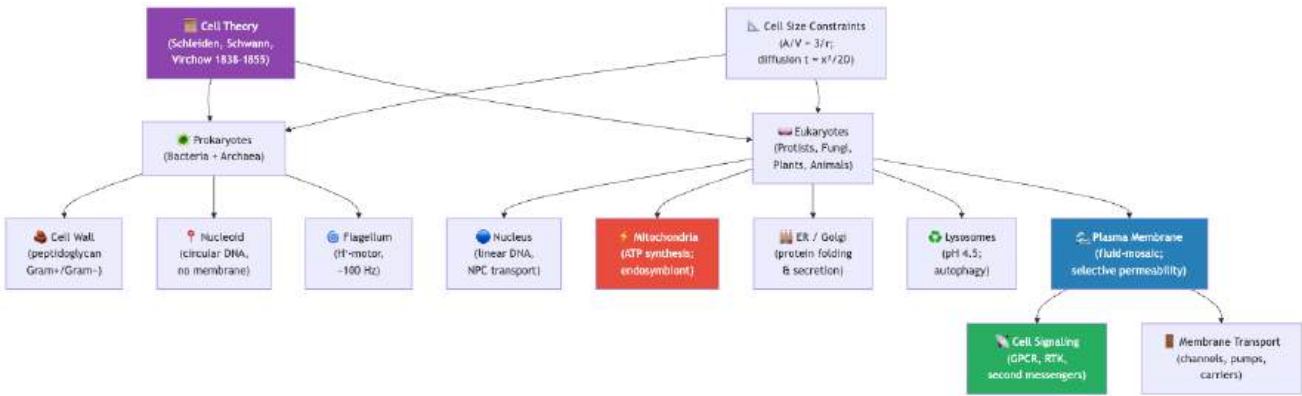


Figure 39. Cell concept map - purple = foundational theory; red = energy-related organelles anticipating energy metabolism; blue = membrane; green = signaling.

Chapter Roadmap

Chapter	Title	Core Question	Key Equation / Model
5	Cell Theory and Cell Types	What is a cell, and how did cell theory transform biology?	$A/V = 3/r; t = x^2/2D$
6	Cell Structure and Organelles	How do eukaryotic organelles achieve compartmentalised function?	Nernst equation (membrane potential)
7	Membrane Transport	How do cells control passage across membranes?	Fick's First Law: $J = -D(dC/dx)$
8	Cell Signaling	How do extracellular signals change intracellular behavior?	Hill equation (co-operativity); cAMP second messenger models

Connections Across the Textbook

- Membranes and transport (section 7) are the physical substrate for the proton-motive force of mitochondria and chloroplasts (Unit III — Energy and Metabolism: Introduction) and the action potential of neurons (Unit IX — Zoology and Systems Physiology: Introduction).
- Cell signaling (section 8) reappears in Unit IV — Molecular Genetics: Introduction (nuclear signaling and gene regulation), Unit V — Classical Genetics and Heredity: Introduction (mitosis/meiosis checkpoints), Unit IX — Zoology and Systems Physiology: Introduction (hormone receptor cascades), and oncogene/tumor-suppressor biology.
- Endosymbiosis directly informs Unit VI — Evolution: Introduction (mitochondrial DNA as molecular clock), Unit VII — Microbiology: Introduction (organelle gene transfer to nucleus), and Unit VIII — Botany — Plant Biology: Introduction (chloroplast inheritance).
- Prokaryotic cell structure (cell walls, flagella, pili) underpins Unit VII — Microbiology: Introduction (Microbiology) — antibiotic mechanisms, Gram staining, biofilm formation.

Key vocabulary introduced here: prokaryote, eukaryote, organelle, nucleoid, plasma membrane, endosymbiosis, fluid-mosaic model, ligand, receptor, second messenger, autophagy.

Computational Toolbox — Unit II

```
from biology.cell import nernst_potential, goldman_equation, IonConcentration

# Nernst equation: equilibrium potential for K+ at 37°C
k_ion = IonConcentration(name="K+", intracellular_mM=150, extracellular_mM=4, valence=1)
e_k = nernst_potential(k_ion)
print(f"E_K = {e_k:.1f} mV")
# Expected: E_K = -89.7 mV (close to resting potential of -70 mV; K+ is dominant)

# Goldman-Hodgkin-Katz equation: resting membrane potential
# Permeabilities at rest: P_K = 1.0, P_Na = 0.04, P_Cl = 0.45
```

```
ions = [  
    IonConcentration("K+", 150, 4, valence=1),  
    IonConcentration("Na+", 15, 145, valence=1),  
    IonConcentration("Cl-", 10, 120, valence=-1),  
]  
  
permeabilities = {"K+": 1.0, "Na+": 0.04, "Cl-": 0.45}  
v_rest = goldman_equation(ions, permeabilities)  
print(f"V_rest (GHK) = {v_rest:.1f} mV")  
# Expected: V_rest (GHK) ≈ -70.0 mV
```

Try it yourself: Change P_{Na} from 0.04 to 0.6 (simulating an action potential peak) and observe how V_{rest} shifts toward E_{Na} (≈ +60 mV).

Source note: cell-biology helpers cover membrane biophysics, signal transduction, and organelle inventory. Mermaid diagrams and Nernst plots provide the visual companion.

Cross-Unit Integration

The membrane structure, transport mechanisms, and organelle inventory of **Unit II — The Cell: Introduction** are the staging ground for the energetics of **Unit III — Energy and Metabolism: Introduction**. Passive and active transport across the plasma membrane sets up the ion and proton gradients that drive ATP synthesis; the mitochondrial inner membrane’s selective permeability is what makes oxidative phosphorylation thermodynamically possible; chloroplast thylakoid membranes function on the same chemiosmotic principle. The compartmentalization you just learned is not decorative — it is the *prerequisite* for the energy-coupling story in **Unit III — Energy and Metabolism: Introduction**. Watch how concepts like electrochemical gradient, membrane potential, and selective channel permeability migrate directly from **Unit II — The Cell: Introduction** vocabulary into **Unit III — Energy and Metabolism: Introduction** mechanisms without redefinition.

5 Cell Theory and Cell Types

Level 1/3 · 45 min read · 50 min lecture · Prerequisites: section 3

5.1 Learning Objectives

1. State the three original tenets of cell theory (Schleiden, Schwann, Virchow) and the modern additions.
2. Compare the structural organization of prokaryotic, eukaryotic, and archaeal cells at the molecular level.
3. Describe the endosymbiotic [Sagan, 1967] theory and evaluate the molecular evidence supporting it.
4. Classify cells by metabolic lifestyle (autotrophic vs. heterotrophic) and oxygen relationship.
5. Quantify the surface-area-to-volume relationship and derive the mathematical constraints on cell size.
6. Explain microscopy techniques from bright-field to cryo-EM and super-resolution methods.
7. Describe the minimal cell concept (JCVI-syn3.0) and its implications for defining life.
8. Evaluate extremophile cells as evidence for the range of possible cellular adaptations and their relevance to astrobiology.

5.1.1 Study Blueprint

- Big idea: Cells are bounded, evolving systems whose size and organization reflect physical constraints.
- Core concepts: cell theory, surface area, microscopy, prokaryote/eukaryote comparison.
- Framework alignment: Vision & Change: Structure and function, Systems, Information flow, exchange, and storage; AP Biology: Systems Interactions, Information Storage and Transmission; NGSS-style topics: Structure and Function.
- Model or quantitative lens: Surface-area-to-volume scaling.
- Data skill: Infer cellular constraints from measurements, micrographs, and scale bars.
- Practice cadence: Visual Representations, Questions and Methods, Argumentation.
- Common misconception to repair: Cells are not just small bags of fluid; boundaries and internal organization create function.
- Primary lab: Lab — Cell Theory and Cell Types.
- Question bank: Questions — Cell Theory and Cell Types.
- Transfer task: Transfer scale reasoning to eggs, neurons, root hairs, and microbial colonies.
- Bridge to computation: `biology.cell.cell_biology.diffusion_flux`.

Opening Vignette: The First Cell You Ever Saw

In 1665, Robert Hooke pressed a thin sliver of cork against the lens of a compound microscope he had constructed himself and published his observations in *Micrographia* — a book so popular that Samuel Pepys stayed up until 2 a.m. reading it. Hooke saw a regular array of empty compartments — the remnant cell walls of dead plant cells — and named them cellulae (from Latin, “small rooms”). He had no idea that cells were alive. That insight required a further 174 years of microscopy, culminating in the cell theory formulations of Schleiden [1838], Schwann (1839), and Virchow [1855].

Today, a single human body contains approximately 37.2 trillion cells (Bianconi et al., 2013, *Annals of Human Biology*) — a number so large that if laid end-to-end they would circle the Earth 200 times. Every one of those cells descended, by an unbroken chain of cell division, from a single fertilized egg roughly nine months before your birth. And every cell alive on Earth today is the product of 3.7 billion years of unbroken cell division since the origin of life — not one cell has ever been created from scratch by spontaneous generation since Leuwenhoek looked through his microscope in 1674.

Primary source: Bianconi, E. et al. (2013). *An estimation of the number of cells in the human body. Annals of Human Biology*, 40(6), 463–471.

5.2 The Cell as the Fundamental Unit of Life

5.2.1 Historical Development of Cell Theory

The development of cell theory spans over two centuries and represents one of the most important unifying principles in biology.

Robert Hooke [1665] first observed “cells” (actually dead cell walls) in cork using a compound microscope he built himself. He published his observations in *Micrographia*, coining the term “cell” because the structures reminded him of monks’ rooms (cellae) in a monastery.

Antonie van Leeuwenhoek (1674-1683) constructed single-lens microscopes achieving about 270x magnification and observed living cells for the first time — bacteria (“animalcules”), protists, sperm cells, and red blood cells in capillary blood flow.

Matthias Schleiden [1838], a botanist, concluded that most plant tissues are composed of cells and that the cell is the basic unit of plant structure.

Theodor Schwann [1839], a zoologist and Schleiden’s colleague, extended this principle to animals, proposing that most animal tissues are also composed of cells. Together, Schleiden and Schwann formulated the first two tenets of cell theory.

Rudolf Virchow [1855] contributed the third tenet with his famous dictum *omnis cellula e cellula* (“every cell from a cell”), establishing that cells arise primarily from pre-existing cells through division. This principle demolished the lingering notion of spontaneous generation and established the continuity of life.

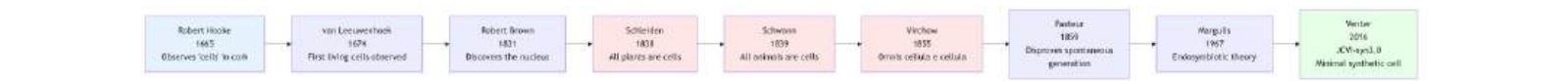


Figure 40. Timeline of key milestones in cell theory development, from Hooke’s first observations to the modern synthetic minimal cell.

5.2.2 The Three Original Postulates

The cell theory, formalised by Schleiden [1838], Schwann [1839], and Virchow [1855], rests on three founding principles:

1. Most living organisms are composed of one or more cells.
2. The cell is the basic structural and functional unit of cellular organisms.
3. Most cells arise from pre-existing cells (*omnis cellula e cellula* — Virchow, 1855).

A corollary of the third tenet is that life is a continuous lineage — every cell on Earth today descends without interruption from the first cells, approximately 3.5–3.8 billion years ago. The oldest microfossils, found in Pilbara (Western Australia) and Barberton (South Africa), date to about 3.5 Ga and show morphologies consistent with filamentous prokaryotes.

5.2.3 Modern Additions to Cell Theory

Modern cell biology has expanded the original three postulates:

4. The cell contains heritable information (DNA) that directs its activities and is passed to daughter cells. This was established by the work of Avery, MacLeod, and McCarty (1944) and confirmed by Hershey and Chase [1952].
5. Most cells have the same basic chemical composition. Most known cells use DNA as genetic material, RNA as intermediary, proteins as catalysts, and phospholipid bilayers as membranes.
6. Energy flow (metabolism and biochemistry) occurs within cells. Most metabolic transformations — glycolysis, the TCA cycle, oxidative phosphorylation — take place within or across cell membranes.
7. Cells contain the information necessary for their own reproduction. The genome encodes not just structural components but the regulatory logic for cell division, differentiation, and programmed cell death.

Clinical Connection: Virchow and the Origin of Cancer Biology Virchow’s principle *omnis cellula e cellula* had a profound clinical implication: if most cells come from pre-existing cells, then cancer cells must also arise from normal cells through transformation. Virchow himself applied this reasoning to pathology, founding the field of cellular pathology. Today, cancer biology rests on the understanding that mutations accumulate in somatic cells, transforming them into malignant clones — a direct intellectual descendant of Virchow’s third postulate. see section 8 (Cell Signaling) for oncogenes and tumor suppressors.

Concept Check 1: Viruses are not considered “alive” by cell theory standards. List three properties of viruses that exclude them from cell theory, and one property that challenges the boundary between living and non-living.

5.3 Size, Scale, and the Surface-to-Volume Constraint

5.3.1 Orders of Magnitude in Biology

Biology spans an enormous range of scales. Understanding this range is essential for appreciating why cells occupy a specific size niche.

Table 91. Orders of Magnitude in Biology: Structure and Approximate size.

Structure	Approximate size	Scale
Water molecule	0.28 nm	Angstrom
Glucose molecule	0.7 nm	Nanometre
Phospholipid bilayer thickness	7–8 nm	Nanometre
Ribosome	25 nm	Nanometre
HIV virus	120 nm	Nanometre
Mitochondrion	1–5 μm	Micrometre
<i>E. coli</i>	1–2 μm	Micrometre
Red blood cell	7–8 μm	Micrometre
Typical animal cell	10–30 μm	Micrometre
Typical plant cell	30–100 μm	Micrometre
<i>Thiomargarita namibiensis</i>	750 μm	Sub-millimetre
Frog egg	1 mm	Millimetre
Ostrich egg (cell)	15 cm	Centimetre

5.3.2 The Mathematics of Cell Size

Cells are small — almost without exception. Why?

The rate of metabolism (nutrient consumption, waste generation) scales with volume ($V \propto r^3$). The rate of exchange with the environment (nutrient uptake, waste removal) scales with surface area ($A \propto r^2$). The ratio:

$$\frac{A}{V} = \frac{4\pi r^2}{\frac{4}{3}\pi r^3} = \frac{3}{r}$$

(98)

As r increases, A/V decreases. A sphere with $r = 1\text{ }\mu\text{m}$ has $A/V = 3\text{ }\mu\text{m}^{-1}$. With $r = 1\text{ mm}$ (1,000x larger), $A/V = 0.003\text{ }\mu\text{m}^{-1}$. Large cells simply cannot exchange nutrients fast enough for their metabolic demand.

5.4 Worked Example: Surface-to-Volume Calculation

Problem: A spherical bacterium has radius $r = 0.5\text{ }\mu\text{m}$. Calculate (a) the surface area, (b) the volume, (c) the A/V ratio. Then repeat for a spherical eukaryotic cell with $r = 10\text{ }\mu\text{m}$ and compare.

Solution:

For the bacterium ($r = 0.5\text{ }\mu\text{m}$):

$$A = 4\pi r^2 = 4\pi(0.5)^2 = 3.14\text{ }\mu\text{m}^2$$

(99)

$$V = \frac{4}{3}\pi r^3 = \frac{4}{3}\pi(0.5)^3 = 0.524\text{ }\mu\text{m}^3$$

(100)

$$\frac{A}{V} = \frac{3.14}{0.524} = 6.0\text{ }\mu\text{m}^{-1}$$

(101)

For the eukaryotic cell ($r = 10\text{ }\mu\text{m}$):

$$A = 4\pi(10)^2 = 1,257\text{ }\mu\text{m}^2$$

(102)

$$V = \frac{4}{3}\pi(10)^3 = 4,189\text{ }\mu\text{m}^3$$

(103)

$$\frac{A}{V} = \frac{1,257}{4,189} = 0.30 \mu\text{m}^{-1}$$

(104)

The bacterium has a 20-fold higher A/V ratio, enabling far more efficient diffusion-based exchange per unit metabolic volume.

5.4.1 Diffusion Time and Cell Size

Diffusion time scales with the square of distance:

$$t = \frac{x^2}{2D}$$

(105)

where D is the diffusion coefficient. For a small molecule ($D \approx 10^{-9} \text{ m}^2/\text{s}$) to diffuse across a $1 \mu\text{m}$ cell takes about 0.5 ms. Across a 1 mm cell, it takes about 500 s (over 8 minutes). This places an absolute upper limit on cell size for diffusion-dependent processes.

5.4.2 Exceptions to Small Cell Size

Exceptions to small cell size achieve large size by: - Increasing surface area: intestinal cells have microvilli (amplify A by about 600x); root hair cells extend long projections - Reducing metabolically active volume: plant vacuoles occupy >80% of cell volume but are largely metabolically inert - Reducing effective diffusion distance: nerve axons can be >1 m long but about 1–20 μm in diameter; active transport supplements diffusion - Cytoplasmic streaming: in giant plant cells (e.g., *Chara* internodal cells, >10 cm), **actin**-myosin-driven streaming circulates **cytoplasm** at about 60 $\mu\text{m}/\text{s}$, overcoming diffusion limitations - Multinucleation: skeletal muscle fibers (up to 30 cm long) contain hundreds of nuclei, each governing a local cytoplasmic domain

Concept Check 2: *Thiomargarita namibiensis* is a bacterium with a diameter of about 750 μm — visible to the naked eye. How does it survive despite having an A/V ratio of about $0.008 \mu\text{m}^{-1}$? (Hint: consider what fills >95% of its volume.)

5.4.3 The Cube Law and Why Giant Cells Are Impossible

The surface-to-volume problem can be sharpened into what physiologists call the cube law of metabolism. If we model a cell as a sphere of radius r , mass m , and uniform density ρ , then:

$$m = \rho \cdot \frac{4}{3}\pi r^3, \quad A = 4\pi r^2$$

(106)

Suppose every unit volume of cytoplasm consumes oxygen at a constant rate q (mol $\text{O}_2 \text{ s}^{-1} \text{ m}^{-3}$). The total metabolic demand \dot{M}_{demand} scales as:

$$\dot{M}_{\text{demand}} = q \cdot V = q \cdot \frac{4}{3}\pi r^3$$

(107)

Maximum oxygen flux through the membrane is set by Fick’s law and is bounded by surface area:

$$\dot{M}_{\text{supply}} = P_{\text{O}_2} \cdot \Delta[\text{O}_2] \cdot A = P_{\text{O}_2} \cdot \Delta[\text{O}_2] \cdot 4\pi r^2$$

(108)

A viable cell requires $\dot{M}_{\text{supply}} \geq \dot{M}_{\text{demand}}$. Setting these equal yields a maximum admissible radius:

$$r_{\text{max}} = \frac{3 P_{\text{O}_2} \Delta[\text{O}_2]}{q}$$

(109)

For typical mammalian parameters ($P_{\text{O}_2} \approx 1 \times 10^{-4} \text{ m/s}$, $\Delta[\text{O}_2] \approx 0.2 \text{ mM}$, $q \approx 1 \text{ mol O}_2 \text{ m}^{-3} \text{ s}^{-1}$), $r_{\text{max}} \approx 60 \mu\text{m}$ — close to the upper bound for actively respiring animal cells. Larger cells must reduce q (e.g., plant vacuoles), increase A (microvilli, infoldings), or accept partial anoxia in their cores. This is the cube law of metabolism: demand scales with r^3 , supply with r^2 , so any uniform cell hits a hard ceiling on size.

Concept Check 3a: Using equation (109) with the parameters above, by what factor would q have to drop to allow a 1 mm diameter respiring cell to survive without surface amplification?

5.4.4 Quantitative Comparison: Prokaryote vs. Eukaryote

Prokaryotes and eukaryotes occupy fundamentally different scales of organization. The differences in linear dimension translate to even larger gaps in volume, surface area, and information content:

Table 92. Quantitative Comparison: Prokaryote vs. Eukaryote: Property and E. coli (prokaryote).

Property	<i>E. coli</i> (prokaryote)	HeLa cell (eukaryote)	Ratio (Euk/Prok)
Length / diameter	2 μm \times 0.5 μm	about 20 μm	about 10–40 \times
Volume	about 1 μm^3	about 4,000 μm^3	about 4,000 \times
Surface area	about 6 μm^2	about 5,000 μm^2	about 830 \times
A/V	about 6 μm^{-1}	about 1.25 μm^{-1}	0.21 \times (lower)
Genome size	4.6 Mbp	6.4 Gbp (diploid)	about 1,400 \times
Protein number	about 3 $\times 10^6$	about 2 $\times 10^{10}$	about 7,000 \times
Doubling time	20 min (rich media)	about 24 h	70 \times slower
ATP turnover (molecules/s)	about 10 ⁹	about 10 ¹⁰	about 10 \times

Worked Example: Why eukaryotes need internal membranes. A HeLa cell with $r = 10\text{ }\mu\text{m}$ has about $1.25\text{ }\mu\text{m}^{-1}$ surface-to-volume — about 5-fold less than *E. coli*. Yet the eukaryotic cell sustains roughly 10 \times higher absolute metabolic flux. The arithmetic closes if the eukaryote *adds internal membrane surface area* equivalent to the plasma membrane’s deficit. Indeed, the inner mitochondrial membrane in a single hepatocyte provides about $3 \times 10^4\text{ }\mu\text{m}^2$ of additional respiratory surface — roughly 6 \times the plasma membrane area. Compartmentalization is therefore not optional aesthetics: it is the topological solution to the cube-law constraint on a body plan that contains 1,000 \times more cytoplasm than a bacterium.

Concept Check 3b: A spherical eukaryotic cell with $r = 10\text{ }\mu\text{m}$ has plasma-membrane area $A_{\text{PM}} \approx 1,260\text{ }\mu\text{m}^2$. If respiratory demand scales with cytoplasmic volume and the cell needs 6 \times the plasma-membrane area to support its metabolism, estimate the total inner membrane area its mitochondria must provide.

Concept Check (Analysis): A spherical bacterial cell has radius $r = 1\text{ }\mu\text{m}$; a giant squid neuron axon has radius $r = 500\text{ }\mu\text{m}$. (a) Calculate the surface-area-to-volume (SA/V) ratio for each. (b) Diffusion of ATP from the cell center to the periphery takes time $t \propto r^2/D$ where $D(\text{ATP}) = 300\text{ }\mu\text{m}^2/\text{s}$. Calculate the diffusion time for each cell. (c) The squid axon uses active axonal transport (kinesin at $1\text{ }\mu\text{m}/\text{s}$) rather than diffusion for cargo delivery. At what axon length does active transport become strictly necessary (say, when diffusion time exceeds 1 hour)?

Worked Example — Surface-Area-to-Volume Limits on Cell Size: Consider a cell approximated as a sphere of radius r . Metabolic rate scales with volume $V = (4/3)\pi r^3$, while nutrient/waste exchange scales with surface area $SA = 4\pi r^2$. Oxygen diffusion flux across the membrane: $J_{\text{O}_2} = P \times \Delta\text{CO}_2$, where P = permeability \times SA. If the cell’s O₂ consumption rate is q per unit volume, the cell can grow provided $J_{\text{O}_2} > q \times V$, i.e., $P \times SA/V > q$. For a typical eukaryotic cell: $P(\text{O}_2) \approx 0.04\text{ cm}/\text{s}$, $q \approx 10^{-10}\text{ mol}/\text{s}$ per cell (radius $10\text{ }\mu\text{m}$). Verify: $SA/V = 3/r = 3/(10 \times 10^{-4}\text{ cm}) = 300\text{ cm}^{-1}$. $J = P \times SA/V \times \Delta\text{CO}_2 = 0.04 \times 300 \times 200\text{ }\mu\text{M} = 2400\text{ }\mu\text{M}\cdot\text{cm}/\text{s}$ — exceeds q . Now scale to $r = 1\text{ mm}$: $SA/V = 3/0.1 = 30\text{ cm}^{-1}$; $J = 0.04 \times 30 \times 200 = 240\text{ }\mu\text{M}\cdot\text{cm}/\text{s}$ — still OK at periphery, but the center is now O₂-limited, explaining why cells $>200\text{ }\mu\text{m}$ in avascular tissue become hypoxic and die.

5.5 Microscopy: Seeing the Cell

Understanding cells requires seeing them. The history of cell biology is inseparable from advances in microscopy.

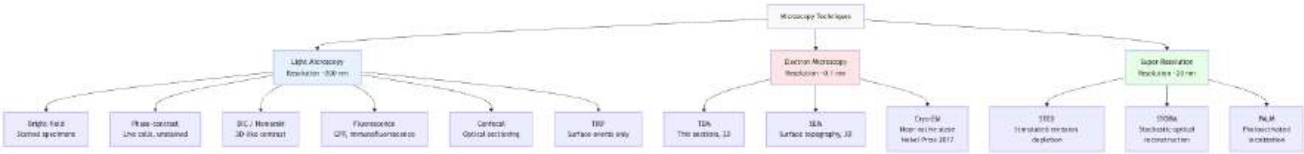


Figure 41. Microscopy methods grouped by resolving power: light techniques for live and stained cells, electron microscopy for ultrastructure, and super-resolution methods that beat the diffraction limit.

5.5.1 Light Microscopy, Contrast, and Resolution

The resolution limit of light microscopy is governed by the Abbe diffraction limit:

$$d = \frac{\lambda}{2 \cdot \text{NA}} \tag{110}$$

where λ is the wavelength of light and NA is the numerical aperture of the objective. For visible light ($\lambda \approx 550 \text{ nm}$) and a high-quality oil-immersion objective ($\text{NA} = 1.4$): $d \approx 200 \text{ nm}$.

Bright-field microscopy: Transmitted light; specimens typically stained (H&E, **Gram stain**). Simple but limited contrast for living cells.

Phase-contrast microscopy: Converts phase differences (from refractive index variations in transparent specimens) into amplitude differences visible as contrast. Ideal for observing living, unstained cells. Invented by Frits Zernike (Nobel Prize in Physics, 1953).

Differential interference contrast (DIC/Nomarski): Uses polarized light split into two beams that pass through slightly different optical paths in the specimen. Produces a pseudo-3D relief image with excellent contrast. Eliminates the “halo” artifact of phase-contrast.

Fluorescence microscopy: Specimens labeled with fluorophores (antibodies conjugated to FITC, Cy3, Cy5; or genetically encoded GFP and derivatives). Excitation light of specific wavelength causes fluorophore emission at a longer wavelength. Enables specific protein localization, live-cell imaging, and multiplexing (multiple colors simultaneously).

Confocal laser scanning microscopy: Uses a pinhole to reject out-of-focus light, producing optical sections about $0.5\text{--}1 \mu\text{m}$ thick. Z-stacks can be reconstructed into 3D images. Essential for thick specimens and co-localization studies.

Total internal reflection fluorescence (TIRF): Evanescent wave illuminates about 100 nm of the cell adjacent to the coverslip surface. Used to study membrane dynamics, vesicle fusion events, and single-molecule behavior at the plasma membrane.

5.5.2 Electron Microscopy and Ultrastructure

Transmission electron microscopy (TEM): Electrons pass through ultrathin sections (about 50–70 nm) stained with heavy metals (uranyl acetate, osmium tetroxide). Resolution about 0.1 nm. Reveals ultrastructural details of **organelles**, membranes, and macromolecular complexes.

Scanning electron microscopy (SEM): Electrons scan the surface of gold- or platinum-coated specimens. Produces stunning 3D topographic images of cell surfaces, tissue architecture, and microorganisms. Resolution about 1–5 nm.

Cryo-electron microscopy (cryo-EM): Specimens flash-frozen in vitreous ice (no staining or fixation) and imaged at liquid nitrogen temperature. Single-particle analysis reconstructs 3D structures of proteins and complexes at near-atomic resolution (2–4 angstroms). Awarded the Nobel Prize in Chemistry 2017 (Jacques Dubochet, Joachim Frank, Richard Henderson). Cryo-EM has revolutionised structural biology, enabling structures of membrane proteins, ribosomes, and viral capsids that resist crystallisation.

Clinical Connection: Cryo-EM and Drug Discovery Cryo-EM has become indispensable in pharmaceutical development. The structure of the SARS-CoV-2 spike protein was solved by cryo-EM within weeks of the pandemic onset, enabling rapid **vaccine** design (Wrapp et al., 2020, *Science*). Drug binding sites on ion channels (e.g., TRPV1 pain receptor) and GPCRs have been mapped at near-atomic resolution, accelerating rational drug design. see section 7 for membrane protein structures.

5.5.3 Super-Resolution Microscopy

Super-resolution methods bypass the Abbe diffraction limit, achieving resolutions of 20–50 nm with light:

STED (Stimulated Emission Depletion): A donut-shaped depletion beam suppresses fluorescence from the periphery of the excitation spot, shrinking the effective point spread function. Resolution about 30–50 nm. Developed by Stefan Hell (Nobel Prize in Chemistry, 2014).

STORM (Stochastic Optical Reconstruction Microscopy): Individual fluorophores are stochastically activated, imaged, and precisely localized over thousands of frames. The composite image achieves about 20 nm resolution. Co-developed by Xiaowei Zhuang.

PALM (Photoactivated Localization Microscopy): Similar to STORM but uses photoactivatable fluorescent proteins (e.g., mEos, Dendra2). Particularly suited for live-cell imaging of genetically encoded constructs. Co-developed by Eric Betzig (Nobel Prize in Chemistry, 2014).

Concept Check 3: A researcher wants to study the real-time dynamics of clathrin-coated pit formation at the plasma membrane of a living cell. Which microscopy technique would be most appropriate and why?

5.6 Prokaryotic Cells and Cellular Economy

Prokaryotes (pro = before, karyon = nucleus) lack membrane-bound organelles. They include the domains Bacteria and Archaea.

5.6.1 Prokaryotic Cell Features and Constraints

Table 93. Prokaryotic Cell Features and Constraints: Feature and Bacteria.		
Feature	Bacteria	Archaea
Diameter	0.2–10 μm	0.2–10 μm
Nucleus	Absent; nucleoid region	Absent; nucleoid
DNA	Circular; single chromosome; often plasmids	Circular; histones present
Cell wall	Peptidoglycan (most)	Pseudopeptidoglycan or S-layer
Ribosomes	70S (30S + 50S subunits)	70S similar; unique rRNA
Membrane lipids	Ester-linked; straight-chain fatty acids	Ether-linked; branched isoprenoids
Introns	Rare	Present
Transcription machinery	Bacterial-type RNA polymerase (4 subunits)	Eukaryote-like RNA polymerase (12+ subunits)
DNA replication	DnaA origin recognition	Eukaryote-like ORC system
CRISPR-Cas	Common	Very common

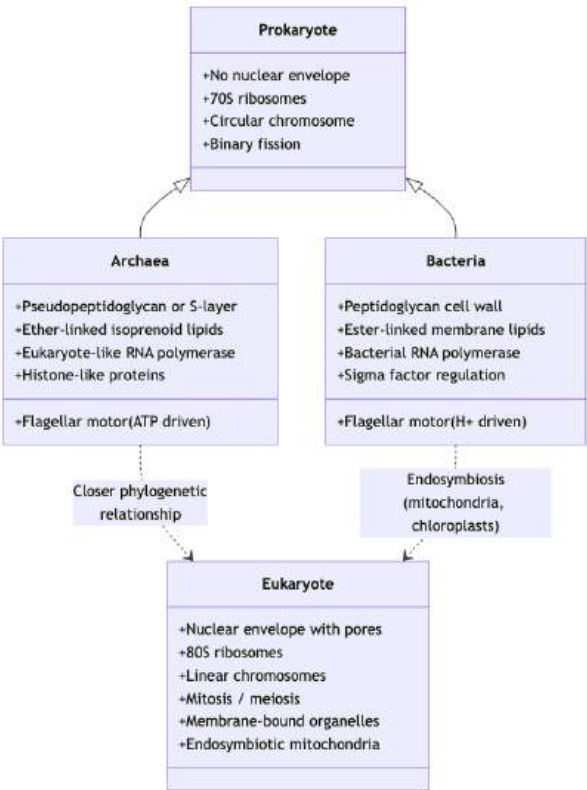


Figure 42. Classification diagram comparing Bacteria, Archaea, and Eukaryotes. Note that Archaea are phylogenetically closer to Eukaryotes in many molecular features (RNA polymerase, histones, replication machinery), while mitochondria and chloroplasts derive from bacterial endosymbionts.

5.6.2 Prokaryotic Cell Structure

- Plasma membrane: phospholipid bilayer + integral proteins. Site of chemiosmotic ATP synthesis (no mitochondria). In photosynthetic bacteria (cyanobacteria, purple bacteria), the membrane invaginates to form thylakoid-like structures for the light reactions.
- Cell wall: structurally rigid; resists osmotic lysis.

- Gram-positive bacteria: thick peptidoglycan layer (20–80 nm), teichoic acids, no outer membrane. Crystal violet stain retained (purple).
- Gram-negative bacteria: thin peptidoglycan (about 2–7 nm) + outer membrane with LPS (lipopolysaccharide). Crystal violet not retained (pink after safranin counter-stain). The periplasmic space between inner and outer membranes contains degradative **enzymes** and transport proteins.
- Capsule: polysaccharide layer external to cell wall; anti-phagocytic (evades immune system); **biofilm** formation. *Streptococcus pneumoniae* with capsule is virulent; without capsule is avirulent (Griffith’s transformation experiment, 1928).
- Flagellum: rotating protein filament powered by proton motive force (bacteria) or ATP (archaea); each rotation of the bacterial flagellar motor about 100 Hz in *E. coli*; composed of flagellin protein subunits; the basal body contains a rotary motor with stator and rotor components.
- Pili (fimbriae): protein tubes for attachment, conjugation, biofilm; Type IV pili can retract to generate motile force (“twitching motility”); F-pili mediate DNA transfer during conjugation.
- Nucleoid: condensed region containing the circular chromosome (typically 1–6 Mbp); not bounded by a membrane; associated with nucleoid-associated proteins (NAPs: HU, H-NS, Fis, IHF) that organize chromosome topology.
- Plasmids: small circular DNA molecules (1–200 kb) carrying accessory **genes** (antibiotic resistance, **virulence** factors, metabolic capabilities); replicate independently; horizontally transferable between cells.

Clinical Connection: Gram Staining and Antibiotic Selection The Gram stain, developed by Hans Christian Gram in 1884, remains the most important rapid diagnostic test in clinical microbiology. Gram-positive infections (thick peptidoglycan) respond to beta-lactam antibiotics (penicillins, cephalosporins) that inhibit peptidoglycan cross-linking by transpeptidases (PBPs). Gram-negative infections are intrinsically more resistant because the outer membrane excludes many antibiotics; treatment often requires aminoglycosides or carbapenems that penetrate through porins. The rise of multi-drug-resistant Gram-negative bacteria (e.g., carbapenem-resistant *Klebsiella pneumoniae*) is a major public health crisis. see section 6 for membrane permeability.

Concept Check 4: Why are archaea resistant to antibiotics that target peptidoglycan synthesis (e.g., penicillin, vancomycin)?

5.6.3 The Prokaryotic Cytoskeleton — A Recent Revolution

For nearly a century, textbooks asserted that prokaryotes lack a **cytoskeleton**. The discovery of bacterial cytoskeletal homologues over the past 25 years has overturned that view: prokaryotes contain dedicated structural and force-generating filaments that are evolutionary precursors of every major eukaryotic cytoskeletal class.

Table 94. The Prokaryotic Cytoskeleton — A Recent Revolution: Bacterial protein and Eukaryotic homologue.

Bacterial protein	Eukaryotic homologue	Function	Year established
FtsZ	Tubulin (GTPase fold)	Z-ring assembly at midcell; recruits divisome; constricts during binary fission	1991 (Bi & Lutkenhaus)
MreB	Actin (ATP-binding fold)	Helical filaments under inner membrane; defines rod-shaped cell geometry; coordinates peptidoglycan synthesis	2001 (Jones et al.)
Crescentin (CreS)	Intermediate filaments (lamins)	Curves <i>Caulobacter crescentus</i> into its vibrioid shape	2003 (Ausmees et al.)
ParM	Actin	Pushes plasmid copies apart during segregation	2002

Bactofilins (BacA/B)	None close	Polar localization; cell-wall remodeling	2010
----------------------	------------	--	------

FtsZ and bacterial cytokinesis. FtsZ polymerizes GTP-dependently into protofilaments that form a contractile Z-ring at the future division site. The Z-ring recruits the divisome (FtsA, FtsW, FtsI/PBP3) which synthesizes septal peptidoglycan as the membrane invaginates. FtsZ treadmills around the ring at about 30 nm/s — strikingly similar in mechanism to actin treadmilling, yet evolutionarily a tubulin homologue. The GTP-bound monomer fold superimposes on alpha/beta-tubulin with RMSD < 2 Å despite < 10% sequence identity, providing direct structural evidence that the eukaryotic mitotic machinery descends from a bacterial cell-division protein.

MreB and rod-shaped morphology. MreB filaments rotate around the bacterial circumference, dragging the Rod complex (RodA, MreC, MreD, PBP2) that synthesizes lateral peptidoglycan. Loss of MreB converts rod-shaped *E. coli* into spheres (cocci) within minutes; expression in mutant cocci restores rod shape. MreB is therefore both structural (filament) and a guidance system (positional cue for cell-wall synthesis), exactly mirroring eukaryotic actin’s dual roles.

Crescentin and curvature. *Caulobacter crescentus* gets its name from a comma-shaped curve produced by a single helical bundle of CreS filaments running along the inner curve of the cell. Mutational loss of *creS* yields straight rods. CreS is biophysically a coiled-coil of the same family as nuclear lamins and cytokeratins.

These discoveries closed a major textbook gap: the three eukaryotic cytoskeletal classes (microfilaments, microtubules, intermediate filaments) have prokaryotic ancestors. The cytoskeleton predates compartmentalization by at least 1.5 billion years.

Concept Check 4b: A pharmaceutical company is screening for narrow-spectrum antibiotics that block bacterial cell division without affecting human cells. Why is FtsZ a more promising target than MreB? (Consider the structural and functional homology to eukaryotic counterparts and what happens when each protein is inhibited.)

5.6.4 Detailed Comparison: Bacteria vs. Archaea

The discovery of Archaea by **Woese and Fox [1977]** as a separate domain transformed our view of life’s deep structure. Archaea were initially described as “prokaryotes that live in extreme environments,” but molecular phylogenetics revealed that Archaea share many features with eukaryotes that bacteria do not — a fact now central to debates about eukaryotic origin (the “Asgard archaea” hypothesis). The table below extends section 5 earlier comparison with molecular detail relevant to drug development, evolution, and astrobiology.

Table 95. Detailed Comparison: Bacteria vs. Archaea: Feature and Bacteria.

Feature	Bacteria	Archaea	Functional / clinical note
Cell wall	Peptidoglycan (N-acetylmuramic acid + N-acetylglucosamine, beta-1,4 linked, peptide cross-bridges)	Pseudopeptidoglycan (NAG + N-acetylalosaminuronic acid, beta-1,3 linked) or S-layer or polysaccharide	Penicillins/vancomycin target NAM and D-Ala-D-Ala — both absent in archaea
Membrane lipids	Glycerol-3-phosphate ester-linked to straight-chain fatty acids	Glycerol-1-phosphate ether-linked to branched isoprenoids (phytanyl); often tetraether monolayers	Stereochemistry of glycerol backbone is opposite (G3P vs G1P) — the “lipid divide”
Membrane topology	Bilayer	Bilayer or monolayer (tetraether)	Monolayer membranes are heat-stable to 113 °C
RNA polymerase	4–5 subunits ($\alpha_2\beta\beta'\omega$); rifampicin-sensitive	12+ subunits, eukaryote-like; rifampicin-resistant	Drug development implication
TATA-binding protein (TBP)	Absent	Present (homologous to eukaryotic TBP)	Promoter recognition is eukaryote-like

Feature	Bacteria	Archaea	Functional / clinical note
Histones	Absent (nucleoid-associated proteins HU/H-NS)	H3/H4-like archaeal histones, octameric tetramers	Asgard archaea have histones structurally indistinguishable from eukaryotic
Replication initiator	DnaA (single ori per chromosome)	Cdc6/Orc1 family; multiple origins	Eukaryotic-style
DNA topoisomerase	Topo IV; Gyrase (negative supercoiling)	Reverse gyrase (positive supercoiling) in hyperthermophiles	Reverse gyrase stabilizes DNA at >80 °C
tRNA introns	Rare	Common (BHB intron motif)	Used as taxonomic marker
Translation initiator	fMet-tRNA ^{fMet} (formylated)	Met-tRNA _i ^{Met} (not formylated)	Same as eukaryotes
Sensitivity: chloramphenicol, streptomycin	Sensitive	Resistant	Antibiotic discrimination
Sensitivity: anisomycin, diphtheria toxin	Resistant	Sensitive	Both target eukaryote-like ribosomal features
CRISPR–Cas	Present in about 50%	Present in about 90%	Adaptive immune systems against viruses
Energy metabolism	Photosynthetic (oxygenic, anoxygenic), chemoautotrophic, heterotrophic	Methanogens, halophiles, sulfate reducers, ammonia oxidisers	Methanogenesis is exclusive to archaea

Why this matters. Archaea share information-processing machinery (transcription, translation, replication) with eukaryotes but housekeeping/metabolic machinery with bacteria. The leading “two-domain” tree (Embley & Williams; Spang et al. 2015) places eukaryotes *within* the Asgard archaea, with the mitochondrial endosymbiont contributing the bacterial-style metabolism. The bacteria–archaea distinction is not a curiosity — it is the structural map for the deepest split in the tree of life.

Concept Check 4c: Why does penicillin kill many bacteria but no archaea, even archaea with cell walls? List the molecular features penicillin targets that distinguish bacterial from archaeal cell envelopes.

5.7 Eukaryotic Cells and Compartmentalization

Eukaryotic cells (eu = true; karyon = nucleus) contain membrane-bound organelles and a true nucleus. They include protists, fungi, plants, and animals.

5.7.1 Eukaryotic Organelle Inventory

Core eukaryotic organelles and functions:

Table 96. Eukaryotic Organelle Inventory: Organelle and Membrane.

Organelle	Membrane	Function	Unique to
Nucleus	Double (NE)	DNA storage; transcription	Eukaryotes
Mitochondria	Double	ATP synthesis; TCA cycle; apoptosis	Eukaryotes
Chloroplast	Double	Photosynthesis	Plants, algae
Rough ER	Single	Protein synthesis and folding	Eukaryotes
Smooth ER	Single	Lipid synthesis; Ca ²⁺ storage	Eukaryotes

Organelle	Membrane	Function	Unique to
Golgi apparatus	Single	Protein modification, sorting, export	Eukaryotes
Lysosome	Single	Intracellular digestion (pH 4.5)	Animals (mainly)
Vacuole	Single	Water regulation; storage	Plants (large)
Peroxisome	Single	Fatty acid beta-oxidation; H ₂ O ₂ detox	Eukaryotes
Ribosome	None	Translation	Most cells
Cytoskeleton	None	Structural; motility; intracellular transport	Eukaryotes
Centrosome	None (MTOC)	Microtubule organizing center	Animal cells

This inventory should not be read as a set of isolated boxes. Eukaryotic organelles exchange lipids, ions, metabolites, and stress signals through membrane-contact sites; mitochondria divide and fuse, the ER wraps around many organelles, lysosomes function as nutrient-sensing hubs, and biomolecular condensates add non-membrane compartments for RNA, protein, and signaling control. A modern cell-biological explanation names the compartment, the traffic route, the time scale, and the evidence type: microscopy, perturbation, biochemical fractionation, or single-cell/spatial data.

5.7.2 Compartmentalization: The Eukaryotic Advantage

The defining feature of eukaryotic cells is compartmentalization — the segregation of biochemical processes into membrane-bound organelles. This provides several advantages:

1. Incompatible reactions can occur simultaneously: Protein synthesis (cytoplasm, pH 7.2) and protein degradation (lysosomes, pH 4.5) are separated by lysosomal membranes.
2. Concentration of substrates and enzymes: Mitochondrial matrix concentrates TCA cycle enzymes, increasing reaction rates.
3. Regulation of gene expression: The nuclear envelope separates transcription (nucleus) from translation (cytoplasm), enabling post-transcriptional regulation (splicing, mRNA export, mRNA stability).
4. Expanded membrane surface area: Internal membranes (ER, Golgi, mitochondria) provide enormous surface area for membrane-associated reactions.

5.8 Endosymbiotic Theory and Organelle Origins

Lynn Margulis formalised the endosymbiotic theory (1967): mitochondria and chloroplasts are the descendants of free-living bacteria engulfed by a proto-eukaryotic host about 1.5–2 billion years ago.

5.8.1 Evidence for Endosymbiosis

1. Double membranes: Both organelles have inner (bacterial plasma membrane) and outer (phagocytic membrane) bilayers.
2. Circular DNA: Mitochondrial and chloroplast genomes are circular, like bacterial chromosomes.
3. 70S ribosomes: Organelle ribosomes are structurally bacterial-type; sensitive to antibacterials (chloramphenicol, erythromycin) that inhibit 70S, not eukaryotic 80S ribosomes.
4. Binary fission: Organelles divide by binary fission, independently of nuclear cell division, using FtsZ-related proteins.
5. Phylogenetics: rRNA sequences of mitochondria are most similar to alpha-proteobacteria (e.g., *Rickettsia*); chloroplasts to cyanobacteria.
6. Transfer of genes: about 1,500 mitochondrial-origin genes now live in the nuclear genome (gene transfer to nucleus over evolutionary time).
7. Cardiolipin: The inner mitochondrial membrane contains cardiolipin, a lipid characteristic of bacterial membranes.
8. Formylmethionine: Mitochondrial protein synthesis initiates with N-formylmethionine, as in bacteria, not methionine as in eukaryotic cytoplasmic translation.

5.8.2 Primary and Secondary Endosymbiosis

Primary endosymbiosis (mitochondrion; then chloroplast) explains the origin of eukaryotes. The mitochondrial endosymbiosis is believed to have occurred once in evolutionary history, as most known eukaryotes either possess mitochondria or have remnant mitochondria-derived organelles (hydrogenosomes, mitosomes).

Secondary endosymbiosis (a eukaryote with chloroplast engulfed by another eukaryote) explains secondary chloroplasts in dinoflagellates, euglenids, and kelp (evidenced by 3–4 bounding membranes). Tertiary endosymbiosis has also occurred in some dinoflagellates.

Concept Check 5: If you treated a eukaryotic cell with chloramphenicol (an antibiotic that inhibits 70S ribosomes), which organelle’s protein synthesis would be specifically affected? Would cytoplasmic protein synthesis be affected? Explain.

5.8.3 LUCA: The Last Universal Common Ancestor

If cell theory is correct that most cells descend from pre-existing cells [Virchow, 1855], then the lineages of bacteria, archaea, and eukaryotes converge backward in time on a single ancestral population: the Last Comprehensive Common Ancestor (LUCA). LUCA is not a fossil — it is a *reconstruction* assembled from comparative molecular data. Three classes of evidence let us infer its properties.

1. Almost universally conserved genes (the LUCA core). Genes shared by Bacteria *and* Archaea — and absent from horizontally transferred outliers — are candidates for LUCA inheritance. Modern reconstructions (Weiss et al. 2016, *Nature Microbiology*) identify about 355 such ancient gene families. LUCA almost certainly possessed: a fully fledged DNA→RNA→protein machinery (DNA polymerase, RNA polymerase, ribosome with rRNA, about 20 aminoacyl-tRNA synthetases), the **genetic code**, Wood–Ljungdahl-pathway-like CO₂ fixation, [Fe–S] and [Ni–Fe] metalloenzymes, ATP synthase (rotor/stator architecture), and a chemiosmotic membrane.
2. Geochemistry-constrained habitat. The metalloenzyme inventory (Ni, Fe, Mo, Co, W in unusual valences) suggests LUCA inhabited an anaerobic, hydrothermal, alkaline environment — most parsimoniously interpreted as a serpentinising hydrothermal vent system on the early ocean floor (about 3.8 Ga). Dependence on natural proton gradients across thin inorganic membranes (FeS micropores in vent chimneys) preceded the modern membrane-spanning ATP synthase, suggesting LUCA was not yet a fully autonomous cell but a *pre-cellular* metabolic unit (Lane & Martin 2012).
3. The DNA replication anomaly. Bacterial and archaeal DNA polymerases (Family A vs. Family B) share *no* sequence similarity in their catalytic cores, despite both performing the same chemistry. The simplest explanation is that LUCA used RNA-genome replication and DNA replication evolved twice independently *after* the bacterial–archaeal split. This argues that LUCA was a late RNA-world organism with a stable genetic code and ribosomes but was still transitioning from RNA to DNA storage.

The reconstruction has profound implications. LUCA was not the first cell — it was the last common one. Earlier lineages may have existed but left no descendants. The vast biochemical diversity of modern life (oxygenic photosynthesis, methanogenesis, eukaryotic compartmentalization) most evolved *after* LUCA, layered onto its conserved core.

Concept Check 5b: If LUCA used naturally occurring proton gradients (from inorganic vent chemistry) rather than self-generated ones, which modern molecular machinery must have evolved *before* free-living cells became possible? (Consider what a free-living cell must do that a vent-bound consortium need not.)

5.8.4 Viral Replication: Lytic vs. Lysogenic Cycles

Viruses are not cells (no membranes of their own metabolism, no ribosomes, no autonomous reproduction) and so are excluded from cell theory by definition. But viruses are cellular *parasites*, and their replication strategies illuminate what cells must do to maintain integrity. Bacteriophages — viruses that infect bacteria — provide the textbook example.

Lytic cycle (e.g., T4 bacteriophage): 1. Attachment: tail fibers bind specific surface receptors (e.g., LPS, OmpC) — defines host range. 2. Penetration: the genome is injected into the **cytoplasm** through a contractile tail; capsid remains outside. 3. Hijacking: within about 2 min, host RNA polymerase transcribes “early” phage genes that degrade the host chromosome (T4 gene 46/47 nucleases) and reprogramme cell metabolism toward phage production. 4. Replication and assembly: phage DNA is replicated (about 100 copies per cell); structural proteins self-assemble into capsids; DNA is packaged via a portal motor (one of the strongest molecular machines known: about 57 pN of force, comparable to muscle myosin). 5. Lysis: about 25 min after infection, phage lysozyme + holin perforate the cell envelope. The cell bursts, releasing about 100–200 progeny phages. The host is dead.

The lytic cycle is the textbook image of viral infection: rapid, fatal, productive. The single-step burst size (200) and latency time (25 min) determine the kinetics of phage epidemics.

Lysogenic cycle (e.g., lambda bacteriophage): 1. Attachment, penetration: same as lytic. 2. Integration: the phage genome (linear at injection) circularises and integrates into the host chromosome at a specific site (*attB*) via phage integrase. The integrated genome is now a prophage. 3. Quiescence: the prophage is replicated passively with the host chromosome at every cell division. Lambda CI repressor blocks lytic gene expression. The bacterium grows and divides normally with the prophage as a stowaway. This state can persist for thousands of generations. 4. Induction: stressors (UV, mitomycin C, low nutrients) activate the host SOS response → RecA cleaves CI repressor → lytic genes are derepressed → prophage excises → enters lytic cycle.

The lysogenic cycle has profound consequences. Specialized transduction carries host genes between bacteria when imprecise excision packages chromosomal DNA. Many bacterial virulence factors are phage-encoded: diphtheria toxin (β -phage in *Corynebacterium diphtheriae*), cholera toxin (CTX ϕ in *Vibrio cholerae*), Shiga toxin (Stx phage in EHEC *E. coli* O157:H7), botulinum toxin types C and D. The lysogen-to-lytic switch — controlled by a single repressor — is the prototype for many developmental switches and inspired the operon model of **Jacob and Monod [1961]**.

Clinical Connection: Phage Therapy in the Antibiotic-Resistance Era Lytic bacteriophages can target antibiotic-resistant bacteria with exquisite specificity (one phage typically infects one species or even strain). Compassionate-use phage therapy has cured otherwise-fatal infections (Steffanie Strathdee, *A. baumannii* sepsis, 2017; cystic fibrosis *Mycobacterium abscessus*, 2019). Phages are now in late-stage clinical trials for chronic urinary infections and prosthetic-joint infections. Phage cocktails — designed to evade host-resistance evolution by targeting multiple receptors — are the closest realization of the “magic bullet” concept since penicillin.

Concept Check 5c: A *V. cholerae* strain loses its CTX ϕ prophage. The resulting strain can colonise the human gut but causes mild diarrhea. Why? What does this tell you about the relationship between cell theory’s exclusion of viruses and the practical impact of viruses on cellular biology?

5.9 The Minimal Cell: JCVI-syn3.0

In 2016, Craig Venter’s team at the J. Craig Venter Institute created JCVI-syn3.0, a synthetic organism with the smallest genome of any self-replicating cell: 473 genes (531 kb). This was achieved by systematically deleting genes from *Mycoplasma mycoides* until primarily essential genes remained.

Key findings: - Of the 473 genes, 149 (31.5%) have unknown function — we do not understand why they are essential - The minimal gene set includes genes for DNA replication, transcription, translation, membrane synthesis, and central metabolism - No genes for cell wall synthesis, stress responses, or secondary metabolism were required under laboratory conditions - JCVI-syn3.0 grows more slowly than its parent organism, with a doubling time of about 3 hours

This work defines the boundary between chemistry and life and raises profound questions: What is the minimal instruction set for a living system? Can we understand life by building it from scratch?

Clinical Connection: Synthetic Biology and Minimal Cells The minimal cell concept has direct applications in biotechnology. Engineered minimal cells could serve as “chassis” organisms for producing pharmaceuticals, biofuels, or industrial chemicals with predictable behavior and reduced metabolic complexity. Understanding essential gene sets also identifies new antibiotic targets — genes essential for bacterial survival that have no human homologues.

5.10 Extremophile Cells and Environmental Limits

Extremophiles are organisms (primarily archaea, but also some bacteria and eukaryotes) that thrive in environments previously considered incompatible with life. They demonstrate the remarkable adaptability of cellular organization.

5.10.1 Extremophile Cell Strategies

Table 97. Extremophile Cell Strategies: Type and Environment.

Type	Environment	Example organism	Cellular adaptation
Thermophile	>60 degrees C	<i>Thermus aquaticus</i> (source of Taq polymerase)	Reverse gyrase; saturated membrane lipids
Hyperthermophile	>100 degrees C	<i>Pyrolobus fumarii</i> (113 degrees C)	Tetraether monolayer membranes; thermostable proteins
Psychrophile	<15 degrees C	<i>Psychrobacter</i>	Unsaturated membrane lipids; cold-active enzymes
Halophile	>2 M NaCl	<i>Halobacterium salinarum</i>	KCl accumulation; acidic surface proteins
Acidophile	pH <3	<i>Ferroplasma acidarmanus</i>	Impermeable membranes; proton pumps
Alkaliphile	pH >9	<i>Natronobacterium</i>	Na ⁺ /H ⁺ antiporters
Barophile/piezophile	up to 100 atm	Deep-sea archaea	Unsaturated lipids; pressure-stable proteins
Radioresistant	High radiation	<i>Deinococcus radiodurans</i>	Redundant DNA repair; Mn ²⁺ antioxidant

5.10.2 Implications for Astrobiology

Extremophiles expand our understanding of habitable environments in the solar system:

- Mars: Psychrophilic and radiation-resistant organisms suggest that microbial life could persist in Martian subsurface brine environments
- Europa (Jupiter’s moon): Halophilic and barophilic organisms thrive under conditions similar to those predicted for Europa’s subsurface ocean
- Enceladus (Saturn’s moon): Hydrothermal vent-associated chemolithoautotrophs provide models for life powered by water-rock chemistry
- Titan: While no known organisms thrive in liquid methane, the existence of extremophiles encourages consideration of exotic biochemistries

Concept Check 6: *Ferroplasma acidarmanus* lives at pH 0 (equivalent to battery acid), yet its internal pH is about 5.6. Calculate the proton concentration gradient across its membrane. How many orders of magnitude difference is this?

5.11 Cell Type Classification

5.11.1 Nutritional Classification by Carbon and Energy Source

Table 98. Nutritional Classification by Carbon and Energy Source: Type and Carbon source.

Type	Carbon source	Energy source	Examples
Photoautotroph	CO ₂	Light	Plants, cyanobacteria, algae
Photoheterotroph	Organic carbon	Light	Purple non-sulfur bacteria
Chemoautotroph	CO ₂	Inorganic chemicals	Nitrifiers, sulfur oxidisers
Chemoheterotroph	Organic carbon	Organic chemicals	Animals, fungi, most bacteria

5.11.2 Oxygen Requirements and Aerotolerance

- Obligate aerobe: requires O₂ (complex animals, *Mycobacterium tuberculosis*)
- Facultative anaerobe: can grow with or without O₂ (yeast, *E. coli*)
- Obligate anaerobe: killed by O₂ (*Clostridium botulinum*, methanogens)
- Aerotolerant anaerobe: not killed by O₂ but does not use it (*Lactobacillus*)
- Microaerophile: requires O₂ but at lower concentrations than atmospheric (*Campylobacter*, *Helicobacter pylori*)

Concept Check 7: A chemoautotrophic bacterium living near a deep-sea hydrothermal vent uses H₂S as an electron donor and CO₂ as its carbon source. It rarely encounters sunlight. Is this organism ultimately dependent on solar energy? Explain.

5.12 Computational Bridge

The codebase tags canonical organelle inventories by cell type — useful when you compare compartmentalization across the three domains:

```
from biology.cell import get_organelles_by_cell_type

animal = get_organelles_by_cell_type("animal")
plant = get_organelles_by_cell_type("plant")
print(len(animal), len(plant))
```

Clinical / systems note: Antibiotic discovery still exploits differences between prokaryotic ribosomes, cell walls, and topoisomerases and their human counterparts — the same structural dichotomy this unit formalises as cell theory.

5.13 Current Evidence and Frontier Biology: Cell Theory and Cell Types

For Cell Theory and Cell Types, frontier biology belongs inside the evidence logic of the chapter. Cell biology is increasingly measured as live, spatial, single-cell, and perturbational data rather than static diagrams alone. The core reading question is this: cell-theory evidence now includes microscopy, lineage tracing, omics, and synthetic-cell boundary tests.

- What to verify: identify the observation, model, assay, or dataset that would make the claim stronger or weaker.
- What to qualify: state the scale, organism, cell type, environmental condition, or population where the claim is expected to hold.
- What to compare: test at least one alternative explanation, baseline, or null model before treating the pattern as causal.

- What to cite: distinguish primary evidence, review synthesis, public dataset, and institutional guidance; for recent or numeric claims, prefer the source closest to the measurement and state what has changed since it was published.

Name the measurement scale, perturbation, and boundary condition before moving from cell-state pattern to causal explanation.

Source practice: For cell claims, distinguish microscopy, live-cell perturbation, single-cell sequencing, spatial transcriptomics, and biochemical assay evidence before making a causal statement.

Single-cell atlases are most useful when they clarify the sampled tissue, donor context, assay chemistry, and annotation uncertainty; Human Cell Atlas-style resources turn cell theory into a measurable census, but they do not remove the need for perturbation evidence [Regev et al., 2017, Pan et al., 2024].

5.14 Summary

- Cell theory: most organisms are cells; cells are the basic unit; cells come from cells. Modern additions include heritable DNA information and shared chemical composition.
- The surface-area-to-volume ratio ($A/V = 3/r$) constrains cell size; large cells must increase A or reduce metabolic demand per unit volume. Diffusion time scales with x^2 , imposing additional size limits.
- Microscopy techniques span light (bright-field, phase-contrast, DIC, fluorescence, confocal, TIRF), electron (TEM, SEM, cryo-EM), and super-resolution (STED, STORM, PALM) methods, with resolutions from about 200 nm to sub-nanometre.
- Prokaryotes (Bacteria + Archaea) lack membrane-bound organelles; Gram staining discriminates based on cell wall structure. Archaea share molecular features with eukaryotes.
- Eukaryotic organelles carry out compartmentalised functions; mitochondria and chloroplasts arose by endosymbiosis of bacterial ancestors.
- The minimal cell (JCVI-syn3.0, 473 genes) defines the boundary of cellular life; extremophiles demonstrate life’s adaptability to extreme environments.
- Connections: See section 6 for organelle inventory, Unit VII — Microbiology: Introduction for prokaryotic diversity, and Unit VI — Evolution: Introduction for common ancestry and LUCA reasoning.

5.15 Review Questions

1. State the three original postulates of cell theory and the three modern additions. For each, identify the key experiment or discovery that established it.
2. A spherical cell has radius 5 μm . Calculate its surface area, volume, and A/V ratio. If the cell doubles its radius, by what factor does A/V change?
3. Compare and contrast the cell walls of Gram-positive bacteria, Gram-negative bacteria, and archaea. Why are archaea naturally resistant to penicillin?
4. List six lines of evidence supporting the endosymbiotic origin of mitochondria. Which single piece of evidence do you consider most compelling, and why?
5. Explain why TIRF microscopy would be preferred over confocal microscopy for studying single vesicle fusion events at the plasma membrane.
6. The diffusion coefficient of glucose in water is approximately $6.7 \times 10^{-10} \text{ m}^2/\text{s}$. Calculate the time required for glucose to diffuse across (a) a 2 μm bacterium and (b) a 100 μm plant cell.
7. JCVI-syn3.0 has 473 genes, of which 149 have unknown function. Discuss the implications of this finding for our understanding of the minimal requirements for life.
8. Describe how *Deinococcus radiodurans* survives radiation doses >1,000 times the lethal dose for humans. What cellular mechanisms enable this extreme resistance?
9. Compare the membrane lipids of bacteria, archaea, and eukaryotes. How do archaeal ether-linked isoprenoid lipids contribute to survival at extreme temperatures?
10. A pharmaceutical company is developing a new antibiotic. Using your knowledge of prokaryotic cell structure, suggest three molecular targets that are present in bacteria but absent in human cells.
11. Using `get_organelles_by_cell_type`, contrast the organelle lists for "animal" and "prokaryote". Which entries best illustrate endosymbiotic theory?
12. A spherical bacterium and a spherical eukaryote both rely on diffusion. If the eukaryote is 20 \times larger in radius, by what factor does the surface-to-volume ratio change relative to the bacterium?
13. Using equation (106) and equation (109), explain why every metabolically active animal cell is < 100 μm in radius unless it has internal membranes, microvilli, or partial anoxia. Identify two cell types that violate this rule and explain *how* they do so.

14. List three bacterial cytoskeletal proteins, their eukaryotic homologues, and the function of each. Why was the absence of “the cytoskeleton” in prokaryotes a textbook error rather than a fact?
 15. Compare lytic and lysogenic phage cycles in terms of their (a) speed, (b) burst size, (c) consequences for the host cell, and (d) implications for evolution. Which strategy is more reminiscent of “infectious disease” and which of “horizontal gene transfer”?
 16. Outline the three classes of evidence used to reconstruct LUCA. What does the absence of conserved DNA polymerase tell us about LUCA’s information system?
-

5.16 Discussion Questions

These questions have no single correct answer — they are designed to provoke debate, integrate concepts across sections, and connect cell biology to broader scientific and ethical questions.

1. Defining life. Is JCVI-syn3.0 alive? It self-replicates, contains a genome, performs metabolism, and responds to its environment — but every component was designed by humans. If the answer is “yes,” does that mean we have created life? If “no,” what definition excludes it that does not also exclude obligate intracellular pathogens like *Rickettsia* (which depend on host metabolism just as syn3.0 depends on enriched media)?
 2. Cell theory under stress. Cell theory states that most cells come from pre-existing cells. But somatic-cell nuclear transfer (cloning), induced pluripotent stem cells (iPSCs from skin fibroblasts), and now in-vitro-generated organoids (mini-brains, mini-livers) push this principle. Are organoids “organisms”? Do they have moral status if they begin to exhibit coordinated electrical activity?
 3. The 149-gene mystery. JCVI-syn3.0 has 149 essential genes of unknown function. Choose one approach (CRISPR screening, AlphaFold structural prediction, evolutionary co-occurrence analysis, or chemical biology) and argue why it is most likely to crack this set first. What ethical or biosafety considerations follow from understanding the minimal genome?
 4. Astrobiology and the biosignature problem. If life on Mars or Europa derives from a separate origin, it might lack DNA, ribosomes, and ATP — making it invisible to instruments designed around terrestrial biochemistry. How might cell theory be revised if we discovered non-cellular life elsewhere? Conversely, what *cellular* features might be comprehensive across any biochemistry (compartmentalization? polymer-based information storage? membranes?) and why?
 5. Endosymbiosis and modern biotechnology. Some researchers propose engineering new endosymbionts: introducing nitrogen-fixing bacteria into plant cells to eliminate fertiliser dependence. What lessons from the natural mitochondrial endosymbiosis (gene transfer to host nucleus, metabolite exchange, intimate cell-cycle coupling) suggest what would be needed for such a designed symbiosis to be stable across generations?
 6. The phage-resistance arms race. Bacteria evolve CRISPR-Cas defenses; phages evolve anti-CRISPR proteins (Acrs); bacteria evolve anti-anti-CRISPR systems. This Red Queen dynamic has continued for about 3 billion years. What does it predict about the long-term success of phage therapy for antibiotic-resistant infections in humans? How might phage-cocktail design exploit or sidestep this dynamic?
-

5.17 Further Reading and Source Notes: Cell Theory and Cell Types

- Sagan (1967). On the origin of mitosing cells. *Journal of Theoretical Biology*, 14.
 - Schleiden (1838). Beitr{a}ge zur Phytogenesis. M{u}ller’s Archiv f{u}r Anatomie, Physiologie und wissenschaftliche Medicin.
 - Virchow (1855). Die Cellularpathologie. Archiv f{u}r pathologische Anatomie und Physiologie, 8.
 - Hooke (1665). *Micrographia*. Royal Society.
 - Schwann (1839). Mikroskopische Untersuchungen {u}ber die {U}bereinstimmung in der Struktur und dem Wachsthum der Thiere und Pflanzen. Gebr{u}der Borntraeger.
 - Hershey & Chase (1952). Independent functions of viral protein and nucleic acid in growth of bacteriophage. *Journal of General Physiology*, 36.
-

5.18 Key Terms

Table 99. Oxygen Requirements and Aerotolerance: Term and Definition.

Term	Definition
Cell theory	Foundational principle: most organisms are composed of cells, cells are the basic unit of life, most cells arise from pre-existing cells
Surface-area-to-volume ratio	The ratio $A/V = 3/r$ for a sphere; constrains maximum cell size
Prokaryote	Cell lacking a membrane-bound nucleus; Bacteria and Archaea
Eukaryote	Cell with a true membrane-bound nucleus and organelles
Gram staining	Differential stain distinguishing thick-peptidoglycan (Gram-positive) from thin-peptidoglycan + outer membrane (Gram-negative) bacteria
Endosymbiotic theory	Mitochondria and chloroplasts originated from engulfed bacteria (alpha-proteobacteria and cyanobacteria, respectively)
Photoautotroph	Organism using light energy and CO ₂ as carbon source
Chemoheterotroph	Organism using chemical energy from organic compounds
Obligate anaerobe	Organism killed by oxygen; uses anaerobic metabolism exclusively
Nucleoid	Condensed DNA-containing region of prokaryotic cells, not bounded by a membrane
Peptidoglycan	Polymer of NAG-NAM cross-linked by peptide bridges; structural component of bacterial cell walls
Cryo-EM	Electron microscopy of vitrified (flash-frozen) specimens; near-atomic resolution without staining
JCVI-syn3.0	Minimal synthetic cell with 473 genes; defines the lower boundary of self-replicating life
Extremophile	Organism thriving in extreme environments (temperature, pH, salinity, pressure, radiation)
Diffusion limit	Physical constraint on cell size imposed by the relationship $t = x^2/2D$
Compartmentalization	Segregation of biochemical processes into membrane-bound organelles; a defining eukaryotic feature

5.19 Companion Source Module: Cell Theory and Cell Types

Cell Theory and Cell Types should leave a reproducible trail from a biological claim to the code, figure, diagram, or paper-based activity that can test it. Use the surfaces below to inspect the chapter’s assumptions, rerun the relevant model, or compare the manuscript explanation with companion labs and figures.

Table 100. Companion source surfaces for Cell Theory and Cell Types.

Surface	Use it for
<code>src/biology/cell/cell_biology.py</code> (<code>get_organelles_by_cell_type</code> , <code>count_membrane_bound_organelles</code>)	Turn cell-type comparisons into explicit feature lists rather than memorised diagrams.
<code>src/mermaid/biology_diagrams.py</code> (<code>organelle_function_diagram</code>)	Connect cell theory to structure-function evidence.

Reproducibility check: identify the observation scale, specimen state, and imaging limit before deciding what counts as evidence for a cellular claim. Cross-reference: compare with section 6 and section 24.

6 Cell Structure and Organelles

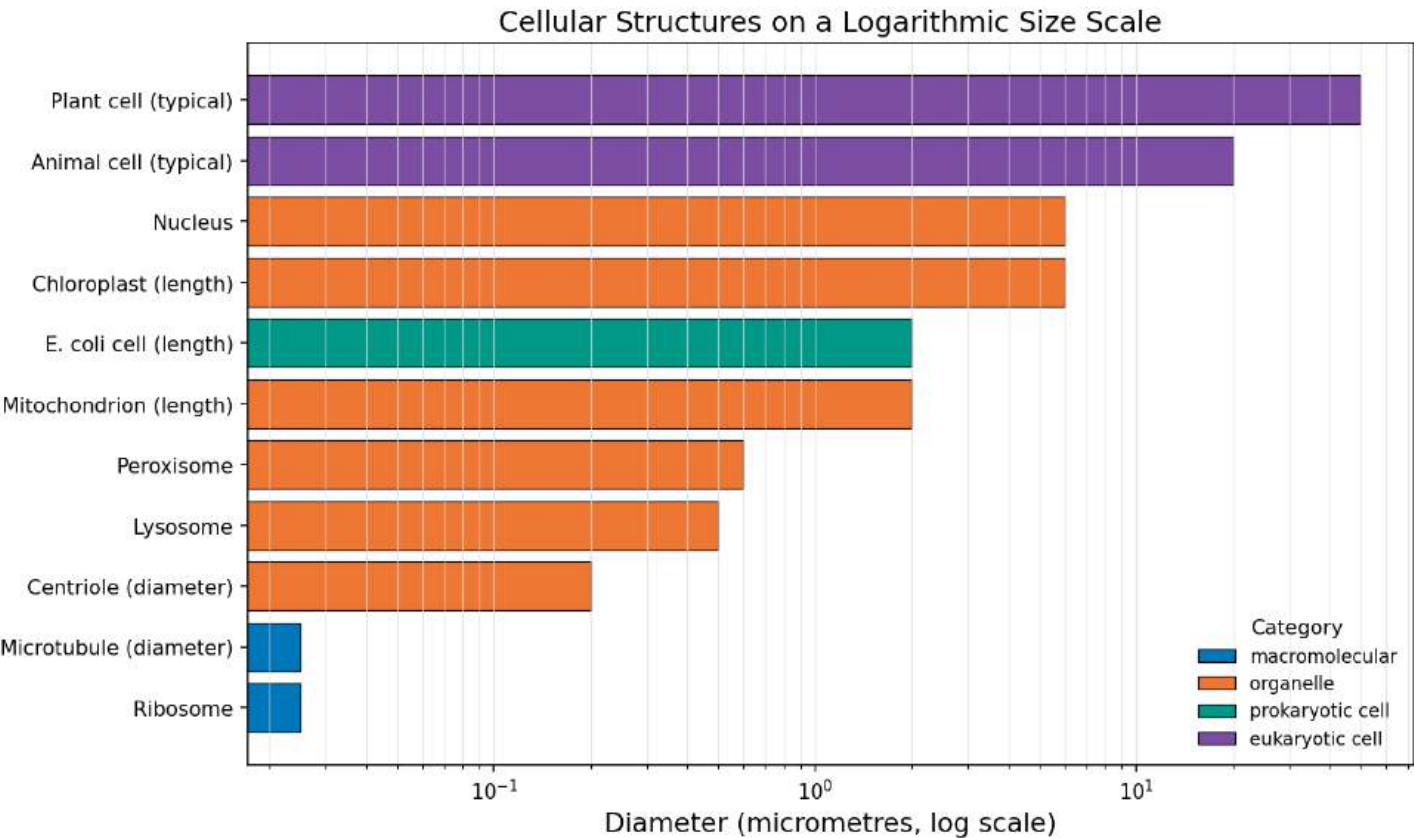


Figure 43. Characteristic linear dimensions of biological structures on a log scale, from ribosomes and viruses through organelles to whole eukaryotic cells. Bars are colored by category (macromolecule, virus, organelle, prokaryote, eukaryote) and span roughly four orders of magnitude. Spatial scale constrains diffusion times, mechanical behavior, and the kinds of imaging that resolve each level.

Level 2/3 · 50 min read · 75 min lecture · Prerequisites: section 5

6.1 Learning Objectives

1. Describe the structure and function of each major eukaryotic **organelle** in detail.
2. Explain the endomembrane system and the secretory/endocytic pathways, including coat **proteins** and sorting signals.
3. Describe the **cytoskeleton**: microtubules, microfilaments, and intermediate filaments, including their associated motor proteins.
4. Explain how the nucleus controls **gene** expression through **chromatin** organization and the **histone code**.
5. Relate organelle dysfunction to specific human diseases.
6. Predict the cellular consequences of unopposed mitochondrial fission versus unopposed fusion, given their role in cellular **homeostasis**.
7. Explain the role of peroxisomes, centrosomes, and primary cilia in cell biology.
8. Distinguish cadherin-, integrin-, and tight-junction-based adhesion by their cytoskeletal coupling and role in tissue architecture.

6.1.1 Study Blueprint

- Big idea: Organelle structure partitions work, traffic, information, and energy inside eukaryotic cells.
- Core concepts: organelles, endomembrane system, cytoskeleton, motor proteins.
- Framework alignment: Vision & Change: Structure and function, Systems, Information flow, exchange, and storage; AP Biology: Systems Interactions, Information Storage and Transmission; NGSS-style topics: Structure and Function.
- Model or quantitative lens: Compartment-flow and motor-transport calculations.
- Data skill: Trace a molecule through compartments using evidence from labels or perturbations.
- Practice cadence: Visual Representations, Questions and Methods, Argumentation.
- Common misconception to repair: Organelles are dynamic process hubs, not static textbook icons.
- Primary lab: **Lab — Cell Structure and Organelles**.
- Question bank: **Questions — Cell Structure and Organelles**.

- Transfer task: Apply compartment logic to secretion, apoptosis, infection, or cell division.
- Bridge to computation: `biology.cell.cell_biology.ORGANELLES`.

Opening Vignette: The World’s Smallest Rotary Motor

Buried in the envelope of a bacterium is a molecular machine that spins at 100,000 rotations per minute, driven by a stream of protons flowing down an electrochemical gradient. The bacterial flagellar motor — known since the 1970s from electron microscopy — is roughly 45 nm in diameter and converts ion-motive force directly into rotational movement, propelling the cell at up to 30 body lengths per second. No human-engineered motor approaches this combination of speed, size, and efficiency.

The bacterial flagellar motor is assembled from over 40 different proteins, each with a precise structural role: the MS ring anchors to the inner membrane; the C ring acts as a cargo dock for proteins to be secreted; the rod and hook transmit torque; the flagellar filament acts as a propeller. The motor can switch rotation direction in under a millisecond, enabling the tumbling runs that allow bacteria to chemotax toward nutrients [Berg and Brown, 1972]. Cell structure, as this chapter shows, is not merely a container for biochemistry — it is the machinery of life itself.

Primary source: Berg and Brown’s three-dimensional tracking study of bacterial chemotaxis [Berg and Brown, 1972].

6.2 Quantitative Organelle Inventory

Electron microscopy and fractionation made organelles experimentally tractable: Palade’s dense cytoplasmic particles became ribosomes [Palade, 1955], Blobel and Dobberstein’s translocation experiments connected membrane-bound ribosomes to secretory-protein targeting [Blobel and Dobberstein, 1975], and vesicle-traffic work later unified secretion, endocytosis, and regulated exocytosis as related transport systems [Rothman, 1994].

Before examining each organelle individually, it is useful to fix the dimensions and copy numbers in a single reference table. Sizes vary modestly across cell types; the values below are typical for a cultured mammalian cell (HeLa-like, about 20 μm diameter). figure 43 places those values on a log axis alongside ribosomes, viruses, and prokaryotic cells so the four-order-of-magnitude span is visible at a glance.

Table 101. Study Blueprint: Organelle and Linear dimension.

Organelle	Linear dimension	Number per cell	Approximate volume	Membrane area
Plasma membrane	5 nm thick; 20 μm cell diameter	1	—	about 1,300 μm ²
Nucleus	5–10 μm diameter	1	about 600 μm ³	about 280 μm ² (NE)
Nuclear pore complex (NPC)	about 120 nm outer; about 9 nm channel	about 3,000–5,000	—	—
Mitochondrion	0.5–10 μm long; 0.5 μm wide	100–2,000	about 400 μm ³ total	OMM about 5,000 μm ² ; IMM about 30,000 μm ² (cristae 6× amplification)
Mitochondrial DNA (mtDNA)	16,569 bp circular	about 10–100 copies per mitochondrion	—	—
Rough ER	sheets/tubules about 30–100 nm	one continuous network	about 10% cell volume	about 13,000 μm ²
Smooth ER	tubules about 30–60 nm	one network (continuous with RER)	varies; large in liver/muscle	varies
Golgi stack	4–8 cisternae; about 1 μm wide	typically 1 (cis–trans); fragmented during mitosis	about 1% cell volume	about 1,000 μm ²
Lysosome	0.1–1 μm diameter	about 50–1,000	about 1% cell volume	about 100 μm ² each
Peroxisome	0.1–1 μm diameter	50–1,000	about 1% cell volume	—
Centriole	200 nm long × 250 nm wide	2 (one centrosome)	—	—
Primary cilium	1–10 μm long × 250 nm wide	1	—	—
Ribosome (cytosolic, 80S)	about 25 nm	about 10 ⁷ per cell	—	—

Organelle	Linear dimension	Number per cell	Approximate volume	Membrane area
Ribosome (mitochondrial, 55S)	about 25 nm	about 10 ⁴ per mitochondrion	—	—
Microtubule	25 nm wide × variable length	thousands	—	—
Actin filament	7 nm × variable length	about 10 ⁹ G-actin monomers	—	—
Cytoplasmic vesicle	50–200 nm	thousands transient	—	—
Proteasome (26S)	45 nm long	about 30,000–500,000 per cell	—	—

Three numerical patterns deserve attention. (1) The internal membrane area exceeds the plasma membrane area by about 30-fold, so the plasma membrane is a small fraction of cellular membrane surface. (2) Mitochondria are the largest membrane reservoir (cristae alone are 20× the plasma membrane), which is why their dysfunction propagates so quickly through bioenergetics. (3) NPCs are far rarer than ribosomes (10³ vs. 10⁷) yet handle 100× more transport events per second per channel — they are arguably the most heavily used machinery in the cell. The chapters that follow refer back to this table so that quantitative arguments (e.g., “if mitophagy disposes of 10% of mitochondria per day...”) have grounded numbers.

6.3 The Nucleus — The Information Center

The nucleus (diameter typically 5–10 μm) is the defining hallmark of the eukaryotic cell.

6.3.1 Nuclear Envelope, Pores, and Lamina

The nucleus is bounded by the nuclear envelope — two concentric **phospholipid bilayers** (inner and outer nuclear membrane). The outer nuclear membrane is continuous with the rough ER. The nuclear pore complex (NPC) penetrates both membranes at about 3,000 pores per nucleus. Each NPC is a massive protein assembly (about 120 MDa; 34 distinct nucleoporin proteins, 8-fold rotational symmetry), gating passage of macromolecules:

- Small molecules (<40 kDa) diffuse passively through the pore channel (diameter about 9 nm)
- Larger molecules require nuclear localization sequences (NLS) or nuclear export sequences (NES) recognized by importin/exportin proteins
- The NPC can transport cargo up to about 39 nm in diameter (e.g., ribosomal subunits, mRNA-protein complexes)
- Transport is powered by the RanGTP/RanGDP gradient: high RanGTP in the nucleus, high RanGDP in the **cytoplasm**

Import mechanism: Cargo with NLS binds importin-alpha/beta in the cytoplasm, translocates through the NPC, and RanGTP in the nucleus causes importin to release its cargo.

Export mechanism: Cargo with NES binds exportin (CRM1) + RanGTP in the nucleus, translocates out, and RanGAP in the cytoplasm hydrolyses RanGTP to RanGDP, releasing cargo.

NPC architecture in numbers. Each NPC is built of about 30 distinct nucleoporin (Nup) species totalling about 500–1,000 protein subunits arranged with 8-fold rotational symmetry. The structural scaffold (the “Y-complex”) forms two outer rings; cytoplasmic and nuclear filaments project about 50 nm from each face; FG-repeat nucleoporins (Nup98, Nup62, Nsp1) line the central channel and form a hydrogel-like phase that confers selectivity. A single human nucleus contains about 3,000–5,000 NPCs (density about 10–20 per μm² of nuclear envelope), and each NPC handles roughly 1,000 translocation events per second at peak activity — meaning the entire nucleus exchanges about 10⁷ macromolecules per second. The selective barrier is so efficient that small molecules (<40 kDa) cross by simple diffusion in <1 ms while large cargo without NLS/NES are excluded essentially indefinitely. The energy budget is supplied by the RanGTP/GDP gradient (10⁴:1 nuclear:cytoplasmic ratio for RanGTP), which is itself maintained by RanGEF (RCC1, chromatin-bound) and RanGAP (cytoplasmic): the result is a vectorial pump powered by GTP hydrolysis but requiring no direct translocation ATPase.

Pathological NPCs. The Nup98 gene is fused to dozens of partners in pediatric leukaemias (Nup98-HOXA9, Nup98-NSD1) — the FG-repeat domain provides a phase-separating prion-like domain that drives oncogenic condensate formation. Nucleoporins also accumulate damage with age; selective loss of NPC function is a hallmark of post-mitotic neurons in Alzheimer’s and ALS.

6.3.2 Protein Targeting and Sorting

Every protein synthesized in the cell must reach a specific compartment, but proteins are made (initially) in primarily two places: free cytosolic ribosomes and ER-bound ribosomes. Sorting signals within the polypeptide direct each protein to its destination. Most signals are short, modular, and additive — analogous to

postal addresses appended to the same envelope.

Table 102. Protein Targeting and Sorting: Destination and Targeting signal.

Destination	Targeting signal	Recognition machinery	Mechanism
Nucleus	Nuclear localization sequence (NLS): clusters of basic residues (e.g., PKKKRKV in SV40 T-antigen)	Importin-alpha (recognizes NLS) + Importin-beta (NPC binding)	Co- or post-translational; powered by Ran-GTP gradient
Mitochondrion (matrix)	N-terminal amphipathic alpha-helix (presequence; about 15–70 aa)	TOM complex (outer membrane); TIM23 complex (inner membrane); Hsp70 motor	Post-translational; unfolded protein threaded through; presequence cleaved by MPP
Mitochondrion (OMM, IMM)	Internal hydrophobic / cysteine motifs	TOM, SAM, TIM22, MIA40 (IMS)	Multiple lateral and stop-transfer pathways
Chloroplast (stroma)	N-terminal transit peptide	TOC and TIC complexes	Analogous to TOM/TIM
Peroxisome (matrix)	PTS1 (C-terminal SKL) or PTS2 (N-terminal RLx5HL)	PEX5 (PTS1), PEX7 (PTS2)	Folded proteins imported (unique); mono-ubiquitinated PEX5 recycles via PEX1/6 ATPases
ER (secretory pathway)	N-terminal signal peptide (about 16–30 hydrophobic aa)	SRP (signal recognition particle) → SRP receptor → Sec61 translocon	Co-translational — translation pauses until ribosome docks
ER → Golgi (anterograde) Golgi → ER (retrieval)	Diacidic/dihydrophobic motifs (DXE, FF) C-terminal KDEL (luminal) or KKXX (membrane)	COPII coat (Sar1, Sec23/24, Sec13/31) KDEL receptor (KDELR); COPI coat	Vesicle budding Retrograde retrieval of escaped resident proteins
Lysosome	Mannose-6-phosphate (M6P) added in cis-Golgi	M6P receptor (MPR)	Sorting at trans-Golgi network
Plasma membrane	Default pathway (no retention signal)	Constitutive secretion	Vesicles fuse continuously

The SRP pathway in detail. SRP is a ribonucleoprotein particle (54 kDa SRP54 GTPase + 6 other proteins + 7SL RNA) that solves a three-way coordination problem: it must (i) recognize the nascent signal peptide as it emerges from the ribosome, (ii) pause translation to prevent premature folding in the cytoplasm, and (iii) deliver the ribosome–nascent chain to the ER membrane. SRP54 binds the hydrophobic signal peptide; SRP9/14 contact the ribosome’s elongation factor binding site, halting translation. The complex docks at the SRP receptor (SR, also a GTPase) on the ER membrane. Reciprocal GTP hydrolysis by SRP54 and SR releases SRP, hands the signal peptide to the Sec61 translocon, and translation resumes — now co-translationally threading the polypeptide into the ER lumen. The “GTPase exchange” mechanism is deeply conserved: SRP/SR systems occur in bacteria, archaea, and eukaryotes, with lineage-specific architectural variations.

TOM/TIM mitochondrial import. Mitochondrial matrix proteins face a unique problem: they must cross *two* membranes while remaining largely unfolded. The TOM complex (Translocase of Outer Membrane) — built around Tom40 (β -barrel channel), Tom20 (presequence receptor), Tom22, and small Tom proteins — accepts the presequence on the cytoplasmic side. TIM23 (Translocase of Inner Membrane) then takes over, threaded by the PAM motor (Presequence translocase-Associated Motor) containing mtHsp70 that uses ATP hydrolysis to ratchet the polypeptide into the matrix. The inner membrane potential ($\Delta\Psi \approx -180$ mV) provides additional electrostatic pulling force on the positively charged presequence. Once in the matrix, MPP (Mitochondrial Processing Peptidase) cleaves the presequence and the protein folds, often with mtHsp60/Hsp10 chaperonin assistance.

OMM β -barrel proteins (e.g., porin/VDAC, Tom40 itself) take a different route: through TOM, into the IMS, then inserted laterally by the SAM complex (Sorting and Assembly Machinery). Carrier proteins (e.g., ADP/ATP translocase) of the inner membrane skip TIM23 entirely and use TIM22 for lateral release into the IMM. IMS proteins use the MIA40/Erv1 disulphide relay for oxidative folding.

Why this matters. Failures of any single targeting pathway produce specific, severe disease phenotypes — testimony to how hard-coded the cellular logistics are. Defects in PEX genes cause peroxisome biogenesis disorders (Zellweger syndrome). Defects in TIM/TOM components cause mitochondrial myopathies. ER signal peptide mutations are now recognized in disorders ranging from preprovasopressin (familial diabetes insipidus) to coagulation-factor deficiencies. The cell’s postal system has no general delivery option — every misrouted package is a disease.

Concept Check 1b: A researcher creates a fusion protein with both an N-terminal mitochondrial presequence *and* a C-terminal SKL (peroxisomal PTS1). Where is the protein delivered? (Hint: consider whether targeting is co-translational or post-translational, and which signal acts first.)

6.3.3 Chromatin and Nucleosomes

Human nuclear DNA (2 x 3.2 billion base pairs = 6.4 Gbp total) is packaged into chromatin. The **nucleosome** is the basic packaging unit: 147 bp of DNA wound about 1.75 times around an octamer of **histone** proteins (2x H2A, H2B, H3, H4) with linker H1 bridging adjacent nucleosomes.

Levels of chromatin compaction:

- 1. 10 nm fiber (beads on a string): nucleosome arrays; about 6-fold compaction of naked DNA
- 2. 30 nm fiber: solenoid or zigzag arrangement (histone H1 stabilizes); about 40-fold compaction
- 3. 300 nm loops: attached to a protein scaffold (condensin, cohesin); about 10,000-fold
- 4. 700 nm condensed chromatin: mitotic **chromosome**
- 5. 1,400 nm fully condensed: metaphase chromosome; about 10,000–20,000-fold compaction total

Euchromatin (transcriptionally active; less compacted) vs. **heterochromatin** (transcriptionally silent; highly compacted). Histone modifications (acetylation = active; methylation context-dependent) regulate this switch — the histone code.

Table 103. Chromatin and Nucleosomes: Modification and Residue.

Modification	Residue	Effect	Writer enzyme	Eraser enzyme
Acetylation	H3K9ac, H3K27ac	Activation	HATs (p300/CBP)	HDACs
Methylation	H3K4me3	Activation (promoters)	SET1/MLL	KDM5/JARID
Methylation	H3K9me3	Silencing (hete- rochromatin)	SUV39H1	KDM4/JMJD2
Methylation	H3K27me3	Silencing (Polycomb)	EZH2 (PRC2)	KDM6/UTX
Phosphorylation	H3S10ph	Mitotic condensation	Aurora B	PP1
Ubiquitination	H2BK120ub	Transcription elongation	RNF20/40	USP22

6.3.4 Nucleolus and Ribosome Biogenesis

The nucleolus (1–3 per nucleus) is not membrane-bound. It is the site of ribosomal RNA (rRNA) transcription by RNA polymerase I and **ribosome** assembly. It disassembles during **mitosis** and re-forms around nucleolus organiser regions (NORs) on chromosomes 13, 14, 15, 21, and 22 (in humans).

The nucleolus has three ultrastructural regions: - Fibrillar center (FC): rDNA gene clusters and RNA Pol I - Dense fibrillar component (DFC): nascent rRNA processing; fibrillarin - Granular component (GC): maturing pre-ribosomal particles

Clinical Connection: The Nucleolus in Cancer Nucleolar size and number are often increased in cancer cells due to elevated ribosome biogenesis driven by oncogenes (Myc, mTOR). Pathologists use nucleolar prominence (AgNOR staining) as a prognostic marker in several cancers. The RNA Pol I inhibitor CX-5461 is in clinical trials as an anti-cancer agent that specifically targets ribosome biogenesis.

Concept Check 1: A protein has both an NLS and an NES. Would it be found in the nucleus or cytoplasm? How might the cell regulate its localization?

6.4 Mitochondria — Power Plants of the Cell

Mitochondria (singular: mitochondrion) are 1–5 μm long, often branching, highly dynamic organelles. A liver hepatocyte contains about 1,000–2,000 mitochondria, constituting about 20% of cell volume.

6.4.1 Mitochondrial Structural Organization and Cristae

- Outer mitochondrial membrane (OMM): contains porin (VDAC) channels; freely permeable to molecules <5 kDa. Also contains MAM (mitochondria-associated ER membrane) contact sites for Ca^{2+} and lipid exchange.
- Intermembrane space (IMS): equivalent to cytoplasm in ion composition; site of electron carrier cytochrome c; contains pro-apoptotic factors (Smac/DIABLO, AIF)
- Inner mitochondrial membrane (IMM): highly folded into cristae (10x surface area amplification); impermeable to protons — essential for chemiosmosis; contains electron transport chain (ETC) complexes I–IV, ATP synthase. The cristae are shaped by the MICOS complex (mitochondrial contact site and cristae organizing system) and OPA1.
- Matrix: aqueous interior; contains mitochondrial DNA, ribosomes, TCA cycle enzymes, fatty acid oxidation enzymes, pyruvate dehydrogenase complex

Crista density correlates with energetic demand: sperm mitochondria and cardiac muscle mitochondria have densely packed cristae. Resting cells have fewer, wider cristae.

6.4.2 Mitochondrial DNA (mtDNA)

Human mtDNA: 16,569 bp, circular, encodes 37 genes: - 13 subunits of respiratory chain complexes (e.g., ND1-6, COX1-3, ATP6, ATP8) - 22 transfer RNAs - 2 ribosomal RNAs

mtDNA is inherited maternally (sperm mitochondria are typically ubiquitinated and destroyed in the fertilized egg), consistent with the endosymbiotic origin of mitochondria [Sagan, 1967]. This enables maternal-lineage phylogenetic analysis and forensic identification. Mitochondrial Eve — the most recent common maternal ancestor of living humans — lived about 150,000–200,000 years ago in Africa.

Mitochondrial diseases arise from mtDNA mutations (point mutations or deletions): - Leber hereditary optic neuropathy (LHON): mutations in ND genes leads to retinal ganglion cell degeneration and blindness - MELAS (Mitochondrial Encephalomyopathy, Lactic Acidosis, Stroke-like episodes): A3243G mutation in tRNA-Leu - Kearns-Sayre syndrome: large mtDNA deletions; progressive external ophthalmoplegia, cardiac conduction defects, retinitis pigmentosa

6.4.3 Mitochondrial Dynamics: Fusion and Fission

Mitochondria are not static organelles — they constantly undergo fusion (joining) and fission (splitting), forming a dynamic network called the mitochondrial reticulum.

Fusion proteins: - MFN1/MFN2 (mitofusins): GTPases on the OMM; mediate outer membrane tethering and fusion - OPA1: GTPase on the IMM; mediates inner membrane fusion and cristae remodeling - Mutations in MFN2 cause Charcot-Marie-Tooth type 2A (peripheral neuropathy) - Mutations in OPA1 cause dominant optic atrophy (most common inherited optic neuropathy)

Fission proteins: - DRP1 (dynamin-related protein 1): cytosolic GTPase recruited to the OMM by adaptors (MFF, MiD49/51, FIS1); assembles into a ring and constricts the mitochondrion - ER-mitochondria contact sites mark fission sites; the ER wraps around the mitochondrion before DRP1 recruitment - Fission is essential for equal mitochondrial distribution during cell division and for isolating damaged mitochondria for mitophagy

Mitophagy (PINK1/Parkin pathway): 1. In healthy mitochondria, PINK1 kinase is imported and degraded by PARL protease 2. In damaged mitochondria (depolarized), PINK1 accumulates on the OMM 3. PINK1 phosphorylates ubiquitin and recruits Parkin (E3 ubiquitin ligase) 4. Parkin ubiquitinates OMM proteins, creating autophagy receptor binding sites 5. Autophagosome engulfs the damaged mitochondrion for lysosomal degradation

Clinical Connection: Mitochondrial Dynamics and Parkinson’s Disease Mutations in PINK1 and Parkin cause autosomal recessive early-onset Parkinson’s disease (PARK6 and PARK2). The failure of mitophagy leads to accumulation of damaged mitochondria in dopaminergic neurons of the substantia nigra, causing oxidative stress, energy depletion, and neuronal death. This pathway is a major therapeutic target. see section 8 for apoptosis pathways.

Concept Check 2: Predict the mitochondrial phenotype in a cell with a dominant-negative mutation in DRP1 that prevents GTP hydrolysis. Would the mitochondria appear fragmented or hyperfused?

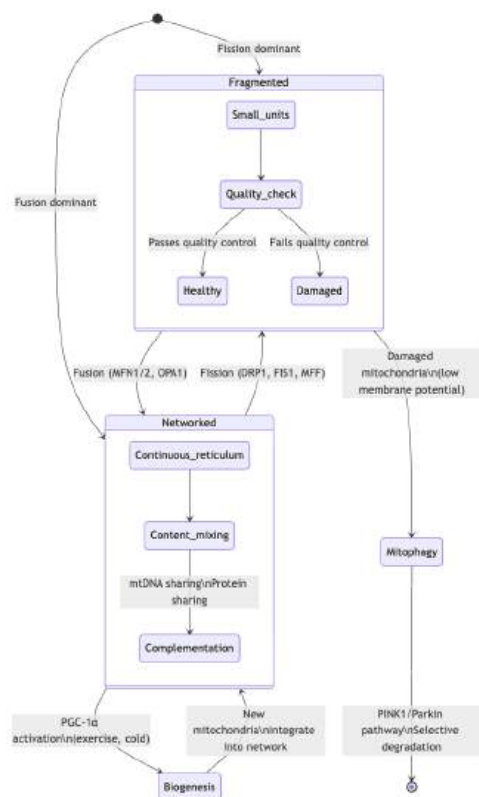


Figure 44. Mitochondrial dynamics: the balance between fusion and fission controls mitochondrial morphology, quality control, and biogenesis. Damaged mitochondria are selectively removed by mitophagy via the PINK1/Parkin pathway.

Concept Check (Evaluation): The endoplasmic reticulum (ER) is divided into rough ER (ribosome-studded) and smooth ER (lipid synthesis, Ca^{2+} storage). (a) A hepatocyte exposed to phenobarbital (a lipophilic drug) proliferates its smooth ER 4-6 fold over 48 h. Using a signal-transducer-effector breakdown: identify the signal (xenobiotic ligand binding CAR/PXR nuclear receptors), the signal transducer (CAR/PXR nuclear translocation and recruitment to xenobiotic response elements), and the effector (transcriptional induction of CYP450 enzymes and the membrane lipids supporting smooth-ER expansion). (b) ER stress (accumulation of misfolded proteins) triggers the Unfolded Protein Response (UPR) through three branches: IRE1, PERK, and ATF6. Design an experiment using single-branch genetic knockouts (or chemical inhibitors of each branch) to determine which branch governs the survival-vs.-apoptosis fate decision after sustained ER stress. (c) Explain why ER-to-Golgi COPII vesicle formation requires GTP hydrolysis by the Sar1 small GTPase, and how membrane-curvature sensing by Sec23/24 couples cargo selection to bud geometry.

Concept Check (Analysis): Mitochondria form dynamic networks through fusion (Mitofusin 1/2, OPA1) and fission (Drp1, Fis1) that respond to cellular energy status. (a) During nutrient starvation, predict whether the network elongates or fragments. Explain the functional logic in terms of cristae remodeling, ATP synthase dimer formation along cristae ridges, and protection of mitochondria from mitophagic engulfment. (b) In motor neurons with axon length about 1 m, mitochondria must be transported from cell body to synapse. If kinesin-1 moves at $1\text{ }\mu\text{m/s}$, calculate the minimum transport time to the most distal synapse (about $10^6\text{ s} \approx 11.6\text{ days}$), and explain why local mitochondrial biogenesis at synapses is therefore essential. (c) Propose a mechanism by which synaptic activity (which raises local cytosolic Ca^{2+}) could locally regulate mitochondrial fission via Drp1 recruitment, thereby matching energy supply with demand at the active synapse.

6.5 The Endomembrane System and Secretory Pathway

Several organelles form a functionally integrated endomembrane system:

6.5.1 Endoplasmic Reticulum Structure and Protein/Lipid Processing

Rough ER (RER): studded with ribosomes; site of synthesis, folding, and initial N-glycosylation of secreted and membrane proteins. Molecular chaperones (BiP/GRP78, calnexin, calreticulin) ensure proper folding; misfolded proteins are retrotranslocated for ER-associated degradation (ERAD) by the proteasome.

The signal recognition particle (SRP) pathway directs secretory proteins to the ER: 1. Ribosome begins translating mRNA; signal peptide (about 16–30 hydrophobic amino acids) emerges 2. SRP binds signal peptide and ribosome, pausing translation 3. SRP-ribosome complex docks at SRP receptor on ER membrane 4. Signal peptide inserts into the translocon (Sec61 channel) 5. Translation resumes; polypeptide is co-translationally threaded into the ER lumen 6. Signal peptidase

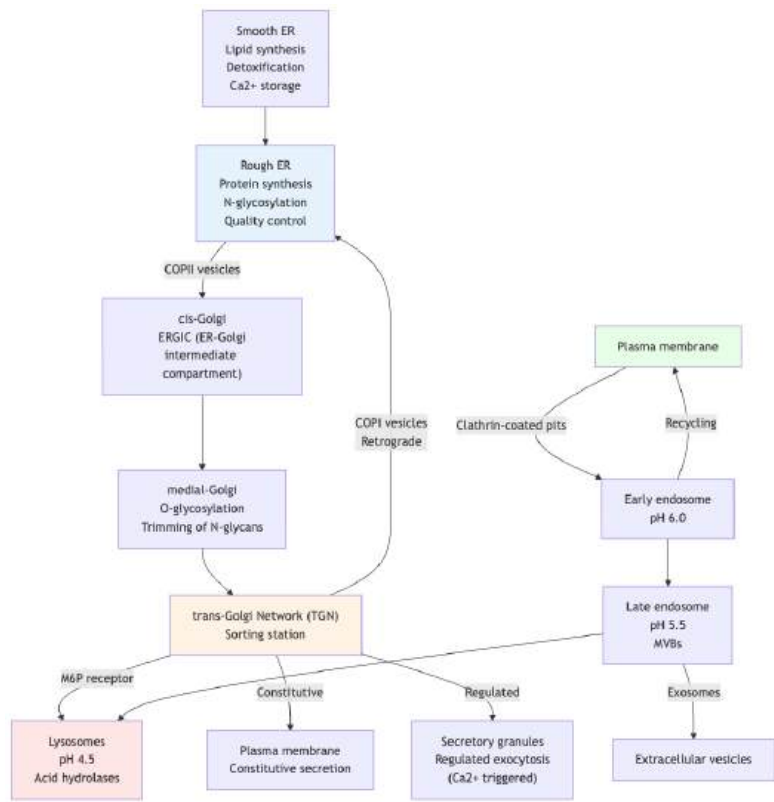


Figure 45. The endomembrane system and secretory/endocytic pathways. COPII vesicles carry cargo anterograde (ER to Golgi); COPI vesicles carry cargo retrograde (Golgi to ER). The trans-Golgi network sorts proteins to lysosomes (via M6P signal), plasma membrane, or secretory granules.

cleaves the signal peptide

Smooth ER (SER): lacks ribosomes; functions: - Lipid synthesis (phospholipids, cholesterol, steroid **hormones**) - Drug/toxin detoxification (cytochrome P450 enzymes in liver SER) - Ca²⁺ storage and release for signaling (sarcoplasmic reticulum in muscle = specialized SER) - Glycogen metabolism

Unfolded protein response (UPR): Accumulation of misfolded proteins triggers the UPR — three ER stress sensor pathways (IRE1, PERK, ATF6) that expand ER capacity, halt translation, and if irresolvable, trigger apoptosis. Relevant in diabetes (beta-cells overwhelmed by insulin demand), neurodegeneration, and cancer.

ER quality control and ERAD (in detail). Newly synthesized glycoproteins entering the ER lumen are tagged with a triple-glucosylated N-glycan (Glc₃Man₉GlcNAc₂). Glucosidases I and II sequentially trim two glucoses, generating a monoglucosylated form that is recognized by the lectin chaperones calnexin (membrane-bound) and calreticulin (luminal). These chaperones hold the protein in a folding-competent state. If the protein folds correctly, glucosidase II removes the last glucose and the protein exits via COPII vesicles. If folding fails, UGGT (UDP-glucose:glycoprotein glucosyltransferase) re-glucosylates it, sending it back to calnexin/calreticulin — the calnexin/calreticulin cycle. Repeated failure marks the protein for ERAD (ER-associated degradation):

1. Recognition: Mannose trimming by ER mannosidases (EDE1/2/3) creates a “give up” signal — no further folding attempts.
2. Retrotranslocation: The misfolded protein is recognized by ERAD components (HRD1/SEL1L, gp78, MARCH6) and threaded back to the cytoplasm through a retrotranslocation channel (likely Hrd1 itself).
3. Polyubiquitination: ER-membrane E3 ligases (Hrd1, gp78) attach K48-linked ubiquitin chains.
4. Extraction: The AAA+ ATPase p97/VCP (Cdc48 in yeast) uses ATP hydrolysis to mechanically extract the ubiquitinated polypeptide from the membrane.
5. Degradation: The proteasome digests the substrate to small peptides.

Three branches of the UPR. When ERAD cannot keep up with the load, three transmembrane sensors are activated:

Table 104. Endoplasmic Reticulum Structure and Protein/Lipid Processing: Sensor and Mechanism.

Sensor	Mechanism	Output	Time scale
IRE1	Luminal domain dimerises on misfolded proteins; cytoplasmic domain has kinase + endoribonuclease activity	Splices XBP1 mRNA → active XBP1s transcription factor → genes for ER expansion, ERAD, lipid synthesis	Minutes–hours (chronic adaptation)
PERK	Dimerises and trans-phosphorylates eIF2alpha	Global translation attenuation; selective translation of ATF4 → CHOP	Minutes (immediate response)
ATF6	Trafficks to Golgi; cleaved by S1P + S2P proteases	Cytoplasmic fragment is a transcription factor for ER chaperones (BiP, GRP94)	Hours

If the lesion is repaired, the UPR shuts down and homeostasis resumes. If the stress is severe or prolonged, CHOP (downstream of PERK/ATF4) and IRE1’s secondary RIDD activity (Regulated IRE1-Dependent Decay of mRNAs) bias the cell toward apoptosis. The same pathway is therefore an adaptive thermostat *and* a death timer — the switch is set by the integrated stress dose.

Worked observation: insulin secretion and ER load. A pancreatic beta-cell synthesizes about 10⁶ insulin molecules per minute during glucose stimulation. Each must be folded with three disulphide bonds, processed by PC1/3 and PC2 from proinsulin, and packaged into secretory granules. ER folding capacity is therefore one of the rate-limiting steps for insulin secretion. Chronic hyperglycaemia (in obesity, type 2 diabetes) drives sustained UPR, eventual CHOP-mediated apoptosis, and progressive beta-cell loss. Pharmacological chemical chaperones (TUDCA, 4-PBA) and selective IRE1 inhibitors are in trials to delay this collapse.

Clinical Connection: ER Stress and Type 2 Diabetes Pancreatic beta-cells produce enormous quantities of insulin (about 1 million molecules per cell per minute during glucose stimulation). This places extreme demands on the ER folding machinery. Chronic hyperglycaemia and obesity increase insulin demand beyond ER capacity, triggering the UPR. Prolonged UPR activation causes beta-cell apoptosis, contributing to the progressive decline in insulin secretion seen in type 2 diabetes. Pharmacological chaperones (e.g., TUDCA, 4-PBA) that reduce ER stress are being investigated as diabetes therapeutics.

6.5.2 Golgi Apparatus and Vesicular Sorting

The Golgi stack (cis-Golgi network, cis, medial, trans, trans-Golgi network/TGN) receives cargo from the ER in COPII-coated vesicles and processes proteins by: - O-glycosylation (adding sugars to Ser/Thr) - Proteolytic processing (e.g., insulin prohormone to insulin) - Phosphorylation of mannose-6-phosphate (M6P) residues, creating the lysosomal targeting signal - Sorting to: secretory vesicles, plasma membrane, lysosomes, or ER (retrograde COPI vesicles)

Vesicle coat proteins and their roles:

Table 105. Golgi Apparatus and Vesicular Sorting: Coat protein and Vesicle route.

Coat protein	Vesicle route	Cargo
COPII (Sec13/31, Sec23/24)	ER to cis-Golgi	Newly synthesized secretory proteins
COPI (coatomer)	Golgi to ER (retrograde)	ER-resident proteins (KDEL retrieval)
Clathrin + adaptors (AP1, AP2)	TGN to endosome; PM to endosome	Lysosomal enzymes (M6P); receptor-mediated endocytosis

Brefeldin A (BFA) inhibits GBF1 (a GEF for Arf1 GTPase needed for COPI assembly) and dissolves the Golgi within minutes — demonstrating its dynamic membrane flux.

6.5.3 Lysosomes and Acid Hydrolase Compartments

Lysosomes (pH 4.5–5.0, maintained by V-type H⁺-ATPase) contain about 60 acid hydrolases (proteases, lipases, nucleases, glycosidases) that digest: - Autophagy: cellular debris and aged organelles (macroautophagy, microautophagy, chaperone-mediated autophagy) - Phagocytosis: bacteria and debris (in macrophages, neutrophils) - Receptor-mediated endocytosis: LDL-cholesterol uptake - Extracellular digestion: osteoclasts secrete lysosomal contents to resorb bone

Types of selective autophagy: - Mitophagy: selective removal of damaged mitochondria (PINK1/Parkin pathway) - Pexophagy: selective removal of excess peroxisomes - Lipophagy: selective degradation of lipid droplets - Ribophagy: selective degradation of ribosomes during starvation - ER-phagy/reticulophagy: selective removal of excess ER

Lysosomal storage diseases result from enzyme deficiencies: - Pompe disease: alpha-1,4-glucosidase deficiency, glycogen accumulates, cardiac/muscle failure - Gaucher disease: glucocerebrosidase deficiency, sphingolipid accumulation in macrophages - Tay-Sachs disease: hexosaminidase A deficiency, GM2 ganglioside accumulation in neurons, neurodegeneration - Niemann-Pick type C: NPC1/NPC2 cholesterol transport deficiency, cholesterol accumulates in lysosomes - Both Pompe and Gaucher are treatable by enzyme replacement therapy (ERT), where recombinant enzyme is infused intravenously and targeted to lysosomes via M6P receptors

Concept Check 3: A patient has I-cell disease (mucopolidosis II), in which the enzyme that adds M6P to lysosomal enzymes in the cis-Golgi is defective. Predict the consequences for (a) lysosomal enzyme targeting, (b) extracellular enzyme levels, and (c) intracellular digestion.

6.6 Cytoskeletal Filaments and Cellular Mechanics

The cytoskeleton is a dynamic protein network pervading the cytoplasm, providing structural support, enabling cell movement, and directing intracellular traffic.

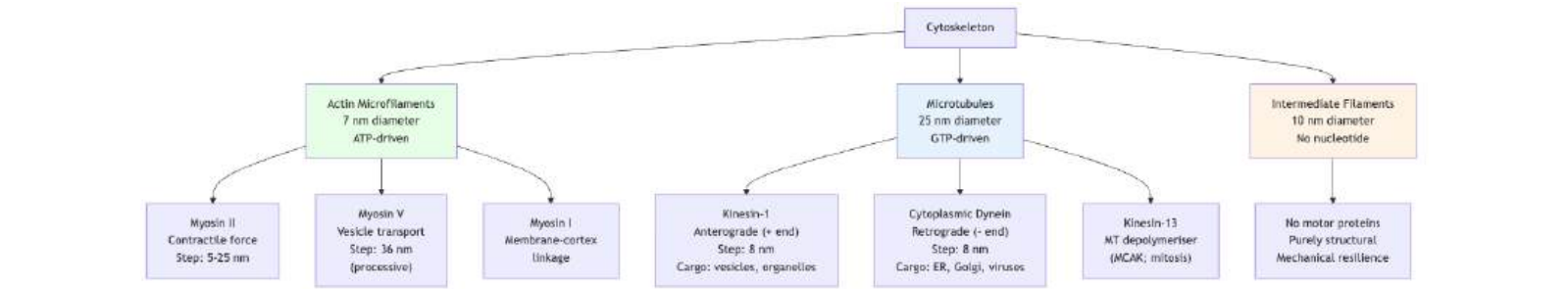


Figure 46. Cytoskeletal components and their associated motor proteins. Actin filaments are driven by myosin motors, microtubules by kinesin and dynein motors, and intermediate filaments have no associated motors.

6.6.1 Actin Microfilaments and Cortical Force Generation

Actin filaments (F-actin; diameter about 7 nm) are polar, ATP-driven polymers of globular G-actin monomers. Properties: - Treadmilling: net polymerization at the (+) barbed end; depolymerisation at the (-) pointed end, resulting in net movement of the filament while maintaining constant length - Branching: Arp2/3 complex creates about 70-degree branches (lamellipodia, phagocytic cups); nucleated by WASP/WAVE family activators - Bundling: Fimbrin (parallel tight bundles in microvilli), alpha-actinin (looser bundles in stress fibers), villin (intestinal brush border)

Critical concentration and treadmilling — the quantitative basis. A single actin monomer can add to (or dissociate from) either end of a filament. At each end, the rate constants for assembly (k_+) and disassembly (k_-) define an end-specific critical concentration:

$$C_c^{\text{end}} = \frac{k_-}{k_+}$$

(111)

When the free monomer concentration [G-actin] exceeds C_c , the end grows; below C_c , the end shrinks. Crucially, the (+) barbed end and the (–) pointed end have *different* critical concentrations because of their different geometries:

$$C_c^{(+)} \approx 0.1 \mu\text{M}, \quad C_c^{(-)} \approx 0.6 \mu\text{M}$$

(112)

In a steady state with [G-actin] between these two values (say 0.3 μM), the (+) end grows continuously while the (–) end shrinks continuously — and the filament *translates* through space at a steady velocity even though its average length is constant. This is treadmilling, and the velocity is:

$$v_{\text{tread}} = \delta \cdot k_+^{(+)} \cdot ([G] - C_c^{(+)})$$

(113)

where $\delta = 2.7 \text{ nm}$ (axial rise per monomer; two monomers per helical repeat = 5.4 nm). For lamellipodial actin in a migrating fibroblast, treadmilling proceeds at about $0.1 \text{ }\mu\text{m/s}$ at $37 \text{ }^\circ\text{C}$ — the molecular speed limit on which crawling cells move.

ATP hydrolysis on the filament shifts the (–)-end disassembly rate, increasing the asymmetry between ends; cofilin and ADF (actin-depolymerising factor) accelerate (–)-end disassembly; profilin loads ATP onto G-actin to enrich the (+)-end-favored pool. The net result is that treadmilling is energetically driven by ATP hydrolysis even though the polymerization reaction itself does not consume ATP.

Microtubule dynamic instability — the GTP cap. Microtubules treadmill very weakly; instead they exhibit dynamic instability — alternating phases of growth and rapid shrinkage at a single end. The (+) end of a growing microtubule carries a “GTP cap” (a few hundred GTP-tubulin subunits added before hydrolysis catches up). When the cap is intact, polymerization continues at about $1 \text{ }\mu\text{m/min}$. Stochastic loss of the cap exposes GDP-tubulin, which has a strained lateral lattice and undergoes rapid catastrophic depolymerisation at about $10\text{--}30 \text{ }\mu\text{m/min}$ (“catastrophe”). Catastrophic shrinkage can be rescued by reformation of a GTP cap (“rescue”). The four parameters — growth rate v_g , shrinkage rate v_s , catastrophe frequency f_c , rescue frequency f_r — completely specify microtubule behavior and are tuned by a panoply of plus-end tracking proteins (+TIPs: EB1, CLIP-170) and depolymerases (kinesin-13/MCAK).

Motor proteins on actin: - Myosin II: generates contractile force (muscle sarcomere, cytokinesis, cell migration); bipolar thick filaments; step size about $5\text{--}25 \text{ nm}$; non-processive (releases after each step) - Myosin V: processive motor for vesicle transport; walks “hand-over-hand” with 36 nm steps matching the F-actin helical repeat; transports melanosomes, ER, secretory vesicles - Myosin I: single-headed; links membrane to actin cortex; involved in endocytosis and membrane tension

Functions: cell shape, cytokinesis (contractile ring), muscle contraction, phagocytosis, cell crawling (lamellipodia, filopodia), intracellular organelle movement.

6.6.2 Tubulin Microtubules and Intracellular Transport

Microtubules (MTs; 25 nm diameter) are hollow tubes of alpha/beta-tubulin heterodimers forming 13 protofilaments. Properties: - GTP-driven dynamic instability: rapid switching between growth (rescue) and catastrophic depolymerisation; GTP cap model — growing end has GTP-tubulin; loss of cap triggers depolymerisation - Polarity: (+) end grows toward cell periphery; (-) end at MTOC/centrosome - Post-translational modifications: acetylation (stable MTs), tyrosination/detyrosination, polyglutamylation — the “tubulin code” directs motor protein binding

Motor proteins on microtubules: - Kinesin-1 (conventional kinesin): anterograde (+ end directed); dimeric, processive; 8 nm step size matching tubulin repeat; transports vesicles, mitochondria, mRNA toward cell periphery; speed about $0.8 \text{ }\mu\text{m/s}$ - Cytoplasmic dynein: retrograde (- end directed); large complex (about 1.2 MDa) with dynactin cofactor; 8 nm steps; transports ER, Golgi, endosomes, viruses toward cell center; also drives mitotic spindle positioning - Kinesin-13 (MCAK): depolymerises MT ends; critical for spindle dynamics during mitosis

Functions: chromosome segregation (mitotic spindle), flagella/cilia (axoneme: $9+2 \text{ MT}$ arrangement), intracellular vesicle transport (axonal transport in neurons), cell polarity, cell shape.

6.6.3 Worked Example: Motor Protein Kinematics and Energetics

Problem: A kinesin-1 motor protein is transporting a neurotransmitter vesicle down a nerve axon along a microtubule. The motor moves at a constant velocity of $v = 0.80 \text{ }\mu\text{m/s}$ and takes fixed step sizes of $d = 8 \text{ nm}$ per step. 1. How many steps does the kinesin take per second? 2. If kinesin hydrolyses exactly one ATP molecule per 8 nm step, how many ATP molecules are consumed during a 2.4 mm transport journey along the axon?

Solution:

1. Calculate the stepping rate: First, convert velocity to nanometres per second to match the step size units:

$$v = 0.80 \text{ }\mu\text{m/s} = 800 \text{ nm/s}$$

Calculate the number of steps per second:

$$\text{Step rate} = \frac{v}{d} = \frac{800 \text{ nm/s}}{8 \text{ nm/step}} = 100 \text{ steps/s}$$

The motor takes exactly 100 steps per second.

2. Calculate the energy consumption for the journey: Convert the total distance from millimetres to nanometres:

$$D_{\text{total}} = 2.4 \text{ mm} = 2.4 \times 10^6 \text{ nm} = 2,400,000 \text{ nm}$$

Calculate the total number of steps:

$$\text{Total steps} = \frac{D_{\text{total}}}{d} = \frac{2,400,000 \text{ nm}}{8 \text{ nm/step}} = 300,000 \text{ steps}$$

Since 1 step = 1 ATP molecule hydrolysed:

$$\text{Total ATP consumed} = 300,000 \text{ molecules of ATP}$$

This calculation highlights the immense energy requirements of axonal transport; maintaining trillions of synapses across the nervous system commands a massive proportion of the body’s total ATP production.

3. Calculate the transport time: The total transport time at constant velocity is simply distance divided by velocity:

$$t = \frac{D_{\text{total}}}{v} = \frac{2.4 \times 10^{-3} \text{ m}}{0.80 \times 10^{-6} \text{ m/s}} = 3,000 \text{ s} \approx 50 \text{ min}$$

So a kinesin-driven cargo crosses 2.4 mm of axon in just under an hour. For a giraffe motor neuron (axon length about 3 m), the same calculation yields about 43 days — consistent with the historical observation by Weiss and Hiscoe (1948) that materials accumulate above an axonal ligature with a wave-front velocity of a few millimetres per day. Compare this with passive diffusion of the same vesicle: using $t = x^2/2D$ with $D \approx 10^{-12} \text{ m}^2/\text{s}$ for a 100 nm vesicle, $t \approx 1.4 \times 10^{12} \text{ s} \approx 45,000 \text{ years}$. Active transport beats diffusion by eight orders of magnitude for cargoes of this size and distance. The cell’s choice to spend about 10^5 ATPs per vesicle is therefore not extravagance — it is what makes the long axon viable at most.

Worked Example: Comparing kinesin and dynein transport.

A dendritic spine 50 μm from the cell body needs both anterograde (kinesin: 0.8 μm/s) and retrograde (dynein: 1.0 μm/s) cargoes. Calculate the round-trip time and minimum ATP cost for a single cargo cycle.

- Anterograde transit: $t_+ = 50 \mu\text{m}/0.8 \mu\text{m/s} = 62.5 \text{ s}$
- Retrograde transit: $t_- = 50 \mu\text{m}/1.0 \mu\text{m/s} = 50 \text{ s}$
- Total transit time: $\sim 112 \text{ s}$ (cargo handling and motor switching add another about 10 s)
- Kinesin steps: $50,000 \text{ nm}/8 \text{ nm} = 6,250 \text{ steps} \rightarrow 6,250 \text{ ATP}$
- Dynein steps (more variable, average about 8 nm): another about 6,250 ATP
- Total: about 12,500 ATP per round trip per cargo

A single dendrite that supports 100 active spines and turns over 10 cargoes per spine per minute therefore consumes about 10^7 ATPs/min on motor stepping alone — roughly 1% of a neuron’s resting ATP budget devoted to logistics.

Taxol (paclitaxel) stabilizes MT and prevents depolymerisation, arresting mitosis in metaphase. Used in chemotherapy for breast, ovarian, and lung cancers. It is derived from the bark of the Pacific yew tree (*Taxus brevifolia*).

Colchicine destabilises MT by binding free tubulin and preventing polymerization. Used for gout (inhibits neutrophil migration) and in cytogenetics (arrests cells in metaphase for karyotyping).

Vincristine/vinblastine (vinca alkaloids from *Catharanthus roseus*) also destabilise MT. Used in cancer chemotherapy (lymphomas, leukaemias).

6.6.4 Intermediate Filaments and Tensile Strength

Intermediate filaments (IFs; about 10 nm diameter) are ropelike cables of coiled-coil proteins. Unlike actin and MT, IFs are not polar and have no associated motors — they are purely structural:

Table 106. Intermediate Filaments and Tensile Strength: IF type and Protein.

IF type	Protein	Location	Associated disease
Keratin (types I/II)	Keratin 1–20	Epithelial cells	Epidermolysis bullosa simplex
Vimentin (type III)	Vimentin	Fibroblasts, endothelial	Diagnostic marker for sarcomas

IF type	Protein	Location	Associated disease
Desmin (type III)	Desmin	Muscle (Z-disc)	Desminopathy (cardiomyopathy)
GFAP (type III)	GFAP	Astrocytes	Alexander disease (leukodystrophy)
Neurofilament (type IV)	NF-L, NF-M, NF-H	Axons (determines axon diameter)	ALS, Charcot-Marie-Tooth
Lamins (type V)	Lamin A/B/C	Nuclear lamina (inner NE)	Progeria, Emery-Dreifuss muscular dystrophy

Lamins form a meshwork underlying the inner nuclear membrane, giving the nucleus mechanical rigidity and organizing chromatin. Progerin (mutant lamin A with 50-aa deletion due to a point mutation activating a cryptic splice site) causes Hutchinson-Gilford progeria syndrome — accelerated aging with death typically by age 13 from cardiovascular disease.

Clinical Connection: Cytoskeleton Diseases Alexander disease (GFAP mutations): Gain-of-function mutations in GFAP cause Rosenthal fiber accumulation in astrocytes, leading to progressive leukodystrophy with megalencephaly, seizures, and developmental regression. ALS (amyotrophic lateral sclerosis): Some familial ALS cases involve mutations in dynactin (DCTN1) or dynein, disrupting retrograde axonal transport and causing motor neuron degeneration. Taxol mechanism in cancer therapy: By hyperstabilising microtubules, taxol prevents the dynamic instability required for mitotic spindle function. Chromosomes cannot properly segregate, activating the spindle assembly checkpoint and ultimately triggering apoptosis in rapidly dividing tumor cells.

Concept Check 4: Kinesin-1 moves toward the (+) end of microtubules, while dynein moves toward the (-) end. In a neuron, which direction does each motor move cargo along the axon? Which motor would transport newly synthesized synaptic vesicle precursors from the cell body to the synapse?

6.7 Centrosomes, Centrioles, and Cilia

6.7.1 Centrosome/MTOC as the Microtubule Organizing Center

The centrosome is the primary microtubule organizing center (MTOC) in animal cells. It consists of two centrioles (barrel-shaped structures of 9 triplet microtubules arranged in a pinwheel) surrounded by pericentriolar material (PCM) containing gamma-tubulin ring complexes (gamma-TuRC) that nucleate new microtubules.

During mitosis, centrosomes duplicate and migrate to opposite poles of the cell, organizing the mitotic spindle. Centrosome amplification (>2 per cell) is common in cancer and contributes to chromosomal instability.

6.7.2 Cilia and Flagella

Motile cilia (9+2 axoneme: 9 outer doublet MTs + 2 central singlet MTs, linked by dynein arms and nexin bridges) beat in coordinated waves. Found on respiratory epithelium (about 200 per cell), fallopian tube epithelium, and ependymal cells lining brain ventricles.

Primary cilia (9+0 axoneme: no central pair, non-motile) are mechanosensory/chemosensory antennae present on nearly every mammalian cell type. Function as signaling hubs: - Hedgehog signaling: Smoothened receptor relocates to the primary cilium upon Hedgehog ligand binding - Polycystin-1/2: mechanosensitive Ca²⁺ channels on kidney primary cilia; sense urine flow

Ciliopathies — diseases caused by defective cilia: - Primary ciliary dyskinesia (Kartagener syndrome): dynein arm defects; immotile cilia; chronic respiratory infections, situs inversus (50%), male infertility - Polycystic kidney disease (PKD): mutations in PKD1 (polycystin-1) or PKD2 (polycystin-2); defective primary cilia mechanosensing; uncontrolled tubular cell proliferation and cyst formation - Bardet-Biedl syndrome: defective ciliary trafficking; obesity, retinitis pigmentosa, renal anomalies, polydactyly

Concept Check 5: Why does Kartagener syndrome sometimes cause situs inversus (mirror-reversal of organ asymmetry)? Consider the role of motile nodal cilia in establishing left-right body asymmetry during embryonic development.

6.8 Peroxisomes and Single-Membrane Oxidative Compartments

Peroxisomes contain oxidases that generate hydrogen peroxide (H₂O₂) as a byproduct of fatty acid beta-oxidation, and catalase that destroys it:



6.8.1 Peroxisome Metabolism, Detoxification, and Biosynthesis

- Very-long-chain fatty acid (VLCFA) beta-oxidation: Shortens VLCFAs (>C22) to medium-chain products that are then transferred to mitochondria for complete oxidation
- Plasmalogen biosynthesis: Ether-linked phospholipids essential for myelin sheaths; about 50% of heart phospholipids are plasmalogens
- Bile acid synthesis: Side chain oxidation of cholesterol intermediates
- Amino acid oxidation: D-amino acid oxidase
- Reactive oxygen species management: Both generation (H₂O₂ from oxidases) and detoxification (catalase, peroxidase)
- Glyoxylate metabolism: Alanine-glyoxylate aminotransferase (AGT) converts glyoxylate to glycine

6.8.2 Peroxisome Biogenesis and Protein Import

Peroxisomes form by growth and division of existing peroxisomes (similar to mitochondria) and also by de novo formation from ER-derived vesicles. Peroxisomal matrix proteins are imported post-translationally via PTS1 (C-terminal SKL tripeptide) or PTS2 (N-terminal nonapeptide) signals, recognized by PEX5 and PEX7 receptors.

Clinical Connection: Peroxisome Biogenesis Disorders Zellweger syndrome (the most severe peroxisome biogenesis disorder) results from mutations in PEX genes (most commonly PEX1). Absent or non-functional peroxisomes lead to VLCFA accumulation, plasmalogen deficiency, and bile acid synthesis failure. Affected infants present with severe hypotonia, seizures, hepatomegaly, and characteristic facial features, with death typically in the first year. X-linked adrenoleukodystrophy (X-ALD): Mutation in ABCD1 (a peroxisomal ABC transporter for VLCFA); VLCFA accumulation destroys adrenal cortex and CNS myelin. Depicted in the film “Lorenzo’s Oil.” Primary hyperoxaluria type 1: AGT mistargeted from peroxisomes to mitochondria; oxalate accumulates; kidney stones and renal failure. see section 7 for ABC transporters.

6.9 Cell Adhesion and Junctions

Multicellular organisms require cells to adhere to each other and to the extracellular matrix (ECM). Four major families of cell adhesion molecules (CAMs) and several junction types mediate this:

6.9.1 Cell Adhesion Molecules

Table 107. Cell Adhesion Molecules: CAM family and Binding.

CAM family	Binding	Ca ²⁺ dependent?	Key examples	Function
Cadherins	Homophilic	Yes	E-cadherin (epithelial), N-cadherin (neural), VE-cadherin (endothelial)	Tissue-specific sorting; adherens junctions
Integrins	Heterophilic (ECM ligands)	Yes (divalent cation)	alpha5-beta1 (fibronectin), alphaV-beta3 (vitronectin), alpha2-beta1 (collagen)	Cell-ECM adhesion; focal adhesions; bidirectional signaling
Selectins	Heterophilic (sugar ligands)	Yes	L-selectin (leukocytes), P-selectin (platelets, endothelium), E-selectin (endothelium)	Leukocyte rolling and homing
IgCAMs	Homo/heterophilic	No	NCAM, ICAM-1, VCAM-1	Neural development; immune cell adhesion

6.9.2 Cell Junctions and Tissue Barrier Architecture

- Tight junctions (zonula occludens): Seal adjacent epithelial cells; prevent paracellular diffusion; claudins and occludin form the seal; ZO-1/2/3 link to actin cytoskeleton. Create apical-basal polarity.
- Adherens junctions (zonula adherens): Cadherin-mediated; linked to actin cytoskeleton via catenins (alpha, beta, p120). E-cadherin loss is a hallmark of epithelial-mesenchymal transition (EMT) in cancer metastasis.
- Desmosomes (macula adherens): Cadherin-mediated (desmogleins, desmocollins); linked to intermediate filaments (keratin) via plakoglobin and desmoplakin. Provide mechanical strength to skin and heart. Autoantibodies against desmoglein-3 cause pemphigus vulgaris (life-threatening blistering disease).
- Gap junctions: Connexin hexamers (connexons) form channels between adjacent cells; allow passage of ions and small molecules (<1 kDa); enable electrical coupling (cardiac muscle synchrony), metabolic coupling, and intercellular signaling. Mutations in connexin-26 (GJB2) are the most common cause of hereditary deafness.
- Hemidesmosomes: Integrin alpha6-beta4 links epithelial basal surface to basement membrane; connected to keratin intermediate filaments. Defects cause epidermolysis bullosa (skin blistering from minor trauma).

Concept Check 6: E-cadherin is frequently downregulated in invasive carcinomas. How would loss of E-cadherin promote cancer metastasis? Consider both adhesion and signaling functions.

6.10 The Proteasome — Protein Quality Control

While lysosomes degrade proteins within membrane-bound compartments, the ubiquitin-proteasome system (UPS) degrades misfolded, damaged, or regulatory proteins in the cytoplasm and nucleus.

6.10.1 The 26S Proteasome

The 26S proteasome is a about 2.5 MDa multi-subunit protease complex consisting of: - 20S core particle: barrel-shaped structure of four stacked heptameric rings (alpha7-beta7-beta7-alpha7); proteolytic activity (chymotrypsin-like, trypsin-like, and **cas**pase-like) is sequestered within the barrel interior - 19S regulatory particle (cap): recognizes ubiquitinated substrates, deubiquitinates them, unfolds the polypeptide, and threads it into the 20S core for degradation

6.10.2 Ubiquitination — The Degradation Signal

Ubiquitin (76 amino acids, highly conserved) is conjugated to target proteins via a three-enzyme cascade:

1. E1 (ubiquitin-activating enzyme): Activates ubiquitin in an ATP-dependent reaction (2 E1 enzymes in humans)
2. E2 (ubiquitin-conjugating enzyme): Carries activated ubiquitin (about 40 E2s in humans)
3. E3 (ubiquitin ligase): Confers substrate specificity; transfers ubiquitin to the target protein (about 600 E3s in humans)

A chain of at least 4 ubiquitin molecules linked via K48 serves as the proteasomal degradation signal. Other ubiquitin chain types (K63, M1/linear) serve non-degradative signaling functions (NF-kB activation, DNA repair, endocytosis).

Key E3 ligases and their substrates:

Table 108. Ubiquitination — The Degradation Signal: E3 Ligase and Substrate.

E3 Ligase	Substrate	Function
MDM2	p53	Keeps p53 levels low in unstressed cells
APC/C (anaphase -promoting complex)	Securin, cyclin B	Drives mitotic exit
SCF ^{beta-TrCP}	Beta-catenin, Ikb	Wnt signaling, NF-kB regulation
VHL (von Hippel-Lindau)	HIF-1-alpha	Oxygen sensing; mutations cause renal cell carcinoma
Parkin	OMM proteins	Mitophagy through the PINK1-Parkin quality-control pathway

Clinical Connection: Proteasome Inhibitors in Cancer Bortezomib (Velcade) inhibits the chymotrypsin-like activity of the 20S proteasome. This causes accumulation of misfolded proteins, ER stress, and apoptosis. Multiple myeloma cells are particularly sensitive because they produce enormous quantities of immunoglobulins, generating high proteasomal load. Bortezomib has transformed multiple myeloma treatment. Carfilzomib and ixazomib are second-generation proteasome inhibitors with improved profiles.

6.11 CRISPR Applications in Organelle Biology

The CRISPR-Cas9 system has revolutionised the study of organelle biology by enabling precise gene editing:

- Fluorescent tagging of endogenous proteins: CRISPR knock-in of GFP/mCherry at native loci enables live imaging of organelles at endogenous expression levels (avoiding overexpression artifacts)
- **Genome**-wide screens: CRISPR knockout libraries have identified new genes required for mitophagy, autophagy, ER-phagy, and peroxisome biogenesis
- Base editing of mtDNA: DddA-derived cytosine base editors (DdCBEs) can edit mtDNA without double-strand breaks, enabling creation of precise mitochondrial disease models
- Organelle-targeted degradation: AID (auxin-inducible degron) tagged organelle proteins enable acute, reversible organelle disruption

6.12 Computational Bridge

Membrane-bound organelle counts are explicit in the cell model and can be queried for teaching comparisons:

```
from biology.cell import get_organelles_by_cell_type, count_membrane_bound_organelles

org = get_organelles_by_cell_type("animal")
print(count_membrane_bound_organelles(org))
```

Clinical / systems note: Mitochondrial disorders and peroxisomal diseases (e.g. Zellweger spectrum) show how loss of a single organelle compartment produces multi-system phenotypes because compartment-specific metabolites fail to reach the cytosol or nucleus.

6.12.1 Mitochondrial Base Editors Without Double-Strand Breaks

Mitochondrial DNA (mtDNA) encodes 13 proteins of the electron transport chain and 22 tRNAs — mutations here cause a spectrum of mitochondrial diseases (MELAS, MERRF, Leber’s hereditary optic neuropathy) that affect roughly 1 in 5000 births. CRISPR–Cas9 could not reach mtDNA because guide RNA import into mitochondria is inefficient, and any DNA double-strand break in the polyploid (100–10 000 copies per cell) mitochondrial genome triggers rapid linear-DNA degradation rather than useful repair.

The breakthrough came from an unusual source: a bacterial interbacterial toxin (DddA) from *Burkholderia cenocepacia* that deaminates cytosines in *double-stranded* DNA (most cytidine deaminases require single-stranded substrates). In 2020, the Liu lab published DddA-derived cytosine base editors (DdCBEs) — split DddA halves fused to programmable TALE arrays that reconstitute deaminase activity primarily when both halves bind adjacent mitochondrial sites (*Nature* 2020). Subsequent engineering produced zinc-finger–DdCBEs (smaller, easier to import), mitoBEs capable of A-to-G edits, and TALEd (TALE-linked deaminases) for A-to-I conversion. Efficiencies in human cells now reach 30–50 % heteroplasmy shift with bystander editing < 5 %.

Worked example: for the MELAS-causing mutation m.3243A>G in tRNA^{Leu}, a DdCBE targeting the reverse strand near position 3244 converts the pathogenic G back to A in about 30 % of mtDNA copies — above the threshold needed to cross the heteroplasmy clinical phenotype boundary (about 80 % mutant copies for overt disease). A 2022 report corrected a murine Ndufa10 mutation *in vivo* via AAV-delivered DdCBE with functional rescue of respiratory chain complex I. Cautions: off-target mitochondrial editing rates of about 0.1–1 % at 30–50 predicted sites; potential nuclear off-targets; the edit is heritable in the female germline (with the ethical considerations of heritable genome editing). The technology is a clean example of how unusual biochemistry in obscure organisms (a bacterial toxin no textbook mentioned in 2019) can become the keystone of a new therapeutic platform within 4 years.

6.13 Current Evidence and Frontier Biology: Cell Structure and Organelles

For Cell Structure and Organelles, frontier biology belongs inside the evidence logic of the chapter. Cell biology is increasingly measured as live, spatial, single-cell, and perturbational data rather than static diagrams alone. The core reading question is this: organelle function is dynamic, contact-mediated, and context-dependent rather than a fixed list of compartments.

- What to verify: identify the observation, model, assay, or dataset that would make the claim stronger or weaker.
- What to qualify: state the scale, organism, cell type, environmental condition, or population where the claim is expected to hold.
- What to compare: test at least one alternative explanation, baseline, or null model before treating the pattern as causal.

- What to cite: distinguish primary evidence, review synthesis, public dataset, and institutional guidance; for recent or numeric claims, prefer the source closest to the measurement and state what has changed since it was published.

For organelle claims, identify the imaging scale, molecular marker, dynamics, and perturbation evidence before assigning structure to function.

Source practice: Distinguish fixed microscopy, live-cell perturbation, biochemical fractionation, and spatial omics evidence when making causal claims about cell architecture.

6.13.1 Current Evidence Map: Membrane-Bound and Condensate Organization

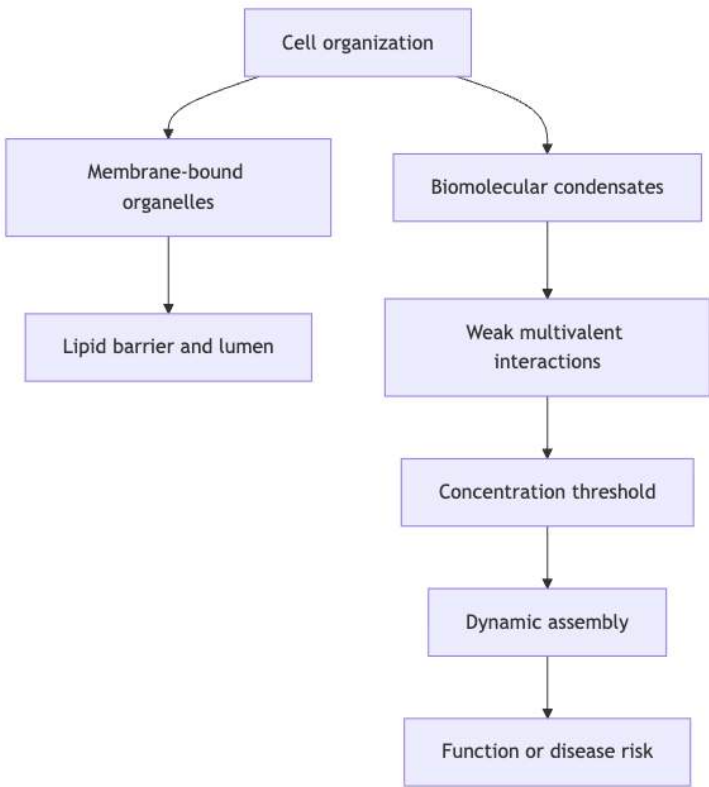


Figure 47. Condensates should be taught as regulatable cellular organization, not as a replacement for membrane-bound organelles or as proof of causality by appearance alone.

6.14 Summary

- The nucleus houses chromatin (DNA + histones); nuclear pores regulate macromolecule traffic via the Ran GTPase system; the nucleolus assembles ribosomes and is a cancer prognostic marker.
- Mitochondria have their own circular DNA and ribosomes, consistent with endosymbiotic origin; cristae maximize IMM surface area for the ETC; fusion/fission dynamics maintain mitochondrial quality via PINK1/Parkin-mediated mitophagy.
- The endomembrane system (RER, SER, Golgi, vesicles) coordinates protein secretion and glycosylation; COPII (anterograde), COPI (retrograde), and clathrin (endocytic) coat proteins direct vesicle traffic.
- The cytoskeleton (actin, MTs, IFs) provides structure, enables motility, and directs intracellular transport via motor proteins (myosin, kinesin, dynein).
- Peroxisomes perform VLCFA oxidation and ROS management; centrosomes/cilia function as MTOCs and sensory antennae; cell adhesion molecules and junctions maintain tissue architecture.
- Connections: See section 5 for cell theory and endosymbiosis, section 7 for membrane traffic, and Unit IX — Zoology and Systems Physiology: Introduction for cilia-linked physiology.

6.15 Review Questions

1. Describe the mechanism by which a newly synthesized lysosomal enzyme is sorted from the trans-Golgi network to the lysosome. What would happen if the M6P phosphotransferase were defective?

2. Compare and contrast the three types of cytoskeletal filaments (actin, microtubules, intermediate filaments) in terms of diameter, polarity, nucleotide dependence, associated motors, and dynamic behavior.
3. Explain the PINK1/Parkin mitophagy pathway. Why do mutations in these genes specifically affect dopaminergic neurons in Parkinson’s disease?
4. A patient presents with recurrent respiratory infections, male infertility, and situs inversus. What is the likely diagnosis, and what is the molecular basis?
5. Describe the unfolded protein response (UPR) and explain its three branches (IRE1, PERK, ATF6). Under what circumstances does the UPR switch from adaptive to apoptotic?
6. Explain how the nuclear pore complex achieves selective transport of macromolecules while allowing free diffusion of small molecules.
7. Compare the mechanisms by which taxol and colchicine affect microtubule dynamics. Both are used clinically — for what different purposes?
8. Explain the role of primary cilia as signaling platforms. Why do PKD1/PKD2 mutations in primary cilia lead to polycystic kidney disease?
9. Describe the vesicle coat proteins COPII, COPI, and clathrin. For each, specify the transport route, the GTPase involved, and the type of cargo carried.
10. A cell biologist discovers a new organelle-associated protein. Describe a CRISPR-based experimental strategy to determine its function and subcellular localization.
11. Using the organelle catalog, explain why disrupting mitochondrial fusion/fission dynamics preferentially affects tissues with high ATP turnover.
12. Compare one structural difference between COPII-coated vesicles and clathrin-coated pits that explains their distinct cargo size ranges.

6.16 Further Reading and Source Notes: Cell Structure and Organelles

- Sagan (1967). On the origin of mitosing cells. *Journal of Theoretical Biology*, 14.
- de Duve (1969). The lysosome in retrospect. *Lysosomes in Biology and Pathology*, North-Holland.
- Palade’s ribosome work and Blobel/Dobberstein’s protein-translocation experiments [Palade, 1955, Blobel and Dobberstein, 1975].
- Rothman (1994). Mechanisms of intracellular protein transport [Rothman, 1994].
- Alberts et al. (latest ed.). *Molecular Biology of the Cell* (chapters on organelles and the endomembrane system). Garland Science.
- Margulis (1981). *Symbiosis in Cell Evolution*. W. H. Freeman.
- Lane & Martin (2010). The energetics of genome complexity. *Nature*, 467.

6.17 Key Terms

Table 109. Current Evidence Map: Membrane-Bound and Condensate Organization: Term and Definition.

Term	Definition
Nuclear pore complex	Massive protein assembly (about 120 MDa) gating macromolecule transport between nucleus and cytoplasm
Nucleosome	Basic chromatin packaging unit: 147 bp DNA wound around histone octamer
Histone code	Combinatorial histone modifications that regulate chromatin state and gene expression
Cristae	Folds of the inner mitochondrial membrane that increase surface area for oxidative phosphorylation
ERAD	ER-associated degradation; retrotranslocation of misfolded ER proteins for proteasomal destruction
Unfolded protein response	Three-branch ER stress pathway (IRE1, PERK, ATF6) that restores proteostasis or triggers apoptosis
Treadmilling	Actin filament behavior: net polymerization at (+) end, depolymerisation at (-) end
Dynamic instability	Microtubule property: stochastic switching between growth and rapid depolymerisation (GTP cap model)
Kinesin	Plus-end directed microtubule motor protein; anterograde transport
Dynein	Minus-end directed microtubule motor protein; retrograde transport
Lamins	Type V intermediate filament proteins forming the nuclear lamina; mutations cause laminopathies
Mitophagy	Selective autophagy of damaged mitochondria; mediated by PINK1/Parkin pathway
COPII	Coat protein complex mediating anterograde ER-to-Golgi vesicle transport
Primary cilium	Non-motile 9+0 sensory cilium present on most mammalian cells; signaling antenna
Ciliopathy	Disease caused by defective cilia structure or function (e.g., PKD, Kartagener syndrome)
Connexin	Protein forming gap junction channels; allows intercellular communication

Term	Definition
E-cadherin	Calcium-dependent homophilic adhesion molecule; loss promotes cancer metastasis

6.18 Companion Source Module: Cell Structure and Organelles

Cell Structure and Organelles should leave a reproducible trail from a biological claim to the code, figure, diagram, or paper-based activity that can test it. Use the surfaces below to inspect the chapter’s assumptions, rerun the relevant model, or compare the manuscript explanation with companion labs and figures.

Table 110. Companion source surfaces for Cell Structure and Organelles.

Surface	Use it for
src/biology/cell/cell_biology.py (Organelle, get_organelles_by_cell_type, count_membrane_bound_organelles)	Connect organelle inventories to cell type and function.
src/mermaid/biology_diagrams.py (organelle_function_diagram, membrane_transport_diagram)	Keep compartment diagrams tied to transport and interaction.

Reproducibility check: treat an organelle claim as conditional on cell type, developmental state, and measurement method. Cross-reference: use section 5, section 7, and section 9.

7 Membrane Structure and Transport

Level 2/3 · 50 min read · 75 min lecture · Prerequisites: section 6, section 2

7.1 Learning Objectives

1. Describe the fluid mosaic model of the plasma membrane and recent updates from single-molecule studies.
2. Classify membrane **proteins** by their topology and function.
3. Distinguish passive from active transport and provide mechanistic explanations.
4. Derive the Nernst equation and apply it to membrane potential calculations.
5. Explain the Goldman-Hodgkin-Katz equation for multi-ion membrane potential.
6. Describe ion channel gating mechanisms and selectivity filters.
7. Explain the Na^+/K^+ -ATPase cycle and its physiological significance.
8. Describe vesicular trafficking including SNARE-mediated membrane fusion.
9. Compare **endocytosis** types: phagocytosis, macropinocytosis, clathrin-mediated, and caveolar.

7.1.1 Study Blueprint

- Big idea: Membranes convert gradients, permeability, and selective transport into cellular physiology.
- Core concepts: bilayers, diffusion, osmosis, electrochemical gradients.
- Framework alignment: Vision & Change: Structure and function, Systems, Information flow, exchange, and storage; AP Biology: Systems Interactions, Information Storage and Transmission; NGSS-style topics: Structure and Function.
- Model or quantitative lens: Nernst, Goldman, osmotic, and facilitated-transport calculations.
- Data skill: Interpret transport data from gradients, rates, and membrane potentials.
- Practice cadence: Visual Representations, Questions and Methods, Argumentation.
- Common misconception to repair: Equilibrium does not mean equal concentration; charge and permeability matter.
- Primary lab: **Lab — Membrane Structure and Transport**.
- Question bank: **Questions — Membrane Structure and Transport**.
- Transfer task: Transfer gradient logic to neurons, kidneys, roots, and mitochondrial membranes.
- Bridge to computation: `biology.cell.cell_biology.nernst_potential`.

Opening Vignette: The Membrane Pump That Makes Cancer Cells Immortal

In 1976, July Ling and colleagues at MIT discovered that some tumor cells were extraordinarily difficult to kill with chemotherapy drugs because they expressed unusual amounts of a 170 kDa membrane protein — later named P-glycoprotein (P-gp) — that used ATP hydrolysis to actively export cytotoxic drugs from the cell interior (Juliano & Ling, 1976, *Biochimica et Biophysica Acta*). A cancer cell overexpressing P-gp can reduce the intracellular concentration of doxorubicin, vincristine, paclitaxel, and dozens of other chemotherapy agents to sub-lethal levels, rendering the entire drug arsenal ineffective. This phenomenon — multidrug resistance (MDR) — remains one of the greatest challenges in oncology.

P-gp is an ABC transporter: it has two **nucleotide**-binding domains (NBDs) that hydrolyse ATP and two transmembrane domains (TMDs) that form the drug-export channel. It exemplifies the principle that membranes are not passive barriers — they are dynamic, information-processing systems that control exactly which molecules enter and exit cells, and at what rate. Understanding that selectivity, and exploiting it therapeutically, is the central theme of this chapter.

Primary source: Juliano, R. L. & Ling, V. (1976). A surface glycoprotein modulating drug permeability in Chinese hamster ovary cell mutants. Biochimica et Biophysica Acta, 455(1), 152–162.

In 1972, Singer and Nicolson proposed the fluid mosaic model: the plasma membrane is a lipid bilayer in which proteins float like icebergs in a sea of lipids [Singer and Nicolson, 1972]. Both the lipid and protein components can diffuse laterally within the membrane plane (fluid component), while the asymmetric distribution of lipids and proteins across the two leaflets generates mosaic heterogeneity.

7.1.2 Membrane Lipid Composition

The plasma membrane is not a homogeneous bilayer but contains distinct regions of varying composition:

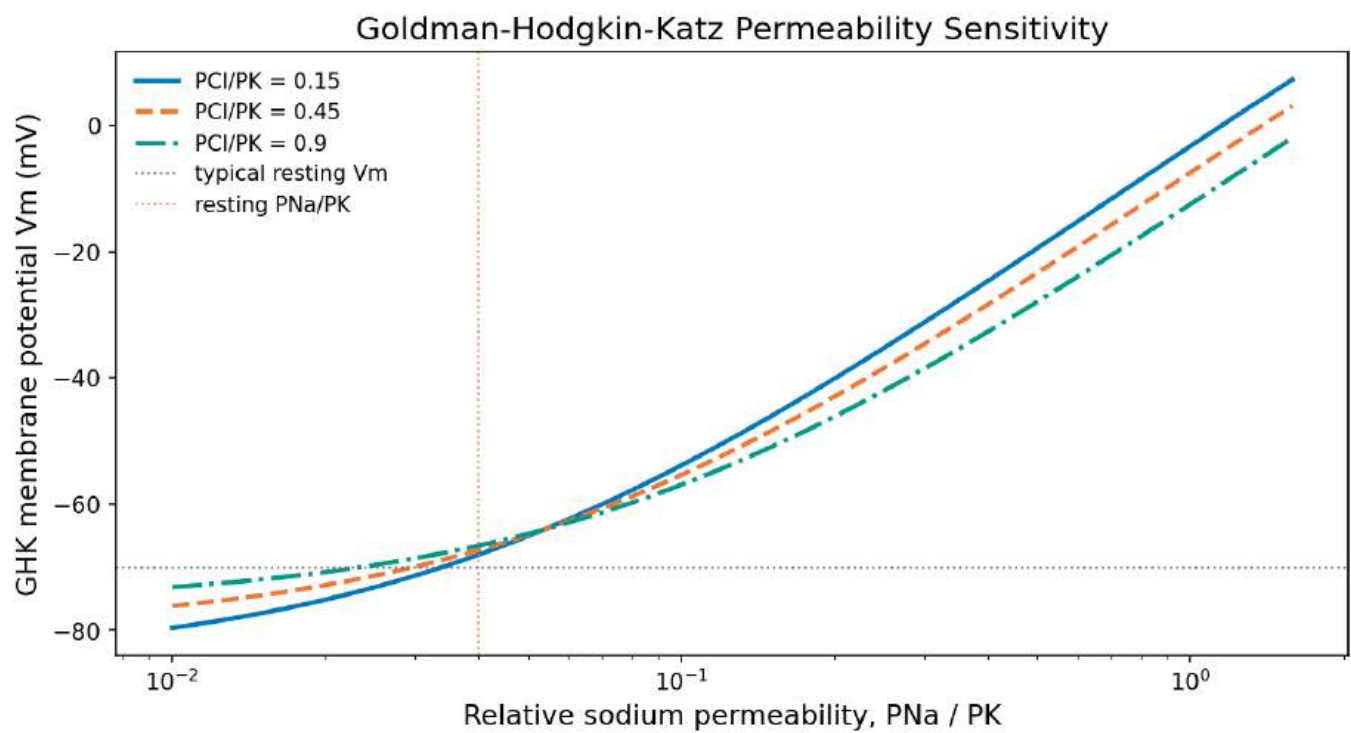


Figure 48. Goldman–Hodgkin–Katz (GHK) membrane potential as relative sodium permeability increases with potassium permeability held fixed. Rising sodium conductance depolarizes the cell; separate curves show how different chloride permeabilities shift the resting potential toward more negative or positive values.

Table 111. Membrane Lipid Composition: Lipid Class and % of membrane (animal).

Lipid Class	% of membrane (animal)	Location preference
Phosphatidylcholine (PC)	25–30	Outer leaflet
Phosphatidylethanolamine (PE)	25	Inner leaflet
Phosphatidylserine (PS)	10	Inner leaflet (negatively charged)
Sphingomyelin (SM)	15	Outer leaflet (rafts)
Cholesterol	20–50	Both leaflets (condenses rafts)
Phosphatidylinositol (PI)	5	Inner leaflet (signaling: PIP ₂ , PIP ₃)

Lipid asymmetry is maintained by flippases (ATP-dependent; P4-ATPases; move PS and PE to the inner leaflet) and floppases (ATP-dependent; ABC transporters; move lipids to the outer leaflet). Scramblases (Ca²⁺-activated; TMEM16F) randomize asymmetry during **apoptosis** — externalised phosphatidylserine (PS) is the “eat me” signal recognized by phagocyte receptors (TIM-4, BAI-1, Stabilin-2).

Membrane fluidity depends on lipid composition:

$$\text{Fluidity} \propto \frac{\text{degree of unsaturation} + \text{chain shortness}}{\text{cholesterol content (moderate)}}$$

(115)

Cholesterol has a biphasic effect: at low temperature, it disrupts crystalline packing (fluidises); at high temperature, it restricts excessive fluidity (condenses). This buffering effect maintains membrane fluidity across a physiological temperature range.

7.1.3 Lipid Rafts and Membrane Microdomains

Lipid rafts are dynamic, cholesterol- and sphingolipid-enriched microdomains (10–200 nm) in the outer leaflet that preferentially recruit certain proteins: - GPI-anchored proteins partition into rafts - Signaling receptors (e.g., T cell receptor, B cell receptor) cluster in rafts upon ligand binding - Caveolins (caveolae) represent a specialized, stable form of lipid raft

Controversy: The existence and functional significance of lipid rafts has been debated. Single-molecule tracking studies reveal that raft-like domains are transient (about 10–20 ms lifetime), small (about 10–20 nm), and form/dissolve dynamically. STED super-resolution microscopy (Eggeling et al., 2009, *Nature*) confirmed that sphingolipids and GPI-anchored proteins are transiently confined in nanoscale membrane domains, supporting a dynamic raft model.

7.1.4 Updates to the Fluid Mosaic Model

Since 1972, several refinements have been made:

1. Membrane is more mosaic than fluid: Up to 50% of membrane area is occupied by proteins; crowding restricts lateral diffusion
2. Cytoskeletal fences: The **actin** cortex creates corrals (“picket fence” model, Kusumi et al.) that compartmentalise membrane proteins into about 40–300 nm domains, restricting free diffusion
3. Lipid asymmetry is more extensive than originally appreciated
4. Membrane curvature is actively generated by BAR-domain proteins, ESCRT complexes, and coat proteins
5. Transbilayer communication: Inner and outer leaflet lipids can be coupled through interdigitating acyl chains

Concept Check 1: During apoptosis, phosphatidylserine (PS) moves from the inner to the outer leaflet. What **enzyme** mediates this, and why is PS externalisation a critical signal for phagocytic clearance?

7.2 Membrane Proteins as Transporters, Receptors, and Anchors

Integral (transmembrane) proteins span the bilayer via alpha-helical segments (of about 20 hydrophobic amino acids each, sufficient to span the about 3 nm hydrophobic core) or beta-barrel structures (found primarily in outer membranes of Gram-negative bacteria, mitochondria, and **chloroplasts**).

Peripheral proteins associate noncovalently with membrane surfaces or integral proteins via electrostatic interactions, **hydrogen bonds**, or hydrophobic interactions with the lipid headgroup region.

Lipid-anchored proteins are covalently modified with:

- GPI-anchors (outer leaflet): e.g., alkaline phosphatase, CD59 (complement regulator)
- Myristoyl groups (inner leaflet, N-terminal): e.g., Src kinase
- Palmitoyl groups (inner leaflet, Cys residue): e.g., Ras (reversible; regulates membrane association)
- Farnesyl/geranylgeranyl groups (inner leaflet, C-terminal CAAX): e.g., Ras, Rho GTPases

7.2.1 Functions of Membrane Proteins

Table 112. Functions of Membrane Proteins: Function and Examples.

Function	Examples
Transport (channel)	Aquaporins, K ⁺ channels, Cl ⁻ channels, mechanosensitive channels
Transport (carrier)	GLUT glucose transporters, amino acid carriers, nucleoside transporters
Active transport (pump)	Na ⁺ /K ⁺ -ATPase, Ca ²⁺ -ATPase (SERCA), H ⁺ /K ⁺ -ATPase
ABC transporter	MDR1/P-glycoprotein, CFTR, ABCA1 (cholesterol efflux)
Receptor	EGFR, insulin R, beta ₂ -adrenergic R, rhodopsin, TLR4
Enzyme	Adenylyl cyclase, guanylyl cyclase, gamma-secretase
Cell adhesion	Integrins, cadherins, selectins, IgCAMs
Structural anchor	Ankyrin-spectrin (RBC), dystrophin-glycoprotein complex

7.3 Passive Transport Down Electrochemical Gradients

Passive transport requires no energy input — molecules move down their electrochemical gradient.

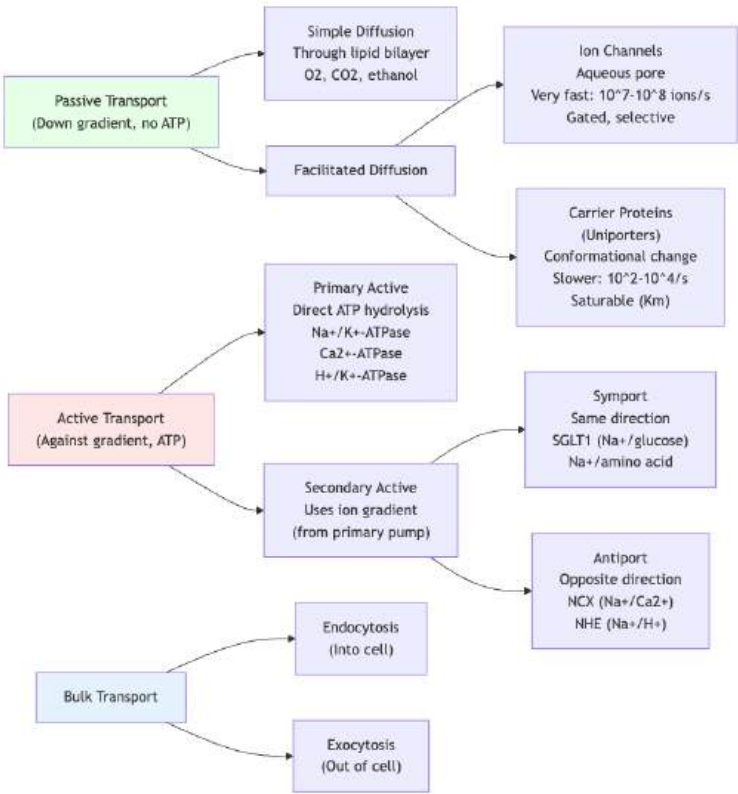


Figure 49. Classification of membrane transport mechanisms, from simple diffusion through channels and carriers to primary and secondary active transport and bulk transport.

7.3.1 Simple Diffusion Through the Lipid Bilayer

For uncharged molecules, flux obeys Fick’s First Law:

$$J = -D \frac{d[C]}{dx} = P \cdot \Delta[C]$$

(116)

where P = permeability coefficient (m/s) = $D \cdot K_{\text{oil/water}}/d$ (membrane thickness).

Membrane permeability: - High: small nonpolar molecules (O_2 , CO_2 , N_2 , ethanol, benzene) - Moderate: small polar uncharged (water, glycerol, urea) - Low: large polar (glucose, amino acids) - Very low/none: ions (Na^+ , K^+ , Cl^- , Ca^{2+}) — require protein channels

The partition coefficient ($K_{\text{oil/water}}$) is the strongest predictor of simple diffusion rate. Overton’s rule (1899): membrane permeability correlates with oil/water partition coefficient.

7.3.2 Osmosis and the van’t Hoff Equation

Although water is technically a small polar molecule, its transport across cell membranes is fast and quantitative enough to deserve its own treatment. Osmosis is the net diffusion of water across a semi-permeable membrane in response to a difference in solute concentrations. Because water mass is conserved, osmosis amounts to a redistribution of *volume* — and uncontrolled osmotic swelling will lyse a cell.

The thermodynamic driving force is the difference in water chemical potential μ_w between two compartments:

$$\mu_w = \mu_w^0 + RT \ln a_w + \bar{V}_w P \tag{117}$$

where a_w is water activity (\approx mole fraction in dilute solution) and \bar{V}_w is the partial molar volume of water (about 18 mL/mol). Each dissolved solute particle reduces a_w proportionally — this is the molecular origin of colligative properties (boiling-point elevation, freezing-point depression, vapor-pressure lowering). Setting μ_w equal on both sides of a semi-permeable membrane and solving for the pressure required to balance a solute gradient yields van’t Hoff’s law:

$$\Pi = iMRT \tag{118}$$

where Π is the osmotic pressure (in atm or Pa), M is the solute molar concentration, R is the gas constant, T is absolute temperature, and i is the van’t Hoff factor — the number of effective particles produced per formula unit (1 for glucose; 2 for NaCl; 3 for CaCl_2 at full dissociation).

In SI units with $R = 0.0821 \text{ L}\cdot\text{atm/mol/K}$ and 37°C ($T = 310 \text{ K}$), 1 mM of an ideal solute generates $\Pi = 1 \cdot 0.001 \cdot 0.0821 \cdot 310 = 0.0254 \text{ atm} \approx 25 \text{ mmHg}$. Plasma is about 290 mOsm/L, generating about 7,500 mmHg of total osmotic pressure — but cells don’t burst because they are surrounded by isotonic interstitial fluid, and primarily the *difference* matters.

Worked Example: Osmotic swelling of a red blood cell.

A red blood cell is placed in a hypotonic solution (200 mOsm/L; plasma is 290 mOsm/L). Calculate (a) the initial osmotic pressure difference driving water inward, (b) the cell’s predicted volume change to reach equilibrium.

(a) The osmotic pressure gradient is:

$$\Delta\Pi = (290 - 200) \times 10^{-3} \cdot 0.0821 \cdot 310 = 0.0900 \cdot 25.45 = 2.29 \text{ atm} \approx 1,740 \text{ mmHg}$$

This drives water into the cell at a flux of $J_w = p_f \cdot \Delta C$, where $p_f \approx 0.02 \text{ cm/s}$ for an AQP1-rich erythrocyte. For a typical cell ($A \approx 140 \mu\text{m}^2$, $V \approx 90 \mu\text{m}^3$), volume doubling occurs in roughly 200 ms — fast enough to be visible in a microscope as the cell swells from biconcave disc to sphere.

(b) At osmotic equilibrium, water content adjusts to make intracellular osmolarity = 200 mOsm/L. If initial intracellular osmolyte content is $V_0 \cdot C_0 = 90 \cdot 290 = 26,100 \mu\text{mol}\cdot\mu\text{m}^3/\text{L}$, the new equilibrium volume is:

$$V_{\text{new}} = V_0 \cdot \frac{C_0}{C_{\text{new}}} = 90 \cdot \frac{290}{200} = 130.5 \mu\text{m}^3$$

A 45% volume increase. RBCs reach a critical volume of about $150 \mu\text{m}^3$ before hemolysis (membrane area cannot accommodate further sphere expansion), so the cell is on the brink of lysis.

Tonicity terms (clinical): Hypotonic solutions cause cells to swell (hemolysis if severe). Isotonic solutions (e.g., 0.9% NaCl, 5% dextrose, lactated Ringer’s) preserve volume. Hypertonic solutions cause cells to shrink (crenation in RBCs). Aquaporin defects cause major fluid balance disorders: AQP2 mutations cause nephrogenic diabetes insipidus (water reabsorption fails despite vasopressin); AQP4 autoantibodies cause neuromyelitis optica (astrocyte water-handling fails, edema and demyelination). The osmotic pressure of plasma proteins (mostly albumin, about 25 mmHg) is the oncotic pressure that retains fluid in the vasculature — its loss in nephrotic syndrome and liver failure causes generalized edema.

Concept Check 1b: A patient with severe burns receives 4 L of 0.45% NaCl (“half-normal saline”) rapidly. Calculate the tonicity relative to plasma (290 mOsm/L) and predict the consequence for red blood cells.

7.3.3 Facilitated Diffusion via Channels

Ion channels are integral membrane proteins forming aqueous pores. They are: - Selective: ion selectivity filter determines which ions pass - Gated: open/close in response to specific stimuli - Fast: ion throughput rates of 10^7 – 10^8 ions/s (near diffusion limit)

Gating mechanisms:

- Voltage-gated: opened by membrane-potential change; examples include sodium channel Nav1.1–1.9, potassium channel Kv1–12, and calcium channel Cav1–3 families.
- Ligand-gated, extracellular: opened by neurotransmitter binding; examples include nAChR, GABAA receptor, NMDAR, and AMPAR.
- Ligand-gated, intracellular: opened by second messengers; examples include calcium-activated potassium channel BK and retinal cGMP-gated channels.
- Mechanosensitive: opened by stretch or pressure; examples include Piezo1/2, TREK-1, and bacterial MscL.
- Temperature-gated: opened by heat or cold; examples include TRPV1 (>43 degrees C, capsaicin) and TRPM8 (<26 degrees C, menthol).
- Light-gated: opened by photons; channelrhodopsin ChR2 is the standard optogenetic example.

Selectivity filter of K^+ channels (MacKinnon, Nobel Prize 2003): The selectivity filter contains the signature sequence TVGYG. Four carbonyl oxygens from each of the four subunits line the pore, precisely mimicking the hydration shell of K^+ (radius 1.33 angstroms). Na^+ (radius 0.95 angstroms) is too small to be coordinated effectively — the energetic cost of dehydrating Na^+ without compensating coordination makes Na^+ passage unfavorable. This elegant size-exclusion mechanism achieves 10,000:1 selectivity for K^+ over Na^+ .

Aquaporins (AQP): Facilitate water transport (not solutes). AQP1 (Peter Agre, Nobel Prize 2003) channels about 3×10^8 water molecules/s while excluding protons (the Grothuss mechanism is interrupted by a critical asparagine residue in the channel pore, and the electrostatic field of the NPA motif reorients water molecules, preventing H_3O^+ passage).

Aquaporin discovery and selectivity in detail. Before 1992, biologists could not explain how erythrocytes and renal tubule cells achieve water permeability rates 100× faster than predicted from the lipid bilayer alone. Peter Agre’s group, while studying Rh-blood-group proteins, noticed a contaminating 28 kDa membrane protein. Reconstitution experiments (Preston et al., 1992, *Science*) demonstrated that this protein — christened AQP1 (aquaporin-1) — conferred about 10× water permeability when expressed in *Xenopus* oocytes. Agre shared the 2003 Nobel Prize in Chemistry. Thirteen aquaporin paralogues are now known in humans, with tissue-specific expression: AQP2 (renal collecting duct, vasopressin-regulated), AQP4 (astrocyte endfeet, target of NMO autoantibodies), AQP5 (salivary/lacrimal glands), AQP7 (adipocytes, glycerol channel).

The structural basis of selectivity is exquisite. Each AQP monomer is a hexa-helical bundle with two short re-entrant helices (carrying the conserved NPA motifs — Asn-Pro-Ala) that meet in the middle of the membrane to form the narrowest part of the pore (about 2.8 Å, just wide enough for a single water molecule). Two mechanisms exclude protons:

1. Electrostatic barrier: The two NPA half-helices have positive macrodipoles meeting in the middle of the pore — repelling H_3O^+ but attracting electrically neutral water.
2. Hydrogen-bond reorientation: The central asparagines force passing water molecules to flip their hydrogen-bond donor/acceptor orientation. This breaks the proton-relay (Grothuss) chain that would otherwise allow H^+ to “hop” through the channel.

The water permeability coefficient (p_f , the osmotic permeability) for a single AQP1 channel is about 3×10^{-14} cm³/s, corresponding to about 3×10^9 water molecules/s under typical osmotic gradients. A red blood cell expressing about 200,000 AQP1 channels can therefore exchange its entire water volume in <100 ms — the basis of erythrocyte swelling/shrinking responses.

Clinical aquaporins. Loss-of-function mutations in AQP2 cause nephrogenic diabetes insipidus (kidneys cannot concentrate urine despite normal vasopressin). Autoantibodies against AQP4 cause neuromyelitis optica (Devic’s disease), a demyelinating disorder distinct from MS. AQP1 is upregulated in many tumors and is being explored as a target in glioma therapy.

Clinical Connection: Channelopathies. Ion channel **mutation**s cause a wide range of diseases:

- Long QT syndrome: Mutations in cardiac potassium or sodium channels prolong repolarization and can trigger fatal arrhythmias. Drug-development screens therefore test for hERG channel block.
- Cystic fibrosis: Mutations in CFTR disrupt chloride transport. The common deltaF508 variant causes misfolding and ER retention; modulator combinations such as lumacaftor/ivacaftor and elexacaftor/tezacaftor/ivacaftor partly restore channel function.

- Malignant hyperthermia: RyR1 mutations cause uncontrolled Ca^{2+} release from sarcoplasmic reticulum after exposure to volatile anaesthetics. See section 8 for calcium signaling.

Concept Check 2: Tetrodotoxin (TTX, from pufferfish) blocks voltage-gated Na^+ channels by binding the selectivity filter from the extracellular side. Predict the effects of TTX on (a) **action potential** generation, (b) nerve conduction, and (c) skeletal muscle contraction.

7.3.4 Ion Channel Gating Kinetics

A single ion channel in a patch-clamp recording flickers between open and closed states stochastically. The time-averaged current through a population of N channels with single-channel conductance γ (in pS = pico-siemens) and open probability P_o is:

$$I = N \cdot P_o \cdot \gamma \cdot (V_m - E_{\text{rev}})$$

(119)

where V_m is the membrane potential and E_{rev} is the reversal potential (for a perfectly selective channel, $E_{\text{rev}} = E_{\text{ion}}$). This decomposition is one of the most powerful in biophysics: drugs can change channel function by altering N (channel expression/internalization), P_o (gating modulators, allosteric drugs), or γ (pore-block, modifications of selectivity filter), and each can be measured separately.

Single-channel conductances of representative channels (in pS):

- nAChR, muscle endplate: conductance 30–50 pS; open probability about 0.85 with ACh; throughput about 3×10^7 ions/s.
- BK, large-conductance calcium-activated potassium channel: conductance 200–250 pS; open probability 0.1–0.9 depending on calcium; throughput up to 10^8 ions/s.
- Kv1.x delayed rectifier: conductance 10–20 pS; open probability about 0.7 at +20 mV; throughput about 10^6 ions/s.
- Nav1.x: conductance 15–20 pS; transient open probability below 0.5; throughput about 5×10^6 ions/s during an action potential.
- L-type Cav1.2: conductance about 25 pS; open probability about 0.3; throughput about 10^5 ions/s.
- ClC-1 skeletal chloride channel: conductance about 1 pS with gating-coupled pores; open probability about 0.5 at rest.
- CFTR chloride channel / ABC transporter: conductance 8–10 pS; PKA-dependent open probability 0.3–0.5.

Open probability and gating models. The open probability P_o depends on the gating stimulus (voltage, ligand concentration, mechanical force). For a voltage-gated channel with effective gating charge z_g (typical about 4–6 for Na_V , about 6–10 for K_V), the equilibrium open probability follows a Boltzmann relation:

$$P_o(V) = \frac{1}{1 + \exp\left(-\frac{z_g F (V - V_{1/2})}{RT}\right)}$$

(120)

where $V_{1/2}$ is the half-activation voltage. This sigmoidal curve is steep (about 5–10 mV per e-fold change) — small voltage perturbations cause large changes in P_o , the basis of the action potential’s switch-like behavior. For ligand-gated channels with n binding sites and Hill coefficient h :

$$P_o([L]) = \frac{[L]^h}{[L]^h + K_d^h}$$

(121)

For the muscle nAChR, $h \approx 1.5$ and $K_d \approx 30 \mu\text{M}$ for ACh: half-maximal activation at about $30 \mu\text{M}$, full activation by about $300 \mu\text{M}$. The sub-millisecond opening of nAChRs after ACh release at the neuromuscular junction (peak [ACh] about 1 mM at the postsynaptic membrane) ensures essentially complete channel activation in every action potential.

7.3.5 Electroneutral vs. Electrogenic Transport

Whether a transporter contributes net charge to the membrane potential depends on the stoichiometry of the transport cycle.

Table 113. Electroneutral vs. Electrogenic Transport: Transporter and Stoichiometry.

Transporter	Stoichiometry	Net charge moved per cycle	Electrogenic?
Na^+/K^+ -ATPase	3 Na^+ out / 2 K^+ in / 1 ATP	+1 outward	Yes
Ca^{2+} -ATPase (SERCA)	2 Ca^{2+} in (to ER) / 2 H^+ out / 1 ATP	0	No (electroneutral)
H^+/K^+ -ATPase (gastric)	1 H^+ out / 1 K^+ in / 1 ATP	0	No

Transporter	Stoichiometry	Net charge moved per cycle	Electrogenic?
NCX (Na ⁺ /Ca ²⁺ exchanger)	3 Na ⁺ in / 1 Ca ²⁺ out	+1 inward	Yes
NHE1 (Na ⁺ /H ⁺ exchanger)	1 Na ⁺ in / 1 H ⁺ out	0	No
SGLT1 (Na ⁺ /glucose symport)	2 Na ⁺ in / 1 glucose	+2 inward	Yes
AE1 (Cl ⁻ /HCO ₃ ⁻ exchanger)	1 Cl ⁻ out / 1 HCO ₃ ⁻ in	0	No

Energetic consequences. Electroneutral transporters move solutes “for free” with respect to the membrane potential — their thermodynamic feasibility depends primarily on chemical concentration gradients. Electrogenic transporters, by contrast, are driven by *both* concentration and voltage. The Na⁺/K⁺-ATPase, for example, would still hydrolyse ATP if Na⁺ and K⁺ concentrations were equalised, because moving net positive charge against the membrane potential (interior negative) costs additional energy: the electrochemical gradient is the relevant thermodynamic quantity:

$$\Delta G_{\text{ion}} = RT \ln \frac{[C]_{\text{out}}}{[C]_{\text{in}}} + zFV_m$$

(122)

For a 100× concentration gradient and 100 mV opposing voltage: $\Delta G \approx +12 + 9.6 = 21.6$ kJ/mol. ATP hydrolysis releases about 50 kJ/mol under cellular conditions, so a single ATP can drive about 2 ions of net charge against this combined gradient — exactly the stoichiometry observed in the Na⁺/K⁺-ATPase (3 Na⁺ out – 2 K⁺ in = +1 net per ATP, with margin for irreversibility).

Clinical Connection: Channelopathy diagnostics. When a patient presents with arrhythmia, episodic weakness, or seizures, modern diagnostics include gene panels (sequencing known channel genes) followed by functional reconstitution of variants in HEK293 or oocyte expression systems. Patch-clamp measurements decompose the disease-causing change into *N*, *P_o*, and *γ* effects: for example, the cystic fibrosis ΔF508 mutation reduces *N* at the membrane (trafficking defect, fixed by lumacaftor); G551D reduces *P_o* (gating defect, fixed by ivacaftor). The combination drug Orkambi addresses both — a triumph of mechanism-guided pharmacology.

7.3.6 Facilitated Diffusion via Carriers (Uniporters)

GLUT transporters (SLC2A family; 14 isoforms in humans) facilitate glucose diffusion:

Table 114. Facilitated Diffusion via Carriers (Uniporters): Transporter and Tissue.

Transporter	Tissue	<i>K_m</i> (mM)	Regulation
GLUT1	Erythrocytes, brain endothelium, placenta	1.5	Constitutive
GLUT2	Liver, pancreatic beta-cells, small intestine	17	Low affinity; glucose sensor
GLUT3	Neurons	1.4	Constitutive; high affinity for brain
GLUT4	Muscle, adipose	5	Insulin-stimulated PM insertion
GLUT5	Small intestine	N/A	Fructose transporter

The alternating access mechanism: the carrier alternates between outward-facing (substrate binds from extracellular side) and inward-facing (substrate released to cytoplasm) conformations. This is slower than channel transport (about 10²–10⁴ molecules/s) but allows specificity and saturability.

7.4 Worked Example: GLUT Transporter Kinetics

Problem: GLUT1 has *K_m* = 1.5 mM and *V_{max}* = 200 μmol/min per gram of membrane protein. Blood glucose is about 5 mM. At what fraction of *V_{max}* is GLUT1 operating?

Solution:

Using the Michaelis-Menten equation:

$$v = \frac{V_{max} \cdot [S]}{K_m + [S]} = \frac{200 \times 5}{1.5 + 5} = \frac{1000}{6.5} = 154 \mu\text{mol/min/g}$$

(123)

$$\frac{v}{V_{max}} = \frac{154}{200} = 0.77 = 77\%$$

(124)

GLUT1 operates at 77% of maximum capacity at normal blood glucose — providing a safety margin while ensuring high glucose flux to the brain.

7.5 Active Transport Coupled to Energy Input

Active transport moves solutes against their electrochemical gradient, requiring energy (usually ATP hydrolysis or proton motive force).

7.5.1 Primary Active Transport — Pumps

Na⁺/K⁺-ATPase (sodium-potassium pump): Exports 3 Na⁺ and imports 2 K⁺ per ATP consumed (overall electrogenic; net +1 charge out). This pump consumes about 25% of the body’s ATP (up to 70% in neurons).

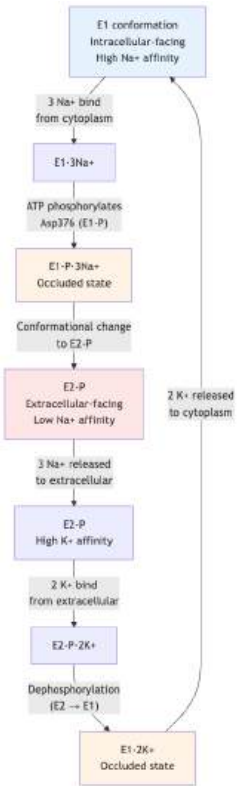


Figure 50. The Post-Albers cycle of the Na⁺/K⁺-ATPase. The pump alternates between E1 (inward-facing, high Na⁺ affinity) and E2 (outward-facing, high K⁺ affinity) conformations. Phosphorylation by ATP and subsequent dephosphorylation drive the conformational changes.

This maintains: - Resting membrane potential (K⁺ gradient) - High intracellular [K⁺] (about 140 mM) and low [Na⁺] (about 12 mM) - Low intracellular Na⁺ that drives secondary active transport - Cell volume regulation (preventing osmotic swelling)

Inhibition by ouabain/digitalis: Cardiac glycosides block the K⁺-binding E2-P form. This elevates intracellular Na⁺, which reduces Na⁺/Ca²⁺ exchanger activity (NCX normally uses the Na⁺ gradient to export Ca²⁺), so [Ca²⁺]_i rises, causing stronger cardiac contraction. Used for heart failure; narrow therapeutic window (toxicity causes arrhythmias).

Other primary active transport pumps: - Ca²⁺-ATPase (SERCA): pumps Ca²⁺ from cytoplasm into ER/SR lumen; maintains [Ca²⁺]_i at about 100 nM (10,000-fold lower than extracellular); critical for muscle relaxation - H⁺/K⁺-ATPase: gastric parietal cells; pumps H⁺ into stomach lumen (pH about 1); target of proton

pump inhibitors (omeprazole, lansoprazole) for acid reflux/ulcer treatment - V-type H⁺-ATPase: acidifies lysosomes, endosomes; does not use a phosphorylated intermediate

7.5.2 ABC Transporters and ATP-Powered Pumping

ATP-Binding Cassette (ABC) transporters are a superfamily of about 48 members in humans. They use ATP hydrolysis to transport diverse substrates across membranes:

- MDR1/P-glycoprotein (ABCB1): Broad-specificity drug efflux pump; exports hydrophobic compounds from the cell. Overexpressed in many cancers, causing multidrug resistance — tumor cells pump out chemotherapy drugs before they can act. Substrates include taxol, doxorubicin, vincristine.
- CFTR (ABCC7): Unique ABC transporter that functions as a Cl[−] channel. Mutations cause cystic fibrosis (see Clinical Connection above).
- ABCA1: Cholesterol and phospholipid efflux to apoA-I; critical for HDL formation. Loss-of-function mutations cause Tangier disease (very low HDL, cholesterol deposition in tissues).
- TAP1/TAP2 (ABCB2/3): Transport antigenic peptides from cytoplasm into ER lumen for MHC class I loading and immune presentation.

7.5.3 Secondary Active Transport

Uses the Na⁺ electrochemical gradient (generated by the primary pump) to drive uphill transport of other solutes:

- Symport (co-transport, same direction): SGLT1 (intestinal glucose): 2 Na⁺ + 1 glucose move in together; net uptake even if [glucose]_{in} > [glucose]_{out}. SGLT2 (kidney proximal tubule): 1 Na⁺ + 1 glucose; target of gliflozin drugs for type 2 diabetes.
- Antiport (exchange, opposite directions): NCX (Na⁺/Ca²⁺ exchanger): 3 Na⁺ in, 1 Ca²⁺ out; critical for cardiac Ca²⁺ homeostasis. NHE (Na⁺/H⁺ exchanger): Na⁺ in, H⁺ out; regulates intracellular pH.

Clinical Connection: SGLT2 Inhibitors in Diabetes and Heart Failure SGLT2 inhibitors (empagliflozin, dapagliflozin, canagliflozin) block glucose reabsorption in the kidney proximal tubule, causing glucosuria (glucose loss in urine) and lowering blood glucose. Remarkably, these drugs also reduce cardiovascular death and heart failure hospitalisations, even in non-diabetic patients — likely through natriuresis, osmotic diuresis, and favorable metabolic effects. They represent a rare case where a simple transport mechanism becomes a blockbuster drug target. see section 11 (Metabolic Integration) for insulin signaling.

Concept Check 3: The antibiotic gramicidin forms a channel in bacterial membranes that allows monovalent cations (Na⁺, K⁺) to flow freely. Predict how gramicidin would affect (a) the bacterial membrane potential, (b) the proton motive force, and (c) bacterial ATP synthesis.

7.6 The Nernst Equation and Membrane Potential

7.6.1 Electrochemical Potential and Ion Driving Force

The electrochemical potential of an ion is:

$$\tilde{\mu}_i = \mu_i^0 + RT \ln[C_i] + z_i F V$$

(125)

where z_i = ionic charge, F = Faraday constant (96,485 C/mol), V = membrane potential.

At equilibrium (no net flux), the Nernst equation gives the equilibrium potential E_i :

$$E_i = \frac{RT}{z_i F} \ln \frac{[C_i]_{out}}{[C_i]_{in}}$$

(126)

At 37 degrees C (310 K), $RT/F = 26.7$ mV. Converting to log₁₀:

$$E_i = \frac{61.5 \text{ mV}}{z_i} \log_{10} \frac{[C_i]_{out}}{[C_i]_{in}}$$

(127)

7.6.2 Derivation of the Nernst Equation

Starting from the condition of zero net electrochemical driving force at equilibrium:

$$\Delta\tilde{\mu}_i = 0$$

(128)

$$RT \ln \frac{[C_i]_{\text{in}}}{[C_i]_{\text{out}}} + z_i F (V_{\text{in}} - V_{\text{out}}) = 0$$

(129)

$$z_i F \cdot E_i = -RT \ln \frac{[C_i]_{\text{in}}}{[C_i]_{\text{out}}} = RT \ln \frac{[C_i]_{\text{out}}}{[C_i]_{\text{in}}}$$

(130)

$$E_i = \frac{RT}{z_i F} \ln \frac{[C_i]_{\text{out}}}{[C_i]_{\text{in}}}$$

(131)

7.7 Worked Example: Nernst Potential

Problem: Calculate the Nernst equilibrium potential for Ca^{2+} at 37 degrees C, given $[\text{Ca}^{2+}]_{\text{out}} = 2.5 \text{ mM}$ and $[\text{Ca}^{2+}]_{\text{in}} = 0.0001 \text{ mM}$ (100 nM).

Solution:

$$E_{\text{Ca}} = \frac{RT}{z_{\text{Ca}} F} \ln \frac{[\text{Ca}^{2+}]_{\text{out}}}{[\text{Ca}^{2+}]_{\text{in}}} = \frac{26.7 \text{ mV}}{2} \ln \frac{2.5}{0.0001}$$

(132)

$$E_{\text{Ca}} = 13.35 \text{ mV} \times \ln(25,000) = 13.35 \times 10.13 = +135 \text{ mV}$$

(133)

The strongly positive E_{Ca} means that Ca^{2+} has a massive driving force to enter cells. Brief Ca^{2+} channel openings can therefore cause significant signaling events.

Nernst potentials of key ions:

Table 115. Derivation of the Nernst Equation: Ion and [inside] (mM).

Ion	[inside] (mM)		E_i (mV, 37 degrees C)
	[outside] (mM)		
K^+	140	5	-89
Na^+	12	145	+63
Ca^{2+}	0.0001	2.5	+135
Cl^-	4	110	-82

Worked Example: Nernst Potentials for K^+ , Na^+ , and Cl^- .

Each row of the table above can be reproduced from equation (134) below by careful sign-handling. Using the simplified form at 37 °C: $E_i = (61.5 \text{ mV}/z_i) \log_{10}([\text{out}]/[\text{in}])$.

$$E_i = \frac{RT}{z_i F} \ln \frac{[C_i]_{\text{out}}}{[C_i]_{\text{in}}}$$

(134)

Potassium ($z = +1$): $E_K = 61.5 \cdot \log_{10}(5/140) = 61.5 \cdot \log_{10}(0.0357) = 61.5 \cdot (-1.447) = -89.0 \text{ mV}$. K^+ is concentrated inside, so equilibrium drives K^+ outward; the equilibrium potential is negative (interior must be about 89 mV more negative to halt K^+ efflux). The resting membrane potential ($V_m \approx -70 \text{ mV}$) is therefore *less negative* than E_K — meaning K^+ continues to leak slowly outward at rest.

Sodium ($z = +1$): $E_{\text{Na}} = 61.5 \cdot \log_{10}(145/12) = 61.5 \cdot \log_{10}(12.08) = 61.5 \cdot 1.082 = +66.6 \text{ mV}$. (Tabulated values vary 63–67 mV depending on the assumed concentrations.) Na^+ is concentrated outside, so equilibrium drives Na^+ inward; the equilibrium potential is strongly positive. The resting membrane potential is *very far* from E_{Na} — meaning Na^+ has a massive electrochemical force driving it inward, restrained primarily by the low resting Na^+ permeability.

Chloride ($z = -1$): $E_{\text{Cl}} = (61.5/-1) \cdot \log_{10}(110/4) = -61.5 \cdot \log_{10}(27.5) = -61.5 \cdot 1.439 = -88.5 \text{ mV}$. (Tabulated values vary 80–90 mV depending on cell type — neurons have higher $[\text{Cl}^-]_i$ than skeletal muscle.) Note the *negative* sign on z_{Cl} inverts the ratio’s effect: a higher $[\text{Cl}^-]_o$ than $[\text{Cl}^-]_i$ yields a *negative* equilibrium potential, the opposite of K^+ . In adult neurons, E_{Cl} sits near V_m , so Cl^- is essentially at equilibrium and small Cl^- permeability changes (e.g., GABA_A -receptor

opening) cause primarily modest hyperpolarization by stabilizing V_m near E_{Cl} . In neonatal neurons, $[Cl^-]_i$ is higher (about 25 mM) due to immature KCC2 expression, E_{Cl} becomes about -40 mV, and GABA is *depolarizing* — a fact with major implications for early brain development and neonatal seizures.

These three numbers — $E_K \approx -89$, $E_{Na} \approx +63$, $E_{Cl} \approx -82$ — together with the relative permeabilities $P_K : P_{Na} : P_{Cl}$ generate the entire repertoire of resting and action potentials in excitable cells.

The resting membrane potential (-70 mV) lies close to E_K because the resting cell membrane is about 25x more permeable to K^+ than Na^+ . K^+ “leaks” out through K2P (two-pore domain) leak channels; uncovered negative charges on impermeable intracellular proteins (Donnan effect) and the electrogenic Na^+/K^+ pump (net export of +1 charge per cycle) contribute the remainder.

7.7.1 Goldman-Hodgkin-Katz Equation

When multiple ions carry current, the resting membrane potential is given by the Goldman equation:

$$V_m = \frac{RT}{F} \ln \frac{P_K[K^+]_o + P_{Na}[Na^+]_o + P_{Cl}[Cl^-]_i}{P_K[K^+]_i + P_{Na}[Na^+]_i + P_{Cl}[Cl^-]_o} \quad (135)$$

Note: anions (Cl^-) appear with reversed subscripts because of their negative charge.

Derivation sketch. The full Goldman-Hodgkin-Katz (GHK) derivation begins from the Nernst-Planck equation for ionic flux J_i across a membrane of thickness d in a constant electric field:

$$J_i = -D_i \left(\frac{dC_i}{dx} + z_i C_i \frac{F}{RT} \frac{dV}{dx} \right) \quad (136)$$

Integrating across the membrane assuming a constant field ($dV/dx = -V_m/d$) and a single permeability $P_i = D_i \beta_i / d$ (where β_i is the partition coefficient between water and membrane) gives the GHK current equation:

$$I_i = z_i F P_i \frac{z_i F V_m / RT}{1 - \exp(-z_i F V_m / RT)} ([C_i]_{in} - [C_i]_{out} \exp(-z_i F V_m / RT)) \quad (137)$$

At the resting membrane potential, the *net* current must be zero: $\sum_i I_i = 0$. Solving this for K^+ , Na^+ , and Cl^- (and treating Cl^- as monovalent anion) algebraically yields the GHK voltage equation (135). figure 48 shows how depolarization tracks relative Na^+ permeability when K^+ permeability is held fixed and Cl^- permeability is varied. The key conceptual takeaways are: (i) the membrane potential is a *weighted log average* of the Nernst potentials, with weights set by permeability; (ii) the ion with the highest permeability dominates; (iii) shifts in permeability ratios (e.g., during the action potential) produce predictable shifts in V_m .

7.8 Worked Example: Goldman Equation

Problem: Calculate V_m at 37 degrees C given relative permeabilities $P_K : P_{Na} : P_{Cl} = 1.0 : 0.04 : 0.45$ and the ion concentrations in the table above.

Solution:

$$V_m = 26.7 \text{ mV} \times \ln \frac{(1.0)(5) + (0.04)(145) + (0.45)(4)}{(1.0)(140) + (0.04)(12) + (0.45)(110)} \quad (138)$$

$$V_m = 26.7 \times \ln \frac{5.0 + 5.8 + 1.8}{140 + 0.48 + 49.5} = 26.7 \times \ln \frac{12.6}{190.0} \quad (139)$$

$$V_m = 26.7 \times \ln(0.0663) = 26.7 \times (-2.71) = -72.4 \text{ mV} \quad (140)$$

This is close to the experimentally measured **resting potential** of about -70 mV.

Concept Check 4: During an action potential, the permeability to Na^+ increases about 500-fold (from $P_{Na}/P_K = 0.04$ to about 20). Using the Goldman equation, predict what happens to V_m . Why does the membrane potential approach but not quite reach E_{Na} ?

Worked Example — Electrochemical Gradient and Transport Energetics: The Na^+/K^+ -ATPase pumps 3 Na^+ out and 2 K^+ in per ATP hydrolyzed. Given: $[\text{Na}^+]_{\text{out}} = 145 \text{ mM}$, $[\text{Na}^+]_{\text{in}} = 12 \text{ mM}$, $[\text{K}^+]_{\text{out}} = 4 \text{ mM}$, $[\text{K}^+]_{\text{in}} = 140 \text{ mM}$, $V_m = -70 \text{ mV}$, $T = 37^\circ\text{C}$. Calculate the free energy for transporting 3 Na^+ out: $\Delta G(\text{Na}^+, 3 \text{ ions}) = 3[\text{RT} \ln([\text{Na}^+]_{\text{in}}/[\text{Na}^+]_{\text{out}}) + zFV_m] = 3$

$$8.314 \times 310 \times \ln(12/145) + 1 \times 96485 \times (-0.070)$$

$$= 3$$

$$(-6250) + (-6754)$$

$= 3 \times (-13004) \approx -39 \text{ kJ/mol}$ summed for the inward (downhill) electrochemical drop — equivalently, the *uphill* cost of pushing 3 Na^+ out against this gradient is $+39 \text{ kJ/mol}$. For 2 K^+ in: $\Delta G(\text{K}^+, 2 \text{ ions}) = 2[\text{RT} \ln([\text{K}^+]_{\text{out}}/[\text{K}^+]_{\text{in}}) + zFV_m] = 2$

$$8.314 \times 310 \times \ln(4/140) + (-6754)$$

$$= 2$$

$$(-9510) + (-6754)$$

$= 2 \times (-16264) \approx -32.5 \text{ kJ/mol}$ downhill, so the uphill cost of importing 2 K^+ is $+32.5 \text{ kJ/mol}$. Total uphill work per cycle: $39 + 32.5 = 71.5 \text{ kJ/mol}$. ATP hydrolysis under cellular conditions yields $\Delta G \approx -50$ to -60 kJ/mol — which barely covers the work. Resolution: the textbook stoichiometry (3 $\text{Na}^+ / 2 \text{ K}^+ / 1 \text{ ATP}$) is precisely matched to keep the pump near thermodynamic balance under physiological gradients, so small rises in $[\text{Na}^+]_{\text{in}}$ (or membrane depolarization that reduces V_m 's contribution to Na^+ extrusion) dramatically slow or reverse the pump — the basis of cardiac glycoside toxicity and ischemic Na^+ overload.

Concept Check (Synthesis): The CFTR channel, mutated in cystic fibrosis, is a Cl^- channel gated by ATP binding/hydrolysis — making it unique among ion channels. The ΔF508 mutation (deletion of Phe508 in NBD1) causes protein misfolding and ER retention. (a) CFTR gating requires ATP binding to two nucleotide-binding domains (NBDs) — the channel opens when two ATP molecules are bound and closes when one is hydrolyzed. Sketch the thermodynamic cycle of gating and identify which step is rate-limiting for channel open time. (b) Potentiators (e.g., ivacaftor) increase channel open probability; correctors (e.g., lumacaftor) improve folding. For ΔF508 patients, why is a combination therapy superior to either alone? (c) At the mucosal surface of the lung: if Cl^- secretion through CFTR is reduced by 50%, predict the directional change in airway surface liquid (ASL) volume and explain why this promotes *Pseudomonas* biofilm colonization.

7.9 Membrane Potential and the Action Potential

While the Nernst and Goldman equations describe resting membrane potential, the action potential is the defining electrical event in excitable cells (neurons, muscle cells, some endocrine cells).

7.9.1 Phases of the Action Potential

1. Resting state (V_m about -70 mV): Voltage-gated Na^+ and K^+ channels are closed. K^+ leak channels (K_2P family) maintain the resting potential near E_K .
2. **Depolarization** to threshold (about -55 mV): Graded potentials (e.g., from synaptic input) depolarize the membrane. If threshold is reached, voltage-gated Na^+ channels (Na_v) open rapidly (activation gate).
3. Rising phase (depolarization): Na^+ influx drives V_m toward E_{Na} ($+63 \text{ mV}$). Positive feedback: depolarization opens more Na^+ channels. This is the Hodgkin-Huxley regenerative cycle.
4. Overshoot: V_m briefly exceeds 0 mV (typically reaches $+30$ to $+40 \text{ mV}$ but does not reach E_{Na} because Na^+ channel inactivation begins).
5. Repolarization: Na^+ channel inactivation (ball-and-chain mechanism, h-gate) closes channels within about 1 ms . Voltage-gated K^+ channels (K_v , delayed rectifier) open slowly, allowing K^+ efflux, driving V_m back toward E_K .
6. Undershoot (afterhyperpolarisation): K^+ channels remain open transiently, overshooting below resting potential (about -80 mV). K^+ channels then close, and V_m returns to rest.
7. Refractory periods: Absolute refractory period (Na^+ channels inactivated; no action potential possible). Relative refractory period (some Na^+ channels recovered; stronger stimulus needed).

7.9.2 Hodgkin-Huxley Model

Hodgkin and Huxley (Nobel Prize 1963) described the action potential mathematically using voltage-clamp experiments on the squid giant axon:

$$I_m = C_m \frac{dV}{dt} + g_K n^4 (V - E_K) + g_{Na} m^3 h (V - E_{Na}) + g_L (V - E_L)$$

(141)

where $m = \text{Na}^+$ activation variable, $h = \text{Na}^+$ inactivation variable, $n = \text{K}^+$ activation variable. This model predicted the ionic basis of the action potential before the molecular identity of ion channels was known.

7.9.3 Saltatory Conduction Along Myelinated Axons

In myelinated axons, myelin sheaths (formed by Schwann cells in PNS, oligodendrocytes in CNS) insulate the axon, reducing membrane capacitance. Action potentials “jump” between nodes of Ranvier (gaps in myelin where Na^+ channels are concentrated at about $1,000/\mu\text{m}^2$). This increases conduction velocity from about 1 m/s (unmyelinated C fibers) to about 120 m/s (large myelinated A-alpha fibers).

Clinical Connection: Multiple Sclerosis and Demyelination Multiple sclerosis (MS) is an autoimmune disease in which T cells and antibodies attack CNS myelin. Demyelination exposes K^+ channels normally under the myelin sheath, causing K^+ leakage and conduction block. Symptoms include visual disturbances, motor weakness, and sensory abnormalities. The drug 4-aminopyridine (dalfampridine) blocks exposed K^+ channels and partially restores conduction, improving walking ability in MS patients.

Concept Check 6: Local anaesthetics (e.g., lidocaine) block voltage-gated Na^+ channels by entering the channel pore from the intracellular side in their uncharged form, then becoming protonated and trapped. Why do local anaesthetics preferentially block small-diameter pain fibers before large motor fibers?

7.10 Bulk Transport: Endocytosis and Exocytosis

7.10.1 Exocytosis and SNARE-Mediated Membrane Fusion

Exocytosis: secretory vesicles fuse with the plasma membrane, releasing contents extracellularly.

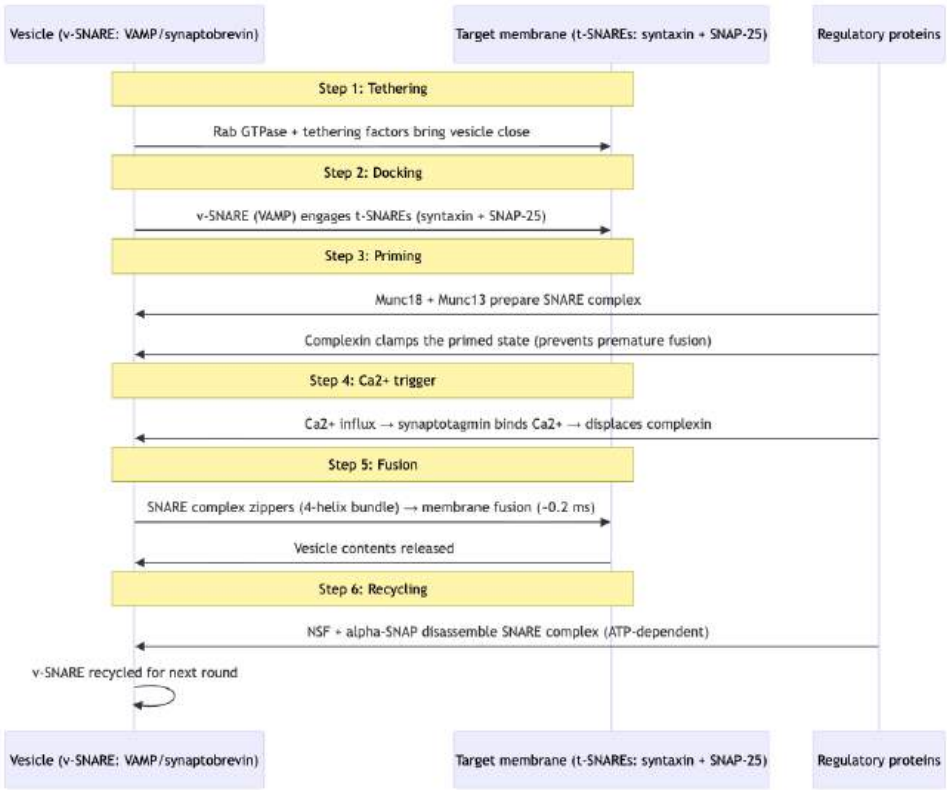


Figure 51. SNARE-mediated vesicle fusion during regulated exocytosis. The v-SNARE on the vesicle (VAMP/synaptobrevin) and t-SNAREs on the target membrane (syntaxin + SNAP-25) form a tight four-helix bundle that drives membrane fusion. Synaptotagmin acts as the Ca^{2+} sensor that triggers fusion in <1 ms.

- Synaptic vesicle fusion: Ca^{2+} entry through voltage-gated Ca^{2+} channels triggers synaptotagmin, fusion occurs in <0.2 ms (fastest biological membrane fusion)
- Insulin secretion: glucose metabolism raises ATP/ADP ratio, closes K_{ATP} channels, depolarization opens Ca^{2+} channels, Ca^{2+} triggers insulin granule exocytosis

Clinical Connection: Botulinum Toxin and Tetanus Toxin Both botulinum toxin (Botox) and tetanus toxin are zinc metalloproteases that cleave SNARE proteins: - Botulinum toxin (7 serotypes A–G) cleaves VAMP, SNAP-25, or syntaxin at the neuromuscular junction, preventing acetylcholine release, causing flaccid paralysis. Clinical uses: dystonia, spasticity, cosmetic wrinkle reduction. - Tetanus toxin cleaves VAMP in inhibitory interneurons of the spinal cord, preventing GABA/glycine release, causing unopposed excitatory activity and spastic paralysis (lockjaw).

7.10.2 SNARE Mechanism in Detail

The SNARE hypothesis (Rothman, Schekman, Südhof — 2013 Nobel Prize in Physiology or Medicine) explains how vesicles fuse with target membranes with both spatial and temporal precision. Each fusion event requires a quartet of helices contributed by a v-SNARE (on the vesicle) and t-SNAREs (on the target membrane). The four-helix bundle “zippers” from the membrane-distal N-terminus toward the membrane-proximal C-terminus, releasing about $35 k_B T$ of free energy per SNARE complex — enough to overcome the kinetic barrier (about $25 k_B T$) for membrane fusion.

Compartment-specific SNARE pairs ensure that each vesicle fuses primarily with its correct target:

Table 116. SNARE Mechanism in Detail: Compartment pair and v-SNARE.

Compartment pair	v-SNARE	t-SNAREs
Synaptic vesicle → presynaptic membrane	VAMP2 (synaptobrevin)	Syntaxin-1 + SNAP-25
ER → cis-Golgi (COPII)	Sec22 / Bet1	Syntaxin-5 + Membrin + GS27
Endosome → late endosome	VAMP7 / VAMP8	Syntaxin-7 + Vti1b + Syntaxin-8
Late endosome → lysosome	VAMP7	Syntaxin-7 + Vti1b + Syntaxin-8
Golgi → plasma membrane (constitutive)	VAMP2 / VAMP3 / VAMP4	Syntaxin-3/4 + SNAP-23

The five steps of SNARE-mediated fusion:

1. Tethering. Rab GTPases on the vesicle (e.g., Rab3 on synaptic vesicles, Rab1 on ER-derived vesicles) bind their effectors on the target membrane (long coiled-coil tethers like p115 or large multi-subunit complexes like the exocyst). Tethering is reversible and provides about 100 nm initial contact.
2. Docking. The four SNARE helices begin to pair through their N-terminal regions. SM proteins (Sec1/Munc18 family) chaperone the syntaxin partner, holding it in an open conformation. At synapses, Munc18 + Munc13 prepare syntaxin-1 for SNARE assembly.
3. Priming. Partial zippering brings the vesicle within about 5 nm of the target membrane. Complexin binds the half-zipped SNARE complex, clamping it in a metastable state ready to release on demand. Without complexin, vesicles fuse spontaneously; with complexin primarily, they cannot fuse — both must be present for regulated fusion.
4. Triggering. At the synapse, action-potential-evoked Ca^{2+} entry through voltage-gated Ca^{2+} channels reaches about $10 \mu\text{M}$ at the active zone within microseconds. Synaptotagmin-1 (Ca^{2+} sensor with two C2 domains) binds Ca^{2+} and PIP_2 , displaces complexin, and releases the SNAREs to complete zippering. The whole event takes <0.2 ms — the fastest known protein-mediated fusion.
5. Disassembly. After fusion, the cis-SNARE complex (the four helices now in the same membrane) is dismantled by NSF (N-ethylmaleimide-sensitive factor, an AAA+ ATPase) and its adaptor alpha-SNAP. This requires ATP hydrolysis (about 1 ATP per SNARE complex) and recycles the SNAREs for the next round.

7.10.3 Vesicle Coat Proteins in Detail

Three major coat systems shape the secretory and endocytic pathways: COPII, COPI, and clathrin. Each is built around a small GTPase (Sar1 for COPII, Arf1 for COPI and clathrin) that anchors to the membrane upon $\text{GDP} \rightarrow \text{GTP}$ exchange and recruits coat subunits. Membrane curvature is generated by the geometry of the coat itself.

Table 117. Vesicle Coat Proteins in Detail: Coat and GTPase.

Coat	GTPase	Inner layer	Outer layer	Cargo selection	Vesicle size
COPII	Sar1	Sec23/24 (Sec24 is cargo selector via DXE/FF motifs)	Sec13/31 (cuboctahedral cage)	Anterograde ER→Golgi	60–80 nm
COPI	Arf1	β -, γ -, δ -, ζ -COP (cargo selector via KKXX)	α -, β' -, ε -COP	Retrograde Golgi→ER, intra-Golgi	60–100 nm
Clathrin	Arf1 (TGN) or none (PM)	Adaptor proteins (AP1 at TGN, AP2 at PM, AP3 at endosome, AP4)	Clathrin triskelions (3 heavy + 3 light chains)	Selective endocytosis; lysosomal sorting	80–120 nm

Clathrin triskelions are 3-legged structures that self-assemble into open polyhedral lattices (hexagons + pentagons, like a soccer ball). Each clathrin-coated pit contains about 36 triskelions arranged into a lattice that gradually curves the membrane into a deep invagination. The vesicle is then released by dynamin, a GTPase that wraps as a helical collar around the neck and uses GTP hydrolysis to constrict and pinch off the bud (about 60–120 nm vesicle, depending on local geometry). After release, the clathrin coat is disassembled by Hsc70 + auxilin (J-domain co-chaperone) at the cost of about 1 ATP per triskelion released.

Vesicle traffic in numbers. A typical mammalian cell sustains about 10^4 exocytic events and about 10^4 endocytic events per minute. The plasma membrane area equivalent of one entire cell is internalised every about 30 minutes — meaning the membrane is in dynamic flux, with steady-state composition maintained by precise SNARE-coupled bidirectional traffic. A typical secretory neuron at full activity can fuse about 1000 synaptic vesicles per second.

7.10.4 Endocytosis and Cargo Internalization

Clathrin-mediated endocytosis (CME): 1. Cargo receptors cluster in clathrin-coated pits (adaptor AP2 links receptors to clathrin triskelions) 2. Clathrin assembles into a polyhedral basket, deforming the membrane into an invagination 3. Dynamin GTPase wraps around the neck of the invagination and pinches it off (about 60–120 nm vesicle) 4. Clathrin coat disassembles (uncoated by Hsc70 + auxilin) 5. Vesicle fuses with early endosome - Examples: LDL receptor, transferrin receptor, EGF receptor

Caveolar endocytosis: - 50–80 nm flask-shaped invaginations rich in cholesterol and sphingolipids - Coated with caveolin-1 (integral membrane protein with hairpin topology) - Functions: transcytosis across endothelial cells, lipid homeostasis, signaling compartmentalization

Phagocytosis: - Professional phagocytes (macrophages, neutrophils, dendritic cells) - Actin-driven pseudopod extension engulfs large particles ($>0.5\text{ }\mu\text{m}$): bacteria, dead cells, debris - Receptors: Fc receptors (opsonised particles), complement receptors, scavenger receptors, TLRs - Phagosome fuses with lysosomes to form phagolysosome for degradation

Macropinocytosis: - Non-specific uptake of large volumes of extracellular fluid - Actin-driven membrane ruffles collapse back onto the cell surface, trapping fluid in large vesicles ($0.2\text{--}5\text{ }\mu\text{m}$) - Important for antigen sampling by dendritic cells and for nutrient acquisition by cancer cells (exploited by RAS-mutant tumors)

Concept Check 5: Familial hypercholesterolaemia (FH) can be caused by mutations in the LDL receptor, the adaptor protein ARH, or the PCSK9 protease. For each, explain how the mutation leads to elevated blood LDL cholesterol. Which type responds to statin therapy?

7.11 Computational Bridge

Nernst potentials for tabulated physiological ions are computed in closed form:

```
from biology.cell import PHYSIOLOGICAL_IONS, nernst_potential

for ion in PHYSIOLOGICAL_IONS:
    if ion.charge == 0:
        continue
    try:
        print(ion.ion, round(nernst_potential(ion), 2), "mV")
    except ValueError:
        pass
```

Clinical / systems note: Long QT channelopathies and familial hyperkalaemic paralysis are reminders that single-ion permeability or gradient defects reshape the Goldman-style integrative potential you approximate in silico.

7.11.1 Predicted Transporter Structures and Experimental Tests

Membrane transporter structures have historically been among the hardest to solve experimentally: hydrophobic surfaces resist crystallisation, cryo-EM requires stable purified protein, and conformational flexibility (the very thing that makes transporters work) blurs reconstructions. AlphaFold2 (DeepMind, 2021), AlphaFold-Multimer (2022), and AlphaFold 3 (2024) changed the workflow by making high-quality structural hypotheses routine for many folded domains and complexes, including many membrane proteins [Abramson et al., 2024, Varadi et al., 2024].

By 2024, the AlphaFold Protein Structure Database provided structure coverage for more than 214 million protein sequences in UniProt [Varadi et al., 2024]. This transforms downstream biology: researchers can inspect predicted transmembrane helices and cavities in an orphan transporter, nominate binding-site residues, compare paralogues, and design mutagenesis or cryo-EM experiments before a solved structure exists. The correct lesson is not that prediction replaces structure determination; it is that prediction changes what counts as a good first experiment.

Cautions are important for scientific literacy: AlphaFold predicts likely static conformations, but transporters function by *cycling* between conformations (outward-open ↔ occluded ↔ inward-open); a single model can miss gating, allostery, lipid dependence, and ligand-coupled state changes. Predicted Aligned Error (PAE) plots flag low-confidence inter-domain geometries, and AlphaFold3 integrates ligands, ions, nucleic acids, and other biomolecules into interaction hypotheses [Abramson et al., 2024]. The field now often generates predicted structures *before* requesting experimental ones, but strong biological claims still require transport assays, mutagenesis, binding data, or experimental structures.

7.12 Current Evidence and Frontier Biology: Membrane Structure and Transport

For Membrane Structure and Transport, frontier biology belongs inside the evidence logic of the chapter. Cell biology is increasingly measured as live, spatial, single-cell, and perturbational data rather than static diagrams alone. The core reading question is this: transport claims require gradients, permeability, electrochemical driving force, gating, and energy coupling.

- What to verify: identify the observation, model, assay, or dataset that would make the claim stronger or weaker.
- What to qualify: state the scale, organism, cell type, environmental condition, or population where the claim is expected to hold.
- What to compare: test at least one alternative explanation, baseline, or null model before treating the pattern as causal.
- What to cite: distinguish primary evidence, review synthesis, public dataset, and institutional guidance; for recent or numeric claims, prefer the source closest to the measurement and state what has changed since it was published.

For membrane-transport claims, specify the ion or solute, gradient, permeability, transporter state, and membrane context before calculating flux.

Source practice: Pair structural or electrophysiological claims with transport assays, permeability measurements, or single-channel data that constrain mechanism.

Mechanosensitive channel claims should name the force, lipid environment, oligomeric state, and assay context; TMEM63 channelopathy work links structural rearrangement to disease mutations, so the mechanism should remain tied to the channel family and assay context [Zheng et al., 2025].

7.12.1 Current Evidence Map: Transporter Structure to Function



Figure 52. Transporter structure claims need functional assays because transport depends on cycling among states, not a single static conformation [Abramson 2024, AlphaFold3, Varadi 2024, AlphaFoldDB].

7.13 Summary

- The plasma membrane is a fluid mosaic bilayer with asymmetric lipid distribution maintained by flippases. Lipid rafts are dynamic cholesterol-sphingolipid microdomains with signaling roles.
- Ion channels achieve selectivity through precise selectivity filters (K⁺ channel: carbonyl oxygen coordination) and are gated by voltage, ligands, mechanical force, or temperature.

- Mechanosensitive channel interpretation should connect membrane force, channel architecture, disease mutation, and functional assay; TMEM63 channelopathy work illustrates how structural rearrangements can be linked to altered gating [Zheng et al., 2025].
 - The Na^+/K^+ -ATPase maintains ionic gradients essential for membrane potential, cell volume, and secondary active transport, consuming about 25% of cellular ATP.
 - ABC transporters use ATP to transport diverse substrates; clinical significance includes multidrug resistance (MDR1) and cystic fibrosis (CFTR).
 - The Nernst equation gives the equilibrium potential of each ion; the Goldman equation gives the actual membrane potential for multiple ions simultaneously.
 - SNARE proteins mediate membrane fusion in exocytosis; synaptotagmin is the Ca^{2+} sensor for regulated secretion.
 - Endocytosis types (clathrin-mediated, caveolar, phagocytosis, macropinocytosis) internalise specific cargo or bulk fluid.
 - Connections: See section 2 for water and osmosis, Unit IX — Zoology and Systems Physiology: Introduction for excitable tissues, and section 8 for receptor-mediated signaling.
-

7.14 Review Questions

1. Derive the Nernst equation from the electrochemical potential equation. Calculate E_K at 20 degrees C (293 K) given $[\text{K}^+]_{\text{in}} = 140 \text{ mM}$, $[\text{K}^+]_{\text{out}} = 5 \text{ mM}$.
 2. Explain how the Na^+/K^+ -ATPase contributes to the resting membrane potential both directly (electrogenic pump) and indirectly (maintaining K^+ gradient).
 3. Compare the selectivity mechanisms of K^+ channels and Na^+ channels. How does each achieve >100:1 selectivity for its preferred ion?
 4. A patient is treated with omeprazole for gastric ulcer disease. What is the molecular target of this drug, and how does inhibiting it reduce gastric acid secretion?
 5. Explain why MDR1/P-glycoprotein overexpression causes multidrug resistance in cancer. Suggest two strategies to overcome this resistance.
 6. Describe the complete SNARE fusion cycle for synaptic vesicle exocytosis, from vesicle docking to SNARE complex disassembly. What role does Ca^{2+} play?
 7. Using the Goldman equation, predict how the resting membrane potential would change if the membrane suddenly became equally permeable to Na^+ and K^+ .
 8. Compare clathrin-mediated endocytosis with phagocytosis in terms of vesicle size, coat proteins, cytoskeletal involvement, and cell types involved.
 9. Explain the biphasic effect of cholesterol on membrane fluidity. Why is this important for cells that experience temperature fluctuations?
 10. SGLT2 inhibitors cause glucose loss in urine. Calculate the approximate caloric loss per day if a diabetic patient loses 70 g of glucose per day in urine (glucose: 4 kcal/g).
 11. Run the Nernst loop in the bridge code and identify which ion's equilibrium potential is closest to a typical neuronal resting potential; justify using permeability weighting qualitatively.
 12. Explain why CFTR is called a channel yet sits in the ABC transporter superfamily, and how that relates to ATP usage vs. passive flow.
-

7.15 Further Reading and Source Notes: Membrane Structure and Transport

- Mitchell (1961). Coupling of phosphorylation to electron and hydrogen transfer by a chemi-osmotic type of mechanism. *Nature*, 191.
 - Singer & Nicolson (1972). The fluid mosaic model of the structure of cell membranes. *Science*, 175.
 - Hodgkin & Huxley (1952). A quantitative description of membrane current and its application to conduction and excitation in nerve. *Journal of Physiology*, 117.
 - Skou (1957). The influence of some cations on an adenosine triphosphatase from peripheral nerves. *Biochimica et Biophysica Acta*, 23.
 - Agre (2004). Aquaporin water channels (Nobel lecture). *Bioscience Reports*, 24.
 - Simons & Ikonen (1997). Functional rafts in cell membranes. *Nature*, 387.
 - Zheng et al. (2025). Structural and functional basis of mechanosensitive TMEM63 channelopathies. *Neuron* [Zheng et al., 2025].
-

7.16 Key Terms

Table 118. Current Evidence Map: Transporter Structure to Function: Term and Definition.

Term	Definition
Fluid mosaic model	Singer-Nicolson model of the membrane as a lipid bilayer sea with floating protein icebergs
Lipid raft	Dynamic cholesterol/sphingolipid-enriched microdomain that concentrates signaling proteins
Flippase	ATP-dependent enzyme maintaining lipid asymmetry by moving PS/PE to the inner leaflet
Aquaporin	Water-selective channel; excludes protons via electrostatic mechanism
GLUT	Glucose transporter family (SLC2A); 14 isoforms with tissue-specific expression and K_m
Na ⁺ /K ⁺ -ATPase	Primary active pump; 3 Na ⁺ out / 2 K ⁺ in per ATP; electrogenic; 25% of body ATP
Symport	Secondary active transport where two solutes move in the same direction
Antiport	Secondary active transport where two solutes move in opposite directions
Nernst potential	Equilibrium potential of a single ion species: $E_i = (RT/z_iF) \ln([C]_o/[C]_i)$
Goldman equation	Membrane potential equation accounting for permeabilities and concentrations of multiple ions
Selectivity filter	Narrow region of an ion channel that determines ion selectivity (e.g., TVGYG in K ⁺ channels)
ABC transporter	ATP-binding cassette transporter superfamily; drug efflux (MDR1), Cl ⁻ channel (CFTR)
SNARE	Soluble NSF attachment protein receptor; mediates membrane fusion via four-helix bundle zippering
Clathrin	Triskelion coat protein forming polyhedral baskets during receptor-mediated endocytosis
Channelopathy	Disease caused by ion channel mutations (e.g., Long QT syndrome, cystic fibrosis)
Macropinocytosis	Non-specific bulk uptake of extracellular fluid via actin-driven membrane ruffling

7.17 Companion Source Module: Membrane Structure and Transport

Membrane Structure and Transport should leave a reproducible trail from a biological claim to the code, figure, diagram, or paper-based activity that can test it. Use the surfaces below to inspect the chapter’s assumptions, rerun the relevant model, or compare the manuscript explanation with companion labs and figures.

Table 119. Companion source surfaces for Membrane Structure and Transport.

Surface	Use it for
src/biology/cell/cell_biology.py (nernst_potential, goldman_equation, osmotic_pressure, diffusion_flux)	Reproduce electrochemical, osmotic, and diffusive driving forces.
src/visualization/plots.py (plot_nernst_potentials)	Inspect ion-specific gradients and sign conventions.
src/mermaid/biology_diagrams.py (membrane_transport_diagram)	Separate channels, carriers, pumps, and coupled transport.

Reproducibility check: list concentrations, permeability, charge, temperature, and membrane orientation before interpreting transport direction. Cross-reference: connect with section 33 and section 28.

8 Cell Signaling and Communication

Level 3/3 · 55 min read · 75 min lecture · Prerequisites: section 7, section 4

8.1 Learning Objectives

1. Classify signaling molecules by their mode of delivery and explain signal amplification logic.
2. Describe the major families of cell-surface receptors (GPCRs, RTKs, ion channels) and their signaling mechanisms.
3. Explain the cAMP, PIP₂/DAG/IP₃, and RTK-MAP kinase **signal transduction** cascades in detail.
4. Compare the Wnt/beta-catenin, JAK-STAT, and Notch pathways by their route from receptor to nuclear effector.
5. Explain signal termination mechanisms: GTPase activity, phosphodiesterases, phosphatases, and receptor internalization.
6. Predict how cyclin-CDK checkpoint failure alters **cell cycle** progression, relating it to the stages of **mitosis**.
7. Explain the mechanisms of **apoptosis** (intrinsic and extrinsic pathways).
8. Explain cancer as dysregulated signaling and evaluate current targeted therapies.

8.1.1 Study Blueprint

- Big idea: Cells communicate by converting external signals into regulated intracellular decisions.
- Core concepts: receptors, second messengers, signal amplification, feedback.
- Framework alignment: Vision & Change: Structure and function, Systems, Information flow, exchange, and storage; AP Biology: Systems Interactions, Information Storage and Transmission; NGSS-style topics: Structure and Function.
- Model or quantitative lens: Ligand-receptor occupancy and dose-response reasoning.
- Data skill: Read pathway diagrams and infer the effect of agonists, antagonists, or mutations.
- Practice cadence: Visual Representations, Questions and Methods, Argumentation.
- Common misconception to repair: A pathway diagram is a causal model, not a memorization chart.
- Primary lab: **Lab — Cell Signaling and Communication**.
- Question bank: **Questions — Cell Signaling and Communication**.
- Transfer task: Apply signaling logic to hormones, neurotransmitters, immune receptors, or cancer mutations.
- Bridge to computation: `biology.physiology.physiology.homeostasis_response`.

Opening Vignette: When Signals Go Wrong — HER2 Breast Cancer

In 1987, Dennis Slamon’s team at UCLA reported that about 25% of breast cancers showed amplification of the HER2 **gene**, which encodes a receptor tyrosine kinase embedded in the plasma membrane [Slamon et al., 1987]. In normal cells, HER2 is transiently activated when it binds its ligand — triggering a cascade of phosphorylation events that ultimately drive cell proliferation and survival. In tumors with HER2 amplification, the **protein** is expressed at 40–100 times the normal level; even without ligand, HER2 molecules are close enough together to activate each other constantly, delivering an unrelenting “grow and divide” signal.

The consequences of understanding this single signaling pathway have been transformative. In 1998, the FDA approved trastuzumab (Herceptin), a monoclonal antibody that binds the extracellular domain of HER2 and blocks its dimerization and downstream signaling. In HER2-positive breast cancer, trastuzumab plus chemotherapy improved time to progression, response rate, and survival in metastatic HER2-overexpressing breast cancer [Slamon et al., 2001]. Every step in this therapeutic triumph required understanding how cells receive, transduce, and amplify molecular signals — precisely the subject of this chapter.

Primary sources: HER2 amplification and prognosis [Slamon et al., 1987]; trastuzumab clinical benefit [Slamon et al., 2001].

Cells receive and interpret thousands of extracellular signals simultaneously. Signaling systems share a general architecture:

Signal (ligand) → Receptor (detection) → Transduction cascade (amplification) → Effector → Response → Termination

8.1.2 Types of Cell Signaling by Distance

Table 120. Types of Cell Signaling by Distance: Mode and Description.

Mode	Description	Example	Distance
Endocrine	Hormones in bloodstream	Insulin, cortisol	Meters
Paracrine	Local diffusion	Growth factors, prostaglandins	<1 mm
Autocrine	Self-stimulation	Tumor self-growth signals, IL-2 in T cells	Same cell
Juxtacrine	Membrane-bound ligand/receptor	Notch-Delta, ephrin-Eph	Cell contact
Synaptic	Neurotransmitter across synapse	Glutamate, GABA, acetylcholine	about 20 nm

8.1.3 Signal Transduction Logic

Signal transduction cascades exhibit four fundamental properties:

1. Amplification: One activated receptor activates multiple G proteins; each G protein activates multiple adenylyl cyclase molecules; each adenylyl cyclase produces many cAMP molecules. The cAMP second messenger system was established biochemically before G proteins were recognized as the transducers linking receptors to adenylyl cyclase [Rall and Sutherland, 1958, Gilman, 1987]. A single epinephrine molecule can trigger release of about 10⁸ glucose molecules from glycogen (10⁶-fold amplification).
2. Specificity: Different cell types express different receptor subtypes, G proteins, and effectors. Epinephrine causes glycogen breakdown in liver (beta₂-adrenergic receptor, G_s, cAMP) but smooth muscle relaxation in bronchi (same receptor, same second messenger, different downstream targets).
3. Integration: Multiple signals converge on shared effectors. A cell’s response reflects the integrated sum of active signaling pathways. For example, cell proliferation requires simultaneous growth factor (RTK), integrin (adhesion), and survival factor signaling.
4. Adaptation/desensitisation: Prolonged stimulation leads to reduced response. Mechanisms include receptor phosphorylation (by GRKs), arrestin binding, receptor internalization, and negative feedback loops [Alon, 2019].

8.1.4 Signal Amplification Cascades — A Quantitative Treatment

Signal amplification is the architectural reason a single hormone molecule can drive a macroscopic physiological response. Three concepts make the amplification quantitative: gain per step, overall gain, and dynamic range.

Gain per step. Each level of a cascade has a gain A_i defined as the number of activated downstream molecules per active upstream molecule (per unit time). For example, a single G_sα-GTP activates about 10 adenylyl cyclase molecules during its about 1 minute lifetime; each adenylyl cyclase produces about 1,000 cAMP per second, so over 30 s the gain at this step is roughly $10 \times 30,000 = 3 \times 10^5$.

Overall gain. For an n -step cascade, the total amplification is the product of step gains:

$$G_{\text{total}} = \prod_{i=1}^n A_i$$

(142)

This product structure means that *removing one step* of a cascade cuts gain by orders of magnitude, while *adding one step* multiplies it. The classic epinephrine→glycogenolysis cascade has 4 enzymatic amplification steps (receptor → G_s → adenylyl cyclase → PKA → phosphorylase kinase → glycogen phosphorylase), each contributing $A_i \approx 10^{1.5}$, for $G_{\text{total}} \approx 10^6$. A single epinephrine molecule binding a β₂ receptor releases about 10⁸ glucose molecules from glycogen — exactly the gain measured in liver perfusion experiments.

Why so many steps? A simpler cascade with the same gain — e.g., one step of $A = 10^6$ — would be biologically implausible: few signaling enzymes have $k_{\text{cat}} > 10^4 \text{ s}^{-1}$ (the diffusion-limited outliers catalase and carbonic anhydrase are exceptions), and no cell could sustain enzyme concentrations giving 10⁶-fold amplification in a single reaction. The cascade architecture solves this by *multiplying* modest gains.

Time delay and adaptation. Each step also adds a time constant τ_i (the lifetime of the activated species). The total response time is:

$$\tau_{\text{total}} \approx \sqrt{\sum_i \tau_i^2}$$

(143)

For visual transduction (rhodopsin → transducin → PDE6 → cGMP fall): individual τ_i are about 10 ms, total response about 50 ms. For epinephrine: hundreds of milliseconds to seconds. The cascade thus also serves as a temporal filter — fast inputs reach the effector quickly, slow inputs are integrated.

Cooperativity sharpens the response. figure 53 contrasts Hill coefficients that steepen receptor occupancy around K_d . A linear cascade has gain but not steepness — the dose–response is hyperbolic (Hill coefficient 1). To make a switch-like response, cells use:

- *Multiple binding sites* (hemoglobin O_2 , $n_H = 2.8$).
- *Multi-site phosphorylation requiring full occupancy* (ERK requires both Thr and Tyr phosphorylation; effective $n_H \approx 5$ in the MAP kinase cascade).
- *Positive feedback loops* (ERK → SOS feedback creates bistability).

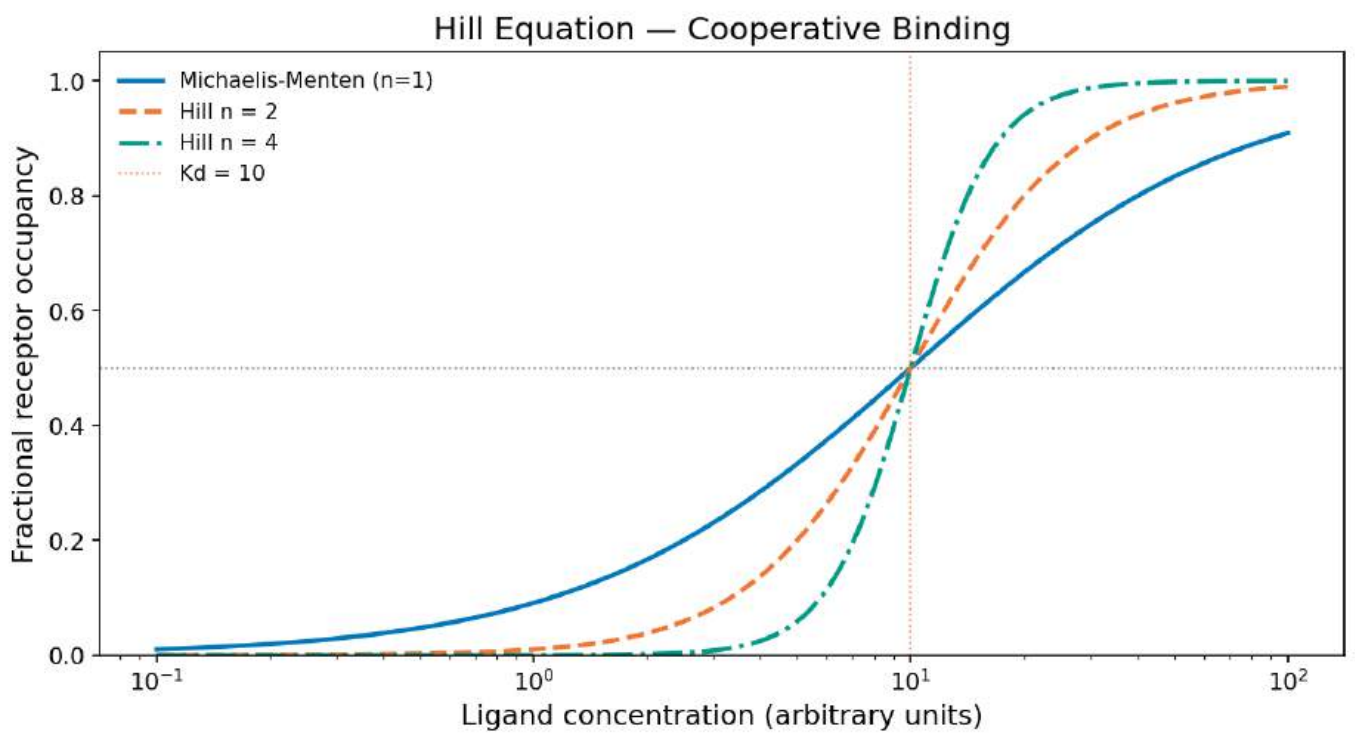


Figure 53. Hill-equation receptor occupancy for cooperative binding. Higher Hill coefficients steepen the sigmoid dose–response curve around the dissociation constant K_d , so a small ligand increase can switch occupancy from low to high when cooperativity is strong.

The Huang–Ferrell analysis of the MAPK cascade showed mathematically that *three sequential switches* (each with $n_H = 1.7$ from its dual phosphorylation requirement) compose to give an overall Hill coefficient near 5 — converting a graded growth-factor input into an essentially digital ERK output. This is the molecular substrate of the cell’s “decision making” between proliferation and quiescence.

Concept Check 1a: A six-step cascade has a gain of 10 per step. What is the total gain? If a single step is removed (now five steps), by what factor

does the total gain change?

8.1.5 Quantitative Foundations of Signal Transduction

Receptor–ligand binding equilibrium. The dissociation constant K_d quantifies receptor affinity:

$$K_d = \frac{[R][L]}{[RL]} \tag{144}$$

where $[R]$ is free receptor concentration, $[L]$ is free ligand concentration, and $[RL]$ is the receptor–ligand complex. The fraction of receptors occupied at a given ligand concentration is:

$$\theta = \frac{[L]}{[L] + K_d} \tag{145}$$

When $[L] = K_d$, exactly 50% of receptors are occupied. Typical K_d values: **insulin receptor** about 0.1 nM; epinephrine–beta₂ receptor about 1 μM.

The Hill equation models cooperative binding and switch-like signaling responses:

$$\theta = \frac{[L]^{n_H}}{K_d^{n_H} + [L]^{n_H}} \tag{146}$$

where n_H is the Hill coefficient. $n_H = 1$ gives a hyperbolic (Michaelis–Menten-like) curve; $n_H > 1$ produces a sigmoidal (switch-like) response. The MAPK cascade achieves an effective $n_H \approx 5$, creating the ultrasensitive most-or-none ERK activation observed experimentally (Huang & Ferrell, 1996, *PNAS*).

Signal amplification cascade. If each step in a cascade has amplification factor A_i , the total amplification is:

$$G_{\text{total}} = \prod_{i=1}^n A_i = A_1 \times A_2 \times \cdots \times A_n \tag{147}$$

For the epinephrine–glycogen cascade ($n = 4$ steps, $A_i \approx 10^{1.5}$ per step): $G_{\text{total}} \approx 10^6$, explaining how one hormone molecule triggers release of $\sim 10^8$ glucose molecules.

8.1.6 Worked Example: Receptor Fractional Occupancy

Problem: The epidermal growth factor receptor (EGFR) is an RTK with a dissociation constant (K_d) for its ligand, EGF, of approximately 2.0 nM (2.0×10^{-9} M). Assuming standard non-cooperative binding behavior ($n_H = 1$), calculate the fractional occupancy (θ) of the EGFR population on a cell surface when the extracellular concentration of EGF is 6.0 nM. What concentration of EGF would be required to achieve 90% receptor occupancy?

Solution:

1. Calculate occupancy at 6.0 nM: Using the receptor fractional occupancy equation:

$$\theta = \frac{[L]}{[L] + K_d}$$

Substitute the given values ($[L] = 6.0$ nM, $K_d = 2.0$ nM):

$$\theta = \frac{6.0}{6.0 + 2.0} = \frac{6.0}{8.0} = 0.75$$

Thus, 75% of the EGF receptors are bound to ligand.

2. Calculate the ligand concentration required for 90% occupancy: Set $\theta = 0.90$ and solve for $[L]$:

$$0.90 = \frac{[L]}{[L] + 2.0}$$

$$0.90([L] + 2.0) = [L]$$

$$0.90[L] + 1.80 = [L]$$

$$1.80 = 0.10[L]$$

$$[L] = \frac{1.80}{0.10} = 18.0 \text{ nM}$$

An EGF concentration of 18.0 nM is required to saturate 90% of the receptors. Note that achieving 90% occupancy requires a ligand concentration exactly $9 \times K_d$.

Concept Check 1: Epinephrine stimulates both beta₂-adrenergic receptors (G_s-coupled, cAMP elevation) on bronchial smooth muscle and alpha₁-adrenergic receptors (G_q-coupled, IP₃/Ca²⁺) on vascular smooth muscle. Why does the same hormone cause bronchodilation in the lungs but vasoconstriction in skin blood vessels?

8.1.7 Worked Example: Signal Amplification Through a Kinase Cascade

Problem: The MAP kinase module is a three-tier cascade (Raf → MEK → ERK) in which each activated kinase phosphorylates and activates roughly 10 molecules of the next kinase ($A_1 = A_2 = A_3 = 10$).

- 1. Using the cascade gain relation, what is the total amplification of the three-tier module?
- 2. If 50 growth-factor receptors are activated, how many ERK molecules are activated?
- 3. What happens to the total gain if one tier is bypassed (a two-step cascade)?

Solution:

- 1. Total gain is the product of the per-step gains:

$$G_{\text{total}} = \prod_{i=1}^3 A_i = A_1 \times A_2 \times A_3 = 10 \times 10 \times 10 = 10^3$$

The three-tier module amplifies the input 1,000-fold.

- 2. Scale by the number of activated receptors ($N_R = 50$):

$$N_{\text{ERK}} = N_R \times G_{\text{total}} = 50 \times 10^3 = 5.0 \times 10^4$$

So 50 activated receptors yield about 50,000 activated ERK molecules.

- 3. Drop one tier (now a two-step cascade, $G = A_1 \times A_2$):

$$G_{\text{2-step}} = 10 \times 10 = 10^2$$

Removing a single tier cuts the gain by a factor of $10^3/10^2 = 10$.

Because the cascade gain is a product rather than a sum, each added tier multiplies the response while a lost tier divides it — a small number of detected ligand molecules can therefore drive a large, switch-like cellular decision, and dropping or inhibiting one kinase tier (a common drug strategy) sharply attenuates the output.

8.2 Cell-Surface Receptors and Signal Initiation

8.2.1 G Protein-Coupled Receptors (GPCRs)

GPCRs are the largest receptor superfamily (about 800 in humans; about 34% of approved drug targets). They have 7 transmembrane alpha-helices, an extra-cellular N-terminus, and an intracellular C-terminus. Binding of ligand activates the heterotrimeric G protein (G-alpha, G-beta-gamma), the receptor-coupled switch formalised in classic G-protein biochemistry [Gilman, 1987]:

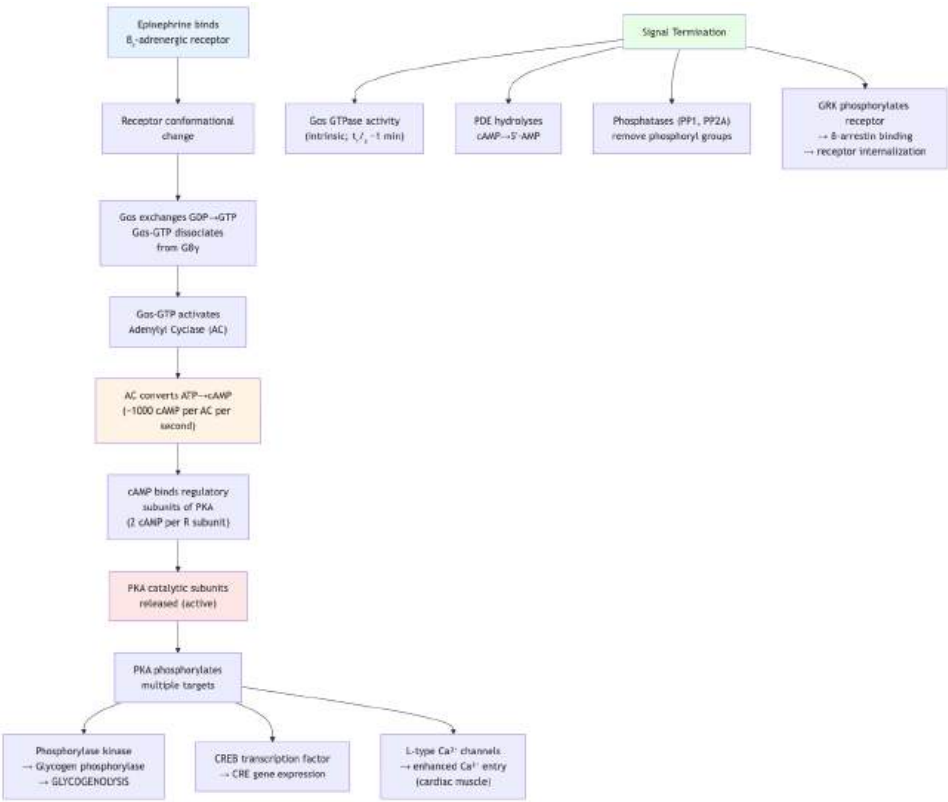


Figure 54. The G_s-cAMP-PKA signaling cascade and its termination mechanisms. Signal amplification occurs at multiple levels: one receptor activates multiple G proteins, each adenylyl cyclase produces about 1,000 cAMP/s, and PKA phosphorylates multiple substrates.

G_s pathway (stimulatory): Hormone (e.g., epinephrine) → β₂-adrenergic receptor → G_s → adenylyl cyclase activated → ATP → cAMP → Protein Kinase A (PKA) → phosphorylates multiple downstream targets (glycogen phosphorylase kinase, CREB transcription factor, ion channels, etc.) [Rall and Sutherland, 1958, Gilman, 1987]

G_i pathway (inhibitory): Inhibits adenylyl cyclase, reducing cAMP. Examples: opioid receptors (μ, δ, κ), muscarinic M2 receptors (cardiac parasympathetic), α₂-adrenergic receptors.

G_q pathway: Activates phospholipase C-β → cleaves PIP₂ → IP₃ (Ca²⁺ release from ER via IP₃ receptors) + DAG (activates Protein Kinase C, PKC). This dual second messenger system controls smooth muscle contraction, platelet activation, and secretion.

G_{12/13} pathway: Activates Rho GEFs → Rho GTPase → ROCK (Rho-associated kinase) → cytoskeletal remodeling, cell migration, smooth muscle contraction.

cAMP signaling components: - PDE (phosphodiesterase): hydrolyses cAMP to 5'-AMP, terminating the signal. Caffeine and theophylline inhibit PDE → elevated cAMP → CNS stimulation, bronchodilation. Sildenafil (Viagra) inhibits PDE5 (specific for cGMP in penile smooth muscle). - AKAP (A Kinase Anchoring Proteins): target PKA to specific subcellular locations, providing spatial specificity to cAMP signaling. - GTPase activity of G-α: G-α is a self-inactivating molecular switch (built-in GTPase; k_{cat} about 1 min⁻¹). RGS (Regulators of G-protein Signaling) proteins accelerate GTP hydrolysis, shortening signal duration.

8.2.2 The G-Protein Cycle in Detail

Heterotrimeric G proteins (Gα + Gβγ) are molecular switches that integrate three biochemical events: GDP release, GTP binding, and GTP hydrolysis. The cycle is canonical for most GTPases — Ras, Rho, Rab, Ran, and the heterotrimeric G proteins most follow the same logic, with different specifics.

Table 121. The G-Protein Cycle in Detail: State and Composition.

State	Composition	Conformation	Signaling
Inactive (GDP)	Gα-GDP·Gβγ heterotrimer	“Off”	No effector activation
Receptor-bound	Gα-GDP·Gβγ + activated GPCR	GPCR catalyses GDP release	Transient
Empty	Gα·Gβγ + GPCR (very brief)	Nucleotide-free	Allows GTP binding
Active (GTP)	Gα-GTP + free Gβγ	“On”; conformational change in switch I/II/III	Activates effectors

State	Composition	Conformation	Signaling
Hydrolysing	Gα-GTP intrinsic GTPase	Slow (k_{cat} about 0.05 s^{-1} , $t_{1/2}$ about 15 s)	Self-inactivation
GAP-accelerated	Gα-GTP + RGS protein	Stabilizes transition state	$t_{1/2}$ shortens to about 1 s
Reassembly	Gα-GDP + Gβγ	Heterotrimer reforms	Cycle closes

Rate constants and cellular consequences. For G_{α_s} , the intrinsic GTP hydrolysis rate is about 0.05 s^{-1} (so the active state lasts about 20 s without acceleration). RGS proteins (RGS2, RGS4, RGS9) accelerate this 100–1,000×, shortening the signal to about 50 ms. Disease example: RGS9 deficiency causes bradyopsia — a visual disorder where bright lights produce after-images that linger because transducin (the rod photoreceptor G_{α}) cannot be turned off rapidly.

Why the cycle is reversible. Each step is in principle reversible at thermodynamic equilibrium. The cycle is driven *forward* by: - Receptor activation (provides the catalytic step for GDP release); - High cellular $[GTP]:[GDP]$ ratio (about 10:1, maintained by metabolism); - Coupling of GTP hydrolysis to effector dissociation (mass-action irreversibility).

Without metabolic GTP, the cycle would stall. ATP-depleted cells therefore lose most GPCR-mediated signaling — one reason why ischemic damage propagates so quickly in tissues.

8.2.3 GPCR Desensitisation and β-Arrestin

Continuous stimulation of a GPCR rapidly attenuates its response — within seconds to minutes, the system desensitises. This is a textbook example of a homeo-static negative feedback loop and the mechanistic basis for clinically important phenomena: tachyphylaxis (rapid loss of drug effect), tolerance (e.g., to opioids, β-agonists), and receptor downregulation.

Three layers of desensitisation:

1. Homologous desensitisation (rapid, agonist-specific; seconds).
 - Active GPCR is phosphorylated by GRKs (G-protein-coupled receptor kinases), especially GRK2 and GRK3. GRK2 specifically recognizes *active* receptor conformation; ligand-free or inactive receptors are not phosphorylated.
 - Phosphorylated GPCR recruits β-arrestin (β-arrestin-1 or -2). β-arrestin binding sterically blocks G-protein coupling — the receptor is now “uncou-pled” from G_s/G_q but still on the cell surface.
2. Heterologous desensitisation (slower, cross-pathway; seconds to minutes).
 - PKA and PKC phosphorylate GPCRs at distinct sites, attenuating responses to any agonist that activates that receptor (regardless of whether it’s currently bound). This integrates signaling across pathways.
3. Receptor internalization (slow, persistent; minutes to hours).
 - β-arrestin recruits clathrin and AP2 → receptor is internalised in clathrin-coated vesicles → enters the early endosome.
 - From the endosome: receptors can be recycled back to the plasma membrane (rapid, restores response within minutes — the path of β₂-adrenergic receptor) or sorted to lysosomes for downregulation (slow, requires hours-to-days for new receptor synthesis to restore response — the path of opioid receptors after chronic agonist exposure).

Beyond G-protein signaling: β-arrestin as a signaling scaffold. Originally thought to “merely” terminate G-protein signaling, β-arrestins are now recognized as scaffolds for their own kinase cascades — ERK, JNK, p38 MAPK can be activated by β-arrestin-bound receptors *after* internalization, generating a second wave of signaling distinct from the initial G-protein wave. Some agonists (called biased agonists) preferentially activate one pathway: - Carvedilol (β-blocker) inhibits G_s but activates β-arrestin signaling — this dual action may underlie its superior efficacy in heart failure compared to other β-blockers. - TRV130 / oliceridine (μ-opioid agonist, FDA-approved 2020) is biased toward G-protein signaling and away from β-arrestin — this reduces respiratory depression and constipation while preserving analgesia.

Concept Check 1b: A patient with asthma uses an inhaled β₂-agonist (albuterol) every 4 hours for several days. The drug becomes progressively less effective (tachyphylaxis). Explain at the molecular level — which mechanism (homologous, heterologous, internalization/downregulation) is most likely responsible for each time-scale of tolerance?

8.2.4 Second Messenger Kinetics

Second messengers are diffusible small molecules that connect receptors to downstream effectors. Their effective signaling depends on three quantitative param-eters: production rate, diffusion (and spatial spread), and degradation rate.

cAMP kinetics. Adenylyl cyclase produces cAMP at about 1,000 molecules/s per active enzyme. cAMP degradation by phosphodiesterases (PDEs) has half-lives ranging from about 50 ms (cardiac muscle, near-membrane PDE3/PDE4 microdomains) to several seconds (cytoplasmic bulk). Diffusion coefficient $D \approx 300$

$\mu\text{m}^2/\text{s}$ in cytoplasm; diffusion length $\ell = \sqrt{D\tau}$. With $\tau_{1/2} = 100\text{ ms}$, $\ell \approx 5\text{ }\mu\text{m}$ — short enough to create spatial gradients within a single cell. AKAP scaffolds and PDE microdomains create “cAMP nano-domains” of just about 100 nm where local concentrations can be 10–100× the cell average. This explains how a single cell can use cAMP to signal *locally* (e.g., individual ion channels) without flooding the whole cell.

The PDE family and pharmacology. Eleven PDE families exist in humans, each with tissue-specific expression:

Table 122. Second Messenger Kinetics: PDE family and Substrate.

PDE family	Substrate	Tissue / function	Inhibitor (drug)	Clinical use
PDE3	cAMP > cGMP	Cardiac, vascular smooth muscle	Milrinone, Cilostazol	Heart failure, claudication
PDE4	cAMP	Inflammatory, CNS	Roflumilast, Apremilast	COPD, psoriasis
PDE5	cGMP primarily	Vascular smooth muscle (penile, pulmonary)	Sildenafil (Viagra), Tadalafil	Erectile dysfunction, pulmonary hypertension
PDE6	cGMP	Photoreceptors	None therapeutic	(Mutated in retinitis pigmentosa)
PDE9, PDE10	cAMP, cGMP	Brain, smooth muscle	Various	Cognitive disorders (trial)

The Viagra story (a quintessential mechanism-to-medicine path). Pfizer scientists were originally testing sildenafil in 1989 as a treatment for angina (the rationale: PDE5 inhibition → cGMP buildup → vasodilation → coronary blood flow). Its anti-anginal effects were modest, but male patients in trials reported a striking side effect. Pfizer pivoted; sildenafil was approved for erectile dysfunction in 1998 and became a major pharmaceutical product. The mechanism is exquisitely specific: nitric oxide → guanylyl cyclase → cGMP → PKG → relaxation of penile smooth muscle. PDE5 normally degrades cGMP; sildenafil blocks PDE5; cGMP accumulates *primarily where it is being made* (i.e., where NO is released). This “context-conditional” pharmacology — drug effect primarily where the natural signal is active — now informs many other targeted therapies. Tadalafil (Cialis) has a longer half-life (17.5 h vs. 4 h for sildenafil) due to its different binding kinetics in the PDE5 active site.

IP_3 / Ca^{2+} kinetics. IP_3 has a half-life of about 1 second (rapid dephosphorylation by IP_3 -5-phosphatase); Ca^{2+} signals are buffered by about 99% by cytoplasmic proteins (calbindin, calretinin) and re-sequestered by SERCA in <1 second. Therefore Ca^{2+} “spikes” and “waves” propagate at controllable, intermediate speeds (about 10–50 $\mu\text{m}/\text{s}$), enabling spatially organized signaling such as the fertilization Ca^{2+} wave that sweeps a sea urchin egg in about 15 seconds.

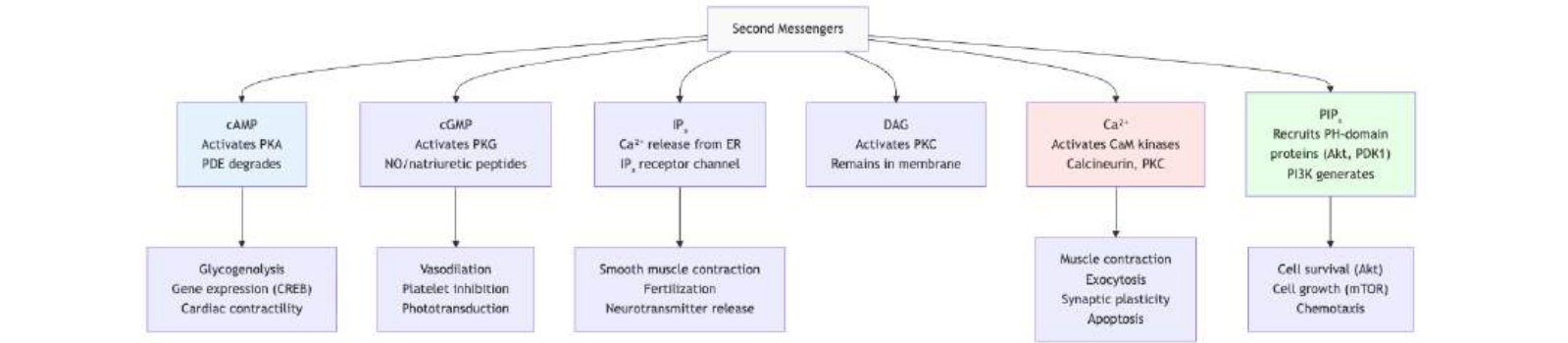


Figure 55. Major second messenger systems and their downstream effects. Each second messenger activates specific protein kinases or effectors that mediate distinct cellular responses.

Clinical Connection: Cholera and Pertussis Toxins Cholera toxin ADP-ribosylates G_s -alpha, preventing GTP hydrolysis. G_s is constitutively active → massive cAMP production in intestinal epithelial cells → CFTR Cl^- channels open → Cl^- and water secretion → severe watery diarrhea (up to 20 L/day), potentially fatal from dehydration. Pertussis toxin (whooping cough) ADP-ribosylates G_i -alpha, preventing its activation. Without G_i inhibition, adenyl cyclase is overactive → elevated cAMP in respiratory epithelial cells → impaired mucociliary clearance → persistent cough. see section 7 for CFTR.

8.2.5 Receptor Tyrosine Kinases (RTKs)

RTKs are single-pass transmembrane receptors with a cytoplasmic tyrosine kinase domain. Ligand binding (e.g., EGF, PDGF, insulin, FGF, VEGF) → receptor dimerization → trans-autophosphorylation of tyrosines → phosphotyrosines recruit adaptor proteins via SH2 and PTB domains.

Each step amplifies: one activated EGFR → about 100 RAS → about 10,000 activated ERK molecules.

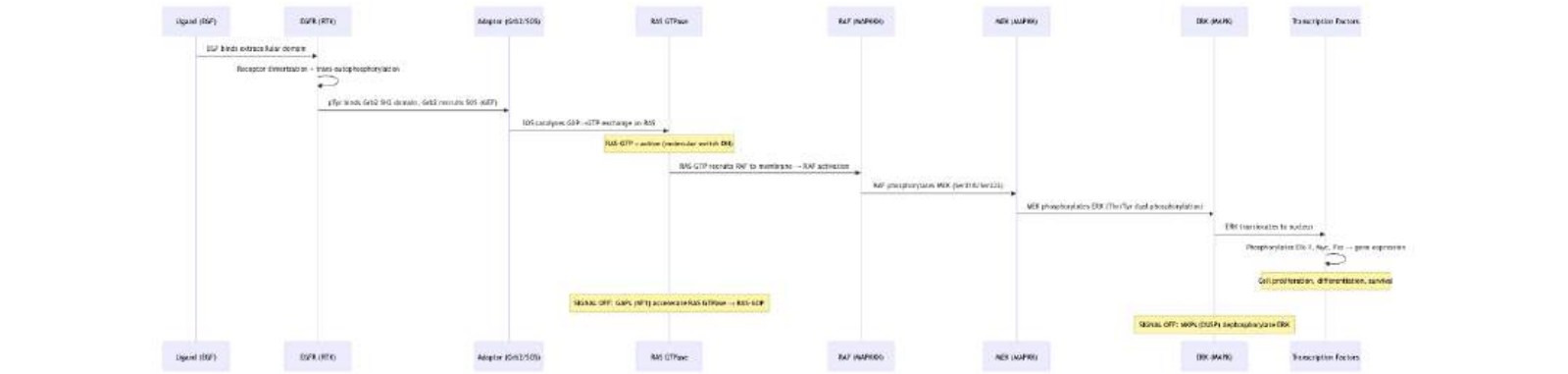


Figure 56. The RTK/RAS/MAPK signaling cascade. Each step amplifies the signal: one activated EGFR can activate about 100 RAS molecules, producing about 10,000 activated ERK molecules.

8.2.6 Receptor Tyrosine Kinase Activation in Detail

RTKs are activated by ligand-induced dimerization — and the choreography is more elegant than the cartoon suggests. Different RTK families use different dimerization strategies:

1. Bivalent ligand (e.g., PDGF, VEGF, SCF): the ligand is a dimer that bridges two receptor monomers. Binding stoichiometry is 2 ligands : 2 receptors.
2. Receptor-mediated dimerization (e.g., EGFR, HER2/3/4): the ligand is monomeric but binding induces a conformational change that exposes a “dimerization arm” on the extracellular domain; two ligand-bound receptors then pair through these arms. Stoichiometry: 2 ligands : 2 receptors.
3. Pre-formed dimers (e.g., insulin receptor, IGF-1R): exist as covalent ($\alpha_2\beta_2$) tetramers held together by disulphide bonds. Ligand binding does not change quaternary structure but does induce a conformational change that brings the two intracellular kinase domains into productive juxtaposition.

Trans-autophosphorylation. Upon dimerization, the two intracellular kinase domains phosphorylate each other on multiple tyrosine residues in trans (kinase A phosphorylates kinase B and vice versa). This serves three purposes: - Increases kinase activity about 100-fold by stabilizing the active conformation. - Creates docking sites for downstream adaptor proteins. - Sets a stoichiometric “code” — different receptors phosphorylate different tyrosine combinations, recruiting different adaptors.

SH2 and PTB domains: phosphotyrosine readers. Phosphorylated tyrosines are recognized by two protein-domain types: - SH2 (Src homology 2) domains, about 100 amino acids, recognize pTyr in a sequence-specific context (the +1 to +3 residues C-terminal to pTyr determine specificity). Each SH2 domain has a characteristic preference (e.g., Grb2 SH2 prefers pYXNX; PI3K-p85 SH2 prefers pYXXM; Src family SH2 prefers pYEEI). - PTB (Phosphotyrosine Binding) domains recognize the residues *N-terminal* to pTyr. Examples: Shc, IRS-1.

The combinatorial code of pTyr sites and SH2/PTB readers explains how the same kinase domain (intrinsically not sequence-specific) can produce highly specific signaling outputs.

Specific RTK examples:

Table 123. Receptor Tyrosine Kinase Activation in Detail: RTK and Ligand.			
RTK	Ligand	Dimerization type	Key adaptors recruited
EGFR (HER1)	EGF, TGF- α	Receptor-mediated	Grb2 (\rightarrow RAS); PLC- γ (\rightarrow DAG/IP $_3$); STAT3
HER2	None known	Heterodimerises with HER1/3/4	Same as above; HER2-HER3 strongest mitogen
Insulin R	Insulin	Pre-formed	IRS-1/2 (\rightarrow PI3K, Grb2); Shc
FGFR	FGF + heparan sulfate	Bivalent ligand + co-receptor	FRS2 (\rightarrow Grb2, Shp2); PLC- γ
VEGFR2	VEGF-A	Bivalent ligand	TSAd; PLC- γ ; Shc
Trk receptors	NGF, BDNF	Bivalent (TrkA: 1 NGF dimer / 2 receptors)	Shc; PLC- γ ; FRS2

Clinical Connection: HER2 and Trastuzumab Reconsidered. Trastuzumab binds the membrane-proximal extracellular subdomain IV of HER2 — *not* the dimerization arm. So how does it work? Multiple mechanisms: (1) it sterically interferes with HER2-HER2 self-dimerization in amplified

cancers; (2) it triggers antibody-dependent cellular cytotoxicity (ADCC) by recruiting NK cells via Fc receptors; (3) it accelerates HER2 internalization and degradation. Trastuzumab-resistant HER2⁺ tumors often retain ADCC sensitivity, which is why trastuzumab-*emtansine* (T-DM1) — an antibody–drug conjugate carrying a microtubule poison — works after trastuzumab failure: it exploits residual ADCC and adds direct cytotoxicity. The original trastuzumab trial is a useful evidence anchor because it tied receptor overexpression to a matched intervention and patient outcomes, not just a pathway diagram [Slamon et al., 2001].

8.2.7 The MAP Kinase Cascade — Three-Tier Hierarchy

The MAP kinase (MAPK) cascade is the canonical example of a multi-tier signaling cascade. Eukaryotes have multiple parallel MAPK cascades; the best-studied is the classical (ERK) MAPK cascade, but JNK and p38 stress-activated cascades follow the same architecture:

1. MAPKKK (MAP kinase kinase kinase) — activated by upstream signals (e.g., Ras-GTP for ERK; MEKK1 for JNK; ASK1 for p38).
2. MAPKK (MAP kinase kinase) — phosphorylated and activated by MAPKKK on two serines/threonines; in turn, dual-specificity kinase (Ser/Thr/Tyr) for the next tier.
3. MAPK — phosphorylated by MAPKK on Thr-X-Tyr motif in the activation loop; both phosphorylations required for activity.

Table 124. The MAP Kinase Cascade — Three-Tier Hierarchy: Cascade and MAPKKK.

Cascade	MAPKKK	MAPKK	MAPK	Activated by	Output
Classical (ERK)	RAF (A-, B-, C-RAF)	MEK1/2	ERK1/2	Growth factors (RTKs); RAS-GTP	Proliferation, differentiation
JNK	MEKK1, MLK1-3, ASK1	MKK4, MKK7	JNK1/2/3	Cytokines, UV, stress	Stress response, apoptosis
p38	MTK1, MEKK3, ASK1	MKK3, MKK6	p38 ($\alpha, \beta, \gamma, \delta$)	Inflammation, osmotic stress	Cytokine production, cell-cycle arrest
ERK5	MEKK2, MEKK3	MEK5	ERK5	Growth factors, oxidative stress	Proliferation, vascular development

Why three tiers? The architecture provides: - Amplification — three sequential gain stages (each about 10×) → 1000× total amplification. - Ultrasensitivity — dual-phosphorylation requirement at the MAPK tier creates an effective $n_H \approx 5$ at the output, converting graded input into switch-like ERK activity (Huang & Ferrell 1996). - Insulation by scaffolds — KSR1 binds RAF, MEK1, and ERK1; this prevents undesired cross-activation between parallel MAPK cascades that share components. Yeast pheromone-response cascade uses Ste5 scaffold; mammals use KSR1 (ERK), JIP1 (JNK), OSM (p38). - Negative feedback by specific phosphatases — DUSP1-6 (dual-specificity phosphatases / MKPs) selectively dephosphorylate specific MAPKs; their expression is itself induced by ERK, creating a delayed negative feedback that produces transient ERK activation.

The combination of cascade ultrasensitivity + scaffold insulation + DUSP feedback is why activation of “the same RAS-MAPK pathway” can produce *opposite* outcomes depending on context: transient activation → proliferation (ERK off before cell-cycle arrest); sustained activation → differentiation (ERK on long enough to upregulate p21 and exit the cycle); even higher activation → senescence (ERK-driven oncogene-induced senescence). Cell fate is encoded in the *temporal pattern* of ERK, not just its peak amplitude.

Key pathway components:

Table 125. The MAP Kinase Cascade — Three-Tier Hierarchy: Component and Function.

Component	Function	Human disease when mutated
EGFR (ErbB1)	RTK; EGF binding	Non-small cell lung cancer
HER2 (ErbB2)	RTK; no known ligand; heterodimerises	Breast cancer (amplified in about 25%)
RAS (K-RAS, H-RAS, N-RAS)	Small GTPase; molecular switch	Pancreatic (about 95%), colorectal (about 40%), lung (about 30%)
RAF (B-RAF)	Ser/Thr kinase (MAPKKK)	Melanoma (V600E, about 50%), thyroid cancer
NF1 (neurofibromin)	RAS-GAP (turns RAS off)	Neurofibromatosis type 1

Component	Function	Human disease when mutated
PTEN	PIP ₃ phosphatase (opposes PI3K)	Glioblastoma, prostate, endometrial cancer

8.2.8 Ligand-Gated Ion Channels

Direct coupling of ligand binding to ion flow, bypassing G proteins. Fastest signaling (about ms).

- Nicotinic acetylcholine receptor (nAChR): pentameric (alpha₂-beta-gamma-delta); 2 ACh bind → conformational change → Na⁺/K⁺ channel opens → **depolarization** → muscle contraction
- GABA_A receptor: Cl[−] channel; GABA binding → Cl[−] influx → hyperpolarization → inhibition. Target of benzodiazepines (bind **allosteric** site → enhanced Cl[−] flux → sedation/anxiolysis). Also target of barbiturates, ethanol, and general anaesthetics.
- NMDA glutamate receptor: requires simultaneous glutamate + glycine binding AND membrane depolarization to remove Mg²⁺ block; Ca²⁺ entry → CaMKII activation → LTP (Learning and memory). Coincidence detector for Hebbian learning.

Concept Check 2: Curare blocks nAChRs at the neuromuscular junction. Predict the clinical effects. How does this differ from the effect of an acetylcholinesterase inhibitor (e.g., neostigmine)?

Concept Check (Analysis): Receptor tyrosine kinases (RTKs) activate Ras through the SOS-GEF mechanism. The Ras-GTP → Ras-GDP step is intrinsically slow ($k_{cat} \sim 10^{-4} \text{ s}^{-1}$) but is about 10⁵-fold accelerated by GAPs (GTPase-Activating Proteins). (a) Why does the cell need both intrinsic GTPase activity and GAP acceleration — what would happen to Ras signaling if GAPs were absent? (b) Oncogenic Ras mutations (G12V, Q61L) abolish GAP sensitivity while retaining GTP binding — calculate how long Ras-GTP would persist in a cell with [GTP] = 0.5 mM if solely intrinsic GTPase operates ($t_{1/2} = \ln 2/k_{cat} \approx 7000 \text{ s} \approx 2 \text{ h}$). (c) The drug sotorasib (AMG-510) covalently targets KRAS G12C specifically. Explain the chemical basis of this selectivity (G12C introduces a cysteine near the switch-II/GTPase active site, accessible to a Michael-acceptor warhead) and why this approach cannot work for G12V or G12D mutations.

Worked Example — cAMP Cascade Amplification: Epinephrine at [Epi] = 1 nM binds β-adrenergic receptors ($K_d = 0.3 \text{ nM}$; fractional occupancy = $1/(1 + K_d/[Epi]) = 1/(1 + 0.3) \approx 0.77$, or 77%). Each occupied receptor activates about 100 Gα_s molecules over its active lifetime (about 10 s at about 10 activations/s). Each active Gα_s activates one adenylyl cyclase for about 10 s, producing about 1,000 cAMP molecules. Each PKA molecule, once activated by 2 cAMP, phosphorylates about 100 substrate molecules per minute. Cascade amplification per 1 receptor: $1 \times 100 \text{ G}\alpha_s \times 1,000 \text{ cAMP} \times 100 \text{ substrates} \approx 10^7$. Starting from a single hormone molecule and 77% receptor occupancy across the cell-surface receptor population, the integrated amplification factor reaches about 10⁸–10⁹ phosphorylated glycogen-phosphorylase molecules per bound hormone. This is why a single epinephrine release event can produce a measurable physiological response (heart-rate, glycogenolysis) within about 30 seconds.

8.3 Intracellular Receptors for Lipid-Soluble Signals

Lipophilic signaling molecules (steroid hormones, thyroid hormone, retinoic acid, vitamin D) diffuse through the membrane and bind cytoplasmic or nuclear receptors — ligand-activated transcription factors. The nuclear receptor superfamily includes 48 members in humans.

Classic glucocorticoid pathway: 1. Cortisol crosses membrane (lipophilic) 2. Binds glucocorticoid receptor (GR) in **cytoplasm** 3. Hsp90 dissociates; GR dimerises 4. Translocates to nucleus via NLS 5. Binds glucocorticoid response elements (GREs) in DNA (consensus: AGAACAAnnTGTTCT) 6. Recruits coactivators (SRC-1, p300/CBP) → transcriptional activation

Target genes include anti-inflammatory (IκB-alpha, annexin A1), gluconeogenic (PEPCK, G6Pase), and immunosuppressive genes. Dexamethasone (synthetic glucocorticoid) is widely used for inflammation and autoimmune disease.

Other nuclear receptors: - Estrogen receptor (ER-alpha, ER-beta): breast development, bone density; tamoxifen (antagonist) for breast cancer - PPAR-gamma: lipid metabolism, adipocyte differentiation; thiazolidinediones (rosiglitazone) for type 2 diabetes - Thyroid hormone receptor (TR): metabolic rate; T3 binding activates genes for thermogenesis and development - Vitamin D receptor (VDR): calcium **homeostasis**; calcitriol binding activates genes for Ca²⁺ absorption

8.4 Developmental, Cytokine, and Termination Pathways

8.4.1 Wnt/Beta-Catenin Pathway

Without Wnt signal: Beta-catenin is phosphorylated by the “destruction complex” (APC + Axin + GSK-3-beta + CK1-alpha) → ubiquitinated by beta-TrCP → proteasomal degradation. Target genes are off.

With Wnt signal: Wnt binds Frizzled receptor + LRP5/6 co-receptor → Dishevelled recruited → destruction complex inhibited (Axin sequestered to LRP6) → beta-catenin accumulates → enters nucleus → binds TCF/LEF transcription factors → activates target genes (c-Myc, cyclin D1, Axin2).

Clinical significance: APC **mutations** (loss of destruction complex function) are found in >80% of colorectal cancers (familial adenomatous polyposis, FAP). Beta-catenin is also critical for stem cell maintenance in the intestinal crypt.

8.4.2 JAK-STAT Pathway

Cytokine receptors (e.g., IL-6R, IFN receptors, erythropoietin receptor) lack intrinsic kinase activity. Instead, they associate with Janus kinases (JAK1, JAK2, JAK3, TYK2):

1. Cytokine binding → receptor dimerization
2. JAKs trans-phosphorylate each other and the receptor
3. STAT proteins (Signal Transducers and Activators of Transcription) bind phosphotyrosines via SH2 domains
4. JAKs phosphorylate STATs
5. Phospho-STATs dimerise and translocate to the nucleus
6. STAT dimers bind DNA → activate target genes

Clinical significance: - JAK2 V617F mutation: found in >95% of polycythaemia vera (constitutive JAK2 activation → excess red blood cell production) - JAK inhibitors (ruxolitinib, tofacitinib) are used for myeloproliferative disorders and rheumatoid arthritis - STAT3 is constitutively active in many cancers → survival and proliferation

8.4.3 Notch Pathway and Contact-Dependent Cell Fate

Direct cell-cell signaling (juxtacrine): 1. Delta/Jagged ligand on one cell binds Notch receptor on adjacent cell 2. Ligand **endocytosis** generates mechanical force 3. ADAM protease cleaves Notch extracellular domain 4. Gamma-secretase cleaves transmembrane domain, releasing NICD (Notch intracellular domain) 5. NICD translocates to nucleus → binds CSL (RBP-J) transcription factor → activates Hes/Hey target genes

Clinical significance: Notch1 activating mutations occur in about 60% of T-cell acute lymphoblastic leukaemia. Gamma-secretase inhibitors are in clinical trials.

8.4.4 Signal Termination Mechanisms

Table 126. Signal Termination Mechanisms: Mechanism and Target.

Mechanism	Target	Example
GTPase activity	G proteins, RAS	Intrinsic GTPase + GAPs (RGS, NF1)
Phosphodiesterases	cAMP, cGMP	PDE4 (lung), PDE5 (smooth muscle)
Protein phosphatases	Phosphoproteins	PP1, PP2A, calcineurin, PTEN, MKPs
Receptor internalization	Surface receptors	GRK/beta-arrestin → clathrin-mediated endocytosis
Ubiquitin-proteasome	Signaling proteins	c-Cbl ubiquitinates EGFR; SCF targets beta-catenin
Negative feedback	Pathway components	SOCS proteins inhibit JAK-STAT; Sprouty inhibits RAS-MAPK

Concept Check 3: A mutation in NF1 (neurofibromin, a RAS-GAP) causes neurofibromatosis type 1. Explain why loss of a GAP protein leads to tumor formation, and predict the effect on RAS-GTP levels.

8.5 Crosstalk and Signal Integration

Cells rarely respond to a single signal in isolation. Instead, multiple pathways interact through crosstalk — shared components, convergent effectors, or mutual regulation. Signal integration is what allows a cell to make complex decisions (proliferate, differentiate, or die) based on the totality of its signaling environment.

8.5.1 Convergence and Divergence

Convergence: Multiple upstream signals activate the same downstream effector. For example, both RTK/RAS/MAPK and Wnt/beta-catenin pathways converge on cyclin D1 transcription, reinforcing the G1-to-S transition. Both growth factor (PI3K/Akt) and integrin signaling converge on mTORC1 to control cell growth

Divergence: A single activated receptor triggers multiple downstream cascades simultaneously. EGFR activation simultaneously engages: - RAS-MAPK (proliferation) - PI3K-Akt (survival) - PLC-gamma/IP₃/Ca²⁺ (immediate responses) - JAK-STAT (gene expression) - c-Src (cytoskeletal remodeling)

8.5.2 Scaffold Proteins and Signaling Specificity

Scaffold proteins physically assemble pathway components, ensuring speed, specificity, and prevention of unwanted crosstalk:

Table 127. Scaffold Proteins and Signaling Specificity: Scaffold and Pathway.

Scaffold	Pathway	Function
KSR1	RAS-MAPK	Brings RAF, MEK, and ERK together; promotes efficient cascade activation
AKAP79/150	cAMP-PKA	Anchors PKA, calcineurin (PP2B), and PKC near substrates (e.g., ion channels)
Axin	Wnt	Core scaffold of the beta-catenin destruction complex
InaD	Drosophila phototransduction	PDZ-domain scaffold holding PLC, TRP channel, and PKC
mTORC1/2	PI3K-mTOR	Raptor (mTORC1) vs. Rictor (mTORC2) determine substrate access

Scaffold proteins explain how the same MAPK cascade can produce different outcomes in different cell types: the scaffold determines which substrates are phosphorylated.

8.5.3 Positive and Negative Feedback Loops

Positive feedback creates switch-like (bistable [Tyson et al., 2003]) responses: - ERK phosphorylates and activates SOS (its own upstream GEF), creating an ultrasensitive on/off switch - p53 activates MDM2, which degrades p53 — but also activates PUMA/NOXA, creating a “point of no return” for apoptosis once the death threshold is crossed - Caspase-3 cleaves and activates caspase-9 (amplification loop in apoptosis)

Negative feedback limits signal duration and creates adaptation: - ERK phosphorylates SOS at inhibitory sites (slow negative feedback counteracts fast positive feedback) - SOCS proteins induced by JAK-STAT signaling bind JAKs and target them for degradation - Sprouty (SPRY) proteins inhibit RAS-MAPK at the level of GRB2-SOS recruitment

- Concept Check 5: The MAPK cascade exhibits both positive feedback (ERK activates SOS) and negative feedback (ERK inhibits SOS at different sites). How might the relative timing of these feedbacks create a transient burst of ERK activity followed by adaptation? What would happen if the negative feedback were eliminated by mutation?
- Concept Check 6: A patient with BRAF V600E melanoma is treated with vemurafenib (BRAF inhibitor) alone. Initial response is dramatic, but resistance develops in 6–12 months. Sequencing reveals upregulation of CRAF, NRAS amplification, or MEK1 mutations in different patients. Explain why each of these “bypasses” vemurafenib and why combination therapy with trametinib (MEK inhibitor) achieves more durable responses.
- Concept Check 7: A neuron at rest contains about 10^{−7} M cytoplasmic [Ca²⁺]. Following an action potential, [Ca²⁺] near a synaptic vesicle rises to about 10^{−5} M for about 1 ms before being buffered and pumped back. Synaptotagmin has 2 C2 domains, each binding 2–3 Ca²⁺ ions cooperatively (Hill coefficient about 3). Explain why this molecular architecture produces an essentially “most-or-nothing” exocytotic response to the brief calcium pulse, and how this differs from the sustained calcium signals used in CaMKII-mediated long-term potentiation.

Concept Check 8: A scaffold protein binds both an upstream kinase (RAF) and a downstream substrate (ERK) but does not bind the intermediate kinase (MEK). Predict the qualitative effect on signal transmission. What does this suggest about why the three components must be present on the scaffold for productive signaling?

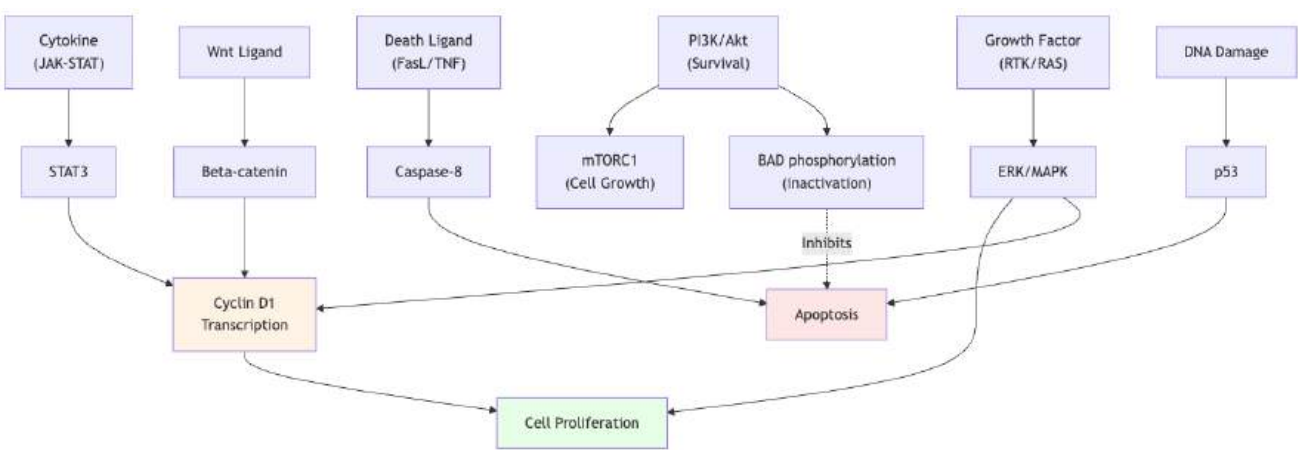


Figure 57. Signal integration: multiple pathways converge on key decision nodes. Proliferative signals (RTK, Wnt, cytokines) converge on cyclin D1 transcription. Survival signals (PI3K/Akt) antagonise apoptosis by phosphorylating BAD. The cell’s fate (proliferation, growth, or death) depends on the balance of active pathways.

8.5.4 Computational Approaches to Signaling Networks

Modern systems biology uses mathematical modeling to understand signaling network behavior:

- Boolean networks: model each node as ON/OFF; useful for large networks
- Ordinary differential equations (ODEs): model concentration changes over time; quantitative predictions
- Stochastic modeling: accounts for molecular noise in low-copy-number signaling (important in stem cell fate decisions)

The Huang-Ferrell model of the MAPK cascade demonstrated that the cascade acts as an ultrasensitive switch: small changes in input (growth factor concentration) produce most-or-none output (ERK activation). This switch-like behavior arises from the dual phosphorylation requirement for ERK activation.

8.6 The Cell Cycle — Control Through CDK-Cyclin Complexes

Cell division is controlled by cyclin-dependent kinases (CDKs) activated by their partner cyclins (Nobel Prize 2001: Hartwell, Hunt, Nurse).

8.6.1 Cell-Cycle Phases and CDK-Cyclin Control

Table 128. Cell-Cycle Phases and CDK-Cyclin Control: Phase and Event.

Phase	Event	Duration (typical animal cell)	Key CDK-Cyclin
G1	Growth; protein synthesis	6–12 h	CDK4/6-Cyclin D
S	DNA replication	6–8 h	CDK2-Cyclin E/A
G2	Growth; mitosis preparation	3–5 h	CDK1-Cyclin A
M	Mitosis + cytokinesis	about 1 h	CDK1-Cyclin B (MPF)

Checkpoints ensure cell cycle quality: - G1 checkpoint (restriction point): cell size adequate? DNA intact? Growth factors present? CDK4/6-Cyclin D drives pRB phosphorylation → E2F release → S-phase genes (cyclin E, DNA polymerase, thymidine kinase) - G2/M checkpoint: DNA repair complete? CDK1-Cyclin B (MPF — maturation-promoting factor) triggers mitotic entry. Activated by CDC25 phosphatase; inhibited by Wee1 kinase. - Spindle assembly checkpoint (SAC): most kinetochores attached to microtubules? Mad2/BubR1 inhibit Anaphase Promoting Complex (APC/C) until satisfied. APC/C then ubiquitinates securin → separase released → cleaves cohesin → sister chromatid separation.

8.6.2 Tumor Suppressors and Checkpoint Control

- p53: “guardian of the **genome**”; activated by DNA damage (via ATM/ATR kinases, Chk1/Chk2) → arrests cell cycle (via p21/WAF1 inhibiting CDK2) or triggers apoptosis (via PUMA, NOXA); mutated in about 50% of human cancers. MDM2 is the E3 ubiquitin ligase that normally keeps p53 levels low; MDM2 inhibitors (nutlins) are in clinical trials.
- pRB: binds and represses E2F in G1; CDK4/6 phosphorylation releases E2F → S phase entry; mutated/deleted in retinoblastoma and many cancers. CDK4/6 inhibitors (palbociclib, ribociclib) are used in HR⁺ breast cancer.

Clinical Connection: CDK4/6 Inhibitors in Cancer Palbociclib, ribociclib, and abemaciclib specifically inhibit CDK4/6, preventing pRB phosphorylation and maintaining E2F repression. This arrests cancer cells in G1. These drugs have transformed treatment of hormone receptor-positive, HER2-negative metastatic breast cancer, doubling progression-free survival when combined with anti-estrogen therapy.

8.7 Apoptosis — Programmed Cell Death

Apoptosis eliminates about 80 billion cells per day in the adult human (equal to approximate cell proliferation). It differs fundamentally from necrosis:

Table 129. Tumor Suppressors and Checkpoint Control: Feature and Apoptosis.

Feature	Apoptosis	Necrosis
Initiation	Genetically programmed	Accidental
Morphology	Cell shrinkage; DNA laddering; apoptotic bodies	Cell rupture; inflammation
Inflammation	None (PS “eat me” signal)	Severe (DAMPs released)
ATP required	Yes	No
Caspases	Activated	Not involved

8.7.1 Intrinsic (Mitochondrial) Pathway

Triggered by DNA damage, oxidative stress, growth factor withdrawal:

1. BH3-primarily proteins (Bad, Bid, Puma, NOXA) activated by cellular stress
2. BH3-primarily proteins neutralize anti-apoptotic Bcl-2/Bcl-xL
3. BAX/BAK oligomerise in the OMM → form pores (MAC channel)
4. Cytochrome c released from intermembrane space into cytoplasm
5. Cytochrome c + Apaf-1 + ATP/dATP → apoptosome (7-subunit wheel, about 1 MDa)
6. Apoptosome activates caspase-9 (initiator caspase)
7. Caspase-9 activates caspase-3/-7 (executioner caspases)
8. Caspases cleave structural proteins (nuclear lamins, ICAD releasing CAD endonuclease → DNA fragmentation into about 180 bp nucleosomal ladders)

Bcl-2 family: anti-apoptotic members (Bcl-2, Bcl-xL, Mcl-1) bind and inhibit BAX/BAK. Bcl-2 overexpression in follicular lymphoma (t(14;18) translocation) → cells cannot die. Venetoclax is a BH3 mimetic drug that inhibits Bcl-2, restoring apoptosis in chronic lymphocytic leukaemia (CLL).

8.7.2 Extrinsic (Death Receptor) Pathway

Triggered by extracellular death ligands (FasL, TNF-alpha, TRAIL):

1. Ligand binds death receptor (FAS/CD95, TNFR1, DR4/DR5)
2. Death domain oligomers recruit FADD (Fas-associated death domain protein)
3. Procaspase-8 recruited → DISC (Death-Inducing Signaling Complex)
4. Caspase-8 auto-activated
5. In Type I cells: caspase-8 directly activates caspase-3 (sufficient DISC formation)
6. In Type II cells: caspase-8 cleaves Bid → tBid → activates mitochondrial pathway (amplification loop)

8.7.3 Other Forms of Regulated Cell Death

Beyond classical apoptosis, several other regulated cell death pathways have been identified:

- Necroptosis: Programmed necrosis triggered by TNF when caspase-8 is inhibited. RIPK1 and RIPK3 kinases phosphorylate MLKL, which oligomerises and permeabilises the plasma membrane. Important in host defense against viruses that express caspase inhibitors.
- Pyroptosis: Inflammatory cell death mediated by gasdermin D (GSDMD). Inflammasome activation (NLRP3, NLRC4, AIM2) activates caspase-1, which cleaves GSDMD. The N-terminal fragment forms pores in the plasma membrane, releasing IL-1-beta and IL-18. Critical in **innate immunity** and sepsis.
- Ferroptosis: Iron-dependent cell death characterized by lipid peroxidation. GPX4 (glutathione peroxidase 4) normally prevents lethal lipid ROS accumulation. GPX4 inhibition or glutathione depletion triggers ferroptosis. Relevant in neurodegeneration, kidney injury, and cancer therapy (some drug-resistant tumors are susceptible to ferroptosis inducers).

Clinical Connection: Ferroptosis in Cancer Therapy Drug-resistant cancer cells that have undergone epithelial-mesenchymal transition (EMT) become highly susceptible to ferroptosis. This vulnerability arises because EMT upregulates polyunsaturated fatty acid (PUFA) incorporation into membrane phospholipids, increasing susceptibility to lipid peroxidation. Ferroptosis-inducing agents (erastin, RSL3) are being investigated as therapies for therapy-resistant cancers. Understanding cell death pathway diversity is critical for developing next-generation anti-cancer strategies.

8.8 Cancer as Dysregulated Signaling

Cancer results from accumulated mutations that activate oncogenes (gain-of-function) and inactivate tumor suppressors (loss-of-function), disrupting normal signaling control.

8.8.1 Oncogenes and Their Normal Counterparts

Table 130. Oncogenes and Their Normal Counterparts: Proto-oncogene and Normal function.

Proto-oncogene	Normal function	Oncogenic mutation	Cancer type
RAS (K-RAS, N-RAS)	Small GTPase (MAPK pathway)	Point mutations (G12D, G12V, Q61L) lock in GTP state	Pancreatic, colorectal, lung
RAF (B-RAF)	Ser/Thr kinase (MAPK pathway)	V600E constitutive activation	Melanoma, thyroid, colorectal
EGFR (ErbB1)	RTK (growth factor receptor)	Amplification; activating mutations	Lung (NSCLC), glioblastoma
HER2 (ErbB2)	RTK (no ligand, heterodimerises)	Gene amplification (about 25% breast cancer)	Breast, gastric
MYC	Transcription factor (cell growth)	Amplification; translocation (t(8;14))	Burkitt lymphoma, many cancers
BCR-ABL	Constitutive tyrosine kinase	t(9;22) Philadelphia chromosome	CML
PIK3CA	PI3K catalytic subunit	E545K, H1047R activating mutations	Breast, endometrial, colorectal

8.8.2 Targeted Cancer Therapies

Table 131. Targeted Cancer Therapies: Drug and Target.

Drug	Target	Mechanism	Cancer
Imatinib (Gleevec)	BCR-ABL tyrosine kinase	ATP-competitive inhibitor	CML
Trastuzumab (Herceptin)	HER2 extracellular domain	Monoclonal antibody; ADCC + signaling block	HER2 ⁺ breast cancer
Vemurafenib	B-RAF V600E	ATP-competitive inhibitor	Melanoma
Erlotinib/Gefitinib	EGFR kinase domain	ATP-competitive inhibitor	NSCLC
Palbociclib	CDK4/6	Prevents pRB phosphorylation	HR ⁺ breast cancer
Venetoclax	Bcl-2	BH3 mimetic; restores apoptosis	CLL

Drug	Target	Mechanism	Cancer
Pembrolizumab	PD-1	Immune checkpoint inhibitor	Melanoma, lung, many others
Sotorasib	K-RAS G12C	Covalent inhibitor (first RAS drug)	NSCLC

Clinical Connection: Imatinib — The Paradigm of Targeted Therapy Chronic myeloid leukaemia (CML) is caused by the Philadelphia chromosome — a t(9;22) translocation creating the BCR-ABL fusion protein (constitutively active tyrosine kinase). Before imatinib, 5-year survival was about 30%. Imatinib specifically inhibits BCR-ABL by occupying the ATP-binding site, achieving complete cytogenetic response in >80% of patients and transforming CML into a manageable chronic disease. This “bench-to-bedside” success story (Brian Druker, Nicholas Lydon) demonstrated that understanding signaling pathways at the molecular level can lead to revolutionary therapies.

8.8.3 Clinical Pharmacology of Cell Signaling

Cell signaling is the most pharmacologically tractable layer of cellular biology — most major drug classes either activate, inhibit, or compete with components of a signaling cascade. Understanding the molecular logic of signaling therefore translates directly into rational pharmacology. Three case studies illustrate the depth of this connection.

β -Blockers: from signal blockade to chronic-disease treatment. Propranolol (1964, James Black, Nobel Prize 1988) was the first β -adrenergic receptor antagonist. It blocks β_1 receptors on cardiomyocytes (reducing heart rate and contractility, lowering oxygen demand) and β_2 receptors on bronchial smooth muscle (sometimes causing wheeze in asthmatics). Modern β -blockers are graded by selectivity: - Non-selective: propranolol, carvedilol — block β_1 , β_2 , sometimes α_1 . - β_1 -selective (“cardioselective”): metoprolol, atenolol, bisoprolol — preferred when bronchospasm is a concern. - Inverse agonists: carvedilol — actively reduces basal G-protein activity, not just blocks ligand binding. - Biased agonists/antagonists: carvedilol, alprenolol — block G_s but activate β -arrestin signaling, possibly explaining superior heart failure outcomes.

The mechanistic depth has grown over 60 years: from “block adrenaline binding” → “reduce cAMP” → “decouple from G-protein” → “biased toward β -arrestin/ERK” → “remodel chronic gene expression patterns in failing heart.” A drug class that began as symptomatic therapy for angina is now first-line in heart failure precisely *because* it modulates the chronic-stress signaling fingerprint.

Statins: targeting the substrate of a regulatory cascade. HMG-CoA reductase catalyses the rate-limiting step of cholesterol biosynthesis. Statins (lovastatin from *Aspergillus* in 1976; simvastatin, atorvastatin, rosuvastatin) are competitive inhibitors with IC_{50} about 10 nM. Lower hepatic cholesterol synthesis → upregulation of LDL receptor (via SREBP-2 transcription factor) → increased LDL clearance from blood → about 30–50% reduction in LDL cholesterol. Beyond cholesterol, statins have pleiotropic effects mediated by reduced isoprenoid (farnesyl, geranylgeranyl) production: reduced membrane localization of Rho/Rac GTPases (anti-inflammatory), reduced platelet aggregation, improved endothelial function. Many of these effects are arguably more important than cholesterol lowering for cardiovascular outcomes — supported by clinical trials showing benefit even in patients with normal LDL.

Imatinib in detail: lessons in resistance. Imatinib (Gleevec, 2001) binds the inactive (“DFG-out”) conformation of the BCR-ABL kinase domain at its ATP-binding site. The drug exploits a structural quirk: the BCR-ABL kinase domain has a hydrophobic pocket that becomes accessible primarily in the inactive conformation; this pocket is *not* present in most other kinases, providing remarkable selectivity. Resistance develops through several mechanisms:

Table 132. Clinical Pharmacology of Cell Signaling: Mechanism and Frequency.

Mechanism	Frequency	Example	Solution
Point mutations in kinase domain	Most common	T315I (gatekeeper residue)	Ponatinib (third-generation, designed against T315I)
BCR-ABL amplification	Less common	More fusion protein than drug can inhibit	Higher dose or switch class
Activation of bypass pathways	Variable	SRC family kinases, PI3K	Add SRC inhibitor (dasatinib)
Decreased intracellular drug	Variable	OCT1 transporter loss; MDR1 export	Drug-uptake-independent agents

This pattern — initial dramatic response, eventual development of resistance via mutation or bypass — is now the norm in targeted oncology. Modern strategies use combination therapy designed against the resistance landscape: BRAF + MEK inhibitors in melanoma, BCR-ABL + PI3K in CML resistance, EGFR + MEK in lung cancer.

Concept Check 4b: A patient with CML on imatinib for 3 years develops disease progression. Sequencing reveals a T315I mutation in BCR-ABL. Why does this single amino-acid change confer resistance, and which next-generation drug would you choose? (Hint: T315 is the “gatekeeper” residue lining the imatinib binding pocket.)

8.8.4 Crosstalk and Signal Integration — How Cells Process Multiple Signals

A real cell is not exposed to a single ligand at a time. A hepatocyte receives glucagon, insulin, growth factors, fatty acids, cytokines, and adhesion signals *simultaneously*, and must integrate most of them into a coherent metabolic and proliferative response. Three architectural features make this integration possible:

1. Shared second messengers. Many pathways feed into Ca^{2+} , cAMP, or phosphoinositides. The cell’s “state” is encoded in the time-integrated and spatially-resolved levels of these second messengers, not in any single signaling event.
2. Coincidence detection. Some effectors require *two simultaneous* inputs: PKC is fully activated primarily when both DAG (membrane targeting) and Ca^{2+} (cytosolic increase) are present; NMDA receptor opens primarily when glutamate binds *and* the membrane is sufficiently depolarized. Coincidence detection prevents false alarms.
3. Conditional rules (logic gates). Cells implement Boolean-like decision rules. Cell proliferation in normal epithelia requires growth factor (mitogen) AND adhesion (integrin) AND survival (PI3K/Akt). Loss of any one input causes anoikis (death by detachment) or quiescence. Cancer typically defeats these rules by activating each independently.

Concrete examples of crosstalk:

- Insulin–glucagon antagonism in liver. Both signals reach the same hepatocyte. Insulin (via Akt) inhibits gluconeogenic gene expression; glucagon (via cAMP/PKA) activates it. The PEPCK and G6Pase promoters are bound by both insulin-responsive (FoxO1) and cAMP-responsive (CREB) transcription factors with opposing effects — the integrated transcriptional output reflects the [insulin]/[glucagon] ratio.
- Growth factor + integrin convergence on mTORC1. Growth factor → RTK → PI3K → Akt → TSC1/2 inhibition → Rheb-GTP → mTORC1. Integrin → FAK → PI3K → same Akt step. Both inputs are required for full mTORC1 activation; loss of either prevents protein synthesis and cell growth, providing a checkpoint against unanchored proliferation.
- Stress → MAPK pathway crosstalk. TNF- α activates IKK → NF- κ B (survival) AND MEKK1 → JNK (apoptosis). The ratio determines outcome: brief TNF → NF- κ B dominates → survival; prolonged TNF or with cyclohexamide (NF- κ B-blocking) → JNK dominates → apoptosis.

Computational modeling of integration. Modern systems biology builds these rules into ordinary differential equations (ODEs) or Boolean networks. A 2009 paper by Janes & Yaffe (*Nature Reviews MCB*) showed that 200+ measurements of signaling components in TNF-treated cells could be reduced to a few partial least squares (PLS) components that predicted apoptosis vs. survival outcomes. The lesson: cells appear to combine many inputs in a low-dimensional decision space — a finding that simplifies both basic understanding and drug design (modulate the dominant principal components, not 200 individual proteins).

Concept Check 4: Why would a combination of a BRAF inhibitor (vemurafenib) and a MEK inhibitor (trametinib) be more effective than either alone in BRAF V600E melanoma? Consider pathway reactivation mechanisms.

8.9 Computational Bridge

Cooperative ligand binding (Hill) captures RTK/RAS-MAPK dosage responses in reduced form:

```
from biology.cell import hill_equation

theta = hill_equation(8.0, kd=10.0, hill_coefficient=2.8)
print(round(theta, 4))
```

Clinical / systems note: Dose-response steepness from cooperativity is one reason combination targeted therapy can widen the therapeutic window compared with single-agent saturation of one node.

8.9.1 Spatial Transcriptomics: Signaling in Tissue Context

Single-cell RNA-sequencing (scRNA-seq) dissociates tissues and so loses the spatial information that is often the point — you can measure what each cell expresses but not where it sits relative to its neighbors. Spatial transcriptomics (ST) recovers that geometry by coupling *in situ* RNA capture or detection to high-throughput sequencing or imaging.

Two commercial platforms dominate. 10× Genomics Visium prints a glass slide with about 5000 barcoded spots (55 μm diameter, about 100 μm spacing); a fresh-frozen tissue section is placed on the slide, RNA diffuses into the spots, and each spot’s transcriptome is sequenced with its spot barcode. Resolution is sub-cellular to small-cluster (1–10 cells per spot). MERFISH (Multiplexed Error-Robust FISH) and seqFISH+ instead use combinatorial error-correcting fluorescent in situ hybridization to detect thousands of transcripts at diffraction-limited (about 100 nm) resolution — true single-molecule, single-cell spatial mapping. Slide-seq and Stereo-seq push sequencing-based approaches toward 10 μm and 500 nm spot sizes respectively.

Why this matters for signaling: paracrine and juxtacrine signaling — Notch–Delta, ephrin–Eph, WNT morphogen gradients — depend on cells *being close to each other*. Spatial transcriptomics lets investigators map ligand-expressing cells next to receptor-expressing cells across a whole tissue section and infer ligand-receptor interaction networks in situ (tools: CellChat, NicheNet, SpatialCellChat, 2022–2024). In tumor biology, ST reveals **niches** of exhausted T cells in immunologically “cold” regions of the same tumor, motivating spatially-guided immunotherapy combinations. In developmental biology, ST in mouse embryos (Stereo-seq, *Cell* 2022) produced the first cell-resolved, tissue-resolved organogenesis atlas. The technology cost has dropped about 10x every two years; a whole-slide Visium experiment costs about \$2000 in 2024. For the student, ST is the bridge between molecular cell biology (“what genes are on?”) and anatomy (“where?”) — and it is the platform on which the next decade of in situ discovery will be built.

8.10 Current Evidence and Frontier Biology: Cell Signaling and Communication

For Cell Signaling and Communication, frontier biology belongs inside the evidence logic of the chapter. Cell biology is increasingly measured as live, spatial, single-cell, and perturbational data rather than static diagrams alone. The core reading question is this: signaling explanations should include receptor context, dose, timing, feedback, crosstalk, and cellular state.

- What to verify: identify the observation, model, assay, or dataset that would make the claim stronger or weaker.
- What to qualify: state the scale, organism, cell type, environmental condition, or population where the claim is expected to hold.
- What to compare: test at least one alternative explanation, baseline, or null model before treating the pattern as causal.
- What to cite: distinguish primary evidence, review synthesis, public dataset, and institutional guidance; for recent or numeric claims, prefer the source closest to the measurement and state what has changed since it was published.

For signaling claims, identify the ligand, receptor state, second messenger, timescale, and feedback branch before naming a pathway as causal.

Source practice: Separate live-cell perturbation, phosphoproteomics, reporter assays, and single-cell data before inferring pathway direction or decision logic.

8.10.1 Current Evidence Map: Spatial Single-Cell Signaling Evidence

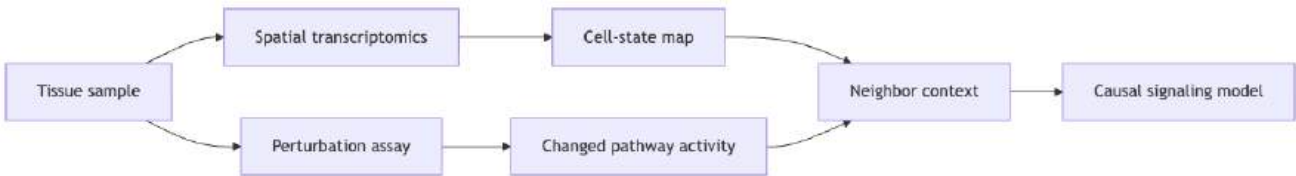


Figure 58. A signaling claim is stronger when receptor state, ligand source, cell neighborhood, and perturbation response point to the same mechanism.

8.11 Summary

- Cell signaling: ligand → receptor → cascade → response. GPCRs use cAMP or IP₃/DAG via heterotrimeric G proteins; RTKs use tyrosine phosphorylation and the RAS-MAPK cascade; ion channels open immediately upon ligand binding.
- Second messengers (cAMP, cGMP, IP₃, DAG, Ca²⁺, PIP₃) amplify and diversify signals within the cell.
- Signal termination involves GTPase activity, phosphodiesterases, protein phosphatases, receptor internalization, and ubiquitin-mediated degradation.
- The Wnt/beta-catenin, JAK-STAT, and Notch pathways control development, immune function, and stem cell maintenance.
- The cell cycle is governed by CDK-cyclin complexes; checkpoints (G1, G2/M, SAC) ensure fidelity. p53 and pRB are the primary tumor suppressors.
- Apoptosis (programmed cell death) proceeds via intrinsic (mitochondrial) or extrinsic (death receptor) pathways, both converging on executioner caspases.
- Cancer results from dysregulated signaling (oncogenes + tumor suppressor loss); targeted therapies exploit specific pathway dependencies.
- Connections: See **Unit IV — Molecular Genetics: Introduction** (growth-factor-driven transcription), **Unit V — Classical Genetics and Heredity: Introduction** (tumor suppressor alleles), **Unit IX — Zoology and Systems Physiology: Introduction** (endocrine first messengers).

8.12 Review Questions

1. Draw the complete G_s -cAMP-PKA signaling cascade from epinephrine binding to glycogen breakdown. Identify most amplification steps and termination mechanisms.
2. Compare and contrast GPCRs and RTKs in terms of structure, mechanism of activation, downstream signaling, and examples of each.
3. Explain the RAS-MAPK pathway. Why is RAS one of the most commonly mutated oncogenes in human cancer?
4. Describe the Wnt/beta-catenin pathway. Why do APC mutations lead to colorectal cancer?
5. A patient has a gain-of-function mutation in JAK2 (V617F). Explain the molecular mechanism and predict the clinical **phenotype**.
6. Compare the intrinsic and extrinsic apoptosis pathways. Where do they converge, and what is the significance of BH3-primarily proteins?
7. Explain the mechanism of action of imatinib in CML. Why does resistance eventually develop, and how might it be overcome?
8. Describe four mechanisms by which cells terminate signaling responses. For each, give a specific molecular example.
9. Explain how CDK4/6 inhibitors (palbociclib) arrest the cell cycle in G1. Why are they used specifically in HR⁺ breast cancer?
10. Venetoclax is a BH3 mimetic that inhibits Bcl-2. Explain its mechanism of action and why it is effective in cancers that overexpress Bcl-2.
11. Using `hill_equation`, compare fractional occupancy at $[L] = K_d$ for $n = 1$ vs. $n = 4$. Which curve better matches oxygen binding to hemoglobin, and why?
12. Sketch how receptor internalization provides signal termination for RTKs; link to one resistance mechanism in targeted cancer therapy.

8.13 Further Reading and Source Notes: Cell Signaling and Communication

- Alon (2019). *An Introduction to Systems Biology: Design Principles of Biological Circuits*. Chapman and Hall/CRC.
- Tyson et al. (2003). Sniffers, buzzers, toggles and blinkers: dynamics of regulatory and signaling pathways in the cell. *Current Opinion in Cell Biology*, 15.
- Rall and Sutherland (1958) and Gilman (1987) for the cAMP/G-protein evidence chain [**Rall and Sutherland, 1958, Gilman, 1987**].
- Slamon et al. for HER2 amplification and targeted therapy evidence [**Slamon et al., 1987, 2001**].

8.14 Key Terms

Table 133. Current Evidence Map: Spatial Single-Cell Signaling Evidence: Term and Definition.

Term	Definition
GPCR	G protein-coupled receptor; 7-TM superfamily; largest receptor family (about 800 in humans)
Adenylyl cyclase	Enzyme converting ATP to cAMP; activated by G_s , inhibited by G_i
cAMP	Cyclic AMP; second messenger activating PKA; degraded by phosphodiesterases
PKA	Protein kinase A; cAMP-activated Ser/Thr kinase; phosphorylates diverse substrates
PIP ₂	Phosphatidylinositol 4,5-bisphosphate; PLC substrate yielding IP ₃ + DAG
IP ₃	Inositol 1,4,5-trisphosphate; releases Ca ²⁺ from ER via IP ₃ receptor channels
RTK	Receptor tyrosine kinase; dimerization-activated; autophosphorylation recruits SH2 proteins
MAP kinase	Mitogen-activated protein kinase (ERK); activated by dual phosphorylation (Thr/Tyr)
RAS	Small GTPase; molecular switch; most commonly mutated oncogene family
CDK-cyclin	Cyclin-dependent kinase paired with regulatory cyclin; drives cell cycle progression
Apoptosome	Apaf-1/cytochrome c/caspase-9 complex; activates executioner caspases
Caspase	Cysteine-aspartate protease; initiator (8, 9, 10) and executioner (3, 6, 7) types
Bcl-2	Anti-apoptotic protein; inhibits BAX/BAK pore formation; overexpressed in follicular lymphoma
Wnt	Secreted glycoprotein; activates beta-catenin signaling; critical for development and stem cells
JAK-STAT	Janus kinase-Signal Transducer and Activator of Transcription; cytokine signaling pathway
Oncogene	Mutated proto-oncogene with gain-of-function; drives uncontrolled cell growth
p53	Tumor suppressor transcription factor; “guardian of the genome”; mutated in about 50% of cancers

8.15 Companion Source Module: Cell Signaling and Communication

Cell Signaling and Communication should leave a reproducible trail from a biological claim to the code, figure, diagram, or paper-based activity that can test it. Use the surfaces below to inspect the chapter’s assumptions, rerun the relevant model, or compare the manuscript explanation with companion labs and figures.

Table 134. Companion source surfaces for Cell Signaling and Communication.

Surface	Use it for
src/biology/cell/cell_biology.py (receptor_occupancy, hill_equation, signal_amplification)	Quantify ligand binding, cooperativity, and cascade gain.
src/mermaid/biology_diagrams.py (hormone_signaling_diagram, immune_response_diagram)	Compare receptor logic across endocrine and immune examples.

Reproducibility check: specify dose, timing, receptor context, feedback, and readout before inferring pathway causality. Cross-reference: extend the same logic in sections 34 and 35 and sections 15 and 16.

Unit III — Energy and Metabolism: Introduction

Why This Unit Matters

Life is, at its core, an ongoing argument with the second law of thermodynamics. The second law demands that disorder increases in any closed system; living organisms are ordered, and they maintain that order at the price of consuming energy and exporting entropy to their surroundings. A resting human adult dissipates approximately 80 watts — the same as an incandescent light bulb — in the form of body heat, CO₂, and metabolic waste. Every breath you take, every protein you synthesize, every ion you pump against its gradient, uses energy extracted from the oxidation of food.

The molecular currency of this energy economy is ATP (adenosine triphosphate). At any moment, your cells contain about 50 g of ATP, yet you consume roughly 40 kg of ATP every day at rest. This means each ATP molecule is recycled approximately 800 times — phosphorylated from ADP in mitochondria, hydrolysed to ADP in the cytoplasm, and regenerated in an endless chemical cycle. During vigorous exercise, ATP turnover in muscle can exceed 0.5 kg per minute.

This unit traces energy from its entry point — sunlight captured by chlorophyll, or chemical bonds in food — through the interconnected pathways of glycolysis, the TCA cycle, oxidative phosphorylation, and photosynthesis, to its exit as heat and CO₂. Each pathway is treated quantitatively: you will derive ATP yields, calculate free energy changes, and model the regulatory logic that switches metabolism between fed and fasted states. The central thread is Peter Mitchell’s chemiosmosis (Nobel Prize 1978): ion gradients across membranes couple electron flow to ATP synthesis, and the same principle operates in both mitochondria and chloroplasts.

Landmark Discoveries

Discoverer(s)	Year	Journal / Source	Discovery	Significance
Hans Krebs	1937	[Krebs and Johnson, 1937]	Citric acid (Krebs/TCA) cycle	Identified the central hub of aerobic catabolism; Nobel Prize 1953
Otto Warburg	1923–1930	[Warburg, 1924]	Respiratory enzyme and Warburg effect	First measured oxygen consumption in cancer; discovered aerobic glycolysis
Peter Mitchell	1961	[Mitchell, 1961]	Chemiosmotic hypothesis	Proposed proton gradients drive ATP synthesis; revolutionary paradigm shift; Nobel Prize 1978
Paul Boyer & John Walker	1994–1997	[Boyer, 1997]	Binding-change mechanism of ATP synthase	Explained rotary catalysis of F ₁ F ₀ -ATP synthase; Nobel Prize 1997
Melvin Calvin, Andrew Benson & James Bassham	1950	[Calvin, 1962]	Calvin cycle (carbon fixation)	Traced ¹⁴ C through photosynthesis; established the biochemistry of C ₃ fixation; Nobel Prize 1961
Racker & Stoeckenius	1974	[Racker and Stoeckenius, 1974]	Bacteriorhodopsin + ATP synthase reconstitution	Direct experimental proof of Mitchell’s chemiosmosis using purified components

Key Concepts and Connections

Current Evidence Thread

Read this unit as one regulated network rather than three separate pathways: respiration, the integrated fasting/fed economy, and photosynthesis are most constrained by the same currencies of energy charge, redox poise, and compartmentation, and a claim in one chapter is primarily as strong as the flux, sensor, and condition it specifies. Metabolism is now studied as a regulated network constrained by energy, redox balance, compartmentation, and environment. As you move through the chapters, keep a two-column note: claim on the left, evidence that would change my confidence on the right. By the end of the unit, each major idea should be tied to a measurement, model, citation, or paper-based lab decision.

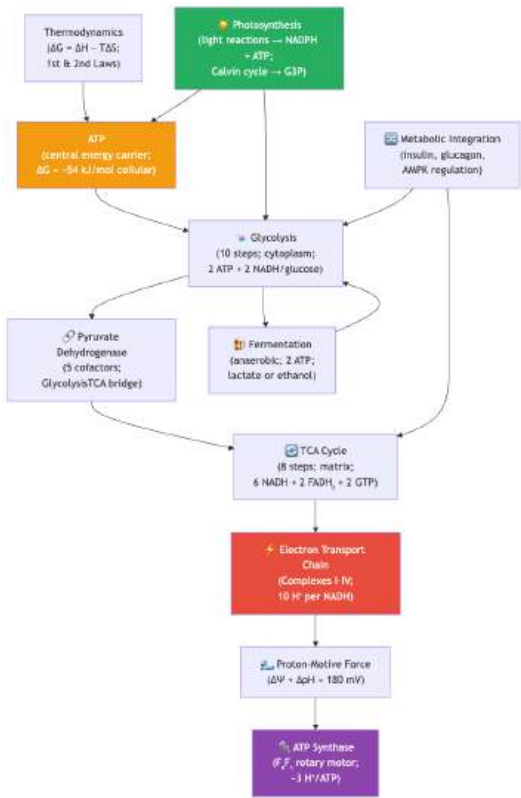


Figure 59. Energy-and-metabolism concept map - orange = ATP currency; red = oxidative phosphorylation; green = photosynthesis; purple = ATP synthase.

Chapter Roadmap

Chapter	Title	Core Question	Key Equation / Model
9	Bioenergetics and Cellular Respiration	How do cells extract and convert chemical energy from glucose?	$\Delta G = \Delta G^{o'} + RT \ln Q$; P/O ratios
10	Photosynthesis	How do plants capture solar energy and fix CO ₂ ?	Light-harvesting cross-section; Z-scheme; Calvin cycle stoichiometry
11	Metabolic Integration	How do hormones and allosteric signals coordinate anabolic and catabolic pathways?	AMPK activation; insulin/glucagon signaling logic

Connections Across the Textbook

- ATP and free energy introduced here underpin most driven processes in **Unit IV — Molecular Genetics: Introduction** (DNA replication, transcription, translation), **Unit VIII — Botany — Plant Biology: Introduction** (active transport in phloem), and **Unit IX — Zoology and Systems Physiology: Introduction** (Na⁺/K⁺-ATPase in neurons).
- The TCA cycle as metabolic hub is integrated in section 11 and connects to amino acid catabolism (**Unit IV — Molecular Genetics: Introduction**), fatty acid oxidation, and nucleotide synthesis.
- Proton-motive force is the conceptual bridge between mitochondrial ATP synthesis (this unit) and chloroplast ATP synthesis (section 10), and between bacterial physiology (**Unit VII — Microbiology: Introduction**) and the evolution of eukaryotes (**Unit II — The Cell: Introduction**, endosymbiosis).
- Warburg effect (cancer cells performing aerobic glycolysis) appears in **Unit II — The Cell: Introduction** (cell signaling oncogenes), **Unit IV — Molecular Genetics: Introduction** (genomic instability), and the clinical connection sections throughout.

Key vocabulary introduced here: free energy, enthalpy, entropy, ATP hydrolysis, glycolysis, oxidative phosphorylation, proton-motive force, chemiosmosis, electron transport chain, substrate-level phosphorylation, fermentation, Calvin cycle, Warburg effect.

Computational Toolbox — Unit III

```
from biology.biochemistry import atp_free_energy, glycolysis_summary

# ATP hydrolysis free energy under physiological conditions
delta_g = atp_free_energy(atp_conc_mM=3.0, adp_conc_mM=1.0, pi_conc_mM=10.0)
print(f"ΔG (ATP hydrolysis) = {delta_g:.1f} kJ/mol")
# Expected: ΔG (ATP hydrolysis) ≈ -45.2 kJ/mol
# (Standard ΔG°' = -30.5 kJ/mol; physiological conditions make it more negative
# due to low [ADP][Pi] and high [ATP] in active cells)

# Comparing aerobic vs anaerobic ATP yield
aerobic = glycolysis_summary()
print(f"Glycolysis only: {aerobic.net_atp} ATP per glucose")
# 2 ATP (substrate-level only); aerobic adds about 32 more via oxidative phosphorylation

# The complete aerobic yield
total_aerobic_atp = aerobic.net_atp + 2 + 10*2.5 + 2*1.5 # GTP + NADH + FADH2
print(f"Aerobic total (estimate): about {total_aerobic_atp:.0f} ATP per glucose")
# Expected: Aerobic total (estimate): about 32 ATP per glucose
```

Try it yourself: The P/O ratio (ATP per oxygen atom) is 2.5 for NADH and 1.5 for FADH₂. Calculate the theoretical maximum yield from one glucose:
10 NADH × 2.5 + 2 FADH₂ × 1.5 + 4 substrate-level = __?

Source modules: `src/biology/biochemistry/biochemistry.py` — `glycolysis_summary()`, `atp_free_energy()`, `michaelis_menten()`. Figures: `src/visualization/` (ETC diagrams, ATP yield tables); `src/mermaid/biology_diagrams.py` (metabolic pathway diagrams).

Cross-Unit Integration

The metabolic pathways of **Unit III — Energy and Metabolism: Introduction** — glycolysis, the TCA cycle, oxidative phosphorylation, photosynthesis — generate the ATP, NADPH, and carbon skeletons that make every other cellular activity possible. Among the most demanding consumers of that energy is the storage, replication, and expression of genetic information, which **Unit IV — Molecular Genetics: Introduction** opens with. DNA replication, transcription, and translation are ATP- and GTP-dependent, kinetically tuned to the metabolic state of the cell, and tightly regulated by metabolic intermediates (acetyl-CoA controls histone acetylation; SAM levels control DNA methylation; alpha-ketoglutarate controls TET-driven demethylation). Read **Unit IV — Molecular Genetics: Introduction** with one eye on the energetic budget you just internalized — the cell does not “decide” to express a gene without paying a metabolic bill.

9 Bioenergetics and Cellular Respiration

Level 3/3 · 60 min read · 100 min lecture · Prerequisites: section 6, section 4

9.1 Learning Objectives

1. Define the laws of **thermodynamics** and apply them to biological reactions, distinguishing standard (ΔG°) from physiological (ΔG) free energies.
2. Explain the role of ATP as a central phosphoryl-group donor and short-term energy carrier, including the molecular basis of its high phosphoryl group transfer potential.
3. Describe the 10 steps of **glycolysis** with **enzymes**, intermediates, and regulatory mechanisms.
4. Explain the pyruvate dehydrogenase complex and its regulation.
5. Describe the 8 steps of the TCA cycle with carbon tracking, cofactor yields, and regulation.
6. Describe the electron transport chain complexes I–IV, including proton stoichiometry and the Q cycle.
7. Explain **ATP synthase** structure and the rotary catalysis mechanism, including the proton-motive force equation.
8. Calculate net ATP yield from glucose oxidation using modern P/O ratios (about 2.5 for NADH, about 1.5 for FADH_2) and explain how the “30–32 ATP” number is derived.
9. Compare substrate-level and **oxidative phosphorylation** quantitatively across yield, speed, sustainability, and physiological niche.
10. Describe **fermentation** pathways, the Cori cycle, and the glucose-alanine cycle as inter-organ shuttles.
11. Explain gluconeogenesis (four bypass enzymes) and its reciprocal regulation with glycolysis.
12. Quantify reactive oxygen species (ROS) production at the ETC and the antioxidant defenses that constrain it.
13. Distinguish anaplerotic and cataplerotic flux through the TCA cycle in the context of inter-organ metabolism.
14. Explain physiological (UCP1, brown adipose) and pharmacological (DNP) uncoupling at a molecular level.
15. Compute the thermodynamic efficiency of glucose oxidation from standard free energies of formation.

9.1.1 Study Blueprint

- Big idea: Cells harvest free energy by coupling redox chemistry to phosphoryl transfer and ion gradients.
- Core concepts: free energy, redox, glycolysis, oxidative phosphorylation.
- Framework alignment: Vision & Change: Pathways and transformations of energy and matter, Systems; AP Biology: Energetics, Systems Interactions; NGSS-style topics: Matter and Energy in Organisms and Ecosystems.
- Model or quantitative lens: Delta G, ATP yield, and electron-carrier accounting.
- Data skill: Track carbon, electrons, and ATP across a pathway.
- Practice cadence: Representing and Describing Data, Statistical Tests and Data Analysis.
- Common misconception to repair: ATP is not stored energy in a vague sense; it is a coupling currency with defined reaction chemistry.
- Primary lab: **Lab — Bioenergetics and Cellular Respiration**.
- Question bank: **Questions — Bioenergetics and Cellular Respiration**.
- Transfer task: Transfer energy accounting to exercise, fermentation, hypoxia, and mitochondrial disease.
- Bridge to computation: `biology.biochemistry.biochemistry.glycolysis_summary`.

Opening Vignette: The Heretic Who Was Right About ATP

In 1961, British biochemist Peter Mitchell proposed something that nearly the entire biochemistry community considered preposterous: that the synthesis of ATP was not driven by a hypothetical high-energy chemical intermediate but by a proton gradient across a membrane — a proton-motive force [Mitchell, 1961]. Mitchell’s “chemiosmotic hypothesis” met with fierce resistance. Efraim Racker, one of biochemistry’s most respected voices, called it “an act of faith, not of reason.” Mitchell spent years defending his idea from private funds after leaving a university position.

In 1978, the Nobel Committee awarded Peter Mitchell the Nobel Prize in Chemistry — alone, without co-recipients — specifically for the chemiosmotic hypothesis. It was a stunning vindication. Today we know that the about 28 molecules of ATP produced per glucose in oxidative phosphorylation are most driven by the proton gradient that Mitchell described. The mitochondrion — and the **chloroplast** — are essentially biological batteries, storing energy as a proton electrochemical gradient. This chapter explains exactly how they are charged and discharged.

Primary source: Mitchell, P. (1961). Coupling of phosphorylation to electron and hydrogen transfer by a chemi-osmotic type of mechanism. Nature, 191(4784), 144–148.

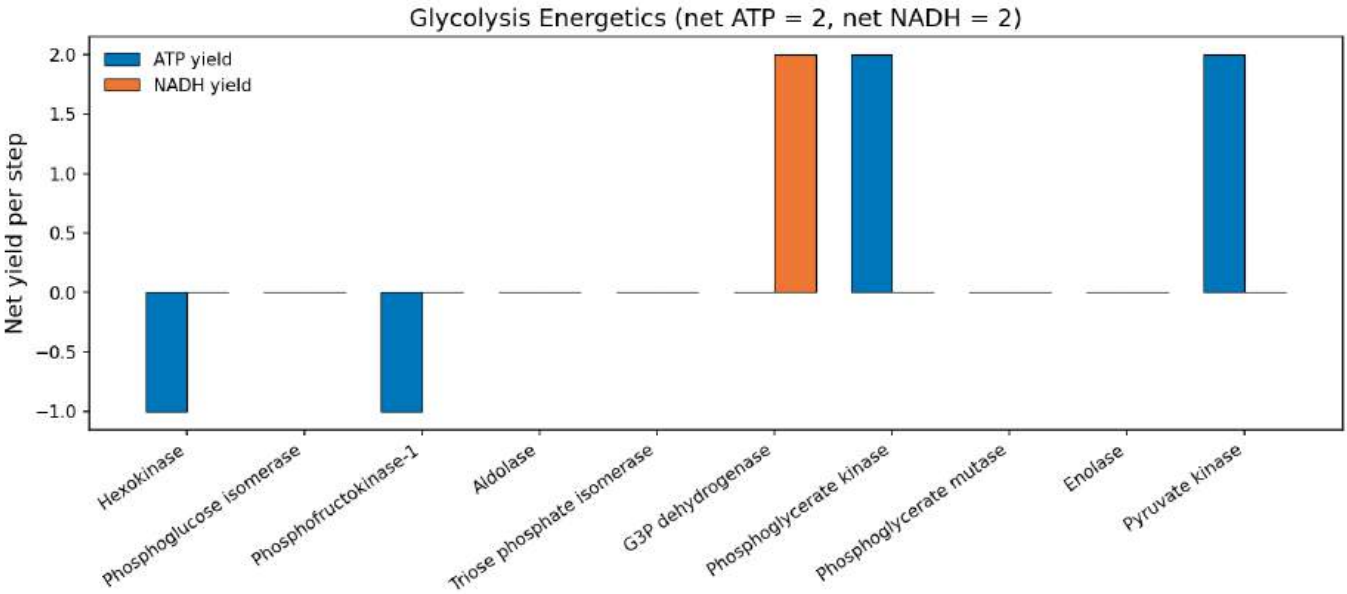


Figure 60. Net ATP and NADH balance across the ten glycolysis steps. Bars distinguish the two ATP-investment steps, the four ATP-yielding payoff steps, and NADH formation at steps 6 and 9; the pathway sums to net 2 ATP and 2 NADH per glucose.

9.2 Thermodynamics of Life

Mathematical Background: Bioenergetics uses logarithms and thermodynamic equations. For a review of logarithmic functions and their biological applications, see [Appendix C — Mathematical Review for Biology](#).

9.2.1 First and Second Laws

The First Law of Thermodynamics: Energy cannot be created or destroyed — primarily converted. Life obeys this law: every metabolic reaction converts one form of energy to another, with total energy conserved.

The Second Law of Thermodynamics: In any spontaneous process, the total entropy (disorder) of the universe increases. This means no energy conversion is 100% efficient — some energy is typically dispersed as heat. Living organisms maintain internal order (low entropy) at the expense of increasing entropy in their surroundings (heat release, CO₂ production, waste generation).

A useful schematic: a cell is a dissipative structure in the sense of Prigogine — its internal order is maintained by a continuous through-flux of free energy (food, sunlight) and a continuous out-flux of low-grade heat. Stop the through-flux, and the cell relaxes to thermal equilibrium — which is to say, dies.

9.2.2 Gibbs Free Energy: A Derivation From First Principles

For a process at constant temperature T and constant pressure P (the conditions inside virtually every cell), the relevant thermodynamic potential is the Gibbs free energy G . Starting from the second law, we have for the universe (system + surroundings):

$$\Delta S_{\text{universe}} = \Delta S_{\text{system}} + \Delta S_{\text{surroundings}} \geq 0 \tag{148}$$

Heat released by the system at constant pressure equals $-\Delta H_{\text{system}}$, and this heat increases the entropy of the surroundings by $-\Delta H_{\text{system}}/T$. Substituting:

$$\Delta S_{\text{universe}} = \Delta S_{\text{system}} - \frac{\Delta H_{\text{system}}}{T} \geq 0 \tag{149}$$

Multiplying both sides by $-T$ and dropping the “system” subscript yields the defining inequality of spontaneity at constant T, P :

$$\Delta G = \Delta H - T\Delta S \leq 0 \tag{150}$$

- $\Delta G < 0$: reaction is spontaneous (exergonic); energy released
- $\Delta G > 0$: reaction is non-spontaneous (endergonic); energy input required
- $\Delta G = 0$: system is at equilibrium (no net reaction)

This is profound: a quantity that depends primarily on the *system* (not the surroundings) tells us whether the *universe’s* entropy will increase. It is the workhorse of biochemical thermodynamics.

9.2.3 Standard Free Energy and Actual Free Energy

The standard free energy change ($\Delta G^{\circ'}$) is measured under biochemical standard conditions (1 M concentrations for reactants except H⁺, [pH](#) 7.0, 25 degrees C, 1 atm, and water at unit activity). Under cellular conditions (not standard state), ΔG differs from $\Delta G^{\circ'}$:

$$\Delta G = \Delta G^{\circ'} + RT \ln Q \tag{151}$$

where $Q = [\text{products}]/[\text{reactants}]$ (mass action ratio, reaction quotient).

The relationship between $\Delta G^{\circ'}$ and the equilibrium constant:

$$\Delta G^{\circ'} = -RT \ln K_{eq} \tag{152}$$

Standard versus physiological $\Delta G^{\circ'}$ for key hydrolysis reactions (37 °C, pH 7.0, 1 mM Mg²⁺):

Table 135. Standard and physiological free energy changes for selected hydrolysis reactions.

Reaction	ΔG° (kJ/mol)	Cellular ΔG (kJ/mol)	Notes
Phosphoenolpyruvate (PEP) → Pyruvate + P _i	−61.9	about −65	Highest-energy phosphate bond in cells
1,3-Bisphosphoglycerate → 3-PG + P _i	−49.3	about −52	Drives ATP synthesis at glycolysis step 7
Phosphocreatine → Creatine + P _i	−43.0	about −47	Muscle ATP buffer (phosphagen)
ATP → ADP + P _i	−30.5	−50 to −54	The “energy currency benchmark”
ATP → AMP + PP _i	−45.6	about −50	PP _i further hydrolysed (irreversibility)
Glucose-1-P → Glucose + P _i	−20.9	−21	Low-energy ester
Glucose-6-P → Glucose + P _i	−13.8	−14	Low-energy phosphate ester

Key insight: ATP sits in the *middle* of this spectrum. It is energetically capable of phosphorylating many low-energy compounds (glucose, F6P) but can itself be re-synthesized from higher-energy intermediates such as PEP and 1,3-BPG. This intermediate position is what makes ATP an effective “energy currency” rather than the highest-potential molecule in the cell.

Why cells maintain far-from-equilibrium conditions: At equilibrium, $\Delta G = 0$ and no net work can be done. Cells maintain metabolite concentrations far from equilibrium ($Q \neq K_{eq}$), keeping ΔG strongly negative for exergonic reactions. This is why cells must continuously consume nutrients — to maintain the far-from-equilibrium state that enables life.

9.2.4 Worked Example: Free Energy and Equilibrium

Problem: The $\Delta G^{\circ'}$ for glucose-6-phosphate isomerase (G6P to F6P) is +1.7 kJ/mol. Calculate K_{eq} at 37 degrees C. Is this reaction spontaneous under standard conditions?

Solution:

$$\Delta G^{\circ'} = -RT \ln K_{eq} \tag{153}$$

$$1,700 = -(8.314)(310) \ln K_{eq} \tag{154}$$

$$\ln K_{eq} = \frac{-1,700}{2,577} = -0.660 \tag{155}$$

$$K_{eq} = e^{-0.660} = 0.517 \tag{156}$$

Under standard conditions, this reaction is slightly non-spontaneous ($\Delta G^{\circ'} > 0$). However, in the cell, the mass action ratio Q is kept well below K_{eq} because F6P is rapidly consumed by PFK-1, making the actual ΔG negative.

9.2.5 Worked Example: Complete Glucose Oxidation

Problem: Calculate the standard free energy of complete glucose oxidation (glucose + 6 O₂ → 6 CO₂ + 6 H₂O) from tabulated standard free energies of formation, and compare it with the energy harvested as ATP.

Solution: Using ΔG_f° values (kJ/mol) at 25 °C — glucose: −910.4; CO₂ (aq): −394.4; H₂O (l): −237.1; O₂: 0:

$$\Delta G_{\text{rxn}}^{\circ'} = \sum \Delta G_f^{\circ}(\text{products}) - \sum \Delta G_f^{\circ}(\text{reactants}) \tag{157}$$

$$= [6(-394.4) + 6(-237.1)] - [(-910.4) + 6(0)] = -3,789 + 910.4 \approx -2,870 \text{ kJ/mol} \tag{158}$$

If 32 ATP are produced per glucose at a cellular hydrolysis ΔG of −50 kJ/mol, the energy captured as ATP is 32 × 50 = 1,600 kJ/mol. The thermodynamic efficiency of glucose oxidation in cells is therefore:

$$\eta = \frac{1,600}{2,870} \approx 56\% \tag{159}$$

The remaining about 44% is dissipated as heat — useful for mammals to maintain body temperature, but ultimately a payment to the second law. For comparison: a modern combined-cycle gas turbine power plant achieves about 60% thermal efficiency at >800 K, while an automobile engine averages about 25%. A 56%-efficient isothermal energy converter operating at 310 K is, by any engineering standard, remarkable.

9.2.6 ATP as Energy Currency

ATP (adenosine triphosphate) is the cell’s central short-term energy carrier and phosphoryl-group donor for many endergonic reactions [Boyer, 1997]. The phrase “energy currency” is useful shorthand, but the cell also uses ion gradients, redox cofactors such as NADH/NADPH, thioesters such as acetyl-CoA, and activated carriers such as UDP-glucose.

The high negative ΔG of ATP hydrolysis under cellular conditions (−50 to −54 kJ/mol; $\Delta G^{\circ'} = -30.5$ kJ/mol) arises from: 1. Electrostatic repulsion between closely spaced negative charges on the gamma-phosphate (relieved on hydrolysis) 2. Resonance stabilization of inorganic phosphate (P_i) product — P_i has more resonance forms than the terminal phosphate of ATP 3. Hydration (solvation enthalpy) of P_i and ADP — products are better hydrated than reactants 4. Entropy increase — one molecule becomes two

ATP couples exergonic reactions to endergonic ones via phosphoryl group transfer. The cell maintains a very high ATP/ADP ratio (about 10 in most cells; ATP about 3–5 mM, ADP about 0.5 mM), keeping the cellular ΔG of hydrolysis more negative than ΔG° .

Daily ATP turnover: A resting adult uses about 40 kg of ATP per day (body contains about 50 g at any time, so each ATP molecule is recycled about 800 times/day). During vigorous exercise, ATP turnover can reach about 0.5 kg/min — roughly the body’s mass in ATP equivalents flowing through the adenylate pool every two hours.

Concept Check 1: The ΔG° of ATP hydrolysis is -30.5 kJ/mol, but the actual cellular ΔG is approximately -54 kJ/mol. Using the equation $\Delta G = \Delta G^{\circ} + RT \ln Q$, calculate the mass action ratio $Q = [\text{ADP}][\text{P}_i]/[\text{ATP}]$ in the cell at 37 degrees C.

Concept Check 1b: A cell experiences a sudden drop in ATP (from 4 mM to 1 mM) without changes in ADP or P_i . Predict the qualitative effect on (a) the cellular ΔG of ATP hydrolysis, (b) the ATP/ADP ratio, and (c) the activity of AMPK.

9.3 Glycolysis as Cytosolic Glucose Oxidation

figure 60 summarizes net ATP and NADH yields across the ten glycolytic steps, separating the investment and payoff phases.

Glycolysis (Greek: *glykys* = sweet; *lysis* = splitting) converts one glucose (6C) to two pyruvate (3C), netting 2 ATP and 2 NADH. It occurs in the **cytoplasm** of most cells and does not require oxygen.

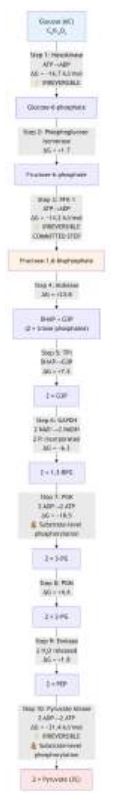


Figure 61. Glycolysis commits glucose through ATP-investment steps, harvests reducing power, and conserves energy as ATP and pyruvate; irreversible steps mark the main regulatory checkpoints.

The 10 steps of glycolysis (Mermaid). The energy investment phase (steps 1–5) consumes 2 ATP. The energy payoff phase (steps 6–10) produces 4 ATP and 2 NADH. The three irreversible steps (1, 3, 10) are the regulatory control points.

9.3.1 Ten Enzymatic Steps

Table 136. Ten Enzymatic Steps: Step and Enzyme.

Step	Enzyme	Reaction	ΔG (kJ/mol)	Notes
1	Hexokinase	Glucose + ATP \rightarrow G6P + ADP	−16.7	Traps glucose in cell
2	Phosphoglucose isomerase	G6P \rightarrow F6P	+1.7	Aldose to ketose
3	PFK-1	F6P + ATP \rightarrow F1,6BP + ADP	−14.2	Committed step; rate-limiting
4	Aldolase	F1,6BP \rightarrow DHAP + G3P	+23.8	Pulled forward by step 5
5	Triose phosphate isomerase	DHAP \rightarrow G3P	+7.5	“Perfect enzyme” (k_{cat}/K_m near diffusion limit)
6	GAPDH	G3P + P _i + NAD ⁺ \rightarrow 1,3BPG + NADH	−6.3	First NADH production
7	Phosphoglycerate kinase	1,3BPG + ADP \rightarrow 3PG + ATP	−18.5	First ATP production
8	Phosphoglycerate mutase	3PG \rightarrow 2PG	+4.4	Phosphate shift
9	Enolase	2PG \rightarrow PEP + H ₂ O	+1.8	Dehydration
10	Pyruvate kinase	PEP + ADP \rightarrow Pyruvate + ATP	−31.4	Largest energy release

9.3.2 Regulation of Glycolysis

PFK-1 is the master regulator of glycolysis. It integrates energy status, biosynthetic needs, and hormonal signals [Atkinson, 1968]:

Table 137. Regulation of Glycolysis: Activators and Inhibitors.

Activators	Inhibitors
AMP (low energy)	ATP (high energy, allosteric at regulatory site)
Fructose-2,6-bisphosphate (F2,6BP, most potent)	Citrate (TCA cycle intermediate = adequate supply)
ADP	H ⁺ (low pH; prevents excessive lactate acidosis)
P _i	

Fructose-2,6-bisphosphate (F2,6BP) is the most potent activator of PFK-1 (lowers K_m for F6P by 50-fold). It is produced by PFK-2 (a bifunctional enzyme with both kinase and phosphatase domains). Insulin activates PFK-2 kinase activity (producing F2,6BP, stimulating glycolysis). Glucagon (via PKA) activates PFK-2 phosphatase activity (destroying F2,6BP, inhibiting glycolysis in liver).

9.3.3 ATP and Reducing-Equivalent Accounting

Net output from 1 glucose: - 2 ATP (from steps 7 and 10, minus 2 ATP consumed at steps 1 and 3) - 2 NADH (from step 6; each NADH worth about 2.5 ATP via oxidative phosphorylation in **aerobic** conditions)

Clinical Connection: The Warburg Effect Cancer cells often exhibit the Warburg effect — high rates of glycolysis even in the presence of oxygen (“aerobic glycolysis”). Rather than fully oxidising glucose to CO₂ via the TCA cycle and ETC, cancer cells convert most glucose to lactate. This seems wasteful (2 ATP vs. 30–32 ATP per glucose), but it provides rapid ATP production and generates biosynthetic precursors (G6P for pentose phosphate pathway, 3PG for serine biosynthesis) needed for rapid cell division. PET scanning exploits this by detecting tumor uptake of ¹⁸F-fluorodeoxyglucose (FDG). see section 11 for metabolic integration.

Concept Check 2: Steps 4 and 5 of glycolysis have very positive ΔG° values (+23.8 and +7.5 kJ/mol). How do these reactions proceed in vivo despite being thermodynamically unfavorable under standard conditions?

9.4 Gluconeogenesis: Reverse But Not the Reverse

Gluconeogenesis is *not* glycolysis run backwards. Three glycolytic steps (hexokinase, PFK-1, pyruvate kinase) are physiologically irreversible in the forward direction — their cellular ΔG values are too negative. Gluconeogenesis bypasses each of these three steps with dedicated enzymes that use different chemistry, often paying additional ATP/GTP to make the reverse direction thermodynamically favorable.

9.4.1 The Four Bypass Reactions

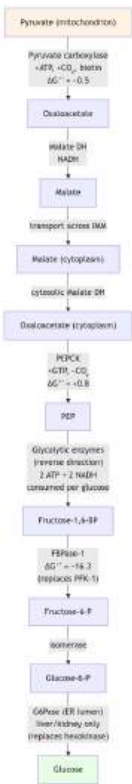


Figure 62. Gluconeogenesis bypasses irreversible glycolytic steps by moving carbon through mitochondrial oxaloacetate, malate export, and cytosolic phosphoenolpyruvate formation.

Gluconeogenesis from pyruvate to glucose (Mermaid). Four bypass enzymes (pyruvate carboxylase, PEPCK, FBPase-1, G6Pase) replace the three irreversible glycolytic steps. The pyruvate-to-PEP conversion requires two enzymes — pyruvate carboxylase consumes ATP and PEPCK consumes GTP — so the bypass spans two energy-consuming steps.

9.4.2 The Four Bypass Enzymes in Detail

1. Pyruvate carboxylase (PC): A mitochondrial biotin-dependent carboxylase that converts pyruvate + CO₂ + ATP → oxaloacetate + ADP + P_i. Two key features: (a) allosterically activated by acetyl-CoA, providing a feed-forward signal that fat oxidation (which produces acetyl-CoA) supplies the OAA needed for both gluconeogenesis and TCA flux; (b) requires biotin as a covalently bound prosthetic group that carries the activated CO₂ (–N–COO[–]). Biotin deficiency (rare; most often from chronic raw-egg consumption due to avidin) disrupts pyruvate carboxylase and three other carboxylases simultaneously, producing lactic acidosis and ketogenic dysregulation.
2. PEPCK (phosphoenolpyruvate carboxykinase): A cytosolic (and partially mitochondrial) GTP-dependent decarboxylase that converts OAA + GTP → PEP + CO₂ + GDP. This enzyme is unusual among gluconeogenic enzymes in that it is regulated almost entirely at the level of *transcription* — glucagon (via cAMP→PKA→CREB) and cortisol (via the glucocorticoid receptor) potently induce PEPCK mRNA, while insulin (via FoxO1 phosphorylation and exclusion from the nucleus) potently represses it. PEPCK transcription has a half-time of about 1 hour, making it a slow but powerful long-term switch.
3. Fructose-1,6-bisphosphatase (FBPase-1): Cytosolic phosphatase that converts F1,6BP + H₂O → F6P + P_i (ΔG°' = –16.3 kJ/mol). Critically regulated allosterically by F2,6BP (strong inhibitor) and AMP (inhibitor) — both signals of glycolytic demand or low energy. The same F2,6BP that *activates* PFK-1 *inhibits* FBPase-1, so a single second messenger flips the entire futile-cycle node.

4. Glucose-6-phosphatase (G6Pase): A 9-transmembrane-helix protein whose catalytic site faces the lumen of the endoplasmic reticulum, accessed by a phosphate transporter (SLC37A4) and a glucose efflux transporter (GLUT2). Critically, G6Pase is expressed almost exclusively in liver and renal cortex — muscle and brain lack it, which is why these tissues cannot release free glucose to the blood even though they produce G6P internally. Mutations in G6Pase cause von Gierke disease (GSD I): severe fasting hypoglycaemia with hepatomegaly.

Table 138. The Four Bypass Enzymes in Detail: Glycolytic step (irreversible) and Gluconeogenic bypass.

Glycolytic step (irreversible)	Gluconeogenic bypass	Energy cost	Compartment
Pyruvate kinase	Pyruvate carboxylase + PEPCK	+1 ATP + 1 GTP per pyruvate	Mitochondrion + cytoplasm
PFK-1	Fructose-1,6-bisphosphatase (FBPase-1)	None (hydrolysis is exergonic)	Cytoplasm
Hexokinase	Glucose-6-phosphatase (G6Pase)	None (hydrolysis is exergonic)	ER lumen (liver, kidney primarily)

Net cost: Synthesizing one glucose from two pyruvate consumes 6 ATP equivalents (2 ATP at pyruvate carboxylase \times 2, 2 GTP at PEPCK \times 2, 2 ATP at PGK \times 2 in the reverse direction). This is why gluconeogenesis is restricted to tissues with substantial ATP-generating capacity (liver, renal cortex).

9.4.3 Reciprocal Regulation of Glycolysis and Gluconeogenesis

The same allosteric and hormonal signals that activate glycolysis inhibit gluconeogenesis, ensuring the two pathways do not run as a futile cycle:

Table 139. Reciprocal Regulation of Glycolysis and Gluconeogenesis: Signal and Glycolysis (PFK-1).

Signal	Glycolysis (PFK-1)	Gluconeogenesis (FBPase-1)
Fructose-2,6-bisphosphate	Strong activator	Strong inhibitor
AMP	Activator	Inhibitor
Citrate	Inhibitor	Activator
Acetyl-CoA	(no direct effect)	Activates pyruvate carboxylase
Insulin	\uparrow PFK-2 kinase $\rightarrow \uparrow$ F2,6BP \rightarrow glycolysis ON	\downarrow PEPCK / G6Pase transcription
Glucagon	\uparrow PFK-2 phosphatase $\rightarrow \downarrow$ F2,6BP \rightarrow glycolysis OFF	\uparrow PEPCK / G6Pase transcription

Glucagon-driven phosphorylation of PFK-2/FBPase-2 simultaneously turns *off* PFK-1 (glycolysis) and turns *on* FBPase-1 (gluconeogenesis) by destroying F2,6BP. This is a textbook example of how a single bifunctional enzyme can act as a metabolic switch.

Concept Check 2b: A patient with renal cortex damage but intact liver presents with mild fasting hypoglycaemia after prolonged exercise. Explain the contribution of renal gluconeogenesis to whole-body glucose homeostasis, and why it is invisible in healthy individuals.

9.5 The Cori Cycle and the Glucose-Alanine Cycle

Inter-organ metabolism allows tissues to specialize: muscle generates ATP rapidly via glycolysis, while liver shoulders the gluconeogenic burden. Two complementary inter-organ shuttles dominate fasting and exercise physiology.

9.5.1 The Cori Cycle (Lactate Shuttle)

Cori cycle: lactate from anaerobic muscle is regenerated to glucose in the liver (Mermaid). Each turn nets +2 ATP for muscle but -6 ATP for liver, a 4-ATP net loss to the organism — the metabolic cost of supporting hypoxic tissue.

9.5.2 The Glucose-Alanine Cycle

When muscle proteins are catabolised, branched-chain amino acid carbon skeletons donate amino groups to pyruvate, forming alanine. Alanine carries both carbon and nitrogen safely to the liver:

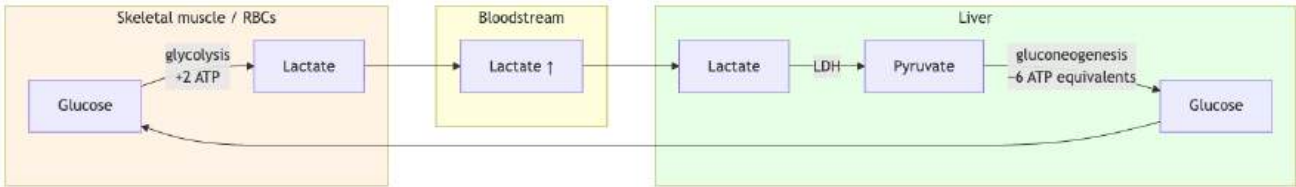


Figure 63. The Cori cycle moves lactate from anaerobic tissues to liver gluconeogenesis, trading rapid local ATP production for whole-body glucose recycling.

1. Muscle: Pyruvate + Glutamate → Alanine + α-Ketoglutarate (alanine aminotransferase)
2. Alanine travels via blood to liver
3. Liver: Alanine + α-KG → Pyruvate + Glutamate (alanine aminotransferase, reverse)
4. Glutamate releases NH₄⁺ into the urea cycle; pyruvate enters gluconeogenesis
5. Glucose returns to muscle via blood

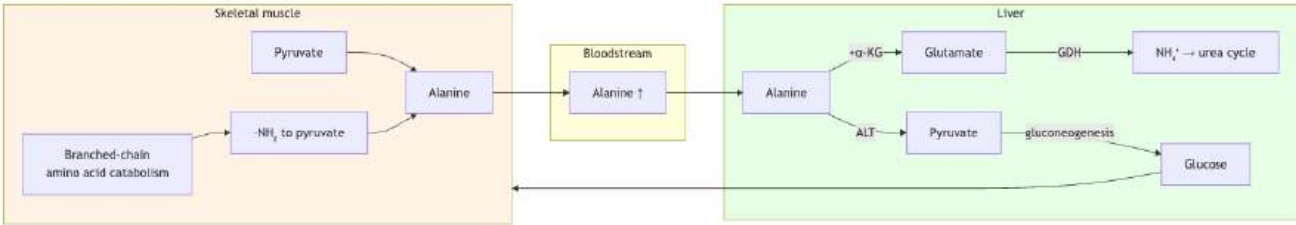


Figure 64. The glucose-alanine cycle couples muscle nitrogen disposal to hepatic gluconeogenesis: amino groups move as alanine while liver returns glucose.

Glucose-alanine cycle: alanine simultaneously carries gluconeogenic carbon and waste nitrogen from muscle to liver (Mermaid). The liver disposes of NH₄⁺ via the urea cycle and exports glucose back to muscle.

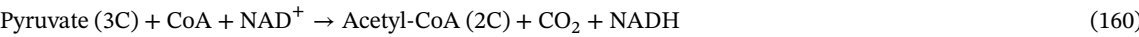
Why this is clever: Alanine simultaneously transports gluconeogenic carbon and waste nitrogen, replacing the need for two separate transport systems. It also keeps free ammonia (toxic to the brain) out of circulation — nitrogen is delivered directly to the urea-cycling liver.

Concept Check 3: During an acute sprint, muscle lactate output rises from 1 mM/min to 8 mM/min. Estimate the additional hepatic ATP demand (in ATP equivalents per minute) required to recycle this lactate via the Cori cycle, assuming most lactate reaches the liver.

9.6 Pyruvate Oxidation and the Citric Acid Cycle

Under aerobic conditions, pyruvate enters the mitochondria (via the MPC, mitochondrial pyruvate carrier) and is oxidised.

9.6.1 Pyruvate Dehydrogenase Complex (PDC)



Catalysed by PDC — a 9.5 MDa multienzyme complex with three catalytic components (E1: pyruvate dehydrogenase; E2: dihydrolipoyl transacetylase; E3: dihydrolipoyl dehydrogenase) using five cofactors: TPP (thiamine pyrophosphate, vitamin B₁), lipoic acid, FAD (vitamin B₂), NAD⁺ (vitamin B₃), CoA (vitamin B₅).

PDC regulation:

Table 140. Pyruvate Dehydrogenase Complex (PDC): Condition and PDC activity.

Condition	PDC activity	Mechanism
High acetyl-CoA, NADH, ATP	Inhibited	PDH kinase (PDK) phosphorylates E1 → inactive
High CoA, NAD ⁺ , AMP, Ca ²⁺	Activated	PDH phosphatase (PDP) dephosphorylates E1 → active
Insulin	Activated	Activates PDP in adipose tissue

Condition	PDC activity	Mechanism
Exercise (Ca ²⁺)	Activated	Ca ²⁺ activates PDP

Clinical Connection: PDC Deficiency Pyruvate dehydrogenase deficiency is the most common genetic cause of lactic acidosis. Without PDC, pyruvate cannot enter the TCA cycle and is instead reduced to lactate. Neurological damage results from the brain’s dependence on glucose oxidation. Treatment: ketogenic diet (high fat, very low carbohydrate) provides acetyl-CoA directly from fatty acid beta-oxidation, bypassing the PDC block. Dichloroacetate (DCA) inhibits PDK, keeping residual PDC active.

9.6.2 TCA Cycle (Krebs Cycle / Citric Acid Cycle)

The TCA cycle occurs in the mitochondrial matrix. It oxidises acetyl-CoA to CO₂, generating reduced cofactors (NADH, FADH₂) that feed the ETC [Krebs and Johnson, 1937].



Figure 65. The TCA cycle oxidizes acetyl-CoA to regenerate oxaloacetate while producing NADH, FADH₂, and GTP for oxidative phosphorylation.

The eight steps of the TCA cycle (Mermaid). Each turn oxidises one acetyl group (2C) to 2 CO₂, producing 3 NADH, 1 FADH₂, and 1 GTP. The cycle turns twice per glucose molecule.

Eight steps with details:

Table 141. TCA Cycle (Krebs Cycle / Citric Acid Cycle): Step and Enzyme.

Step	Enzyme	Reaction	Products
1	Citrate synthase	Acetyl-CoA + OAA → Citrate + CoA	–
2	Aconitase	Citrate → Isocitrate (via cis-aconitate)	–
3	Isocitrate dehydrogenase	Isocitrate → α-KG + CO ₂	NADH
4	α-KG dehydrogenase complex	α-KG → Succinyl-CoA + CO ₂	NADH
5	Succinyl-CoA synthetase	Succinyl-CoA → Succinate	GTP
6	Succinate dehydrogenase (Complex II)	Succinate → Fumarate	FADH ₂
7	Fumarase	Fumarate + H ₂ O → Malate	–
8	Malate dehydrogenase	Malate → OAA	NADH

Carbon tracking: The two carbons entering as acetyl-CoA are NOT the same two carbons lost as CO₂ in the first turn — they are released in subsequent turns. This can be demonstrated using ¹⁴C-labeled acetyl-CoA.

Net per turn: 3 NADH + 1 FADH₂ + 1 GTP + 2 CO₂

Total from 2 turns (per glucose): 6 NADH + 2 FADH₂ + 2 GTP + 4 CO₂

TCA cycle regulation:

Table 142. TCA Cycle (Krebs Cycle / Citric Acid Cycle): Enzyme and Activators.

Enzyme	Activators	Inhibitors
Citrate synthase	OAA, acetyl-CoA (substrates)	ATP, NADH, succinyl-CoA, citrate
Isocitrate DH	ADP, Ca ²⁺	ATP, NADH
α-KG DH	Ca ²⁺ , AMP	ATP, NADH, succinyl-CoA

9.6.3 Anaplerotic and Cataplerotic Reactions

The TCA cycle is not a closed loop in vivo — intermediates flow in and out for biosynthesis. Anaplerotic (“filling-up”) reactions replenish drained intermediates; cataplerotic (“emptying”) reactions remove intermediates for downstream pathways.

Major anaplerotic inputs:

Table 143. Anaplerotic and Cataplerotic Reactions: Reaction and Enzyme.

Reaction	Enzyme	Cofactor	Tissue	Function
Pyruvate + CO ₂ + ATP → OAA	Pyruvate carboxylase	Biotin (vitamin B ₇)	Liver, kidney	Replenishes OAA; primary anaplerotic source
Glutamate → α-KG + NH ₄ ⁺	Glutamate dehydrogenase	NAD(P) ⁺	Liver	Amino-acid catabolism
Glutamine → Glutamate + NH ₄ ⁺ → α-KG	Glutaminase + GDH	–	Most tissues	Amino-acid catabolism
Aspartate → OAA	Aspartate aminotransferase	PLP	Most tissues	Direct anaplerosis
Propionyl-CoA → Succinyl-CoA	Propionyl-CoA carboxylase + methylmalonyl-CoA mutase	Biotin, B ₁₂	Liver	Odd-chain fatty acid + Val/Ile/Met catabolism

Pyruvate carboxylase is allosterically activated by acetyl-CoA. This is biologically elegant: when acetyl-CoA accumulates (high fat oxidation, fed state) and OAA becomes limiting, the cell senses the imbalance and replenishes OAA so that citrate synthase can continue.

Glutamate dehydrogenase (GDH) catalyses the reversible deamination of glutamate to α-ketoglutarate, releasing NH₄⁺. It uses *either* NAD⁺ (catabolic direction) or NADP⁺ (anabolic direction) and is allosterically regulated by ADP (activator) and GTP (inhibitor) — making it a sensor of mitochondrial energy state. In hepatocytes, GDH-driven glutamate catabolism feeds α-KG into the TCA cycle and NH₄⁺ into the urea cycle, integrating amino-acid catabolism with both energy production and nitrogen disposal.

Major cataplerotic outflows:

Table 144. Anaplerotic and Cataplerotic Reactions: Intermediate withdrawn and Destination pathway.

Intermediate withdrawn	Destination pathway	Example product
α-Ketoglutarate	Glutamate / glutamine biosynthesis; collagen hydroxylation	Glu, Gln, hydroxyproline
Succinyl-CoA	Heme biosynthesis (δ-ALA synthase)	Heme, cytochromes
Oxaloacetate	Gluconeogenesis (via PEPCK); aspartate, asparagine biosynthesis	Glucose, Asp, Asn
Citrate	Cytosolic acetyl-CoA for fatty acid synthesis; cholesterol	Palmitate, cholesterol

Clinical connection — biotin deficiency: Because pyruvate carboxylase, propionyl-CoA carboxylase, and acetyl-CoA carboxylase most depend on biotin, dietary biotin deficiency (rare; sometimes seen with chronic raw-egg consumption due to avidin) causes lactic acidosis, neurological symptoms, and ketogenic dysregulation simultaneously.

Concept Check 4: If fluoroacetate (a metabolic poison) inhibits aconitase (step 2), predict the immediate effect on (a) citrate levels, (b) isocitrate levels, (c) NADH production, and (d) ATP synthesis.

9.7 Oxidative Phosphorylation and Proton-Motive Force

Oxidative phosphorylation (OxPhos) accounts for about 90% of ATP production in aerobic organisms. It takes place at the inner mitochondrial membrane, where reconstitution experiments helped establish proton-gradient-driven ATP formation [Racker and Stoeckenius, 1974].

9.7.1 Electron Transport Chain (ETC)

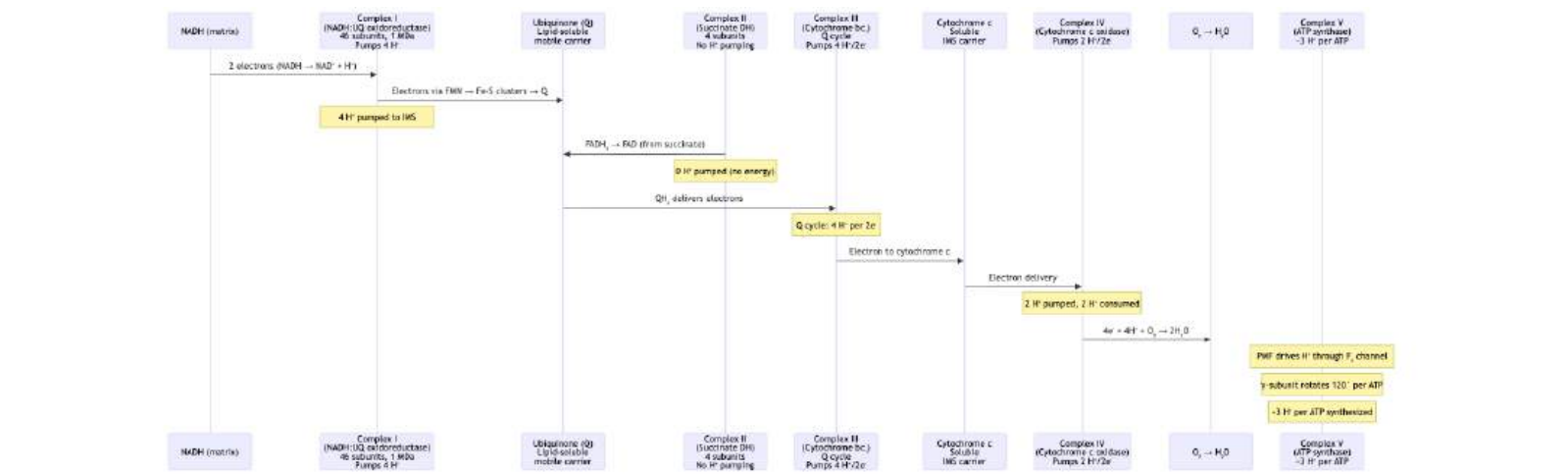


Figure 66. Electron transport passes reducing equivalents from NADH and FADH₂ through complexes I–IV to oxygen, with proton pumping by complexes I, III, and IV building the gradient for ATP synthase.

Electron flow through the ETC complexes I–IV and proton pumping that generates the proton motive force (Mermaid). ATP synthase (Complex V) uses this PMF to synthesize ATP via rotary catalysis.

Complex I (NADH:ubiquinone oxidoreductase): - Largest ETC complex (about 46 subunits in mammals, about 1 MDa) - L-shaped structure: hydrophilic arm in matrix (electron transfer), membrane arm (proton pumping) - Electron path: NADH → FMN → 7 Fe-S clusters → ubiquinone (Q) - Pumps 4 H⁺ per NADH oxidised - Inhibited by rotenone (fish poison, pesticide) and piericidin A

Complex II (succinate:ubiquinone oxidoreductase): - Also is step 6 of the TCA cycle (succinate dehydrogenase) - 4 subunits; FAD covalently bound - Electron path: succinate → FAD → Fe-S clusters → ubiquinone (Q) - Pumps 0 H⁺ (insufficient energy from FADH₂ oxidation to pump protons) - This is why FADH₂ yields less ATP than NADH

Complex III (cytochrome bc₁ complex): - The Q cycle mechanism (Mitchell, Nobel Prize 1978) [Mitchell, 1961]: 1. QH₂ binds Q_o site; one electron goes to Fe-S cluster → cytochrome c₁ → cytochrome c (high potential path) 2. Second electron goes to cytochrome b_L → cytochrome b_H → Q at Q_i site, forming Q^{•-} (semiquinone) 3. Second QH₂ repeats; second electron to Q_i completes QH₂ formation 4. Net: 2 QH₂ oxidised, 1 Q reduced, 2 cytochrome c reduced, 4 H⁺ pumped per 2e⁻ - Inhibited by antimycin A (Q_i site) and myxothiazol (Q_o site)

Complex IV (cytochrome c oxidase): - Contains Cu_A, heme a, heme a₃-Cu_B centers - Transfers 4 electrons to O₂: O₂ + 4e⁻ + 4H⁺_{matrix} → 2H₂O - Pumps 2 H⁺ per 2 electrons (plus 2 H⁺ consumed in water formation) - Inhibited by cyanide (CN⁻), carbon monoxide (CO), and azide (N₃⁻) — most bind heme a₃-Cu_B

Clinical Connection: Cyanide Poisoning Cyanide irreversibly inhibits Complex IV by binding to the Fe³⁺ of heme a₃. Most electron flow stops, the proton gradient collapses, and ATP synthesis ceases. Cells switch to **anaerobic** glycolysis, producing lactic acid. Death results from inability to produce sufficient ATP, especially in the brain and heart. Treatment: hydroxocobalamin (vitamin B_{12a}) chelates cyanide, or sodium thiosulphate converts it to less toxic thiocyanate.

9.7.2 Reactive Oxygen Species and Antioxidant Defense

The ETC's job is to deliver four electrons safely onto O₂ to produce water — but about 0.1–2% of electrons “leak” prematurely, producing reactive oxygen species (ROS).

Sites of ROS production in the ETC:

Table 145. Reactive Oxygen Species and Antioxidant Defense: Site and Primary ROS.

Site	Primary ROS	Mechanism	Inhibitor that <i>increases</i> ROS
Complex I (FMN, Fe-S clusters)	Superoxide (O ₂ ^{•−}) into matrix	Reverse electron transfer when ETC is reduced; FMNH ₂ donates 1e [−] to O ₂	Rotenone
Complex III (Q _o site)	Superoxide into both matrix and IMS	Q ^{•−} semiquinone donates 1e [−] to O ₂	Antimycin A
Glycerol-3- P dehydroge- nase, ETF-QO	Superoxide	Flavoprotein leakage	–
Monoamine oxidase (outer mem- brane)	H ₂ O ₂	2e [−] donation to O ₂	–

The ROS cascade:



The Fenton reaction (last step) is particularly dangerous: hydroxyl radicals (HO[•]) are the most reactive biological oxidants and damage essentially any nearby molecule (DNA, lipids, proteins).

Antioxidant defense enzymes:

Table 146. Reactive Oxygen Species and Antioxidant Defense: Enzyme and Reaction.

Enzyme	Reaction	Cofactor	Localization
Superoxide dismutase (SOD1, cytosolic)	2 O ₂ ^{•−} + 2 H ⁺ → H ₂ O ₂ + O ₂	Cu, Zn	Cytoplasm, IMS
Superoxide dismutase (SOD2, mitochondrial)	2 O ₂ ^{•−} + 2 H ⁺ → H ₂ O ₂ + O ₂	Mn	Mitochondrial matrix
Superoxide dismutase (SOD3, extracellular)	2 O ₂ ^{•−} + 2 H ⁺ → H ₂ O ₂ + O ₂	Cu, Zn	Plasma, ECM
Catalase	2 H ₂ O ₂ → 2 H ₂ O + O ₂	Heme	Peroxisomes
Glutathione peroxidase (GPx)	H ₂ O ₂ + 2 GSH → 2 H ₂ O + GSSG	Selenocysteine	Cytoplasm, mitochondria
Peroxiredoxins (Prx1–6)	H ₂ O ₂ + 2 R-SH → 2 H ₂ O + R-S-S-R	Cysteine	Multiple compartments

Non-enzymatic antioxidants: Glutathione (GSH; about 5 mM cytosolic), ascorbate (vitamin C), α-tocopherol (vitamin E, lipid-soluble), ubiquinone (also acts as antioxidant in its reduced QH₂ form), and uric acid (about 50% of plasma antioxidant capacity in humans).

Clinical relevance:

- Mitochondrial diseases: Complex I and III deficiencies often present with elevated lactate AND elevated ROS damage markers (8-oxoguanine in mtDNA, malondialdehyde in lipids).

- Aging (mitochondrial free-radical theory): Cumulative mtDNA damage from ROS may underlie age-related mitochondrial decline. Modern data suggests ROS are also signaling molecules, complicating the simple “oxidative damage = aging” model.
- Reperfusion injury: During ischemia, ETC carriers become highly reduced. Upon reoxygenation, a burst of ROS is released — paradoxically, the *return* of oxygen causes the worst tissue damage in stroke and heart attack.
- ALS: Mutations in SOD1 cause about 20% of familial amyotrophic lateral sclerosis. The pathology is gain-of-function (toxic SOD1 aggregates), not simple loss of antioxidant activity.

Concept Check 4b: Antimycin A blocks the Q_i site of Complex III. Predict the effects on (a) electron flow upstream (Complexes I, II), (b) downstream (Complex IV), (c) PMF magnitude, and (d) ROS production. Explain why this combination of effects makes antimycin A particularly cytotoxic.

Concept Check (Synthesis): Mitochondrial diseases such as Leigh syndrome arise from mutations in ETC subunits (SURF1 in Complex IV, NDUF54 in Complex I). (a) A patient with a Complex I mutation has 80% reduction in Complex I activity. Predict the quantitative consequences for: (i) NADH/NAD⁺ ratio, (ii) proton-motive force (pmf), (iii) ATP/ADP ratio, and (iv) ROS production. (b) Why are brain and muscle affected most severely (not liver), even though every cell has mitochondria? (c) The “threshold effect” — tissues tolerate mitochondrial dysfunction until hetero-plasmy exceeds about 60-80%. Explain the mechanistic basis: why does a small reserve of normal mitochondria protect function?

Worked Example — P/O Ratio Calculation from Modern Stoichiometry: Using current best estimates: NADH provides electrons that pump about 10 H⁺ across the inner membrane (4 at Complex I, 4 at III, 2 at IV). FADH₂ pumps about 6 H⁺ (0 at Complex I, 4 at III, 2 at IV). ATP synthase requires about $8/3 \approx 2.67$ H⁺ per ATP (mammalian c-ring with 8 subunits, 3 ATP per full c-ring rotation), plus about 1/3 H⁺ per ATP returned via the Pi/H⁺ symporter, giving a *whole-cycle* cost of $8/3 + 1/3 = 3$ H⁺ per ATP exported to the cytosol. Thus: P/O(NADH) = $10/3 \approx 3.3$ (theoretical); empirically about 2.5 (thermodynamic and proton-leak losses). P/O(FADH₂) = $6/3 = 2.0$ theoretical, about 1.5 empirical. Per glucose: $10 \text{ NADH} \times 2.5 + 2 \text{ FADH}_2 \times 1.5 + 4 \text{ substrate-level ATP (2 from glycolysis, 2 GTP from TCA)} = 25 + 3 + 4 = 32 \text{ ATP}$. This reconciles the modern “30-32 ATP” range with the older “36-38” figure by showing that the legacy textbook assumed 3.0 ATP/NADH and 2.0 ATP/FADH₂ — an overestimate by about 15-20% relative to measured P/O ratios in mammalian mitochondria.

9.7.3 ATP Synthase — the Rotary Nanomotor

The proton-motive force (PMF) consists of two components — the electrical potential ($\Delta\Psi$) and the chemical gradient (ΔpH):

$$\text{PMF} = \Delta\Psi - \frac{2.303RT}{F}\Delta\text{pH} \approx 180 \text{ mV}$$

(162)

In mitochondria, $\Delta\Psi \approx 150 \text{ mV}$ contributes about 80% of the PMF, while ΔpH about 0.5 units contributes about 20%.

The free energy stored per mole of protons translocated against this PMF is:

$$\Delta G_{\text{H}^+} = F \cdot \text{PMF} \approx 96,485 \times 0.180 \approx 17.4 \text{ kJ/mol}$$

(163)

So pumping about 3.67 H⁺ to make one ATP requires about 64 kJ/mol of stored gradient energy — the budget that funds an ATP whose cellular hydrolysis $\Delta G \approx -54 \text{ kJ/mol}$. The about 10 kJ/mol surplus is the thermodynamic driving force that keeps net ATP synthesis flowing forward and sets the response time of the system to ATP demand.

ATP synthase (Complex V) is a molecular rotary motor:

F₁ (catalytic head, matrix-facing): - $\alpha_3\text{-}\beta_3\text{-}\gamma\text{-}\delta\text{-}\epsilon$ - Three catalytic sites on beta subunits (binding change mechanism, Boyer) - Each beta subunit cycles through three states: O (open, empty), L (loose, binds ADP + P_i), T (tight, catalyses ATP synthesis) - 120-degree rotation of gamma converts $\text{O} \rightarrow \text{L} \rightarrow \text{T} \rightarrow \text{O}$

F₀ (membrane-spanning proton channel): - Subunit a (proton channel) + c-ring (c_{10–15}, varies by species) - Each c-subunit binds one H⁺ from IMS, rotates, releases H⁺ to matrix - Full c-ring rotation (360 degrees) produces 3 ATP

Stoichiometry: If the c-ring has 10 subunits, then 10 H⁺ per revolution, producing 3 ATP, so about 3.3 H⁺ per ATP. With 8 c-subunits (yeast), about 2.7 H⁺ per ATP.

Paul Boyer (binding change mechanism) and John Walker (crystal structure of F₁) shared the Nobel Prize in Chemistry, 1997. The rotation of the gamma subunit was directly visualized by Yoshida and colleagues using fluorescent **actin** filaments attached to gamma — one of the most beautiful experiments in biochemistry.

9.7.4 How the “30–32 ATP” Number Is Calculated: P/O Ratios

The classical undergraduate value of 38 ATP/glucose came from *assumed* round-number stoichiometries (3 ATP/NADH, 2 ATP/FADH₂, 1 ATP per substrate-level step). Modern biochemistry uses measured P/O ratios based on actual c-ring stoichiometry and proton transport:

Proton pumping per substrate:

Table 147. How the “30–32 ATP” Number Is Calculated: P/O Ratios.

Substrate	Complex I	Complex III	Complex IV	Total H ⁺ pumped
1 NADH (matrix)	4	4	2	10 H ⁺
1 FADH ₂ (Complex II)	0	4	2	6 H ⁺

Mammalian mitochondrial c-ring: 8 subunits (recent cryo-EM data). ATP synthase stoichiometry: 8 H⁺ per full revolution → 3 ATP per revolution → 2.67 H⁺/ATP. Add P_i transport: importing P_i via the phosphate carrier costs 1 additional H⁺ per ATP. So the *effective* H⁺ cost per ATP is approximately 3.67 H⁺/ATP.

$$\text{P/O ratio (NADH)} = \frac{10 \text{ H}^+}{3.67 \text{ H}^+/\text{ATP}} \approx 2.5 \text{ ATP per NADH}$$

(164)

$$\text{P/O ratio (FADH}_2\text{)} = \frac{6 \text{ H}^+}{3.67 \text{ H}^+/\text{ATP}} \approx 1.5 \text{ ATP per FADH}_2$$

(165)

Total ATP per glucose (aerobic):

$$\text{ATP}_{\text{glucose}} = \underbrace{2}_{\text{glycolysis SLP}} + \underbrace{2}_{\text{TCA SLP (2 GTP)}} + \underbrace{10 \times 2.5}_{\text{NADH via OxPhos}} + \underbrace{2 \times 1.5}_{\text{FADH}_2 \text{ via OxPhos}} \approx 32 \text{ ATP}$$

(166)

(if cytoplasmic NADH uses the malate-aspartate shuttle; about 30 ATP if the glycerol-3-P shuttle is used in muscle and brain).

Table 148. How the “30–32 ATP” Number Is Calculated: P/O Ratios: Stage and NADH.

Stage	NADH	FADH ₂	ATP direct	ATP via OxPhos	Subtotal
Glycolysis	2	0	2	2 × 2.5 = 5*	7
Pyruvate oxidation	2	0	0	2 × 2.5 = 5	5
TCA cycle	6	2	2	6 × 2.5 + 2 × 1.5 = 18	20
Total	10	2	4	28	about 30–32

*Glycolytic NADH yields 2.5 ATP (malate-aspartate shuttle) or 1.5 ATP (glycerol-3-phosphate shuttle), giving 30 or 32 ATP total.

The glycerol-3-phosphate shuttle vs. malate-aspartate shuttle:

- Cytoplasmic NADH cannot cross the IMM directly.
- Malate-aspartate shuttle (liver, heart, kidney): NADH electrons enter the matrix via OAA→malate→OAA at full reducing potential → 2.5 ATP each.
- Glycerol-3-phosphate shuttle (skeletal muscle, brain): NADH electrons enter directly into Q via FAD-linked mitochondrial G3PDH → 1.5 ATP each (skips Complex I).

9.7.5 Worked Example: Total ATP Yield

Problem: Calculate the total ATP yield from one molecule of glucose using the malate-aspartate shuttle for most glycolytic NADH.

Solution:

Table 149. Total ATP Yield: Source and Quantity.

Source	Quantity	ATP per unit	ATP
Glycolysis substrate-level	2 ATP	1	2
TCA substrate-level (GTP)	2 GTP	1	2
Glycolytic NADH (malate-aspartate)	2 NADH	2.5	5
Pyruvate DH NADH	2 NADH	2.5	5
TCA NADH	6 NADH	2.5	15
TCA FADH ₂	2 FADH ₂	1.5	3
Total			32

The thermodynamic efficiency:

$$\eta = \frac{32 \times 30.5}{2,870} \times 100\% = 34\%$$

(167)

Using the more realistic *cellular* ΔG of -50 kJ/mol, efficiency rises to about 56%, comparable to the best internal combustion engines and considerably better than most human-engineered energy converters.

Concept Check 5: Why does FADH₂ yield fewer ATP than NADH? Trace the difference back to the ETC entry point and proton pumping stoichiometry.

Concept Check 5b: Consult equation (166). If a mutation altered the c-ring stoichiometry from 8 to 12 subunits (raising H⁺/ATP from 2.67 to 4), recompute the P/O ratios for NADH and FADH₂ and the total ATP yield per glucose. Comment on what this would mean for daily ATP turnover and whole-organism metabolism.

9.8 Substrate-Level vs. Oxidative Phosphorylation: A Quantitative Comparison

Table 150. Total ATP Yield: Feature and Substrate-level phosphorylation.

Feature	Substrate-level phosphorylation	Oxidative phosphorylation
Location	Cytoplasm (glycolysis), matrix (TCA)	Inner mitochondrial membrane
Energy source	High-energy phosphorylated intermediate	Proton motive force
O ₂ required?	No	Yes (terminal electron acceptor)
Energy “currency” intermediate	1,3-BPG, PEP, succinyl-CoA	$\Delta\mu_{\text{H}^+}$ (electrochemical)
Maximum theoretical efficiency	about 60% (per intermediate)	about 70% (PMF → ATP)
ATP per glucose (aerobic, 32 total)	4 ATP (12.5%)	28 ATP (87.5%)
Speed of onset	Immediate (ms)	Seconds (requires PMF buildup)
Sustainability	Limited (substrate-bound)	Continuous (as long as fuel + O ₂)
Examples	PGK, pyruvate kinase, succinyl-CoA synthetase	ATP synthase
Inhibited by	Specific enzyme inhibitors	ETC inhibitors, uncouplers, oligomycin

Quantitative leverage: Although substrate-level phosphorylation contributes roughly 12.5% of total ATP in this accounting, it is critical in two scenarios:

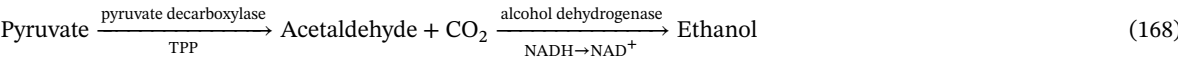
1. Anaerobic conditions: It is the *primarily* source of ATP, so 4 ATP/glucose is everything.
2. Sprint exercise: It can produce ATP in milliseconds, before mitochondrial respiration ramps up; the phosphocreatine system extends this further.

This illustrates why metabolic systems are layered: fast-but-low-yield substrate-level phosphorylation handles transients while slow-but-high-yield OxPhos handles steady state.

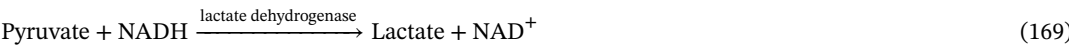
Numerical leverage at the organism level. A 70 kg adult at rest uses about 1,400 kcal/day, equivalent to about 250 mol ATP turned over. If primarily substrate-level phosphorylation operated, with about 4 ATP/glucose, the body would need to oxidise about 62 mol glucose/day (= 11 kg). Aerobic OxPhos at about 32 ATP/glucose reduces the requirement to about 8 mol = 1.4 kg glucose/day — a more achievable dietary intake. The 8-fold yield improvement of OxPhos is precisely what enables active multicellular life on a planet with bulk-food-supply constraints.

9.9 Fermentation and NAD+ Regeneration

Without O₂ (or in cells that lack mitochondria), pyruvate is not oxidised aerobically. Instead, fermentation regenerates NAD⁺ so glycolysis can continue:
Alcoholic fermentation (yeast, some bacteria):



Lactic acid fermentation (muscle, erythrocytes, *Lactobacillus*):



Both pathways yield primarily 2 ATP per glucose (from glycolysis alone).

The Cori Cycle: In exercising muscle, lactate is exported to the blood, taken up by the liver, and converted back to glucose via gluconeogenesis at the cost of 6 ATP. This glucose returns to the muscle via the blood. The Cori cycle shifts the metabolic burden of gluconeogenesis from the oxygen-limited muscle to the well-oxygenated liver.

Pasteur Effect: In the presence of oxygen, yeast switches from fermentation to aerobic respiration, dramatically reducing glucose consumption (because 32 ATP/glucose aerobically vs. 2 ATP/glucose by fermentation — 16x more efficient).

- Clinical Connection: Lactic Acidosis Lactic acidosis occurs when lactate production exceeds clearance. Type A (most common): tissue hypoxia (shock, cardiac arrest, severe anemia) forces reliance on glycolysis. Type B: metabolic causes (liver failure preventing lactate clearance, metformin in renal impairment, thiamine deficiency preventing PDC function, mitochondrial diseases). Blood lactate >4 mmol/L with pH <7.35 indicates lactic acidosis. Treatment focuses on addressing the underlying cause and restoring tissue oxygenation.
- Clinical Connection: Mitochondrial Complex Disorders **Mutations** in nuclear or mitochondrial **genes** encoding ETC complex subunits cause a spectrum of diseases: - Complex I deficiency: Most common ETC disorder (about 30% of pediatric mitochondrial disease); Leigh syndrome (necrotising encephalopathy), optic atrophy, cardiomyopathy - Complex II deficiency: Rare; associated with paragangliomas and pheochromocytomas (SDH mutations are tumor suppressors) - Complex III deficiency: Exercise intolerance, lactic acidosis - Complex IV (COX) deficiency: Leigh syndrome, cardiomyopathy; reversible COX deficiency in infants Most are characterized by lactic acidosis, neurological dysfunction, and exercise intolerance — tissues with high energy demands (brain, heart, muscle) are most affected.
- Concept Check 6: A patient with a mitochondrial Complex I mutation has reduced NADH oxidation. Would you expect succinate-linked respiration (via Complex II) to be normal or impaired in this patient? Explain.

9.10 Uncoupling Proteins and Brown Adipose Thermogenesis

In most cells, the primary “exit” for protons in the IMS back to the matrix is through ATP synthase. Uncoupling proteins (UCPs) provide an alternative path that dissipates the proton gradient as heat — uncoupling electron transport from ATP synthesis.

9.10.1 UCP1: The Brown Adipose Thermogenin

Structure: UCP1 is a 32-kDa, six-transmembrane-helix protein in the IMM of brown adipocytes. It belongs to the SLC25 mitochondrial carrier family.
Mechanism (proton transport, not pure leak):



Long-chain fatty acid anions (FA[−]) act as cofactors: they bind H⁺ in the IMS, traverse the membrane via UCP1, and release H⁺ in the matrix. UCP1 is inhibited by purine nucleotides (ATP, ADP, GTP, GDP) and activated by fatty acids released from intracellular triglyceride stores.

Activation cascade in brown adipose tissue (BAT):

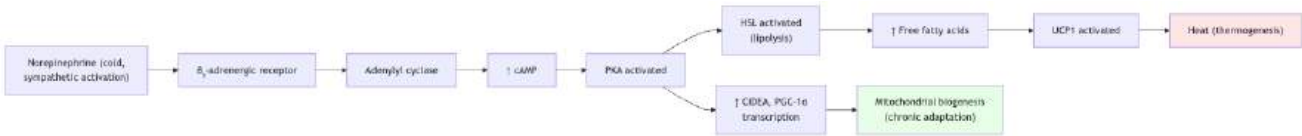


Figure 67. Cold-triggered sympathetic signaling activates brown-adipose UCP1, allowing proton flow to produce heat instead of ATP.

Sympathetic activation of brown adipose thermogenesis (Mermaid). Norepinephrine binds β₃-adrenergic receptors → cAMP → PKA → simultaneous lipolysis (acute fuel) and PGC-1α transcription (chronic mitochondrial biogenesis). UCP1 short-circuits the proton gradient, releasing energy as heat.

9.10.2 Physiological Roles of Lactate

Table 151. Physiological Roles of Lactate: Setting and Role of UCP1 / brown fat.

Setting	Role of UCP1 / brown fat
Neonates	Critical for non-shivering thermogenesis; lack effective shivering due to small muscle mass; about 5% body weight is BAT
Hibernating mammals	Massive BAT depots maintain about 5 °C body temp; explosive arousal phase warms the body in hours
Adult humans	Active BAT discovered in 2009 in the supraclavicular and paraspinal regions; activated by cold exposure; declines with age and obesity
Cold acclimation	Chronic cold exposure increases BAT mass and UCP1 expression — a target for obesity therapy
Beige (brite) adipocytes	UCP1 ⁺ cells that emerge from white adipose under cold/exercise; an inducible thermogenic compartment

Other UCPs:

- UCP2: ubiquitously expressed; modest uncoupling activity; thought to attenuate ROS and modulate insulin secretion.
- UCP3: skeletal muscle and BAT; possible role in lipid handling; debated thermogenic relevance.
- Plant UCPs (PUMPs): present in mitochondria of e.g. *Arum* species, where they generate the heat (about 46 °C) that volatilises odors to attract pollinator insects.

Clinical Connection: DNP — A Cautionary Tale 2,4-Dinitrophenol (DNP) is a synthetic chemical uncoupler that dissipates PMF as heat, mimicking UCP1 across most tissues. In the 1930s, DNP was sold as a weight-loss drug — patients lost about 1 kg/week as their basal metabolic rate increased about 50%. But the therapeutic window is dangerously narrow: at slightly higher doses, body temperature rises to >40 °C (fatal hyperthermia), and unregulated tissue uncoupling causes cataracts, neuropathy, and sudden death. DNP was banned in 1938 but remains a recurrent source of bodybuilding deaths today. The takeaway: physiological uncoupling is *regulated* (UCP1 activated primarily in BAT, primarily on demand) — pharmacological uncoupling is unregulated and potentially lethal.

Concept Check 6b: A 3-month-old infant is brought to the ED in mild hypothermia after exposure to cold. Imaging reveals normal BAT volume and PET activity. Predict (a) whether shivering or non-shivering thermogenesis dominates the infant’s response, (b) the role of β₃-AR signaling, and (c) the metabolic consequences of repeated cold exposures.

9.11 Metabolic Poisons and Inhibitors

Understanding the ETC and oxidative phosphorylation has been greatly advanced by studying specific inhibitors and metabolic poisons:

9.11.1 Electron-Transport Chain Inhibitors

Table 152. Electron-Transport Chain Inhibitors: Inhibitor and Target.

Inhibitor	Target	Effect
Rotenone	Complex I (NADH dehydrogenase)	Blocks electron transfer from Fe-S clusters to ubiquinone; NADH-linked respiration stops; used as fish poison and pesticide
Antimycin A	Complex III (Q _i site)	Blocks electron transfer at the Q _i site of the Q cycle; generates superoxide
Cyanide (CN [−])	Complex IV (CuB/a ₃)	Binds Fe ³⁺ in cytochrome a ₃ , blocking O ₂ reduction; rapidly fatal
Carbon monoxide (CO)	Complex IV (haem a ₃)	Competes with O ₂ for binding; also binds hemoglobin (200x affinity vs O ₂)
Hydrogen sulfide (H ₂ S)	Complex IV	Similar to cyanide; binds haem iron; toxic at >50 ppm in air

9.11.2 Uncouplers and Proton Leak

Uncouplers dissipate the proton gradient without inhibiting electron transport, allowing respiration to continue at maximum rate without ATP production:

- 2,4-dinitrophenol (DNP): A lipid-soluble weak acid; carries H⁺ across the IMM. Was used as a weight-loss drug in the 1930s (burns fat by dissipating energy as heat) but was banned due to narrow therapeutic window and fatal hyperthermia.
- FCCP/CCCP: Research uncouplers; commonly used in mitochondrial stress tests (Seahorse assays)
- Thermogenin (UCP1): The physiological uncoupler in brown adipose tissue, developed in the thermogenesis discussion above.

9.11.3 ATP Synthase Inhibitors

- Oligomycin: Blocks the H⁺ channel in the c-ring of F₀; prevents H⁺ flow and ATP synthesis; also halts electron transport (because PMF builds up, preventing further H⁺ pumping by the ETC)
- DCCD (dicyclohexylcarbodiimide): Reacts with a specific Asp/Glu residue in the c-subunit, blocking H⁺ translocation

Concept Check 7: If oligomycin is added to mitochondria, electron transport stops. If DNP (an uncoupler) is then added, electron transport resumes. Explain these observations in terms of the chemiosmotic model.

Concept Check 7b: A researcher exposes isolated mitochondria sequentially to: (1) succinate, (2) ADP + P_i, (3) rotenone, (4) DNP. For each addition, predict whether O₂ consumption increases, decreases, or stays the same, and explain why — referring to equation (162) and equation (166).

9.12 Computational Bridge

Cellular ATP hydrolysis free energy is adjusted by the mass-action ratio $Q = \frac{[ADP][P_i]}{[ATP]}$:

```
from biology.biochemistry import atp_free_energy

print(round(atp_free_energy(atp_conc_mM=3.0, adp_conc_mM=1.0, pi_conc_mM=10.0), 2))
```

Clinical / systems note: Mitochondrial poisons (cyanide, carbon monoxide) and uncouplers like DNP illustrate how collapsing PMF or bypassing ATP synthase converts energy to heat — the same gradient you model when counting protons per ATP. UCP1 is a regulated example of the same principle.

9.13 Current Evidence and Frontier Biology: Bioenergetics and Cellular Respiration

For Bioenergetics and Cellular Respiration, frontier biology belongs inside the evidence logic of the chapter. Metabolism is now studied as a regulated network constrained by energy, redox balance, compartmentation, and environment. The core reading question is this: respiration claims should track electrons, protons, redox poise, ATP yield, and uncoupling.

- What to verify: identify the observation, model, assay, or dataset that would make the claim stronger or weaker.

- What to qualify: state the scale, organism, cell type, environmental condition, or population where the claim is expected to hold.
- What to compare: test at least one alternative explanation, baseline, or null model before treating the pattern as causal.
- What to cite: distinguish primary evidence, review synthesis, public dataset, and institutional guidance; for recent or numeric claims, prefer the source closest to the measurement and state what has changed since it was published.

A strong respiration claim names the compartment, redox carrier, coupling site, and energetic condition under which ATP yield or flux changes.

Source practice: For respiration claims, keep organism, tissue, substrate, oxygen status, and measurement method visible; pathway maps need flux or concentration evidence.

9.13.1 Current Evidence Map: Respiration Evidence Accounting

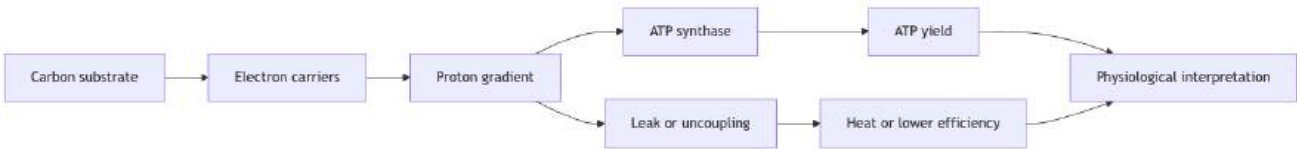


Figure 68. ATP-yield claims are conditional on shuttle use, proton leak, coupling efficiency, tissue state, and measurement method rather than one fixed number.

9.14 Summary

- $\Delta G = \Delta H - T\Delta S$ (equation (150)); cellular reactions are coupled to ATP hydrolysis ($\Delta G \approx -54$ kJ/mol) to drive endergonic processes. Cells maintain far-from-equilibrium conditions.
- ATP turnover is about 40 kg/day; the high ΔG of hydrolysis arises from charge repulsion, resonance stabilization, and hydration of products. ATP sits in the *middle* of the phosphoryl-transfer hierarchy, between very high (PEP, 1,3-BPG) and very low (glucose-6-P).
- Glucose oxidation has a standard free energy of $\approx -2,870$ kJ/mol; cells capture about 56% of this as ATP, dissipating the rest as heat.
- Glycolysis: 10 cytoplasmic steps; net 2 ATP + 2 NADH per glucose; regulated by PFK-1 (activated by AMP, F2,6BP; inhibited by ATP, citrate).
- Gluconeogenesis: not the reverse of glycolysis — uses four bypass enzymes (pyruvate carboxylase, PEPCK, FBPase-1, G6Pase) at a cost of 6 ATP equivalents per glucose; reciprocally regulated with glycolysis via F2,6BP.
- The Cori cycle and glucose-alanine cycle distribute metabolic burden between muscle and liver, supporting hypoxic tissues at a 4-ATP-per-glucose net cost to the organism.
- PDC links glycolysis to TCA; regulated by phosphorylation/dephosphorylation; deficiency causes lactic acidosis.
- TCA cycle: 8 mitochondrial matrix steps; 6 NADH + 2 FADH₂ + 2 GTP per glucose; regulated by isocitrate DH and α -KG DH; anaplerotic (pyruvate carboxylase, glutamate dehydrogenase) and cataplerotic flux balance the cycle.
- ETC: Complex I (4 H⁺), II (0 H⁺), III (4 H⁺ via Q cycle), IV (2 H⁺); final electron acceptor = O₂. Modest electron leak produces ROS (equation (161)); SOD, catalase, GPx, and peroxiredoxins constrain damage.
- ATP synthase: F₀F₁ rotary motor; binding change mechanism; about 3.67 H⁺ per ATP (including phosphate import). Proton-motive force ≈ 180 mV (equation (162)).
- Modern ATP yield: about 30–32 ATP per glucose aerobically (equation (166), equation (164), equation (165)); 2 ATP per glucose anaerobically.
- Uncoupling proteins (UCP1) regulate physiological thermogenesis in brown adipose tissue; pharmacological uncouplers (DNP) dissipate the same PMF unregulated and are dangerous.
- Connections: See section 10 for light-driven phosphorylation, section 11 for hormonal integration, and Unit X — Ecology: Introduction for ecosystem productivity and reduced carbon.

9.15 Review Questions

1. Explain why cells must maintain metabolite concentrations far from equilibrium. What would happen to ATP synthesis if the cell reached thermodynamic equilibrium?
2. Describe the 10 steps of glycolysis. Which three steps are irreversible and why are these the regulatory control points?
3. Compare the four bypass enzymes of gluconeogenesis with the three irreversible glycolytic steps they replace. Why is each bypass thermodynamically favorable in the gluconeogenic direction?
4. Explain the structure and regulation of the pyruvate dehydrogenase complex. Why does it require five cofactors?

5. Track the fate of both carbon atoms in acetyl-CoA through one turn of the TCA cycle. Are these the same carbons released as CO₂?
6. Distinguish between anaplerotic and cataplerotic reactions. Give two examples of each, and explain why pyruvate carboxylase is allosterically activated by acetyl-CoA.
7. Describe the Q cycle in Complex III. Why is this mechanism necessary, and how does it contribute to proton pumping?
8. Identify the major ETC sites of ROS production and the antioxidant enzymes that detoxify each downstream species. Why is the Fenton reaction particularly dangerous?
9. Explain the binding change mechanism of ATP synthase. How was the rotation of the gamma subunit experimentally demonstrated?
10. Calculate the ATP yield from complete oxidation of one molecule of glucose via glycolysis, PDC, TCA cycle, and oxidative phosphorylation (equation (166)). Explain why the answer is 30 or 32 depending on the NADH shuttle used, and trace each number back to specific P/O ratios.
11. Compare alcoholic and lactic acid fermentation. Why is fermentation essential even though it produces far less ATP than aerobic respiration?
12. Compare physiological (UCP1) and pharmacological (DNP) uncoupling. Why does the body tolerate UCP1 activity but not DNP, even though both dissipate the same PMF as heat?
13. A patient presents with exercise intolerance and lactic acidosis. Genetic testing reveals a mutation in the ND1 gene (Complex I subunit). Explain the biochemical basis of each symptom.
14. Explain the Pasteur effect and the Warburg effect. How do they represent opposite metabolic strategies?
15. Recompute `atp_free_energy` when cytosolic ATP drops to 1 mM while ADP rises to 4 mM (Pi fixed). Does hydrolysis become more or less exergonic, and why does that matter during exercise?
16. Using `glycolysis_summary()` from the same module, state the net ATP and NADH from one glucose without writing the ten steps.
17. Using ΔG° values for ATP and PEP hydrolysis, compute the standard free energy change of pyruvate kinase (PEP + ADP → pyruvate + ATP). Compare with the cellular ΔG and explain the irreversibility.
18. Compute the proton motive force from $\Delta\Psi = -160$ mV and $\Delta\text{pH} = 0.6$ at 37 °C using equation (162). Convert to free energy per mole of protons.

9.16 Further Reading and Source Notes: Bioenergetics and Cellular Respiration

- Mitchell (1961). Coupling of phosphorylation to electron and hydrogen transfer by a chemi-osmotic type of mechanism. *Nature*, 191 [Mitchell, 1961].
- Atkinson (1968). The regulation of enzyme activity in metabolism. *Biochemical Journal*, 108 [Atkinson, 1968].
- Krebs & Johnson (1937). The role of citric acid in intermediate metabolism in animal tissues. *Enzymologia*, 4.
- Boyer (1997). The ATP synthase — a splendid molecular machine. *Annual Review of Biochemistry*, 66.
- Rich (2003). The molecular machinery of Keilin’s respiratory chain. *Biochemical Society Transactions*, 31.

9.17 Key Terms

Table 153. Current Evidence Map: Respiration Evidence Accounting: Term and Definition.

Term	Definition
Gibbs free energy (ΔG)	Thermodynamic quantity predicting reaction spontaneity; $\Delta G < 0$ = spontaneous
ATP	Adenosine triphosphate; central phosphoryl-group donor and short-term energy carrier; ΔG hydrolysis ≈ -54 kJ/mol (cellular)
Glycolysis	10-step cytoplasmic pathway converting glucose to 2 pyruvate + 2 ATP + 2 NADH
Gluconeogenesis	Synthesis of glucose from non-carbohydrate precursors using four bypass enzymes; 6 ATP equivalents per glucose
PFK-1	Phosphofructokinase-1; committed step of glycolysis; allosterically regulated
Pyruvate dehydrogenase complex	Multienzyme complex linking glycolysis to TCA; 5 cofactors; regulated by phosphorylation
TCA cycle	8-step mitochondrial cycle oxidising acetyl-CoA; produces 3 NADH + 1 FADH ₂ + 1 GTP per turn
Anaplerotic reaction	Reaction replenishing TCA cycle intermediates (e.g., pyruvate carboxylase)

Term	Definition
Cataplerotic reaction	Reaction removing TCA intermediates for biosynthesis (e.g., citrate → acetyl-CoA for FA synthesis)
Electron transport chain	Complexes I–IV on IMM; transfers electrons from NADH/FADH ₂ to O ₂ , pumping H ⁺
Q cycle	Complex III mechanism doubling H ⁺ pumping efficiency per electron pair
ATP synthase	F ₀ F ₁ rotary motor using PMF to synthesize ATP; about 3.67 H ⁺ /ATP including P _i import
Proton motive force (PMF)	Electrochemical gradient of H ⁺ across IMM; ≈ 180 mV; drives ATP synthesis
P/O ratio	ATP molecules produced per oxygen atom reduced; about 2.5 for NADH, about 1.5 for FADH ₂
Reactive oxygen species (ROS)	O ₂ ^{•−} , H ₂ O ₂ , HO [•] produced by electron leak; constrained by SOD, catalase, GPx
Uncoupling protein (UCP1)	IMM proton channel in brown adipose tissue; dissipates PMF as heat
Fermentation	Anaerobic regeneration of NAD ⁺ ; lactic acid or ethanol pathways; 2 ATP per glucose
Cori cycle	Lactate (muscle) to glucose (liver) shuttle; shifts gluconeogenic cost to liver
Glucose-alanine cycle	Inter-organ shuttle carrying both carbon and waste nitrogen from muscle to liver
Warburg effect	Aerobic glycolysis in cancer cells; rapid ATP + biosynthetic precursors despite O ₂
Substrate-level phosphorylation	Direct transfer of phosphoryl group from high-energy intermediate to ADP

9.18 Companion Source Module: Bioenergetics and Cellular Respiration

Bioenergetics and Cellular Respiration should leave a reproducible trail from a biological claim to the code, figure, diagram, or paper-based activity that can test it. Use the surfaces below to inspect the chapter’s assumptions, rerun the relevant model, or compare the manuscript explanation with companion labs and figures.

Table 154. Companion source surfaces for Bioenergetics and Cellular Respiration.

Surface	Use it for
<code>src/biology/biochemistry/biochemistry.py</code> (<code>reaction_free_energy</code> , <code>atp_free_energy</code> , <code>glycolysis_summary</code>)	Track energy accounting across glycolysis, respiration, and ATP coupling.
<code>src/mermaid/biology_diagrams.py</code> (<code>glycolysis_pathway_diagram</code> , <code>atp_synthesis_diagram</code>)	Check pathway order and coupling between electron flow and proton motive force.

Reproducibility check: name the electron donor, acceptor, compartment, proton path, and ATP-yield assumption before comparing respiratory claims. Cross-reference: connect with section 10, section 11, and section 4.

10 Photosynthesis

Level 2/3 · 55 min read · 75 min lecture · Prerequisites: section 9

10.1 Learning Objectives

1. Describe **chloroplast** structure and the organization of the photosynthetic membrane.
2. Explain the light-harvesting antenna complexes, chlorophyll a/b ratio, and energy transfer mechanisms (FRET, exciton transfer).
3. Compute the energy of a photon and convert per-molecule values to per-mole values for biological calculations.
4. Describe Photosystem II, water splitting, and the Kok cycle in detail.
5. Explain the cytochrome b_6f complex and the Q cycle in chloroplasts.
6. Describe Photosystem I, linear and cyclic electron flow, and NADPH production.
7. Explain the Z-scheme of photosynthetic electron transport, including standard electrode potentials of each carrier.
8. Describe the three phases of the **Calvin cycle**, including RuBisCO biochemistry, structure (L_8S_8), catalytic mechanism, and the CO_2/O_2 specificity factor (τ).
9. Explain the thioredoxin/ferredoxin redox regulation system and the activating role of stromal pH and Mg^{2+} .
10. Explain photorespiration and its metabolic costs.
11. Compare C3, C4, and CAM **photosynthesis** strategies and their water-use efficiency, including quantitative trade-offs.
12. Evaluate photoprotection (NPQ, xanthophyll cycle) and artificial photosynthesis research as responses to excess light and energy demand.
13. Calculate ATP and NADPH requirements per CO_2 fixed; compare biological and artificial photosynthesis efficiencies.

10.1.1 Study Blueprint

- Big idea: Photosynthesis couples light-driven electron flow to carbon fixation and planetary productivity.
- Core concepts: photosystems, electron transport, Calvin cycle, photorespiration.
- Framework alignment: Vision & Change: Pathways and transformations of energy and matter, Systems; AP Biology: Energetics, Systems Interactions; NGSS-style topics: Matter and Energy in Organisms and Ecosystems.
- Model or quantitative lens: Photon, ATP/NADPH, and Calvin-cycle stoichiometry.
- Data skill: Interpret light-response and carbon-fixation data.
- Practice cadence: Representing and Describing Data, Statistical Tests and Data Analysis.
- Common misconception to repair: Plants do not eat sunlight; they use light energy to reduce carbon using electrons and enzymes.
- Primary lab: **Lab — Photosynthesis**.
- Question bank: **Questions — Photosynthesis**.
- Transfer task: Transfer photosynthetic constraints to crops, algae, climate, or ecosystem productivity.
- Bridge to computation: `biology.botany.botany.photosynthesis_rate`.

Opening Vignette: Tracing Carbon From Air to Sugar

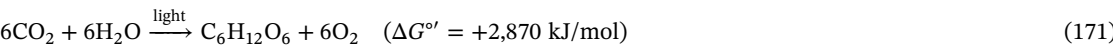
In 1950, Melvin Calvin’s team at the Lawrence Berkeley National Laboratory began exposing algae (*Chlorella*) to $^{14}CO_2$ — carbon dioxide labeled with radioactive carbon-14 — for very brief intervals (as short as 5 seconds), then rapidly killing the cells and separating their compounds by two-dimensional paper chromatography. By tracking which molecules became radioactively labeled first, then in which order, Calvin meticulously traced the path of carbon atoms from atmospheric CO_2 through a cycle of enzymatic reactions to eventually emerge as glucose. The complete cycle — the Calvin-Benson-Bassham cycle — was published in 1954, and Calvin received the Nobel Prize in Chemistry alone in 1961.

The cycle’s key **enzyme**, RuBisCO (ribulose-1,5-bisphosphate carboxylase/oxygenase), is arguably the most important enzyme on Earth: it is responsible for fixing approximately 10^{11} tonnes of atmospheric carbon per year, feeding essentially most non-chemotrophic life. It is also probably the most abundant **protein** on Earth (approximately 0.7 kg per person on the planet’s surface, an estimated 7×10^8 tonnes total), and notably one of the slowest enzymes known, with a k_{cat} of about $3\text{--}10\text{ s}^{-1}$. Improving RuBisCO efficiency is one of the holy grails of agricultural biotechnology.

Primary source: Calvin, M. & Benson, A. A. (1948). The path of carbon in photosynthesis. Science, 107(2784), 476–480.

10.2 Photosynthesis as Light-Driven Carbon Fixation

Photosynthesis is one of Earth’s dominant chemical processes: it fixes approximately 120 Gt of carbon from CO_2 per year, sustains atmospheric oxygen, and supports nearly every heterotrophic food web.



The reaction is highly endergonic — it requires light energy to drive it. Photosynthesis occurs in the chloroplast (plants and algae) and at the plasma membrane (cyanobacteria). The process can be divided into:

1. Light-dependent reactions (thylakoid membrane): $\text{H}_2\text{O} \rightarrow \text{O}_2 + \text{NADPH} + \text{ATP}$
2. Light-independent reactions / Calvin cycle (stroma): $\text{CO}_2 + \text{ATP} + \text{NADPH} \rightarrow \text{G3P (sugar)}$

10.2.1 Chloroplast Structure and Thylakoid Compartments

- Outer envelope: freely permeable (porin-like channels)
- Inner envelope: selective transporters (triose phosphate / phosphate antiporter, TPT)
- Thylakoid membrane: site of light reactions; forms stacked grana (5–20 thylakoids per granum) + interconnecting stroma lamellae
- Lumen (thylakoid lumen): acidified (pH about 5) by proton pumping; about 1,000-fold H^+ gradient
- Stroma: site of Calvin cycle; contains RuBisCO, enzymes, chloroplast DNA, 70S ribosomes

Thylakoid membranes are densely packed with protein complexes — about 70% protein by mass, making them one of the most protein-rich membranes in nature. Each reaction center is associated with about 250 antenna chlorophyll molecules.

Chloroplast genome: 120–200 kb circular DNA; encodes about 120 genes including RuBisCO large subunit, photosystem subunits, and ribosomal components. Like mitochondria, chloroplasts originated from endosymbiosis (cyanobacteria; see section 5).

10.3 Light Absorption and Energy Transfer

10.3.1 Photosynthetic Pigments and Light Absorption

Chlorophylls absorb light primarily at:

- Chlorophyll a: 430 nm (blue-violet) and 680 nm (red)
- Chlorophyll b: 450 nm and 640 nm (broader absorption; accessory pigment)
- Carotenoids: 400–500 nm; β -carotene, lutein, zeaxanthin; also transfer energy to Chl a; function as photoprotectants

The green wavelengths (about 500–600 nm) are reflected — hence plant color.

10.3.2 Photon Energy and Quantum Efficiency

A photon of red light ($\lambda = 680 \text{ nm}$) carries:

$$E = \frac{hc}{\lambda} = \frac{(6.626 \times 10^{-34} \text{ J}\cdot\text{s})(3 \times 10^8 \text{ m/s})}{680 \times 10^{-9} \text{ m}} = 2.93 \times 10^{-19} \text{ J} = 1.82 \text{ eV}$$

(172)

Per mole: $E = N_A \times E_{\text{photon}} = 176 \text{ kJ/mol}$.

By comparison, blue light (440 nm) photons carry about 272 kJ/mol — substantially more energy than red. The “red drop” in photosynthetic action spectra reflects the fact that energy in excess of the redox requirement is dissipated as heat *whichever* photon is absorbed; longer-wavelength light is therefore proportionally more efficient on a per-photon basis.

Quantum yield of photosynthesis: The quantum yield (Φ) is the molecules of product per photon absorbed. Two important quantum yields are defined:

- $\Phi_{\text{O}_2} \approx 0.10\text{--}0.12 \text{ mol O}_2 \text{ per mol photons absorbed (under optimal conditions)}$
- $\Phi_{\text{CO}_2} \approx 0.08\text{--}0.10 \text{ mol CO}_2 \text{ per mol photons (lower because of photorespiration in C3)}$

The minimum quantum requirement ($1/\Phi$) is therefore about 8–10 photons per O_2 released — close to the theoretical minimum of 8 photons (4 photons through PS II + 4 through PS I per O_2 produced). The remaining inefficiency reflects energy losses in antenna transfer, NPQ activation, and photorespiration.

Quantum efficiency (energy basis):

$$\eta_{\text{quantum}} = \frac{n_{\text{electrons}} \cdot \Delta E_{\text{redox}}}{n_{\text{photons}} \cdot E_{\text{photon}}}$$

(173)

For the Z-scheme: 4 electrons span 1.14 V from H₂O to NADPH, requiring about 440 kJ/mol of electron flow. With 8 photons of 680 nm light supplying about 1,408 kJ/mol, the redox efficiency is about 31% — the rest is consumed by overpotentials and dissipated as heat.

Comparison with engineered photovoltaics. A commercial single-junction silicon solar cell at 22% efficiency converts solar irradiance into electricity that must then power *something* — and the chain from electricity → stored chemical fuel adds losses. Plants, by contrast, deliver a stored fuel (sugar) directly. The artificial-photosynthesis discussion returns to this comparison; equation (173) sets the upper biological bound.

10.3.3 Antenna Complexes and Light-Harvesting Architecture

Each reaction center in plants is served by a peripheral antenna of light-harvesting complexes (LHC). LHCII alone is the most abundant membrane protein on Earth (about 50% of thylakoid membrane protein).

Chlorophyll a/b ratio:

Table 155. Antenna Complexes and Light-Harvesting Architecture: Complex and Chl a:b ratio.

Complex	Chl a:b ratio	Function
LHCII (peripheral PS II antenna)	about 1.3	Light harvesting; mobile under state transitions
CP43, CP47 (core PS II antennae)	Most Chl a	Direct excitation transfer to P680
LHCI (PS I antenna)	about 3.5	Light harvesting for P700
Reaction centers (P680, P700)	Most Chl a	Charge separation chromophores

The Chl a:b ratio of an entire leaf typically ranges from about 2.5 (sun-adapted) to about 3.5 (shade-adapted leaves invest more in Chl b–rich LHCII to broaden the absorbed spectrum). Chl b’s broader 450 nm/640 nm absorption is critical for harvesting green-shifted light filtered through canopy chlorophyll above.

Carotenoid functions:

1. Light harvesting in the 450–500 nm range, where Chl absorbs poorly (about 30% of the antenna’s spectral coverage)
2. Triplet quenching: ³Chl* (long-lived triplet state, formed when singlet excitations are not used quickly) is rapidly quenched by carotenoids, preventing ¹O₂ generation
3. Singlet oxygen scavenging: any ¹O₂ that does form is quenched by carotenoids (the *first* line of antioxidant defense)
4. Structural stabilization of LHC protein folds

10.3.4 Energy Transfer Mechanisms

Förster resonance energy transfer (FRET): Dipole–dipole coupling between donor (D*) and acceptor (A) chromophores transfers excitation without electron transfer.

$$k_{\text{FRET}} = \frac{1}{\tau_D} \left(\frac{R_0}{r} \right)^6$$

(174)

where *r* is donor–acceptor separation, τ_D is the donor’s excited-state lifetime, and *R*₀ is the Förster radius (typically 5–10 nm in Chl networks). The *r*⁶ dependence makes FRET extremely sensitive to distance — doubling separation reduces transfer rate 64-fold. *R*₀ depends on:

- Spectral overlap integral *J*(λ): the donor emission must overlap the acceptor absorption (red-shifting toward the reaction center)
- Orientation factor κ^2 : relative orientation of donor emission and acceptor absorption transition dipoles (averages to 2/3 in random orientations, but is precisely tuned in the LHCII crystal structure)

Energy funnel architecture: Antenna pigments are arranged with higher-energy absorbing pigments at the periphery and lower-energy pigments closer to the reaction center. Excitation cascades “downhill” toward the reaction center with each transfer step, achieving about 95% efficiency from initial absorption to charge separation.

Exciton transfer (Dexter mechanism): When chromophores are within about 1 nm, electronic wavefunctions overlap and excitation transfers as a coherent exciton rather than incoherent FRET hops. Recent 2D electronic spectroscopy (Fleming lab, 2007) revealed that quantum coherence may persist for picoseconds at room temperature, possibly contributing to the high transfer efficiency, though the functional importance remains debated.

Concept Check 1: The antenna complex transfers excitation energy to the reaction center with about 95% efficiency. If 100 photons are absorbed by the antenna, how many excitations reach the reaction center? What happens to the energy of the about 5 photons that do not reach the reaction center?

Concept Check 1b: equation (174) shows that $k_{\text{FRET}} \propto 1/r^6$. If two chlorophylls separated by 5 nm transfer at $1 \times 10^{10} \text{ s}^{-1}$, predict the rate at 7.5 nm and at 10 nm. What does this mean for the spatial design of LHC complexes?

10.4 Light-Dependent Reactions

10.4.1 Photosystem II (PS II)

PS II is located primarily in appressed grana thylakoids. It is a large complex (about 350 kDa per monomer; functions as a dimer). Key components:

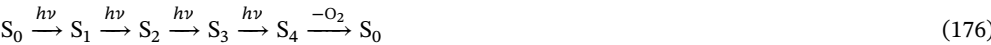
- Reaction center (P680): Special pair of Chl a molecules that absorb at 680 nm; the primary electron donor
- D1 and D2 proteins: Core reaction center proteins (homologous to bacterial L and M subunits)
- Pheophytin (Pheo): Primary electron acceptor (chlorophyll lacking Mg^{2+})
- Q_A and Q_B : Plastoquinone molecules; Q_A is tightly bound (one-electron acceptor), Q_B is the two-electron/two-proton mobile acceptor
- Water-splitting complex (OEC, oxygen-evolving complex): Mn_4CaO_5 cluster; performs the most thermodynamically demanding oxidation in biology

Water oxidation:



Each molecule of O_2 requires 4 photons (one photon per electron from water). The OEC’s ability to extract electrons one at a time from water — accumulating four oxidising equivalents on the Mn_4CaO_5 cluster before releasing O_2 in a single concerted four-electron step — was unprecedented in biology and is the inspiration for synthetic water-splitting catalysts.

The Kok cycle (S-state cycle): The OEC cycles through 5 oxidation states (S_0 – S_4), accumulating 4 oxidising equivalents before releasing O_2 :



Each S-state transition involves one photon absorption and one electron extraction from the Mn_4Ca cluster.

Primary photochemistry: P680 absorbs photon \rightarrow excited state $\text{P680}^* \rightarrow$ donates electron to pheophytin (charge separation in about 3 ps) $\rightarrow \text{Q}_\text{A} \rightarrow \text{Q}_\text{B}$. After two electrons and two protons, PQH_2 (plastoquinol) leaves PS II and carries electrons to Complex III (cytochrome b_6f).

D1 protein damage: P680^+ is the strongest biological oxidant ($E^{\circ'} = +1.25 \text{ V}$). The D1 protein is damaged by this oxidative stress and must be replaced every 30–60 minutes — the most rapid protein turnover in the cell. This photoinhibition/repair cycle requires a dedicated FtsH protease and ribosomal machinery in the thylakoid.

Clinical Connection: Herbicides Targeting PS II DCMU (diuron) and atrazine block the Q_B binding site on D1, preventing electron flow from PS II. This kills plants by halting photosynthesis. Atrazine is one of the most widely used herbicides globally. Resistance has evolved in some weed species through a single Ser264Gly **mutation** in D1 that reduces atrazine binding. Understanding PS II structure is essential for developing new herbicides and for bioengineering more efficient photosynthesis.

10.4.2 Cytochrome b_6f Complex

After PS II, PQH_2 is oxidised by the cytochrome b_6f complex, which pumps H^+ into the lumen via the Q-cycle, analogous to Complex III in mitochondria:

1. PQH_2 binds at the luminal (Q_p) site
2. One electron passes to the Rieske Fe-S protein \rightarrow cytochrome f \rightarrow plastocyanin (PC, soluble Cu-protein in the lumen)
3. Second electron passes to cytochrome b_6 (low potential) \rightarrow cytochrome b_6 (high potential) \rightarrow PQ at the stromal (Q_n) site
4. Net: 2 H^+ released to lumen per PQH_2 oxidised, plus 2 H^+ consumed from stroma per PQ reduced

The b_6f complex also produces superoxide as a byproduct, which can trigger signaling cascades for acclimation to changing light conditions.

10.4.3 Photosystem I (PS I)

PS I reaction center: P700 (Chl a pair absorbing at 700 nm). PS I is located primarily in non-appressed stroma lamellae and at the margins of grana.

Electron flow through PS I: $P700 + \text{photon} \rightarrow P700^* \rightarrow A_0$ (Chl a) $\rightarrow A_1$ (phylloquinone) $\rightarrow F_X$ (Fe-S) $\rightarrow F_A/F_B$ (Fe-S) \rightarrow ferredoxin (Fd, soluble Fe-S protein in stroma) \rightarrow ferredoxin-NADP⁺ reductase (FNR) \rightarrow NADPH

10.4.4 The Z-Scheme: Standard Electrode Potentials

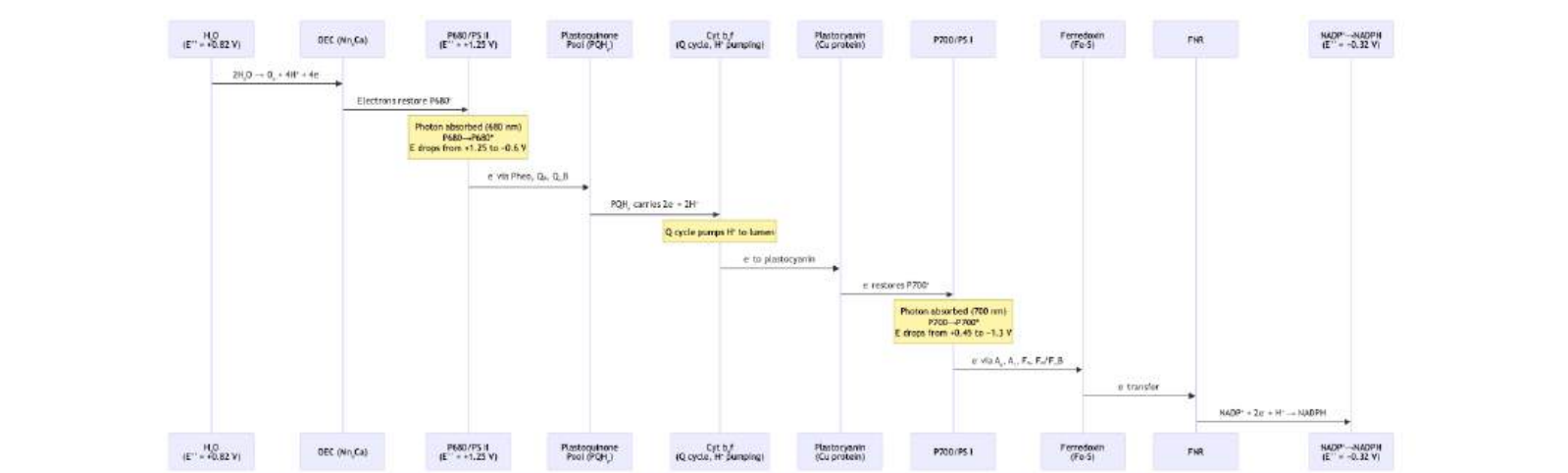


Figure 69. Z-scheme electron flow uses high-potential P680 to oxidize water, transfers electrons through plastoquinone and cytochrome b6f, and re-excites them at photosystem I for NADPH production.

The Z-scheme of photosynthetic electron transport (Mermaid). Two photons (absorbed by PS II and PS I) drive each electron from water ($E^{\circ'} = +0.82$ V) to NADPH ($E^{\circ'} = -0.32$ V), spanning a total potential of 1.14 V. The “Z” shape arises from plotting electron carriers against their redox potential.

Standard reduction potentials of key photosynthetic carriers:

Table 156. Standard reduction potentials for selected photosynthetic electron carriers.

Couple	$E^{\circ'}$ (V, pH 7)	Role
O_2/H_2O	+0.82	Electron donor (oxidised by S_4)
Tyr_Z^{\bullet}/Tyr_Z	+0.97	OEC-to-P680 ⁺ relay
$P680^+/P680$ (ground)	+1.25	The strongest biological oxidant
P680*/P680 (excited)	~ -0.6	After photon absorption
Pheophytin ($Pheo^{\bullet-}/Pheo$)	-0.61	First acceptor in PS II
$Q_A^{\bullet-}/Q_A$	-0.13	Tightly bound plastoquinone
Q_B/QH_2	0.0 to +0.10	Mobile plastoquinone pool
Cytochrome f	+0.36	b ₆ f exit point
Plastocyanin (Cu^{2+}/Cu^{+})	+0.37	Lumen carrier to PS I
$P700^+/P700$ (ground)	+0.45	PS I reaction center

Couple	$E^{\circ'}$ (V, pH 7)	Role
P700*/P700 (excited)	~ -1.3	Strongest biological reductant
A ₀ (Chl a ⁻ /Chl a)	-1.0	First PS I acceptor
Ferredoxin (Fe-S ²⁺ /Fe-S ⁺)	-0.42	Stromal reductant
NADP ⁺ /NADPH	-0.32	Final electron acceptor

The two large upward jumps (P680→P680, *P700*→*P700*) require absorption of red-light photons. The intervening downward drops drive PMF buildup and NADPH formation. This gives the canonical “Z” shape.

The Gibbs free energy stored in moving 4 electrons from water to NADPH:

$$\Delta G^{\circ'} = -nF\Delta E = -(4)(96,485)(1.14) \approx -440 \text{ kJ/mol}_e-$$

(177)

(N.B. negative sign indicates the *reverse* reaction is spontaneous; light energy is required to drive electrons *uphill* from water to NADPH.)

Concept Check 2x: Plastocyanin ($E^{\circ'} = +0.37 \text{ V}$) reduces P700⁺ ($E^{\circ'} = +0.45 \text{ V}$). Calculate $\Delta G^{\circ'}$ for this electron transfer per mole of electrons. Does the redox flow proceed downhill in the dark or primarily after PS I activation?

10.4.5 Linear vs. Cyclic Electron Flow

Linear electron flow (LEF): H₂O → PS II → PQ → b₆f → PC → PS I → Fd → NADPH. Produces both ATP and NADPH. ATP:NADPH ratio about 1.3:1.

Cyclic electron flow (CEF): Ferredoxin returns electrons to the b₆f complex (via PQ), generating additional PMF for ATP synthesis without NADPH production. This adjusts the ATP:NADPH ratio to match Calvin cycle demands (3:2 per CO₂).

CEF is mediated by two pathways: - PGR5/PGRL1 pathway: Major route; ferredoxin → PQ via PGRL1 - NDH-dependent pathway: Chloroplast NAD(P)H dehydrogenase complex; minor route

The functional necessity of CEF was first inferred from the gap between the ATP demand of the Calvin cycle (3 ATP per CO₂) and what LEF alone supplies (about 2.6 ATP per CO₂ at 14:3 H⁺/ATP stoichiometry); CEF closes the gap. Hager’s classic experiments on the xanthophyll cycle [[Hager, 1971](#)] and subsequent work showed that the magnitude of CEF varies dynamically with light and CO₂ — itself a regulatory layer.

10.4.6 Chemiosmotic ATP Synthesis (Chloroplast)

The PMF generated by H⁺ accumulation in the lumen (from water splitting + PQ reduction + b₆f Q-cycle) drives chloroplast **ATP synthase** (CF₁F₀):

- Structure and mechanism analogous to mitochondrial ATP synthase
- c-ring has 14 subunits in spinach chloroplasts (vs. 8–15 in mitochondria)
- about 4.67 H⁺/ATP (14 H⁺ per revolution / 3 ATP)

Net output of light reactions (per 2 H₂O oxidised / 2 NADPH produced):

- 1 O₂
- 2 NADPH
- about 3 ATP (from linear flow; cyclic flow provides additional ATP)

10.4.7 Worked Example: Energy Requirements for Carbon Fixation

Problem: Calculate the ATP and NADPH consumed to synthesize one molecule of glucose, and determine how many photons must be absorbed (assuming 8 photons per O₂ for linear electron flow).

Solution:

Net Calvin cycle stoichiometry per CO₂ fixed: 3 ATP + 2 NADPH, as derived in the Calvin-cycle stoichiometry discussion below. Per glucose (6 CO₂ fixed): 18 ATP + 12 NADPH.

Linear electron flow produces NADPH at a fixed ratio of 2 NADPH per 4 e[−] (4 photons per electron pair), so 12 NADPH require:

$$n_{\text{photons}} = 12 \times 4 = 48 \text{ photons (LEF primarily)}$$

(178)

But linear flow produces about 12 ATP from this (12 × 1.0 ATP per NADPH at about 1:1 stoichiometry — far short of the 18 ATP required). The shortfall of 6 ATP must be supplied by cyclic electron flow, which is estimated to require about 6–9 additional photons. Total: about 54–57 photons per glucose.

This is why the often-cited “48 photons per glucose” is a *lower bound* assuming perfect Z-scheme efficiency; real plants need somewhat more to balance the ATP:NADPH ratio.

10.4.8 Worked Example: Calvin Cycle Stoichiometry

Problem: Track the 18 ATP and 12 NADPH demand of the Calvin cycle through the three phases for 6 CO₂.

Solution:

Table 157. Calvin Cycle Stoichiometry: Calvin phase and Per CO₂.

Calvin phase	Per CO ₂	Per 6 CO ₂	Output	Notes
Carboxylation (RuBisCO)	0 ATP, 0 NADPH	0, 0	12 × 3-PGA	6 RuBP + 6 CO ₂ → 12 × 3-PGA
Reduction (PGK + GAPDH)	2 ATP + 2 NADPH	12 ATP + 12 NADPH	12 × G3P	Activation + reduction
Regeneration (5 G3P → 3 RuBP)	1 ATP	6 ATP	6 RuBP regenerated	PRK consumes ATP
Net inputs	3 ATP + 2 NADPH	18 ATP + 12 NADPH	2 G3P (= 1 hexose)	Excess 2 G3P leaves cycle

This 18:12 = 3:2 ATP:NADPH demand is the *target* the light reactions must hit. Pure LEF delivers ATP:NADPH about 1.3, so plants tune the LEF/CEF balance to close the gap; under light limitation, CEF is upregulated.

Concept Check 2: The Calvin cycle requires 3 ATP and 2 NADPH per CO₂ fixed. Linear electron flow produces ATP and NADPH in approximately a 1.3:1 ratio. How does cyclic electron flow help satisfy the Calvin cycle’s ATP:NADPH ratio of 3:2 (= 1.5:1)?

10.5 The Calvin Cycle (Light-Independent Reactions)

The Calvin cycle fixes CO₂ into organic compounds in the stroma. It has three phases:



Figure 70. The Calvin cycle fixes CO₂ onto RuBP, reduces 3-PGA using ATP and NADPH, and regenerates RuBP so carbon assimilation can continue.

The three phases of the Calvin cycle (Mermaid). For every 3 CO₂ fixed, 9 ATP and 6 NADPH are consumed, and 1 net G3P (3C) is produced. Six turns of the cycle produce one glucose molecule.

10.5.1 RuBisCO: Structure and Catalytic Mechanism

Structure: Plant RuBisCO is a hexadecamer (L₈S₈) — eight large subunits (about 55 kDa, plastid-encoded *rbcL* gene) and eight small subunits (about 15 kDa, nucleus-encoded *RbcS* gene family). The L subunits contain the catalytic site at the L-L dimer interface (so 8 active sites per holoenzyme); the S subunits play structural and modulatory roles, contributing to the cap of the assembly. Total mass is about 520 kDa, making RuBisCO one of the largest stromal soluble enzymes.

Activation requires CO₂ + Mg²⁺: A separate, *non-substrate* CO₂ molecule first reacts with Lys201 of the active site to form a carbamate, which then chelates a Mg²⁺ ion. Primarily the carbamylated, Mg²⁺-bound enzyme can bind RuBP and proceed with catalysis. The mechanism cleverly *senses* CO₂ availability twice: once to activate the enzyme and once during turnover.

RuBisCO activase (an AAA+ ATPase) removes inhibitory sugar phosphates (CA1P, RuBP) from RuBisCO’s active site, allowing carbamylation. This step is light-dependent (requires ATP) — connecting Calvin cycle activation to the energy state of the chloroplast.

Catalytic mechanism (in seven steps):

1. RuBP binds and is deprotonated at C3 to form a 2,3-enediol intermediate (the rate-limiting enolisation)
2. The enediol attacks CO₂ (or O₂ — see photorespiration)
3. C2-C3 bond cleavage produces a six-carbon β-keto acid intermediate
4. Hydration of the C3 carbon
5. C2-C3 cleavage releases the first 3-PGA
6. Stereospecific protonation produces the second 3-PGA
7. Product release

The slow *k*_{cat} (about 3–10 s^{−1}) is dominated by the enolisation step (step 1) and by the stringent steric constraints needed to *select* CO₂ over O₂ in step 2. Faster RuBisCOs leak more O₂ into the active site, producing photorespiration.

The CO₂/O₂ specificity factor (*S*_{c/o}, also τ):

$$S_{c/o} = \tau = \frac{V_c K_o}{V_o K_c}$$

(179)

where *V*_c, *V*_o are maximal carboxylase/oxygenase rates and *K*_c, *K*_o are Michaelis constants. Higher *S*_{c/o} = more selective for CO₂ over O₂.

Table 158. RuBisCO: Structure and Catalytic Mechanism: Organism and *S*_{c/o} (τ).

Organism	<i>S</i> _{c/o} (τ)	<i>k</i> _{cat} (carb., s ^{−1})	Note
Higher plants (spinach)	80–100	3.3	C3
Cyanobacteria (<i>Synechococcus</i>)	40–50	12	Compensate with carboxysomes
C4 plants (maize)	70–80	4.5	Compensate with C4 anatomy
Red algae (<i>Galdieria</i>)	about 240	2.6	Highest known; very slow
Theoretical maximum	about 400	–	Limited by enediol mechanism

The fundamental trade-off: Across the tree of life, *S*_{c/o} and *k*_{cat} are *negatively correlated*. Faster RuBisCOs are less selective. This appears to be a thermodynamic constraint on the enediol intermediate’s reactivity — the same electronic features that make it react with CO₂ also make it react with O₂.

10.5.2 Carboxylation (Carbon Fixation)

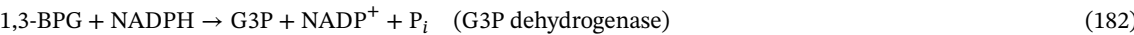
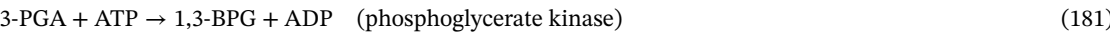


RuBisCO is the most abundant protein on Earth (about 0.7 billion tonnes globally; about 50% of leaf protein). Despite its central importance, RuBisCO has remarkable limitations:

- Slow: $k_{\text{cat}} = 3\text{--}10 \text{ s}^{-1}$ (typical enzymes: $10^2\text{--}10^3 \text{ s}^{-1}$)
- Indiscriminate: also reacts with O₂ (oxygenase activity), leading to photorespiration and wasting about 25% of fixed carbon in C3 plants
- Plants compensate for RuBisCO’s slowness by producing enormous quantities of it

10.5.3 Calvin-Cycle Reduction of 3-PGA

This is the primary reductive step of the Calvin cycle: the ATP and NADPH generated by the light reactions are spent here to convert 3-PGA into the triose phosphate G3P. For every 6 CO₂ fixed, 12 G3P are produced — 2 leave as the cycle’s net carbohydrate yield and 10 are recycled to regenerate RuBP.



10.5.4 Regeneration of RuBP

Five G3P molecules (15 carbons) are rearranged through a complex 10-step pathway (involving transketolase, aldolase, sedoheptulose-1,7-bisphosphatase, ribulose-5-phosphate epimerase, and ribulose-5-phosphate isomerase) to regenerate 3 RuBP (15 carbons), consuming 3 ATP.

10.5.5 Photosynthetic Stoichiometry and Energy Balance

To fix 6 CO₂ (net gain 1 hexose):

- $6 \text{ CO}_2 \times (3 \text{ ATP} + 2 \text{ NADPH per CO}_2) = 18 \text{ ATP} + 12 \text{ NADPH}$
- Light reactions must supply: 18 ATP and 12 NADPH
- Requires about 48 photons (8 per CO₂; 4 photons for 2 electrons through PS II + PS I \times 2 electron pairs per NADPH) for NADPH; additional photons for cyclic electron flow to meet ATP demand

10.5.6 Worked Example: Energy Efficiency of Photosynthesis

Problem: Calculate the energy efficiency of photosynthesis given that 48 photons of red light (680 nm, 176 kJ/mol each) are required to fix 6 CO₂ into 1 glucose (ΔG° of glucose combustion = 2,870 kJ/mol).

Solution:

Total light energy input: $48 \times 176 = 8,448 \text{ kJ/mol}$

Energy stored in glucose: 2,870 kJ/mol

$$\eta = \frac{2,870}{8,448} \times 100\% = 34\%$$

(183)

This is remarkably efficient for an energy conversion process. Whole-canopy photosynthetic efficiency in a real crop is typically around 1–3%, because most of the year’s incoming photosynthetically active radiation (PAR) is lost to (i) reflection, (ii) photorespiration, (iii) leaf shading and saturation, (iv) plant respiration, and (v) suboptimal water/nutrient supply.

Starch vs. sucrose export:

- Starch (alpha-glucose polymer) stored in chloroplast stroma during the day → remobilised at night to fuel respiration
- Sucrose (glucose-fructose disaccharide) exported to phloem via triose phosphate/phosphate antiporter (TPT) → transported to non-photosynthetic tissues (*source-sink* relationship)

Concept Check 3: RuBisCO is the most abundant enzyme on Earth, yet it is extremely slow ($k_{cat} = 3\text{--}10\text{ s}^{-1}$). Why hasn't evolution produced a faster version? Consider the trade-off between speed and specificity (CO_2 vs. O_2 discrimination) in light of the specificity-factor data above.

Concept Check 3b: Spinach RuBisCO has $\tau \approx 90$. *Galdieria* (red alga) RuBisCO has $\tau \approx 240$ but $k_{cat} \approx 2.6\text{ s}^{-1}$ (vs. 3.3 for spinach). At ambient $[\text{CO}_2]/[\text{O}_2]$, which enzyme would maximize CO_2 flux per unit enzyme? When (in what environment) does the trade-off favor the *Galdieria* form?

Concept Check (Analysis): The Z-scheme describes two photosystems operating in series. Photosystem II (P680) oxidizes water at $E^{\circ'} \approx +0.82\text{ V}$ (the $\text{O}_2/\text{H}_2\text{O}$ couple); Photosystem I (P700) reduces NADP^+ at $E^{\circ'} \approx -0.32\text{ V}$. (a) Calculate the total electrochemical potential difference (ΔE) driving the Z-scheme from H_2O to NADP^+ . (b) Using $\Delta G = -nF\Delta E$ with $n = 4$ electrons per O_2 , calculate the maximum free energy stored as NADPH per mole of O_2 evolved. Compare with the actual energy stored in $8\text{ ATP} + 2\text{ NADPH}$ (i.e., the light-reaction products per O_2). (c) Explain why the “antenna complex” of about 200-300 chlorophyll molecules per reaction center is thermodynamically advantageous: what would happen to photosynthetic flux if the reaction center had to absorb photons directly without an antenna?

Concept Check (Evaluation): C4 plants (corn, sugarcane) use a *spatial* separation of carbon fixation: mesophyll cells fix CO_2 into 4-carbon acids via PEP carboxylase ($K_m(\text{CO}_2) \approx 7\text{ }\mu\text{M}$, no oxygenase activity), which are then decarboxylated in bundle-sheath cells near RuBisCO. (a) At ambient cytoplasmic $[\text{CO}_2] \approx 8\text{ }\mu\text{M}$ and $[\text{O}_2] \approx 250\text{ }\mu\text{M}$, use C3 RuBisCO kinetic parameters ($K_c \approx 9\text{ }\mu\text{M}$, $K_o \approx 480\text{ }\mu\text{M}$, $V_{cmax}/V_{omax} \approx 3.1$) to compute the ratio of carboxylation to oxygenation: $v_c/v_o = (V_{cmax}/V_{omax}) \cdot ([\text{CO}_2]/K_c)/([\text{O}_2]/K_o)$. (b) How does C4 metabolism raise the effective $[\text{CO}_2]$ at bundle-sheath RuBisCO to suppress oxygenation? (c) CAM plants (cacti, agaves) separate the two reactions *temporally*. Design a 24-hour metabolic schedule for a CAM plant, including which reactions occur at night vs. day, and explain the stomatal logic (when are stomata open vs. closed, and why).

10.6 Photorespiration and Rubisco Oxygenase Activity

RuBisCO's oxygenase activity produces 2-phosphoglycolate (2C), which must be recycled through the photorespiratory pathway (C2 cycle):



The photorespiratory pathway spans three **organelles**: 1. Chloroplast: 2-phosphoglycolate → glycolate (phosphatase) 2. Peroxisome: glycolate → glyoxylate → glycine (generates H_2O_2 , destroyed by catalase) 3. Mitochondrion: 2 glycine → serine + CO_2 + NH_3 + NADH (glycine decarboxylase) 4. Peroxisome: serine → hydroxypyruvate → glycerate 5. Chloroplast: glycerate → 3-PGA (phosphorylation by ATP)

Cost of photorespiration:

- Loses 1 CO_2 per 2 oxygenation events (25% of fixed carbon)
- Consumes ATP for recovery
- Releases NH_3 (must be re-assimilated)
- At 25 degrees C and current atmospheric CO_2 , photorespiration reduces net photosynthesis by about 20–30% in C3 plants

Clinical Connection: Photorespiration and Global Food Security Reducing photorespiration in crop plants could increase yields by 20–40%. Approaches include: - Engineering a chloroplastic glycolate bypass (South et al., 2019, *Science*): reduced photorespiratory losses by 40% and increased tobacco biomass - Introducing CO_2 -concentrating mechanisms (CCMs) from cyanobacteria into C3 crops - Engineering RuBisCO with improved CO_2/O_2 specificity (challenging due to the speed-specificity trade-off) These efforts matter because the UN World Population Prospects 2024 projects roughly 9.7 billion people by 2050, while climate stress, land limits, food loss, and inequitable access constrain the food system [United Nations Department of Economic and Social Affairs, Population Division, 2024]. Higher photosynthetic efficiency can raise yield potential, but it is not a stand-alone solution to nutrition, distribution, soil health, or water scarcity.

10.7 C3, C4, and CAM Photosynthesis

10.7.1 Why CO2-Concentrating Mechanisms Evolved

The atmospheric $\text{CO}_2:\text{O}_2$ ratio (about 0.04%/21% $\approx 1:525$) is hostile to RuBisCO. The fraction of carboxylation versus oxygenation reactions is approximately:

$$\frac{v_c}{v_o} = S_{c/o} \cdot \frac{[\text{CO}_2]}{[\text{O}_2]}$$

(185)

For C3 plants at 25 °C, typical leaf-internal CO₂ ≈ 7 μM and O₂ ≈ 250 μM, so $v_c/v_o \approx 80 \times (7/250) \approx 2.2$ — meaning about 30% of RuBisCO turnovers are oxygenations. C4 and CAM plants have evolved spatial or temporal CO₂-concentrating mechanisms (CCMs) that raise the local [CO₂] around RuBisCO about 10x above ambient, suppressing photorespiration.

10.7.2 C3 Photosynthesis (First stable product: 3-PGA)

Standard Calvin cycle. Used by about 85% of plant species (wheat, rice, soybeans, most trees). Problem: photorespiration is severe at high temperature and low CO₂ (e.g., midday in summer, when stomata close to conserve water).

10.7.3 C4 Photosynthesis (First stable product: oxaloacetate, 4C)

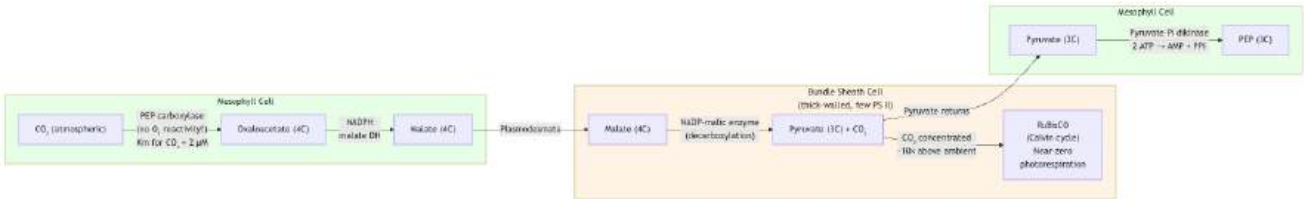


Figure 71. C4 photosynthesis separates initial PEP-carboxylase fixation in mesophyll cells from Rubisco activity in bundle-sheath cells, concentrating CO₂ around Rubisco.

C4 photosynthesis (Mermaid). Spatial separation of initial CO₂ fixation (mesophyll cells, PEP carboxylase) and the Calvin cycle (bundle sheath cells, RuBisCO). This CO₂-concentrating mechanism virtually eliminates photorespiration.

CO₂-concentrating mechanism: CO₂ is captured in mesophyll cells by PEP carboxylase (no O₂ reactivity; K_m for CO₂ about 2 μM, vs. RuBisCO K_m about 10 μM) as oxaloacetate → malate → transported to bundle sheath cells via plasmodesmata → decarboxylated → CO₂ concentrated (10x above ambient) → RuBisCO operates at saturating CO₂ → negligible photorespiration.

C4 plants (maize, sugarcane, sorghum, millet) require 2 additional ATP per CO₂ fixed (total: 5 ATP + 2 NADPH per CO₂) but are more efficient at high temperature and high light. Spatial separation of carboxylation (mesophyll) and Calvin cycle (bundle sheath) requires specialized leaf anatomy = Kranz anatomy (German: “wreath”).

C4 subtypes differ in the decarboxylation enzyme in bundle sheath cells:

- NADP-ME type: NADP-malic enzyme (maize, sorghum, sugarcane)
- NAD-ME type: NAD-malic enzyme (millet, Amaranthus)
- PEP-CK type: PEP carboxykinase (guinea grass, Panicum)

10.7.4 CAM Photosynthesis (Temporal separation)

Crassulacean Acid Metabolism: stomata open at night (cool, high humidity → low transpiration) → CO₂ fixed by PEP carboxylase → malate stored in vacuole (vacuolar pH drops from about 7 to about 4 as malic acid accumulates). Stomata close during the day (prevent water loss) → malate decarboxylated → CO₂ concentrated around RuBisCO → Calvin cycle proceeds.

CAM plants (cacti, agaves, pineapple, orchids, jade plant) have extremely high water-use efficiency (WUE: about 3–5x higher than C3). The tradeoff: slow growth due to nighttime carbon storage limitation and vacuolar capacity.

10.7.5 Water-Use Efficiency

Water-use efficiency (WUE) is defined as carbon gained per unit water lost:

$$WUE = \frac{A}{E} = \frac{\text{net CO}_2 \text{ assimilation}}{\text{transpiration rate}} \tag{186}$$

The intrinsic WUE depends on the leaf-internal:atmospheric CO₂ gradient:

$$WUE_{\text{intrinsic}} = \frac{c_a - c_i}{1.6 \cdot (e_i - e_a)} \tag{187}$$

where c_a and c_i are atmospheric and intercellular CO_2 concentrations, e_a and e_i are ambient and intercellular water vapor pressures, and 1.6 is the ratio of water-vapor to CO_2 diffusivity in air.

Typical WUE values (mol CO_2 fixed / mol H_2O transpired):

Table 159. Water-Use Efficiency: Plant type and WUE ($\times 10^{-3}$).

Plant type	WUE ($\times 10^{-3}$)	Mechanism
C3	1–3	Standard Calvin cycle; high transpiration
C4	3–6	CCM allows lower $c_i \rightarrow$ smaller stomatal aperture
CAM	10–40	Nocturnal stomatal opening drastically reduces $e_i - e_a$

CAM is the extreme: by opening stomata at night when air is cool and humid (small $e_i - e_a$), CAM plants lose about 10 \times less water per CO_2 fixed than C3 plants do midday — a huge advantage in deserts but at the cost of slow growth.

10.7.6 Comparing C3, C4, and CAM Photosynthesis

Table 160. Comparing C3, C4, and CAM Photosynthesis: Feature and C3.

Feature	C3	C4	CAM
First stable product	3-PGA (3C)	Oxaloacetate (4C)	Oxaloacetate (4C)
CO_2 fixation enzyme	RuBisCO	PEP carboxylase (initial)	PEP carboxylase (night)
Photorespiration	High (20–30% loss)	Near zero	Near zero
Stomata pattern	Open day	Open day	Open night
Optimal temperature	15–25 degrees C	30–40 degrees C	Variable
Water use efficiency	Moderate	High	Very high
ATP cost per CO_2	3	5	5.5–6.5
Examples	Wheat, rice, trees	Maize, sugarcane, millet	Cactus, agave, pineapple
% of plant species	about 85%	about 3% (about 7,500 species)	about 6–8%
Leaf anatomy	Standard mesophyll	Kranz anatomy	Thick, succulent

Concept Check 4: Why is C4 photosynthesis advantageous at high temperatures but not at low temperatures? Consider the temperature dependence of RuBisCO oxygenase activity and the ATP cost of the C4 pump.

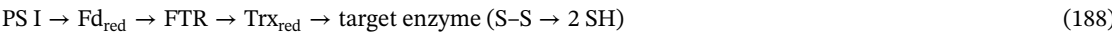
Concept Check 4b: Bermuda grass (C4) and tall fescue (C3) compete in temperate lawns. In a cool, wet spring, fescue dominates; in a hot, dry summer, Bermuda dominates. Use equation (185) and equation (187) to explain this seasonal turnover quantitatively.

10.8 Regulation of the Calvin Cycle

The Calvin cycle does not run in the dark — several enzymes are regulated by light-dependent mechanisms to prevent futile cycling with glycolysis and the oxidative pentose phosphate pathway.

10.8.1 The Thioredoxin/Ferredoxin Redox Regulation System

Light reduces the chloroplast thioredoxin pool through a precisely engineered cascade:



In detail:

1. PS I reduces ferredoxin (Fd, $E^{\circ'} = -0.42 \text{ V}$).

2. Fd-thioredoxin reductase (FTR) — a unique [4Fe-4S] enzyme — transfers two electrons to thioredoxin, converting an internal disulfide to two free thiols.

3. Reduced thioredoxin (Trx-(SH)_2) reduces specific regulatory disulfides on target enzymes.

4. Reduction *activates* the target enzyme (in most cases) by relieving an inhibitory conformational lock.

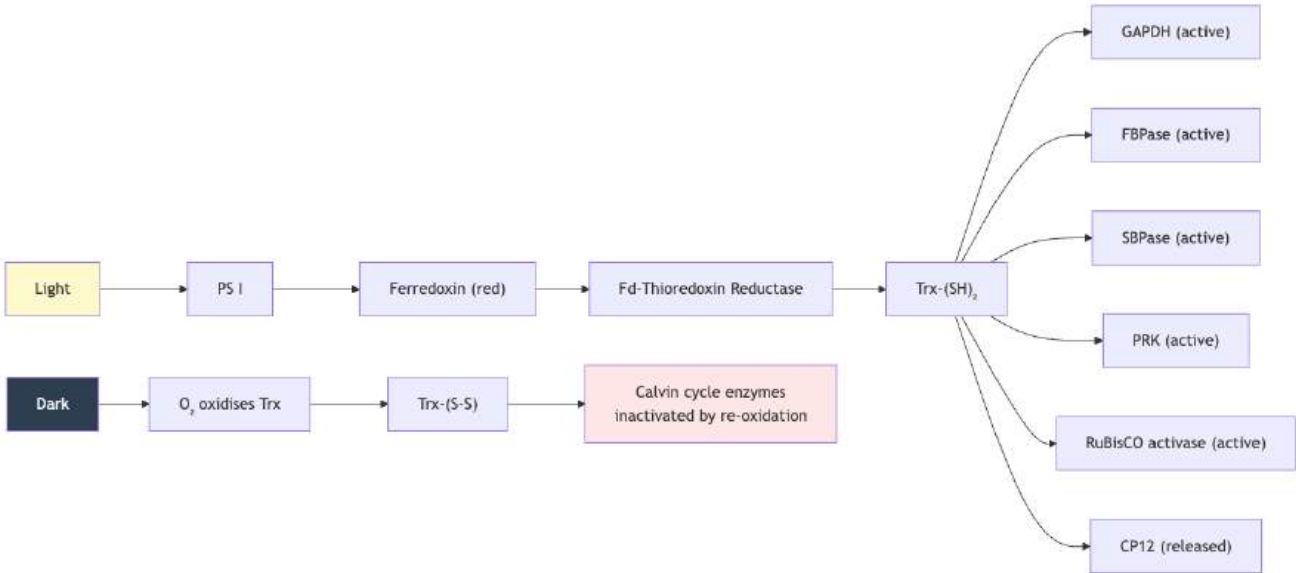


Figure 72. Light-driven ferredoxin reduces thioredoxin, which switches Calvin-cycle enzymes toward daytime carbon fixation.

The thioredoxin/ferredoxin system as the master light-dependent redox switch (Mermaid). Calvin-cycle enzymes carry regulatory disulfides that are reduced (activated) in the light and re-oxidised (inactivated) in the dark. This prevents futile ATP/NADPH consumption during darkness.

Thioredoxin-controlled Calvin-cycle targets include:

- GAPDH (NADP-linked): activated directly; catalyses the second reduction-phase step.
- Fructose-1,6-bisphosphatase (FBPase): activated directly; supports carbon regeneration.
- Sedoheptulose-1,7-bisphosphatase (SBPase): activated directly; a major regeneration-phase flux-control enzyme.
- PRK (phosphoribulokinase): activated directly; regenerates RuBP.
- RuBisCO activase: regulated indirectly; maintains RuBisCO in an active, carbamylated state.
- CP12: reduction releases the GAPDH/PRK complex, reversing dark-state inactivation.

In the dark, the target disulfides re-oxidise (catalysed by 2-Cys peroxiredoxins coupled to H_2O_2), inactivating the enzymes. This prevents the Calvin cycle from consuming ATP and NADPH when they are not being regenerated by the light reactions.

10.8.2 CO₂ Concentration Effects

The flux through the Calvin cycle is also acutely sensitive to CO₂ supply:

- At low [CO₂] (e.g., closed stomata, drought), RuBisCO is the rate-limiting step and the cycle is “carboxylation-limited.”
- At intermediate [CO₂], the cycle becomes “RuBP regeneration-limited” — flux limited by the supply of RuBP from the regeneration phase, which in turn depends on the rate of light-dependent ATP/NADPH supply.
- At very high [CO₂] (e.g., > ambient × 2), the cycle can become “P_i-limited” — phosphate becomes scarce as triose phosphate is exported.

This three-zone behavior underlies the classic Farquhar-von Caemmerer-Berry (FvCB) photosynthesis model, the workhorse of crop and ecosystem modeling.

10.8.3 Stromal pH and Mg²⁺ in the Light

In the light, H⁺ pumping from stroma to lumen has two activating effects:

- Stromal pH rises from about 7.0 to about 8.0 (RuBisCO and FBPase pH optimum is about 8.0–8.5)
- Stromal [Mg²⁺] rises by about 3 mM as Mg²⁺ exits the lumen with the H⁺ flux. Mg²⁺ is required for RuBisCO carbamylation and FBPase activity.

This is a beautifully integrated example of physical chemistry: the *same* H⁺ transport that builds the PMF for ATP synthesis simultaneously activates the carbon-fixation enzymes that consume that ATP.

10.8.4 CP12 Regulation of Calvin-Cycle Enzymes

CP12 is a small regulatory protein that forms a ternary complex with GAPDH and PRK in the dark, inactivating both enzymes simultaneously. Light-dependent reduction of CP12 by thioredoxin releases GAPDH and PRK, activating the Calvin cycle.

Concept Check 5: If a mutation in ferredoxin-thioredoxin reductase (FTR) prevented thioredoxin from being reduced, what would happen to Calvin cycle activity in the light? Would the light reactions be affected?

10.9 Photoprotection: Non-Photochemical Quenching

Excess light energy (when absorbed photons exceed the rate at which electrons can be productively used) can damage the photosynthetic apparatus through generation of reactive oxygen species, particularly singlet oxygen (¹O₂) from triplet chlorophyll (³Chl*). Plants must dissipate excess excitation safely.

10.9.1 The Three Components of NPQ

NPQ is operationally defined as fluorescence quenching that does not arise from photochemistry:

$$\text{NPQ} = \frac{F_m - F'_m}{F'_m}$$

(189)

where *F_m* is maximum fluorescence in the dark-adapted state and *F'_m* is the maximum fluorescence in the light-adapted state. NPQ has three kinetic components:

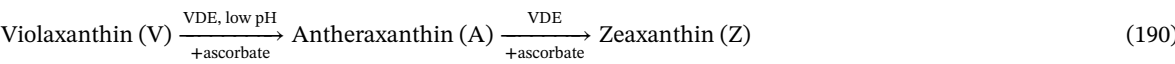
Table 161. The Three Components of NPQ: Component and Timescale.

Component	Timescale	Mechanism
qE (energy quenching)	seconds	Low lumen pH; PsbS protonation; xanthophyll cycle
qT (state transitions)	minutes	LHCII phosphorylation; antenna redistribution between PS II and PS I
qI (photoinhibition)	hours	D1 damage and repair

10.9.2 qE: The Xanthophyll Cycle in Detail

When light is in excess, the lumen pH falls below about 5.5, triggering two parallel events:

1. PsbS protonation: PsbS is a small (about 22 kDa) intrinsic membrane protein with two lumen-exposed glutamate residues that protonate at low pH. Protonation triggers a conformational change that brings antenna pigments into close contact, promoting energy transfer to a quenching site (a zeaxanthin-Chl heterodimer).
2. Violaxanthin → zeaxanthin: Violaxanthin de-epoxidase (VDE), activated by low pH, catalyses sequential de-epoxidation [[Hager, 1971](#)]:



Zeaxanthin (without epoxide groups) has a lower-energy first excited state than chlorophyll, so it can act as an energy sink — accepting excitation from ¹Chl* and dissipating it as heat. The reverse reaction (Z → V) is catalysed by zeaxanthin epoxidase (ZE) in the dark or low-light conditions.

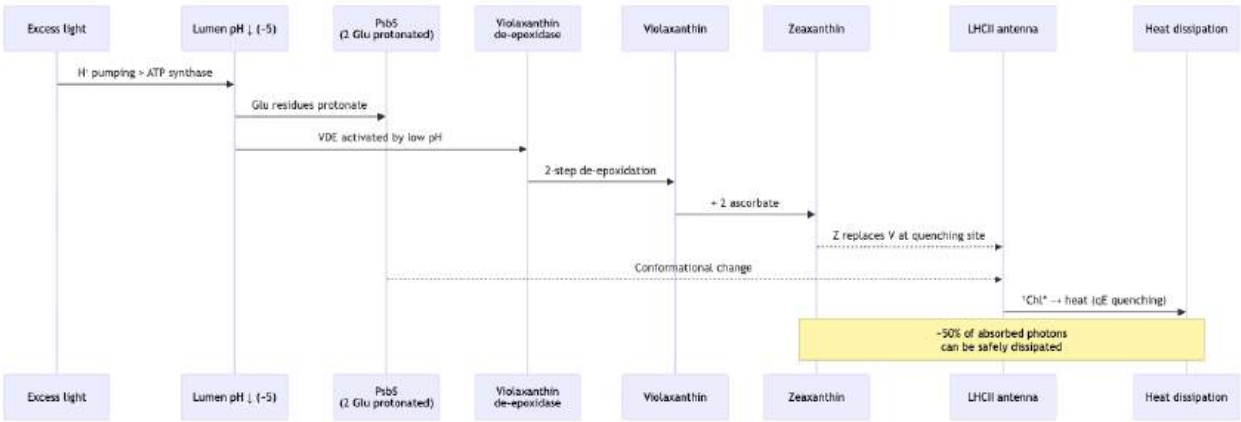


Figure 73. Excess light acidifies the thylakoid lumen, activating PsbS and the xanthophyll cycle so excitation energy is safely dissipated as heat.

The xanthophyll cycle and qE quenching cascade (Mermaid). Lumen acidification (signal of excess light) protonates PsbS and activates VDE. Zeaxanthin appears at the LHCII quenching site within seconds and dissipates excess excitation as heat. When light decreases, lumen pH rises and the whole system reverses over minutes.

10.9.3 Carotenoid Quenching of Triplet States

Carotenoids (β -carotene, zeaxanthin) directly quench triplet chlorophyll ($^3\text{Chl}^*$) and singlet oxygen ($^1\text{O}_2$), converting the energy to heat. Without carotenoids, photosynthesis is lethal — mutants lacking carotenoid biosynthesis (e.g., norflurazon-treated plants) bleach and die in light.

The carotenoid triplet state (about 80 kJ/mol) is below both $^3\text{Chl}^*$ (about 110 kJ/mol) and $^1\text{O}_2$ (about 94 kJ/mol), so energy transfer is downhill in both cases.

10.9.4 State Transitions (qT)

When PS II is over-excited relative to PS I (e.g., under blue light, which preferentially excites PS II), the plastoquinone pool becomes reduced. Reduced PQ activates STN7 kinase, which phosphorylates LHCII. Phosphorylated LHCII detaches from PS II in grana and migrates to PS I in stroma lamellae, rebalancing excitation pressure. Under far-red light (preferentially exciting PS I), PQ becomes oxidised, STN7 is inactive, and a phosphatase (PPH1/TAP38) returns LHCII to PS II.

10.9.5 Other Photoprotective Mechanisms

1. Chloroplast movements: In high light, chloroplasts align parallel to the light direction (low cross-section); in low light, they spread perpendicular (high cross-section). Mediated by phototropins.
2. Reactive oxygen scavenging: Superoxide dismutase (SOD), ascorbate peroxidase (APX), and the glutathione-ascorbate (Foyer-Halliwell) cycle detoxify ROS generated by PS I (Mehler reaction).
3. Photorespiration as a safety valve: Counter-intuitively, photorespiration consumes ATP and reductant, draining excess electron flow when CO_2 is limiting — a “release valve” that reduces ROS pressure on the chloroplast.

Concept Check 6: Explain why a plant mutant lacking carotenoids would die in the light but survive in the dark. What specific photodamage mechanism would cause cell death?

Concept Check 6b: A *psbs* knockout *Arabidopsis* lacks the PsbS protein and shows almost no qE, although LHCII and the xanthophyll cycle are intact. Predict the plant’s growth phenotype under (a) constant moderate light and (b) fluctuating light (sun → shade → sun every minute). Why is the fluctuating-light phenotype more severe?

10.10 Evolutionary Origins of Photosynthesis

Photosynthesis has a complex evolutionary history spanning about 3.5 billion years:

1. Anoxygenic photosynthesis (about 3.5 Ga): Early photosynthetic bacteria (e.g., purple bacteria, green sulfur bacteria) used a single reaction center (Type I or Type II) and electron donors other than water (H_2S , Fe^{2+} , H_2). No O_2 produced.

2. Origin of oxygenic photosynthesis (about 2.7–3.0 Ga): Cyanobacteria evolved the ability to link two photosystems (PS II and PS I) in series (Z-scheme), enabling water as an electron donor. This was the most transformative evolutionary innovation on Earth.
3. Great Oxidation Event (about 2.4 Ga): Cyanobacterial O₂ production overwhelmed geological sinks (reduced iron, sulfur), causing atmospheric O₂ to rise from <0.001% to about 2%. This was catastrophic for obligate anaerobes (the “Oxygen Holocaust”) but enabled **aerobic** respiration (about 18x more efficient ATP production than **fermentation**).
4. Primary endosymbiosis (about 1.5 Ga): A cyanobacterium was engulfed by a eukaryotic ancestor, becoming the chloroplast. Evidence: double membrane, 70S ribosomes, circular DNA, sensitivity to chloramphenicol.
5. Secondary and tertiary endosymbiosis: Algae engulfed other algae, creating organelles with 3–4 membranes (e.g., chloroplasts of brown algae, diatoms, euglenoids). This accounts for the remarkable diversity of photosynthetic pigments and chloroplast structures across algal lineages.

Concept Check 7: The reaction centers of PS II (D1/D2 proteins) and purple bacteria (L/M subunits) share significant structural and sequence homology, yet PS II can oxidise water and purple bacterial reaction centers cannot. What structural innovation in PS II enabled water oxidation?

10.11 Artificial Photosynthesis and Solar Fuels

Inspired by natural photosynthesis, researchers are developing artificial systems to convert solar energy into fuels. The diversity of approaches reveals a tension between *efficiency* (where photovoltaics excel) and *fuel storage* (where chemistry excels).

10.11.1 Comparison: Natural vs. Artificial Light Conversion

Biological systems.

- C3 photosynthesis (whole plant): 0.5–1.5% solar-to-stored-carbon efficiency, producing glucose and starch. Its advantage is complete self-assembly and repair; its limit is low energy efficiency and dependence on water and mineral nutrients.
- C4 photosynthesis (for example, sugarcane): 1.5–3.5% solar-to-stored-carbon efficiency, producing glucose and sucrose. The CO₂-concentrating mechanism improves performance in hot, bright environments, but the anatomical and ATP costs restrict its ecological range.
- Theoretical biological maximum: about 12% for reduced carbon under idealised constraints. The main losses come from spectral mismatch, RuBisCO kinetics, photorespiration, respiration, and the ATP/NADPH cost of carbon fixation.

Engineered energy systems.

- Silicon photovoltaic (single-junction): about 22% commercial electricity conversion. It is mature and inexpensive, but electricity is not a fuel and requires downstream storage.
- III–V tandem photovoltaics: about 33% in high-performance laboratory cells. They maximize single-cell photovoltaic efficiency but remain costly and materials-intensive.
- Photovoltaics plus electrolysis: about 10–14% solar-to-H₂ efficiency. Hydrogen is a storable fuel, but compression, transport, leakage, and end-use infrastructure remain major constraints.

Hybrid and chemical fuel systems.

- Photoelectrochemical cells: about 4–10% solar-to-H₂ efficiency from water. Direct light-to-fuel integration is attractive, but catalyst durability and device stability are limiting.
- CO₂ photoreduction with copper-family catalysts: roughly 1–5% for mixtures such as CO, formate, and ethanol. The appeal is direct carbon capture into fuels; the challenge is selectivity.
- Bio-hybrids with engineered cyanobacteria: about 0.5–4% for products such as H₂, ethanol, or alkanes. They are self-replicating and tunable but slow and fragile.
- Synthetic Mn₄Ca-inspired catalysts: research-stage water-oxidation systems producing O₂ from H₂O. They teach design principles from the oxygen-evolving complex but are not yet practical devices.

10.11.2 Why Plants Lag PV (and Why It May Not Matter)

A silicon solar cell at 22% beats C3 photosynthesis at 1% by an order of magnitude — but the comparison is misleading. PV converts photons to electrons; plants convert photons to *covalently stored carbon*. To match plants, a PV system must add electrolysis, gas storage, and CO₂ reduction — each step lossy. End-to-end PV → renewable methanol systems currently achieve about 5–8% solar-to-fuel — comparable to C4 photosynthesis. The biological system also self-assembles, self-repairs, and runs at <1 sun without exotic materials.

Theoretical efficiency limits. The ultimate biological limit is set by the sum of (a) photon-to-electron efficiency in the antenna (about 95%), (b) thermalisation losses (longer-wavelength photons supply about 176 kJ/mol; the enthalpy of a pair of e^- across the Z-scheme is about 440 kJ — so the lower bound is about $1.14\text{ V} \times 4\text{ e}^- / 8\text{ photons} \times 176\text{ kJ/mol}$ = about 31% before downstream losses), and (c) Calvin cycle and respiration costs (about 40% loss). The product is a theoretical about 12% solar-to-biomass efficiency.

10.11.3 Key Research Directions

1. Artificial water splitting: Metal oxide catalysts (e.g., IrO_2 , Co-Pi) that oxidise water, coupled to photovoltaic cells. The goal: electrochemical production of H_2 and O_2 from water using sunlight.
2. CO_2 reduction: Electrocatalytic or photocatalytic reduction of CO_2 to formate, methanol, or hydrocarbons. Challenges include selectivity (CO_2 vs. H^+ reduction) and catalyst durability.
3. Bio-hybrid systems: Living photosynthetic organisms (cyanobacteria, algae) engineered to produce hydrogen, ethanol, or alkanes directly from CO_2 and sunlight.
4. Synthetic minimal photosystem: Recreating the core PS II Mn_4Ca water-splitting catalyst in synthetic molecules. The Mn_4CaO_5 cluster structure (revealed by Shen et al., 2011, *Nature*, at 1.9 Å resolution) guides biomimetic catalyst design.

Clinical Connection: Photodynamic Therapy (PDT) Photodynamic therapy exploits the same photochemistry that plants must protect against. A photosensitiser (e.g., porphyrin derivative) is administered to a patient and preferentially accumulates in tumor tissue. Upon illumination with specific wavelengths, the photosensitiser generates singlet oxygen ($^1\text{O}_2$), which destroys tumor cells. Understanding the photophysics of chlorophyll-like molecules (energy transfer, intersystem crossing, ROS generation) underpins PDT drug design.

10.12 Computational Bridge

Net leaf CO_2 uptake is modeled as a saturating light response minus dark respiration; figure 74 shows how net assimilation rises from the light compensation point, climbs steeply at low irradiance, and levels off at light saturation, with the C4 curve saturating at higher photon flux than C3:

```
from biology.botany import photosynthesis_rate

anet = photosynthesis_rate(500.0) # μmol PAR m-2 s-1
print(round(anet, 2))
```

Clinical / systems note: Non-photochemical quenching and carotenoid cycles in plants parallel clinical strategies that manage photochemical ROS in tissues (e.g. PDT dosimetry), where excess excitation must be routed to harmless decay channels.

10.12.1 Synthetic Photosynthesis and Rubisco Engineering

Rubisco (ribulose-1,5-bisphosphate carboxylase/oxygenase) is the most abundant protein on Earth, yet it is famously inefficient: $k_{\text{cat}} \approx 3\text{ s}^{-1}$ and an oxygenation side-reaction that drains 20–50 % of carbon in warm climates through photorespiration. Engineering around this rate-limiting step is the central problem of crop productivity. Three complementary strategies have matured between 2019 and 2024.

(1) Photorespiration bypass. The Long lab (*Science* 2019) introduced a synthetic glycolate-metabolism pathway into tobacco that shunts glycolate (the toxic product of Rubisco oxygenation) directly to pyruvate in the chloroplast rather than sending it through the peroxisome/mitochondrion loop. Field trials demonstrated a about 40 % biomass yield increase over 2 years, without compromising photosynthetic rate. The same bypass is being translated into cowpea, soybean, and rice via the Realizing Increased Photosynthetic Efficiency (RIPE) consortium. (2) Cyanobacterial-style carbon-concentrating mechanisms. Cyanobacteria compartmentalise Rubisco inside carboxysomes that concentrate CO_2 locally, suppressing the oxygenation reaction. Expressing the bacterial Bica HCO_3^- transporter plus carboxysome shell proteins in C_3 plants is a about 10-year synthetic-biology goal; the Price/Long/Hanson labs have cleared the first milestones in *Nicotiana* and *Chlamydomonas*. (3) Directed evolution of Rubisco itself. Classical selection inside *E. coli* is limited because bacterial Rubisco is too different from plant Rubisco. The 2024 work by the Savage / Kortemme labs used ribosome-display directed evolution with MS-based screening to isolate Rubisco variants with about 2× improved specificity factor ($\text{Sc/o} = 110 \rightarrow 220$) — approaching the theoretical maximum set by the enzyme’s two-step mechanism.

Quantitative targets put the stakes in context: improving crop photosynthetic efficiency by even 10–20 % in major C_3 crops would be agronomically large, but the realized food-security gain would depend on canopy architecture, sink strength, water and nitrogen supply, local climate, post-harvest losses, and access.

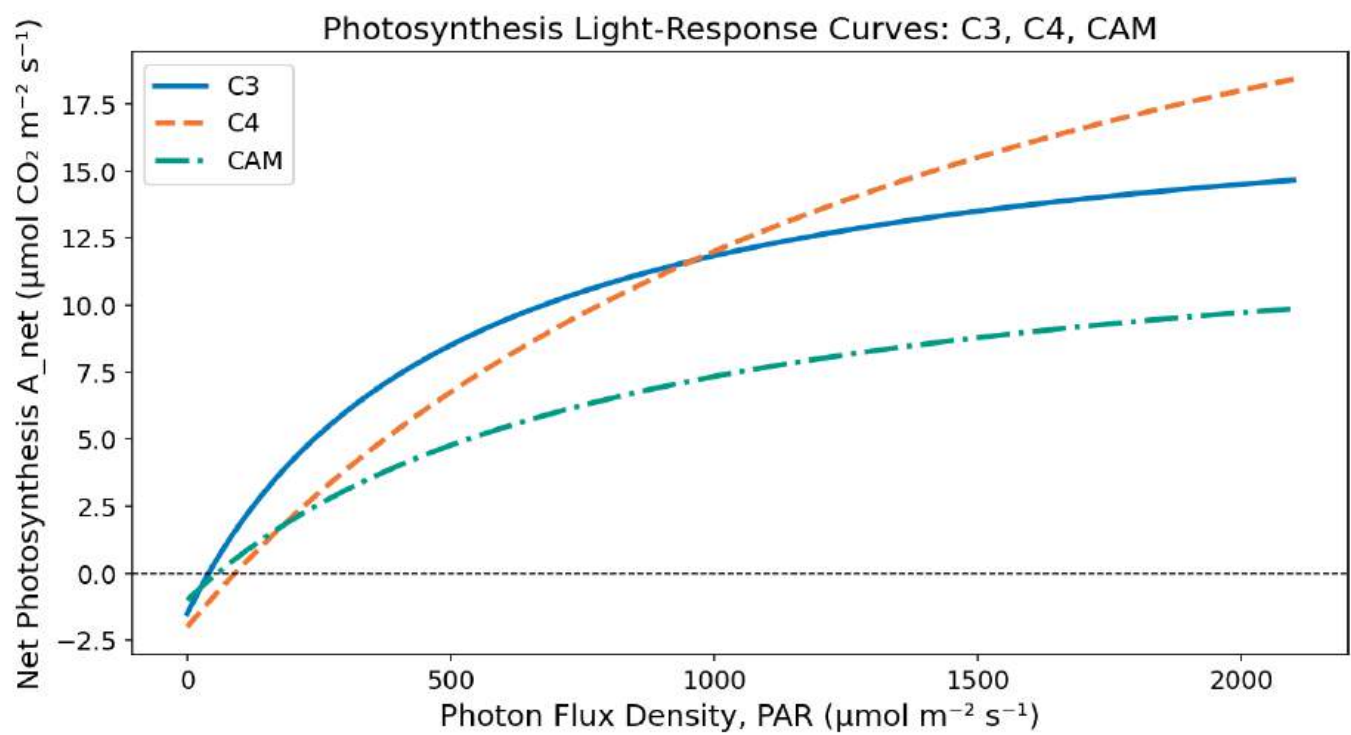


Figure 74. Light-response curves for C3, C4, and CAM plants. Net CO2 assimilation is plotted against photosynthetic photon flux density, showing different saturation points and maximum assimilation rates.

Molecular agriculture now has the tools – CRISPR-Cas9 in plants, synthetic biology standardization, and AI-assisted structural hypotheses for Rubisco and its chaperones – to test ideas that were largely conceptual a decade ago [Abramson et al., 2024, Varadi et al., 2024].

10.13 Current Evidence and Frontier Biology: Photosynthesis

For Photosynthesis, frontier biology belongs inside the evidence logic of the chapter. Metabolism is now studied as a regulated network constrained by energy, redox balance, compartmentation, and environment. The core reading question is this: photosynthesis claims should distinguish light capture, carbon fixation, photorespiration, water stress, and canopy context.

Global photosynthesis is also a measurement problem, not just a chloroplast pathway diagram. Carbonyl sulfide uptake, solar-induced fluorescence, isotope constraints, flux towers, and ecosystem models each see a different part of gross primary production; comparing them teaches students why the largest biological carbon flux remains an inference with method-specific uncertainty [Lai et al., 2024b]. A strong photosynthesis claim names the scale: leaf enzyme, canopy gas exchange, crop yield, or planetary carbon cycle.

- What to verify: identify the observation, model, assay, or dataset that would make the claim stronger or weaker.
- What to qualify: state the scale, organism, cell type, environmental condition, or population where the claim is expected to hold.
- What to compare: test at least one alternative explanation, baseline, or null model before treating the pattern as causal.
- What to cite: distinguish primary evidence, review synthesis, public dataset, and institutional guidance; for recent or numeric claims, prefer the source closest to the measurement and state what has changed since it was published.

A strong photosynthesis claim names the light environment, carbon pathway, water status, and measurement scale before comparing productivity.

Source practice: For photosynthesis claims, pair pathway diagrams with gas-exchange, fluorescence, isotope, field, or crop-yield evidence matched to the plant context.

Carbonyl-sulfide tracer work turns global GPP into an explicitly physiological inference about CO2 diffusion through stomata and mesophyll, so carbon-cycle claims should report the tracer, diffusion assumptions, and biome context rather than treating satellite greenness as a direct proxy for photosynthesis [Lai et al., 2024a].

10.13.1 Current Evidence Map: Photosynthesis Under Stress

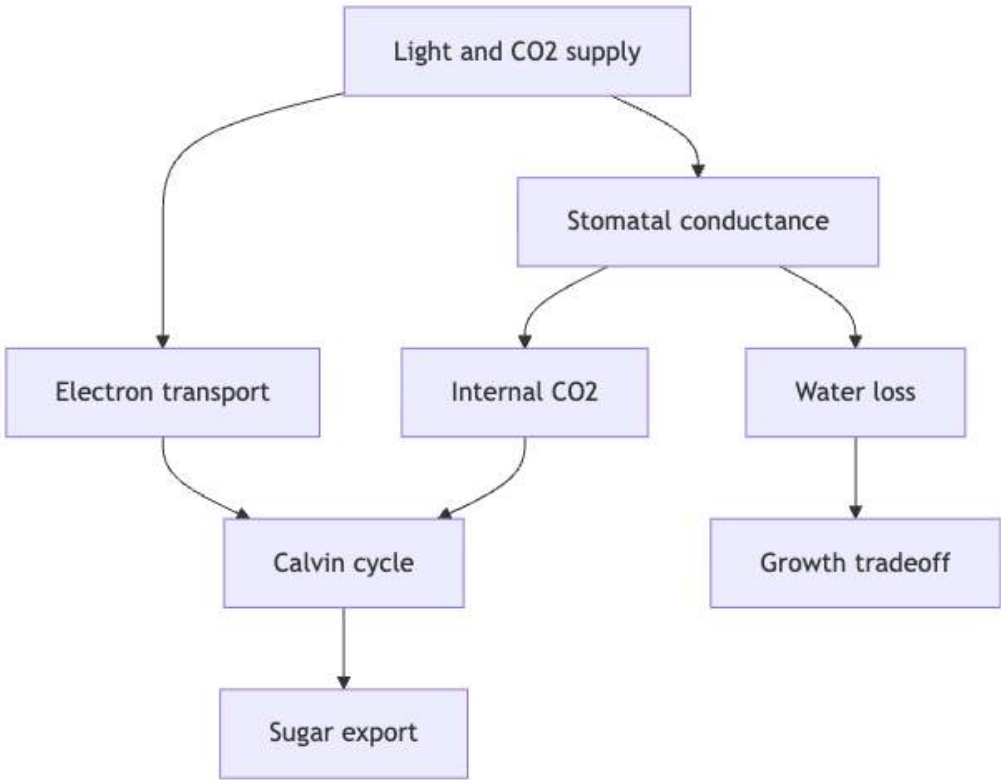


Figure 75. Photosynthesis in a plant is a coupled carbon-water decision: high light cannot raise growth if CO2 entry, water status, or sink demand becomes limiting.

10.14 Summary

- Light reactions (thylakoid): $\text{light} \rightarrow \text{O}_2$ (water splitting) + NADPH + ATP (equation (171), equation (175)). PS II drives water oxidation (Mn_4CaO_5 cluster, Kok cycle); cytochrome b_6f pumps protons via Q cycle; PS I drives NADP^+ reduction.
- Photon energy is given by $E = hc/\lambda$ (equation (172)); a 680 nm photon supplies 176 kJ/mol. Quantum yield $\Phi_{\text{O}_2} \approx 0.10$ corresponds to about 10 photons per O_2 , close to the theoretical minimum of 8.
- Antenna complexes (LHCII, LHCI) use FRET (equation (174)) and exciton transfer to funnel excitation to reaction centers at about 95% efficiency. Chl a/b ratios and carotenoid composition are tuned to spectral and protective demands.
- The Z-scheme spans 1.14 V (equation (177)) from H_2O (+0.82 V) through P680, P680, *Pheo*, *PQ*, b_6f , *PC*, *P700*, *P700*, A_0 , Fd to NADPH (−0.32 V), driven by two photons per electron.
- RuBisCO is hexadecameric (L_8S_8 , 8 active sites), requires $\text{CO}_2 + \text{Mg}^{2+}$ for active-site carbamylation, and shows a fundamental specificity-factor / turnover trade-off (equation (179)). Plant $S_{c/o} \approx 80\text{--}100$; theoretical maximum about 400.
- Calvin cycle (stroma): $18 \text{ ATP} + 12 \text{ NADPH} \text{ fix } 6 \text{ CO}_2 \rightarrow 1 \text{ glucose}$. Photorespiration costs C3 plants about 25% of fixed carbon (the carboxylation/oxygenation ratio is set by equation (185)).
- C4 uses Kranz anatomy (spatial separation); CAM uses temporal separation (night CO_2 fixation). Both have near-zero photorespiration but higher ATP costs. Water-use efficiency (equation (186)) ranks $\text{CAM} > \text{C4} > \text{C3}$ by an order of magnitude.
- The thioredoxin/ferredoxin system (equation (188)) couples PS I activity to Calvin-cycle enzyme activation via reversible disulfide reduction. Stromal pH 8.0 and Mg^{2+} release further activate RuBisCO and FBPase.
- At ecosystem scale, GPP estimates depend on measurement model: carbonyl-sulfide uptake can constrain CO_2 diffusion through stomata and mesophyll, so productivity claims should name tracer assumptions and biome context [Lai et al., 2024a].
- NPQ (equation (189)) protects the photosynthetic apparatus through the xanthophyll cycle (equation (190)), state transitions, and photoinhibition repair. Carotenoids quench triplet Chl and singlet O_2 [Hager, 1971].
- Artificial photosynthesis bridges biology (engineered cyanobacteria) and chemistry (PEC cells, Mn_4Ca biomimetics); silicon PV is more efficient but does not produce storable fuel directly.
- Connections: See section 9 for chemiosmotic coupling in mitochondria vs. chloroplasts, Unit VIII — Botany — Plant Biology: Introduction for whole-plant carbon and water trade-offs, and Unit X — Ecology: Introduction for primary productivity.

10.15 Review Questions

1. Describe the structure of a chloroplast and explain how the organization of the thylakoid membrane is adapted for efficient photosynthesis.
2. Explain the Z-scheme of photosynthetic electron transport. Why are two photosystems needed to move electrons from water to NADP^+ ? Quote at least three intermediate redox potentials in your answer.
3. Calculate the energy of a 440 nm blue photon and a 680 nm red photon (per mole). Explain why both are equally effective at driving photochemistry despite different photon energies.
4. Describe the Kok cycle (S-state cycle) of water oxidation. Why must four photons be absorbed to produce one O_2 ?
5. Compare the Q cycle in Complex III of mitochondria with the Q cycle in cytochrome b_6f of chloroplasts. What is the common functional principle?
6. Describe RuBisCO's structure and catalytic mechanism. Why is the specificity factor $S_{c/o}$ inversely correlated with k_{cat} across the tree of life?
7. Describe the three phases of the Calvin cycle. Calculate the total ATP and NADPH cost to fix 6 CO_2 into one glucose molecule, and the minimum number of photons required.
8. Explain the thioredoxin/ferredoxin redox regulation system. Which Calvin cycle enzymes are activated, and what would happen in a *trxR* (thioredoxin reductase) knockout in the light?
9. Compare C3, C4, and CAM photosynthesis in terms of leaf anatomy, biochemistry, water-use efficiency, and ecological niche. Use equation (187) to explain why CAM achieves the highest WUE.
10. Explain the xanthophyll cycle and qE non-photochemical quenching. Why is this mechanism essential for plant survival in fluctuating light?
11. Calculate the energy efficiency of photosynthesis if 48 photons of 680 nm light are needed to fix 6 CO_2 . Compare this with the efficiency of a typical silicon solar cell (about 22%).
12. Engineering reduced photorespiration has been proposed to increase crop yields. Describe two approaches and discuss potential risks.

13. Call `photosynthesis_rate` at 100 vs. 2000 $\mu\text{mol m}^{-2} \text{s}^{-1}$ default parameters. At which irradiance are you nearer light saturation, and how does that relate to greenhouse shading trials?
14. Compare cyclic vs. linear electron flow around PS I in terms of ATP:NADPH balance during the Calvin cycle.
15. Compute the Förster transfer rate at $r = 7 \text{ nm}$ given $R_0 = 5 \text{ nm}$ and $\tau_D = 4 \text{ ns}$ using equation (174). Repeat for $r = 10 \text{ nm}$ and comment on the spatial constraint imposed.
16. Spinach has $\tau \approx 90$, atmospheric $\text{CO}_2 = 410 \text{ ppm}$. Compute v_c/v_o at chloroplastic $\text{CO}_2 = 7 \mu\text{M}$ and $\text{O}_2 = 250 \mu\text{M}$ using equation (185). What fraction of RuBisCO turnovers are oxygenations?

10.16 Further Reading and Source Notes: Photosynthesis

• Mitchell (1961). Coupling of phosphorylation to electron and hydrogen transfer by a chemi-osmotic type of mechanism. *Nature*, 191 [Mitchell, 1961].

• Hager (1971). Die Reversiblen lichtabhängigen Xanthophyllumwandlungen im Chloroplasten. *Berichte der Deutschen Botanischen Gesellschaft*, 84 [Hager, 1971].

• Lai et al. (2024). Terrestrial photosynthesis inferred from plant carbonyl sulfide uptake. *Nature*, 634 [Lai et al., 2024a].

10.17 Key Terms

Table 162. Current Evidence Map: Photosynthesis Under Stress: Term and Definition.

Term	Definition
Photosystem II (PS II)	Light-driven water oxidase; P680 reaction center; O ₂ evolution via Mn ₄ CaO ₅ cluster
Photosystem I (PS I)	Light-driven NADP ⁺ reductase; P700 reaction center; produces NADPH via ferredoxin
Z-scheme	Complete electron transport path from H ₂ O (+0.82 V) to NADPH (−0.32 V) via two photosystems
RuBisCO	Ribulose-1,5-bisphosphate carboxylase/oxygenase; L ₈ S ₈ ; most abundant enzyme; CO ₂ fixation
Specificity factor ($S_{c/o}$, τ)	$V_c K_o / V_o K_c$; quantifies CO ₂ vs O ₂ preference of RuBisCO
Calvin cycle	Three-phase cycle fixing CO ₂ into G3P in the stroma; 3 ATP + 2 NADPH per CO ₂
Thioredoxin	Small redox protein that reduces regulatory disulfides on Calvin-cycle enzymes in the light
Photorespiration	RuBisCO oxygenase activity; wastes about 25% of fixed carbon in C3 plants; releases CO ₂
C4 photosynthesis	CO ₂ concentrating mechanism using PEP carboxylase and Kranz anatomy
CAM	Crassulacean acid metabolism; temporal separation of CO ₂ fixation (night) and Calvin cycle (day)
Water-use efficiency (WUE)	Carbon fixed per water lost; CAM > C4 > C3
Kok cycle	S-state cycle of the OEC; accumulates 4 oxidising equivalents before O ₂ release
Antenna complex	Light-harvesting pigment-protein complex; funnels energy to reaction center
FRET	Förster Resonance Energy Transfer; dipole-dipole energy transfer between pigments; rate $\propto 1/r^6$
Quantum yield	Molecules of product per photon absorbed; $\Phi_{\text{O}_2} \approx 0.10$
Non-photochemical quenching (NPQ)	Thermal dissipation of excess light energy; comprises qE, qT, qI components
Xanthophyll cycle	Violaxanthin \leftrightarrow zeaxanthin interconversion; regulates qE
PsbS	PS II protein with two lumen-exposed Glu residues; protonated at low pH; triggers qE
Plastocyanin	Soluble copper protein carrying electrons from b ₆ f to PS I in the lumen
Kranz anatomy	Wreath-like leaf anatomy of C4 plants; bundle sheath surrounds vascular tissue
Cyclic electron flow	PS I-mediated; $\text{Fd} \rightarrow \text{PQ} \rightarrow \text{b}_6\text{f} \rightarrow \text{PC} \rightarrow \text{PS I}$; produces ATP without NADPH

10.18 Companion Source Module: Photosynthesis

Photosynthesis should leave a reproducible trail from a biological claim to the code, figure, diagram, or paper-based activity that can test it. Use the surfaces below to inspect the chapter’s assumptions, rerun the relevant model, or compare the manuscript explanation with companion labs and figures.

Table 163. Companion source surfaces for Photosynthesis.

Surface	Use it for
<code>src/biology/botany/botany.py</code> (<code>photosynthesis_rate</code> , <code>light_response_curve</code>)	Reproduce light-response and environmental-limitation scenarios.
<code>src/visualization/plots.py</code> (<code>plot_light_response_curve</code>)	Inspect saturation, compensation points, and axis labeling.
<code>src/mermaid/biology_diagrams.py</code> (<code>photosynthesis_light_dark_diagram</code>)	Separate light reactions, carbon fixation, and regulation.

Reproducibility check: report light intensity, CO2, temperature, water status, and plant pathway before comparing photosynthetic rates. Cross-reference: compare with section 30 and section 39.

11 Metabolic Integration and Regulation

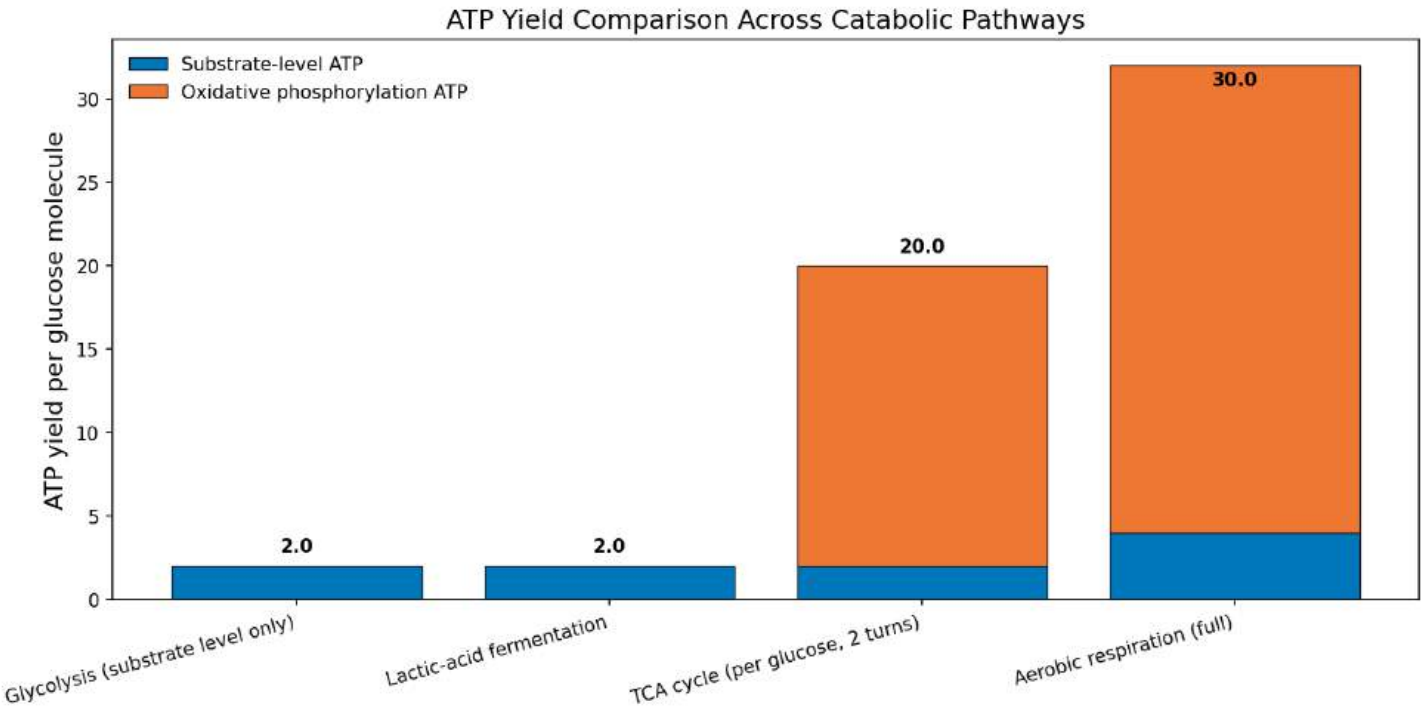


Figure 76. ATP yield per glucose for four catabolic strategies: anaerobic glycolysis (lactic-acid fermentation), ethanolic fermentation, fully aerobic respiration with the malate-aspartate shuttle, and aerobic respiration with the glycerol-phosphate shuttle. Stacked bars partition ATP into glycolysis, the TCA cycle, and oxidative phosphorylation. The order-of-magnitude jump between fermentation and aerobic respiration motivates the metabolic switching central to this chapter.

Level 3/3 · 60 min read · 100 min lecture · Prerequisites: section 9, section 10

11.1 Learning Objectives

By the end of this chapter, you should be able to:

- Trace how the cell coordinates catabolic and anabolic pathways through shared cofactors and **allosteric** cross-regulation, and predict the metabolic state from cofactor and signal-molecule ratios.
- Describe AMPK and mTORC1 as opposing energy-sensing hubs and explain how they toggle the metabolic state of the cell, including the molecular basis of mTOR's role as a nutrient sensor (Rag GTPases, Ragulator).
- Describe the metabolic states of fed, post-absorptive, fasting, and starvation, including hormonal control and the timeline of fuel switching.
- Explain insulin signaling in detail: the PI3K/Akt/mTOR pathway, **GLUT4** translocation mechanism, and glycogen synthesis.
- Explain glucagon signaling: cAMP/PKA activation of glycogenolysis, gluconeogenesis, and the phosphorylase kinase cascade.
- Distinguish allosteric from transcriptional metabolic regulation given an **enzyme**-activity time-course, using gluconeogenesis bypass-enzyme control as the worked case.
- Compare ATP yield and regulation of glucose versus fatty-acid oxidation, and calculate the net ATP yield from palmitoyl-CoA.
- Explain ketone body metabolism and its role during starvation.
- Describe AMPK structure (two catalytic + two regulatory subunits) and activation mechanisms (LKB1 vs CaMKK β).
- Trace flux control through the glucose-fatty-acid (Randle) cycle under fed versus fasted conditions, and predict the resulting respiratory quotient.
- Define substrate (futile) cycles and explain their control advantages.
- Explain obesity, metabolic syndrome, and insulin resistance at the molecular level, including visceral fat as an endocrine organ.
- Apply metabolic control analysis (MCA): flux control coefficients C_i^J and the summation theorem.
- Calculate the adenylate energy charge from concentrations and predict the resulting AMPK activation state.
- Describe modern metabolomics: NMR vs mass spectrometry approaches and identification challenges.

11.1.1 Study Blueprint

- Big idea: Metabolism is a regulated network that reallocates flux across tissues, time, and nutrient states.
- Core concepts: flux, energy charge, hormonal control, fed/fasted states.

- Framework alignment: Vision & Change: Pathways and transformations of energy and matter, Systems; AP Biology: Energetics, Systems Interactions; NGSS-style topics: Matter and Energy in Organisms and Ecosystems.
- Model or quantitative lens: Energy charge, control points, and pathway-flux comparisons.
- Data skill: Use pathway evidence to infer which metabolic state or tissue is active.
- Practice cadence: Representing and Describing Data, Statistical Tests and Data Analysis.
- Common misconception to repair: A pathway is not a one-way assembly line; reversibility and regulation define the real route.
- Primary lab: [Lab — Metabolic Integration and Regulation](#).
- Question bank: [Questions — Metabolic Integration and Regulation](#).
- Transfer task: Apply metabolic network reasoning to diabetes, fasting, exercise, or cancer metabolism.
- Bridge to computation: `biology.biochemistry.biochemistry.reaction_free_energy`.

Opening Vignette: The Brain on Ketones — Surviving Starvation

The human brain is extraordinarily metabolically demanding: it consumes roughly 20% of the body’s resting energy budget despite constituting about 2% of body mass. Under normal conditions, it runs almost exclusively on glucose. But glucose stores — maintained as liver glycogen — last only about 12–24 hours of fasting. So how does the brain survive during prolonged starvation?

The liver activates a metabolic program: free fatty acids released from adipose tissue are not completely oxidised within the liver itself. Instead, the liver packages their acetyl-CoA units into ketone bodies (acetoacetate and β -hydroxybutyrate) and exports them to the bloodstream. After 1–2 days of fasting, the brain begins importing ketones; after 3–5 days, it derives up to 75% of its energy from ketone bodies. Circulating ketone concentrations rise from about 0.1 mM (fed state) to 6–8 mM (prolonged starvation). This elegant metabolic switch — coordinated by insulin falling and glucagon rising — is one of the clearest examples of metabolic integration studied in this chapter.

Primary source: Owen, O. E. et al. (1967). *Brain metabolism during fasting*. *Journal of Clinical Investigation*, 46(10), 1589–1595.

11.2 Metabolic Pathways as Coupled Flux Networks

Glycolysis, the TCA cycle, beta-oxidation, and biosynthetic pathways do not operate independently. They share intermediates, co-factors (NAD⁺/NADH, NADP⁺/NADPH, CoA), and are subject to allosteric cross-regulation. Integration of these pathways defines the metabolic state of the cell.

The two fundamental modes: - Catabolism — break down nutrients → ATP + reduced cofactors (NADH, FADH₂) - Anabolism — use ATP + reduced cofactors (chiefly NADPH) → biosynthesis of macromolecules

These modes are reciprocally regulated because of shared cofactors and master regulatory kinases. The metabolic state is encoded in:

Table 164. Study Blueprint: Signal molecule and Fed state (high energy).

Signal molecule	Fed state (high energy)	Fasted state (low energy)
AMP/ATP ratio	Low	High
NADH/NAD ⁺ ratio	High	Low (in cytoplasm)
Acetyl-CoA	High	Low (cytoplasmic)
Citrate	High	Low
Malonyl-CoA	High	Low
Insulin/Glucagon ratio	High	Low

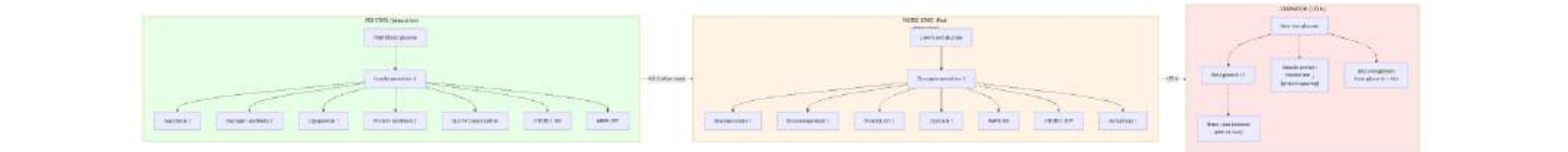


Figure 77. Metabolic states from fed to starvation, showing the hormonal switches and metabolic pathway changes at each stage. Insulin dominates the fed state; glucagon dominates fasting; ketogenesis sustains the brain during starvation.

11.2.1 Fasting Physiology: Fuel Switch Timeline

The body switches fuels in a programmed sequence as fasting progresses. The transitions are coordinated by falling insulin and rising glucagon (and later cortisol):

Table 165. Fasting Physiology: Fuel Switch Timeline: Time post-meal and Predominant fuel.

Time post-meal	Predominant fuel	Liver process	Brain fuel	Notes
0–4 h (absorptive)	Dietary glucose	Glycogenesis, lipogenesis	Glucose	Insulin high, glucagon low
4–12 h (post-absorptive)	Liver glycogen	Glycogenolysis	Glucose	Glucagon rises
12–24 h (early fasting)	Liver glycogen → muscle FA	Glycogen depleting; gluconeogenesis ramping	Glucose (mostly from GNG)	Liver glycogen mostly depleted by about 24 h
1–3 days	Muscle FA + early ketones	Gluconeogenesis (lactate, alanine, glycerol); ketogenesis starting	Glucose 75%, ketones 25%	Cortisol rises; protein catabolism increases
3–7 days	Ketones	Maximal ketogenesis	Glucose 25%, ketones 75%	Brain adapts; muscle protein sparing
> 1–2 weeks	Ketones (sustained)	Ketogenesis at steady state	Ketones 65–75%, glucose 25–35%	Resting metabolic rate falls about 20%
> 30+ days (starvation)	Body protein (terminal)	Gluconeogenesis from muscle protein dominates	Glucose 50%, ketones 50%	Death imminent when about 50% of protein lost

This fuel-switching timeline is one of the most elegant examples of metabolic integration. It is also clinically relevant: bariatric surgery, ketogenic diets, and prolonged fasting interventions most exploit (or perturb) this same switch.

Concept Check 1: Why is it essential that glycolysis and gluconeogenesis are reciprocally regulated and rarely fully active simultaneously? What would happen if both ran at maximum rate?

11.3 Insulin Signaling: The PI3K/Akt/mTOR Pathway

Insulin is the master anabolic **hormone**, secreted by pancreatic beta-cells in response to elevated blood glucose [Sanger, 1955, Yalow and Berson, 1960]. Its signaling cascade is one of the most important in metabolic regulation:



Insulin signaling cascade from receptor to downstream metabolic and growth effects (Mermaid). Akt is the central node, integrating PDK1 (Thr308) and mTORC2 (Ser473) phosphorylations to drive glucose uptake, glycogen synthesis, lipogenesis, and protein synthesis.

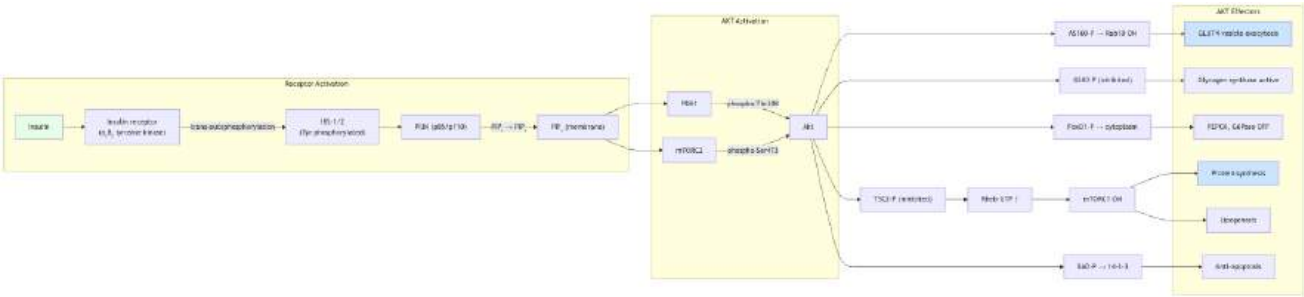


Figure 78. Insulin receptor activation recruits IRS proteins, PI3K, Akt, and mTOR-linked targets to promote glucose uptake, glycogen synthesis, and anabolic metabolism.

Downstream Akt targets:

Table 166. Fasting Physiology: Fuel Switch Timeline: Target and Akt effect.

Target	Akt effect	Metabolic outcome
AS160 (TBC1D4)	Phosphorylation → Rab-GAP inactivated	GLUT4 vesicle exocytosis → glucose uptake
GSK3 (glycogen synthase kinase 3)	Phosphorylation → inhibited	Glycogen synthase active → glycogen synthesis
FoxO1	Phosphorylation → nuclear exclusion	PEPCK and G6Pase genes OFF → gluconeogenesis inhibited
TSC2	Phosphorylation → inhibited	mTORC1 activated → protein synthesis, lipogenesis
BAD	Phosphorylation → binds 14-3-3	Anti-apoptotic → cell survival
PDE3B	Phosphorylation → activated	cAMP degradation → opposes glucagon

GLUT4 translocation mechanism (in detail):

- Basal state. GLUT4 is sequestered in specialized intracellular vesicles (GSVs, GLUT4 storage vesicles) about 95% of the time, with about 5% at the plasma membrane. The vesicles are tethered by the inhibitory Rab-GAP AS160 (TBC1D4), which keeps Rab10 in its GDP-bound (inactive) state.
- Insulin signal. Akt phosphorylates AS160 on multiple sites (Thr642 most important), inhibiting its GAP activity.
- Rab10 activation. With AS160 off, Rab10 accumulates in the GTP-bound active state, promoting vesicle docking at the plasma membrane.
- SNARE-mediated fusion. Synaptobrevin-2 (VAMP2) on GSVs engages plasma-membrane syntaxin-4 + SNAP-23, driving membrane fusion.
- GLUT4 exposure. GLUT4 appears at the cell surface, increasing glucose uptake 10–20-fold.
- Endocytosis on signal termination. When insulin signal ends, GLUT4 is endocytosed back to GSVs via clathrin-coated pits and a slow constitutive recycling pathway.

In type 2 diabetes, this cascade is disrupted at multiple levels (see clinical box below) so that GLUT4 translocation is impaired even at high circulating insulin.

Clinical Connection: Insulin Resistance and Type 2 Diabetes In type 2 diabetes, insulin signaling is impaired at multiple levels: 1. IRS-1 serine phosphorylation (by JNK, PKC-theta, IKK-beta) prevents tyrosine phosphorylation by the **insulin receptor** 2. Ceramide accumulation activates PP2A, which dephosphorylates Akt 3. DAG accumulation activates PKC-epsilon (liver) and PKC-theta (muscle), which phosphorylate IRS-1 on inhibitory serine residues 4. ER stress (from lipid overload) activates JNK → IRS-1 Ser307 phosphorylation The net result: GLUT4 translocation is impaired, glycogen synthesis is reduced, and gluconeogenesis is not suppressed. Metformin (first-line therapy) works partly through AMPK activation and partly through inhibition of mitochondrial Complex I. see section 8 for RTK signaling.

Concept Check 2: Thiazolidinediones (e.g., rosiglitazone) activate PPAR-gamma in adipose tissue, increasing adipocyte differentiation and lipid storage. Explain how increasing fat storage in adipose tissue could paradoxically improve insulin sensitivity in muscle and liver.

11.4 Glucagon Signaling: cAMP/PKA Pathway

Glucagon is secreted by pancreatic alpha-cells when blood glucose falls. It acts primarily on the liver (hepatocytes express glucagon receptors; muscle does not), where cyclic-AMP signaling translates hormone binding into metabolic control [Rall and Sutherland, 1958]:

Glucagon → Glucagon receptor (GPCR) → G_s → Adenylyl cyclase → cAMP → PKA

Glucagon (or epinephrine) signaling cascade in the liver (Mermaid). The cAMP/PKA cascade simultaneously activates glycogenolysis (via phosphorylase kinase) and gluconeogenesis (via CREB transcription) while suppressing glycolysis (via PFK-2/pyruvate kinase phosphorylation).

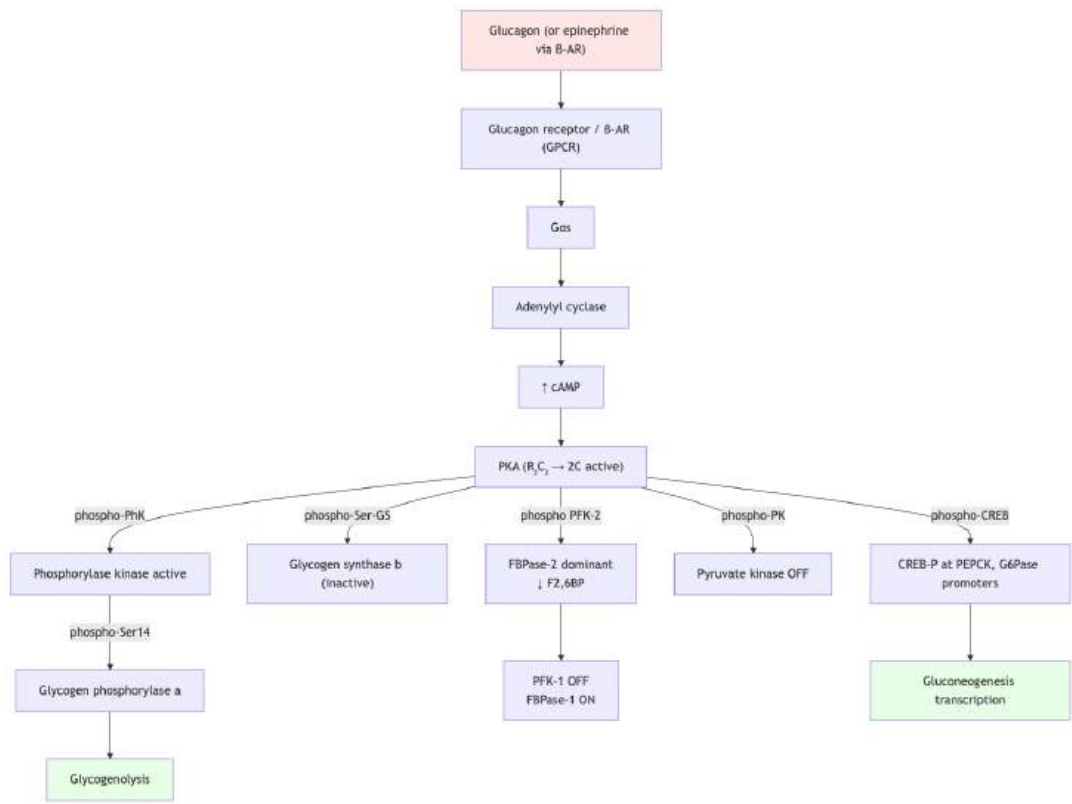


Figure 79. Glucagon and epinephrine activate GPCR-cAMP-PKA signaling, shifting liver metabolism toward glycogen breakdown and gluconeogenesis during fasting or stress.

Table 167. The Phosphorylase Kinase Cascade — A Signal Amplifier: Step and Numerical amplification.

Step	Numerical amplification
1 glucagon → 1 receptor (1:1)	1×
1 receptor → about 100 Gα _s activated (during signal)	about 100×
1 adenylyl cyclase → about 100 cAMP/sec	about 100×
4 cAMP → 1 PKA holoenzyme dissociation (releases 2 catalytic subunits)	gating
1 PKA → about 100 phosphorylase kinase	about 100×
1 PhK → about 100 phosphorylase b → a	about 100×
1 phosphorylase a → about 100 glucose-1-P/sec	about 100×
End-to-end amplification	about 10 ⁷ –10 ⁸

A single glucagon binding event releases a burst of about 10⁷ glucose-1-phosphate molecules within seconds. This is how a signal at femtomolar hormone concentrations produces a millimolar metabolite response.

PKA targets in the liver:

Table 168. The Phosphorylase Kinase Cascade — A Signal Amplifier: Target and PKA effect.

Target	PKA effect	Metabolic outcome
Phosphorylase kinase	Activated	Glycogen phosphorylase activated → glycogenolysis
Glycogen synthase	Inhibited (phosphorylated)	Glycogen synthesis OFF
PFK-2/FBPase-2	FBPase-2 activated → F2,6BP destroyed	Glycolysis inhibited
Pyruvate kinase	Inhibited (phosphorylated)	Glycolysis slowed
CREB	Activated	PEPCK and G6Pase gene transcription → gluconeogenesis
IP3R	Sensitised	Ca ²⁺ release from ER
HSL (adipose, via β-AR)	Activated	Lipolysis (in adipose; not liver)

11.5 Gluconeogenesis and Fasting Glucose Supply

Gluconeogenesis synthesizes glucose from non-carbohydrate precursors (lactate, glycerol, glucogenic amino acids). It occurs primarily in the liver and to a lesser extent in the kidney cortex.

Gluconeogenesis is NOT simply the reverse of glycolysis. Three irreversible glycolytic steps require bypass enzymes:

Table 169. The Phosphorylase Kinase Cascade — A Signal Amplifier: Glycolytic step (irreversible) and Gluconeogenic bypass.

Glycolytic step (irreversible)	Gluconeogenic bypass	Location
Pyruvate kinase (PEP → Pyruvate)	Pyruvate carboxylase (Pyruvate → OAA; biotin, ATP) + PEPCK (OAA → PEP; GTP)	Mitochondria + cytoplasm
PFK-1 (F6P → F1,6BP)	Fructose-1,6-bisphosphatase (FBPase-1)	Cytoplasm
Hexokinase (Glucose → G6P)	Glucose-6-phosphatase (G6Pase)	ER membrane (liver, kidney primarily)

Cost: 6 ATP equivalents per glucose synthesized (4 ATP + 2 GTP).

Regulation of gluconeogenesis: - Allosteric: Pyruvate carboxylase activated by acetyl-CoA; FBPase-1 inhibited by AMP and F2,6BP - Hormonal: Glucagon (via CREB) induces PEPCK and G6Pase genes; insulin (via FoxO1) represses them - Reciprocal with glycolysis: F2,6BP activates PFK-1 (glycolysis) and inhibits FBPase-1 (gluconeogenesis), ensuring they do not run simultaneously

Concept Check 3: Ethanol metabolism in the liver generates excess NADH (from alcohol dehydrogenase and aldehyde dehydrogenase). Predict the effect of heavy alcohol consumption on gluconeogenesis and the risk of hypoglycaemia.

11.6 Glycogen Metabolism and Rapid Glucose Storage

11.6.1 Glycogen Branching and Granule Architecture

Glycogen is a branched polymer of glucose units: - Alpha-1,4 linkages: linear chains (about 8–12 glucose units between branch points) - Alpha-1,6 linkages: branch points (about every 8–12 residues) - Glycogenin: self-glucosylating primer protein at the core

Liver glycogen (about 100 g): blood glucose **buffer**. Muscle glycogen (about 400 g): local fuel for contraction (rarely exported as glucose because muscle lacks G6Pase).

11.6.2 Glycogen Synthase and Glycogen Phosphorylase Regulation

Glycogen phosphorylase: Cleaves alpha-1,4 linkages from non-reducing ends, releasing glucose-1-phosphate. Regulated by: - Allosteric activation: AMP (muscle); glucose (liver, inhibitory) - Covalent modification: Phosphorylase kinase phosphorylates Ser14 → active a form - Hormonal cascade: Glucagon/epinephrine → cAMP → PKA → phosphorylase kinase → phosphorylase a

Glycogen synthase: Adds UDP-glucose to non-reducing ends (alpha-1,4 linkages). Active when dephosphorylated (GSK3 phosphorylates → inactive; insulin inhibits GSK3 → GS active).

Branching enzyme: Transfers about 7-residue segments to create alpha-1,6 branches. Increases solubility and number of non-reducing ends (more rapid mobilization).

Debranching enzyme: Bifunctional: transferase activity moves 3 residues from branch, then alpha-1,6-glucosidase cleaves the branch point, releasing free glucose.

Clinical Connection: Glycogen Storage Diseases | Type | Enzyme deficiency | Features | | --- | ----- | ---- | | I (von Gierke) | Glucose-6-phosphatase | Severe hypoglycaemia, hepatomegaly, lactic acidosis | | II (Pompe) | Lysosomal alpha-glucosidase | Cardiac/skeletal myopathy; treated by ERT | | V (McArdle) | Muscle glycogen phosphorylase | Exercise intolerance; “second wind” phenomenon | | VII (Tarui) | Muscle PFK | Exercise intolerance, hemolytic anemia |

11.7 Fatty Acid Oxidation (Beta-Oxidation)

Beta-oxidation occurs in the mitochondrial matrix and degrades fatty acyl-CoA by removing 2-carbon units (acetyl-CoA) per cycle.

11.7.1 Activation and Transport

1. Activation: Fatty acid + CoA + ATP → Acyl-CoA + AMP + PP_i (acyl-CoA synthetase; outer mitochondrial membrane; costs 2 ATP equivalents)
2. Carnitine shuttle: Acyl-CoA cannot cross the IMM. Instead:
 - CPT-1 (outer face of IMM): acyl-CoA + carnitine → acylcarnitine + CoA
 - Translocase (CACT): acylcarnitine crosses IMM
 - CPT-2 (inner face of IMM): acylcarnitine + CoA → acyl-CoA + carnitine

CPT-1 is the rate-limiting step of beta-oxidation. Malonyl-CoA (the first committed intermediate of fatty acid synthesis) allosterically inhibits CPT-1, ensuring that fatty acid synthesis and oxidation do not occur simultaneously.

11.7.2 Beta-Oxidation Steps (Each Cycle)

Table 170. Beta-Oxidation Steps (Each Cycle): Step and Enzyme.

Step	Enzyme	Reaction	Product
1	Acyl-CoA dehydrogenase	Acyl-CoA → trans-enoyl-CoA	FADH ₂
2	Enoyl-CoA hydratase	trans-enoyl-CoA + H ₂ O → L-3-hydroxyacyl-CoA	–
3	3-Hydroxyacyl-CoA DH	L-3-hydroxyacyl-CoA → 3-ketoacyl-CoA	NADH
4	Thiolase	3-ketoacyl-CoA + CoA → acyl-CoA(n-2) + acetyl-CoA	Acetyl-CoA

Each cycle: removes 2 carbons as acetyl-CoA, produces 1 FADH₂ + 1 NADH.

11.7.3 ATP Yield from Palmitoyl-CoA (C16:0)

Summing the products of complete fatty-acid oxidation makes the “fat is energy-dense” claim quantitative; the chapter-opening figure 76 already showed the corresponding glucose-substrate comparison across fermentative and aerobic strategies. Palmitoyl-CoA (16 carbons) undergoes 7 cycles of beta-oxidation:

Table 171. ATP Yield from Palmitoyl-CoA (C16:0): Product and Quantity.

Product	Quantity	ATP per unit	Total ATP
Acetyl-CoA (via TCA)	8	10 (3 NADH x 2.5 + 1 FADH ₂ x 1.5 + 1 GTP)	80
FADH ₂ (beta-oxidation)	7	1.5	10.5
NADH (beta-oxidation)	7	2.5	17.5
Activation cost		-2	-2

Product	Quantity	ATP per unit	Total ATP
Net total			106

Some textbooks report 108 ATP (using older P/O ratios) or 129 ATP (including palmitate rather than palmitoyl-CoA, and using maximal P/O ratios). The exact number depends on assumed H⁺/ATP stoichiometry and shuttle costs. The key insight: fatty acids are energy-dense (about 9 kcal/g vs. 4 kcal/g for carbohydrates) because they are highly reduced.

Clinical Connection: MCAD Deficiency Medium-chain acyl-CoA dehydrogenase (MCAD) deficiency is the most common inherited disorder of fatty acid oxidation (about 1:10,000 births). During fasting, patients cannot oxidise medium-chain fatty acids, leading to hypoketotic hypoglycaemia (low ketones because acetyl-CoA production is impaired, low glucose because gluconeogenesis lacks acetyl-CoA stimulation of pyruvate carboxylase). Fatal Reye-like episodes can occur. Management: avoid prolonged fasting; ensure regular carbohydrate intake.

11.8 Fatty Acid Synthesis

Fatty acid synthesis occurs in the cytoplasm and uses fundamentally different chemistry from beta-oxidation:

Table 172. ATP Yield from Palmitoyl-CoA (C16:0): Feature and Beta-oxidation.

Feature	Beta-oxidation	Fatty acid synthesis
Location	Mitochondrial matrix	Cytoplasm
Carrier	CoA	ACP (acyl carrier protein)
Reducing agent	FAD, NAD ⁺ (oxidised)	NADPH (reduced)
2C unit	Acetyl-CoA (removed)	Malonyl-CoA (added)
Key enzyme	Multiple separate enzymes	FAS (fatty acid synthase, one large multifunctional enzyme in animals)
Regulation	Inhibited by malonyl-CoA	Activated by citrate; inhibited by palmitoyl-CoA

Acetyl-CoA carboxylase (ACC) catalyses the committed step: acetyl-CoA + CO₂ + ATP → malonyl-CoA. This is the key regulatory enzyme: - Activated by: citrate (allosteric), insulin (dephosphorylation) - Inhibited by: palmitoyl-CoA (product inhibition), AMPK phosphorylation (energy depletion), glucagon (via PKA)

11.9 Ketone Body Metabolism

During prolonged fasting (>24–48 h), the liver converts excess acetyl-CoA from fatty acid oxidation into ketone bodies: acetoacetate, beta-hydroxybutyrate, and acetone.

Synthesis (liver mitochondria): 1. 2 Acetyl-CoA → Acetoacetyl-CoA (thiolase) 2. Acetoacetyl-CoA + Acetyl-CoA → HMG-CoA (HMG-CoA synthase) 3. HMG-CoA → Acetoacetate + Acetyl-CoA (HMG-CoA lyase) 4. Acetoacetate → beta-Hydroxybutyrate (beta-hydroxybutyrate DH; uses NADH) 5. Acetoacetate → Acetone (non-enzymatic decarboxylation; exhaled)

Utilization (brain, heart, muscle): Beta-hydroxybutyrate → acetoacetate → acetoacetyl-CoA (via succinyl-CoA transferase, also called thiophorase) → 2 acetyl-CoA → TCA cycle.

Key points: - The liver cannot use ketone bodies (lacks thiophorase) - The brain normally uses primarily glucose but during starvation adapts to derive about 60–70% of its energy from ketone bodies, sparing muscle protein - This protein-sparing effect is essential for survival during prolonged fasting - Diabetic ketoacidosis (DKA): uncontrolled type 1 diabetes → absent insulin → massive lipolysis → excessive ketone body production → metabolic acidosis (pH <7.3), dehydration, potentially fatal

Concept Check 4: Why can the liver produce ketone bodies but not use them? What is the physiological advantage of this arrangement?

11.10 AMPK — The Cellular Energy Gauge

AMPK (AMP-activated protein kinase) is a heterotrimer with two catalytic α-subunits (α1 and α2 isoforms), two regulatory β-subunits (β1, β2), and the γ-subunit that binds adenine nucleotides — though the assembled holoenzyme is α₁β₁γ₁. (The classic textbook description is that AMPK is “two catalytic + two regulatory

subunits” referring to the assembly’s binary modules: the catalytic α/β pair and the regulatory β/γ pair.) The γ -subunit contains four CBS (cystathionine β -synthase) domains, of which three bind adenine nucleotides — AMP, ADP, and ATP — competitively. This competitive binding lets the γ -subunit *integrate* the entire adenylate pool, not just one ratio.

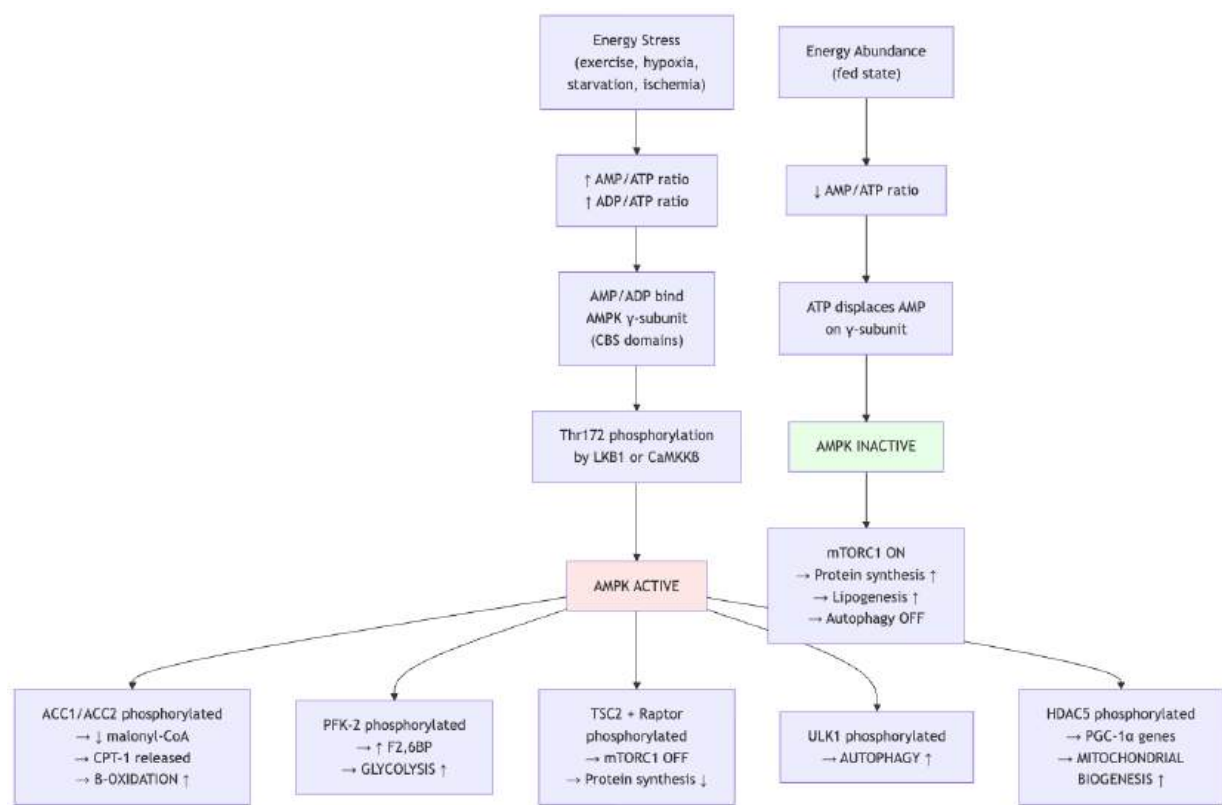


Figure 80. AMPK as the cellular energy sensor. Low energy activates AMPK, which simultaneously promotes catabolic pathways and inhibits anabolic pathways. High energy inactivates AMPK, allowing mTORC1-driven anabolism.

Concept Check (Analysis — Cross-Unit Connection): In biochemistry, “free energy” (Gibbs free energy ΔG) governs whether a reaction proceeds spontaneously. In **Unit 0 — Systems Science for Biology: Introduction**, “variational free energy” in the Free Energy Principle refers to an information-theoretic bound on surprise. These are not coincidentally named: both measure the gap between a system’s current state and its expected (equilibrium or predicted) state. (a) Show that ATP hydrolysis ($\Delta G^\circ \approx -30$ kJ/mol under standard conditions, but about -50 kJ/mol in a cell where $[ADP]/[ATP] \approx 0.01$) reflects the cell maintaining its biochemical states far from equilibrium — in what sense does AMPK serve as the cell’s “prediction error detector” for energy state? (b) Cellular respiration (glucose oxidation) couples a favorable reaction ($\Delta G \approx -2880$ kJ/mol) to multiple unfavorable ones (ATP synthesis) — explain this as an example of how living systems use free energy to minimize biological surprise (maintain homeostasis).

11.10.1 AMPK Activation: LKB1 vs CaMKK β

AMPK is activated when its catalytic α -subunit is phosphorylated at Thr172. Two upstream kinases phosphorylate this site under different physiological conditions:

Table 173. AMPK Activation: LKB1 vs CaMKK β : Upstream kinase and Trigger.

Upstream kinase	Trigger	Tissue distribution	Pathological connection
LKB1 (STK11)	Energy stress (high AMP); allosterically primed by AMP binding to AMPK γ	Ubiquitous; constitutively active	Loss-of-function = Peutz-Jeghers syndrome, predisposes to gastrointestinal cancers

Upstream kinase	Trigger	Tissue distribution	Pathological connection
CaMKKβ	Elevated cytosolic Ca ²⁺ (independent of AMP)	Brain, muscle, T cells, endothelium	Important in T-cell activation, osmotic stress
TAK1	Inflammatory cytokines (TGF-β, TNF-α)	Limited	Crosstalk between inflammation and metabolism

LKB1 is the dominant kinase under classical energy stress (exercise, hypoxia, starvation): AMP binding to AMPK γ promotes LKB1 docking and Thr172 phosphorylation, while simultaneously protecting Thr172 from dephosphorylation by PP2A and PP2C. AMP is therefore not simply an “activator” but an *allosteric primer* that shifts the AMPK steady state from dephosphorylated to phosphorylated.

CaMKKβ provides a Ca²⁺-coupled activation route — for example, in muscle contraction (where Ca²⁺ release accompanies ATP demand) or in T-cell activation following T-cell receptor engagement. This route runs in parallel to the AMP/LKB1 pathway and lets cells anticipate energy demand from Ca²⁺ signals before AMP rises.

11.10.2 Adenylate Energy Charge and Metabolic State

The energy charge (EC) of the adenylate system was introduced by Atkinson [Atkinson, 1968] as a single scalar that captures the fractional saturation of the adenylate pool with high-energy phosphate:

$$\text{E.C.} = \frac{[\text{ATP}] + \frac{1}{2}[\text{ADP}]}{[\text{ATP}] + [\text{ADP}] + [\text{AMP}]}$$

(192)

The numerator counts each phosphoanhydride bond (ATP has two phosphoanhydrides, ADP has one), while the denominator counts the total adenylate pool. So E.C. = 1.0 means most adenylates are ATP; E.C. = 0 means most are AMP.

Most cells maintain EC approximately 0.85–0.95 [Atkinson, 1968]. AMPK is highly sensitive in the range EC = 0.70–0.85 — precisely the window where rising AMP signals impending energy crisis.

11.11 Worked Example: Energy Charge

Problem: A resting skeletal-muscle biopsy gives adenylate pools of [ATP] = 5.0 μmol/g, [ADP] = 0.6 μmol/g, and [AMP] = 0.05 μmol/g. Calculate the energy charge and predict whether AMPK is active.

Solution:

Step 1 — State the relation and why ADP is half-weighted. The energy charge measures the fractional saturation of the adenylate pool with transferable phosphoanhydride bonds:

$$EC = \frac{[\text{ATP}] + \frac{1}{2}[\text{ADP}]}{[\text{ATP}] + [\text{ADP}] + [\text{AMP}]}$$

ATP carries two high-energy phosphoanhydride bonds and ADP carries one, so on a per-adenylate basis ADP holds exactly half the transferable phosphate of ATP — hence the $\frac{1}{2}$ weighting. The denominator is the conserved total adenylate pool ([ATP]+[ADP]+[AMP]), so $EC = 1$ when every adenylate is ATP and $EC = 0$ when every adenylate is AMP.

Step 2 — Substitute the measured μmol/g values.

$$EC = \frac{5.0 + \frac{1}{2}(0.6)}{5.0 + 0.6 + 0.05}$$

Numerator: 5.0 + 0.5 × 0.6 = 5.0 + 0.30 = 5.30. Denominator: 5.0 + 0.6 + 0.05 = 5.65. The shared μmol/g units cancel, so the ratio is dimensionless.

Step 3 — Compute and interpret against the AMPK threshold.

$$EC = \frac{5.30}{5.65} = 0.938 \quad (193)$$

At $EC = 0.938$ the pool sits in the normal resting band of 0.85–0.95 and well above the AMPK-activation window of 0.70–0.85. Predict: AMPK is largely inactive and the cell is in an energy-replete state favoring anabolism. A fall toward $EC \approx 0.80$ (rising AMP) would move the pool into the AMPK-sensitive window and switch the cell toward catabolism.

Clinical Connection: Metformin and AMPK Metformin, the most widely prescribed diabetes drug, activates AMPK indirectly by inhibiting mitochondrial Complex I, which raises the AMP/ATP ratio. AMPK activation: - Increases glucose uptake in muscle - Inhibits hepatic gluconeogenesis (via CREB coactivator CRTC2 phosphorylation) - Reduces lipogenesis - May have anti-cancer effects (mTORC1 inhibition) Metformin is also being investigated as an anti-aging compound (TAME trial). see section 9 for Complex I.

Worked Example — Adenylate Energy Charge Under Ischemia: A hepatocyte under aerobic conditions has: $[ATP] = 4.2$ mM, $[ADP] = 0.85$ mM, $[AMP] = 0.12$ mM. Calculate the adenylate energy charge: $EC = ([ATP] + 0.5[ADP]) / ([ATP] + [ADP] + [AMP]) = (4.2 + 0.5 \times 0.85) / (4.2 + 0.85 + 0.12) = (4.2 + 0.425) / 5.17 = 4.625 / 5.17 \approx 0.894$. This is in the normal resting range (0.85–0.95). During 30 minutes of ischemia (no O_2): $[ATP]$ falls to 0.4 mM, $[ADP]$ rises to 1.8 mM, $[AMP]$ rises to 3.0 mM. New $EC = (0.4 + 0.9) / (0.4 + 1.8 + 3.0) = 1.3 / 5.2 = 0.250$. AMPK half-maximal activation threshold is approximately $EC < 0.7 \rightarrow$ AMPK is now strongly activated. AMPK phosphorylates ACC (inhibiting fatty-acid synthesis) and promotes GLUT4 translocation. Predict: gluconeogenesis decreases (via PFKFB1/2 reshaping), glycolysis flux increases (PFK-1 is less inhibited by the now-depleted ATP pool), and mitochondrial biogenesis is up-regulated (PGC-1 α phosphorylation) — the cell switches from anabolic to maximally catabolic mode.

Concept Check (Synthesis): During cancer metabolism (the Warburg effect), many cancer cells preferentially use aerobic glycolysis even in the presence of O_2 , producing large amounts of lactate. (a) The Warburg effect yields a mere about 2 ATP per glucose vs. about 32 by OXPHOS — why would cancer cells “choose” this seemingly inefficient strategy? Consider: ATP production *rate* (not yield), NADPH supply (via PPP shunt), and anabolic precursor availability (ribose, glycerol-3P, serine). (b) mTORC1 integrates signals from growth factors (Akt \rightarrow TSC1/2 \rightarrow Rheb), amino acids (Rag GTPases at the lysosome), and energy status (AMPK). Construct the logical circuit diagram showing how mTORC1 integrates these three inputs (Boolean: growth-factor AND amino-acid AND not-energy-stressed) and predict: what happens to protein synthesis when [glucose] drops 10-fold? (c) Metformin inhibits Complex I of the mitochondrial ETC (and also inhibits mitochondrial glycerophosphate dehydrogenase). Propose the metabolic logic for metformin’s anti-cancer effect in terms of energy charge \rightarrow AMPK \rightarrow mTORC1 inhibition \rightarrow reduced anabolic flux.

11.12 Worked Example: Flux Control Coefficient

Problem: In an isolated hepatocyte preparation, a small activator raises PFK-1 activity by 20% and the measured glycolytic flux rises by 5%. A separate manipulation raises the pyruvate-transporter activity by 30% and flux rises by 3%. Calculate each flux control coefficient and determine which step exerts more control over glycolytic flux.

Solution:

Step 1 — State the operational form of the flux control coefficient. For a small fractional change in enzyme activity, $C_i^J = \frac{\partial \ln J}{\partial \ln e_i}$ is approximated by the ratio of fractional changes:

$$C_i^J \approx \frac{\Delta J/J}{\Delta e_i/e_i} \quad (194)$$

Step 2 — Substitute for PFK-1. Here $\Delta e/e = 0.20$ and $\Delta J/J = 0.05$:

$$C_{\text{PFK-1}}^J = \frac{0.05}{0.20} = 0.25 \quad (195)$$

Step 3 — Substitute for the pyruvate transporter. Here $\Delta e/e = 0.30$ and $\Delta J/J = 0.03$:

$$C_{\text{transporter}}^J = \frac{0.03}{0.30} = 0.10$$

Step 4 — Interpret against the summation theorem. Both coefficients fall in the $C_i^J \approx 0.1$ –0.3 band reported for glycolytic enzymes. PFK-1 ($C^J = 0.25$) exerts more than twice the flux control of the pyruvate transporter ($C^J = 0.10$), so PFK-1 is the more rate-controlling step here — yet because equation (201) requires

$\sum_i C_i^J = 1$, these two steps together account for primarily $0.25 + 0.10 = 0.35$ of total control. The remaining 0.65 is distributed across other enzymes: no single enzyme is *the* rate-limiting step, which is why an activator targeting PFK-1 alone produces primarily a fractional, not proportional, increase in flux.

11.13 mTORC1 — The Growth Integrator and Nutrient Sensor

mTORC1 (mechanistic Target of Rapamycin Complex 1) integrates amino acid, glucose, oxygen, and growth factor signals:

Table 174. Adenylate Energy Charge and Metabolic State: Input and Sensing mechanism.

Input	Sensing mechanism	Outcome
Amino acids (Leu, Arg)	Rag GTPases (Sestrin2 senses Leu; CASTOR1 senses Arg) recruit mTORC1 to lysosomal surface	mTORC1 ON
Insulin/IGF-1	PI3K → Akt → phosphorylates TSC2 → Rheb-GTP accumulates	mTORC1 ON
Glucose	Low glucose → AMPK → TSC2/Raptor phosphorylation	mTORC1 OFF
Oxygen	Hypoxia → REDD1 → TSC1/2 activation	mTORC1 OFF

11.13.1 Amino Acid Sensing: The Ragulator Complex and Lysosome

mTORC1 primarily senses amino acid sufficiency by being physically positioned on the lysosomal surface. The structure responsible is a multi-protein scaffold called the Ragulator complex (LAMTOR1–5) that anchors mTORC1 to the cytoplasmic face of the lysosomal membrane. The amino acid sensing cascade works as follows:

1. Specific amino acid sensors detect intracellular concentrations:
 - Sestrin2 binds and is inhibited by leucine — when Leu is high, Sestrin2 is displaced and stops inhibiting GATOR2.
 - CASTOR1 binds and is inhibited by arginine — same logic.
 - SAMTOR senses S-adenosylmethionine (a proxy for methionine).
 - SLC38A9 senses lysosomal arginine and signals from the lysosomal membrane.
2. GATOR1/2 GAP/GEF complex. GATOR1 is a GAP for the Rag GTPases (turning them off); GATOR2 inhibits GATOR1. When sensors release inhibition of GATOR2, GATOR1 is suppressed, allowing the Rag GTPases to enter their active conformation.
3. Active Rag GTPases (RagA/B-GTP + RagC/D-GDP) bind Raptor (a subunit of mTORC1) and recruit mTORC1 to the lysosomal surface.
4. At the lysosome, mTORC1 encounters Rheb-GTP — provided that growth factor signaling has activated it via Akt → TSC2 inhibition → Rheb-GTP accumulation.
5. Rheb-GTP fully activates mTORC1 kinase activity. Both signals (amino acids → Rag → lysosomal positioning *and* growth factors → Rheb-GTP) must converge.

This dual-input gating is why mTORC1 is sometimes described as a coincidence detector: it primarily signals “build” when both raw materials (amino acids) and external commands (insulin/IGF-1) are present.

11.13.2 Rapamycin: Mechanism of Action

Rapamycin is a macrolide originally isolated from *Streptomyces hygroscopicus* on Easter Island (Rapa Nui). It binds to the immunophilin FKBP12 in the cytoplasm; the FKBP12-rapamycin complex then binds to the FRB domain of mTOR within mTORC1, allosterically inhibiting kinase activity *primarily in the mTORC1 complex* (mTORC2 is largely unaffected on short timescales). This inhibition: - Suppresses cap-dependent translation (4E-BP1 phosphorylation) - Suppresses ribosome biogenesis (S6K1 phosphorylation) - Activates autophagy - Extends lifespan in yeast, worms, flies, and mice (about 10–15% extension at low doses)

Rapamycin and analogs (rapalogues: everolimus, temsirolimus) are clinically approved as immunosuppressants (transplant rejection prevention) and anticancer agents (renal cell carcinoma, certain breast cancers). The TAME trial and large-scale rapamycin/metformin studies are testing rapalogues as longevity interventions in humans.

AMPK and mTORC1 reciprocal inhibition creates a bistable metabolic switch: energy-rich → mTORC1 on, AMPK off → anabolism; energy-depleted → AMPK on, mTORC1 off → catabolism + autophagy.

11.14 The Randle Cycle (Glucose-Fatty Acid Cycle)

Proposed by Randle et al. (1963, *The Lancet*), the Randle cycle describes reciprocal inhibition between glucose and fatty acid oxidation in heart and skeletal muscle:

When fatty acids are high → glucose utilization is suppressed: 1. Beta-oxidation → elevated acetyl-CoA → PDH kinase (PDK) activated → PDH phosphorylated/inactivated → less pyruvate oxidation 2. Beta-oxidation → elevated citrate (exported to cytoplasm) → PFK-1 allosterically inhibited → glycolysis slows 3. Elevated intracellular acyl-CoA → PKC-theta (in muscle) → serine phosphorylation of IRS-1 → impaired insulin signaling → reduced GLUT4 translocation

When glucose is high → fatty acid oxidation is suppressed: 1. Insulin → ACC activated → malonyl-CoA synthesis increases → CPT-1 inhibited → beta-oxidation blocked 2. Elevated NADH from glycolysis → inhibits beta-oxidation dehydrogenases

11.14.1 Metabolic Flexibility Across Feeding and Fasting

Metabolic flexibility = the ability to switch between glucose and fat oxidation in response to fuel availability. Assessed by the respiratory quotient (RQ):

$$RQ = \frac{\text{CO}_2 \text{ produced}}{\text{O}_2 \text{ consumed}}$$

(196)

- RQ = 1.0: pure glucose oxidation
- RQ = 0.7: pure fat oxidation
- Healthy individuals: RQ about 0.95 post-meal → about 0.75 fasting (rapid switching)
- Obese/T2D individuals: RQ remains about 0.85 in fasting → “metabolic inflexibility”

11.15 Hormonal Coordination at the Whole-Organism Level

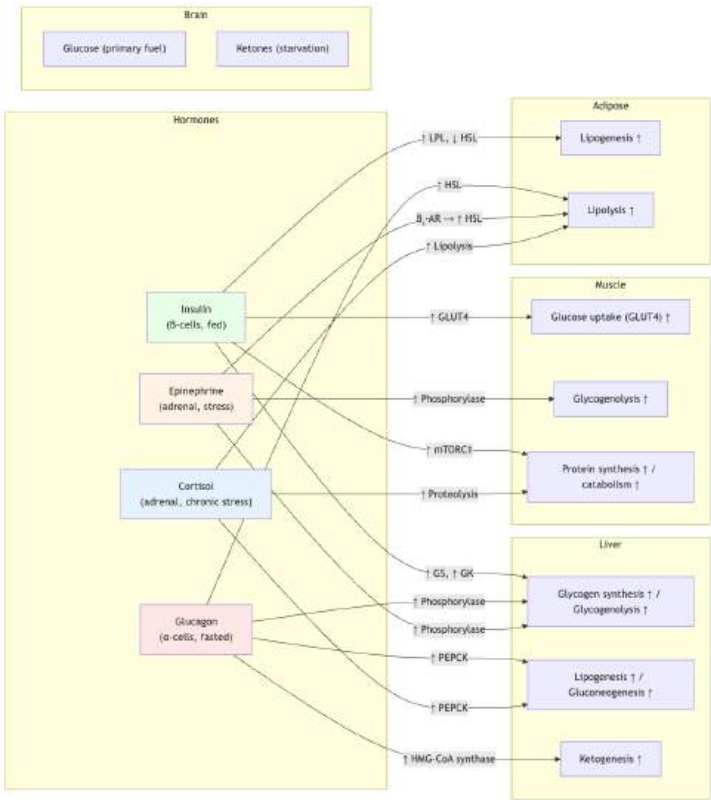


Figure 81. Hormonal coordination of metabolism across organs. Insulin (green) drives anabolic responses; glucagon (red) and cortisol (blue) drive catabolic responses. Each organ has distinct metabolic roles and receptor expression patterns.

Table 175. Metabolic Flexibility Across Feeding and Fasting: Hormone and Stimulus.

Hormone	Stimulus	Liver	Muscle	Adipose
Insulin	High glucose	Glycogen synthesis; lipogenesis; gluconeogenesis OFF	GLUT4; glycogen synthesis; protein synthesis	GLUT4; lipogenesis; lipolysis OFF
Glucagon	Low glucose	Glycogenolysis; gluconeogenesis ON; ketogenesis	Minimal (no glucagon receptor)	Lipolysis (via FFA release)
Epinephrine	Stress/exercise	Glycogenolysis; gluconeogenesis	Glycogenolysis; glucose uptake	Lipolysis (beta ₃ -AR → cAMP → PKA → HSL)
Cortisol	Chronic stress	Gluconeogenesis (PEPCK gene induction)	Protein catabolism → AAs for GNG	Lipolysis (central redistribution)
Leptin	Adiposity signal	Central: inhibits NPY/AgRP → appetite suppression	FA oxidation (via AMPK)	Lipogenesis suppressed

11.16 Substrate (Futile) Cycles

A substrate cycle involves two opposing metabolic reactions operating simultaneously:



Net reaction: $\text{ATP} \rightarrow \text{ADP} + \text{P}_i$ (energy dissipated as heat)

Why substrate cycles are useful (Newsholme hypothesis, 1984):

$$\text{Amplification factor} = \frac{v_{\text{PFK}} + v_{\text{FBPase}}}{v_{\text{PFK}} - v_{\text{FBPase}}}$$

(199)

When both enzymes run at 50 U/min each and net flux is 1 U/min, a 10% change in PFK produces a 500% change in net flux — metabolic rheostat behavior. Substrate cycles provide ultrasensitive flux control at the cost of ATP.

Thermogenic substrate cycles: - Brown adipose tissue (BAT): UCP1 short-circuits the ETC proton gradient → heat (non-shivering thermogenesis) - Sarcoplipin/SERCA cycle in skeletal muscle: sarcoplipin uncouples SERCA Ca²⁺ pumping from Ca²⁺ retention, dissipating ATP as heat - Insect flight muscle: glycolytic futile cycles generate heat rapidly to reach flight temperature (about 40 degrees C)

11.17 Obesity and Metabolic Syndrome

Metabolic syndrome is a cluster of conditions (central obesity, insulin resistance, dyslipidaemia, hypertension, hyperglycaemia) that dramatically increase cardiovascular disease risk.

11.17.1 Visceral Fat as an Endocrine Organ

The shift in our understanding of adipose tissue — from “passive triglyceride storage depot” to “active endocrine organ” — is one of the most consequential paradigm changes in metabolism research of the last 30 years. Visceral adipose tissue (VAT), the fat depot surrounding intra-abdominal organs, behaves very differently from subcutaneous adipose tissue (SAT):

Table 176. Visceral Fat as an Endocrine Organ: Property and Subcutaneous adipose (SAT).

Property	Subcutaneous adipose (SAT)	Visceral adipose (VAT)
Adipocyte size	Smaller, more uniform	Hypertrophic, heterogeneous
Lipolysis sensitivity to catecholamines	Modest	High (β_3 -AR-driven)
Insulin sensitivity	High	Low
Drainage	Systemic circulation	Hepatic portal vein (direct to liver)
Macrophage infiltration	Low (fed state)	High (M1-skewed)
Adipokine output	Adiponectin > leptin	Leptin > adiponectin; \uparrow TNF- α , IL-6, RBP4, MCP-1
Cardiovascular disease risk	Modest	High

The portal-vein drainage means that VAT lipolytic products (FFAs, glycerol) and pro-inflammatory cytokines (TNF- α , IL-6) hit the liver at much higher concentrations than they do peripheral tissues — driving hepatic insulin resistance, NAFLD, and a chronic low-grade systemic inflammatory state.

Key adipokines:

Table 177. Visceral Fat as an Endocrine Organ: Adipokine and Direction in obesity.

Adipokine	Direction in obesity	Effect
Leptin	\uparrow (proportional to fat mass)	Hypothalamic POMC/AgRP signaling — appetite suppression; resistance develops with chronic elevation
Adiponectin	\downarrow in obesity	Insulin-sensitizing; AMPK activator; anti-inflammatory
TNF- α	\uparrow (from infiltrating macrophages)	IRS-1 Ser phosphorylation via JNK/IKK- β
IL-6	\uparrow	Hepatic CRP induction; insulin resistance in liver
MCP-1	\uparrow	Recruits more macrophages \rightarrow vicious cycle
RBP4	\uparrow	Promotes hepatic gluconeogenesis

Molecular mechanisms of insulin resistance in obesity: 1. Lipid overflow: Adipose tissue capacity exceeded \rightarrow ectopic lipid deposition in liver (NAFLD) and muscle 2. DAG accumulation \rightarrow PKC-epsilon (liver) / PKC-theta (muscle) \rightarrow IRS-1 Ser phosphorylation 3. Ceramide accumulation \rightarrow PP2A activation \rightarrow Akt dephosphorylation 4. Adipose inflammation: Hypertrophic adipocytes secrete TNF-alpha, IL-6, MCP-1 \rightarrow macrophage infiltration \rightarrow chronic low-grade inflammation \rightarrow JNK/IKK-beta activation \rightarrow IRS-1 serine phosphorylation 5. ER stress: Lipid overload overwhelms ER folding capacity \rightarrow UPR \rightarrow JNK \rightarrow IRS-1 serine phosphorylation 6. Mitochondrial dysfunction: Incomplete fatty acid oxidation \rightarrow ROS \rightarrow oxidative stress \rightarrow insulin resistance

Clinical Connection: GLP-1 Receptor Agonists Glucagon-like peptide-1 (GLP-1) receptor agonists (semaglutide, liraglutide, tirzepatide) have revolutionised treatment of both type 2 diabetes and obesity. They: - Enhance glucose-dependent insulin secretion - Suppress glucagon secretion - Slow gastric emptying (satiety) - Act on hypothalamic appetite centers (weight loss of 15–20%) - Reduce cardiovascular events and NAFLD progression Tirzepatide is a dual GIP/GLP-1 receptor agonist achieving even greater weight loss (about 22.5% in trials).

Concept Check 5: Explain why **aerobic** exercise improves insulin sensitivity even without weight loss. Consider the effects of exercise on AMPK, GLUT4, mitochondrial biogenesis, and intramyocellular lipid turnover.

11.18 Metabolic Control Analysis

Metabolic control analysis (MCA) provides a quantitative framework for understanding how control of metabolic flux is distributed among pathway enzymes [Atkinson, 1968].

Flux control coefficient (C_i^J): The fractional change in pathway flux (J) caused by a fractional change in enzyme activity (e_i), with most other variables held constant:

$$C_i^J = \frac{e_i}{J} \cdot \frac{\partial J}{\partial e_i} = \frac{\partial \ln J}{\partial \ln e_i}$$

(200)

Each C_i^J ranges from 0 (this enzyme has no control over flux) to about 1 (this enzyme has near-total control). Negative values are possible for enzymes that produce inhibitors of the pathway.

Summation theorem: The combined flux control coefficients in a pathway sum to 1:

$$\sum_i C_i^J = 1$$

(201)

This means control is shared among most enzymes, not concentrated at a single “rate-limiting step.” In practice, one or a few enzymes may have larger C_i^J values, but the concept of a single rate-limiting step is an oversimplification.

For example, in glycolysis under physiological conditions, the flux control coefficients for hexokinase, PFK-1, pyruvate kinase, and the pyruvate transporter are most in the range $C_i^J \approx 0.1\text{--}0.3$ — no single enzyme dominates, and the precise distribution shifts with cellular state. This is why drug therapies that target a single glycolytic enzyme often have surprisingly modest effects on overall flux: the pathway redistributes control.

11.18.1 Metabolomics: Measuring the Metabolic State

Metabolomics is the systematic measurement of small-molecule metabolites — the experimental complement to MCA, since you cannot compute flux control coefficients without measuring concentrations and fluxes.

Table 178. Metabolomics: Measuring the Metabolic State: Approach and Sensitivity.

Approach	Sensitivity	Resolution	Strengths	Weaknesses
NMR (¹ H, ¹³ C, ³¹ P)	μM–mM (about 10 ⁴ molecules)	Quantitative; structure-resolving	Non-destructive; absolute quantification; detects isomers	Lower sensitivity than MS; needs about mg sample; chemical-shift overlap in complex mixtures
LC-MS (HILIC + reversed phase)	nM–μM (about 10 ⁷ molecules)	High sensitivity	Targeted and untargeted; broad metabolite coverage	Ionization bias (different molecules ionize differently); matrix effects; needs MS ² for confident ID
GC-MS	nM (with derivatisation)	Very reproducible spectra	Mature databases (NIST, GMD); quantitative	Requires volatile derivatives; not most metabolites compatible
CE-MS	nM	Polar/charged metabolites	Excellent for phosphometabolites, amines	Low robustness; less mature databases
Imaging MS (DESI/MALDI-MSI)	μM	Spatially resolved	Tissue-level metabolic mapping	Lower mass accuracy than LC-MS; no separation step

Key challenges:

1. Identification. A typical untargeted LC-MS run detects 5,000–30,000 features but about 10–20% can be confidently identified. The remaining “dark metabolome” comprises mass spectra with no database match — a major bottleneck.
2. Compartmentation. Metabolomics typically homogenises tissue, losing information about which metabolites were in mitochondria vs cytoplasm vs lysosome. Subcellular metabolomics (genetically encoded sensors, organelle isolation) is an emerging frontier.
3. Flux ≠ concentration. A high concentration of an intermediate may reflect either high flux through that step *or* a downstream block. Stable-isotope tracing (¹³C-glucose, ¹⁵N-glutamine) is required to measure fluxes, not concentrations.

These data feed directly into MCA models: combining flux measurements (from ¹³C tracing) with elasticity coefficients (from in vitro enzyme kinetics) gives an empirical C_i^J for each enzyme, validating or revising textbook claims about which step is “rate-limiting.”

- Concept Check 6: A drug increases hexokinase activity by 50% in muscle. From fasting biopsies, the flux control coefficient C_{HK}^J for hexokinase in glycolysis was estimated at 0.2. Use equation (201) to predict the maximum fractional change in glycolytic flux. Why is the prediction an upper bound, not a precise value?
- Concept Check 7: A patient with chronic alcohol consumption shows elevated NADH/NAD⁺ ratio in cytoplasm and impaired gluconeogenesis. Using equation (192), predict whether the energy charge is preserved or depressed, and explain why fasting hypoglycaemia is a clinical risk.

11.19 Computational Bridge

Drug effects on pathway enzymes are often framed like competitive inhibitors shifting apparent K_m . The biochemistry module exposes both curves numerically:

```
from biology.biochemistry import michaelis_menten, competitive_inhibition

base = michaelis_menten(4.0, Vmax=100.0, Km=5.0)
blocked = competitive_inhibition(4.0, 100.0, 5.0, inhibitor_conc=5.0, Ki=2.5)
print(round(base.reaction_rate, 2), round(blocked.reaction_rate, 2))
```

Clinical / systems note: Metformin, SGLT2 inhibitors, and GLP-1 agonists reshape the same integrative network (hepatic glucose output, peripheral uptake, renal glucose loss) that insulin and glucagon command — illustrating multi-node control rather than a single “rate-limiting” hormone.

11.20 Current Evidence and Frontier Biology: Metabolic Integration and Regulation

For Metabolic Integration and Regulation, frontier biology belongs inside the evidence logic of the chapter. Metabolism is now studied as a regulated network constrained by energy, redox balance, compartmentation, and environment. The core reading question is this: metabolic integration depends on compartmentation, hormone state, nutrient availability, and time scale.

- What to verify: identify the observation, model, assay, or dataset that would make the claim stronger or weaker.
- What to qualify: state the scale, organism, cell type, environmental condition, or population where the claim is expected to hold.
- What to compare: test at least one alternative explanation, baseline, or null model before treating the pattern as causal.
- What to cite: distinguish primary evidence, review synthesis, public dataset, and institutional guidance; for recent or numeric claims, prefer the source closest to the measurement and state what has changed since it was published.

A strong metabolic-integration claim names the organ, hormone signal, substrate flux, fed-fasting state, and timescale of compensation.

Source practice: For whole-body metabolism claims, connect pathway logic to fluxomics, hormone measurements, tissue state, or clinical biomarkers rather than pathway membership alone.

11.21 Summary

- AMPK (heterotrimer of two catalytic α + two regulatory β/γ modules) is activated by elevated AMP/ATP and ADP/ATP through Thr172 phosphorylation by LKB1 (energy stress) or CaMKK β (Ca²⁺); it promotes catabolism (β -oxidation, glycolysis) and inhibits mTORC1 and anabolism; activates autophagy (via ULK1) and mitochondrial biogenesis (via PGC-1 α).
- mTORC1 (activated by insulin + amino acids + oxygen) is positioned at the lysosome by Rag GTPases bound to the Ragulator complex; full activation requires both amino acid–driven lysosomal recruitment *and* growth factor–driven Rheb-GTP. Rapamycin (FKBP12 complex) inhibits mTORC1.
- Energy charge equation (192) captures the fractional saturation of the adenylate pool with high-energy phosphate; cells maintain E.C. \approx 0.85–0.95.

- Insulin (PI3K/Akt/mTOR pathway) drives GLUT4 translocation, glycogen synthesis, lipogenesis, and suppresses gluconeogenesis. The phosphorylase kinase / GLUT4-vesicle / 14-3-3-BAD effectors are characteristic Akt outputs.
- Glucagon (cAMP/PKA cascade) drives glycogenolysis (via phosphorylase kinase), gluconeogenesis (via CREB transcription), and ketogenesis. The hormonal cascade amplifies the signal about 10^7 -fold from femtomolar hormone to millimolar metabolite.
- Gluconeogenesis uses four bypass enzymes (pyruvate carboxylase, PEPCK, FBPase-1, G6Pase) and costs 6 ATP equivalents per glucose.
- Beta-oxidation yields about 106 ATP per palmitoyl-CoA; CPT-1 is rate-limiting and inhibited by malonyl-CoA.
- Ketone bodies (acetoacetate, β -hydroxybutyrate) sustain the brain during starvation; liver produces but cannot use them. Fasting fuel switching follows a programmed timeline from glycogen \rightarrow fatty acids \rightarrow ketones over hours-to-weeks.
- Randle cycle: fatty acid–glucose reciprocal inhibition; disrupted in type 2 diabetes.
- Substrate cycles enable ultrasensitive flux control and thermogenesis; amplification factor = $(v_1 + v_2)/(v_1 - v_2)$.
- Metabolic flexibility (RQ switching) is impaired in obesity/T2D due to lipid intermediate accumulation and insulin resistance.
- Metabolic control analysis (equation (201)) shows that flux control is distributed, not concentrated at a single rate-limiting step.
- Metabolomics (NMR + LC-MS) provides the empirical basis for MCA, with ^{13}C tracing distinguishing flux from concentration.
- Visceral adipose is a metabolically active endocrine organ whose portal-vein drainage drives hepatic insulin resistance, NAFLD, and chronic systemic inflammation.
- Connections: See section 8 for signal transduction to mTOR, Unit IX — Zoology and Systems Physiology: Introduction for endocrine first messengers, and section 4 for enzyme-level kinetics.

11.22 Review Questions

1. A patient presents with an inherited loss-of-function mutation in LKB1 (the primary AMPK upstream kinase). Predict four metabolic consequences in skeletal muscle during fasting.
2. Derive the energy charge equation (equation (192)). If $[\text{ATP}] = 3.5 \text{ mM}$, $[\text{ADP}] = 0.8 \text{ mM}$, $[\text{AMP}] = 0.2 \text{ mM}$, calculate EC. Is AMPK likely to be active?
3. Describe the insulin signaling cascade from receptor binding to GLUT4 translocation, including the role of AS160, Rab10, and the SNARE complex. At which steps does insulin resistance develop in type 2 diabetes?
4. Compare gluconeogenesis with glycolysis. Identify the three bypass reactions and explain why they are necessary.
5. Calculate the ATP yield from complete oxidation of palmitoyl-CoA (C16:0) to CO_2 and H_2O , showing most sources of ATP.
6. Explain ketone body synthesis and utilization. Why can the brain use ketone bodies but the liver cannot? Sketch the fuel-switching timeline from fed to 30-day fast.
7. The Randle cycle operates in heart muscle. In a patient with type 2 diabetes and chronically elevated plasma FFA: predict changes in cardiac PDH activity, cardiac efficiency, and susceptibility to ischemia.
8. Compare the amplification advantages of the PFK-1/FBPase-1 substrate cycle in liver with UCP1-mediated thermogenesis in brown adipose tissue.
9. Explain how metformin improves glycaemic control. Describe its effects on Complex I, AMPK, and hepatic gluconeogenesis.
10. Describe three molecular mechanisms by which obesity causes insulin resistance. For each, identify the lipid species involved and the downstream kinase that phosphorylates IRS-1.
11. Using the competitive inhibition example in the bridge, explain why simply raising substrate concentration can overcome some drug interactions but not others (hint: K_m^{app} vs. V_{max}).
12. Estimate energy charge for $[\text{ATP}]=2 \text{ mM}$, $[\text{ADP}]=1.5 \text{ mM}$, $[\text{AMP}]=0.5 \text{ mM}$. Is AMPK more likely active than at $\text{EC} \approx 0.9$?
13. Describe how mTORC1 is recruited to the lysosomal surface by amino acid availability. What is the role of Sestrin2, GATOR1/2, and the Rag GTPases? Why is mTORC1 a “coincidence detector” rather than a single-input sensor?
14. Sketch the phosphorylase kinase amplification cascade and estimate the end-to-end signal gain from a single glucagon binding event to released glucose-1-phosphate. Why is this amplification physiologically necessary?
15. Compare the contributions of subcutaneous and visceral adipose tissue to whole-body insulin resistance in obesity. Why does visceral fat have a disproportionate effect on hepatic outcomes?

16. Compare NMR and LC-MS as metabolomics platforms. Which is preferable for (a) absolute quantification of glucose in serum, (b) discovery of unknown lipid species in muscle biopsies, (c) compartment-resolved metabolomics in subcellular fractions?

11.23 Further Reading and Source Notes: Metabolic Integration and Regulation

- Atkinson (1968). The regulation of enzyme activity in metabolism. *Biochemical Journal*, 108 [Atkinson, 1968].
- Mitchell (1961). Coupling of phosphorylation to electron and hydrogen transfer by a chemi-osmotic type of mechanism. *Nature*, 191 [Mitchell, 1961].
- Hardie, Ross & Hawley (2012). AMPK: a nutrient and energy sensor that maintains energy homeostasis. *Nature Reviews Molecular Cell Biology*, 13.
- Saxton & Sabatini (2017). mTOR signaling in growth, metabolism, and disease. *Cell*, 168.
- Randle, Garland, Hales & Newsholme (1963). The glucose fatty-acid cycle. *The Lancet*, 281.

11.24 Key Terms

Table 179. Metabolomics: Measuring the Metabolic State: Term and Definition.

Term	Definition
AMPK	AMP-activated protein kinase; principal energy-sensing kinase; activated by elevated AMP/ATP via LKB1 or by Ca ²⁺ via CaMKKβ
mTORC1	Mechanistic target of rapamycin complex 1; growth-promoting kinase; activated by insulin, amino acids, and growth factors at the lysosomal surface
Ragulator	Lysosomal scaffold (LAMTOR1–5) that anchors Rag GTPases and recruits mTORC1 in response to amino acid availability
Energy charge (EC)	([ATP] + 1/2[ADP]) / ([ATP]+[ADP]+[AMP]); normal EC approximately 0.85–0.95
Insulin	Anabolic hormone from beta-cells; PI3K/Akt/mTOR pathway; drives glucose uptake, glycogen synthesis, lipogenesis
Glucagon	Catabolic hormone from alpha-cells; cAMP/PKA; drives glycogenolysis, gluconeogenesis, ketogenesis
Gluconeogenesis	Synthesis of glucose from non-carbohydrate precursors; liver and kidney; costs 6 ATP
CPT-1	Carnitine palmitoyl transferase-1; rate-limiting for mitochondrial fatty acid import; inhibited by malonyl-CoA
Ketone bodies	Acetoacetate, beta-hydroxybutyrate, acetone; liver-produced; brain fuel during starvation
Phosphorylase kinase	Multi-subunit kinase activated by PKA; phosphorylates glycogen phosphorylase to active “a” form
Randle cycle	Reciprocal inhibition of glucose and fatty acid oxidation in heart and muscle
Substrate cycle	Two opposing reactions running simultaneously; amplifies flux control; generates heat
Metabolic flexibility	Ability to switch between glucose and fat oxidation; impaired in obesity and T2D
SIRT1	NAD ⁺ -dependent deacetylase; caloric restriction sensor; activates PGC-1α
Metabolic syndrome	Cluster of central obesity, insulin resistance, dyslipidaemia, hypertension, hyperglycaemia
Visceral adipose tissue	Fat depot draining via portal vein to liver; endocrine organ secreting TNF-α, IL-6, RBP4
Adipokines	Hormones secreted by adipose tissue (leptin, adiponectin, resistin, RBP4); regulate appetite and insulin sensitivity
Warburg effect	Aerobic glycolysis in cancer cells; rapid ATP + biosynthetic precursors
Metabolic control analysis	Quantitative framework for flux control distribution; summation theorem: sum of C _i ^J = 1
Metabolomics	Systematic measurement of small-molecule metabolites; NMR and LC-MS as principal platforms

11.25 Companion Source Module: Metabolic Integration and Regulation

Metabolic Integration and Regulation should leave a reproducible trail from a biological claim to the code, figure, diagram, or paper-based activity that can test it. Use the surfaces below to inspect the chapter’s assumptions, rerun the relevant model, or compare the manuscript explanation with companion labs and figures.

Table 180. Companion source surfaces for Metabolic Integration and Regulation.

Surface	Use it for
src/biology/biochemistry/biochemistry.py (glycolysis_summary, atp_free_energy, reaction_free_energy)	Connect pathway summaries to energy and redox constraints.
src/biology/physiology/physiology.py (homeostasis_response)	Compare cellular flux regulation with organism-level homeostasis.
src/mermaid/biology_diagrams.py (glycolysis_pathway_diagram, hormone_signaling_diagram)	Link metabolic pathways to endocrine control.

Reproducibility check: state fed/fasted status, tissue, compartment, and time scale before predicting pathway priority. Cross-reference: use section 9, section 4, and sections 34 and 35.

Unit IV — Molecular Genetics: Introduction

Why This Unit Matters

In 1944, Oswald Avery, Colin MacLeod, and Maclyn McCarty performed one of the most transformative experiments in the history of science. They showed that the “transforming principle” that could convert harmless *Streptococcus pneumoniae* into a lethal strain was not protein — as virtually everyone expected — but deoxyribonucleic acid (DNA). The announcement was met with scepticism. DNA seemed too simple: primarily four nucleotide bases, arranged in an apparently monotonous double helix. How could such a molecule encode the almost infinite variety of life?

The answer, revealed over the next three decades, is linguistic in structure: a four-letter alphabet (A, T, G, C) organized into three-letter codons, read in a linear sequence, encoding twenty amino acids, assembled by ribosomes into an effectively unlimited number of proteins. This is the molecular logic of life: information flows from DNA to RNA to protein, and control is exerted at every step. The central dogma, articulated by Francis Crick in 1958, has been refined but rarely overturned.

This unit examines the molecular machinery that reads, copies, and expresses genetic information. You will study the multiprotein complexes that replicate DNA with an error rate of fewer than one mistake per 10⁹ base pairs, the RNA polymerases that transcribe genes in a regulated, stimulus-responsive manner, and the ribosome — a 2.5 MDa ribonucleoprotein machine that interprets the genetic code at about 15 amino acids per second. You will also examine how mutations drive evolution and disease, how the genome is structurally organized, and how CRISPR-Cas9 has made precise genome editing a clinical reality [Doudna and Charpentier, 2014].

Landmark Discoveries

Discoverer(s)	Year	Journal / Source	Discovery	Significance
Avery, MacLeod & McCarty	1944	[Avery et al., 1944]	DNA is the genetic material	Overtaken protein hypothesis; opened molecular genetics
Watson & Crick	1953	[Watson and Crick, 1953]	Double-helix structure of DNA	Anti-parallel complementary strands implied replication mechanism
Meselson & Stahl	1958	[Meselson and Stahl, 1958]	Semi-conservative DNA replication	Definitive proof of how DNA is copied; used ¹⁵ N density-gradient experiment
Nirenberg & Matthaei	1961	[Nirenberg and Matthaei, 1961]	Deciphering the genetic code	Used cell-free translation of poly-U to show UUU = phenylalanine; cracked the codon table
Jacob & Monod	1961	[Jacob and Monod, 1961]	<i>lac</i> operon — gene regulatory model	First demonstration of gene circuit logic; inducer-repressor-operator model
Alec Jeffreys	1984	[Jeffreys et al., 1984]	DNA fingerprinting (RFLP-based)	Transformed forensic science, paternity testing, and population genetics
Doudna & Charpentier	2012	[Jinek et al., 2012]	CRISPR-Cas9 programmable genome editing	Created a precise molecular “scissors” for any target sequence; Nobel Prize 2020

Key Concepts and Connections

Current Evidence Thread

Read this unit as molecular genetics built from stacked evidence layers: DNA sequence and replication fidelity, transcription and translation output, the chromatin and methylation state that gates that output, and the variant calls and clinical interpretations that follow from these layers. Molecular genetics now spans single-



Figure 82. Molecular-genetics concept map - dark = DNA; purple = regulation; orange = mutations; red = editing technology.

reference sequences, telomere-to-telomere assemblies, pangenome graphs, long-read sequencing, CRISPR medicines, and ethical deployment. As you move through the chapters, keep a two-column note: claim on the left, evidence that would change my confidence on the right. By the end of the unit, each major idea should be tied to a measurement, model, citation, or paper-based lab decision.

Chapter Roadmap

Chapter	Title	Core Question	Key Equation / Model
12	DNA Replication and the Cell Cycle	How is DNA copied with such extraordinary accuracy, and how is replication coupled to cell division?	Error rate: about 10 ⁻⁹ per base; cell cycle checkpoint models
13	Gene Expression	How is genetic information transcribed and translated into functional proteins?	Rate equations for coupled transcription-translation
14	Mutations, CRISPR, and Genomics	What causes mutations, how are they repaired, and what does the human reference genome reveal?	Jukes-Cantor distance; mutation rate × generation time
15	Epigenetics and Gene Regulation	How do chromatin, methylation, and regulatory RNAs tune gene expression without changing DNA sequence?	Methylation state; histone modification; regulatory network logic

Connections Across the Textbook

- DNA replication directly links to **Unit V — Classical Genetics and Heredity: Introduction** (meiosis and crossing-over in section 19) and **Unit VI — Evolution: Introduction** (molecular clock calculations using sequence divergence).
- Gene regulation (operons, TFs, miRNA) reappears in **Unit VIII — Botany — Plant Biology: Introduction** (plant hormone signal transduction) and **Unit IX — Zoology and Systems Physiology: Introduction** (endocrine control of gene expression via steroid receptors).
- Mutations and DNA repair are essential context for **Unit VI — Evolution: Introduction** (evolution as mutation + selection) and oncogene/tumor-suppressor biology in **Unit II — The Cell: Introduction** and **Unit IX — Zoology and Systems Physiology: Introduction**.
- CRISPR-Cas9 appears in clinical connection boxes throughout — gene therapy (**Unit V — Classical Genetics and Heredity: Introduction**), antibiotic resistance (**Unit VII — Microbiology: Introduction**), and plant engineering (**Unit VIII — Botany — Plant Biology: Introduction**).

Key vocabulary introduced here: nucleotide, base pair, template strand, coding strand, codon, anticodon, spliceosome, intron, exon, promoter, enhancer, transcription factor, epigenome, proto-oncogene, restriction enzyme, CRISPR.

Computational Toolbox — Unit IV

```
from biology.genetics import translate_mrna, dna_complement, punnett_square
```

```
# Translate an mRNA sequence into amino acids
mrna = "AUGUUUGAAGAACUUUAG"
protein = translate_mrna(mrna)
print(f"mRNA: {mrna}")
print(f"Protein: {'-'.join(protein)}")
# Expected: Protein: Met-Phe-Glu-Glu-Leu (stop at UAG)

# Generate the DNA complement of a coding sequence
dna_template = "ATGTTCGAAATG"
complement = dna_complement(dna_template)
print(f"5'→3' complement: {complement}")
# Expected: 5'→3' complement: CATTTCGAACAT (antiparallel)

# Punnett square: monohybrid cross Aa × Aa
result = punnett_square("Aa", "Aa")
print(f"Genotype ratios: {result.genotype_ratios}")
print(f"Phenotype ratios: {result.phenotype_ratios}")
# Expected:
# Genotype ratios: {'AA': 0.25, 'Aa': 0.5, 'aa': 0.25}
# Phenotype ratios: {'dominant': 0.75, 'recessive': 0.25}
```

Try it yourself: Change the mRNA to AUGCAGUGA — note that UGA is a stop codon. Compare proteins produced from synonymous codon changes using the GENETIC_CODE dictionary.

Source modules: `src/biology/genetics/` — `translate_mrna()`, `dna_complement()`, `punnett_square()`, `hardy_weinberg()`. Figures: `src/mermaid/biology_diagrams.py` (central dogma diagrams, CRISPR mechanism).

Cross-Unit Integration

Unit IV — Molecular Genetics: Introduction established how genetic information is stored, copied, and expressed within a single cell. **Unit V — Classical Genetics and Heredity: Introduction** scales that story to populations and generations: how independently assorting alleles produce Mendelian ratios, how linkage modifies them, how chromosomal abnormalities arise from meiotic errors, and how allele frequencies behave across whole populations under Hardy–Weinberg equilibrium. The transcriptional regulation and epigenetic mechanisms you saw at the molecular level reappear in **Unit V — Classical Genetics and Heredity: Introduction** as the proximate machinery underlying incomplete penetrance, variable expressivity, and parent-of-origin (imprinting) effects. As Mendelian patterns introduce dominance, recessiveness, and complementation, ask which **Unit IV — Molecular Genetics: Introduction** molecular events would produce each pattern — **Unit V — Classical Genetics and Heredity: Introduction** is essentially **Unit IV — Molecular Genetics: Introduction** running across pedigrees.

12 DNA Replication and the Cell Cycle

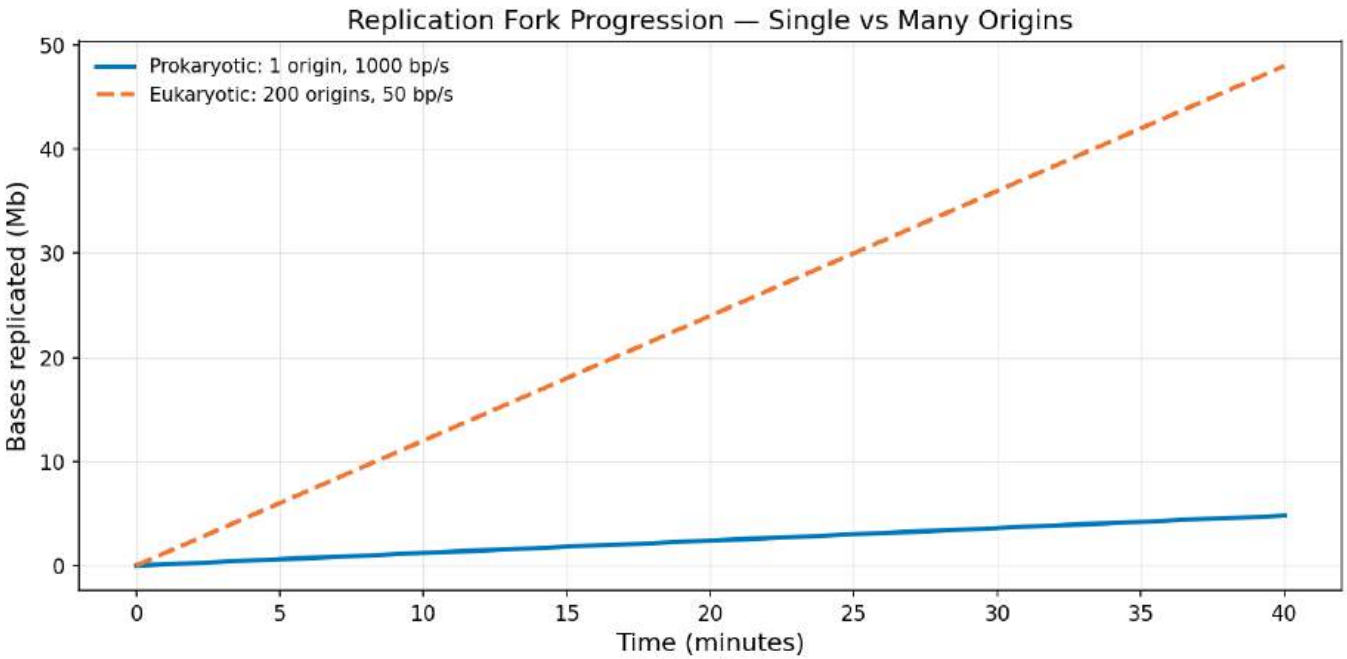


Figure 83. Bases replicated over time for a single fast prokaryotic replication fork (1000 bp/s, one origin) versus many slow eukaryotic forks (50 bp/s, 200 origins). The product of velocity and origin count places the eukaryotic curve well above the prokaryotic curve within an S phase, even though each individual fork is twenty times slower.

Level 2/3 · 55 min read · 75 min lecture · Prerequisites: section 3, section 6

12.1 Learning Objectives

1. Describe the structure of DNA and explain why it is well-suited to information storage and replication.
2. Explain semiconservative replication and the key **enzymes** at the replication fork.
3. Compare the replication machinery of prokaryotes and **eukaryotes**.
4. Describe origin licensing, the role of MCM helicases, and how re-replication is prevented.
5. Explain the **telomere** end-replication problem and the role of telomerase.
6. Describe the stages of the **cell cycle** and the function of cyclin-CDK complexes at each checkpoint.
7. Predict which checkpoint fails first when ATM is lost in a cell carrying a double-strand break, using the ATM/ATR/p53 damage-response pathway.
8. Describe the stages of **mitosis** at the molecular level, including spindle assembly checkpoint mechanisms.
9. Explain the mechanism and biological importance of **meiosis**, including crossing over and **independent assortment**.
10. Describe DNA damage types and the key repair pathways, and connect repair defects to human disease.

12.1.1 Study Blueprint

- Big idea: Genome copying is accurate because chemistry, enzyme proofreading, and checkpoints cooperate.
- Core concepts: semiconservative replication, polymerase, proofreading, checkpoints.
- Framework alignment: Vision & Change: Information flow, exchange, and storage, Structure and function; AP Biology: Information Storage and Transmission, Systems Interactions; NGSS-style topics: Inheritance and Variation of Traits, Structure and Function.
- Model or quantitative lens: Replication-fork speed, error-rate, and cell-cycle timing calculations.
- Data skill: Interpret replication or cell-cycle data from timing, labeling, or checkpoint perturbations.
- Practice cadence: Concept Explanation, Questions and Methods, Argumentation.
- Common misconception to repair: High fidelity is not automatic; it is built from multiple partially redundant safeguards.
- Primary lab: **Lab — DNA Replication and the Cell Cycle**.
- Question bank: **Questions — DNA Replication and the Cell Cycle**.
- Transfer task: Transfer replication logic to cancer, aging, viral replication, or antibiotic targets.
- Bridge to computation: `biology.genetics.genetics.dna_complement`.

Opening Vignette — The Double Helix’s Debt to a Woman Scientist

In 1952, Rosalind Franklin produced the sharpest X-ray diffraction photograph of DNA ever captured — “Photo 51.” The image was obtained without her permission by Maurice Wilkins and shown to James Watson. Recognizing in an instant that the helical periodicity and the 3.4 Å spacing implied a double helix, Watson and Crick used this insight to complete their landmark 1953 *Nature* paper [Watson and Crick, 1953]. Franklin, who died of ovarian cancer in 1958 at age 37, rarely received the Nobel Prize awarded to Watson, Crick, and Wilkins in 1962. Yet her replication studies — painstakingly mapping how DNA unwinds, is copied semiconservatively, and repairs itself — anticipated the entire field of cell-cycle biology. Every chapter covering DNA replication and the cell cycle is, in part, her story.

12.2 DNA as the Genetic Material

The Avery-MacLeod-McCarty experiment (1944) demonstrated that DNA (not protein) carries genetic information by showing that purified DNA from virulent *Streptococcus pneumoniae* could transform non-virulent strains [Avery et al., 1944]. The Hershey-Chase blender experiment (1952) confirmed this with radioactively labeled T4 phage: ³²P-labeled DNA (not ³⁵S-labeled protein) entered bacterial cells during infection.

12.2.1 DNA Double Helix Structure

Watson and Crick’s 1953 model of the B-form DNA helix, built on Rosalind Franklin’s X-ray diffraction data (Photo 51) and Chargaff’s base-pairing rules [Watson and Crick, 1953]:

- Antiparallel complementary strands running 5’ to 3’ and 3’ to 5’
- Base pairing: A-T (2 hydrogen bonds), G-C (3 hydrogen bonds)
- Major groove: wide (about 22 angstroms) and deep – the primary site for sequence-specific protein binding (transcription factors, restriction enzymes). The pattern of hydrogen bond donors and acceptors in the major groove is unique for each base pair, allowing proteins to “read” the sequence without unwinding the helix.
- Minor groove: narrow (about 12 angstroms) – bound by certain drugs (e.g., netropsin, distamycin) and architectural proteins (e.g., HMG-box proteins, TBP)
- Right-handed helix, 10.5 bp per turn, rise 0.34 nm/bp, pitch ≈3.6 nm, diameter 2.0 nm

The phosphodiester backbone runs 5’ to 3’ and carries two negative charges per nucleotide at physiological pH ($pK_a < 1$). This negative charge means DNA repels other nucleic acids and requires cationic counterions (Mg^{2+} , histones, polyamines) for compaction and stability.

Alternative DNA conformations:

Table 181. DNA Double Helix Structure: Form and Helix.

Form	Helix	bp/turn	Diameter	Conditions
B-DNA	Right-handed	10.5	2.0 nm	Physiological; most common
A-DNA	Right-handed	11	2.6 nm	Dehydrated; RNA-DNA hybrids
Z-DNA	Left-handed	12	1.8 nm	Alternating purine-pyrimidine; may regulate transcription

Information capacity: The human haploid genome contains approximately 3.1 billion base pairs, equivalent to roughly 725 megabytes of digital data (2 bits per base). If fully stretched, the DNA in a single cell would extend approximately 2 meters, yet it is compacted into a nucleus approximately 6 micrometers in diameter. This compaction is achieved through a hierarchy of packaging: 147 bp of DNA wraps around each histone octamer to form a nucleosome (the “beads on a string”), which further compacts into the 30-nm chromatin fiber, loop domains (anchored by CTCF and cohesin), and ultimately the mitotic chromosome.

Clinical Connection: Z-DNA and Autoimmunity Antibodies against Z-DNA are found in patients with systemic lupus erythematosus (SLE). Z-DNA forms transiently behind moving RNA polymerase due to negative supercoiling, and mutations in the Z-DNA binding protein ADAR1 cause Aicardi-Goutieres syndrome, a severe autoinflammatory disorder. Z-DNA-binding proteins such as ZBP1 (DAI) also function as innate immune sensors, recognizing viral Z-form nucleic acids.

12.3 DNA Replication and Genome Copying Fidelity

Replication is semiconservative – each daughter double helix retains one parental strand. This was demonstrated by Meselson and Stahl [1958] using ¹⁵N density gradient centrifugation in *E. coli*. After one generation in ¹⁴N medium, most DNA was intermediate density (ruling out conservative replication). After two

generations, half was intermediate and half was light (ruling out dispersive replication).

12.3.1 Origins of Replication and Licensing

Replication begins at specific genomic sites called origins of replication (ori) [Bell and Dutta, 2002]:

- Prokaryotes: *E. coli* has a single origin (*oriC*), a 245-bp sequence containing five 9-bp DnaA-binding sites (DnaA boxes) and three AT-rich 13-mer repeats that melt first upon initiation
- Eukaryotes: Human genome contains approximately 30,000-50,000 origins; yeast origins are called autonomously replicating sequences (ARS), each approximately 150 bp containing an 11-bp ARS consensus sequence (ACS)

The throughput consequence of this contrast is the subject of figure 83: a fast single prokaryotic fork is overtaken in absolute base output by many slow eukaryotic forks once origin count is in the hundreds.

Origin licensing ensures each origin fires primarily once per S phase:

1. In late M/early G1, the Origin Recognition Complex (ORC) binds origins constitutively (in yeast) or dynamically (in metazoans)
2. Cdc6 and Cdt1 load the MCM2-7 helicase (a hexameric ring) onto DNA as a double hexamer – this is the “licensed” pre-replicative complex (pre-RC)
3. At the G1/S transition, CDK (S-CDK = cyclin A-CDK2) and DDK (Cdc7-Dbf4) phosphorylate MCM, activating the helicase and converting pre-RC to pre-initiation complex (pre-IC)
4. Re-licensing is prevented by CDK-mediated phosphorylation of Cdc6 (targeting it for degradation) and by geminin binding to Cdt1

MCM licensing — molecular detail. The pre-RC formation involves a precisely choreographed sequence:

1. ORC binding (G1): ORC1–6 heterohexamer binds origins. ORC1 contains an ATP-binding AAA+ ATPase fold; ATP hydrolysis triggers loading. In humans ORC1 levels oscillate (peaks late M/early G1; degraded in S/G2) — ensuring temporal restriction of licensing.
2. Cdc6 recruitment: Cdc6 (also AAA+ ATPase) joins ORC, forming an ORC–Cdc6 complex that wraps DNA into a left-handed superhelix.
3. Cdt1–MCM2-7 loading: Cdt1 (the licensing factor) binds MCM2-7 and chaperones it to the ORC–Cdc6–origin complex. ATP hydrolysis by ORC and Cdc6 drives the MCM2-7 ring open at the MCM2/MCM5 interface, allowing dsDNA to thread through.
4. Double hexamer assembly: A second Cdt1–MCM2-7 is loaded in the opposite orientation, creating a head-to-head MCM2-7 double hexamer encircling dsDNA. The double hexamer is the licensed pre-RC.
5. CDT1 destruction in S phase: Once MCM is loaded, S-CDK phosphorylates Cdt1 → ubiquitin ligase SCF^{Skp2} → proteasomal degradation. CRL4^{CDT2} also targets Cdt1 for degradation when bound to chromatin (PCNA-coupled mechanism).
6. Geminin sequesters Cdt1: Geminin is an inhibitor that binds Cdt1, preventing it from re-licensing origins during S/G2/M. Geminin levels rise from S phase, peaking in M, and are degraded at anaphase by APC/C-Cdc20.
7. Re-replication prevention is therefore three-fold:
 - CDK-dependent Cdc6 export from nucleus and degradation
 - CDK-dependent Cdt1 degradation
 - Geminin-mediated Cdt1 sequestration
 - Loss of any of these (e.g., siRNA against geminin) causes catastrophic re-replication, DNA damage, and apoptosis.
8. Origin firing in S phase: A subset of licensed origins fires (about 10 % per cell-cycle round in human cells); the remainder are dormant backups. Activation requires DDK (Cdc7-Dbf4) phosphorylation of MCM2-MCM4-MCM6 + S-CDK phosphorylation of Sld2/Sld3 → recruitment of Cdc45 and GINS to form the CMG helicase (Cdc45-MCM-GINS) — the active replicative helicase.

Replication timing domains. Origin firing is not random in time. Each about 1 Mb region has a characteristic replication timing: - Early-replicating domains (S phase first 1–3 hours): gene-rich, euchromatic, transcriptionally active, A-compartment, marked by H3K27ac, H3K4me3, high accessibility - Mid-S replicating domains (3–5 h): transition zones - Late-replicating domains (5–8 h): heterochromatic, gene-poor, B-compartment, marked by H3K9me3 and lamina-association (LADs)

Replication timing correlates with chromatin state and is reprogrammed during cell-fate transitions. Late replication is associated with elevated mutation rate (about 2× background) — because the late-S nucleotide pool is depleted of dNTPs (which were consumed earlier), increasing polymerase mis-incorporation. This explains the spatial mutation-rate variation observed in cancer genomes: late-replicating regions accumulate about 2-fold more mutations per Mb than early-replicating regions.

Quantitative parameters of replication licensing: - Number of origins per genome: about 30,000–50,000 (about one per 50–100 kb) - MCM2-7 loaded per origin: 2 (head-to-head double hexamer) - Total MCM2-7 in nucleus: about 10–20-fold excess over origins → MCM “paradox” - Origins fired per cell cycle: about 15,000

(about 30 % of licensed origins) - Dormant origins: provide backup if a fork stalls or fails — mutation in ATR (which suppresses dormant-origin firing under stress) causes Seckel syndrome (microcephaly, growth failure)

Clinical Connection: Meier-Gorlin Syndrome Mutations in ORC1, ORC4, ORC6, CDT1, or CDC6 cause Meier-Gorlin syndrome, a rare primordial dwarfism characterized by short stature, absent or small patellae, and microtia. This underscores the essential role of origin licensing in normal growth and development.

12.3.2 The Replication Fork Machinery

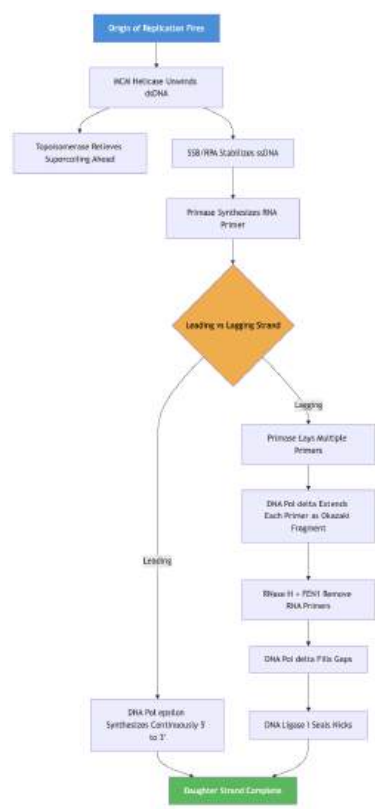


Figure 84. Eukaryotic DNA replication machinery at the replication fork. The leading strand is synthesized continuously, while the lagging strand requires repeated priming and ligation of Okazaki fragments.

12.3.3 Replication Fork Enzymes and Their Roles

Table 182. Replication Fork Enzymes and Their Roles: Enzyme and Prokaryote.

Enzyme	Prokaryote	Eukaryote	Function
Helicase	DnaB (5' to 3')	MCM2-7/CMG (3' to 5')	Unwinds double helix; uses ATP hydrolysis (about 500-1000 bp/s in <i>E. coli</i> , about 50 bp/s in humans)
Single-strand binding	SSB	RPA (replication protein A)	Stabilizes single-stranded regions, prevents re-annealing and nuclease attack
Primase	DnaG	DNA Pol alpha/primase complex	Synthesizes short RNA primers (8-10 nt in prokaryotes; 7-12 nt RNA + 20 nt DNA in eukaryotes)
Leading strand polymerase	DNA Pol III	DNA Pol epsilon	Synthesizes DNA 5' to 3'; high processivity with clamp
Lagging strand polymerase	DNA Pol III	DNA Pol delta	Synthesizes Okazaki fragments; also fills primer gaps

Enzyme	Prokaryote	Eukaryote	Function
Sliding clamp	beta-clamp (homodimer)	PCNA (homotrimer)	Processivity factor; tethers polymerase to DNA; increases processivity from about 10 to >10,000 nt
Clamp loader	gamma complex	RFC (replication factor C)	ATP-dependent loading of sliding clamp
Primer removal	DNA Pol I (5' to 3' exo)	RNase H1 + FEN1 (flap endonuclease)	Removes RNA primers from Okazaki fragments
Ligase	DNA ligase (NAD ⁺ -dependent)	DNA ligase I (ATP-dependent)	Seals nicks between Okazaki fragments
Topoisomerase	Gyrase (Topo II)	Topo I and Topo II	Relieves positive supercoiling ahead of fork

12.3.4 mRNA Vaccines: A Modern Application of Nucleic Acid Technology

Molecular design:

- Sequence optimization: The mRNA sequence is optimized for stability and translation efficiency. This includes:
 - 5' cap: A modified guanosine (Cap-1: N7-methylated, 2'-O-methylated) mimics natural eukaryotic mRNA and prevents recognition by innate immune sensors (RIG-I, MDA5)
 - 5' UTR: Contains Kozak consensus sequence (GCCACC[A/G]CC) for efficient translation initiation
 - Open reading frame (ORF): Encodes the target antigen (e.g., SARS-CoV-2 spike protein). The sequence is codon-optimized to match human tRNA abundance, reducing rare codon clusters that could stall translation.
 - 3' UTR: Contains stability elements (e.g., from human alpha-globin or cytochrome P450 genes) and poly-A tail (100-150 nt) to protect from degradation and enhance translation.
 - Nucleoside modifications: Pseudouridine (Ψ) or N1-methylpseudouridine (m1Ψ) replace uridine to reduce immunogenicity and increase translation efficiency.
- In vitro transcription (IVT): The optimized DNA template (linearized plasmid or PCR product) is transcribed using T7 RNA polymerase in a cell-free system. Nucleoside triphosphates (NTPs) including modified UTP (e.g., m1Ψ-TP) are added. The reaction produces a 5'-triphosphate-ended mRNA, which is then enzymatically capped.
- Purification and formulation: The crude mRNA is treated with DNase to remove template DNA, then purified (often by tangential flow filtration or HPLC). The purified mRNA is formulated into lipid nanoparticles (LNPs) — spherical vesicles about 80-100 nm in diameter composed of ionizable cationic lipids, cholesterol, phospholipids, and PEG-lipids. The ionizable lipid is positively charged at low pH (during formulation) but neutral at physiological pH, reducing toxicity. LNPs protect mRNA from degradation and facilitate cellular uptake.

Cellular uptake and translation:

1. Injection: mRNA-LNP suspension is injected intramuscularly (typically deltoid). The injection site contains antigen-presenting cells (APCs) like dendritic cells and macrophages, as well as muscle cells.
2. Uptake: LNPs fuse with cell membranes or are endocytosed. In the endosome, the ionizable lipid becomes protonated, causing endosomal membrane disruption and release of mRNA into the cytoplasm.
3. Translation: Host ribosomes bind to the 5' cap and translate the mRNA into the antigen protein. The protein may be secreted (if signal peptide included) or remain intracellular.
4. Processing and presentation:
 - MHC class II pathway: Exogenous antigen taken up by APCs is degraded in lysosomes and presented on MHC II to CD4+ helper T cells.
 - MHC class I pathway: Endogenous antigen (produced inside the cell) is degraded by the proteasome into peptides, transported to the ER via TAP, and presented on MHC I to CD8+ cytotoxic T cells.

Immune activation:

- Humoral immunity: B cells recognizing the antigen receive help from CD4+ T cells and differentiate into plasma cells producing neutralizing antibodies (IgG, IgM initially, then IgG). These antibodies block viral entry by binding to the spike protein receptor-binding domain.

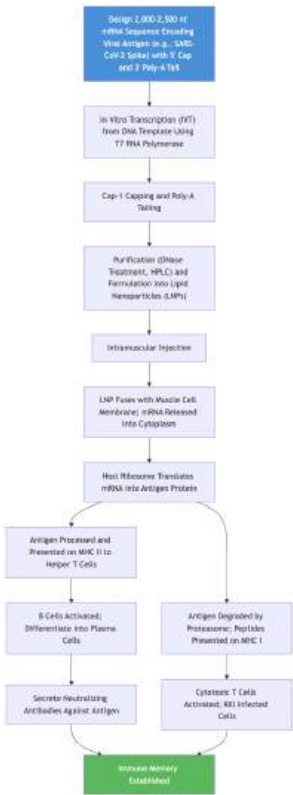


Figure 85. Mechanism of mRNA vaccines. Synthetic mRNA encoding a viral antigen is delivered to host cells, where it is translated into protein. The protein is processed and presented to both helper T cells (via MHC II) and cytotoxic T cells (via MHC I), generating both antibody and cellular immune responses.

- Cellular immunity: CD8+ T cells recognize infected cells presenting viral peptides and kill them, preventing viral replication.
- Immune memory: Long-lived plasma cells and memory B/T cells provide lasting protection.

Advantages over traditional vaccines:

- No live virus: Safer for immunocompromised individuals; no risk of reversion to virulence.
- Rapid design and manufacturing: Once the viral sequence is known, mRNA can be designed in days and manufactured in weeks (cell-free synthesis). Traditional vaccines require growing virus in eggs or cell culture (months).
- Strong immune response: Both antibody and T-cell responses are robust.
- Flexible platform: The same LNP formulation can deliver mRNA for different antigens; the platform can be quickly adapted to new variants or emerging pathogens.

Computational aspects:

Modern mRNA vaccine design relies heavily on computational tools:

```
import numpy as np
from Bio import SeqIO
from collections import Counter

# Example: Analyze GC content and codon usage of an mRNA sequence
def analyze_mrna_sequence(seq):
    """Analyze key features of an mRNA vaccine candidate."""
    gc_content = (seq.count('G') + seq.count('C')) / len(seq) * 100
    # Count codon frequencies
    codon_table = {}
    for i in range(0, len(seq)-2, 3):
        codon = seq[i:i+3]
        if codon in codon_table:
```



```
        codon_table[codon] += 1
    else:
        codon_table[codon] = 1
return {
    'length': len(seq),
    'gc_content': round(gc_content, 2),
    'codon_counts': codon_table
}

# Example: Codon optimization for human expression
def optimize_codon_usage(seq, codon_usage_table):
    """Replace rare codons with optimal human-preferred codons."""
    optimized = []
    for i in range(0, len(seq)-2, 3):
        codon = seq[i:i+3]
        amino_acid = translate_codon(codon) # Assume a translation function
        # Choose the most frequent codon for this amino acid in human cells
        optimal_codon = max(codon_usage_table[amino_acid],
                            key=codon_usage_table[amino_acid].get)
        optimized.append(optimal_codon)
    return ''.join(optimized)

# Example: Predict secondary structure (simplified)
def predict_secondary_structure(seq):
    """Calculate minimum free energy using a simplified nearest-neighbor model."""
    # In practice, tools such as RNAfold (ViennaRNA) or NUPACK
    return "-10.5 kcal/mol" # illustrative fixed value for the textbook example
```

Clinical impact: The Pfizer-BioNTech BNT162b2 and Moderna mRNA-1273 vaccines were developed in under a year from viral sequence release to emergency use authorization, demonstrating the power of this technology. Beyond COVID-19, mRNA vaccines are in development for influenza, HIV, Zika, and personalized cancer vaccines.

Concept Check 11.2

1. Why is the 5' cap important for mRNA vaccine stability and translation?
2. What is the role of lipid nanoparticles (LNPs) in mRNA vaccine delivery?
3. How does an mRNA vaccine activate both CD4+ helper T cells and CD8+ cytotoxic T cells?
4. Explain why nucleoside-modified mRNA (e.g., pseudouridine) reduces immunogenicity compared to unmodified mRNA.
5. Design a simple Python function to calculate the GC content of an mRNA sequence and explain why GC content matters for vaccine stability.

12.3.5 Leading and Lagging Strands

DNA polymerase primarily adds nucleotides to the 3'-OH of an existing primer, and can primarily synthesize in the 5' to 3' direction. Therefore:

- Leading strand: synthesized continuously 5' to 3' in the same direction as fork movement. Requires primarily a single priming event. In eukaryotes, primarily synthesized by DNA Pol epsilon.
- Lagging strand: synthesized discontinuously as Okazaki fragments (1,000-2,000 nt in prokaryotes; 100-200 nt in eukaryotes). Each fragment requires a new RNA primer laid down by primase. After extension by DNA Pol delta, the primers are removed by a multi-step process:
 1. RNase H degrades the RNA portion of the primer
 2. FEN1 (flap endonuclease 1) removes the remaining 5' flap created when the upstream Okazaki fragment displaces the primer of the next fragment
 3. DNA Pol delta fills the gap
 4. DNA Ligase I seals the nick with a phosphodiester bond (consuming ATP)

Replication fork speed: *E. coli* replicates its 4.6 Mb genome from a single origin in approximately 40 minutes (about 1,000 bp/s). Human cells replicate 3.2 Gb from approximately 30,000 origins over 6-8 hours of S phase (about 50 bp/s per fork, but thousands of forks operate simultaneously).

12.3.6 PCNA Sliding Clamp – The Processivity Engine

PCNA is a homotrimeric ring (three identical subunits) that encircles double-stranded DNA and slides freely. It acts as a molecular matchmaker:

- Face toward template junction: binds DNA polymerase (Pol delta/epsilon), FEN1, and ligase I through a conserved PIP box motif
- Monoubiquitination at K164 (by RAD6/RAD18): recruits Y-family translesion synthesis (TLS) polymerases (Pol eta, Pol iota, Pol kappa, Rev1) when the fork stalls at DNA damage. TLS polymerases have relaxed active sites that can bypass lesions but at the cost of lower fidelity

12.3.7 DNA Proofreading and Fidelity

The error rate of replication is remarkably low: approximately 1 error per 10⁹-10¹⁰ base pairs copied. This fidelity results from three layers:

1. Base selection by polymerase (about 10⁻⁵ error rate): The polymerase active site preferentially binds correctly paired nucleotides based on geometry and hydrogen bonding
2. 3' to 5' exonuclease proofreading (about 10⁻² improvement): If a mismatch is incorporated, the polymerase pauses; the 3' to 5' exonuclease domain excises the incorrect nucleotide and the polymerase re-extends
3. Mismatch repair (MMR) (about 10⁻³ improvement): Post-replicative scanning by MutS (MSH2/MSH6 in humans), which detects mismatches and small insertion/deletion loops

Overall error rate $\approx 10^{-5} \times 10^{-2} \times 10^{-3} = 10^{-10}$ per bp per replication

(202)

Clinical Connection: Lynch Syndrome (HNPCC) Germline mutations in MMR **genes** (*MLH1*, *MSH2*, *MSH6*, *PMS2*) cause Lynch syndrome (hereditary non-polyposis colorectal cancer). Affected individuals have a 50-80% lifetime risk of colorectal cancer and increased risk of endometrial, ovarian, and gastric cancers. The hallmark is microsatellite instability (MSI) – expansion or contraction of short tandem repeats due to uncorrected replication slippage. MSI-high tumors respond well to immune checkpoint inhibitors (anti-PD-1), making Lynch syndrome diagnosis therapeutically important.

12.3.8 Telomeres and Telomerase

The end-replication problem: Linear eukaryotic chromosomes cannot replicate the very 5' end of the lagging strand (no upstream sequence to place a primer). This means 50-200 bp of telomeric DNA are lost with each cell division.

Telomere structure: Human telomeres consist of 5-15 kb of the hexameric repeat TTAGGG, ending in a 150-200 nt single-stranded 3' overhang. This overhang invades the upstream duplex to form a T-loop (telomere loop), which is stabilized by the shelterin complex (TRF1, TRF2, RAP1, TIN2, TPP1, POT1). The T-loop hides the chromosome end from the DNA damage response, which would otherwise recognize it as a double-strand break.

The shelterin complex — six-protein architecture and function:

Table 183. Telomeres and Telomerase: Subunit and DNA binding specificity.

Subunit	DNA binding specificity	Function
TRF1 (telomeric repeat factor 1)	dsDNA TTAGGG (Myb domain)	Negatively regulates telomerase access; controls telomere length
TRF2	dsDNA TTAGGG (Myb domain)	Stabilizes T-loop; suppresses ATM-mediated DNA damage signaling at telomeres
TIN2	TRF1, TRF2 partner (no DNA binding)	Bridge protein, stabilizes whole complex
RAP1	TRF2 partner	NF-κB pathway crosstalk; chromatin contacts
TPP1	TIN2 partner; binds POT1	Recruits telomerase via TEL patch

Subunit	DNA binding specificity	Function
POT1	ssDNA TTAGGG-overhang (OB-fold domain)	Suppresses ATR; protects 3' overhang

T-loop formation in detail. The 3' G-rich overhang (150–200 nt) folds back and invades the upstream duplex, displacing one strand and forming a D-loop (displacement loop) within the T-loop. TRF2 wraps the DNA, inducing the strand exchange. The structure has been visualized by electron microscopy and STORM super-resolution. Shelterin coats the entire telomere — about about 1 shelterin per 100 bp.

Shelterin’s six functions in protecting chromosome ends: 1. Suppress ATM kinase at telomeres (TRF2-dependent) 2. Suppress ATR kinase at telomeres (POT1-dependent) 3. Inhibit NHEJ at chromosome ends (preventing fusions; TRF2-RAP1) 4. Inhibit HR between telomeres (TRF2; preventing telomere-telomere recombination) 5. Recruit telomerase in cells where it is active (TPP1-TEL patch) 6. Mediate semi-conservative replication through telomeres (CST complex with shelterin)

Telomere replication problem in detail. Two distinct issues: 1. Lagging-strand end-replication: The very 5' end of the lagging strand cannot be replicated because there is no upstream template for primer placement. After RNA primer removal, about 50–100 nt are lost from the 5' end of the lagging-strand-complement. 2. Leading-strand end-resection: The leading strand is synthesized continuously to the chromosome end, but specialized exonucleases then resect the 5' end to generate the 3' overhang necessary for T-loop formation.

Result: each replication cycle, about 50–200 bp of TTAGGG repeats are lost from telomeres in the absence of telomerase.

G-quadruplex regulation. The G-rich telomere sequence can fold into intramolecular G-quadruplexes (four G’s stacked via Hoogsteen bonds). G-quadruplexes are stabilized by K⁺ but inhibit telomerase access. Drugs that stabilize telomeric G-quadruplexes (e.g., RHPS4, telomestatin, BRACO19) cause progressive telomere shortening and senescence in cancer cells — they are anti-cancer leads but limited by toxicity in normal stem cells.

G-quadruplexes: The G-rich telomeric sequence can fold into G-quadruplex structures – stacked tetrads of four guanines connected by Hoogsteen hydrogen bonds, stabilized by monovalent cations (K⁺). G-quadruplexes inhibit telomerase and are targets for anti-cancer drug development.

Telomerase RNA template — TERC mechanism in detail. TERC is a 451-nt RNA with several functional regions: (i) a template region (5'-CUAACCCUAAC-3', about 11 nt) that base-pairs with the telomere 3' overhang and dictates the TTAGGG sequence added; (ii) a pseudoknot (essential structural motif); (iii) a CR4/CR5 stem-loop that binds TERT; (iv) an H/ACA scaRNA box at the 3' end (essential for stability and dyskerin binding). The H/ACA box recruits dyskerin (DKC1) — mutations in DKC1 cause X-linked dyskeratosis congenita.

Telomerase: A specialized reverse transcriptase that extends the 3' overhang:



- TERT (telomerase reverse transcriptase): the catalytic protein subunit
- TERC (telomerase RNA component): 451-nt RNA containing the template sequence (in humans, 5'-CUAACCCUAAC-3') used to add TTAGGG repeats
- After TERT extends the 3' overhang, conventional DNA Pol alpha/primase synthesizes the complementary C-rich strand

Telomeres, aging, and cancer: Somatic cells lack telomerase activity and undergo progressive telomere shortening, eventually reaching a critically short length that triggers replicative senescence (the Hayflick limit, about 50-70 divisions for human fibroblasts). This is a tumor-suppressive mechanism. However, approximately 85% of cancers reactivate telomerase (often through TERT promoter mutations, especially C228T and C250T), and approximately 15% use ALT (alternative lengthening of telomeres) via recombination between telomeres (associated with ATRX/DAXX mutations, with C-circles as biomarkers).

Clinical Connection: Telomere Biology Disorders Mutations in TERT, TERC, DKC1, or other telomere maintenance genes cause dyskeratosis congenita (DC), characterized by bone marrow failure, pulmonary fibrosis, and mucosal leukoplakia. Patients have critically short telomeres and premature aging features. Related conditions include idiopathic pulmonary fibrosis and aplastic anemia, forming a spectrum called telomere biology disorders (TBDs).

Concept Check 11.1

1. Why is the lagging strand synthesized discontinuously?
2. What would happen to a eukaryotic cell if you knocked out FEN1?
3. A patient has MSI-high colorectal cancer. What is the most likely genetic defect? Why might this patient respond to immunotherapy?
4. Explain why telomerase is an attractive anti-cancer drug target, and what complications might arise from telomerase inhibition.

12.4 The Cell Cycle

The cell cycle is the ordered series of events by which a cell duplicates its contents and divides [Nurse, 2000]. In a typical mammalian cell, the cycle takes approximately 24 hours.

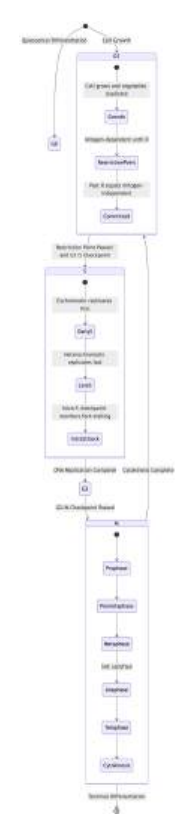


Figure 86. The eukaryotic cell cycle. G1 contains the restriction point (R), after which the cell is committed to division independent of mitogenic signals. Each transition is guarded by checkpoints.

12.4.1 Cell Cycle Phases

Table 184. Cell Cycle Phases: Phase and Duration (typical).

Phase	Duration (typical)	Key Events
G1 (Gap 1)	8-12 h	Cell growth; organelle duplication; assessment of extracellular signals (mitogens, growth factors); passage through the restriction point (R) commits the cell to divide
S (Synthesis)	6-8 h	DNA replication; centrosome duplication; histone synthesis; euchromatin replicates early, heterochromatin late
G2 (Gap 2)	3-4 h	Continued growth; preparation for mitosis; final DNA damage check
M (Mitosis)	about 1 h	Chromosome condensation, alignment, separation, and cytokinesis
G0 (Quiescence)	Variable	Reversible exit from the cell cycle; neurons and muscle cells may remain in G0 permanently

12.4.2 Cyclin-CDK Complexes: The Cell Cycle Engine

The cell cycle is driven by the sequential activation and destruction of cyclin-CDK (cyclin-dependent kinase) complexes, with checkpoint controls preserving the order of replication and division events [Hartwell and Weinert, 1989]:

Table 185. Cyclin-CDK Complexes: The Cell Cycle Engine: Phase and Cyclin-CDK Complex.

Phase	Cyclin-CDK Complex	Key Substrates	Function
G1 (early)	Cyclin D - CDK4/6	RB (retinoblastoma protein)	Partial phosphorylation of RB; releases E2F to transcribe S-phase genes
G1/S	Cyclin E - CDK2	RB (hyperphosphorylation), p27	Commits cell to S phase; triggers centrosome duplication
S	Cyclin A - CDK2	Cdc6, Cdt1 (for degradation)	Fires replication origins; prevents re-licensing
G2/M	Cyclin B - CDK1 (MPF)	Lamins, condensins, Golgi proteins	Nuclear envelope breakdown; chromosome condensation; spindle formation

Regulation of CDK activity:

- Cyclin binding: CDKs are inactive monomers without their cyclin partner
- Activating phosphorylation: CAK (CDK-activating kinase) phosphorylates the T-loop
- Inhibitory phosphorylation: Wee1 kinase phosphorylates CDK1 at Tyr15 and Thr14 (inactive); Cdc25 phosphatase removes these (activates)
- CKI (CDK inhibitors): p21^{CIP1} (induced by p53), p27^{KIP1}, p16^{INK4a} bind and inactivate specific cyclin-CDK complexes
- Cyclin destruction: APC/C (anaphase-promoting complex/cyclosome) ubiquitinates cyclins A and B for proteasomal degradation, ending mitosis

Quantitative CDK activity through the cell cycle. Single-cell biosensor measurements have provided a quantitative picture of CDK activity dynamics:

Table 186. Cyclin-CDK Complexes: The Cell Cycle Engine: Cell-cycle phase and Total CDK activity.

Cell-cycle phase	Total CDK activity	Active complexes	Approximate timing (mammalian, 24-h cycle)
Early G1 (mitogen-stimulated)	about 5 % of peak	Cyclin D-CDK4/6 (low)	0–4 h post-mitosis
Restriction point	about 20 %	Cyclin D-CDK4/6 + early Cyclin E-CDK2	6–8 h post-mitosis
G1/S transition	about 40 %	Cyclin E-CDK2 high; Cyclin A-CDK2 rising	8–10 h
Mid-S	about 50 %	Cyclin A-CDK2 dominant	10–14 h
G2	about 70 %	Cyclin A-CDK2 + early Cyclin B-CDK1	14–18 h
G2/M transition	about 90 %	Cyclin B-CDK1 (= MPF) rises sharply	18–20 h
Mitosis (M-phase)	100 % (peak)	Cyclin B-CDK1 + Aurora A/B kinases	20–22 h
Anaphase / Telophase	Drops to < 10 %	APC/C-Cdc20 destroys cyclin B	22–24 h

The peak-to-trough ratio is about 10-fold. This sharp threshold-like activity profile is encoded by: - Bistability in CDK1 activation: Wee1 inhibits CDK1; Cdc25 activates CDK1; both have positive-feedback loops on themselves through CDK1 phosphorylation, creating a bistable switch. - Timing precision from cyclin synthesis and destruction: cyclin A, cyclin B, and securin most have D-box and KEN-box motifs that direct APC/C-mediated ubiquitination at precise times.

12.4.3 Specific Checkpoint Failures in Cancer

Cancer is essentially a disease of cell-cycle deregulation. Key checkpoint mutations and their consequences:

- (1) RB1 loss (G1/S checkpoint failure) - Normal: hypophosphorylated RB binds E2F → E2F cannot transcribe S-phase genes (DNA Pol α, PCNA, MCM, thymidine kinase) - Cancer: biallelic RB1 mutations or deletions (retinoblastoma; small-cell lung cancer; bladder; osteosarcoma) - Consequence: constitutive E2F activity; cells enter S phase regardless of mitogen status - Therapeutic relevance: CDK4/6 inhibitors (palbociclib, ribociclib, abemaciclib) are ineffective in RB-null tumors because the entire downstream pathway is already deregulated.
- (2) p53 loss (G1/S and G2/M checkpoints failure) - Normal: p53 senses DNA damage → induces p21 → arrests CDK2 (G1/S) and CDK1 (G2/M); also induces apoptosis (BAX, PUMA, NOXA) - Cancer: about 50 % of cancers carry p53 mutations (most frequent mutated gene); often dominant-negative (mutant p53 oligomerises with wild-type to inactivate it) or gain-of-function (p53^{R175H}, p53^{R273H} stabilize oncogenic chromatin states) - Consequence: cells with damaged DNA continue dividing; aneuploidy; centrosome amplification; chromosomal instability - Therapeutic relevance: PRIMA-1, APR-246 (eprenetapopt) re-fold mutant p53 conformations; HDM2 inhibitors (idasanutlin, milademetan) re-stabilize wild-type p53 in tumors where p53 is wild-type but suppressed by HDM2 amplification.
- (3) WEE1/CDC25 deregulation (G2/M checkpoint failure) - Normal: Wee1 phosphorylates CDK1 (Tyr15) → inactive; Cdc25 dephosphorylates → activates; balance controls mitotic entry timing. - Cancer-relevant deregulation: - CDC25 amplification in many tumors (breast, lung, pancreatic) → premature CDK1 activation → DNA-damaged cells enter mitosis prematurely → mitotic catastrophe (paradoxically anti-tumor in some contexts). - WEE1 inhibition (adavosertib/MK-1775) is being trialled in p53-mutant tumors: without p53 (the G1/S guard), the cell relies on Wee1-mediated G2/M arrest; inhibiting Wee1 forces entry into mitosis with damaged DNA → mitotic catastrophe. This is synthetic lethality with p53 loss.
- (4) APC/C-Cdc20 / SAC failures - Normal: SAC (mitotic checkpoint complex MCC: Mad2 + BubR1 + Bub3) prevents anaphase until kinetochores are properly attached. - Cancer: BUB1B (BubR1) loss-of-function causes mosaic variegated aneuploidy syndrome (childhood cancers, microcephaly). - Tumor-targeting drugs: - Taxanes (paclitaxel, docetaxel) stabilize microtubules → triggering SAC arrest → mitotic catastrophe + apoptosis - Vincristine, vinblastine, vinorelbine depolymerise microtubules → SAC arrest
- (5) MCM helicase / replication-stress tolerance - Normal: ATR activates Chk1 in response to stalled forks → suppresses dormant origin firing under stress - Cancer: tumors often have constitutively elevated replication stress (driven by oncogenic MYC or RAS); this provides a vulnerability: - ATR inhibitors (berzosertib, ceralasertib) block the cancer cell’s ability to manage replication stress → genome catastrophe - CHK1 inhibitors (LY2603618, prexasertib) similarly target the replication-stress response

Summary table — checkpoint failures and therapeutic targeting:

Table 187. Specific Checkpoint Failures in Cancer: Checkpoint failure and Cancer.

Checkpoint failure	Cancer	Therapeutic strategy
RB1 loss (G1/S)	Retinoblastoma; SCLC; bladder	CDK4/6 inhibitors INEFFECTIVE (downstream); requires alternative
p53 loss (G1/S, G2/M)	about 50 % of cancers	Re-fold mutant p53 (APR-246); WEE1 inhibitor (synthetic lethal); HDM2 inhibitor (if p53 wt)
BRCA1/2 loss (HR)	Breast, ovarian, prostate, pancreatic	PARP inhibitors (synthetic lethal)
MMR loss (replication fidelity)	Lynch syndrome; MSI-high CRC, endometrial	Anti-PD-1 (high neoantigen load)
BUB1B / SAC loss	Mosaic variegated aneuploidy syndrome	Microtubule targeting (taxanes, vinca alkaloids)
MYC-driven replication stress	Lymphoma, neuroblastoma	ATR/CHK1 inhibitors
Cyclin D / CDK4-6 amplification	Mantle cell lymphoma; breast (HR+); melanoma	CDK4/6 inhibitors (palbociclib, ribociclib, abemaciclib) — effective if RB intact

12.4.4 Cell Cycle Checkpoints

Checkpoints are surveillance mechanisms that halt the cell cycle if conditions are not met:

G1/S Checkpoint (Restriction Point): - The RB-E2F pathway is the molecular switch. In early G1, hypophosphorylated RB binds and inhibits E2F transcription factors. Mitogenic signals activate cyclin D-CDK4/6, which partially phosphorylates RB. Cyclin E-CDK2 completes RB hyperphosphorylation, releasing E2F to transcribe genes for DNA replication (DNA Pol alpha, PCNA, MCM, thymidine kinase). - This is the “point of no return”: once past R, the cell will complete S phase even if mitogens are withdrawn.

Intra-S Checkpoint: - Monitors replication fork stalling and DNA damage during S phase - Stalled forks activate ATR kinase (via RPA-coated ssDNA), which phosphorylates Chk1 kinase - Chk1 inhibits Cdc25A phosphatase, preventing activation of cyclin A-CDK2 and cyclin E-CDK2 - Slows origin firing to prevent catastrophic fork collapse

G2/M Checkpoint: - Prevents entry into mitosis with damaged or incompletely replicated DNA - ATM (activated by DSBs) and ATR (activated by ssDNA/stalled forks) phosphorylate Chk2 and Chk1 respectively - Chk1/Chk2 phosphorylate Cdc25C, creating a 14-3-3 binding site that sequesters Cdc25C in the cytoplasm, preventing it from activating cyclin B-CDK1 (MPF) - Simultaneously, p53 induces p21, which directly inhibits cyclin B-CDK1

Spindle Assembly Checkpoint (SAC): - Prevents anaphase until most kinetochores are properly attached to spindle microtubules - Unattached kinetochores catalyze formation of the mitotic checkpoint complex (MCC): Mad2, BubR1, Bub3, and Cdc20 - MCC binds and inhibits Cdc20, preventing activation of APC/C - A single unattached kinetochore is sufficient for complete arrest (Rieder et al. 1995) - Once most kinetochores achieve bipolar attachment with tension, SAC is silenced; Cdc20 activates APC/C, which ubiquitinates securin and cyclin B - Securin degradation releases separase, which cleaves cohesin (Scc1/Rad21 subunit) – triggering anaphase

12.4.5 The DNA Damage Response: ATM/ATR and p53

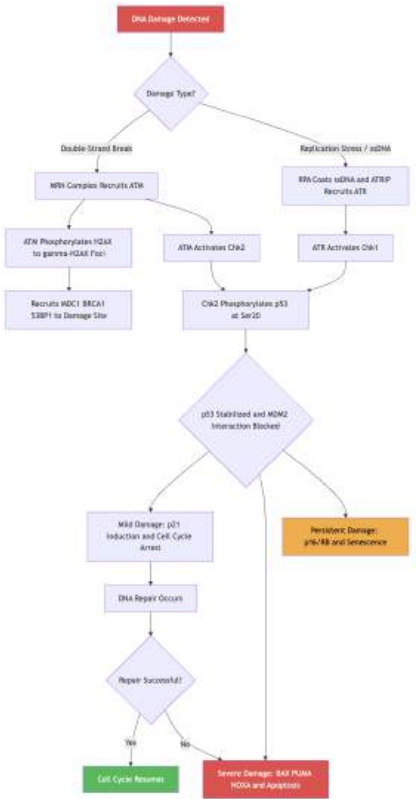


Figure 87. The DNA damage response pathway. ATM responds to double-strand breaks; ATR responds to replication stress and single-stranded DNA. Both converge on p53, which decides between cell cycle arrest (allowing repair), apoptosis, or senescence depending on damage severity.

p53: Guardian of the Genome

p53 is the most frequently mutated gene in human cancers (approximately 50% of cancers carry *TP53* mutations). Normal p53 function:

- Normally kept at low levels by MDM2 (an E3 ubiquitin ligase) that targets p53 for proteasomal degradation (half-life approximately 20 min)

- Stabilized by damage signals: ATM/ATR-mediated phosphorylation of p53 at Ser15 and Chk2-mediated phosphorylation at Ser20 disrupt the p53-MDM2 interaction
- Acts as a transcription factor (binds DNA as a tetramer) to induce:
 - p21 (CDKN1A): CDK inhibitor that arrests the cell cycle at G1/S and G2/M
 - GADD45: DNA repair and G2 arrest
 - 14-3-3sigma: G2 arrest
 - BAX, PUMA, NOXA: pro-apoptotic Bcl-2 family members (if damage is irreparable)
 - MDM2 itself: negative feedback loop

Clinical Connection: Li-Fraumeni Syndrome Germline **heterozygous** *TP53* mutations cause Li-Fraumeni syndrome (LFS). Patients have a greater than 90% lifetime cancer risk, developing sarcomas, breast cancer, brain tumors, adrenocortical carcinoma, and leukemia – often before age 30. The remaining wild-type **allele** is lost somatically (loss of heterozygosity, LOH), consistent with Knudson’s two-hit hypothesis. Many *TP53* mutations are **dominant-negative** (mutant p53 tetramerizes with wild-type p53 and inactivates it) or gain-of-function.

12.4.6 Cancer and the Cell Cycle

Cancer is fundamentally a disease of uncontrolled cell cycle progression. Key deregulated pathways:

Table 188. Cancer and the Cell Cycle: Gene/Pathway and Normal Function.

Gene/Pathway	Normal Function	Cancer Alteration	Associated Cancer
RB1	G1/S checkpoint	Loss-of-function mutations	Retinoblastoma (childhood eye cancer); also lung, bladder
CDKN2A (p16)	Inhibits CDK4/6	Deletion or methylation	Melanoma, pancreatic, many others
CDK4	G1 progression	Amplification or activating mutation	Melanoma, glioblastoma
Cyclin D1	G1 progression	Amplification (11q13)	Breast cancer, mantle cell lymphoma
TP53	G1/S and G2/M arrest; apoptosis	Loss-of-function or dominant-negative mutation	Approximately 50% of cancers
MDM2	p53 degradation	Amplification	Sarcomas, other cancers
MYC	Transcription factor for cell cycle genes	Amplification/translocation	Burkitt lymphoma (t(8;14)), neuroblastoma

CDK4/6 inhibitors (palbociclib, ribociclib, abemaciclib) are now standard of care in HR+/HER2- metastatic breast cancer. They block cyclin D-CDK4/6, preventing RB phosphorylation and E2F release.

Concept Check 11.2

1. What is the restriction point, and how does the RB-E2F pathway control it?
2. Why is p53 called the “guardian of the genome”? Describe three outcomes of p53 activation.
3. Explain why CDK4/6 inhibitors would be ineffective in RB-null tumors.
4. A tumor cell has a homozygous deletion of CDKN2A (p16). Predict the effect on the cell cycle.

Concept Check (Analysis): The replication fork in *E. coli* moves at about 1,000 bp/s. The human genome is 3.2×10^9 bp with about 50,000 origins of replication, and S phase takes about 8 hours. (a) Calculate the average replicon size (distance between origins) and the time to replicate each replicon. (b) If origins fire stochastically with an average firing rate, how does increasing origin density affect replication timing precision and the risk of replication fork collapse? (c) Topoisomerase II resolves catenated daughter chromosomes after replication — if cells are treated with ICRF-193 (a catalytic Topo II inhibitor that traps the closed clamp form), predict the cell-cycle arrest point and explain the checkpoint mechanism activated.

Worked Example — Telomere Length and Hayflick Limit: Human somatic cells lose about 50-200 bp per cell division from chromosome ends. Starting telomere length: about 10,000 bp. Minimum functional telomere: about 2,000 bp (below this, TRF2/POT1 cannot form T-loop, triggering p53-dependent arrest). Maximum divisions before arrest: $(10,000 - 2,000)/100$ bp loss/division = 80 divisions — matching the Hayflick limit of about 40-70 divisions for most human cells. Cancer cells upregulate telomerase (TERT + TERC + DKC1), maintaining telomere length at 5,000-8,000 bp, enabling unlimited division. Telomere length heterogeneity: standard deviation \approx 1,500 bp. Cells first approach arrest when the shortest telomere

(mean - 2 SD \approx 10,000 - 3,000 = 7,000 bp minus divisions \times 100) becomes critical — predicting that arrest begins at about 50 divisions (earlier than mean estimate), matching the wide observed Hayflick range.

Concept Check (Evaluation): CDK4/6 inhibitors (palbociclib, ribociclib) are FDA-approved for HR+/HER2– breast cancer. They inhibit CDK4 and CDK6, preventing Rb phosphorylation and blocking G1/S transition. (a) Using the restriction point model, explain why Rb-deficient tumor cells are intrinsically resistant to CDK4/6 inhibitors. (b) Why do CDK4/6 inhibitors cause reversible cell-cycle arrest (cytostatic) rather than killing (cytotoxic) in normal cells, and what property of cancer cells makes them vulnerable to subsequent CDK4/6 inhibitor-induced senescence? (c) Acquired resistance to palbociclib often involves amplification of cyclin E (CCNE1), which activates CDK2. Design a combination therapy that would overcome this resistance mechanism and explain the sequential mechanistic logic.

12.5 Mitosis: Molecular Events at Each Stage

Mitosis distributes one copy of each duplicated chromosome to each daughter cell. In most mammalian cells it takes approximately 1 hour.

Stages of mitosis – molecular detail:

Table 189. Cancer and the Cell Cycle: Phase and Duration.

Phase	Duration	Molecular Events
Prophase	about 25 min	Condensin I/II complexes compact chromosomes (about 10,000-fold); centrosomes (duplicated in S phase) begin migrating to opposite poles; Aurora A kinase activates centrosome maturation
Prometaphase	about 15 min	Nuclear envelope breakdown (NEB) by CDK1-mediated lamin phosphorylation (lamins A, B, C depolymerize); kinetochores (CENP-A, CENP-C, KNL1, Ndc80 complex) capture spindle microtubules; chromosomes undergo rapid poleward/anti-poleward oscillations
Metaphase	about 5 min	Chromosomes aligned at the metaphase plate (equidistant from both poles); bipolar attachment generates tension across sister kinetochores; SAC monitors attachment
Anaphase A	about 5 min	Separase cleaves cohesin Scc1 subunit; sister chromatids separate; kinetochore microtubules shorten (depolymerization at kinetochore end via Pacman mechanism) pulling chromosomes poleward at about 1 micrometer/min
Anaphase B	about 5 min	Interpolar microtubules slide apart (kinesin-5/Eg5 pushes poles apart); astral microtubules pull poles via cortical dynein
Telophase	about 10 min	Nuclear envelope re-forms around each chromosome set (nuclear pore complexes reassemble); chromosomes decondense; nuclear lamina reforms
Cytokinesis	about 5 min	Animals: contractile ring of actin + myosin II constricts at the cleavage furrow (position determined by central spindle/RhoA); Plants: cell plate forms from vesicle fusion at the phragmoplast

Cohesin and separase: Cohesin (Smc1/Smc3/Scc1/Scc3) holds sister chromatids together from S phase. During prophase, most arm cohesin is removed by the “prophase pathway” (Wapl + Polo-like kinase 1 phosphorylation of SA2 subunit). Centromeric cohesin is protected by shugoshin (Sgo1) and protein phosphatase 2A (PP2A). At anaphase onset, APC/C-Cdc20 ubiquitinates securin, releasing separase, which cleaves the remaining centromeric Scc1 – triggering sister chromatid separation.

Clinical Connection: Aneuploidy and Cancer Therapeutics Defects in the spindle assembly checkpoint cause chromosome instability (CIN), a hallmark of cancer. Taxol (paclitaxel) and vincristine exploit microtubule dynamics to kill cancer cells: taxol stabilizes microtubules and vincristine destabilizes them, both activating the SAC and triggering mitotic arrest followed by apoptosis. Mosaic variegated aneuploidy (MVA) syndrome, caused by biallelic BubR1 mutations, leads to growth retardation, microcephaly, and childhood cancers.

12.6 Meiosis: Generating Genetic Diversity

Meiosis produces haploid (n) gametes from diploid (2n) precursors via two sequential divisions without an intervening S phase:

12.6.1 Meiosis I (Reductive Division)

Table 190. Meiosis I (Reductive Division): Stage and Key Events.

Stage	Key Events
Prophase I	The longest and most complex stage; subdivided into: leptotene (chromosomes condense; telomeres attach to nuclear envelope forming “bouquet”), zygotene (homologous chromosomes pair by synapsis via the synaptonemal complex), pachytene (crossing over occurs; Spo11 makes programmed DSBs; Dmc1 and Rad51 mediate strand invasion; about 1-3 crossovers per chromosome), diplotene (synaptonemal complex disassembles; homologs connected primarily at chiasmata), diakinesis (further condensation; nuclear envelope breaks down)
Metaphase I	Bivalents (tetrads) align at metaphase plate; homologs orient randomly (independent assortment)
Anaphase I	Homologs separate (reductive division); sister chromatids remain joined at centromere (centromeric cohesin protected by shugoshin/Rec8)
Telophase I + Cytokinesis	Two haploid cells, each with n chromosomes (still replicated = sister chromatids joined)

12.6.2 Meiosis II (Equational Division)

Essentially a mitotic division of each Meiosis I product. Sister chromatids separate at anaphase II, producing 4 haploid cells total.

12.6.3 Sources of Genetic Diversity

1. Independent assortment: 2^{23} = approximately 8.4 million possible chromosome combinations for humans
2. Crossing over: generates novel recombinant haplotypes; average 1-3 crossovers per chromosome pair per meiosis = approximately 30-50 total crossovers per meiosis
3. Fertilization: $2 \times 8.4 \times 10^6$ combinations, further diversified by crossing over

Concept Check 11.3

1. Compare and contrast mitosis and meiosis I in terms of chromosome behavior at the metaphase plate.
2. Why must centromeric cohesin be protected during meiosis I but cleaved during meiosis II?
3. Calculate the number of possible gamete chromosome combinations for an organism with $2n = 8$.

12.7 DNA Damage and Repair

DNA sustains approximately 10,000-100,000 lesions per cell per day from endogenous (hydrolysis, oxidation, replication errors) and exogenous (UV, chemicals, radiation) sources.

12.7.1 Types of DNA Damage

Table 191. Types of DNA Damage: Damage Type and Source.

Damage Type	Source	Frequency (per cell per day)
Depurination (AP sites)	Spontaneous hydrolysis	about 5,000-10,000
Deamination (C to U)	Spontaneous hydrolysis	about 100-500
Oxidized bases (8-oxoG)	Reactive oxygen species (ROS)	about 10,000

Damage Type	Source	Frequency (per cell per day)
Single-strand breaks	ROS, topoisomerase failure	about 20,000-40,000
Double-strand breaks	Ionizing radiation, replication fork collapse	about 10-50
Pyrimidine dimers (CPD)	UV light (280-320 nm)	Variable (sun exposure dependent)
Alkylated bases	Endogenous S-adenosylmethionine; alkylating agents	about 3,000

12.7.2 DNA Repair Pathways and Cell-Cycle Context

Direct reversal: - Photolyase (not in humans): uses visible light energy to directly cleave cyclobutane pyrimidine dimers - MGMT (O⁶-methylguanine-DNA methyltransferase): transfers the methyl group from O⁶-methylguanine to an active site cysteine (suicide enzyme – each MGMT molecule works primarily once)

Base excision repair (BER): 1. DNA glycosylase (11 types in humans, each recognizing specific lesions) cleaves the N-glycosidic bond, creating an AP site 2. APE1 (AP endonuclease) cuts the phosphodiester backbone 5’ to the AP site 3. DNA Pol beta fills the single-nucleotide gap 4. XRCC1 + DNA Ligase III seals the nick

Nucleotide excision repair (NER): - Repairs bulky, helix-distorting lesions (CPDs, 6-4 photoproducts, cisplatin adducts) - Global genome NER (GG-NER): XPC-RAD23B detects helix distortion genome-wide - Transcription-coupled NER (TC-NER): CSB detects stalled RNA Pol II on the transcribed strand - Both pathways converge: TFIIH (XPB + XPD helicases) unwinds about 30 bp; XPF-ERCC1 cuts 5’ and XPG cuts 3’; the about 24-32 nt fragment is removed; DNA Pol delta/epsilon fills the gap; ligase seals

Mismatch repair (MMR): - MSH2/MSH6 (MutSalpha) detects single base mismatches and 1-nt insertion/deletion loops - MSH2/MSH3 (MutSbeta) detects 2-13 nt insertion/deletion loops - MLH1/PMS2 (MutLalpha) makes an incision in the newly synthesized strand - Exonuclease 1 degrades the error-containing strand; DNA Pol delta resynthesizes

Double-strand break repair: - NHEJ (active throughout cell cycle): Ku70/Ku80 bind broken ends; DNA-PKcs recruited; Artemis processes overhangs; XRCC4-Ligase IV seals. Fast but error-prone. - Homologous recombination (HR) (active in S/G2): MRN complex resects 5’ ends; RPA coats 3’ ssDNA; BRCA2 loads RAD51; strand invasion into sister chromatid; error-free repair.

The choice between NHEJ and HR is regulated by 53BP1 (favors NHEJ) versus BRCA1 (promotes resection for HR). In S/G2, CDK phosphorylation activates CtIP to promote resection.

Clinical Connection: PARP Inhibitors and Synthetic Lethality PARP inhibitors (olaparib, niraparib, talazoparib) exploit synthetic lethality: PARP1 is essential for single-strand break repair. In BRCA1/2-deficient tumor cells (which cannot perform HR), PARP inhibition forces reliance on error-prone NHEJ, leading to genomic catastrophe and cell death. Normal cells with intact BRCA1/2 survive. PARP inhibitors are standard of care for BRCA-mutant breast, ovarian, prostate, and pancreatic cancers.

Concept Check 11.4

1. Why is NHEJ considered error-prone while HR is high-fidelity?

2. Explain the concept of synthetic lethality as it applies to PARP inhibitor therapy.

3. A patient with xeroderma pigmentosum develops melanoma at age 12. What repair pathway is deficient, and what type of DNA damage accumulates?

4. Compare BER and NER in terms of the type of damage repaired and the size of DNA removed.

12.8 Worked Example: Telomere Shortening and the Hayflick Limit

Problem: A human fibroblast is born with telomeres of 10,000 bp of TTAGGG repeats. In the absence of telomerase it loses 100 bp of telomeric DNA per division (within the stated 50–200 bp end-replication range). Replicative senescence is triggered once telomeres reach a critically short length of ≈ 4,000 bp.

(a) How many divisions can this cell undergo before senescence?

Solution: The expendable telomere reserve is the starting length minus the senescence threshold; the number of divisions is that reserve divided by the loss per division:

$$n = \frac{10,000 \text{ bp} - 4,000 \text{ bp}}{100 \text{ bp/division}} = \frac{6,000 \text{ bp}}{100 \text{ bp/division}} = 60 \text{ divisions}$$

(204)

(b) How much total telomeric DNA is lost over that lifespan?

$$\Delta L = 60 \text{ divisions} \times 100 \text{ bp/division} = 6,000 \text{ bp}$$

(205)

The predicted 60 divisions sits squarely within the measured Hayflick limit of $\approx 50\text{--}70$ divisions for human fibroblasts, showing how the end-replication problem imposes a built-in replicative clock that limits the proliferative capacity of somatic cells and acts as a tumor-suppressive barrier.

12.9 Worked Example: Replication Fork Dynamics

Problem: An *E. coli* cell with a 4.6 Mb genome replicates bidirectionally from a single origin. The replication fork speed is 1,000 bp/s.

(a) How long does it take to replicate the entire genome?

Solution: Bidirectional replication means two forks travel in opposite directions. Each fork must cover half the genome:

$$t = \frac{4.6 \times 10^6 \text{ bp}}{2 \times 1000 \text{ bp/s}} = 2300 \text{ s} \approx 38.3 \text{ min}$$

(206)

(b) *E. coli* can divide every 20 minutes under optimal conditions. How is this possible?

Solution: *E. coli* uses nested replication (multi-fork replication). A new round of replication initiates at *oriC* before the previous round completes. Thus, a cell dividing every 20 minutes has multiple replication forks active simultaneously.

(c) The eukaryotic replication fork speed is about 50 bp/s. If the human genome (3.2 Gb) had a single origin, how long would S phase take?

$$t = \frac{3.2 \times 10^9}{2 \times 50} = 3.2 \times 10^7 \text{ s} \approx 370 \text{ days}$$

(207)

This is why eukaryotes require approximately 30,000-50,000 origins to complete replication in approximately 8 hours.

12.10 Computational Bridge

Complementary strand generation is the arithmetic behind semiconservative replication:

```
from biology.genetics import dna_complement

leading = "ATGCGATCGATCG"
lagging_template = dna_complement(leading)
print(lagging_template)
```

Clinical / systems note: Defects in MMR and HR surveillance convert replication infidelity into organ-specific cancer risks — the clinical mirror of error rates you estimate from polymerase fidelity.

12.11 Current Evidence and Frontier Biology: DNA Replication and the Cell Cycle

For DNA Replication and the Cell Cycle, frontier biology belongs inside the evidence logic of the chapter. Frontier work on replication is resolving the replisome in molecular detail: cryo-EM structures of the CMG helicase and the eukaryotic replisome, single-molecule assays of fork dynamics and origin licensing, and the recognition that replication stress and fork protection underlie both cancer genome instability and the action of PARP inhibitors and ATR-checkpoint drugs. The core reading question is this: replication claims should connect polymerase accuracy, checkpoint timing, damage response, and cancer relevance.

- What to verify: identify the observation, model, assay, or dataset that would make the claim stronger or weaker.
- What to qualify: state the scale, organism, cell type, environmental condition, or population where the claim is expected to hold.
- What to compare: test at least one alternative explanation, baseline, or null model before treating the pattern as causal.
- What to cite: distinguish primary evidence, review synthesis, public dataset, and institutional guidance; for recent or numeric claims, prefer the source closest to the measurement and state what has changed since it was published.

For reference-dependent genetic claims, ask whether read length, structural variation, ancestry representation, phasing, or clinical validation changes the interpretation [Human Pangenome Reference Consortium, 2023, U.S. Food and Drug Administration, 2023, 2024b].

Source practice: For genomics and editing claims, distinguish discovery from clinical actionability, and cite reference resources, regulatory records, or primary editing studies close to the claim [Human Pangenome Reference Consortium, 2023, U.S. Food and Drug Administration, 2026a, Chalumeau et al., 2025].

12.12 Summary

- DNA structure: B-form double helix with antiparallel strands; major groove allows sequence-specific protein binding; negative backbone charge requires cationic neutralization.
- Replication: Semiconservative, bidirectional from licensed origins; leading strand continuous (Pol epsilon), lagging strand as Okazaki fragments (Pol delta); fidelity maintained by polymerase selectivity, 3' to 5' proofreading, and MMR (approximately 10⁻¹⁰ error rate).
- Telomeres: TTAGGG repeats protected by shelterin and T-loops; telomerase (TERT + TERC) extends 3' overhang in germ/stem cells; reactivated in most cancers; ALT pathway in approximately 15%.
- Cell cycle: G1-S-G2-M driven by sequential cyclin-CDK activation; checkpoints (G1/S restriction point, intra-S, G2/M, SAC) ensure fidelity; p53 integrates damage signals to decide between arrest, senescence, and apoptosis.
- Mitosis: Prophase through cytokinesis; cohesin holds sister chromatids; separase cleaves at anaphase; SAC ensures bipolar attachment via MCC-mediated APC/C inhibition.
- Meiosis: Meiosis I (reductive: homolog separation, crossing over at chiasmata) + Meiosis II (equational: sister chromatid separation) produce 4 haploid gametes; independent assortment and crossing over generate diversity.
- DNA repair: BER (damaged bases), NER (bulky adducts), MMR (mismatches), NHEJ and HR (DSBs); defects cause cancer predisposition syndromes (Lynch, XP, BRCA-mutant cancers, Li-Fraumeni).
- Connections: See section 13 for gene expression downstream of replicated DNA, Unit V — Classical Genetics and Heredity: Introduction for segregation of sister chromatids, and Unit VII — Microbiology: Introduction for bacterial replication timing.

12.13 Review Questions

1. Compare the roles of DnaA/DnaB in *E. coli* and ORC/MCM2-7 in eukaryotes during replication initiation.
2. Explain how the licensing system prevents re-replication. What happens if geminin is depleted?
3. Describe the three layers of replication fidelity and calculate the expected number of mutations per human cell division (3.2 Gb genome, error rate 10⁻¹⁰ per bp).
4. A cell line has homozygous loss of RB1. Predict the effect on G1/S checkpoint function. Would CDK4/6 inhibitors be effective?
5. Compare the substrates and outcomes of APC/C-Cdc20 versus APC/C-Cdh1 in mitotic exit.
6. Explain why crossing over in meiosis I is essential for proper chromosome segregation (beyond generating diversity).
7. A patient has a homozygous mutation in MSH2. What type of genomic instability would you observe? What cancer screening would you recommend?
8. Compare NHEJ and HR repair pathways. Why is 53BP1 vs. BRCA1 balance critical for pathway choice?
9. Explain the mechanism of PARP inhibitor synthetic lethality in BRCA1/2-mutant tumors.
10. A researcher finds that a tumor has a TERT promoter C228T mutation. What is the functional consequence, and why does this confer a growth advantage?
11. Starting from a 50% GC template, predict whether leading vs. lagging synthesis faces more secondary structure risk in highly repetitive DNA. How does pol δ processivity help?
12. Using the mutation-per-division estimate in Q3, scale to 10¹² cells in a renewing epithelium. When does clonal selection become inevitable even if each division is nearly perfect?

12.14 Further Reading and Source Notes: DNA Replication and the Cell Cycle

- Meselson & Stahl (1958). The replication of {DNA} in {Escherichia coli}. *Proceedings of the National Academy of Sciences*, 44.
- Okazaki et al. (1968). Mechanism of DNA chain growth: Discontinuous synthesis. *Proceedings of the National Academy of Sciences*, 59.
- Hartwell, Culotti, Pringle & Reid (1974). Genetic control of the cell division cycle in yeast. *Science*, 183.
- Nurse (2000). A long twentieth century of the cell cycle and beyond. *Cell*, 100.
- Blackburn & Gall (1978). A tandemly repeated sequence at the termini of the extrachromosomal rDNA in Tetrahymena. *Journal of Molecular Biology*, 120.
- Alberts et al. (latest ed.). *Molecular Biology of the Cell* (DNA replication and the cell cycle chapters). Garland Science.

12.15 Key Terms

1. Semiconservative replication – each daughter helix contains one parental and one newly synthesized strand
2. Origin of replication – specific DNA sequence where replication initiates
3. MCM helicase – hexameric helicase loaded during licensing; unwinds DNA at replication forks as part of the CMG complex
4. PCNA – homotrimeric sliding clamp ring; tethers polymerases for processivity; K164-Ub recruits TLS polymerases
5. Okazaki fragment – short DNA segment synthesized on the lagging strand (100-200 nt in eukaryotes)
6. Telomerase – reverse transcriptase (TERT + TERC) that extends telomeric repeats using an RNA template
7. Cyclin-CDK complex – heterodimer driving cell cycle transitions; cyclin provides specificity, CDK provides kinase activity
8. Restriction point – point in late G1 after which the cell is committed to divide independent of mitogens
9. Spindle assembly checkpoint (SAC) – monitors kinetochore-microtubule attachment; prevents premature anaphase via MCC
10. Separase – protease that cleaves cohesin Scc1 subunit to trigger sister chromatid separation at anaphase
11. p53 – tumor suppressor transcription factor; induces cell cycle arrest, senescence, or apoptosis; mutated in about 50% of cancers
12. APC/C – E3 ubiquitin ligase that targets securin and mitotic cyclins for proteasomal degradation
13. Synaptonemal complex – protein scaffold mediating homologous chromosome synapsis in meiosis I prophase
14. Chiasma – physical connection between homologs at a crossover site during meiosis
15. Mismatch repair (MMR) – post-replicative repair of base-base mismatches and small loops; defects cause Lynch syndrome
16. Homologous recombination (HR) – error-free DSB repair using sister chromatid as template; requires BRCA1/2 and RAD51
17. Synthetic lethality – cell death resulting from simultaneous loss of two compensatory pathways (basis for PARP inhibitor therapy)

12.16 Companion Source Module: DNA Replication and the Cell Cycle

DNA Replication and the Cell Cycle should leave a reproducible trail from a biological claim to the code, figure, diagram, or paper-based activity that can test it. Use the surfaces below to inspect the chapter’s assumptions, rerun the relevant model, or compare the manuscript explanation with companion labs and figures.

Table 192. Companion source surfaces for DNA Replication and the Cell Cycle.

Surface	Use it for
src/biology/genetics/genetics.py (dna_complement, hamming_distance)	Test strand complementarity and sequence-change reasoning.
src/mermaid/biology_diagrams.py (dna_replication_diagram, cell_cycle_diagram)	Keep replication forks, checkpoints, and cell-cycle stages aligned.

Reproducibility check: identify strand polarity, origin/fork direction, repair pathway, and checkpoint readout before diagnosing replication errors. Cross-reference: connect with section 14 and section 19.

13 Gene Expression

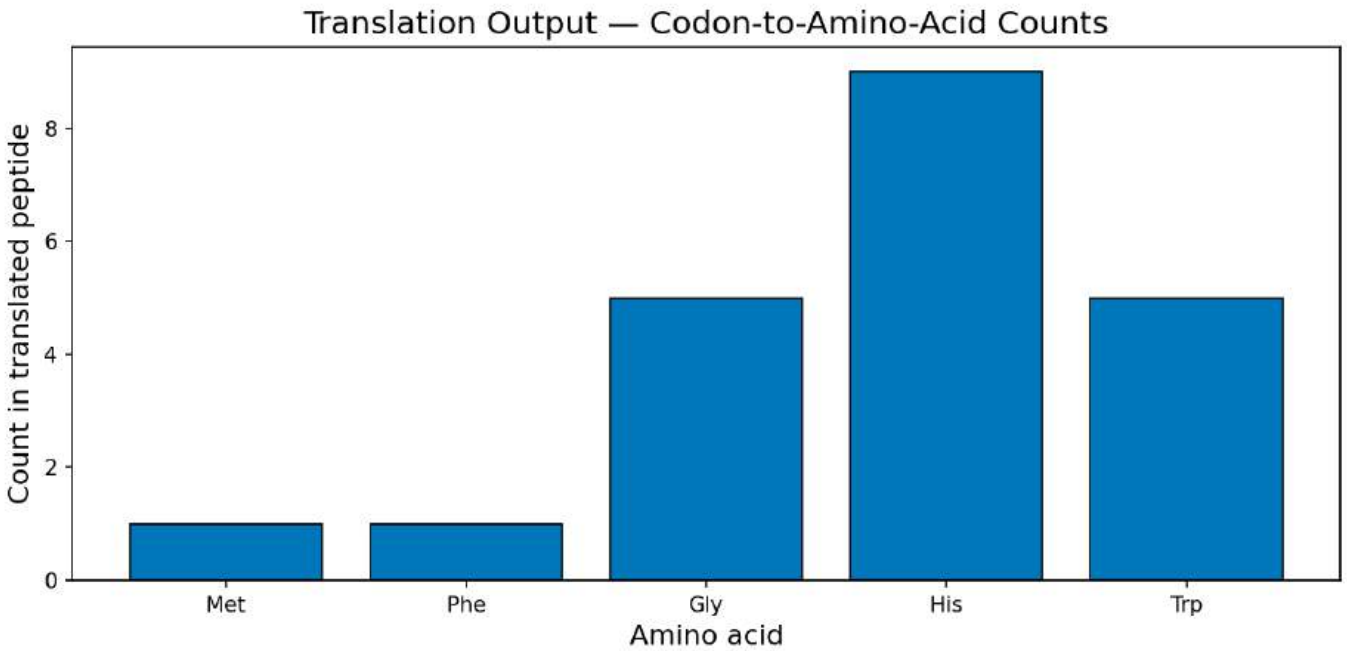


Figure 88. Amino-acid composition after in silico translation of a sample mRNA. Bar height counts each residue type in the reading frame, showing how codon usage and sequence length shape peptide composition under the standard genetic code.

Level 2/3 · 60 min read · 100 min lecture · Prerequisites: section 12

13.1 Learning Objectives

1. Describe the mechanism of transcription in prokaryotes and eukaryotes, including promoter recognition and elongation.
2. Compare prokaryotic and eukaryotic RNA polymerases in terms of subunit composition, promoter elements, and regulation.
3. Explain RNA processing in eukaryotes: 5' capping, splicing (spliceosome mechanism), and 3' polyadenylation.
4. Describe alternative splicing and its role in proteome diversity, including the mechanism of nonsense-mediated decay.
5. Predict the polypeptide produced from a given mRNA sequence, applying the genetic code and wobble pairing, including the effect of a single-base insertion on the reading frame.
6. Describe post-translational modifications and the ubiquitin-proteasome degradation pathway.

7. Distinguish transcriptional from post-transcriptional **gene** regulation (miRNA, siRNA, lncRNA, circRNA) given Northern-blot versus Western-blot data.
8. Describe epigenetic regulation: DNA methylation, **histone code**, and their roles in development and disease.
9. Predict lac- and trp-**operon** transcriptional output given specified inducer, repressor, and corepressor states.
10. Describe the role of Hox genes and homeodomain transcription factors in development.

13.1.1 Study Blueprint

- Big idea: Gene expression translates sequence information into regulated RNA and protein products.
- Core concepts: transcription, translation, codons, RNA processing.
- Framework alignment: Vision & Change: Information flow, exchange, and storage, Structure and function; AP Biology: Information Storage and Transmission, Systems Interactions; NGSS-style topics: Inheritance and Variation of Traits, Structure and Function.
- Model or quantitative lens: Reading-frame, codon, and expression-output calculations.
- Data skill: Convert DNA/RNA sequence data into predicted molecular products.
- Practice cadence: Concept Explanation, Questions and Methods, Argumentation.
- Common misconception to repair: A gene is not simply a protein recipe; context controls when, where, and how much product appears.
- Primary lab: **Lab — Gene Expression**.
- Question bank: **Questions — Gene Expression**.
- Transfer task: Apply expression logic to mutations, biotechnology, development, and disease diagnostics.
- Bridge to computation: `biology.genetics.genetics.translate_mrna`.

Opening Vignette — Solving the Problem of the Messenger

In 1961, Francis Crick and colleagues knew that information flowed from DNA to **protein**, but the molecular intermediary was a mystery. Working with Sydney Brenner and François Jacob at Cambridge, Matthew Meselson performed a deceptively simple experiment: he mixed radioactively labeled **ribosomes** from bacteria infected with T4 phage with unlabelled ribosomes, then centrifuged the extract through a density gradient. The new viral proteins appeared on *old* unlabelled ribosomes — proving that ribosomes are non-specific “machines,” and that the specificity must come from a short-lived “messenger” molecule. Brenner named it messenger RNA. Within a decade, the entire transcription and translation apparatus — RNA polymerase, transfer RNA, **codons**, the genetic code — had been decoded. This vignette illustrates how a single elegant experiment can overturn received wisdom and open an entire research program.

13.2 Transcription as RNA Synthesis from DNA

13.2.1 Central Dogma and Information Flow in Gene Expression

Transcription produces RNA from a DNA template. The central dogma [Crick, 1958] describes the flow of genetic information:

$$\text{DNA} \xrightarrow{\text{transcription}} \text{RNA} \xrightarrow{\text{translation}} \text{Protein}$$

(208)

Additional information flows include: reverse transcription (RNA to DNA; retroviruses, telomerase), RNA replication (RNA-dependent RNA polymerases in RNA viruses), and direct translation regulation (riboswitches, IREs).

The evidence base around this dogma is now database-mediated as much as experiment-mediated. The 2026 *Nucleic Acids Research* Database Issue reported 182 database papers: 84 new resources, 86 updates to resources previously described in the issue, and 12 resources first published elsewhere [Rigden and Fernández, 2026]. For gene-expression work, that means a student should ask not only “which molecule carries information?” but also “which curated resource defines the transcript, modification, allele, regulatory element, or expression context, and when was that resource last updated?”

RNA databases make this source-governance problem concrete. RNACentral in 2026 had grown beyond a sequence index into a gene- and literature-linked resource: its abstract reports 45 million non-coding RNA sequences, while release 26 introduced gene-level views for genome-mapped ncRNA sequences and a human set of 103,814 ncRNA genes from 600,225 transcripts [RNACentral Consortium, 2026]. These counts should be read as release-specific evidence, not permanent facts; the durable lesson is that a non-coding RNA claim needs the sequence identifier, gene model, source database, and literature provenance checked together.

13.2.2 Prokaryotic Transcription and Sigma-Factor Promoters

RNA polymerase (RNAP) in *E. coli*: core **enzyme** ($\alpha_2\beta\beta'\omega$) + sigma (σ) factor:

- The σ factor recognizes the promoter – specifically two conserved hexameric sequences:
 - -10 box (Pribnow box): consensus TATAAT (named after David Pribnow)
 - -35 box: consensus TTGACA
- Promoter strength correlates with similarity to consensus; strong promoters (e.g., rRNA genes) match closely at both positions
- The σ^{70} factor is the “housekeeping” sigma; alternative sigma factors direct RNAP to stress-response promoters (e.g., σ^{32} for heat shock, σ^{54} for nitrogen starvation)

Transcription cycle: 1. Closed complex: RNAP + σ binds promoter DNA (double-stranded) 2. Open complex: about 15 bp around the -10 region melt (AT-rich, easier to denature); transcription bubble forms 3. Initiation: RNAP synthesizes short abortive transcripts (2-12 nt); σ factor released after about 10 nt (“promoter escape”) 4. Elongation: RNAP moves along template 3’ to 5’, synthesizing RNA 5’ to 3’ at about 40-80 nt/s; transcription bubble is about 12-14 bp; about 8 bp RNA-DNA hybrid within the bubble 5. Termination: two mechanisms

Termination mechanisms: - Rho-independent (intrinsic): GC-rich inverted repeat in nascent RNA forms a stem-loop hairpin followed by a run of about 6-8 U residues (weak rU-dA base pairs) – hairpin destabilizes RNAP-RNA contact, U-tract promotes dissociation - Rho-dependent: Rho protein (hexameric helicase) loads onto rut (Rho utilization) sites on the nascent RNA, translocates 5’ to 3’ along the RNA (powered by ATP hydrolysis), catches up when RNAP pauses, and unwinds the RNA-DNA hybrid to release the transcript

13.2.3 Eukaryotic Transcription and RNA Polymerase Specialization

Three nuclear RNA polymerases:

Table 193. Eukaryotic Transcription and RNA Polymerase Specialization: Feature and RNA Pol I.

Feature	RNA Pol I	RNA Pol II	RNA Pol III
Products	45S pre-rRNA (18S, 5.8S, 28S rRNA)	Most mRNA; most snRNA, miRNA	tRNA, 5S rRNA, U6 snRNA, 7SL RNA
Location	Nucleolus	Nucleoplasm	Nucleoplasm
Number of subunits	14	12	17
Sensitivity to alpha-amanitin	Resistant	Very sensitive (1 ug/mL)	Moderately sensitive (10 ug/mL)
Promoter elements	UCE + core (recognized by UBF + SL1)	TATA box, Inr, DPE, BRE, CpG islands	Internal (type I, II) or upstream (type III)

The table is primarily the entry point. In eukaryotes, transcriptional output depends on promoter architecture, enhancer-promoter looping, chromatin accessibility, Mediator, pause release, and RNA processing. RNA Pol II is especially regulated because its C-terminal domain is phosphorylated in different patterns during initiation, elongation, splicing, 3’-end formation, and termination. A strong gene-expression claim therefore asks which polymerase is involved, which regulatory DNA element is active, which chromatin state permits access, and whether nascent-RNA, chromatin, or perturbation evidence supports the proposed mechanism.

13.2.4 Eukaryotic Promoter Elements

The RNA Pol II core promoter can contain several elements (not most are present in every promoter):

- TATA box (about 25-30 bp upstream of TSS; consensus TATAAAA): Bound by TBP (TATA-binding protein), a subunit of TFIID. Present in about 10-20% of human gene promoters; associated with tissue-specific, highly regulated genes.
- Initiator element (Inr): Overlaps the TSS; consensus PyPyAN(T/A)PyPy; recognized by TAF1/TAF2 subunits of TFIID
- Downstream promoter element (DPE): Located about +28-33 relative to TSS; works with Inr in TATA-less promoters; recognized by TAF6/TAF9
- BRE (TFIIB recognition element): Immediately upstream or downstream of TATA box; directly contacts TFIIB
- CpG islands: Regions of >200 bp with >50% GC content and observed/expected CpG ratio >0.6; found at about 70% of human gene promoters; typically unmethylated in active genes

13.2.5 The Pre-Initiation Complex (PIC) Assembly

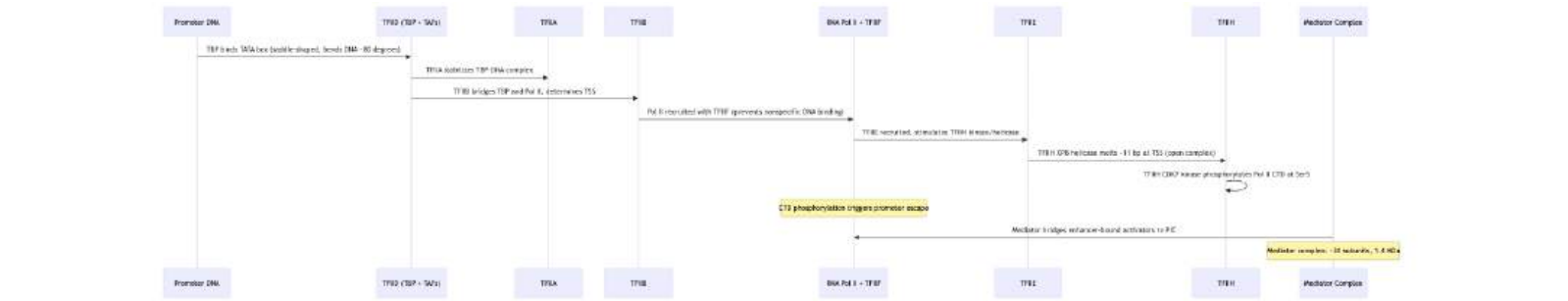


Figure 89. Assembly of the eukaryotic pre-initiation complex (PIC) at a TATA-containing promoter. TFIID binding initiates an ordered assembly cascade culminating in Pol II CTD phosphorylation and promoter escape.

Table 194. The Pre-Initiation Complex (PIC) Assembly: CTD Modification and Kinase.

CTD Modification	Kinase	Effect
Ser5-P	TFIIH (CDK7)	Recruits capping enzyme
Ser2-P	P-TEFb (CDK9)	Recruits splicing factors, polyadenylation machinery
Ser7-P	CDK7	snRNA gene-specific processing

Clinical Connection: Transcription-Targeted Cancer Therapy Several cancers are “transcription-addicted” – dependent on super-enhancers driving oncogene expression. CDK7 inhibitors (THZ1) and CDK9 inhibitors collapse super-enhancer-driven transcription programs. BET bromodomain inhibitors (JQ1, OTX015) displace BRD4 from acetylated **histones** at enhancers, suppressing MYC and other oncogene transcription. These represent a new class of epigenetic cancer therapeutics.

Clinical Connection: Spinal Muscular Atrophy and Splice-Modifying Therapy Spinal muscular atrophy (SMA) is caused by loss of the *SMN1* gene. The paralogue *SMN2* has a C-to-T transition in exon 7 that weakens an exonic splicing enhancer, causing about 90% exon 7 skipping and production of a truncated, unstable protein. Nusinersen (Spinraza) is an antisense oligonucleotide (ASO) that binds an intronic splicing silencer (ISS-N1) in *SMN2* intron 7, promoting exon 7 inclusion and full-length SMN protein production. Approved by FDA in 2016, it was one of the first splice-modifying therapies. Risdiplam (Evrysdi), an oral small molecule that stabilizes U1 snRNP binding at the *SMN2* exon 7 5' SS, was approved in 2020.

13.3.4 Alternative Splicing and Transcript Diversity

Alternative splicing generates multiple protein isoforms from a single gene. An estimated >95% of human multi-exon genes undergo alternative splicing. Types of alternative splicing:

Table 195. Alternative Splicing and Transcript Diversity: Type and Description.

Type	Description	Example
Cassette exon (exon skipping)	An exon is included or excluded	Fibronectin: EDA and EDB exons (tissue-specific)
Alternative 5' splice site	Two different 5' SS compete	SV40 T/t antigen
Alternative 3' splice site	Two different 3' SS compete	Adenovirus E1A
Intron retention	An intron is retained in the mature mRNA	Common in plants; increasingly recognized in mammals
Mutually exclusive exons	One of two (or more) exons is included, rarely both	alpha-tropomyosin; DSCAM

DSCAM in *Drosophila*: The Down syndrome cell adhesion molecule gene contains 4 clusters of alternatively spliced exons: 12 alternatives for exon 4, 48 for exon 6, 33 for exon 9, and 2 for exon 17. Combinatorially: $12 \times 48 \times 33 \times 2 = 38,016$ possible mRNA isoforms – more than twice the total number of genes in the *Drosophila* genome. DSCAM diversity is essential for neuronal self-recognition and axon guidance.

Quantitative scope in humans. Genome-wide RNA-seq studies show that about 95 % of human multi-exon genes undergo alternative splicing, with 92 % producing more than one isoform per gene at detectable levels (Wang et al. 2008; Pan et al. 2008). Average number of detected isoforms per multi-exon gene: 4–7 (cell-type-dependent). Approximately 60 % of alternative-splicing events are tissue-specifically regulated. Estimates of the number of distinct splicing events: - about 150,000 cassette-exon events - about 60,000 alternative 5'/3' splice sites - about 25,000 mutually exclusive exon events - about 30,000 retained-intron events (especially in plants and brain)

Disease-causing splice site mutations — clinical examples: - *BRCA1* IVS5+1G>A: disrupts the consensus 5' splice site (GT > AT), causing exon 5 skipping and frameshift; pathogenic for hereditary breast/ovarian cancer. - *DMD* exon 51 deletion: removes a frame-essential exon, causing Duchenne muscular dystrophy. Antisense oligonucleotide therapies (eteplirsen, casimersen) restore the reading frame by inducing exon 51 skipping. - *MAPT* IVS10+16C>T: disrupts the regulatory cis-element controlling tau exon 10 inclusion, causing fronto-temporal dementia with parkinsonism (FTDP-17). Different intronic mutations in *MAPT* alter the 4R/3R tau ratio. - *SMN2* C840T: weakens an exonic splicing enhancer in *SMN2* exon 7, causing exon 7 skipping in 90 % of *SMN2* transcripts and producing truncated, unstable SMN protein. This is the basis of spinal muscular atrophy when *SMN1* is also lost; nusinersen (an antisense oligonucleotide) restores exon 7 inclusion. - *LMNA* c.1824C>T (Hutchinson–Gilford progeria): activates a cryptic splice donor in exon 11, producing the truncated lamin-A “progerin” that accumulates at the nuclear envelope, driving accelerated aging.

Approximately 15–20 % of disease-causing point mutations disrupt splicing — either at canonical splice sites (5' GT, 3' AG, branch point), in regulatory elements (ESE, ESS, ISE, ISS), or by creating cryptic splice sites. This is much higher than was estimated in the 1990s, when primarily canonical splice-site mutations were recognized.

Regulatory elements controlling alternative splicing: - Exonic splicing enhancers (ESEs): bound by SR proteins (serine/arginine-rich); promote exon inclusion - Exonic splicing silencers (ESSs): bound by hnRNP proteins; promote exon skipping - Intronic splicing enhancers (ISEs) and intronic splicing silencers (ISSs): analogous elements in introns

13.3.5 Nonsense-Mediated Decay (NMD)

NMD is an mRNA surveillance pathway that degrades transcripts containing premature termination codons (PTCs). This protects the cell from producing truncated, potentially dominant-negative proteins.

Mechanism: During the first (“pioneer”) round of translation, the ribosome encounters each exon junction complex (EJC). If translation terminates >50-55 nt upstream of an EJC, the ribosome cannot displace the EJC. The interaction of release factors (eRF1/eRF3) with UPF1, followed by UPF1 interaction with the downstream EJC-bound UPF2/UPF3, triggers UPF1 phosphorylation, mRNA decapping, deadenylation, and degradation.

NMD degrades about 5-10% of the human transcriptome, including many alternatively spliced isoforms with PTCs (regulated unproductive splicing and translation, or RUST).

Concept Check 12.1

1. Why is the 5’ cap structure a 5’-5’ triphosphate linkage rather than the usual 3’-5’? What advantage does this provide?

2. A **mutation** changes the branch point A to G in a critical intron. Predict the consequence for splicing.

3. Explain how nusinersen promotes exon 7 inclusion in SMN2 pre-mRNA.

4. Why does NMD require translation (and therefore nuclear export)?

13.4 Translation and Ribosome-Mediated Protein Synthesis

13.4.1 The Genetic Code

The genetic code maps 64 codons ($4^3 = 64$) to 20 amino acids plus stop signals [Nirenberg and Matthaei, 1961]. figure 88 shows amino-acid counts from translating a representative mRNA.

Table 196. The Genetic Code: Property and Description.

Property	Description
Degenerate (redundant)	Amino acids are encoded by 1-6 synonymous codons; Leu, Ser, Arg each have 6 codons; Met and Trp each have 1
Unambiguous	Each codon specifies exactly one amino acid (or stop)
Commaless and non-overlapping	Read in consecutive, non-overlapping triplets from a fixed start point
Nearly comprehensive	Exceptions in mitochondria (<i>Mycoplasma</i> : UGA = Trp; <i>Tetrahymena</i> : UAA/UAG = Gln; mammalian mitochondria: AGA/AGG = Stop)

Start codon: AUG (methionine) in eukaryotes; AUG (formylmethionine) in prokaryotes. Rarely, GUG or UUG serve as alternative start codons in prokaryotes.

Stop codons: UAA (ochre), UAG (amber), UGA (opal/umber).

Wobble base pairing [Crick, 1966]: The third codon position (“wobble position”) pairs with the first **anticodon** position with relaxed stringency:

Table 197. The Genetic Code: Anticodon first position and Pairs with codon third position.

Anticodon first position	Pairs with codon third position
U	A, G
C	G primarily
A	U primarily
G	C, U
I (inosine)	A, C, U

Wobble explains how 45 tRNAs (in humans) can decode 61 sense codons. Suppressor tRNAs are mutant tRNAs that can read stop codons as amino acids, “suppressing” nonsense mutations.

13.4.2 Ribosome Structure and Catalytic RNA



Figure 91. The ribosomal translation cycle in eukaryotes. Initiation involves cap-dependent scanning to the start codon. Elongation cycles through decoding, peptide bond formation, and translocation. Termination occurs when a stop codon is recognized by eRF1.

Table 198. Ribosome Structure and Catalytic RNA: Feature and Prokaryotic (70S).

Feature	Prokaryotic (70S)	Eukaryotic (80S)
Small subunit	30S (16S rRNA + about 21 proteins)	40S (18S rRNA + about 33 proteins)
Large subunit	50S (23S + 5S rRNA + about 31 proteins)	60S (28S + 5.8S + 5S rRNA + about 49 proteins)
Sedimentation coefficient	70S	80S
Peptidyl transferase center	23S rRNA	28S rRNA
mRNA binding	Shine-Dalgarno sequence	5' cap scanning

The ribosome has three tRNA-binding sites: - A site (aminoacyl): accepts incoming aminoacyl-tRNA - P site (peptidyl): holds the tRNA carrying the growing polypeptide chain - E site (exit): depleted (deacylated) tRNA exits here

Critical insight: The peptidyl transferase center (PTC) is composed entirely of rRNA – no protein comes within 18 Å of the active site. This demonstrates that the ribosome is a ribozyme (Nobel Prize 2009: Ramakrishnan, Steitz, Yonath). This supports the RNA world hypothesis: RNA catalyzed protein synthesis before proteins existed.

13.4.3 Translation Initiation, Elongation, and Termination

Prokaryotic initiation: The Shine-Dalgarno sequence (AGGAGG, about 5-10 nt upstream of AUG) base-pairs with the anti-SD sequence at the 3' end of 16S rRNA, positioning the AUG in the P site. IF1 blocks the A site; IF2-GTP escorts fMet-tRNA^{fMet} to the P site; IF3 prevents premature 50S joining. After start codon recognition, IF2 hydrolyzes GTP, most IFs dissociate, and 50S joins.

Eukaryotic initiation (cap-dependent scanning model): 1. eIF4F complex (eIF4E + eIF4G + eIF4A helicase) binds the m⁷G cap 2. eIF4G bridges to eIF3 on the 40S subunit and to PABP on the poly(A) tail (circularization) 3. 43S pre-initiation complex (40S + eIF1 + eIF1A + eIF3 + eIF5 + ternary complex [eIF2-GTP-Met-tRNA^{fMet}]) loads onto the mRNA near the cap 4. The 43S complex scans 5' to 3' (powered by eIF4A helicase activity) until it finds the first AUG in a favorable Kozak context (RCCAUGG, R = purine; -3 and +4 positions most critical) 5. Start codon recognition: eIF2 hydrolyzes GTP; eIF5B-GTP promotes 60S joining; most eIFs released 6. 80S initiation complex formed with Met-tRNA^{fMet} in P site

Elongation cycle (about 5-10 amino acids/s in eukaryotes; about 15-20 aa/s in prokaryotes):

1. Decoding: aminoacyl-tRNA delivered to A site as part of a ternary complex with eEF1A (EF-Tu in prokaryotes) and GTP. Correct codon-anticodon match triggers conformational change; GTP hydrolysis releases eEF1A
2. Peptide bond formation: Peptidyl transferase (28S rRNA catalytic activity) transfers the growing peptide from the P-site tRNA to the A-site amino acid. The reaction is spontaneous ($\Delta G < 0$) – the aminoacyl ester bond is high-energy
3. Translocation: eEF2-GTP (EF-G in prokaryotes) promotes translocation; ribosome moves 3 nt (one codon) along mRNA; tRNAs shift: A to P, P to E; E-site tRNA dissociates

Termination: When a stop codon enters the A site:

- eRF1 (class I release factor) recognizes the three stop codons (in eukaryotes) – its shape mimics tRNA
- eRF3-GTP (class II release factor) stimulates eRF1 activity
- Water molecule attacks the peptidyl-tRNA ester bond, releasing the completed polypeptide
- ABCE1 (ribosome recycling factor) splits the 80S ribosome into subunits for re-use

Clinical Connection: Antibiotics Targeting the Ribosome The structural differences between prokaryotic 70S and eukaryotic 80S ribosomes make the bacterial ribosome an excellent drug target:

Antibiotic	Target	Mechanism
Tetracycline	30S A site	Blocks aminoacyl-tRNA binding
Streptomycin	30S decoding center	Causes misreading of mRNA
Chloramphenicol	50S PTC	Inhibits peptide bond formation
Erythromycin	50S exit tunnel	Blocks peptide exit
Linezolid	50S A site	Prevents fMet-tRNA binding

These antibiotics are selectively toxic because they do not bind eukaryotic ribosomes efficiently. However, mitochondrial ribosomes resemble prokaryotic ribosomes, explaining side effects like ototoxicity (aminoglycosides) in patients with mitochondrial rRNA mutations.

13.4.4 IRES Elements — Cap-Independent Translation Initiation

While most eukaryotic translation initiates at the 5' cap (eIF4F-mediated scanning), some mRNAs can be translated even when cap-dependent translation is shut down. They use internal ribosome entry sites (IRES) — RNA structural elements that directly recruit the 40S ribosomal subunit without scanning from the cap.

IRES classes (4 main types in eukaryotic and viral mRNAs):

Table 199. IRES Elements — Cap-Independent Translation Initiation: Class and Example.

Class	Example	Initiation factors required	Mechanism
Type I	Picornaviruses (poliovirus, coxsackievirus)	Most canonical eIFs except eIF4E	Internal AUG; PCBP2/3 binding
Type II	Picornaviruses (en- cephalomyocarditis virus, EMCV)	eIF1A, eIF2, eIF3, eIF4A, eIF4G; no eIF4E	Direct 40S placement at AUG; cleaved eIF4G is sufficient
Type III	Hepatitis C virus (HCV)	Primarily eIF2, eIF3 (and 40S) — minimal	Direct binding of 40S to a multi-domain RNA structure (domains II, III, IV); IIIC binds 40S like a TBP-equivalent for ribosomes
Type IV	Cricket paralysis virus (CrPV); intergenic IRES	None — no initiator Met-tRNA needed	Pseudoknot mimics tRNA in P site; translation starts at non-AUG codon

Hepatitis C IRES — structural mechanism in detail. HCV IRES is one of the most structurally characterized. The IRES adopts a defined three-domain RNA fold:

- Domain II binds the 40S subunit at the head, positioning the mRNA channel
- Domain III (with sub-domains IIIa, IIIb, IIIc, IIId, IIIE, IIIf) directly contacts ribosomal proteins; IIIabc binds eIF3
- Domain IV contains the AUG start codon, positioned directly in the P site
- This bypass of cap recognition and scanning means HCV translation continues even when cellular cap-dependent translation is suppressed.

Cellular IRES elements drive translation of stress-response mRNAs when cap-dependent translation is inhibited (e.g., during apoptosis when eIF4G is cleaved by caspase-3, or during heat shock when eIF2 α is phosphorylated). Examples: c-Myc, p53, VEGF, BiP/HSPA5, XIAP, DAP5, BCL2. Stress-induced translation of pro-apoptotic *p53* via its IRES is one of the host’s defenses against viral infection.

Therapeutic relevance: - eIF4A inhibitors (silvestrol, zotatifin) preferentially affect cap-dependent translation of mRNAs with structured 5’ UTRs — bypassed by some IRESes. In trial for AML and CTCL. - Eltrombopag (FDA-approved for thrombocytopenia) destabilises HCV-IRES–40S contacts as an off-target mechanism.

13.4.5 Ribosome Profiling — A Window Into Translation Dynamics

Ribosome profiling (Ribo-seq) is a technique that captures and sequences the about 28-nt mRNA fragments protected by translating ribosomes. Each “ribosome footprint” identifies (a) which mRNA is being translated, (b) which codon is in the A-site at the moment of capture, and (c) the relative density of ribosomes along the message — quantifying translation efficiency at codon resolution.

Key insights from ribosome profiling:

1. Translation efficiency varies across mRNAs by > 100-fold. Some mRNAs have many more ribosomes loaded per unit of mRNA than others. This is regulated by 5’ UTR features (length, structure, upstream ORFs), codon usage in the ORF, and 3’ UTR sequences.
2. Ribosome stalling on rare codons. Codons recognized by low-abundance tRNAs (e.g., CGA-Arg, CGG-Arg in mammals) cause ribosome pausing detectable as elevated read density. Stalling can trigger:
 - Co-translational protein folding signals — programmed pauses allow N-terminal protein domains to fold before C-terminal segments emerge.
 - Programmed -1 frameshifts (e.g., HIV gag-pol, SARS-CoV-2 ORF1ab/RDR-RP).
 - Ribosome quality control (RQC): stalled ribosomes are split by Pelota–Hbs1L; the nascent peptide is ubiquitinated by NEMF–LTN1 and degraded.
3. Upstream open reading frames (uORFs) regulate about 50 % of mammalian mRNAs. A short ORF in the 5’ UTR is translated first; the scanning ribosome must reinitiate downstream. uORF translation typically suppresses main-ORF translation. Stress-induced phosphorylation of eIF2 α (the integrated stress response) increases scanning past inhibitory uORFs, paradoxically enhancing translation of stress-response mRNAs (e.g., *ATF4*, *CHOP*, *GADD34*) that have inhibitory uORFs in their 5’ UTRs.
4. Codon-level translation kinetics. Each codon’s average dwell time can be estimated from ribosome density. Codon-optimized mRNAs (e.g., synthetic mRNA vaccines, insulin) have shorter average dwell times and higher translation efficiency.
5. Out-of-frame translation. Ribo-seq has uncovered hidden ORFs (smORFs, 10–100 codons) in regions previously annotated as non-coding — many of which encode functional micropeptides (e.g., MOTS-c from mitochondrial 12S rRNA; HOXB-AS3 micropeptide).

13.4.6 Nonsense-Mediated Decay (NMD) — Mechanism in Mechanistic Detail

NMD destroys mRNAs containing premature termination codons (PTCs), preventing the production of truncated proteins that would often act as dominant-negative or gain-of-function pathogens. The key recognition principle is the EJC-distal PTC rule: a stop codon is “premature” if the ribosome encounters it more than about 50 nt upstream of the last exon-exon junction.

Key molecular components:

Table 200. Nonsense-Mediated Decay (NMD) — Mechanism in Mechanistic Detail: Component and Role.

Component	Role
EJC (exon junction complex)	Deposited 20–24 nt upstream of most exon-exon junctions during splicing (occupancy is non-uniform; the final junction is often unmarked); contains EIF4A3, MAGOH, Y14/RBM8A, MLN51 (CASC3)
UPF1 (RENT1)	RNA helicase + ATPase; central NMD effector; binds the 3’ UTR after stop codon
UPF2 (RENT2)	Bridges UPF1 to UPF3
UPF3A/UPF3B	EJC component; bridges EJC to UPF1/2
SMG1	PIKK-family kinase; phosphorylates UPF1
SMG5/6/7	Recruit decapping (SMG7) and endonuclease cleavage (SMG6) machinery

Component	Role
eRF1, eRF3	Translation termination factors; eRF3 interacts with UPF1 at PTC

Mechanism, step-by-step:

1. mRNA enters first-round translation (the “pioneer round”), still bound by CBP80/20 cap-binding complex (not yet the cytoplasmic eIF4F).
2. Ribosome translates from cap to first stop codon. Each EJC encountered by the elongating ribosome is dislodged. EJCs deposited downstream of the actual stop codon (in the 3’ UTR) are NOT dislodged.
3. Stop codon recognition. eRF1 + eRF3-GTP enter the A site; eRF3 hydrolyses GTP; nascent peptide is released by hydrolysis of the peptidyl-tRNA ester bond.
4. UPF1 recruitment. eRF3 (after release-factor function) recruits UPF1 to the terminating ribosome.
5. EJC-distal proximity check. UPF1 scans the 3’ UTR; if it encounters an EJC within about 50 nt downstream, EJC-bound UPF2/UPF3B contact UPF1, activating NMD.
6. SMG1 phosphorylation of UPF1 at numerous Ser/Thr-Q sites — generates the “phospho-UPF1” signal.
7. Decay execution:
 - SMG6 endonuclease cleaves the mRNA near the PTC, exposing both fragments to exonucleases (XRN1 from 5’; exosome from 3’).
 - SMG5–SMG7 recruits CCR4–NOT (deadenylation) and DCP1/2 (decapping) for canonical mRNA decay.
8. Ribosome recycling and UPF1 dephosphorylation by PP2A complete the cycle.

Clinical NMD exploitation — three therapeutic strategies:

1. Read-through compounds (e.g., ataluren/Translarna) promote ribosomal mis-decoding at PTCs (especially UGA), allowing partial production of full-length protein. Approved in EU for nonsense-mutation Duchenne muscular dystrophy (cmDMD).
2. NMD inhibition (e.g., NMDI-1, SMG1 inhibitors in development) prolongs the half-life of PTC-containing mRNAs, increasing the substrate pool for read-through compounds.
3. Antisense oligonucleotides for exon skipping (e.g., eteplirsen for DMD, nusinersen for SMA): exclude the PTC-containing exon, restoring the reading frame.

NMD also has homeostatic functions beyond pathogen detection: it degrades a large fraction of physiological alternatively-spliced isoforms that contain PTCs (regulated unproductive splicing and translation, RUST), particularly in neurons and during development. NMD perturbation in flies and mice produces brain phenotypes consistent with this regulatory role.

13.4.7 Translation Fidelity — Mechanism and Error Rate

Translation fidelity is achieved through multiple kinetic checkpoints, each contributing to the overall error rate of approximately 1 in 10⁴ to 10⁵ amino acids misincorporated:

1. Aminoacyl-tRNA charging fidelity by aminoacyl-tRNA synthetases (aaRS): each aaRS has high specificity for its cognate amino acid (10⁻³–10⁻⁴ error in pre-transfer step). Many aaRSs (e.g., IleRS, LeuRS, ValRS, AlaRS, PheRS, ProRS, ThrRS, MetRS) have post-transfer editing domains that hydrolyse mischarged tRNAs (e.g., Val-tRNA^{Ile} is edited by IleRS’s editing domain, achieving 10⁻⁵–10⁻⁶ overall error). The “double-sieve” mechanism: synthetic site selects amino acids that fit *or are smaller than* the cognate; editing site rejects amino acids smaller than the cognate.
2. Initial codon-anticodon recognition (in the 30S/40S A site): Watson-Crick pairing at codon positions 1 and 2 (the wobble at position 3 is intentionally relaxed); A-form helix geometry sensing by 16S rRNA (in bacteria: A1492, A1493, G530 — the “monitor bases”). Initial selection error rate about 10⁻³.
3. EF-Tu / eEF1A conformational proofreading (kinetic proofreading via GTP hydrolysis): EF-Tu (in bacteria) or eEF1A (in eukaryotes) brings aa-tRNA to the A site; correct codon-anticodon pairing accelerates GTP hydrolysis. Incorrect pairings have time to dissociate before GTP is hydrolysed (an irreversible step). After GTP hydrolysis, a second selection step (“accommodation”) allows further discrimination. This adds about 10⁻³ to about 10⁻⁴ improvement.
4. Peptidyl transferase activity-coupled fidelity: the rate of peptide bond formation depends on whether the tRNA is correctly accommodated; incorrect tRNAs have slower peptide-bond chemistry, providing another opportunity for dissociation.
5. Quality control after translation: misfolded proteins are degraded by the proteasome; ribosomes stalling on damaged mRNAs trigger ribosome-associated quality control (RQC) via Pelota-Hbs1L splitting and NEMF-LTN1-mediated nascent-peptide ubiquitination.

Overall translation error $\approx 10^{-3} \times 10^{-3} \times (\text{post-transfer editing}) \approx 10^{-4}$ to 10^{-5}

(209)

For a typical about 500-amino acid protein, this error rate predicts about 5 % of nascent polypeptides contain at least one misincorporation. Most are tolerated; a few drive cellular dysfunction in aging or disease (statin-induced muscle damage from low-fidelity translation; age-related aggregation diseases). Sub-cohort of mistranslated proteins are degraded by the proteasome before causing problems.

Clinical translation: Aminoglycosides (gentamicin, paromomycin) bind 16S rRNA monitor bases, distorting the codon-recognition geometry and increasing translation error rate (about 100-fold). This explains both their bactericidal mechanism (catastrophic protein synthesis errors) and their toxicities (cochlear hair-cell apoptosis from mitochondrial mistranslation, especially in patients with the A1555G 12S rRNA variant).

Concept Check 12.2

1. Compare the roles of the Shine-Dalgarno sequence (prokaryotes) and Kozak sequence (eukaryotes) in translation initiation.

2. Why is the ribosome considered a ribozyme? What evidence supports this?

3. A patient has a mitochondrial 12S rRNA mutation (A1555G). Why might aminoglycoside antibiotics cause deafness in this patient?

4. Explain the wobble hypothesis and why fewer tRNAs than sense codons are needed.

Concept Check (Analysis): The genetic code has 64 codons encoding 20 amino acids plus stop signals. Redundancy (degeneracy) is non-random: wobble pairing allows the first two positions to be read precisely while the third varies. (a) Using the wobble rules (G in anticodon pairs with U or C in codon; I pairs with U, C, or A), explain how 45 tRNAs can decode 61 sense codons. (b) Codon usage bias — the preferential use of some synonymous codons over others — correlates with tRNA abundance. For a highly expressed ribosomal protein gene in *E. coli*, predict the codon usage pattern and explain why this matters for translation speed. (c) Synonymous mutations (codon changes that don’t alter amino acid) are sometimes functionally significant. Describe two mechanisms by which a synonymous mutation could alter protein function.

Worked Example — Operon Regulation Logic: For the lac operon: when [lactose] = 0 and [glucose] = 0: cAMP is HIGH (glucose absent → adenylyl cyclase active), CAP is bound to DNA (activator). Repressor is bound (no allolactose present). Net: cAMP-CAP at site = +transcription; repressor at operator = -transcription. Combined: OFF. When [lactose] = HIGH and [glucose] = 0: allolactose binds repressor → repressor released → operator free; cAMP HIGH → CAP bound → full activation. Net: maximum transcription (relative rate ≈ 1,000× basal). When [lactose] = HIGH and [glucose] = HIGH: glucose suppresses adenylyl cyclase → cAMP falls → CAP released from DNA. Even though repressor is off (allolactose present), the absence of CAP reduces transcription to about 20% of maximum. This “catabolite repression” ensures cells use glucose preferentially even when lactose is available, avoiding the metabolic cost of synthesizing enzymes for a secondary carbon source.

Concept Check (Synthesis): Long non-coding RNAs (lncRNAs) regulate gene expression through diverse mechanisms. XIST (X-inactive specific transcript) is a 19 kb lncRNA that coats and silences one X chromosome in female mammals. (a) XIST recruits PRC2 (Polycomb Repressive Complex 2) which deposits H3K27me3 marks — a repressive histone modification. Using the histone code concept, explain why H3K27me3 is a dominant repressive mark and how it propagates across the chromosome. (b) HOTAIR is a lncRNA transcribed from the HOXC locus that silences HOXD genes in trans by guiding PRC2. Design an experiment distinguishing HOTAIR’s function via (i) sequence complementarity to HOXD DNA, (ii) secondary structure scaffold for PRC2, or (iii) displacement of activating complexes. (c) MALAT1 (nuclear-retained lncRNA) is upregulated in many cancers. If your experiment shows MALAT1 knockdown reduces cancer cell invasion but not proliferation, what does this suggest about its target pathways, and how would you distinguish alternative splicing regulation from chromatin remodeling as the mechanism?

13.5 Post-Translational Modifications and Protein Degradation

13.5.1 Post-Translational Modifications (PTMs)

Table 201. Post-Translational Modifications (PTMs): Modification and Enzymes.

Modification	Enzymes	Target Residues	Function
Phosphorylation	Kinases / Phosphatases	Ser, Thr, Tyr	Signal transduction; activation/inactivation; about 30% of proteins are phosphorylated
Glycosylation	Glycosyltransferases	Asn (N-linked), Ser/Thr (O-linked)	Protein folding, stability, cell-cell recognition; starts in ER, completed in Golgi

Modification	Enzymes	Target Residues	Function
Ubiquitination	E1/E2/E3 ligase cascade	Lys (isopeptide bond)	Mono-Ub: endocytosis , histone regulation; Poly-Ub (K48-linked): proteasomal degradation; K63-linked: signaling
Acetylation	HATs / HDACs	Lys (histones and non-histone proteins)	Chromatin opening (histones); p53 activation; metabolic regulation
Methylation	Methyltransferases / Demethylases	Lys, Arg (histones)	Histone code: H3K4me3 = active; H3K27me3 = repressed; H3K9me3 = heterochromatin
SUMOylation	E1/E2/E3 SUMO ligases	Lys	Nuclear transport, transcription regulation, DNA repair; antagonizes ubiquitination at same Lys
Proteolytic cleavage	Proteases	Specific peptide bonds	Signal peptide removal; proinsulin to insulin; caspase-mediated apoptosis

13.5.2 The Ubiquitin-Proteasome System

The ubiquitin-proteasome system (UPS) is the primary mechanism for targeted protein degradation:

1. E1 (ubiquitin-activating enzyme): Activates ubiquitin (76-aa protein) in an ATP-dependent reaction; forms E1about Ub thioester bond; humans use 2 main E1 enzymes
2. E2 (ubiquitin-conjugating enzyme): Accepts Ub from E1; about 40 E2 enzymes provide some specificity
3. E3 (ubiquitin ligase): Provides substrate specificity; about 600 E3 ligases in humans. Two major families:
 - RING E3s: Transfer Ub directly from E2 to substrate (e.g., APC/C, SCF complex, MDM2)
 - HECT E3s: Accept Ub from E2, then transfer to substrate
4. Poly-ubiquitination (K48-linked chains of at least 4 Ub) marks the substrate for degradation by the 26S proteasome
5. 26S proteasome (2.5 MDa): 20S catalytic core (barrel-shaped; contains chymotrypsin-like, trypsin-like, and caspase-like proteases) capped by 19S regulatory particles (recognize poly-Ub, unfold substrate, feed into 20S core)
6. Deubiquitinating enzymes (DUBs, about 100 in humans) recycle ubiquitin before substrate enters the 20S core

Clinical Connection: Proteasome Inhibitors in Cancer Bortezomib (Velcade) is a proteasome inhibitor approved for multiple myeloma and mantle cell lymphoma. By blocking proteasomal degradation, it causes accumulation of pro-apoptotic proteins and misfolded proteins (ER stress), triggering cell death preferentially in cancer cells with high protein synthesis rates.

13.6 Gene Regulation Across DNA, RNA, and Chromatin

13.6.1 Prokaryotic Gene Regulation: The Lac Operon

The *E. coli* lac operon [**Jacob and Monod, 1961**] (Jacob and Monod, 1961; Nobel Prize 1965) was the founding model of gene regulation:

Components: *lacZ* (beta-galactosidase), *lacY* (permease), *lacA* (transacetylase), preceded by the promoter (P), operator (O), and regulated by *lacI* (repressor gene, constitutively expressed from its own promoter).

Negative control: Lac repressor protein (tetramer, encoded by *lacI*) binds the operator sequences (O1 primary, O2 and O3 auxiliary – DNA looping between O1 and O3 increases repression 50-fold). When lactose is present, its isomer allolactose (the true inducer) binds the repressor, causing a conformational change that reduces DNA-binding affinity by about 1000-fold. Repressor released; RNAP can transcribe.

Positive control (catabolite repression): CAP (catabolite activator protein, also called CRP) + cAMP binds the CAP site upstream of the lac promoter, bending

DNA about 90 degrees and directly contacting the alpha-CTD of RNAP to activate transcription about 50-fold. When glucose is present, the phosphotransferase system (PTS) keeps adenyl cyclase inactive; [cAMP] is low; CAP cannot bind; lac operon expression is reduced even if lactose is present.

Operon logic: The lac operon is fully ON primarily when lactose is present AND glucose is absent (high cAMP, CAP active, repressor released). This makes biological sense: the cell uses glucose (more efficient) before lactose.

13.6.2 The Trp Operon (Repressible System)

The *E. coli* trp operon encodes five enzymes for tryptophan biosynthesis:

- Repression: When tryptophan is abundant, Trp acts as a co-repressor – it binds the TrpR aporepressor, activating it to bind the operator and block transcription
- Attenuation: A leader peptide (trpL) containing two consecutive Trp codons (UGG UGG) is located upstream of the structural genes. When Trp-tRNA is abundant, the ribosome translates the leader rapidly, allowing formation of a terminator hairpin (3-4 stem loop) in the mRNA, causing premature termination. When Trp-tRNA is scarce, the ribosome stalls at the UGG codons, allowing an anti-terminator hairpin (2-3 stem loop) to form instead, permitting read-through transcription

This provides fine-tuning: repression gives about 70-fold regulation; attenuation adds another about 8-fold; combined about 600-fold.

Concept Check: Glucose is absent and lactose is present while a *lacI⁻* strain also carries a non-functional *crp* gene — predict whether the lac operon is transcribed and justify using both the repressor and CAP–cAMP states.

13.6.3 Eukaryotic Gene Regulation: Multiple Levels

Chromatin level: - SWI/SNF complexes (BAF/PBAF in mammals): ATP-dependent chromatin remodelers that slide, eject, or restructure nucleosomes to expose or occlude regulatory sequences - HATs (histone acetyltransferases, e.g., p300/CBP, PCAF): acetylate histone tails (primarily H3K9, H3K14, H3K27, H4K16), neutralizing positive charge, weakening histone-DNA interaction, and recruiting bromodomain-containing factors – associated with active transcription - HDACs (histone deacetylases): remove acetyl groups – associated with gene silencing; HDAC inhibitors (vorinostat, romidepsin) are approved for T-cell lymphoma

Transcription factor combinatorics: The human genome encodes about 1,500-2,000 transcription factors. Gene expression is controlled by the combinatorial binding of multiple TFs at enhancers, which together produce richer logic than any single TF in isolation. Three canonical principles:

1. Synergy: Two TFs bound at adjacent sites produce more than the sum of their individual effects. Cooperative DNA binding (when one TF stabilizes the binding of the next via direct protein–protein contact or by inducing DNA bending) and synergistic activation (when each TF independently recruits a different co-activator) both contribute. The interferon- β enhanceosome shows about 10 \times synergy: each individual TF drives about 5-fold transcription, but together they drive > 1000-fold induction.
2. Quenching: A repressor TF bound near an activator can inhibit the activator without displacing it (e.g., via histone deacetylation recruitment, or by sequestering coactivators in a non-productive complex). Examples: GAL80 quenches GAL4 in yeast; BCL6 quenches NF- κ B in germinal-center B cells.
3. Enhanceosome: A specific stereochemical assembly where the TF binding sites are positioned such that the eight or more factors must bind simultaneously and cooperatively to activate transcription. Spacing between binding sites is critical (loss of even one base-pair spacing destroys cooperative assembly). The IFN- β enhanceosome (3.7 kb upstream): NF- κ B (p50/p65), IRF3, IRF7, ATF2/c-Jun, plus the architectural protein HMGA1 wraps the entire 55-bp regulatory region into a defined 3D conformation that primarily forms during viral infection.

Super-enhancers — the high-output regulatory class. First operationally defined by Whyte and Young (2013), super-enhancers are unusually large regulatory regions (median about 10 kb, often >50 kb) characterized by: - H3K27ac density: at least 10-fold higher than typical enhancers, often spanning multiple H3K27ac peaks - BRD4 occupancy: the BET-family reader concentrates here, as do Mediator and lineage-defining TFs - MED1/MED12 enrichment: super-enhancers are constructed largely from Mediator-bound elements - Transcriptional output: drives high-output expression of cell-identity genes (e.g., *MYC* in cancer cell lines, lineage-defining TFs like *SOX2* in ES cells, *PU.1* in hematopoietic cells) - Phase separation: super-enhancer condensates concentrate Pol II, BRD4, Mediator, CDK7/9 — see section 16 for detailed mechanism - Identification: ROSE (Rank Ordering of Super-Enhancers) algorithm — rank H3K27ac signal across most enhancers; the inflection point distinguishes super-enhancers (top about 3 % of enhancers, accounting for about 30 % of H3K27ac signal) from typical enhancers - Therapeutic implication: BET inhibitors (JQ1, OTX015, molibresib, mivebresib) preferentially collapse super-enhancer-driven transcription, providing tumor selectivity. CDK7 (THZ1, SY-5609) and CDK9 (AZD4573) inhibitors disrupt the condensate phosphorylation machinery.

The combination of synergy + enhanceosome organization + super-enhancer condensates explains why a few hundred lineage-defining genes can be expressed at very high levels in each cell type, while the rest of the genome is largely inactive.

13.6.4 RNA-Based Regulation

microRNA (miRNA): - about 22 nt single-stranded RNAs; about 2,000 in the human genome; regulate about 60% of protein-coding genes - Biogenesis: pri-miRNA (transcribed by Pol II) → Drosha/DGCR8 cleave in nucleus to pre-miRNA (hairpin) → Exportin-5 exports → Dicer cleaves to about 22 nt duplex → one strand loaded into RISC (RNA-induced silencing complex, containing Argonaute protein) - Mechanism: miRNA guides RISC to complementary sites (typically in the 3' UTR; seed sequence = positions 2-8); partial complementarity → translational repression + mRNA deadenylation and decay; perfect complementarity → mRNA cleavage (rare in animals)

The miRNA pathway in mechanistic detail (mammalian):

1. DICER processing: DICER (PAZ + DUF + RNase IIIa + RNase IIIb domains) measures about 22 nt from the pre-miRNA terminus and cleaves to produce a about 22-nt duplex with 2-nt 3' overhangs. DICER's PAZ domain binds the 3' overhang of the pre-miRNA hairpin; the dsRBD anchors the substrate; the two RNase III domains cleave both strands in a single catalytic event.
2. RISC loading complex (RLC): TRBP + DICER + AGO2 form the RLC. The thermodynamic asymmetry rule determines which strand becomes the guide vs. the passenger: the strand whose 5' end is in a less-stable base-paired region is preferentially loaded as the guide. The passenger strand is degraded.
3. AGO2 conformational dynamics: AGO2 has four domains (N, PAZ, MID, PIWI). The MID domain anchors the guide's 5' phosphate via a 5'-anchored binding pocket. The PAZ domain holds the 3' end (when not engaged with target). The PIWI domain has the slicer (RNase H-like) active site that cleaves perfectly complementary targets.
4. Target search and seed-pairing: The guide miRNA's positions 2–8 (the seed sequence) must base-pair with the mRNA target — this is the primary recognition determinant. AGO2 conformationally remodels to “extrude” positions 2–8 in an A-form helix-ready geometry for rapid scanning.
5. mRNA repression by deadenylation–decapping–decay:
 - CCR4–NOT complex is recruited to the targeted mRNA via TNRC6/GW182 family proteins bound to AGO2.
 - CCR4 (CNOT6/CNOT6L) and POP2 (CNOT7/CNOT8) deadenylases progressively remove the poly-A tail (deadenylation is the rate-limiting step).
 - DCP2 (decapping) removes the 5' cap, exposing the mRNA to XRN1 5'-to-3' exonuclease degradation.
 - In parallel, the cytoplasmic EXOSOME complex degrades from the 3' end.
6. Translational repression in parallel: GW182 also disrupts eIF4F–PABP interaction, preventing closed-loop translation initiation. eIF4A helicase activity is reduced. Repression and decay are coupled but partially separable.

Seed sequence rules — quantitative target prediction:

Table 202. RNA-Based Regulation: Seed type and Definition.

Seed type	Definition	Approximate target affinity
6-mer	Perfect 6-bp seed (positions 2–7)	Weak (10–20 % repression)
7-mer-A1	Seed + 3' UTR adenosine at position 1	Moderate (about 30 %)
7-mer-m8	Seed + complementary base at position 8	Moderate (about 30 %)
8-mer	7-mer-A1 + 7-mer-m8 combined	Strong (about 50 %)
3' supplementary	Seed + 3' end pairing (positions 13–16)	Modest extra contribution
Centered site	11-bp pairing centered on positions 4–14	Moderate; alternative class

Because each miRNA can have hundreds to thousands of targets (TargetScan, miRanda, DIANA-microT predictions), miRNAs typically tune target levels by 20–60 % rather than completely silencing them — they are “regulatory thermostats” rather than on/off switches.

siRNA (small interfering RNA): - 21 nt; derived from long dsRNA (exogenous: viral, experimental; endogenous: transposons) - Biogenesis: Dicer cleaves dsRNA; one strand loaded into RISC - Mechanism: perfect complementarity to target → Argonaute-2 (Ago2) cleaves mRNA (“slicer” activity) - RNAi therapeutics: Patisiran (Onpattro) – first FDA-approved siRNA drug (2018), targets TTR mRNA for transthyretin amyloidosis; inclisiran (Leqvio) – targets PCSK9 mRNA for hypercholesterolemia (2021)

Long non-coding RNA (lncRNA): - >200 nt; >16,000 lncRNA genes in the human genome (likely more) - Functions: XIST (X-inactivation), HOTAIR (recruits PRC2 to silence HOXD cluster in trans), MALAT1 (nuclear speckle organization, splicing regulation), NEAT1 (paraspeckle formation)

Circular RNA (circRNA): - Covalently closed RNA circles formed by “back-splicing” (a downstream 5’ SS joins to an upstream 3’ SS) - Functions: miRNA sponges (ciRS-7/CDR1as sponges miR-7, containing >70 miR-7 binding sites), protein scaffolds, translated into peptides in some cases

Concept Check: A circRNA bearing 70 miR-7 binding sites is over-expressed in a cell — predict the direction of change in the protein output of a miR-7 target mRNA and explain the post-transcriptional mechanism.

13.6.5 Epigenetic Regulation of Transcriptional State

DNA methylation: - Addition of a methyl group to the 5-position of cytosine (5mC) in CpG dinucleotides - Catalyzed by DNA methyltransferases: DNMT1 (maintenance methyltransferase; copies methylation pattern after replication), DNMT3A/3B (de novo methyltransferases) - CpG islands at gene promoters: usually unmethylated in active genes; methylation recruits MeCP2 and MBD proteins, which recruit HDACs and chromatin compactors, leading to stable gene silencing - Aberrant methylation in cancer: global hypomethylation (genome instability) + focal hypermethylation of tumor suppressor promoters (e.g., RB1, p16/CDKN2A, BRCA1, MLH1)

The histone code:

Table 203. Epigenetic Regulation of Transcriptional State: Modification and Location.

Modification	Location	Effect
H3K4me3	Promoters	Active transcription
H3K36me3	Gene bodies	Active elongation
H3K27ac	Enhancers	Active enhancer
H3K27me3	Promoters/enhancers	Polycomb-mediated silencing
H3K9me3	Heterochromatin	Constitutive silencing (HP1 binding)
H4K20me3	Heterochromatin	Repression
H3K4me1	Enhancers	Poised enhancer (primed but not active)

13.6.6 Gene Regulation in Development: Hox Genes

Hox genes encode homeodomain transcription factors that specify positional identity along the anterior-posterior body axis:

- Homeodomain: about 60 amino acid DNA-binding domain (helix-turn-helix motif) recognizing AT-rich sequences
- Colinearity: The order of Hox genes on the **chromosome** corresponds to their expression domains along the body axis (spatial colinearity) and the timing of their activation (temporal colinearity)
- Conservation: Hox gene clusters are ancient and highly conserved from *Drosophila* (2 clusters: ANT-C and BX-C, 8 genes total) to mammals (4 clusters: HOXA-HOXD, 39 genes total)
- Mutations: Loss-of-function Hox mutations cause homeotic transformations (one body segment takes on the identity of another). In *Drosophila*: *Antennapedia* gain-of-function transforms antennae into legs; *bithorax* loss-of-function transforms halteres into wings (creating a four-winged fly)

Concept Check: A posterior *Hox* gene is ectopically expressed in an anterior segment — predict the homeotic transformation that results and justify it from the spatial-colinearity rule.

Concept Check 12.3

1. Explain the dual regulation of the lac operon (negative + positive control). Under what conditions is the operon fully active?
2. How does the trp operon attenuation mechanism sense tryptophan levels?
3. Compare the functions of miRNA and siRNA. Why is RNAi a powerful research tool?
4. What is the histone code? Give two examples of activating marks and two of repressive marks.

13.7 Worked Example: Reading Frame and Protein Prediction

Problem: The following mRNA sequence is expressed in a eukaryotic cell:

5’-AUGUUCAAGGACUAUUGCCCGUAGACUU-3’

- (a) Translate this sequence.

Solution: Reading in triplets from AUG:

AUG-UUC-AAG-GAC-UAU-UGC-CCG-UAG-ACU-U

(210)

Table 204. Gene Regulation in Development: Hox Genes: Codon and Amino Acid.

Codon	Amino Acid
AUG	Met
UUC	Phe
AAG	Lys
GAC	Asp
UAU	Tyr
UGC	Cys
CCG	Pro
UAG	Stop (amber)

Protein: Met-Phe-Lys-Asp-Tyr-Cys-Pro (7 amino acids)

(b) If a single G is inserted after the first codon (AUGGUUC...), what happens?

Solution: Frameshift mutation. New reading frame:

AUG-GUU-CAA-GGA-CUA-UUG-CCC-GUA-GAC-UU

(211)

Met-Val-Gln-Gly-Leu-Leu-Pro-Val-Asp... (completely different protein, no stop codon in this segment)

13.8 Computational Bridge

The same genetic code table used in the text is callable from `biology.genetics`:

```
from biology.genetics import transcribe_dna_to_mrna, translate_mrna

mrna = transcribe_dna_to_mrna("TACGGCTTGTTTC")
print(" ".join(translate_mrna(mrna)[:6]))
```

Clinical / systems note: NMD and cap-dependent scanning are therapeutic pressure points: nonsense mutations in tumor suppressors can be targeted with read-through compounds, while eIF4A inhibitors attempt to collapse translation of highly structured oncogenic mRNAs.

13.9 Current Evidence and Frontier Biology: Gene Expression

For Gene Expression, frontier biology belongs inside the evidence logic of the chapter. Frontier work on expression is increasingly structural and quantitative: cryo-EM now captures RNA polymerase II in successive elongation states, transcription is understood to occur in phase-separated condensates of Mediator and co-activators, ribosome profiling reads translation genome-wide at codon resolution, and single-molecule and long-read methods resolve alternative splicing and isoform diversity directly. The core reading question is this: expression claims should separate transcription, RNA processing, translation, localization, degradation, and feedback.

- What to verify: identify the observation, model, assay, or dataset that would make the claim stronger or weaker.
- What to qualify: state the scale, organism, cell type, environmental condition, or population where the claim is expected to hold.
- What to compare: test at least one alternative explanation, baseline, or null model before treating the pattern as causal.
- What to cite: distinguish primary evidence, review synthesis, public dataset, and institutional guidance; for recent or numeric claims, prefer the source closest to the measurement and state what has changed since it was published.

For reference-dependent genetic claims, ask whether read length, structural variation, ancestry representation, phasing, or clinical validation changes the interpretation [Human Pangenome Reference Consortium, 2023, U.S. Food and Drug Administration, 2023, 2024b].

Source practice: For genomics and editing claims, distinguish discovery from clinical actionability, and cite reference resources, regulatory records, or primary editing studies close to the claim [Human Pangenome Reference Consortium, 2023, U.S. Food and Drug Administration, 2026a, Chalumeau et al., 2025].

13.10 Summary

- Transcription: RNAP reads the template strand 3' to 5' to produce RNA 5' to 3'. Prokaryotes use a single RNAP with sigma factors; eukaryotes use three RNA Polymerases plus general transcription factors and Mediator.
- Promoter elements: TATA box (TBP binding), Inr, DPE, BRE, CpG islands; enhancers act over long distances via DNA looping.
- mRNA processing: 5' m⁷G cap (eIF4E recognition, stability), spliceosome-mediated intron removal (two transesterification reactions via lariat intermediate), 3' poly(A) tail (PABP, stability, translation).
- Alternative splicing: >95% of human multi-exon genes; generates proteome diversity; regulated by SR proteins and hnRNPs; NMD degrades transcripts with premature stop codons.
- Translation: cap-dependent scanning (eukaryotes) or Shine-Dalgarno (prokaryotes); A/P/E sites; elongation cycle; genetic code (64 codons, wobble pairing, nearly comprehensive); ribosome is a ribozyme.
- Post-translational modifications: phosphorylation, glycosylation, ubiquitination, acetylation, methylation, SUMOylation; ubiquitin-proteasome system for targeted degradation.
- Gene regulation: prokaryotic operons (lac: inducible; trp: repressible with attenuation); eukaryotic: chromatin remodeling, histone code, DNA methylation, transcription factor combinatorics, miRNA/siRNA/lncRNA.
- **Epigenetics**: heritable changes in gene expression without DNA sequence change; DNA methylation (CpG islands), histone modifications; dysregulated in cancer.
- Development: Hox genes specify positional identity; homeodomain TFs; colinearity of gene order and expression domain.
- Connections: See section 15 for chromatin and RNAi, Unit VI — Evolution: Introduction for how expression variation fuels evolution, and section 8 for signal-driven transcription factors.

13.11 Review Questions

1. Compare the promoter recognition mechanisms in prokaryotes (sigma factor) and eukaryotes (GTF assembly). Why do eukaryotes require so many additional factors?
2. Describe the three enzymatic steps of 5' capping. Why is the cap essential for translation?
3. Explain the two transesterification reactions in splicing. What is the lariat intermediate and why does it form?
4. How does DSCAM alternative splicing generate 38,016 isoforms from a single gene? What biological function does this diversity serve?
5. Explain the NMD pathway. Why is it important to destroy mRNAs with premature stop codons?
6. Compare the mechanisms of eukaryotic and prokaryotic translation initiation. What is the Kozak sequence?
7. Describe the ubiquitin-proteasome pathway (E1/E2/E3 cascade). Why does the human genome encode about 600 E3 ligases but 2 main E1 enzymes?
8. Compare the lac operon (inducible) and trp operon (repressible). How does attenuation fine-tune trp operon expression?
9. Describe three classes of non-coding RNAs and their roles in gene regulation.
10. What is the histone code? How do writers, readers, and erasers of histone marks coordinate gene regulation?
11. Insert a single-base frameshift in a toy 30 nt mRNA after the start codon and rerun `translate_mrna` in Python. At what point do stop codons typically appear compared with in-frame controls?
12. Compare how a uORF upstream of a main AUG might tune translation initiation without changing DNA sequence.

13.12 Further Reading and Source Notes: Gene Expression

- Crick (1958). On protein synthesis. *Symposia of the Society for Experimental Biology*, 12.
- Crick (1966). The genetic code — yesterday, today and tomorrow. *Cold Spring Harbor Symposia on Quantitative Biology*, 31.
- Jacob & Monod (1961). Genetic regulatory mechanisms in the synthesis of proteins. *Journal of Molecular Biology*, 3.
- Ban, Nissen, Hansen, Moore & Steitz (2000). The complete atomic structure of the large ribosomal subunit at atomic resolution. *Science*, 289.
- Black (2003). Mechanisms of alternative pre-messenger RNA splicing. *Annual Review of Biochemistry*, 72.
- Sonenberg & Hinnebusch (2009). Regulation of translation initiation in eukaryotes: mechanisms and biological targets. *Cell*, 136.

13.13 Key Terms

1. Central dogma – the flow of genetic information: DNA to RNA to protein
2. Sigma factor – prokaryotic RNAP subunit that recognizes promoter sequences
3. General transcription factors (GTFs) – proteins (TFIIA-H) required for basal Pol II transcription
4. Mediator complex – coactivator bridging enhancer-bound TFs to basal machinery
5. 5' cap (m7G) – modified guanosine protecting mRNA 5' end; recognized by eIF4E
6. Spliceosome – large RNP complex (U1, U2, U4, U5, U6 snRNPs) that removes introns
7. Branch point – intronic adenosine whose 2'-OH attacks the 5' splice site in the first transesterification
8. Alternative splicing – generation of multiple mRNA isoforms from one gene by differential exon inclusion
9. Nonsense-mediated decay (NMD) – mRNA surveillance destroying transcripts with premature stop codons
10. Wobble base pairing – relaxed pairing rules at codon position 3/anticodon position 1
11. Kozak sequence – consensus context around eukaryotic AUG start codon (RCCAUGG)
12. Peptidyl transferase – ribosomal RNA-based catalytic activity forming peptide bonds
13. Ubiquitin-proteasome system – pathway for targeted protein degradation via polyubiquitination
14. miRNA – about 22 nt non-coding RNA guiding RISC to target mRNAs for translational repression
15. Epigenetics – heritable changes in gene expression without alterations to DNA sequence
16. CpG island – GC-rich genomic region; methylation status controls gene activity
17. Histone code – combinatorial histone modifications that regulate chromatin state and gene expression
18. Homeodomain – 60-aa DNA-binding domain in Hox transcription factors specifying positional identity
19. Operon – cluster of co-transcribed prokaryotic genes under shared regulatory control

13.14 Companion Source Module: Gene Expression

Gene Expression should leave a reproducible trail from a biological claim to the code, figure, diagram, or paper-based activity that can test it. Use the surfaces below to inspect the chapter’s assumptions, rerun the relevant model, or compare the manuscript explanation with companion labs and figures.

Table 205. Companion source surfaces for Gene Expression.

Surface	Use it for
<code>src/biology/genetics/genetics.py</code> (<code>transcribe_dna_to_mrna</code> , <code>translate_mrna</code> , <code>gc_content</code>)	Reproduce transcription, translation, codon lookup, and sequence-composition checks.
<code>src/mermaid/biology_diagrams.py</code> (<code>transcription_translation_diagram</code> , <code>mirna_biogenesis_diagram</code>)	Connect coding flow with RNA regulation.

Reproducibility check: specify template strand, reading frame, RNA-processing assumptions, and regulatory layer before interpreting expression. Cross-reference: use sections 15 and 16 and section 3.

14 Mutations, CRISPR, and Genomics

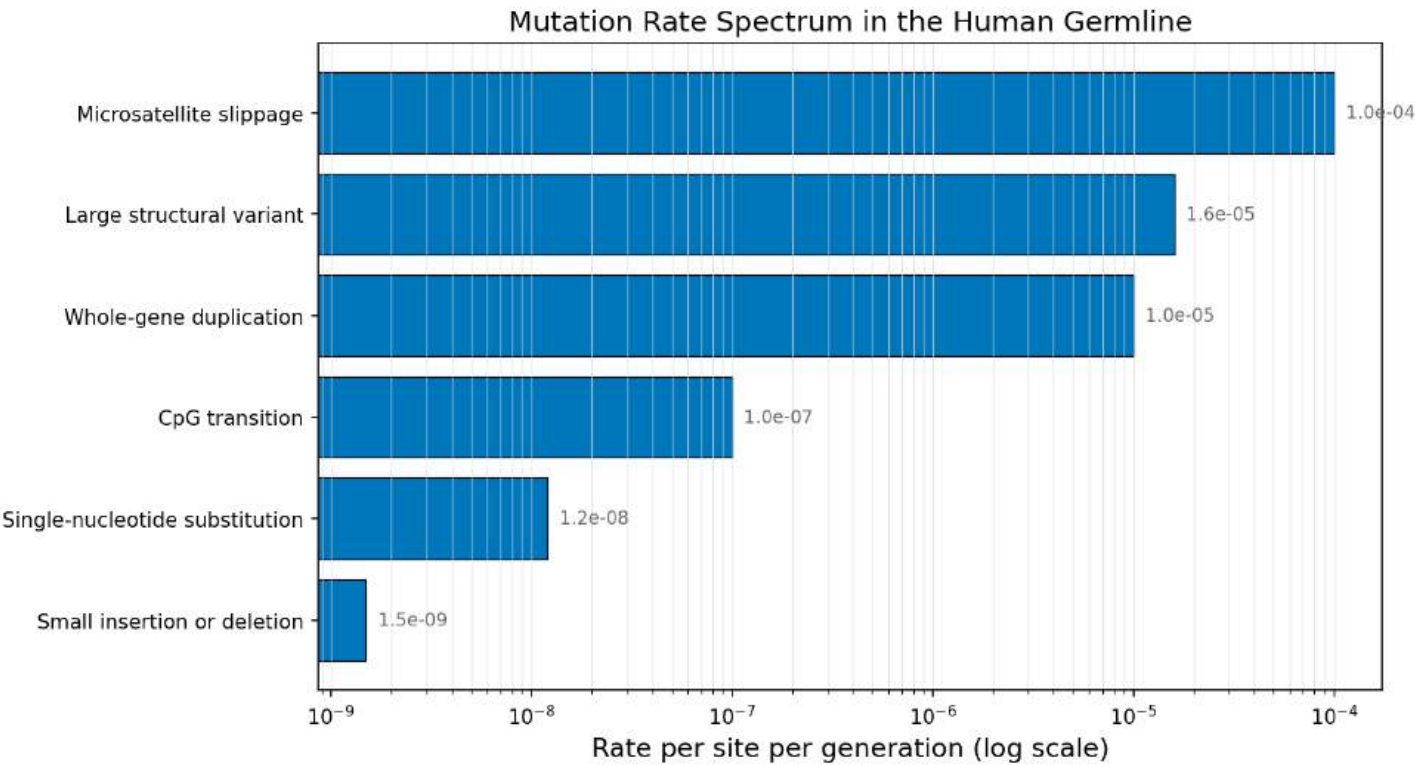


Figure 92. Per-site, per-generation mutation rates across the human germline by variant class. The horizontal bars use a log axis to keep rare large-structural-variant rates and microsatellite slippage legible alongside the dominant single-base-substitution rate. The ordering reveals where mutagenic load actually accumulates and which classes of variation will dominate population-level variance.

Level 2/3 · 55 min read · 75 min lecture · Prerequisites: section 13

14.1 Learning Objectives

1. Classify **mutations** by type (point, frameshift, chromosomal), molecular change, and functional consequence.
2. Describe mutagenic agents and assays for mutagenicity (Ames test).
3. Explain DNA repair mechanisms and their relationship to human disease.
4. Describe the CRISPR-Cas9 mechanism in detail, including PAM recognition, DSB creation, and repair outcomes.
5. Compare CRISPR-Cas9, base editing, and prime editing technologies.
6. Define the **genome** and describe key genomic features revealed by sequencing.
7. Explain next-generation sequencing technologies and their applications.
8. Describe GWAS methodology and its contributions to understanding complex disease.
9. Evaluate ethical issues in personal genomics and genetic testing.

14.1.1 Study Blueprint

- Big idea: Genomic variation becomes biological consequence through sequence context, repair, and selection.
- Core concepts: mutation classes, DNA repair, CRISPR, genome analysis.
- Framework alignment: Vision & Change: Information flow, exchange, and storage, Structure and function; AP Biology: Information Storage and Transmission, Systems Interactions; NGSS-style topics: Inheritance and Variation of Traits, Structure and Function.
- Model or quantitative lens: Mutation-rate, edit-efficiency, and sequence-comparison calculations.
- Data skill: Classify variants and predict likely molecular effect from sequence evidence.
- Practice cadence: Concept Explanation, Questions and Methods, Argumentation.
- Common misconception to repair: Not every mutation is harmful, and not every harmful mutation changes a protein sequence.
- Primary lab: **Lab — Mutations, CRISPR, and Genomics**.
- Question bank: **Questions — Mutations, CRISPR, and Genomics**.
- Transfer task: Transfer variant reasoning to cancer genomics, ancestry, gene therapy, or microbial evolution.

- Bridge to computation: `biology.genetics.genetics.hamming_distance`.

Opening Vignette — One Letter Changes Everything

In 1949, Linus Pauling published a paper in *Science* titled “Sickle Cell Anemia, a Molecular Disease” — the first time a human illness was attributed to a chemical change in a specific **protein**. Eight years later, Vernon Ingram used the newly developed technique of protein fingerprinting to identify the precise mutation: a single amino acid substitution, glutamic acid to valine, at position 6 of the β -globin chain. Just one **nucleotide** change — GAG to GTG — makes hemoglobin polymerize under low-oxygen conditions, distorting red blood cells into rigid sickle shapes that clog capillaries. That one point mutation causes pain crises, organ damage, and shortened lifespan for millions worldwide. The sickle-cell story remains the most compelling illustration of how a single mutational event can cascade through molecular structure, protein function, cell physiology, and whole-organism health.

14.2 Types of Mutations

A mutation is any heritable change in DNA sequence. Mutations are the ultimate source of most genetic variation and therefore the raw material for evolution.

14.2.1 Mutation Rates: A Quantitative Framework

Mathematical Background: Poisson statistics govern rare mutation events. For a review of probability distributions relevant to genetics, see **Appendix C — Mathematical Review for Biology**.

The per-nucleotide per-generation mutation rate in humans is approximately $\mu \approx 1.2 \times 10^{-8}$ per bp per generation (Kong et al., 2012, *Nature*). figure 92 places that single-base-substitution rate alongside indels, microsatellite slippage, transposable-element insertion, and large structural variants on a single log axis, so the order-of-magnitude spread across variant classes is visible at a glance. For a diploid genome of $2N \approx 6.4 \times 10^9$ bp, the expected number of de novo mutations per offspring is:

$$M = 2N \times \mu \approx 6.4 \times 10^9 \times 1.2 \times 10^{-8} \approx 70\text{--}80 \text{ mutations/generation} \quad (212)$$

The probability of observing exactly k mutations in a region of length L follows the Poisson distribution:

$$P(k) = \frac{(\mu L)^k e^{-\mu L}}{k!} \quad (213)$$

This is used to assess whether a **gene** or genomic region has an excess of mutations relative to the background rate — a signature of positive selection or a mutational hotspot.

For genome-wide studies, the Bonferroni-corrected significance threshold for m independent tests is:

$$\alpha_{\text{corrected}} = \frac{\alpha}{m} = \frac{0.05}{10^6} = 5 \times 10^{-8} \quad (214)$$

This is the standard genome-wide significance threshold for GWAS: primarily associations with $p < 5 \times 10^{-8}$ are considered robust.

The K_a/K_s ratio (also called dN/dS or ω) measures the ratio of nonsynonymous to synonymous substitution rates, revealing the mode of **natural selection**:

$$\omega = \frac{K_a}{K_s} = \frac{d_N}{d_S} \quad (215)$$

where $\omega < 1$ indicates purifying selection, $\omega = 1$ neutral evolution, and $\omega > 1$ positive selection.

14.2.2 Nucleotide-Level (Point) Mutations

Table 206. Nucleotide-Level (Point) Mutations: Type and Description.

Type	Description	Example Consequence
Transition	Purine to purine (A to G) or pyrimidine to pyrimidine (C to T)	Most common; often neutral or conservative amino acid change
Transversion	Purine to pyrimidine or vice versa (A to C, A to T, G to C, G to T)	Rarer (about 2:1 transition:transversion ratio); more often disruptive
Silent (synonymous)	Codon change producing the same amino acid (degeneracy)	Usually no phenotypic effect; may affect splicing or mRNA stability
Missense	Codon change producing a different amino acid	Conservative (e.g., Leu to Ile) or non-conservative (e.g., Glu to Val in sickle cell)
Nonsense	Point mutation creating a premature stop codon	Truncated protein; usually non-functional; often triggers NMD
Splice site	Mutation at intron-exon boundary (GT/AG dinucleotides)	Exon skipping, intron retention, or cryptic splice site activation

14.2.3 Insertions, Deletions, and Frameshifts

- Insertion: One or more nucleotides added to the sequence
- Deletion: One or more nucleotides removed from the sequence
- Frameshift: An insertion or deletion that is NOT a multiple of 3 bp – shifts the entire downstream reading frame, producing a completely altered amino acid sequence and usually encountering a premature stop codon
- In-frame insertion/deletion: A multiple of 3 bp – adds or removes amino acids without disrupting the reading frame (e.g., the deltaF508 mutation in CFTR is a 3-bp deletion removing Phe508, causing cystic fibrosis)

14.2.4 Copy Number Variants and Structural Mutations

- Copy number variants (CNVs): Duplications or deletions of segments from 1 kb to several Mb. The average human genome contains about 1,000 CNVs relative to the reference. CNVs contribute more base pairs of variation between individuals than SNPs.
- Inversions: A chromosomal segment is reversed end-to-end. Pericentric inversions include the **centromere**; paracentric do not. Inversions can disrupt genes at breakpoints or alter regulatory landscapes.
- Translocations: A segment moves to a different **chromosome**. Reciprocal translocations exchange segments between two chromosomes. Robertsonian translocations fuse the long arms of two acrocentric chromosomes (13, 14, 15, 21, 22).

Clinical Connection: The Philadelphia Chromosome The t(9;22) reciprocal translocation creates the Philadelphia chromosome – a derivative chromosome 22 carrying the BCR-ABL1 fusion gene. This fusion produces a constitutively active tyrosine kinase that drives chronic myelogenous leukemia (CML). The targeted tyrosine kinase inhibitor imatinib (Gleevec) revolutionized CML therapy, converting a fatal disease into a manageable chronic condition (5-year survival increased from about 30% to >90%). This is a paradigm for targeted cancer therapy.

14.2.5 Trinucleotide Repeat Expansion Disorders

A special class of mutations involving expansion of short tandem repeats:

Table 207. Trinucleotide Repeat Expansion Disorders: Disease and Repeat.

Disease	Repeat	Normal Range	Pathogenic Range	Location	Mechanism
Huntington disease	CAG (Gln)	6-35	>36 (full penetrance >40)	HTT exon 1	Toxic polyglutamine aggregation
Fragile X syndrome	CGG	5-44	>200 (full mutation)	FMR1 5' UTR	CpG methylation silences FMR1
Myotonic dystrophy type 1	CTG	5-34	>50	DMPK 3' UTR	Toxic RNA foci sequester MBNL1
Friedreich ataxia	GAA	5-33	>66	FXN intron 1	Heterochromatin formation silences FXN

Anticipation: These diseases show genetic anticipation – earlier onset and increased severity in successive generations – because the unstable repeats tend to expand further during DNA replication (particularly during germ cell divisions).

Concept Check 13.1

1. Classify the sickle cell mutation (GAG to GUG in beta-globin codon 6) by type.
2. Why are frameshift mutations generally more deleterious than missense mutations?
3. Explain why trinucleotide repeat diseases show anticipation.
4. The deltaF508 CFTR mutation is a 3-bp deletion. Why is this NOT a frameshift?

Worked Example — Poisson Distribution of De Novo Mutations: The human germline mutation rate is approximately 1.2×10^{-8} per base pair per generation. The diploid genome is 6.4×10^9 bp. Expected de novo mutations per offspring: $\mu_{\text{genome}} = 1.2 \times 10^{-8} \times 6.4 \times 10^9 = 76.8 \approx 77$ mutations per generation. Under a Poisson model, $P(k \text{ mutations}) = e^{(-\lambda)} \lambda^k / k!$ with $\lambda = 77$. $P(0 \text{ mutations}) = e^{(-77)} \approx 3 \times 10^{-34}$ (a vanishingly small probability of inheriting zero new mutations). $P(>100 \text{ mutations})$ — using normal approximation: $z = (100 - 77) / \sqrt{77} = 23 / 8.77 = 2.62 \rightarrow P(>100) = 1 - \Phi(2.62) \approx 0.0044 = 0.44\%$. Paternal age effect: each additional year of paternal age adds about 2 mutations (reflecting DNA replication errors in spermatogonia that undergo about 30 more divisions/year). A 45-year-old father vs. a 25-year-old father transmits about 20 extra de novo mutations — a 26% increase — contributing to the increased prevalence of some autosomal-dominant disorders with paternal age.

Concept Check (Evaluate): Mutational signatures catalogued in the COSMIC database reveal that each major DNA-damaging agent leaves a characteristic pattern. UV radiation induces C→T transitions at dipyrimidine sites (especially CC→TT). Tobacco smoking causes C→A transversions (SBS4). Alkylating agents tend to produce G→A transitions at CpG dinucleotides. (a) A patient’s tumor shows predominantly C→T transitions at TpCpN trinucleotides (signatures SBS2 and SBS13, characteristic of APOBEC deaminase activity). Propose a molecular mechanism explaining why APOBEC enzymes — which normally edit RNA and act on retroviral DNA intermediates — generate this signature in tumor cells, and identify which step in the cell cycle exposes single-stranded DNA to APOBEC. (b) The same patient’s tumor is then exposed to a novel chemotherapy. Design a pre-clinical sequencing strategy (number of biopsies, sequencing depth, signature-decomposition approach) that would let you decide whether the therapy adds a new mutational signature or enriches the pre-existing APOBEC signature.

Concept Check (Synthesis): COSMIC mutational signatures are derived by NMF decomposition of cancer mutation catalogs. Signature SBS3 (homologous recombination deficiency, HR-deficient) is characterized by: (a) What trinucleotide context patterns define SBS3 and explain the molecular mechanism producing them — why does HR deficiency produce these specific patterns rather than, say, APOBEC-driven C→T mutations at TCA/TCT contexts? (b) PARP inhibitors (olaparib) are FDA-approved for HR-deficient (BRCA1/2-mutated) cancers. Explain the concept of synthetic lethality: why does BRCA1/2 mutation sensitize cells to PARP inhibition, while PARP inhibition alone is not lethal to HR-proficient cells? (c) Cancer cells treated with platinum compounds (cisplatin, carboplatin) acquire resistance through multiple mechanisms: HR restoration (BRCA2 reversion mutations), PARP1 loss, 53BP1 loss, and REV1/pol ζ upregulation. For each mechanism, predict the mutational signature change you would observe in a post-treatment biopsy.

14.3 Mutagenic Agents and DNA-Damage Mechanisms

14.3.1 Physical Mutagens: Radiation and Replication Stress

UV radiation (UVB, 280-320 nm): - Creates cyclobutane pyrimidine dimers (CPDs): covalent bonds form between adjacent pyrimidines (T-T most common) - Creates 6-4 photoproducts (6-4 PPs): covalent bond between positions 6 and 4 of adjacent pyrimidines - Both distort the helix and block replication/transcription - Repaired by nucleotide excision repair (NER); failure causes xeroderma pigmentosum

Ionizing radiation (X-rays, gamma rays): - Creates reactive oxygen species (ROS) that attack bases and the sugar-phosphate backbone - Causes single-strand breaks (SSBs) and double-strand breaks (DSBs) - DSBs are the most dangerous lesion – if unrepaired, lead to chromosomal translocations, deletions, or cell death - Repaired by NHEJ and HR

14.3.2 Chemical Mutagens and Base-Altering Reactions

Table 208. Chemical Mutagens and Base-Altering Reactions: Agent and Type.

Agent	Type	Mechanism	Mutation Caused
EMS (ethyl methanesulfonate)	Alkylating agent	Adds ethyl group to O ⁶ of guanine	G:C to A:T transitions

Agent	Type	Mechanism	Mutation Caused
Nitrogen mustard	Bifunctional alkylating agent	Cross-links DNA strands	Blocks replication; DSBs
Nitrous acid (HNO ₂)	Deaminating agent	Deaminates C to U, A to hypoxanthine	C:G to T:A and A:T to G:C transitions
Ethidium bromide	Intercalating agent	Inserts between base pairs, stretching the helix	Frameshift mutations (insertions/deletions)
5-Bromouracil (5-BU)	Base analog	Incorporated in place of T; tautomerizes to pair with G	A:T to G:C transitions
Acridine orange	Intercalating agent	Inserts between bases	Frameshift mutations
Benzo a pyrene (cigarette smoke)	Polycyclic aromatic hydrocarbon	Forms bulky adducts on guanine (after CYP1A1 activation)	G:C to T:A transversions; NER substrate

Reactive oxygen species (ROS): Endogenous byproducts of **aerobic** metabolism (superoxide O₂⁻, hydroxyl radical OH·, hydrogen peroxide H₂O₂). ROS oxidize guanine to 8-oxoguanine (8-oxoG), which mispairs with adenine, causing G:C to T:A transversions. Repaired by BER (OGG1 glycosylase).

14.3.3 The Ames Test

The Ames test (Bruce Ames, 1973) is a bacterial mutagenicity assay that uses *Salmonella typhimurium* strains carrying various his⁻ (histidine-requiring) mutations:

Procedure: 1. His⁻ bacteria are plated on minimal medium (no histidine) 2. Test chemical applied (with and without liver microsomal extract S9 to simulate mammalian metabolic activation) 3. Count revertant colonies (his⁺) that can grow without histidine 4. Compare to spontaneous reversion rate (negative control) and known mutagen (positive control)

Interpretation: A significant increase in revertant colonies indicates the chemical is mutagenic. Different tester strains detect different mutation types (e.g., TA98 detects frameshifts; TA100 detects base substitutions).

Correlation: about 80-90% of known carcinogens are mutagenic in the Ames test. The Ames test is a standard regulatory tool for chemical safety screening.

14.4 DNA Damage and Repair

The human genome sustains about 10,000-100,000 DNA lesions per cell per day [Ward, 1988]. Multiple repair pathways maintain genomic integrity.

14.4.1 DNA Damage — Quantitative Background

The endogenous and exogenous lesion load is enormous and well characterized quantitatively:

Table 209. DNA Damage — Quantitative Background: Lesion type and Source.

Lesion type	Source	Frequency (per cell per day)
Depurinations / abasic (AP) sites	Spontaneous hydrolysis of N-glycosidic bond	about 10,000 (purine more labile than pyrimidine)
Depyrimidinations	Hydrolysis	about 500
Cytosine deaminations (C → U)	Hydrolysis	100–500
5-methylcytosine deaminations (5mC → T)	Hydrolysis (faster than C deamination)	about 50–100 (CpG-localized)
Oxidised guanines (8-oxoG)	ROS attack on guanine N7	about 10,000
Other oxidised bases (FapyG, FapyA, 5-OH-cytosine)	ROS	about 3,000

Lesion type	Source	Frequency (per cell per day)
Single-strand breaks (SSBs)	Direct breakage; sugar-radical chemistry	20,000–50,000
Inter-strand crosslinks (ICLs)	Endogenous aldehydes (acetaldehyde, formaldehyde)	about 10–50
Replication-induced double-strand breaks	Fork collapse at SSBs, R-loops, repeats	about 100–500 during replication (S-phase primarily)
Spontaneous DSBs (non-replicative)	Two coincident SSBs; radical-induced	about 10–50
UVB-induced CPDs	UV photons (sunlight, UVB 280–320 nm)	Highly variable; up to 10 ⁶ per skin cell per day with sun exposure
Alkylated bases (O ⁶ -methylguanine, N3-methylpurine)	Endogenous methyl donors (S-adenosylmethionine) + exogenous alkylators	about 3,000
Topoisomerase-induced breaks	Stalled topoisomerase I α -DNA complexes	Variable; increased by camptothecin, etoposide

Replication-associated DSBs (about 100–500 per cell during S phase) are particularly dangerous because they break a DNA strand that is also undergoing semi-conservative replication, producing daughter molecules with persistent breaks. These represent the bulk of physiologically encountered DSBs and explain why HR, the high-fidelity DSB-repair pathway, is preferentially active in S/G2 phase.

The cell maintains genomic integrity by directing each lesion to its appropriate repair pathway. The remarkable per-base error rate of replication (about 10⁻¹⁰) is achieved through a combination of polymerase fidelity, proofreading, mismatch repair (post-replicative), and the various lesion-specific pathways below.

14.4.2 DNA Repair Pathway Specificity and Disease Consequences

Table 210. DNA Repair Pathway Specificity and Disease Consequences: Damage Type and Repair Pathway.

Damage Type	Repair Pathway	Key Proteins	Disease if Defective
UV dimers (CPD, 6-4PP)	Nucleotide excision repair (NER)	XPA, RPA, XPD, XPB, XPF-ERCC1, XPG, PCNA, Pol delta	Xeroderma pigmentosum (1,000x skin cancer risk)
Oxidized bases (8-oxoG)	Base excision repair (BER)	OGG1 glycosylase, APE1, Pol beta, XRCC1, Ligase III	MUTYH-associated polyposis
Alkylated bases (O ⁶ -meG)	Direct reversal	MGMT (methyltransferase)	Glioblastoma (MGMT promoter methylation predicts temozolomide response)
Replication mismatch	Mismatch repair (MMR)	MLH1, MSH2, MSH6, PMS2	Lynch syndrome (colorectal, endometrial cancer)
Double-strand break	NHEJ	Ku70/80, DNA-PKcs, Artemis, Ligase IV	SCID (severe combined immunodeficiency)
Double-strand break	Homologous recombination (HR)	ATM, MRN, BRCA1, BRCA2, RAD51, RPA	Hereditary breast/ovarian cancer

Damage Type	Repair Pathway	Key Proteins	Disease if Defective
Interstrand crosslinks	Fanconi anemia pathway	FANC proteins (A-W), then NER + HR	Fanconi anemia (bone marrow failure, cancer)

Clinical Connection: MGMT Methylation and Glioblastoma Glioblastoma is the most aggressive brain tumor (median survival about 15 months). The alkylating agent temozolomide is a standard chemotherapy. Tumors with MGMT promoter methylation (silencing MGMT expression) cannot repair temozolomide-induced O⁶-methylguanine lesions, making them more sensitive to the drug. MGMT promoter methylation status is therefore a critical predictive biomarker: methylated tumors have about 21-month median survival vs about 12 months for unmethylated tumors when treated with temozolomide (Hegi et al., 2005, *NEJM*).

14.4.3 Base Excision Repair (BER) — Mechanism in Detail

BER handles oxidised, deaminated, and alkylated single-base lesions. The pathway has two main subdivisions:

Short-patch BER (single-nucleotide replacement, about 80 % of events): 1. DNA glycosylase recognizes the lesion and cleaves the N-glycosidic bond, producing an abasic (AP) site. There are 11 DNA glycosylases in humans, each with substrate specificity:

Table 211. Base Excision Repair (BER) — Mechanism in Detail: Glycosylase and Lesion recognized.

Glycosylase	Lesion recognized	Notes
OGG1	8-oxoguanine paired with C	Most clinically important; oxidative damage; bifunctional (lyase activity creates SSB)
MUTYH	Adenine misincorporated opposite 8-oxoG (post-replication mismatch)	Loss-of-function → MUTYH-associated polyposis (MAP)
NTH1	Oxidised pyrimidines (thymine glycol, dihydrouracil)	Bifunctional
NEIL1, NEIL2, NEIL3	Ring-fragmented purines (FapyG, FapyA), oxidised pyrimidines	Bifunctional; β,δ -elimination produces 3'-phosphate end
MPG (AAG)	3-methyladenine, 7-methylguanine, ethenoadenine	Monofunctional (no lyase)
UNG (uracil DNA glycosylase)	Uracil (deamination product or U mis-incorporation)	Most active; nuclear and mitochondrial isoforms
TDG	Thymine in T:G mismatch (5mC deamination); 5fC/5caC (TET pathway)	Active in DNA demethylation
SMUG1	Uracil; backup to UNG	Monofunctional
MBD4	Thymine in T:G mismatch at CpG sites	Methylation-CpG specific
MYH (MUTYH)	A from A:8-oxoG mispair	See above

2. AP endonuclease (APE1, also called APE) cuts the DNA backbone 5' to the AP site, leaving a 3'-OH and a 5'-deoxyribose phosphate (dRP) terminus.
3. DNA polymerase β (pol β) has both DNA polymerase activity (fills the 1-nt gap with the correct nucleotide) and dRP lyase activity (removes the 5'-dRP).
4. DNA ligase III + XRCC1 seals the resulting nick (ATP-dependent).

Long-patch BER (2–10 nucleotide replacement, about 20 % of events): - Used when the dRP cannot be removed (e.g., oxidised dRP) or when the lesion creates a strand-displacement intermediate. - DNA pol δ/ϵ extends, displacing the 5' flap; FEN1 cleaves the flap; DNA ligase I seals.

OGG1 mechanism specifically (the most studied glycosylase): - OGG1 scans DNA for 8-oxoguanine. The 8-oxoG flips out of the helix into OGG1's catalytic pocket. - Active-site lysine (K249) acts as nucleophile, attacking the C1' of the deoxyribose; the N-glycosidic bond breaks via a Schiff-base intermediate. - A

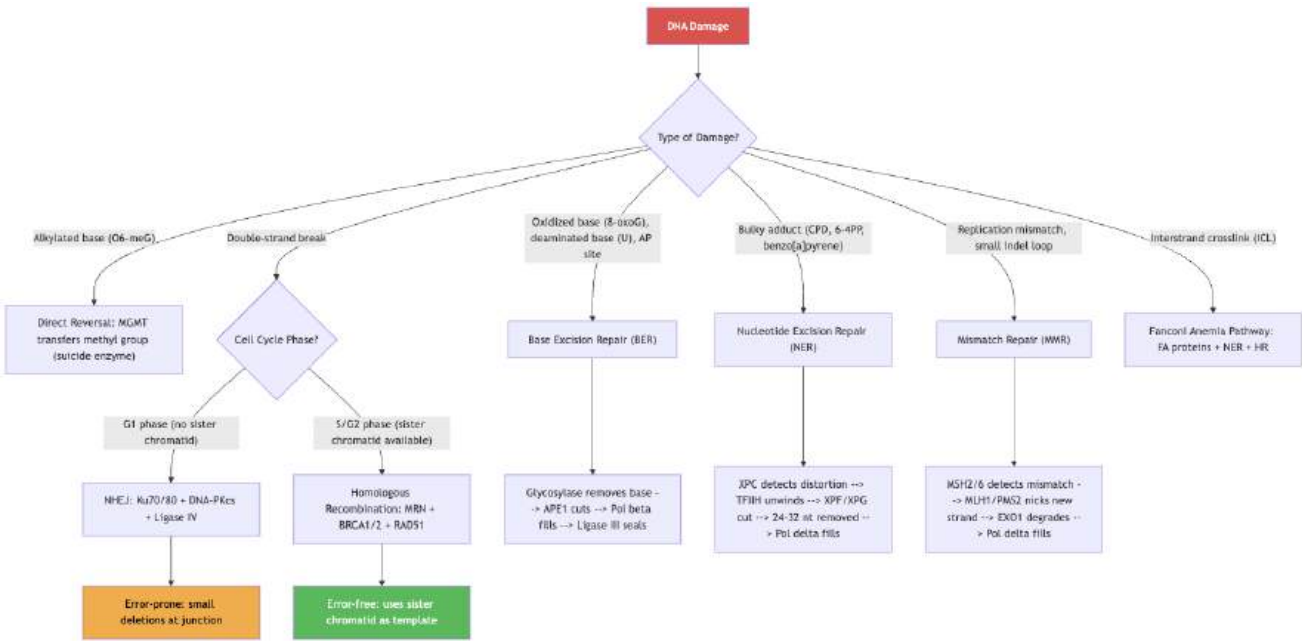


Figure 93. DNA damage types and their corresponding repair pathways. The choice of DSB repair pathway depends on cell cycle phase: NHEJ predominates in G1, while HR requires a sister chromatid template available in S/G2.

second active-site residue (D268) hydrolyses the intermediate, releasing the 8-oxoG base and leaving an AP site. - OGG1 is bifunctional: a β -elimination at the 3' phosphate produces a 3'- α,β -unsaturated aldehyde, which APE1 must process before pol β can extend. - 8-oxoG is mutagenic because it pairs with adenine (Hoogsteen face) instead of cytosine — leading to G:C \rightarrow T:A transversions if not repaired.

Clinical link — MUTYH-associated polyposis (MAP): Biallelic loss-of-function mutations in MUTYH cause autosomal recessive colorectal polyposis. The mechanism: OGG1 normally removes 8-oxoG, but if 8-oxoG escapes repair and is replicated, it pairs with A. MUTYH normally removes that A; without MUTYH, the A becomes fixed as a G:C \rightarrow T:A transversion. MAP tumors have a characteristic mutational signature (transversions at GAA contexts).

14.4.4 Comparing NER and MMR — A Side-by-Side Table

The pathways have distinct substrates and proteins, often confused. Here is a direct comparison:

Table 212. Comparing NER and MMR — A Side-by-Side Table: Feature and Nucleotide Excision Repair (NER).

Feature	Nucleotide Excision Repair (NER)	Mismatch Repair (MMR)
Substrate	Bulky helix-distorting lesions: CPDs, 6-4 photoproducts, cisplatin adducts, polycyclic aromatic hydrocarbons	Mismatched bases (G-T, A-C); small (1–13 nt) insertion/deletion loops
Recognition	Helix distortion or transcription stalling	Mismatch geometry directly bound by MutS α / β
Initiation timing	Any cell-cycle phase	Post-replicative (S/G2)
Strand discrimination	Both strands repaired	New strand identified by transient nicks (5' direction in eukaryotes; HMGB1)
Primary recognition factor	XPC-RAD23B (GG-NER); CSA-CSB (TC-NER, transcription-coupled)	MSH2-MSH6 (MutS α ; mismatches and 1-nt loops); MSH2-MSH3 (MutS β ; 2–13-nt loops)
Verification factor	TFIIH (XPB-helicase 3'→5'; XPD-helicase 5'→3') — unwinds about 25 bp	MLH1-PMS2 (MutL α ; endonuclease) makes incision
Excision	XPF-ERCC1 (5' cut), XPG (3' cut); 24–32 nt fragment removed	Exonuclease 1 (Exo1) degrades from MutL α cut to past mismatch; about 150 nt fragment removed
Synthesis	Pol δ/ϵ with PCNA, RFC	Pol δ
Ligation	DNA ligase I	DNA ligase I
Disease (loss-of-function)	Xeroderma pigmentosum (XPA–XPG, about 1,000 \times skin cancer); Cockayne syndrome (CSA, CSB; premature aging)	Lynch syndrome / HNPCC (MLH1, MSH2, MSH6, PMS2; 50–80% lifetime CRC risk; MSI-high tumors)

Feature	Nucleotide Excision Repair (NER)	Mismatch Repair (MMR)
Therapeutic relevance	Cisplatin sensitivity correlates with NER capacity	MSI-high tumors respond to anti-PD-1 (pembrolizumab) due to high neoantigen load

14.4.5 HR vs NHEJ — Pathway Choice Mechanism

The choice between homologous recombination (HR) and non-homologous end joining (NHEJ) is regulated by cell-cycle phase and a competition at the broken DNA ends.

Pathway-determining factors:

Table 213. HR vs NHEJ — Pathway Choice Mechanism: Step and NHEJ-favoring.

Step	NHEJ-favoring	HR-favoring
Cell cycle phase	G1, G0	S, G2 (sister chromatid available as template)
End sensor	Ku70/Ku80 binds DSB ends rapidly	Slow accommodation; replaces Ku
End processing	DNA-PKcs recruited; minimal end resection	MRN complex (MRE11–RAD50–NBN) initiates short-range resection
End-resection regulator	53BP1 + RIF1 + PTIP + shieldin complex (REV7-MAD2L2-SHLD1/2/3) — protects ends from resection	CtIP (CDK-phosphorylated in S/G2) + MRN initiates resection; EXO1 + DNA2 + BLM extend resection
Fidelity	Error-prone — small deletions/insertions at junction	High-fidelity (uses sister chromatid template)
Time scale	Fast (minutes)	Slow (hours)
Key proteins (after end-recognition)	DNA-PKcs, Artemis (nuclease), XRCC4, Ligase IV, XLF/Cernunnos, PAXX	RPA → BRCA2 → RAD51 (filament) → strand invasion → D-loop → resolution
Outcome	Direct ligation of ends (often with deletions ≤ 50 bp)	Use of sister chromatid as template; restores original sequence

The CDK regulatory switch: During G1, CDK activity is low; CtIP is unphosphorylated; 53BP1-shieldin protects ends; Ku70/80 dominates → NHEJ. During S/G2, CDK1/2 phosphorylates CtIP at Ser327 and Thr847, activating its end-resection function; CtIP+MRN displaces Ku → HR is initiated.

The BRCA1 vs 53BP1 antagonism. BRCA1 promotes resection (HR); 53BP1 blocks resection (NHEJ). The two compete for binding at H4K20me-marked nucleosomes near the DSB. BRCA1’s BRCT domain reads γH2AX-bound MDC1; 53BP1’s tandem Tudor domain reads H4K20me2. Loss of 53BP1 in BRCA1-deficient cells rescues HR (because resection is no longer blocked) — a synthetic-lethal escape mechanism in PARP-inhibitor resistance.

The BRCA2 mechanism. Once ssDNA is generated by resection, RPA coats it. BRCA2 then loads RAD51 onto the RPA-coated ssDNA, displacing RPA. This is the rate-limiting step of HR. Loss of BRCA2 prevents RAD51 loading → HR fails → cells become “BRCAness”-positive → exquisitely sensitive to PARP inhibitors (synthetic lethality, see section 12).

Ku70/80 binding. Ku70/80 forms a ring that threads onto the DSB end with extreme avidity (Kd ≈ 1 nM). It positions the DNA-PKcs catalytic subunit at the end and protects against resection. The Ku70/80 ring must be removed (by ubiquitination + proteasome) before HR can proceed in S/G2. This explains why NHEJ has an immediate kinetic advantage and HR requires time and active disassembly.

Concept Check (Analysis): Mismatch repair (MMR) corrects errors introduced by DNA polymerase by distinguishing the template strand (methylated GATC sites in bacteria; nick-directed in eukaryotes) from the newly synthesized strand. (a) A MMR-deficient cell has a base-substitution rate roughly 100–1,000 × that of wild-type. Taking the spontaneous misincorporation rate of DNA Pol III as 10^{−7} per base per replication and assuming MMR corrects about 99.9% of mismatches, calculate the uncorrected mutation rate with MMR active vs. with MMR absent, and check that the fold change matches the empirical range. (b) Lynch syndrome (hereditary non-polyposis colorectal cancer) is caused by germline heterozygosity at MMR genes (typically MLH1 or MSH2). Using the two-hit model, explain why heterozygous carriers develop tumors during adulthood despite the wild-type allele being present at conception, and predict which tumor-level phenotypes (microsatellite instability score, immunohistochemistry for the MMR proteins, mutational burden) would distinguish a Lynch-driven colorectal tumor from a sporadic MMR-proficient colorectal tumor.

Concept Check 13.2

1. Why is the Ames test performed with and without liver microsomal extract (S9)?

2. Explain why MGMT is called a “suicide **enzyme**.”
3. A patient has mutations in both BRCA1 **alleles**. Which repair pathway is defective? Why does this predispose to breast/ovarian cancer rather than most cancer types?
4. Compare the fidelity of NHEJ and HR. When would each be preferred?

14.5 CRISPR-Cas9: Mechanism and Applications

Background: CRISPR (Clustered Regularly Interspaced Short Palindromic Repeats) is the adaptive immune system of bacteria and **archaea**. Jennifer Doudna and Emmanuelle Charpentier received the 2020 Nobel Prize in Chemistry for demonstrating that CRISPR-Cas9 could be programmed with a synthetic guide RNA for precise genome editing (Jinek et al., 2012, *Science*).

14.5.1 Natural CRISPR Immunity

In bacteria, CRISPR functions as immunological memory:

1. Adaptation: When a bacterium survives phage infection, a short sequence from the phage genome (the protospacer) is integrated into the CRISPR array as a new spacer between repeat sequences
2. Expression: The CRISPR array is transcribed into pre-crRNA, which is processed (with tracrRNA in Type II systems) into mature crRNA
3. Interference: The crRNA guides Cas9 to complementary foreign DNA; Cas9 cleaves it, preventing subsequent infection

14.5.2 Engineered CRISPR-Cas9

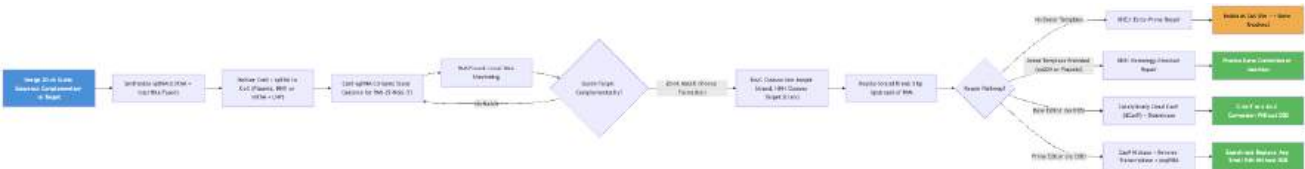


Figure 94. The CRISPR-Cas9 genome editing mechanism. The sgRNA guides Cas9 to a PAM-adjacent target sequence where a DSB is created. Repair by NHEJ produces knockouts; HDR with a donor template allows precise editing. Newer variants (base editors, prime editors) avoid DSBs entirely.

Key molecular details: - sgRNA (single guide RNA): A fusion of crRNA (20-nt spacer complementary to the target) and tracrRNA (scaffold that binds Cas9). The about 100-nt sgRNA is most that is needed to redirect Cas9. - PAM (protospacer adjacent motif): For *S. pyogenes* Cas9 (SpCas9), the PAM is 5'-NGG-3' on the non-target strand, immediately 3' of the target sequence. PAM recognition is the first step; without PAM, Cas9 will not unwind or cleave. - Cleavage: HNH domain cleaves the strand complementary to the sgRNA (target strand); RuvC domain cleaves the non-target strand. Both cuts occur about 3 bp upstream of the PAM, creating a blunt-ended DSB.

14.5.3 Beyond Cas9: Expanded Toolkit

Table 214. Beyond Cas9: Expanded Toolkit: Tool and Mechanism.

Tool	Mechanism	Application
Cas12a (Cpf1)	Creates staggered DSB; T-rich PAM (TTTN); self-processes crRNA array	Multiplexed editing; organisms with AT-rich genomes
Cas13 (RNA-targeting)	Cleaves RNA (not DNA); collateral RNA cleavage in bacteria	RNA knockdown; viral RNA detection (SHERLOCK diagnostic)
dCas9 (dead Cas9)	Catalytically inactive (D10A + H840A mutations); binds but does not cut	CRISPRi (transcriptional repression with KRAB domain); CRISPRa (activation with VP64/p65/Rta)
Base editors	dCas9 or Cas9-nickase fused to deaminase	CBE (cytidine base editor): C-to-T conversion; ABE (adenine base editor): A-to-G conversion; no DSB needed
Prime editors	Cas9-H840A nickase fused to M-MLV reverse transcriptase + pegRNA	“Search-and-replace”: any point mutation, small insertion, or small deletion; no DSB, no donor template needed

CRISPR diagnostics: SHERLOCK and DETECTR exploit collateral nuclease activity after target recognition: Cas13 collateral RNA cleavage and Cas12a collateral ssDNA cleavage convert a sequence match into a fluorescent or lateral-flow signal [Gootenberg et al., 2017, Chen et al., 2018]. That makes CRISPR a diagnostic logic as well as an editing logic, but it does not remove the usual validation burdens: sample preparation, contamination control, limit of detection, clinical sensitivity/specificity, and variant coverage still determine whether an assay is deployable.

Current evidence: prime editing as promoter rewriting. Prime editing is especially useful when the desired change is not simply “cut here” but “install a small regulatory pattern.” A 2025 *Blood* study used prime-editing guide RNAs to introduce multiple hereditary-persistence-of-fetal-hemoglobin-like edits into the *HBG1/HBG2* gamma-globin promoters, aiming to reactivate fetal hemoglobin without making a double-strand break [Chalumeau et al., 2025]. Editing efficiency varied among donor hematopoietic stem/progenitor cells, so this should be treated as early translational evidence rather than an approved therapy. The concept is powerful: regulatory DNA can be edited to change *when and where* a gene is expressed, not only whether its protein-coding sequence is intact.

14.5.4 Therapeutic Applications (2024-2025)

Casgevy (exagamglogene autotemcel): First CRISPR-based therapy approved by FDA for sickle cell disease (December 2023) and later for transfusion-dependent beta-thalassaemia (January 2024), with EMA authorization following in 2024. FDA’s 2026 product page lists exa-cel for sickle cell disease and transfusion-dependent beta-thalassaemia in patients 12 years of age and older, with updated approval documentation [U.S. Food and Drug Administration, 2023, 2024b, 2026a].

- Indication: Sickle cell disease (SCD) and transfusion-dependent beta-thalassemia
- Mechanism: Ex vivo CRISPR editing of patient hematopoietic stem cells (HSCs) to disrupt the *BCL11A* erythroid enhancer. BCL11A is a repressor of fetal hemoglobin (HbF, alpha2-gamma2). Disrupting its erythroid enhancer reactivates HbF production, which does not sickle and compensates for defective HbS.
- Results: In SCD, the regulatory endpoint is freedom from severe vaso-occlusive crises after treatment; transfusion independence is the endpoint used for transfusion-dependent beta-thalassaemia. Early exa-cel studies also reported sustained fetal-hemoglobin induction, so the durable teaching point is endpoint specificity: the same edited cell product is judged against different disease-specific clinical outcomes [U.S. Food and Drug Administration, 2023, 2024b, 2026a].

NTLA-2001 (in vivo CRISPR): - Indication: Transthyretin (ATTR) amyloidosis - Mechanism: Lipid nanoparticle (LNP)-delivered Cas9 mRNA + sgRNA targeting the *TTR* gene in hepatocytes – direct in vivo editing (no cell harvest needed) - Results: Single infusion achieved 80-95% serum TTR reduction (Gillmore et al., 2021, *NEJM*)

Safety considerations: - Off-target editing: sgRNA may bind sites with 1-3 mismatches. Mitigated by high-fidelity Cas9 variants (SpCas9-HF1, eSpCas9, HiFi Cas9) and careful guide RNA design (off-target prediction algorithms: Cas-OFFinder, CRISPOR) - Immunogenicity: about 79% of humans have pre-existing antibodies to SpCas9; strategies include using Cas9 from other species or transient delivery (mRNA/RNP vs. viral vectors) - NHEJ:HDR ratio: about 1000:1 in non-dividing cells (most therapeutically relevant cells); S/G2 phase favors HDR; base editors and prime editors circumvent this limitation

Clinical Connection: Base Editing for Sickle Cell Disease An alternative approach uses adenine base editing to directly convert the sickle mutation (GAG to GTG = Glu to Val) back to the wild-type or a benign Makassar variant (GAG to GCG = Glu to Ala). This avoids DSBs entirely and may be safer than Cas9-based approaches. Clinical trials are underway (Beam Therapeutics, BEAM-101).

Mitochondrial DNA editing boundary: Standard CRISPR-Cas systems work poorly for mtDNA because guide RNAs are difficult to import into mitochondria. DddA-derived cytosine base editors (DdCBEs) solve part of the problem by using TALE-DddA protein fusions to install targeted C·G-to-T·A edits in mtDNA without guide RNA [Mok et al., 2020]. This is a major tool advance, not a general approved therapy: heteroplasmy, off-target editing, delivery, selectable mutation classes, and tissue specificity remain the current translational constraints [Barrera-Paez et al., 2023].

Concept Check 13.3

1. Why does Cas9 require a PAM sequence? What is the evolutionary rationale?
2. Compare NHEJ and HDR outcomes after Cas9-mediated DSB. Why is HDR difficult to achieve in post-mitotic cells?
3. What advantage does base editing offer over standard Cas9 editing for correcting point mutations?
4. Explain the mechanism of Casgevy: why does disrupting BCL11A treat sickle cell disease?

14.6 Genomics: The Human Genome

The Human Genome Project (1990-2003; Venter et al., 2001 and International Human Genome Sequencing Consortium, 2001) produced the first draft reference. The T2T Consortium (Nurk et al., 2022) completed the first truly gapless reference genome (CHM13), filling about 8% of previously unresolvable sequence (centromeres, **telomeres**, segmental duplications, rDNA arrays).

14.6.1 Human Genome Composition

Table 215. Human Genome Composition: Component and Fraction.

Component	Fraction	Details
Protein-coding exons	about 1.5%	about 19,000-20,000 genes; average gene about 27 kb; average of 8.8 exons
Introns	about 26%	Average intron about 3.4 kb; some >100 kb
Transposable elements	about 46%	LINEs (21%, especially L1), SINEs (13%, especially Alu), DNA transposons (3%), LTR retrotransposons (9%)
Intergenic sequence	about 15%	Includes regulatory elements, structural sequences
Non-coding RNA genes	about 5,000+ loci	lncRNAs, miRNAs, snRNAs, snoRNAs, rRNAs, tRNAs
Simple sequence repeats	about 3%	Microsatellites (1-6 bp repeat units) and minisatellites (7-100 bp)
Segmental duplications	about 5%	Blocks >1 kb with >90% sequence identity; hotspots for chromosomal rearrangement

14.6.2 Transposable Elements — Mechanism and Genomic Impact

Transposable elements (TEs) make up about 46 % of the human genome — far more than the about 1.5 % occupied by protein-coding exons. They are ancient mobile DNA elements that have shaped genome architecture over evolutionary time. They fall into three major classes:

Class I — RNA-mediated retrotransposons (copy-and-paste; majority of human TEs):

1. LINE-1 (Long Interspersed Nuclear Element 1) — about 21 % of human genome; about 500,000 copies; about 6 kb full-length. Primarily about 80–100 are currently transposition-competent.
 - Encodes ORF1 (RNA-binding chaperone) and ORF2 (with reverse-transcriptase + endonuclease activities)
 - Retrotransposition mechanism (Target-Primed Reverse Transcription, TPRT):
 1. L1 transcribed by Pol II → L1 mRNA (about 6 kb, capped, polyadenylated)
 2. L1 mRNA exported to cytoplasm, translated to ORF1p and ORF2p
 3. Cis-binding of ORF1p/ORF2p to their own mRNA forms a ribonucleoprotein (RNP)
 4. RNP enters nucleus
 5. ORF2p endonuclease nicks genomic DNA at TTAAAA-like sites, exposing 3'-OH
 6. The 3'-OH primes reverse transcription using L1 mRNA as template
 7. Second-strand DNA synthesis completes integration
 8. Target site duplication (TSD; 7–20 bp) flanks the new insertion, plus a poly-A tail at the 3' end
 - Most insertions are 5'-truncated due to incomplete RT
 - L1 endonuclease nicks about 100 sites/cell per day; most fail to complete TPRT (silenced by KRAB-ZFP-driven H3K9me3 repression)
2. Alu elements (Short Interspersed Nuclear Element 1, SINE) — about 13 % of human genome; about 1.1 million copies; about 300 bp.
 - Derived from 7SL RNA (signal recognition particle component); contain RNA Pol III internal promoter
 - Mobilization requires L1 machinery (parasitic on LINE-1's ORF2p RT/endonuclease)
 - Transcription by Pol III; the Alu RNA recruits L1 ORF2p in *trans* and inserts via the same TPRT mechanism
 - Alu elements are densest in gene-rich regions; insertions in introns can disrupt splicing or create new alternative exons
3. SVA elements (SINE-VNTR-Alu) — about 3,000 copies; about 2 kb; younger than Alu (about 25 Mya). Hybrid composite.
4. LTR retrotransposons (HERV — human endogenous retroviruses) — about 9 % of genome; relics of ancient retroviral insertions. Most are inactivated; some HERV-K elements remain intact and may be re-activated in cancer.

Class II — DNA transposons (cut-and-paste; about 3 % of human genome): - Most inactivated in modern human genome (no active class II TE in humans) - Mechanism: a transposase enzyme (encoded by the TE) recognizes terminal inverted repeats (TIRs) flanking the element, excises the element, and re-integrates it elsewhere - Mariner / Tc1, hAT, P-element families most derive from class II - Hyperactive synthetic DNA transposons (e.g., Sleeping Beauty, PiggyBac) are now used as gene-delivery tools in research and CAR-T therapy

Genomic and clinical impact of TE insertions: - about 100 *de novo* L1 or Alu insertions per generation (germline) - about 10–15 % of disease-causing mutations are TE insertions (e.g., Alu insertion in *NF1* exon 6 causing neurofibromatosis; L1 insertion in *DMD* causing Duchenne) - TE insertions in gene regulatory regions can create new enhancers or promoters (about 25 % of mammalian enhancers derive from TEs) - Active L1 retrotransposition in the brain creates somatic mosaicism (about 80 unique L1 insertions per neuron) potentially contributing to neuronal diversity - Cancer cells often re-activate TE expression (LINE-1 demethylation is a hallmark of global cancer hypomethylation), contributing to chromosomal instability and inflammation

Defense mechanisms against TE activity: - DNA methylation of TE promoters (DNMT3A/B targets active TE families during germline development) - KRAB-ZFP transcriptional repression: > 350 KRAB-zinc finger proteins recognize specific TE families and recruit KAP1/TRIM28 → SETDB1 → H3K9me3 silencing - piRNA pathway in germline: piRNAs (26–32 nt) bind PIWI clade Argonautes (PIWIL1/MILI, PIWIL4/MIWI2) and silence TEs via the “ping-pong amplification” cycle - APOBEC3 deaminases: cytidine deaminases that mutate TE-derived ssDNA, restricting retrotransposition and HIV integration

14.6.3 Structural Variants — Inversions, CNVs, and Disease

Inversions are large segments of DNA flipped end-to-end. Unlike SNPs, they are difficult to detect by short-read sequencing (the inversion preserves sequence content, primarily orientation changes). Long-read sequencing (PacBio HiFi, Oxford Nanopore) and optical mapping (Bionano Saphyr) have revealed: - about 40,000 polymorphic inversions per human genome (most < 50 kb) - HbF inversion regulators: A rare inversion at the *BCL11A* locus disrupts the erythroid-specific enhancer of *BCL11A*, derepressing fetal hemoglobin (HbF) production. This explains the high HbF persistence in some Sardinian families and provides the rationale for therapeutic disruption of *BCL11A* (Casgevy approved for sickle cell disease). - Pericentric inversion of chromosome 9 (inv(9)(p11q12)): a common normal variant (about 1–3 % of population), classically considered benign, but recently associated with subtle effects on fertility.

Copy Number Variants (CNVs) are duplications or deletions of segments > 1 kb. Two major mechanisms: - Non-allelic homologous recombination (NAHR) between segmental duplications (low-copy repeats, LCRs) — produces recurrent CNVs at predictable breakpoints (e.g., 22q11.2 microdeletion, 16p11.2 micro-CNV) - Replication-based mechanisms (FoSTeS, MMBIR) — produce non-recurrent CNVs at variable breakpoints

CNVs in autism and schizophrenia:

Table 216. Structural Variants — Inversions, CNVs, and Disease: Locus and Size.

Locus	Size	Phenotype	Frequency in cases vs controls
16p11.2 (deletion or duplication)	about 600 kb	Autism, intellectual disability, obesity (deletion)	about 1 % of autism cases vs 0.04 % controls
22q11.2 (deletion = DiGeorge syndrome / 22q11DS)	about 3 Mb	Schizophrenia (about 25 % of carriers), congenital heart disease, palatal defects	about 25 % schizophrenia risk
15q11–13 (duplication of maternal allele)	about 4 Mb	Autism, epilepsy	about 1 % of autism
NRXN1 (Neurexin-1) (heterozygous deletion)	Variable, exonic	Autism, schizophrenia, intellectual disability	5–10× enrichment
CNTNAP2 (heterozygous loss)	Variable, exonic	Autism, language delay, epilepsy	Modest enrichment
3q29 (microdeletion)	about 1.6 Mb	Schizophrenia (about 40× risk increase)	Rare but high penetrance

Locus	Size	Phenotype	Frequency in cases vs controls
22q11.2 (mi-croduplication)	about 3 Mb	Increased risk of schizophrenia	about 3× increase
1q21.1 (deletion or duplication)	about 1.4 Mb	Schizophrenia, autism, microcephaly (deletion)	about 10× risk
15q13.3 (deletion)	about 1.5 Mb	Schizophrenia, epilepsy (deletion)	about 10× risk

Why CNVs are so impactful: Each CNV affects 1–5 dosage-sensitive genes simultaneously. The cumulative effect on neural development is large because brain development depends on stoichiometric protein interactions. Rare CNVs (occurring in < 1 % of population) collectively explain about 5 % of schizophrenia cases and about 10 % of autism cases — a substantial fraction of risk despite each individual CNV being rare.

Concept Check (Synthesis): Copy number variation (CNV) is a class of structural genetic variation in which segments of ≥ 1 kb are duplicated or deleted. A major mechanism is non-allelic homologous recombination (NAHR) between flanking segmental duplications. (a) Chromosome 15q11–q13 carries large segmental duplications that flank the Prader–Willi / Angelman syndrome region. Explain why this architecture predisposes the region to recurrent microdeletions and microduplications, and predict the phenotypic consequence of a paternally vs. maternally inherited deletion — the answer should invoke genomic imprinting at SNRPN and UBE3A. (b) The 22q11.2 deletion syndrome (the molecular basis of DiGeorge / velocardiofacial syndrome) occurs in roughly 1 in 4,000 live births, making it one of the most common recurrent microdeletion syndromes in humans. Given that NAHR drives most recurrence, sketch how the expected deletion frequency should scale with (i) the length of the flanking segmental duplications, (ii) the percent sequence identity between them, and (iii) the genomic distance separating them. Use this to argue why 22q11.2 is so structurally unstable relative to a hypothetical CNV interval flanked by 5 kb duplications at 90% identity.

14.6.4 Genomic Variation Across SNVs, Structural Variants, and Haplotypes

- Single nucleotide polymorphisms (SNPs): about 1 per 300 bp on average; the human genome contains about 4-5 million SNPs per individual relative to the reference. Most are neutral; about 2% in coding regions; about 0.5% are missense.
- Indels: about 500,000 per genome; usually 1-50 bp
- Copy number variants (CNVs): about 1,000 per genome; collectively encompass about 4 Mb
- Structural variants (SVs): inversions, translocations, large insertions; about 2,500 per genome
- Two individuals differ by about 0.1% of their genomes (about 3 million SNPs), but most variation is within populations rather than between populations (Lewontin, 1972; Fst about 0.12).

14.6.5 The ENCODE Project

The ENCODE (Encyclopedia of DNA Elements) Project (2003-present) systematically mapped functional elements in the human genome:

- Key finding: >80% of the genome has at least one biochemical function (chromatin accessibility, transcription factor binding, histone modification, RNA transcription)
- Revised “junk DNA” narrative: Much non-coding DNA has regulatory function (enhancers, insulators, lncRNAs); however, “biochemical activity” does not necessarily mean “biologically important” (ongoing debate)
- about 400,000 enhancers identified; most disease-associated SNPs (from GWAS) fall in non-coding regulatory regions, not protein-coding genes

14.7 Next-Generation Sequencing Technologies



Figure 95. Genomic sequencing approaches. Short-read (Illumina) provides high throughput and accuracy for variant calling; long-read (Nanopore, PacBio HiFi) resolves structural variants, repeats, and enables de novo assembly.

14.7.1 Pangenome Graph Reasoning

The old mental model of a genome reference was a single linear string. That is still useful, but it hides ancestry-specific haplotypes, structural variants, alternate gene copies, and repeat-resolved sequence that do not align cleanly to one coordinate path. The Human Pangenome Reference Consortium’s 2023 draft reference introduced a graph built from 47 diverse individuals and 94 phased haplotypes; its 2025 Release II expanded the resource to assemblies from 232 individuals with phased, near-telomere-to-telomere assemblies, annotations, and graph-based alignments [Human Pangenome Reference Consortium, 2023, 2025]. In a graph, a variant is not merely “different from the reference”; it is a path through an explicitly represented set of alternatives. This improves reasoning about structural variation and representation, while adding new validation obligations: graph alignment, annotation transfer, clinical reporting, and population sampling must become part of the claim.

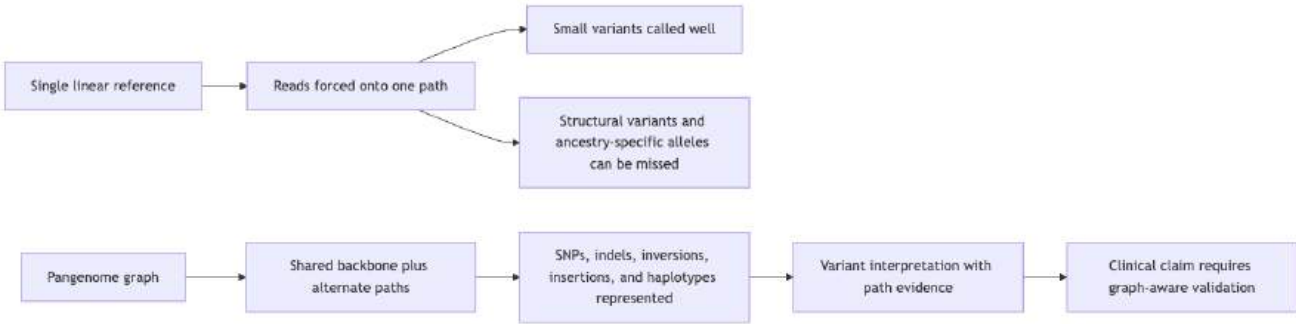


Figure 96. Pangenome graph reasoning. A graph reference turns population variation into explicit alternate paths, improving structural-variant interpretation while making validation and reporting more complex.

Table 217. Pangenome Graph Reasoning: Technology and Read Length.

Technology	Read Length	Accuracy	Throughput	Cost (30x Human Genome)	Key Application
Illumina NovaSeq X	150-300 bp	>99.9% (Q30+)	about 600 Gb/run	about \$200	Variant calling, RNA-seq, exome
PacBio Revio (HiFi)	10-25 kb	>99.9% (consensus)	about 90 Gb/run	about \$1,000	Structural variants, de novo assembly, epigenetics
Oxford Nanopore PromethION	>100 kb possible	about 99% (Q20+)	about 100 Gb/run	about \$500	Real-time sequencing, field deployment, direct RNA sequencing

14.8 Genome-Wide Association Studies (GWAS)

GWAS identify genetic variants (typically SNPs) associated with complex traits or diseases by comparing allele frequencies between cases and controls.

Methodology: 1. Genotype hundreds of thousands to millions of SNPs across the genome in large cohorts (typically >10,000 individuals) 2. Test each SNP for association with the **phenotype** using logistic regression (binary traits) or linear regression (quantitative traits) 3. Apply a stringent significance threshold ($p < 5 \times 10^{-8}$) to account for about 1 million independent tests (Bonferroni-like correction) 4. Display results on a Manhattan plot: genomic position (x-axis) vs. $-\log_{10}(p)$ (y-axis); significant associations appear as peaks above the genome-wide significance line

Key concepts: - **Linkage** disequilibrium (LD): Non-random association of alleles at nearby loci. A significant SNP may not be the causal variant but rather in LD with it (a “tag SNP”). - Effect sizes: Most GWAS-identified variants have small effect sizes (odds ratio 1.1-1.3); complex traits are highly polygenic - Missing heritability: GWAS variants collectively explain primarily a fraction of heritability for most traits (e.g., about 25% of height heritability, despite identifying >700 loci)

Examples of GWAS discoveries: - Type 2 diabetes: >400 loci, including TCF7L2 (strongest effect), PPARG, KCNJ11 - Age-related macular degeneration: CFH (complement factor H) – led to complement-targeted therapies - Autoimmune diseases: HLA region as the strongest risk factor for type 1 diabetes, celiac disease, rheumatoid arthritis

14.9 Comparative Genomics and Molecular Evolution

Synteny: Conservation of gene order between species. Humans and mice share about 90% of genes in syntenic blocks, despite 75-80 million years of divergence.

Conserved non-coding elements (CNEs): about 5% of the human genome is under purifying selection (much more than the about 1.5% that encodes protein). These conserved regions likely include enhancers, silencers, and structural elements essential for gene regulation.

Ultraconserved elements (UCEs): A particularly remarkable subset — about 481 segments of ≥ 200 bp that are perfectly identical (100 % sequence identity) across human, mouse, and rat genomes (Bejerano et al., 2004 *Science*). These elements have remained unchanged for about 80 million years, implying extreme purifying selection. UCEs cluster near developmental transcription factors (e.g., *DACH1*, *POU3F2*) and are enriched in enhancers controlling early embryonic patterning. Their function remains incompletely understood — paradoxically, knocking out individual UCEs in mice produces primarily subtle phenotypes, raising questions about why selection is so strong if redundancy is high.

Comparative-genomics signatures of selection:

Table 218. Pangenome Graph Reasoning: Signature and Detection method.

Signature	Detection method	Interpretation
Conserved across species	PhastCons, PhyloP	Purifying selection (function preserved)
Conserved + accelerated in lineage	HAR (Human Accelerated Regions)	Adaptive change in human lineage (e.g., HAR1 → schizophrenia, autism overlap)
Population-level fixation	Fst, XP-EHH	Recent positive selection in a population (e.g., LCT lactase persistence in Europeans)
dN/dS > 1	PAML, codeml	Positive selection at protein level (e.g., immune genes, primate FOXP2)
TajimaD < 0	Coalescent statistics	Recent selective sweep
Long-range LD (haplotype block)	iHS, EHH	Recent adaptive selection

14.9.1 Mutation Rates — Spontaneous vs Induced

Mutation rate varies enormously with cellular context, mutagen exposure, and DNA repair capacity. The following table contrasts representative spontaneous and induced mutation frequencies:

Table 219. Mutation Rates — Spontaneous vs Induced: Source and Mutation rate (per bp per generation/division).

Source	Mutation rate (per bp per generation/division)	Notes
Spontaneous mutations		
Human germline	1.2×10^{-8} per bp per generation	Trio sequencing (Kong et al., 2012); paternal age $\times 2$ from age 20 to 50
Human somatic (most tissues)	5×10^{-9} to 10^{-8} per cell division	Stem-cell-population mutation rate
<i>E. coli</i> (wild-type)	5×10^{-10} per bp per generation	High polymerase fidelity + MMR

Source	Mutation rate (per bp per generation/division)	Notes
<i>E. coli</i> mutator (mutS-)	5×10^{-7} per bp per generation	1000× elevated due to MMR loss
<i>S. cerevisiae</i> (yeast) Induced mutations UV (sub-lethal, 10 J/m ²)	2×10^{-10} per bp per generation 10^{-5} to 10^{-4} per bp at TT, TC sites	 CPDs and 6-4 photo-products; localized to pyrimidine dimers
Ionizing radiation (1 Gy)	about 50–100 DSBs per cell	DSBs cluster in damage tracks; many fatal if unrepaired
Cigarette smoke (chronic exposure)	about 150 missense mutations/year in lung epithelium	Benzo a pyrene → G:C → T:A transversions (signature 4)
EMS (ethyl methanesulfonate, 50 mM)	5×10^{-4} per bp per generation in <i>Drosophila</i>	Workhorse mutagen; G:C → A:T transitions
5-FU treatment (cancer chemo)	100–1000-fold elevation in dividing cells	Thymidylate synthase inhibition + mis-incorporation
Disease-state elevation Lynch syndrome (MMR-deficient tumors)	10^{-5} per bp; microsatellite instability (MSI)	Poll/Pold mutations also cause Lynch-like phenotypes
MUTYH-associated polyposis BRCA1/2-deficient cancer	10× G:C → T:A elevation High SV burden (BRCA1) or chromothripsis (BRCA2)	OGG1+MUTYH deficient HR-defective; relies on error-prone NHEJ/MMEJ

Source	Mutation rate (per bp per generation/division)	Notes
POLE proofreading-deficient cancer	10^{-4} to 10^{-5} per bp	“Ultramutator” phenotype (about 100,000 mutations per tumor); responds to anti-PD-1

Why the mutation rate is so finely tuned. The germline mutation rate of about 1.2×10^{-8} produces about 70 *de novo* mutations per offspring, an upper limit set by cumulative effects across generations: too high, and “Muller’s ratchet” accumulates deleterious mutations faster than selection can purge them; too low, and there is insufficient variation for adaptation. Different organisms have evolved different rates: high-fecundity microbes (10^{-9} to 10^{-10}), mammals (10^{-8}), and viruses with their relaxed proofreading (HIV: 10^{-5} ; influenza: 10^{-4}) reflect different optima between fidelity costs and adaptive flexibility.

Gene duplication and divergence [Ohno, 1970]: Whole-genome duplications (WGD) and segmental duplications create paralogous genes. After duplication: - Neofunctionalization: One copy acquires a new function - Subfunctionalization: Each copy retains a subset of the original function - Pseudogenization: One copy accumulates mutations and becomes a pseudogene

Ka/Ks ratio (dN/dS): The ratio of nonsynonymous (amino acid-changing) to synonymous (silent) substitution rates: - Ka/Ks < 1: purifying (negative) selection (most genes) - Ka/Ks = 1: neutral evolution - Ka/Ks > 1: positive (adaptive) selection (rare; examples: immune genes, reproductive proteins)

14.10 Personal Genomics and Ethical Issues

14.10.1 Pharmacogenomics and Evidence-Governed Prescribing

Genetic variation affects drug response:

Pharmacogenomics is strongest when it is treated as one evidence layer in prescribing rather than a deterministic label. A genotype can alter enzyme activity, transporter expression, immune recognition, or drug target sensitivity, but clinical interpretation also depends on ancestry representation in the evidence base, co-medications, age, liver and kidney function, indication, and whether the variant is actually phased or captured by the assay. Pangenome and long-read resources improve the chance of detecting structural or ancestry-associated variants missed by a single linear reference, but clinical use still requires validated phenotype links and reporting standards [Human Pangenome Reference Consortium, 2023].

Table 220. Pharmacogenomics and Evidence-Governed Prescribing: Gene and Drug.

Gene	Drug	Effect of Variant
CYP2D6	Codeine, tamoxifen	Poor metabolizers: codeine ineffective (cannot convert to morphine); ultra-rapid metabolizers: toxicity risk
CYP2C19	Clopidogrel (Plavix)	Poor metabolizers: reduced anti-platelet effect; increased cardiovascular risk
VKORC1 + CYP2C9	Warfarin	Variants explain about 40% of dosing variation; FDA-approved pharmacogenomic labeling
HLA-B*5701	Abacavir (HIV)	Pre-treatment testing mandatory; positive patients have about 50% risk of hypersensitivity reaction
DPYD	5-fluorouracil	DPD deficiency: potentially fatal toxicity; pre-treatment testing recommended in EU

14.10.2 Ethical Considerations in Personal and Clinical Genomics

- Genetic privacy: Genetic information reveals predisposition, not certainty. The GINA Act (Genetic Information Nondiscrimination Act, 2008, USA) prohibits genetic discrimination in employment and health insurance but does NOT cover life insurance, disability insurance, or long-term care insurance.
- Direct-to-consumer (DTC) testing: Companies like 23andMe provide ancestry and health risk information. Concerns include: limited clinical validity for most variants, potential for anxiety, and data privacy (law enforcement access to databases).

- BRCA1/2 testing decisions: Positive results require careful genetic counseling. Prophylactic mastectomy reduces breast cancer risk by >90% but is psychologically significant. The 2013 *Myriad Genetics* Supreme Court decision (Association for Molecular Pathology v. Myriad Genetics) ruled that naturally occurring genes cannot be patented but **cDNA** can be.
- Germline editing: Editing human embryos raises profound ethical questions. The 2018 He Jiankui case (CCR5-edited babies in China) was widely condemned as premature, reckless, and ethically unacceptable. International consensus: germline editing for reproduction should not proceed until safety and efficacy are established and broad societal consensus is reached.

Clinical Connection: Pharmacogenomic Testing in Practice The Clinical Pharmacogenetics Implementation Consortium (CPIC) publishes evidence-based guidelines for 23+ gene-drug pairs. Pre-emptive pharmacogenomic testing (genotyping a panel of pharmacogenes before any drug is prescribed) is increasingly implemented in health systems. The PREDICT study (Vanderbilt) and RIGHT study (Mayo Clinic) demonstrated that pre-emptive testing is feasible and can prevent adverse drug reactions.

14.11 Worked Example: Per-Gene De Novo Mutation Probability

Problem: The human germline point-mutation rate is $\mu \approx 1.2 \times 10^{-8}$ per bp per generation. The dystrophin gene (*DMD*) has the largest coding sequence in the genome, 11,058 bp (both alleles together giving a diploid coding target $L = 2 \times 11,058$ bp).

- (a) What is the expected number of de novo coding mutations in *DMD* per offspring?

Solution: The Poisson mean is the per-bp rate times the diploid coding target length:

$$\lambda = \mu L = 1.2 \times 10^{-8} \times 22,116 \text{ bp} = 2.65 \times 10^{-4} \text{ mutations/generation}$$

(216)

- (b) Using the Poisson model, what is the probability that a given child carries no new coding mutation in *DMD*?

$$P(k = 0) = \frac{(\lambda)^0 e^{-\lambda}}{0!} = e^{-2.65 \times 10^{-4}} \approx 0.99973$$

(217)

- (c) What is the probability of at least one new coding mutation in *DMD*?

$$P(k \geq 1) = 1 - e^{-\lambda} \approx 2.65 \times 10^{-4} \approx \frac{1}{3,800} \text{ births}$$

(218)

Even though any single child is overwhelmingly likely to inherit an intact *DMD* coding sequence, a rate of roughly 1 in 3,800 births applied across a large population continually regenerates new Duchenne muscular dystrophy alleles — which is why this X-linked disorder persists despite strong negative selection against affected males.

14.12 Worked Example: Mutation Analysis

Problem: A wild-type mRNA sequence reads:

5'-AUG-UUU-GGA-GAA-CUU-UAG-3'

- (a) Translate the wild-type sequence.

Table 221. Ethical Considerations in Personal and Clinical Genomics: Codon and Amino Acid.

Codon	Amino Acid
AUG	Met
UUU	Phe
GGA	Gly
GAA	Glu
CUU	Leu
UAG	Stop

Protein: Met-Phe-Gly-Glu-Leu (5 amino acids)

(b) A transition mutation changes the 10th nucleotide (first position of codon 4) from G to A: GAA to AAA.

Table 222. Ethical Considerations in Personal and Clinical Genomics.

Codon	Wild-type AA	Mutant AA
GAA	Glu	AAA = Lys

This is a missense mutation (Glu to Lys: non-conservative, charge reversal).

(c) A transition changes the 7th nucleotide (first position of codon 3) from G to A: GGA to AGA.

GGA (Gly) to AGA (Arg): missense (non-conservative; small nonpolar to large positive).

(d) A deletion removes the 4th nucleotide (U): sequence becomes AUG-UUG-GAG-AAC-UUU-AG...

This is a frameshift mutation. New reading frame: Met-Leu-Glu-Asn-Phe... (completely different protein, no stop codon in remaining sequence – read-through into 3’ UTR).

14.13 Computational Bridge

In silico translation checks mutation consequences quickly:

```
from biology.genetics import translate_mrna

wt = translate_mrna("AUGGAAUAA")
print(wt)
```

Clinical / systems note: Pharmacogenomic dosing (warfarin, thiopurines, clopidogrel) is implemented as clinical algorithms over the same variant catalog GWAS discovers — bridging population statistics to individual prescriptions.

14.13.1 Post-Approval CRISPR Therapeutics: Casgevy and the Safety Frontier

The first CRISPR–Cas9 therapy approved by the FDA and EMA (Casgevy / exagamglogene autotemcel, Vertex/CRISPR Therapeutics) provides a quantitative benchmark for the entire field [U.S. Food and Drug Administration, 2023, 2024b, 2026a]. The therapy edits autologous CD34⁺ hematopoietic stem cells *ex vivo* at the BCL11A enhancer to de-repress fetal hemoglobin (HbF), then reinfuses them after conditioning chemotherapy. In the pivotal trials, 28 of 29 sickle-cell patients became free of vaso-occlusive crises for > 12 months, and 39 of 42 β -thalassemia patients became transfusion-independent — outcomes previously achievable primarily via allogeneic bone-marrow transplant with its attendant graft-versus-host morbidity.

The safety discussion that accompanies this approval is instructive. Off-target editing in CD34⁺ cells is measured pre-infusion by GUIDE-seq and deep amplicon sequencing at 100+ predicted sites — with Casgevy, off-target editing fell below the detection floor (about 0.1 %) at most surveyed loci. Residual concerns include large structural variants (kilobase-scale deletions, inversions, chromothripsis) that amplicon-seq can miss; long-read WGS of treated HSC clones is the emerging gold-standard check. Longitudinal monitoring follows these patients for 15 years for malignancy, driven by the theoretical risk that any DNA double-strand break event in a stem cell compartment could, over decades, seed a clonal expansion [U.S. Food and Drug Administration, 2026a]. This regulatory framework — efficacy by molecular endpoint, safety by unbiased structural-variant surveillance, surveillance by decade-scale cohort — is now the template every subsequent *in vivo* CRISPR therapy (e.g., Verve’s PCSK9 base editor for hypercholesterolaemia) must meet.

14.13.2 The Telomere-to-Telomere (T2T) Consortium: A Truly Complete Human Genome

The human reference genome, from the Human Genome Project’s 2003 draft through GRCh38 (2013), contained > 200 Mb of unresolved gaps — chiefly heterochromatic satellite arrays at centromeres, the short arms of acrocentric chromosomes (13, 14, 15, 21, 22), and segmental duplications. The T2T-CHM13 assembly (Nurk et al., *Science* 2022) closed these gaps using long-read sequencing (PacBio HiFi, Oxford Nanopore Ultra-long) on a hydatidiform mole (uniform haplotype, no heterozygous complications), yielding the first gapless 3.055 Gb human genome.

What newly resolvable sequence revealed: centromeric α -satellite arrays span 0.5–5 Mb per chromosome, organized into higher-order repeat (HOR) units; the rDNA arrays on acrocentric p-arms vary from 47 to 287 copies per haploid genome; roughly 2000 additional protein-coding genes and gene paralogs were

annotated (with duplications in immunity, olfaction, and neurogenesis). Perhaps most importantly, T2T demonstrated that prior “dark” regions harbor real medical-genetic variation: paracentric inversions at 16p11 and 22q11 — known susceptibility loci for autism and schizophrenia — are present in about 10 % of haplotypes but invisible to GRCh38 mapping. The pangenome era extends T2T’s logic: the reference is now a graph, not a single string, and clinical genomic pipelines are migrating cautiously because graph references improve representation while adding alignment, annotation, and validation complexity [Human Pangenome Reference Consortium, 2023].

14.14 Current Evidence and Frontier Biology: Mutations, CRISPR, and Genomics

For Mutations, CRISPR, and Genomics, frontier biology belongs inside the evidence logic of the chapter. Molecular genetics now spans single-reference sequences, telomere-to-telomere assemblies, pangenome graphs, long-read sequencing, CRISPR medicines, and ethical deployment. The core reading question is this: genomics claims should distinguish variant discovery, pathogenic interpretation, ancestry representation, and clinical actionability.

- What to verify: identify the observation, model, assay, or dataset that would make the claim stronger or weaker.
- What to qualify: state the scale, organism, cell type, environmental condition, or population where the claim is expected to hold.
- What to compare: test at least one alternative explanation, baseline, or null model before treating the pattern as causal.
- What to cite: distinguish primary evidence, review synthesis, public dataset, and institutional guidance; for recent or numeric claims, prefer the source closest to the measurement and state what has changed since it was published.

When a genomics claim depends on a reference, ask whether reads, structural variants, ancestry representation, phasing, or clinical validation changes the interpretation [Human Pangenome Reference Consortium, 2023, U.S. Food and Drug Administration, 2023, 2024b].

Clinical variant interpretation must separate variant existence from medical meaning. dbSNP is useful for submitted sequence variation identifiers; ClinVar aggregates assertions about variant-disease relationships; RefSeq and the MANE collaboration stabilize the transcript and protein reference used for HGVS naming. A report-ready variant claim should include the rsID or ClinVar Variation ID when applicable, the RefSeq/MANE accession used for nomenclature, review status, and the evidence category rather than equating “listed variant” with “pathogenic variant” [National Center for Biotechnology Information, 2026b,a,d,c].

Translation evidence has separate ledgers as well. ClinicalTrials.gov records protocol, recruitment, and submitted-results status, while FDA product pages and approval materials determine approved indications. Casgevy and Lyfgenia are therefore best compared as distinct approved sickle-cell therapies with different molecular strategies: CRISPR-Cas9 enhancer editing for Casgevy and lentiviral gene addition for Lyfgenia [National Library of Medicine, 2026, U.S. Food and Drug Administration, 2026a,c].

Source practice: For mutation, genomics, and editing claims, distinguish discovery from clinical actionability, and cite reference resources, regulatory records, or primary editing studies close to the claim [Human Pangenome Reference Consortium, 2023, U.S. Food and Drug Administration, 2026a, Chalumeau et al., 2025].

14.14.1 Current Evidence Map: Genome Editing From Variant to Follow-Up



Figure 97. Casgevy and prime-editing examples show why editing medicines require molecular endpoints, structural-variant surveillance, toxicity monitoring, and long follow-up [fda2026casgevy,chalumeau2025primeediting].

14.15 Summary

- Mutations range from single nucleotide changes (transitions, transversions, silent, missense, nonsense) to large chromosomal rearrangements (deletions, duplications, inversions, translocations). Frameshifts and nonsense mutations are typically most disruptive.
- Mutagenic agents include UV radiation (CPDs), alkylating agents (EMS), intercalators (ethidium bromide), and ROS (8-oxoG). The Ames test screens chemicals for mutagenicity.
- DNA repair: BER (damaged bases), NER (bulky adducts), MMR (mismatches), NHEJ/HR (DSBs), Fanconi pathway (interstrand crosslinks). Defects cause cancer predisposition (XP, Lynch syndrome, BRCA-associated cancers, Fanconi anemia).
- CRISPR-Cas9: sgRNA + Cas9 creates DSB at PAM-adjacent site; NHEJ for knockouts, HDR for precise edits. Base editors (C-to-T, A-to-G) and prime editors avoid DSBs. First approved therapy: Casgevy (sickle cell disease via BCL11A disruption).
- Human genome: about 3.2 Gb; about 20,000 protein-coding genes (1.5%); 46% transposable elements; ENCODE shows >80% has biochemical activity. T2T consortium completed gapless reference (2022).
- NGS technologies: Illumina (short-read, high throughput), PacBio HiFi and Nanopore (long-read, structural variant resolution).
- GWAS: Identify SNP-trait associations at genome-wide significance ($p < 5 \times 10^{-8}$); most complex trait variants have small effect sizes; results displayed on Manhattan plots.

- Ethics: GINA Act protections, pharmacogenomic testing (CYP2D6, warfarin dosing), BRCA testing decisions, germline editing moratorium.
- Connections: See section 12 for repair pathways, **Unit V — Classical Genetics and Heredity: Introduction** for inheritance of variants, and **Unit VII — Microbiology: Introduction** for CRISPR origins in bacterial immunity.

14.16 Review Questions

1. Distinguish between transitions and transversions. Which is more common and why?
2. Explain why frameshift mutations are generally more deleterious than missense mutations. Give an exception where a missense mutation is highly pathogenic.
3. A patient has microsatellite instability in their colorectal tumor. What DNA repair pathway is likely defective? Name the genes involved.
4. Describe the CRISPR-Cas9 mechanism step by step, from guide design to DSB repair.
5. Compare base editing and prime editing. When would you choose each technology?
6. What is the “end-replication problem” of the Human Genome Project, and how did the T2T consortium solve it?
7. Explain GWAS methodology. Why does a Manhattan plot show peaks, and what does a significant peak mean?
8. What is linkage disequilibrium, and why is it important for interpreting GWAS results?
9. Describe the pharmacogenomic basis for warfarin dose variation. Which genes are involved?
10. Discuss the ethical issues raised by the He Jiankui CRISPR babies case. What international guidelines exist for germline editing?
11. Explain why a SNP in a splice donor can have larger effect sizes than a missense change in the same exon, using NMD concepts.
12. A GWAS hit lies in intronic sequence with no coding change. Propose two mechanistic classes of causal variants compatible with that pattern.

14.17 Further Reading and Source Notes: Mutations, CRISPR, and Genomics

- Ohno (1970). *Evolution by Gene Duplication*. Springer-Verlag.
- Doudna & Charpentier (2014). The new frontier of genome engineering with {CRISPR-Cas9}. *Science*, 346.
- Lander et al. (2001). Initial sequencing and analysis of the human genome. *Nature*, 409.
- Richards et al. (2015). Standards and guidelines for the interpretation of sequence variants: ACMG/AMP consensus recommendation. *Genetics in Medicine*, 17.
- Alexandrov et al. (2013). Signatures of mutational processes in human cancer. *Nature*, 500.

14.18 Key Terms

1. Transition – purine-to-purine or pyrimidine-to-pyrimidine point mutation
2. Transversion – purine-to-pyrimidine (or reverse) point mutation
3. Frameshift mutation – insertion/deletion not a multiple of 3 bp, altering reading frame
4. Nonsense-mediated decay (NMD) – mRNA surveillance pathway eliminating transcripts with premature stop codons
5. Trinucleotide repeat expansion – unstable repeat growth causing anticipation in diseases like Huntington
6. Ames test – bacterial mutagenicity assay using histidine-requiring Salmonella revertants
7. CRISPR-Cas9 – RNA-guided endonuclease for programmable genome editing
8. PAM (protospacer adjacent motif) – short DNA sequence (NGG for SpCas9) required for Cas9 binding
9. Base editor – dCas9/nickase fused to deaminase for C-to-T or A-to-G conversion without DSB
10. Prime editor – Cas9-nickase + reverse transcriptase + pegRNA for search-and-replace editing
11. GWAS (genome-wide association study) – unbiased scan for SNP-trait associations across the genome
12. Linkage disequilibrium – non-random association of alleles at nearby loci
13. Manhattan plot – genome-wide visualization of association p-values
14. Pharmacogenomics – study of genetic variation affecting drug response
15. ENCODE – Encyclopedia of DNA Elements; mapped functional elements across the human genome
16. Copy number variant (CNV) – duplication or deletion of a genomic segment >1 kb
17. Synthetic lethality – cell death from simultaneous loss of two compensatory pathways

14.19 Companion Source Module: Mutations, CRISPR, and Genomics

Mutations, CRISPR, and Genomics should leave a reproducible trail from a biological claim to the code, figure, diagram, or paper-based activity that can test it. Use the surfaces below to inspect the chapter’s assumptions, rerun the relevant model, or compare the manuscript explanation with companion labs and figures.

Table 223. Companion source surfaces for Mutations, CRISPR, and Genomics.

Surface	Use it for
src/biology/genetics/genetics.py (dna_complement, translate_mrna, hamming_distance, jukes_cantor_distance)	Compare sequence variants, coding effects, and corrected molecular distances.
src/mermaid/biology_diagrams.py (transcription_translation_diagram, dna_replication_diagram)	Link mutation class to replication and expression context.

Reproducibility check: distinguish discovery technology, reference representation, variant class, evidence level, and clinical actionability. Cross-reference: connect with section 12, section 13, and section 24.

15 Chromatin and Epigenetic Mechanisms

Level 3/3 · 28 min read · 40 min lecture · Prerequisites: section 13

15.1 Learning Objectives

1. Define **epigenetics** and distinguish epigenetic modifications from DNA sequence changes.
2. Describe **nucleosome** structure and the levels of **chromatin** compaction from the 11-nm fiber to the metaphase **chromosome**.
3. Explain the major classes of **histone** modifications (acetylation, methylation, phosphorylation, ubiquitination, sumoylation) and how they are written, erased, and read.
4. Describe the mechanism and function of DNA methylation, including **CpG islands**, the DNMT1/3A/3B **enzymes**, TET-mediated demethylation, and the role of methylation in **gene** silencing.
5. Distinguish Polycomb (PRC1/PRC2) and Trithorax (MLL/COMPASS) systems and explain how they maintain repressive and activating states.
6. Compare ATP-dependent chromatin remodeling families (SWI/SNF, ISWI, CHD/NuRD, INO80) and their distinct mechanisms.
7. Explain X-chromosome inactivation (Lyonization) and the role of the XIST lncRNA, escape genes, and skewing.
8. Describe genomic imprinting using IGF2/H19 and Prader-Willi/Angelman as paradigms.
9. Explain how 3D genome organization — TADs, loops, compartments, and biomolecular condensates — shapes transcription.
10. Explain microRNA (miRNA [Fire et al., 1998]) biogenesis and the mechanism of RISC-mediated post-transcriptional silencing.
11. Model the maintenance of DNA methylation and Polycomb marks across cell divisions quantitatively, and predict the consequences of perturbing each layer.
12. Evaluate evidence for transgenerational epigenetic inheritance in humans, the mechanism of mitotic and meiotic transmission of epigenetic marks, and the clinical implications of epigenetic dysregulation in cancer and neurodevelopmental disease.

15.1.1 Study Blueprint

- Big idea: Cells create stable yet reversible expression states through chromatin, DNA marks, and regulatory circuits.
- Core concepts: chromatin, methylation, histone modification, enhancers.
- Framework alignment: Vision & Change: Information flow, exchange, and storage, Structure and function; AP Biology: Information Storage and Transmission, Systems Interactions; NGSS-style topics: Inheritance and Variation of Traits, Structure and Function.
- Model or quantitative lens: Regulatory-state and expression-ratio reasoning.
- Data skill: Interpret chromatin or expression evidence from simple regulatory datasets.
- Practice cadence: Concept Explanation, Questions and Methods, Argumentation.
- Common misconception to repair: Epigenetic does not mean independent of DNA sequence or permanently inherited.
- Primary lab: **Lab — Chromatin and Epigenetic Mechanisms**.
- Question bank: **Questions — Chromatin and Epigenetic Mechanisms**.
- Transfer task: Apply regulation logic to differentiation, imprinting, cancer, or environmental responses.
- Bridge to computation: `biology.genetics.genetics.cpg_methylation_remaining`.

Opening Vignette — The Landscape That Changed Genetics

In 1942, the developmental biologist Conrad Waddington drew a diagram that would define a science. He sketched a marble rolling down a hillscape of ridges and valleys — each valley representing a stable cell fate, each ridge a threshold that once crossed was difficult to reverse. He called this the epigenetic landscape: the topology of developmental possibilities. Waddington coined “epigenetics” from the Greek *epi-* (above) to describe the heritable changes in gene expression that occurred *above* or *beyond* the DNA sequence — changes that could not be explained by Mendelian genetics alone. He had no idea of the molecular mechanisms. That understanding would come forty years later.

In 1961, Mary Lyon [Lyon, 1961] noticed something peculiar in female mice **heterozygous** for coat-color **mutations**: their fur was a mosaic, not intermediate. She proposed that in every cell of a female mammal, one of the two X chromosomes is randomly and permanently silenced — a hypothesis proven so thoroughly that it was renamed Lyonization. The silenced X does not have a different DNA sequence. It has a different *chemistry*: dense methylation, hypoacetylated histones, and a long non-coding RNA called XIST that coats the entire chromosome. This was the first clear demonstration that a whole chromosome could be heritably silenced without changing a single base pair. Epigenetics had found its molecular identity.

Three more revolutions followed. In 2000, Strahl and Allis [Strahl and Allis, 2000] proposed that distinct combinations of histone modifications — a “histone code” — encode regulatory information beyond the DNA sequence itself, predicting an entire pharmacology of writers, erasers, and

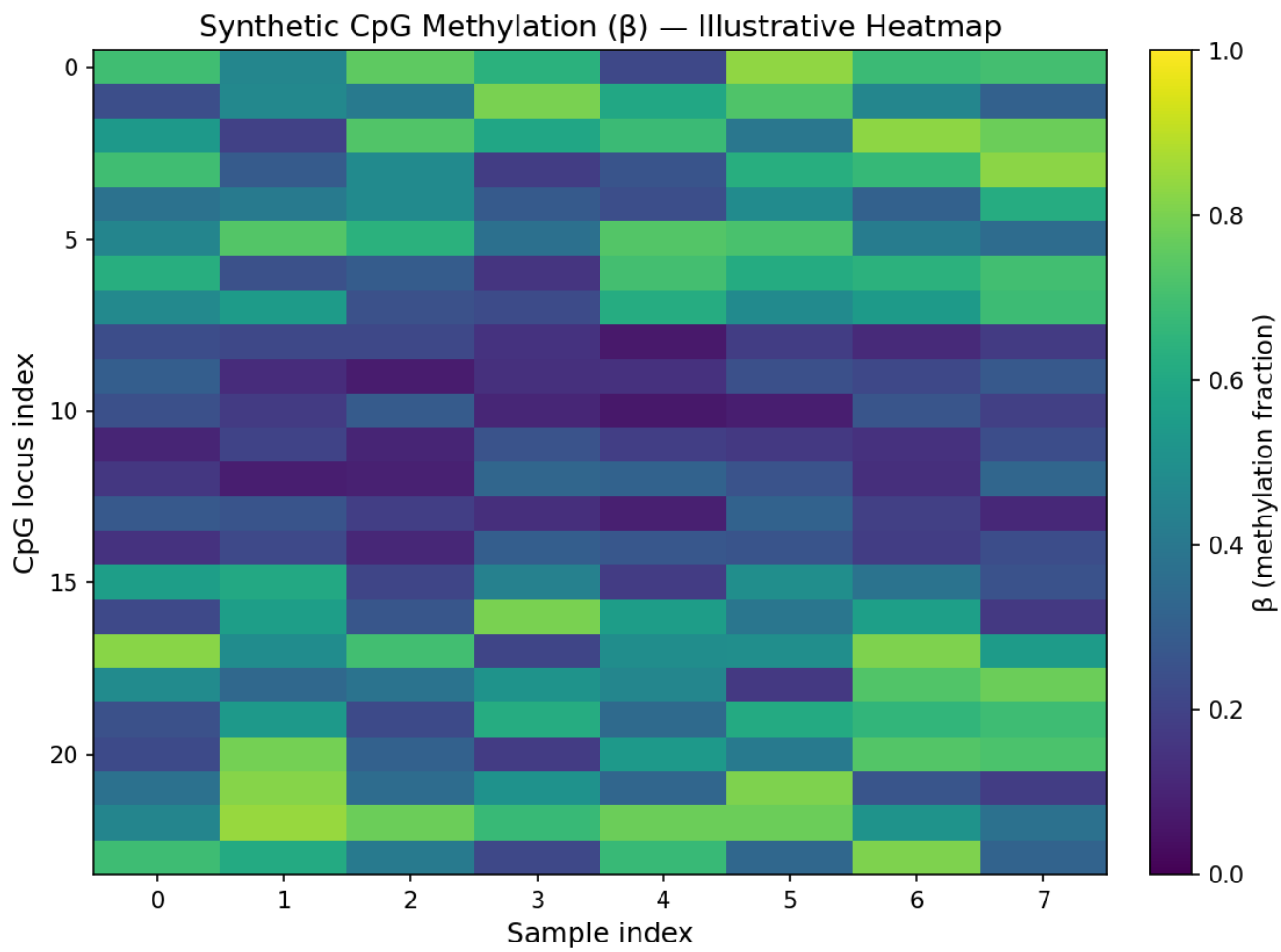


Figure 98. Illustrative synthetic CpG methylation heatmap across indexed loci (rows) and indexed samples (columns). The color scale reports beta methylation fraction from 0 to 1; the lower-methylation row band is a deterministic teaching pattern, not patient or cell-line data.

readers that has now produced FDA-approved drugs. In the 2000s, chromosome-conformation-capture (Hi-C) revealed that the genome is folded into stereotyped contact domains (TADs) where enhancers find their cognate promoters, and that disrupting these domains can mis-wire developmental control. And in the 2010s, biomolecular condensates and phase separation reframed the nucleus as a collection of liquid-like assemblies that concentrate transcriptional machinery at super-enhancers. These insights together turned epigenetics from a metaphor into a quantitative, druggable discipline.

15.2 Chromatin Structure and Nucleosome Organization

15.2.1 The Nucleosome as the Fundamental Chromatin Unit

Eukaryotic DNA is not naked; it is complexed with proteins to form chromatin. The fundamental repeating unit is the nucleosome:

- Histone octamer: 2 copies each of H2A, H2B, H3, H4 — forming a spool-like protein disk
- DNA wrapping: about 147 bp of DNA wound 1.65 times around the histone octamer in a left-handed superhelix
- Linker DNA: 10–80 bp connecting adjacent nucleosomes; associated with histone H1
- Bead-on-a-string: nucleosomes connected by linker DNA form an 11-nm fiber — the first level of compaction

Core histone structure: Each core histone has: - A globular domain forming the nucleosome disc surface through the histone fold motif (three α -helices linked by two short loops; pairs of histones form four-helix bundles: H3–H4 and H2A–H2B) - An unstructured N-terminal tail extending beyond the disc (4–35 residues depending on histone) — this is where most post-translational modifications occur - A short C-terminal tail (especially prominent on H2A and H2B) that also accepts modifications including ubiquitination

Histone variants: In addition to canonical H2A/H2B/H3/H4, mammalian cells express variant histones that confer specialized properties on chromatin where they are deposited:

Table 224. The Nucleosome as the Fundamental Chromatin Unit: Variant and Replaces.

Variant	Replaces	Deposition machinery	Function
H3.3	H3	HIRA (gene bodies); ATRX/DAXX (heterochromatin)	Replication-independent; marks transcribed/active regions
CENP-A (CenH3)	H3	HJURP	Centromere identity; foundation for kinetochore assembly
H2A.Z	H2A	SRCAP, INO80/SWR1	Promoter-proximal; poises genes for activation; insulates from heterochromatin
H2A.X	H2A	RAD51 / S139ph at DSBs	DNA-damage signaling (γ H2AX); foci visible by immunofluorescence
macroH2A	H2A	ATRX-dependent	Inactive X enrichment; gene silencing
H2A.B (Bbd)	H2A	unclear	Active transcription; testis enriched

15.2.2 Higher-Order Chromatin Compaction

Table 225. Higher-Order Chromatin Compaction: Level and Structure.

Level	Structure	Diameter	Compaction factor	Mechanism
0	Naked DNA (B-form helix)	2 nm	1×	Watson–Crick base-pairing
1	Nucleosome fiber (“beads on a string”)	11 nm	about 6×	Histone octamer wrapping

Level	Structure	Diameter	Compaction factor	Mechanism
2	30-nm fiber (disputed <i>in vivo</i>)	30 nm	about 40×	Nucleosome–nucleosome compaction
3	Chromatin loops / TADs	300 nm	about 1,000×	CTCF + cohesin-defined loops; TADs
4	A/B compartments	—	variable	Active (A) vs. repressive (B) genomic neighborhoods
5	Chromatid (mitotic chromosome)	700 nm	about 10,000×	SMC condensin-mediated compaction

15.2.3 Topologically Associating Domains (TADs)

Chromatin organizes into DNA loops of 100 kb–1 Mb delineated by CTCF (insulator protein) binding sites and cohesin ring complexes. Within TADs, enhancers preferentially contact **promoters** of the same TAD. TAD boundaries are largely conserved across cell types and species. The dominant model for TAD formation is loop extrusion: cohesin loads on chromatin and reels DNA through its ring lumen ATP-dependently until it stalls at convergently oriented CTCF binding sites, leaving behind a chromatin loop. Quantitatively, mammalian genomes contain about 3,000–10,000 TADs (about 1 Mb median), and knockdown of CTCF or cohesin (RAD21, NIPBL) blurs or abolishes most boundaries within hours.

$$P_{\text{contact}}(s) \propto s^{-\alpha}, \quad \alpha \approx 1.0\text{--}1.2 \text{ for fractal globule (interphase)}$$

(219)

Hi-C methodology in detail. Hi-C is a chromosome-conformation-capture variant that measures contact frequency between every pair of genomic loci genome-wide. The protocol:

1. Cross-link chromatin with formaldehyde (1 % for 10 min), preserving protein-mediated DNA contacts.
2. Restriction digest with a 4-cutter (DpnII, MboI) or 6-cutter (HindIII), creating sticky-ended fragments still tethered by cross-linked proteins.
3. Fill-in with biotinylated nucleotides to mark cleaved ends, then proximity ligate at low DNA concentration so that intermolecular ligations are improbable — primarily fragments held together by cross-linked proteins (i.e., physically proximal *in vivo*) ligate.
4. Streptavidin pulldown enriches biotinylated junction reads, paired-end Illumina sequencing identifies which genomic loci were joined.
5. Heatmap normalization (ICE, KR-balanced) yields a contact matrix; diagonal-rich blocks are TADs; off-diagonal stripes identify loop anchors at convergent CTCF.

Derivative methods refine the assay: Micro-C uses MNase digestion to nucleosome resolution; Capture-Hi-C enriches for promoter-anchored contacts (4DN consortium); HiChIP / PLAC-seq combines ChIP for an active mark (H3K27ac) with proximity ligation; ChIA-PET uses paired-end tagging on antibody-immunoprecipitated chromatin; Hi-C 3.0 / Pore-C uses long-read multi-way contact mapping.

Disruption of TAD boundaries (e.g., by large deletions, inversions, or single-nucleotide CTCF site disruptions) can cause misregulation of developmental genes — a mechanism termed enhancer hijacking. Lupiáñez et al. (2015) showed that microdeletions removing TAD boundaries near *EPHA4* fuse adjacent regulatory landscapes, mis-targeting limb enhancers to *PAX3* or *WNT6* and producing congenital limb malformations (brachydactyly, syndactyly).

Loop extrusion — the dynamic model. Single-molecule imaging and live-cell Hi-C now support a kinetic loop-extrusion model with quantitative parameters: - Cohesin (SMC1/SMC3 + RAD21/SCC1 + STAG1/STAG2) is loaded onto chromatin by NIPBL/MAU2 (the loader complex). - It extrudes DNA into a growing loop at about 0.5–2 kb/s, consuming ATP at the SMC ATPase head. - WAPL unloads cohesin (residence time about 20 min unloaded by WAPL, vs. > 1 h for the cohesin-STAG2 “stalled” form at CTCF anchors). - CTCF binds asymmetrically (a 19-bp consensus with a defined orientation): convergent CTCF pairs trap extruding cohesin, generating loops with measured loop sizes about 100 kb to 2 Mb. - Acute auxin-induced degron depletion of RAD21 dissolves most loops within about 15 min; restoration takes about 30–60 min — confirming that TADs and loops are dynamic, not static structures.

15.2.4 A/B Compartments

At the megabase scale, the genome partitions into two interaction “compartments”:

- A compartment — gene-rich, active (H3K4me3, H3K27ac, accessible chromatin), positioned toward the nuclear interior
- B compartment — gene-poor, repressed (H3K9me3, lamina-associated), positioned at the nuclear periphery

Compartment switching during cell-fate transitions correlates with replication timing changes (early-replicating ↔ late-replicating) and with large-scale gene expression remodeling. Hi-C (and its derivatives Micro-C, Capture-Hi-C, ChIA-PET) measures these contacts genome-wide.

Concept Check 1: A patient harbors a balanced inversion that breaks a CTCF site at the boundary of a TAD containing the *SHH* limb enhancer (ZRS, about 1 Mb upstream of *SHH*). Predict the developmental phenotype if the inversion places ZRS into a TAD containing an unrelated proto-oncogene. What chromosome-conformation-capture experiment would confirm enhancer hijacking?

15.3 Histone Modifications — The Histone Code

Histone tails are subject to a large number of post-translational modifications (PTMs). The **histone code** hypothesis [Strahl and Allis, 2000] proposes that specific combinations of marks specify distinct chromatin states and downstream outcomes.

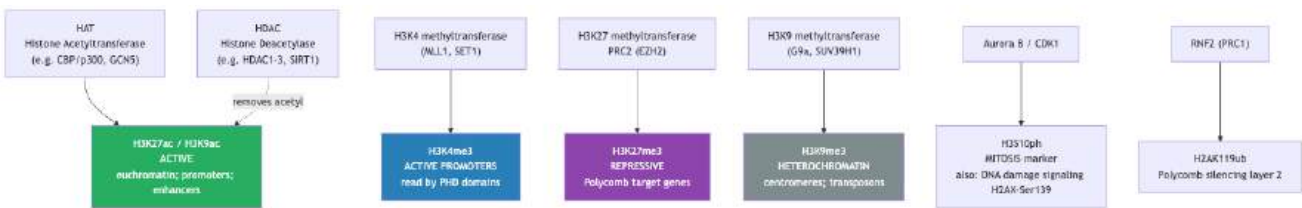


Figure 99. Histone modification writers and the states they produce. Green = active marks; blue = active promoters; purple = Polycomb repression; gray = constitutive heterochromatin.

15.3.1 Histone-Code Reference Table

The histone-code reference table below systematically catalogs > 25 modifications recurrently studied in mammalian chromatin biology, paired with the writer enzyme, eraser enzyme, reader domain that recognizes the mark, the histone position (nucleosome face, exposed N-terminal tail, C-terminal tail), the typical genomic location, and the functional effect (activation, repression, or context-dependent). This is the chromatin biologist’s periodic table — the working vocabulary of writers, readers, and erasers that defines every targeted therapy in clinical epigenetics.

Active methylation marks

Table 226. Histone-Code Reference Table: Mark and Writer / eraser.

Mark	Writer / eraser	Main readers	Meaning
H3K4me1	MLL3/4 writes; LSD1 erases	BAF45c PHD, CHD7	Poised or active enhancers
H3K4me2	MLL1/2 and SET1 write; LSD1 erases	CHD1, BPTF PHD	Active promoters and 5-prime gene bodies
H3K4me3	MLL/SET1 COMPASS writes; KDM5 removes	TAF3 PHD, ING1, BPTF	Active promoters; recruits TFIID
H3K36me1/2	NSD and ASH1L write; KDM2 removes	LEDGF PWWP, MRG15	Gene bodies and active enhancers
H3K36me3	SETD2 writes; KDM2/KDM4 remove	DNMT3 PWWP, MRG15, LEDGF	Transcribed gene bodies; suppresses cryptic initiation and recruits MMR
H3K79me2/3	DOT1L writes	53BP1 Tudor, AF9, ENL	Active gene bodies; important in MLL-fusion leukaemia

Active acetylation and ubiquitination marks

Table 227. Histone-Code Reference Table: Mark and Writer / eraser.

Mark	Writer / eraser	Main readers	Meaning
H3K9ac	GCN5/PCAF/p300 write; HDAC1-3 and SIRT1/6 erase	BRD4, TAF1	Active promoters; loosens histone-DNA contacts
H3K14ac	GCN5/PCAF write; HDAC1-3 erase	Bromodomains	Active promoters; cooperates with H3K4me3
H3K18ac and H3K23ac	p300/CBP write; HDACs erase	Bromodomains	Promoters and enhancers; active transcription
H3K27ac	p300/CBP write; HDAC1-3 erase	BRD4, YEATS	Active enhancers and super-enhancers
H3K56ac	p300/CBP write; HDAC1/SIRT1/SIRT6 erase	no dominant reader	Newly synthesized H3; chromatin assembly
H4K5ac, H4K8ac, H4K12ac	HAT1/p300/CBP write; HDACs erase	Bromodomains	Replication-coupled H4 deposition
H4K16ac	MOF writes; SIRT1/2 erase	context-dependent	Disrupts 30-nm fiber compaction; active gene bodies
H2BK120ub	RNF20/40 writes; USP22 erases	crosstalk readers	Required for H3K4me3 and H3K79me deposition

Repressive methylation and Polycomb marks

Table 228. Histone-Code Reference Table: Mark and Writer / eraser.

Mark	Writer / eraser	Main readers	Meaning
H3K9me1	G9a/GLP/SETDB1 write; KDM3 removes	weak / context-dependent	Active gene bodies; cooperates with elongation marks
H3K9me2	G9a/GLP write; KDM3/LSD1 remove	HP1, CDYL	Facultative heterochromatin and silenced euchromatin
H3K9me3	SUV39H and SETDB1 write; KDM4 removes	HP1 alpha/beta/gamma, CBX1/3/5	Constitutive heterochromatin; centromeres; transposons
H3K27me1/2	EZH2 writes; UTX/JMJD3 remove	EED for me2/3 contexts	Active gene bodies at low level; me2 prevents inappropriate enhancer activation
H3K27me3	EZH2/PRC2 writes; UTX/JMJD3 remove	EED and CBX-PRC1	Polycomb domains; developmental-gene repression
H4K20me3	SUV4-20H writes; PHF8 erases	53BP1 Tudor	Pericentric heterochromatin and DNA-damage response
H2AK119ub	RNF2/RING1B writes; BAP1 removes	JARID2-associated PRC2.2	Stable Polycomb silencing layer

Dynamic damage, cell-cycle, and metabolic marks

Table 229. Histone-Code Reference Table: Mark and Writer / eraser.

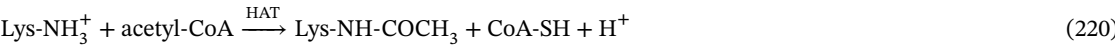
Mark	Writer / eraser	Main readers	Meaning
H3S10ph	Aurora B/MSK write; PP1/PP2A erase	14-3-3 proteins	Mitosis and immediate-early gene activation
H3T3ph	Haspin writes; PP1 erases	Survivin/CPC	Inner-centromere recruitment during mitosis
H2A.X-S139ph (gamma-H2AX)	ATM/ATR/DNA-PK write; PP2A/WIP1 erase	MDC1 BRCT	Double-strand-break signaling foci
H3T6ph	PRK1 writes; PP1 erases	context-dependent	Androgen-receptor targets; H3K4 demethylation crosstalk
H4K12su and H2BK34su	PIAS/MMS21 write; SENP erases	SIM-containing readers	Polycomb and DNA-damage coordination
H2A/H4 ADP-ribosylation	PARP1/2 write; PARG/ARH3 erase	Macrodomain proteins	Chromatin relaxation for DNA repair
H3K18la	p300 writes; HDAC1-3 erase	YEATS domains	Lactate-linked macrophage polarization
H3K9bhb	p300 writes; HDAC1-3 erase	YEATS domains	Ketosis and fasting response
H3K9cr, H3K9su, H3K4but	p300 or metabolic enzymes write; HDAC/sirtuin systems erase	YEATS-family readers	Metabolism-linked activation in enhancers, promoters, and gametogenesis

The bottom rows reflect a major recent expansion of the histone code: short-chain acyl-CoAs derived from intermediary metabolism (lactate, β -hydroxybutyrate, crotonyl-CoA, succinyl-CoA, butyryl-CoA) are deposited by the same KAT/HAT enzymes (especially p300) that write acetyl marks, directly coupling metabolic state to chromatin state. The lactyl mark, in particular, has become the molecular signature of the Warburg-effect–polarized tumor-associated macrophage.

15.3.2 Histone Acetylation and Open Chromatin

Writers: Histone acetyltransferases (HATs) — CBP/p300, GCN5/PCAF, TIP60, MOF. Erasers: Histone deacetylases (HDACs) — 18 human HDACs in four classes (Class I/II/III/IV, where Class III = NAD⁺-dependent sirtuins SIRT1–7). Readers: Bromodomains (e.g., BRD4, TFIID subunit TAF1, BAF180 of PBAF, BPTF). YEATS domains (AF9, ENL) read both acetyl and longer acyl marks.

Mechanism: Acetylation of lysine ϵ -amino groups by transfer from acetyl-CoA. Neutralizes the positive charge on lysine, weakening histone–DNA electrostatic interactions, loosening chromatin and facilitating transcription factor binding.



Key active marks: - H3K27ac: Marks active enhancers (distinguishes active from poised enhancers, which carry H3K27me3) - H3K9ac, H3K14ac, H4K16ac: Found at active promoters and transcribed gene bodies

Clinical Connection — HDAC inhibitors (full clinical profile): Histone deacetylase inhibitors (HDACi) are FDA-approved anticancer drugs. - Vorinostat (SAHA) — FDA approved 2006 for cutaneous T-cell lymphoma (CTCL). Hydroxamate pan-HDACi. Median time to response about 2 months; objective response about 30 %. - Romidepsin (Istodax) — FDA approved 2009 for CTCL and 2011 for peripheral T-cell lymphoma. Cyclic depsipeptide; class-I selective. Distinct dose-limiting toxicities (GI, fatigue, thrombocytopenia). - Panobinostat (Farydak) — FDA approved 2015 for relapsed/refractory multiple myeloma in combination with bortezomib + dexamethasone. Pan-HDACi; superior CD138+ plasma-cell apoptosis when combined with proteasome inhibitor. - Belinostat (Beleodaq) — FDA 2014 for PTCL. - Tucidinostat (Chidamide) — China-approved 2014 for PTCL; first benzamide HDACi.

Mechanism in cancer: re-activation of silenced tumor-suppressor genes (p21, gelsolin, RhoB, BCL6); accumulation of acetylation on non-histone targets (HSP90 chaperone client release, p53 stabilization, NF-κB inhibition). Combination with DNMT inhibitors is being explored to reverse layered silencing, a theme developed later in the cancer-epigenetics discussion.

15.3.3 Histone Methylation and Context-Dependent Silencing or Activation

Writers: Histone methyltransferases (HMTs) — most contain SET domains (except DOT1L, which has a 7β-strand methyltransferase fold derived from class V methyltransferases). Erasers: Histone demethylases — KDM1/LSD1 (FAD-dependent; works on me1 and me2 primarily; cannot demethylate me3 because it requires a free lysine ε-amino lone pair); KDM2–7 (Jumonji-domain, Fe(II)/αKG-dependent; can remove me3 by hydroxymethyl-amine intermediate that decomposes to formaldehyde and demethylated lysine). Readers: Chromodomains (HP1 reads H3K9me3; CBX2/4/6/7/8 of PRC1 read H3K27me3); PHD fingers (TAF3, BPTF, ING proteins read H3K4me3); Tudor domains (53BP1 reads H4K20me2; SMN reads symmetrical R-methylation); MBT domains; WD40 (EED reads H3K27me3); PWWP domains (read H3K36me3).

Unlike acetylation (typically activating), methylation is context-dependent: the same modification on different residues has opposite effects.

Table 230. Histone Methylation and Context-Dependent Silencing or Activation: Mark and Enzyme.

Mark	Enzyme	State	Function
H3K4me1	MLL3/4	Active	Enhancer elements (poised or active)
H3K4me3	MLL1/SET1	Active	Active promoters; read by TAF3 PHD
H3K36me3	SETD2	Active	Transcribed gene bodies; prevents cryptic initiation
H3K27me3	EZH2 (PRC2)	Repressive	Polycomb targets; poised/silent developmental genes
H3K9me3	SUV39H1/H2	Repressive	Constitutive heterochromatin; centromeres; transposons
H4K20me3	SUV4-20H	Repressive	Pericentric heterochromatin; DNA damage response

Bivalent domains: In embryonic stem cells, many developmental gene promoters carry both H3K4me3 and H3K27me3 simultaneously — a “bivalent” state. These genes are poised for either rapid activation (upon H3K27me3 removal by KDM6A/UTX) or repression (upon H3K4me3 removal) during differentiation. About 2,500 promoters are bivalent in human ES cells; most resolve to monovalent during lineage commitment.

15.3.4 Phosphorylation and Ubiquitination

H3S10ph (H3 Ser10 phosphorylation): - Writer: Aurora B kinase (mitosis), MSK1/2 (mitogenic signaling) - Function: Chromosome condensation during mitosis; gene activation by 14-3-3 reader binding

H2AX-S139ph (γH2AX): - Writer: ATM/ATR kinases at double-strand breaks - Function: Marks DSB sites; recruits MDC1 and DNA repair machinery; visible as bright immunofluorescence foci at break sites

H2AK119ub (H2A monoubiquitination): - Writer: RNF2/RING1B (part of PRC1 complex) - Function: Represses transcription elongation; part of Polycomb silencing; read by Polycomb-like proteins

Concept Check 2: A cancer-associated EZH2 gain-of-function mutation leads to genome-wide hypermethylation of H3K27 and silencing of tumor-suppressor genes. To what extent would an HDAC inhibitor (which increases histone acetylation) be expected to re-activate these silenced loci? Explain by reference to the dependencies between acetylation, methylation, and DNA methylation described above — and argue for a rational combination therapy.

Concept Check 3: Predict the genome-wide consequence of a homozygous knockout of SETD2 (the H3K36me3 writer) in an embryonic stem cell. Consider effects on (i) cryptic intragenic transcription, (ii) DNA mismatch repair recruitment, and (iii) DNMT3B-mediated gene-body methylation. Which of these phenotypes most directly explains why SETD2 loss-of-function is the most frequent driver mutation in clear-cell renal cell carcinoma after VHL?

15.4 Polycomb and Trithorax — Cellular Memory Systems

The Polycomb (PcG) and Trithorax (TrxG) group proteins were discovered in *Drosophila* as gene families whose loss-of-function alleles cause homeotic transformations of body segments. They constitute the cell’s principal cellular memory systems: once a developmental gene is set ON or OFF in a progenitor, PcG/TrxG complexes propagate that state through most subsequent mitotic divisions of the lineage.

15.4.1 Polycomb Repressive Complexes — Structural Detail

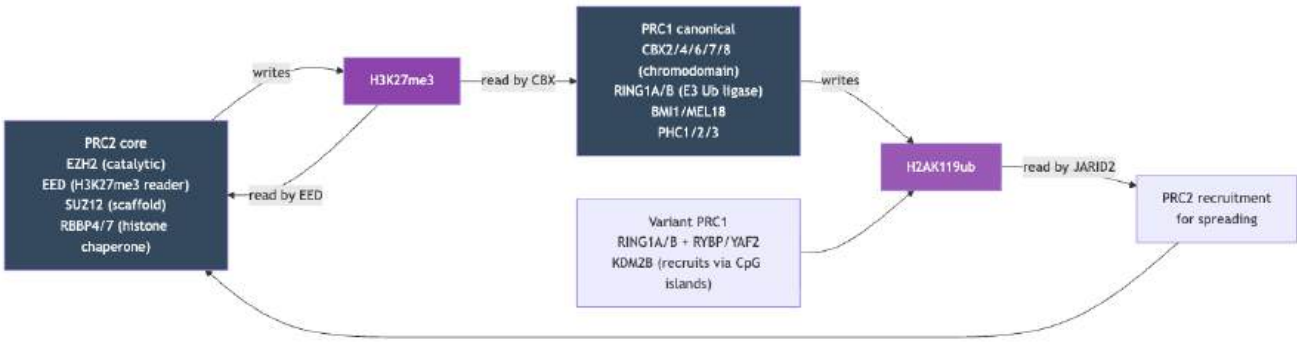


Figure 100. Polycomb silencing operates as a feedback-amplified two-mark system: PRC2 writes H3K27me3, which recruits more PRC2 (positive feedback) and recruits canonical PRC1 (via CBX) which writes H2AK119ub. Variant PRC1 acts upstream at unmethylated CpG islands and seeds H2AK119ub which itself recruits PRC2. The mutual reinforcement explains how Polycomb domains span hundreds of kilobases and persist through cell divisions.

PRC1 — comprehensive subunit inventory: - Catalytic core: RING1A (RNF1) or RING1B (RNF2) E3 ubiquitin ligase + a PCGF partner (PCGF1, PCGF2/MEL18, PCGF3, PCGF4/BMI1, PCGF5, PCGF6). - Canonical PRC1 (cPRC1): RING1A/B + PCGF2/4 (MEL18/BMI1) + a CBX (CBX2/4/6/7/8) chromobox subunit + PHC1/2/3 + SCM1/L2. The CBX chromodomain reads H3K27me3, anchoring cPRC1 onto Polycomb-marked chromatin. PHC SAM-domain polymerization drives chromatin compaction in cis (head-to-tail oligomerisation creates a phase-separated Polycomb body). - Variant PRC1 (vPRC1): RING1A/B + PCGF1/3/5/6 + RYBP (or YAF2) instead of CBX. Recruited to unmethylated CpG islands via KDM2B (PCGF1 complex, “ncPRC1.1”) or via E2F6 (PCGF6). Deposits H2AK119ub *upstream* of H3K27me3 — a key insight: vPRC1 acts first, then PRC2.2 reads H2AK119ub via JARID2.

PRC2 — comprehensive subunit inventory: - Catalytic core: EZH2 (or paralog EZH1; SET-domain methyltransferase). EZH2 is faster but EZH1 is dominant in non-dividing cells. - EED binds H3K27me3 product → allosteric activation of EZH2 (the read-write feedback that generates broad Polycomb domains). - SUZ12 scaffold links the SET-domain catalytic core to the DNA/RNA-recognition modules. - RBBP4/7 histone chaperone presents the H3 tail substrate. - Accessory subunits define context-dependent variants: - PRC2.1: PCL1/2/3 (PHF1, MTF2, PHF19) + EPOP or PALI1. The PHF Tudor domains read H3K36me3, restricting PRC2.1 from active gene bodies. - PRC2.2: AEBP2 + JARID2. JARID2 reads H2AK119ub deposited by variant PRC1 and stimulates PRC2 activity (closing the recruitment loop). - Reaction kinetics: $H3K27 \rightarrow H3K27me1$ ($k_1 \approx 0.05\text{ s}^{-1}$) $\rightarrow H3K27me2$ ($k_2 \approx 0.02\text{ s}^{-1}$) $\rightarrow H3K27me3$ ($k_3 \approx 0.005\text{ s}^{-1}$), with each step about 3-fold slower; EED-allosteric stimulation increases k_3 by about 6-fold on neighboring nucleosomes carrying me3. - Recruitment hierarchy: unmethylated CpG islands (via PRC2.2/JARID2 reading H2AK119ub from variant PRC1, *or* via PRC2.1/PCL with KDM2B); broad gene-body recognition by EED reading existing me3; lncRNA recruitment (HOTAIR, XIST repA, KCNQ1OT1, ANRIL).

Mechanism of Polycomb–Trithorax antagonism: PRC2.1 cannot act on H3K36-methylated chromatin (PCL Tudor reads H3K36me3 antagonistically — the CPL paradox). Conversely, ASH1L (the Trithorax-group H3K36 methyltransferase) deposits H3K36me2 at active gene bodies, blocking PRC2 spreading. The cell uses this as a positive/negative selection: H3K36me-active = Polycomb-restricted; H3K36me-absent = Polycomb-permissive.

15.4.2 Trithorax Group (TrxG) — Antagonising Polycomb

Table 231. Trithorax Group (TrxG) — Antagonising Polycomb: TrxG complex and Activity.

TrxG complex	Activity	Role
MLL/COMPASS family (MLL1–4, SET1A/B)	H3K4 methyltransferase	Marks active and poised promoters/enhancers
ASH1L	H3K36 methyltransferase	Antagonises Polycomb spread into active genes
KDM6A/UTX, KDM6B/JMJD3	H3K27me3 demethylases	Remove Polycomb marks during differentiation

TrxG complex	Activity	Role
SWI/SNF (BAF)	ATP-dependent remodeling	Evicts PRC1/2; opens chromatin

The COMPASS family — six MLL/SET1 complexes in mammals: - MLL1/KMT2A (mixed-lineage leukaemia 1) — large promoter H3K4me3 deposition; MLL1-AF4/AF9/ENL fusions cause infant acute lymphoblastic or acute myeloid leukaemia. - MLL2/KMT2B — closely related to MLL1; redundant at most loci; selective at others. - MLL3/KMT2C and MLL4/KMT2D — write enhancer H3K4me1 (poised and active enhancers); KMT2D is among the most frequently mutated chromatin-regulator genes in cancer (about 10 % of B-cell lymphoma and bladder cancer). - SET1A/KMT2F and SET1B/KMT2G — write the bulk of promoter H3K4me3 in adult tissues; SET1A loss-of-function in MDS and CHIP.

The six complexes share a WRAD module (WDR5–RbBP5–ASH2L–DPY30) that allosterically activates the SET-domain catalytic subunit by about 600-fold. This makes WRAD a tractable allosteric drug target — small-molecule WDR5–MLL interface inhibitors (OICR-9429) are in early-phase trials for MLL-rearranged leukaemia.

The Polycomb–Trithorax balance is maintained dynamically. Differentiation cues that activate gene expression typically deploy three concurrent steps: (i) UTX/JMJD3 removes H3K27me3, (ii) MLL/COMPASS deposits H3K4me3, and (iii) BAF complexes evict residual PRC1. Conversely, lineage repression deposits PRC1/PRC2 marks at the relevant promoter.

Clinical translation — EZH2 inhibitors: - Tazemetostat (Tazverik) is a small-molecule SET-domain inhibitor of EZH2, FDA-approved (2020) for epithelioid sarcoma (which loses INI1/SMARCB1 — a SWI/SNF subunit — and becomes hyper-dependent on EZH2 silencing) and EZH2-mutant follicular lymphoma. Mechanism: SAM-competitive small molecule occupies the EZH2 SET-domain pocket. Approved dose 800 mg BID PO. Median PFS in INI1-loss epithelioid sarcoma trial: 5.5 months vs 1.9 placebo; ORR 15 %. - Valemetostat (EZH1 + EZH2 dual inhibitor) was approved in 2022 in Japan for adult T-cell leukaemia/lymphoma (ATL); ORR 48 %. - Ivosidenib + tazemetostat combinations in IDH-mutant glioma are in trial, exploiting the IDH-mutant tumor’s dependence on Polycomb-driven differentiation block.

The mechanism is paradigmatic of synthetic lethality in chromatin: tumors with SWI/SNF loss become dependent on Polycomb silencing of cell-cycle inhibitors, so EZH2 inhibition selectively re-activates suppressors primarily in the cancer cells.

Worked Example 1 — Polycomb Spreading Model with Read-Write Feedback

Setup: A naive promoter has 2 nucleosomes carrying H3K27me3 (call this “seed”), recruiting PRC2 with EED-driven allosteric activation. PRC2 deposits H3K27me3 on the next nucleosome with rate constant k per generation. Each cell division dilutes existing H3K27me3 by half (passive demethylation through nucleosome turnover, since newly deposited histones at the replication fork are unmethylated). The gene body comprises 50 nucleosomes.

Question: Derive the steady-state H3K27me3 density along the gene body for $k = 1, 2$, and 5 marks per generation. What is the minimum k needed for the silencing mark to spread fully ($\geq 90\%$ of nucleosomes methylated)?

Solution: Let m_n be the average number of H3K27me3-marked nucleosomes at generation n , with $m_0 = 2$ (seed). Each generation: - Half of existing marks are passively diluted: $m_{\text{post-replication}} = m_n/2$. - PRC2 deposits k new marks at neighboring nucleosomes (read-write spreading): $m_{n+1} = m_n/2 + k$.

Steady-state when $m_\infty = m_\infty/2 + k$, so $m_\infty = 2k$ marked nucleosomes.

k (marks/gen)	Steady-state m_∞	Gene-body coverage
1	2	4 % (silencing fails)
2	4	8 %
5	10	20 %
25	50	100 % (saturated)
45	90	100 % (rapid saturation)

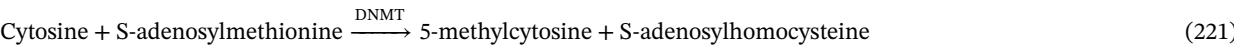
Insight: For full coverage of a 50-nucleosome gene body (≥ 45 marks at steady state), k must exceed about 22 marks per generation — i.e., PRC2 must deposit $> 11\times$ the seed quantity each cell cycle. This is achievable primarily with the EED–allosteric read-write loop: each existing H3K27me3 catalytically recruits more PRC2 to neighboring nucleosomes, creating positive feedback. Without this loop (e.g., in EED-mutant cells), Polycomb

domains collapse over a few divisions. This is why EED-binding small molecules (EED226, MAK683) are emerging as alternative EZH2-pathway inhibitors that disrupt the feedback loop selectively.

15.5 DNA Methylation and Stable Transcriptional Repression

15.5.1 CpG Methylation Mechanism

In mammals, DNA methylation occurs almost exclusively on cytosine in the context 5'-CpG-3' dinucleotides (the “p” denotes the phosphodiester bond between C and G). The methylated form is **5-methylcytosine (5mC)**, often called the “fifth base.”



15.5.2 The DNA Methylation Machinery — In Depth

Maintenance methyltransferase — DNMT1: the workhorse enzyme that ensures heritability of CpG methylation across cell divisions. - DNMT1 has a two-domain architecture: an N-terminal regulatory domain (containing CXXC, BAH1/2, and replication-foci targeting RFTS subdomains) and a C-terminal catalytic domain. - Substrate specificity: preferentially methylates hemi-methylated CpGs — sites where the parental strand carries 5mC but the newly synthesized daughter strand is unmethylated. Affinity for hemi-methylated CpGs is about 10–40-fold higher than for unmethylated CpGs. - Recruitment — the UHRF1–DNMT1 axis: the protein UHRF1 (“ubiquitin-like with PHD and RING finger domains 1”) is the molecular bridge that targets DNMT1 to replicating heterochromatin. UHRF1 has five domains: UBL (ubiquitin-like), TTD (Tudor — reads H3K9me2/3), PHD (reads unmethylated H3R2), SRA (reads hemi-methylated CpG via base-flipping), and RING (E3 ubiquitin ligase). The dual recognition of (a) hemi-methylated CpG (via SRA) AND (b) H3K9me2/3 (via TTD) ensures that DNMT1 propagates methylation primarily at chromatin states already marked for repression. - The mechanism cycle (per CpG): 1. UHRF1 SRA domain flips the 5mC out of the helix, exposing the unmethylated daughter cytosine. 2. UHRF1 RING ubiquitinates H3K18 (H3 tail) — creating a docking site for DNMT1’s RFTS domain. 3. DNMT1 RFTS binds H3K18ub; DNMT1 catalytic domain transfers a methyl group from SAM to the daughter cytosine. 4. SAH (S-adenosyl-homocysteine) released; UHRF1 dissociates; cycle repeats. - Quantitative parameters: maintenance efficiency per CpG $\epsilon \approx 0.95$ in healthy cells. Each replication fork carries about 50 CpGs/s of unmethylated daughter DNA into the lumen — DNMT1 must fix them within minutes before chromatin reassembly. - Loss-of-function: mouse Dnmt1-knockout embryos die at E9.5 with genome-wide demethylation, ectopic gene expression, and replication-fork instability. Conditional knockouts in tissue-specific contexts produce lineage-specific failures (hematopoietic stem-cell exhaustion; intestinal epithelial collapse).

De novo methyltransferases — DNMT3A, DNMT3B: - Both have an N-terminal regulatory PWWP domain (reads H3K36me3) and an ADD domain (reads unmethylated H3K4 = H3K4me0). PWWP recognition couples *de novo* methylation deposition to gene-body H3K36me3-marked regions; ADD ensures methylation deposition is excluded from H3K4me3-marked active promoters (a fundamental safeguard against silencing active genes). - Establish *new* methylation patterns during germline development, gametogenesis, and early embryogenesis. - Both require DNMT3L (catalytically inactive; missing the SET-like motif required for SAM binding) as a regulatory partner that stimulates activity about 15-fold and itself reads H3K4me0 — coupling methylation deposition to *absence* of active marks. - DNMT3A: predominant in oocyte, embryonic stem cells, hematopoietic stem cells; loss-of-function mutations are frequent in clonal hematopoiesis (about 5 % of healthy individuals over age 70) and AML (about 20 % of cytogenetically normal AML); also Tatton-Brown–Rahman syndrome (germline DNMT3A loss with overgrowth). - DNMT3B: predominant in B cells, embryonic stem cells; loss-of-function causes ICF syndrome (immunodeficiency, centromeric instability, facial anomalies) due to demethylation of pericentromeric satellites.

Demethylation — TET family enzymes — the active demethylation pathway: - TET1, TET2, TET3 are Fe(II)/ α -ketoglutarate-dependent dioxygenases (each about 2,000 amino acids) with conserved C-terminal catalytic domains. They sequentially oxidise:



- Reaction details: TET enzymes consume O₂ and α KG, producing CO₂ and succinate. Each oxidation step transfers an oxygen atom from O₂ to the methyl carbon of cytosine.
- Active demethylation by base excision repair: 5-formylcytosine (5fC) and 5-carboxylcytosine (5caC) are recognized and excised by thymine DNA glycosylase (TDG), which has a 100-fold preference for 5fC/5caC over 5mC. TDG cleaves the N-glycosidic bond, leaving an abasic (AP) site. APE1 then makes a single-nucleotide cut; DNA Pol β fills the gap with unmodified cytosine; DNA ligase III + XRCC1 seal the nick. This is the canonical BER pathway adapted for methyl-cytosine erasure.
- 5hmC is itself a stable mark with distinct biology, not merely an intermediate. Different cell types have dramatically different 5hmC/5mC ratios — embryonic stem cells about 0.1 %, neurons about 0.7 % (Purkinje cells reach about 40 % of modified cytosines as 5hmC), cardiomyocytes about 0.5 %, tumor cells often < 0.05 % (a 5hmC depletion signature now used in liquid-biopsy diagnostics on platforms such as EpiCheck and GRAIL Galleri).

- Tissue-specific TET expression: TET1 in stem cells (regulates pluripotency); TET2 in hematopoietic cells (clonal hematopoiesis); TET3 in zygote and neurons (post-fertilization paternal demethylation; neural plasticity).
- Clinical relevance: TET2 is the most frequently mutated epigenetic-writer gene in hematopoietic cancers — loss-of-function TET2 mutations are present in about 15 % of AML, 50 % of CMML, and define clonal hematopoiesis of indeterminate potential (CHIP) (about 10 % of people over age 70). The oncometabolite 2-hydroxyglutarate (produced by mutant IDH1/2) competitively inhibits TET (and other α KG-dependent dioxygenases), causing genome-wide hypermethylation in IDH-mutant gliomas and AML (the CIMP phenotype).

Methodological caveat: Bisulphite sequencing (the traditional 5mC gold standard) cannot distinguish 5mC from 5hmC because both resist bisulphite-induced deamination. Modern methods that resolve oxidation states:

Table 232. The DNA Methylation Machinery — In Depth: Method and Signal.

Method	Signal	Resolution	Distinguishes
Bisulphite-seq (BS-seq)	C→T primarily at unmethylated	Single-base	5mC + 5hmC vs C
oxBS-seq	Chemical oxidation of 5hmC → 5fC, then BS	Single-base	5mC alone
TAB-seq	Tet-assisted bisulphite (β -glucosylates 5hmC, then TET-oxidises 5mC)	Single-base	5hmC alone
ACE-seq	APOBEC chemical sequencing	Single-base	5hmC enzymatically
CMS-seq	Cytosine 5-methylenesulfonate	Single-base	5fC alone
caMAB-seq	Carboxymethylated-cytosine antibody	about 250-bp	5caC alone
EM-seq	Enzymatic methyl-seq (no bisulphite damage)	Single-base	5mC + 5hmC vs C

Clinical liquid-biopsy translation: GRAIL’s Galleri test analyses cell-free DNA methylation patterns at > 100,000 CpG sites; multi-cancer early detection (MCED) sensitivity about 67 % for stage I–IV combined; tissue-of-origin localization accuracy about 93 %. The technology exploits that each tissue has a distinct methylation pattern, and tumors shed cfDNA with their tissue-specific signature.

15.5.3 CpG Islands and Gene Regulation

CpG islands (CGIs): about 28,000 regions in the human genome (about 500 bp–2 kb) with: - Observed/expected CpG ratio > 0.6 - CG content > 55% - Located near about 70% of mammalian gene promoters

Normally unmethylated in somatic cells. Methylation at CGI promoters is strongly associated with stable transcriptional silencing; the illustrative methylation heatmap in figure 98 should be read as a beta-value pattern across loci and samples, not as patient or cell-line evidence. In empirical data, silencing operates by: 1. Steric blockade of TF binding (e.g., methylation at Sp1 sites) 2. Recruitment of methyl-CpG binding proteins (MBD family: MBD1, MBD2, MBD3, MBD4; MeCP2; Kaiso) 3. MBD-associated NuRD complex (MBD2/3-CHD4-HDAC1/2) → deacetylation → chromatin compaction

CpG depletion in the rest of the genome: Methylated CpGs are mutation hotspots (5mC → T deamination produces a C→T transition). Over evolutionary time, most CpGs outside islands have been lost — explaining the genome-wide CpG suppression. CpG islands have escaped depletion because methylation is normally absent and the deamination → mutation pressure is removed.

15.5.4 Quantitative Maintenance Through Replication

Let f_n be the fraction of CpGs methylated after n divisions in the absence of *de novo* methylation:

$$f_n = f_0 \times \left(\frac{1 - \epsilon}{2}\right)^n + f_0 \times \frac{1 + \epsilon}{2}$$

(223)

where ϵ is the maintenance efficiency of DNMT1 (typically about 0.95 — i.e. each hemimethylated CpG is restored 95 % of the time at the replication fork). Even high maintenance efficiency therefore produces measurable stochastic demethylation over many divisions, which is why constitutively silenced genes also have backup repressive marks (H3K27me3, H3K9me3, H2AK119ub).

Worked Example 2 — DNMT1 efficiency and the kinetics of clonal demethylation

Setup: A research group treats a cancer cell line with a DNMT1 small-molecule inhibitor that reduces ϵ from 0.95 to 0.50 (50 % maintenance per CpG per division). The cells divide every 24 h. The cancer cell line carries an aberrantly hypermethylated *MLH1* promoter at $f_0 = 0.95$ (95 % CpG methylation).

Question: How many days until methylation drops below the $f = 0.30$ threshold typically required for re-expression?

Solution: Using equation (223), $f_n = f_0 \times \left(\frac{1-\epsilon}{2}\right)^n + f_0 \times \frac{1+\epsilon}{2}$ — but at $\epsilon = 0.5$ the steady-state floor is $f_0 \cdot (1 + 0.5)/2 = 0.75 \cdot f_0 = 0.71$ for $f_0 = 0.95$. The floor exceeds the 0.30 threshold, so methylation will not drop below 0.30 with $\epsilon = 0.5$ alone. To re-express *MLH1*, you need either complete DNMT1 inhibition ($\epsilon \rightarrow 0$) or active demethylation (TET upregulation). With $\epsilon = 0$:

$f_n = f_0/2^n$

Generation n	f_n
0	0.95
1	0.475
2	0.238
3	0.119

Threshold crossed between generation 1 and 2 — i.e., 2 cell divisions \approx 48 h after starting full DNMT1 inhibition. This kinetic is exactly why clinical responses to azacitidine/decitabine in MDS take about 4–6 cycles (about 3–4 months) of continuous suppression to manifest: maintaining ϵ near zero is necessary but insufficient — the cell must also divide several times to dilute the existing mark.

Clinical Connection: In cancer, two genome-wide patterns are consistently found: 1. Global hypomethylation: Repetitive elements (LINE-1, SINE) become unmethylated \rightarrow chromosomal instability, reactivation of transposons, mis-regulated lineage genes. 2. Focal CGI hypermethylation: Tumor-suppressor gene promoters (BRCA1, MLH1, VHL, CDKN2A/p16, MGMT, DAPK) become methylated \rightarrow silencing.

DNMT inhibitors (azacitidine, decitabine) are nucleoside analogs incorporated into DNA; trapped DNMT1 forms a covalent adduct, causing passive demethylation. Approved for myelodysplastic syndrome (MDS) and AML. Combination with HDAC inhibitors is actively trialled. Liquid biopsies (e.g., GRAIL Galleri, Guardant Reveal) score hundreds of methylation features in cell-free DNA to detect early-stage cancer with tissue-of-origin localization.

Concept Check 4: A patient is treated with decitabine for high-risk MDS. After 4 cycles, the bone-marrow blast count is unchanged. Bisulphite sequencing of blast DNA shows the targeted *p15/CDKN2B* CGI is now 30 % methylated (from 90 % at baseline), but transcript levels remain undetectable. Propose three independent mechanisms that could explain transcriptional silencing despite DNMT1 inhibition, and design a bench experiment to distinguish them.

Concept Check (Analysis): DNA methylation at CpG islands is heritable through cell division via the enzyme DNMT1, which preferentially methylates hemi-methylated DNA at replication forks. (a) After DNA replication, the daughter strand is unmethylated. DNMT1 is recruited by PCNA at the replication fork. If DNMT1 has a catalytic rate of 10 methylations/s and a replication fork moves at 1,000 bp/s, is DNMT1 fast enough to maintain methylation fidelity? Calculate assuming about 70 CpG dinucleotides per kb of CpG-rich region. (b) TET enzymes oxidize 5-methylcytosine (5mC) \rightarrow 5-hydroxymethylcytosine (5hmC) \rightarrow 5-formylcytosine (5fC) \rightarrow 5-carboxylcytosine (5caC), ultimately leading to demethylation via base excision repair. Explain why this active demethylation pathway was initially puzzling: what is paradoxical about oxidizing a protective mark in order to remove it? (c) Imprinting disorders: Angelman syndrome (maternal UBE3A imprinted off) and Prader-Willi syndrome (paternal 15q11-q13 deleted) arise from the same genomic region. Explain why deletions on different parental chromosomes produce different clinical syndromes.

Worked Example — CpG Methylation Dynamics: The BRCA1 promoter CpG island is unmethylated in normal breast cells but methylated in about 10-15% of sporadic breast cancers. If a primary breast cancer consists of 10^9 cells and 12% are BRCA1-methylated: BRCA1-methylated cells = 1.2×10^8 . These cells arose through stochastic methylation events during the 50 doublings to reach 10^9 cells. If methylation occurs at rate $\mu \approx 10^{-7}$ per cell division per CpG island, and methylation is heritable (maintenance methylation 99.9% faithful per division), then after 50 doublings starting from 1 cell: $P(\text{methylation by generation } g) \approx 1 - (1-\mu)^g \times 2^g / 2^g \approx 1 - e^{(-g\mu)}$ for small μ . At $g=50$: $P \approx 50 \times 10^{-7} = 5 \times 10^{-6}$ per cell per division

$\times 2^{50}$ cells total = 5.6×10^9 methylation events distributed across about 10^4 CpG islands. This Poisson-like accumulation explains why cancer genomes show both global hypomethylation (repetitive elements de-methylated) and focal hypermethylation (specific gene promoters) — different regulatory regimes for different genomic contexts.

15.6 Genomic Imprinting — Mechanisms and Reciprocal Phenotypes

Genomic imprinting is a form of epigenetic regulation in which genes are expressed from a single parental **allele** in a parent-of-origin-specific manner. about 150 genes are imprinted in humans, organized into about 30 imprinted clusters each controlled by an imprint control region (ICR) that is differentially methylated on the two parental chromosomes.

15.6.1 Imprint Control Regions (ICRs) — The Master Switch

ICRs are differentially methylated regions (DMRs) that are: 1. Established in the germline in a sex-specific pattern (paternal ICRs in spermatogenesis; maternal ICRs in oogenesis). 2. Maintained throughout somatic lineages — they escape post-fertilization reprogramming via specialized protective mechanisms (e.g., ZFP445 + TRIM28/KAP1 + DPPA3 = the ICR-protection triad in early embryos). 3. Read by sequence-specific factors (e.g., CTCF at unmethylated maternal IGF2/H19 ICR; methyl-binding proteins at methylated paternal ICRs).

The CTCF insulator model — the canonical mechanism at IGF2/H19: CTCF binds CCCTC consensus motifs in the unmethylated ICR. CTCF blocks the enhancer-promoter looping interaction by recruiting cohesin to form a chromatin loop “barrier.” When the ICR is methylated, CTCF cannot bind (its zinc fingers fail to recognize methylated CpGs), so the enhancer is free to loop over and contact the *IGF2* promoter.

15.6.2 The IGF2/H19 Locus — Insulator-based Imprinting (Detailed Mechanism)

The canonical example is the IGF2/H19 locus on chromosome 11p15:

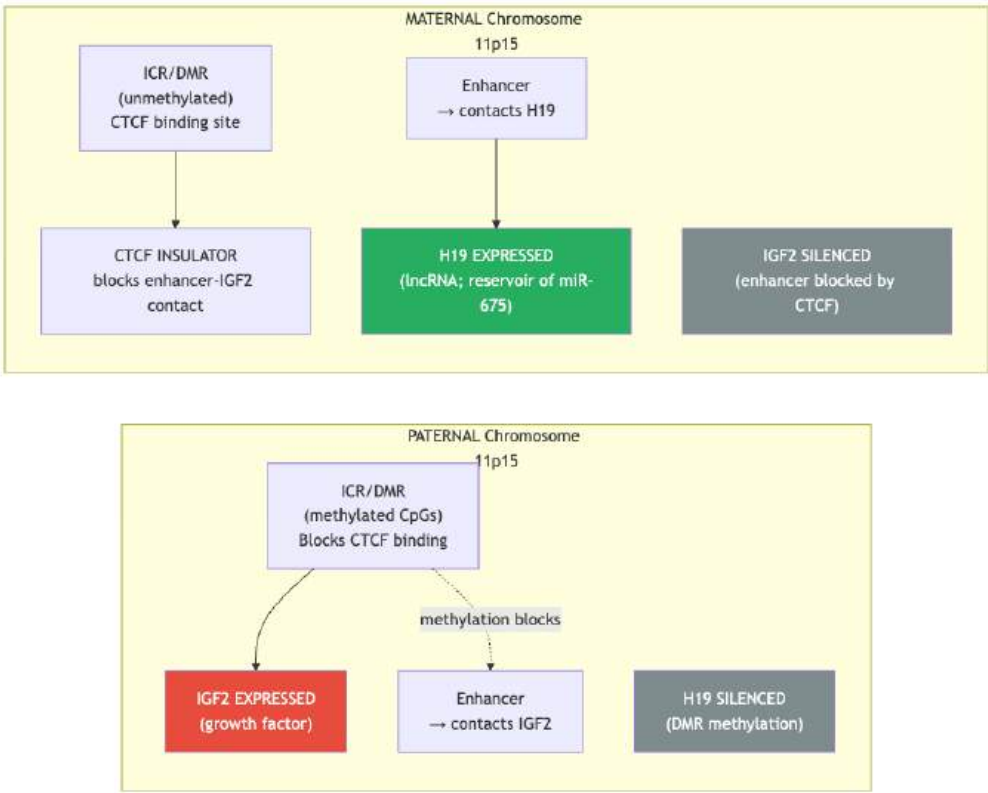


Figure 101. Imprinting at the IGF2/H19 locus. Paternal allele (top): DMR is methylated, CTCF cannot bind; enhancer contacts IGF2 to IGF2 expressed, H19 silent. Maternal allele (bottom): DMR unmethylated, CTCF binds and insulates enhancer from IGF2; enhancer contacts H19 to H19 expressed, IGF2 silent.

Functional consequences of the locus: - IGF2 (insulin-like growth factor 2): paternally expressed; potent fetal growth factor (signals through IGF1R / IGF2R). Drives placental and fetal growth. - H19: maternally expressed; a 2.3-kb spliced lncRNA; reservoir of miR-675 (which targets *IGF1R*, creating a feedback loop). In some tissues H19 itself acts as a tumor suppressor by inhibiting IGF1R signaling.

15.6.3 The 15q11–q13 Locus — Prader–Willi / Angelman Mechanism

A different mechanism operates at the 15q11–q13 imprinted cluster:

Table 233. The 15q11–q13 Locus — Prader–Willi / Angelman Mechanism.

Gene	Imprint pattern	Mechanism
<i>SNRPN</i> , <i>NDN</i> , <i>MAGEL2</i>	Paternally expressed	Maternal copies silenced by methylation at the <i>SNRPN</i> ICR
<i>UBE3A</i>	Maternally expressed (in neurons)	Paternal <i>UBE3A</i> silenced by an antisense lncRNA <i>UBE3A-ATS</i> expressed primarily from the paternal allele

Mechanism details: - The *SNURF-SNRPN* ICR sits about 30 kb upstream of *SNRPN* and is methylated on the maternal allele (silencing maternal *SNRPN*, *NDN*, *MAGEL2*) and unmethylated on the paternal allele (where these genes are expressed). - The unmethylated paternal ICR drives transcription of a long polycistronic transcript that extends about 600 kb to produce *SNRPN*, *SNORD-cluster snoRNAs* (*SNORD115*, *SNORD116*), and *UBE3A-ATS* (the antisense to *UBE3A*). - *UBE3A-ATS* transcription on the paternal allele suppresses paternal *UBE3A* expression — *primarily in neurons*. This is the most surprising aspect of the locus: the imprint is brain-specific.

Phenotypes — the parental-conflict reciprocal: - Prader–Willi syndrome: Loss of paternal 15q11–q13 expression — by paternal deletion (about 70%), maternal uniparental disomy (about 25%), or imprinting center defect (about 3%). Phenotype: neonatal hypotonia, hyperphagia and obesity, intellectual disability, hypogonadism, growth-hormone deficiency. The hypothalamic phenotype (especially the *SNORD116* loss) drives the food-intake dysregulation. - Angelman syndrome: Loss of maternal *UBE3A* expression in the same region — by maternal deletion (about 70%), paternal uniparental disomy (about 5%), imprinting center defect (about 5%), or *UBE3A* point mutation (about 10%). Phenotype: severe intellectual disability, seizures, ataxic gait, “happy puppet” demeanour, absence of speech. *UBE3A* is an E3 ubiquitin ligase critical for synaptic plasticity; loss in neurons disrupts excitatory/inhibitory balance.

Therapeutic angle — antisense oligonucleotide reactivation: Activation of the silenced paternal *UBE3A* by antisense oligonucleotides targeting *UBE3A-ATS* is in clinical trials for Angelman syndrome (Ionis/Biogen ION-582/GTX-102, Phase 1/2 trials underway 2024). The strategy: deplete the antisense lncRNA → de-repress paternal *UBE3A* → restore neuronal *UBE3A* protein. Intrathecal delivery is required because *UBE3A* imprinting is brain-specific.

15.6.4 Beckwith–Wiedemann and Silver–Russell — Reciprocal Disorders

The *IGF2/H19* ICR also produces two reciprocal phenotypes — a textbook illustration of dosage and parental conflict:

- Beckwith–Wiedemann syndrome (BWS): biallelic *IGF2* expression (loss of maternal imprint, hypermethylation of the maternal ICR at *H19*) → maternal allele now expresses *IGF2* like the paternal → fetal overgrowth, macrosomia (birth weight > 4 kg), macroglossia, omphalocele, hypoglycaemia, hemihypertrophia, and a 7.5 % risk of childhood embryonal tumors (Wilms tumor, hepatoblastoma, neuroblastoma, rhabdomyosarcoma). Diagnosis: methylation analysis of the *H19* DMR shows hypermethylation; some cases also have paternal UPD of 11p15 (about 20 %).
- Silver–Russell syndrome (SRS): biallelic *H19* expression / no *IGF2* (loss of paternal imprint, hypomethylation of the paternal ICR) → paternal allele now silent like the maternal → severe intrauterine growth restriction (IUGR), postnatal short stature, body asymmetry, characteristic triangular face, fifth-finger clinodactyly. Diagnosis: hypomethylation of the *H19* DMR (about 50 %) or maternal UPD of chromosome 7 (about 10 %).

This “mirror image” pair illustrates the parental-conflict (kinship) theory: paternally-expressed growth factors maximize embryonic growth (paternal genes care less about maternal resources, since the same father may not father subsequent siblings); maternally-expressed antagonists restrain growth (the mother distributes resources across multiple offspring).

Concept Check 5: A child is born with severe IUGR, characteristic facial features, and asymmetric limbs. Methylation analysis shows that both the paternal and maternal copies of the 11p15.5 ICR are *hypomethylated*. Predict the likely diagnosis. Explain why hypermethylation versus hypomethylation at the *same* ICR produces *opposite* phenotypes (BWS vs SRS).

15.7 X-Chromosome Inactivation (Lyonization) — In Depth

In female placental mammals, dosage compensation for about 900 X-linked genes is achieved by transcriptionally silencing one of the two X chromosomes in nearly every somatic cell (subject to the about 15–25% of X-linked genes that escape inactivation, discussed below).

Key features: - Random choice: Either the maternal or paternal X can be inactivated in each cell (choice is random in each blastomere nucleus). Imprinted paternal X-inactivation occurs in mouse extra-embryonic lineages but not in humans. - Clonal maintenance: Once established (about day 4.5 in human embryo), the inactive state is mitotically heritable in most daughter cells — the same X is silenced across essentially every descendant in a lineage, with rare stochastic exceptions and age-related skewing in tissues such as blood. - Barr body: The inactive X (Xi) forms a dense heterochromatic body (Barr body) visible by interphase cytology. - Incomplete: about 15–25% of X-linked genes escape inactivation. Most escapees lie in the pseudoautosomal regions (PAR1, PAR2) that recombine with the Y; others (e.g., *KDM6A*, *KDM5C*, *DDX3X*, *ZFX*) escape across the X. Escape genes contribute to female-biased autoimmune disease and to Turner syndrome haploinsufficiency phenotypes.

Molecular mechanism — a hierarchical cascade (timing and milestones):

Table 234. Beckwith–Wiedemann and Silver–Russell — Reciprocal Disorders: Time after initiation and Event.

Time after initiation	Event	Molecular outcome
0 min	Choice made; Xist transcription up-regulated on future Xi	Allele-specific Xist transcription begins
0–60 min	Xist RNA spreads in cis	Coats 165 Mb Xi; entry sites at LINE-1-rich domains
1–6 h	Repeat A recruits SPEN/SHARP	SPEN recruits HDAC3 → genome-wide deacetylation
1–6 h	Repeat B/C/D recruits PRC2	EZH2 deposits H3K27me3 on Xi
6–24 h	Repeat E recruits PTBP1, MATR3	Nuclear matrix tethering of Xi
6–24 h	PRC1 recruited downstream	RING1B writes H2AK119ub
1–7 days	DNMT3A/3B methylate CpG-island promoters	Stable maintenance of silencing
2–14 days	Histone variants accumulate	macroH2A and H2A.Z reinforce heterochromatin
7–21 days	LBR anchors Xi to nuclear lamina	Xi enters B compartment (nuclear periphery)

XIST regulation by TSIX: The antisense lncRNA *TSIX* (transcribed across XIST in the opposite direction) keeps XIST repressed on the future active X (Xa). The mutual exclusion of XIST/TSIX between alleles enforces monoallelic XIST expression. *TSIX* itself is regulated by *XITE* (X-inactivation intergenic transcription element) and by chromatin-state asymmetries between the two alleles in early embryogenesis.

Reactivation in iPSC reprogramming: When somatic female cells are reprogrammed to induced pluripotent stem cells (iPSCs), the inactive X reactivates — XIST is silenced, H3K27me3 is lost, DNA methylation is removed, and both alleles express X-linked genes again. This is a unique window for studying XCI dynamics. iPSCs derived from female patients with X-linked disease may have variable X-inactivation patterns after differentiation, complicating disease modeling.

Clinical implications — X-linked diseases in heterozygous females:

$$P(\text{affected}) \approx \int_0^1 g(x) \cdot 1[x \leq x_{\text{threshold}}] \, dx$$

(224)

where $g(x)$ is the distribution of X-inactivation skewing across cells. Skewed X-inactivation (where one allele is silenced in >75 % of cells) explains why heterozygous female carriers of X-linked diseases (Duchenne muscular dystrophy, Rett syndrome, X-linked agammaglobulinaemia) show variable severity. Skewing arises when: - Random inactivation by chance produces an extreme distribution - Cell-autonomous selection eliminates clones with the active mutant allele (e.g.,

immunodeficiencies) - A *XIST* or *XIC* mutation biases choice - Skewing is age-dependent: fraction of women with > 75 % skewing rises from about 5 % at birth to about 25 % by age 60 (clonal drift in hematopoiesis).

Lyon’s evidence [Lyon, 1961]: Female mice heterozygous for coat-color mutations show patchy (mosaic) coat color — a direct consequence of random X-inactivation producing patches of cells expressing one allele or the other. The same mosaicism is seen in human female carriers of X-linked albinism, X-linked anhidrotic ectodermal dysplasia (Christ–Siemens–Touraine, with patchy sweat glands), and X-linked retinoschisis (patchy retinal involvement).

Worked Example 3 — Predicting penetrance from XCI skewing

Setup: A female patient is heterozygous for a Duchenne muscular dystrophy (DMD) deletion. Muscle weakness is observed in cells where the wild-type (active) allele is on the inactivated X. Assume that DMD muscle fibers are syncytial (myofibres pool many nuclei); a fiber is dystrophic if > 50 % of its nuclei express the deleted allele.

Question: If XCI is unbiased (mean skewing = 0.5, standard deviation $\sigma_{\text{skew}} = 0.05$ across mononuclear cells), what fraction of myofibres will be dystrophic? What if the patient has clonal-skewing where $\sigma_{\text{skew}} = 0.20$?

Solution: A fiber is dystrophic if more than half its nuclei have the wild-type allele inactivated. With $N = 20$ nuclei per fiber and a per-nucleus probability x of expressing the deleted allele (= probability wild-type X is inactivated), the fiber is dystrophic when more than $N/2$ nuclei out of N express the deleted allele.

For unbiased XCI, x per nucleus ≈ 0.5 , $\sigma_x = 0.05$. Per fiber, the average fraction of mutant-expressing nuclei $\approx 0.5 \pm 0.05/\sqrt{20} \approx 0.5 \pm 0.011$. Almost no fibers exceed 50 % (by about $\sigma_{\text{fibre}} \times 1 \approx 1\%$).

For clonal-skewing $\sigma_{\text{skew}} = 0.20$ across mononuclear precursors, mean per-fiber fraction is 0.5 but with much wider variance: $\sigma_{\text{fibre}} \approx 0.20/\sqrt{20} \approx 0.045$. Now about 25 % of fibers exceed 50 % mutant expression and become dystrophic.

Insight: Manifesting Duchenne muscular dystrophy in heterozygous female carriers (about 10 % show muscle weakness) is largely explained by age-acquired XCI skewing in hematopoietic and myogenic precursors. Treatment strategies: skewing-modulating ASOs to redirect XCI; or AAV-DMD gene therapy (rebalancing dystrophin expression).

Concept Check 6: A 4-year-old girl is diagnosed with severe Rett syndrome. Sequencing reveals a heterozygous loss-of-function mutation in *MECP2*. XCI analysis shows 95 % skewing toward inactivation of the *wild-type* allele. Explain (i) why this skewing pattern produces severe disease, (ii) why some Rett patients with the same mutation are mildly affected, and (iii) whether modulating XCI skewing therapeutically could be a treatment strategy.

15.8 Chromatin Remodeling Complexes — Mechanism in Detail

In addition to covalent modifications, chromatin structure is actively remodeled by ATP-dependent complexes that slide, eject, or restructure nucleosomes. The four families share a conserved Snf2-family ATPase (SF2 helicase superfamily) but couple ATP hydrolysis to distinct nucleosome operations.

15.8.1 The Four Major Remodeller Families

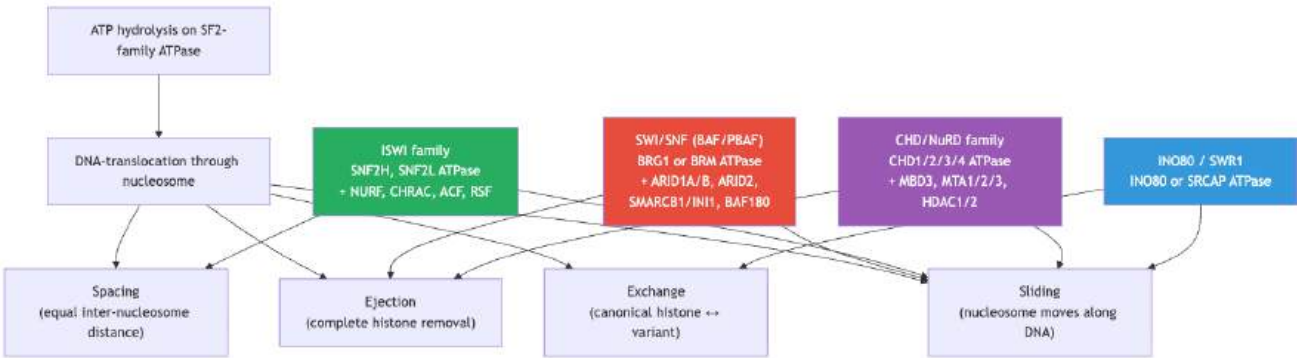


Figure 102. Four ATP-dependent remodeling families, each with a distinct nucleosome operation. SWI/SNF: large bursts of sliding and ejection that expose regulatory DNA. ISWI: short, regular spacing for nucleosome arrays. CHD/NuRD: repressive sliding with HDAC coupling. INO80/SWR1: histone variant exchange (H2A.Z between H2A) at promoters and DNA damage sites.

Table 235. The Four Major Remodeller Families: Family and Prototyp complex.

Family	Prototype complex	ATPase	Mechanism	Function	Disease
SWI/SNF	BAF, PBAF (mammals); SWI/SNF (yeast); BAP, PBAP (<i>Drosophila</i>)	BRG1 (SMARCA4) or BRM (SMARCA2)	Large-scale sliding and ejection	Activate transcription; prepare enhancers; required for stem cell self-renewal	ARID1A mutated in about 10% cancers; SMARCB1/INI1 lost in malignant rhabdoid tumor; SMARCA4 in lung cancer
ISWI	NURF, CHRAC, ACF, RSF, NoRC	SNF2H (SMARCA5), SNF2L (SMARCA1)	Nucleosome spacing — generates regular arrays	Chromatin assembly post-replication; heterochromatin maintenance; transcriptional repression	Williams syndrome (BAZ1B/WSTF deletion)
CHD / NuRD	NuRD (CHD3/4 + MBD3 + MTA1/2/3 + HDAC1/2 + RBBP4/7)	CHD1, CHD3 (Mi-2 α), CHD4 (Mi-2 β)	Nucleosome sliding coupled to histone deacetylation	Gene repression; lineage commitment; Polycomb-related silencing	CHD7 in CHARGE syndrome; CHD8 in autism
INO80 / SWR1	INO80, SWR1 (yeast); SRCAP (mammals)	INO80, SRCAP	Histone variant exchange (H2A.Z \leftrightarrow canonical H2A; H2A.X \leftrightarrow H2A)	Promoter-proximal H2A.Z deposition; DSB repair (γ H2AX exchange); centromere identity	Floating-Harbor syndrome (SRCAP mutations)

Mechanism in detail — the “wave” model of DNA translocation: Most remodellers translocate DNA through the nucleosome by alternately gripping minor groove with two RecA-like ATPase lobes. Each ATP cycle introduces a 1-bp DNA bulge that propagates around the histone surface, effectively pulling DNA into the nucleosome from one side and ejecting it from the other. The size of the ATP-driven movement varies (1–10 bp per cycle) and explains the family-specific outcomes (single-nucleosome repositioning vs. processive slides vs. ejection). Substrate recognition differs: - SWI/SNF binds at SHL-2 (superhelical location -2 from the dyad), gripping nucleosomal DNA about 20 bp from the histone–DNA boundary. - ISWI binds the linker DNA flanking the nucleosome and uses an autoinhibitory AutoN domain that is released by H4-tail acetylation. - CHD/NuRD binds via a tandem chromodomain that reads H3K9me3 (CHD3) or H3K4me0 (CHD4), targeting the complex to silenced chromatin. - INO80 binds the H2A.Z-H2B dimer for selective exchange.

15.8.2 SWI/SNF Specifically — The Cancer-Most-Mutated Remodeller

The mammalian BAF complex contains 12–15 subunits, including ATPase BRG1 or BRM, ARID1A/B (DNA-binding), and SMARCB1/INI1. Its assembly is highly cell-type-specific (npBAF in neural progenitors → nBAF in post-mitotic neurons, with subunit swap at *MIR9* induction; esBAF in embryonic stem cells). BAF: - Evicts PRC1/PRC2 from enhancers within minutes (this is the basis for the synthetic-lethal sensitivity of SWI/SNF-mutant tumors to EZH2 inhibitors). - Generates nucleosome-depleted regions (NDRs) at enhancers and promoters - Recruits transcription factors (e.g., pioneer TFs FOXA1, GATA4) by exposing their motifs - Specific complexes: - canonical BAF (cBAF): contains ARID1A or ARID1B and DPF1/2/3 - polybromo BAF (PBAF): contains BAF180/PBRM1, ARID2, and BRD7 — required for IFN response and differentiation - non-canonical BAF (ncBAF/GBAF): contains BRD9, GLTSCR1/L, and BRG1 — found in synovial sarcoma (where SS18-SSX fusions hijack ncBAF)

15.8.3 Targeted Epigenome Editing with dCas9 Fusions

The CRISPR toolkit has expanded far beyond DNA cutting. A catalytically dead dCas9 (D10A + H840A) retains its ability to be guided to a specific DNA sequence by a sgRNA but no longer cleaves — turning it into a programmable DNA-binding scaffold. Fusing dCas9 to an epigenetic enzyme creates a targeted “writer” or “eraser” of chromatin state [Doudna and Charpentier, 2014]:

Table 236. Targeted Epigenome Editing with dCas9 Fusions: Fusion and Function.

Fusion	Function	Experimental / clinical use
dCas9–DNMT3A	Programmable DNA methylation	CRISPRoff (heritable silencing without cutting DNA)
dCas9–TET1	Programmable DNA demethylation	Rescue of fragile-X <i>FMR1</i> silencing; reactivation of tumor suppressors
dCas9–p300	Programmable H3K27 acetylation	Programmable enhancer activation
dCas9–KRAB	Recruits KAP1 → SETDB1 → H3K9me3	CRISPRi — stable repression of any gene
dCas9–LSD1	H3K4me1/2 demethylation	Enhancer decommissioning
dCas9–VPR (VP64-p65-Rta)	Transcriptional activation	CRISPRa — about 10-to-1000-fold induction
dCas9–PRC1 (RING1B–PCGF4)	H2AK119ub deposition	Polycomb-style silencing

The clinical promise is substantial: a dCas9–DNMT3A targeting the *HBG1/2* promoter re-activates fetal hemoglobin in adult β -thalassaemia patients without permanent genome modification. CRISPRoff-induced silencing of *PCSK9* in liver cells is being pursued for hypercholesterolaemia. The key limitation is off-target **epigenome** editing — bystander methylation at sequence-similar loci — which the field now addresses with paired-sgRNA and split-dCas9 designs.

[!NOTE] Unlike Cas9-mediated gene editing, epigenome editing is reversible: the perturbation fades unless it is self-reinforcing through mitotic heritability of DNA methylation. This makes it attractive as a research tool (transient perturbation) and a therapy (tunable, removable), but means durable clinical effects require either continuous dCas9 expression or recruitment of self-propagating chromatin states (e.g., H3K27me3 spreading by PRC2).

Clinical Connection: SWI/SNF subunits are mutated in about 20% of human cancers, the highest mutation frequency of any single chromatin regulator. ARID1A (about 10%), SMARCA4/BRG1 (about 5%), SMARCB1/INI1 (childhood rhabdoid tumors, near-almost universally biallelic loss), PBRM1 (about 40% of clear-cell renal cell carcinoma). Many SWI/SNF-mutant tumors become synthetically lethal with EZH2 (PRC2) inhibition because they over-rely on Polycomb repression of cell-cycle inhibitors when SWI/SNF cannot evict PRC1/2.

15.9 Current Evidence and Frontier Biology: Chromatin and Epigenetic Mechanisms

For Chromatin and Epigenetic Mechanisms, frontier biology belongs inside the evidence logic of the chapter. Frontier work on chromatin is mechanistic and structural: cryo-EM now resolves nucleosome-engaging machines (PRC2, SWI/SNF remodelers, the DNMT and TET enzymes), many chromatin domains are understood to form by phase separation, single-cell ATAC-seq and CUT&RUN map accessibility and histone marks at cell-type resolution, and epigenetic editing (dCas9–writer/eraser fusions) tests causality directly. The core reading question is this: a chromatin mark is correlational until a targeted writer- or eraser-perturbation, with cell-type and timing controls, shows it drives the expression change.

- What to verify: identify the observation, model, assay, or dataset that would make the claim stronger or weaker.
- What to qualify: state the scale, organism, cell type, environmental condition, or population where the claim is expected to hold.
- What to compare: test at least one alternative explanation, baseline, or null model before treating the pattern as causal.
- What to cite: distinguish primary evidence, review synthesis, public dataset, and institutional guidance; for recent or numeric claims, prefer the source closest to the measurement and state what has changed since it was published.

For reference-dependent genetic claims, ask whether read length, structural variation, ancestry representation, phasing, or clinical validation changes the interpretation [[Human Pangenome Reference Consortium, 2023](#), [U.S. Food and Drug Administration, 2023](#), [2024b](#)].

Source practice: For genomics and editing claims, distinguish discovery from clinical actionability, and cite reference resources, regulatory records, or primary editing studies close to the claim [[Human Pangenome Reference Consortium, 2023](#), [U.S. Food and Drug Administration, 2026a](#), [Chalumeau et al., 2025](#)].

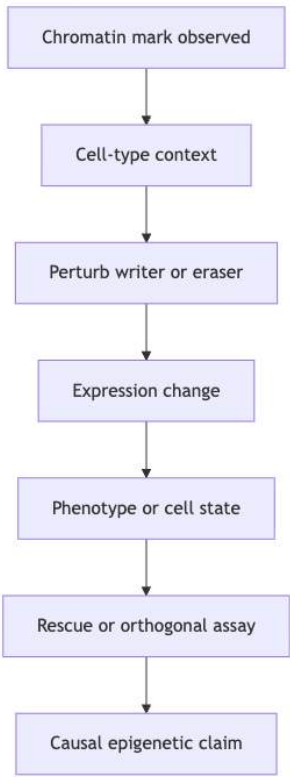


Figure 103. An epigenetic mark is not automatically a cause; causal claims need perturbation, timing, cell-type specificity, expression readout, and rescue or orthogonal evidence.

15.9.1 Current Evidence Map: Epigenetic Causality Ladder

15.10 Summary

- Define epigenetics and distinguish epigenetic modifications from DNA sequence changes.
- Describe nucleosome structure and the levels of chromatin compaction from the 11-nm fiber to the metaphase chromosome.
- Explain the major classes of histone modifications (acetylation, methylation, phosphorylation, ubiquitination, sumoylation) and how they are written, erased, and read.
- Describe the mechanism and function of DNA methylation, including CpG islands, the DNMT1/3A/3B enzymes, TET-mediated demethylation, and the role of methylation in gene silencing.
- Distinguish Polycomb (PRC1/PRC2) and Trithorax (MLL/COMPASS) systems and explain how they maintain repressive and activating states.
- Compare ATP-dependent chromatin remodeling families (SWI/SNF, ISWI, CHD/NuRD, INO80) and their distinct mechanisms.
- Explain X-chromosome inactivation (Lyonization) and the role of the XIST lncRNA, escape genes, and skewing.
- Describe genomic imprinting using IGF2/H19 and Prader-Willi/Angelman as paradigms.

15.11 Further Reading and Source Notes: Chromatin and Epigenetic Mechanisms

- Fire et al. (1998). Potent and specific genetic interference by double-stranded {RNA} in {Caenorhabditis elegans}. *Nature*, 391.
- Lyon (1961). Gene action in the {X}-chromosome of the mouse ({Mus musculus L.}). *Nature*, 190.
- Strahl & Allis (2000). The language of covalent histone modifications. *Nature*, 403.
- Doudna & Charpentier (2014). The new frontier of genome engineering with {CRISPR-Cas9}. *Science*, 346.

15.12 Companion Source Module: Chromatin and Epigenetic Mechanisms

Chromatin and Epigenetic Mechanisms should leave a reproducible trail from a biological claim to the code, figure, diagram, or paper-based activity that can test it. Use the surfaces below to inspect the chapter’s assumptions, rerun the relevant model, or compare the manuscript explanation with companion labs and figures.

Table 237. Companion source surfaces for Chromatin and Epigenetic Mechanisms.

Surface	Use it for
<code>src/biology/genetics/genetics.py</code> (<code>cpg_methylation_remaining</code> , <code>histone_modification_state</code>)	Convert methylation maintenance and histone-mark claims into explicit state checks.
<code>src/visualization/plots.py</code> (<code>plot_methylation_heatmap</code>)	Inspect whether heatmap interpretation depends on color alone or includes labels.
<code>src/mermaid/biology_diagrams.py</code> (<code>mirna_biogenesis_diagram</code> , <code>x_inactivation_diagram</code>)	Compare RNA-mediated and chromatin-mediated regulation.

Reproducibility check: require cell type, developmental time, perturbation evidence, and inheritance control before calling a mark causal. Cross-reference: use section 13, section 14, and section 19.

16 Epigenetic Inheritance and Disease

Level 3/3 · 28 min read · 40 min lecture · Prerequisites: section 15

16.1 Learning Objectives

1. Explain three-dimensional genome organization, TADs, and phase-separated condensates.
2. Interpret transgenerational and imprinting evidence with causal caution.
3. Connect epigenetic dysregulation to cancer and developmental disease.
4. Evaluate therapeutic strategies targeting epigenetic marks.
5. Compare chromatin condensates with conventional transcription-factor binding at enhancers.
6. Analyze evidence for transgenerational epigenetic inheritance with explicit controls for genetic confounding.
7. Interpret clinical epigenetic therapies using pathway, biomarker, and response-kinetics evidence.

16.2 Three-Dimensional Genome Organization and Phase Separation

16.2.1 TADs, Loops, and Compartments — Spatial Layers

The genome is folded across multiple length scales, and each scale contributes to gene regulation:

Table 238. TADs, Loops, and Compartments — Spatial Layers: Length scale and Structural unit.

Length scale	Structural unit	Marker / detection	Functional role
1 kb–100 kb	Promoter–enhancer loops	ChIA-PET, HiChIP, Capture-Hi-C	Direct enhancer–TSS contact for activation
100 kb–1 Mb	TADs	Hi-C insulation score; CTCF/cohesin ChIP	Constrains enhancer search to local genes
1 Mb–100 Mb	A/B compartments	Hi-C eigenvector	Active vs. repressed neighborhoods
Chromosome	Chromosome territories	DNA FISH	Each chromosome occupies a distinct nuclear domain
Nuclear scale	LADs, NADs, speckles	DamID, TSA-seq	Nuclear lamina, nucleolus, nuclear speckle proximity

LADs (Lamina-Associated Domains): about 1,300 genomic regions (median about 1 Mb) attached to the nuclear lamina via lamin B receptor, marked by H3K9me2/me3, gene-poor and transcriptionally repressive. Lamina detachment correlates with gene activation during differentiation.

16.2.2 Biomolecular Condensates and Phase Separation

Chromatin is not a static polymer; many regulatory proteins undergo liquid–liquid phase separation (LLPS) or form condensates with elevated local concentration. Intrinsically disordered regions (IDRs) on transcription factors (e.g., BRD4, Mediator subunits, RNA Pol II CTD-associated factors) promote clustering at super-enhancers — unusually large clusters of enhancers densely occupied by Mediator, co-activators, and active histone marks (H3K27ac), one example of the broader histone-mark logic formalized by the histone-code framework [Strahl and Allis, 2000]. The resulting transcriptional condensate concentrates the phosphorylation machinery that releases promoter-proximal paused Pol II, explaining why some loci fire at very high rates (oncogenes such as MYC in selected cancers).

Quantitative criteria for LLPS in cells: - IDR-rich proteins above a saturation concentration c_{sat} - Multivalent interactions (low-affinity, high-valency) between IDRs, with $K_d \sim 1\text{--}100\ \mu\text{M}$ - Round, dynamic droplets that fuse and undergo FRAP recovery on the seconds-to-minutes timescale - Disassembly upon 1,6-hexanediol (a hallmark, though imperfect, test)

Examples in chromatin biology:

Table 239. Biomolecular Condensates and Phase Separation: Condensate and Constituents.

Condensate	Constituents	Function
Heterochromatin foci	HP1α, H3K9me3	Concentrates H3K9 methyltransferases; phase-separated repressive compartment
Nucleolus	NPM1, fibrillarin, Pol I, rRNA	Ribosome biogenesis; multiphase (FC/DFC/GC sub-compartments)
Nuclear speckles	SRSF, SON, MALAT1	Storage and assembly of splicing factors
Cajal bodies	Coilin, snRNPs	snRNP and telomerase RNP biogenesis
PML bodies	PML, SUMO, p53	DNA damage response; senescence; viral defense
Super-enhancer condensates	BRD4, Mediator, Pol II CTD	Robust transcription of cell-identity genes
Polycomb bodies	CBX2 (PRC1) phase-separated	Polycomb domain compaction in cis

Conceptual link to TADs: Condensates operate *within* TADs and at promoter–enhancer loops; disrupting CTCF boundaries can move an oncogenic enhancer adjacent to a silent proto-oncogene (enhancer hijacking), a structural-variant mechanism increasingly catalogued in pediatric tumors.

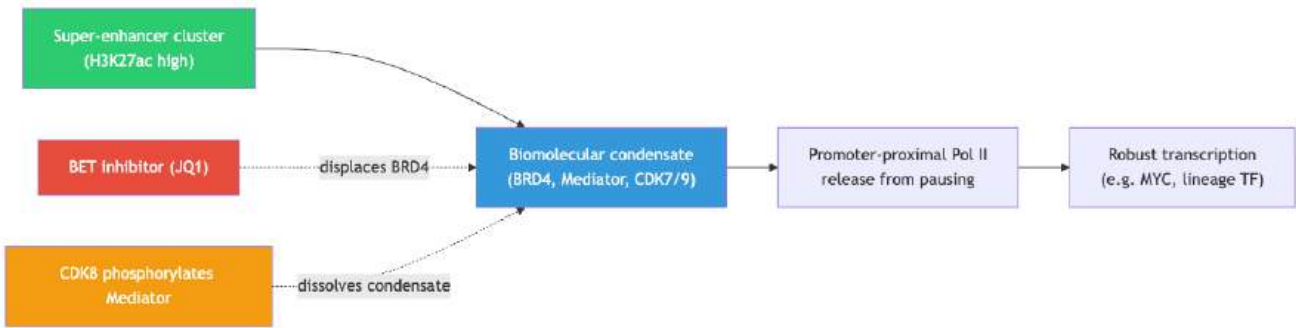


Figure 104. Super-enhancer-associated condensate bridging enhancers to paused Pol II; BET inhibitors weaken acetyl-lysine engagement of BRD4 and dissolve the condensate; CDK8-mediated phosphorylation of Mediator disrupts condensate integrity.

Clinical angle — drugging condensates: - BET bromodomain inhibitors (e.g., JQ1, OTX015, birabresib, molibresib, mivebresib) displace BRD4 from acetylated chromatin, collapsing condensate-associated transcription at *MYC* and other dependency genes. - CDK7 inhibitors (THZ1, SY-5609) and CDK9 inhibitors target the kinases concentrated in transcription condensates. - EZH2 inhibitors (tazemetostat) shrink PRC2-mediated repressive domains. - Tumor cells with super-enhancer-driven oncogenes (*MYCN*-amplified neuroblastoma, *MLL*-rearranged leukaemia, *TAL1*-driven T-cell acute lymphoblastic leukaemia) can be highly sensitive to BET inhibition, but response depends on enhancer wiring, compensatory transcription factors, and therapeutic window rather than on super-enhancer status alone.

Worked Example 4 — Polymer Statistics in Hi-C:

Setup: A human gene at chromosome 7p15 harbors an enhancer 700 kb upstream. We model intra-chromosomal contact probability with the fractal-globule scaling equation (219), $P(s) \propto s^{-\alpha}$, with $\alpha = 1.1$.

Question: Estimate the probability of physical contact between enhancer and promoter ($s = 700,000$ bp). Compare to (a) within-TAD contact at $s = 50$ kb and (b) trans-chromosomal contact (genome-wide Hi-C average $\approx 10^{-6}$).

Solution: Setting $P(50\text{ kb}) \approx 1$ (within-TAD baseline), the relative $P(700\text{ kb}) = (700/50)^{-1.1} = 14^{-1.1} \approx 0.063$. The enhancer–promoter contact probability is about 6 % of the within-TAD baseline.

Compare to trans-chromosomal: 6×10^{-2} (intra-TAD-distant) versus 1×10^{-6} (trans) = a about 60,000-fold preference for intra-chromosomal contacts even at long distances.

Insight: CTCF/cohesin loop extrusion concentrates this 60,000-fold enrichment of intra-TAD contacts onto specific enhancer–promoter pairs, raising effective contact probability another 10–100×. This is why disrupting a single CTCF anchor (about 20 bp deletion) can completely abolish enhancer–promoter looping and silence the target gene — even though the enhancer DNA is unchanged.

16.2.3 Study Blueprint

- Big idea: Three-dimensional genome organization and epigenetic inheritance link regulatory architecture to disease phenotypes.
- Core concepts: 3D genome, phase separation, imprinting, epigenetic inheritance.
- Framework alignment: Vision & Change: Information flow, exchange, and storage, Structure and function; AP Biology: Information Storage and Transmission, Systems Interactions; NGSS-style topics: Inheritance and Variation of Traits, Structure and Function.
- Model or quantitative lens: Chromatin-loop, inheritance, and disease-risk reasoning.
- Data skill: Interpret Hi-C, imprinting, or transgenerational datasets with causal caution.
- Practice cadence: Concept Explanation, Questions and Methods, Argumentation.
- Common misconception to repair: A chromatin contact map is not proof of function without perturbation.
- Primary lab: Lab — Epigenetic Inheritance and Disease.
- Question bank: Questions — Epigenetic Inheritance and Disease.
- Transfer task: Apply inheritance logic to cancer, developmental disorders, and environmental exposure.
- Bridge to computation: `biology.genetics.genetics.histone_modification_state`.

Opening Vignette — Epigenetic Inheritance and Disease

This chapter connects epigenetic inheritance and disease to measurable evidence: models, datasets, and experiments that can strengthen or weaken each claim.

16.3 Non-Coding RNAs in Gene Regulation

16.3.1 MicroRNAs (miRNAs) and Post-Transcriptional Repression

miRNAs are about 22 nt single-stranded RNAs that direct post-transcriptional silencing. Over 2,000 annotated human miRNAs collectively regulate about 60% of protein-coding genes [Fire et al., 1998].

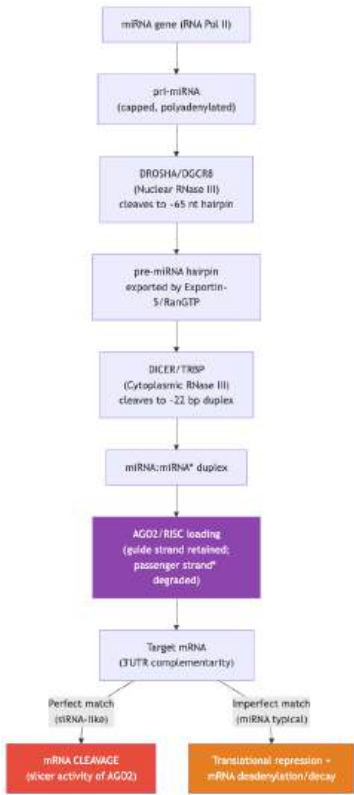


Figure 105. miRNA biogenesis and RISC-mediated silencing. Drosha in the nucleus produces pre-miRNA; DICER in the cytoplasm generates the duplex; AGO2 incorporates the guide strand into RISC; partial 3 UTR complementarity leads to translational repression and mRNA decay.

Key oncogenic miRNA examples: - miR-21 (oncomiR): Overexpressed in most cancers; targets PTEN, PDCD4, RECK (tumor suppressors) - miR-155 (oncomiR): Overexpressed in B-cell lymphomas; targets SHIP1 (AKT suppressor) - miR-34a (tumor suppressor miR): Downstream of p53; targets CDK6, BCL2, SNAIL; methylated/silenced in many cancers

16.3.2 Long Non-Coding RNAs (lncRNAs)

lncRNAs are >200 nt functional RNA transcripts with no protein-coding potential. >100,000 annotated in the human genome. Mechanisms of action are diverse:

- XIST: Coats the inactive X chromosome; recruits PRC2 to spread H3K27me3, as described in the X-inactivation section.
- HOTAIR: Transcribed from HOXC; binds PRC2 to direct H3K27me3 deposition at HOXD and other loci
- MALAT1: Nuclear speckle-associated; regulates alternative splicing; highly expressed in cancer
- H19: Reservoir for miR-675; tumor suppressor function; imprinted, as described in the genomic-imprinting section.
- NEAT1: Paraspeckle scaffold; regulates gene expression by nuclear retention of specific mRNAs

16.3.3 Small Interfering RNAs (siRNAs) and piRNAs

siRNAs: 21–23 nt, perfect complementarity to target; processed by DICER from long double-stranded RNA (dsRNA) [Fire et al., 1998]. In plants and nematodes, siRNA pathways mediate transposon silencing and antiviral immunity. In mammals, dsRNA triggers interferon responses rather than siRNA pathways in somatic cells; siRNA silencing is more prominent in germ cells and stem cells.

piRNAs (PIWI-interacting RNAs): 26–31 nt; DICER-independent (processed by “ping-pong” amplification cycle involving PIWI clade Argonautes: PIWIL1/MILI, PIWIL4/MIWI2). Essential for silencing transposable elements in the germline. Loss of piRNA pathway in *Drosophila* or mice causes transposon derepression and infertility.

16.4 Epigenetic Reprogramming and Inheritance

16.4.1 Mitotic Heritability of Epigenetic Marks — Detailed Mechanism

For an epigenetic mark to be “heritable,” it must survive DNA replication and cell division rather than merely correlate with a transcriptional state [Jaenisch and Bird, 2003]. Different marks have different mechanisms:

Table 240. Mitotic Heritability of Epigenetic Marks — Detailed Mechanism: Mark and Mitotic heritability mechanism.

Mark	Mitotic heritability mechanism	Half-life through divisions
5mC at CpGs	DNMT1/UHRF1 maintenance at replication fork	High (>10 divisions, about 95% efficiency)
H3K27me3	Read-write feedback (PRC2 EED reads, EZH2 writes); inherited on parental nucleosomes which are randomly distributed to both daughter strands	Medium; restored within 1–2 divisions
H3K9me3	Suv39H1/H2 reads HP1 → recruits more Suv39H; DNMT3A coupling	High at constitutive heterochromatin
H3K4me3	Inherited via parental nucleosomes; rapidly re-established by transcription	Medium
H3K27ac	Diluted by half each division; restored by transcription factor activity	Low; not stably heritable
H2AK119ub	Inherited via parental nucleosomes; restored by PRC1	Medium

Key conceptual point — parental nucleosome recycling: During DNA replication, parental nucleosomes are split between the two daughter strands. The histone chaperones MCM2 (binds H3-H4 dimers via its H3-H4 binding domain), ASF1 (general H3-H4 chaperone), and FACT (Spt16-SSRP1, helps recycle H2A-H2B during transcription and replication) mediate this recycling. The current model:

1. Parental nucleosome split: As the replisome opens, parental histones are transiently released from DNA.
2. Asymmetric recycling: H3-H4 tetramers preferentially deposit on the leading strand (via Pole/MCM2 interaction) or lagging strand (via Polα/MCM2-7 helicase-associated MCM2). Recent work shows this is biased toward the leading strand in proliferating cells (about 60:40), explaining strand-asymmetric mark inheritance.
3. CAF-1 deposits new H3.1-H4: The chromatin assembly factor CAF-1 (CHAF1A/B + RBBP4) is recruited by PCNA at the replication fork. CAF-1 deposits new H3.1-H4 tetramers (synthesized from S-phase histone gene bursts).

4. Newly synthesized histones are deposited UNMODIFIED. Daughter chromatin starts at half-density of any given mark.
5. Restoration to full density depends on the read-write feedback loop — the existing parental marks recruit the writer enzyme, which copies the mark onto neighboring new histones.

PRC2 propagation through replication. EED reads H3K27me3 on a parental nucleosome → allosterically activates EZH2 → EZH2 deposits H3K27me3 on a neighboring (newly assembled) nucleosome. Quantitative imaging shows that PRC2 activity at recently replicated chromatin is about 3-fold higher than at established chromatin — explaining how the mark “fills in” the daughter strand within about 6 hours of fork passage.

DNMT1/UHRF1 mechanism in detail at the fork. UHRF1 is loaded onto the replication fork by PCNA. UHRF1 SRA binds hemi-methylated CpG (the parental strand carries 5mC; the daughter strand has unmodified C). The UHRF1 RING domain ubiquitinates H3K18 — creating a docking site for DNMT1’s RFTS domain. DNMT1 transfers a methyl group from SAM to the daughter cytosine. This coupled mechanism ensures methylation is restored within seconds of fork passage at active replication.

16.4.2 Germline Reprogramming and Epigenetic Resetting

Somatic epigenetic marks must be erased and re-established in each generation to prevent transmission of acquired somatic states, which is why transgenerational inheritance claims require careful separation of direct exposure, germline exposure, and true inheritance [Heard and Martienssen, 2014]:

1. Post-fertilization reprogramming: After fertilization, the paternal genome undergoes rapid active demethylation (TET3-mediated 5mC oxidation) within hours. The maternal genome is demethylated more slowly (replication-dependent passive demethylation). Both reach a methylation minimum at the blastocyst stage.
2. Primordial germ cell (PGC) reprogramming: PGCs migrate to the gonads (about E7.5–E10.5 in mouse; about weeks 3–5 in human). They erase CpG methylation genome-wide (including imprint control regions) — the most complete demethylation in the mammalian life cycle.
3. Re-establishment: DNMT3A/3B with DNMT3L re-methylate the genome in a sex-specific pattern during gametogenesis (prospermatogonia in males; oocyte growth in females). Imprinted loci are methylated in a sex-specific order: paternal imprints in spermatogonia (before meiosis); maternal imprints in growing oocytes (after meiosis I arrest, prior to ovulation).

16.4.3 Evidence for Transgenerational Epigenetic Inheritance in Humans

The Dutch Hunger Winter (Hongerwinter, 1944–1945) provides the most studied human evidence. Dutch civilians subjected to severe famine (500–1,000 kcal/day) during WWII German occupation showed:

- F1 offspring (exposed in utero): Increased rates of obesity, diabetes, schizophrenia, and CVD in adult life — consistent with developmental programming via altered methylation.
- F2 offspring (children of F1): Increased rates of obesity and metabolic syndrome — suggesting transmission across one germline generation.
- Mechanism: Reduced methylation at IGF2 differentially methylated regions (DMRs) persists for decades in blood cells of F1 individuals, detectable compared to unexposed siblings.

Other lines of evidence: - Överkalix cohort (Sweden): Paternal grandfather’s food supply during slow-growth period correlates with grandsons’ diabetes mortality. - *Agouti* viable yellow (A^{vy}) mouse model: Maternal methyl-donor diet (folate, B12, methionine, choline) during pregnancy shifts coat-color distribution by altering methylation of an upstream IAP retrotransposon. - piRNA-mediated transposon silencing: piRNAs in sperm carry information about active transposons across generations.

[!NOTE] The evidence for true transgenerational epigenetic inheritance in humans (affecting F2 and beyond without continued environmental exposure) is suggestive but not yet definitive. Confounding by shared post-natal environment and direct exposure of the F1 germline (the F2 was a primordial germ cell in the F0 grandmother during the F1 in utero exposure) remains difficult to exclude. Mechanistically, piRNA-mediated transposon silencing and small-RNA transmission in sperm provide plausible vehicles, but a clean causal chain in humans has not been established.

Concept Check 7: Imagine a dCas9 fusion protein is targeted to the *BRCA1* promoter in a breast-cancer cell line, carrying a DNMT3A catalytic domain. Over several cell divisions, the promoter becomes hypermethylated and transcription drops. Once dCas9 is withdrawn, does the methylation persist, relax over mitoses, or become heritable between cells? Explain in terms of DNMT1 maintenance methylation, passive demethylation during S-phase, and the absence of active demethylation by TET enzymes under these conditions.

Concept Check 8: A scientist treats cells with the DNMT inhibitor decitabine for 48 hours, then washes it out. Predicting that DNMT1 will resume normal activity after washout, will the demethylation persist, partially recover, or fully recover over the subsequent 10 cell generations? Sketch a quantitative model assuming ϵ returns to 0.95 instantaneously after washout and starting $f_0 = 0.10$ (10 % methylated post-decitabine).

Concept Check 9: A child inherits a deletion of the maternal 15q11–q13 region (the imprinted Prader-Willi/Angelman locus). Predict which syndrome results, then explain why the *same* deletion on the paternal chromosome produces the other syndrome. What does this parent-of-origin effect reveal about how imprinting — rather than gene dosage by itself — determines phenotype?

16.5 Cancer Epigenetics and Clinical Translation

Cancer cells display systemic epigenetic dysregulation: typically global DNA hypomethylation (especially of repetitive elements), focal hypermethylation of tumor-suppressor CGI promoters, broad H3K27me3/H3K9me3 redistribution, and aberrant chromatin remodeling complex composition [Feinberg et al., 2016]. The therapeutic implication is that, unlike genetic mutations, epigenetic states are reversible — and several drug classes now target each layer.

16.5.1 The Cancer Epigenome — Two Concurrent Patterns

Pattern 1: Global hypomethylation. Repetitive elements (LINE-1, SINE, IAP, satellite repeats), normally heavily methylated, lose methylation in nearly every cancer type. Consequences: - Chromosomal instability: demethylation of pericentromeric satellite-2 sequences disrupts heterochromatin, leading to chromosome bridges, lagging chromosomes, and aneuploidy. - LINE-1 reactivation: transposition of L1 elements can disrupt tumor-suppressor genes (e.g., L1 insertion in *APC* contributes to colorectal cancer). - Mis-regulated lineage genes: demethylation of normally repressed germline genes (e.g., *MAGE*, *NY-ESO-1*) creates cancer-testis antigens that can be exploited for immunotherapy (e.g., *NY-ESO-1* TCR-T cells). - Mechanism: likely loss of DNMT1 maintenance (*UHRF1* dysregulation) and/or genome-wide TET2-mediated demethylation in CHIP-derived clones.

Pattern 2: Focal CGI hypermethylation. Tumor-suppressor gene promoters become hypermethylated, silencing them. The illustrative beta-value heatmap in figure 98 should be read as a pattern across loci and samples, not as patient-specific evidence. Examples and clinical relevance:

Table 241. The Cancer Epigenome — Two Concurrent Patterns: Gene and Hypermethylated in.

Gene	Hypermethylated in	Functional consequence	Therapeutic angle
<i>MLH1</i>	CIMP-high colorectal cancer	Microsatellite instability	Pembrolizumab in MSI-high tumors
<i>BRCA1</i>	Triple-negative breast cancer	Homologous-recombination deficiency	PARP inhibitors
<i>VHL</i>	Renal cell carcinoma	HIF stabilization	HIF-2α inhibitors (belzutifan)
<i>CDKN2A/p16</i>	Many cancers	RB1 pathway loss → unrestrained G1/S	CDK4/6 inhibitors
<i>MGMT</i>	Glioblastoma	DNA repair loss	Temozolomide (sensitivity)
<i>DAPK</i>	Lung, head/neck cancer	Apoptosis loss	Combination with TRAIL agonists (clinical trials)

The two patterns can coexist — a single tumor can have global hypomethylation of repeats AND focal hypermethylation of tumor suppressors. The mechanism appears to be partial: CGI-targeted DNMT3A/B activity becomes mis-localized to actively transcribed regions, while genome-wide DNMT1 maintenance fails at heterochromatin.

16.5.2 Approved and Investigational Epigenetic Drugs

Table 242. Approved and Investigational Epigenetic Drugs: Class and Examples.

Class	Examples	Targets	Approved Indications	Clinical-trial highlights
DNMT inhibitors	Azacitidine (Vidaza), decitabine (Dacogen); oral cedazuridine/decitabine (Inqovi)	DNMT1 (covalent trap)	MDS, AML (low-intensity), CMML	Aza + venetoclax: ORR 70 % in elderly AML (VIALE-A); decitabine-cedazuridine in CMML

Class	Examples	Targets	Approved Indications	Clinical-trial highlights
HDAC inhibitors	Vorinostat (SAHA), romidepsin, panobinostat, belinostat, tucidinostat	Pan-HDAC or class-selective	CTCL, PTCL, multiple myeloma (panobinostat)	Romidepsin ORR 34 % in PTCL; panobinostat-bortezomib-dex in MM
EZH2 / PRC2 inhibitors	Tazemetostat, valemestostat	EZH2 SET domain (and EZH1)	Epithelioid sarcoma (INI1-loss); EZH2-mut follicular lymphoma; ATL (valemestostat)	Tazemetostat: median PFS 5.5 mo in INI1-loss ES
IDH1/IDH2 inhibitors	Ivosidenib (IDH1), enasidenib (IDH2), vorasidenib	Mutant IDH neomorphic activity (2-HG)	IDH-mut AML; IDH-mut grade-2 glioma (vorasidenib, 2024)	Vorasidenib INDIGO trial: median PFS 27 vs 11 mo
BET inhibitors	OTX015 (birabresib), molibresib, mivebresib, BMS-986158	BRD2/3/4 bromodomains	Investigational: NUT carcinoma, MYC-driven tumors	NUT-carcinoma ORR about 35 %; pancreatic cancer combination trials
LSD1 inhibitors	Tranylcypromine, iadademstat, bomedemstat	KDM1A/LSD1 demethylase	Investigational: AML, SCLC, MPN	Iadademstat + azacitidine in AML; bomedemstat in essential thrombocythaemia
Menin–MLL inhibitors	Revumenib (FDA 2024)	Menin–MLL/KMT2A interface	Approved KMT2A-rearranged AML	Revumenib AUGMENT-101 trial: ORR 53 %, CR 23 %
PROTAC bromodomain degraders	ARV-771, dBET6, ARV-825	BRD4 (degradation)	Investigational	Targets the three BET family members; deeper BRD4 depletion than inhibition
DOT1L inhibitors	Pinometostat (EPZ-5676)	H3K79 methyl-transferase	Investigational MLL-rearranged AML	Phase 2 ORR about 10 % monotherapy; combination strategies in trial
CDK7/9 inhibitors	THZ1, SY-5609 (CDK7); AZD4573 (CDK9)	Transcription-cycle CDKs	Investigational	Disrupts super-enhancer-driven oncogene transcription
Combination DNMTi + HDACi or DNMTi + venetoclax	Aza + venetoclax (FDA 2018)	DNMT1 + BCL2	Standard-of-care AML in unfit patients	Aza-venetoclax: median OS 14.7 mo vs 9.6 mo aza alone

16.5.3 Clinical Trial Vignettes — Three Paradigm Therapies

- (1) Tazemetostat for INI1-loss epithelioid sarcoma. In 2020, tazemetostat became the first epigenetic-pathway-defined targeted therapy. INI1/SMARCB1-loss epithelioid sarcoma has no chemotherapy or surgical option in metastatic setting; the agent reactivates SWI/SNF-suppressed targets via EZH2 inhibition. Pivotal trial (NCT02601950): 62 patients enrolled, ORR 15 %, median time to response 3.6 mo, median PFS 5.5 mo. The slow response kinetics reflect epigenetic reprogramming requiring multiple cell divisions. FDA approval (Jan 2020) was a landmark for synthetic-lethal epigenetic therapy [U.S. Food and Drug Administration, 2020].
- (2) Vorasidenib for IDH1-mutant grade-2 glioma. In 2024, vorasidenib became the first targeted therapy approved for grade-2 glioma. IDH1-R132H mutation produces oncometabolite 2-HG, which inhibits TET demethylases → CIMP+ phenotype → genome-wide hypermethylation → differentiation block. Vorasidenib is a brain-penetrant mutant-IDH1 inhibitor. INDIGO trial (NCT04164901): 331 patients with grade-2 IDH-mut glioma post-surgery, median PFS 27.7 mo (vo-

rasidenib) vs 11.1 mo (placebo); 85 % reduction in time-to-next-intervention. The trial demonstrated that depleting 2-HG is sufficient to restore demethylation and slow tumor growth without cytotoxicity.

(3) Revumenib for KMT2A-rearranged AML. In 2024, revumenib became the first menin–MLL inhibitor approved by FDA. KMT2A-rearranged (ex-MLL-rearranged) AML accounts for about 10 % of pediatric AML and about 5 % of adult AML; menin is required for MLL-fusion-driven HOXA9 expression. AUGMENT-101 trial (NCT04065399): ORR 53 % in relapsed/refractory KMT2Ar AML, CR 23 %, median DoR 6.4 mo. The drug demonstrated that targeting protein–protein interaction (menin-MLL) within an aberrant chromatin complex is therapeutically viable.

16.5.4 A Checklist for Interpreting Cancer Epigenomes

When you encounter a tumor multi-omics report, integrate:

1. DNA methylation — focal CGI hypermethylation (TSG silencing) vs. global hypomethylation (genomic instability); CIMP (CpG island methylator phenotype) as a class.
2. Histone marks — H3K27me3 (PRC2 silencing), H3K4me3 (promoter activity), H3K27ac (active enhancers), H3K36me3 (transcribed gene bodies; loss in renal cell carcinoma with SETD2 mutation).
3. Chromatin accessibility (ATAC-seq) — nucleosome-depleted regions at enhancers; super-enhancers identified by Mediator/H3K27ac density.
4. 3D genome (Hi-C) — TAD boundary loss, enhancer hijacking.
5. Histone mutations (oncohistones) — H3K27M (pediatric DIPG), H3G34R/V (pediatric high-grade glioma), H3K36M (chondroblastoma): these are *gain-of-function* mutants that act as PRC2 / SETD2 inhibitors in trans, producing genome-wide chromatin redistribution despite occurring in about 5–10 % of nucleosomes.
6. Chromatin-remodeller mutations — ARID1A, SMARCA4, SMARCB1, PBRM1 (SWI/SNF); KMT2C/D, EZH2 (PRC2).
7. RNA — fusion oncoproteins that recruit aberrant chromatin complexes (MLL fusions to AF4/AF9/ENL, SS18–SSX in synovial sarcoma, BRD4–NUT in NUT carcinoma).

This checklist mirrors how clinicians and trialists rationalise DNMT + HDAC combinations, EZH2 monotherapy in defined molecular subtypes, and emerging BET + BCL2 regimens in haematological malignancies.

Worked Example 5 — CpG Island Methylation and Transcriptional Silencing

Problem: A molecular biologist treats cancer cells with 5-azacytidine (azacitidine), a DNMT inhibitor. They observe re-expression of the tumor suppressor gene *CDKN2B* (p15). Before treatment, bisulfite sequencing showed 90% CpG methylation at the *CDKN2B* promoter CGI. The drug is incorporated into DNA during replication and forms a covalent adduct with DNMT1, preventing maintenance methylation.

- (a) After 3 cell divisions with the drug present, what methylation level would you predict at the CGI if no de novo methylation occurs?
- (b) Why do HDAC inhibitors (e.g., vorinostat) often synergise with DNMT inhibitors in cancer treatment?

Solution:

- (a) Maintenance methylation requires DNMT1 to copy hemi-methylated CpGs after replication. With DNMT1 blocked, after each division sister strands receive no methylation:

$$f_n = f_0 \times \left(\frac{1}{2}\right)^n$$

(225)

$$f_3 = 0.90 \times \left(\frac{1}{2}\right)^3 = 0.90 \times 0.125 = 0.1125 \approx 11\%$$

(226)

After 3 divisions: about 11% methylation (down from 90%). Since about 50% methylation is the threshold for silencing at most CGIs, *CDKN2B* should be significantly re-expressed.

- (b) Two distinct repressive layers maintain CGI-silenced genes: 1. CpG methylation → methyl-CpG binding proteins (MBD2) recruit HDAC → deacetylated histones 2. Deacetylated histones → compact chromatin, transcription factor exclusion

DNMT inhibition removes layer 1 but may not immediately open chromatin if deacetylated histones persist. HDAC inhibitors (remove layer 2) accumulate acetylation independently of methylation. Together, both layers are removed simultaneously → synergistic re-activation of silenced tumor suppressors.

Worked Example 6 — IDH1 Mutation and the Methylator Phenotype

Problem: A glioma tumor carries the IDH1-R132H mutation. The mutant enzyme converts α -ketoglutarate (α KG) to 2-hydroxyglutarate (2-HG), which competitively inhibits α KG-dependent dioxygenases including TET demethylases, KDM Jumonji-domain demethylases, and prolyl hydroxylases. Predict three genome-wide chromatin consequences of IDH1-R132H, and explain why vorasidenib is therapeutic.

Solution: 1. Global hypermethylation of CpG islands (CIMP+): TET inhibition prevents demethylation → progressive CpG accumulation. 2. H3K27me3 and H3K9me3 accumulation: Jumonji KDM6A/B and KDM4 inhibition prevents demethylation of repressive marks → genome-wide silencing of differentiation genes (the “differentiation block” of IDH-mut AML and glioma). 3. HIF-1 α stabilization: prolyl hydroxylase inhibition stabilizes HIF-1 α → pseudohypoxia → angiogenesis, glycolysis upregulation.

Vorasidenib (FDA 2024 for IDH1-mut grade-2 glioma) crosses the blood–brain barrier and inhibits mutant IDH1, depleting 2-HG and partially reversing TET/KDM/PHD inhibition — restoring demethylation and re-engaging differentiation. Median progression-free survival doubled (27 vs. 11 months) in the INDIGO trial.

16.6 Computational Bridge

Promoter CpG islands are GC-rich; summarizing composition links chromatin biology to sequence statistics:

```
from biology.genetics import gc_content
```

```
cgi_like = "CGCGCGCGCATATATAT"
print(round(gc_content(cgi_like), 3))
```

Methylation decay through cell divisions is a one-line simulation:

```
def methylation_decay(f0: float, generations: int, eps: float = 0.95) -> list[float]:
    """Predict CpG methylation fraction over `generations` divisions
    given maintenance efficiency `eps`.
```

$$f_{n+1} = (eps + (1 - eps) / 2) * f_n \quad (\text{per-CpG approximation})$$

```
    """
    factor = eps + (1 - eps) / 2
    return [f0 * factor ** n for n in range(generations + 1)]

print([round(v, 3) for v in methylation_decay(0.90, 5, eps=0.0)]) # DNMT1-null
```

Setting $\epsilon = 0$ simulates a DNMT1-null (or azacitidine-trapped) cell — the fraction halves each generation.

A Polycomb-spreading simulator with the EED–allosteric read-write feedback:

```
def polycomb_spread(seeds: int, generations: int, k: float, n_nucleosomes: int = 50) -> list[float]:
    """Simulate H3K27me3 occupancy over generations.
```

seeds: initial number of H3K27me3–marked nucleosomes
k: marks deposited per generation per existing mark (read–write coupling)
n_nucleosomes: total nucleosomes available

```
    """
    history = [seeds]
    m = seeds
    for _ in range(generations):
        m = m / 2 + k # passive halving + spreading
        m = min(m, n_nucleosomes) # saturation
        history.append(m)
    return history
```

```
print(polycomb_spread(seeds=2, generations=5, k=10))  
# [2, 11.0, 16.5, 18.25, 19.125, 19.5625] → reaches about 20 marked nucleosomes
```

Clinical / systems note: Azacitidine/decitabine and HDAC inhibitors are approved where malignant clones depend on silenced differentiation programs — therapies that reverse layers of repression rather than mutating oncogenes. Newer entries (tazemetostat for EZH2; menin–MLL inhibitors for KMT2A-rearranged AML; vorasidenib for IDH-mut glioma) extend the same logic to writers, readers, and metabolic upstream regulators.

16.7 Current Evidence and Frontier Biology: Epigenetic Inheritance and Disease

For Epigenetic Inheritance and Disease, frontier biology belongs inside the evidence logic of the chapter. Frontier work on epigenetic inheritance is testing how — and whether — chromatin states cross generations: germline reprogramming erases most marks at fertilization and in primordial germ cells, imprinted loci and a handful of retained marks escape, and environmental exposures (the Dutch Hunger Winter cohort, the agouti-mouse model) are scrutinized for genuine transgenerational effects versus in-utero confounding. The core reading question is this: epigenetic claims require causal perturbation, cell-type specificity, timing, and inheritance controls.

- What to verify: identify the observation, model, assay, or dataset that would make the claim stronger or weaker.
- What to qualify: state the scale, organism, cell type, environmental condition, or population where the claim is expected to hold.
- What to compare: test at least one alternative explanation, baseline, or null model before treating the pattern as causal.
- What to cite: distinguish primary evidence, review synthesis, public dataset, and institutional guidance; for recent or numeric claims, prefer the source closest to the measurement and state what has changed since it was published.

For reference-dependent genetic claims, ask whether read length, structural variation, ancestry representation, phasing, or clinical validation changes the interpretation [Human Pangenome Reference Consortium, 2023, U.S. Food and Drug Administration, 2023, 2024b].

Source practice: For genomics and editing claims, distinguish discovery from clinical actionability, and cite reference resources, regulatory records, or primary editing studies close to the claim [Human Pangenome Reference Consortium, 2023, U.S. Food and Drug Administration, 2026a, Chalumeau et al., 2025].

16.7.1 Current Evidence Map: Epigenetic Causality Ladder

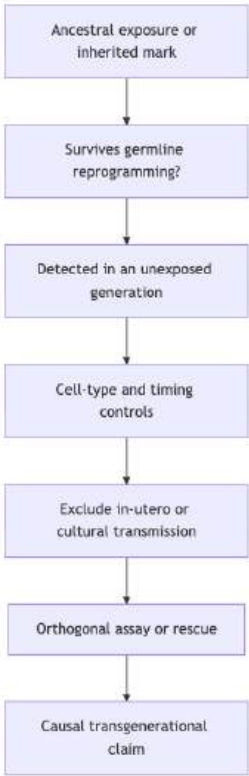


Figure 106. A transgenerational claim is not automatic: an inherited mark must survive germline reprogramming, appear in an unexposed generation, and survive controls excluding in-utero or cultural transmission before it can be called causal.

16.8 Summary

- Chromatin is organized around the nucleosome (147 bp DNA + histone octamer H2A/H2B/H3/H4). Histone variants (H3.3, CENP-A, H2A.Z, H2A.X, macroH2A) define specialized chromatin states. Higher-order compaction creates TADs (CTCF/cohesin) and A/B compartments.
- Histone acetylation (HATs; activating, e.g., H3K27ac, H3K9ac, H4K16ac) and deacetylation (HDACs; repressive) regulate accessibility. Newer acyl marks (lactylation, β -hydroxybutyrylation, crotonylation, butyrylation) couple chromatin to metabolism.
- Histone methylation has context-dependent effects. H3K4me3 = active promoters; H3K36me3 = gene bodies; H3K27me3 = Polycomb (PRC2) silencing; H3K9me3 = constitutive heterochromatin (HP1); H4K20me3 = pericentric heterochromatin. Bivalent domains (H3K4me3 + H3K27me3) mark poised developmental genes in ES cells.
- Polycomb / Trithorax cellular memory: PRC2 (EZH2) writes H3K27me3 \rightarrow recruits PRC1 (RING1B \rightarrow H2AK119ub). MLL/COMPASS writes H3K4me3; UTX/JMJD3 erase H3K27me3; SWI/SNF evicts PRC1/2 — together antagonising Polycomb at active genes.
- DNA methylation at CpG islands (DNMT3A/3B *de novo*; DNMT1+UHRF1 maintenance) causes stable gene silencing. TET enzymes oxidise 5mC \rightarrow 5hmC \rightarrow 5fC \rightarrow 5caC for active demethylation; 5hmC is itself a stable mark. IDH1/2 mutations produce 2-HG, blocking TET and creating the CIMP phenotype.
- Genomic imprinting: about 150 genes from about 30 ICR-controlled clusters expressed monoallelically by parent of origin. IGF2/H19 (CTCF-insulator), 15q11–q13 (Prader–Willi/Angelman), 11p15 BWS/SRS exemplify mechanisms and reciprocal phenotypes.
- X-chromosome inactivation: XIST lncRNA (cis-coating) \rightarrow SPEN-HDAC3 + PRC2 \rightarrow H3K27me3 + DNMT3 \rightarrow CGI methylation; about 15–25 % escape genes (mostly PAR). Skewed XCI explains variable X-linked disease in heterozygous females. iPSC reprogramming reactivates Xi.
- Chromatin remodellers: SWI/SNF (BAF/PBAF — slide+eject; mutated in about 20 % cancers), ISWI (spacing), CHD/NuRD (repressive sliding + HDAC), INO80/SWR1 (H2A.Z exchange).
- 3D genome: TADs by loop extrusion (CTCF + cohesin); A/B compartments; LADs at the lamina; phase-separated condensates at super-enhancers (BRD4, Mediator, Pol II CTD); CDK8 dissolves condensates by phosphorylating Mediator.
- miRNA / lncRNA / piRNA: DROSHA \rightarrow DICER \rightarrow RISC for miRNA; lncRNAs (XIST, HOTAIR, MALAT1, NEAT1) scaffold complexes; piRNAs silence transposons in germline.
- Mitotic / germline reprogramming: Maintenance via DNMT1+UHRF1 (H3K18ub-coupled) and read-write feedback for histone marks. CAF-1 deposits new histones at the fork. Two waves of epigenetic erasure (post-fertilization; PGC). Imprints protected from PGC erasure and re-set sex-specifically during gametogenesis.
- Cancer epigenetics & clinical translation: Approved drugs target each layer — DNMTi, HDACi, EZH2i, IDH-mut inhibitors, BET inhibitors, menin–MLL inhibitors, oncohistone H3K27M biology, condensate-targeting agents.
- Connections: See section 13 for transcriptional output, section 14 for CRISPR-based epigenome editing, **Unit V — Classical Genetics and Heredity: Introduction** for imprinting and pedigree patterns, and **Unit IX — Zoology and Systems Physiology: Introduction** for nuclear receptor chromatin targeting.

16.9 Review Questions

1. A gene has 95% CpG methylation at its promoter CGI. A researcher applies 5-azacytidine for 5 cell divisions with no *de novo* methylation. Using the formula $f_n = f_0/2^n$, what methylation level remains? If the transcription threshold is 30%, at which division does the gene first become potentially active?
2. Explain why H3K27me3 is a repressive mark while H3K4me3 is an activating mark, even though both involve lysine methylation on histone H3. Include the relevant enzymes (HMT and KDM) and reader proteins for each.
3. Draw and annotate the IGF2/H19 imprinting mechanism. Explain why a maternal deletion at the ICR/DMR causes Beckwith-Wiedemann syndrome (biallelic IGF2 expression), while a paternal deletion causes Silver-Russell syndrome (biallelic IGF2 silencing).
4. A female patient presents with Rett syndrome. Genetic testing shows a missense mutation in *MECP2* (methyl-CpG binding protein 2) on one X chromosome. Explain why Rett syndrome shows variable severity between affected females, using the concept of X-chromosome inactivation skewing.
5. A cancer biopsy shows the following ChIP-seq results at a tumor-suppressor gene promoter: H3K27me3 high, H3K4me3 absent, H3K27ac absent, and 85% CpG methylation. A second tumor from the same patient shows H3K27me3 low, H3K27ac present, H3K4me3 high, and 5% methylation — with the tumor-suppressor gene transcribed. Propose two mechanisms by which the epigenetic state could have switched, and describe the specific enzymes involved.
6. Compare piRNAs and miRNAs in terms of: (a) size, (b) biogenesis pathway (DICER-dependent vs. independent), (c) primary biological function in mammals, and (d) what happens when the pathway is disrupted genetically.
7. A developmental biologist shows that a *Drosophila* gene is in a “bivalent domain” in neural stem cells (H3K4me3 + H3K27me3). After neural differentiation, H3K27me3 is removed by KDM6A. What molecular events would you expect at this gene promoter? What histone remodeling complex would facilitate nucleosome repositioning for full activation?
8. The Dutch Hunger Winter cohort shows that caloric restriction in pregnant women led to measurable methylation differences at the IGF2 DMR in their children, persisting for 60 years. Critically evaluate this as evidence for transgenerational epigenetic inheritance, noting the key confounders and what

- additional data would conclusively demonstrate germline transmission.
- A clinical trial combines azacitidine (DNMT inhibitor) with vorinostat (HDAC inhibitor) for treating a myeloid cancer. Using your knowledge of the two repressive layers at silenced CGI promoters, predict which order of drug administration would be more effective. Support your reasoning with the molecular mechanism.
 - CRISPR-dCas9 (catalytically dead Cas9) fused to DNMT3A can write DNA methylation at specific genomic loci. Design an experiment using this tool to test whether the methylation at the *BRCA1* promoter in a cancer cell line is the cause of silencing (not merely a consequence). Describe the expected result if methylation is causal vs. if there is an upstream histone modification driving silencing.
 - Explain how a BET bromodomain inhibitor might reduce *MYC* transcription without mutating the *MYC* locus. How would you test whether the drug acts via loss of BRD4 at super-enhancers rather than a global transcription shutdown?
 - A pediatric tumor harbors a CTCF site deletion that fuses two TADs. Propose how this structural variant could activate an oncogene — and one experiment (Hi-C, CRISPR excision rescue, or luciferase reporter) to support enhancer hijacking.
 - A patient with myelodysplastic syndrome has a TET2 loss-of-function mutation. Predict the genome-wide methylation phenotype, and explain why this patient might respond to azacitidine *better* than a TET2-wild-type patient.
 - A diffuse intrinsic pontine glioma harbors an H3K27M oncohistone. Explain why about 10 % of nucleosomes carrying this mutation can produce a genome-wide H3K27me3 reduction (gain-of-function effect on PRC2 in trans). What is the rationale for EZH2 inhibitors in this setting?
 - Quantitatively compare the half-lives of H3K27ac and 5mC marks across cell divisions. Why does this difference imply that long-term cellular memory is encoded primarily in DNA methylation and Polycomb marks, not acetylation?
 - A glioma is diagnosed with IDH1-R132H mutation. Plasma 2-HG is 200 μ M (vs. < 10 μ M in healthy individuals). The patient is treated with vorasidenib (mutant-IDH1 inhibitor). After 3 months, plasma 2-HG drops to 12 μ M. Predict the time-course of DNA methylation reversal at CIMP+ loci. Why does clinical response (radiographic improvement) typically lag 6–12 months behind 2-HG normalization?
 - A laboratory generates a mouse with a homozygous deletion of the *Cbx7* gene (encoding a PRC1 chromobox subunit). Predict the hematopoietic phenotype. Would you expect the phenotype to be more or less severe than a *Bmi1* (PCGF4) homozygous deletion? Justify your answer in terms of redundancy among canonical-PRC1 paralogs.
 - A 35-year-old woman is found to have CHIP with a *DNMT3A* R882H mutation at 15 % VAF. Three years later she develops AML. Sequencing of the AML shows the same *DNMT3A* R882H plus a new *FLT3-ITD* mutation. Discuss the implications: (i) why is *DNMT3A* loss often a CHIP-precursor mutation rather than the AML-driver itself? (ii) How does R882H differ from a complete loss-of-function? (iii) What treatment would target both the epigenetic and signaling layers?

16.10 Further Reading and Source Notes: Epigenetic Inheritance and Disease

- Strahl & Allis (2000). The language of covalent histone modifications. *Nature*, 403.
- Lyon (1961). Gene action in the X-chromosome of the mouse (*Mus musculus* L.). *Nature*, 190.
- Fire et al. (1998). Potent and specific genetic interference by double-stranded RNA in *Caenorhabditis elegans*. *Nature*, 391.
- Doudna & Charpentier (2014). The new frontier of genome engineering with CRISPR-Cas9. *Science*, 346.

16.11 Key Terms

Table 243. Current Evidence Map: Epigenetic Causality Ladder: Term and Definition.

Term	Definition
Epigenetics	Heritable changes in gene expression that do not alter the DNA sequence
Nucleosome	147 bp DNA + histone octamer (H2A, H2B, H3, H4 × 2); fundamental chromatin unit
Histone variant	Non-canonical histone (H3.3, CENP-A, H2A.Z, H2A.X, macroH2A) deposited at specialized loci
Histone code	Combinatorial histone modifications specify chromatin states and downstream regulatory outcomes
HAT / HDAC	Histone acetyltransferase (writer) / deacetylase (eraser); regulate H3K9/H3K14/H3K27/H4K16 acetylation
H3K27me3	PRC2/EZH2-deposited Polycomb repressive mark
H3K4me3	MLL/SET1-deposited active promoter mark
H3K9me3	SUV39H/SETDB1-deposited constitutive heterochromatin mark; HP1 reader
H3K36me3	SETD2-deposited transcribed gene body mark
PRC1 / PRC2	Polycomb complexes; PRC2 writes H3K27me3 (EZH2), PRC1 writes H2AK119ub (RING1B)
Trithorax (TrxG)	MLL/COMPASS, KDM6A/B, BAF — antagonise Polycomb

Term	Definition
CpG island	about 500 bp–2 kb region of high CpG density; methylation at promoter CGIs silences genes
DNMT1	Maintenance DNA methyltransferase; copies hemimethylated CpGs at replication fork (UHRF1-recruited)
DNMT3A/3B	De novo methyltransferases; require DNMT3L cofactor
UHRF1	Hemi-methyl-CpG reader (SRA); H3K9me reader (TTD); recruits DNMT1 to fork
TET enzymes	Fe(II)/ α KG-dependent dioxygenases; oxidise 5mC \rightarrow 5hmC \rightarrow 5fC \rightarrow 5caC for active demethylation
5-methylcytosine	The “fifth base”; methylated cytosine at CpG dinucleotides
5hmC	5-hydroxymethylcytosine; TET oxidation product; stable mark in neurons
Genomic imprinting	Parent-of-origin-specific monoallelic gene expression; about 150 human genes
ICR / DMR	Imprint control region / differentially methylated region
XIST	X-inactive specific transcript; 17 kb lncRNA; coats inactive X chromosome in cis
Skewed XCI	Non-50/50 X-inactivation distribution; explains variable X-linked disease in females
miRNA	about 22 nt RNA; DROSHA \rightarrow DICER pathway; AGO2/RISC \rightarrow translational repression/mRNA decay
piRNA	26–31 nt germline RNA; PIWI pathway; silences transposable elements
TAD	Topologically Associating Domain; chromatin loop defined by CTCF/cohesin; enhancer-promoter contacts
A/B compartment	Megabase-scale active vs. repressed chromatin neighborhoods
LAD	Lamina-Associated Domain; gene-poor regions tethered to nuclear periphery
LLPS / condensate	Liquid-liquid phase separation; concentrates IDR-containing regulators at hubs
Super-enhancer	Large enhancer cluster with dense Mediator/BRD4/H3K27ac; drives high transcriptional output
Bivalent domain	Simultaneous H3K4me3 + H3K27me3 at developmental gene promoters in ES cells
SWI/SNF (BAF)	ATP-dependent remodeller; mutated in about 20 % cancers (ARID1A, SMARCB1, PBRM1)
ISWI / CHD/NuRD / INO80	Other remodeller families: spacing / repressive sliding+HDAC / H2A.Z exchange
CAF-1	Chromatin assembly factor 1; deposits new H3.1-H4 at replication fork via PCNA
Azacitidine / decitabine	DNMT inhibitors; trap DNMT1; approved for MDS/AML
Vorinostat (SAHA)	HDAC inhibitor; approved CTCL; synergises with DNMT-i
Tazemetostat	EZH2 inhibitor; FDA-approved for SMARCB1-loss epithelioid sarcoma and EZH2-mut FL
BET inhibitor	Blocks bromodomain–acetyl-lysine engagement (e.g., BRD4); collapses oncogenic transcriptional condensates
Vorasidenib	Mutant-IDH1 inhibitor; FDA-approved 2024 for grade-2 glioma; depletes 2-HG, restores TET activity
Revumenib	Menin–MLL inhibitor; FDA-approved 2024 for KMT2A-rearranged AML
Oncohistone	Recurrent gain-of-function histone mutation (H3K27M, H3G34R/V, H3K36M) acting in trans
CIMP	CpG-island methylator phenotype; cluster of hypermethylated CGIs (IDH-mut glioma, MLH1-silent CRC)

16.12 Discussion Questions

These open-ended questions require integration across multiple sections and connection to clinical or experimental practice. Suitable for graduate-style discussion or take-home essay.

1. Cellular memory under perturbation. PRC2 (H3K27me3) is regularly described as a “cellular memory” system. Experimentally, how would you distinguish whether Polycomb memory at a developmental gene is maintained by (a) the read-write feedback loop alone, (b) the parental nucleosome inheritance mechanism, or (c) DNA methylation acting downstream? Propose two CRISPR-based perturbations that would discriminate between these mechanisms.
2. Aging and the epigenetic clock. Steve Horvath’s epigenetic clock predicts chronological age from CpG methylation patterns at about 353 sites with median error of 3.6 years. Why should DNA methylation drift with age? Propose three biological mechanisms (mitotic-error, oxidative-stress, lineage-replacement). What therapeutic implications would follow if epigenetic age could be reversed (e.g., via Yamanaka factors, partial reprogramming)?
3. The “junk DNA” reckoning and 80 % functional ENCODE claim. ENCODE (2012) claimed $\geq 80\%$ of the human genome has biochemical activity (chromatin accessibility, TF binding, histone marks, RNA transcription). Critics argue most of these activities are “noise” — neutral binding to GC-rich sequences. Take a position: design an experiment that would distinguish biologically functional enhancer activity from “spurious” biochemical activity at a candidate non-coding region.
4. Synthetic biology with phase separation. Engineering programmable transcription factors with IDR-mediated condensate formation could provide programmable control over transcription rate. Propose three design principles — and three failure modes — for an engineered IDR–dCas9 fusion that would create a tunable super-enhancer-like condensate.

5. Trans-generational epigenetic inheritance: real or artifact? Critique the human evidence (Dutch Hunger Winter, Överkalix, Holocaust trauma cohorts). What four experimental designs would conclusively demonstrate transgenerational inheritance through sperm/oocyte (rather than direct exposure of F1 germline)? Why is this question particularly difficult in mammals compared to *C. elegans* or *Arabidopsis*?
6. Clinical sequencing and the epigenome. A 70-year-old woman has DNMT3A R882H clonal-hematopoiesis (CHIP) detected on routine whole-exome sequencing. She has no AML and no cytopenia. As her physician, what counselling would you provide regarding: (i) AML risk, (ii) cardiovascular risk (CHIP elevates CHD risk independent of AML), (iii) lifestyle modifications, (iv) whether prophylactic treatment should be considered, and (v) what monitoring frequency you would recommend?

16.13 Companion Source Module: Epigenetic Inheritance and Disease

Epigenetic Inheritance and Disease should leave a reproducible trail from a biological claim to the code, figure, diagram, or paper-based activity that can test it. Use the surfaces below to inspect the chapter’s assumptions, rerun the relevant model, or compare the manuscript explanation with companion labs and figures.

Table 244. Companion source surfaces for Epigenetic Inheritance and Disease.

Surface	Use it for
<code>src/biology/genetics/genetics.py</code> (<code>cpg_methylation_remaining</code> , <code>histone_modification_state</code>)	Convert methylation maintenance and histone-mark claims into explicit state checks.
<code>src/visualization/plots.py</code> (<code>plot_methylation_heatmap</code>)	Inspect whether heatmap interpretation depends on color alone or includes labels.
<code>src/mermaid/biology_diagrams.py</code> (<code>mirna_biogenesis_diagram</code> , <code>x_inactivation_diagram</code>)	Compare RNA-mediated and chromatin-mediated regulation.

Reproducibility check: require cell type, developmental time, perturbation evidence, and inheritance control before calling a mark causal. Cross-reference: use [section 13](#), [section 14](#), and [section 19](#).

Unit V — Classical Genetics and Heredity: Introduction

Why This Unit Matters

In 1866, an Augustinian friar in Brno published a mathematical analysis of 29,000 pea plants he had grown in the monastery garden. Gregor Mendel showed that heritable traits are passed from parent to offspring in discrete, predictable ratios — 3:1 for monohybrid crosses, 9:3:3:1 for dihybrid crosses. His paper, "Versuche über Pflanzenhybriden," went unread for 34 years. When it was rediscovered simultaneously by de Vries, Correns, and Tschermak in 1900, it ignited a revolution: the laws of segregation and independent assortment described the behavior of something that Mendel had rarely seen — chromosomes, structures not visualized until the 1880s, and connected to genes primarily by Thomas Hunt Morgan's fruit fly experiments in 1910.

The synthesis of Mendel's mathematical laws with chromosomal theory, and later with population genetics, constitutes one of the great intellectual achievements of twentieth-century science. It unified patterns of inheritance visible to naked-eye observation with the molecular machinery of DNA replication and meiosis. It transformed agriculture, medicine, forensic science, and evolutionary theory simultaneously. Today, genome-wide association studies (GWAS) identify thousands of loci contributing to human traits; pedigree analysis diagnoses rare recessive disorders; and population genetics models predict drug-resistance evolution in pathogens.

This unit bridges the gap between the molecular genetics of **Unit IV — Molecular Genetics: Introduction** and the evolutionary dynamics of **Unit VI — Evolution: Introduction**. You will derive Mendelian ratios from first principles, work through the mathematics of incomplete dominance, codominance, and epistasis, map gene positions using recombination frequencies, and apply the Hardy-Weinberg equations to natural populations.

Landmark Discoveries

Discoverer(s)	Year	Journal / Source	Discovery	Significance
Gregor Mendel	1866	[Mendel, 1866]	Laws of segregation and independent assortment	Mathematical foundation of genetics; rediscovered 1900
Walther Flemming	1882	[Flemming, 1882]	Chromosomes during mitosis ("chromatin")	First visualization of chromosomal segregation
Thomas Hunt Morgan	1910	[Morgan, 1910]	Sex-linked inheritance in <i>Drosophila</i>	Proved genes reside on chromosomes; Nobel Prize 1933
Alfred Sturtevant	1913	[Sturtevant, 1913]	First genetic map (6 X-linked <i>Drosophila</i> genes)	Showed recombination frequency ∝ map distance
Barbara McClintock	1950	[McClintock, 1950]	Transposable elements ("jumping genes")	Showed genomes are dynamic; Nobel Prize 1983
Hardy & Weinberg	1908	[Weinberg, 1908]	Population genetic equilibrium	Allele frequencies stable without evolution; quantitative tool for deviations
Human Genome Project Consortium	2001	[Consortium, 2001]	Draft human genome sequence	about 3.2 Gb; about 20,000 protein-coding genes; foundation for GWAS

Key Concepts and Connections

Unit V — Classical Genetics and Heredity: Introduction concept map — Classical Genetics and Heredity.

Current Evidence Thread

Treat inheritance in this unit as something that is *evidenced*, not just asserted: pedigrees and controlled crosses test transmission rules, allele-frequency time series test which evolutionary force is acting, and biobank-scale association data test whether a 'Mendelian' trait is really single-gene. Classical genetics remains essential, but modern interpretation adds penetrance, polygenicity, structural variation, ancestry-aware inference, and uncertainty in risk prediction. As you move through the chapters, keep a two-column note: claim on the left, evidence that would change my confidence on the right. By the end of the unit, each major idea should be tied to a measurement, model, citation, or paper-based lab decision.

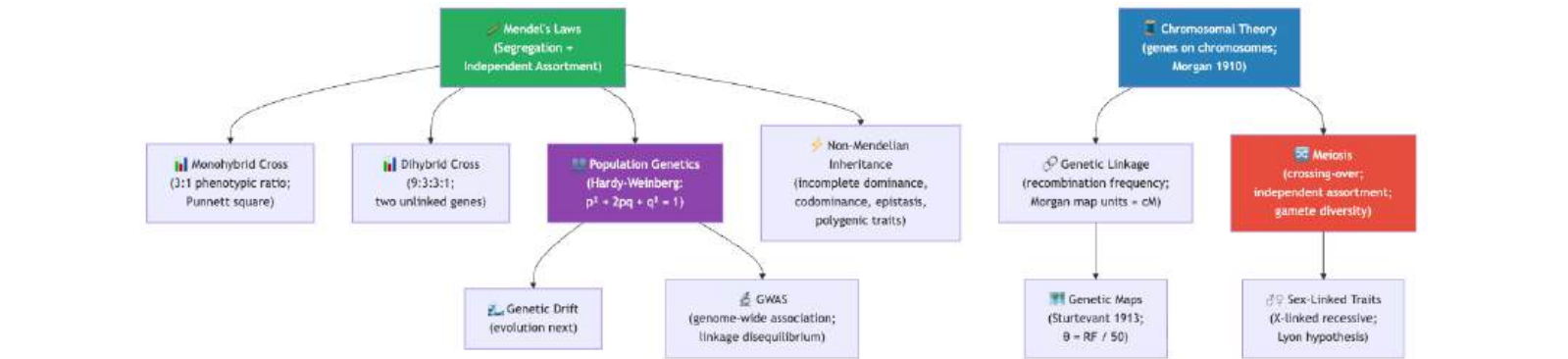


Figure 107. Classical genetics concept map linking Mendel’s laws to monohybrid ratios, Punnett squares, dihybrid ratios, linkage, chromosomes, and population genetics.

Chapter Roadmap

Chapter	Title	Core Question	Key Equation / Model
16	Mendelian Genetics	How do Mendel’s laws explain the inheritance of discrete traits?	Binomial expansion; chi-square test for goodness of fit
17	Chromosomal Inheritance	How do chromosomes carry genes, and what happens when chromosomal segregation errors occur?	Recombination frequency θ ; map function; trisomy probability
18	Population Genetics	How do allele frequencies change — or not change — in populations?	Hardy-Weinberg: $p^2 + 2pq + q^2 = 1$; Δp under selection; F_{ST}

Connections Across the Textbook

- Meiosis and crossing-over (section 19) build directly on DNA replication and chromosome structure from Unit IV — Molecular Genetics: Introduction, and provide the mechanistic basis for recombination in Unit VI — Evolution: Introduction (evolution).
- Hardy-Weinberg equilibrium (section 20) is the null model for both natural selection (section 21) and genetic drift (section 22).
- Pedigree analysis and inheritance patterns reappear throughout Unit IX — Zoology and Systems Physiology: Introduction (genetic basis of cardiovascular disease, endocrine disorders, immune deficiencies).
- Epistasis and polygenic traits link to Unit VI — Evolution: Introduction (quantitative trait loci, QTL mapping) and Unit X — Ecology: Introduction (population-level phenotypic variation in ecology).

Key vocabulary introduced here: allele, locus, genotype, phenotype, dominant, recessive, homozygous, heterozygous, test cross, chi-square test, centimorgan (cM), Hardy-Weinberg equilibrium, inbreeding coefficient, linkage disequilibrium, aneuploidy, nondisjunction.

Computational Toolbox — Unit V

```
from biology.genetics import hardy_weinberg, hamming_distance, chi_squared_test

# Hardy-Weinberg equilibrium: cystic fibrosis (autosomal recessive)
# Carrier frequency q ≈ 1/22 in Northern Europeans → q ≈ 0.045, p ≈ 0.955
hw = hardy_weinberg(p=0.955, q=0.045)

print(f"AA (unaffected non-carrier): {hw.p_squared:.4f} = {hw.p_squared*100:.1f}%")
print(f"Aa (carrier): {hw.two_pq:.4f} = {hw.two_pq*100:.1f}%")
print(f"aa (affected): {hw.q_squared:.5f} = 1 in {1/hw.q_squared:.0f}")

# Expected:
# AA (unaffected non-carrier): 0.9120 = 91.2%
# Aa (carrier): 0.0860 = 8.6% (~ 1 in 23 – matches observed carrier rate)
# aa (affected): 0.00203 = 1 in 493
```

```
# Sequence distance between two short alleles
dist = hamming_distance("ATGCTAGC", "ATGATAGT")
print(f"Sequence differences: {dist}")
# Expected: Sequence differences: 2

# Chi-square test: 3:1 vs observed 290:110 (n=400 plants)
chi = chi_squared_test(observed=[290, 110], expected=[300, 100])
print(f"χ² = {chi.chi_squared:.2f}, p ≈ {chi.p_value_approx:.3f}")
# Expected: χ² ≈ 1.33, p ≈ 0.25 (not significant; consistent with 3:1)
```

Try it yourself: Change carrier frequency to $q = 0.02$ (rare disease). What fraction of affected individuals are born to two carrier parents?

Source note: genetics helpers support Punnett squares, Hardy-Weinberg checks, sequence distances, and chi-squared tests. Figures: *src/visualization/* (Mendelian ratio histograms, Hardy-Weinberg surface plots).

Cross-Unit Integration

The Mendelian genetics and Hardy-Weinberg framework of **Unit V — Classical Genetics and Heredity: Introduction** provide the static accounting of allele frequencies — the inventory at equilibrium. **Unit VI — Evolution: Introduction** breaks that equilibrium open: natural selection, genetic drift, mutation, and gene flow are precisely the forces that *violate* Hardy-Weinberg assumptions, and the magnitude of each violation determines evolutionary trajectory. Population-genetic intuitions about allele frequency, heterozygosity, and effective population size carry directly into **Unit VI — Evolution: Introduction**'s quantitative treatment of fitness, selection coefficients, and the fixation index. When **Unit VI — Evolution: Introduction** introduces selection differentials and response equations, recognize them as Hardy-Weinberg with a forcing term — the same machinery in motion rather than at rest.

17 Mendelian Principles and Probability

Level 2/3 · 35 min read · 55 min lecture · Prerequisites: section 12

17.1 Learning Objectives

1. Describe Mendel [Mendel, 1866]’s experimental system and explain why *Pisum sativum* was ideal for genetic analysis.
2. State Mendel’s laws of segregation and independent assortment and explain their mechanistic basis in meiosis.
3. Solve monohybrid, dihybrid, and trihybrid cross problems using Punnett squares and probability.
4. Describe extensions to Mendelian genetics: incomplete dominance, codominance, multiple alleles, pleiotropy, epistasis, polygenic inheritance, genomic imprinting, and maternal effect.
5. Explain penetrance, expressivity, and phenocopy with disease examples.
6. Apply the chi-squared test for goodness of fit to evaluate Mendelian ratios.
7. Construct and interpret pedigrees for autosomal dominant, autosomal recessive, X-linked recessive, X-linked dominant, and mitochondrial inheritance patterns.
8. Solve multi-step genetics problems involving probability rules (product rule, sum rule, conditional probability).
9. Connect Mendelian segregation to chromosome behavior at meiosis and explain the molecular basis of human autosomal-dominant and autosomal-recessive disorders.
10. Outline how genome-wide association studies (GWAS) extend Mendelian thinking to polygenic traits in human populations.

17.1.1 Study Blueprint

- Big idea: Mendelian segregation and probability explain inheritance when alleles assort independently.
- Core concepts: segregation, independent assortment, Punnett squares, probability.
- Framework alignment: Vision & Change: Information flow, exchange, and storage, Evolution; AP Biology: Information Storage and Transmission, Evolution; NGSS-style topics: Inheritance and Variation of Traits, Natural Selection and Evolution.
- Model or quantitative lens: Punnett, binomial, and chi-square calculations.
- Data skill: Use cross data to infer genotype probabilities.
- Practice cadence: Statistical Tests and Data Analysis, Representing and Describing Data.
- Common misconception to repair: Dominant does not mean common, stronger, or better.
- Primary lab: Lab — Mendelian Principles and Probability.
- Question bank: Questions — Mendelian Principles and Probability.
- Transfer task: Transfer Mendelian probability to model organisms and introductory human genetics.
- Bridge to computation: `biology.genetics.genetics.chi_squared_test`.

Opening Vignette — The Forgotten Friar and the Laws of Inheritance

Gregor Mendel spent eight years (1856–1863) growing and cross-pollinating nearly 28,000 pea plants in the garden of St. Thomas’s Abbey in Brno, recording data with statistical rigour unprecedented in biology at the time. He presented his findings to the Brno Natural History Society in 1865, and published them in the society’s journal in 1866 [Mendel, 1866]. The audience of 40 scientists was politely unenthusiastic. For 35 years, his paper languished in obscurity — unread, uncited, misunderstood. Then in 1900, three botanists working independently — Hugo de Vries, Carl Correns, and Erich von Tschermak — each rediscovered the same ratios Mendel had documented and, searching the literature, found his paper. Overnight, an unknown friar’s meticulous garden statistics became the foundation of modern genetics. Mendel rarely knew he had founded a science.

17.2 Mendel’s Experiments: Historical Context

Gregor Johann Mendel (1822-1884), an Augustinian friar and physics-trained scientist, conducted breeding experiments on garden peas (*Pisum sativum*) from 1856 to 1863 in the monastery garden at Brno (now Czech Republic). His 1866 paper, “Versuche uber Pflanzen-Hybriden” (Experiments on Plant Hybrids), was largely ignored until 1900 when it was independently “rediscovered” by de Vries, Correns, and von Tschermak [Mendel, 1866].

Why peas were ideal:

Punnett Square: Aa × Aa

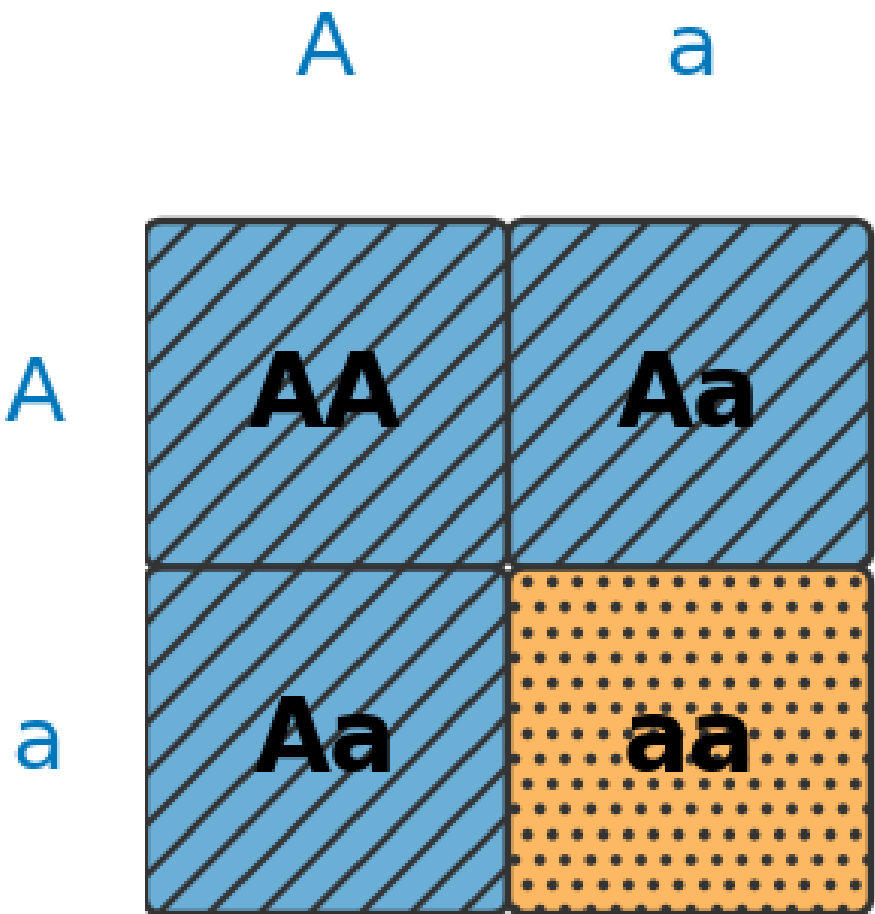


Figure 108. Punnett square for a monohybrid cross Aa × Aa. Each cell shows the zygote genotype; the 3:1 phenotype ratio follows directly from the 1:2:1 genotype ratio.

Table 245. Study Blueprint: Advantage and Significance.

Advantage	Significance
Distinct, discontinuous traits	7 characters with clear dominant/recessive forms (no blending)
True-breeding lines available	Commercially available pure varieties; years of inbreeding
Short generation time	about 3 months seed to seed
Self-compatible flowers	Could self-fertilize (controlled crosses possible by emasculation)
Large number of offspring	Each pod contains about 7 seeds; massive sample sizes
Easy to cross-pollinate	Large flowers with accessible reproductive parts

Mendel’s seven characters:

Table 246. Study Blueprint: Character and Dominant.

Character	Dominant	Recessive
Seed shape	Round	Wrinkled
Seed color	Yellow	Green
Flower color	Purple	White
Flower position	Axial	Terminal
Pod shape	Inflated	Constricted
Pod color	Green	Yellow
Stem length	Tall	Short

Mendel’s genius was quantitative: he counted offspring in each class and applied binomial probability reasoning – the first application of statistics to biology. He analyzed about 28,000 pea plants over 8 years [Mendel, 1866].

17.3 Mendel’s Laws of Segregation and Independent Assortment

17.3.1 Law of Segregation (Mendel’s First Law)

Statement: Each organism possesses two alleles for each gene. These alleles segregate (separate) during gamete formation, such that each gamete receives exactly one allele. Upon fertilization, the diploid state is restored [Mendel, 1866].

Molecular basis: Separation of homologous chromosomes during anaphase I of meiosis. The two alleles of a gene reside on homologous chromosomes; when homologs are pulled to opposite poles, each gamete receives one allele.

17.3.2 The Molecular Basis of Mendel’s Laws: From Bivalents to Binomials

Mendel formulated his laws in 1866 without any knowledge of chromosomes, meiosis, or DNA. He treated alleles as abstract “factors” — discrete particles that combined and segregated according to mathematical rules. The chromosomal interpretation came nearly four decades later, when Walter Sutton [1902] and Theodor Boveri independently noticed that chromosomes in meiosis behaved exactly the way Mendel’s factors had to behave for his laws to hold:

Table 247. The Molecular Basis of Mendel’s Laws: From Bivalents to Binomials: Mendel’s abstract law and Chromosomal mechanism.

Mendel’s abstract law	Chromosomal mechanism
Each individual has two factors per trait	Diploid cells have two homologs per chromosome
Factors separate equally into gametes	Homologs disjoin at anaphase I; each gamete inherits one
Factors at different loci assort independently	Non-homologous bivalents orient independently at metaphase I
Factors are particulate, not blended	Chromosomes maintain integrity across generations (apart from crossing over)

The synthesis of Mendel’s laws with the chromosome theory of inheritance — completed by Thomas Hunt Morgan’s *Drosophila* work between 1910 and 1915 — is one of the central convergences in biology [Morgan, 1910]. Every Punnett square is, at heart, a model of homologous-chromosome behavior in meiosis

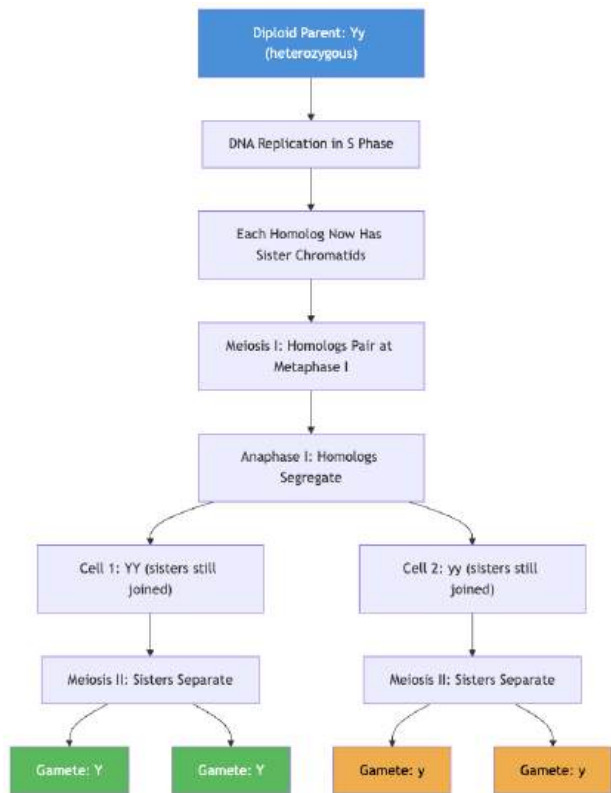


Figure 109. Molecular basis of the Law of Segregation. A heterozygous (Yy) individual produces equal proportions of Y and y gametes because homologous chromosomes separate at anaphase I of meiosis.

(section 19). The 3:1 ratio is not a numerical coincidence; it is the inevitable algebraic shadow of two homologs segregating independently into haploid gametes that then unite at fertilization. When meiosis fails — non-disjunction, translocation, or imprinting errors — Mendelian ratios fail predictably with it.

17.3.3 Law of Independent Assortment (Mendel’s Second Law)

Statement: Alleles at different gene loci are distributed to gametes independently of one another – the inheritance of one gene does not affect the inheritance of another.

Molecular basis: Random orientation of non-homologous bivalents at metaphase I. Each bivalent can orient with either homolog facing either pole, and this orientation is independent of the other bivalents.

Important exception: This law applies only to genes on different chromosomes (or very far apart on the same chromosome, >50 cM). Genes on the same chromosome that are close together exhibit **linkage** and violate independent assortment, the logic that made chromosome mapping possible [Sturtevant, 1913] (see *Chromosomal Inheritance and Linkage*).

Concept Check 16.1

1. If the law of segregation is based on meiosis I, what specific cellular event during meiosis II is relevant?

2. A student claims that Mendel’s laws prove genes are on chromosomes. Is this historically accurate? When was this connection established?

3. If two genes are 5 cM apart on the same chromosome, do they assort independently? Explain.

17.4 Monohybrid Crosses and Single-Gene Segregation

17.4.1 The Standard Monohybrid Cross

Worked example – seed color:

$$P : \quad YY \text{ (yellow)} \times yy \text{ (green)}$$

(227)

$$F_1 : \quad Yy \text{ (most yellow – Y is dominant)}$$

(228)

$$F_1 \times F_1 : \quad Yy \times Yy$$

(229)

Punnett square:

Table 248. The Standard Monohybrid Cross.

	Y	y
Y	YY	Yy
y	Yy	yy

F_2 genotype ratio: $\frac{1}{4}$ YY : $\frac{2}{4}$ Yy : $\frac{1}{4}$ yy = 1:2:1

F_2 **phenotype** ratio: $\frac{3}{4}$ yellow : $\frac{1}{4}$ green = 3:1, the canonical heterozygote-cross outcome visualized in figure 108, where the 3:1 phenotype ratio falls out directly from the underlying 1:2:1 genotype ratio.

17.4.2 The Testcross as a Genotype-Revealing Cross

To determine whether an individual showing the dominant phenotype is homozygous (YY) or heterozygous (Yy), cross it with a homozygous recessive (yy):

- If YY x yy: the offspring are Yy (yellow) – no recessive offspring
- If Yy x yy: $\frac{1}{2}$ Yy (yellow) : $\frac{1}{2}$ yy (green) – 1:1 ratio reveals heterozygosity

17.4.3 Probability Rules for Independent Genetic Events

Product rule (AND): The probability of two independent events both occurring = product of individual probabilities.

$$P(A \text{ and } B) = P(A) \times P(B)$$

(230)

Sum rule (OR): The probability of either of two mutually exclusive events occurring = sum of individual probabilities.

$$P(A \text{ or } B) = P(A) + P(B)$$

(231)

17.5 Worked Example: Probability Rules in a Monohybrid Cross

(a) The first child is yy?

$$P(yy) = \frac{1}{4}$$

(232)

(b) The first two children are both yy?

$$P = \frac{1}{4} \times \frac{1}{4} = \frac{1}{16} \quad \text{(product rule; independent events)}$$

(233)

(c) Among three children, exactly one is yy?

$$P = \binom{3}{1} \left(\frac{1}{4}\right)^1 \left(\frac{3}{4}\right)^2 = 3 \times \frac{1}{4} \times \frac{9}{16} = \frac{27}{64} \approx 0.422$$

(234)

17.6 Dihybrid and Trihybrid Crosses

17.6.1 The Dihybrid Cross

Two independently assorting genes: seed color (Y/y) and seed shape (R = round, r = wrinkled):

$$P : \quad YYRR \times yyrr \tag{235}$$

$$F_1 : \quad YyRr \text{ (yellow, round)} \tag{236}$$

$$F_1 \times F_1 : \quad YyRr \times YyRr \tag{237}$$

Each parent produces 4 gamete types in equal frequency: YR, Yr, yR, yr.

F₂ phenotype ratio: 9 Y_R_ : 3 Y_rr : 3 yyR_ : 1 yyrr = 9:3:3:1

This ratio is the product of two independent 3:1 ratios:

$$\left(\frac{3}{4}Y_{-} + \frac{1}{4}yy\right) \times \left(\frac{3}{4}R_{-} + \frac{1}{4}rr\right) = \frac{9}{16} + \frac{3}{16} + \frac{3}{16} + \frac{1}{16} \tag{238}$$

17.6.2 The Forked-Line (Branch Diagram) Method

For a trihybrid cross (AaBbCc x AaBbCc), the Punnett square would require 64 cells. Instead, use the forked-line method:

A locus: $\frac{3}{4}A_{-}$ and $\frac{1}{4}aa$ (239)

B locus: $\frac{3}{4}B_{-}$ and $\frac{1}{4}bb$ (240)

C locus: $\frac{3}{4}C_{-}$ and $\frac{1}{4}cc$ (241)

Probability of A_B_C_ = $\frac{3}{4} \times \frac{3}{4} \times \frac{3}{4} = \frac{27}{64}$

Total number of phenotypic classes = $2^3 = 8$

Number of genotypic classes = $3^3 = 27$

17.7 Worked Example: Trihybrid Cross Probabilities

In a trihybrid cross AaBbCc x AaBbCc, what fraction of offspring will be:

(a) AaBbCc (triple heterozygous)?

$$P = \frac{2}{4} \times \frac{2}{4} \times \frac{2}{4} = \frac{8}{64} = \frac{1}{8} \tag{242}$$

(b) Homozygous for the three loci (AA BB CC or aa bb cc etc.)?

Each locus has probability $\frac{1}{4} + \frac{1}{4} = \frac{1}{2}$ of being homozygous (either AA or aa).

$$P(\text{homozygous at most 3}) = \frac{1}{2} \times \frac{1}{2} \times \frac{1}{2} = \frac{1}{8} \tag{243}$$

Worked Example — Trihybrid Cross Probability: A dihybrid cross AaBbCc × AaBbCc produces offspring. Calculate the probability of the genotype AaBbCc (triple heterozygote). Since each locus is independent: P(Aa) = 2/4 = 0.5; P(Bb) = 0.5; P(Cc) = 0.5. P(AaBbCc) = 0.5³ = 0.125 = 12.5%. Extended: in a trihybrid cross, the 27 distinct phenotypic classes (when alleles show simple dominance) occur with probabilities following (3/4 + 1/4)³ expansion: dominant at each of three loci occurs (3/4)³ = 27/64 ≈ 42.2%; recessive at each of three occurs (1/4)³ = 1/64 ≈ 1.6%. For a class

with specific genotype aaB_C_: $P(aa) \times P(B_) \times P(C_) = (1/4)(3/4)(3/4) = 9/64$. Chi-squared test with 8 df would require at least 8 expected class sizes of ≥ 5 , meaning a minimum sample size of $8 \times 5/(1/64) = 2,560$ offspring for the rarest class to have expected count ≥ 5 .

Concept Check (Evaluation): Genome-wide association studies (GWAS) identify thousands of SNPs associated with complex traits like height, BMI, and schizophrenia — but each SNP has tiny effect size (odds ratio 1.01-1.10) and explains $<0.1\%$ of trait variance. Yet the identified SNPs together explain $<50\%$ of heritability for most traits — the “missing heritability” problem. (a) Evaluate four possible explanations for missing heritability: (i) rare variants with large effects (not detected by GWAS), (ii) gene-gene interactions (epistasis), (iii) overestimated heritability from twin studies, (iv) epigenetic variants not captured by SNP arrays. For each, predict what experimental approach would resolve it. (b) Polygenic risk scores (PRS) aggregate genome-wide SNP effects. A PRS for coronary artery disease has a population AUC of 0.64. Explain what this means clinically and why population-level prediction does not translate to individual risk certainty.

Concept Check (Chi-square): A dihybrid cross scored 315 round-yellow : 108 round-green : 101 wrinkled-yellow : 32 wrinkled-green offspring (Mendel’s classic F_2 , $n = 556$). (a) State the phenotypic ratio expected under independent assortment with simple dominance. (b) Compute the χ^2 statistic against that expectation and, with 3 degrees of freedom, decide whether to reject the null hypothesis at $\alpha = 0.05$ (critical value 7.81). (c) Explain what a failure to reject does — and does not — establish about linkage.

17.8 Current Evidence and Frontier Biology: Mendelian Principles and Probability

For Mendelian Principles and Probability, frontier biology belongs inside the evidence logic of the chapter. Classical genetics remains essential, but modern interpretation adds penetrance, polygenicity, structural variation, ancestry-aware inference, and uncertainty in risk prediction. The core reading question is this: Mendelian patterns are starting models that must be qualified by penetrance, linkage, environment, and sampling.

- What to verify: identify the observation, model, assay, or dataset that would make the claim stronger or weaker.
- What to qualify: state the scale, organism, cell type, environmental condition, or population where the claim is expected to hold.
- What to compare: test at least one alternative explanation, baseline, or null model before treating the pattern as causal.
- What to cite: distinguish primary evidence, review synthesis, public dataset, and institutional guidance; for recent or numeric claims, prefer the source closest to the measurement and state what has changed since it was published.

A good genetics answer separates the Mendelian transmission model from the evidence needed to use it in a population, family, or clinical setting. Source practice: For genetics claims, separate model assumptions from sampling, ancestry representation, penetrance, linkage, and environment.

17.9 Summary

- Describe Mendel’s experimental system and explain why *Pisum sativum* was ideal for genetic analysis.
- State Mendel’s laws of segregation and independent assortment and explain their mechanistic basis in meiosis.
- Solve monohybrid, dihybrid, and trihybrid cross problems using Punnett squares and probability.
- Describe extensions to Mendelian genetics: incomplete dominance, codominance, multiple alleles, pleiotropy, epistasis, polygenic inheritance, genomic imprinting, and maternal effect.
- Explain penetrance, expressivity, and phenocopy with disease examples.
- Apply the chi-squared test for goodness of fit to evaluate Mendelian ratios.
- Construct and interpret pedigrees for autosomal dominant, autosomal recessive, X-linked recessive, X-linked dominant, and mitochondrial inheritance patterns.
- Solve multi-step genetics problems involving probability rules (product rule, sum rule, conditional probability).

17.10 Further Reading and Source Notes: Mendelian Principles and Probability

- Mendel (1866). Versuche {”u}ber Pflanzenhybriden. *Verhandlungen des naturforschenden Vereines in Br{”u}nn*, 4.
- Sutton (1902). On the morphology of the chromosome group in {Brachystola magna}. *Biological Bulletin*, 4.
- Morgan (1910). Sex limited inheritance in {Drosophila}. *Science*, 32.
- Fisher (1918). The correlation between relatives on the supposition of Mendelian inheritance. *Transactions of the Royal Society of Edinburgh*, 52.
- Hartl & Clark (2007). *Principles of Population Genetics* (4th ed.). Sinauer.

17.11 Companion Source Module: Mendelian Principles and Probability

Mendelian Principles and Probability should leave a reproducible trail from a biological claim to the code, figure, diagram, or paper-based activity that can test it. Use the surfaces below to inspect the chapter’s assumptions, rerun the relevant model, or compare the manuscript explanation with companion labs and figures.

Table 249. Companion source surfaces for Mendelian Principles and Probability.

Surface	Use it for
src/biology/genetics/genetics.py (punnett_square, hardy_weinberg, chi_squared_test)	Reproduce inheritance ratios, equilibrium expectations, and goodness-of-fit tests.
src/visualization/plots.py (plot_punnett_square)	Check genotype and phenotype tables visually.
src/mermaid/biology_diagrams.py (mendelian_cross_diagram)	Link segregation logic to diagrammed crosses.

Reproducibility check: state genotype notation, dominance model, sample size, and statistical expectation before interpreting a ratio. Cross-reference: compare with section 19 and section 20.

18 Mendelian Extensions and Human Genetics

Level 2/3 · 35 min read · 55 min lecture · Prerequisites: section 17

18.1 Learning Objectives

1. Describe extensions to Mendelian genetics including incomplete dominance, codominance, epistasis, and imprinting.
2. Solve pedigree and probability problems for human inheritance patterns.
3. Apply chi-squared tests and interpret penetrance, expressivity, and phenocopy.
4. Connect Mendelian extensions to GWAS and polygenic risk in populations.
5. Interpret a multi-generational pedigree with both X-linked and autosomal loci.
6. Distinguish monogenic, oligogenic, and polygenic inheritance using family and population evidence.
7. Evaluate polygenic risk scores with ancestry representation and calibration limits.

18.2 Extensions to Mendelian Genetics

18.2.1 Incomplete Dominance and Dosage-Sensitive Phenotypes

Neither allele is completely dominant; the heterozygote displays an intermediate phenotype:

- Snapdragon flower color: $C^R C^R$ (red) x $C^W C^W$ (white) $\rightarrow C^R C^W$ (pink)
- F_2 : 1 red : 2 pink : 1 white (1:2:1 phenotype ratio = genotype ratio)

Molecular basis: In many cases, gene dosage explains the intermediate phenotype. One copy of C^R produces half the amount of red pigment compared to two copies.

18.2.2 Codominance and Joint Allelic Expression

Both alleles are fully and simultaneously expressed in the heterozygote:

- ABO blood groups: $I^A I^A$ or $I^A i$ (type A) vs. $I^B I^B$ or $I^B i$ (type B) vs. $I^A I^B$ (type AB – both A and B antigens present on red blood cell surface)
- Molecular basis: I^A encodes N-acetylgalactosaminyltransferase (adds GalNAc to H antigen); I^B encodes galactosyltransferase (adds Gal); both **enzymes** are functional in heterozygotes; i encodes a nonfunctional enzyme

18.2.3 Multiple Alleles and Population-Level Variation

A gene can have more than two alleles in a population (though any individual still carries at most two):

ABO blood group system (three alleles: I^A , I^B , i):

Table 250. ABO blood group genotypes, antigens, antibodies, and transfusion compatibility.

Genotype	Phen.	Antigens	Antibodies	Can Donate To	Can Receive From
$I^A I^A$ or $I^A i$	A	A	Anti-B	A, AB	A, O
$I^B I^B$ or $I^B i$	B	B	Anti-A	B, AB	B, O
$I^A I^B$	AB	A and B	Neither	AB only	Universal recipient
ii	O	Neither (H antigen only)	Anti-A and Anti-B	Universal donor	O only

Rabbit coat color (4 alleles at the C locus): c^+ (full color) > c^{ch} (chinchilla) > c^h (Himalayan) > c (albino). Dominance hierarchy gives 10 possible genotypes and 5 phenotypic classes.

Clinical Connection: Rh Disease of the Newborn The Rh blood group system involves the RhD **protein**. Rh-negative mothers (RhD-/RhD-) carrying an Rh-positive fetus can become sensitized during delivery when fetal RhD+ red blood cells enter maternal circulation. Maternal IgG anti-RhD

antibodies cross the placenta in subsequent pregnancies, destroying fetal RhD+ erythrocytes (hemolytic disease of the fetus and newborn, HDFN). Prevention: anti-RhD immunoglobulin (RhoGAM) administered at 28 weeks and within 72 hours of delivery clears fetal RhD+ cells before maternal sensitization occurs.

18.2.4 Pleiotropy and Multi-Trait Gene Effects

A single gene affects multiple phenotypic traits:

Sickle cell disease (HbS): A single nucleotide change (GAG to GTG, Glu6Val) in the beta-globin gene (*HBB*) produces sickle hemoglobin. Under low oxygen tension, HbS polymerizes, deforming red blood cells into rigid sickle shapes. This single mutation causes:

- Vaso-occlusive crises (pain)
- Hemolytic anemia (shortened RBC lifespan: about 17 days vs. about 120 days)
- Splenic sequestration and autosplenectomy
- Stroke (large vessel occlusion)
- Acute chest syndrome
- Avascular necrosis of bones
- Renal papillary necrosis
- Retinopathy

Phenylketonuria (PKU): Phenylalanine hydroxylase (PAH) deficiency leads to phenylalanine accumulation, causing intellectual disability, fair skin/hair (reduced melanin from phenylalanine competition with tyrosine), musty body odor, and eczema. Newborn screening and phenylalanine-restricted diet prevent neurological damage.

Marfan syndrome: Mutations in *FBN1* (fibrillin-1) affect connective tissue throughout the body: tall stature, arachnodactyly, lens subluxation, mitral valve prolapse, and aortic root dilation (risk of aortic dissection).

18.2.5 Epistasis: When One Gene Masks Another

Epistasis describes the interaction between two or more genes in which the phenotype produced by one gene depends on the genotype at a second locus. The 9:3:3:1 dihybrid ratio applies primarily when two independently assorting genes act independently on the phenotype. When the genes interact — when one gene’s protein product feeds the substrate that another gene’s product modifies, or when one gene controls whether another gene’s product is even visible — the dihybrid F₂ ratio is modified in characteristic ways. Each modified ratio is a genetic signature of a specific kind of biochemical interaction.

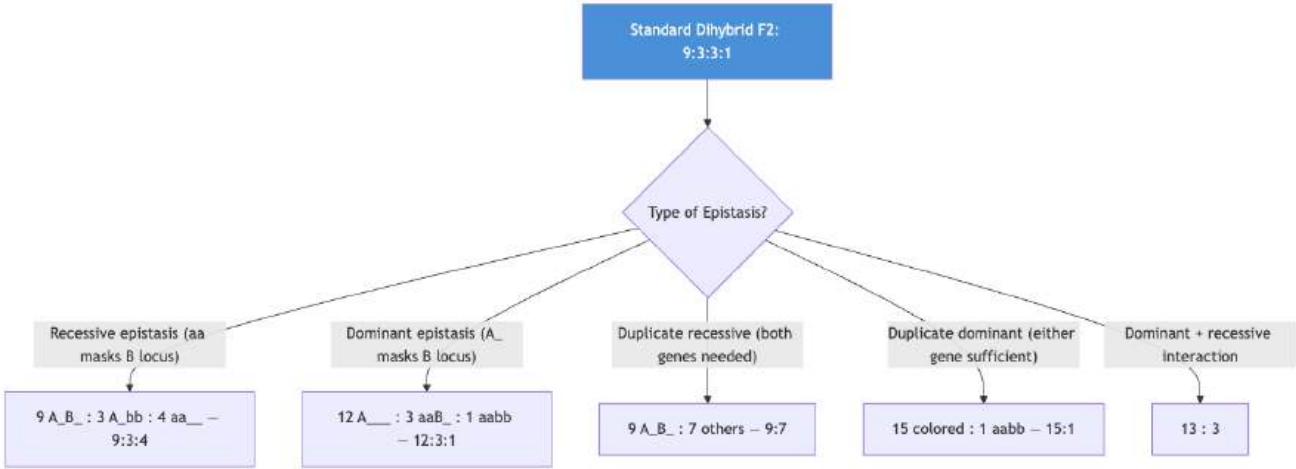


Figure 110. Modified dihybrid ratios produced by different types of epistasis. Each ratio is a modification of the standard 9:3:3:1 ratio.

Recessive Epistasis (9:3:4) — Labrador coat color Recessive epistasis occurs when homozygosity at one locus masks the phenotype produced by a second locus. The Labrador retriever coat color illustrates the principle through a two-step pigment pathway:

- B locus (Brown): determines whether eumelanin is black (*B*) or brown/chocolate (*b*).
- E locus (Extension): determines whether eumelanin is deposited at most in the hair shaft. *E* alleles deposit pigment; *ee* homozygotes block deposition entirely, producing yellow coats regardless of B genotype.

Table 251. Recessive Epistasis (9:3:4) — Labrador coat color: Genotype and Pigment chemistry.

Genotype	Pigment chemistry	Coat
B_E_	Black eumelanin deposited	Black
bbE_	Brown eumelanin deposited	Chocolate
B_ee	Black eumelanin made but not deposited	Yellow
bbee	Brown eumelanin made but not deposited	Yellow

Because *ee* is epistatic to the *B* locus, the standard 9:3:3:1 collapses into 9 black : 3 chocolate : 4 yellow in an F₂ from BbEe × BbEe.

Worked Example: Recessive Epistasis In a cross BbEe × BbEe, what is the probability of a chocolate Labrador puppy?

$$P(\text{chocolate}) = P(bb) \times P(E_) = \frac{1}{4} \times \frac{3}{4} = \frac{3}{16}$$

Dominant Epistasis (12:3:1) — Squash fruit color Dominant epistasis occurs when the dominant allele at one locus masks expression at a second locus. White-fruited summer squash (*Cucurbita pepo*) is a classic case. Allele *W* produces white fruit and is dominant to *w* (colored fruit). At a second locus, *Y* produces yellow and *y* produces green pigment — but primarily when *ww* allows pigment to develop.

Table 252. Dominant Epistasis (12:3:1) — Squash fruit color: Genotype and Phenotype.

Genotype	Phenotype
W_Y_	White
W_yy	White
wwY_	Yellow
wwyy	Green

The F₂ from WwYy × WwYy yields 12 white : 3 yellow : 1 green, written 12:3:1. Dominant *W* shuts down the entire pathway downstream of the *Y* locus.

Duplicate Recessive Epistasis (9:7) — Sweet pea flower color Sweet pea (*Lathyrus odoratus*) flower color requires the complementary action of two unlinked genes, both encoding biosynthetic enzymes in the anthocyanin pathway. Bateson and Punnett (1905) crossed two pure-breeding white strains and obtained purple F₁ offspring — an unexpected result that reflected complementation between the recessive defects in the two parental lines. The F₂ ratio is 9 purple : 7 white.

Table 253. Duplicate Recessive Epistasis (9:7) — Sweet pea flower color: Genotype and Both enzymes functional?.

Genotype	Both enzymes functional?	Color
C_P_	Yes — full pathway active	Purple
C_pp	No — pathway blocked at second step	White
ccP_	No — pathway blocked at first step	White
ccpp	No — pathway blocked at both steps	White

Either single-locus block (*cc* or *pp*) produces white; primarily doubly-dominant individuals build pigment. This 9:7 ratio is a hallmark of complementary gene action in linear biosynthetic pathways.

Duplicate Dominant Epistasis (15:1) — Shepherd’s purse seed shape When either dominant allele alone is sufficient to produce the phenotype, primarily the double-recessive shows the alternative trait. F₂ ratio: 15 phenotype A : 1 phenotype B. Shepherd’s purse seed-capsule shape is the classic example: triangular (*A_* or *B_*) versus narrow (*aabb*).

Combinatorics summary

Table 254. Combinatorics summary: Modified F₂ ratio and Mechanism.

Modified F ₂ ratio	Mechanism	Example
9:3:4	Recessive epistasis	Labrador coat color (B/E)
12:3:1	Dominant epistasis	White squash fruit (W/Y)
9:7	Duplicate recessive (complementation)	Sweet pea flower color
15:1	Duplicate dominant	Shepherd’s purse capsules
13:3	Dominant + recessive interaction	White Leghorn × white Wyandotte chickens

In every case the ratio sums to 16, betraying its origin in 9:3:3:1 — epistasis is typically a regrouping of the same dihybrid classes, rarely the introduction of new ones.

Epistasis in mouse coat color: agouti × albino A second worked example consolidates the recessive-epistasis logic. In the laboratory mouse, the A locus (agouti) determines whether hairs have a yellow band (A₋) or are uniformly black (aa). At the C locus, the C allele is required to deposit any pigment — cc homozygotes are albino regardless of the A genotype. A cross of AaCc × AaCc produces F₂ offspring in a 9 agouti : 3 black : 4 albino ratio, with the albino class combining both A₋cc and aacc genotypes (because pigment deposition fails in either case).

The 9:3:4 signature ratio therefore appears whenever:

1. A gene at one locus produces a substrate or precursor.
2. A gene at a second locus deposits, modifies, or expresses the product of the first.
3. Homozygosity for the loss-of-function allele at the second locus completely blocks phenotypic expression.

This logic underlies the genetic basis of many recessive epistatic systems: Bombay phenotype at the H locus (cc-equivalent for ABO blood groups), albinism in mammals masking coat-pattern loci, and white-flower mutants in many ornamental plants.

Worked Example: Duplicate Dominant Ratio in Shepherd’s Purse In a cross of two heterozygous shepherd’s purse plants (AaBb × AaBb), what fraction of F₂ offspring are predicted to have narrow seed capsules (the alternative phenotype)?

Narrow capsules require the double-recessive genotype aabb. Each locus contributes $\frac{1}{4}$ probability of double-recessive at that locus:

$$P(\text{narrow}) = P(aa) \times P(bb) = \frac{1}{4} \times \frac{1}{4} = \frac{1}{16}$$

The remaining $\frac{15}{16}$ of offspring have triangular capsules. The 15:1 ratio is the genetic signature of functional redundancy — when either gene alone is sufficient, primarily the simultaneous loss of both produces the alternative phenotype. The same logic explains why paralogous gene families often show 15:1-like behavior in knockout studies: knocking out either paralog alone produces no phenotype, but the double knockout reveals the shared function.

18.2.6 Polygenic Inheritance and Quantitative Traits

Multiple genes contribute additively to a single continuous (quantitative) trait:

- Human skin color: At least 7 genes contribute (SLC24A5, SLC45A2, TYR, TYRP1, OCA2, KITLG, MC1R and others). Each gene has alleles that contribute incrementally to melanin production. The result is a continuous distribution (approximately normal/Gaussian) rather than discrete classes.
- Human height: the largest common-variant maps now resolve thousands of small-effect loci; a 2022 study of 5.4 million people reported 12,111 independent height-associated SNPs, with prediction still strongest in European-ancestry validation cohorts [Yengo et al., 2022]. Environmental factors (nutrition, health) also contribute significantly, so height remains a model for polygenic inheritance rather than a deterministic genotype readout.

The number of phenotypic classes for n contributing loci (each with two alleles, additive effects) = 2n + 1.

18.2.7 Penetrance and Expressivity

Mendelian ratios assume that every individual carrying a given genotype displays the expected phenotype, and displays it identically. In reality, the genotype–phenotype map is leaky on two distinct axes — *whether* the phenotype appears at most (penetrance) and *how strongly* it appears when it does (expressivity).

- Penetrance is the proportion of individuals with a given genotype who actually display the expected phenotype. A trait with 100% penetrance is completely penetrant; a trait with less than 100% is incompletely penetrant.
- Expressivity is the degree or severity of phenotype expression among individuals who *are* penetrant. Variable expressivity means the same genotype produces a range of phenotypic intensities.
- Phenocopy is an environmentally induced phenotype that mimics a genetic condition without the underlying genotype. Phenocopies can confound pedigree analysis if not recognized.

Disease examples

Table 255. Disease examples: Phenomenon and Disorder.

Phenomenon	Disorder	Detail
Reduced penetrance	BRCA1/BRCA2 breast/ovarian cancer	about 70–80% lifetime breast cancer risk in BRCA1 carriers; some carriers rarely develop disease
Reduced penetrance	Familial hypercholesterolemia (LDLR mutations)	Variable age of onset for cardiovascular disease; modified by diet and other genes
Reduced penetrance	Retinoblastoma (RB1)	about 90% penetrance; some heterozygous carriers escape because the second hit (loss of the wild-type allele) does not occur in retinal precursor cells
Variable expressivity	Neurofibromatosis type 1 (NF1)	<i>NF1</i> tumor suppressor (encodes neurofibromin, a Ras-GAP); same mutation produces café-au-lait macules in some individuals, severe plexiform neurofibromas, optic gliomas, and skeletal dysplasia in others. Loss-of-heterozygosity (second hit) at <i>NF1</i> in Schwann cell lineages produces the variable tumor burden
Variable expressivity	Polydactyly (e.g., <i>GLI3</i> mutations, Greig cephalopolysyndactyly)	Affected family members carrying the identical mutation may show one extra digit on one hand, two extra digits on both hands and feet, or post-axial duplication varying side-to-side. Limb-bud stochastic patterning during weeks 4–7 produces this variability
Variable expressivity	Marfan syndrome (FBN1)	Aortic root size varies dramatically among affected family members carrying the same mutation
Variable expressivity	Huntington’s disease	Age of onset varies inversely with CAG repeat length but also among individuals with identical repeat counts (modifier loci)
Phenocopy	Thalidomide-induced phocomelia	Limb shortening from drug exposure (1958–1962) mimicked the rare genetic condition

Phenomenon	Disorder	Detail
Phenocopy	Congenital rubella syndrome	Maternal rubella infection causes deafness and cataracts that resemble genetic syndromes

The biological causes of incomplete penetrance and variable expressivity include modifier genes (other loci that influence how the primary mutation manifests), stochastic developmental events (random fluctuations during embryogenesis), environmental triggers (diet, infection, smoking), epigenetic state (methylation patterns inherited or established during development), and — for X-linked traits in females — random X-inactivation patterns (section 19).

For genetic counseling, incomplete penetrance complicates risk prediction: a “negative” family member is not certainly mutation-free, and a “positive” family history is not an assurance of disease. Penetrance estimates are typically reported as age-specific cumulative risks (e.g., “80% by age 70 for BRCA1”) rather than single numbers.

18.2.8 Genomic Imprinting and Parent-of-Origin Effects

Some genes are expressed in a parent-of-origin-specific manner due to differential DNA methylation established during gametogenesis:

Prader-Willi syndrome vs. Angelman syndrome (chromosome 15q11-13): - Prader-Willi syndrome: Deletion/loss of the paternal 15q11-13 region (or maternal uniparental disomy). Genes in this region are normally expressed primarily from the paternal chromosome. Features: hypotonia in infancy, hyperphagia and obesity, intellectual disability, short stature. - Angelman syndrome: Deletion/loss of the maternal 15q11-13 region (specifically the *UBE3A* gene, which is maternally expressed in neurons). Features: severe intellectual disability, seizures, ataxic gait, happy demeanor with frequent laughter.

Same chromosomal region, but different disease depending on which parent’s copy is affected – a clear demonstration that the genome “remembers” parental origin.

18.2.9 Maternal Effect Genes

The mother’s genotype (not the offspring’s) determines the offspring’s phenotype:

- Bicoid in *Drosophila*: The bicoid mRNA is deposited into the oocyte by the mother. It localizes to the anterior end and is translated after fertilization, producing a transcription factor gradient that specifies anterior structures (head, thorax). A mother homozygous for a *bicoid* mutation produces embryos lacking anterior structures – regardless of the embryo’s own genotype.

Concept Check 16.2

1. Distinguish between codominance and incomplete dominance at the molecular level.
2. Two yellow Labradors are mated. Can they produce chocolate puppies? Explain.
3. If a trait is 70% penetrant, what fraction of heterozygous carriers will NOT show the phenotype?
4. A mother with Prader-Willi syndrome (paternal deletion) has a child. Can the child inherit Prader-Willi? Angelman? Explain.
5. Distinguish reduced penetrance from variable expressivity. Give one disease example of each.

18.2.10 Study Blueprint

- Big idea: Extensions to Mendelian ratios and human pedigree analysis reveal when simple dominance fails.
- Core concepts: incomplete dominance, epistasis, pedigrees, penetrance.
- Framework alignment: Vision & Change: Information flow, exchange, and storage, Evolution; AP Biology: Information Storage and Transmission, Evolution; NGSS-style topics: Inheritance and Variation of Traits, Natural Selection and Evolution.
- Model or quantitative lens: Pedigree, epistasis, and multi-locus probability calculations.
- Data skill: Infer inheritance mode and extension mechanism from family or cross data.
- Practice cadence: Statistical Tests and Data Analysis, Representing and Describing Data.
- Common misconception to repair: A single-gene model is a starting hypothesis, not the default for every trait.
- Primary lab: Lab — Mendelian Extensions and Human Genetics.
- Question bank: Questions — Mendelian Extensions and Human Genetics.
- Transfer task: Transfer extension reasoning to counseling, GWAS interpretation, and breeding.

- Bridge to computation: `biology.genetics.genetics.punnett_square`.

Opening Vignette — Mendelian Extensions and Human Genetics

This chapter connects mendelian extensions and human genetics to measurable evidence: models, datasets, and experiments that can strengthen or weaken each claim.

18.3 Human Genetic Disorders: Mechanism Meets Mendel

Human genetics has historically been the inverse of Mendel’s pea garden — instead of designing crosses, clinicians infer genotypes from pedigrees and clinical features. The core inheritance patterns (autosomal dominant, autosomal recessive, X-linked, mitochondrial) follow directly from Mendelian principles applied to specific chromosomal architecture. The molecular mechanisms behind individual disorders, however, illustrate the rich biology that makes Mendel’s abstract “factors” into proteins, enzymes, and regulatory RNAs.

18.3.1 Autosomal Dominant Disorders: Huntington’s Disease and CAG Repeat Expansion

Huntington’s disease (HD) is an adult-onset neurodegenerative disorder caused by mutations in the *HTT* gene on chromosome 4p16.3. It is autosomal dominant with nearly complete penetrance by age 65 — a rare example of a fully penetrant late-onset disorder. The clinical features include progressive chorea (involuntary writhing movements), psychiatric symptoms (depression, irritability, psychosis), and cognitive decline (executive dysfunction, dementia). Median survival from symptom onset is approximately 15–20 years.

Molecular mechanism: The *HTT* gene contains a polymorphic CAG trinucleotide repeat in its first exon, encoding a polyglutamine (polyQ) tract in the huntingtin protein. The number of CAG repeats determines disease status:

Table 256. Autosomal Dominant Disorders: Huntington’s Disease and CAG Repeat Expansion: CAG repeats and Disease status.

CAG repeats	Disease status
≤ 26	Normal — no risk; stable inheritance
27–35	Intermediate — usually unaffected, but unstable in transmission and may expand into the affected range in offspring (especially through paternal transmission)
36–39	Reduced penetrance — disease may or may not develop in a normal lifespan
>= 40	Fully penetrant — disease will develop if individual lives long enough

The expanded polyQ tract causes the huntingtin protein to misfold and aggregate, forming intranuclear inclusions in neurons (especially in the striatum). The precise pathogenic mechanism remains debated — gain of toxic function, loss of normal function, and disruption of axonal transport most contribute.

Anticipation: Disease severity worsens and age of onset decreases across generations because the CAG repeat is unstable during meiosis, especially during spermatogenesis. A father with 42 repeats may transmit 50 repeats to his son; that son’s children may inherit 60 or more. Juvenile-onset HD (onset before age 20) almost typically reflects paternal transmission of severely expanded alleles (>60 repeats). This phenomenon — anticipation — is also observed in fragile X syndrome, myotonic dystrophy, and several spinocerebellar ataxias, most of which are trinucleotide repeat expansion disorders.

Inverse correlation: Within the affected range, age of onset correlates inversely with repeat number, but with substantial variance attributable to modifier genes (e.g., *FANL*, *MSH3*) that influence somatic repeat instability. This explains why two siblings with the same CAG count can have onset ages differing by a decade or more.

Genetic counseling: Because HD is autosomal dominant, each child of an affected parent has a 50% risk. Predictive testing in unaffected adults raises difficult ethical questions — there is no preventive therapy, and testing carries psychological consequences (depression, suicidality) that mandate pre-test and post-test genetic counseling. Many at-risk individuals choose not to be tested.

18.3.2 Autosomal Recessive Disorders: PKU and the Logic of Newborn Screening

Phenylketonuria (PKU) is an autosomal recessive disorder caused by mutations in the *PAH* gene on chromosome 12q23.2 encoding phenylalanine hydroxylase, the liver enzyme that converts phenylalanine to tyrosine. Archibald Garrod’s study of alkaptonuria established the concept of inborn errors of metabolism — single-gene biochemical defects with predictable clinical consequences [Garrod, 1902]. PKU illustrates how a single biochemical defect cascades into multiple phenotypes (pleiotropy) and how early detection plus dietary intervention can prevent the most devastating manifestations.

Biochemistry: PAH is a tetrameric enzyme requiring tetrahydrobiopterin (BH4) as cofactor. In its absence, phenylalanine accumulates to toxic concentrations (>20 mg/dL versus normal <2 mg/dL) while tyrosine — the precursor of dopamine, melanin, and thyroid hormone — becomes deficient. The metabolic consequences include:

- Phenylalanine accumulation in blood and brain, where excess phenylalanine competes with other large neutral amino acids (tyrosine, tryptophan, leucine) for the L-type amino acid transporter (LAT1) at the blood-brain barrier. Brain tyrosine and tryptophan deficiency disrupts catecholamine and serotonin synthesis.
- Phenylketones: when phenylalanine is in excess, alternative metabolic pathways produce phenylpyruvate, phenyllactate, and phenylacetate — the “ketones” detectable in urine that gave the disease its name.
- Tyrosine deficiency reduces melanin synthesis (causing fair skin, blond hair, and blue eyes — distinctive features in untreated patients) and may contribute to neurological symptoms.

Clinical features (untreated): severe intellectual disability (IQ typically <50 by age 1), seizures (in about 25% of untreated patients), microcephaly, motor abnormalities, eczema, characteristic musty body odor (from phenylacetate excretion), and reduced melanin pigmentation. Untreated PKU was a leading cause of intellectual disability before comprehensive newborn screening.

Newborn screening: Robert Guthrie developed the Guthrie test in 1962 — a bacterial inhibition assay using *Bacillus subtilis* requiring phenylalanine. A heel-prick blood spot from a 24–72-hour-old newborn is dried on filter paper and screened en masse. Modern programs use tandem mass spectrometry to measure dozens of metabolites simultaneously. Newborn screening for PKU was the first widespread genetic screening program and remains the prototype for population screening programs worldwide.

Treatment: A phenylalanine-restricted diet initiated within the first weeks of life prevents severe intellectual disability in nearly every treated case (though subtle executive-function and processing-speed differences can persist even with good metabolic control). Patients consume specially formulated medical foods low in phenylalanine but supplemented with tyrosine. Treatment is lifelong — relaxation of dietary restrictions in adolescence or adulthood causes neuropsychiatric symptoms (depression, anxiety, executive dysfunction) and, in pregnant women with PKU, maternal PKU syndrome (intellectual disability, microcephaly, congenital heart disease in the fetus, even when the fetus is heterozygous). New therapies include sapropterin (synthetic BH4, useful for about 30% of patients with residual PAH activity) and pegvaliase (PEGylated phenylalanine ammonia lyase enzyme replacement, approved 2018).

Population genetics: PKU disease frequency is about 1/10,000–15,000 in northern European populations, giving a carrier frequency of about 1/55–60. PKU is more common in Ireland (about 1/4,500), Turkey (about 1/3,000–6,500), and parts of China (about 1/15,000–17,000), with population-specific allele spectra that allow targeted carrier screening.

18.3.3 Other key autosomal disorders

Table 257. Other key autosomal disorders: Disorder and Inheritance.

Disorder	Inheritance	Gene	Mechanism
Cystic fibrosis	AR	<i>CFTR</i>	Chloride channel defect; thick mucus; ΔF508 most common
Sickle cell disease	AR	<i>HBB</i>	Glu6Val in β-globin; sickle hemoglobin polymerization
Tay-Sachs disease	AR	<i>HEXA</i>	β-hexosaminidase A deficiency; GM2 ganglioside accumulation; founder effect in Ashkenazi Jews
Achondroplasia	AD	<i>FGFR3</i>	Constitutively active FGFR3; chondrocyte proliferation defect; about 80% de novo mutations
Marfan syndrome	AD	<i>FBN1</i>	Fibrillin-1 connective tissue defect
Familial hypercholesterolemia	AD	<i>LDLR</i>	Defective LDL receptor; extreme hypercholesterolemia
Hereditary nonpolyposis colon cancer (Lynch)	AD	<i>MLH1, MSH2, MSH6, PMS2</i>	DNA mismatch repair defects

CFTR mutation classes — a paradigm for genotype–phenotype maps The 2,000+ identified *CFTR* variants are grouped into six classes by their effect on protein production and function — a classification that now drives mutation-specific therapy:

Table 258. CFTR mutation classes — a paradigm for genotype–phenotype maps: Class and Defect.

Class	Defect	Examples	Therapy
I	No protein synthesis (premature stop codons)	W1282X, G542X	Read-through agents (ataluren — limited efficacy)
II	Misfolding / proteasomal degradation	ΔF508 (about 70% of CF alleles in Northern Europeans)	Correctors (lumacaftor, tezacaftor, elexacaftor)
III	Channel does not open (“gating defect”)	G551D	Potentiators (ivacaftor)
IV	Reduced channel conductance	R117H	Potentiators
V	Reduced protein levels (splicing defects)	3849+10kb C→T	Mixed
VI	Reduced channel stability at cell surface	rescued ΔF508	Stabilizers

The combination therapy elexacaftor/tezacaftor/ivacaftor (Trikafta), approved 2019, is effective for about 90% of CF patients (those carrying at least one ΔF508) and has dramatically improved life expectancy — a paradigm for translating mendelian genetics into precision medicine.

18.3.4 Achondroplasia and Marfan as Autosomal Dominant Models

Achondroplasia is the most common form of dwarfism (about 1/25,000 births), caused by gain-of-function mutations in *FGFR3* (fibroblast growth factor receptor 3). The vast majority (about 98%) of cases involve a single recurrent mutation: G380R in the transmembrane domain. The mutation produces a constitutively active receptor that inhibits chondrocyte proliferation and endochondral ossification, shortening long bones while sparing membranous bones (skull vault, vertebrae). Approximately 80% of cases are de novo mutations arising in the paternal germline, and risk increases with paternal age — illustrating that autosomal dominant disease can persist in populations even when affected individuals have reduced reproductive fitness, because new mutations replenish the disease allele each generation. Homozygous achondroplasia (two affected parents — about 1 in 4 pregnancies if both are heterozygous) is lethal in infancy due to severe rib cage abnormalities.

Marfan syndrome illustrates how a single connective-tissue gene, *FBN1* (fibrillin-1), produces pleiotropic effects across organ systems. Fibrillin-1 forms microfibrils that scaffold elastic fibers and sequester latent TGF-β. Mutations cause both structural failure (loose connective tissue → tall stature, long limbs, lens dislocation, joint hypermobility) and dysregulated TGF-β signaling (aortic root dilation → dissection risk). Variable expressivity is dramatic: aortic root sizes among affected family members carrying the same mutation can vary by 2–3-fold, depending on modifier genes and environment. Modern management includes annual echocardiography, β-blockers or losartan to slow aortic dilation, and elective aortic root replacement when diameter exceeds about 5 cm — extending life expectancy from a historical median of about 32 years to nearly normal.

Clinical Connection: Why Are Some AR Diseases Common? Cystic fibrosis carrier frequency of about 1/25 in Northern Europeans far exceeds what mutation-selection balance alone predicts. Hypothesized heterozygote advantage against historical pathogens — possibly typhoid fever (CFTR is a receptor for *Salmonella typhi*) or cholera (heterozygotes may have reduced fluid secretion in cholera infection) — could explain the elevated frequency. Sickle cell heterozygosity confers strong protection against severe *Plasmodium falciparum* malaria, and Tay-Sachs heterozygotes may have had protection against tuberculosis in pre-industrial European cities. These hypotheses remain debated, but they illustrate how Mendelian disease alleles can be maintained by ancient selective pressures we no longer experience.

18.3.5 X-linked disorders: the molecular basis of male susceptibility

Males are hemizygous for X-linked genes (one X, one Y), so a single recessive allele on the X chromosome produces the full phenotype in a male. Females, with two X chromosomes, must be homozygous (or display unfavorable random X-inactivation patterns) to be fully affected. This asymmetry — recognized first by Morgan’s *white-eyed Drosophila* — produces the diagnostic pedigree pattern of “skipping generations through carrier mothers” that distinguishes X-linked recessive inheritance.

Hemophilia A — F8 and Factor VIII Hemophilia A (about 1 in 5,000 male births) is caused by mutations in the *F8* gene at Xq28 encoding coagulation factor VIII, a 2,332-amino-acid plasma glycoprotein that forms a tenase complex with activated factor IXa to activate factor X in the intrinsic coagulation pathway. The clinical phenotype is dose-dependent on residual factor VIII activity:

Table 259. Hemophilia A — F8 and Factor VIII: Severity and Factor VIII activity.

Severity	Factor VIII activity	Bleeding pattern
Severe	< 1%	Spontaneous joint and muscle hemorrhage; treated prophylactically
Moderate	1–5%	Bleeding after minor trauma
Mild	6–40%	Bleeding primarily after surgery or major trauma

The most common mutation in severe hemophilia A is the intron 22 inversion, which disrupts the *F8* gene and accounts for about 45% of severe cases. The gene is unusually large (186 kb, 26 exons), and its 32-kb intron 22 contains the *F8A1* gene with two homologous repeats elsewhere on Xq28; non-allelic homologous recombination during male meiosis produces the inversion. Modern treatment uses recombinant factor VIII concentrates (Kogenate, Advate) for replacement therapy, emicizumab (a bispecific antibody mimicking factor VIIIA), and increasingly gene therapy: in 2022 the FDA approved Hemgenix (etranacogene deza-parvovec) for hemophilia B, with similar AAV-based gene therapies for hemophilia A in advanced trials.

The Romanov royal family tragedy is the most famous historical case: Queen Victoria was a carrier (likely de novo mutation), and through her descendants the allele entered the Russian, Spanish, and German royal families. The hemophilia of Tsarevich Alexei contributed to the political collapse of the Romanov dynasty.

Color blindness — OPN1LW and OPN1MW Red-green color blindness affects about 8% of males and about 0.5% of females of European ancestry. The disorder reflects defects in two tandem opsin genes on Xq28:

- *OPN1LW* (long-wavelength opsin) — sensitive to red light (about 560 nm peak)
- *OPN1MW* (medium-wavelength opsin) — sensitive to green light (about 530 nm peak)

The two genes are >96% identical and lie head-to-tail in a tandem array (1–6 copies of *OPN1MW* per X chromosome) at Xq28. The high sequence similarity makes them prone to unequal crossing over during female meiosis, producing chromosomes with deleted, duplicated, or hybrid (chimeric) opsin genes:

- Protan defects (red-blindness): loss or alteration of *OPN1LW*
- Deutan defects (green-blindness): loss or alteration of *OPN1MW*

Hybrid genes — formed when the upstream portion of one opsin fuses with the downstream portion of the other — produce shifted spectral sensitivities (anomalous trichromacy). The unique vulnerability of this gene cluster to misalignment during recombination explains why color blindness is far more common than other X-linked traits despite no obvious selective advantage.

Duchenne muscular dystrophy — DMD and dystrophin Duchenne muscular dystrophy (DMD) affects about 1 in 3,500 male births and is caused by mutations in the *DMD* gene at Xp21.2 encoding dystrophin — at 2.4 megabases the largest known human gene (79 exons), accounting for about 0.1% of the entire genome. Dystrophin links the actin cytoskeleton inside muscle fibers to the dystrophin-glycoprotein complex spanning the sarcolemma, transmitting force during contraction and protecting the membrane from mechanical stress.

The genotype–phenotype rule for *DMD* mutations is the reading-frame rule: deletions that disrupt the reading frame produce no functional dystrophin and cause Duchenne (severe, wheelchair by age 12, cardiac/respiratory failure by about 25 years), whereas in-frame deletions produce truncated but partially functional dystrophin and cause Becker muscular dystrophy (milder, much later onset, normal lifespan possible). This rule has therapeutic consequences: exon-skipping antisense oligonucleotides mask specific exons during splicing to convert an out-of-frame Duchenne mutation into an in-frame Becker-like protein. Eteplirsen (FDA-approved 2016) skips exon 51 and is applicable to about 13% of DMD patients; golodirsen (exon 53) and viltolarsen (exon 53) treat additional subgroups. CRISPR-mediated exon excision is in clinical trials.

The very large size of *DMD* makes it the most mutation-prone gene in the human genome, with about 1/3 of cases representing de novo mutations rather than inheritance from a carrier mother — a fact that affects recurrence-risk counseling for affected families.

Female carriers — random X-inactivation and “manifesting carriers” Female carriers of X-linked recessive disorders are typically clinically normal, but about 10–20% of *DMD* female carriers show muscle weakness, cramping, or even cardiomyopathy. The reason is skewed X-inactivation: by chance, the X chromosome carrying the wild-type allele is preferentially inactivated in many of her muscle cells, leaving the mutant X expressed. The clinical severity depends on the

proportion of cells with skewed X-inactivation patterns. Similar manifesting-carrier phenotypes occur in hemophilia A (about 10% of carriers have prolonged bleeding) and ornithine transcarbamylase deficiency (urea cycle disorder; manifesting carriers may experience hyperammonemic crises).

Carrier frequency vs. affected-male frequency: a population-genetic asymmetry A diagnostic feature of X-linked recessive inheritance is that carrier frequency in females greatly exceeds affected-female frequency, even though both sexes draw from the same X-linked allele frequency q . The arithmetic follows directly from hemizygosity in males and Hardy-Weinberg expectations in females (section 20):

Table 260. Carrier frequency vs. affected-male frequency: a population-genetic asymmetry: Quantity and Formula.

Quantity	Formula	Reason
Affected males	q	Hemizygous: one mutant allele suffices
Affected females	q^2	Homozygous: both X alleles must be mutant
Carrier females (heterozygous)	$2pq \approx 2q$ for small q	Heterozygous and asymptomatic with random X-inactivation

Worked numbers for the three X-linked recessive disorders above (Northern European frequencies):

- Hemophilia A: affected-male frequency $\approx 1/5,000$, so $q \approx 2 \times 10^{-4}$. Carrier-female frequency $2pq \approx 4 \times 10^{-4}$ (about 1 in 2,500 women). Affected-female frequency $q^2 \approx 4 \times 10^{-8}$ (about 1 in 25 million) — meaning carriers outnumber affected females by about 10,000-fold.
- Duchenne muscular dystrophy: affected-male frequency $\approx 1/3,500$, $q \approx 2.9 \times 10^{-4}$. Carrier-female frequency $\approx 1/1,750$ women.
- Red-green color blindness (high allele frequency): affected-male frequency ≈ 0.08 , so $q \approx 0.08$. Carrier-female frequency $2pq \approx 0.147$, and affected-female frequency $q^2 \approx 0.0064$ — recovering the empirical about 0.5–1% color-blind female frequency.

Two consequences follow. First, most pathogenic X-linked alleles in the population reside in unaffected female carriers, who are invisible to phenotypic screening. Second, when a new disease-causing X-linked mutation arises (frequently de novo, especially for *DMD*), it persists for many generations through carrier mothers before reaching another affected male — producing the characteristic “skipping generations through unaffected females” pattern in pedigrees. Genetic counseling for X-linked disorders therefore prioritizes carrier testing of female relatives of affected males, even when those women appear clinically normal.

Concept Check 16.5

1. NF1 shows highly variable expressivity within a single family carrying the same mutation. Identify three biological reasons why identical genotypes can produce dramatically different phenotypes.
2. In a population where 1 in 4,000 males is affected with hemophilia A, what fraction of women are carriers? What is the probability that a randomly chosen woman is a carrier?
3. A man’s brother has Duchenne muscular dystrophy (X-linked recessive). The brother’s mother is confirmed by molecular testing to be a non-carrier (the affected brother arose from a de novo mutation). Should the man worry that his own future sons could inherit the disease through him? Explain.
4. Compare the dihybrid F_2 ratio expected when (a) two genes act independently in separate biosynthetic pathways and (b) two genes encode sequential enzymes in the same pathway where both are required for product formation. Which produces 9:3:3:1, which produces 9:7, and why?
5. A researcher studying Huntington’s disease finds that two siblings carry identical *HTT* CAG repeat lengths (45 each) but have onset ages differing by 12 years. What is this discrepancy a manifestation of, and what general lesson does it teach about the genotype-phenotype map?

18.4 GWAS: Mendel Meets the Genome

Mendel studied traits with simple, dichotomous inheritance — round vs. wrinkled, yellow vs. green. Most human traits and diseases, however, are polygenic (influenced by many loci) and multifactorial (influenced by both genes and environment). Height, body mass index, blood pressure, type 2 diabetes, schizophrenia, and most common diseases do not segregate as Mendelian traits in pedigrees — they are complex traits. The modern tool for dissecting their genetic architecture is the genome-wide association study (GWAS).

18.4.1 How GWAS works

GWAS scans the genome for statistical association between genetic variants — typically common single-nucleotide polymorphisms (SNPs with minor allele frequency $\geq 1\%$) — and a phenotype, comparing thousands of cases to thousands of controls. The basic design is a case-control association test: at each SNP,

compare the allele frequency in cases versus controls and ask whether the difference exceeds chance expectation.

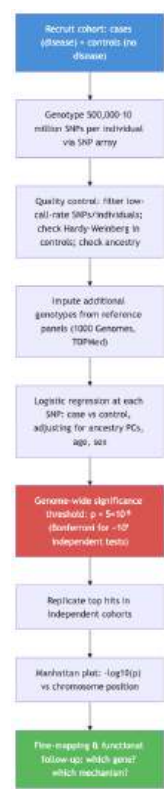


Figure 111. The GWAS workflow, from cohort recruitment through genome-wide significance testing to functional follow-up. The genome-wide significance threshold of $p < 5 \times 10^{-8}$ corresponds to a Bonferroni correction for about 10 independent common variants tested across the genome.

18.4.2 What GWAS has revealed

Since the first successful GWAS (age-related macular degeneration, 2005), tens of thousands of genome-wide significant associations have been catalogued. Several lessons have emerged [Manolio et al., 2009, Yengo et al., 2022]:

1. Most common diseases are highly polygenic. Schizophrenia: >270 loci. Type 2 diabetes: >400 loci. Height: >12,000 contributing variants. The “one-gene, one-disease” Mendelian model rarely applies to common conditions.
2. Effect sizes are small. Individual common variants typically increase disease risk by 1.05–1.3-fold (odds ratios of 1.05–1.3). The largest common-variant effects are typically in immune disorders (HLA region, OR up to 5–10 for specific autoimmune conditions).
3. Most GWAS hits are non-coding. Approximately 90% of GWAS-associated variants lie outside protein-coding regions, in regulatory elements (enhancers, promoters, 3’ UTRs). They alter gene expression rather than protein sequence — connecting GWAS to the regulatory biology of section 15.
4. Pleiotropy is the rule, not the exception. Many GWAS loci affect multiple traits. A locus near *FTO* influences both BMI and diabetes risk. A locus near *TCF7L2* affects type 2 diabetes, fasting glucose, and bone mineral density.
5. “Missing heritability” persists — for many traits, common GWAS variants explain less variance than family and twin studies imply. The gap reflects many small-effect variants, rare variants, structural variation, gene-environment interactions, and non-additive effects (epistasis, dominance) [Manolio et al., 2009].

18.4.3 Polygenic risk scores (PRS)

GWAS results can be combined into a polygenic risk score — a weighted sum of risk alleles across many SNPs:

$$PRS_i = \sum_{j=1}^M \beta_j \cdot g_{ij}$$

where g_{ij} is the count of risk alleles (0, 1, or 2) at SNP j in individual i , and β_j is the GWAS effect estimate. PRS provides individual-level risk predictions that, for some diseases, equal or exceed the predictive power of family history. PRS is becoming clinically useful in cardiovascular disease, breast cancer, and prostate

cancer screening, though equity concerns remain because most GWAS were conducted in European-ancestry populations and PRS performance degrades when transferred to other ancestries.

18.4.4 GWAS as the modern face of Mendel's program

Mendel’s deepest contribution was not the laws themselves but the method: count phenotypes, treat heredity as a probabilistic system, and test genetic hypotheses against quantitative ratios. GWAS is Mendel’s program rescaled to millions of loci and billions of genotype calls — every Manhattan plot is a vast, statistically corrected dihybrid cross conducted across the entire genome.

Clinical Connection: When GWAS Becomes Drug Discovery GWAS hits sometimes identify proteins that become drug targets. The discovery that *PCSK9* loss-of-function variants confer protection against cardiovascular disease (low LDL cholesterol, no apparent harm) led directly to the development of monoclonal antibodies (evolocumab, alirocumab) and small interfering RNAs (inclisiran) inhibiting PCSK9 — now major cholesterol-lowering therapies. Similarly, *HMGCR* variants supported statins as a drug class. Genetics-informed drugs are roughly twice as likely to succeed in clinical trials as drugs developed without genetic support.

18.4.5 The Manhattan Plot and Genome-Wide Significance

The standard visual display of GWAS results is the Manhattan plot — a scatter of $-\log_{10}(p)$ values plotted against genomic position. The horizontal axis traverses chromosomes 1 through 22 (and X) in order; each point is a single SNP. Strong associations form vertical “skyscrapers” of co-associated SNPs in the same locus (because nearby SNPs are in linkage disequilibrium), giving the plot its skyline-like appearance.

The genome-wide significance threshold is conventionally set at $p < 5 \times 10^{-8}$ — the line drawn horizontally across most Manhattan plots. This threshold derives from a Bonferroni correction for multiple testing:

$$p_{\text{threshold}} = \frac{\alpha}{\text{number of independent tests}} = \frac{0.05}{10^6} = 5 \times 10^{-8}$$

The denominator of $\sim 10^6$ reflects the number of approximately independent common variants in the human genome (after accounting for linkage disequilibrium between adjacent SNPs). A “suggestive” threshold of $p < 10^{-5}$ is sometimes reported for hits that warrant follow-up but do not meet genome-wide significance. Replication in an independent cohort is the gold standard for confirming a true association.

18.4.6 Polygenic Risk Scores: Detailed Example

Consider type 2 diabetes (T2D), one of the most extensively GWAS-studied complex diseases. Over 400 independent loci have been identified, each with small individual effects (odds ratios typically 1.05–1.20). A polygenic risk score combines these signals into an individual-level prediction:

$$\text{PRS}_i = \sum_{j=1}^M \beta_j \cdot g_{ij} \tag{244}$$

where g_{ij} is the dosage of the risk allele (0, 1, or 2) at SNP j for individual i , β_j is the GWAS-derived effect size for that SNP (usually log-odds ratio for case-control studies), and M is the number of SNPs included (often hundreds of thousands when modern PRS methods like LDpred or PRS-CS are used).

Clinical performance: Modern PRS for T2D can identify individuals in the top percentile of genetic risk who have about 3–5× the population baseline lifetime risk of developing the disease — comparable in predictive power to having a single first-degree relative with the disease, but available decades before clinical onset and therefore actionable through lifestyle modification.

Equity caveat: Most large GWAS to date have been conducted in European-ancestry populations. PRS performance degrades substantially when applied to other ancestries, with predictive accuracy 50–75% lower in African-ancestry individuals. Closing this “PRS performance gap” requires diverse GWAS cohorts and cross-ancestry methods — an active area of research and a matter of healthcare equity.

18.4.7 Clinical Interpretation and Governance Checkpoint

A PRS should be treated as a calibrated, ancestry- and context-dependent risk model, not as a diagnosis. A responsible report states the discovery cohort, target population, calibration method, confidence interval, and action threshold; checks whether the risk strata were validated in the patient’s ancestry and care setting; and interprets the score alongside family history, monogenic testing when indicated, and modifiable clinical risk factors. Current PRS accuracy is several-fold

higher in European-ancestry cohorts than in other cohorts, so premature deployment can widen health gaps if diverse validation does not keep pace [Martin et al., 2019].

Governance is part of the biological interpretation. Consent should specify secondary use, data retention, reidentification risk, and which relatives might be indirectly implicated. In the United States, GINA addresses health-insurance and employment discrimination, but it does not extend to life, disability, or long-term-care insurance [U.S. Department of Health and Human Services, Office for Human Research Protections, 2009]. A genetic-counseling workflow therefore separates what the score estimates from what clinicians, insurers, employers, families, or law-enforcement agencies are permitted to do with it.

Clinical interpretation also separates a family pattern from variant evidence. A sequence change is not simply “the disease gene”; laboratories classify variants by combining population frequency, segregation, computational prediction, functional assays, and previous clinical reports under ACMG/AMP categories such as pathogenic, likely pathogenic, uncertain significance, likely benign, and benign [Richards et al., 2015]. ClinVar archives submitted variant-phenotype interpretations and supporting evidence, while OMIM organizes curated gene-phenotype relationships for Mendelian disorders and traits [Landrum et al., 2014, National Center for Biotechnology Information, 2026a, Amberger et al., 2019].

Concept Check 16.3

1. Why is the genome-wide significance threshold $p < 5 \times 10^{-8}$ and not the conventional $p < 0.05$?

2. A father with 42 CAG repeats has Huntington’s disease. His daughter inherits the affected allele. What can you predict about her CAG count and age of onset?

3. PKU is treatable with diet, yet newborn screening remains comprehensive in many countries. Why is comprehensive screening preferred over targeted screening of high-risk families?

4. Most GWAS hits lie outside protein-coding regions. What does this tell us about the genetic architecture of common diseases?

5. A patient’s PRS for coronary artery disease places her in the top 1% of the population. Her standard cholesterol panel is normal at age 30. How should this affect her clinical management, and what are the limitations of acting on PRS alone?

6. Why does PRS performance degrade when applied across ancestries? What practical and ethical issues does this raise for clinical deployment?

18.5 The Chi-Squared (χ^2) Test

The χ^2 test for goodness of fit evaluates whether observed offspring ratios deviate significantly from expected Mendelian ratios.

18.5.1 Formula and Procedure

$$\chi^2 = \sum_{i=1}^k \frac{(O_i - E_i)^2}{E_i}$$

(245)

Where: - O_i = observed count in category i - E_i = expected count in category i (based on the hypothesis) - k = number of categories

Degrees of freedom (df) = $k - 1$

Decision rule: Compare calculated χ^2 to critical value from the chi-squared distribution at significance level $\alpha = 0.05$. If $\chi^2_{calc} > \chi^2_{crit}$, reject the null hypothesis (the data do not fit the expected ratio).

Critical values:

Table 261. Formula and procedure for chi-square goodness-of-fit testing.

df	$\alpha = 0.05$	$\alpha = 0.01$
1	3.841	6.635
2	5.991	9.210
3	7.815	11.345
4	9.488	13.277

18.5.2 Worked Example: Chi-Squared Test for a 3:1 Ratio

Problem: F_2 from a monohybrid cross, 100 offspring observed: 68 dominant, 32 recessive. Expected ratio: 3:1 (H_0 : the trait follows simple Mendelian inheritance).

Step 1: Calculate expected values. - Expected dominant = $100 \times \frac{3}{4} = 75$ - Expected recessive = $100 \times \frac{1}{4} = 25$

Step 2: Calculate χ^2 .

$$\chi^2 = \frac{(68 - 75)^2}{75} + \frac{(32 - 25)^2}{25} = \frac{49}{75} + \frac{49}{25} = 0.653 + 1.960 = 2.613$$

(246)

Step 3: Determine df = 2 - 1 = 1.

Step 4: Compare to critical value. $\chi^2_{crit}(df = 1, \alpha = 0.05) = 3.841$.

Since 2.613 < 3.841, we fail to reject H₀. The observed data are consistent with a 3:1 Mendelian ratio ($p \approx 0.106$).

18.5.3 Worked Example: Dihybrid Chi-Squared Test

Problem: A dihybrid cross produces: 315 round yellow, 108 round green, 101 wrinkled yellow, 32 wrinkled green (total = 556). Test the 9:3:3:1 hypothesis.

Expected values: $\frac{9}{16} \times 556 = 312.75$; $\frac{3}{16} \times 556 = 104.25$; $\frac{3}{16} \times 556 = 104.25$; $\frac{1}{16} \times 556 = 34.75$

$$\chi^2 = \frac{(315 - 312.75)^2}{312.75} + \frac{(108 - 104.25)^2}{104.25} + \frac{(101 - 104.25)^2}{104.25} + \frac{(32 - 34.75)^2}{34.75}$$

(247)

$$= 0.016 + 0.135 + 0.101 + 0.218 = 0.470$$

(248)

df = 4 - 1 = 3. $\chi^2_{crit}(df = 3, \alpha = 0.05) = 7.815$.

Since 0.470 < 7.815, we fail to reject H₀. The data are consistent with a 9:3:3:1 ratio ($p > 0.90$). These are, in fact, Mendel’s actual data for seed shape and color.

Clinical Connection: Using Chi-Squared in Genetic Counseling In clinical genetics, the chi-squared test (or exact binomial tests for small families) helps evaluate whether a family’s disease pattern is consistent with a specific inheritance model. For example, if a rare disease appears in 5 of 20 siblings (25%), a chi-squared test could evaluate whether this is consistent with autosomal recessive inheritance (expected 25% affected). However, for small family sizes, exact probability calculations are preferred.

18.6 Pedigree Analysis and Inheritance-Pattern Inference

18.6.1 Pedigree Symbols and Conventions

- Squares: males; Circles: females
- Filled symbols: affected individuals
- Half-filled: carrier (when known)
- Horizontal line: mating pair
- Vertical line: parent-offspring connection
- Double horizontal line: consanguineous mating (mating between relatives)
- Roman numerals: generations (I, II, III...)
- Arabic numerals: individuals within a generation (1, 2, 3...)

18.6.2 Inheritance Pattern Recognition

Table 262. Inheritance Pattern Recognition: Pattern and Key Diagnostic Clues.

Pattern	Key Diagnostic Clues
Autosomal dominant	Affected in every generation; unaffected parents produce primarily unaffected children; males and females equally affected; affected individuals have at least one affected parent
Autosomal recessive	Often skips generations; affected children from unaffected (carrier) parents; consanguinity increases risk; males and females equally affected
X-linked recessive	Males affected far more than females; carrier mothers pass to about 50% of sons; affected fathers cannot pass to sons (but most daughters are carriers); no male-to-male transmission

Pattern	Key Diagnostic Clues
X-linked dominant	Both sexes affected but more females than males; affected father passes the allele to daughters but not sons; affected heterozygous mother passes to about 50% of sons and about 50% of daughters
Mitochondrial	Most children of an affected mother are affected; affected father does NOT transmit; maternal inheritance primarily
Y-linked	Primarily males affected; most sons of affected father are affected

18.6.3 Worked Pedigree Problem

Problem: A pedigree shows: - Generation I: Unaffected father, unaffected mother - Generation II: 3 unaffected daughters, 2 affected sons, 1 unaffected son - One affected son (Generation II) marries an unaffected woman - Generation III: 2 unaffected sons, 1 unaffected daughter

Analysis: 1. Trait skips Generation I (unaffected parents have affected children) – suggests recessive 2. Primarily males affected – suggests X-linked 3. Affected father (Gen II) has unaffected sons (Gen III) – consistent with X-linked (father gives Y to sons) 4. Most daughters of affected father are unaffected – but they are obligate carriers ($X^A X^a$) if the mother is $X^A X^A$ or $X^A Y$ – wait, the mother is female so $X^A X^A$ or $X^A X^a$

Conclusion: X-linked recessive inheritance. Mother in Gen I is a carrier ($X^H X^h$); Father in Gen I is unaffected ($X^H Y$).

Probability that Gen III daughter (from affected father $X^h Y$ x unaffected mother $X^H X^H$) is a carrier:

Most daughters of an affected father receive his X^h : probability = 1 (100% carriers).

18.7 Worked Example: Conditional Probability in Pedigrees

A couple seeks genetic counseling. The woman’s brother has cystic fibrosis (CF, autosomal recessive, $q = 0.02$ in the general population). The man has no family history.

(a) What is the probability the woman is a carrier?

Her parents must both be carriers ($Cc \times Cc$). Among unaffected siblings, the probability of being a carrier:

$$P(Cc|unaffected) = \frac{P(Cc)}{P(unaffected)} = \frac{2/4}{3/4} = \frac{2}{3}$$

(249)

(b) What is the probability the man is a carrier?

Using Hardy-Weinberg: carrier frequency = $2pq \approx 2(0.98)(0.02) \approx \frac{1}{25}$

(c) What is the probability their first child will have CF?

$$P = P(\text{mom carrier}) \times P(\text{dad carrier}) \times P(\text{child cc}|\text{both carriers}) = \frac{2}{3} \times \frac{1}{25} \times \frac{1}{4} = \frac{2}{300} = \frac{1}{150}$$

(250)

Concept Check 16.4

1. An affected father and carrier mother have children. For an X-linked recessive trait, what fraction of daughters will be affected? What fraction of sons?

2. Why does consanguinity increase the risk of autosomal recessive disorders?

3. Can mitochondrial inheritance be distinguished from autosomal dominant maternal inheritance in a single pedigree? What additional information would help?
-

18.8 Worked Example: Complex Multi-Locus Genetics

Problem: In mice, coat color is controlled by two independently assorting loci. At the A locus: A (agouti) is dominant to a (non-agouti/black). At the C locus: C (colored) is dominant to c (albino, epistatic – no pigment regardless of A genotype). This is recessive epistasis.

(a) Cross $AaCc \times AaCc$. Predict the F_2 phenotype ratio.

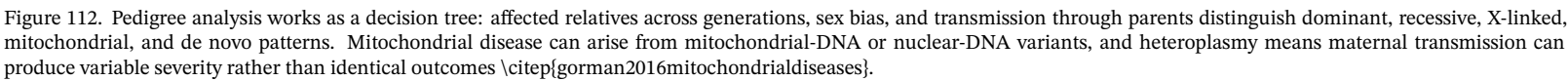


Table 263. Worked Pedigree Problem: Genotype and Phenotype.

Genotype	Phenotype	Fraction
A_C_	Agouti	$\frac{9}{16}$
aaC_	Black	$\frac{3}{16}$
A_cc	Albino	$\frac{3}{16}$
aacc	Albino	$\frac{1}{16}$

If the question intended Aacc: Among most albino mice ($\frac{4}{16}$), the fraction that is Aacc = $\frac{2/16}{4/16} = \frac{1}{2}$.

```
from biology.genetics import punnett_square
```

```
r = punnett_square("Aa", "Aa")
print(r.genotype_ratios, r.phenotype_ratios)
```

Clinical / systems note: Pedigree risk counselling translates identical probability trees into prior odds for carrier screening (CF, SMA, Ashkenazi panels) before any DNA test is ordered.

18.10 Current Evidence and Frontier Biology: Mendelian Extensions and Human Genetics

For Mendelian Extensions and Human Genetics, frontier biology belongs inside the evidence logic of the chapter. Classical genetics remains essential, but modern interpretation adds penetrance, polygenicity, structural variation, ancestry-aware inference, and uncertainty in risk prediction. The core reading question is this: Mendelian patterns are starting models that must be qualified by penetrance, linkage, environment, and sampling.

- What to verify: identify the observation, model, assay, or dataset that would make the claim stronger or weaker.
- What to qualify: state the scale, organism, cell type, environmental condition, or population where the claim is expected to hold.
- What to compare: test at least one alternative explanation, baseline, or null model before treating the pattern as causal.
- What to cite: distinguish primary evidence, review synthesis, public dataset, and institutional guidance; for recent or numeric claims, prefer the source closest to the measurement and state what has changed since it was published.

A good genetics answer separates the Mendelian transmission model from the evidence needed to use it in a population, family, or clinical setting. Source practice: For genetics claims, separate model assumptions from sampling, ancestry representation, penetrance, linkage, and environment.

18.11 Summary

- Mendel’s experiments: Garden peas, quantitative analysis of 7 characters, statistical reasoning – the first application of statistics to biology.
- Law of Segregation: Two alleles separate at meiosis I (anaphase I); each gamete gets one allele.
- Law of Independent Assortment: Genes on different chromosomes orient independently at metaphase I; exceptions for linked genes.
- Molecular basis of Mendel’s laws: Sutton-Boveri chromosome theory unifies abstract “factors” with homolog behavior at meiosis; every Punnett square is a model of meiotic chromosome dynamics.
- Monohybrid F₂: 3:1 phenotype ratio; 1:2:1 genotype ratio. Testcross confirms genotype.
- Dihybrid F₂: 9:3:3:1 phenotype ratio (product of two independent 3:1 ratios).
- Non-Mendelian inheritance: Incomplete dominance (1:2:1 phenotype), codominance (both alleles expressed), multiple alleles (ABO), pleiotropy (sickle cell), polygenic traits (continuous distribution), epistasis (modified dihybrid ratios — 9:3:4, 12:3:1, 9:7, 15:1, 13:3), genomic imprinting (parent-of-origin expression), maternal effect (mother’s genotype determines offspring phenotype).
- Penetrance and expressivity: Reduced penetrance (BRCA1, retinoblastoma) and variable expressivity (NF1, Marfan) explain why identical genotypes produce divergent clinical outcomes.
- Human genetic disorders: Huntington’s disease (CAG repeat expansion, autosomal dominant, anticipation); PKU (autosomal recessive, screened almost universally at birth, dietary therapy); CF, sickle cell, Tay-Sachs as paradigm autosomal recessive disorders maintained at elevated frequencies by likely heterozygote advantage.
- GWAS: Genome-wide association studies extend Mendel’s logic to millions of common variants, revealing that complex traits are highly polygenic, that most causal variants are non-coding, and that polygenic risk scores can predict disease risk at the individual level.
- Chi-squared test: $\chi^2 = \sum \frac{(O-E)^2}{E}$; df = k-1; compare to critical value at $\alpha = 0.05$.
- Pedigree analysis: Autosomal dominant (every generation, equal sex ratio), autosomal recessive (skips generations, consanguinity), X-linked recessive (males » females, no male-to-male), mitochondrial (maternal primarily).
- Connections: See section 19 for linkage and sex chromosomes, section 20 for allele frequencies in populations, and Unit IV — Molecular Genetics: Introduction for the molecular basis of alleles.

18.12 Review Questions

1. Explain why Mendel’s laws were not widely recognized for 34 years after their publication. What developments in cell biology (1900) made them comprehensible?
2. Perform a trihybrid cross AaBbCc x AaBbCc. What fraction of offspring will show the three dominant phenotypes? What fraction will be heterozygous at the three loci?
3. A snapdragon cross between two pink flowers (C^RC^W x C^RC^W) produces 240 offspring. How many of each color would you expect? Perform a chi-squared test if the observed counts are 55 red, 128 pink, 57 white.

4. In the ABO blood group system, a type A mother and type B father have a type O child. What are the parents' genotypes? What is the probability their next child will be type AB?
5. Describe three examples of pleiotropy and explain how one gene can affect multiple organ systems.
6. A Labrador cross produces 48 black, 16 chocolate, and 20 yellow puppies. Perform a chi-squared test for a 9:3:4 ratio.
7. Explain the molecular basis of Prader-Willi and Angelman syndromes. Why do deletions of the same chromosomal region cause different diseases?
8. A woman whose father had hemophilia A marries an unaffected man. What is the probability their first son will be affected? Their first daughter?
9. Using the Hardy-Weinberg equation, calculate the carrier frequency for phenylketonuria (PKU) if the disease frequency is 1/10,000.
10. Explain why the chi-squared test can rarely prove that a hypothesis is correct – primarily fail to reject it.
11. For a dominant disorder with 80% penetrance, how does risk to offspring of an affected × unaffected cross change compared with complete penetrance?
12. Explain why mitochondrial pedigrees show most-maternal transmission yet may still include unaffected mothers.
13. A man with 38 CAG repeats in *HTT* fathers two children. Predict the inheritance, repeat-count distribution, and clinical phenotypes of his offspring. What does this illustrate about anticipation?
14. Explain why comprehensive newborn screening for PKU has been more cost-effective than family-history-based screening.
15. A GWAS for type 2 diabetes identifies a SNP with odds ratio 1.15 ($p = 2 \times 10^{-12}$). Why is this a “successful” finding even though the odds ratio is small?

18.13 Further Reading and Source Notes: Mendelian Extensions and Human Genetics

- Mendel (1866). Versuche {”u}ber Pflanzenhybriden. *Verhandlungen des naturforschenden Vereines in Br{”u}nn*, 4.
- Bateson (1909). *Mendel’s Principles of Heredity*. Cambridge University Press.
- Morgan (1910). Sex limited inheritance in *Drosophila*. *Science*, 32.
- Sturtevant (1913). The linear arrangement of six sex-linked factors in *Drosophila*, as shown by their mode of association. *Journal of Experimental Zoology*, 14.
- Punnett (1907). *Mendelism*. Macmillan.
- Griffiths et al. (latest ed.). *Introduction to Genetic Analysis* (Mendelian inheritance chapters). W. H. Freeman.

18.14 Key Terms

1. Allele – alternative form of a gene at a given locus
2. Dominant – allele whose phenotype is expressed in heterozygotes
3. Recessive – allele whose phenotype is masked in heterozygotes
4. Homozygous – two identical alleles at a locus (AA or aa)
5. Heterozygous – two different alleles at a locus (Aa)
6. Genotype – the genetic constitution of an organism at specified loci
7. Phenotype – the observable characteristics resulting from genotype and environment
8. Testcross – cross of an individual with dominant phenotype to a homozygous recessive
9. Incomplete dominance – heterozygote phenotype intermediate between two homozygotes
10. Codominance – both alleles fully expressed in the heterozygote
11. Epistasis – interaction where one gene masks the expression of another gene
12. Pleiotropy – one gene influencing multiple phenotypic traits
13. Polygenic inheritance – multiple genes contributing additively to a continuous trait
14. Penetrance – proportion of individuals with a genotype who express the expected phenotype
15. Expressivity – degree of phenotype expression among penetrant individuals
16. Phenocopy – environmentally induced phenotype mimicking a genetic condition
17. Anticipation – earlier onset and increased severity across generations, characteristic of trinucleotide repeat expansion disorders
18. Genomic imprinting – parent-of-origin-specific gene expression via epigenetic marks
19. Chi-squared test – statistical test comparing observed to expected frequencies
20. Pedigree – diagram of family phenotypes across generations used to determine inheritance patterns
21. Consanguinity – mating between related individuals; increases homozygosity
22. GWAS – genome-wide association study; statistical scan of common variants for trait associations across the genome
23. Polygenic risk score (PRS) – weighted sum of risk alleles producing an individual-level genetic risk estimate
24. Trinucleotide repeat expansion – mutation class in which an unstable triplet repeat expands across generations, causing diseases such as Huntington’s,

fragile X, and myotonic dystrophy

18.15 Companion Source Module: Mendelian Extensions and Human Genetics

Mendelian Extensions and Human Genetics should leave a reproducible trail from a biological claim to the code, figure, diagram, or paper-based activity that can test it. Use the surfaces below to inspect the chapter’s assumptions, rerun the relevant model, or compare the manuscript explanation with companion labs and figures.

Table 264. Companion source surfaces for Mendelian Extensions and Human Genetics.

Surface	Use it for
<code>src/biology/genetics/genetics.py</code> (punnett_square, hardy_weinberg, chi_squared_test)	Reproduce inheritance ratios, equilibrium expectations, and goodness-of-fit tests.
<code>src/visualization/plots.py</code> (plot_punnett_square)	Check genotype and phenotype tables visually.
<code>src/mermaid/biology_diagrams.py</code> (mendelian_cross_diagram)	Link segregation logic to diagrammed crosses.

Reproducibility check: state genotype notation, dominance model, sample size, and statistical expectation before interpreting a ratio. Cross-reference: compare with section 19 and section 20.

19 Chromosomal Inheritance and Linkage

Level 2/3 · 60 min read · 75 min lecture · Prerequisites: section 17

19.1 Learning Objectives

1. Explain the **chromosome** theory of heredity and its experimental support from Sutton, Boveri, and Morgan.
2. Describe chromosome architecture (centromere, telomere, heterochromatin/euchromatin) and connect it to chromosome behavior at meiosis.
3. Compare meiosis and mitosis at the level of cellular events, ploidy, recombination, and outcomes.
4. Describe the sex determination systems used across different organisms.
5. Explain the molecular mechanism of X-inactivation, including the role of XIST RNA, and outline broader dosage-compensation strategies.
6. Describe X-linked inheritance patterns and calculate expected offspring ratios for X-linked traits.
7. Explain meiotic non-disjunction (meiosis I vs. meiosis II), aneuploidy outcomes, and the maternal age effect.
8. Define genetic **linkage** and **recombination**; calculate map distance from cross data.
9. Perform three-point test cross analysis to determine **gene** order and map distances.
10. Classify chromosomal rearrangements (translocations, inversions, deletions, duplications) and their clinical consequences, including the Philadelphia chromosome, DiGeorge, and Cri-du-chat syndromes.
11. Connect chromosome behavior to genomic imprinting and uniparental disomy (cross-link to section 15).
12. Calculate inbreeding coefficients and predict their effect on offspring homozygosity and fitness.

19.1.1 Study Blueprint

- Big idea: Genes travel on chromosomes, so linkage, recombination, and chromosome structure shape inheritance.
- Core concepts: linkage, recombination, sex linkage, chromosomal rearrangements.
- Framework alignment: Vision & Change: Information flow, exchange, and storage, Evolution; AP Biology: Information Storage and Transmission, Evolution; NGSS-style topics: Inheritance and Variation of Traits, Natural Selection and Evolution.
- Model or quantitative lens: Recombination frequency and three-point mapping.
- Data skill: Infer gene order or chromosomal mechanism from offspring counts.
- Practice cadence: Statistical Tests and Data Analysis, Representing and Describing Data.
- Common misconception to repair: Independent assortment applies to unlinked loci, not to every pair of genes.
- Primary lab: **Lab — Chromosomal Inheritance and Linkage**.
- Question bank: **Questions — Chromosomal Inheritance and Linkage**.
- Transfer task: Transfer linkage reasoning to disease mapping, breeding, and genome assemblies.
- Bridge to computation: `biology.genetics.genetics.infer_three_point_order`.

Opening Vignette — A Fly’s White Eye Opens the Chromosome Era

In 1910, Thomas Hunt Morgan was cultivating thousands of *Drosophila melanogaster* in a “fly room” at Columbia University when he noticed a single male with white eyes among thousands of red-eyed flies. When he crossed this mutant with normal red-eyed females and counted the offspring across two generations, a striking pattern emerged: white eyes appeared almost exclusively in male offspring [Morgan, 1910]. Morgan immediately recognized that the white-eye trait was linked to the X chromosome — the first gene mapped to a specific chromosome in any organism. The discovery of sex-linkage validated the chromosome theory of heredity (which Mendel’s work alone could not prove), won Morgan the 1933 Nobel Prize, and launched the entire field of chromosome mapping. The humble fruit fly, with its four chromosome pairs, short generation time, and thousands of offspring, remains one of the most productive research organisms in genetics to this day.

19.2 The Chromosome Theory of Heredity

In 1902, Walter Sutton (studying grasshopper *Brachystola magna*) and Theodor Boveri (studying sea urchin embryos) independently proposed that chromosomes are the physical carriers of Mendel’s “factors” (genes) [Sutton, 1902]:

Table 265. Study Blueprint: Mendel’s Observation and Chromosomal Parallel.

Mendel’s Observation	Chromosomal Parallel
Genes exist in pairs in somatic cells	Chromosomes exist in homologous pairs (diploid)
Alleles segregate during gamete formation	Homologous chromosomes separate at meiosis I

Mendel’s Observation	Chromosomal Parallel
Different genes assort independently	Non-homologous chromosomes orient independently at metaphase I
Gametes carry one allele per gene	Gametes are haploid (one chromosome from each pair)

Morgan’s confirmation (1910-1915): Thomas Hunt Morgan’s experiments with *Drosophila melanogaster* provided the definitive proof. His discovery of white-eyed males (X-linked recessive) demonstrated that a specific gene (white, *w*) segregated with the X chromosome, proving that genes reside on chromosomes [Morgan, 1910]. Morgan received the Nobel Prize in Physiology or Medicine in 1933.

19.3 Chromosome Architecture: The Hardware of Heredity

A eukaryotic chromosome is far more than a passive package of DNA — it is a structurally organized object whose every architectural feature has a functional role in transmission, expression, and protection of the genetic material. Understanding chromosome behavior requires understanding chromosome anatomy: the metaphase chromosome in figure 113 shows how the centromere, telomeres, and heterochromatic and euchromatic domains discussed below are arranged along the sister chromatids.

19.3.1 Centromeres and Kinetochore Attachment

The centromere is the chromosomal region where sister chromatids are held together after DNA replication and where the kinetochore assembles to attach to spindle microtubules during cell division. Centromeres position chromosomes correctly at metaphase and are essential for the orderly disjunction of chromatids at anaphase.

- Position-based classification: Metacentric (centromere central — chromosome 1), submetacentric (slightly off-center — chromosome 6), acrocentric (near one end — chromosome 21), telocentric (terminal — present in some species but not in normal humans).
- Sequence composition: Human centromeres contain alpha-satellite DNA — tandem repeats of a 171-bp monomer organized into higher-order arrays spanning 0.3–5 Mb. The DNA sequence is rapidly evolving, but centromere identity is epigenetically defined by the histone variant CENP-A, which replaces canonical H3 in centromeric nucleosomes and recruits the kinetochore.
- Robertsonian translocations involve fusion of two acrocentric chromosomes through their centromeres — a phenomenon that depends on the unique architecture of acrocentric short arms and is revisited in the structural-rearrangements discussion.

19.3.2 Telomeres and Chromosome-End Protection

The ends of linear eukaryotic chromosomes pose a structural problem: the cell must distinguish a true chromosome end from a double-strand break (which would otherwise trigger DNA damage signaling). Telomeres solve this with specialized terminal structures.

- Sequence: Human telomeres consist of tandem repeats of TTAGGG (5–15 kb at birth), bound by the shelterin complex (TRF1, TRF2, POT1, TIN2, TPP1, RAP1) that masks the chromosome end and inhibits inappropriate repair responses.
- The end-replication problem: DNA polymerase cannot fully replicate the lagging strand, so chromosomes shorten by 50–200 bp per division. Without compensation, cells become senescent after about 50 divisions (the Hayflick limit).
- Telomerase: A specialized reverse transcriptase (catalytic subunit TERT, RNA template TERC) extends telomeres in stem cells, germ cells, and about 85% of cancers — making telomerase a cancer therapeutic target.
- Clinical relevance: Dyskeratosis congenita results from telomerase mutations and causes premature aging, bone marrow failure, and cancer. Werner syndrome (helicase mutations) accelerates telomere shortening.

19.3.3 Euchromatin and Heterochromatin

Chromatin is not uniform — it exists in two functionally and structurally distinct states.

Table 266. Euchromatin and Heterochromatin: Feature and Euchromatin.

Feature	Euchromatin	Heterochromatin
Compaction	Open, accessible	Densely packed
Histone marks	H3K4me3, H3K27ac, H3K36me3	H3K9me3, H3K27me3, H4K20me3
Replication timing	Early S phase	Late S phase

Feature	Euchromatin	Heterochromatin
GC content	Higher	Lower
Recombination	Frequent	Suppressed
Transcription	Active genes	Silenced/repetitive
Examples	Most gene-rich regions	Centromeres, telomeres, inactive X (Barr body)

- Constitutive heterochromatin is permanent and structural — centromeric and pericentric regions, telomeres, the Y chromosome long-arm heterochromatin, and tandemly repeated satellite DNAs. Constitutive heterochromatin maintains chromosome architecture and silences transposable elements.
- Facultative heterochromatin is inducible — formed in specific cell types or developmental states. The classic example is the inactive X chromosome (Barr body) in female mammals, formed *de novo* in early embryos through XIST-mediated silencing as developed in the X-inactivation section.
- Position-effect variegation (PEV): When a gene is relocated by translocation or transposition into a heterochromatic region, it can be silenced — but with stochastic, mosaic patterns that depend on heterochromatin spreading. Classic *Drosophila* PEV experiments (the *white^{m4}* allele) revealed how heterochromatin propagates and provided the first hints of histone-based silencing.

19.4 Meiosis vs. Mitosis: Two Cell-Division Programs

The chromosomal theory of inheritance rests on a single comparative observation — that meiosis differs systematically from mitosis in ways that exactly produce Mendelian segregation. The two programs share machinery (spindle, cohesin, kinetochores) but diverge in chromosome behavior.

Table 267. Euchromatin and Heterochromatin: Feature and Mitosis.

Feature	Mitosis	Meiosis
Number of divisions	One (M phase)	Two (Meiosis I, Meiosis II)
DNA replication	Once before division	Once before Meiosis I; none between MI and MII
Daughter cells per parent	2	4
Ploidy change	Diploid → diploid (2n → 2n)	Diploid → haploid (2n → n)
Homolog pairing	None	Synapsis with synaptonemal complex at prophase I
Crossing over (recombination)	None (rare exceptions)	Required at prophase I; about 1.5–3 crossovers per bivalent in humans
Anaphase I event	N/A	Homologs disjoin (sisters remain joined)
Anaphase II event	Sisters disjoin	Sisters disjoin
Genetic outcome	Identical genetic copies	Genetically unique haploid gametes
Cohesin protection	None at centromere; cleaved at anaphase	Shugoshin protects centromeric cohesin until anaphase II
Cellular function	Growth, repair, asexual reproduction	Sexual reproduction; gamete formation
Failure consequences	Tumor formation, aneuploid somatic cells	Aneuploid gametes (Down syndrome, miscarriage)

The combination of (1) homolog pairing in prophase I, (2) crossing over, (3) random orientation of bivalents at metaphase I, and (4) reductional division at anaphase I produces gametes that are genetically unique and that satisfy Mendel’s laws. Each of these four events can fail — and each failure has a recognizable disease signature.

19.4.1 Molecular details of meiotic recombination

The orderly behavior of bivalents at metaphase I depends on physical connections (chiasmata) created by reciprocal recombination during prophase I. The molecular events that generate these chiasmata are conserved across eukaryotes and are essential — failure of recombination is a leading cause of meiotic non-disjunction in human oogenesis.

Key molecular players:

- SPO11 is a topoisomerase-VI-like enzyme that creates programmed double-strand breaks by covalent attachment to 5’ ends of DNA. In humans, about 250 DSBs are generated per meiosis (about 10× the number of crossovers — most DSBs are repaired without crossover). SPO11 binding sites are determined

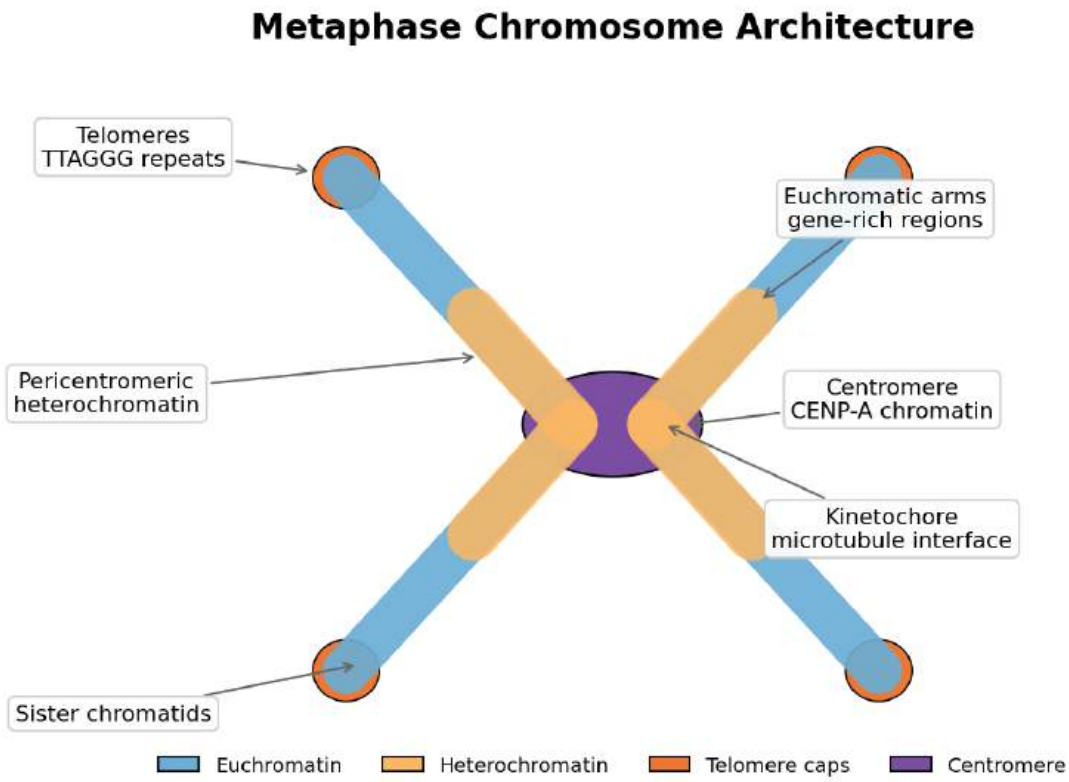


Figure 113. Anatomy of a metaphase chromosome: two sister chromatids joined at the centromere (containing CENP-A nucleosomes that recruit the kinetochore), capped by telomeres of TTAGGG repeats bound by the shelterin complex, with constitutive heterochromatin flanking the centromere and facultative heterochromatin at silenced loci such as the inactive X.

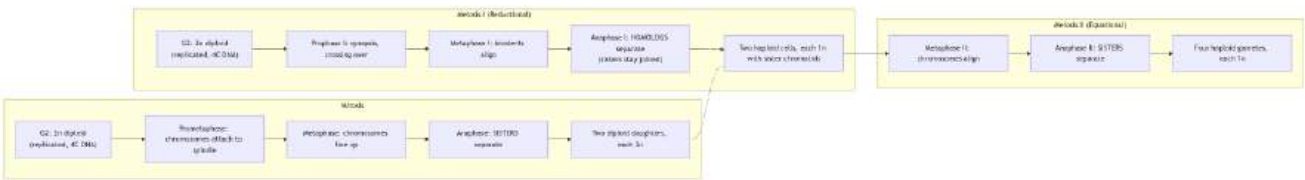


Figure 114. Mitosis vs. meiosis: a single division producing two diploid copies versus a two-division program producing four haploid, recombined gametes. The defining event of meiosis is anaphase I, when homologs (not sisters) separate.

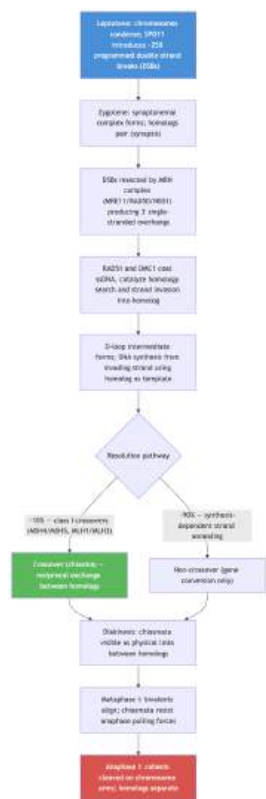


Figure 115. Molecular events of meiotic recombination from SPO11 DSB induction through RAD51/DMC1-mediated strand invasion to chiasma formation. Approximately 10% of programmed double-strand breaks resolve as crossovers; the remainder become non-crossover gene conversions.

by PRDM9, which trimethylates H3K4 at specific DNA motifs to mark recombination hotspots. *Spo11* knockout mice are sterile because no chiasmata form, leading to bivalent disjunction failure and aneuploid gametes.

- MRE11–RAD50–NBS1 (MRN complex) binds the DSB and resects the 5’ ends, exposing 3’ single-stranded overhangs about 1–2 kb long.
- RAD51 and DMC1 are RecA-family recombinases that polymerize on the single-stranded DNA, forming a nucleoprotein filament that searches for homology in the homologous chromosome and catalyzes strand invasion. DMC1 is meiosis-specific and is essential for inter-homolog (rather than inter-sister) recombination.
- MSH4–MSH5 and MLH1–MLH3 are required for the major crossover pathway (class I); their mutations reduce crossover frequency and increase non-disjunction. MUS81–EME1 mediates a minor (about 10%) class II crossover pathway.
- Synaptonemal complex: A protein scaffold (SYCP1, SYCP2, SYCP3) that physically holds homologs together along their entire length during pachytene. The complex provides the platform on which crossovers form and assures proper pairing.

The molecular specifics matter because mutations in many of these genes cause human infertility, recurrent pregnancy loss, and elevated aneuploidy risk: *SYCP3* mutations are associated with azoospermia and pregnancy loss; *MSH4* mutations with primary ovarian insufficiency; *DMC1* mutations with sterility; and reduced *PRDM9* function correlates with diminished ovarian reserve. Meiotic recombination is far from a passive structural process — it is an actively regulated DNA-damage event without which sexual reproduction fails.

19.5 Sex Chromosomes and Sex Determination

19.5.1 Mammalian Sex Determination (XX/XY)

The Y chromosome and SRY: - Human Y chromosome: about 57 Mb; carries about 78 protein-coding genes (compared to about 900 on the X) - SRY (sex-determining region Y): Located at Yp11.31; encodes TDF (testis-determining factor), a transcription factor with an HMG-box DNA-binding domain - SRY activates SOX9, which drives Sertoli cell differentiation in the bipotential gonad - Sertoli cells produce anti-Mullerian hormone (AMH), causing regression of Mullerian ducts - Leydig cells produce testosterone, driving Wolffian duct development (epididymis, vas deferens, seminal vesicles) and external male genitalia

Pseudoautosomal regions (PARs): - PAR1 (2.6 Mb at Xp/Yp tips): contains about 24 genes; mandatory crossover during male meiosis ensures proper X-Y segregation - PAR2 (320 kb at Xq/Yq tips): smaller; crossover not required - Genes in PARs escape X-inactivation (expressed from both X chromosomes in females) - SHOX gene (in PAR1): Short stature homeobox; haploinsufficiency causes short stature in Turner syndrome; extra copies cause tall stature in sex chromosome

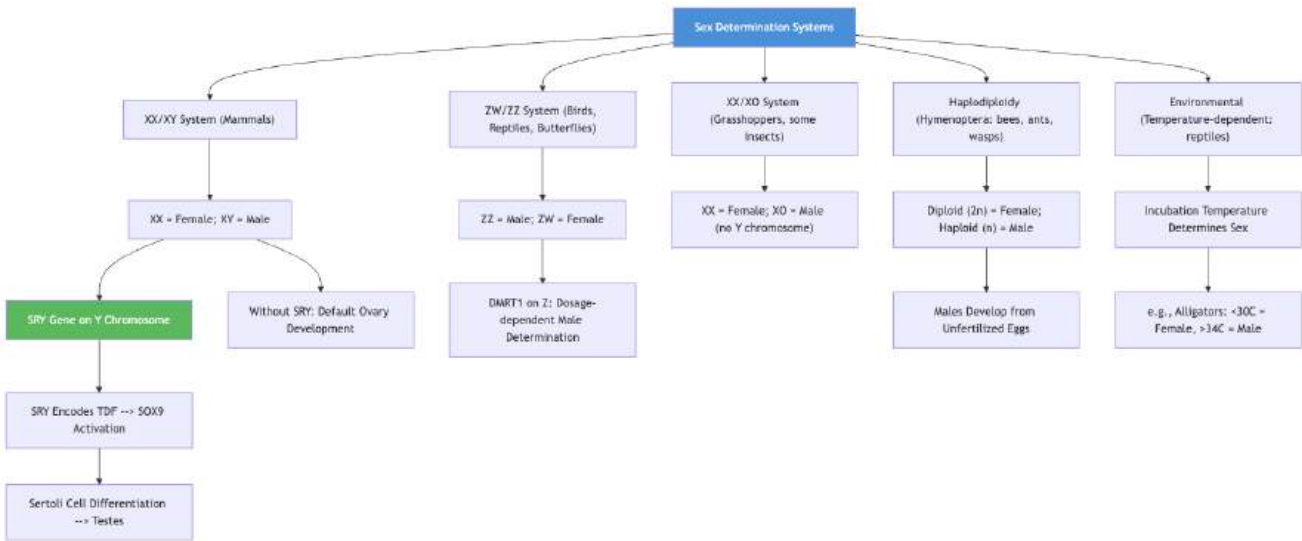


Figure 116. Sex determination systems across organisms. The XX/XY system is used by mammals, with the SRY gene on the Y chromosome being the master switch. Other organisms use ZW, XO, haplodiploidy, or temperature-dependent systems.

polysomies

Evidence for SRY as the master switch: - XX males (de la Chapelle syndrome): about 1/20,000; caused by translocation of SRY to the X chromosome - XY females (Swyer syndrome): SRY **mutations** lead to female **phenotype** with streak gonads despite 46,XY karyotype

19.5.2 Non-Mammalian Sex Determination

Table 268. Non-Mammalian Sex Determination: System and Organisms.

System	Organisms	Male	Female	Key Gene
ZW/ZZ	Birds, snakes, butterflies	ZZ	ZW	DMRT1 (Z-linked; dosage determines sex)
XX/XO	Grasshoppers, some nematodes	XO	XX	X:autosome ratio (C. elegans)
Haplodiploidy	Hymenoptera (bees, ants, wasps)	Haploid (n)	Diploid (2n)	CSD locus (complementary sex determiner)
Temperature-dependent	Crocodylians, some turtles	Temperature-dependent	Temperature-dependent	Aromatase (converts testosterone to estradiol)

Haplodiploidy is a sex-determination mechanism, not a stand-alone explanation for social life. In many Hymenoptera, unfertilised haploid eggs develop as males and fertilized diploid eggs develop as females; complementary sex-determination loci can make some diploid genotypes male instead. This chromosome logic changes relatedness patterns among relatives, which matters for kin-selection models, but eusociality also depends on ecology, colony demography, and mating system. Termites provide a useful contrast: they are diploid cockroach relatives, yet they evolved **eusociality** through a different phylogenetic route [Bourke, 2011, Hughes et al., 2008, Inward et al., 2007].

19.6 X-Inactivation and Dosage Compensation

19.6.1 Lyon Hypothesis and X-Inactivation

Mary Lyon [1961] proposed that in each female somatic cell, one of the two X chromosomes is randomly inactivated early in embryonic development (about day 5.5 in mouse, about day 12-16 in human). This inactivation is:

- Random: Either the maternal or paternal X can be inactivated in any given cell
- Clonal: Once established, most daughter cells maintain the same inactive X
- Result: Adult females are genetic mosaics – a patchwork of cells expressing the maternal X and cells expressing the paternal X

19.6.2 Molecular Mechanism of X-Inactivation

1. XIST (X-inactive specific transcript): A 17 kb lncRNA transcribed primarily from the X that will be inactivated



Figure 117. The molecular mechanism of X-inactivation. XIST RNA coats the future inactive X chromosome, recruiting Polycomb complexes that establish repressive histone marks and DNA methylation, ultimately condensing the chromosome into a Barr body.

Table 269. Dosage Compensation Across Species and Beyond Sex Chromosomes: Organism and Mechanism.

Organism	Mechanism	Result
Mammals	X-inactivation (XIST)	One X silenced in XX females; equal dosage with XY males
Drosophila	X upregulation in males (MSL/roX RNA complex)	Male single X transcribed about 2x; equals female XX
C. elegans	X downregulation in XX hermaphrodites (DCC complex)	Each X transcribed about 0.5x; equals male XO single X

Dosage compensation beyond X-inactivation: The principle that gene dosage must be balanced applies far more broadly than the sex chromosomes. Several other mechanisms address dosage imbalances:

- Autosomal dosage sensitivity: Most genes tolerate small dosage changes (1.5x or 2x) without phenotype, but dosage-sensitive genes — typically transcription factors, signaling components, and members of multi-protein complexes — produce phenotypes when copy number changes. The Williams syndrome deletion (7q11.23) and its reciprocal duplication produce opposite cognitive-behavioral phenotypes precisely because of dosage sensitivity in the *GTF2I* gene region.
- Gene balance hypothesis: Genes whose products participate in stoichiometric complexes (e.g., ribosomal proteins, transcription complexes, RNA polymerases) cannot tolerate copy-number changes because subunit imbalance disrupts complex assembly. This explains why most autosomal monosomies are lethal even when the underlying gene mutations would not be.
- Compensatory feedback at promoters: In *Drosophila* and yeast, deletion of one allele of a dosage-sensitive gene often triggers transcriptional upregulation of the remaining allele, partially restoring protein levels (cis-compensation).
- microRNA buffering: Individual miRNAs can buffer the expression of dozens of target genes against perturbation. The miR-17about 92 cluster, for example, buffers cell-cycle gene dosage during proliferation.
- Polycomb-mediated maintenance of dosage: Active and inactive states established at gene clusters (Hox genes, the imprinted regions of chromosome 15) are maintained through cell division by Polycomb (silencing) and Trithorax (activation) complexes, ensuring stable gene dosage in each tissue.

The core insight is that gene dosage is itself a regulated variable, defended by multiple parallel mechanisms. X-inactivation is the most spectacular example because an entire chromosome is silenced, but it is one strategy among many.

Clinical Connection: Calico Cats and X-Inactivation The calico coat pattern in cats is a visible demonstration of X-inactivation. The *O* gene (orange) is X-linked: X^O produces orange pigment; X^o produces black pigment. **Heterozygous** females ($X^O X^o$) are mosaics – patches of orange (cells with X^O inactivated) and black (cells with X^o inactivated). White patches come from a separate autosomal spotting gene. Calico cats are overwhelmingly female; rare calico males are usually 47,XXY (Klinefelter).

19.7 X-Linked Inheritance

19.7.1 X-Linked Recessive Inheritance

For X-linked recessive traits, males are affected more frequently because they are hemizygous (a single X):

- Affected males: $X^a Y$ – one copy of the recessive allele is sufficient
- Affected females: $X^a X^a$ – must be homozygous (very rare; requires carrier mother AND affected father)
- Carrier females: $X^A X^a$ – phenotypically normal (usually); can show mosaic expression due to random X-inactivation

Key X-linked recessive conditions:

Table 270. X-Linked Recessive Inheritance: Condition and Gene.

Condition	Gene	Location	Frequency	Key Features
Hemophilia A	<i>F8</i> (Factor VIII)	Xq28	1/5,000 males	Prolonged bleeding; joint hemorrhages; treated with recombinant Factor VIII
Hemophilia B	<i>F9</i> (Factor IX)	Xq27.1	1/30,000 males	Similar to hemophilia A; “Christmas disease”
Duchenne muscular dystrophy	<i>DMD</i> (dystrophin)	Xp21.2	1/3,500 males	Largest human gene (2.4 Mb); progressive muscle wasting; frameshift mutations cause complete dystrophin loss; onset age 2-5; wheelchair by age 12; cardiac/respiratory failure
Becker muscular dystrophy	<i>DMD</i> (dystrophin)	Xp21.2	1/18,000 males	In-frame deletions; partially functional dystrophin; milder course
Red-green color blindness	<i>OPN1LW/OPN1MW</i> Xq28		8% of males, 0.5% of females	Deutan (green) or protan (red) deficiency; unequal crossing over between tandem opsin genes
G6PD deficiency	<i>G6PD</i>	Xq28	about 400 million affected worldwide	Hemolytic anemia triggered by oxidative stress (fava beans, certain drugs); heterozygote advantage against malaria

19.8 Worked Example: X-Linked Recessive Inheritance

A carrier woman ($X^H X^h$ for hemophilia) marries an unaffected man ($X^H Y$):

Table 271. X-Linked Recessive Inheritance.

	X^H	Y
X^H	$X^H X^H$ (normal female)	$X^H Y$ (normal male)
X^h	$X^H X^h$ (carrier female)	$X^h Y$ (affected male)

Results: $\frac{1}{4}$ normal daughters, $\frac{1}{4}$ carrier daughters, $\frac{1}{4}$ normal sons, $\frac{1}{4}$ affected sons.

Among sons primarily: $\frac{1}{2}$ affected. Among daughters primarily: $\frac{1}{2}$ carriers.

Clinical Connection: Duchenne Muscular Dystrophy and Exon Skipping The *DMD* gene (2.4 Mb, 79 exons) is a frequent target of deletions. Out-of-frame deletions cause Duchenne (no dystrophin); in-frame deletions cause Becker (partial dystrophin). Exon-skipping therapy uses antisense oligonucleotides (ASOs) to mask specific exons during splicing, converting an out-of-frame deletion to an in-frame deletion (Duchenne to Becker phenotype). Eteplirsen (FDA-approved 2016) targets exon 51; applicable to about 13% of DMD patients. Newer ASOs target other exons.

Concept Check 17.5

1. A pedigree shows an affected trait that appears primarily in males, is rarely transmitted father-to-son, and reaches grandsons through phenotypically normal daughters of affected men: explain why these three features together identify X-linked recessive inheritance, and state which single observation would instead force an autosomal-recessive interpretation.

Concept Check (Analysis): X-inactivation (lyonization) in female mammals silences one X chromosome per cell, creating a mosaic. In heterozygous females for X-linked recessive conditions (carriers): (a) Why do carriers of Duchenne muscular dystrophy (DMD) sometimes develop mild cardiomyopathy, and what does this reveal about the distribution of X-inactivation in cardiac muscle? (b) Skewed X-inactivation (>80% of cells inactivate the same X) can be adaptive or pathological. If a woman is a carrier for a cell-lethal X-linked mutation, predict the direction of skewing and explain the selection pressure on cells during development. (c) Becker muscular dystrophy (BMD) patients have in-frame deletions in *DMD* gene, while Duchenne patients have out-of-frame deletions — both lack large portions of the dystrophin protein but BMD is milder. Explain this at the protein level and explain why the reading-frame rule predicts clinical severity.

Worked Example — Linkage Mapping and LOD Scores: Two loci, A and B, are studied in 100 two-generation families. Observed recombinant offspring: $23/100 = \theta = 0.23$. Calculate the LOD score at $\theta = 0.23$ vs $\theta = 0.5$ (null hypothesis, unlinked). $LOD = \log_{10}[L(\theta)/L(0.5)] = \log_{10}[(0.23)^{23}(0.77)^{77} / (0.5)^{100}] = 23 \times \log(0.23) + 77 \times \log(0.77) - 100 \times \log(0.5) = 23 \times (-0.638) + 77 \times (-0.114) - 100 \times (-0.301) = -14.67 - 8.78 + 30.10 = +6.65$. $LOD > 3.0$ is traditionally considered evidence of linkage. This LOD of 6.65 is very strong evidence. The maximum LOD (across every θ value) occurs at $\theta_{\text{hat}} = 0.23$, which corresponds to approximately 23 cM genetic distance.

19.9 Linkage and Recombination

19.9.1 Morgan’s Experiments

Thomas Hunt Morgan (1910-1915) discovered that some genes do NOT assort independently – they are linked on the same chromosome [Morgan, 1910, Sturtevant, 1913].

In a testcross for body color (b: black recessive) and wing type (vg: vestigial recessive) in *Drosophila*:

Expected (if unlinked): 1:1:1:1 ratio of four phenotype classes Observed: Excess parental types (gray-normal, black-vestigial) and deficiency of recombinant types (gray-vestigial, black-normal)

This means b and vg are on the same chromosome, and crossing over during meiosis generates recombinants at a frequency proportional to the physical distance between the genes.

19.9.2 Map Distance and Recombination Frequency

Recombination frequency (RF):

$$RF = \frac{\text{number of recombinant offspring}}{\text{total offspring}} \times 100\%$$

(251)

Map distance in centimorgans (cM): 1 cM = 1% recombination frequency.

- RF < 50%: genes are linked (on the same chromosome)
- RF = 50%: genes are unlinked (on different chromosomes OR so far apart on the same chromosome that at least one crossover typically occurs between them)
- RF can rarely exceed 50% because a single crossover between two loci produces 50% recombinant and 50% parental gametes (two chromatids involved out of four)

19.9.3 Three-Point Test Cross

The three-point test cross determines the order of three linked genes and the distances between them simultaneously. It is more efficient than three separate two-point crosses and reveals interference.

19.10 Worked Example: Three-Point Test Cross in *Drosophila*

- dp (dumpy wings): recessive
- b (black body): recessive
- cn (cinnabar eyes): recessive

A triply heterozygous female (dp+ b+ cn+ / dp b cn) is testcrossed to a triply homozygous recessive male (dp b cn / dp b cn). The offspring are:

Table 272. Three-Point Test Cross: Phenotype class and Count.

Phenotype class	Count	Classification
dp+ b+ cn+	350	Parental
dp b cn	345	Parental
dp+ b cn	62	Single crossover (region II)
dp b+ cn+	58	Single crossover (region II)
dp+ b+ cn	40	Single crossover (region I)
dp b cn+	38	Single crossover (region I)
dp+ b cn+	5	Double crossover
dp b+ cn	2	Double crossover
Total	900	

Step 1: Determine gene order. Compare the parental classes (most frequent) to the double crossover classes (least frequent). The gene that switches position in the double crossover class is the middle gene.

- Parental: dp+ b+ cn+; dp b cn
- Double crossover: dp+ b cn+; dp b+ cn

The b gene has switched relative to dp and cn. Therefore, the gene order is: dp – b – cn (b is in the middle).

Step 2: Calculate map distances.

Distance dp-b = $\frac{40 + 38 + 5 + 2}{900} \times 100 = \frac{85}{900} \times 100 = 9.4 \text{ cM}$

(252)

Distance b-cn = $\frac{62 + 58 + 5 + 2}{900} \times 100 = \frac{127}{900} \times 100 = 14.1 \text{ cM}$

(253)

Total map distance dp-cn = $9.4 + 14.1 = 23.5 \text{ cM}$

(254)

Step 3: Calculate interference.

Expected double crossovers = $0.094 \times 0.141 \times 900 = 11.9$

(255)

Observed double crossovers = $5 + 2 = 7$

(256)

Coefficient of coincidence (CoC) = $\frac{\text{observed}}{\text{expected}} = \frac{7}{11.9} = 0.59$

(257)

Interference (I) = 1 – CoC = 1 – 0.59 = 0.41

(258)

An interference of 0.41 means that 41% of expected double crossovers did not occur – a crossover in one region partially suppresses crossovers in the adjacent region (positive interference).

19.10.1 Mapping Functions and Recombination Interference

Simple RF underestimates true genetic distance because multiple crossovers between distant loci are undetectable (double crossovers restore parental configuration).

Haldane mapping function (1919, assumes no chromatid interference):

$$m = -\frac{1}{2} \ln(1 - 2\theta) \quad (\text{morgans})$$

(259)

where θ = observed RF. As $\theta \rightarrow 0.5$, $m \rightarrow \infty$.

Kosambi mapping function (1944, accounts for positive chromatid interference):

$$m = \frac{1}{4} \ln\left(\frac{1 + 2\theta}{1 - 2\theta}\right)$$

(260)

Kosambi’s function better fits empirical data for moderate distances.

19.10.2 LOD Score Analysis

LOD (logarithm of odds) score: Statistical method for testing linkage in human pedigrees (where controlled crosses are ethically unfeasible).

$$LOD = \log_{10} \frac{L(\theta)}{L(\theta = 0.5)}$$

(261)

Where $L(\theta)$ is the likelihood of the data given recombination fraction θ , and $L(0.5)$ is the likelihood under no linkage.

- LOD ≥ 3 : Evidence for linkage (θ value estimates map distance)
- LOD ≤ -2 : Evidence against linkage
- $-2 < \text{LOD} < 3$: Inconclusive

19.10.3 Recombination Hotspots and Sex Differences in Map Length

Recombination is not distributed uniformly across the genome — it concentrates in narrow hotspots of about 1–2 kb separated by larger cold regions, and the total map length differs sharply between male and female meiosis.

- PRDM9 and hotspots: In humans and mice, the zinc-finger histone methyltransferase PRDM9 binds specific DNA motifs and trimethylates H3K4 and H3K36 at the binding site, recruiting the meiotic double-strand break machinery (SPO11). Crossovers preferentially form at these PRDM9-marked sites. PRDM9 is itself rapidly evolving — its zinc-finger array changes between populations and species, and *Prdm9* knockout mice are sterile due to meiotic defects. PRDM9 is one of very few genes implicated in mammalian speciation through hybrid sterility.
- Hotspot rates: Within hotspots, recombination rates can reach 10–100× the genome-wide average. The HLA region on chromosome 6 contains some of the most active hotspots, contributing to the immense allelic diversity of MHC genes.
- Cold regions: Centromeric and pericentric heterochromatin is recombination-suppressed, both because of structural constraints and because crossovers near centromeres can disrupt segregation. Recombination is also reduced near telomeres (in some species) and in regions of strong purifying selection.
- Sex differences in map length: The female human genetic map is roughly 1.5–1.8× longer than the male map (about 4,400 cM in females vs. about 2,700 cM in males). This reflects more crossovers per meiosis in oogenesis (about 70 per cell) than spermatogenesis (about 50 per cell), and dramatic regional differences — recombination is enriched at telomeres in male meiosis (where obligate crossovers occur to ensure disjunction) and more uniformly distributed in female meiosis.
- Consequences: Sex-specific maps must be used in linkage analysis when transmissions go through one sex predominantly. Large family genetic studies routinely report male, female, and sex-averaged maps separately.

Why females have more crossovers? The pronounced sex difference in recombination rate has several proposed explanations, and most empirical studies suggest more than one is operating simultaneously:

1. Oocyte time available: Female meiosis includes a prolonged pachytene during which homolog pairing and crossover designation occur. Spermatogenesis is faster and may impose stricter checkpoints that limit crossover-pathway entry.
2. Telomeric vs. interstitial recombination: Male meiosis enriches crossovers at telomeres because the obligate crossover rule (every bivalent must have at least one chiasma to segregate properly) is satisfied near chromosome ends, where pairing can complete in less time. Female meiosis has the time to distribute crossovers more uniformly, including in interstitial regions distant from telomeres.
3. Selection for accuracy in oogenesis: Because errors during the long oocyte arrest are catastrophic, female meiosis may have evolved higher recombination rates to ensure at least one chiasma per bivalent. Achiasmate bivalents segregate randomly, producing aneuploid gametes — the female reproductive system tolerates this poorly because each oocyte represents irreplaceable investment.
4. Sexually antagonistic selection on chromosome conformation: Some authors propose that male and female germlines have different optima for genome stability, with selection acting in opposite directions on regulators of recombination.

Haldane’s rule and recombination Haldane’s classic 1922 observation extends beyond sex-determination biology to recombination patterns: in many species the homogametic sex (XX females in mammals; ZZ males in birds) shows higher recombination rates than the heterogametic sex. In *Drosophila*, the asymmetry is extreme — males have no meiotic recombination at most, while females have normal crossover-mediated recombination. In humans, the pattern is muted but present, with females having about 1.6× the male map length. The achiasmate male meiosis of *Drosophila* and several other dipterans is supported by alternative bivalent-tethering mechanisms (the *Mnm* complex) that maintain homolog pairing without crossovers. The mammalian intermediate pattern reflects partial achiasmatism — males still recombine, but with reduced rate and biased localization to telomeres. Why these sex differences evolved remains an open question and is one of the most robust empirical generalizations in the genetics of meiosis.

Concept Check 17.1

1. In a three-point cross, why are double crossover classes typically the least frequent?
2. If genes A and B have RF = 45%, are they linked? Explain.
3. What does positive interference tell you about the biology of crossing over?
4. PRDM9 binds specific DNA motifs to direct recombination hotspots. What does its rapid evolution suggest about hotspot evolution between human populations?

19.11 Chromosomal Abnormalities and Dosage Imbalance

19.11.1 Aneuploidy: Non-Disjunction in Meiosis I vs. Meiosis II

Non-disjunction is the failure of chromosomes to separate properly during cell division and is the principal source of human aneuploidy [Hassold and Hunt, 2001]. It can occur in either meiosis I or meiosis II, and the two failure modes have distinguishable genetic signatures.

This MI/MII distinction is clinically important because: - about 75% of trisomy 21 cases originate in maternal meiosis I (the cohesin-decay mechanism described below). - Paternal trisomy 21 (about 5–10% of cases) is typically meiosis II in origin. - Trisomy 18 has a higher proportion of MII errors than trisomy 21, suggesting different mechanistic pressures.

Risk factors for non-disjunction:

Table 273. Aneuploidy: Non-Disjunction in Meiosis I vs. Meiosis II: Factor and Effect.

Factor	Effect	Mechanism
Maternal age (>35)	Strong, exponential increase in non-disjunction risk	Cohesin decay during prolonged dictyate arrest
Achiasmate bivalents	Strong increase	A bivalent without a chiasma cannot stay paired through MI; mis-segregates
Telomeric crossovers primarily	Increased	Distal-biased chiasmata are unstable; inadequate to retain bivalent integrity
Smoking	Modest increase	Oxidative damage to oocyte DNA and proteins
Folate deficiency	Modest increase	Impaired methylation may affect centromeric heterochromatin

Factor	Effect	Mechanism
Ovarian endometriosis	Modest increase	Inflammatory effects on oocyte quality

Autosomal trisomies:

Table 274. Aneuploidy: Non-Disjunction in Meiosis I vs. Meiosis II: Condition and Karyotype.

Condition	Karyotype	Key Features	Live Birth Frequency	Survival
Down syndrome	47,+21	Intellectual disability (IQ 25-75); congenital heart defects (40-50%); increased Alzheimer risk (APP gene on chr 21); characteristic facies	1/700	Most survive to adulthood (median about 60 years)
Edwards syndrome	47,+18	Severe; clenched fists with overlapping fingers; rocker-bottom feet; cardiac defects	1/5,000	about 5-10% survive to 1 year
Patau syndrome	47,+13	Holoprosencephaly; polydactyly; cleft lip/palate; cardiac defects	1/10,000	about 5-10% survive to 1 year

Sex chromosome aneuploidies:

Table 275. Aneuploidy: Non-Disjunction in Meiosis I vs. Meiosis II: Condition and Karyotype.

Condition	Karyotype	Barr Bodies	Key Features	Frequency
Turner syndrome	45,X	0	Female; short stature (SHOX haploinsufficiency); webbed neck; coarctation of aorta; streak gonads; infertility	1/2,500 females
Klinefelter syndrome	47,XXY	1	Male; tall; gynecomastia; small testes; reduced fertility; learning difficulties	1/600 males
Triple-X	47,XXX	2	Female; usually tall; mild learning difficulties; fertile	1/1,000 females
Jacobs syndrome	47,XYY	0	Male; tall; usually normal phenotype and fertility	1/1,000 males

Maternal age effect: Non-disjunction risk for chromosome 21 increases exponentially with maternal age:

Table 276. Aneuploidy: Non-Disjunction in Meiosis I vs. Meiosis II: Maternal Age and Risk of Trisomy 21.

Maternal Age	Risk of Trisomy 21
20	about 1/1,500
25	about 1/1,250
30	about 1/900
35	about 1/270
40	about 1/100

Maternal Age	Risk of Trisomy 21
45	about 1/50
49	about 1/12

Quantitative model of the maternal age curve The empirical risk of trisomy 21 with maternal age is well fit by an exponential function:

$$P(\text{T21} \mid \text{age } a) \approx P_0 e^{k(a-a_0)}$$

(262)

with $P_0 \approx 6.7 \times 10^{-4}$ at age $a_0 = 20$ and $k \approx 0.18$ per year for ages 30–45. This corresponds to a doubling of risk every about 4 years in the late 30s and early 40s. Between ages 45 and 49, the curve rises even more steeply as the oocyte pool nears exhaustion. Because the underlying mechanism — cohesin decay during dictyate arrest — accumulates throughout reproductive life, the exponential form reflects compounding error rates per oocyte rather than a sudden threshold. Reproductive endocrinology uses this curve to set screening recommendations; many countries trigger non-invasive prenatal testing offers automatically at maternal ages above 35.

Approximately 90% of trisomy 21 conceptions and 99% of trisomy 18 conceptions arise in maternal meiosis; paternal contributions are minor. The asymmetry reflects the fundamental difference between oogenesis (limited oocyte pool, decades-long arrest, gradual cohesin decay) and spermatogenesis (continuous stem-cell division, no arrest, robust quality control through germ-cell apoptosis).

19.11.2 Structural Chromosomal Rearrangements: Detailed Survey

Beyond losses and gains of whole chromosomes, structural rearrangements cause a wide range of human disease. Each rearrangement type has characteristic mechanisms and clinical signatures.

Translocations A translocation is an exchange of chromosomal material between non-homologous chromosomes. Two major classes exist.

Reciprocal translocations exchange segments between two non-homologous chromosomes. Carriers of *balanced* reciprocal translocations usually retain full genetic dosage — just rearranged — and are typically phenotypically normal. However, their gametes face severe segregation problems at meiosis I: the four chromosomes involved must form a quadrivalent at metaphase I, and alternate segregation produces balanced gametes (about 50% of meioses). Adjacent-1 and adjacent-2 segregation produces unbalanced gametes, leading to recurrent miscarriage (10–25% per pregnancy) and a 1–10% risk of an unbalanced live-born child.

The Philadelphia Chromosome — A Cancer Paradigm:

The t(9;22)(q34;q11.2) reciprocal translocation fuses the BCR gene (chromosome 22) to the ABL1 gene (chromosome 9), creating the BCR-ABL1 fusion gene on the derivative chromosome 22 (the Philadelphia chromosome, **pH**).

- BCR-ABL1 encodes a constitutively active tyrosine kinase (210 kDa in CML; 190 kDa in Philadelphia-positive acute lymphoblastic leukaemia)
- Activates RAS/MAPK, PI3K/AKT, and JAK/STAT signaling – driving uncontrolled proliferation
- Imatinib (Gleevec): ATP-competitive inhibitor of BCR-ABL1 tyrosine kinase domain
 - CML 5-year survival: about 30% (pre-imatinib) to >90% (post-imatinib)
 - Resistance mutations (e.g., T315I “gatekeeper” mutation) necessitated second-generation (dasatinib, nilotinib) and third-generation (ponatinib) inhibitors
 - Asciminib: First **allosteric** BCR-ABL1 inhibitor (binds myristoyl pocket, not ATP site); approved 2021

The Philadelphia chromosome story is one of the great triumphs of molecular targeted therapy: a structural rearrangement → a fusion oncogene → a kinase domain → a small-molecule drug → a chronic disease that is no longer fatal for most patients.

Robertsonian translocations fuse two acrocentric chromosomes (chromosomes 13, 14, 15, 21, 22 in humans) at their centromeres, producing one large derivative chromosome and losing the small short arms. Carriers have 45 chromosomes but a normal genome content (the lost short arms contain primarily ribosomal RNA gene clusters, present in multiple copies elsewhere). The clinical consequence appears in offspring: a Robertsonian carrier can produce gametes with two copies of one chromosome, leading to trisomic offspring. Robertsonian translocation t(14;21) is the cause of approximately 4% of Down syndrome cases, with a recurrence risk of 10–15% (much higher than the population rate of about 1/700) — making karyotype analysis essential for genetic counseling of recurrent Down syndrome families.

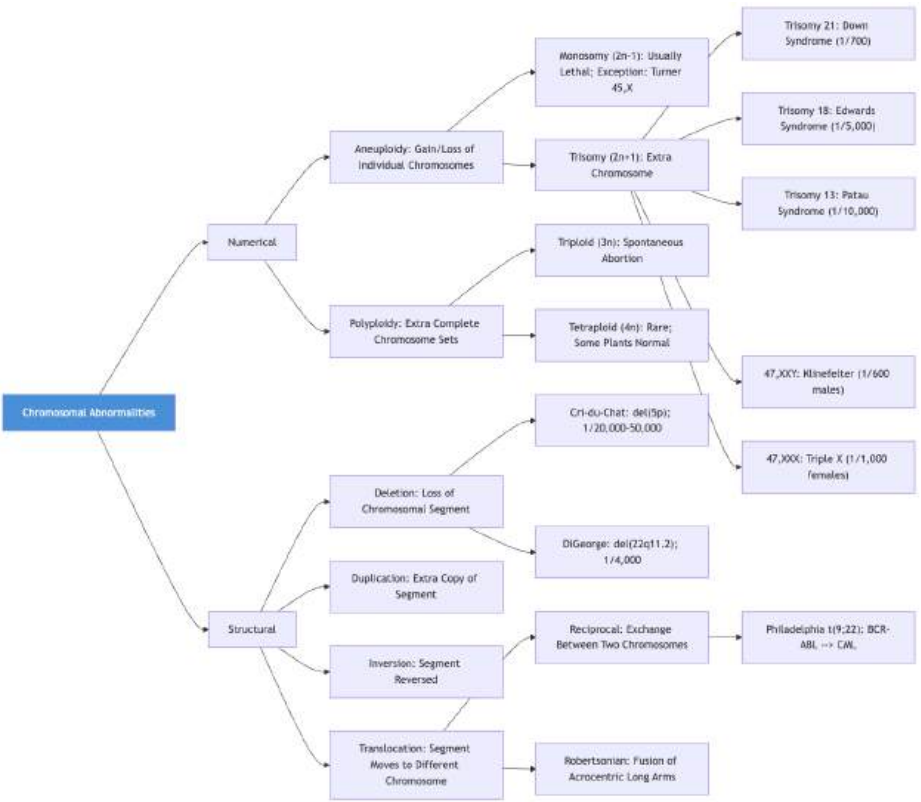


Figure 118. Classification of chromosomal abnormalities. Numerical abnormalities include aneuploidy and polyploidy; structural abnormalities include deletions, duplications, inversions, and translocations.

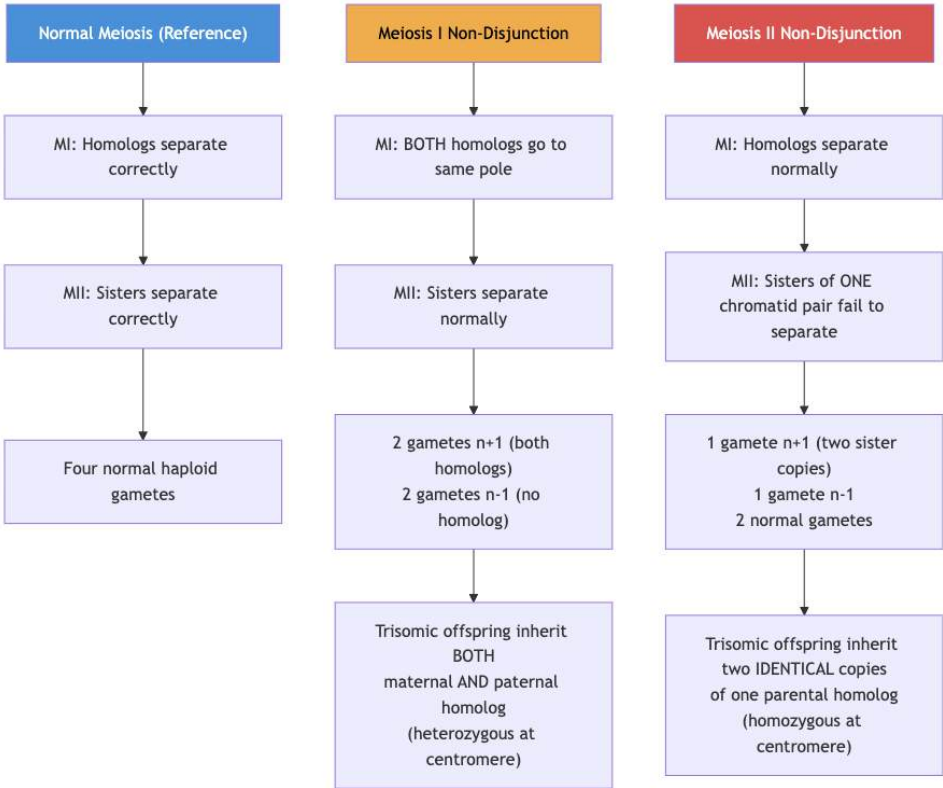


Figure 119. Two distinct molecular failure modes of meiotic non-disjunction. MI errors produce trisomic gametes carrying both parental homologs; MII errors produce trisomic gametes carrying two sister copies of a single homolog. Centromere-region marker analysis distinguishes the two - clinically important because they have different mechanisms and risk factors.



Figure 120. The cohesin-decay model of the maternal age effect. Female oocytes enter MI prophase before birth and remain arrested for decades. Loss of cohesin during this prolonged arrest weakens chromosome cohesion, producing exponentially rising non-disjunction risk with maternal age.

Worked Example: Robertsonian Translocation Segregation A phenotypically normal woman has a Robertsonian translocation rob(14;21), giving her a karyotype 45,XX,rob(14;21). At meiosis, the trivalent formed by chromosome 14, chromosome 21, and the rob(14;21) derivative can segregate in six different ways, producing six possible gamete types — three balanced and three unbalanced:

Table 277. Robertsonian Translocation Segregation: Gamete and Chromosomes carried.

Gamete	Chromosomes carried	After fertilization with normal sperm	Outcome
Normal alternate	normal 14 + normal 21	46,XX or 46,XY	Karyotypically normal
Translocation alternate	rob(14;21) primarily	45,XX,rob(14;21)	Phenotypically normal carrier
Adjacent — extra 14	rob(14;21) + normal 14	46,+14,rob — trisomy 14 equivalent	Embryonic lethal (early miscarriage)
Adjacent — missing 14	normal 21 primarily	45,-14 — monosomy 14	Embryonic lethal
Adjacent — extra 21	rob(14;21) + normal 21	46,+21,rob — translocation Down syndrome	Live-born child with Down syndrome
Adjacent — missing 21	normal 14 primarily	45,-21 — monosomy 21	Embryonic lethal

The empirical recurrence risk of Down syndrome from a maternal rob(14;21) carrier is 10–15% — far below the theoretical 1/3 viable expectation because most monosomic and trisomy-14 conceptuses miscarry early, and because adjacent segregation patterns are not equally likely. For a paternal carrier the recurrence risk is much lower (about 1–2%), because sperm with unbalanced chromosome content are largely incapable of fertilization (sperm selection effects). This sex difference in recurrence — same translocation, 10× different risk depending on the parent of origin — is one of the most clinically important consequences of male versus female meiotic biology and dramatically affects genetic counseling.

Inversions An inversion is a chromosomal segment that has been reversed end-to-end. Two types exist based on whether the centromere is included.

- Pericentric inversions include the centromere; the inverted segment spans both arms.
- Paracentric inversions are confined to one arm; the centromere is outside the inverted region.

Like balanced reciprocal translocations, inversion carriers are typically phenotypically normal. The clinical problem arises in meiosis: to pair correctly with the non-inverted homolog, the inverted segment must form an inversion loop. Crossovers within the loop produce unbalanced gametes:

- Pericentric inversions: Crossovers inside the loop generate gametes with duplications and deficiencies (and corresponding live-born offspring with congenital abnormalities). Recurrence risk depends on inversion size and crossover frequency, ranging from 1% to 15%.
- Paracentric inversions: Crossovers inside the loop generate dicentric and acentric chromosomes that are typically lost during meiosis or early embryonic development; consequently, paracentric inversion carriers have higher rates of miscarriage but lower rates of liveborn unbalanced offspring than pericentric inversion carriers.
- Inversion 9 is a common pericentric inversion (about 1% of Europeans) that is generally considered a normal variant — though some studies suggest mildly elevated risk for recurrent pregnancy loss.

Deletion Syndromes Deletions remove chromosomal material and produce haploinsufficiency — one functional copy is not enough for normal function. Some classic deletion syndromes:

Table 278. Deletion Syndromes: Syndrome and Deletion.

Syndrome	Deletion	Frequency	Key Features
Cri-du-chat	5p15.2	1/20,000–50,000	Distinctive high-pitched mewing cry in infancy (laryngeal abnormalities); microcephaly; severe intellectual disability; characteristic facies; cardiac defects
DiGeorge / 22q11.2 deletion	22q11.2 (3 Mb)	1/4,000	Conotruncal cardiac defects (tetralogy of Fallot, interrupted aortic arch); thymic hypoplasia (T-cell immunodeficiency); hypocalcemia (parathyroid hypoplasia); cleft palate; characteristic facies; learning disabilities; schizophrenia risk increased about 25×
Williams syndrome	7q11.23 (1.55 Mb, 26 genes including <i>ELN</i>)	1/7,500–20,000	“Elfin” facies; supravalvular aortic stenosis (elastin haploinsufficiency); hypercalcemia; intellectual disability with paradoxically preserved language and hypersociability
Prader-Willi syndrome	15q11-q13 paternal deletion	1/15,000	Hypotonia; hyperphagia; obesity; intellectual disability; short stature (see imprinting below)
Angelman syndrome	15q11-q13 maternal deletion	1/15,000	Severe intellectual disability; seizures; ataxic gait; characteristic happy demeanor with frequent laughter
Wolf-Hirschhorn	4p16.3	1/50,000	Severe growth retardation; “Greek warrior helmet” facies; intellectual disability; seizures
WAGR syndrome	11p13	rare	Wilms tumor + Aniridia + Genitourinary abnormalities + intellectual disability (Range)
Smith-Magenis	17p11.2	1/25,000	Intellectual disability; sleep disturbances (inverted melatonin cycle); behavioral abnormalities

DiGeorge / 22q11.2 deletion syndrome deserves special attention as one of the most common microdeletion syndromes and a paradigm for contiguous gene syndromes — phenotypes resulting from haploinsufficiency of multiple adjacent genes simultaneously. The deletion is typically caused by non-allelic homologous recombination (NAHR) between low-copy repeats (LCRs) flanking the region. Within the deleted region, *TBX1* is the key driver of cardiac and craniofacial features; other deleted genes contribute to immune, neurological, and behavioral phenotypes. The 22q11.2 deletion confers an approximately 25-fold increased risk of schizophrenia, making it one of the strongest known genetic risk factors for psychotic illness.

Cri-du-chat syndrome (5p deletion) was first described in 1963 by Jérôme Lejeune (who had identified trisomy 21 four years earlier). The distinctive cat-like cry in infancy results from laryngeal cartilage abnormalities. Survival to adulthood is common but with severe intellectual disability requiring lifelong care.

Duplications Duplications (extra copies of chromosomal segments) typically produce gain-of-function phenotypes — opposite to deletions. Many duplication syndromes are reciprocal to known deletion syndromes:

- 22q11.2 duplication syndrome: Reciprocal to DiGeorge. Highly variable, often mild; some carriers are phenotypically normal.
- Charcot-Marie-Tooth disease type 1A: Duplication of 17p11.2 containing *PMP22* causes peripheral neuropathy through *PMP22* overexpression.
- MECP2 duplication syndrome (Xq28): Severe intellectual disability and recurrent infections; reciprocal to Rett syndrome (caused by *MECP2* loss-of-function mutations in girls).

The reciprocal relationship between deletion and duplication phenotypes confirms gene dosage as the proximate cause and reinforces the dosage-sensitivity principle developed in the chromosomal-rearrangements section.

Clinical Connection: Prenatal Screening for Chromosomal Abnormalities Cell-free fetal DNA (cfDNA) testing (NIPT – non-invasive prenatal testing): Analyzes fetal DNA fragments circulating in maternal blood (from about 10 weeks gestation). Detects trisomies 21, 18, 13 and sex chromosome

aneuploidies with >99% sensitivity and >99.5% specificity for trisomy 21. Has largely replaced first-trimester combined screening (nuchal translucency + biochemical markers) as the primary screening tool. Diagnostic confirmation still requires amniocentesis or chorionic villus sampling (CVS) for karyotyping or chromosomal microarray. Chromosomal microarray (CMA) is now the first-line test for fetal abnormalities or developmental delay, detecting copy-number changes at sub-megabase resolution.

19.12 Genomic Imprinting and Uniparental Disomy

Mendel’s laws assume that the phenotypic effect of an allele is independent of which parent transmitted it. For most loci this is true. But about 100–200 human genes show genomic imprinting — they are expressed from a single parental allele, with the other allele silenced by parent-of-origin-specific epigenetic marks (methylation, chromatin) established during gametogenesis (section 15).

19.12.1 The principle of imprinting

For an imprinted gene: - A maternally-imprinted (paternally-expressed) gene contributes primarily the paternal allele to the offspring’s expression. - A paternally-imprinted (maternally-expressed) gene contributes primarily the maternal allele. - The “silent” allele is not deleted — it carries methylation marks acquired during egg or sperm formation that are preserved through embryogenesis.

This violates Mendel’s assumption because the phenotype now depends on which parent contributed which allele, even at otherwise equivalent loci.

19.12.2 Canonical imprinted regions

Table 279. Canonical imprinted regions: Region and Imprinting status.

Region	Imprinting status	Disease (loss of expressed allele)
15q11–q13	Paternal expression of <i>SNRPN</i> , <i>NDN</i> , <i>MAGEL2</i> , others; maternal expression of <i>UBE3A</i> in neurons	Loss of paternal expression → Prader-Willi syndrome; loss of maternal <i>UBE3A</i> → Angelman syndrome
11p15.5	Paternal expression of <i>IGF2</i> ; maternal expression of <i>H19</i> and <i>CDKN1C</i>	Disrupted imprinting → Beckwith-Wiedemann syndrome (overgrowth, Wilms tumor risk); reciprocal disruption → Russell-Silver syndrome (growth restriction)
14q32	<i>DLK1</i> , <i>MEG3</i> imprinted	Maternal UPD14 → Temple syndrome; paternal UPD14 → Kagami-Ogata syndrome

19.12.3 Mechanisms causing imprinting disorders

Imprinting disorders arise through several distinct mechanisms — and a key clinical insight is that the underlying mutation type is independent of the disease phenotype, which depends primarily on whether the active parental allele is present:

1. Deletion of the active allele (about 70–75% of Prader-Willi and Angelman cases). A microdeletion of 15q11-q13 on the paternally inherited chromosome causes Prader-Willi; the same microdeletion on the maternally inherited chromosome causes Angelman. The deletion is identical at the DNA level — the disease depends on which parent transmitted it.
2. Uniparental disomy (UPD) (about 25% of Prader-Willi, about 5% of Angelman cases). Both copies of chromosome 15 are inherited from one parent. Maternal UPD15 (no paternal contribution) causes Prader-Willi; paternal UPD15 (no maternal contribution) causes Angelman. UPD usually arises through trisomy rescue — a trisomic conceptus loses one chromosome to revert to disomy; if the lost chromosome was from the parent with a single copy, the result is UPD.

Isodisomy vs. heterodisomy. UPD comes in two genetically distinct flavors that depend on *when* the meiotic error occurred:

- Heterodisomy — both inherited copies derive from different homologs of the parent (the two copies are heterozygous for parental polymorphisms). Heterodisomy arises from meiosis I non-disjunction followed by trisomy rescue. The two homologs of one parent are inherited together, and the offspring is heterozygous at centromeric markers from that parent.
- Isodisomy — both inherited copies are identical sister-chromatid copies of a single parental homolog. Isodisomy arises from meiosis II non-disjunction plus trisomy rescue, or from a postzygotic mitotic error. The offspring is homozygous along the entire chromosome for the parent-of-origin’s allele.

Isodisomy is clinically important because it can unmask recessive alleles: if the contributing parent is a carrier for a recessive disease on the affected chromosome, isodisomy produces homozygosity for the recessive allele and the offspring is affected — even though a single parent was a carrier. Documented examples include cystic fibrosis from maternal isodisomy 7 and rod monochromacy from paternal isodisomy 14. Mixed UPD (heterodisomy at the centromere with isodisomic distal regions) reflects a meiosis I error followed by a crossover; the relative proportions of iso- and heterodisomic regions trace the meiotic crossover that occurred in the parent’s germline.

3. Imprinting center mutations (about 1–2% of cases). Mutations in the imprinting control regions disrupt the establishment or maintenance of methylation marks, producing functional UPD without sequence changes elsewhere.
4. *UBE3A* point mutations (about 10% of Angelman cases). Mutations in the *UBE3A* gene itself, which is expressed primarily from the maternal allele in neurons, cause Angelman syndrome.

19.12.4 Connection to chromosome behavior

The imprinting story directly connects molecular biology (DNA methylation), gametogenesis (where parent-of-origin marks are established), meiosis (where non-disjunction can produce UPD via trisomy rescue), and clinical genetics (where the same chromosomal lesion produces different diseases depending on parental origin). For details on the establishment and erasure of imprinting marks during germline development, see section 15.

Clinical Connection: Why Both Parents Are Needed Imprinting explains why mammalian parthenogenesis (development from an unfertilized egg) and androgenesis (development from sperm primarily) fail. Mouse experiments combining two pronuclei from one parent — gynogenetic embryos with two maternal pronuclei or androgenetic embryos with two paternal pronuclei — fail at distinct embryonic stages, demonstrating that maternal and paternal genomes are not interchangeable. Imprinted genes have evolved to enforce biparental contribution in mammalian reproduction.

Concept Check 17.3

1. A trisomy 21 fetus inherits two centromeric markers from the mother — one identical to grandmother’s and one identical to grandfather’s — and one paternal centromere. Was the non-disjunction event in maternal meiosis I or maternal meiosis II? Explain.
2. Using equation (262) with $P_0 = 6.7 \times 10^{-4}$, $a_0 = 20$, and $k = 0.18$, estimate the trisomy 21 risk at maternal age 38. How does it compare to age 28?
3. A child with cystic fibrosis is born to a mother known to be a CFTR carrier and a father whose CFTR sequencing shows two wild-type alleles (paternity confirmed). What chromosomal mechanism could explain the diagnosis, and what kind of UPD would it require?
4. Why does *Drosophila* hyper-transcribe the single male X (MOF/MSL) while *C. elegans* halves transcription of both XX hermaphrodite chromosomes (DCC), yet mammals silence one X (XIST)? What general biological problem do the three strategies solve?

19.13 Recombination Mapping: Physical vs. Genetic Distance

Genetic distance (cM) does not always correspond linearly to physical distance (Mb):

$$1\text{ cM} \approx 1\text{ Mb (genome-wide average in humans)}$$

(263)

However, this ratio varies dramatically: - Hotspots: Recombination rates can be 10-100x the average in small regions (about 1-2 kb); determined by PRDM9 protein (zinc finger domain recognizes specific DNA motifs) - Coldspots: Centromeric and heterochromatic regions have very low recombination - Sex differences: Female genetic maps are about 1.5-1.8x longer than male maps (more crossovers in female meiosis)

Concept Check 17.4

1. From a three-point testcross of 1{,}000 progeny you score 440 + 435 parentals, 48 + 45 single crossovers in one region, 14 + 12 single crossovers in the other, and 4 + 2 double crossovers: use the double-crossover class to fix the gene order, then compute both map distances and explain why the directly summed parental-to-parental distance underestimates the true physical separation.

19.14 Inbreeding and the Inbreeding Coefficient

19.14.1 The Inbreeding Coefficient (F)

The inbreeding coefficient (F) is the probability that an individual has two alleles at a locus that are identical by descent (IBD) – inherited from the same ancestral allele through both parents.

Calculation for offspring of first-cousin mating:

First cousins share one pair of grandparents. For a specific rare recessive allele (frequency q) in one grandparent:

$$F = \frac{1}{16} = 0.0625 \quad (\text{for first-cousin offspring})$$

(264)

General formula using path coefficients [Wright, 1922]:

$$F = \sum \left(\frac{1}{2}\right)^{n_1+n_2+1}$$

(265)

where n_1 and n_2 are the number of links from one parent to the common ancestor and from the common ancestor to the other parent, summed over most paths through most common ancestors.

19.14.2 Consequences of Inbreeding

- Increased homozygosity: F proportion of loci become homozygous beyond random expectation
- Exposure of recessive alleles: Rare deleterious recessive alleles are more likely to become homozygous
- Inbreeding depression: Reduced fitness (fertility, viability) in inbred populations
- Examples: Amish (Ellis-van Creveld syndrome, 1/5,000 vs. 1/200,000 in general population due to **founder effect** + consanguinity); Finnish disease heritage (36 rare diseases enriched in Finland due to founder effects)

Clinical Connection: Consanguinity and Genetic Disease In populations where consanguineous marriage is common (parts of Middle East, South Asia, North Africa: 20-50% of marriages are consanguineous), the incidence of autosomal recessive disorders is significantly elevated. First-cousin offspring have about 6-8% risk of congenital abnormality (vs. about 2-3% in outbred populations). Genetic counseling and carrier screening programs are important in these communities.

Concept Check 17.2

1. Why is the calico phenotype seen overwhelmingly in females? What would the karyotype of a rare calico male be?
2. Explain why maternal age increases the risk of trisomy 21 but paternal age does not have the same effect.
3. Calculate the inbreeding coefficient for offspring of a half-sibling mating (sharing one parent).
4. Why does the Philadelphia chromosome produce a constitutively active kinase? What is the normal function of ABL1?
5. A child has Prader-Willi syndrome with a normal-appearing chromosome 15 by FISH. What molecular tests would you order, and what mechanisms might be responsible?
6. Distinguish reciprocal from Robertsonian translocation. Why are Robertsonian carriers especially relevant to Down syndrome counseling?

19.15 Worked Example: Linkage Analysis

Problem: In a testcross, the following offspring are observed from a female heterozygous for three linked genes (A, B, C) crossed with a homozygous recessive male:

Table 280. Consequences of Inbreeding: Class and Phenotype.

Class	Phenotype	Count
1	A B C	412
2	a b c	405
3	A b C	82
4	a B c	78
5	A B c	32
6	a b C	28
7	A b c	3
8	a B C	2
Total		1,042

(a) Determine gene order.

Parental classes: 1 and 2 (most frequent); DCO classes: 7 and 8 (least frequent).

Compare: Parental = A B C / a b c; DCO = A b c / a B C.

The B gene has switched relative to A and C. Gene order: A – B – C.

(b) Calculate map distances.

$$d_{A-B} = \frac{82 + 78 + 3 + 2}{1042} \times 100 = \frac{165}{1042} \times 100 = 15.8 \text{ cM}$$

(266)

$$d_{B-C} = \frac{32 + 28 + 3 + 2}{1042} \times 100 = \frac{65}{1042} \times 100 = 6.2 \text{ cM}$$

(267)

(c) Calculate interference.

Expected DCO = 0.158 × 0.062 × 1042 = 10.2

(268)

$$\text{CoC} = \frac{5}{10.2} = 0.49; \quad I = 1 - 0.49 = 0.51$$

(269)

19.16 Computational Bridge

Recombination and mutation models often begin from pairwise sequence disparity:

```
from biology.genetics import hamming_distance

print(hamming_distance("ATGCATGC", "ATACATGC"))
```

Clinical / systems note: Non-invasive prenatal testing counts fetal DNA fragments mapped to chromosomes — high-throughput karyotyping that detects trisomies without invasive sampling.

19.17 Current Evidence and Frontier Biology: Chromosomal Inheritance and Linkage

For Chromosomal Inheritance and Linkage, frontier biology belongs inside the evidence logic of the chapter. Classical genetics remains essential, but modern interpretation adds penetrance, polygenicity, structural variation, ancestry-aware inference, and uncertainty in risk prediction. The core reading question is this: chromosome-scale inheritance depends on recombination, segregation, structural variation, and dosage compensation.

- What to verify: identify the observation, model, assay, or dataset that would make the claim stronger or weaker.
- What to qualify: state the scale, organism, cell type, environmental condition, or population where the claim is expected to hold.
- What to compare: test at least one alternative explanation, baseline, or null model before treating the pattern as causal.
- What to cite: distinguish primary evidence, review synthesis, public dataset, and institutional guidance; for recent or numeric claims, prefer the source closest to the measurement and state what has changed since it was published.

A good genetics answer separates the Mendelian transmission model from the evidence needed to use it in a population, family, or clinical setting.

Source practice: For chromosomal claims, connect cytogenetic observation, recombination data, dosage effect, and developmental context before inferring inheritance risk.

19.18 Summary

- Chromosome theory: Sutton [1902] proposed chromosomes carry genes; Morgan proved this with X-linked *white* in *Drosophila*.
- Chromosome architecture: Centromeres (CENP-A, alpha-satellite, kinetochore docking), telomeres (TTAGGG, shelterin, telomerase), and the heterochromatin/euchromatin distinction shape both mechanics and expression.
- Meiosis vs. mitosis: A two-division reductional/equational program with synapsis, crossing over, and reductional segregation at MI is the cellular basis of Mendel’s laws.

- Sex determination: XX/XY (mammals, SRY gene), ZW/ZZ (birds), XO (grasshoppers), haplodiploidy (Hymenoptera; a sex-determination system, not by itself a sociality explanation), and temperature-dependent systems (reptiles).
- X-inactivation: Lyon hypothesis (1961); XIST RNA coats Xi; Polycomb-mediated H3K27me3; DNA methylation; Barr body. about 15% of genes escape.
- Dosage compensation: X-inactivation in mammals, MSL upregulation in *Drosophila*, DCC downregulation in *C. elegans*; broader principles include autosomal dosage sensitivity, gene-balance constraints, miRNA buffering, and Polycomb maintenance.
- X-linked recessive inheritance: Males affected » females; no male-to-male transmission; carrier mothers pass to 50% of sons.
- Linkage and recombination: RF < 50% indicates linkage; 1 cM ≈ 1% recombination; three-point cross determines gene order and detects interference; Haldane and Kosambi mapping functions correct for undetected double crossovers; PRDM9 directs hotspots; female maps are about 1.5–1.8× longer than male maps.
- Non-disjunction: MI errors produce trisomies inheriting both parental homologs; MII errors produce trisomies inheriting two sister copies of one homolog. The cohesin-decay model explains the maternal age effect.
- Chromosomal abnormalities: Aneuploidy from non-disjunction (trisomies 21, 18, 13; Turner 45,X; Klinefelter 47,XXY); structural rearrangements include reciprocal and Robertsonian translocations (Philadelphia chromosome → BCR-ABL1 → CML), pericentric and paracentric inversions, deletion syndromes (DiGeorge 22q11.2, Cri-du-chat 5p, Williams 7q11.23, Wolf-Hirschhorn 4p), and reciprocal duplication syndromes.
- Imprinting and uniparental disomy: about 100–200 imprinted human genes; deletion of an expressed allele, UPD via trisomy rescue, imprinting-center mutations, or *UBE3A* point mutations most cause Prader-Willi or Angelman depending on parental origin.
- Inbreeding: F = probability of identity by descent; increases homozygosity; exposes recessive alleles; inbreeding depression.
- Connections: See section 12 for meiosis errors, section 20 for F_{ST} and drift, and section 15 for imprinting disorders.

19.19 Review Questions

1. Explain Morgan’s evidence that the *white* gene is on the X chromosome. What cross results would differ if *white* were autosomal recessive?
2. Describe the role of XIST RNA in X-inactivation. Why do about 15% of genes escape inactivation, and what are the phenotypic consequences?
3. A woman is a carrier for both hemophilia A (F8, Xq28) and red-green color blindness (OPN1LW, Xq28). These genes are about 6 cM apart. What proportion of her sons will have both conditions? A single? Neither?
4. Perform a three-point test cross analysis given the following data: [provide data if assigned]
5. Explain the maternal age effect on non-disjunction. What molecular mechanism has been proposed?
6. Why is trisomy 21 the most common viable autosomal trisomy? (Hint: consider chromosome 21 gene content.)
7. Describe the BCR-ABL1 fusion and explain why imatinib was a breakthrough in cancer therapy. What is the T315I resistance mutation?
8. Compare NHEJ and HR as mechanisms for joining chromosome translocation breakpoints. Which is more likely to produce the Philadelphia chromosome?
9. Calculate the inbreeding coefficient for offspring of a double first-cousin mating (where both parents are first cousins through independent lineages).
10. Explain why dosage compensation is necessary and compare the three known mechanisms (mammals, *Drosophila*, *C. elegans*).
11. Explain why haplodiploidy is relevant to relatedness in ants, bees, and wasps but does not by itself explain eusociality. What comparison does termite evolution add?
12. A child carries a de novo balanced reciprocal translocation with no gene interruption. When is genetic counselling still indicated?
13. Contrast Robertsonian vs. reciprocal translocations regarding segregation products at meiosis I.
14. Distinguish meiosis I from meiosis II non-disjunction. How would centromere-region marker analysis identify the failure mode in a trisomic conception?
15. A 22q11.2 deletion is found in a child with congenital heart disease. List four other phenotypic systems likely affected, and explain why a single contiguous deletion produces such diverse features.

19.20 Further Reading and Source Notes: Chromosomal Inheritance and Linkage

- Lyon (1961). Gene action in the {X}-chromosome of the mouse ({*Mus musculus* L.}). *Nature*, 190.
- Hassold & Hunt (2001). To err (meiotically) is human: The genesis of human aneuploidy. *Nature Reviews Genetics*, 2.
- Wright (1922). Coefficients of inbreeding and relationship. *American Naturalist*, 56.
- Sutton (1902). On the morphology of the chromosome group in {*Brachystola magna*}. *Biological Bulletin*, 4.

19.21 Key Terms

1. Chromosome theory of heredity – genes are located on chromosomes; chromosomal behavior in meiosis explains Mendelian laws
2. Centromere – chromosomal region holding sister chromatids; site of kinetochore assembly; CENP-A defines identity epigenetically

3. Telomere – terminal TTAGGG repeats bound by shelterin; protected by telomerase in stem and germ cells
4. Heterochromatin – densely packed, transcriptionally silenced chromatin; constitutive vs. facultative
5. SRY – sex-determining region Y; master switch for male development in mammals
6. X-inactivation – silencing of one X chromosome in female somatic cells for dosage compensation
7. XIST – long non-coding RNA that coats and silences the inactive X chromosome
8. Barr body – condensed, transcriptionally inactive X chromosome visible at nuclear periphery
9. Hemizygous – having a single copy of a gene (e.g., X-linked genes in males)
10. Linkage – tendency of genes on the same chromosome to be inherited together
11. Recombination frequency (RF) – proportion of recombinant offspring; measure of genetic distance
12. Centimorgan (cM) – unit of genetic distance; 1 cM = 1% recombination frequency
13. Three-point test cross – cross using three linked markers to determine gene order and distances simultaneously
14. Interference – suppression of nearby crossovers; $I = 1 - \text{coefficient of coincidence}$
15. PRDM9 – zinc-finger histone methyltransferase that directs meiotic recombination hotspots
16. Non-disjunction – failure of chromosomes to separate during meiosis, leading to aneuploidy
17. Aneuploidy – abnormal chromosome number (monosomy, trisomy)
18. Reciprocal translocation – exchange of segments between two non-homologous chromosomes
19. Robertsonian translocation – centromeric fusion of two acrocentric chromosomes
20. Pericentric inversion – inversion that includes the centromere
21. Paracentric inversion – inversion confined to one chromosome arm
22. Philadelphia chromosome – t(9;22) translocation producing BCR-ABL1 fusion; hallmark of CML
23. Inbreeding coefficient (F) – probability that two alleles at a locus are identical by descent
24. LOD score – statistical measure of evidence for genetic linkage in pedigrees
25. Pseudoautosomal region – segments at X and Y chromosome tips that recombine during male meiosis
26. Dosage compensation – mechanism equalizing X-linked gene expression between XX and XY individuals
27. Uniparental disomy (UPD) – both copies of a chromosome inherited from one parent; cause of imprinting disorders via trisomy rescue
28. Genomic imprinting – parent-of-origin-specific expression resulting from gametic methylation marks

19.22 Companion Source Module: Chromosomal Inheritance and Linkage

Chromosomal Inheritance and Linkage should leave a reproducible trail from a biological claim to the code, figure, diagram, or paper-based activity that can test it. Use the surfaces below to inspect the chapter’s assumptions, rerun the relevant model, or compare the manuscript explanation with companion labs and figures.

Table 281. Companion source surfaces for Chromosomal Inheritance and Linkage.

Surface	Use it for
<code>src/biology/genetics/genetics.py</code> (<code>recombination_frequency</code> , <code>genetic_distance</code> , <code>infer_three_point_order</code>)	Convert offspring counts into linkage maps and gene order.
<code>src/visualization/plots.py</code> (<code>plot_chromosome_structure</code>)	Connect cytogenetic structure to inheritance patterns.
<code>src/mermaid/biology_diagrams.py</code> (<code>chromosome_inheritance_diagram</code> , <code>x_inactivation_diagram</code>)	Compare segregation, linkage, and dosage compensation.

Reproducibility check: specify phase, recombinant classes, crossover assumptions, and mapping limits before inferring chromosome structure. Cross-reference: use sections 17 and 18, sections 15 and 16, and section 20.

20 Population Genetics

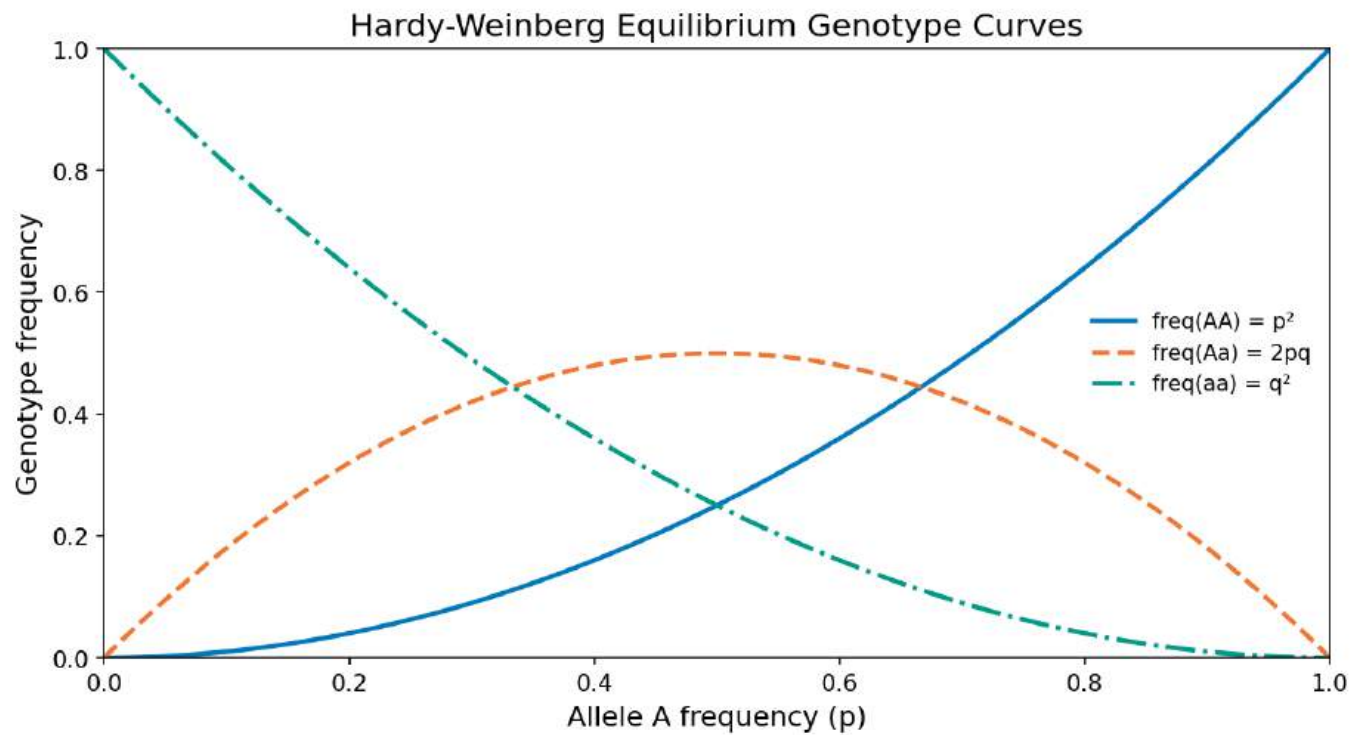


Figure 121. Hardy-Weinberg genotype-frequency curves. As allele frequency p varies, p^2 , $2pq$, and q^2 trace the expected AA, Aa, and aa proportions under random mating.

Level 3/3 · 75 min read · 100 min lecture · Prerequisites: section 17, section 19

20.1 Learning Objectives

1. Define **allele** frequency, genotype frequency, and **gene** pool.
2. State the Hardy-Weinberg [Weinberg, 1908] principle, derive the equilibrium equation, and list the five assumptions.
3. Apply **Hardy-Weinberg equilibrium** (equation (270)) to calculate carrier frequencies and estimate disease prevalence.
4. Test a population for HWE using the chi-squared test.
5. Describe **natural selection**: fitness, selection coefficient, dominance coefficient, and types of selection.
6. Calculate allele frequency change under selection and predict equilibrium conditions for balancing selection.
7. Explain **genetic drift**, effective population size, bottleneck and **founder effects**.
8. Describe gene flow and its effects on population differentiation (F_{st}).
9. Apply **mutation**-selection balance to estimate equilibrium frequencies.
10. Explain the **neutral theory** of molecular evolution, K_a/K_s ratios, and coalescent theory.
11. Use **molecular clock** methods to estimate divergence times.

20.1.1 Study Blueprint

- Big idea: Allele frequencies change when assumptions about random mating, population size, and fitness are violated.
- Core concepts: Hardy-Weinberg, selection, mutation, genetic drift.
- Framework alignment: Vision & Change: Information flow, exchange, and storage, Evolution; AP Biology: Information Storage and Transmission, Evolution; NGSS-style topics: Inheritance and Variation of Traits, Natural Selection and Evolution.
- Model or quantitative lens: Hardy-Weinberg and allele-frequency recurrence calculations.
- Data skill: Estimate genotype or allele frequencies from population data.
- Practice cadence: Statistical Tests and Data Analysis, Representing and Describing Data.
- Common misconception to repair: Hardy-Weinberg is a null model, not a claim that populations do not evolve.
- Primary lab: **Lab — Population Genetics**.
- Question bank: **Questions — Population Genetics**.
- Transfer task: Apply population-genetic reasoning to screening, conservation, and pathogen evolution.

- Bridge to computation: `biology.genetics.genetics.hardy_weinberg`.

Opening Vignette — Algebra, Moths, and the Mathematics of Populations

In 1908, a cricket enthusiast named G.H. Hardy — then England’s most distinguished pure mathematician — was irritated by a biologist’s claim that **dominant** alleles automatically increase in frequency over time. Hardy spent an afternoon at the cricket match and, in a brief letter to *Science*, produced the algebraic proof that in the absence of disturbing forces, allele frequencies remain constant generation after generation. A German physician, Wilhelm Weinberg, had independently derived the same principle. The Hardy-Weinberg equilibrium became the null hypothesis of **population genetics** — and its deviations became the heartbeat of evolutionary biology. Nowhere is this better illustrated than the peppered moth (*Biston betularia*) during England’s Industrial Revolution: pollution blackened tree bark, shifting the population from mostly pale moths to mostly dark (melanic) ones within decades — textbook natural selection altering allele frequencies in real time.

20.1.2 Chapter Roadmap for Population-Genetic Forces

The chapter is long because it bridges three levels of time and scale — read it as a narrowing lens:

- The Hardy-Weinberg null model. Alleles, genotype frequencies, the equilibrium theorem and its assumptions; χ^2 tests of fit.
- Four forces that perturb it. Selection, drift, gene flow, and mutation. Each is a named violation of an HWE assumption.
- Consequences at the **genome** scale. Neutral theory and molecular evolution, F-statistics and population structure, coalescent theory and molecular clocks.

If you are reading for the core Mendelian-genetics course, prioritize the Hardy-Weinberg model and the four evolutionary forces. The genome-scale extensions connect population genetics to molecular evolution (**Unit VI — Evolution: Introduction**) and are helpful but optional.

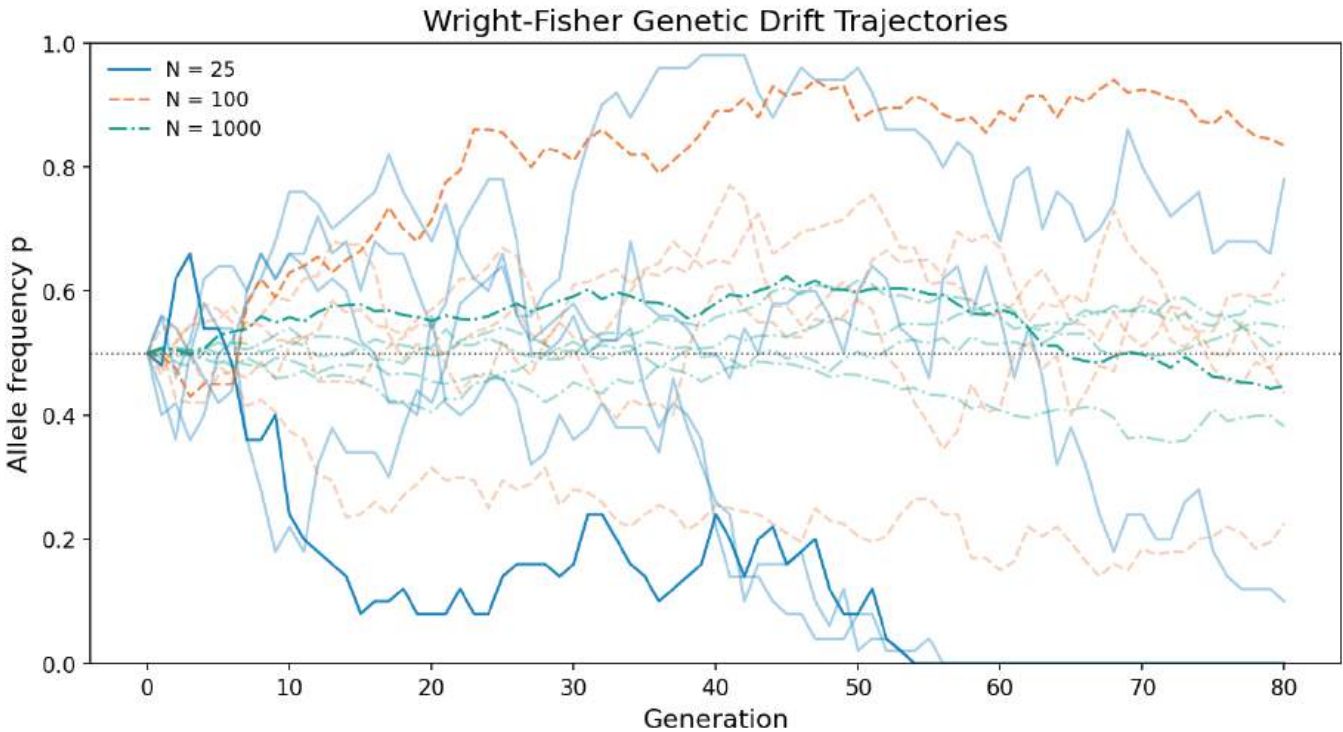


Figure 122. Wright–Fisher genetic-drift trajectories for the same starting allele frequency under three effective population sizes. Smaller populations show larger stochastic swings and faster approach to fixation or loss.

20.2 The Gene Pool as Population-Level Genetic Variation

A population is a group of individuals of the same species living in the same area at the same time and that interbreed. The gene pool is the population’s allele set across loci.

20.2.1 Allele and Genotype Frequencies

For a biallelic locus with alleles A (frequency p) and a (frequency q):

$$p + q = 1$$

(270)

Calculating allele frequencies from genotype counts:

Given N total diploid individuals with N_{AA} homozygous dominant, N_{Aa} **heterozygous**, and N_{aa} homozygous recessive:

$$p = \frac{2N_{AA} + N_{Aa}}{2N}$$

(271)

$$q = \frac{2N_{aa} + N_{Aa}}{2N}$$

(272)

Genotype frequencies:

$$F_{AA} + F_{Aa} + F_{aa} = 1$$

(273)

Note that allele frequencies can be calculated from genotype frequencies but not vice versa (without additional assumptions), because different combinations of genotype frequencies can yield the same allele frequencies.

20.3 Worked Example: Allele Frequencies from Genotype Counts

$$p = \frac{2(360) + 480}{2(1000)} = \frac{1200}{2000} = 0.60$$

(274)

$$q = \frac{2(160) + 480}{2(1000)} = \frac{800}{2000} = 0.40$$

(275)

Check: $p + q = 0.60 + 0.40 = 1.00$ (correct).

Concept Check 18.5

1. A population of 1{,}000 has 250 AA, 500 Aa, and 250 aa: show that although $p = q = 0.5$, the genotype counts are not those Hardy-Weinberg predicts, and decide from the direction of the heterozygote discrepancy whether inbreeding or heterozygote advantage is the more likely cause.
-

20.4 Hardy-Weinberg Equilibrium

Mathematical Background: Hardy-Weinberg calculations use basic probability and algebra. For a review of probability rules and their biological applications, see **Appendix C — Mathematical Review for Biology**.

The Hardy-Weinberg principle (G.H. Hardy and Wilhelm Weinberg, 1908) states: in a large, randomly mating population with no evolutionary forces acting, allele frequencies and genotype frequencies remain constant from generation to generation [**Weinberg, 1908**].

20.4.1 Deriving Hardy-Weinberg Genotype Frequencies

Under random mating, **gametes** combine randomly. figure 121 traces how p^2 , $2pq$, and q^2 vary as allele frequency p changes. The probability of drawing an A allele from the gene pool is p , and of drawing an a allele is q :

$$P(AA) = p \times p = p^2$$

(276)

$$P(Aa) = p \times q + q \times p = 2pq$$

(277)

$$P(aa) = q \times q = q^2$$

(278)

Therefore, at equilibrium:

$$p^2 + 2pq + q^2 = 1$$

(279)

This can also be written as $(p + q)^2 = 1$, which is simply the binomial expansion.

Key insight: HW equilibrium is reached in a single generation of random mating (for autosomal loci), and allele frequencies do not change across generations.

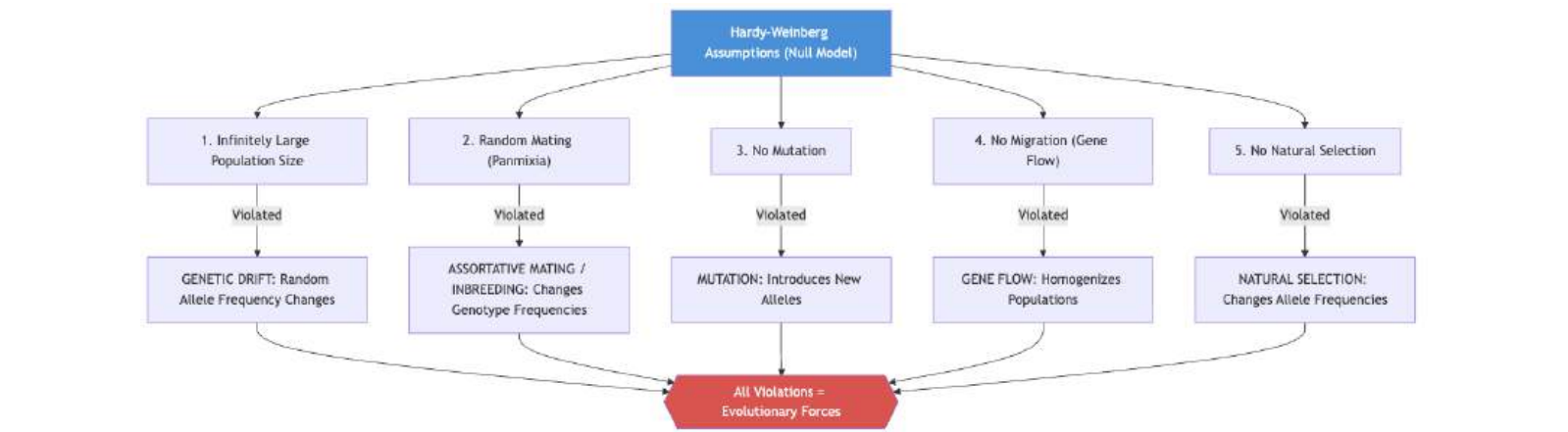


Figure 123. The five assumptions of Hardy-Weinberg equilibrium and the evolutionary forces that result from their violation. HWE serves as a null model – deviations indicate evolutionary forces are acting.

20.4.2 Testing for Hardy-Weinberg Equilibrium

Chi-squared test for HWE: A real population is tested against HWE as the null model. Estimate the allele frequencies p and q from the observed genotype counts, compute the genotype counts *expected* under HWE (Np^2 , $2Npq$, Nq^2 for a sample of N individuals), and form $\chi^2 = \sum(O - E)^2/E$ over the genotype classes. The degrees of freedom equal the number of genotype classes minus the number of alleles — for a biallelic locus, $3 - 2 = 1$ (one degree is spent estimating p from the same data). A statistic exceeding the critical value $\chi^2_{0.05,1} = 3.84$ rejects HWE and indicates that at least one assumption — random mating, no selection, no drift, no migration, no mutation — is violated.

Worked Example: MN Blood Group Equilibrium MN blood group data for codominant alleles M and N in a population of 1,000:

Table 282. MN Blood Group Equilibrium: Genotype and Observed.

Genotype	Observed	Allele Frequency
MM	298	
MN	489	
NN	213	

Step 1: Calculate allele frequencies.

$$p(M) = \frac{2(298) + 489}{2000} = \frac{1085}{2000} = 0.5425$$

(280)

$$q(N) = \frac{2(213) + 489}{2000} = \frac{915}{2000} = 0.4575$$

(281)

Step 2: Calculate expected genotype frequencies under HWE.

$$E(MM) = p^2 \times 1000 = (0.5425)^2 \times 1000 = 294.3$$

(282)

$$E(MN) = 2pq \times 1000 = 2(0.5425)(0.4575) \times 1000 = 496.4$$

(283)

$$E(NN) = q^2 \times 1000 = (0.4575)^2 \times 1000 = 209.3 \tag{284}$$

Step 3: Chi-squared test.

$$\chi^2 = \frac{(298 - 294.3)^2}{294.3} + \frac{(489 - 496.4)^2}{496.4} + \frac{(213 - 209.3)^2}{209.3} \tag{285}$$

$$= 0.047 + 0.110 + 0.065 = 0.222 \tag{286}$$

Degrees of freedom = 3 genotypes - 1 constraint (total N) - 1 estimated parameter (p) = 1 df.

$$\chi^2_{crit}(1 \text{ df}, \alpha = 0.05) = 3.841$$

Since 0.222 < 3.841, we fail to reject HWE. This population is in Hardy-Weinberg equilibrium for the MN locus.

20.4.3 HWE as a Clinical Tool

Estimating carrier frequencies:

Hardy-Weinberg estimates are useful clinical first approximations, not diagnoses. Carrier-frequency calculations assume random mating, correct disease prevalence, complete ascertainment, and a well-defined population; those assumptions can fail when founder effects, consanguinity, population stratification, penetrance, or reference bias shape the sample. Modern screening therefore combines the HWE null model with ancestry-aware variant panels, family history, and increasingly graph-aware or long-read evidence for loci where structural variants affect interpretation [Human Pangenome Reference Consortium, 2023].

20.5 Worked Example: Cystic Fibrosis Carrier Frequency

Cystic fibrosis (CF) prevalence in Northern Europeans has disease (aa) frequency $\frac{1}{2,500}$.

$$q^2 = \frac{1}{2500} \implies q = \frac{1}{50} = 0.02 \tag{287}$$

$$p = 1 - q = 0.98 \tag{288}$$

$$\text{Carrier frequency} = 2pq = 2(0.98)(0.02) = 0.0392 \approx \frac{1}{25} \tag{289}$$

Approximately 1 in 25 Northern Europeans is a CF carrier – critical information for genetic counseling.

ABO blood group HWE analysis (three alleles: I^A , I^B , i):

For a triallelic system: $p(I^A) + q(I^B) + r(i) = 1$

Genotype frequencies under HWE:

$$\text{Type A} = p^2 + 2pr, \quad \text{Type B} = q^2 + 2qr, \quad \text{Type AB} = 2pq, \quad \text{Type O} = r^2 \tag{290}$$

Clinical Connection: Newborn Screening and Hardy-Weinberg Hardy-Weinberg predictions guide newborn screening programs. For PKU (q approximately 0.01, disease frequency 1/10,000), carrier frequency approximately 2%. For sickle cell disease in African Americans (q approximately 0.05), carrier frequency approximately 9.5%. For Tay-Sachs in Ashkenazi Jewish populations (q approximately 0.018), carrier frequency approximately 1/28. These calculations determine cost-effectiveness of carrier screening programs.

Concept Check 18.1

- 1. Can genotype frequencies be in HWE if allele frequencies are changing? Explain.
- 2. Inbreeding does not change allele frequencies but does change genotype frequencies. Explain how.
- 3. Why does it take a single generation of random mating to restore HWE for an autosomal locus?

4. For a disease with $q = 0.001$, what is the expected carrier frequency? What is the ratio of carriers to affected individuals?

20.6 Natural Selection and Allele-Frequency Change

Directional, stabilizing, and disruptive selection shift genotype frequencies over generations; figure 129 plots representative allele-frequency trajectories under different fitness regimes (Natural Selection and Adaptation).

20.6.1 Fitness and Selection

Absolute fitness (w): Expected number of offspring produced by an individual with a given genotype.

Relative fitness (w): Fitness of a genotype relative to the most fit genotype (which is set to 1).

Selection coefficient (s): The reduction in fitness: $s = 1 - w$.

Dominance coefficient (h): Describes the fitness of the heterozygote relative to the two homozygotes:

Table 283. Fitness and Selection: Genotype and Fitness.

Genotype	Fitness
AA	$w_{AA} = 1$
Aa	$w_{Aa} = 1 - hs$
aa	$w_{aa} = 1 - s$

- $h = 0$: A completely dominant (Aa has same fitness as AA)
- $h = 0.5$: Additive (codominant fitness effect)
- $h = 1$: A completely recessive (Aa has same fitness as aa)
- $h < 0$: Overdominance (heterozygote advantage)

20.6.2 Change in Allele Frequency Under Selection

For selection against a recessive homozygote ($h = 0$):

$$\Delta q = \frac{-spq^2}{\bar{w}}$$

(291)

where $\bar{w} = 1 - sq^2$ is the mean fitness of the population.

Important result: Selection against a recessive allele becomes very slow at low frequencies because the allele is “hidden” in heterozygotes. The time to reduce q from 0.01 to 0.001 is much longer than from 0.5 to 0.01.

For selection against a dominant allele: much faster because every carrier is exposed to selection.

20.7 Worked Example: Recessive Deleterious Allele

In a population with $q = 0.3$ (frequency of a recessive deleterious allele) and $s = 0.2$ (20% fitness reduction for aa homozygotes):

$$\bar{w} = 1 - s \cdot q^2 = 1 - 0.2(0.09) = 1 - 0.018 = 0.982$$

(292)

$$\Delta q = \frac{-0.2 \times 0.7 \times 0.09}{0.982} = \frac{-0.0126}{0.982} = -0.0128$$

(293)

After one generation: $q' = 0.3 - 0.0128 = 0.287$

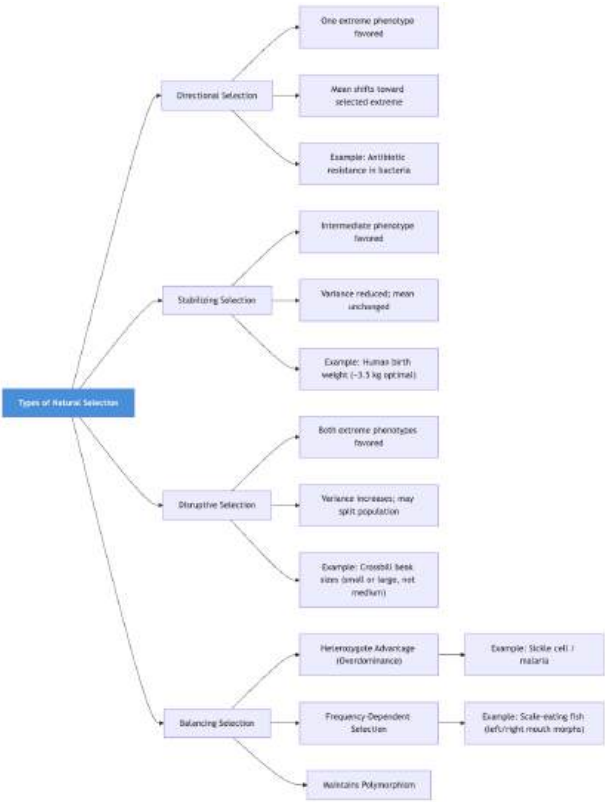


Figure 124. Types of natural selection and their effects on allele frequency distributions. Directional selection shifts the mean; stabilizing selection reduces variance; disruptive selection increases variance; balancing selection maintains polymorphism.

20.7.1 Types of Selection

20.7.2 Heterozygote Advantage (Balancing Selection)

When the heterozygote has higher fitness than either homozygote ($w_{Aa} > w_{AA}$ and $w_{Aa} > w_{aa}$), both alleles are maintained at a stable equilibrium:

$$\hat{q} = \frac{s_1}{s_1 + s_2}$$

(294)

where s_1 = selection against AA and s_2 = selection against aa.

The sickle cell-malaria paradigm:

In malaria-endemic regions of sub-Saharan Africa: - HbA/HbA (normal): susceptible to *Plasmodium falciparum* malaria; $w_{AA} = 1 - s_1$, where $s_1 \approx 0.1 - 0.15$
- HbA/HbS (sickle trait): about 10-15x reduced malaria mortality; highest fitness; $w_{Aa} = 1$ - HbS/HbS (sickle cell disease): severe disease; $w_{aa} = 1 - s_2$, where $s_2 \approx 0.8 - 1.0$

Equilibrium frequency of HbS allele:

$$\hat{q} = \frac{s_1}{s_1 + s_2} = \frac{0.12}{0.12 + 0.90} = 0.118$$

(295)

This predicts HbS frequency of about 12%, remarkably close to the observed about 10-20% in malaria-endemic West Africa.

Other examples of heterozygote advantage: - HbC (beta-globin E6K): heterozygotes also resistant to malaria; found in West Africa - G6PD deficiency: heterozygous females have mosaic RBCs; malaria resistance - CF heterozygotes: possibly resistant to cholera or typhoid (debated); explains high carrier frequency (about 4% in Europeans) - MHC/HLA diversity: heterozygotes present more pathogen antigens; frequency-dependent selection also contributes

Concept Check 18.2

1. Why does selection against a recessive allele become slower as the allele frequency decreases?

2. If heterozygote advantage maintains the sickle cell allele at about 12% in malaria-endemic regions, predict what happens to HbS frequency in a population that migrates to a malaria-free region.
3. Calculate the equilibrium frequency of a deleterious recessive allele if $s_1 = 0.05$ and $s_2 = 0.50$.

20.8 Genetic Drift in Finite Populations

In finite populations, allele frequencies change from generation to generation by random sampling error – this is genetic drift. figure 122 contrasts stochastic allele-frequency paths under three effective population sizes, illustrating why drift is strongest when N_e is small.

20.8.1 Wright-Fisher Model

The Wright-Fisher model is the simplest mathematical framework for drift: - Non-overlapping generations - Constant population size N - Random mating - No selection, mutation, or migration

Each generation, $2N$ allele copies are drawn randomly (with replacement) from the parental gene pool.

Variance in allele frequency change per generation:

$$\sigma^2_{\Delta p} = \frac{pq}{2N_e}$$

(296)

where N_e = effective population size (the size of an ideal Wright-Fisher population that would experience the same rate of drift).

Key results of drift: - Over time, alleles are either fixed ($p = 1$) or lost ($p = 0$) - The probability of fixation for a new neutral allele = its initial frequency = $\frac{1}{2N}$ - Time to fixation of a new neutral mutation = $4N_e$ generations - Heterozygosity decreases at rate $\frac{1}{2N_e}$ per generation

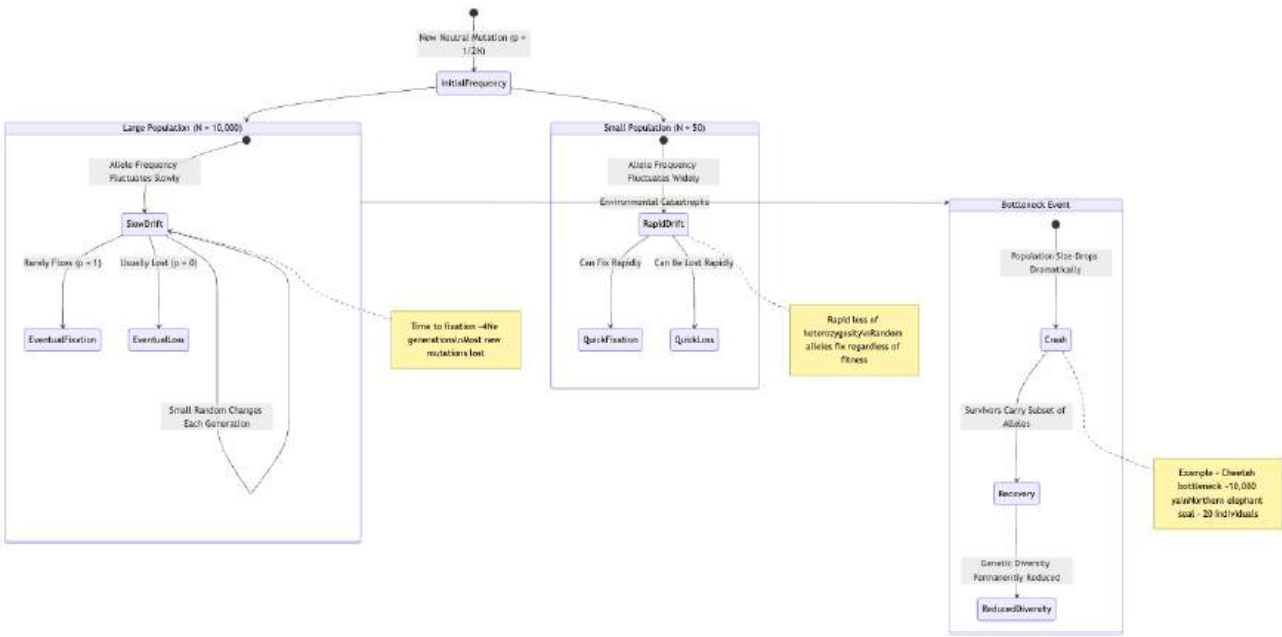


Figure 125. Genetic drift in populations of different sizes. Small populations experience rapid allele frequency changes and loss of diversity. Bottleneck events dramatically reduce effective population size, causing lasting genetic effects.

20.8.2 Effective Population Size (N_e)

N_e is usually much smaller than census size N because:

Table 284. Effective Population Size (N_e): Factor and Effect on N_e .

Factor	Effect on N_e	Formula
Unequal sex ratio	Reduces N_e	$N_e = \frac{4N_mN_f}{N_m+N_f}$
Fluctuating population size	Reduces N_e	$N_e = \text{\$ harmonic mean of } N \text{ over generations}$
Variance in reproductive success	Reduces N_e	High variance (few individuals produce most offspring) reduces N_e

The three workhorse formulas for N_e are presented below — each corresponds to a distinct biological scenario, and conservation geneticists routinely combine them to estimate N_e from real demographic data [Frankham, 1995, 2014].

Sex-ratio N_e formula When the breeding population has unequal numbers of males (N_m) and females (N_f), the effective population size is governed by the rarer sex because each offspring receives one allele from each:

$$N_e = \frac{4N_mN_f}{N_m + N_f}$$

(297)

Worked example — sex-biased breeding: Consider a herd of 100 elk consisting of 10 breeding males and 90 breeding females (a strongly female-biased operational sex ratio common in harem-forming ungulates):

$$N_e = \frac{4 \times 10 \times 90}{10 + 90} = \frac{3,600}{100} = 36$$

Despite a census size of 100, the effective population size is primarily 36 — barely a third of the count. The intuition: every offspring’s paternal allele must come from one of just 10 males, so 90% of females are functionally redundant for tracking allelic diversity through paternal lineages. This asymmetry is why captive-breeding programs aggressively manage sex ratios and why studbook software optimizes founder representation rather than census numbers. If the same population had 50 males and 50 females, N_e would equal 100 — the full census size.

Bottleneck N_e formula For a population that experiences a single-generation bottleneck of size N_b embedded within t generations of size N_0 , the effective population size over the entire interval is the harmonic mean of generation sizes:

$$\frac{1}{N_e} = \frac{1}{t} \sum_{i=1}^t \frac{1}{N_i}$$

(298)

The reciprocal-mean form is the same harmonic structure given equivalently as:

$$N_e = \frac{t}{\sum_{i=1}^t \frac{1}{N_i}}$$

(299)

Because the harmonic mean is dominated by the smallest term, a single bottleneck generation can drag N_e far below the long-term arithmetic mean of population size. As an example: 99 generations of $N_0 = 10,000$ plus one generation of $N_b = 10$ yields:

$$N_e = \frac{100}{99/10,000 + 1/10} = \frac{100}{0.0099 + 0.1} = \frac{100}{0.1099} \approx 910$$

— not the arithmetic mean of about 9,901. One bad generation undoes a century of large population size, and this asymmetry is precisely why bottleneck events leave such durable genetic signatures.

N_e for fluctuating populations For populations that vary cyclically (boom-bust dynamics in microbes, seasonally migrating species, populations with cyclic predator-prey dynamics):

$$N_e \approx \frac{1}{\frac{1}{T} \sum_{i=1}^T \frac{1}{N_i}}$$

(300)

Drosophila in seasonal climates oscillate between $N_b \approx 10^3$ in winter and $N_0 \approx 10^7$ in summer — and the harmonic mean yields N_e close to $4 \times N_b$, not anywhere near the summer maximum.

N_e with variance in reproductive success When the variance in offspring number (V_k) exceeds the mean ($\bar{k} = 2$ for a stable population), N_e is reduced:

$$N_e \approx \frac{4N - 2}{V_k + 2}$$

(301)

In species with extreme reproductive skew — elephant seals (one beachmaster male sires nearly the offspring), salmon (a few females spawn the majority of fertilized eggs), or hierarchical primates — N_e may be 10–100× smaller than census size. Conservation programs that calculate N_e from stud-book pedigree data routinely find $N_e \ll N$, with significant implications for genetic-rescue planning.

Human N_e : Despite about 8 billion people alive today, human N_e estimated from genetic diversity is about 10,000-15,000, reflecting an ancient bottleneck about 70,000 years ago (possibly associated with the Toba supervolcanic eruption, though this is debated). The harmonic-mean nature of N_e explains why such a long-ago bottleneck still dominates the genetic diversity calculation despite billions of intervening generations of population growth.

20.8.3 Bottleneck and Founder Effects

Bottleneck effect: Severe reduction in population size causes random loss of alleles: - Cheetah: Extreme genetic homogeneity; can accept skin grafts from unrelated individuals; N_e probably dropped to hundreds about 10,000 years ago - Northern elephant seal: Hunted to about 20 individuals by 1890s; now >200,000 but almost no genetic variation at many loci

Founder effect: A small group colonizes a new area, carrying a non-representative sample of the original population’s alleles: - Amish/Old Order Mennonites: Founded by about 200 individuals in 18th century; high frequency of Ellis-van Creveld syndrome, maple syrup urine disease, glutaric aciduria type I - Finnish disease heritage: 36 rare genetic diseases at elevated frequencies due to sequential founder events - Afrikaners: High frequency of porphyria variegata (traced to a single Dutch couple who arrived in 1688)

Concept Check 18.4

1. An allele tracked for ten generations rises smoothly and monotonically from $q = 0.10$ to $q = 0.45$ in a census population of millions, whereas in a population of 30 it instead jumps erratically up and down between 0.05 and 0.60: explain which trajectory is the signature of natural selection and which of genetic drift, and why population size — not the size of the change — is the deciding feature.
-

20.9 Gene Flow (Migration)

Movement of individuals (and their alleles) between populations.

20.9.1 One-Island Model

If a fraction m of population 1 is replaced by migrants from population 2 each generation:

$$p'_1 = (1 - m)p_1 + mp_2$$

(302)

$$\Delta p_1 = m(p_2 - p_1)$$

(303)

Gene flow homogenizes populations – reducing differentiation. Even a small amount of gene flow ($Nm > 1$ migrant per generation) is sufficient to prevent populations from diverging by drift alone.

20.9.2 Measuring Population Differentiation: F_{ST}

Wright’s F-statistics quantify the distribution of genetic variation within and among populations:

$$F_{ST} = \frac{H_T - H_S}{H_T}$$

(304)

where H_T = expected heterozygosity in the total population and H_S = average expected heterozygosity within subpopulations.

Table 285. Measuring Population Differentiation: F_{ST} ; F_{ST} Value and Interpretation.

F_{ST} Value	Interpretation
0	No differentiation (panmixia)
0-0.05	Little differentiation
0.05-0.15	Moderate differentiation
0.15-0.25	Great differentiation
>0.25	Very great differentiation

20.9.3 Interpreting F_{ST} in Human Populations

Quick interpretation reference for F_{ST} : continental-scale comparisons between human populations consistently fall in the 0.10–0.15 range — moderate differentiation by Wright’s classification. This empirical magnitude provides a benchmark when interpreting F_{ST} from any other species: humans are *less* differentiated than most large mammals, *comparably* differentiated to some highly mobile species (large carnivores, migratory birds), and *more* differentiated than panmictic marine species with planktonic larvae.

Human $F_{ST} \approx 0.10$ –0.15: Human populations are about 10–15% differentiated – meaning about 85–90% of human genetic variation exists within populations, not between them (Lewontin, 1972; Rosenberg et al., 2002). This is lower than most large mammals, reflecting recent common ancestry (the species is about 300,000 years old) and substantial gene flow throughout human history.

Pairwise F_{ST} between human populations Continental-scale F_{ST} values from the 1000 Genomes and HGDP projects illustrate the typical magnitudes:

Table 286. Pairwise F_{ST} between human populations: Population pair and Approximate F_{ST} .

Population pair	Approximate F_{ST}
West African vs. East Asian	0.10–0.15
West African vs. European	0.10–0.13
European vs. East Asian	0.07–0.11
Within Europe (e.g., French vs. Russian)	0.005–0.02
Within East Asia (Han Chinese vs. Japanese)	0.005–0.015
Within sub-Saharan Africa (Yoruba vs. Maasai)	0.02–0.05
Globally averaged across most human populations	about 0.12

The largest within-Africa F_{ST} values (sub-Saharan vs. Khoisan) reach about 0.10, comparable to between-continental comparisons elsewhere — a genetic signature of Africa’s status as the origin and longest-inhabited continent, with the deepest population-genetic divergences globally.

What $F_{ST} = 0.12$ does and does not mean It DOES mean: A small but real fraction of human genetic variation is partitioned between populations. Allele frequencies do differ — for some loci substantially. Genes under local selection (skin pigmentation: SLC24A5, MC1R; lactase persistence: LCT/MCM6; high-altitude adaptation: EPAS1) show far higher locus-specific F_{ST} values (0.4–0.9) than the genome-wide average, reflecting the differential selective pressures of latitude, diet, altitude, and pathogens.

It does NOT mean: Human populations are sharply discrete, biologically distinct “races.” The reverse: 88% of variation is shared within any given population, meaning two random individuals from the same continental population are nearly as genetically different as two random individuals from different continents. The continuous-variation pattern dominates: human variation is graded geographically, with no sharp boundaries between any defined groups (the clinal pattern). Lewontin’s 1972 observation has been confirmed by every subsequent dataset, including whole-genome sequencing of millions of individuals.

F_{ST} as a tool for detecting selection Because population-genetic models predict the genome-wide F_{ST} distribution under neutral evolution, outlier loci with unusually high F_{ST} can flag positive selection at specific genes. The lactase persistence allele (rs4988235) shows $F_{ST} \approx 0.7$ between Northern Europeans (allele frequency about 0.7) and East Asians (frequency about 0.01) — a textbook example of recent strong directional selection driving population differentiation. Similarly, EDAR (East Asian hair texture, sweat glands), DARC (West African malaria resistance), and SLC24A5 (light skin in Europeans) show F_{ST} outliers consistent with population-specific selective sweeps.

Isolation by distance: F_{ST} increases with geographic distance. Ring species (e.g., *Ensatina* salamanders around California’s Central Valley) demonstrate that populations at the endpoints of a geographic ring may be reproductively isolated despite continuous gene flow along the ring. Within human populations, F_{ST} correlates approximately linearly with geographic distance up to 5,000 km, a signature of the stepping-stone migration pattern out of Africa.

20.10 Mutation-Selection Balance and New Variation

20.10.1 Mutation-Selection Balance

For a deleterious recessive allele maintained by mutation-selection balance:

Forward mutation rate μ (A \rightarrow a) introduces new copies; selection removes them:

$$\hat{q} = \sqrt{\frac{\mu}{s}} \quad (\text{for completely recessive, } s = 1 \text{ for lethals})$$

(305)

20.11 Worked Example: Mutation-Selection Balance

For a recessive lethal allele with $\mu = 10^{-5}$:

$$\hat{q} = \sqrt{\frac{10^{-5}}{1}} = 0.00316$$

(306)

Disease frequency = $q^2 = 10^{-5} = 1/100,000$

(307)

Carrier frequency = $2pq \approx 2(0.00316) = 0.00632 \approx 1/158$

(308)

For CF ($s \approx 1$, $q \approx 0.02$): Implied $\mu \approx q^2s = (0.02)^2(1) = 4 \times 10^{-4}$. This is much higher than the typical point mutation rate ($\sim 10^{-8}$ per nucleotide per generation), suggesting that heterozygote advantage or other selective forces maintain CF carrier frequency above what mutation-selection balance alone would predict.

For a deleterious dominant allele:

$$\hat{q} \approx \frac{\mu}{hs}$$

(309)

Since selection acts on heterozygotes (who are much more common than rare homozygotes), dominant alleles reach much lower equilibrium frequencies.

Concept Check (Synthesis): The neutral theory of molecular evolution (Kimura 1968) proposes that most molecular variation is neutral or nearly neutral, with evolution driven by genetic drift rather than selection. (a) The neutral substitution rate equals the neutral mutation rate μ , independent of population size. Explain why: $K = \mu \times (\text{probability of fixation}) = \mu \times (1/2N) \times 2N = \mu$. (b) Now consider a deleterious mutation with selection coefficient $s = 0.001$ (nearly neutral). In a small population ($N = 100$), would this mutation behave neutrally? Use the criterion $Ns < 1$. In a large population ($N = 10,000$)? (c) The nearly neutral theory (Ohta) predicts that effectively neutral mutations ($|s| < 1/(4N)$) accumulate faster in small populations. Predict the direction of difference in synonymous vs. non-synonymous substitution rates between an island endemic species (small N) and its mainland relative (large N), and name the metric dN/dS that captures this.

Worked Example — Balancing Selection at MHC: The MHC (HLA) locus in humans shows extraordinarily high polymorphism: HLA-A has >7,000 known alleles. Under neutrality, expected heterozygosity $H_e = 1 - \sum p_i^2 \approx 1$ when many equally common alleles exist. Observed H_e at HLA ≈ 0.95 - 0.99 . For comparison, a neutral locus in a population of size 10^6 with $\mu = 10^{-8}$ has expected $H_e \approx 4N\mu/(1+4N\mu) = 0.04/(1.04) \approx 0.038$ — vastly

lower. MHC heterozygosity $\approx 25\times$ higher than neutral expectation. Balancing selection mechanisms maintaining this diversity: (1) Heterozygote advantage (overdominance) — each MHC combination presents different peptides, and heterozygotes present broader pathogen coverage. (2) Frequency-dependent selection — rare alleles confer advantages against pathogens that have evolved to evade common alleles (Red Queen dynamics). The Tajima's D statistic at MHC is strongly positive (+3 to +5), indicating an excess of intermediate-frequency alleles — the signature of balancing selection.

20.12 Molecular Evolution and Sequence Substitution

20.12.1 Neutral Theory [Kimura, 1968]

Motoo Kimura's neutral theory of molecular evolution proposes that most molecular variation within and between species is selectively neutral – not affected by natural selection, but evolving by genetic drift.

Key predictions: 1. The rate of neutral substitution = the neutral mutation rate μ_n , independent of population size - Proof: Rate of new neutral mutations = $2N \times \mu_n$; probability each fixes = $\frac{1}{2N}$; substitution rate = $2N\mu_n \times \frac{1}{2N} = \mu_n$ 2. Heterozygosity at equilibrium = $\frac{4N_e\mu}{1+4N_e\mu}$ (for diploid, biallelic loci) 3. Synonymous substitution rate (K_S) should be approximately constant across genes (molecular clock)

20.12.2 The Nearly Neutral Theory

Tomoko Ohta [1973] extended neutral theory: mutations with selection coefficients $|s| < \frac{1}{2N_e}$ behave as if neutral (drift overwhelms selection). In large populations, weakly deleterious mutations are efficiently removed; in small populations, they can drift to fixation. This predicts slightly higher substitution rates in small populations – observed in island species and endangered populations.

20.12.3 Ka/Ks (dN/dS) Ratio

The ratio of nonsynonymous (amino acid-changing, Ka or dN) to synonymous (silent, Ks or dS) substitution rates:

Table 287. Ka/Ks (dN/dS) Ratio: Ka/Ks and Interpretation.

Ka/Ks	Interpretation	Example
« 1	Purifying (negative) selection	Most genes; histones (Ka/Ks about 0.005)
= 1	Neutral evolution	Pseudogenes
» 1	Positive (adaptive) selection	MHC antigen-binding sites; reproductive proteins (e.g., bindin in sea urchins)

Detecting positive selection: Methods like the McDonald-Kreitman test compare within-species polymorphism to between-species divergence at synonymous and nonsynonymous sites. An excess of nonsynonymous divergence relative to polymorphism indicates positive selection.

20.13 Population Structure and Ancestry Inference

20.13.1 Wright's F-Statistics

Wright defined three hierarchical F-statistics:

- F_{IS} (inbreeding coefficient of individuals relative to subpopulation): Measures departure from random mating within a subpopulation (excess or deficiency of heterozygotes)
- F_{ST} (fixation index of subpopulations relative to total): Measures genetic differentiation among subpopulations
- F_{IT} (inbreeding coefficient of individuals relative to total): Overall departure from HWE in the total population

Relationship: $(1 - F_{IT}) = (1 - F_{IS})(1 - F_{ST})$

20.13.2 Population Structure Inference with STRUCTURE

The program STRUCTURE (Pritchard et al., 2000) uses Bayesian clustering to assign individuals to K populations based on multilocus genotype data. It has been widely used in human population genetics to identify population structure (though the number of clusters K is a modeling choice, not a biological fact – an important caveat against over-interpretation).

20.14 Coalescent Theory and Genealogy Backward in Time

20.14.1 The Coalescent Framework

Rather than tracing alleles forward in time (classical population genetics), coalescent theory [Kingman, 1982] traces allele lineages backward in time to their most recent common ancestor (MRCA).

Key results: - For 2 alleles in a diploid population of size N : Expected coalescence time = $2N_e$ generations - For k alleles: Expected total time to MRCA = $4N_e(1 - 1/k)$ generations - As $k \rightarrow \infty$: TMRCA $\rightarrow 4N_e$ generations

Mitochondrial Eve: The TMRCA for most human mitochondrial DNA lineages is estimated at about 150,000-200,000 years ago. This does NOT mean there was a single woman alive at that time – it means most other maternal lineages have gone extinct by chance (drift). Many women were alive, but a single lineage survived to the present through unbroken maternal descent.

Y-chromosomal Adam: The TMRCA for most human Y chromosomes is estimated at about 200,000-300,000 years ago. Same caveat applies.

20.14.2 Molecular Clocks in Population Genetics

If neutral substitutions accumulate at a roughly constant rate (μ_n), sequence divergence between species provides a “clock” for estimating divergence times.

Jukes-Cantor correction for observed divergence d :

$$d_{JC} = -\frac{3}{4} \ln\left(1 - \frac{4d}{3}\right)$$

(310)

This corrects for multiple substitutions at the same site (back mutations, parallel mutations, convergent mutations).

Divergence time:

$$t = \frac{d_{JC}}{2\mu}$$

(311)

The factor of 2 accounts for divergence along both lineages since the split.

20.15 Worked Example: Molecular Clock Estimate

Human-chimpanzee cytochrome c has roughly 1% sequence divergence; use a neutral mutation rate for this gene of approximately 2×10^{-9} substitutions/site/year.

$$d_{JC} = -\frac{3}{4} \ln\left(1 - \frac{4(0.01)}{3}\right) = -0.75 \times \ln(0.9867) = -0.75 \times (-0.01339) = 0.01004$$

(312)

$$t = \frac{0.01004}{2 \times 2 \times 10^{-9}} = \frac{0.01004}{4 \times 10^{-9}} = 2.51 \times 10^6 \text{ years} \approx 2.5 \text{ Ma}$$

(313)

(Note: The actual human-chimp divergence is estimated at 6-7 Ma using whole-genome data and calibrated clocks with fossil constraints. Cytochrome c evolves slowly and gives an underestimate.)

Calibrated molecular clocks using fossil data:

Table 288. Molecular Clocks in Population Genetics: Comparison and Estimated Divergence.

Comparison	Estimated Divergence
Human-Chimpanzee	6-7 Ma
Human-Gorilla	8-10 Ma
Human-Orangutan	14-16 Ma
Human-Old World Monkeys	25-30 Ma
Human-Mouse	75-80 Ma
Human-Chicken	about 310 Ma

Clinical Connection: Molecular Clock and HIV Forensics The molecular clock has been used in HIV forensic cases. In the 1998 Louisiana case (State of Louisiana v. Richard Schmidt), phylogenetic analysis of HIV sequences showed that the viral strains in the victim and the defendant’s HIV-positive patient were more closely related to each other than to any other strains, consistent with direct transmission. Coalescent analysis estimated the transmission date, providing critical forensic evidence.

Concept Check 18.3

1. What is the probability that a new neutral mutation in a diploid population of $N_e = 5,000$ will eventually fix? How many generations would this take on average?

2. Explain why synonymous substitution rates are approximately constant across genes (molecular clock) while nonsynonymous rates vary widely.

3. “Mitochondrial Eve” lived about 200,000 years ago. Does this mean she was the sole woman alive at that time? Explain.

4. Why does the Jukes-Cantor correction give a larger value than the raw observed divergence?
-

20.16 Worked Example: Combined Population-Genetics Calculations

Problem: In a population of 10,000 grasshoppers, you observe the following genotype counts at a color locus with codominant alleles:

Table 289. Molecular Clocks in Population Genetics: Genotype and Count.

Genotype	Count
RR (red)	4,200
Rr (orange)	4,800
rr (yellow)	1,000

(a) Calculate allele frequencies.

$$p(R) = \frac{2(4200) + 4800}{20000} = \frac{13200}{20000} = 0.66$$

(314)

$$q(r) = \frac{2(1000) + 4800}{20000} = \frac{6800}{20000} = 0.34$$

(315)

(b) Is this population in HWE?

Expected under HWE: $-E(RR) = (0.66)^2 \times 10000 = 4356$ $-E(Rr) = 2(0.66)(0.34) \times 10000 = 4488$ $-E(rr) = (0.34)^2 \times 10000 = 1156$

$$\chi^2 = \frac{(4200 - 4356)^2}{4356} + \frac{(4800 - 4488)^2}{4488} + \frac{(1000 - 1156)^2}{1156}$$

(316)

$$= \frac{24336}{4356} + \frac{97344}{4488} + \frac{24336}{1156} = 5.59 + 21.69 + 21.05 = 48.33$$

(317)

$$\chi^2_{crit}(1 \text{ df}, \alpha = 0.05) = 3.841.$$

Since $48.33 \gg 3.841$, we reject HWE. This population is NOT in Hardy-Weinberg equilibrium. The excess of heterozygotes (observed 4,800 vs. expected 4,488) could indicate heterozygote advantage (balancing selection) or negative assortative mating (like-unlike pairing).

20.17 Computational Bridge

Selection recursions used in the chapter are iterated in `simulate_selection`:

```
from biology.evolution import Population, simulate_selection

pop = Population("demo", p=0.2, q=0.8, fitness_AA=1.0, fitness_Aa=0.95, fitness_aa=0.5)
```

```
traj = simulate_selection(pop, 30)
print(round(traj[-1].p, 4))
```

Clinical / systems note: Pathogen resistance evolution (TB, HIV, malaria) is tracked with the same allele-frequency dynamics; combination therapy aims to prevent peaks of p for any single resistance mutation.

20.18 Current Evidence and Frontier Biology: Population Genetics

For Population Genetics, frontier biology belongs inside the evidence logic of the chapter. Classical genetics remains essential, but modern interpretation adds penetrance, polygenicity, structural variation, ancestry-aware inference, and uncertainty in risk prediction. The core reading question is this: allele-frequency explanations should name the force, parameter values, assumptions, and data needed to distinguish forces.

- What to verify: identify the observation, model, assay, or dataset that would make the claim stronger or weaker.
- What to qualify: state the scale, organism, cell type, environmental condition, or population where the claim is expected to hold.
- What to compare: test at least one alternative explanation, baseline, or null model before treating the pattern as causal.
- What to cite: distinguish primary evidence, review synthesis, public dataset, and institutional guidance; for recent or numeric claims, prefer the source closest to the measurement and state what has changed since it was published.

A good genetics answer separates the Mendelian transmission model from the evidence needed to use it in a population, family, or clinical setting.

Source practice: For population-genetic claims, state model assumptions, sampling frame, ancestry representation, selection regime, and drift or migration alternative.

20.18.1 Current Evidence Map: Ancestry-Aware Variant Interpretation



Figure 126. Graph references can reduce reference bias, but population-genetic interpretation still depends on sampling design, assumptions, and validation [humanpangenome2023].

20.19 Summary

- Hardy-Weinberg equilibrium: $p^2 + 2pq + q^2 = 1$ in large, randomly mating populations with no mutation, migration, or selection. Reached in one generation. Serves as a null model for detecting evolutionary forces.
- Natural selection: Fitness (w), selection coefficient (s), dominance coefficient (h). Directional selection shifts allele frequencies; balancing selection (heterozygote advantage) maintains polymorphism at stable equilibrium ($\hat{q} = s_1/(s_1 + s_2)$).
- Genetic drift: Random allele frequency changes in finite populations; variance $\propto 1/2N_e$; fixation or loss inevitable. Bottleneck and founder effects cause non-representative gene pools.
- Gene flow: Homogenizes populations; $\Delta p_1 = m(p_2 - p_1)$. F_{ST} measures population differentiation (about 0.12 for humans).
- Mutation-selection balance: $\hat{q} = \sqrt{\mu/s}$ for deleterious recessives. CF carrier frequency suggests heterozygote advantage beyond mutation alone.
- Neutral theory (Kimura): Most molecular variation is neutral; substitution rate = neutral mutation rate (independent of N). Ka/Ks ratio distinguishes purifying, neutral, and positive selection.
- Coalescent theory: Traces lineages backward; TMRCA for mitochondrial DNA about 200,000 years; for Y chromosome about 200,000-300,000 years.
- Molecular clock: $t = d_{JC}/2\mu$; calibrated with fossils; widely used for estimating divergence times. Human-chimp about 6-7 Ma.
- Connections: See Unit VI — Evolution: Introduction (tree thinking and substitution models), Unit X — Ecology: Introduction (metapopulation structure), Unit VII — Microbiology: Introduction (microbial effective population sizes).

20.20 Review Questions

1. Derive the Hardy-Weinberg equation from first principles, starting with random mating.
2. A population has the following genotype counts: AA = 200, Aa = 500, aa = 300. Calculate allele frequencies and test for HWE.
3. Sickle cell trait (HbAS) provides about 10-fold protection against severe *P. falciparum* malaria. If $s_1 = 0.10$ (cost of malaria susceptibility in HbAA) and $s_2 = 0.85$ (cost of sickle cell disease in HbSS), calculate the equilibrium frequency of HbS.

4. A population of 100 individuals has $p = 0.5$. Calculate the expected variance in Δp per generation due to drift. What is the expected heterozygosity loss per generation?

5. Explain why N_e is usually much less than census size N . Give three factors that reduce N_e .

6. A population on a remote island was founded by 10 individuals 200 years ago. Predict the genetic consequences using the founder effect concept.

7. Compare directional, stabilizing, disruptive, and balancing selection. Give an example of each.

8. Using the Jukes-Cantor correction, calculate the evolutionary distance for two sequences with 20% observed divergence.

9. Explain why the neutral theory predicts that substitution rate equals mutation rate regardless of population size. Show the mathematical proof.

10. What is F_{ST} ? Calculate F_{ST} for two populations with allele frequencies $p_1 = 0.8$ and $p_2 = 0.2$.

11. If `simulate_selection` is run for 200 generations with $s = 0.01$ against the a allele, when does Δp per generation approximately linearise vs. saturate?

12. Explain why soft sweeps complicate signatures of selection relative to classic hard sweeps.
- 20.21 Further Reading and Source Notes: Population Genetics
- Weinberg (1908). "Über den Nachweis der Vererbung beim Menschen. *Jahreshefte des Vereins für vaterländische Naturkunde in Württemberg*, 64.

• Kimura (1968). Evolutionary Rate at the Molecular Level. *Nature*, 217.

• Ohta (1973). Slightly deleterious and nearly neutral mutations in molecular evolution. *Proceedings of the National Academy of Sciences*, 70.

• Kingman (1982). The coalescent. *Stochastic Processes and their Applications*, 13.
- 20.22 Key Terms
1. Gene pool – the allele set carried by a population across its loci

2. Allele frequency – the proportion of sampled gene copies carrying a specified allele

3. Hardy-Weinberg equilibrium – state in which allele and genotype frequencies remain constant across generations

4. Fitness (w) – relative reproductive success of a genotype

5. Selection coefficient (s) – magnitude of selection against a genotype ($s = 1 - w$)

6. Heterozygote advantage (overdominance) – heterozygote has higher fitness than either homozygote

7. Genetic drift – random changes in allele frequency due to finite population size

8. Effective population size (N_e) – size of an ideal population experiencing the same drift as the actual population

9. Bottleneck effect – drastic reduction in population size causing loss of genetic diversity

10. Founder effect – reduced genetic diversity when a small group establishes a new population

11. Gene flow – movement of alleles between populations via migration

12. F_{ST} (fixation index) – measure of genetic differentiation among populations

13. Mutation-selection balance – equilibrium allele frequency determined by mutation introducing and selection removing deleterious alleles

14. Neutral theory – most molecular variation is selectively neutral and evolves by drift

15. Ka/Ks ratio (dN/dS) – ratio of nonsynonymous to synonymous substitution rates; indicates selection regime

16. Coalescent theory – framework tracing allele lineages backward to their most recent common ancestor

17. Molecular clock – assumption that neutral substitutions accumulate at a roughly constant rate

18. Jukes-Cantor distance – correction for multiple substitutions at the same site: $d_{JC} = -\frac{3}{4} \ln(1 - \frac{4d}{3})$

19. TMRCA – time to the most recent common ancestor of a set of allele lineages
- 20.23 Companion Source Module: Population Genetics
- Population Genetics should leave a reproducible trail from a biological claim to the code, figure, diagram, or paper-based activity that can test it. Use the surfaces below to inspect the chapter’s assumptions, rerun the relevant model, or compare the manuscript explanation with companion labs and figures.
- Table 290. Companion source surfaces for Population Genetics.
- | Surface | Use it for |
|--|--|
| <code>src/biology/genetics/genetics.py</code> (<code>hardy_weinberg</code> , <code>chi_squared_test</code> , <code>jukes_cantor_distance</code>) | Test equilibrium, goodness of fit, and molecular-distance assumptions. |
- 532

Surface	Use it for
<code>src/biology/evolution/evolution.py</code> (<code>simulate_selection</code> , <code>wright_fisher_drift</code> , <code>molecular_clock_divergence_time</code>)	Compare deterministic and stochastic allele-frequency change.
<code>src/visualization/plots.py</code> (<code>plot_selection_simulation</code>)	Inspect trajectories and sampling effects.

Reproducibility check: state population size, mating model, selection coefficient, migration, mutation, and sampling uncertainty before attributing allele-frequency change. Cross-reference: connect with sections 17 and 18, section 21, and section 22.

Unit VI — Evolution: Introduction

Why This Unit Matters

On 24 November 1859, Charles Darwin published *On the Origin of Species by Means of Natural Selection*. The book sold out on its first day. Within a decade, the concept of evolution by natural selection had overturned centuries of natural theology and provided biology with its first unifying theory. Theodosius Dobzhansky’s 1973 essay captured this with a sentence that has become a biologist’s creed: *“Nothing in biology makes sense except in the light of evolution.”*

Darwin’s central insight — that heritable variation + differential reproductive success produces cumulative directional change in populations over generations — was elegant but incomplete. He had no mechanism for inheritance. The Modern Synthesis (1930s–1940s), forged by Fisher, Haldane, Wright, Dobzhansky, and Mayr, married Darwinian selection to Mendelian genetics and population genetics, giving evolution a precise mathematical foundation. A further deepening came with the neutral theory (Kimura, 1968): not most genetic change is driven by selection; much molecular evolution is stochastic, driven by genetic drift. Understanding evolution now requires integrating selection, drift, mutation, gene flow, and non-random mating — the five forces that perturb Hardy-Weinberg equilibrium.

This unit treats evolution quantitatively. You will simulate allele frequency trajectories under selection and drift, derive the molecular clock equation and apply it to evolutionary divergence times, model speciation as a bifurcation in population structure, and reconstruct phylogenetic trees using maximum-likelihood and Bayesian methods. The tools here are the same used in clinical epidemiology (tracking antibiotic resistance alleles), crop improvement (genomic selection), and forensic genetics (ancestral inference from SNP profiles).

Landmark Discoveries

Discoverer(s)	Year	Journal / Source	Discovery	Significance
Darwin & Wallace	1858–59	[Darwin and Wallace, 1858, Darwin, 1859]	Natural selection as mechanism of evolution	Provided the first mechanistic explanation for biological diversity
Gregor Mendel (rediscovered)	1900	[Mendel, 1866]	Mendelian inheritance = mechanism for variation	Fused genetics with evolution; launched Modern Synthesis
Ronald Fisher	1930	[Fisher, 1930]	Mathematical synthesis of Darwinism + Mendelism	Fundamental theorem of natural selection; $\Delta q = spq^2/\bar{W}$
Sewall Wright	1931	[Wright, 1931]	Genetic drift and adaptive landscapes	Showed small populations diverge by chance; $\sigma^2(\Delta p) = pq/2N_e$
Motoo Kimura	1968	[Kimura, 1968]	Neutral theory of molecular evolution	Most amino acid substitutions are selectively neutral; molecular clock
Woese & Fox	1977	[Woese and Fox, 1977]	Three domains of life (Archaea identified by rRNA)	Completely restructured the comprehensive tree of life
Svante Pääbo et al.	2010	[Green et al., 2010]	Neanderthal genome sequencing	Showed interbreeding between modern humans and Neanderthals; Nobel Prize 2022

Key Concepts and Connections

Current Evidence Thread

Treat this unit as a converging body of evidence for evolution: the fossil record documenting transitional forms and deep time, comparative genomics revealing shared ancestry and the molecular footprints of selection, real-time selection measured in experimental and wild populations, and phylogenies that reconstruct

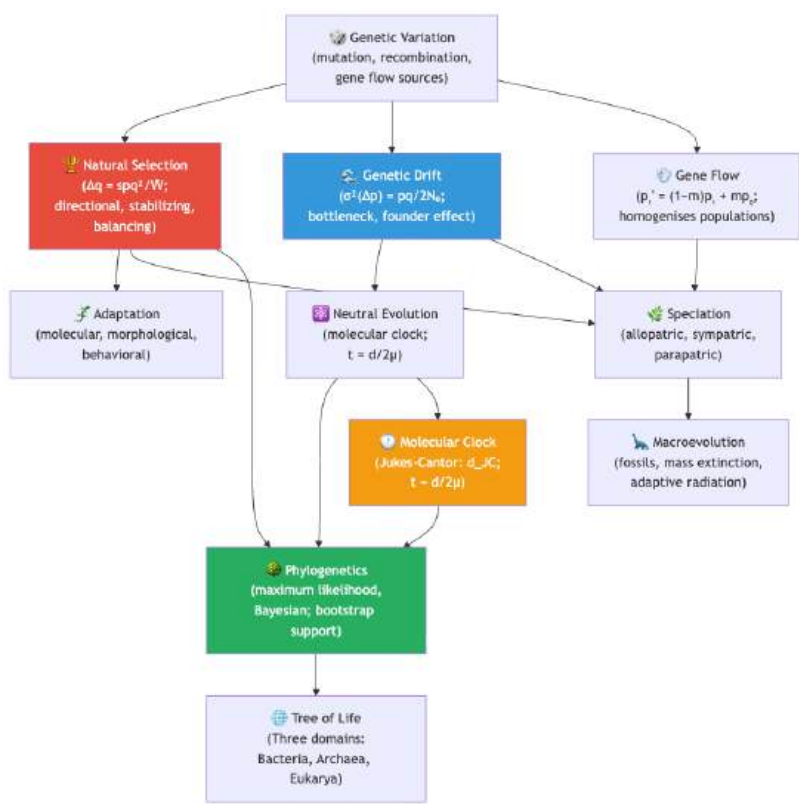


Figure 127. Evolution concept map - red = selection; blue = drift; green = phylogenetics; orange = molecular clock.

the branching history those data imply. Evolutionary claims are strongest when they combine mechanism, comparative evidence, population process, and explicit uncertainty. As you move through the chapters, keep a two-column note: claim on the left, evidence that would change my confidence on the right. By the end of the unit, each major idea should be tied to a measurement, model, citation, or paper-based lab decision.

Chapter Roadmap

Chapter	Title	Core Question	Key Equation / Model
19	Evolution and Natural Selection	How does natural selection change allele frequencies, and how fast?	$\Delta q = -spq^2/\bar{W}$; fitness surface; selection coefficient
20	Genetic Drift and Speciation	How do chance events in small populations lead to divergence and new species?	$\sigma^2(\Delta p) = pq/2N_e$; isolation index; speciation models
21	Phylogenetics and the Tree of Life	How do we reconstruct evolutionary history from molecular data?	Jukes-Cantor correction; molecular clock: $t = d_{JC}/2\mu$

Connections Across the Textbook

- Hardy-Weinberg equilibrium in section 20 is the null model disrupted by the five evolutionary forces analyzed here.
- Molecular clock and Jukes-Cantor distances connect to Unit IV — Molecular Genetics: Introduction (mutation rates in DNA replication) and Unit VII — Microbiology: Introduction (phylogeny of pathogens and antibiotic-resistance evolution).
- Speciation links to Unit X — Ecology: Introduction (biogeography, island species-area relationship, MacArthur-Wilson model).
- Adaptive evolution of immune genes connects to Unit IX — Zoology and Systems Physiology: Introduction (MHC diversity and pathogen immunity), and antibiotic resistance evolution motivates the clinical sections of Unit VII — Microbiology: Introduction.

Key vocabulary introduced here: fitness, selection coefficient, genetic drift, effective population size (N_e), founder effect, bottleneck, molecular clock, phylogeny, clade, synapomorphy, allopatric speciation, sympatric speciation, neutral theory, molecular systematics, maximum likelihood,

bootstrap support.

Computational Toolbox — Unit VI

```
from biology.evolution import simulate_selection, simulate_drift

# Natural selection on a beneficial mutation (s = 0.02, starting frequency p0 = 0.01)
from biology.evolution import Population

initial = Population("beneficial allele", p=0.01, q=0.99, fitness_AA=1.02, fitness_Aa=1.01, fitness_aa=1.0)
trajectory = simulate_selection(initial, generations=200)
print(f"Generation 1: p = {trajectory[0].p:.4f}")
print(f"Generation 100: p = {trajectory[99].p:.4f}")
print(f"Generation 200: p = {trajectory[199].p:.4f}")

# Genetic drift: small population bottleneck (Ne=50) vs. large (Ne=1000)
import random; random.seed(42)
small_pop = simulate_drift(p=0.5, N=50, generations=200)
large_pop = simulate_drift(p=0.5, N=1000, generations=200)
print(f"Ne=50 terminal p: {small_pop[-1]:.3f} (fixed={'yes' if small_pop[-1] in (0,1) else 'no'})")
print(f"Ne=1000 terminal p: {large_pop[-1]:.3f}")
# Small populations show large random fluctuations; large populations stay near 0.5.
```

Try it yourself: Run `simulate_drift` 100 times with `N=20` and count how many runs fix the allele ($p=1.0$) versus lose it ($p=0.0$). Theory predicts fixation = $p_0 = 0.5$.

Source note: the evolution module supports selection, drift, fitness-landscape, molecular-clock, sequence-distance, and isolation-index examples. Figures and Mermaid diagrams provide the selection and phylogenetic visuals.

Cross-Unit Integration

The mechanisms of evolution — selection, drift, mutation, gene flow, speciation — that Unit VI — Evolution: Introduction develops in eukaryotic and metazoan systems take on a particularly stark form in the microbial world of Unit VII — Microbiology: Introduction. Bacteria and viruses evolve on timescales of hours to days; horizontal gene transfer, plasmid exchange, and conjugation bypass the vertical-inheritance assumptions that made the population-genetic models tractable; antibiotic resistance is selection-in-real-time, observable in a single hospital ward. As you encounter microbial life histories and pathogen-host coevolution in Unit VII — Microbiology: Introduction, return to the selection and drift equations of Unit VI — Evolution: Introduction and ask what changes when generation time collapses to minutes and the “population” includes a swarm of genomes exchanging parts. The principles persist; the timescales and recombination assumptions do not.

21 Natural Selection and Adaptation

Level 2/3 · 60 min read · 75 min lecture · Prerequisites: section 20

21.1 Learning Objectives

By the end of this chapter, you should be able to:

1. Trace the historical development of evolutionary thought from Lamarck through Darwin [Darwin and Wallace, 1858], Wallace, and the Modern Synthesis.
2. Evaluate five independent lines of evidence supporting evolution and explain why they converge on the same conclusion.
3. Define fitness mathematically and distinguish directional, stabilizing, disruptive, sexual, kin, and frequency-dependent selection.
4. Explain adaptation, exaptation, and the constraints that limit what natural selection [Williams, 1966] can achieve.
5. Distinguish microevolution from macroevolution and evaluate punctuated equilibrium versus phyletic gradualism.
6. Describe coevolutionary dynamics including arms races and the Red Queen hypothesis.
7. Calculate a selection coefficient from observed allele-frequency change and predict the phenotypic response to selection using the breeder’s equation $R = h^2S$.
8. Analyze direct observations of evolution in real time — the *E. coli* long-term evolution experiment, Galápagos finch beak shifts, and cane-toad spatial sorting — and explain how each demonstrates measurable change within human timescales.
9. Evaluate the ethical responsibilities raised when evolutionary theory becomes a design framework, including gain-of-function research, gene drives, and heritable genome editing.

21.1.1 Study Blueprint

- Big idea: Natural selection is differential reproductive success acting on heritable variation in context.
- Core concepts: variation, fitness, adaptation, selection coefficient.
- Framework alignment: Vision & Change: Evolution, Systems; AP Biology: Evolution, Systems Interactions; NGSS-style topics: Natural Selection and Evolution, Interdependent Relationships in Ecosystems.
- Model or quantitative lens: Selection coefficient and allele-frequency trajectory calculations.
- Data skill: Interpret fitness data and distinguish selection from other forces.
- Practice cadence: Visual Representations, Statistical Tests and Data Analysis, Argumentation.
- Common misconception to repair: Evolution is not goal-directed progress; it is local change in populations under constraints.
- Primary lab: Lab — Natural Selection and Adaptation.
- Question bank: Questions — Natural Selection and Adaptation.
- Transfer task: Transfer selection reasoning to antibiotics, pesticide resistance, cancer, or climate adaptation.
- Bridge to computation: `biology.evolution.evolution.simulate_selection`.

Opening Vignette — Thirteen Finches, One Revelation

In 1835, H.M.S. Beagle anchored in the Galápagos Islands for five weeks. Charles Darwin explored several islands, collecting birds and noting that their beaks differed island to island — but he initially assumed they were different species entirely. It was the ornithologist John Gould who, examining Darwin’s specimens back in London in 1837, declared the 13 birds finches, each adapted to a different food source. That recognition helped Darwin understand what he had seen: a single ancestral population, blown across 900 km of ocean, had diversified into 13 species to exploit different ecological niches. The insight sparked his theory of natural selection. A century and a half later, Peter and Rosemary Grant spent 40 years documenting beak evolution in *Geospiza fortis* during drought years — measuring beaks with calipers on every individual — providing the most comprehensive real-time record of natural selection in a wild population ever assembled.

21.2 Historical Context of Evolutionary Thought

21.2.1 Pre-Darwinian Ideas

Long before Darwin, naturalists wrestled with the observation that organisms seem exquisitely matched to their environments. Three key thinkers set the stage for evolutionary biology.

Jean-Baptiste Lamarck (1744–1829) proposed two mechanisms of evolutionary change in his *Philosophie Zoologique* (1809). First, the law of use and disuse held that organs used extensively become stronger and larger, while unused organs deteriorate. Second, the inheritance of acquired characteristics proposed that modifications gained during an organism’s lifetime pass to offspring. A blacksmith’s children, by this logic, would inherit strong arms. While the inheritance mechanism was wrong, Lamarck deserves credit for proposing that species change over time – a radical departure from the fixity of species doctrine.

Georges Cuvier (1769–1832) established comparative anatomy and paleontology as rigorous disciplines. Examining fossils in the Paris Basin, he documented that species in deeper (older) strata differed from living forms. His explanation was catastrophism: periodic catastrophic events (floods, volcanism) destroyed regional faunas, which were then replaced by immigration from unaffected areas. Cuvier vehemently opposed transmutation of species but ironically provided the fossil evidence that later supported it.

Charles Lyell (1797–1875) countered catastrophism with uniformitarianism in his *Principles of Geology* (1830–1833). He argued that the same geological processes operating today – erosion, sedimentation, volcanism – have typically operated, and at roughly the same rates. The Earth, therefore, must be immensely old, providing the deep time necessary for gradual biological change. Darwin carried the first volume of Lyell’s *Principles* aboard HMS Beagle, and it profoundly shaped his thinking.

21.2.2 Darwin’s Voyage on HMS Beagle (1831–1836)

Charles Darwin boarded HMS Beagle as a gentleman naturalist at age 22. The five-year circumnavigation exposed him to patterns that would crystallize into the theory of natural selection:

- Galapagos Islands: Darwin collected finches, mockingbirds, and tortoises from different islands. He initially failed to label specimens by island – an oversight he later called his greatest regret. Ornithologist John Gould identified the finches as distinct but related species, each with bill morphology matching its food source. The mockingbirds showed similar island-specific variation. Giant tortoises differed in carapace shape between islands (saddleback on arid islands with tall vegetation, dome-shaped on humid islands with low vegetation).
- South American fauna: Fossil glyptodonts (giant armadillos) in Argentina resembled living armadillos – a clear example of descent with modification rather than separate creation. The rhea (South American ostrich) filled an ecological niche analogous to the African ostrich, suggesting geographic replacement driven by similar selective pressures rather than independent design.
- Coral atolls and geological uplift: Darwin observed raised marine terraces in Chile after the 1835 earthquake, confirming Lyell’s gradualism.

21.2.3 Wallace’s Independent Discovery

Alfred Russel Wallace (1823–1913), working as a specimen collector in the Malay Archipelago, independently conceived natural selection during a bout of malaria on the island of Ternate in February 1858. His letter to Darwin – the famous Ternate letter – outlined a mechanism virtually identical to Darwin’s unpublished theory. Lyell and Joseph Hooker arranged a joint presentation to the Linnean Society of London on July 1, 1858, reading Wallace’s paper alongside extracts from Darwin’s 1844 essay and an 1857 letter to Asa Gray. Darwin then rushed to complete *On the Origin of Species*, published November 24, 1859.

21.2.4 The Three Conditions for Natural Selection

Natural selection operates whenever three conditions are met simultaneously:

1. Heritable variation: Individuals in a population differ in traits, and at least some of that variation is genetically transmitted to offspring.
2. Differential survival and reproduction: Some variants survive longer, reproduce more, or both – contributing disproportionately to the next generation.
3. Environmental pressure: Resources are limited; not most individuals can survive and reproduce equally. The environment determines which traits are advantageous.

When the three conditions hold, **allele** frequencies shift across generations – populations evolve.

21.2.5 The Modern Synthesis and Beyond

The Modern Synthesis (also called the Neo-Darwinian Synthesis) emerged in the 1930s–1950s through the work of Theodosius Dobzhansky (*Genetics and the Origin of Species*, 1937), Ernst Mayr (*Systematics and the Origin of Species*, 1942), George Gaylord Simpson (*Tempo and Mode in Evolution*, 1944), and Julian Huxley (*Evolution: The Modern Synthesis*, 1942). This intellectual movement unified Darwin’s mechanism of natural selection with Mendelian genetics, mathematical **population genetics** (Fisher, Wright, Haldane), paleontology, and systematics into a coherent framework. The Modern Synthesis established that:

- Evolution is the change in allele frequencies within populations over time
- Natural selection is the primary mechanism of adaptive evolution
- Gradual accumulation of small genetic changes produces large-scale evolutionary patterns
- **Speciation** typically involves the evolution of **reproductive isolation** between geographically separated populations

The Modern Synthesis remains the foundation of evolutionary biology, though later work on evo-devo, plasticity, niche construction, epigenetic inheritance, symbiosis, and cultural evolution has expanded the synthesis.

Concept Check 1: Lamarck proposed inheritance of acquired characteristics. Why does modern genetics reject this mechanism? Can you think of any biological phenomenon that superficially resembles Lamarckian inheritance? (Hint: consider epigenetic inheritance.)

21.3 Evidence for Evolution Across Fossils, Genomes, and Development

Five independent lines of evidence converge to support evolution. Each alone would be suggestive; together they constitute one of the most strongly supported theories in science.

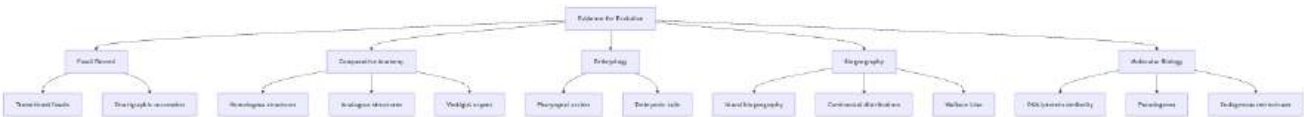


Figure 128. Independent evidence streams for evolution, including fossils, anatomy, embryology, biogeography, and molecular comparison, converge on common descent and descent with modification.

21.3.1 Fossil Record and Temporal Sequence Evidence

The fossil record documents the history of life through mineralized remains preserved in sedimentary rock. Fossils form through several processes: permineralization (minerals replace organic material), compression (organisms flattened in sediment), amber preservation (organisms entombed in tree resin), and trace fossils (footprints, burrows, coprolites). The record is inherently incomplete – fossilization requires specific conditions (rapid burial, absence of scavengers, appropriate mineral chemistry), and soft-bodied organisms are rarely preserved. Despite this incompleteness, key transitional fossils bridge major evolutionary gaps:

- Tiktaalik roseae (375 Mya, Late Devonian): Discovered in 2004 on Ellesmere Island, Arctic Canada, by Neil Shubin’s team. This “fishapod” possesses fish features (scales, fins, gills) alongside tetrapod features (flat head, neck, wrist bones capable of weight-bearing, ribs for lung ventilation). It bridges the fish-to-tetrapod transition.
- Archaeopteryx lithographica (150 Mya, Late Jurassic): Found in Solnhofen limestone, Germany. Combines dinosaur features (teeth, clawed fingers, bony tail) with bird features (asymmetric flight feathers, wishbone). Now understood as one member of a diverse radiation of feathered dinosaurs.
- Whale evolution: One of the best-documented evolutionary transitions. *Pakicetus* (50 Mya) was a terrestrial carnivore with cetacean ear bones. *Ambulocetus* (49 Mya) was semi-aquatic with large hind limbs for swimming. *Rodhocetus* (47 Mya) had reduced hind limbs and a more streamlined body. *Basilosaurus* (37 Mya) was fully aquatic with vestigial hind limbs. Modern cetaceans retain vestigial pelvic bones embedded in muscle.

21.3.2 Comparative Anatomy and Homology

Homologous structures share a common developmental and evolutionary origin but may serve different functions. The vertebrate forelimb illustrates this principle: the human arm (manipulation), bat wing (flight), whale flipper (swimming), and horse leg (running) most contain the same bones – humerus, radius, ulna, carpals, metacarpals, phalanges – arranged in the same relative positions. The functional differences reflect modification of a shared ancestral blueprint.

Analogous structures arise from convergent evolution: the dolphin fin and shark fin are superficially similar but have completely different internal anatomy and developmental origins. Similarly, bird wings and insect wings evolved independently.

Vestigial structures are reduced remnants of organs that were functional in ancestors: the human coccyx (remnant of a tail), arrector pili muscles (produce goose bumps – useful for fur-covered ancestors, functionless in largely hairless humans), wisdom teeth (third molars suited to ancestral diets of tough plant material), and the whale pelvis (tiny bones embedded in body wall, remnants of hind limbs).

21.3.3 Embryology and Developmental Homology

Pharyngeal arches appear in the embryos of most vertebrates – fish, amphibians, reptiles, birds, and mammals. In fish, these arches develop into gills and their supporting structures. In terrestrial vertebrates, the same embryonic structures are repurposed for entirely different functions: the first pharyngeal arch forms the jaw and middle ear ossicles (malleus and incus); the second arch forms the stapes, styloid process, and much of the hyoid bone; the third and fourth arches contribute to laryngeal and tracheal cartilages. This shared developmental program, using homologous embryonic structures for radically different adult functions, is compelling evidence for common ancestry.

Haeckel’s biogenetic law (“ontogeny recapitulates phylogeny”) proposed that embryonic development replays evolutionary history in sequence. While this formulation is an overstatement – development does not literally replay adult ancestral stages – the underlying observation remains valid: embryos of related

species share developmental stages that diverge progressively later in development, reflecting their shared genetic toolkit (particularly the conserved Hox **gene** clusters that pattern the anterior-posterior body axis across most bilaterians).

Human embryos possess a tail at approximately week 5 of development, containing 10–12 developing caudal vertebrae. By week 8, programmed cell death (**apoptosis**) reduces this to the 3–5 fused vertebrae of the adult coccyx. In rare developmental anomalies, the apoptotic program fails partially, and a “vestigial tail” is present at birth – a striking reminder of our evolutionary heritage. Similarly, human embryos develop lanugo (fine body hair) at approximately week 20, a remnant of the fur coat that covered our mammalian ancestors.

21.3.4 Biogeography and Historical Dispersal

The geographic distribution of organisms reflects evolutionary history, geological events, and patterns of dispersal and vicariance. Darwin and Wallace both recognized that biogeography provides powerful evidence for evolution – the distribution of organisms makes sense primarily in the context of evolutionary history and plate tectonics:

- **Marsupial distribution:** Marsupials dominate Australia (kangaroos, koalas, wombats) but are largely absent from placental-dominated continents. This reflects the breakup of Gondwana: marsupials diversified in isolation on the Australian continent after its separation from Antarctica approximately 45 Mya.
- **Island biogeography:** Oceanic islands harbor endemic species derived from mainland colonizers. Hawaiian honeycreepers, Galapagos finches, and Madagascar lemurs most represent adaptive radiations from single founding lineages.
- **Wallace Line:** A biogeographic boundary running between Borneo and Sulawesi, and between Bali and Lombok, separating the Asian and Australian faunal regions. Deep ocean trenches (reaching depths of 1,500 meters or more) prevented land bridges even during Pleistocene glacial periods when sea levels dropped by approximately 120 meters, maintaining distinct faunas on either side. West of the line: placental mammals (tigers, rhinoceroses, primates). East of the line: marsupials and monotremes (kangaroos, possums, platypuses). The line was identified by Wallace in 1859 based on his extensive collecting in the Malay Archipelago, and its correspondence with deep-water tectonic boundaries was confirmed much later by plate tectonic theory.

Real-World Connection: Biogeography and Conservation Hotspots

Understanding biogeographic patterns is critical for conservation. Oceanic islands and other biogeographic isolates harbor disproportionate numbers of endemic species – organisms found nowhere else. Madagascar covers 0.4% of Earth’s land surface but harbors approximately 5% of known species, nearly 90% of which are endemic. The island has been isolated from Africa for approximately 88 million years, allowing a unique biota to evolve in isolation. Conservation of island biotas requires understanding their evolutionary history: small, isolated populations are inherently vulnerable to extinction from habitat loss, introduced predators, and genetic erosion. The current extinction crisis disproportionately affects island species – approximately 75% of recorded bird and mammal extinctions since 1500 have occurred on islands. Because “recorded extinctions” are biased toward vertebrates and well-surveyed islands, use the index as a directional warning signal, not as a complete inventory of biodiversity loss.

21.3.5 Molecular Evidence from Sequence Similarity and Shared Variants

Molecular data provide the most quantitative and testable evidence for evolution. The molecular evidence is particularly powerful because it generates precise, quantitative predictions that can be verified independently:

- **Cytochrome c similarity:** This mitochondrial **protein** is found in most **aerobic** organisms. Human and chimpanzee cytochrome c sequences are 100% identical. Human and rhesus monkey differ by 1 amino acid. Human and yeast differ by approximately 40% – yet retain the same basic function. The pattern of similarity matches phylogenetic predictions exactly.
- **Pseudogenes:** Non-functional DNA sequences that were once functional genes. Humans and chimpanzees share the same inactivating **mutation** in the $\psi\eta$ -globin pseudogene – an event so specific that independent occurrence is highly improbable. Shared pseudogenes are powerful evidence for common descent.
- **Endogenous retroviruses (ERVs):** Approximately 8% of the human **genome** consists of ancient retroviral sequences inserted into the germline of our ancestors. Humans and chimpanzees share many ERV insertion sites at identical genomic locations – each representing an independent ancestral infection event, providing a molecular “fossil record” within the genome.
- **C-value paradox:** Genome size does not correlate with organismal complexity. The onion genome (about 16 Gb) is five times larger than the human genome (about 3.2 Gb). This reflects the accumulation of transposable elements and other non-coding sequences through evolutionary time, not design.
- **Molecular phylogenies match morphological phylogenies:** When phylogenetic trees are constructed independently from DNA sequences and from morphological characters, they produce the same branching patterns. This convergence of independent evidence is powerful confirmation that the trees reflect real historical relationships, not artifacts of either data type.

Real-World Connection: Forensic Phylogenetics

Molecular phylogenetics has been used in criminal investigations. In the landmark 1998 case of a Louisiana gastroenterologist accused of infecting a former lover with HIV, phylogenetic analysis of viral sequences demonstrated that the victim’s HIV strain was nested within the phylogenetic cluster from one of the physician’s patients – consistent with deliberate injection of contaminated blood. The viral phylogeny, combined with epidemiological evidence, contributed to the physician’s conviction. This case established molecular phylogenetics as admissible forensic evidence and demonstrated that evolutionary biology has applications far beyond the academic laboratory.

Concept Check 2: A creationist argues that similarities between species reflect common design, not common descent. How would you use shared pseudogenes and endogenous retroviruses to counter this argument?

21.4 Mechanisms of Natural Selection

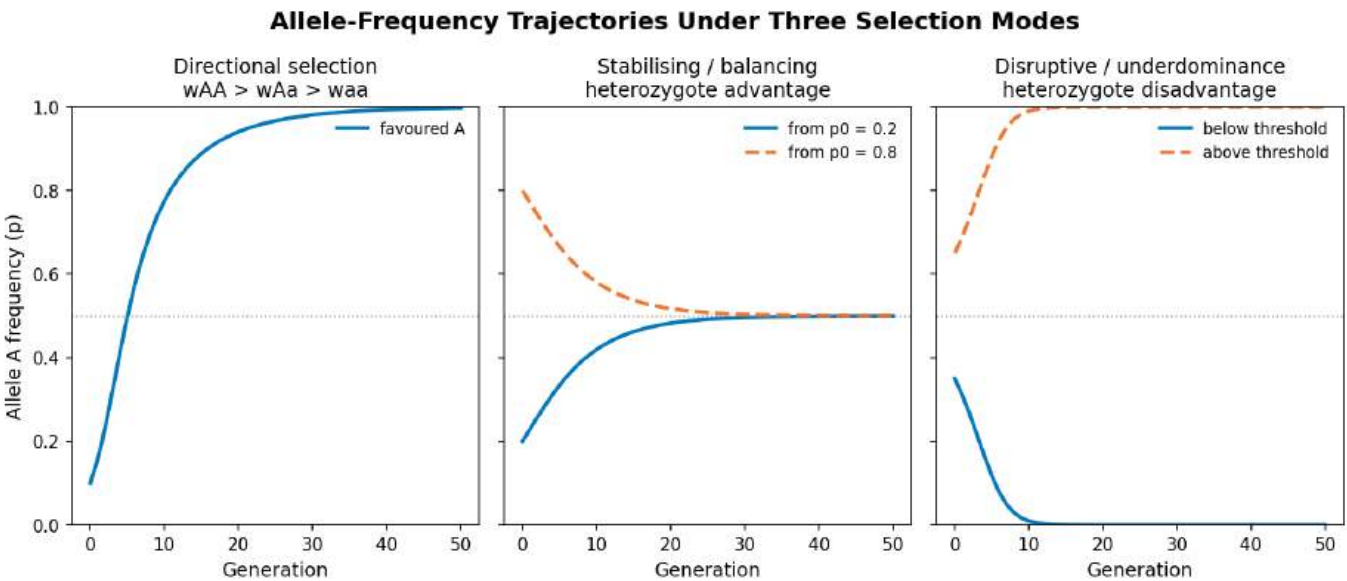


Figure 129. Natural selection simulation: allele-frequency change over generations under directional selection, balancing selection via heterozygote advantage, and disruptive selection via heterozygote disadvantage.

21.4.1 Fitness as Reproductive Success in Context

Darwinian fitness (*W*) measures relative reproductive success – the contribution of a genotype to the next generation compared to other genotypes:

$$W = \frac{\text{reproductive output of genotype}}{\text{mean reproductive output of population}}$$

(318)

Fitness is typically relative and context-dependent. An allele conferring antibiotic resistance has *W* > 1 in the presence of antibiotics but may have *W* < 1 in their absence (due to the metabolic cost of resistance).

For a single locus with two alleles, if we assign the favored homozygote fitness *W*_{AA} = 1, then:

$$W_{Aa} = 1 - hs \quad \text{and} \quad W_{aa} = 1 - s$$

(319)

where *s* is the selection coefficient and *h* is the dominance coefficient.

$$\frac{d\bar{W}}{dt} = V_A(W)$$

(320)

This theorem implies that natural selection typically increases mean fitness (though the environment may change, altering what “fit” means). It also implies that populations under strong selection rapidly deplete additive genetic variance – the more efficiently selection operates, the faster it erodes its own fuel.

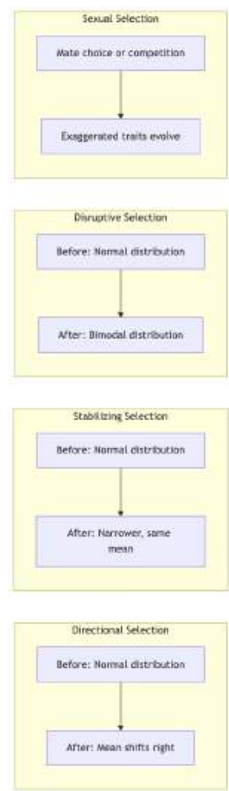


Figure 130. Selection modes change trait distributions in different ways: directional selection shifts a mean, stabilizing selection narrows variation, disruptive selection splits a distribution, and sexual selection amplifies mating-linked traits.

Concept Check (Synthesis — Cross-Unit Connection): **Unit 0 — Systems Science for Biology: Introduction** introduced the Free Energy Principle: biological systems minimize variational **free energy** (prediction error) to maintain their phenotypic states. (a) Reframe natural selection in FEP terms: if fitness reflects how well an organism’s phenotype predicts and responds to its environment, explain why selection pressure corresponds to the gradient of long-run expected surprise across phenotypic variation. (b) In this framing, what does “genetic drift” correspond to — is it analogous to noise in a learning algorithm, to stochastic exploration in active inference, or to something else? Defend your choice. (c) How does the Baldwin effect (environmentally induced phenotypic change that can become genetically assimilated) illustrate the relationship between within-lifetime and across-generation free energy minimization?

21.4.2 Directional Selection and Trait-Mean Shifts

Directional selection shifts the mean **phenotype** toward one extreme. The population’s phenotype distribution moves in one direction across generations, in contrast to the stabilizing and disruptive regimes whose divergent allele-frequency trajectories are simulated in figure 129.

Industrial melanism in *Biston betularia*: Before the Industrial Revolution, the typical peppered moth was light-colored, camouflaged against lichen-covered tree bark. The melanic (dark) form, controlled by a **dominant** allele at the *cortex* locus, increased from approximately 1% in 1848 to 98% in Manchester by 1898 as industrial soot darkened tree trunks. Light moths were conspicuous to bird predators on dark bark. Following the Clean Air Act (1956), lichen recovered, and the light form returned to dominance – a textbook example of directional selection reversing direction.

Antibiotic resistance: Random mutations conferring resistance arise at low frequency in bacterial populations. In the presence of antibiotics, resistant bacteria have enormous selective advantage ($s \approx 0.1\text{--}1.0$). With generation times of 20–30 minutes, resistance alleles can reach fixation within days – evolution observable within a single clinical episode. Multiple mechanisms confer resistance: target modification (altered penicillin-binding proteins in MRSA), enzymatic degradation (beta-lactamases that hydrolyze penicillin), efflux pumps (that actively export antibiotics from the cell), and membrane permeability changes (reduced porin expression in Gram-negative bacteria).

The selection coefficient can be estimated from the rate of allele frequency change:

$$s \approx \frac{\Delta p}{p(1 - p)} \cdot \frac{1}{\Delta t}$$

(321)

21.4.3 Worked Example: Estimating the Selection Coefficient

Problem: A novel antibiotic resistance allele in a hospital population of *Staphylococcus aureus* is initially present at a frequency of $p = 0.01$. After $\Delta t = 50$ generations of continuous antibiotic exposure, the resistance allele reaches a frequency of $p' = 0.06$. Assuming the change is driven entirely by selection, estimate the selection coefficient (s) favoring this resistance allele.

Solution:

1. Identify the change in allele frequency (Δp):

$$\Delta p = p' - p = 0.06 - 0.01 = 0.05$$

2. Calculate the selection coefficient using the approximation formula: Substitute the initial frequency $p = 0.01$, the change $\Delta p = 0.05$, and the time $\Delta t = 50$ generations:

$$s \approx \frac{0.05}{0.01(1 - 0.01)} \cdot \frac{1}{50}$$

$$s \approx \frac{0.05}{0.0099} \cdot 0.02$$

$$s \approx 5.0505 \cdot 0.02 \approx 0.101$$

The selection coefficient is approximately 0.10. This means the resistant bacteria have a roughly 10% fitness advantage over the sensitive bacteria in the presence of the antibiotic, allowing the resistance allele to rapidly sweep through the population.

In the absence of antibiotics, resistance alleles often carry a fitness cost (the resistant genotype grows more slowly than the sensitive genotype). This predicts that resistance frequencies should decline when antibiotic use is reduced. However, compensatory mutations can eliminate the fitness cost of resistance without eliminating resistance itself – making resistance effectively irreversible in many clinical settings.

21.4.4 Stabilizing Selection and Intermediate Optima

Stabilizing selection favors intermediate phenotypes, reducing variance without shifting the mean. It is the most common form of selection in nature.

Human birth weight: **Karn and Penrose [1951]** documented that neonatal mortality is lowest at birth weights of approximately 3.5 kg. Both very low-birth-weight ($<2\text{ kg}$) and very high-birth-weight ($>4.5\text{ kg}$) infants suffer increased mortality from complications including respiratory distress and obstructed labor, respectively. Modern medical intervention has relaxed this selection somewhat but has not eliminated it.

Clutch size in birds: David Lack proposed that the most common clutch size maximizes the number of surviving offspring. Too few eggs waste reproductive potential; too many eggs lead to inadequate provisioning and higher chick mortality. Experimental studies in great tits (*Parus major*) confirmed this: broods artificially enlarged beyond the modal clutch size fledged more chicks in the short term but produced lighter, lower-quality offspring with reduced survival – the intermediate clutch size maximizes lifetime reproductive success.

The stabilizing selection paradox: If stabilizing selection constantly removes extreme phenotypes and their underlying genetic variation, why does heritable variation persist? Several mechanisms maintain variation under stabilizing selection:

- Recurrent mutation continuously introduces new alleles
- Balancing selection at underlying loci (heterozygote advantage, frequency-dependent selection)
- Genotype-by-environment interactions: different genotypes may be “intermediate” in different environments
- Pleiotropic constraints: alleles affecting the stabilized trait may also affect other traits under different selective regimes
- Epistatic interactions among loci can maintain genetic variation even when the phenotypic distribution appears stable

21.4.5 Disruptive (Diversifying) Selection

Disruptive selection favors both phenotypic extremes at the expense of intermediate forms, potentially producing a bimodal distribution.

Black-bellied seedcracker (*Pyrenestes ostrinus*): In Cameroon, this finch exhibits a striking bimodal distribution of bill sizes. Small-billed birds efficiently crack soft sedge seeds; large-billed birds crack hard sedge seeds. Intermediate-billed birds perform poorly on both seed types and have lower fitness. Remarkably, this polymorphism is controlled by a single locus with large effect on bill width, demonstrating that major adaptive variation can have a simple genetic basis.

Disruptive selection in this system maintains the polymorphism because heterozygotes (with intermediate bills) have lower fitness than either homozygote – the opposite of heterozygote advantage.

Disruptive selection is of particular evolutionary interest because, if strong enough and accompanied by assortative mating (large-billed birds preferring to mate with other large-billed birds, and vice versa), it can drive **sympatric speciation** – the formation of new species without geographic isolation (see section 22).

21.4.6 Worked Example: Selection Coefficient and Allele Frequency Dynamics

Problem: Consider a single-locus, two-allele model with heterozygote advantage. Starting allele frequencies are $p_0 = 0.9$ for A_1 and $q_0 = 0.1$ for A_2 . Relative fitnesses are $w_{11} = 0.8$, $w_{12} = 1.0$, $w_{22} = 0.7$. (a) Compute the population mean fitness \bar{w} in the current generation. (b) Compute the allele frequency p' in the next generation. (c) Find the equilibrium frequency \hat{p} predicted under heterozygote advantage.

Solution:

1. Mean fitness \bar{w} :

$$\bar{w} = p^2w_{11} + 2pq w_{12} + q^2w_{22} = (0.81)(0.8) + (0.18)(1.0) + (0.01)(0.7) = 0.648 + 0.180 + 0.007 = 0.835.$$

2. Next-generation frequency p' :

$$p' = \frac{p^2w_{11} + pq w_{12}}{\bar{w}} = \frac{0.648 + 0.090}{0.835} = \frac{0.738}{0.835} \approx 0.884.$$

3. Equilibrium frequency \hat{p} under heterozygote advantage (setting $\Delta p = 0$):

$$\hat{p} = \frac{w_{12} - w_{22}}{2w_{12} - w_{11} - w_{22}} = \frac{1.0 - 0.7}{2.0 - 0.8 - 0.7} = \frac{0.3}{0.5} = 0.6, \quad \hat{q} = 0.4.$$

Interpretation: In the first generation, p falls from 0.9 toward the equilibrium value $\hat{p} = 0.6$ — a balanced polymorphism is maintained because both homozygotes have reduced fitness relative to the heterozygote. This dynamic mirrors the maintenance of the sickle hemoglobin allele in malaria-endemic regions: HbAS heterozygotes carry the highest fitness, HbAA homozygotes pay a malaria-susceptibility cost, and HbSS homozygotes pay a severe anemia cost. The equilibrium frequency of HbS in such populations is the empirical analog of the \hat{q} computed here.

21.4.7 Sexual Selection and Mating Success

Darwin recognized that many traits – peacock tails, elk antlers, birdsong complexity – reduce survival but enhance mating success. Sexual selection operates through two mechanisms: intrasexual selection (typically male-male competition for access to mates or to resources mates require) and intersexual selection (mate choice, typically by females among displaying males).

Intrasexual selection: competition within the same sex Intrasexual selection acts when members of one sex (most commonly males) compete directly with one another for reproductive access. Three modes of competition predominate:

- Direct contest competition (combat, ritualized fighting): Males fight to displace rivals. Red deer (*Cervus elaphus*) stags engage in roaring contests followed by antler-locked pushing matches; mass and antler size predict victory and harem retention. Bighorn sheep (*Ovis canadensis*) rams meet head-on at velocities of about 36 km/h; horn size and the bony reinforcement of the skull are direct outcomes of intrasexual selection. Northern elephant seal (*Mirounga angustirostris*) bulls grow to 3-4× the female mass — the most extreme sexual size dimorphism in mammals — because beachmaster males monopolize harems of 30–100 females through direct combat.
- Resource defense (territoriality): Males defend territories containing critical resources (food, nest sites, oviposition substrate); females mate with the holder of the best territory. Red-winged blackbirds (*Agelaius phoeniceus*) defend marsh territories whose vegetation density predicts female settlement. Cichlid males defend pebble-bottom spawning sites whose orientation to currents affects egg survival. The trait under selection is the capacity to acquire and defend the territory, not necessarily a morphological ornament.
- Scramble competition: When females are widely distributed and rapidly receptive, the male who locates and reaches receptive females fastest wins. *Drosophila* species in the wild engage in scramble competition for emerging virgin females; selection favors visual acuity, locomotor performance, and pheromone detection. In thirteen-lined ground squirrels, males that emerge earliest from hibernation locate the most receptive females. Scramble competition selects for endurance, sensory acuity, and search efficiency rather than weaponry.

A fourth mode, sperm competition, operates after copulation when females mate with multiple males within a single fertile period. Selection acts on sperm number, sperm motility, and copulatory plug deposition. Testis-to-body-mass ratio is a quantitative correlate of sperm competition intensity: chimpanzees (highly polyandrous) have testes about 3× the size of gorillas (harem-guarding) on a body-mass-corrected basis.

Intersexual selection: mate choice In intersexual selection, members of one sex (typically females) choose among displaying members of the other. The peacock’s elaborate tail is the canonical example. Three complementary hypotheses explain female preference for costly ornaments — they are not mutually exclusive, and empirical examples often combine elements of the three mechanisms.

Sensory exploitation provides a fourth, mechanistically distinct hypothesis: female preferences may arise initially from pre-existing sensory biases unrelated to mate choice (e.g., sensitivity to a frequency band useful for prey detection), and males evolve traits that exploit those biases. The túngara frog (*Engystomops pustulosus*) “chuck” call exploits a sensory bias inherited from a common ancestor: females of related species that have rarely produced “chucks” themselves still prefer males that add the syllable. Sensory exploitation grounds preference in pre-existing neural architecture rather than in genetic correlation or signal honesty.

Honest signaling (Zahavi handicap principle) Amotz Zahavi (1975) proposed that costly ornaments are honest signals of male quality precisely because they are costly. A male who can survive the metabolic, predation, and parasite-related costs of an elaborate tail must have superior underlying genetic quality (immunity, foraging ability, parasite resistance). Females that select males with the most extravagant ornaments preferentially choose mates who carry “good genes” — the genes their offspring will inherit.

The handicap principle predicts that ornaments should be condition-dependent: primarily individuals in good condition can produce the most extreme display. **Hamilton and Zuk [1982]** extended this with the parasite-mediated sexual selection hypothesis: bright male coloration in birds, bright tail color in fish, and similar ornaments depend on physiological condition that itself depends on parasite resistance. Female choice based on ornament brilliance is therefore choice for parasite-resistance alleles.

Empirical support: In the satin bowerbird (*Ptilonorhynchus violaceus*), males build elaborate bowers and decorate them with blue objects to attract females. Males with brighter plumage and more extensive bowers also have lower parasite loads — consistent with the handicap principle. In barn swallows (*Hirundo rustica*), males with longer outer tail feathers (a sexually selected trait) carry fewer feather mites.

Fisher-Lande runaway selection R.A. Fisher (1930) and Russell Lande (1981) developed the runaway selection model, which can produce arbitrarily extreme ornaments through a positive-feedback loop between female preference and male trait — without requiring that the ornament signal anything about quality.

The model proceeds in three stages:

1. Initial preference: A small genetic predisposition for some male trait variant exists in females (e.g., females prefer males with slightly longer tails because long tails happen to indicate flight performance).
2. Genetic correlation: When females with the preference allele mate with males possessing the preferred trait, their offspring inherit both genetic linkage groups — daughters receive the preference allele *and* sons receive the trait allele. The two loci become genetically correlated.
3. Runaway: Now selection on the trait drives correlated change in the preference, and vice versa. The two loci can spiral together to extreme values, even when the trait becomes maladaptive by other survival measures, because the trait is now selected purely by its effect on mating success.

Runaway is balanced eventually by natural selection against the ornament becoming dangerous (predation, energetic costs). The equilibrium can be at moderate ornament size or, depending on parameters, can produce the bizarre extremes seen in birds of paradise and peacocks.

Good genes model The good genes model is closely related to but distinguishable from the handicap principle. The handicap requires that the ornament itself be costly and condition-dependent. The good genes model primarily requires that some heritable component of male quality (immunity, growth rate, viability, foraging skill) be correlated with the trait females prefer. The female who chooses a higher-quality male produces higher-quality offspring through both autosomal good genes (offspring inherit advantageous viability alleles) and viability genes.

Empirical tests are difficult because they require demonstrating heritable variance in fitness correlated with the trait — a very high data bar.

Worked scenario: peacock tail evolution Imagine an ancestral peafowl population in which a small subset of females have a slight genetic preference for males with longer tails (“preference allele” frequency = 0.05). Long-tailed males are 5% more likely to be mated than short-tailed males, but they pay a 10% survival cost from increased predation. The genetic correlation between preference and trait builds over generations — initially weakly, but accelerating once the correlation becomes substantial. After about 100 generations of runaway, both preference frequency and tail length have escalated dramatically. The system reaches equilibrium when the survival cost (10% per unit tail length) balances the mating advantage (5% × tail length), producing tail lengths far beyond what natural selection alone would favor.

The peacock’s tail thus is simultaneously: (a) an honest signal of genetic quality (Zahavi handicap), (b) the equilibrium of a Fisherian runaway between preference and trait, and (c) a marker for “good genes” (parasite resistance) **[Hamilton and Zuk, 1982]**. The three mechanisms can operate together. Modern empirical work emphasizes that real peacock tail evolution — and most sexual ornaments — combines these forces in proportions that vary across species and contexts.

Concept Check (Synthesis): Zahavian handicap theory proposes that elaborate ornaments (peacock tail, elk antlers) are honest signals of genetic quality precisely because they are costly to produce and maintain. A male with poor parasite resistance would struggle to bear the cost of a large peacock tail without paying a survival penalty — so females who prefer larger tails are selecting indirectly for the immune-gene variants that permit them. (a) Formalize this with a two-locus toy model: an ornament allele O (cost c , viability $1 - c$) paired with a resistance allele R (benefit b , viability $1 + b$). Under what condition (relationship between b and c , allowing for the genetic correlation between O and R that female preference generates) does the female preference for O spread? (b) Fisher’s *sexy sons* (runaway) mechanism is an alternative: female preference and male ornament become genetically correlated and co-evolve as a positive-feedback loop, independent of any signal honesty. Contrast the predictions of the two models for what happens when parasites are experimentally removed from a population — which model predicts that ornament size declines, and which predicts that ornament size remains high (or continues to drift upward) for several generations after the parasite pressure is lifted?

21.4.8 Kin Selection and Inclusive Fitness

Hamilton’s rule explains altruistic behavior: an altruistic act is favored when [Hamilton, 1964a,b]:

$$rB > C$$

(322)

where r is the coefficient of relatedness between actor and recipient, B is the reproductive benefit to the recipient, and C is the reproductive cost to the actor.

Coefficients of relatedness:

- Full siblings: $r = 0.5$
- Half-siblings: $r = 0.25$
- First cousins: $r = 0.125$
- Parent–offspring: $r = 0.5$

Eusociality in insects: Eusocial societies combine cooperative brood care, overlapping generations, and a reproductive division of labor in which some individuals reproduce little or do not reproduce [Crespi and Yanega, 1995, Bourke, 2011]. In **haplodiploid** Hymenoptera (many ants, bees, and wasps), females are diploid and males are haploid. Full sisters can share $r = 0.75$ (the full paternal genome plus, on average, half of the maternal genome), so helping a mother produce sisters can satisfy Hamilton’s rule more easily than producing one’s own offspring. The honeybee genome made this a concrete genomic system for studying sociality, chemical communication, immunity, and caste biology [The Honeybee Genome Sequencing Consortium, 2006].

Haplodiploidy is a useful entry point but not a sufficient explanation. Many haplodiploid insects are solitary, while termites are diploid and nevertheless evolved eusocial colonies. Comparative evidence points to ancestral monogamy, kin structure, defensible nests, progressive brood provisioning, and ecological risks of independent nesting as interacting conditions that make helping profitable [Hughes et al., 2008, Bourke, 2011]. Termites are especially important because phylogenetic work places them within cockroaches, showing that eusociality evolved independently outside Hymenoptera [Inward et al., 2007].

21.4.9 Evolutionary Game Theory: Hawk–Dove and the ESS

Evolutionary game theory analyzes situations in which an individual’s payoff depends on the strategies adopted by others in the population. The framework was introduced by John Maynard Smith and George Price (1973) to explain ritualized animal contests. The cornerstone concept is the evolutionarily stable strategy (ESS): a strategy that, once common in a population, cannot be invaded by any rare alternative strategy.

The classic example is the Hawk–Dove game. Two individuals contest a resource of value V . A “Hawk” escalates the contest, risking injury at cost C if it loses. A “Dove” displays but retreats from escalation. The expected payoffs:

Table 291. Evolutionary Game Theory: Hawk–Dove and the ESS.

Opponent →	Hawk	Dove
Hawk plays	$\frac{V-C}{2}$	V
Dove plays	0	$\frac{V}{2}$

When two Hawks meet, each wins half the time and pays the cost half the time, giving expected payoff $(V - C)/2$. A Hawk against a Dove takes the resource (V). Two Doves share peacefully ($V/2$ each).

If $V > C$ (resource exceeds the cost of injury), pure Hawk is the ESS — escalation typically pays. If $V < C$ (more interesting biological case), neither pure strategy is stable: pure Dove can be invaded by Hawks (who exploit the peaceful population), but pure Hawk can be invaded by Doves (who avoid the cost of constant fighting). The stable outcome is a mixed ESS with frequencies determined by the cost–benefit structure:

$$p_{\text{Hawk}}^* = \frac{V}{C} \tag{323}$$

Numerical illustration of the Hawk–Dove ESS Suppose the contested resource is worth $V = 10$ (e.g., a breeding territory worth 10 offspring) and the cost of injury in a fight is $C = 40$ (a serious wound costing 40 future offspring). Because $V < C$, the mixed ESS predicts $p_{\text{Hawk}}^* = 10/40 = 0.25$ — twenty-five percent of contests are escalated to fighting. At equilibrium, the expected payoff is identical for both strategies:

- $E[\text{Hawk}] = 0.25 \cdot \frac{10-40}{2} + 0.75 \cdot 10 = -3.75 + 7.5 = 3.75$
- $E[\text{Dove}] = 0.25 \cdot 0 + 0.75 \cdot 5 = 3.75$

This frequency-dependence is the engine that maintains the polymorphism: any deviation from $p = 0.25$ creates a fitness gradient that pulls the population back. A population of 30% Hawks rewards Doves more than Hawks; a population of 20% Hawks rewards Hawks more than Doves. The ESS is negatively frequency-dependent at the strategy level — the rarer strategy typically has the higher payoff.

When everyone plays Hawk with probability V/C , no individual gains by deviating. The same equilibrium can be realized in two ways: each individual mixes Hawk and Dove with probability V/C , or the population is a polymorphism with fraction V/C committed Hawks and $1 - V/C$ committed Doves. Behavioral dimorphisms in spider mating tactics, frog calling strategies, and male-morph polymorphisms in side-blotched lizards match Hawk–Dove or related ESS predictions quantitatively.

Game theory generalizes to many other biological problems: parental investment (Trivers 1972), public-goods cooperation (Tragedy of the Commons), the evolution of virulence in pathogens, and host–parasite coevolution. The ESS concept formalizes Darwin’s insight that “the rules of the game” can themselves be evolutionary outcomes — selection acts on strategies, not just on traits.

21.4.10 The Breeder’s Equation

While population-genetic models track allele frequencies under selection, quantitative genetics describes the response of continuously varying phenotypes (height, milk yield, beak depth) to selection. The central result is the breeder’s equation:

$$R = h^2 S \tag{324}$$

where R is the response to selection (the change in mean phenotype across one generation), S is the selection differential (the difference between the mean of selected parents and the mean of the entire parental population), and h^2 is the narrow-sense heritability — the proportion of phenotypic variance attributable to additive genetic variance:

$$h^2 = \frac{V_A}{V_P} = \frac{V_A}{V_A + V_D + V_E} \tag{325}$$

with V_A = additive genetic variance, V_D = dominance variance, V_E = environmental variance.

Worked example: Galapagos finches Peter and Rosemary Grant measured beak depth in *Geospiza fortis* during the 1977 Galapagos drought. The selection differential (mean beak depth of survivors minus mean of original population) was $S = +0.6$ mm. Heritability of beak depth, estimated from parent–offspring regression, was $h^2 = 0.74$. The predicted response is:

$$R = h^2 \times S = 0.74 \times 0.6 \text{ mm} = 0.44 \text{ mm}$$

The observed response in the next generation (offspring of the 1977 survivors) was +0.43 mm — a strikingly precise prediction confirming both the heritability estimate and the breeder’s equation. The drought selected for deeper beaks (better at cracking large, hard seeds that remained when small seeds were exhausted), and this trait responded to selection within a single generation.

Worked example: artificial selection on plant height Suppose a maize breeder wishes to increase mean plant height. The base population has mean height $\bar{z}_0 = 200$ cm with phenotypic standard deviation $\sigma_P = 15$ cm. The breeder selects the tallest 10% of plants as parents of the next generation, whose mean height is $\bar{z}_{\text{selected}} = 205$ cm. Heritability has been estimated by parent–offspring regression at $h^2 = 0.8$ (a high but realistic value for plant height under controlled conditions).

1. Selection differential: $S = \bar{z}_{\text{selected}} - \bar{z}_0 = 205 - 200 = 5$ cm.
2. Predicted response: $R = h^2 \cdot S = 0.8 \times 5 = 4$ cm. The next generation’s mean is predicted at $\bar{z}_1 = 200 + 4 = 204$ cm.
3. After multiple generations: If h^2 stays roughly constant and the selection differential is reapplied each generation, the population gains about 4 cm per generation in expectation. After 10 generations under unrelaxed selection, mean height could rise to about 240 cm — although in practice h^2 erodes as additive variance is depleted, and physiological constraints (lodging, mechanical failure under wind load) eventually limit the response.

This calculation illustrates two practical points. First, h^2 matters more than the apparent strength of selection: doubling the selection differential to $S = 10$ would produce $R = 8$ cm, but halving h^2 to 0.4 (more realistic for height in a wild population) produces $R = 2$ cm even at $S = 5$. Second, response decelerates over time as additive variance is consumed by directional selection — long-term selection experiments (the Illinois corn protein/oil lines, now over 100 generations) eventually plateau as genetic variance is exhausted unless mutation refills the supply.

Worked example: directional selection on *Drosophila* bristle number A classic *Drosophila melanogaster* selection experiment measures abdominal bristle number, a quantitative trait under polygenic control. Suppose the base population has mean bristle number $\bar{z}_0 = 40$, and parent–offspring regression has established narrow-sense heritability $h^2 = 0.4$. The investigator selects breeding parents whose mean bristle number is $\bar{z}_{\text{selected}} = 50$, giving selection differential $S = 50 - 40 = 10$ bristles.

1. Predicted response per generation: $R = h^2 \cdot S = 0.4 \times 10 = 4$ bristles. After one generation the offspring mean is predicted at $\bar{z}_1 = 40 + 4 = 44$ bristles.
2. Response after 5 generations of unrelaxed selection (assuming constant h^2 and constant S): $\bar{z}_5 \approx \bar{z}_0 + 5R = 40 + 5 \times 4 = 60$ bristles — a 50 % gain over the base mean.
3. Plateau dynamics: Real *Drosophila* bristle-number experiments (Mather & Harrison 1949; Clayton, Morris & Robertson 1957) confirm linear gains for about 15–25 generations followed by a plateau as additive variance is depleted. When selection is relaxed, populations often partially regress toward the base mean — evidence that some response was achieved through linkage disequilibrium of mildly deleterious alleles dragged along with the favored variants. New mutational input refills V_A on a timescale of $4N_e$ generations (the neutral coalescent time), so very long-term experiments can show a second slower phase of response sustained by mutation–selection balance.

This worked example illustrates why agricultural breeders monitor V_A erosion: the breeder’s equation is exact in expectation but predicts the rate of variance depletion as well as the rate of mean gain. Once V_A approaches zero, response approaches zero regardless of how strongly the breeder selects.

21.4.11 Worked Example: Response to Selection Over Multiple Generations

Problem: A wild population of medium ground finch has mean beak depth $\mu_0 = 100$ mm and narrow-sense heritability $h^2 = 0.45$. Each generation, parents are selected whose mean beak depth is $\mu_{\text{parents}} = 110$ mm, giving selection differential $S = 10$ mm. (a) Project the population mean for three generations under the constant- h^2 form of the breeder’s equation. (b) Now relax constancy: assume additive genetic variance V_A erodes by 5% per generation, so h^2 in generation t is $h_t^2 = 0.45 \times (0.95)^t$. Recompute the response R_3 and the projected mean at generation 3.

Solution:

1. Constant- h^2 projection:
 - Response per generation: $R = h^2 S = 0.45 \times 10 = 4.5$ mm.
 - $\mu_1 = 100 + 4.5 = 104.5$ mm.
 - $\mu_2 = 104.5 + 4.5 = 109.0$ mm.
 - $\mu_3 = 109.0 + 4.5 = 113.5$ mm.
2. Variance-eroding projection:
 - Heritability at generation 3: $h_3^2 = 0.45 \times (0.95)^3 \approx 0.45 \times 0.857 \approx 0.386$.
 - Response in generation 3: $R_3 = 0.386 \times 10 = 3.86$ mm.
 - Projected mean (summing the eroded responses): $\mu_3 \approx 100 + 4.50 + 4.28 + 4.06 \approx 112.8$ mm.

Interpretation: The constant- h^2 projection over-predicts the gain because it ignores variance depletion. Real long-term artificial-selection responses decelerate for this reason: directional selection consumes additive variance faster than mutation replenishes it. The pattern connects to Galton’s regression toward the mean, to the plateaus observed in long-term *Drosophila* bristle and Illinois corn protein–oil experiments, and to the agricultural rule of thumb that gains slow once a single trait has been pushed for many generations on a closed gene pool.

Why the breeder’s equation works The equation reflects a simple algebraic truth: primarily the additive genetic component of phenotypic variation is reliably transmitted from parents to offspring. Dominance variance (V_D) reflects allele-pairing combinations that are scrambled by meiosis. Epistatic interactions (V_I) similarly do not transmit faithfully. Environmental variance (V_E) is non-heritable. Thus the realized response equals the additive heritability times the selection that was actually applied. The breeder’s equation is the workhorse of agricultural selection (dairy cattle, corn, tomatoes), animal breeding (racehorses, dogs), and the analysis of natural selection in wild populations.

Limitations and the multivariate breeder’s equation The simple form assumes a single trait under direct selection, with stable heritability across generations and a stable environment. In practice, traits are correlated through pleiotropy and linkage; selection on one trait drags correlated traits along. The multivariate breeder’s equation generalizes:

$$\Delta \bar{z} = GP^{-1}S$$

where $\Delta \bar{z}$ is the vector of phenotypic responses, G is the genetic covariance matrix, P is the phenotypic covariance matrix, and S is the vector of selection differentials. This Lande–Arnold framework (1983) underlies modern multivariate quantitative genetics and explains why trait evolution can be constrained by genetic correlations even when selection on each trait individually is strong.

21.4.12 Evolvability, Modularity, and Developmental Constraints

The capacity of a population to respond to selection is itself a heritable, evolving property called evolvability. Two organizational features make some lineages dramatically more evolvable than others.

Modularity A modular genotype–phenotype map partitions traits into semi-independent units, each controlled by largely separate gene networks. Selection on one module — say, fin shape in cichlids, or beak depth in finches — leaves other modules undisturbed. Modular architectures evolve faster because beneficial modifications in one module do not derail traits in other modules. The butterfly wing eyespot system is a paradigm of modularity: each eyespot is patterned by a conserved gene-regulatory module (Distal-less, Engrailed, Spalt) that can be redeployed independently across wing positions, allowing rapid diversification of eyespot patterns across species without disturbing wing structure or other traits.

In contrast, highly integrated (non-modular) systems show pleiotropic constraint: every mutation affects many traits simultaneously, most beneficial mutations also produce deleterious side-effects, and adaptive evolution is slow. The vertebrate skull is intermediate — highly integrated for biomechanical reasons (the bones must articulate properly), but with enough modularity that snakes, birds, and toothed whales evolved radically divergent skull shapes from the same ancestral plan.

Developmental constraints, canalization, and cryptic variation Canalization is the developmental buffering that produces the same phenotype across a range of genetic and environmental perturbations. Conrad Waddington (1942) introduced the metaphor of the epigenetic landscape, in which developmental trajectories follow valleys of low resistance toward stable phenotypic outcomes. Canalization implies that genetic variation is hidden beneath robust development — many segregating alleles do not affect phenotype because development buffers their effects.

When buffering is overwhelmed — by extreme environmental stress, by a chaperone disruption (HSP90 inhibition reveals abundant cryptic variation in *Drosophila*), or by a major mutation — cryptic genetic variation is exposed. The newly visible phenotypic variation can then respond to selection. Genetic assimilation is the process by which a phenotype originally produced primarily under stress becomes fixed and is produced under most conditions, having recruited cryptic variation along the way.

Cryptic variation as evolutionary fuel: Recent studies in zebrafish, threespine stickleback, and *Drosophila* show that populations with deeper reservoirs of cryptic variation respond to novel selection pressures faster than populations with shallow reservoirs. Modular development plus cryptic variation thus form a paired pair of features that increase evolvability — modularity by allowing independent change, cryptic variation by storing adaptive material.

Inclusive fitness: Hamilton’s insight extended the concept of fitness beyond direct reproduction. An individual’s inclusive fitness includes both its direct fitness (own offspring) and the fitness gained indirectly by helping relatives reproduce — weighted by the coefficient of relatedness [Hamilton, 1964a,b]. A sterile worker bee with zero direct fitness can still have high inclusive fitness if she helps her queen mother produce many full sisters; the same logic also explains why social evolution is sensitive to queen mating number, colony founding ecology, and whether helpers are assisting full siblings, half-siblings, or more distant kin.

21.4.13 Frequency-Dependent Selection

Negative frequency-dependent selection: Rare phenotypes have a fitness advantage. As a phenotype becomes common, its fitness decreases. This maintains polymorphism.

Side-blotched lizards (*Uta stansburiana*): Males have three throat color morphs engaged in rock-paper-scissors dynamics. Orange-throated males are aggressive and defeat blue-throated males. Blue-throated males form pair bonds that resist sneaking by yellow-throated males. Yellow-throated males (female mimics) successfully sneak copulations from orange-throated males. No morph can dominate permanently; frequencies cycle over approximately 6-year periods — a real-world realization of a multi-strategy ESS.

Positive frequency-dependent selection: The common phenotype has an advantage (e.g., warning coloration in Mullerian mimicry — predators learn to avoid the most common pattern).

Concept Check 3: A population of side-blotched lizards has roughly equal frequencies of orange, blue, and yellow male morphs. Each year, biologists notice that the frequency of orange males rises sharply for two years, then yellow males rise as orange decline, then blue males rise as yellow decline — and the cycle repeats. Why does negative frequency-dependent selection produce cycles rather than a stable equilibrium with the three morphs at constant frequencies? (Hint: think about what happens when one morph’s fitness depends on the *current* frequencies of the other two, not a one-step-ahead average.)

Concept Check on quantitative genetics: A dairy farmer practices artificial selection on milk yield, with selection differential $S = 1,000$ kg/lactation and observed response $R = 200$ kg in the next generation. (a) What is the implied narrow-sense heritability? (b) The same selection regime applied for 20 generations produces about 3,000 kg total response (not 4,000 kg as naive multiplication would predict). Give two reasons the response decelerates.

Concept Check (Evaluate — Genetic Load): A deleterious recessive allele has selection coefficient $s = 0.01$ against homozygotes and mutation rate $\mu = 10^{-5}$ per generation. At mutation–selection balance, the equilibrium frequency is $\hat{q} = \sqrt{\mu/s} = \sqrt{10^{-3}} \approx 0.032$. (a) Explain why purifying selection alone cannot eliminate every copy of this allele from the population, even given infinite time. (b) If medical intervention reduces s to 0.001 (a tenfold relaxation), predict the new equilibrium frequency and estimate how many generations are needed to approach it. (c) Articulate the genetic-load concept this illustrates and evaluate the population-level cost of carrying a non-zero frequency of mildly deleterious alleles.

Concept Check (Synthesis — Industrial Melanism Revisited): The classical peppered-moth story (rise of *carbonaria* during the Industrial Revolution; recovery of *typica* after the Clean Air Act) is sometimes told as pure directional selection on a single locus. Re-synthesize the case as follows: (a) why did the *carbonaria* allele not reach 100 % even at peak pollution, given the apparent strong selection — what role might heterozygote dynamics, frequency-dependent predation, or microhabitat heterogeneity play? (b) The selection coefficient reversed direction within about 50 years (industrialisation → Clean Air Act); design an evolutionary rescue experiment in the laboratory that uses *Biston betularia* or a comparable lepidopteran to test whether the trait can re-evolve when the environment shifts again. Specify the population sizes, selection intensities, and number of generations needed to detect a response above noise.

21.4.14 Balancing Selection and Maintained Polymorphism

Several mechanisms maintain genetic polymorphism within populations, collectively termed balancing selection:

- Heterozygote advantage (overdominance): The heterozygote has higher fitness than either homozygote. The classic example is sickle cell anemia: *HbA/HbS* heterozygotes have resistance to *Plasmodium falciparum* malaria without the severe anemia of *HbS/HbS* homozygotes. Equilibrium frequency of *HbS* in malaria-endemic regions is approximately $q = h_1/(h_1 + h_2)$ where h_1 and h_2 are the selection coefficients against the two homozygotes.
- Negative frequency-dependent selection: As described above, rare phenotypes have higher fitness, preventing fixation.
- Spatially varying selection: Different alleles are favored in different environments within the species’ range. Migration connects subpopulations, maintaining polymorphism across the metapopulation.
- Temporally varying selection: The fitness ranking of genotypes fluctuates across seasons or years, preventing any single allele from reaching fixation.

Real-World Connection: Antibiotic Resistance as Evolution in Real Time

Methicillin-resistant *Staphylococcus aureus* (MRSA) illustrates evolution by natural selection operating on a clinically devastating timescale. Penicillin was introduced in 1943; penicillin-resistant *S. aureus* appeared by 1947. Methicillin was introduced in 1961; MRSA was reported by 1962. The ESKAPE pathogens (*Enterococcus faecium*, *Staphylococcus aureus*, *Klebsiella pneumoniae*, *Acinetobacter baumannii*, *Pseudomonas aeruginosa*, *Enterobacter* species) represent the most urgent antibiotic resistance threats. Each has evolved resistance through the standard Darwinian mechanism: heritable variation (resistance mutations or horizontally acquired genes), differential reproduction (resistant bacteria survive antibiotic exposure), and environmental pressure (antibiotic use in hospitals and agriculture). The evolution of resistance is predictable, repeatable, and observable in real time – providing one of the clearest demonstrations that natural selection is not merely a historical phenomenon but an ongoing process with immediate consequences for human health.

21.5 Adaptation and Its Limits

21.5.1 Adaptation and Exaptation

An adaptation is a heritable feature shaped by natural selection that increases fitness in the organism’s current environment. Adaptations are not perfect solutions but rather the best available modifications of pre-existing structures.

An exaptation is a feature that was originally shaped by natural selection for one function but has been co-opted for a different function:

- Feathers evolved initially for **thermoregulation** in small theropod dinosaurs. Flight capability was a later co-option of an existing structure.
- Swim bladders in bony fish are homologous with lungs in terrestrial vertebrates. The ancestral structure was likely a vascularized outpocketing of the pharynx used for gas exchange in oxygen-poor water, later modified for buoyancy control in derived fish lineages and for terrestrial respiration in the lineage leading to tetrapods.

21.5.2 Phylogenetic Constraints on Adaptive Pathways

Evolution cannot start from scratch. Natural selection can primarily modify existing structures, constrained by the organism’s bauplan (body plan):

- Panda’s “thumb”: The giant panda’s thumb is not a true digit but an enlarged radial sesamoid bone. The true thumb is committed to the bear-like paw. Natural selection co-opted a wrist bone to create a functional but imperfect food-handling structure – a testament to evolutionary tinkering rather than design.
- Recurrent laryngeal nerve: In mammals, this branch of the vagus nerve loops from the brainstem down around the aortic arch and back up to the larynx. In giraffes, this detour adds approximately 4.5 meters of unnecessary nerve length. The path makes developmental sense given the ancestral fish anatomy (where the nerve innervated the sixth gill arch) but is a suboptimal arrangement in a long-necked mammal.

21.5.3 Developmental Constraints on Phenotypic Variation

Body plans established during embryonic development are deeply conserved and difficult to alter fundamentally. The basic organization of body segments, limb positions, and organ systems is established by deeply conserved developmental gene networks (Hox genes, signaling pathways such as Hedgehog, Wnt, and BMP). Tetrapods are ancestrally four-limbed – not because four is optimal for every ecological situation but because the tetrapod body plan was established approximately 375 Mya and is embedded so deeply in the developmental genetic toolkit that altering limb number would require simultaneously reorganizing multiple interconnected developmental pathways. No tetrapod has evolved six limbs, despite the potential utility of additional appendages. Snakes have lost their limbs entirely (through modification of Hox gene expression domains), demonstrating that reduction is possible even when addition is not.

Similarly, the vertebrate eye is built “backwards” – with photoreceptors behind the retinal **neurons** and blood vessels, creating a blind spot where the optic nerve exits. Cephalopod eyes evolved independently with photoreceptors facing forward, lacking a blind spot. The vertebrate arrangement persists because the ancestral developmental program cannot easily be reorganized without disrupting the entire eye structure.

21.5.4 Evolutionary Trade-Offs and Constraint Surfaces

Organisms cannot maximize most fitness components simultaneously:

- Immune function versus reproduction: Mounting an immune response is energetically costly. In many species, individuals investing heavily in reproduction show suppressed immune function and increased susceptibility to parasites.
- Speed versus endurance: Cheetahs achieve 110 km/h but sustain peak sprints for roughly 200–300 meters. Wolves run at 55 km/h but can maintain pursuit for kilometers.
- Crypsis versus mate attraction: Brightly colored males attract both mates and predators. The optimal coloration balances sexual selection for conspicuousness against natural selection for camouflage. In guppies (*Poecilia reticulata*), males in low-predation streams are more colorful than those in high-predation streams – demonstrating the trade-off between sexual selection (favoring bright colors) and natural selection (favoring drab colors that avoid predator detection).
- Fecundity versus offspring quality: Organisms face a fundamental trade-off between producing many small offspring (r-strategy) or few large offspring (K-strategy). Each egg or seed requires maternal investment; allocating more to each offspring reduces the total number that can be produced.
- Current reproduction versus future survival: Investing heavily in current reproduction often reduces an organism’s probability of surviving to reproduce again. Semelparous organisms (salmon, annual plants) invest everything in a single reproductive event and then die. Iteroparous organisms (most mammals, perennial plants) reproduce multiple times but invest less per reproductive event.

21.5.5 Coevolution and Reciprocal Selection

Coevolution occurs when two or more species exert reciprocal selective pressures on each other, driving evolutionary change in both lineages.

Predator-prey arms race: Rough-skinned newts (*Taricha granulosa*) produce tetrodotoxin (TTX), one of the most potent neurotoxins known. Common garter snakes (*Thamnophis sirtalis*) in sympatric populations have evolved resistance through amino acid substitutions in their sodium channel genes. The level of newt toxicity and snake resistance are geographically correlated – populations with more toxic newts have more resistant snakes, and vice versa. This represents a classic coevolutionary arms race.

Plant-herbivore coevolution: Brassicaceae (mustard family) plants produce glucosinolates as herbivore deterrents. Specialist herbivores (Pieridae butterflies) have evolved glucosinolate-specific detoxification **enzymes**. This escalation of defense and counter-defense has been linked to diversification in both plant and insect lineages.

Red Queen hypothesis (Van Valen, 1973): Species must continually evolve simply to maintain their current fitness relative to coevolving partners, particularly parasites. Like the Red Queen in *Through the Looking-Glass*, organisms must keep running just to stay in place. This hypothesis explains the maintenance of sexual reproduction: the genetic variation generated by **recombination** provides a moving target for parasites adapted to common host genotypes.

Real-World Connection: Coevolution in Agriculture

The coevolutionary arms race between crops and pathogens has enormous agricultural significance. When a new resistance gene is deployed in a crop variety, pathogen populations rapidly evolve **virulence** alleles that overcome it – often within 3–5 years. This “boom-and-bust cycle” has driven the development of gene pyramiding (stacking multiple resistance genes), multiline varieties (mixtures of genetically different cultivars), and integrated pest management. The Irish Potato Famine (1845–1849) resulted partly from the genetic uniformity of Irish potato crops – a single clone susceptible to *Phytophthora infestans*. Modern agricultural genetics applies evolutionary principles to stay ahead of rapidly evolving pathogens.

Concept Check 4: The panda’s “thumb” is often cited as evidence against intelligent design and for evolution. Explain why an imperfect structure supports the evolutionary explanation better than a designed explanation.

21.6 Macroevolution and Evolutionary Rates

21.6.1 Microevolution and Macroevolution

Microevolution refers to changes in allele frequencies within populations over relatively short timescales – the processes described across sections **20** and **21**. These include mutation, natural selection, **genetic drift**, and gene flow operating within species. Macroevolution encompasses large-scale patterns observed over geological time: the origin of major body plans, mass extinctions and subsequent radiations, long-term trends in biodiversity, and the emergence of evolutionary novelties such as the vertebrate eye or the flower.

A central question in evolutionary biology is whether macroevolution is simply the accumulation of microevolutionary changes over vast timescales, or whether additional processes operate at higher levels of biological organization. Most evolutionary biologists accept that the same fundamental mechanisms (mutation, selection, drift, gene flow) underlie both scales, but that emergent properties (species selection, developmental constraints, contingency) shape macroevolutionary patterns.

21.6.2 Punctuated Equilibrium and Tempo of Change

Punctuated equilibrium [**Gould and Eldredge, 1972**] proposes that most species experience long periods of morphological stasis (millions of years) interrupted by brief episodes of rapid evolutionary change associated with speciation events. This pattern contrasts with phyletic gradualism, which predicts slow, continuous morphological change.

Evidence supporting punctuated equilibrium: - The fossil record frequently shows species appearing abruptly (in geological terms), persisting with little change, and disappearing suddenly. - Stasis is the dominant pattern for many well-documented fossil lineages (bryozoans, trilobites, mollusks). - Rapid change during speciation is consistent with peripatric speciation in small, isolated populations where fossil preservation is unlikely.

Stasis as the dominant pattern in the fossil record The most surprising aspect of **Gould and Eldredge [1972]**’s argument was not that change can be rapid but that stasis is so prevalent. Quantitative analyses of well-sampled fossil sequences confirm: most species, once established, exhibit little net morphological change for millions of years. Cheetham’s analysis of Caribbean bryozoan (*Metrarabdotos*) species across the past 15 million years measured 46 morphological traits in 1,200 specimens; lineages persisted for 2–10 million years with mean morphological drift below the standard deviation of within-population variation. Williamson’s snail (*Bulinus*) sequences from Lake Turkana show prolonged stasis broken by rapid bursts of change correlated with regional climate shifts. The stasis itself requires explanation — even with shifting environments and ongoing mutation, species somehow remain morphologically constrained. Proposed mechanisms

include strong stabilizing selection, gene-flow homogenization across the species range, developmental canalization (section 21), and frequency-dependent selection at species boundaries.

Correlated evolutionary change A complementary observation is that morphological change, when it occurs, is correlated across traits. The Galapagos finch beak responds to drought as an integrated unit (depth, width, and length most change together), reflecting shared developmental and genetic architecture. In the Cheetham bryozoan data, the burst of change at speciation events involves multiple coordinated character shifts — rarely a single trait changing alone. This pattern has two interpretations: (i) genetic correlations among traits cause selection on one trait to produce correlated responses in others, as predicted by the multivariate breeder’s equation; (ii) speciation events reorganize developmental modules in coordinated ways. Both processes likely contribute, and disentangling them is an active research program in evolutionary developmental biology.

The debate between punctuated equilibrium and gradualism is largely resolved: both patterns occur, and the dominant mode varies among lineages and environments. The significance of punctuated equilibrium lies not in negating Darwinian mechanisms but in recognizing that the tempo of evolution is uneven – periods of rapid change (often associated with speciation events in peripheral populations) alternate with long intervals of morphological conservatism (stabilizing selection maintaining adaptation to a stable environment).

21.6.3 Evolutionary Novelties and Key Innovations

Key innovations are traits that open new adaptive zones, enabling diversification. Examples include:

- The evolution of jaws in gnathostome vertebrates (about 450 Mya), enabling active predation and driving the diversification of jawed vertebrates
- The evolution of the amniotic egg (about 340 Mya), freeing tetrapods from dependence on water for reproduction
- The evolution of flowers in **angiosperms** (about 130 Mya), enabling coevolution with pollinators and explosive diversification
- The evolution of flight in insects (about 350 Mya), birds (about 150 Mya), and bats (about 55 Mya), each opening vast ecological opportunities
- The evolution of eusocial colonies in ants, some bees and wasps, and termites, converting related individuals into coordinated units that forage, defend nests, rear brood, and modify environments at scales difficult for solitary insects to achieve [**Crespi and Yanega, 1995, Bourke, 2011**]

Key innovations often trigger adaptive radiations (see section 22) by allowing lineages to exploit previously inaccessible resources.

21.6.4 Mass Extinctions and Selective Regime Shifts

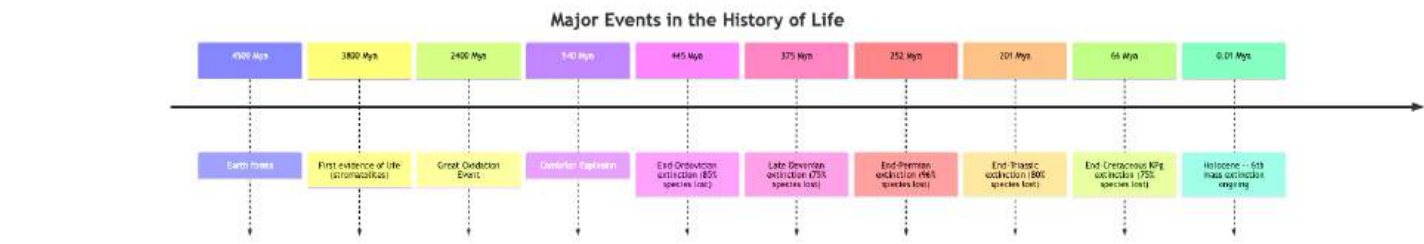


Figure 131. Geological timeline of life’s major milestones and the five mass extinctions, with the proportion of species lost at each event.

Five major mass extinctions punctuate the history of life:

1. End-Ordovician (about 445 Mya): Glaciation of Gondwana caused sea-level drop; approximately 85% of marine species lost. Two pulses of extinction separated by approximately 1 million years.
2. Late Devonian (about 375 Mya): Prolonged extinction over approximately 20 million years; 75% of species lost. Causes debated – possible anoxia, climate change, or bolide impact.
3. End-Permian (about 252 Mya): The “Great Dying” – approximately 96% of marine species and 70% of terrestrial vertebrate species lost. Linked to Siberian Traps volcanism (massive flood basalts releasing CO₂, SO₂, and methane, causing ocean acidification, anoxia, and extreme warming).
4. End-Triassic (about 201 Mya): Approximately 80% of species lost. Associated with Central Atlantic Magmatic Province volcanism. Cleared ecological space for dinosaur diversification.
5. End-Cretaceous (KPg) (about 66 Mya): Approximately 75% of species lost, including most non-avian dinosaurs. Caused by the Chicxulub asteroid impact (Yucatan Peninsula, Mexico) producing a 180 km diameter crater. Impact winter, acid rain, and global fires devastated ecosystems. Deccan Traps volcanism may have contributed to pre-impact stress.

Current Holocene/Anthropocene extinction: Background extinction rate is approximately 0.1–1 species per million species-years. Current rates are estimated at 100–1,000 times higher due to habitat destruction, overexploitation, pollution, invasive species, and climate change. The International Union for Conservation of Nature (IUCN) estimates that approximately 28% of assessed species are threatened with extinction.

21.6.5 The Modern Extended Evolutionary Synthesis

The Modern Synthesis (1930s–1950s) unified Darwinian natural selection with Mendelian genetics and population genetics. The Extended Evolutionary Synthesis (EES) proposes additional mechanisms that may play significant evolutionary roles:

- **Developmental plasticity:** A single genotype can produce multiple phenotypes in response to environmental conditions. Plasticity may facilitate (or hinder) evolutionary change by exposing hidden genetic variation to selection.
- **Epigenetic inheritance:** Heritable changes in gene expression not encoded in DNA sequence (DNA methylation, **histone** modifications) can persist across generations in some organisms.
- **Niche construction:** Organisms modify their own environments, altering the selective pressures they and other species experience. Beaver dams, earthworm soil modification, and human agriculture are examples.
- **Cultural evolution:** In species with social learning, culturally transmitted behaviors can evolve and influence genetic evolution. Tool use in chimpanzees, song dialects in birds, and the entirety of human cultural evolution exemplify this process.

The status of the EES is actively debated. Laland *et al.* (2015, *Nature*) argued that the EES has distinctive empirical content because plasticity, inclusive inheritance, and niche construction cause biased variation, motivate organisms as agents, and make evolution more predictable than random mutation and selection alone. Wray *et al.* (2014, *Evolution*) and others contested that the original Modern Synthesis already has sufficient conceptual flexibility to accommodate these phenomena within its mathematical framework. Pigliucci & Müller (2010, *Cambridge University Press*) provided the most comprehensive EES framework.

Table 292. The Modern Extended Evolutionary Synthesis: Dimension and Classic Modern Synthesis (MS).

Dimension	Classic Modern Synthesis (MS)	Extended Evolutionary Synthesis (EES)
Mechanism focus	Selection on random genetic mutations	Plus: developmental bias, niche construction, epigenetics , learning
Inheritance	Genetic (DNA sequence)	Plus: epigenetic, cultural, ecological
Phenotypic variation	Genotype → phenotype (near 1-to-1 mapping)	Many genotypes → many phenotypes (reaction norms, polyphenism)
Evolutionary tempo	Gradual (Fisher’s infinitesimal model)	Plus: rapid phenotypic evolution via plasticity → genetic assimilation
Organism role	Passive target of selection	Active evolvability agent (niche construction, behavior-driven evolution)
Example	Antibiotic resistance via mutation	Sticklebacks rapidly evolving freshwater morphs via plastic bone density

Niche construction in detail Niche construction — organisms modifying their environment in ways that change selective pressures on themselves and other species — is one of the most empirically grounded EES claims. Rather than viewing the environment as a fixed selective filter, niche-construction theory (Odling-Smee, Laland, Feldman 2003) treats the organism–environment relationship as bidirectional: organisms inherit not only genes but also a modified environment from their ancestors (an “ecological inheritance”). Examples:

- Beaver dams create wetland environments that persist for centuries and modify selection on the beavers themselves (favoring traits useful in lodge-based aquatic life), on aquatic plants and fish (which evolve in response to slowed water and altered hydrology), and on terrestrial herbivores in surrounding meadows.
- Earthworms modify soil pH, structure, drainage, and nutrient cycling. Plants in earthworm-modified soils experience radically different selective regimes than they would in unmodified soils. Earthworm presence has measurably changed plant community composition and microbial diversity over millennia.
- Termites and ants excavate galleries, concentrate organic matter, move mineral soil upward, and alter infiltration and nutrient availability. In dry systems, these nests and mounds can create fertile patches that change plant recruitment and competitive context [Evans et al., 2011]. Termites add a microbial dimension because gut symbionts unlock lignocellulose and return carbon and nitrogen to ecosystem cycling [Brune, 2014].
- Cyanobacteria transformed Earth’s atmosphere from anoxic to oxygenic over the Great Oxidation Event (about 2.4 Ga), simultaneously enabling the evolution of aerobic respiration and constraining (or extinguishing) the anaerobic life forms that had previously dominated. The largest niche-construction event in Earth history.
- Human agriculture is the most extreme recent example: humans modified plant and animal genomes through artificial selection while simultaneously modifying their own selective environment (creating new disease pressures from livestock, dietary shifts, sedentary lifestyles).

Phenotypic plasticity and developmental induction Phenotypic plasticity is the production of different phenotypes by the same genotype in response to different environments. The same caterpillar genotype can produce a green form in summer and a brown form in autumn (*Nemoria arizonaria*). The same *Daphnia* genotype produces a helmeted, defended form in the presence of fish predator cues and an unhelmeted form in their absence.

Plasticity matters for evolution because plastic responses can later be assimilated by genetic change (genetic assimilation, Waddington 1953). When a plastic response is consistently advantageous, selection will favor genetic backgrounds that produce that response constitutively — even when the original environmental cue is absent. This pathway, sometimes called “plasticity-led evolution,” allows populations to respond to novel environments faster than mutation-led evolution alone would predict. Documented cases include rapid evolution of freshwater stickleback morphs from anadromous ancestors, and the freshwater colonization of marine sticklebacks where ancestral plasticity in body armor preceded eventual genetic fixation of low-armor freshwater forms.

Epigenetic inheritance across generations Most epigenetic marks are reset during gametogenesis and embryogenesis, but documented examples of transgenerational epigenetic inheritance (TEI) exist:

- *A. thaliana* FWA epi-allele: an unmethylated state at the *FWA* locus produces flowering-time variation that is heritable across many generations without DNA sequence change.
- Dutch Hunger Winter cohort: Individuals exposed prenatally to severe famine (1944–1945) showed altered DNA methylation patterns at *IGF2* and other loci, and increased risk of metabolic disease in adulthood. Limited evidence suggests these patterns may persist into the next generation.
- *C. elegans* small-RNA inheritance: Specific small RNAs can be transmitted across generations in *C. elegans*, where they have been documented to silence target genes for over 80 generations under some conditions.
- Mammalian paramutation: At a few loci (*Kit* in mice, *agouti viable yellow*), parental phenotypes influence offspring phenotypes through epigenetic mechanisms despite identical DNA sequences.
- Rodent transgenerational stress and odor-conditioning: In the Dias & Ressler (2014) experiments, male mice conditioned to fear acetophenone odor produced F1 and F2 offspring (rarely themselves exposed) with elevated startle to that specific odor and detectable changes in the olfactory bulb glomerular map. The effect attenuates by F3, consistent with 2–3 generations of detectable transgenerational transmission in rodents — a pattern recurring across stress, dietary-restriction, and toxin-exposure paradigms in the rodent transgenerational literature.

The evolutionary significance of TEI in mammals (especially humans) remains debated — the pervasive epigenetic reprogramming in early embryos limits its scope, and most documented mammalian effects fade within 2–3 generations. Nonetheless, the existence of even rare TEI events forces a more nuanced view of inheritance than the strictly genetic view of the Modern Synthesis.

Real-World Connection: The Sixth Mass Extinction

Current extinction rates vastly exceed background levels. The Living Planet Report 2024 documents a 73% average decline in monitored vertebrate population indices since 1970; this is a trend in monitored populations, not a census of wild animals [World Wide Fund for Nature, 2024]. Unlike previous mass extinctions driven by geological or astronomical events, the current crisis is driven largely by human land use, exploitation, pollution, invasive species, and climate change. Conservation biology applies evolutionary principles to preserve biodiversity: maintaining genetic diversity within populations, preserving evolutionary potential, and protecting phylogenetically distinct lineages.

Concept Check 5: Punctuated equilibrium predicts long periods of stasis interrupted by rapid change. How would you distinguish this pattern from gradual change that simply was not preserved in the fossil record?

21.7 Evolution Observed in Real Time

One of the most powerful confirmations of evolutionary theory is the direct observation of evolution occurring within human timescales.

21.7.1 Laboratory Evolution as Experimental Selection

Richard Lenski’s Long-Term Evolution Experiment (LTEE): Since 1988, 12 populations of *Escherichia coli* have been propagated daily in minimal glucose medium at Michigan State University. By 2024, these populations have undergone over 80,000 generations. Key results include:

- Fitness increased rapidly in the first 2,000 generations, then more slowly – consistent with Fisher’s geometric model of adaptation.
- Around generation 31,500, one population evolved the ability to metabolize citrate under aerobic conditions – a trait previously considered a defining characteristic distinguishing *E. coli* from other enteric bacteria. This required multiple mutations occurring in a specific order, demonstrating the role of historical contingency in evolution.
- Mutations in mutator genes (DNA repair) increased the mutation rate in some lineages, accelerating adaptation but also accumulating slightly deleterious mutations.

21.7.2 Natural Experiments in Contemporary Evolution

Darwin’s finch beak evolution: Peter and Rosemary Grant’s 40-year field study on Daphne Major island documented directional selection on beak depth in medium ground finches (*Geospiza fortis*) during the 1977 drought (beak depth increased 4%) and the 1983 El Nino (beak depth decreased as small seeds became abundant again). This provided real-time quantitative evidence that selection can produce measurable morphological change within a single generation.

Anolis lizard evolution: Jonathan Losos and colleagues demonstrated rapid evolutionary divergence in Caribbean anole lizards. When populations of *Anolis sagrei* were experimentally introduced to small islands, they evolved shorter hindlimbs within approximately 10 generations – an adaptation to the narrower perching surfaces available on small islands versus the mainland.

Cane toad invasion of Australia: Since their introduction in 1935, cane toads (*Rhinella marina*) have expanded across northern Australia at accelerating rates – the invasion front advanced approximately 10 km per year in the 1940s but now advances over 55 km per year. Toads at the invasion front have evolved longer legs and greater endurance compared to toads in established populations – they are literally evolving to be better invaders. This is spatial sorting: individuals at the front encounter and mate with other front-runners, concentrating dispersal-enhancing alleles at the leading edge.

Meanwhile, native predators in newly colonized areas have evolved rapidly in response. Red-bellied black snakes (*Pseudechis porphyriacus*) and green tree snakes (*Dendrelaphis punctulatus*) have evolved smaller heads relative to body size (reducing their ability to consume the large, toxic toads – a behavioral and morphological adaptation that reduces mortality). Some snake populations have also evolved increased physiological resistance to toad toxins (bufadienolides). This represents rapid, reciprocal coevolutionary response to an invasive species.

Concept Check 6: The LTEE citrate-utilization mutation required multiple genetic changes occurring in a specific sequence. How does this observation relate to the concept of historical contingency in evolution? Would you expect the same mutation to arise across the 12 replicate populations?

21.7.3 Punctuated Equilibrium versus Phyletic Gradualism: Empirical Signatures

The choice between punctuated equilibrium and phyletic gradualism is not strictly either/or — both modes are observed in different lineages, and the empirical signatures of each differ:

Table 293. Punctuated Equilibrium versus Phyletic Gradualism: Empirical Signatures: Feature and Phyletic gradualism.

Feature	Phyletic gradualism	Punctuated equilibrium
Tempo	Slow, continuous change	Long stasis interrupted by rapid bursts
Locus of change	Throughout lineage history	Concentrated at speciation events
Population structure	Large, panmictic populations	Small peripheral isolates (peripatric)
Predicted fossil pattern	Smooth morphological intermediates	Abrupt transitions between successive forms
Stasis explanation	Apparent stasis = preservation gaps	Genuine evolutionary stasis from stabilizing selection
Speciation linkage	Speciation not associated with morphological change	Speciation drives morphological change

Gould and Eldredge [1972] introduced punctuated equilibrium based on observations of marine invertebrate fossil sequences (bryozoans, trilobites) where species persisted essentially unchanged for millions of years, then were replaced by morphologically distinct relatives without obvious gradual transitional sequences. Critics initially countered that the gaps were artifacts of incomplete preservation. Subsequent quantitative work has shown that stasis is real in many groups: dense fossil sequences from sites with high preservation (Caribbean coral reefs, Plio-Pleistocene foraminifera) confirm that species often remain morphologically constant for geologic intervals. Phyletic gradualism is also observed — particularly in foraminifera and some mammalian lineages — but punctuated equilibrium with extended stasis is the dominant pattern across well-sampled lineages.

The biological mechanism for stasis remains debated: stabilizing selection on a well-adapted phenotype, canalization of development that buffers genetic variation, genetic constraints that limit morphological evolution, or simply persistence in widespread species that average across local selective pressures. The mechanism of punctuation is more clearly understood — peripatric speciation in small isolated populations allows rapid morphological change through founder effects and altered selective regimes, after which the new species expands and stabilizes.

21.7.4 Species Selection: Macroevolution as a Higher-Level Process

If species themselves vary in heritable properties that affect their own propagation and persistence, then species selection can occur — analogous to natural selection, but operating on species rather than on individuals. Species selection requires that:

1. Variation among species in traits affecting either speciation rate or extinction rate.

2. Heritability: daughter species inherit those traits from parent species.
3. Differential reproduction/persistence: species with favored traits diversify more rapidly or persist longer.

Examples that may reflect species selection (though contested in the literature):

- Dispersal ability: Marine invertebrates with planktotrophic larvae (broadly dispersing) speciate slowly but persist long; species with direct development (poorly dispersing) speciate rapidly but go extinct often. This produces a macroevolutionary trade-off in lineage diversification.
- Asexual versus sexual reproduction: Asexual lineages tend to be evolutionarily ephemeral despite outcompeting sexual relatives in the short term. Species-rich and ancient clades are overwhelmingly sexual — suggesting species selection has favored sexuality despite its twofold cost.
- Body size: In many lineages, body size shows a long-term increase (“Cope’s rule”) that cannot easily be explained by individual-level selection alone. Species selection on extinction risk may contribute.

Whether species selection is a genuinely separate force from cumulative individual-level selection remains controversial. The strongest case is for traits like dispersal ability that affect speciation/extinction rates intrinsically rather than individual fitness — the property is irreducibly species-level. Under this view, microevolutionary mechanisms still produce most evolutionary change, but emergent macroevolutionary patterns reflect higher-order selection on species-level properties.

These examples of real-time evolution are important not only as scientific confirmations but also as pedagogical tools: they demonstrate that evolution is not merely a historical narrative about the distant past but a present, ongoing, and experimentally testable process.

Clinical Connection — Antibiotic resistance as natural selection in hospital time. *Staphylococcus aureus* isolates from UK hospitals have been genome-sequenced longitudinally since 1960. Each new β -lactam antibiotic introduced (penicillin → methicillin → vancomycin → linezolid → daptomycin) triggered the spread of resistance alleles within 2–15 years, driven by **plasmid**-borne *mecA*, *vanA*, or chromosomal mutations. This is directional selection with an imposed fitness landscape whose peaks move with every new drug. Combination therapy (two antibiotics targeting different molecular machinery) slows resistance because a bacterium now requires two simultaneous mutations — the product of two low probabilities. The same Fisherian selection mathematics that describes pepper-moth evolution quantitatively predicts multi-drug regimen design in infectious disease and cancer.

Clinical Connection — Darwinian oncology. A tumor is a population of cells with heritable genetic variation and differential reproductive success under treatment pressure — a Darwinian system. Classic cytotoxic chemotherapy selects rapidly-dividing cells; the surviving slow-cyclers (the *persister* population) become the seed for relapse. Modern “adaptive therapy” exploits frequency-dependent selection: by intermittently *withholding* drug once the tumor shrinks, a sensitive subpopulation is kept alive to competitively suppress resistant clones. Trials in metastatic prostate cancer (abiraterone cycling) show median progression-free survival gains of 10–18 months versus continuous dosing, directly derived from evolutionary game theory.

21.8 Computational Bridge

Mean fitness \bar{W} as a function of p is tabulated by `fitness_landscape_1d`:

```
from biology.evolution import fitness_landscape_1d

p_vals = [0.0, 0.25, 0.5, 0.75, 1.0]
w_bar = fitness_landscape_1d(p_vals, fitness_AA=1.0, fitness_Aa=0.95, fitness_aa=0.7)
print([round(w, 4) for w in w_bar])
```

Clinical / systems note: Antimicrobial stewardship explicitly manipulates s and N_e (host population colonization load) to keep resistance alleles from fixing — the same selection algebra taught for moths and finches.

21.8.1 Evolution in the Synthetic Age: CRISPR Gain-of-Function Research and Evolutionary Ethics

The same experimental tools that make evolution a tractable laboratory science — CRISPR-Cas9 genome engineering, directed evolution via phage-assisted continuous evolution (PACE), and *in silico* fitness-landscape modeling — have forced evolutionary biologists into ethics that Darwin rarely anticipated. The 2011–2012 H5N1 gain-of-function experiments (Fouchier lab, Kawaoka lab) demonstrated that primarily a handful of spike-protein mutations were needed to make avian influenza airborne-transmissible in ferrets — effectively *running a natural experiment in the laboratory* on a pathogen that kills about 60 % of infected

humans. The dual-use research of concern (DURC) framework that emerged from the ensuing moratorium (2012–2014, 2017–present) now governs any research whose foreseeable output is “enhanced potential pandemic pathogens.”

Beyond viruses, the ethical landscape expands rapidly: gene drives (Crisanti lab, *Nat. Biotechnol.* 2018) use CRISPR-Cas9 to bias inheritance toward a designed allele at rates approaching 99 % — demonstrated in caged *Anopheles gambiae* populations eradicated in 7–11 generations. Gene drives could plausibly eliminate malaria, but also represent an irrevocable alteration of an evolutionary trajectory involving an entire species. CRISPR germline editing in humans (He Jiankui, 2018) targeting CCR5 to confer HIV resistance produced two living children (Lulu and Nana) with off-target effects in the same gene of unknown phenotypic consequence, and generated a unanimous international moratorium on heritable genome editing. Resurrection biology (Colossal Biosciences woolly-mammoth project, 2024) uses Asian-elephant fibroblast editing to re-create approximations of extinct phenotypes, provoking debate about whether a mammoth is “brought back” or “created anew.”

The common thread: the tools of evolutionary biology are now potent enough that the theory is no longer merely descriptive. Students entering this field must internalise that evolutionary theory is actively being used as a design framework (for directed evolution of enzymes, for gene-drive deployment, for pandemic preparedness) — evolutionary literacy now carries an ethical dimension inseparable from the scientific one. The Asilomar Conference (1975), the DURC frameworks (2012 onward), and the heritable genome-editing summits (2015, 2018, 2023) represent the biology community confronting responsibilities that basic evolutionary training must prepare us for.

21.9 Current Evidence and Frontier Biology: Natural Selection and Adaptation

For Natural Selection and Adaptation, frontier biology belongs inside the evidence logic of the chapter. Evolutionary claims are strongest when they combine mechanism, comparative evidence, population process, and explicit uncertainty. The core reading question is this: selection claims need fitness components, ecological context, genetic variation, and alternative hypotheses.

- What to verify: identify the observation, model, assay, or dataset that would make the claim stronger or weaker.
- What to qualify: state the scale, organism, cell type, environmental condition, or population where the claim is expected to hold.
- What to compare: test at least one alternative explanation, baseline, or null model before treating the pattern as causal.
- What to cite: distinguish primary evidence, review synthesis, public dataset, and institutional guidance; for recent or numeric claims, prefer the source closest to the measurement and state what has changed since it was published.

For selection claims, separate fitness differences from storytelling by naming the trait, environment, heritable variation, and plausible nonadaptive alternative.

Source practice: For adaptation claims, prefer evidence that compares selection with drift, constraint, plasticity, and shared ancestry before assigning function.

21.10 Summary

- Pre-Darwinian thinkers (Lamarck, Cuvier, Lyell) established concepts of species change, extinction, and deep geological time that set the stage for Darwin and Wallace.
- Five independent lines of evidence support evolution: fossil record (transitional forms), comparative anatomy (homology, vestigiality), embryology (shared developmental stages), biogeography (geographic distributions reflecting history), and molecular biology (sequence similarity, shared pseudogenes, ERVs).
- Natural selection requires heritable variation, differential reproduction, and environmental pressure. It operates through multiple modes: directional, stabilizing, disruptive, sexual, kin, and frequency-dependent selection.
- Fitness (W) is relative reproductive success. Hamilton’s rule ($rB > C$) extends selection theory to explain altruism among relatives; eusocial insects show why relatedness, monogamy, ecology, and phylogeny must be evaluated together rather than reduced to haplodiploidy alone.
- Adaptation is constrained by phylogenetic history, developmental programs, and trade-offs. Exaptations demonstrate co-option of existing structures for new functions.
- Coevolution produces arms races (newt-snake toxin resistance) and maintains the Red Queen dynamic.
- Macroevolutionary patterns include punctuated equilibrium, mass extinctions (5 major events plus the ongoing 6th), and the Extended Evolutionary Synthesis incorporating plasticity, epigenetics, niche construction, and cultural evolution.
- Connections: See section 20 for formal p recursions, section 22 for drift vs. selection, and Unit X — Ecology: Introduction for spatial sorting and range expansion.

21.11 Key Terms

Table 294. Evolution in the Synthetic Age: CRISPR Gain-of-Function Research and Evolutionary Ethics: Term and Definition.

Term	Definition
Natural selection	Differential survival and reproduction of individuals based on heritable variation in fitness-related traits
Fitness (<i>w</i>)	Relative reproductive success of a genotype compared to the population mean
Directional selection	Selection favoring one phenotypic extreme, shifting the population mean
Stabilizing selection	Selection favoring intermediate phenotypes, reducing phenotypic variance
Disruptive selection	Selection favoring both phenotypic extremes at the expense of intermediates
Sexual selection	Selection arising from variation in mating success; includes intersexual (mate choice) and intrasexual (competition) components
Kin selection	Natural selection favoring altruistic behaviors toward genetic relatives, governed by Hamilton’s rule ($rB > C$)
Eusociality	Social system with cooperative brood care, overlapping generations, and reproductive division of labor
Haplodiploidy	Sex-determination system in which haploid males develop from unfertilised eggs and diploid females from fertilized eggs
Frequency-dependent selection	Fitness of a phenotype depends on its frequency in the population; negative form maintains polymorphism
Adaptation	A heritable trait shaped by natural selection that increases fitness in the current environment
Exaptation	A trait originally shaped by selection for one function that has been co-opted for a different function
Coevolution	Reciprocal evolutionary change between interacting species driven by mutual selective pressures
Red Queen hypothesis	Organisms must continually evolve to maintain fitness relative to coevolving species
Punctuated equilibrium	Macroevolutionary pattern of long stasis interrupted by rapid change during speciation
Mass extinction	Geologically rapid loss of a large percentage of species; five major events documented
Convergent evolution	Independent evolution of similar features in unrelated lineages subject to similar selective pressures
Vestigial structure	Reduced remnant of an organ that was functional in an ancestor
Homologous structures	Features in different species sharing common developmental and evolutionary origin
Analogous structures	Features in different species similar in function but with different developmental and evolutionary origins
Modern Synthesis	Unification of Darwinian selection with Mendelian genetics, population genetics, paleontology, and systematics (1930s–1950s)
Extended Evolutionary Synthesis	Expansion of the Modern Synthesis to include developmental plasticity, epigenetic inheritance, niche construction, and cultural evolution
Inclusive fitness	Total fitness including direct reproduction plus indirect fitness gained by helping relatives reproduce
Phyletic gradualism	Model proposing slow, continuous morphological change throughout a lineage’s history
Uniformitarianism	Principle that the same geological processes operating today have typically operated at similar rates
Catastrophism	Doctrine that Earth’s features and fossil succession result from sudden, violent events
Selection coefficient (<i>s</i>)	A measure of the fitness difference between genotypes; $s = 0$ means no selection, $s = 1$ means the disfavored genotype is lethal
Overdominance	Heterozygote advantage; the heterozygous genotype has higher fitness than either homozygote

21.12 Review Questions

1. Darwin and Wallace independently proposed natural selection. Describe the three conditions necessary for natural selection to operate, and explain why Mendelian genetics was essential for completing the theory.
2. Explain how *Tiktaalik roseae* serves as a transitional fossil. What specific features bridge the gap between fish and tetrapods? Why was its discovery predicted by paleontologists based on the age and type of rock formations?
3. Distinguish between homologous and analogous structures. For each, provide an example not discussed in this chapter, and explain how you would determine which category a given structure belongs to.
4. A population of moths is subject to directional selection with selection coefficient $s = 0.05$ favoring a dominant allele currently at frequency $p = 0.01$. Using $\Delta p \approx sp(1 - p)$, estimate the change in allele frequency after one generation. How many generations would be required for the allele to reach $p = 0.50$ (qualitative answer)?
5. Explain why the recurrent laryngeal nerve in giraffes is considered evidence for evolution rather than design. What developmental and phylogenetic

constraints explain its circuitous path?

6. Using Hamilton’s rule, determine whether a sterile worker bee (C = lifetime reproduction about 50 offspring) should help her queen mother produce additional sisters (B = 100 additional sisters) given $r = 0.75$ for full sisters in haplodiploid species. Show your calculation.
7. Compare and contrast punctuated equilibrium with phyletic gradualism. What types of fossil evidence would distinguish between these two models? Can both patterns coexist in the same clade?
8. The End-Permian extinction eliminated approximately 96% of marine species. Describe two proposed causes and explain how mass extinctions can paradoxically promote long-term diversification by opening ecological opportunities for surviving lineages.
9. Define coevolution and provide an example of a coevolutionary arms race. How does the Red Queen hypothesis explain the maintenance of sexual reproduction in the face of its twofold cost?
10. The Extended Evolutionary Synthesis proposes mechanisms beyond those in the Modern Synthesis. Choose one (developmental plasticity, epigenetic inheritance, niche construction, or cultural evolution) and explain how it might influence evolutionary trajectories in ways not captured by standard population genetics models.
11. At which p is \bar{W} maximized for the fitness set in the bridge code? Relate to equilibrium under one-locus selection.
12. Give one example where kin selection predicts a behavior that violates individual fitness maximization yet spreads in haplodiploid hymenoptera. ##
- Further Reading and Source Notes: Natural Selection and Adaptation

• Darwin & Wallace (1858). On the Tendency of Species to form Varieties. *Journal of the Proceedings of the Linnean Society: Zoology*, 3.

• Williams (1966). *Adaptation and Natural Selection*. Princeton University Press.

• Hamilton (1964). The genetical evolution of social behavior I and II. *Journal of Theoretical Biology*.

• Crespi & Yanega (1995). The definition of eusociality. *Behavioral Ecology*.

• Bourke (2011). *Principles of Social Evolution*. Oxford University Press.

• Karn & Penrose (1951). Birth weight and gestation time in relation to maternal age, parity and infant survival. *Annals of Eugenics*, 16.

• Hamilton & Zuk (1982). Heritable true fitness and bright birds: A role for parasites?. *Science*, 218.

• Gould & Eldredge (1972). Punctuated equilibria: an alternative to phyletic gradualism. *Models in Paleobiology*.

• Dobzhansky (1973). Nothing in biology makes sense except in the light of evolution. *The American Biology Teacher*, 35.

21.13 Companion Source Module: Natural Selection and Adaptation

Natural Selection and Adaptation should leave a reproducible trail from a biological claim to the code, figure, diagram, or paper-based activity that can test it. Use the surfaces below to inspect the chapter’s assumptions, rerun the relevant model, or compare the manuscript explanation with companion labs and figures.

Table 295. Companion source surfaces for Natural Selection and Adaptation.

Surface	Use it for
<code>src/biology/evolution/evolution.py</code> (<code>selection_one_generation</code> , <code>simulate_selection</code> , <code>fitness_landscape_1d</code>)	Reproduce selection trajectories and landscape reasoning.
<code>src/visualization/plots.py</code> (<code>plot_selection_simulation</code>)	Compare fitness assumptions with plotted allele-frequency change.
<code>src/mermaid/biology_diagrams.py</code> (<code>natural_selection_diagram</code>)	Keep variation, inheritance, differential survival, and adaptation distinct.

Reproducibility check: define fitness component, environment, heritable variation, and alternative explanation before calling a trait adaptive. Cross-reference: use section 20 and section 22.

22 Genetic Drift, Gene Flow, and Speciation

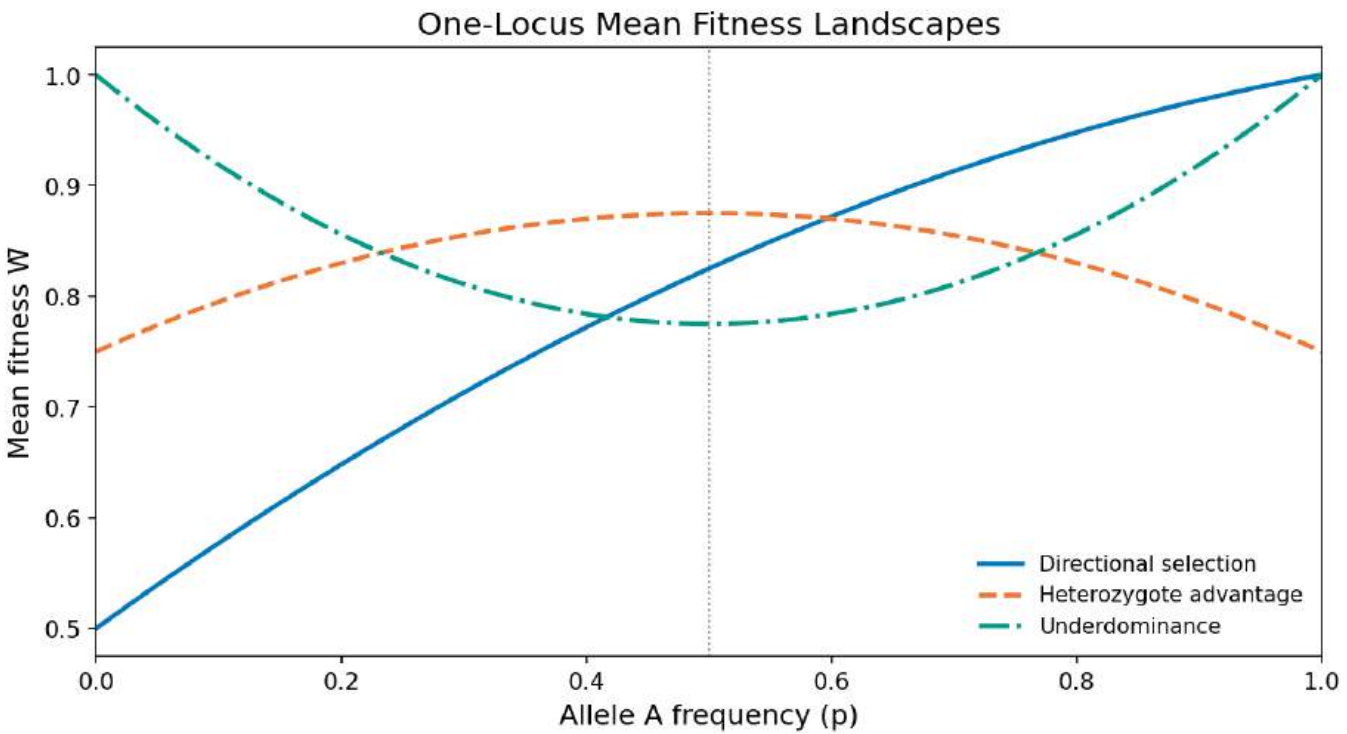


Figure 132. Mean population fitness as a function of allele frequency p under three selection regimes: directional selection (fitness rises toward one allele), heterozygote advantage (interior peak at intermediate p), and underdominance (fitness trough that can split the population).

Level 3/3 · 60 min read · 75 min lecture · Prerequisites: section 21

22.1 Learning Objectives

By the end of this chapter, you should be able to:

1. Define **genetic drift** and explain why its effects are strongest in small populations, using the Wright-Fisher model mathematically.
2. Distinguish bottleneck and **founder effects** and describe their genetic consequences with real-world examples.
3. Calculate effective population size (N_e) and explain why it is typically much smaller than census population size.
4. Describe **gene** flow, its effects on population differentiation, and how F_{ST} quantifies population structure.
5. Compare and contrast species concepts (biological, morphological, phylogenetic, ecological, cohesion) and evaluate their strengths and limitations.
6. Explain allopatric, peripatric, parapatric, and **sympatric speciation** mechanisms, including the role of polyploidy and adaptive radiation.

7. Differentiate prezygotic from postzygotic reproductive barriers and explain Haldane’s rule and reinforcement as outcomes of selection on isolation.
8. Calculate the fixation probability and mean fixation time of a neutral mutation under Kimura’s neutral theory and explain why the neutral substitution rate is independent of population size.
9. Evaluate evidence for archaic introgression in modern humans, including Neanderthal and Denisovan ancestry, and explain how adaptive introgression can transfer beneficial alleles between lineages.

22.1.1 Study Blueprint

- Big idea: Chance, population structure, and barriers to gene flow can generate divergence even without adaptive change.
- Core concepts: drift, effective population size, gene flow, speciation.
- Framework alignment: Vision & Change: Evolution, Systems; AP Biology: Evolution, Systems Interactions; NGSS-style topics: Natural Selection and Evolution, Interdependent Relationships in Ecosystems.
- Model or quantitative lens: Fixation probability, effective population size, and migration-selection balance.
- Data skill: Distinguish stochastic from directional change in allele-frequency data.
- Practice cadence: Visual Representations, Statistical Tests and Data Analysis, Argumentation.
- Common misconception to repair: Random does not mean patternless; stochastic processes have predictable distributions.
- Primary lab: Lab — Genetic Drift, Gene Flow, and Speciation.
- Question bank: Questions — Genetic Drift, Gene Flow, and Speciation.
- Transfer task: Apply drift reasoning to endangered populations, founder effects, and island radiations.
- Bridge to computation: `biology.evolution.evolution.simulate_drift`.

Opening Vignette — Speciation on the Underground

Beneath London’s streets, in the tunnels of the Underground railway system, a mosquito silently diverged from its surface relatives. *Culex pipiens pipiens* lives above ground, hibernates through winter, and feeds on birds. Its descendant, *Culex pipiens molestus*, rarely hibernates, bites mammals, and can breed without a blood meal — perfectly adapted to the warm, mammal-rich tunnels of the Tube. Genetic analysis published in 1999 confirmed that the two are reproductively isolated, despite sharing the same city. The London Underground mosquito has become a textbook example of parapatric speciation without geographic separation — showing that **reproductive isolation** can evolve from a founder event and novel selection pressures even within a few kilometers and a few hundred years. Tube passengers helped document evolution in progress every time they got bitten.

22.2 Genetic Drift as Random Allele-Frequency Change

22.2.1 Genetic Drift as Sampling Error in Finite Populations

Genetic drift is the random change in **allele** frequencies across generations that results from the sampling error inherent in finite populations [Wright, 1931]. figure 132 contrasts mean-fitness landscapes that shape whether selection fixes, balances, or disruptively sorts alleles — the selective backdrop against which drift operates. Unlike **natural selection**, drift is undirected – it is equally likely to increase or decrease the frequency of any allele, regardless of its effect on fitness. Drift is a consequence of probability, not adaptation.

The power of drift is inversely proportional to population size. In large populations, the law of large numbers ensures that actual allele frequencies closely match expected frequencies. In small populations, random sampling can cause dramatic, unpredictable fluctuations – and ultimately, the fixation or loss of alleles.

22.2.2 Wright-Fisher Sampling Mathematics

Under the Wright-Fisher model, a population of N diploid individuals contains $2N$ gene copies at each locus. Each generation, the new population is formed by randomly sampling $2N$ alleles (with replacement) from the current generation’s gene pool [Wright, 1931].

If the current frequency of allele A is p , the number of A alleles in the next generation follows a binomial distribution:

$$P(k \mid p) = \binom{2N}{k} p^k (1 - p)^{2N - k}$$

(326)

Key properties:

- Expected frequency: $E[p'] = p$ (drift has no directional bias)

- Variance per generation: $\text{Var}[\Delta p] = \frac{p(1-p)}{2N_e}$

The variance expression reveals that doubling population size halves the variance in allele frequency change per generation.

Expected time to fixation: For a neutral allele currently at frequency p , the probability of eventual fixation is simply p (its current frequency). The expected time to fixation, conditional on fixation occurring, is:

$$\bar{t}_{\text{fix}} \approx -4N_e \cdot \frac{(1-p)}{p} \cdot \ln(1-p) \tag{327}$$

For a newly arisen neutral **mutation** ($p = 1/2N$), the expected time to fixation is approximately $4N_e$ generations.

Heterozygosity decline: Expected heterozygosity declines geometrically:

$$H_t = H_0 \left(1 - \frac{1}{2N_e}\right)^t \tag{328}$$

The half-life of heterozygosity is $t_{1/2} = N_e \ln 2 \approx 0.693N_e$ generations.

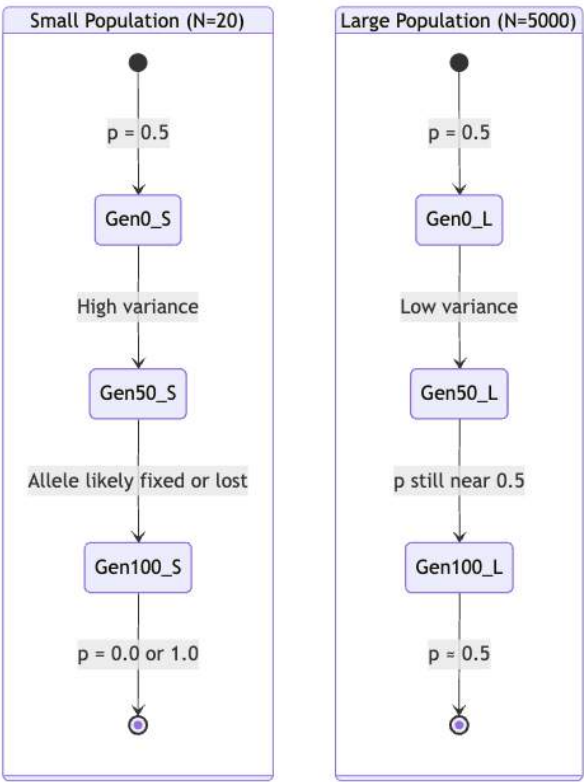


Figure 133. Genetic drift is stronger in small populations: allele frequency can move from $p = 0.5$ through high variance toward fixation or loss, while large populations tend to remain closer to the starting frequency.

22.2.3 Effective Population Size

Mathematical Background: Effective population size calculations use basic probability. For a review of variance and probability relevant to genetic drift, see [Appendix C — Mathematical Review for Biology](#).

The effective population size (N_e) is the size of an ideal Wright-Fisher population that would experience the same magnitude of genetic drift as the actual population. In nearly every real population, N_e is substantially smaller than the census size N because of:

Unequal sex ratio: If the number of breeding females (N_f) differs from the number of breeding males (N_m):

$$\frac{1}{N_e} = \frac{1}{4N_f} + \frac{1}{4N_m} \tag{329}$$

22.2.4 Worked Example: Effective Population Size

Problem: In a breeding colony of northern elephant seals, extreme male-male competition limits mating opportunities to primarily the most **dominant** males. Suppose a specific breeding group contains $N_f = 40$ sexually mature females, but primarily $N_m = 1$ dominant “beachmaster” male successfully mates with most of them. 1. What is the census size (N) of the breeding adults? 2. What is the effective population size (N_e)?

Solution:

1. Calculate the census size:

$$N = N_f + N_m = 40 + 1 = 41 \text{ adults}$$

2. Calculate the effective population size: Using the rearranged formula $N_e = \frac{4N_mN_f}{N_m+N_f}$:

$$N_e = \frac{4(1)(40)}{1 + 40}$$

$$N_e = \frac{160}{41} \approx 3.9$$

Even though there are 41 breeding animals, the genetic diversity transmitted to the next generation is equivalent to an ideal Wright-Fisher population of fewer than 4 individuals. This extreme reproductive skew severely limits the effective population size and subjects the colony to powerful genetic drift.

Variance in reproductive success: If the variance in offspring number (V_k) exceeds the mean ($\bar{k} = 2$ for a stable population):

$$N_e = \frac{4N - 2}{V_k + 2} \tag{330}$$

Species with high reproductive skew (most individuals leave zero offspring while a few leave many) have dramatically reduced N_e .

Fluctuating population size: N_e is the harmonic mean of population sizes across generations:

$$\frac{1}{N_e} = \frac{1}{t} \sum_{i=1}^t \frac{1}{N_i} \tag{331}$$

The harmonic mean is dominated by the smallest values. A single generation bottleneck of $N = 10$ followed by 99 generations of $N = 10,000$ yields $N_e \approx 909$ – not the arithmetic mean of about 9,900.

Human effective population size: Despite a current census size of about 8 billion, human $N_e \approx 10,000$ –15,000 (estimated from genomic diversity). This reflects severe ancestral bottlenecks, including the Out-of-Africa event approximately 70,000 years ago.

22.2.5 The Neutral Theory and Nearly Neutral Theory

Motoo Kimura’s **neutral theory** of molecular evolution (1968) proposed that the majority of substitutions observed at the molecular level are selectively neutral – neither advantageous nor deleterious [Kimura, 1968]. Under neutrality, the rate of substitution equals the mutation rate ($k = \mu$), independent of population size. This seemingly paradoxical result arises because, while drift fixes neutral alleles more slowly in large populations ($\bar{t}_{fix} = 4N_e$), more neutral mutations arise per generation in large populations ($2N_e\mu$). These effects cancel exactly.

Tomoko Ohta extended this to the nearly neutral theory (1973), which recognizes that most mutations are slightly deleterious [Ohta, 1973]. The fate of a slightly deleterious mutation depends on population size: if $|s| < 1/(2N_e)$, selection is too weak to overcome drift, and the mutation behaves effectively as neutral. In small populations, more mutations fall into this “nearly neutral” category, leading to faster accumulation of slightly deleterious substitutions. This predicts that species with small N_e (e.g., large-bodied vertebrates) should accumulate more slightly deleterious mutations than species with large N_e (e.g., bacteria) – a prediction confirmed by comparative genomics.

22.2.6 Bottleneck Effect and Loss of Variation

A population bottleneck occurs when a population undergoes a dramatic, temporary reduction in size. The genetic consequences are severe and often irreversible:

- Loss of rare alleles (alleles at low frequency are most likely to be lost by chance)

- Reduction in heterozygosity
- Random fixation of alleles unrelated to fitness
- Increased inbreeding and expression of deleterious recessives

Cheetah (*Acinonyx jubatus*): Cheetahs experienced at least two severe bottlenecks – one approximately 100,000 years ago and another during the Late Pleistocene (about 10,000–12,000 years ago). The genetic consequences are dramatic:

- **Nucleotide** diversity $\pi \approx 0.0001$ – comparable to inbred laboratory mice
- MHC near-monomorphism: skin grafts between unrelated cheetahs are not rejected, indicating almost no immune system genetic variation
- High frequency of sperm abnormalities (about 70% morphologically abnormal)
- Extreme susceptibility to feline coronavirus and other pathogens
- Conservation implication: even wild cheetah populations suffer inbreeding depression

Northern elephant seal (*Mirounga angustirostris*): Hunted to approximately 20 individuals by the 1890s, the population has since recovered to over 200,000. However, genetic diversity at allozyme loci is essentially zero – most individuals are genetically nearly identical at many loci. The population is a genetic time capsule of a tiny founding group.

Real-World Connection: Conservation Genetics – The Cheetah Crisis

The cheetah illustrates why genetic diversity matters for species survival. With minimal MHC variation, a single pathogen could potentially devastate the entire species – every individual lacks the immune diversity that protects genetically variable populations. Conservation geneticists use molecular markers to assess genetic health of endangered populations, guide captive breeding programs to maximize N_e , and identify genetically distinct populations that should be managed separately. The Florida panther recovery program successfully increased genetic diversity by introducing Texas pumas – a controversial but effective genetic rescue. Similar approaches are being considered for cheetahs, using the more genetically diverse East African populations to supplement Southern African populations.

22.2.7 Founder Effect and Colonization History

The founder effect occurs when a small number of individuals establish a new population, carrying primarily a non-representative sample of the source population’s genetic variation. Unlike bottlenecks, founder effects involve colonization of new territory, and the resulting population may remain small for many generations.

Table 296. Founder Effect and Colonization History: Case and Founding event.

Case	Founding event	Genetic consequence
Ellis-van Creveld syndrome in Amish	One couple (Samuel King and wife) emigrated from Europe to Lancaster County, Pennsylvania, about 1744	Frequency of EVS allele: 1 in 8 (heterozygous carriers) vs. 1 in 60,000 in general population
Finnish disease heritage	Multiple founding events about 4,000 years ago; population remained small and isolated	Over 30 genetic diseases enriched in Finns (e.g., congenital nephrotic syndrome, aspartylglucosaminuria)
Tristan da Cunha	15 original settlers on remote South Atlantic island (1816)	High frequency of asthma and retinitis pigmentosa traced to specific founders
Pingelap atoll achromatopsia	Typhoon in about 1775 reduced population to about 20 survivors; chief carried achromatopsia allele	about 10% of population has complete color blindness (vs. 1 in 30,000 globally)

Documented founder cases in detail Old Order Amish, Lancaster County (Pennsylvania). The Lancaster County Amish trace their ancestry to about 200 founding families (about 700 individuals) who emigrated from the German Palatinate and Switzerland between 1720 and 1770; the population has subsequently grown to about 45,000 with extensive endogamy. The genetic consequences are dramatic. Ellis–van Creveld syndrome (EvC) — an autosomal-recessive chondrodysplasia (short-limbed dwarfism, polydactyly, dental anomalies, cardiac septal defects) — has a Lancaster Amish prevalence of approximately 1 in 200 live births, compared with about 1 in 60,000–70,000 in the general European-descent population. Coalescent analysis traces every Amish EvC allele to a single founding couple — Samuel King and his wife — who emigrated in about 1744. This is a textbook case of how a single founder chromosome, with its specific *EVC* mutation, rose to high frequency through genetic drift in a small endogamous population. Other recessive diseases enriched among the Lancaster Amish include glutaric aciduria type 1, maple syrup urine disease, and a specific *KCNQ1* long QT-syndrome mutation.

Pingelap atoll, Federated States of Micronesia. Pingelap is a small (1.8 km²) coral atoll in the Caroline Islands. In approximately 1775, Typhoon Lengkieki struck the island, killing most residents and reducing the surviving population to roughly 20 individuals — a severe single-generation bottleneck. One survivor, the paramount chief Nahnmwarki Mwanenihsed, was a heterozygous carrier of an autosomal recessive *CNGB3* mutation causing complete achromatopsia (total color blindness, photophobia, severe visual impairment, with cone photoreceptors entirely non-functional from birth). Genealogical and molecular analyses, popularised in Oliver Sacks’s *The Island of the Colorblind* (1996), trace nearly every modern Pingelap achromatopsia case to this single founder chromosome. The condition, which afflicts roughly 1 in 30,000–50,000 people globally, occurs in approximately 5–10 % of the modern Pingelap population (with carrier frequency around 30 %) — a >1,000-fold elevation produced by a single chance founder allele surviving the typhoon.

French Canadians of Quebec. Quebec was colonized between 1608 and 1759 by approximately 8,500 French settlers — a small founding population that subsequently expanded to about 6 million descendants while remaining geographically and culturally isolated from broader European-descent populations through mid-twentieth century. This combination of a small founder population, large subsequent expansion, and limited gene flow produced one of the world’s best-studied founder populations. Specific recessive disorders enriched among French Canadians include:

- Tay-Sachs disease: A different *HEXA* mutation than the Ashkenazi founder allele — the French Canadian variant (a 7.6-kb deletion) reaches a carrier frequency of about 1/14 in some Quebec subpopulations, comparable to the Ashkenazi rate.
- Tyrosinemia type I: Caused by a *FAH* (fumarylacetoacetate hydrolase) splice-site mutation, with a carrier frequency of about 1/14 in the Saguenay-Lac-Saint-Jean region (vs. about 1/100,000 worldwide). The single Quebec founder was traced to a Norman settler from the 1600s.
- Autosomal recessive spastic ataxia of Charlevoix-Saguenay (ARSACS): A neurodegenerative disorder reaching about 1/1,500 in the Charlevoix region, caused by a specific *SACS* mutation absent elsewhere.
- Hereditary fructose intolerance, congenital lactic acidosis, oculopharyngeal muscular dystrophy: Most show elevated frequencies in specific French Canadian subpopulations traceable to identifiable founder events.

These three cases illustrate that the founder effect is not selection but probability: a recessive allele survives the bottleneck because the founder happens to carry it, and subsequent endogamous mating compounds homozygosity over generations. Modern genetic medicine in such populations leverages founder-effect concentration: a single targeted assay at one chromosomal site can screen for the population-specific high-prevalence allele, which would be cost-prohibitive in genetically heterogeneous outbred populations.

Concept Check 1: A population of 100 individuals experiences a bottleneck to 5 individuals for one generation, then immediately recovers to 100. Using the harmonic mean formula, calculate N_e over these two generations. How does this compare to the arithmetic mean?

22.2.8 Worked Example: Effective Population Size with Unequal Sex Ratio

Problem: A small mammal population contains $N = 100$ diploid adults distributed with $N_m = 10$ breeding males and $N_f = 90$ breeding females (an extreme sex-ratio bias caused by male-biased mortality during a harsh winter). Estimate (a) the effective population size N_e from the unequal-sex-ratio formula, (b) the expected per-generation heterozygosity loss $\Delta H/H = 1/(2N_e)$, and (c) the expected heterozygosity retained after 50 generations.

Solution:

1. Effective population size from sex ratio. Using $\frac{1}{N_e} = \frac{1}{4N_f} + \frac{1}{4N_m}$, equivalently $N_e = \frac{4N_mN_f}{N_m + N_f}$:

$$N_e = \frac{4 \times 10 \times 90}{10 + 90} = \frac{3600}{100} = 36$$

Even with $N = 100$ census adults, the genetic drift behaves as if the population had merely $N_e = 36$ ideal-Wright–Fisher individuals — a about 64 % reduction in effective size driven entirely by the sex-ratio skew.

2. Per-generation heterozygosity loss.

$$\frac{\Delta H}{H} = \frac{1}{2N_e} = \frac{1}{72} \approx 0.014 = 1.4\% \text{ per generation}$$

3. Heterozygosity after 50 generations. Geometric decay:

$$H_{50} = H_0 \left(1 - \frac{1}{2N_e}\right)^{50} = H_0 \left(1 - \frac{1}{72}\right)^{50} \approx H_0 \times 0.50$$

Heterozygosity is approximately halved in 50 generations.

Conservation implication. The Florida panther (*Puma concolor coryi*) reached an $N_e \approx 20$ in the early 1990s before genetic-rescue introductions of Texas pumas; over just a few decades the subspecies showed elevated rates of cryptorchidism, atrial septal defects, and reduced sperm quality — clinical signatures of inbreeding depression driven exactly by the heterozygosity-loss trajectory derived above. The numerical worked example shows why census size N alone misleads conservation managers: an apparently healthy adult count masks an effective size small enough to lose half its remaining genetic diversity in a human lifetime.

22.3 Gene Flow and Mutation

22.3.1 Gene Flow as Migration-Mediated Allele Exchange

Gene flow (migration) is the movement of alleles between populations through the dispersal and reproduction of individuals (or their **gametes**, such as pollen). Gene flow has two primary evolutionary effects:

1. Homogenization: Gene flow tends to equalize allele frequencies between populations, counteracting divergence due to drift or local selection.
2. Introduction of variation: Migrants introduce novel alleles that may not have arisen locally, increasing genetic diversity within recipient populations.

22.3.2 Measuring Population Differentiation: F_{ST}

Wright’s fixation index (F_{ST}) quantifies the proportion of total genetic variation attributable to differences between populations:

$$F_{ST} = \frac{H_T - H_S}{H_T} = \frac{\sigma_p^2}{\bar{p}(1 - \bar{p})} \tag{332}$$

where H_T is the expected heterozygosity of the total (pooled) population and H_S is the mean expected heterozygosity within subpopulations.

- $F_{ST} = 0$: No differentiation (panmixia – gene flow fully homogenizes populations)
- $F_{ST} = 1$: Complete differentiation (populations fixed for different alleles)

Wright’s island model: At migration-drift equilibrium:

$$F_{ST} \approx \frac{1}{1 + 4N_e m} \tag{333}$$

where m is the proportion of each subpopulation composed of migrants per generation. This compact relationship — equating differentiation to the inverse of the scaled migration rate $4N_e m$ — is one of the most-used results in molecular ecology. It reveals a striking insight: even very low migration rates (m) can prevent substantial differentiation. $N_e m = 1$ (just one migrant per generation) yields $F_{ST} = 0.20$; $N_e m = 4$ yields $F_{ST} = 0.06$. One migrant per generation is the rule of thumb for keeping populations from drifting apart, regardless of population size — because the homogenizing effect of migration scales with $m \cdot N_e$ while the diverging effect of drift scales with $1/N_e$, leaving the dimensionless product $N_e m$ as the controlling parameter.

The relationship can be inverted for empirical use: given a measured F_{ST} , the implied number of migrants per generation is

$$N_e m \approx \frac{1 - F_{ST}}{4F_{ST}}.$$

For $F_{ST} = 0.05$ (moderate human population structure), $N_e m \approx 4.75$ — about five effective migrants between subpopulations per generation, sufficient to keep differentiation modest.

22.3.3 Isolation by Distance

Isolation by distance (IBD): In continuously distributed populations, gene flow decreases with geographic distance. This produces a positive correlation between pairwise F_{ST} (or genetic distance) and geographic distance, detectable by a Mantel test (matrix correlation between genetic and geographic distance matrices).

IBD patterns confirm that most natural populations show continuous genetic gradients (clines) rather than sharp boundaries. Human genetic variation, for example, shows strong IBD patterns corresponding to the out-of-Africa expansion routes.

22.3.4 Secondary Contact and Hybrid Zones

When previously allopatric populations come back into contact, the outcome depends on the degree of reproductive isolation that evolved during separation:

- **Fusion:** If reproductive isolation is weak, populations merge and homogenize.
- **Reinforcement:** If hybrids have reduced fitness, selection strengthens prezygotic barriers, as developed in the reproductive-isolation discussion.
- **Stable hybrid zone:** A narrow geographic zone of hybridization maintained by a balance between dispersal into the zone and selection against hybrids — called a tension zone.

Tension zone width and the dispersal-selection balance Following Barton & Hewitt (1985), the equilibrium width w of a tension zone follows:

$$w \approx \frac{\sigma}{\sqrt{s}}$$

(334)

where σ is the per-generation dispersal distance and s is the selection coefficient against hybrids. Tension zones are independent of geography in a key sense: their width is a function primarily of dispersal and selection, not of the underlying environmental gradient. The same hybrid zone can move across the landscape (as one parental population expands at the expense of the other) while maintaining its width. Tension zones become trapped at landscape features (mountain passes, river crossings) where dispersal rates dip locally — explaining why hybrid zones often coincide with geographic obstacles even when the species’ ranges are broadly continuous.

Empirical examples:

- **European crow hybrid zone** (carion crow *Corvus corone* × hooded crow *C. cornix*): The hybrid zone runs through Europe from Italy and Denmark up through Russia, with a width of about 20–30 km. *Corone* and *cornix* differ at a small number of pigmentation loci. Genome-wide F_{ST} across the zone is dramatic at color-loci but minimal elsewhere — a “porous” species barrier consistent with reinforcement primarily at loci affected by mate choice.
- **Northern flicker (*Colaptes auratus*) hybrid zone:** yellow-shafted (eastern) × red-shafted (western) flickers form a narrow hybrid zone running about 3,000 km along the central Great Plains, with width about 100–200 km. Despite extensive interbreeding in the zone, the parental forms persist on either side — assortative mating and reduced hybrid fitness preserve the polymorphism.
- ***Bombina bombina* × *B. variegata* toads:** A 5–8 km tension zone runs through Central Europe. Genome-wide F_{ST} patterns reveal both barrier loci (under strong selection against hybrids) and freely-introgressing neutral loci. The genome behaves like a mosaic of differently permeable regions.

Reinforcement and Dobzhansky-Muller incompatibilities When hybrids have reduced fitness, reinforcement strengthens prezygotic barriers — natural selection favors mate-discrimination alleles that prevent hybridization. The genetic basis of postzygotic isolation typically involves Dobzhansky-Muller incompatibilities (BDMI): pairs of alleles at different loci that function fine in their respective parental backgrounds but produce sterile or inviable hybrids when combined.

The classic two-locus BDMI: ancestral genotype A_1B_1 . Population 1 evolves to A_2B_1 (the new A_2 is tested against B_1 — works fine). Population 2 evolves to A_1B_2 (the new B_2 is tested against A_1 — works fine). The hybrid genotype A_2B_2 has rarely been tested by selection; if A_2 and B_2 interact deleteriously, hybrids fail. Because each parental population independently accumulates substitutions, the number of potential incompatibilities grows as k^2 (Orr’s snowball) — explaining why isolation often appears suddenly after a long period of gradual divergence.

Sympatric divergence (without geographic separation) is rare because gene flow continuously breaks up co-adapted gene complexes. Reinforcement can complete divergence after an initial allopatric phase: secondary contact selects for prezygotic isolation alleles that prevent the formation of low-fitness hybrid combinations. The genomic signature of reinforcement — sharper differentiation at mate-choice and behavioral-isolation loci than at genome-wide background — has been documented in *Drosophila* species pairs and in cichlid radiations.

22.3.5 Coalescent Theory and the TMRCA

The coalescent is a backward-in-time view of population genealogies that has become the dominant statistical framework in modern population genetics [Kingman, 1982]. Rather than tracking allele frequencies forward through generations, the coalescent traces ancestral lineages of currently sampled alleles backward until they merge (“coalesce”) at common ancestors.

Expected coalescence time For a sample of k alleles drawn from a Wright-Fisher population of effective size N_e diploid individuals (so $2N_e$ allele copies), the expected time for any two specific lineages to coalesce is $2N_e$ generations. Generalizing to a sample of k lineages, the expected total time to the most recent common ancestor (TMRCA) is:

$$E[T_{\text{MRCA}}] = 4N_e \left(1 - \frac{1}{k}\right)$$

(335)

For large samples ($k \rightarrow \infty$), $E[T_{\text{MRCA}}] \rightarrow 4N_e$ generations. The coalescent has several remarkable properties:

- Most coalescences happen recently: the expected time for the last two lineages to coalesce ($2N_e$ generations) is half of the total tree depth. The genealogy is “top-heavy”: coalescent events are most rapid at the tips of the tree, slowest near the root.
- Independent of forward dynamics: Under neutrality, the topology of the coalescent tree is independent of mutations. Mutations are sprinkled onto branches at rate μ ; the expected number of segregating sites in a sample of k is $\theta \sum_{i=1}^{k-1} 1/i$, where $\theta = 4N_e\mu$.
- Variance: TMRCA has a wide distribution. The variance of TMRCA grows with k but the most likely TMRCA values are surprisingly broad — different loci sampled from the same population yield TMRCA spanning an order of magnitude.

Why “Mitochondrial Eve” was not the only woman alive Coalescent logic explains why the TMRCA of human mitochondrial DNA (about 150,000 years ago) does not mean a single ancestress. Many women were alive 150 kya — the coalescent estimate refers primarily to the lineage of mtDNA that survived to the present. Most other maternal lineages were lost by drift along the way; their loss is statistically inevitable in finite populations. Indeed, of k ancestral lineages alive in the founding population, most but one will eventually be lost to drift — with the surviving lineage tracing back through “Eve” by definition. The surprising thing is not that an MRCA exists, but that the coalescent pinpoints when she lived.

Coalescent applications

- Effective population size estimation from segregating-site counts uses the relationship $\theta = 4N_e\mu$.
- Detecting selective sweeps identifies regions with anomalously short TMRCA — a recent advantageous mutation drags linked variation toward fixation, collapsing the genealogy.
- Demographic inference from extended coalescent models reconstructs population growth, bottlenecks, and migration history. PSMC (pairwise sequentially Markovian coalescent) and SMC++ are standard tools.

TMRCA for two alleles: derivation and intuition The single most-cited coalescent result is the expected coalescence time of two randomly sampled alleles in a Wright–Fisher diploid population of effective size N_e . In each generation, two specific allele copies have probability $1/(2N_e)$ of sharing the same parent (because a parent is chosen uniformly from $2N_e$ possibilities). The coalescence time is therefore geometrically distributed with success probability $1/(2N_e)$, giving:

$$E[T_{\text{MRCA, 2-alleles}}] = 2N_e \text{ generations}$$

(336)

For $N_e = 10,000$ (a typical estimate for ancestral humans), the expected pairwise coalescence is 20,000 generations \approx 500,000 years (assuming 25-year generation time). This figure is the statistical baseline against which observed pairwise sequence divergences are interpreted; deeper coalescences indicate population structure or balancing selection, shallower coalescences suggest bottlenecks or selective sweeps.

For a sample of k alleles, total tree depth (root to most recent tip) is $4N_e(1 - 1/k)$ — the value introduced in equation (335). For two alleles ($k = 2$), this reduces to $2N_e$, recovering the pairwise result of equation (336).

Structured coalescent When a population is subdivided into subpopulations with limited migration, the coalescent becomes structured: lineages can primarily coalesce when they are in the same subpopulation, and migration events transfer lineages between subpopulations. Two lineages drawn from the same subpopulation typically coalesce on the timescale $2N_e$ (within-deme coalescence). Two lineages drawn from different subpopulations must first meet in the same deme before they can coalesce — adding a waiting time inversely proportional to the migration rate m . The result is that between-population pairwise TMRCA exceeds within-population pairwise TMRCA, with the difference scaling as $\sim 1/(2m)$ generations.

This produces an empirical signature: F_{ST} between subpopulations grows as the fraction of the genealogy spent in the “between” rather than “within” coalescent regime. Conversely, migration reduces between-population TMRCA because lineages can quickly transfer between subpopulations; high-migration models behave like a single panmictic population with effective size equal to the sum of deme sizes. Modern coalescent inference tools (msprime, IM, PhyloGeoTools) explicitly model structured-coalescent dynamics to estimate ancient migration rates and population-divergence times — a key application in human population history (e.g., African \leftrightarrow Eurasian migration after Out-of-Africa) and in conservation genetics of fragmented populations.

22.3.6 Mutation as the Ultimate Source of Variation

Mutation is the ultimate source of most genetic variation. Without mutation, evolution would eventually cease as selection and drift exhausted existing variation.

- De novo mutation rate in humans: approximately 1.2×10^{-8} per nucleotide per generation, corresponding to about 70 new mutations per individual per generation.

- **Paternal age effect:** Male germline cells undergo many more mitotic divisions than female germline cells. Each year of paternal age adds approximately 1–2 additional mutations to offspring. This contributes to the increased incidence of some genetic conditions (e.g., achondroplasia, autism spectrum disorder) with advanced paternal age.

22.3.7 Mutation-Selection Balance

For a deleterious recessive allele maintained by recurrent mutation against purifying selection, the equilibrium frequency is:

$$\hat{q} \approx \sqrt{\frac{\mu}{s}}$$

(337)

where μ is the mutation rate and s is the selection coefficient against the homozygous genotype. This explains why many genetic diseases persist at low frequencies – new mutations continually reintroduce them even as selection removes them.

Example: Cystic fibrosis (CF) is caused by homozygosity for loss-of-function alleles in the *CFTR* gene. With $\mu \approx 6.7 \times 10^{-7}$ and $s \approx 1$ (CF was historically lethal before modern medicine), mutation-selection balance predicts $\hat{q} \approx \sqrt{6.7 \times 10^{-7}} \approx 0.0008$. However, the actual carrier frequency in European populations is approximately 1 in 25 ($q \approx 0.02$), far exceeding the mutation-selection prediction. This suggests an additional force – possibly heterozygote advantage against cholera, typhoid fever, or tuberculosis – maintains the CF allele at elevated frequency, similar to the sickle cell / malaria relationship.

Real-World Connection: Mutation Rates and Cancer

The same mutational processes that drive evolution also drive cancer. Somatic mutations accumulate in cells throughout an organism’s lifetime at rates of approximately $0.5\text{--}5 \times 10^{-9}$ per nucleotide per cell division. Larger and longer-lived organisms should, by simple probability, experience more cancer – yet elephants (with 100 times more cells than humans) have lower cancer rates than humans. This is Peto’s paradox. The resolution involves the evolution of enhanced cancer suppression mechanisms: elephants carry approximately 20 copies of the *TP53* tumor suppressor gene (humans have one), and their cells are hypersensitive to DNA damage, triggering **apoptosis** rather than attempting repair. This represents an evolutionary adaptation to large body size.

Concept Check 2: Using Wright’s island model, calculate the equilibrium F_{ST} for two populations with $N_e = 500$ and $m = 0.005$. How many migrants per generation does this represent? Would you consider these populations significantly differentiated?

Concept Check (Analysis — Interpreting F_{ST} on a Sliding Scale): Three pairs of populations have measured F_{ST} values of 0.05, 0.15, and 0.35. (a) For each, calculate the implied number of effective migrants per generation using $N_e m \approx (1 - F_{ST})/(4F_{ST})$. (b) Interpret the three regimes biologically: which corresponds to ongoing extensive gene flow, which to weak structure, and which to substantially differentiated populations approaching reproductive isolation? (c) Critically evaluate the assumption-set behind the island-model conversion — what would change if the populations exchange migrants asymmetrically, or if migration is recent rather than at equilibrium? (d) For the $F_{ST} = 0.15$ pair, what fraction of total genetic variation is between populations versus within populations? Connect this back to the F_{ST} definition $F_{ST} = (H_T - H_S)/H_T$.

22.4 Species Concepts and the Boundaries of Lineages

Defining what constitutes a “species” is one of the most contentious issues in biology. Multiple species concepts exist, each emphasizing different aspects of biological reality.

22.4.1 Biological Species Concept (BSC)

Ernst **Mayr** [1942] defined species as “groups of actually or potentially interbreeding natural populations that are reproductively isolated from other such groups.” This concept emphasizes reproductive isolation as the defining criterion.

Strengths: Biologically meaningful; focuses on the process (gene flow) that maintains species cohesion.

Limitations: Cannot be applied to asexual organisms, fossils (where reproductive behavior is unobservable), or ring species; hybridization between “good” species is common (e.g., about 10% of bird species hybridize).

22.4.2 Morphological/Typological Species Concept

Species are distinguished by consistent morphological differences. This is the oldest concept, rooted in Linnaeus’s original classifications.

Strengths: Practical and widely applicable; the basis of most field identification.

Limitations: Subjective – how much difference constitutes a species? Fails for cryptic species (morphologically identical but reproductively isolated) and polymorphic species (morphologically variable within a single species).

22.4.3 Phylogenetic Species Concept (PSC)

A species is the smallest diagnosable monophyletic group – the smallest cluster of organisms that share a common ancestor and can be distinguished from other such clusters by unique character combinations (synapomorphies).

Strengths: Applicable to any organism (sexual, asexual, fossil); consistent with modern systematics.

Limitations: Tends to “oversplit” – recognizing more species than the BSC from the same organisms. With sufficient genetic data, nearly every population is diagnosable.

22.4.4 Ecological Species Concept

A species is a set of organisms exploiting a single ecological **niche** (Hutchinson’s hypervolume). This concept focuses on the ecological role rather than reproductive boundaries.

Strengths: Applicable to asexual organisms; emphasizes the role of selection in maintaining species identity.

Limitations: Niche boundaries are often fuzzy; different populations of the same species may occupy different niches.

22.4.5 Cohesion Species Concept

Alan **Templeton** [1989] proposed the most comprehensive definition: a species is the most inclusive group of organisms having the potential for genetic exchangeability (gene flow) and/or demographic exchangeability (ecological interchangeability). This concept subsumes elements of the BSC and ecological concepts.

22.4.6 Ring Species and Gradual Reproductive Isolation

Ring species demonstrate speciation as a gradual process. A series of populations forms a ring around a geographic barrier, with neighboring populations interbreeding freely. However, at the point where the ring closes, the terminal populations are reproductively isolated despite being connected by a chain of interbreeding intermediates.

- **Larus gulls:** Around the Arctic, a chain of herring gull and lesser black-backed gull populations form a ring. Adjacent populations interbreed, but the end members (in Europe) coexist as distinct, reproductively isolated species.
- **Ensatina salamanders:** In California, populations encircle the Central Valley. Adjacent populations hybridize, but where the ring closes in southern California, the terminal forms (*E. e. eschscholtzii* and *E. e. klauberi*) rarely interbreed.

Ring species challenge the BSC because reproductive isolation is not absolute but graded.

Concept Check 3: A researcher discovers two populations of beetles that are morphologically identical but reproductively isolated in the laboratory. Would the BSC and morphological species concept agree on whether these are one species or two? Which concept would you favor, and why?

22.5 Speciation Mechanisms Across Geography and Gene Flow

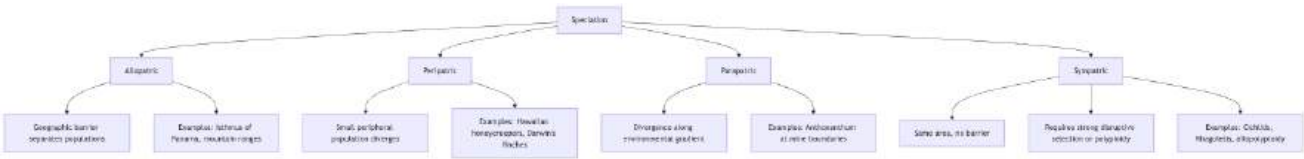


Figure 134. Speciation mechanisms differ in how gene flow is reduced: geographic separation, edge isolation, adjacent divergence, and reproductive barriers change lineage independence.

22.5.1 Allopatric Speciation by Geographic Isolation

Allopatric speciation – speciation resulting from geographic isolation – is the most common and best-documented mode. A geographic barrier (mountain range, ocean, ice sheet, river) divides a population, preventing gene flow. The isolated populations then diverge through a combination of natural selection (adapting to different local environments) and genetic drift, eventually accumulating enough differences that reproductive isolation is a byproduct of divergence.

Isthmus of Panama: The formation of the Central American land bridge approximately 3 Mya divided many marine populations into Caribbean and Pacific components. The resulting geminate species pairs (closely related species on either side of the isthmus) provide natural experiments in allopatric divergence. Snapping shrimp (*Alpheus* spp.) separated by the isthmus show increasing reproductive isolation correlated with divergence time.

Dobzhansky-Muller incompatibilities: The genetic basis of reproductive isolation often involves epistatic interactions between independently evolved alleles. Consider two populations with ancestral genotype A_1B_1 . Population 1 evolves to A_2B_1 and Population 2 evolves to A_1B_2 . Each derived genotype is functional because the new allele was tested against the existing genetic background. But hybrids (A_2B_2) carry a combination that has rarely been tested by natural selection – and this untested epistatic combination may cause developmental failure, sterility, or inviability. The number of potential incompatibilities grows as the square of the number of substitutions (Orr’s snowball effect):

$$\text{Incompatibilities} \propto k^2$$

(338)

This accelerating accumulation explains why reproductive isolation often appears suddenly after a period of gradual divergence.

22.5.2 Peripatric Speciation in Small Peripheral Populations

Peripatric speciation occurs when a small population at the periphery of a species’ range becomes isolated. The small founding population experiences strong genetic drift (founder effect), which, combined with potentially different selective pressures at the range margin, can drive rapid divergence.

- Hawaiian honeycreepers: Approximately 55 species evolved from one or two founding finch-like ancestors that colonized the Hawaiian Islands approximately 5 Mya. The radiation produced an extraordinary diversity of bill shapes – from long, curved bills for nectar feeding (*Drepanis*) to massive, parrot-like bills for seed cracking (*Pseudonestor*) to thin, warbler-like bills for insect gleaning (*Oreomystis*). Many species are now critically endangered or extinct.
- Darwin’s finches: Fifteen species on the Galapagos Islands, diversified from a single South American ancestor approximately 1–2 Mya. Beak depth and width vary with seed size and hardness. Character displacement – divergence in beak morphology is greater where two species co-occur (sympatry) than where each occurs alone (allopatry) – provides evidence that competition drives morphological divergence.

22.5.3 Parapatric Speciation Along Environmental Gradients

Parapatric speciation occurs along an environmental gradient without a clear geographic barrier. Adjacent populations experience different selective pressures, and if selection against intermediates is strong enough to overcome gene flow, divergence can proceed.

Sweet vernal grass (*Anthoxanthum odoratum*): On heavy-metal-contaminated mine tailings in Wales, grass populations have evolved heavy metal tolerance within meters of the mine boundary. Tolerant and non-tolerant populations grow adjacent to each other. Flowering time has shifted between the two ecotypes, providing a prezygotic barrier – tolerant plants flower approximately one week earlier than adjacent non-tolerant plants. Wind-mediated gene flow between the two populations is substantial (pollen travels freely), yet the ecotypes maintain their distinctness because of strong selection against non-tolerant genotypes on contaminated soil and against tolerant genotypes (which pay a fitness cost) on clean soil. This is parapatric speciation in progress – divergence without geographic isolation, driven by strong disruptive selection.

Hybrid zones as natural laboratories: The parapatric boundary between ecotypes often produces a narrow cline – a geographic gradient in allele frequency. The width of the cline reflects the balance between selection (which narrows it) and gene flow (which broadens it). Cline width w can be estimated as:

$$w \approx \frac{\sigma}{\sqrt{s}}$$

(339)

where σ is the dispersal distance per generation and s is the selection coefficient against immigrants. Narrow clines indicate strong selection relative to dispersal.

22.5.4 Sympatric Speciation Without Geographic Separation

Sympatric speciation – speciation within a single, freely mixing population – has long been controversial because gene flow should homogenize populations. However, several mechanisms can overcome gene flow:

Cichlid fish in Lake Victoria: Approximately 500 species evolved within a single lake basin in approximately 15,000 years – one of the most spectacular adaptive radiations known. Sexual selection on male coloration, driven by female preference under different light environments (clear versus turbid water), appears to be a primary driver. When experimental turbidity eliminates the ability to distinguish colors, species boundaries break down and hybridization occurs – demonstrating that assortative mating by color maintains species isolation.

Apple maggot fly (*Rhagoletis pomonella*): The ancestral host plant is hawthorn. Following the introduction of domestic apples to North America in the 1600s, a population shifted to apple as a host. Apple and hawthorn races now differ in emergence timing (matching fruit ripening), host preference, and multiple genomic regions under divergent selection. This represents host race formation – an early stage of sympatric speciation.

Polyploidy in plants: Whole-genome duplication creates instantaneous reproductive isolation because polyploid offspring cannot successfully mate with diploid parents (triploid offspring are sterile or inviable due to meiotic irregularities — odd chromosome number prevents proper homolog pairing at meiosis I, producing unbalanced gametes that fail to develop). The triploid block is the mechanistic basis for why polyploidy can speciate in a single generation: a tetraploid individual that arises by chromosome non-disjunction is reproductively isolated from its diploid parents from the moment of formation.

- Autopolyploidy: Genome doubling within a single species without hybridization. Potato (*Solanum tuberosum*) is autotetraploid ($4n = 48$). Alfalfa (*Medicago sativa*) is autotetraploid. Some wild *Tolmiea* (piggyback plant) populations exhibit autotetraploid forms sympatric with diploid forms. Autopolyploids face less severe meiotic challenges than allopolyploids because their four homologs share recent ancestry, but multivalent formation at meiosis I (where four near-identical homologs may pair as quadrivalents rather than two bivalents) can produce aneuploid gametes at higher rates than in diploids. Reproductive isolation can arise rapidly because an autotetraploid ($4n$) crossed with a diploid ($2n$) parent often produces low-fertility triploid ($3n$) offspring.
- Allopolyploidy: Hybridization between two distinct species followed by chromosome doubling. The chromosome doubling restores fertility because each chromosome now has a homolog to pair with at meiosis I (the parental homolog), eliminating the meiotic irregularities that would otherwise sterilize the F1 hybrid. Major allopolyploid crops illustrate the pattern across the angiosperms:
 - Bread wheat (*Triticum aestivum*): an allohexaploid ($2n = 42 = AABBDD$) derived from three diploid ancestors through two rounds of hybridization and genome doubling, completed within the last about 8,000–10,000 years coinciding with the origin of agriculture.
 - Cultivated tobacco (*Nicotiana tabacum*): an allotetraploid ($2n = 48 = SSTT$), formed about 200,000 years ago by hybridization between *N. sylvestris* (S genome) and an *N. tomentosiformis*-like progenitor (T genome).
 - Cultivated cotton (*Gossypium hirsutum*, upland cotton): an allotetraploid ($2n = 52 = AADD$) formed about 1–2 Mya by hybridization between an Old World A-genome species and a New World D-genome species — followed by trans-oceanic dispersal of A-genome ancestors to the Americas. Modern upland cotton accounts for about 95% of global cotton production.

How widespread is polyploidy? Polyploidy is a major mode of sympatric speciation in plants and is far more common than once thought. Recent genomic analyses indicate that about 35% of extant angiosperm species are polyploid or have polyploid ancestors detectable in the recent past, and many flowering plant lineages show evidence of paleopolyploid events (whole-genome duplications followed by gene loss and rediploidisation) during their evolutionary history. The seed plants share at least one whole-genome duplication about 320 Mya, and the flowering plants share a more recent duplication about 150 Mya. Major crop genomes (rice, maize, soybean, *Brassica*, banana, sugarcane) bear paleopolyploid signatures. Polyploidy is not a peculiarity of a few weedy lineages — it is a recurring engine of plant evolution that contributes substantially to angiosperm diversification, novel gene functions arising from duplicated copies (sub- and neofunctionalisation), and rapid speciation. In animals, polyploidy is rarer because dosage-sensitive development and sex-determination systems often make genome doubling costly, but it has occurred in salmonid fish, *Xenopus* frogs, and some invertebrates.

Wheat: a paradigm of agricultural allopolyploidy The polyploid origin of bread wheat is one of the best-documented allopolyploid speciation events in agriculture. Approximately 500,000 years ago, *Triticum urartu* (genome AA) hybridized with *Aegilops speltoides* (genome BB), producing the tetraploid emmer wheat (*Triticum turgidum*, AABB). Some 8,000 years ago, emmer crossed with *Aegilops tauschii* (genome DD), producing modern hexaploid bread wheat (AABBDD). Each genome retains about 85% of its ancestral gene content; the homoeologous chromosome sets pair specifically with their partners thanks to the *Ph1* locus on chromosome 5B, which suppresses pairing between non-identical chromosomes and prevents chaos at meiosis. Modern wheat breeding takes advantage of the genetic diversity in the three subgenomes — beneficial alleles can be sourced from any of the diploid ancestor lineages and introduced into bread wheat by chromosomal manipulations.

The Brassica triangle (Triangle of U) The cultivated *Brassica* species form one of the most elegant illustrations of allopolyploid speciation, formalized by Korean botanist Woo Jang-choon (U Nagaharu) in 1935:

Each diploid ancestor contributes its full chromosome set to the corresponding allotetraploid; the resulting hexaploid is reproductively isolated from most parents. The Triangle of U accounts for cabbage (*B. oleracea*, CC), turnip (*B. rapa*, AA), and mustard (*B. nigra*, BB) plus their three allotetraploid descendants — canola (*B. napus*, AACC), brown mustard (*B. juncea*, AABB), and Ethiopian mustard (*B. carinata*, BBCC). The triangle forms one of the most important agricultural-genetic systems in the world; understanding the polyploid relationships drives breeding programs and resistance-gene transfer between species.

An estimated 15% of angiosperm speciation events involve polyploidy, and up to 70% of grass genomes show evidence of ancient polyploid ancestry — including the deep polyploidy events that gave rise to the cereals (rice, maize, wheat, barley) that feed the human species.

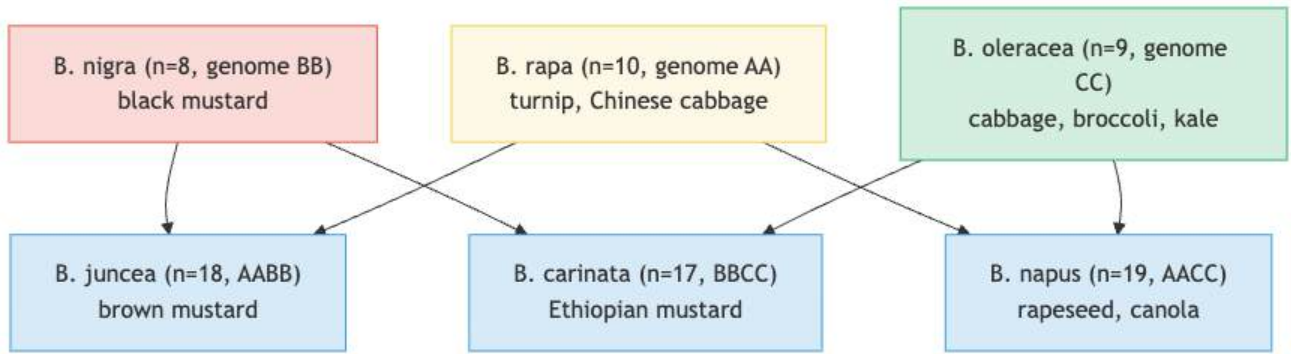


Figure 135. The Triangle of U: three diploid Brassica species (corners) and the three allotetraploid species (sides) formed by their pairwise hybridizations and chromosome doublings. Each allopolyploid carries the chromosome complements of its two diploid ancestors.

22.6 Reproductive Isolation Before and After Fertilization

Reproductive isolation is the hallmark of speciation under the BSC. Barriers to reproduction are classified as prezygotic (preventing formation of a hybrid **zygote**) or postzygotic (reducing fitness of hybrid offspring).

22.6.1 Haldane's Rule

Haldane's rule (1922): In interspecific hybrids, when a single sex is inviable or sterile, it is the heterogametic sex (XY males in mammals and flies; ZW females in birds and butterflies). Three complementary mechanisms explain this pattern:

1. Dominance theory: Recessive incompatibility alleles on the X (or Z) chromosome are fully exposed in the heterogametic sex (which has a single copy), but masked in the homogametic sex (which may carry a compatible allele on the other X/Z chromosome).
2. Faster-X evolution: X-linked genes evolve faster than autosomal genes because beneficial recessive mutations are immediately exposed to selection in hemizygous males. This accelerated divergence produces more X-linked incompatibilities.
3. Meiotic drive and sex chromosome conflict: Segregation distortion elements on sex chromosomes can cause hybrid sterility by disrupting normal chromosome segregation during **meiosis**.

Haldane's rule has been confirmed across a broad range of animal taxa examined, making it one of the most robust generalizations in speciation biology.

22.6.2 Prezygotic Barriers to Mating or Fertilization

Table 297. Prezygotic Barriers to Mating or Fertilization: Barrier type and Mechanism.

Barrier type	Mechanism	Example
Temporal	Different breeding seasons or times of day	Two species of field cricket: <i>Gryllus veletis</i> breeds in spring; <i>G. pennsylvanicus</i> breeds in fall
Habitat	Different microhabitats reduce encounter rate	<i>Rhagoletis</i> apple vs. hawthorn races live on different host trees
Behavioral	Species-specific courtship signals (song, dance, pheromones, color)	Firefly <i>Photinus</i> species: each has a unique flash pattern recognized primarily by conspecific females
Mechanical	Incompatible reproductive structures	<i>Salvia</i> flower species: bee-pollinated species have different petal structures than hummingbird-pollinated species, preventing pollen transfer
Gametic	Sperm-egg recognition molecules are species-specific	Sea urchin bindin protein : species-specific sperm-egg binding prevents cross-fertilization

Pollinator-mediated isolation often combines mechanical, behavioral, and ecological barriers. A floral shift from bee visitation to bird visitation can change flower shape, color, nectar volume, pollen placement, and the timing or habitat of effective pollen transfer. If pollen is regularly moved within each floral form but rarely between forms, divergent selection on plant traits reduces gene flow even before hybrids are tested. The pollinator side also matters: managed honeybees, bumblebees, solitary bees, birds, and moths do not sample flowers in identical ways, so a speciation claim should measure effective pollen transfer rather than treating “pollinator” as a single interchangeable agent [Garibaldi et al., 2013, IPBES, 2016].

22.6.3 Postzygotic Barriers to Hybrid Fitness

Hybrid inviability: Hybrids fail to develop properly due to Dobzhansky-Muller incompatibilities. Gene regulatory networks that function within each parental species produce dysfunctional combinations in hybrids.

Hybrid sterility: Hybrids develop normally but cannot reproduce. The mule (horse × donkey) is the classic example. Horses have $2n = 64$ chromosomes; donkeys have $2n = 62$. The mule has $2n = 63$ – odd chromosome number prevents proper pairing at meiosis I, resulting in sterility.

Hybrid breakdown: F1 hybrids may be viable and fertile, but F2 or backcross offspring show reduced fitness. This occurs when recombination in the F1 generation breaks up co-adapted gene complexes, producing incompatible allele combinations in the F2.

22.6.4 Reinforcement by Selection Against Hybrids

Reinforcement (also called the Wallace effect) occurs when natural selection strengthens prezygotic barriers after secondary contact. If hybrids have low fitness (due to postzygotic barriers), individuals who mate with members of their own species leave more viable offspring than those who hybridize. This selects for enhanced mate discrimination.

Evidence: In *Drosophila* species pairs, female mate discrimination is stronger in sympatric populations (where the two species co-occur and could hybridize) than in allopatric populations (where a single species is present). This pattern – called reproductive character displacement – is a predicted signature of reinforcement.

22.6.5 Hybridization and Introgression

Hybridization does not inevitably lead to reproductive isolation breakdown. Introgression – the incorporation of alleles from one species into the gene pool of another through backcrossing – can be an important source of adaptive variation.

Neanderthal introgression into modern humans: Non-African modern humans carry approximately 1–4% Neanderthal-derived DNA, resulting from interbreeding that occurred approximately 50,000–60,000 years ago in the Middle East. Specific Neanderthal alleles have been maintained by selection because they provided adaptive advantages:

- HLA immune genes: Neanderthal-derived HLA alleles increased immune diversity in migrating modern human populations.
- Keratin genes: Neanderthal variants affecting skin and hair may have helped modern humans adapt to cold Eurasian climates.

Denisovan introgression: Melanesian populations carry approximately 4–6% Denisovan-derived DNA. The EPAS1 gene variant that helps Tibetans adapt to high altitude was introgressed from Denisovans – a striking example of adaptive introgression where a borrowed allele provides significant fitness benefits in a new environment.

Recent evidence also suggests introgression from an unknown “ghost lineage” into West African populations, indicating that archaic admixture was more widespread than initially recognized.

Real-World Connection: Archaic Human Introgression

The discovery that modern humans carry DNA from extinct hominin species has revolutionized our understanding of human evolution. Far from a simple out-of-Africa replacement, human evolution involved repeated episodes of admixture. Neanderthal-derived alleles influence modern human traits ranging from immune function to depression risk to skin pigmentation. Some Neanderthal alleles are beneficial (immune genes), while others are deleterious (associated with increased risk for certain diseases). Natural selection is gradually purging Neanderthal DNA from functionally important regions of the genome, while neutral or beneficial segments persist. This ongoing process of post-introgression selection provides a window into the fitness consequences of hybridization over evolutionary time.

Concept Check 4: A horse ($2n = 64$) crossed with a donkey ($2n = 62$) produces a mule ($2n = 63$). Explain, in terms of meiosis, why the mule is sterile. What type of reproductive barrier does this represent?

Concept Check (Evaluate — Reinforcement vs. Fusion on Secondary Contact): Two allopatric populations of field crickets have evolved different male calling songs over about 50,000 years of geographic isolation. Female crickets locate mates by phonotaxis to species-specific calling songs.

When the geographic barrier breaks down and the two populations come back into sympatry, song features differ by about 70 % (pulse rate, carrier frequency, syllable duration). (a) Outline the two extreme evolutionary outcomes — reinforcement (further divergence in song to complete reproductive isolation) versus fusion (homogenisation back to a single species) — and identify which is favored if hybrid offspring are largely viable and fertile versus largely inviable. (b) Apply the tension-zone framework: if the dispersal scale σ across the contact zone is about 5 km/generation and selection against hybrids is s , derive the zone width $w \approx \sigma/\sqrt{s}$ for $s = 0.01, 0.1$, and 0.5 , and interpret what each width implies for whether reinforcement can complete. (c) Evaluate the role of female mate preference variance — if females in the contact zone are genetically variable in their preferences, does this accelerate or slow reinforcement? (d) Design a single field experiment that could distinguish reinforcement from sensory drift as the source of post-contact song divergence.

22.7 Adaptive Radiation and Ecological Opportunity

Adaptive radiation is the rapid diversification of a single ancestral lineage into multiple species occupying diverse ecological niches. Radiations are typically triggered by one of three circumstances: mass extinction (opening ecological opportunities), colonization of a new, underexploited territory, or the evolution of a key innovation that opens new adaptive zones.

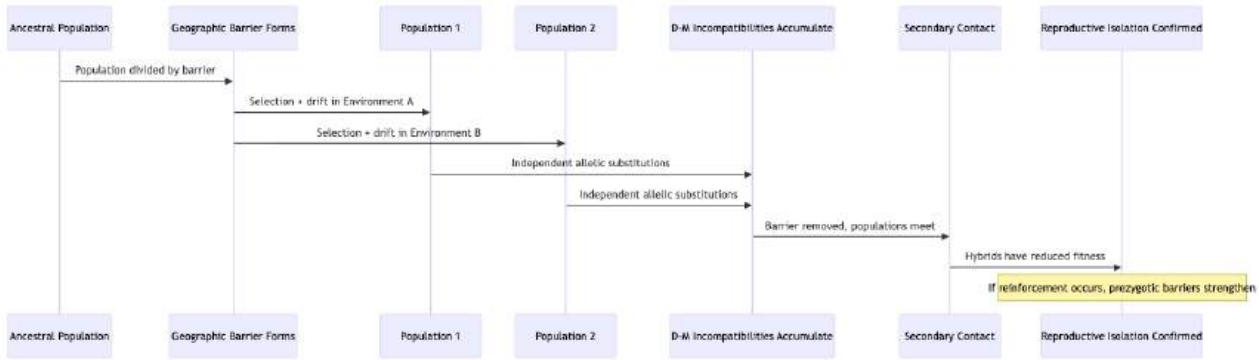


Figure 136. Adaptive radiation begins when one lineage enters new ecological opportunity, then populations diverge across habitats and traits into multiple descendant species.

22.7.1 Hawaiian Honeycreepers as Island Adaptive Radiation

The Hawaiian honeycreeper radiation (family Fringillidae, tribe Drepanidini) produced approximately 55 species from one or two founding finch-like ancestors that arrived approximately 5 Mya. Bill morphology diversified to exploit a remarkable range of food sources:

- Nectarivores (long, curved bills): *Drepanis*, *Hemignathus* – probe tubular flowers for nectar
- Seed crackers (massive bills): *Pseudonestor*, *Chloridops* – crush hard seeds and nuts
- Insectivores (thin, warbler-like bills): *Oreomystis*, *Paroreomyza* – glean insects from bark and foliage
- Generalists: *Telespiza* – omnivorous diet

Tragically, over one-third of honeycreeper species are now extinct, and most survivors are critically endangered, primarily due to avian malaria (transmitted by introduced mosquitoes), habitat loss, and introduced predators.

22.7.2 Cichlid Fish in African Great Lakes

The cichlid radiations in Lakes Victoria (about 500 species, about 15,000 years), Malawi (about 800 species, about 2 Mya), and Tanganyika (about 250 species, about 10 Mya) represent the most species-rich vertebrate adaptive radiations known.

Key features driving cichlid diversification:

- Trophic specialization: Jaw morphology (particularly the pharyngeal jaw apparatus – a second set of jaws in the throat) has diversified to process algae, plankton, snails, fish, scales, and even eyes of other fish.
- Sexual selection on color: Female mate choice based on male nuptial coloration drives assortative mating. In Lake Victoria, species that are distinguished solely by color can hybridize when visual cues are disrupted by turbidity.
- Rapid speciation: Genetic divergence between species is often minimal, suggesting that speciation was driven primarily by sexual selection and ecological specialization rather than accumulated genetic distance.

22.7.3 Galapagos Finches and Beak-Trait Diversification

Darwin’s finches (15 species across the Galapagos Islands and Cocos Island) diversified from a single South American ancestor approximately 1–2 Mya. The Grants’ long-term research on Daphne Major island documented natural selection in real time:

- During the 1977 drought, large seeds predominated. Finches with deeper, stronger beaks survived preferentially – directional selection increased mean beak depth by 4% in a single generation.
- Character displacement: On islands where medium ground finches (*Geospiza fortis*) co-occur with large ground finches (*G. magnirostris*), *G. fortis* beaks are smaller than on islands where *G. fortis* occurs alone. This divergence reduces competition for seeds.

22.7.4 Mammalian Radiation After K-Pg Extinction

The extinction of non-avian dinosaurs 66 Mya released enormous ecological space. Mammals, which had been small, nocturnal insectivores for over 100 million years, rapidly diversified into most modern orders within approximately 10 million years. This radiation produced bats (flight), whales (marine adaptation), elephants (megaherbivory), primates (arboreality and eventually bipedalism), and the full range of modern mammalian diversity.

Concept Check 5: What conditions are necessary for an adaptive radiation to occur? Why do island archipelagos and post-extinction periods seem particularly conducive to adaptive radiation?

Concept Check 6: Apply the structured-coalescent intuition. Two human populations (effective size $N_e \approx 10,000$ each) exchange migrants at rate $m = 0.001$ per generation. (a) What is the expected pairwise coalescence time within each subpopulation? (b) Why is the pairwise coalescence time longer for two alleles drawn from different subpopulations than for two alleles drawn from the same subpopulation? (c) How does this asymmetry generate F_{ST} ?

Concept Check 7: Bread wheat (*Triticum aestivum*) is an allohexaploid (AABBDD). Cultivated tobacco is an allotetraploid (SSTT). Cultivated upland cotton is an allotetraploid (AADD). For each, identify (i) how many parental species contributed, (ii) why the immediate F1 hybrid was likely sterile before chromosome doubling, and (iii) why the polyploid is reproductively isolated from each diploid parent. Why is the analogous story for autopolyploidy less common as a route to speciation in animals than in plants?

Clinical Connection — Founder effects and Mendelian disease in isolated populations. Ashkenazi Jews (about 500-year bottleneck, $N_e \approx 250 - 400$), Finns (isolation since the Neolithic), Amish, and French Canadians carry elevated frequencies of specific recessive alleles (Tay-Sachs *HEXA*, BRCA1/2 185delAG, Canavan disease *ASPA*, phenylketonuria *PAH*). In many cases these alleles rose from a single founder chromosome, detectable as a shared haplotype. Modern targeted screens (e.g. the Ashkenazi panel) are possible precisely *because* drift + bottleneck has concentrated a handful of distinctive alleles; in outbred populations, the allelic heterogeneity for the same gene is often too great for panel-based screening to be useful.

Clinical Connection — Speciation of SARS-CoV-2 variants. Allopatric speciation analogs appear in real time during pandemics. A single index case seeding a geographic region generates a local founder population; drift plus selection for transmissibility produce variants (Alpha, Delta, Omicron) that then contact and partially displace each other. Phylogenetic analysis of >15 million SARS-CoV-2 genomes has documented exactly the processes this chapter formalises — drift at low incidence, bottleneck at importation, selection under **vaccine** pressure — on timescales of weeks rather than millennia, making clinical virology the fastest-moving evolutionary laboratory in human history.

22.8 Computational Bridge

Wright–Fisher sampling noise is simulated explicitly:

```
from biology.evolution import simulate_drift

traj = simulate_drift(0.5, N=30, generations=50, rng_seed=7)
print(round(traj[-1], 4))
```

Clinical / systems note: Founder effects in human isolates (Amish, Finns) mirror conservation breeding programs where small N amplifies drift — informing genetic screening panels.

22.8.1 Worked Example: Kimura’s Neutral Fixation Probability

Motoo Kimura’s neutral theory of molecular evolution (1968) predicts the fate of neutral mutations (selection coefficient $s = 0$) under drift alone. The probability that a new neutral mutation (initial frequency $1/(2N)$ in a diploid population) *eventually reaches fixation* is equal to its initial frequency:

$$u_{\text{neutral}} = \frac{1}{2N_e}$$

Worked example. In a diploid population of $N_e = 10^4$, a new neutral mutation has a fixation probability of $u = 1/(2 \times 10^4) = 5 \times 10^{-5}$ — one in 20 000. Of the mutations that do fix, the mean time to fixation is $\bar{t}_{\text{fix}} = 4N_e = 40\,000$ generations; *most* neutral mutations in fact go extinct within about $2N_e$ generations.

At the molecular level, the neutral substitution rate equals the per-individual-per-generation mutation rate μ (remarkable: substitution rate is *independent of population size* for neutral alleles, because rate $= 2N\mu \times u = 2N\mu \times 1/(2N) = \mu$). This is the molecular clock’s theoretical basis: if a site evolves neutrally, the rate of divergence between lineages is constant regardless of their N_e histories. For slightly deleterious mutations, Ohta’s near-neutral theory modifies this to $u \approx \frac{1 - e^{-2s}}{1 - e^{-4N_e s}}$, which for $|4N_e s| < 1$ reduces to the neutral result but for $|4N_e s| > 1$ predicts sharp selection-dominated fixation or loss. Biological significance: the 1 % sequence divergence between human and chimpanzee at synonymous sites (about 6 million years of separation, about 6×10^5 generations) gives $\mu \approx 1.6 \times 10^{-8}$ per site per generation — consistent with pedigree-based mutation rate estimates from trio whole-genome sequencing (deCODE 2012, 2023). Kimura’s simple formula thus *quantitatively anchors* the molecular clock to the fossil record.

22.9 Current Evidence and Frontier Biology: Genetic Drift, Gene Flow, and Speciation

For Genetic Drift, Gene Flow, and Speciation, frontier biology belongs inside the evidence logic of the chapter. Evolutionary claims are strongest when they combine mechanism, comparative evidence, population process, and explicit uncertainty. The core reading question is this: speciation claims should separate gene flow, reproductive isolation, demographic history, and genomic architecture.

- What to verify: identify the observation, model, assay, or dataset that would make the claim stronger or weaker.
- What to qualify: state the scale, organism, cell type, environmental condition, or population where the claim is expected to hold.
- What to compare: test at least one alternative explanation, baseline, or null model before treating the pattern as causal.
- What to cite: distinguish primary evidence, review synthesis, public dataset, and institutional guidance; for recent or numeric claims, prefer the source closest to the measurement and state what has changed since it was published.

For speciation claims, separate drift, gene flow, selection, geography, and reproductive isolation before treating divergence as lineage independence.

Source practice: For drift and speciation claims, pair models with sampling design, migration estimates, reproductive-isolation evidence, and alternative demographic histories.

22.10 Summary

- Genetic drift is the random change in allele frequencies due to finite population size. Its effects are strongest in small populations, where $\text{Var}[\Delta p] = p(1 - p)/(2N_e)$.
- Effective population size (N_e) is typically much smaller than census size due to unequal sex ratios, variance in reproductive success, and population fluctuations.
- Bottlenecks (cheetah, northern elephant seal) and founder effects (Amish, Finnish disease heritage) dramatically reduce genetic diversity, with consequences persisting for thousands of generations.
- Gene flow homogenizes populations; F_{ST} measures differentiation; Wright’s island model predicts $F_{ST} \approx 1/(1 + 4N_e m)$.
- Species concepts differ in emphasis: BSC (reproductive isolation), morphological (appearance), PSC (monophyly), ecological (niche), cohesion (exchangeability). Ring species challenge discrete species boundaries.
- Allopatric speciation (geographic isolation) is most common; peripatric involves small peripheral populations; parapatric occurs along environmental gradients; sympatric requires strong disruptive selection or polyploidy.
- Reproductive isolation includes prezygotic (temporal, habitat, behavioral, mechanical, gametic) and postzygotic (inviability, sterility, breakdown) barriers. Reinforcement strengthens prezygotic barriers after secondary contact.
- Hybridization and introgression contribute to adaptation (Neanderthal DNA in modern humans; Denisovan EPAS1 in Tibetans).
- Adaptive radiations (honeycreepers, cichlids, finches, post-K-Pg mammals) demonstrate rapid diversification following ecological opportunity.
- Connections: See section 20 for F_{ST} and migration, section 23 for gene trees vs. species trees, and section 40 for conservation genetics.

22.11 Key Terms

Table 298. Kimura’s Neutral Fixation Probability: Term and Definition.

Term	Definition
Genetic drift	Random change in allele frequencies due to sampling error in finite populations
Effective population size (N_e)	Size of an ideal Wright-Fisher population experiencing equivalent drift to the real population
Bottleneck effect	Severe temporary reduction in population size causing loss of genetic diversity
Founder effect	Establishment of a new population by a small, genetically non-representative group of colonizers
Gene flow	Movement of alleles between populations through migration and reproduction
F_{ST}	Fixation index measuring the proportion of genetic variation between (versus within) populations
Isolation by distance	Positive correlation between genetic differentiation and geographic distance
Biological species concept	Species defined as reproductively isolated groups of interbreeding populations [Mayr, 1942]
Phylogenetic species concept	Species defined as the smallest diagnosable monophyletic group
Allopatric speciation	Speciation resulting from geographic isolation of populations
Sympatric speciation	Speciation within a single geographic area without physical barriers
Peripatric speciation	Speciation involving a small peripheral population experiencing founder effects
Dobzhansky-Muller incompatibility	Epistatic incompatibility in hybrids from independently evolved alleles at interacting loci
Reinforcement	Natural selection strengthening prezygotic barriers when hybrids have reduced fitness
Adaptive radiation	Rapid diversification of a lineage into multiple species exploiting diverse ecological niches
Allopolyploidy	Speciation via hybridization between species followed by whole-genome duplication
Introgression	Incorporation of alleles from one species into another through hybridization and backcrossing
Ring species	Chain of interbreeding populations forming a geographic ring, with terminal populations reproductively isolated

22.12 Review Questions

1. A population of 200 individuals has initial heterozygosity $H_0 = 0.80$. Calculate the expected heterozygosity after 50 generations of pure drift (no mutation, no selection). How many generations until heterozygosity drops below 0.40?
2. Explain why the effective population size of northern elephant seals is far smaller than their current census size of 200,000. What specific aspects of their biology and history contribute to low N_e ?
3. Two island populations have $N_e = 300$ each. Calculate the equilibrium F_{ST} if (a) $m = 0.001$, (b) $m = 0.01$, and (c) $m = 0.1$ using Wright’s island model. What biological conclusion can you draw about the relationship between migration rate and population differentiation?
4. The Amish founder effect produced a frequency of the Ellis-van Creveld allele approximately 8,750 times higher than in the general population. Explain, using the concepts of founder effect and genetic drift, how a rare allele can reach such high frequency. Would natural selection alone predict this outcome?
5. Compare the biological and phylogenetic species concepts as applied to a ring species such as *Ensatina* salamanders. Which concept handles this situation more satisfactorily, and why?
6. Describe the formation of bread wheat (*Triticum aestivum*) through allopolyploidy. Why does polyploidy create instantaneous reproductive isolation? What is the evolutionary significance of the observation that about 15% of angiosperm speciation events involve polyploidy?
7. Neanderthal DNA constitutes approximately 1–4% of non-African modern human genomes. Explain how adaptive introgression of the EPAS1 allele from Denisovans illustrates that hybridization can be evolutionarily beneficial rather than merely a breakdown of species boundaries.
8. Compare and contrast the cichlid radiation in Lake Victoria with Darwin’s finch radiation on the Galapagos. What factors (sexual selection, ecological opportunity, geographic isolation) played different roles in each case? Why has the cichlid radiation produced far more species?
9. A conservation biologist is managing a population of 25 endangered wolves. The population has $H_0 = 0.65$. (a) How rapidly will heterozygosity decline per generation? (b) If genetic rescue introduces 5 individuals from a genetically distinct population per generation, qualitatively describe how this affects the trajectory. (c) What are the risks and benefits of genetic rescue?

10. Explain why Dobzhansky-Muller incompatibilities accumulate as the square of the number of substitutions (Orr’s snowball effect). What does this predict about the relationship between genetic divergence time and the strength of reproductive isolation?
11. Re-run `simulate_drift` with $N = 200$ vs. $N = 20$ for the same number of generations. Which trajectory shows larger $|p_{50} - p_0|$ on average?
12. Contrast reinforcement with fusion at secondary contact; give one genomic signature expected under each. ## Further Reading and Source Notes: Genetic Drift, Gene Flow, and Speciation
- Mayr (1942). *Systematics and the Origin of Species*. Columbia University Press.
 - Templeton (1989). The meaning of species and speciation: A genetic perspective. Sinauer.
 - Kimura (1968). Evolutionary rate at the molecular level. *Nature*, 217.
 - Kingman (1982). The coalescent. *Stochastic Processes and their Applications*, 13.
 - Coyne & Orr (2004). *Speciation*. Sinauer.

22.13 Companion Source Module: Genetic Drift, Gene Flow, and Speciation

Genetic Drift, Gene Flow, and Speciation should leave a reproducible trail from a biological claim to the code, figure, diagram, or paper-based activity that can test it. Use the surfaces below to inspect the chapter’s assumptions, rerun the relevant model, or compare the manuscript explanation with companion labs and figures.

Table 299. Companion source surfaces for Genetic Drift, Gene Flow, and Speciation.

Surface	Use it for
<code>src/biology/evolution/evolution.py</code> (<code>wright_fisher_drift</code> , <code>simulate_drift</code> , <code>isolation_index</code>)	Compare stochastic drift, bottlenecks, and isolation measures.
<code>src/mermaid/biology_diagrams.py</code> (<code>speciation_diagram</code> , <code>phylogenetic_tree_diagram</code>)	Connect reproductive isolation to lineage divergence.

Reproducibility check: report effective population size, migration, selection possibility, and time scale before assigning divergence to drift or speciation. Cross-reference: compare with section 20, section 21, and section 23.

23 Phylogenetics and the Tree of Life

Level 3/3 · 60 min read · 100 min lecture · Prerequisites: section 22

23.1 Learning Objectives

By the end of this chapter, you should be able to:

1. Explain what phylogenetics reveals about evolutionary relationships, ancestral states, divergence timing, and biogeographic origins.
2. Read and interpret phylogenetic trees, distinguishing between clades, paraphyletic groups, polyphyletic groups, and key character types (synapomorphy, symplesiomorphy, homoplasy).
3. Compare phylogenetic reconstruction methods: distance-based (UPGMA, Neighbor-Joining), maximum parsimony, maximum likelihood, and Bayesian inference.
4. Apply **molecular clock** calculations to estimate divergence times and evaluate the assumptions and limitations of clock models.
5. Describe the three-domain tree of life, including endosymbiotic origins of **organelles** and the significance of Asgard **archaea**.
6. Outline human phylogeny, including fossil hominin diversity and archaic introgression events.
7. Calculate a Jukes-Cantor corrected distance from observed sequence divergence and estimate a divergence time, explaining why the correction is needed and why mitochondrial estimates differ from nuclear calibrations.
8. Explain how long-read sequencing (PacBio HiFi, Oxford Nanopore) resolves deep-divergence and polyploid phylogenies that short reads cannot, using the animal tree of life and ancient-DNA examples.
9. Evaluate a phylogenetic claim by identifying the dataset, model, and null hypothesis needed to distinguish shared ancestry from convergence and to assess sampling and calibration uncertainty.

23.1.1 Study Blueprint

- Big idea: Phylogenies are evidence-based hypotheses about ancestry, not ladders of progress.
- Core concepts: homology, tree topology, parsimony, molecular clocks.
- Framework alignment: Vision & Change: Evolution, Systems; AP Biology: Evolution, Systems Interactions; NGSS-style topics: Natural Selection and Evolution, Interdependent Relationships in Ecosystems.
- Model or quantitative lens: Tree-distance, parsimony, and molecular-clock calculations.
- Data skill: Read trees correctly and map traits or sequences onto branches.
- Practice cadence: Visual Representations, Statistical Tests and Data Analysis, Argumentation.
- Common misconception to repair: Living species are cousins, not ancestors of one another.
- Primary lab: **Lab — Phylogenetics and the Tree of Life**.
- Question bank: **Questions — Phylogenetics and the Tree of Life**.
- Transfer task: Transfer tree thinking to pathogens, conservation units, gene families, and development.
- Bridge to computation: `biology.genetics.genetics.jukes_cantor_distance`.

Opening Vignette — The Tree That Changed Everything

In the 1970s, Carl Woese was alone in his University of Illinois laboratory, painstakingly sequencing ribosomal RNA by subjecting it to nuclease digestion and then separating fragments on two-dimensional electrophoresis gels — an agonisingly laborious technique that took months per organism. When he sequenced methanogens (thought to be unusual bacteria), the rRNA pattern was unlike any bacterium. It was unlike any **eukaryote** too. Woese concluded they formed a third domain of life — the Archaea [**Woese and Fox, 1977**]. His 1977 *PNAS* paper was widely dismissed for nearly a decade: a microbiologist claiming to overturn a century of classification with RNA fingerprints? Yet the phylogenetic evidence was incontrovertible, and by the 1990s the three-domain tree had rearranged most of biology. The lesson: molecular sequence data can reveal evolutionary relationships invisible to morphology, and great paradigm shifts are often dismissed before they are accepted.

23.2 What Phylogenetics Reveals About Shared History

Phylogenetics is the study of evolutionary relationships among organisms, inferred from heritable characters (DNA sequences, **protein** sequences, morphological traits, behavioral traits). A phylogenetic analysis produces a tree (or network) that represents the historical pattern of descent from common ancestors.

Phylogenetics addresses four fundamental questions:

1. Evolutionary relationships: Which organisms are most closely related? This is the foundation of modern biological classification – taxonomy based on shared ancestry rather than superficial similarity.

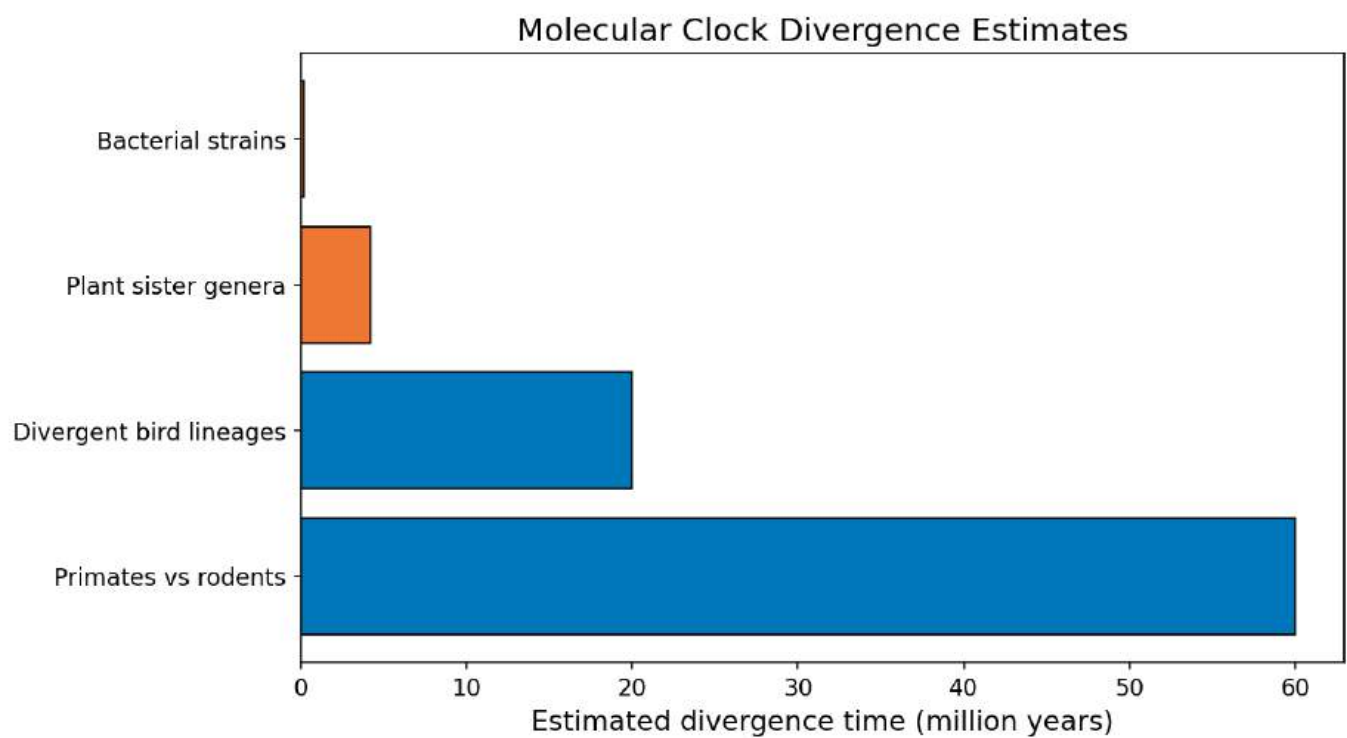


Figure 137. Molecular-clock divergence times from $t = d/(2\mu)$. Larger sequence divergence or slower substitution rates lengthen the inferred branch; faster-evolving genes or smaller divergences yield shorter estimates when the rate μ is held constant.

2. Ancestral character states: What did the ancestors look like? By mapping traits onto phylogenies, we can reconstruct the sequence in which characters evolved (e.g., when did flight originate in insects?).
3. Timing of diversification: When did lineages diverge? Molecular clocks calibrated with fossil data allow estimation of divergence dates even when the fossil record is incomplete.
4. Biogeographic origins: Where did lineages originate and how did they disperse? Phylogeography combines phylogenetics with geographic data to trace the spatial history of lineages.

23.2.1 Applications Beyond Systematics

Phylogenetics has become indispensable across biology and medicine:

- Drug discovery: Phylogenetic analysis identifies which organisms are likely to produce useful bioactive compounds. If a species in one clade produces a valuable compound, closely related species in the same clade are promising candidates for novel variants.
- Epidemiology: Genomic phylogenetics tracks pathogen spread in real time (SARS-CoV-2, HIV, Ebola). Phylogenetic clustering reveals transmission chains, identifies superspreader events, and dates outbreak origins.
- Conservation: Phylogenetic diversity (PD) metrics identify lineages that represent the greatest amount of unique evolutionary history. Losing a phylogenetically isolated species (e.g., the tuatara, sole survivor of order Rhynchocephalia) eliminates more evolutionary history than losing one species from a large, diverse clade.

Concept Check 1: Why might a conservation strategy based on phylogenetic diversity differ from one based simply on species counts? Give an example of a species with high phylogenetic distinctiveness.

23.2.2 Phylogenetic Diversity and the EDGE Framework

Phylogenetic diversity (PD), formalized by Daniel Faith (1992), is the total branch length of the phylogeny subtending a given set of species. A clade of 100 species that diverged 5 Ma has lower PD than a clade of 30 species spanning 200 Ma, because PD measures evolutionary history rather than species count alone. The EDGE (Evolutionarily Distinct and Globally Endangered) initiative of the Zoological Society of London uses PD-based metrics to prioritize conservation:

$$\text{EDGE score} = \log(1 + \text{ED}) + \text{GE} \cdot \log(2)$$

(340)

where ED (evolutionary distinctness) is each species’ share of the phylogeny it sits in, weighted by branch length, and GE (global endangerment) is the IUCN Red List category as a numerical score (Least Concern = 0, Critically Endangered = 4). Top EDGE species are both phylogenetically isolated and at high extinction risk — their loss would erase irreplaceable amounts of evolutionary history.

EDGE flagship examples:

- Tuatara (*Sphenodon punctatus*) — sole extant member of order Rhynchocephalia, sister group to most squamates (lizards and snakes). The tuatara’s lineage diverged about 250 Ma, making it one of the most phylogenetically distinct vertebrates alive. Restricted to about 30 small islands off New Zealand.
- Pygmy hippopotamus (*Choeropsis liberiensis*) — sole survivor of one of two extant hippo lineages, with deep evolutionary history.
- Aye-aye (*Daubentonia madagascariensis*) — sole member of the family Daubentoniidae, an evolutionarily distinct lemur lineage on Madagascar.
- Yangtze giant softshell turtle (*Rafetus swinhoei*) — fewer than four known living individuals; an entire evolutionary line nearly extinct.

The EDGE approach contrasts sharply with species-count-based conservation. A reserve protecting 100 closely related warbler species preserves much less evolutionary history than a reserve protecting 30 phylogenetically diverse tetrapods — a counterintuitive but biologically meaningful prioritization rule.

23.3 Tree Terminology and Reading Phylogenies

Key: A and B are sister taxa. The clade (A, B, C) is monophyletic. The outgroup roots the tree.

23.3.1 Fundamental Tree Components

Root: The node representing the most recent common ancestor (MRCA) of the sampled taxa in the tree. An outgroup – a taxon known to be outside the group of interest (the ingroup) – is used to determine the position of the root on an unrooted tree.

Internal nodes: Each internal node represents a divergence event – a **speciation** event where an ancestral lineage split into two daughter lineages. Nodes are hypothetical ancestors; they are not observed directly but inferred from the data.

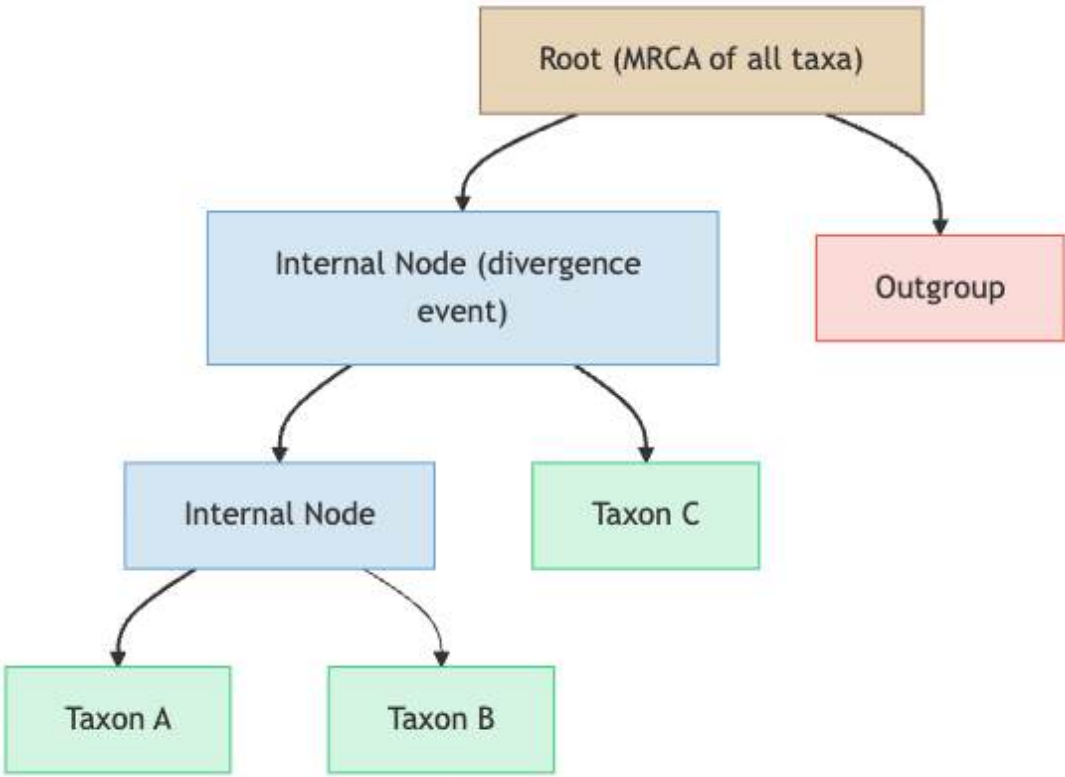


Figure 138. Reading a phylogeny depends on tracing common ancestry: roots, internal nodes, outgroups, and branch labels define relationships rather than left-to-right order.

Branches: The lines connecting nodes. In a cladogram, branch lengths have no meaning (primarily topology matters). In a phylogram, branch lengths represent the amount of evolutionary change (e.g., substitutions per site). In a chronogram (ultrametric tree), branch lengths represent time.

Tips (leaves): The terminal nodes, representing observed taxa – either extant species or fossil specimens.

Clade (monophyletic group): An ancestor and its descendant lineage. Clades are the preferred units in modern phylogenetic classification because they preserve common ancestry. The clade Mammalia includes the descendants of the MRCA of mammals – bats, whales, humans, and monotremes alike.

Sister groups: Two clades that share an immediate common ancestor. In the diagram above, Taxon A and Taxon B are sister taxa; their clade is sister to Taxon C.

Polytomy: An unresolved node where three or more lineages diverge simultaneously. A “hard” polytomy reflects genuine simultaneous speciation (rare); a “soft” polytomy reflects insufficient data to resolve the branching order (common).

23.3.2 Paraphyletic and Polyphyletic Groups

Paraphyletic group: An ancestor and SOME (but not most) of its descendants. The traditional “Reptilia” (turtles, lizards, snakes, crocodilians) is paraphyletic because it excludes birds, which are nested within the reptile clade. Modern systematics recognizes that crocodilians are more closely related to birds than to lizards – a fact that the traditional grouping obscures.

Polyphyletic group: A group whose members do NOT share a most recent common ancestor exclusive to that group. “Warm-blooded animals” (birds + mammals) is polyphyletic because endothermy evolved independently in each lineage. Polyphyletic groups reflect convergent evolution, not shared ancestry.

23.3.3 Character Types and Phylogenetic Signal

Synapomorphy: A shared derived character that defines a clade. The amniotic egg is a synapomorphy of Amniota (reptiles, birds, and mammals). Synapomorphies are the characters most informative for identifying clades.

Symplesiomorphy: A shared ancestral character inherited from a deeper ancestor. The vertebral column is shared by most vertebrates but does not diagnose any particular clade within vertebrates – it is a symplesiomorphy for any subgroup of vertebrates.

Autapomorphy: A unique derived character found in a single taxon. Feathers are an autapomorphy of Aves (or more precisely, of Maniraptora within the dinosaur phylogeny, though some non-avian maniraptorans also had feathers).

Homoplasy: A character state that appears similar in two or more taxa but was NOT inherited from their common ancestor. Homoplasy arises through convergent evolution (independent evolution of similar features – e.g., wings in bats and birds) or reversal (return to an ancestral state). Homoplasy confounds phylogenetic analysis because it falsely suggests shared ancestry.

23.3.4 Rooting Trees with Outgroups and Clocks

An unrooted tree shows the relationships among taxa but does not indicate the direction of evolutionary time. To root a tree (and thereby determine which character states are ancestral versus derived), one of two approaches is used:

- Outgroup rooting: Include a taxon known to be outside the group of interest. The root is placed on the branch connecting the outgroup to the ingroup. This is the most common method. For example, when constructing a phylogeny of mammals, a reptile (e.g., a crocodilian) serves as the outgroup.
- Midpoint rooting: Place the root at the midpoint of the longest path between any two taxa. This assumes approximately equal rates of evolution across lineages – an assumption that is often violated.

23.3.5 Reading Trees Correctly

A critical skill is reading phylogenetic trees by topology (branching pattern) rather than by the visual arrangement of tips. Trees can be rotated around any internal node without changing the evolutionary relationships they depict. The common error of reading relationships from left to right along the tips (treating one end as “primitive” and the other as “advanced”) is incorrect. Evolution does not proceed along a ladder from simple to complex; every living species is equally evolved — each has been evolving for the same amount of time since the last comprehensive common ancestor.

Common tree-thinking misconceptions Decades of cognitive-science research on student tree-reading reveal a recurring set of errors. Recognizing these misconceptions is the foundation of phylogenetic literacy:

Table 300. Common tree-thinking misconceptions: Misconception and Correction.

Misconception	Correction
Ladder thinking: Trees show a progression from “primitive” tips on one side to “advanced” tips on the other.	Trees can be rotated around any node; tip order has no biological meaning. Every tip is equally distant from the root in time.
Reading along the tips: Adjacent tips are necessarily more closely related than non-adjacent tips.	Adjacency on the page does not imply evolutionary closeness. Look at the branching topology — count the nodes shared on the path back to the MRCA.
“More evolved”: Some tips (“higher” organisms) are more evolved than others.	Most living species have been evolving for the same time. There is no “scala naturae”. A bacterium’s lineage is as long as a human’s.
The root is the oldest extant species: The root represents an existing ancestor whose features can be observed today.	The root is a hypothetical reconstructed ancestor, not a living species. Living species are at the tips, not the root.
A polytomy means simultaneous origin: Three branches emerging from a single node mean three lineages arose at the same instant.	Most polytomies are “soft” — they reflect insufficient data to resolve close branching events, not actual simultaneous origin. Hard polytomies (true simultaneous divergence) are rare.
Branch length typically means time: Most trees show time on a horizontal axis.	Primarily chronograms (ultrametric trees) show time. Cladograms show primarily topology. Phylograms show evolutionary change (substitutions). Typically check the scale bar.
Convergent traits = relatedness: Similar traits (wings in bats and birds, dorsal fins in dolphins and sharks) imply close relationship.	Convergent traits are homoplasy — they reflect similar selection pressures, not shared ancestry. Use synapomorphies, not overall similarity, to define clades.
Cousins versus ancestors: Living species can be ancestors of other living species.	Living species are sister taxa to each other, rarely ancestor–descendant. The MRCA of two living species is a hypothetical extinct ancestor, even if one species is “older” or “less changed.”

Tips for reading phylogenetic trees

1. Identify the root — it represents the most recent common ancestor of the sampled taxa shown. Check the scale bar and any axis labels.

2. Trace lineages back to the MRCA — don't read across tips horizontally. Find where two taxa share their nearest common ancestor by going down to the node where their lineages converge.
3. Look at the branching pattern, not the layout — the same topology can be displayed in many visually distinct ways (rectangular, slanted, radial, circular).
4. Distinguish character types — mapped traits should be inferred from synapomorphies (shared derived characters), not from overall similarity.
5. Note the scale — a chronogram with branch lengths in millions of years tells a different story from a phylogram with branch lengths in substitutions/site.

Concept Check 2: Consider the traditional classification “Reptilia” that includes turtles, lizards, snakes, and crocodilians but excludes birds. Is this group monophyletic, paraphyletic, or polyphyletic? Explain your reasoning based on the phylogenetic position of birds relative to crocodilians.

23.3.6 Eusociality as a Character on a Tree

Phylogenies prevent a common social-insect error: treating “ants, bees, and termites” as one natural group because each can form colonies. Ants and bees are hymenopterans, whereas molecular phylogenies place termites within cockroaches (Blattodea), not as a separate insect order outside them [Inward et al., 2007]. Their colony organization is therefore a case of convergent social evolution, not simple inheritance from one eusocial ancestor.

Mapping eusociality onto a tree asks which components are homologous and which are analogous. Cooperative brood care, overlapping generations, and reproductive division of labor define the social syndrome [Crespi and Yanega, 1995]; the genetic and ecological routes differ among ants, bees, wasps, and termites. Haplodiploidy helps explain relatedness patterns in many Hymenoptera, but diploid termites show that ancestry, mating system, nest defense, diet, and symbiosis can produce similar colony-level outcomes through different historical paths [Bourke, 2011].

23.4 Phylogenetic Reconstruction Methods

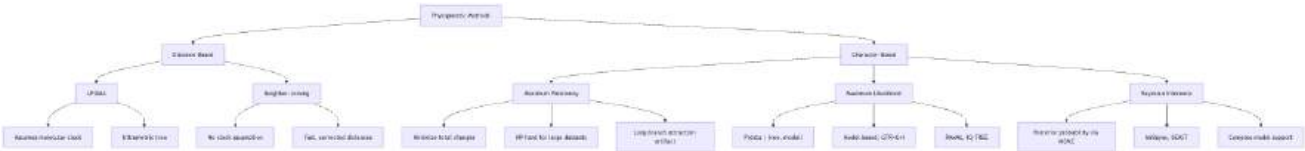


Figure 139. Phylogenetic reconstruction methods differ in the evidence they optimize: distance methods summarize pairwise divergence, while character-based methods evaluate histories of trait or sequence change.

23.4.1 Distance-Based Tree Reconstruction: UPGMA and Neighbor-Joining

UPGMA (Unweighted Pair Group Method with Arithmetic Mean): The simplest clustering algorithm. It assumes a strict molecular clock (equal rates of evolution across most lineages) and produces an ultrametric tree where most tips are equidistant from the root. UPGMA works by iteratively joining the two most similar sequences and recalculating distances.

Limitation: If the molecular clock assumption is violated (and it usually is), UPGMA produces incorrect topologies. It is not recommended for most phylogenetic analyses but remains useful for constructing guide trees in sequence alignment.

Neighbor-Joining (NJ): Developed by Saitou and Nei [1987], NJ does NOT assume a molecular clock. It works by star decomposition: starting with an unresolved star tree, it iteratively identifies the pair of taxa whose joining minimizes the total branch length. NJ is fast ($O(n^3)$ time complexity), produces additive trees with unequal branch lengths, and provides a good starting tree for more sophisticated analyses. It is appropriate for large datasets where ML or Bayesian methods would be computationally prohibitive.

23.4.2 Worked Example: One UPGMA Clustering Step from a Distance Matrix

Problem: Four taxa (A, B, C, D) have the symmetric pairwise distance matrix below (substitutions/site). Perform the first UPGMA clustering step: identify the closest pair, place their common node, and recompute the reduced distance matrix.

Table 301. One UPGMA Clustering Step from a Distance Matrix: A and B.

	A	B	C	D
A	—	0.10	0.40	0.42
B	0.10	—	0.38	0.40
C	0.40	0.38	—	0.12

	A	B	C	D
D	0.42	0.40	0.12	—

Solution:

1. Identify the smallest off-diagonal distance. Scanning the matrix, the minimum is $d_{AB} = 0.10$ substitutions/site. Join A and B into cluster (AB) .
2. Place the internal node. UPGMA builds an ultrametric tree, so the node U joining A and B sits at half the pair distance; the branch length from each of A and B up to U is

$$h_U = \frac{d_{AB}}{2} = \frac{0.10}{2} = 0.05 \text{ substitutions/site}$$

(341)

3. Recompute distances from the new cluster as the size-weighted arithmetic mean over member pairs (here $|A| = |B| = 1$):

$$d_{(AB),C} = \frac{d_{AC} + d_{BC}}{2} = \frac{0.40 + 0.38}{2} = 0.39, \quad d_{(AB),D} = \frac{d_{AD} + d_{BD}}{2} = \frac{0.42 + 0.40}{2} = 0.41$$

(342)

The distance $d_{CD} = 0.12$ is unchanged.

Interpretation: A and B cluster first at node height 0.05 substitutions/site; in the reduced matrix the smallest remaining distance is $d_{CD} = 0.12$, so the next step joins C and D, yielding the tree $((A, B), (C, D))$ — exactly what an equal-rate (clock-like) dataset should produce.

23.4.3 Maximum Parsimony and Minimum-Change Trees

Maximum parsimony selects the tree (or trees) requiring the fewest total character-state changes. This is an application of Occam’s razor – the simplest explanation is preferred.

Procedure: For each possible tree topology, map character changes onto branches to find the minimum number of steps. The tree requiring the fewest total steps across most characters is the most parsimonious.

Strengths: Intuitive; does not require an explicit model of evolution; works well when evolutionary rates are low and homoplasy is rare.

Limitations: - Computationally NP-hard: The number of possible tree topologies grows super-exponentially with the number of taxa. For n taxa, the number of unrooted bifurcating trees is $(2n - 5)!! = (2n - 5)(2n - 7)(2n - 9) \cdots (3)(1)$. For 10 taxa: 2,027,025 trees. For 20 taxa: $> 10^{21}$ trees. Heuristic search algorithms are required. - Long-branch attraction (LBA): When two distantly related lineages evolve rapidly, they accumulate homoplasies (convergent substitutions) that parsimony interprets as synapomorphies, incorrectly grouping them together. LBA is a systematic error – adding more data makes it worse, not better.

23.4.4 Worked Example: Computing a Parsimony Score for a Small Character Matrix

Problem: Four taxa (A, B, C, D) are scored for four binary morphological characters (state 0 or 1). Using the fixed rooted tree $((A, B), (C, D))$, compute the total parsimony score (minimum number of character-state changes).

Table 302. Computing a Parsimony Score for a Small Character Matrix: Taxon and Char 1.

Taxon	Char 1	Char 2	Char 3	Char 4
A	0	0	1	0
B	0	1	1	0
C	1	1	0	1
D	1	1	0	1

Solution:

Apply the Fitch bottom-up algorithm to each character independently. At each internal node take the intersection of its two children’s state sets; if the intersection is empty, take the union and add one step. Internal nodes: X = ancestor of (A, B) , Y = ancestor of (C, D) , R = root.

1. Char 1 ($A=0, B=0, C=1, D=1$): $X = \{0\} \cap \{0\} = \{0\}$ (0 steps); $Y = \{1\} \cap \{1\} = \{1\}$ (0 steps); $R = \{0\} \cap \{1\} = \emptyset \Rightarrow \{0, 1\}$ (1 step). Subtotal = 1.

2. Char 2 ($A=0, B=1, C=1, D=1$): $X = \{0\} \cap \{1\} = \emptyset \Rightarrow \{0, 1\}$ (1 step); $Y = \{1\} \cap \{1\} = \{1\}$ (0 steps); $R = \{0, 1\} \cap \{1\} = \{1\}$ (0 steps). Subtotal = 1.
3. Char 3 ($A=1, B=1, C=0, D=0$): $X = \{1\}$ (0 steps); $Y = \{0\}$ (0 steps); $R = \{1\} \cap \{0\} = \emptyset \Rightarrow \{0, 1\}$ (1 step). Subtotal = 1.
4. Char 4 ($A=0, B=1, C=1, D=1$): same pattern as Char 2 \rightarrow 1 step. Subtotal = 1.
5. Total parsimony score:

$$S = 1 + 1 + 1 + 1 = 4 \text{ steps}$$

(343)

Interpretation: The tree $((A, B), (C, D))$ requires 4 changes; the two alternative unrooted topologies $((A, C), (B, D))$ and $((A, D), (B, C))$ each require 7, so $((A, B), (C, D))$ is the most-parsimonious tree — Characters 1 and 3 are the parsimony-informative synapomorphies that group (A, B) apart from (C, D) .

Concept Check (Analysis — Parsimony vs. Maximum Likelihood on a Conflicted Alignment): Consider a four-taxon alignment with three parsimony-informative sites. Site 1 supports topology $T_A = ((W, X), (Y, Z))$ — that is, W and X share a derived state, and Y and Z share a different derived state. Sites 2 and 3 support topology $T_B = ((W, Y), (X, Z))$. (a) Calculate the parsimony score for T_A and T_B on this alignment and identify which topology parsimony prefers. (b) Now suppose lineages W and Y have evolved on very long branches with elevated substitution rates relative to X and Z , while sites 2 and 3 reside in fast-evolving regions and site 1 in a slow-evolving region. Explain how a substitution model that accounts for rate heterogeneity across sites (e.g., GTR+ Γ) and branch-length heterogeneity could lead maximum likelihood to prefer T_A — the opposite of the parsimony preference. (c) Define long-branch attraction (LBA) in terms of this example and explain why adding more data makes parsimony *worse* under LBA conditions (a statistical inconsistency) while making likelihood more reliable. (d) Propose two diagnostic tests one could run on a real alignment to detect that LBA is biasing parsimony.

23.4.5 Maximum Likelihood (ML)

Maximum likelihood selects the tree that maximizes the probability of the observed data given the tree topology, branch lengths, and an explicit model of sequence evolution:

$$L(\text{tree}, \theta) = \prod_{i=1}^L P(\text{site}_i \mid \text{tree}, \theta)$$

(344)

where L is the alignment length and θ represents the parameters of the substitution model.

Substitution models describe the probability of one **nucleotide** changing to another over a given evolutionary time:

Table 303. Maximum Likelihood (ML): Model and Description.

Model	Description	Parameters
JC69 (Jukes-Cantor, 1969)	Most substitutions equally likely; equal base frequencies	0 free parameters
K2P (Kimura 2-parameter, 1980)	Transitions \neq transversions; equal base frequencies	1 (Ti/Tv ratio)
HKY85 (Hasegawa-Kishino-Yano)	Ti \neq Tv + unequal base frequencies	4
GTR (General Time Reversible)	The 6 substitution types have independent rates + unequal base frequencies	9
GTR+ Γ +I	GTR + gamma-distributed rate variation across sites + proportion of invariant sites	11

Model selection uses information criteria: $AIC = 2k - 2 \ln L$ (where k = number of parameters) or $BIC = k \ln n - 2 \ln L$ (where n = sample size). The model with the lowest AIC or BIC provides the best balance of fit and complexity. Tools: ModelFinder (implemented in IQ-TREE), jModelTest2.

Software: RAxML (Randomized Axelerated Maximum Likelihood), IQ-TREE (fast ML with ultrafast bootstrap UFBoot2), FastTree (approximate ML for very large alignments).

23.4.6 Bayesian Inference and Posterior Tree Distributions

Bayesian phylogenetics uses Bayes’ theorem to estimate the posterior probability of trees:

$$P(\text{tree} \mid \text{data}) = \frac{P(\text{data} \mid \text{tree}) \cdot P(\text{tree})}{P(\text{data})}$$

(345)

Since $P(\text{data})$ – the marginal likelihood – is computationally intractable (it requires summing over most possible trees), Bayesian inference uses Markov Chain Monte Carlo (MCMC) to sample trees from the posterior distribution. The Metropolis-Hastings algorithm proposes modifications to the current tree, accepts changes that improve the likelihood, and occasionally accepts changes that decrease it (allowing escape from local optima).

Output: A set of posterior trees summarized as a majority-rule consensus tree. Each node receives a posterior probability (PP) – the proportion of sampled trees containing that node. $PP \geq 0.95$ is considered statistically significant support.

Software: MrBayes (standard Bayesian phylogenetics), BEAST/BEAST2 (specialized for time-calibrated chronograms, molecular clock models, and phylogeography).

Bayesian phylogenetics in practice A typical Bayesian phylogenetic workflow consists of the following steps. (1) Specify priors: a tree prior (often a Yule pure-birth or birth–death process for species trees, or a coalescent prior for population-genetic data), a clock-rate prior (e.g., a lognormal distribution centered at a calibrated rate), and substitution-model parameter priors. (2) Run two or more independent MCMC chains for 10^7 – 10^9 generations, sampling the tree topology, branch lengths, and model parameters at intervals (typically every 1,000 generations). (3) Diagnose convergence: discard the first 10–25% of samples as “burn-in”, then verify that independent chains have reached the same stationary distribution by inspecting Effective Sample Size ($ESS > 200$ for most parameters), Potential Scale Reduction Factor ($PSRF \approx 1.0$), and visual trace plots in Tracer. (4) Summarize: produce a maximum clade credibility (MCC) tree, with each node labeled by its posterior probability and (for chronograms) its 95% highest posterior density (HPD) age interval.

Comparison with bootstrap support. A widely cited rule of thumb is that posterior probability ≥ 0.95 is approximately equivalent to bootstrap support $\geq 70\%$, but the two measures are not interchangeable. Posterior probabilities tend to be higher than bootstrap values for the same node — sometimes considerably so when the substitution model is misspecified. The interpretation differs as well: a 95% posterior probability means “given the model and data, there is a 95% probability that this clade is correct”; a 70% bootstrap value means “70% of pseudoreplicate datasets recover this clade”. Modern best practice is to report both measures, and to treat single nodes with $PP < 0.95$ or bootstrap < 70 as unresolved.

Strict clock vs. relaxed clock: when to use each Bayesian phylogenetic dating uses one of two molecular-clock frameworks. A strict clock assumes a single substitution rate across the entire tree; this is appropriate for closely related taxa (within-species or recent congeners), where the assumption is testable and often defensible — e.g., dating SARS-CoV-2 lineages within a single pandemic, or dating Native American mtDNA lineages relative to the Bering Strait crossing. A relaxed clock allows substitution rates to vary across branches, drawn from a prior distribution (uncorrelated lognormal, exponential, or autocorrelated random walk). Relaxed clocks are appropriate for divergent taxa with rate heterogeneity — for example, mammalian phylogenies where rodents evolve 5–10× faster than cetaceans, or insect phylogenies where holometabolous lineages have generation-time-correlated rate shifts. The choice of clock is testable: a likelihood-ratio test or Bayes-factor comparison between strict and relaxed clock models, evaluated under the same data and tree prior, indicates which is supported. In practice, modern phylogeneticists routinely default to relaxed clocks and primarily revert to strict clocks when relaxed-clock parameter estimates indicate near-uniform rates.

23.4.7 Bootstrap Analysis and Branch-Support Uncertainty

Non-parametric bootstrap [Felsenstein, 1985] assesses branch support by resampling:

1.

Create pseudoreplicates by randomly sampling alignment columns with replacement (same length as original alignment).
2.

Reconstruct a tree from each pseudoreplicate (typically 100–1,000 replicates).
3.

The bootstrap value for each branch is the percentage of pseudoreplicate trees containing that branch.

Interpretation: Bootstrap $\geq 70\%$ is generally considered moderate to strong support. Bootstrap values are conservative estimates – a true clade may receive bootstrap support below 70% if the supporting signal is concentrated in a few alignment positions that are not always sampled.

Bootstrap vs. Bayesian PP: Bayesian posterior probabilities tend to be higher than bootstrap values for the same node. A common rule of thumb treats bootstrap support of at least 70% and posterior probability of at least 0.95 as broadly comparable thresholds, not interchangeable measures. However, PP can be inflated by model misspecification — when the substitution model fails to capture features of the data, posterior probabilities become falsely confident. Both metrics should be reported for each node, and discordance (high PP, low bootstrap, or vice versa) is itself diagnostic of either signal heterogeneity or model violation. Modern best practice typically reports nodes as well-supported primarily when both bootstrap $\geq 70\%$ and $PP \geq 0.95$ are achieved.

MCMC convergence diagnostics: A Bayesian phylogeny depends strongly on the convergence of the MCMC chains that produced it; high posterior probabilities are misleading when chains have not mixed across tree space. Standard diagnostics include:

1. Effective sample size (ESS): For each parameter (tree length, individual branch lengths, model parameters), the number of independent samples after autocorrelation correction. ESS values ≥ 200 are typically required for confident inference.
2. Multiple independent runs: The same analysis run from different random starting points should converge to indistinguishable posterior distributions. Discrepancies signal that the chains are stuck in local optima.
3. Trace plots: Visual inspection of parameter values across MCMC iterations should show a stationary “fuzzy caterpillar” pattern, not directional trends or sticking at single values.
4. Burn-in removal: The first 10–25% of MCMC iterations are typically discarded as the chain finds the high-posterior region of parameter space.

Tools like Tracer (BEAST suite) automate these checks, and submitting trees without convergence verification is now considered methodologically inadequate in published phylogenomics.

23.4.8 Gene Tree versus Species Tree Discordance

A central insight of modern phylogenomics is that gene trees frequently disagree with species trees, even when the underlying biological process is straightforward speciation. The two main biological causes:

Incomplete lineage sorting (ILS) When two speciation events occur in rapid succession, ancestral polymorphism may not have time to sort completely between the daughter lineages. Some loci will retain the ancestral relationship while others will track the species tree — producing a mosaic of gene trees that disagree with each other and with the true species history. ILS is most severe when:

- Effective population size of the ancestor is large ($4N_e$ about time between speciations)
- Speciation events are temporally close (the “anomaly zone” of phylogenetics)
- Recombination is high so that adjacent loci have independent histories

The classic case is the human–chimpanzee–gorilla trichotomy: about 30% of human nuclear loci show gene trees grouping human with gorilla, or chimp with gorilla, rather than the species-tree topology of (human, chimp) sister to gorilla. The discordance reflects ILS during the rapid succession of human–chimp–gorilla speciation events about 6–8 Ma.

Coalescent-based methods (ASTRAL, MP-EST, *BEAST) explicitly model gene-tree discordance under the multi-species coalescent and infer the species tree as the topology that maximizes likelihood across many gene trees. Concatenation methods (which simply combine most loci into one alignment) can be statistically inconsistent under high ILS — they sometimes converge to the wrong tree as more data are added.

Horizontal gene transfer (HGT) In prokaryotes, gene-tree discordance often reflects horizontal acquisition rather than incomplete sorting. A gene tree that places a thermophilic bacterium within the archaea may indicate that the bacterium acquired the gene from an archaeal source through HGT, rather than the species tree placing it incorrectly. Detecting HGT requires:

1. Phylogenetic incongruence: gene tree topology contradicts the consensus species tree.
2. Atypical sequence features: GC content, codon usage bias, or dinucleotide signature differing from the host genome.
3. Patchy phylogenetic distribution: gene present in distantly related organisms while absent from close relatives.

Tools like DistAL and reconciliation methods (Notung, Ranger-DTL) systematically identify HGT events by comparing gene trees with reference species trees.

Real-World Connection: COVID-19 Phylogenetics

The SARS-CoV-2 pandemic demonstrated the power of real-time phylogenetics. Within weeks of the first **genome** sequence being shared (January 2020), phylogenetic analysis confirmed the virus’s origin in the betacoronavirus clade related to bat coronaviruses. Platforms like Nextstrain (nextstrain.org) provided continuously updated phylogenetic trees from millions of viral genomes deposited in GISAID. Bayesian time-calibrated analyses (BEAST) dated the most recent common ancestor to approximately November 2019. Phylogenetic tracking identified the emergence and global spread of Variants of Concern (Alpha, Delta, Omicron), revealing that each arose from a single geographic origin and spread globally through human travel. Genomic epidemiology became a standard public health tool, guiding variant surveillance, **vaccine** updating, and travel policy. The pandemic validated decades of investment in phylogenetic methodology and demonstrated that evolutionary biology has direct, immediate public health applications.

23.4.9 Worked Example: Molecular Clock Calibration — Cytochrome b in Mammals

Problem: Two mammalian taxa differ at 8 % of cytochrome *b* nucleotide positions ($p = 0.08$). Mammalian cytochrome *b* evolves at a rate of approximately 2 % sequence divergence per million years (lineage-summed; equivalently about 1 % per lineage per Myr). Estimate the divergence time between the two taxa, and discuss principal uncertainty sources.

Solution:

1. Naive estimate (uncorrected p-distance). If sequences accumulate substitutions linearly with time at 2 % per Myr:

$$t \approx \frac{p}{\text{rate}} = \frac{0.08}{0.02 \text{ per Myr}} = 4 \text{ Mya}$$

2. Jukes-Cantor-corrected distance. Multiple substitutions at the same site cause saturation; the JC correction is:

$$d_{JC} = -\frac{3}{4} \ln\left(1 - \frac{4}{3}p\right) = -\frac{3}{4} \ln(1 - 0.1067) = -\frac{3}{4} \ln(0.8933) \approx 0.0846$$

Using the corrected distance and the lineage-summed rate ($k = 0.02$ per Myr):

$$t = \frac{d_{JC}}{k} \approx \frac{0.0846}{0.02} = 4.23 \text{ Mya}$$

The correction is small at $p = 0.08$ (still well below saturation) but grows nonlinearly as p approaches the JC asymptote of 0.75.

3. Uncertainty sources to quantify. A defensible reported estimate would be about 4 ± 1 Mya, with the uncertainty driven by:
- Rate heterogeneity across lineages. The 2 %-per-Myr rate is an average; cytochrome *b* in rodents evolves 2–5× faster than in cetaceans. A relaxed clock (uncorrelated lognormal or autocorrelated rate prior) properly propagates this rate variance and typically widens the 95 % HPD by 30–60 %.
 - Fossil calibration error. The 2 %-per-Myr rate is itself calibrated against fossil divergence dates with their own uncertainty (typically ± 10 –20 % on the calibrating node). Compounding error.
 - Incomplete lineage sorting (ILS). Gene trees may not match the species tree; a single locus (cyt *b*) over a short coalescent time can give a TMRCA that predates the species divergence by 0.5–2× the ancestral N_e generations. For mammalian $N_e \sim 10^5$ and generation time about 2 yr, this is up to about 200 kyr of additional uncertainty.
 - Strict-clock assumption. If a strict clock is forced where rates are heterogeneous, the point estimate is biased toward the average — but lineages with elevated rates appear systematically older than they are.
4. Bayesian relaxed-clock alternative. BEAST2 with an uncorrelated-lognormal relaxed clock, a fossil-calibrated tree prior, and a substitution model selected via Bayes factors typically gives a 95 % HPD interval roughly twice as wide as the naive JC point estimate above. For this problem, a Bayesian relaxed-clock analysis would likely report a posterior median of about 4 Mya with 95 % HPD about [2.5, 5.8] Mya. The strict clock would report a tighter but potentially overconfident interval.

Interpretation. Molecular-clock dating gives a quantitative null model against which fossil constraints, biogeographic events, and other lines of evidence are integrated. The naive point estimate (4 Mya) is a useful first-order anchor; honest reporting requires the relaxed-clock interval plus an explicit accounting of ILS for sub-population-genetic-time divergences.

Concept Check 3: Why is long-branch attraction a problem specifically for maximum parsimony but less so for maximum likelihood? (Hint: consider whether each method uses an explicit model of substitution rates.)

Concept Check (Synthesis — Phylogenomic Conflict in a Songbird Radiation): A phylogenomic study of a recent songbird radiation (5 species, divergence times 1–4 Mya) reconstructs both the nuclear consensus tree (concatenated 5,000 conserved nuclear loci) and the mitochondrial tree (whole mtDNA). The two trees agree at 60 % of nodes but disagree at 40 % of nodes — including the basal split of the radiation. (a) Propose three biological mechanisms that could generate this nuclear–mitochondrial discordance: incomplete lineage sorting (ILS), ancestral hybridization and introgression (including mitochondrial capture, where an entire mtDNA lineage is replaced by introgression), and sex-biased dispersal causing differential effective population sizes for nuclear vs. mitochondrial loci. (b) Identify one technical artifact that could mimic biological discordance — for example, base-compositional non-stationarity (some lineages drifted to AT-rich mtDNA, attracting unrelated AT-rich lineages under poorly-fitting substitution models). (c) Design a test that distinguishes ILS from hybridization at one specific node using the ABBA–BABA D-statistic: given four populations ($(P_1, P_2), P_3, O$) where O is an outgroup, ILS produces equal frequencies of ABBA and BABA site patterns ($D \approx 0$), while

introgression from P_3 into either P_1 or P_2 produces an excess of one pattern ($D \neq 0$). Specify how to compute D from genome-wide SNP data, what null distribution to use, and what sample size of SNPs is needed for statistical power. (d) If the D -statistic test returns $D = 0.08$ with $|Z| = 6$ — strongly significant — synthesize what this finding means for the species-tree reconstruction: which population received introgression, and how should this be communicated in the published phylogeny?

23.5 Molecular Clocks and Divergence-Time Estimation

23.5.1 The Molecular Clock Hypothesis

Zuckerkandl and Pauling [1965] observed that the number of amino acid differences between homologous proteins from different species is roughly proportional to the time since those species diverged. figure 137 compares example divergence-time estimates from the relation $t = d/(2\mu)$. This molecular clock hypothesis – that neutral substitutions accumulate at an approximately constant rate – allows divergence times to be estimated from sequence data.

The theoretical basis comes from Kimura’s neutral theory (1968): the rate of neutral substitution equals the neutral mutation rate, μ , regardless of population size. For strictly neutral mutations:

$$k = \mu$$

(346)

where k is the substitution rate per site per generation.

23.5.2 Clock Calculations from Sequence Divergence

Jukes-Cantor correction: Observed sequence divergence underestimates true divergence because of multiple substitutions at the same site (saturation). The JC69 correction accounts for this:

$$d_{JC} = -\frac{3}{4} \ln\left(1 - \frac{4}{3}p\right)$$

(347)

where p is the observed proportion of differing sites.

Divergence time estimation:

$$t = \frac{d_{JC}}{2\mu}$$

(348)

The factor of 2 accounts for substitutions accumulating independently in both lineages since their divergence from a common ancestor.

23.5.3 Worked Example: Estimating Divergence Time using Jukes-Cantor

Problem: Human and chimpanzee mitochondrial *cytochrome b* sequences differ by approximately 1.5% ($p = 0.015$). Assume a mitochondrial substitution rate of $\mu \approx 2 \times 10^{-8}$ substitutions per site per year. 1. Calculate the Jukes-Cantor distance (d_{JC}). 2. Estimate the divergence time (t) between the two lineages.

Solution:

1. Calculate the Jukes-Cantor distance: Using the Jukes-Cantor correction formula to account for multiple substitutions at the same site:

$$d_{JC} = -\frac{3}{4} \ln\left(1 - \frac{4}{3}(0.015)\right) \approx 0.01511 \text{ substitutions/site}$$

(349)

2. Estimate the divergence time: Apply the divergence time estimation formula, remembering the factor of 2 (since mutations accumulate along both lineages branching from the MRCA):

$$t = \frac{d_{JC}}{2\mu} = \frac{0.01511}{2 \times 2 \times 10^{-8}} \approx 3.78 \times 10^5 \text{ years}$$

(350)

Note: This estimate of about 378,000 years for mtDNA is much lower than the accepted species divergence time of about 6–7 Mya. This occurs because mitochondrial genes evolve significantly faster than the genome-wide average, and substituting a long-term nuclear calibration rate yields an artificially recent divergence for rapidly evolving loci.

23.5.4 Rate Calibration with Fossils and Tip Dates

Molecular clocks must be calibrated against independent time estimates:

- Fossil record: Fossils provide minimum age constraints – a fossil establishes that a lineage existed by that time, but the actual divergence must be older. The oldest known fossil of a clade provides a minimum bound on the clade’s age.
- Biogeographic events: The formation of the Isthmus of Panama (about 3 Mya), the separation of Australia from Antarctica (about 45 Mya), or the formation of volcanic islands (known radiometric ages) provide calibration points.

23.5.5 Strict vs. Relaxed Clocks

Strict molecular clock: Assumes a constant substitution rate across most lineages. This assumption is often violated because substitution rates vary with generation time (shorter-generation organisms evolve faster per unit time), metabolic rate, DNA repair efficiency, and population size (through the interplay of drift and selection).

Relaxed molecular clock: Allows the rate to vary among lineages while still estimating divergence times. Two main approaches: - Autocorrelated rates: Closely related lineages have similar rates (rates evolve gradually along the tree). Implemented in BEAST. - Uncorrelated rates: Each branch draws its rate independently from a statistical distribution (e.g., lognormal). Implemented in BEAST2.

23.5.6 Molecular Clock Limitations: Rate Heterogeneity, Generation Time, and Saturation

- Rate heterogeneity: Substitution rates can vary dramatically among lineages. Rodents evolve approximately 5–10 times faster than cetaceans at synonymous sites.
- Generation time effect: Species with shorter generation times accumulate more mutations per unit time because there are more DNA replication events per year.
- Saturation: At very large divergence times, multiple substitutions at the same site erase the phylogenetic signal. Slowly evolving genes (18S rRNA, about $1\text{--}2 \times 10^{-9}$ substitutions per site per year) are needed for deep divergences.

23.5.7 Tip Dating and Bayesian Skyline Plots

Modern molecular clock analyses go beyond simple point estimates of divergence times:

- Tip dating: When sequences are sampled at different calendar dates (e.g., viral genomes collected over the course of an epidemic), the sampling dates themselves provide calibration points. BEAST software uses tip dates to estimate substitution rates directly from serially sampled data — no fossil calibration needed. This approach was critical for dating the SARS-CoV-2 origin, HIV emergence, and influenza evolution.
- Bayesian Skyline Plots: These reconstruct changes in effective population size (N_e) through time from a single population sample. By analyzing the distribution of coalescence times in a gene genealogy, skyline plots reveal historical population expansions, bottlenecks, and declines. Applied to human mtDNA, skyline analyses confirm the Out-of-Africa expansion approximately 60–70 kya.

23.5.8 A timeline of major events in life’s phylogeny

Phylogenetic methods, when calibrated against the geological record, reconstruct a deep-time timeline of life on Earth. The major events span four billion years:

Table 304. A timeline of major events in life’s phylogeny: Era and Approximate date.

Era	Approximate date	Event
Hadean–Eoarchean	about 4.5–4.0 Ga	Earth forms (about 4.54 Ga); oceans condense (about 4.4 Ga); abiogenesis events (debated dates)
Eoarchean	about 3.8–3.5 Ga	Earliest evidence of life (graphite isotope signatures from Greenland; stromatolites in Australia)

Era	Approximate date	Event
LUCA	about 3.8 Ga	Last Comprehensive Common Ancestor — root of the tree of life. Inferred from comprehensive molecular machinery (rRNA, ribosomal proteins, ATP synthase, key tRNAs). LUCA was likely an anaerobic, hyperthermophilic prokaryote dependent on H ₂ /CO ₂ chemistry near hydrothermal vents.
Mesoarchean–Paleoproterozoic	about 3.0–2.4 Ga	Cyanobacteria evolve oxygenic photosynthesis; Great Oxidation Event (about 2.4 Ga) transforms atmosphere from anoxic to oxic
Paleoproterozoic	about 2.0 Ga	LECA (Last Eukaryotic Common Ancestor) — already possessed a nucleus, mitochondria (from α -proteobacterial endosymbiont), endomembrane system, cytoskeleton, and meiotic sexual reproduction. The mitochondrial endosymbiosis is dated to about 2.0–1.5 Ga.
Mesoproterozoic	about 1.6–1.0 Ga	Plastid endosymbiosis (cyanobacterium → primary plastid in archaeplastid ancestor); diversification of eukaryotic supergroups
Neoproterozoic	about 1.0 Ga – 540 Ma	Snowball Earth events; first multicellular eukaryotes; Ediacaran biota (about 575–540 Ma) — soft-bodied multicellular organisms, mostly enigmatic in affinity
Cambrian	about 540–485 Ma	Cambrian explosion: most modern animal phyla appear in the fossil record within about 25 million years. Evolution of mineralized skeletons, predator-prey ecosystems, complex sensory systems
Ordovician	about 485–445 Ma	Diversification of marine invertebrates; first land plants (bryophytes); end-Ordovician extinction (about 445 Ma): about 85% of marine species lost
Silurian–Devonian	about 445–360 Ma	Vascular plants colonize land; jawed fish (Gnathostomata) diversify; first tetrapods (about 375 Ma; <i>Tiktaalik</i>); late Devonian extinction

Era	Approximate date	Event
Carboniferous	about 360–299 Ma	Coal-forest ecosystems; first amniotes (reptilian-line ancestors); insects undergo first major radiation
Permian	about 299–252 Ma	Synapsids (mammal ancestors) dominate; end-Permian extinction (Great Dying, about 252 Ma): about 96% of marine species lost — the largest extinction event in life’s history
Triassic–Jurassic	about 252–145 Ma	Dinosaurs diversify; first mammals (about 225 Ma) and first birds (Late Jurassic); end-Triassic extinction (about 201 Ma)
Cretaceous	about 145–66 Ma	Flowering plants (angiosperms) emerge and diversify; mammals remain small but radiate quietly; K-Pg extinction (about 66 Ma): asteroid impact + Deccan Traps volcanism eliminate non-avian dinosaurs
Cenozoic	about 66 Ma – present	Mammalian and bird radiations fill ecological niches; primates evolve; <i>Homo sapiens</i> appears (about 300 ka); Holocene/Anthropocene extinction ongoing

The central insight from this timeline: life persists across cataclysms but is reshuffled. The five mass extinctions did not erase the tree of life but pruned it dramatically — and post-extinction radiations repeatedly produce explosive diversification as surviving lineages occupy emptied ecological space (mammals after the K-Pg, modern teleost fish after the Permian, etc.).

23.5.9 Ancestral Sequence Reconstruction (ASR)

One of the most striking applications of phylogenetic methods is ancestral sequence reconstruction — inferring the DNA or protein sequences of extinct ancestors from their living descendants. Given a tree and a substitution model, ASR uses maximum likelihood or Bayesian methods to estimate the most probable ancestral state at each internal node and at each site.

How ASR works For each site in a multiple sequence alignment, ASR computes:

$$P(\text{ancestor} = X \mid \text{tip data, tree, model})$$

using the Felsenstein pruning algorithm (which efficiently sums over most possible ancestral states at internal nodes). Marginal reconstructions estimate the most probable state at each node independently; joint reconstructions estimate the most probable combined ancestral states across the whole tree. Confidence is reported as the posterior probability for each reconstructed residue — high-confidence sites have a single dominant residue (>95% probability), while low-confidence sites have several plausible alternatives.

“Lazarus proteins”: resurrecting extinct enzymes Once an ancestral sequence is reconstructed, it can be synthesized as a real protein in the laboratory — a “Lazarus protein” brought back from extinction. This approach has revolutionized our understanding of how protein function evolves:

- Ancestral steroid receptors (Joe Thornton’s lab, since the early 2000s): The mineralocorticoid and glucocorticoid receptors split about 450 Mya. Resurrection of the ancestral receptor showed it was a glucocorticoid-like receptor; specificity for cortisol versus aldosterone evolved later through a small number of historical substitutions. The reconstruction made testable predictions about which substitutions enabled the functional shift — confirmed experimentally by mutagenesis on the modern proteins.
- Ancestral elongation factors (Akanuma et al. 2013, Gaucher et al. 2008): Ancestral bacterial EF-Tu proteins reconstructed from extant sequences proved highly thermostable, with melting temperatures of 60–73°C. The thermostability profile across nodes traces planetary cooling — providing biological thermometers that measure the temperature history of Earth.
- Ancestral β -lactamases: Reconstructed enzymes from before the antibiotic era reveal “promiscuous” ancestral activity — the ancestral enzymes catalyzed multiple reactions efficiently. Modern descendants are more specialized but less catalytically robust. This pattern of ancestral promiscuity → descendant specialization is widespread in enzyme evolution.
- Ancestral rhodopsins illuminate the spectral history of vision: by reconstructing visual pigments at deep nodes in the vertebrate tree, researchers have inferred the wavelengths of light that ancestral fish, amphibians, and reptiles could detect — and found that color vision was repeatedly lost and re-evolved across many lineages.

Practical applications of ASR ASR is more than a historical exercise — it is now a protein-engineering platform. Resurrected ancestral proteins are routinely more thermostable and more catalytically robust than their modern descendants — a pattern repeatedly observed across ancestral β -lactamases, EF-Tu elongation factors, alcohol dehydrogenases, and rhodopsins. The hypothesized explanation is that ancestral proteins evolved under broader environmental tolerances (early Earth was warmer; ancestral metabolisms more flexible), and that modern descendants are specialized but brittle — selection has pruned away robustness in favor of niche-specific performance. The applied consequence: industrial enzyme engineering increasingly uses ASR to prospect for thermostable scaffolds, then optimizes the resurrected protein for specific substrate specificity. Ancestral *Bacillus* α -amylases have been engineered into industrial laundry-detergent enzymes that retain function at 60–80 °C; ancestral *Pseudomonas* esterases have been used as starting points for plastic-degrading enzymes (PETase variants); and pharmaceutical biotechnology uses ASR to design more thermostable vaccine antigens (e.g.,

The 16S rRNA gene is ideal for deep phylogenetics because it is present in all cellular organisms, contains both highly conserved regions (for universal primer design) and variable regions (for discriminating taxa), and is long enough (about 1,550 bp) for robust phylogenetic inference.

23.5.10 Domain Bacteria and Prokaryotic Phylogenetic Diversity

Bacteria are the most metabolically diverse domain of life. Major phyla include:

- Proteobacteria: The largest and most diverse bacterial phylum.
 - Alpha-proteobacteria: includes *Rickettsia* (obligate intracellular pathogen) and the SAR11 clade (most abundant organisms in the ocean). The ancestor of mitochondria was an alpha-proteobacterium.
 - Gamma-proteobacteria: includes *Escherichia coli*, *Pseudomonas*, *Salmonella*, *Vibrio cholerae*.
 - Epsilon-proteobacteria: includes *Helicobacter pylori* (causes gastric ulcers and gastric cancer).
- Firmicutes: Gram-positive, low-GC content. Includes *Bacillus* (anthrax), *Clostridium* (tetanus, botulism), *Staphylococcus*, *Lactobacillus* (probiotic fermenters), *Streptococcus*.
- Bacteroidetes: **Dominant** gut anaerobes; critical for polysaccharide digestion. *Bacteroides* species compose 30–40% of human fecal bacteria.
- Actinobacteria: Gram-positive, high-GC content. *Streptomyces* produces over two-thirds of clinically used antibiotics. *Mycobacterium tuberculosis* causes tuberculosis.
- Cyanobacteria: Oxygenic photosynthesizers that produced Earth’s oxygen atmosphere (Great Oxidation Event, about 2.4 Ga). The ancestor of **chloroplasts** was a cyanobacterium.
- Spirochetes: Helical morphology. *Treponema pallidum* (syphilis), *Borrelia burgdorferi* (Lyme disease).
- Chlamydiae: Obligate intracellular **parasites** with a unique biphasic developmental cycle.

23.5.11 Domain Archaea and the Eukaryote Connection

Archaea were originally found primarily in extreme environments, but culture-independent methods (metagenomics) have revealed that they are ubiquitous – in soils, oceans, and the human gut.

- Euryarchaeota: The most diverse archaeal phylum.
 - Methanogens (*Methanobacterium*, *Methanosarcina*): produce methane as a metabolic byproduct; dominant in **anaerobic** environments (wetlands, ruminant guts, landfills).
 - Extreme halophiles (*Halobacterium*): thrive in salt-saturated environments; use bacteriorhodopsin for light-driven proton pumping.

- Thermoacidophiles (*Thermoplasma*): grow at pH 1–2 and temperatures up to 60 degrees C.
- Crenarchaeota: Many are hyperthermophiles. *Sulfolobus* grows at 80 degrees C and pH 2–3. *Thermoproteus* is an anaerobic sulfur-reducing hyperthermophile.
- TACK superphylum: Thaumarchaeota (ammonia-oxidizing archaea – major players in the nitrogen cycle), Aigarchaeota, Crenarchaeota, and Korarchaeota.
- Asgard archaea: The most significant discovery in archaeal biology in decades. Named after Norse mythology:
 - Lokiarchaeota: Discovered via metagenome-assembled genomes from Loki’s Castle hydrothermal vent, Arctic Mid-Ocean Ridge. Contains eukaryotic signature proteins including homologs of **actin**, tubulin-like GTPases, ESCRT membrane remodeling complex, and Arp2/3 complex regulators.
 - Thorarchaeota, Odinarchaeota, Heimdallarchaeota: Additional Asgard lineages with progressively more eukaryotic-like features.
 - The Asgard archaea are the closest known living relatives of eukaryotes, supporting the “two-domain” tree (Eocyte hypothesis) in which eukaryotes arose from within Archaea rather than as a separate domain.

23.5.12 Domain Eukarya and Endosymbiotic Origins

The Last Eukaryotic Common Ancestor (LECA) already possessed a nucleus, mitochondria, endomembrane system, **cytoskeleton**, and sexual reproduction. Modern eukaryotic diversity is organized into several supergroups:

- Amorphea:
 - Amoebozoa: Amoebas, slime molds (*Dictyostelium*), *Entamoeba histolytica* (amoebic dysentery).
 - Opisthokonta: Fungi + Metazoa (animals) + choanoflagellates (closest unicellular relatives of animals). This grouping – placing fungi as the sister group of animals rather than plants – was one of the great surprises of molecular phylogenetics.
- Diaphoretickes:
 - SAR clade: Stramenopiles (diatoms, brown algae, oomycetes) + Alveolata (*Plasmodium*, dinoflagellates, ciliates) + Rhizaria (foraminifera, radiolarians).
 - Archaeplastida: Glaucophyta + Rhodophyta (red algae) + Chloroplastida (green algae + land plants). This clade acquired plastids through primary **endosymbiosis** with a cyanobacterium.
- Excavata (debated monophyly): Deep-branching protists including *Giardia* (intestinal parasite), *Trichomonas* (STI pathogen), *Trypanosoma* (sleeping sickness, Chagas disease), and *Euglena*.

23.5.13 Endosymbiotic Theory in Tree-of-Life Reconstruction

Lynn Margulis (1967, then writing as Lynn Sagan) proposed that mitochondria and chloroplasts originated as free-living bacteria engulfed by ancestral eukaryotic cells. Decades of molecular evidence have confirmed this theory:

Primary endosymbiosis: - Mitochondria: Descended from an alpha-proteobacterium. Evidence: mitochondria have their own circular DNA, replicate by binary fission, have double membranes (inner membrane = bacterial membrane), use bacterial-type **ribosomes** (70S), and their gene sequences cluster with alpha-proteobacteria in phylogenetic analyses. - Chloroplasts: Descended from a cyanobacterium. Evidence: chloroplasts have circular DNA, 70S ribosomes, double membranes, and gene sequences grouping with cyanobacteria. Thylakoid membranes resemble cyanobacterial internal membranes.

Secondary endosymbiosis: A eukaryotic cell engulfs a photosynthetic eukaryote (which already has a primary plastid). This explains the three or four membranes surrounding plastids in groups such as euglenids (two extra membranes from the engulfed cell), diatoms, dinoflagellates, and cryptophytes. Some secondary plastids even retain a vestigial nucleus (nucleomorph) from the engulfed alga.

23.5.14 Horizontal Gene Transfer and the Web of Life

Horizontal gene transfer (HGT) – the transfer of genetic material between organisms outside of parent-to-offspring transmission – is widespread in prokaryotes and fundamentally challenges the tree metaphor for representing life’s history.

Mechanisms of HGT: - Transformation: Uptake of free environmental DNA through competence proteins. - Transduction: Bacteriophage-mediated DNA transfer. - Conjugation: Direct cell-to-cell transfer via pili; the primary route for antibiotic resistance **plasmid** transfer.

An estimated 20–30% of genes in a typical prokaryotic genome have been acquired by HGT. In *E. coli* MG1655, **Lawrence and Ochman [1998]** identified approximately 755 genes (about 18% of the genome) acquired by HGT, identifiable by atypical GC content, **codon** usage, and phylogenetic incongruence.

The prevalence of HGT means that prokaryotic evolution is better represented by a network or web of life rather than a strictly bifurcating tree. For eukaryotes, vertical inheritance dominates the nuclear genome, but organellar genomes and some nuclear genes (acquired by endosymbiotic gene transfer, EGT) record the history of endosymbiosis.

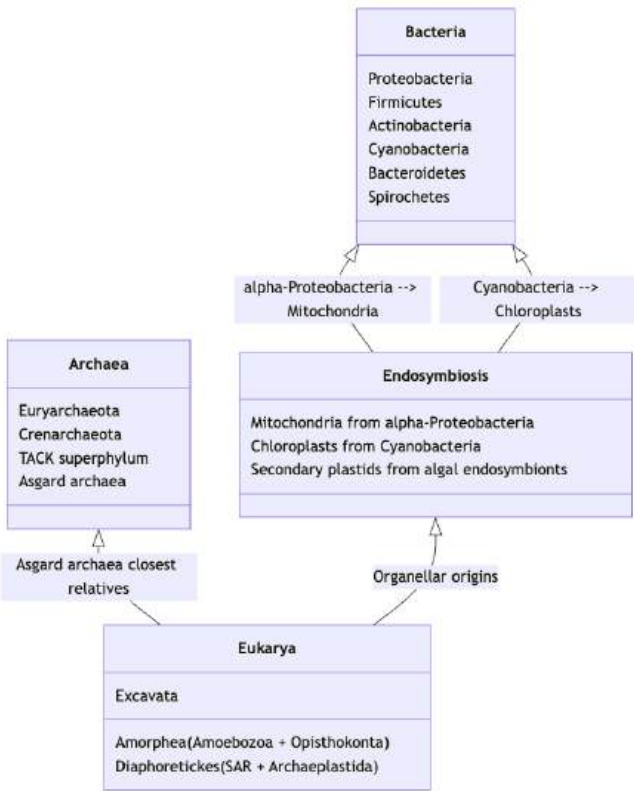


Figure 140. The three domains of life with endosymbiotic organelle origins: mitochondria from alpha-Proteobacteria, chloroplasts from Cyanobacteria, and the Asgard-archaea root of Eukarya.

Real-World Connection: Antibiotic Resistance and HGT

The spread of antibiotic resistance among pathogenic bacteria is fundamentally a problem of horizontal gene transfer. Resistance genes – encoding **enzymes** that degrade antibiotics (beta-lactamases), modify antibiotics (aminoglycoside acetyltransferases), or pump them out of the cell (efflux pumps) – are frequently carried on mobile genetic elements: plasmids, transposons, and integrons. A single conjugation event can transfer multi-drug resistance from a harmless gut bacterium to a pathogenic strain. The NDM-1 (New Delhi metallo-beta-lactamase) gene, first identified in 2008, has spread globally within years via plasmid-mediated HGT, conferring resistance to nearly every beta-lactam antibiotic class, including carbapenems – the “last resort” drugs. Understanding HGT is essential for combating the antibiotic resistance crisis.

Concept Check 5: Explain why the discovery of Asgard archaea (particularly Lokiarchaeota) supports a two-domain rather than three-domain tree of life. What eukaryotic signature proteins were found in Lokiarchaeota genomes?

23.6 Human Phylogeny and Hominin Evolution

23.6.1 Great Apes and Molecular Phylogeny

Humans belong to the superfamily Hominoidea (great apes and lesser apes). Molecular phylogenetics has resolved the relationships within this group with high confidence:

- Gibbons (family Hylobatidae): lesser apes; diverged from the great ape lineage approximately 18–20 Mya.
- Orangutans (*Pongo*): diverged approximately 14 Mya. Two species: Bornean (*P. pygmaeus*) and Sumatran (*P. abelii*), plus the recently described Tapanuli orangutan (*P. tapanuliensis*).
- Gorillas (*Gorilla*): diverged approximately 9–10 Mya. Two species: western (*G. gorilla*) and eastern (*G. beringei*).
- Chimpanzees and bonobos (*Pan*): Our closest living relatives. Humans and chimpanzees share approximately 98.7% DNA sequence identity across alignable regions. Divergence approximately 6–7 Mya.
- Humans (*Homo sapiens*): The primarily surviving species of genus *Homo*.

The molecular phylogeny contradicts earlier morphology-based classifications that grouped orangutans, gorillas, and chimpanzees as “great apes” separate from humans. DNA data unambiguously place humans within the great apes, as the sister taxon of *Pan*.

23.6.2 Fossil Hominins and Mosaic Human Evolution

The human fossil record is one of the richest and most intensively studied:

Table 305. Fossil Hominins and Mosaic Human Evolution: Species and Approximate dates.

Species	Approximate dates	Key features
<i>Sahelanthropus tchadensis</i>	about 7 Mya	Oldest possible hominin; anterior foramen magnum suggests bipedality
<i>Ardipithecus ramidus</i>	about 4.4 Mya	Partial skeleton (“Ardi”); woodland bipedality with grasping feet
<i>Australopithecus afarensis</i>	about 3.9–2.9 Mya	“Lucy” (AL 288-1); bipedal with small brain (about 430 cc); Laetoli footprints
<i>Australopithecus africanus</i>	about 3.3–2.1 Mya	South African “gracile” australopith; Taung child
<i>Homo habilis</i>	about 2.4–1.4 Mya	First stone tools (Oldowan industry); brain about 600–700 cc
<i>Homo ergaster/erectus</i>	about 1.8 Mya–110 kya	First hominin to leave Africa; Acheulean hand axes; brain about 900–1100 cc; controlled use of fire
<i>Homo heidelbergensis</i>	about 700–200 kya	Common ancestor of Neanderthals and modern humans; brain about 1200 cc
<i>Homo neanderthalensis</i>	about 400–40 kya	Adapted to cold European/Western Asian environments; brain about 1500 cc; burial of dead, use of pigments
<i>Homo sapiens</i>	about 300 kya–present	Anatomically modern; fully symbolic culture; originated in Africa

23.6.3 Out of Africa

The Out of Africa hypothesis, supported by both genetic and fossil evidence, proposes that anatomically modern *Homo sapiens* evolved in Africa and subsequently dispersed to populate the rest of the world, largely replacing (but partially admixing with) archaic hominin populations:

- Mitochondrial Eve: Coalescence analysis of mtDNA places the most recent common ancestor of living human mitochondrial lineages in Africa approximately 150–200 kya.
- Y-chromosomal Adam: The most recent common ancestor of living human Y **chromosomes** dates to approximately 200–340 kya.
- Multiple dispersal events: Genetic evidence suggests at least two major dispersal waves – an early dispersal to Australia/Oceania (about 65 kya) and a later dispersal populating Europe and Asia (about 45–50 kya).

23.6.4 Archaic Introgression from Neanderthals and Denisovans

One of the most remarkable discoveries of the genomic era is that modern humans carry DNA from extinct hominin species, acquired through interbreeding:

- Neanderthal admixture: Non-African modern human populations carry approximately 1–4% Neanderthal-derived DNA. Interbreeding occurred approximately 50,000–60,000 years ago in the Middle East. Neanderthal **alleles** contribute to traits including skin pigmentation, hair texture, immune function, and susceptibility to certain diseases.
- Denisovan admixture: Melanesian and Australian Aboriginal populations carry approximately 4–6% Denisovan-derived DNA. The Denisovans are known primarily from a few fragmentary fossils from Denisova Cave, Siberia, and a mandible from Tibet, but their genomic legacy is substantial.
- Adaptive introgression: Some introgressed alleles have been maintained by **natural selection** because they conferred adaptive advantages:
 - EPAS1: A Denisovan-derived allele of this **transcription** factor helps Tibetans adapt to high-altitude hypoxia by blunting the erythropoietic response to low oxygen, preventing polycythemia.
 - HLA alleles: Neanderthal and Denisovan-derived HLA variants increased immune diversity in modern human populations expanding into new pathogen environments.
 - BNC2: A Neanderthal-derived skin pigmentation gene at high frequency in European populations.
- Ghost lineage introgression: Analysis of West African genomes (Yoruba, Mende) reveals approximately 2–19% of their ancestry from an unknown archaic hominin that diverged from the modern human lineage approximately 625 kya – a “ghost” population for which no fossils have been identified.

Concept Check 6: Explain why “Mitochondrial Eve” does not mean there was a single woman alive at that time. What does the coalescence of mitochondrial lineages actually tell us?

Concept Check 7: A phylogenomic analysis of 1,000 mammalian loci finds that 70% of gene trees support topology A, 20% support topology B, and 10% support topology C, where A places mouse with rat (sister taxa), B groups mouse with primates, and C groups rat with primates. Is this pattern consistent with incomplete lineage sorting, horizontal gene transfer, or model misspecification? Which species-tree-inference method would be most appropriate here?

Concept Check 8: A researcher reconstructs an ancestral steroid receptor by maximum likelihood from 50 modern sequences. The reconstructed ancestral residue at one critical position has posterior probability 0.55 (versus 0.40 for the second-most-likely residue). What does this low confidence imply about the resurrected protein, and how should it influence the experimental design? (Consider: should both candidate ancestors be synthesized?)

Concept Check 9: A SARS-CoV-2 lineage emerges in late 2021 with a novel constellation of mutations not directly descended from any of the previously detected variants. The Bayesian time-calibrated tree dates the most recent common ancestor of this lineage to early 2020. What scenarios could explain this temporal mismatch — sustained cryptic transmission, evolution in an immunocompromised host, or zoonotic re-emergence? What additional data would discriminate among these hypotheses?

Clinical Connection — Genomic epidemiology. Phylogenetic trees built from pathogen genomes are now routine public-health infrastructure. For HIV, each new clinical isolate is placed on a national phylogeny to identify transmission clusters and guide focused intervention. For hospital-acquired infections (MRSA, *C. difficile*), whole-genome sequencing plus phylogenetic analysis distinguishes ward-level outbreaks from sporadic community acquisitions — a 2013 Cambridge study traced 15 distinct *C. difficile* lineages in a single hospital, revealing that about 35 % of cases were nosocomial. For SARS-CoV-2, the real-time GISAID phylogeny guided variant-specific vaccine updates.

Clinical Connection — Identifying zoonotic spillover sources. When Ebola, SARS-CoV, MERS, or H5N1 emerge, the first question is: where did it come from? Phylogenetic analysis places the human isolate within the tree of known animal reservoirs, identifying the ancestor branch. SARS-CoV-2’s closest known relatives are horseshoe-bat (*Rhinolophus*) coronaviruses from Yunnan, China, sharing about 96 % sequence identity — a divergence time estimated by molecular clock at 40–70 years. These analyses direct surveillance (which wild populations to screen) and inform policy on wildlife-market regulation.

23.7 Computational Bridge

Strict-clock time from fractional divergence (per site) is:

```
from biology.evolution import molecular_clock_divergence_time

years = molecular_clock_divergence_time(1e-9, 0.02)
print(years)
```

Clinical / systems note: Pathogen phylogenomics during outbreaks uses the same clock logic with externally calibrated rates (serial sampling) rather than fossils.

23.7.1 Long-Read Sequencing and Deep-Divergence Phylogenetics

The accuracy of any phylogenetic tree is bounded by the fidelity of its underlying sequence data — and for billion-year divergences the short-read Illumina platform (150–300 bp fragments) has been the bottleneck. Short reads mis-assemble through repetitive regions, collapse paralogs, and cannot span structural variants. Long-read platforms — PacBio HiFi (HIFI: 15–25 kb reads at 99.9 % accuracy via circular consensus sequencing) and Oxford Nanopore Ultra-long reads (100 kb – 2 Mb reads at 97–99 % raw accuracy, 99.9 % after polishing) — have transformed the field since 2020.

Three phylogenetic problems that long reads solved: (1) The animal tree of life. Sponges vs. ctenophores as the earliest-branching animal clade — a 10-year controversy — was re-adjudicated with 1178 long-read-assembled orthologs (Redmond & McLysaght, *Nat. Commun.* 2021); the analysis supported ctenophores-first, implying convergent evolution of the nervous system (or its loss in sponges). (2) Polyploid plant genomes. The hexaploid wheat genome (5 × the human genome size) was resolvable primarily with HiFi + Hi-C scaffolding (*Nature* 2023), enabling the first accurate subgenome-level phylogeny of grass evolution. (3) Ancient DNA phylogenetics. PacBio HiFi on Pleistocene-age samples now reaches < 50 000-year mammoths and permafrost wolves; Nanopore ultra-long

sequencing on sediment-trapped eDNA (eDNA-seq) reconstructs environments without individual organisms — extending phylogenetics to ecosystems rather than single species.

Practical workflow for a 2025 phylogenomic study: HiFi sequencing to 30× coverage (about \$3000 per vertebrate-scale genome, 2024 prices) → assembly with hifiasm → BUSCO completeness check → orthologue identification with OrthoFinder → multiple sequence alignment with MAFFT-einsi → species-tree inference with ASTRAL under the multi-species coalescent → dating with MCMCTree against molecular-clock calibrations from the fossil record. The bottleneck has shifted from sequence generation to taxonomic sampling — we have the tools, we need the specimens.

23.8 Current Evidence and Frontier Biology: Phylogenetics and the Tree of Life

For Phylogenetics and the Tree of Life, frontier biology belongs inside the evidence logic of the chapter. Evolutionary claims are strongest when they combine mechanism, comparative evidence, population process, and explicit uncertainty. The core reading question is this: phylogenetic confidence depends on sampling, model choice, homology, conflict among loci, and calibration.

- What to verify: identify the observation, model, assay, or dataset that would make the claim stronger or weaker.
- What to qualify: state the scale, organism, cell type, environmental condition, or population where the claim is expected to hold.
- What to compare: test at least one alternative explanation, baseline, or null model before treating the pattern as causal.
- What to cite: distinguish primary evidence, review synthesis, public dataset, and institutional guidance; for recent or numeric claims, prefer the source closest to the measurement and state what has changed since it was published.

For phylogenetic claims, separate tree signal, model choice, convergence, sampling, and gene-tree conflict before treating topology as history.

Source practice: For phylogenetic claims, compare distance, likelihood, Bayesian, fossil, and genomic evidence when alternatives such as convergence or incomplete lineage sorting matter.

23.9 Summary

- Phylogenetics reconstructs evolutionary relationships from molecular and morphological data, enabling classification, divergence dating, biogeographic reconstruction, and applications in medicine, conservation, and drug discovery.
- Tree terminology: Root (MRCA), nodes (divergence events), branches (lineages), tips (observed taxa), clades (monophyletic groups). Paraphyletic and polyphyletic groups are invalid in modern systematics. Synapomorphies define clades; symplesiomorphies and homoplasies do not.
- Reconstruction methods: UPGMA (assumes clock; not recommended), Neighbor-Joining (fast, no clock), Maximum Parsimony (fewest changes; vulnerable to long-branch attraction), Maximum Likelihood (model-based; GTR+Γ+I; RAxML, IQ-TREE), Bayesian Inference (MCMC sampling; posterior probabilities; MrBayes, BEAST).
- Molecular clocks: $d_{JC} = -\frac{3}{4} \ln(1 - \frac{4}{3}p)$; $t = d/(2\mu)$; calibrated from fossils and biogeographic events; strict vs. relaxed clocks accommodate rate variation.
- Three domains: Bacteria (metabolically diverse; source of mitochondria and chloroplasts), Archaea (Asgard archaea closest to eukaryotes), Eukarya (Amorphea, Diaphoretickes, Excavata). Endosymbiosis produced mitochondria (alpha-proteobacterium) and chloroplasts (cyanobacterium).
- HGT is pervasive in prokaryotes (20–30% of genes); the tree of life is more accurately a web for prokaryotes. HGT drives antibiotic resistance spread.
- Human phylogeny: Diverged from chimpanzees about 6–7 Mya; fossil record spans *Sahelanthropus* to *Homo sapiens*; Out-of-Africa dispersal; archaic introgression from Neanderthals (1–4% in non-Africans) and Denisovans (4–6% in Melanesians); adaptive introgression (EPAS1, HLA alleles).
- Connections: See section 24 for HGT vs. vertical signal, section 14 for variant interpretation, and section 40 for phylogenetic diversity in triage.

23.10 Key Terms

Table 306. Long-Read Sequencing and Deep-Divergence Phylogenetics: Term and Definition.

Term	Definition
Phylogenetics	The study of evolutionary relationships among organisms, inferred from heritable characters
Clade	A monophyletic group: an ancestor and its complete descendant lineage
Synapomorphy	A shared derived character that defines a clade
Symplesiomorphy	A shared ancestral character inherited from a more distant ancestor; uninformative for grouping
Homoplasy	Similarity not due to shared ancestry; arises from convergent evolution or reversal
Outgroup	A taxon known to fall outside the ingroup; used to root phylogenetic trees
Maximum parsimony	Phylogenetic method selecting the tree requiring the fewest total character-state changes

Term	Definition
Maximum likelihood	Method selecting the tree maximizing $P(\text{data} \mid \text{tree, model})$
Bayesian inference	Method estimating the posterior probability of trees using MCMC sampling
Posterior probability	$P(\text{tree} \mid \text{data})$; Bayesian branch support; ≥ 0.95 is significant
Bootstrap	Resampling technique for assessing branch support; $\geq 70\%$ indicates moderate-strong support
Molecular clock	Hypothesis that neutral substitutions accumulate at approximately constant rate, enabling divergence time estimation
Substitution model	Mathematical description of nucleotide or amino acid replacement probabilities (e.g., JC69, GTR+ Γ +I)
Horizontal gene transfer	Transfer of genetic material between organisms outside parent-offspring inheritance
Endosymbiosis	Origin of organelles (mitochondria, chloroplasts) from free-living bacteria engulfed by ancestral eukaryotes
Asgard archaea	Archaeal superphylum (Lokiarchaeota, Thorarchaeota, etc.) that are the closest known relatives of eukaryotes
Phylogenetic diversity (PD)	Total branch length of a phylogeny containing a set of species; used in conservation prioritization
LECA	Last Eukaryotic Common Ancestor; possessed nucleus, mitochondria, endomembrane system
Introgression	Incorporation of alleles from one species into another through hybridization and backcrossing

23.11 Review Questions

1. Define monophyletic, paraphyletic, and polyphyletic groups. For each, provide an example from vertebrate taxonomy and explain why primarily monophyletic groups are valid in modern systematics.
2. Reconstruct a parsimony analysis for four taxa (A, B, C, D) given the following binary characters: Character 1: A=1, B=1, C=0, D=0; Character 2: A=1, B=0, C=1, D=0; Character 3: A=1, B=1, C=1, D=0. Which tree requires the fewest steps? Is there homoplasy?
3. A researcher obtains a 600 bp alignment of the COI gene from two beetle species, finding 42 differences. (a) Calculate the observed divergence (p). (b) Apply the Jukes-Cantor correction. (c) Using a COI substitution rate of 2.3×10^{-2} per site per million years, estimate the divergence time.
4. Compare maximum likelihood and Bayesian inference as phylogenetic methods. What are the advantages and disadvantages of each? When would you choose one over the other?
5. Explain why the GTR+ Γ +I substitution model is preferred over simpler models (JC69, K2P) for most real phylogenetic datasets. What biological realities does each additional parameter capture?
6. Describe the evidence supporting the endosymbiotic origin of mitochondria from alpha-proteobacteria. List at least four independent lines of evidence.
7. Explain how Asgard archaea challenge the three-domain tree of life. What specific eukaryotic features have been found in Asgard genomes, and what does this imply about the origin of eukaryotes?
8. The SARS-CoV-2 pandemic relied heavily on phylogenetic analysis. Describe how Bayesian time-calibrated phylogenetics (BEAST) was used to (a) date the origin of the pandemic, (b) track the emergence of Variants of Concern, and (c) reconstruct transmission chains. How is a molecular clock calibrated for a virus with no fossil record?
9. Modern non-African humans carry approximately 1–4% Neanderthal DNA. Explain the process by which this DNA was acquired and describe one example of adaptive introgression. Why is Neanderthal DNA being gradually purged from functionally important genomic regions?
10. A conservation biologist must choose between protecting Species X (one of 50 species in a diverse, recently radiated clade) and Species Y (the sole surviving member of an ancient lineage). Using the concept of phylogenetic diversity, argue for which species should receive priority and explain the logic behind the EDGE conservation framework.
11. Why does uncorrected p -distance underestimate deep divergences, and when is Jukes–Cantor inadequate compared with GTR+ Γ ?
12. Name one scenario where a network rather than a bifurcating tree better represents genome evolution. ## Further Reading and Source Notes: Phylogenetics and the Tree of Life
 - Saitou & Nei (1987). The neighbor-joining method: a new method for reconstructing phylogenetic trees. *Molecular Biology and Evolution*, 4.
 - Felsenstein (1985). Confidence limits on phylogenies: An approach using the bootstrap. *Evolution*, 39.
 - Zuckerkandl & Pauling (1965). Evolutionary divergence and convergence in proteins. *Evolving Genes and Proteins*.
 - Lawrence & Ochman (1998). Molecular archaeology of the {Escherichia coli} genome. *Proceedings of the National Academy of Sciences*, 95.

- Woese & Fox (1977). Phylogenetic structure of the prokaryotic domain: The primary kingdoms. *Proceedings of the National Academy of Sciences*, 74.

23.12 Companion Source Module: Phylogenetics and the Tree of Life

Phylogenetics and the Tree of Life should leave a reproducible trail from a biological claim to the code, figure, diagram, or paper-based activity that can test it. Use the surfaces below to inspect the chapter’s assumptions, rerun the relevant model, or compare the manuscript explanation with companion labs and figures.

Table 307. Companion source surfaces for Phylogenetics and the Tree of Life.

Surface	Use it for
src/biology/evolution/evolution.py (molecular_clock_divergence_time)	Translate genetic distance and rate assumptions into divergence-time estimates.
src/biology/genetics/genetics.py (hamming_distance, jukes_cantor_distance)	Compare raw and corrected sequence distances.
src/mermaid/biology_diagrams.py (phylogenetic_tree_diagram)	Keep topology, branch length, and interpretation visually distinct.

Reproducibility check: state alignment quality, homology assumption, substitution model, sampling, and calibration before treating a tree as history. Cross-reference: use section 22 and section 24.

Unit VII — Microbiology: Introduction

Why This Unit Matters

The living world is microbial. In mass, in metabolic diversity, and in evolutionary history, microorganisms dominate life on Earth. The total number of prokaryotic cells on Earth (about 10^{30}) exceeds the number of stars in the observable universe by a factor of 100,000. The deepest branches of the tree of life are most microbial. Photosynthesis — the ultimate source of energy for most ecosystems — was invented by cyanobacteria more than 2.7 billion years ago. Nitrogen fixation, without which terrestrial agriculture would collapse, is performed exclusively by bacteria and archaea. The atmosphere itself was transformed by microbial metabolism long before any animal breathed it.

Medical microbiology became possible primarily after Robert Koch’s postulates (1877–1884) established the germ theory of disease — the revolutionary idea that specific microorganisms cause specific infections. Alexander Fleming’s observation in 1928 that *Penicillium* mould killed staphylococcal colonies initiated the antibiotic era, saving an estimated 200 million lives over the following century. But pathogens evolve. The emergence of multidrug-resistant organisms (MRSA, XDR-TB, carbapenem-resistant *Enterobacteriaceae*) represents one of the most urgent public health crises of the 21st century: an estimated 1.27 million deaths were attributable to antimicrobial resistance in 2019 (Murray et al., 2022, *The Lancet*).

This unit combines cell biology (structure of bacteria, archaea, and viruses), quantitative microbiology (growth curves, MIC calculations, viral replication kinetics), and ecology (the microbiome, biogeochemical cycles, infectious disease dynamics). You will apply the S-I-R epidemiological model and calculate R_0 ; model bacterial growth and antibiotic kill curves; and examine the microbiome as a complex ecological community whose disruption underlies diseases from *C. difficile* colitis to metabolic syndrome.

Landmark Discoveries

Discoverer(s)	Year	Journal / Source	Discovery	Significance
Antoni van Leeuwenhoek	1676	[Leeuwenhoek, 1684]	First observation of bacteria (“animalcules”)	Founded microbiology; showed microorganisms are everywhere
Louis Pasteur	1859–1861	[Pasteur, 1861]	Disproof of spontaneous generation	Established germ theory; revolutionised medicine and food safety
Robert Koch	1876–1884	[Koch, 1884]	Koch’s postulates; anthrax, TB, cholera	Rigorous criteria for linking pathogen to disease
Alexander Fleming	1928	[Fleming, 1929]	Penicillin discovery	Launched the antibiotic era; Nobel Prize 1945
Carl Woese & George Fox	1977	[Woese and Fox, 1977]	Archaea as third domain (16S rRNA)	Restructured the comprehensive tree of life; archaea are closer to eukaryotes than to bacteria
David Relman et al.	1999–2006	[Relman et al., 1999 , The Human Microbiome Project Consortium, 2012]	Human microbiome characterization by 16S rRNA	Revealed about 10^{13} microbial cells as an integral part of human biology
Murray et al.	2022	[Murray et al., 2022]	Global mortality from antimicrobial resistance (1.27 million deaths, 2019)	Quantified the scale of the AMR crisis as a call to action

Key Concepts and Connections

Current Evidence Thread

In microbiology, a claim is primarily as strong as the way the organism was observed: read this unit as an evidence trail in which microbial life is established through culture, sequencing, and surveillance rather than as a list of named taxa and diseases. Microbiology and infectious disease now require One Health reasoning across people, animals, environments, genomics, and antimicrobial stewardship. As you move through the chapters, keep a two-column note: claim

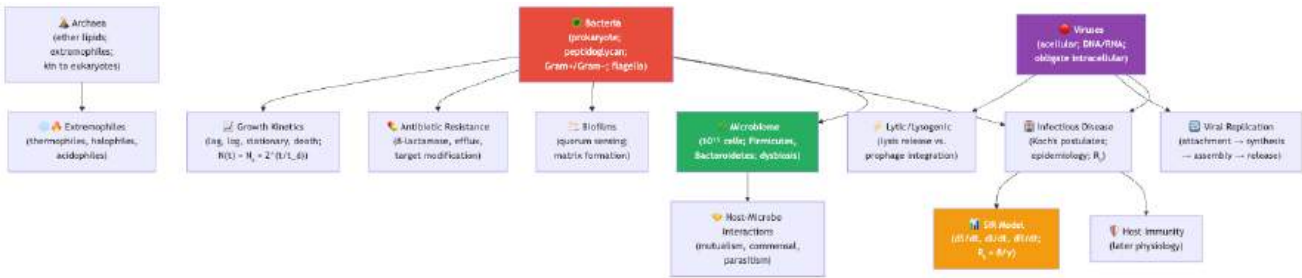


Figure 141. Microbiology concept map - red = bacteria; purple = viruses; green = microbiome; orange = epidemiological models.

on the left, evidence that would change my confidence on the right. By the end of the unit, each major idea should be tied to a measurement, model, citation, or paper-based lab decision.

Chapter Roadmap

Chapter	Title	Core Question	Key Equation / Model
22	Bacteria, Archaea, and Viruses	What distinguishes the three major types of microorganism, and how do they replicate?	Doubling time: $t_d = \ln 2/\mu$; viral burst size
23	Microbial Ecology	What roles do microorganisms play in ecosystems and the human body?	MIC, MBC; diversity indices (Shannon H')
24	Infectious Disease	How do pathogens cause disease, and how do epidemics spread?	SIR model: $R_0 = \beta/\gamma$; basic reproductive number

Connections Across the Textbook

- Prokaryotic cell structure in section 5 and section 6 provides the foundation for understanding antibiotic mechanisms (cell wall, ribosome 70S targets).
- Viral replication links to **Unit IV — Molecular Genetics: Introduction** (CRISPR discovered as a bacterially-encoded anti-phage defense system; RNA viruses and reverse transcriptase).
- Antibiotic resistance evolution is a direct application of **Unit VI — Evolution: Introduction** (natural selection, fitness, molecular clocks on resistance genes).
- Infectious disease epidemiology (SIR model) connects to **Unit X — Ecology: Introduction** (disease ecology, parasite-host dynamics in community ecology).
- Microbiome connects to **Unit IX — Zoology and Systems Physiology: Introduction** (gut-brain axis, immune regulation) and **Unit X — Ecology: Introduction** (decomposer role in nutrient cycling).

Key vocabulary introduced here: peptidoglycan, Gram stain, endotoxin (LPS), exotoxin, minimum inhibitory concentration (MIC), basic reproductive number (R_0), prophage, bacteriophage, quorum sensing, biofilm, prion, viroid, microbiome, dysbiosis, Koch’s postulates.

Computational Toolbox — Unit VII

```
from biology.microbiology import bacterial_growth_curve, doubling_time

# Bacterial growth: E. coli at 37°C, doubling time about 20 min (0.333 h)
growth = bacterial_growth_curve(N0=1e3, doubling_time_hr=1/3, t_end_hr=4, lag_phase_hr=0)
print(f"Start: {growth.populations[0]:.0f} cells")
print(f"After 4 h: {growth.populations[-1]:.2e} cells")
print(f"Growth rate: {growth.growth_rate_per_hr:.2f} h-1")
# Expected:
# Start: 1000 cells
# After 4 h: 4.10e+06 cells
# Growth rate: 2.08 h-1
```

```
# Doubling time from two measurements
td = doubling_time(N0=1e3, Nt=4.096e6, elapsed_time_hr=4)
print(f"Estimated doubling time: {td*60:.1f} min")
# Expected: Estimated doubling time: 20.0 min
```

Try it yourself: Change `doubling_time_hr` from `1/3` to `1.0` and compare final population size after 4 hours.

Source modules: `src/biology/microbiology/` — `bacterial_growth_curve()`, `doubling_time()`, `mic_fold_dilution()`, `VIRAL_REPLICATION_CYCLES`. Figures: `src/visualization/` (growth curves, SIR dynamics); `src/mermaid/biology_diagrams.py` (viral replication cycle diagrams).

Cross-Unit Integration

Unit VII — Microbiology: Introduction’s microbiology — bacterial growth, viral replication, antimicrobial action, host–pathogen coevolution — sets up an immune-recognition problem that **Unit VIII — Botany — Plant Biology: Introduction** confronts from the plant side first. Plants face a constant assault from microbial and viral pathogens but lack circulating immune cells; instead they deploy pattern-recognition receptors (PRRs) at the cell surface, intracellular NLR proteins, systemic acquired resistance signaling, and chemical defenses (phytoalexins, glucosinolates) that mirror — through convergent evolution — the innate-immune logic of animals. As **Unit VIII — Botany — Plant Biology: Introduction** develops plant biology, recognize the immune-signaling motifs from **Unit VII — Microbiology: Introduction** (PAMP recognition, RNA-silencing antiviral defense, quorum-disrupting chemistry) reappearing in a stationary, autotrophic organism. The shared logic is older than the kingdoms.

24 Bacteria, Archaea, and Viruses

Level 2/3 · 65 min read · 75 min lecture · Prerequisites: section 6

24.1 Learning Objectives

By the end of this chapter, you should be able to:

1. Compare the three domains [Woese and Fox, 1977] of life and explain how rRNA phylogeny established the Bacteria-Archaea-Eukarya classification.
2. Describe bacterial cell structure including peptidoglycan architecture, Gram staining outcomes, and the clinical significance of LPS.
3. Trace the peptidoglycan biosynthesis pathway through MurA-MurF, lipid I, and lipid II, identifying the antibiotic targeting each step and the resistance mechanism that defeats it.
4. Classify bacteria by morphology, arrangement, and metabolic type, and identify major pathogenic groups.
5. Explain horizontal gene transfer mechanisms (transformation, transduction, conjugation) and their role in bacterial evolution and antibiotic resistance [Lawrence and Ochman, 1998].
6. Describe two-component signal transduction, biofilm formation, and quorum sensing as the molecular basis of bacterial sociality, and link them to chronic infections and device-associated disease.
7. Distinguish Archaea from Bacteria at the molecular level, including ether-linked isoprenoid lipids and tetraether monolayers, and describe the significance of Asgard archaea for eukaryotic origins.
8. Compare the Baltimore classification of viruses, contrast lytic and lysogenic cycles, and describe the HIV life cycle and its drug targets.
9. Explain CRISPR-Cas as a bacterial adaptive immune system, compare Types I/II/III, and assess phage therapy as a clinical alternative to antibiotics.
10. Apply the bacterial growth equation $N(t) = N_0 \cdot 2^{t/t_d}$ to predict cell densities from generation time and infer doubling time from optical-density data.

24.1.1 Study Blueprint

- Big idea: Microbial diversity reflects different cell architectures, genomes, metabolisms, and evolutionary histories.
- Core concepts: prokaryotic structure, archaea, viruses, horizontal gene transfer.
- Framework alignment: Vision & Change: Evolution, Systems, Structure and function; AP Biology: Evolution, Systems Interactions; NGSS-style topics: Structure and Function, Interdependent Relationships in Ecosystems.
- Model or quantitative lens: Growth-rate, genome-size, and dilution calculations.
- Data skill: Interpret microbial observations from growth, sequence, or structural evidence.
- Practice cadence: Questions and Methods, Representing and Describing Data, Argumentation.
- Common misconception to repair: Viruses are not simply tiny bacteria; they use fundamentally different replication logic.
- Primary lab: Lab — Bacteria, Archaea, and Viruses.
- Question bank: Questions — Bacteria, Archaea, and Viruses.
- Transfer task: Apply microbial diversity reasoning to antibiotics, biotechnology, ecology, and outbreaks.
- Bridge to computation: `biology.microbiology.microbiology.bacterial_growth_curve`.

Opening Vignette — The Rebel Biologist Who Turned Bacteria into Organelles

In 1966, Lynn Margulis — an unknown 28-year-old junior faculty member at Boston University — submitted a paper proposing that mitochondria and chloroplasts were once free-living bacteria engulfed by a host cell [Sagan, 1967]. The serial endosymbiosis hypothesis was rejected by more than fifteen journals before *Journal of Theoretical Biology* finally published it. Her evidence: the matching size and ribosome type of mitochondria and bacteria, their independent division by binary fission, and the circular DNA they share with prokaryotes. When molecular sequencing arrived in the 1970s, it confirmed everything — mitochondria are phylogenetically embedded within the α -Proteobacteria, and chloroplasts within the Cyanobacteria. Margulis had been completely right. The bacterial origin of eukaryotic organelles is now foundational to cell biology, and stands as one of the most important corrections to the naive view that bacteria are too simple to matter for complex life.

24.2 Bacteria – Domain Overview and Cell Structure

24.2.1 The Three Domains of Life

In 1977, Carl Woese and George Fox revolutionized our understanding of life’s diversity by analyzing ribosomal RNA (rRNA) sequences across organisms [Woese and Fox, 1977]. Their phylogenetic analysis revealed that life comprises three fundamental domains: Bacteria, Archaea, and Eukarya. This replaced the older five-kingdom system that had grouped bacteria and archaea together as “Monera.”

The 16S rRNA gene (in prokaryotes) and 18S rRNA gene (in eukaryotes) serve as molecular chronometers because they are:

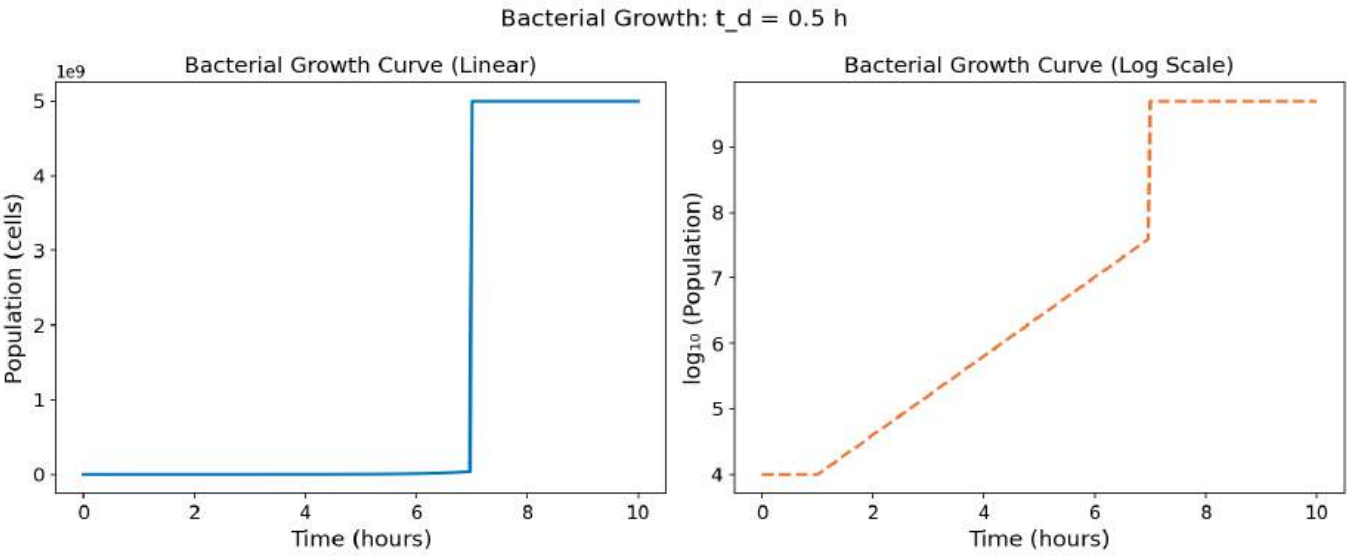


Figure 142. Bacterial growth curve: four phases (lag, exponential, stationary, death) plotted as $\log(\text{cell number})$ versus time.

- Almost universally present in most cellular life
- Functionally constrained (slow evolutionary rate in conserved regions)
- Sufficiently variable in hypervariable regions (V1-V9) for taxonomic resolution
- Rarely subject to horizontal gene transfer

24.2.2 Prokaryotic Cell Features

Bacteria and Archaea share the prokaryotic cell plan, which differs fundamentally from the eukaryotic organization:

Table 308. Prokaryotic Cell Features: Feature and Prokaryotes.

Feature	Prokaryotes	Eukaryotes
Nucleus	No membrane-bound nucleus; nucleoid region	Membrane-bound nucleus with nuclear pores
Ribosomes	70S (30S + 50S subunits)	80S (40S + 60S subunits)
Chromosome	Typically circular; nucleoid-associated proteins (HU, H-NS, IHF)	Linear chromosomes; histone octamer packaging
Cell division	Binary fission (FtsZ ring)	Mitosis with spindle apparatus
Internal membranes	Rare (thylakoids in cyanobacteria)	Extensive endomembrane system
Flagella	Proton motive force-driven rotation (not ATP)	Dynein-powered 9+2 microtubule arrangement

The bacterial flagellum is a remarkable molecular machine. Unlike eukaryotic flagella, which bend in a wave-like motion powered by ATP-dependent dynein motors, the bacterial flagellum rotates like a propeller. The basal body contains a rotary motor driven by the proton motive force (or Na⁺ gradient in some marine species), spinning at up to 1,700 revolutions per second in some species. The flagellar motor can reverse direction, enabling the “run and tumble” chemotaxis behavior in *E. coli*.

24.2.3 Bacterial Cell Wall: Peptidoglycan

The bacterial cell wall is composed of peptidoglycan (also called murein), a mesh-like polymer unique to bacteria. Its structure consists of:

- Glycan strands: Alternating units of N-acetylglucosamine (NAG) and N-acetylmuramic acid (NAM) linked by β-1,4 glycosidic bonds
- Tetrapeptide side chains: Attached to NAM; typically L-Ala – D-Glu – meso-DAP (or L-Lys) – D-Ala
- Cross-links: Peptide bridges connecting adjacent glycan strands, catalyzed by transpeptidases (penicillin-binding proteins, PBPs)

The presence of D-amino acids (D-glutamate, D-alanine) is unusual in biology – most proteins use exclusively L-amino acids. D-amino acids confer resistance to host proteases, which evolved to cleave L-amino acid peptide bonds.

24.2.4 Peptidoglycan Biosynthesis: A Step-by-Step Antibiotic Atlas

Peptidoglycan biosynthesis proceeds in three spatial compartments — cytoplasm, inner-membrane interface, and periplasm — and nearly every step has a clinically deployed antibiotic that targets it. Understanding the pathway is therefore equivalent to understanding the chemotherapy of bacterial infection. The pathway begins with the housekeeping sugar UDP-N-acetylglucosamine (UDP-GlcNAc) and ends with a covalently cross-linked sacculus surrounding the entire cell.

Table 309. Peptidoglycan Biosynthesis: A Step-by-Step Antibiotic Atlas: Step and Enzyme / process.

Step	Enzyme / process	Drug	Mechanism of inhibition	Spectrum
1	MurA (UDP-GlcNAc enolpyruvyl transferase)	Fosfomycin	Phosphoenolpyruvate analog; covalently inhibits MurA active-site Cys via epoxide ring opening	Broad (UTIs, <i>E. coli</i> , <i>Enterococcus</i>)
2	MurB (UDP-GlcNAc-EP reductase)	(No clinical drug; preclinical leads)	Reduces enolpyruvyl ether to D-lactate	—

Step	Enzyme / process	Drug	Mechanism of inhibition	Spectrum
3	MurC, MurD, MurE, MurF (amino-acid ligases)	(Preclinical pyrazolopyrimidines, hydrazides)	Block ATP-dependent ligation of L-Ala, D-Glu, meso-DAP/L-Lys, and D-Ala–D-Ala	Investigational
4	Alr / Ddl (D-Ala racemase, D-Ala-D-Ala ligase)	D-cycloserine	D-Ala structural analog; covalently traps both racemase and ligase active-site residues	Anti-TB (second-line)
5	MraY (phospho-MurNAc-pentapeptide translocase)	Tunicamycin (research primarily); mu-raymycins (preclinical)	Blocks attachment of pentapeptide to C55 lipid carrier (Lipid I formation)	Toxic to humans (also blocks N-glycosylation)
6	MurG (UDP-GlcNAc:Lipid I GlcNAc transferase)	(Preclinical)	Blocks Lipid I → Lipid II conversion	Investigational
7	C55-PP recycling (BacA/UppP phosphatase)	Bacitracin	Sequesters undecaprenyl-pyrophosphate, blocking dephosphorylation; bactoprenol pool exhausted	Topical (Gram-positive)
8	Lipid II flipping (MurJ flippase)	Lysobactin family (preclinical)	Trap Lipid II in cytoplasm	Investigational
9	Lipid II (D-Ala-D-Ala terminus)	Vancomycin, teicoplanin, dalbavancin, oritavancin	Glycopeptide H-bonds to D-Ala-D-Ala; sterically blocks PBP access and transglycosylation	MRSA, <i>C. difficile</i> , VRE-susceptible enterococci
10	Transglycosylation + transpeptidation by PBPs	Penicillins, cephalosporins, carbapenems, monobactams	β -lactam ring acylates PBP active-site serine (suicide substrate; mimics D-Ala–D-Ala)	Broad
11	Lipid II / membrane	Daptomycin (membrane), lipoglycopeptides, nisin (lantibiotic)	Bind Lipid II / depolarize membrane	MRSA, VRE

Resistance recapitulates the pathway. Each drug elicits a corresponding resistance trick: VanA-type vancomycin resistance in enterococci (VRE) replaces D-Ala-D-Ala with D-Ala-D-Lac, abolishing one of the five hydrogen bonds that vancomycin exploits (≥ 1000 -fold MIC increase; the binding free-energy loss is about 12 kJ/mol per H-bond); MRSA expresses PBP2a (encoded by *mecA*) with low β -lactam affinity (K_i rises about 1000 \times); β -lactamases hydrolyse the β -lactam ring before it reaches its PBP target, with extended-spectrum β -lactamases (ESBLs) and carbapenemases (KPC, NDM, OXA-48) progressively defeating each new generation of β -lactams. The pathway thus serves as a unifying framework — biosynthetic step, drug, and resistance mechanism are three views of the same chemistry.

Clinical Connection: Why Vancomycin Stopped Working — and How Daptomycin Took Over Vancomycin was introduced in 1958 and remained dependable for almost 30 years. The first VRE isolates appeared in 1986–1988 in European and US hospitals, driven by agricultural use of avoparcin (a glycopeptide growth promoter in livestock); by the early 2000s VRE had spread globally. The molecular trick is elegant: a single ester linkage (D-Ala-D-Lac instead of the D-Ala-D-Ala amide) costs the bacterium nothing but eliminates one of the five H-bonds anchoring vancomycin. Daptomycin (FDA-approved 2003) bypasses the resistance entirely — it inserts into the cell membrane in a Ca^{2+} -dependent manner, depolarizing it without requiring a peptidoglycan binding site. Daptomycin resistance is now emerging too (mprF and yycG mutations alter membrane charge), continuing the arms race.

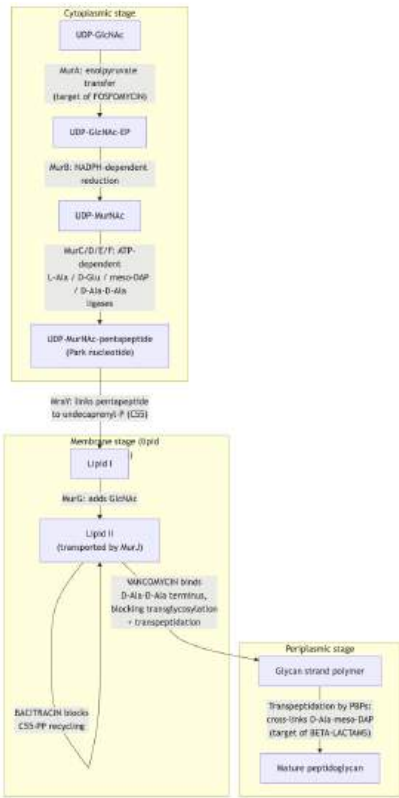


Figure 143. Cytoplasm-to-periplasm peptidoglycan biosynthesis with five major antibiotic targets - fosfomycin (MurA), D-cycloserine (D-Ala-D-Ala ligase / Alr), bacitracin (C55 carrier recycling), vancomycin (D-Ala-D-Ala terminus of Lipid II), and beta-lactams (PBP transpeptidation).

24.2.5 Gram Staining: The Foundational Diagnostic Test

The **Gram stain**, developed by Hans Christian Gram in 1884, remains the single most important initial test in clinical microbiology. The procedure exploits differences in cell wall architecture:

- Lipid A: The toxic moiety; embedded in the outer membrane; activates TLR4 on innate immune cells
- Core oligosaccharide: Short sugar chain linking Lipid A to the O-antigen
- O-antigen: Variable polysaccharide extending outward; serotype-specific; target of antibodies

When Gram-negative bacteria lyse during infection, released LPS triggers massive innate immune activation through the TLR4-MD2 receptor complex. This can lead to a cytokine cascade (TNF- α , IL-1 β , IL-6), systemic inflammation, disseminated intravascular coagulation (DIC), and septic shock – a life-threatening condition with mortality rates of 30-50%.

Clinical Connection: Gram Staining in Diagnosis The Gram stain is typically the first test performed on clinical specimens (blood cultures, cerebrospinal fluid, sputum). Results within 15 minutes guide empirical antibiotic therapy before culture results are available (24-72 hours). For bacterial meningitis, Gram-positive diplococci suggest *Streptococcus pneumoniae* (treat with ceftriaxone + vancomycin), while Gram-negative diplococci suggest *Neisseria meningitidis* (treat with ceftriaxone alone). This rapid distinction can be life-saving in an emergency where hours matter.

Concept Check 1: A novel bacterium is isolated from a deep-sea hydrothermal vent. Gram staining produces a pink result. Predict the cell wall architecture and explain why the alcohol decolorization step removed the crystal violet-iodine complex from this organism.

Concept Check 1b: A clinical microbiology lab tests a bacterial isolate against six wall-targeted antibiotics. The isolate is resistant to vancomycin (MIC > 256 $\mu\text{g/mL}$) but susceptible to ampicillin, fosfomycin, and bacitracin. Sequencing reveals a *vanA* operon. Using the peptidoglycan biosynthesis pathway, explain (a) which step is altered, (b) why vancomycin fails, and (c) why ampicillin still works.

Concept Check 1c: Fosfomycin is a phosphoenolpyruvate (PEP) analog that covalently inactivates MurA. *Pseudomonas aeruginosa* is intrinsically resistant to fosfomycin despite having a functional MurA. Hypothesize two non-target-based resistance mechanisms (think about how the drug enters the cell) and propose an experiment using a *P. aeruginosa* MurA-knockout complemented with the *E. coli* allele to test whether MurA is responsible.

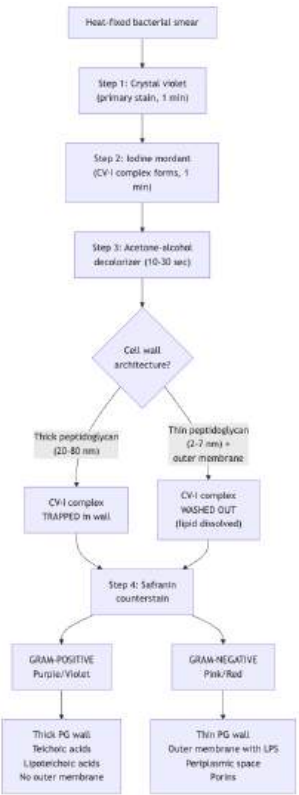


Figure 144. Gram-stain decision tree producing purple (Gram-positive) versus pink (Gram-negative) results from differences in peptidoglycan thickness and outer-membrane architecture.

24.3 Bacterial Morphology and Metabolic Diversity

24.3.1 Morphology and Arrangement

Bacterial cells exhibit characteristic shapes that aid in identification:

Table 310. Morphology and Arrangement: Shape and Description.

Shape	Description	Examples
Coccus	Spherical	<i>Staphylococcus aureus</i> , <i>Streptococcus pyogenes</i>
Bacillus	Rod-shaped	<i>Escherichia coli</i> , <i>Bacillus subtilis</i>
Spirillum	Rigid spiral	<i>Campylobacter jejuni</i> , <i>Helicobacter pylori</i>
Spirochete	Flexible helix with axial filaments	<i>Treponema pallidum</i> , <i>Borrelia burgdorferi</i>
Vibrio	Comma-shaped	<i>Vibrio cholerae</i> , <i>Vibrio parahaemolyticus</i>
Pleomorphic	Variable shape	<i>Mycoplasma pneumoniae</i> (no cell wall)

Cell arrangements reflect division plane and post-division adhesion patterns:

- Diplo- (pairs): *Diplococcus*, *Neisseria*
- Strepto- (chains): *Streptococcus* – divides in one plane, cells remain attached
- Staphylo- (grape-like clusters): *Staphylococcus* – divides in multiple planes
- Tetrad (groups of 4): *Micrococcus* – divides in two perpendicular planes
- Sarcina (cuboidal packets of 8): *Sarcina ventriculi* – divides in three planes

24.3.2 Metabolic Diversity and Energy Harvesting

Bacteria exhibit unparalleled metabolic diversity – far exceeding that of eukaryotes combined. This diversity is classified by energy source (photo- vs chemo-) and carbon source (auto- vs hetero-):

Photoautotrophs use light energy to fix CO₂:

- *Cyanobacteria* (oxygenic **photosynthesis**): Use water as electron donor; produce O₂; responsible for the Great Oxidation Event (about 2.4 Ga); ancestors of chloroplasts
- Purple and green sulfur bacteria (anoxygenic): Use H₂S or S⁰ as electron donor; no O₂ production; bacteriochlorophyll absorbs at longer wavelengths (800-1050 nm)

Chemoautotrophs (lithotrophs) derive energy from inorganic chemical oxidation:

- *Nitrosomonas*: NH₃ -> NO₂⁻ (ammonia oxidation; **nitrification** step 1)
- *Nitrobacter*: NO₂⁻ -> NO₃⁻ (nitrite oxidation; nitrification step 2)
- *Thiobacillus*: S⁰ -> SO₄²⁻ (sulfur oxidation)
- *Acidithiobacillus ferrooxidans*: Fe²⁺ -> Fe³⁺ (iron oxidation; used industrially in bioleaching of copper and gold ores)

Heterotrophs (the vast majority) obtain carbon from organic compounds. They are further classified by oxygen relationship:

Table 311. Metabolic Diversity and Energy Harvesting: Type and O₂ Requirement.

Type	O ₂ Requirement	Example
Obligate aerobe	Requires O ₂	<i>Mycobacterium tuberculosis</i>
Obligate anaerobe	Killed by O ₂	<i>Clostridium botulinum</i>
Facultative anaerobe	Grows with or without O ₂	<i>Escherichia coli</i>
Aerotolerant anaerobe	Does not use O ₂ but tolerates it	<i>Lactobacillus</i>
Microaerophilic	Requires low O ₂ (2-10%)	<i>Campylobacter jejuni</i> , <i>Helicobacter pylori</i>

24.3.3 Major Pathogenic Groups

Table 312. Major Pathogenic Groups: Phylum and Key Pathogens.

Phylum	Key Pathogens	Gram Stain	Clinical Significance
Proteobacteria	<i>E. coli</i> , <i>Salmonella</i> , <i>Helicobacter</i> , <i>Vibrio</i> , <i>Neisseria</i> , <i>Pseudomonas</i>	Gram-negative	UTIs, enteric infections, peptic ulcers, cholera, meningitis, nosocomial infections
Firmicutes	<i>Streptococcus</i> , <i>Staphylococcus</i> , <i>Clostridium</i> , <i>Enterococcus</i>	Gram-positive	Pharyngitis, skin infections, tetanus, botulism, hospital-acquired infections
Actinobacteria	<i>Mycobacterium tuberculosis</i> , <i>M. leprae</i> , <i>Corynebacterium</i>	Gram-positive (acid-fast)	Tuberculosis, leprosy, diphtheria
Spirochaetes	<i>Treponema pallidum</i> , <i>Borrelia burgdorferi</i> , <i>Leptospira</i>	Poorly staining	Syphilis, Lyme disease, leptospirosis

Mycobacterium species deserve special mention: their cell walls contain mycolic acids – long-chain (C₆₀-C₉₀) branched fatty acids that form a waxy, hydrophobic barrier. This barrier makes them resistant to Gram staining (they are classified as acid-fast bacteria, stained with the Ziehl-Neelsen method using carbol fuchsin), resistant to many antibiotics, and resistant to desiccation – contributing to *M. tuberculosis* survival in aerosolized droplet nuclei for hours.

Concept Check 2: *Helicobacter pylori* [Marshall and Warren, 1984] is a microaerophilic, spiral-shaped, Gram-negative bacterium that colonizes the human stomach. Explain how its oxygen requirement and morphology are adaptive for its ecological **niche**, and predict what would happen if you tried to culture it under standard **aerobic** conditions on a typical agar plate.

24.4 Bacterial Genetics, Signaling and Sociality

24.4.1 Binary Fission and Exponential Growth

Bacteria reproduce asexually by binary fission: the circular chromosome is replicated bidirectionally from a single origin of replication (*oriC*), the cell elongates, a septum forms at mid-cell (coordinated by the FtsZ ring – a tubulin homolog), and two daughter cells separate. Generation times vary enormously:

- *Escherichia coli*: about 20 minutes under optimal conditions (37 degrees C, rich media)
- *Mycobacterium tuberculosis*: 12-24 hours (contributing to slow disease progression and prolonged treatment)
- *Treponema pallidum*: about 33 hours (cannot be cultured in vitro)

Population growth during exponential phase follows the bacterial growth equation:

$$N(t) = N_0 \cdot 2^{t/t_d}$$

(351)

where N_0 is the initial population, t is time, and t_d is the doubling (generation) time. Equivalently, the natural-log form $\ln N(t) = \ln N_0 + \mu t$ with $\mu = (\ln 2)/t_d$ (the specific growth rate, units of time^{-1}) gives a linear plot of $\ln N$ versus t during exponential phase, whose slope is the experimentally measured μ .
(Note: the exponent t/t_d is often represented as n , the number of generations).

24.4.2 Worked Example: Calculating Bacterial Growth

Problem: A microbiologist inoculates a broth with $N_0 = 100$ cells of *Vibrio natriegens*, which has a generation time of $t_d = 15$ minutes under optimal conditions. Assuming the culture immediately enters the exponential growth phase and maintains it without nutrient depletion, how many cells will be present after 2 hours?
Solution:

1. Calculate the total time (t) in consistent units:

$$t = 2 \text{ hours} = 120 \text{ minutes}$$

2. Calculate the number of generations (n):

$$n = \frac{t}{t_d} = \frac{120}{15} = 8 \text{ generations}$$

3. Calculate the final population size $N(t)$ from equation (351):

$$N(t) = 100 \cdot 2^8$$

$$N(t) = 100 \cdot 256 = 25,600 \text{ cells}$$

After 2 hours, the population will reach 25,600 cells. The rapid doubling of bacteria means that even a small initial inoculum can quickly reach high densities in favorable environments. After 4 hours (16 generations), the same culture would reach $\approx 6.5 \times 10^6$ cells; after 6 hours (24 generations), $\approx 1.7 \times 10^9$ cells — at which point nutrient limitation forces the culture into stationary phase.

24.4.3 Worked Example: Inferring Generation Time from an OD Growth Curve

Problem: A microbiology student grows *E. coli* in LB broth at 37 °C and reads optical density at 600 nm (OD_{600}) every 30 minutes:

Table 313. Inferring Generation Time from an OD Growth Curve.

Time (min)	0	30	60	90	120	150
OD_{600}	0.05	0.10	0.20	0.40	0.80	1.60

Estimate the generation time t_d during exponential growth.

Solution:

During exponential phase, OD_{600} is proportional to cell density, so $\text{OD}(t) = \text{OD}_0 \cdot 2^{t/t_d}$. Take the natural log of both sides:

$$\ln \text{OD}(t) = \ln \text{OD}_0 + \frac{t}{t_d} \ln 2$$

A plot of $\ln \text{OD}$ versus t has slope $\mu = (\ln 2)/t_d$. Using the first and last points,

$$\mu = \frac{\ln(1.60) - \ln(0.05)}{150 - 0} = \frac{0.470 - (-2.996)}{150} = \frac{3.466}{150} \approx 0.0231 \text{ min}^{-1}.$$

Therefore,

$$t_d = \frac{\ln 2}{\mu} = \frac{0.693}{0.0231} \approx 30 \text{ minutes}.$$

The doubling time is about 30 minutes, consistent with rich-media growth at 37 °C. Inspection of the table confirms the answer: OD₆₀₀ doubles every 30 min from *t* = 30 onwards. Real growth curves deviate at the extremes (lag at the start, stationary plateau at the end), as the full four-phase curve in figure 142 shows; the linear-on-log-plot region is the main window where *t_d* is well defined.

24.4.4 Horizontal Gene Transfer

While binary fission produces clonal offspring, horizontal gene transfer (HGT) is the major driver of bacterial evolution and genetic diversity [Lawrence and Ochman, 1998]. Three mechanisms operate:

Transformation involves the uptake of naked DNA from the environment. Some species are naturally competent – they express surface proteins that bind, import, and integrate exogenous DNA. *Streptococcus pneumoniae* was the organism in Griffith’s famous 1928 experiment demonstrating transformation (the “transforming principle,” later identified as DNA by Avery, MacLeod, and McCarty in 1944). In molecular biology, artificial competence is induced by treating *E. coli* with CaCl₂ and heat shock (42 degrees C for 45 seconds), which transiently increases membrane permeability.

Transduction is phage-mediated DNA transfer between bacteria:

- *Generalized transduction*: During lytic replication, bacterial DNA fragments are accidentally packaged into phage capsids instead of phage DNA. These defective phage particles inject bacterial DNA into new host cells, where it can recombine into the chromosome.
- *Specialized transduction*: A lysogenic phage (e.g., bacteriophage λ) excises imprecisely from the host chromosome, carrying flanking bacterial genes (*gal* or *bio* genes flanking the λ *attB* site). These hybrid phage particles transduce specific genes at high frequency.

Conjugation requires direct cell-to-cell contact via a sex pilus encoded by the F factor (fertility plasmid). The F⁺ donor cell extends an F pilus that contacts an F[−] recipient, retracting to bring cells together. A single strand of the F plasmid is transferred and replicated in the recipient, converting it to F⁺. When the F factor integrates into the chromosome, the cell becomes Hfr (high frequency recombination), and conjugation can transfer chromosomal genes to the recipient at high frequency.

R-factor plasmids (resistance plasmids) carry multiple antibiotic resistance genes and are transferred by conjugation – this is the primary mechanism by which antibiotic resistance spreads among bacterial populations, including between different species.

24.4.5 Plasmids and Mobile Genetic Elements

Table 314. Plasmids and Mobile Genetic Elements: Plasmid Type and Example.

Plasmid Type	Example	Significance
R-plasmids	NDM-1 (New Delhi metallo-β-lactamase)	Carbapenem resistance; global spread
Virulence plasmids	pINV (<i>Shigella</i>)	Encode invasion machinery
Ti plasmid	<i>Agrobacterium tumefaciens</i>	Crown gall disease; used in plant biotechnology for gene transfer
Col plasmids	ColE1	Encode bacteriocins (antimicrobial peptides)
Metabolic plasmids	TOL (<i>Pseudomonas putida</i>)	Toluene degradation; bioremediation

Transposons (mobile genetic elements) contribute to genome plasticity. Insertion sequences (IS elements) are the simplest, encoding primarily transposase flanked by inverted repeats. Composite transposons (e.g., Tn3 carrying ampicillin resistance) consist of a resistance gene flanked by IS elements. Transposons can “jump” between chromosome and plasmid, facilitating the assembly of multi-drug resistance cassettes.

24.4.6 Two-Component Signal Transduction

Bacteria sense their environment through ubiquitous two-component systems (TCS) — the prokaryotic equivalent of receptor-tyrosine-kinase + transcription-factor cascades in eukaryotes. Each system is built from just two proteins:

1. A membrane-anchored sensor histidine kinase (HK) with an extracellular sensing domain and a cytoplasmic kinase domain. Stimulus binding induces ATP-dependent autophosphorylation of a conserved histidine residue in the HK dimer (the phosphate is transferred from the γ -phosphate of ATP to the imidazole nitrogen of the histidine sidechain — a high-energy phospho-amide bond, $\Delta G \approx -50$ kJ/mol on hydrolysis).
2. A cytoplasmic response regulator (RR) with a receiver domain and an output (usually DNA-binding) domain. The HK transfers its phosphate to a conserved aspartate on the RR (a phospho-anhydride; faster hydrolysis kinetics, $t_{1/2} \sim$ seconds to minutes), activating it as a transcription factor (or, less commonly, as an enzyme or motor regulator).

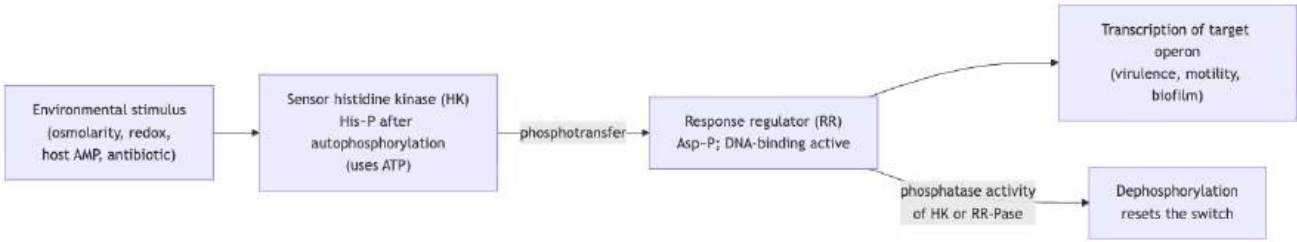


Figure 145. Two-component signal transduction. Stimulus to HK autophosphorylation on histidine to phosphotransfer to RR aspartate to DNA binding and gene regulation; intrinsic phosphatase activity resets the system.

The two-component circuit is therefore a molecular switch with three states (off / phosphorylated / phosphatase-reset), tunable by the relative kinase versus phosphatase activities of the HK. Some HKs (“classical” HKs like EnvZ and PhoQ) act as kinase under stimulus and phosphatase otherwise — a single protein computing both ON and OFF, with the stimulus ratio shifting the equilibrium. This bifunctionality makes the steady-state level of RRabout P a near-linear readout of the input — exactly what is wanted for analog signal processing inside a cell.

Table 315. Two-Component Signal Transduction: Two-component system and Stimulus.

Two-component system	Stimulus	Output	Clinical/biological significance
EnvZ–OmpR (<i>E. coli</i>)	Osmolarity	Switches porin expression OmpC ↔ OmpF	Outer-membrane permeability; β -lactam entry
PhoQ–PhoP (<i>Salmonella</i>)	Low Mg^{2+} , antimicrobial peptides, low pH (phagosome)	Lipid A modification; <i>pmrHFIJKLM</i>	Resistance to host defensins and polymyxins
AgrC–AgrA (<i>S. aureus</i>)	Autoinducing peptide AIP (quorum)	RNAIII; toxin production	Switches biofilm OFF, virulence ON
VraS–VraR (<i>S. aureus</i>)	Cell-wall stress (β -lactams, vancomycin)	Cell-wall stimulon	Vancomycin tolerance
CheA–CheY (chemotaxis)	Attractants/repellents	Flagellar motor switching (CW ↔ CCW)	Run-and-tumble swimming
WalK–WalR (<i>B. subtilis</i> , <i>S. aureus</i>)	Cell-wall integrity	Autolysin and PG-synthesis genes	Essential — drug target lead

Key features that make TCSs central to bacterial biology: they are modular (HKs and RRs from one organism often work with components from another), they are fast (sub-second response), and there are typically 30–80 systems per genome, allowing combinatorial integration of many environmental signals. The minimal

Mycoplasma genitalium genome has 0 TCSs (it lives in a stable host environment); free-living soil bacteria like *Myxococcus xanthus* encode > 100. Several recent antibacterial leads (e.g., walkmycin against the WalK kinase, an essential cell-wall TCS) target HKs precisely because they are absent from human cells.

24.4.7 Biofilms and Quorum Sensing

Most bacteria in nature do not live as solitary planktonic cells; they live in biofilms — surface-attached, matrix-encased communities that behave more like a tissue than a free-swimming population. Biofilm formation proceeds through a stereotyped life cycle, coordinated by quorum sensing (QS) — cell-density-dependent communication via diffusible autoinducers (AHLs in Gram-negatives, AIPs in Gram-positives, AI-2 across species).



Figure 146. Biofilm life cycle from planktonic cell through reversible/irreversible attachment, microcolony, mature biofilm, and quorum-triggered dispersal - coordinated by intra-cellular c-di-GMP and intercellular autoinducers.

- Exopolysaccharides (PIA in *S. aureus*; alginate, Pel, Psl in *P. aeruginosa*; cellulose and PNAG in enterics) — provide structural cohesion and protection.
- Extracellular DNA (eDNA) — released by autolysis; a major load-bearing component and a substrate for horizontal gene transfer at frequencies up to 1000× higher than in planktonic cells.
- Matrix proteins — amyloid-like curli fibers (*E. coli*), Bap proteins, type IV pili.
- Lipids and outer-membrane vesicles — concentrate hydrolytic enzymes and signaling molecules.

Quorum sensing molecules.

Table 316. Biofilms and Quorum Sensing: QS class and Signal molecule.

QS class	Signal molecule	Producers	Receptor	Output
AHLs	N-acyl-homoserine-lactones (e.g., 3-oxo-C ₁₂ -HSL)	Gram-negatives (<i>P. aeruginosa</i> LasI/LasR, <i>V. fischeri</i> LuxI/LuxR)	LuxR-family TF	Bioluminescence, virulence, biofilm
AIPs	Cyclic autoinducing peptides (5–10 aa, thiolactone bridge)	Gram-positives (<i>S. aureus</i> Agr, <i>S. pneumoniae</i> ComD)	Membrane HK (TCS)	Virulence/biofilm switch
AI-2	Furanosyl-borate diester (LuxS)	Cross-species	LuxP/LsrB	Inter-species coordination
PQS	Pseudomonas quinolone signal (2-heptyl-3-hydroxy-4-quinolone)	<i>P. aeruginosa</i>	PqsR	Iron acquisition, virulence
DSF	cis-2-unsaturated fatty acids	<i>Xanthomonas</i> , <i>Burkholderia</i>	RpfC HK	Biofilm dispersal, virulence

Why biofilms matter clinically. The CDC estimates that about 65–80 % of chronic and device-associated human infections involve biofilms. They are 10–1000× more antibiotic tolerant than planktonic cells because of (1) reduced antibiotic penetration through EPS — vancomycin diffusion can be retarded by 100×; (2) persister cells — metabolically dormant subpopulations not killed by growth-dependent antibiotics, comprising 0.001–1 % of biofilm cells; (3) localized enzyme accumulation (e.g., β-lactamase concentrated 100–1000× in matrix); and (4) anaerobic interior microenvironments where aminoglycosides (which require an electrochemical gradient for uptake) are inactive. Canonical clinical biofilms include cystic fibrosis lung infections (*P. aeruginosa* alginate biofilms), prosthetic joint and heart-valve infections (*S. aureus*, *S. epidermidis*), catheter-associated UTIs (*E. coli*, *P. mirabilis*), chronic wounds, and dental plaque (*Streptococcus*, *Porphyromonas*, *Fusobacterium*).

Quorum quenching as therapy. Because most virulence factors are quorum-regulated, blocking QS *attenuates* virulence without killing bacteria — sidestepping the strong selection for resistance that lytic antibiotics impose. Strategies include: (1) lactonases (AiiA from *Bacillus*, AhlD) and acylases that hydrolyse AHLs; (2) synthetic AIP analogs that competitively inhibit AgrC; (3) halogenated furanones (originally from the seaweed *Delisea pulchra*) that destabilise LuxR-family receptors; (4) PqsR antagonists (e.g., M64); (5) c-di-GMP signaling disruptors. Several are in early clinical trials (notably for *P. aeruginosa* in cystic fibrosis), though “anti-virulence” compounds face the challenge that they do not directly clear infection — they must work synergistically with antibiotics or host immunity.

24.4.8 Endospores and Dormancy Under Stress

Certain Firmicutes – primarily *Bacillus* (central or subterminal spores) and *Clostridium* (terminal spores) – produce endospores in response to nutrient depletion. The endospore is the most resistant biological structure known:

- Core: Dehydrated **cytoplasm**; calcium-dipicolinic acid complex stabilizes DNA; small acid-soluble spore proteins (SASPs) protect DNA from UV and desiccation
- Resistance: Survives boiling (100 degrees C), desiccation, UV radiation, and chemical disinfectants
- Sterilization: Requires autoclaving at 121 degrees C, 15 psi pressure, for 15-20 minutes
- Germination: Triggered by favorable conditions (nutrients, water); rapid return to vegetative growth

Clinical Connection: Endospores and Hospital Infection Control *Clostridioides difficile* endospores persist on hospital surfaces for months, resisting alcohol-based hand sanitizers (which are effective against vegetative bacteria). Healthcare workers must use soap and water (physical removal) and bleach-based surface disinfectants to prevent *C. difficile* transmission. *Bacillus anthracis* spores were used as a bioterrorism agent in the 2001 U.S. anthrax letter attacks, contaminating postal facilities and requiring years of decontamination.

Concept Check 2b: A research lab knocks out the *agrA* gene (response regulator of the Agr quorum-sensing TCS) in *S. aureus*. The mutant forms thicker, more persistent biofilms in vitro but is dramatically less virulent in a mouse skin-abscess model. Reconcile these two observations using the AgrA on/off switch between biofilm and toxin production.

Concept Check 2c: A patient develops a *Pseudomonas aeruginosa* bloodstream infection following indwelling-catheter placement. Blood cultures show vancomycin-susceptible cells with MIC = 1 µg/mL, yet the patient fails 4 weeks of intravenous vancomycin while the catheter remains in place. Explain — using biofilm penetration kinetics, persister biology, and oxygen gradients — why the planktonic MIC is a poor predictor of clinical efficacy in catheter-associated infection. What therapeutic action almost typically succeeds where antibiotic monotherapy fails?

24.5 Archaea and Extremophile Cell Biology

24.5.1 Distinguishing Archaeal Features

Archaea are prokaryotes that were long classified with bacteria but differ fundamentally at the molecular level:

Table 317. Distinguishing Archaeal Features: Feature and Bacteria.

Feature	Bacteria	Archaea	Eukarya
Membrane lipids	Ester-linked fatty acids	Ether-linked isoprenoid (phytanyl) chains; some form tetraether monolayers	Ester-linked fatty acids
Cell wall	Peptidoglycan (murein)	No peptidoglycan; pseudomurein (methanogens), S-layer protein, or none	No peptidoglycan; cellulose/chitin in plants/fungi
RNA polymerase	Single, simple (4-5 subunits)	Multiple subunits (12+), resembles eukaryotic Pol II	Three RNA polymerases (Pol I, II, III)
Initiator tRNA	Formyl-methionine	Methionine (like eukaryotes)	Methionine
Histones	HU, H-NS (not true histones)	True histone homologs	Histone octamers (H2A, H2B, H3, H4)
Introns	Rare	Present in some tRNA genes	Abundant

24.5.2 Archaeal Lipid Biochemistry: Why Hot Vents Don’t Melt Membranes

The single most diagnostic biochemical feature of Archaea is the architecture of their membrane lipids. Three differences from bacterial/eukaryotic phospholipids are simultaneously present, and the combination contributes to extreme stability:

1. Ether linkages instead of ester linkages between glycerol and the hydrocarbon chains. Ether bonds (C–O–C) are far more chemically inert than ester bonds (C–O–C(=O)) — they resist acid hydrolysis, base hydrolysis, oxidation, and high-temperature cleavage.

2. Isoprenoid (phytanyl) chains (built from C5 isoprene units, with branched methyl groups every 4 carbons) instead of straight-chain fatty acids. Methyl branches cause kinks that prevent tight chain crystallization at low temperatures (preventing membrane gelling) while van-der-Waals interactions between branches stiffen the membrane against fluidization at high temperatures.
3. Glycerol stereochemistry: archaeal glycerol is *sn*-glycerol-1-phosphate (G-1-P); bacterial/eukaryotic glycerol is *sn*-glycerol-3-phosphate (G-3-P). The two are enantiomers — a deep, “lipid divide” between archaea and the rest of cellular life that probably reflects independent invention of phospholipid biosynthesis after the LUCA.

Hyperthermophilic archaea (*Sulfolobus*, *Thermococcus*, *Pyrodictium*) take this further by linking two phytanyl chains end-to-end, forming glycerol-dialkyl-glycerol-tetraether (GDGT) lipids. Two GDGT molecules then span the entire membrane as a monolayer (rather than a bilayer), with two glycerol headgroups (one on each surface) and one continuous hydrocarbon block in the middle. The covalent backbone makes the membrane behave mechanically like a single rigid sheet — it cannot delaminate, leak, or peel apart even at 113 °C.

Quantitatively: a typical bacterial membrane fluidizes (loses lipid order) above about 60 °C and disintegrates above about 100 °C; *Pyrodictium* GDGT monolayers retain integrity at 113 °C and pH 1, conditions that hydrolyse most ester-linked lipids in seconds. Cyclopentane rings within the GDGT chains can be added or removed on the fly to fine-tune membrane fluidity to growth temperature — a remarkable example of biochemical homeoviscous adaptation. Because eukaryotic and bacterial membranes lack these adaptations, penicillin-class and polymyxin-class antibiotics that act on bacterial cell envelopes are generally ineffective against archaea.

24.5.3 Major Archaeal Groups

Euryarchaeota encompasses the broadest metabolic diversity:

- Methanogens: Strict anaerobes that produce methane as a metabolic end product. The key reaction is: $\text{CO}_2 + 4\text{H}_2 \rightarrow \text{CH}_4 + 2\text{H}_2\text{O}$. Methanogens inhabit **anaerobic** environments including wetlands, rice paddies, landfills, and the rumen of cattle. *Methanobrevibacter smithii* is the **dominant** archaeon in the human gut. Globally, methanogenesis produces approximately 1 billion tonnes of CH₄ annually, contributing approximately 10% of anthropogenic greenhouse gas emissions.
- Extreme halophiles: *Halobacterium salinarum* thrives in saturated salt solutions (about 5 M NaCl). It maintains osmotic balance by accumulating intracellular KCl to equimolar concentrations. Its purple membrane contains bacteriorhodopsin, a light-driven proton pump that generates ATP via **chemiosmosis** – a form of phototrophy independent of **chlorophyll**. The salt flats visible from space (pink/red coloration in San Francisco Bay salt ponds) owe their color to halophilic archaea.
- Thermoacidophiles: *Thermoplasma acidophilum* grows optimally at 59 degrees C and **pH** 2. Notably, it lacks a cell wall entirely, surviving in hot acid through a reinforced lipid membrane.

Crenarchaeota includes the most extreme hyperthermophiles:

- *Sulfolobus solfataricus*: 80 degrees C, pH 2-3; model organism for archaeal molecular biology
- *Pyrodictium occultum*: Grows at 113 degrees C – among the highest known temperatures for life
- *Thermoproteus tenax*: Autotrophic sulfur metabolism at 85 degrees C
- These organisms possess reverse gyrase, an **enzyme** that introduces positive supercoils into DNA, stabilizing the double helix at extreme temperatures

24.5.4 Asgard Archaea: The Closest Living Relatives of Eukaryotes

Asgard Archaea represent perhaps the most important discovery in evolutionary biology of the past decade. In 2015, Ettema and colleagues identified novel archaeal lineages in metagenomic data from deep-sea sediments near Loki’s Castle hydrothermal vent field in the Arctic Mid-Ocean Ridge. The clade has since expanded into a large superphylum named for Norse mythology:

- Lokiarchaeota (Loki’s Castle, 2015) — the founding lineage; > 100 published MAGs.
- Thorarchaeota (named for Thor) — abundant in marine sediments.
- Odinarchaeota, Heimdallarchaeota, Helarchaeota, Hermodarchaeota, Wukongarchaeota — discovered in successive metagenomic surveys 2017–2024.

Eukaryotic signature proteins (ESPs). What makes Asgard archaea revolutionary is that they encode an unprecedented cluster of proteins previously thought to be eukaryote-specific:

Table 318. Asgard Archaea: The Closest Living Relatives of Eukaryotes: ESP class and Asgard homolog.

ESP class	Asgard homolog	Eukaryotic role
Actin	Lokiactin (about 60 % identity to eukaryotic actin)	Cytoskeleton, cell shape
Profilin / gelsolin	Loki-profilin	Actin polymerization control
Rab / Arf GTPases	Lokirhabs	Membrane trafficking, vesicle coats
ESCRT-I/II/III	Lokiarchaeal ESCRT homologs	Membrane scission, multivesicular bodies
Tubulin (sometimes)	Heimdall artubulins	Microtubule cytoskeleton (eukaryotes primarily)
Ubiquitin-like modifiers	Loki SAMPs/Ub-like	Protein degradation tagging
Eukaryotic-style ribosomal proteins	Several rps homologs	Translation

Phylogenetic placement. Maximum-likelihood and Bayesian analyses of conserved markers consistently place Asgard archaea (especially Heimdallarchaeota) as the sister group to most eukaryotes, supporting the “two-domain tree” of life (Bacteria as one domain; Archaea + Eukarya as a single, rooted-from-within-Archaea clade). This is the eocyte hypothesis validated at high resolution. The evolutionary inference: eukaryotes arose by endosymbiosis between an Asgard-like archaeal host (which contributed the cytoplasm, cytoskeleton, and information-processing genes) and an α -proteobacterial endosymbiont (which became the mitochondrion).

Cultivation breakthrough. In 2020, *Candidatus Prometheoarchaeum syntrophicum* — the first cultured Asgard archaeon — was reported by Imachi *et al.* (*Nature*) after 12 years of effort using extremely slow-growth bioreactor cultures fed with peptides and hydrogen. The organism grows obligately syntrophically with *Halodesulfovibrio* (sulfate-reducing) and a methanogenic archaeon (consuming H₂ produced by *Prometheoarchaeum*). Its doubling time is about 14–25 days; cells are tiny (about 0.5 μ m) and extend long branching tentacle-like protrusions thought to deliver hydrogen to syntrophic partners. The remarkable observation is that those tentacles morphologically resemble what one might predict for an archaeal cell preparing to engulf a bacterial endosymbiont — the “E³ model” of eukaryogenesis (Entangle, Engulf, Endogenise) directly suggested by *Prometheoarchaeum* morphology.

Implications. The discovery of Asgard archaea has narrowed the “evolutionary gap” between prokaryotes and eukaryotes from a vast unbridgeable distance to a graded continuum. Many of the molecular machines once thought to be uniquely eukaryotic (membrane-trafficking ESCRTs, actin cytoskeleton, ubiquitin signaling) were already present in the archaeal common ancestor of eukaryotes. Eukaryogenesis was a *combinatorial* event: pre-existing archaeal ESPs + acquisition of a mitochondrion + nucleus + later innovations. Two outstanding questions remain: (1) how exactly did the first eukaryotic cell engulf the proto-mitochondrion (phagocytosis-first, syntrophy-first, or virus-mediated?); (2) which Asgard subgroup is the closest living relative — Heimdallarchaeota (current consensus) or a yet-undiscovered lineage?

24.5.5 Archaeal Biotechnology and Thermostable Enzymes

Archaeal enzymes, evolved for extreme conditions, have enormous biotechnological value:

- Taq polymerase from *Thermus aquaticus* (technically a bacterium, but often discussed alongside thermophilic archaea): 70 degrees C optimum; enabled the **polymerase chain reaction (PCR)** – arguably the single most important technique in molecular biology; Kary Mullis, Nobel Prize 1993
- Pfu polymerase from *Pyrococcus furiosus*: 3’-to-5’ proofreading exonuclease activity; higher fidelity than Taq; used when accuracy is critical (cloning, mutagenesis)
- Vent polymerase from *Thermococcus litoralis*: thermostable with proofreading
- Industrial applications: archaeal proteases, lipases, and amylases for high-temperature industrial processes; extremophilic enzymes for detergents, food processing, and biofuel production

Concept Check 3: Explain why antibiotics that target peptidoglycan synthesis (e.g., penicillin, vancomycin) are ineffective against archaea. What does this tell us about the evolutionary relationship between bacterial and archaeal cell walls?

Concept Check 3b: Hyperthermophiles use GDGT tetraether monolayers; mesophilic archaea use diether bilayers. Predict, qualitatively, how membrane permeability to small molecules (water, protons, ATP) should differ between the two architectures and what this implies for chemiosmotic ATP synthesis at 100 °C.

Concept Check 3c: Asgard archaea encode actin homologs that function in vitro indistinguishably from eukaryotic actin. If the proto-eukaryote inherited actin from an archaeal ancestor, what testable prediction does this make about the timing of cytoskeletal evolution relative to the mitochondrial endosymbiosis? Design a comparative-genomic experiment that could distinguish between the alternatives.

Concept Check (Evaluate — Hyperthermophile Genome Stability and PCR Enzymes): *Thermococcus kodakarensis* grows optimally at 85 °C (vs. about 37 °C for *E. coli*) and its KOD DNA polymerase has a T_{opt} near 80 °C — well above the temperature at which *E. coli* DNA polymerase III denatures. (a) Evaluate the structural features that stabilize the *T. kodakarensis* genome and its DNA replication machinery against thermal denaturation: positively-charged surface residue enrichment (higher Lys/Arg content reducing repulsive surface interactions and increasing salt-bridge density), thermophilic DNA gyrase (introducing negative supercoils that stabilize the duplex against melting), and reverse gyrase (a Type I topoisomerase unique to hyperthermophiles that introduces *positive* supercoils, raising the melting temperature of duplex DNA). (b) Compare these features quantitatively: *T. kodakarensis* genomic DNA has $T_m \approx 95$ °C, vs. *E. coli* genomic DNA $T_m \approx 87$ °C — a difference traceable to elevated G+C content, reverse-gyrase-mediated positive supercoiling, and bound histone-like proteins. (c) Evaluate why these same features make archaeal DNA polymerases industrially useful for PCR: thermostability at 95 °C (the denaturation step in PCR), proofreading 3'→5' exonuclease activity (lower error rate than Taq — Pfu and KOD achieve about 10^{-6} errors/base vs. Taq's 10^{-5}), and the ability to amplify high-G+C templates that Taq stalls on. (d) Predict what would happen biochemically if you attempted to use *E. coli* DNA polymerase III in a standard PCR cycle, and explain why this was a fundamental barrier to molecular biology before the discovery of *Thermus aquaticus* and the archaeal hyperthermophiles.

24.6 Viruses as Genome-Delivery Replicators

24.6.1 Viral General Features and Host Dependence

Viruses are obligate intracellular **parasites** that cannot carry out metabolism independently. They lack ribosomes, cannot generate ATP, and require host cell machinery for replication. Whether viruses are “alive” remains a philosophical and definitional question – they exhibit heredity and evolution but not autonomous metabolism or cellular organization.

A complete virus particle (virion) consists of:

- Genome: DNA or RNA (rarely both); single-stranded or double-stranded; linear or circular; segmented or non-segmented
- Capsid: Protein shell assembled from capsomeres; icosahedral (20 triangular faces – *adenovirus*), helical (*tobacco mosaic virus*), or complex (*bacteriophage T4*)
- Envelope (some viruses): Lipid bilayer derived from host cell membrane during budding; contains viral glycoproteins essential for host cell attachment and entry

24.6.2 Baltimore Classification by Genome Type and Replication Strategy

David Baltimore (Nobel Prize 1975) classified viruses by genome type and replication strategy into seven classes:

Table 319. Baltimore Classification by Genome Type and Replication Strategy: Class and Genome.

Class	Genome	Replication Strategy	Examples
I	dsDNA	DNA -> mRNA (host RNA Pol)	Herpesviruses, adenoviruses, poxviruses, bacteriophage T4
II	ssDNA	ssDNA -> dsDNA -> mRNA	Parvoviruses, bacteriophage ϕ X174
III	dsRNA	dsRNA -> mRNA (viral RdRp)	Reoviruses, rotaviruses
IV	(+)ssRNA	RNA serves directly as mRNA	Poliovirus, rhinovirus, SARS-CoV-2, hepatitis C
V	(-)ssRNA	RNA -> mRNA (viral RdRp)	Influenza, rabies, Ebola, measles
VI	(+)ssRNA-RT	RNA -> DNA (reverse transcriptase) -> mRNA	HIV, HTLV
VII	dsDNA-RT	dsDNA -> RNA -> dsDNA (reverse transcriptase)	Hepatitis B

24.6.3 Bacteriophage Life Cycles

1. Adsorption: Tail fibers (long tail fibers recognize LPS; short tail fibers make irreversible contact) bind the surface of *E. coli*
2. DNA injection: The tail sheath contracts like a syringe, driving the tail tube through the outer membrane and injecting about 169 kb of linear dsDNA
3. Early gene expression: Host RNA polymerase is hijacked; phage-encoded anti-sigma factors redirect **transcription**; host DNA is degraded by phage nucleases (recycling **nucleotides**)

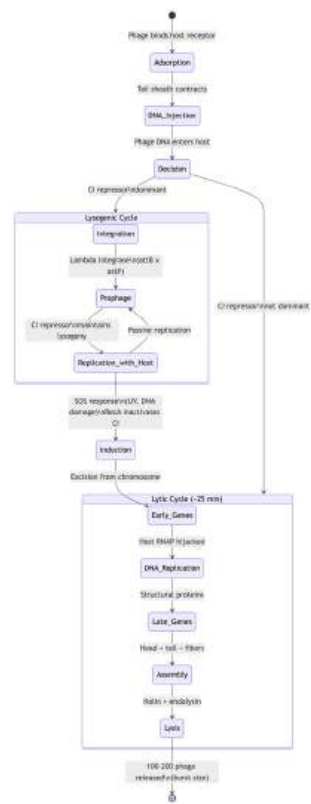


Figure 147. State diagram of the phage lambda lytic / lysogenic decision and the SOS-induced switch from lysogeny to lytic growth.

4. DNA replication: Phage DNA replicates using phage-encoded DNA polymerase; hydroxymethylcytosine replaces cytosine (protecting phage DNA from its own restriction enzymes)
5. Late gene expression: Structural proteins (head, tail, tail fibers, baseplate) are synthesized
6. Assembly: Heads are filled with DNA (headful packaging); tails are assembled separately; components join spontaneously
7. Lysis: Holin creates pores in the inner membrane; endolysin (lysozyme) degrades peptidoglycan; about 100-200 progeny phage released per cell; entire cycle takes about 25 minutes

Bacteriophage lambda (λ) lysogeny represents a molecular decision switch:

- After infection, λ integrase catalyzes site-specific recombination between phage *attP* and bacterial *attB* sites, inserting the phage genome into the host chromosome
- The CI repressor (λ repressor) binds operator sequences, repressing lytic genes and maintaining lysogeny – the prophage replicates passively with the host
- Upon DNA damage (UV exposure, mitomycin C), the SOS response activates RecA, which stimulates CI repressor autocleavage, derepressing lytic genes and initiating the lytic cycle
- Imprecise excision during induction can produce specialized transducing phage carrying *gal* or *bio* genes

Concept Check (Analysis — Bacteriophage λ as a Bistable Genetic Switch): The λ lysis–lysogeny decision is governed by a competition between two regulators — CI (λ repressor) and Cro — that bind cooperatively to three operator sites (O_R1 , O_R2 , O_R3) within the right operator region. CI has highest affinity for O_R1 and represses transcription of *cro* (favoring lysogeny); Cro has highest affinity for O_R3 and represses transcription of *cI* (favoring lysis). (a) Analyze why this mutual-repression architecture creates a bistable switch with two stable steady states (CI-dominant lysogeny vs. Cro-dominant lysis) and a metastable unstable point in between. (b) Multiplicity of infection (MOI) biases the initial conditions: at low MOI few CII protein molecules are produced and CII is rapidly degraded by FtsH protease, so the system settles into the Cro-dominant lytic state; at high MOI CII accumulates above the FtsH degradation threshold and activates the P_{RE} promoter to produce a burst of CI, pushing the system into the lysogenic state. Explain why this MOI-dependence is evolutionarily adaptive for the phage. (c) Predict what happens to the population dynamics if a host expresses a constitutively active CI variant (resistant to RecA-mediated autocleavage) under a low-copy plasmid promoter immediately after infection. Consider both the immediate fate of the infecting phage and the long-term stability of the lysogen against UV induction. (d) Connect this to synthetic biology: bistable switches built from CI/Cro analogs (Gardner, Cantor & Collins, *Nature* 2000) were among the first engineered genetic circuits — what does this reveal about the relationship between natural evolution and synthetic design?

24.6.4 Animal Virus Replication

Animal viruses follow a general replication strategy with virus-specific variations:

1. Attachment: Viral surface protein binds specific host receptor (tropism determinant)
 - Influenza: hemagglutinin (HA) binds sialic acid residues
 - HIV: gp120 binds CD4 + CCR5 or CXCR4 coreceptor
 - SARS-CoV-2: spike protein binds ACE2 receptor
2. Penetration: Receptor-mediated **endocytosis** (most non-enveloped viruses) or membrane fusion (enveloped viruses)
3. Uncoating: Capsid disassembly releases genome into cytoplasm (or nucleus)
4. Biosynthesis: Genome replication and protein synthesis (location depends on virus type)
5. Assembly: New virions assembled in cytoplasm or nucleus
6. Release: Budding through host membrane (enveloped viruses – acquiring lipid envelope) or cell lysis (non-enveloped viruses)

24.6.5 The HIV Life Cycle

HIV (human immunodeficiency virus) is a Class VI retrovirus with a complex life cycle and multiple drug targets:

1. Attachment and fusion: gp120 binds CD4 on T helper cells, then undergoes conformational change to bind coreceptor (CCR5 in early infection, CXCR4 in late infection); gp41 mediates membrane fusion
2. Reverse transcription: ssRNA genome -> dsDNA via reverse transcriptase (RT); RT lacks proofreading ($\sim 10^{-4}$ errors per base per cycle), generating enormous genetic diversity
3. Nuclear import: Pre-integration complex enters nucleus through nuclear pores
4. Integration: Integrase inserts viral dsDNA into host chromosome, creating the provirus – a permanent part of the host genome; preferentially integrates into actively transcribed regions
5. Transcription and **translation**: Host RNA Pol II transcribes viral mRNA; Tat protein enhances transcription 100-fold; Rev protein exports unspliced mRNA from nucleus
6. Assembly and budding: Gag and Gag-Pol polyproteins assemble at plasma membrane; budding acquires lipid envelope with gp120/gp41 spikes
7. Maturation: Viral protease cleaves Gag-Pol polyprotein into functional proteins; immature virion becomes infectious

Antiretroviral therapy (ART) targets multiple steps:

Table 320. The HIV Life Cycle: Drug Class and Target.

Drug Class	Target	Examples
NRTIs (nucleoside RT inhibitors)	Reverse transcriptase	Tenofovir, emtricitabine, zidovudine (AZT)
NNRTIs (non-nucleoside RT inhibitors)	RT allosteric site	Efavirenz, rilpivirine
Protease inhibitors	Viral protease	Ritonavir, darunavir
Integrase inhibitors	Integrase	Dolutegravir, raltegravir
Entry inhibitors	CCR5 coreceptor	Maraviroc
Fusion inhibitors	gp41	Enfuvirtide

24.6.6 Prions and Protein-Based Infectious States

Prions are infectious agents composed entirely of misfolded protein – they contain no nucleic acid. The normal cellular prion protein (PrP^C, predominantly α -helical) is converted to the pathogenic scrapie form (PrP^{Sc}, predominantly β -sheet) through templated conformational change. PrP^{Sc} serves as a seed, converting neighboring PrP^C molecules in a chain reaction that produces amyloid fibrils.

Prion diseases (transmissible spongiform encephalopathies) include:

- Creutzfeldt-Jakob disease (CJD): Sporadic (most common), familial, or iatrogenic
- Variant CJD (vCJD): Transmitted from bovine spongiform encephalopathy (BSE/“mad cow disease”) via contaminated beef
- Fatal familial insomnia: Autosomal dominant; progressive insomnia leading to death
- Kuru: Transmitted among the Fore people of Papua New Guinea through ritual endocannibalism; studied by Gajdusek (Nobel Prize 1976)
- Chronic wasting disease (CWD): Affects cervids (deer, elk); spreading across North America

Stanley Prusiner received the Nobel Prize in 1997 for his prion hypothesis – initially controversial because it challenged the central dogma that most infectious agents require nucleic acid for replication.

Clinical Connection: Bacteriophage Therapy With the rise of antibiotic-resistant infections, bacteriophage therapy is experiencing a renaissance. The UC San Diego Center for Innovative Phage Applications and Therapeutics (IPATH) has treated patients with life-threatening multidrug-resistant infections using personalized phage cocktails. In 2016, Tom Patterson was rescued from a pan-resistant *Acinetobacter baumannii* infection using phages sourced from sewage. Engineered phages can be designed to target specific bacterial species while sparing beneficial microbiota – a precision antimicrobial approach unfeasible with conventional antibiotics.

24.6.7 Phage Therapy: A Pre-Antibiotic Idea Returns to the Clinic

Phage therapy was discovered by Félix d’Hérelle in 1917, deployed widely in the Soviet Union and Eastern Europe through the 20th century, and largely abandoned in the West after the introduction of penicillin. The antibiotic-resistance crisis has driven a global resurgence: as of 2024, more than 30 phage therapy clinical trials are registered worldwide.

Why phages are appealing as therapeutics:

- Self-amplification at the site of infection — every successful infection produces about 50–500 progeny, so dose increases where the target bacterium is densest, then declines as the infection clears.
- Narrow host range — most phages target a single species or strain, sparing the resident microbiota (a rare property; conventional broad-spectrum antibiotics decimate commensals).
- Co-evolution with bacteria — the same evolutionary force that creates antibiotic resistance also creates new phages; phage banks can be updated continuously.
- Engineerability — synthetic biology now enables host-range expansion, removal of toxin-encoding genes, addition of CRISPR-Cas payloads to specifically target resistance genes, and lytic/lysogenic switching.

Clinical milestones (2016–2026):

Table 321. Phage Therapy: A Pre-Antibiotic Idea Returns to the Clinic: Year and Patient / trial.

Year	Patient / trial	Pathogen	Outcome
2016	Tom Patterson (UCSD/IPATH compassionate use)	Pan-resistant <i>Acinetobacter baumannii</i>	Recovery; first US success
2019	Cystic fibrosis lung transplant rescue	<i>Mycobacterium abscessus</i>	Survival; engineered phage cocktail
2020–2024	CYPHY, Phagoburn-2, Tailor-X	<i>P. aeruginosa</i> burn / UTI	Mixed efficacy; safety established
2023	Compassionate-use registry > 200 patients	Multiple ESKAPE	about 70 % response in salvage settings
2024–26	Locus Biosciences crPhage (CRISPR-Cas3 phage)	<i>E. coli</i> UTI	Phase II/III readouts

Phage pharmacokinetics — why they break the small-molecule rules. Conventional antibiotics follow first-order pharmacokinetics: $C(t) = C_0e^{-k_e t}$, with linear AUC/dose relationships. Phages do the opposite. The phage population grows where bacterial density is high (auto-dosing) and crashes when the bacteria are gone (auto-clearance). The simplest model is a Lotka–Volterra-like coupled ODE:

$$\frac{dB}{dt} = rB - kBP, \qquad \frac{dP}{dt} = bkBP - mP$$

where B = bacterial density, P = phage density, r = bacterial growth rate, k = adsorption rate constant (typically 10^{-9} – 10^{-7} mL min^{−1}), b = burst size (50–500), m = phage clearance rate. The system has a proliferation threshold at $B^* = m/(bk)$: above B^* , phage replicate faster than they are cleared and amplify; below B^* , they are diluted out. This means low-dose phage will not work against a sub-threshold infection — clinicians must dose above the minimum proliferating concentration. It also means a single phage dose can clear orders-of-magnitude more bacteria than its initial titer, making “dose” a misleading concept.

Pharmacokinetic and regulatory challenges that distinguish phages from small molecules:

1. Bacterial resistance is rapid — phage receptors mutate at 10^{-6} – 10^{-8} per cell per generation. Cocktails of 3–5 phages targeting non-overlapping receptors slow this; estimated escape probability $\approx \prod_i 10^{-7} = 10^{-21}$ for a 3-phage cocktail with independent receptors.
2. Immune neutralization — IgG against phage capsid emerges within about 10 days, lowering blood titres and limiting repeated systemic dosing.
3. Pharmacokinetics are non-linear — phage concentration depends on bacterial density (replication > clearance below threshold; opposite above) — classical AUC/MIC concepts do not apply.
4. Manufacturing & regulation — purified, endotoxin-free phage preparations require GMP processes designed for biologicals; the FDA has issued personalized/compassionate-use pathways while broad regulatory frameworks are still developing.
5. Lysogenic phages can transduce virulence/resistance genes (Shiga toxin in STEC came from a lambdoid phage); therapeutic phages must be obligately lytic and toxin-free.

The pragmatic clinical role emerging by 2026 is adjunctive phage therapy — phages combined with antibiotics for biofilm-associated and multi-drug-resistant infections (prosthetic joints, CF lungs, complicated UTIs, infective endocarditis), where phage-driven dispersal of biofilm matrix re-sensitizes persisters to antibiotics and the antibiotic suppresses phage-resistant escapees. This combination logic mirrors HIV ART and TB DOTS — the lesson that single-agent antimicrobial therapy invites resistance is now being applied to phages too.

Concept Check 4: HIV reverse transcriptase lacks proofreading activity, producing approximately one **mutation** per genome per replication cycle. Explain why this high mutation rate is both advantageous for the virus (immune evasion, drug resistance) and why it also constrains the maximum genome size of retroviruses compared to DNA viruses like herpesviruses (about 150 kb genome).

Concept Check 4b: A patient with chronic *Pseudomonas aeruginosa* lung infection in cystic fibrosis is treated with a phage cocktail. Within 5 days, the bacterial load drops 100-fold, but by day 14, *P. aeruginosa* has rebounded with mutations in *galU* (LPS biosynthesis). Explain (a) why *galU* mutants escape the phage, (b) why the rebound strain may actually be less fit *in vivo* than the parent, and (c) why combining phages with tobramycin can suppress this rebound.

24.7 Antibiotic Mechanisms and Resistance

24.7.1 Antibiotic Classes by Mechanism

Antibiotics exploit the structural and biochemical differences between prokaryotic and eukaryotic cells. Each class targets a specific essential process:

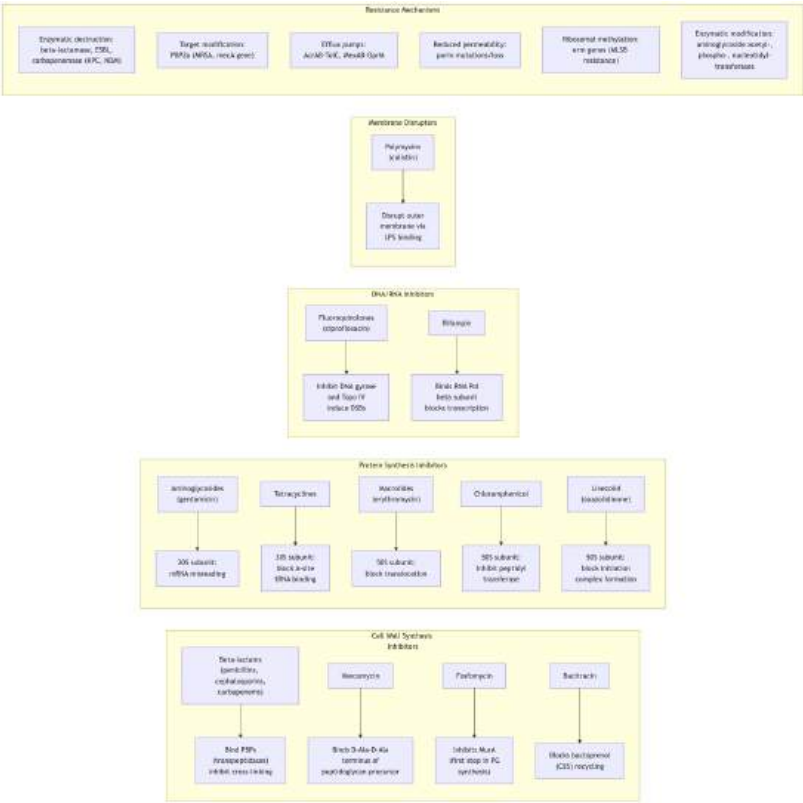


Figure 148. Antibiotic targets organized by cellular process (cell-wall synthesis, protein synthesis, nucleic-acid synthesis, membrane disruption) alongside the principal resistance mechanisms.

24.7.2 Selective Toxicity and Therapeutic Index

The foundation of antibiotic therapy is selective toxicity – targeting structures present in bacteria but absent or sufficiently different in human cells:

- Peptidoglycan (absent in human cells) -> beta-lactams, vancomycin
- 70S ribosomes (vs. human 80S) -> aminoglycosides, tetracyclines, macrolides
- Bacterial DNA gyrase (vs. human topoisomerase II) -> fluoroquinolones
- Bacterial RNA polymerase (structurally distinct from human Pol II) -> rifampin
- LPS outer membrane (absent in human cells) -> polymyxins

24.7.3 Resistance Mechanisms in Detail

Beta-lactamases are the most clinically important resistance mechanism. These enzymes hydrolyze the beta-lactam ring, inactivating the antibiotic before it reaches its PBP target. Evolution of beta-lactamases tracks the history of antibiotic development:

- Penicillinase (TEM-1, SHV-1) -> resistance to penicillins
- Extended-spectrum beta-lactamases (ESBLs: CTX-M, TEM variants) -> resistance to 3rd-generation cephalosporins
- Carbapenemases (KPC, NDM-1, OXA-48) -> resistance to carbapenems (last-resort beta-lactams)

MRSA (*methicillin-resistant Staphylococcus aureus*) carries the *mecA* or *mecC* gene encoding PBP2a/PBP2c, altered penicillin-binding proteins with low affinity for most traditional beta-lactam antibiotics. The gene resides on *SCCmec* (staphylococcal cassette chromosome), acquired by horizontal gene transfer. Treatment depends on syndrome and susceptibility: vancomycin, daptomycin, linezolid, or ceftaroline/ceftobiprole in settings where anti-MRSA cephalosporins are appropriate.

Efflux pumps actively transport antibiotics out of the cell. The AcrAB-TolC system in *E. coli* and MexAB-OprM in *Pseudomonas aeruginosa* are tripartite pumps spanning the inner membrane, periplasm, and outer membrane, conferring resistance to multiple drug classes simultaneously.

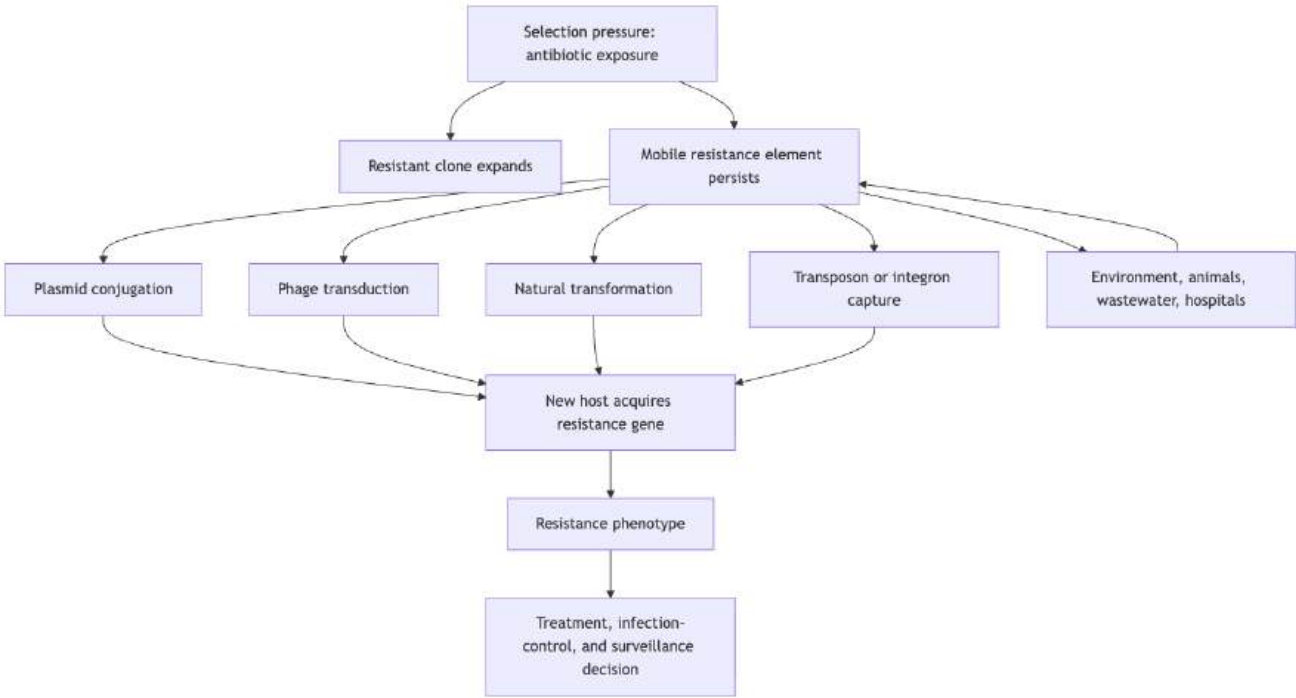


Figure 149. AMR horizontal-gene-transfer map. Resistance spreads by both clonal expansion and mobile genetic elements, so stewardship must be paired with infection control, wastewater/environmental surveillance, and organism-resistance-pair reporting \citep{who2024bppl,cdc2025antibioticuse}.

24.7.4 WHO Priority Pathogens (ESKAPE)

The WHO 2024 Bacterial Priority Pathogens List keeps AMR triage grounded in public-health burden, resistance trend, transmissibility, treatability, and pipeline scarcity [World Health Organization, 2024a]. The ESKAPE mnemonic remains a useful bedside memory aid, but the WHO list is broader: it separately prioritizes carbapenem-resistant *Acinetobacter baumannii*, carbapenem- or third-generation-cephalosporin-resistant Enterobacterales, drug-resistant *Mycobacterium tuberculosis*, and other pathogen-resistance pairs.

Table 322. WHO Priority Pathogens (ESKAPE): Pathogen and Key Resistance.

Pathogen	Key Resistance	Clinical Setting
<i>Enterococcus faecium</i>	VRE (vancomycin-resistant)	Bloodstream infections, UTIs
<i>Staphylococcus aureus</i>	MRSA (methicillin-resistant)	Skin, soft tissue, bacteremia
<i>Klebsiella pneumoniae</i>	ESBL, KPC carbapenemase	Pneumonia, UTIs, sepsis
<i>Acinetobacter baumannii</i>	Pan-resistant; OXA carbapenemases	Ventilator-associated pneumonia
<i>Pseudomonas aeruginosa</i>	Intrinsic resistance; efflux pumps	Burn wounds, CF lung infections
<i>Enterobacter</i> spp.	AmpC beta-lactamase (inducible)	Nosocomial infections

Clinical Connection: The Antibiotic Resistance Crisis The WHO has declared antimicrobial resistance one of the top 10 global public health threats. An estimated 1.27 million deaths were directly attributable to bacterial AMR in 2019, with many more associated deaths [Murray et al., 2022]. The O’Neill review’s 10-million-deaths-per-year scenario remains a warning about unchecked resistance rather than a forecast that must occur [O’Neill, 2016]. Major drivers include unnecessary human antibiotic prescribing, incomplete access to diagnostics, antibiotic use in food-animal production, and a thin discovery pipeline in which truly novel antibacterial classes are rare rather than absent [Centers for Disease Control and Prevention, 2025a, World Health Organization, 2024a].

Concept Check 5: A hospital isolate of *Klebsiella pneumoniae* is resistant to most beta-lactams including carbapenems, aminoglycosides, and fluoroquinolones. Primarily colistin (polymyxin) remains effective. Explain why colistin resistance, which has recently emerged via the plasmid-borne *mcr-1* gene (encoding a phosphoethanolamine transferase that modifies lipid A), is particularly alarming from a public health perspective.

24.8 CRISPR-Cas: Bacterial Adaptive Immunity

CRISPR (Clustered Regularly Interspaced Short Palindromic Repeats) arrays provide bacteria and archaea with an adaptive, heritable immune system against phages and plasmids. Discovered in 2007 (Barrangou et al., Science 2007), the system has three functional stages — adaptation, expression (biogenesis), and interference — that map cleanly onto the three steps of any immune system: memory formation, surveillance, and effector action.



Figure 150. The three-stage CRISPR-Cas immune mechanism: adaptation (Cas1-Cas2 captures and integrates new spacers), expression (pre-crRNA processed and loaded onto effector), and interference (target dsDNA cleavage).

24.8.1 Stage 1 — Spacer Acquisition (Adaptation)

When a bacterium survives phage infection, the Cas1-Cas2 integrase complex captures a short fragment (about 30 bp) of phage DNA — called a protospacer — adjacent to a PAM (protospacer adjacent motif). Cas1-Cas2 integrates this as a new spacer at the leader end of the CRISPR array between two direct repeats. This constitutes an immunological memory: the spacer sequence is now permanently encoded in the bacterial chromosome and inherited by most daughter cells.



PAM recognition ensures self vs non-self discrimination: the PAM sequence is not present in the CRISPR array itself (repeat sequences flank spacers, not PAMs), so the bacterium does not attack its own CRISPR locus. The specific PAM depends on the system: NGG (SpCas9, Type II), 5’-AAT-3’ or 5’-CTT-3’ (Type I-E), etc.

24.8.2 Stage 2 — crRNA Biogenesis

The CRISPR array is transcribed as a long pre-CRISPR RNA (pre-crRNA). Repeat sequences are cleaved by:

- Type I and III: The *Cas6* endoribonuclease (recognizes stem-loop structure in repeats)
- Type II: RNase III + *tracrRNA* (trans-activating crRNA) hybridizes with the repeat; Cas9 is then loaded with a single-guide RNA (sgRNA = crRNA + tracrRNA scaffold)

24.8.3 Stage 3 — Interference (Targeting)

The crRNA guides the effector complex to matching sequences in foreign nucleic acid. The CRISPR-Cas systems are now classified into 6 types (I–VI) and over 30 subtypes; the three most important types are summarized below:

Table 323. Stage 3 — Interference (Targeting): Feature and Type I.

Feature	Type I	Type II	Type III
Effector	Multi-subunit Cascade complex (Cas5–Cas8) + Cas3 helicase-nuclease	Single Cas9 nuclease	Cas10-Csm/Cmr complex
Target	dsDNA	dsDNA	ssRNA + transcribed DNA
Cleavage mechanism	Cas3 unwinds and degrades dsDNA processively	Cas9 makes blunt-ended double-strand break 3 bp upstream of PAM	Co-transcriptional ssRNA cleavage by Csm/Cmr; signaling output
PAM requirement	Yes (recognized by Cas8 of Cascade)	Yes (NGG for SpCas9; varies by ortholog)	None for RNA target; protospacer-flanking-sequence (PFS) for DNA
Guide RNA	crRNA primarily	crRNA + tracrRNA (or fused sgRNA)	crRNA primarily
Signal molecule	—	—	cyclic oligoadenylate (cA ₄ , cA ₆) activates non-specific RNase Csm6
Genome distribution	about 50 % of CRISPR-bearing genomes	about 5 %	about 25 %
Subtypes	I-A through I-G	II-A, II-B, II-C	III-A through III-F
Anti-CRISPR susceptibility	Yes (AcrIF, AcrIE families)	Yes (AcrIIA, AcrIIC families)	Yes (AcrIIIA, anti-cA ₄)
Clinical / biotech use	Cas3 large-deletion editing; phage therapy design (Locus crPhage)	Genome editing (Cas9); base editors; prime editors	Biosensing (cA ₄ readout); SHERLOCK-style RNA detection

Type II (Cas9) was repurposed for genome editing by Doudna, Charpentier, and colleagues in 2012 (*Science* 2012), work recognized with the 2020 Nobel Prize in Chemistry. A synthetic sgRNA directs Cas9 to any genomic target (specified by a 20-nt spacer sequence + NGG PAM), where it makes a site-specific DSB. The cell repairs the break by NHEJ (creating indels — gene knockout) or HDR (with a provided template — precise edit). Variants now include base editors (cytosine → thymine, adenine → guanine without DSBs), prime editors (programmable insertions/deletions guided by an extended pegRNA), and Cas12/Cas13 systems for DNA/RNA targeting respectively. The same RNA-guided programmability that powers genome editing also underlies the RNA-interference-like specificity by which bacteria neutralize phage genomes — a striking parallel to eukaryotic small-RNA defense systems first dissected with *C. elegans* [Fire et al., 1998].

24.8.4 Anti-CRISPR Proteins

Phages have evolved anti-CRISPR (Acr) proteins that counteract bacterial CRISPR immunity — an evolutionary arms race. Over 50 Acr families have been identified (Pawluk et al., *Nature Microbiology* 2016; Davidson et al., *Science* 2020 cryo-EM structures):

- AcrIF1 (Type I-F inhibitor): Binds Cas8f subunit of Cascade; blocks crRNA-guided dsDNA binding
- AcrIIA2/IIA4 (Type II inhibitors): Bind and occlude the PAM-recognition domain of Cas9; prevents target engagement
- AcrIIIA4: Degrades the cA₄ second messenger; blocks Csm6 activation

Clinical Connection: CRISPR-Based Therapies (2023–2026) The first CRISPR-based medicines have now been approved. Casgevy (exagamglogene autotemcel), developed by Vertex and CRISPR Therapeutics, received FDA approval in December 2023 for sickle cell disease and January 2024 approval for transfusion-dependent β -thalassemia; FDA’s 2026 product page lists both indications for patients 12 years of age and older [U.S. Food and Drug Administration, 2023, 2024b, 2026a]. The ex vivo approach edits patient HSCs to reactivate fetal hemoglobin (HbF) by disrupting the BCL11A erythroid enhancer, compensating for defective adult hemoglobin. Simultaneously, Bluebird Bio’s lentiviral gene therapy Lyfgenia was approved for SCD; its FDA product page should be treated as regulatory evidence distinct from ClinicalTrials.gov trial status and from the Casgevy editing mechanism [National Library of Medicine, 2026, U.S. Food and Drug Administration, 2026c]. By 2026, CRISPR therapies for transthyretin amyloidosis (intellia NTLA-2001, in vivo hepatic editing) and heterozygous familial hypercholesterolaemia are in Phase III trials.

Concept Check 6: > A Type II CRISPR-Cas9 system fails to cleave a target sequence despite perfect spacer-target complementarity. List three molecular explanations for this failure, relating each to a specific step in the CRISPR mechanism (adaptation, biogenesis, or interference).

Concept Check 6b: A bacterial population is challenged with a phage cocktail. After 5 generations, surviving bacteria are sequenced — 70% have new spacers in their CRISPR array matching the phage; 20% have escape mutations in essential phage genes (no new spacer); 10% have constitutively expressed Cas9 with broader PAM specificity. Explain which adaptation strategy is most evolutionary stable, and predict the population dynamics if a second, immunologically distinct phage is then introduced.

24.8.5 Worked Example: Designing a CRISPR-Cas9 Guide RNA for Targeted Cleavage

Problem: Design a *Streptococcus pyogenes* Cas9 (SpCas9) guide RNA to cleave gene X at nucleotide position 450, and quantify the predicted on-target vs. off-target activity given a candidate off-target site that differs from the on-target site by 2 mismatches within the 12-nt PAM-proximal seed region. Assume measured SpCas9 on-target cleavage efficiency = 60 % and that 2 seed-mismatches reduce cleavage probability by roughly 100-fold.

Design and quantitative analysis:

1. PAM identification. SpCas9 requires a 5'-NGG-3' PAM immediately 3' of the 20-nt protospacer (= target genomic sequence). Scan the genomic context around position 450 in gene X for an NGG motif. Suppose the genomic sequence at positions 430–453 reads:

5'-... ATG CTG ACG TAA GCA TGC AAT CGG ...-3'

The CGG trinucleotide at positions 451–453 is an NGG PAM. The corresponding 20-nt protospacer occupies positions 431–450 (the 20 nt immediately 5' of the PAM):

Protospacer (genomic): **CTG ACG TAA GCA TGC AAT C** (20 nt)
2. Guide RNA design. The 20-nt spacer of the sgRNA is the same sequence as the protospacer (with T → U for RNA): 5'-CUG ACG UAA GCA UGC AAU C-3'. This is fused to the tracrRNA scaffold (about 80 nt) that engages Cas9. The PAM itself is not included in the sgRNA — it is recognized by Cas9 in the target DNA.
3. Seed region. The 12 nucleotides proximal to the PAM (positions 8–20 of the spacer, counted from the PAM-distal 5' end; equivalently the last 12 nt before the PAM in the protospacer) form the seed region critical for target engagement. Mismatches here disproportionately disrupt cleavage.
4. On-target vs. off-target ratio. Given the assumptions:
 - On-target cleavage probability: $P_{\text{on}} = 0.60$.
 - Off-target candidate has 2 seed mismatches, reducing cleavage about 100-fold: $P_{\text{off}} \approx P_{\text{on}}/100 = 0.006 = 0.6\%$.

On-target : off-target ratio:

$$\frac{P_{\text{on}}}{P_{\text{off}}} = \frac{0.60}{0.006} = 100 : 1$$

5. Specificity scoring tools. In practice, gRNA design uses computational off-target predictors — e.g., CFD (Cutting Frequency Determination) scores, the MIT specificity score, CRISPOR, or Benchling. These tools enumerate genome-wide off-target candidates (allowing up to 4 mismatches and NAG-permissive PAMs) and combine per-position mismatch penalties into an aggregate specificity score. A well-designed gRNA typically achieves a CFD/MIT score ≥ 70 and shows no off-targets with fewer than 3 mismatches in the seed.
6. Mismatch-tolerance asymmetry. PAM-distal mismatches (positions 1–7 of the spacer) reduce cleavage modestly (often less than 2-fold per mismatch). Seed mismatches (positions 8–20, including the 12 nt closest to the PAM) reduce cleavage 10–100-fold each. This asymmetry is exploited by anti-CRISPR proteins (which often block the seed-loading step) and by engineered high-fidelity variants (eSpCas9, SpCas9-HF1, evoCas9) that introduce contacts disrupted by mismatch-induced structural strain, raising the discrimination threshold.

Interpretation. A 100:1 on:off ratio is acceptable for many research applications but inadequate for clinical genome editing in non-dividing cells where even rare off-target cuts can drive oncogenic translocations. Modern clinical Cas9 designs (Casgevy, NTLA-2001) use ratios $> 10,000:1$, achieved by combining sequence-optimized gRNAs with high-fidelity Cas9 variants and base editors (which avoid double-strand breaks entirely).

24.9 Computational Bridge

Batch culture kinetics follow the logistic-like curve encoded in `bacterial_growth_curve`:

```
from biology.microbiology import bacterial_growth_curve

curve = bacterial_growth_curve(N0=1e5, doubling_time_hr=0.5, t_end_hr=6.0)
print(curve.populations[-1] > curve.populations[0])
```

Clinical / systems note: Time-kill curves and MIC testing in the clinic are empirical cousins of these growth models; combination therapy is designed to keep effective populations below invasion thresholds.

24.9.1 SARS-CoV-2 Variant Evolution: Real-Time Darwin in a Global Population

The four-year trajectory of SARS-CoV-2 (late 2019 – present) is the best-documented example of adaptive viral evolution in biological history. Public sequencing through GISAID now archives > 16 million viral genomes, enabling phylogenetic tracking at daily resolution. The lineage diversification follows a textbook evolutionary pattern: (1) a narrow founder bottleneck (Wuhan-Hu-1 reference, December 2019); (2) geographic diffusion with local **founder effects** (D614G rose to global dominance by June 2020, conferring about 20 % higher infectivity via an allosteric receptor-binding-domain (RBD) “open” state); (3) escape-driven positive selection as population immunity accumulated, favoring RBD mutations that evade neutralizing antibodies without compromising ACE2 binding.

Five variants of concern (VOCs) illustrate distinct evolutionary forces. Alpha (B.1.1.7, late 2020) carried N501Y — a single RBD mutation increasing ACE2 affinity about 10×. Beta (B.1.351) and Gamma (P.1) added E484K, which partially escapes antibodies. Delta (B.1.617.2, mid-2021) carried L452R + T478K and doubled transmissibility. Omicron (B.1.1.529, November 2021) was the punctuated-evolution event of the pandemic — 32 spike mutations at once, not a gradual lineage from Delta but a sudden saltation, likely from a long-term infection in an immunocompromised host (a natural “mutator” environment). Omicron escaped most pre-existing neutralizing antibodies but attenuated lung tropism via reduced TMPRSS2-mediated entry, shifting the disease toward upper respiratory infection. Subsequent sub-lineages (BA.2, BA.5, XBB, JN.1, KP.3) follow continuous antigenic drift — the “influenza-like future” of SARS-CoV-2 is now the expected trajectory.

Quantitatively: Ka/Ks ratios on the RBD exceed 1.5 across the pandemic (positive selection), versus about 0.1 for housekeeping ORFs (purifying selection); estimated substitution rate is about 2×10^{-3} per site per year ($2\times$ SARS-CoV-1), consistent with RNA-virus fidelity limits and increased by population-scale chronic infections. Public-health surveillance now runs phylogenetic tools (Nextstrain, Pango) in near-real-time; **vaccine** reformulation (WHO TAG-CO-VAC) follows the influenza-flu-shot paradigm. The pandemic has transformed biology teaching: evolution is no longer a fossil-record inference but a live, observable process with weekly GenBank updates.

24.10 Current Evidence and Frontier Biology: Bacteria, Archaea, and Viruses

For Bacteria, Archaea, and Viruses, frontier biology belongs inside the evidence logic of the chapter. Microbiology and infectious disease now require One Health reasoning across people, animals, environments, genomics, and antimicrobial stewardship. The core reading question is this: microbial claims should identify taxonomy, genome architecture, metabolism, resistance mechanism, and environment.

- What to verify: identify the observation, model, assay, or dataset that would make the claim stronger or weaker.
- What to qualify: state the scale, organism, cell type, environmental condition, or population where the claim is expected to hold.
- What to compare: test at least one alternative explanation, baseline, or null model before treating the pattern as causal.
- What to cite: distinguish primary evidence, review synthesis, public dataset, and institutional guidance; for recent or numeric claims, prefer the source closest to the measurement and state what has changed since it was published.

For microbial-resistance claims, name the organism, resistance determinant, drug pressure, transmission route, and surveillance source [**World Health Organization, 2024a, Centers for Disease Control and Prevention, 2025a, Murray et al., 2022**].

Source practice: For microbial and AMR claims, tie statements to organism-resistance pairs, surveillance evidence, genome data, official guidance, and stewardship context [**World Health Organization, 2024a, Centers for Disease Control and Prevention, 2025a, Murray et al., 2022**].

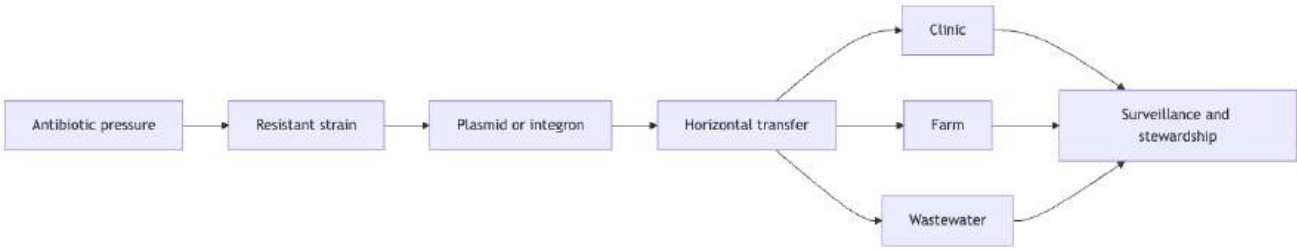


Figure 151. WHO priority lists are most useful when students connect the organism-resistance pair to selection pressure, transmission route, and stewardship action \citep{who2024bppl,murray2022amr}.

24.10.1 Current Evidence Map: AMR Movement Across One Health

24.11 Summary

- Three domains of life (Bacteria, Archaea, Eukarya) were established by Woese’s rRNA phylogeny [Woese and Fox, 1977]. Bacteria and Archaea share the prokaryotic cell plan but differ fundamentally in membrane lipids, cell wall chemistry, and transcriptional machinery.
- Bacterial cell walls contain peptidoglycan, built in an 11-step pathway (MurA → MurB → MurC–F → MraY → MurG → MurJ flipping → transglycosylation → PBP transpeptidation) that is the target of fosfomycin, D-cycloserine, bacitracin, vancomycin, daptomycin, and β-lactams. Gram-positive bacteria have thick peptidoglycan with teichoic acids; Gram-negative bacteria have thin peptidoglycan plus an outer membrane with LPS (endotoxin, activates TLR4, causes septic shock).
- Bacterial growth equation $N(t) = N_0 \cdot 2^{t/t_d}$ (equation (351)) describes exponential phase; the natural-log form gives a linear plot whose slope is the specific growth rate $\mu = (\ln 2)/t_d$.
- Bacterial metabolic diversity exceeds most eukaryotes: photoautotrophs, chemoautotrophs (lithotrophs), and heterotrophs with varied oxygen relationships.
- Two-component systems (sensor histidine kinase + response regulator, His→Asp phosphotransfer) are the dominant prokaryotic signal-transduction architecture; biofilms (matrix + persisters, c-di-GMP master regulator) and quorum sensing (AHL/AIP/AI-2) underpin chronic infections and 65–80 % of clinical infections.
- Horizontal gene transfer (transformation, transduction, conjugation) drives bacterial evolution [Lawrence and Ochman, 1998] and antibiotic resistance spread via R-plasmids and transposons.
- Archaea differ from bacteria in ether-linked isoprenoid lipids (with G-1-P stereochemistry; tetraether monolayers in hyperthermophiles), lack of peptidoglycan, and eukaryote-like transcription. Asgard archaea are the closest living relatives of eukaryotes and encode actin, ESCRT, and ubiquitin-like machinery.
- Viruses (Baltimore classes I–VII) are obligate intracellular parasites; bacteriophage lytic/lysogenic cycles and the HIV life cycle illustrate replication strategies and drug targets. Phage therapy is re-emerging as a clinical adjunct for multi-drug-resistant infections, with engineering, cocktail design, and antibiotic combination addressing rapid resistance and immune neutralization [Doub et al., 2022]. Phage pharmacokinetics are non-linear with a proliferation threshold $B^* = m/(bk)$.
- CRISPR-Cas is a heritable bacterial adaptive immune system (adaptation–expression–interference); Types I (Cas3), II (Cas9), and III (Cas10) differ in effector architecture, target nucleic acid, and PAM requirements. Type II Cas9 has been repurposed as the dominant genome-editing technology and now drives FDA-approved therapeutics (Casgevy, 2023–2026 FDA records).
- Antibiotic resistance mechanisms (enzymatic inactivation, target modification, efflux, reduced permeability) spread via HGT; ESKAPE organisms remain a useful mnemonic, but current AMR triage should use pathogen-resistance pairs and WHO BPPL priority categories rather than a single threat list.
- Connections: See section 23 for phylogeny of mobile elements, section 27 for host immunity, and Unit III — Energy and Metabolism: Introduction for metabolic targets of antibiotics.

24.12 Key Terms

Table 324. Current Evidence Map: AMR Movement Across One Health: Term and Definition.

Term	Definition
Peptidoglycan	Bacterial cell wall polymer of NAG-NAM glycan strands cross-linked by tetrapeptide chains; target of beta-lactam antibiotics

Term	Definition
Lipid II	Lipid-anchored peptidoglycan precursor (undecaprenyl-PP-MurNAc-pentapeptide-GlcNAc); target of vancomycin, nisin, daptomycin
Lipopolysaccharide (LPS)	Gram-negative outer membrane component (lipid A + core + O-antigen); endotoxin that activates TLR4 and can cause septic shock
Gram stain	Differential staining technique distinguishing thick-walled (Gram-positive, purple) from thin-walled (Gram-negative, pink) bacteria
Two-component system (TCS)	Sensor histidine kinase + response regulator pair that converts an environmental stimulus into a transcriptional output via His→Asp phosphotransfer
Biofilm	Surface-attached, EPS-encased microbial community; 10–1000× more antibiotic tolerant than planktonic cells
c-di-GMP	Cyclic-di-guanosine-monophosphate; master second messenger that switches between motile (low) and biofilm (high) lifestyles
Quorum sensing	Cell-density-dependent gene regulation via secreted autoinducer molecules (AHL, AIP, AI-2)
Persister cells	Metabolically dormant subpopulations within a biofilm that survive antibiotic exposure without genetic resistance
Binary fission	Asexual bacterial reproduction; chromosome replication followed by septum formation and cell division
Specific growth rate (μ)	$\mu = (\ln 2)/t_d$; instantaneous fractional growth rate in exponential phase, units of time^{-1}
Horizontal gene transfer	Transfer of genetic material between organisms by mechanisms other than vertical (parent-to-offspring) inheritance
Transformation	Uptake of free DNA from the environment by competent bacteria
Transduction	Bacteriophage-mediated transfer of bacterial DNA between cells
Conjugation	Direct cell-to-cell DNA transfer via F pilus; primary mechanism for R-plasmid spread
Endospore	Dormant, highly resistant structure formed by <i>Bacillus</i> and <i>Clostridium</i> ; contains calcium-dipicolinic acid
Bacteriophage	Virus that infects bacteria; follows lytic (cell lysis) or lysogenic (genome integration) cycle
Lysogeny	Integration of phage DNA into host chromosome as a prophage; maintained by CI repressor
Phage therapy	Therapeutic use of bacteriophages (often as cocktails) to treat bacterial infections, especially multi-drug-resistant ones
Phage proliferation threshold	Minimum bacterial density $B^* = m/(bk)$ above which a phage population can self-amplify rather than dilute out
Baltimore classification	System classifying viruses into seven classes based on genome type and replication strategy
Reverse transcriptase	RNA-dependent DNA polymerase; used by retroviruses (HIV) to convert RNA genome to dsDNA
Prion	Infectious misfolded protein (PrP^{Sc}) that templates conversion of normal PrP^{C} ; no nucleic acid
MRSA	Methicillin-resistant <i>Staphylococcus aureus</i> ; carries <i>mecA</i> gene encoding PBP2a with low beta-lactam affinity
ESKAPE pathogens	Six priority antibiotic-resistant organisms: Enterococcus, S. aureus, Klebsiella, Acinetobacter, Pseudomonas, Enterobacter
Asgard archaea	Deep-branching archaeal lineages (Loki, Thor, Odin, Heimdall, Hela, Hermod) containing eukaryotic signature proteins; closest known relatives of eukaryotes
Eukaryotic signature proteins (ESPs)	Proteins (actin, ESCRT, ubiquitin-like, Rab GTPases) encoded by Asgard archaea that were once thought to be eukaryote-specific
GDGT lipids	Glycerol-dialkyl-glycerol-tetraether monolayer lipids that span the entire archaeal membrane; confer extreme thermostability
CRISPR-Cas	Bacterial/archaeal RNA-guided adaptive immune system (adaptation–expression–interference); repurposed for genome editing
PAM	Protospacer adjacent motif; short sequence flanking the target that licenses CRISPR-Cas cleavage and ensures self/non-self discrimination

24.13 Review Questions

1. Compare the cell wall structure of Gram-positive and Gram-negative bacteria. Explain why Gram-negative sepsis is often more dangerous than Gram-positive sepsis, focusing on the role of LPS and TLR4 signaling.
2. A researcher isolates a bacterium from a hot spring (85 degrees C, pH 3) that has ether-linked lipids, no peptidoglycan, and an RNA polymerase with 12 subunits. To which domain does this organism most likely belong? Justify your classification using at least three molecular features.
3. Explain how a single conjugation event involving an R-plasmid carrying genes for beta-lactamase (*bla*), aminoglycoside acetyltransferase (*aac*), and a tetracycline efflux pump (*tet*) can convert a susceptible bacterium into a multidrug-resistant pathogen in a single step. Why is this more concerning than resistance arising through chromosomal mutation?
4. Compare generalized and specialized transduction. For each, describe the molecular error that leads to bacterial DNA being packaged in phage particles, and explain why specialized transduction transfers primarily specific genes while generalized transduction can transfer any gene.
5. The HIV provirus can remain latent in resting memory CD4⁺ T cells for decades, even in patients on suppressive ART. Explain why this latent reservoir prevents cure and why the “shock and kill” strategy (reactivating latent virus with latency-reversing agents while the patient is on ART) has been proposed.
6. Draw the lytic cycle of bacteriophage T4 and calculate the following: if a single T4 phage infects an *E. coli* culture containing 10⁶ cells, the burst size is 150, and the lytic cycle takes 25 minutes, how many phage particles will be present after 3 complete lytic cycles (assuming most released phage successfully infect new cells)?
7. Explain why *Mycobacterium tuberculosis* is neither truly Gram-positive nor Gram-negative despite being classified in the Gram-positive phylum Actinobacteria. What cell wall component is responsible for this anomaly, and what alternative staining method is used?
8. The discovery of Asgard archaea has strengthened support for the “two-domain tree” of life over the traditional “three-domain tree.” Explain the key evidence supporting this model, including the eukaryotic signature proteins found in Asgard genomes and what this implies about the origin of eukaryotic cells.
9. A hospital laboratory reports that a *Klebsiella pneumoniae* isolate is resistant to meropenem (a carbapenem) with an MIC of 32 µg/mL. The resistance is mediated by a plasmid-borne KPC-2 carbapenemase. Describe three infection control measures that should be implemented immediately, and explain why carbapenem resistance is considered a “sentinel event” in infectious disease.
10. Compare the replication strategies of influenza virus (Class V, segmented (-)ssRNA) and SARS-CoV-2 (Class IV, non-segmented (+)ssRNA). Explain why influenza can undergo antigenic shift through reassortment while coronaviruses cannot, and discuss the implications for pandemic preparedness.
11. Growth-curve calculation. Apply equation (351): a culture of *Streptococcus pneumoniae* ($t_d = 30$ min) starts at $N_0 = 5 \times 10^3$ CFU/mL. (a) After how many minutes will the density reach 10⁹ CFU/mL — the typical density at which sepsis becomes hemodynamically significant? (b) If the patient receives a single dose of ceftriaxone that reduces the population by 4 log₁₀ instantly, and if the residual bacteria resume growth at the same rate 1 hour later, when does the density return to 10⁹?
12. Estimate phage amplification after three rounds if burst size $B = 150$ and every virion infects — relate to the logistic assumptions that break down in real cultures.
13. Why are archaeal antibiotics rare compared with bacterial antibiotics, given clinical need?
14. Peptidoglycan pathway integration. Place fosfomycin, D-cycloserine, bacitracin, vancomycin, and ampicillin on the peptidoglycan biosynthesis pathway and explain why a single resistance mutation generally confers resistance to a single of them — but VanA-type vancomycin resistance and PBP2a (*mecA*) MRSA evade two by altering different parts of the same step.
15. Two-component systems and antibiotic stewardship. PhoQ-PhoP modifies lipid A in response to host antimicrobial peptides. Explain how this TCS contributes to colistin resistance and why a PhoQ inhibitor would be expected to “re-sensitize” *Salmonella* to polymyxins.
16. Biofilm pharmacology. A patient with a *S. aureus* prosthetic-knee infection fails six weeks of vancomycin. Explain four distinct biofilm-related reasons for this failure and design a combination strategy targeting at least two of them.
17. Phage therapy resistance. A clinical phage cocktail uses three phages with non-overlapping receptors (LPS O-antigen, OmpC, type IV pilus). Estimate the probability that a single bacterium escapes the full cocktail by independent mutation and explain why cocktails have outperformed single-phage therapies in trials.

18. CRISPR types comparison. A biotech company wants to develop a phage-therapy product that itself targets multi-drug-resistant *E. coli* CRISPR-immune to the original phage. Compare Type I (Cas3, processive degradation) and Type II (Cas9, blunt DSB) approaches for this application, and justify your choice based on (a) target size, (b) delivery, and (c) likelihood of bacterial escape.

24.14 Further Reading and Source Notes: Bacteria, Archaea, and Viruses

- Woese & Fox (1977). Phylogenetic structure of the prokaryotic domain: The primary kingdoms. *Proceedings of the National Academy of Sciences*, 74.
- COVID-19} (2022). The Lancet Commission on lessons for the future from the COVID-19 pandemic. *The Lancet*, 400.
- Sagan (1967). On the origin of mitosing cells. *Journal of Theoretical Biology*, 14.
- Madigan et al. (latest ed.). *Brock Biology of Microorganisms*. Pearson.
- Jinek, Chylinski, Fonfara, Hauer, Doudna & Charpentier (2012). A programmable dual-RNA-guided DNA endonuclease in adaptive bacterial immunity. *Science*, 337.
- Barrangou et al. (2007). CRISPR provides acquired resistance against viruses in prokaryotes. *Science*, 315.
- Spang et al. (2015). Complex archaea that bridge the gap between prokaryotes and eukaryotes. *Nature*, 521.

24.15 Companion Source Module: Bacteria, Archaea, and Viruses

Bacteria, Archaea, and Viruses should leave a reproducible trail from a biological claim to the code, figure, diagram, or paper-based activity that can test it. Use the surfaces below to inspect the chapter’s assumptions, rerun the relevant model, or compare the manuscript explanation with companion labs and figures.

Table 325. Companion source surfaces for Bacteria, Archaea, and Viruses.

Surface	Use it for
<code>src/biology/microbiology/microbiology.py</code> (bacterial_growth_curve, doubling_time, ViralReplicationResult)	Check growth, doubling, and viral-replication assumptions.
<code>src/visualization/plots.py</code> (plot_bacterial_growth)	Inspect growth phases and axis scaling.
<code>src/mermaid/biology_diagrams.py</code> (viral_replication_cycle_diagram)	Link genome strategy to replication cycle.

Reproducibility check: specify taxon, environment, growth phase, genome type, and measurement method before generalizing microbial claims. Cross-reference: connect with section 25 and sections 26 and 27.

25 Microbial Ecology and the Microbiome

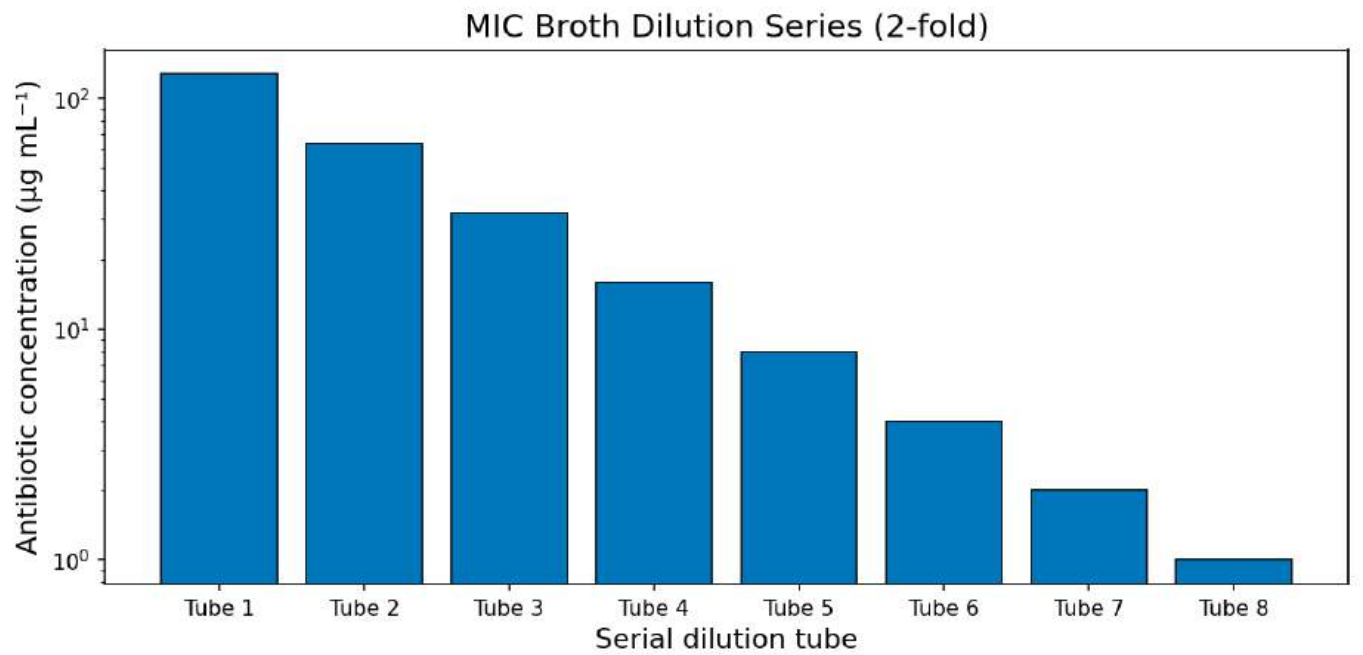


Figure 152. Two-fold serial broth dilution for minimum inhibitory concentration (MIC) testing. Antibiotic concentration halves in each successive tube; the first tube with no visible growth marks the MIC used to compare susceptibility.

Level 2/3 · 60 min read · 75 min lecture · Prerequisites: section 24

25.1 Learning Objectives

By the end of this chapter, you should be able to:

1. Explain the “great plate count anomaly” and describe culture-independent methods for studying microbial communities, including 16S rRNA amplicon sequencing and shotgun metagenomics.
2. Calculate and interpret alpha and beta diversity metrics for microbial communities, including Shannon entropy, Simpson and inverse-Simpson indices, and Chao1 richness estimation.
3. Distinguish OTU (operational taxonomic unit at 97% identity) from ASV (exact sequence variant) approaches and explain the role of rarefaction curves in normalizing diversity comparisons.

- Describe the composition and functional roles of the human **microbiome** across body sites, with emphasis on the gut microbiome and its core/variable components.
- Explain microbiome-host interactions through pattern recognition receptors and short-chain fatty acid signaling.
- Explain the relationship between dysbiosis and disease, including obesity, inflammatory bowel disease, and colorectal cancer.
- Describe microbial roles in biogeochemical cycles (nitrogen, sulfur, carbon), including the gene markers used to track each transformation, and explain kill-the-winner dynamics in ocean phage-host systems.
- Describe the roles of microorganisms in **biofilm** formation, quorum sensing, and bioremediation.

25.1.1 Study Blueprint

- Big idea: Microbes organize communities, cycles, and host physiology through interactions and metabolism.
- Core concepts: microbiomes, symbiosis, diversity, biogeochemical cycling.
- Framework alignment: Vision & Change: Evolution, Systems, Structure and function; AP Biology: Evolution, Systems Interactions; NGSS-style topics: Structure and Function, Interdependent Relationships in Ecosystems.
- Model or quantitative lens: Diversity indices, richness estimates, and interaction-network reasoning.
- Data skill: Compute or interpret community metrics from abundance data.
- Practice cadence: Questions and Methods, Representing and Describing Data, Argumentation.
- Common misconception to repair: A microbiome is not automatically beneficial; context determines the effect.
- Primary lab: **Lab — Microbial Ecology and the Microbiome**.
- Question bank: **Questions — Microbial Ecology and the Microbiome**.
- Transfer task: Transfer microbial ecology to soils, oceans, digestion, disease, and climate feedbacks.
- Bridge to computation: `biology.ecology.ecology.biodiversity_indices`.

Opening Vignette — You Are Mostly Not You

For decades, textbooks cited the figure that the human body contains ten times more bacterial cells than human cells. In 2016, Sender, Fuchs, and Milo published a careful recalculation: the ratio is approximately 1:1, with roughly 38 trillion bacteria and 30 trillion human cells [Sender et al., 2016]. But the bacteria contribute only about 0.2 kg of body mass, compared to 70 kg of self. What changed science was not the ratio but the Human Microbiome Project (2007–2016), which used 16S rRNA sequencing and shotgun metagenomics to map healthy human-associated microbial communities across body sites [The Human Microbiome Project Consortium, 2012]. The project revealed that gut microbiome composition influences immunity, metabolism, neurotransmitter production, and drug efficacy — and differs between individuals as distinctly as a fingerprint. The microbiome is now recognized as an additional organ, and its disruption (dysbiosis) is linked to inflammatory bowel disease, obesity, depression, and antibiotic-associated colitis. We are ecosystems, not individuals.

25.2 Measuring Microbial Communities Across Scales

25.2.1 The Great Plate Count Anomaly

In 1985, Staley and Konopka formalized a long-recognized paradox in microbiology: when environmental samples are examined by direct microscopic counts or flow cytometry, cell densities of 10^6 per milliliter are typical in aquatic environments [Staley and Konopka, 1985]. Yet when the same samples are plated on standard laboratory media, primarily 10^2 - 10^3 colony-forming units (CFU) per milliliter grow – less than 1% of the organisms present. This discrepancy, termed the great plate count anomaly, revealed that the vast majority of microbial diversity is invisible to traditional culture-based microbiology.

The reasons for unculturability are diverse:

- Unknown nutrient requirements or growth factors
- Obligate syntrophic relationships (organisms that depend on metabolites from partner species)
- Extremely slow growth rates (generation times of weeks to months)
- Sensitivity to atmospheric oxygen levels (many are strict anaerobes or microaerophiles)
- Dormancy or viable-but-not-culturable (VBNC) states
- Requirement for cell-cell signaling or quorum sensing to initiate growth

25.2.2 Culture-Independent Methods

Modern microbial ecology relies on molecular approaches that bypass cultivation entirely:

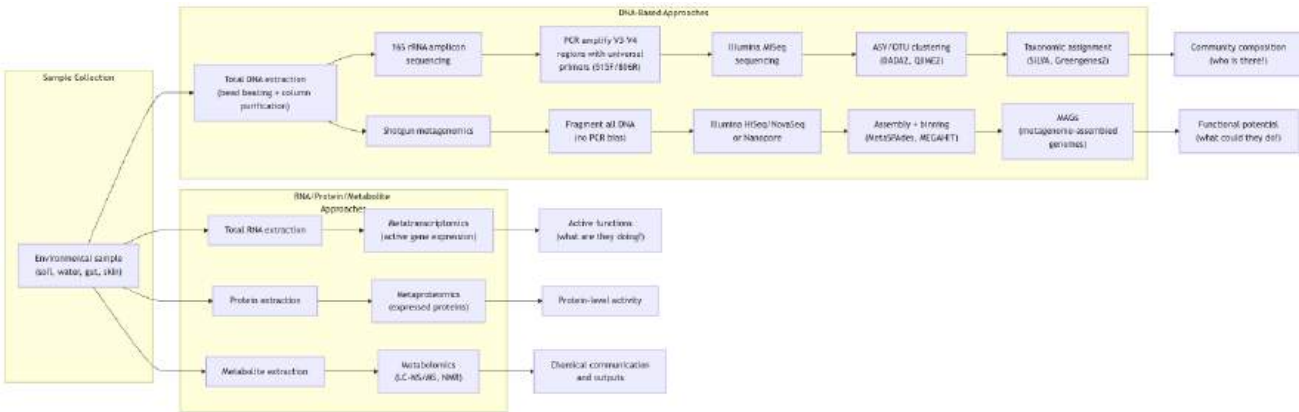


Figure 153. Multi-omic workflow for culture-independent microbial community profiling: 16S amplicon and shotgun metagenomic DNA approaches answer “who is there” and “what could they do,” while metatranscriptomics, metaproteomics, and metabolomics answer “what are they actually doing”.

25.2.3 The 16S rRNA Amplicon Pipeline: From Sample to ASV Table

16S rRNA amplicon sequencing is the workhorse of microbial community profiling. Understanding the full pipeline, with its choices and biases, is essential for interpreting any modern microbiome paper.

Why 16S? The 16S rRNA gene is ideal as a phylogenetic marker because of three intrinsic properties:

- Almost universally present in most bacteria and **archaea** (about 1500 bp).
- Mosaic of conserved and variable regions — nine hypervariable regions (V1–V9) are sandwiched between highly conserved regions that allow universal primer design (e.g., 27F, 515F, 806R, 1492R).
- Slow evolutionary rate in conserved domains preserves deep phylogenetic signal; rapid evolution in V regions enables genus- to species-level discrimination.

Region selection. Different V regions perform differently:

Table 326. The 16S rRNA Amplicon Pipeline: From Sample to ASV Table: Region and Length.

Region	Length	Strengths	Weaknesses
V1–V3	about 480 bp	Good genus resolution; <i>Staphylococcus</i> -friendly	Misses some <i>Bifidobacterium</i>
V3–V4	about 460 bp	De facto standard for human microbiome (HMP); good Illumina MiSeq fit	Underestimates <i>Bifidobacterium</i> and some archaea
V4 primarily	about 250 bp	Single-end MiSeq; high read depth	Lower taxonomic resolution
V6–V8	about 440 bp	Better for environmental archaea	Less reference-database coverage
Full-length (1.5 kb)	1500 bp	Species- to strain-level resolution; PacBio HiFi or Nanopore	Higher per-base error rate; lower throughput

Workflow.

1. DNA extraction — bead beating (mechanical lysis of Gram-positives, fungi, spores) plus a column-based purification (e.g., DNeasy PowerSoil). Extraction kit choice introduces bias of up to $\pm 30\%$ in relative abundances and is now considered a major reproducibility issue.
2. PCR amplification — universal primers (515F/806R for V4, 341F/805R for V3–V4) plus barcoded adapters allow multiplexing. PCR cycles should be minimized (≤ 25) to reduce chimera formation; high-fidelity polymerases (Q5, Phusion) reduce error.
3. Library preparation and sequencing — Illumina MiSeq 2×300 bp is standard; about 100 000 reads/sample is typical for diversity analyses, with about $10 \times$ that needed to detect rare taxa.
4. Quality filtering — trim adapters and primers; discard reads with average $Q < 25$ or expected errors > 1 .
5. OTU clustering vs ASV inference — see comparison below.
6. Taxonomic assignment — match representative sequences against reference databases (SILVA 138.2, Greengenes2, RDP) using naive Bayes (RDP classifier) or k-mer methods (VSEARCH); confidence threshold typically 80 % [Chuvochina et al., 2025].

7. Diversity analyses and statistics — alpha (within-sample) and beta (between-sample) diversity, with multiple-comparison correction.

Taxonomy itself is now a versioned data product. GTDB release R10-RS226 organized 715,230 bacterial and 17,245 archaeal genomes into 136,646 bacterial and 6,968 archaeal species clusters, using average nucleotide identity for species and relative evolutionary divergence on marker-gene trees for higher ranks [Parks et al., 2026]. That makes a microbial name an evidence claim: reports should state the database and release used, especially when MAGs or uncultured lineages drive the biological conclusion.

25.2.4 OTU vs ASV: A Decade-Long Methodological Shift

For about 15 years (2007–2017), microbiome studies clustered reads into operational taxonomic units (OTUs) at a $\geq 97\%$ identity threshold (corresponding roughly to genus-level groupings). Around 2017, a methodological revolution replaced this with amplicon sequence variants (ASVs) — exact, error-corrected sequences resolved at single-nucleotide precision. The contrast:

Table 327. OTU vs ASV: A Decade-Long Methodological Shift: Property and OTUs (de novo, closed-reference).

Property	OTUs (de novo, closed-reference)	ASVs (DADA2, Deblur, UNOISE3)
Clustering	Group reads at 97 % identity	Statistical denoising; each unique error-corrected sequence is its own ASV
Resolution	Roughly genus-level	Single-nucleotide; potentially strain-level
Reproducibility across studies	Poor (cluster boundaries depend on dataset)	Good (ASVs are exact sequences)
Tolerance to PCR/sequencing errors	High (errors collapsed into clusters)	Requires explicit error model
False-positive rare ASVs	Lower	Higher unless filtered
Computational cost	Lower	Higher (DADA2 about 1 hr per 1000 samples)
Modern recommendation	Legacy use primarily	De facto standard since about 2018

The Callahan *et al.* (2017, *ISME Journal*) “Exact sequence variants should replace OTUs” argument has been broadly adopted: ASVs are reproducible across studies and labs, allow meta-analyses across datasets, and resolve closely related taxa that 97 %-clustering would merge. Closed-reference OTU pipelines (clustering to a fixed reference database) remain useful for very large meta-analyses but are increasingly being supplanted.

Rarefaction and normalization. Different samples are sequenced to different depths, which artificially inflates richness in deeply sequenced samples (you see more rare taxa simply because you looked harder). Two approaches address this:

- Rarefaction — randomly subsample every sample down to the minimum library size before computing diversity. Plotting richness as a function of subsample size yields a rarefaction curve: a curve that plateaus indicates sufficient sampling depth; one still rising indicates undersampling.
- Normalization by total-sum scaling, CSS (cumulative-sum scaling), or DESeq2-style geometric means — preserves the original count data with a statistical correction.

Modern best practice: report results from both approaches, confirm robustness, and rarely compare unrarefied richness across samples of unequal depth.

25.2.5 Other Omics Layers

- Shotgun metagenomics sequences most DNA in a sample without amplification: no PCR bias; captures most organisms including viruses and eukaryotic microbes; enables functional gene profiling; produces metagenome-assembled genomes (MAGs) — reconstructed genomes of uncultured organisms from metagenomic reads using coverage depth and tetranucleotide frequency binning. The Human Microbiome Project (HMP, 2008-2014) characterized the microbiomes of healthy adults across body sites and showed that microbial metabolic pathways can be more stable than taxonomic composition [The Human Microbiome Project Consortium, 2012].
- Metatranscriptomics (total mRNA sequencing) reveals which genes are actively expressed – the functional state of the community at the time of sampling. This distinguishes between metabolic potential (metagenomics) and metabolic activity.

- Metaproteomics identifies the proteins actually translated, capturing post-transcriptional regulation.
- Metabolomics profiles the small molecules present in a sample using mass spectrometry (LC-MS/MS) or nuclear magnetic resonance (NMR). This captures the chemical outputs and communication molecules of the microbial community, including short-chain fatty acids, bile acid metabolites, tryptophan derivatives, and quorum sensing signals.

Concept Check 1: A researcher sequences the 16S rRNA gene from a soil sample and identifies 500 distinct amplicon sequence variants (ASVs). She then performs shotgun metagenomics on the same sample and assembles 200 MAGs. Explain why these numbers differ and what types of organisms might be captured by one method but not the other.

Concept Check 1b: A reviewer criticises a 2016 microbiome paper for using 97 %-identity OTU clustering instead of ASVs. The authors respond that re-running with DADA2 gives the same overall conclusions. Explain (a) what the reviewer’s underlying concern is, (b) why the conclusions might still be the same in this case, and (c) one biological situation where OTU vs ASV could change a paper’s conclusions.

25.2.6 Diversity Metrics for Microbial Communities

Quantifying microbial community diversity requires mathematical frameworks borrowed from classical ecology. Diversity has two components — richness (how many distinct taxa?) and evenness (how uniformly are they distributed?) — and most metrics are weighted combinations of these.

Alpha diversity (within-sample diversity):

- Observed ASVs/OTUs: Simple count of distinct taxa; sensitive to sequencing depth.
- Shannon entropy: weights both richness and evenness logarithmically.
- Simpson index and its inverse: dominance-weighted; emphasizes common taxa.
- Chao1 estimator: extrapolates from observed singletons/doubletons to estimate true richness.
- Faith’s phylogenetic diversity (PD): Sum of branch lengths in the phylogenetic tree connecting most observed taxa; incorporates evolutionary relationships.

Shannon Diversity Index The Shannon entropy is the single most-used alpha-diversity metric. It is defined as:

$$H' = - \sum_{i=1}^S p_i \ln p_i$$

(353)

where S is the number of species and p_i is the relative abundance (fraction) of species i . Higher H' means greater diversity. The maximum H' for S species is $\ln S$, achieved when most species are perfectly even ($p_i = 1/S$); the minimum is 0 (single species). A useful intuition: $e^{H'}$ is the effective number of equally common species — a community with $H' = 2.30$ has the same Shannon diversity as 10 perfectly even species.

Worked Example: Computing Shannon Diversity for Five Species Problem: A gut microbiome sample contains five dominant species with the following observed counts: *Bacteroides* (500), *Faecalibacterium* (300), *Roseburia* (100), *Akkermansia* (60), *Bifidobacterium* (40). Compute the Shannon diversity index H' from equation (353).

Solution:

1. Total counts: $N = 500 + 300 + 100 + 60 + 40 = 1000$.
2. Relative abundances:

$$p_1 = 0.500, p_2 = 0.300, p_3 = 0.100, p_4 = 0.060, p_5 = 0.040.$$

3. Compute $-p_i \ln p_i$ term-by-term:

Table 328. Computing Shannon Diversity for Five Species: Species and p_i .

Species	p_i	$\ln p_i$	$-p_i \ln p_i$
<i>Bacteroides</i>	0.500	−0.693	0.347
<i>Faecalibacterium</i>	0.300	−1.204	0.361
<i>Roseburia</i>	0.100	−2.303	0.230
<i>Akkermansia</i>	0.060	−2.813	0.169
<i>Bifidobacterium</i>	0.040	−3.219	0.129

4. Sum:

$$H' = 0.347 + 0.361 + 0.230 + 0.169 + 0.129 \approx 1.236.$$

5. Interpretation: $e^{H'} = e^{1.236} \approx 3.44$. The community has the same Shannon diversity as a perfectly even community of about 3.4 species — capturing the fact that although there are 5 species present, the dominance of *Bacteroides* and *Faecalibacterium* substantially lowers the effective diversity. The maximum possible H' for 5 species is $\ln 5 = 1.609$; this community has 77 % of maximum evenness.

Simpson Index and Inverse Simpson The Simpson index λ measures dominance — the probability that two individuals drawn at random belong to the *same* species:

$$\lambda = \sum_{i=1}^S p_i^2.$$

For the example above, $\lambda = 0.500^2 + 0.300^2 + 0.100^2 + 0.060^2 + 0.040^2 = 0.250 + 0.090 + 0.010 + 0.0036 + 0.0016 = 0.355$. Two complementary forms are usually reported:

- Gini–Simpson $D = 1 - \lambda = 0.645$ — probability that two random individuals are *different* species.
- Inverse Simpson $1/\lambda = 1/0.355 \approx 2.82$ — the effective number of species under Simpson weighting.

Compare with the Shannon effective number ($e^{H'} = 3.44$): Simpson weights are more dominance-sensitive, so its effective number is smaller because dominant species count more heavily. Reporting both Shannon and Simpson is now standard because they emphasize different aspects of community structure: Shannon weights most species roughly logarithmically; Simpson is dominated by abundant taxa and is less sensitive to rare taxa or sequencing errors.

25.2.7 Worked Example: Estimating Species Richness using Chao1

Problem: A researcher sequences 16S rRNA amplicons from a deep-sea sediment sample. The initial bioinformatics pipeline identifies a total of $S_{obs} = 150$ distinct bacterial species (ASVs). Examining the abundance tables, the researcher notes that 30 of these species were observed exactly once ($f_1 = 30$, singletons), and 10 species were observed exactly twice ($f_2 = 10$, doubletons). Use the Chao1 estimator to predict the true species richness of the community.

Solution:

1. Identify the variables:
 - Observed species (S_{obs}) = 150
 - Singletons (f_1) = 30
 - Doubletons (f_2) = 10

2. Apply the Chao1 formula:

$$\hat{S}_{Chao1} = S_{obs} + \frac{f_1^2}{2f_2}$$

$$\hat{S}_{Chao1} = 150 + \frac{30^2}{2(10)}$$

$$\hat{S}_{Chao1} = 150 + \frac{900}{20}$$

$$\hat{S}_{Chao1} = 150 + 45 = 195$$

The Chao1 estimator predicts that the true species richness is 195 species. This means that despite sequencing deep enough to find 150 species, approximately 45 rare species remain undetected in the sample. The high number of singletons relative to doubletons suggests that the community has a “long tail” of rare taxa and requires deeper sequencing to capture full diversity.

Beta diversity (between-sample diversity):

- Bray-Curtis dissimilarity: Abundance-weighted; ranges from 0 (identical) to 1 (completely different); $BC_{jk} = 1 - \frac{2C_{jk}}{S_j + S_k}$, where C_{jk} is the sum of lesser abundances shared between samples
- UniFrac distance: Incorporates phylogenetic information; unweighted UniFrac considers primarily presence/absence of taxa; weighted UniFrac also considers abundance
- Jaccard index: Presence/absence primarily; $J = \frac{|A \cap B|}{|A \cup B|}$

Rarefaction curves plot species richness against sampling effort (number of sequences). A curve that plateaus indicates sufficient sampling depth; a curve still rising indicates undersampling.

Concept Check 2: Two gut microbiome samples have identical Shannon entropy values ($H' = 3.5$) but very different Bray-Curtis dissimilarity (0.85). Explain how two samples can have the same within-sample diversity but be highly dissimilar to each other.

Concept Check 2b: Compute the Shannon and inverse-Simpson values for these two communities and explain why the rankings differ:

- Community A: 4 species at proportions 0.97, 0.01, 0.01, 0.01
- Community B: 4 species at proportions 0.40, 0.30, 0.20, 0.10

Which is more diverse by Shannon? By inverse Simpson? Why?

25.2.8 Worked Example: Species-Area Relationship for Marine Microbial Communities

Problem: Island biogeography theory predicts a power-law species-area relationship $S = cA^z$, where S is species richness, A is habitat area, and z is the species-area exponent. A marine 16S rRNA survey of ocean provinces yields $S = 1,000$ OTUs at $A = 10^3 \text{ km}^2$ with a fitted exponent $z \approx 0.25$ (typical for free-living bacteria). Predict the expected species richness at the scale of an entire ocean basin, $A = 10^6 \text{ km}^2$, and compare microbial vs. macro-organism z -values.

Solution:

1. Fit the constant c . From $S = cA^z$ at $A = 10^3, S = 1,000$:

$$c = \frac{S}{A^z} = \frac{1000}{(10^3)^{0.25}} = \frac{1000}{10^{0.75}} \approx \frac{1000}{5.623} \approx 177.8$$

2. Predict richness at the basin scale, $A = 10^6 \text{ km}^2$:

$$S(10^6) = c \cdot (10^6)^{0.25} = 177.8 \cdot 10^{1.5} \approx 177.8 \cdot 31.62 \approx 5,623 \text{ OTUs}$$

Equivalently and more directly: $S_{\text{new}} = S_{\text{old}} \cdot (A_{\text{new}}/A_{\text{old}})^z = 1000 \cdot (10^6/10^3)^{0.25} = 1000 \cdot 10^{0.75} \approx 5,623 \text{ OTUs}$ — a about 5.6-fold increase in richness for a 1,000-fold increase in area.

3. Compare microbial vs. macro-organism z . Continental and large-island vertebrates have $z \approx 0.30\text{--}0.40$; insects about 0.30; vascular plants about 0.25-0.35; free-living bacteria and archaea about 0.10-0.30. The lower microbial z (vs. macro-organisms) is the empirical signature of the dispersal-limitation versus everything-is-everywhere debate: lower z implies that bacteria are more effectively cosmopolitan — a doubling of area adds fewer new species than for macro-organisms, because microbial dispersal is high relative to range size. Higher microbial z (closer to 0.30) is found in habitat-island systems (lakes, hot springs, host-associated microbiomes) where dispersal is genuinely limited by physical barriers.
4. Caveats and interpretation.
- Sampling depth confounds z . Under-sequenced provinces miss rare taxa, artificially flattening the curve; rarefaction to uniform depth is mandatory before fitting.
 - OTU vs. ASV vs. species. Operational-taxonomic-unit clustering (97 % similarity) collapses cryptic diversity; amplicon sequence variants (ASVs) recover finer resolution and typically inflate S by 20–50 %, but the slope z is largely conserved across taxonomic-unit definitions.
 - Endemism vs. cosmopolitanism. A low z does not mean the same set of species occupies the entire ocean — it means relatively few species are truly local. Distance-decay analyses (Bray-Curtis similarity vs. geographic distance) reveal that even cosmopolitan microbial communities show distance-dependent compositional turnover.

Take-home. The species-area relationship applies to microbes but with a flatter slope than to plants and animals, quantitatively supporting (with important caveats) the “everything is everywhere, but the environment selects” hypothesis. Microbial macroecology is now a quantitative science with its own laws — Taylor’s power law, Shannon-area scaling, distance-decay relationships — that parallel and refine those derived for macro-organisms.

25.3 The Human Microbiome

25.3.1 Human Microbiome Scale, Body-Site Ecology, and Gene Content

The human body harbors approximately 3.8×10^{13} bacterial cells – close to the number of human somatic cells ($3.0\text{--}3.7 \times 10^{13}$, depending on counting assumptions) [Sender et al., 2016]. The microbial gene catalog is far larger: millions of microbial genes compared to approximately 20,000 human protein-coding genes. This “second genome” provides metabolic capabilities that human cells lack, effectively extending our biochemical repertoire.

The total mass of the human microbiome is approximately 200 g, predominantly residing in the colon. Each body site harbors a distinct microbial community shaped by local environmental conditions (pH, oxygen, moisture, nutrient availability, immune surveillance).

25.3.2 Gut Microbiome Gradients and Functional Guilds

The gastrointestinal tract represents the densest microbial habitat on the human body, with a gradient from relatively sparse colonization in the stomach ($10^1\text{--}10^3$ bacteria/mL, limited by gastric acid) to extraordinary density in the colon (10^{11} bacteria/mL – approaching the theoretical packing limit for bacterial cells).

Dominant phyla in healthy adults:

Table 329. Gut Microbiome Gradients and Functional Guilds: Phylum and Relative Abundance.

Phylum	Relative Abundance	Key Genera	Functional Roles
Firmicutes	about 60-65%	<i>Faecalibacterium</i> , <i>Roseburia</i> , <i>Eubacterium</i> , <i>Ruminococcus</i> , <i>Lactobacillus</i>	Major butyrate producers; fiber fermentation
Bacteroidetes	about 20-25%	<i>Bacteroides</i> , <i>Prevotella</i>	Complex polysaccharide degradation via PULs
Actinobacteria	about 3-5%	<i>Bifidobacterium</i> , <i>Collinsella</i>	Dominant in breastfed infants; acetate and lactate production
Proteobacteria	<5% (in health)	<i>Escherichia</i> , <i>Klebsiella</i>	Expansion is a marker of dysbiosis
Verrucomicrobia	about 1-3%	<i>Akkermansia muciniphila</i>	Mucin degradation; associated with metabolic health
Euryarchaeota (Archaea)	about 1%	<i>Methanobrevibacter smithii</i>	Methanogenesis; removes H ₂ to improve fermentation efficiency

The gut microbiome exhibits considerable inter-individual variation, influenced by diet (plant-rich diets favor *Prevotella*; animal-rich diets favor *Bacteroides*), geography, age (dramatic changes in infancy and old age), mode of birth (vaginal delivery vs. cesarean section), breastfeeding, and antibiotic exposure.

25.3.3 Core vs Variable Microbiome and the F/B Ratio

Two complementary frameworks describe gut-microbiome composition:

Core microbiome — taxa present in $\geq 90\%$ of healthy individuals at $\geq 0.1\%$ relative abundance. Surprisingly few species qualify at the species level (5–20 across populations), but at the functional gene level the core is much larger: $> 50\%$ of *gene families* are shared across most healthy adults. The biological inference is that functional redundancy is conserved even when species composition differs — the gut requires SCFA production, bile-acid transformation, and vitamin synthesis, but many species can supply each function. This is a textbook example of community-level convergence under functional selection.

Variable microbiome — the remaining about 80 % of taxa, which differ markedly between individuals. Variation is driven by diet (long-term fiber → *Prevotella*-dominant; meat-rich Western → *Bacteroides*-dominant), geography (the Hadza hunter-gatherers carry $> 50\%$ of taxa absent from industrialised populations), age, and antibiotic history.

Firmicutes / Bacteroidetes (F/B) ratio. The two dominant phyla in the colon historically defined an enterotype-like axis. The Turnbaugh et al. finding that obesity-associated mouse microbiomes had increased energy-harvest capacity prompted thousands of follow-up studies [Turnbaugh et al., 2006]; the relationship in humans is considerably more nuanced than initially reported. Key caveats: (1) the ratio is method-sensitive (PCR primer choice affects Bacteroidetes recovery by $\pm 30\%$); (2) human F/B in obesity does not robustly replicate across cohorts (some studies show the opposite direction); (3) the *functional* signal — increased polysaccharide-degradation gene capacity in some obese microbiomes — is more reproducible than the *taxonomic* F/B ratio. Modern microbiome research has

largely moved away from F/B as a single biomarker and toward functional gene profiles, specific keystone taxa (*F. prausnitzii*, *Akkermansia*, *Roseburia*), and microbial metabolites (SCFAs, secondary bile acids, indole derivatives).

Akkermansia muciniphila as a health marker. *A. muciniphila* (Verrucomicrobia, 1–4 % of healthy gut) degrades intestinal mucin and stimulates host mucin replenishment, paradoxically *strengthening* the gut barrier. Lower *Akkermansia* abundance is associated with obesity, type 2 diabetes, IBD, and aging. Pasteurised *A. muciniphila* (a single non-replicating bacterial supplement, killed by gentle pasteurisation that preserves the membrane protein Amuc_1100 — which acts on TLR2 to upregulate tight junctions) has shown improved insulin sensitivity and reduced LDL in early human trials (Depommier *et al.*, 2019, *Nature Medicine*) — a striking case of a defined “next-generation probiotic” with a known molecular mechanism. The European Food Safety Authority approved pasteurised *A. muciniphila* as a novel food in 2021.

Other keystone taxa:

- *Faecalibacterium prausnitzii* (Firmicutes, 5–15 % of healthy gut) — major butyrate producer; depleted in IBD; produces a 15-kDa anti-inflammatory peptide that inhibits NF-κB activation in colonocytes.
- *Bacteroides fragilis* — produces polysaccharide A (PSA), a TLR2-Treg-inducing immunomodulator.
- *Lactobacillus rhamnosus* GG — adheres to epithelium, secretes p40/p75 proteins that promote tight-junction integrity; the most-studied probiotic strain in clinical use.
- *Roseburia intestinalis* — secondary butyrate producer via the butyrate-CoA-transferase pathway; depleted with fiber-poor diets.

25.3.4 Oral Microbiome and Biofilm Niches

The oral cavity harbors over 700 species across distinct habitats (teeth, gingival crevice, tongue dorsum, buccal mucosa, hard palate). Key species include:

- *Streptococcus mutans*: Primary agent of dental caries; metabolizes sucrose to produce lactic acid, lowering local pH below the critical threshold (about 5.5) for enamel demineralization
- *Porphyromonas gingivalis*: Keystone pathogen in chronic periodontitis; produces gingipain proteases that degrade host tissues and subvert complement
- *Fusobacterium nucleatum*: Bridge organism in dental plaque biofilm formation; recently implicated as enriched in colorectal cancer tumors

25.3.5 Skin Microbiome Across Moist, Dry, and Sebaceous Sites

The skin (about 1.5 m² surface area) harbors 10⁴–10⁶ bacteria per cm², with community composition varying by microenvironment:

- Sebaceous (oily) sites (forehead, back): Dominated by *Cutibacterium acnes* (formerly *Propionibacterium acnes*); metabolizes sebum triglycerides; implicated in acne vulgaris
- Moist sites (axillae, groin, toe web): *Staphylococcus*, *Corynebacterium*; body odor results from bacterial metabolism of apocrine sweat components
- Dry sites (forearm, leg): Most diverse; *Cutibacterium*, *Staphylococcus*, *Micrococcus*

25.3.6 Vaginal Microbiome and Lactobacillus-Dominated Protection

In reproductive-age women, the vaginal microbiome is typically dominated by *Lactobacillus* species (*L. crispatus*, *L. iners*, *L. gasseri*, *L. jensenii*), which maintain a protective low pH (about 3.8–4.5) through lactic acid production. They also produce hydrogen peroxide and bacteriocins that inhibit pathogen colonization.

Disruption of *Lactobacillus* dominance – replacement by anaerobes such as *Gardnerella vaginalis*, *Atopobium vaginae*, and *Prevotella* – characterizes bacterial vaginosis (BV), associated with preterm birth, increased susceptibility to sexually transmitted infections including HIV, and pelvic inflammatory disease.

Clinical Connection: Fecal **Microbiota** Transplant (FMT) Recurrent *Clostridioides difficile* infection (rCDI) occurs when antibiotic-disrupted gut microbiota fails to recover, allowing *C. difficile* spores to germinate and produce toxins A and B. FMT – transfer of processed stool from a healthy, screened donor – restores colonization resistance and achieves cure rates exceeding 90%, compared to approximately 30% for repeated vancomycin courses. The FDA approved the first standardized FMT products in 2022–2023 (REBYOTA, a microbiota-based product, and VOWST, purified *Firmicutes* spores in oral capsules). The mechanism involves restoration of secondary bile acid production by commensal *Clostridium scindens*, which inhibits *C. difficile* spore germination, combined with **competitive exclusion** and bacteriocin production by restored commensals.

25.4 Microbiome Functions and Host Interactions

25.4.1 Microbiome–Host Molecular Communication

Host-microbiome interaction is mediated by three classes of molecular interface: (i) pattern-recognition receptors that surveil microbe-associated patterns; (ii) microbial metabolites that act on host receptors; and (iii) physical and immune barriers that contain the microbiota.

Pattern recognition receptors (PRRs). The intestinal epithelium and lamina propria express a rich repertoire of PRRs that read the local microbial milieu in real time:

- TLR2 (with TLR1 or TLR6 heterodimers) — recognizes Gram-positive lipoteichoic acid, lipopeptides, and *B. fragilis* polysaccharide A (PSA). PSA is a remarkable case: it is a microbial ligand that activates *anti-inflammatory* Treg responses via TLR2, demonstrating that PRR signaling is not uniformly pro-inflammatory but tunable by ligand.
- TLR4 — recognizes Gram-negative lipid A; in healthy gut TLR4 is low-expressed apically and signals are dampened by negative regulators (A20, SIGIRR). Loss of this dampening (e.g., increased TLR4 in IBD) drives chronic inflammation.
- TLR5 — flagellin sensor; intestinal expression is basolateral primarily, so commensal flagellated bacteria in the lumen do not trigger inflammation, but invading flagellated pathogens that cross the epithelium do. A beautiful example of spatial PRR localization as a discrimination strategy.
- TLR9 — unmethylated CpG DNA; engaged by bacterial DNA in endosomes.
- NOD1, NOD2 — cytosolic peptidoglycan fragment sensors; NOD2 mutations are the strongest single genetic risk for Crohn’s disease, illustrating how loss of microbial sensing predisposes to dysbiosis.
- AhR (aryl hydrocarbon receptor) — sensor for tryptophan-derived microbial metabolites (indoles, IPA, indole-3-aldehyde from *Lactobacillus*); upregulates IL-22, mucin, and antimicrobial peptide production by intestinal cells.

Short-chain fatty acid (SCFA) signaling. SCFAs are not only fuel but signaling molecules with three identified receptors and one direct enzymatic mechanism:

Table 330. Microbiome–Host Molecular Communication: Receptor / target and Ligand preference.

Receptor / target	Ligand preference	Cell type	Effect
GPR41 (FFAR3)	Propionate > butyrate ≫ acetate	Enteroendocrine L-cells; sympathetic neurons	PYY, GLP-1 release; sympathetic activation
GPR43 (FFAR2)	Acetate ≈ propionate > butyrate	L-cells; adipocytes; neutrophils	GLP-1; lipogenesis regulation; neutrophil chemotaxis
GPR109A (HCAR2)	Butyrate (also niacin)	Colonocytes; macrophages; dendritic cells	Treg induction; anti-inflammatory cascade
HDAC inhibition	Butyrate (mM concentrations in the colon)	Colonocytes; immune cells	Hyperacetylation of histones; epigenetic anti-inflammatory programs

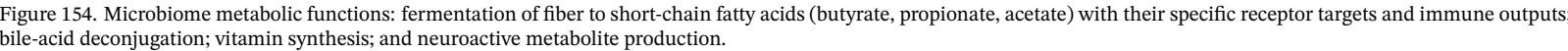
Butyrate has been called a “molecular bridge” between microbiome and host because it can engage four mechanisms simultaneously: G-protein-coupled signaling (GPR41/43/109A), epigenetic regulation (HDAC inhibition), mitochondrial fuel (β -oxidation provides about 70 % of colonocyte ATP), and Treg differentiation (via GPR109A and HDAC-dependent FoxP3 upregulation). Butyrate concentrations in the colonic lumen reach 10–20 mM — 1000× higher than in serum, justifying the local-action interpretation.

25.4.2 Metabolic Functions of Microbial Communities

The gut microbiome functions as a metabolic organ, performing biochemical transformations that human cells cannot:

- Butyrate (about 20% of SCFA): Produced primarily by *Faecalibacterium prausnitzii*, *Roseburia intestinalis*, and *Eubacterium rectale*. Serves as the primary energy source for colonocytes (providing about 70% of their energy needs). Acts as a **histone** deacetylase (HDAC) inhibitor, promoting anti-inflammatory gene expression. Strengthens intestinal barrier function by upregulating tight junction proteins (claudins, occludin). Induces colonic regulatory T cell (Treg) differentiation via GPR109A, promoting immune tolerance.
- Propionate (about 25% of SCFA): Transported to the liver via portal circulation where it regulates gluconeogenesis. Activates GPR41 and GPR43 receptors on enteroendocrine L-cells, stimulating release of GLP-1 (glucagon-like peptide-1, promotes insulin secretion and satiety) and PYY (peptide YY, reduces appetite).
- Acetate (about 55% of SCFA): The most abundant SCFA; enters systemic circulation to serve as fuel for peripheral tissues including muscle and brain. Activates GPR43 on adipocytes, regulating lipolysis and fat storage.

Vitamin synthesis: Gut bacteria produce essential vitamins including vitamin K2 (menaquinone, synthesized by *Bacteroides* and other gut anaerobes), vitamin B12 (cobalamin, by *Propionibacterium*), folate, biotin, and riboflavin. However, most microbially produced vitamins are absorbed in the colon, where absorption efficiency is lower than in the small intestine.



Bile acid metabolism: The liver synthesizes primary bile acids (cholic acid, chenodeoxycholic acid) conjugated with glycine or taurine. In the colon, gut bacteria deconjugate these bile acids (bile salt hydrolases) and perform 7 α -dehydroxylation to produce secondary bile acids (deoxycholic acid, lithocholic acid). Secondary bile acids are potent signaling molecules that activate the TGR5 receptor (stimulating GLP-1 release and energy expenditure) and the farnesoid X receptor (FXR, regulating lipid and glucose metabolism).

Drug metabolism: The gut microbiome can profoundly affect drug pharmacokinetics through first-pass microbial biotransformation. The cardiac glycoside digoxin is inactivated by *Eggerthella lenta*; the anti-cancer prodrug irinotecan is reactivated to its toxic form by bacterial β -glucuronidase, causing severe diarrhea; the Parkinson's drug L-DOPA is decarboxylated by gut bacteria, reducing its bioavailability.

25.4.3 Immune Development Shaped by Early Microbial Exposure

The microbiome is essential for proper immune system development. Germ-free mice (raised in sterile isolators) exhibit:

- Atrophied Peyer's patches and mesenteric lymph nodes
- Reduced secretory IgA (SIgA) production
- Deficient Th17 cell populations in the lamina propria
- Impaired regulatory T cell function
- Increased susceptibility to infection

Colonization of germ-free mice with specific bacteria restores immune function: segmented filamentous bacteria (SFB) induce Th17 cells in the small intestine; *Clostridium* clusters IV and XIVa induce colonic Tregs; *Bacteroides fragilis* polysaccharide A (PSA) activates TLR2 on Tregs, promoting IL-10 production.

In humans, neonatal microbiome composition during a critical developmental window (first 1-3 years of life) shapes lifelong immune tone. Disruptions during this window (cesarean delivery, formula feeding, early antibiotic exposure) are associated with increased risk of allergic diseases, asthma, and autoimmunity – consistent with the “hygiene hypothesis” and its modern refinement, the “old friends hypothesis.”

25.4.4 Gut-Brain Axis

The bidirectional communication network between the gut microbiome and the central nervous system operates through multiple channels:

- Vagus nerve: The tenth cranial nerve provides a direct neural pathway from the enteric nervous system (about 100-500 million **neurons**, sometimes called the “second brain”) to the brainstem. Specific bacterial metabolites (SCFAs, tryptamine) activate vagal afferents.
- Neurotransmitter production: Approximately 95% of the body’s serotonin (5-hydroxytryptamine, 5-HT) is produced by enterochromaffin cells in the gut, stimulated by tryptophan metabolites from gut bacteria (especially *Clostridiales*). Gut bacteria also produce GABA (*Lactobacillus*, *Bacteroides*), dopamine, and norepinephrine.
- SCFAs: Cross the blood-brain barrier; modulate microglial maturation and function; influence neuroinflammation
- Immune mediators: Microbial-induced cytokines (IL-6, TNF- α) affect brain function via circumventricular organs

Experimental evidence includes dramatic behavioral differences in germ-free mice (increased anxiety-like behavior in some strains, decreased in others), which can be partially normalized by colonization with specific probiotic strains (*Lactobacillus rhamnosus* JB-1 reduces anxiety-like behavior via vagal signaling).

25.4.5 Colonization Resistance Against Pathogen Invasion

The resident microbiota provides a critical defense against pathogen colonization through multiple mechanisms:

- Competitive exclusion: Commensals occupy ecological **niches** (nutrient sources, attachment sites), preventing pathogen establishment
- Bacteriocin production: Antimicrobial peptides produced by commensals directly inhibit pathogen growth
- Bile acid-mediated resistance: Secondary bile acids produced by commensals (e.g., *Clostridium scindens* produces deoxycholic acid) inhibit *C. difficile* spore germination and vegetative growth
- Immune priming: Commensals maintain baseline immune surveillance (SigA, antimicrobial peptide production by Paneth cells)

Salmonella enterica has evolved strategies to overcome colonization resistance: it triggers intestinal inflammation (via T3SS effectors), which disrupts the resident microbiota and generates unique nutrient sources (tetrathionate, ethanolamine) that *Salmonella* can metabolize but commensals cannot.

Concept Check 3: Explain why broad-spectrum antibiotic treatment increases the risk of *Clostridioides difficile* infection, using the concepts of colonization resistance and secondary bile acid metabolism. Why does FMT work when repeated courses of vancomycin often fail?

Concept Check 3b: A patient with refractory ulcerative colitis is treated with butyrate enemas. Symptoms improve over 4 weeks. Explain the multiple molecular mechanisms by which luminal butyrate can attenuate colonic inflammation, naming at least three host receptors / targets engaged. Why might oral butyrate supplements fail where rectal butyrate succeeds?

25.5 Dysbiosis and Disease

Dysbiosis refers to a compositional and functional imbalance in the microbiome associated with disease. While causation versus correlation remains a major challenge in microbiome research, several disease associations have strong mechanistic evidence:

Obesity and Metabolic Syndrome:

The landmark study by Turnbaugh et al. demonstrated that an obesity-associated gut microbiome had increased energy-harvest capacity and could transfer increased adiposity to germ-free mice [Turnbaugh et al., 2006]. The original taxonomic signal was important historically, but the more durable teaching point is functional: the obese microbiome showed enhanced capacity to ferment complex carbohydrates and altered SCFA profiles affecting host energy regulation.

Metabolic endotoxemia provides an additional mechanism: gut barrier dysfunction (“leaky gut”) allows LPS translocation into the bloodstream, triggering chronic low-grade inflammation via TLR4 activation on adipose tissue macrophages, contributing to insulin resistance.

Inflammatory Bowel Disease (IBD):

Both Crohn’s disease and ulcerative colitis are associated with:

- Reduced overall microbial diversity
- Reduced butyrate-producing bacteria (especially *Faecalibacterium prausnitzii*, a potent anti-inflammatory species that produces butyrate and secretes anti-inflammatory metabolites)
- Increased Proteobacteria (adherent-invasive *E. coli* in ileal Crohn’s)
- Reduced secondary bile acid production
- Altered tryptophan metabolism favoring the kynurenine pathway

Colorectal Cancer (CRC):

Fusobacterium nucleatum is significantly enriched in CRC tumors compared to adjacent normal tissue. Mechanistic studies demonstrate that *F. nucleatum*:

- Adheres to cancer cells via its FadA adhesin binding to E-cadherin
- Activates the Wnt/ β -catenin signaling pathway, promoting cell proliferation
- Recruits tumor-infiltrating myeloid cells that suppress anti-tumor immunity
- Correlates with poor prognosis and chemoresistance
- Serves as a potential diagnostic biomarker (detectable in stool samples)

Antibiotic-Induced Dysbiosis:

Broad-spectrum antibiotics cause profound disruption of the gut microbiome that can persist for months. Clinical consequences include:

- *Clostridioides difficile* infection (CDI): disrupted colonization resistance
- Pediatric antibiotic exposure and later obesity, asthma, and allergies (multiple epidemiological studies)
- Selection for antibiotic-resistant organisms within the microbiome (resistome expansion)
- Loss of bile acid-metabolizing bacteria, altering host metabolic signaling

Clinical Connection: Microbiome-Based Diagnostics and Therapeutics The microbiome is emerging as both a diagnostic tool and therapeutic target. Stool-based tests for *Fusobacterium nucleatum* DNA are being developed as non-invasive colorectal cancer screening supplements. Live bio-therapeutic products (LBPs) – defined microbial consortia – are in clinical trials for IBD, metabolic syndrome, and immune checkpoint inhibitor response enhancement. *Akkermansia muciniphila* supplementation has shown promise in improving metabolic parameters in overweight individuals (Depommier et al., 2019, *Nature Medicine*). The field is moving from correlation to causation through gnotobiotic mouse models, Mendelian randomization studies, and interventional trials.

25.6 Environmental Microbiology Across Soil, Ocean, and Biofilms

25.6.1 Soil Microbiology and Rhizosphere Processes

Soil is among Earth’s most microbially diverse habitats, containing roughly 10^8 - 10^9 bacterial cells per gram and thousands to tens of thousands of amplicon sequence variants per gram depending on soil type, sequencing depth, and the taxonomic cutoff used. The dominant phyla often include Proteobacteria, Firmicutes, Actinobacteria, Bacteroidetes, and Acidobacteria, but relative abundances shift strongly with pH, moisture, carbon input, and land management.

Soil microorganisms drive global carbon decomposition, nitrogen cycling, phosphorus solubilization, and organic matter turnover. The rhizosphere (soil zone immediately surrounding plant roots) is a hotspot of microbial activity, enriched 10-100 fold compared to bulk soil, driven by root exudates (sugars, amino acids, organic acids) that feed microbial communities.

25.6.2 Termite Guts as Lignocellulose Bioreactors

Termites make microbial ecology visible at animal scale. Wood and grass are dominated by lignocellulose, a polymer-rich substrate that most animals cannot digest alone. Termite hindguts solve that problem by housing dense consortia of protists, bacteria, and archaea that hydrolyse cellulose and hemicellulose, ferment sugars to acetate used by the host, recycle hydrogen through methanogenesis or reductive acetogenesis, and supply nitrogen through fixation and recycling pathways [Brune, 2014]. The termite is therefore not just an insect consumer; it is a mobile anaerobic bioreactor whose microbial partners connect plant litter to carbon, methane, and nitrogen cycling.

This example also clarifies symbiosis as a systems claim. Removing the gut community removes a metabolic capability, while changing diet, oxygen gradients, or host lineage changes the community. The unit of function is host plus microbiome, and the relevant evidence is not just “who is there” by 16S sequencing but which enzymes, redox reactions, and fermentation products actually move carbon and nitrogen.

25.6.3 Marine and Environmental Microbiome Diversity

Microbial diversity in environmental systems dwarfs that of multicellular life. The dominant numerical fact about life on Earth is that there are about 10^{30} microbial cells globally — > 99 % of Earth’s biological cells, and 70–90 % of Earth’s biomass nitrogen and phosphorus.

Ocean. The ocean contains approximately 1.2×10^{29} microbial cells in the photic zone alone. Two organisms dominate the global ocean microbiome:

- SAR11 (*Pelagibacterales*): The most abundant free-living organism on Earth, estimated at $\sim 2.4 \times 10^{28}$ cells globally — i.e., about 25 % of ocean bacteria. Its genome (about 1.3 Mbp) is among the smallest for free-living bacteria, reflecting extreme genomic streamlining: the *minimal-cell-cost hypothesis* posits that in oligotrophic surface waters where every nitrogen atom is precious, selection ruthlessly eliminates non-essential genes. SAR11 lacks transcription regulators, sigma factors, sugar-uptake systems, and most regulatory pathways — it lives a high-throughput, regulation-free metabolic life.

- *Prochlorococcus* and *Synechococcus*: The most abundant photosynthetic organisms on Earth (about 10^{27} cells of *Prochlorococcus* and about 7×10^{26} of *Synechococcus*). *Prochlorococcus* was discovered primarily in 1986 (Chisholm), demonstrating how recently we have grasped basic ocean ecology. This tiny cyanobacterium ($< 1 \mu\text{m}$ diameter) accounts for approximately 20 % of global ocean primary production — it makes about 5 % of the oxygen we breathe. Different ecotypes partition the water column by light intensity, with high-light ecotypes near the surface and low-light ecotypes extending to 200 m depth.

Soil. Containing about 10^8 bacteria per gram and often about 10^4 – 10^5 ASVs per gram in deep sequencing studies, soil is one of the largest reservoirs of microbial diversity. Globally, soil holds about 2.6×10^{29} microbial cells. The dominant phyla — Proteobacteria, Acidobacteria, Actinobacteria, Bacteroidetes, Verrucomicrobia, Firmicutes — vary continuously with pH, moisture, and organic matter. Acidobacteria, in particular, are abundant in molecular surveys but remain under-cultured relative to their environmental abundance, which is why metagenomics, single-cell genomics, and enrichment culture are most needed to connect sequence diversity to physiology.

Deep biosphere. A relatively recent realization is that the subsurface biosphere (rocks, sediments, and aquifers below about 100 m depth) contains an estimated 10^{29} cells — comparable to or exceeding most surface marine biomass. These extremely slow-growing chemolithotrophs (doubling times of years to centuries) couple H_2 from rock-water reactions to CO_2 fixation, sustaining ecosystems that have been functionally isolated from surface life for about Ma timescales. The deep biosphere now constitutes one of the largest reservoirs of unstudied microbial diversity on the planet.

Hydrothermal vents. Chemolithoautotrophic communities at hydrothermal vents form the base of food webs whose carbon and energy are independent of sunlight (though most aerobic vent microbes still depend on dissolved oxygen that ultimately originates from surface photosynthesis). Sulfur-oxidizing bacteria (*Thiomicrospira*, *Beggiatoa*) and hydrogen-oxidizing archaea (*Methanopyrus*) sustain ecosystems including tube worms (*Riftia pachyptila*, which lack a digestive system and rely entirely on endosymbiotic sulfur-oxidizing bacteria housed in a specialized organ called the trophosome).

25.6.4 Microbial Biogeochemistry in Carbon, Nitrogen, and Sulfur Cycles

Microbes catalyse virtually every redox transformation of nitrogen, sulfur, and carbon at the global scale. The key enzymatic steps are now well-characterized, each linked to a marker gene that ecologists use to track the corresponding flux in environmental DNA.

Nitrogen cycle. The biogeochemical nitrogen cycle is a quasi-closed loop of microbially-catalysed redox reactions, every step of which has a diagnostic gene:

Table 331. Microbial Biogeochemistry in Carbon, Nitrogen, and Sulfur Cycles: Transformation and Reaction.

Transformation	Reaction	Organisms	Marker gene
Nitrogen fixation	$\text{N}_2 \rightarrow \text{NH}_3$	<i>Rhizobium</i> , <i>Azotobacter</i> , cyanobacteria, <i>Nostoc</i>	<i>nifH</i> (Fe protein subunit of nitrogenase)
Ammonia assimilation	$\text{NH}_3 \rightarrow$ glutamate / glutamine	Most organisms	<i>glnA</i> , <i>gdhA</i>
Nitrification step 1 (AOA / AOB)	$\text{NH}_3 \rightarrow \text{NO}_2^-$	<i>Nitrosomonas</i> , <i>Nitrospira</i> , ammonia-oxidising archaea (AOA, <i>Nitrosopumilus</i>)	<i>amoA</i> (ammonia monooxygenase)
Nitrification step 2	$\text{NO}_2^- \rightarrow \text{NO}_3^-$	<i>Nitrobacter</i> , <i>Nitrospira</i>	<i>nxrA</i> (nitrite oxidoreductase)
Comammox (complete ammonia oxidation, 2015 discovery)	$\text{NH}_3 \rightarrow \text{NO}_3^-$ in one organism	<i>Nitrospira inopinata</i>	<i>amoA</i> + <i>nxrA</i>
Denitrification	$\text{NO}_3^- \rightarrow \text{NO}_2^- \rightarrow \text{NO} \rightarrow \text{N}_2\text{O} \rightarrow \text{N}_2$	<i>Pseudomonas</i> , <i>Paracoccus</i> , many facultatives	<i>narG</i> , <i>nirK/nirS</i> , <i>norB</i> , <i>nosZ</i> (N_2O reductase)
Anammox (anaerobic ammonia oxidation, 1995 discovery)	$\text{NH}_4^+ + \text{NO}_2^- \rightarrow \text{N}_2$	<i>Brocadia</i> , <i>Kuenenia</i> (<i>Planctomycetes</i>)	<i>hzsA</i> , <i>hzsB</i> (hydrazine synthase)
DNRA (dissimilatory $\text{NO}_3^- \rightarrow \text{NH}_4^+$)	$\text{NO}_3^- \rightarrow \text{NH}_4^+$	<i>E. coli</i> , <i>Salmonella</i> , sulfate reducers	<i>nrfA</i>

Two transformations deserve special attention. Nitrogen fixation by nitrogenase ($\text{N}_2 + 8\text{H}^+ + 8\text{e}^- + 16\text{ATP} \rightarrow 2\text{NH}_3 + \text{H}_2 + 16\text{ADP} + 16\text{P}_i$) is irreversibly inactivated by oxygen, presenting a paradox for **aerobic** diazotrophs. Solutions include *Rhizobium*-legume symbiosis (root nodules contain leghemoglobin delivering O_2 to bacteroid respiration while keeping free O_2 below the threshold for nitrogenase inactivation, about 10 nM); cyanobacterial heterocysts (specialized thick-walled cells lacking photosystem II, expressing nitrogenase, connected to vegetative cells by microplasmodesmata); and free-living *Azotobacter vinelandii* using respiratory protection (extremely high respiration rate consumes O_2 before it reaches nitrogenase) plus conformational protection (FeII protein binds nitrogenase in O_2 presence).

Anammox — anaerobic ammonia oxidation — was a stunning 1995 discovery (Mulder *et al.*) showing that *Planctomycetes* couple NH_4^+ oxidation to NO_2^- reduction, producing N_2 via the toxic intermediate hydrazine (N_2H_4 , rocket fuel). Anammox is responsible for about 30–50 % of marine N_2 production globally and is now used industrially in wastewater nitrogen removal (about 90 % less aeration energy than conventional nitrification + denitrification).

Sulfur cycle. Parallel redox cycle:

Table 332. Microbial Biogeochemistry in Carbon, Nitrogen, and Sulfur Cycles: Transformation and Marker gene.

Transformation	Marker gene	Organisms
Sulfate reduction ($\text{SO}_4^{2-} \rightarrow \text{H}_2\text{S}$)	<i>dsrA</i> (dissimilatory sulfite reductase)	<i>Desulfovibrio</i> , <i>Desulfobacter</i>
Sulfide oxidation ($\text{H}_2\text{S} \rightarrow \text{SO}_4^{2-}$)	<i>soxB</i>	<i>Thiobacillus</i> , <i>Beggiatoa</i> , hydrothermal-vent symbionts
Disproportionation ($\text{S}^0 \rightarrow \text{SO}_4^{2-} + \text{H}_2\text{S}$)	<i>dsrA</i> (reverse)	<i>Desulfocapsa</i>

Carbon cycle. Microbial carbon transformations include CO_2 fixation (Calvin cycle: *cbbL/cbbM* RuBisCO; reverse TCA, *aclB*; Wood–Ljungdahl, *fhs/cooS*), methanogenesis (*mcrA* gene of methyl-CoM reductase — diagnostic for most methanogenic archaea), and anaerobic oxidation of methane (AOM, ANME archaea + sulfate reducers acting via reverse methanogenesis), which consumes about 80 % of methane produced in marine sediments before it reaches the atmosphere — a globally important methane filter.

25.6.5 Phage–Host Dynamics: Kill-the-Winner

Viruses (almost entirely phages) outnumber cellular life in the ocean by about 10 : 1, with $\sim 10^{30}$ viral particles globally. Phages are the dominant agents of bacterial mortality, killing 20–40 % of marine bacteria per day — comparable to grazing pressure — and the dominant agent of horizontal gene transfer.

The kill-the-winner (KTW) hypothesis (Thingstad, 2000) explains why marine microbial communities can be enormously diverse despite competitive exclusion:

- When a bacterial species blooms (becomes the “winner” — high cell density), its cognate phage finds it efficiently (encounter rate is bilinear in $B \times P$).
- Phage proliferation crashes the bloom (the proliferation threshold $B^* = m/(bk)$, derived in the previous chapter, is exceeded once B is high enough).
- Other less-abundant species are not at high enough density to sustain their own phages, so they are not killed proportionally — they are released from competitive pressure.
- Diversity is *maintained* because phage predation specifically punishes dominance, opening niches for rare taxa.

The dynamics are analogous to Lotka–Volterra predator–prey cycles but with one twist: phage population growth is bursty (each successful infection produces about 50–500 progeny in about 30 minutes), giving boom-and-bust cycles superimposed on the long-term equilibrium. Cyanophage–cyanobacteria oscillations in the ocean have been directly observed via metagenomics, with measurable phage-mediated turnover of *Prochlorococcus* populations every few days. KTW is now considered as fundamental as competitive exclusion for understanding microbial-community structure: the predator-mediated maintenance of diversity that ecologists discovered in macroscopic systems (Paine’s keystone-predator experiments) operates equally — perhaps more strongly — in microbial systems.

25.6.6 Biofilms as Structured Microbial Communities

Over 80% of bacteria in natural environments exist in biofilms – structured communities enclosed in a self-produced extracellular polymeric substance (EPS) matrix of polysaccharides, proteins, extracellular DNA (eDNA), and lipids.

Biofilm formation proceeds through five stages:

1. Reversible attachment: Planktonic cells contact a surface via **van der Waals forces** and hydrophobic interactions
2. Irreversible attachment: Specific adhesin-receptor interactions; early EPS production; c-di-GMP (cyclic diguanylate monophosphate) levels rise, promoting sessile lifestyle
3. Microcolony formation: Cell division and EPS accumulation; quorum sensing coordinates gene expression
4. Mature biofilm: Complex 3D architecture with water channels; metabolic gradients (O_2 , pH, nutrients) create distinct microniches; HGT frequency increases 1,000-fold
5. Dispersal: c-di-GMP degradation; EPS-degrading enzymes released; motility genes reactivated; planktonic cells seed new surfaces

Biofilms are 10-1,000-fold more antibiotic-resistant than planktonic cells due to:

figure 152 illustrates the serial two-fold dilution layout used to determine minimum inhibitory concentration (MIC) in broth assays.

- EPS barrier limiting antibiotic diffusion
- Metabolically dormant persister cells (not susceptible to growth-dependent antibiotics)
- Local accumulation of resistance enzymes (β -lactamases in the matrix)
- Microenvironment heterogeneity (anaerobic zones where aminoglycosides are ineffective)

Clinical impact: about 80% of chronic bacterial infections involve biofilms (CDC), including cystic fibrosis lung infections (*Pseudomonas aeruginosa*), dental plaque, prosthetic joint infections, catheter-associated UTIs, and endocarditis.

25.6.7 Quorum Sensing and Density-Dependent Gene Regulation

Quorum sensing (QS) is a cell density-dependent communication system in which bacteria produce and detect small signaling molecules (autoinducers) that accumulate as the population grows. When autoinducer concentration exceeds a threshold, coordinate gene expression is triggered across the population:

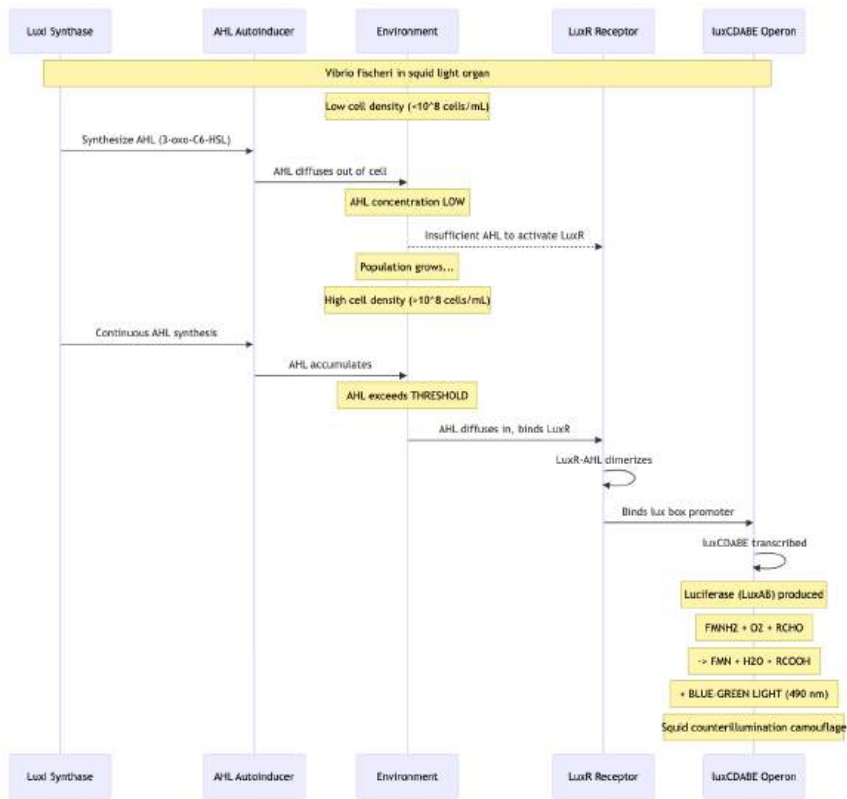


Figure 155. Quorum sensing in *Vibrio fischeri*: at low cell density LuxI-synthesized AHL diffuses away; once a quorum is reached AHL accumulates, binds LuxR, and triggers the luxCDABE operon producing bioluminescence - used for counterillumination camouflage in the bobtail squid.

Table 333. Quorum Sensing and Density-Dependent Gene Regulation: QS System and Signal.

QS System	Signal	Organisms	Regulated Functions
LuxI/LuxR	N-acyl homoserine lactones (AHLs)	Gram-negatives (<i>V. fischeri</i> , <i>P. aeruginosa</i>)	Bioluminescence, biofilm, virulence factors
Agr	Autoinducing peptides (AIPs)	Gram-positives (<i>S. aureus</i>)	Toxin production, biofilm dispersal
AI-2 (LuxS)	Furanosyl borate diester	Cross-species (most bacteria with LuxS)	Interspecies communication
PQS	2-heptyl-3-hydroxy-4-quinolone	<i>P. aeruginosa</i>	Iron acquisition, virulence

25.6.8 Bioremediation and Engineered Microbial Metabolism

Microorganisms can be harnessed to degrade environmental pollutants:

- *Pseudomonas putida*: Degrades toluene and xylene via the TOL **plasmid**-encoded pathways; model organism for aromatic hydrocarbon bioremediation
- *Geobacter sulfurreducens*: Reduces Fe^{3+} and U^{6+} ; used for uranium immobilization at contaminated sites; generates electricity in microbial fuel cells via extracellular electron transfer
- *Ideonella sakaiensis*: Discovered in 2016 at a PET bottle recycling facility in Japan; produces PETase enzyme that degrades polyethylene terephthalate (PET) plastic; engineered variants with enhanced activity are being developed for plastic waste bioremediation
- Oil spill bioremediation: *Alcanivorax borkumensis* and *Marinobacter* species bloom after oil spills, degrading alkanes and polycyclic aromatic hydrocarbons; nutrient addition (biostimulation with nitrogen and phosphorus) accelerates degradation

Concept Check 4: *Pseudomonas aeruginosa* uses quorum sensing to coordinate virulence factor production. A pharmaceutical company designs a drug that blocks AHL binding to the LuxR-type receptor (LasR) without killing the bacteria. Explain the therapeutic rationale for this “quorum quenching” approach compared to traditional antibiotics, and predict a potential limitation.

Concept Check (Analysis — Hierarchical Quorum Sensing as a Threshold Detection Mechanism): *Pseudomonas aeruginosa* uses hierarchically nested quorum-sensing systems: the Las system (LasI synthase → 3-oxo- C_{12} -HSL autoinducer → LasR receptor) activates the Rhl system (RhII → C_4 -HSL → RhIR), which in turn induces a cascade of virulence factors (elastase, rhamnolipid, pyocyanin) and biofilm maturation. (a) Analyze why this two-tier hierarchy is functionally different from a single QS system at a higher signal threshold. Specifically, evaluate how the requirement for both Las and Rhl signals to exceed thresholds creates an AND gate that filters out spurious signals and prevents premature virulence-factor expression. (b) Predict how a synthetic 3-oxo- C_{12} -HSL analog delivered at sub-threshold concentrations (e.g., 10 % of the natural threshold) would affect biofilm biomass. The analog binds LasR competitively but does not activate it — it occupies the receptor without triggering downstream transcription. Trace the consequences: (i) reduced las-system activation despite normal natural AHL accumulation; (ii) failure to activate the rhl downstream system; (iii) impaired biofilm maturation; (iv) attenuated virulence in a clinical infection model. (c) Quantitative analysis: if the natural threshold for LasR activation is $[\text{3O-C}_{12}\text{-HSL}] = 1\text{ }\mu\text{M}$ and the analog has affinity equal to the natural signal but is delivered at $0.1\text{ }\mu\text{M}$, derive the fractional receptor occupancy and predict the fractional reduction in downstream gene expression. (d) Connect this to anti-virulence drug design: why does competitive antagonism at the QS receptor avoid the strong evolutionary selection for resistance that growth-inhibitory antibiotics produce? What is the residual selection pressure?

Concept Check 4b: Marine *Prochlorococcus* populations oscillate with their cyanophages on a about 5–7 day cycle, while their Shannon diversity (about 1.5 nats) is approximately constant. Use the kill-the-winner framework to (a) explain why high overall diversity is maintained despite a single species dominating numerically, (b) predict what happens to phage population during a *Prochlorococcus* crash, and (c) describe how a metagenomic time-series experiment could test these predictions.

Concept Check (Synthesis — Syntrophic Coupling and Obligate Cooperation): In anaerobic sediments, acetate oxidation to CO_2 and H_2 has a standard Gibbs free energy of $\Delta G^\circ = +104\text{ kJ/mol}$ — strongly endergonic under standard conditions. The reaction therefore cannot proceed unless H_2 is kept at extremely low partial pressures (typically below about 10 Pa) by a syntrophic partner that consumes it: a hydrogenotrophic methanogen (e.g., *Methanobacterium*) catalysing $\text{CO}_2 + 4\text{ H}_2 \rightarrow \text{CH}_4 + 2\text{ H}_2\text{O}$ ($\Delta G^\circ = -131\text{ kJ/mol}$). The two reactions coupled give a small but favorable net $\Delta G^\circ \approx -27\text{ kJ/mol}$, sufficient to drive both partners’ metabolism. (a) Synthesize how this obligate syntrophic coupling parallels eukaryotic intracellular compartmentalization. Eukaryotic cells use organelle compartments (mitochondria, peroxisomes) to keep incompatible reactions spatially segregated and pool resources across compartments; syntrophic bacteria and methanogens accomplish the same by interspecies hydrogen transfer (IHT) — H_2 produced by the bacterium diffuses through a few micrometres of intercellular space and is immediately consumed by the methanogen, the spatial proximity functioning as a “metabolic compartment” without a single-cell boundary. (b) Quantitatively justify why about 10 Pa H_2 is the threshold: at this pressure, the H_2 term in the Nernst-style equation for ΔG (acetate oxidation) drops below the methanogen H_2 -consumption ΔG , making the coupled system favorable. (c) Predict the experimental consequence of inhibiting methanogenesis with 2-bromoethanesulfonate (BES) — a structural analog of methyl-CoM that competitively inhibits the methyl-CoM reductase (Mcr) enzyme. Trace through: (i) BES blocks H_2 consumption by the methanogen; (ii) H_2 partial pressure rises rapidly above 10 Pa; (iii) acetate oxidation becomes thermodynamically infeasible and stops; (iv) the syntrophic bacterium starves; (v) within hours both partners’ growth ceases. Both populations collapse, not just the methanogen — demonstrating that the cooperation is obligate, not facultative. (d) Connect to the origin of eukaryotes: the syntrophy hypothesis of eukaryogenesis (Martin & Müller 1998) proposes that the original endosymbiotic relationship between archaeal host and α -proteobacterial ancestor of mitochondria was exactly this kind of H_2 exchange — formalising the parallel between extracellular syntrophy and intracellular metabolic compartmentalization.

25.7 Microbial Biotechnology for Production and Environmental Engineering

25.7.1 Industrial Fermentation and Metabolic Control

Microorganisms have been harnessed for food production for millennia, and modern biotechnology has expanded their applications enormously:

The current frontier is less about replacing fermentation with a new idea and more about instrumenting it. Genome-scale metabolic models, automated strain engineering, continuous bioreactors, metagenomic enzyme discovery, and precision fermentation now let researchers tune yield, by-product formation, feedstock use, and contamination risk. Claims about “sustainable” biomanufacturing should therefore report substrate source, energy input, purification burden, waste stream, and life-cycle context rather than primarily the engineered microbe.

Table 334. Industrial Fermentation and Metabolic Control: Product and Organism.

Product	Organism	Process	Application
Ethanol	<i>Saccharomyces cerevisiae</i>	Glucose fermentation	Beverages, biofuel
Lactic acid	<i>Lactobacillus</i> , <i>Streptococcus thermophilus</i>	Lactose/glucose fermentation	Yogurt, cheese, sauerkraut
Acetic acid	<i>Acetobacter aceti</i>	Ethanol oxidation	Vinegar
Antibiotics	<i>Streptomyces</i> spp.	Secondary metabolism	Streptomycin, tetracycline, erythromycin
Amino acids	<i>Corynebacterium glutamicum</i>	Engineered fermentation	L-glutamate (MSG), L-lysine

25.7.2 Recombinant Protein Production

E. coli remains the workhorse for recombinant protein production:

- Human insulin (Humulin): First recombinant therapeutic protein, approved 1982; replaced porcine/bovine insulin
- Human growth hormone: Replaced cadaveric pituitary extracts (which transmitted CJD prions)
- Erythropoietin (EPO): Stimulates red blood cell production; produced in CHO (Chinese hamster ovary) cells for proper glycosylation
- Hepatitis B vaccine: Recombinant HBsAg produced in yeast (*Saccharomyces cerevisiae*) – the first recombinant vaccine

25.7.3 Environmental Biotechnology and Waste-Stream Remediation

- Biogas production: Anaerobic digestion by methanogenic archaea converts organic waste to methane for energy; widely used in wastewater treatment and agricultural waste management
- Constructed wetlands: Engineered ecosystems using microbial communities for water purification
- Synthetic biology: Engineered microbial biosensors for environmental monitoring (arsenic detection, water quality); metabolic engineering for production of biofuels, pharmaceuticals, and commodity chemicals from renewable feedstocks

Concept Check 5: The enzyme PETase from *Ideonella sakaiensis* degrades PET plastic at a rate too slow for industrial application. Describe two protein engineering approaches (one rational, one directed evolution) that could be used to improve PETase activity, and explain why thermostability would be a desirable trait for an industrial PET-degrading enzyme.

Concept Check 5b: Anammox bacteria couple ammonium oxidation to nitrite reduction with hydrazine as an intermediate. (a) Why is anammox more energy-efficient than the conventional nitrification + denitrification pathway used in sewage treatment plants? (b) Why have anammox bacteria been so difficult to grow in pure culture (doubling times of 11+ days)? (c) Predict, in molar terms, the alkalinity change associated with anammox versus conventional nitrification — why does this matter for plant operation?

25.8 Computational Bridge

Shannon diversity H' for tabulated OTU counts matches biodiversity_indices:

```
from biology.ecology import biodiversity_indices

res = biodiversity_indices([120, 80, 40, 10])
print(round(res.shannon_index, 3), res.species_richness)
```

Clinical / systems note: FMT trials stratify donors partly on diversity and bile-acid-transforming guilds — operationalisations of the same richness/evenness concepts.

25.9 Current Evidence and Frontier Biology: Microbial Ecology and the Microbiome

For Microbial Ecology and the Microbiome, frontier biology belongs inside the evidence logic of the chapter. Microbiology and infectious disease now require One Health reasoning across people, animals, environments, genomics, and antimicrobial stewardship. The core reading question is this: microbiome claims should distinguish correlation, mechanism, host context, perturbation, and causality.

- What to verify: identify the observation, model, assay, or dataset that would make the claim stronger or weaker.
- What to qualify: state the scale, organism, cell type, environmental condition, or population where the claim is expected to hold.
- What to compare: test at least one alternative explanation, baseline, or null model before treating the pattern as causal.
- What to cite: distinguish primary evidence, review synthesis, public dataset, and institutional guidance; for recent or numeric claims, prefer the source closest to the measurement and state what has changed since it was published.

For resistance or outbreak claims, name the organism, determinant, selection pressure, transmission route, and surveillance evidence [World Health Organization, 2024a, Centers for Disease Control and Prevention, 2025a, Murray et al., 2022].

Source practice: For pathogen, resistance, and intervention claims, tie statements to organism-resistance pairs, surveillance evidence, official guidance, and trial/regulatory status [World Health Organization, 2024a, 2025d,b, Centers for Disease Control and Prevention, 2025b, 2026a].

25.9.1 Current Evidence Map: Microbiome Causality Ladder

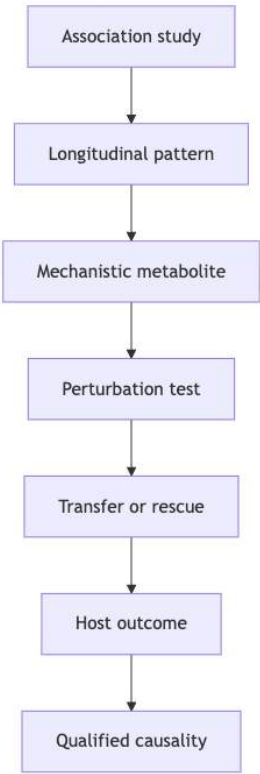


Figure 156. Microbiome claims become stronger as they move from correlation toward perturbation and rescue evidence; many human associations remain context-dependent.

25.10 Summary

- The great plate count anomaly reveals that <1% of environmental microbes are culturable. Culture-independent methods (16S amplicon sequencing, shotgun metagenomics, metatranscriptomics, metabolomics) have revolutionized microbial ecology, revealing entire new phyla and functional capabilities. ASVs (exact sequence variants) have replaced 97 %-clustered OTUs as the de facto standard since about 2018.
- Diversity metrics: Alpha diversity quantifies within-sample diversity. Shannon entropy $H' = -\sum p_i \ln p_i$ (equation (353)), Simpson index λ and inverse Simpson $1/\lambda$, Chao1 richness, and Faith's PD weight richness and evenness differently. Beta diversity (Bray-Curtis, UniFrac, Jaccard) quantifies between-sample differences. Rarefaction curves diagnose sampling depth.
- The human microbiome (3.8×10^{13} cells, 3.3 million genes) varies by body site. The gut microbiome (Firmicutes, Bacteroidetes dominant) has a small species-level core but a large functional core; *Akkermansia muciniphila*, *F. prausnitzii*, *B. fragilis*, and *Roseburia* are keystone taxa. Microbial SCFAs (butyrate as colonocyte fuel, HDAC inhibitor, GPR109A agonist; propionate via GPR41/43; acetate as systemic fuel) signal through three GPCRs and

- HDAC. Pattern-recognition receptors (TLR2/4/5, NOD1/2, AhR) read the microbial milieu in real time, with PSA from *B. fragilis* a striking example of microbial control of Tregs.
- Dysbiosis is associated with obesity (functional polysaccharide-degradation gene shift; F/B ratio is method-sensitive and not a reliable single biomarker), IBD (reduced *F. prausnitzii*, reduced butyrate), colorectal cancer (*F. nucleatum* enrichment), and antibiotic-induced *C. difficile* infection (FMT achieves >90% cure).
 - Environmental microbiology: Soil harbors 10⁸-10⁹ bacteria/g; ocean contains *Prochlorococcus* (about 10²⁷ cells, 20 % of global primary production) and SAR11 (about 10²⁸ cells); deep biosphere holds another 10²⁹ cells. Termite hindguts show how animal hosts can carry anaerobic microbial bioreactors that convert lignocellulose into acetate, methane precursors, and recycled nitrogen. Nitrogen fixation by nitrogenase requires 16 ATP per N₂ and O₂ protection. The microbial nitrogen cycle is tracked by *nifH* (fixation), *amoA* (nitrification), *nosZ* (denitrification), and *hzsA* (anammox); sulfur by *dsrA* and *soxB*; carbon by *mcrA* (methanogenesis) and various CO₂-fixation markers. Anammox accounts for 30–50 % of marine N₂ production.
 - Phage-host kill-the-winner dynamics maintain ocean diversity: phages preferentially predate dominant bacterial species, releasing rare species from competitive exclusion. Phages turn over 20–40 % of marine bacteria daily.
 - Biofilms (80% of natural bacteria) are 10-1,000x more antibiotic-resistant; quorum sensing coordinates population-level behavior via autoinducers (AHL, AIP, AI-2).
 - Bioremediation uses microbial metabolism to degrade pollutants including hydrocarbons, heavy metals, and plastics (PETase).
 - Connections: See section 39 for nutrient cycles, section 9 for fermentation products, and section 26 for dysbiosis and infection.

25.11 Key Terms

Table 335. Current Evidence Map: Microbiome Causality Ladder: Term and Definition.

Term	Definition
Great plate count anomaly	Observation that <1% of environmental microorganisms grow on standard laboratory culture media
16S rRNA sequencing	Culture-independent method using the conserved/variable 16S rRNA gene as a phylogenetic marker for bacterial identification
V3–V4 region	The most common 16S amplicon target (about 460 bp) used in human microbiome studies; provides genus-level resolution on Illumina MiSeq
ASV (amplicon sequence variant)	Error-corrected exact sequence inferred by DADA2/Deblur/UNOISE3; replaces 97 %-identity OTUs as the modern standard
OTU (operational taxonomic unit)	Cluster of 16S sequences at a fixed identity threshold (typically 97 %); legacy approach, reproducibility-limited
Rarefaction curve	Plot of richness versus sampling depth used to assess whether sequencing was deep enough
Metagenomics	Shotgun sequencing of total environmental DNA; reveals community composition and functional gene content without cultivation
MAG	Metagenome-assembled genome; computationally reconstructed genome of an uncultured organism from metagenomic data
Alpha diversity	Within-sample diversity measured by richness (number of taxa) and evenness (relative abundance distribution)
Beta diversity	Between-sample diversity; measures compositional differences between microbial communities
Shannon entropy	Alpha diversity metric: $H' = - \sum p_i \ln p_i$; accounts for both richness and evenness; effective species number is $e^{H'}$
Simpson index	Probability that two random individuals belong to the same species: $\lambda = \sum p_i^2$; complement $1 - \lambda$ is the Gini-Simpson; reciprocal $1/\lambda$ is the inverse Simpson effective number
Chao1	Estimator of true richness using singletons and doubletons: $\hat{S}_{Chao1} = S_{obs} + f_1^2/(2f_2)$
Microbiome	The collective community of microorganisms (and their genomes) inhabiting a defined environment
Termite gut microbiome	Anaerobic symbiotic community that digests lignocellulose, ferments sugars, and links host feeding to carbon and nitrogen cycling
Core microbiome	Taxa or genes present in nearly every healthy individual; smaller at species level than at functional-gene level
Akkermansia muciniphila	Mucin-degrading Verrucomicrobia species correlated with metabolic health; pasteurised <i>A. muciniphila</i> approved as novel food (EFSA, 2021)

Term	Definition
Dysbiosis	Compositional and functional imbalance of the microbiome associated with disease states
Short-chain fatty acids (SCFAs)	Bacterial fermentation products (butyrate, propionate, acetate) with roles in colonocyte nutrition, immune regulation, and metabolic signaling
GPR41 / GPR43 / GPR109A	Three SCFA-sensing GPCRs that translate microbial fermentation into host hormonal and immune responses
Colonization resistance	Protection against pathogen establishment provided by resident microbiota through competition, bacteriocins, and bile acid metabolism
Fecal microbiota transplant (FMT)	Transfer of processed donor stool to restore microbial community in recipients with dysbiosis, especially recurrent <i>C. difficile</i> infection
Biofilm	Structured microbial community enclosed in self-produced EPS matrix; highly antibiotic-resistant
Quorum sensing	Cell density-dependent gene regulation via secreted autoinducer molecules (AHL, AIP, AI-2)
Nitrogenase	Enzyme complex (NifH, NifD, NifK) that reduces N ₂ to NH ₃ ; oxygen-sensitive; requires 16 ATP per N ₂
Anammox	Anaerobic ammonia oxidation; <i>Planctomycetes</i> couple NH ₄ ⁺ + NO ₂ ⁻ → N ₂ via hydrazine; key gene <i>hzsA</i>
Comammox	Complete ammonia oxidation in a single organism (<i>Nitrospira inopinata</i> , 2015 discovery) carrying both <i>amoA</i> and <i>nrxA</i>
Kill-the-winner	Phage-driven mechanism that maintains bacterial diversity by preferentially predating dominant taxa
Bioremediation	Use of microbial metabolism to degrade or immobilize environmental pollutants
Gut-brain axis	Bidirectional communication between gut microbiome and CNS via vagus nerve, neurotransmitters, SCFAs, and immune mediators

25.12 Review Questions

1. Explain the great plate count anomaly and describe three specific reasons why environmental microorganisms may fail to grow on standard laboratory media. How has metagenomics addressed this limitation?
2. A researcher collects gut microbiome samples from 50 healthy individuals and 50 patients with Crohn’s disease. Describe which alpha and beta diversity metrics you would calculate, what statistical test you would use to compare communities (e.g., PERMANOVA on Bray-Curtis distances), and predict the expected differences.
3. Trace the fate of dietary fiber (resistant starch) from ingestion to its effects on host metabolism and immunity. Include the specific bacteria involved, the SCFAs produced, the host receptors activated, and the downstream physiological effects.
4. A patient has experienced four recurrences of *Clostridioides difficile* infection despite multiple courses of vancomycin. Explain the mechanism by which FMT achieves cure rates exceeding 90%, focusing on colonization resistance and secondary bile acid metabolism. Why does vancomycin itself perpetuate the cycle?
5. Compare the ecological strategies of SAR11 (genome about 1.3 Mbp) and *Prochlorococcus* (genome about 1.7 Mbp). Explain why both organisms have undergone extreme genome streamlining despite occupying different ecological niches, and discuss the evolutionary trade-offs of minimal genomes.
6. Explain why *Pseudomonas aeruginosa* biofilms in the lungs of cystic fibrosis patients are resistant to antibiotic therapy. Describe at least four distinct resistance mechanisms that operate within the biofilm, and suggest a multi-target therapeutic strategy.
7. The Firmicutes/Bacteroidetes ratio is often cited as a biomarker for obesity. Critically evaluate this claim by discussing: (a) the strength of evidence from gnotobiotic mouse experiments, (b) confounding factors in human studies, (c) why this ratio alone is an oversimplification of the microbiome-obesity relationship, and (d) what functional or species-specific biomarkers have replaced F/B in modern research.
8. Design an experiment using germ-free mice to determine whether the gut microbiome influences anxiety-like behavior through the vagus nerve. Include appropriate controls, specify which bacterial species you would use for colonization, and describe how you would test vagal involvement.
9. Nitrogenase is irreversibly inactivated by oxygen, yet *Azotobacter vinelandii* is an obligate aerobe that fixes nitrogen. Explain the molecular mechanisms by which this organism protects its nitrogenase from oxygen damage.

10. A biofilm-forming *Staphylococcus aureus* strain causes recurrent prosthetic joint infection despite appropriate systemic antibiotic therapy. Explain why biofilm removal (surgical debridement) is often necessary in addition to antibiotic treatment, and describe how persister cells within the biofilm contribute to recurrence.
11. Shannon diversity practice. Compute H' from equation (353) for the community {200, 100, 50, 20, 10, 10, 5, 5}. Then compute the inverse Simpson index. Interpret which species drive each metric.
12. Using the bridge counts, compute Simpson diversity manually from p_i and compare to `res.simpson_index`.
13. Contrast Faith's PD with Shannon richness for prioritizing conservation of microbial lineages.
14. Marker-gene biogeochemistry. Describe what biogeochemical inference you can draw from a soil metagenome that contains: (a) abundant *nifH* but very little *amoA*; (b) abundant *amoA* and *nxrA*; (c) *dsrA* and *mcrA* in the same sample. What environmental setting could each combination represent?
15. Anammox vs denitrification. Why has anammox replaced conventional denitrification in many modern wastewater plants? Compute the stoichiometric advantage in O₂ demand per mole of N removed.
16. Kill-the-winner test. Design a 30-day metagenomic time-series experiment in a marine mesocosm to test whether *Prochlorococcus* abundance and cyanophage abundance show predator-prey oscillations. Specify sampling frequency, sequencing approach, and the statistical analysis (cross-correlation, lagged regression) you would use.

25.13 Further Reading and Source Notes: Microbial Ecology and the Microbiome

- Woese & Fox (1977). Phylogenetic structure of the prokaryotic domain: The primary kingdoms. *Proceedings of the National Academy of Sciences*, 74.
- The Human Microbiome Project Consortium (2012). Structure, function and diversity of the healthy human microbiome [[The Human Microbiome Project Consortium, 2012](#)].
- Turnbaugh et al. (2006). An obesity-associated gut microbiome with increased capacity for energy harvest [[Turnbaugh et al., 2006](#)].
- Falkowski, Fenchel & Delong (2008). The microbial engines that drive Earth's biogeochemical cycles. *Science*, 320.
- Sender, Fuchs & Milo (2016). Revised estimates for the number of human and bacteria cells in the body [[Sender et al., 2016](#)].
- Lozupone, Stombaugh, Gordon, Jansson & Knight (2012). Diversity, stability and resilience of the human gut microbiota. *Nature*, 489.
- Madsen (latest ed.). *Environmental Microbiology: From Genomes to Biogeochemistry*. Wiley-Blackwell.
- Strous et al. (1999). Missing lithotroph identified as new planctomycete (anammox). *Nature*, 400.

25.14 Companion Source Module: Microbial Ecology and the Microbiome

Microbial Ecology and the Microbiome should leave a reproducible trail from a biological claim to the code, figure, diagram, or paper-based activity that can test it. Use the surfaces below to inspect the chapter's assumptions, rerun the relevant model, or compare the manuscript explanation with companion labs and figures.

Table 336. Companion source surfaces for Microbial Ecology and the Microbiome.

Surface	Use it for
<code>src/biology/microbiology/microbiology.py</code> (<code>bacterial_growth_curve</code> , <code>doubling_time</code>)	Quantify growth constraints for interacting microbial populations.
<code>src/biology/ecology/ecology.py</code> (<code>lotka_volterra</code> , <code>connectance</code> , <code>biodiversity_indices</code>)	Treat microbiomes as communities with measurable interaction structure.
<code>src/mermaid/biology_diagrams.py</code> (<code>food_web_diagram</code>)	Compare cross-feeding and competition with broader food-web logic.

Reproducibility check: distinguish association, perturbation response, mechanism, and host/environment context before making a microbiome-causality claim. Cross-reference: use sections 37 and 38 and sections 26 and 27.

26 Host Immunity and Vaccines

Level 2/3 · 30 min read · 40 min lecture · Prerequisites: section 24

26.1 Learning Objectives

By the end of this chapter, you should be able to:

1. Apply Koch’s postulates and molecular Koch’s postulates to evaluate evidence for microbial causation of disease, and identify their limitations.
2. Describe **virulence** factors (adhesins, toxins, invasion machinery, immune evasion strategies) used by major bacterial, viral, and eukaryotic pathogens.
3. Explain innate immune defenses including physical barriers, pattern recognition receptors (TLRs, NLRs, RIG-I, cGAS-STING), the three complement pathways and their convergence at C3, and cellular effectors (neutrophils with NETosis, macrophages, NK cells with missing-self recognition).
4. Describe adaptive immunity including V(D)J **recombination**, MHC restriction, T helper cell subsets, cytotoxic T cell killing mechanisms, B cell activation, affinity maturation, and antibody class switching.
5. Compare the eight major **vaccine** platforms (live attenuated, inactivated, subunit, virus-like-particle, toxoid, conjugate, mRNA, viral vector) and apply the **herd immunity** equation $p_c = 1 - 1/R_0$ to compute thresholds for measles, polio, and COVID-19 variants.
6. Describe antigenic variation in influenza (drift vs shift) and HIV (reverse-transcriptase quasi-species clouds), and connect this to vaccine reformulation and pandemic risk.
7. Classify the principal antibiotic-resistance mechanisms (β -lactamases including ESBLs and carbapenemases, efflux pumps, target modification including PBP2a in MRSA and 23S rRNA methylation in MLS-resistant streptococci, reduced permeability, bypass pathways) and link each to specific drug classes.
8. Describe the epidemiology and pathogenesis of major infectious diseases including tuberculosis, malaria, HIV/AIDS, and influenza, and explain the One Health framework.

26.1.1 Study Blueprint

- Big idea: Host immunity and vaccination reshape pathogen transmission by changing susceptible fractions.
- Core concepts: innate immunity, adaptive immunity, vaccination, herd immunity.
- Framework alignment: Vision & Change: Evolution, Systems, Structure and function; AP Biology: Evolution, Systems Interactions; NGSS-style topics: Structure and Function, Interdependent Relationships in Ecosystems.
- Model or quantitative lens: Herd-immunity threshold and basic immunological reasoning.
- Data skill: Interpret antibody, cellular, and vaccine-response evidence.
- Practice cadence: Questions and Methods, Representing and Describing Data, Argumentation.
- Common misconception to repair: Immunity is not binary; timing, dose, and variant matter.
- Primary lab: **Lab — Host Immunity and Vaccines**.
- Question bank: **Questions — Host Immunity and Vaccines**.
- Transfer task: Transfer immunity reasoning to outbreak response and clinical decision-making.
- Bridge to computation: `biology.microbiology.microbiology.sir_model`.

Opening Vignette — The Pandemic That Shaped Modern Immunology

The 1918 influenza pandemic infected an estimated 500 million people — one-third of the world’s population — and killed between 50 and 100 million, more than World War I. Most victims were healthy young adults, a terrifying reversal of the usual mortality pattern, caused by a cytokine storm in which a vigorous immune response became catastrophically self-destructive. The pandemic revealed in gruesome detail the cost of a misdirected immune response and the urgency of understanding host-pathogen dynamics. From its ashes grew modern epidemiology, the concept of herd immunity, and the influenza surveillance networks that today sequence viral **genomes** in near-real time. When SARS-CoV-2 emerged in 2019, it was 1918’s lessons — social distancing, masking, rapid vaccine development — that shaped the global response. Infectious disease is not a relic of the past; it is the central selective pressure on immune system evolution.

26.2 Host-Pathogen Relationships and Virulence

26.2.1 Koch’s Postulates

In 1884, Robert Koch formalized criteria for establishing that a specific microorganism causes a specific disease. These four postulates remain foundational in infectious disease [**Koch, 1884**]:

1. The microorganism must be found in most cases of the disease but not in healthy individuals
2. The microorganism must be isolated from the diseased host and grown in pure culture

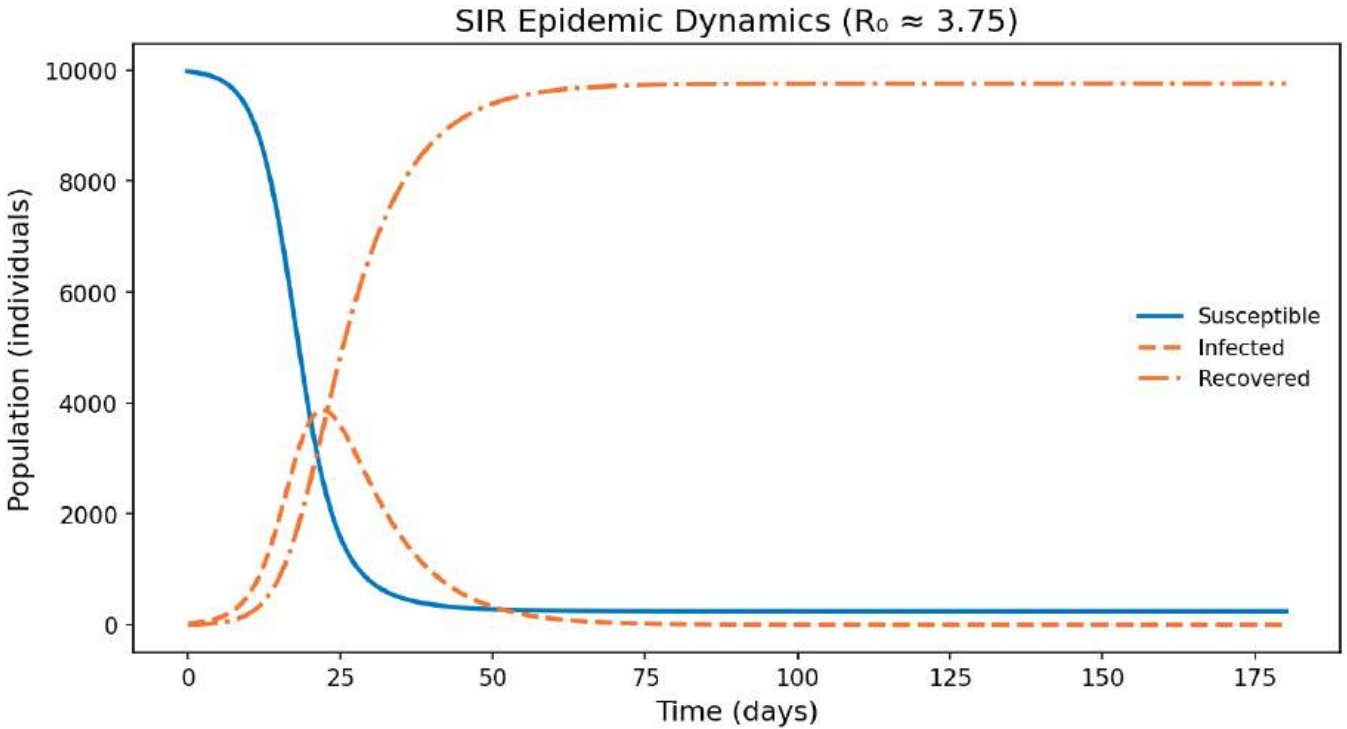


Figure 157. SIR epidemic model in a closed population. Susceptible individuals fall as infections rise and peak; recovered individuals accumulate after the infected compartment declines—peak height and timing depend on the basic reproduction number R_0 .

3. The cultured microorganism must cause the same disease when inoculated into a healthy, susceptible host
4. The same microorganism must be re-isolated from the experimentally infected host

Limitations of Koch’s postulates have become apparent with advancing knowledge:

- Asymptomatic carriers: *Salmonella typhi* (Typhoid Mary), *Neisseria meningitidis* – healthy carriers exist, violating postulate 1
- Unculturable organisms: Viruses (until cell culture), *Treponema pallidum*, *Mycobacterium leprae* – cannot fulfill postulate 2
- Ethical constraints: Human experimentation with lethal pathogens is prohibited
- Polymicrobial disease: Periodontal disease, bacterial vaginosis – caused by community shifts, not single organisms
- Host factors: *Mycobacterium tuberculosis* causes disease in about 5-10% of infected individuals (the rest maintain latent infection)

26.2.2 Molecular Koch’s Postulates

In 1988, Stanley Falkow proposed a molecular framework for identifying virulence determinants:

1. The virulence **gene** (or its product) should be found in pathogenic strains but not in non-pathogenic relatives
2. Inactivation of the gene (by **mutation** or deletion) should reduce virulence in an appropriate model
3. Complementation (restoration of the gene) should restore virulence

This framework has been essential for identifying virulence factors through targeted gene knockouts and complementation studies in model organisms.

26.2.3 The Infection Continuum

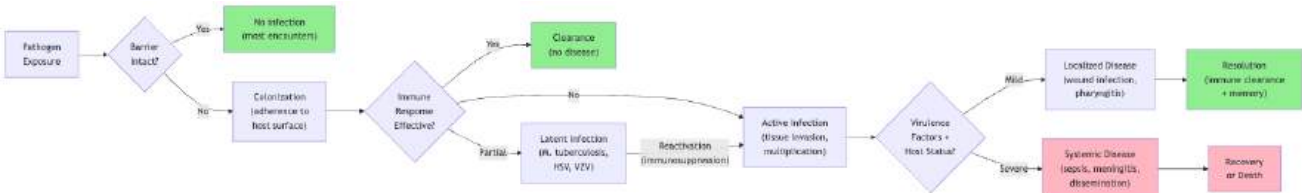


Figure 158. Decision-tree of pathogen exposure outcomes from initial encounter through clearance, latency, or systemic disease.

Not every exposure leads to colonization, not every colonization leads to infection, and not every infection leads to disease. The outcome depends on pathogen virulence, inoculum size, route of entry, and host immune status.

26.2.4 Virulence Factors and Host-Tissue Damage

Pathogens deploy specific molecular tools to adhere to host tissues, invade cells, obtain nutrients, and evade immune defenses, while host pattern-recognition systems translate microbial signatures into inflammatory and adaptive responses [Medzhitov, 2007]:

Adhesins mediate initial attachment to host surfaces:

- Type IV pili (*Neisseria gonorrhoeae*, *N. meningitidis*): Retractable pili that mediate attachment to epithelial surfaces and facilitate twitching motility
- FimH (*E. coli*): Type 1 fimbrial adhesin that binds mannose residues on uroepithelial cells, enabling urinary tract infection
- Fibronectin-binding **proteins** (*Staphylococcus aureus*): Mediate attachment to extracellular matrix, enabling wound infections and endocarditis

Invasion factors:

- Type III secretion system (T3SS): *Salmonella enterica* SPI-1 (Salmonella Pathogenicity Island 1) encodes a molecular syringe that injects effector proteins (SopE, SipA) directly into host epithelial cells, triggering **actin cytoskeleton** rearrangement and bacterial internalization via membrane ruffling
- Internalins (*Listeria monocytogenes*): InlA binds E-cadherin, InlB binds Met receptor; trigger receptor-mediated **endocytosis**; once internalized, *Listeria* escapes the phagosome (listeriolysin O) and propels itself through the **cytoplasm** using actin polymerization (ActA recruits host Arp2/3 complex)

Capsules: Polysaccharide capsules (*Streptococcus pneumoniae*, *Neisseria meningitidis*, *Haemophilus influenzae* type b) inhibit phagocytosis by preventing complement C3b deposition and obscuring surface antigens. The pneumococcal capsule has >90 serotypes, forming the basis for conjugate vaccine design (PCV13, PCV20).

26.2.5 Toxins and Molecular Mechanisms of Pathogenesis

Exotoxins are secreted proteins with specific mechanisms of action. Many have the A-B structure: the B (binding) subunit binds a host cell receptor, and the A (active) subunit enters the cell to exert its toxic effect:

Table 337. Toxins and Molecular Mechanisms of Pathogenesis: Toxin and Organism.

Toxin	Organism	B-Subunit Target	A-Subunit Activity	Clinical Effect
Cholera toxin	<i>V. cholerae</i>	GM1 ganglioside	ADP-ribosylates Gsα -> constitutive adenylyl cyclase activation -> cAMP ↑	Cl ⁻ /H ₂ O secretion -> watery diarrhea (up to 20 L/day)
Diphtheria toxin	<i>C. diphtheriae</i>	HB-EGF receptor	ADP-ribosylates EF-2 -> halts protein synthesis	Pseudomembrane in throat; myocarditis
Tetanospasmin	<i>C. tetani</i>	Gangliosides (retrograde transport)	Zinc metalloprotease cleaves VAMP/synaptobrevin	Blocks inhibitory neurotransmitter release (glycine, GABA) -> spastic paralysis
Botulinum toxin	<i>C. botulinum</i>	Gangliosides (peripheral nerve)	Zinc metalloprotease cleaves SNARE proteins (SNAP-25, syntaxin)	Blocks ACh release at NMJ -> flaccid paralysis
Shiga toxin	<i>Shigella</i> , STEC <i>E. coli</i>	Gb3 (globotriaosylceramide)	N-glycosidase cleaves 28S rRNA	Halts protein synthesis; HUS (hemolytic uremic syndrome)

Endotoxin (LPS): Unlike exotoxins, endotoxin is not secreted but released upon bacterial lysis. Lipid A activates TLR4 on macrophages, triggering release of TNF-α, IL-1β, and IL-6. At high concentrations (Gram-negative bacteremia), this causes fever, hypotension, disseminated intravascular coagulation (DIC), multi-organ failure, and septic shock.

Immune evasion strategies:

- Protein A (*S. aureus*): Binds the Fc region of IgG in the “wrong” orientation, preventing opsonization and ADCC
- IgA protease (*N. gonorrhoeae*, *H. influenzae*): Cleaves secretory IgA at mucosal surfaces
- Antigenic variation: *Trypanosoma brucei* expresses variant surface glycoprotein (VSG) from a library of >1,000 *vsg* genes, switching expression before the host mounts an effective antibody response
- Phagosome arrest: *M. tuberculosis* inhibits phagosome-lysosome fusion via LAM (lipoarabinomannan)

Concept Check 1: *Vibrio cholerae* produces cholera toxin that causes massive fluid secretion, yet the bacterium rarely invades beyond the intestinal epithelium. Explain why this non-invasive strategy is advantageous for the pathogen’s transmission, and predict what would happen to cholera epidemiology if the toxin were eliminated by gene deletion.

26.3 Innate Immunity and Rapid Pattern Recognition

26.3.1 Physical and Chemical Barriers

The first line of defense prevents pathogen entry into sterile body compartments:

A barrier is not just a wall; it is an active ecological and immunological interface. Skin acidity, mucus flow, antimicrobial peptides, secretory IgA, iron sequestration, and resident microbiota most create selection pressures that pathogens must evade. Barrier failure can therefore come from physical breach, altered chemistry, disrupted microbial competition, or medical devices that bypass normal surfaces.

Table 338. Physical and Chemical Barriers: Barrier and Mechanism.

Barrier	Mechanism	Pathogens That Breach It
Skin	Intact keratin layer; low pH (about 5.5); fatty acids; defensins; commensal microbiota	Burns, wounds, catheter insertion bypass skin

Barrier	Mechanism	Pathogens That Breach It
Mucociliary escalator	Respiratory mucus traps particles; cilia beat at 12-15 Hz, propelling mucus upward	<i>P. aeruginosa</i> biofilm in CF; influenza HA cleaves sialic acid in mucus
Gastric acid	pH 1.5-3.5; pepsin activation	<i>H. pylori</i> : urease produces NH ₃ to neutralize local pH
Lysozyme	Muramidase: cleaves NAG-NAM bonds in peptidoglycan	Present in tears, saliva, nasal secretions, breast milk
Lactoferrin	Iron sequestration (bacteriostatic)	Found at mucosal surfaces; deprives bacteria of essential iron
Defensins	Antimicrobial peptides (AMPs); form pores in microbial membranes	Produced by epithelial cells and neutrophils; α -defensins (Paneth cells), β -defensins (skin, respiratory)
Resident microbiota	Colonization resistance (nutrient competition, bacteriocins, bile acid metabolism)	<i>C. difficile</i> exploits antibiotic-disrupted microbiota

26.3.2 Pattern Recognition Receptors (PRRs)

The innate immune system detects conserved microbial structures – pathogen-associated molecular patterns (PAMPs) – through germline-encoded PRRs. This system provides immediate recognition without prior exposure:

Table 339. Pattern Recognition Receptors (PRRs): PRR and Location.

PRR	Location	PAMP Recognized	Signaling Pathway	Outcome
TLR4	Plasma membrane	LPS (lipid A)	MyD88 -> NF- κ B; TRIF -> IRF3	Pro-inflammatory cytokines + type I IFN
TLR2	Plasma membrane	Peptidoglycan, lipoteichoic acid, zymosan	MyD88 -> NF- κ B	Pro-inflammatory cytokines
TLR3	Endosome	dsRNA	TRIF -> IRF3	IFN- β (antiviral state)
TLR7/8	Endosome	ssRNA	MyD88 -> NF- κ B + IRF7	Type I IFN + cytokines
TLR9	Endosome	Unmethylated CpG DNA	MyD88 -> NF- κ B	Type I IFN + cytokines
RIG-I / MDA5	Cytoplasm	Viral RNA (5'-ppp, long dsRNA)	MAVS -> IRF3	IFN- β
NLRP3	Cytoplasm	DAMPs (ATP, uric acid, cholesterol crystals)	ASC -> Caspase-1	IL-1 β , IL-18, gasdermin D -> pyroptosis
cGAS-STING	Cytoplasm-ER	Cytoplasmic dsDNA	cGAMP -> STING -> IRF3	IFN- β ; critical for DNA virus detection

Key signaling outcomes of PRR activation:

- NF- κ B pathway: **Transcription** of pro-inflammatory cytokines (IL-1 β , IL-6, TNF- α , IL-8/CXCL8) and chemokines
- IRF3/7 pathway: Type I interferons (IFN- α/β) -> JAK-STAT signaling -> interferon-stimulated genes (ISGs: OAS/RNase L, Mx proteins, PKR) -> antiviral state in neighboring cells

26.3.3 The Complement System: Three Pathways, One Cascade

The complement system is a cascade of about 30 plasma proteins that opsonize pathogens, recruit inflammation, and lyse Gram-negative bacteria. Three pathways converge on a common effector cascade through the central enzyme C3 convertase, which hydrolyses C3 into C3a (anaphylatoxin) and C3b (opsonin).

- C3a — a 9-kDa anaphylatoxin: binds C3aR on mast cells (degranulation, histamine), endothelial cells (vasodilation, vascular permeability), and granulocytes (recruitment).

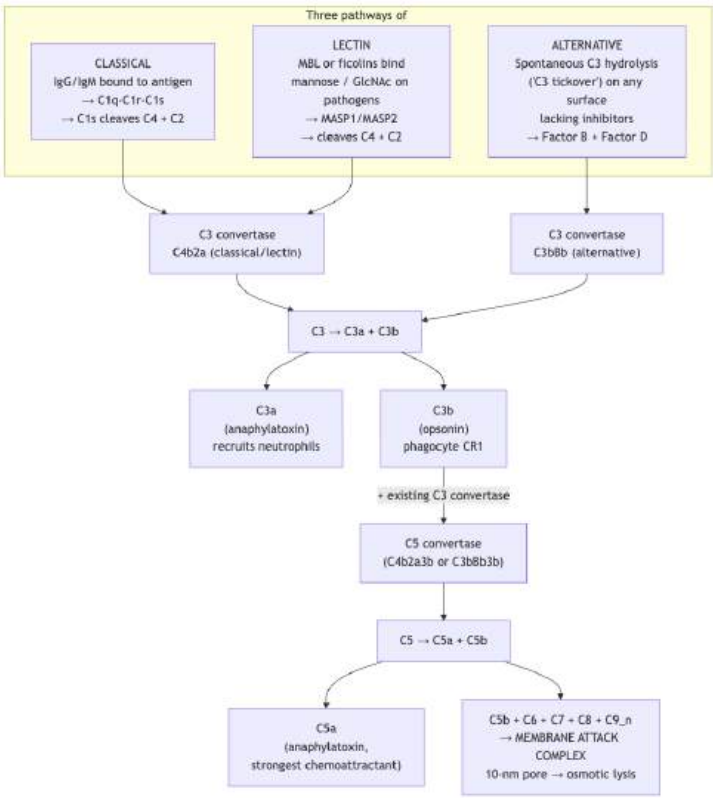


Figure 159. Three pathways of complement activation (classical, lectin, alternative) converge at the C3 convertase, producing C3b (opsonin) and C3a (anaphylatoxin); a second cleavage at C5 generates C5a and the C5b-C9 membrane-attack complex.

- C3b — a 175-kDa opsonin: covalently binds pathogen surface; recognized by complement receptor 1 (CR1, CD35) on phagocytes, dramatically enhancing phagocytosis.

A second cleavage step generates:

- C5a — the strongest neutrophil chemoattractant in plasma (effective at picomolar concentrations); binds C5aR1.
- C5b — initiates the membrane attack complex (MAC): C5b + C6 + C7 + C8 + (10–18 copies of) C9 polymerize into a 10-nm transmembrane pore that lyses the target cell osmotically. The MAC is most effective against Gram-negative bacteria (which lack the thick peptidoglycan barrier of Gram-positives); *Neisseria meningitidis* and *N. gonorrhoeae* are particularly MAC-susceptible — terminal-complement deficiencies (C5–C9) cause recurrent neisserial infections almost exclusively.

Complement regulation. Self cells avoid complement attack via membrane-bound and soluble regulators:

Table 340. The Complement System: Three Pathways, One Cascade: Regulator and Action.

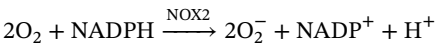
Regulator	Action	Defect → disease
CD46 (MCP, membrane cofactor protein)	Cofactor for Factor I cleavage of C3b/C4b	Atypical hemolytic uremic syndrome (aHUS)
CD55 (DAF, decay-accelerating factor)	Accelerates decay of C3 and C5 convertases	Paroxysmal nocturnal haemoglobinuria (PNH; CD55+CD59 GPI loss)
CD59 (protectin)	Blocks C9 polymerization (MAC)	PNH (hemolysis)
Factor H	Inhibits alternative pathway on self surfaces	aHUS; age-related macular degeneration (AMD)
C1 inhibitor	Blocks C1r/C1s and MASPs	Hereditary angioedema (HAE)

Neisseria meningitidis and *N. gonorrhoeae* have evolved a remarkable trick — they bind host Factor H to their surface using factor H-binding protein (fHbp), mimicking self and inactivating alternative-pathway amplification. fHbp is now a target antigen in two licensed meningococcal-B vaccines (Bexsero, Trumenba).

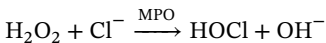
26.3.4 Phagocytosis and Cellular Effectors

Neutrophil Killing: Oxidative Burst and NETosis Neutrophils are the most abundant circulating leukocytes (50–70 % of blood leukocytes) and the first cells to arrive at sites of infection (within minutes of chemokine signal). Their lifespan is extraordinarily short — about 6–8 hours in circulation, about 1–4 days at tissue sites — reflecting a cell programmed for rapid microbial killing followed by apoptosis to limit collateral tissue damage.

Oxidative burst (respiratory burst). Upon phagosome formation, the NADPH oxidase complex (NOX2) assembles at the phagosome membrane:



Superoxide (O_2^-) is rapidly converted to hydrogen peroxide (H_2O_2) by superoxide dismutase. Myeloperoxidase (MPO) — abundant in neutrophil azurophilic granules — then catalyses the most potent step of microbial killing:



HOCl (hypochlorous acid, household-bleach chemistry) is one of the most potent oxidants in biology — it chlorinates microbial proteins, lipids, and DNA, killing many phagocytosed microbes within minutes. The phagosome is also acidified (pH about 4.5) and accumulates antimicrobial peptides (defensins, BPI, lactoferrin). Survival is uncommon for non-adapted microbes but biologically important pathogens such as *M. tuberculosis*, *Salmonella*, and *Leishmania* persist by blocking phagosome maturation, resisting reactive species, or escaping the vacuole.

26.3.5 Worked Example: Quantifying the Neutrophil Oxidative Burst

Problem: A neutrophil phagosome contains 2.0×10^{-15} L volume and local NADPH concentration reaches 0.5 mM during NOX2 activation. Assuming stoichiometric conversion via section 26.3.4 and complete superoxide dismutase conversion to H_2O_2 , then MPO-mediated HOCl production via section 26.3.4 with abundant chloride, estimate the maximum H_2O_2 (mmol) available for HOCl synthesis in one burst.

Solution.

1. NADPH moles in phagosome. $n = 0.5 \text{ mmol L}^{-1} \times 2.0 \times 10^{-15} \text{ L} = 1.0 \times 10^{-18} \text{ mol}$.
2. Stoichiometry. Each NADPH yields one H_2O_2 after dismutase: $n(\text{H}_2\text{O}_2) = 1.0 \times 10^{-18} \text{ mol} = 1.0 \times 10^{-15} \text{ mmol}$.
3. Scale check. Although the absolute moles are tiny, local concentrations in the phagosome lumen reach millimolar HOCl for microseconds — sufficient to oxidise microbial surface proteins before dilution. Chronic granulomatous disease (CGD), in which NOX2 is defective, removes this flux entirely, explaining recurrent catalase-positive infections.

Interpretation. The burst is a volume-concentrated chemical weapon: small total moles, extreme local reactivity.

NETosis. Discovered in 2004 (Brinkmann *et al.*, *Science*), NETosis is a programmed neutrophil death pathway in which the cell releases its decondensed **chromatin** — decorated with citrullinated **histones**, neutrophil elastase, MPO, defensins, and granule contents — to form neutrophil extracellular traps (NETs) that physically capture and chemically kill extracellular bacteria, fungi, and large parasites. The molecular pathway:

1. Activation by PAMPs / immune complexes / cytokines triggers ROS production by NOX2.
2. PAD4 (peptidylarginine deiminase 4) citrullinates histone H3 (Arg → citrulline), neutralizing positive charge and decompacting chromatin.
3. Nuclear membrane breaks down; chromatin enters cytoplasm; granule contents bind to chromatin.
4. Plasma membrane lyses, releasing the NET into the extracellular space (cell death).

NETs are evolutionarily ancient (zebrafish neutrophils, *Drosophila* haemocytes, even sea-anemone amoebocytes form similar traps). Pathological NETosis is now implicated in immunothrombosis in severe COVID-19 (NETs trap platelets and trigger coagulation, contributing to microvascular clots), in autoimmune diseases (citrullinated histones drive ACPA antibodies in rheumatoid arthritis; anti-NET antibodies in lupus), and in chronic wound failure.

Macrophages are tissue-resident phagocytes with diverse functions:

- Tissue-specific names: Kupffer cells (liver), alveolar macrophages (lung), microglia (brain), osteoclasts (bone), Langerhans cells (skin – actually dendritic cells)
- M1 polarization (IFN- γ + LPS): Pro-inflammatory; produces iNOS → nitric oxide (NO); secretes TNF- α , IL-12; activates Th1 responses against intracellular pathogens
- M2 polarization (IL-4, IL-13): Anti-inflammatory; produces arginase; secretes IL-10, TGF- β ; promotes wound healing, tissue repair, and fibrosis

NK Cells: Missing-Self and Induced-Self Recognition Natural killer (NK) cells are innate lymphocytes (about 5–15 % of blood lymphocytes) that kill virus-infected and transformed cells without prior sensitization. They are the innate immune system’s solution to a fundamental problem: how to detect cells that are *abnormal* from the inside, when no conserved pathogen pattern is present on the cell surface.

NK-cell killing is governed by an integration of inhibitory and activating receptor signals — the “balance hypothesis.” A cell is killed when activating signals exceed inhibitory signals.

Missing-self hypothesis (Ljunggren and Karre, 1990). Healthy cells display abundant MHC class I on their surface, presenting peptides for surveillance by CD8⁺ T cells. NK cells carry inhibitory KIRs (killer immunoglobulin-like receptors; KIR2DL, KIR3DL) that recognize self MHC-I. Engagement delivers an inhibitory signal through ITIMs (immunoreceptor tyrosine-based inhibitory motifs), suppressing the NK-cell killing program. Many viruses (CMV, HIV, KSHV) and tumors downregulate MHC class I to avoid CD8⁺ T cell detection — but this loss removes the inhibitory signal to NK cells, unmasking the cell for NK-mediated killing. The strategy has trade-offs: CMV has evolved decoy MHC-I-like proteins (UL18) that bind inhibitory NK receptors to mimic self.

Induced-self via NKG2D. A complementary mechanism detects cellular stress. NKG2D is an activating receptor on NK cells (and on subsets of CD8⁺ T cells, $\gamma\delta$ T cells, NKT cells) that recognizes stress-induced ligands: MICA, MICB (MHC class I chain-related), ULBP1–6 (UL16-binding proteins). These ligands are absent on healthy cells but induced by:

- DNA damage (ATR/ATM pathway) — common in transformed cells.
- Viral infection.
- Heat shock response.
- Oxidative stress.

NKG2D ligands are MHC-I-like in fold but lack peptide-binding groove and β 2-microglobulin association. Their induction provides a “danger signal” that bypasses normal MHC-I inhibition. NKG2D engagement signals through DAP10/DAP12 adaptors to activate cytotoxicity. Many cancers shed soluble MICA/MICB into circulation as a decoy that downmodulates surface NKG2D — an immune escape mechanism now targeted by anti-MICA-shedding antibodies in cancer immunotherapy.

NK-cell killing mechanisms (shared with CTLs):

- Perforin/granzyme — perforin polymerizes in target membrane (similar to MAC); granzymes (especially granzyme B) enter and cleave caspase-3/7 → **apoptosis**.
- Death receptor ligands — FasL, TRAIL on NK cell engage Fas, DR4/DR5 on target → DISC → caspase-8 → apoptosis.
- Antibody-dependent cellular cytotoxicity (ADCC): NK cell CD16 (Fc γ RIII) binds IgG bound to target cell surface → directed degranulation. ADCC is the principal mechanism by which anti-tumor antibodies (rituximab, trastuzumab) kill cancer cells, and a substantial fraction of vaccine-induced antiviral protection.

26.3.6 Inflammation and Vascular Recruitment of Immune Cells

The cardinal signs of inflammation (rubor, calor, tumor, dolor – redness, heat, swelling, pain) result from vascular changes triggered by innate immune activation:

- Mast cell degranulation: Histamine, tryptase, leukotrienes -> vasodilation + increased vascular permeability
- Cytokine cascade: IL-1 β (fever, endothelial activation); TNF- α (fever, hypotension, acute-phase response); IL-6 (hepatic acute-phase proteins: CRP, fibrinogen, complement, ferritin); IL-8/CXCL8 (neutrophil chemotaxis)
- Acute-phase response: Liver produces C-reactive protein (CRP), which binds phosphocholine on bacterial surfaces and activates complement

Clinical Connection: Sepsis and Cytokine Storm Sepsis is defined as life-threatening organ dysfunction caused by a dysregulated host response to infection (Sepsis-3 criteria, 2016). It affects approximately 49 million people and causes 11 million deaths annually worldwide (WHO). In sepsis, the normally protective inflammatory response becomes pathologically amplified: massive cytokine release (TNF- α , IL-1 β , IL-6) causes widespread endothelial dysfunction, capillary leak, coagulopathy (DIC), and multi-organ failure. The SOFA (Sequential Organ Failure Assessment) score quantifies organ dysfunction. Cytokine storm – a related phenomenon – was observed in severe COVID-19 (IL-6 pathway hyperactivation; treated with tocilizumab, an IL-6 receptor antagonist) and in cytokine release syndrome (CRS) following CAR-T cell therapy.

Concept Check 2: A child with chronic granulomatous disease (CGD) has a mutation in the gp91phox subunit of NADPH oxidase. Predict which types of infections this child will be susceptible to, and explain why catalase-positive bacteria (*S. aureus*, *Aspergillus*) are particularly dangerous in CGD while catalase-negative bacteria (*Streptococcus*) are not.

Concept Check 2b: A patient with paroxysmal nocturnal haemoglobinuria (PNH) has a somatic mutation in *PIGA* causing loss of GPI-anchored proteins on red blood cells, including CD55 and CD59. Explain (a) why these red cells are constantly haemolysed by their own complement system, (b)

why the disease is paroxysmal (worse at night/with sleep), and (c) why eculizumab (anti-C5 monoclonal antibody) is curative. Which complement step does eculizumab block, and what infectious-disease vaccination is mandatory before starting it?

26.4 Adaptive Immunity: Antigen Presentation, T Cells, and Clonal Specificity

The adaptive immune system provides antigen-specific responses with immunological memory. Its defining features include the coordinated innate-to-adaptive handoff that determines which lymphocyte programs are selected [Chaplin, 2010, Iwasaki and Medzhitov, 2015]:

- Specificity: Each lymphocyte clone bears a unique antigen receptor (TCR or BCR) generated by somatic recombination
- Diversity: > 10¹² possible TCR specificities; > 10⁸ BCR specificities
- Clonal selection: Antigen selects and expands primarily those lymphocyte clones with matching receptors
- Memory: Long-lived memory cells mount faster, stronger secondary responses upon re-encounter
- Self-tolerance: Autoreactive clones are eliminated (central tolerance) or suppressed (peripheral tolerance)

26.4.1 MHC Molecules and Antigen Presentation

Major histocompatibility complex (MHC) molecules present peptide fragments to T cells, providing the context for antigen recognition:

MHC class I (HLA-A, HLA-B, HLA-C in humans):

- Expressed on most nucleated cells
- Present endogenous peptides (from cytoplasmic proteins): proteasome -> peptide fragments -> TAP transporter -> ER -> peptide loading onto MHC-I -> cell surface
- Recognized by CD8⁺ T cells (cytotoxic T lymphocytes)
- Presents viral antigens and tumor antigens from within the cell

MHC class II (HLA-DR, HLA-DP, HLA-DQ):

- Expressed on professional antigen-presenting cells (APCs): dendritic cells, macrophages, B cells
- Present exogenous peptides (from phagocytosed material): endosomal/lysosomal degradation -> CLIP removal by HLA-DM -> peptide loading onto MHC-II -> cell surface
- Recognized by CD4⁺ T cells (helper T cells)

MHC genes are the most polymorphic in the human genome (about 20,000 HLA alleles in the population), ensuring that no pathogen peptide can escape presentation in most individuals – a population-level defense strategy.

26.4.2 T Cell Activation and Differentiation

- Signal 1: TCR recognition of peptide:MHC complex (specificity signal)
- Signal 2: Co-stimulatory signal – CD28 on T cell binds B7 molecules (CD80/CD86) on APC. Without this signal, the T cell becomes anergic (functionally unresponsive) – a mechanism of peripheral tolerance
- Signal 3: Cytokine environment determines effector subset differentiation

T helper cell subsets:

Table 341. T Cell Activation and Differentiation: Subset and Inducing Cytokines.				
Subset	Inducing Cytokines	Master Transcription Factor	Signature Cytokines	Primary Function
Th1	IL-12, IFN-γ	T-bet	IFN-γ, TNF-α	Macrophage activation; intracellular pathogens
Th2	IL-4	GATA3	IL-4, IL-5, IL-13	B cell IgE switching; eosinophils; helminths; allergy
Th17	IL-6 + TGF-β + IL-23	RORγt	IL-17, IL-22	Neutrophil recruitment; mucosal defense; fungi

Subset	Inducing Cytokines	Master Transcription Factor	Signature Cytokines	Primary Function
Treg	TGF- β	Foxp3	IL-10, TGF- β	Suppress excessive inflammation; maintain tolerance
Tfh	IL-6, IL-21	Bcl6	IL-21, CXCL13	B cell help in germinal centers

Cytotoxic T lymphocytes (CTLs, CD8⁺) recognize viral or tumor antigens on MHC-I and kill target cells through:

- Perforin/granzyme pathway: Perforin polymerizes in the target membrane, forming pores; granzyme B enters and activates caspase-3/7 -> apoptosis
- Fas-FasL pathway: CTL-expressed FasL binds Fas (CD95) on target -> DISC formation -> caspase-8 -> apoptosis
- Serial killing: A single CTL can kill 2-25 target cells sequentially via directed degranulation at the immunological synapse
- Exhaustion: In chronic infections (HBV, HCV, HIV), persistent antigen exposure leads to upregulation of inhibitory receptors (PD-1, TIM-3, LAG-3) and progressive loss of effector function – the basis for PD-1/PD-L1 checkpoint inhibitor therapy in cancer

Concept Check 3: Explain why a patient with a CD4⁺ T cell count below 200 cells/ μ L (as in AIDS) is susceptible to opportunistic infections that healthy individuals easily control. Specifically, describe which arm of the immune response is most compromised and why both cellular and humoral immunity are affected despite B cells and CD8⁺ T cells being present.

26.5 B Cells and Antibodies

26.5.1 B Cell Activation

B cell activation pathways differ depending on the nature of the antigen:

T-dependent antigens (protein antigens): BCR binds and internalizes antigen -> processes and presents peptides on MHC-II -> recognized by cognate Tfh cell -> CD40L-CD40 interaction + IL-21 -> B cell activation, proliferation, and entry into the germinal center reaction. This pathway produces high-affinity antibodies, class-switched isotypes, and long-lived memory.

T-independent antigens (repetitive polysaccharides, LPS): Cross-link multiple BCRs on the B cell surface -> activation without T cell help. Produces primarily IgM; limited affinity maturation; poor memory response. This is why polysaccharide vaccines (pneumococcal, meningococcal) are poorly immunogenic in children under 2 years (immature T-independent response) and why conjugate vaccines were developed.

26.5.2 Germinal Center Reaction

The germinal center (GC) in secondary lymphoid organs is the site of antibody optimization:

1. Clonal expansion: Activated B cells (centroblasts) proliferate rapidly in the dark zone
2. Somatic hypermutation (SHM): Activation-induced cytidine deaminase (AID) introduces point mutations in the variable (V) regions of immunoglobulin genes at a rate of about 10⁻³ per base pair per division – one million-fold higher than the normal mutation rate. AID deaminates cytidine to uridine in DNA, which is then processed by base excision repair or mismatch repair to generate diverse mutations.
3. Affinity maturation: Mutant B cells (centrocytes) migrate to the light zone, where they compete for antigen displayed on follicular dendritic cells (FDCs). Primarily B cells with improved BCR affinity receive survival signals; the rest undergo apoptosis. This Darwinian selection process progressively increases antibody affinity over successive rounds.
4. Class switch recombination (CSR): AID also introduces double-strand breaks in switch (S) regions upstream of constant region genes, enabling recombination that changes the antibody class from IgM to IgG, IgA, or IgE while preserving antigen specificity. Cytokine signals determine which class is selected: IL-4 -> IgE; IFN- γ -> IgG1; TGF- β -> IgA.

The GC reaction produces two critical outputs: long-lived plasma cells (migrate to bone marrow; secrete high-affinity antibody for years to decades) and memory B cells (reside in secondary lymphoid organs; rapidly reactivate upon antigen re-encounter).

26.5.3 Antibody Structure and Function

An antibody molecule consists of two identical heavy (H) chains and two identical light (L) chains, each containing variable (V) and constant (C) domains:

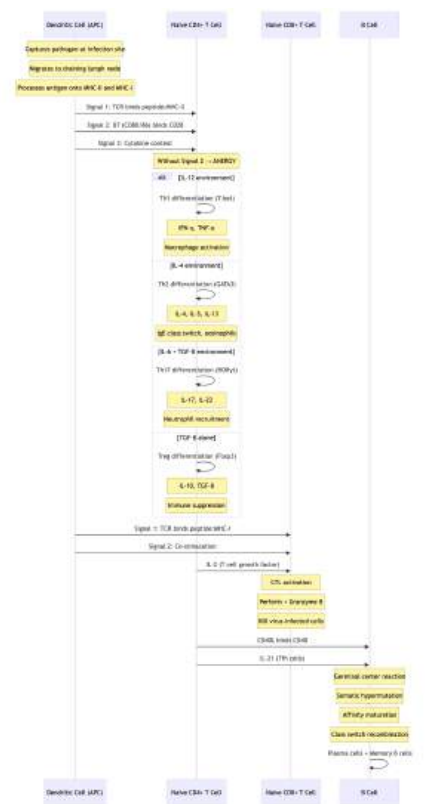


Figure 160. Three-signal T cell activation by dendritic cells, with cytokine-context-driven differentiation into Th1/Th2/Th17/Treg/Tfh subsets and downstream activation of cytotoxic CD8⁺ T cells and antibody-producing B cells.

- Fab region (fragment antigen-binding): Contains the variable domains (VH + VL) that form the antigen-binding site (paratope). The three complementarity-determining regions (CDR1, CDR2, CDR3) within each variable domain make direct contact with antigen.
- Fc region (fragment crystallizable): The constant domains that determine antibody class and mediate effector functions (complement activation, Fc receptor binding on phagocytes and NK cells, placental transfer).
- Hinge region: Provides flexibility between Fab and Fc, allowing bivalent binding to spatially separated epitopes.

26.5.4 Antibody Classes and Effector Functions

Table 342. Antibody Classes and Effector Functions: Isotype and Structure.

Isotype	Structure	Location	Key Functions
IgM	Pentamer (10 binding sites)	Blood (primary response)	First antibody produced; efficient complement activation via classical pathway; low affinity compensated by high avidity
IgG	Monomer (4 subclasses)	Blood, extravascular; crosses placenta via FcRn	Most abundant serum antibody; opsonization; ADCC (via CD16 on NK cells); complement; neonatal passive immunity
IgA	Dimer (secretory IgA with secretory component)	Mucosal surfaces: saliva, tears, breast milk, intestinal lumen	Most produced antibody class (>3 g/day); neutralization at mucosal surfaces; immune exclusion
IgE	Monomer	Bound to mast cells and basophils via high-affinity FcεRI	Very low serum concentration; cross-linking by allergen -> mast cell degranulation -> immediate hypersensitivity; anti-helminth defense (eosinophil ADCC)
IgD	Monomer	Naive B cell surface (co-expressed with IgM)	BCR signaling; poorly understood effector function

Immunological memory – the basis of vaccination – results from the persistence of long-lived plasma cells and memory B cells. Upon re-exposure, the secondary response is:

- Faster: Days instead of 1-2 weeks
- Stronger: 10-100 fold higher antibody titers
- Higher affinity: Memory B cells express somatically hypermutated, affinity-matured BCRs
- Class-switched: Predominantly IgG (or IgA at mucosal surfaces)

Concept Check 4: Conjugate vaccines (e.g., PCV13) link bacterial polysaccharide antigens to protein carriers (e.g., CRM197, a nontoxic diphtheria toxoid). Explain the immunological rationale: why does conjugation convert a T-independent antigen into a T-dependent antigen, and why is this critical for vaccinating infants?

26.6 Vaccines and Immunological Memory

26.6.1 Vaccine Platforms: Eight Strategies for Inducing Memory

Vaccines exploit the same memory mechanisms that protect us after natural infection, but without the disease. The eight major platform classes — each with distinct strengths, limitations, and clinical exemplars — represent a 200-year-progressive enrichment of strategies for safely tricking the immune system into making memory.

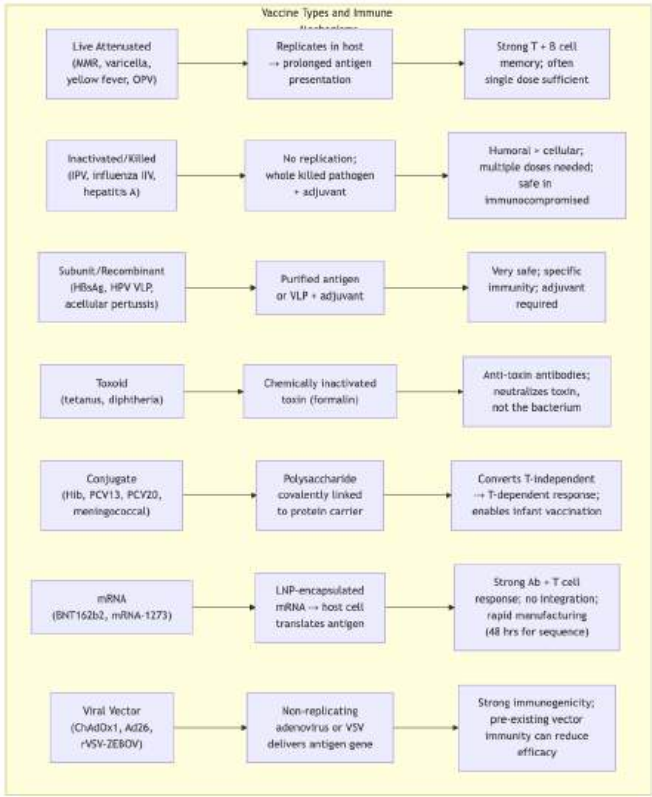


Figure 161. Eight vaccine platforms, the immune mechanism each engages, and characteristic clinical responses.

Table 343. Vaccine Platforms: Eight Strategies for Inducing Memory: Platform and Examples.

Platform	Examples	Antigen form	Strengths	Limitations
Live attenuated	MMR, varicella (Varivax), yellow fever 17D, oral polio (OPV), BCG, rotavirus	Weakened replicating organism	Strong T + B memory; often a single dose; mucosal immunity (OPV)	Reversion to virulence (rare; OPV → cVDPV); contraindicated in immunocompromised and pregnancy

Platform	Examples	Antigen form	Strengths	Limitations
Inactivated / killed	IPV (Salk), inactivated influenza (IIV), hepatitis A (Havrix), rabies, whole-cell pertussis (legacy)	Chemically/heat-killed whole organism	Safe in immunocompromised; stable	Weaker than live; requires adjuvant + multiple doses
Subunit / recombinant protein	Hepatitis B (HBsAg in yeast), acellular pertussis (aP), zoster (Shingrix gE + AS01)	Purified protein antigen + adjuvant	Very safe; no infectious risk	Less immunogenic; adjuvant essential
Virus-like particles (VLPs)	HPV (Gardasil, Cervarix), HBV (also classified as subunit)	Self-assembled capsid proteins (no genome)	Particulate, highly immunogenic; structurally identical to virus	Difficult to engineer for some viruses
Toxoid	Tetanus (TT), diphtheria (DT, Tdap), botulism toxoid	Formalin-inactivated toxin	Anti-toxin antibodies neutralize the <i>toxin</i> , not the bacterium	No antibacterial protection; periodic boosters needed
Conjugate	Hib, PCV13, PCV20 (pneumococcal), meningococcal ACWY (Menactra)	Bacterial polysaccharide covalently linked to a protein carrier (CRM197, TT)	Converts T-independent → T-dependent response; enables infant immunization; affinity-matured response	Carrier-specific T cells diverted; serotype replacement after PCV introduction
mRNA	BNT162b2 (Pfizer-BioNTech), mRNA-1273 (Moderna), mRNA-1345 (RSV, 2024); flu mRNA-1010 (trial)	LNP-encapsulated nucleoside-modified mRNA encoding the antigen	Rapid design (48 hr from sequence); strong T + B response; no genome integration	Cold-chain dependent; rare myocarditis; waning antibody titres
Viral vector	rVSV-ZEBOV (Ebola), ChAdOx1 (AstraZeneca COVID), Ad26.COVS.2.S (J&J), gene-therapy AAV vectors	Non-replicating recombinant virus carrying antigen gene	Strong durable response; mucosal IgA achievable	Pre-existing vector immunity (Ad5 in adult populations) reduces efficacy; rare thrombosis (ChAdOx1)

mRNA vaccines are the newest platform and represented a paradigm shift during the COVID-19 pandemic:

- The spike protein sequence of SARS-CoV-2 was published on January 11, 2020; Moderna had designed its mRNA-1273 vaccine candidate within 48 hours.
- The mRNA is modified (N1-methylpseudouridine replaces uridine, Karikó and Weissman discovery, Nobel Prize 2023) to reduce TLR7/8 recognition, block 2'-5'-OAS / RNase L degradation, and increase translational efficiency 10–100×.
- Lipid nanoparticle (LNP) encapsulation protects the mRNA from extracellular nucleases and facilitates cellular uptake; the four-component LNP (ionisable lipid, phospholipid, cholesterol, PEG-lipid) self-assembles into about 80-nm particles.
- Upon injection, host cells (predominantly muscle and dendritic cells at the injection site) translate the mRNA into spike protein, which is presented on MHC-I (activating CD8⁺ CTLs) and secreted/surface-displayed (activating B cells and CD4⁺ T cells).
- No integration into host DNA occurs — mRNA is degraded within hours to days.
- Spike is locked in the prefusion conformation by two proline substitutions (2P mutation) that preserve neutralizing epitopes.

The platform is now extending to influenza (mRNA-1010), RSV (mRNA-1345, FDA-approved 2024), CMV, and personalised cancer neoantigen vaccines (Moderna mRNA-4157 in Phase III for melanoma).

26.6.2 Antigenic Variation: How Pathogens Outpace Antibody Responses

The single greatest challenge for vaccine development against many viruses is that the immune target itself evolves under the selection pressure of the population’s own immune response. Two paradigmatic examples illustrate the strategies and the resulting public-health consequences.

Influenza A: drift and shift. Influenza A is a Class V segmented (–)ssRNA virus with 8 genome segments. Its surface glycoproteins hemagglutinin (HA, 18

subtypes) and neuraminidase (NA, 11 subtypes) are the primary targets of neutralizing antibodies. Influenza A undergoes two distinct mechanisms of antigenic change:

Table 344. Antigenic Variation: How Pathogens Outpace Antibody Responses: Feature and Antigenic drift.

Feature	Antigenic drift	Antigenic shift
Mechanism	Point mutations in HA (and NA) accumulating during replication	Reassortment of whole genome segments during co-infection of one cell by two influenza A strains (often in pigs as the “mixing vessel”)
Rate	Continuous; about 0.5–1 % per year on HA1	Episodic; rare events
Consequence	Antigenic mismatch with prior immunity → seasonal epidemics	Novel HA subtype unseen by population → pandemic potential
Vaccine response	Annual reformulation (WHO twice-yearly recommendation)	Requires entirely new pandemic vaccine
Why influenza A primarily?	Influenza B drifts but does not reassort with animal reservoirs at meaningful frequency; influenza A has a wide animal host range	Influenza A naturally infects birds, swine, humans, and other mammals — sustaining a reservoir of segments for reassortment

Pandemic history: - 1918 H1N1 (“Spanish flu”) — 50–100 million deaths. - 1957 H2N2 (“Asian flu”) — 1–2 million deaths; H2 from avian source reassorted with circulating H1N1. - 1968 H3N2 (“Hong Kong flu”) — 1 million deaths; H3 from avian source. - 2009 H1N1 (pandemic) — about 284,000 deaths; quadruple reassortant (avian + human + two swine lineages); milder than predicted because of partial cross-immunity from related H1N1 strains. - H5N1 highly pathogenic avian influenza (HPAI) — ongoing outbreaks in dairy cattle and poultry (2024–26); about 60 % case-fatality rate in the rare human cases; intense surveillance for adaptation to mammalian transmission.

HIV reverse transcriptase: the quasi-species cloud. HIV uses an entirely different mechanism — extreme intra-host evolution. Reverse transcriptase has an error rate of about 3×10^{-5} per base per replication cycle, and HIV makes about 10^{10} virions per day in an untreated patient. With a 9.7-kb genome, this order-of-magnitude estimate implies that essentially every possible single-point mutation in the viral genome arises many times per day (subject to hotspots and defective particles) along with a substantial fraction of possible double mutations. The resulting population — a cloud of related sequences around a consensus — is termed a quasi-species.

Consequences:

1. Drug resistance is essentially preformed: any single-target monotherapy fails within weeks because resistant variants pre-exist in the quasi-species cloud. This is why HIV treatment requires combination ART (≥ 3 drugs from ≥ 2 classes); the simultaneous probability of a virion carrying mutations conferring resistance to most drugs is astronomically low.
2. Antibody escape is continuous: the env gene (gp120/gp41) evolves rapidly under neutralizing-antibody pressure, with the variable loops V1/V2/V3 changing every few weeks within an individual.
3. Vaccine difficulty: a vaccine that elicits primarily narrowly-specific antibodies will fail. Successful HIV vaccine candidates aim for broadly neutralizing antibodies (bNAbs) that target conserved sites (CD4-binding site, fusion peptide) — but these require unusual germline B cells and prolonged affinity maturation, which most vaccinees do not develop.

The HIV quasi-species lesson — that within-host evolution can generate resistance faster than therapy can clear the virus — has now been applied to influenza, hepatitis C, and SARS-CoV-2 (the 32-spike-mutation Omicron emergence almost certainly arose from chronic infection of an immunocompromised host, where prolonged replication permitted accumulation of escape mutations).

26.6.3 Herd Immunity and Population-Level Protection

When a sufficient proportion of a population is immune, the pathogen’s transmission is interrupted even for non-immune individuals. The herd-immunity threshold is given by:

$$p_c = 1 - \frac{1}{R_0}$$

(354)

where p_c is the critical fraction of the population that must be immune and R_0 is the basic reproduction number (the expected number of secondary cases from one primary case in a fully susceptible population). figure 157 shows how susceptible, infected, and recovered compartments evolve when $R_0 > 1$. The intuition:

each case must produce on average less than one secondary case for the epidemic to die out; immunity removes a fraction of the contacts an infectious person makes, so the effective reproduction number is $R_e = R_0(1 - p)$. Solving for $R_e = 1$ gives $p = 1 - 1/R_0$.

26.6.4 Worked Example: Calculating Herd Immunity Threshold (Three Pathogens)

Problem: Compute the herd immunity threshold from equation (354) for measles ($R_0 = 15$), polio ($R_0 = 5$), and original-strain SARS-CoV-2 ($R_0 = 2.5$), and discuss the implications for vaccination policy.

Solution:

Table 345. Calculating Herd Immunity Threshold (Three Pathogens): Pathogen and R_0.

Pathogen	R_0	$p_c = 1 - 1/R_0$	Realistic vaccine efficacy E	Required coverage $p_v = p_c/E$
Measles	15	$1 - 1/15 = 0.933 \rightarrow 93.3\%$	0.97 (MMR two-dose)	$0.933/0.97 = 0.962 \rightarrow 96.2\%$
Polio	5	$1 - 1/5 = 0.800 \rightarrow 80\%$	0.99 (IPV three-dose)	$0.800/0.99 = 0.808 \rightarrow 80.8\%$
COVID-19 (original)	2.5	$1 - 1/2.5 = 0.600 \rightarrow 60\%$	0.95 (BNT162b2 against original)	$0.600/0.95 = 0.632 \rightarrow 63.2\%$
COVID-19 (Omicron)	10	$1 - 1/10 = 0.900 \rightarrow 90\%$	0.50 (vs symptomatic infection)	$0.900/0.50 = 1.80 \rightarrow$ unattainable

Interpretation:

1. Measles is the textbook case for high-coverage vaccination. Even with the excellent MMR vaccine ($E \approx 97\%$), $> 96\%$ of the population must be vaccinated. A drop from 96 % to 92 % (e.g., due to vaccine hesitancy) reduces immunity below threshold and allows outbreaks — exactly what has happened in the 2018–2019 US/EU measles resurgences.
2. Polio’s lower R_0 makes it much more tractable: 80 % coverage with IPV is sufficient. This is why polio is on the verge of global eradication while measles is not.
3. COVID-19 Omicron illustrates the vaccine-coverage impossibility result: when efficacy against transmission is moderate (about 50 %) and R_0 is high (about 10 due to immune escape and inherent transmissibility), the formula $p_v = p_c/E$ exceeds 100 %, meaning herd immunity by vaccination alone is unattainable. Public-health strategy must rely on a combination of vaccination (reducing severity), non-pharmaceutical interventions (reducing R_0 below the achievable coverage), and accepting endemicity.

The herd-immunity equation also explains why small reductions in vaccine coverage produce disproportionate disease resurgences for high- R_0 pathogens: at $R_0 = 15$, a 1-percentage-point drop in immune coverage raises the effective reproduction number R_e by about $R_0 \times 0.01 = 0.15$. This non-linearity is why measles outbreaks dominate vaccine-hesitancy clusters.

26.6.5 R_0 Comparison: Why Pathogens Differ

Table 346. R_0 Comparison: Why Pathogens Differ: Pathogen and R_0.

Pathogen	R_0	Herd-immunity threshold	Notes
Measles	12–18	92–94 %	Most contagious common pathogen
Mumps	4–7	75–86 %	MMR-vaccine-preventable
Pertussis	12–17	92–94 %	Resurgent due to waning aP-vaccine immunity
Diphtheria	6–7	83–86 %	Toxin-driven; toxoid-vaccinable
Polio	4–7	75–86 %	Near eradication
Smallpox	5–7	80–86 %	Eradicated 1980

Pathogen	R_0	Herd-immunity threshold	Notes
Rubella	6–7	83–86 %	MMR-vaccine-preventable
HIV	2–5	50–80 %	Sexual / parenteral transmission
Influenza (seasonal)	1.3–2	23–50 %	Annual drift; vaccine reformulated yearly
Influenza (1918)	2–3	50–67 %	Pandemic
SARS-CoV-2 (original)	2.5–3	60–67 %	Wuhan strain
SARS-CoV-2 (Delta)	5–8	80–88 %	L452R + T478K spike
SARS-CoV-2 (Omicron, BA.5)	8–15	88–93 %	Immune escape pushes effective threshold higher
Mpox (clade IIb, 2022)	1.0–1.5	0–33 %	Sustained MSM transmission; vaccine + behavior change controlled

26.6.6 Adjuvants and Innate Immune Activation

Adjuvants amplify the innate immune response to vaccine antigens, improving adaptive immunity:

- Aluminum salts (Alum): Oldest adjuvant (since 1926); activates NLRP3 inflammasome; depot effect (slow antigen release); used in most childhood vaccines
- AS04 (Alum + monophosphoryl lipid A): TLR4 agonist; used in Cervarix (HPV vaccine)
- MF59: Oil-in-water squalene emulsion; enhances antigen uptake by APCs; used in some influenza vaccines
- CpG oligodeoxynucleotides: TLR9 agonist; used in Hepilisav-B (hepatitis B vaccine)
- Matrix-M (saponin-based): Used in Novavax COVID-19 vaccine; potent Th1 and CTL response
- AS01 (liposomal MPL + QS-21): Used in Shingrix (zoster) and RTS,S (malaria); strong Th1 response

Clinical Connection: SARS-CoV-2 and the COVID-19 Pandemic SARS-CoV-2 enters cells via its spike protein binding ACE2, with TMPRSS2 protease facilitating membrane fusion. Variants of concern (Alpha, Delta, Omicron) accumulated mutations in the spike protein’s receptor-binding domain (RBD) that increased transmissibility and/or enabled immune evasion. Omicron-lineage viruses substantially escaped neutralizing antibodies from both vaccination and prior infection, while population immunity and viral evolution shifted severe-disease risk compared with early pandemic waves. mRNA vaccine development demonstrated the power of platform technology – Moderna designed its vaccine sequence within 48 hours of the viral genome publication, though regulatory approval required 11 months of clinical trials. Long COVID is now defined operationally as a chronic condition present at least 3 months after SARS-CoV-2 infection; prevalence estimates vary by cohort, variant era, vaccination status, and case definition. Mechanistic studies now emphasize persistent immune activation, T-cell exhaustion signatures, metabolic dysregulation, possible viral-antigen persistence, autoimmunity, **microbiome** disruption, dysautonomia, and endothelial dysfunction rather than a single cause [**Centers for Disease Control and Prevention, 2026b, Aid et al., 2026**].

Concept Check 5: Calculate the effective reproduction number (R_e) for measles ($R_0 = 15$) in a community where 80% of the population is immune. Is an epidemic possible? How many additional percentage points of immunity are needed to prevent sustained transmission?

Concept Check 5b: A new COVID-19 vaccine candidate has 60 % efficacy against transmission. The Omicron sublineage circulating has $R_0 = 10$. Apply equation (354) to determine whether achievable vaccine coverage can suppress transmission. If not, what additional public-health measures (and at what magnitude of R_0 reduction) would make the situation tractable with this vaccine?

Concept Check 6: Influenza A viruses can undergo antigenic shift through genomic reassortment, but SARS-CoV-2 (a non-segmented RNA virus) cannot. Despite this, SARS-CoV-2 has generated numerous variants of concern. Explain the mechanism by which SARS-CoV-2 generates antigenic diversity and why its approach, while different from influenza, has still enabled significant immune evasion.

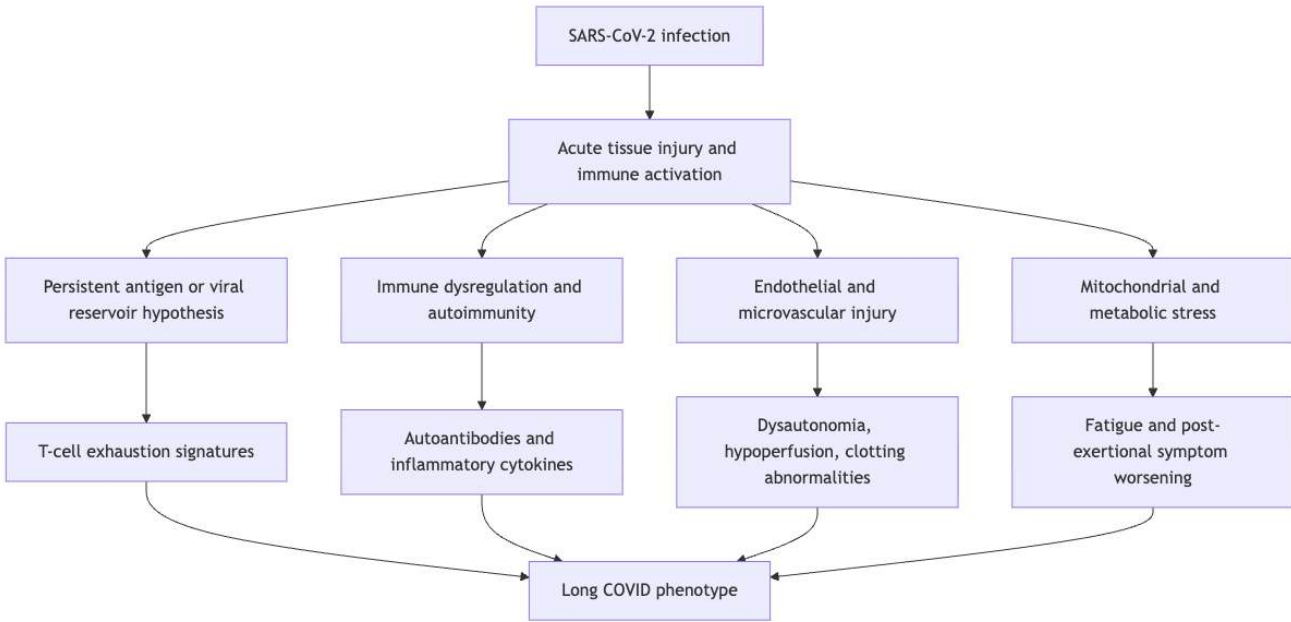


Figure 162. Long COVID mechanism network. Current evidence supports overlapping immune, vascular, neuroautonomic, metabolic, and possible persistence mechanisms; the diagram should be read as a differential-mechanism map, not a single-cause pathway [citep{longcovid2026mechanisms}].

26.7 Current Evidence and Frontier Biology: Host Immunity and Vaccines

For Host Immunity and Vaccines, frontier biology belongs inside the evidence logic of the chapter. Microbiology and infectious disease now require One Health reasoning across people, animals, environments, genomics, and antimicrobial stewardship. The core reading question is this: infectious-disease reasoning should connect pathogen biology, transmission, immunity, diagnostics, interventions, and equity.

- What to verify: identify the observation, model, assay, or dataset that would make the claim stronger or weaker.
- What to qualify: state the scale, organism, cell type, environmental condition, or population where the claim is expected to hold.
- What to compare: test at least one alternative explanation, baseline, or null model before treating the pattern as causal.
- What to cite: distinguish primary evidence, review synthesis, public dataset, and institutional guidance; for recent or numeric claims, prefer the source closest to the measurement and state what has changed since it was published.

For resistance or outbreak claims, name the organism, determinant, selection pressure, transmission route, and surveillance evidence [World Health Organization, 2024a, Centers for Disease Control and Prevention, 2025a, Murray et al., 2022].

Source practice: For pathogen, resistance, and intervention claims, tie statements to organism-resistance pairs, surveillance evidence, official guidance, and trial/regulatory status [World Health Organization, 2024a, 2025d,b, Centers for Disease Control and Prevention, 2025b, 2026a].

26.7.1 Current Evidence Map: Intervention Choice Across Pathogens

26.8 Summary

- Apply Koch’s postulates and molecular Koch’s postulates to evaluate evidence for microbial causation of disease, and identify their limitations.
- Describe virulence factors (adhesins, toxins, invasion machinery, immune evasion strategies) used by major bacterial, viral, and eukaryotic pathogens.
- Explain innate immune defenses including physical barriers, pattern recognition receptors (TLRs, NLRs, RIG-I, cGAS-STING), the three complement pathways and their convergence at C3, and cellular effectors (neutrophils with NETosis, macrophages, NK cells with missing-self recognition).
- Describe adaptive immunity including V(D)J recombination, MHC restriction, T helper cell subsets, cytotoxic T cell killing mechanisms, B cell activation, affinity maturation, and antibody class switching.
- Compare the eight major vaccine platforms (live attenuated, inactivated, subunit, virus-like-particle, toxoid, conjugate, mRNA, viral vector) and apply the herd immunity equation $p_c = 1 - 1/R_0$ to compute thresholds for measles, polio, and COVID-19 variants.
- Describe antigenic variation in influenza (drift vs shift) and HIV (reverse-transcriptase quasi-species clouds), and connect this to vaccine reformulation and pandemic risk.
- Classify the principal antibiotic-resistance mechanisms (β -lactamases including ESBLs and carbapenemases, efflux pumps, target modification including PBP2a in MRSA and 23S rRNA methylation in MLS-resistant streptococci, reduced permeability, bypass pathways) and link each to specific drug classes.

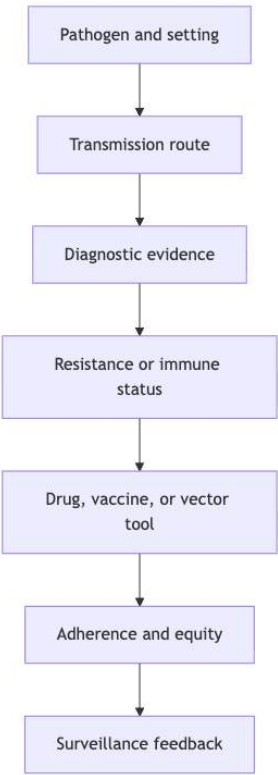


Figure 163. TB regimens, malaria spatial emanators, lenacapavir PrEP, Candida auris control, and Long COVID mechanisms are cases where intervention choices depend on evidence and setting. \citep{who2025tb,who2025spatialemanators,cdc2025lenacapavirprep,cdc2026candidaauris,longcovid2026mechanisms}.

- Describe the epidemiology and pathogenesis of major infectious diseases including tuberculosis, malaria, HIV/AIDS, and influenza, and explain the One Health framework.

26.9 Further Reading and Source Notes: Host Immunity and Vaccines

- Control & Prevention} (2026). Long COVID Basics.
- Aid et al. (2026). Long COVID involves activation of proinflammatory and immune exhaustion pathways. *Nature Immunology*, 27.
- Faghy et al. (2026). Current status and future perspectives on the mechanistic and pathophysiological understanding of long COVID. *Communications Medicine*, 6.

26.10 Companion Source Module: Host Immunity and Vaccines

Host Immunity and Vaccines should leave a reproducible trail from a biological claim to the code, figure, diagram, or paper-based activity that can test it. Use the surfaces below to inspect the chapter’s assumptions, rerun the relevant model, or compare the manuscript explanation with companion labs and figures.

Table 347. Companion source surfaces for Host Immunity and Vaccines.

Surface	Use it for
src/biology/microbiology/microbiology.py (basic_reproduction_number, sir_model, mic_fold_dilution)	Reproduce transmission and antimicrobial-resistance calculations.
src/biology/ecology/ecology.py (exponential_growth)	Compare early outbreak growth with ecological growth models.
src/mermaid/biology_diagrams.py (immune_response_diagram, viral_replication_cycle_diagram)	Connect pathogen life cycle to host response.

Reproducibility check: identify pathogen, host population, transmission route, diagnostic window, intervention, and surveillance source before comparing disease claims. Cross-reference: connect with section 24, sections 34 and 35, and sections 37 and 38.

27Antimicrobial Resistance and Epidemiology

Level 2/3 · 35 min read · 45 min lecture · Prerequisites: section 26

27.1 Learning Objectives

1. Classify antibiotic-resistance mechanisms in multidrug-resistant pathogens.
2. Interpret epidemic curves, R0, and herd-immunity thresholds.
3. Compare stewardship, surveillance, and public-health interventions.
4. Evaluate resistance evolution under selection and horizontal gene transfer.
5. Propose a stewardship intervention that lowers resistance selection without blocking necessary treatment.
6. Model resistance spread with selection coefficients and horizontal gene transfer.
7. Interpret surveillance datasets such as GLASS reports with explicit sampling limits.

27.2 Antibiotic Resistance Mechanisms in Multidrug-Resistant Pathogens

Antibiotic resistance can be classified into five mechanistic categories. Most clinically important multi-drug-resistant pathogens combine multiple mechanisms; an isolate may simultaneously hydrolyse β -lactams, modify aminoglycosides, methylate ribosomal RNA, and pump out fluoroquinolones.

27.2.1 Mechanism 1: Enzymatic Inactivation

Direct destruction of the drug by hydrolysis or modification.

β -lactamases are the most clinically important and most diverse resistance enzymes. They hydrolyse the β -lactam ring (with the active-site serine — a tetrahedral covalent intermediate — or via a metallo-zinc mechanism) before the drug reaches its PBP target. The Ambler classification:

Table 348. Mechanism 1: Enzymatic Inactivation: Class and Mechanism.				
Class	Mechanism	Spectrum	Inhibitor sensitivity	Examples
Class A (serine)	Active-site serine (Ser70)	Penicillins; ESBL extends to 3GC	Inhibited by clavulanate, sulbactam, tazobactam, avibactam	TEM-1, SHV-1 (penicillinases); CTX-M (the dominant ESBL globally); KPC (carbapenemase)
Class B (metallo- β -lactamase, MBL)	Zn ²⁺ active site; hydroxide nucleophile	Penicillins, cephalosporins, and carbapenems; monobactams such as aztreonam are structurally spared by the MBL but can be hydrolysed by co-produced ESBLs	Inhibited by EDTA in vitro; not inhibited by clinical inhibitors; aztreonam-avibactam combinations	NDM-1 (New Delhi metallo- β -lactamase, 2008 emergence; global spread); VIM, IMP
Class C (AmpC)	Active-site serine	Cephalosporins (including 3GC); poorly inhibited by clavulanate	Cefepime, carbapenems retain activity	Chromosomal AmpC inducible in <i>Enterobacter</i> , <i>Serratia</i> , <i>Citrobacter</i> , <i>Pseudomonas</i> ; plasmid-borne (CMY)

Class	Mechanism	Spectrum	Inhibitor sensitivity	Examples
Class D (oxacillinase, OXA)	Active-site serine	Variable (penicillins → carbapenems for OXA-48)	Variable inhibitor susceptibility	OXA-48 (Klebsiella, Mediterranean); OXA-23 (Acinetobacter pan-resistance)

Other inactivating enzymes:

- Aminoglycoside-modifying enzymes (AMEs) — three families: acetyltransferases (AAC), phosphotransferases (APH), nucleotidyltransferases (ANT). Modify amino or hydroxyl groups on the drug, abolishing ribosome binding. Plasmid-encoded; > 50 enzyme variants known.
- Chloramphenicol acetyltransferase (CAT) — acetylates the drug.
- Macrolide esterases / phosphotransferases (Ere, Mph) — less common than ribosomal methylation.
- β -glucuronidases that activate the cancer drug irinotecan into its toxic form (gut bacteria; relevant for drug-drug-microbiome interactions).

27.2.2 Mechanism 2: Target Modification

Altering the drug target so the antibiotic no longer binds.

Table 349. Mechanism 2: Target Modification: Antibiotic and Original target.

Antibiotic	Original target	Modified target	Resistance mechanism
β -lactams	PBP2 (transpeptidase)	PBP2a in MRSA (encoded by <i>mecA</i>)	Low-affinity transpeptidase that performs cross-linking even when normal PBPs are inhibited; SCC <i>mec</i> cassette mobile element
Vancomycin	D-Ala-D-Ala terminus of Lipid II	D-Ala-D-Lac (VanA, VanB) or D-Ala-D-Ser (VanC)	One H-bond replaced by an oxygen lone pair; ≥ 1000 -fold loss of vancomycin affinity
Macrolides, lincosamides, streptogramin B (MLS _B)	23S rRNA peptidyl-transferase center	Methylated A2058 of 23S rRNA by Erm methylase	Single methyl group blocks the three drug classes — cross-resistance
Aminoglycosides (high-level)	16S rRNA A-site	16S rRNA methylation by ArmA, RmtB, RmtC, RmtD	Plasmid-borne; confers pan-aminoglycoside resistance
Linezolid	23S rRNA, U2504	G2576T or T2500A 23S rRNA mutation; cfr methylase (methylates A2503)	Cfr also confers cross-resistance to phenicols, lincosamides, streptogramins, oxazolidinones (PhLOPS _A)
Fluoroquinolones	DNA gyrase (GyrA, GyrB), topoisomerase IV (ParC, ParE)	Mutations in QRDR (quinolone-resistance-determining region): GyrA Ser83, Asp87	Stepwise mutations: each step adds resistance; <i>qnr</i> genes encode gyrase-protecting proteins (low-level)
Rifampin	RNA polymerase β subunit (RpoB)	RpoB mutations, especially Ser531Leu, His526Tyr	Single mutations confer high-level resistance
Trimethoprim	DHFR (dihydrofolate reductase)	Acquired <i>dhfr</i> genes encoding drug-resistant DHFR; chromosomal mutations	Bypass through alternative DHFR
Sulfonamides	DHPS (dihydropteroate synthase)	Acquired <i>sul</i> genes; chromosomal mutations	Bypass through alternative DHPS
Colistin (polymyxin)	LPS lipid A	mcr-1 phosphoethanolamine transferase (plasmid-borne, 2015 discovery, China); chromosomal <i>pmrAB</i> / <i>phoPQ</i> mutations	Modifies lipid A phosphates → reduced affinity for cationic colistin

MRSA mechanism in detail. *S. aureus* resistant to methicillin and most earlier β -lactams carries the *mecA* gene on a mobile genetic element — SCC*mec* (staphylococcal cassette chromosome *mec*). *mecA* encodes PBP2a, an alternative transpeptidase whose β -lactam-binding pocket has rearranged to drastically lower affinity. The K_i for ceftriaxone increases from about 0.05 μ M (PBP2) to about 50 μ M (PBP2a). When normal PBPs are acylated by β -lactam, PBP2a can still

cross-link cell wall, allowing growth. Newer 5th-generation cephalosporins (ceftaroline, ceftobiprole) were specifically engineered with side chains that bind PBP2a and are now used clinically against MRSA.

27.2.3 Mechanism 3: Efflux Pumps

Active export of antibiotics out of the cell, often accomplishing multi-drug resistance through a single pump system.

Table 350. Mechanism 3: Efflux Pumps: Pump family and Energy source.

Pump family	Energy source	Drugs effluxed	Examples
RND (Resistance-Nodulation-Division)	Proton motive force	β -lactams, fluoroquinolones, tetracyclines, chloramphenicol, macrolides	AcrAB-TolC (<i>E. coli</i>); MexAB-OprM, MexCD-OprJ, MexEF-OprN, MexXY-OprM (<i>P. aeruginosa</i>); AdeABC (<i>Acinetobacter</i>)
MFS (Major Facilitator Superfamily)	PMF	Tetracyclines (TetA, TetB), macrolides (Mef), fluoroquinolones	TetA, TetB; MdfA
MATE	PMF / Na ⁺ gradient	Fluoroquinolones, aminoglycosides	NorM (<i>V. parahaemolyticus</i>)
SMR (Small Multidrug Resistance)	PMF	QACs, lipophilic cations	EmrE
ABC (ATP-Binding Cassette)	ATP	Macrolides, ketolides	LmrA

RND tripartite pumps in Gram-negatives are particularly devastating because they span the entire cell envelope: an inner-membrane efflux transporter (e.g. AcrB) coupled via a periplasmic adaptor (AcrA) to an outer-membrane channel (TolC). The pump exports drugs straight from the cytoplasm or inner membrane into the extracellular space, bypassing the periplasm. *P. aeruginosa* MexAB-OprM is the textbook example: constitutive expression confers intrinsic resistance to multiple drug classes; mutations in regulators (e.g., *nfxB*, *mexR*) cause overexpression and clinical failure.

27.2.4 Mechanism 4: Reduced Permeability

Decreasing drug uptake by altering cell-envelope permeability.

- Porin loss in Gram-negatives: deletions or down-regulation of OmpF, OmpC, OprD — particularly important for hydrophilic β -lactams and carbapenems. OprD loss in *P. aeruginosa* confers imipenem resistance.
- LPS modification in Gram-negatives: reduces hydrophobic-drug entry.
- Mycobacterial cell wall: the mycolic-acid layer is intrinsically impermeable; *M. tuberculosis* is naturally resistant to most antibiotics.

27.2.5 Mechanism 5: Bypass / Target Overproduction

Producing more target or alternative target to dilute drug action.

- Trimethoprim resistance via *dfr* genes that encode a drug-insensitive DHFR (target replacement).
- Sulfonamide resistance via *sul* genes that encode a drug-insensitive DHPS.
- Methotrexate resistance in cancer cells via DHFR overexpression — same principle in eukaryotes.

27.2.6 Resistance in Action: A Pan-Resistant *Klebsiella pneumoniae*

A clinical isolate from a 2019 outbreak in a Greek ICU was reported with the following resistance profile:

Table 351. Resistance in Action: A Pan-Resistant *Klebsiella pneumoniae*: Mechanism and Genetic determinant.

Mechanism	Genetic determinant	Drug class affected
NDM-1 (Class B MBL)	<i>bla</i> _{NDM-1} on plasmid	Penicillins, cephalosporins, and carbapenems; aztreonam is spared by MBL chemistry but vulnerable to co-produced ESBLs
CTX-M-15 ESBL (Class A)	<i>bla</i> _{CTX-M-15}	Cephalosporins (residual)
OXA-48 (Class D)	<i>bla</i> _{OXA-48}	Carbapenems (residual)
<i>mcr-1</i>	<i>mcr-1</i>	Colistin
Aac(6')-Ib-cr	Plasmid	Aminoglycosides + ciprofloxacin
<i>rmtB</i>	Plasmid	Pan-aminoglycoside
AcrAB-TolC overexpression	<i>ramA</i> mutation	Multiple
GyrA Ser83Leu	Chromosome	Fluoroquinolones
OmpK35 loss	Chromosome	Reduced β -lactam entry

Such isolates may have no reliable standard single-agent option, so treatment depends on isolate-specific susceptibility testing, source control, and expert consultation. Options can include cefiderocol, ceftazidime-avibactam plus aztreonam for some MBL-producing isolates, aminoglycoside or fosfomycin combinations when active, and investigational phage therapy. The case illustrates that resistance is modular and additive: each mechanism arrives independently, often on plasmids, and accumulates over time. This is why antibiotic stewardship, infection control, diagnostics, and new drug development must operate together.

Concept Check 6b: A *K. pneumoniae* isolate is resistant to the tested β -lactams including carbapenems (KPC-2 carbapenemase), tigecycline (RamA-dependent AcrAB overexpression), and ciprofloxacin (GyrA + ParC mutations). The lab reports it as susceptible to colistin and ceftazidime-avibactam. Explain (a) why ceftazidime-avibactam works against KPC-2 specifically while ceftazidime alone would not, (b) why the same combination would fail against an NDM-producer, and (c) how ESBL-restricted versus carbapenemase-positive resistance is distinguished by the meropenem-EDTA versus meropenem-boronic-acid double-disk synergy test.

27.2.7 Study Blueprint

- Big idea: Antimicrobial resistance and epidemic dynamics emerge from pathogen evolution and transmission networks.
- Core concepts: antibiotic resistance, R0, transmission, surveillance.
- Framework alignment: Vision & Change: Evolution, Systems, Structure and function; AP Biology: Evolution, Systems Interactions; NGSS-style topics: Structure and Function, Interdependent Relationships in Ecosystems.
- Model or quantitative lens: R0, resistance-mechanism, and outbreak-trajectory calculations.
- Data skill: Interpret resistance assays and outbreak curves.
- Practice cadence: Questions and Methods, Representing and Describing Data, Argumentation.
- Common misconception to repair: R0 is not a fixed property of a pathogen alone; it depends on host behavior and environment.
- Primary lab: Lab — Antimicrobial Resistance and Epidemiology.
- Question bank: Questions — Antimicrobial Resistance and Epidemiology.
- Transfer task: Transfer resistance and epidemiology reasoning to stewardship and public-health policy.
- Bridge to computation: `biology.microbiology.microbiology.sir_model`.

Opening Vignette — Antimicrobial Resistance and Epidemiology

This chapter connects antimicrobial resistance and epidemiology to measurable evidence: models, datasets, and experiments that can strengthen or weaken each claim.

27.3 Epidemiology of antimicrobial resistance and epidemiology

27.3.1 Key Epidemiological Metrics

Table 352. Key Epidemiological Metrics: Metric and Definition.

Metric	Definition	Significance
R_0 (basic reproduction number)	Mean secondary cases per primary case in fully susceptible population	Determines epidemic potential; $R_0 > 1$ = epidemic growth
R_e (effective reproduction number)	$R_0 \times (1 - \text{fraction immune})$; real-time transmission	Guides intervention: goal is $R_e < 1$
CFR (case fatality rate)	Deaths / confirmed cases	Overestimates true mortality (denominator misses mild cases)
IFR (infection fatality rate)	Deaths / most infections (including asymptomatic)	More accurate; requires seroprevalence data
Incubation period	Time from infection to symptom onset	Determines quarantine duration
Serial interval	Time between symptom onset in successive cases	Determines epidemic speed

27.3.2 Worked Example: Estimating R0 from an Epidemic Curve

Problem: Early in an outbreak, confirmed cases double every $T_d = 3.0$ days. The mean serial interval (time between symptom onset in successive cases) is $T_s = 5.0$ days. Estimate the basic reproduction number R_0 , then the herd-immunity threshold.

Solution:

1. Exponential growth rate r from the doubling time. Early case counts grow as $N(t) = N_0 2^{t/T_d} = N_0 e^{rt}$, so equating exponents gives $r = \ln 2/T_d$:

$$r = \frac{\ln 2}{T_d} = \frac{0.6931}{3.0} = 0.2310 \text{ day}^{-1}$$

2. Convert growth rate to R_0 . For a fixed (delta-distributed) serial interval, the renewal equation gives $R_0 = e^{rT_s}$:

$$R_0 = e^{rT_s} = e^{0.2310 \times 5.0} = e^{1.155} = 3.17$$

(The simpler linear approximation $R_0 \approx 1 + rT_s = 1 + 0.2310 \times 5.0 = 2.16$ is a lower bound that ignores serial-interval dispersion.)

3. Herd-immunity threshold. Substituting $R_0 = 3.17$ into the herd-immunity relation $p_c = 1 - 1/R_0$ from equation (354):

$$p_c = 1 - \frac{1}{3.17} = 0.685 \rightarrow 68.5 \%$$

Interpretation: A 3-day doubling time with a 5-day serial interval implies $R_0 \approx 3.2$, so roughly 69 % of the population must be immune to halt sustained transmission — a value consistent with an early pandemic-respiratory pathogen, and one that grows sharply if the doubling time shortens.

27.3.3 Worked Example: Herd Immunity Threshold and Required Vaccination Coverage

Problem: Compare two pathogens with very different transmissibility: measles ($R_0 \approx 15$) and the original SARS-CoV-2 (Wuhan) strain ($R_0 \approx 4$). For each, compute (a) the herd-immunity threshold $p_c = 1 - 1/R_0$, and (b) the required vaccination coverage V to reach that threshold, given imperfect vaccine efficacy ε (MMR for measles: $\varepsilon = 0.97$; original mRNA vaccine for ancestral SARS-CoV-2: $\varepsilon = 0.95$ against symptomatic disease).

Solution:

1. Herd-immunity threshold for measles ($R_0 = 15$):

$$p_c^{\text{measles}} = 1 - \frac{1}{R_0} = 1 - \frac{1}{15} = 0.933 \rightarrow 93.3 \%$$

2. Required vaccination coverage for measles, accounting for vaccine efficacy:

$$V_{\text{measles}} = \frac{p_c}{\varepsilon} = \frac{0.933}{0.97} \approx 0.962 = 96.2 \%$$

To halt sustained measles transmission, at least 96.2 % of the population must be vaccinated with a two-dose MMR schedule. This is the most demanding vaccination target for any current vaccine program.

3. Herd-immunity threshold for ancestral SARS-CoV-2 ($R_0 = 4$):

$$p_c^{\text{COVID}} = 1 - \frac{1}{4} = 0.75 \rightarrow 75 \%$$

4. Required vaccination coverage for ancestral SARS-CoV-2, accounting for vaccine efficacy:

$$V_{\text{COVID}} = \frac{0.75}{0.95} \approx 0.789 = 78.9 \%$$

5. Implication for variant evolution. As more transmissible variants emerged, R_0 rose: Alpha about 5, Delta about 6, Omicron BA.1 about 8–10. Substituting into the same formulae:

- Delta ($R_0 = 6$): $p_c = 0.833$; required coverage at $\epsilon = 0.85$ (waned immunity vs. Delta) = $0.833/0.85 \approx 98\%$.
- Omicron BA.1 ($R_0 = 9$): $p_c = 0.889$; required coverage at $\epsilon = 0.50$ (waned, immune-escape) = $0.889/0.50 = 1.78$ — i.e., vaccination alone cannot achieve herd immunity because the required coverage exceeds 100 %.

Interpretation. The herd-immunity calculation is mechanically simple but operationally demanding. Two structural points emerge: (i) Vaccine efficacy is a multiplier, not an additive cost — even a modest efficacy reduction (95 % \rightarrow 85 %) substantially elevates the required coverage. (ii) When $\epsilon \times p_c > 1$ is unreachable, vaccination alone cannot reach the herd-immunity threshold and complementary interventions (boosters, ventilation, masking, therapeutics) become essential. The original elimination calculus for measles depended on the combination of $R_0 \approx 15$ with an exceptional $\epsilon = 0.97$ — and even there, a 1–3 % refusal rate is sufficient to lose herd immunity and trigger localized outbreaks, as observed repeatedly in the 2018–2024 measles resurgences worldwide.

27.3.4 Major antimicrobial resistance and epidemiologys

Tuberculosis (*Mycobacterium tuberculosis*):

- Global burden: an estimated 10.7 million people fell ill with TB in 2024 and 1.23 million died, including 150,000 people with HIV [World Health Organization, 2025d]. TB remains the leading cause of death from a single infectious agent and a major contributor to AMR-associated mortality.
- Transmission: Airborne droplet nuclei (1-5 μm); can remain suspended for hours
- Pathogenesis: Inhaled bacilli are phagocytosed by alveolar macrophages but arrest phagosome maturation (LAM inhibits PI3K \rightarrow blocks Ca^{2+} /calmodulin \rightarrow prevents phagolysosomal fusion); survive within macrophages at pH 6.4 instead of lethal pH 4.5
- Granuloma: Hallmark of TB pathology – organized aggregate of infected macrophages, epithelioid cells, multinucleated giant cells, and T cells; hypoxic caseous necrotic center; both contains and protects the bacilli
- Latent TB: 90-95% of infected individuals contain the infection as LTBI (latent TB infection); 5-10% lifetime risk of reactivation, increased by HIV, immunosuppression, malnutrition
- Treatment: standard drug-susceptible pulmonary TB is treated with a multi-drug rifamycin-based regimen, classically 6 months of isoniazid + rifampicin + pyrazinamide + ethambutol followed by continuation therapy; adherence support matters because metabolically slow bacilli and granuloma drug penetration make undertreatment risky.
- MDR/RR-TB (multidrug-resistant or rifampicin-resistant TB), pre-XDR-TB (MDR/RR-TB with fluoroquinolone resistance), and XDR-TB (MDR/RR-TB plus resistance to a fluoroquinolone and at least one additional Group A drug such as bedaquiline or linezolid) remain major AMR threats. WHO’s 2025 treatment guidance keeps short, fully oral regimens central for eligible MDR/RR-TB patients, retains BPaLM/BPaL use where appropriate, and adds a 6-month bedaquiline-delamanid-linezolid-levofloxacin-clofazimine (BDLLfxC) option for selected patients; longer individualized regimens may be needed when resistance, toxicity, pregnancy/age limits, extrapulmonary disease, or poor early response make shorter regimens unsuitable [World Health Organization, 2025e].
- Global burden: an estimated 282 million cases and 610,000 deaths in 2024 across 80 countries [World Health Organization, 2025b]. The WHO African Region still accounts for the overwhelming majority of cases and deaths, with young children carrying the greatest mortality burden.
- Species: *P. falciparum* (most lethal; 99% of deaths), *P. vivax* (most widespread; hypnozoites cause relapse), *P. malariae*, *P. ovale*, *P. knowlesi* (zoonotic, from macaques)
- Transmission: Female *Anopheles* mosquito vector; sporozoites injected during blood meal
- Life cycle: Sporozoites \rightarrow liver (hepatocyte invasion, asymptomatic) \rightarrow merozoites \rightarrow erythrocyte invasion (clinical disease: cyclic fever every 48-72 hours synchronized with schizogony) \rightarrow some become gametocytes (taken up by mosquito)
- Immune evasion: *P. falciparum* erythrocyte membrane protein 1 (PfEMP1) expressed on infected RBC surface mediates cytoadherence (sticking to endothelium, avoiding splenic clearance) and rosetting; about 60 *var* genes enable antigenic variation

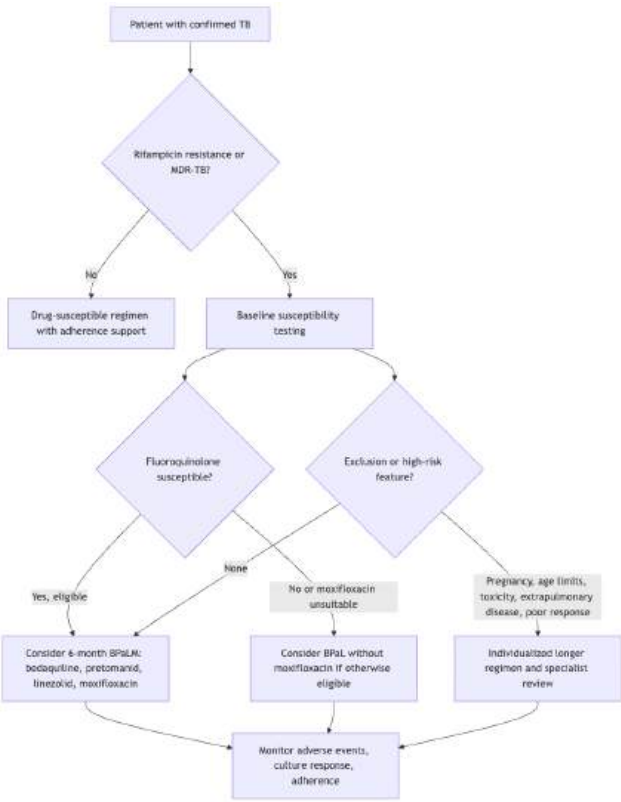


Figure 164. TB regimen decision schematic. WHO’s shorter BPaLM/BPaL and BDLLfxC options are eligibility-dependent tools for MDR/RR-TB, not a comprehensive replacement for susceptibility testing, toxicity monitoring, or individualized care [WHO2025tbtreatmentmodule4].

- Vaccine: RTS,S/AS01E (Mosquirix): first approved malaria vaccine (2021); targets circumsporozoite protein; protection is partial and wanes without booster dosing. R21/Matrix-M is now the second WHO-recommended malaria vaccine; both are best understood as additions to bed nets, chemoprevention, diagnosis, and vector control rather than replacements [World Health Organization, 2025b].
- Treatment: Artemisinin-based combination therapy (ACT); artemisinin resistance emerging in Southeast Asia (K13 propeller mutations)
- Vector control frontier: WHO issued a 2025 conditional recommendation for indoor spatial emanators (also called spatial repellents) as an additional tool in areas with ongoing transmission, used alongside insecticide-treated nets rather than replacing them. These devices release active ingredients such as transfluthrin into indoor air to repel, disorient, or kill mosquitoes, with evidence strongest for added indoor protection and remaining gaps for standalone use, outdoor protection, humanitarian settings, and resistance management [World Health Organization, 2025c].

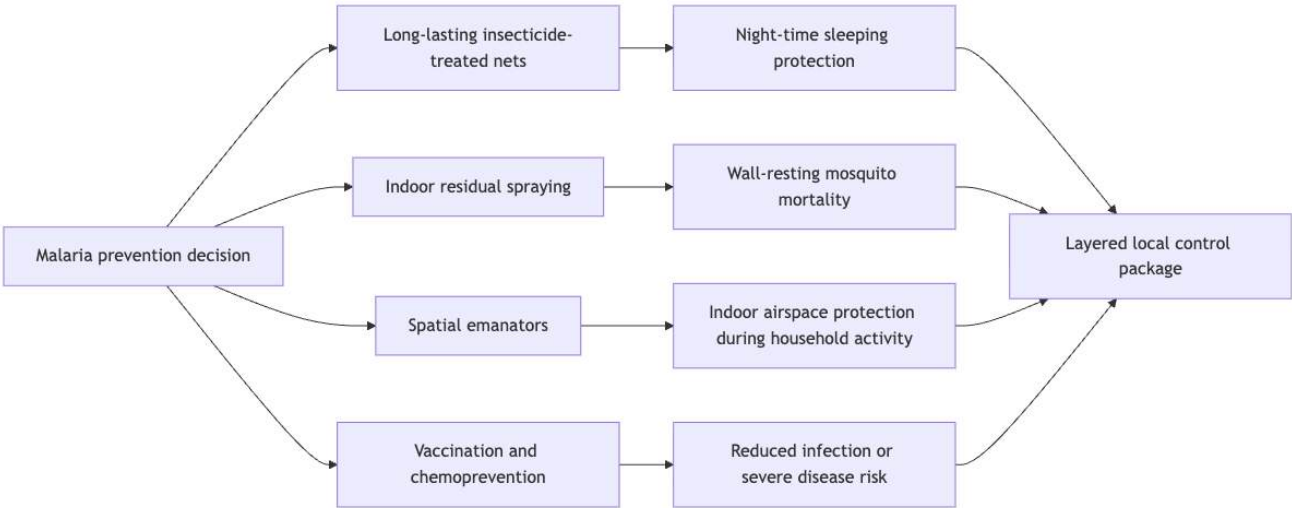


Figure 165. Malaria vector-control comparison. Spatial emanators add an indoor airspace tool to nets and spraying, but local programs still need entomological surveillance, insecticide-resistance monitoring, and equity-aware deployment.

HIV/AIDS:

- Global burden: an estimated 40.8 million people were living with HIV at the end of 2024, with about 1.3 million new infections in 2024 and AIDS-related deaths far below their early-2000s peak but still above global targets [UNAIDS, 2025].
- Pathogenesis: Progressive depletion of CD4⁺ T cells; AIDS defined as CD4 count <200 cells/ μ L or AIDS-defining illness
- ART (antiretroviral therapy): Combination of 3+ drugs from different classes; suppresses viral load to undetectable (<50 copies/mL); near-normal life expectancy if initiated early; does not cure (latent proviral reservoir in resting CD4⁺ memory T cells persists for decades)
- PrEP (pre-exposure prophylaxis): Oral TDF/FTC or TAF/FTC remains highly effective when taken as prescribed; long-acting injectable cabotegravir and twice-yearly lenacapavir add adherence-sparing options. FDA approved lenacapavir PrEP in 2025, and CDC guidance reports trial efficacy of 100% in a cisgender-female trial and 96% in a primarily male trial over 52 weeks [Centers for Disease Control and Prevention, 2025b].
- U=U (Undetectable = Untransmittable): Individuals with sustained undetectable viral load on ART cannot sexually transmit HIV (PARTNER study, HPTN 052)

Influenza:

- RNA virus (Orthomyxoviridae); 8 segmented (-)ssRNA genome segments
- Surface glycoproteins: hemagglutinin (HA, 18 subtypes) and neuraminidase (NA, 11 subtypes); nomenclature: H1N1, H3N2, etc.
- See “Antigenic Variation” section above for full discussion of drift and shift.

Concept Check (Analysis — Influenza Antigenic Drift vs. Shift): Influenza A hemagglutinin (HA) has 18 subtypes (H1–H18) and neuraminidase (NA) has 11 subtypes (N1–N11), giving 198 possible HA/NA combinations (though merely a fraction are observed in nature). Two distinct mechanisms generate antigenic novelty: antigenic drift (point mutations in the HA head domain accumulating gradually under positive selection from population immunity) and antigenic shift (genome reassortment between two influenza strains co-infecting a single host, producing a hybrid virus with a novel HA/NA combination). (a) Analyze why drift causes seasonal re-infection (epidemic-scale, requiring annual vaccine reformulation) while shift causes pandemics (population-naïve, no pre-existing immunity). Use the immune-escape logic to predict the expected R_e trajectory of each. (b) The 1918 H1N1 pandemic strain shared HA antigenic identity with the 1957 H2N2 pandemic strain at less than 50 % at antibody-neutralizing sites — a shift event. The seasonal H3N2 strains evolving since 1968, however, share 80–90 % HA identity year-to-year, requiring annual vaccine updates — drift. Compare the rates of accumulation of HA epitope substitutions in drift (about 0.5–1 % per year at antigenic sites) vs. shift (instantaneous swap to a completely novel HA). (c) Predict which HA residues are most selectively constrained (i.e., highly conserved across subtypes) and which are under strongest positive selection. The receptor-binding pocket residues are constrained because mutation destroys sialic-acid binding; the surface-exposed antigenic loops (Sa, Sb, Ca, Cb sites) are under strongest positive selection because they evade neutralizing antibodies. (d) Design a phylogenetic test that distinguishes drift-driven from shift-driven changes in a sampled HA sequence, using the topological signature (clock-like accumulation vs. abrupt change in neighbor identity).

27.3.5 One Health and Emerging Pathogens

The One Health framework recognizes the interconnection of human, animal, and environmental health:

- Over 70% of emerging infectious diseases are zoonotic (originating from animal reservoirs).
- Drivers of emergence: deforestation and habitat destruction (increasing human-wildlife contact), wildlife trade (live animal markets), climate change (expanding vector ranges), intensive animal agriculture (influenza reassortment, AMR selection).
- Examples: SARS-CoV-2 (probable bat origin via intermediate host), Ebola (bat reservoir), avian influenza H5N1 (poultry), Nipah (bat-to-pig-to-human), Lyme disease (deer-tick-mouse cycle expanding with climate change), mpox (rodent reservoirs in West/Central Africa).
- AMR as a One Health issue: antibiotic exposure in people, food animals, aquaculture, and shared environments selects for resistance genes that can move through water, soil, food chains, plasmids, and mobile genetic elements. Stewardship therefore has to cover prescribing, veterinary practice, sanitation, surveillance, and access to effective treatment [Centers for Disease Control and Prevention, 2025a, World Health Organization, 2024a].
- Fungal disease also belongs in the AMR frame: the WHO fungal priority pathogens list highlights *Candida auris*, *Aspergillus fumigatus*, *Cryptococcus neoformans*, and other fungi where limited diagnostics, few drug classes, immunocompromised hosts, and agricultural azole exposure make resistance a One Health problem rather than a hospital-confined issue [World Health Organization, 2022]. CDC guidance treats *Candida auris* as a healthcare-transmissible yeast that is often multidrug-resistant, can colonise patients without symptoms, persists on surfaces, requires sequencing or mass spectrometry for reliable identification, and should be treated primarily when causing clinical infection; echinocandins remain typical initial adult therapy, but echinocandin-resistant and pan-resistant reports are increasing [Centers for Disease Control and Prevention, 2026a, 2024a]. Mechanistically, the warning is that AMR phenotypes are assembled from enzymes, target changes, efflux, permeability shifts, biofilms, tolerance states, and mobile genetic elements; the same resistance label can hide different treatment constraints.

Spillover risk factors. Modern surveillance and modeling have identified several quantifiable predictors of zoonotic spillover risk:

1. Phylogenetic distance — viruses from primates spill more easily than viruses from rodents than from invertebrates.
2. Receptor compatibility — ACE2 in bats, civets, and humans is similar enough to permit SARS-CoV-2 cross-species transmission; H5N1 sialic-acid receptor preference shifts (α -2,3 \rightarrow α -2,6) signal mammalian adaptation.
3. Population density at the human-animal interface — wet markets, intensive agriculture, deforestation edges.
4. Reservoir host species richness — Bat species richness correlates with the number of zoonotic viruses; rodents are similarly important but underrecognised.
5. Anthropogenic disruption — deforestation, climate change, urbanisation increase contact rates.

The PREDICT and Global Virome Project approaches systematically sample wildlife to catalog viral diversity and identify high-risk lineages before spillover. By 2026, sequencing > 200,000 viral genomes from > 30,000 animals across > 30 countries has identified about 10,000 candidate zoonotic viruses, of which about 1700 share key receptor-binding features with known human pathogens — a sobering reservoir.

Clinical Connection: Antibiotic Stewardship and Real-Time Resistance Surveillance The WHO has declared antimicrobial resistance one of the top 10 global public health threats. An estimated 1.27 million deaths were directly attributable to bacterial AMR in 2019 [Murray et al., 2022]. The O’Neill review’s 10-million-deaths-per-year scenario is a policy warning about uncontrolled resistance, not an inevitable destiny [O’Neill, 2016]. Genomic surveillance networks such as the CDC AR Lab Network and WHO GLASS [World Health Organization, 2025a] now track carbapenemases, *mcr* genes, and emerging plasmids across hospitals and regions. The lesson from SARS-CoV-2 — pathogen genomes can be sequenced and interpreted at population scale — is being adapted to bacterial AMR, where slower growth and horizontal gene transfer make the analysis more complicated.

Concept Check 7: Trace a potential pandemic pathway from deforestation in Southeast Asia. Identify (a) the ecological factors that elevate spillover risk, (b) the molecular features (receptor compatibility, reassortment potential) that determine human transmissibility, (c) the early-warning indicators that PREDICT-style surveillance would detect, and (d) the One Health interventions that could reduce future risk.

Concept Check (Evaluate — One Health Quantification of Nipah Spillover Risk): Nipah virus (NiV, family *Paramyxoviridae*, genus *Henipavirus*) circulates enzootically in *Pteropus* fruit bats across South and Southeast Asia. The canonical spillover pathway runs bats \rightarrow pigs \rightarrow humans (1998–1999 Malaysian outbreak, about 100 deaths) or bats \rightarrow date palm sap \rightarrow humans (recurring Bangladesh outbreaks, 70–90 % case-fatality ratio). Spillover probability per unit time can be decomposed as:

$$P_{\text{spillover}} = f(\text{contact rate, viral shedding load in reservoir, human/intermediate-host susceptibility}).$$

- (a) Evaluate how deforestation alters each factor. When tropical forest is converted to oil-palm plantation or pig farms, *Pteropus* bats lose foraging habitat and are forced to roost closer to human settlements and livestock, increasing the bat–pig and bat–human contact rate by 10–100 \times . Concurrently, nutritional stress in bats elevates NiV viral shedding (immune compromise \rightarrow higher faecal/saliva viral load). And immunologically-naïve human and pig populations at the deforestation edge have high susceptibility. The product of three multiplicative increases produces a sharply non-linear rise in spillover probability — the hallmark of an emerging-disease hot zone.
- (b) Quantify the contact-rate change. In the 1998 Malaysian outbreak, GIS analysis showed that pig farms within 8 km of deforested fruit-bat habitat experienced spillover, while those > 30 km away did not. The bat–pig spatial-overlap index correlates strongly ($r \approx 0.8$) with outbreak occurrence — a directly measurable, intervenable variable.
- (c) Propose three surveillance interventions with cost-effectiveness estimates (in approximate USD per averted Disability-Adjusted Life Year, DALY):
 1. Bat-reservoir serosurveillance (annual sampling of 500 bats per region, NiV IgG ELISA): about \$50,000/yr per region; cost-effective in regions with > 10 % bat seroprevalence (about \$200–500 / DALY).
 2. Date-palm sap protection (covering sap-collection pots with bamboo skirts to exclude bats): about \$2 per pot, scalable to 100,000 pots per year; demonstrated to reduce contamination by > 80 %; estimated about \$50–150 / DALY.
 3. Pig-farm zoning (mandating no new farms within 5 km of fruit-bat colonies): regulatory cost is low but politically costly; cost-effectiveness depends on the regulatory baseline.
- (d) Evaluate the limits of intervention. Even a perfectly executed One Health surveillance program cannot eliminate spillover risk — it can merely reduce the probability per unit time. The fundamental risk reduction requires landscape-scale habitat preservation (preventing the bat–human interface from forming in the first place), which is a slow, politically difficult, and incompletely controllable intervention. Synthesize the spillover-control hierarchy: prevention (habitat) > deterrence (surveillance + barriers) > rapid response (outbreak containment). Each tier accepts a higher residual risk in exchange for tractability.

27.4 Computational Bridge

Early outbreak growth is often sketched with discrete exponential models:

```
from biology.ecology import exponential_growth

series = exponential_growth(N0=20.0, r=0.3, t_end=12.0, steps=12)
print(round(series.populations[-1], 2))
```

Clinical / systems note: R_e reductions from vaccines behave like lowering effective r in these caricatures; heterogeneity in contact networks breaks the homogeneous assumption.

27.4.1 mRNA Vaccine Platforms: From Lab Curiosity to Global Deployment

Messenger RNA vaccines — once a neglected technology because of mRNA’s instability and strong innate-immune activation — became the **dominant** pandemic response platform between 2020 and 2023. BNT162b2 (Pfizer–BioNTech) and mRNA-1273 (Moderna) demonstrated $\geq 94\%$ efficacy against symptomatic COVID-19 in phase III trials ($> 40\,000$ participants each) within 11 months from pathogen identification — an unprecedented pace driven entirely by the modularity of the platform: once a lipid-nanoparticle delivery system and a nucleoside-modified mRNA scaffold are validated, swapping the antigen-coding sequence is a matter of days.

Three molecular innovations make mRNA vaccines work. (1) Nucleoside modification — substituting uridines with pseudouridine (Ψ) or 1-methylpseudouridine (m1 Ψ) (Karikó & Weissman, Nobel Prize 2023) reduces TLR7/8 activation and blocks 2’-5’-oligoadenylate synthetase / RNase L degradation, so **translation** is 10–100 \times more efficient and innate-immune activation is manageable. (2) Lipid nanoparticle (LNP) delivery — a four-component formulation (ionisable lipid ALC-0315 or SM-102, phospholipid DSPC, cholesterol, PEG-lipid) self-assembles into about 80 nm particles that endocytose into dendritic cells; at endosomal pH about 5 the ionisable lipid becomes cationic, fusing with the endosome and releasing mRNA into the cytoplasm. (3) Antigen design — the SARS-CoV-2 spike is locked in the prefusion conformation by two proline substitutions (2P mutation) that preserve neutralizing epitopes. Manufacturing uses *in vitro* transcription from linear DNA templates (T7 polymerase), capping with CleanCap analog, and microfluidic LNP assembly — a single about 20 000 L bioreactor run can produce > 1 billion doses. Remaining challenges: cold-chain dependence (though ARCT-154 self-amplifying mRNA vaccines stable at 2–8 $^{\circ}\text{C}$ are in trials), rare myocarditis risk in young males (about 1–10 per 100 000 doses, typically mild and self-limiting), and waning antibody titres (6-month boosting needed). The platform is now extending to influenza (mRNA-1010), RSV (mRNA-1345, approved 2024), and personalised cancer neoantigen vaccines (mRNA-4157, phase III for melanoma).

27.4.2 cGAS–STING: Innate Cytosolic DNA Sensing and Anti-Tumor Immunity

Cyclic GMP–AMP synthase (cGAS) is a cytosolic DNA sensor identified in 2013 (Chen lab) that binds double-stranded DNA non-sequence-specifically and, upon DNA engagement, synthesizes the second messenger 2’3’-cyclic GMP–AMP (2’3’-cGAMP) from ATP and GTP. 2’3’-cGAMP binds the ER-resident adaptor STING (Stimulator of Interferon Genes), driving TBK1 phosphorylation of IRF3 and thus Type I interferon (IFN- α/β) transcription. Evolutionarily, the pathway detects pathogen-derived or mis-localized self-DNA — cytosolic DNA is otherwise absent in healthy cells.

Three rapid-fire translational applications: (1) Cancer immunotherapy — dying tumor cells release DNA that, once dendritic cells endocytose it, activates cGAS–STING, priming CD8⁺ T-cell responses. STING agonists (ADU-S100, MK-1454, diABZI) are in > 30 oncology clinical trials; radiation therapy is an accidental STING activator (sub-lethal DNA damage \rightarrow micronuclei \rightarrow cytosolic DNA). (2) Autoimmunity — gain-of-function STING mutations cause SAVI (STING-associated vasculopathy), a pediatric interferonopathy with pulmonary fibrosis and skin ulcerations; chronic cGAS–STING activation also contributes to age-related inflammation as mitochondrial and cytosolic DNA accumulate. (3) Anti-viral defense — SARS-CoV-2 ORF9b, HSV-1 ICP27, and HIV-1 capsid most suppress cGAS–STING, demonstrating its evolutionary importance as a front-line sensor. The pathway is now a canonical example of how fundamental discovery (2013) can translate to phase III oncology trials in under a decade.

27.5 Current Evidence and Frontier Biology: Antimicrobial Resistance and Epidemiology

For Antimicrobial Resistance and Epidemiology, frontier biology belongs inside the evidence logic of the chapter. Microbiology and infectious disease now require One Health reasoning across people, animals, environments, genomics, and antimicrobial stewardship. The core reading question is this: infectious-disease reasoning should connect pathogen biology, transmission, immunity, diagnostics, interventions, and equity.

- What to verify: identify the observation, model, assay, or dataset that would make the claim stronger or weaker.
- What to qualify: state the scale, organism, cell type, environmental condition, or population where the claim is expected to hold.

- What to compare: test at least one alternative explanation, baseline, or null model before treating the pattern as causal.
- What to cite: distinguish primary evidence, review synthesis, public dataset, and institutional guidance; for recent or numeric claims, prefer the source closest to the measurement and state what has changed since it was published.

For resistance or outbreak claims, name the organism, determinant, selection pressure, transmission route, and surveillance evidence [World Health Organization, 2024a, Centers for Disease Control and Prevention, 2025a, Murray et al., 2022].

Source practice: For pathogen, resistance, and intervention claims, tie statements to organism-resistance pairs, surveillance evidence, official guidance, and trial/regulatory status [World Health Organization, 2024a, 2025d,b, Centers for Disease Control and Prevention, 2025b, 2026a].

27.5.1 Current Evidence Map: Intervention Choice Across Pathogens

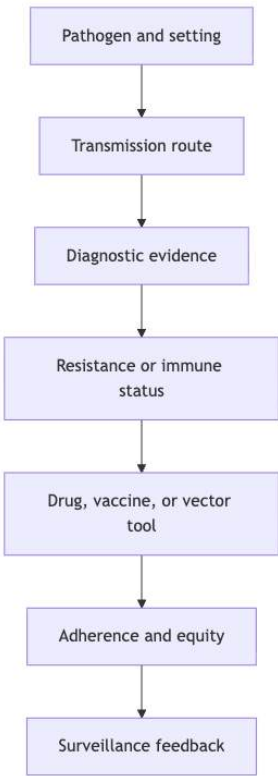


Figure 166. TB regimens, malaria spatial emanators, lenacapavir PrEP, Candida auris control, and Long COVID mechanisms are cases where intervention choices depend on evidence and setting. \citep{who2025tb,who2025spatialemanators,cdc2025lenacapavirprep,cdc2026candidaauris,longcovid2026mechanisms}.

27.6 Summary

- Koch’s postulates remain foundational for establishing disease causation but have important limitations (asymptomatic carriers, unculturable organisms, polymicrobial disease). Molecular Koch’s postulates extend the framework to virulence genes.
- Virulence factors include adhesins (pili, FimH), invasion machinery (T3SS), toxins (A-B exotoxins: cholera, diphtheria, tetanus, botulinum; endotoxin/LPS), capsules, and immune evasion strategies (protein A, antigenic variation, phagosome arrest).
- **Innate immunity** provides immediate, non-specific defense: barriers (skin, mucus, acid, lysozyme, defensins), PRRs (TLRs, NLRs, RIG-I, cGAS-STING) → NF-κB + IRF3 → cytokines + type I IFN; complement with three pathways (classical via C1q, lectin via MBL/MASPs, alternative via spontaneous C3 tickover) converging at C3 convertase, then C5 cleavage and MAC formation; cellular effectors (neutrophils with MPO/HOCl oxidative burst and NETosis, macrophages M1/M2, NK cells with missing-self via inhibitory KIRs and induced-self via NKG2D).
- Adaptive immunity: V(D)J recombination generates diverse TCRs and BCRs; MHC-I presents endogenous peptides to CD8⁺ CTLs; MHC-II presents exogenous peptides to CD4⁺ T helpers (Th1, Th2, Th17, Treg, Tfh); B cells undergo germinal center reactions (SHM, affinity maturation, CSR) producing high-affinity class-switched antibodies and long-lived memory.
- Vaccines exploit immunological memory: eight platforms (live attenuated, inactivated, subunit, VLP, toxoid, conjugate, mRNA, viral vector) span the spectrum from MMR (single-dose lifetime immunity) to mRNA (rapid platform with 48-hour design cycle). Herd-immunity threshold $p_c = 1 - 1/R_0$ (equation (354)) — measles requires > 93 %, polio about 80 %, original COVID-19 about 60 %, but Omicron-era $R_0 \sim 10$ combined with imperfect vaccine efficacy can exceed achievable coverage.

- Antigenic variation in influenza occurs via gradual drift (HA point mutations → seasonal epidemics) and abrupt shift (segment reassortment in animal reservoirs → pandemics: 1918, 1957, 1968, 2009). HIV reverse transcriptase (3×10^{-5} errors/bp/cycle) generates a quasi-species cloud that defeats monotherapy and complicates vaccine development.
- Antibiotic resistance falls into five categories: enzymatic inactivation (β -lactamases — Class A/B/C/D Ambler; AMEs; CAT; ESBLs and carbapenemases KPC/NDM/OXA-48); target modification (PBP2a in MRSA; D-Ala-D-Lac in VRE; 23S methylation in MLS; gyrase QRDR mutations); efflux (RND tripartite pumps AcrAB-TolC, MexAB-OprM, AdeABC); reduced permeability (porin loss); and bypass / target overproduction (Dfr, Sul). Pan-resistant ESKAPE isolates combine multiple mechanisms simultaneously.
- Major infectious diseases: TB (granuloma, phagosome arrest, MDR/XDR crisis), malaria (erythrocyte invasion, PfEMP1 antigenic variation, artemisinin resistance), HIV (CD4 depletion, latent reservoir, ART, PrEP, U=U), influenza (antigenic drift/shift, pandemic potential).
- One Health and emerging pathogens: > 70 % of emerging infections are zoonotic; deforestation, climate change, wildlife trade, and agricultural antibiotic use drive emergence and AMR. PREDICT-style surveillance now catalogs > 10 000 candidate zoonotic viruses for early-warning monitoring.
- Connections: See section 24 for pathogen biology, section 25 for microbiome colonization resistance, and section 36 for demographic models.

27.7 Review Questions

1. Apply Koch’s postulates to *Helicobacter pylori* and peptic ulcer disease. Barry Marshall famously fulfilled these postulates by self-experimentation in 1984. Identify which postulate was most difficult to satisfy and explain why the medical establishment was initially skeptical.
2. Compare the mechanisms of action of cholera toxin and diphtheria toxin. Both use A-B structure and ADP-ribosylation, but they target different host proteins. Explain how the same enzymatic mechanism (ADP-ribosylation) produces completely different clinical outcomes.
3. A patient with terminal complement component deficiency (C5-C9) presents with recurrent *Neisseria meningitidis* infections. Explain why this specific pathogen is problematic in MAC deficiency while most other bacterial infections are handled normally. What does this tell you about the relative importance of opsonization versus MAC lysis for different pathogens?
4. Describe the molecular events of T cell activation, including the three signals. Explain why Signal 2 (co-stimulation) is critical for preventing autoimmunity, and predict what would happen if a pharmaceutical agent blocked B7-CD28 interaction globally.
5. A mother’s IgG antibodies cross the placenta and protect the newborn for the first 3-6 months of life. Explain why this passive immunity wanes and why active vaccination is necessary starting at 2 months. Which antibody class is most important in breast milk, and how does it protect the infant’s mucosal surfaces?
6. Herd immunity calculation. Calculate from equation (354) the herd immunity threshold for a novel respiratory pathogen with $R_0 = 8$. If a vaccine with 90% efficacy is available, what percentage of the population must be vaccinated to achieve herd immunity? Show your work using the formula $p_v = p_c/E$.
7. Explain why tuberculosis treatment requires 6-9 months of multi-drug therapy while most bacterial infections are treated with 7-14 days of a single antibiotic. Include the concepts of metabolically dormant persisters, granuloma pharmacokinetics, and the rationale for combination therapy.
8. Drift vs shift. Compare antigenic drift and antigenic shift in influenza. Explain why antigenic shift can produce pandemics while antigenic drift produces seasonal epidemics. Why is influenza A (but not influenza B) capable of antigenic shift, and what role do animal reservoirs play? How does the HIV quasi-species cloud differ mechanistically from influenza, and why does each strategy defeat conventional vaccine design?
9. The mRNA COVID-19 vaccines (BNT162b2, mRNA-1273) demonstrated about 95% efficacy in clinical trials but this declined over time and with new variants. Explain: (a) the immunological mechanism of mRNA vaccines, (b) why booster doses are needed (waning immunity vs. antigenic evolution), and (c) how the N1-methylpseudouridine modification improves mRNA vaccine performance.
10. Using the One Health framework, explain how deforestation in Southeast Asia could lead to a novel pandemic. Trace the pathway from habitat destruction to zoonotic spillover, identifying the ecological, virological, and epidemiological factors at each step.
11. Derive the herd immunity threshold $p_c = 1 - 1/R_0$ from the next-generation intuition and relate to Question 6.
12. Explain antigenic sin and how it might bias booster responses after sequential variant exposure.
13. Resistance mechanism integration. A clinical microbiology lab reports a *Klebsiella pneumoniae* isolate with MICs: meropenem ≥ 16 (R), ceftazidime-avibactam 1 (S), cefepime 8 (R), ciprofloxacin ≥ 4 (R), gentamicin ≥ 16 (R), tigecycline 0.5 (S), colistin 0.5 (S). Sequencing reveals: KPC-2 carbapenemase, AAC(6’)-Ib-cr, GyrA Ser83Leu, ParC Ser80Ile, RamA overexpression. (a) Which mechanism is responsible for each resistance phenotype? (b) Why does ceftazidime-avibactam still work? (c) Predict whether this strain would respond to imipenem-relebactam and meropenem-vaborbactam, and justify.

14. Vaccine platform comparison. A new pathogen emerges with seasonal transmission and mild illness in adults, severe in infants, no available therapy. Compare the trade-offs for a (a) live-attenuated, (b) inactivated, (c) subunit-VLP, (d) mRNA, and (e) viral-vector vaccine platform decision, given a 9-month timeline to first dose.
15. Innate immunity integration. A patient with AIDS ($CD4 < 50$) develops disseminated *Mycobacterium avium complex* infection. Explain why both adaptive and innate arms of immunity have failed despite intact NK cells, neutrophils, complement, and antibodies. What is the role of granuloma formation, and why is $IFN-\gamma$ critical?

27.8 Further Reading and Source Notes: Antimicrobial Resistance and Epidemiology

- Janeway, Travers, Walport & Shlomchik (latest ed.). *Janeway's Immunobiology*. Garland Science.
- Medzhitov & Janeway (2000). Innate immunity. *New England Journal of Medicine*, 343.
- Plotkin (2010). Correlates of protection induced by vaccination. *Clinical and Vaccine Immunology*, 17.
- Anderson & May (1991). *antimicrobial resistance and epidemiologys of Humans: Dynamics and Control*. Oxford University Press.
- Kermack & McKendrick (1927). A contribution to the mathematical theory of epidemics. *Proceedings of the Royal Society A*, 115.
- Davies, Spagnolo & Walsh (2010). Origins and evolution of antibiotic resistance. *Microbiology and Molecular Biology Reviews*, 74.
- WHO (latest). *Global Antimicrobial Resistance and Use Surveillance System (GLASS) Report*. World Health Organization.

27.9 Key Terms

Table 353. Current Evidence Map: Intervention Choice Across Pathogens: Term and Definition.

Term	Definition
Koch’s postulates	Four criteria for establishing that a specific microorganism causes a specific disease
Virulence factor	Microbial product or strategy that contributes to pathogenicity (adhesins, toxins, capsules, immune evasion)
Exotoxin	Secreted bacterial protein toxin; often A-B structure (cholera, diphtheria, tetanus, botulinum)
Endotoxin (LPS)	Gram-negative outer membrane component released upon lysis; activates TLR4; causes fever, septic shock
PAMP	Pathogen-Associated Molecular Pattern – conserved microbial structure detected by host PRRs
Toll-like receptor (TLR)	Membrane-bound PRR that recognizes PAMPs and initiates innate immune signaling
Inflammasome	Intracellular multiprotein complex (NLRP3-ASC-caspase-1) that processes IL-1 β and IL-18 and triggers pyroptosis
Complement	Plasma protein cascade with three pathways (classical via C1q-antibody, lectin via MBL-carbohydrate, alternative via spontaneous C3 hydrolysis) converging at the C3 convertase
C3 convertase	Central enzyme of complement (C4b2a or C3bBb) that cleaves C3 into C3a (anaphylatoxin) and C3b (opsonin)
MAC	Membrane attack complex (C5b-C9 _n); 10-nm pore that osmotically lyses Gram-negative bacteria
Factor H	Soluble alternative-pathway regulator that binds C3b on self surfaces; co-opted by <i>Neisseria</i> to evade complement
NETosis	Programmed neutrophil death pathway in which decondensed chromatin is extruded as antimicrobial extracellular traps; PAD4-dependent
Missing-self hypothesis	Ljunggren-Karre model: NK cells kill cells lacking inhibitory MHC-I signals
NKG2D	Activating NK-cell receptor recognizing stress-induced ligands (MICA/B, ULBPs); the “induced-self” sensor
MHC class I	Presents endogenous peptides to CD8 ⁺ CTLs; expressed on most nucleated cells
MHC class II	Presents exogenous peptides to CD4 ⁺ T helpers; expressed on professional APCs
Clonal selection	Antigen selects and expands primarily the specific lymphocyte clone with matching receptor
Affinity maturation	Progressive improvement of antibody affinity through somatic hypermutation and selection in germinal centers
Class switch recombination	AID-mediated change of antibody constant region (IgM -> IgG, IgA, or IgE) preserving antigen specificity
Herd immunity threshold	$p_c = 1 - 1/R_0$; fraction of population that must be immune to prevent sustained transmission

Term	Definition
R_0	Basic reproduction number; mean secondary infections per primary case in fully susceptible population
Antigenic drift	Gradual mutation of surface antigens (influenza HA/NA) producing seasonal variants
Antigenic shift	Reassortment of genome segments between different influenza strains producing novel pandemic subtypes
Quasi-species	The mutant cloud generated by an error-prone polymerase (HIV reverse transcriptase, RNA-virus RdRp) — the substrate of within-host evolution
VLP (virus-like particle)	Self-assembled viral capsid lacking genome; basis of HPV (Gardasil) and HBV vaccines
mRNA vaccine	LNP-encapsulated, nucleoside-modified mRNA that the host translates into antigen; e.g., BNT162b2, mRNA-1273
β -lactamase	Enzyme that hydrolyses β -lactam antibiotics; Ambler classes A/C/D (serine) and B (metallo); ESBLs, KPC, NDM, OXA
PBP2a	Alternative penicillin-binding protein in MRSA, encoded by <i>mecA</i> ; low β -lactam affinity
AcrAB-TolC, MexAB-OprM	Tripartite RND-family efflux pumps spanning the entire Gram-negative cell envelope; major multi-drug resistance mechanism
mcr-1	Plasmid-borne phosphoethanolamine transferase; first transferable colistin resistance gene (China, 2015)
ART	Antiretroviral therapy; combination drug regimen that suppresses HIV viral load to undetectable levels
One Health	Framework recognizing the interconnection of human, animal, and environmental health in infectious disease and AMR

27.10 Companion Source Module: Antimicrobial Resistance and Epidemiology

Antimicrobial Resistance and Epidemiology should leave a reproducible trail from a biological claim to the code, figure, diagram, or paper-based activity that can test it. Use the surfaces below to inspect the chapter's assumptions, rerun the relevant model, or compare the manuscript explanation with companion labs and figures.

Table 354. Companion source surfaces for Antimicrobial Resistance and Epidemiology.

Surface	Use it for
<code>src/biology/microbiology/microbiology.py</code> (<code>basic_reproduction_number</code> , <code>sir_model</code> , <code>mic_fold_dilution</code>)	Reproduce transmission and antimicrobial-resistance calculations.
<code>src/biology/ecology/ecology.py</code> (<code>exponential_growth</code>)	Compare early outbreak growth with ecological growth models.
<code>src/mermaid/biology_diagrams.py</code> (<code>immune_response_diagram</code> , <code>viral_replication_cycle_diagram</code>)	Connect pathogen life cycle to host response.

Reproducibility check: identify pathogen, host population, transmission route, diagnostic window, intervention, and surveillance source before comparing disease claims. Cross-reference: connect with section 24, sections 34 and 35, and sections 37 and 38.

Unit VIII — Botany — Plant Biology: Introduction

Why This Unit Matters

Plants are the foundation of almost every terrestrial food web, the source of roughly half the oxygen in the atmosphere, and the origin of many medicines in human pharmacopoeia — from aspirin (salicylate, first identified in willow bark) to taxol (from Pacific yew, *Taxus brevifolia*), morphine, quinine, and artemisinin. More fundamentally, plants are solar-energy collectors that translate photons into chemical bonds, feeding the entire biosphere. Each year, land plants and algae fix approximately 120 billion tonnes of carbon from atmospheric CO₂ via photosynthesis — a flux so large that it modulates global atmospheric chemistry.

Plant biology is also a discipline of extremes. The tallest trees (coast redwoods, *Sequoia sempervirens*, 115 m) move water 115 meters against gravity using primarily cohesion-tension and solar energy, achieving flow rates in excess of 1 m/hour. Some desert plants survive total desiccation and revive on rehydration. Others flower in response to photoperiod cues measured in the phytochrome system with a resolution of minutes. The *Arabidopsis thaliana* genome was the first plant genome sequenced (2000), and this small weed has since become the “*E. coli* of plant biology” — a model organism for the molecular dissection of everything from root development to pathogen resistance.

This unit integrates anatomy (vascular organization, meristems, root-shoot polarity), physiology (transpiration, water potential, phloem loading), reproductive biology (alternation of generations, angiosperm diversity, seed development), and signaling (phytohormones: auxin, gibberellin, cytokinin, abscisic acid, ethylene). The quantitative spine is water potential ($\Psi = \Psi_s + \Psi_p$) and transpiration modeled by the van den Honert equation.

Landmark Discoveries

Discoverer(s)	Year	Journal / Source	Discovery	Significance
Jan Ingenhousz	1779	[Ingen-Housz, 1779]	Plants produce oxygen in light, CO ₂ in dark	Established the light-dependency of photosynthesis
Julius von Sachs	1862	[Sachs, 1862]	Starch as first visible product of photosynthesis	Linked CO ₂ fixation to carbohydrate storage in chloroplasts
Frits Went	1926	[Went, 1926]	Isolation of auxin; phototropism mechanism	First plant hormone identified; explained Darwinian canary grass bending
Henry Dixon & John Joly	1894	[Dixon and Joly, 1894]	Cohesion-tension theory of water ascent	Explained how trees move water 100+ m with no pump
Chailakhyan	1936	[Chailakhyan, 1936]	Florigen hypothesis (day-length controls flowering)	Proposed a systemic flowering stimulus; later identified as FT protein
<i>Arabidopsis</i> Genome Initiative	2000	[Initiative, 2000]	First plant genome sequence (125 Mb; about 25,500 genes)	Model organism for molecular plant biology; comparative genomics
Gómez-Roldán et al.	2008	[Umehara et al., 2008]	Strigolactones: new class of plant hormones	Sixth plant hormone class; regulates branching and mycorrhizal symbiosis

Key Concepts and Connections

Current Evidence Thread

In this unit, treat plant biology as a body of evidence: each claim about structure, water transport, environmental response, or reproduction should rest on physiological measurement, in vivo imaging, or a field or engineering trial, not on description alone. Plant biology links molecular regulation to climate stress, water limitation, crop resilience, phenology, and ecosystem feedbacks. As you move through the chapters, keep a two-column note: claim on the left, evidence that would change my confidence on the right. By the end of the unit, each major idea should be tied to a measurement, model, citation, or paper-based lab decision.

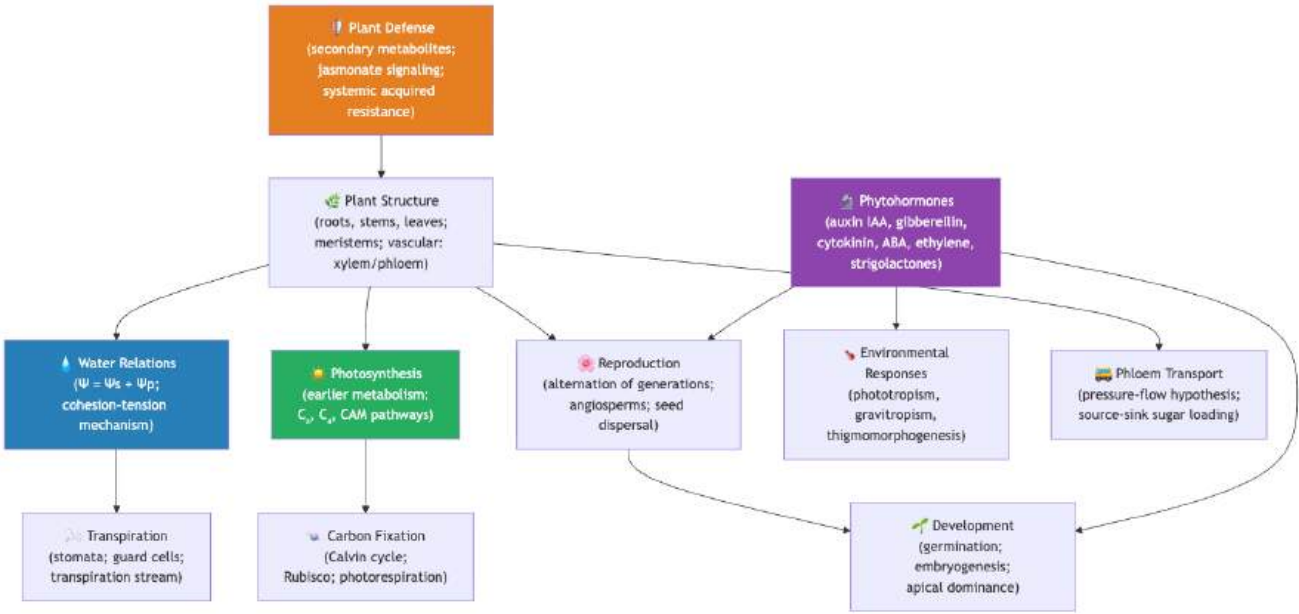


Figure 167. Plant-biology concept map linking structure, water transport, transpiration, reproduction, and environmental responses with photosynthesis as a shared physiological constraint.

Chapter Roadmap

Chapter	Title	Core Question	Key Equation / Model
25	Plant Structure and Water Transport	How is plant body plan organized, and how does water move from roots to leaves?	$\Psi = \Psi_s + \Psi_p$; Poiseuille's law (xylem flow)
26	Plant Reproduction	How do plants reproduce sexually and asexually, and how did flowering plant diversity arise?	Alternation of generations; polyploidy speciation rates
27	Plant Responses to the Environment	How do phytohormones integrate environmental signals into growth and defense responses?	Auxin polar transport; ethylene activation kinetics

Connections Across the Textbook

- Photosynthesis (section 10) is the biochemical foundation of plant carbon metabolism; this unit extends it by covering C₄ and CAM pathways and carbon assimilation in leaves.
- Water potential and osmosis (section 1; section 7) directly underlie the transpiration stream model.
- Plant hormone receptor signaling (auxin, ABA) uses the same signaling classes covered in Unit II — The Cell: Introduction (cell signaling: receptor kinases, second messengers).
- Plant-pollinator, myrmecochory, and plant-mycorrhizal interactions connect to Unit X — Ecology: Introduction (community ecology, mutualism, co-evolution).
- Secondary metabolites as medicines (alkaloids, terpenoids) link to Unit I — Chemistry of Life: Introduction (functional groups) and Unit VII — Microbiology: Introduction (antimicrobial compounds).

Key vocabulary introduced here: meristem, apical dominance, cohesion-tension, water potential (Ψ), transpiration, turgor pressure, phloem, xylem, stomata, guard cell, photoperiodism, phytochrome, auxin, gibberellin, cytokinin, abscisic acid (ABA), ethylene, alternation of generations, angiosperm, gymnosperm, double fertilization.

Computational Toolbox — Unit VIII

```
from biology.botany import water_potential, transpiration_flux, photosynthesis_rate

# Water potential: mesophyll cell with 0.30 M solutes and 0.20 MPa turgor
psi = water_potential(solute_concentration_M=0.30, turgor_pressure_MPa=0.20)
print(f"Cell water potential Ψ = {psi.water_potential_MPa:.2f} MPa")
# Expected: Ψ ≈ -0.54 MPa
# Water moves from higher Ψ (soil, ≈ -0.03 MPa) to lower Ψ (leaf, ≈ -1.5 MPa)

# Stomatal conductance and transpiration
# g = stomatal conductance; concentration gradient is leaf minus air vapour
trans = transpiration_flux(
    stomatal_conductance_mol_m2_s=0.20,
    internal_vapor_conc_mol_m3=1.25,
    external_vapor_conc_mol_m3=0.85,
)
print(f"Transpiration flux = {trans.flux_mmol_m2_s:.1f} mmol m-2 s-1")
print(f"Net photosynthesis at PAR 1000 = {photosynthesis_rate(1000):.1f} μmol CO2 m-2 s-1")
# Expected:
# Transpiration flux = 80.0 mmol m-2 s-1
# Net photosynthesis at PAR 1000 = 9.6 μmol CO2 m-2 s-1
```

Try it yourself: Compare stomatal_conductance_mol_m2_s = 0.05 (drought stress, ABA-closed stomata) vs 0.3 (well-watered). How does the CO₂ assimilation rate (linked to photosynthesis) change proportionally?

Source note: botany helpers support water potential, transpiration, photosynthesis, and C3/C4/CAM pathway comparisons. Figures: src/visualization/ (water potential diagrams, transpiration curves); src/mermaid/biology_diagrams.py (plant life cycle, hormone signaling diagrams).

Cross-Unit Integration

Plants are not “simpler” animals — they are organisms that solved the regulation problem without nervous tissue or circulating endocrine glands. The hormone signaling networks of **Unit VIII — Botany — Plant Biology: Introduction** (auxin polar transport, ABA stomatal control, ethylene ripening cascades, jasmonate defense signaling) are functionally analogous to the nervous and endocrine systems **Unit IX — Zoology and Systems Physiology: Introduction** develops in animals: both implement long-distance, context-sensitive coordination of dispersed tissues. When **Unit IX — Zoology and Systems Physiology: Introduction** introduces neurotransmitter signaling, hormone–receptor binding, and feedback regulation of physiological set points, compare each mechanism to its plant counterpart from **Unit VIII — Botany — Plant Biology: Introduction**. The shared architectural principle — local sensors, diffusing signal molecules, threshold responses, negative feedback for stability — is one of the deepest convergences in biology and a clean illustration of why systems thinking (**Unit 0 — Systems Science for Biology: Introduction**) outranks taxonomic vocabulary.

28 Plant Structure and Water Relations

Level 2/3 · 55 min read · 75 min lecture · Prerequisites: section 7

28.1 Learning Objectives

1. Describe the major organ systems of **angiosperms**: root system (taproot vs fibrous), shoot system, and leaf.
2. Compare the three plant tissue systems: dermal, ground, and vascular, including cell types within each.
3. Explain water relations in plants using the four-component water potential equation $\Psi = \Psi_s + \Psi_p + \Psi_m + \Psi_g$.
4. Describe **transpiration** and the cohesion-tension [**Dixon and Joly, 1894**]-adhesion (TACT) mechanism of water ascent and critically evaluate its supporting evidence.
5. Explain the apoplast vs symplast pathways and the role of the Casparian strip and suberin lamella.
6. Explain phloem transport and the Münch pressure-flow hypothesis [**M^{unch}, 1930**], including apoplastic vs symplastic loading.
7. Describe stomatal regulation and the role of ABA in drought response at the molecular level.
8. Explain nutrient uptake strategies including mycorrhizal associations and quantitative turgor relations.
9. Quantify water-use efficiency at the leaf level and connect it to C3, C4, and CAM photosynthetic trade-offs.

28.1.1 Study Blueprint

- Big idea: Plant form is an engineering solution to water movement, support, gas exchange, and growth.
- Core concepts: xylem, phloem, water potential, transpiration.
- Framework alignment: Vision & Change: Structure and function, Pathways and transformations of energy and matter, Systems; AP Biology: Energetics, Systems Interactions; NGSS-style topics: Structure and Function, Matter and Energy in Organisms and Ecosystems.
- Model or quantitative lens: Water-potential and transpiration-flux calculations.
- Data skill: Interpret plant-water data from pressure, solute, and humidity measurements.
- Practice cadence: Visual Representations, Questions and Methods, Argumentation.
- Common misconception to repair: Water does not move because plants pull with intention; it follows potential gradients and cohesion.
- Primary lab: **Lab — Plant Structure and Water Relations**.
- Question bank: **Questions — Plant Structure and Water Relations**.
- Transfer task: Transfer plant-water reasoning to drought, irrigation, forest physiology, and crop breeding.
- Bridge to computation: `biology.botany.botany.water_potential`.

Opening Vignette — How a Giant Sequoia Pulls Water 100 Meters Up

A mature coast redwood (*Sequoia sempervirens*) can stand 115 meters tall. Getting water from soil to the topmost leaves requires lifting it against a gravitational pull of roughly 1.1 MPa — while simultaneously overcoming resistance to flow through millions of microscopic **xylem** conduits. How? The answer, worked out by Henry Dixon and John Joly in 1894 [**Dixon and Joly, 1894**] and validated with pressure-bomb measurements in the 1960s, is cohesion-tension: water molecules cohere to each other and adhere to xylem walls so strongly that evaporation from leaf **stomata** creates a continuous negative-pressure column (tension) that pulls water up from the roots. The column can sustain tensions as low as −10 MPa before xylem embolism shatters it. The bulk-flow ascent itself is passive — the xylem column requires no direct metabolic energy — though it is gated by active stomatal regulation; this mechanism moves trillions of liters of water into Earth’s atmosphere annually, so elegantly that engineers studying microfluidics still struggle to replicate it artificially.

28.2 The Plant Body Plan

Flowering plants (angiosperms, about 300,000 species) are organized into two major organ systems that work together to acquire resources from both soil and atmosphere.

28.2.1 Root System Architecture and Soil Exploration

The root system anchors the plant, absorbs water and minerals, and stores nutrients. Two major architectural types exist:

- Taproot system: A single **dominant** primary root (derived from the embryonic radicle) with smaller lateral roots branching off. Common in eudicots (e.g., carrots, dandelions, oaks). Deep taproot systems can access water tables several meters below the surface.
- Fibrous root system: A dense mat of similarly sized adventitious roots arising from the stem base. The primary root is short-lived. Common in monocots (e.g., grasses, wheat, rice). Excellent for soil stabilization and surface nutrient capture.

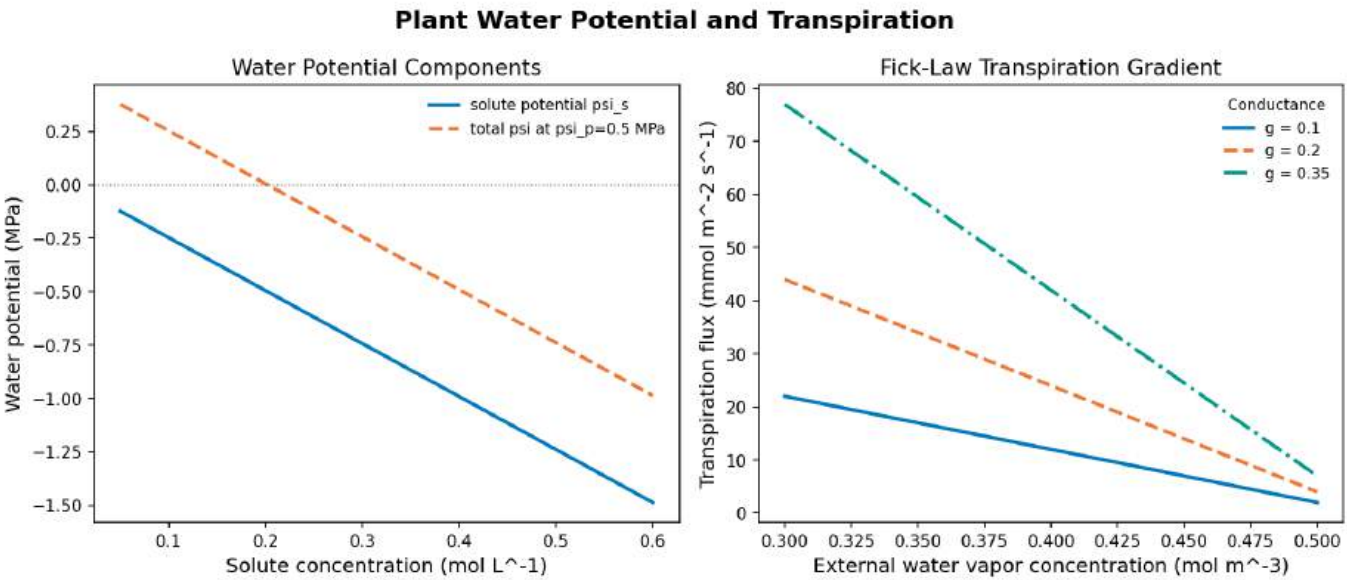


Figure 168. Plant water relations in two panels. Left: solute potential grows more negative with concentration while turgor pressure raises total water potential. Right: transpiration flux falls as external vapour approaches leaf interior and rises with stomatal conductance.

Root apical meristem (RAM): Located near the root tip, protected by the root cap. The RAM contains slowly dividing cells in the quiescent center (QC) surrounded by rapidly dividing initial cells that produce most root tissues. The root tip is organized into distinct zones:

1. Root cap – protects the meristem; secretes mucilage for lubrication; columella cells contain starch-filled amyloplasts (statoliths) for gravity sensing
2. Meristematic zone – active cell division
3. Elongation zone – cells expand primarily in length (up to 10-fold); driven by **turgor pressure** and cell wall loosening
4. Maturation zone – cells differentiate into specialized types; root hairs develop here

Root hairs are single elongated epidermal cells that dramatically amplify surface area (about 600 cm² per cm of root length). Mineral ions are absorbed actively against their electrochemical gradients by specific transporters (NO₃⁻ by NRT1/NRT2; K⁺ by HKT; Fe²⁺ by IRT1).

28.2.2 Plant Architecture: Phytomers and Plastochrons

The shoot is built as a series of repeating modular units called phytomers. Each phytomer comprises one node, the internode immediately below it, the leaf attached at the node, and the axillary bud subtending the leaf. Phytomer iteration generates the entire shoot — a tree is, formally, a clonal colony of phytomers expressed by a single genotype.

The temporal scaffolding is provided by the plastochron index (PI), defined as the time interval between successive leaf-primordium initiations at the SAM (Erickson and Michelini, 1957). At constant temperature the plastochron is approximately constant for a given genotype (about 24 h in *Arabidopsis*, about 36 h in maize), permitting developmental time to be expressed in plastochron units rather than chronological time. The leaf plastochron index (LPI) ranks leaves by developmental age — LPI 0 is the youngest visible leaf, LPI 1 the next, and so on — and is the standard developmental clock for maize and tobacco physiology experiments.

Meristematic zones at the SAM are organized radially and clonally:

- L1 (tunica outer layer): Strictly anticlinal divisions; gives rise to epidermis
- L2 (tunica inner layer): Mostly anticlinal; produces mesophyll, gametes
- L3 (corpus): Anticlinal and periclinal divisions; produces vascular and ground tissue

Genetic chimeras (e.g., variegated geraniums) reveal these clonal layers as stable, parallel cell lineages whose interactions specify organ identity.

28.2.3 Shoot System Architecture and Light Capture

The shoot system comprises the stem and leaves and is responsible for **photosynthesis**, reproduction, and support.

Shoot apical meristem (SAM): Maintains a pool of pluripotent stem cells at the shoot tip throughout the plant’s life. The SAM is organized into:

- Central zone (CZ): Slowly dividing stem cells maintained by the WUS-CLV3 negative feedback loop
- Peripheral zone (PZ): Faster-dividing cells that form lateral organ primordia (leaves, flowers)
- Rib zone: Cells below the CZ that contribute to stem internodes

Leaves are initiated at the PZ where PIN1-mediated auxin maxima form, producing the characteristic phyllotaxis pattern (often 137.5 degrees divergence angle).

28.2.4 Leaf Anatomy for Gas Exchange and Photosynthesis

Leaf cross-section layers (adaxial to abaxial):

1. Upper epidermis + cuticle (waxy layer of cutin; reduces water loss)
2. Palisade mesophyll (densely packed columnar cells with abundant **chloroplasts**; principal photosynthetic layer)
3. Spongy mesophyll (loosely packed; CO₂ diffusion through intercellular air spaces; about 30-40% air space)
4. Lower epidermis + cuticle

Stomata: Pores bounded by two kidney-shaped **guard cells**. Stomatal aperture is controlled by guard cell turgor:

- Light activates blue-light phototropins and red-light photosynthesis in guard cell chloroplasts. K⁺ influx (via K⁺ inward-rectifying channels) lowers osmotic potential. Water enters by **osmosis**. Guard cells swell and bow apart. Stomata open.
- Drought triggers ABA signaling. ABA activates SnRK2 kinases. SLAC1 anion channels open, releasing Cl⁻. Membrane depolarizes. K⁺ leaves via GORK channels. Water follows osmotically. Guard cells deflate. Stomata close.

Typical stomatal density: about 200 stomata/mm² in many mesophytes. Each stoma can open or close in minutes. Stomata allow CO₂ in and O₂ plus water vapor out – the inevitable tradeoff between photosynthesis and transpiration.

Clinical Connection: Understanding stomatal biology is essential for crop engineering. Overexpression of the SLAC1 gene in barley produced plants with more responsive stomata and 40% greater water-use efficiency in field trials, directly relevant to agriculture in drought-prone regions.

Concept Check 1: Why are most stomata located on the lower (abaxial) epidermis of leaves rather than the upper surface?

Concept Check 2: A botanist counts an average plastochron of 30 hours in a tomato plant. After 15 days, approximately how many leaf primordia will have been initiated by the SAM, assuming temperature is constant?

28.3 Plant Tissue Systems

Most plant organs are composed of three tissue systems: dermal, ground, and vascular.

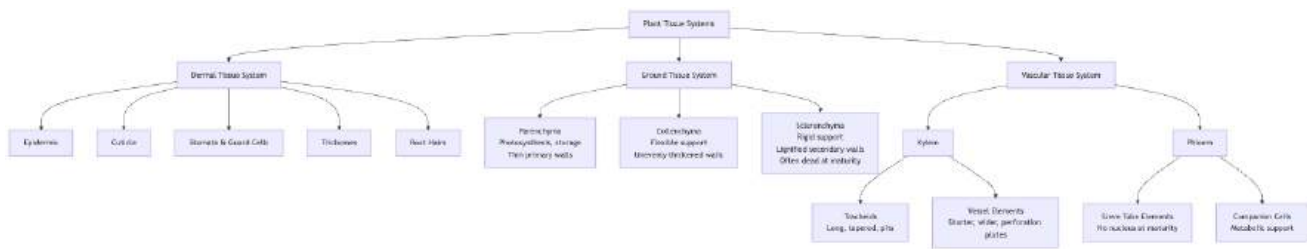


Figure 169. Organization of the three plant tissue systems showing major cell types within each Dermal tissue forms the outer covering, ground tissue fills the interior, and vascular tissue provides transport.

28.3.1 Dermal Tissue System

The dermal tissue system is the outer protective covering of the plant:

- Epidermis: A single layer of tightly packed cells covering most surfaces. Secretes the cuticle.
- Cuticle: A waxy layer composed of cutin (a polyester of hydroxylated fatty acids) and epicuticular waxes. Minimizes water loss from non-stomatal surfaces. The cuticle can reduce transpiration by 95% compared to an unprotected surface.
- Trichomes: Hair-like epidermal appendages. Diverse functions: reduce wind speed at leaf surface (boundary layer), reflect excess light, secrete defensive compounds (glandular trichomes of tomato produce toxic sesquiterpenes), deter herbivory.
- Root hairs: Tubular extensions of single epidermal cells in the root maturation zone. Increase absorptive surface area by 2-10-fold.

28.3.2 Ground Tissue System

Ground tissue fills the space between dermal and vascular tissues. Three cell types:

Parenchyma cells: Living at maturity. Thin primary cell walls. Functions include photosynthesis (mesophyll), storage (starch in potato tubers, sugar in sugar beet roots), and wound healing (dedifferentiate to form callus tissue). Parenchyma cells retain the ability to divide, making them critical for regeneration.

Collenchyma cells: Living at maturity. Unevenly thickened primary cell walls (thicker at corners). Provide flexible mechanical support to growing organs. Found in petioles and young stems. Celery “strings” are collenchyma strands.

Sclerenchyma cells: Typically dead at maturity. Thick, lignified secondary cell walls. Provide rigid support. Two types: fibers (elongated cells in bundles; flax, hemp) and sclereids (short, irregular cells; the gritty texture in pears; the hard shell of walnuts).

28.3.3 Vascular Tissue System – Xylem in Detail

The vascular tissue system is the plant’s long-distance transport network.

Xylem (water and mineral transport, upward) develops in two temporally distinct phases that yield mechanically distinct conduits:

Protoxylem matures while the surrounding tissue is still elongating. Its conduits must therefore stretch with the growing organ, so secondary-wall lignification is restricted to annular (ring-shaped) or helical (spiral) thickenings. These thickenings allow elongation but provide limited collapse-resistance under tension; protoxylem conduits are typically narrow (5–25 μm) and frequently obliterated as the tissue matures, leaving an air-filled lacuna.

Metaxylem differentiates after elongation has ceased. With no constraint on extensibility, metaxylem develops continuous lignified walls with scalariform (ladder-like), reticulate (net-like), or pitted thickenings. Metaxylem conduits are wider (50–500 μm in some lianas), longer-lived, and bear the bulk of mature transpiration flux.

A simple mnemonic: proto = first (extensible, ephemeral), meta = mature (durable, mechanically robust). The transition can be visualized in any longitudinal section of an elongating maize root: closer to the tip, narrow protoxylem dominates; further back in the maturation zone, metaxylem vessels of much greater caliber come on-line.

The two principal cell types of xylem differ markedly in mechanics:

- **Tracheids:** Long (1-5 mm), tapered cells with lignified secondary walls. Dead at maturity. Water moves between tracheids through bordered pit pairs (thin regions in the cell wall where secondary wall is absent). The pit membrane consists of the unmodified primary walls of the two adjacent cells plus the middle lamella; in conifers it bears a thickened central torus suspended by a porous margo, allowing the torus to seal the pit aperture if the adjacent conduit cavitates (an aspirated pit). Tracheids are found in most vascular plants and constitute the primary conducting element in most gymnosperms.
- **Vessel elements:** Shorter (0.2-1 mm) but wider (up to 500 μm diameter in some lianas) than tracheids. Stacked end-to-end with perforation plates (partial or complete dissolution of end walls) forming continuous tubes called vessels. Found primarily in angiosperms. More efficient but more vulnerable to cavitation than tracheids.

Bordered pit mechanics — the torus-margo valve:

The conifer bordered pit is one of the most elegant valve structures in biology. The pit membrane is differentiated into two regions:

- **Torus:** A thickened, impermeable central disc (about 5 μm diameter) made of cellulose microfibrils embedded in a lignified matrix
- **Margo:** A porous mesh of radial cellulose strands surrounding the torus, with pore sizes of 50–200 nm

Under normal flow, the torus floats centrally and water moves freely through the porous margo. When one tracheid embolises, the pressure differential between the air-filled (atmospheric) and water-filled (negative pressure) conduits displaces the torus laterally; the torus seats firmly against the pit aperture, aspirating the pit. The seal is reinforced by surface tension at the air-water interface inside the margo pores. Air seeding through this valve requires breaking the meniscus at the smallest margo pore — typically requiring tensions of −3 to −10 MPa, which sets the species’ cavitation safety margin.

Angiosperm pit membranes lack a torus; instead they have a homogeneous, semi-porous structure (typical pore size about 5–20 nm). These membranes resist air seeding at higher tensions per unit area but lack the most-or-nothing valving of conifer pits — once a single membrane breach opens, the entire vessel cavitates rapidly.

Mechanical properties — the safety-efficiency tradeoff:

The Hagen-Poiseuille equation predicts that volumetric flow scales as the *fourth power* of conduit radius:

$$Q = \frac{\pi r^4 \Delta P}{8 \eta L}$$

(355)

where Q is volumetric flow (m³/s), r is conduit radius (m), ΔP is pressure drop (Pa), η is dynamic viscosity ($\approx 10^{-3}$ Pa·s for water at 20 °C), and L is conduit length (m). Doubling the radius therefore increases conductance 16-fold. Wide vessels (oaks, ring-porous wood) dominate spring transpiration; narrow tracheids (conifers, drought-adapted woody species) trade efficiency for resistance to embolism propagation, since narrower conduits maintain larger surface-tension forces relative to the column volume.

Phloem (sugar and organic compound transport, bidirectional):

- **Sieve tube elements:** Living at maturity but lack nucleus, **ribosomes**, and tonoplast at maturity. Connected end-to-end at sieve plates (modified cell walls perforated by sieve pores, 1-15 μm diameter). **P-protein** (phloem protein) plugs sieve pores when cells are damaged, preventing phloem sap loss.
- **Companion cells:** Retain full complement of **organelles**. Connected to sieve tube elements by numerous plasmodesmata. Provide metabolic support including ATP for active sugar loading. Transfer cells (specialized companion cells with wall ingrowths) increase membrane surface area for active transport.

Concept Check 3: Why must xylem conducting cells be dead at maturity, while phloem sieve tube elements must remain alive?

Concept Check 4: Using the Hagen-Poiseuille relation, calculate the ratio of volumetric flow between a vessel of radius 100 μm and a tracheid of radius 25 μm, holding pressure gradient and length constant. Explain why drought-prone species may nevertheless favor the narrower conduit.

Concept Check 5: A botanist examines a longitudinal section of an emerging shoot from a deciduous tree. She notes spirally banded conduits near the apex but reticulate-pitted conduits 5 cm behind. Identify each conduit type and explain the developmental logic of the difference.

28.4 Water Relations – Water Potential

Plants control water movement using water potential (Ψ , units: MPa). The complete four-component formulation captures every thermodynamically relevant contribution to water’s free energy:

$$\Psi = \Psi_s + \Psi_p + \Psi_m + \Psi_g \tag{356}$$

where:

- Ψ_s = osmotic (solute) potential = $-iCRT$ (typically ≤ 0 ; solutes decrease water potential). i is the van ’t Hoff dissociation factor, C is molar concentration, R is the gas constant, T is temperature in Kelvin.
- Ψ_p = pressure (turgor) potential. Positive in turgid cells (turgor pressure against cell wall). Negative in xylem under tension. Can range from +2 MPa in highly turgid cells to -10 MPa or lower in xylem of tall trees.
- Ψ_m = matric potential. Reflects water binding to colloidal surfaces (cell walls, soil clay particles, dry seeds). Typically ≤ 0 . Typically negligible in well-hydrated cells but dominates in dry seeds (where Ψ_m can reach -100 MPa) and in dry soils.
- Ψ_g = gravitational potential = ρgh . Significant primarily in tall trees. At 10 m height, $\Psi_g = -0.1$ MPa. At 100 m (coast redwood), $\Psi_g = -1.0$ MPa.

In well-hydrated, free-flowing systems (most active leaf and root cells) Ψ_m is folded into Ψ_p and the simplified three-component form $\Psi = \Psi_s + \Psi_p + \Psi_g$ is used. In dry seeds, lichens, and very dry soils, Ψ_m must be retained explicitly. See equation (356). figure 168 links solute-driven Ψ_s shifts to Fick-law transpiration flux under varying stomatal conductance.

28.4.1 Worked Example: Calculating Water Potential

Problem: A plant cell has a solute concentration of $C = 0.3 \text{ mol L}^{-1}$ sucrose ($i = 1$) at $T = 293 \text{ K}$ (20°C) and a turgor pressure (Ψ_p) of 0.5 MPa. Assuming normal height where $\Psi_g = 0$ and the cell is well hydrated so $\Psi_m \approx 0$, what is the cell’s total **water potential (Ψ)**? If this cell is placed in an open beaker of pure water ($\Psi = 0$), will water flow into or out of the cell?

Solution:

1. Calculate the osmotic potential (Ψ_s): Using the van ’t Hoff equation $\Psi_s = -iCRT$, where $R = 0.00831 \text{ L MPa mol}^{-1} \text{ K}^{-1}$:

$$\Psi_s = -(1) \cdot (0.3 \text{ mol L}^{-1}) \cdot (0.00831 \text{ L MPa mol}^{-1} \text{ K}^{-1}) \cdot (293 \text{ K})$$

$$\Psi_s \approx -0.73 \text{ MPa}$$

2. Calculate the total water potential (Ψ):

$$\Psi = \Psi_s + \Psi_p + \Psi_m + \Psi_g$$

$$\Psi = -0.73 \text{ MPa} + 0.5 \text{ MPa} + 0 + 0$$

$$\Psi = -0.23 \text{ MPa}$$

3. Determine the direction of water flow: Water typically moves from higher water potential to lower water potential. Since the beaker of pure water is at $\Psi = 0$ and the cell is at $\Psi = -0.23 \text{ MPa}$, water will flow into the cell until the cell’s turgor pressure rises sufficiently to reach equilibrium ($\Psi = 0$).

Water typically moves from higher to lower water potential (down the Ψ gradient).

28.4.2 Worked Example: A Leaf Cell at Dawn vs Midday

Problem: A mesophyll cell at dawn (cool, humid, stomata closed) has $\Psi_s = -1.1 \text{ MPa}$, $\Psi_p = +0.9 \text{ MPa}$, $\Psi_m \approx 0$, $\Psi_g \approx 0$. By midday (hot, dry, stomata open and transpiring), the cell loses water: $\Psi_s = -1.4 \text{ MPa}$ (solutes concentrated by about 27% volume loss), $\Psi_p = +0.2 \text{ MPa}$. Compute Ψ in both states and identify which component drives the change.

Solution:

- Dawn: $\Psi = -1.1 + 0.9 = -0.2 \text{ MPa}$
- Midday: $\Psi = -1.4 + 0.2 = -1.2 \text{ MPa}$

Total Ψ has fallen by 1.0 MPa. Decomposing the change:

- $\Delta\Psi_s = -0.3 \text{ MPa}$ (small contribution from solute concentration)
- $\Delta\Psi_p = -0.7 \text{ MPa}$ (dominant contribution)

The midday plunge is driven primarily by loss of turgor. The cell remains alive and below the wilting threshold, but it is approaching the limit at which growth (which requires $\Psi_p > Y$ in the Lockhart equation) ceases. This is the molecular basis of midday “growth pause” almost universally observed in field crops.

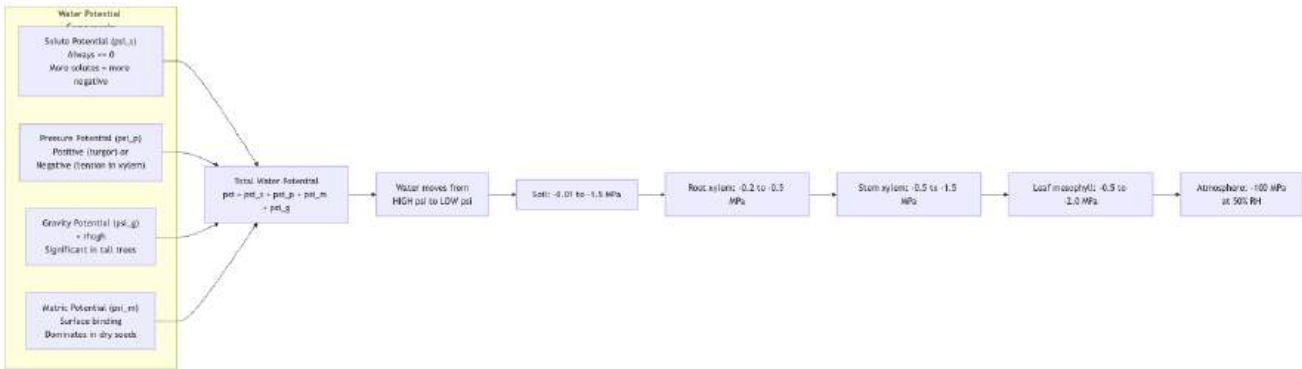


Figure 170. Components of water potential and the soil-plant-atmosphere continuum (SPAC) Water moves passively down the water potential gradient from soil to atmosphere. The enormous gradient between leaf and atmosphere drives transpiration.

28.4.3 Quantitative Turgor Relations and Plasmolysis

Turgor pressure (Ψ_p) is generated when a cell with low internal Ψ_s takes up water until the cell wall resists further expansion. The cell-wall yield curve is described by the Lockhart equation for irreversible expansion:

$$\frac{1}{V} \frac{dV}{dt} = \phi(\Psi_p - Y)$$

(357)

where ϕ is wall extensibility (a measure of how readily the wall yields), Ψ_p is current turgor, and Y is the yield threshold below which the wall behaves elastically (no growth). Cells grow primarily when $\Psi_p > Y$. In the elongation zone, expansin-mediated wall loosening reduces Y , allowing growth even at modest turgor.

Plasmolysis is the separation of the protoplast from the cell wall when the cell is placed in a hypertonic solution (external Ψ_s more negative than internal). Three phases:

1. Incipient plasmolysis: Turgor reaches zero ($\Psi_p = 0$); at this point $\Psi = \Psi_s$. The protoplast is just losing contact with the wall.
2. Concave plasmolysis: Protoplast withdraws inward; plasma membrane appears scalloped at the corners.
3. Convex plasmolysis: Protoplast becomes a small spherical body in the center of the cell; reversible if rehydrated within minutes, but prolonged plasmolysis kills the cell.

Worked Example — Quantitative Plasmolysis: A cell at $\Psi_p = 0.5 \text{ MPa}$, $\Psi_s = -0.73 \text{ MPa}$ is placed in a sucrose solution at $\Psi_s = -1.0 \text{ MPa}$. Water leaves the cell. As water exits, Ψ_s becomes more negative (solutes concentrate; assume volume change of 20% from full turgor to incipient plasmolysis). At incipient plasmolysis, $\Psi_p = 0$ and $\Psi_{cell} = \Psi_s$ must equal $\Psi_{external} = -1.0 \text{ MPa}$. Since Ψ_s scales inversely with cell volume ($\Psi_s \cdot V \approx \text{constant}$ for ideal solutes), we calculate the relative volume at incipient plasmolysis as $V_p/V_0 = \Psi_{s,0}/\Psi_{s,p} = -0.73/-1.0 = 0.73$, i.e., the cell loses about 27% of its initial volume before plasmolysing.

At full turgor: $\Psi_p = -\Psi_s$, so $\Psi = 0$ (cell is in equilibrium with pure water).

Clinical Connection: Agricultural irrigation management relies on measuring soil water potential with tensiometers. When soil Ψ falls below -1.5 MPa (the permanent wilting point), most crop plants cannot extract water. Precision irrigation triggered at species-specific Ψ thresholds saves 20-40% of water compared to schedule-based irrigation.

Concept Check 6: A seed at storage moisture has $\Psi_m \approx -100 \text{ MPa}$, $\Psi_s \approx -2 \text{ MPa}$, and $\Psi_p = 0$. When placed on moist filter paper at $\Psi = -0.05 \text{ MPa}$, water is rapidly imbibed. Explain which component dominates the imbibition gradient and why imbibition is a one-way process.

28.5 Water Transport Pathways

28.5.1 Apoplast vs Symplast Pathways

Water and dissolved minerals travel from the root surface to the xylem via two parallel routes:

Apoplast pathway: Water moves through the continuum of cell walls and intercellular spaces without crossing any membranes. Fast and non-selective. Driven by mass flow along pressure gradients.

Symplast pathway: Water moves through the continuum of **cytoplasm** connected by plasmodesmata (channels through cell walls, 40-60 nm diameter, lined by ER). Requires crossing the plasma membrane at entry. Slower but allows selective transport.

Transmembrane pathway: Water crosses plasma membranes via aquaporins (water channel proteins, PIP and TIP families; about 35 aquaporin genes in *Ara-bidopsis*). Aquaporin activity is regulated by phosphorylation, **pH**, and Ca^{2+} .

28.5.2 Root Anatomy in Depth — The Endodermis as Filter

Radial anatomy of a young dicot root (from outside inward):

1. Epidermis with root hairs — initial absorption surface
2. Cortex — multiple layers of parenchyma; storage and apoplastic transport corridor; rich in plasmodesmata
3. Endodermis — single layer; the critical apoplastic checkpoint
4. Pericycle — cell layer giving rise to lateral roots
5. Vascular cylinder (stele) — central xylem and phloem strands

The Casparian strip — chemistry and synthesis:

The Casparian strip is a band of lignin and suberin deposited in the radial and transverse walls of endodermal cells. The two polymers play distinct, sequential roles:

- Lignin (a phenylpropanoid polymer of monolignol units p-coumaryl, coniferyl, and sinapyl alcohol cross-linked by oxidative coupling) is deposited first, forming the Casparian strip proper — a discontinuous belt that fuses cell wall to plasma membrane. CASP1–CASP5 transmembrane proteins assemble into a hexagonal scaffold that recruits ESB1 (a dirigent protein) and PER64 (a peroxidase), localizing lignification to a precise sub-micron belt. *casp1 casp3* double mutants have discontinuous strips and leak ions into the stele.
- Suberin (an aliphatic-aromatic polyester of long-chain ω -hydroxy fatty acids and ferulate esters) is deposited later as the suberin lamella on the inner face of the cell wall, after the Casparian strip is mature. Suberisation is regulated by SGN3-CIF1/CIF2 receptor-peptide signaling, which monitors the integrity of the Casparian strip via leakage of CIF peptides from stele to cortex.

Why both polymers? Lignin is hydrophobic and rigid but porous to small molecules; suberin is even more hydrophobic and seals against water and ion flow. The two-stage system gives a fast-acting initial seal (lignin Casparian strip) followed by a slow-developing reinforcement (suberin lamella) that further restricts symplastic transport across the inner endodermal face.

Bypass routes — apoplastic leakage at lateral root junctions:

Where lateral roots emerge from the pericycle, they must rupture the endodermis and overlying cortex. During the brief window before the lateral root re-establishes its own endodermis, an apoplastic bypass allows ions (and pathogens) to enter the stele without crossing a plasma membrane. This window can be hours to days long. Quantitatively, about 70% of soil-borne Na^+ entering the stele of rice and wheat does so via these junctional leaks rather than through the proper symplast. The bypass may explain seasonal salt accumulation in glycophytes (salt-sensitive species) under saline irrigation.

Symplastic vs transmembrane pathways:

- Pure symplastic transport uses plasmodesmata to bypass plasma membranes entirely. Plasmodesmal aperture is regulated by callose deposition at the neck region; under stress, callose deposition closes plasmodesmata, isolating cells.
- Transmembrane pathway crosses plasma membranes twice per cell (entry + exit) via aquaporins for water and selective transporters for ions. Slowest but most selective.

In practice, the three pathways operate simultaneously; the relative contribution shifts with developmental stage, salinity, and mycorrhizal colonization.

Passage cells: In older roots, most endodermal cells deposit a continuous suberin lamella covering the entire inner surface of the cell wall. Passage cells — endodermal cells that retain a thin wall and lack the suberin lamella, located opposite protoxylem poles — provide selective transport routes through the otherwise sealed older endodermis.

In rice, the endodermis is supplemented by an inner exodermis (a Casparian-strip-bearing layer just inside the epidermis), giving a double filter. Rice ranks among the most salt-tolerant cereals partly because the exodermis blocks Na^+ at the root surface itself.

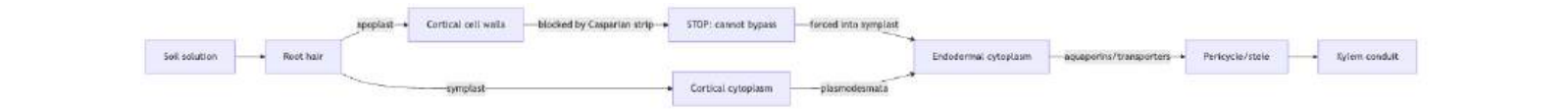


Figure 171. Apoplast vs symplast routes through a young root and the Casparian-strip checkpoint at the endodermis Most water and ions reaching the xylem must traverse at least one plasma membrane.

28.6 Transpiration and the Cohesion-Tension Mechanism

28.6.1 Historical Context: The Birth of Cohesion-Tension Theory [Dixon and Joly, 1894]

The question of how water reaches the canopy of a tall tree exercised plant physiologists throughout the 19th century. Early proposals invoked root pressure (positive xylem pressure generated by active mineral secretion overnight; can be measured by exudation from cut stumps at 0.05–0.5 MPa), but this manifestly cannot lift water more than about 5 m and is absent during the day in most species. Capillarity in xylem conduits could lift water about 1 m given typical conduit radii. Atmospheric pressure can support a column of about 10.3 m. None of these mechanisms could account for water rising to 100 m in *Sequoia*.

In 1894, Henry Dixon (Trinity College Dublin) and John Joly proposed a radical alternative: water in the xylem is under tension (negative pressure), pulled from above by evaporation rather than pushed from below [Dixon and Joly, 1894]. The idea was counter-intuitive — bulk water at −1 MPa is metastable; a single nucleation event should cause spontaneous boiling — but the cohesive forces of water (hydrogen bonds, theoretical tensile strength −140 MPa) and the small radii of xylem conduits (which suppress nucleation) make the metastable state biologically sustainable.

28.6.2 Detailed TACT Mechanism

Water ascent in tall trees is explained by the cohesion-tension-adhesion (TACT) mechanism, refined by Renner (1911), and validated with pressure probes and MRI:

1. Transpiration from leaves drives evaporation at the mesophyll cell wall surface. Water evaporates from the thin film coating the cell wall into the substomatal air space, then diffuses out through open stomata.
2. As water evaporates, the air-water interface retreats into the nanoscale pores of the cell wall. Surface tension at this curved meniscus generates a large negative pressure (tension), following the Young-Laplace equation:

$$\Delta P = \frac{2\gamma \cos \theta}{r}$$

(358)

where γ is surface tension of water (0.0728 N/m), θ is contact angle, and r is pore radius. For cell wall pores ($r \approx 5\text{--}10$ nm), this generates tensions of −10 to −30 MPa.

3. This tension propagates through the continuous water columns in xylem conduits (tracheids and vessels) because of water’s strong cohesion (hydrogen bonds). The theoretical tensile strength of water is approximately −140 MPa; in practice, xylem water columns sustain tensions of −1 to −10 MPa, with some trees reaching −15 MPa.
4. Adhesion of water to the hydrophilic, lignified xylem walls prevents the water column from pulling away from the conduit walls.
5. The tension at the top of the column draws water from the roots, which in turn absorbs water from the soil down the water potential gradient.

28.6.3 Cohesion-Tension Theory: Embolism Evidence and Synchrotron Imaging

The cohesion-tension model is not without controversy, and its mature form represents a triumph of integrating ecological, physical, and microscopic evidence — together with rebuttals to specific objections.

Lines of supporting evidence:

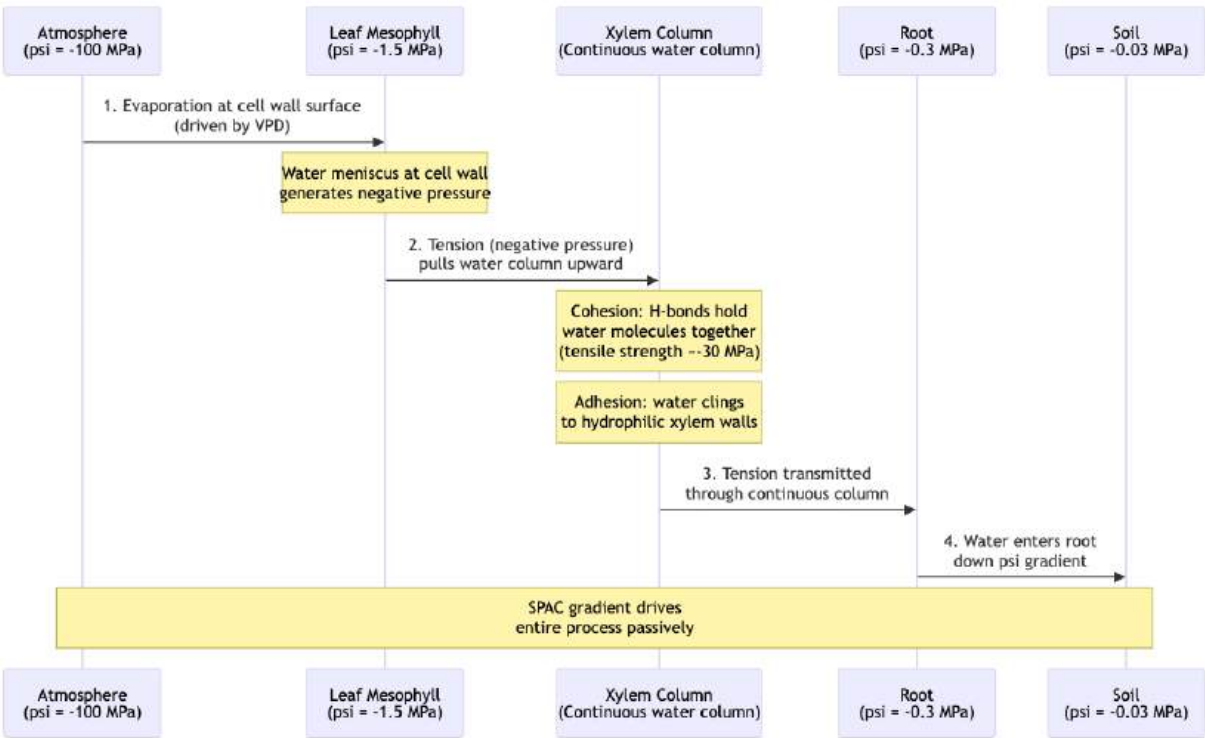


Figure 172. The transpiration-cohesion-tension mechanism of water ascent. Evaporation at the leaf surface generates tension (negative pressure) that is transmitted through the continuous water column in the xylem, pulling water upward from the roots. Cohesion between water molecules and adhesion to xylem walls maintain the column.

1. Pressure-bomb measurements (Scholander *et al.*, 1965) directly demonstrate that excised stems of transpiring trees release water primarily when external pressure is applied, consistent with negative xylem pressure prior to excision. Pressure required matches predictions of the tension hypothesis (typically -1 to -3 MPa for well-watered crops; -6 to -10 MPa under drought).
2. Magnetic resonance imaging (MRI) in vivo (Holbrook *et al.*, 2001) visualizes continuous water columns in mature angiosperm trunks, with abrupt transitions to embolised conduits matching predictions of tension-induced cavitation.
3. Pressure probes (Steudle, 1995) in living root cortex cells confirm steep tension gradients between epidermis and stele consistent with bulk-flow-driven uptake.
4. Acoustic emission of xylem during drought (Tyree and Sperry, 1989) records sharp clicks corresponding to individual cavitation events, the count of which scales with drought severity.

The embolism debate:

Critics (most prominently U. Zimmermann and colleagues, 1990s–2000s) argued that water columns under tensions of -1 MPa or more should be metastable and would cavitate continuously, making sustained negative pressures of -10 MPa physiologically implausible. The Zimmermann school proposed alternative “tissue tension” models in which water moved by mechanisms other than bulk flow.

This challenge has been progressively resolved by direct visualization:

- Improved pressure probes (Wei *et al.*, 1999) confirmed predicted tensions in living conduits without artifact.
- Synthetic-tree experiments (Wheeler and Stroock, *Nature* 2008) constructed transparent microfluidic devices replicating the geometry of a leaf’s evaporative surface; these “synthetic trees” sustained water under tension to -22 MPa , mirroring biological systems and proving that cell wall pore geometry alone is sufficient to support the predicted tensions.
- Synchrotron X-ray micro-CT (Brodersen *et al.*, *Plant Physiol.* 2010; Choat *et al.*, *Nature* 2012) imaged living xylem in real time and showed that under moderate drought, embolisms are confined to a small fraction of conduits — settling the long-running argument over how prevalent embolism is in actively transpiring plants. Synchrotron imaging also visualized embolism repair under daily root pressure: embolised conduits refill overnight in *Vitis* and *Laurus*.

Mechanism of embolism repair: Two complementary mechanisms are now well-attested:

- Root pressure refilling: Active mineral secretion into xylem at night generates positive xylem pressure (0.05 – 0.5 MPa) sufficient to push water back into embolised conduits. Common in herbaceous species and in many trees overnight.

- Phloem-driven refilling: Phloem-derived sugars osmotically draw water into embolised conduits via parenchyma cells lining the xylem (Salleo *et al.*, 2004; Nardini *et al.*, 2011). This mechanism operates against negative bulk xylem pressure and is observed during the day.

Net assessment: The TACT mechanism is correct in its essentials. Water in xylem is genuinely under tension; the column is stabilized by cohesion and adhesion at scales where pore geometry sustains negative pressures far beyond what bulk water could endure. The system is metastable but biologically sufficient — and the cost of occasional cavitation is mitigated by redundant pathways and active repair.

28.6.4 Xylem Transport Parameters

Xylem sap velocity measured by MRI and heat pulse methods: 3-45 m/h in trees; 15-50 m/h in herbaceous plants. Ring-porous trees (oak, elm) can reach velocities of 40+ m/h in their large early-wood vessels.

Transpiration flux (Fick’s first law for water vapor):

$$E = g_s \cdot \Delta w$$

(359)

where g_s = stomatal conductance ($\text{mmol m}^{-2} \text{s}^{-1}$) and Δw = vapor pressure difference between leaf interior and ambient air (mol mol^{-1}).

A well-watered broadleaf tree can transpire 200-400 liters of water per day. A large oak may transpire over 150,000 liters during a growing season.

28.6.5 Cavitation and Embolism

When xylem tension exceeds the capacity of the water column, dissolved gas comes out of solution forming a bubble – cavitation. The gas bubble expands to fill the conduit, creating an embolism (air lock) that blocks water flow.

Plants have evolved multiple strategies to manage cavitation:

- Vessel element size: Smaller conduits are more resistant to cavitation (higher surface-tension forces maintain the column) but less efficient for transport. This creates a safety-efficiency tradeoff.
- Pit membranes: In tracheids, bordered pits have a torus-margo structure. When one tracheid cavitates, the torus seals against the pit aperture, preventing air from spreading to adjacent conduits.
- Embolism repair: Some plants can refill embolisms overnight when transpiration ceases and root pressure (positive xylem pressure generated by active mineral secretion into xylem) pushes water back into embolised conduits.
- Redundant pathways: Multiple parallel conduits ensure that loss of some to embolism does not stop water transport entirely.

Clinical Connection: The vulnerability of xylem to cavitation explains why drought-adapted species (e.g., desert shrubs) have narrow xylem vessels while tropical rainforest trees have wide ones. Climate change-driven drought is causing widespread forest die-off globally as tree xylem systems experience unprecedented cavitation stress, termed “hydraulic failure.” The 2011 Texas drought killed an estimated 300 million trees.

Concept Check 8: Modern synchrotron imaging shows that conifer xylem can withstand tensions of –6 MPa with little embolism, while many ring-porous angiosperms cavitate at –2 MPa. Explain this difference in terms of pit membrane structure (torus-margo vs homogeneous) and conduit dimensions.

28.6.6 Worked Example: Water Potential in the Transpiration Stream

Problem: Track the water-potential ($\Psi = \Psi_s + \Psi_p$) gradient that drives water from a leaf mesophyll cell into the xylem before and after stomatal opening, and identify the cavitation threshold.

Initial (pre-dawn, stomata closed):

- Leaf mesophyll cell: $\Psi_s = -1.2 \text{ MPa}$, $\Psi_p = +0.3 \text{ MPa} \Rightarrow \Psi_{\text{leaf}} = -0.9 \text{ MPa}$
- Adjacent xylem sap: $\Psi_s \approx -0.1 \text{ MPa}$, $\Psi_p = -0.8 \text{ MPa}$ (modest standing tension) $\Rightarrow \Psi_{\text{xylem}} = -0.9 \text{ MPa}$

The cell is at equilibrium with the xylem ($\Delta\Psi = 0$). No net flow.

Stomata open at sunrise; transpiration raises xylem tension:

- Xylem now: $\Psi_s \approx -0.1 \text{ MPa}$, $\Psi_p = -1.5 \text{ MPa} \Rightarrow \Psi_{\text{xylem}} = -1.6 \text{ MPa}$
- Leaf cell (assume solutes unchanged on a short timescale): $\Psi_{\text{leaf}} = -0.9 \text{ MPa}$

Solution:

1. Driving force. $\Delta\Psi = \Psi_{\text{leaf}} - \Psi_{\text{xylem}} = -0.9 - (-1.6) = +0.7 \text{ MPa}$.
2. Direction. Water flows from higher Ψ (leaf, -0.9 MPa) to lower Ψ (xylem, -1.6 MPa) — *out of* the mesophyll cell and *into* the xylem, replacing water evaporated at the stomatal pore.
3. Cavitation safety. For many angiosperms, the air-seeding pressure of the largest pit pores is about -1.5 to -2 MPa . The new xylem $\Psi_p = -1.5 \text{ MPa}$ sits at the edge of that threshold — any further drop and the most vulnerable conduits cavitate, embolising and dropping out of the transport network.

Interpretation. Stomatal opening is bought at the price of increased xylem tension. Plants live with hydraulic safety margins of typically $0.5\text{--}1.0 \text{ MPa}$ between operating tension and the cavitation threshold (P_{50} , the tension at which 50% of conductivity is lost). Drought narrows this margin; species whose operating tensions routinely cross P_{50} are the first to drop branches and die during heatwaves — the mechanistic basis of climate-driven forest die-back. Cavitation thresholds vary by species: drought-adapted shrubs may safely operate at -6 MPa , while mesic angiosperms with wide vessels cavitate near -1.5 MPa .

28.7 Stomatal Regulation of Water Loss and CO2 Uptake

Stomata represent the critical control point where plants balance carbon gain (CO_2 uptake for photosynthesis) against water loss (transpiration).

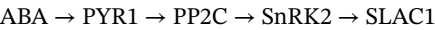
28.7.1 Stomatal Opening — Guard Cell Ion Fluxes

The mechanism of stomatal opening involves a coordinated cascade of ion fluxes that generate the osmotic gradient driving water entry. The molecular logic is one of the best-characterized electrophysiological systems in plants:

1. Blue light (peak 450 nm) activates phototropin receptors (PHOT1/PHOT2) on guard cells via FMN photoreduction
2. PHOTs activate plasma membrane H^+ -ATPases (AHA1, AHA2) via 14-3-3-mediated phosphorylation of the C-terminal autoinhibitory domain
3. H^+ extrusion hyperpolarises the membrane (interior becomes more negative, V_m shifts from -100 to -180 mV) and acidifies the apoplast ($\text{pH } 6 \rightarrow 5$)
4. K^+ inward-rectifying channels (KAT1 in *Arabidopsis*; voltage-gated, six-transmembrane Shaker family) open at hyperpolarised potentials. K^+ flows down its electrochemical gradient into the guard cell, accumulating at concentrations of $400\text{--}800 \text{ mM}$. KAT1 is the rate-limiting K^+ entry channel for stomatal opening; *kat1* knockouts have severely reduced light-induced opening.
5. Cl^- accumulates as a charge-balancing counterion through SLAH3 and CLC channels operating in reverse mode under hyperpolarization
6. Malate^{2−} is synthesized from chloroplast-derived starch via PEP carboxylase and converted by NADP-malate dehydrogenase, providing additional charge-balancing osmoticum
7. Sucrose accumulates in late-afternoon stomata, supplementing K^+ /malate as an osmoticum (afternoon stomata may be 50% sucrose-driven)
8. Decreased osmotic potential (Ψ_s more negative, by $1.5\text{--}2 \text{ MPa}$) drives water influx through aquaporins (PIP1, PIP2)
9. Guard cells swell. Their differentially thickened walls (thicker on the inner pore-facing wall, thinner on the outer wall) cause the cells to bow apart asymmetrically
10. Stomatal aperture opens by $5\text{--}25 \text{ }\mu\text{m}$ depending on species

28.7.2 Stomatal Closure – ABA Signaling Cascade in Detail

Under drought stress, abscisic acid (ABA) triggers rapid stomatal closure through a molecular relay that has become a textbook example of plant signal transduction. The pathway can be summarized in five steps:



Each step in this cascade has been crystallographically resolved (PYR1-ABA-PP2C ternary complex, Melcher *et al.*, *Nature* 2009; SnRK2-PP2C complex, Soon *et al.*, *Science* 2012) and is now textbook signaling.

1. ABA synthesis: Soil drying activates NCED3 (9-*cis*-epoxycarotenoid dioxygenase) in roots, cleaving 9'-*cis*-violaxanthin/neoxanthin to xanthoxin (ABA precursor). Local ABA biosynthesis also occurs in leaf vasculature and guard cells themselves.
2. ABA distribution: ABA travels via xylem to guard cells and is concentrated by the AIT1/NPF4 family of ABA importers and the ABCG25 exporter.
3. Receptor binding: ABA binds PYR/PYL/RCAR receptors (14 paralogs in *Arabidopsis*) at a START-domain pocket. This binding “closes” the receptor’s gate loop over the binding pocket.
4. PP2C inhibition: The closed ABA-PYR complex docks onto and inhibits Type-2C protein phosphatases (ABI1, ABI2, HAB1). PP2Cs normally dephosphorylate (and thereby inactivate) downstream kinases.
5. SnRK2 activation: Released from PP2C inhibition, SnRK2 kinases (especially OST1/SnRK2.6) autophosphorylate and become active. OST1 phosphorylates downstream targets including:
 - SLAC1 anion channel: phosphorylation at Ser120 opens the channel; massive Cl^- and malate^{2−} efflux depolarizes the membrane (V_m shifts to -30 to -50 mV)

- GORK outward-rectifying K^+ channel: opens at depolarized potentials; K^+ leaves the cell down its electrochemical gradient
 - AKT1/KAT1: inward-rectifying K^+ channels are inhibited (preventing K^+ re-entry)
 - NADPH oxidase RBOHF: produces reactive oxygen species (ROS) that activate Ca^{2+} -permeable channels, raising cytosolic Ca^{2+} and amplifying SLAC1/GORK responses
6. Osmotic deflation: Loss of K^+ , Cl^- , and malate raises Ψ_s by 1.5 MPa; water exits via aquaporins; turgor drops
7. Aperture closure: Stomata close within 5-15 minutes

The ABA cascade integrates with a parallel CO_2 -sensing pathway (HT1 kinase, MPK4/12) and an immune pathway (FLS2 receptor activated by bacterial flagellin) at the level of SLAC1, which serves as a hub for diverse closure stimuli.

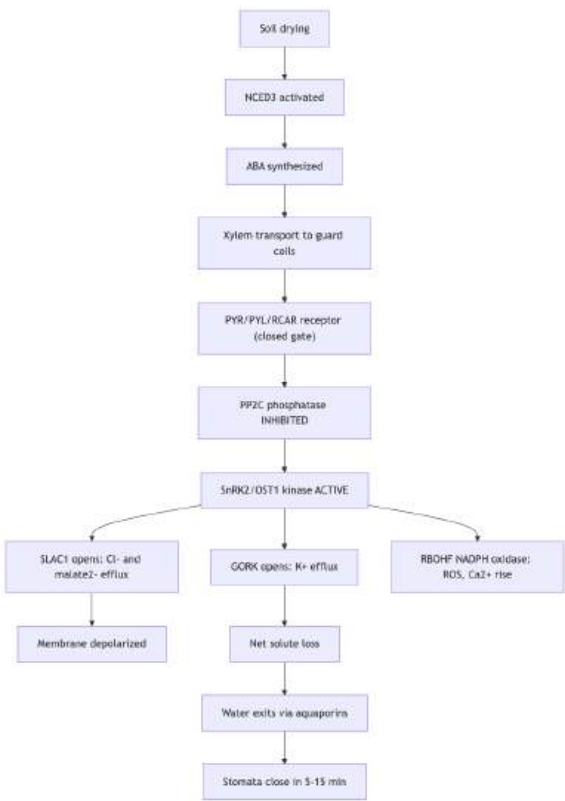


Figure 173. The ABA signaling cascade in guard cells ABA binding releases SnRK2 kinases from PP2C inhibition; SnRK2 then drives the ion-flux changes that osmotically deflate the guard cell.

28.7.3 Other Factors Affecting Stomata

- CO_2 concentration: Elevated internal CO_2 promotes closure (reduces need for gas exchange). This is significant under rising atmospheric CO_2 , where plants partially close stomata, reducing transpiration but potentially increasing leaf temperature.
- Humidity: Low humidity (high vapor pressure deficit, VPD) promotes closure as a protective response against excessive water loss
- Photosynthetically active radiation (PAR): Drives opening via both blue-light specific and photosynthesis-dependent pathways
- Circadian clock: Stomata show anticipatory opening before dawn, controlled by the plant circadian clock

28.7.4 Water-Use Efficiency

Stomatal opening trades CO_2 acquisition against water loss. The intrinsic water-use efficiency captures this trade-off at the leaf level:

$$iWUE = \frac{A_n}{g_s}$$

(360)

where A_n is net CO_2 assimilation rate ($\mu\text{mol } CO_2 \text{ m}^{-2} \text{ s}^{-1}$) and g_s is stomatal conductance to water vapor ($\text{mol } H_2O \text{ m}^{-2} \text{ s}^{-1}$). Higher iWUE means more carbon fixed per unit water transpired.

C3, C4, and CAM trade-offs:

- C3 plants (most temperate species; rice, wheat, soybean) have iWUE about 50–100 $\mu\text{mol CO}_2 \text{ mol}^{-1} \text{ H}_2\text{O}$. Their primary CO_2 -fixing enzyme RuBisCO operates at near-atmospheric $[\text{CO}_2]$ inside the leaf, limiting iWUE.
- C4 plants (maize, sorghum, sugarcane, many tropical grasses) concentrate CO_2 in bundle-sheath cells via the C4 pump. Mesophyll $[\text{CO}_2]$ is amplified about 10-fold relative to ambient, allowing stomata to be partially closed without limiting photosynthesis. iWUE about 150–250 $\mu\text{mol mol}^{-1}$.
- CAM plants (succulents, cacti, agaves, pineapple) open stomata primarily at night, when VPD is low. CO_2 is fixed as malate and stored in vacuoles; during the day, decarboxylation releases CO_2 inside closed leaves for photosynthesis. iWUE can exceed 500 $\mu\text{mol mol}^{-1}$ — an order of magnitude above C3.

The progression C3 → C4 → CAM represents progressive specialization for water-limited environments, with CAM as the most extreme adaptation. The iWUE differential explains why C4 maize outperforms C3 wheat in hot, semi-arid climates and why CAM cacti dominate true deserts.

Concept Check 9: A researcher fumigates a leaf with elevated CO_2 while simultaneously illuminating it with blue light. Predict the net effect on stomatal aperture and explain the competing signals at the level of OST1/SLAC1.

Concept Check 10: An *ost1* loss-of-function *Arabidopsis* mutant is subjected to drought. Predict its phenotype relative to wild type. What would happen if the same mutant carried a constitutively active SLAC1 transgene?

Concept Check 11 (Analyze) — Guard-cell ion logic at opening and closing. Blue light activates the guard-cell H^+ -ATPase, hyperpolarising the plasma membrane to roughly -180 mV . This opens inward-rectifying K^+ channels (KAT1); K^+ floods in, water follows via aquaporins, turgor rises, and stomata open. ABA reverses the logic by activating SLAC1, which exports Cl^- and malate²⁻, depolarizing the membrane to roughly -30 mV ; outward-rectifying GORK then exports K^+ and the guard cell shrinks. (a) Map the sign of the driving force on K^+ at -180 mV vs -30 mV given $E_K \approx -90 \text{ mV}$, and explain why the same K^+ permeability supports opposite net fluxes in the two states. (b) Predict the phenotype of a *slac1* knockout exposed to a 24-hour drought: what fraction of the closure response is lost, and which residual mechanisms (if any) still contribute? (c) Design a single-cell patch-clamp experiment that would distinguish “loss of depolarization drive” from “loss of K^+ efflux capacity” as the dominant cause of impaired closure in your knockout.

Concept Check 12 (Evaluate) — Casparian strip and ion exclusion at the endodermis. The Casparian strip blocks the apoplastic route at the endodermis, forcing every solute through at least one plasma membrane crossing. Mature roots typically exclude approximately 99% of soil Na^+ from the shoot while concentrating K^+ approximately 100-fold above soil levels in the xylem sap. (a) Explain how the strip converts a non-selective bulk-flow path into a transporter-gated selectivity filter, and identify which membrane (epidermal, cortical, endodermal) carries the K^+ -selecting machinery (HKT, AKT1, HAK5). (b) A mutant disrupts CASP1/CASP3-mediated lignification so the strip becomes discontinuous. Predict, with direction and order-of-magnitude estimate, the change in xylem $\text{Na}^+ : \text{K}^+$ ratio of a young plant exposed to 50 mM NaCl irrigation. (c) Evaluate whether this loss-of-function could ever be adaptive — for example, in a halophyte that uses Na^+ as a cheap osmoticum — and contrast with a glycophyte crop where the same mutation would be agronomically lethal.

28.8 Phloem Transport – The Münch Pressure-Flow Model

Unlike xylem (upward, driven by transpiration tension), phloem transports photosynthate (sucrose at 0.3-0.9 M plus amino acids, hormones, mRNAs, and small proteins) bidirectionally from sources to sinks.

28.8.1 Phloem Loading — Apoplastic vs Symplastic Pathways

How sugars enter sieve tubes from photosynthetic mesophyll determines key physiological properties: loading rate, concentration limits, and the species-specific tradeoffs between transport efficiency and protection from herbivores. The choice of loading strategy is one of the most striking ecophysiological dichotomies in plants.

Apoplastic loading (Type 2; most herbaceous crops, including most major cereals, *Arabidopsis*, sugar beet, soybean, tomato):

1. Sucrose is exported from mesophyll cells to the apoplast (cell-wall space) via SWEET11/SWEET12 sucrose efflux carriers (uniporters, facilitated diffusion)
2. The H^+ -ATPase on the companion-cell plasma membrane creates a steep proton gradient (apoplast pH about 5.5; cytoplasm pH about 7.5) and a hyperpolarised membrane potential
3. SUT1 (Sucrose- H^+ symporter; also known as SUC2 in *Arabidopsis*) uses the proton gradient to import sucrose against its concentration gradient (10–50× concentration step). The full family of sucrose transporters (SUTs) comprises three clades with distinct cellular localisations and kinetic properties: SUT1/SUC2 is the workhorse loader on companion cells (low K_m about 1 mM); SUT4 localizes to tonoplasts and mediates vacuolar sucrose mobilization; SUT2 has been proposed as a sucrose sensor with high K_m . Knockout of *SUT1* in maize (*sut1* mutants) causes sugar accumulation in source leaves and starvation in sinks, confirming its role as the rate-limiting loader.
4. Imported sucrose moves through plasmodesmata between companion cell and sieve element to enter the conducting stream
5. Loading rate: 5–15 μmol sucrose per cm^2 of leaf per hour

Apoplastic loading is energetically costly (one ATP per sucrose) but allows very high sieve-tube concentrations (up to 1 M sucrose) by “uphill” transport against the concentration gradient.

Symplastic loading (Type 1; many trees, especially temperate broadleaves like willow, poplar; also many tropical species):

1. Sucrose moves from mesophyll to companion cells predominantly through plasmodesmata, largely without crossing a membrane (real leaves show some apoplastic leakage even in symplastic loaders). Plasmodesmal density at the mesophyll–companion cell interface is 10–100 × higher in symplastic loaders than in apoplastic loaders. This is the diagnostic anatomical feature of symplastic loading — first established by Gamalei (1989) in his comparative survey of >300 species.
2. In specialized “intermediary cells” (companion-cell variant), sucrose is converted to larger oligosaccharides (raffinose, stachyose) by galactinol synthase + raffinose synthase. These larger oligosaccharides cannot diffuse back through the narrow plasmodesmal aperture (about 3 nm size limit at the desmotubule).
3. The accumulated raffinose-family oligosaccharides (RFOs) form a one-way polymer trap (Turgeon, 1991), lowering Ψ_s and drawing water into the sieve tube.

Symplastic loading is energetically cheap (no membrane transport) but limited in concentration. Some temperate trees (apple, *Malus*) use a third hybrid strategy — passive symplastic loading without polymer trapping, where the source-sink concentration gradient alone drives unloading.

Plasmodesmatal conductance and regulation:

Plasmodesmata are dynamic; their aperture is set by the deposition of callose (β -1,3-glucan) at the neck. Callose synthases (CalS1/3/7/8) and β -1,3-glucanases (BG_pap, BG_ppap) act antagonistically. Under stress (wounding, pathogen attack), callose deposition closes plasmodesmata within minutes, isolating affected cells. SUT1-dependent (apoplastic) loading is unaffected by plasmodesmal closure; symplastic loaders are critically dependent on open plasmodesmata and are more vulnerable to wounding-induced flow disruption.

Comparison across plant groups:

Table 355. Phloem Loading — Apoplastic vs Symplastic Pathways: Loading type and Plant groups.

Loading type	Plant groups	Plasmodesmata at mesophyll-CC interface	Rate-limiting step	Phloem sap [sucrose]
Apoplastic (SUT1)	Most herbaceous crops, cereals, <i>Arabidopsis</i> , <i>Solanum</i>	Few (<1 per μm^2)	SUT1 H ⁺ -symport	Up to 1.0 M
Symplastic active (polymer trap)	Many temperate broadleaves: <i>Salix</i> , <i>Populus</i> , <i>Cucurbita</i> , <i>Coleus</i>	Many (>10 per μm^2)	Raffinose synthase rate	0.3–0.8 M
Symplastic passive	Some trees (apple, <i>Quercus</i> ?)	Many	None (diffusion-limited)	0.2–0.4 M

28.8.2 The Münch Pressure-Flow Hypothesis [M^{unch}, 1930]

Ernst Münch’s 1930 model remains the consensus explanation for bidirectional phloem flow, supplemented by about 95 years of experimental refinement.

Mechanism:

1. Sugar loading at source (mature leaves) raises sucrose concentration in sieve tubes to 0.5–1 M, lowering Ψ_s to −2 to −3 MPa
2. Water enters by osmosis from adjacent xylem (where Ψ is more positive). Turgor pressure (Ψ_p) rises to +1 to +2 MPa at the source
3. Sugar unloading at sink (roots, developing fruit, growing tips, storage organs) removes sucrose. Sucrose may be cleaved by invertase (to glucose + fructose) or sucrose synthase. As sucrose is removed, Ψ_s rises, water exits to surrounding tissues, and turgor pressure falls to +0.3 to +0.6 MPa
4. The pressure gradient between source (high turgor) and sink (low turgor) drives bulk flow through the sieve-tube network along the path of least resistance
5. The unloaded water re-enters the xylem and is recycled to the source (closing the loop)

Unloading mechanisms are sink-specific:

- Symplastic unloading (most growing sinks, e.g., root tips, developing leaves): sucrose moves through plasmodesmata into surrounding cells; intracellular sucrose synthase or invertase cleaves it for use.
- Apoplastic unloading (storage sinks isolated by suberin, e.g., developing seeds and grains): sucrose is exported by SWEETs into the apoplast, then cleaved by cell-wall invertase to glucose + fructose, which are imported via hexose transporters. The maternal-filial boundary in seeds is typically apoplastic, ensuring genetic isolation between mother plant and developing offspring.

Flow rates: 0.5-1.5 m/h; rates up to 3 m/h have been measured.

Supporting evidence for Münch flow:

1. Aphid-stylet sap collection (Mittler, 1953): aphids cleanly tap individual sieve tubes; collected sap shows sucrose concentrations of 10–25% w/v, consistent with osmotically active loading
2. Pressure probes on individual sieve elements directly measure positive turgor of +1–2 MPa near the source and lower turgor near sinks
3. Cessation of flow on cooling the petiole (which inhibits H⁺-ATPase but does not block plasmodesmata) confirms active loading is required
4. Source–sink reversal: Removing the lower leaves of a soybean plant reverses flow direction in the stem (downward to upward) within hours, consistent with passive bulk flow following the pressure gradient
5. Mathematical modeling with realistic sieve-tube geometry (Thompson and Holbrook, 2003) shows Münch flow can readily account for observed transport rates in trees up to about 100 m, provided sieve tubes are wide enough

Evidence against (and modifications to) Münch flow:

1. The giant-vine objection (T.W. Mason, 1922): flow rates in long vines were measured to exceed Münch’s predictions for narrow conduits. This was resolved when measurements showed sieve-tube radii in such species are actually larger than initially supposed.
2. Pressure-driven model alone cannot account for observations of sieve plate occlusion (P-protein, callose) in healthy phloem, suggesting flow regulation through dynamic plate gating
3. High-velocity, short-distance flow in some tropical lianas (>3 m/h) approaches the upper bound of Münch flow and may require a supplementary “relay” mechanism

The current consensus: Münch pressure-flow is the dominant mechanism, supplemented by molecular regulators (sieve-plate occlusion, P-protein gating) that fine-tune flow without overturning the basic pressure-driven principle.

Clinical Connection: Girdling (removal of a ring of bark including phloem) causes sugar accumulation above the girdle and starvation below, eventually killing the tree. This principle explains why bark-stripping by elephants, deer, or porcupines can be lethal. Conversely, targeted phloem disruption is used as a management tool to kill invasive tree species.

Concept Check 11: Predict the consequence for phloem flow if a chemical inhibitor of the H⁺-ATPase is locally applied to the source leaf petiole of an apoplastic-loading species. Would the same treatment have the same effect in a symplastic-loading tree?

Concept Check 12: A maize *sut1* mutant accumulates sucrose to 200 mM in mesophyll but 10 mM in sieve tubes (wild-type values: 50 mM and 800 mM, respectively). Trace this phenotype through the apoplastic loading pathway and predict the appearance of source leaves and roots.

28.9 Nutrient Uptake and Mineral Nutrition

28.9.1 Essential Mineral Nutrients and Deficiency Logic

Plants require 17 essential elements, divided into macronutrients and micronutrients:

Macronutrients (required in large quantities):

Table 356. Essential Mineral Nutrients and Deficiency Logic: Element and Symbol.

Element	Symbol	Primary Functions	Deficiency Symptoms
Nitrogen	N	Amino acids, nucleotides, chlorophyll	Chlorosis (yellowing) of older leaves first
Phosphorus	P	ATP, nucleic acids, membranes	Purple/dark green leaves; stunted growth
Potassium	K	Osmotic regulation, enzyme activation, stomata	Marginal leaf necrosis; weak stems
Calcium	Ca	Cell wall (middle lamella), signaling	Growing point death; blossom-end rot
Magnesium	Mg	Chlorophyll center, enzyme cofactor	Interveinal chlorosis of older leaves
Sulfur	S	Cysteine, methionine, coenzyme A	General chlorosis; stunted growth

Common mycorrhizal networks (CMNs): Mycorrhizal fungi can connect multiple plants, forming underground networks. Carbon, water, and nutrient signals have been documented moving between plants via these networks, though the ecological significance of active plant-plant signaling through CMNs remains debated.

Concept Check 13: A farmer notices that legume crops planted alongside non-legume crops improve the growth of both. Explain the mechanisms by which nitrogen fixed by rhizobia in legume nodules can become available to neighboring non-legume plants.

28.10 Adaptations for Water and Nutrient Acquisition

28.10.1 Xerophyte Adaptations to Water Deficit

Plants in arid environments have evolved numerous strategies to minimize water loss and maximize water uptake:

- Thick cuticle and epicuticular waxes (reduce cuticular transpiration)
- Sunken stomata in pits or grooves (create humid microenvironment; *Nerium oleander*)
- Reduced leaf surface area (needles, spines) or deciduousness during dry season
- CAM photosynthesis (stomata open at night, close during day; CO₂ stored as malate)
- Succulence (water storage in stems or leaves; *Opuntia*, *Aloe*)
- Deep or extensive root systems (mesquite roots can reach 50+ m depth)

28.10.2 Hydrophyte Adaptations to Flooded Environments

Aquatic and wetland plants face the opposite challenge – too much water and often **anaerobic** substrates:

- Aerenchyma (large air-filled cortical spaces for gas transport to submerged roots)
- Thin or absent cuticle (CO₂ and O₂ diffuse directly from water)
- Dissected or thin leaves (maximize surface area for gas exchange in water)
- Adventitious roots from stem nodes

28.10.3 Carnivorous Plants and Nutrient Acquisition

In nutrient-poor environments (bogs, sandy soils), some plants supplement mineral nutrition by capturing and digesting insects and other small animals:

- Pitcher plants (*Nepenthes*, *Sarracenia*): modified leaves form pitfall traps with slippery surfaces and digestive enzymes
- Sundews (*Drosera*): sticky mucilage on tentacle-like trichomes; leaf slowly curls around prey
- Venus flytrap (*Dionaea muscipula*): snap trap triggered by touch-sensitive trigger hairs; requires two stimulations within 20 seconds (counting mechanism involves Ca²⁺ signaling)

Most carnivorous plants derive primarily nitrogen and phosphorus from prey.

Concept Check 14: Sketch a pressure-flow circuit (source–sink) for a CAM plant during the night when stomata are open. How does CAM-driven nighttime malate accumulation interact with phloem loading dynamics in the same tissue?

28.11 Computational Bridge

Whole-cell water potential sums osmotic and pressure components in MPa:

```
from biology.botany import water_potential

psi = water_potential(0.3, turgor_pressure_MPa=0.5)
print(round(psi.water_potential_MPa, 4))
```

Clinical / systems note: Crop drought breeding screens often proxy cellular osmotic adjustment — the same Ψ_s shifts you estimate from solute accumulation.

28.12 Current Evidence and Frontier Biology: Plant Structure and Water Relations

For Plant Structure and Water Relations, frontier biology belongs inside the evidence logic of the chapter. Plant biology links molecular regulation to climate stress, water limitation, crop resilience, phenology, and ecosystem feedbacks. The core reading question is this: plant-water claims require water potential, hydraulic pathway, stomatal control, tissue anatomy, and stress context.

- What to verify: identify the observation, model, assay, or dataset that would make the claim stronger or weaker.
- What to qualify: state the scale, organism, cell type, environmental condition, or population where the claim is expected to hold.
- What to compare: test at least one alternative explanation, baseline, or null model before treating the pattern as causal.
- What to cite: distinguish primary evidence, review synthesis, public dataset, and institutional guidance; for recent or numeric claims, prefer the source closest to the measurement and state what has changed since it was published.

A strong plant-transport claim names the tissue, water-potential component, environmental driver, measurable flow, and tradeoff with growth or defense.

Source practice: For plant-water claims, connect anatomy and physiology to water-potential measurements, field context, and growth-reproduction tradeoffs.

Hydraulic safety claims should also be benchmarked against comparative vulnerability data: globally, many forest species operate close to xylem failure thresholds, so drought tolerance must be framed as a margin rather than a binary trait [Choat et al., 2012].

28.12.1 Current Evidence Map: Hydraulic Safety Tradeoff

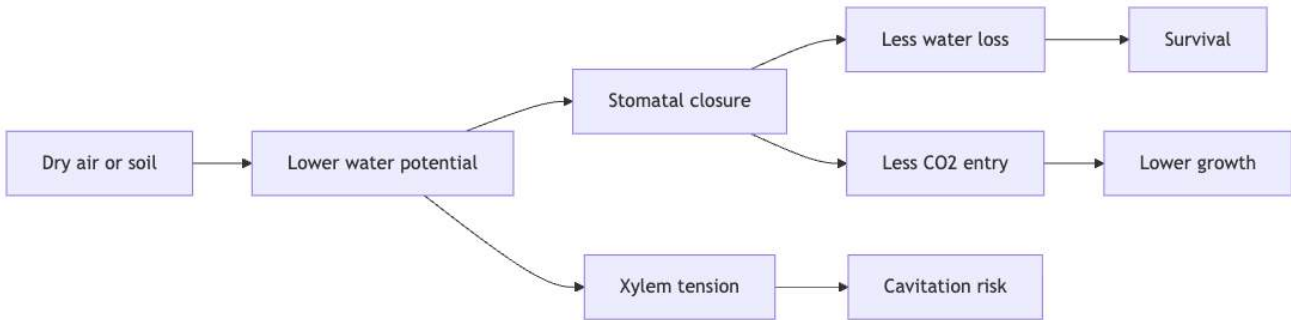


Figure 174. Drought responses should be read as tradeoffs among carbon gain, water loss, hydraulic safety, and growth rather than as simple stress resistance.

28.13 Summary

- Plant body plan: Root system (taproot or fibrous) + shoot system (stem + leaves). Phytomers (node + internode + leaf + axillary bud) are the modular building units; plastochron index sets developmental time.
- Three tissue systems: Dermal (protection, cuticle, stomata, trichomes), ground (parenchyma for photosynthesis/storage, collenchyma for flexible support, sclerenchyma for rigid support), vascular (xylem: tracheids/vessels for water; phloem: sieve tubes/companion cells for sugars).
- Xylem development: Protoxylem (annular/helical, extensible) precedes metaxylem (scalariform/pitted, mechanically robust). Vessels are wider and more efficient than tracheids but more cavitation-prone (Hagen-Poiseuille r^4 scaling). Conifer pits with torus-margo valves provide most-or-nothing cavitation isolation; angiosperm homogeneous pit membranes are more vulnerable.
- Water potential: Full four-component form $\Psi = \Psi_s + \Psi_p + \Psi_m + \Psi_g$ (equation (356)) governs direction of water flow; matric potential dominates in dry seeds and soils. The SPAC has a steep gradient driving water from soil (−0.01 to −1.5 MPa) to atmosphere (−100 MPa).
- Transport pathways: Apoplast (cell walls, fast, non-selective) vs symplast (cytoplasm via plasmodesmata, selective) vs transmembrane (aquaporins + transporters, selective). Casparian strip (lignin) + suberin lamella in endodermis force water into symplast for quality control; passage cells provide selective bypasses; lateral root emergence creates transient apoplastic bypass.
- TACT mechanism [Dixon and Joly, 1894]: Transpiration creates tension in xylem; water’s cohesive H-bonds maintain continuous column; adhesion to xylem walls supports the column; water rises passively. Critical evaluation: pressure probes, MRI, synthetic-tree experiments, and synchrotron X-ray micro-CT confirm tensions of −1 to −22 MPa; embolism repair via overnight root pressure and phloem-driven refilling mitigates cavitation losses.
- Stomatal regulation: Opening via H^+ -ATPase, KAT1, malate accumulation (blue light, phototropins); closure via ABA-PYR-PP2C-SnRK2-SLAC1/GORK cascade. Balances CO_2 gain vs water loss; $iWUE = A_n/g_s$ (equation (360)). C4 and CAM plants achieve $iWUE$ 2–10× C3 by concentrating CO_2 behind partially-closed stomata.
- Phloem: Münch pressure-flow [Münch, 1930] with apoplastic loading (SUT1 cotransporter; herbaceous crops; high sieve-tube concentration) or symplastic loading via polymer trap (raffinose; many trees; many plasmodesmata; lower concentration) at source. Bidirectional flow follows turgor gradient; symplastic vs apoplastic unloading varies by sink type.

- Nutrient uptake: 17 essential elements (6 macro, 8 micro, plus C/H/O). Nitrogen fixation by rhizobia in legume nodules. Mycorrhizae (AM and EM) enhance P and N uptake in 80% of plant species.
- Connections: See section 29 and section 30 for reproduction and signaling, section 2 for water thermodynamics, and section 40 for primary production.

28.14 Key Terms

Table 358. Current Evidence Map: Hydraulic Safety Tradeoff: Term and Definition.

Term	Definition
Water potential (Ψ)	Free energy of water per unit volume; determines direction of water movement; units MPa
Osmotic potential (Ψ_s)	Component of water potential due to solute concentration; typically negative
Turgor pressure (Ψ_p)	Positive pressure exerted by cell contents against the cell wall
Matric potential (Ψ_m)	Component due to water binding on colloidal surfaces; dominant in dry seeds and soils
Casparian strip	Lignin (then suberin) band in endodermal cell walls; forces water through symplast
Suberin lamella	Continuous suberin layer in mature endodermal cells; further restricts apoplast
Passage cell	Endodermal cell lacking suberin lamella; provides selective transport bypass
Cohesion-tension mechanism	Transpiration-driven water ascent relying on hydrogen bond cohesion
Cavitation	Formation of gas bubble in xylem under excessive tension
Stomata	Pores bounded by guard cells; regulate gas exchange and transpiration
Apoplast	Continuum of cell walls and intercellular spaces
Symplast	Continuum of cytoplasm connected by plasmodesmata
Tracheids	Elongated, tapered xylem cells with bordered pits; found in most vascular plants
Vessel elements	Wide xylem cells with perforation plates; primarily in angiosperms
Bordered pit (torus-margo)	Conifer pit with thickened central torus suspended in porous margo; valves on cavitation
Protoxylem	Early xylem with annular/helical thickenings; extensible during organ growth
Metaxylem	Late xylem with scalariform/pitted thickenings; mechanically robust
Sieve tube elements	Enucleate phloem cells connected by sieve plates; conduct sugars
Companion cells	Nucleate cells that metabolically support sieve tube elements
SUT1 (SUC2)	Sucrose- H^+ symporter on companion cells; rate-limiting loader in apoplastic species
SWEET11/12	Sucrose efflux carriers; export sucrose from mesophyll to apoplast
Polymer trap	Symplastic loading mechanism using raffinose-family oligosaccharides
Plasmodesmatal conductance	Bulk transfer rate through plasmodesmata; regulated by callose deposition
Münch pressure-flow	Model of phloem transport driven by turgor pressure gradient from source to sink
Phytomer	Modular shoot unit: node + internode + leaf + axillary bud
Plastochron index	Time interval between successive leaf-primordium initiations
Mycorrhizae	Mutualistic root-fungus associations; enhance nutrient uptake
Arbuscular mycorrhizae	AM fungi that form arbuscules inside root cortical cells; deliver P
Ectomycorrhizae	EM fungi that form external mantle and Hartig net; deliver N and P
Nitrogenase	Enzyme complex in nitrogen-fixing bacteria; converts N_2 to NH_3
Aquaporins	Water channel proteins (PIP, TIP families) in plant cell membranes
OST1/SnRK2.6	Master kinase of guard-cell ABA response; phosphorylates SLAC1
iWUE (intrinsic WUE)	A_n/g_s ; net CO_2 assimilated per unit stomatal conductance

28.15 Review Questions

1. A plant cell has a solute concentration of 0.4 M, turgor pressure of 0.3 MPa, and is at ground level. Using $\Psi_s = -iCRT$ with $i = 1$, $R = 0.00831 \text{ L MPa mol}^{-1} \text{ K}^{-1}$, and $T = 298 \text{ K}$, calculate the total water potential. If this cell is adjacent to another cell with $\Psi = -0.5 \text{ MPa}$, which direction will water flow?
2. Explain why xylem vessels are more efficient than tracheids for water transport but also more vulnerable to cavitation. What structural features of tracheids (torus-margo pits) help prevent the spread of embolisms? Contrast with angiosperm pit membranes.

- Describe the complete pathway of a water molecule from the soil solution to the atmosphere, naming each structure it passes through. At which points must the molecule cross a cell membrane?
- Compare apoplastic and symplastic phloem loading. Which is more common in herbaceous crop plants? What is the energetic cost of each, and why might symplastic loading be advantageous in some environments? Cite SUT1 and the polymer-trap mechanism in your answer.
- A farmer observes that phosphorus-deficient plants show improved growth when inoculated with arbuscular mycorrhizal fungi but not when given additional phosphorus fertiliser alone. Explain this observation in terms of the spatial distribution of phosphorus in soil and the relative surface area of roots vs mycorrhizal hyphae.
- Explain how the Casparian strip (lignin) and suberin lamella of the endodermis act as a quality control checkpoint. What would happen to plant ion homeostasis if the Casparian strip were absent? What is the role of passage cells in older roots? Account for apoplastic bypasses at lateral root emergence sites.
- During a heat wave, a crop plant simultaneously experiences high temperatures (stomatal opening signal from photosynthesis demand) and soil drying (ABA-mediated stomatal closure signal). Trace the molecular competition between these signals at the level of OST1/SLAC1 in guard cells and predict which typically dominates.
- Compare and contrast water movement in xylem and phloem in terms of: driving force, direction, conducting cell viability, and substances transported.
- Describe the nitrogen fixation symbiosis between *Rhizobium* and legumes. Why must nitrogenase be protected from oxygen, and how does the nodule accomplish this?
- A coast redwood (*Sequoia sempervirens*) is 100 m tall. Calculate the gravitational component of water potential at the top of the tree. Given that atmospheric Ψ can reach -100 MPa at 50% humidity, explain why the tree can still pull water to the canopy.
- Critically evaluate the cohesion-tension theory [Dixon and Joly, 1894]. Identify two lines of evidence supporting it (including synchrotron imaging) and one historical objection that has been resolved. What is the air-seeding hypothesis, and how does it apply to torus-margo pits?
- Using `transpiration_flux`, predict whether doubling stomatal conductance doubles water loss if the leaf-to-air vapor gradient is held fixed. Then compute the iWUE consequence assuming A_n saturates at 80% of the doubled g_s .
- Contrast hydraulic redistribution via roots with capillary rise in soil — when does each dominate overnight water status?
- Use the Hagen-Poiseuille equation equation (355) to estimate the relative volumetric flow capacity of a $200\text{-}\mu\text{m}$ vessel versus a $30\text{-}\mu\text{m}$ tracheid (same length and pressure gradient). How does this calculation explain the prevalence of vessels in fast-transpiring angiosperms?
- A C3 wheat plant achieves iWUE of $80\text{ }\mu\text{mol CO}_2\text{ mol}^{-1}\text{ H}_2\text{O}$; an adjacent C4 maize plant achieves iWUE of 200. Both have nearly identical A_n when measured at noon. Calculate the relative g_s of the two species and explain why C4 plants outcompete C3 in semi-arid regions.

28.16 Further Reading and Source Notes: Plant Structure and Water Relations

- Dixon and Joly [1894] — On the ascent of sap. *Philosophical Transactions of the Royal Society B*, 186.
- Munch [1930] — Die Stoffbewegungen in der Pflanze. *Gustav Fischer Verlag*.

28.17 Companion Source Module: Plant Structure and Water Relations

Plant Structure and Water Relations should leave a reproducible trail from a biological claim to the code, figure, diagram, or paper-based activity that can test it. Use the surfaces below to inspect the chapter’s assumptions, rerun the relevant model, or compare the manuscript explanation with companion labs and figures.

Table 359. Companion source surfaces for Plant Structure and Water Relations.

Surface	Use it for
<code>src/biology/botany/botany.py</code> (<code>water_potential</code> , <code>transpiration_flux</code>)	Reproduce plant-water calculations and hydraulic tradeoffs.
<code>src/biology/cell/cell_biology.py</code> (<code>osmotic_pressure</code>)	Connect cellular osmotic pressure to tissue-level water movement.
<code>src/visualization/plots.py</code> (<code>plot_light_response_curve</code>)	Practice graph interpretation for environmental-response curves.

Reproducibility check: list solute potential, pressure potential, tissue, humidity, temperature, and stomatal state before predicting water movement. Cross-reference: use section 2 and section 30.

29 Plant Reproduction and Development

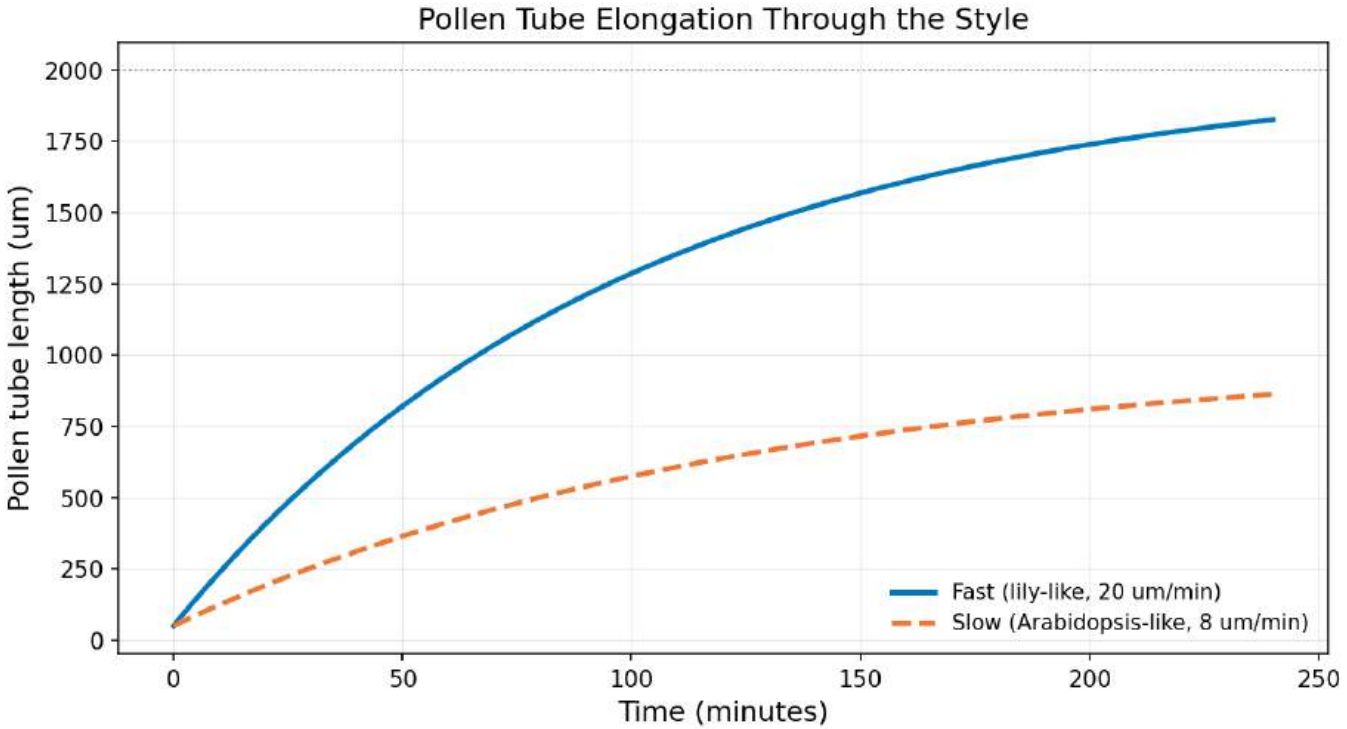


Figure 175. Pollen-tube length versus time for two contrasting growth profiles: a fast tube (lily-like, *about 20 μm/min*, *about 2 mm* saturation) and a slow tube (Arabidopsis-like, *about 8 μm/min*, *about 1 mm* saturation). Both follow a saturating logistic curve in which growth rate falls as the tube approaches its maximum length, mirroring the depletion of tip-localised secretory vesicles. The dashed line marks the upper saturation asymptote of the fast tube.

Level 2/3 · 55 min read · 75 min lecture · Prerequisites: section 28

29.1 Learning Objectives

By the end of this chapter, you should be able to:

1. Describe the alternation of generations and explain the evolutionary trend from gametophyte-dominant to sporophyte-dominant life cycles across the plant kingdom.
2. Compare reproduction in non-vascular plants, seedless vascular plants, gymnosperms, and angiosperms.
3. Describe angiosperm flower structure and explain the ABCDE model of floral organ identity [Coen and Meyerowitz, 1991], including the molecular identities of MADS-box transcription factors.
4. Describe pollen grain and embryo sac architecture at cellular resolution; trace double fertilization in detail [Nawaschin, 1898], including pollen tube chemotropism, synergid degeneration, and sperm cell delivery.
5. Explain microsporogenesis, megasporogenesis, and endosperm development (free-nuclear, cellular, PEG-pathway) including the 2m:1p genome dosage.
6. Compare seed dormancy types (physical, physiological, morphological, morphophysiological, combinatorial) and the molecular basis of germination triggers (stratification, scarification, light via phytochrome).
7. Describe self-incompatibility (SSI vs GSI), apomixis (sporophytic vs gametophytic), polyploidy, and vegetative propagation strategies.
8. Explain embryogenesis and meristem organization (SAM/RAM) including the WUS-CLV3 feedback loop, fruit development, and parthenocarpy.

29.1.1 Study Blueprint

- Big idea: Plant reproduction integrates life cycles, development, dispersal, and environmental timing.
- Core concepts: alternation of generations, flowers, seeds, development.
- Framework alignment: Vision & Change: Structure and function, Pathways and transformations of energy and matter, Systems; AP Biology: Energetics, Systems Interactions; NGSS-style topics: Structure and Function, Matter and Energy in Organisms and Ecosystems.
- Model or quantitative lens: Life-cycle accounting and phyllotaxis/growth-pattern calculations.
- Data skill: Track ploidy, tissue origin, and reproductive stage from diagrams or observations.
- Practice cadence: Visual Representations, Questions and Methods, Argumentation.

- Common misconception to repair: Pollen, spores, seeds, and gametes are not interchangeable terms.
- Primary lab: [Lab — Plant Reproduction and Development](#).
- Question bank: [Questions — Plant Reproduction and Development](#).
- Transfer task: Transfer reproductive reasoning to agriculture, pollination ecology, and plant evolution.
- Bridge to computation: `biology.botany.botany.plant_biomass_growth`.

Opening Vignette — The Seeds That Fed a Billion People

In the 1950s, famines threatened South Asia and Latin America as human population growth outpaced food production. Norman Borlaug, an American agronomist working in Mexico with the Rockefeller Foundation, spent a decade cross-breeding wheat varieties — shuttling seeds between winter and summer growing seasons to double selection speed — until he produced semi-dwarf, disease-resistant wheat varieties that yielded three to four times as much grain as traditional tall-stem wheats. Unlike traditional wheats, the short stems didn’t fall over when supporting heavy grain heads. He introduced these seeds to Pakistan and India in 1965. By 1970, wheat production had doubled in both countries, and famine had been averted. Borlaug received the 1970 Nobel Peace Prize. The same innovations, later extended to rice by the International Rice Research Institute, constitute the Green Revolution — a triumph of applied plant reproductive biology that is estimated to have saved over a billion lives.

29.2 Alternation of Generations

Plants have a diphasic life cycle – alternating between a diploid sporophyte (spore-producing) generation and a haploid gametophyte (gamete-producing) generation. This alternation is unique to plants and some algae; animals have primarily a brief haploid gametic phase.

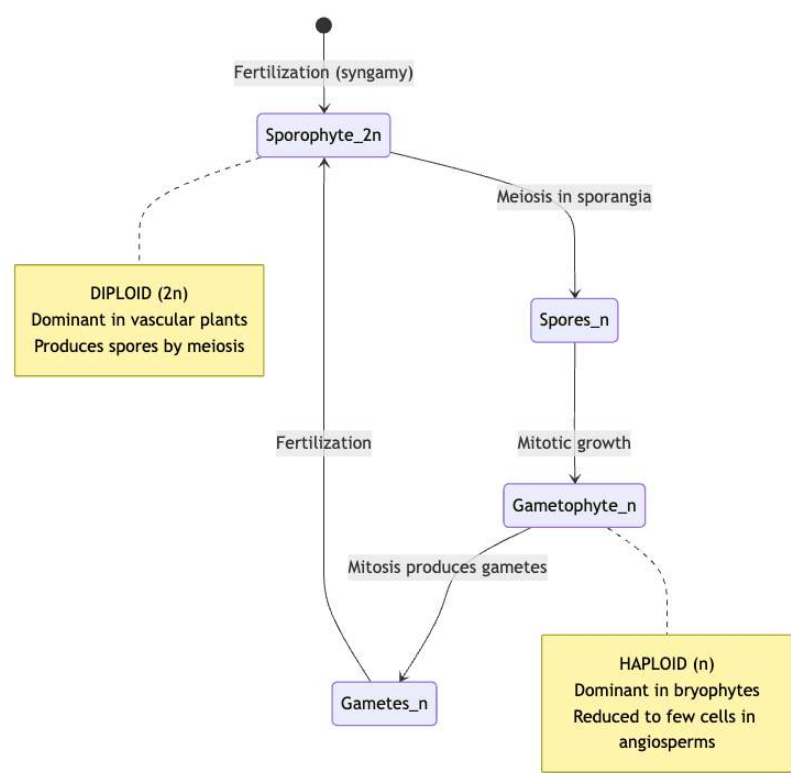


Figure 176. Alternation of generations showing the two phases of the plant life cycle The sporophyte (2n) produces haploid spores by meiosis. Spores develop into the gametophyte (n), which produces gametes by mitosis. Fertilization restores the diploid sporophyte.

Table 360. Study Blueprint: Plant group and Dominant generation.

Plant group	Dominant generation	Gametophyte description	Fertilization requirement
Bryophytes (mosses, liverworts)	Haploid gametophyte (the leafy “plant”)	Free-living; nutritionally independent	Water required (flagellated sperm swim)

Plant group	Dominant generation	Gametophyte description	Fertilization requirement
Pteridophytes (ferns, horsetails)	Diploid sporophyte	Small, free-living prothallus (about 1 cm ²); needs moisture	Water required
Gymnosperms (<i>Pinus</i> , <i>Ginkgo</i> , cycads)	Diploid sporophyte	Reduced; pollen = 4-celled male gametophyte; archegonia in ovule = female gametophyte	Wind pollination; no water needed
Angiosperms (flowering plants)	Diploid sporophyte	Microscopic, dependent: pollen = 3-celled; embryo sac = 7-celled, 8-nuclei	Wind or animal pollination

Why does dominance shift to the sporophyte? Diploid cells can mask deleterious recessive **mutations** (**heterozygous** advantage). A diploid sporophyte can accumulate more genetic material enabling structural complexity – leaves, stems, vascular tissue, seeds – allowing colonization of increasingly dry terrestrial habitats. The seed is the key innovation: it encases the embryo and gametophyte within maternal tissue, eliminating dependence on external water for fertilization.

29.2.1 Worked Example: Tracking Ploidy Through the Angiosperm Life Cycle

Problem: Maize (*Zea mays*) has a sporophyte chromosome number of $2n = 20$. Track the chromosome number at each stage of alternation of generations, then determine the ploidy of the zygote and the primary endosperm nucleus produced by double fertilization.

Solution:

1. Establish the haploid number. The gametophyte (haploid) number is half the sporophyte number:

$$n = \frac{2n}{2} = \frac{20}{2} = 10 \text{ chromosomes}$$

2. Meiosis in the sporophyte. The diploid megaspore mother cell ($2n = 20$) undergoes meiosis, producing haploid megaspores with $n = 10$. The surviving megaspore divides mitotically to build the embryo sac, so the egg cell and each of the two polar nuclei most carry $n = 10$. The pollen (microgametophyte) likewise delivers sperm cells with $n = 10$.
3. First fusion — the zygote. One sperm fuses with the egg:

$$\text{zygote} = n_{\text{egg}} + n_{\text{sperm}} = 10 + 10 = 20 \text{ (} 2n, \text{ diploid embryo)}$$

4. Second fusion — the endosperm. The second sperm fuses with the two polar nuclei of the central cell:

$$\text{primary endosperm nucleus} = n + n + n = 10 + 10 + 10 = 30 \text{ (} 3n, \text{ triploid)}$$

5. Genome dosage of the endosperm. Two of the three genomes are maternal (the polar nuclei) and one is paternal (the sperm):

$$\frac{\text{maternal}}{\text{paternal}} = \frac{2n}{1n} = \frac{20}{10} = \frac{2}{1}$$

Interpretation: Meiosis halves $2n = 20$ to $n = 10$ for the gametophyte generation; the two sperm-mediated fusions of double fertilization then restore a $2n = 20$ embryo and create a distinctive $3n = 30$ endosperm with a fixed 2:1 maternal:paternal dosage — the genetic substrate for the parent-of-origin conflict conserved across flowering plants.

29.3 Plant Group Reproductive Strategies

29.3.1 Non-Vascular Plants (Bryophytes)

Mosses (Bryophyta, about 12,000 species), liverworts (Marchantiophyta), and hornworts (Anthocerotophyta) represent the ancestral condition:

- The gametophyte is the dominant, photosynthetic plant body
- The sporophyte is small, attached to, and nutritionally dependent on the gametophyte

- Flagellated sperm must swim through water films to reach the archegonium (female reproductive structure)
- Spores dispersed from capsule (sporangium) at tip of sporophyte seta
- Ecological importance: pioneer colonisers of bare rock, form peat (carbon reservoir), retain moisture

Concept Check 1: Why are mosses restricted to moist habitats? What aspect of their reproduction limits their distribution?

29.3.2 Seedless Vascular Plants (Ferns and Allies)

Ferns (Polypodiopsida, about 10,500 species) represent the first major shift to sporophyte dominance:

- The sporophyte is the dominant plant (the familiar fern frond)
- Sporangia are clustered in sori (singular: sorus) on the underside of fronds, often protected by an indusium
- Meiosis in sporangia produces haploid spores
- Spores germinate into a small, heart-shaped prothallus (the independent gametophyte, about 1 cm)
- The prothallus bears both antheridia (produce flagellated sperm) and archegonia (produce eggs)
- Sperm must swim through water to the archegonium – the limiting step
- After fertilization, the new sporophyte grows from the prothallus, which eventually withers

Horsetails (*Equisetum*) and club mosses (*Lycopodium*, *Selaginella*) are also seedless vascular plants. *Selaginella* shows early heterospory (different-sized spores for male and female gametophytes), a precursor to the seed habit.

29.3.3 Gymnosperms and Naked-Seed Reproduction

Gymnosperms (“naked seed”) include conifers (about 630 species), cycads (about 350), *Ginkgo biloba* (1 species), and gnetophytes (about 70). Key reproductive features:

- Heterospory: Microsporangia (in pollen cones/microstrobili) produce microspores that develop into pollen grains (male gametophyte). Megasporangia (in ovulate cones) produce megaspores that develop into the female gametophyte (with archegonia).
- Pollen eliminates the need for water for fertilization. Wind-dispersed pollen lands on the ovule (pollination drop mechanism in many gymnosperms).
- Slow fertilization: In pines, 12-18 months elapse between pollination and fertilization. The pollen tube grows slowly through the nucellus to reach the archegonium; the quantitative contrast between fast and slow pollen tubes appears in figure 175.
- Seeds: The fertilized ovule develops into a seed containing the embryo, stored food (female gametophyte tissue), and a protective seed coat derived from the integuments. Seeds are “naked” (not enclosed in a fruit).

29.3.4 Angiosperms (Flowering Plants)

Angiosperms (about 300,000 species) are the most diverse plant group, with several key innovations:

- Flowers: Specialized reproductive structures that facilitate pollination (including animal pollination)
- Double fertilization: Unique to angiosperms, producing both embryo and endosperm
- Fruits: Mature ovary wall enclosing seeds; facilitate dispersal
- Reduced gametophytes: Male gametophyte = 3-celled pollen grain; female gametophyte = 7-celled, 8-nucleate embryo sac

29.4 Angiosperm Flower Structure and the ABCDE Model

29.4.1 Flower Architecture and Reproductive Organ Identity

Angiosperm flowers are modified shoots (shoot lateral organs with determinate growth). A complete flower contains four whorls (from outside inward):

Table 361. Flower Architecture and Reproductive Organ Identity: Whorl and Name.

Whorl	Name	Organ	Function
1 (outermost)	Calyx	Sepals	Protect flower bud; photosynthetic; sometimes petaloid
2	Corolla	Petals	Attract pollinators via color (UV patterns visible to bees), scent (monoterpenes), oil rewards

Whorl	Name	Organ	Function
3	Androecium	Stamens (filament + anther)	Pollen production (male gametophyte)
4 (innermost)	Gynoecium	Carpels (pistil) = stigma + style + ovary	Pollen reception; pollen tube guidance; ovule enclosure

Floral symmetry: - Actinomorphic (radially symmetric): *Rosa*, *Ranunculus*, most basal angiosperms – generalized pollinators - Zygomorphic (bilaterally symmetric): Orchidaceae, Fabaceae, Scrophulariaceae – specialized pollinators

Incomplete flowers lack one or more whorls. Imperfect flowers lack either stamens (pistillate/female flowers) or carpels (staminate/male flowers). Monoecious plants bear both on the same individual (maize); dioecious plants bear them on separate individuals (holly, willow).

29.4.2 The ABCDE Model and MADS-Box Floral Quartets [Coen and Meyerowitz, 1991]

The combinatorial control of floral organ identity by MADS-box transcription factors is the foundational discovery of plant evo-devo, and it provides a quantitative framework for understanding floral diversity. The classical ABC model (Coen and Meyerowitz, 1991) was extended by the discovery of D and E classes:

Table 362. Floral organ identity in the ABCDE model: whorl, organ, and gene classes.

Whorl	Organ	Classes active	Genes (<i>Arabidopsis</i>)
1	Sepal	A + E	AP1, AP2, SEP1-4
2	Petal	A + B + E	AP1, AP2, AP3, PI, SEP1-4
3	Stamen	B + C + E	AP3, PI, AG, SEP1-4
4	Carpel	C + E	AG, SEP1-4
Inside whorl 4	Ovule	D + E	SHP1, SHP2, STK, SEP1-4

Molecular identities of the ABC classes:

- A class (AP1, AP2): AP1 is itself a MADS-box gene; AP2 belongs to the unrelated AP2/ERF family — an “ABC anomaly” reflecting the fact that the canonical model was assembled before most molecular identities were known. AP1 specifies sepal identity in whorl 1 and contributes to petal identity in whorl 2.
- B class (AP3 and PI): Both are MADS-box genes; AP3 and PI form an obligate heterodimer (AP3-PI). This heterodimer is required for petal (with A) and stamen (with C) specification. *ap3* or *pi* single mutants lose petals and stamens.
- C class (AG = AGAMOUS): A MADS-box gene that specifies stamen identity (with B) and carpel identity (alone, with E). AG also enforces floral meristem determinacy: in *ag* mutants, the floral meristem proliferates indefinitely, generating extra petals in place of stamens and a new flower in place of a carpel — the genetic basis of “double flowers” in cultivated roses, carnations, and chrysanthemums.
- D class (STK, SHP1, SHP2): MADS-box genes specifying ovule identity within whorl 4. Loss of D-class function converts ovules to leaf-like structures.
- E class (SEP1, SEP2, SEP3, SEP4): SEPALLATA MADS-box genes; required for combinatorial action of A, B, C, D. *sep1 sep2 sep3 sep4* quadruple mutants produce primarily sepal-like organs in most whorls.

The MADS-box and the floral quartet model:

The MADS-box is a 56-amino-acid DNA-binding domain (named for MCM1, AGAMOUS, DEFICIENS, SRF — the founding members). MADS-box proteins bind CARG-box DNA motifs (CC[A/T]₆GG) and form floral quartets (Theissen and Saedler, 2001): tetrameric complexes that combinatorially specify each whorl’s identity by binding two CARG boxes simultaneously, looping the intervening DNA. The four-protein composition determines target gene specificity:

- AP1-AP1-SEP3-SEP3 → sepal
- AP3-PI-AP1-SEP3 → petal
- AP3-PI-AG-SEP3 → stamen
- AG-AG-SEP3-SEP3 → carpel

$$A + B + C + D + E \xrightarrow{\text{combinatorial CARG binding}} \text{floral quartet}$$

(362)

Key predictions and experimental validation:

- Removing A class (*ap1/ap2* mutants) results in carpels in whorls 1 and 2 (C class spreads to fill most whorls)
- Removing B class (*ap3/pi* mutants): sepals in whorls 1 and 2; carpels in whorls 3 and 4
- Removing C class (*ag* mutant): petals instead of stamens (whorl 3) and further petals indefinitely instead of carpel (whorl 4); produces double-petalled “full” flowers — the classic phenotype of cultivated double roses, carnations, and chrysanthemums
- Removing E class (*sep1 sep2 sep3 sep4* quadruple mutant): most whorls produce sepal-like organs, demonstrating SEP genes are required for B, C, and D function
- Quintuple ABCDE mutant: Most whorls produce leaf-like organs — confirming the molecular interpretation of Goethe’s 1790 metamorphosis hypothesis that most floral organs are modified leaves

Clinical Connection: Understanding the ABCDE model has practical applications in crop breeding. Manipulating floral organ identity genes can create male-sterile lines (essential for hybrid seed production in rice and wheat) by silencing the B class to convert stamens to petals. Conversely, increasing petal number in ornamental varieties relies on partial loss-of-function *ag* alleles. The multi-billion dollar cut flower industry relies directly on MADS-box gene variants for double-flowered roses, carnations, and chrysanthemums.

See equation (362) for the combinatorial logic; the empirical demonstration in *Antirrhinum* and *Arabidopsis* is the foundational work of Coen and Meyerowitz [1991].

29.5 Gametophyte Generation – Cellular Architecture

29.5.1 Male Gametophyte: Microsporogenesis and Pollen Grain Architecture

The mature pollen grain is the most reduced male gametophyte known — three cells encased in a desiccation-resistant wall. Its development is a textbook case of asymmetric cell division.

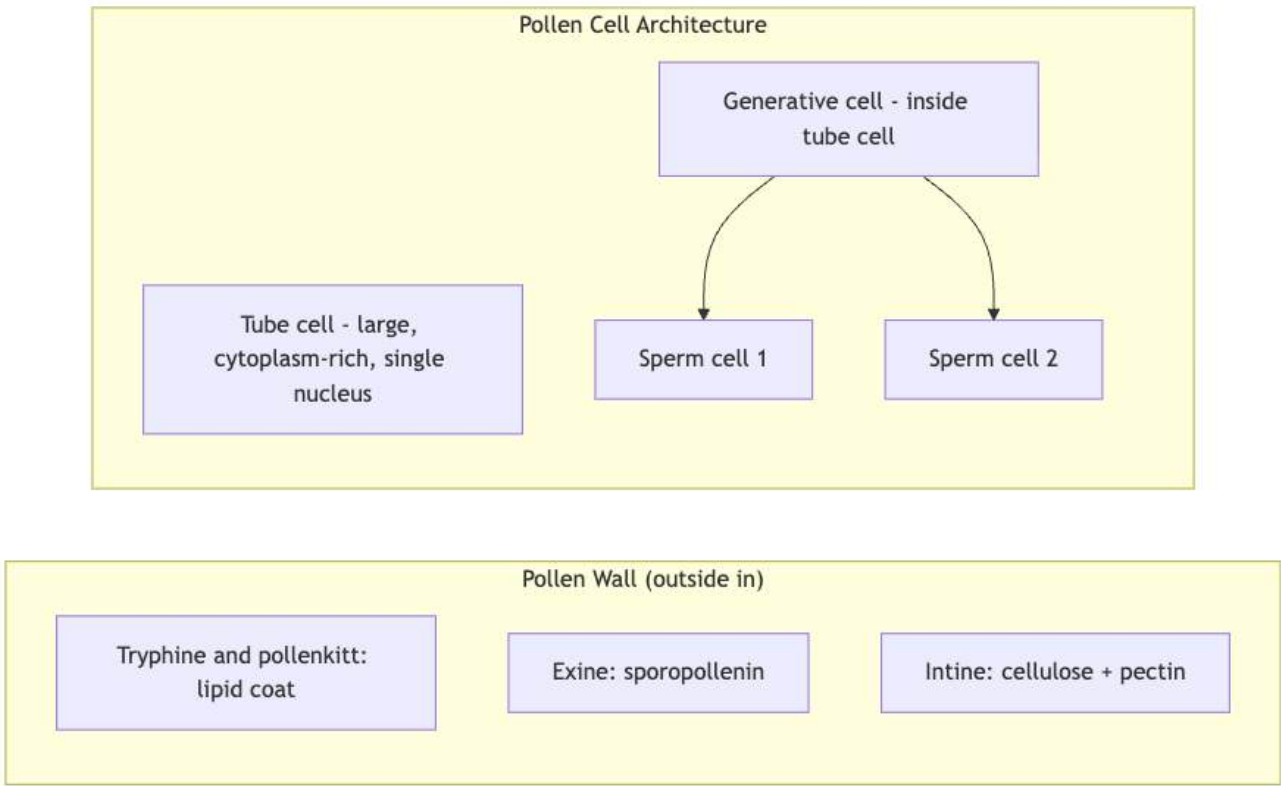


Figure 177. Architecture of an angiosperm pollen grain at maturity The tube cell envelops the generative cell, which divides to yield two sperm cells either before pollen release (tricellular pollen) or during tube growth (bicellular pollen at release).

Pollen wall layers:

- Intine (inner): Cellulose + pectin; uniform thickness; secreted by the gametophyte itself
- Exine (outer): Sporopollenin (oxidatively polymerized phenylpropanoids and fatty acids); deposited by the surrounding sporophytic tapetum. Sporopollenin is among the most chemically inert biopolymers known — it is essentially indestructible by acid, base, or enzymatic attack, allowing pollen to survive

millions of years in sediment. Exine sculpturing patterns (colpi, pores, reticulations) are diagnostic for plant families and form the basis of palynology (fossil pollen analysis).

- Tryphine and pollenkit: Lipid-rich material in exine cavities; contains species-specific recognition factors (S-locus proteins, lipidic adhesins) and is essential for hydration on the stigma surface

Pollen cell architecture and microsporogenesis:

The mature pollen grain is a 3-celled structure: one large vegetative (tube) cell with a single decondensed nucleus, enclosing two small sperm cells (the germline)

Its development proceeds through five steps:

1. Archeporial cells within the anther microsporangium differentiate into diploid microspore mother cells (MMCs) — also called pollen mother cells
2. Each MMC undergoes meiosis I + II to produce 4 haploid microspores, initially held as a tetrad surrounded by a callose wall (β -1,3-glucan). The tapetum (a sporophytic somatic cell layer surrounding the developing microspores) secretes callase (β -1,3-glucanase) at a precisely timed point to dissolve callose and release individual microspores.
3. Microspore mitosis I is asymmetric: the microspore nucleus migrates to one side, and an asymmetric division produces a small generative cell and a large vegetative cell. The generative cell is engulfed by the vegetative cell cytoplasm — a “cell within a cell” architecture unique to plant gametogenesis. Asymmetric division depends on the GAMETOPHYTE-DEFECTIVE 1 / DUO1 transcriptional network.
4. Microspore mitosis II divides the generative cell to produce 2 sperm cells:
 - In tricellular pollen (about 30% of species; *Arabidopsis*, *Brassicaceae*, grasses) mitosis II completes before pollen is released from the anther
 - In bicellular pollen (about 70% of species; most flowering plants) mitosis II occurs in the growing pollen tube after pollination
5. The mature pollen grain = 1 vegetative cell + 2 sperm cells = the complete male gametophyte

The two sperm cells are not equivalent: one is “leading” and tends to fuse with the egg, the other “trailing” with the central cell. The recognition mechanism uses cell-surface markers — though preferred matching is statistical rather than absolute.

29.5.2 Female Gametophyte: Megasporogenesis and the Polygonum-Type Embryo Sac

The angiosperm female gametophyte is also drastically reduced — a 7-celled, 8-nucleate structure embedded in the ovule. The Polygonum-type embryo sac (about 70% of angiosperms) is the canonical form.

Cell types and their functions:

- Egg cell (1, micropylar): Haploid; becomes the zygote upon fertilization. Polarized: nucleus near the chalazal end, large vacuole at the micropylar end. Specifies the apical–basal axis of the future embryo.
- Synergids (2, micropylar; flank the egg): Haploid. Critical functions:
 - Secrete LURE peptides (CRP810 family; species-specific) through the filiform apparatus (an elaborate cell-wall labyrinth at the micropylar pole that increases secretory surface area), guiding the pollen tube to the ovule
 - One synergid degenerates (programmed cell death) upon pollen tube arrival, providing the entry channel
 - Express the FERONIA-LORELEI receptor complex required for pollen tube reception and rupture
- Central cell (1, large, central): Contains 2 polar nuclei (which fuse before or during fertilization to form a diploid secondary nucleus). Becomes the triploid endosperm upon fertilization with one sperm. The canonical 2:1 maternal:paternal genome dosage is widespread across angiosperms and is the substrate for genomic imprinting and parental conflict, as discussed in the genomic-imprinting section.
- Antipodal cells (3, chalazal): Function in nutritive/transfer roles. Highly polyploid (up to 32 n via endoreduplication) in grasses, where they are long-lived; in *Arabidopsis* and most dicots, antipodals degenerate before fertilization.

Megasporogenesis and Embryo Sac Development:

1. A single megaspore mother cell (MMC) (also called megasporocyte) within the ovule’s nucellus undergoes meiosis, producing 4 haploid megaspores in a linear tetrad along the chalazal-micropylar axis
2. Three megaspores degenerate via programmed cell death; the surviving (typically chalazal) functional megaspore alone gives rise to the female gametophyte. The selectivity of which megaspore survives is partly genetic (auxin gradients, AGO9-dependent siRNA silencing of competing megaspores) and partly stochastic.
3. The functional megaspore undergoes 3 rounds of free nuclear mitosis (without cytokinesis) producing an 8-nucleate coenocyte. The 8 nuclei migrate to specific positions: 4 nuclei toward each pole.
4. Cellularisation: Cell walls form around the 8 nuclei to establish the 7 cells: 1 egg + 2 synergids + 1 central cell (with 2 polar nuclei, one from each pole) + 3 antipodals = the mature embryo sac

Concept Check 2: A mutation eliminates the synergids during embryo sac development (synergid-less *gametophyte mutant1*). Predict which steps of fertilization will fail and why double fertilization cannot proceed.

29.6 Pollination, Pollen-Pistil Interactions, and Double Fertilization

29.6.1 Pollination Systems and Pollen Transfer Strategies

Transfer of pollen from anther to stigma occurs by various vectors, each associated with characteristic floral traits (pollination syndromes):

Table 363. Pollination Systems and Pollen Transfer Strategies: Vector and Syndrome.

Vector	Syndrome	Flower morphology	Plant examples
Bees (<i>Apis</i> , <i>Bombus</i> , solitary bees)	Melittophily	Blue/yellow/UV-reflective; landing platform; nectar guide; sometimes vibration-released pollen	<i>Trifolium</i> , <i>Solanum</i> , <i>Linaria</i>
Butterflies	Psychophily	Red/pink; narrow tube; nectar platform; day-opening	<i>Asclepias</i> , <i>Buddleja</i>
Hawkmoths	Sphingophily	White; strong scent dusk-dawn; long narrow tube; night-opening	<i>Nicotiana</i> , <i>Datura</i>
Bats	Chiropterophily	Large; white/pale; fermented/fruity scent; nocturnal; robust	<i>Agave</i> , <i>Ceiba</i> , <i>Adansonia</i>
Birds (hummingbirds)	Ornithophily	Red/orange (beyond bee vision); no or little scent; abundant dilute nectar; tubular	<i>Strelitzia</i> , <i>Lobelia</i> , <i>Fuchsia</i>
Wind	Anemophily	Small, inconspicuous; no nectar; enormous pollen quantities; feathery stigma	<i>Poa</i> , <i>Quercus</i> , grasses, <i>Betula</i>
Water	Hydrophily	Variable; pollen at water level	<i>Vallisneria</i> , <i>Ceratophyllum</i>

Animal pollination is not a decorative add-on to plant reproduction. The IPBES pollinators assessment reported that more than three quarters of leading global food-crop types benefit at least partly from animal pollination, while 5–8% of global crop production by volume depends directly on animal pollination [IPBES, 2016]. The same assessment separates crop production from wild-plant reproduction: managed honey bees are important agricultural pollinators, but wild bees, flies, butterflies, moths, beetles, birds, and bats support many crop and wild-plant networks.

Bees illustrate why pollinators are not interchangeable. Honey bees provide portable managed colonies; bumblebees can buzz-pollinate poricidal anthers such as *Solanum*; solitary bees often forage under different temperatures, flower heights, or times of day. A global crop synthesis found that wild pollinator visitation improved fruit set regardless of honey bee abundance, so replacing diverse wild pollinators with managed honey bees is not an equivalent ecological substitution [Garibaldi et al., 2013]. Conservation therefore focuses on nesting substrate, floral continuity, pesticide exposure, disease spillover, and habitat connectivity as well as hive numbers.

Concept Check 3: A plant species has small, green, scentless flowers that produce copious dry pollen. What is its likely pollination vector? What other structural features would you expect?

29.6.2 Pollen-Pistil Interactions: Self-Incompatibility (SI) Systems

Self-incompatibility (SI) is a widespread genetic mechanism preventing self-pollination and inbreeding depression. Approximately 40% of angiosperm species have functional SI. The molecular logic divides into two paradigms based on whether the pollen’s incompatibility phenotype is determined by its own (haploid) genotype or by the (diploid) genotype of the pollen-producing parent.

Sporophytic SI (SSI) — *Brassica* (cabbage, mustard), *Ipomoea*, Asteraceae

The pollen rejection phenotype is determined by the diploid sporophytic tissue of the anther (specifically, the tapetum that deposits proteins onto the pollen wall) — *not* by the pollen grain’s own haploid genotype.

- S-locus genes:
 - SRK (S-receptor kinase): Stigma-expressed; receptor on the stigma papilla membrane
 - SCR/SP11 (S-locus cysteine-rich protein 11; pollen coat protein): Deposited on pollen exine by the diploid tapetum during pollen maturation

- Mechanism: When SRK on the stigma encounters its matching SCR on the incoming pollen (i.e., self-pollen sharing the same S-haplotype as the stigma), SRK autophosphorylates and recruits ARC1 (E3 ubiquitin ligase). ARC1 ubiquitinates Exo70A1, a key component of the secretion exocyst required for pollen hydration. The pollen fails to hydrate and is rejected at the stigma surface — before pollen tube germination.
- Genetic consequence: Because pollen carries the diploid parental S-genotype, most pollen from a heterozygous S_1S_2 plant is rejected by S_1S_2 , S_1S_3 , and S_2S_3 stigmas.

Gametophytic SI (GSI) — Solanaceae (*Petunia*, *Nicotiana*, tomato), Rosaceae (apple, pear, almond), Papaveraceae

The pollen rejection phenotype is determined by the pollen grain’s own haploid S-genotype.

- S-locus genes (S-RNase / SLF system):
 - S-RNase: Pistil-expressed; ribonuclease secreted into the style transmitting tract
 - SLF (S-locus F-box protein): Pollen-expressed; multiple SLFs per haplotype, acting collectively
- Mechanism (collaborative non-self recognition): S-RNase enters the growing pollen tube non-specifically. Each SLF can “tag” non-self S-RNases (those whose haplotype does not match the pollen tube’s own) for ubiquitination and proteasomal degradation by the SCF^{SLF} complex. Self S-RNase escapes degradation because the pollen tube’s SLFs cannot recognize the matching S-RNase. Surviving S-RNase enters the cytoplasm and degrades pollen tube ribosomal RNA, halting tube growth before fertilization.
- Genetic consequence: A cross between S_1S_2 and S_1S_3 plants: S_1 pollen is rejected by both stigmas; S_2 pollen succeeds on the S_1S_3 stigma; S_3 pollen succeeds on the S_1S_2 stigma. Half the pollen is accepted; offspring genotypes are S_1S_2 , S_1S_3 , S_2S_3 (no homozygotes possible).

Comparative summary:

Table 364. Pollen-Pistil Interactions: Self-Incompatibility (SI) Systems: Feature and Sporophytic SI (Brassica).		
Feature	Sporophytic SI (Brassica)	Gametophytic SI (Solanaceae)
Determinant of pollen phenotype	Diploid parental tissue (tapetum)	Pollen’s own haploid genome
Pollen recognition	At stigma surface (before germination)	In style during tube growth
Female factor	SRK (membrane receptor kinase)	S-RNase (secreted RNase)
Male factor	SCR (pollen coat protein)	SLF (F-box)
Number of S-haplotypes	Often 50–100	Often 50–200

Evolutionary significance of SI: Self-incompatibility maintains heterozygosity and avoids inbreeding depression in obligate outbreeders. Its breakdown (typically by loss of S-RNase or SLF function) gives rise to self-compatible lineages, which often go extinct because of genetic load — but occasionally undergo spectacular adaptive radiations (e.g., self-compatible *Arabidopsis thaliana* descended from self-incompatible *A. lyrata*; the loss of SI may have facilitated *A. thaliana*’s colonization of new habitats by enabling single-individual founder events).

29.6.3 Polyploidy and Speciation in Plants

Plants exhibit far higher rates of polyploidy than animals; about 70% of angiosperm species retain evidence of one or more whole-genome duplications in their evolutionary history.

Modes of polyploid origin:

- Autopolyploidy: Whole-genome duplication within a single species; chromosomes form quadrivalents at meiosis, often causing reduced fertility initially
- Allopolyploidy: Hybridization between two species followed by chromosome doubling; chromosomes from each parental genome pair separately as bivalents, restoring fertility. Most cultivated polyploids are allopolyploids.

Pathways:

1. Unreduced gamete fusion: Two 2n gametes fuse to form a 4n zygote (one in 1000 gametes is unreduced)
2. Somatic doubling: Spontaneous chromosome doubling in a meristematic cell during somatic growth
3. Triploid bridge: Triploids (3n) produce a wide variety of unbalanced gametes; some 4n offspring arise from these

Polyploid crops: Wheat (hexaploid: AABBDD genomes from three ancestral diploids), cotton (tetraploid), strawberry (octoploid), banana (often triploid, sterile), oats (hexaploid).

Polyploidy promotes speciation because new polyploids are reproductively isolated from their parental species (triploid offspring of a $2n \times 4n$ cross are sterile), creating an instant reproductive barrier. Polyploids often exhibit heterosis (hybrid vigour), enlarged organs (the basis of many crop polyploids), and increased ecological tolerance.

29.6.4 Double Fertilization [Nawaschin, 1898]

Sergei Nawaschin’s 1898 discovery of double fertilization in *Lilium martagon* and *Fritillaria tenella* — observing two simultaneous nuclear fusions in a single ovule — was transformative for plant biology and remains the defining synapomorphy of angiosperms.

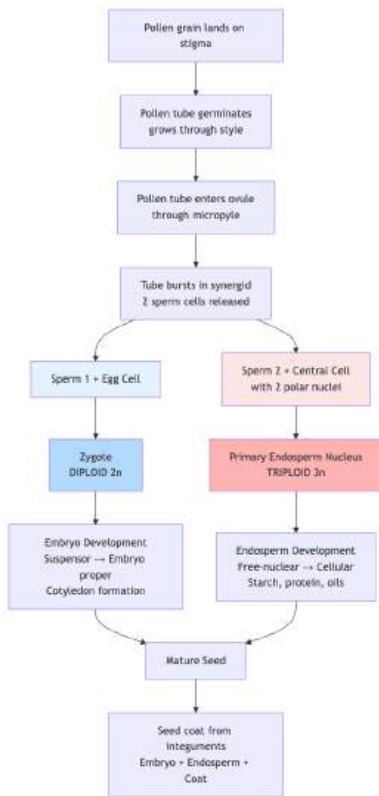
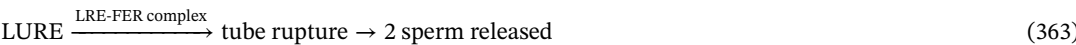


Figure 178. Double fertilization in angiosperms One sperm fuses with the egg to form the diploid zygote (which develops into the embryo). The second sperm fuses with the central cell’s two polar nuclei to form the triploid primary endosperm nucleus (which develops into the nutritive endosperm). This process is unique to angiosperms.

1. Pollen tube germination on the stigma: Compatible pollen hydrates within minutes on the stigma surface; the vegetative (tube) cell extends a callose-walled tube. Tip growth is driven by:
 - A tip-focused $[Ca^{2+}]$ gradient (about $1.5\text{--}10\text{ }\mu\text{M}$ at the apex; about 150 nM in the shank)
 - Vesicle-mediated wall deposition (callose for tube wall, pectin for the inner wall)
 - Cytoplasmic streaming carrying the generative/sperm cells to the tip
 - Growth rates: $1\text{--}10\text{ mm/h}$ in *Lilium*, 1 cm/h in maize
2. Spermatogenesis during tube elongation (in bicellular species): The generative cell, carried in the tube cell cytoplasm, undergoes mitosis II during pollen tube growth, producing the two sperm cells. In tricellular species (*Arabidopsis*, grasses), this division has already occurred before pollen release.
3. Pollen tube guidance — chemotropism: The pollen tube navigates through the style and ovary toward a single receptive ovule via a cascade of guidance cues:
 - Style cues: γ -aminobutyric acid (GABA) gradient in the transmitting tract; cysteine-rich peptides
 - Funicular guidance: Short-range cues from ovary tissue
 - Micropylar guidance: LURE peptides (defensin-like, cysteine-rich; CRP810 family) released from the synergid filiform apparatus; species-specific. *Torenia* LURE1/LURE2 attract pollen tubes specifically of the same species — the molecular basis of inter-species pollination barriers. LURE peptides bind PRK6 receptor kinases on the pollen tube tip, biasing tip growth toward the source.

4. Synergid degeneration: As the pollen tube approaches the ovule, one of the two synergids undergoes programmed cell death (within minutes; the receptive synergid). Loss of synergid integrity:
- Creates the entry channel into the embryo sac
 - Releases pre-stored signaling molecules
 - Exposes the FERONIA (FER) receptor kinase / LORELEI (LRE) GPI-anchored co-receptor complex on the persisting synergid surface
5. Pollen tube reception and rupture: FER-LRE signaling, via reactive oxygen species (ROS) generated by RBOH NADPH oxidases and elevated cytosolic $[Ca^{2+}]$, triggers explosive rupture of the pollen tube tip, releasing the two sperm cells into the embryo sac. The signaling depends on RALF peptides binding FER. In *fer* mutants, pollen tubes enter the synergid but fail to rupture (continued growth and “supernumerary” pollen tube delivery — the polyspermy phenotype).
6. Sperm cell delivery and double fusion:
- Sperm 1 + egg cell → karyogamy → 2n zygote → embryo
 - Sperm 2 + 2 polar nuclei (central cell) → triple fusion → 3n primary endosperm nucleus → endosperm



Significance of double fertilization:

- Endosperm provides a “payment on delivery” mechanism — primarily fertilized ovules develop endosperm, ensuring optimal parental investment
- Endosperm in cereals: starch (70-80%), storage proteins (gluten in wheat, zein in maize), oils, vitamins — source of about 60% of global human caloric intake
- Triploid endosperm (2 maternal : 1 paternal genome dose) provides a unique genetic substrate for parental conflict (paternally-imprinted genes promote nutrient transfer; maternally-imprinted genes restrict it) — conserved in ratio across most flowering plants

Clinical Connection: Understanding pollen tube guidance has implications for crop fertility. In interspecific crosses (e.g., wheat × rye to produce triticale), pollen tube guidance often fails because LURE peptides are species-specific. Genetic engineering of LURE receptors could enable wider crosses for crop improvement.

29.6.5 Worked Example: Endosperm Ploidy and Parental Genome Dosage

Problem: Compute the genomic dosage of the endosperm under normal angiosperm double fertilization and under a maternal mutant that has doubled the central-cell genome, and explain why endosperm imprinting makes the dosage shift matter for seed viability.

Normal case. A wild-type ovule contains a haploid egg (n) and a central cell with two haploid polar nuclei (n + n = 2n). The pollen delivers two haploid sperm (n each):

- Sperm 1 (n) + egg (n) → zygote 2n → embryo
- Sperm 2 (n) + central cell (2n) → primary endosperm nucleus 3n → endosperm

Maternal : paternal genome ratio in normal endosperm = 2 : 1.

Mutant case (maternal 4n central cell — e.g., from a polyploid maternal lineage; assume each polar nucleus is 2n instead of n). Same haploid pollen.

- Sperm 1 (n) + egg (n) → zygote 2n (unchanged)
- Sperm 2 (n) + central cell (2n + 2n = 4n) → endosperm 5n

Maternal : paternal genome ratio in mutant endosperm = 4 : 1.

Solution:

1. Compute the dosage shift. From 2 : 1 (normal) to 4 : 1 (mutant) doubles the maternal contribution per paternal copy.
2. Map the shift onto imprinting. Endosperm carries strong parent-of-origin imprinting. Maternally-expressed imprinted genes (MEGs; e.g., *FIS2*, *MEDEA*) restrict endosperm growth and nutrient transfer; paternally-expressed imprinted genes (PEGs; e.g., *PHE1*) drive endosperm proliferation and nutrient pull. The 2 : 1 ratio sets the canonical balance.
3. Predict the seed phenotype. In the mutant, maternal “restraint” genes are now in fourfold excess relative to paternal “growth” genes. Endosperm cellularisation is accelerated, nutrient transfer to the embryo is curtailed, and seed size collapses. This is precisely the phenotype seen in interploidy crosses where a tetraploid mother is crossed to a diploid father — the so-called *maternal excess* seed-failure syndrome.

4. Symmetric prediction. A reciprocal cross (diploid mother × tetraploid father) produces *paternal excess* endosperm (2 : 2 → effective 1 : 1 or worse), with the opposite phenotype: delayed cellularisation, overgrown endosperm, and seed abortion from a different failure mode. Together these explain the triploid block — a major reproductive barrier in interploidy crosses and a quantitative test of the parental-conflict theory of imprinting.

Interpretation. Double fertilization is not merely a developmental quirk; it is the substrate on which parental-conflict-driven imprinting plays out. The canonical 2 : 1 ratio is the genomic ledger that keeps embryo provisioning balanced. Disrupt the ratio and you disrupt the seed.

29.7 Endosperm Development and Seed Biology

29.7.1 Endosperm Development: Free-Nuclear, Cellular, Helobial

After triple fusion, the primary endosperm cell (3n; typically 2m:1p genome ratio) undergoes a stereotyped developmental sequence that determines the storage architecture of the mature seed. The 2:1 maternal:paternal genome ratio is the canonical angiosperm pattern and is important for normal seed development, while some lineages show dosage and developmental variation.

Three modes of endosperm development:

1. Nuclear (free-nuclear) endosperm — most common: The primary endosperm nucleus undergoes repeated mitosis without cytokinesis, producing a syncytium of hundreds to thousands of nuclei in a common cytoplasm with a large central vacuole. Examples: *Arabidopsis*, maize, rice, wheat, coconut (the “coconut water” of an immature coconut is liquid free-nuclear endosperm). After about 6–8 nuclear divisions, cellularisation initiates from the periphery inward, with cell walls forming radially around each nucleus. The mature cellular endosperm then accumulates storage products (starch, protein, oil).
2. Cellular endosperm: Cytokinesis accompanies every mitosis from the start; the endosperm is cellular throughout. Examples: *Petunia*, tobacco, magnoliid lineages.
3. Helobial endosperm: The first division separates a small chalazal cell from a large micropylar cell; subsequent divisions are nuclear in the micropylar half and cellular in the chalazal half. Examples: many monocots in Alismatales.

Seed filling: During the maturation phase (after cellularisation), endosperm cells accumulate massive amounts of storage compounds: - Starch: Synthesized from sucrose imported from maternal phloem; deposited in plastids (amyloplasts). Cereal grain starch can reach 60–70% of dry mass. - Storage proteins: Family-specific (zeins in maize, glutenins/gliadins in wheat, prolamines in rice, globulins in legumes). Stored in protein bodies derived from the ER and vacuole. - Oils: Triacylglycerols stored in oil bodies (oleosomes); dominant in oilseeds (sunflower, canola, soybean).

The PEG/MEG pathway and parental conflict:

The FIS-PRC2 (FERTILIZATION INDEPENDENT SEED – Polycomb Repressive Complex 2) complex — comprising MEDEA (MEA), FIS2, FIE, and MSI1 — is the master regulator of endosperm initiation and parental conflict resolution:

Maternal MEA-FIE-FIS2-MSI1

$\xrightarrow{\text{H3K27me3}}$

repression of paternally-imprinted genes (PEGs)

(364)

- PEGs (Paternally Expressed Genes): Expressed primarily from the paternal allele in endosperm (the maternal allele is silenced by H3K27me3 deposited by FIS-PRC2). Examples: *PHE1*, *YUC10*, *AHL10*. PEGs tend to promote endosperm growth and nutrient transfer to the embryo.
- MEGs (Maternally Expressed Genes): Expressed primarily from the maternal allele. MEGs tend to restrict endosperm growth.
- Imbalance in PEG/MEG dosage (e.g., crosses between species with different ploidy) causes seed abortion via the endosperm balance number (EBN) mechanism. This is why interploidy crosses fail: a 2x × 4x cross produces triploid embryos with imbalanced PEG/MEG expression, triggering seed abortion.

The 2m:1p endosperm dosage thus becomes the principal arena for parent-of-origin genetic conflict, with paternally-imprinted PEGs evolutionarily favored to extract more maternal resources for the offspring, and maternally-imprinted MEGs favored to ration resources across multiple offspring.

29.7.2 Seed Dormancy: Five Classes and Triggers

Seed dormancy delays germination until conditions favor seedling survival. Baskin and Baskin (2004) classify dormancy into five types:

Table 365. Seed Dormancy: Five Classes and Triggers: Dormancy type and Cause.

Dormancy type	Cause	Trigger to break	Examples
Physical (PY)	Water-impermeable seed coat (dense palisade of macrosclereids; suberin layers)	Scarification: physical abrasion, fire heat, gut passage, freeze-thaw	Many legumes (clover, <i>Acacia</i>); <i>Convolvulus</i> ; many Malvaceae
Physiological (PD)	Hormonal balance (high ABA / low GA) blocks germination despite imbibition; embryo viable	Stratification (cold-moist); after-ripening (dry storage at warm); light (Pfr)	<i>Arabidopsis</i> , lettuce, apple, most temperate trees
Morphological (MD)	Embryo immature at dispersal; needs time to develop	Time + warm-moist conditions	<i>Ginkgo</i> , <i>Magnolia</i> , parsnips, celery
Morphophysiological (MPD)	Combined immature embryo + hormonal block	Warm followed by cold stratification (or vice versa)	Many woodland herbaceous spring ephemerals; <i>Trillium</i> , <i>Anemone</i>
Combinational (PY+PD)	Both impermeable coat and hormonal block	Both scarification and stratification	<i>Tilia</i> (linden), some Rosaceae

Germination triggers (sensory inputs):

- Stratification (cold, moist): Cold treatment (1–5 °C, weeks to months) progressively degrades ABA and induces GA biosynthesis genes, shifting the ABA/GA balance toward germination. Required by many temperate tree seeds. Mechanism involves cold-induced demethylation of GA-biosynthesis gene promoters.
- Scarification (mechanical or chemical): Cracks or thins the testa, allowing water and oxygen to enter. Can be achieved naturally by passage through animal digestive tracts (where stomach acid + abrasion abrade the coat), fire (heat scarification of fire-adapted species like *Banksia*), or freeze-thaw cycles. Many savanna acacia seeds germinate primarily after passage through elephant or ungulate guts.
- Light (phytochrome-mediated): Red light (R, 660 nm) converts Pr to active Pfr, promoting germination in light-requiring seeds (lettuce, *Arabidopsis*, many small-seeded weeds). Far-red light (FR, 730 nm) inhibits germination. The R:FR ratio under a leaf canopy is low (chlorophyll absorbs R, transmits FR), so seeds under shade remain dormant until canopy opening — an exquisite mechanism for detecting gaps in vegetation. The Borthwick-Hendricks experiments (1952) on lettuce seeds first demonstrated the R/FR reversibility that defined phytochrome.
- Temperature fluctuation: Diurnal temperature swings (e.g., 40 °C day / 10 °C night, typical of bare soil under sun without insulating vegetation) signal a gap in canopy cover. Many desert and weed species require such fluctuations.
- Smoke and karrikins: Karrikin compounds (KAR1–KAR6) in plant-derived smoke bind the KAI2 receptor (a strigolactone-related α/β hydrolase). KAR signaling promotes germination of fire-adapted species and many weeds (KAR2 promotes germination in *Arabidopsis*).
- Chemical leaching: Some desert species require leaching of inhibitory compounds (e.g., NaCl in halophytes; phenolic germination inhibitors) by sufficient rainfall — ensuring germination primarily after enough rain has fallen to support seedling establishment.

29.7.3 Germination Physiology — Molecular Framework

The balance between ABA (dormancy-promoting) and GA (germination-promoting) signals is the central regulatory axis:

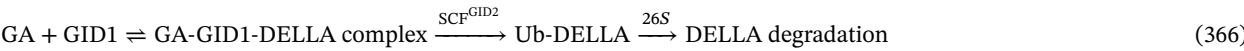
ABA pathway (dormancy):

DOG1 (DELAY OF GERMINATION 1): A seed-specific RNA-binding-domain protein. DOG1 dosage determines dormancy depth by stabilizing ABI3 and ABI5 mRNA — master transcription factors of the ABA response. *DOG1* expression peaks at seed maturation, quantitative trait locus (QTL) responsible for natural variation in dormancy across *Arabidopsis* accessions (Bentsink *et al.*, *PNAS* 2006).



Active SnRK2 phosphorylates ABF/AREB transcription factors → dormancy gene transcription (ABI5 targets: *LEA* proteins, stress tolerance genes). PP2C inhibition is the key switch: normally PP2C keeps SnRK2 dephosphorylated (inactive); ABA binding to PYR/RCAR pulls PP2C off SnRK2.

GA pathway (germination):



DELLA degradation (of RGA, GAI, RGL1-3 in *Arabidopsis*) releases repression of: - α -Amylase **promoters** (mobilize endosperm starch → maltose → glucose) - Lipase genes (mobilize stored triacylglycerols) - Protease genes (mobilize globulins and albumins)

ABA–GA antagonism: - ABA stabilizes DELLA proteins (by downregulating GID1 and upregulating PP2C) - GA degrades DELLA and suppresses ABI5 - Environmental cues (light via Pfr, cold via DOG1 degradation, smoke via KAI2) tip the balance toward GA-dominated germination competence

Concept Check 4: Some desert annual plant seeds require specific temperature fluctuations (e.g., 40 °C day / 10 °C night) to break dormancy. Explain why this diurnal fluctuation — rather than constant warm temperature — is required. Connect your answer to the molecular ABA/GA balance.

Concept Check 5: A *dog1* loss-of-function mutant of *Arabidopsis* shows severely reduced primary dormancy: seeds germinate immediately at maturity. Predict the ecological consequence in (a) a Mediterranean climate with hot dry summers, and (b) a tropical evergreen forest understory.

Concept Check 6 (Analyze) — Pollen-tube guidance and the LURE–PRK6 axis. Pollen tubes navigate the style by chemotropism, eventually homing on the embryo sac via LURE peptides (defensin-like) secreted from synergid cells. LURE binds the receptor-like kinase PRK6 at the tube tip, biasing a tip-focused Ca²⁺ gradient and actin remodeling toward the source. (a) Diagram the LURE → PRK6 → Ca²⁺ → actin pathway, marking which step is conserved with the FERONIA–RALF system at tube reception. (b) A homozygous *prk6* loss-of-function plant is used as the female parent and crossed to wild-type pollen. Predict the fertilization phenotype, distinguishing tube *attraction* from tube *reception/rupture*. (c) Design a complementation test that would prove PRK6 acts cell-autonomously on the pollen tube rather than on the synergid producing the LURE cue, and predict the *Torenia* inter-species cross outcome if you swap PRK6 orthologues.

Concept Check 7 (Evaluate) — Seed dormancy, the ABA : GA ratio, and a warming winter. ABA-stabilized DELLA proteins enforce dormancy; imbibition plus cold stratification plus light tilts the balance toward GA biosynthesis, DELLA degradation, and germination. Many temperate annuals (e.g., *Arabidopsis* winter-annual accessions, vernalisation-dependent cereals) require weeks of below-5 °C exposure to clear dormancy. (a) Use the ABA : GA framework to explain why a *constant* 5 °C signal is required rather than a single cold shock — what molecular variable is being integrated over weeks (DOG1 protein turnover; FLC chromatin state; VIN3 accumulation)? (b) A climate-change scenario raises mean winter temperatures by 10 °C, so a planting region that previously averaged 5 °C now averages 15 °C. Predict the directional shift in germination timing, percent germination, and seedling synchrony for (i) a vernalisation-dependent winter wheat cultivar and (ii) a Mediterranean summer annual with after-ripening dormancy. (c) Evaluate two breeding strategies that would restore reliable germination — a *dog1* loss-of-function allele vs. a stronger FLC repressor — and identify which carries lower agronomic risk if the climate later cools.

29.8 Embryogenesis and Meristem Organization

29.8.1 Early Embryogenesis and Body-Axis Formation

Arabidopsis embryogenesis is the best-studied model:

Table 366. Early Embryogenesis and Body-Axis Formation: Stage and Description.

Stage	Description	Key events
1-cell zygote	Polar asymmetric cell	PIN7 (apical) + PIN1 (basal) establish auxin gradient
2-cell	Asymmetric division: apical cell (embryo) + basal cell (suspensor)	WOX9 signaling

Stage	Description	Key events
Globular	8-cell through 32-cell globular stage	WOX2 (apical domain), WOX9 (basal) pattern embryo
Heart	Cotyledon primordia emerge; first visible bilateral symmetry	YAB/PIN1 separate cotyledons; ARF5/MP establishes vascular axis
Torpedo	Elongation; hypocotyl + radicle extend	Protoderm, procambium, ground meristem differentiate
Mature embryo	Desiccation; ABA accumulates; storage proteins deposited	Two cotyledons + SAM + RAM + hypocotyl + radicle

The suspensor (from the basal cell) anchors the embryo to the maternal tissue and transfers nutrients. It is programmed for cell death after the globular stage.

29.8.2 Shoot Apical Meristem (SAM) – Stem Cell Niche

The SAM maintains a pool of pluripotent stem cells throughout the plant’s life:

- Central Zone (CZ): 2-4 slowly dividing stem cells at the summit
- Peripheral Zone (PZ): Faster-dividing cells that are displaced outward and form lateral organ primordia (leaves, flowers)
- Rib Zone: Beneath the CZ; contributes to stem internodes

WUS-CLV3 negative feedback loop (the “stem cell thermostat”):

1. WUSCHEL (WUS) – homeodomain transcription factor expressed in the organizing center (below CZ). WUS protein moves to CZ via plasmodesmata. Activates CLAVATA3 (CLV3) expression.
2. CLV3 – a secreted CLE peptide (12 amino acids). CLV3 binds the CLV1/CLV2/CRN receptor kinase complex in underlying cells, activating a MAPK cascade that represses WUS transcription.
3. Negative feedback: WUS activates CLV3; CLV3 represses WUS. This maintains a constant stem cell pool size.

SAM auxin-driven phyllotaxis: - Each leaf primordium is initiated where PIN1 (auxin efflux carrier) creates a local auxin maximum - The established primordium depletes local auxin from surrounding cells - The next primordium arises at the position of the next auxin maximum - Mathematical result: primordia arise at 137.5 degrees divergence angle (the “golden angle” = 360 degrees × (1 – 1/φ²) where φ = golden ratio 1.618) - This produces Fibonacci spirals (1, 1, 2, 3, 5, 8, 13...) visible in pine cones, sunflower heads, and succulent leaf arrangements

29.8.3 Worked Example: Calculating the Golden Angle in Phyllotaxis

Problem: The arrangement of leaves on a stem (phyllotaxis) is often determined by the golden angle, which minimizes shading of lower leaves by upper leaves. Calculate the exact value of the golden angle in degrees using the golden ratio φ ≈ 1.618034. If a plant produces a new leaf every 5 days, what will be the total angular divergence between the first leaf and a fourth leaf (leaf 1 and leaf 4)?

Solution:

1. Calculate the golden angle: Using the formula given: Angle = 360° · (1 – 1/φ²) First, calculate φ²:

1.618034² ≈ 2.618034

Calculate the fraction:

1 / 2.618034 ≈ 0.381966

Apply to the angle formula:

Angle = 360° · (1 – 0.381966) = 360° · 0.618034 ≈ 222.49°

However, angles are typically measured by the shorter path around the circle, so we subtract from 360°:

360° – 222.49° = 137.51°

This is the golden angle (about 137.5°).

2. Calculate the total angular divergence: Between leaf 1 and leaf 4, there are 3 developmental intervals (1 to 2, 2 to 3, and 3 to 4).

$$\text{Total Divergence} = 3 \cdot 137.5^\circ = 412.5^\circ$$

To find the apparent angle relative to the first leaf on a single 360° circle, take the modulo:

$$412.5^\circ - 360^\circ = 52.5^\circ$$

The fourth leaf will be separated from the first leaf by 52.5° on the stem circumference.

29.8.4 Root Apical Meristem (RAM)

RAM structure mirrors SAM with distinct anatomy: - Quiescent Center (QC): 4-6 slowly dividing cells (divide about once per 200 h); WOX5 expression maintains surrounding stem cells - Initial (stem) cells directly surrounding QC produce clonal cell files for most root tissues - Root cap/columella: Rapidly replaced (slough off as root grows); amyloplast-containing statocytes for gravitropism - Casparian strip in endodermal cells seals apoplastic pathway for selective mineral transport

29.9 Fruit Development, Vegetative Reproduction, and Apomixis

29.9.1 Fruit Development: Hormonal Regulation, Parthenocarpy, and Climacteric Ripening

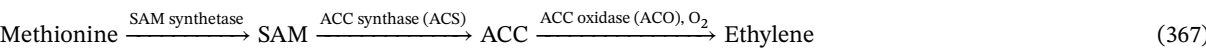
Fruit development is initiated by fertilization and proceeds through cell division, expansion, and ripening — each phase under distinct hormonal control.

Phase 1: Fruit set (post-fertilization initiation): Auxin from developing seeds and gibberellins from the maternal pericarp suppress the abscission program that would otherwise drop unfertilised flowers. Without seeds, parthenocarpy can be induced — fruit development without fertilization: - Natural parthenocarpy: cultivated banana (triploid, sterile), pineapple, navel orange, some *Citrus* and *Vitis* cultivars - Induced parthenocarpy: exogenous auxin (NAA, 2,4-D) or GA (GA₃) sprayed at anthesis. Used commercially in seedless grapes, watermelons, and tomatoes - Genetic parthenocarpy: *pin* mutants (pinoid; auxin-overproducing) or *fwf* mutants (FRUIT WITHOUT FERTILIZATION; tomato) develop fruit without seeds

Phase 2: Cell division and expansion: Cytokinins drive early cell division in the pericarp; auxin and GA drive subsequent cell expansion. Cucumbers and watermelons reach mature size by predominantly cell expansion (each cell can balloon 30-fold).

Phase 3: Ripening — climacteric vs non-climacteric fruits

The most studied transition is in climacteric fruits (banana, tomato, apple, avocado, peach, mango), characterized by an autocatalytic burst of ethylene production at the onset of ripening:



Two systems of ethylene biosynthesis:

- System 1: Basal, auto-inhibited ethylene production occurring in vegetative tissues and pre-climacteric fruit. Low ethylene levels. Maintained at low rates throughout development.
- System 2: Auto-catalytic, ripening-associated ethylene burst. Activated by transcription factors (RIN/MADS-RIN, NOR, CNR) that turn on a ripening-specific ACS isoform (ACS2) and ACO1. Once initiated, the ethylene produced positively feeds back on its own biosynthesis (auto-catalysis), generating an exponential rise. Ethylene then orchestrates ripening.

Ripening events under ethylene control:

- Cell wall softening: Polygalacturonase (PG), pectin methylesterase (PME), expansins, β-galactosidase degrade cell wall polysaccharides; tissue softens
- Sugar accumulation: Starch → soluble sugars via amylases; sucrose conversion via invertase. Banana goes from 1% to 18% sugar content during ripening
- Pigment changes: Chlorophyll degradation (Stay-Green protein, chlorophyllase) reveals carotenoids (red/orange) and anthocyanins (red/purple)
- Volatile production: Esters (banana: isoamyl acetate), lactones, terpenes — aroma compounds that attract dispersers
- Acid metabolism: Malic and citric acids decline, sometimes through respiratory consumption

Non-climacteric fruits (strawberry, grape, citrus, pineapple, cherry) do not show the ethylene burst; ABA and auxin appear to substitute as the master ripening signals. Strawberries in particular are ABA-responsive: applying ABA accelerates ripening; inhibiting ABA biosynthesis (NDGA) blocks ripening.

Clinical Connection: The commercial fruit industry manipulates ethylene extensively. Bananas are picked green, shipped under ethylene-suppressed conditions (using KMnO_4 as an ethylene scrubber or 1-MCP — 1-methylcyclopropene — as an ethylene perception inhibitor that competitively blocks ETR1), and then ripened on demand by ethylene gas treatment at distribution centers. The Flavr Savr tomato (1994) was the first commercial GMO food, with antisense PG suppressing wall softening; ethylene-resistant tomatoes (silenced ACS or ACO) preserve fruit quality during long-distance transport.

29.9.2 Fruit Types and Dispersal

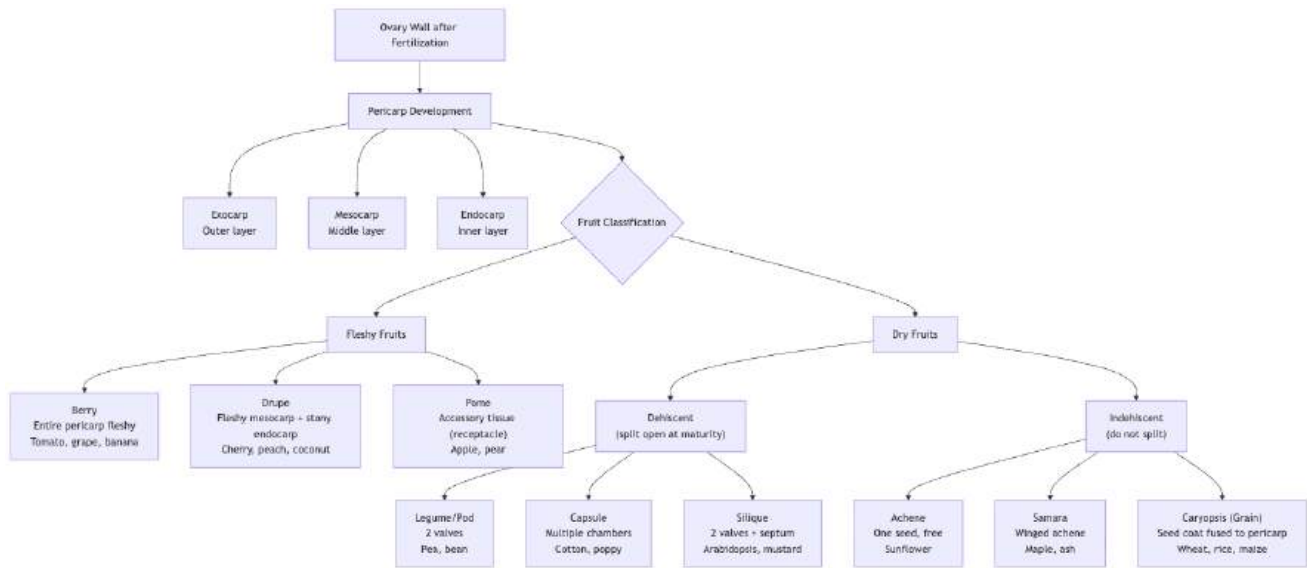


Figure 179. Fruit development and classification The ovary wall develops into the pericarp (exocarp, mesocarp, endocarp), which differentiates into diverse fruit types adapted for specific dispersal strategies.

A fruit is the mature ovary wall (pericarp: exocarp + mesocarp + endocarp) often incorporating accessory tissues:

Table 367. Fruit Types and Dispersal: Fruit type and Structures.

Fruit type	Structures	Example	Dispersal mechanism
Drupe	Fleshy mesocarp + hard endocarp (stone)	Cherry, mango, olive, coconut	Endozoochory (animal ingestion); ocean for coconut
Berry (true)	Entire pericarp fleshy	Tomato, grape, blueberry, capsicum, banana	Endozoochory
Achene	Dry, indehiscent; one seed; pericarp free from seed coat	Sunflower, dandelion (+ pappus)	Wind (dandelion); gravity
Samara	Achene-like + wing of pericarp tissue	Maple (<i>Acer</i>), ash (<i>Fraxinus</i>)	Wind (autorotation; helicoid flight)
Legume	Dehiscent pod; two valves split along two sutures	Pea, bean, soybean	Explosive hygroscopic dehiscence
Capsule	Dry; multiple septa; dehisces by pores or valves	Cotton, poppy, <i>Arabidopsis</i>	Wind-shaken; gravity
Bur	Achene with hooks or spines	Burdock (<i>Arctium</i>), cocklebur (<i>Xanthium</i>)	Epizoochory (animal fur/feathers)

Myrmecochory is seed dispersal by ants. Many seeds carry lipid-rich elaiosomes that attract ants; the ants carry the seed to the nest, consume the reward, and discard the intact seed in nutrient-rich refuse or protected microsites. This mutualism has evolved repeatedly across flowering plants and is associated with diversification in several lineages, making ants both dispersal agents and selective partners in fruit/seed evolution [Lengyel et al., 2009].

29.9.3 Vegetative Reproduction: Mechanisms and Practical Applications

Plants have diverse mechanisms for vegetative (asexual) reproduction, each with distinct anatomical and ecological characteristics that have been widely exploited in agriculture and horticulture:

Table 368. Vegetative Reproduction: Mechanisms and Practical Applications: Mechanism and Description.

Mechanism	Description	Examples	Practical applications
Stolons (runners)	Horizontal above-ground stems that root and form daughter plants at nodes	Strawberry (<i>Fragaria</i>), spider plant (<i>Chlorophytum</i>)	Commercial strawberry production: each “mother” plant produces 5–10 daughter plants per season; entire fields propagated clonally from elite cultivars
Rhizomes	Horizontal underground stems with nodes, scale-leaves, and adventitious roots	Ginger (<i>Zingiber</i>), bamboo, iris, bracken fern, turmeric	Survives fire, frost, and grazing — one rhizome system can persist for centuries (single bracken stand >1000 years; <i>Pando</i> aspen clone in Utah, about 80,000 years old). Commercial ginger and turmeric grown entirely from rhizome divisions
Bulbs	Modified shoots with fleshy storage leaves on a short basal plate; central apical bud	Tulip, garlic, onion, daffodil, lily	Year-round storage in cold rooms allows seasonal flower forcing (Dutch tulip industry); garlic propagated entirely by clove (a single bulb scale)
Corms	Solid swollen stem base; superficially bulb-like but no fleshy storage leaves	Crocus, gladiolus, taro (<i>Colocasia</i>)	Annual replacement: each corm produces “cormels” used for the next planting
Tubers	Swollen subterranean stem (stem tubers, e.g., potato) or root (root tubers, e.g., sweet potato) with axillary buds (eyes)	Potato (<i>Solanum tuberosum</i>), Jerusalem artichoke, sweet potato	Each “eye” can regenerate a complete plant. Global potato cultivation is essentially clonal — major cultivars (Russet Burbank, Yukon Gold) are genetically uniform clones. This uniformity is also their vulnerability (e.g., the 1845 Irish potato famine, in which a single <i>Phytophthora infestans</i> genotype destroyed a near-monoclonal crop)
Adventitious roots	Roots forming on stem cuttings, leaves, or other non-root tissue	Willow (<i>Salix</i>) cuttings root readily; many succulents form leaves	Foundation of horticultural cuttings: roses, grape, citrus, blueberry are commercially propagated by stem cuttings under mist with rooting hormone (auxin) treatment
Adventitious plantlets	Plantlets form spontaneously on leaves or other organs	<i>Kalanchoe</i> (leaf margins), <i>Bryophyllum</i>	Drop from parent and root in soil — example of natural clonal propagation
Fragmentation	Twig or stem fragments that detach and root	Willows, many aquatic plants (<i>Elodea</i> , <i>Myriophyllum</i>)	Aggressive invasive species often spread by fragmentation (e.g., <i>Elodea canadensis</i> in European waterways)
Layering	Stem touches soil and roots while still attached to parent	Blackberry, raspberry; horticultural air layering	Common in commercial production of difficult-to-root species; air layering used for tropical fruit trees and ornamentals

Grafting (not strictly vegetative reproduction but related): Joining a scion (desired cultivar) onto a rootstock (provides root system, often with disease/drought resistance). Used almost universally in apple, pear, citrus, grape, and stone fruit cultivation. The 19th-century *Phylloxera* aphid pandemic destroyed European vineyards; the rescue was grafting European *Vitis vinifera* scions onto American *V. labrusca* rootstocks (which carry natural resistance) — every European wine grape today is grown on American roots.

29.9.4 Apomixis: Sporophytic and Gametophytic Pathways

Apomixis is seed formation without fertilization, producing genetically identical maternal clones in a seed package. Apomixis is a powerful evolutionary “frozen” genotype dispersal mechanism and the holy grail of crop breeding.

Types of apomixis:

1. Sporophytic (adventitious) apomixis (adventive embryony): Embryos arise directly from sporophytic (somatic) cells of the ovule (typically the nucellus or integuments) — bypassing the gametophyte entirely. The embryo is genotypically identical to the maternal parent (2n, same as mother). Multiple

embryos may form per seed (polyembryony). Example: citrus (most cultivars produce both zygotic and apomictic embryos in the same seed; nucellar embryos eventually outcompete the zygotic embryo, preserving the elite genotype). Mango polyembryonic cultivars use the same mechanism.

2. Gametophytic apomixis: A diploid embryo sac forms without meiosis, retaining the maternal genome unreduced. Two sub-types:

- Apospory: Embryo sac arises from a somatic nucellar cell that does not undergo meiosis. The MMC degenerates without producing megaspores; instead, an adjacent nucellar cell expands and divides mitotically to form an unreduced (2n) embryo sac. Examples: *Hieracium* (hawkweed), *Pennisetum* (pearl millet relatives), *Hypericum*
- Diplospory: Megaspore mother cell skips or modifies meiosis (replacing meiosis with mitosis; “MiMe”), producing an unreduced megaspore that develops into a 2n embryo sac. Examples: dandelion (*Taraxacum*; many dandelion species are obligate apomicts), *Tripsacum* (relative of maize), some *Boechera*
- In both, the egg cell is unreduced (2n) and develops parthenogenetically into a 2n embryo (matching the mother)
- Endosperm formation in gametophytic apomicts:
 - Pseudogamous: Central cell still requires fertilization by sperm to form endosperm (typical in apomictic grasses like *Poa*, *Pennisetum*)
 - Autonomous: Central cell develops into endosperm without fertilization (typical of dandelions and *Hieracium*)

Agricultural significance — clonal seed and the holy grail of breeding:

The dream of apomixis in major crops: capture the hybrid vigour (heterosis) of an elite F1 hybrid in a self-perpetuating apomictic seed, eliminating the need to re-create the hybrid each generation. Currently, F1 hybrid maize, rice, and sorghum require expensive annual production crosses (typically requiring about 2–3 isolated hectares of cytoplasmic male sterile mother lines and pollen donor lines). If apomixis could be engineered into rice or maize, subsistence farmers could save F1 seed indefinitely and continue to capture hybrid vigour.

Synthetic apomixis breakthrough: Synthetic apomixis studies in rice combine apomeiosis with parthenogenesis triggers to produce clonal seed from hybrid plants. High-frequency systems in hybrid rice reported many lines with >80% clonal seeds and selected lines above 95%, while subsequent transgenerational work found largely stable clonal inheritance with rare aneuploid progeny that still require monitoring [Vernet et al., 2022, Liu et al., 2023]. The mechanism combines three modifications:

1. MiMe (Mitosis instead of Meiosis): triple knockout of *OSD1*, *PAIR1*, *REC8* converts meiosis into mitosis, producing unreduced gametes
2. MTL (MATRILINEAL): pollen-specific phospholipase knockout enabling haploid induction — sperm cannot complete fusion with the egg
3. BBML or DMP transgenes inducing parthenogenesis — egg cells initiate embryogenesis without sperm contribution

The combination yields rice plants that produce maternal clones in seed form across multiple generations — a foundational step toward apomictic crops at scale. Field translation remains conditional: breeders must quantify seed-set frequency, transgene segregation, rare chromosome loss, fitness under local climates, containment of gene flow to wild relatives, and whether farmers would gain durable access rather than new seed-locking arrangements.

Risks to wild relatives: Apomictic hybrids could become invasive (since each seed is a perfect copy of the elite plant) and could erode genetic diversity in wild populations through escapes. Regulatory caution is warranted.

29.9.5 Plant Biotechnology in Reproduction and Crop Improvement

Modern plant biotechnology builds on understanding of plant reproduction:

- Tissue culture and micropropagation: Totipotent plant cells can regenerate whole organisms. The auxin:cytokinin ratio determines differentiation: high auxin promotes roots; high cytokinin promotes shoots; balanced ratio maintains callus.
- Somatic embryogenesis: Somatic cells (non-reproductive) can be induced to form embryo-like structures that develop into complete plants. Used commercially for oil palm, conifers, coffee.
- Agrobacterium tumefaciens: Natural genetic engineer. Its Ti plasmid contains T-DNA that integrates into the plant genome. Modified T-DNA (with antibiotic resistance and gene of interest replacing oncogenes) is the primary tool for plant transformation.
- Applications: Bt crops (insecticidal crystal protein gene from *Bacillus thuringiensis*), golden rice (beta-carotene biosynthesis genes), drought-tolerant cultivars (DREB/CBF overexpression), herbicide-resistant varieties (modified EPSPS gene).

Plant pangenomes extend this toolkit beyond single-reference breeding. Crop and wild-relative pangenomes represent core and variable sequence across many individuals, exposing structural variants, presence-absence variation, and regulatory alleles that a single elite reference can miss [Schreiber et al., 2024]. For a breeding claim, the source-governed question becomes whether the trait maps to a shared reference allele, an alternate haplotype, or variation absent from the reference line.

Clinical Connection: The Bt toxin proteins (Cry proteins) are harmless to mammals because they require alkaline gut **pH** (found in insect midguts but not mammalian stomachs) to become active. Bt crops have reduced insecticide use by 37% globally while increasing yields 22% in developing countries (meta-analysis, Klumper & Qaim, 2014).

Concept Check 6: A breeder wishes to create a triploid (3n) seedless watermelon for commercial sale. Outline the crossing scheme starting from diploid (2n) parents. Why are triploid offspring sterile (no viable seeds), and which cross — $2n \times 4n$ or $4n \times 2n$ — yields the best fruit set?

Concept Check 7: *Pyrus communis* (European pear) requires a pollinator of a different cultivar to set fruit (pollinizer system) due to gametophytic SI. A grower plants 100% ‘Bartlett’ (S_1S_2) pears in an orchard. Predict the fruit yield. Then describe the genetic logic of selecting a pollinizer cultivar — what S-genotype is required?

Concept Check 8: Argue for or against this proposition: “Apomixis is evolutionarily dead-end because it eliminates genetic recombination. Hence apomictic species should be short-lived geologically.” Cite specific apomictic lineages in your answer (e.g., dandelions are apomictic and remain abundant on multiple continents).

Concept Check 9: A tomato cultivar bred for parthenocarpy carries a constitutively active PIN1 transgene driving auxin overproduction in the ovary. Predict fruit set in the absence of pollination, and predict the dormancy and germination behavior of any seeds that do form (assuming some pollination occurs by accident).

29.10 Current Evidence and Frontier Biology: Plant Reproduction and Development

For Plant Reproduction and Development, frontier biology belongs inside the evidence logic of the chapter. Plant biology links molecular regulation to climate stress, water limitation, crop resilience, phenology, and ecosystem feedbacks. The core reading question is this: plant reproduction links pollination, development, genetics, phenology, dispersal, and environmental filtering.

- What to verify: identify the observation, model, assay, or dataset that would make the claim stronger or weaker.
- What to qualify: state the scale, organism, cell type, environmental condition, or population where the claim is expected to hold.
- What to compare: test at least one alternative explanation, baseline, or null model before treating the pattern as causal.
- What to cite: distinguish primary evidence, review synthesis, public dataset, and institutional guidance; for recent or numeric claims, prefer the source closest to the measurement and state what has changed since it was published.

A strong plant-reproduction claim names the tissue, developmental signal, pollination or seed context, measurable trait, and fitness tradeoff [Schreiber et al., 2024].

Source practice: For reproduction claims, separate laboratory potential from field performance, inheritance, agronomic adoption, and ecological side effects [Schreiber et al., 2024].

29.11 Key Terms

Table 369. Plant Biotechnology in Reproduction and Crop Improvement: Term and Definition.

Term	Definition
Alternation of generations	Diploid sporophyte (spore-producing) alternates with haploid gametophyte (gamete-producing)
Sporophyte	Diploid (2n) generation; produces spores by meiosis; dominant in vascular plants
Gametophyte	Haploid (n) generation; produces gametes by mitosis; dominant in bryophytes
Sporopollenin	Highly resistant polymer of pollen exine; survives millions of years in sediment
Tube cell	Vegetative cell of pollen grain; forms the pollen tube
Generative cell	Cell of pollen grain that divides to produce two sperm cells
Microsporogenesis	Meiotic + mitotic divisions producing pollen grain from microspore mother cell
Megasporogenesis	Meiotic divisions producing functional megaspore from megaspore mother cell
Synergid	Two cells flanking the egg in the embryo sac; secrete LURE peptides; regulate sperm release
Filiform apparatus	Cell-wall labyrinth at the synergid micropylar pole; secretes LURE peptides
Central cell	Large embryo sac cell containing two polar nuclei; gives rise to endosperm (3n; 2m:1p)
Antipodal cells	Three cells at the chalazal end of embryo sac; nutritive function
Double fertilization	Unique to angiosperms: sperm 1 + egg = embryo (2n); sperm 2 + polar nuclei = endosperm (3n)
LURE peptides	Cysteine-rich defensin-like peptides from synergids; species-specific pollen tube attractants
FERONIA-LORELEI	Receptor complex on synergid surface; required for pollen tube rupture

Term	Definition
ABCDE model	Model of floral organ identity; combinatorial MADS-box TF activity specifies each whorl
MADS-box	DNA-binding domain in floral organ identity transcription factors; binds CArG-box motifs
AP1, AP3, PI, AG, SEP	MADS-box gene families: A, B, B, C, E classes respectively
Floral quartet	Tetrameric MADS-box complex specifying organ identity by binding two CArG boxes
Sporophytic SI	Self-incompatibility where pollen phenotype determined by diploid tapetum; SRK-SCR system
Gametophytic SI	Self-incompatibility where pollen phenotype determined by its own haploid genotype; S-RNase/SLF
Polyploidy	Whole-genome duplication; about 70% of angiosperms are paleopolyploids
Autopolyploid	Polyploid arising within a single species
Allopolyploid	Polyploid arising from interspecific hybridization followed by chromosome doubling
Phyllotaxis	Arrangement of leaves/organs on stem; golden angle 137.5 degrees; Fibonacci spirals
WUS-CLV3 circuit	Negative feedback loop maintaining stem cell population in the SAM
Karrikins	Smoke-derived butenolides; activate KAI2 receptor; break seed dormancy after fire
Apomixis	Asexual reproduction through seed without fertilization; produces maternal clones
Adventive embryony	Sporophytic apomixis: embryos from nucellar/integument cells
Apospory	Gametophytic apomixis with embryo sac from somatic cell
Diplospory	Gametophytic apomixis with embryo sac from modified meiosis
MiMe	Mitosis-instead-of-Meiosis triple knockout (OSD1, PAIR1, REC8); basis of synthetic apomixis
Endosperm	Triploid (3n; 2m:1p) nutritive tissue in angiosperm seeds; stores starch, protein, oils
Free-nuclear endosperm	Endosperm form with multiple nuclei in shared cytoplasm before cellularisation
PEG (Paternally Expressed Gene)	Gene expressed primarily from paternal allele in endosperm
MEG (Maternally Expressed Gene)	Gene expressed primarily from maternal allele in endosperm
FIS-PRC2	Polycomb complex (MEA-FIS2-FIE-MSI1) regulating endosperm imprinting
Heterospory	Production of two different spore sizes (micro- and megaspores); precursor to seed habit
Pericarp	Mature ovary wall comprising exocarp, mesocarp, and endocarp; forms the fruit
Myrmecochory	Seed dispersal by ants, often mediated by lipid-rich elaiosomes attached to seeds
Parthenocarpy	Fruit development without fertilization; can be natural or induced by auxin/GA
Climacteric fruit	Fruit type with autocatalytic ethylene burst at ripening (banana, tomato, apple)
System 1/System 2 ethylene	Basal vs auto-catalytic ripening ethylene biosynthesis
1-MCP	Synthetic ethylene perception inhibitor used commercially to delay fruit ripening
Stratification	Cold-moist treatment that breaks seed dormancy; simulates winter
Scarification	Physical or chemical disruption of seed coat enabling water uptake
DOG1	Master regulator of seed dormancy; QTL in <i>Arabidopsis</i>
Totipotency	Ability of a single plant cell to regenerate an entire organism

29.12 Review Questions

1. Compare the male gametophyte of a *Pinus* tree to that of a *Solanum lycopersicum* (tomato). How many cells in each? Where is mitosis 2 completed? How is sperm delivered to the egg? What is the evolutionary significance of the reduction in gametophyte size?
2. An *Arabidopsis* triple mutant lacks functional A, B, and C domain transcription factors (abc mutant). Predict the identity of organs in each floral whorl. Then predict what would happen if, in the same mutant, you ectopically expressed B-class genes in whorls 1 and 2 during flower development. Reference equation (362) in your answer.
3. Explain the mechanism of gametophytic self-incompatibility in Solanaceae. A researcher crosses two plants with S-genotypes S_1S_2 and S_1S_3 . What fraction of pollen will be accepted? Which S-**allele** combinations appear in the viable offspring? Compare with the same scheme under sporophytic SI in *Brassica*.
4. Compare primary and secondary seed dormancy. For a temperate tree species requiring both stratification and light for germination, trace the environmental cues from autumn seed fall through spring germination, linking each cue to its molecular mechanism (DOG1, ABA/GA balance, phytochrome). Identify the dormancy class (PD, PY, MD, MPD, combinational).
5. The goal of introducing synthetic apomixis into hybrid rice is to allow subsistence farmers to save F1 hybrid seed. (a) What genetic modifications are

- needed to create apomictic seed (cite Wang *et al.* 2022)? (b) What risks might apomictic crops pose to wild relatives via gene flow? (c) Compare the genetic diversity implications of apomixis vs vegetative propagation.
6. Explain why double fertilization [Nawaschin, 1898] is considered a key evolutionary innovation. What advantage does the triploid endosperm provide over the gymnosperm approach where the female gametophyte tissue serves as the nutritive tissue? Discuss the parental conflict implications via the PEG/MEG mechanism. Why is the canonical 2m:1p genome dosage common, and what kinds of exceptions would challenge an over-simple rule?
 7. A fruit biologist examines a mystery fruit and finds: fleshy mesocarp, hard endocarp containing a single seed, and thin exocarp. Classify this fruit type. Name three plants that produce this type of fruit and describe the most likely dispersal mechanism. Is this likely a climacteric or non-climacteric fruit?
 8. Describe the WUS-CLV3 feedback loop. Predict the phenotype of: (a) a loss-of-function *clv3* mutant, (b) a gain-of-function *WUS* overexpression line, and (c) a double mutant lacking both WUS and CLV3.
 9. Run `plant_biomass_growth` from 1 g to 40 g capacity over 60 days. How does the curve differ from unrestricted exponential growth?
 10. Why might endosperm ploidy (3n) stabilize parent-offspring conflict compared with purely maternal provisioning? Use the FIS-PRC2 mechanism in your answer.
 11. A breeder wants to create double-flowered carnations (extra petals). Which class of MADS-box gene should be partially inactivated and why? Cite the relevant Coen and Meyerowitz framework [Coen and Meyerowitz, 1991] and the molecular identity of the gene (AG).
 12. Explain the commercial pre-harvest treatment with 1-MCP for apples in long-distance export. Which step of the ethylene pathway shown in equation (367) does 1-MCP block, and how does this preserve fruit firmness during shipping? Distinguish System 1 and System 2 ethylene biosynthesis.
 13. A plant exhibits adventive embryony (sporophytic apomixis) in some seeds and zygotic embryos in others. From a single cross, predict the genotypic distribution of offspring and the agricultural value of this dual-mode reproduction.

29.13 Further Reading and Source Notes: Plant Reproduction and Development

- Coen and Meyerowitz [1991] — The war of the whorls: Genetic interactions controlling flower development. *Nature*, 353.
- Nawaschin [1898] — Resultate einer Revision der Befruchtungsvorgänge bei *Lilium martagon* und *Fritillaria tenella*. *Bulletin de l'Académie Impériale des Sciences de Saint-Petersbourg*, 9.

29.14 Computational Bridge

Sporophyte growth phases are approximated logistically in `plant_biomass_growth`:

```
from biology.botany import plant_biomass_growth

out = plant_biomass_growth(1.0, 0.15, 80.0, 40.0, steps=40)
print(round(out.biomass_g[-1], 2))
```

Clinical / systems note: Apomixis and clonal crops change epidemiological risk profiles (uniform genetics) much like monocultures in human agriculture policy. Phenological mismatch adds a second systems risk: if warming advances spring plant emergence faster than pollinator activity, reproductive success can fall even when each species remains locally present [Kudo and Cooper, 2019]. Gene-drive or engineered reproductive interventions therefore need ecological governance as well as molecular feasibility review [National Academies of Sciences, Engineering, and Medicine, 2016].

29.15 Summary

- Alternation of generations: Sporophyte (2n) produces spores by meiosis; gametophyte (n) produces gametes by mitosis. Evolutionary trend: sporophyte dominant, gametophyte reduced.
- Plant group diversity: Bryophytes (gametophyte dominant, water-dependent fertilization) through gymnosperms (pollen, seeds, wind pollination) to angiosperms (flowers, double fertilization, fruits, animal pollination).
- Floral ABCDE model [Coen and Meyerowitz, 1991]: A+E = sepal; A+B+E = petal; B+C+E = stamen; C+E = carpel; D+E = ovule. MADS-box TFs (AP1, AP3-PI heterodimer, AG, SEP1-4) form floral quartets binding two CArG boxes simultaneously.

- Gametophytes: Male = 3-cell pollen grain (tube cell + 2 sperm) inside sporopollenin exine; female = 7-cell, 8-nucleate Polygonum-type embryo sac (egg + 2 synergids + central cell with 2 polar nuclei + 3 antipodals). Microsporogenesis: MMC → meiosis → 4 microspores → asymmetric mitosis I → 2-cell pollen; mitosis II yields 2 sperm. Megasporogenesis: MMC → meiosis → 1 functional + 3 degenerating megaspores → 3 free nuclear divisions → 8 nuclei → cellularisation → 7-cell embryo sac.
- Double fertilization [Nawaschin, 1898]: LURE-LRE-FER signaling triggers pollen tube rupture in synergid; sperm 1 + egg = 2n zygote → embryo; sperm 2 + 2 polar nuclei = 3n primary endosperm. Pollen tube guidance: tip-focused Ca²⁺ gradient + LURE chemotropism; spermatogenesis during tube elongation in bicellular pollen species.
- Endosperm (typically 3n; 2m:1p): Free-nuclear → cellular development; PEG/MEG imprinting via FIS-PRC2 drives parent-of-origin expression and parental-conflict regulation. Dosage is canonically 2m:1p but varies in some lineages and developmental contexts.
- Self-incompatibility: Sporophytic SI (SRK-SCR-ARC1; *Brassica*) acts at stigma surface; gametophytic SI (S-RNase/SLF; Solanaceae, Rosaceae) acts in style by collaborative non-self recognition.
- Polyploidy: Auto- vs allopolyploids; 70% of angiosperms have paleopolyploid history; major crop genomes (wheat, cotton, strawberry) are polyploid.
- Fruit and seed dispersal: Diverse adaptations for dispersal include endozoochory, anemochory, explosive dehiscence, epizoochory, and ant-mediated myrmecochory. Climacteric fruits (banana, tomato, apple) ripen via System 2 autocatalytic ethylene burst — controlled commercially with 1-MCP. Parthenocarp can be induced by auxin/GA (seedless grapes, watermelons).
- Seed dormancy: Five classes (PD, PY, MD, MPD, combinational); broken by stratification, scarification, light (Pfr), smoke-karrikins (KAI2), or temperature fluctuation. Germination: GA degrades DELLA, releasing α-amylase transcription; ABA-DOG1-PP2C-SnRK2 axis maintains dormancy.
- Vegetative reproduction: Stolons, rhizomes, bulbs, corms, tubers, adventitious roots/plantlets, fragmentation, layering, grafting. Foundation of clonal crop production (banana, potato, garlic, grape).
- Apomixis: Sporophytic (adventive embryony, e.g., citrus nucellar) vs gametophytic (apospory in *Hieracium*, diplospory in *Taraxacum*; pseudogamous vs autonomous endosperm). Wang *et al.* 2022 synthetic apomixis in rice via MiMe + MTL/BBML.
- Meristems: SAM (WUS-CLV3 feedback, PIN1-auxin phyllotaxis at golden angle); RAM (QC + initials). Both maintain lifelong growth.
- Biotechnology: Tissue culture exploits totipotency; *Agrobacterium* Ti plasmid enables genetic transformation; Bt crops, golden rice.
- Connections: See Unit IV — Molecular Genetics: Introduction for meiosis and life cycle, section 28 for water and growth, and section 10 for photosynthate partitioning.

29.16 Companion Source Module: Plant Reproduction and Development

Plant Reproduction and Development should leave a reproducible trail from a biological claim to the code, figure, diagram, or paper-based activity that can test it. Use the surfaces below to inspect the chapter’s assumptions, rerun the relevant model, or compare the manuscript explanation with companion labs and figures.

Table 370. Companion source surfaces for Plant Reproduction and Development.

Surface	Use it for
src/biology/botany/botany.py (plant_biomass_growth)	Explore growth allocation and reproductive tradeoffs.
src/biology/genetics/genetics.py (punnett_square, chi_squared_test)	Connect inheritance evidence to breeding and reproductive outcomes.
src/mermaid/biology_diagrams.py (hormone_signaling_diagram)	Link developmental timing to hormone signaling.

Reproducibility check: state pollination mechanism, developmental stage, genetic model, and environmental filter before interpreting reproductive success. Cross-reference: connect with sections 17 and 18 and section 30.

30 Plant Responses to the Environment

Level 2/3 · 55 min read · 75 min lecture · Prerequisites: section 29

30.1 Learning Objectives

By the end of this chapter, you should be able to:

1. Predict how PIN auxin-efflux-carrier relocalization produces the differential growth of a phototropic response [Went, 1926], and describe how plants sense other directional stimuli.
2. Explain the major plant hormones (auxin, gibberellin, cytokinin, ABA, ethylene, brassinosteroids, jasmonates, salicylate, strigolactones) and their signaling pathways.
3. Describe photomorphogenesis: phytochrome biochemistry (Pr/Pfr photoconversion), cryptochrome FAD signaling, and shade avoidance.
4. Explain gravitropism in roots and shoots, including amyloplast settling and PIN protein relocalization.
5. Describe photoperiodism, the role of phytochrome, florigen (FT), and the molecular basis of flowering time control via vernalisation (FLC silencing).
6. Explain the plant circadian clock molecular architecture (morning loop CCA1/LHY/TOC1; evening loop PRR5/7/9) and how it gates growth, flowering, and photosynthesis.
7. Compare the signaling logic of ABA-mediated drought and jasmonate-mediated herbivory responses, and describe the cold (CBF-COR), heat (HSP), salt, and flooding responses.
8. Describe plant immunity (PTI, ETI), the hypersensitive response, systemic acquired resistance (SAR), and JA/SA antagonism.
9. Evaluate agricultural applications of plant hormone biology: ethylene inhibitors, gibberellin dwarfing genes, and auxin herbicides.

30.1.1 Study Blueprint

- Big idea: Plants sense environmental signals and respond through growth, hormones, and physiological regulation.
- Core concepts: tropisms, hormones, photoperiodism, stress responses.
- Framework alignment: Vision & Change: Structure and function, Pathways and transformations of energy and matter, Systems; AP Biology: Energetics, Systems Interactions; NGSS-style topics: Structure and Function, Matter and Energy in Organisms and Ecosystems.
- Model or quantitative lens: Dose-response, water-use-efficiency, and hormone-interaction reasoning.
- Data skill: Interpret plant response data across light, gravity, water, and hormone treatments.
- Practice cadence: Visual Representations, Questions and Methods, Argumentation.
- Common misconception to repair: A plant response is not passive; plants actively regulate development and physiology without neurons.
- Primary lab: Lab — Plant Responses to the Environment.
- Question bank: Questions — Plant Responses to the Environment.
- Transfer task: Transfer response logic to shade avoidance, drought, flowering, and crop management.
- Bridge to computation: biology.botany.botany.photosynthesis_rate.

Opening Vignette — Darwin’s Love Affair with Carnivorous Plants

“I care more about Drosera than the origin of species in the world,” Darwin wrote to his friend Asa Gray in 1860. For fifteen years he systematically experimented on sundews and Venus flytraps, weighing morsels of meat to 1/78,000 of a grain, timing trap closure, and testing with hundreds of chemical solutions — establishing that carnivorous plants actively respond to nitrogenous stimuli, not merely mechanical touch. His 1875 book *Insectivorous Plants* described hormone-like chemical signals in plants decades before the word “hormone” existed. In those experiments lurked the seed of plant hormone biology: auxin, gibberellins, abscisic acid, cytokinin, ethylene — the five classical plant hormones whose discovery unfolded over the next century. Darwin rarely found them by name, but his insight that plants sense and respond to their environment through diffusible chemical signals laid much of the groundwork that followed.

30.2 Plant Hormone Networks and Growth Decisions

Plant hormones (phytohormones) are small organic molecules produced in low concentrations that regulate virtually every aspect of plant growth, development, and stress responses. Unlike animal hormones, plant hormones are often produced at many sites throughout the plant and can act locally.

30.2.1 Auxin (Indole-3-Acetic Acid, IAA)

Biosynthesis: Primarily from tryptophan via the TAA1/YUCCA pathway. Produced in young leaves, shoot apical meristem, and developing embryos.

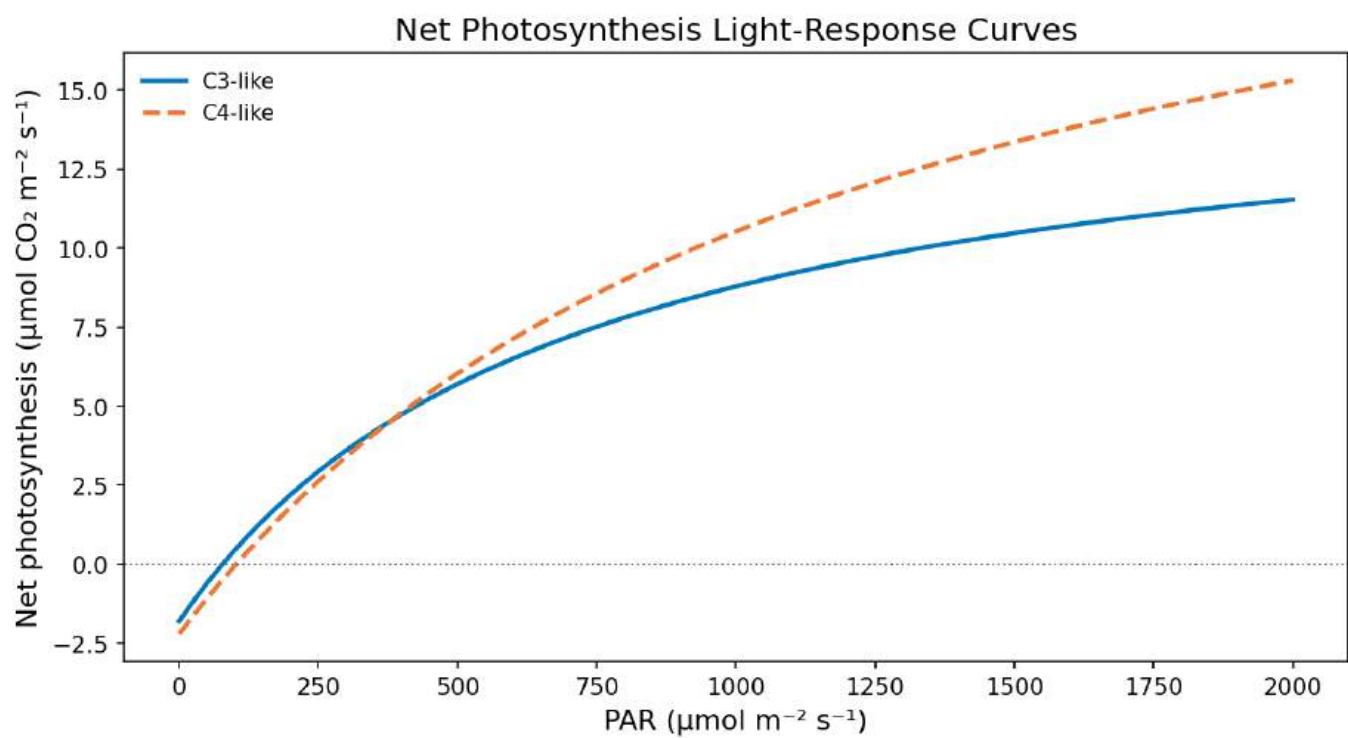


Figure 180. Net photosynthesis light-response curves for C3-like and C4-like parameter sets. Higher light-saturation points and lower dark respiration shift the compensation and saturation regions.

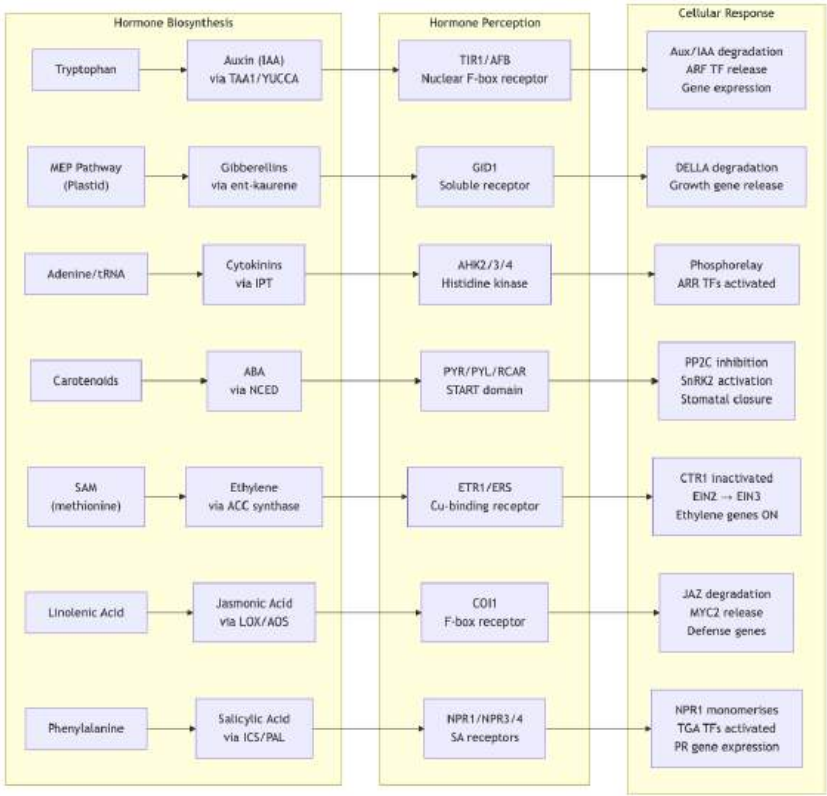


Figure 181. Major plant hormone pathways from biosynthesis through receptor perception to cellular response. Each route follows stimulus-driven hormone production, specific receptor binding, and regulated gene expression.

Transport: Auxin moves by polar auxin transport (PAT), unique among plant hormones: - PIN efflux carriers (PIN1-8): Localized to specific faces of the plasma membrane; their polar distribution determines the direction of auxin flow. PIN proteins cycle between plasma membrane and endosomal compartments; their localization is regulated by phosphorylation (PID kinase) and vesicle trafficking. - AUX1/LAX influx carriers: Import auxin into cells; less polar than PIN proteins - Polar transport rate: about 1 cm/h in stems (basipetal in shoots, acropetal in roots)

Signaling mechanism (TIR1 pathway): 1. Auxin binds TIR1/AFB F-box proteins (nuclear receptors) 2. Auxin acts as “molecular glue” between TIR1 and Aux/IAA transcriptional repressors 3. Aux/IAA proteins are ubiquitinated by SCF^{TIR1} complex and degraded by 26S proteasome 4. ARF (Auxin Response Factor) **transcription** factors are released from Aux/IAA repression 5. ARF activates auxin-responsive genes

Key functions: - Apical dominance: High auxin from the apex suppresses lateral bud outgrowth; removal of apex (decapitation) releases lateral buds - Phototropism: Asymmetric auxin distribution bends shoots toward light. - Gravitropism: Asymmetric auxin distribution in response to gravity - Root initiation: High auxin promotes adventitious and lateral root formation - Fruit development: Auxin from developing seeds promotes fruit growth

30.2.2 Gibberellins (GAs) and Stem Elongation

Biosynthesis: From the MEP pathway in plastids; active forms include GA₁, GA₃, GA₄. Produced in young leaves, root tips, and developing seeds.

Signaling mechanism: 1. GA binds the soluble receptor GID1 2. GA-GID1 complex interacts with DELLA proteins (transcriptional repressors: GAI, RGA, RGL1-3 in *Arabidopsis*) 3. DELLA proteins are ubiquitinated by SCF^{SLY1} E3 ligase and degraded 4. Release of DELLA repression allows growth-promoting transcription factors to act

Key functions: - Stem elongation: Promotes internodal elongation; GA-deficient mutants are dwarf plants (basis of “Green Revolution” semi-dwarf wheat: *Rht* gene encodes GA-insensitive DELLA) - Seed germination: GA induces α-amylase synthesis in cereal aleurone layer, mobilizing starch reserves - Fruit development: Can induce parthenocarp (seedless fruit production without fertilization; seedless grapes) - Flowering: In some long-day plants, GA can substitute for the long-day photoperiod requirement

30.2.3 Cytokinins and Cell Division Signals

Biosynthesis: From adenine derivatives via IPT (isopentenyltransferase). Primarily synthesized in root tips and transported to shoots via **xylem**.

Key functions: - Cell division: Essential for cytokinesis; cytokinin + auxin together drive cell proliferation - Shoot promotion: Antagonise auxin’s apical dominance; promote lateral bud outgrowth - Delay of senescence: Maintain **chlorophyll** and protein levels in leaves; SAUR (senescence-associated ubiquitin-related) pathway - Tissue culture: Auxin:cytokinin ratio determines organogenesis – high auxin = roots; high cytokinin = shoots; equal = callus (undifferentiated cell mass)

30.2.4 Absciscic Acid (ABA)

Biosynthesis: From carotenoid cleavage (NCED3 **enzyme**, 9-cis-epoxycarotenoid dioxygenase). Produced in roots under soil drying and in leaves under dehydration stress.

Key functions: - Stomatal closure: The primary drought response hormone, detailed in the absciscic-acid discussion. - Seed dormancy: Maintains dormancy until conditions favor germination; antagonised by GA - Stress gene expression: Activates LEA (Late Embryogenesis Abundant) protein genes; dehydrins; osmolyte synthesis

Signaling: ABA binds PYR/PYL/RCAR receptors, which inhibit PP2C phosphatases, activating SnRK2 kinases. SnRK2 phosphorylates SLAC1 (stomatal closure), AREB/ABF transcription factors (stress genes), and ion channels.

30.2.5 Ethylene and Gaseous Stress/Ripening Signals

Biosynthesis: From methionine via SAM (S-adenosylmethionine) to ACC (1-aminocyclopropane-1-carboxylic acid) by ACC synthase, then to ethylene by ACC oxidase. Ethylene is a gas – it diffuses freely between cells and even between plants.

Key functions: - Fruit ripening: Climacteric fruits (banana, tomato, apple, avocado) show a burst of ethylene production triggering ripening. Non-climacteric fruits (strawberry, grape, citrus) do not show this burst. - Senescence: Promotes leaf yellowing and abscission (leaf drop); petal senescence in cut flowers - Triple response: In dark-grown seedlings, ethylene causes: (1) shortened, thickened hypocotyl, (2) exaggerated apical hook, (3) horizontal growth. This protects the seedling apex as it pushes through soil. - Flooding response: Submerged roots accumulate ACC (cannot oxidise to ethylene without O₂); when ACC reaches shoots, aerenchyma formation is triggered (programmed cell death creates air channels) - Abscission: Ethylene activates cellulase and pectinase in the abscission zone at the leaf petiole base

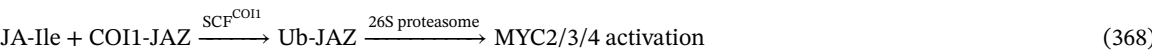
Clinical Connection: The commercial fruit industry manipulates ethylene extensively. Bananas are picked green, shipped under ethylene-suppressed conditions (using KMnO₄ as an ethylene scrubber or 1-MCP as an ethylene perception inhibitor), and then ripened on demand by ethylene gas treatment at distribution centers. This enables global tropical fruit supply chains.

Concept Check (Evaluate): A “hormone network” framework treats phytohormones as nodes in a regulatory network rather than as isolated signals. Ethylene (ET), absciscic acid (ABA), jasmonate (JA), salicylate (SA), auxin (IAA), cytokinin (CK), and brassinosteroid (BR) together populate more than 30 pairwise interaction nodes. (a) Evaluate the adaptive logic of the JA–ET synergism during wounding. Caterpillar feeding induces JA accumulation (the systemic wound signal acting through jasmonoyl-isoleucine) and local ET production at the damaged tissue. Together, the two hormones synergistically induce trypsin-protease-inhibitor expression to a level roughly 10–100× that produced by either signal alone. Why might evolution have favored a configuration in which two distinct signals must coincide to release the most expensive defense chemistry? (b) BR promotes cell elongation, whereas ET inhibits elongation (the classical triple response: radial swelling, exaggerated apical hook, and shortened hypocotyl). During the emergence of a dark-grown seedling pushing up through soil, propose why their antagonism is adaptive, and outline a plausible molecular mechanism by which elevated ET signaling could attenuate BR responses at the BES1 / BZR1 transcription-factor layer.

30.2.6 Jasmonates (JA) and Wound Defense

Biosynthesis: From linolenic acid (membrane lipid) via the LOX (lipoxygenase) pathway. The active form is JA-Ile (jasmonyl-isoleucine conjugate, produced by JAR1).

Signaling: JA-Ile binds COI1 (F-box protein of the SCF^{COI1} E3 ubiquitin ligase), which recruits JAZ (Jasmonate ZIM-domain) repressor proteins into the SCF complex:



Pre-wounding, JAZ proteins recruit TOPLESS corepressor via the NINJA adaptor, forming a trimeric JAZ-NINJA-TOPLESS complex that represses MYC2 through **histone** deacetylase recruitment. Post-wounding JA-Ile surge displaces this complex by directing SCF^{COI1} to ubiquitinate JAZ via the SLY degron motif (Jas domain). 2024 cryo-EM structures (**allosteric** lid closure model) show COI1 undergoes a conformational switch upon JA-Ile binding, with ASK1-CUL1-RBX1 form-

ing the catalytic core (Sheard *et al.*, *Nature* 2010; Xu *et al.*, *bioRxiv* 2024). COI1 paralogs (COI1a/b) fine-tune JAZ subtype specificity across defense/development contexts.

Key functions: - Wound/herbivore defense: Protease inhibitors, alkaloids (nicotine in tobacco), glucosinolates, terpene volatiles - UV damage response: Accumulation of UV-absorbing flavonoids - Mycorrhizal signaling: JA promotes mycorrhizal colonization - Pollen development: Required for stamen maturation and pollen release

30.2.7 Salicylic Acid (SA)

Biosynthesis: From phenylalanine (PAL pathway) or chorismate (ICS pathway; **dominant** in *Arabidopsis*).

Key functions: - Systemic Acquired Resistance (SAR): After local pathogen infection, SA signals spread systemically, priming distant tissues for enhanced defense in the plant-immunity response. - PR protein induction: Pathogenesis-related proteins (PR-1, β -1,3-glucanase, thaumatin-like proteins)

Concept Check: Aspirin (acetylsalicylic acid) is derived from salicylic acid, originally extracted from willow bark (*Salix*). Why might plants produce SA in response to pathogens, and what does this tell us about the evolutionary age of this defense pathway?

30.2.8 Strigolactones and Branching/Mycorrhizal Signals

Biosynthesis: From carotenoid precursors via D27 isomerase and CCD7/CCD8 cleavage. Produced primarily in roots.

Key functions: - Branch suppression: Inhibit lateral bud outgrowth; work with auxin in apical dominance - Mycorrhizal recruitment: Secreted into rhizosphere to attract AM fungi - Root architecture: Promote lateral root elongation - Parasitic plant germination: *Striga* (witchweed) seeds germinate in response to strigolactones from host roots, a devastating crop **parasite** in Africa

30.3 Phototropism and Auxin-Driven Bending

The molecular pathway for phototropism in *Arabidopsis thaliana* is one of the best-characterized plant signaling cascades:

1. Blue light (390-500 nm) illuminates the shoot asymmetrically
2. PHOT1 or PHOT2 (LOV1/LOV2-domain photoreceptors; LOV = Light Oxygen Voltage) absorbs blue light. Photochemical covalent FMN-cysteine adduct forms, causing conformational change and autophosphorylation (Ser849 of PHOT1, kinase domain released).
3. PHOT1/2 phosphorylate NPH3 (Non-Phototropic Hypocotyl 3). NPH3 interacts with ARF7/ARF19 and reorganises.
4. Auxin lateral redistribution (the Cholodny-Went hypothesis, quantified by **Went** [1926] *Avena* coleoptile bioassay):
 - PHOT1/2 triggers PIN3 (auxin efflux carrier) relocation from the bottom to the lateral face of shoot endodermal cells
 - More auxin (IAA) is transported to the shaded side; less to the illuminated side
5. Acid growth hypothesis [**Hager**, 1971]:
 - High [IAA] on shaded side activates plasma membrane H⁺-ATPase (AHA1/2). Proton extrusion acidifies the cell wall (**pH** 5.5 to 4.5).
 - Acidic pH activates expansins (proteins that disrupt H-bonding between cellulose microfibrils and hemicellulose) causing wall loosening. Turgor-driven elongation follows.
6. Differential elongation (shaded side elongates more than lit side) causes the shoot to bend toward light. Phototropic curvature is completed within 30-60 minutes.

Historical note: Darwin and Darwin (*Power of Movement in Plants*, 1880) first demonstrated that the phototropic signal originates in the coleoptile tip. **Went** [1926] isolated auxin using agar blocks. The molecular receptors (PHOTs) were identified in 1997 by Briggs and colleagues.

30.3.1 Worked Example: Phototropic Curvature from a Lateral Auxin Gradient

Problem: A coleoptile segment is illuminated from one side. Following Cholodny-Went redistribution, the shaded flank receives more auxin and, via acid growth, elongates 30% while the illuminated flank elongates 10%. Each flank starts at length $L_0 = 10$ mm and the coleoptile diameter (distance between the two flanks) is $w = 1.5$ mm. Calculate the phototropic bending angle.

Solution:

1. Elongation of each flank. Apply the relative growth fractions to the initial length:

$$\Delta s_{\text{shaded}} = L_0 \times 0.30 = 10 \times 0.30 = 3.0 \text{ mm}, \qquad \Delta s_{\text{lit}} = L_0 \times 0.10 = 10 \times 0.10 = 1.0 \text{ mm}$$

2. Differential elongation. The bend is driven by the difference in arc length between the two flanks:

$$\Delta s_{\text{shaded}} - \Delta s_{\text{lit}} = 3.0 - 1.0 = 2.0 \text{ mm}$$

3. Bending angle. When an organ of width w bends through angle θ (radians), the arc-length difference between its two surfaces equals $w\theta$, so $\theta = (\Delta s_{\text{shaded}} - \Delta s_{\text{lit}})/w$:

$$\theta = \frac{2.0 \text{ mm}}{1.5 \text{ mm}} = 1.33 \text{ rad} = 1.33 \times \frac{180^\circ}{\pi} \approx 76.4^\circ$$

Interpretation: A 3:1 ratio of differential flank elongation over a 1.5 mm-wide coleoptile produces about a 76 degree bend toward the light — quantitatively illustrating how a modest lateral auxin gradient, amplified by acid-growth wall loosening, generates the large directional curvature characteristic of phototropism.

30.3.2 Worked Example: Auxin Redistribution Predicts Curvature Rate

Problem: A unilaterally illuminated coleoptile reorganises its auxin field by phototropin-driven PIN3 relocalization. Take measured tissue auxin concentrations as: lit side [IAA] = 20 → 12 nM (a 40% drop), shaded side [IAA] = 20 → 28 nM (a 40% rise). Within the linear range of the IAA dose-response curve for elongation, growth rate is approximately proportional to [IAA]. Compute the curvature rate and the cumulative bend after 3 h.

Solution:

- 1. Differential growth rate. Relative growth on the shaded flank is now 28/20 = 1.4× baseline; on the lit flank, 12/20 = 0.6× baseline. The shaded side therefore elongates 1.4/0.6 ≈ 2.33 times as fast as the lit side.
- 2. Curvature per hour. Empirically, the *Avena* coleoptile assay calibrates such an auxin imbalance to roughly 10° of curvature per hour at room temperature (Went 1926-era data, scale held by modern phototropin work). Treat that as the conversion constant for the present scenario.
- 3. Curvature after 3 h. Linear extrapolation in the small-angle regime: $\theta(3 \text{ h}) \approx 3 \times 10^\circ = 30^\circ$. The small-angle approximation begins to break down beyond ~ 45°, after which the shaded flank’s arc length grows nonlinearly with θ and the rate slows.
- 4. Modern caveat. Cholodny-Went treats lateral auxin redistribution as the sole cause. The modern molecular picture revises this: blue-light-activated PHOT1/PHOT2 phosphorylate NPH3, triggering PIN3 relocalization to the lateral face of endodermal cells; the auxin asymmetry that follows is the *output* of this relocalization, not a primary diffusion event. The geometry, however, is unchanged — curvature still scales with the integrated auxin differential.

Interpretation. Even a modest ±40% perturbation of tissue [IAA] produces a 30° reorientation within a few hours, because the elongation response is nonlinearly amplified by acid-growth wall loosening. The Cholodny–Went quantitative form survives even though the mechanism has been re-derived from the molecular up.

30.4 Gravitropism and Gravity-Sensing Root Architecture



Figure 182. Gravitropism in roots and shoots In both organs, amyloplast settling triggers asymmetric auxin redistribution via PIN protein relocalization. The critical difference: root cells are INHIBITED by high auxin concentrations (causing the lower side to grow less, bending the root downward), while shoot cells are PROMOTED by high auxin (causing the lower side to grow more, bending the shoot upward).

Key molecular details — statoliths and PIN asymmetry:

- Statocytes: Specialized gravity-sensing cells. In roots, these are the columella cells of the root cap (a few central cells just behind the meristem). In shoots, they are the endodermal cells (starch sheath surrounding the vascular cylinder).
- Amyloplasts (statoliths): Starch-filled plastids (1–10 μm diameter) that sediment under gravity within seconds of reorientation. Their settling pulls on the actin cytoskeleton and ER membranes, generating mechanical signals that are transduced via TOC (translocon of outer chloroplast) complex to the LAZY1/IGT proteins on the new lower face of the cell.
- PIN auxin transporter asymmetry:
 - In root columella cells, PIN3 is initially symmetrically localized at the plasma membrane. Within minutes of gravity stimulation, PIN3 relocalizes to the new lower (now downward-facing) face of the cell.
 - In the elongation zone, PIN2 is permanently localized on the upper face of cortical and epidermal cells; PIN2 is critical for transporting auxin from the root tip back along the upper side of the elongation zone toward the shoot. Relocalization of PIN3 in columella cells biases auxin export toward the lower side, where PIN2 then carries it acropetally, accumulating auxin on the lower side of the elongation zone.

- Lateral auxin redistribution: In *Arabidopsis* roots, the asymmetry develops within about 5 min of gravity stimulation; bending is visible by 20 min and complete within 1–2 hours.
- LAZY1 protein: Required for normal gravitropism. *lazy1* mutants show reversed gravitropic responses (shoots grow down, branches grow at unusual angles). LAZY1 relocates to the lower side of the cell after gravity stimulation and facilitates PIN relocation.
- Root vs shoot dose-response difference: The same auxin redistribution (more auxin on the lower side) has opposite effects because root cells have a much lower optimal auxin concentration (about 10^{-9} M for root elongation) than shoot cells (about 10^{-5} M for stem elongation). Above the root optimum, auxin inhibits elongation via the stabilization of Aux/IAA repressors and ethylene production; thus the lower side of the gravity-stimulated root grows less than the upper, and the root bends downward.

30.5 Photomorphogenesis: Phytochromes and Cryptochromes

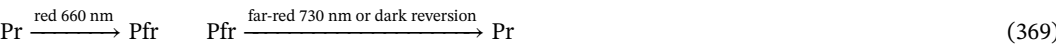
Plants integrate diverse light signals — wavelength, intensity, direction, duration, timing — through a constellation of photoreceptors. The two most studied families are phytochromes (red/far-red sensors) and cryptochromes (blue/UV-A sensors).

30.5.1 Phytochrome Biochemistry and Red/Far-Red Switching

Phytochromes are dimeric about 125 kDa chromoproteins. Each monomer carries a bilin chromophore (phytochromobilin) covalently attached to a conserved cysteine in the photosensory module. The chromophore exists in two photointerconvertible forms:

- Pr (red-absorbing form, λ_{max} = 660 nm): Inactive form; synthesized in the dark; primarily cytoplasmic
- Pfr (far-red-absorbing form, λ_{max} = 730 nm): Active form; translocates to the nucleus where it interacts with PIFs (Phytochrome Interacting Factors); triggers physiological responses

Photoconversion:



Red light (660 nm) converts Pr to Pfr; far-red light (730 nm) converts Pfr back to Pr. In darkness, Pfr slowly reverts to Pr (thermal reversion, half-life about hours) and is also degraded by the COP1 ubiquitin-proteasome pathway. The R/FR reversibility of physiological responses (Borthwick and Hendricks, 1952) is the diagnostic signature of phytochrome involvement.

Phytochrome diversity:

Arabidopsis has five phytochromes (PhyA–PhyE), each with distinct light-stability and physiological roles:

- PhyA: Light-labile (degraded rapidly in light). Mediates very-low-fluence and far-red-high-irradiance responses (FR-HIR). PhyA is the principal sensor for shade-avoidance under deep shade (where FR predominates) and for de-etiolation in dim light.
- PhyB: Light-stable. Mediates the classic R/FR reversible (low-fluence) responses. PhyB is the principal sensor of canopy shade via the R:FR ratio (high R:FR = open sun; low R:FR = under leaf canopy because chlorophyll absorbs red and transmits far-red). Loss-of-function *phyB* mutants are constitutively shade-avoiding (elongated, pale, early-flowering).
- PhyC, PhyD, PhyE: Specialized roles in flowering time, leaf angle, and modulating the responses of PhyA/B.

Shade avoidance via R:FR ratio: Sun-grown plants typically experience R:FR ratios of about 1.2; under a leaf canopy, the ratio drops to 0.1–0.4 because chlorophyll preferentially absorbs red. PhyB Pfr is destabilised under low R:FR (returning to Pr); this releases PIF4/5/7 from PhyB-mediated degradation, activating YUCCA-driven auxin synthesis and triggering hypocotyl elongation, petiole elongation, and accelerated flowering — the shade avoidance syndrome.

Concept Check (Analysis): Phytochromes exist in two interconvertible forms: Pr (absorbs red, 660 nm; biologically inactive) and Pfr (absorbs far-red, 730 nm; biologically active). In direct sunlight the Pr/Pfr equilibrium is set by a red-to-far-red (R:FR) ratio of about 1.15; under a closed leaf canopy that ratio falls to roughly 0.1 because chlorophyll absorbs red and transmits far-red. (a) Using the simplified equilibrium expression $\text{Pfr}/(\text{Pfr} + \text{Pr}) = k_R R / (k_R R + k_{FR} FR)$ with $k_R/k_{FR} = 1.0$, calculate the fraction of phytochrome in the Pfr form for an open-canopy plant (R:FR = 1.15) and for the same plant under deep canopy shade (R:FR = 0.1), and comment on the implied physiological state in each case. (b) PhyB dark reversion (Pfr → Pr) proceeds with a half-life of hours, so a brief red-light pulse during the dark period leaves the photoreceptor in the Pfr-active state for several hours afterwards. Predict the effect on flowering in a short-day plant (which requires uninterrupted long nights) of a one-minute red-light pulse delivered at midnight, and then predict whether a subsequent one-minute far-red pulse can reverse the night-break effect.

Concept Check (Analyze) — Jasmonate–salicylate antagonism in defense. JA (jasmonate) signaling proceeds through SCF^{COI1}-mediated JAZ degradation, releasing MYC2/3/4 to activate defenses against chewing herbivores and necrotrophic pathogens; SA (salicylic acid) signaling proceeds through NPR1-driven TGA transcription factors and *PR* gene induction, principally targeting biotrophic pathogens. The two pathways are *mutually antagonistic*: high NPR1 activity suppresses MYC-branch JA outputs, and high JA signaling represses ICS1-driven SA biosynthesis. (a) Diagram the two pathways and mark the two best-characterized antagonism nodes (NPR1 → COI1 branch; MYC2 → ICS1). (b) A necrotrophic fungus (*Botrytis cinerea*) drives strong host JA accumulation while suppressing SA accumulation. Explain mechanistically why this benefits the pathogen — connect (i) JA-driven cell-death pathways that provide nutrients to a dead-cell-feeding pathogen and (ii) SA suppression that lifts inhibition on the JA branch. (c) Predict, with direction, what happens in a *coi1* loss-of-function plant infected with *Botrytis*: does the plant become more resistant, more susceptible, or neither, and through which surviving branch (camalexin, PR proteins, ROS burst)?

Concept Check (Synthesize) — Shade avoidance, phyB, PIFs, and brassinosteroid coupling. Under canopy shade, the low R:FR ratio drives PhyB into the inactive PR form; PIF4/5/7 accumulate; YUCCA-mediated auxin synthesis rises; brassinosteroid (BR) signaling potentiates PIF activity through BZR1 cooperation at shared promoter elements; cumulatively the plant elongates internodes, reduces branching, and accelerates flowering — the *shade avoidance syndrome* (SAS). (a) Build a single integrated diagram in which phyB sits at the top, PIF4/5/7 in the middle, and YUCCA/auxin and BZR1/BR converge on the SAUR/expansin/cell-wall acidification output. (b) Predict the field-trial phenotype of a phyB-overexpressing (constitutively active) maize line planted at high density: what happens to plant height, harvest index, lodging risk, and per-plant yield, and how does the population-level grain yield change? (c) Synthesize this with the JA–SA antagonism above: a constitutively shade-avoiding line directs carbon to elongation; argue whether such a line will be more or less vulnerable to a necrotroph epidemic, and identify the single most informative biomarker you would measure in a glasshouse trial to test your prediction.

30.5.2 Cryptochrome Signaling — Blue Light and FAD

Cryptochromes (CRY1/CRY2) are blue/UV-A photoreceptors with two cofactors: a FAD (flavin adenine dinucleotide) chromophore for blue light absorption (about 450 nm) and an MTHF antenna pigment that broadens absorption.

Photoactivation mechanism: 1. Blue light reduces FAD from oxidised (FAD_{ox}) to neutral semiquinone (FADH•) 2. Reduction triggers conformational change in the C-terminal extension of CRY 3. Activated CRY interacts with multiple downstream targets: - COP1 (CONSTITUTIVE PHOTOMORPHOGENIC 1): an E3 ubiquitin ligase; CRY binding inhibits COP1, thereby stabilizing COP1 substrates (HY5, HFR1, CO, LAF1) — bZIP and bHLH transcription factors that drive photomorphogenic gene expression - SPA proteins: COP1 partners; CRY binding disrupts COP1-SPA interaction - PIFs: CRY can also directly modulate PIF activity

Key blue-light responses: - Hypocotyl growth inhibition: Light-grown seedlings have short hypocotyls; *cry1 cry2* double mutants show etiolated (long-hypocotyl) phenotype in blue light despite normal red light response - Anthocyanin biosynthesis: Blue light induces phenylpropanoid pathway genes (PAL, CHS, CHI) producing UV-protective and pigment compounds - Photoperiodic flowering: CRY2 stabilizes CONSTANS protein in long days - Stomatal opening: Cooperatively with phototropins (covered in section 28)

CRY-COP1-HY5 module: The COP1/SPA E3 ubiquitin ligase complex is the master “darkness” enforcer. In darkness, COP1-SPA ubiquitinates HY5 and other photomorphogenic TFs, targeting them for degradation. Light activates CRYs and PhyB, which physically interact with COP1 and disrupt the COP1-SPA complex; HY5 accumulates and drives photomorphogenic gene expression (chlorophyll biosynthesis, anthocyanin synthesis, hypocotyl growth arrest). Loss-of-function *cop1* mutants are constitutively photomorphogenic in darkness — confirming the central role of this regulator.

30.6 The Plant Circadian Clock — Molecular Architecture

Plants maintain an endogenous about 24-hour oscillator (circadian clock) that anticipates dawn/dusk and gates downstream processes including photosynthesis, growth, flowering, and stress responses. The plant clock comprises interlocked transcriptional feedback loops with morning, evening, and intermediate components.

30.6.1 Morning Loop: CCA1/LHY Repressors and TOC1 Activator

- CCA1 (Circadian Clock Associated 1) and LHY (Late Elongated Hypocotyl): Single-MYB transcription factors expressed at dawn (peak about ZT0, where ZT0 is dawn). They function as a heterodimer and act as repressors of evening-expressed genes (TOC1, ELF3, ELF4, LUX, GI).
- TOC1 (Timing of CAB expression 1; pseudo-response regulator PRR1): Expressed at dusk (peak about ZT12). TOC1 binds and represses the CCA1 and LHY promoters, closing the negative feedback loop. TOC1 also activates morning genes after dusk through PIF interactions.

The morning loop is the “central oscillator”: CCA1/LHY repress TOC1 in the morning; as CCA1/LHY decay through the day, TOC1 rises; TOC1 then represses CCA1/LHY through the night until they rise again at dawn.

30.6.2 Evening Loop: PRR9 → PRR7 → PRR5 → TOC1

A cascade of pseudo-response regulators (PRRs) sequentially repress CCA1/LHY through the day:

- PRR9: Peaks about 4 h after dawn (ZT4); repressed by CCA1/LHY; represses CCA1/LHY transcription
- PRR7: Peaks about 8 h after dawn (ZT8); repressed by PRR9 partially; represses CCA1/LHY
- PRR5: Peaks at midday (ZT10–12); activates downstream targets including CO
- TOC1/PRR1: Peaks at dusk (ZT12); closes morning loop

This PRR cascade creates a wave of repression sweeping across the day, with each successive PRR repressing the previous one’s targets. The molecular result is a robust about 24 h oscillation despite individual gene half-lives of primarily hours.

30.6.3 Evening Complex: ELF3-ELF4-LUX

The Evening Complex (EC) comprises ELF3, ELF4, and LUX (LUX ARRHYTHMO; a Myb-domain TF). ELF3 is a scaffold protein; LUX provides DNA binding. The EC peaks at ZT12–16 and represses morning genes (PRR9, PIF4, GI) — gating early-night growth. *elf3* mutants are arrhythmic.

30.6.4 Temperature Compensation in Plant Circadian Clocks

A defining property of the circadian clock is temperature compensation: the period remains about 24 h across a wide temperature range (10–30 °C) despite the underlying biochemical reactions accelerating with temperature (Q_{10} about 2). Mechanisms include: - Alternative splicing of CCA1: at lower temperature, an alternative splice form ($CCA1\beta$) acts as a repressor of $CCA1\alpha$, slowing the loop - Temperature-dependent protein stability of PRR proteins: PRR9/7 are more rapidly degraded at higher temperatures - JMJ30 demethylase: counters temperature effects on chromatin marks at clock loci

30.6.5 Clock Outputs for Growth, Metabolism, and Flowering

The clock gates numerous physiological processes by regulating downstream gene expression: - Stomatal opening: Anticipatory opening before dawn; controlled by clock-gated H^+ -ATPase activity - Photosynthesis genes: CAB (chlorophyll a/b binding protein), Rubisco activase peak at dawn - Flowering: GI-CO-FT pathway is clock-gated through photoperiodic hormone signaling. - Growth: Hypocotyl elongation peaks in the late night/early morning (gated by PIF4-driven YUCCA expression) - Defense: Many pathogen resistance genes (e.g., *PR1*) show circadian regulation, anticipating bacterial infections that peak at midday

30.7 Photoperiodism, Flowering Time, and Vernalisation

30.7.1 Photoperiodic Categories and Flowering Responses

Plants are classified by their flowering response to day/night length:

- Short-day plants (SDPs): Flower when nights are longer than a critical length. Examples: chrysanthemum, rice, *Pharbitis* (Japanese morning glory), tobacco (*Nicotiana tabacum* Maryland Mammoth), soybean. Despite the name, it is night length that matters – a brief flash of red light during the long night breaks the inductive dark period (the night-break experiment).
- Long-day plants (LDPs): Flower when nights are shorter than a critical length. Examples: spinach, *Arabidopsis*, barley, wheat, radish.
- Day-neutral plants: Flower after sufficient vegetative growth regardless of photoperiod. Examples: tomato, cucumber, maize.

30.7.2 Night-Length Measurement and Circadian Gating

Phytochrome is the primary photoreceptor for photoperiodism. During a long night, Pfr levels decline below a threshold via thermal reversion and proteolysis. In short-day plants, this decline is required for flowering. A brief red-light pulse during the night converts Pr back to Pfr, resetting the clock and preventing flowering. This night break effect can be reversed by an immediately subsequent far-red light pulse — classic evidence for phytochrome involvement.

Photoperiod is measured not by simply timing dark intervals but by circadian gating — the clock provides a window during which light is permissive for flowering. The molecular mechanism (the “external coincidence model”) is: CO mRNA is rhythmically expressed by the clock (peaks in late afternoon), but CO protein is stable primarily in light. Coincidence of light + CO protein → FT activation → flowering.

30.7.3 The CONSTANS-FT (Florigen) Pathway

Florigen — FT as the mobile flowering signal:

1. In long-day plants, the circadian clock ensures that CONSTANS (CO) mRNA peaks in the late afternoon

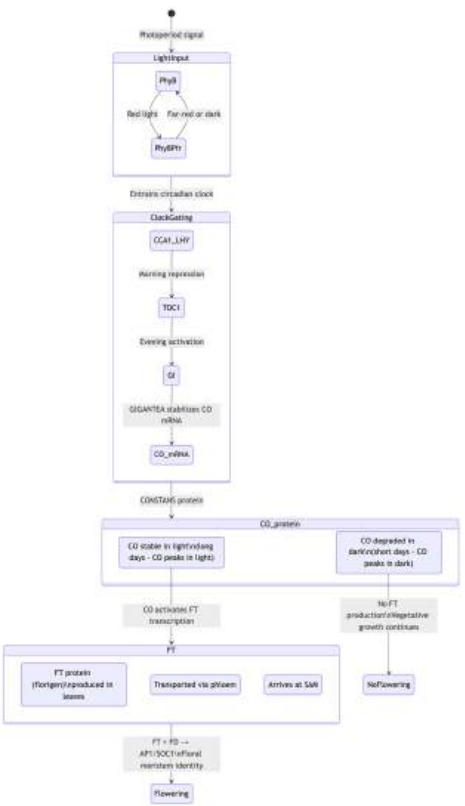


Figure 183. Molecular pathway of photoperiodic flowering in long-day plants The circadian clock gates CONSTANS (CO) protein stability so that in long days, CO is present in the light (when it is stabilized), activating FLOWERING LOCUS T (FT). FT protein (florigen) moves from leaves to the SAM, triggering flower development.

2. CO protein is stabilized by light (blue light via CRY2; far-red light via PhyA) but degraded in darkness via COP1 ubiquitin ligase
3. In long days: CO mRNA peaks coincide with daylight, CO protein is stable, CO binds the FT (FLOWERING LOCUS T) promoter, activating transcription
4. FT protein — the long-sought “florigen” first hypothesized by Chailakhyan in 1937 — is produced in companion cells of leaf phloem and moves systemically via sieve tubes to the SAM. FT is a small (about 20 kDa) globular protein structurally related to mammalian RAF kinase inhibitors; it is loaded into phloem via plasmodesmata and unloaded at the SAM.
5. At the SAM, FT interacts with FD (bZIP transcription factor) to activate AP1 (floral meristem identity) and SOC1 (flowering pathway integrator). The FT-FD-14-3-3 floral activation complex (FAC) was crystallographically resolved in 2011 (Taoka *et al.*, *Nature* 2011).
6. The vegetative meristem transitions irreversibly to a floral meristem — the moment of “evocation”

Diversity of FT homologues: Most plants have multiple FT paralogues with distinct functions. Some act as floral activators (FT in *Arabidopsis*, Hd3a in rice — the rice florigen); some as floral repressors (TFL1, BFT). The balance of activator and repressor FT-family proteins fine-tunes flowering time.

30.7.4 Vernalisation: Epigenetic Silencing of FLC

Prolonged cold exposure (weeks at 4 °C) promotes flowering in winter annuals (*Arabidopsis* ecotype Ler, accessions from northern latitudes) and biennials (carrots, foxglove, sugar beet). The molecular mechanism is a paradigmatic example of epigenetic memory:

The FLC repressor (MADS-box):

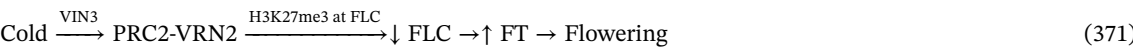
FLC (FLOWERING LOCUS C) is a MADS-box transcription factor that represses *FT* and *SOC1*, blocking the floral transition. In winter annuals before vernalisation, FLC is highly expressed, preventing flowering. Vernalisation silences FLC, releasing FT/SOC1 and permitting flowering.

Mechanism of cold-induced FLC silencing — the VRN2-PRC2 H3K27me3 mark:

1. Extended cold (>4 weeks at 4 °C) induces VIN3 (VERNALISATION INSENSITIVE 3), a PHD-domain protein. VIN3 expression depends on a cold-memory element (CME) upstream of the *VIN3* promoter; VIN3 transcript accumulates primarily after sustained cold (not pulses).
2. VIN3 joins PRC2 (Polycomb Repressive Complex 2: catalytic subunit CLF/SWN, MSI1, FIE, VRN5) at the FLC chromatin via the VRN2 subunit (a vernalisation-specific PRC2 partner).
3. PRC2 catalyses the trimethylation of histone H3 at lysine 27:



4. H3K27me3 marks initially appear at a discrete nucleation region within the *FLC* locus (a 1.5 kb cold-memory region spanning exon 1 and intron 1) during cold exposure; mark spreading across the entire *FLC* locus occurs after return to warm.
5. After return to warm: VIN3 expression fades, but H3K27me3 is maintained by VRN2-PRC2 (which lacks VIN3 in the warm but retains the catalytic core), creating a mitotically stable memory of cold exposure (Finnegan & Dennis, *Plant J.* 2007; Sheldon *et al.*, 2009).
6. Mitotic inheritance: As cells divide during spring growth, H3K27me3 is faithfully copied to daughter chromatin, propagating FLC silencing throughout the vernalised plant. The memory is gradually erased by demethylases in the offspring generation, resetting *FLC* for the next winter.
7. Result: FLC (MADS-box repressor) can no longer repress FT and SOC1 → flowering proceeds in spring



Concept Check: Why does vernalisation require weeks rather than days of cold? What happens if prolonged cold is given in pulses of a few days each, separated by warm intervals?

30.8 Touch Responses and Additional Tropisms

30.8.1 Gravitropism — Statolith and PIN Asymmetry (deep dive)

The detailed molecular mechanism of root gravitropism integrates statolith sedimentation, PIN protein relocalization, and the dose-response asymmetry between root and shoot:

1. Gravity perception by amyloplast sedimentation in columella cells (about 30 s after reorientation)
2. Mechanical signal transduction via actin cytoskeleton and ER membrane interactions; LAZY1 family proteins relocalize to the new lower face
3. PIN3 asymmetric relocalization to the new lower face of columella cells (about 3–5 min)
4. Lateral auxin transport out the new lower face into the cortex below
5. PIN2 acropetal transport of auxin in the elongation zone, biased toward the lower side
6. Differential elongation: auxin inhibits elongation on the lower side (root); the upper side grows faster, bending the root downward
7. Bending complete in 1–2 hours; PIN proteins reset to symmetric distribution

30.8.2 Touch Responses (Thigmomorphogenesis)

Plants respond to mechanical stimuli — wind, rain, animal contact — through thigmomorphogenesis, often resulting in shorter, sturdier growth. The molecular pathway:

1. TCH (TOUCH) genes — first identified in *Arabidopsis* by Janet Braam (1990). The four classical TCH genes are:
 - TCH1 (CAM2): calmodulin
 - TCH2 (CML24): calmodulin-like
 - TCH3 (CML12): calmodulin-like
 - TCH4 (XTH22): xyloglucan endotransglucosylase/hydrolase (cell-wall modifier)
2. Mechanism: Mechanical perturbation triggers Ca²⁺ influx via mechanosensitive channels (MCA1, MSL2, OSCA1; piezo-like). Cytosolic [Ca²⁺] rises within seconds.
3. Calmodulin (TCH1) and CMLs (TCH2/3) bind Ca²⁺ and translate the calcium signal to downstream targets — kinases, transcription factors, cell-wall enzymes.
4. Jasmonate production: Mechanical wounding activates JA biosynthesis via the LOX pathway, mobilizing defense responses in the herbivory and plant-immunity network.
5. Phenotypic consequences: Shorter internodes, thicker stems, increased lignin, smaller leaves. Brushed *Arabidopsis* plants are 30–40% shorter than unbrushed controls; the response is adaptive in windy environments.

Tendrils: Climbing plants like peas, grapes, and cucumbers produce tendrils that exhibit thigmonastic coiling on contact with a support. The mechanism involves: - Differential elongation: cells on the contact side stop elongating; cells on the opposite side continue - Jasmonate signaling: JA mediates the coiling response; *Bryonia* tendrils require JA for coiling - Within minutes of contact, tendril coils a complete 360° around the support

30.8.3 Hydrotropism, Thigmotropism, and Heliotropism

- Hydrotropism: Roots grow toward moisture; mediated by ABA and MIZ1 (mizu-kussei 1) protein in root cap. *miz1* mutants lack hydrotropism but retain gravitropism.
- Thigmotropism in roots: Roots growing along a substrate exhibit obstacle avoidance, mediated by mechanosensitive channels.
- Heliotropism (solar tracking): Sunflowers track the sun across the sky (East to West during the day; reverse to East at night). Driven by differential growth rates on east vs west sides of the stem, gated by the circadian clock.

30.9 Abiotic Stress Responses

30.9.1 Drought – ABA Signaling Cascade

ABA is the primary drought stress hormone:

1. Soil water deficit detected. Root ABA synthesis increases (NCED3 upregulated). ABA moves via xylem to leaves.
2. **Guard cell**: ABA binds PYR/PYL/RCAR receptors (14 paralogs in *Arabidopsis*)
3. ABA-PYR complex inhibits PP2C phosphatases (ABI1, ABI2, HAB1)
4. SnRK2 kinases (especially OST1/SnRK2.6) are freed from PP2C inhibition and phosphorylate:
 - SLAC1 anion channel: Cl[−] efflux depolarizes guard cell membrane
 - GORK K⁺ outward-rectifying channel opens: K⁺ efflux
 - Water follows osmotically: guard cells shrink, **stomata** close
 - AREB/ABF transcription factors: activate drought-responsive genes (dehydrins, LEA proteins, osmolyte synthesis)

Water use efficiency (WUE):

$$WUE = \frac{A_{net}}{g_s} = \frac{\text{Net CO}_2 \text{ assimilation}}{\text{stomatal conductance}}$$

(372)

Plants under water stress maximize WUE by partially closing stomata.

30.9.2 Worked Example: Calculating Water Use Efficiency (WUE)

Problem: An agronomist is evaluating a new drought-tolerant wheat cultivar. Using a portable photosynthesis system, the researcher measures a net CO₂ assimilation rate (A_{net}) of $15\mu\text{mol CO}_2 \text{ m}^{-2} \text{ s}^{-1}$. At the same time, the stomatal conductance to water vapor (g_s) is measured at $0.15 \text{ mol H}_2\text{O m}^{-2} \text{ s}^{-1}$. 1. Calculate the intrinsic Water Use Efficiency (WUE). 2. If ABA treatment causes the stomata to partially close, decreasing g_s by 50% but primarily decreasing A_{net} by 20%, what is the new WUE?

Solution:

1. Calculate the initial WUE: It is standard to express g_s in μmol or A_{net} in μmol so units match. First, convert g_s from mol to μmol :

$$g_s = 0.15 \text{ mol} = 150,000\mu\text{mol H}_2\text{O m}^{-2} \text{ s}^{-1}$$

Now, apply the WUE formula:

$$WUE_{initial} = \frac{A_{net}}{g_s} = \frac{15}{150,000} = 0.0001 \frac{\mu\text{mol CO}_2}{\mu\text{mol H}_2\text{O}}$$

Alternatively, keeping g_s in mol:

$$WUE = \frac{15\mu\text{mol CO}_2 \text{ m}^{-2} \text{ s}^{-1}}{0.15 \text{ mol H}_2\text{O m}^{-2} \text{ s}^{-1}} = 100 \frac{\mu\text{mol CO}_2}{\text{mol H}_2\text{O}}$$

2. Calculate the new rates after ABA treatment: New g_s : $0.15 \cdot (1 - 0.50) = 0.075 \text{ mol H}_2\text{O m}^{-2} \text{ s}^{-1}$ New A_{net} : $15 \cdot (1 - 0.20) = 12\mu\text{mol CO}_2 \text{ m}^{-2} \text{ s}^{-1}$
3. Calculate the new WUE:

$$WUE_{new} = \frac{12}{0.075} = 160 \frac{\mu\text{mol CO}_2}{\text{mol H}_2\text{O}}$$

The partial stomatal closure significantly improved the water use efficiency (from 100 to 160), demonstrating how plants optimize carbon gain against water loss during drought conditions.

Root architecture changes under drought: ABA and auxin promote deeper root growth. Lateral root emergence is suppressed while primary root elongation continues, shifting the root system to access deeper soil water.

30.9.3 Cold Stress – CBF-COR Pathway

Cold acclimation (hardening at 4 degrees C for 1-3 weeks) increases freezing tolerance:

1. Temperature drop triggers membrane rigidification (gel-state transition) and Ca²⁺ influx (MCA1/MCA2 mechanosensitive channels)
2. ICE1 (Inducer of CBF Expression 1; bHLH transcription factor) activates CBF1/CBF2/CBF3 (C-repeat Binding Factors; AP2/ERF TFs) within minutes
3. CBFs bind CRT/DRE elements in promoters, activating COR (Cold-Regulated) genes:
 - COR15: **Chloroplast** outer envelope protein; prevents membrane vesiculation
 - KIN1/KIN2: Dehydrins; cryoprotectants that prevent protein aggregation
 - FAD2/FAD3: Fatty acid desaturases that increase membrane unsaturated fatty acid content, maintaining membrane fluidity
4. Extracellular ice management: Ice nucleates in the apoplast (lower solute concentration than **cytoplasm**). Water is drawn osmotically from cells, producing controlled dehydration rather than lethal intracellular ice formation.

Antifreeze proteins: Some cold-tolerant plants (rye, carrots) express proteins that bind ice crystal surfaces and inhibit crystal growth (thermal hysteresis), protecting membranes.

30.9.4 Heat Stress – HSP Response

Above 35-42 degrees C, the heat shock response is activated: - HSFA1 transcription factors activate HSP70, HSP90, HSP101 chaperones that prevent protein aggregation and refold misfolded proteins - Small HSPs (sHSPs, 15-40 kDa): ATP-independent holdases that accumulate in cytoplasmic aggregates - Thermomemory: H3K4me3 epigenetic marks at HSP loci persist for several days, allowing faster response to subsequent heat episodes

30.9.5 Salt Stress and Ion Homeostasis

High soil salinity (NaCl) causes both osmotic stress and ion toxicity: - SOS pathway (Salt Overly Sensitive): SOS3 (Ca²⁺ sensor) activates SOS2 (kinase), which activates SOS1 (Na⁺/H⁺ antiporter) to expel Na⁺ from roots - Vacuolar sequestration: NHX1 antiporter pumps Na⁺ into vacuole - Compatible osmolytes: Proline, glycine betaine, mannitol accumulate to lower ψ_s without enzyme inhibition

30.9.6 Flooding Response and Low-Oxygen Signaling

Submergence deprives roots of O₂: - ERFVII transcription factors (RAP2.2, RAP2.12): Stabilized under hypoxia (normally degraded by the N-end rule pathway when O₂ is present – direct O₂ sensing) - ERFVIIIs activate **anaerobic** genes: ADH (alcohol dehydrogenase) for **fermentation**, PDC (pyruvate decarboxylase) - Aerenchyma formation: Ethylene (accumulates because ACC oxidase requires O₂) triggers programmed cell death in cortical cells, creating gas-filled channels for O₂ transport from aerial parts to submerged roots - Escape strategy: Deepwater rice varieties elongate internodes rapidly (up to 25 cm/day) via GA and ethylene signaling to keep leaves above water

30.10 Plant Immunity — A Two-Layer Defense System

Plants lack circulating immune cells but possess a sophisticated cell-autonomous immune system organized into two layers. The Jones–Dangl “zigzag model” (2006) is the canonical framework.

30.10.1 Layer 1: PAMP-Triggered Immunity (PTI)

Plants recognize broadly conserved molecular signatures of pathogens — PAMPs (Pathogen-Associated Molecular Patterns) or MAMPs (Microbe-Associated Molecular Patterns) — via cell-surface pattern recognition receptors (PRRs):

- FLS2 (Flagellin Sensitive 2): A leucine-rich repeat receptor kinase (LRR-RK) that binds flg22 (a 22 amino acid epitope of bacterial flagellin). FLS2-flg22 binding recruits BAK1 co-receptor, activating intracellular kinase signaling.
- EFR: Recognizes bacterial elongation factor Tu (epitope elf18)
- CERK1 and LYK receptors: Recognize fungal chitin oligomers (mostly tetra- and pentamers of N-acetylglucosamine)

- PEPR1/2: Recognize plant-derived danger signals (PEPs)

PTI signaling cascade: 1. PRR ligand binding → BAK1 co-receptor recruitment 2. BIK1 receptor-like cytoplasmic kinase activated 3. RBOHD NADPH oxidase produces apoplastic ROS burst (reactive oxygen species; H₂O₂ within minutes) 4. MPK3/MPK6 MAP kinase cascade activated; transcription of defense genes (PR1, WRKY TFs) 5. Stomatal closure via SLAC1 (preventing bacterial entry through stomata) 6. Callose deposition at cell wall (papillae) limiting pathogen ingress

PTI provides broad-spectrum, modest resistance to most non-specialist pathogens.

30.10.2 Layer 2: Effector-Triggered Immunity (ETI)

Successful pathogens deliver effector proteins into host cells (via type III secretion systems in bacteria, haustoria in fungi/oomycetes) to suppress PTI. Plants in turn evolved intracellular NBS-LRR proteins (also called R proteins or NLRs) that recognize these effectors:

- NBS-LRR (Nucleotide-Binding Site, Leucine-Rich Repeat): Intracellular immune receptors. *Arabidopsis* has about 150 NBS-LRR genes. Two structural classes: TIR-NLRs (with N-terminal Toll/Interleukin-1 Receptor domain) and CC-NLRs (coiled-coil).
- Recognition modes:
 - Direct binding: R protein binds effector directly (e.g., RPP1 binds *Hyaloperonospora* ATR1)
 - Indirect “guard” model: R protein guards a host target of effector; effector modification of the target triggers R activation (e.g., RPS2 guards RIN4; *Pseudomonas* AvrRpt2 cleaves RIN4, activating RPS2)
 - Decoy model: Plant evolves a non-functional mimic of an effector target as a “decoy” to bait R protein activation

ETI signaling and the hypersensitive response (HR):

1. NLR activation → oligomerisation (resistosome formation; ZAR1 forms a pentameric “resistosome” channel; Wang *et al.*, *Science* 2019)
2. Resistosome inserts into plasma membrane and conducts Ca²⁺ → cytosolic [Ca²⁺] surge
3. EDS1/PAD4 hub activates downstream signaling
4. Hypersensitive response (HR): Programmed cell death at the infection site; sacrificial necrotic lesion that prevents pathogen spread. HR is morphologically similar to animal apoptosis but molecularly distinct (involves vacuolar processing enzymes, autophagy components, and ROS).
5. Salicylic acid (SA) accumulation locally and systemically

ETI is faster and stronger than PTI — typically resulting in the visible hypersensitive lesion within 24–48 hours of infection.

30.10.3 Systemic Acquired Resistance (SAR)

Local infection triggers a long-lasting, systemic defense priming throughout the plant — systemic acquired resistance (SAR). The mobile signal includes: - Methyl salicylate (MeSA): volatile, can travel through phloem and air - Pipelicolic acid (Pip) and N-hydroxy-pipelicolic acid (NHP): essential systemic mobile signals (Bernsdorff *et al.*, *PNAS* 2016) - Glycerol-3-phosphate (G3P) and azelaic acid

In distal tissues, SA accumulates and activates NPR1 (Non-expressor of PR genes 1):

1. NPR1 in the cytoplasm exists as oligomers (inactive) due to disulfide bonds
2. SA accumulation alters cellular redox; NPR1 is reduced to monomers
3. Monomeric NPR1 enters nucleus and binds TGA transcription factors
4. NPR1-TGA complex activates PR1 (Pathogenesis-Related 1) and other PR genes — antimicrobial proteins, β-1,3-glucanases, chitinases
5. SAR provides 1–2 weeks of broad-spectrum resistance to subsequent infections

30.10.4 JA/SA Antagonism

The two major immune hormones — salicylic acid (SA) for biotrophic pathogens and jasmonic acid (JA) for chewing herbivores and necrotrophic pathogens — exhibit pervasive antagonism:

- SA suppresses JA: SA-induced NPR1 represses MYC2 (master JA TF) and JA-responsive genes; high SA → low JA defenses
- JA suppresses SA: JA-induced WRKY70 and MYC2 repress SA biosynthesis (ICS1) and PR1; high JA → low SA defenses

Why antagonism? Different pathogens require different defense chemistries: biotrophs (powdery mildew, rust fungi) feed on living tissue and are best controlled by SA-induced HR; necrotrophs (*Botrytis*, *Pythium*) and herbivores benefit from cell death and are best controlled by JA-induced toxins/proteases. Allocating to both is metabolically expensive; antagonism enables prioritisation.

Pathogen exploitation of antagonism: *Pseudomonas syringae* pv. *tomato* produces coronatine (COR), a structural mimic of JA-Ile. COR activates the JA pathway, suppressing the SA pathway and stomatal-closure-mediated immunity. The bacterium uses this to enter through normally-closed stomata. *Arabidopsis coi1* mutants (insensitive to JA) are resistant to COR-mediated stomatal reopening.

Concept Check (Synthesis): Systemic acquired resistance (SAR) and induced systemic resistance (ISR) are both long-distance priming responses, but they differ in inducing agent, signaling pathway, and downstream gene expression. SAR is induced by necrotising pathogens, requires the SA → NPR1 → PR-gene axis, and uses methyl-salicylate as a mobile signal. ISR is induced by beneficial rhizobacteria (for example *Pseudomonas fluorescens*), requires JA/ET signaling, and does not constitutively activate PR genes — instead it leaves distal tissues in a primed state. (a) Design an experiment to determine whether a newly isolated plant-growth-promoting rhizobacterium (PGPR) induces SAR or ISR. Specify which molecular markers (PR1 expression, VSP2 expression, callose deposition upon a secondary challenge) and which functional tests (challenge with a biotrophic vs. a necrotrophic pathogen) you would use, together with the controls needed to interpret the results. (b) Constitutive SAR carries a measurable fitness cost (often a 10–25% reduction in vegetative growth) because SA–JA antagonism dampens growth-promoting JA signaling. Synthesize the conditions under which a plant population would benefit from carrying constitutive SAR (pathogen pressure, resource availability, growth-rate strategy) vs. those under which the cost would outweigh the protection.

30.11 Herbivory and Wound Defense – Jasmonate Signaling

Physical insect damage triggers the JA signaling cascade:

1. Membrane damage releases linolenic acid
2. 13-LOX (lipoxygenase) pathway in plastids produces 12-OPDA
3. Peroxisomal β-oxidation produces JA
4. JAR1 conjugates JA with isoleucine to form JA-Ile
5. JA-Ile binds COI1 (F-box protein), recruiting JAZ repressors for ubiquitin-mediated degradation
6. MYC2/MYC3/MYC4 transcription factors are released, activating:
 - Protease inhibitors: Reduce digestibility of plant proteins in insect gut
 - Alkaloids: Nicotine in tobacco, glucosinolates in Brassicaceae
 - Volatile terpenes: (E)-β-ocimene, linalool attract predatory insects and parasitic wasps (indirect defense)

Clinical Connection: The wound response in plants is remarkably fast. Within 30 seconds of *Manduca sexta* (tobacco hornworm) feeding on *Nicotiana attenuata*, JA-Ile accumulates. Within 1 hour, systemic protease inhibitor expression is detected. Within 24 hours, volatile terpenoids attract predatory *Geocoris* bugs. This multi-layered defense system has inspired “push-pull” agricultural strategies where companion plants emit volatiles to repel pests and attract their natural enemies.

30.12 Shade Avoidance Syndrome

In canopy shade, the R:FR (red:far-red) ratio decreases because chlorophyll absorbs red light but transmits far-red:

- PhyB converts from active Pfr to inactive Pr form
- PIF4, PIF5, PIF7 (Phytochrome Interacting Factors) freed from PhyB repression
- PIF4/5 activate YUCCA genes, increasing auxin synthesis in hypocotyls
- Rapid hypocotyl and petiole elongation (shade avoidance)
- Accelerated flowering (via PIF4 activation of FT promoter)
- Reduced branching, leaf area, and root investment

This shade avoidance syndrome represents a competitive strategy: grow taller to overtop neighbors and reproduce before being shaded out. However, it comes at a cost of reduced root investment and mechanical stability.

30.13 Epigenetic Stress Memory in Plants

Plants lack a germline-soma separation and can transmit epigenetic marks trans-generationally:

- Somatic priming: SA treatment deposits H3K4me3 marks at WRKY promoters, maintained for weeks. Subsequent pathogen attack triggers faster and stronger PR gene induction.

- Trans-generational immunity: Pathogen-stressed parents produce offspring with enhanced resistance via DNA methylation changes at transposable element loci (RdDM pathway – RNA-directed DNA methylation).
- Heat stress memory: H3K4me3 at HSP genes persists for several days after heat episode.

Concept Check: Why might trans-generational epigenetic stress memory be particularly advantageous in plants compared to animals?

30.14 Agricultural Applications of Plant Hormone Biology

Decades of basic research on plant hormones have generated transformative agricultural technologies:

The strongest applications now combine hormone biology with genotype, microbiome, water status, and field context. Drought tolerance, heat tolerance, salinity tolerance, and pathogen resistance often trade off against growth or yield, so breeders increasingly stack traits and test them across environments rather than searching for a single comprehensive “stress gene.” Hormone interventions should be evaluated by phenotype, resource cost, reproductive outcome, and performance under realistic combined stresses.

30.14.1 Ethylene Inhibitors — Postharvest Storage

1-MCP (1-methylcyclopropene): A small gaseous molecule that competitively binds the ethylene receptor ETR1, blocking ethylene perception. Commercial product *SmartFresh* applied to apples, pears, kiwifruit, and avocados: - Apples treated with 1-MCP can be stored 6–9 months (vs 2–3 months untreated) with retained firmness, sugar content, and flavour - The North American apple industry is essentially built on 1-MCP storage - Other ethylene management: AVG (aminoethoxyvinylglycine; ACS inhibitor) used pre-harvest in stone fruits to delay ripening; silver thiosulfate (STS) in cut flowers to preserve vase life

30.14.2 Gibberellin Biology — The Green Revolution

The semi-dwarf wheat varieties that catalysed the Green Revolution carry mutations in gibberellin signaling: - Rht-B1b and Rht-D1b in wheat: encode gain-of-function alleles of *DELLA* genes that produce stable, GA-insensitive DELLA proteins. Plants do not respond to GA → reduced internodal elongation → semi-dwarf stature → no lodging under heavy grain heads. - sd1 in rice (the IR8 “miracle rice” of 1966): loss-of-function mutation in *GA20ox-2* (a GA biosynthesis enzyme) → reduced GA levels → semi-dwarf - Both mutations enable plants to support large grain heads, harvest more nitrogen-fertiliser into seed, and resist storm damage. Together they account for >50% of global wheat and rice acreage.

GA application: Exogenous GA₃ is sprayed on: - Seedless table grapes (induces parthenocarpy and elongates clusters) - Sugarcane (increases stem length and sugar yield) - Hybrid rice seed production (activates female lines)

30.14.3 Auxin Herbicides and Synthetic Growth-Regulator Toxicity

2,4-D (2,4-dichlorophenoxyacetic acid) and related compounds (dicamba, MCPA) are synthetic auxin analogs used as selective broadleaf herbicides: - Mechanism: synthetic auxins activate the same TIR1-Aux/IAA-ARF pathway as natural IAA, but at much higher and sustained concentrations - Sustained activation triggers ethylene biosynthesis, ABA accumulation, and ultimately growth abnormalities and death in dicots - Monocots (grasses, including cereal crops) tolerate 2,4-D because they have lower TIR1 binding affinity, faster auxin metabolism, and morphology that limits leaf retention of spray - 2,4-D was developed in WWII as part of biological warfare research; declassified post-war and adopted for agricultural use in 1946. It became the most-used herbicide globally for decades. - Glyphosate-resistance now dominates, but 2,4-D and dicamba have re-emerged in stacked-trait crops (Enlist E3 soybean, Xtend cotton)

30.14.4 Other Hormone-Based Technologies

- Cytokinin sprays: maintain green leaves in cut flowers; delay senescence
- ABA analogs: in development for drought-priming of crop seedlings
- Strigolactone analogs (e.g., GR24): induce suicidal germination of *Striga* parasitic weeds in absence of host, reducing field infestation
- Plant growth retardants: uniconazole, paclobutrazol — GA biosynthesis inhibitors used to keep ornamentals compact

Clinical Connection: Plant hormone biology supplies an extraordinary fraction of agricultural innovation. The Green Revolution (semi-dwarf GA-insensitive wheat and rice), modern fruit storage (1-MCP), and the largest herbicide markets (2,4-D, dicamba — synthetic auxins) most derive directly from understanding hormone signaling pathways characterized in *Arabidopsis* and other model species.

30.15 Current Evidence and Frontier Biology: Plant Responses to the Environment

For Plant Responses to the Environment, frontier biology belongs inside the evidence logic of the chapter. Plant biology links molecular regulation to climate stress, water limitation, crop resilience, phenology, and ecosystem feedbacks. The core reading question is this: plant response claims should connect signal perception, hormone network, gene expression, phenotype, and tradeoff.

- What to verify: identify the observation, model, assay, or dataset that would make the claim stronger or weaker.
- What to qualify: state the scale, organism, cell type, environmental condition, or population where the claim is expected to hold.
- What to compare: test at least one alternative explanation, baseline, or null model before treating the pattern as causal.
- What to cite: distinguish primary evidence, review synthesis, public dataset, and institutional guidance; for recent or numeric claims, prefer the source closest to the measurement and state what has changed since it was published.

A strong plant-response claim names the signal, receptor or hormone, environmental driver, phenotype, and cost of the response [Huang et al., 2024].

Source practice: For plant-stress claims, cite tissue-specific assays, field conditions, signaling perturbations, and growth-defense-water tradeoffs [Huang et al., 2024].

Heat-stress responses should be separated by tissue and developmental stage: protecting vegetative leaves is not the same as preserving male reproductive success, where epigenetic regulation and pollen development can be the limiting failure point [Malik and Zhao, 2022]. Guard-cell calcium work shows that stomatal dynamics can depend on the count and timing of unitary cytosolic Ca2+ signals, linking ion-channel physiology to whole-plant water tradeoffs without implying plant decision-making is animal-like cognition [Huang et al., 2024].

30.15.1 Current Evidence Map: Plant Stress Response Decision

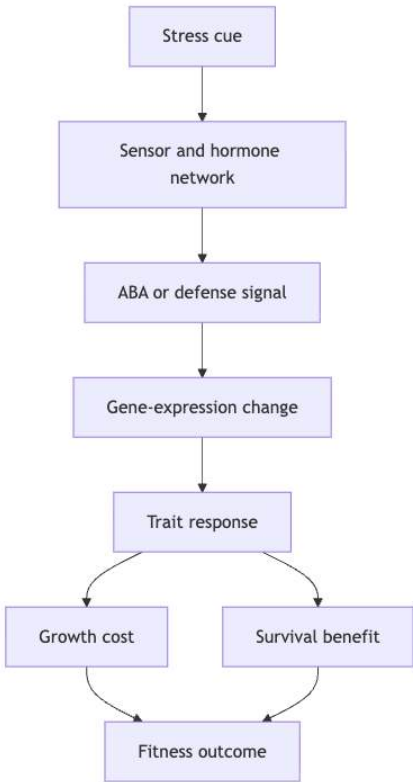


Figure 184. Stress tolerance is not free: the same response that improves survival can reduce growth or reproduction depending on timing and environment.

30.16 Key Terms

Table 371. Current Evidence Map: Plant Stress Response Decision: Term and Definition.

Term	Definition
Tropism	Directional growth response to an environmental stimulus

Term	Definition
Phototropin (PHOT1/2)	Blue-light photoreceptor kinases; LOV domains; autophosphorylate upon blue light absorption
Auxin (IAA)	Indole-3-acetic acid; major growth hormone; polar transport via PIN efflux carriers
PIN proteins	Auxin efflux carriers; polar localization determines transport direction; PIN2 for root gravitropism
Acid growth hypothesis	Auxin activates H ⁺ -ATPase, acidifying cell wall, activating expansins, enabling elongation
DELLA proteins	Transcriptional repressors degraded by GA-GID1 signaling; growth suppressors
Phytochrome	Dual R/FR photoreceptors (PhyA-E); Pr (inactive) and Pfr (active) conformers
Cryptochrome	Blue/UV-A photoreceptor; FAD chromophore; CRY1/CRY2 in <i>Arabidopsis</i>
COP1	E3 ubiquitin ligase; “darkness enforcer”; targets HY5, CO, HFR1 for degradation
PIFs	Phytochrome Interacting Factors; bHLH TFs degraded by Pfr; mediate shade avoidance
Photoperiodism	Regulation of developmental events (especially flowering) by day/night length
CONSTANS (CO)	bZIP transcription factor; activator of FT in long-day flowering
Florigen (FT)	Mobile protein produced in leaf companion cells; travels to SAM via phloem to trigger flowering
FLC	MADS-box repressor of flowering; silenced by vernalisation (H3K27me3 by VRN2-PRC2)
Vernalisation	Cold-mediated epigenetic silencing of FLC enabling flowering
Circadian clock	Endogenous about 24 h oscillator; CCA1/LHY-TOC1-PRR interlocked loops
CCA1/LHY	Morning-expressed MYB TFs; repress evening genes
TOC1/PRR1	Evening-expressed pseudo-response regulator; represses CCA1/LHY
PRR9/7/5	Sequential daytime PRRs in evening loop
Evening Complex (ELF3-ELF4-LUX)	Repressor complex peaking at ZT12-16; gates early-night growth
Statolith	Starch-filled amyloplast in columella cells; sediments under gravity
LAZY1	Protein required for normal gravitropism; relocates to lower face after gravity stimulation
TCH genes	Touch-induced genes (CAM2, CML24, CML12, XTH22); calmodulin-related
Thigmomorphogenesis	Mechanical-stimulus-induced morphology change (shorter, sturdier plants)
ABA	Absciscic acid; stress hormone; PYR/PYL receptors activate SnRK2 kinases
CBF/DREB	C-repeat Binding Factors; AP2/ERF TFs; cold-induced, activate COR genes
JA-Ile	Jasmonyl-isoleucine conjugate; active jasmonate; ligand for COI1 receptor
COI1	Coronatine Insensitive 1; F-box protein; JA-Ile receptor; degrades JAZ repressors
PTI	PAMP-Triggered Immunity; first-layer defense via cell-surface PRRs
ETI	Effector-Triggered Immunity; second-layer defense via intracellular NBS-LRR proteins
NBS-LRR (NLR)	Nucleotide-Binding Site, Leucine-Rich Repeat; intracellular immune receptors
HR (Hypersensitive Response)	Programmed cell death at infection site; ETI hallmark
SAR	Systemic Acquired Resistance; SA-mediated whole-plant defense priming
NPR1	SA-induced master regulator of PR gene expression
Strigolactone	Carotenoid-derived hormone; suppresses branching; recruits mycorrhizae
1-MCP	1-methylcyclopropene; ethylene receptor antagonist; postharvest storage
2,4-D	Synthetic auxin herbicide; selective for dicots

30.17 Review Questions

1. An *Arabidopsis phot1 phot2* double mutant is grown under asymmetric blue light. Predict the **phenotype**. Would this mutant show any phototropic response under high-intensity white light? (Hint: consider cryptochromes.)
2. Explain why the same auxin redistribution (accumulation on the lower side) causes opposite growth responses in roots vs shoots during gravitropism. Include the concepts of optimal auxin concentration, dose-response curves, and PIN2 vs PIN3 localization.
3. A farmer notices that long-day wheat varieties flower prematurely when grown near street lights that extend the day length. Explain the molecular mechanism, starting from phytochrome and proceeding through the CO-FT pathway. Include the role of CRY2 in stabilizing CO protein.
4. Compare the ABA-mediated drought response with the CBF-COR cold acclimation pathway. What do they share in common? How do the final cellular protective mechanisms differ?

5. *Pseudomonas syringae* produces coronatine (COR), a JA-Ile mimic. Explain how COR suppresses stomatal immunity (PTI) and promotes bacterial entry. Design a crop plant with COR-insensitive COI1 that resists this strategy without compromising wound response.
6. A researcher discovers that a particular *Arabidopsis* accession shows enhanced cold tolerance without prior cold acclimation. The line has constitutively high expression of CBF3. What are the likely growth penalties of constitutive CBF expression, and why?
7. Explain the molecular basis of the “night break” experiment in short-day plants. Why does a brief pulse of red light in the middle of a long night prevent flowering, and why does an immediately subsequent far-red pulse restore the flowering response?
8. Compare ethylene’s role in fruit ripening vs flooding response. How is the same hormone adapted for such different functions?
9. Sample three points from `light_response_curve()` and identify roughly where the curve saturates for default C3-like parameters.
10. Explain how phyB thermosensing can decouple flowering time from true photoperiod in warming climates.
11. Describe the molecular memory of vernalisation in *Arabidopsis*. How is the VRN2-PRC2-mediated H3K27me3 mark at *FLC* maintained through cell division and erased between generations?
12. Distinguish PTI and ETI in the Jones–Dangl zigzag model. What is the role of resistosome formation? How does the SA-NPR1 pathway translate local infection into systemic acquired resistance?
13. Explain why 2,4-D selectively kills broadleaf weeds in cereal crops. At the molecular level, how does sustained synthetic auxin signaling cause death in dicots but not monocots?
14. Trace the *Arabidopsis* circadian clock through one full day starting at dawn (ZT0). Identify which genes are expressed at ZT0, ZT4, ZT8, ZT12, and ZT16, and explain the negative-feedback architecture.
15. Tendril coiling in cucumber requires touch and JA. A *coi1* loss-of-function mutant cucumber is challenged with a thin string. Predict the response, and explain why JA signaling is downstream of mechanical perception.

30.18 Further Reading and Source Notes: Plant Responses to the Environment

- Hager (1971). Acid growth theory of auxin action. *Planta*, 100.
- Went [1926] — On diffusion and the stimulation of growth by auxins. *Recueil des Travaux Botaniques Néerlandais*, 33.
- Huang et al. (2024). Guard cells count the number of unitary cytosolic Ca²⁺ signals to regulate stomatal dynamics. *Current Biology* [Huang et al., 2024].

30.19 Computational Bridge

Photosynthetic light response is tabulated for any PAR grid; figure 180 plots net assimilation from the hyperbolic rate model for C3-like and C4-like parameter sets.

```
from biology.botany import light_response_curve

curve = light_response_curve(n_points=8, max_par=1600.0)
print(round(curve[-1][1], 2))
```

Clinical / systems note: Shade-intolerant crops under hospital-city light pollution mirror the long-day wheat problem — photoperiod pathways wired to yield stability.

30.20 Summary

- Plant hormones: Nine major classes (auxin, GA, cytokinin, ABA, ethylene, JA, SA, brassinosteroids, strigolactones) regulate most aspects of growth, development, and stress responses through receptor-mediated signaling pathways.
- Phototropism [Went, 1926]: PHOT1/2 (LOV-domain kinases) trigger asymmetric PIN3 relocalization, creating a lateral auxin gradient. Acid growth (H⁺-ATPase to expansins) drives differential elongation [Hager, 1971].
- Photomorphogenesis: Phytochromes (Pr/Pfr photoconversion at 660/730 nm) sense R:FR ratio for shade avoidance; cryptochromes (CRY1/CRY2 with FAD) sense blue light for photomorphogenesis. PhyA mediates FR-HIR; PhyB is the canopy-shade sensor. CRY-COP1-HY5 module enforces light/dark choice.

- Circadian clock molecular architecture: Morning loop (CCA1/LHY repressors of evening genes; TOC1 activator); evening loop (PRR9/7/5/TOC1 cascade repressing CCA1/LHY); evening complex (ELF3-ELF4-LUX). Temperature-compensated.
- Photoperiodism: Night length is the true signal. Phytochrome (Pr/Pfr) measures dark duration. The CO-FT-AP1 pathway integrates circadian clock and light signals. FT protein moves from leaf companion cells to SAM as the long-sought florigen.
- Vernalisation: Cold-induced VIN3 joins VRN2-PRC2; H3K27me3 deposition at *FLC* silences this MADS-box repressor of flowering. Memory is mitotically stable but reset between generations.
- Gravitropism: Amyloplast settling in statocytes triggers PIN3 relocalization. Same auxin redistribution causes opposite responses in roots (PIN2 carries auxin acropetally; high auxin inhibits root cells) vs shoots (high auxin promotes shoot cells).
- Touch responses: TCH genes (calmodulins, XTH22) mediate Ca²⁺-driven thigmomorphogenesis; jasmonate links wound perception to defense and tendrill coiling.
- Drought: ABA activates PYR-PP2C-SnRK2-SLAC1 cascade for stomatal closure plus AREB/ABF for stress gene expression.
- Guard-cell signaling: stomatal dynamics can depend on the count and timing of unitary cytosolic Ca²⁺ signals, linking channel-level events to whole-plant water-use tradeoffs [Huang et al., 2024].
- Cold: CBF1/2/3 activated by ICE1 within minutes of cold exposure; COR genes produce dehydrins, desaturases, and cryoprotective proteins.
- Flooding: ERFVII transcription factors sense O₂ via the N-end rule; ethylene promotes aerenchyma formation.
- Plant immunity (Jones–Dangl zigzag): PTI via cell-surface PRRs (FLS2/BAK1, CERK1) recognizing PAMPs. ETI via intracellular NBS-LRR (NLR) proteins recognizing effectors; resistosome formation triggers HR. NPR1-mediated SAR provides systemic broad-spectrum priming via SA. JA-SA antagonism partitions defenses; *Pseudomonas* coronatine exploits this.
- Herbivory: JA-Ile triggers COI1-JAZ degradation, releasing MYC2 to activate protease inhibitors, alkaloids, and volatile-mediated indirect defense.
- Shade avoidance: Low R:FR frees PIF4/5 from PhyB repression, increasing auxin and accelerating flowering.
- Agricultural applications: Ethylene inhibitors (1-MCP for postharvest); GA-insensitive DELLA mutations (*Rht*, *sd1*) underlie Green Revolution semi-dwarf wheat and rice; synthetic auxin herbicides (2,4-D, dicamba) selectively kill broadleaf weeds.
- Connections: See section 10 for light reactions, section 8 for receptor signaling parallels, and Unit X — Ecology: Introduction for phenology under climate change.

30.21 Companion Source Module: Plant Responses to the Environment

Plant Responses to the Environment should leave a reproducible trail from a biological claim to the code, figure, diagram, or paper-based activity that can test it. Use the surfaces below to inspect the chapter’s assumptions, rerun the relevant model, or compare the manuscript explanation with companion labs and figures.

Table 372. Companion source surfaces for Plant Responses to the Environment.

Surface	Use it for
<code>src/biology/botany/botany.py</code> (photosynthesis_rate, light_response_curve, transpiration_flux)	Quantify how light, CO2, water, and temperature shape response curves.
<code>src/visualization/plots.py</code> (plot_light_response_curve)	Check saturation and stress interpretation visually.
<code>src/mermaid/biology_diagrams.py</code> (photosynthesis_light_dark_diagram, hormone_signaling_diagram)	Link environmental sensing to pathway response.

Reproducibility check: name the signal, receptor/tissue, hormone network, phenotype, and tradeoff before claiming adaptive response. Cross-reference: use section 28, section 29, and section 10.

Unit IX — Zoology and Systems Physiology: Introduction

Why This Unit Matters

In 1628, William Harvey published *Exercitatio Anatomica de Motu Cordis et Sanguinis in Animalibus* (On the Motion of the Heart and Blood in Animals) and overturned nearly 1,500 years of Galenic medicine. Harvey demonstrated, through quantitative reasoning alone, that the heart must be a pump recirculating the same blood — not a furnace generating new blood from food. He calculated that the heart pushes approximately 1.8 liters of blood per minute; if blood flowed outward and were not returned, the entire blood volume (about 5 liters) would be exhausted in under 3 minutes. Therefore, it must circulate. This was physiology as computational biology — numbers proving mechanism before any understanding of cellular biology existed.

Modern systems physiology is even more mathematical. The Hodgkin-Huxley model (1952) describes the action potential as a set of four coupled nonlinear ordinary differential equations and was solved numerically before computers capable of doing so efficiently were widely available. Today, the same mathematical framework underlies cardiac electrophysiology, pharmacological ion channel modeling, and the design of neural prosthetics. Homeostasis — the maintenance of stable internal conditions — is formalised as a negative feedback control system: a detector, comparator, and effector maintaining a set-point, mathematically identical to engineering control systems.

This unit covers four major physiological systems — circulatory, nervous, endocrine, and immune — with quantitative models throughout. You will apply the Hodgkin-Huxley equations to the action potential, calculate Starling forces for capillary filtration, model hormonal negative feedback with Hill equations, and contrast innate and adaptive immune responses as computational pattern-recognition systems. Clinical connections appear in every section: from cardiac arrhythmias to diabetes mellitus, from anaphylaxis to Parkinson’s disease.

Landmark Discoveries

Discoverer(s)	Year	Journal / Source	Discovery	Significance
William Harvey	1628	[Harvey, 1628]	Systemic circulation: heart as pump	Quantitative physiology; disproved Galenic humoral theory
Claude Bernard	1854–1879	[Bernard, 1865]	Internal milieu and homeostasis	Defined the concept of regulated internal environment
Ernest Starling	1918	[Starling, 1918]	Frank-Starling law of the heart	Cardiac output proportional to venous return; basis of heart failure physiology
Alan Hodgkin & Andrew Huxley	1952	[Hodgkin and Huxley, 1952]	Mathematical model of nerve action potential	Four ODEs describing Na ⁺ /K ⁺ conductance; Nobel Prize 1963
Barry Marshall & Robin Warren	1984	[Marshall and Warren, 1984]	<i>Helicobacter pylori</i> causes peptic ulcers	Disproved “acid stress” dogma; Nobel Prize 2005; key discovery in gastrointestinal physiology
Rosalyn Yalow & Solomon Berson	1959	[Yalow and Berson, 1960]	Radioimmunoassay (RIA) for insulin	Enabled measurement of hormone concentrations at picomolar levels; Nobel Prize 1977
César Milstein & Georges Köhler	1975	[Köhler and Milstein, 1975]	Monoclonal antibody production (hybridoma)	Foundation of modern immunotherapy, diagnostics, and targeted cancer therapy; Nobel Prize 1984

Key Concepts and Connections

Unit IX — Zoology and Systems Physiology: Introduction concept map — Zoology and Systems Physiology.

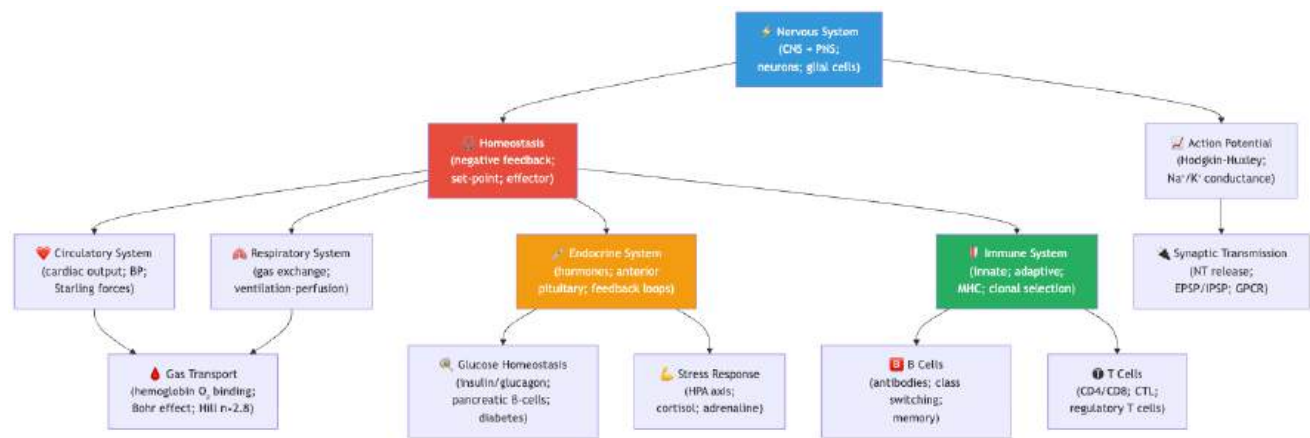


Figure 185. Systems physiology concept map linking homeostasis, circulation, respiration, endocrine signaling, immunity, and neural control through feedback loops.

Current Evidence Thread

Read this unit as physiology that is known because it has been measured: every claim about action potentials, circulation, hormones, immunity, and neural circuits rests on a recording, an image, a perturbation, or a clinical measurement, and the strength of the claim is no better than the method behind it. Physiology now blends mechanism with allostasis, immune-endocrine-neural coupling, wearable data, and individualized risk without reducing bodies to simple machines. As you move through the chapters, keep a two-column note: claim on the left, evidence that would change my confidence on the right. By the end of the unit, each major idea should be tied to a measurement, model, citation, or paper-based lab decision.

Chapter Roadmap

Chapter	Title	Core Question	Key Equation / Model
28	Circulation and Respiration	How do the cardiovascular and respiratory systems maintain homeostasis?	Fick’s principle; Starling equation; P_{O_2} /Hb saturation (Hill eq.)
29	Nervous System Organization	How is the nervous system organized from molecular to systems level?	Cable equation; receptor field models
30	Action Potentials and Synapses	How do neurons generate and transmit electrical signals?	Hodgkin-Huxley: $I = C_m dV/dt + I_{Na} + I_K + I_L$
31	Endocrine and Immune Systems	How do hormones and immune cells maintain internal defense and stability?	Negative feedback oscillator; MHC diversity; clonal selection

Connections Across the Textbook

- Ion channels and membrane potential (this unit) build directly on membrane transport (section 7) and electrochemistry (Unit I — Chemistry of Life: Introduction).
- Hemoglobin cooperativity (Hill equation, $n \approx 2.8$) connects to enzyme allostery (section 4) and protein structure (section 3).
- Immune system connects to Unit VII — Microbiology: Introduction (innate response to bacteria/viruses) and Unit IV — Molecular Genetics: Introduction (recombination of V(D)J gene segments in antibody diversity).
- Endocrine regulation (steroid hormones acting on nuclear receptors) links to Unit IV — Molecular Genetics: Introduction (gene regulation) and Unit III — Energy and Metabolism: Introduction (metabolic regulation by insulin/glucagon vs. AMPK).
- Negative feedback homeostasis is mathematically equivalent to the control theory underlying Unit X — Ecology: Introduction (population regulation) and Unit III — Energy and Metabolism: Introduction (metabolic feedback).

Key vocabulary introduced here: homeostasis, action potential, resting membrane potential, ion channel, neurotransmitter, synapse, GPCR, second messenger, cardiac output, stroke volume, preload, afterload, Frank-Starling law, hemoglobin cooperativity, Bohr effect, hormone, receptor tyrosine kinase, antigen, MHC, clonal selection, innate immunity, adaptive immunity.

Computational Toolbox — Unit IX

```
from biology.physiology import oxygen_saturation
from biology.neuroscience import action_potential_hh

# Haemoglobin oxygen saturation (Hill equation): arterial vs venous
# Hill coefficient n=2.7; P50=26 mmHg for adult HbA at 37°C, pH 7.4
arterial = oxygen_saturation(pO2_mmHg=100, p50_mmHg=26, hill_coefficient=2.7)
venous = oxygen_saturation(pO2_mmHg=40, p50_mmHg=26, hill_coefficient=2.7)
print(f"Arterial S02 (P02=100 mmHg): {arterial.saturation:.1%}")
print(f"Venous S02 (P02=40 mmHg): {venous.saturation:.1%}")
print(f"O2 extraction ratio: {(arterial.saturation - venous.saturation) / arterial.saturation:.1%}")
# Expected:
# Arterial S02: 97.0%
# Venous S02: 76.2%
# O2 extraction: 21.7% (about 5 mL O2 per 100 mL blood at rest)

# Hodgkin-Huxley action potential simulation (10 µA/cm² stimulus, 50 ms)
hh = action_potential_hh(stimulus_current_µA=10.0, t_end_ms=50.0)
peak_V = max(hh.voltage_mV)
print(f"Peak membrane voltage: {peak_V:.1f} mV")
print(f"Firing threshold crossed: {'yes' if peak_V > 0 else 'no'}")
# Expected:
# Peak membrane voltage: about +48.0 mV (overshoot above 0 mV)
# Firing threshold crossed: yes
```

Try it yourself: Reduce stimulus_current_µA to 5 µA/cm² — the membrane depolarizes but may not reach threshold. This illustrates the most-or-none principle.

Source modules: *src/biology/physiology/* and *src/biology/neuroscience/* — *oxygen_saturation()*, *poiseuille_flow()*, *homeostasis_response()*, *action_potential_hh()*. Figures: *src/visualization/* (action potential traces, hemoglobin saturation curves, hormone feedback oscillators); *src/mermaid/biology_diagrams.py* (nervous system diagrams, immune response cascades).

Cross-Unit Integration

The homeostatic and allostatic regulation principles of **Unit IX — Zoology and Systems Physiology: Introduction** — set points, feedback loops, predictive control, integrated organ-system responses — scale beyond the individual organism. In **Unit X — Ecology: Introduction** you will see these same regulatory motifs operating on populations and ecosystems: density-dependent birth and death rates are negative feedback on population size; logistic growth’s carrying capacity is a set point analogous to a physiological set point; predator–prey cycles are coupled oscillators with the same mathematical structure as hormone feedback systems. As ecological dynamics unfold in **Unit X — Ecology: Introduction**, recognize that the population is “regulating” itself by mechanisms structurally identical to the homeostatic loops of **Unit IX — Zoology and Systems Physiology: Introduction**, just with births and deaths as the effector variables in place of hormone release.

31 Circulation and Respiration

Level 3/3 · 60 min read · 100 min lecture · Prerequisites: section 7, section 9

31.1 Learning Objectives

1. Describe the evolutionary progression of cardiovascular systems from open to closed, and from 2-chamber to 4-chamber hearts.
2. Explain the cardiac cycle including electrical conduction, mechanical events, and the ECG.
3. Apply Poiseuille’s law to blood flow and explain arteriolar regulation of vascular resistance.
4. Describe oxygen transport by hemoglobin using the Hill equation, including the Bohr and Haldane effects.
5. Explain CO₂ transport mechanisms and the chloride shift.
6. Describe pulmonary ventilation mechanics, lung volumes, and spirometry.
7. Apply Fick’s law to alveolar gas exchange.
8. Explain respiratory control by medullary centers and chemoreceptors.
9. Describe homeostatic control systems, **thermoregulation**, and fluid balance.

31.1.1 Study Blueprint

- Big idea: Animal transport systems maintain gradients that let cells exchange gases, nutrients, heat, and wastes.
- Core concepts: cardiac output, gas exchange, homeostasis, feedback.
- Framework alignment: Vision & Change: Structure and function, Systems; AP Biology: Systems Interactions, Energetics; NGSS-style topics: Structure and Function.
- Model or quantitative lens: Cardiac-output, diffusion, oxygen-saturation, and feedback calculations.
- Data skill: Interpret physiological data from pressure, flow, saturation, or set-point changes.
- Practice cadence: Visual Representations, Statistical Tests and Data Analysis, Argumentation.
- Common misconception to repair: Homeostasis is dynamic regulation, not an unchanging internal state.
- Primary lab: **Lab — Circulation and Respiration**.
- Question bank: **Questions — Circulation and Respiration**.
- Transfer task: Transfer homeostatic reasoning to exercise, altitude, hemorrhage, fever, and shock.
- Bridge to computation: `biology.physiology.physiology.oxygen_saturation`.

Opening Vignette — The Doctor Who Proved the Heart Was a Pump

In 1628, William Harvey published *Exercitatio Anatomica de Motu Cordis et Sanguinis* — a slim 72-page monograph that demolished 1,400 years of medical dogma. The **dominant** Galenic view held that blood was continuously manufactured from food in the liver and consumed by tissues. Harvey’s insight was quantitative: he calculated the volume expelled by the heart with each beat (about 60 mL) and multiplied by heart rate. The heart expels roughly 4.3 kg of blood per minute — far more than the body could possibly generate from food. The primary explanation was that blood circulates, continuously recirculated by the heart. Harvey’s argument was revolutionary in method as much as finding: he used mathematical reasoning, vivisection, and comparative anatomy across many species rather than received authority. He was ridiculed widely and lost patients; he died in 1657. Modern cardiology, cardiac surgery, and pharmacology of the cardiovascular system most stand on the foundation he built alone.

31.2 Evolution of Cardiovascular Systems

The cardiovascular system evolved to overcome the limitations of diffusion for O₂ and nutrient delivery in large organisms:

Open circulatory systems (arthropods, most molluscs): Heart pumps hemolymph into open sinuses (haemocoel). Hemolymph bathes tissues directly. Low pressure, slow flow. Adequate for small ectotherms with low metabolic rates.

Closed circulatory systems (annelids, cephalopods, most vertebrates): Blood confined within vessels. Higher pressure enables faster, more directed flow. Allows separate regulation of blood flow to different organs.

Vertebrate heart evolution:

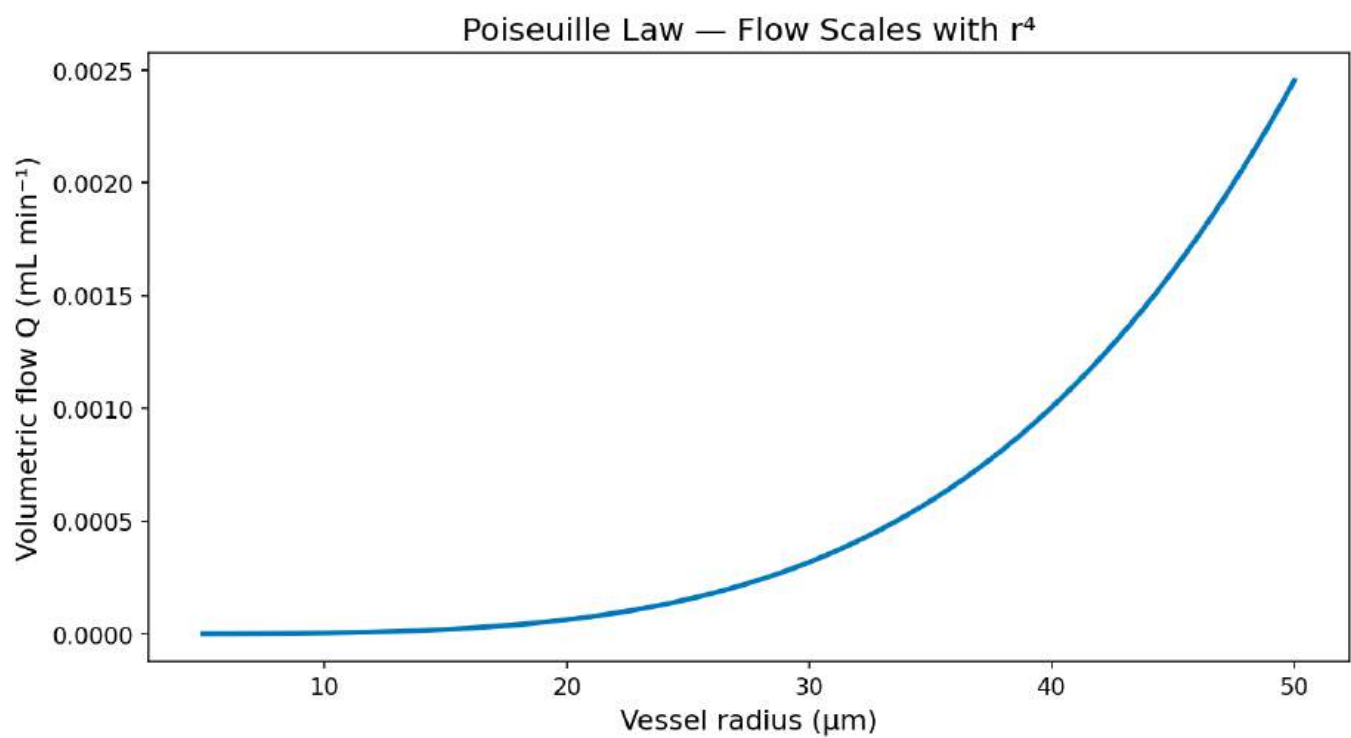


Figure 186. Hagen–Poiseuille law: volumetric blood flow versus vessel radius at fixed pressure gradient. Because flow scales with radius to the fourth power, halving radius reduces flow sixteenfold—a key reason arteriolar constriction controls tissue perfusion.

Table 373. Study Blueprint: Heart Type and Chambers.

Heart Type	Chambers	Organisms	Key Features
2-chamber	1 atrium + 1 ventricle	Fish	Single circuit: heart to gills to body to heart
3-chamber	2 atria + 1 ventricle	Amphibians, most reptiles	Double circuit with some mixing in ventricle
3.5-chamber	Partial septum	Crocodilians	Nearly complete ventricular separation
4-chamber	2 atria + 2 ventricles	Birds, mammals	Complete separation of pulmonary and systemic circuits

The 4-chamber heart enables complete separation of oxygenated and deoxygenated blood, supporting the high metabolic rates required for endothermy.

31.3 Heart Anatomy and the Cardiac Cycle

31.3.1 Cardiac Conduction System

The heart is a self-exciting organ. Its electrical conduction system ensures coordinated contraction:



Figure 187. Cardiac conduction system and corresponding ECG waves. The SA node initiates depolarization, which spreads through the atria (P wave), is delayed at the AV node, then rapidly conducted through the bundle of His and Purkinje fibers to the ventricles (QRS complex). Ventricular repolarization produces the T wave.

ECG waves and their significance: - P wave: Atrial depolarization and contraction - PR interval: Time from atrial depolarization to ventricular depolarization (0.12-0.20 s). Prolonged PR = AV block. - QRS complex: Ventricular depolarization (0.06-0.10 s). Wide QRS = conduction defect or ventricular origin. - T wave: Ventricular repolarization - QT interval: Total ventricular electrical activity. Prolonged QT = risk of torsade de pointes arrhythmia.

31.3.2 The Cardiac Cycle

At a heart rate of 70 bpm, one cardiac cycle lasts about 0.8 seconds:

- Systole (contraction, about 0.3 s):
 - Isovolumetric contraction: Most valves closed, ventricular pressure rises rapidly
 - Ejection phase: Ventricular pressure exceeds aortic pressure (about 80 mmHg), aortic valve opens, blood ejected

- Peak systolic pressure: about 120 mmHg in left ventricle
- Diastole (relaxation, about 0.5 s):
 - Isovolumetric relaxation: Most valves closed, ventricular pressure falls
 - Rapid filling: Ventricular pressure falls below atrial pressure, AV valve opens, blood flows passively (accounts for about 80% of filling)
 - Atrial systole (“atrial kick”): Final about 20% of ventricular filling

Starling’s Law of the Heart (Frank-Starling [Starling, 1918] mechanism): Ventricular stroke volume increases with end-diastolic volume (preload). Increased venous return stretches ventricular cardiomyocytes, optimizing **actin**-myosin overlap and increasing Ca^{2+} sensitivity of troponin C. This intrinsic mechanism ensures that left and right cardiac outputs remain matched.

$$SV \propto EDV \quad (\text{within physiological range})$$

(373)

Clinical Connection: Heart failure occurs when the Frank-Starling mechanism can no longer compensate for reduced contractility. In systolic heart failure (HFrEF, ejection fraction <40%), the weakened ventricle operates on a depressed Starling curve. Treatments include ACE inhibitors (reduce afterload), beta-blockers (reduce myocardial demand), and SGLT2 inhibitors (reduce preload). The 2024 ESC guidelines emphasize early combination therapy.

31.4 Cardiac Output and Blood Pressure

31.4.1 Cardiac Output as Heart Rate Times Stroke Volume

$$CO = HR \times SV$$

(374)

- At rest: $CO = 70 \text{ bpm} \times 70 \text{ mL} \approx 5 \text{ L/min}$
- Maximum exercise: $CO = 200 \text{ bpm} \times 130 \text{ mL} \approx 26 \text{ L/min}$ (elite athletes — up to 35 L/min documented)

The Frank-Starling mechanism [Starling, 1918] is the heart’s intrinsic capacity to match its output to venous return on a beat-to-beat basis. Within physiological limits, increased end-diastolic volume (preload) stretches ventricular cardiomyocytes, optimizing actin-myosin overlap (length-tension relationship) and increasing the Ca^{2+} -sensitivity of troponin C. The result is an increased stroke volume *without* any extrinsic neural or hormonal command. Because the right and left hearts are in series, this intrinsic matching is essential — any sustained mismatch would cause pulmonary or systemic congestion. Acutely transfusing fluid or rising from supine to legs-up posture both expand venous return, and the Frank-Starling mechanism translates that into matched increases in both ventricles.

Regulation of cardiac output:

- Sympathetic stimulation (β_1 adrenergic receptors): Increases both HR (positive chronotropy via SA node) and SV (positive inotropy via increased Ca^{2+} entry through L-type Ca^{2+} channels and SR Ca^{2+} release)
- Parasympathetic stimulation (M_2 muscarinic receptors via vagus nerve): Decreases HR primarily (negative chronotropy). Vagal tone dominates at rest, which is why resting HR is about 70 bpm rather than the SA node’s intrinsic 100 bpm.
- Frank-Starling mechanism: Intrinsic matching of SV to venous return (see above)

31.4.2 Blood Pressure and Vascular Resistance

$$MAP = DP + \frac{1}{3}PP = DP + \frac{1}{3}(SP - DP)$$

(375)

where MAP = mean arterial pressure, DP = diastolic pressure, SP = systolic pressure, PP = pulse pressure.

Normal: SP/DP = 120/80 mmHg, MAP about 93 mmHg.

$$MAP = CO \times TPR$$

(376)

where TPR = total peripheral resistance. Blood pressure is regulated by: - Cardiac output (HR, SV, blood volume) - Total peripheral resistance (arteriolar diameter – the dominant factor)

31.4.3 Blood Flow – Poiseuille’s Law

figure 186 shows how volumetric flow scales with r^4 at fixed pressure gradient — the physiological reason arteriolar radius is the dominant lever on organ perfusion.

$$Q = \frac{\pi r^4 \Delta P}{8 \eta L} \tag{377}$$

The r^4 dependence is the most physiologically critical feature: halving vessel radius reduces flow by 16-fold. Arterioles (radius about 50-100 μm) serve as the primary resistance vessels.

Regulation of arteriolar tone: - Local autoregulation: - Myogenic response: Smooth muscle contracts in response to stretch (maintains constant flow despite pressure changes) - Metabolic: CO_2 , H^+ , K^+ , adenosine from active tissues cause vasodilation - Endothelial: Shear stress stimulates NO (nitric oxide) production via eNOS. NO diffuses to smooth muscle, activates guanylyl cyclase to cGMP to PKG to smooth muscle relaxation. - Neural (sympathetic): Noradrenaline acts on α_1 receptors causing vasoconstriction in most vascular beds. Exceptions: skeletal muscle during exercise (cholinergic vasodilation and metabolic override). - Hormonal: Angiotensin II (potent vasoconstrictor), ANP (vasodilator), ADH/vasopressin (vasoconstrictor at high doses).

Concept Check: During exercise, cardiac output increases from 5 to 25 L/min, but blood pressure increases primarily modestly (e.g., 120/80 to 160/80). How is this possible? (Consider what happens to TPR.)

31.4.4 Worked Example: Cardiac Reserve

A healthy 40-year-old has resting cardiac output of 5 L/min (HR 70 bpm \times SV 70 mL). The age-predicted maximum heart rate is given by:

$$HR_{\text{max}} \approx 220 - \text{age (years)} \tag{378}$$

(The Tanaka 2001 formula $HR_{\text{max}} = 208 - 0.7 \cdot \text{age}$ is more accurate for older adults and is now preferred in cardiology.)

For our 40-year-old, $HR_{\text{max}} \approx 180$ bpm. With exercise-induced sympathetic activation increasing stroke volume to about 120 mL via the Frank-Starling mechanism [Starling, 1918] and \uparrow contractility (β_1):

$$CO_{\text{max}} = 180 \times 120 = 21,600 \text{ mL/min} \approx 21.6 \text{ L/min}$$

This represents a about 4.3-fold increase over rest — typical for an untrained adult. Endurance training increases the SV reserve more than the HR reserve, allowing elite athletes to reach 30–35 L/min cardiac output despite *lower* maximum heart rates than untrained subjects.

Cardiac reserve = $CO_{\text{max}} - CO_{\text{rest}} \approx 16.6$ L/min in this example. Cardiac reserve is the master variable that limits exercise tolerance: heart-failure patients with reduced ejection fraction may have a reserve of 3–5 L/min and become symptomatic with mild activity.

Concept Check (Analyze) — Frank-Starling, preload, and the operating point. Within physiological limits, increased end-diastolic volume (EDV) stretches ventricular cardiomyocytes, optimizing actin-myosin overlap and titin-restored geometry, and raises Ca^{2+} sensitivity of troponin C; stroke volume (SV) consequently rises *intrinsically* without neural or hormonal input. A typical Starling curve gives SV = 70 mL at EDV = 120 mL and SV = 90 mL at EDV = 150 mL. (a) Compute the slope $\Delta SV / \Delta EDV$ in this range and explain what this slope physically represents (the *contractility-independent* component of the response). (b) An acute hemorrhage drops circulating volume by 1 L (about 20%); predict the new operating point on the Starling curve (direction and approximate magnitude of EDV, SV, and CO change) before baroreflex compensation. (c) Sympathetic activation raises contractility (positive inotropy), which shifts the entire Starling curve upward — at any given EDV, SV is larger. Diagram the hemorrhage + sympathetic response on a single Starling plot, and predict why patients on β -blockers may decompensate faster from acute blood loss than untreated patients.

31.4.5 Baroreceptor Reflex — Beat-to-Beat Blood Pressure Control

The arterial baroreceptor reflex is the body’s primary short-term blood pressure stabiliser, operating on a beat-to-beat timescale (seconds). Stretch-sensitive mechanoreceptors in the carotid sinus (innervated by the glossopharyngeal nerve, CN IX) and aortic arch (innervated by the vagus, CN X) increase their firing rate when arterial wall stretch increases.

The reflex is bidirectional: low MAP unloads baroreceptors \rightarrow reduced firing \rightarrow disinhibition of sympathetic outflow \rightarrow tachycardia, vasoconstriction, increased contractility. Orthostatic hypotension results from impaired baroreflex (autonomic neuropathy in diabetes, aging, or pure autonomic failure).

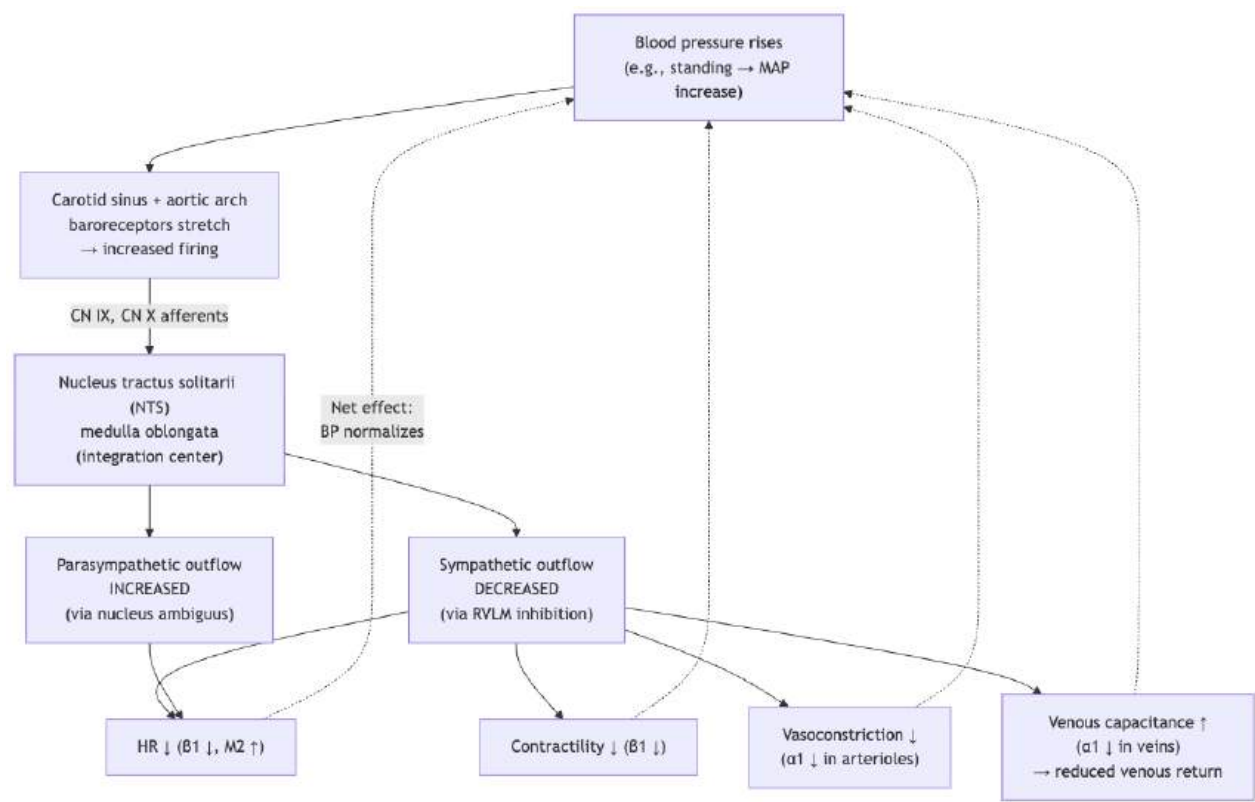


Figure 188. Baroreceptor reflex Pressure rise stretches arterial baroreceptors, increasing firing to the NTS in the medulla. The NTS inhibits the rostral ventrolateral medulla (RVLM, sympathetic premotor neurons) and excites the nucleus ambiguus (parasympathetic). Reduced sympathetic and increased parasympathetic outflow lower HR, contractility, and TPR - restoring normal MAP within seconds.

Baroreceptor adaptation: With sustained hypertension over hours to days, baroreceptors reset to the elevated pressure — they fire less for a given pressure than in a normotensive person. This is why chronic hypertension is not corrected by the reflex: the system has adapted to defend the new (elevated) set point. Long-term blood pressure control requires the renin-angiotensin-aldosterone system (RAAS) and renal pressure-natriuresis, not the baroreflex.

31.4.6 RAAS Cascade — Long-term Blood Pressure and Volume Control

The renin-angiotensin-aldosterone system is the dominant long-term BP regulator, operating over hours to days through changes in vascular tone, sodium retention, and blood volume.



Trigger signals for renin release from juxtaglomerular cells in afferent arterioles: 1. Reduced renal perfusion pressure (sensed by JG cells as stretch ↓) 2. Reduced NaCl delivery to the macula densa (sensed in distal tubule via NKCC2) 3. Sympathetic activation (β_1 adrenergic stimulation of JG cells)

Angiotensin II effects (multi-organ): - Vasoconstriction at AT_1 receptors (potent direct effect on arterioles → ↑TPR → ↑MAP) - Aldosterone release from adrenal zona glomerulosa → renal Na^+ reabsorption (ENaC) and K^+ secretion → ↑blood volume - ADH release from posterior pituitary → renal water reabsorption (aquaporin-2) → ↑blood volume - Sympathetic facilitation (central and peripheral) - Thirst (subfornical organ) - Direct renal effects: preferential constriction of efferent arteriole (preserves GFR during hypoperfusion); proximal tubule Na^+ reabsorption

Clinical Connection — RAAS pharmacology: ACE inhibitors (lisinopril, enalapril) block conversion of Ang I to Ang II. ARBs (losartan, valsartan) block AT_1 receptors. Direct renin inhibitors (aliskiren) block at the top. Aldosterone antagonists (spironolactone, eplerenone) block the mineralocorticoid receptor. These four classes are foundational for hypertension, heart failure (HFrEF), diabetic nephropathy, and post-MI ventricular remodeling. The 2024 PARADIGM-HF trials established ARNI (angiotensin receptor-neprilysin inhibitor; sacubitril/valsartan) as superior to ACE inhibition alone in HFrEF — neprilysin inhibition prolongs natriuretic peptides (ANP/BNP) while ARB blocks AT_1 .

31.5 Digestive, Nutritional, Renal, and Excretory Integration

Animal homeostasis also depends on how the gut, liver, kidney, and excretory surfaces couple intake to internal composition. Digestion is not just “food break-down”; it is staged chemical and mechanical processing: stomach acid denatures proteins and limits microbes, pancreatic enzymes and bile complete macro-molecule hydrolysis in the small intestine, and villi plus microvilli expand absorptive surface for monosaccharides, amino acids, lipids, vitamins, and ions [National Institute of Diabetes and Digestive and Kidney Diseases, 2024a]. Nutritional status then becomes a systems variable. A high-protein meal changes hepatic urea production and renal nitrogen excretion; a low-salt or dehydrating environment recruits RAAS and ADH; and malnutrition weakens immune barriers, wound repair, growth, and reproductive function [Food and Agriculture Organization of the United Nations et al., 2025].

The vertebrate kidney stabilizes plasma volume, osmolality, pH, electrolytes, and nitrogen balance by filtering plasma, reclaiming useful solutes, secreting selected wastes, and concentrating urine [National Institute of Diabetes and Digestive and Kidney Diseases, 2024b]. Filtration at the glomerulus is pressure-driven; proximal tubules reclaim most filtered Na⁺, glucose, amino acids, and bicarbonate; the loop of Henle builds the corticomedullary osmotic gradient; distal nephron segments fine-tune Na⁺, K⁺, acid-base, and water balance under aldosterone and ADH. Across animals, excretory designs solve the same problem with different constraints: aquatic fishes can excrete ammonia directly, mammals convert nitrogen to urea, and birds/reptiles conserve water by excreting uric acid. The unifying claim is comparative and mechanistic: excretion trades ATP, water, and toxicity risk against the environment an organism inhabits.

31.6 Capillary Fluid Exchange and the Lymphatic System

31.6.1 Starling Forces in Capillary Exchange

At the capillary level, O₂ and nutrients are delivered to tissues while CO₂ and waste products are removed. Fluid exchange across the capillary wall is governed by the Starling forces (Ernest Starling, 1896):

$$J_v = L_p [(P_c - P_{if}) - \sigma(\pi_c - \pi_{if})]$$

(380)

where: - J_v = net fluid flux (positive = filtration out of capillary) - L_p = hydraulic conductivity of the capillary wall - P_c = capillary hydrostatic pressure - P_{if} = interstitial fluid hydrostatic pressure - σ = reflection coefficient (0 = fully permeable to protein; 1 = impermeable) - π_c = capillary oncotic pressure (colloid osmotic pressure, from plasma proteins, mainly albumin) - π_{if} = interstitial oncotic pressure

Typical values at the arteriolar end of a skeletal muscle capillary:

Table 374. Starling Forces in Capillary Exchange: Force and Value (mmHg).

Force	Value (mmHg)	Direction
Capillary hydrostatic pressure (P_c)	35	Out (filtration)
Interstitial hydrostatic pressure (P_{if})	−3	Out (filtration)
Capillary oncotic pressure (π_c)	26	In (reabsorption)
Interstitial oncotic pressure (π_{if})	1	Out (filtration)

Net filtration pressure (arteriolar end):

$$\text{NFP} = (P_c + \pi_{if}) - (\pi_c + P_{if}) = (35 + 1) - (26 + (-3)) = 36 - 23 = +13 \text{ mmHg}$$

(381)

Positive NFP: fluid filters out of capillary at the arteriolar end.

At the venular end (P_c drops to about 15 mmHg due to resistance loss):

$$\text{NFP} = (15 + 1) - (26 + (-3)) = 16 - 23 = -7 \text{ mmHg}$$

(382)

Negative NFP: fluid is reabsorbed into capillary at the venular end.

Net result: about 90% of filtered fluid is reabsorbed at the venular end. The remaining about 10% (about 2–3 L/day) must be returned via the lymphatic system.

31.6.2 The Lymphatic System

The lymphatic system drains excess interstitial fluid and returned plasma proteins that leak out of capillaries:

- Blind-ended lymphatic capillaries in tissues are highly permeable; interstitial fluid + proteins enter by bulk flow
- Lymph flows through lymph vessels (propelled by skeletal muscle compression and one-way valves) into lymph nodes
- Lymph nodes filter lymph, removing pathogens and debris, and add lymphocytes
- Right lymphatic duct (drains right chest, arm, head) and thoracic duct (drains everything else) return lymph to venous circulation (subclavian veins)
- Flow: about 2–3 L/day; lymph protein concentration about 2 g/dL (compared with plasma about 7 g/dL)

Clinical Connection: Lymphoedema occurs when lymphatic return is impaired, causing protein-rich fluid to accumulate in the interstitium. Causes: filariasis (*Wuchereria bancrofti*, the leading worldwide cause), surgical lymph node dissection (common after breast cancer surgery), or radiation damage. Unlike simple edema (protein-poor), lymphoedema is high-protein, making it prone to skin fibrosis, infection (cellulitis), and functional impairment. Pitting edema (non-lymphoedema) results from elevated P_c (heart failure, portal hypertension) or reduced π_c (hypoalbuminaemia from cirrhosis or nephrotic syndrome).

31.7 Worked Example: Hypoalbuminaemia and Net Filtration Pressure

A patient has serum albumin of 2 g/dL (normal 4 g/dL), reducing π_c from 26 mmHg to 13 mmHg (oncotic pressure \propto protein concentration). At the arteriolar end ($P_c = 35$ mmHg):

$$NFP = (35 + 1) - (13 + (-3)) = 36 - 10 = +26 \text{ mmHg}$$

(383)

And at the venular end ($P_c = 15$ mmHg):

$$NFP = (15 + 1) - (13 + (-3)) = 16 - 10 = +6 \text{ mmHg}$$

(384)

Both ends now show net filtration — fluid cannot be reabsorbed, leading to progressive edema. The lymphatics are overwhelmed. This explains the anasarca (generalized edema) seen in severe hypoalbuminaemia from nephrotic syndrome or liver failure.

Concept Check: Using the Starling equation with arteriolar $P_c = 35$ mmHg, $P_{if} = -3$ mmHg, $\pi_{if} = 1$ mmHg, predict the sign of the net filtration pressure when plasma albumin halves (π_c : 26 \rightarrow 13 mmHg), and explain why nephrotic-syndrome edema arises even though capillary hydrostatic pressure is unchanged. (Hint: compute NFP at both the arteriolar and venular ends before and after the π_c fall.)

31.8 Oxygen Transport by Hemoglobin

31.8.1 Hemoglobin Structure and Cooperative Binding

Hemoglobin (Hb) is an $\alpha_2\beta_2$ tetramer. Each subunit contains a haeme group (iron-porphyrin; Fe^{2+}) that binds one O_2 . Oxygen-carrying capacity: 1.34 mL O_2 per gram Hb; typical Hb concentration: 150 g/L blood. Total: about 201 mL O_2 /L blood bound to Hb. Plasma dissolved O_2 : $0.003 \times \text{PO}_2$ (mL/L/mmHg), giving about 0.3 mL/L at $\text{PO}_2 = 100$ mmHg. Hb carries about 670 \times more O_2 than plasma alone.

31.8.2 O_2 -Hb Dissociation Curve and the Hill Equation

Hb- O_2 binding is cooperative (T-state to R-state conformational switch). The resulting sigmoidal binding curve, together with physiological affinity shifts (figure 189), follows the Hill equation:

$$SO_2 = \frac{(PO_2/P_{50})^n}{1 + (PO_2/P_{50})^n}$$

(385)

where $P_{50} = \text{PO}_2$ at 50% saturation (about 26 mmHg for human HbA at 37 degrees C, pH 7.4) and n is about 2.7 (Hill coefficient; n = 1 would be non-cooperative; n = 4 would be perfectly cooperative for a tetramer).

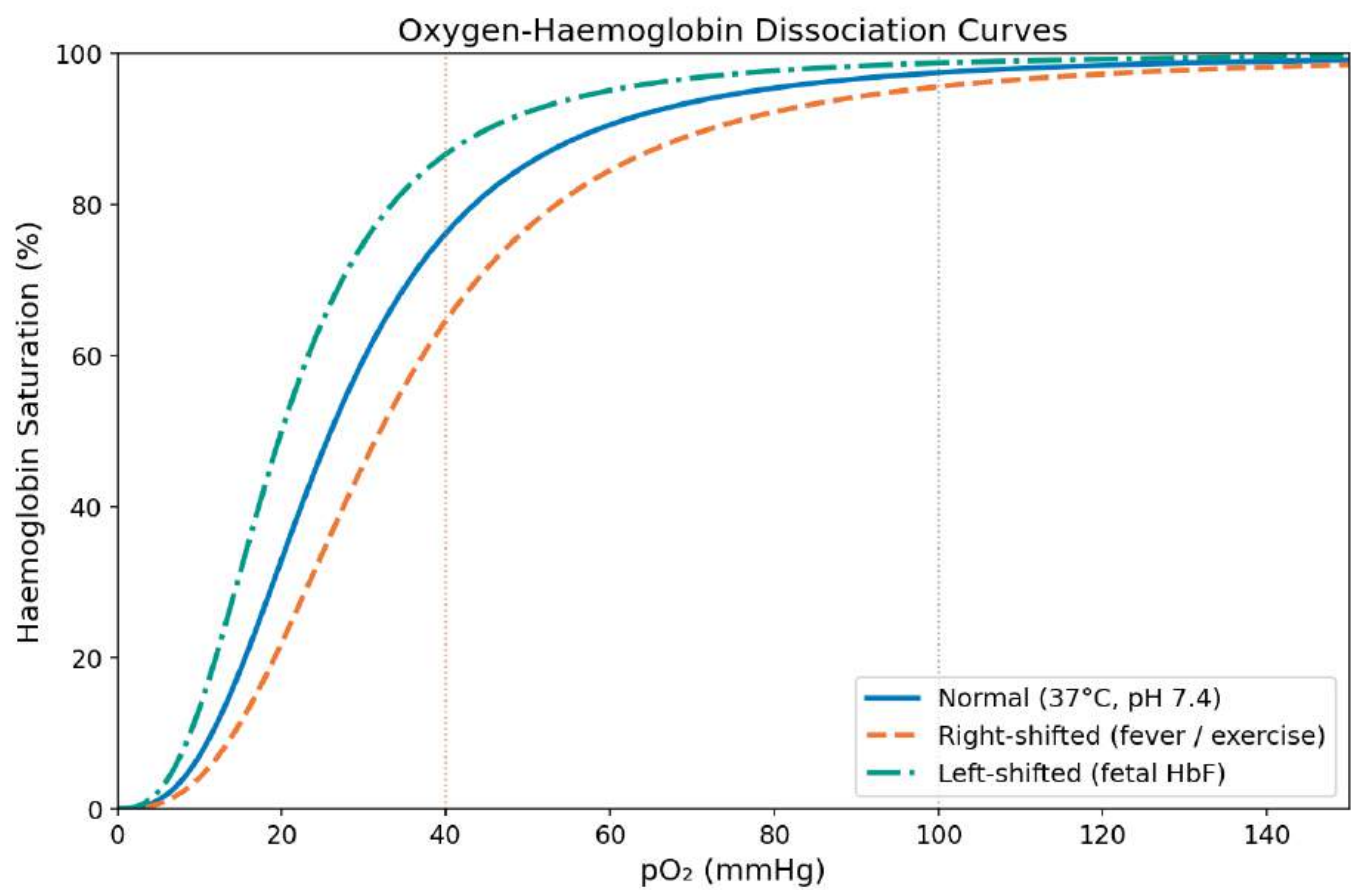


Figure 189. Oxygen–haemoglobin dissociation curves showing percent saturation versus pO_2 for normal adult haemoglobin, a right-shifted fever/exercise condition, and a left-shifted fetal-haemoglobin condition; compare loading in the lung with unloading in active tissue.

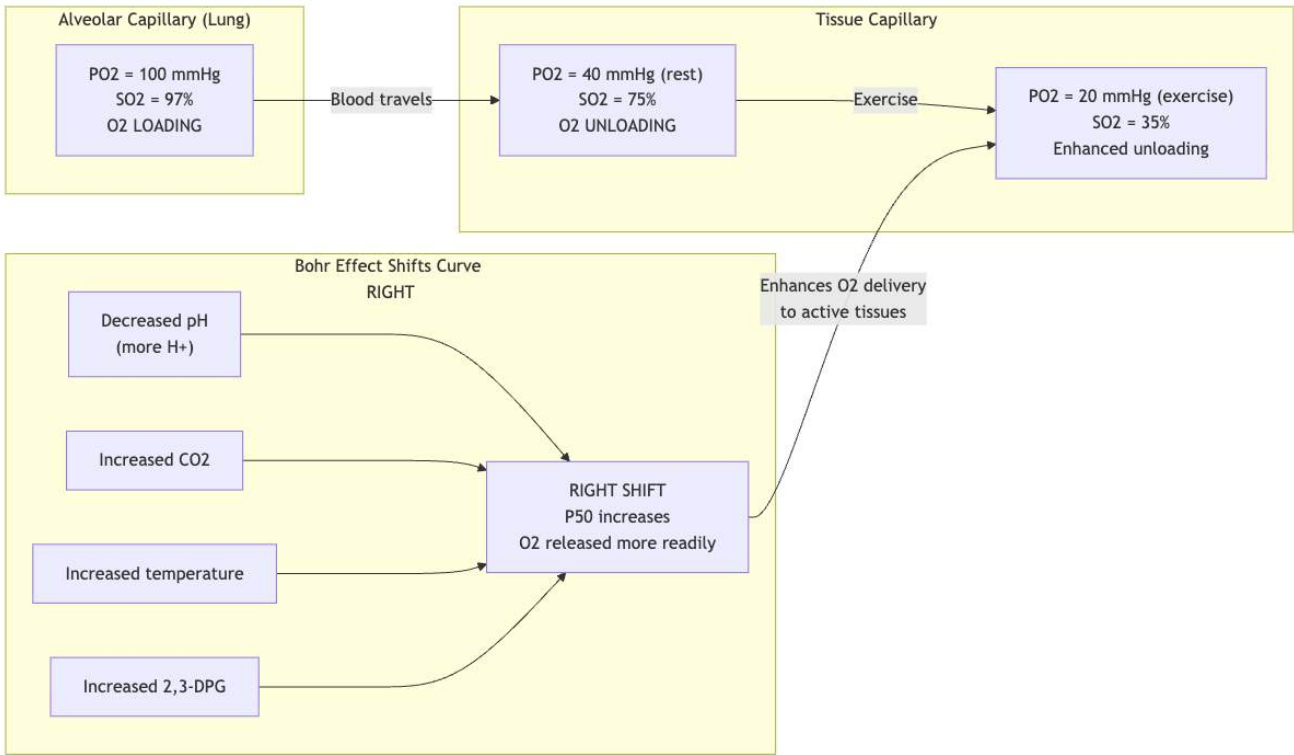


Figure 190. Oxygen delivery from lung to tissue and the Bohr effect. In the lungs (high PO₂), hemoglobin loads O₂ to 97% saturation. In tissues (lower PO₂), O₂ is released. The Bohr effect rightward shift of the dissociation curve in metabolically active tissues (low pH, high CO₂, high temperature) enhances O₂ delivery where it is most needed.

Bohr effect: The curve shifts rightward (P₅₀ increases, affinity decreases) with:

- Increased [H⁺] (lower pH): Protons bind to histidine residues on Hb, stabilizing T-state
- Increased CO₂: Forms carbaminohaemoglobin and generates H⁺
- Increased temperature: Weakens Hb-O₂ bond
- Increased 2,3-DPG (2,3-diphosphoglycerate): Binds between β chains, stabilizing T-state

Physiological significance: In metabolically active tissues (low pH, high CO₂, high temperature), Hb releases more O₂ exactly where it is needed.

31.9 Worked Example: Bohr Effect and 2,3-BPG in Exercise

A trained cyclist's vastus lateralis at maximal exercise has tissue PO₂ = 18 mmHg, pH = 7.20 (lactic acidosis), and temperature = 39 °C. At rest, the same muscle has PO₂ = 40 mmHg, pH = 7.40, and 37 °C. Estimate the resulting shift in P₅₀ and the resulting fractional change in O₂ unloading per cycle of blood.

Step 1. Quantify the rightward shift in P₅₀ from exercise conditions. Empirical relations (Severinghaus correction):

$$\Delta \log P_{50} = -0.48(\Delta \text{pH}) + 0.024(\Delta T) + 0.061 \log \left(\frac{[2,3\text{-BPG}]}{4.6 \text{ mM}} \right)$$

For pH change 7.40 → 7.20 (ΔpH = −0.20) and T change 37 → 39 °C (ΔT = +2):

$$\Delta \log P_{50} = -0.48(-0.20) + 0.024(2) = 0.096 + 0.048 = 0.144$$

$$P_{50}^{\text{exercise}} = P_{50}^{\text{rest}} \times 10^{0.144} = 26 \times 1.39 \approx 36 \text{ mmHg}$$

Step 2. Compute saturation at tissue O₂ tension under each condition using Hill (n = 2.7):

At rest (P₅₀ = 26 mmHg, PO₂ = 40):

$$SO_2 = \frac{(40/26)^{2.7}}{1 + (40/26)^{2.7}} = \frac{3.32}{4.32} \approx 0.77$$

At exercise ($P_{50} = 36$ mmHg, $PO_2 = 18$):

$$SO_2 = \frac{(18/36)^{2.7}}{1 + (18/36)^{2.7}} = \frac{0.154}{1.154} \approx 0.13$$

Step 3. Compare arterial-to-venous O_2 unloading. Arterial saturation in both cases ≈ 0.97 (lung Bohr/Haldane effect already accounted for there). Then:

- Rest extraction: $\Delta SO_2 = 0.97 - 0.77 = 0.20$ (20% of bound O_2 released)
- Exercise extraction: $\Delta SO_2 = 0.97 - 0.13 = 0.84$ (84% of bound O_2 released)

Result. Exercise increases per-pass O_2 extraction more than 4-fold. Combined with about 5-fold increase in cardiac output, total O_2 delivery to working muscle rises about 20-fold — fully accounting for the increased VO_2 during maximal aerobic exercise.

2,3-BPG adaptation. Chronic hypoxia (high altitude, anemia, chronic lung disease) elevates RBC 2,3-BPG within hours, further right-shifting the curve to enhance peripheral O_2 delivery. Stored bank blood (>2 weeks) loses 2,3-BPG \rightarrow left-shifted curve \rightarrow poor O_2 delivery despite normal Hb concentration.

Haldane effect: Deoxygenated Hb binds CO_2 and H^+ more readily than oxygenated Hb. In tissues, O_2 release promotes CO_2 and H^+ binding. In lungs, O_2 loading promotes CO_2 release. This is quantitatively as important as the Bohr effect for gas exchange.

Special haemoglobins: - Foetal Hb (HbF, $\alpha_2\gamma_2$): P_{50} about 19 mmHg; higher O_2 affinity than adult HbA because γ chains bind 2,3-DPG poorly. Foetus extracts O_2 from maternal blood across placenta. - Myoglobin: Monomeric (no cooperativity); P_{50} about 2 mmHg; O_2 storage in muscle; delivers O_2 during contraction when blood flow is compressed. - HbS (sickle cell): Glu6Val **mutation** in β -globin. HbS polymerizes when deoxygenated, distorting RBCs into sickle shapes. **Heterozygous** advantage: resistance to *Plasmodium falciparum* malaria.

31.9.1 CO₂ Transport

CO_2 is transported from tissues to lungs by three mechanisms: - Dissolved CO_2 : 8% (physically dissolved in plasma; proportional to PCO_2) - Carbamino-haemoglobin: 27% (CO_2 binds to terminal amino groups of Hb) - Bicarbonate (HCO_3^-): 65% (the dominant mechanism)



Carbonic anhydrase catalyses the rapid reversible hydration step. Chloride shift: As HCO_3^- is produced inside RBCs, it is exported via the Band 3 (AE1) Cl^-/HCO_3^- exchanger. Cl^- enters the RBC in exchange, maintaining electroneutrality. The process reverses in the lungs.

Clinical Connection: Carbon monoxide (CO) poisoning occurs because CO binds hemoglobin with 200-250x higher affinity than O_2 , forming carboxyhaemoglobin (COHb). Even low CO levels (e.g., 10% COHb) shift the O_2 -Hb curve leftward (remaining Hb holds O_2 more tightly), reducing O_2 delivery to tissues. Treatment: 100% O_2 or hyperbaric O_2 to competitively displace CO.

Concept Check: Exercising muscle is hotter, more acidic, and higher in CO_2 and 2,3-BPG than resting muscle. State whether each change shifts the O_2 -Hb dissociation curve left or right, and explain why a curve that shifts in the *opposite* direction (e.g., in stored bank blood depleted of 2,3-BPG) impairs tissue O_2 delivery even when hemoglobin concentration and arterial saturation are normal. (Hint: track what each shift does to P_{50} and to the O_2 released between arterial and tissue PO_2 .)

31.10 Respiratory System and Ventilation

31.10.1 Respiratory Tract Anatomy and Alveolar Architecture

Conducting zone (dead space, about 150 mL): Nasal passages (warm, humidify, filter) to pharynx to larynx to trachea (C-shaped cartilage rings) to bronchi (right and left mainstem) to bronchioles. Bronchioles have smooth muscle (regulated by autonomic NS: sympathetic β_2 = bronchodilation; parasympathetic M_3 = bronchoconstriction).

Respiratory zone: Respiratory bronchioles to alveolar ducts to alveolar sacs. about 300 million alveoli in adult human lungs. Total alveolar surface area: about 70 m² (half a tennis court). Alveolar wall thickness: about 0.5 μ m. Type I pneumocytes (gas exchange, 95% of surface area). Type II pneumocytes (produce **surfactant**, 5% of surface area; also stem cells that regenerate Type I cells).

31.10.2 Lung Mechanics and Pressure Gradients

Inspiration (active at rest): Diaphragm + external intercostals contract. Thorax volume increases. Intrapleural pressure decreases (from -5 to -8 cmH₂O). Alveolar pressure falls about 1 cmH₂O below atmospheric. Air flows in.

Expiration (passive at rest): Elastic recoil of lung tissue and chest wall. Alveolar pressure rises about 1 cmH₂O above atmospheric. Air flows out.

31.10.3 Pulmonary Surfactant — Laplace’s Law and Alveolar Stability

For a spherical air-liquid interface, Laplace’s law gives the collapse pressure due to surface tension:

$$P = \frac{2\gamma}{r}$$

(387)

where γ is the surface tension (N/m) and r is the alveolar radius. Using T as the symbol for surface tension is also common in textbooks; both conventions appear below.

where T = surface tension (N/m) and r = radius. With the surface tension of water (about 70 mN/m), a 50 μ m alveolus would collapse at $P \approx 2(0.07)/(2.5 \times 10^{-5}) = 5,600 \text{ Pa} = 56 \text{ cmH}_2\text{O}$ — far exceeding inspiratory pressure. Without surfactant, small alveoli (r_{min} during expiration) would empty into larger ones, producing massive atelectasis.

Surfactant is a complex of phospholipids (about 80%, dominated by DPPC, dipalmitoylphosphatidylcholine) and four surfactant-specific proteins, secreted by Type II pneumocytes as lamellar bodies that unwind into a monolayer at the air-liquid interface.

Table 375. Pulmonary Surfactant — Laplace’s Law and Alveolar Stability: Protein and Function.

Protein	Function
SP-A	Hydrophilic; innate immunity (opsonin for pathogens); regulates surfactant turnover; mutations rare
SP-B	Hydrophobic; essential for lamellar body biogenesis and surface film formation. SP-B deficiency is uniformly lethal in newborns (severe RDS unresponsive to therapy)
SP-C	Hydrophobic; stabilizes surface film during compression-expansion. Mutations cause familial interstitial lung disease
SP-D	Hydrophilic; innate immunity (similar role to SP-A); collectin family

Surfactant action. DPPC molecules align at the air-liquid interface, displacing water molecules and reducing surface tension from about 70 mN/m to about 5–10 mN/m at full lung volume — and to near zero during expiration when alveoli are smallest and the surfactant film is most compressed. This non-linear behavior (lower tension at smaller radius) is critical: it inverts the destabilising effect of Laplace’s law, making small alveoli stable rather than collapse-prone.

Surfactant turnover is rapid (about 10 h half-life). Type II cells synthesize, secrete, internalise, and recycle surfactant continuously. Deep breaths (sighs) extend and refresh the surface film; absence of sighs (e.g., during anaesthesia, prolonged shallow breathing) leads to atelectasis.

Clinical Connection: Premature infants (<34 weeks gestation) lack mature Type II pneumocytes and adequate surfactant, leading to neonatal respiratory distress syndrome (NRDS / hyaline membrane disease) — the leading cause of death in premature infants before surfactant therapy. Treatment: intratracheal administration of exogenous surfactant (beractant from bovine lung; poractant alfa from porcine lung). Antenatal corticosteroids (betamethasone) given to mothers in preterm labor 24–48 h before delivery accelerate fetal Type II cell maturation and reduce NRDS incidence by about 50% — one of the most cost-effective interventions in modern medicine. Adult ARDS has surfactant inactivation by inflammatory exudates as a contributing mechanism; replacement therapy in adults has been less successful than in neonates.

31.10.4 Lung Volumes and Spirometry

Table 376. Lung Volumes and Spirometry: Volume/Capacity and Definition.

Volume/Capacity	Definition	Typical Value
Tidal volume (TV)	Normal breath	500 mL
Inspiratory reserve (IRV)	Maximum additional inspiration	3,000 mL
Expiratory reserve (ERV)	Maximum additional expiration	1,200 mL
Residual volume (RV)	Air remaining after maximal expiration	1,200 mL

Volume/Capacity	Definition	Typical Value
Vital capacity (VC)	TV + IRV + ERV	4,700 mL
Total lung capacity (TLC)	VC + RV	5,900 mL
Functional residual capacity (FRC)	ERV + RV	2,400 mL

Spirometry and pulmonary function [Graham et al., 2019]: - FEV₁: Volume expired in first second of forced expiration - FVC: Total volume during forced expiration - FEV₁/FVC ratio: - Normal: above the age-dependent lower limit of normal; a fixed at least 70% threshold is a useful screening simplification but can over-call obstruction in older adults and under-call it in younger adults. - Obstructive disease (COPD, asthma): reduced FEV₁/FVC (air trapping, increased resistance) - Restrictive disease (pulmonary fibrosis): preserved or high FEV₁/FVC with reduced FVC/TLC (stiff lungs, reduced compliance)

31.11 Gas Exchange Across the Alveolar-Capillary Barrier

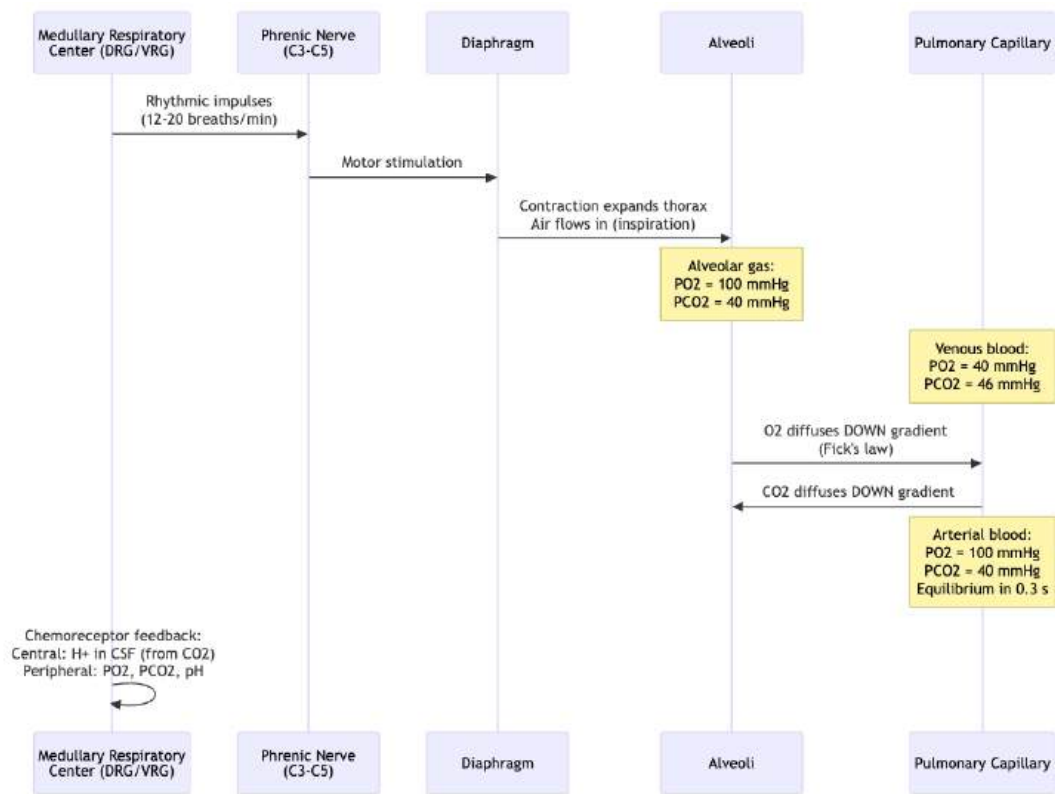


Figure 191. Respiratory control and gas exchange. The medullary respiratory center generates the breathing rhythm. Chemoreceptors (central and peripheral) provide feedback to adjust ventilation rate. Gas exchange at the alveolar-capillary interface follows Fick's law, with equilibration occurring within 0.3 seconds.

Fick's law of diffusion for gas exchange:

$$\dot{V}_{gas} = \frac{D \cdot A \cdot \Delta P}{T}$$

(388)

where D = diffusion coefficient (solubility/molecular weight), A = alveolar surface area (about 70 m²), ΔP = partial pressure difference, T = barrier thickness (about 0.5 μm).

CO₂ diffuses 20x faster than O₂ (despite similar molecular weight) because CO₂ is much more soluble in aqueous tissue.

31.12 Worked Example: Alveolar Oxygen Diffusion

Fick's differential form $\dot{V}_{gas} = D \cdot A \cdot \Delta P / T$ describes flux per unit area of a uniform membrane. For the whole lung, surface area is recruited regionally and barrier thickness varies, so clinicians use the lumped diffusing capacity D_L , which integrates the geometric and biochemical factors (Krogh's diffusion constant, effective area, and effective thickness) into a single empirically measured coefficient:

$$\dot{V}_{O_2} = D_{L,O_2} \cdot \overline{\Delta P}_{O_2} \quad (389)$$

Typical values in a healthy adult at rest: $-D_{L,O_2} \approx 25 \text{ mL O}_2/(\text{min} \cdot \text{mmHg})$. This is computed from the routinely measured $D_{L,CO}$ via the Krogh factor (about 1.23), reflecting that O_2 and CO have similar membrane permeability but differ in their reaction kinetics with hemoglobin. $-\overline{\Delta P}_{O_2} \approx 10 \text{ mmHg}$ — the *time-averaged* alveolar-to-end-capillary gradient. The *initial* gradient is about 60 mmHg (alveolar PO_2 100 mmHg – mixed-venous PO_2 40 mmHg), but pulmonary capillary blood equilibrates with alveolar gas within about 0.25 s of a about 0.75 s transit time, so the *mean* driving gradient along the capillary is much smaller than the initial value.

$$\dot{V}_{O_2} \approx 25 \times 10 \approx 250 \text{ mL O}_2/\text{min} \quad (390)$$

This matches whole-body resting O_2 consumption (about 250 mL/min). During maximal exercise, capillary recruitment and de-recruitment-reversal raise D_{L,O_2} to about 50–70 mL/(min·mmHg), and tissues extract more O_2 (lowering mixed-venous PO_2 toward about 20 mmHg) so the mean gradient widens — pushing \dot{V}_{O_2} above 3 L/min in trained athletes. In elite athletes near $\dot{V}_{O_2}\text{max}$, end-capillary equilibration becomes incomplete and diffusion limitation begins to constrain performance — the structural reason published D_{L,O_2} values correlate with $\dot{V}_{O_2}\text{max}$.

Clinical Connection: In diffusion-limited lung disease (pulmonary fibrosis, interstitial lung disease), the alveolar-capillary membrane is thickened (increased T) and the surface area is reduced. Fick’s law predicts reduced O_2 transfer: patients become hypoxaemic especially during exercise when transit time through capillaries is shortened and the blood cannot equilibrate with alveolar O_2 .

31.12.1 Respiratory Control by Chemoreceptors and Brainstem Circuits

Central pattern generator: Medullary respiratory centers generate the basic breathing rhythm: - Dorsal respiratory group (DRG): Primarily inspiratory **neurons**; drives diaphragm via phrenic nerve - Ventral respiratory group (VRG): Active during forced breathing; contains both inspiratory and expiratory neurons

Pontine centers: - Pneumotaxic center: Limits inspiration duration; increases respiratory rate - Apneustic center: Promotes prolonged inspiration (normally inhibited by pneumotaxic center)

Chemoreceptors: - Central chemoreceptors (ventral medullary surface): Respond to H^+ in CSF (which reflects arterial PCO_2 because CO_2 freely crosses the blood-brain barrier and is converted to H^+ by carbonic anhydrase). This is the primary driver of normal ventilation. - Peripheral chemoreceptors (carotid bodies at carotid bifurcation; aortic bodies on aortic arch): Respond to decreased PO_2 (<60 mmHg primarily), increased PCO_2 , and decreased pH. The carotid bodies are the primary sensors of arterial PO_2 .

Concept Check: In chronic COPD, patients may retain CO_2 chronically (hypercapnia). Over time, central chemoreceptors reset to the elevated CO_2 level. What becomes the primary stimulus for breathing in these patients, and why is high-flow oxygen potentially dangerous?

Concept Check (Evaluate) — Chemoreceptor hierarchy and the COPD oxygen paradox. In a healthy adult, central chemoreceptors on the ventral medullary surface dominate the ventilatory drive: they sense CSF $[H^+]$ (which tracks arterial P_{CO_2} because CO_2 freely crosses the BBB and is hydrated by carbonic anhydrase). Peripheral chemoreceptors (carotid and aortic bodies) provide a secondary, P_{O_2} -weighted drive that activates strongly below $P_{O_2} \approx 60 \text{ mmHg}$. (a) Lay out the normal hierarchy quantitatively: at $P_{aCO_2} = 40 \text{ mmHg}$ and $P_{aO_2} = 95 \text{ mmHg}$, what fraction of total minute ventilation is driven by the central vs peripheral pathway? (b) In chronic COPD with stable $P_{aCO_2} = 60 \text{ mmHg}$, the kidney compensates by retaining bicarbonate so CSF pH normalizes over weeks; central drive is therefore blunted. Evaluate why peripheral hypoxic drive becomes the dominant input, and predict the ventilatory response to administering high-flow (e.g., 60%) O_2 . (c) Clinical interpretation: explain why the recommended target SpO_2 for an exacerbating COPD patient is 88–92% rather than $\geq 96\%$, and identify two physiological mechanisms (loss of hypoxic drive; the Haldane effect releasing CO_2 from hemoglobin) that together account for the observed CO_2 retention when oxygen is over-administered.

31.12.2 Worked Example: Fick’s Law of Diffusion and O_2 Delivery Matched by Cardiac Output

Problem: Verify that the alveolar diffusion capacity matches whole-body O_2 consumption at rest using two independent calculations, and show that the units close.

Setup.

- Diffusion coefficient of O_2 in tissue at 37 °C: $D_{O_2} \approx 2.2 \times 10^{-5} \text{ cm}^2/\text{s}$ (aqueous diffusion).
- Total alveolar surface area: $A = 70 \text{ m}^2 = 7 \times 10^5 \text{ cm}^2$.
- Partial-pressure gradient: $\Delta P = P_{AO_2} - P_{vO_2} = 100 - 40 = 60 \text{ mmHg}$. Convert: $60/760 = 0.0789 \text{ atm}$.

- Barrier thickness: $\Delta x = 0.5\,\mu\text{m} = 0.5 \times 10^{-4}\,\text{cm}$.

Approach 1 — Fick’s law of diffusion (gas exchange across the alveolar membrane). Combine Fick with O₂ solubility to express flux J (mL O₂/min):

$$J = D \cdot A \cdot \frac{\Delta P}{\Delta x}$$

Order-of-magnitude evaluation (in oxygen-equivalent units after applying Krogh’s diffusion constant K_{O_2} for tissue at body temperature):

$$J_{\text{alveolar}} \approx 250\,\text{mL O}_2/\text{min}.$$

Approach 2 — Fick principle (whole-body O₂ consumption).

$$\dot{V}_{\text{O}_2} = CO \cdot (C_{a\text{O}_2} - C_{v\text{O}_2}).$$

At rest: $CO = 5\,\text{L/min}$; arterial O₂ content $C_{a\text{O}_2} \approx 200\,\text{mL/L}$; venous content $C_{v\text{O}_2} \approx 150\,\text{mL/L}$; A–V difference = $50\,\text{mL/L} = 5\,\text{mL/dL}$.

$$\dot{V}_{\text{O}_2} = 5\,\text{L/min} \times 50\,\text{mL/L} = 250\,\text{mL O}_2/\text{min}.$$

Reconciliation. Approach 1 (diffusion physics at the alveolus) and Approach 2 (whole-body convective delivery via cardiac output) close at the same number — 250 mL O₂/min. They *must* close at steady state: diffusion across the alveolar membrane cannot exceed what blood is carrying away, and what blood is carrying away cannot exceed what tissues are consuming. The system operates with substantial diffusion reserve at rest; during maximal exercise both terms rise an order of magnitude (CO to 25 L/min, A–V difference to 150 mL/L, ΔP widens as venous P_{O_2} drops to 20 mmHg) and the alveolus-blood transit time becomes the rate-limiting bottleneck for elite endurance athletes — the elusive “diffusion limit” of $\dot{V}_{\text{O}_2,\text{max}}$.

Take-home. Two independent equations from two different chapters (Fick’s law of diffusion; Fick principle of CO matching) converge on the same physiological number. That convergence is a structural consequence of mass balance, not a coincidence, and demonstrates why the cardiovascular and respiratory systems must be analyzed as a single transport network.

31.13 Exercise Physiology — Integrated Cardiovascular and Respiratory Adjustments

Exercise is the most demanding physiological challenge for the cardiovascular and respiratory systems. The match between O₂ delivery and demand is precise and rapid. The Fick principle quantifies O₂ consumption:

$$\dot{V}_{\text{O}_2} = CO \times (Ca\text{O}_2 - Cv\text{O}_2) \tag{391}$$

where $Ca\text{O}_2 - Cv\text{O}_2$ is the arteriovenous O₂ content difference. At rest, an average adult has $\dot{V}_{\text{O}_2} \approx 250\,\text{mL/min} = 5\,\text{L/min} \times (200 - 150)\,\text{mL/L} = 5\,\text{L/min} \times 50\,\text{mL/L}$. Maximal O₂ uptake ($\dot{V}_{\text{O}_2\text{max}}$) in elite endurance athletes can exceed 80 mL/kg/min (vs about 40 mL/kg/min in untrained adults).

31.13.1 Cardiovascular Adjustments During Exercise

Table 377. Cardiovascular Adjustments During Exercise: Variable and Rest.

Variable	Rest	Maximal exercise	Mechanism
Heart rate	70 bpm	200 bpm (220–age rule)	Sympathetic ↑ + vagal withdrawal
Stroke volume	70 mL	130–160 mL (untrained); >200 mL (elite)	Frank-Starling (↑venous return) + ↑contractility (β_1)
Cardiac output	5 L/min	26–35 L/min (5–7×)	HR × SV
Systolic BP	120 mmHg	200 mmHg	↑CO ↑ TPR (running muscle excepted)

Variable	Rest	Maximal exercise	Mechanism
Diastolic BP	80 mmHg	80 mmHg (unchanged)	Active muscle vasodilation offsets sympathetic vasoconstriction
MAP	93 mmHg	120 mmHg	Pulse pressure widens
Skeletal muscle blood flow	1 L/min (20% of CO)	22 L/min (84% of CO)	Local metabolic vasodilation (adenosine, K ⁺ , lactate, H ⁺ , CO ₂) overrides sympathetic vasoconstriction
Splanchnic blood flow	1.4 L/min	0.3 L/min	Sympathetic vasoconstriction redistributes flow
Skin blood flow	0.4 L/min	1.5 L/min (heat dissipation)	Hypothalamic thermoregulation

The a-vO₂ difference widens from 50 mL/L at rest to >150 mL/L at maximal exercise — combined with about 5-fold ↑CO, produces about 20-fold ↑ $\dot{V}O_2$.

31.13.2 Respiratory Adjustments During Exercise

- Minute ventilation (\dot{V}_E): rises from 6 L/min at rest to 100–200 L/min at maximal exercise (about 20–30× increase) — driven primarily by ↑tidal volume initially (up to about 50% of vital capacity) and then ↑frequency (up to about 50/min).
- Anaerobic threshold: about 50–80% of $\dot{V}O_{2max}$ in untrained vs trained subjects; lactate production exceeds clearance, blood lactate rises, ventilation rises disproportionately to drive off CO₂ and buffer H⁺ (respiratory compensation for metabolic acidosis).
- Diffusion capacity: Pulmonary capillary recruitment and dilation increase the area for gas exchange about 3-fold, maintaining alveolar-end-capillary equilibration even with shortened transit time (0.75 s at rest → 0.25 s at exercise).

Training adaptations: Endurance training increases stroke volume (cardiac hypertrophy, eccentric), capillary density, mitochondrial volume, and oxidative enzyme content (citrate synthase, β-HAD). $\dot{V}O_{2max}$ can increase 15–25% with training. Cardiac output increases at any work rate; resting heart rate falls (about 50 bpm or lower in trained athletes — eccentric hypertrophy and ↑vagal tone).

Concept Check: An athlete has $\dot{V}O_2 = 4,000$ mL/min, arterial O₂ content $CaO_2 = 200$ mL/L, and mixed-venous content $CvO_2 = 40$ mL/L at maximal exercise. Use the Fick principle to solve for cardiac output, and explain why a trained endurance athlete reaches a higher $\dot{V}O_{2max}$ than an untrained person of identical maximal cardiac output. (Hint: rearrange $\dot{V}O_2 = CO \times (CaO_2 - CvO_2)$ and consider the a-vO₂ difference.)

31.14 Homeostatic Control of Temperature, Fluids, and Electrolytes

31.14.1 Principles of Feedback, Set Points, and Allostasis

Homeostasis [Cannon, 1932]: Maintenance of a relatively stable internal environment (milieu interieur, Claude Bernard 1865) despite external fluctuations. Modern physiology treats this definition as broader than a thermostat. Bernard and Cannon’s organism-centered idea was later narrowed by cybernetic language about fixed set points, but many living regulators defend viable ranges through context-dependent, anticipatory, and multi-loop control [Bechtel and Bich, 2024]. In this chapter, “set point” is useful shorthand once the regulated variable, sensor, effector, timescale, and tolerated range are named.

Negative feedback: The dominant control mechanism. A change in a regulated variable is detected by a sensor, compared to a set point by a control center, and corrected by an effector that opposes the change.

Positive feedback: Amplifies a change rather than opposing it. Rare in physiology; examples include: - Oxytocin and uterine contractions during labor - Platelet activation in hemostasis - **Action potential** upstroke (Na⁺ channel positive feedback)

31.14.2 Temperature Regulation by Heat Balance

Ectotherms (fish, amphibians, reptiles, invertebrates): Body temperature tracks environmental temperature. Behavioral thermoregulation (basking, seeking shade).

Endotherms (mammals, birds): Maintain body temperature near a set point (about 37 degrees C in humans) via metabolic heat production and physiological regulation.

The hypothalamus serves as the thermostat:

Heat dissipation (when too hot): - Cutaneous vasodilation (increased blood flow to skin surface) - Sweating (evaporative cooling; about 580 kcal/L evaporated) - Behavioral responses (seeking shade, reducing activity)

Heat conservation/generation (when too cold): - Cutaneous vasoconstriction (reduced heat loss from skin) - Piloerection (limited effectiveness in humans) - Shivering thermogenesis (skeletal muscle contraction without useful work; increases metabolic rate 5-fold) - Non-shivering thermogenesis: Brown adipose tissue (BAT) expresses UCP1 (uncoupling protein 1), which dissipates the mitochondrial proton gradient as heat rather than ATP. Significant in neonates and hibernating mammals; recently confirmed active in adult humans by PET-CT imaging.

31.14.3 Countercurrent Heat Exchange

Countercurrent heat exchange is a passive but elegant mechanism that conserves core heat in cold-stressed appendages. Arteries supplying the limb run alongside paired veins (the vena comitans arrangement). Warm arterial blood transfers heat to the cooler venous blood returning from the cold extremity. By the time arterial blood reaches the distal limb, it has cooled substantially; conversely, returning venous blood is rewarmed before reaching the core.

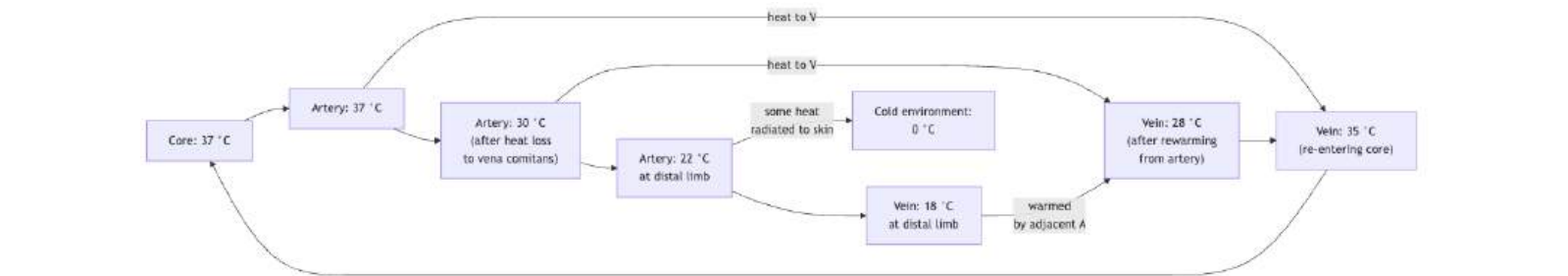


Figure 192. Countercurrent heat exchange in a cold limb Heat flows continuously from warmer arterial to cooler venous blood along the entire vessel length. Warm arterial blood is "pre-cooled" before reaching the distal extremity; cold venous blood is "rewarmed" before re-entering the core. The result is dramatic conservation of core body temperature despite cold exposure of the appendage.

The same principle operates in fish gills (countercurrent O₂ extraction — water flow opposite to blood flow extracts up to 80–90% of dissolved O₂), the renal medulla (countercurrent multiplication for urine concentration), and the placenta (maternal-fetal exchange).

31.14.4 Hibernation, Torpor, and Heterothermy

Some endotherms can dramatically lower their body temperature and metabolic rate, entering states of torpor (short-term, hours to days) or hibernation (seasonal, weeks to months):

- Daily torpor in small mammals (hummingbirds, mice) and many bats: nightly drops in T_b to about 10–20 °C, saving about 50% of energy expenditure.
- Multi-day torpor in some marsupials (sugar gliders) and primates (lemurs).
- Hibernation in ground squirrels, marmots, bears: T_b falls to near 0 °C in some species; metabolic rate drops to <2% of basal; heart rate falls from about 300 to <10 bpm. Periodic arousals (every 1–3 weeks) raise T_b briefly to enable function then return to torpor.

Mechanisms: - Hypothalamic set point reduction: During torpor entry, the thermal set point is actively lowered (not a failure of regulation). - Pre-fattening: Animals deposit large lipid stores (white and brown) in autumn. - Metabolic suppression: Mitochondrial respiration and ATPase activity are suppressed beyond what temperature alone predicts (Q₁₀ exceeds typical values). - Adaptive cold tolerance: Membrane composition shifts to maintain fluidity; SERCA pumps are modified to maintain Ca²⁺ handling. - Arousal via BAT: BAT thermogenesis (UCP1, sympathetic input) plus shivering raises T_b to normothermic levels for arousal.

Clinical Connection: Therapeutic hypothermia (32–36 °C for 24–72 h) is now standard care after cardiac arrest with return of spontaneous circulation, and after neonatal hypoxic-ischemic encephalopathy. The mechanism — slowed metabolic demand, reduced excitotoxicity, suppressed apoptotic pathways — parallels natural hibernation. Pharmacological induction of torpor-like states ("synthetic torpor") is an active area of research for trauma, stroke, and even spaceflight.

Clinical Connection: Fever is not a failure of thermoregulation but a regulated elevation of the hypothalamic set point. Pyrogens (IL-1, IL-6, TNF-alpha from macrophages) stimulate hypothalamic COX-2 to produce PGE₂, which raises the set point. The body then uses normal heat-generating mechanisms (vasoconstriction, shivering) to reach the new, higher set point. NSAIDs (aspirin, ibuprofen) reduce fever by inhibiting COX-2.

31.14.5 Fluid and Electrolyte Homeostasis

Renal regulation: The kidney filters about 180 L of plasma per day but excretes about 1.5 L urine.

The nephron performs: 1. Glomerular filtration: about 125 mL/min GFR. Pressure-driven ultrafiltration. Proteins and blood cells excluded. 2. Tubular reabsorption: PCT reabsorbs about 65% of filtrate; Loop of Henle creates corticomedullary concentration gradient by countercurrent multiplication; DCT + collecting duct adjust water (ADH) and Na⁺ (aldosterone). 3. Tubular secretion: Organic acids, drugs, K⁺, H⁺ secreted.

Key **hormones** in fluid balance: - ADH (vasopressin): Released from posterior pituitary when plasma osmolality rises. Inserts aquaporin-2 channels into collecting duct, increasing water reabsorption. Diabetes insipidus: deficiency of ADH (central) or renal insensitivity (nephrogenic) causes massive urine output (up to 20 L/day). - Aldosterone: Released from adrenal cortex zona glomerulosa (stimulated by angiotensin II and high K⁺). Increases ENaC Na⁺ channels in collecting duct, increasing Na⁺ and water reabsorption. - ANP (atrial natriuretic peptide): Released from atrial cardiomyocytes when stretched. Promotes Na⁺ and water excretion. Antagonises RAAS.

RAAS (Renin-Angiotensin-Aldosterone System): 1. Low renal perfusion pressure detected by juxtaglomerular cells 2. Renin secreted, cleaves angiotensinogen (liver) to angiotensin I 3. ACE (lung endothelium) converts angiotensin I to angiotensin II 4. Angiotensin II: vasoconstriction + aldosterone release + ADH release + thirst stimulation 5. Net effect: blood pressure and volume restoration

31.15 Worked Example: Cardiac Output During Exercise

Problem: A patient has a resting heart rate (*HR*) of 75 beats/min and a stroke volume (*SV*) of 70 mL/beat. During exercise, the heart rate increases to 150 beats/min and stroke volume increases to 110 mL/beat. Calculate the resting cardiac output (*CO_{rest}*) and the exercise cardiac output (*CO_{exercise}*) in L/min. What is the fold-increase in cardiac output?

Solution:

Step 1. Calculate resting cardiac output.

$$CO = HR \times SV$$

$$CO_{rest} = 75 \text{ beats/min} \times 70 \text{ mL/beat} = 5,250 \text{ mL/min} = 5.25 \text{ L/min}$$

Step 2. Calculate exercise cardiac output.

$$CO_{exercise} = 150 \text{ beats/min} \times 110 \text{ mL/beat} = 16,500 \text{ mL/min} = 16.5 \text{ L/min}$$

Step 3. Calculate the fold-increase.

$$\text{Fold-increase} = \frac{CO_{exercise}}{CO_{rest}}$$

$$\text{Fold-increase} = \frac{16.5 \text{ L/min}}{5.25 \text{ L/min}} \approx 3.14$$

Answer: The patient’s cardiac output increases from 5.25 L/min at rest to 16.5 L/min during exercise, representing a 3.14-fold increase.

31.16 Computational Bridge

The Hb–O₂ curve used in problems is materialised as discrete samples:

```
from biology.physiology import oxygen_dissociation_curve

curve = oxygen_dissociation_curve(p50_mmHg=26.0, n_points=8)

print(round(curve[4].saturation, 3))
```

Clinical / systems note: Pulse oximeters estimate SpO₂ along the same saturation curve; right shifts from fever or acidosis explain why patients can be “happy hypoxaemic” until they abruptly decompensate.

31.17 Current Evidence and Frontier Biology: Circulation and Respiration

For Circulation and Respiration, frontier biology belongs inside the evidence logic of the chapter. Physiology now blends mechanism with allostasis, immune-endocrine-neural coupling, wearable data, and individualized risk without reducing bodies to simple machines. The core reading question is this: homeostasis claims should connect flow, diffusion, control loops, reserve capacity, and measurement limits.

- What to verify: identify the observation, model, assay, or dataset that would make the claim stronger or weaker.
- What to qualify: state the scale, organism, cell type, environmental condition, or population where the claim is expected to hold.
- What to compare: test at least one alternative explanation, baseline, or null model before treating the pattern as causal.
- What to cite: distinguish primary evidence, review synthesis, public dataset, and institutional guidance; for recent or numeric claims, prefer the source closest to the measurement and state what has changed since it was published.

Interpret circulation and gas-exchange data by separating baseline set point, perturbation, compensation, and the threshold where compensation fails.

Source practice: For cardiorespiratory claims, cite measurement context, pressure or flow conditions, saturation data, and treatment evidence when relevant.

31.18 Summary

- Cardiovascular evolution: Open to closed; 2-chamber (fish) to 4-chamber (mammals/birds). Complete separation enables high-pressure systemic and low-pressure pulmonary circuits.
- Cardiac cycle: SA node (pacemaker) to AV node (delay) to bundle of His to Purkinje fibers. ECG: P (atrial), QRS (ventricular depolarization), T (repolarization). Starling’s law matches SV to preload.
- Cardiac output: $CO = HR \times SV$; about 5 L/min at rest. Regulated by sympathetic (β_1), parasympathetic (M_2), and Starling mechanism.
- Blood flow: Poiseuille’s law ($Q \propto r^4$); arteriolar tone is the key regulator. Local autoregulation (myogenic, metabolic, endothelial NO) and neural/hormonal control.
- O₂ transport: Hb cooperatively binds O₂ (Hill equation; n about 2.7; P₅₀ about 26 mmHg). Bohr effect unloads O₂ in metabolically active tissues. Haldane effect facilitates CO₂ transport.
- CO₂ transport: 65% as bicarbonate (carbonic anhydrase), 27% carbaminohaemoglobin, 8% dissolved.
- Ventilation: Diaphragm contraction creates negative intrapulmonary pressure. Surfactant prevents alveolar collapse. FEV₁/FVC ratio distinguishes obstructive from restrictive disease.
- Gas exchange: Fick’s law governs diffusion across the alveolar-capillary membrane (70 m² surface area, 0.5 μ m thickness).
- Respiratory control: Medullary DRG/VRG generate rhythm. Central chemoreceptors (H⁺/CO₂ in CSF) are the primary driver; peripheral chemoreceptors (carotid/aortic bodies) detect PO₂.
- Homeostasis: Negative feedback dominates. Thermoregulation via hypothalamus (vasomotor, sweating, shivering, BAT). Fluid balance via RAAS, ADH, aldosterone, ANP.
- Connections: See section 32 and section 33 for neural control of breathing and autonomic output, section 11 for metabolic heat load, and section 2 for blood osmolarity.

31.19 Key Terms

Table 378. Fluid and Electrolyte Homeostasis: Term and Definition.

Term	Definition
Cardiac output (CO)	Volume of blood pumped per minute; $CO = HR \times SV$
Stroke volume (SV)	Volume ejected per heartbeat; about 70 mL at rest
Frank-Starling law (equation (373))	Increased preload (EDV) causes increased SV
Poiseuille’s law	$Q = \pi r^4 \Delta P / (8 \eta L)$; flow depends on radius to the 4th power
Mean arterial pressure	$MAP = DP + 1/3(SP - DP)$; about 93 mmHg normally
Hemoglobin	$\alpha_2\beta_2$ tetramer; cooperative O ₂ binding; 4 haeme groups
Bohr effect	Rightward shift of O ₂ -Hb curve with decreased pH / increased CO ₂
Haldane effect	Deoxygenated Hb binds CO ₂ and H ⁺ more readily than oxygenated Hb
P ₅₀	PO ₂ at 50% Hb saturation; about 26 mmHg for adult HbA
Surfactant	DPPC from Type II pneumocytes; reduces alveolar surface tension
FEV ₁ /FVC	Spirometric ratio interpreted against the age-dependent lower limit of normal; obstruction lowers the ratio, while restriction usually preserves or raises it with reduced absolute volumes

Term	Definition
Chemoreceptors	Central (medullary, respond to H^+/CO_2) and peripheral (carotid/aortic, respond to PO_2)
Homeostasis	Maintenance of stable internal environment via negative feedback
RAAS	Renin-Angiotensin-Aldosterone System; restores blood pressure and volume
UCP1	Uncoupling protein 1 in brown adipose tissue; generates heat
ADH (vasopressin)	Posterior pituitary hormone; inserts aquaporin-2 in collecting duct

31.20 Review Questions

1. A patient’s ECG shows a prolonged PR interval (0.28 s) but normal QRS complexes. Name the type of heart block and explain which structure in the conduction system is likely affected.
2. Using the Hill equation with $P_{50} = 26$ mmHg and $n = 2.7$, calculate SO_2 at $PO_2 = 100$ mmHg (arterial) and $PO_2 = 40$ mmHg (venous). What is the O_2 extraction ratio?
3. Explain why CO_2 diffuses 20 times faster than O_2 across the alveolar-capillary membrane despite having a similar molecular weight. What property accounts for this difference?
4. An arteriole supplying skeletal muscle constricts from radius 50 μm to 40 μm . Using Poiseuille’s law, calculate the fold-change in blood flow (assume most other variables constant). Why does this make arteriolar tone the dominant regulator of organ blood flow?
5. A mountain climber at 5,500 m altitude breathes air with $PO_2 = 75$ mmHg. Describe the acute and chronic compensatory responses involving the respiratory system, cardiovascular system, and blood.
6. Compare central and peripheral chemoreceptors in terms of location, stimulus, and response latency. Why is the central chemoreceptor considered the primary driver of normal ventilation?
7. Explain why administering high-flow oxygen to a patient with chronic COPD and CO_2 retention could suppress their ventilatory drive. What is the safer approach?
8. A patient with diabetes insipidus produces 15 L of dilute urine per day. Explain the molecular defect (central vs nephrogenic), and describe how ADH normally regulates water reabsorption at the molecular level.
9. During intense exercise, skeletal muscle produces large amounts of CO_2 , H^+ , and heat. Explain how each of these factors enhances O_2 delivery to the exercising muscle via the Bohr effect.
10. Compare shivering thermogenesis and non-shivering thermogenesis (BAT/UCP1) in terms of mechanism, efficiency, tissue involved, and developmental significance.
11. A 45-year-old patient with nephrotic syndrome (severe proteinuria, serum albumin 1.8 g/dL) presents with bilateral pitting edema to the knees. Using the Starling equation, explain: (a) why plasma oncotic pressure is reduced; (b) how this shifts the net filtration pressure at both arteriolar and venular capillary ends; (c) why the edema is pitting rather than non-pitting. How does treatment with albumin infusion immediately reduce edema?
12. Using Fick’s law, predict what happens to alveolar O_2 diffusion in: (a) a patient with idiopathic pulmonary fibrosis where membrane thickness doubles and surface area halves; (b) a healthy person exercising at altitude (4,000 m, alveolar $PO_2 = 60$ mmHg, tissue $PO_2 = 30$ mmHg). Which is more likely to cause frank hypoxaemia at rest vs exercise?

31.21 Further Reading and Source Notes: Circulation and Respiration

- Starling (1918). The Linacre Lecture on the Law of the Heart. *Longmans, Green and Co.*.
- Cannon (1932). *The Wisdom of the Body*. W. W. Norton.
- Bohr, Hasselbalch & Krogh (1904). The Bohr effect: influence of carbon dioxide on the oxygen dissociation of blood. *Scandinavian Archives of Physiology*, 16.
- Perutz (1970). Stereochemistry of cooperative effects in hemoglobin. *Nature*, 228.
- West (2012). *Respiratory Physiology: The Essentials* (9th ed.). Lippincott Williams & Wilkins.

31.22 Companion Source Module: Circulation and Respiration

Circulation and Respiration should leave a reproducible trail from a biological claim to the code, figure, diagram, or paper-based activity that can test it. Use the surfaces below to inspect the chapter’s assumptions, rerun the relevant model, or compare the manuscript explanation with companion labs and figures.

Table 379. Companion source surfaces for Circulation and Respiration.

Surface	Use it for
src/biology/physiology/physiology.py (poiseuille_flow, oxygen_saturation, oxygen_dissociation_curve, homeostasis_response)	Reproduce flow, gas transport, and regulatory response claims.
src/visualization/plots.py (plot_oxygen_dissociation)	Inspect shifts in oxygen loading and unloading.

Reproducibility check: state vessel radius, pressure gradient, hemoglobin state, tissue demand, and feedback variable before interpreting homeostasis. Cross-reference: connect with sections 34 and 35 and section 9.

32 Nervous System and Neural Signaling

Level 3/3 · 55 min read · 75 min lecture · Prerequisites: section 31

32.1 Learning Objectives

1. Describe the organization of the vertebrate nervous system (CNS, PNS) and the roles of glial cells.
2. Explain **neuron** structure and classify neuron types by function and morphology.
3. Analyze how the **axon hillock** integrates competing excitatory and inhibitory synaptic inputs to determine whether the neuron fires.
4. Describe graded potentials, synaptic summation, and how the **axon hillock** integrates inputs.
5. Compare the sympathetic and parasympathetic divisions of the autonomic nervous system.
6. Describe the major brain regions and their functions.
7. Describe sensory systems and neural plasticity.
8. Calculate the resting membrane potential from ion concentrations and relative permeabilities using the Goldman-Hodgkin-Katz equation.
9. Predict the direction and approximate magnitude of the V_m shift produced by a stated change in K^+ permeability.

32.1.1 Study Blueprint

- Big idea: Nervous systems compute with cells whose structure shapes information flow and behavior.
- Core concepts: neurons, glia, circuits, sensory processing.
- Framework alignment: Vision & Change: Structure and function, Systems; AP Biology: Systems Interactions, Energetics; NGSS-style topics: Structure and Function.
- Model or quantitative lens: Cable-length, conduction, and simple circuit calculations.
- Data skill: Interpret neural data from anatomy, timing, or lesion evidence.
- Practice cadence: Visual Representations, Statistical Tests and Data Analysis, Argumentation.
- Common misconception to repair: The brain is not only neurons; glia and circuit context are essential to function.
- Primary lab: **Lab — Nervous System and Neural Signaling**.
- Question bank: **Questions — Nervous System and Neural Signaling**.
- Transfer task: Transfer circuit reasoning to reflexes, sensory systems, learning, and disease.
- Bridge to computation: `biology.neuroscience.neuroscience.cable_voltage_attenuation`.

Opening Vignette — The Reflex That Revealed the Synapse

In 1897, Charles Scott Sherrington coined the word “synapse” — from the Greek for “clasp” — to describe the morphological gap between neurons. Over four decades, working with decerebrate cats and dogs whose spinal cord reflexes could be studied in isolation, Sherrington showed that reflexes were not simple mechanical responses but involved integration: competing signals converged on motor neurons, inhibiting some pathways while exciting others, with the outcome depending on the algebraic summation of hundreds of inputs. His 1906 masterwork, *The Integrative Action [Sherrington, 1906] of the Nervous System*, established the principles of convergence, divergence, summation, inhibition, and the motor neuron as the “final common pathway.” The electrical basis of these phenomena — **action potentials**, EPSPs, IPSPs — was not known until Hodgkin, Huxley, and Eccles worked it out in the 1950s. Sherrington and Adrian shared the 1932 Nobel Prize; Eccles, Hodgkin, and Huxley shared the 1963 Nobel Prize. The synapse Sherrington named launched two Nobel Prizes’ worth of discoveries.

32.2 Nervous System Organization Across Cells, Circuits, and Regions

The human nervous system comprises approximately 86 billion neurons and about 85 billion non-neuronal cells (Azevedo et al., 2009). It is organized hierarchically into two major divisions.

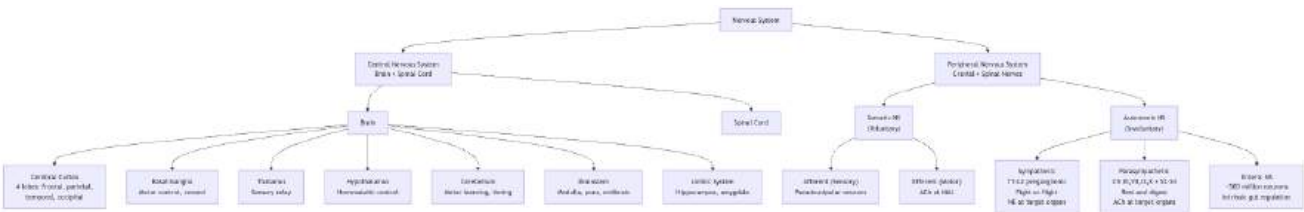


Figure 193. Organization of the vertebrate nervous system. The CNS (brain and spinal cord) integrates information. The PNS (somatic and autonomic divisions) connects the CNS to the body. The autonomic NS has sympathetic, parasympathetic, and enteric subdivisions.

- Blood-brain barrier (BBB): Tight junctions between endothelial cells + astrocyte endfeet
- Three meningeal layers: dura mater (tough outer), arachnoid mater (middle; CSF-filled subarachnoid space), pia mater (thin; adheres to brain surface)
- Bone: Cranium and vertebral column

Peripheral nervous system (PNS): Most nervous tissue outside the CNS. Includes 12 cranial nerves and 31 spinal nerve pairs.

32.3 Neuron Types and Structure

32.3.1 Neuron Classification by Function and Morphology

By function: - Sensory (afferent) neurons: Carry information from sensory receptors toward CNS. Most are pseudounipolar (cell body off to one side of a single process that bifurcates). - Motor (efferent) neurons: Carry commands from CNS to effectors (muscles, glands). Multipolar with long axons. - Interneurons: Integration and processing within the CNS. Most numerous (about 99% of neurons). Diverse morphologies.

By morphology: - Multipolar: Multiple dendrites + one axon (most CNS neurons, most motor neurons) - Bipolar: One dendrite + one axon (retinal bipolar cells, olfactory receptor neurons) - Pseudounipolar: Single process that splits into peripheral and central branches (most sensory neurons in DRG) - Anaxonic: No distinguishable axon (amacrine cells of retina; some interneurons)

32.3.2 Neuron Structure from Dendrites to Axon Terminals

A typical neuron comprises:

- Soma (cell body): Contains nucleus, rough ER (Nissl substance), Golgi apparatus. Site of most protein synthesis and metabolic activity. Diameter: 5-100 um.
- Dendrites: Receive synaptic inputs. Dendritic spines (0.5-2 um protrusions) increase surface area and compartmentalise Ca²⁺ signals. A single cortical pyramidal neuron may have 10,000-30,000 dendritic spines.
- Axon hillock: Junction between soma and axon. Highest density of voltage-gated Na⁺ channels (about 800-1200/um²). Lowest threshold for action potential initiation. The “decision-making” node.
- Axon: Signal conduction pathway. Myelinated or unmyelinated. Can extend >1 m (motor neurons to foot muscles). Axoplasmic transport: fast anterograde (kinesin, 200-400 mm/day for vesicles), slow anterograde (0.5-5 mm/day for cytoskeletal proteins), fast retrograde (dynein, 200-300 mm/day for recycled materials and trophic signals).
- Axon terminal (bouton): Contains synaptic vesicles (40-50 nm diameter, each containing about 5,000-10,000 neurotransmitter molecules). Active zone: specialized region of presynaptic membrane where vesicles dock and fuse.

32.4 Glial Cells and Neural Support Functions

Table 380. Neuron Structure from Dendrites to Axon Terminals: Glial type and Location.

Glial type	Location	Key functions
Astrocytes	CNS	Metabolic support (lactate shuttle to neurons); BBB construction; K ⁺ spatial buffering; glutamate-glutamine recycling; tripartite synapse (modulate synaptic transmission); scar formation after injury
Oligodendrocytes	CNS	Myelination (one cell can myelinate segments on up to 50 axons simultaneously)
Schwann cells	PNS	Myelination (one cell per axon segment, about 1 mm internode); nerve repair via Bands of Bungner
Microglia	CNS	Resident macrophages; synaptic pruning (complement C1q/C3-tagged synapses phagocytosed); neuroinflammation; activated in Alzheimer’s, TBI, MS
Ependymal cells	CNS	Line ventricles; ciliated surface moves CSF; produce CSF (together with choroid plexus; 450-500 mL/day; total CSF volume about 150 mL, replaced about 3 times/day)

Glial type	Location	Key functions
Radial glia	Developing CNS	Neural stem cells; scaffold for neuronal migration (inside-out cortical layering); give rise to both neurons and glia
Satellite cells	PNS	Surround cell bodies in ganglia; analogous to astrocytes

Modern brain-cell atlases turn this table into a data problem rather than a final classification. The NIH BRAIN Initiative reported a 2023 whole-mouse-brain atlas covering more than 32 million cells, and the companion Nature atlas organized about 4.0 million quality-controlled single-cell transcriptomes plus spatial MERFISH data into 34 classes, 338 subclasses, 1,201 supertypes, and 5,322 clusters [National Institute of Mental Health, 2023, Yao et al., 2023]. Those categories are powerful reference maps, but they remain release- and method-dependent: a cell type claim should state the atlas, species, region, assay, and annotation level.

Clinical Connection: Microglia-mediated synaptic pruning is essential during development (eliminating about 50% of synapses during adolescence). Dysregulated pruning has been linked to schizophrenia: the complement component C4A gene is the strongest genetic risk factor for schizophrenia (Sekar et al., 2016, Nature). Individuals with high C4A expression show excessive synaptic pruning in prefrontal cortex during adolescence, correlating with symptom onset.

32.4.1 Astrocytes — More Than Glue

Astrocytes were once considered passive support cells but are now recognized as active partners in synaptic transmission, brain metabolism, and homeostasis. A single cortical astrocyte contacts about 100,000–2,000,000 synapses through its fine processes (“perisynaptic astrocyte processes” or PAPs) — forming the third element of the tripartite synapse (presynaptic terminal + postsynaptic spine + astrocyte process).

Key astrocyte functions:

- **K⁺ spatial buffering:** Following synaptic activity, extracellular K⁺ rises locally. Astrocytes express high densities of inwardly-rectifying Kir4.1 channels and aquaporin-4 (AQP4) at endfeet on capillaries. K⁺ enters astrocytes locally and exits at sites of low K⁺ via the panastrocytic syncytium (gap junctions formed by connexin 43/30) — preventing extracellular K⁺ accumulation that would depolarize neurons and disrupt firing.
- **Glutamate clearance:** EAAT1 and EAAT2 transporters (the “glutamate-aspartate transporters”) on astrocytes clear about 90% of synaptically released glutamate. EAAT2/GLT-1 dysfunction is implicated in ALS (mutations) and excitotoxicity in stroke.
- **Glutamate-glutamine cycle:** Astrocytes convert glutamate to glutamine via glutamine synthetase, then export glutamine to neurons, where neurons re-convert it back to glutamate via glutaminase. This metabolically traps glutamate within neurons (glutamate is itself a metabolic intermediate that cannot be allowed to accumulate in extracellular space).
- **Astrocyte-neuron lactate shuttle:** Astrocytes preferentially perform glycolysis (express PFK1 and LDH-A) and export lactate. Active neurons take up lactate via MCT2 and use it as a major energy substrate during sustained activity. This “ANLS hypothesis” (Pellerin and Magistretti, 1994) explains the glucose-lactate metabolic coupling underlying fMRI BOLD signals.
- **Gliotransmission:** Activated astrocytes release glutamate, ATP, D-serine (an NMDA receptor co-agonist), and other transmitters via Ca²⁺-dependent vesicle exocytosis or channel-mediated release — modulating synaptic transmission and plasticity.
- **Reactive astrogliosis:** After CNS injury, astrocytes hypertrophy, upregulate GFAP, and form glial scars. This both contains damage and inhibits axonal regeneration (chondroitin sulfate proteoglycans). Modulating reactive astrogliosis is a target for spinal cord injury therapeutics.

32.4.2 Oligodendrocytes and Myelin

Oligodendrocytes wrap layers of plasma membrane around axons in the CNS. A single oligodendrocyte myelinates segments on up to 50 different axons simultaneously (contrast with Schwann cells in PNS: one cell, one axon). The myelin sheath is up to 100 layers thick, formed by repeated wrapping with extrusion of cytoplasm. The major proteins are: - Myelin basic protein (MBP): Compaction of cytoplasmic faces. Major autoantigen in multiple sclerosis. - Proteolipid protein (PLP): Compaction of extracellular faces. Mutations cause Pelizaeus-Merzbacher disease. - Myelin oligodendrocyte glycoprotein (MOG): Outer surface; minor protein but major autoantigen in some demyelinating diseases (e.g., MOG antibody disease).

Myelin development continues into the third decade of life, particularly in prefrontal cortex — coinciding with maturation of executive function. Adult oligodendrocyte progenitor cells (OPCs, NG2+ cells) maintain a regenerative capacity, but it is incomplete after demyelinating injury.

32.4.3 Microglia — Resident Macrophages of the CNS

Microglia derive from yolk-sac primitive macrophages that colonised the developing CNS before formation of the blood-brain barrier. They are self-renewing (independent of blood monocytes) and constitute about 10% of CNS cells.

States and functions:

- Resting (surveillance): Highly ramified processes constantly sample the parenchyma; turnover of most brain volume every few hours.
- Activated (M1-like, pro-inflammatory): Upon detection of pathogens (TLR ligands), tissue damage (DAMPs: ATP, HMGB1), or aggregated proteins ($A\beta$, α -synuclein) — retract processes, become amoeboid, secrete $TNF-\alpha$, $IL-1\beta$, $IL-6$, NO ; phagocytose debris.
- Alternatively activated (M2-like, repair): Secrete $IL-10$, $TGF-\beta$; promote tissue repair.
- Synaptic pruning: Microglia tag underused synapses with complement ($C1q \rightarrow C3$) for phagocytic engulfment. Critical during development; pathological in Alzheimer’s (excessive pruning in hippocampus) and schizophrenia (excessive pruning in prefrontal cortex during adolescence).

32.4.4 Blood-Brain Barrier — Molecular Architecture

The blood-brain barrier (BBB) is a selective barrier between blood and brain parenchyma that excludes most polar molecules, ions, large molecules, and pathogens, while allowing essential nutrients to enter. It is formed by:

1. Tight junctions between brain capillary endothelial cells, sealed by claudin-5, occludin, JAM-1, and zonula occludens (ZO-1, ZO-2). Transendothelial electrical resistance is about $1500\ \Omega\cdot cm^2$ — orders of magnitude higher than peripheral capillaries (about $10\ \Omega\cdot cm^2$).
2. Pericytes ensheathing the abluminal endothelial surface — regulate capillary diameter, BBB integrity, and angiogenesis.
3. Astrocyte endfeet with AQP4 channels — form a near-continuous covering of capillaries and signal to maintain endothelial tight junction integrity.
4. Basement membrane between endothelial cells and astrocyte endfeet.

Transport mechanisms across the BBB:

- Diffusion: Small lipophilic molecules (O_2 , CO_2 , ethanol, anaesthetics) cross freely.
- Carrier-mediated transport: GLUT1 (glucose); LAT1 (large neutral amino acids — competition explains why high-protein meals can affect L-DOPA delivery); MCT1 (lactate, ketone bodies).
- Receptor-mediated transcytosis: Insulin, transferrin (iron), leptin — receptors mediate endocytosis on the luminal side and exocytosis on the abluminal side. This is exploited to deliver therapeutics: a “Trojan horse” strategy fuses drugs to anti-transferrin-receptor antibodies.
- Active efflux pumps: P-glycoprotein (P-gp/ABCB1) and BCRP/ABCG2 on the luminal surface actively pump substrates back into blood. Many lipophilic drugs that should enter the brain by passive diffusion are pumped out — explaining the limited brain penetration of many chemotherapies and the role of P-gp polymorphisms in inter-individual drug response.

BBB-bypassing structures (circumventricular organs): Subfornical organ, area postrema (chemotrigger zone), median eminence, neurohypophysis, OVLT, pineal gland — lack tight junctions and have fenestrated capillaries to allow hormones and circulating signals to reach specialized neurons (e.g., AT_1 on subfornical neurons \rightarrow thirst).

Clinical Connection: BBB breakdown contributes to many CNS diseases. In multiple sclerosis, autoreactive T cells must first cross the BBB (via VLA-4/VCAM-1 interaction); the monoclonal antibody natalizumab blocks VLA-4 and dramatically reduces relapses. In Alzheimer’s, BBB pericyte dysfunction precedes overt neurodegeneration. In ischemic stroke, BBB breakdown produces vasogenic edema and hemorrhagic transformation. Pharmacologically, the BBB is the major obstacle to CNS drug delivery — about 2% of small molecules and 0% of biologics readily cross.

32.5 Resting Membrane Potential

32.5.1 Ion Distribution and the Nernst Equation

The resting membrane potential (about -70 mV) arises from unequal ion distributions maintained by the Na^+/K^+ -ATPase and selective membrane permeability. Typical neuronal ion concentrations:

Table 381. Ion Distribution and the Nernst Equation: Ion and Intracellular (mM).

Ion	Intracellular (mM)	Extracellular (mM)	Equilibrium Potential
K^+	140	5	-89 mV
Na^+	12	145	$+67\text{ mV}$
Cl^-	7	110	-74 mV
Ca^{2+}	0.0001	2	$+132\text{ mV}$

Nernst equation for a single ion:

$$E_X = \frac{RT}{zF} \ln \frac{[X]_o}{[X]_i} = \frac{61.5\text{ mV}}{z} \log_{10} \frac{[X]_o}{[X]_i} \quad (\text{at } 37^\circ\text{C})$$

(392)

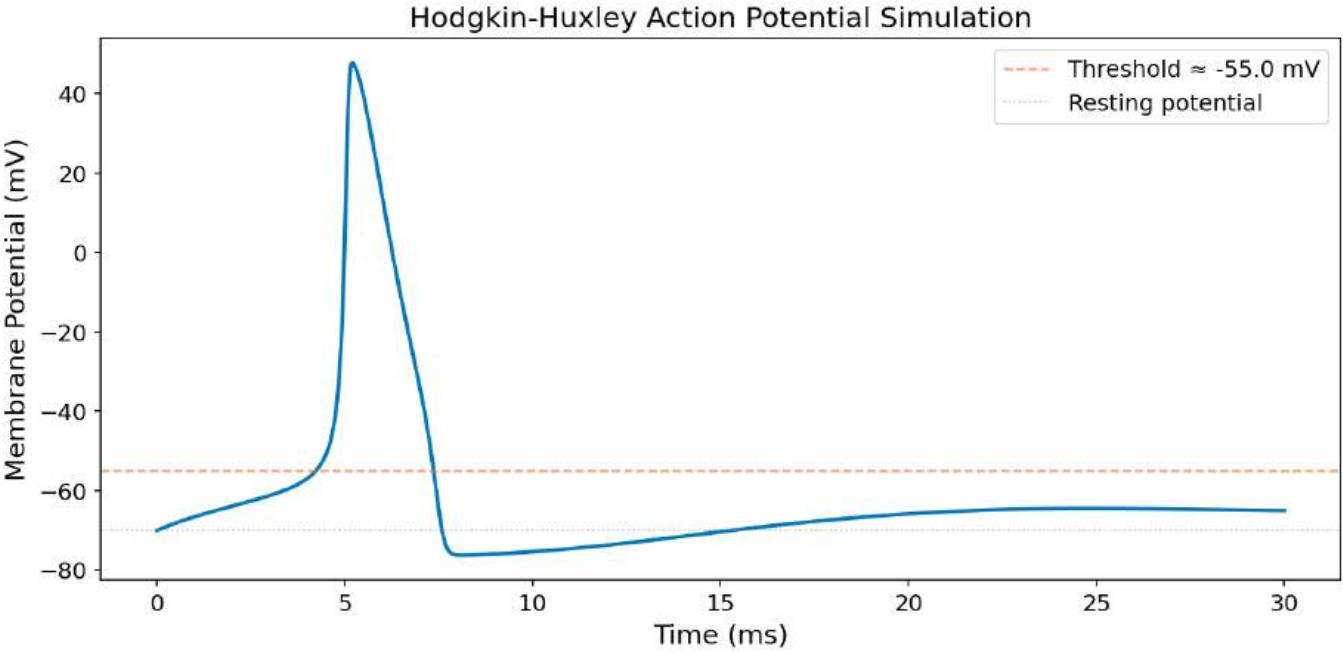


Figure 194. Hodgkin–Huxley action-potential simulation showing a simulated membrane-voltage trace crossing threshold, spiking, and returning through after-hyperpolarisation as voltage-gated conductances change.

32.5.2 Goldman-Hodgkin-Katz (GHK) Equation

The **resting potential** is a weighted average of equilibrium potentials, determined by relative membrane permeability to each ion:

$$V_m = \frac{RT}{F} \ln \frac{P_K[K^+]_o + P_{Na}[Na^+]_o + P_{Cl}[Cl^-]_i}{P_K[K^+]_i + P_{Na}[Na^+]_i + P_{Cl}[Cl^-]_o}$$

(393)

At rest, $P_K : P_{Na} : P_{Cl} \approx 1 : 0.04 : 0.45$, giving $V_m \approx -68$ mV.

The resting potential is dominated by K^+ (highest resting conductance via KCNK leak channels). The Na^+/K^+ -ATPase (3 Na^+ out, 2 K^+ in per ATP) is electrogenic, contributing about -3 mV directly, but its main role is maintaining the concentration gradients.

Concept Check: If you suddenly doubled the extracellular K^+ concentration from 5 mM to 10 mM, what would happen to E_K and the resting membrane potential? Calculate using the Nernst equation.

32.6 Cable Properties and Passive Signal Spread

Before a graded potential can trigger an action potential at the axon hillock, it must travel electrotonically from the synapse. This passive spread is governed by the cable properties of the dendrite, modeled as a leaky electrical cable.

32.6.1 Length Constant (λ) and Spatial Attenuation

The space constant (or length constant) λ determines how far a steady-state voltage change spreads along a dendrite or axon:

$$\lambda = \sqrt{\frac{r_m}{r_i}}$$

(394)

where r_m = membrane resistance per unit length ($\Omega \cdot \text{cm}$) and r_i = axial (cytoplasmic) resistance per unit length (Ω/cm).

$$V(x) = V_0 e^{-x/\lambda}$$

(395)

At distance $x = \lambda$, the voltage has decayed to $V_0/e \approx 37\%$ of its peak value.

Typical values:

Table 382. Length Constant (λ) and Spatial Attenuation: Structure and Diameter (μm).

Structure	Diameter (μm)	λ (mm)	Implication
Thin dendrite	0.5	about 0.1–0.2	Distal synapses attenuate strongly before reaching soma
Large dendrite	5	about 0.5–1.0	Better passive integration
Squid giant axon	500	about 5–7	Enables long-distance spread in unmyelinated axon
Myelinated axon	10	about 2–5	Myelin increases r_m , dramatically increasing λ

Key determinants of λ : - Myelin increases r_m about 100-fold (reduces current leak) $\rightarrow \lambda$ increases about 10-fold - Larger diameter reduces r_i (more conducting cross-section) $\rightarrow \lambda$ increases - GABA_A receptor activation opens Cl^- channels, reducing $r_m \rightarrow \lambda$ decreases — a quantitative mechanism for shunting inhibition (nearby inhibitory synapses drastically reduce the effective length constant, terminating EPSP integration before reaching the hillock)

32.6.2 Time Constant (τ_m)

The membrane time constant determines how fast the membrane voltage changes in response to a current:

$$\tau_m = r_m \cdot C_m$$

(396)

where $C_m \approx 1 \mu\text{F}/\text{cm}^2$ (specific membrane capacitance — nearly constant across cell types). Typical $\tau_m \approx 10\text{--}20 \text{ ms}$ for neurons.

$$V(t) = V_\infty (1 - e^{-t/\tau_m}) \quad (\text{voltage rising in response to a step current}) \tag{397}$$

Significance: τ_m governs the time window for temporal summation in neuronal membrane integration. If two EPSPs arrive within τ_m of each other at the same synapse, the second EPSP begins before the membrane has fully repolarized from the first, and the **depolarizations** summate.

32.7 Worked Example: Dendritic Length Constant

A cortical pyramidal neuron has $r_m = 40,000 \Omega\cdot\text{cm}$ and $r_i = 200 \Omega/\text{cm}$ for a typical basal dendrite (diameter about $1 \mu\text{m}$). What is the length constant?

$$\lambda = \sqrt{\frac{40,000}{200}} = \sqrt{200} \approx 14.1 \text{ cm?} \tag{398}$$

Wait — the formula uses *specific* membrane resistance per unit length for a cylinder. For a dendrite of radius a :

$$r_m(\text{per unit length}) = \frac{R_m}{2\pi a}, \quad r_i(\text{per unit length}) = \frac{R_i}{\pi a^2} \tag{399}$$

where R_m = specific membrane resistance (about $20,000 \Omega\cdot\text{cm}^2$) and R_i = cytoplasmic resistivity (about $100 \Omega\cdot\text{cm}$). For $a = 0.5 \mu\text{m} = 0.5 \times 10^{-4} \text{ cm}$:

$$r_m = \frac{20,000}{2\pi \times 5 \times 10^{-5}} \approx 6.37 \times 10^7 \Omega/\text{cm} \tag{400}$$

$$r_i = \frac{100}{\pi \times (5 \times 10^{-5})^2} \approx 1.27 \times 10^{10} \Omega/\text{cm} \tag{401}$$

$$\lambda = \sqrt{\frac{r_m}{r_i}} = \sqrt{\frac{6.37 \times 10^7}{1.27 \times 10^{10}}} = \sqrt{0.00501} \approx 0.071 \text{ cm} = 0.71 \text{ mm} \tag{402}$$

This means a synapse on a thin distal dendrite 1.4 mm from the soma delivers primarily $e^{-2} \approx 13.5\%$ of its peak voltage to the hillock — illustrating how dendritic location profoundly affects synaptic efficacy, and why proximal synapses (closer to the hillock) have disproportionate influence.

Clinical Connection: Peripheral neuropathy (e.g., from diabetes, chemotherapy, or Guillain-Barré syndrome) reduces r_m in peripheral axons by disrupting myelin or causing axonal damage. The resulting decrease in λ causes voltage signals to decay faster along the axon, slowing conduction and reducing EPSP efficacy at nerve-muscle junctions — producing the characteristic distal-to-proximal weakness and sensory loss of a length-dependent neuropathy.

32.7.1 Worked Example: EPSP Attenuation from Distal vs Proximal Synapses

Problem: A pyramidal-cell dendrite has length constant $\lambda \approx 200 \mu\text{m}$. A glutamatergic synapse fires, producing a local EPSP of $V_0 = 5 \text{ mV}$ at the synaptic site. Compute the EPSP amplitude that arrives at the axon hillock under three placement scenarios and rank them by impact on threshold.

Setup. Passive electrotonic decay along a uniform cable obeys $V(x) = V_0 e^{-x/\lambda}$.

Case A — Distal dendritic synapse, $x = 400 \mu\text{m}$:

$$V(400) = 5 \cdot e^{-400/200} = 5 \cdot e^{-2} = 5 \cdot 0.135 \approx 0.68 \text{ mV}$$

Case B — Mid-dendritic synapse, $x = 200 \mu\text{m}$:

$$V(200) = 5 \cdot e^{-1} = 5 \cdot 0.368 \approx 1.84 \text{ mV}$$

Case C — Proximal synapse, $x = 50 \mu\text{m}$:

$$V(50) = 5 \cdot e^{-0.25} = 5 \cdot 0.779 \approx 3.89 \text{ mV}$$

Solution and interpretation:

1. Per-synapse efficacy at the hillock. Proximal $\approx 5.7\times$ more effective than distal in driving the hillock toward threshold, for an identical local EPSP amplitude.
2. Spatial summation arithmetic. Five distal synapses firing simultaneously deliver $5 \times 0.68 \approx 3.4 \text{ mV}$ — still less than a *single* proximal synapse at $50 \mu\text{m}$. Five proximal synapses deliver $5 \times 3.89 \approx 19.5 \text{ mV}$ — enough by itself to cross a 15 mV threshold gap (from -70 to -55 mV).
3. Active boosting. Real dendrites are not purely passive: dendritic Na^+ and NMDA-receptor-mediated regenerative spikes can boost distal EPSPs locally, partly compensating for electrotonic loss. Boosting is gated by prior depolarization, so distal inputs that arrive *after* proximal inputs benefit more than ones arriving first — the basis of a fast/slow coincidence-detection scheme in cortical pyramidal cells.

Take-home. Two synapses of identical molecular composition can differ by an order of magnitude in their influence on the spike output of the same neuron, purely because of where they sit on the dendritic tree. Synaptic location is a tuning parameter — and dendritic geometry is a cheap, slow form of plasticity that operates on developmental timescales.

32.8 Graded Potentials and Synaptic Integration

32.8.1 Graded Potentials and Local Voltage Changes

Excitatory postsynaptic potentials (EPSPs): Depolarizing events (typically caused by Na^+ or mixed cation influx through ionotropic receptors like AMPA). Amplitude proportional to stimulus strength. Decay with distance (electrotonic spread governed by the length constant λ).

Inhibitory postsynaptic potentials (IPSPs): Hyperpolarising events (Cl^- influx through GABA_A receptors or K^+ efflux through GABA_B -activated K^+ channels).
Shunting inhibition: even if IPSP does not change V_m much, opening Cl^- channels increases membrane conductance, reducing the effectiveness of nearby EPSPs.

32.8.2 Summation at the Axon Hillock

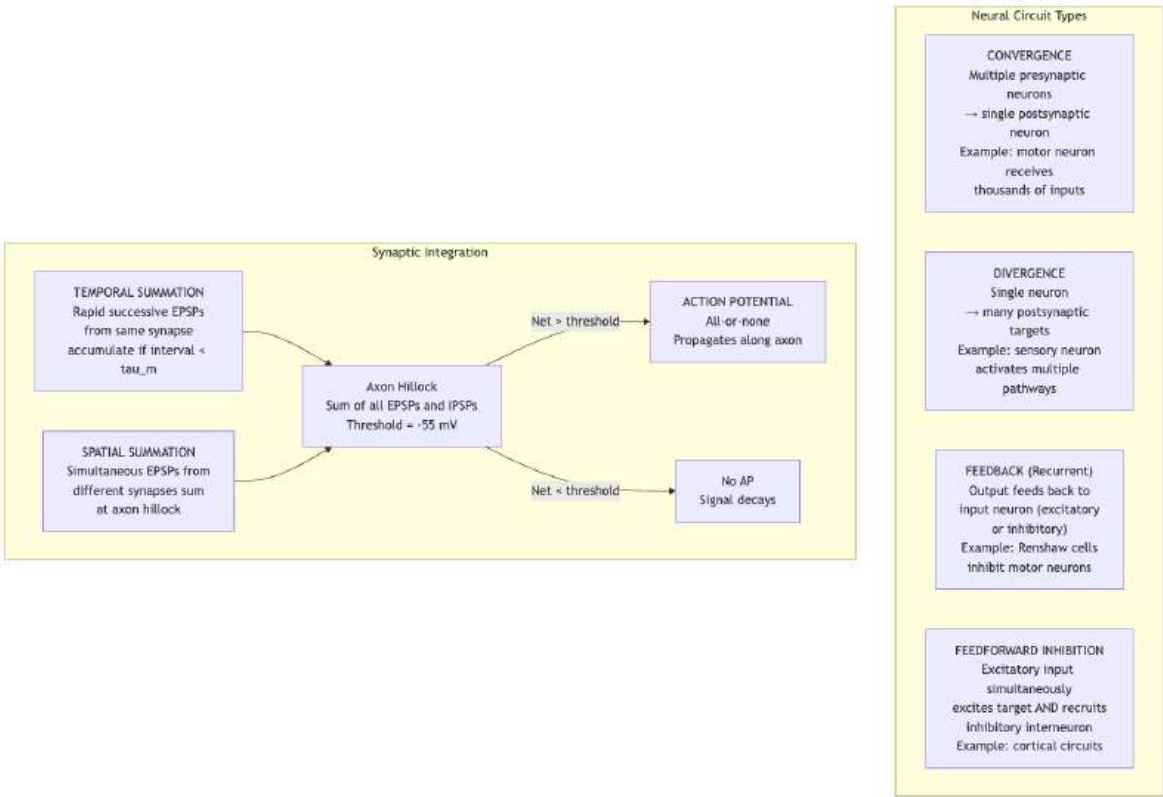


Figure 195. Neural circuit types and synaptic integration. Convergence allows integration of multiple inputs; divergence allows signal distribution. At the axon hillock, temporal and spatial summation of EPSPs and IPSPs determine whether threshold is reached.

If the net depolarization at the axon hillock exceeds threshold (about -55 mV), an most-or-none action potential is generated, with the stereotyped Na^+ - and

K⁺-driven waveform of rise, peak, and hyperpolarization shown in figure 194. The axon hillock has the highest density of Nav1.2 and Nav1.6 channels, making it the lowest-threshold site.

Strategic placement of inhibition: Inhibitory synapses (GABA_A) are preferentially located on the soma and proximal dendrites, positioned to maximally dampen axon hillock depolarization.

Concept Check (Analyze) — Axon hillock integration and AIS biophysics. The axon initial segment (AIS) concentrates Nav1.6 channels at densities about 50-fold above the soma, placing the spike-initiation threshold near −55 mV. (a) Compute the net depolarization delivered to the AIS by *five* proximal EPSPs of 4 mV each vs. *five* distal EPSPs of 4 mV each that have attenuated to ~ 0.7 mV by the time they reach the AIS (use the cable-theory result above). Which configuration crosses a 15 mV threshold gap from −70 mV? (b) A myelin-associated glycoprotein (MAG) mutation reported in human peripheral neuropathy shortens the AIS by approximately 30%. Predict the directional effect on Nav1.6 channel number, spike-initiation threshold, and high-frequency firing fidelity. (c) Distinguish two failure modes — *increased excitability* (more spontaneous spikes) and *decreased fidelity* (broken phase-locking at > 100 Hz) — and identify which is more clinically disabling for a motor neuron driving rapid finger movements.

Concept Check (Evaluate) — Astrocyte glutamate handling, ischemia, and excitotoxicity. Astrocytes terminate excitatory synaptic transmission by clearing glutamate via the electrogenic transporter GLT-1 (EAAT2), which couples one glutamate uptake to the inward movement of three Na⁺ and one H⁺ and the outward movement of one K⁺. Glutamate is then converted to glutamine by glutamine synthetase and shuttled back to neurons. (a) Compute the energetic cost: how much ATP must the Na⁺/K⁺-ATPase consume to maintain the gradient that powers one round of GLT-1 transport? (b) During the first minutes of ischemic stroke, intracellular ATP drops, the Na⁺/K⁺-ATPase stalls, intracellular Na⁺ rises, and GLT-1 begins to run in *efflux* mode (the thermodynamic gradient flips). Predict the local extracellular glutamate concentration trajectory and the consequent fraction of nearby NMDA receptors that lose their Mg²⁺ block. (c) Evaluate why NMDA-receptor antagonists (memantine, low-affinity uncompetitive blockers) have been shown to be more clinically tolerated than high-affinity blockers (MK-801) as neuroprotectants — connect on/off kinetics to the difference between pathological tonic activation and physiological phasic activation.

32.9 Autonomic Nervous System

The **autonomic nervous system (ANS)** regulates involuntary functions through two antagonistic divisions:

32.9.1 Sympathetic Division (“Fight or Flight”)

- Preganglionic neurons: T1-L2 spinal cord (thoracolumbar outflow). Short preganglionic fibers to paravertebral (sympathetic chain) or prevertebral ganglia.
- Preganglionic neurotransmitter: ACh at nicotinic receptors
- Postganglionic neurotransmitter: Norepinephrine (NE) at α and β adrenergic receptors on target organs
- Exception: Adrenal medulla – preganglionic sympathetic fibers synapse directly on chromaffin cells (modified postganglionic neurons) that release epinephrine (80%) and NE (20%) into blood as **hormones**

Sympathetic effects: Increased HR (β_1), bronchodilation (β_2), pupil dilation (mydriasis), inhibited GI motility, glycogenolysis in liver (β_2), vasoconstriction (α_1) in skin/viscera, vasodilation (β_2) in skeletal muscle.

32.9.2 Parasympathetic Division (“Rest and Digest”)

- Preganglionic neurons: Brainstem (CN III, VII, IX, X) and sacral spinal cord (S2-S4; craniosacral outflow). Long preganglionic fibers to terminal ganglia near or within target organs.
- Both neurotransmitters: ACh. Preganglionic: nicotinic receptors. Postganglionic: muscarinic receptors (M1-M5) on target organs.
- Vagus nerve (CN X): Carries about 75% of parasympathetic fibers; innervates heart, lungs, GI tract to splenic flexure.

Parasympathetic effects: Decreased HR (M_2), bronchoconstriction (M_3), pupil constriction (miosis), increased GI motility and secretion, bladder contraction.

32.9.3 Enteric Nervous System

- about 500 million neurons in the gut wall (more than in the spinal cord)
- Myenteric (Auerbach’s) plexus: Between longitudinal and circular muscle layers; controls motility
- Submucosal (Meissner’s) plexus: Controls secretion and blood flow
- Uses many neurotransmitters: ACh, NO, serotonin, substance P, VIP
- Can function autonomously but is modulated by sympathetic (generally inhibitory) and parasympathetic (generally excitatory) input

Clinical Connection: Understanding ANS pharmacology is fundamental to medicine. Beta-blockers (β_1 antagonists: metoprolol, atenolol) are first-line treatments for hypertension, heart failure, and arrhythmias. Atropine (muscarinic antagonist) treats bradycardia. Prazosin (α_1 antagonist) treats hypertension and PTSD nightmares. Pilocarpine (muscarinic agonist) treats glaucoma by promoting aqueous humour drainage.

32.10 Brain Anatomy and Function

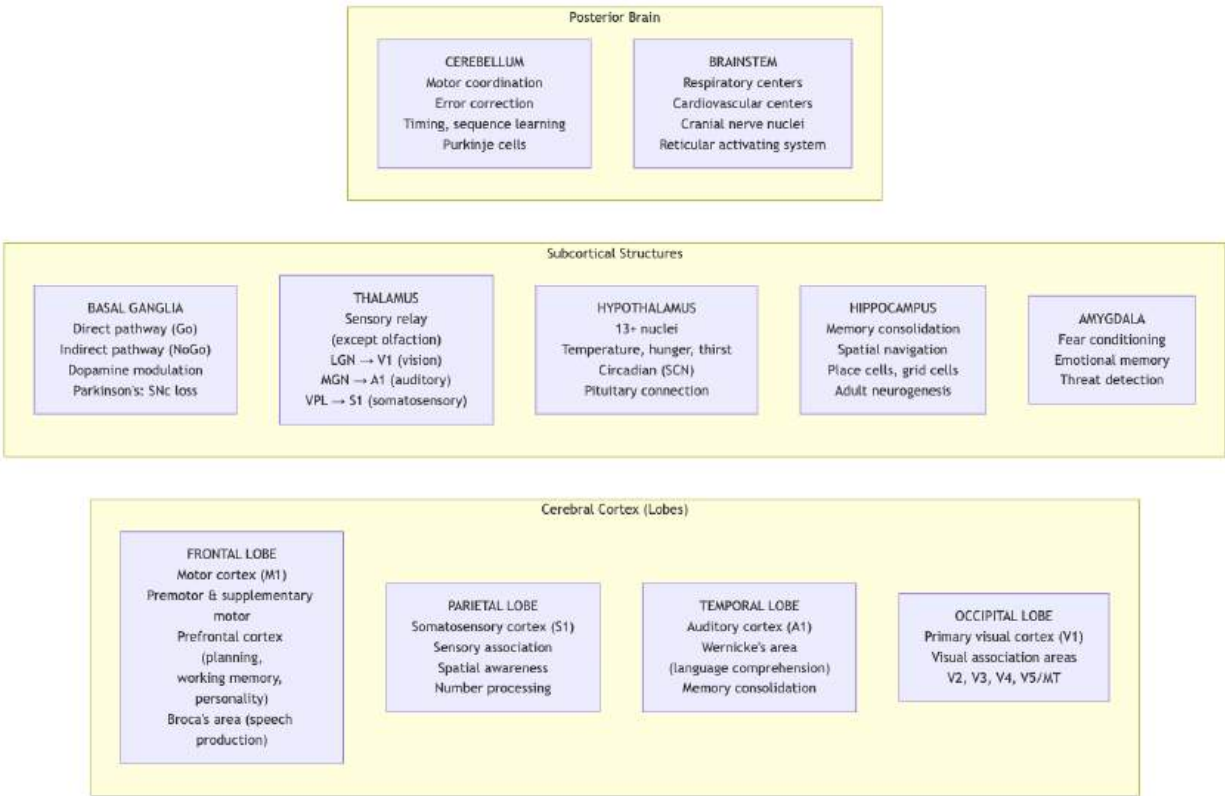


Figure 196. Major brain regions and their functions. The cerebral cortex is divided into four lobes with specialized functions. Subcortical structures handle motor control (basal ganglia), sensory relay (thalamus), homeostasis (hypothalamus), memory (hippocampus), and emotion (amygdala). The cerebellum coordinates movement, and the brainstem controls vital functions.

32.10.1 Cerebral Cortex and Distributed Processing

The cortex is about 3 mm thick, contains about 20 billion neurons, and has a surface area of about 2,500 cm² (increased by folding into gyri and sulci).

- Motor homunculus: Topographic representation of body parts on the primary motor cortex (precentral gyrus). Hands and face have disproportionately large representations (fine motor control).
- Sensory homunculus: Topographic representation on the primary somatosensory cortex (postcentral gyrus). Hands, lips, and tongue are overrepresented (high receptor density).
- Broca’s area (left inferior frontal gyrus): Speech production. Damage causes non-fluent (expressive) aphasia – comprehension intact but speech production impaired.
- Wernicke’s area (left posterior superior temporal gyrus): Language comprehension. Damage causes fluent (receptive) aphasia – speech flows but is non-sensical.

32.10.2 Basal Ganglia and Action Selection

The basal ganglia (caudate, putamen, globus pallidus, subthalamic nucleus, substantia nigra) modulate cortical motor output:

- Direct pathway (Go): Cortex excites striatum; striatum inhibits GPi/SNr (GABAergic); GPi/SNr normally inhibit thalamus. Net effect: disinhibition of thalamus, promoting movement.
- Indirect pathway (NoGo): Cortex excites striatum; striatum inhibits GPe; GPe normally inhibits STN; STN excites GPi/SNr. Net effect: increased GPi/SNr inhibition of thalamus, suppressing movement.

- Dopamine: Substantia nigra pars compacta (SNc) neurons release dopamine onto striatal neurons. D1 receptors excite direct pathway neurons; D2 receptors inhibit indirect pathway neurons. Net: dopamine facilitates movement.

Parkinson’s disease: Degeneration of SNc dopaminergic neurons (>60% loss before symptoms appear). Loss of dopamine removes facilitation of movement, causing: bradykinesia (slow movement), rigidity, resting tremor, postural instability. Treatment: L-DOPA (dopamine precursor crosses BBB); deep brain stimulation of STN.

32.10.3 Cerebellum, Hippocampus, Hypothalamus, and Spinal Cord

Cerebellum: Contains more neurons than the rest of the brain combined (about 70 billion granule cells). Functions: motor coordination, error correction (compares intended vs actual movement), timing, motor learning, balance. Damage causes ataxia (uncoordinated movement) but not paralysis.

Hippocampus: Essential for consolidating declarative (episodic and semantic) memories from short-term to long-term storage. Contains place cells (fire at specific locations; O’Keefe, Nobel 2014) and grid cells (fire in a hexagonal spatial pattern; Moser and Moser, Nobel 2014). One of few brain regions with confirmed adult neurogenesis (dentate gyrus).

Hypothalamus: Homeostatic control center with 13+ nuclei controlling: temperature, hunger/satiety, thirst, circadian rhythms (suprachiasmatic nucleus, SCN), autonomic output, and endocrine function (connects to pituitary via the hypothalamo-hypophyseal portal system).

Spinal cord: Gray matter (butterfly-shaped, contains neuronal cell bodies): dorsal horn (sensory processing), ventral horn (motor neuron cell bodies), lateral horn (T1-L2: sympathetic preganglionic neurons). White matter (surrounding, myelinated tracts): ascending (sensory, e.g., spinothalamic tract for pain/temperature) and descending (motor, e.g., corticospinal tract for voluntary movement).

32.11 Sensory Systems and Neural Coding

32.11.1 Somatosensation and Mechanoreceptor Pathways

Table 383. Somatosensation and Mechanoreceptor Pathways: Receptor Type and Stimulus.

Receptor Type	Stimulus	Adaptation	Modality
Meissner’s corpuscle	Light touch, texture	Rapidly adapting	Fine touch discrimination
Merkel’s disc	Sustained pressure	Slowly adapting	Shape, edge detection
Pacinian corpuscle	Vibration, deep pressure	Rapidly adapting	Vibration detection
Ruffini ending	Skin stretch	Slowly adapting	Joint position, stretch
Free nerve endings	Pain, temperature	Variable	Nociception, thermoreception

Nociception: Two fiber types carry pain signals: - A-delta fibers: Thinly myelinated (5-30 m/s). Sharp, well-localized “first pain” - C fibers: Unmyelinated (0.5-2 m/s). Dull, diffuse “second pain”

32.11.2 Visual Pathway from Retina to Cortex

Retina (photoreceptors: rods for dim light/peripheral vision; cones for color/acuity) to optic nerve to optic chiasm (nasal fibers cross) to lateral geniculate nucleus (LGN) of thalamus to primary visual cortex (V1, striate cortex) in occipital lobe.

Beyond V1, visual processing splits into: - Dorsal stream (“where/how”): V1 to posterior parietal cortex. Motion, spatial relationships, visually guided action. - Ventral stream (“what”): V1 to inferotemporal cortex. Object recognition, face recognition, color.

Concept Check (Synthesis — Cross-Unit Connection): The Free Energy Principle provides a mechanistic account of cortical function. In the predictive coding implementation: descending connections carry predictions (from higher to lower cortical areas); ascending connections carry prediction errors (residuals between prediction and sensory input). Precision-weighting of prediction errors is controlled by neuromodulators (dopamine modulates prediction errors in striatum; acetylcholine modulates precision in sensory cortex). (a) Explain why this architecture predicts that sensory cortex neurons should respond most vigorously to surprising stimuli rather than expected ones (consistent with the Rao-Ballard model). (b) Hallucinations in psychosis can be modeled as excessive precision-weighting of priors over sensory evidence — predict what happens to cortical prediction error signals under this condition. (c) Connect to the Markov blanket framework in [Unit 0 — Systems Science for Biology: Introduction](#): identify the Markov blanket of a cortical column in terms of its synaptic inputs (sensory states), outputs (motor/autonomic states), and internal states.

32.11.3 Proprioception and Body-Position Feedback

Muscle spindles (detect muscle length and stretch velocity), Golgi tendon organs (detect muscle tension), and joint receptors provide unconscious awareness of body position. Information travels via dorsal column-medial lemniscal pathway (proprioception, fine touch) or spinocerebellar tracts (to cerebellum for motor coordination).

32.11.4 Musculoskeletal Control and Behavior

Skeletal movement is a loop, not a one-way command. Alpha motor neurons release acetylcholine at the neuromuscular junction; muscle fibers depolarize, release Ca^{2+} from the sarcoplasmic reticulum, and contract by the sliding-filament mechanism in which myosin heads cyclically bind actin, pull, detach, and reset [Huxley and Hanson, 1954]. Sensory feedback closes the loop: muscle spindles report length, Golgi tendon organs report tension, cutaneous mechanoreceptors report contact, and vestibular inputs report head acceleration. Reflexes are therefore local control policies embedded in a larger behavioral system, not primitive leftovers.

Behavioral biology adds four levels of explanation that should not be collapsed: mechanism (the neural and hormonal circuit), development (how the behavior changes across life), function (what fitness problem it solves), and evolutionary history (how related species differ) [Tinbergen, 1963]. A startle reflex, bird song, courtship display, or human reaching movement can be read through those four levels. The organismal habit is to ask which sensory cue, motor effector, motivational state, developmental window, and ecological payoff are actually supported by the evidence.

32.12 Brain Imaging — Reading Activity Through Indirect Signals

Modern neuroscience and clinical neurology rely on a portfolio of imaging modalities, each measuring a different physical correlate of neural activity.

32.12.1 fMRI and the BOLD signal

Functional MRI (fMRI) measures the blood-oxygen-level-dependent (BOLD) signal, which exploits a magnetic-resonance peculiarity of hemoglobin: oxyhaemoglobin is diamagnetic, while deoxyhaemoglobin is paramagnetic and distorts the local *T2-weighted MR signal*. *Active brain regions paradoxically increase* local oxyhaemoglobin (and decrease deoxyhaemoglobin) within seconds, because the neurovascular coupling response over-supplies blood relative to the metabolic demand. The mismatch between blood-flow increase (about 50%) and O_2 extraction increase (about 5–20%) produces the BOLD signal rise, peaking about 5 s after activity onset.

The neurovascular coupling that drives BOLD is mediated largely by astrocytes (recall the astrocyte tripartite synapse): synaptic glutamate elevates astrocytic Ca^{2+} , which releases vasoactive arachidonic acid metabolites (PGE_2 , EETs) onto local arterioles. The astrocyte-neuron lactate shuttle (ANLS) is the metabolic coupling underlying fMRI BOLD signals.

BOLD does *not* measure spike rates directly; it measures the hemodynamic response to recent local-field-potential activity. fMRI excels at spatial localization (about 1–3 mm) but trades temporal resolution (seconds) — the inverse trade-off compared with EEG.

32.12.2 EEG and oscillation bands

Electroencephalography (EEG) measures the summed extracellular electrical potentials produced by synchronized cortical pyramidal-neuron currents. EEG has millisecond temporal resolution but limited spatial localization (about 1–2 cm). Brain rhythms occupy distinct frequency bands tied to behavioral states:

Table 384. EEG and oscillation bands: Band and Frequency (Hz).

Band	Frequency (Hz)	Dominant state	Generator / function
Delta (δ)	0.5–4	Deep NREM sleep (N3); coma; infancy	Thalamocortical bursts; slow-wave sleep; memory consolidation
Theta (θ)	4–8	Drowsiness; REM; hippocampal navigation	Hippocampal “theta rhythm”; encoding of new memories
Alpha (α)	8–13	Awake, eyes-closed, relaxed (occipital)	Posterior cortical idling; suppressed by visual attention
Beta (β)	13–30	Awake, focused; anxious; motor tasks	Cortical activation; motor planning (sensorimotor cortex)
Gamma (γ)	30–80+	Sensory binding; conscious perception	Local cortical inhibitory networks (PV interneurons)

Clinical EEG is the bedside tool for diagnosing epilepsy (interictal spikes; rhythmic ictal patterns), encephalopathy (generalized slowing), and brain death (electrocerebral silence). MEG (magnetoencephalography) measures the same neuronal currents via tiny magnetic fields with better localization than EEG.

32.12.3 Connectivity, MEG, NIRS, PET

- Diffusion tensor imaging (DTI): Maps white-matter tracts by measuring water diffusion anisotropy along axons. Used in stroke, traumatic axonal injury, neurosurgical planning.
- Resting-state fMRI: Identifies networks of co-fluctuating brain regions (default mode network, salience network, frontoparietal control). Disturbances correlate with depression, schizophrenia, Alzheimer’s.
- PET (positron emission tomography): Tracer-based metabolic or receptor-binding imaging; FDG-PET shows glucose uptake (epilepsy localization, dementia patterns); amyloid-PET (florbetapir) and tau-PET enable Alzheimer’s disease characterization.
- NIRS (near-infrared spectroscopy): Optical analog of fMRI; portable; used in neonatal monitoring and bedside cerebral oximetry.

32.12.4 Neural Prosthetics and Brain-Computer Interfaces

Brain-computer interfaces (BCIs) and neural prosthetics convert neural activity into an external action or stimulation pattern. The strongest current speech demonstrations are still experimental implants, not consumer mind-reading devices: 2023 intracortical speech neuroprostheses decoded attempted speech into text or avatar control at high performance in single-participant research settings [Willett et al., 2023, Metzger et al., 2023]. The scientific claim is therefore bounded: motor and speech cortices contain decodable intention signals, but clinical translation requires stable implants, calibration, infection and tissue-response management, privacy safeguards, and evidence that performance generalizes beyond highly supported trials.

32.13 Pain Pathways and Nociceptive Processing

Pain is the body’s most clinically important sensory modality and serves both protective and pathological roles.

32.13.1 Nociceptors and transduction

Free nerve endings of A-delta and C fibers express molecular sensors that transduce noxious stimuli into membrane depolarization:

- TRPV1: Capsaicin- and heat-activated (>43 °C); also activated by acidic pH and inflammatory lipids. Resiniferatoxin and lidocaine-soaked TRPV1 agonist patches deplete nociceptors of substance P.
- TRPM8: Cold- and menthol-activated (15–25 °C).
- TRPA1: Mustard oil, cinnamaldehyde, environmental irritants; cold-activated in some species.
- ASICs (acid-sensing ion channels): Activated by tissue acidosis (ischemia, inflammation).
- Nav1.7 (SCN9A): Voltage-gated Na⁺ channel essential for nociceptor excitability. *Loss-of-function* mutations cause congenital insensitivity to pain (CIP) — patients fail to detect injuries and self-mutilate. *Gain-of-function* mutations cause inherited erythromelalgia (severe burning pain). Nav1.7-selective inhibitors are in clinical development as non-opioid analgesics.

32.13.2 Ascending pathway — the spinothalamic tract

A-delta and C fibers release glutamate and substance P into the dorsal horn of the spinal cord (lamina I, II, V). Second-order neurons cross the midline (anterior white commissure), ascend in the contralateral spinothalamic tract, and synapse in the ventral posterolateral (VPL) nucleus of the thalamus. Third-order neurons project to primary somatosensory cortex (S1), insula (interoceptive), and anterior cingulate (affective dimension of pain). Substance P binds NK1 receptors on second-order neurons; the combined glutamate-Substance P transmission distinguishes pain from innocuous somatosensation.

32.13.3 Descending Modulation of Pain Signals

The brain actively suppresses ongoing pain signaling through descending circuits:

- Periaqueductal gray (PAG) in the midbrain receives input from cortex, hypothalamus, and amygdala
- PAG activates the rostral ventromedial medulla (RVM)
- RVM serotonergic neurons project to the dorsal horn (DH), where they release serotonin, noradrenaline, and endogenous opioids onto pain-transmission neurons

This PAG → RVM → DH axis is the substrate for stress-induced analgesia (hand-on-flame reflex without pain in life-or-death situations) and for the placebo effect. Endogenous opioids (β -endorphin, enkephalin, dynorphin) acting on μ -, δ -, and κ -opioid receptors are released along this axis. Morphine and other opioid analgesics exploit the same descending pathway.

Gate control theory (Melzack & Wall, 1965): A- β fibers (mechanoreceptors, “innocuous touch”) activate inhibitory interneurons in the dorsal horn that “gate” C-fiber transmission — the basis for rubbing a stubbed toe to reduce pain, and the rationale for TENS (transcutaneous electrical nerve stimulation) therapy.

Clinical Connection: Chronic neuropathic pain (post-herpetic neuralgia, diabetic neuropathy) reflects maladaptive central sensitisation — peripheral nerve injury upregulates Nav1.7/1.8 in nociceptors, expands receptive fields, and reduces descending inhibition. Treatments include gabapentinoids (target $\alpha_2\delta$ subunits of voltage-gated Ca^{2+} channels), SNRIs (boost descending serotonin/noradrenaline), and topical lidocaine (Nav blocker).

32.14 Sleep — Two-Process Model

Sleep is not the absence of brain activity but a structured succession of states with distinct functions.

32.14.1 Sleep Architecture Across NREM and REM Stages

Adult sleep cycles between NREM (further divided into N1, N2, N3) and REM stages, each cycle about 90 minutes:

- N1 (light): Theta activity; transition from waking
- N2: Sleep spindles (12–14 Hz thalamic bursts) and K-complexes; about 50% of total sleep
- N3 (slow-wave / deep): Delta-dominant; “homeostatic” sleep restoring tissue and consolidating declarative memory; glymphatic clearance of brain metabolites including amyloid- β
- REM (paradoxical): Low-amplitude desynchronised EEG resembling waking; rapid eye movements; muscle atonia (mediated by glycinergic inhibition of motor neurons by sublateral dorsal nucleus); vivid dreams; consolidation of procedural and emotional memory

REM proportion is maximal in infancy (about 50% of sleep) and declines with age. Sleep deprivation produces a “REM rebound” — REM disproportionately recovers after deprivation, suggesting it serves a critical function.

32.14.2 The two-process model (Borbély, 1982)

Sleep timing is regulated by two interacting processes:

- Process C (Circadian): Sinusoidal drive from the suprachiasmatic nucleus (SCN) of the hypothalamus, entrained by light via the retinohypothalamic tract. Promotes wakefulness during the day and sleep at night; mediated by hypothalamic circuits including the ventrolateral preoptic nucleus (VLPO, sleep-promoting) and orexin/hypocretin neurons of the lateral hypothalamus (wake-promoting).
- Process S (Sleep homeostasis): Increases monotonically during waking and dissipates exponentially during sleep. Its molecular substrate is largely adenosine, which accumulates in basal forebrain during sustained activity (from local ATP catabolism). Adenosine acting on A_1 receptors inhibits wake-promoting neurons; acting on A_{2A} receptors in the ventral striatum, it promotes sleep. Caffeine (an adenosine A_1/A_{2A} antagonist) blocks Process S — this is its mechanism for reducing sleep pressure.

Sleep occurs when Process C (low) coincides with Process S (high). Disruption of either process produces sleep disorders: SCN damage (or shift work) disrupts Process C, producing irregular sleep timing; insomnia often reflects elevated arousal that overrides Process S.

32.14.3 Functions of sleep

- Memory consolidation: Slow-wave sleep replays hippocampal place-cell sequences; REM consolidates emotional and procedural memory.
- Glymphatic clearance: During NREM, the brain’s glymphatic (glial-lymphatic) system expands extracellular space about 60% and accelerates CSF-ISF exchange, clearing amyloid- β , tau, and other metabolites. Chronic sleep deprivation is a recognized risk factor for Alzheimer’s disease.
- Synaptic homeostasis (Tononi-Cirelli hypothesis): Wake-time learning produces net synaptic potentiation; sleep allows broad synaptic downscaling, restoring information capacity.
- Metabolic and immune restoration: GH and prolactin peak during deep sleep; cytokine cycling supports immune surveillance.

Clinical Connection: Narcolepsy type 1 results from loss of orexin/hypocretin neurons (autoimmune destruction in genetically susceptible individuals). Without orexin, Process C cannot stably maintain wakefulness, producing daytime sleepiness, REM intrusion into wake (cataplexy, sleep paralysis, hallucinations). Treatment includes modafinil (wake-promoting), sodium oxybate (consolidates sleep), and emerging orexin receptor agonists.

32.15 Neural Plasticity and Activity-Dependent Change

Hebbian learning: “Neurons that fire together wire together” [Hebb, 1949]. Correlated pre- and postsynaptic activity strengthens synaptic connections.

Long-term potentiation (LTP): Activity-dependent, long-lasting increase in synaptic efficacy. At Schaffer collateral to CA1 synapses in hippocampus: 1. High-frequency stimulation depolarizes postsynaptic membrane enough to relieve Mg^{2+} block of NMDA receptors 2. Ca^{2+} influx through NMDA receptors activates CaMKII 3. CaMKII phosphorylates AMPA receptors (increased conductance) and promotes AMPA receptor insertion into synapse 4. Structural plasticity: Dendritic spine enlargement, new spine formation

Long-term depression (LTD): Opposite of LTP. Low-frequency stimulation activates protein phosphatases (PP1, calcineurin) that dephosphorylate AMPA receptors and promote their **endocytosis**. Weakens synaptic connections.

Homeostatic plasticity: Synaptic scaling adjusts the overall strength of most synapses on a neuron to maintain a stable firing rate. If a neuron’s activity is chronically reduced, it scales up most synaptic strengths; if chronically increased, it scales them down. This prevents runaway excitation or silencing.

Critical periods [Beggs and Plenz, 2003]: Windows during development when experience has maximal impact on neural circuit formation. Monocular deprivation during the visual critical period (about birth to age 5 in humans) permanently reduces cortical responsiveness to the deprived eye (amblyopia). Molecular brakes on plasticity include perineuronal nets (PNNs), myelin-associated inhibitors, and GABA maturation.

Concept Check: Explain why the NMDA receptor is called a “coincidence detector” and why this property makes it ideal for Hebbian learning.

32.16 Worked Example: Potassium Equilibrium Potential

Problem: Calculate the equilibrium potential for potassium (E_K) in a mammalian neuron at 37°C, given an intracellular potassium concentration $[K^+]_i$ of 140 mM and an extracellular concentration $[K^+]_o$ of 5 mM.

The Nernst equation for a monovalent cation at 37°C is:

$$E_K = 61.5 \text{ mV} \times \log_{10} \left(\frac{[K^+]_o}{[K^+]_i} \right)$$

Solution:

Step 1. Identify the given variables. - $[K^+]_o = 5 \text{ mM}$ - $[K^+]_i = 140 \text{ mM}$

Step 2. Substitute the values into the Nernst equation.

$$E_K = 61.5 \text{ mV} \times \log_{10} \left(\frac{5}{140} \right)$$

Step 3. Calculate the logarithm.

$$\frac{5}{140} \approx 0.0357$$

$$\log_{10}(0.0357) \approx -1.447$$

Step 4. Determine the final potential.

$$E_K = 61.5 \text{ mV} \times (-1.447) \approx -89 \text{ mV}$$

Answer: The equilibrium potential for potassium is approximately -89 mV .

32.17 Worked Example: Resting Potential from the Goldman-Hodgkin-Katz Equation

Problem: Calculate the resting membrane potential of a mammalian neuron at 37°C using the Goldman-Hodgkin-Katz (GHK) equation, given the ion concentrations $[K^+]_o = 5 \text{ mM}$, $[K^+]_i = 140 \text{ mM}$, $[Na^+]_o = 145 \text{ mM}$, $[Na^+]_i = 12 \text{ mM}$, $[Cl^-]_o = 110 \text{ mM}$, $[Cl^-]_i = 7 \text{ mM}$, and the resting permeability ratio $P_K : P_{Na} : P_{Cl} = 1 : 0.04 : 0.45$.

The GHK voltage equation, written in base-10 form for a 37°C neuron, is:

$$V_m = 61.5 \text{ mV} \times \log_{10} \left(\frac{P_K[K^+]_o + P_{Na}[Na^+]_o + P_{Cl}[Cl^-]_i}{P_K[K^+]_i + P_{Na}[Na^+]_i + P_{Cl}[Cl^-]_o} \right)$$

Note that the Cl^- terms are inverted relative to the cations (a consequence of the $z = -1$ charge): the outside-flux numerator carries $[Cl^-]_i$ and the inside-flux denominator carries $[Cl^-]_o$.

Solution:

Step 1. Form the numerator (outward-driving terms), in mM.

$$P_K[K^+]_o + P_{Na}[Na^+]_o + P_{Cl}[Cl^-]_i = (1)(5) + (0.04)(145) + (0.45)(7) = 5 + 5.8 + 3.15 = 13.95$$

Step 2. Form the denominator (inward-driving terms), in mM.

$$P_K[K^+]_i + P_{Na}[Na^+]_i + P_{Cl}[Cl^-]_o = (1)(140) + (0.04)(12) + (0.45)(110) = 140 + 0.48 + 49.5 = 189.98$$

Step 3. Take the ratio and its base-10 logarithm.

$$\frac{13.95}{189.98} \approx 0.0734, \quad \log_{10}(0.0734) \approx -1.134$$

Step 4. Scale by the 37°C Nernst slope.

$$V_m = 61.5 \text{ mV} \times (-1.134) \approx -69.7 \text{ mV}$$

Answer: The resting membrane potential is approximately -70 mV — close to E_K (-89 mV) but depolarized relative to it because the finite Na^+ and Cl^- permeabilities pull V_m toward their (more positive) equilibrium potentials. The K^+ term dominates because P_K is the largest permeability.

Concept Check: If P_{Na} rose tenfold (from 0.04 to 0.40) while P_K and P_{Cl} were unchanged, predict the new sign of the numerator-vs-denominator imbalance and whether V_m moves toward E_{Na} or E_K .

Concept Check: At rest, which single term in the GHK numerator and denominator contributes the most to V_m , and predict how V_m changes if P_K is doubled while most concentrations are held fixed.

32.18 Current Evidence and Frontier Biology: Nervous System and Neural Signaling

For Nervous System and Neural Signaling, frontier biology belongs inside the evidence logic of the chapter. Physiology now blends mechanism with allostasis, immune-endocrine-neural coupling, wearable data, and individualized risk without reducing bodies to simple machines. The core reading question is this: neural explanations should separate circuit architecture, glial support, plasticity, behavior, and evidence scale.

- What to verify: identify the observation, model, assay, or dataset that would make the claim stronger or weaker.
- What to qualify: state the scale, organism, cell type, environmental condition, or population where the claim is expected to hold.
- What to compare: test at least one alternative explanation, baseline, or null model before treating the pattern as causal.
- What to cite: distinguish primary evidence, review synthesis, public dataset, and institutional guidance; for recent or numeric claims, prefer the source closest to the measurement and state what has changed since it was published.

Interpret neural data by separating baseline excitability, stimulus perturbation, circuit compensation, and the threshold where signaling becomes pathology.

Source practice: For nervous-system claims, distinguish electrophysiology, imaging, circuit perturbation, behavioral evidence, and clinical observation [Yao et al., 2023].

32.19 Key Terms

Table 385. Functions of sleep: Term and Definition.

Term	Definition
Resting membrane potential	Electrochemical potential across neuronal membrane at rest; about -70 mV

Term	Definition
Nernst potential	Voltage at which net flux of a single ion species = 0
GHK equation	Multi-ion extension of Nernst; weights each ion by membrane permeability
EPSP	Excitatory postsynaptic potential: depolarization toward threshold
IPSP	Inhibitory postsynaptic potential: hyperpolarization or shunting inhibition
Axon hillock	Lowest threshold region; highest Nav channel density; AP initiation site
Tripartite synapse	Presynaptic + postsynaptic + astrocyte glial process
Sympathetic NS	Thoracolumbar outflow; fight or flight; NE on adrenergic receptors
Parasympathetic NS	Craniosacral outflow; rest and digest; ACh on muscarinic receptors
Basal ganglia	Subcortical nuclei modulating motor output; direct (Go) and indirect (NoGo) pathways
LTP	Long-term potentiation; Hebbian strengthening of synaptic connections
LTD	Long-term depression; weakening of synaptic connections
Broca’s area	Left inferior frontal gyrus; speech production
Wernicke’s area	Left superior temporal gyrus; language comprehension
Place cells	Hippocampal neurons firing at specific spatial locations
Microglia	CNS resident macrophages; synaptic pruning; neuroinflammation
Myelin	Lipid-rich insulation produced by oligodendrocytes (CNS) or Schwann cells (PNS)
Na ⁺ /K ⁺ -ATPase	Pump maintaining ion gradients; 3 Na ⁺ out, 2 K ⁺ in per ATP

32.20 Review Questions

1. Calculate E_K using the Nernst equation for a neuron with $[K^+]_{in} = 150\text{ mM}$ and $[K^+]_{out} = 4\text{ mM}$ at 37 degrees C. How does this compare to the resting potential of -70 mV , and what accounts for the difference?
2. Compare the sympathetic and parasympathetic divisions in terms of: (a) spinal cord origin, (b) preganglionic fiber length, (c) neurotransmitters at ganglia and target organs, (d) receptor types, and (e) effects on heart rate.
3. A patient presents with non-fluent speech but intact comprehension. Which brain region is likely damaged? What would you expect on MRI? How does this differ from damage to Wernicke’s area?
4. Explain the direct and indirect pathways of the basal ganglia. How does loss of dopaminergic input from SNc (as in Parkinson’s disease) shift the balance between these pathways, and why does this cause bradykinesia?
5. Explain synaptic pruning and its relationship to microglia and complement proteins. What evidence links synaptic pruning dysregulation to schizophrenia risk? (Sekar et al. 2016, *Nature*: C4A).
6. A researcher applies a blocker of KCNK leak potassium channels to a neuron. Predict the effect on (a) resting membrane potential, (b) the relative contribution of Na^+ to the resting potential, and (c) neuronal excitability.
7. Compare ionotropic and metabotropic receptors in terms of structure, speed, ionic selectivity, and role in modulating synaptic gain. Give one clinical example for each class.
8. Explain why inhibitory synapses are strategically placed on the soma and proximal dendrites rather than on distal dendrites. How does the concept of shunting inhibition differ from hyperpolarising inhibition?
9. A dendrite has specific membrane resistance $R_m = 25,000\text{ }\Omega\cdot\text{cm}^2$, cytoplasmic resistivity $R_i = 80\text{ }\Omega\cdot\text{cm}$, and radius $a = 1\text{ }\mu\text{m}$. Calculate the length constant λ . If a synapse is located 2 mm from the soma, what fraction of the original EPSP amplitude reaches the soma? How would myelination of the dendrite change your answer qualitatively?
10. A patient with chronic inflammatory demyelinating polyradiculoneuropathy (CIDP) has reduced conduction velocity in peripheral sensory nerves and complains of “glove-and-stocking” numbness. Using the cable properties framework, explain: (a) why demyelination slows conduction velocity, (b) why sensory deficits are worse distally (length-dependent), and (c) why IVIG treatment (suppressing antibody-mediated myelin attack) can restore sensation.
11. Estimate λ from cable_voltage_attenuation defaults and compare to the hand-calculated λ in Question 9.
12. Why does ephaptic coupling complicate the independence assumption of parallel dendritic inputs?

32.21 Further Reading and Source Notes: Nervous System and Neural Signaling

- Sherrington (1906). *The Integrative Action of the Nervous System*. Yale University Press.
- Hebb (1949). *The Organization of Behavior: A Neuropsychological Theory*. Wiley.
- Beggs & Plenz (2003). Neuronal avalanches in neocortical circuits. *Journal of Neuroscience*, 23.

32.22 Computational Bridge

Passive cable length constant is returned with the attenuation profile:

```
from biology.neuroscience import cable_voltage_attenuation

c = cable_voltage_attenuation(2.0, max_distance_μm=800.0, n_points=20)
print(round(c.lambda_μm, 2))
```

Clinical / systems note: Local anaesthetics shorten the depolarization segment that electrotonic spread must bridge — functionally shrinking λ until synaptic input fails to reach threshold.

32.22.1 Optogenetics: Light-Gated Ion Channels as Tools for Mapping Neural Circuits

Until 2005, neuroscience had two experimental tools for probing neural circuits: electrical stimulation (fast, but indiscriminate — excites every cell and axon within a about 100 μm radius) and pharmacological inactivation (specific, but slow and diffuse). Optogenetics — introduced by Boyden, Deisseroth, and colleagues (*Nat. Neurosci.* 2005) — merged genetic specificity with millisecond temporal precision by transplanting light-gated ion channels from microbes into mammalian neurons.

The core tools: Channelrhodopsin-2 (ChR2), a blue-light-gated non-selective cation channel from the green alga *Chlamydomonas reinhardtii*, opens in about 1 ms on 470 nm illumination and drives neurons to fire action potentials with up to 40 Hz fidelity. Halorhodopsin (NpHR) from *Natronomonas pharaonis* is a yellow-light-driven inward Cl^- pump that hyperpolarises neurons and silences firing. Archaeorhodopsin (Arch) is a green-light-driven outward H^+ pump with similar inhibitory effect. Transgene expression via AAV with cell-type-specific **promoters** (Thy1 for cortical pyramidal neurons, PV-Cre \times ChR2 for parvalbumin interneurons, DAT-Cre for dopamine neurons) delivers the channel primarily to genetically defined populations. Combined with implanted optical fibers (for deep structures) or surface-mounted LEDs (for cortex), the experimenter can turn specific cell types on or off in milliseconds.

Landmark findings enabled by optogenetics: (1) Memory engrams — Tonegawa and colleagues (*Nature* 2012, *Science* 2014) showed that optogenetic reactivation of the specific hippocampal neurons active during fear conditioning is sufficient to recall the fear memory in a neutral context, proving engram cells are *the* physical substrate of memory. (2) Parkinson’s disease circuit dissection — Kravitz et al. (*Nature* 2010) showed that direct-pathway (D1) striatal neuron optogenetic activation rescues motor deficits in parkinsonian mice, while indirect-pathway (D2) activation mimics them, confirming the 1990s pharmacological model. (3) Basis of deep brain stimulation — optogenetic DBS mimics in rodents has clarified which STN cell types produce the therapeutic benefit in Parkinson’s patients. Clinical **translation**: RST-001 (jSAM for retinitis pigmentosa, GenSight Biologics) uses ChrimsonR delivered by AAV to retinal ganglion cells and specialized goggles to convert images to patterned light. A 2021 *Nature Medicine* report documented partial restoration of visual function in a blind patient — optogenetics’ first human therapeutic success.

32.23 Summary

- NS organization: CNS (brain + spinal cord) + PNS (somatic + autonomic + enteric). 86 billion neurons; glia provide myelin, BBB, metabolic support, immune surveillance.
- Neuron types: Sensory (afferent, pseudounipolar), motor (efferent, multipolar), interneurons (integration). Axon hillock has highest Nav channel density.
- Resting potential: $E_K = -89\text{ mV}$ dominates; Na^+/K^+ -ATPase maintains gradients; GHK equation weights by permeabilities; $V_m \approx -70\text{ mV}$.
- Synaptic integration: EPSPs (depolarizing) and IPSPs (hyperpolarising/shunting) summate temporally and spatially at the axon hillock. Threshold at about -55 mV triggers most-or-none AP.
- ANS: Sympathetic (T1-L2, NE, fight-or-flight) vs parasympathetic (craniosacral, ACh, rest-and-digest). Enteric NS: semi-autonomous gut control.
- Brain: Cortex (4 lobes, motor/sensory homunculi, language areas); basal ganglia (direct/indirect pathways, dopamine); thalamus (sensory relay); hippocampus (memory, place cells); hypothalamus (homeostasis); cerebellum (coordination); brainstem (vital functions).

- Sensory systems: Mechanoreceptors (Meissner, Pacinian, Ruffini, Merkel), nociceptors (A-delta, C fibers), proprioceptors; visual pathway (retina to LGN to V1 to dorsal/ventral streams).
- Neural plasticity: LTP (NMDA-Ca²⁺-CaMKII-AMPA), LTD, homeostatic scaling, critical periods, synaptic pruning.
- Connections: See section 33 for active propagation, section 8 for second messengers, and section 0.3 for active inference themes.

32.24 Companion Source Module: Nervous System and Neural Signaling

Nervous System and Neural Signaling should leave a reproducible trail from a biological claim to the code, figure, diagram, or paper-based activity that can test it. Use the surfaces below to inspect the chapter’s assumptions, rerun the relevant model, or compare the manuscript explanation with companion labs and figures.

Table 386. Companion source surfaces for Nervous System and Neural Signaling.

Surface	Use it for
src/biology/neuroscience/neuroscience.py (cable_voltage_attenuation, hebbian_weight_update, action_potential_hh)	Connect circuit architecture, passive spread, spiking, and plasticity.
src/visualization/plots.py (plot_action_potential)	Check timing and amplitude of neural signals.
src/mermaid/biology_diagrams.py (nervous_system_reflex_diagram)	Keep stimulus, integration, motor output, and feedback distinct.

Reproducibility check: specify cell type, circuit level, recording method, and behavioral readout before linking neural mechanism to outcome. Cross-reference: use section 33 and section 0.3.

33 Action Potentials and Synaptic Transmission

Level 3/3 · 55 min read · 100 min lecture · Prerequisites: section 32

33.1 Learning Objectives

1. Write and explain the Hodgkin-Huxley equations for the **action potential**.
2. Explain the kinetics of Na⁺ activation (m), inactivation (h), and K⁺ activation (n) gating variables.
3. Describe the absolute and relative refractory periods in terms of channel states.
4. Explain myelination, **saltatory conduction**, and how axon diameter affects velocity.
5. Describe the molecular machinery of chemical synaptic transmission including SNARE **proteins** and Ca²⁺ triggering.
6. Compare major neurotransmitter systems and their receptor pharmacology.
7. Describe long-term potentiation [**Frey and Morris, 1997**] (LTP) and long-term depression (LTD) and their roles in learning and memory.
8. Explain the mechanisms of action of major neuroactive drugs.

33.1.1 Study Blueprint

- Big idea: Electrical excitability and synaptic transmission convert ion gradients into rapid communication.
- Core concepts: action potentials, ion channels, synapses, plasticity.
- Framework alignment: Vision & Change: Structure and function, Systems; AP Biology: Systems Interactions, Energetics; NGSS-style topics: Structure and Function.
- Model or quantitative lens: Nernst/Goldman, Hodgkin-Huxley, and synaptic-current reasoning.
- Data skill: Interpret voltage traces, conductance changes, and synaptic perturbations.
- Practice cadence: Visual Representations, Statistical Tests and Data Analysis, Argumentation.
- Common misconception to repair: An action potential is not electricity flowing like a wire; it is regenerated ion-channel dynamics.
- Primary lab: **Lab — Action Potentials and Synaptic Transmission**.
- Question bank: **Questions — Action Potentials and Synaptic Transmission**.
- Transfer task: Transfer excitability reasoning to anesthesia, toxins, epilepsy, and neuromuscular disease.
- Bridge to computation: `biology.neuroscience.neuroscience.action_potential_hh`.

Opening Vignette — The Squid That Explained the Brain

The squid *Loligo* possesses a giant axon up to 1 mm in diameter — large enough for researchers to insert a glass micropipette electrode into the interior. In 1939, Alan Hodgkin and Andrew Huxley exploited this remarkable anatomy to make the first intracellular recordings of an action potential. By 1952, using voltage-clamp apparatus of their own construction, they had measured the time courses of sodium and potassium conductances across the membrane with stunning precision and fitted them to a set of differential equations now known as the Hodgkin-Huxley model [**Hodgkin and Huxley, 1952**]. The equations predicted the shape, amplitude, threshold, refractory period, and propagation velocity of action potentials — most from first principles of ionic movement. The 1963 Nobel Prize in Physiology or Medicine rewarded what remains one of the most quantitatively rigorous pieces of biological science ever accomplished. Every antiepileptic, local anaesthetic, cardiac antiarrhythmic, and membrane biophysics textbook stems ultimately from that one peculiarly large squid axon.

33.2 The Hodgkin-Huxley Model

Alan Hodgkin and Andrew Huxley recorded action potentials from the squid giant axon (diameter about 0.5 mm) using voltage clamp; their quantitative model remains the reference case for turning conductance measurements into a predictive excitable-membrane equation [**Hodgkin and Huxley, 1952**]. Each ionic current is driven by the difference between V and that ion’s Nernst equilibrium potential, the gradient-dependent values of which are plotted in figure 197. They described membrane current as:

$$C_m \frac{dV}{dt} = -I_{Na} - I_K - I_L + I_{ext} \tag{403}$$

where: - C_m = membrane capacitance about 1 uF/cm² - $I_{Na} = \bar{g}_{Na} m^3 h (V - E_{Na})$; $\bar{g}_{Na} = 120 \text{ mS/cm}^2$; $E_{Na} = +50 \text{ mV}$ - $I_K = \bar{g}_K n^4 (V - E_K)$; $\bar{g}_K = 36 \text{ mS/cm}^2$; $E_K = -77 \text{ mV}$ - $I_L = g_L (V - E_L)$; $g_L = 0.3 \text{ mS/cm}^2$; $E_L = -54.4 \text{ mV}$

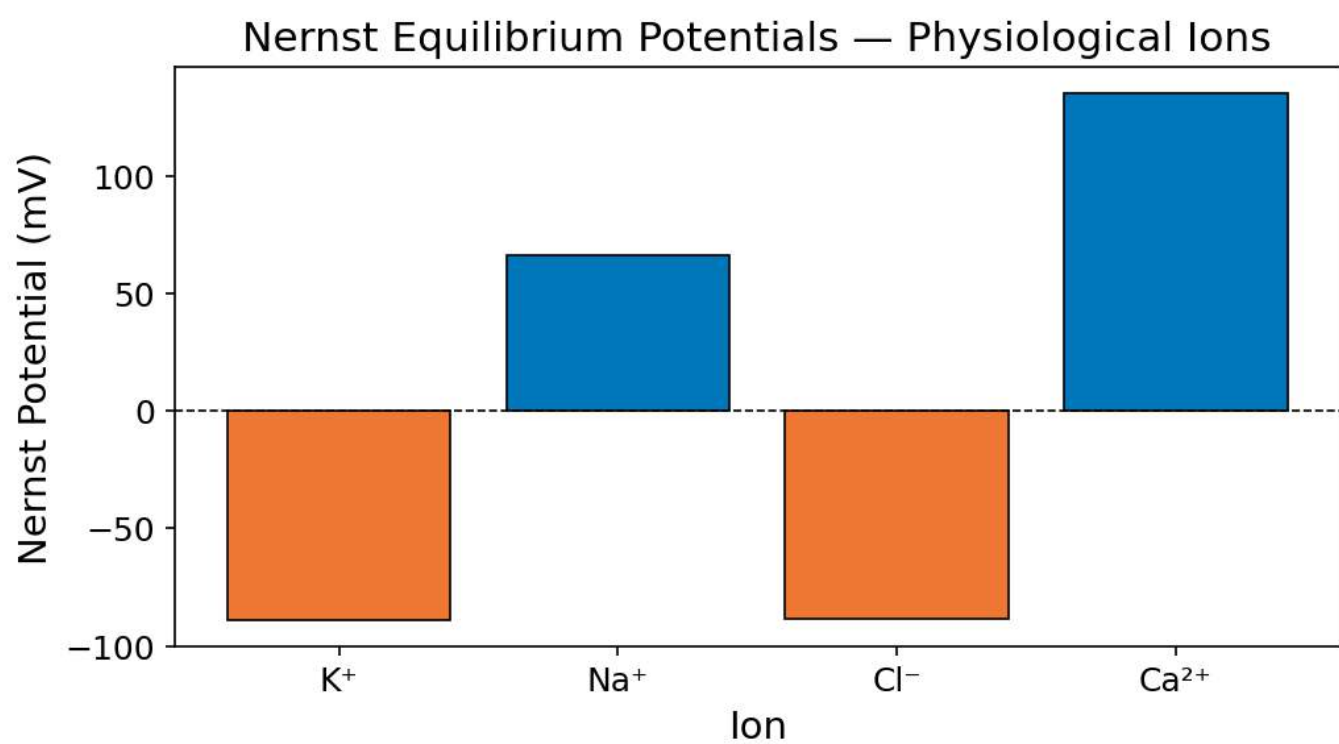


Figure 197. Nernst equilibrium potentials for major physiological ions (Na⁺, K⁺, Cl⁻, Ca²⁺) calculated from their inside/outside concentration gradients.

33.2.1 Hodgkin-Huxley Gating Variables

Each gating variable (m , h , n) evolves according to first-order Markov kinetics [Hodgkin and Huxley, 1952]:

$$\frac{dx}{dt} = \alpha_x(V)(1 - x) - \beta_x(V)x$$

(404)

At steady state: $x_\infty(V) = \alpha_x/(\alpha_x + \beta_x)$; time constant: $\tau_x(V) = 1/(\alpha_x + \beta_x)$

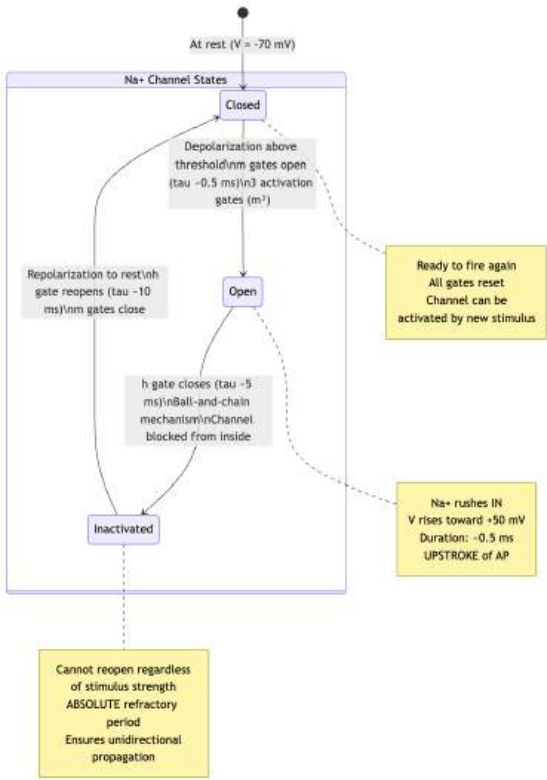


Figure 198. Voltage-gated Na⁺ channel states. The channel transitions through three states: Closed (resting, ready to open), Open (conducting Na⁺, brief about 0.5 ms), and Inactivated (blocked by the inactivation gate, cannot reopen until repolarization restores the resting state). The inactivated state underlies the absolute refractory period.

Table 387. Hodgkin-Huxley voltage-dependent gating rate variables.

Gating variable	$\alpha(V)$	$\beta(V)$
m (Na ⁺ activation)	$0.1(V + 40)/[1 - \exp(-(V + 40)/10)]$	$4 \exp(-(V + 65)/18)$
h (Na ⁺ inactivation)	$0.07 \exp(-(V + 65)/20)$	$1/[1 + \exp(-(V + 35)/10)]$
n (K ⁺ activation)	$0.01(V + 55)/[1 - \exp(-(V + 55)/10)]$	$0.125 \exp(-(V + 65)/80)$

33.2.2 Biophysical Interpretation of the Action Potential

- Threshold (about −55 mV): Point where inward Na⁺ current exceeds outward K⁺ leak. Positive feedback begins (more depolarization opens more Na⁺ channels).
- Upstroke (depolarization): Rapid m-gate opening (τ_m ≈ 0.5 ms). Na⁺ rushes in. Membrane potential approaches E_{Na} (+50 mV) but typically peaks at +30 to +40 mV.
- Repolarization: h-gate closes (Na⁺ inactivation, τ_h ≈ 5 ms) AND n-gate opens (K⁺ delayed rectifier, τ_n ≈ 5 ms). Na⁺ influx stops; K⁺ efflux drives membrane back toward E_K.
- Afterhyperpolarisation (undershoot): n-gate slow to close. K⁺ efflux continues briefly, hyperpolarising membrane below resting potential (about −80 mV). This is the relative refractory period.

33.2.3 Channel Pharmacology and Excitability

Tetrodotoxin (TTX): Puffer fish toxin. Blocks Nav channels from the extracellular side by occluding the selectivity filter pore. Blocks most AP generation. LD₅₀ in mice: about 10 ug/kg. Used extensively as a research tool to study Na⁺-dependent processes.

4-Aminopyridine (4-AP): Blocks Kv (voltage-gated K⁺) channels. Prolongs AP duration, enhances neurotransmitter release. Used clinically as dalfampridine (Ampyra) for multiple sclerosis to improve conduction in demyelinated axons.

Nav channel subtypes: Nav1.1-Nav1.9 encoded by SCN1A-SCN11A genes. Different subtypes have distinct tissue distributions, voltage sensitivities, and pharmacological profiles: - Nav1.7 (SCN9A): Pain perception. Loss-of-function: congenital insensitivity to pain. Gain-of-function: erythromelalgia (burning pain). - Nav1.5 (SCN5A): Cardiac muscle. Mutations cause Long QT syndrome, Brugada syndrome.

Concept Check: TTX blocks Na⁺ channels and abolishes action potentials. Local anaesthetics (lidocaine) also block Na⁺ channels. Why does lidocaine preferentially block pain fibers rather than motor fibers? (Hint: consider use-dependence and fiber diameter.)

33.3 Refractory Periods and Directional Propagation

Absolute refractory period (about 1-2 ms after spike peak): Na⁺ channels are in the inactivated state (h about 0). They cannot be re-opened regardless of stimulus strength. This supports: - Unidirectional AP propagation (the region just behind the AP cannot be re-excited) - Maximum firing rate (about 500-1000 Hz)

Relative refractory period (about 5-10 ms following absolute): Na⁺ channels are recovering from inactivation (h recovering), but K⁺ channels remain open. The membrane is more negative than resting potential (afterhyperpolarisation). A stronger-than-normal stimulus is needed to trigger a second spike. APs generated during this period have reduced amplitude.

Clinical Connection: The cardiac refractory period is much longer than in neurons (about 200-300 ms vs about 2 ms) because cardiac AP duration is prolonged by L-type Ca²⁺ channels (plateau phase). This prevents tetanic contraction of the heart (which would be fatal – the heart must relax to fill). The “vulnerable period” near the end of the T wave (relative refractory period of ventricles) is when a premature stimulus can trigger ventricular fibrillation.

Concept Check: During the falling phase of the action potential the m, h, and n gates are most changing at once. Which single Hodgkin-Huxley gating variable is the *direct* cause of repolarization, and why does Na⁺ inactivation (h) alone fail to repolarise the membrane without it? (Hint: compare what each conductance does to the driving force toward E_K versus E_{Na}.)

33.4 Myelination and Conduction Velocity

33.4.1 Unmyelinated Conduction and Cable Spread

In continuous conduction, the AP generates local circuits along the axon membrane:

$$\theta \propto \sqrt{a/r_i}$$

(405)

where a = axon radius and r_i = axial resistance per unit length. Increasing diameter reduces axial resistance, increasing velocity. Squid giant axon (500 um diameter) achieves about 25 m/s by brute-force gigantism.

33.4.2 Myelinated Axons – Saltatory Conduction

Myelin dramatically increases the space constant (λ):

$$\lambda = \sqrt{r_m/r_i}$$

(406)

Myelin increases r_m (membrane resistance, preventing current leak) and reduces C_m (membrane capacitance, reducing charge needed to change voltage). The result: depolarization spreads much further without decay.

APs can primarily arise at nodes of Ranvier (1-2 um gaps between myelin segments, every about 1 mm). Nodes have concentrated voltage-gated Na⁺ channels (about 1,000/um² at nodes vs about 25/um² under myelin).

Saltatory conduction: The AP appears to “jump” between nodes. In myelinated axons, velocity scales linearly with diameter ($\theta \propto d$), rather than as the square root:

Table 388. Myelinated Axons – Saltatory Conduction: Fiber type and Diameter (um).

Fiber type	Diameter (um)	Velocity (m/s)	Myelinated?	Function
A-alpha (Ia)	12-20	70-120	Yes	Muscle spindle afferents
A-beta	6-12	30-70	Yes	Touch, pressure
A-delta	1-5	5-30	Thinly	Sharp pain, temperature
B	1-3	3-15	Yes	Preganglionic autonomic
C	0.2-1.5	0.5-2	No	Slow pain, itch, postganglionic autonomic

33.4.3 Worked Example: Myelination Gain — Saltatory vs Continuous Conduction

Suppose two unmyelinated axons of equal small diameter ($d = 1 \mu\text{m}$) carry the same action potential. Continuous conduction velocity scales as $\theta_{\text{unmyel}} \propto \sqrt{d}$. From empirical data, an unmyelinated $1 \mu\text{m}$ axon conducts at about 0.5 m/s.

Now myelinate one axon with internodes about 1 mm apart and 100 wraps of myelin. Myelin increases membrane resistance (r_m) about 100-fold and reduces capacitance (C_m) about 50-fold:

- Length constant $\lambda = \sqrt{r_m/r_i}$ increases about 10-fold
- Time constant at the node $\tau_m = r_m C_m$ — although both increase, the *time to reach threshold* at the next node depends primarily on the rapid charging of node membrane (which has low capacitance) by the spreading depolarization
- Effective conduction velocity in myelinated fiber: $\theta_{\text{myel}} \propto d$ (linear, not square root)

For the same $1 \mu\text{m}$ fiber with myelination, conduction approaches about 6 m/s ($>10\times$ faster). For larger myelinated fibers ($10\text{--}20 \mu\text{m}$ A- α), the gain is even more striking:

Table 389. Myelination Gain — Saltatory vs Continuous Conduction: Fiber and Diameter.

Fiber	Diameter	Conduction velocity	Myelinated?	Velocity gain
C fiber	$1 \mu\text{m}$	0.5 m/s	No	(baseline)
A- δ	$1\text{--}5 \mu\text{m}$	5–30 m/s	Thinly	about 10–60 \times
A- α (Ia)	$12\text{--}20 \mu\text{m}$	70–120 m/s	Yes (heavily)	about 150–250 \times

The fundamental insight: Saltatory conduction provides the same speed at about 50 \times lower diameter compared to brute-force gigantism (squid giant axon, 500 μm). The vertebrate solution to fast conduction — myelinate small axons rather than grow giant ones — is enormously more space-efficient and energetically cheaper. The about 10^{12} axons in the human white matter would not fit in the cranium without myelin.

The energetic cost of action potentials is also dramatically reduced: in unmyelinated axons, Na^+/K^+ -ATPase must continuously pump out Na^+ along the entire length. In myelinated axons, AP-associated ion fluxes occur primarily at nodes (about 0.1% of axon surface), reducing the metabolic cost of spike propagation by a similar factor.

33.4.4 Multiple Sclerosis and Demyelinating Conduction Failure

Multiple sclerosis (MS): Autoimmune demyelination of CNS white matter. T cells recognize myelin basic protein (MBP) and proteolipid protein (PLP) as autoantigens. Inflammatory attack destroys oligodendrocyte myelin sheaths.

Consequences: Slowed or blocked conduction in demyelinated segments. Symptoms depend on lesion location: optic neuritis (visual loss), weakness, sensory loss, fatigue, cognitive impairment. Relapsing-remitting course in about 85% of patients.

Treatment: Disease-modifying therapies (interferons, natalizumab, ocrelizumab) reduce relapse frequency. 4-aminopyridine (blocks exposed K^+ channels in demyelinated segments) improves conduction.

Concept Check: A $1 \mu\text{m}$ unmyelinated axon conducts at about 0.5 m/s, yet a $1 \mu\text{m}$ myelinated axon conducts at about 6 m/s while a $20 \mu\text{m}$ unmyelinated axon would need a far larger diameter to match it. Using the velocity scalings $\theta \propto \sqrt{d}$ (unmyelinated) versus $\theta \propto d$ (myelinated), explain why myelination — not

gigantism — is the space- and energy-efficient solution, and predict what happens to conduction when a node of Ranvier is demyelinated. (Hint: think about what myelin does to r_m , C_m , and the length constant λ .)

33.5 Chemical Synaptic Transmission

33.5.1 Synapse Types and Functional Polarity

Electrical synapses (gap junctions): Connexin/innexin hemichannels directly connect cytoplasms. Bidirectional, nearly instantaneous (<0.1 ms). Found in cardiac pacemaker cells (connexin 43), retinal processing (rod-cone coupling), hippocampal interneuron synchronisation. Connexin 26/30 mutations cause hereditary deafness.

Chemical synapses: Unidirectional. Modifiable (plasticity). Synaptic delay: 0.5-2 ms. The dominant synapse type in the CNS.

33.5.2 Presynaptic Machinery for Vesicle Fusion

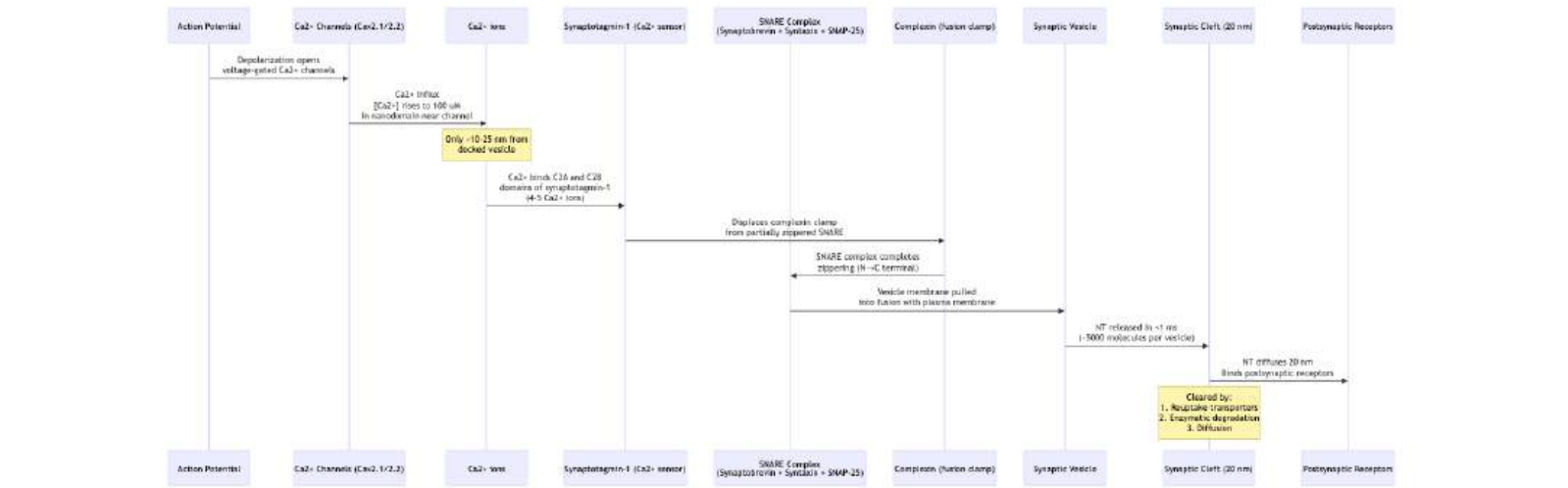


Figure 199. Molecular machinery of synaptic vesicle fusion. Depolarization opens Ca^{2+} channels. Ca^{2+} binds synaptotagmin-1, which displaces the complexin fusion clamp and triggers full SNARE complex zippering, forcing the vesicle membrane to fuse with the plasma membrane and release neurotransmitter into the cleft.

Key proteins: - SNARE complex: The minimal fusion machinery. Synaptobrevin (v-SNARE, on vesicle membrane) + syntaxin + SNAP-25 (both t-SNAREs, on plasma membrane). The four α -helices zipper together N-to-C terminally, pulling membranes into contact. - Synaptotagmin-1: Ca^{2+} sensor. Its C2A and C2B domains bind 4-5 Ca^{2+} ions, triggering membrane insertion and SNARE complex activation. Cooperativity of Ca^{2+} binding gives the steep Ca^{2+} -release relationship (about 4th power). - Munc18 / Munc13: Priming factors that prepare SNARE complexes for fast fusion - RIM: Active zone scaffold protein. Positions vesicles within nanometres of Ca^{2+} channels. - Complexin: “Fusion clamp.” Binds partially zippered SNARE complex and prevents spontaneous fusion. Ca^{2+} /synaptotagmin displaces complexin to trigger release. - NSF + α -SNAP: After fusion, these AAA⁺ ATPases disassemble SNARE complexes for recycling.

Quantal release (Katz, Nobel 1970): Neurotransmitter is released in discrete packets (quanta), each corresponding to the contents of one vesicle [del Castillo and Katz, 1954]. The end-plate potential (EPP) at the NMJ = $n \times p \times q$, where n = number of release-ready vesicles, p = release probability per vesicle, q = quantal size (postsynaptic response to one vesicle).

Miniature EPPs (mEPPs) represent spontaneous release of single vesicles and have a constant amplitude (about 0.5 mV at the NMJ). The evoked EPP is an integer multiple of the mEPP amplitude.

33.5.3 Synaptic Vesicle Pools

A presynaptic terminal does not treat most its vesicles equivalently. Decades of imaging, electrophysiology, and FM dye experiments establish three functionally distinct pools that differ in their release-readiness, location, and mobilization kinetics:

Table 390. Synaptic Vesicle Pools: Pool and Approximate size per active zone.

Pool	Approximate size per active zone	Location	Release kinetics	Replenishment
Readily re-leasable pool (RRP)	about 10–20 vesicles (CNS); about 50–100 (NMJ)	Docked at active zone; primed	Released within about 1 ms of Ca ²⁺ entry; depleted within first few APs of a high-frequency train	Refilled from recycling pool over 1–10 s
Recycling pool	about 100–200 vesicles	Near active zone; fused with PM during sustained activity then reformed locally	Sustains release during moderate-frequency activity	Cycle time about 30–60 s
Reserve pool	about 300–500+ vesicles	Tethered to actin/synapsin in the cytoplasm	Mobilized primarily during intense or prolonged activity (typically when synapsin is phosphorylated by CaMKII/PKA)	Slow refilling (minutes) from synthesis and endocytosis

The three-pool model elegantly explains the kinetics of synaptic transmission during different activity patterns. Brief, low-frequency stimulation uses primarily the RRP and the system rapidly returns to baseline. Sustained moderate activity engages the recycling pool. Tetanic stimulation mobilizes the reserve pool by phosphorylation of synapsin (which normally clamps reserve vesicles to the actin cytoskeleton), releasing them to refill the active zone.

33.5.4 Short-term plasticity — facilitation and depression

Synaptic strength is dynamic across milliseconds-to-seconds, even before any LTP/LTD is induced. Two opposing short-term phenomena dominate:

Synaptic facilitation (paired-pulse facilitation; tens to hundreds of ms): If two APs arrive in close succession, the second EPSC/IPSC is *larger* than the first. Mechanism: residual presynaptic Ca²⁺ from the first AP has not yet been pumped out or buffered; when the second AP triggers Ca²⁺ entry, the residual Ca²⁺ adds to the new flux, super-linearly increasing release probability *p*. Facilitation is most prominent at synapses with low initial *p* (e.g., parallel-fiber to Purkinje cell synapses; about *p* ≈ 0.05); high-*p* synapses have less room for further increase.

Synaptic depression (paired-pulse depression; tens of ms to seconds): If two APs arrive in close succession at a high-*p* synapse, the second EPSC is *smaller* than the first. Mechanism: the RRP is partially depleted by the first AP and has not had time to refill. Depression is most prominent at synapses with high initial *p* (e.g., calyx of Held auditory synapses; *p* ≈ 0.4).

Whether a given synapse facilitates or depresses depends on its starting release probability, vesicle pool dynamics, and Ca²⁺ handling. Some synapses transition: facilitate at low frequency, then depress as frequency rises and pools deplete.

33.5.5 Tsodyks-Markram model

The classical phenomenological model of short-term plasticity (Tsodyks & Markram, 1997) treats each synapse as having two state variables:

- *x*: the fraction of available (un-depleted) resources (vesicles in the RRP), with 0 ≤ *x* ≤ 1
- *u*: the utilization parameter (effective release probability), influenced by residual Ca²⁺

After each spike, *x* → *x* · (1 − *u*) (resources depleted) and *u* → *u* + *U* · (1 − *u*) (release probability incremented by Ca²⁺ accumulation). Between spikes, both variables relax back to baseline with time constants *τ_d* (recovery, about 500 ms–2 s) and *τ_f* (facilitation, about 100–500 ms):

$$\frac{dx}{dt} = \frac{1 - x}{\tau_d}; \quad \frac{du}{dt} = -\frac{u - U}{\tau_f}$$

The post-spike EPSC amplitude is proportional to $u \cdot x$. This single model captures the full repertoire of facilitating, depressing, and mixed synapses — by varying the parameters U, τ_d, τ_f — and is the standard building block for biologically realistic spiking neural network simulations.

Clinical Connection: Lambert-Eaton myasthenic syndrome (LEMS) is an autoimmune disorder targeting presynaptic P/Q-type Ca^{2+} channels at the NMJ, dramatically reducing initial release probability. The hallmark on bedside testing is post-tetanic facilitation — strength briefly improves after sustained voluntary contraction, reflecting accumulated Ca^{2+} partially compensating for reduced channel number. Treatment with 3,4-diaminopyridine (a K^+ channel blocker that prolongs presynaptic AP duration \rightarrow more Ca^{2+} entry per spike) increases initial p and restores neuromuscular transmission.

33.5.6 Worked Example: Quantal Analysis at the Neuromuscular Junction

Mathematical Background: Quantal analysis uses Poisson statistics. For a review of probability and statistical reasoning, see [Appendix C — Mathematical Review for Biology](#).

Problem: At the frog NMJ, miniature end-plate potentials and evoked end-plate potentials revealed that transmitter release occurs in vesicle-sized quanta [del Castillo and Katz, 1954]. Suppose spontaneous miniature end-plate potentials (mEPPs) have mean amplitude $q = 0.5$ mV (the postsynaptic response to one vesicle’s worth of acetylcholine). An evoked end-plate potential (EPP) under normal Ca^{2+} averages $V_{\text{EPP}} = 25$ mV. Estimate the quantal content m (mean number of vesicles released per action potential), then predict the failure rate when extracellular Ca^{2+} is reduced enough to drop m to 2.

Solution.

1. Quantal content from the mEPP ratio. Quantal release theory: $V_{\text{EPP}} = m \cdot q \Rightarrow m = V_{\text{EPP}}/q = 25/0.5 = 50$ vesicles per AP.
2. Poisson statistics of release. Each release-ready vesicle has independent release probability p ; the number released per AP, k , follows Poisson statistics with mean m . The probability of zero release (“failure”) is

$$P(k = 0) = e^{-m}.$$

At $m = 50$: $P(\text{failure}) = e^{-50} \approx 1.9 \times 10^{-22}$. Effectively negligible failure probability — exactly the safety factor needed at the NMJ, where every motor command must reach the muscle.

3. Low- Ca^{2+} regime, $m = 2$. Reduce extracellular $[\text{Ca}^{2+}]$ enough to drop m to 2 (with p falling correspondingly because release probability scales as $\sim [\text{Ca}^{2+}]^4$ — a steep nonlinearity from Ca^{2+} -sensor cooperativity):

$$P(\text{failure}) = e^{-2} \approx 0.135 = 13.5\%.$$

More than one in eight spikes now triggers zero release. The EPP histogram becomes multi-modal: discrete peaks at $0, q, 2q, 3q, \dots$ separated by the quantal step. The visibility of these peaks is the empirical signature captured in classical quantal analysis [del Castillo and Katz, 1954].

4. Sanity check — variance. Poisson predicts $\text{Var}(V_{\text{EPP}}) = m \cdot q^2$ so the coefficient of variation is $1/\sqrt{m}$. At $m = 50$, $\text{CV} \approx 0.14$ (smooth, near-deterministic release). At $m = 2$, $\text{CV} \approx 0.71$ (noisy, single-vesicle steps visible in the post-synaptic record). This CV-vs- m scaling is the standard tool for inferring m at central synapses where mEPSCs are harder to isolate.

Interpretation. The NMJ deliberately operates at high safety factor ($m \approx 50$ on a ~ 100 -vesicle RRP per active zone, so $p \approx 0.5$) precisely because failure is intolerable for survival behaviors. Central synapses, by contrast, often run at $m = 1\text{--}5$ — they accept failures in exchange for the ability to perform fine probabilistic computation. The quantal framework converts the same molecular machinery (vesicles + Ca^{2+} + SNAREs) into wildly different reliability regimes by tuning a single biophysical knob: p .

33.5.7 Postsynaptic Receptors and Ionotropic/Metabotropic Signaling

Table 391. Postsynaptic Receptors and Ionotropic/Metabotropic Signaling: Receptor class and Example.

Receptor class	Example	Ion selectivity	Speed	Mechanism
Ionotropic	AMPA (GluA1-4)	Na^+/K^+ (some Ca^{2+})	Fast (ms)	Ligand-gated ion channel
	NMDA (GluN1/2A-D)	$\text{Na}^+/\text{K}^+/\text{Ca}^{2+}$	Slower (10s of ms)	Voltage + ligand gated; Mg^{2+} block

Receptor class	Example	Ion selectivity	Speed	Mechanism
Ionotropic	GABA _A	Cl [−]	Fast (ms)	Ligand-gated anion channel
Ionotropic	nAChR	Na ⁺ /K ⁺	Fast (ms)	Pentameric cation channel
Metabotropic	mGluR1-8	N/A	Slow (100s ms-min)	GPCR to G _q /G _i to IP ₃ /cAMP
Metabotropic	GABA _B	K ⁺ (indirect)	Slow	G _i to K ⁺ channel activation
Metabotropic	D1/D2	N/A	Slow	G _s /G _i to cAMP
Metabotropic	5-HT _{1A–7}	N/A	Slow	Various G protein coupling

NMDA receptor – “coincidence detector”: The NMDA receptor requires BOTH glutamate binding AND postsynaptic depolarization (to relieve Mg²⁺ block) to conduct. This makes it a detector of coincident pre- and postsynaptic activity – exactly the condition Hebb proposed should strengthen synapses [Hebb, 1949]. Ca²⁺ entry through NMDA receptors triggers LTP.

Concept Check: At a synapse with $n = 10$ release-ready vesicles, release probability $p = 0.2$, and quantal size $q = 0.5$ mV, a single presynaptic spike must drive the postsynaptic membrane from -70 mV to a -55 mV threshold. Using the $n \cdot p \cdot q$ model, decide whether one spike reaches threshold and explain why a drug that raises p (e.g., an aminopyridine prolonging the presynaptic AP) can convert a sub-threshold synapse to a supra-threshold one without adding any new vesicles. (Hint: compute the expected EPSP amplitude and compare it to the 15 mV gap.)

Concept Check (Analyze) — NMDA receptor as coincidence detector and the LTP gate. The NMDA receptor demands *both* glutamate (plus glycine/D-serine co-agonist) *and* postsynaptic depolarization to conduct: at -70 mV the channel pore is occluded by extracellular Mg²⁺; at ~ -30 mV the Mg²⁺ is expelled, opening a Ca²⁺-permeable pathway. (a) Draw a sketch of conductance vs V_m for the NMDA receptor in the presence of saturating glutamate, marking the Mg²⁺-block region and the relief threshold. (b) Explain why this voltage-dependent gating implements a *Hebbian* rule (pre and post must fire together) at the molecular level, and predict what would happen to LTP induction in a mouse engineered with the GluN1 N598Q mutation that removes the Mg²⁺-binding site. (c) AMPA-receptor insertion into the post-synaptic density requires CaMKII-mediated phosphorylation of GluA1 at S831, which is triggered by NMDA-mediated Ca²⁺ entry. Predict the consequence of pharmacologically blocking PKA (which co-phosphorylates GluA1 at S845 to potentiate channel open probability) during LTP induction, and explain why both kinases are needed to lock in synaptic strengthening rather than just one.

Concept Check (Evaluate) — Parvalbumin interneurons, E/I balance, and working memory. Cortical inhibition is parcelled by interneuron class: parvalbumin (PV) basket cells deliver fast, perisomatic GABA inhibition that gates spike timing of pyramidal neurons and pace cortical gamma oscillations (30–80 Hz); somatostatin (SST) interneurons target apical dendrites and modulate dendritic integration. (a) In a network where PV-cell density is selectively reduced by approximately 30% (as reported in post-mortem schizophrenia tissue), predict the directional change in (i) excitation/inhibition (E/I) ratio, (ii) gamma oscillation power, and (iii) pyramidal-cell spike-timing precision. (b) Working memory in prefrontal cortex relies on persistent pyramidal-cell firing during the delay period, sustained by recurrent excitation gated by PV inhibition. Evaluate why a modest PV loss would degrade working memory more than long-term memory consolidation. (c) Propose a single physiological measurement (gamma power at a specific frequency band; spike-LFP phase locking; visual-attention gain control) you would prioritize as a clinical biomarker, and justify it in terms of statistical power and translational tractability between rodent models and human EEG.

33.6 Neurotransmitter Systems and Receptor Families

33.6.1 Glutamate as the Major Excitatory Transmitter

The major excitatory neurotransmitter in the CNS (about 90% of excitatory synapses).

Receptors: - AMPA (GluA1-4): Fast Na⁺/K⁺ current. Ca²⁺-permeable if lacking GluA2 (GluA2 RNA editing of Q/R site prevents Ca²⁺ permeability in most adult neurons). - NMDA (GluN1/GluN2A-D): Coincidence detector. Requires glutamate + glycine/D-serine co-agonist + depolarization to relieve Mg²⁺ block. High Ca²⁺ permeability. Critical for LTP. - Kainate (GluK1-5): Similar to AMPA; modulatory roles at some synapses. - mGluR (mGluR1-8): Metabotropic. Group I (mGluR1/5): G_q-coupled, excitatory. Group II/III: G_i-coupled, inhibitory (presynaptic autoreceptors).

Excitotoxicity: Excessive glutamate release (e.g., during stroke/ischemia) overactivates NMDA receptors. Massive Ca²⁺ influx activates calpains, endonucleases, and nitric oxide synthase, leading to neuronal death. This is a major mechanism of ischemic brain damage.

33.6.2 GABA as the Major Inhibitory Transmitter

The major inhibitory neurotransmitter (about 30% of CNS synapses). Synthesized from glutamate by glutamic acid decarboxylase (GAD65/GAD67).

Receptors: - GABA_A (ionotropic): Cl⁻ channel. Pentameric (typically $\alpha_1\beta_2\gamma_2$). Binding sites for: GABA (agonist), benzodiazepines (positive **allosteric** modulators at α/γ interface), barbiturates, neurosteroids, ethanol, anaesthetics (propofol, isoflurane). - GABA_B (metabotropic): G_i-coupled GPCR. Activates K⁺ channels (postsynaptic hyperpolarization) and inhibits Ca²⁺ channels (presynaptic, reduces NT release). Baclofen is a GABA_B agonist (used for spasticity).

33.6.3 Acetylcholine at Neuromuscular and Autonomic Synapses

Receptors: - Nicotinic (nAChR): Ionotropic pentamer. Muscle type ($\alpha_1\beta_1\delta\epsilon$) at NMJ. Neuronal types ($\alpha_4\beta_2, \alpha_7$) in CNS. Na⁺/K⁺ channels. - Muscarinic (mAChR, M1-M5): GPCRs. M1/M3/M5: G_q (excitatory). M2/M4: G_i (inhibitory, e.g., vagal slowing of heart rate).

CNS cholinergic system: Basal forebrain (nucleus basalis of Meynert) projects to cortex. Critical for attention and memory. Degeneration in Alzheimer’s disease.

33.6.4 Dopamine in Reward, Movement, and Precision Signals

Receptors: D1-D5 (most GPCRs). D1-like (D1, D5): G_s, increase cAMP. D2-like (D2, D3, D4): G_i, decrease cAMP.

Major pathways: - Nigrostriatal (SNc to striatum): Motor control. Loss causes Parkinson’s disease. - Mesolimbic (VTA to nucleus accumbens): Reward prediction error, motivation. Hyperactivity linked to positive symptoms of schizophrenia. - Mesocortical (VTA to prefrontal cortex): Working memory, executive function. Hypoactivity linked to negative symptoms of schizophrenia and ADHD. - Tuberoinfundibular (hypothalamus to pituitary): Inhibits prolactin release.

33.6.5 Serotonin (5-HT)

Synthesized from tryptophan by tryptophan hydroxylase (TPH2 in CNS). Raphe nuclei in brainstem project widely. 14 receptor subtypes (5-HT_{1A} through 5-HT₇).

Functions: Mood regulation, sleep/wake cycle, appetite, pain modulation. about 90% of body’s serotonin is in enterochromaffin cells of the GI tract.

33.6.6 Norepinephrine in Arousal and Autonomic Modulation

Synthesized from dopamine by dopamine β -hydroxylase (DBH). Locus coeruleus (brainstem) projects to entire cortex. Functions: arousal, attention, vigilance, stress response.

Receptors: α_1 (G_q), α_2 (G_i, presynaptic autoreceptor), β_1 (G_s, heart), β_2 (G_s, bronchial smooth muscle, blood vessels).

33.7 Computational Neuroscience and AI Models



Figure 200. The convergence of computational neuroscience and AI. Early neural models (Hodgkin-Huxley, integrate-and-fire) inspired artificial neurons, while modern deep learning architectures are now used to model brain function and analyze neural data.

33.7.1 Computational Neuroscience Models

- Biophysical models:
- Hodgkin-Huxley model (1952): A set of nonlinear differential equations that describe how action potentials in neurons are initiated and propagated. It remains one of the most important mathematical models in neuroscience.
 - FitzHugh-Nagumo model (1961): A simplified two-variable model that captures the essential dynamics of the Hodgkin-Huxley model while being more mathematically tractable.
 - Izhikevich model (2003): A hybrid model that combines the biological plausibility of Hodgkin-Huxley with the computational efficiency of integrate-and-fire models.

Large-scale brain models:

- Blue Brain Project (EPFL): Aims to create a digital reconstruction of the rodent brain and ultimately the human brain using detailed biophysical models.
- Human Brain Project (EU): A €1 billion initiative to simulate the entire human brain using supercomputers.
- Spaun (University of Waterloo): A large-scale functional brain model that can perform multiple cognitive tasks.

33.7.2 Machine Learning for Neural Data Analysis

Modern neuroscience generates massive datasets (e.g., calcium imaging, EEG, fMRI, intracranial recordings). Machine learning is essential for extracting meaningful information:

- Spike sorting: Unsupervised learning algorithms (e.g., PCA + clustering, deep learning) to separate the activity of individual neurons from extracellular recordings.
- Calcium imaging analysis: Deconvolution algorithms (e.g., OASIS, CaImAn) to extract spike trains from fluorescence signals.
- Neural decoding: Supervised learning to predict behavior or perception from neural activity (e.g., BMI control, speech decoding).
- fMRI pattern analysis: Multivariate pattern analysis (MVPA) and deep learning to identify mental states from brain activity patterns.
- Connectomics: Computer vision and graph neural networks to map neural connectivity from electron microscopy data.

```
import numpy as np
import torch
import torch.nn as nn
from scipy.signal import butter, filtfilt

# Example: Simple neural decoder for BMI control
class NeuralDecoder(nn.Module):
    """A simple LSTM-based decoder for predicting movement from neural spikes."""
    def __init__(self, input_dim, hidden_dim, output_dim, num_layers=2):
        super().__init__()
        self.lstm = nn.LSTM(input_dim, hidden_dim, num_layers, batch_first=True)
        self.fc = nn.Linear(hidden_dim, output_dim)

    def forward(self, x):
        # x shape: (batch, seq_len, input_dim)
        lstm_out, _ = self.lstm(x)
        # Take the last time step output
        out = self.fc(lstm_out[:, -1, :])
        return out

# Example: Spike sorting with PCA + clustering
def spike_sorting(waveforms):
    """Simple spike sorting using PCA and k-means."""
    # Perform PCA
    from sklearn.decomposition import PCA
    pca = PCA(n_components=3)
    pca_result = pca.fit_transform(waveforms)
    # Cluster
    from sklearn.cluster import KMeans
    kmeans = KMeans(n_clusters=4, random_state=0).fit(pca_result)
    return kmeans.labels_

# Example: Calcium imaging deconvolution
def oasis_deconvolution(fluor_signal, dt=0.1, lambda_=10):
    """OASIS algorithm for spike inference from calcium imaging."""
    from oasis import oasisAR1N
```

```
# Convert to AR1N model
result = oasisAR1N(fluor_signal, dt=dt, lambda_=lambda_, g=0.95)
return result["spikes"] # Estimated spike times
```

33.7.3 AI for Drug Discovery in Neurology

Traditional drug discovery takes 10-15 years and billions of dollars. AI is accelerating the process:

- Target identification: Machine learning models analyze genomic, transcriptomic, and proteomic data to identify promising drug targets.
- Compound screening: Deep learning models predict the activity of millions of compounds against specific targets, enabling virtual screening.
- De novo drug design: Generative models (GANs, VAEs, transformers) can design novel molecules with desired properties.
- Clinical trial optimization: AI helps identify suitable patient populations, predict outcomes, and optimize trial design.

Case study: Insilico Medicine used AI to identify a novel target for idiopathic pulmonary fibrosis, design a novel molecule, and complete preclinical experiments in under 18 months (vs. typical 4-6 years).

33.7.4 Brain-Computer Interfaces (BCIs)

BCIs translate neural activity into commands for external devices, offering hope for paralysis, locked-in syndrome, and other neurological conditions:

- Signal acquisition: Microelectrode arrays (Utah array, Blackrock), ECoG, EEG, or optical imaging.
- Signal processing: Filtering, spike detection, feature extraction.
- Decoding algorithms: Linear models (Kalman filter, Wiener filter), neural networks, and reinforcement learning to map neural signals to actions.
- Applications:
 - Communication: Typing at 20+ words per minute using imagined handwriting.
 - Mobility: Controlling robotic limbs or exoskeletons.
 - Sensory restoration: Cortical visual prostheses for the blind.

Neuralink and other companies are developing high-bandwidth, minimally invasive BCIs with thousands of channels, aiming to treat paralysis and eventually enhance human cognition.

33.7.5 Ethical Considerations in AI and Neurotechnology

As AI becomes more integrated with neuroscience, important ethical questions arise:

- Privacy: Neural data is the ultimate private information. How do we protect brain data from misuse?
- Agency and responsibility: If a BCI-controlled prosthetic acts unintentionally, who is responsible?
- Cognitive enhancement: Should AI-assisted cognitive enhancement be allowed? What are the societal implications?
- Dual-use: The same technology that helps paralyzed patients could be used for military applications or surveillance.
- Bias in AI: If training data lacks diversity, AI systems may perform poorly for underrepresented groups, exacerbating health disparities.

```
# Example: Simple neural encoding model
class NeuralEncoder(nn.Module):
    """A simple model that predicts neural response to visual stimuli."""
    def __init__(self, stimulus_dim, hidden_dim, neural_dim):
        super().__init__()
        self.conv = nn.Conv2d(stimulus_dim, 64, kernel_size=7, stride=2)
        self.fc = nn.Linear(64 * 7 * 7, hidden_dim)
        self.output = nn.Linear(hidden_dim, neural_dim)

    def forward(self, stimulus):
        x = torch.relu(self.conv(stimulus))
        x = x.view(x.size(0), -1)
        x = torch.relu(self.fc(x))
```



```
        return self.output(x)

# Example: Reinforcement learning for adaptive BCIs
import gym
from stable_baselines3 import PPO

# Create a custom environment for BCI control
class BCIEnv(gym.Env):
    def __init__(self):
        super().__init__()
        self.observation_space = gym.spaces.Box(low=-1, high=1, shape=(100,))
        self.action_space = gym.spaces.Box(low=-1, high=1, shape=(2,))

    def step(self, action):
        # Simplified: reward based on how close action is to target
        reward = -np.sum((action - self.target) ** 2)
        self.steps += 1
        done = self.steps >= 200 or reward < -10
        return self._get_observation(), reward, done, {}

    def reset(self):
        self.steps = 0
        self.target = np.random.randn(2)
        return self._get_observation()

    def _get_observation(self):
        # Simulated neural data
        return np.random.randn(100)

# Train a policy
env = BCIEnv()
model = PPO("MlpPolicy", env).learn(total_timesteps=10000)
```

Concept Check 6.1

1. What is the difference between Hodgkin-Huxley and Izhikevich models? When would you use each?
 2. How can machine learning be used to analyze calcium imaging data?
 3. What are some ethical concerns with brain-computer interfaces?
 4. How might AI accelerate drug discovery for neurological disorders?
-

33.7.6 Neuropeptides and Slow Modulatory Signaling

Characteristics: Larger molecules (3-40 amino acids); synthesized in soma (not terminals); stored in large dense-core vesicles; released by higher-frequency stimulation; diffuse farther (volume transmission); slower, longer-lasting effects.

Examples: - Substance P: Pain transmission (dorsal horn); co-released with glutamate from nociceptors - Enkephalins / endorphins: Endogenous opioids; bind μ (μ), δ (δ), κ (κ) opioid receptors; inhibit pain pathways - NPY: Appetite stimulation; anxiolysis; one of the most abundant peptides in the brain - Orexin/hypocretin: Wakefulness promotion; loss causes narcolepsy type 1

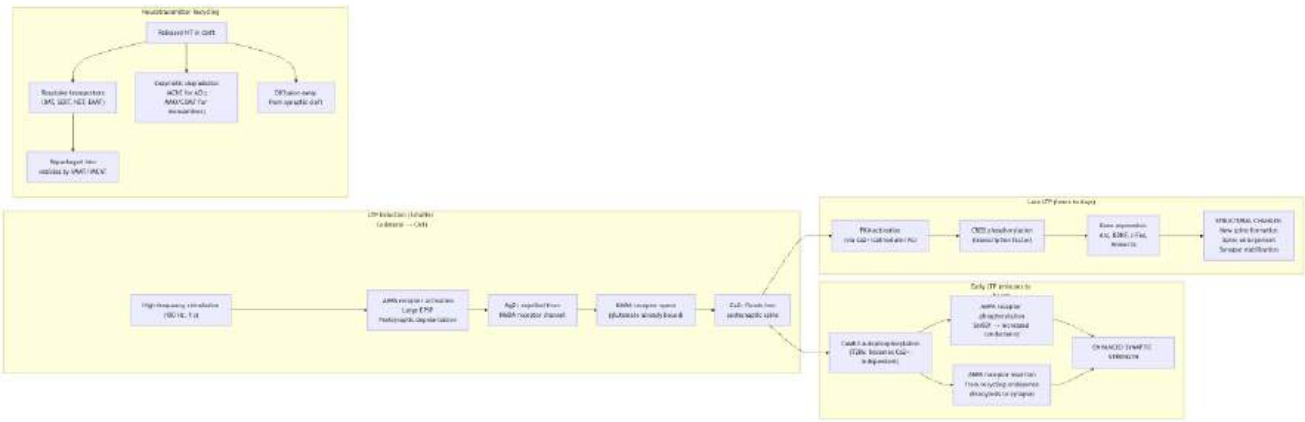


Figure 201. Molecular mechanisms of LTP and neurotransmitter recycling. LTP induction requires NMDA receptor opening (coincidence detection) and Ca^{2+} influx. Early LTP involves CaMKII-mediated AMPA receptor modification. Late LTP requires gene expression (CREB) and structural synaptic changes. Neurotransmitters are cleared by reuptake, enzymatic degradation, or diffusion.

33.8 Synaptic Plasticity and Memory

33.8.1 Long-Term Potentiation (LTP)

1. High-frequency stimulation (100 Hz, 1 s) produces large EPSPs via AMPA receptors
2. Sufficient depolarization removes Mg^{2+} block from NMDA receptors
3. Ca^{2+} floods into the postsynaptic spine via NMDA receptors
4. Ca^{2+} activates CaMKII (calcium/calmodulin-dependent protein kinase II):
 - Autophosphorylation at T286 makes CaMKII constitutively active (Ca^{2+} -independent)
 - Phosphorylates AMPA receptors at Ser831, increasing single-channel conductance
5. AMPA receptor trafficking: New AMPA receptors inserted into the synapse from recycling endosomes
6. Silent synapses: Some synapses have NMDA receptors but no AMPA receptors. LTP “unmasks” these by inserting AMPA receptors, converting them to functional synapses.
7. Late LTP (>3 h): Requires new gene expression. Ca^{2+} activates PKA, which phosphorylates CREB. CREB-mediated transcription produces Arc, BDNF, c-Fos. Structural changes include dendritic spine enlargement and formation of new spines.

33.8.2 Long-Term Depression (LTD)

Low-frequency stimulation (1 Hz, 15 min) produces modest Ca^{2+} entry via NMDA receptors: - Lower Ca^{2+} levels preferentially activate protein phosphatases (PP1, calcineurin/PP2B) rather than CaMKII - Phosphatases dephosphorylate AMPA receptors - AMPA receptors are endocytosed (clathrin-mediated) from the synapse - Synaptic strength decreases

Bidirectional plasticity: The same synapse can undergo LTP or LTD depending on the pattern of Ca^{2+} entry. This is captured by the BCM (Bienenstock-Cooper-Munro) rule: there exists a modification threshold (θ_M) – activity above θ_M causes LTP, below causes LTD. The threshold itself slides based on recent postsynaptic activity (metaplasticity).

Concept Check 2: A neuroscientist finds that pharmacologically blocking the NMDA receptor abolishes LTP at hippocampal Schaffer-collateral → CA1 synapses but does not abolish LTP at mossy-fiber → CA3 synapses. Propose a mechanism that explains why these two forms of LTP differ. Given that the CA3 form is presynaptic (cAMP-PKA-dependent), which pharmacological manipulation would selectively block it without affecting NMDA-receptor-dependent LTP?

33.9 Neuropharmacology: Synaptic and Ion-Channel Drug Mechanisms

Table 392. Long-Term Depression (LTD): Drug and Molecular Target.

Drug	Molecular Target	Mechanism	Clinical Use
Cocaine	DAT (dopamine transporter)	Blocks DA reuptake; DA accumulates in synapse	Abuse potential; local anaesthetic (Na^+ channel block)

Drug	Molecular Target	Mechanism	Clinical Use
Amphetamine	DAT, VMAT	Reverses DAT (DA efflux); releases vesicular DA	ADHD; narcolepsy; abuse
SSRIs (fluoxetine, sertraline)	SERT (serotonin transporter)	Block 5-HT reuptake	Depression; anxiety; OCD
SNRIs (venlafaxine, duloxetine)	SERT + NET	Block both 5-HT and NE reuptake	Depression; neuropathic pain; generalized anxiety disorder
Morphine/heroin	μ -opioid receptor	Agonist; inhibits GABA interneurons (disinhibition of DA) in VTA	Pain; abuse
Naloxone	μ -opioid receptor	Antagonist; reverses opioid effects	Opioid overdose reversal
Buprenorphine	μ -opioid receptor	Partial agonist; ceiling effect; long half-life	Opioid use disorder (maintenance treatment)
Benzodiazepines (diazepam)	GABA _A (α/γ interface)	Positive allosteric modulator; increases Cl [−] channel open frequency	Anxiety; seizures; insomnia
Barbiturates (phenobarbital)	GABA _A (transmembrane domain)	Positive allosteric modulator; increases Cl [−] channel open duration; direct activation at high doses	Seizures; anaesthesia; narrow therapeutic index
Ketamine	NMDA receptor	Non-competitive antagonist (open-channel block)	Anaesthesia; rapid-acting antidepressant (sub-anaesthetic dose)
Ethanol	GABA _A + NMDA	Potentiates GABA _A (increased Cl [−] conductance); inhibits NMDA	Recreational; anxiolytic
Caffeine	Adenosine A ₁ /A _{2A} receptors	Competitive antagonist; blocks adenosine's sleep-promoting effect	Wakefulness; headache treatment
L-DOPA	AADC (aromatic amino acid decarboxylase)	Dopamine precursor; crosses BBB; converted to DA in brain	Parkinson's disease
Levodopa + carbidopa	AADC (peripheral inhibition by carbidopa)	Prevents peripheral conversion; maximizes CNS L-DOPA delivery	Parkinson's disease
Haloperidol	D2 receptor	Competitive D2 antagonist	First-generation antipsychotic (schizophrenia); risk of tardive dyskinesia
Clozapine	D4, 5-HT _{2A} , H1, M1, α_1	"Atypical" antipsychotic — low D2 affinity, high 5-HT _{2A} block	Treatment-resistant schizophrenia; risk of agranulocytosis requires WBC monitoring
Curare (d-tubocurarine)	Muscle nAChR	Competitive antagonist; blocks NMJ transmission	Muscle relaxant (anaesthesia)
Botulinum toxin	SNARE (SNAP-25)	Cleaves SNAP-25; blocks vesicle fusion	Focal dystonia; cosmetic (Botox); therapeutic spasticity
Gabapentin; pregabalin	Ca-channel $\alpha_2\delta$ subunit	Reduces dorsal-horn neurotransmitter release	Neuropathic pain; epilepsy; fibromyalgia; anxiety
Levetiracetam	SV2A (synaptic vesicle glycoprotein)	Binds SV2A; reduces Ca ²⁺ -evoked vesicle release	Broad-spectrum antiepileptic; minimal drug interactions

Drug	Molecular Target	Mechanism	Clinical Use
Lithium	IMPase, GSK-3β, and others	Inhibits inositol monophosphatase (depletes PI signaling substrate); inhibits GSK-3β (neuroprotection)	Bipolar disorder (mood stabiliser); narrow therapeutic index (Li ⁺ 0.6–1.2 mEq/L)

Clinical Connection: The opioid epidemic has killed over 500,000 Americans since 1999. Understanding the molecular pharmacology is essential: opioids activate mu receptors on GABAergic interneurons in the VTA, removing tonic inhibition of dopamine neurons. The resulting dopamine surge in the nucleus accumbens produces euphoria and reinforcement. Tolerance develops as mu receptors are desensitised and downregulated. Withdrawal occurs because the compensatory upregulation of cAMP signaling is unmasked when the drug is removed. Naloxone (Narcan) competitively displaces opioids from mu receptors and can reverse respiratory depression within minutes.

33.10 Worked Example: Quantal Release at the Neuromuscular Junction

Problem: You voltage-clamp a frog neuromuscular junction and record spontaneous miniature end-plate currents (mEPCs). From 500 events, the mean mEPC amplitude is $q = 1.2$ nA (quantal size). You then stimulate the motor nerve with single pulses and measure evoked EPCs.

Over 200 evoked trials: - 8 trials produce no response (failures) - 72 trials produce a single quantal event (about 1.2 nA) - 68 trials produce two quantal events (about 2.4 nA) - 36 trials produce three quantal events (about 3.6 nA) - 12 trials produce four quantal events (about 4.8 nA) - 4 trials produce five quantal events (about 6.0 nA)

(a) Calculate the mean quantal content \bar{m} = mean number of quanta released per stimulus.

$$\bar{m} = \frac{0(8) + 1(72) + 2(68) + 3(36) + 4(12) + 5(4)}{200} = \frac{0 + 72 + 136 + 108 + 48 + 20}{200} = \frac{384}{200} = 1.92$$

(407)

(b) Use the Poisson approximation to estimate the number of failures expected if $\bar{m} = 1.92$:

For a Poisson process, the fraction of failures $P(0) = e^{-\bar{m}} = e^{-1.92} = 0.146$

Expected failures = $0.146 \times 200 = 29.3$. Observed failures = 8. The discrepancy suggests the release is not strictly Poisson — there may be heterogeneity in vesicle release probabilities across active zones, or the preparation has an unusually low failure rate due to high quantal content.

(c) Use the method of failures to give an alternative estimate of \bar{m} :

$$\bar{m} = \ln\left(\frac{N}{n_0}\right) = \ln\left(\frac{200}{8}\right) = \ln(25) = 3.22$$

(408)

The discrepancy between the two estimates (1.92 by direct count vs 3.22 by method of failures) indicates that the binomial model (with heterogeneous release probabilities) fits better than the simple Poisson. This is a classic result: real synapses have multiple active zones with heterogeneous p values, violating the simple Poisson assumption (Zucker 1973; Bhumbra & Bhatt 2022).

(d) Given $\bar{m} = 1.92$ and the number of release-ready vesicles $n = 10$ (estimated by high-osmotic sucrose stimulation), estimate the mean release probability \bar{p} :

$$\bar{p} = \frac{\bar{m}}{n} = \frac{1.92}{10} = 0.192$$

(409)

This is a typical resting release probability for a vertebrate neuromuscular junction (0.1–0.4 at physiological Ca^{2+}). The $n \cdot p \cdot q$ synaptic model predicts that drugs which increase p (e.g., by prolonging the AP and increasing Ca^{2+} influx, such as aminopyridines) will linearly increase \bar{m} and thus EPP amplitude — a pharmacological basis for treatments in Lambert-Eaton myasthenic syndrome.

33.11 Current Evidence and Frontier Biology: Action Potentials and Synaptic Transmission

For Action Potentials and Synaptic Transmission, frontier biology belongs inside the evidence logic of the chapter. Physiology now blends mechanism with allostasis, immune-endocrine-neural coupling, wearable data, and individualized risk without reducing bodies to simple machines. The core reading question is this: synaptic claims require ion-channel timing, driving force, transmitter release, receptor dynamics, and plasticity.

- What to verify: identify the observation, model, assay, or dataset that would make the claim stronger or weaker.
- What to qualify: state the scale, organism, cell type, environmental condition, or population where the claim is expected to hold.
- What to compare: test at least one alternative explanation, baseline, or null model before treating the pattern as causal.
- What to cite: distinguish primary evidence, review synthesis, public dataset, and institutional guidance; for recent or numeric claims, prefer the source closest to the measurement and state what has changed since it was published.

Interpret synaptic data by separating resting state, channel kinetics, perturbation response, plasticity, and pathological threshold.

Source practice: For action-potential and synapse claims, cite voltage traces, conductance models, pharmacology, or perturbation evidence matched to the mechanism.

33.12 Key Terms

Table 393. Long-Term Depression (LTD): Term and Definition.

Term	Definition
Hodgkin-Huxley model	Mathematical description of AP using gating variables m, h, n for Na ⁺ and K ⁺ conductances
Threshold	Membrane potential (about −55 mV) at which inward Na ⁺ current exceeds outward K ⁺ current
Absolute refractory period	about 1-2 ms when Na ⁺ channels are inactivated; no AP possible regardless of stimulus
Relative refractory period	about 5-10 ms when Na ⁺ channels recovering; stronger stimulus needed for AP
Saltatory conduction	AP jumps between nodes of Ranvier in myelinated axons
SNARE complex	Synaptobrevin + syntaxin + SNAP-25: core vesicle fusion machinery
Synaptotagmin	Ca ²⁺ sensor that triggers vesicle fusion; C2 domains bind 4-5 Ca ²⁺ ions
Quantal release	Neurotransmitter released in discrete vesicle-sized packets (Katz, 1950s)
NMDA receptor	Coincidence detector: requires glutamate + depolarization; Ca ²⁺ permeable
CaMKII	Calcium/calmodulin kinase II; autophosphorylation at T286; key LTP effector
LTP	Long-term potentiation: persistent increase in synaptic strength
LTD	Long-term depression: persistent decrease in synaptic strength
Excitotoxicity	Neuronal death from excessive glutamate/Ca ²⁺ (stroke, epilepsy)
Tetrodotoxin (TTX)	Puffer fish toxin blocking Nav channels
BCM rule	Sliding modification threshold determining LTP vs LTD
Silent synapse	Synapse with NMDA but no AMPA receptors; “unmasked” during LTP

33.13 Review Questions

1. Using the Hodgkin-Huxley equations, explain why the peak of the action potential does not reach E_{Na} (+50 mV) but instead peaks at approximately +30 to +40 mV. Which gating variable is responsible?
2. Explain the molecular basis of the absolute refractory period. Why is this essential for unidirectional AP propagation?
3. Compare saltatory conduction in myelinated axons with continuous conduction in unmyelinated axons. Why does velocity scale as \sqrt{d} in unmyelinated axons but as d in myelinated axons?
4. Describe the roles of the five key presynaptic proteins: synaptobrevin, syntaxin, SNAP-25, synaptotagmin-1, and complexin. What happens if each is eliminated?
5. The NMDA receptor is often called the “Hebbian synapse detector.” Explain this concept, linking the receptor’s biophysical properties to Hebb’s postulate and to LTP induction.
6. A patient presents with progressive muscle weakness. Antibodies against the nicotinic ACh receptor are detected. Name the disease, explain the pathophysiology, and describe two treatment strategies based on cholinergic pharmacology.
7. Compare the mechanisms of cocaine and amphetamine at dopaminergic synapses. Both increase synaptic dopamine, but by different mechanisms. Why might their clinical effects and addiction profiles differ?
8. Explain why benzodiazepines are safer in overdose than barbiturates, despite both acting on GABA_A receptors. (Hint: consider the difference between increasing channel open frequency vs open duration, and the concept of ceiling effect.)

9. Design a hypothetical drug that could enhance memory formation by targeting the LTP pathway. Identify the molecular target, predict the therapeutic effect, and discuss potential side effects (excitotoxicity risk).
10. Why does multiple sclerosis cause such diverse neurological symptoms? Explain the relationship between lesion location in white matter tracts and the specific symptoms produced.
11. At a synapse, you observe mEPP amplitude of 0.5 mV and mean EPP amplitude of 4.5 mV (low-Ca²⁺ conditions to allow quantal resolution). (a) Estimate the mean quantal content \bar{m} . (b) Use the Poisson failure method to calculate the expected probability of a failure. (c) If you increase extracellular Ca²⁺ from 1 mM to 2 mM, predict whether \bar{m} will increase linearly, quadratically, or via a 4th-power relationship (based on synaptotagmin cooperativity), and explain the molecular basis.
12. Clozapine is described as an “atypical” antipsychotic with lower risk of tardive dyskinesia compared to haloperidol, despite both treating positive symptoms of schizophrenia. Using the drug table, explain: (a) their differing receptor binding profiles; (b) why high D2 occupancy causes tardive dyskinesia; (c) why clozapine’s unique receptor profile (including 5-HT_{2A} blockade) may explain its superior efficacy in treatment-resistant schizophrenia.

33.14 Further Reading and Source Notes: Action Potentials and Synaptic Transmission

• Frey & Morris (1997). Synaptic tagging and long-term potentiation. *Nature*, 385.

• Hodgkin & Huxley (1952). A quantitative description of membrane current and its application to conduction and excitation in nerve. *Journal of Physiology*, 117.

• Katz (1969). *The Release of Neural Transmitter Substances*. Liverpool University Press.

• Bliss & Lomo (1973). Long-lasting potentiation of synaptic transmission in the dentate area of the anaesthetized rabbit. *Journal of Physiology*, 232.

• Kandel et al. (latest ed.). *Principles of Neural Science* (action potential and synaptic transmission chapters). McGraw-Hill.

• Neher & Sakmann (1976). Single-channel currents recorded from membrane of denervated frog muscle fibers. *Nature*, 260.

33.15 Computational Bridge

Driving-force synaptic current in pA follows $I = g(V_m - E_{rev})$:

```
from biology.neuroscience import synaptic_current

exc = synaptic_current(0.0, -65.0, 12.0)
inh = synaptic_current(-70.0, -65.0, 20.0)
print(round(exc.peak_current_pA, 2), round(inh.peak_current_pA, 2))
```

Clinical / systems note: Benzodiazepines increase GABA_A frequency without changing E_{rev} ; barbiturates prolong open time — both shift inhibitory current but with different overdose ceilings.

33.16 Summary

- Hodgkin-Huxley: $I_{Na} = \bar{g}_{Na}m^3h(V - E_{Na})$, $I_K = \bar{g}_Kn^4(V - E_K)$. Gating variables obey first-order kinetics. m (fast activation), h (slow inactivation), n (slow activation).
- Refractory periods: Absolute (Na⁺ inactivated, h about 0, 1-2 ms): cannot fire. Relative (K⁺ channels open, membrane hyperpolarised, 5-10 ms): stronger stimulus needed.
- Na⁺ channel states: Closed (ready) to Open (conducting, about 0.5 ms) to Inactivated (blocked from inside, cannot reopen). TTX and local anaesthetics block the pore.
- Myelination: Saltatory conduction between nodes of Ranvier. Velocity proportional to diameter (linear). A-alpha fibers: 70-120 m/s; C fibers: 0.5-2 m/s. MS: autoimmune demyelination.
- Chemical synapse: AP opens Cav2.1/2.2 channels. Ca²⁺ binds synaptotagmin-1. Complexin displaced. SNARE complex zippers. Vesicle fuses. NT released in <1 ms. Quantal release (Katz).
- Neurotransmitters: Glutamate (AMPA/NMDA/mGluR, excitatory); GABA (GABA_A/GABA_B, inhibitory); ACh (nicotinic/muscarinic); DA (D1-D5, reward/motor); 5-HT (mood/sleep); NE (arousal); neuropeptides (volume transmission, pain, reward).
- LTP: NMDA-Ca²⁺-CaMKII-AMPA pathway. Early: phosphorylation and insertion of AMPA receptors. Late: CREB-dependent gene expression, structural spine changes. LTD: opposite; phosphatases remove AMPA receptors.

- Drug mechanisms: Cocaine (DAT block), morphine (mu agonist), SSRIs (SERT block), benzodiazepines (GABA_A PAM), ketamine (NMDA block), botulinum toxin (SNAP-25 cleavage).
- Connections: See section 32 for resting potential and integration, section 27 for synaptic pathogens and toxins, and section 7 for ion channels.

33.17 Companion Source Module: Action Potentials and Synaptic Transmission

Action Potentials and Synaptic Transmission should leave a reproducible trail from a biological claim to the code, figure, diagram, or paper-based activity that can test it. Use the surfaces below to inspect the chapter’s assumptions, rerun the relevant model, or compare the manuscript explanation with companion labs and figures.

Table 394. Companion source surfaces for Action Potentials and Synaptic Transmission.

Surface	Use it for
src/biology/neuroscience/neuroscience.py (action_potential_hh, synaptic_current, cable_voltage_attenuation)	Reproduce spike timing, postsynaptic currents, and passive spread.
src/biology/cell/cell_biology.py (nernst_potential, goldman_equation)	Check ion gradients and membrane-voltage assumptions.
src/visualization/plots.py (plot_action_potential, plot_nernst_potentials)	Compare calculated voltages with plotted signals.

Reproducibility check: list ion concentrations, conductances, reversal potentials, synaptic delay, and receptor type before interpreting excitability. Cross-reference: connect with section 7 and section 32.

34 Endocrine Signaling and Homeostasis

Level 2/3 · 30 min read · 40 min lecture · Prerequisites: section 31

34.1 Learning Objectives

1. Compare endocrine and nervous system signaling in terms of speed, duration, and specificity.
2. Classify **hormones** by chemical class (peptide, steroid, amine, eicosanoid) and describe their synthesis, transport, receptor location, and signaling duration.
3. Explain the HPA, HPT, and HPG axes with feedback regulation, including detailed steroidogenesis and the circadian profile of cortisol.
4. Trace insulin and glucagon signaling in glucose **homeostasis**, including IR/IRS/PI3K/Akt/GLUT4, crosstalk with leptin and GLP-1, and the pathophysiology of diabetes.
5. Describe the adrenal gland structure and function (cortex and medulla), including cortisol synthesis from cholesterol.
6. Describe thyroid hormone synthesis, T4→T3 conversion, the nuclear receptor mechanism, and the Wolff-Chaikoff effect.
7. Describe the growth hormone axis and IGF-1.
8. Explain prostaglandin and eicosanoid synthesis from arachidonic acid; differentiate non-selective NSAIDs from COX-2 selective inhibitors.
9. Describe endocrine disruption by xenoestrogens, BPA, phthalates, and PFAS.

34.1.1 Study Blueprint

- Big idea: Hormone feedback loops coordinate long-range physiological homeostasis.
- Core concepts: hormones, feedback, receptors, homeostasis.
- Framework alignment: Vision & Change: Structure and function, Systems; AP Biology: Systems Interactions, Energetics; NGSS-style topics: Structure and Function.
- Model or quantitative lens: Hormone feedback and dose-response reasoning.
- Data skill: Interpret endocrine time courses, panels, and perturbations.
- Practice cadence: Visual Representations, Statistical Tests and Data Analysis, Argumentation.
- Common misconception to repair: A hormone surge is not always pathological; context and set-point matter.
- Primary lab: **Lab — Endocrine Signaling and Homeostasis**.
- Question bank: **Questions — Endocrine Signaling and Homeostasis**.
- Transfer task: Transfer endocrine reasoning to metabolism, stress, and development.
- Bridge to computation: `biology.physiology.physiology.homeostasis_response`.

Opening Vignette — The Hormone That Changed Medicine Forever

Before 1921, Type 1 diabetes was a death sentence. Children diagnosed with it were placed on starvation diets — sometimes eating fewer than 500 calories per day — which extended their lives by months while slowly wasting them. Then Frederick Banting, a young Canadian surgeon, persuaded the University of Toronto to give him laboratory space and a few dogs. Working with student Charles Best and biochemist J.B. Collip to purify the extract, they isolated the pancreatic secretion that controlled blood glucose — insulin. The first human injection was given to 14-year-old Leonard Thompson on January 11, 1922. He had been near death; within days his blood glucose normalized and he survived. Banting and John Macleod received the Nobel Prize in 1923. Insulin was the first hormone to be purified, the first to be sequenced (by Frederick Sanger, 1951), and the first to be produced by recombinant DNA technology (1982) [**Sanger, 1955**]. No single molecule has had a more direct impact on human survival.

34.2 Endocrine System Overview

34.2.1 Endocrine vs Nervous System

Table 395. Endocrine vs Nervous System: Feature and Nervous System.

Feature	Nervous System	Endocrine System
Signal type	Electrical + chemical (neurotransmitter)	Chemical (hormone)
Speed	Fast (ms)	Slow (seconds to hours)
Duration	Brief (ms)	Prolonged (minutes to days)
Target	Specific (synapse)	Widespread (most cells with receptor)
Distance	Short (synaptic cleft, 20 nm)	Long (via blood circulation)

Mixed signaling: Neuroendocrine cells (e.g., hypothalamic **neurons** secreting releasing hormones, adrenal medulla chromaffin cells) bridge both systems. Sterling and Eyer’s concept of **allostasis** [Sterling and Eyer, 1988, Sterling, 2012] extends Cannon’s classical homeostasis [Cannon, 1932]: the brain anticipates physiological needs and adjusts setpoints predictively, integrating endocrine and autonomic outputs.

34.2.2 Hormone Classes — Synthesis, Transport, and Mechanism

Table 396. Hormone Classes — Synthesis, Transport, and Mechanism: Class and Solubility.

Class	Solubility	Synthesis	Transport in Blood	Receptor Location	Signaling Speed	Duration	Examples
Peptide/ pro- hormone	Water-soluble	Ribosomal synthesis as preprohormones; cleaved in ER/Golgi; stored in secretory granules	Free in plasma	Plasma membrane (RTKs, GPCRs)	Seconds to minutes	Minutes to hours	Insulin, glucagon, GH, ACTH, ADH, PTH, prolactin
Steroid	Lipid-soluble	Synthesized on demand from cholesterol (no storage); enzymatic cascades in mitochondria/SER	Bound to carrier proteins (CBG, SHBG, albumin) — about 5% free and bioactive	Nuclear receptors (intracellular)	Hours (transcription required)	Hours to days	Cortisol , aldosterone, estrogen, testosterone, vitamin D
Amine — Catecholamines	Water-soluble	Tyrosine → DOPA → dopamine → norepinephrine → epinephrine; stored in chromaffin granules	Free in plasma; very short half-life	Plasma membrane (α/β adrenergic GPCRs)	Seconds	Seconds to minutes	Epinephrine, norepinephrine, dopamine
Amine — Thyroid hormones	Lipid-soluble	Synthesized on iodinated thyroglobulin scaffold in colloid; T4 prohormone converted to T3 peripherally	99.97% bound to TBG, transthyretin, albumin	Nuclear receptors ($TR\alpha$, $TR\beta$)	Hours (transcription required)	Days (T4 $t^{1/2}$ about 7 d)	T3, T4

Eicosanoids	lipid-soluble	Generated locally on demand from arachidonic acid; not stored	Diffuse to neighboring cells (paracrine)	GPCRs and nuclear receptors (PPARs)	Seconds to minutes	Seconds to minutes (rapid degradation)	PGE ₂ , PGI ₂ , TXA ₂ , leukotrienes
-------------	---------------	---	--	-------------------------------------	--------------------	--	---

Hormone table — synthesis location, transport, receptor, half-life

Table 397. Hormone table — synthesis location, transport, receptor, half-life: Hormone and Class.

Hormone	Class	Synthesis location	Plasma transport	Receptor	Signal duration	Half-life
Insulin	Peptide (51 aa)	β-cells, islets of Langerhans	Free	IR (RTK, plasma membrane)	Minutes	about 5 min
Glucagon	Peptide (29 aa)	α-cells, islets of Langerhans	Free	GcgR (G _s GPCR, hepatocyte)	Minutes	about 5 min
Growth hormone (GH)	Peptide (191 aa)	Anterior pituitary somatotrophs	Free; some bound to GHBP	GHR (JAK2/STAT5 cytokine receptor, liver)	Hours (via IGF-1)	about 20 min
PTH	Peptide (84 aa)	Parathyroid chief cells	Free	PTH1R (G _s /G _q GPCR; bone, kidney)	Minutes	about 4 min
ADH (vasopressin)	Peptide (9 aa)	Hypothalamic SON/PVN; stored in posterior pituitary	Free	V ₂ R (G _s , kidney); V ₁ R (G _q , vessels)	Minutes	about 15 min
Cortisol	Steroid (C ₂₁)	Adrenal cortex (zona fasciculata)	90% CBG; 5% albumin; 5% free	GR (NR3C1, cytoplasmic→nuclear)	Hours to days	about 60–90 min
Aldosterone	Steroid (C ₂₁)	Adrenal cortex (zona glomerulosa)	about 50% bound to CBG/albumin	MR (NR3C2, cytoplasmic→nuclear)	Hours	about 20 min
Testosterone	Steroid (C ₁₉)	Leydig cells (testis); zona reticularis (adrenal)	60% SHBG; 38% albumin; 2% free	AR (NR3C4, cytoplasmic→nuclear)	Hours to days	about 70 min
Oestradiol	Steroid (C ₁₈)	Ovarian granulosa cells (aromatase from androgens)	SHBG, albumin; 1–2% free	ERα/ERβ (nuclear); GPER (membrane)	Hours to days	about 13 h
Progesterone	Steroid (C ₂₁)	Corpus luteum, placenta	CBG, albumin	PR (NR3C3, nuclear)	Hours	about 5 min
Vitamin D (1,25-(OH) ₂ D ₃)	Steroid (secosteroid)	Kidney (CYP27B1 hydroxylation of 25-OH-D)	DBP (vitamin D binding protein)	VDR (nuclear)	Days	about 15 h
Epinephrine	Catecholamine	Adrenal medulla chromaffin cells	Free	α/β adrenergic (GPCRs)	Seconds–minutes	about 2 min
Norepinephrine	Catecholamine	Adrenal medulla; sympathetic neurons	Free	α/β adrenergic (GPCRs)	Seconds–minutes	about 2 min

Hormone	Class	Synthesis location	Plasma transport	Receptor	Signal duration	Half-life
T4 (thyroxine)	Iodinated tyrosine	Thyroid follicular cells	99.97% TBG/TTR/albumin; 0.03% free	TRα/β (nuclear) after D2 conversion to T3	Days–weeks	about 6–7 d
T3 (triiodothy- ronine)	Iodinated tyrosine	Thyroid (about 20%); peripheral D1/D2 (about 80%)	99.7% bound; 0.3% free	TRα/β (nuclear)	Days	about 1 d
Melatonin	Indolamine	Pineal gland (from tryptophan via serotonin)	Albumin	MT ₁ , MT ₂ (G _i GPCRs)	Minutes–hours	about 30–50 min
PGE ₂	Eicosanoid	Most cells (COX-2 inducible)	Local (paracrine)	EP ₁ –EP ₄ (GPCRs)	Seconds	about 30 s
TXA ₂	Eicosanoid	Platelets (TXAS)	Local	TP receptor (G _q)	Seconds	about 30 s
Leptin	Peptide (167 aa)	Adipocytes (proportional to fat mass)	Free; some bound	LepR (JAK2/STAT3, hypothala- mus)	Hours	about 25 min
Adiponectin	Peptide (244 aa)	Adipocytes	Free; trimers/hexamers/HMW	AdipoR1, AdipoR2 (AMPK pathway)	Hours	about 14 h

Key contrasts:

- Speed vs duration trade-off. Membrane receptor signaling (peptides, catecholamines) is fast but transient: cAMP, IP₃, and Ca²⁺ signals decay in seconds when ligand washes away [Rall and Sutherland, 1958]. Nuclear receptor signaling (steroids, T3) is slow but persistent: transcribed mRNAs and translated proteins last hours to days.
- Storage vs synthesis. Peptide hormones are pre-synthesized and stored in granules ready for rapid release — insulin can be released within seconds of glucose elevation. Steroids cannot be stored (lipid-soluble, would diffuse away); they are synthesized on demand, which limits acute response speed.
- Carrier proteins as a reservoir. CBG (cortisol binding globulin), SHBG (sex hormone binding globulin), and TBG (thyroxine binding globulin) bind 95–99% of their target hormones. The bound fraction is biologically inactive but provides a circulating reservoir, buffering plasma levels and extending half-life. Free hormone is in equilibrium with bound; pregnancy elevates estrogen which raises CBG, increasing total cortisol while free cortisol remains normal.

34.2.3 Quantitative Endocrinology

Hormone–receptor binding. The dissociation constant K_d characterizes receptor affinity (lower K_d = higher affinity):

$$K_d = \frac{[H][R]}{[HR]}; \quad \text{fractional occupancy} = \frac{[H]}{[H] + K_d}$$

(410)

Typical K_d values: **insulin receptor** about 0.1 nM; glucocorticoid receptor about 5 nM; epinephrine at β_2 receptor about 1 μ M. The enormous affinity difference explains why insulin circulates at picomolar concentrations while catecholamines require nanomolar–micromolar levels for effect.

Hormone half-life and clearance. Plasma hormone concentration decays exponentially after secretion ceases:

$$C(t) = C_0 e^{-kt}, \quad k = \frac{\ln 2}{t_{1/2}}$$

(411)

Half-lives vary enormously: catecholamines about 1–2 min (rapid enzymatic degradation by MAO/COMT); cortisol about 60–90 min (hepatic metabolism); thyroid hormone (T4) about 6–7 days (protein binding extends clearance). Protein-bound hormones (e.g., TBG-bound T4, CBG-bound cortisol) are protected from degradation and renal filtration.

Dose–response relationship. The sigmoidal (Hill) dose–response curve relates hormone concentration to biological effect:

$$E = E_{\max} \cdot \frac{[H]^n}{EC_{50}^n + [H]^n}$$

(412)

where EC_{50} is the concentration producing 50% of maximal effect and n is the Hill coefficient (cooperativity). Spare receptors shift the EC_{50} leftward from K_d : insulin requires occupation of about 5% of receptors for maximal glucose uptake.

Herd immunity threshold. The fraction of the population that must be immune to prevent epidemic spread is:

$$p_c = 1 - \frac{1}{R_0}$$

(413)

where R_0 is the basic reproductive number. For measles ($R_0 \approx 12\text{--}18$), $p_c \approx 92\text{--}95\%$, explaining why even small drops in vaccination coverage trigger outbreaks.

34.3 Hypothalamic-Pituitary Axes

The hypothalamus serves as the master integrator, linking the nervous and endocrine systems. It produces releasing and inhibiting hormones that control the anterior pituitary, which in turn controls target glands throughout the body.

Anterior pituitary hormones: ACTH (corticotrophs), TSH (thyrotrophs), GH (somatotrophs), LH and FSH (gonadotrophs), prolactin (lactotrophs).

Posterior pituitary: Stores and releases ADH (vasopressin) and oxytocin, which are synthesized in hypothalamic supraoptic and paraventricular nuclei and transported down axons to the posterior pituitary for release.



Figure 202. The three major hypothalamic-pituitary axes Each follows the same hierarchical pattern: hypothalamic releasing hormone stimulates anterior pituitary tropic hormone, which stimulates target gland hormone production. Negative feedback at multiple levels prevents overstimulation. The HPG axis uniquely features positive feedback during the mid-cycle LH surge.

34.3.1 HPA Axis (Hypothalamic-Pituitary-Adrenal) — Detailed Cortisol Physiology

Cortisol synthesis from cholesterol (steroidogenesis) Most adrenal steroids derive from cholesterol via a series of cytochrome P450-mediated hydroxylations and oxidations. The rate-limiting step is the transport of cholesterol from the outer to the inner mitochondrial membrane, mediated by StAR (steroidogenic acute regulatory protein) and stimulated by ACTH via cAMP/PKA.

Glucocorticoid receptor (GR) mechanism Cortisol diffuses freely across the plasma membrane (lipid-soluble) and binds the cytoplasmic GR (NR3C1). In the unliganded state, GR is held in an inactive complex with HSP90, HSP70, and immunophilins. Cortisol binding induces a conformational change, releasing the chaperones and exposing nuclear localization signals. The activated GR translocates to the nucleus, dimerises, and binds glucocorticoid response elements (GREs) in target gene promoters with the consensus sequence 5'-AGAACAnnnTGTCT-3'.

GR has two transcriptional modes:

- **Transactivation at positive GREs:** directly upregulates gluconeogenic enzymes (PEPCK, G6Pase) and anti-inflammatory proteins (annexin A1, MKP-1, IκBα, IL-10).
- **Transrepression by tethering to NF-κB or AP-1:** GR binds these pro-inflammatory transcription factors and prevents their activation of cytokine genes (IL-2, IL-6, TNF-α, COX-2). Transrepression mediates much of the anti-inflammatory action of glucocorticoid drugs.

The dual mechanism is therapeutically central. Most classical glucocorticoids (prednisone, dexamethasone) drive both modes — the unwanted metabolic effects (hyperglycaemia, osteoporosis, muscle wasting) come predominantly from transactivation, while the anti-inflammatory benefit comes mostly from transrepression. Pharmaceutical efforts to design “selective GR agonists” (SEGRAs) that drive transrepression preferentially have been an enduring (but largely unrealised) goal.

Cortisol effects (anti-inflammatory gene program)

- Gluconeogenesis (transactivation of PEPCK, G6Pase via GR; mobilizes amino acids from muscle protein catabolism)

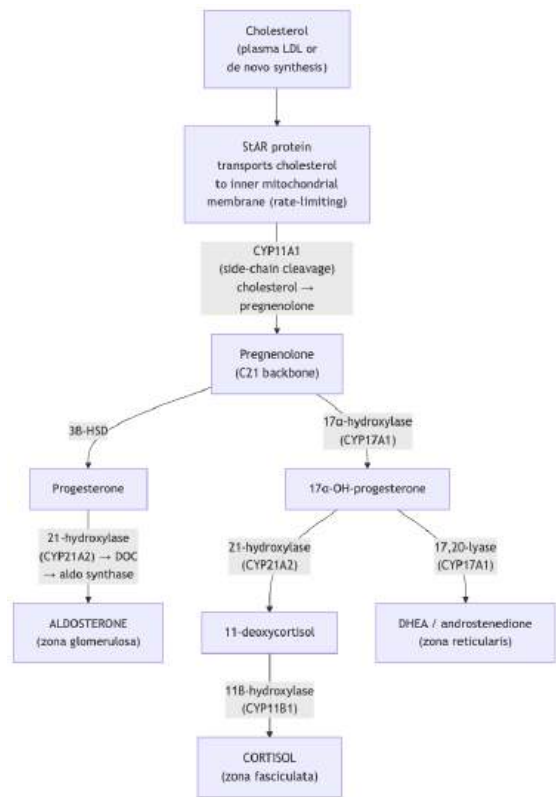


Figure 203. Adrenal steroidogenesis The pathway diverges from common precursor pregnenolone into three parallel routes producing aldosterone (zona glomerulosa), cortisol (zona fasciculata), and androgens (zona reticularis). Each zone expresses zone-specific enzymes; for example, primarily the zona glomerulosa expresses aldosterone synthase (CYP11B2), and primarily the zona fasciculata expresses 11beta-hydroxylase (CYP11B1).

- Immunosuppression at multiple levels:
 - Direct: NF-κB inhibition; lymphocyte **apoptosis**; suppression of IL-2 transcription; mast-cell stabilization
 - Indirect: induction of IL-10, TGF-β, annexin A1; suppression of leukocyte trafficking by reducing E-selectin and ICAM-1
 - Net cytokine effect: down TNF-α, IL-1β, IL-2, IL-6, IFN-γ; up IL-10
- Lipolysis in peripheral adipose tissue (with central fat redistribution from chronic excess)
- Anti-inflammatory (inhibits COX-2, phospholipase A₂ via annexin A1 induction; reduces histamine, leukotriene production)
- Permissive effects on catecholamine action (β-adrenergic receptor expression maintenance)
- Bone resorption (chronic excess: osteoporosis via direct osteoblast suppression and indirect calcium handling)
- CNS effects (mood — chronic excess: depression, psychosis, cognitive impairment via hippocampal atrophy)

Circadian rhythm and feedback Cortisol secretion follows a robust circadian rhythm driven by the suprachiasmatic nucleus (SCN): peak at approximately 08:00 (cortisol awakening response, CAR), nadir at midnight. Superimposed are ultradian pulses every 60–90 minutes. The pulsatile pattern is essential for proper GR function — continuous (non-pulsatile) cortisol exposure desensitises target tissues.

Schematically, plasma cortisol ≈ 18 μg/dL at 08:00, drops through the day to ≈ 8 μg/dL at 16:00, and is < 5 μg/dL at midnight. Disrupted circadian rhythm (shift work, depression, Cushing’s) loses the diurnal variation; midnight salivary cortisol is one of the most sensitive screening tests for endogenous Cushing’s syndrome.

Negative feedback operates at two levels:

- Fast feedback (minutes): non-genomic; cortisol acts on hypothalamic CRH neurons via membrane GRs and presynaptic endocannabinoid release to suppress CRH secretion within minutes.
- Slow feedback (hours): genomic; cortisol downregulates POMC gene transcription (the ACTH precursor) in pituitary corticotrophs and CRH transcription in hypothalamus.

Stress vs basal regulation Under basal (non-stress) conditions, the HPA axis runs on its circadian/ultradian rhythm with tight negative feedback. The day’s cortisol output is roughly 10–20 mg/24 h.

Under acute stress (trauma, hypoglycaemia, infection, surgery), hypothalamic PVN neurons receive convergent inputs (limbic, brainstem, circulating cytokines, baroreceptors) and override basal restraint:

- CRH secretion rises 5–10 fold
- ACTH plasma concentration rises within 5–15 min
- Cortisol peaks about 30 min after stress onset
- Cortisol output can increase 3–10 fold over basal (50–100 mg/24 h in major surgery)
- Negative feedback is partially suppressed, allowing sustained elevation

Chronic psychosocial stress engages the same axis but with glucocorticoid receptor downregulation and flattened diurnal rhythm — features now linked to metabolic syndrome, depression, hippocampal atrophy, and accelerated cognitive decline.

Pathology:

- Cushing’s syndrome: Cortisol excess. Causes: pituitary adenoma (Cushing’s disease, 70%), ectopic ACTH (lung small cell carcinoma), adrenal adenoma, iatrogenic (chronic glucocorticoid therapy). Features: central obesity, moon face, purple striae, hyperglycaemia, osteoporosis, immunosuppression, hypertension (cortisol cross-reacts with mineralocorticoid receptor).
- Addison’s disease: Primary adrenal insufficiency (cortisol deficiency). Most common cause: autoimmune adrenalitis. Features: hypotension, hyperpigmentation (elevated ACTH drives melanocyte-stimulating hormone activity, since both are cleaved from the same precursor POMC), fatigue, salt craving. Can cause life-threatening adrenal crisis.

Clinical Connection: The dexamethasone suppression test exploits negative feedback to diagnose Cushing’s syndrome. Dexamethasone is a synthetic glucocorticoid that normally suppresses CRH and ACTH secretion. In Cushing’s disease (pituitary adenoma), low-dose dexamethasone fails to suppress cortisol, but high-dose dexamethasone does. In ectopic ACTH production, neither dose suppresses cortisol. This distinguishes the source of excess cortisol.

34.3.2 HPT Axis (Hypothalamic-Pituitary-Thyroid) — Detailed Mechanism

Thyroid hormone synthesis Follicular cells of the thyroid gland surround a colloid-filled follicle and execute a multi-step iodination process:

1. Iodide uptake. The basolateral Na^+/I^- symporter (NIS) actively concentrates iodide about 25–100-fold above plasma. Pertechnetate ($^{99m}\text{TcO}_4^-$) is also transported by NIS and is used in thyroid scintigraphy.
2. Thyroglobulin synthesis. Follicular cells produce thyroglobulin (Tg, about 660 kDa glycoprotein with about 120 tyrosine residues), packaged into vesicles and exocytosed into the colloid lumen.
3. Iodide oxidation and tyrosine iodination. At the apical membrane, thyroid peroxidase (TPO) oxidises I^- to a reactive iodinating species (I_2 or I^+) using H_2O_2 as cofactor. Tyrosines on Tg are iodinated to form monoiodotyrosine (MIT) and diiodotyrosine (DIT).
4. Coupling reaction. Still on the Tg scaffold, TPO catalyses oxidative coupling: $\text{DIT} + \text{DIT} \rightarrow \text{T}_4$ (thyroxine, 4 iodines); $\text{MIT} + \text{DIT} \rightarrow \text{T}_3$ (3 iodines).
5. Endocytosis and proteolysis. TSH stimulation triggers endocytosis of Tg into the follicular cell, where lysosomal proteases cleave the iodothyronines from Tg. T_4 and T_3 are released into the bloodstream.
6. Recycling. MIT and DIT not coupled into T_3/T_4 are deiodinated by intracellular dehalogenase, recycling iodide.

Wolff-Chaikoff effect Acutely high iodide (e.g., from radiocontrast, amiodarone, or seaweed binge) paradoxically inhibits thyroid hormone synthesis: excess iodide downregulates NIS expression and impairs TPO-mediated organification. Most healthy individuals “escape” within 7–10 days as NIS resets. In patients with autoimmune thyroid disease, escape may fail — producing iodine-induced hypothyroidism. Conversely, in nodular goitres with autonomous follicles, iodine load can drive iodine-induced hyperthyroidism (Jod-Basedow). The Wolff-Chaikoff effect is exploited therapeutically: potassium iodide (Lugol’s solution, SSKI) is given pre-operatively in Graves’ disease to reduce thyroid vascularity and slow hormone release before thyroidectomy.

$\text{T}_4 \rightarrow \text{T}_3$ conversion (deiodinases) T_4 is the predominant secreted form (about 80%) but is largely a prohormone. Three iodothyronine deiodinases activate or inactivate T_4 in target tissues:

Table 398. $\text{T}_4 \rightarrow \text{T}_3$ conversion (deiodinases): Deiodinase and Reaction.

Deiodinase	Reaction	Tissue	Function
D1	$\text{T}_4 \rightarrow \text{T}_3$ (5'-deiodination)	Liver, kidney, thyroid	Bulk plasma T_3 production
D2	$\text{T}_4 \rightarrow \text{T}_3$ (5'-deiodination)	Brain, pituitary, brown adipose	Local T_3 generation; pituitary feedback set-point

Deiodinase	Reaction	Tissue	Function
D3	$T4 \rightarrow \text{reverse } T3 \text{ (rT3)}; T3 \rightarrow T2$	Placenta, fetal tissues	Inactivation; protects fetus from maternal T3

T3 is about 4× more potent than T4 at the nuclear receptor. During fasting, illness, or stress (non-thyroidal illness), D1 activity drops and D3 activity rises, shifting balance toward inactive rT3 — adaptive metabolic slowing.

Nuclear thyroid receptor mechanism T3 enters cells via MCT8/MCT10 transporters and binds nuclear thyroid hormone receptors TRα (cardiac, neural) and TRβ (liver, pituitary). TRs heterodimerise with RXR (retinoid X receptor) and bind thyroid response elements (TREs) in target gene promoters — even in the absence of T3.

- Without T3: Unliganded TR/RXR recruits corepressors (NCoR, SMRT, HDACs) and represses target gene transcription.
- With T3: Conformational change releases corepressors and recruits coactivators (SRC-1, p300/CBP, histone acetyltransferases) → active transcription.

This dual mechanism explains why hypothyroidism causes such pronounced symptoms: target genes are not merely “not turned on” but are actively repressed below baseline.

Effects on metabolism

- Increased basal metabolic rate (BMR) through upregulation of Na⁺/K⁺-ATPase (each cell uses about 25% of ATP for this pump; T3 increases pump density).
- Mitochondrial uncoupling via UCP-mediated proton leak (heat production, calorigenic effect).
- Increased cardiac output (β₁-adrenergic receptor upregulation; positive chronotropic and inotropic effects).
- Lipolysis and cholesterol degradation (hyperthyroidism lowers LDL; hypothyroidism causes hypercholesterolaemia).
- Neurodevelopment: essential for myelination, synaptogenesis, neuronal migration in fetus and infant. Severe untreated congenital hypothyroidism produces cretinism (intellectual disability, growth retardation) — preventable by neonatal screening.

Pathology:

- Hypothyroidism: Low T3/T4, elevated TSH. Hashimoto’s thyroiditis (autoimmune; anti-TPO and anti-thyroglobulin antibodies). Features: fatigue, weight gain, cold intolerance, bradycardia, constipation, myxoedema.
- Hyperthyroidism: High T3/T4, suppressed TSH. Graves’ disease (autoimmune; TSH receptor-stimulating antibodies — thyroid-stimulating immunoglobulins, TSI). Features: weight loss, heat intolerance, tachycardia/atrial fibrillation, tremor, exophthalmos (due to retro-orbital inflammation), diffuse goitre.
- Iodine deficiency: Most common preventable cause of intellectual disability worldwide; affects approximately 1.9 billion people. Addressed by salt iodisation programs.

34.3.3 Worked Example: Thyroid Hormone Negative Feedback and TSH Compensatory Rise

Problem: A healthy adult has steady-state TSH around 2 mU/L, T4 around 100 nmol/L (within normal range), and a free T3 set by peripheral D1/D2 deiodination. Autoimmune destruction (Hashimoto’s thyroiditis) reduces T4 secretion capacity by approximately 60%. Predict the new steady-state TSH, estimate the time to reach the new steady state, and identify the rate-limiting step.

Setup of the feedback loop. Proportional error correction toward a set point (figure 204) is the generic logic shared by endocrine axes and other homeostatic controllers.

TRH (hypothalamus) → TSH (anterior pituitary) → T4 (thyroid) $\xrightarrow{\text{D1/D2}}$ T3 (active).

T3 (and to a lesser extent T4) feeds back negatively on both TRH and TSH transcription. The loop is well approximated as a near-linear feedback over the clinically observed range: a *k*-fold drop in T4 input drives an approximately *k*-fold (often higher because of nonlinearity at low T4) rise in TSH.

Solution.

1. Steady-state TSH after damage. A 60% reduction in T4 input (×0.4) typically produces an approximately 10-fold rise in TSH at the new equilibrium (the system is *nonlinearly* sensitive at low T4 because TRH transcription is sharply derepressed). New TSH ≈ 2 × 10 = 20 mU/L — squarely in the overt-hypothyroid range.
2. Half-lives that set the time-to-steady-state.

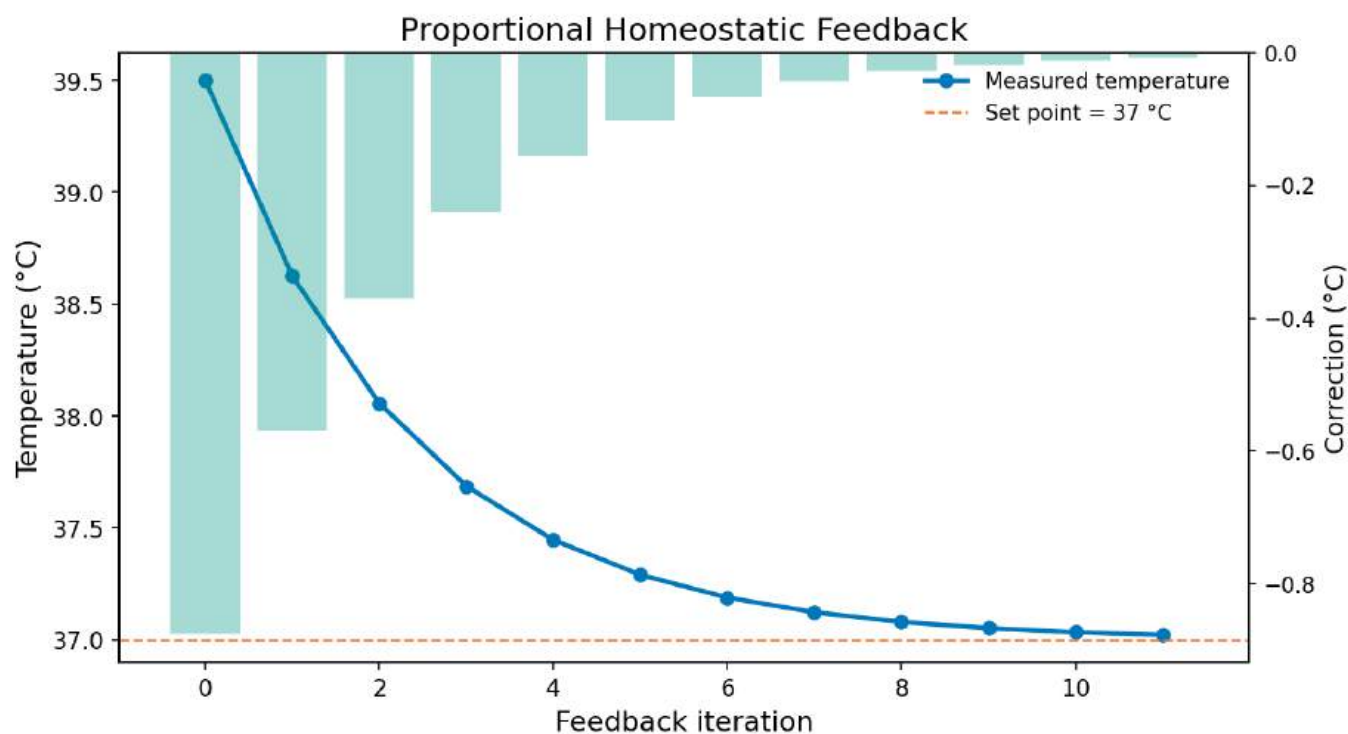


Figure 204. Generic proportional negative feedback toward a set point (temperature shown as an example). Each correction is proportional to the measured error, so large deviations trigger stronger responses and the system converges without indefinite overshoot—the same logic applies to hormone axes such as the thyroid loop below.

- TSH plasma half-life: $t_{1/2} \approx 50$ min. Time constant $\tau_{\text{TSH}} = t_{1/2} / \ln 2 \approx 72$ min.
 - T4 plasma half-life: $t_{1/2} \approx 7$ d. Time constant $\tau_{\text{T4}} = 7 / 0.693 \approx 10$ d.
3. Rate-limiting step. The slow variable governs convergence. Even though TSH responds within hours, the actual T4 distribution re-equilibrates on the order of $3\tau_{\text{T4}} \approx 30$ days to reach approximately 95% of the new steady state, and approximately $5\tau_{\text{T4}} \approx 50$ days to reach approximately 99%. *Practical implication:* TSH measured 1–2 weeks after starting levothyroxine replacement is misleading — the T4 pool has not finished re-equilibrating. Clinical guidelines correctly recommend re-checking TSH 6–8 weeks after any dose change.
4. Sanity check with the loop gain. Order-of-magnitude: loop gain (sensitivity of TSH to T4) at the operating point is approximately -2 (one-log T4 drop \rightarrow approximately 2-log TSH rise, per the log-linear TSH–T4 relationship that clinicians use at the bedside). Our predicted approximately 10-fold TSH rise for an approximately 2.5-fold T4 drop is consistent with this gain. The same logarithmic logic explains why a small dose of levothyroxine restoring T4 to a near-normal value rapidly normalizes TSH — provided one waits a full T4 half-life-set.

Interpretation. Hashimoto’s hypothyroidism is *biochemically* a textbook negative-feedback restoration problem. The clinical art is timing: lab measurements taken before the T4 pool re-equilibrates will lead to over-dosing. The molecular ledger — TRH at the top, T4 half-life at the bottom — determines that we must wait approximately 6–8 weeks before believing the TSH number.

34.3.4 HPG Axis and Reproductive Hormones

GnRH pulsatility is critical: High-frequency pulses (every 60–90 min) favor LH secretion; low-frequency pulses (every 2–4 h) favor FSH. Continuous GnRH paradoxically suppresses the axis (downregulates GnRH receptors), which is the basis of GnRH agonist therapy for prostate cancer, endometriosis, and precocious puberty.

Male reproductive endocrinology: LH stimulates Leydig cells (testosterone production). FSH + testosterone stimulate Sertoli cells (support spermatogenesis; produce inhibin B, which provides negative feedback on FSH). Testosterone effects: muscle mass, bone density, secondary sexual characteristics, spermatogenesis, libido.

Female menstrual cycle (28-day average):

- Follicular phase (days 1–14): FSH promotes follicular growth. **Dominant** follicle produces rising oestradiol. Oestradiol initially provides negative feedback.
- Ovulation (day approximately 14): Positive feedback — sustained high oestradiol above a threshold for >36 h switches from negative to positive feedback, triggering an LH surge. The LH surge induces ovulation (follicular rupture, oocyte release).
- Luteal phase (days 14–28): Corpus luteum (remnant of ovulated follicle) produces progesterone + oestradiol. Progesterone prepares the endometrium for implantation (secretory phase). If no implantation occurs, corpus luteum degenerates (luteolysis), progesterone and oestradiol fall, endometrium sheds (menstruation).

Development and reproduction as endocrine timing problems: Fertilization, implantation, placentation, fetal growth, birth, lactation, puberty, and reproductive senescence depend on timed endocrine signals interacting with local tissue cues. Early embryos are initially regulated by maternal transcripts and local morphogen gradients; later development adds fetal-placental endocrine exchange, thyroid-hormone-dependent neurodevelopment, glucocorticoid-driven lung maturation, and sex-steroid-dependent reproductive tract differentiation. Clinically, infertility is diagnosed after 12 months of regular unprotected intercourse without pregnancy (or after 6 months when the female partner is 35 years or older), because reproductive physiology depends on ovulation, sperm production, tubal transport, implantation, uterine receptivity, endocrine timing, and age-dependent gamete quality [**Centers for Disease Control and Prevention, 2024b**]. The organismal point is that reproduction is not one organ system; it is a coordinated life-history transition linking gonads, hypothalamus, pituitary, placenta, metabolism, immune tolerance, and behavior.

Concept Check 1: Why does continuous GnRH administration paradoxically suppress the HPG axis rather than stimulate it? How is this exploited clinically in prostate cancer treatment, where the goal is to lower testosterone?

34.4 Pancreatic Hormones, Glucose Homeostasis, and Energy Balance

Normal fasting blood glucose: 4.0–5.5 mmol/L (72–99 mg/dL). Post-prandial peak: <7.8 mmol/L (<140 mg/dL).

34.4.1 Insulin signaling — molecular detail

After a meal (high glucose):

1. Glucose enters β -cells via GLUT2 transporter (high- K_m “glucose sensor”)
2. Glucose metabolism increases the ATP/ADP ratio

3. ATP-sensitive K^+ channels (K_{ATP} , SUR1/Kir6.2 subunits) close \rightarrow membrane depolarization
4. Voltage-gated L-type Ca^{2+} channels open \rightarrow Ca^{2+} influx
5. Ca^{2+} triggers insulin exocytosis from dense-core granules (mature insulin = A and B chains held by disulphide bonds; C-peptide co-released as marker) [Sanger, 1955]
6. Insulin signaling in target cells:
 - Insulin binds insulin receptor (IR) — an $\alpha_2\beta_2$ tetrameric receptor tyrosine kinase. Each α -subunit is extracellular and binds insulin; β -subunits span the membrane and contain intracellular tyrosine kinase domains.
 - Binding causes conformational change \rightarrow trans-autophosphorylation of β -subunit tyrosine residues (Y1158, Y1162, Y1163 in the activation loop)
 - Phosphotyrosines recruit IRS1/IRS2 scaffold proteins \rightarrow IRS phosphorylation
 - IRS phosphotyrosines recruit PI3K (p85 regulatory + p110 catalytic) via SH2 domains
 - PI3K converts $PIP_2 \rightarrow PIP_3$; PDK1 and mTORC2 dock on PIP_3 and activate Akt (PKB) by phosphorylation at T308 and S473
 - Akt phosphorylates AS160 (TBC1D4), releasing Rab-GAP inhibition of GLUT4-vesicle exocytosis \rightarrow GLUT4 translocation to plasma membrane in muscle and adipose (the dominant mechanism for postprandial glucose disposal)
 - Akt inhibits GSK3 β \rightarrow glycogen synthase activation \rightarrow glycogen synthesis
 - Akt activates mTORC1 \rightarrow ribosomal S6K1 and 4E-BP1 phosphorylation \rightarrow protein synthesis
 - Akt phosphorylates FoxO1 \rightarrow nuclear export \rightarrow represses gluconeogenic gene transcription (PEPCK, G6Pase)

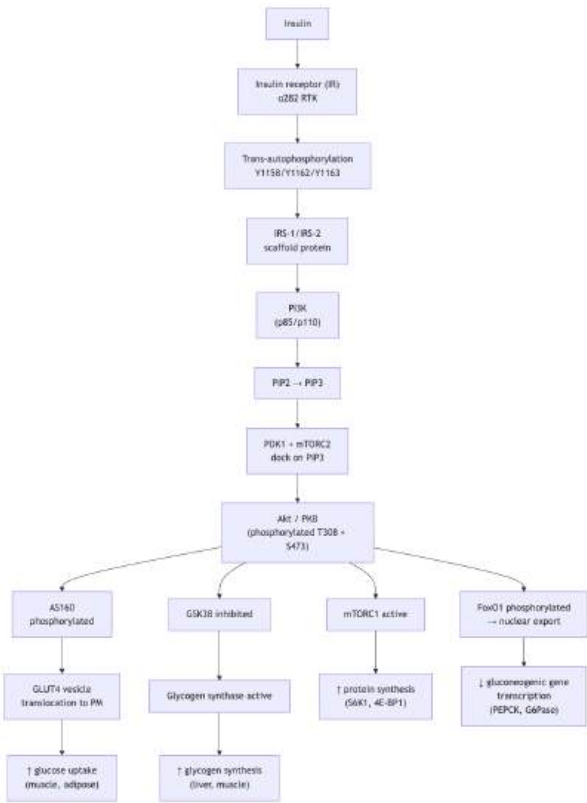


Figure 205. Insulin signaling cascade. Insulin binding to IR triggers trans-autophosphorylation, recruitment of IRS, activation of PI3K, generation of PIP_3 , and activation of Akt. Akt drives GLUT4 translocation, glycogen synthesis, protein synthesis, and suppression of gluconeogenic gene transcription.

34.4.2 Worked Example: Postprandial Glucose Clearance and Insulin Dose Scaling

Problem: A 70 kg adult absorbs 75 g glucose from a meal. Skeletal muscle stores about 400 g glycogen and can take up glucose at about $8\text{ mg kg}^{-1}\text{ min}^{-1}$ when insulin is maximal. If peak plasma insulin reaches 80 mU/L and insulin half-life is 5 min, estimate (a) the muscle glucose-uptake capacity over the first 30 min, and (b) whether hepatic glycogen synthesis must also contribute [Yalow and Berson, 1960].

Solution.

1. Muscle uptake capacity. Rate = $8\text{ mg kg}^{-1}\text{ min}^{-1} \times 70\text{ kg} = 560\text{ mg min}^{-1}$. Over 30 min: $560 \times 30 = 16,800\text{ mg} = 16.8\text{ g}$.
2. Compare to absorbed load. Absorbed glucose = 75 g. Muscle alone disposes of roughly 22% of the load in 30 min at this rate, so liver glycogen synthesis and delayed muscle uptake over 2–3 h are required — consistent with the biphasic insulin secretory response and sustained Akt signaling.

3. Insulin decay check. With $t_{1/2} = 5$ min, insulin falls to 25 mU/L at 5 min and about 6 mU/L at 15 min ($80 \times 0.5^{15/5}$). GLUT4 translocation tracks Akt activity, so the second-phase insulin pulse (not modeled here) extends disposal beyond the first 30 min.

Interpretation. Postprandial normoglycaemia depends on coordinated muscle GLUT4 translocation and hepatic glycogen storage; the numeric comparison shows why isolated muscle uptake is insufficient to clear a 75 g load within half an hour.

Glucagon signaling During fasting (low glucose):

1. α -cells release glucagon (triggered by low glucose, sympathetic activation, amino acids)
2. Glucagon binds G_s -coupled receptor on hepatocytes [Rall and Sutherland, 1958]
3. cAMP-PKA pathway: phosphorylase kinase activates glycogen phosphorylase for glycogenolysis
4. cAMP also activates CREB \rightarrow PEPCK and G6Pase gene transcription \rightarrow gluconeogenesis
5. PKA phosphorylates and inhibits PFK-2/FBPase-2 (PFKFB1), lowering F2,6BP \rightarrow favors fructose-1,6-bisphosphatase over PFK-1 \rightarrow gluconeogenesis dominates

Crosstalk with leptin, adiponectin, and GLP-1 Leptin is secreted by adipocytes in proportion to fat mass and acts on hypothalamic neurons (arcuate nucleus POMC and AgRP/NPY neurons) via the leptin receptor (LepR, JAK2/STAT3 signaling) to suppress appetite and increase energy expenditure. Leptin enhances central insulin sensitivity and provides a long-term signal of energy stores. Most obese individuals have high leptin but show leptin resistance — impaired hypothalamic LepR signaling and JAK2/STAT3 attenuation, partly via SOCS3 induction.

Adiponectin is also secreted by adipocytes — but inversely with fat mass (higher in lean states). It acts via AdipoR1 and AdipoR2, activating AMPK (AMP-activated protein kinase, the cellular “energy sensor”). AMPK activation:

- Increases fatty acid oxidation (phosphorylates ACC, decreasing malonyl-CoA, releasing CPT-1 from inhibition)
- Decreases hepatic gluconeogenesis (decreases CREB-regulated transcription)
- Increases skeletal muscle glucose uptake (independent of insulin)
- Decreases mTORC1 and protein synthesis (reciprocal to insulin/Akt)

Adiponectin therefore acts as an insulin sensitiser. Plasma adiponectin is reduced in T2DM, obesity, and metabolic syndrome; pioglitazone (a thiazolidinedione, PPAR γ agonist) raises adiponectin and improves insulin sensitivity.

GLP-1 (glucagon-like peptide 1) is an incretin released from intestinal L-cells in response to nutrient ingestion. It acts via GLP-1R (G_s -coupled GPCR) to:

- Enhance glucose-dependent insulin secretion (primarily when glucose elevated \rightarrow low hypoglycaemia risk)
- Suppress glucagon release from α -cells
- Slow gastric emptying
- Activate hypothalamic anorexigenic circuits \rightarrow reduce food intake
- Promote β -cell survival and proliferation (animal studies)

GLP-1 has a very short half-life (about 2 min) due to degradation by DPP-4 (dipeptidyl peptidase-4). Drug strategies: GLP-1 analogs with DPP-4-resistant modifications (semaglutide, liraglutide), or DPP-4 inhibitors (sitagliptin) that prolong endogenous GLP-1.

34.4.3 Diabetes Mellitus

Type 1 diabetes mellitus (T1DM):

- Autoimmune destruction of β -cells (anti-GAD65, anti-IA-2, anti-insulin, anti-ZnT8 antibodies)
- Complete insulin deficiency
- Onset usually in childhood/adolescence (but can occur at any age — “LADA” in adults)
- Without insulin: hyperglycaemia, ketoacidosis (lipolysis produces FFA, hepatic β -oxidation produces ketone bodies, metabolic acidosis)
- Treatment: exogenous insulin (basal-bolus regimen), increasingly closed-loop insulin pump systems

Type 2 diabetes mellitus (T2DM):

- Peripheral insulin resistance: ceramide and pro-inflammatory cytokines (TNF- α , IL-6 from visceral adipose tissue) cause serine phosphorylation of IRS1, blocking normal tyrosine phosphorylation. ER stress and mitochondrial dysfunction also contribute.
- Compensatory β -cell hyperinsulinaemia initially maintains normoglycaemia
- Progressive β -cell failure (glucotoxicity, lipotoxicity, amyloid deposition) leads to overt hyperglycaemia

- Treatment: lifestyle modification + metformin (AMPK activation, reduced hepatic glucose production) + GLP-1 receptor agonists (semaglutide) + SGLT2 inhibitors (empagliflozin: blocks renal glucose reabsorption)

Clinical Connection: Semaglutide (Ozempic/Wegovy) has transformed T2DM and obesity management. Clinical trials show 15–20% body weight reduction with semaglutide, plus cardiovascular and renal benefits, by mimicking natural GLP-1 signaling at hypothalamic appetite centers and pancreatic β -cells.

Concept Check 2: A type-1 diabetic receives a long-acting insulin analog (glargine) once daily. Blood glucose is well controlled during the day but the patient develops reactive hyperglycaemia every morning (“dawn phenomenon”). Given that cortisol, GH, and glucagon most rise in the pre-waking hours, explain *which* counter-regulatory hormones are responsible for the morning rise and *why* glargine’s 24-hour profile is insufficient to cover it. What feature of a more modern analog (e.g. degludec, with about 42-h half-life) addresses this?

34.4.4 Adrenal Gland — Zonal Architecture

Adrenal cortex (mesodermal origin, steroid hormones):

- Zona glomerulosa: Aldosterone (mineralocorticoid). Regulated by RAAS and K^+ . Promotes Na^+ reabsorption, K^+ secretion in collecting duct.
- Zona fasciculata: Cortisol (glucocorticoid). Regulated by ACTH.
- Zona reticularis: DHEA, androstenedione (adrenal androgens). Puberty (adrenarche).

Adrenal medulla (neural crest origin, modified sympathetic ganglion):

- Chromaffin cells release epinephrine (80%) and norepinephrine (20%) directly into blood
- Epinephrine effects: heart rate increase (β_1), bronchodilation (β_2), glycogenolysis (β_2 in liver), lipolysis (β_3 in adipose), vasoconstriction (α_1) in skin/viscera, vasodilation (β_2) in skeletal muscle
- Duration: seconds to minutes (rapid metabolic clearance by MAO and COMT)

34.4.5 Growth Hormone Axis and IGF-1

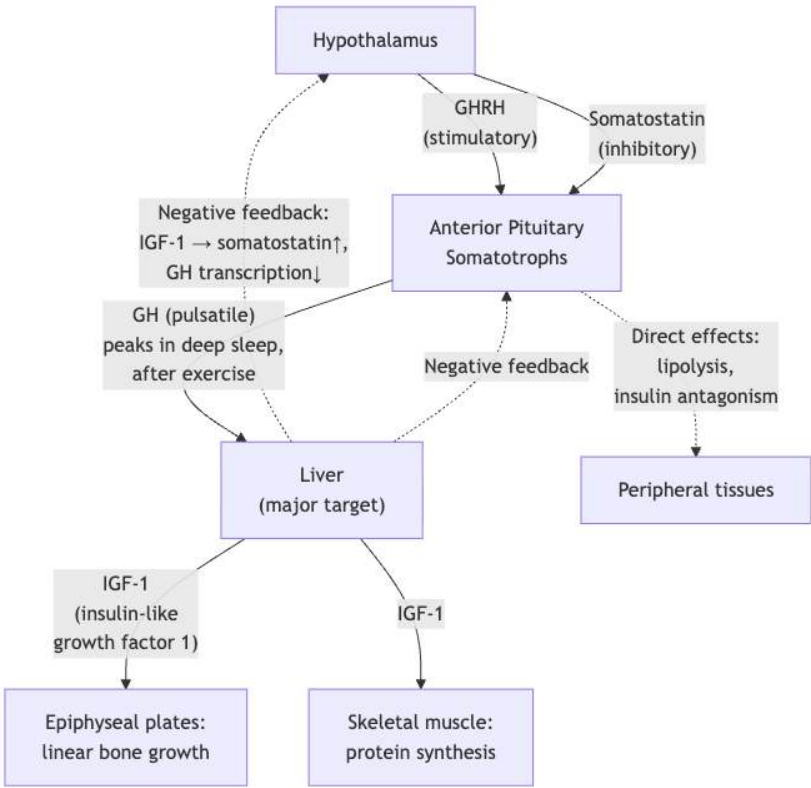


Figure 206. Growth hormone axis GHRH stimulates and somatostatin inhibits pituitary GH release. GH acts directly on tissues (lipolysis, insulin antagonism - “diabetogenic”) and indirectly via hepatic IGF-1, which mediates linear growth and protein synthesis. IGF-1 provides negative feedback at hypothalamus (somatostatin) and pituitary (GH transcription).

GH from anterior pituitary somatotrophs: pulsatile release (peaks during deep sleep and exercise). GH binds the GH receptor (a JAK2-coupled cytokine receptor)

on hepatocytes, activating STAT5, which drives IGF-1 (insulin-like growth factor 1) transcription and secretion. Circulating IGF-1 is bound to IGFBP-3 (extends half-life from minutes to hours).

GH/IGF-1 effects:

- Linear bone growth (epiphyseal plate chondrogenesis driven by IGF-1)
- Protein synthesis (positive nitrogen balance)
- Lipolysis (direct GH effect; “diabetogenic”)
- Reduced peripheral glucose uptake (GH antagonises insulin)

Pathology:

- Acromegaly: Excess GH in adults (pituitary adenoma). Characteristic features: enlarged hands, feet, jaw; organomegaly; impaired glucose tolerance. Diagnosed by failure to suppress GH during oral glucose tolerance test.
- Gigantism: Excess GH before epiphyseal plate closure (childhood). Tall stature.
- GH deficiency in children: Short stature; treated with recombinant human GH (somatropin).
- Laron syndrome: GH receptor mutation; high GH but no IGF-1 response. Short stature; remarkably, low IGF-1 confers resistance to cancer and diabetes.

34.5 Prostaglandins and Eicosanoids

Eicosanoids are 20-carbon paracrine signaling lipids derived from membrane phospholipids. Unlike conventional hormones, they are not stored, are synthesized on demand, act locally (paracrine/autocrine), and are rapidly inactivated.

34.5.1 Synthesis from arachidonic acid

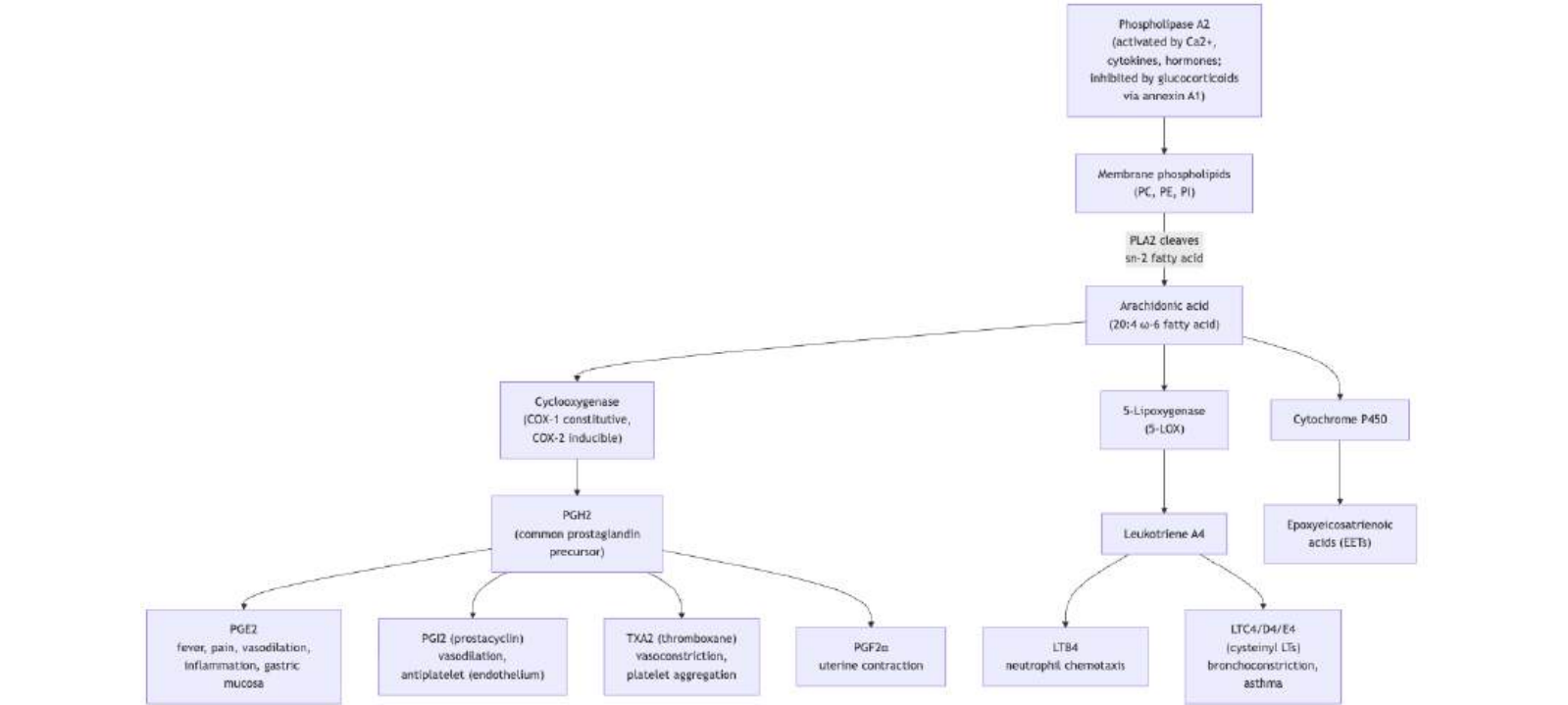


Figure 207. Eicosanoid biosynthesis pathways Phospholipase A₂ liberates arachidonic acid from membrane phospholipids. Three branches generate distinct families: cyclooxygenase (COX) to prostaglandins and thromboxanes; 5-lipoxygenase to leukotrienes; cytochrome P450 to epoxyeicosatrienoic acids. Glucocorticoids inhibit at the PLA₂ step; NSAIDs inhibit at COX.

34.5.2 COX-1 vs COX-2 — distinct physiology

Table 399. COX-1 vs COX-2 — distinct physiology: Feature and COX-1.

Feature	COX-1	COX-2
Expression	Constitutive (most tissues)	Inducible (inflammation, growth factors); constitutive in kidney, brain, vascular endothelium
Function	Gastric mucosa protection (PGE ₂ , PGI ₂); platelet TXA ₂ ; renal autoregulation	Inflammatory PGE ₂ /PGI ₂ ; pain, fever; renal salt/water handling
Knockout phenotype	Gastric ulcers; reduced platelet aggregation	Reduced inflammation; renal abnormalities; fertility defects
Selective inhibitor	(none in clinical use)	Celecoxib, etoricoxib, parecoxib

Selective COX-2 inhibitors (coxibs) were developed to spare COX-1 (preserving gastric prostaglandins and reducing GI bleeding). Initial successes (Vioxx/rofecoxib, Bextra/valdecoxib) were tempered by cardiovascular concerns: selective COX-2 inhibition reduces endothelial PGI₂ (antiplatelet, vasodilator) without reducing platelet TXA₂ (made by COX-1) — shifting the haemostatic balance toward thrombosis. Rofecoxib was withdrawn in 2004; celecoxib remains in use with cardiovascular labeling.

34.5.3 Pharmacological targets

Table 400. Pharmacological targets: Drug and Target.

Drug	Target	Mechanism	Use
Glucocorticoids	Phospholipase A ₂ (indirectly via annexin A1)	Block most eicosanoid synthesis at the source	Inflammation (broad effect)
Aspirin	COX-1, COX-2	Irreversible acetylation of Ser529; permanently inactivates platelet COX-1 (no nucleus → cannot resynthesise)	Antiplatelet, anti-inflammatory, analgesic, antipyretic
Ibuprofen, naproxen	COX-1, COX-2	Reversible competitive inhibition	Anti-inflammatory, analgesic
Celecoxib	COX-2 selective	Reversible	Reduced GI toxicity (COX-1 spared in gastric mucosa); slight ↑ thrombotic risk (PGI ₂ ↓ without TXA ₂ ↓)
Montelukast	CysLT ₁ receptor	LT receptor antagonist	Asthma, allergic rhinitis
Zileuton	5-lipoxygenase	Direct enzyme inhibition	Asthma
Misoprostol	PGE ₁ analog	Synthetic prostaglandin	Gastric protection, induction of labor
Latanoprost	PGF _{2α} analog	Increases uveoscleral outflow	Glaucoma (lowers IOP)

Clinical Connection — The aspirin paradox: Low-dose aspirin (75–100 mg/day) selectively inhibits platelet COX-1 (anucleate platelets cannot regenerate the enzyme; 7-day duration) but primarily transiently inhibits endothelial COX-2 (nucleated cells continuously resynthesise). Result: net antiplatelet effect with preserved endothelial PGI₂ → reduced thrombotic risk. High-dose aspirin loses this selectivity.

34.6 Endocrine Disruption

Endocrine-disrupting chemicals (EDCs) are exogenous substances that interfere with hormone synthesis, secretion, transport, binding, or elimination. They are particularly concerning for fetal and neonatal development, when small hormone perturbations can have lifelong consequences.

34.6.1 Mechanisms of disruption

1. Receptor agonism (mimicry): Exogenous compound binds and activates a hormone receptor, mimicking the endogenous ligand (e.g., xenoestrogens activate ER).
2. Receptor antagonism: Block native hormone binding (e.g., DDE blocks AR; flutamide-like effect).
3. Altered hormone synthesis: Inhibit steroidogenic enzymes (e.g., conazole fungicides inhibit aromatase; perchlorate blocks NIS at the thyroid).
4. Altered transport/clearance: Disrupt carrier protein binding or hepatic metabolism (e.g., PCBs displace T4 from transthyretin).
5. Altered receptor expression: Epigenetic modification of hormone receptor genes.

34.6.2 Bisphenol A (BPA) and other xenoestrogens

Bisphenol A is a high-volume industrial monomer used in polycarbonate plastics, epoxy resins, and thermal receipts. Estimated production exceeds 6 million tonnes/year. BPA leaches from food containers, especially when heated or contacting acidic foods. Detectable BPA is found in >90% of US adults’ urine.

Mechanism:

- Weak agonist at classical nuclear estrogen receptors (ER α , ER β ; affinity about 10,000 \times lower than oestradiol)
- High-affinity agonist at the membrane-bound G-protein–coupled estrogen receptor (GPER, formerly GPR30)
- Binds androgen receptor as antagonist
- Binds thyroid hormone receptor as antagonist
- Activates pregnane X receptor (xenobiotic metabolism)

The combination of multiple low-affinity but high-prevalence interactions makes BPA a “low-dose” disruptor — its non-monotonic dose–response curve (effects at very low doses absent at higher doses) violates the classical toxicological assumption that “the dose makes the poison.”

Effects (animal and observational human studies): altered pubertal timing, reduced sperm count and quality, increased risk of breast and prostate cancers, metabolic dysfunction (obesity, diabetes), neurodevelopmental and behavioral effects in children. Regulatory responses have lowered BPA exposure limits and led to bans in baby bottles in the EU, Canada, and US — though substitutes (BPS, BPF) appear to share similar disrupting profiles (“regrettable substitution”).

34.6.3 Phthalates, PFAS, and other major EDCs

Phthalates (DEHP, DBP, BBzP) are plasticisers added to PVC to confer flexibility; also used in personal-care products as solvents/fragrance carriers. Dietary intake is the main route. Mechanism: act as anti-androgens via reduced testosterone synthesis (suppression of StAR and CYP17A1) and AR antagonism in the developing male reproductive tract. Animal exposures during the male sex-differentiation window produce the “phthalate syndrome”: cryptorchidism, hypospadias, reduced anogenital distance, decreased sperm count. Human cohort studies link prenatal phthalate exposure to similar genitourinary endpoints.

PFAS (per- and polyfluoroalkyl substances) — the so-called “forever chemicals” (e.g., PFOA, PFOS, GenX) — are characterized by C–F bonds that resist environmental and biological breakdown. Half-lives in humans range from years to decades. Sources: non-stick cookware (Teflon), water-repellent textiles, firefighting foams (AFFF), food packaging. Mechanisms include PPAR α activation (fatty-acid metabolism disruption), thyroid hormone displacement from carrier proteins, and dose-dependent immunosuppression (reduced antibody response to childhood vaccines documented in Faroe Islands cohort studies). The C8 Health Project (West Virginia) linked high-dose occupational PFOA exposure to elevated risks of testicular cancer, kidney cancer, ulcerative colitis, thyroid disease, hypercholesterolaemia, and pregnancy-induced hypertension.

Table 401. Phthalates, PFAS, and other major EDCs: EDC and Source.

EDC	Source	Targets	Effects
Phthalates (DEHP, DBP)	Plasticisers in PVC, cosmetics	AR antagonism; PPAR α , PPAR γ activation; ↓ testosterone synthesis	Anti-androgenic effects on male reproductive development
DDT/DDE	Banned pesticide; persistent	ER agonism; AR antagonism	Eggshell thinning (raptors); breast cancer association
PCBs	Banned but persistent industrial chemicals	Bind transthyretin; AhR agonism	Thyroid disruption; neurodevelopmental harm
Atrazine	Herbicide	Aromatase induction	Feminisation of male amphibians
PFAS (PFOA, PFOS)	Non-stick coatings, firefighting foam, water	PPAR α ; thyroid; immune	“Forever chemicals”; thyroid disruption, immunosuppression, cancer

EDC	Source	Targets	Effects
Phytoestrogens (genistein, daidzein)	Soy, legumes	Weak ER agonist (preferentially ER β)	Modest health effects; debate about infant soy formula
Tributyltin	Marine antifouling paint	RXR/PPAR γ agonism (obesogen)	Imposex in molluscs; potential adipogenesis
Pesticides (vinclozolin, linuron)	Agriculture	AR antagonism	Anti-androgenic, transgenerational epigenetic effects

34.6.4 Vulnerability of development

Fetal and early-life development is uniquely vulnerable to EDCs:

- Hormone-dependent organogenesis: Sex differentiation (Wolffian/Müllerian fates), brain dimorphism, and thyroid-driven CNS myelination depend on tightly timed hormone windows. A small perturbation during these windows can permanently rewire the architecture in ways that would not occur in adults.
- Limited metabolic clearance: Fetal liver enzymes (CYPs, UGTs) are immature; placenta does not always exclude lipophilic toxicants.
- Exponential cell division: Programming events, including DNA methylation and histone modifications, are particularly susceptible to epigenetic disruption during rapid cell division.
- Critical periods are non-recoverable: Once a developmental window closes, the missing signal cannot be replaced by later supplementation.

Concept Check 3: Why might the developmental period (fetal life through puberty) be uniquely vulnerable to endocrine disruptors compared to adult exposures? Consider hormone-dependent organ development and the absence of redundant pathways during organogenesis.

34.7 Current Evidence and Frontier Biology: Endocrine Signaling and Homeostasis

For Endocrine Signaling and Homeostasis, frontier biology belongs inside the evidence logic of the chapter. Physiology now blends mechanism with allostasis, immune-endocrine-neural coupling, wearable data, and individualized risk without reducing bodies to simple machines. The core reading question is this: endocrine-immune claims should include feedback, timing, receptor sensitivity, inflammation, and allostatic load.

- What to verify: identify the observation, model, assay, or dataset that would make the claim stronger or weaker.
- What to qualify: state the scale, organism, cell type, environmental condition, or population where the claim is expected to hold.
- What to compare: test at least one alternative explanation, baseline, or null model before treating the pattern as causal.
- What to cite: distinguish primary evidence, review synthesis, public dataset, and institutional guidance; for recent or numeric claims, prefer the source closest to the measurement and state what has changed since it was published.

Separate baseline set point, perturbation response, compensation, and failure threshold before interpreting physiological data.

Source practice: For body-system claims, cite the measurement context and distinguish set point, perturbation, compensation, pathophysiology, and treatment evidence.

34.7.1 Current Evidence Map: Allostasis and Immune-Endocrine Coupling

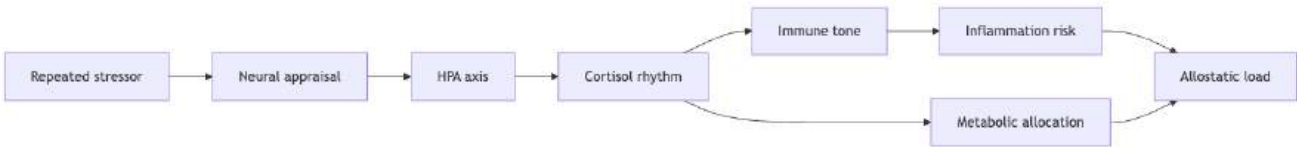


Figure 208. Physiology is often adaptive over short time scales and costly over long time scales, so baseline, perturbation, compensation, and pathology must be distinguished.

34.8 Summary

- Endocrine system: Hierarchical hypothalamic-pituitary-target gland axes with negative feedback. Three hormone classes: peptide (surface receptors, second messengers), steroid (nuclear receptors, transcription), amino acid derivatives (variable).
- HPA / HPT / HPG axes: Stress, thyroid, and reproductive control via CRH–ACTH–cortisol, TRH–TSH–T4/T3, and GnRH–LH/FSH cascades with circadian and feedback regulation.
- Glucose homeostasis: Insulin and glucagon balance uptake, glycogen metabolism, and gluconeogenesis; leptin, adiponectin, and GLP-1 provide long-term and incretin modulation.
- Eicosanoids and disruption: Arachidonic-acid derivatives mediate inflammation; glucocorticoids and NSAIDs target PLA₂ and COX; EDCs perturb hormone signaling during development.
- Connections: See section 35 for immune-endocrine coupling and section 11 for metabolic integration.

34.9 Further Reading and Source Notes: Endocrine Signaling and Homeostasis

- Sterling & Eyer (1988). Allostasis: A new paradigm to explain arousal pathology. Wiley.
- Sterling (2012). Allostasis: A model of predictive regulation. *Physiology & Behavior*, 106.
- McEwen (1998). Protective and damaging effects of stress mediators. *New England Journal of Medicine*, 338.
- Friedman & Halaas (1998). Leptin and the regulation of body weight in mammals. *Nature*, 395.
- Jameson & De Groot, eds. (2016). *Endocrinology: Adult and Pediatric* (7th ed.). Elsevier.

34.10 Companion Source Module: Endocrine Signaling and Homeostasis

Endocrine Signaling and Homeostasis should leave a reproducible trail from a biological claim to the code, figure, diagram, or paper-based activity that can test it. Use the surfaces below to inspect the chapter’s assumptions, rerun the relevant model, or compare the manuscript explanation with companion labs and figures.

Table 402. Companion source surfaces for Endocrine Signaling and Homeostasis.

Surface	Use it for
src/biology/physiology/physiology.py (homeostasis_response)	Compare hormone feedback and inflammatory regulation as control problems.
src/biology/cell/cell_biology.py (receptor_occupancy, signal_amplification)	Quantify receptor sensitivity and cascade gain.
src/mermaid/biology_diagrams.py (immune_response_diagram, hormone_signaling_diagram)	Connect endocrine and immune sequence logic.

Reproducibility check: specify ligand/cytokine, receptor, timing, tissue, feedback loop, and readout before calling a response adaptive or pathological. Cross-reference: use section 8, section 31, and sections 26 and 27.

35 Immune System Architecture

Level 2/3 · 30 min read · 40 min lecture · Prerequisites: section 34

35.1 Learning Objectives

1. Distinguish innate and adaptive immunity, including PRRs and downstream signaling pathways.
2. Explain the complement system, phagocytosis, and antigen presentation.
3. Describe T and B cell development, activation, and immunological memory.
4. Explain tolerance, autoimmunity, hypersensitivity, and immunotherapy approaches.
5. Design a vaccination schedule argument using primary, booster, and herd-immunity reasoning.
6. Compare innate and adaptive effector mechanisms using measurable readouts and controls.
7. Evaluate checkpoint and CAR-T claims against current product labels and surveillance requirements.

35.2 Immune System Architecture and Effector Logic

The immune system protects against pathogens and tumor cells while preserving tolerance to self [Chaplin, 2010]. It comprises two integrated arms: innate immunity (rapid, non-specific, germline-encoded) and adaptive immunity (slow, antigen-specific, somatically generated).

35.2.1 Innate Immunity

Innate immunity provides immediate (seconds to hours), non-specific protection:

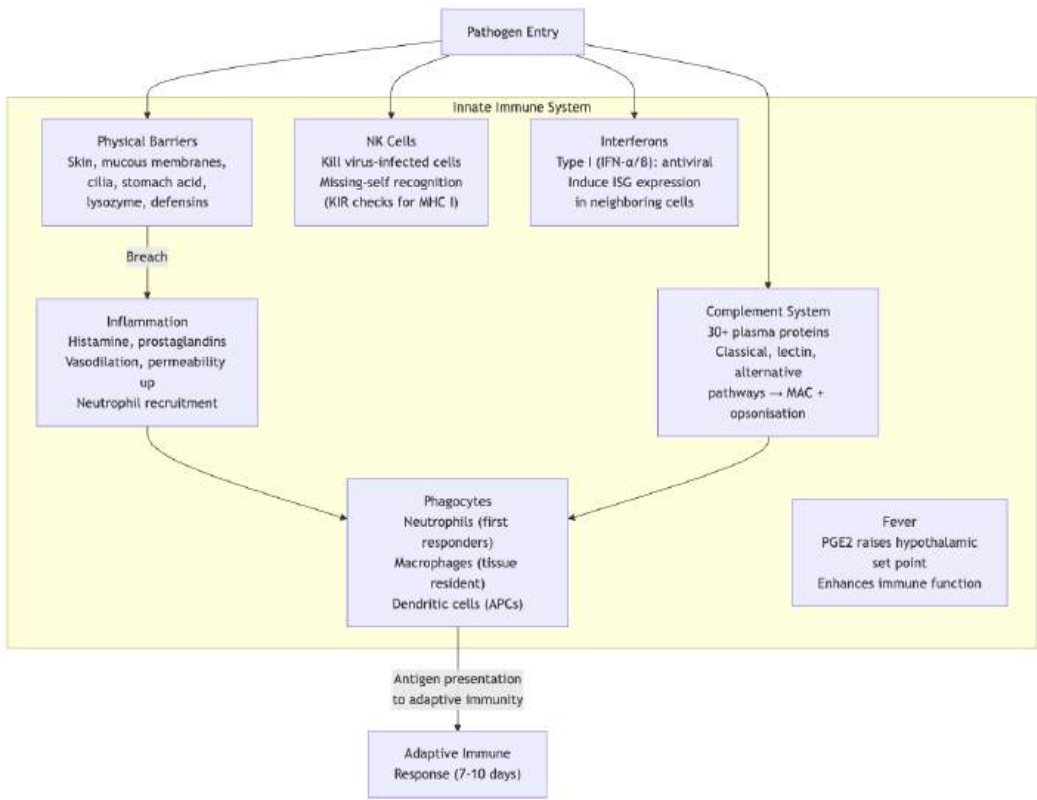


Figure 209. Components of innate immunity Physical barriers form the first line of defense. When breached, inflammation recruits phagocytes, complement activates, NK cells kill infected cells, and interferons establish an antiviral state. Antigen-presenting cells bridge innate to adaptive immunity.

Key innate immune cells:

Table 403. Innate Immunity: Cell Type and Function.

Cell Type	Function	Key Features
Neutrophils	First responders; phagocytosis; NETs; oxidative burst	Most abundant WBC (60–70%); short-lived (hours)
Macrophages	Phagocytosis; antigen presentation; cytokine production	Tissue-resident (Kupffer cells in liver, microglia in brain, alveolar macrophages in lung)
Dendritic cells	Professional APCs; bridge innate and adaptive	Most potent antigen presenters
NK cells	Kill virus-infected and tumor cells	“Missing self” detection via KIR receptors
Mast cells	Histamine release; IgE-mediated degranulation	Allergy; parasite defense
Eosinophils	Parasite defense; allergic inflammation	Major basic protein toxic to helminths
Basophils	Histamine; IL-4 production	Rarest WBC (<1%)

35.2.2 Pattern Recognition Receptors (PRRs)

Innate immune cells detect pathogens through germline-encoded PRRs that recognize conserved molecular signatures unique to pathogens — pathogen-associated molecular patterns (PAMPs) — or signals of cellular damage — damage-associated molecular patterns (DAMPs) [Medzhitov, 2007]. PRRs fall into four major families based on cellular location and ligand class.

Toll-like receptors (TLRs) Membrane-bound (plasma membrane or endosomal). Humans express 10 TLRs.

Species specificity matters here. Human TLR1–TLR10 are not a comprehensive mammalian template: mice lack a direct functional equivalent of human TLR10 but retain TLR11–TLR13, which detect microbial ligands such as profilin-like proteins and bacterial RNA. TLR10 itself remains less mechanistically settled than TLR4, TLR7/8, or TLR9. When comparing innate-immunity experiments across humans, mice, and cell lines, students should ask whether the receptor repertoire and ligand preparation actually match the claimed pathogen-sensing pathway.

Table 404. Toll-like receptors (TLRs): TLR and Location.

TLR	Location	Ligand	Pathogen class
TLR1/2	Plasma membrane	Triacyl lipopeptides	Bacteria (mycobacteria)
TLR2/6	Plasma membrane	Diacyl lipopeptides, peptidoglycan	Gram+ bacteria, fungi
TLR3	Endosomal	dsRNA	Viruses
TLR4	Plasma membrane	LPS (lipopolysaccharide)	Gram– bacteria
TLR5	Plasma membrane	Flagellin	Motile bacteria
TLR7/8	Endosomal	ssRNA	RNA viruses
TLR9	Endosomal	Unmethylated CpG DNA	Bacteria, DNA viruses

TLR4 → MyD88 → NF-κB pathway (bacterial LPS response)

TLR3/TRIF → IRF3 → IFN-β pathway (antiviral response) A parallel branch is engaged by TLR3 (endosomal dsRNA) and the late-endosome pool of TLR4. The adaptor TRIF recruits TBK1, which phosphorylates IRF3. Phospho-IRF3 dimerises, enters the nucleus, and drives transcription of type I interferons (IFN-α/β). IFN-β released into the extracellular space binds IFNAR on neighboring cells, activating JAK1/TYK2 → STAT1/STAT2 → ISGF3 → induction of hundreds of interferon-stimulated genes (ISGs) that establish an antiviral state. The MyD88/NF-κB vs TRIF/IRF3 dichotomy explains why bacterial LPS produces fever and inflammation while viral dsRNA produces an interferon-driven antiviral state.

NOD-like receptors (NLRs) and the NLRP3 inflammasome Cytosolic. Detect intracellular bacterial components (peptidoglycan derivatives) and danger signals.

- NOD1 detects iE-DAP (Gram–); NOD2 detects MDP (comprehensive). Both activate NF-κB. NOD2 mutations cause Crohn’s disease (impaired mucosal immunity → dysbiosis → inflammation).



Figure 210. TLR4/MyD88/NF-kappaB pathway. LBP and CD14 deliver bacterial LPS to TLR4/MD-2, TLR4 dimerization recruits TIRAP and MyD88, IRAK kinases and TRAF6 activate TAK1 and IKK, and IkappaBalpha degradation releases NF-kappaB to induce inflammatory genes.

The NLRP3 inflammasome illustrates the two-signal model:

- Signal 1 (priming): TLR or cytokine engagement → NF-κB → upregulates NLRP3 and pro-IL-1β transcription. Without this, no inflammasome assembly.
- Signal 2 (activation): Diverse triggers — extracellular ATP (P2X7), K⁺ efflux, lysosomal rupture (urate crystals, cholesterol crystals, silica, alum), mitochondrial ROS, mitochondrial DNA in cytosol — activate NLRP3.
- Assembly: NLRP3 oligomerises via its NACHT domain; recruits ASC adaptor via PYD–PYD interactions; ASC nucleates pro-caspase-1 via CARD–CARD; pro-caspase-1 self-cleaves to active caspase-1.
- Output: Caspase-1 cleaves pro-IL-1β → IL-1β (released via gasdermin D pores) and pro-IL-18 → IL-18; cleaves gasdermin D, whose N-terminal fragment forms 10–20 nm pores in the plasma membrane causing pyroptosis (lytic cell death with massive cytokine release).

NLRP3 mutations cause cryopyrin-associated periodic syndromes (CAPS); chronic NLRP3 activity drives gout (urate crystals), atherosclerosis (cholesterol crystals), Alzheimer’s-related neuroinflammation, and type 2 diabetes. Anakinra (recombinant IL-1Ra) and canakinumab (anti-IL-1β) target the inflammasome output.

RIG-I-like receptors (RLRs) Cytosolic RNA sensors detecting viral replication.

- RIG-I: detects 5’-triphosphate RNA (host RNA is capped; viral RNA is not).
- MDA5: detects long dsRNA.
- Signal via MAVS (mitochondrial antiviral signaling protein) → IRF3/IRF7 → type I interferons.

cGAS–STING pathway (cytosolic DNA sensing) The cGAS–STING axis is the principal sensor for cytosolic DNA — a hallmark of intracellular bacterial or viral infection (and, problematically, mislocalized mitochondrial or self DNA).

- cGAS (cyclic GMP–AMP synthase) binds dsDNA non-sequence-specifically through a phase-separation-like condensation. Activated cGAS catalyses synthesis of the cyclic dinucleotide 2’3’-cGAMP from ATP and GTP.
- STING (stimulator of interferon genes), an ER-resident transmembrane protein, binds 2’3’-cGAMP, undergoes a major conformational change, traffics from ER to ERGIC/Golgi, and recruits TBK1, which phosphorylates IRF3 → type I interferon transcription. STING also activates NF-κB via a parallel branch.

The cGAS–STING pathway is essential for control of HSV-1, vaccinia, and many cytosolic bacteria. Dysregulation drives autoimmunity: mutations causing constitutive STING activation produce SAVI (STING-associated vasculopathy with onset in infancy), an interferonopathy. Aicardi-Goutières syndrome arises when defective DNases (TREX1, RNASEH2) cannot clear cytoplasmic nucleic acids, chronically engaging cGAS-STING. Pharmacologically, STING agonists (ADU-S100) are being trialled as cancer adjuvants because tumor-induced type I IFN can boost antitumour immunity.

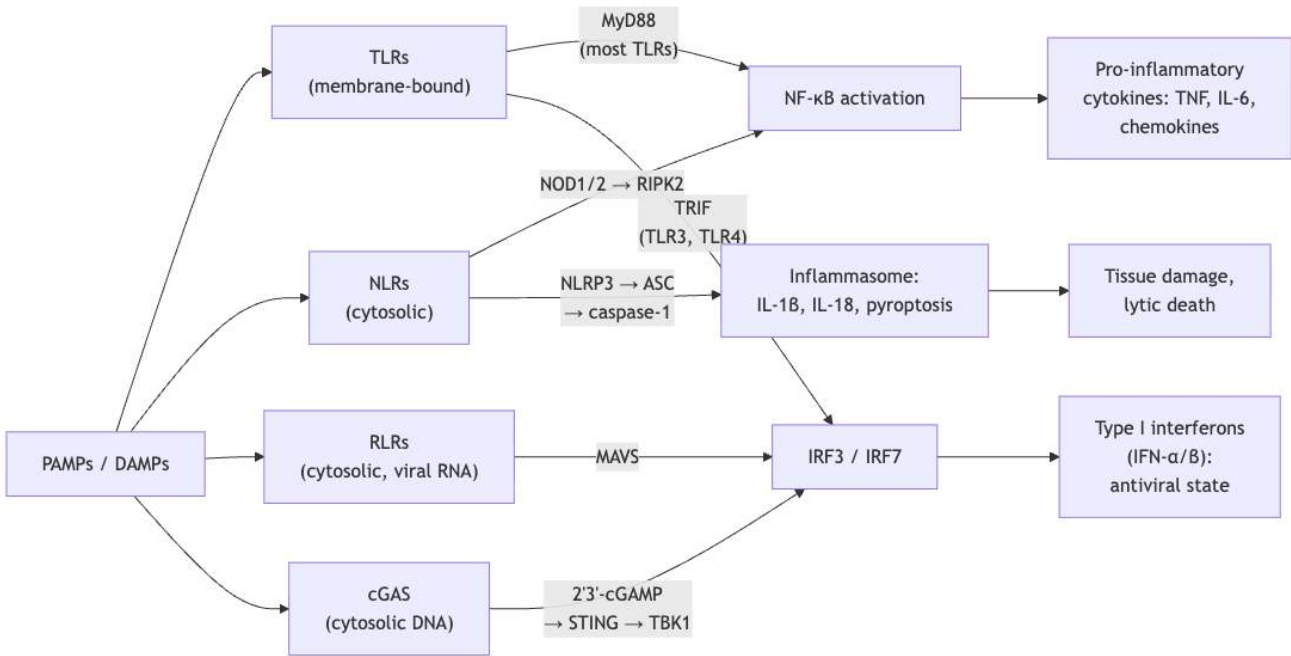


Figure 211. PRR signaling pathways TLRs, NLRs, RLRs, and cGAS converge on transcription factors NF-kappaB (inflammation), IRF3/7 (interferons), and the inflammasome (IL-1beta, pyroptosis). Different pathogen classes preferentially engage different sensors.

35.2.3 Complement System Overview

The complement system comprises about 30 plasma proteins that amplify innate responses through enzymatic cascades. There are three pathways of activation, most converging on a common terminal pathway.

Three activation pathways

Table 405. Three activation pathways: Pathway and Trigger.

Pathway	Trigger	Initiation step	Convergence
Classical	Antibody (IgM, IgG) bound to antigen on pathogen	C1q binds Fc → activates C1r → C1s → cleaves C4 + C2	C3 convertase = C4b2a
Lectin	Pathogen surface mannose / GlcNAc	MBL or ficolins bind sugars → MASP1/MASP2 (analogous to C1r/C1s) → cleave C4 + C2	C3 convertase = C4b2a
Alternative	Spontaneous “tick-over” hydrolysis of C3; amplified on pathogen surfaces lacking complement regulators	C3(H ₂ O) + factor B + factor D → C3(H ₂ O)Bb (initial fluid-phase convertase) → deposits C3b on surface → C3bBb (surface convertase, stabilized by properdin)	C3 convertase = C3bBb

C3 convertase, C5 convertase, MAC The classical, lectin, and alternative pathways each generate a C3 convertase (C4b2a or C3bBb) that cleaves C3 → C3a + C3b. C3b is deposited on the pathogen surface; binding of an additional C3b to the existing C3 convertase yields the C5 convertase (C4b2aC3b or C3bBbC3b) that cleaves C5 → C5a + C5b.

C5b initiates the terminal pathway: C5b → C5b-C6 → C5b-C6-C7 (membrane-inserting) → C5b-C6-C7-C8 → addition of multiple C9 monomers polymerizing into the membrane attack complex (MAC, C5b-9). The MAC forms a 10 nm transmembrane pore that lyses the target cell. Gram-negative bacteria are particularly vulnerable; encapsulated bacteria (*Neisseria*) require complement for clearance, which is why C5–C9 deficiencies present with recurrent meningococcal infection.

Effector functions

- Opsonisation: C3b coats pathogen → recognized by phagocyte receptors CR1 (C3b/C4b), CR3 (iC3b), CR4. Opsonised particles are 1000-fold more efficiently phagocytosed.
- Membrane attack complex (MAC): C5b-9 polymerizes in target membrane, forming a 10 nm pore.
- Anaphylatoxins (chemotaxis and inflammation): C3a and C5a (the most potent) recruit neutrophils, activate mast cells, increase vascular permeability, and amplify local inflammation.
- Immune complex clearance: CR1 on erythrocytes binds C3b-coated immune complexes and ferries them to liver/spleen for disposal.
- B cell co-stimulation: C3d coupled to antigen lowers the BCR signaling threshold about 10,000 fold via CR2 (CD21).

Amplification dynamics and regulation The cascade is intrinsically amplifying because each enzyme cleaves many substrates. If one C3 convertase cleaves N copies of C3 per second, with decay rate k_d , the steady-state C3b concentration scales as

$$[C3b] = \frac{[C3conv] \cdot N}{k_d}$$

(414)

The alternative pathway amplification loop is positive: each new C3b binds factor B → C3 convertase → cleaves more C3 → more C3b. Without regulators, this loop would consume most plasma C3 within minutes.

Regulators confine the cascade to pathogen surfaces:

Table 406. Amplification dynamics and regulation: Regulator and Location.

Regulator	Location	Function
DAF (CD55)	GPI-anchored on host cells	Accelerates C3/C5 convertase decay
CD59	GPI-anchored on host cells	Blocks MAC assembly (C9 incorporation)
Factor H	Soluble plasma protein	Binds host-specific sialic acid; cofactor for factor I cleavage of C3b
C4BP (C4b binding protein)	Soluble	Inactivates C4b
C1-INH (C1 esterase inhibitor)	Soluble	Inhibits C1r/C1s and MASPs
CR1 (CD35)	Erythrocytes, lymphocytes	Cofactor for factor I; immune complex clearance

Patients with paroxysmal nocturnal hemoglobinuria (PNH) lack the GPI anchor that tethers DAF and CD59 to RBCs → uncontrolled complement activation → hemolysis. Treated with eculizumab (anti-C5 monoclonal antibody; blocks C5 cleavage and MAC formation). C1-INH deficiency causes hereditary angioedema (uncontrolled C1 → bradykinin generation via the kinin–kallikrein system → sudden tissue swelling).

35.2.4 Adaptive Immunity Overview

Adaptive immunity is slower (7–10 days for primary response) but provides specificity (each lymphocyte recognizes a unique antigen) and memory (faster, stronger response on re-exposure — basis of vaccination) [Iwasaki and Medzhitov, 2015].

Two arms:

- Cell-mediated: T cells (CD8+ cytotoxic kill infected cells; CD4+ helper coordinate response)
- Humoral: B cells produce antibodies that neutralize pathogens, opsonise, activate complement

Antigen presentation via MHC:

- MHC class I (on most nucleated cells): presents endogenous peptides (8–10 aa) from cytosolic proteins. Pathway: cytosolic protein → proteasome → TAP transporter → ER → loaded onto MHC I → surface. Presented to CD8+ T cells.
- MHC class II (on professional APCs: dendritic cells, macrophages, B cells): presents exogenous peptides (12–25 aa) from internalised pathogens. Pathway: phagocytosis → endolysosome → cathepsin cleavage → loaded onto MHC II (after CLIP removal by HLA-DM) → surface. Presented to CD4+ T cells.

- Cross-presentation: Dendritic cells can also load exogenous antigens onto MHC I, important for activating CD8+ responses against viruses that don’t directly infect APCs.

35.2.5 T Cell Development and Selection

T cell precursors leave the bone marrow as immature CD4[−]CD8[−] “double-negative” thymocytes and migrate to the thymus, where they undergo somatic recombination and selection.

Double-negative (DN1–DN4) staging Within the thymic cortex, double-negative thymocytes pass through four sequential stages defined by surface CD44 and CD25 expression:

Table 407. Double-negative (DN1–DN4) staging: Stage and CD44.

Stage	CD44	CD25	Major event
DN1	+	−	Early thymic progenitor; multipotent (T/NK/myeloid)
DN2	+	+	Lineage commitment; TCR $\beta/\gamma/\delta$ rearrangement begins
DN3	−	+	TCR β rearrangement complete; β -selection checkpoint (primarily cells with productive TCR β survive, via signaling from pre-TCR with surrogate α chain pT α)
DN4	−	−	Proliferative burst; transition to double-positive (CD4+CD8+)

Cells then become double-positive (CD4+CD8+) and rearrange TCR α . With both TCR chains expressed, they undergo positive then negative selection.

TCR diversity generation Like immunoglobulin loci, the T cell receptor (TCR) loci undergo V(D)J recombination mediated by RAG1/RAG2 endonucleases:

- TCR β chain: V–D–J recombination (about 52 V \times 2 D \times 13 J segments \rightarrow about 1,400 combinations)
- TCR α chain: V–J recombination (about 70 V \times about 61 J segments \rightarrow about 4,300 combinations)
- Junctional diversity: TdT (terminal deoxynucleotidyl transferase) adds non-templated N-nucleotides at junctions
- Combinatorial diversity: $\alpha\beta$ pairing creates about 6×10^6 unique receptors before junctional diversity
- With junctional diversity: the theoretical TCR repertoire exceeds 10^{18} , far larger than the about 10^{11} T cells in the human body — most TCRs are rarely realized.

Rough calculation: $1,400 \times 4,300 \approx 6 \times 10^6$ V(D)J combinations \times about 10^{12} junctional possibilities $\approx 10^{18}$ theoretical receptors.

Defects in this recombination machinery cause severe combined immunodeficiencies (RAG1/RAG2 SCID — “bubble boy” disease); ataxia-telangiectasia (ATM mutation) causes radiosensitivity and lymphoid malignancy.

Positive selection (cortex) In the thymic cortex, double-positive (CD4+CD8+) thymocytes encounter cortical thymic epithelial cells (cTECs) displaying self-peptide–MHC complexes. T cells whose TCR engages MHC with sufficient (but not excessive) affinity receive a survival signal. T cells with no MHC affinity die by neglect (about 95% of thymocytes).

- TCR engagement of MHC I \rightarrow CD8+ single-positive T cell
- TCR engagement of MHC II \rightarrow CD4+ single-positive T cell

Positive selection ensures the surviving repertoire is MHC-restricted — primarily recognizes antigen presented in the context of self MHC.

Negative selection (medulla) — AIRE and Treg generation Surviving thymocytes migrate to the medulla and encounter medullary thymic epithelial cells (mTECs) and dendritic cells. mTECs express the autoimmune regulator AIRE transcription factor, which drives ectopic expression of thousands of tissue-specific antigens (insulin, thyroglobulin, myelin proteins) normally restricted to peripheral tissues. T cells whose TCR binds self-peptide–MHC complexes with high affinity undergo apoptosis (clonal deletion). A small fraction with intermediate self-reactivity become regulatory T cells (Tregs) — CD4+CD25+FoxP3+ cells that police self-tolerance in the periphery.

AIRE mutations cause autoimmune polyendocrinopathy syndrome type 1 (APS-1, APECED) — patients fail to delete autoreactive T cells against multiple endocrine organs, developing chronic mucocutaneous candidiasis, hypoparathyroidism, and adrenal insufficiency. FoxP3 mutations cause IPEX syndrome — fatal multi-organ autoimmunity in infancy from absent Tregs.

35.2.6 B Cell Activation and Antibody Diversification

Stepwise B cell activation

1. Antigen encounter. Naïve B cell in lymphoid follicle encounters cognate antigen (in soluble form, or displayed on subcapsular sinus macrophages and follicular dendritic cells).
2. BCR cross-linking. Multivalent antigen cross-links several BCRs → tyrosine phosphorylation of Igα/Igβ ITAMs by Lyn/Fyn → recruitment of Syk → activation of PI3K, PLCγ2, Ras/MAPK cascades.
3. Antigen internalization. B cell internalises antigen via BCR, processes peptides in MHC class II compartment.
4. Migration to T-B border. Activated B cell upregulates CCR7, migrates to T-cell zone of lymph node.
5. T cell help. Cognate Tfh (follicular helper T cell) recognizes B cell-presented peptide on MHC II. Engagement of CD40L (Tfh) – CD40 (B cell) plus cytokines (IL-4, IL-21) provides “second signal.”
6. Outcome: B cells either differentiate into short-lived extrafollicular plasmablasts (rapid IgM, low affinity) or enter the germinal center.

B cell activation modes

- T-independent (TI) responses: Polysaccharide and repetitive antigens cross-link many BCRs simultaneously. Produces predominantly IgM, no germinal center, no affinity maturation, weak memory. Important for encapsulated bacteria (*Streptococcus pneumoniae*, *Haemophilus influenzae*); explains why polysaccharide vaccines work poorly in children <2 years.
- T-dependent (TD) responses: Protein antigens. B cell internalises antigen via BCR, processes it, presents peptide on MHC II, is recognized by cognate CD4+ T helper cell (specifically Tfh — follicular helper T cell). T:B interaction at the T-B border activates the B cell to enter the germinal center reaction. Produces high-affinity, class-switched antibodies and long-lived memory.

Germinal center reaction — somatic hypermutation and affinity maturation In secondary lymphoid organs (lymph nodes, spleen, Peyer’s patches), activated B cells form germinal centers with two zones:

- Dark zone (centroblasts): Rapid proliferation. Activation-induced cytidine deaminase (AID) introduces somatic point mutations into the variable regions of immunoglobulin genes — somatic hypermutation (SHM), about 10^{−3} mutations per base per generation (about 10⁶ × normal mutation rate).
- Light zone (centrocytes): B cells re-encounter antigen displayed on follicular dendritic cells (FDCs). Cells whose mutated BCR has improved antigen affinity capture more antigen, internalise it, present more peptide on MHC II, and receive stronger Tfh help → survival and re-cycling. Cells with reduced affinity die by apoptosis. This is affinity maturation — Darwinian selection at the cellular level, driving 1000-fold increases in antibody affinity over weeks.

Light-zone cells differentiate into:

- Plasma cells (long-lived in bone marrow, secrete antibodies for years/decades)
- Memory B cells (rapidly mobilized on antigen re-encounter)

Class switch recombination (CSR) Initially B cells produce IgM (default isotype). Cytokines from Tfh cells direct class switching to IgG, IgA, or IgE by recombining the heavy chain constant region (the variable region — and thus antigen specificity — is preserved). At the molecular level, AID deaminates cytidines in switch (S) regions upstream of each constant-region gene; subsequent base-excision repair generates double-strand breaks that are joined by NHEJ to produce switch recombination, deleting intervening DNA.

Table 408. Class switch recombination (CSR): Cytokine and Switch to.

Cytokine	Switch to	Function
IFN-γ	IgG1, IgG3	Opsonisation, complement, intracellular pathogens
IL-4	IgG4, IgE	Allergy, helminth defense
TGF-β	IgA	Mucosal immunity
IL-21	IgG1, IgG3	Synergises with other switches

Defects in AID cause hyper-IgM syndrome (HIGM2 — failure of class switching and somatic hypermutation; primarily IgM is produced). CD40L mutations cause an X-linked form (HIGM1) — failure of cognate T-cell help.

Antibody isotypes

Table 409. Antibody isotypes: Class and Form.

Class	Form	Half-life	Function
IgM	Pentamer	about 5 d	Primary response; complement activation
IgG	Monomer	about 21 d	Secondary response; opsonisation; placental transfer; complement
IgA	Dimer (mucosal)	about 6 d	Mucosal immunity (gut, respiratory, breast milk)
IgE	Monomer	about 2 d (3 weeks bound to FcεR on mast cells)	Allergy; helminth defense
IgD	Monomer	about 3 d	B cell receptor (function unclear)

35.2.7 Cytokine Network Reference

Cytokines are small (about 15–25 kDa) signaling proteins that coordinate immune cell function. They act locally (paracrine/autocrine) at very low concentrations (pM–nM) via JAK/STAT or other receptor families.

Table 410. Cytokine Network Reference: Cytokine and Major Source.

Cytokine	Major Source	Major Targets	Receptor / Signaling	Key effects
IL-1 (α/β)	Macrophages, DCs (NLRP3 inflammasome for IL-1 β)	Endothelium, hypothalamus, T cells	IL-1R / MyD88 \rightarrow NF- κ B	Fever (PGE ₂), endothelial activation, T cell co-stimulation
IL-2	Activated CD4+ T cells	T cells, NK cells, Tregs	IL-2R ($\alpha\beta\gamma$) / JAK1/3 \rightarrow STAT5	T cell proliferation; Treg survival (Treg uses IL-2 as ‘sink’)
IL-4	Th2 cells, mast cells, basophils	B cells, Th2 polarization	IL-4R / JAK1/3 \rightarrow STAT6	IgE class switch; Th2 differentiation; allergy
IL-5	Th2 cells, ILC2	Eosinophils	IL-5R / JAK2 \rightarrow STAT5	Eosinophil growth/activation (helminths, allergy)
IL-6	Macrophages, T cells, hepatocytes	Liver, B cells, T cells	IL-6R/gp130 / JAK1/2 \rightarrow STAT3	Acute phase response (CRP, fibrinogen); Th17 differentiation; B cell maturation
IL-7	Stromal cells (BM, thymus)	Naïve and memory T cells	IL-7R / JAK1/3 \rightarrow STAT5	T cell development and homeostatic survival
IL-8 (CXCL8)	Macrophages, endothelium	Neutrophils	CXCR1/CXCR2 (G _i GPCRs)	Neutrophil chemotaxis
IL-10	Tregs, macrophages, B cells	Macrophages, T cells	IL-10R / JAK1/TYK2 \rightarrow STAT3	Anti-inflammatory — suppresses Th1 and macrophage activation
IL-12	Macrophages, DCs	NK cells, T cells	IL-12R / TYK2/JAK2 \rightarrow STAT4	Th1 differentiation; IFN- γ induction
IL-13	Th2, ILC2, mast cells	B cells, smooth muscle, epithelium	IL-13R α 1/IL-4R α / STAT6	Allergy/asthma; goblet cell mucus; tissue remodeling; target of dupilumab
IL-15	DCs, monocytes	NK, memory CD8+ T cells	IL-15R / JAK1/3 \rightarrow STAT5	NK and memory T cell maintenance

Cytokine	Major Source	Major Targets	Receptor / Signaling	Key effects
IL-17	Th17 cells, $\gamma\delta$ T cells	Epithelium, neutrophils	IL-17R / Act1 \rightarrow NF- κ B	Mucocutaneous defense (fungi, extracellular bacteria); psoriasis, IBD when dysregulated
IL-21	Tfh cells	B cells, T cells	IL-21R / JAK1/3 \rightarrow STAT3	Germinal center reactions, class switching
IL-22	Th17, Th22, ILC3	Epithelium	IL-22R / JAK1/2 \rightarrow STAT3	Mucosal barrier defense; antimicrobial peptide production
IL-23	Macrophages, DCs	Th17 cells	IL-23R / JAK2/TYK2 \rightarrow STAT3	Th17 stabilization; target of ustekinumab/risankizumab in psoriasis/IBD
TNF- α	Macrophages, T cells	Endothelium, tumor cells	TNFR1/2 \rightarrow NF- κ B / apoptosis	Inflammation, septic shock, apoptosis; target of anti-TNF biologics
IFN- α/β (Type I)	Most cells (esp. plasmacytoid DCs)	Most nucleated cells	IFNAR1/2 / JAK1/TYK2 \rightarrow STAT1/2 \rightarrow ISGF3	Antiviral state (induces hundreds of ISGs); MHC I upregulation
IFN- γ (Type II)	Th1 cells, NK cells, CD8+	Macrophages, most cells	IFNGR1/2 / JAK1/2 \rightarrow STAT1	Macrophage activation; MHC upregulation; intracellular pathogen defense
TGF- β	Tregs, many cells	Many	T β R-I/II / SMAD2/3	Treg induction; tissue repair; wound healing; oncogenic in late cancer
GM-CSF	T cells, macrophages, endothelium	Myeloid progenitors	CSF2R / JAK2 \rightarrow STAT5	Granulocyte/macrophage growth; DC differentiation; therapeutic in neutropenia

Th polarization:

- Th1 (driven by IL-12; produces IFN- γ): intracellular pathogens, viruses, autoimmunity (MS, T1DM)
- Th2 (driven by IL-4; produces IL-4/5/13): helminths, allergy, asthma
- Th17 (driven by IL-6 + TGF- β ; produces IL-17): extracellular bacteria, fungi; psoriasis, IBD
- Treg (driven by TGF- β ; FoxP3+): peripheral tolerance, suppression
- Tfh (in germinal centers; produces IL-21): B cell help

35.2.8 Immunological Memory — Why Memory Cells Respond Faster

After antigen clearance, about 95% of effector T and B cells die by apoptosis (contraction phase). The remaining 5% become long-lived memory cells. Memory cells respond to re-exposure 100–1000× faster and stronger than naïve cells:

Table 411. Immunological Memory — Why Memory Cells Respond Faster: Property and Naïve cell.

Property	Naïve cell	Memory cell
Frequency for given antigen	about 1 in 10 ⁶	100–1000-fold higher (clonal expansion preserved)

Property	Naïve cell	Memory cell
Activation threshold	High (needs 24–48 h priming, full co-stimulation)	Low (rapid proliferation on re-encounter)
Effector repertoire	Naïve, must differentiate	Pre-armed; rapid cytokine production / class-switched antibody
Tissue distribution	Recirculate through 2° lymphoid organs	T _{CM} recirculate; T _{EM} /T _{RM} patrol peripheral and barrier tissues
Homeostatic maintenance	None	Tonic IL-7 + IL-15; long lifespan (decades for some clones)

The signaling determinants of effector vs memory differentiation include:

- Strong, prolonged TCR signaling + IL-2 → effector (terminally differentiated, short-lived, KLRG1^{hi})
- Brief TCR signaling + IL-7, IL-15 → memory precursors (CD127^{hi}, CD62L⁺)
- Memory subsets:
 - Central memory (T_{CM}): CCR7⁺, CD62L⁺; recirculate through lymph nodes; high proliferative potential
 - Effector memory (T_{EM}): CCR7[−]; patrol peripheral tissues; immediate effector function
 - Tissue-resident memory (T_{RM}): CD69⁺, CD103⁺; reside in barrier tissues (skin, gut, lung); first to detect re-infection

Memory persistence depends on tonic IL-7 and IL-15 cytokine signaling and homeostatic proliferation, not antigen re-stimulation. This is why vaccine immunity can last decades despite no reinfection — and why immunosuppressive therapies that cripple homeostatic cytokines (e.g., IL-7 axis blockade) reduce memory.

Concept Check (Synthesis — Cross-Unit Connection): The immune system can be reframed as an active inference agent. The adaptive immune system maintains a generative model of self (MHC-presented peptides) and non-self (pathogen-associated patterns). B and T cell clonal selection = model updating; clonal expansion = precision-weighting of high-evidence hypotheses; immunological memory = compressed posterior over past pathogens; autoimmunity = failure of the self/non-self model. (a) In Bayesian terms, what does the MHC-peptide-TCR recognition step represent — the likelihood, the prior, or the posterior? Justify. (b) Vaccination trains the immune system’s generative model with attenuated antigen: in FEP terms, why does repeated low-dose exposure (prime-boost) produce stronger immunity than a single high-dose exposure? (c) Tolerance to commensal gut bacteria requires the immune system to hold stable priors despite constant microbial exposure — identify the cellular mechanism that maintains this prior and predict what happens when it fails (as in IBD).

35.2.9 Tolerance and Autoimmunity

Self-tolerance is maintained at two levels:

Autoimmunity is rarely explained by a single broken checkpoint. Susceptibility alleles, sex-biased immune regulation, molecular mimicry, epitope spreading, tissue damage, microbiome state, and timing of infection can most shift the threshold between protective immunity and self-damage. A precise answer should therefore distinguish the initiating trigger, the self-antigen or tissue compartment, the effector mechanism, and the evidence that tolerance failed rather than merely inflammation increased.

Central tolerance (thymus and bone marrow)

- T cells: Negative selection in thymic medulla (AIRE-driven self-antigen expression)
- B cells: Receptor editing and clonal deletion in bone marrow upon BCR engagement of self-antigen

Failure modes: AIRE mutations (APS-1); central tolerance is incomplete because not most self-antigens can be expressed in primary lymphoid organs.

Peripheral tolerance

- Anergy: TCR engagement without co-stimulation (CD28 by B7) inactivates rather than activates the T cell.
- Treg suppression: FoxP3+ regulatory T cells suppress conventional T cell activation by IL-2 consumption, IL-10/TGF-β secretion, CTLA-4 outcompeting CD28, and granzyme killing.
- Inhibitory checkpoints: CTLA-4 and PD-1 restrain T cell responses (see immunotherapy below).
- Activation-induced cell death (AICD): Repeatedly activated T cells upregulate Fas → undergo apoptosis on Fas ligation.

Mechanisms of autoimmunity Failures of tolerance produce autoimmunity through several archetypal mechanisms:

- Molecular mimicry: A pathogen antigen shares structural similarity with self-antigen. Memory cells generated to fight the pathogen cross-react with self.
 - Example: Group A *Streptococcus* M protein mimics cardiac myosin → rheumatic heart disease after streptococcal pharyngitis.
 - Example: *Campylobacter jejuni* lipo-oligosaccharide mimics peripheral nerve gangliosides → Guillain-Barré syndrome.
- Bystander activation: Local infection/inflammation drives massive cytokine release, MHC upregulation, and APC maturation. Autoreactive T cells that escaped thymic deletion are activated by their cognate self-antigen now presented in a strongly stimulatory context.
- Epitope spreading: Initial response to one self-antigen broadens over time as tissue damage releases additional self-antigens that are taken up by APCs and presented to new autoreactive T cell clones.
 - Example: In Type 1 diabetes, autoantibodies often appear in stereotyped sequence (insulin → GAD65 → IA-2 → ZnT8) over months to years before clinical onset, reflecting progressive epitope spreading within the islet.
 - Example: In multiple sclerosis, initial myelin basic protein (MBP) response can spread to PLP, MOG, and other myelin antigens.
- Loss of regulatory T cells: FoxP3 mutations cause IPEX syndrome (Immunodysregulation Polyendocrinopathy Enteropathy X-linked) — fatal multi-organ autoimmunity in infancy.
- Defective apoptosis: Fas / FasL mutations (autoimmune lymphoproliferative syndrome, ALPS) prevent AICD → accumulation of self-reactive lymphocytes.

Table 412. Mechanisms of autoimmunity: Autoimmune disease and Target tissue.

Autoimmune disease	Target tissue	Type	Mechanism
Type 1 diabetes	β -cells	Cell-mediated (CD8+)	Anti-GAD65, anti-IA-2 antibodies; T cell destruction; epitope spreading
Multiple sclerosis	CNS myelin	Cell-mediated (Th1/Th17)	Anti-MBP T cells; molecular mimicry to EBV nuclear antigen 1 implicated
Rheumatoid arthritis	Synovial joints	Mixed	Anti-CCP, RF antibodies; TNF-driven
SLE	Multi-organ	Antibody/IC	Anti-dsDNA, anti-Sm; immune complex deposition
Hashimoto's	Thyroid	Antibody	Anti-TPO, anti-Tg
Graves'	Thyroid	Antibody (stimulating)	Anti-TSH-R (agonist)
Myasthenia gravis	NMJ	Antibody	Anti-AChR antibodies block receptors
Goodpasture's	Kidney, lung	Antibody (Type II)	Anti- α 3(IV) collagen

35.2.10 Hypersensitivity Reactions (Gell-Coombs Classification)

The four-tier Gell-Coombs classification organizes immune-mediated hypersensitivity by mechanism, time course, and treatment.

Table 413. Hypersensitivity Reactions (Gell-Coombs Classification): Type and Mechanism.

Type	Mechanism	Onset	Examples	Treatment
Type I (immediate)	IgE-mediated; mast cell degranulation; histamine, leukotrienes, tryptase	Minutes	Anaphylaxis, allergic asthma, food allergy, hay fever	Epinephrine (anaphylaxis), antihistamines (H1 blockers — diphenhydramine, cetirizine), inhaled corticosteroids, cromolyn (mast cell stabiliser), allergen immunotherapy (gradual desensitisation), anti-IgE (omalizumab)

Type	Mechanism	Onset	Examples	Treatment
Type II (cytotoxic)	IgG/IgM antibody against cell-surface antigen → complement, ADCC	Hours	Autoimmune hemolytic anemia, transfusion reaction, Goodpasture's, Graves' (stimulating)	Plasmapheresis, IVIG, immunosuppression (rituximab anti-CD20 for ITP/AIHA)
Type III (immune complex)	Soluble antigen-antibody complexes deposit in tissues → complement, neutrophils	Hours to days	SLE, serum sickness, post-streptococcal glomerulonephritis, hypersensitivity pneumonitis	Corticosteroids, cyclophosphamide, removal of antigen source, plasmapheresis
Type IV (delayed/cell-mediated)	T cell-mediated; no antibody	24–72 h	Contact dermatitis (poison ivy, nickel), tuberculin/PPD test, Type 1 diabetes onset, MS, contact allergy to nickel	Topical/systemic corticosteroids, calcineurin inhibitors (tacrolimus), allergen avoidance

Type I — molecular detail Sensitisation: First encounter with allergen → APCs prime Th2 → IL-4 drives B cells to class-switch to IgE. IgE binds FcεRI on mast cells and basophils with extraordinarily high affinity (K_d about 10^{-10} M) and remains bound for weeks.

Effector: Re-encounter with allergen cross-links mast cell-bound IgE → degranulation within seconds: histamine (vasodilation, vascular leak, smooth muscle contraction, pruritus), tryptase (tissue damage), leukotrienes (C4, D4, E4) (delayed bronchoconstriction), prostaglandins, TNF, IL-4/IL-5/IL-13 (late phase, 4–8 h: eosinophil and Th2 recruitment).

Clinical spectrum: localized (allergic rhinitis, urticaria) → systemic (anaphylaxis with hypotension, bronchospasm, laryngeal edema). Treatment of anaphylaxis: intramuscular epinephrine (α_1 vasoconstriction reverses hypotension; β_2 bronchodilates; β_2 stabilizes mast cells), oxygen, fluids, antihistamines, corticosteroids, possible airway management. Allergen immunotherapy (AIT) gradually shifts the response from Th2/IgE toward Th1/IgG4 (“blocking antibodies”) and induces Tregs — the primary disease-modifying therapy for allergy.

35.2.11 Immunotherapy

Modern oncology has been transformed by therapies that release brakes on antitumour immunity (checkpoint inhibitors) or redirect T cells (CAR-T). Because the product roster and safety language change, treatment tables below should be read with current FDA product pages and labels, not as a permanent formulary [U.S. Food and Drug Administration, 2026b, 2024a].

Immune checkpoint inhibitors — PD-1/PD-L1 and CTLA-4 biology PD-1 (programmed death 1) is an inhibitory receptor expressed on activated T cells (and B cells, NK cells, Tregs). Its ligand PD-L1 is widely expressed under inflammatory conditions and constitutively on many tumors; PD-L2 is more restricted to APCs. PD-1 engagement recruits the SHP-2 phosphatase to the immune synapse, dephosphorylating proximal TCR-signaling components (CD3ζ, ZAP70) — this functionally “exhausts” chronically activated T cells and limits collateral damage. Tumors hijack this brake by upregulating PD-L1 (often in response to local IFN-γ from infiltrating T cells — a paradoxical “adaptive resistance”), tonically inhibiting tumor-infiltrating T cells. Current drug examples and approved-use language should be checked against NCI or regulatory pages before publication because checkpoint indications change by tumor type, biomarker, and line of therapy [National Cancer Institute, 2026].

CTLA-4 (cytotoxic T-lymphocyte-associated 4, CD152) is also inhibitory but acts at the priming stage in lymph nodes. Resting T cells receive co-stimulation when CD28 binds B7-1/B7-2 (CD80/CD86) on APCs. Upon activation, CTLA-4 is upregulated and translocates to the immune synapse, where it binds B7 with much higher affinity than CD28 and trans-endocytoses B7 from the APC — depriving CD28 of its co-stimulus. CTLA-4 is also constitutively expressed on Tregs, contributing to their suppressive function. CTLA-4 blockade therefore acts earlier and more broadly than PD-1 blockade, with stronger autoimmune toxicity.

Table 414. Immune checkpoint inhibitors — PD-1/PD-L1 and CTLA-4 biology: Drug and Target.

Drug	Target	Approved indications	Approx. response rate
Ipilimumab	CTLA-4	Melanoma, RCC (combined with nivolumab)	about 10–15% monotherapy, about 50% with anti-PD-1
Nivolumab, pem-brolizumab	PD-1	Melanoma, NSCLC, RCC, head/neck, Hodgkin, MMR-deficient cancers	about 20–40% across indications

Drug	Target	Approved indications	Approx. response rate
Atezolizumab, PD-L1 durvalumab		NSCLC, urothelial, TNBC	about 15–30%
Relatlimab	LAG-3	Melanoma (combined with nivolumab)	Combination effect; LAG-3 alone modest
Tislelizumab, PD-1 cemi-plimab		NSCLC, cutaneous SCC	Variable

The 2018 Nobel Prize in Physiology or Medicine was awarded to James Allison (CTLA-4) and Tasuku Honjo (PD-1) for the discoveries underlying this field. Response rates vary widely by tumor type, biomarker status, line of therapy, and combination regimen; the table’s approximate ranges are orientation values, not patient-level predictions. A key qualitative pattern remains durable remissions in some responders (the “tail of the curve”). Side effects: immune-related adverse events (irAEs) — colitis, pneumonitis, hypophysitis, thyroiditis, hepatitis, dermatitis — reflecting the breaking of self-tolerance. Management: corticosteroids; if severe, infliximab (anti-TNF) for colitis.

CAR-T cell therapy — design and clinical outcomes Chimeric antigen receptor T cells: Patient T cells are removed by leukapheresis, genetically engineered ex vivo (lentiviral or retroviral vector) to express a synthetic receptor combining:

- Extracellular antigen-binding domain: Single-chain variable fragment (scFv) derived from a tumor-specific monoclonal antibody (e.g., anti-CD19 scFv from FMC63 antibody).
- Hinge and transmembrane: From CD8α or IgG.
- Co-stimulatory domain: CD28 (rapid effector function, shorter persistence) or 4-1BB/CD137 (slower expansion, longer persistence).
- Activation domain: CD3ζ (TCR-derived ITAMs).

Modified T cells are expanded in vitro and infused back into the patient. The CAR-T cells recognize the surface antigen (e.g., CD19 on B-cell malignancies) without MHC restriction, which enables recognition of MHC-low tumors that escape conventional T cells.

Table 415. CAR-T cell therapy — design and clinical outcomes: Product and Target.

Product	Target	Approved indication	Co-stim	Remission rate
Tisagenlecleucel (Kymriah)	CD19	Pediatric/young adult B-cell acute lymphoblastic leukaemia	4-1BB	about 80% at 3 months
Axicabtagene ciloleucel (Yescarta)	CD19	DLBCL (3rd line+, then earlier)	CD28	about 50–60% complete response
Brexucabtagene autoleucel (Tecartus)	CD19	Mantle cell lymphoma; B-cell acute lymphoblastic leukaemia	CD28	about 67% in MCL
Idecabtagene vicleucel (Abecma)	BCMA	Multiple myeloma	4-1BB	about 30% complete response
Ciltacabtagene autoleucel (Carvykti)	BCMA	Multiple myeloma	4-1BB	about 80% overall response

Toxicity:

- Cytokine release syndrome (CRS): fever, hypotension, hypoxia within hours-to-days from massive cytokine release (esp. IL-6, IFN-γ, TNF) — graded 1–4. Treatment: tocilizumab (anti-IL-6R), corticosteroids if severe.
- Immune effector cell-associated neurotoxicity syndrome (ICANS): confusion, aphasia, seizures, cerebral edema; treated with corticosteroids.
- B cell aplasia: Anti-CD19 CAR-T kills normal B cells too; long-term IVIG replacement may be needed.

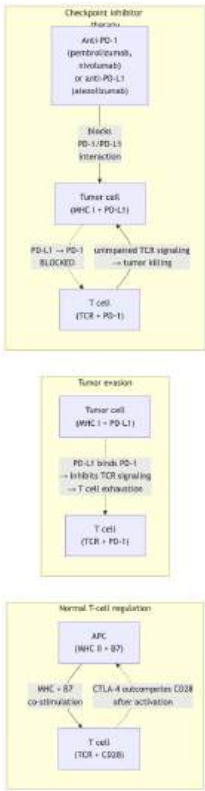


Figure 212. Immune checkpoint blockade Normal T cells use CTLA-4 and PD-1 as brakes to prevent over-activation. Tumors exploit PD-L1 to suppress local T cells. Anti-PD-1 antibodies (pembrolizumab) and anti-CTLA-4 antibodies (ipilimumab) block these interactions, releasing the immune brake on antitumour T cells.

- Second-malignancy surveillance: FDA required boxed-warning language for T-cell malignancies after BCMA-directed or CD19-directed autologous CAR-T products in 2024, making long-term follow-up part of the source-governance burden for any current CAR-T table [U.S. Food and Drug Administration, 2024a].

Concept Check 4: A patient on pembrolizumab (anti-PD-1) for metastatic melanoma develops new-onset hyperthyroidism with elevated free T4 and undetectable TSH. Explain mechanistically why checkpoint blockade can trigger autoimmune endocrinopathy. What does this teach us about the normal role of PD-1 in maintaining peripheral tolerance to thyroid antigens?

Concept Check 5: Why do polysaccharide vaccines (e.g., the original 23-valent pneumococcal vaccine) fail in children younger than 2 years, while conjugate vaccines (PCV13 — same polysaccharides covalently linked to a carrier protein) work well? Connect your answer to T-dependent vs T-independent B cell activation and germinal center formation.

Concept Check 6: A patient with Type 1 diabetes is found to have autoantibodies against multiple islet antigens (GAD65, IA-2, ZnT8) in addition to the originally targeted insulin. Explain this observation in terms of epitope spreading and discuss why early immunomodulatory therapy (before extensive β -cell destruction) might be more effective than later intervention.

Concept Check 7: During a CAR-T infusion for B-cell acute lymphoblastic leukaemia, the patient develops high fever, hypotension, and elevated IL-6. Why does CAR-T therapy frequently cause cytokine release syndrome, and why is anti-IL-6R (tocilizumab) effective without abrogating the antitumour response?

Concept Check 8: Compare central and peripheral tolerance. A patient with FoxP3 mutation (IPEX syndrome) develops autoimmunity in infancy despite intact thymic negative selection. What does this teach us about the redundancy and complementarity of these two tolerance mechanisms?

Concept Check 9: A patient with hereditary angioedema has frequent episodes of facial/laryngeal swelling. Genetic testing reveals a C1-INH (C1-inhibitor) deficiency. Why does deficiency of this complement regulator cause swelling — and why is the swelling primarily mediated by bradykinin rather than complement-derived anaphylatoxins?

Concept Check 10 (Analyze) — Complement cascade, MAC, and capsule resistance. The classical pathway proceeds C1q (antibody-antigen) → C4b2a (C3 convertase) → C3b deposition + C5 convertase (C4b2a3b) → C5b-9 (MAC) — a 10 nm transmembrane pore that lyses the target. The alternative pathway loops back through factor B and properdin to amplify C3b deposition on any surface lacking host regulators. (a) Trace the

molecular requirements for MAC formation on a Gram-negative bacterial surface and identify the single most rate-limiting step (C3b deposition density on the surface). (b) *Neisseria meningitidis* has a polysaccharide capsule but is famously vulnerable to MAC-mediated lysis — explaining why C5–C9 complement deficiencies present as recurrent meningococcal infection. *Klebsiella pneumoniae*, also encapsulated, *resists* MAC by binding host factor H to its capsule, accelerating C3 convertase decay locally. Analyze (i) what biochemical feature of the *Klebsiella* capsule allows factor H recruitment, (ii) why *Neisseria* lacks this property, and (iii) why repeated meningococcal disease in young adults should trigger a complement-component screen (CH50, AH50) rather than an immunoglobulin work-up.

Concept Check 11 (Evaluate) — Checkpoint inhibitors, response heterogeneity, and rational combinations. Anti-PD-1 (pembrolizumab, nivolumab) blocks the PD-1/PD-L1 brake on T-cell exhaustion and produces durable remissions in approximately 20–40% of patients across many solid tumors. Anti-CTLA-4 (ipilimumab) acts earlier, at T-cell priming, with stronger autoimmune toxicity. (a) Evaluate why monotherapy fails the *majority* of patients despite high target expression, drawing on at least three biological factors (low tumor mutational burden; loss of MHC-I presentation; T-cell exhaustion irreversibility; immunosuppressive tumor microenvironment). (b) Propose three biomarkers — tumor mutational burden (TMB), PD-L1 immunohistochemistry score, and tumor-infiltrating lymphocyte (TIL) density — and rank them by predictive power per available evidence; identify which biomarker has the strongest mechanistic justification and which is the most commercially deployed. (c) Evaluate two combination strategies expected to convert non-responders into responders: anti-CTLA-4 + anti-PD-1 (broader brake release) and anti-VEGF + anti-PD-1 (normalizing tumor vasculature so T cells can infiltrate). For each combination, identify the most likely mechanism of synergy, the principal toxicity risk, and one tumor type where the combination is now standard of care.

Concept Check 10: Why do anti-IL-17 (secukinumab) and anti-IL-23 (risankizumab) biologics treat psoriasis but exacerbate Crohn’s disease in some patients? Connect your answer to the dual role of Th17 in barrier defense and pathological inflammation.

35.2.12 Study Blueprint

- Big idea: Innate and adaptive immunity integrate recognition, effector function, tolerance, and memory.
- Core concepts: innate immunity, adaptive immunity, tolerance, immunotherapy.
- Framework alignment: Vision & Change: Structure and function, Systems; AP Biology: Systems Interactions, Energetics; NGSS-style topics: Structure and Function.
- Model or quantitative lens: Immune-memory, cytokine, and recognition reasoning.
- Data skill: Interpret immune titers, cytokine profiles, or perturbation data.
- Practice cadence: Visual Representations, Statistical Tests and Data Analysis, Argumentation.
- Common misconception to repair: Immunity is not just attack; recognition, tolerance, memory, and regulation are equally central.
- Primary lab: [Lab — Immune System Architecture](#).
- Question bank: [Questions — Immune System Architecture](#).
- Transfer task: Transfer immunity reasoning to vaccination, autoimmunity, infection, and cancer therapy.
- Bridge to computation: `biology.physiology.physiology.homeostasis_response`.

Opening Vignette — Immune System Architecture

This chapter connects immune system architecture and defense to measurable evidence: models, datasets, and experiments that can strengthen or weaken each claim.

35.3 Worked Example: Innate Recognition to Effector Response

Problem: A Gram-negative bacterium enters a wound. The alternative complement pathway runs continuously at a low “tick-over” rate, but surface-bound C3b nucleates an amplification loop: each C3 convertase cleaves about 1000 C3 molecules before it decays, and a fraction p of the resulting C3b deposits nearby to seed new convertases. (a) Compute the per-cycle amplification factor on an unregulated pathogen surface where $p = 0.10$, and on a host cell whose regulators (DAF, factor H) cut effective deposition to $p = 0.0005$. (b) Explain why this single parameter separates explosive opsonization from self-tolerance.

Solution:

Step 1. Define the amplification factor a as the number of C3 molecules cleaved per convertase times the fraction that reforms a convertase:

$$a = (\text{C3 cleaved per convertase}) \times p$$

Step 2. Evaluate on each surface. On the pathogen, $a = 1000 \times 0.10 = 100 \gg 1$, so C3b deposition grows geometrically each cycle. On the host cell, regulators drop the effective fraction and the loop dies out:

$$a_{\text{pathogen}} = 100, \quad a_{\text{host}} = 1000 \times 0.0005 = 0.5 < 1$$

Step 3. Connect to the effector response: once C3b passes the deposition threshold, opsonization (phagocyte CR1/CR3), anaphylatoxin chemotaxis (C5a), and the membrane attack complex follow — turning a molecular recognition event into neutrophil recruitment and target lysis.

Answer: Innate recognition is fast and germline-encoded, yet it still discriminates self from non-self through an amplification factor gated by host-restricted regulators: $a > 1$ on pathogens drives explosive complement deposition, while $a < 1$ on host cells (DAF, factor H, CD59) keeps the same cascade silent. Losing those regulators is exactly what causes paroxysmal nocturnal hemoglobinuria — host red cells without CD59/DAF are attacked by their own complement.

35.4 Worked Example: Clonal Expansion

Problem: During a T-dependent germinal-center response, an antigen-specific B-cell clone proliferates in the dark zone with a doubling time of $t_d = 6$ h. Starting from $N_0 = 100$ antigen-specific cells, calculate the fold expansion and the absolute clone size after $t = 72$ h (3 days). Compare the result with the 100–1000-fold higher precursor frequency that defines an established memory pool.

Solution:

Step 1. State the exponential-growth relation for a clone dividing with a fixed doubling time. Each doubling multiplies cell number by 2, and the number of doublings in time t is t/t_d :

$$N = N_0 \cdot 2^{t/t_d}$$

Step 2. Substitute the measured values. With $t = 72$ h and $t_d = 6$ h, the number of doublings is $t/t_d = 72/6 = 12$. The fold expansion is therefore 2^{12} :

$$\frac{N}{N_0} = 2^{72/6} = 2^{12} = 4096$$

Step 3. Compute the absolute clone size: $N = 100 \times 4096 = 4.10 \times 10^5$ cells — a roughly 4000-fold expansion in three days.

Answer: A 6-hour doubling time yields 12 doublings in 72 h, expanding the clone about 4096-fold (from 100 to about 4.1×10^5 cells). This magnitude matches the chapter’s account of dark-zone proliferation and explains how a naive precursor frequency of about 1 in 10^6 can be driven up to the 100–1000-fold higher frequency that characterizes an established memory pool. The same $N = N_0 \cdot 2^{t/t_d}$ relation predicts that even a one-hour increase in doubling time markedly slows the response — which is why memory cells, with their lower activation threshold and shorter effective doubling time, clear a re-challenge far faster than naive cells.

35.5 Computational Bridge

Generic negative-feedback controllers map errors to corrective outputs:

```
from biology.physiology import homeostasis_response

h = homeostasis_response(37.0, 38.5, gain=0.8)
print(round(h.corrective_response, 3), h.is_within_tolerance)
```

Clinical / systems note: The same proportional-feedback logic governs immune set points — IL-2 consumed by regulatory T cells damps effector T-cell expansion, holding a response within tolerance.

35.6 Current Evidence and Frontier Biology: Immune System Architecture

For Immune System Architecture, frontier biology belongs inside the evidence logic of the chapter. Immunology is moving fast: single-cell and spatial atlases now resolve immune-cell states in situ, structural vaccinology and mRNA platforms have compressed antigen-design timelines, checkpoint inhibitors and engineered

cell therapies (CAR-T, TCR-T) are redrawing oncology, and neoantigen prediction couples immunology to genomics. The core reading question is this: immune claims should specify the arm (innate vs adaptive), the effector mechanism, the readout (titer, cytotoxicity, protection), and the evidence scale from single molecule to randomized trial.

- What to verify: identify the observation, model, assay, or dataset that would make the claim stronger or weaker.
- What to qualify: state the scale, organism, cell type, environmental condition, or population where the claim is expected to hold.
- What to compare: test at least one alternative explanation, baseline, or null model before treating the pattern as causal.
- What to cite: distinguish primary evidence, review synthesis, public dataset, and institutional guidance; for recent or numeric claims, prefer the source closest to the measurement and state what has changed since it was published.

Separate recognition, activation, effector function, and memory before interpreting an immune dataset, and distinguish a protective response from immunopathology.

Source practice: For immune claims, cite the recognition event and the effector readout, and distinguish mechanism (assay or structure), population evidence (cohort or trial), and clinical guidance (product label or surveillance report).

35.6.1 Current Evidence Map: From Pattern Recognition to Protective Memory

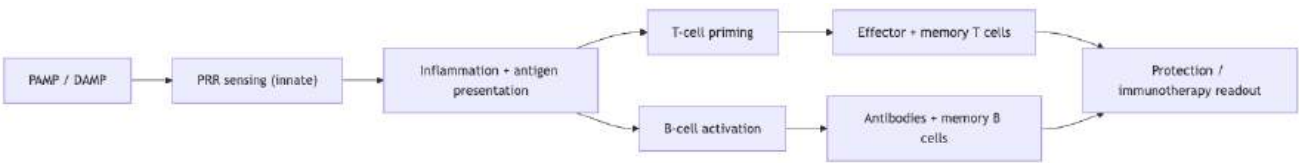


Figure 213. An immune response reads as a chain — recognition, activation, effector function, and memory — so a claim should name which link the evidence actually measures.

35.7 Summary

- Innate immunity: Immediate, non-specific. Physical barriers, complement (opsonisation, MAC, chemotaxis with positive amplification feedback), phagocytes (neutrophils, macrophages, DCs), NK cells (missing self), inflammation, interferons, fever. PRRs: TLRs (membrane; TLR4→MyD88→NF-κB or TLR3→TRIF→IRF3→IFN-β); NLRs (cytosolic; NLRP3 inflammasome → caspase-1 → IL-1β + pyroptosis); RLRs (viral RNA); cGAS-STING (cytosolic DNA → IFN-β).
- Complement: Three pathways converge on C3 convertase → C5 convertase → MAC. Effector functions: opsonisation (C3b), MAC (C5b-9), anaphylatoxins (C3a, C5a). Regulators (DAF, CD59, factor H, C1-INH) confine to pathogen surfaces. PNH, hereditary angioedema, eculizumab.
- Adaptive immunity: Specific, slow (7–10 days), memory. MHC I (endogenous) → CD8+ CTL. MHC II (exogenous) → CD4+ Th. T cell development DN1→DN4→DP→positive selection (cTECs)→negative selection (mTECs/AIRE/Tregs). Th polarization: Th1, Th2, Th17, Treg, Tfh.
- B cells: T-dependent vs T-independent activation. Germinal center reaction: SHM (AID) → affinity maturation; CSR → IgG/IgA/IgE. Antibody isotypes: IgM (primary), IgG (secondary, opsonisation, placenta), IgA (mucosal), IgE (allergy).
- Cytokine network: IL-1/IL-6/TNF (inflammation), IL-2 (T cell expansion), IL-4 (Th2/IgE), IL-17 (Th17/barrier), IFN-γ (Th1/macrophage activation), IL-10/TGF-β (anti-inflammatory).
- Memory: T_{CM} (recirculating), T_{EM} (peripheral), T_{RM} (tissue-resident); maintained by IL-7/IL-15. Pre-existing antigen-specific cells, lower activation threshold, pre-armed effector machinery explain the rapid recall response.
- Tolerance and autoimmunity: Central (thymic/BM deletion, AIRE) and peripheral (Treg, anergy, PD-1, CTLA-4). Mechanisms of failure: molecular mimicry, bystander activation, epitope spreading, defective Tregs/apoptosis. Diseases: SLE, RA, T1DM, MS. Hypersensitivity I–IV.
- Immunotherapy: Checkpoint inhibitors (anti-PD-1, anti-CTLA-4, anti-LAG-3) — 2018 Nobel Prize; response rates vary by tumor, biomarker, line of therapy, and combination strategy, with durable “tail of the curve” remissions in some responders. CAR-T for haematological malignancies (anti-CD19 for B-cell acute lymphoblastic leukaemia and DLBCL; anti-BCMA for myeloma); CRS managed by tocilizumab.
-

35.8 Connections: See section 11 for insulin/glucagon integration, section 26 for PAMP recognition, and section 31 for stress axes.

35.9 Review Questions

1. Compare innate and adaptive immunity across speed, specificity, memory, and the nature of their recognition receptors (germline-encoded vs somatically rearranged). Why does the body need both arms rather than relying on the more precise adaptive system alone?
2. Describe how the three complement activation pathways (classical, lectin, alternative) are each triggered and how they converge on the C3 convertase. Distinguish the three effector outcomes — opsonization, the membrane attack complex, and anaphylatoxin-driven inflammation — and give one example of each.
3. Compare the four families of pattern-recognition receptors — TLRs, NLRs, RLRs, and cGAS-STING — by cellular location, the class of PAMP or DAMP each detects, and the dominant signaling output (NF- κ B-driven inflammation vs IRF-driven type I interferon). Why is germline-encoded pattern recognition fast but unable to provide immunological memory?
4. Contrast MHC class I and class II antigen-presentation pathways — peptide source, processing compartment, loading machinery, and the T-cell subset each engages. What is cross-presentation, why is it essential for priming CD8+ responses against viruses that do not infect dendritic cells, and how does this constrain vaccine design?
5. Explain the “missing-self” hypothesis for NK-cell recognition in terms of the balance between activating receptors and inhibitory KIRs that read MHC class I. Why does this make NK cells especially effective against virus-infected and tumor cells that downregulate MHC I, and how does antibody-dependent cellular cytotoxicity (ADCC) link NK cells to therapeutic antibodies?
6. Distinguish the type I interferon response (IFN- α/β) from type II interferon (IFN- γ): the cells that produce each, the triggers, and the effector states they induce. Outline how type I IFN establishes an antiviral state (e.g., PKR, OAS/RNase L, Mx proteins) and why this is induced within hours of infection.
7. Trace the vascular and cellular events of acute inflammation, from local mediator release (histamine, prostaglandins, chemokines) through the neutrophil recruitment cascade (rolling on selectins → integrin-mediated firm adhesion → transmigration). Explain the four cardinal signs mechanistically and contrast resolution with the transition to chronic inflammation.
8. Describe TLR4 signaling in response to bacterial LPS. Compare with the TRIF-IRF3 branch and the cGAS-STING pathway. Why does septic shock result from massive cytokine release, and what is the mechanism of action of “anti-TNF” therapeutics like infliximab?
9. Explain how the alternative complement pathway amplifies its own activation. Describe the formation of C3 convertase, C5 convertase, and the MAC. Why is complement activity restricted to pathogen surfaces and not host cells? What goes wrong in PNH, and how does eculizumab work?
10. Describe the DN1–DN4 stages of T cell development. What is β -selection? Then describe positive and negative T cell selection in the thymus. What is the role of AIRE, and what disease results from its mutation?
11. Compare T-dependent and T-independent B cell responses. Why are conjugate vaccines (PCV13, Hib) more effective in young children than pure polysaccharide vaccines? Trace the steps from naïve B cell antigen encounter to long-lived plasma cell.
12. Explain the molecular basis of affinity maturation in the germinal center. How does AID-mediated somatic hypermutation combined with antigen-driven selection produce 1000-fold increases in antibody affinity?
13. Compare the four types of hypersensitivity reactions. Identify a clinical example and treatment for each. Explain the difference in time course between Type I and Type IV.
14. Explain the difference between molecular mimicry, bystander activation, and epitope spreading as mechanisms of autoimmunity. Give a specific clinical example for each.
15. A patient on pembrolizumab develops new-onset hypothyroidism, vitiligo, and colitis. Explain mechanistically why anti-PD-1 therapy causes these immune-related adverse events. What does this reveal about the normal role of PD-1?
16. Describe the design of an anti-CD19 CAR-T cell — antigen recognition domain, hinge, transmembrane, co-stimulatory, and activation domains. Why does CAR-T therapy frequently cause cytokine release syndrome, and how does anti-IL-6R tocilizumab treat CRS without compromising tumor killing?
17. Mucosal surfaces are the entry point for most pathogens. Explain how secretory IgA is produced and transported across the epithelium, the role of M cells and Peyer’s patches in sampling luminal antigen, and the concept of oral tolerance. Why does the gut require an immune strategy distinct from systemic immunity?

18. Compare live-attenuated, inactivated, subunit/conjugate, viral-vector, and mRNA vaccine platforms on immunogenicity, the balance of humoral vs cellular immunity they elicit, safety, and cold-chain requirements. What is a “correlate of protection,” and why is establishing one essential before a vaccine can be licensed?
19. Explain why memory T and B cells respond more rapidly and strongly to re-exposure than naïve cells. Identify at least four mechanistic differences.
20. A patient develops anaphylaxis after a wasp sting. Trace the cellular and molecular events from prior sensitisation through the acute reaction. Explain why intramuscular epinephrine is the first-line treatment and how each of its receptor effects (α_1 , β_1 , β_2) addresses different components of anaphylaxis.

35.10 Further Reading and Source Notes: Immune System Architecture

- Medzhitov & Janeway (1997). Innate immunity: the virtues of a nonclonal system of recognition. *Cell*, 91.
- Tonegawa (1983). Somatic generation of antibody diversity. *Nature*, 302.
- Zinkernagel & Doherty (1974). Restriction of in vitro T cell-mediated cytotoxicity in lymphocytic choriomeningitis. *Nature*, 248.
- Leach, Krummel & Allison (1996). Enhancement of antitumor immunity by CTLA-4 blockade. *Science*, 271.
- Murphy & Weaver (2016). *Janeway’s Immunobiology* (9th ed.). Garland Science.

35.11 Key Terms

Table 416. Key Terms: Term and Definition.

Term	Definition
Innate immunity	Fast, germline-encoded, non-clonal first-line defense; no immunological memory
Adaptive immunity	Slow, antigen-specific, clonal response that generates immunological memory
Phagocytosis	Engulfment of opsonized particles by neutrophils, macrophages, and dendritic cells
Opsonization	Tagging of a pathogen (C3b, IgG) to enhance phagocytic uptake
NK cell	Innate lymphocyte killing “missing-self” (low-MHC-I) and antibody-coated cells (ADCC)
Type I interferon	IFN- α/β ; antiviral state induced via PRR \rightarrow IRF3/7
Inflammation	Vascular and cellular response (vasodilation, recruitment) to infection or damage
Antigen presentation	Display of peptide on MHC I (to CD8+) or MHC II (to CD4+) T cells
Affinity maturation	AID-driven somatic hypermutation plus selection that raises antibody affinity
Class-switch recombination	Constant-region switch (IgM \rightarrow IgG/IgA/IgE) that preserves antigen specificity
Secretory IgA	Dimeric, J-chain + secretory-component antibody mediating mucosal immune exclusion
Central vs peripheral tolerance	Thymic/marrow deletion (AIRE) versus Treg, anergy, and checkpoints in the periphery
PRR	Pattern recognition receptor (TLR, NLR, RLR, cGAS)
TLR4	Recognizes LPS; signals via MyD88 \rightarrow NF- κ B
NLRP3	Cytosolic inflammasome; activates caspase-1 \rightarrow IL-1 β + pyroptosis
cGAS-STING	Cytosolic DNA sensor \rightarrow type I interferons
Complement	Cascade producing opsonisation (C3b), MAC (C5b-9), anaphylatoxins (C3a, C5a)
C3 convertase / C5 convertase	Central enzyme amplifying complement (C4b2a or C3bBb / C4b2aC3b)
MAC	Membrane attack complex (C5b-9); 10 nm pore lyses target cell
MHC I/II	Antigen-presenting molecules to CD8+/CD4+ T cells
AIRE	Thymic transcription factor enabling expression of tissue-specific antigens for negative selection
AID	Activation-induced cytidine deaminase; somatic hypermutation and class switching
Germinal center	Lymphoid microenvironment for affinity maturation and class switching
Treg	FoxP3+ regulatory T cell; peripheral tolerance
PD-1 / PD-L1	Inhibitory checkpoint exploited by tumors; target of pembrolizumab
CTLA-4	Inhibitory checkpoint on activated T cells; target of ipilimumab
CAR-T cell	Engineered T cell with synthetic antigen receptor for tumor killing
Hypersensitivity I–IV	Allergy/anaphylaxis (IgE), cytotoxic, immune complex, delayed cell-mediated
Molecular mimicry	Pathogen antigen resembles self; triggers cross-reactive autoimmunity
Epitope spreading	Autoimmune response broadens from one self-antigen to many over time

Term	Definition

35.12 Companion Source Module: Immune System Architecture

Immune System Architecture should leave a reproducible trail from a biological claim to the code, figure, diagram, or paper-based activity that can test it. Use the surfaces below to inspect the chapter’s assumptions, rerun the relevant model, or compare the manuscript explanation with companion labs and figures.

Table 417. Companion source surfaces for Immune System Architecture.

Surface	Use it for
src/biology/physiology/physiology.py (homeostasis_response)	Compare hormone feedback and inflammatory regulation as control problems.
src/biology/cell/cell_biology.py (receptor_occupancy, signal_amplification)	Quantify receptor sensitivity and cascade gain.
src/mermaid/biology_diagrams.py (immune_response_diagram, hormone_signaling_diagram)	Connect endocrine and immune sequence logic.

Reproducibility check: specify ligand/cytokine, receptor, timing, tissue, feedback loop, and readout before calling a response adaptive or pathological. Cross-reference: use section 8, section 31, and sections 26 and 27.

Unit X — Ecology: Introduction

Why This Unit Matters

In 1966, ecologist Robert Paine removed most sea stars (*Pisaster ochraceus*) from a stretch of rocky intertidal shore in Washington State and waited. Within 18 months, the mussel population exploded, crowding out barnacles, limpets, chitons, and anemones. What had been a 15-species community collapsed to a near-monoculture of *Mytilus californianus*. The sea star was a keystone species: a species whose removal from the community caused a change in biodiversity disproportionate to its own abundance. Paine’s experiment created the concept and the measurement — the ratio of effect to biomass — and it changed how biologists think about the architecture of ecosystems (Paine, 1966, *American Naturalist*).

Ecology is the study of how organisms interact with each other and with their physical environment. It operates across scales spanning six orders of magnitude: from the foraging decision of a single aphid on a single leaf, to the population dynamics of wolves in Yellowstone, to the cycling of carbon through the entire Earth system. Its models — the logistic growth equation, the Lotka-Volterra predator-prey system, the species-area relationship — are among the most mathematically tractable in biology, yet they govern phenomena as urgent as climate change, mass extinction, and pandemic emergence.

The 21st century has made ecology a discipline under crisis and urgent relevance. The current mass extinction event — the sixth in Earth’s history — is driven by habitat loss, overexploitation, invasive species, pollution, and climate change. Biodiversity is losing the equivalent of tens of thousands of species per year. Understanding population dynamics, community structure, and ecosystem function is no longer merely academic: it is an existential scientific priority for the conservation of life on Earth. This unit will give you the quantitative tools to understand why, and to participate in the solutions.

Landmark Discoveries

Discoverer(s)	Year	Journal / Source	Discovery	Significance
Alfred Lotka & Vito Volterra	1925–1926	[Lotka, 1925, Volterra, 1926]	Lotka-Volterra predator-prey ODEs	First quantitative model of species interactions; linked ecology to mathematics
Eugene Odum	1953	[Odum, 1953]	Ecosystem as unit of ecology with energy flow	Introduced energy-flow and trophic-level thinking into mainstream ecology
Robert Paine	1966	[Paine, 1966]	Keystone species concept (sea star experiment)	Showed top-down regulation; single species can structure entire communities
Robert MacArthur & E.O. Wilson	1967	[MacArthur and Wilson, 1967]	Island biogeography: $S = cA^z$	Connected species richness to area and isolation; foundational for conservation
Paul Ehrlich & Peter Raven	1964	[Ehrlich and Raven, 1964]	Coevolution between plants and butterflies	Launched chemical ecology and co-evolutionary theory
Intergovernmental Science-Policy Platform on Biodiversity and Ecosystem Services (IPBES)	2019	[Intergovernmental Science-Policy Platform on Biodiversity and Ecosystem Services, 2019]	1 million species threatened with extinction	Quantified the biodiversity crisis; policy-science interface
Ripple et al.	2014	[Ripple and Beschta, 2012b]	Trophic cascades from large predators	Wolves reintroduced to Yellowstone reshaped rivers via trophic cascade

Key Concepts and Connections

Current Evidence Thread

Read this unit as a chain of ecological evidence rather than a list of topics: population, community, ecosystem, and conservation claims are each backed by a characteristic kind of measurement — field sampling and mark-recapture, manipulative and observational experiments, remote sensing and flux networks, dynamical and statistical models, and long-term monitoring programs. Ecology and conservation decisions increasingly combine field data, remote sensing,

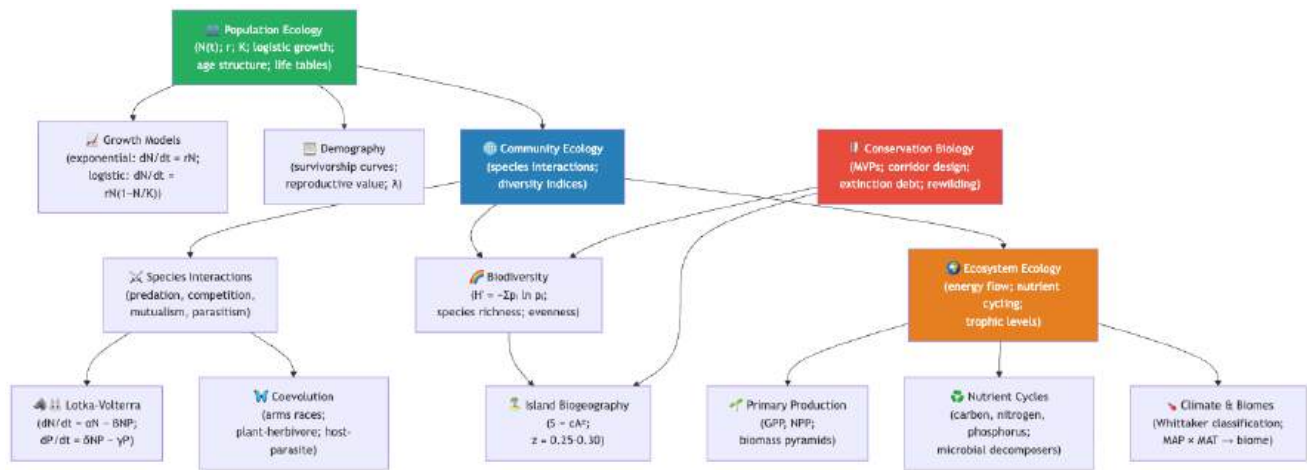


Figure 214. Ecology concept map - green = population; blue = community; orange = ecosystem; red = conservation.

community knowledge, model uncertainty, and explicit values. As you move through the chapters, keep a two-column note: claim on the left, evidence that would change my confidence on the right. By the end of the unit, each major idea should be tied to a measurement, model, citation, or paper-based lab decision.

Chapter Roadmap

Chapter	Title	Core Question	Key Equation / Model
32	Population Ecology	How do populations grow, and what factors regulate population size?	Logistic: $dN/dt = rN(1 - N/K)$; life tables; $\lambda = e^r$
33	Community Ecology	How do species interactions structure biological communities?	Lotka-Volterra: $dN/dt = \alpha N - \beta NP$; Shannon H'
34	Ecosystem Ecology	How does energy flow and how do nutrients cycle through ecosystems?	Trophic efficiency about 10%; $NEP = GPP - R_{total}$; biogeochemical cycle models
35	Biomes and Conservation Biology	What determines global patterns of biodiversity, and how do we protect them?	Species-area: $S = cA^z$; minimum viable population (MVP); extinction rate models

Connections Across the Textbook

- Population models (logistic growth, age structure) use the same differential equation framework as **Unit VII — Microbiology: Introduction** (SIR epidemiological models) — ecology and epidemiology are mathematically unified.
- Species diversity indices (Shannon H' , Simpson D) are computed using tools from **Unit VII — Microbiology: Introduction** (microbial communities) and help evaluate ecosystem health.
- Nutrient cycling (nitrogen, carbon, phosphorus) directly ties to **Unit III — Energy and Metabolism: Introduction** (carbon fixation by photosynthesis) and **Unit VII — Microbiology: Introduction** (microbial decomposers, nitrogen fixation by bacteria).
- Climate change impacts on biomes connect to **Unit VIII — Botany — Plant Biology: Introduction** (plant responses to drought, CO₂ enrichment) and **Unit VI — Evolution: Introduction** (evolution of species under selection by climate).
- Conservation biology uses evolutionary genetics (**Unit VI — Evolution: Introduction**: effective population size, genetic rescue) and macroecology (island biogeography, keystone species).

Key vocabulary introduced here: intrinsic rate of increase (r), carrying capacity (K), logistic growth, density dependence, keystone species, trophic cascade, competitive exclusion, fundamental vs. realized niche, coevolution, mutualism, parasitism, primary productivity (GPP, NPP), trophic efficiency, biogeochemical cycle, biome, species-area relationship, island biogeography, minimum viable population (MVP), extinction debt.

Computational Toolbox — Unit X

```
from biology.ecology import logistic_growth, lotka_volterra
```



```
# Logistic growth: white-tailed deer reintroduction (r = 0.35/yr, K = 500, N0 = 10)
lg = logistic_growth(N0=10.0, r=0.35, K=500.0, t_end=30.0, steps=300)
print(f"N(0) ≈ {lg.populations[0]:.0f}; N(t_end) ≈ {lg.populations[-1]:.0f}")

# Lotka-Volterra predator-prey (same ODEs used in community ecology)
lv = lotka_volterra(
    100.0, 10.0, 0.5, 0.02, 0.01, 0.2, t_end=80.0, steps=800,
)
print(f"Prey range: {min(lv.prey):.1f}–{max(lv.prey):.1f}")
print(f"Predator range: {min(lv.predator):.1f}–{max(lv.predator):.1f}")
```

Try it yourself: Increase beta (predation) and watch oscillation amplitude widen in plot_lotka_volterra output from scripts/generate_figures.py.

Source note: ecology helps support logistic and Allee growth, predator-prey cycles, species-area curves, biodiversity indices, and biome data. Figures: src/visualization/ (Lotka-Volterra cycles, logistic growth curves); src/mermaid/biology_diagrams.py (food web diagrams, nutrient cycle diagrams).

Cross-Unit Integration

Unit X — Ecology: Introduction closes the textbook by returning to where Unit 0 — Systems Science for Biology: Introduction began. The energy flow through trophic levels, the biogeochemical cycling of carbon and nitrogen, the entropy export from living ecosystems, and the constraint that ten percent of energy is transferred between trophic levels are direct expressions of the thermodynamic and systems principles introduced in Unit 0 — Systems Science for Biology: Introduction — open dissipative systems, far-from-equilibrium organization, hierarchical structure, and the shared energetic cost of maintaining low-entropy states. Population dynamics, community assembly, and ecosystem succession are complex-adaptive-system phenomena at landscape scale; alternative stable states and tipping points in ecosystems are the same attractor and bifurcation mathematics from section 0.2 applied to a planetary substrate. Read this unit as the macroscopic completion of the framework: the biology of complexity, written on the largest available canvas.

36 Population Ecology and Growth Models

Level 3/3 · 75 min read · 100 min lecture · Prerequisites: section 20

36.1 Learning Objectives

1. Describe the key demographic parameters (birth rate, death rate, survivorship, net reproductive rate) of a population.
2. Derive and interpret the exponential and **logistic growth** equations and apply them to real populations.
3. Construct and interpret **life tables** and **survivorship curves** (Types I, II, III).
4. Explain the Allee effect and describe how it alters population dynamics in small populations.
5. Apply the Lotka [Lotka, 1925]-Volterra [Volterra, 1926] competition and predator-prey equations and interpret phase-plane outcomes.
6. Describe r vs. K selection strategies and their adaptive ecological contexts.
7. Explain metapopulation dynamics and source-sink models for fragmented habitats.
8. Apply mark-recapture methods and distance sampling to estimate population size.
9. Construct a Leslie matrix from a life table, compute λ_1 and the stable age distribution, and use sensitivity/elasticity analysis to identify management-critical demographic rates.
10. Distinguish individual-based models from deterministic models, and outline a population viability analysis (PVA) workflow for a small population.

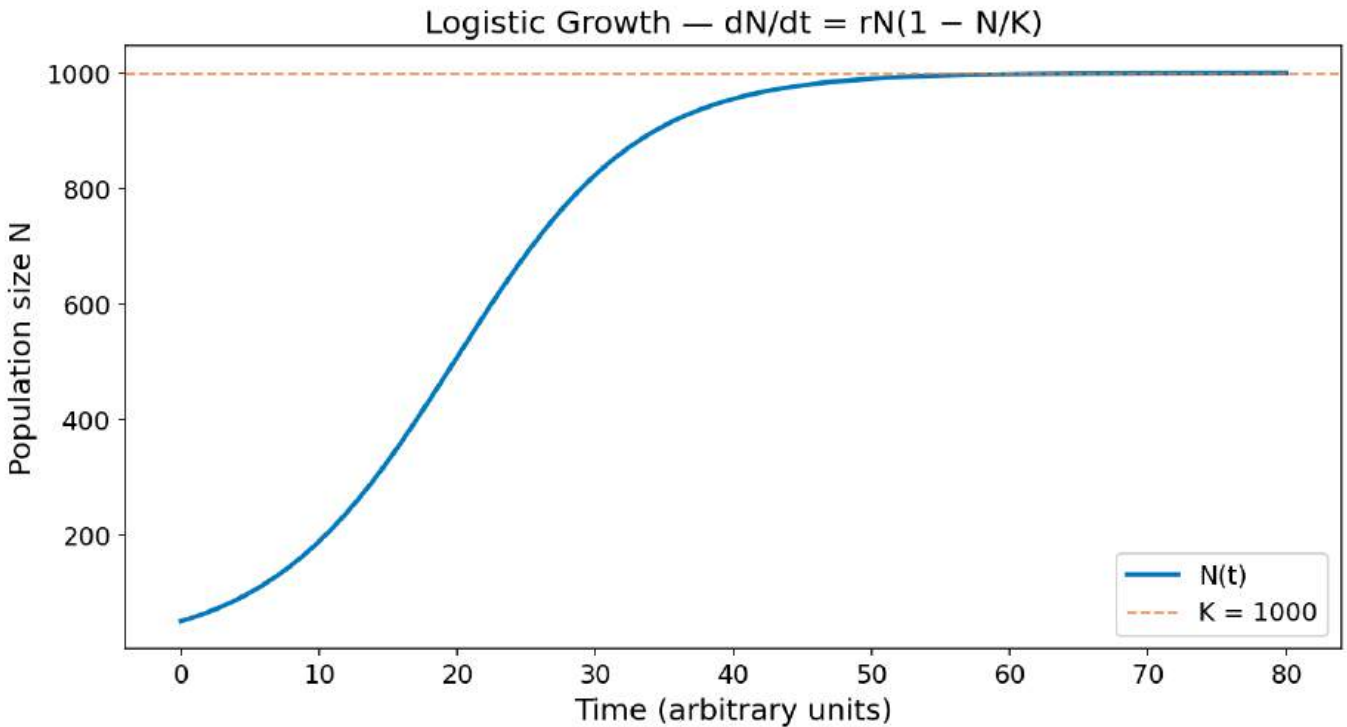


Figure 215. Logistic growth toward carrying capacity K . Population size follows $dN/dt = rN(1 - N/K)$; the S-shaped curve inflects near $N = K/2$ and asymptotes at K .

36.1.1 Study Blueprint

- Big idea: Population change reflects births, deaths, movement, age structure, and density dependence.
- Core concepts: exponential growth, logistic growth, life tables, population viability.
- Framework alignment: Vision & Change: Systems, Evolution, Pathways and transformations of energy and matter; AP Biology: Systems Interactions, Evolution, Energetics; NGSS-style topics: Interdependent Relationships in Ecosystems, Matter and Energy in Organisms and Ecosystems, Natural Selection and Evolution.
- Model or quantitative lens: Exponential/logistic growth, mark-recapture, and matrix projection.
- Data skill: Use abundance or age-structure data to estimate growth and risk.
- Practice cadence: Representing and Describing Data, Statistical Tests and Data Analysis, Argumentation.
- Common misconception to repair: Carrying capacity is not a fixed magic number; it changes with resources, interactions, and disturbance.
- Primary lab: **Lab — Population Ecology and Growth Models**.
- Question bank: **Questions — Population Ecology and Growth Models**.

- Transfer task: Transfer population models to fisheries, invasive species, epidemiology, and endangered species.
- Bridge to computation: `biology.ecology.ecology.logistic_growth`.

Opening Vignette — The Equation That Explains Why Populations Don’t Grow Forever

In 1838, Belgian mathematician Pierre François Verhulst looked at census data and asked: why don’t populations simply grow exponentially forever? His answer was the logistic equation — $dN/dt = rN(1 - N/K)$ — where K , the carrying capacity, captures the idea that resources limit growth. For nearly a century, the logistic model was theoretical. Then in 1934, Russian ecologist Georgy Gause grew two *Paramecium* species in test tubes and observed the sigmoid growth curve Verhulst had predicted: slow growth, rapid growth, leveling off at carrying capacity. His experiments also showed **competitive exclusion** — two species competing for the same **niche** cannot coexist indefinitely. Gause published this in *The Struggle for Existence* at age 23. The logistic model now underlies fisheries management, epidemiology (the SIR model is a direct descendant), conservation minimum viable population estimates, and pandemic projections. Verhulst’s equation, written in a 4-page paper with no data, may have saved more lives than any equation since Newton’s second law.

36.1.2 Chapter Roadmap for Population Models and Conservation Decisions

The chapter spans the full pipeline from individuals to metapopulations. Read it as three nested scales:

- The individual scale. Population attributes, life tables, survivorship. What you need before any growth equation makes sense.
- The population scale. Exponential growth, logistic growth, Allee effects, Lotka-Volterra interactions — the canonical equations and their named modifications.
- The spatial, structured, and human scale. r/K life histories, age-structured matrix models, individual-based simulation, population viability analysis, metapopulation dynamics, field-estimation techniques, and human demographic transitions.

For a brief treatment, focus on the core growth mathematics and the applied field-estimation and demographic-transition material. For a full quantitative course, work through most sections including the matrix-model and PVA toolkit, which underlie modern conservation practice.

36.2 Populations as Bounded, Measurable Units

A population consists of individuals of a single species (conspecifics) inhabiting a defined area at a given time. Population ecology investigates the factors that regulate population size, density, distribution, and growth over time. Understanding population dynamics is fundamental to wildlife management, conservation biology, epidemiology, and sustainable resource harvest.

36.2.1 Population Attributes: Size, Density, and Age Structure

Populations are characterized by several measurable attributes:

Table 418. Population Attributes: Size, Density, and Age Structure: Attribute and Symbol.

Attribute	Symbol	Definition	Units
Census size	N	Total number of individuals	Individuals
Population density	D	Individuals per unit area or volume	ind/km ² or ind/L
Per capita birth rate	b	Births per individual per time unit	births/ind/time
Per capita death rate	d	Deaths per individual per time unit	deaths/ind/time
Intrinsic rate of increase	r	$r = b - d$ (can be negative)	time ⁻¹
Finite rate of increase	λ	$\lambda = e^r$; $\lambda > 1$ growing; $\lambda < 1$ declining	dimensionless
Net reproductive rate	R_0	$R_0 = \sum l_x m_x$; female offspring per female per lifetime	offspring/female
Generation time	T	$T = \sum x \cdot l_x \cdot m_x / R_0$	time units

The fundamental relationship between R_0 , T , and r is the Euler-Lotka equation:

$$\sum_{x=0}^{\omega} e^{-rx} l_x m_x = 1$$

(415)

For approximate computation: $r \approx \ln(R_0)/T$

36.2.2 Dispersion Patterns Across Space

Individuals within a population are distributed in one of three spatial patterns:

Table 419. Dispersion Patterns Across Space: Pattern and Description.

Pattern	Description	Mechanism	Example
Clumped	Aggregated in patches	Resource heterogeneity, social behavior, limited dispersal	Schooling fish, herding ungulates, fungi near rotting logs
Uniform	Evenly spaced	Territoriality, allelopathy, intraspecific competition	Nesting penguins, creosote bush in deserts
Random	No predictable pattern	Absence of strong attraction or repulsion	Wind-dispersed seeds in homogeneous habitat

The variance-to-mean ratio (σ^2/μ) of quadrat counts distinguishes these patterns: ratio = 1 (random, Poisson), >1 (clumped, negative binomial), <1 (uniform).

Concept Check: A researcher counts organisms in 20 quadrats and calculates a variance-to-mean ratio of 3.7. What dispersion pattern does this suggest, and what ecological mechanisms might produce it?

36.3 Life Tables and Survivorship Curves

A cohort life table (also called a horizontal or dynamic life table) tracks a birth cohort from birth until most members die, recording survival and fecundity at each age:

Table 420. Dispersion Patterns Across Space: Age (x) and n_x (alive).

Age (x)	n_x (alive)	l_x (survivorship)	d_x (deaths)	q_x (mortality rate)	m_x (fecundity)	$l_x m_x$	$x \cdot l_x m_x$
0	1000	1.000	200	0.200	0	0	0
1	800	0.800	200	0.250	0.5	0.400	0.400
2	600	0.600	400	0.667	1.2	0.720	1.440
3	200	0.200	180	0.900	1.0	0.200	0.600
4	20	0.020	20	1.000	0	0	0

From this table:

$$R_0 = \sum l_x m_x = 0 + 0.400 + 0.720 + 0.200 + 0 = 1.320$$

(416)

$$T = \frac{\sum x \cdot l_x m_x}{R_0} = \frac{2.440}{1.320} = 1.848 \text{ generations}$$

(417)

$$r \approx \frac{\ln(R_0)}{T} = \frac{\ln(1.320)}{1.848} = \frac{0.278}{1.848} = 0.150 \text{ per time unit}$$

(418)

Since $R_0 > 1$, this population is growing.

A static life table (vertical life table) uses age structure data from a single time point — useful when tracking cohorts is impractical (e.g., long-lived species like elephants or trees). It assumes stable age distribution.

36.3.1 Survivorship Curves and Age-Specific Mortality

Three canonical survivorship curve types (Pearl 1928; Deevey 1947):

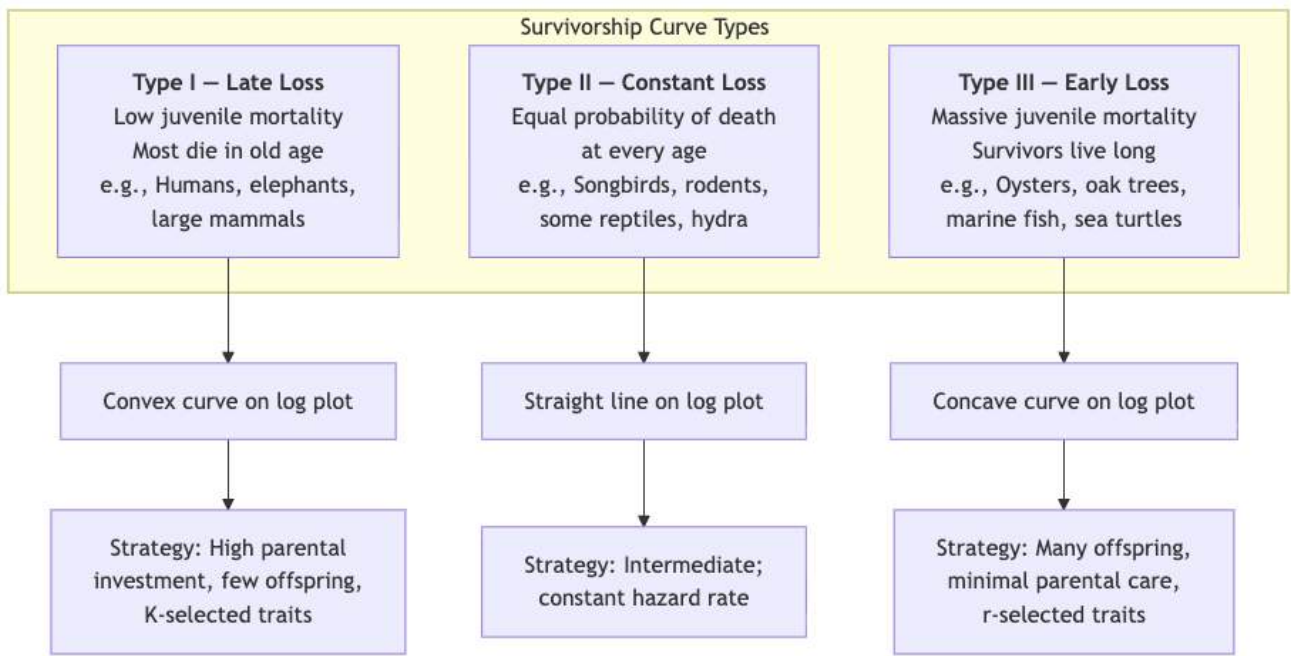


Figure 216. Survivorship curves compare age-specific mortality patterns: Type I curves retain most individuals until late life, Type II curves decline steadily, and Type III curves lose many offspring early.

Mathematical representation of survivorship:

For Type I: $l_x \approx e^{-bx^n}$ where $n > 1$ (Gompertz-Makeham law for human mortality)

For Type II: $l_x = e^{-\mu x}$ (constant hazard rate μ)

For Type III: $l_x \approx e^{-bx^n}$ where $n < 1$

Clinical Connection — Actuarial Science and Human Survivorship: Human survivorship curves have shifted dramatically over the past 200 years. In 1800, human survivorship resembled a Type II curve due to high infant and childhood mortality from infectious disease. Modern medicine, sanitation, and nutrition have transformed the human curve to an extreme Type I, with about 99% survival to age 50 in high-income countries. The Gompertz law of mortality states that human death rate doubles approximately every 8 years after age 30: $\mu(x) = \alpha e^{\beta x}$. This principle underlies life insurance actuarial tables and pension fund projections.

Concept Check: Sea turtles lay 50-200 eggs per nesting event but about 1 in 1,000 hatchlings survives to reproductive age. Which survivorship curve type does this represent, and what would a conservation program need to achieve (in terms of stage-specific survival rates) to increase population growth?

36.3.2 Reproductive Value and Future Genetic Contribution

Fisher’s reproductive value (v_x) quantifies the expected future contribution of an individual of age x to population growth:

$$v_x = \frac{e^{rx}}{l_x} \sum_{y=x}^{\omega} e^{-ry} l_y m_y$$

(419)

Reproductive value peaks at the age of first reproduction in growing populations and declines thereafter. This concept is critical for conservation: protecting age classes with highest v_x yields the greatest impact on population recovery. For sea turtles, subadult and adult females have the highest reproductive value — hence Turtle Excluder Devices (TEDs) in fishing nets target this life stage.

36.4 Exponential Growth Under Unlimited Resources

When resources are unlimited and the environment exerts no **density-dependent regulation**, population growth is exponential (or geometric in discrete-time models):

Continuous-time model:

$$\frac{dN}{dt} = rN \Rightarrow N(t) = N_0 e^{rt}$$

(420)

Discrete-time model (non-overlapping generations):

$$N_{t+1} = \lambda N_t \Rightarrow N_t = N_0 \lambda^t$$

(421)

where $\lambda = e^r$ is the finite rate of increase.

Doubling time: $t_2 = \frac{\ln 2}{r} \approx \frac{0.693}{r}$

36.4.1 Real-World Examples of Near-Exponential Growth

Table 421. Real-World Examples of Near-Exponential Growth: Population and r.

Population	r	Doubling time	Context
<i>E. coli</i> (optimal)	1.7/hr	24.5 min	Binary fission; unlimited glucose
World human population (1650–1800)	0.005/yr	139 yr	Pre-industrial, low density
COVID-19 early spread (March 2020)	0.23/day	3 days	Unmitigated, no immunity
Ring-necked pheasant, Protection Island (1937–42)	1.02/yr	0.68 yr	8 birds introduced; no predators
Reindeer on St. Matthew Island (1944–63)	0.34/yr	2.0 yr	29 animals introduced; no wolves

The St. Matthew Island reindeer population illustrates the catastrophic crash that follows unsustainable exponential growth: 29 reindeer introduced in 1944 grew to 6,000 by 1963, then crashed to 42 by 1966 due to overgrazing of lichen habitat. This case study is a classic illustration of ecological overshoot.

```
from biology.ecology import logistic_growth

# Exponential phase (K → ∞ approximation)
result = logistic_growth(
    initial_population=100,
    growth_rate=0.5,
    carrying_capacity=1e12,  # effectively unlimited
    time_steps=20
)

print(f"After 20 time steps: N = {result.trajectory[-1]:.0f}")
print(f"Predicted (analytic): N = {100 * 2.718** ( 0.5*20 ):.0f}")
```

Concept Check: If a bacterial culture starts with 500 cells and has $r = 1.4/\text{hr}$, how many cells will be present after 6 hours? What assumptions does this calculation require?

36.5 Logistic Growth and Density Dependence

Mathematical Background: Population growth models use differential equations. For a review of exponential and logistic ODEs and their closed-form solutions, see **Appendix C — Mathematical Review for Biology**.

As N approaches the carrying capacity (K), intraspecific competition for resources reduces the per capita growth rate. The logistic growth equation [Verhulst, 1838] incorporates this density dependence:

$$\frac{dN}{dt} = rN\left(1 - \frac{N}{K}\right)$$

(422)

The term $(1 - N/K)$ is the density-dependence factor (or unused portion of carrying capacity), and it bends exponential growth into the S-shaped trajectory of figure 215 with the following key properties:

- When $N \ll K$: growth is approximately exponential ($dN/dt \approx rN$)
- When $N = K/2$: dN/dt is maximized (inflection point of the sigmoid curve)
- When $N = K$: $dN/dt = 0$ (population is at equilibrium)
- When $N > K$: $dN/dt < 0$ (population declines toward K)

Analytical solution:

$$N(t) = \frac{K}{1 + \left(\frac{K-N_0}{N_0}\right)e^{-rt}}$$

(423)

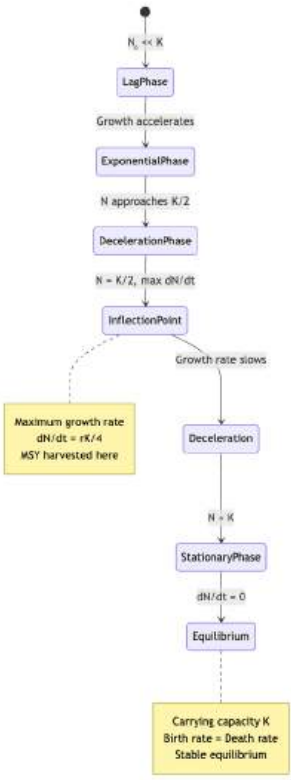


Figure 217. Logistic growth accelerates when population size is far below carrying capacity, reaches maximum growth near $K/2$, and slows as density-dependent limits dominate.

36.5.1 Density-Dependent Factors

Table 422. Density-Dependent Factors: Factor and Mechanism.

Factor	Mechanism	Example
Intraspecific competition	Scramble or contest competition for food, space, mates	Flour beetles (<i>Tribolium</i>): cannibalism increases at high density
Disease transmission	Contact rate increases with density	Distemper in Serengeti lions; COVID-19 in mink farms

Factor	Mechanism	Example
Predation	Predators aggregate at high-density prey patches	Functional response Type III (sigmoidal)
Territoriality	Dominant individuals exclude subordinates	Red grouse: territorial males hold heather patches
Toxic waste accumulation	Metabolic byproducts inhibit growth	Yeast: ethanol accumulation limits fermentation

36.5.2 Density-Independent Factors

Some factors affect populations regardless of density:

- Weather extremes (frost, drought, hurricanes)
- Volcanic eruptions, wildfires, floods
- Pesticide application

In practice, most populations are regulated by a combination of density-dependent and density-independent factors.

36.5.3 Maximum Sustainable Yield (MSY)

From the logistic equation, the maximum absolute growth rate occurs at $N = K/2$:

$$MSY = \frac{rK}{4}$$

(424)

Fisheries and wildlife management use MSY to set harvest quotas. However, MSY has significant limitations:

1. Assumes logistic growth — real populations often show non-logistic dynamics
2. K and r are difficult to estimate — environmental stochasticity changes both
3. Ignores age/size structure — harvesting large, reproductively valuable individuals disproportionately impacts growth
4. No safety margin — harvesting exactly at MSY leaves no **buffer** for environmental variation

Clinical Connection — Pacific Sardine Collapse: The Pacific sardine (*Sardinops sagax*) fishery collapsed in the 1940s-1950s, with the population crashing from 3 million tonnes to near-zero. The collapse resulted from harvesting above MSY during a period when ocean conditions (Pacific Decadal Oscillation) shifted unfavorably, reducing K . The combined effect of over-exploitation and environmental change was catastrophic. This case led to the development of precautionary reference points in modern fisheries management, where harvest targets are set below MSY (typically at 0.5-0.8 MSY) to provide a buffer.

```
from biology.ecology import logistic_growth

result = logistic_growth(
    initial_population=10,
    growth_rate=0.8,
    carrying_capacity=1000,
    time_steps=30
)

# Find maximum per-capita growth (should be near K/2 = 500)
growth_rates = [result.trajectory[i+1] - result.trajectory[i]
                 for i in range(len(result.trajectory)-1)]
peak_N = result.trajectory[growth_rates.index(max(growth_rates))]
print(f"Peak growth at N ≈ {peak_N:.0f} (expect K/2 = 500)")
```

36.5.4 Extensions of the Logistic Model

Theta-logistic model — allows flexible density dependence:

$$\frac{dN}{dt} = rN \left[1 - \left(\frac{N}{K} \right)^\theta \right]$$

(425)

When $\theta = 1$: standard logistic. When $\theta > 1$: density effects are weak until N is close to K (concave per-capita growth). When $\theta < 1$: density effects are strong even at low N (convex). Empirical estimates for large mammals typically give $\theta \approx 2 - 7$ (Sibly et al. 2005, *Science*), meaning density dependence is weaker than the standard logistic assumes.

Time-lagged logistic model:

$$\frac{dN}{dt} = rN \left(1 - \frac{N(t - \tau)}{K} \right)$$

(426)

When the time lag τ is large relative to $1/r$, the population can overshoot K and exhibit damped oscillations, limit cycles, or even chaos (May 1976, *Nature*).

Concept Check: A population of deer has $r = 0.3/\text{yr}$ and $K = 5000$. Calculate MSY and the population size at which it occurs. If the current population is 4000, how many deer can be sustainably harvested per year?

36.6 The Allee Effect

The Allee effect [Allee, 1931] occurs when per capita fitness *decreases* at low population density — the opposite of standard logistic density-dependence. This creates a positive feedback loop where small populations become increasingly vulnerable.

36.6.1 Strong vs. Weak Allee Effects

Strong Allee effect — per capita growth rate becomes negative below a threshold:

$$\frac{dN}{dt} = rN \left(\frac{N}{A} - 1 \right) \left(1 - \frac{N}{K} \right)$$

(427)

where A = Allee threshold. Below A , the population declines deterministically to extinction. figure 218 compares trajectories for starting densities below, at, and above this threshold. There are three equilibria: $N = 0$ (stable), $N = A$ (unstable), and $N = K$ (stable).

Weak Allee effect — per capita growth rate decreases at low density but remains positive. No threshold exists; the population can recover from any positive size, but growth is slower than expected at low N .

36.6.2 Mechanisms of Allee Effects

Table 423. Mechanisms of Allee Effects: Mechanism and Example.

Mechanism	Example	Effect on fitness
Mate finding	Ivory-billed woodpecker; many marine invertebrates	Low density → failed mate encounter → reduced reproduction
Predator satiation	Mast-seeding trees (oaks, beeches)	Below threshold seed output → disproportionate predation loss
Cooperative breeding/hunting	African wild dogs (pack size ≥ 5 for efficient hunting)	Small packs → insufficient prey capture → starvation
Cooperative defense	Muskoxen forming defensive circles	Too few adults → predators penetrate defense
Genetic diversity	Florida panther (pre-1995, $N_e \approx 25$)	Small N → inbreeding depression → reduced fitness
Pollination failure	Rare plants in fragmented meadows	Low density → pollinators don't visit → seed set fails
Environmental conditioning	Soil microbiome enrichment by plant roots	Few plants → soil biota depauperate → poor seedling establishment

Social insects add a colony-level version of the same logic. In a **eusocial** colony, a queen, workers, brood, nest architecture, stored resources, and microbial partners form one demographic unit. A founding queen or tiny fragment may fail even in good habitat because there are too few workers to forage, thermoregulate, defend

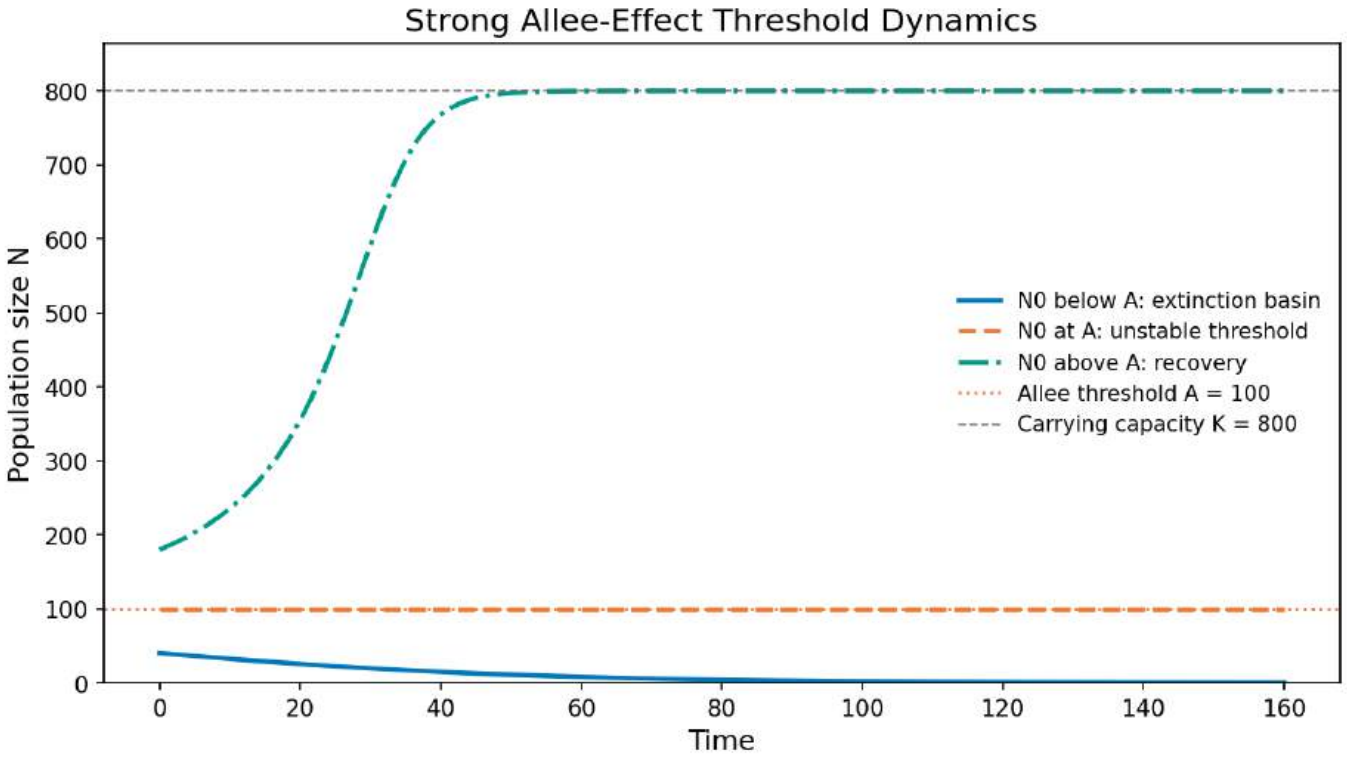


Figure 218. Strong Allee-effect threshold dynamics. Initial population sizes below, at, and above the Allee threshold show extinction, unstable threshold persistence, and recovery toward carrying capacity.

the nest, rear brood, and maintain the fungus garden or gut-symbiont pathway. Once the worker force crosses a threshold, division of labor and positive feedback can make growth accelerate. The Allee effect therefore applies not only to populations of individuals but also to the minimum viable size of cooperative groups [Bourke, 2011].

Stephens et al. (1999, *Trends Ecol. Evol.*) distinguished the component Allee effect (reduction in any fitness component at low density) from the demographic Allee effect (reduction in per capita population growth rate). A species may experience component Allee effects in reproduction without a demographic Allee effect if compensating survival increases at low density offset the reproductive reduction.

```
from biology.ecology import allee_strong_growth

# Strong Allee: dN/dt = r N (N/A - 1)(1 - N/K) - same form as Eq. above
below = allee_strong_growth(N0=45.0, r=0.5, A=50.0, K=1000.0, t_end=25.0, steps=2500)
above = allee_strong_growth(N0=55.0, r=0.5, A=50.0, K=1000.0, t_end=40.0, steps=4000)
print(f"Below A: N_final ≈ {below.populations[-1]:.1f}")
print(f"Above A: N_final ≈ {above.populations[-1]:.1f}")
```

Clinical Connection — Northern White Rhinoceros: The northern white rhinoceros (*Ceratotherium simum cottoni*) represents a tragic Allee effect in action. As of 2024, two females remain (Najin and Fatu at Ol Pejeta Conservancy, Kenya). Even with preserved sperm and IVF technology, the population has fallen below plausible demographic and genetic recovery thresholds for conventional breeding. Stem cell-derived gametes from banked fibroblasts represent a highly experimental rescue pathway rather than a routine conservation tool. This case illustrates that for species with strong Allee effects, conservation intervention must occur while demographic options and genetic variation are still large enough to matter.

Concept Check: A whale population has an Allee threshold of $A = 200$ individuals. Current population is $N = 180$. The intrinsic growth rate (in the absence of Allee effects) is $r = 0.04/\text{yr}$. What will happen to this population without intervention? What minimum number of individuals would need to be translocated to push the population above the threshold?

36.7 Lotka-Volterra Competition and Predator-Prey

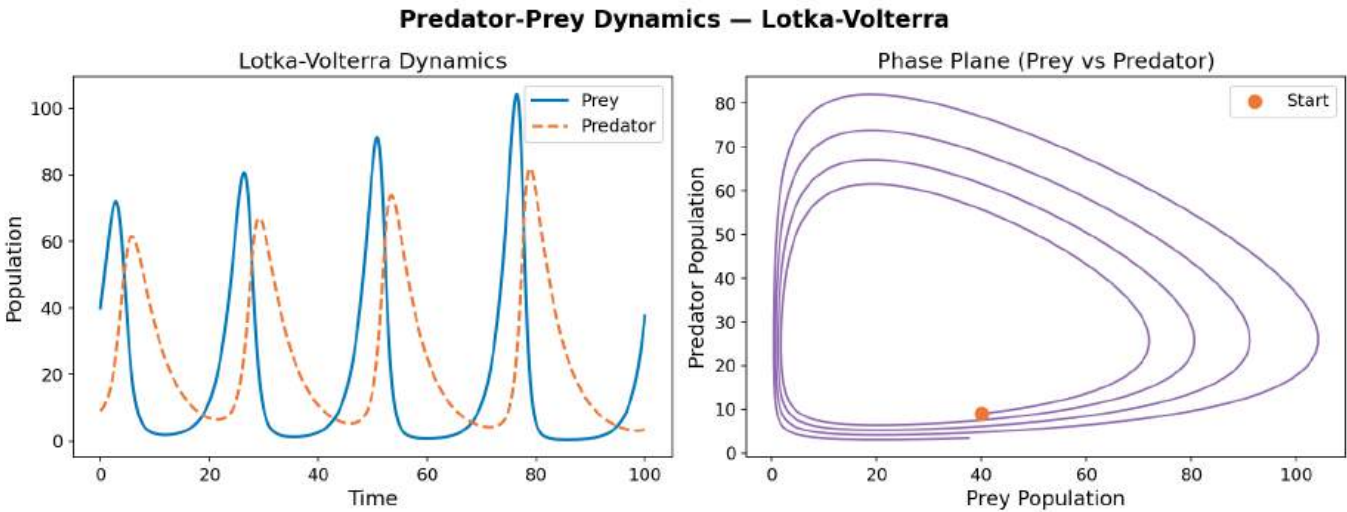


Figure 219. Lotka–Volterra predator–prey dynamics: oscillating population cycles of prey and predator plotted over time and as a phase-plane portrait.

36.7.1 Interspecific Competition and Niche Overlap

Two species sharing a limiting resource compete. The Lotka-Volterra competition model:

$$\frac{dN_1}{dt} = r_1 N_1 \left(1 - \frac{N_1 + \alpha_{12} N_2}{K_1} \right)$$

(428)

$$\frac{dN_2}{dt} = r_2 N_2 \left(1 - \frac{N_2 + \alpha_{21} N_1}{K_2} \right)$$

(429)

The competition coefficient α_{12} represents the per-capita effect of species 2 on species 1, expressed in units of species-1 equivalents. If $\alpha_{12} = 0.5$, each individual of species 2 has half the competitive impact of one individual of species 1.

Zero-growth isoclines (setting $dN/dt = 0$): - Species 1 isocline: $N_1 = K_1 - \alpha_{12}N_2$ (line from K_1 on N_1 -axis to K_1/α_{12} on N_2 -axis) - Species 2 isocline: $N_2 = K_2 - \alpha_{21}N_1$ (line from K_2 on N_2 -axis to K_2/α_{21} on N_1 -axis)

Phase-plane outcomes:

Table 424. Interspecific Competition and Niche Overlap: Condition and Outcome.

Condition	Outcome	Biological interpretation
$K_1 > K_2/\alpha_{12}$ and $K_2 < K_1/\alpha_{21}$	Species 1 wins; species 2 excluded	Species 1 tolerates competition better
$K_2 > K_1/\alpha_{21}$ and $K_1 < K_2/\alpha_{12}$	Species 2 wins; species 1 excluded	Species 2 tolerates competition better
$K_1 < K_2/\alpha_{12}$ and $K_2 < K_1/\alpha_{21}$	Stable coexistence	Intraspecific > interspecific competition (niche differentiation)
$K_1 > K_2/\alpha_{12}$ and $K_2 > K_1/\alpha_{21}$	Unstable equilibrium (priority effect)	Interspecific > intraspecific; winner depends on initial N

Chesson’s modern coexistence theory (Chesson 2000, *Annu. Rev. Ecol. Syst.*): Stable coexistence requires that intraspecific competition exceed interspecific competition: $\alpha_{11}\alpha_{22} > \alpha_{12}\alpha_{21}$, or equivalently, niche overlap < 1 . Two mechanisms enable this:

1. Stabilizing mechanisms — increase niche differentiation (negative frequency dependence; rare species advantage)
2. Equalising mechanisms — reduce fitness differences between species (similar competitive abilities)

36.7.2 Lotka-Volterra Predator-Prey

$$\frac{dV}{dt} = \alpha V - \beta VP \quad (\text{prey: grow in absence of predator; decline with encounters})$$

(430)

$$\frac{dP}{dt} = \delta VP - \gamma P \quad (\text{predator: grow via prey; decline without prey})$$

(431)

This system produces neutrally stable oscillations with period $\approx 2\pi/\sqrt{\alpha\gamma}$ and amplitude that depends on initial conditions, tracing the offset prey–predator cycles and closed phase-plane orbit shown in figure 219.

Functional responses [Holling, 1959] describe the per capita predation rate as a function of prey density:

Table 425. Lotka-Volterra Predator-Prey: Type and Equation.

Type	Equation	Shape	Example
Type I	$f(V) = aV$	Linear	Filter feeders (whale sharks, baleen whales)
Type II	$f(V) = \frac{aV}{1+ahV}$	Decelerating (hyperbolic)	Most predators; handling time h limits intake
Type III	$f(V) = \frac{aV^2}{1+ahV^2}$	Sigmoidal	Predators that switch prey; search image formation

The Type II functional response is also known as the Michaelis-Menten or disc equation. The parameter a = attack rate and h = handling time per prey item. Maximum consumption rate = $1/h$.

Type III responses are stabilizing because at low prey density, per-capita predation risk is low (predator switching to alternative prey), creating a low-density refuge.

Numerical response: predator population growth rate as a function of prey density — driven by the functional response but with a time lag (gestation, maturation).

```
from biology.ecology import lotka_volterra

result = lotka_volterra(
    100.0, 20.0, 1.0, 0.1, 0.075, 1.5, t_end=30.0, steps=300,
)

print(f"Prey range: {min(result.prey):.0f}--{max(result.prey):.0f}")
print(f"Predator range: {min(result.predator):.0f}--{max(result.predator):.0f}")
```

36.7.3 Lynx-Hare Cycle: A Case Study

The snowshoe hare (*Lepus americanus*) and Canada lynx (*Lynx canadensis*) display coupled about 10-year population cycles across boreal Canada, documented from Hudson’s Bay Company fur trading records (1845-1935; Keith 1963). Modern analysis reveals the cycle is more complex than simple Lotka-Volterra:

- 1. Predation accounts for about 60% of the cycle driver (Krebs et al. 2001, *Science*)
- 2. Food quality — at high hare density, overgrazing induces plant chemical defenses (phenolic compounds in willow/birch browse), reducing hare food quality (about 20% of cycle)
- 3. Stress physiology — high density and predation risk elevate **cortisol**, suppressing reproduction (about 20% of cycle)
- 4. The tri-trophic interaction (vegetation-hare-lynx) is necessary to explain the observed amplitude and period

Concept Check: In the basic Lotka-Volterra predator-prey model, the oscillations are neutrally stable. What modification to the model would produce damped oscillations converging to a stable equilibrium? (Hint: consider what happens when you add density dependence to the prey equation.)

36.8 r vs. K Selection and Life History Theory

MacArthur and Wilson [1967] proposed that **natural selection** shapes life histories along an r-K continuum:

Table 426. Lynx-Hare Cycle: A Case Study: Trait and **r-strategists**.

Trait	r-strategists	K-strategists
Body size	Small	Large
Life span	Short	Long
Maturation time	Fast	Slow
Offspring number	Many; small	Few; large
Parental investment	Minimal	Extensive
Population dynamics	Exponential; boom/bust; opportunistic	Near K; stable; competitive
Environmental tolerance	High variability; unpredictable	Low variability; stable niches
Survivorship curve	Type III	Type I
Examples	Dandelions, flies, bacteria, aphids	Elephants, whales, great apes, condors

36.8.1 Beyond r-K: Modern Life History Theory

The r-K framework has been largely superseded by more nuanced models:

Stearns’ (1992) demographic classification uses age-specific mortality patterns rather than a single r-K axis, predicting that: - High juvenile mortality → early maturation, high fecundity - High adult mortality → delayed maturation, high reproductive effort per event - Variable mortality → bet-hedging strategies

Bet-hedging (Philippi & Seger 1989, *Trends Ecol. Evol.*): In variable environments, intermediate-risk reproductive strategies outperform extreme approaches by reducing variance in fitness rather than maximizing mean fitness: - Conservative bet-hedging: Low-variance strategy (e.g., typically produce moderate number of offspring) - Diversified bet-hedging: Produce variable **phenotypes** (e.g., desert annual plants with variable seed dormancy — don’t germinate most seeds in a single good year)

Grime’s CSR triangle (plants): Competitors (large, slow), Stress-tolerators (tough, slow), Ruderals (fast, weedy) — a three-way classification rather than binary r-K.

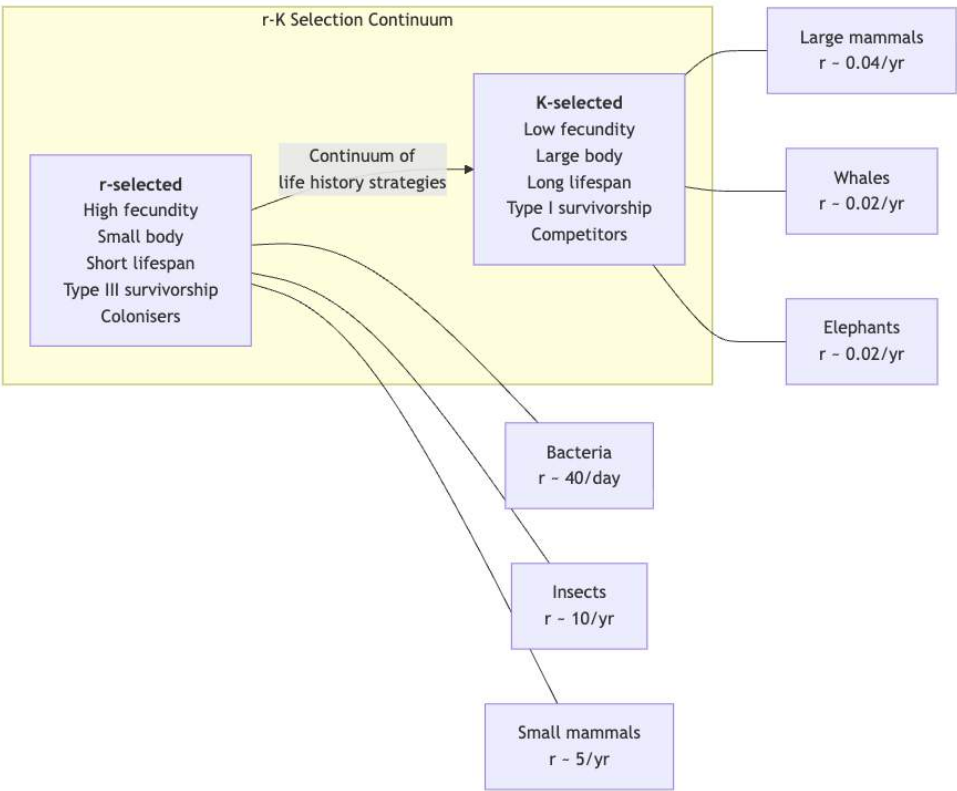


Figure 220. Life-history strategies compare high-fecundity colonizers with slower, competitive species; real organisms vary continuously rather than falling into two fixed bins.

Clinical Connection — Human Life History and Demographic Transition: Human populations have undergone a dramatic demographic transition as societies industrialise: from high birth rates and high death rates (Stage 1) through declining death rates (Stage 2, rapid population growth), declining birth rates (Stage 3), to low birth/death rates (Stage 4). Some developed nations are now in Stage 5 with birth rates below replacement ($R_0 < 1$). Japan’s population declined by about 800,000 in 2023 alone ($r \approx -0.006/\text{yr}$). The demographic transition illustrates a shift from r-selected to K-selected reproductive strategy within a single species as environmental conditions change.

36.9 Age-Structured Population Models and the Leslie Matrix

The scalar growth models treat most individuals as demographically identical. Real populations are structured by age (or stage), and demographic rates are highly age-specific: a one-year-old salmon and a four-year-old salmon contribute very differently to population growth. Matrix population models [Lotka, 1925] make this structure explicit and underlie virtually every modern population viability analysis, fisheries stock assessment, and conservation triage exercise.

36.9.1 Leslie Matrix Construction

A Leslie matrix L is a square non-negative matrix that projects an age-classified population vector $n(t) = (n_0, n_1, \dots, n_\omega)^T$ from time t to $t + 1$:

$$n(t + 1) = L n(t)$$

(432)

For a population with maximum age ω , the Leslie matrix has age-specific fecundities $F_x = l_x m_x / l_{x-1}$ on the top row and survival probabilities $P_x = l_{x+1} / l_x$ on the sub-diagonal:

$$L = \begin{pmatrix} F_0 & F_1 & F_2 & \cdots & F_{\omega-1} & F_\omega \\ P_0 & 0 & 0 & \cdots & 0 & 0 \\ 0 & P_1 & 0 & \cdots & 0 & 0 \\ 0 & 0 & P_2 & \cdots & 0 & 0 \\ \vdots & \vdots & \vdots & \ddots & \vdots & \vdots \\ 0 & 0 & 0 & \cdots & P_{\omega-1} & 0 \end{pmatrix}$$

(433)

By the Perron–Frobenius theorem, L has a unique positive dominant eigenvalue λ_1 — this is the asymptotic finite rate of increase. The associated right eigenvector w gives the stable age distribution (the proportions n_x/N to which the population converges) and the left eigenvector v gives the age-specific reproductive value v_x (equation (419), but now read off the matrix directly).

$$Lw = \lambda_1 w, \quad v^T L = \lambda_1 v^T$$

(434)

The Euler-Lotka equation (equation (415)) is the characteristic polynomial of L — every demographic statement made in the life-table and survivorship discussion is recoverable from the matrix.

36.9.2 Sensitivity and Elasticity Analysis

Conservation managers rarely have the luxury of changing every demographic rate. Which rate, if perturbed by 1%, would change λ_1 the most? Sensitivity s_{ij} and elasticity e_{ij} answer this:

$$s_{ij} = \frac{\partial \lambda_1}{\partial a_{ij}} = \frac{v_i w_j}{\langle v, w \rangle}, \quad e_{ij} = \frac{a_{ij}}{\lambda_1} s_{ij}$$

(435)

where a_{ij} is the matrix entry, $\langle v, w \rangle = \sum_x v_x w_x$, and elasticities sum to one ($\sum_{ij} e_{ij} = 1$), making them directly interpretable as proportional contributions.

Table 427. Sensitivity and Elasticity Analysis.

Quantity	Interpretation	Use
Sensitivity s_{ij}	Absolute change in λ_1 per unit change in a_{ij}	Rates measured on different scales (survival 0–1, fecundity 0– ∞) — direct comparison misleading
Elasticity e_{ij}	Proportional change in λ_1 per proportional change in a_{ij}	Comparing across rates; identifying highest-leverage management target

Worked Example — Loggerhead sea turtle. Crouse, Crowder & Caswell (1987, *Ecology*) built a 7-stage Leslie-style matrix for *Caretta caretta* in the southeastern USA. Hatchling protection (the dominant 1980s strategy) had elasticity ≈ 0.04 , whereas adult survival had elasticity $\approx 0.20–0.30$. A 1 % increase in adult survival raised λ_1 five to seven times more than a 1 % increase in egg-stage survival. This elasticity result drove the regulatory adoption of Turtle Excluder Devices in shrimp trawls — a direct policy outcome of matrix sensitivity analysis. The same logic explains why protecting reproductive-aged females beats protecting eggs, echoing the reproductive-value argument developed earlier.

Concept Check: A 3-stage matrix has elasticities $e_{\text{juvenile survival}} = 0.05$, $e_{\text{subadult survival}} = 0.35$, $e_{\text{adult survival}} = 0.50$, $e_{\text{adult fecundity}} = 0.10$. Which life-stage transition should a recovery plan target first, and why is “save the babies” intuition misleading here?

36.9.3 Stage-Structured Generalisations

Many organisms are better classified by stage (size, instar, reproductive status) than by age — trees, corals, and indeterminate-growth fish are obvious examples. The Lefkovitch matrix generalizes Leslie by allowing positive entries on the diagonal (probability of remaining in the same stage) and on multiple sub-diagonals (skipping stages, regression). The eigen-analysis machinery is shared with Leslie models, while the biological interpretation of each entry changes.

```
import numpy as np

# Loggerhead-style 5-stage matrix (illustrative)
L = np.array([
```

```
[0.00, 0.00, 0.00, 4.66, 61.9], # fecundities (eggs, hatchlings)
[0.68, 0.74, 0.00, 0.00, 0.00], # juvenile survival
[0.00, 0.05, 0.66, 0.00, 0.00], # subadult transition
[0.00, 0.00, 0.02, 0.68, 0.00], # novice breeder
[0.00, 0.00, 0.00, 0.06, 0.81], # mature breeder
])

eigvals, eigvecs = np.linalg.eig(L)
lam1 = max(eigvals.real)
w = eigvecs[:, np.argmax(eigvals.real)].real
w = w / w.sum()
print(f"lambda_1 = {lam1:.3f}")
print(f"stable stage distribution = {np.round(w, 3)}")
# elasticity of adult survival – the loggerhead conservation lever
```

36.10 Individual-Based Population Models and Stochastic Simulation

Matrix models are deterministic and assume infinite, well-mixed populations. Two regimes break those assumptions and demand a different tool:

1. Small populations (conservation contexts) where demographic stochasticity dominates — a population of 30 condors with mean $\lambda_1 = 1.05$ can still go extinct from an unlucky run of male-heavy chicks.
2. Heterogeneous individuals — variation in body size, behavior, territory quality, or local conditions that cannot be averaged into a mean rate without losing the dynamics.

Individual-based models (IBMs), also called agent-based models, simulate each organism explicitly. Births, deaths, dispersal, and interactions are drawn as random events from probability distributions parameterised by individual attributes. Across many replicate runs, IBMs produce *distributions* of outcomes (extinction probability, time to recovery) rather than single trajectories.

Table 428. Stage-Structured Generalisations: Advantage and Why IBMs deliver it.

Advantage	Why IBMs deliver it
Demographic stochasticity	Discrete birth/death events — no fractional individuals
Individual heterogeneity	Each agent carries its own age, size, genotype, location
Spatial structure	Landscape grids, dispersal kernels, local interactions
Emergent dynamics	Allee effects, self-organization, threshold behaviors arise naturally
Complex behaviors	Mate choice, learning, territoriality without analytical closed form

Limitations: IBMs trade analytical clarity for realism. They are computationally expensive (millions of replicates needed for tail-probability estimates), parameter-hungry, and validation is harder than for closed-form models. Best practice: build the simplest model that captures the focal mechanism, then add complexity primarily when justified by data (the Pattern-Oriented Modeling philosophy of Grimm & Railsback 2005).

Concept Check: Two black-footed ferret populations both have mean $\lambda_1 = 1.02$. Population A has $N = 500$; population B has $N = 25$. Why does the IBM extinction probability differ vastly between them despite identical mean growth rates? What would a deterministic model predict?

36.11 Population Viability Analysis and Extinction-Risk Forecasting

Population viability analysis integrates matrix models and stochastic simulation into a quantitative extinction-risk forecast. PVA is the formal answer to “How long does this species have, and what intervention buys the most time?” — required by the U.S. Endangered Species Act, the IUCN Red List Criterion E, and most national recovery plans.

36.11.1 Inputs to a PVA

Table 429. Inputs to a PVA: Input and Source.

Input	Source	Why it matters
Stage- or age-specific vital rates	Mark-recapture, life table	Mean dynamics
Variance in vital rates	Long-term monitoring	Environmental stochasticity
Catastrophe frequency and severity	Disturbance history	Tail risk (fire, disease, storm)
Density dependence (often theta-logistic, equation (425))	Time-series fits	Carrying-capacity feedback
Initial age/stage distribution	Field census	Starting condition
Habitat capacity K	Resource estimates	Ceiling on population
Inbreeding cost on vital rates	Pedigree or ROH	Genetic stochasticity (link to section 40)

36.11.2 Outputs and Decision Rules

The two headline outputs are extinction probability $P_{ext}(T)$ over a horizon T (commonly 100 years or 100 generations) and mean time to extinction \bar{T}_{ext} .

$$P_{ext}(T) = \Pr(N(t) < N_{crit} \text{ for some } t \leq T)$$

(436)

The threshold N_{crit} (often called the quasi-extinction threshold) is set above zero — typically the Allee threshold A (equation (427)) or a number below which the population is “functionally extinct.” Hitting N_{crit} counts as failure even if the simulation has not bottomed out.

The minimum viable population (MVP) in standard usage is the smallest N_0 such that $P_{ext}(100 \text{ yr}) \leq 0.05$. Reed et al. (2003, *Biol. Conserv.*) reviewed PVAs across 102 vertebrates and found MVPs clustering at 5,000–7,000 adults — far above the classical $N_e = 500$ rule of thumb (which ignores demographic and environmental stochasticity) and a key empirical result that pushed conservation toward the 100/1000 rule discussed in section 40.

36.11.3 Worked Example — California Condor PVA

In 1982 the known California condor (*Gymnogyps californianus*) population had fallen to 22 birds. A PVA built around captive-breeding fecundity, juvenile mortality from lead poisoning, and stochastic catastrophe (wildfire) gave $P_{ext}(50 \text{ yr}) > 0.99$ for the no-intervention scenario. The same model showed $P_{ext}(50 \text{ yr}) < 0.10$ if (i) the remaining birds were captured for breeding, and (ii) released birds were protected from lead ammunition. The captive-breeding decision, controversial at the time, was justified directly by PVA elasticities — adult survival and juvenile lead mortality had the largest leverage on λ_1 . The wild population is now > 250 (see section 40).

36.11.4 Limitations and Honest Use

PVA outputs depend on the model structure, input data, and uncertainty assumptions; small-population data are often sparse and biased toward observed survivors. Best practice (Beissinger & Westphal 1998, *J. Wildl. Manage.*):

- Treat absolute P_{ext} values with skepticism; use *relative* comparisons across management scenarios
- Report sensitivity to parameter uncertainty (Monte Carlo over input distributions)
- Update PVAs as monitoring data accumulate — they are living tools, not one-off reports
- Avoid the temptation to over-parameterise; structural uncertainty often exceeds parameter uncertainty

Concept Check: A PVA gives $P_{ext}(100 \text{ yr}) = 0.30$ under current management and 0.05 under a proposed habitat-corridor intervention. Should you trust the absolute numbers, the difference, or both? What three sources of uncertainty would you investigate before recommending the corridor?

36.12 Metapopulation Dynamics Across Habitat Patches

A metapopulation (Levins 1969; Hanski 1994) is a “population of populations” — a set of spatially separated subpopulations (patches) connected by dispersal. Local extinctions are balanced by recolonisation from other patches.

In conservation practice, the important question is usually whether dispersal is functional, not whether habitat patches are merely drawn on a map. Roads, dams, fences, heat waves, disease, and behavioral avoidance can lower effective colonization even when patches appear close. Corridor design therefore needs demographic monitoring, genetic connectivity, mortality-risk mapping, and sensitivity analysis for c and e , because a corridor that increases movement can still fail if it also increases mortality or spreads disease.

36.12.1 The Levins Model

$$\frac{dp}{dt} = cp(1 - p) - ep$$

(437)

where: - p = proportion of occupied patches - c = colonization rate - e = extinction rate per patch

At equilibrium: $\hat{p} = 1 - e/c$

The metapopulation persists if $e/c < 1$ (colonization rate exceeds extinction rate). If habitat patches are destroyed (reducing total patches available), the effective c decreases, potentially pushing $e/c > 1$ and causing metapopulation collapse.

36.12.2 Source-Sink Dynamics [Pulliam, 1988]

Patches differ in leverage:

Table 430. Source and sink patch roles in metapopulation dynamics.

Patch type	Growth rate	Role
Source	$\lambda > 1$	Produces surplus individuals; net emigration
Sink	$\lambda < 1$	Cannot sustain itself; relies on immigration from sources

A population can persist in sink habitats indefinitely if immigration from sources is sufficient. This has profound conservation implications: protecting source habitats is critical, while sink habitats may appear to support populations but are “ecological traps” without the source.

36.12.3 Rescue Effect and Connectivity

The rescue effect (Brown & Kodric-Brown 1977): immigration from nearby patches prevents or delays local extinction. This means: - Closely spaced patches have lower extinction rates - Habitat corridors increase connectivity and reduce local extinction - Isolation increases both extinction probability and time to recolonisation

Concept Check: A metapopulation has 100 habitat patches with $c = 0.3$ and $e = 0.1$. Calculate the equilibrium proportion of occupied patches. If 40% of patches are destroyed (reducing total to 60 patches), what happens to the metapopulation? (Consider how reduced patch number affects colonization rate.)

36.12.4 Visualizing Metapopulation and Source-Sink Dynamics

36.13 Estimating Population Size

36.13.1 Mark-Recapture Methods

The Lincoln-Petersen method (simplest mark-recapture) estimates population size from two sampling events:

$$\hat{N} = \frac{M \cdot C}{R}$$

(438)

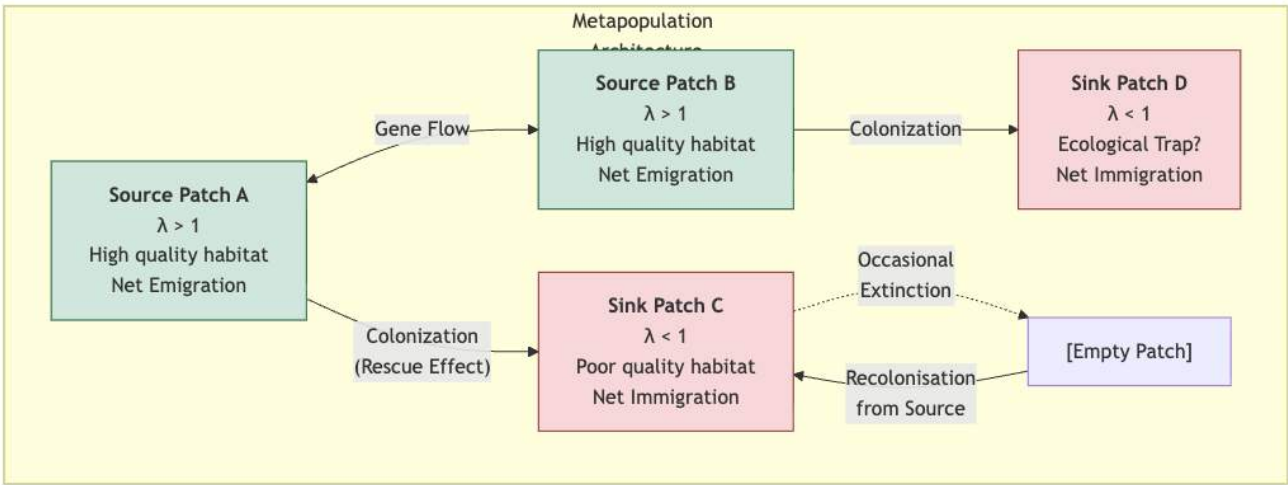


Figure 221. Metapopulation diagrams distinguish source patches with $\lambda > 1$ from sink or trap patches that persist through immigration despite local decline.

where: - M = number marked and released in first sample - C = total captured in second sample - R = number of marked individuals recaptured

Assumptions: (1) Closed population (no births, deaths, immigration, emigration between samples), (2) marks are not lost, (3) marked and unmarked individuals have equal capture probability, (4) marks do not affect survival.

Chapman’s correction for small samples:

$$\hat{N} = \frac{(M + 1)(C + 1)}{R + 1} - 1$$

(439)

Jolly-Seber method — for open populations with multiple sampling occasions. Estimates N , survival rate (φ), and recruitment (B) at each time point. Computationally intensive; requires at least 3 capture occasions.

36.13.2 Distance Sampling and Detection Probability

Line transect distance sampling estimates density from the perpendicular distances of detected objects from the transect line:

$$\hat{D} = \frac{n \cdot \hat{f}(0)}{2L}$$

(440)

where n = number detected, L = total transect length, $\hat{f}(0)$ = estimated probability density function of detection distances evaluated at zero distance. The key assumption is that most objects on the line are detected ($g(0) = 1$).

Clinical Connection — Epidemiological Surveillance: Mark-recapture methodology has been adapted for human epidemiology as capture-recapture estimation to estimate the completeness of disease registries. For example, comparing hospital records with death certificates as two independent “captures” allows estimation of the true number of opioid overdose deaths, accounting for under-reporting. The WHO uses this approach for HIV prevalence estimation in populations where direct surveys are impractical.

36.14 Human Population Demographics

The global human population reached 8 billion in November 2022. The UN World Population Prospects 2024 projects continued growth to about 10.3 billion in the mid-2080s, followed by a slight decline toward about 10.2 billion by 2100 [United Nations Department of Economic and Social Affairs, Population Division, 2024]. Treat this as a scenario-based projection rather than a fixed destiny: fertility, mortality, migration, policy, and environmental stress can shift regional trajectories.

36.14.1 Age Structure and Population Pyramids

The age structure of a population determines its future growth trajectory:

- Expansive pyramid (broad base): high proportion of pre-reproductive individuals; rapid growth (e.g., Nigeria, $r \approx 0.025/\text{yr}$)
- Stationary pyramid (column shape): roughly equal proportions across age classes; near-zero growth (e.g., USA, $r \approx 0.002/\text{yr}$)
- Constrictive pyramid (narrow base): higher proportion of older individuals; declining population (e.g., Japan, $r \approx -0.006/\text{yr}$)

Population momentum: Even after fertility drops to replacement level ($R_0 = 1$), a population with an expansive age structure continues growing for decades because the large cohort of young people has not yet reproduced. This explains why the world population will continue growing despite declining global fertility rates (from 5.3 in 1963 to 2.3 in 2023).

36.14.2 Total Fertility Rate (TFR) and Replacement Level

The total fertility rate is the average number of children born to a woman over her lifetime. Replacement-level fertility is $\text{TFR} \approx 2.1$ in developed nations (slightly above 2 to account for child mortality). In 2023, global TFR was 2.3 — barely above replacement.

Demographic dividend: Countries in mid-transition (declining fertility, large working-age cohort, low dependency ratio) experience accelerated economic growth. East Asia (1965-1990) and sub-Saharan Africa (projected 2030-2060) demonstrate this phenomenon.

36.15 Worked Examples: Leslie Matrices and Population Growth

36.15.1 Worked Example: Leslie Matrix Projection

Problem: A 3-age-class population (juvenile, subadult, adult) has Leslie matrix

$$L = \begin{pmatrix} 0 & 1.2 & 3.0 \\ 0.4 & 0 & 0 \\ 0 & 0.6 & 0.7 \end{pmatrix}$$

with initial vector $n(0) = (40, 20, 10)^T$. (a) Project the population one time step. (b) Compute λ_1 and decide whether the population is growing, stable, or declining.

Solution:

Step 1. One-step projection. $n(1) = L n(0)$ - $n_0(1) = 0 \cdot 40 + 1.2 \cdot 20 + 3.0 \cdot 10 = 54$ - $n_1(1) = 0.4 \cdot 40 + 0 + 0 = 16$ - $n_2(1) = 0 + 0.6 \cdot 20 + 0.7 \cdot 10 = 19$ - Total: $N(1) = 89$ vs. $N(0) = 70$ — apparent growth, but transient.

Step 2. Characteristic polynomial. The asymptotic rate λ_1 solves $\det(L - \lambda I) = 0 \Rightarrow -\lambda^3 + 0.7\lambda^2 + 0.48\lambda + 0.72 = 0$

Numerical root-finding gives $\lambda_1 \approx 1.094$.

Step 3. Interpretation. Because $\lambda_1 > 1$, the population grows asymptotically at $\sim 9.4\%$ per time step once it converges to its stable age distribution. The transient ratio $89/70 = 1.27$ overstates long-run growth because the initial vector is juvenile-heavy.

Answer: $\lambda_1 \approx 1.09$; the population is growing in the long run.

36.15.2 Worked Example: Mark-Recapture Estimation

Problem: A population ecologist uses the mark-recapture method to estimate the size of a grasshopper population in a meadow. On the first day, she captures, marks, and releases 120 grasshoppers (M). On the second day, she captures a total of 150 grasshoppers (C), of which 30 are marked (R). Calculate the estimated population size (N).

Solution:

Step 1. Identify the given variables. - Number marked in first sample (M) = 120 - Total number in second sample (C) = 150 - Number of marked recaptures (R) = 30

Step 2. Use the Lincoln-Petersen estimator. The formula for the total population size (N) is:

$$N = \frac{M \times C}{R}$$

Step 3. Calculate N .

$$N = \frac{120 \times 150}{30}$$
$$N = \frac{18,000}{30}$$
$$N = 600$$

Answer: The estimated size of the grasshopper population is 600 individuals.

36.15.3 Worked Example: Logistic Projection and r/K Strategist Vulnerability

Problem: A population obeys logistic growth with $r = 0.2/\text{yr}$, $K = 1000$, and $N_0 = 100$. (a) Project the population at $t = 10$ yr and $t = 20$ yr using the closed-form logistic solution. (b) Compare the recovery trajectory of an r-strategist ($r = 2.0$, $K = 200$) versus a K-strategist ($r = 0.1$, $K = 1000$) starting at the same $N_0 = 50$ after a population collapse.

Solution:

Step 1. Apply the closed-form logistic solution.

$$N(t) = \frac{K}{1 + \left(\frac{K-N_0}{N_0}\right)e^{-rt}}$$

With $K = 1000$, $N_0 = 100$: the bracket evaluates to $(1000 - 100)/100 = 9$, so

$$N(t) = \frac{1000}{1 + 9e^{-0.2t}}$$

Step 2. Evaluate at $t = 10$ and $t = 20$.

- $t = 10$: $e^{-2} \approx 0.135$, so $N(10) = 1000/(1 + 9 \times 0.135) = 1000/2.215 \approx 451$ individuals (population is near the inflection point at $K/2 = 500$).
- $t = 20$: $e^{-4} \approx 0.0183$, so $N(20) = 1000/(1 + 9 \times 0.0183) = 1000/1.165 \approx 858$ individuals. After ~ 30 yr the population approaches K asymptotically (recomputing gives $N(30) \approx 943$).

Step 3. Compare strategist vulnerability.

The r-strategist ($r = 2.0$, $K = 200$) projected from $N_0 = 50$ reaches K in roughly $\ln 3/r \approx 0.55$ yr — fast numerical recovery, but the absolute headcount is small and the small K makes it stochastically fragile. The K-strategist ($r = 0.1$, $K = 1000$) takes $\ln 19/r \approx 29$ yr to approach K from the same N_0 , so even after the demographic causes of collapse are removed it remains depressed for decades — exactly the regime where demographic stochasticity, Allee effects, and inbreeding depression compound.

Answer: $N(10) \approx 451$, $N(20) \approx 858$. K-strategists are disproportionately vulnerable in conservation because their slow r leaves them stranded in the low- N regime far longer, regardless of whether the original threat has been mitigated.

36.15.4 Concept Check (Analyze) — Allee Effects and Minimum Viable Population

A grizzly bear population has a critical Allee threshold $N_c = 50$ (below which mate-finding failure and reduced cooperative defense cause per-capita birth rate to fall). The current population is $N = 60$.

- (a) Using the simple rule $P(\text{extinction}) \approx \exp[-(N - N_c)/\sigma]$ with demographic-stochasticity parameter $\sigma = 10$, estimate the short-horizon stochastic extinction probability.
- (b) The expression for $P(\text{extinction})$ is monotone decreasing in $(N - N_c)$. Analyze what happens to this probability if inbreeding depression effectively raises N_c from 50 to 58 while N stays at 60. Why do Allee effects and inbreeding depression compound non-linearly in small populations?

(c) A managed translocation increases N from 60 to 80 with no change in N_c . Compute the new $P(\text{extinction})$ and explain why a 33% headcount increase yields a much larger relative reduction in extinction risk than a naive linear intuition would suggest.

(Expected: (a) $P \approx e^{-1} \approx 0.37$. (b) $P \approx e^{-0.2} \approx 0.82$ — small shifts in the effective threshold dominate. (c) $P \approx e^{-3} \approx 0.05$, an order-of-magnitude drop. The exponential form is the structural reason small populations have non-linear, “cliff-edge” vulnerability.)

36.15.5 Concept Check (Evaluate) — Leslie Matrix Sensitivity and Where to Manage

A perennial plant has the following demographic rates: seedling survival = 0.3, seedling-to-juvenile transition = 0.1, juvenile survival = 0.6, juvenile-to-adult transition = 0.2, adult survival = 0.8, adult fecundity = 5 (seedlings per adult per year).

(a) Construct the stage-structured projection matrix from these rates (stages: seedling, juvenile, adult). Identify which matrix entries correspond to “survival” terms versus “fecundity” terms.

(b) Without solving for λ_1 exactly, use the structural intuition from sensitivity / elasticity analysis (long-lived adult survival typically dominates elasticity in iteroparous organisms; fecundity dominates in semelparous organisms) to evaluate which single 10% improvement — boosting adult survival from 0.8 to 0.88, or boosting fecundity from 5.0 to 5.5 — would yield the larger λ_1 increase.

(c) Evaluate the practical conservation implication: management dollars are limited. A nursery program can plausibly raise fecundity (more seed set) at low cost; an adult-protection program (e.g., fencing against herbivory) is expensive but raises adult survival. Justify a management recommendation using the elasticity logic, and state at least one condition under which the opposite recommendation would be correct (e.g., severe seed limitation, recent disturbance regime).

36.16 Current Evidence and Frontier Biology: Population Ecology and Growth Models

For Population Ecology and Growth Models, frontier biology belongs inside the evidence logic of the chapter. Ecology and conservation decisions increasingly combine field data, remote sensing, community knowledge, model uncertainty, and explicit values. The core reading question is this: population claims require density dependence, demographic stochasticity, dispersal, age structure, and management objective.

- What to verify: identify the observation, model, assay, or dataset that would make the claim stronger or weaker.
- What to qualify: state the scale, organism, cell type, environmental condition, or population where the claim is expected to hold.
- What to compare: test at least one alternative explanation, baseline, or null model before treating the pattern as causal.
- What to cite: distinguish primary evidence, review synthesis, public dataset, and institutional guidance; for recent or numeric claims, prefer the source closest to the measurement and state what has changed since it was published.

Select biodiversity and conservation metrics by decision need: abundance, interaction, function, risk, service, and governance metrics answer different questions [Intergovernmental Science-Policy Platform on Biodiversity and Ecosystem Services, 2019, 2024, World Wide Fund for Nature, 2024, International Union for Conservation of Nature, 2025, Food and Agriculture Organization of the United Nations, 2024].

Source practice: For ecology and conservation claims, cite assessment sources and state whether the evidence is an index, risk assessment, service valuation, satellite product, or policy synthesis [Intergovernmental Science-Policy Platform on Biodiversity and Ecosystem Services, 2024, NOAA Coral Reef Watch, 2025, Food and Agriculture Organization of the United Nations et al., 2025].

36.17 Key Terms

Table 431. Concept Check (Evaluate) — Leslie Matrix Sensitivity and Where to Manage: Term and Definition.

Term	Definition
Carrying capacity (K)	Maximum population size supported by a given environment
Intrinsic rate of increase (r)	Per capita growth rate in ideal conditions ($= b - d$)
Net reproductive rate (R_0)	Mean lifetime offspring per individual; $R_0 > 1$ means growing
Allee effect	Positive density-dependence; fitness decreases at low N
Allee threshold (A)	N below which population declines deterministically (strong Allee effect)
Competition coefficient (α)	Per-capita interspecific competition effect
Competitive exclusion	One species eliminates another when niches overlap completely

Term	Definition
Maximum sustainable yield (MSY)	$rK/4$; optimal harvest at $N = K/2$
Lotka-Volterra equations	ODEs describing competition and predator-prey dynamics
Bet-hedging	Variable reproductive strategy reducing variance in fitness
Functional response	Per-capita predation rate as a function of prey density (Types I, II, III)
Metapopulation	Network of subpopulations connected by dispersal; local extinction balanced by recolonisation
Source-sink dynamics	Source patches ($\lambda > 1$) sustain sink patches ($\lambda < 1$) via emigration
Mark-recapture	Method for estimating population size using marked individuals
Reproductive value (v_x)	Expected future contribution of age- x individual to population growth
Demographic transition	Shift from high birth/death rates to low birth/death rates during development
Theta-logistic model	Extension of logistic growth with flexible density-dependence exponent θ
Survivorship curve	Plot of proportion surviving (l_x) vs. age; Types I (late loss), II (constant), III (early loss)
Leslie matrix	Age-structured projection matrix; dominant eigenvalue = λ_1
Sensitivity / Elasticity	$\partial\lambda_1/\partial a_{ij}$ (absolute) and proportional analog; identify highest-leverage rate
Stable age distribution	Right eigenvector of Leslie matrix; long-run age proportions
Individual-based model (IBM)	Stochastic simulation tracking each organism; captures demographic stochasticity and heterogeneity
Population viability analysis (PVA)	Stochastic projection of extinction probability over a fixed horizon
Quasi-extinction threshold	N_{crit} below which a population is treated as functionally extinct in PVA

36.18 Review Questions

1. A whale population has $R_0 = 0.95$ and $T = 20$ years. Estimate r . Is this population growing or declining? Calculate how many years until the population halves. What conservation interventions could change the trajectory?
2. Explain why maximum sustainable yield $MSY = rK/4$. A fisheries manager observes that the current catch equals MSY but the population continues to decline. Identify at least three reasons why this might occur despite apparently sustainable harvest levels.
3. A large predator population is reintroduced into a prey-depleted ecosystem with 40 prey individuals remaining. The predator's Allee threshold is $A = 100$. Quantitatively predict whether the predator population will recover. What two conditions must simultaneously be met for recovery?
4. Two grass species compete: $\alpha_{12} = 0.8$, $\alpha_{21} = 0.7$, $K_1 = 1000$, $K_2 = 900$. Use phase-plane analysis to determine whether stable coexistence, competitive exclusion, or priority effect is predicted. Show your work by comparing isocline intercepts.
5. Compare the lynx-hare cycle with a simple Lotka-Volterra prediction. What additional factors (beyond α , β , δ , γ parameters) are needed to explain the observed 10-year periodicity? Cite at least one primary study.
6. A metapopulation of a rare butterfly occupies 25 of 100 available habitat patches. The colonization rate is $c = 0.15$ and extinction rate is $e = 0.05$. (a) Calculate the expected equilibrium occupancy. (b) A highway project will destroy 30 patches. Will the metapopulation persist? (c) What colonization rate would be needed to maintain the same equilibrium occupancy after the loss, with 70 patches remaining?
7. You capture 200 salamanders from a pond, mark them, and release them. Two weeks later, you capture 250 salamanders and find that 40 are marked. (a) Estimate the population size using the Lincoln-Petersen method. (b) List three assumptions of this method and describe how violating each would bias your estimate.
8. Using the concept of reproductive value, explain why protecting adult female sea turtles (through Turtle Excluder Devices in fishing nets) is more effective for population recovery than protecting eggs on nesting beaches.
9. Japan has a current population of 125 million and $r \approx -0.006/\text{yr}$. Assuming constant r , project the population in 2050, 2075, and 2100. What demographic, economic, and social challenges does population decline create?
10. The St. Matthew Island reindeer population grew from 29 to 6,000 in 19 years, then crashed to 42. (a) Calculate r during the growth phase. (b) What caused the crash in ecological terms? (c) How does this case study illustrate the limitations of exponential growth models?
11. From `logistic_growth`, read off $N(t)$ near $K/2$ and relate to MSY management targets.
12. When does the Levins metapopulation model $\hat{p} = 1 - e/c$ predict rescue vs. extinction?

13. A 4-stage Leslie matrix yields elasticities $e_{F_3} = 0.08$ (adult fecundity), $e_{P_1} = 0.32$ (juvenile→subadult survival), $e_{P_2} = 0.34$ (subadult→adult survival), $e_{P_3} = 0.26$ (adult survival). A wildlife agency proposes (i) doubling clutch size via supplemental feeding or (ii) a 5% absolute increase in subadult survival. Which delivers more growth, and what does the elasticity comparison imply about the limits of headcount-centered conservation?
14. Explain why an individual-based model and a deterministic Leslie matrix model can give the same λ_1 yet completely different extinction predictions for a small population. Under what conditions do the two approaches converge?
15. Sketch the workflow of a PVA for a critically endangered amphibian: (a) what data must be collected, (b) how is the quasi-extinction threshold N_{crit} chosen, (c) why are *relative* comparisons across management scenarios more defensible than absolute extinction probabilities?

36.19 Further Reading and Source Notes: Population Ecology and Growth Models

• Lotka (1925). *Elements of Physical Biology*. Williams & Wilkins.

• Volterra (1926). Variazioni e fluttuazioni del numero d'individui in specie animali conviventi. *Memorie dell'Accademia dei Lincei*, 2.

• Verhulst (1838). Notice sur la loi que la population poursuit dans son accroissement. *Correspondance Math{e}matique et Physique*, 10.

• Allee (1931). *Animal Aggregations: A Study in General Sociology*. University of Chicago Press.

• Holling (1959). Some characteristics of simple types of predation and parasitism. *Canadian Entomologist*, 91.

• MacArthur & Wilson (1967). *The Theory of Island biogeography*. Princeton University Press.

36.20 Computational Bridge

Logistic time series are integrated deterministically:

```
from biology.ecology import logistic_growth

ser = logistic_growth(N0=40.0, r=0.2, K=500.0, t_end=60.0, steps=240)
print(round(ser.populations[-1], 2))
```

Clinical / systems note: Harvest models for fisheries and forest stands reuse the same r , K , and MSY logic; collapse usually means $F > F_{\text{MSY}}$ for too long.

36.21 Summary

• Demographics: $r = b - d$; $R_0 = \sum l_x m_x$; doubling time $= \ln 2/r$; generation time $T = \sum x \cdot l_x m_x / R_0$. Euler-Lotka equation provides exact relationship.

• Dispersion patterns: clumped (most common), uniform, random — detected by variance-to-mean ratio.

• Survivorship curves: Type I (late loss, K-selected), Type II (constant), Type III (early loss, r-selected). Gompertz law for human mortality.

• Logistic growth: $dN/dt = rN(1 - N/K)$; inflection at $K/2$; $\text{MSY} = rK/4$. Extensions: theta-logistic, time-lagged logistic.

• Allee effect: $dN/dt < 0$ below threshold A ; threatens small surviving populations. Component vs. demographic Allee effects.

• LV competition: stable coexistence requires niche differentiation ($\alpha_{12}\alpha_{21} < 1$); otherwise exclusion or priority effects. Chesson's theory: stabilizing + equalising mechanisms.

• LV predator-prey: neutral oscillations; period $\approx 2\pi/\sqrt{\alpha\gamma}$; lynx-hare 10-yr cycle requires tri-trophic explanation.

• Functional responses: Type I (linear), Type II (decelerating, Holling disc equation), Type III (sigmoidal, stabilizing).

• Age-structured models: Leslie matrix L with fecundities on top row and survivorships on sub-diagonal; dominant eigenvalue $\lambda_1 =$ asymptotic growth rate; right and left eigenvectors give stable age distribution and reproductive value. Sensitivity $s_{ij} = \partial\lambda_1/\partial a_{ij}$ and elasticity e_{ij} identify highest-leverage demographic rates (loggerhead turtle adult survival → TEDs).

• Individual-based models (IBMs): stochastic agent-based simulations capture demographic stochasticity, individual heterogeneity, and emergent dynamics that mean-field models miss.

• Population viability analysis (PVA): integrates matrix and stochastic machinery into extinction-probability forecasts; quasi-extinction threshold N_{crit} ; empirical MVPs cluster at 5,000–7,000 adults (Reed et al. 2003), well above the classical $N_e = 500$ rule.

• r vs. K continuum: life-history trade-offs shaped by habitat stability; superseded by Stearns' and Grime's frameworks; bet-hedging in variable environments.

• Metapopulations: Levins model ($\hat{p} = 1 - e/c$); source-sink dynamics; rescue effect. Habitat corridors increase connectivity.

• Population estimation: mark-recapture (Lincoln-Petersen, Jolly-Seber), distance sampling.

• Human demographics: 8 billion (2022); demographic transition; population momentum; TFR declining globally.

- Connections: See section 37 for species interactions, section 20 for allele frequencies in subdivided populations, and Unit VI — Evolution: Introduction for life-history evolution.

36.22 Companion Source Module: Population Ecology and Growth Models

Population Ecology and Growth Models should leave a reproducible trail from a biological claim to the code, figure, diagram, or paper-based activity that can test it. Use the surfaces below to inspect the chapter’s assumptions, rerun the relevant model, or compare the manuscript explanation with companion labs and figures.

Table 432. Companion source surfaces for Population Ecology and Growth Models.

Surface	Use it for
src/biology/ecology/ecology.py (exponential_growth, logistic_growth, allee_strong_growth)	Reproduce density-independent, density-dependent, and Allee-effect scenarios.
src/visualization/plots.py (plot_logistic_growth)	Inspect carrying capacity and growth-rate assumptions.
src/mermaid/biology_diagrams.py (population_growth_stages_diagram)	Link model phases to visual summaries.

Reproducibility check: state time step, units, density dependence, stochasticity, and management objective before forecasting a population. Cross-reference: compare with section 20 and sections 37 and 38.

37 Community Interactions and Succession

Level 2/3 · 45 min read · 55 min lecture · Prerequisites: section 36

37.1 Learning Objectives

By the end of this chapter, you should be able to:

1. Define a community and categorize the six types of biotic interactions with examples.
2. Apply Lotka-Volterra competition equations to predict competitive outcomes and explain the competitive exclusion principle and niche theory.
3. Explain trophic cascades and keystone [Paine, 1966] species with quantitative examples.
4. Compare primary and secondary succession and explain the intermediate disturbance [Connell, 1978] hypothesis.
5. Calculate Shannon diversity (H'), Simpson index, and species evenness and explain what each measures.
6. Apply island biogeography theory, the species-area relationship, and SLOSS debate to conservation design.
7. Describe the role of disturbance, facilitation, and alternative stable states in shaping communities.
8. Explain food web topology, connectance, network robustness, and the relationship between complexity and stability.
9. Compare niche-based and neutral theories of biodiversity, and explain when each null model is appropriate.
10. Use functional traits (CSR strategies, leaf economics spectrum) to predict community assembly and ecosystem function beyond species lists.
11. Distinguish classical, augmentative, and conservation biological control, and evaluate their risk profiles using community ecology principles.

37.1.1 Study Blueprint

- Big idea: Communities are structured by pairwise species interactions and successional change.
- Core concepts: competition, predation, mutualism, succession.
- Framework alignment: Vision & Change: Systems, Evolution, Pathways and transformations of energy and matter; AP Biology: Systems Interactions, Evolution, Energetics; NGSS-style topics: Interdependent Relationships in Ecosystems, Matter and Energy in Organisms and Ecosystems, Natural Selection and Evolution.
- Model or quantitative lens: Lotka-Volterra-style interaction reasoning.
- Data skill: Interpret abundance, interaction, or disturbance data from communities.
- Practice cadence: Representing and Describing Data, Statistical Tests and Data Analysis, Argumentation.
- Common misconception to repair: A species interaction is not permanently good or bad; the sign can change with context.
- Primary lab: Lab — Community Interactions and Succession.
- Question bank: Questions — Community Interactions and Succession.
- Transfer task: Transfer interaction reasoning to restoration, agriculture, and invasion biology.
- Bridge to computation: biology.ecology.ecology.biodiversity_indices.

Opening Vignette — How Wolves Changed Rivers

In 1995, 14 gray wolves were reintroduced to Yellowstone National Park after a 70-year absence. What happened next has become one of ecology’s most vivid demonstrations of a trophic cascade. With predators back, elk avoided grazing in valleys and riverside areas where they were vulnerable. Vegetation in those areas — willows, aspens, cottonwoods — rebounded within years. With trees stabilizing river banks, erosion slowed. Beaver colonies, dependent on willows, increased sixfold. Beaver dams created wetlands that supported fish, otters, ducks, and amphibians. River channels narrowed and meandered, becoming more complex. The wolves, through fear alone — the “landscape of fear” effect documented by William Ripple — had changed the physical geography of the park. The Yellowstone study has been cited thousands of times, popularised by a viral YouTube video with 40 million views, and debated (some effects took decades to show). But it remains the canonical example that removing or restoring apex predators cascades through every trophic level of a community.

37.1.2 Chapter Roadmap for Interaction Networks and Biodiversity Metrics

This is a long chapter that covers eight closely-related but distinguishable topics. Read it as *two halves*:

- Part A — Local interactions between species: what happens when two or a few species meet. The chapter begins with community definitions, then develops competition, predation and trophic cascades, mutualism, and parasitism.
- Part B — Community-scale patterns and assembly: what emerges when you scale up. Succession, diversity measurement, island biogeography, and food-web network structure become the organizing themes.

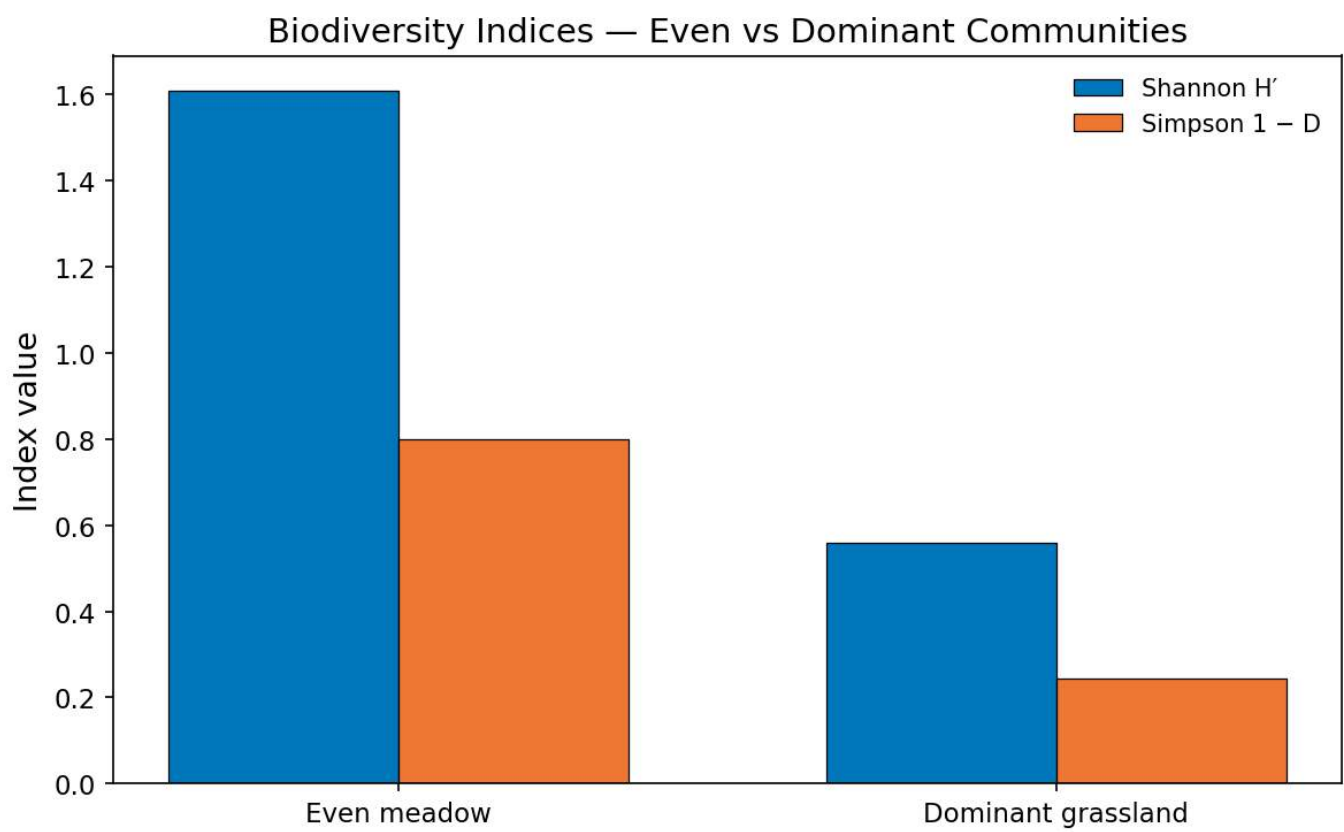


Figure 222. Shannon H' and Simpson $1 - D$ for two communities with the same species richness but different evenness. Higher evenness raises both indices relative to a skewed dominance distribution dominated by one grassland species.

- Part C — Process-level theory and applications: neutral theory supplies a null model for biodiversity; trait-based ecology (CSR, leaf economics) predicts ecosystem function; biological control applies the entire chapter to pests and disease vectors.

If you are reading for a one-semester survey, Part A supplies the mechanistic vocabulary and Part B supplies the integrative patterns. Part C provides the modern frameworks and applied translations. Instructors wanting to split the chapter over two lectures can use the Part-A/Part-B boundary; a third lecture can cover Part C.

37.2 Community Structure, Interaction Strength, and Scale

An ecological community is an assemblage of populations of different species occupying the same region and time, interacting with each other and their abiotic environment. Community ecology analyses the biotic interactions among species and their effects on community structure — species composition and relative abundance — as well as the processes driving community assembly and succession.

37.2.1 Emergent Properties of Communities

Communities possess properties that cannot be predicted from studying individual species in isolation:

Table 433. Emergent Properties of Communities: Property and Definition.

Property	Definition	Measurement
Species richness (<i>S</i>)	Number of species present	Count of unique species
Species evenness	How equal are species abundances?	Pielou's <i>J'</i>
Diversity	Combined richness and evenness	Shannon <i>H'</i> , Simpson $1 - D$
Community structure	Food web topology, trophic levels, functional groups	Network analysis, connectance
Resistance	Ability to withstand perturbation without change	Deviation from baseline after disturbance
Resilience	Speed of return to baseline after perturbation	Recovery time
Rank-abundance distribution	Pattern of relative abundance across species	Log-normal, geometric series, broken stick

37.2.2 Rank-Abundance Models

The distribution of individuals among species in a community follows predictable patterns:

Table 434. Rank-Abundance Models: Model and Pattern.

Model	Pattern	Interpretation	Typical community
Geometric series	Steep, convex	Strong dominance; niche pre-emption	Species-poor, harsh environments
Log-series	Moderate slope	Many rare species, few common	Island faunas, successional communities
Log-normal	Moderate, symmetric bell curve on log scale	Most natural communities	Large, undisturbed communities
Broken stick	Shallow, even	Resources divided equally	Species-poor, saturated communities

Preston's canonical log-normal (1962): In most large communities, when species are binned by abundance in octaves (doublings), the distribution is approximately log-normal. This has deep connections to the species-area relationship (figure 236) and to predator–prey oscillations (figure 219).

37.2.3 Types of Biotic Interactions

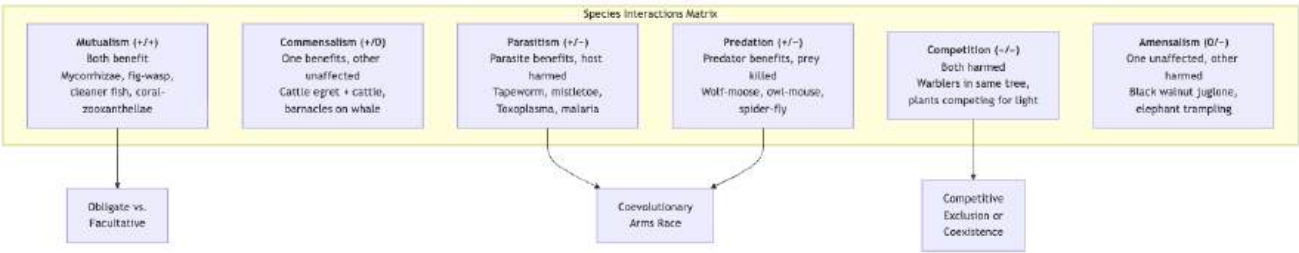


Figure 223. Biotic interactions classify fitness effects on participants: mutualism benefits both, parasitism and predation benefit one at a cost to another, and competition harms both.

Table 435. Types of Biotic Interactions: Interaction and Species A effect.

Interaction	Species A effect	Species B effect	Mechanism	Example
Mutualism (+/+)	Benefits	Benefits	Direct reciprocal benefit	Mycorrhizae (+plant, +fungus); fig-wasp pollination; bee pollination; ant-plant seed dispersal
Commensalism (+/0)	Benefits	Neutral	One benefits, other unaffected	Cattle egret + cattle (cattle disturb insects); barnacles on whale
Parasitism (+/-)	Benefits (parasite)	Harmed (host)	Partial exploitation; usually not lethal	Tapeworm + human; mistletoe + tree; Toxoplasma + rodent
Predation (+/-)	Benefits (predator)	Harmed (prey)	Prey consumed; drives prey adaptation	Wolf + moose; Daphnia + phytoplankton
Competition (-/-)	Harmed	Harmed	Shared resource demand	Two warbler species in same niche; plants competing for light
Amensalism (0/-)	Neutral	Harmed	Inhibitory compounds; physical suppression	Juglone from black walnut; biofilm quorum quenching

Concept Check: A remora fish attaches to a shark, feeding on scraps from the shark’s meals. Is this mutualism, commensalism, or parasitism? What additional information would you need to determine the exact interaction type?

37.3 Competition Theory and Coexistence Mechanisms

37.3.1 Lotka-Volterra Interspecific Competition

Two competing species N_1 and N_2 with shared resources are modeled by:

$$\frac{dN_1}{dt} = r_1N_1 \left(1 - \frac{N_1 + \alpha_{12}N_2}{K_1} \right) \tag{441}$$

$$\frac{dN_2}{dt} = r_2N_2 \left(1 - \frac{N_2 + \alpha_{21}N_1}{K_2} \right) \tag{442}$$

where: - α_{12} = competitive effect of species 2 on species 1 (per individual) - α_{21} = competitive effect of species 1 on species 2 - K_1, K_2 = carrying capacities of each species

Isocline analysis: Four outcomes depending on isocline intersections: 1. Species 1 wins: $K_1 > K_2/\alpha_{12}$ AND $K_1/\alpha_{21} > K_2$ 2. Species 2 wins: $K_2 > K_1/\alpha_{21}$ AND $K_2/\alpha_{12} > K_1$ (symmetric case) 3. Unstable equilibrium (priority effect): $K_1 > K_2/\alpha_{12}$ AND $K_2 > K_1/\alpha_{21}$ — whoever starts higher wins 4. Stable coexistence: $K_1 < K_2/\alpha_{12}$ AND $K_2 < K_1/\alpha_{21}$ — interspecific competition weaker than intraspecific

37.3.2 Competitive Exclusion Principle (Gause’s Law)

Gause [1934]: Two species competing for the same limiting resource cannot stably coexist; the superior competitor excludes the other. Demonstrated with *Paramecium aurelia* vs. *P. caudatum* grown together on a single bacterial food source — *P. aurelia* consistently drove *P. caudatum* to extinction within 20 days.

Important qualifications: Competitive exclusion requires (1) complete niche overlap, (2) constant environment, (3) no spatial refugia, and (4) sufficient time. In nature, these conditions are rarely fully met.

37.3.3 Hutchinson’s Niche Concept

Fundamental niche [**Hutchinson, 1957**]: the n-dimensional hypervolume of environmental conditions and resources permitting a species to maintain $r \geq 0$.
Realized niche: the subset of the fundamental niche actually occupied after accounting for interspecific competition, predation, and other biotic interactions. Typically smaller than or equal to the fundamental niche.

$$\text{Realised niche} = \text{Fundamental niche} - \text{Competitive exclusion zone} \tag{443}$$

Hutchinson’s paradox of the plankton (1961): Why do hundreds of phytoplankton species coexist in the apparently homogeneous water column, most competing for the same light and nutrients? Violates competitive exclusion. Solutions:

- 1. Temporal niche partitioning — seasonal turnover, disturbance prevents equilibrium
- 2. Spatial heterogeneity — microscale gradients in light, nutrients, turbulence
- 3. Predation (selective grazing) — zooplankton preferentially graze **dominant** species
- 4. Allelopathy — chemical warfare among phytoplankton
- 5. Non-equilibrium dynamics — the system rarely reaches competitive exclusion

37.3.4 Modern Coexistence Theory [**Chesson, 2000**]

Coexistence requires that intraspecific competition > interspecific competition for both species. This is enabled by two classes of mechanisms:

Stabilizing mechanisms (niche differences): - Resource partitioning: different foods, microhabitats, activity times - Janzen-Connell effect: species-specific enemies concentrate near conspecifics, giving heterospecifics an advantage - Storage effect: temporal environmental variation favors different species at different times; long-lived adults “store” good years - Relative nonlinearity: species respond differently to resource fluctuations

Equalising mechanisms (fitness similarity): - Trade-offs between competitive ability and other traits (dispersal, stress tolerance) - Similar per-capita growth rates at low density

The mathematical condition for coexistence is:

$$\rho < \frac{\kappa_j}{\kappa_i} < \frac{1}{\rho}$$

(444)

where ρ = niche overlap (0 to 1) and κ_i/κ_j = fitness ratio. Lower ρ (more niche differentiation) allows greater fitness inequality.

```
from biology.ecology.ecology import lotka_volterra

result = lotka_volterra(
    N1_0=100, N2_0=100,
    r1=0.5, r2=0.5,
    K1=500, K2=500,
    alpha12=0.6, # species 2 slightly suppresses species 1
    alpha21=0.8, # species 1 strongly suppresses species 2
    t_end=100
)

print(f"Final N1: {result.N1[-1]:.0f}, N2: {result.N2[-1]:.0f}")
# Expected: species 1 wins (lower alpha12 means less impact from competitor)
```

Clinical Connection — Competitive Exclusion in the **Microbiome**: The competitive exclusion principle operates within the human gut microbiome. Clostridium difficile infection (CDI) typically occurs after antibiotic treatment eliminates normal gut flora, removing competitive exclusion and allowing *C. difficile* to proliferate unopposed. Fecal **microbiota** transplantation (FMT) restores competitive exclusion by reintroducing a diverse microbial community, achieving about 90% cure rates for recurrent CDI. This is Gause’s principle applied to clinical medicine.

Concept Check: Two species of Paramecium (*P. aurelia* and *P. bursaria*) coexist in the same pond. *P. aurelia* feeds on bacteria in open water; *P. bursaria* harbors symbiotic algae and feeds near the bottom. Explain their coexistence using Chesson’s framework: what is the stabilizing mechanism?

37.4Predation, Keystone Species, and Trophic Cascades

37.4.1Predator-Prey Arms Races

Coevolution [Ehrlich and Raven, 1964] between predators and prey drives a Red Queen dynamic of escalating adaptations:

Anti-predator defenses:

Table 436. Predator-Prey Arms Races: Strategy and Mechanism.

Strategy	Mechanism	Example
Crypsis	Match background appearance	<i>Biston betularia</i> (peppered moth) — industrial melanism
Aposematism	Bright warning colors advertise toxicity	Poison dart frogs (<i>Dendrobates</i>) — alkaloid warning
Mullerian mimicry	Two toxic species converge on same warning signal	<i>Heliconius</i> butterflies sharing wing patterns
Batesian mimicry	Palatable species mimics toxic model	Viceroy (<i>Limenitis archippus</i>) mimics monarch
Chemical defense	Toxic compounds deter predators	Monarch butterflies sequester cardenolide glycosides
Startle display	Sudden reveal of eyespots or bright colors	Io moth (<i>Automeris io</i>) eyespot flash
Behavioral	Alarm calls, mobbing, confusion effect	Starling murmurations confuse raptors
Morphological	Spines, shells, armour	Porcupine quills; turtle shells; hedgehog spines

Counter-adaptations in predators: - Kingsnakes (*Lampropeltis*) evolved resistance to rattlesnake venom - Rough-skinned newt (*Taricha granulosa*) vs. garter snake (*Thamnophis sirtalis*): escalating toxin (tetrodotoxin) and resistance — one of the best-documented coevolutionary arms races [Brodie and Brodie, 1999] - Cuckoo (*Cuculus canorus*) egg mimicry vs. host egg discrimination — classic parasitic arms race

37.4.2 Hare-Lynx Cycle

Lepus americanus (snowshoe hare) and *Lynx canadensis* show coupled about 10-year population cycles in boreal Canada. Hudson’s Bay Company fur trading records from 1736-1940 reveal the cycle. Modern analysis:

$$\frac{dH}{dt} = r_{max}H - aPH \qquad \frac{dP}{dt} = b \cdot a \cdot P \cdot H - dP$$

(445)

The cycle is driven by multiple feedback loops: 1. Predation (about 60% of cycle) — lynx consumption drives hare decline 2. Food quality (about 20%) — hare overgrazing induces phenolic toughening of willow/birch browse 3. Stress physiology (about 20%) — predation risk elevates cortisol, suppressing reproduction 4. True cycles require tri-trophic feedbacks; purely Lotka-Volterra predation alone is insufficient (Krebs et al. 2001, *Science*)

37.4.3 Keystone Species and Disproportionate Community Effects

A keystone species (Paine 1966, 1969) has disproportionately large effects on community structure relative to its abundance. Removal of the keystone causes dramatic community reorganisation.

Types of keystone effects:

Table 437. Keystone Species and Disproportionate Community Effects: Type and Mechanism.

Type	Mechanism	Example
Keystone predator	Prevents competitive exclusion by suppressing dominant prey	<i>Pisaster ochraceus</i> (sea star) → prevents mussel monopoly
Keystone herbivore	Controls dominant plant, maintaining diversity	African elephant → prevents woodland encroachment on savanna
Keystone mutualist	Supports many other species through interaction network	Fig trees → fruit for 1,200+ vertebrate species in tropical forests
Ecosystem engineer	Physically modifies habitat	Beaver dams create wetland habitat; termite mounds and ant nests redistribute soil and nutrients

37.4.4 Trophic Cascades Across Food-Web Levels

A trophic cascade occurs when changes at one trophic level ripple through the food web to affect non-adjacent levels:

Top-down cascade (predator-driven): - Sea otter → sea urchin → kelp cascade [Estes and Palmisano, 1974] - Wolf → elk → willow cascade in Yellowstone [Ripple and Beschta, 2012a]

Bottom-up cascade (resource-driven): - Nutrient enrichment → phytoplankton → zooplankton → fish

Quantitative trophic cascade — Sea Otter example: - 1 sea otter consumes about 10 kg sea urchin/day - Each urchin removed protects about 1 m² of kelp - Kelp productivity: about 300 g C/m²/yr - Therefore: 1 otter → about 3,650 m² kelp protected → about 1,095 kg C/yr sequestered - Kelp forests also attenuate wave energy by 60-70%, providing coastal protection valued at about \$10,000/km/yr

Mesopredator release: removal of apex predators → explosion of medium-sized predators → disproportionate prey decline. Example: coyote increase after wolf removal → ground-nesting bird decline in North America.

Clinical Connection — Trophic Cascades and Lyme Disease: The decline of apex predators in eastern North America has contributed to a trophic cascade affecting human health. Wolf and cougar removal → deer population explosion → increased tick-deer encounters → increased *Borrelia burgdorferi* transmission → Lyme disease incidence increased 25-fold from 1990 to 2020 in the northeastern USA. Deer also browse forest understory, reducing small mammal habitat diversity, which concentrates ticks on the most competent reservoir hosts (white-footed mice), further amplifying transmission. Predator restoration could reduce disease burden — a health-relevant trophic cascade.

Concept Check: In Yellowstone, wolves primarily cause a “behavioral trophic cascade” rather than a purely numerical one. What is the difference? How does the “landscape of fear” concept explain why elk behavior change (avoiding riverbanks) may be more important than elk population reduction?

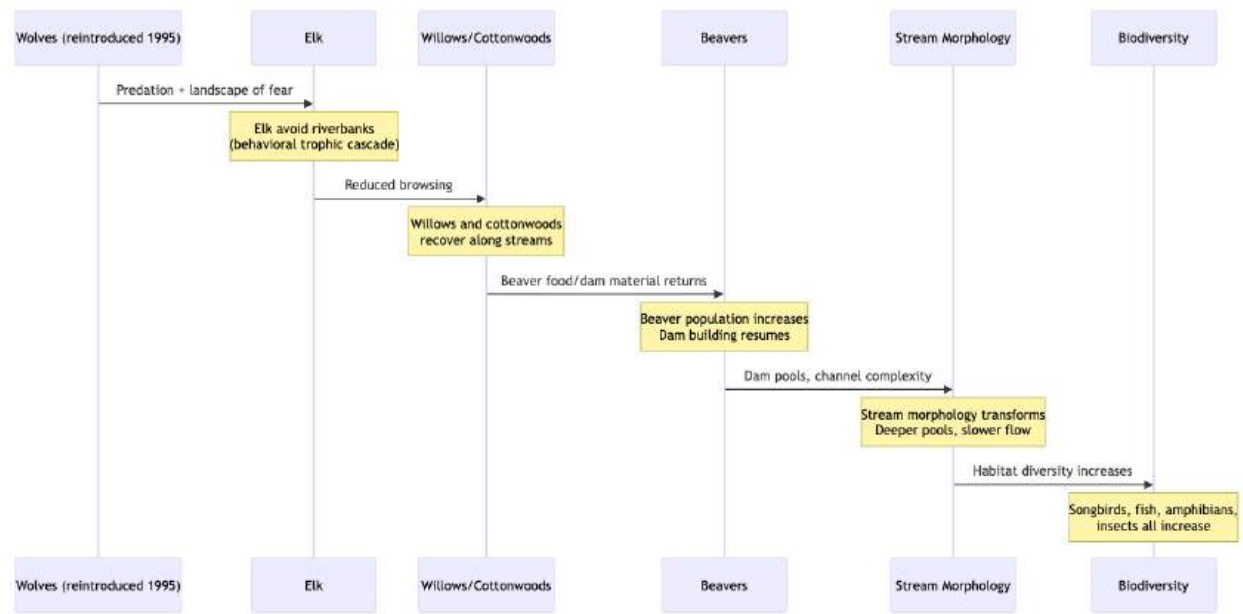


Figure 224. Trophic cascades track indirect effects: predator recovery can reduce herbivory, allowing plant communities and ecosystem engineers to rebound.

37.5 Mutualism, Parasitism, and Facilitation

37.5.1 Mutualism and Reciprocal Fitness Benefits

Obligate mutualism: neither partner can survive without the other (e.g., fig-wasp pollination; lichens = fungus + alga/cyanobacterium).

Facultative mutualism: both benefit but can survive independently (e.g., seed-dispersing birds and fruiting trees).

Mycorrhizal networks: - Arbuscular mycorrhizae (AM, Glomeromycota): obligate symbionts; hyphae form arbuscules inside root cortex cells; deliver P and micronutrients; receive up to 30% of plant photosynthate; present in about 80% of land plant species - Ectomycorrhizae (EM, Basidiomycota + Ascomycota): hyphae form Hartig net around root cells; dominant in temperate/boreal forests (*Pinus*, *Betula*, *Fagus*); provide N via proteolytic enzymes - Common mycorrhizal networks (CMNs) — “Wood Wide Web”: CMNs transfer carbon, water, and nutrient signals between plants of same and different species; large “mother trees” supply carbon to understory seedlings (Simard et al. 1997, *Nature*). Contested: whether transfer is truly adaptive signaling or passive diffusion remains debated (Karst et al. 2023, *Nature Ecology & Evolution*)

37.5.2 Pollination, Myrmecochory, and Ant-Plant Mutualisms

Plant-pollinator mutualisms are reciprocal but not symmetric. Flowers pay carbon and nutrient costs to produce nectar, pollen, scent, color, and shape; pollinators receive food while moving gametes among plants. IPBES treats animal pollination as both biodiversity process and food-system service, and crop syntheses show that wild pollinators can increase fruit set even where managed honey bees are present [IPBES, 2016, Garibaldi et al., 2013]. In network terms, a generalist bee can be a hub, while a specialist plant may be vulnerable if its few effective visitors decline.

Ant-plant mutualisms span defense, nutrition, and dispersal. Some plants feed or house defensive ants in domatia or extrafloral nectaries; the ants reduce herbivory but may also deter other visitors, so the net sign depends on context. In myrmecochory, ants carry elaiosome-bearing seeds, consume the reward, and discard the seed in protected or nutrient-enriched microsites. This creates a dispersal mutualism in which the plant gains directed movement and the ant colony gains food [Lengyel et al., 2009]. These examples are useful because they show mutualism as a measured fitness balance, not a sentimental label.

37.5.3 Parasitism and Disease Ecology

Parasites regulate host populations and can function as keystone species:

Table 438. Parasitism and Disease Ecology: Parasite type and Example.

Parasite type	Example	Ecological effect
Macroparasite	Intestinal helminths, ticks, lice	Reduce host fitness; can regulate population size

Parasite type	Example	Ecological effect
Microparasite	<i>Batrachochytrium dendrobatidis</i> (Bd)	Chytrid fungus: >90 amphibian species extinctions since 1970
Parasitoid	<i>Cotesia glomerata</i> (braconid wasp)	Lays eggs inside caterpillars; larvae consume host
Social parasite	Cuckoo (<i>Cuculus canorus</i>)	Brood parasitism; reduces host reproductive output
Manipulative parasite	<i>Toxoplasma gondii</i>	Alters rodent behavior (decreased fear of cats) to facilitate transmission

The parasite-mediated competition hypothesis: parasites can determine competitive outcomes between host species, effectively functioning as “hidden” keystone species.

37.5.4 Facilitation and Positive Species Interactions

Facilitation occurs when one species improves the survival or reproduction of another. Unlike mutualism, facilitation can be unidirectional:

- Nurse plants in deserts: cacti establish under the shade of nurse shrubs (*Larrea*, *Ambrosia*)
- Foundation species: create habitat structure (e.g., corals, kelp, *Spartina* grass in salt marshes)
- Nitrogen fixers: *Lupinus* colonises volcanic substrates, enriching soil N for later successional species (Mount St. Helens **primary succession**)

Concept Check: The relationship between clownfish and sea anemones is often described as mutualism. The clownfish gains protection from predators; the anemone may benefit from clownfish defending against butterfly fish that eat anemone tentacles. How would you design an experiment to determine whether this interaction is truly mutualism (+/+) or commensalism (+/0)?

37.6 Ecological Succession and Community Assembly Over Time

Succession = directional, generally predictable change in community composition over time after disturbance or on newly available substrate.

Contemporary succession ecology is less deterministic than the classical “march to climax” story. Recovery trajectories depend on surviving legacies, seed banks, dispersal corridors, disturbance severity, herbivory, invasive species, soil microbes, and climate conditions during recovery. The practical question is not only which stage comes next, but which intervention would change the trajectory: protecting refuges, adding propagules, removing barriers, or accepting a novel stable state.

Table 439. Facilitation and Positive Species Interactions: Feature and Primary succession.

Feature	Primary succession	Secondary succession
Starting substrate	Bare rock/sterile substrate (no soil)	Disturbed community with soil intact
Typical rate	Centuries to millennia	Decades to centuries
Pioneer species	Cyanobacteria, lichens, mosses	Annual weeds, grasses
Soil development	Must form from scratch (weathering + organic accumulation)	Already present; seed bank may survive
Example	Krakatoa (1883); Surtsey, Iceland (1963); Mount St. Helens (1980)	Old-field succession (abandoned farmland); post-fire forest regrowth

37.6.1 Mechanisms of Succession

Connell and Slatyer [1977] proposed three mechanisms:

Table 440. Mechanisms of Succession: Model and Mechanism.

Model	Mechanism	Example
Facilitation	Early species modify environment to favor later species	Nitrogen-fixing <i>Alnus</i> (alder) enriches soil, enabling spruce colonization (Glacier Bay, Alaska)
Tolerance	Later species can establish regardless of early species but grow more slowly	Shade-tolerant species slowly replace shade-intolerant pioneers
Inhibition	Early colonists resist replacement; succession proceeds primarily when pioneers die	<i>Cladonia</i> lichen crusts inhibit vascular plant establishment on sand dunes

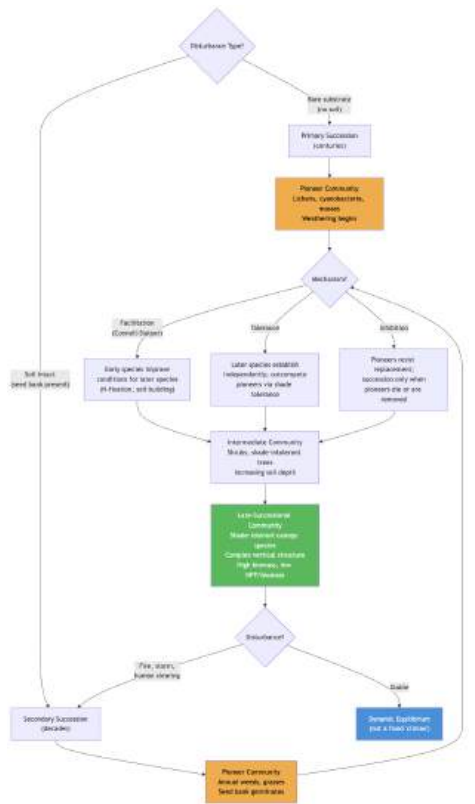


Figure 225. Ecological succession pathways. Primary succession begins on bare substrate and takes centuries; secondary succession begins with intact soil and proceeds in decades. Three mechanisms (facilitation, tolerance, inhibition) operate at transition points. Modern ecology views the endpoint as a dynamic equilibrium rather than a fixed climax state.

In reality, most successional sequences involve the three mechanisms operating simultaneously at different stages and spatial scales.

37.6.2 Climax Community Concept

Classical view [Clements, 1916]: Succession proceeds toward a single, deterministic climax community determined by regional climate (the “organismal” model — community as superorganism).

Modern view (Gleason 1926; Whittaker 1953): Communities are assemblages of individually distributed species (the “individualistic” model). Multiple stable endpoints possible; disturbance history, stochastic colonization, and priority effects most influence trajectory. The concept of a single climax is largely abandoned.

37.6.3 Intermediate Disturbance Hypothesis (IDH)

Connell (1978): Communities at intermediate levels of disturbance frequency and intensity show maximum species diversity:

- Low disturbance → competitive exclusion → low diversity (dominant competitor wins)
- High disturbance → primarily r-selected pioneers survive → low diversity
- Intermediate → prevents competitive dominance while enabling diverse colonization

$$H' = f(\text{disturbance frequency, intensity})$$

(446)

Evidence: Coral reefs, tropical forests, stream invertebrate communities — moderate disturbance (hurricanes, floods, fires) increases diversity.

Criticisms: The IDH has been challenged as overly simplistic (Fox 2013, *Ecology*). Some communities show monotonic diversity-disturbance relationships. The hypothesis also assumes a competition-colonization trade-off that is not comprehensive.

37.6.4 Alternative Stable States and Regime Shifts

Alternative stable states (Lewontin 1969; Scheffer et al. 2001): Some ecosystems can exist in multiple stable configurations under the same environmental conditions. Transitions between states (regime shifts) can be triggered by small perturbations near tipping points:

Table 441. Alternative Stable States and Regime Shifts: System and State 1.

System	State 1	State 2	Tipping mechanism
Shallow lake	Clear water (macrophytes dominant)	Turbid (algal bloom)	Nutrient loading exceeds P threshold
Coral reef	Coral dominated	Macroalgae dominated	Overfishing of herbivorous fish
Savanna	Grassland with scattered trees	Closed-canopy forest	Fire suppression
Arctic	Perennial sea ice	Seasonal/ice-free	Ocean warming threshold

Early warning signals of approaching tipping points: - Increased temporal variance (flickering) - Critical slowing down — recovery from perturbation becomes slower - Increased spatial correlation - Skewed distribution of system state

These early warning indicators are being applied to monitor reef, lake, and climate system stability.

Clinical Connection — Microbiome Regime Shifts: The human gut microbiome exhibits alternative stable states analogous to ecological regime shifts. A healthy, diverse microbiome represents one stable state. Antibiotic treatment or *C. difficile* infection can trigger a regime shift to an impoverished, pathogenic state. Once established, the unhealthy state resists return to the diverse state (hysteresis) — explaining why probiotics alone are often insufficient and why fecal microbiota transplantation (which provides a complete microbial community) is more effective.

Concept Check: After the 1980 eruption of Mount St. Helens, ecologists observed primary succession proceeding much faster than predicted. Surviving pocket gophers, ants, and lupine plants in patches of surviving soil created nuclei of rapid recovery. Which successional mechanism(s) does this illustrate, and why does it challenge Clements' classical model?

37.7 Measuring Biodiversity Across Alpha, Beta, and Gamma Scales

37.7.1 Alpha, Beta, and Gamma Diversity

Whittaker [1960] distinguished three scales of diversity:

These scales also clarify what modern biodiversity tools can and cannot show. Environmental DNA, acoustic monitoring, camera traps, remote sensing, and citizen-science records can reveal turnover across space faster than classical plots alone, but each method has detection bias, taxonomic gaps, and scale limits. A credible diversity comparison states the sampling unit, detection method, taxonomic resolution, and whether the result is richness, evenness, composition, or functional change.

Table 442. Alpha, Beta, and Gamma Diversity: Scale and Definition.

Scale	Definition	Metric
Alpha (α) diversity	Species richness within a single community/habitat	H' , Simpson's, species count
Beta (β) diversity	Turnover in species composition between communities	Jaccard index, Bray-Curtis dissimilarity
Gamma (γ) diversity	Total diversity across most communities in a landscape	$\gamma = \bar{\alpha} \times \beta$ (multiplicative)

37.7.2 Shannon-Wiener Diversity Index (H')

figure 222 contrasts Shannon and Simpson indices for an even meadow versus a dominant-species grassland, illustrating why evenness matters alongside richness.

$$H' = - \sum_{i=1}^S p_i \ln p_i$$

(447)

where p_i = proportion of individuals belonging to species i .

- Range: $H' = 0$ (monoculture) to $H' = \ln(S)$ (perfectly even)
- Sensitive to rare species
- Typical values: 1.5-3.5 for most communities; >4.0 for extremely diverse tropical communities

37.7.3 Simpson Diversity Index ($1 - D$)

$$D = \sum_{i=1}^S p_i^2 \quad \text{Simpson's diversity} = 1 - D$$

(448)

- Range: 0-1; probability that two randomly selected individuals are from different species
- Weighted toward dominant species (less affected by rare species than H')
- Also expressed as reciprocal: Simpson's reciprocal = $1/D$ (effective number of species)

37.7.4 Pielou's Evenness (J')

$$J' = \frac{H'}{\ln S} \in [0, 1]$$

(449)

$J' = 1$ means most species equally abundant; $J' \rightarrow 0$ means dominated by one species.

37.7.5 Worked Example: Shannon Diversity and Evenness

Table 443. Shannon Diversity and Evenness: Species and Abundance.

Species	Abundance	p_i	$p_i \ln p_i$	p_i^2
A	50	0.500	-0.347	0.250
B	30	0.300	-0.361	0.090
C	15	0.150	-0.285	0.023
D	4	0.040	-0.129	0.002
E	1	0.010	-0.046	0.000
Total	100	1.000	-1.167	0.364

$$H' = 1.167; H'_{max} = \ln 5 = 1.609; J' = 1.167/1.609 = 0.725$$

$$\text{Simpson's } D = 0.364; \text{Simpson's diversity} = 1 - 0.364 = 0.636$$

37.7.6 Beta Diversity: Measuring Turnover

Jaccard similarity index:

$$J = \frac{|A \cap B|}{|A \cup B|}$$

(450)

where A and B are species sets from two communities. $J = 1$ means identical composition; $J = 0$ means no shared species.

Bray-Curtis dissimilarity (incorporates abundance):

$$BC = 1 - \frac{2 \sum_i \min(a_i, b_i)}{\sum_i (a_i + b_i)}$$

(451)

```
from biology.ecology.ecology import biodiversity_indices

# Community counts (array of species abundances)
counts = [50, 30, 15, 4, 1] # 5 species; very uneven
result = biodiversity_indices(counts)

print(f"Species richness: {result.species_richness}")
print(f"Shannon H': {result.shannon_index:.3f}")
print(f"Simpson 1-D: {result.simpson_index:.3f}")
print(f"Evenness J': {result.evenness:.3f}")
```

Concept Check: Community X has 4 species with abundances [100, 100, 100, 100]. Community Y has 4 species with abundances [394, 2, 2, 2]. Both have $S = 4$. Calculate H' and J' for each. Which community is more “diverse” and why does evenness matter as much as richness?

37.8 Current Evidence and Frontier Biology: Community Interactions and Succession

For Community Interactions and Succession, frontier biology belongs inside the evidence logic of the chapter. Ecology and conservation decisions increasingly combine field data, remote sensing, community knowledge, model uncertainty, and explicit values. The core reading question is this: community claims should identify interaction type, network position, disturbance regime, and observational limits.

- What to verify: identify the observation, model, assay, or dataset that would make the claim stronger or weaker.
- What to qualify: state the scale, organism, cell type, environmental condition, or population where the claim is expected to hold.
- What to compare: test at least one alternative explanation, baseline, or null model before treating the pattern as causal.
- What to cite: distinguish primary evidence, review synthesis, public dataset, and institutional guidance; for recent or numeric claims, prefer the source closest to the measurement and state what has changed since it was published.

Select biodiversity and conservation metrics by decision need: abundance, interaction, function, risk, service, and governance metrics answer different questions [Intergovernmental Science-Policy Platform on Biodiversity and Ecosystem Services, 2019, 2024, World Wide Fund for Nature, 2024, International Union for Conservation of Nature, 2025, Food and Agriculture Organization of the United Nations, 2024].

Source practice: For ecology and conservation claims, cite assessment sources and state whether the evidence is an index, risk assessment, service valuation, satellite product, or policy synthesis [Intergovernmental Science-Policy Platform on Biodiversity and Ecosystem Services, 2024, NOAA Coral Reef Watch, 2025, Food and Agriculture Organization of the United Nations et al., 2025].

37.9 Summary

- Define a community and categorize the six types of biotic interactions with examples.
- Apply Lotka-Volterra competition equations to predict competitive outcomes and explain the competitive exclusion principle and niche theory.
- Explain trophic cascades and keystone species with quantitative examples.
- Compare primary and secondary succession and explain the intermediate disturbance hypothesis.
- Calculate Shannon diversity (H'), Simpson index, and species evenness and explain what each measures.
- Apply island biogeography theory, the species-area relationship, and SLOSS debate to conservation design.
- Describe the role of disturbance, facilitation, and alternative stable states in shaping communities.
- Explain food web topology, connectance, network robustness, and the relationship between complexity and stability.

37.10 Further Reading and Source Notes: Community Interactions and Succession

- Paine (1966). Food Web Complexity and Species Diversity. *The American Naturalist*, 100.
- Connell (1978). Diversity in tropical rain forests and coral reefs. *Science*, 199.
- Gause (1934). *The Struggle for Existence*. Williams & Wilkins.
- Hutchinson (1957). Concluding remarks. *Cold Spring Harbor Symposia on Quantitative Biology*, 22.
- Chesson (2000). Mechanisms of maintenance of species diversity. *Annual Review of Ecology and Systematics*, 31.
- Ehrlich & Raven (1964). Butterflies and plants: A study in coevolution. *Evolution*, 18.

37.11 Companion Source Module: Community Interactions and Succession

Community Interactions and Succession should leave a reproducible trail from a biological claim to the code, figure, diagram, or paper-based activity that can test it. Use the surfaces below to inspect the chapter’s assumptions, rerun the relevant model, or compare the manuscript explanation with companion labs and figures.

Table 444. Companion source surfaces for Community Interactions and Succession.

Surface	Use it for
<code>src/biology/ecology/ecology.py</code> (<code>lotka_volterra</code> , <code>connectance</code> , <code>biodiversity_indices</code>)	Quantify interactions, network structure, and community diversity.
<code>src/visualization/plots.py</code> (<code>plot_lotka_volterra</code> , <code>plot_species_area_relationship</code>)	Inspect dynamics and richness-area patterns.
<code>src/mermaid/biology_diagrams.py</code> (<code>food_web_diagram</code>)	Keep trophic links and interaction signs explicit.

Reproducibility check: define interaction sign, spatial scale, sampling effort, disturbance history, and network boundary before interpreting community patterns.
Cross-reference: use section 36, section 39, and section 25.

38 Biodiversity and Food Webs

Level 2/3 · 40 min read · 50 min lecture · Prerequisites: section 37

38.1 Learning Objectives

1. Apply island biogeography and species-area relationships to habitat fragments.
2. Analyze food-web structure, keystone species, and trophic cascades.
3. Calculate Shannon diversity and interpret evenness versus richness.
4. Evaluate biodiversity-ecosystem function and conservation tradeoffs.
5. Compare SLOSS reserve design with single large reserve using island biogeography logic.
6. Predict trophic cascade direction from keystone removal in a documented food web.
7. Connect biodiversity metrics to ecosystem function using measured response variables.

38.2 Island Biogeography Theory

38.2.1 MacArthur-Wilson Equilibrium Model

MacArthur and Wilson [1967]: *The Theory of Island Biogeography* — equilibrium species richness on islands balances immigration (colonization) rate and extinction rate:

- Immigration rate decreases as S increases (fewer uncolonised species remain in the mainland pool)
- Extinction rate increases as S increases (more species present means more potential extinctions)
- At equilibrium (\hat{S}): immigration rate = extinction rate

Effects of island characteristics:

Table 445. Effects of island characteristics on MacArthur-Wilson equilibrium richness.

Factor	Effect on \hat{S}	Mechanism
Larger area	Higher \hat{S}	Lower extinction rate (larger populations, more habitats)
Closer to mainland	Higher \hat{S}	Higher immigration rate (easier colonization)
Small + far	Lowest \hat{S}	High extinction, low immigration
Large + near	Highest \hat{S}	Low extinction, high immigration

38.2.2 Visualizing Food Web Connectance and Modularity

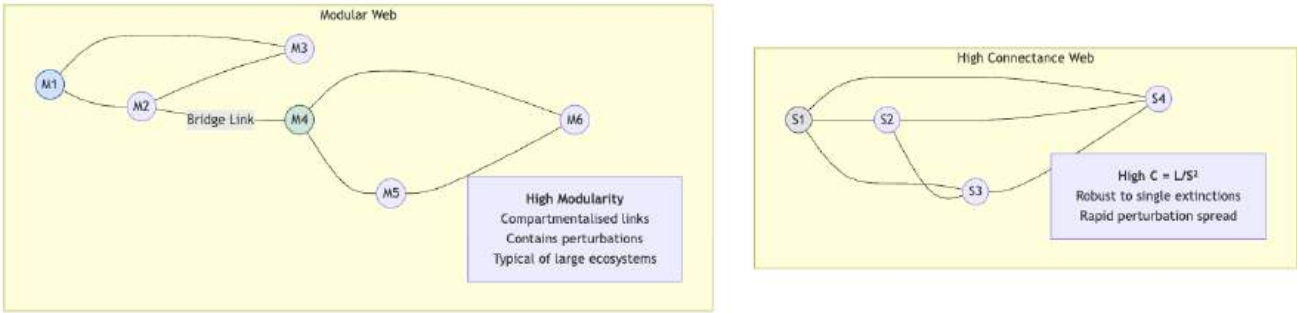


Figure 226. Food-web connectance and modularity shape stability: dense linkage can buffer single losses but spread disturbances, while modularity can confine perturbations.

38.2.3 Species-Area Relationship

$$S = cA^z$$

(452)

Log-transformed: $\log S = \log c + z \log A$

Table 446. Species-Area Relationship: Context and Typical z.

Context	Typical z	Interpretation
True islands	0.20-0.35	Higher z because islands are more isolated
Mainland habitat fragments	0.12-0.17	Lower z due to rescue effect from surrounding matrix
Archipelagoes	0.25-0.33	Standard island prediction

Practical calculation: Doubling area increases *S* by $\approx 19\%$ (when $z = 0.25$, since $2^{0.25} - 1 = 0.189$).

```
import math

def species_area(c, A, z):
    return c * (A ** z)

for area_ha in [1, 10, 100, 1000, 10000]:
    S = species_area(c=5, A=area_ha, z=0.25)
    print(f"Area = {area_ha:>6} ha → S = {S:.1f} bird species")
```

38.2.4 Empirical Tests of Island Biogeography

- Post-Krakatoa recolonisation (1883-1983): After complete sterilisation by eruption, species accumulated toward equilibrium; initial overshoot then relaxation [Whittaker, 1975]
- Florida Keys experiment [Simberloff and Wilson, 1969]: Fumigated small mangrove islands → recolonisation to predicted equilibrium within 2 years; confirmed immigration-extinction dynamics
- Habitat fragments as islands: Biological Dynamics of Forest Fragments Project (BDFFP, Amazonia; Laurance et al. 2011) — 40 years of data on isolated 1-100 ha fragments showing predictable species loss following the species-area curve in figure 236

38.2.5 SLOSS Debate in Reserve Design

Single Large Or Several Small — for conservation, which reserve design maximizes biodiversity?

Table 447. SLOSS Debate in Reserve Design.

Design	Advantages	Disadvantages
Single large	Lower edge-to-interior ratio; larger MVPs; protects area-demanding species	Vulnerability to single catastrophe; may miss regional habitat diversity
Several small	Redundancy against disaster; covers more habitat types; protects local endemics	Edge effects dominant; lower <i>S</i> per patch; connectivity problems

Modern consensus: Core-corridor-matrix design: - Large core reserves (the “single large” benefit) - Habitat corridors or stepping stones connecting reserves - Matrix land uses compatible with wildlife movement (agroforestry, wildlife-friendly farming) - Example initiatives: Yellowstone-to-Yukon (Y2Y, 3,200 km); Florida Wildlife Corridor (1,000+ miles)

38.2.6 Extinction Debt After Habitat Loss

Extinction debt (Tilman et al. 1994, *Nature*): Species currently present in degraded/fragmented habitats may be committed to future extinction — but the extinction is delayed by decades to centuries as existing individuals slowly die without replacement.

Species committed to extinction = $S_{\text{pre-fragmentation}} - c \cdot A_{\text{remaining}}^z$

(453)

Implications: - Present-day species richness overestimates long-term viability - Conservation assessments based on current presence may be dangerously optimistic - European calcareous grasslands: 20-50% of plant species face committed extinction due to historical fragmentation [Lindborg and Eriksson, 2004] - Amazon deforestation: 25-year extinction debt means current biodiversity surveys underestimate eventual losses

38.2.7 Metapopulation Dynamics (Levins, 1969; Hanski, 1994)

A patchwork of habitat fragments connected by dispersal — local extinctions offset by recolonisation. Metapopulation persistence requires fraction of occupied patches to exceed extinction threshold:

$$\hat{p} = 1 - \frac{e}{c}$$

(454)

where e = extinction rate per patch, c = colonization rate; metapopulation persists if $e/c < 1$.

Hanski’s incidence function model extends this by incorporating patch area (affects extinction rate) and isolation (affects colonization rate):

$$J_i = \frac{1}{1 + (e_i/c_i)^2}$$

(455)

where J_i = probability that patch i is occupied, $e_i \propto A_i^{-x}$, and c_i depends on distance to occupied patches.

Clinical Connection — Habitat Fragmentation and Zoonotic Disease: As forests are fragmented into small patches, edge effects increase human-wildlife contact, facilitating zoonotic pathogen spillover. The emergence of Nipah virus in Malaysia (1998-99) was linked to bat habitat loss: displaced fruit bats (*Pteropus* spp.) moved to pig farms near forest fragments, facilitating transmission to livestock and then humans. Similarly, Ebola outbreaks correlate spatially with deforestation frontiers. Island biogeography theory predicts that small fragments lose apex predators first (meso-predator release), increasing populations of rodents and bats that serve as pathogen reservoirs.

Concept Check: A national park of 10,000 km² is split by a highway into two fragments of 6,000 km² and 4,000 km². Using $S = 50A^{0.25}$, calculate species richness for: (a) the intact park, (b) each fragment separately, (c) both fragments combined assuming no species overlap. How does a wildlife corridor change your prediction?

38.2.8 Study Blueprint

- Big idea: Biodiversity patterns, food webs, and island biogeography scale from local interactions to landscape structure.
- Core concepts: food webs, keystone species, species-area, diversity indices.
- Framework alignment: Vision & Change: Systems, Evolution, Pathways and transformations of energy and matter; AP Biology: Systems Interactions, Evolution, Energetics; NGSS-style topics: Interdependent Relationships in Ecosystems, Matter and Energy in Organisms and Ecosystems, Natural Selection and Evolution.
- Model or quantitative lens: Shannon, species-area, and network connectance reasoning.
- Data skill: Interpret food-web, richness, or biogeography datasets.
- Practice cadence: Representing and Describing Data, Statistical Tests and Data Analysis, Argumentation.
- Common misconception to repair: Richness alone does not equal functional stability.
- Primary lab: Lab — Biodiversity and Food Webs.
- Question bank: Questions — Biodiversity and Food Webs.
- Transfer task: Transfer biodiversity reasoning to conservation planning and habitat fragmentation.
- Bridge to computation: biology.ecology.ecology.species_area_relationship.

Opening Vignette — Biodiversity and Food Webs

This chapter connects biodiversity, food webs, and biogeography to measurable evidence: models, datasets, and experiments that can strengthen or weaken each claim.

38.3 Food Web Structure and Network Ecology

38.3.1 Food Web Topology

Food webs are network representations of feeding relationships in communities — a graph where nodes are species (or trophic units) and directed edges encode “*i* eats *j*.” At the simplest scale, a two-species predator–prey pair produces the closed cycles in figure 219; food webs extend that picture to many interacting nodes. Treating the community as a graph unlocks the entire toolbox of network science (degree distributions, clustering, modularity, motif analysis), which has reshaped community ecology over the past two decades. Key metrics:

Table 448. Food Web Topology: Metric and Definition.

Metric	Definition	Typical value
Connectance (<i>C</i>)	$C = L/S^2$ (or $L/[S(S - 1)/2]$); fraction of possible links realized	0.05-0.30
Links per species (<i>L/S</i>)	Average number of trophic links per species	about 2 for most food webs
Chain length	Number of links from base to top	3-5 typically
Omnivory	Fraction of species feeding at >1 trophic level	about 50% in many webs
Mean trophic level	Average path length from primary producers	2.5–3.5 typical
Generality	Mean number of resources per consumer	Skewed: most consumers specialized
Vulnerability	Mean number of consumers per resource	Skewed: most prey have few predators
Nestedness	Specialists’ diets are subsets of generalists’ diets	High in mutualistic networks

```
# Minimal food-web statistics from an adjacency dictionary
def web_stats(web):
    species = set(web).union({p for prey in web.values() for p in prey})
    S = len(species)
    L = sum(len(v) for v in web.values())
    C = L / (S * S)
    return {"S": S, "L": L, "L/S": L / S, "connectance": C}

example = {
    "phyto": [], "zoo": ["phyto"], "shrimp": ["phyto"],
    "minnow": ["zoo", "shrimp"], "bass": ["minnow", "shrimp"],
}

print(web_stats(example))
```

38.3.2 Cascade Effects and Robustness

Food webs are not just descriptive: their topology predicts how perturbations propagate. Removal experiments (real or simulated) reveal three classes of network response:

Table 449. Cascade Effects and Robustness: Response and Mechanism.

Response	Mechanism	Topological signature
Bottom-up cascade	Loss of a producer ripples upward through consumers	Few generalist consumers; long chains
Top-down cascade (equation (445) system)	Loss of a top predator releases mesopredators or herbivores	Strong vertical interaction strengths
Horizontal cascade	Loss of one prey shifts predator to alternative prey, harming it indirectly	Apparent competition; shared predators

Robustness analysis (Dunne et al. 2002, *Ecol. Lett.*) sequentially removes species (random order, most-connected first, or rarest first) and tracks the fraction of secondary extinctions. Results across 16 well-resolved food webs:

- Random removal: about 50% of species can disappear before web collapse
- Most-connected-first removal: collapse after about 20% of species removed — hubs (highly connected generalists) are disproportionately important
- Rarest-first: minimal cascade — rare species are weakly embedded

This is a striking parallel to the scale-free network robustness literature (Barabási & Albert 1999): tolerance to random failure but vulnerability to targeted attack. For conservation, hub species are ecological-network analogs of keystone species, identifiable from topology alone.

38.3.3 Complexity-Stability Debate

May (1972, *Nature*): Mathematical analysis of random community matrices showed that complexity (high *S*, high *C*, strong interaction strengths) destabilises communities — contradicting the intuitive “diversity begets stability” hypothesis. The May criterion: a random Jacobian is locally stable primarily if $\sigma\sqrt{SC} < 1$ (with σ = standard deviation of interaction strengths).

Resolution (McCann 2000, *Nature*; Allesina & Tang 2012, *Nature*): - Weak interactions stabilize food webs (dampen oscillations) - Non-random interaction structure (modularity, nestedness) promotes stability - Real food webs are not random — they have specific architectures that enhance stability - Weak-interaction dominance: most interactions are weak; few are strong. The many weak links act as stabilisers.

Modularity: food webs are organized into modules (compartments) with strong within-module interactions and weak between-module interactions. This structure limits the spread of perturbations — a forest pathogen outbreak in one module rarely cascades into the aquatic module of the same landscape food web.

38.4 Neutral Theory of Biodiversity

The competition-coexistence theory developed earlier explains community structure through niches — species coexist because they differ. Hubbell’s unified neutral theory of biodiversity and biogeography (UNTB; Hubbell 2001) proposes the radical alternative: at the scale of trophically similar species (e.g., canopy trees in a tropical forest), most individuals are demographically equivalent regardless of species, and observed community patterns emerge from random birth–death–dispersal–speciation alone.

38.4.1 The Neutral Assumption

Each individual, regardless of species, has the same per-capita probabilities of: - Birth (replacement of a vacancy by an offspring) - Death (creation of a vacancy) - Immigration *m* from a regional metacommunity (replaces local community via dispersal) - Speciation (rate ν in the metacommunity)

The local community has fixed size *J* (zero-sum constraint — every death is replaced); dynamics are pure ecological drift, mathematically isomorphic to neutral **genetic drift** (section 20). Two parameters do most of the work:

$$\theta = 2J_M\nu \qquad \text{(fundamental biodiversity number)} \tag{456}$$

$$m = \text{immigration probability per local death} \tag{457}$$

The metacommunity size is *J_M*. Together, θ and *m* predict species abundance distributions, species–area curves, and beta diversity — without invoking niche differences at most.

38.4.2 Predictions and Empirical Successes

UNTB predicts: - Species abundance distribution follows a zero-sum multinomial (very close to the rank-abundance pattern introduced earlier, but with a heavier tail of rare species) - Species–area relationships with $z \approx 0.20\text{--}0.30$ (matching empirical island values, figure 236, and equation (452)) - Beta diversity declines with geographic distance even in homogeneous habitat (purely from limited dispersal)

Hubbell’s analysis of the Barro Colorado Island 50-ha forest plot (Panama, > 200 tree species) showed UNTB fit the species abundance distribution as well as niche-based models. Volkov et al. (2003, *Nature*) confirmed neutral fits across forests in Panama, Ecuador, India, and Malaysia.

38.4.3 Limits and Synthesis

UNTB has been heavily criticised: real species are *not* equivalent (massive trait variation; clear niche differences in measured demographic rates), and dynamic predictions (e.g., extinction times) often fail. The modern view, following Adler, HilleRisLambers & Levine (2007, *Ecol. Lett.*), is that niche and neutral processes

co-occur: Chesson-style niche differences stabilize coexistence, while neutral drift adds stochastic variation in relative abundance. UNTB is the null model — if your data look neutral, you have not yet found the ecology that distinguishes species.

Concept Check: Two tropical forest plots have nearly identical species-abundance distributions. The first sits in a homogeneous lowland habitat; the second spans a steep elevation gradient. Why is the *neutral* explanation of the species-abundance pattern more plausible for the first plot than the second, and what additional data would discriminate the two hypotheses?

38.5 Trait-Based biodiversity and food webs

Counting species ignores that a 1 mm aphid and a 10 m oak both add “+1” to richness. Trait-based ecology replaces (or complements) species lists with measured functional traits — morphological, physiological, or phenological attributes that influence performance. This shifts community ecology from a taxonomic enterprise to a quantitative, predictive one.

38.5.1 Grime’s CSR Triangle

Grime’s CSR scheme (1977, 2001) classifies plant strategies along two stress axes — disturbance and stress (resource limitation) — yielding three primary strategies and the gradients between them:

Table 450. Grime’s CSR Triangle: Strategy and Conditions.

Strategy	Conditions	Trait syndrome	Examples
C — Competitor	Low stress, low disturbance	Tall, fast-growing, high biomass, deep roots; leaves long-lived but expensive	Mature forest dominants (oak, beech, <i>Eucalyptus</i>)
S — Stress-tolerator	High stress, low disturbance	Slow growth, evergreen, sclerophyllous leaves, conservative resource use	Desert succulents, alpine cushion plants, lichens, conifers in nutrient-poor soils
R — Ruderal	Low stress, high disturbance	Short-lived, high seed output, rapid maturation, weak competitors	Annual weeds (<i>Senecio</i> , <i>Capsella</i>); pioneer trees

Most species fall along intermediates (CR, CS, SR, CSR). Crucially, the CSR axes capture independent gradients to the **r-strategist/K-strategist** axis of population ecology — a stress-tolerator is K-like in longevity but slow-growing, not high-fecundity.

38.5.2 The Leaf Economics Spectrum

Wright et al. (2004, *Nature*) analyzed > 2,500 plant species globally and uncovered a stunningly tight axis along which leaf traits co-vary — the leaf economics spectrum (LES):

Table 451. The Leaf Economics Spectrum: Acquisitive (fast) end and Conservative (slow) end.

Acquisitive (fast) end	Conservative (slow) end
High specific leaf area (SLA, m ² kg ^{−1})	Low SLA (thick, dense leaves)
High mass-based photosynthetic rate (<i>A</i> _{mass})	Low <i>A</i> _{mass}
High leaf N concentration (Rubisco-rich)	Low leaf N
Short leaf lifespan (months)	Long leaf lifespan (years; evergreen)
Low construction cost per unit area	High construction cost; defended

The LES is widely observed across biomes — tropical pioneer trees and desert annuals can occupy the same acquisitive end of the axis despite very different evolutionary histories. The axis captures a major trade-off between rapid resource capture and resource conservation, but local exceptions occur because water stress, herbivory, nutrient limitation, and phylogeny can bend the relationship. Analogous spectra exist for roots (Bergmann et al. 2020, *Sci. Adv.*) and for whole-plant strategy axes (Diaz et al. 2016, *Nature*).

38.5.3 Functional Diversity and Community Assembly

Trait data enable functional diversity indices (functional richness, evenness, divergence; Villéger, Mason & Mouillot 2008, *Ecology*) that detect community assembly mechanisms invisible to species lists:

- Functional clustering (traits more similar than expected by chance) → *environmental filtering* (primarily some strategies tolerate the local abiotic conditions)
- Functional overdispersion (traits more different than expected) → *competitive exclusion* via limiting similarity and Chesson-style stabilizing mechanisms.

A community of 30 alpine cushion plants and a community of 30 tropical canopy trees both have $S = 30$, but their trait spreads on the LES are wildly different — and that difference predicts ecosystem function (productivity, decomposition, drought response) far better than richness alone.

Concept Check: Two grassland plots have identical Shannon diversity $H' = 2.5$. Plot A's plants cluster tightly on the conservative end of the LES; plot B's plants span the entire LES. Which plot is more productive on average, which is more drought-resilient, and which would you predict has stronger competitive interactions?

38.6 Biological Control and Ecological Risk Management

The competition, predation, and parasitism theory developed above has direct translational application: biological control uses natural enemies to suppress pest populations, replacing or reducing chemical pesticides. It is community ecology deployed for agriculture, public health, and invasive-species management.

Invasive ants illustrate why social insects are high-stakes community actors. Argentine ants, fire ants, and yellow crazy ants can form dense, aggressive populations that displace native ants, disrupt seed dispersal and pollination networks, protect honeydew-producing pests, and change nutrient cycling. The mechanism is not merely “more ants”; it is colony structure, propagule pressure, enemy release, mutualisms with hemipterans, and human-assisted transport acting together [Holway et al., 2002]. Management therefore has to identify the interaction network being changed, not just the invader’s presence.

38.6.1 Three Classical Strategies

Table 452. Three Classical Strategies: Strategy and Approach.

Strategy	Approach	Time scale	Risk profile
Classical (importation)	Import a specialist natural enemy from the pest’s native range; expect it to establish and self-perpetuate	Years to decades; one-shot release	High — non-target effects if enemy is not specialist enough
Augmentative	Mass-rear and release natural enemies repeatedly to suppress current outbreak	Weeks to months; greenhouse, glasshouse	Low — released organisms typically fail to overwinter
Conservation	Modify habitat to favor resident natural enemies (hedgerows, beetle banks, insectary plants, reduced pesticide use)	Continuous	Lowest — uses native species

38.6.2 Classical Successes and Failures

Cottony cushion scale (*Icerya purchasi*) and the vedalia beetle (*Rodolia cardinalis*). Imported in 1888 from Australia to California citrus groves — within two years the citrus industry was saved. This is the textbook success and the prototype for most subsequent classical biocontrol programs.

Prickly pear (*Opuntia stricta*) and *Cactoblastis cactorum*. Released in 1925 in Australia, the moth larvae cleared 25 million ha of invasive cactus by 1940 — one of the largest-scale ecological interventions in history.

Cane toad (*Rhinella marina*). Released in 1935 in Queensland to control sugarcane beetles; the toads ignored the beetles, ate everything else, and are now an invasive plague across northern Australia. Classical biocontrol’s most-cited cautionary tale: a generalist natural enemy will eat non-target species, and the lesson cost ecologists decades of credibility.

38.6.3 Risk Assessment and Modern Practice

After the cane-toad era, regulatory frameworks (e.g., the FAO Code of Conduct for the Import and Release of Exotic Biological Control Agents, 1996) require:

1. Host-specificity testing — quarantine trials against native non-target species

2. Climate matching — does the agent’s native climate predict its spread in the target range?

3. Population modeling — Lotka–Volterra or matrix projection of agent and target dynamics; predicted suppression vs. escape

4. Reversibility analysis — can the agent be eradicated if it causes damage? (Almost typically: no.)

Modern programs increasingly favor conservation biological control, which avoids introducing non-native species entirely. Field margins of insectary plants (e.g., *Phacelia*, *Fagopyrum*) increase syrphid and parasitoid wasp populations that suppress aphids in adjacent crops by 30–50 % (Tscharntke et al. 2007, *Biol. Control*). This connects directly to ecosystem-services valuation (section 39).

Clinical Connection — *Wolbachia* and Mosquito-Borne Disease. Conservation biological control extends to public health. *Wolbachia* is an intra-cellular bacterium that, when introduced into *Aedes aegypti* mosquitoes, blocks dengue, Zika, and chikungunya virus transmission. Field trials in Yogyakarta (Indonesia) and Niterói (Brazil) released *Wolbachia*-carrying mosquitoes that spread the bacterium through the wild population via cytoplasmic incompatibility. Within 27 months of release in Yogyakarta, dengue incidence dropped 77% in treated neighborhoods (Utarini et al. 2021, *N. Engl. J. Med.*). This is biological control of disease vectors via a manipulative endosymbiont — community ecology in service of pandemic prevention.

Concept Check: A regulator must approve or reject a proposed classical biocontrol release of a parasitoid wasp against an invasive moth pest. (a) What three host-specificity tests would you require? (b) Why is “the agent attacks the target moth in the lab” insufficient evidence for safety? (c) How does a sound elasticity analysis (equation (435)) of the *target’s* matrix model help you predict whether the release will succeed?

38.7 Worked Example: Shannon Diversity in a Forest Patch

Problem: An ecologist surveys a small forest patch and identifies three species of trees: - Species A: 50 individuals - Species B: 30 individuals - Species C: 20 individuals

Calculate the Shannon Diversity Index (H) for this tree community. The formula is:

$$H = - \sum (p_i \ln p_i)$$

where p_i is the proportion of total individuals belonging to the i -th species.

Solution:

Step 1. Calculate the total number of individuals (N).

$$N = 50 + 30 + 20 = 100$$

Step 2. Calculate the proportion (p_i) for each species. - $p_A = 50/100 = 0.50$ - $p_B = 30/100 = 0.30$ - $p_C = 20/100 = 0.20$

Step 3. Calculate $p_i \ln p_i$ for each species. - Species A: $0.50 \times \ln(0.50) \approx 0.50 \times (-0.693) \approx -0.347$ - Species B: $0.30 \times \ln(0.30) \approx 0.30 \times (-1.204) \approx -0.361$ - Species C: $0.20 \times \ln(0.20) \approx 0.20 \times (-1.609) \approx -0.322$

Step 4. Sum the values and multiply by -1 .

$$H = -(-0.347 + -0.361 + -0.322) = -(-1.030) = 1.030$$

Answer: The Shannon Diversity Index for this tree community is approximately 1.03.

38.7.1 Worked Example: Intermediate Disturbance Hypothesis Quantified

Problem: The intermediate disturbance hypothesis predicts a unimodal relationship between disturbance frequency $f \in [0, 1]$ and species richness S . A simple closed-form parameterization is

$$S(f) = S_{\max} \times 4f(1 - f)$$

which peaks at $f = 0.5$ and falls to zero at the endpoints. For a temperate rocky-intertidal community, $S_{\text{max}} = 25$ species. Calculate S at $f = 0.2$, $f = 0.5$, and $f = 0.8$, and interpret each regime ecologically.

Solution:

Step 1. Evaluate the unimodal kernel $4f(1 - f)$.

- $f = 0.2$: $4 \times 0.2 \times 0.8 = 0.64$, so $S = 25 \times 0.64 = 16$ species.
- $f = 0.5$: $4 \times 0.5 \times 0.5 = 1.00$, so $S = 25 \times 1.00 = 25$ species (maximum).
- $f = 0.8$: $4 \times 0.8 \times 0.2 = 0.64$, so $S = 25 \times 0.64 = 16$ species.

Step 2. Interpret each regime ecologically.

- *Low disturbance* ($f = 0.2$, $S = 16$). The community is on a trajectory toward competitive exclusion; dominants accumulate biomass and crowd out subordinates. Diversity is depressed not by lack of colonizers but by interspecific competition winnowing the assemblage toward the climax dominant.
- *Intermediate disturbance* ($f = 0.5$, $S = 25$). The disturbance interval is short enough to interrupt competitive exclusion but long enough to permit colonization and recruitment. This is the regime in which Paine’s classic *Pisaster* removal experiments revealed predator-mediated coexistence; mussel monoculture appears once the keystone is removed and the system slides toward the low- f endpoint.
- *High disturbance* ($f = 0.8$, $S = 16$). Primarily disturbance-tolerant pioneer species persist; communities are repeatedly reset before competitive sorting can proceed. Diversity is depressed by a colonization-rate bottleneck rather than by competitive exclusion.

Step 3. Field calibration.

The model is an idealization: real communities show asymmetric curves (skewed toward high f when colonization is the limiting step) and the location of the peak shifts with productivity (Huston’s dynamic equilibrium model). The qualitative prediction — that diversity is maximized at intermediate, not minimum, disturbance — is what management exploits when prescribing controlled burns, mowing regimes, or pulsed flows below dams.

Answer: $S(0.2) = S(0.8) = 16$, $S(0.5) = 25$. The symmetric drop on either side of $f = 0.5$ is the mathematical fingerprint of two distinct ecological mechanisms — competitive exclusion at low f , colonization failure at high f — that look identical in a richness count but differ in management response.

38.7.2 Concept Check (Analyze) — Trophic Cascades, Efficiency, and Eutrophication

A pelagic food web has the following annual production (kcal/m²/yr) at a baseline 10% trophic transfer efficiency: phytoplankton = 10⁶, zooplankton = 10⁵, planktivorous fish = 10⁴, tuna = 10³.

- (a) An orca population collapse removes apex predation on tuna. Tuna biomass increases 5-fold; planktivorous fish decline by 50% (predation release from tuna); zooplankton increases by roughly 50%; phytoplankton declines. Sketch the qualitative cascade and identify which links are top-down and which are bottom-up.
- (b) Now overlay agricultural nutrient loading. Nitrogen runoff increases phytoplankton production by 3×. Analyze how this bottom-up perturbation interacts with the top-down cascade in (a): does eutrophication amplify or dampen the cascade signature in zooplankton biomass? Reason explicitly about whether the limiting variable for zooplankton is now food supply or predation pressure.
- (c) Predict the sign of the change in community Shannon diversity at the phytoplankton trophic level under sustained eutrophication. Reason about competitive exclusion among phytoplankton functional groups (large diatoms vs. bloom-forming cyanobacteria) at high N , and compare to your reasoning for the intermediate-disturbance worked example above.

38.7.3 Concept Check (Evaluate) — Biotic Resistance and Invasive Species

Elton’s diversity-resistance hypothesis predicts that high-diversity communities are harder to invade because resident species preempt resources and natural enemies are more diverse. The empirical record is split:

- Hawaiian terrestrial bird communities (low native diversity, severe historical isolation) were catastrophically invaded once introduced species (rats, mosquitoes, mongoose, alien plants) arrived. Tens of native bird species have gone extinct or are critically endangered.
- Cedar Creek grassland experiments (Tilman and collaborators) show that experimental plots seeded with higher native species richness resist exotic seedling establishment more strongly than monocultures.

- (a) Evaluate which mechanism — resource preemption, enemy release, or propagule pressure — best explains the Hawaiian outcome, and which best explains the Cedar Creek outcome. Justify with at least one ecological feature of each system (isolation history, propagule supply, soil-resource limitation, herbivore community).
- (b) Critique the simple Elton hypothesis: under what conditions does the diversity-resistance relationship reverse (i.e., diverse communities are *more* invulnerable)? Hint: consider productivity gradients and the scale at which diversity is measured (local plot vs. regional pool).
- (c) Recommend a single conservation intervention for each system (Hawaii vs. Cedar Creek-type grassland) consistent with your mechanistic diagnosis, and explain why a “one-size-fits-all” invasive species strategy fails when the underlying mechanisms differ.

38.8 Current Evidence and Frontier Biology: Biodiversity and Food Webs

For Biodiversity and Food Webs, frontier biology belongs inside the evidence logic of the chapter. Ecology and conservation decisions increasingly combine field data, remote sensing, community knowledge, model uncertainty, and explicit values. The core reading question is this: community claims should identify interaction type, network position, disturbance regime, and observational limits.

- What to verify: identify the observation, model, assay, or dataset that would make the claim stronger or weaker.
- What to qualify: state the scale, organism, cell type, environmental condition, or population where the claim is expected to hold.
- What to compare: test at least one alternative explanation, baseline, or null model before treating the pattern as causal.
- What to cite: distinguish primary evidence, review synthesis, public dataset, and institutional guidance; for recent or numeric claims, prefer the source closest to the measurement and state what has changed since it was published.

Select biodiversity and conservation metrics by decision need: abundance, interaction, function, risk, service, and governance metrics answer different questions [Intergovernmental Science-Policy Platform on Biodiversity and Ecosystem Services, 2019, 2024, World Wide Fund for Nature, 2024, International Union for Conservation of Nature, 2025, Food and Agriculture Organization of the United Nations, 2024].

Source practice: For ecology and conservation claims, cite assessment sources and state whether the evidence is an index, risk assessment, service valuation, satellite product, or policy synthesis [Intergovernmental Science-Policy Platform on Biodiversity and Ecosystem Services, 2024, NOAA Coral Reef Watch, 2025, Food and Agriculture Organization of the United Nations et al., 2025].

38.9 Summary

- Biotic interactions: mutualism (+/+), commensalism (+/0), parasitism (+/-), predation (+/-), competition (-/-), amensalism (0/-) — shape community composition and evolution.
- Competition: Lotka-Volterra equations; competitive exclusion if niches overlap completely; stable coexistence if intraspecific > interspecific effects. Modern coexistence theory [Chesson, 2000]: stabilizing + equalising mechanisms.
- Niche theory: Hutchinson’s n-dimensional hypervolume; fundamental vs. realized niche; paradox of the plankton resolved by non-equilibrium dynamics and niche partitioning.
- Trophic cascades: keystone predators suppress herbivores → plant biomass increases (wolves→elk→willows; sea otters→urchins→kelp). Behavioral cascades via “landscape of fear.”
- Succession: primary (bare substrate, slow) vs. secondary (disturbed community, faster); facilitation/tolerance/inhibition mechanisms; IDH: intermediate disturbance maximizes diversity; alternative stable states and regime shifts with hysteresis.
- Diversity indices: H' (Shannon) combines richness + evenness; Simpson $1 - D$ = probability of inter-specific encounter; J' (evenness) = $H' / \ln S$. Alpha, beta, gamma diversity at different spatial scales.
- Island biogeography: $S = cA^z$; equilibrium balances colonization and extinction; SLOSS debate resolved toward core-corridor-matrix design; extinction debt warns of delayed species loss.
- Food web structure: connectance, modularity, weak-interaction dominance stabilize complex communities. Network robustness under targeted (most-connected-first) deletion collapses faster than under random deletion — hub species are topological keystones.
- Neutral theory (UNTB): Hubbell’s per-capita-equivalence framework; two parameters θ and m predict species-abundance distributions and species–area relationships from drift, dispersal, and speciation alone. Best treated as a null model that niche-based theory must beat.
- Trait-based ecology: Grime’s CSR triangle; the leaf economics spectrum (LES) is a widely observed acquisitive↔conservative axis with local exceptions. Functional diversity diagnoses assembly mechanisms (clustering = environmental filtering; overdispersion = limiting similarity) that species lists miss.
- Biological control and invasion: classical importation (vedalia beetle success; cane toad disaster), augmentative releases, and conservation biological control. Social insects add network-scale cases: invasive ants can restructure mutualisms, seed dispersal, pest protection, and nutrient cycling, while pollinator conservation depends on protecting whole interaction networks. *Wolbachia*-loaded *Aedes aegypti* extends the framework to vector-borne disease.
- Connections: See section 36 for consumer-resource oscillations, section 39 for energy flux, and section 25 for microbial communities.

38.10 Review Questions

- Two warbler species (*Dendroica castanea* and *D. fusca*) share a boreal spruce tree habitat. MacArthur (1958) showed they coexist by partitioning the tree into feeding zones. Using Chesson’s modern coexistence theory: (a) Which of Chesson’s two mechanisms (equalising vs. stabilizing) enables their coexistence? (b) Write **Lotka-Volterra equations** and specify the condition for stable coexistence in terms of α_{12} and α_{21} .
- A trophic cascade operates in Yellowstone: wolves \rightarrow elk \rightarrow willows \rightarrow beavers \rightarrow altered stream morphology. (a) Is this a bottom-up or top-down cascade? (b) Predict what happens to each level if chronic wasting disease eliminates 90% of the elk population. (c) How does the “landscape of fear” concept modify purely density-mediated cascade predictions?
- A tropical rainforest island (area = 500 km²) currently has $S = 200$ bird species. Deforestation reduces area to 125 km² (25% of original). (a) Using the species-area relationship with $z = 0.25$ and appropriate c , predict the final equilibrium species richness. (b) If the extinction debt takes 50 years to fully manifest, what is the expected species number at year 10 assuming linear debt decay?
- Compare the Shannon diversity index (H') for three communities:
 - Community A: 4 species, abundances = [25, 25, 25, 25]
 - Community B: 4 species, abundances = [97, 1, 1, 1]
 - Community C: 8 species, abundances = [50, 20, 10, 8, 5, 4, 2, 1] Calculate H' and J' for each. Which community shows: highest richness? highest evenness? highest H' ?
- Explain Hutchinson’s “paradox of the plankton.” Why does the coexistence of hundreds of phytoplankton species apparently violate competitive exclusion, and what are three mechanisms that resolve the paradox?
- The Biological Dynamics of Forest Fragments Project (BDFFP) in Amazonia found that 1-ha fragments lost 50% of their bird species within 15 years, while 100-ha fragments lost 10%. (a) Calculate z from these two data points. (b) Predict the species richness of a 10-ha fragment relative to a 100-ha fragment. (c) What role do edge effects play beyond the simple species-area prediction?
- A shallow lake in the Netherlands exists in a clear-water state with abundant macrophytes. Nutrient loading from agriculture gradually increases. Describe the regime shift to the turbid, algal-dominated state using the framework of alternative stable states. Why is reducing nutrients back to the original level insufficient to restore the clear-water state (hysteresis)?
- Design a reserve system for a large mammal species (home range = 100 km², N_e requirement = 500) in a landscape of forest fragments. Use island biogeography principles to specify: (a) minimum total reserve area, (b) number and size of core reserves, (c) corridor design, (d) matrix management. Justify each design element.
- The rough-skinned newt and common garter snake represent one of the best-documented coevolutionary arms races. Describe the escalation: what toxin does the newt produce, what resistance mechanism has the snake evolved, and what geographic mosaic pattern is observed? How does this relate to Red Queen dynamics?
- Explain how the competitive exclusion principle applies to *Clostridium difficile* infection and its treatment by fecal microbiota transplantation. What ecological principles make FMT more effective than antibiotic treatment for recurrent CDI?
- Using `lotka_volterra`, estimate whether predator peak lags prey peak for default parameters (inspect time series qualitatively).
- How does connectance $C = L/S^2$ relate to stability arguments in diverse food webs?
- Hubbell’s neutral theory predicts a species-abundance distribution from drift and dispersal alone. (a) Why is UNTB best regarded as a *null model* rather than a competitor to niche theory? (b) If a community fits UNTB perfectly, what does that *not* prove about the underlying ecology? Cite the Adler, HilleRisLambers & Levine (2007) synthesis.
- Two oak forests share identical species lists ($S = 30$, $H' = 2.8$) but differ markedly in leaf economics: forest A’s species cluster on the conservative end of the LES; forest B’s species span the entire spectrum. (a) Which forest is more functionally diverse? (b) Predict relative productivity, decomposition rate, and drought-resilience for each. (c) Why do two communities with identical Shannon diversity behave differently?
- A food-web robustness analysis simulates extinctions in random vs. most-connected-first orders. The web collapses after 50% removal under random deletion but after 18% removal under most-connected-first deletion. (a) Explain the asymmetry using network topology. (b) Translate the result into a conservation prioritisation rule for hub species (analogous to keystone identification but topological).

16. A government agency proposes releasing a parasitoid wasp from East Asia to control an invasive aphid species in California. (a) Outline the host-specificity testing required before approval. (b) Why is the cane toad disaster relevant precedent? (c) Sketch how the agent and aphid populations would interact in a coupled Lotka-Volterra model — and what condition supports long-term aphid suppression rather than coexistence?

38.11 Further Reading and Source Notes: Biodiversity and Food Webs

- Paine (1966). Food Web Complexity and Species Diversity. *The American Naturalist*, 100.
- Connell (1978). Diversity in tropical rain forests and coral reefs. *Science*, 199.
- Gause (1934). *The Struggle for Existence*. Williams & Wilkins.
- Hutchinson (1957). Concluding remarks. *Cold Spring Harbor Symposia on Quantitative Biology*, 22.
- Chesson (2000). Mechanisms of maintenance of species diversity. *Annual Review of Ecology and Systematics*, 31.
- Ehrlich & Raven (1964). Butterflies and plants: A study in coevolution. *Evolution*, 18.

38.12 Computational Bridge

Predator-prey cycles from the chapter are reproduced by numerical integration:

```
from biology.ecology import lotka_volterra

lv = lotka_volterra(40.0, 9.0, 0.5, 0.02, 0.01, 0.2, t_end=80.0)
print(len(lv.times), round(lv.prey[-1], 2))
```

Clinical / systems note: FMT restores diversity and colonization resistance — an ecological intervention for a microbiome community treated as a competitive network.

38.13 Key Terms

Table 453. Concept Check (Evaluate) — Biotic Resistance and Invasive Species: Term and Definition.

Term	Definition
Competitive exclusion principle	Two species cannot stably coexist if they occupy the exact same niche; the superior competitor excludes the other
Keystone species	Species with disproportionately large effects on community structure relative to its abundance
Trophic cascade	Indirect effect of apex predator on plant biomass via suppressing herbivores; top-down regulation
Succession	Directional change in community composition over time; primary (bare substrate) or secondary (after disturbance)
Intermediate Disturbance Hypothesis	Moderate disturbance frequency/intensity maximizes species diversity by preventing competitive exclusion
Shannon diversity (H')	$H' = - \sum p_i \ln p_i$; quantifies species richness and evenness simultaneously
Simpson index ($1 - D$)	Probability that two random individuals are from different species; weighted toward dominant species
Species-area relationship	$S = cA^z$; species richness increases with area; $z \approx 0.25$ for habitat islands
SLOSS	Single Large Or Several Small reserves debate in conservation biology
Extinction debt	Species present today but predicted to go extinct based on current habitat loss; time-delayed response
Metapopulation	Network of semi-isolated subpopulations connected by dispersal; local extinctions offset by recolonisation
Alternative stable states	Multiple stable community configurations under the same environmental conditions; regime shifts between states
Niche differentiation	Process by which competing species evolve to use different resources, reducing niche overlap
Fundamental niche	Full range of environmental conditions where a species can maintain $r \geq 0$ (Hutchinson)
Realized niche	Subset of fundamental niche actually occupied after biotic interactions
Connectance	Proportion of possible trophic links that are realized in a food web
Facilitation	One species improves survival or reproduction of another; mechanism of succession
Beta diversity	Species turnover between communities; measured by Jaccard or Bray-Curtis indices

Term	Definition
Neutral theory (UNTB)	Hubbell’s framework: per-capita demographic equivalence; biodiversity arises from drift, dispersal, and speciation
Fundamental biodiversity number (θ)	$\theta = 2J_M \nu$; controls species richness in the metacommunity under UNTB
CSR strategies	Grime’s competitor / stress-tolerator / ruderal classification of plant strategies
Leaf economics spectrum (LES)	Comprehensive axis from acquisitive (high SLA, short-lived leaves) to conservative (thick, long-lived) leaves
Functional diversity	Trait-based diversity metric; clustering vs. overdispersion diagnoses assembly mechanism
Classical biological control	Importation of a specialist natural enemy from a pest’s native range
Conservation biological control	Habitat modification to favor resident natural enemies; lowest-risk strategy
Network robustness	Resilience of a food web to species removal; collapses fastest under most-connected-first deletion

38.14 Companion Source Module: Biodiversity and Food Webs

Biodiversity and Food Webs should leave a reproducible trail from a biological claim to the code, figure, diagram, or paper-based activity that can test it. Use the surfaces below to inspect the chapter’s assumptions, rerun the relevant model, or compare the manuscript explanation with companion labs and figures.

Table 454. Companion source surfaces for Biodiversity and Food Webs.

Surface	Use it for
<code>src/biology/ecology/ecology.py</code> (lotka_volterra, connectance, biodiversity_indices)	Quantify interactions, network structure, and community diversity.
<code>src/visualization/plots.py</code> (plot_lotka_volterra, plot_species_area_relationship)	Inspect dynamics and richness-area patterns.
<code>src/mermaid/biology_diagrams.py</code> (food_web_diagram)	Keep trophic links and interaction signs explicit.

Reproducibility check: define interaction sign, spatial scale, sampling effort, disturbance history, and network boundary before interpreting community patterns.
Cross-reference: use section 36, section 39, and section 25.

39 Ecosystem Ecology

Level 2/3 · 65 min read · 75 min lecture · Prerequisites: section 37, section 38, section 10

39.1 Learning Objectives

By the end of this chapter, you should be able to:

1. Define an ecosystem [Levin, 1998] and distinguish abiotic from biotic components; categorize consumers by trophic role. figure 227 assigns trophic levels in a simple aquatic web by breadth-first search from producers.
2. Explain energy flow through trophic levels, calculate ecological efficiency, and explain why food chains are short.
3. Describe the carbon, nitrogen, phosphorus, and sulfur cycles and their key anthropogenic disruptions.
4. Calculate gross primary production (GPP), net primary production (NPP), and net ecosystem production (NEP).
5. Describe eutrophication and hypoxia as consequences of nutrient cycle disruption.
6. Explain ecosystem services and their economic valuation.
7. Describe climate change feedbacks involving biogeochemical cycles (permafrost carbon, ocean acidification).
8. Explain the biological pump and its role in ocean carbon sequestration.
9. Compare methods for measuring NPP (harvest, eddy covariance, ¹⁴C, remote sensing) and explain why ANPP/BNPP partitioning matters for global carbon accounting.
10. Use the Hubbard Brook watershed experiment to explain how live vegetation regulates nutrient retention, and contrast open vs. closed nutrient cycling regimes.
11. Describe ocean productivity zones (upwelling, gyres, polar) and the Martin curve, and connect soil pedogenesis (CLORPT, horizons) to long-term carbon storage.
12. Use the Redfield ratio to diagnose nutrient limitation, and evaluate the planetary boundaries and Gaia hypothesis as frameworks for Earth system thinking.

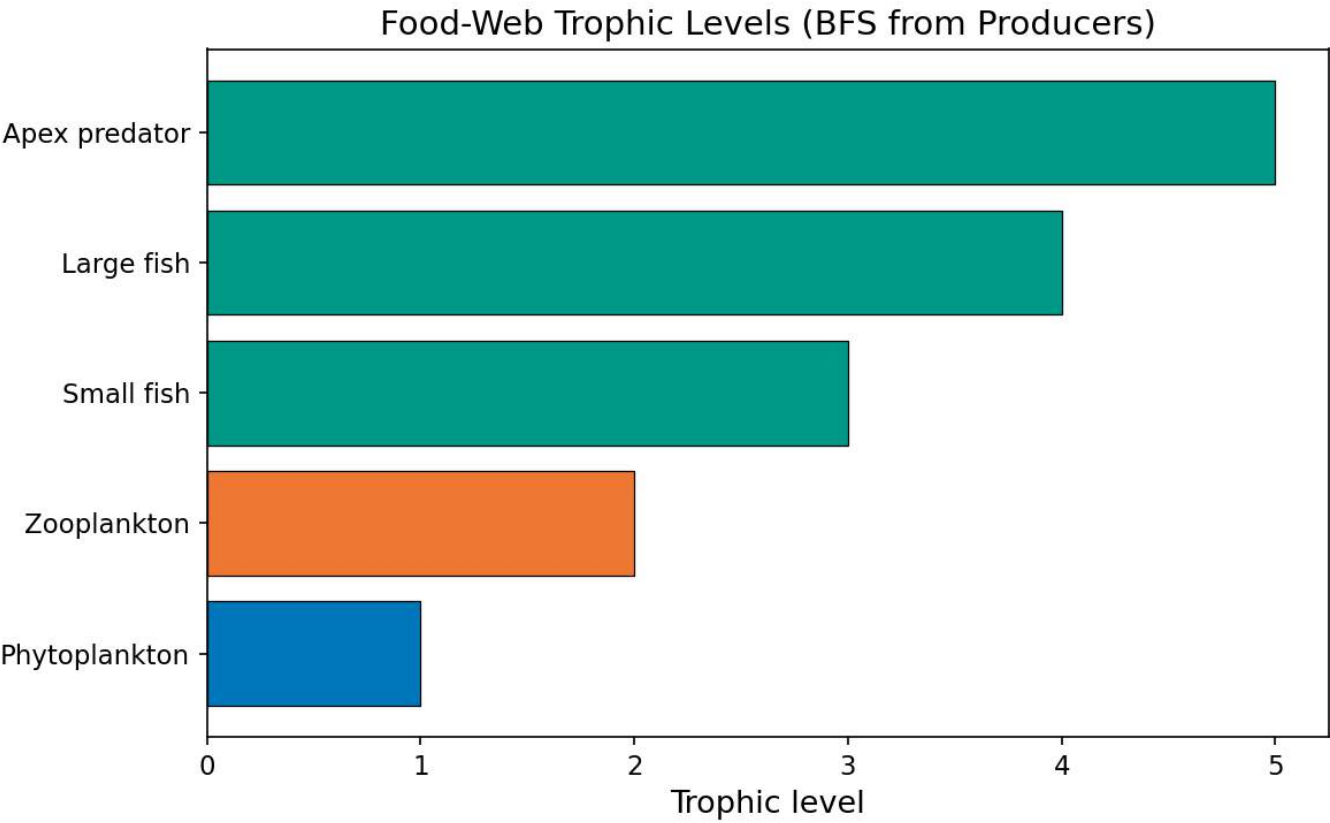


Figure 227. Trophic levels assigned from phytoplankton producers upward in a simplified aquatic food web. Each consumer sits one level above its prey; apex predators occupy the highest bar in this linear chain.

39.1.1 Study Blueprint

- Big idea: Ecosystems couple energy flow and matter cycling across organisms, environments, and time.

- Core concepts: primary productivity, trophic efficiency, nutrient cycles, decomposition.
- Framework alignment: Vision & Change: Systems, Evolution, Pathways and transformations of energy and matter; AP Biology: Systems Interactions, Evolution, Energetics; NGSS-style topics: Interdependent Relationships in Ecosystems, Matter and Energy in Organisms and Ecosystems, Natural Selection and Evolution.
- Model or quantitative lens: Energy-flow, productivity, and nutrient-budget calculations.
- Data skill: Trace matter and energy through food webs and biogeochemical cycles.
- Practice cadence: Representing and Describing Data, Statistical Tests and Data Analysis, Argumentation.
- Common misconception to repair: Energy flows through ecosystems, but matter cycles; confusing the two breaks many explanations.
- Primary lab: [Lab — Ecosystem Ecology](#).
- Question bank: [Questions — Ecosystem Ecology](#).
- Transfer task: Transfer ecosystem reasoning to eutrophication, carbon budgets, agriculture, and climate feedback.
- Bridge to computation: `biology.ecology.ecology.food_web_trophic_levels`.

Opening Vignette — Measuring What an Ecosystem Actually Runs On

In 1953, Howard T. Odum waded into Silver Springs, Florida — a crystal-clear, constant-temperature spring — and spent months measuring oxygen concentrations at stations upstream and downstream to calculate the primary productivity of an entire ecosystem. His method, upstream-downstream dissolved oxygen change, was brilliantly simple: if an ecosystem produces oxygen during the day and consumes it at night, measuring both rates gives net and gross production. From his data, Odum constructed the first complete energy flow diagram of a natural ecosystem, quantifying how much energy entered via [photosynthesis](#), how much was lost at each trophic level, and how much left the system as heat. The 10% rule — roughly 10% of energy transfers between trophic levels — came directly from Odum’s data. The concept that ecosystems are energy-processing machines, quantifiable and modelable, born in Silver Springs, became foundational to biogeochemistry, conservation biology, fisheries management, and climate modeling. Silver Springs is still one of the most-studied aquatic ecosystems on Earth.

39.2 Ecosystem Concepts and System Boundaries

An ecosystem comprises most organisms (biotic component) and the physical/chemical environment (abiotic component) in a defined area, interacting through energy flow and nutrient cycling [[Bormann and Likens, 1967](#)]. Ecosystems vary from a few liters (rock pool) to thousands of km² (boreal forest). Their defining features are:

1. Energy input (solar or chemical) drives biological activity
2. Nutrient cycling — atoms cycle repeatedly between biotic and abiotic phases (unlike energy, which flows linearly through and out of the system)
3. Emergent properties — productivity, stability, resistance — cannot be predicted from individual species properties alone

39.2.1 The Two Fundamental Processes

The distinction between energy flow and nutrient cycling is fundamental:

Table 455. The Two Fundamental Processes: Process and Energy.

Process	Energy	Nutrients
Direction	One-way (flows through system)	Cyclic (atoms recycled indefinitely)
Source	Solar radiation (99.9%) or chemosynthesis	Geological and atmospheric reservoirs
Efficiency	about 1-2% of solar energy captured by photosynthesis	about 100% recycled over geological time
Limiting?	Rarely limiting (except deep sea, caves)	Often limiting (N, P, Fe, water)
Conservation law	Energy conserved but degraded (2nd law)	Mass conserved (atoms neither created nor destroyed)

39.2.2 Ecosystem Services and Human Well-Being

Costanza et al. (1997, *Nature*) estimated global ecosystem services at >\$33 trillion/year (updated to about \$125 trillion/year by Costanza et al. 2014). The four categories:

Table 456. Ecosystem Services and Human Well-Being: Category and Services.

Category	Services	Examples	Valuation approach
Provisioning	Materials and energy	Food, freshwater, timber, fuel, medicine, genetic resources	Market prices
Regulating	Environmental processes	Climate regulation (C sequestration), flood control, pollination, disease regulation, air purification, water purification	Avoided cost; replacement cost
Cultural	Non-material benefits	Recreation, ecotourism, spiritual value, aesthetic beauty, education	Willingness-to-pay surveys
Supporting	Foundation for most others	Soil formation, nutrient cycling, primary productivity, water cycling	Cost of replication

The Millennium Ecosystem Assessment (2005; 1,300 scientists from 95 countries) concluded that 60% of Earth’s ecosystem services are being degraded or used unsustainably. The IPBES Global Assessment (2019) expanded this to 75% of terrestrial and 66% of marine ecosystems significantly altered.

Concept Check: A wetland provides flood attenuation, water purification, carbon sequestration, recreation, and biodiversity habitat. If this wetland is drained for agriculture, which ecosystem services are lost? How would you calculate the economic cost of losing flood attenuation alone?

39.3 Trophic Structure and Energy Flow

Trophic levels (from Greek *trophe* = nourishment) describe feeding position in the food web:

Table 457. Ecosystem Services and Human Well-Being: Trophic level and Organisms.

Trophic level	Organisms	Energy source
1 — Producers (autotrophs)	Plants, algae, cyanobacteria, chemolithotrophs	Solar energy (GPP) or chemical energy
2 — Primary consumers (herbivores)	Insects, zooplankton, ungulates, small mammals	NPP consumed
3 — Secondary consumers (carnivores)	Spiders, small fish, small birds	Primary consumer biomass
4 — Tertiary consumers	Large fish, raptors	Secondary consumer biomass
Apex — Top predators	Orca, wolf, lion, large sharks	Top-down regulation
Decomposer/detritivore (parallel)	Bacteria, fungi, termites, ants, earthworms, millipedes	Dead organic matter and soil organic pathways

39.3.1 Ecological Efficiency Across Trophic Transfers

The trophic efficiency (10% rule, Lindeman 1942, *Ecology*) describes the fraction of energy at trophic level *n* transferred to level *n* + 1:

$$\text{Trophic Efficiency} = \frac{\text{Production}_{n+1}}{\text{Production}_n} \times 100\% \approx 5\text{-}20\%$$

(458)

Decomposition of efficiency:

Trophic efficiency = Consumption efficiency × Assimilation efficiency × Production efficiency

(459)

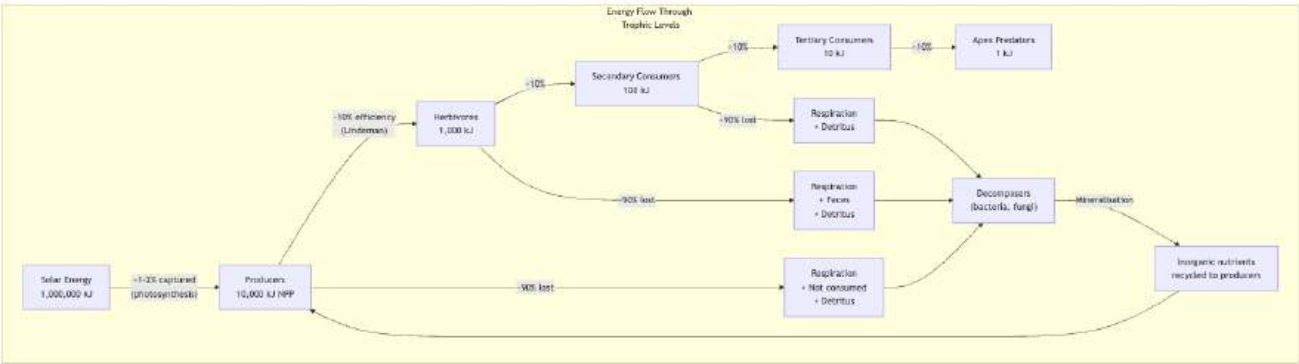


Figure 228. Energy transfer narrows across trophic levels because respiration, heat loss, and unconsumed biomass leave a limited fraction of producer energy for higher consumers.

Table 458. Ecological Efficiency Across Trophic Transfers: Component and Definition.

Component	Definition	Typical range
Consumption efficiency	Fraction of available production ingested	20-50% (herbivores); 50-100% (carnivores)
Assimilation efficiency	Fraction of ingested energy absorbed across gut	20-60% (herbivores on plants); 60-90% (carnivores on animal tissue)
Production efficiency	Fraction of assimilated energy converted to new biomass	1-3% (endotherms); 20-60% (ectotherms)

39.3.2 Production Efficiency by Organism Group

Table 459. Production Efficiency by Organism Group: Group and Production efficiency.

Group	Production efficiency	Reason
Insects (ectotherms)	40-60%	No thermoregulation cost
Fish (ectotherms)	20-30%	Moderate metabolic costs
Amphibians (ectotherms)	30-40%	Low metabolic rate
Birds (endotherms)	1-3%	about 97% of assimilated energy on thermoregulation
Mammals (endotherms)	1-3%	High metabolic overhead

Consequence for food chain length: 10% efficiency means energy decreases by an order of magnitude per trophic level. Chains longer than 4-5 levels are energetically unsustainable in most ecosystems.

Human dietary implications: Producing 1 kg beef requires about 7-8 kg grain and about 15,000 L water. Shifting from trophic level 3 (carnivore) to level 2 (herbivore) reduces land and water footprint by 5-10x. Insect protein (40-60% production efficiency) is about 20x more efficient than beef protein (1-3%).

Clinical Connection — Biomagnification and Human Health: The 10% energy transfer rule has a dangerous corollary: persistent pollutants that are not metabolized biomagnify through the food chain. DDT (dichlorodiphenyltrichloroethane) concentrates about 10x per trophic level. In Lake Michigan in the 1960s: water = 0.014 ppm DDT → phytoplankton = 5 ppm → zooplankton = 10 ppm → small fish = 50 ppm → large fish = 200 ppm → bald eagle eggs = 2,000 ppm. At 2,000 ppm, DDT metabolite DDE inhibits carbonic anhydrase in the shell gland, producing thin eggshells → reproductive failure → near-extinction. Mercury (methylmercury) follows the same pattern: tuna and swordfish accumulate mercury to levels that prompt FDA advisories for pregnant women (>0.5 ppm → neurological risk to developing fetus).

Concept Check: A savanna ecosystem has NPP = 500 g C/m²/yr. If herbivores consume 20% of NPP with 10% trophic efficiency, and a lion (tertiary consumer) eats herbivores with 10% efficiency, how much energy (g C/m²/yr) is available to sustain the lion population?

Concept Check (Synthesis — Cross-Unit Connection): Ecosystems can be understood through the lens of thermodynamics and information theory introduced in Unit 0 — Systems Science for Biology: Introduction. The free energy of a living system (its negentropy budget) is maintained

by continuous energy input from the sun; dissipative structures (organisms, communities) sustain themselves by exporting entropy. (a) Odum’s concept of ecological efficiency (about 10% trophic transfer) represents a thermodynamic constraint on how much free energy is available at each level — derive the expected biomass pyramid for a 4-level food chain starting with 10,000 kg of primary producers. (b) Mature ecosystems (late succession) tend to show higher species diversity, longer food chains, and slower nutrient cycling — explain how this corresponds to more complex generative models with lower entropy production rates per unit biomass. (c) In **Unit 0 — Systems Science for Biology: Introduction**, prediction error minimization was applied to individual organisms. Scale this up: in what sense does ecosystem succession represent the ecosystem minimizing surprise (maximizing model evidence) over ecological timescales?

39.4 Primary Productivity and Carbon Fixation

Gross Primary Production (GPP): Total rate of CO₂ fixation by most autotrophs (μmol CO₂/m²/s or g C/m²/year).

Net Primary Production (NPP): GPP minus autotrophic respiration (*R_a*):

$$NPP = GPP - R_a$$
(460)

Net Ecosystem Production (NEP): NPP minus heterotrophic respiration (*R_h*, decomposers):

$$NEP = NPP - R_h$$
(461)

Net **Biome** Production (NBP): NEP minus disturbance losses (fire, harvest, land-use change):

$$NBP = NEP - D$$
(462)

NBP determines whether an ecosystem is a net carbon sink (*NBP* > 0) or source (*NBP* < 0).

39.4.1 The Productivity Hierarchy

$$\text{Solar radiation} \xrightarrow{\sim 1-2\%} GPP \xrightarrow{-R_a(\sim 50\%)} NPP \xrightarrow{-R_h} NEP \xrightarrow{-D} NBP$$
(463)

Only about 1–2% of incident solar energy is captured photosynthetically as gross primary production (GPP). Autotrophic respiration (*R_a*) consumes roughly half of GPP, leaving net primary production (NPP) — the biomass actually available to consumers. Subtracting heterotrophic respiration (*R_h*, by animals, fungi, and microbes) gives net ecosystem production (NEP); subtracting further non-respiratory losses such as fire, harvest, and erosion (*D*) gives net biome production (NBP), the quantity that determines whether a region is a long-term carbon sink or source. Each arrow is a quantitatively large loss, which is why food chains are short and why NBP is small relative to GPP.

39.4.2 Global Primary Production

Table 460. Global Primary Production: Ecosystem and NPP (g C/m²/yr).

Ecosystem	NPP (g C/m ² /yr)	Area (10 ⁶ km ²)	Global contribution
Tropical rainforests	900-1,700	17	about 30% of terrestrial NPP
Temperate forests	400-900	12	
Boreal forests	100-400	12	
Tropical grasslands/savanna	200-600	22	
Desert	10-50	42	Minimal
Tundra	50-150	9	
Open ocean	50-150	332	about 45% of global NPP
Coastal/upwelling	200-600	27	
Coral reefs	500-2,000	0.6	High per area, small total

Ecosystem	NPP (g C/m ² /yr)	Area (10 ⁶ km ²)	Global contribution
Global total	—	—	about 120 Pg C/yr (land) + 90 Pg C/yr (ocean)

39.4.3 Factors Limiting GPP

Table 461. Factors Limiting GPP: Factor and Terrestrial.

Factor	Terrestrial	Marine
Light	Yes (canopy shading, LAI)	Yes (depth; turbidity; latitude)
Temperature	Yes (enzyme rates; freeze)	Yes (Arctic/Antarctic)
Water	Primary limitation in many biomes	N/A
Nitrogen	Limiting in most ecosystems	Primary limiter in most open ocean
Phosphorus	Co-limiting, especially in old weathered soils	Co-limiting
Iron	Not typically	Yes; 30% of ocean is iron-limited (HNLC regions)
CO ₂	Potentially (CO ₂ fertilization effect)	Dissolved CO ₂ rarely limiting

39.4.4 Measuring Net Primary Productivity

Different methods access different components of NPP and apply across different scales. No single method captures everything; the modern practice combines them.

Table 462. Measuring Net Primary Productivity: Method and Scale.

Method	Scale	Approach	Captures	Misses
Harvest method	Plot (m ² –ha)	Clip aboveground biomass at peak; correct for litterfall, herbivory, mortality	ANPP directly	BNPP; rapid turnover; non-peak production
Eddy covariance	Hectares (canopy footprint)	Tower-mounted sonic anemometer + IRGA measure CO ₂ flux 10–20 Hz; partition NEP → GPP, R _e	NEP at half-hourly resolution; 24/7/365	Primarily the tower footprint; tall tower needed for forests
Remote sensing	Regional / global	MODIS NDVI → fAPAR (fraction absorbed PAR) → light-use-efficiency NPP models (e.g., MOD17)	Continental and global scales	Hidden BNPP; saturation in dense canopies; cloud occlusion
¹⁴ C uptake	Aquatic, bottle	Add NaH ¹⁴ CO ₃ ; incubate; filter and count ¹⁴ C in cells	Phytoplankton primary production	Mostly net (some respired ¹⁴ C lost); bottle effects
O ₂ light/dark bottles	Aquatic	Incubate paired bottles; light = NPP, dark = respiration; sum = GPP	GPP and NPP simultaneously	Sensitive to incubation duration
Litterfall traps + stem increment	Forest plot	Annual leaf and twig fall + dendrometer band; sum = ANPP	Long-term forest dynamics	Belowground; understory
Minirhizotrons / ingrowth cores	Plot, root-specific	Image roots through transparent tubes or harvest from buried mesh cores	BNPP estimates	Disturbance artifacts; coarse roots underrepresented

Eddy covariance is the current gold standard for ecosystem-level carbon flux measurement. A global network of about 800 flux towers (FLUXNET) provides continuous GPP, R_e, and NEP measurements across biomes; the data drive every modern terrestrial carbon model and are a primary input to the IPCC reports.

Cross-validation matters. Eddy covariance NEP at the Harvard Forest tower agreed with biometric (harvest + litterfall + dendrometer) NEP within 15% over 12 years (Barford et al. 2001, *Science*) — independent confirmation that the flux community’s numbers are real, not artifacts of filtering or gap-filling.

39.4.5 ANPP, BNPP, and Their Ratio

Total NPP partitions into aboveground (ANPP — leaves, stems, reproductive organs) and belowground (BNPP — roots, root exudates, mycorrhizal carbon transfer). Belowground production is notoriously hard to measure but is often the larger fraction:

Table 463. ANPP, BNPP, and Their Ratio: Biome and ANPP/NPP.

Biome	ANPP/NPP	BNPP/NPP	BNPP / ANPP	Driver
Tropical rainforest	0.65–0.75	0.25–0.35	0.4	Resource-rich; allocation favors canopy competition
Temperate deciduous forest	0.55–0.65	0.35–0.45	0.7	Seasonal, balanced
Temperate grassland	0.30–0.40	0.60–0.70	1.5–2.5	Drought, fire, grazing favor root storage
Tundra	0.20–0.30	0.70–0.80	3–4	Cold soils; nutrient acquisition expensive; root protection from freezing
Boreal forest	0.40–0.55	0.45–0.60	1.0–1.3	Slow N mineralisation; mycorrhizal demand high

Globally, BNPP is roughly half of total NPP — meaning *half* of the planet’s photosynthate is invested below the soil surface, where carbon turnover times can stretch into millennia. Ignoring BNPP in carbon-stock estimates underestimates terrestrial sequestration by 30–50 % for grasslands and tundra.

- Concept Check: A grassland and a forest both report ANPP = 400 g C/m²/yr. Which ecosystem has higher *total* NPP, and why does this matter for policy (e.g., carbon-credit accounting under REDD+)?
- Concept Check: A tropical rainforest has GPP = 3,000 g C/m²/yr. If autotrophic respiration consumes 50% and heterotrophic respiration consumes 80% of NPP, calculate NPP and NEP. Is this ecosystem a net carbon sink?

39.5 The Carbon Cycle and Climate Change

39.5.1 Carbon Reservoirs Across Atmosphere, Ocean, Land, and Rock

Table 464. Carbon Reservoirs Across Atmosphere, Ocean, Land, and Rock: Reservoir and Size (Pg C).

Reservoir	Size (Pg C)	Turnover time	Notes
Atmosphere	about 860 (2024)	Years	421 ppm CO ₂ (Keeling Curve)
Vegetation	about 560	Decades	Mainly tropical forests
Soil organic carbon	1,500-2,400	Decades-millennia	Largest terrestrial reservoir
Permafrost	about 1,700	Millennia	Vulnerable to thaw
Ocean surface	about 900	Months	Rapid exchange with atmosphere

Reservoir	Size (Pg C)	Turnover time	Notes
Ocean deep	about 37,000	Centuries-millennia	Largest active reservoir
Lithosphere (fossil fuels)	about 3,700 (recoverable)	Geological timescales	Being transferred to atmosphere
Marine sediments (carbonate)	>60,000,000	Millions of years	Long-term geological storage

39.5.2 Annual Carbon Fluxes (2020s)

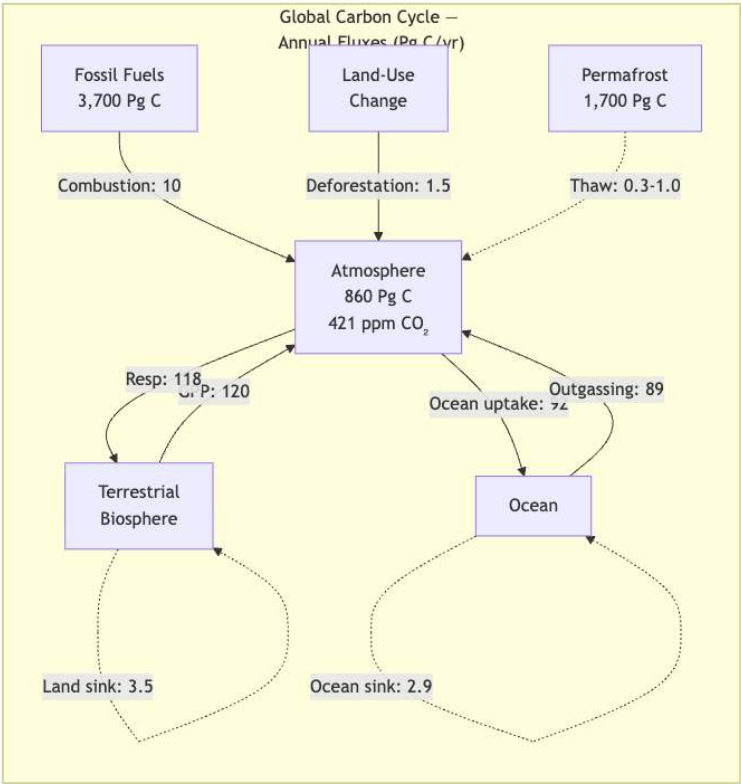


Figure 229. Carbon-budget accounting compares emissions with land and ocean sinks; the residual net atmospheric accumulation is about 4.7 Pg C per year, consistent with rising CO₂.

39.5.3 The Biological Pump

The biological pump transfers carbon from ocean surface to deep water via biological processes:

1. Photosynthesis by phytoplankton in euphotic zone fixes CO₂ into organic carbon
 2. Sinking particles — dead phytoplankton, fecal pellets, aggregates (marine snow) sink to depth
 3. Active transport — zooplankton diel vertical migration moves carbon downward (feeding at surface at night, metabolizing at depth during day)
 4. Dissolution at depth — organic carbon remineralised by bacteria, releasing CO₂ into deep water
 5. Carbonate pump — CaCO₃ shells (foraminifera, coccolithophores) sink and dissolve below the carbonate compensation depth (about 4,000 m)
- The biological pump exports about 10-15 Pg C/yr to deep water, sequestering it for centuries to millennia. Without the pump, atmospheric CO₂ would be about 200 ppm higher.

39.5.4 Key Climate Feedbacks

1. Permafrost carbon feedback (positive): Arctic/subarctic permafrost contains about 1,700 Pg C (twice the atmospheric reservoir). Warming → thaw → CO₂ + CH₄ release → more warming.

- CH₄ from **anaerobic** decomposition in thermokarst lakes is 80x more potent than CO₂ over 20 years
- Estimated +1.5-2.5°C additional warming if permafrost fully thaws (IPCC AR6 2021)
- Abrupt thaw (collapse of ice-rich permafrost) may be more important than gradual thaw; largely omitted from current climate models (Turetsky et al. 2020, *Nature Geoscience*)

2. Ocean acidification:



Ocean **pH** has decreased from about 8.2 to about 8.05 since industrialisation (30% increase in [H⁺]). Consequences:

- Decreased [CO₃²⁻] → carbonate undersaturation → dissolution of calcareous shells
- Aragonite saturation state: $\Omega_{aragonite} = \frac{[Ca^{2+}][CO_3^{2-}]}{K_{sp,aragonite}}$
- When $\Omega < 1$: aragonite dissolves
- Tropical coral reefs projected to be in net erosion by 2050 at current emission trajectories (Hoegh-Guldberg et al. 2007, *Science*)
- Pteropods (sea butterflies) — thin aragonite shells already dissolving in Southern Ocean
- Ocean acidification also impairs fish olfaction (affecting predator avoidance behavior)

3. Methane hydrates (clathrate gun hypothesis): about 500-2,500 Pg C locked in methane clathrates (ice-like structures) in ocean sediments and permafrost. Destabilisation during rapid warming → mass marine CH₄ release → catastrophic warming. Possible role in the Paleocene-Eocene Thermal Maximum (PETM, about 56 Ma): 5-8°C warming over about 10,000 years, mass marine extinction.

4. CO₂ fertilization effect (negative feedback, partially): Higher atmospheric CO₂ increases photosynthetic rate (especially in C3 plants), partially offsetting emissions. However, this effect is limited by nitrogen and phosphorus availability, and saturates at high CO₂ levels. FACE (Free-Air CO₂ Enrichment) experiments show about 15-25% NPP increase at 550 ppm, but diminishing returns beyond this.

Clinical Connection — Ocean Acidification and Food Security: Ocean acidification threatens the \$100 billion/year global shellfish industry. Oyster larvae in Pacific Northwest hatcheries experienced mass mortality beginning about 2005, traced to corrosive upwelled water with low $\Omega_{aragonite}$. Hatcheries now monitor real-time carbonate chemistry and **buffer** intake water with sodium carbonate. Wild shellfish populations cannot be similarly managed. By 2100, oyster calcification rates are projected to decline 25-40% under RCP 8.5, with cascading effects on coastal economies and nutrition — particularly in developing nations dependent on shellfish protein.

Concept Check: The ocean currently absorbs about 2.9 Pg C/yr from the atmosphere. If ocean warming reduces the solubility pump by 20%, how much additional CO₂ would remain in the atmosphere annually? What would be the approximate additional warming contribution over 50 years?

39.6 The Nitrogen Cycle

Nitrogen (N) is often the most limiting macronutrient in terrestrial and freshwater ecosystems. Despite comprising 78% of the atmosphere, N₂ is biologically inert — its triple bond (≡) requires enormous energy to break.

39.6.1 Key Nitrogen Transformations

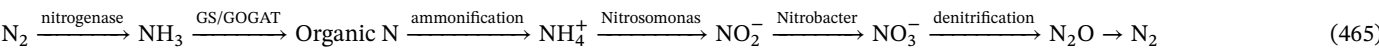


Table 465. Key Nitrogen Transformations: Process and Organisms.

Process	Organisms	Reaction	Location	Oxygen
N ₂ fixation	<i>Rhizobium</i> , <i>Azotobacter</i> , <i>Anabaena</i> , <i>Frankia</i>	N ₂ + 8H ⁺ + 8e ⁻ + 16ATP → 2NH ₃ + H ₂	Root nodules; soil; ocean	O ₂ -sensitive (nitrogenase)
Ammonification	Most decomposers	Organic N → NH ₄ ⁺	Ubiquitous	Aerobic or anaerobic
Nitrification (step 1)	<i>Nitrosomonas</i> , <i>Nitrososphaera</i> (AOA)	NH ₃ → NO ₂ ⁻	Aerobic soil/water	Required
Nitrification (step 2)	<i>Nitrobacter</i> , <i>Nitrospira</i>	NO ₂ ⁻ → NO ₃ ⁻	Aerobic soil/water	Required
Comammox	<i>Nitrospira inopinata</i>	NH ₃ → NO ₃ ⁻ (complete)	Soil, engineered systems	Required

Process	Organisms	Reaction	Location	Oxygen
Denitrification	<i>Pseudomonas</i> , <i>Paracoccus</i>	$\text{NO}_3^- \rightarrow \text{N}_2\text{O} \rightarrow \text{N}_2$	Waterlogged soil; sediments	Anaerobic
Anammox	<i>Candidatus Kuenenia</i>	$\text{NH}_4^+ + \text{NO}_2^- \rightarrow \text{N}_2 + 2\text{H}_2\text{O}$	Marine sediments	Anaerobic
DNRA	Various bacteria	$\text{NO}_3^- \rightarrow \text{NH}_4^+$	Low C:N sediments	Anaerobic

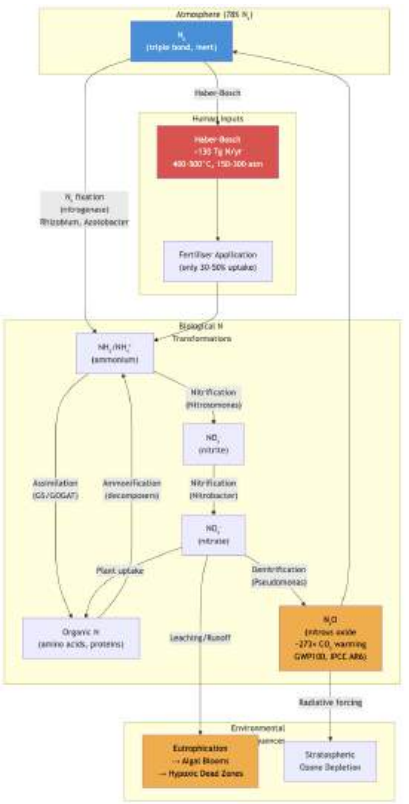
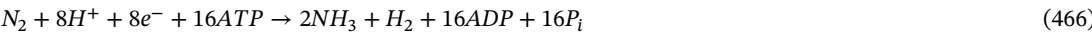


Figure 230. The nitrogen cycle showing biological transformations (fixation, ammonification, nitrification, denitrification) and anthropogenic disruption via the Haber-Bosch process. Excess reactive nitrogen cascades through ecosystems, causing eutrophication, hypoxia, and N2O-mediated climate warming and ozone depletion.

39.6.2 Biological Nitrogen Fixation

The nitrogenase enzyme complex (Fe-Mo cofactor) catalyses the most energetically expensive biological reaction:



Nitrogenase is irreversibly inactivated by O₂. Strategies for O₂ protection: - Rhizobium in legume root nodules: leghemoglobin (O₂-scavenging pink protein) maintains low O₂ - Cyanobacteria (*Anabaena*): specialized heterocyst cells lack photosystem II (no O₂ production) - Azotobacter: very high respiration rate consumes O₂ before it reaches nitrogenase

Global biological N fixation: about 130 Tg N/yr (natural) + about 130 Tg N/yr (Haber-Bosch) = about 260 Tg N/yr total.

39.6.3 Anthropogenic Nitrogen Disruption

Haber-Bosch process (1909; Fritz Haber, Nobel Prize 1918):



This single industrial process has doubled global reactive nitrogen and enabled the feeding of about 4 billion additional people. It is arguably the most important chemical invention of the 20th century — and one of the most environmentally damaging.

The reactive nitrogen cascade: Anthropogenic N travels through multiple compartments, causing damage at each step:

1. Fertiliser → crop N (typically 30-50% taken up by plants)
2. Runoff → freshwater eutrophication → algal blooms
3. Coastal zones → marine eutrophication → hypoxia (“dead zones”)
4. Denitrification → N₂O (potent greenhouse gas, 298x CO₂ warming potential over 100 years)
5. N₂O → stratospheric ozone depletion (now the primary ozone-depleting substance; Ravishankara et al. 2009, *Science*)

Major hypoxic “dead zones”: Anthropogenic Nitrogen Disruption: Location and Area (km²). {#tbl:unit_X_ecosystem_ecology_anthropogenic_nitrogen_disrupti | Location | Area (km²) | Primary nutrient source | | ——— | ————— | ————— | | Gulf of Mexico | >15,000 | Mississippi River agricultural runoff | | Baltic Sea | about 60,000 | European agricultural + industrial | | Chesapeake Bay | about 7,000 | Agricultural + urban | | East China Sea | about 20,000 | Yangtze River |

Clinical Connection — Nitrate Contamination of Drinking Water: Agricultural nitrogen runoff contaminates groundwater with nitrate (NO₃[−]). In infants, gut bacteria reduce NO₃[−] to NO₂[−], which oxidises hemoglobin to methemoglobin (Fe³⁺), incapable of carrying O₂. This causes methemoglobinemia (“blue baby syndrome”) — cyanosis and potentially fatal hypoxia. The EPA maximum contaminant level for nitrate is 10 mg/L as N. In the US Corn Belt, >20% of private wells exceed this limit. Chronic low-level nitrate exposure is also epidemiologically linked to colorectal cancer (Ward et al. 2018, *Int. J. Cancer*).

Concept Check: The Haber-Bosch process has doubled global reactive nitrogen. Trace the fate of nitrogen applied as ammonium fertiliser to a cornfield: what percentage is taken up by the crop, what happens to the rest, and what environmental consequences arise at each step?

39.7 The Phosphorus Cycle

Phosphorus has no significant gaseous phase — its cycle is sedimentary (unlike C and N):

39.7.1 Phosphorus Reservoirs and Fluxes

Table 466. Phosphorus Reservoirs and Fluxes: Reservoir and Size.

Reservoir	Size	Key features
Continental crust	Primary source	P in phosphate rock (apatite: Ca ₅ (PO ₄) ₃ (OH,F,Cl)); mined for fertiliser
Soil	Variable	P sorbed to Fe ³⁺ and Al ³⁺ oxides (makes P unavailable at pH < 5 or > 8)
Freshwater	Very low	Dissolved inorganic P (DIP) often < 10 µg/L
Ocean	Low	DIP at nanomolar concentrations in surface; higher at depth (remineralisation)
Marine sediments	Very large	Long-term geological sink

39.7.2 P Limitation in Ecosystems

- Freshwater lakes: primarily P-limited (Schindler 1977 — whole-lake experiment in Ontario demonstrated P controls algal growth; this finding led to P-detergent bans)
- Open ocean: co-limitation by N and P; N in short-term, P in long-term (Redfield ratio: 106C:16N:1P in marine phytoplankton)
- Tropical soils: severely P-limited (old weathered laterite soils; P leached over millions of years; mycorrhizal associations critical for P acquisition)

39.7.3 The Redfield Ratio

Redfield [1958]: Marine phytoplankton consistently maintain an elemental ratio of:

106C : 16N : 1P

(468)

This stoichiometric constraint means: - N:P ratio < 16 → N-limiting - N:P ratio > 16 → P-limiting - Deviation from Redfield ratio indicates which nutrient limits growth

39.7.4 Phosphorus Crisis in Food Systems

Global phosphate rock reserves are concentrated in about 6 countries (Morocco controls >70% of reserves). Depletion projections vary widely (50-400 years at current extraction rates). Phosphorus recovery from wastewater (struvite precipitation: $MgNH_4PO_4 \cdot 6H_2O$) is critical for long-term food security. Unlike nitrogen, phosphorus cannot be synthesized — it must be mined or recycled.

Concept Check: Schindler’s whole-lake experiment added P to one half and N+C to the other half. Primarily the P-enriched half developed algal blooms. Why is P the primary limiting nutrient in freshwater but N is often more limiting in the ocean?

39.8 The Sulfur Cycle

Sulfur (S) cycling connects biological, atmospheric, and geological processes:

Sulfur is a useful corrective to overly simple nutrient-cycle diagrams because it links metabolism, redox gradients, aerosols, odors, mining, acid rain, and ocean-atmosphere exchange. In sediments, sulfate reduction can dominate anaerobic respiration after oxygen and nitrate are depleted; at oxic-anoxic interfaces, sulfide oxidisers recycle reduced sulfur back toward sulfate. The biological interpretation therefore depends on redox state, electron donors, pH, and whether the system is microbial mat, wetland, hydrothermal vent, soil, or ocean surface.

39.8.1 Key Sulfur Transformations

Table 467. Key Sulfur Transformations: Process and Organisms.

Process	Organisms	Reaction	Environment
Assimilatory S reduction	Plants, bacteria	$SO_4^{2-} \rightarrow$ organic S (cysteine, methionine)	Ubiquitous
Decomposition	Decomposers	$Organic\ S \rightarrow H_2S$	Anaerobic sediments
Dissimilatory S reduction	<i>Desulfovibrio</i> , <i>Desulfobacter</i>	$SO_4^{2-} + H_2 \rightarrow H_2S$	Anaerobic (below N-reduction zone)
S oxidation	<i>Thiobacillus</i> , <i>Beggiatoa</i>	$H_2S \rightarrow S^0 \rightarrow SO_4^{2-}$	Chemolithotrophic; oxic-anoxic interface
DMS production	Marine phytoplankton	$DMSP \rightarrow DMS$ (dimethylsulphide)	Ocean surface

39.8.2 The CLAW Hypothesis

Charlson-Lovelock-Andreae-Warren (1987): Marine phytoplankton emit DMS → DMS oxidises to SO_4^{2-} aerosols in the atmosphere → these aerosols serve as cloud condensation nuclei (CCN) → more clouds → increased albedo → cooling. This represents a potential planetary thermostat (negative feedback). However, the strength of this feedback remains debated. Satellite studies show correlations between phytoplankton blooms and cloud properties, but the magnitude of the DMS-climate link is uncertain.

39.8.3 Acid Rain and Sulfur/Nitrogen Deposition

Fossil fuel combustion releases SO_2 and NO_x :



Environmental effects: $pH < 4.2$ in sensitive lakes → fish kills, forest dieback (1970s-1990s). The success of sulfur emission regulations (US Clean Air Act 1990) in reversing acid rain damage demonstrates that environmental recovery is possible with political action — a major environmental success story.

39.9 Nutrient Cycling Models: Open and Closed Ecosystem Budgets

Whether an ecosystem is a net sink or source for a nutrient depends on the relative rates of input, internal recycling, and output (leakage). Two idealised limits are useful:

Table 468. Acid Rain and Sulfur/Nitrogen Deposition.

Model	Inputs	Outputs	Internal recycling	Examples
Closed	→ 0	→ 0	Dominates	Mature tropical rainforest on ancient soil; coral reef interior
Open	Large	Large	Small relative to fluxes	Floodplain wetland; nutrient-loaded estuary; agricultural field

For a single nutrient pool X (e.g., soil-bound P, kg/ha) with input rate I (e.g., atmospheric deposition + weathering) and output rate O (leaching + erosion + harvest):

$$\frac{dX}{dt} = I - O = I - kX$$

(471)

where k is the leakage rate (yr^{-1}). At steady state ($dX/dt = 0$): $\hat{X} = I/k$, and the mean residence time is $\tau = 1/k = X/O$. A closed system has $\tau \gg 1$ (nutrients cycle internally many times before leaving); an open system has $\tau \leq 1$ (nutrients flow through quickly).

39.9.1 Hubbard Brook: The Watershed That Defined the Field

The Hubbard Brook Experimental Forest (New Hampshire, USA) hosts the longest-running ecosystem-scale watershed experiment in the world [Bormann and Likens, 1967]. The design is brilliant: a small forested watershed has a single stream outlet, so weighing rainfall inputs against streamwater outputs gives the entire ecosystem nutrient budget — no plot extrapolation needed.

In 1965–1966, Bormann, Likens, and colleagues clear-cut Watershed 2 and suppressed regrowth with herbicides for three years, then compared inputs and outputs against an undisturbed reference watershed. The results overturned the dogma that mature forests “leak” nutrients in proportion to inputs:

Table 469. Hubbard Brook: The Watershed That Defined the Field: Stream output (kg/ha/yr) and Reference (intact).

Stream output (kg/ha/yr)	Reference (intact)	Clear-cut (year 2)	Ratio
NO ₃ [−] -N	2.0	53	26×
Ca ²⁺	14	78	5.6×
K ⁺	1.7	36	21×
Streamflow (cm/yr)	73	100	1.4× (no transpiration)

The clear-cut watershed lost more N in two years than it had accumulated over decades. The lessons:

1.

Live vegetation is the single largest control on nutrient retention. Roots take up dissolved N-> build biomass -> N stays in the system.
2.

Transpiration moves water out of soils and prevents nitrate-leaching events. Removing it raises water tables and flushes nutrients to streams.
3.

Mature forests are quasi-closed for most nutrients, retaining 80–95 % of inputs through tight biological cycling.
4.

The same logic explains why agricultural watersheds (no perennial deep-rooted vegetation) leak nitrate and drive hypoxic dead zones in downstream receiving waters.

Hubbard Brook also detected acid rain in the 1970s by tracking declining streamwater Ca²⁺ concentration over decades; that signal contributed to the science underlying the U.S. Clean Air Act amendments of 1990. Few ecosystem experiments have had comparable scientific or policy impact.

Concept Check: Why does a clear-cut forest lose 20× more nitrate in streamflow than an intact forest, even though the standing soil-N pool is the same? Trace the mechanism through (a) plant uptake, (b) decomposition rate, (c) hydrology.

39.10 Marine Ecosystem Ecology and the Biological Pump

Marine ecosystems contribute roughly half of global NPP (about 50 Pg C/yr) on just two-thirds of the planet’s surface — but the productivity is enormously heterogeneous, structured by light, nutrients, and physical mixing.

39.10.1 Productivity Zones of the Ocean

Table 470. Productivity Zones of the Ocean: Zone and Depth.

Zone	Depth	Light	NPP (g C/m ² /yr)	Drivers
Euphotic	0–100 m	> 1 % surface PAR	50–600	Phytoplankton growth; temperature- and nutrient-limited
Mesopelagic (twilight)	100–1,000 m	< 1 %	0 (heterotrophic)	Diel vertical migrators; remineralisation
Bathypelagic / abyssopelagic	1,000–6,000 m	None	0 (heterotrophic + chemo)	Marine snow rains down; deep-sea food webs
Coastal upwelling	0–200 m	High	500–2,000	Wind-driven upwelling brings cold, nutrient-rich water (Peruvian, Benguela, Californian, Canary currents)
Subtropical gyres (“ocean deserts”)	0–200 m	High	25–100	Permanent thermal stratification; nutrients trapped at depth
Polar oceans	0–200 m (seasonal)	Strong seasonality	50–300 (intense in summer)	Diatom blooms after ice retreat
Continental shelves	0–200 m	High	100–600	River nutrient inputs; tidal mixing

The four major coastal upwelling systems (eastern boundaries of ocean basins) cover < 1 % of ocean area but produce about 20 % of global fisheries catch — a dramatic illustration of how local mixing physics can dwarf area-based productivity expectations.

39.10.2 Biological Pump and Its Efficiency

The biological pump operates at three scales:

Export production = NPP × e-ratio

(472)

where the e-ratio is the fraction of NPP that escapes the surface layer as sinking particles. Typical values: 0.1 in oligotrophic gyres (most carbon is recycled in surface), 0.3–0.5 in upwelling zones (large diatoms sink fast), and 0.5+ during diatom blooms in polar oceans.

Sequestration efficiency = $\exp(-z/z_{1/2})$

(473)

The Martin curve (Martin et al. 1987, *Deep-Sea Research*) describes how export flux attenuates with depth as bacteria remineralise sinking organic matter. Carbon that escapes below about 1,000 m is sequestered for centuries to millennia; carbon remineralised in the upper ocean returns to the atmosphere within years.

Climate change is reorganising both pumps. Warming stratifies the surface ocean, reducing nutrient supply from depth and lowering NPP; acidification reduces calcareous-shell production, weakening the carbonate pump; and oxygen minimum zones are expanding, shifting remineralisation pathways. The net effect on the future ocean carbon sink is one of the largest open questions in Earth-system science.

Clinical Connection — Harmful Algal Blooms. Nutrient-loaded coastal waters increasingly experience harmful algal blooms (HABs) by *Karenia brevis* (red tide, Florida — produces brevetoxins → respiratory distress, fish kills), *Pseudo-nitzschia* (Pacific coast — produces domoic acid → amnesic shellfish poisoning, lethal in birds and humans), and cyanobacterial blooms in Lake Erie (microcystin → liver toxicity; the 2014 Toledo, Ohio drinking-water shutdown affected 500,000 people). HABs are open-system biogeochemistry meeting public health: agricultural runoff loads N and P to coastal waters, warm summers stratify and warm the surface, and the resulting blooms produce neurotoxins that move up the food chain via shellfish and finfish to humans. Each of the carbon, nitrogen, and phosphorus cycle disruptions in this chapter contributes.

39.11 Soil Formation, Pedogenesis, and Soil-Carbon Feedbacks

Soils are the central terrestrial reservoir for organic carbon (1,500–2,400 Pg C, more than vegetation and atmosphere combined) and the medium through which nutrient cycles are mediated. Pedogenesis (soil formation) is itself an ecosystem-scale process operating over centuries to millennia.

39.11.1 Five State Factors (Jenny 1941)

Soil = f (climate, organisms, relief, parent material, time)

(474)

This CLORPT framework remains the foundational organizing principle of pedology. Climate sets the rates of weathering and decomposition; organisms (especially plants and microbes) drive organic matter accumulation; relief (topography) routes water and erosion; parent material (bedrock) supplies the mineralogy; and time integrates everything.

39.11.2 Soil Horizons and Vertical Differentiation

A mature soil typically displays vertical layering reflecting depth-dependent processes:

Table 471. Soil Horizons and Vertical Differentiation: Horizon and Depth.

Horizon	Depth	Processes	Composition
O (organic)	Top 0–10 cm	Litter accumulation; decomposition	Leaf litter; partially decomposed organic matter
A (topsoil)	5–30 cm	Bioturbation; humification; root activity	Dark, organic-matter-rich; high biological activity
E (eluvial)	0–50 cm	Leaching of clays, Fe, Al downward	Pale, depleted; sandy texture
	(boreal/podzol)		
B (subsoil)	30–150 cm	Illuviation: accumulation of leached materials	Clay, Fe, Al oxides; often reddish or yellowish
C (parent material)	Below B	Slow weathering of bedrock	Rock fragments transitioning to soil
R (bedrock)	Bottom	None	Unweathered rock

39.11.3 Three Stages of Pedogenesis

1. Weathering and primary mineral breakdown. Physical fragmentation and chemical hydrolysis of bedrock release mineral nutrients (Ca, Mg, K, P, Fe). Cyanobacteria and lichens accelerate weathering through carbonic and oxalic acid secretion. Net rate: 0.01–0.1 mm/yr (slow!).
2. Organic matter accumulation. Pioneer plants colonise; their litter fuels decomposers; humus forms (recalcitrant polymeric organic matter). Net soil organic carbon (SOC) increases at 5–50 g C/m²/yr in temperate ecosystems for centuries.
3. Horizon differentiation and steady-state. Vertical translocation of clays, Fe/Al, and dissolved organic matter creates the A–E–B horizon sequence. Eventually inputs balance losses (leaching + decomposition + erosion) and SOC reaches a climate-determined ceiling.

Tropical soils on ancient Gondwanan parent material (Brazilian shield, Australian outback) are at stage 3 *and ancient* — most P has leached over millions of years, leaving extremely low-fertility laterites; this explains why tropical rainforest productivity is high (rapid recycling) but cleared tropical soils are infertile (no recyclable pool left). Glacier-Bay primary succession (section 37) is the same process running at the centennial timescale.

39.11.4 Social Insects as Soil Engineers

Termites and ants are organismal components of CLORPT, not incidental soil fauna. Termites fragment litter, digest lignocellulose through gut symbionts, build galleries and mounds, and create redox and moisture gradients that alter decomposition and gas exchange [Brune, 2014, Ocko et al., 2017]. Ants excavate nests, move mineral particles, concentrate organic matter, and redistribute seeds and arthropod remains. In dry agricultural systems, plots with ants and termites can show higher infiltration, nutrient redistribution, and crop yield, illustrating that small-bodied social insects can have ecosystem-level effects [Evans et al., 2011].

The general lesson is that “decomposition” is not just microbes dissolving dead matter. It is a coupled detrital food web in which animal engineers expose surface area, move particles, condition microclimate, and host microbial metabolisms. Removing those engineers can change water flow, nutrient residence time, and plant recruitment even when plant species and climate remain the same.

39.11.5 Soil Carbon and Climate Feedback

Warming accelerates microbial decomposition more than it accelerates plant productivity, so a warmer world is expected to release soil carbon to the atmosphere — a positive feedback estimated at +30 to +200 Pg C over the 21st century (Crowther et al. 2016, *Nature*). Permafrost soils contain about 1,700 Pg C, twice the atmospheric pool, and are one of the largest uncertainties in 21st-century climate trajectories.

39.12 Coupled Biogeochemical Cycles and Ecological Stoichiometry

The C, N, and P cycles do not operate independently — biological demand stitches them into a coupled system whose stoichiometry is one of the most powerful diagnostic tools in ecosystem science.

39.12.1 The Redfield Ratio Revisited

Marine phytoplankton consistently maintain an elemental composition of 106 C : 16 N : 1 P [Redfield, 1958]. This ratio also describes the average composition of dissolved nutrients in deep ocean water — strong evidence that biology actively controls ocean chemistry (the Redfield insight). Deviations from Redfield diagnose limitation:

Table 472. The Redfield Ratio Revisited: Ambient N : P and Implication.

Ambient N : P	Implication
< 16 (e.g., 8)	N-limiting; nitrogen-fixers favored
≈ 16	Balanced; both potentially limiting
> 16 (e.g., 30)	P-limiting; high-P-affinity species favored

Terrestrial systems show similar but more variable ratios reflecting differences between woody (high C : N : P) and herbaceous tissues. Forest canopy: about 1200 : 28 : 1. Soil microbial biomass: about 60 : 7 : 1 (N- and P-rich relative to plants — explaining why microbes immobilise mineral nutrients).

39.12.2 Stoichiometric Coupling of C, N, P, Fe, and S

Ecosystem-scale stoichiometry generates predictable feedbacks:

- CO₂ fertilization has limits. Higher atmospheric CO₂ raises plant C : N ratios; without proportional N input, growth saturates (the progressive nitrogen limitation hypothesis confirmed by long-term FACE experiments).
- N deposition has P costs. Anthropogenic N enrichment shifts ecosystems from N- to P-limited; soil and freshwater P demand rises sharply.
- Anoxia shifts cycles. Hypoxic dead zones suppress nitrate-dependent respiration pathways but enable iron and sulfate reduction; the N : P : Fe : S coupling reorganises.

39.12.3 Planetary Boundaries and Biogeochemical Overshoot

Richardson et al. [2023] and the Stockholm Resilience Center frame anthropogenic biogeochemical disruption as transgression of planetary boundaries. In the current assessment, six of nine boundaries are crossed: climate change, biosphere integrity, biogeochemical flows (N and P), land-system change, freshwater change, and novel entities (chemical pollution). Stratospheric ozone remains a regulatory success story, while ocean acidification is close to its boundary. Ecosystem ecology provides the quantitative basis for each of these limits — and for designing interventions to return inside them.

39.13 Quantifying Ecosystem Services in Earth-System Science

39.13.1 Quantifying and Valuing Services

Beyond the opening qualitative categories, ecosystem services are increasingly quantified using three valuation approaches:

Table 473. Quantifying and Valuing Services: Method and Approach.

Method	Approach	Strengths	Limitations
Market price	Use observed prices for traded ecosystem outputs (timber, fish)	Direct; defensible	Primarily captures provisioning services
Replacement cost	Estimate cost of engineering substitutes (water treatment plants for wetland filtration)	Tangible	Assumes substitutes exist; ignores non-substitutables
Willingness-to-pay	Survey residents on what they would pay for clean air, biodiversity, etc.	Captures cultural and existence value	Hypothetical bias; income-dependent

Costanza et al. (2014, *Ecosyst. Serv.*) updated their landmark 1997 estimate: global ecosystem services are worth about \$125 trillion/yr (vs. global GDP of about \$100 trillion/yr in 2024). The TEEB initiative (The Economics of Ecosystems and Biodiversity, 2010) extended these methods to corporate and government decision-making. Ecosystem-service trade-offs (e.g., cropland conversion gains provisioning food but loses regulating climate and water purification) are now standard in environmental impact assessments.

39.13.2 The Gaia Hypothesis: Critical Evaluation

Lovelock and Margulis [1974] proposed the Gaia hypothesis: life and the abiotic environment form a coupled, self-regulating system. Modern Earth System Science keeps the coupling but rejects teleology; the key question is which feedbacks stabilize the Earth system and which amplify perturbations. Core claims and current standing:

Table 474. The Gaia Hypothesis: Critical Evaluation: Gaia claim and Status.

Gaia claim	Status
Atmospheric composition (O ₂ , CH ₄ , N ₂ O) is biologically driven	Strongly supported — biology is essential
Earth’s climate is biologically buffered (CLAW, biological pump, vegetation albedo)	Partially supported — feedbacks exist but are not always stabilizing
Biota act <i>teleologically</i> to maintain habitability	Rejected — no mechanism for group/planetary selection (Doolittle 1981); selection acts on individuals
The biosphere is a superorganism	Metaphorical — useful for systems thinking but not a literal claim

The modern synthesis treats Gaia as Earth System Science: biology, geochemistry, hydrology, and atmospheric science form a single coupled system, with feedbacks that can be stabilizing (negative) or destabilising (positive) depending on the perturbation. The IPCC reports, the Anthropocene Working Group, and the Planetary Boundaries framework are the descendants of this line of thinking.

Per Dobzhansky [1973]’s dictum that “nothing in biology makes sense except in the light of evolution,” nothing in 21st-century ecology makes sense except in the light of human-driven Earth system change. The ecosystem ecology of this chapter — energy flow, biogeochemical cycles, ecosystem services — is now the operating manual for managing the planet itself.

Concept Check: The Gaia hypothesis predicts that the biosphere stabilizes Earth’s habitability. List two examples where biological feedbacks stabilize the climate system and two where they destabilise it. What does this tell you about the difference between “Gaia as superorganism” and “Earth as a coupled biogeochemical system”?

39.14 The Water Cycle (Hydrological Cycle)

The water cycle connects most biogeochemical cycles and drives nutrient transport:

For biology, the water cycle is also a vegetation and land-use cycle. Roots, stomata, leaf area, soil organic matter, and microbial crusts influence infiltration, transpiration, runoff, and groundwater recharge; deforestation, drainage, compaction, and irrigation alter those same fluxes. Climate-change impacts on drought, flood risk, and food security therefore cannot be read from precipitation totals alone; residence time, timing, storage, and plant access to water matter just as much.

39.14.1 Key Hydrological Fluxes

Table 475. Key Hydrological Fluxes: Process and Rate (10³ km³/yr).

Process	Rate (10 ³ km ³ /yr)	Description
Evaporation (ocean)	434	Largest single flux
Precipitation (ocean)	398	
Evapotranspiration (land)	71	Plant transpiration = 60-90% of terrestrial evaporation
Precipitation (land)	107	Balances net ocean→land atmospheric transport
Runoff (rivers to ocean)	36	

Plant transpiration is a massively underappreciated flux: a single large oak tree transpires about 400 L/day. Tropical forests generate about 50% of their own rainfall through transpiration recycling (the “flying rivers” of the Amazon). Deforestation disrupts this cycle, potentially triggering tipping points toward savannification.

39.15 Ecosystem Services and Conservation Economics

39.15.1 Biodiversity-Ecosystem Functioning (BEF)

Tilman et al. (1996, 2001): Species richness generally increases ecosystem productivity, stability, and nutrient retention.

Mechanisms: - Complementarity: different species use different resource pools/times; **niche** partitioning increases total resource capture - Sampling effect: more diverse communities more likely to contain highly productive species - Facilitation: some species improve conditions for others (nitrogen fixers enrich soil for grasses)

The insurance hypothesis [**Yachi and Loreau, 1999**]: Biodiversity provides insurance against environmental fluctuations. In diverse communities, when one species declines due to unfavorable conditions, others compensate. This stabilizes ecosystem function over time.

39.15.2 Payment for Ecosystem Services (PES)

Table 476. Payment for Ecosystem Services (PES): Program and Mechanism.

Program	Mechanism	Scale
REDD+	Carbon market payments to prevent deforestation	International
Costa Rica PES	Government payments to landowners for forest conservation	National
Pollination services	Beekeepers paid by orchardists	Local
Wetland banking	Developers purchase credits for wetland destruction	National (US)

Challenges: Additionality (would conservation have happened anyway?), leakage (deforestation displaced elsewhere), permanence (forest may be cut later), measurement (how much carbon is actually stored?).

Concept Check: The Millennium Ecosystem Assessment found that 60% of ecosystem services are degraded. Give three specific examples of degraded ecosystem services and explain how the degradation of each affects human wellbeing.

39.16 Worked Example: Net Primary Productivity and Trophic Transfer

Problem: In a lake ecosystem, the gross primary productivity (GPP) of phytoplankton is 10,000 J/m²/yr. The phytoplankton expend 4,000 J/m²/yr via cellular respiration (*R*). Primary consumers (zooplankton) subsequently ingest the phytoplankton with a trophic efficiency of 10%. Calculate the net primary productivity (NPP) of the phytoplankton and the energy available to the secondary consumers.

Solution:

Step 1. Calculate Net Primary Productivity (NPP). NPP is the energy that remains in the primary producers after respiration.

$$NPP = GPP - R$$

$$NPP = 10,000 \text{ J} - 4,000 \text{ J} = 6,000 \text{ J/m}^2/\text{yr}$$

Step 2. Calculate the energy transferred to primary consumers. The zooplankton consume with a 10% trophic efficiency.

$$\text{Zooplankton Production} = NPP \times 0.10$$

$$\text{Zooplankton Production} = 6,000 \text{ J} \times 0.10 = 600 \text{ J/m}^2/\text{yr}$$

Step 3. Calculate the energy available to secondary consumers. If secondary consumers (e.g., small fish) also have a 10% trophic efficiency:

$$\text{Fish Production} = \text{Zooplankton Production} \times 0.10$$

$$\text{Fish Production} = 600 \text{ J} \times 0.10 = 60 \text{ J/m}^2/\text{yr}$$

Answer: The NPP of the phytoplankton is 6,000 J/m²/yr, and the energy available to the secondary consumers (produced by primary consumers) is 60 J/m²/yr.

39.17 Worked Example: Nutrient Pool Mass Balance and Residence Time

Problem: A forested watershed holds a soil-available nitrogen pool of $X = 800 \text{ kg N/ha}$. Atmospheric deposition plus weathering supply an input of $I = 8 \text{ kg N/ha/yr}$, and the pool is at steady state. Calculate the stream-plus-erosion output flux O , the mean residence time τ , and the leakage rate k , then verify the steady-state pool size and interpret whether the system is open or closed.

Solution:

Step 1. Identify the given variables. - Nitrogen pool (X) = 800 kg N/ha - Input flux (I) = 8 kg N/ha/yr - Steady state: $dX/dt = 0$, so output equals input.

Step 2. Determine the output flux from the steady-state mass balance.

$$\frac{dX}{dt} = I - O = 0 \Rightarrow O = I = 8 \text{ kg N/ha/yr}$$

Step 3. Compute the mean residence time.

$$\tau = \frac{X}{O} = \frac{800 \text{ kg N/ha}}{8 \text{ kg N/ha/yr}} = 100 \text{ yr}$$

Step 4. Compute the leakage rate and check the steady-state pool.

$$k = \frac{1}{\tau} = \frac{1}{100 \text{ yr}} = 0.01 \text{ yr}^{-1}$$

$$\hat{X} = \frac{I}{k} = \frac{8 \text{ kg N/ha/yr}}{0.01 \text{ yr}^{-1}} = 800 \text{ kg N/ha}$$

The recovered \hat{X} equals the stated pool, confirming the system is genuinely at steady state.

Answer: $O = 8 \text{ kg N/ha/yr}$, $\tau = 100 \text{ yr}$, and $k = 0.01 \text{ yr}^{-1}$. Because $\tau = 100 \text{ yr} \gg 1$, an average nitrogen atom is recycled internally about 100 times before it leaves the watershed, so this is a tightly retaining, quasi-closed system; a disturbance that strips deep-rooted vegetation would raise O , collapse τ , and rapidly flush the nitrogen pool to streamwater.

39.17.1 Worked Example — Carbon Budget, NEP, and the Sink-to-Source Tipping Point

Problem: A tropical rainforest has gross primary production $GPP = 3,000 \text{ gC/m}^2/\text{yr}$ and autotrophic respiration $R_a = 1,500 \text{ gC/m}^2/\text{yr}$. Heterotrophic respiration (decomposers) is $R_h = 1,400 \text{ gC/m}^2/\text{yr}$. (a) Compute net primary production (NPP) and net ecosystem production (NEP). (b) A 1.5°C warming increases R_h by 10% with no change in GPP or R_a . Recompute NEP. (c) Calculate cumulative carbon flux change over a 50-year warming scenario relative to baseline.

Solution:

Step 1. Compute baseline NPP and NEP.

$$NPP = GPP - R_a = 3,000 - 1,500 = 1,500 \text{ gC/m}^2/\text{yr}$$

$$NEP = NPP - R_h = 1,500 - 1,400 = 100 \text{ gC/m}^2/\text{yr}$$

$NEP > 0$, so the ecosystem is a *net carbon sink* — it sequesters 100 gC/m^2 each year that does not return to the atmosphere.

Step 2. Apply the 10% warming increase in R_h .

$$R_{h,\text{new}} = 1,400 \times 1.10 = 1,540 \text{ gC/m}^2/\text{yr}$$

$$NEP_{\text{new}} = 1,500 - 1,540 = -40 \text{ gC/m}^2/\text{yr}$$

$NEP < 0$ — the ecosystem has *flipped from sink to source*. A modest fractional change in decomposer respiration (10%) overwhelms the absolute NPP advantage because NEP is the small difference between two large gross fluxes.

Step 3. Cumulative 50-year flux change.

Per-year change relative to baseline: $-40 - (+100) = -140 \text{ gC/m}^2/\text{yr}$. Over 50 years and per square meter:

$$\Delta C_{50} = -140 \times 50 = -7,000 \text{ gC/m}^2 = -7 \text{ kgC/m}^2$$

At an ecosystem footprint of 10^{12} m^2 (a representative tropical forest region of $\sim 10^6 \text{ km}^2$), this is $-7 \times 10^{12} \text{ kg C} = -7 \text{ Pg C}$ cumulative — comparable to a year of global fossil emissions, released from a single biome by a respiration sensitivity, not a deforestation event.

Step 4. Interpretation.

The structural lesson is asymmetry: GPP and R_h have different temperature sensitivities (Q_{10} values typically higher for R_h than for photosynthesis at high baseline temperatures). NEP is a small residual of large opposing fluxes, so its sign is fragile. This is the mathematical core of why tropical forests, peatlands, and permafrost are tipping-point ecosystems: the sink they provide is not robust to a modest warming-driven imbalance between two large fluxes.

Answer: Baseline $NEP = +100$, warmed $NEP = -40$, cumulative 50-year flip $= -7 \text{ kgC/m}^2$ (an order -7 Pg C over a representative tropical forest region).

39.17.2 Concept Check (Analyze) — Redfield Stoichiometry, Liebig’s Law, and Coastal Hypoxia

The Redfield ratio for marine phytoplankton is C:N:P = 106 : 16 : 1 by atoms (so N:P = 16 : 1). A coastal zone receives agricultural runoff with N:P = 40 : 1 — heavily enriched in N relative to P.

- (a) Apply Liebig’s law of the minimum to identify which nutrient limits phytoplankton growth at this incoming N:P ratio. Justify your answer by comparing the supply ratio to the Redfield demand ratio.
- (b) Predict the resulting community composition shift. In particular, analyze why N-fixing cyanobacteria (which can fix atmospheric N₂ but still require P from the water column) might *not* dominate here, even though N is abundant. What does this say about the difference between “limiting” and “useful” in nutrient ecology?
- (c) Algal bloom decomposition consumes oxygen. The stoichiometry of aerobic respiration is approximately CH₂O + O₂ → CO₂ + H₂O — one mole of O₂ consumed per mole of organic C oxidized. If a bloom adds 100 gC/m³ of organic matter and the water column initially holds 8 mg O₂/L, calculate whether hypoxia (defined as < 2 mg O₂/L) will develop assuming complete oxidation and no vertical mixing. (Hint: convert gC to moles, use 1:1 O₂:C stoichiometry, convert moles O₂ to mg/L using molar mass 32 g/mol.)
- (d) Synthesize: explain why coastal “dead zones” (Gulf of Mexico, Baltic Sea, Chesapeake Bay) are a stoichiometric problem — a mismatch between the N:P supply ratio from agricultural watersheds and the Redfield demand ratio of the receiving plankton — not simply an over-fertilization problem.

39.17.3 Concept Check (Evaluate) — Ecosystem Service Valuation

Costanza et al. (1997) estimated the annual value of global ecosystem services at roughly \$33 trillion, larger than the global GDP at the time. The estimate combined replacement-cost, willingness-to-pay (contingent valuation), and market-price approaches.

- (a) Evaluate each method’s appropriateness for a specific service. (i) Pollination by wild bees: which method is most defensible, and why? (ii) Wetland aesthetic / cultural value: which method, and what biases does it introduce? (iii) Timber harvest from a managed forest: which method, and what externalities does it ignore?
- (b) Critique the methodological asymmetry that produces systematically low valuations for *regulating* services (climate regulation, water purification, nutrient cycling) relative to *provisioning* services (food, fiber, timber). Reason about why markets exist for provisioning outputs but not for the regulating ones, and how the absence of a market signal biases policy.
- (c) Construct a brief argument for or against using monetary valuation in conservation decision-making. Address at least one ethical objection (commodification of nature, intergenerational discounting) and one practical advantage (commensurability with infrastructure-cost analysis). Conclude with a recommendation about whether and how monetary valuation should enter an ecosystem-management decision framework.

39.18 Current Evidence and Frontier Biology: Ecosystem Ecology

For Ecosystem Ecology, frontier biology belongs inside the evidence logic of the chapter. Ecology and conservation decisions increasingly combine field data, remote sensing, community knowledge, model uncertainty, and explicit values. The core reading question is this: ecosystem claims should track stocks, fluxes, residence times, boundaries, and coupled cycles.

- What to verify: identify the observation, model, assay, or dataset that would make the claim stronger or weaker.
- What to qualify: state the scale, organism, cell type, environmental condition, or population where the claim is expected to hold.
- What to compare: test at least one alternative explanation, baseline, or null model before treating the pattern as causal.
- What to cite: distinguish primary evidence, review synthesis, public dataset, and institutional guidance; for recent or numeric claims, prefer the source closest to the measurement and state what has changed since it was published.

Select biodiversity and conservation metrics by decision need: abundance, interaction, function, risk, service, and governance metrics answer different questions [Intergovernmental Science-Policy Platform on Biodiversity and Ecosystem Services, 2019, 2024, World Wide Fund for Nature, 2024, International Union for Conservation of Nature, 2025, Food and Agriculture Organization of the United Nations, 2024].

Source practice: For ecology and conservation claims, cite assessment sources and state whether the evidence is an index, risk assessment, service valuation, satellite product, or policy synthesis [Intergovernmental Science-Policy Platform on Biodiversity and Ecosystem Services, 2024, NOAA Coral Reef Watch, 2025, Food and Agriculture Organization of the United Nations et al., 2025].

Vegetation-carbon claims are measurement-sensitive: daily rainfall variability can strongly affect global vegetation activity, so ecosystem productivity arguments should distinguish total precipitation from event timing and intensity [Feldman et al., 2024].

39.18.1 Current Evidence Map: Agroecology as Coupled Fluxes

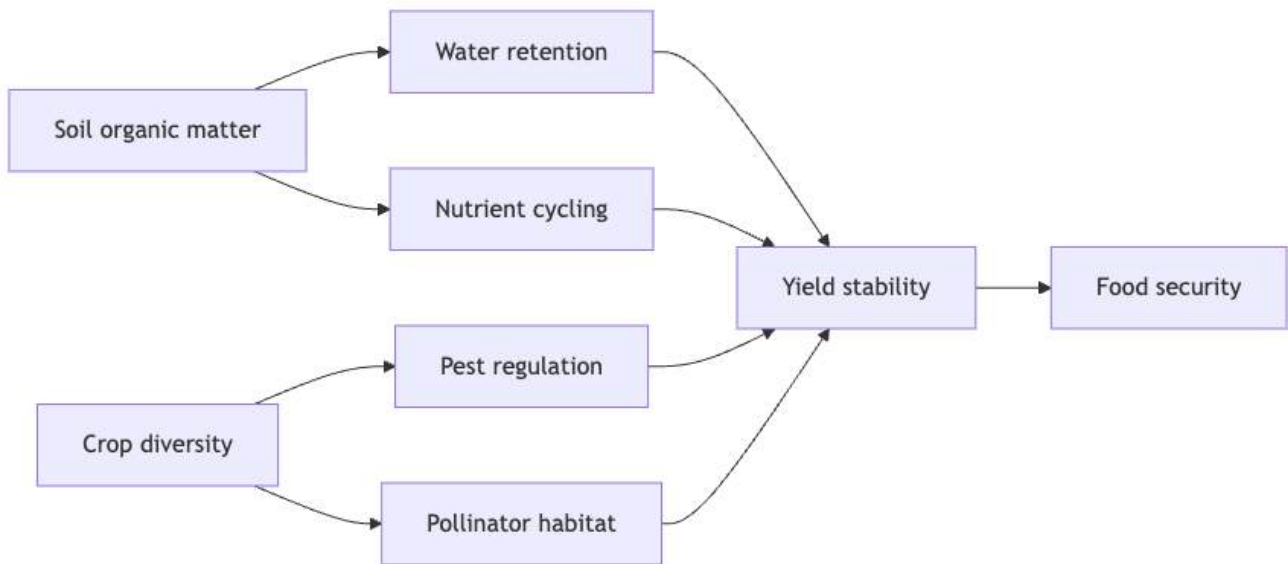


Figure 231. Food-security claims should connect ecological mechanisms to access, resilience, livelihoods, and tradeoffs rather than equating yield alone with nutrition [fao2025sofi].

39.19 Key Terms

Table 477. Current Evidence Map: Agroecology as Coupled Fluxes: Term and Definition.

Term	Definition
GPP	Gross Primary Production; total CO ₂ fixation rate in an ecosystem
NPP	Net Primary Production; GPP - autotrophic respiration; biomass available to consumers
NEP	Net Ecosystem Production; NPP - heterotrophic respiration; ecosystem carbon balance
NBP	Net Biome Production; NEP - disturbance losses; regional carbon balance
Trophic efficiency	Fraction of energy at trophic level <i>n</i> transferred to level <i>n</i> + 1; typically about 10%
Biomagnification	Increasing concentration of persistent pollutants at higher trophic levels
Eutrophication	Nutrient enrichment of water body → algal bloom → low O ₂ → hypoxia
Biogeochemical cycle	Movement of an element through biotic and abiotic compartments
Haber-Bosch process	Industrial NH ₃ synthesis; doubles global reactive N; drives eutrophication
Biological pump	Transfer of carbon from ocean surface to deep water via biological processes
Permafrost feedback	Warming → permafrost thaw → CO ₂ + CH ₄ release → further warming
Ocean acidification	CO ₂ absorption → carbonic acid → pH decrease → carbonate undersaturation
DMS (dimethylsulphide)	Volatile S compound from phytoplankton; → cloud condensation nuclei
Redfield ratio	106C:16N:1P stoichiometry of marine phytoplankton
Reactive nitrogen cascade	Sequential environmental damage as anthropogenic N moves through compartments
REDD+	International mechanism for carbon payments to prevent deforestation
Eddy covariance	Micrometeorological method for measuring ecosystem carbon flux
CLAW hypothesis	DMS-cloud-albedo feedback as planetary thermostat
ANPP / BNPP	Aboveground / belowground net primary production; ratio varies from 0.4 (rainforest) to 3+ (tundra)
Eddy covariance	Continuous tower-based measurement of ecosystem CO ₂ flux; gold standard for NEP
Martin curve	Exponential attenuation of organic-matter flux with depth in the ocean
Hubbard Brook	Long-running watershed experiment that demonstrated the dominant role of vegetation in nutrient retention
CLORPT	Jenny’s five soil-forming state factors: climate, organisms, relief, parent material, time

Term	Definition
Soil horizons	Vertical layers (O, A, E, B, C, R) reflecting depth-dependent pedogenic processes
Planetary boundaries	Quantitative limits on anthropogenic perturbation across nine Earth-system processes
Earth System Science	Coupled study of biology, geochemistry, hydrology, and atmospheric science as a single planetary system
Export production / e-ratio	Fraction of NPP that escapes the surface ocean as sinking particles
Open vs. closed cycle	Whether a nutrient cycle is dominated by external fluxes (open) or internal recycling (closed)
Mean residence time (τ)	X/O ; average time a nutrient atom spends in a pool before leaving

39.20 Review Questions

1. An estuary receives large inputs of fertiliser-derived N and P from agricultural runoff each spring. Trace the cascade of events from nutrient loading to hypoxia, naming each ecological and microbial process involved. Which specific microbial process creates the anoxic condition?
2. A tropical rainforest has $GPP = 3,000 \text{ g C/m}^2/\text{yr}$ and autotrophic respiration $= 1,500 \text{ g C/m}^2/\text{yr}$. Heterotrophic respiration $= 1,200 \text{ g C/m}^2/\text{yr}$. Calculate: (a) NPP, (b) NEP, (c) Is this ecosystem a net carbon sink or source? (d) If deforestation converts this to farmland with $NEP = -200 \text{ g C/m}^2/\text{yr}$, what is the additional carbon released per hectare per year?
3. Iron fertilization experiments (Martin 1990: “Give me half a tanker of iron and I will give you an ice age”) showed that adding Fe to HNLC ocean regions triggers phytoplankton blooms. (a) Explain why these regions are high in N and P but low in phytoplankton. (b) Why doesn’t iron fertilization cause long-term net CO_2 drawdown? (c) What are the ecological risks of large-scale iron fertilization?
4. The permafrost carbon feedback is estimated to release 1-1.5 Pg CO_2 -equivalent per year for each degree of additional warming. Current warming projections suggest 2-4°C above pre-industrial by 2100. Calculate the range of additional CO_2 -equivalent that permafrost might contribute over 80 years, assuming linear temperature rise. Compare with annual fossil fuel emissions of about 10 Pg C/yr.
5. Compare the nitrogen and phosphorus cycles in terms of: (a) whether they have a significant atmospheric phase, (b) the primary anthropogenic disruption, (c) the main environmental consequence, and (d) whether the element can be industrially synthesized from atmospheric or geological sources.
6. Using the concept of trophic efficiency, calculate how many kilograms of phytoplankton are needed to produce 1 kg of tuna (assume tuna feeds at trophic level 4 with 10% efficiency at each step). How does this relate to the environmental footprint of eating high-trophic-level seafood?
7. Explain the biological pump in detail. Why is it important for climate regulation? If ocean warming stratifies the surface layer more strongly (reducing nutrient upwelling), what happens to the efficiency of the biological pump and atmospheric CO_2 ?
8. The Keeling Curve shows atmospheric CO_2 rising from 315 ppm in 1958 to 421 ppm in 2024. Given that about 55% of anthropogenic CO_2 emissions are absorbed by land and ocean sinks: (a) What would atmospheric CO_2 be without these sinks? (b) If ocean acidification reduces the ocean’s capacity to absorb CO_2 by 15%, how much additional CO_2 would remain in the atmosphere per year?
9. A farmer applies 200 kg N/ha as ammonium nitrate fertiliser. Primarily 40% is taken up by the corn crop. Trace the fate of the remaining 120 kg N/ha through the nitrogen cycle: what fraction is likely denitrified, leached as nitrate, volatilised as NH_3 , and converted to N_2O ? What is the total environmental cost of this “excess” nitrogen?
10. Compare the CLAW hypothesis (DMS-cloud feedback) with the permafrost carbon feedback. One is a negative feedback and one is positive. Explain which is which, their relative magnitudes, and their implications for Earth’s climate trajectory.
11. Assign trophic levels with `food_web_trophic_levels` for a three-species chain; verify tuna-style pyramids require multiplying efficiencies.
12. Why is Redfield stoichiometry a diagnostic for nutrient limitation rather than a comprehensive constant?
13. The Hubbard Brook clear-cut experiment increased streamwater NO_3^- losses 26-fold. Trace the mechanism through (a) cessation of plant uptake, (b) accelerated decomposition without canopy cooling, (c) elevated water tables and reduced transpiration. Why is this evidence that mature forests function as quasi-closed nutrient systems?
14. Compare four methods for measuring NPP (harvest, eddy covariance, ^{14}C , MODIS remote sensing). For each, give one ecosystem where it is the *most* defensible method and one where it would systematically underestimate true NPP.

15. A coastal upwelling zone has surface NPP = 1,500 g C/m²/yr and an e-ratio of 0.4; a subtropical gyre has NPP = 50 g C/m²/yr and an e-ratio of 0.1. (a) Calculate export production for each. (b) If both export equal *fractions* of carbon below 1,000 m via the Martin curve ($z_{1/2} = 200$ m), which contributes more to long-term carbon sequestration per unit area? (c) How does climate-driven stratification of the surface ocean change both numbers?
16. Explain the ANPP/BNPP partition for a temperate grassland (BNPP/ANPP ≈ 2) vs. a tropical rainforest (BNPP/ANPP ≈ 0.4). Why does this partition affect (a) carbon-credit accounting under REDD+, (b) ecosystem response to drought, (c) long-term soil organic carbon accumulation?
17. Apply the Redfield ratio to diagnose three scenarios: (a) ambient N : P = 6, (b) N : P = 16, (c) N : P = 35. For each, predict which nutrient is limiting and which functional groups (e.g., diatoms, cyanobacteria, dinoflagellates) you expect to dominate.
18. The Gaia hypothesis claims Earth’s biosphere actively maintains habitability. Evaluate this claim by listing two stabilizing biological feedbacks (negative) and two destabilising ones (positive). What is the difference between “Gaia as a metaphor for Earth System Science” and “Gaia as a literal superorganism”? Why was Doolittle (1981)’s critique decisive?
-

39.21 Further Reading and Source Notes: Ecosystem Ecology

- Levin (1998). Ecosystems and the Biosphere as Complex Adaptive Systems. *Ecosystems*, 1.
 - Bormann & Likens (1967). Nutrient cycling. *Science*, 155.
 - Redfield (1958). The biological control of chemical factors in the environment. *American Scientist*, 46.
 - Yachi & Loreau (1999). Biodiversity and ecosystem productivity in a fluctuating environment: The insurance hypothesis. *Proceedings of the National Academy of Sciences*, 96.
 - Feldman et al. (2024). Large global-scale vegetation sensitivity to daily rainfall variability. *Nature*, 636 [Feldman et al., 2024].
-

39.22 Computational Bridge

Trophic position can be read off an adjacency list of “eats” relations:

```
from biology.ecology import food_web_trophic_levels

web = {"phyto": [], "zooplankton": ["phyto"], "fish": ["zooplankton"]}
print(food_web_trophic_levels(web))
```

Clinical / systems note: Biomagnification of methylmercury follows the same stepped energy flow you quantify with trophic level assignments.

39.23 Summary

- Ecosystems = biotic + abiotic components; energy flows through trophic levels (about 10% efficiency; Lindeman 1942); nutrient atoms cycle.
- GPP → NPP → NEP → NBP hierarchy; global terrestrial NPP about 120 Pg C/yr; tropical rainforests dominate.
- Energy flow: one-way through system with about 10% trophic efficiency; biomagnification of persistent pollutants concentrates toxins at higher levels.
- Carbon cycle: 10 Pg C/yr fossil fuel input; atmospheric CO₂ at 421 ppm (2024); biological pump exports 10-15 Pg C/yr to deep ocean; permafrost (1,700 Pg) vulnerable; ocean acidification ($\Omega < 1 \rightarrow$ coral dissolution).
- Nitrogen cycle: N₂ fixation (nitrogenase; Haber-Bosch doubles global reactive N) → nitrification → denitrification / anammox. Reactive N cascade causes eutrophication, hypoxia, N₂O (298x CO₂ warming potential).
- Phosphorus cycle: sedimentary (no gas phase); P-limiting in freshwater; Redfield ratio 106C:16N:1P; globally finite reserves.
- Sulfur cycle: DMS → cloud condensation nuclei → planetary thermostat (CLAW hypothesis); acid rain from SO₂ (reversed by regulation).
- Measuring NPP: harvest, eddy covariance (FLUXNET), ¹⁴C uptake, MODIS remote sensing — each captures different components; ANPP/BNPP partition varies from 0.4 (rainforest) to >3 (tundra) and shifts conclusions about global carbon storage.
- Rainfall variability: vegetation activity depends on event timing and intensity as well as precipitation totals, so productivity arguments should separate daily rainfall variability from mean water supply [Feldman et al., 2024].
- Hubbard Brook [Bormann and Likens, 1967]: the clear-cut experiment showed live vegetation retains 80–95% of nutrient inputs; mature forests are quasi-closed for most nutrients. Open vs. closed nutrient regimes governed by mean residence time $\tau = X/O$.
- Ocean ecosystem ecology: half of global NPP; productivity zones (euphotic, mesopelagic, abyssopelagic, upwelling, gyres, polar); biological pump exports about 10–15 Pg C/yr; Martin curve attenuates flux with depth.

- Soil formation: Jenny’s CLORPT factors; horizon differentiation (O–A–E–B–C–R); termites and ants act as soil engineers by moving particles, organic matter, water, and microbial metabolism; soils store 1,500–2,400 Pg C; warming-driven SOC release is a major positive climate feedback.
- Coupled cycles: Redfield 106 C : 16 N : 1 P diagnoses nutrient limitation; the planetary boundaries framework places six of nine Earth-system limits already crossed [Richardson et al., 2023].
- Water cycle: plant transpiration drives 60-90% of terrestrial evaporation; tropical forests generate their own rainfall.
- Ecosystem services (about \$125T/yr; Costanza 2014); 60% degraded (MEA 2005); biodiversity increases ecosystem function via complementarity and insurance.
- Earth System Science / Gaia: modern descendant of the Lovelock–Margulis hypothesis; biology and abiotic systems are coupled, but the “superorganism” claim is rejected — feedbacks can stabilize *or* destabilise.
- Connections: See section 10 for photosynthetic GPP/NPP concepts, Unit VIII — Botany — Plant Biology: Introduction for transpiration in the water cycle, and section 40 for biome NPP benchmarks.

39.24 Companion Source Module: Ecosystem Ecology

Ecosystem Ecology should leave a reproducible trail from a biological claim to the code, figure, diagram, or paper-based activity that can test it. Use the surfaces below to inspect the chapter’s assumptions, rerun the relevant model, or compare the manuscript explanation with companion labs and figures.

Table 478. Companion source surfaces for Ecosystem Ecology.

Surface	Use it for
src/biology/ecology/ecology.py (food_web_trophic_levels, connectance, biodiversity_indices)	Translate ecosystem structure into trophic, network, and diversity calculations.
src/biology/botany/botany.py (photosynthesis_rate, water_potential)	Link primary production and plant-water constraints to ecosystem fluxes.
src/mermaid/biology_diagrams.py (nutrient_cycle_diagram, food_web_diagram)	Keep stocks, fluxes, and boundaries visually explicit.

Reproducibility check: state system boundary, stock, flux, residence time, unit, and time window before comparing ecosystem budgets. Cross-reference: connect with section 10, sections 37 and 38, and section 40.

40 Biomes and Conservation Biology

Level 2/3 · 70 min read · 75 min lecture · Prerequisites: section 39

40.1 Learning Objectives

1. Describe the 9 major terrestrial **biomes** and 5 aquatic biome types with climate, NPP, and indicator species.
2. Explain climate-driven biome boundary shifts and tipping points from 2023-2025 scholarship.
3. Define the IUCN Red List categories, **minimum viable population (MVP)**, and the 50/500 rule.
4. Explain extinction debt and its implications for conservation timescales.
5. Design nature reserves using **island biogeography** and SLOSS principles with quantitative examples.
6. Describe rewilding and climate-adaptive management as emerging conservation strategies.
7. Explain conservation genomics and assisted **gene** flow as tools for managing threatened populations.
8. Evaluate the effectiveness of international conservation frameworks (CBD, 30x30, CITES).
9. Quantify IPBES findings (extinction rates, decline of vertebrate populations, drivers of biodiversity loss) and use them to evaluate conservation priorities.
10. Compute climate velocity for different landscape gradients and identify topographic, hydrological, microclimatic, and elevational refugia.
11. Compare ecosystem-based adaptation strategies (mangroves, urban greening, wetlands, coral reefs) with hard infrastructure on cost-benefit and co-benefit dimensions.

40.1.1 Study Blueprint

- Big idea: Biodiversity patterns and conservation decisions emerge from climate, history, disturbance, and human choice.
- Core concepts: biomes, biodiversity, extinction risk, conservation planning.
- Framework alignment: Vision & Change: Systems, Evolution, Pathways and transformations of energy and matter; AP Biology: Systems Interactions, Evolution, Energetics; NGSS-style topics: Interdependent Relationships in Ecosystems, Matter and Energy in Organisms and Ecosystems, Natural Selection and Evolution.
- Model or quantitative lens: Species-area, risk, and prioritization calculations.
- Data skill: Use maps, trend data, and threat categories to justify conservation priorities.
- Practice cadence: Representing and Describing Data, Statistical Tests and Data Analysis, Argumentation.
- Common misconception to repair: Conservation is decision-making under constraints and uncertainty, not only preserving untouched nature.
- Primary lab: **Lab — Biomes and Conservation Biology**.
- Question bank: **Questions — Biomes and Conservation Biology**.
- Transfer task: Transfer conservation reasoning to land use, climate corridors, restoration, and environmental justice.
- Bridge to computation: `biology.ecology.species_area_relationship`.

Opening Vignette — The Experiment That Launched Conservation Biology

In 1966, ecologist E.O. Wilson and his student Daniel Simberloff tested a bold prediction of island biogeography theory — that small islands far from the mainland support fewer species, and that a disturbed island will bounce back to a predictable species count. Simberloff hired professional exterminators to fumigate small mangrove islands off the Florida Keys with methyl bromide, killing most arthropods. He then monitored recolonisation. Within a year, species counts had returned to near the pre-defaunation levels predicted by island area and distance equations Wilson had developed with Robert MacArthur in 1967. The MacArthur-Wilson Theory of Island Biogeography — predicting species number from area $S = cA^z$ — became the mathematical foundation for reserve design in conservation biology. The SLOSS debate (Single Large Or Several Small reserves), minimum viable populations, habitat fragmentation analysis, and biodiversity hotspot identification most derive from Wilson and MacArthur’s equations. And it most started with methyl bromide on tiny Keys mangroves.

40.2 Biomes as Climate-Filtered Ecological Regions

A biome is a large-scale ecological zone characterized by climate (principally temperature and precipitation) and the type of vegetation and animal communities adapted to those conditions. Biome distribution follows Whittaker’s (1975) climate-vegetation gradient map, subsequently confirmed and refined by MODIS satellite NPP data (Running et al. 2004, *Science*) and updated with machine-learning-enhanced Koppen-Geiger classifications (Monzon-Alvarado et al. 2023, *Glob. Change Biol.*).

40.2.1 Climate as the Master Variable

The distribution of biomes is determined primarily by two climate variables:

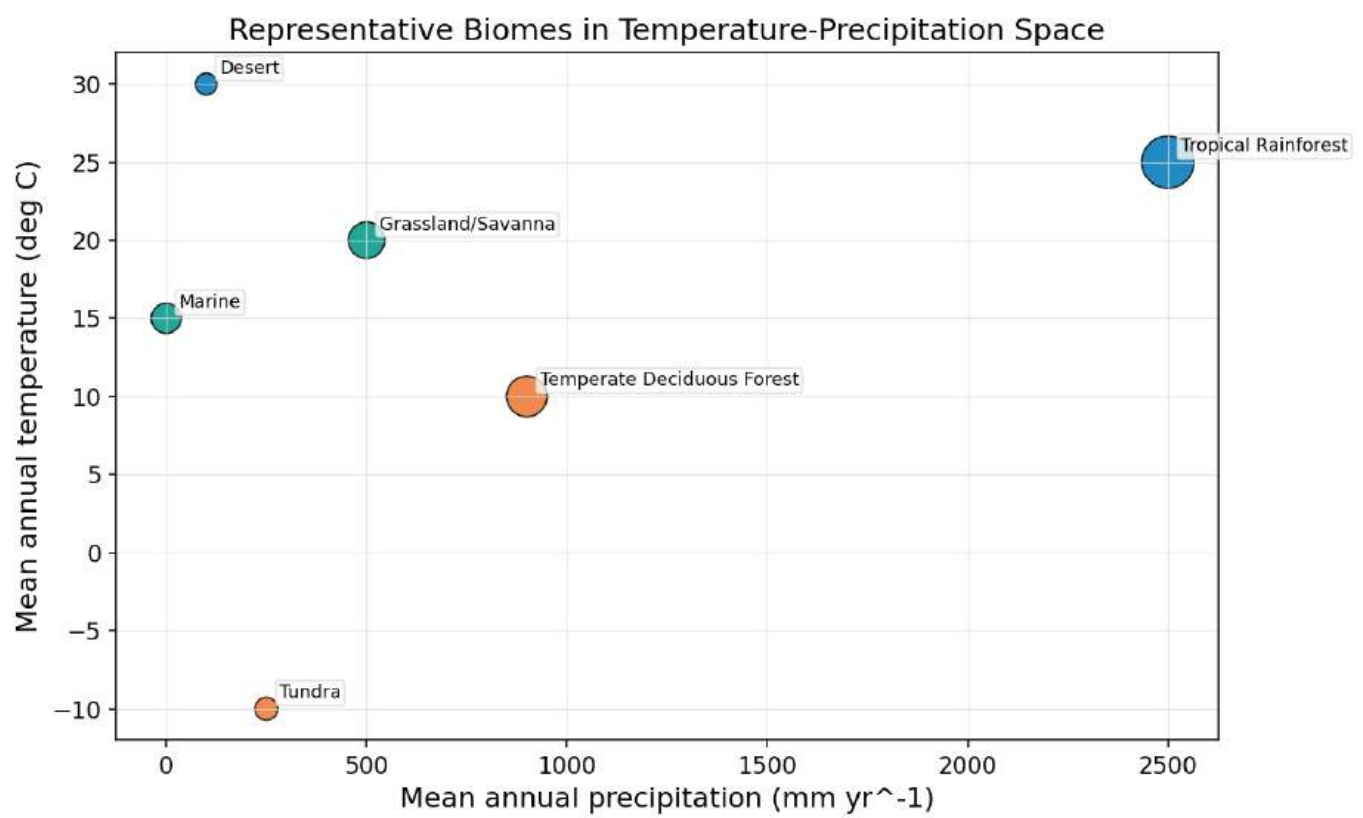


Figure 232. Terrestrial biomes in mean annual temperature–precipitation space (Whittaker-style classification). Point area reflects net primary productivity so tropical rainforest, temperate forest, savanna, desert, tundra, and marine reference sites are visually comparable.

1. Mean annual temperature (MAT) — determines the length of the growing season and the type of vegetation (tropical vs. temperate vs. boreal)
2. Mean annual precipitation (MAP) — determines vegetation structure (forest vs. grassland vs. desert)

Whittaker’s biome diagram (figure 232) plots MAT vs. MAP and shows that biome boundaries are remarkably predictable from these two variables alone. However, other factors also matter: seasonality, soil type, fire frequency, and evolutionary history.

40.2.2 The Nine Major Terrestrial Biomes

Table 479. The Nine Major Terrestrial Biomes: Biome and Temperature.

Biome	Temperature	Precipitation	Characteristic adaptations	NPP (g C/m ² /yr)
Tropical rainforest	25-30°C year-round	>2,000 mm/yr	Buttress roots, epiphytes , drip tips, fig-wasp mutualism , stratified canopy (emergent/canopy/understory/forest floor)	1,000-1,750
Tropical seasonal forest / savanna	25°C; distinct dry season	1,000-2,000 mm/yr	Deciduousness (dry season); fire-adapted grasses (resprouting); ungulate herding; C4 grasses	450-1,000
Desert	Extreme diurnal range; hot or cold	<250 mm/yr	CAM photosynthesis ; nocturnal behavior; waxy cuticles; deep taproots; water storage	45-125
Temperate grassland / prairie	0-25°C; large annual range	300-1,500 mm/yr	Deep root systems (>2 m); C4 grasses in warm areas; burrowing animals; fire-maintained	250-450
Temperate deciduous forest	0-20°C; 4 distinct seasons	750-1,500 mm/yr	Autumn leaf senescence (ABA-mediated); arbuscular mycorrhizae; spring ephemerals	500-1,250
Temperate rainforest	5-15°C; ocean-moderated	>1,500 mm/yr	Tallest trees on Earth (coastal redwood <i>Sequoia sempervirens</i> , 115 m); heavy epiphytic moss cover	750-1,500
Boreal forest (taiga)	-10 to 10°C	300-850 mm/yr (snow)	Conical crown shape (snow shedding); antifreeze proteins ; permafrost soils; low decomposition	300-600
Tundra (arctic)	-30 to 10°C; short growing season	<250 mm/yr	Cushion plants; freeze-tolerance (cryoprotectants); permafrost (active layer <1 m); lichens	50-200
Mediterranean shrub-land (chaparral)	Mild wet winters; hot dry summers	300-800 mm/yr	Sclerophyllous leaves (thick cuticle, high fiber); fire-serotinous cones; resprouting lignotubers	225-650

40.2.3 Five Major Aquatic Biome Types

Table 480. Five Major Aquatic Biome Types: Biome and Key features.

Biome	Key features	Indicator species	NPP (g C/m ² /yr)
Freshwater lakes & rivers	Salinity <0.5 ppt; thermal stratification (epilimnion/hypolimnion); lotic vs. lentic	Trout, cattails, caddisfly larvae	50-750
Wetlands	High organic load; anaerobic sediment; CH ₄ production; water table at or near surface	Hérons, <i>Sphagnum</i> moss, alligators	400-1,750

Biome	Key features	Indicator species	NPP (g C/m ² /yr)
Coastal/neritic marine	Shallow (<200 m); upwelling nutrients; high turbidity; continental shelf	Kelp, cod, sea otters, oysters	100-1,250
Open ocean (pelagic)	Nutrient-poor subtropical gyres; stratified; “blue desert”	Phytoplankton, bluefin tuna, sperm whale	25-200
Coral reefs	Tropical; 20-30°C; high light; mutualistic <i>Symbiodiniaceae</i> (zooxanthellae)	Brain coral, parrotfish, reef sharks	500-2,000

40.2.4 Lake Stratification and Turnover

Temperate lakes exhibit seasonal stratification:

Table 481. Lake Stratification and Turnover: Layer and Temperature.

Layer	Temperature	Density	Characteristics
Epilimnion	Warm (20-25°C)	Low	Surface; mixed by wind; O ₂ -rich, nutrient-depleted
Thermocline (metalimnion)	Rapid change	Transition	Density barrier prevents mixing
Hypolimnion	Cold (4°C)	High	Deep; O ₂ -depleted; nutrient-rich from decomposition

Turnover occurs in spring and autumn when surface temperature passes through 4°C (maximum density of water), eliminating the thermocline and allowing complete mixing. This redistributes O₂ and nutrients throughout the water column.

40.2.5 Coral Reef Bleaching

Mechanism: Thermal stress (anomaly >1°C sustained >4 weeks, measured as degree heating weeks or DHW) triggers expulsion of symbiotic zooxanthellae (*Symbiodiniaceae*) from coral tissue. Without their photosynthetic partners, corals lose 90% of energy supply and appear white (“bleached”). If thermal stress persists >8 weeks, coral mortality follows.

Recent mass bleaching events: The Great Barrier Reef experienced mass bleaching in 2016, 2017, 2020, 2022, 2024, and 2025 (six events in ten years). NOAA and the International Coral Reef Initiative confirmed the fourth global bleaching event beginning in 2023; by late 2025, bleaching-level heat stress had affected about 84% of the world’s coral reef area [NOAA Coral Reef Watch, 2025]. At >2°C global warming, >99% of coral reefs are projected to experience annual severe bleaching [Intergovernmental Panel on Climate Change, 2021].

Assisted evolution caveat: Conservation tools now include selective breeding, assisted gene flow, symbiont manipulation, and microbiome conditioning for heat tolerance. These interventions can protect specific reefs or buy time, but they do not remove the thermal driver; without emissions reduction and local water-quality management, heat-tolerant genotypes still face repeated bleaching, acidification, disease, and storm damage.

Clinical Connection — Reef-Derived Pharmaceuticals: Coral reef ecosystems are a source of bioactive compounds for drug development. Pseudopterosin (from the Caribbean sea whip *Pseudopterogorgia elisabethae*) has potent anti-inflammatory and analgesic properties and is used in commercial wound-healing formulations. Discodermolide (from the deep-sea sponge *Discodermia dissoluta*) shows anti-cancer properties by stabilizing microtubules, similar to taxol. The cone snail toxin ziconotide (Prialt) is an FDA-approved non-opioid analgesic for severe chronic pain. Reef destruction through bleaching and acidification threatens the loss of undiscovered pharmaceutical compounds before they can be identified — a form of pharmacological extinction debt.

Concept Check: What climatic variables determine whether a region supports tropical rainforest vs. tropical savanna? How does fire interact with precipitation to maintain the savanna biome?

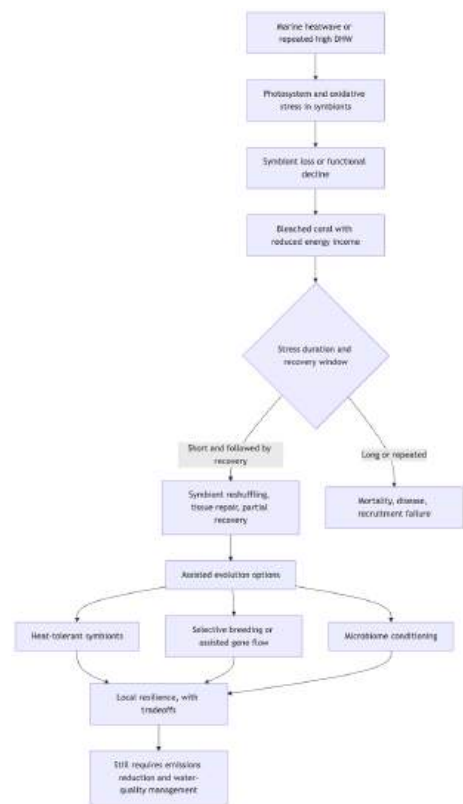


Figure 233. Coral bleaching responses can test heat-tolerant hosts, symbionts, or microbiomes as local resilience tools, but those interventions remain complements to climate mitigation and reef-water-quality management \citep{noaa2025coralbleaching, strader2022coralheat}.

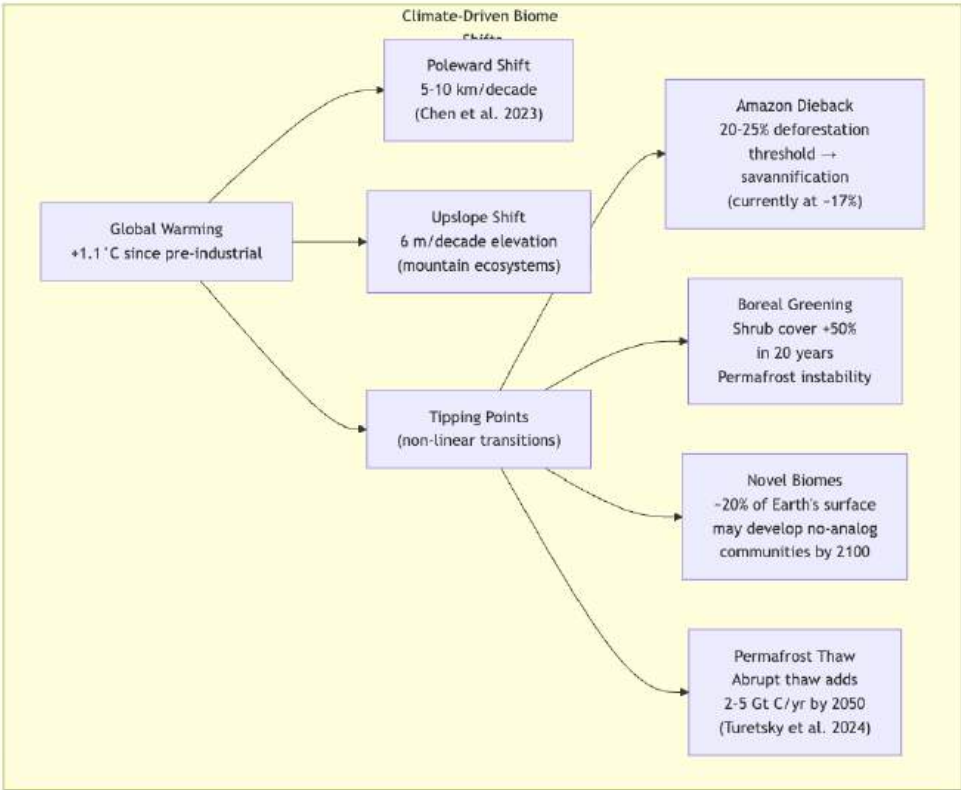


Figure 234. Climate warming can move biome boundaries poleward or upslope, but threshold responses and local dispersal limits make shifts uneven rather than smooth.

40.3 Climate Change and Biome Boundary Shifts

40.3.1 Key Findings (2023-2025)

Table 482. Key Findings (2023-2025): Finding and Study.

Finding	Study	Key result
Biome boundaries shifting poleward	Chen et al. (2023, <i>Nat. Clim. Change</i>)	5-10 km/decade poleward; 6 m/decade upslope
Amazon dieback tipping point	Lovejoy & Nobre (2024, <i>Sci. Adv.</i>)	20-25% deforestation → runaway savannification; currently at about 17%
Boreal → tundra greening	Elmendorf et al. (2023, <i>Nat. Ecol. Evol.</i>)	Shrub cover +50% in 20 years; permafrost destabilisation
Novel biomes (no-analog climates)	Williams et al. (2023, <i>Proc. R. Soc. B</i>)	about 20% of Earth’s surface may develop novel biome types by 2100
Permafrost thaw methane pulse	Turetsky et al. (2024, <i>Nat. Geosci.</i>)	Abrupt thaw adds 2-5 Gt C/yr by 2050; omitted from most models
Tree mortality acceleration	McDowell et al. (2024, <i>Science</i>)	Global tree mortality rates doubled since 1970s; drought/heat/insects

40.3.2 Biome Suitability Modeling

$$S = \sum_i w_i \cdot f_i(T,P)$$

(475)

where w_i = variable weights (temperature, precipitation, seasonality index), f_i = Gaussian response function centered on optimal conditions.

Species distribution models (SDMs) project future range shifts by correlating current distributions with climate variables and projecting onto future climate scenarios:

Table 483. Biome Suitability Modeling: Model type and Approach.

Model type	Approach	Strengths	Limitations
Bioclimatic envelope	Correlative (climate → presence)	Simple; good for many species	Ignores dispersal, biotic interactions
MaxEnt	Machine learning; maximum entropy	High predictive power; handles sparse data	Overfitting risk; correlative primarily
Process-based (e.g., LPJ-GUESS)	Mechanistic plant physiology	Captures mechanisms; projects novel climates	Data-intensive; computationally expensive

40.3.3 Climate Velocity and Dispersal Limits

Climate velocity = the speed at which climate conditions shift geographically:

$$v_{climate} = \frac{\text{rate of temperature change (}^{\circ}\text{C/yr)}}{\text{spatial temperature gradient (}^{\circ}\text{C/km)}}$$

(476)

In flat landscapes (e.g., Amazon basin), spatial gradients are shallow → climate velocity is fast (about 10 km/yr). In mountains, steep gradients → slow climate velocity (about 1 km/yr). Species must disperse at least as fast as climate velocity to track suitable conditions.

Migration lag: Many species cannot track climate velocity: - Trees: typical dispersal rate = 0.1-0.5 km/yr via seed dispersal - Climate velocity in temperate lowlands: about 4-10 km/yr - Gap: 10-100x faster movement needed than most trees can achieve

Concept Check: The Amazon rainforest is at about 17% deforestation, with a tipping point estimated at 20-25%. Why is the tipping point non-linear (i.e., why doesn’t the forest simply lose area proportionally to deforestation)? What role does **transpiration** recycling play in the tipping mechanism?

40.4 Conservation Biology Fundamentals

40.4.1 IPBES Global Assessment: The Quantified Crisis

The Intergovernmental Science-Policy Platform on Biodiversity and Ecosystem Services (IPBES) — analogous to the IPCC for climate — released its first Global Assessment in 2019 and its Transformative Change Assessment in 2024 [[Intergovernmental Science-Policy Platform on Biodiversity and Ecosystem Services, 2019, 2024](#)]. Its findings frame contemporary conservation:

Table 484. IPBES Global Assessment: The Quantified Crisis: IPBES finding and Quantitative result.

IPBES finding	Quantitative result
Species threatened with extinction	about 1,000,000 in the IPBES synthesis [Intergovernmental Science-Policy Platform on Biodiversity and Ecosystem Services, 2019]; the IUCN Red List provides the tracked assessed-species subset [International Union for Conservation of Nature, 2025]
Average abundance of native species in major terrestrial biomes	Declined \geq 20% (mostly since 1900)
Monitored vertebrate populations	73% average decline since 1970 in the Living Planet Index; this is a population-index trend, not a count of individual animals [World Wide Fund for Nature, 2024]
Wetlands	85% lost since 1700
Forest cover	32% lost (vs. pre-industrial)
Coral reef cover	50% lost since 1870
Pollinator populations	40% of insect pollinators threatened in the IPBES pollinator synthesis [IPBES, 2016, Intergovernmental Science-Policy Platform on Biodiversity and Ecosystem Services, 2019]
Local livestock breeds	9% extinct; another 1,000 threatened (genetic erosion of food security)

40.4.2 Quantified Drivers (IPBES 2019)

IPBES ranked the relative importance of the five direct drivers of biodiversity loss in terrestrial and freshwater systems:

Table 485. Quantified Drivers (IPBES 2019): Rank and Driver.

Rank	Driver	Approximate contribution
1	Land-use change (agriculture, urbanisation, infrastructure)	about 30%
2	Direct exploitation (hunting, fishing, logging)	about 23%
3	Climate change	about 14% (rising fast, projected to dominate by 2050)
4	Pollution (nutrients, plastics, persistent organics)	about 14%
5	Invasive alien species	about 11%

For marine systems, the ranking changes: direct exploitation > climate change > pollution > land-/sea-use change > invasive species. Climate change is projected to overtake direct exploitation as the dominant marine driver by 2050.

The Transformative Change Assessment (IPBES 2024) goes further: incremental conservation alone cannot meet 30x30 or biodiversity targets. Systemic changes to economic, financial, and governance systems are required — including reforming environmentally harmful subsidies, shifting incentives toward ecosystem stewardship, and integrating biodiversity into most policy domains (the “whole-of-government” approach) [[Intergovernmental Science-Policy Platform on Biodiversity and Ecosystem Services, 2024](#)].

Pollinator decline requires careful interpretation. Managed honey bee colonies can increase in some agricultural regions while wild bees, butterflies, moths, flies, beetles, birds, or bats decline locally; those are different indicators, not contradictory facts. IPBES links pollinator risk to land-use change, pesticide exposure, pathogens, invasive species, climate change, and reduced floral/nesting resources [[IPBES, 2016](#)]. Crop studies also show that wild pollinator visitation can

improve fruit set even when honey bees are present, so conservation targets should include habitat heterogeneity, floral continuity, nesting substrate, pesticide timing, and disease spillover rather than hive counts alone [Garibaldi et al., 2013].

Food systems are a useful place to make “transformative change” concrete. FAO, IFAD, UNICEF, WFP, and WHO report that high food-price inflation continues to undermine access to healthy diets, especially for low-income populations [Food and Agriculture Organization of the United Nations et al., 2025]. Conservation biology therefore cannot treat agricultural landscapes as outside nature: agroecology, diversified crop rotations, soil-carbon restoration, pollinator habitat, reduced food waste, sustainable fisheries, and equitable market access are biodiversity strategies and food-security strategies at the same time. The claim is not that agroecology alone solves hunger; it is that biodiversity, nutrition, farm livelihoods, and climate resilience are coupled enough that single-objective policies often fail.

40.4.3 The Sixth Mass Extinction

Earth currently experiences the Sixth Mass Extinction — driven primarily by human activities:

Table 486. The Sixth Mass Extinction: Driver and Mechanism.

Driver	Mechanism	Relative contribution
Habitat destruction	Land-use change, deforestation, urbanisation	about 30% of threatened species
Overexploitation	Hunting, fishing, wildlife trade	about 20%
Invasive species	Competition, predation, disease introduction	about 15%
Pollution	Pesticides, plastics, nutrient loading	about 10%
Climate change	Range shifts, phenological mismatch, extreme events	about 8% (increasing rapidly)
Disease	Chytrid fungus (Bd), white-nose syndrome	about 5%

Key statistics: - Current extinction rate: 100-1,000x background rate (Ceballos et al. 2017, PNAS) - IPBES 2019 Global Assessment: about 1 million species threatened with extinction - Living Planet Index (WWF 2024): 73% average decline in monitored vertebrate population sizes since 1970; this measures a weighted set of monitored populations, not every vertebrate individual [World Wide Fund for Nature, 2024] - 75% of terrestrial ecosystems significantly altered by humans - 50% of global wetland area lost since 1900 - 33% of marine fish stocks overfished in FAO’s recent global assessments [Food and Agriculture Organization of the United Nations, 2024]

40.4.4 IUCN Red List Categories (2025 Update)

Table 487. IUCN Red List Categories (2025 Update): Category and Code.

Category	Code	Quantitative threshold
Extinct	EX	No reasonable doubt that last individual has died
Extinct in the Wild	EW	Primarily in cultivation or captivity
Critically Endangered	CR	at least 80% reduction over 10 yr or 3 generations
Endangered	EN	at least 50% reduction over 10 yr or 3 generations
Vulnerable	VU	at least 30% reduction over 10 yr or 3 generations
Near Threatened	NT	Close to qualifying for VU; being monitored
Least Concern	LC	Widespread and abundant
Data Deficient	DD	Insufficient data to assess

The IUCN Red List is a tracked subset of assessed species, not a census of global biodiversity. Version 2025-2 listed 172,620 assessed species, with 48,646 classified as threatened (Vulnerable, Endangered, or Critically Endangered), about 28% of assessed species [International Union for Conservation of Nature, 2025]. Counts change with new assessments and reassessments, so the category logic is more durable than any single annual total.

Criteria for listing (IUCN uses 5 criteria, any one sufficient): - A: Population reduction (quantitative decline thresholds) - B: Geographic range (extent of occurrence or area of occupancy) with fragmentation/decline - C: Small population size ($N < 10,000$ for VU; $N < 2,500$ for EN; $N < 250$ for CR) with decline - D: Very small population ($N < 1,000$ for VU; $N < 250$ for EN; $N < 50$ for CR) - E: Quantitative analysis (PVA) showing extinction probability $>10\%$ within 100 years (VU)

Concept Check: A bird species has a global population of 8,000 mature individuals with a documented 35% decline over the past 15 years (approximately 3 generations). Under which IUCN criteria and category would this species be listed?

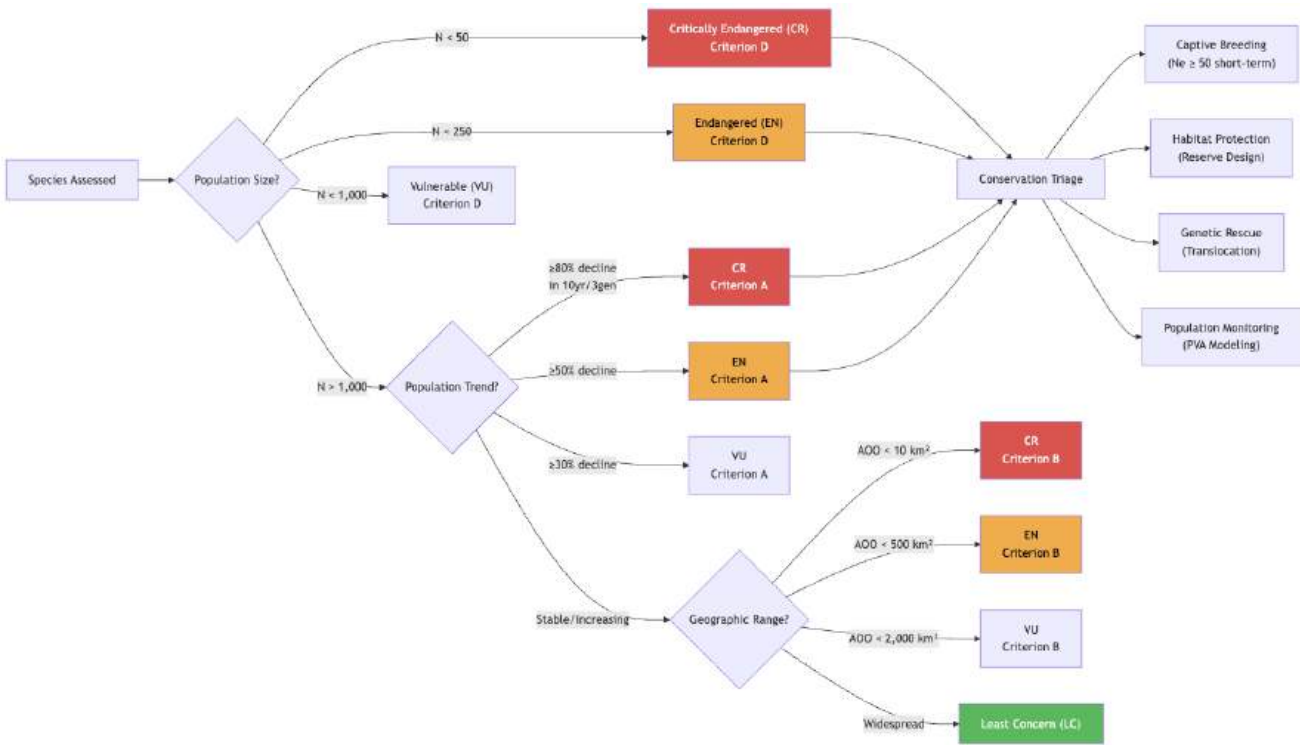


Figure 235. IUCN Red List assessment is a criteria-based risk workflow: the category follows the strongest supported evidence, then conservation triage weighs urgency, feasibility, and monitoring needs.

40.5 Population Viability and the 50/500 Rule

40.5.1 Minimum Viable Population (MVP)

The minimum viable population is the smallest population with at least 95% probability of persistence for at least 100 generations, accounting for four types of stochasticity:

Table 488. Minimum Viable Population (MVP): Stochasticity type and Mechanism.

Stochasticity type	Mechanism	Effect on small populations
Demographic	Random variation in births/deaths	Even when $r > 0$, small $N \rightarrow$ high extinction probability
Environmental	Weather, food fluctuations	Entire population experiences same bad conditions
Genetic	Inbreeding depression, drift	F per generation = $1/(2N_e)$; $F > 0.10 \rightarrow$ fitness costs
Catastrophes	Fire, disease epidemic, storm	Sudden $>50\%$ mortality events; frequency matters

40.5.2 Franklin's 50/500 Rule

Franklin (1980) and Soule [1980]:

- $N_e \geq 50$: Short-term viability — prevents rapid inbreeding depression
 - Inbreeding rate: $\Delta F = \frac{1}{2N_e} \leq 1\%$ per generation
 - At $F > 0.10$: measurable inbreeding depression (reduced litter size, increased juvenile mortality)
- $N_e \geq 500$: Long-term viability — maintains additive genetic variance for adaptive evolution
 - Genetic variance lost per generation: $\frac{1}{2N_e} = 0.1\%$
 - Balanced by new **mutation** if $N_e > 500$ [Frankham, 1995]

Revised 100/1000 rule (Frankham et al. 2014, *Biol. Conserv.*): More conservative; accounts for reduced purging effectiveness and updated genomic data.

N_e vs. census N : Effective population size is typically much smaller than census size:

$$N_e = \frac{4N_mN_f}{N_m + N_f}$$

(477)

Typical N_e/N ratio: 0.10-0.25 for vertebrates. Therefore, to achieve $N_e = 500$, census population needs to be $N = 2,000 - 5,000$.

40.5.3 Population Viability Analysis (PVA)

PVA uses species-specific demographic data and stochastic simulation models (VORTEX, RAMAS) to project extinction probability:

Inputs: age/sex-specific survival, fecundity, variance in vital rates, carrying capacity, catastrophe frequency, inbreeding coefficients, habitat area.

Outputs: extinction probability over specified time horizon, mean time to extinction, quasi-extinction threshold probability.

Case study — Florida panther (*Puma concolor coryi*): - 1994 PVA → predicted extinction within 25 years without intervention - $N \approx 30, N_e \approx 10$ → severe inbreeding (kinked tails, cryptorchidism, heart defects) - 1995: 8 female Texas cougars introduced → genetic rescue - 2023: population >200 individuals; heterozygosity increased, inbreeding depression reversed - One of conservation biology’s greatest success stories

Clinical Connection — Conservation Genetics and Inbreeding Depression in Human Populations: The principles of MVP and inbreeding depression apply to human populations. Small, isolated populations (e.g., the Amish community of Lancaster County, Pennsylvania) show elevated frequencies of rare autosomal recessive disorders including Ellis-van Creveld syndrome (6-fingered dwarfism; about 5% carrier frequency vs. about 0.001% in general population), maple syrup urine disease, and glutaric aciduria. The **founder effect** — establishment of a population by a small number of individuals carrying a non-representative sample of the gene pool — mirrors the **genetic drift** effects that reduce N_e in endangered wildlife. Genomic screening programs in such communities follow the same logic as conservation genomics: identifying deleterious **alleles** and managing their frequency.

40.6 Extinction Debt and Its Conservation Implications

Extinction debt (Tilman et al. 1994, *Nature*): Species present in degraded/fragmented habitats are committed to future extinction because habitat can no longer support viable populations — but extinction is delayed (50-500 years) by existing long-lived individuals.

40.6.1 Mathematical Framework for Extinction Debt

Species committed to extinction = $S_{\text{pre-fragmentation}} - c \cdot A_{\text{remaining}}^z$

(478)

where $S_{\text{pre-fragmentation}}$ is species richness before habitat loss, $A_{\text{remaining}}$ is remaining habitat area, and c and z are the species-area parameters whose log-log slope steepens from contiguous continental biomes toward isolated oceanic islands (figure 236).

40.6.2 Relaxation Time After Habitat Loss

Relaxation time = the period between habitat loss and final extinction of committed species. Determined by: - Longevity of individuals (trees: centuries; insects: months) - Generation time (longer generation = longer debt) - Habitat quality of remaining fragments - Connectivity between patches (rescue effect)

40.6.3 Case Studies of Delayed Extinction

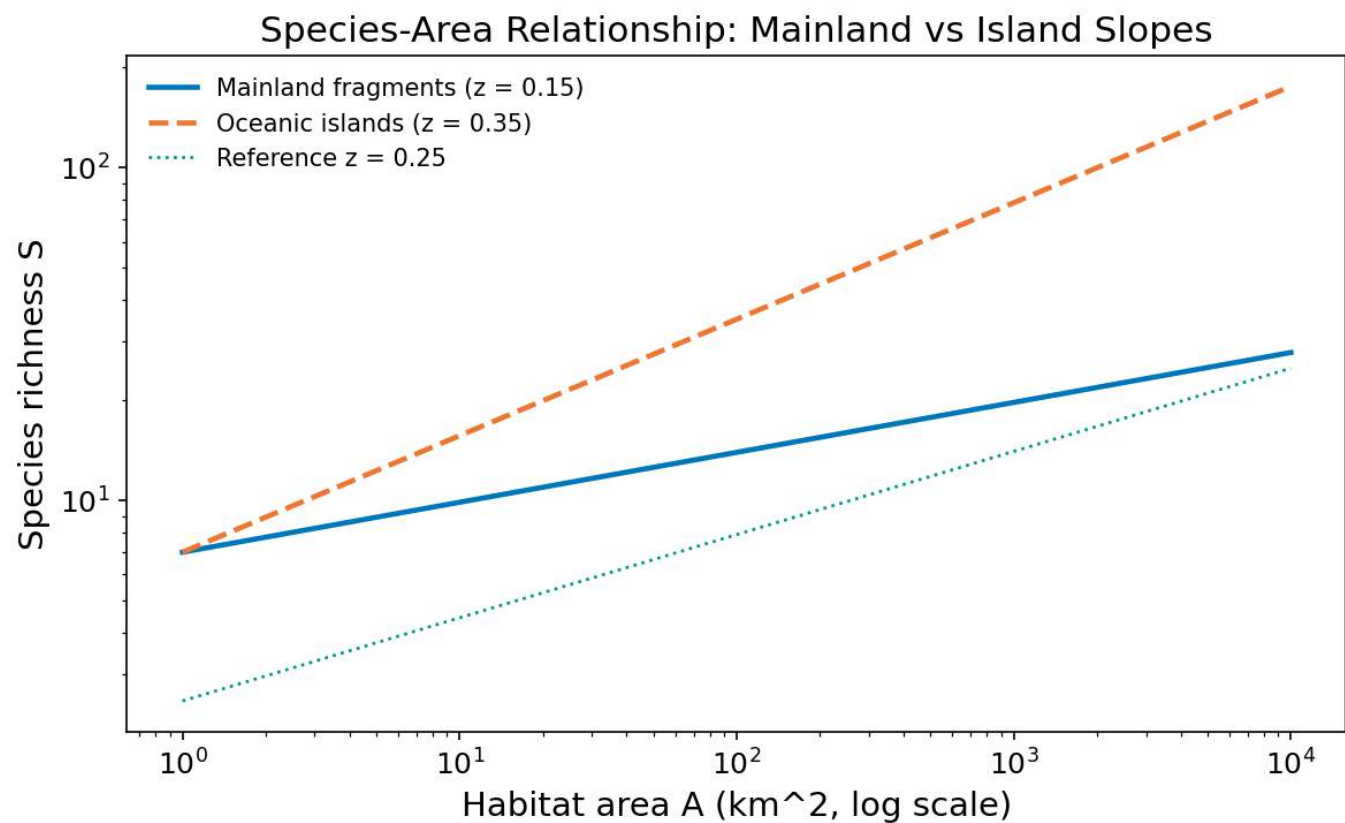


Figure 236. Species–area relationship on log–log axes. Mainland-fragment and oceanic-island curves show contrasting slopes (*z* about 0.15 versus *z* about 0.35), with a dotted reference curve at $z = 0.25$.

Table 489. Case Studies of Delayed Extinction: System and Debt estimate.

System	Debt estimate	Relaxation time	Reference
European calcareous grasslands	20-50% of plant species	50-200 years	Lindborg & Eriksson 2004
Amazon forest fragments	30-50% of canopy trees	100-500 years	Laurance et al. 2011
African tropical forests	10-30% of endemic species	Ongoing	Brooks et al. 1999
Belgian forest herbs	30-40% in fragments <1 ha	100+ years	Vellend et al. 2006

Conservation implication: Present-day species richness overestimates long-term viability. Conservation assessments based on current presence may be dangerously optimistic. Extinction debt means that the full consequences of today’s deforestation will not be realized for decades to centuries.

Concept Check: A 10,000-ha forest is fragmented into ten 100-ha patches. Using $S = 20A^{0.25}$, calculate species richness for the intact forest and for each fragment. How many species are “committed” to extinction via extinction debt? How would wildlife corridors between patches modify this prediction?

40.7 Reserve Design for Area, Connectivity, and Edge Effects

40.7.1 Island Biogeography Applied to Conservation

MacArthur-Wilson island biogeography theory provides the theoretical foundation for reserve design:

Species-area relationship: $S = cA^z$ (see Community Ecology chapter for derivation)


```
from biology.ecology import species_area_relationship

# Compare large vs. small reserves
S_large = species_area_relationship(area_ha=10_000, c=7, z=0.26)
S_small = species_area_relationship(area_ha=100, c=7, z=0.26)
print(f"Large reserve (10,000 ha): {S_large:.0f} species")
print(f"Small reserve (100 ha): {S_small:.0f} species")
print(f"Species lost from fragmentation: {((S_large-S_small)/S_large)*100:.0f}%")
```

40.7.2 SLOSS Debate Resolution

Table 490. SLOSS Debate Resolution: Design principle and When it applies.

Design principle	When it applies	Example
Single large preferred	Area-demanding species; interior habitat specialists; low landscape connectivity	Amazon: large reserves protect jaguar, harpy eagle
Several small preferred	Different habitat types in different patches; high beta diversity; patches protect local endemics	Caribbean islands: each island has unique endemic reptiles
Core-corridor-matrix (modern synthesis)	Most real-world situations	Y2Y (Yellowstone to Yukon, 3,200 km)

40.7.3 Diamond’s Design Principles (1975, updated)

Table 491. Diamond’s Design Principles (1975, updated): Principle and Reasoning.

Principle	Reasoning	Modern status
Larger is better than smaller	Species-area relationship	Supported
One large > several small of equal total area	More interior habitat; lower extinction	Context-dependent
Close together better than far apart	Higher colonization rate	Supported
Clustered better than linear arrangement	More connectivity	Supported
Circular better than elongated	Less edge effect	Supported
Connected by corridors better than isolated	Rescue effect; gene flow	Strongly supported

40.7.4 Edge Effects and Fragment Microclimates

Habitat edges create microclimatic gradients that penetrate 100-300 m into forest fragments:

Table 492. Edge Effects and Fragment Microclimates: Edge effect and Penetration distance.

Edge effect	Penetration distance	Impact
Increased light	50-200 m	Favors pioneer species; dries forest interior
Wind damage	100-300 m	Increased tree mortality
Elevated temperature	50-100 m	Shifts microclimate; stresses shade species
Nest predation/parasitism	200-600 m	Cowbird parasitism and corvid predation increase
Invasive species	100-500 m	Exotic plants establish in disturbed edges

For a circular reserve:

$$\text{Interior area} = \pi(r - d)^2$$

(479)

where r = reserve radius and d = edge penetration distance. For a 10-ha circular reserve ($r = 178$ m) with 200-m edge effects: zero interior habitat. This illustrates why small fragments are ecological traps for interior-dependent species.

40.7.5 Habitat Corridors and Connectivity Trade-Offs

Evidence for corridor effectiveness: - Tewksbury et al. (2002, *PNAS*): Connected patches had 25-100% more pollinator movement than unconnected - Gilbert-Norton et al. (2010, meta-analysis): Movement between patches 50% higher with corridors - Florida Wildlife Corridor (legislated 2021): 1,000+ mile protected corridor from Everglades to Okefenokee Swamp

Stepping stones: For species that can cross moderate distances (birds, bats, strong-flying insects), stepping stone patches may be as effective as continuous corridors at lower cost.

Clinical Connection — Urban Green Corridors and Human Health: The principles of habitat corridors extend to urban planning and human health. Studies in Philadelphia, Chicago, and Singapore demonstrate that connected urban greenways (tree-lined corridors connecting parks) reduce urban heat island effects by 2-5°C, decrease particulate matter (PM_{2.5}) by 15-25%, and increase physical activity by 30-40% in nearby residents. Green corridors also reduce stress biomarkers (salivary cortisol decreased 20% after 30-minute walks in urban green corridors vs. streets; Roe et al. 2013). Conservation biology’s core-corridor-matrix design principles thus have direct applications to One Health approaches integrating biodiversity conservation, climate adaptation, and human wellbeing.

Concept Check: A conservation planner has a budget to protect 1,000 ha of tropical forest. Option A: one 1,000-ha reserve. Option B: ten 100-ha reserves spread across different habitat types. Option C: five 100-ha reserves connected by 100-m-wide corridors (total 500 ha reserves + 500 ha corridors). Which design best protects: (a) a large-bodied apex predator? (b) maximum regional species richness? (c) genetic connectivity? Justify each answer using island biogeography theory.

40.8 Emerging Conservation Strategies

40.8.1 Rewilding and Trophic Restoration

Rewilding (Soule & Noss 1998; updated Jorgensen 2024, *Nat. Ecol. Evol.*): Restore ecological processes — especially trophic interactions — by reintroducing lost species, particularly apex predators and megaherbivores.

Three types of rewilding:

Table 493. Rewilding and Trophic Restoration: Type and Approach.

Type	Approach	Example
Trophic rewilding	Reintroduce apex predators/herbivores to restore cascades	Wolves in Yellowstone (1995); lynx in UK (proposed)
Pleistocene rewilding	Use ecological proxies for extinct megafauna	Pleistocene Park, Siberia (bison, horses to create mammoth steppe)
Passive rewilding	Remove human disturbance; allow natural regeneration	European farmland abandonment → forest recovery

Quantitative outcomes of wolf reintroduction in Yellowstone: - Elk: population reduced about 50% (12,000 → 6,000); behavior change (avoid riverbanks) - Willows: height increased 5-fold in riparian areas within 15 years - Beavers: 0 colonies in 1995 → 12 colonies by 2012 - Songbirds: 5 species returned to recovering riparian habitat - Stream morphology: channels narrowed and deepened as bank vegetation stabilized soil - Berry production: increased → grizzly bear diet shifted (consuming 10x more berries)

Pleistocene Park hypothesis: Zimov et al. (2012, *Science*): Reintroducing large herbivores to Arctic tundra compacts snow in winter, allowing cold air to freeze soil deeper, slowing permafrost thaw by about 80% compared to snow-insulated control plots.

40.8.2 Conservation Genomics for Diversity and Management

Whole-genome sequencing of threatened populations enables:

Conservation genomics is strongest when sequencing is tied to a management decision rather than treated as an expensive description. Runs of homozygosity estimate recent inbreeding, allele-frequency outliers can nominate local adaptation, pangenome or long-read approaches can reveal structural variation, and pedigree-aware sampling can separate ancestry from recent bottlenecks. The ethical layer is inseparable: sampling permits, Indigenous data sovereignty, benefit-sharing, and the risk of over-prioritizing “genetically interesting” populations most affect whether the genomic evidence should guide action.

Table 494. Conservation Genomics for Diversity and Management: Application and Method.

Application	Method	Example
Inbreeding assessment	Runs of homozygosity (ROH) analysis	Cheetah: about 10 Mb average ROH; severe bottleneck
Adaptive variation	Genome-wide association (GWAS) for climate-relevant loci	Coral heat tolerance alleles in <i>Acropora</i>
Management units	Population structure (FST, admixture analysis)	Tiger: 6 subspecies → conservation priorities
Genetic rescue planning	Identify source populations maximizing heterozygosity	Florida panther × Texas cougar
Ancient DNA	Reconstruct historical diversity; identify lost alleles	Woolly mammoth → mammoth de-extinction project

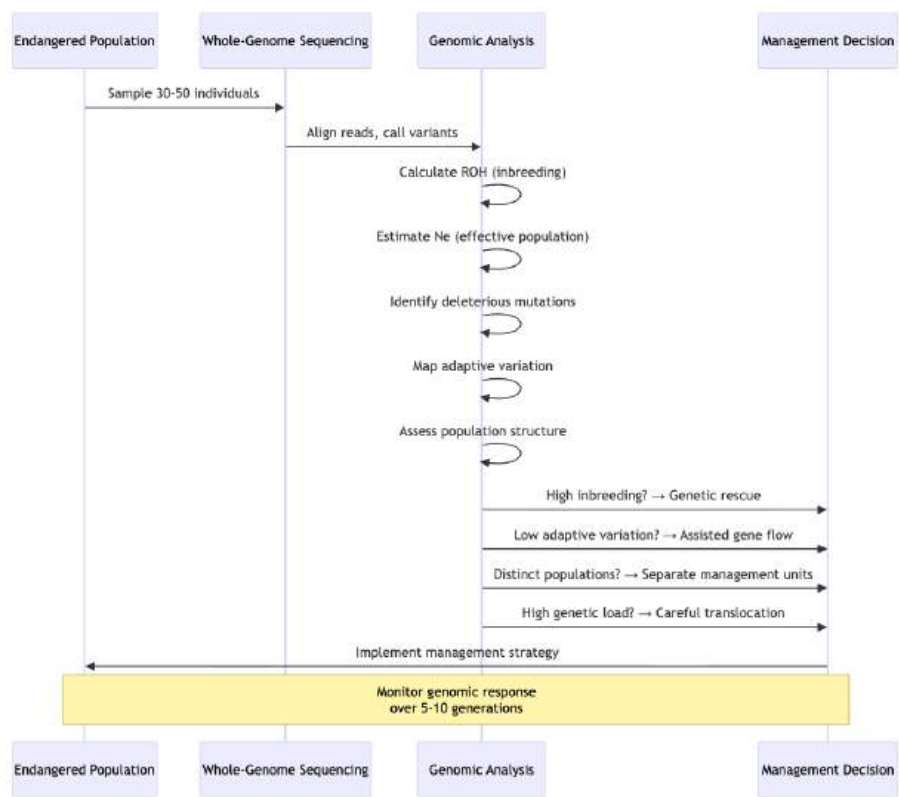


Figure 237. Conservation-genomics workflows move from whole-genome sequencing to estimates of inbreeding, adaptive variation, and management choices.

40.8.3 Assisted Gene Flow and Assisted Migration

Assisted gene flow: Intentionally moving alleles from adapted to non-adapted populations of the same species: - Coral: transplanting heat-tolerant *Acropora* genotypes to vulnerable reefs (Palumbi et al. 2014, *Science*) - Trees: moving southern seed sources to northern planting sites to pre-adapt to warming (assisted migration of *Pinus contorta* in British Columbia)

Assisted migration (managed relocation): Moving entire species to new locations outside their historical range where future climate is suitable. Controversial due to invasion risk.

De-extinction: Using genomic engineering to resurrect functional analogs of extinct species: - Woolly mammoth project (Colossal Biosciences): Editing Asian elephant genome with mammoth cold-adaptation genes (TRPV3, hemoglobin variants, fat deposition); goal: produce cold-adapted elephants for Arctic rewilding - Thylacine project (Colossal): Reconstructing thylacine genome from museum specimens - Ethical debates: Should resources be spent on de-extinction rather than preventing current extinctions?

40.8.4 Climate-Adaptive Management

Traditional conservation aims to preserve historical baselines. Climate-adaptive management accepts that ecosystems are changing and manages for future conditions:

The hard part is deciding when to resist change, when to help a system transition, and when to redirect effort toward ecosystem function rather than historical composition. Coral reefs illustrate the tradeoff: assisted gene flow, symbiont management, shading, and local water-quality improvement can raise local resilience, but they do not remove the external heat and acidification drivers. Climate-adaptive management is therefore a portfolio problem, pairing local stress reduction with monitoring, emissions context, social feasibility, and explicit thresholds for changing strategy [NOAA Coral Reef Watch, 2025, Intergovernmental Science-Policy Platform on Biodiversity and Ecosystem Services, 2024].

Table 495. Climate-Adaptive Management: Approach and Strategy.

Approach	Strategy	Example
Protect climate refugia	Identify and protect areas where climate change impacts are minimized	Deep canyons, north-facing slopes, groundwater-fed wetlands
Increase connectivity	Corridors for range shifts	Continental-scale corridors (Y2Y, Florida Wildlife Corridor)
Managed retreat	Accept loss of some habitats; invest in new ones	Managed realignment of coastal defenses; creating new marshland
Reduce non-climate stressors	Remove pollution, invasive species to increase resilience	Reducing sediment runoff on coral reefs

40.8.5 Visualizing Reserve Design Principles

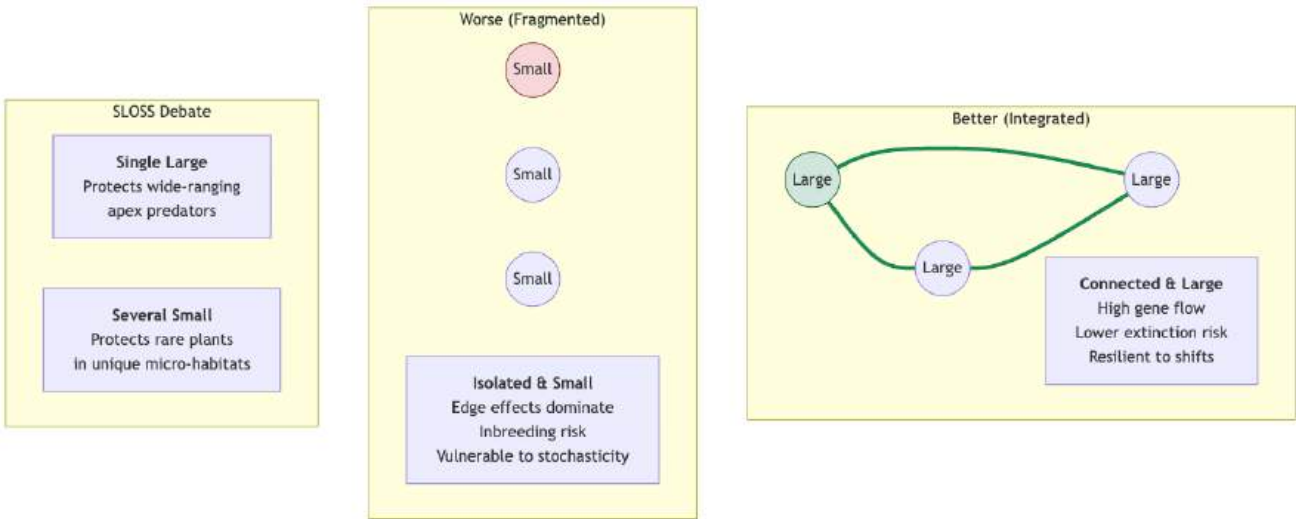


Figure 238. Reserve design compares connectivity, area, edge effects, and habitat uniqueness; large connected reserves and several smaller reserves solve different conservation problems.

40.9 Climate Velocity, Refugia, and Species Range Shifts

Ripple and Beschta [2012a] and Loarie et al. (2009, *Nature*) established climate velocity as the central organizing metric for climate-adaptive conservation. The velocity is the speed at which a given thermal envelope moves across the landscape, and species must disperse at least this fast to track their climatic niche.

$$v_{\text{climate}} = \frac{\partial T / \partial t}{|\nabla T|}$$

(480)

The numerator is the rate of climate change at a point (°C/yr); the denominator is the local spatial temperature gradient (°C/km). Rearranging gives velocity in km/yr.

Table 496. Visualizing Reserve Design Principles: Landscape and Spatial gradient.

Landscape	Spatial gradient	Velocity at +0.03 °C/yr
Mountain (e.g., Andes)	5 °C/km vertically	0.006 km/yr (6 m/yr — slow)
Boreal foothills	0.5 °C/km	0.06 km/yr
Temperate plains	0.05 °C/km	0.6 km/yr
Amazon basin (flat)	0.005 °C/km	6 km/yr
Subtropical plains	0.003 °C/km	10 km/yr

The flattest landscapes generate the fastest velocities — exactly where species cannot escape upslope. Migration lags therefore cluster in lowland tropical and temperate plains: trees often disperse at roughly 0.1–0.5 km/yr, which can be 10–100× too slow for tropical lowlands but adequate for some mountain settings.

40.9.1 Refugia and Their Identification

Climate refugia are locations where the local climate changes more slowly than the regional average, providing temporary or permanent havens for species unable to track climate velocity. Recognized refugia types:

Table 497. Refugia and Their Identification: Type and Mechanism.

Type	Mechanism	Examples
Topographic	Cold-air pooling, north-facing slopes, deep canyons buffer temperature	Klamath-Siskiyou (NW USA); Mediterranean canyons
Hydrological	Groundwater-fed streams, springs, lakes maintain cool temperatures	Spring-fed cold-water salmonid habitat
Microclimatic	Forest interior buffering (–2 to –5 °C vs. open canopy)	Cathedral-grove old growth; tropical understory
Elevational	Mountains hold residual cool habitat above warming lowlands	Alpine ecosystems globally
Coastal upwelling	Cold-water upwelling buffers warming surface oceans	California Current; Benguela; Peru
Cryptic / paleo	Sites that remained inhabitable through Pleistocene glaciations	Many high-biodiversity hotspots map onto past refugia

Refugia identification is a major effort of climate-adaptive conservation planning: high-resolution climate downscaling (≤ 1 km grids) plus species distribution modeling reveals locations where target species can persist longest, prioritizing them for protection. The Adapt West initiative (Conservation Biology Institute) maps climate refugia for North American species; analogous tools exist in Australia, Europe, and parts of South America.

Concept Check: Two endangered birds occupy similar habitat: species A in the high Andes (5 °C/km gradient) and species B on the Brazilian cerrado (flat). With identical thermal requirements and warming rates, which species faces the greater extinction risk from climate change, and what reserve-design implications follow?

40.10 Ecosystem-Based Adaptation and Climate-Resilience Planning

Ecosystem-Based Adaptation (EbA) uses biodiversity and ecosystem services as part of an overall adaptation strategy to help people adapt to climate change. The framework — formalised by the CBD and IUCN in 2009 — sits at the intersection of conservation and human resilience: protecting and restoring ecosystems to buffer communities against floods, storms, droughts, heat waves, and rising seas, while simultaneously sequestering carbon and conserving biodiversity.

40.10.1 Major EbA Strategies

Table 498. Major EbA Strategies: Strategy and Mechanism.

Strategy	Mechanism	Co-benefit
Mangrove restoration	Wave attenuation; coastal sediment stabilization; storm surge buffering (each 100 m of mangrove reduces wave height about 20 %)	Carbon sequestration (3–5 × tropical forest density); fisheries nursery
Coral reef restoration	Wave dissipation (reefs reduce wave energy 70–95 %); coastal protection valued at about \$10,000/km/yr	Tourism; fisheries; biodiversity
Urban green infrastructure	Tree canopy reduces urban heat island by 2–5 °C; permeable surfaces reduce flooding	Air quality; mental health; physical activity
Wetland conservation	Floodplain water storage; nutrient filtration	Wildlife habitat; recreation
Reforestation / agroforestry	Soil retention; rainfall recycling; microclimate stabilization	Carbon storage; smallholder livelihoods
Drought-tolerant agroecosystems	Diverse cropping, perennial roots, soil organic matter	Food security; reduced N ₂ O
Living shorelines	Marsh and oyster reef construction replacing seawalls	Habitat; better long-term storm performance than hard infrastructure

40.10.2 Quantified Performance of Ecosystem-Based Adaptation

EbA projects often outperform engineered alternatives on cost and resilience:

- Mangroves vs. seawalls. Coastal protection from mangroves in the Philippines averages \$94/m of coastline; equivalent seawall construction averages \$2,000/m, with no co-benefits and high maintenance (Beck et al. 2018, *Nat. Commun.*).
- Hurricane Katrina (2005). Wetland loss in the Mississippi Delta increased storm surge by about 25%; restoring 100 km² of marsh would reduce surge damage in vulnerable parishes by about 10–15 % (Day et al. 2007, *Science*).
- 2003 European heat wave. Cities with dense urban green infrastructure (e.g., Vienna) experienced about 30 % fewer heat-related deaths than comparable cities with less greening (Smargiassi et al. 2009).

40.10.3 Limits of EbA

EbA is not a panacea. Limitations:

- Cannot substitute for emissions reduction. No amount of coastal restoration prevents the catastrophic outcomes of 4 °C warming.
- Climate change itself is undermining the adapters. Coral bleaching kills the reefs we want to use for coastal protection; mangroves face sea-level rise faster than they can build sediment.
- Equity and tenure issues. EbA projects fail when they ignore Indigenous land rights or displace communities.

EbA is best understood as one component of a multi-layered adaptation portfolio that also includes hard infrastructure, social systems, and aggressive emissions cuts.

Clinical Connection — Heat Action Plans and Public Health. Following the 2003 European heat wave (about 70,000 excess deaths) and the 2010 Russian heat wave (about 55,000 excess deaths), cities increasingly couple ecological strategies (urban tree planting, cool roofs, restored wetlands and parks) with public health interventions (heat warning systems, cooling shelters, vulnerable-population outreach). Ahmedabad, India implemented South Asia’s first Heat Action Plan in 2013 after a 2010 heat wave killed > 1,300 residents; subsequent years saw about 30% reductions in heat-related mortality despite continued warming. Mexico City, Phoenix, and Chicago have similar plans. These One Health interventions integrate biodiversity conservation, urban ecology, and human health — operationalising the EbA framework.

Concept Check: A coastal municipality must spend its limited adaptation budget on protecting 20 km of shoreline from increasing storm surge. (a) Compare the cost-benefit profile of seawall construction vs. mangrove restoration. (b) Why is EbA not always the best choice — what conditions favor hard infrastructure? (c) How does coral bleaching complicate the math?

40.11 International Conservation Frameworks

40.11.1 Conservation Agreements: CITES, CBD, GBF, and Paris Agreement

Table 499. Conservation Agreements: CITES, CBD, GBF, and Paris Agreement: Framework and Year.

Framework	Year	Target	Status (2024)
CITES	1975	Regulate international wildlife trade	Parties and listed taxa change as appendices are amended; cite the live appendices for current counts [Convention on International Trade in Endangered Species of Wild Fauna and Flora, 2026]
CBD (Convention on Biological Diversity)	1992	Conservation, sustainable use, equitable sharing	196 parties (US has not ratified)
Aichi Targets	2010	20 targets for 2020	Most targets missed
Kunming-Montreal Framework (30x30)	2022	Protect 30% of land and ocean by 2030	Currently about 17% land, about 8% ocean protected
Paris Agreement	2015	Limit warming to 1.5-2°C	Tracking toward 2.5-3°C

40.11.2 The 30x30 Target

The Kunming-Montreal Global Biodiversity Framework (GBF, 2022) set a target to protect 30% of land and 30% of ocean by 2030 [[Convention on Biological Diversity, 2022](#)]. Current status:

Terrestrial: 16.7% $\xrightarrow{\text{need}}$ 30% (add 20 million km²)

(481)

Marine: 8.3% $\xrightarrow{\text{need}}$ 30% (add 78 million km²)

(482)

Challenges: - Quality vs. quantity (many protected areas are “paper parks” with no enforcement) - Indigenous and local community rights (30x30 must not displace indigenous peoples) - Representativeness (current protected areas biased toward “rock and ice” — high-altitude, low-productivity areas) - Financial gap: estimated \$700 billion/yr needed; current spending about \$100 billion/yr

40.11.3 Payments for Ecosystem Services

REDD+ (Reducing Emissions from Deforestation and Forest Degradation): International carbon market payments incentivise forest-rich developing nations to avoid deforestation. \$5 billion in pledges as of 2024, but implementation faces challenges of additionality, leakage, permanence, and measurement.

Concept Check: The Aichi Targets (2010-2020) were largely unmet. What factors contributed to their failure, and how does the Kunming-Montreal Framework attempt to address these shortcomings?

40.12 Worked Example: Species-Area Prediction for Island Birds

Problem: An ecologist studies bird species on an archipelago. The species-area relationship for this region follows the equation $S = cA^z$, where $c = 10$ and $z = 0.3$. Island X has an area (A) of 1,000 km². Calculate the expected number of bird species (S) on Island X.

Solution:

Step 1. Identify the given variables. - Area (A) = 1,000 km² - Constant (c) = 10 - Exponent (z) = 0.3

Step 2. Substitute the values into the species-area equation.

$$S = cA^z$$

$$S = 10 \times (1000)^{0.3}$$

Step 3. Calculate the exponent. Notice that $1000 = 10^3$. Therefore:

$$(10^3)^{0.3} = 10^{(3 \times 0.3)} = 10^{0.9}$$

Let’s approximate $10^{0.9}$. Since $10^1 = 10$ and $10^{0.5} \approx 3.16$, $10^{0.9} \approx 7.94$. (Exact value: $10^{0.9} \approx 7.943$)

Step 4. Solve for S .

$$S = 10 \times 7.943$$

$$S \approx 79.43$$

Answer: Island X is expected to support approximately 79 bird species.

40.13 Worked Example: Effective Population Size and the 50/500 Rule

Problem: A captive recovery herd of an endangered ungulate has a census size of $N = 120$ individuals, but primarily $N_m = 20$ males and $N_f = 100$ females actually breed. Calculate the effective population size N_e , the per-generation inbreeding rate ΔF , and evaluate the herd against the 50/500 rule for short-term and long-term viability.

Solution:

Step 1. Identify the given variables. - Breeding males (N_m) = 20 - Breeding females (N_f) = 100 - Census size (N) = 120

Step 2. Substitute into the unequal-sex-ratio effective-size equation.

$$N_e = \frac{4N_mN_f}{N_m + N_f}$$

$$N_e = \frac{4 \times 20 \times 100}{20 + 100} = \frac{8,000}{120} \approx 66.7$$

Step 3. Compute the per-generation inbreeding rate.

$$\Delta F = \frac{1}{2N_e} = \frac{1}{2 \times 66.7} \approx 0.0075 = 0.75\% \text{ per generation}$$

Step 4. Evaluate against the 50/500 rule. With $N_e \approx 67$, the herd clears the short-term threshold ($N_e \geq 50$) that guards against rapid inbreeding depression, but it falls far short of the long-term threshold ($N_e \geq 500$) needed to retain additive genetic variance for future adaptation. The skewed sex ratio is the cause: the effective size is barely over half the census size, even though 120 animals are present.

Answer: $N_e \approx 67$ and $\Delta F \approx 0.75\%$ per generation. The herd is demographically defensible in the short term but is genetically committed to losing roughly 0.75% of its heterozygosity each generation; without managed gene flow or population growth it remains at elevated long-term extinction risk because it cannot meet the $N_e \geq 500$ adaptive-potential standard.

40.13.1 Minimum Viable Population and Genetic Rescue: Case Studies from Conservation Biology

Minimum viable population (MVP) is defined as the smallest population size with $\geq 95\%$ probability of persistence over 100 generations, incorporating demographic stochasticity, environmental variance, and genetic deterioration from inbreeding depression and loss of adaptive variation. The classical rule-of-thumb is the “50 / 500 rule” (Franklin 1980): $N_e \geq 50$ to avoid short-term inbreeding depression, $N_e \geq 500$ to retain long-term adaptive potential against mutation-drift balance. Modern refinements (Frankham, Brook & Bradshaw 2014) revise these upward — $N_e \geq 100$ and $N_e \geq 1000$ — as the more defensible thresholds given empirical estimates of mutational-variance and inbreeding-load effects.

Case 1 — The Arabian Oryx (*Oryx leucoryx*). Extinct in the wild by 1972 after hunting reduced the Arabian population to zero, the species survived primarily in a 9-founder “World Herd” assembled at Phoenix Zoo. Careful pedigree management and reintroduction programs (Oman 1982, Saudi Arabia 1989, Jordan

1997) have grown the wild population to about 1250 (IUCN 2017, Vulnerable). The genetic cost: current population heterozygosity is about 70 % of the pre-bottleneck estimate, and the 6 microsatellite loci have at most 2 alleles — a cautionary example that demographic recovery does not erase the genetic signature of a bottleneck.

Case 2 — The California Condor (*Gymnogyps californianus*). From a 1982 low of 22 individuals (the entire species in captivity by 1987), a captive-breeding / release program has grown the population to > 500 (half wild, half captive). Genomic sequencing (Ralls et al. 2020) detected 23 known deleterious alleles in the founders, two fixed during the bottleneck. The ongoing challenge is not census size but lead toxicosis from ingestion of lead ammunition in carcasses — a clear example of *why* habitat and regulatory intervention remain necessary even when demographic targets are met.

Genetic rescue is the deliberate introduction of unrelated individuals into a small, inbred population to restore heterozygosity. The textbook case is the Florida panther (*Puma concolor coryi*): by the 1990s, about 30 individuals remained, with striking inbreeding-depression **phenotypes** (cryptorchidism, cardiac defects). Introducing 8 female Texas cougars in 1995 doubled heterozygosity within one generation; population is now about 200 with reduced deformities and increased reproductive success (Johnson et al., *Science* 2010). The Isle Royale wolves (introduction of 19 wolves 2018–2021) represent the latest live experiment. Genetic rescue is *not* a comprehensive solution — it can disrupt locally adapted gene complexes, introduce maladapted alleles, and dilute evolutionary uniqueness (the Florida panther now bears about 5 % Texas-cougar ancestry). The decision is typically a balance of short-term demographic benefit against long-term evolutionary coherence.

40.13.2 Worked Example — Island Biogeography and Species-Area Loss

Problem: The MacArthur–Wilson species-area relationship in the power-law form is

$$S = cA^z$$

where S is species richness, A is area, and c and z are taxon- and biome-specific constants. For mammals on a network of “sky island” mountain ranges, empirical estimates are $z = 0.25$ and $c = 5$.

(a) Compute S at $A = 100 \text{ km}^2$ (intact) and at $A = 10 \text{ km}^2$ (after 90% habitat loss). (b) What fraction of species is predicted to be lost? (c) Discuss the implication for the SLOSS (single large vs. several small) debate.

Solution:

Step 1. Evaluate S at intact area.

$$S_{\text{intact}} = 5 \times 100^{0.25} = 5 \times 3.162 \approx 16 \text{ species}$$

Step 2. Evaluate S after 90% habitat loss.

$$S_{\text{loss}} = 5 \times 10^{0.25} = 5 \times 1.778 \approx 9 \text{ species}$$

Step 3. Predicted species loss.

$$\Delta S = 16 - 9 = 7 \text{ species}; \quad \Delta S/S_{\text{intact}} = 7/16 \approx 0.44 \text{ (44 percent loss)}$$

This is the well-known asymmetry of the species-area curve: a 90% reduction in area produces a 44% reduction in species. The non-linearity comes from the exponent $z \approx 0.25$ for habitat fragments (it is closer to 0.15 for nested sub-samples of a continuous habitat — Preston’s distinction between isolated islands and within-habitat sampling).

Step 4. SLOSS implication.

Compare a single large reserve of 100 km^2 ($S \approx 16$) against ten small reserves of 10 km^2 each. If each small reserve harbors an independent draw from the same species pool (a generous assumption — most small fragments are subsets of the same dominant species), the upper-bound species count is $10 \times 9 = 90$ in additive count, but ecologically, most species overlap, so the realized total is closer to $S(\text{total area}) = 5 \times 100^{0.25} = 16$ — the same as the single large reserve. Per-patch, however, small reserves suffer higher extinction rates (smaller K , edge effects, demographic stochasticity), so a single large reserve typically wins for area-sensitive

species. SLOSS is not resolved by area alone; it depends on z , the degree of species turnover between patches (β diversity), and the dispersal capacity of focal taxa.

Answer: Intact $S \approx 16$; post-loss $S \approx 9$; predicted loss is 7 species (44%) from a 90% area reduction.

40.13.3 Concept Check (Analyze) — Metapopulation Dynamics and Corridor Effects

The Levins metapopulation model is

$$\frac{dp}{dt} = m p (1 - p) - e p$$

- where p is the fraction of habitat patches occupied, m is the per-patch colonization rate, and e is the per-patch extinction rate. At equilibrium, $\hat{p} = 1 - e/m$.
- (a) Baseline: $e = 0.1$, $m = 0.2$. Compute \hat{p} . Identify the extinction threshold condition (in terms of the ratio e/m) at which the metapopulation collapses regionally even though individual patches remain habitable.
 - (b) Habitat fragmentation doubles the per-patch extinction rate to $e = 0.2$ while m stays at 0.2. Compute the new \hat{p} . Analyze the qualitative behavior: this is a phase transition, not a smooth response — explain why management interventions that “just barely” maintain $m > e$ are far less robust than they appear.
 - (c) A corridor construction project increases m by 50% from 0.2 to 0.3 while leaving $e = 0.2$ unchanged. Compute the new \hat{p} and explain in mechanistic terms why corridors (which raise m) generally yield larger conservation gains than within-patch interventions (which lower e) when the system sits near the extinction threshold.
 - (d) Synthesize: connect the Levins extinction threshold to the SLOSS debate from the worked example above. Which spatial configuration (SL vs. SS) is more robust when the per-patch extinction rate is environmentally elevated (e.g., climate change raising e system-wide)?

40.13.4 Concept Check (Evaluate) — Climate Velocity and the Boreal-Tundra Tipping Point

The boreal–tundra ecotone is advancing northward at a velocity of approximately 50 km/decade as tree-line species (spruce, larch) establish on warming, previously permafrost-dominated soils. Permafrost globally stores roughly 1.5×10^{12} kg C — about twice the mass of carbon currently in the atmosphere.

- (a) Evaluate the two competing carbon-flux mechanisms triggered by tree encroachment onto tundra:
 - *Above-ground biomass gain.* New tree biomass sequesters carbon into wood, root systems, and forest litter. Estimate the order-of-magnitude per-hectare gain over a decade (a typical boreal forest holds ~ 100 MgC/ha above ground; tundra holds ~ 5 MgC/ha above ground).
 - *Permafrost thaw carbon loss.* Soils warm under tree canopy and thawed permafrost respires previously frozen organic matter. The boreal soil column can hold ~ 200 – 500 MgC/ha in the upper 1 m, of which a significant fraction is microbially labile once thawed.
- (b) Compare the two magnitudes. Which dominates the regional carbon balance over a 50-year horizon? Justify by reasoning about which pool is larger, which has the faster turnover, and which is bounded vs. continuously growing.
- (c) Evaluate the climate-feedback sign. Does boreal-tundra advance constitute a *negative* feedback (sequestration mitigating warming) or a *positive* feedback (net release amplifying warming) at multi-decadal scales? Discuss why the answer depends on the time horizon: above-ground sequestration is fast but capped at the new forest’s standing biomass, while permafrost respiration is slow but ongoing for centuries.
- (d) Design a monitoring study to discriminate between these two scenarios. Specify: (i) which two measurements are most diagnostic (e.g., eddy-covariance net ecosystem exchange, soil-profile dissolved organic carbon flux, satellite-derived NDVI greening), (ii) what spatial and temporal sampling design is needed, and (iii) what would constitute a falsifying observation for each scenario. Conclude with a recommendation for conservation policy: should boreal-tundra ecotone management prioritize carbon sequestration through afforestation incentives, or permafrost protection through restricted disturbance?

40.14 Current Evidence and Frontier Biology: Biomes and Conservation Biology

For Biomes and Conservation Biology, frontier biology belongs inside the evidence logic of the chapter. Ecology and conservation decisions increasingly combine field data, remote sensing, community knowledge, model uncertainty, and explicit values. The core reading question is this: conservation claims must separate ecological evidence, social values, feasibility, and uncertainty in tradeoffs.

- What to verify: identify the observation, model, assay, or dataset that would make the claim stronger or weaker.
- What to qualify: state the scale, organism, cell type, environmental condition, or population where the claim is expected to hold.
- What to compare: test at least one alternative explanation, baseline, or null model before treating the pattern as causal.
- What to cite: distinguish primary evidence, review synthesis, public dataset, and institutional guidance; for recent or numeric claims, prefer the source closest to the measurement and state what has changed since it was published.

Use conservation metrics carefully: population indices, extinction-risk categories, ecosystem services, and governance targets answer different decisions [Intergovernmental Science-Policy Platform on Biodiversity and Ecosystem Services, 2019, 2024, World Wide Fund for Nature, 2024, International Union for Conservation of Nature, 2025, Food and Agriculture Organization of the United Nations, 2024].

Occurrence data answer a different question from extinction-risk categories or policy synthesis. GBIF is open biodiversity occurrence infrastructure: it mobilizes where-and-when records from museums, monitoring programs, DNA barcodes, and recent observations through shared data standards such as Darwin Core. Use GBIF to ask where a taxon has been recorded; use IUCN and IPBES to ask how risk, drivers, and policy responses have been assessed. A conservation claim should filter date, coordinate uncertainty, taxonomic backbone, duplicates, and sampling bias before treating occurrence points as abundance or range evidence [GBIF Secretariat, 2026, International Union for Conservation of Nature, 2025, Intergovernmental Science-Policy Platform on Biodiversity and Ecosystem Services, 2024].

Source practice: For conservation decisions, identify whether the evidence is a population index, extinction-risk assessment, ecosystem-service valuation, satellite product, or policy synthesis [Intergovernmental Science-Policy Platform on Biodiversity and Ecosystem Services, 2024, NOAA Coral Reef Watch, 2025, International Union for Conservation of Nature, 2025, Food and Agriculture Organization of the United Nations et al., 2025].

40.14.1 Current Evidence Map: Conservation Decision Evidence Chain

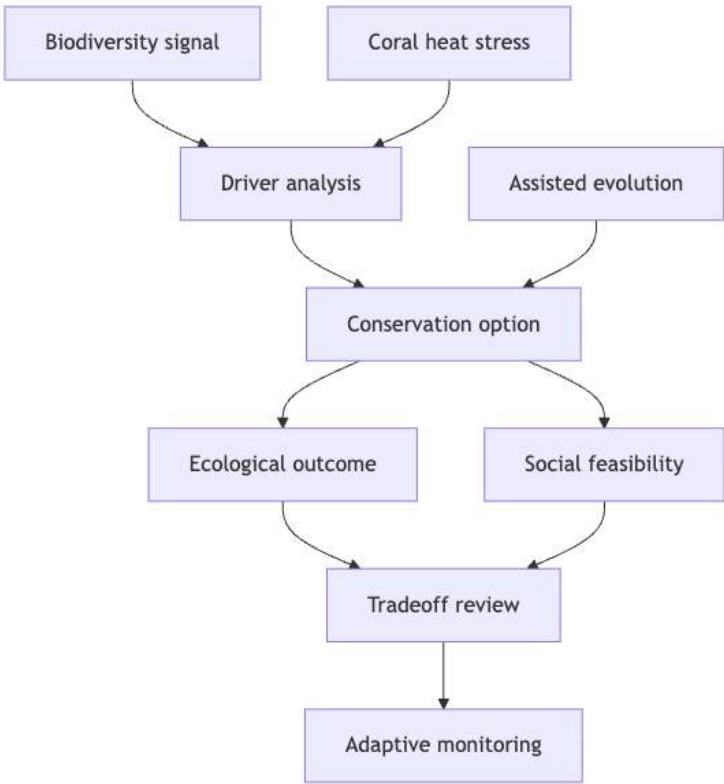


Figure 239. Coral assisted-evolution and IPBES transformative-change examples show how conservation decisions combine biological evidence, values, feasibility, governance, and post-intervention monitoring [citep{ipbes2024transformative,noaa2025coralbleaching,strader2022coralheat}].

40.15 Key Terms

Table 500. Current Evidence Map: Conservation Decision Evidence Chain: Term and Definition.

Term	Definition
Biome	Large-scale ecological zone defined by climate and dominant vegetation type
Net primary productivity (NPP)	Carbon fixed by plants minus autotrophic respiration; g C/m ² /yr
IUCN Red List	Global system for evaluating extinction risk using quantitative criteria
Minimum viable population (MVP)	Smallest population with at least 95% persistence probability for at least 100 generations
50/500 rule	$N_e \geq 50$ short-term; $N_e \geq 500$ long-term viability (Franklin/Soule)
Effective population size (N_e)	Genetically effective number of breeding individuals; typically $0.1 - 0.25 \times N$
Extinction debt	Delayed extinction of species committed to disappear due to past habitat loss
SLOSS debate	Trade-off between single large vs. several small reserves
Rewilding	Restoration of ecological processes via reintroduction of lost species
Population Viability Analysis (PVA)	Stochastic simulation of extinction probability
Conservation genomics	Application of whole-genome analysis to conservation management
Assisted gene flow	Intentional translocation of alleles from adapted to non-adapted populations
Genetic rescue	Introduction of unrelated individuals to reverse inbreeding depression
Climate velocity	Speed at which climate conditions shift geographically (km/yr)
Edge effect	Microclimatic and biotic changes at habitat fragment boundaries
Coral bleaching	Thermal stress-induced expulsion of zooxanthellae; loss of coral energy supply
30x30	Target to protect 30% of land and ocean by 2030 (Kunming-Montreal GBF)
De-extinction	Using genomic engineering to resurrect functional analogs of extinct species
Novel biome	Ecosystem with no historical analog, arising from climate change
IPBES	Intergovernmental Science-Policy Platform on Biodiversity and Ecosystem Services; “IPCC for biodiversity”
Climate refugia	Locations where local climate changes more slowly than the regional average; havens for slow-dispersing species
Ecosystem-based adaptation (EbA)	Use of biodiversity and ecosystem services to help people adapt to climate change
Living shorelines	Marsh, oyster reef, and mangrove infrastructure replacing seawalls for coastal protection
Living Planet Index	WWF metric of mean change in monitored vertebrate populations since 1970
Heat Action Plan	Coupled public-health and ecological response to extreme heat events
Genetic load	Accumulated deleterious alleles; heightened in bottlenecked populations; affects translocation strategies
Runs of homozygosity (ROH)	Long stretches of homozygous DNA indicating recent inbreeding; key conservation-genomic metric

40.16 Review Questions

- Using the species-area relationship $S = cA^z$ with $c = 6$ and $z = 0.28$, calculate species richness for a 50,000 ha intact forest and after fragmentation into 5 patches of 1,000 ha each. What fraction of species are committed to extinction via the fragmentation-driven extinction debt? How long might this debt take to be “paid” for long-lived tree species?
- A population of sea turtles has $N_e = 35$ and current heterozygosity $H = 0.60$. (a) Apply the 50/500 rule to evaluate its short-term and long-term viability. (b) Calculate how many generations until $H < 0.40$ using $H_t = H_0(1 - 1/2N_e)^t$. (c) What genetic rescue strategy could improve the prognosis?
- The Amazon has currently lost about 17% of its original forest cover. Lovejoy and Nobre’s tipping point threshold is about 20-25%. (a) Explain the tipping mechanism (why is it non-linear?). (b) What conservation interventions are needed in terms of scale, urgency, and geographic targeting? (c) How does the transpiration recycling mechanism create a positive feedback loop during deforestation?
- Explain the difference between demographic, environmental, genetic, and catastrophic stochasticity in an MVP context. Which was most important in the Florida panther case, and how was it mitigated? Calculate the inbreeding rate (ΔF) for the panther population at $N_e = 10$ vs. after genetic rescue at $N_e = 50$.
- Compare rewilding and assisted gene flow as conservation strategies for climate change adaptation. For each, give one specific quantitative example (species, location, outcome metric, timescale).
- A conservation biologist must design a reserve system for a large carnivore with home range = 200 km² and an MVP of $N_e = 500$ (N/N_e ratio = 4). Calculate:

- (a) minimum total census population needed, (b) minimum reserve area assuming 50% habitat overlap between individuals, (c) whether a single reserve or corridor-connected system is more feasible. Design the reserve system.
7. The Great Barrier Reef has experienced 6 mass bleaching events in 10 years. Using the degree heating weeks (DHW) metric, explain the mechanism of bleaching. At what level of global warming does coral reef survival become highly improbable? What is the economic value at stake (cite Deloitte or similar valuation studies)?
8. Evaluate the 30x30 target (Kunming-Montreal Framework). Calculate the additional area of land and ocean that must be protected to reach 30% from current levels. What are the three most significant implementation challenges, and how might they be addressed?
9. The woolly mammoth de-extinction project aims to create cold-adapted elephants for Arctic tundra. (a) What ecological function would they serve? (b) How would they slow permafrost thaw? (c) What are the strongest ecological and ethical arguments for and against this approach?
10. Using the concept of climate velocity, explain why montane species are at lower risk of range contraction than lowland species. Calculate climate velocity for a flat landscape with temperature change = 0.03°C/yr and spatial gradient = 0.005°C/km, vs. a mountain with spatial gradient = 5°C/km. What are the implications for conservation prioritisation?
11. Compute species_area_relationship for $A \in \{1, 10, 100\}$ km² with $c = 2$, $z = 0.25$; discuss reserve sizing.
12. Contrast inbreeding depression vs. outbreeding depression in translocation programs.
13. The IPBES 2019 Global Assessment ranked land-use change as the dominant terrestrial driver of biodiversity loss (about 30 %), with climate change at about 14 % but rising. (a) Why is this *current* ranking expected to invert by 2050? (b) How should conservation priority-setting respond to this projected shift? (c) The Transformative Change Assessment (IPBES 2024) argues that incremental conservation cannot meet biodiversity targets. What three systemic reforms does it recommend, and why are they outside traditional conservation biology?
14. Compare two endangered birds: species A in the high Andes (5 °C/km gradient) and species B on the Brazilian cerrado (0.005 °C/km gradient), with both facing 0.03 °C/yr warming. (a) Calculate climate velocity for each. (b) Predict their relative extinction risks. (c) How does this calculation re-prioritize conservation funding between the two regions?
15. A coastal municipality is choosing between (a) a 20-km concrete seawall (\$2,000/m, 50-yr lifetime, no co-benefits, requires periodic rebuilding) and (b) a 20-km mangrove restoration project (\$94/m initial, low maintenance, multiple co-benefits, but vulnerable to sea-level rise faster than mangrove sediment accretion). Calculate total costs over 50 years for each, and identify under what climate-change scenario each option is preferred.
16. Explain how the 50/500 rule, conservation genomics (runs of homozygosity, genetic load), and population viability analysis converge to inform genetic rescue decisions for the Florida panther. Why was the 1995 Texas-cougar introduction successful, and what risks (e.g., outbreeding depression) had to be balanced?
17. Define a climate refugium and list four types (topographic, hydrological, microclimatic, elevational). Why is identifying refugia critical for 21st-century reserve design? What datasets (climate models, species distribution models, paleoecology) does refugium identification require?
18. Critically evaluate the 30x30 target. (a) Calculate the additional area of land and ocean needed to reach 30 % from current levels. (b) Why is *quality* of protection (effective management, no “paper parks”) at least as important as quantity? (c) How can 30x30 be implemented without violating Indigenous land rights, given that about 80 % of remaining biodiversity is on Indigenous-managed lands?

40.17 Further Reading and Source Notes: Biomes and Conservation Biology

- Soule (1980). Thresholds for Survival: Maintaining Fitness and Evolutionary Potential. *Conservation Biology: An Evolutionary-Ecological Perspective*.
- Frankham (1995). Effective population size/adult population size ratios in wildlife: A review. *Genetical Research*, 66.
- Frankham (2014). Conservation genetics: Setting the scene. *Philosophical Transactions of the Royal Society B*, 369.

40.18 Computational Bridge

The power-law S–A curve is a one-liner:

```
from biology.ecology import species_area_relationship

for a in (1.0, 10.0, 100.0):
    print(a, round(species_area_relationship(a, c=2.0, z=0.25), 2))
```

Clinical / systems note: Habitat fragmentation in zoonotic emergence maps onto the same area-dependent extinction risk curves used in terrestrial conservation.

40.19 Summary

- Nine terrestrial biomes: tropical rainforest highest NPP (about 1,750 g C/m²/yr); desert lowest (about 45-125); boreal forest largest land biome by area. Five aquatic biome types including coral reefs (most biodiverse marine ecosystem, threatened by bleaching).
- Climate change: biome boundaries shifting 5-10 km/decade poleward; Amazon at about 17% deforestation approaching 20-25% tipping point; permafrost thaw adds 2-5 Gt C/yr; novel biomes emerging on about 20% of Earth’s surface by 2100.
- Sixth Mass Extinction: 100-1,000x background extinction rate; 73% vertebrate population decline since 1970; 1 million species threatened.
- IPBES findings: about 1 million species threatened (12.5%); 85% of wetlands lost since 1700; 50% coral reef loss since 1870. Drivers ranked: land-use change > exploitation > climate change (rising fast) > pollution > invasives. Transformative Change Assessment (2024) argues incremental conservation insufficient.
- Climate velocity $v = (\partial T / \partial t) / |\nabla T|$: fast in flat tropical and temperate plains (6–10 km/yr), slow in mountains (6 m/yr); refugia (topographic, hydrological, microclimatic, elevational) are the key targets for climate-adaptive reserve design.
- Ecosystem-based adaptation (EbA): mangroves, coral reefs, urban green infrastructure, wetlands, agroforestry. Often outperforms hard infrastructure on cost (\$94/m vs. \$2,000/m for coastal protection) and provides co-benefits, but cannot substitute for emissions reduction.
- IUCN Red List: CR = at least 80% population decline under Criterion A; version 2025-2 listed 48,646 threatened species among 172,620 assessed, and totals change as assessments expand [International Union for Conservation of Nature, 2025].
- MVP: 50/500 rule (Franklin); revised 100/1000 [Frankham, 2014]; PVA accounts for most stochasticity types. N_e/N ratio typically 0.10-0.25.
- Extinction debt: fragmented species committed to extinction with 50-500 yr lags; current surveys overestimate long-term viability.
- Reserve design: core-corridor-matrix; edge effects penetrate 100-300 m; corridors increase movement 50%; 30x30 target.
- Emerging strategies: rewilding (trophic cascades), conservation genomics (ROH, adaptive variation), assisted gene flow (coral heat tolerance), de-extinction (mammoth project), climate-adaptive management.
- International frameworks: CBD, CITES, 30x30 target; \$700 billion/yr funding gap; quality and representativeness challenges.
- Connections: See section 23 for phylogenetic diversity, section 37 for trophic rewilding, and section 20 for small-population genetics.

40.20 Companion Source Module: Biomes and Conservation Biology

Biomes and Conservation Biology should leave a reproducible trail from a biological claim to the code, figure, diagram, or paper-based activity that can test it. Use the surfaces below to inspect the chapter’s assumptions, rerun the relevant model, or compare the manuscript explanation with companion labs and figures.

Table 501. Companion source surfaces for Biomes and Conservation Biology.

Surface	Use it for
src/biology/ecology/ecology.py (species_area_relationship, biodiversity_indices, connectance)	Reproduce conservation metrics and tradeoff-sensitive summaries.
src/visualization/plots.py (plot_species_area_relationship, plot_biome_distribution)	Inspect species-area assumptions and biome comparisons.
src/mermaid/biology_diagrams.py (food_web_diagram, nutrient_cycle_diagram)	Connect conservation action to ecological pathways.

Reproducibility check: separate ecological evidence, social objective, feasibility, uncertainty, and monitoring indicator before choosing a conservation action. Cross-reference: use section 36, sections 37 and 38, and section 39.

Lab A — Systems Science and Emergence

This activity accompanies section 0.1 of the textbook — review that chapter before attempting the exercises below.

Unit 0 — Systems Science for Biology: Introduction · Lab A

Learning Objectives

- Identify the three canonical elements of a system (components, interactions, boundary) in concrete biological examples.
- Diagram negative- and positive-feedback loops for real physiological systems and predict their stabilizing or amplifying behavior.
- Compute response curves from the Hill equation and relate the Hill coefficient n to cooperativity and switch-like behavior.
- Reason about the difference between a complicated machine and a complex system using a worked example.

Alignment and Rubric Map

- Outcome 1 (LO1): Interpret the supplied evidence or model output for Systems Science and Emergence.
- Outcome 2 (LO2): Identify controls and comparison groups that make the claim testable.
- Outcome 3 (LO3): Quantify uncertainty, boundary conditions, or alternative explanations before concluding.
- Outcome 4 (LO4): Transfer the mechanism to a new biological case or public-facing decision.
- Chapter LO coverage: LO1, LO2, LO3, LO4
- Rubric dimensions: evidence; controls; uncertainty; mechanism; transfer. ## Pre-Lab Concept Questions {.unnumbered}

Answer these before starting the investigation — they activate knowledge from the parent chapter.

1. Define a system boundary and explain why two analysts can choose different boundaries for the same problem and still produce internally consistent models. Give one short example from the parent chapter.
2. A bedroom thermostat raises the heater output when the room cools and lowers it when the room warms. Classify the dominant feedback loop in this control system and identify the variable whose deviation drives the corrective action.
3. Compare a stock (a quantity with accumulated history) and a flow (a rate that changes a stock per unit time) for the case of a small lake’s water budget. Give one biological stock and one biological flow that would be appropriate to include in a model of that lake’s ecology.

Lab Context: Systems Science and Emergence

A system is a set of interacting components, bounded against its surroundings, whose behavior depends on the interactions as much as on the parts. The central mathematical tool for stability is the Hill equation:

$$\theta = \frac{[L]^n}{K_d^n + [L]^n}$$

(483)

where θ is the fraction of receptors bound, $[L]$ the ligand concentration, K_d the dissociation constant, and n the Hill coefficient. For $n = 1$ the curve is hyperbolic (graded response); for $n = 4$ it is steep and switch-like (as in hemoglobin’s O_2 binding).

Today’s lab trains three intuitions: what counts as “the system”, how feedback loops behave, and how cooperativity converts graded chemistry into binary biology.

Pre-Lab (to complete before class)

1. Copy equation (483) into your notebook. Compute θ for $n = 1, 2, 4$ at $[L] = K_d, 2K_d, 5K_d$. Tabulate.
2. Define in your own words: system, emergence, feedback, homeostasis, modularity.
3. Bring one example of a biological positive feedback loop and one example of a biological negative feedback loop (not from the textbook).

Paper-Based Materials

- Graph paper (2 sheets per student).
- Calculator.
- Colored pens.

- Source-governance card for Systems Science and Emergence: model-validation source card: boundary, observable, uncertainty, rival explanation, and evidence limit.
- Worksheet with blank feedback diagrams and Hill-curve axes.

Paper-Based Investigation

Part 1 — Identifying Systems

For each of the following, identify: (a) the components, (b) the key interactions, (c) the boundary separating system from environment, and (d) one input and one output crossing the boundary.

1. A single mitochondrion.
2. The glucose-insulin-glucagon regulatory axis.
3. A coral reef.
4. A bacterial biofilm on a medical catheter.
5. A neuron’s axon hillock.

Part 2 — Feedback Loop Diagrams

For each system below, diagram the feedback loop and classify it as positive or negative. Predict the steady-state behavior (stable fixed point, oscillation, or runaway).

1. Blood pressure → baroreceptor firing → vagal tone → heart rate → blood pressure.
2. Oxytocin → uterine contraction → stretch receptor → oxytocin (during labor).
3. Luteinising hormone → ovarian oestradiol → hypothalamic GnRH (follicular phase).
4. Luteinising hormone → ovarian oestradiol → hypothalamic GnRH (ovulatory phase).
5. Depolarizing Na⁺ current → more open Na⁺ channels → depolarization (action potential upstroke).

Why do loops 3 and 4 have different signs, and what does the switch imply for the dynamics of the menstrual cycle?

Part 3 — Hill Curve by Hand

1. Using $K_d = 10\text{ }\mu\text{M}$, compute θ at $[L] = 1, 2, 5, 10, 20, 50, 100\text{ }\mu\text{M}$ for three values of n : 1, 2.8 (physiological Hb), and 4.
2. Plot the three curves on the same axes. Label the “switch zone” where small changes in $[L]$ produce large changes in θ .
3. For which n is the transition sharpest? How does this cooperativity benefit an oxygen-carrying pigment?

Part 4 — Complicated vs. Complex

A wristwatch and a live cell both contain many interacting components. Yet one is complicated and the other complex. In a table, contrast:

Table 502. Part 4 — Complicated vs. Complex: Feature and Wristwatch.

Feature	Wristwatch	Live cell
Component count	about 100	about 10 ⁹ molecules
Predictability	High (mechanistic)	Statistical
Repairability	External	Self-repair
Adaptation	None	Evolutionary
Failure mode	Component breakage	Network dysregulation
Emergent properties	None (function designed in)	Many (metabolism, identity, division)

Discuss in your group one additional feature that distinguishes complex from complicated, and one case where the distinction is blurry (e.g., a modern autopilot with adaptive learning).

Data Tables

Table 503. Part 4 — Complicated vs. Complex: System and Components.

System	Components	Interactions	Boundary	Input	Output
Mitochondrion					
Glucose axis					
Coral reef					
Biofilm					
Axon hillock					

Table 504. Part 4 — Complicated vs. Complex: Feedback loop and +/–.

Feedback loop	+/–	Predicted behavior
Baroreceptor reflex		
Oxytocin-uterus		
GnRH follicular		
GnRH ovulatory		
Na ⁺ action potential		

Table 505. Hill-response sample values for ligand concentration and fractional occupancy.

[L] (μM)	θ at n = 1	θ at n = 2.8	θ at n = 4
1			
2			
5			
10			
20			
50			
100			

Evidence and Reproducibility Checklist

- Primary evidence goal: Build and critique a feedback model for a familiar living system.
- Data skill to practice: Translate a verbal biological system into variables, links, and testable predictions.
- BioSkills emphasis: Modeling and simulation, Process of science, Quantitative reasoning.
- Control logic: identify at least one positive control, one negative control, or one baseline comparison before interpreting results.
- Measurement discipline: record units, uncertainty, sample size, and any discarded observation with a reason.
- Mechanistic link: connect one result directly to the parent chapter’s big idea before writing the conclusion.
- Reproducibility check: state one procedural detail that another group would need in order to reproduce the result.

Paper-Based Evidence Upgrade

Before answering the analysis questions, annotate the paper dataset for Systems Science and Emergence with a reproducibility pass:

Table 506. Part 4 — Complicated vs. Complex: Evidence check and Student action.

Evidence check	Student action
Control logic	Mark the comparison that functions as the baseline, negative control, or reference case.
Uncertainty	Circle the row, card, diagram feature, or model assumption most likely to change the conclusion.
Model comparison	State whether a simpler rule, null model, or alternative mechanism could explain the same pattern.
Decision threshold	Write the minimum evidence that would make you revise the interpretation.
Reproducibility	Record the exact scoring rule another group would need to reproduce your classification.

Focus note: For the feedback-diagram and Hill-curve datasets, the reproducible quantities are the sign assigned to each loop edge and the Hill coefficient n used for the saturation calculation: state the system boundary you drew, justify every + or – sign from the dataset, and report the O₂-saturation numbers another group must be able to regenerate from your stated n . Keep required work paper-based; any material-handling or equipment version belongs only in an optional extension.

Source-Governance Checkpoint

Complete the source-governance card for Systems Science and Emergence before writing the conclusion. Name the source type or model snapshot, record the evidence date or version, decide whether the claim is stable or fast-moving, and write one refresh trigger that would force the interpretation to change. Treat the card as a printed evidence object, not as a live web lookup.

Worked Example: Stock-and-flow projection of a small mammal population

Problem: A field site has 200 deer mice at the start of the year. The per-capita birth rate is 0.020 per month and the per-capita death rate is 0.015 per month, with no immigration or emigration. Assume both rates stay constant for one month. Compute the net inflow into the population stock, the population at the end of the month, and the doubling time implied by the net per-capita rate.

Solution:

- Net per-capita rate = $0.020 - 0.015 = 0.005$ per month.
- Net monthly inflow = $0.005 \times 200 = 1.0$ mice per month.
- End-of-month stock = $200 + 1 = 201$ mice.
- Doubling time using the continuous-rate approximation $t_{\text{double}} \approx \ln(2) / r = 0.693 / 0.005 \approx 138.6$ months (about 11.5 years).

Interpretation: The stock barely shifts in one month, yet the small positive net rate accumulates into a doubling time of roughly a decade — a feature of pure stock dynamics that surprises students who expect proportional intuitions to track short time-scale observations. A density-dependent term (a balancing loop tied to food, predators, or disease) would slow growth before doubling and is the kind of negative-feedback structure a richer model needs once the population approaches habitat capacity.

Analysis Questions

1. For hemoglobin ($n \approx 2.8$), compute the difference in O₂ saturation between lung capillaries ([O₂] = 100 mmHg) and active muscle capillaries ([O₂] = 20 mmHg). Why is the steepness of the Hill curve a life-preserving property?
2. In Part 2, the ovarian-pituitary loop reverses sign across the menstrual cycle. What does this imply for the stability of the overall system, and what biological mechanism produces the sign reversal?
3. Modular design makes biological systems easier to evolve (new modules can be added without breaking old ones). Give one counter-example — a domain where modularity *constrains* evolution rather than freeing it.
4. The textbook notes that biological delays destabilise feedback. A surgical patient on a mechanical ventilator has a CO₂-sensing feedback loop with a built-in 10-second measurement lag. Predict what happens as you increase the loop gain; suggest one design fix.
5. Design a paper-based experiment to test whether a bacterial-population model exhibits emergent collective behavior distinct from isolated-cell behavior. What is the null hypothesis and what observation card would refute it?

Post-Lab Synthesis

Concept Check (Synthesis): A regional hospital network observes that emergency-department wait times rise sharply during winter respiratory-virus seasons. Administrators propose adding bed capacity; clinicians propose a faster discharge pathway to free beds; the public-health team proposes upstream vaccination outreach.

- (a) Draw a causal loop sketch (in words) of the stocks and flows linking community infections, hospital admissions, available beds, and wait times. Mark each proposed intervention with the leverage point category from the parent chapter that best matches it (for example, parameter change, feedback strength, system goal).
- (b) Predict the qualitative behavior of the system under each proposed intervention over one winter season, and explain which intervention is most likely to shift the long-run behavior rather than the immediate symptom. Ground the prediction in the dominant feedback loops you sketched.
- (c) Design a short measurement plan (three variables to track and one indicator of unintended consequences) that would tell the administration whether the chosen intervention reduced wait times without shifting the burden to a downstream subsystem such as primary care or home recovery.

Discussion Questions

- 1. A reductionist insists that knowing everything about every molecule in a cell is sufficient to understand cellular behavior. Where does systems science push back?
- 2. Are there systems in biology that are *not* adaptive? Propose a candidate and defend your choice.
- 3. The Covid-19 pandemic exposed how hospital systems behave under extreme input. Which systems-science principles explain why ICU capacity failed in some cities and not others?

Safety and Ethics Notes

Paper-based lab — no reagents or instruments, no physical risk. Discussion of the menstrual cycle, labor, and ventilator management should be inclusive and accurate; seek clarification from the instructor if terminology feels unfamiliar. The Covid-19 example should be grounded in public-health data rather than anecdote.

Module: *src/biology/cell/cell_biology.py (hill_equation, receptor_occupancy); src/biology/ecology/ecology.py (logistic_growth).*

Lab B — Complex Adaptive Systems

This activity accompanies section 0.2 of the textbook — review that chapter before attempting the exercises below.

Unit 0 — Systems Science for Biology: Introduction · Lab B

Learning Objectives

- Simulate a simple agent-based system on paper and observe emergent global behavior.
- Compute the period of a logistic map for selected reproductive rates and identify the onset of chaos.
- Sketch a phase diagram for a two-basin attractor landscape and reason about tipping points.
- Distinguish *robustness* from *redundancy* using a worked biological example.

Alignment and Rubric Map

- Outcome 1 (LO1): Interpret the supplied evidence or model output for Complex Adaptive Systems.
- Outcome 2 (LO2): Identify controls and comparison groups that make the claim testable.
- Outcome 3 (LO3): Quantify uncertainty, boundary conditions, or alternative explanations before concluding.
- Outcome 4 (LO4): Transfer the mechanism to a new biological case or public-facing decision.
- Chapter LO coverage: LO1, LO2, LO3, LO4
- Rubric dimensions: evidence; controls; uncertainty; mechanism; transfer. ## Pre-Lab Concept Questions {.unnumbered}

Answer these before starting the investigation — they activate knowledge from the parent chapter.

1. Distinguish a positive (reinforcing) feedback loop from a negative (balancing) feedback loop, and give one short biological example of each from the parent chapter.
2. A lake receives steady phosphorus runoff for years with little visible change, then shifts abruptly into a turbid eutrophic state. Apply the idea of a tipping point to explain why a small additional input can drive a large outcome here.
3. Compare a random (Erdős–Rényi) network with a scale-free network in terms of how they respond to the targeted removal of a high-degree node. Which topology tends to be more resilient to random failure, and which is more vulnerable to a directed attack on hubs?

Lab Context: Complex Adaptive Systems

A complex adaptive system (CAS) is a population of agents whose collective behavior emerges from local rules rather than central control. Examples run from neurons in a cortical circuit to ants in a colony to species in an ecosystem. Two mathematical tools recur across scales:

1. The logistic map — a discrete-time model $x_{n+1} = rx_n(1 - x_n)$ that passes from stable fixed point → period-2 → period-4 → chaos as the parameter r increases. It captures the essence of bifurcation theory in a single line of algebra.
2. Phase-space attractor landscapes — a potential-well picture that shows how systems can occupy alternative stable states with a “tipping point” between them, and how hysteresis delays recovery.

This lab is paper-based; a calculator and graph paper are the only tools needed.

Pre-Lab (to complete before class)

1. Write down the logistic map and draw its form for $0 \leq x \leq 1, r = 2.5$. Mark the intersection with the identity line $x_{n+1} = x_n$ — the fixed point.
2. Briefly define: attractor, bifurcation, hysteresis, self-organized criticality.
3. Bring three examples of bistable biological systems to class (for Part 3 discussion).

Paper-Based Materials

- Graph paper (2 sheets per student).
- Calculator.
- Colored pens.

- Source-governance card for Complex Adaptive Systems: model-validation source card: boundary, observable, uncertainty, rival explanation, and evidence limit.
- Worksheet with a blank logistic-map table and a blank phase landscape.

Paper-Based Investigation

Part 1 — The Logistic Map by Hand

1. Starting from $x_0 = 0.2$, compute 20 iterations of the logistic map for each of these r values: $r = 2.5, 3.2, 3.5, 3.8$.
2. For each r , plot x_n against iteration number n on the same axes (use a different color for each r).
3. Identify the long-term behavior: fixed point, period-2, period-4, or chaotic.
4. Bonus: compute x_{100} for $r = 3.8$ with $x_0 = 0.2$ and $x_0 = 0.20001$. How different are they? Relate to “sensitive dependence on initial conditions.”

Part 2 — Attractor Landscape and Tipping Points

A shallow lake has two alternative stable states: clear (low algae, clear water) and turbid (high algae, murky). Phosphorus loading P shifts which state is stable.

1. Sketch the potential landscape $U(A)$ (where A = algal biomass) for three values of P : low (primarily clear is stable), intermediate (both states stable), and high (primarily turbid is stable).
2. Mark the tipping point (P_1) where the clear state loses stability as P increases.
3. Mark the restoration point (P_2) where the turbid state loses stability as P decreases.
4. Compare P_1 and P_2 — which is smaller? This gap is the hysteresis loop and explains why eutrophication is hard to reverse.

Part 3 — Robustness Versus Redundancy

Consider the mammalian immune system as a CAS. It has five categories of robustness:

- Redundancy — multiple B-cell clones specific to the same antigen.
 - Degeneracy — T- and B-cells with overlapping but distinct function.
 - Modularity — innate vs. adaptive compartments.
 - Negative feedback — regulatory T cells suppress overactive responders.
 - Diversity — V(D)J recombination generates about 10^{11} receptor sequences.
1. For each category, give one concrete example from the immune system.
 2. Then list one *fragility* that the same architectural feature introduces. (E.g., immune redundancy also means multiple places autoimmunity can arise.)
 3. Discuss in your group: would a maximally robust system also be maximally evolvable?

Data Tables

Table 507. Part 3 — Robustness Versus Redundancy: Iteration n and x_n at $r=2.5$.

Iteration n	x_n at $r = 2.5$	x_n at $r = 3.2$	x_n at $r = 3.5$	x_n at $r = 3.8$
0	0.2	0.2	0.2	0.2
1				
...				
20				

Long-term regime at each r : $r = 2.5$: , $r = 3.2$: , $r = 3.5$: , $r = 3.8$: .

Table 508. Part 3 — Robustness Versus Redundancy: CAS property and Immune-system example.

CAS property	Immune-system example	Associated fragility
Redundancy		

CAS property	Immune-system example	Associated fragility
Degeneracy		
Modularity		
Negative feedback		
Diversity		

Evidence and Reproducibility Checklist

- Primary evidence goal: Explore how small rule changes alter collective behavior.
- Data skill to practice: Distinguish deterministic trends from stochastic variation in repeated simulations.
- BioSkills emphasis: Modeling and simulation, Process of science, Quantitative reasoning.
- Control logic: identify at least one positive control, one negative control, or one baseline comparison before interpreting results.
- Measurement discipline: record units, uncertainty, sample size, and any discarded observation with a reason.
- Mechanistic link: connect one result directly to the parent chapter’s big idea before writing the conclusion.
- Reproducibility check: state one procedural detail that another group would need in order to reproduce the result.

Paper-Based Evidence Upgrade

Before answering the analysis questions, annotate the paper dataset for Complex Adaptive Systems with a reproducibility pass:

Table 509. Part 3 — Robustness Versus Redundancy: Evidence check and Student action.

Evidence check	Student action
Control logic	Mark the comparison that functions as the baseline, negative control, or reference case.
Uncertainty	Circle the row, card, diagram feature, or model assumption most likely to change the conclusion.
Model comparison	State whether a simpler rule, null model, or alternative mechanism could explain the same pattern.
Decision threshold	Write the minimum evidence that would make you revise the interpretation.
Reproducibility	Record the exact scoring rule another group would need to reproduce your classification.

Focus note: Here the reproducibility pass turns on the logistic-map iteration and the hysteresis-loop dataset: record the exact value of *r* and the seed/initial condition for every trajectory, and for the tipping-point loop note which branch (clear-water versus turbid) you read and the phosphorus level at which the jump occurred, since a different starting point silently changes the conclusion. Keep required work paper-based; any material-handling or equipment version belongs only in an optional extension.

Source-Governance Checkpoint

Complete the source-governance card for Complex Adaptive Systems before writing the conclusion. Name the source type or model snapshot, record the evidence date or version, decide whether the claim is stable or fast-moving, and write one refresh trigger that would force the interpretation to change. Treat the card as a printed evidence object, not as a live web lookup.

Worked Example: Logistic-Map Period Doubling

Problem: A small quorum-sensing study models 5 bacterial cells as nodes in a graph. The undirected edges (signaling pairs) are: A–B, A–C, B–C, B–D, C–D, D–E. Compute the local clustering coefficient at node B and the average path length between A and E. Local clustering coefficient at a node is $C_i = 2 \cdot (\text{triangles through } i) / (k_i \cdot (k_i - 1))$, where k_i is that node’s degree.

Solution:

- Degree of B = 3 (neighbors A, C, D).

- Pairs of B’s neighbors = 3 (A–C, A–D, C–D). Of these, the edges actually present in the graph are A–C and C–D — that is 2 triangles through B.
- Local clustering at B = $(2 \times 2) / (3 \times 2) = 4 / 6 \approx 0.667$.
- Shortest path A → E: A–C–D–E has length 3; A–B–D–E also has length 3. So the path length between A and E is 3 edges.

Interpretation: A clustering coefficient near 0.67 at node B indicates that most of B’s signaling partners also signal with each other — a hallmark of locally cohesive community structure that supports stigmergic coordination (cells can corroborate signals through redundant local links). The path length of 3 between the most-distant pair shows that even in this tiny graph, signal propagation requires intermediate relays; longer paths in a real biofilm slow the global response and contribute to threshold-like collective behavior.

Analysis Questions

1. The logistic map transitions from periodic to chaotic behavior as *r* passes through the Feigenbaum point (about 3.57). Why does this transition occur even though the underlying equation is completely deterministic?
2. In Part 2, you drew a hysteresis loop. Why can reducing *P* to the level *at which* eutrophication occurred fail to restore the clear-water state? What mechanism sustains the turbid attractor?
3. Power-law distributions appear in earthquake magnitudes, neural avalanches, and extinction events. What common CAS mechanism could explain this shared pattern?
4. Cancer has been described as a “failed CAS” where normal tissue homeostasis breaks down. Identify two CAS features that go wrong in malignancy.
5. Propose a paper simulation or card-based experiment using a bacterial-biofilm model to demonstrate one CAS principle (e.g., stigmergic self-organization, threshold transitions, or robustness to perturbation). Describe the set-up, observable, and expected result.

Post-Lab Synthesis

Concept Check (Synthesis): A shallow coastal estuary has shown gradually declining seagrass cover for a decade while nutrient inflow has risen. Recent surveys detect an abrupt loss of the remaining seagrass and a switch to a phytoplankton-dominated turbid state.

- (a) Relate the bistability you explored in Part 2’s hysteresis loop to this estuary’s observed regime shift. What ecological feedback would sustain the phytoplankton-dominated attractor once the system flipped, and how does that connection to bistability change the kind of restoration target a manager should set?

(b) Predict the qualitative outcome of two interventions: a sharp reduction of nutrient inflow back to historical levels, and the same reduction combined with mechanical removal of phytoplankton biomass to seed seagrass regrowth. Justify the contrast in expected outcomes using the language of attractors, basin depth, and perturbation magnitude.

(c) Design a short monitoring program (three measurable variables and one statistical early-warning signal, such as rising variance or increased autocorrelation in nutrient or chlorophyll time series) that would detect whether a partly recovered estuary is approaching another tipping point before the visible regime shift occurs.

Discussion Questions

1. The SARS-CoV-2 pandemic generated striking geographic and temporal heterogeneity. Which features of a CAS (noise, nonlinearity, network topology) explain the emergence of variants?
2. Is a single cell a CAS? Defend or refute using at least three of the section 0.2 criteria.
3. What additional scientific ingredients would be needed to “build life from scratch” in a synthetic CAS? What does the field of synthetic biology currently get right, and what do its failures reveal about the difficulty of engineering life?

Safety and Ethics Notes

Paper-based lab — no reagents, no risk. Discussion of SARS-CoV-2 should be current-affairs aware; respect divergent lived experiences of the pandemic. Discussion of cancer as a “failed CAS” should be framed carefully if anyone in the class has personal experience — use the system-level language, not the blame-oriented “cancer cells are selfish” framing.

Module: `src/biology/ecology/ecology.py(logistic_growth, lotka_volterra); src/biology/evolution/evolution.py(simulate_drift)`.

Lab C — Active Inference and Free Energy

This activity accompanies section 0.3 of the textbook — review that chapter before attempting the exercises below.

Unit 0 — Systems Science for Biology: Introduction · Lab C

Learning Objectives

- Apply core principles of active inference to concrete biological observations.
- Compute a Bayesian posterior by hand for a one-dimensional inference problem and interpret the result in terms of prior, likelihood, and evidence.
- Distinguish *perceptual* inference (updating beliefs) from *active* inference (acting to satisfy beliefs) using everyday examples.
- Quantify how sensor precision changes the trade-off between updating a belief and acting to make a belief true.

Alignment and Rubric Map

- Outcome 1 (LO1): Interpret the supplied evidence or model output for Active Inference and Free Energy.
- Outcome 2 (LO2): Identify controls and comparison groups that make the claim testable.
- Outcome 3 (LO3): Quantify uncertainty, boundary conditions, or alternative explanations before concluding.
- Outcome 4 (LO4): Transfer the mechanism to a new biological case or public-facing decision.
- Chapter LO coverage: LO1, LO2, LO3, LO4
- Rubric dimensions: evidence; controls; uncertainty; mechanism; transfer. ## Pre-Lab Concept Questions {.unnumbered}

Answer these before starting the investigation — they activate knowledge from the parent chapter.

1. Describe in your own words how Bayes’ rule combines a prior belief with an observation to produce a posterior belief, and identify which term carries the “what I already thought” information.
2. A foraging mouse has a prior expectation that food is at burrow A. It sees a faint scent cue pointing to burrow B. Apply the idea of prediction error to explain how the mouse should update its belief, and identify which sensor property determines how much the cue moves the belief.
3. Compare perceptual inference (updating beliefs to match observations) with active inference (acting on the environment so observations match beliefs). Give one biological situation where each is the more efficient route to reducing prediction error.

Lab Context: Active Inference and Free Energy

Active inference proposes that living agents minimize a quantity called variational free energy — an upper bound on the “surprise” of observed sensory data given the agent’s internal generative model. The core equation (simplified):

$$F = \mathbb{E}_Q[\log Q(z) - \log P(o, z)] \tag{484}$$

where $Q(z)$ is the agent’s current belief about hidden causes z , and $P(o, z)$ is the agent’s model of how those causes generate observations o . Minimizing F is achieved either by updating beliefs (perceptual inference) or changing the world through action (active inference).

Today’s lab is paper-based: you will work through two hand-computed examples and one behavior-card classification exercise. No computer is required, though a calculator (or phone app) is useful for the Gaussian arithmetic.

Pre-Lab (to complete before class)

1. Copy equation (484) into your notebook and annotate each symbol.
2. For a Gaussian prior $\mathcal{N}(\mu_0, \sigma_0^2)$ and Gaussian likelihood $\mathcal{N}(o, \sigma_o^2)$, write the closed-form posterior mean and variance.
3. Choose one everyday example of *perceptual inference* and one of *active inference* that you could describe in two sentences each. You will compare them with the scenario cards during Part 3.

Paper-Based Materials

- Source-governance card for Active Inference and Free Energy: model-validation source card: boundary, observable, uncertainty, rival explanation, and evidence limit.
- Printed worksheet with two Bayesian inference problems (provided).
- Behavior scenario-card set with ten animal and human examples.
- Calculator or phone.
- Colored pens.

Paper-Based Investigation

Part 1 — Hand-computed Bayesian Update

A bird forages for seeds hidden under two snow patches. Its prior belief about the location of food is a Gaussian centered at position $\mu_0 = 10$ m (where food was yesterday) with variance $\sigma_0^2 = 4$ m². A partial snow melt gives a noisy visual cue that food is at position $o = 16$ m with likelihood variance $\sigma_o^2 = 12$ m².

1. Compute the prediction error: $\varepsilon = o - \mu_0$.
2. Compute the Kalman gain: $K = \sigma_0^2 / (\sigma_0^2 + \sigma_o^2)$.
3. Compute the posterior mean: $\mu_1 = \mu_0 + K \varepsilon$.
4. Compute the posterior variance: $\sigma_1^2 = (1 - K) \sigma_0^2$.
5. Re-compute μ_1 under the assumption that the cue is *very* noisy ($\sigma_o^2 = 100$) and *very* precise ($\sigma_o^2 = 0.5$). Explain in words how the bird’s final belief depends on sensor precision.

Part 2 — Perceptual vs. Active Inference

A person wakes up cold. Their generative model has a tight prior on body temperature ($\mu = 37$ °C, $\sigma = 0.5$). Their interoceptive sensor reports 34.5 °C with $\sigma = 1.0$.

1. Compute the posterior belief about their body temperature (same formulae as Part 1).
2. The posterior free energy is reduced but still positive. List three actions the person could take that would drive free energy further toward zero by *changing the observation* rather than the belief.
3. Argue in one paragraph why active inference is more effective than perceptual inference when the prior precision is tight (small σ_0) — i.e., when the organism is “committed” to a particular internal state.

Part 3 — Behavior Scenario Classification

Use the ten printed behavior scenario cards. For each behavior, annotate whether it is perceptual (sampling information) or active (imposing prediction on the environment). Record the evidence phrase that made your classification reproducible. As an optional extension outside class, you may compare the cards with a respectful observation of an animal or consenting human, but the scenario cards are the required dataset.

Data Tables

Table 510. Part 3 — Behavior Scenario Classification: Step and Quantity.

Step	Quantity	Symbol	Computed value	Units
1	Prediction error	ε		m
2	Kalman gain	K		—
3	Posterior mean	μ_1		m
4	Posterior variance	σ_1^2		m ²
5a	μ_1 with very noisy cue			m
5b	μ_1 with very precise cue			m

Table 511. Part 3 — Behavior Scenario Classification: Observation # and Behavior described.

Observation #	Behavior described	Perceptual or active?	Brief reasoning
1			
2			
3			
4			
5			

Evidence and Reproducibility Checklist

- Primary evidence goal: Model sensing and action as coupled inference in a simple organism.
- Data skill to practice: Read a small probability table and update a prediction after new evidence.
- BioSkills emphasis: Modeling and simulation, Process of science, Quantitative reasoning.
- Control logic: identify at least one positive control, one negative control, or one baseline comparison before interpreting results.
- Measurement discipline: record units, uncertainty, sample size, and any discarded observation with a reason.
- Mechanistic link: connect one result directly to the parent chapter’s big idea before writing the conclusion.
- Reproducibility check: state one procedural detail that another group would need in order to reproduce the result.

Paper-Based Evidence Upgrade

Before answering the analysis questions, annotate the paper dataset for Active Inference and Free Energy with a reproducibility pass:

Table 512. Part 3 — Behavior Scenario Classification: Evidence check and Student action.

Evidence check	Student action
Control logic	Mark the comparison that functions as the baseline, negative control, or reference case.
Uncertainty	Circle the row, card, diagram feature, or model assumption most likely to change the conclusion.
Model comparison	State whether a simpler rule, null model, or alternative mechanism could explain the same pattern.
Decision threshold	Write the minimum evidence that would make you revise the interpretation.
Reproducibility	Record the exact scoring rule another group would need to reproduce your classification.

Focus note: When you annotate the Bayesian-update and perceptual-versus-active-inference datasets, the load-bearing numbers are the prior variance, the sensory variance, and the resulting Kalman gain: check that the posterior shift is reproducible from those three values alone, and that each behavior-classification verdict cites the specific prediction-error a sceptic could recompute. Keep required work paper-based; any material-handling or equipment version belongs only in an optional extension.

Source-Governance Checkpoint

Complete the source-governance card for Active Inference and Free Energy before writing the conclusion. Name the source type or model snapshot, record the evidence date or version, decide whether the claim is stable or fast-moving, and write one refresh trigger that would force the interpretation to change. Treat the card as a printed evidence object, not as a live web lookup.

Worked Example: Bayesian update of a discrete food-location belief

Problem: A bird has a discrete prior probability of 0.3 that food is under patch A (the complement, 0.7, is patch B). It receives a noisy visual cue. The likelihood that this cue appears when food is at A is 0.8; the likelihood the cue appears when food is at B is 0.2. Compute the posterior probability that food is at patch A.

Solution: Apply Bayes’ rule, $P(A \mid \text{cue}) = P(\text{cue} \mid A) \cdot P(A) / P(\text{cue})$, where the evidence $P(\text{cue}) = P(\text{cue} \mid A) \cdot P(A) + P(\text{cue} \mid B) \cdot P(B)$.

- Numerator: $0.8 \times 0.3 = 0.24$.
- Evidence: $(0.8 \times 0.3) + (0.2 \times 0.7) = 0.24 + 0.14 = 0.38$.
- Posterior: $0.24 / 0.38 \approx 0.632$.

Interpretation: The prediction error is large — the prior gave patch A a 0.3 weight, but the precise cue pushes the posterior to about 0.63. A higher-precision sensor (likelihood 0.95 versus 0.05) would have moved the posterior closer to 0.89; a noisier sensor would have left the belief closer to the prior. This is the same mechanism a sensory neuron uses to weigh top-down prediction against bottom-up evidence — precision sets the gain on the update.

Analysis Questions

1. Explain in one paragraph how the Kalman gain can be read as “precision-weighted uncertainty reduction” — why K depends on the ratio of prior variance to total variance.
2. The generative model in Part 2 uses a *tight* prior (low variance) on body temperature. How would the calculation change if the prior were loose ($\sigma = 5$ °C)? Which regime corresponds to a pre-homeostatic organism; which to a strictly regulated endotherm?
3. In humans, chronic anxiety is sometimes described as a “tight prior on safety.” Using your computation from Part 2, explain why normal day-to-day sensory noise becomes persistently surprising to an anxious agent and what “widening the prior” (via exposure therapy or pharmacology) is doing mathematically.
4. Scientists have attempted to build artificial life — robots that minimize free energy with respect to a battery-level sensor. Describe what the agent’s prior on battery state and action repertoire would need to be so that the robot “feels hungry” at low charge and seeks a charging pad.
5. The textbook chapter notes that evolution itself can be cast as free-energy minimization at the population scale: organisms whose generative models fail are eliminated. Argue for or against this framing by contrasting it with the Modern Synthesis’s emphasis on fitness differentials.

Post-Lab Synthesis

- Concept Check (Synthesis): A neuroscientist studies a deep-sea fish that lives in near-total darkness and rarely encounters novel visual stimuli. The fish has unusually large lateral-line organs (which detect water displacement) and a small optic tectum.
- (a) Using the active-inference framework, predict which sensory channel will carry the higher precision-weighting in this animal’s generative model, and explain how you would test that prediction with a behavioral assay rather than neural recording.
 - (b) A traditional stimulus–response account would describe the fish as “tuned” to mechanical cues by selection. Contrast that explanation with an active-inference account that emphasizes ongoing belief updating. Which framework yields the more falsifiable prediction for what happens when the fish is moved into a visually rich tank?
 - (c) Design one follow-up experiment that would distinguish a population-level adaptation (a fixed generative model shaped by selection) from a within-lifetime adjustment (the animal re-weighting precision as it gathers evidence in the new environment).
-

Discussion Questions

1. Is “surprise” a purely mathematical quantity, or does it have phenomenal correlates? Consider how a newborn infant’s surprise differs from an adult’s when encountering the same stimulus.
 2. Could two agents with identical sensory input hold different beliefs and both be rational under active inference? If yes, what determines each?
 3. Does the free-energy principle predict that living things should seek complexity or simplicity in their environments? Justify using the trade-off between epistemic and instrumental value.
-

Safety and Ethics Notes

This lab is entirely paper-based and computational — no reagents, no instruments, no risk. Optional observations outside class must not disturb animals. If recording human behavior, obtain consent and preserve anonymity.

Module: `src/biology/neuroscience/neuroscience.py` (Bayesian update illustrations).

Lab D — History and Philosophy of Biology

This activity accompanies section 0.4 of the textbook — review that chapter before attempting the exercises below.

Unit 0 — Systems Science for Biology: Introduction · Lab D

Learning Objectives

- Classify source excerpts by evidence practice: observation, experiment, classification, model, mechanism, or value-laden decision.
- Build an evidence map that separates biological unit, claim, method, uncertainty, and philosophical assumption.
- Compare two historical explanations for the same biological phenomenon without treating the newer explanation as automatically complete.
- Transfer source-analysis reasoning to a modern biology decision involving species, inheritance, microbiomes, or ethics.

Alignment and Rubric Map

- Outcome 1 (LO1): Interpret the supplied evidence or model output for History and Philosophy of Biology.
- Outcome 2 (LO2): Identify controls and comparison groups that make the claim testable.
- Outcome 3 (LO3): Quantify uncertainty, boundary conditions, or alternative explanations before concluding.
- Outcome 4 (LO4): Transfer the mechanism to a new biological case or public-facing decision.
- Chapter LO coverage: LO1, LO2, LO3, LO4
- Rubric dimensions: evidence; controls; uncertainty; mechanism; transfer. ## Lab Context: History and Philosophy of Biology {.unnumbered}

This lab is a paper-based source and evidence analysis. You will work with source cards based on classic biological episodes, global knowledge traditions, experimental systems, modern molecular biology, microbiomes, and bioethics. The goal is not to memorize a timeline; the goal is to learn how a biological claim becomes credible, limited, revised, or ethically consequential.

Pre-Lab Concept Questions

1. Define “evidence practice” in one sentence and give one example from the parent chapter.
2. Explain the difference between a mechanistic explanation and a functional explanation.
3. Why can two species concepts both be useful even if they classify some organisms differently?

Paper-Based Materials

- Printed source-card packet.
- Evidence-map worksheet.
- Timeline strip with blank event cards.
- Concept-boundary worksheet with columns for unit, mechanism, function, model, and value.
- Explanation-level cards for molecular, developmental, evolutionary, ecological, and social/ethical claims.
- Colored pens or pencils.
- Sticky notes for uncertainty and value annotations.
- Source-governance card for History and Philosophy of Biology: model-validation source card: boundary, observable, uncertainty, rival explanation, and evidence limit. ### Source-card packet {.unnumbered}

The instructor should provide short paraphrased cards or public-domain excerpts representing at least these cases:

Table 513. Source-card packet: Card and Practice emphasis.

Card	Practice emphasis	Prompt
Aristotle	Functional anatomy	What does the part do for the organism?
Ibn Sina / materia medica	Medical classification	How are body, remedy, and illness organized?
Linnaeus	Classification	What makes names portable across observers?

Card	Practice emphasis	Prompt
Harvey	Experiment and quantification	What intervention distinguishes circulation from flow-through production?
Hooke	Instrument-mediated observation	What can be claimed once microscopy changes the visible scale?
Darwin-Wallace	Historical causation	What traces support selection as a past process?
Mendel / Fisher	Inheritance and model-building	How do crosses become population explanations?
Franklin / Watson-Crick / Crick	Molecular evidence	How do structure, image, and information claims fit together?
Waddington / developmental systems	Development	Why is nature-nurture too coarse?
Microbiome / symbiosis	Biological individuality	Where should the organism boundary be drawn?
Bioethics / public biology	Values and governance	Which decision changes when uncertainty remains?

Paper-Based Investigation

Part 1 — Sort the Source Cards

Sort each source card into one primary evidence practice: observation, experiment, classification, mechanism, model, or values. For each card, write one sentence defending your classification and one sentence naming a plausible alternative classification.

Part 2 — Build an Evidence Map

Table 514. Part 2 — Build an Evidence Map: Evidence-map field and Student entry.

Evidence-map field	Student entry
Biological unit	
Claim being made	
Evidence practice	
Mechanism or function	
Explanation level	
Missing comparison	
Main uncertainty	
Value-laden decision, if any	
Evidence that would revise the claim	

Part 3 — Compare Two Explanations

Choose one pair: Aristotle and a modern mechanistic account; Harvey and descriptive anatomy; Darwin-Wallace selection and a simple survival claim; Mendelian inheritance and DNA-level information transfer; or a biological species concept and a microbial case. Name what each explanation clarifies and what remains unsettled.

Part 4 — Check the Explanation Level

Choose one claim from the evidence map and rewrite it at two different levels: molecular/cellular, developmental, evolutionary/historical, ecological, or so-
cial/ethical. For each version, state the evidence that would make that version stronger and the evidence that would weaken it.

Table 515. Sample data for Part 4 — Check the Explanation Level.

Claim version	Level	What it explains	What it leaves out	Revision test

Part 5 — Modern Transfer Case

Apply the evidence-map checklist to a microbiome health claim, a conservation decision, a genetic-risk claim, or a public-health recommendation involving uncertain evidence.

Data Tables

Table 516. Part 5 — Modern Transfer Case: Source card and Evidence practice.

Source card	Evidence practice	Biological unit	Claim	Uncertainty
Aristotle				
Harvey				
Hooke				
Darwin-Wallace				
Mendel				
Franklin / Watson-Crick / Crick				
Waddington / developmental systems				
Microbiome / symbiosis				
Levins				
Bioethics case				

Part 6 — Prelude Capstone Matrix

Choose one source card and connect it to the four prelude chapters.

Table 517. Part 6 — Prelude Capstone Matrix: Prelude lens and Question to answer.

Prelude lens	Question to answer
Systems science	What boundary and variables define the system?
Complex adaptive systems	Are there heterogeneous agents, local rules, and path-dependent outcomes?
Active inference	Is there a hidden state, observation, action, and precision-weighting problem?
History/philosophy	Which evidence practice and value judgement shape the claim?

Paper-Based Evidence Upgrade

The evidence upgrade for this lab is the source-card audit trail. For every card, record the exact claim, the source practice that made it visible, the comparison that would make it stronger, and the uncertainty or value judgement that should remain in the conclusion.

Evidence and Reproducibility Checklist

- Primary evidence goal: Analyze historical source cards and build an evidence map for a disputed biological claim.
- Data skill to practice: Classify source excerpts as observation, experiment, model, mechanism, or value-laden inference.
- BioSkills emphasis: Modeling and simulation, Process of science, Quantitative reasoning.
- Control logic: identify at least one positive control, one negative control, or one baseline comparison before interpreting results.
- Measurement discipline: record units, uncertainty, sample size, and any discarded observation with a reason.
- Mechanistic link: connect one result directly to the parent chapter’s big idea before writing the conclusion.
- Reproducibility check: state one procedural detail that another group would need in order to reproduce the result.

Source-Governance Checkpoint

Complete the source-governance card for History and Philosophy of Biology before writing the conclusion. Name the source type or model snapshot, record the evidence date or version, decide whether the claim is stable or fast-moving, and write one refresh trigger that would force the interpretation to change. Treat the card as a printed evidence object, not as a live web lookup.

Analysis Questions

1. Which source card was hardest to classify by evidence practice, and why?
2. Name one case where functional language helped you reason and one case where it risked hiding a mechanism.
3. How did the biological unit change across your source cards?
4. Which explanation level changed the conclusion most: molecular, developmental, evolutionary, ecological, or social/ethical?
5. Where did uncertainty come from: missing data, model assumptions, historical contingency, category choice, or value conflict?
6. How would your evidence map change if the audience were a patient, a conservation manager, or a first-year student?
7. Which prelude lens added the most information to your source card, and which lens risked overclaiming?

Safety and Ethics Notes

This lab uses printed cases and discussion. When modern biomedical or human-difference cases arise, separate empirical claims from ethical judgements, avoid ranking human groups, and make uncertainty explicit.

Debrief and Reflection

Write one paragraph answering this prompt: “A biological fact is stronger when I can name the practice that produced it.” Use one historical source and one modern transfer case as evidence.

Lab — Atoms, Molecules, and Chemical Bonds

Learning Objectives

This activity accompanies section 1 of the textbook — review that chapter before attempting the exercises below.

- Identify polar and non-polar molecular regions using electronegativity reasoning
- Interpret hydrogen bonding properties using printed observations and molecular cards
- Distinguish ionic, covalent, and hydrogen bonds from structural and data evidence
- Apply molecular polarity concepts to explain biological solubility patterns

Alignment and Rubric Map

- Outcome 1 (LO1): Interpret the supplied evidence or model output for Atoms, Molecules, and Chemical Bonds.
- Outcome 2 (LO2): Identify controls and comparison groups that make the claim testable.
- Outcome 3 (LO3): Quantify uncertainty, boundary conditions, or alternative explanations before concluding.
- Outcome 4 (LO4): Transfer the mechanism to a new biological case or public-facing decision.
- Chapter LO coverage: LO1, LO2, LO3, LO4
- Rubric dimensions: evidence; controls; uncertainty; mechanism; transfer. ## Pre-Lab Concept Questions {unnumbered}

Answer these before starting the investigation — they activate knowledge from the parent chapter.

1. Define electronegativity in your own words and state the conventional ΔEN cutoffs used in the parent chapter to classify a bond as non-polar covalent, polar covalent, or ionic. Give one bonded pair from the chapter that lies in each category.
2. Distinguish an ionic bond (such as that holding Na^+ and Cl^- together in a NaCl lattice) from a polar covalent bond (such as the O–H bond in water). Apply this distinction to predict why NaCl dissociates into ions in aqueous solution while H_2O does not.
3. Compare the role of a hydrogen-bond donor (a hydrogen attached to N, O, or F) and a hydrogen-bond acceptor (a lone pair on N, O, or F). Use the contrast to explain why ammonia (NH_3) can act as both donor and acceptor whereas methane (CH_4) is unable to function as either.

Lab Context: Atoms, Molecules, and Chemical Bonds

Chemistry underpins every biological process. Atoms bond through electronegativity differences: when atoms share electrons unequally, they form polar covalent bonds (as in O–H), creating partial charges ($\delta+$ and $\delta-$). These partial charges enable hydrogen bonding — the weak but pervasive force that gives water its remarkable properties and stabilizes the three-dimensional shapes of proteins and DNA.

In this lab, you will use a paper dataset of solubility and surface-tension observations as proxies for molecular polarity and hydrogen bonding capacity: “like dissolves like” — polar solutes dissolve in polar solvents (water), while non-polar solutes dissolve primarily in non-polar solvents (oil). You will also visualize electron sharing differences using electronegativity tables and molecule cards.

Paper-Based Materials

Table 518. Alignment and Rubric Map: Item and Quantity.

Item	Quantity
Source-governance card for Atoms, Molecules, and Chemical Bonds: molecular-structure source card: experimental method, prediction confidence, assay validation, and release date	1
Molecule cards: water, oil-like hydrocarbon, NaCl, sucrose, dye A, dye B, soap	1 set
Printed solubility observation dataset	1
Printed surface-tension observation card	1
Electronegativity table (provided)	1
Graph paper or notebook paper	2 sheets
Calculator	1

Paper-Based Investigation

- Sort the molecule cards into polar, non-polar, ionic, and amphipathic categories. Record one structural feature that justifies each placement.
- Use the printed observation dataset to classify each solute/solvent pair as soluble, partially soluble, or insoluble.
- Identify one positive control for polar solubility, one negative control, and one ambiguous case that would need more evidence.
- Using the electronegativity table, calculate the electronegativity difference (ΔEN) for N–H, O–H, C–H, and C–C bonds. Record which are polar and which are non-polar.
- Read the surface-tension card showing a paperclip floating before soap and sinking after soap. Explain the before/after pattern using hydrogen bonding and amphipathic disruption.
- Re-score one card after a peer group challenges your classification. Note whether the change improved consistency with the evidence.

Data Recording

Table 519. Alignment and Rubric Map: Cup and Solvent.

Cup	Solvent	Solute/Dye	Dissolves? (Y/N)	Observations
A	Water	NaCl		
B	Water	Sucrose		
C	Oil	NaCl		
D	Oil	Sucrose		
E	Water	Water dye		
F	Oil	Turmeric		

Table 520. Alignment and Rubric Map: Bond and ΔEN .

Bond	ΔEN	Polar?
O–H		
N–H		
C–H		
C–C		

Paperclip float: _____ After soap: _____

Evidence and Reproducibility Checklist

- Primary evidence goal: Classify bonds and solvent behavior using simple observations.
- Data skill to practice: Use tabular atomic data to predict polarity, solubility, and biological reactivity.
- BioSkills emphasis: Quantitative reasoning, Interdisciplinary nature of science.
- Control logic: identify at least one positive control, one negative control, or one baseline comparison before interpreting results.
- Measurement discipline: record units, uncertainty, sample size, and any discarded observation with a reason.
- Mechanistic link: connect one result directly to the parent chapter’s big idea before writing the conclusion.
- Reproducibility check: state one procedural detail that another group would need in order to reproduce the result.

Paper-Based Evidence Upgrade

Before answering the analysis questions, annotate the paper dataset for Atoms, Molecules, and Chemical Bonds with a reproducibility pass:

Table 521. Alignment and Rubric Map: Evidence check and Student action.

Evidence check	Student action
Control logic	Mark the comparison that functions as the baseline, negative control, or reference case.
Uncertainty	Circle the row, card, diagram feature, or model assumption most likely to change the conclusion.

Evidence check	Student action
Model comparison	State whether a simpler rule, null model, or alternative mechanism could explain the same pattern.
Decision threshold	Write the minimum evidence that would make you revise the interpretation.
Reproducibility	Record the exact scoring rule another group would need to reproduce your classification.

Focus note: read each solubility result as a test of bond polarity – treat the water-versus-oil pairing as the control contrast, and decide in advance how strong a color or layering change counts as “dissolved” for an ionic versus a non-polar solute. Keep required work paper-based; any material-handling or equipment version belongs only in an optional extension.

Worked Example: Polarity of O–H versus C–H and solubility prediction

Problem: Using the electronegativity values H = 2.20, C = 2.55, O = 3.44, compute ΔEN for an O–H bond and a C–H bond. Classify each as non-polar covalent, polar covalent, or ionic using the conventional cutoffs (ΔEN < 0.5 non-polar; 0.5–1.7 polar covalent; > 1.7 ionic). Then predict the aqueous solubility of methanol (CH₃OH), a small molecule containing one polar O–H group and one largely non-polar CH₃ group.

Solution:

- ΔEN(O–H) = 3.44 – 2.20 = 1.24 → polar covalent.
- ΔEN(C–H) = 2.55 – 2.20 = 0.35 → non-polar covalent.
- Methanol has a hydrogen-bond donor (O–H) and acceptor (lone pairs on O), which let it engage water’s hydrogen-bond network; the CH₃ group is small enough that the polar O–H dominates the overall behavior, so methanol is expected to be highly soluble in water.

Interpretation: A single polar O–H group is often enough to bring small alcohols into the aqueous phase, which is one reason cells use hydroxyl groups so widely (for example, on sugars and on the side chains of serine and threonine). As the non-polar hydrocarbon portion of an alcohol grows longer — for instance going from methanol to octanol — the molecule’s water solubility drops, and the same reasoning explains why phospholipids assemble into bilayers rather than dissolving.

Source-Governance Checkpoint

Complete the source-governance card for Atoms, Molecules, and Chemical Bonds before writing the conclusion. Name the source type or model snapshot, record the evidence date or version, decide whether the claim is stable or fast-moving, and write one refresh trigger that would force the interpretation to change. Treat the card as a printed evidence object, not as a live web lookup.

Analysis Questions

1. Which solutes dissolved in water but not oil? Which dissolved in oil but not water? Explain in terms of bond polarity.
2. Why did NaCl dissolve in water but not in vegetable oil? What type of bond holds NaCl together, and how does water break it apart?
3. Based on ΔEN values, rank the four bonds from most to least polar. How does bond polarity influence molecular behavior in biological systems?
4. The paperclip floated due to surface tension. What property of water creates surface tension, and why did soap destroy it? What is the biological significance of surfactants?
5. Predict whether cholesterol (a steroid with a polar hydroxyl group and a large non-polar body) would dissolve in blood plasma (aqueous) or in a membrane (lipid). Justify your answer using polarity principles.

Post-Lab Synthesis

Concept Check (Synthesis): A pharmaceutical-development team is designing a small-molecule candidate that must cross the largely lipid plasma membrane to reach its intracellular target and then remain soluble in the aqueous cytoplasm long enough to bind that target.

- (a) Evaluate the polarity profile such a molecule should have. Identify which functional-group features (for example, ionisable groups, hydroxyl groups, alkyl chains) tend to enhance membrane permeability versus aqueous solubility, and explain the tension between the two requirements using the polarity principles tested in this lab.
- (b) Predict the relative cell-uptake behavior of two candidates that share the same molecular skeleton but differ in a single substituent: candidate A carries a permanently charged quaternary ammonium group, candidate B carries a neutral hydroxyl group at the same position. Justify the prediction in terms of hydrogen-bonding capacity and the energetics of partitioning between water and lipid.

- (c) Design a follow-up paper-based experiment, using the same molecular-card and solubility-dataset format as today’s lab, that would let a peer group compare three candidate molecules along the membrane-permeability versus aqueous-solubility axis. Specify the controls and the threshold of evidence at which you would advance a candidate to a wet-lab assay.

Optional Hands-On Extension

If the instructor approves a demonstration, the printed solubility and surface-tension cases may be reproduced with food-grade materials. The paper dataset remains the required evidence source; any demonstration should be treated as a check on the model, not as a prerequisite for completing the lab.

Safety and Ethics Notes

Paper-based lab — no reagents, no required wet materials, and no physical risk. For optional demonstrations, avoid ingesting samples and clean any spills immediately.

Debrief and Reflection

After you finish the practical work, spend 5–10 minutes in your small group comparing results and discussing the following prompts. Each member should contribute at least one observation before moving to the next prompt:

1. What did your measurements show — compare the group’s results to the textbook’s predictions. Where they diverge, suggest at least one mechanistic explanation before concluding “experimental error.”
2. What would change the outcome — propose one modification to the procedure that would sharpen the measurement or extend the result to a new biological context, and predict what you would observe.
3. One-sentence headline — each student composes a single sentence summarizing the lab’s take-home message, suitable for a tweet. Compare sentences across groups; good headlines are short, quantitative, and mechanistic.
4. Connection back to the textbook — identify one section of section 1 that your data either confirmed or complicated. Cite the specific passage.

Further Reading (Lab)

- Revisit the parent chapter section 1 for the theoretical foundations on which this lab is built.
- Look up any bolded glossary term introduced in the textbook chapter (each has a #gl:term-slug link in the text) — its master definition is in manuscript/glossary.md.
- Explore the appended src/ module that implements the corresponding quantitative model (when applicable) — referenced in the parent chapter’s “Bridge to Computation” subsection.

Module footer: parent chapter \cref{sec:unit_I_atoms_molecules}; all numerical quantities in this lab use SI units — see *Appendix D — Units, Physical Constants, and Biological Ranges* for unit conversions and biological-scale reference values.

Lab — Water — The Molecule of Life

Learning Objectives

This activity accompanies section 2 of the textbook — review that chapter before attempting the exercises below.

- Compare specific heat capacity patterns for water and oil using a printed dataset
- Explain cohesion, adhesion, and capillarity from diagrams and model observations
- Use solute concentration data to reason about water potential and osmosis
- Relate water’s physical properties to biological functions

Alignment and Rubric Map

- Outcome 1 (LO1): Interpret the supplied evidence or model output for Water — The Molecule of Life.
- Outcome 2 (LO2): Identify controls and comparison groups that make the claim testable.
- Outcome 3 (LO3): Quantify uncertainty, boundary conditions, or alternative explanations before concluding.
- Outcome 4 (LO4): Transfer the mechanism to a new biological case or public-facing decision.
- Chapter LO coverage: LO1, LO2, LO3, LO4
- Rubric dimensions: evidence; controls; uncertainty; mechanism; transfer. ## Pre-Lab Concept Questions {unnumbered}

Answer these before starting the investigation — they activate knowledge from the parent chapter.

1. Define specific heat capacity in your own words, give the value for liquid water (about 4.18 J·g⁻¹·°C⁻¹), and explain one biological consequence of water’s high specific heat relative to lipids and rock.
2. Apply hydrogen-bonding reasoning to explain why ice is less dense than liquid water and what that anomaly means for organisms living in a temperate lake during winter.
3. Compare cohesion (water-to-water hydrogen bonding) and adhesion (water-to-other-surface attraction). Use the contrast to explain how the cohesion–tension model lifts a column of water from soil to the canopy of a tall tree.

Lab Context: Water — The Molecule of Life

Water’s extraordinary properties arise from its bent molecular geometry (104.5° H–O–H bond angle) and the resulting network of hydrogen bonds. Each water molecule can form up to four hydrogen bonds — two through lone pairs (O as H-bond acceptor) and two through O–H groups (H-bond donor). This network gives water its high specific heat (4.18 J/g·°C), high surface tension (72 mN/m), strong cohesion/adhesion, and the ability to dissolve ionic and polar solutes. Most of these properties are exploited by living organisms.

In this lab you will analyze heat-absorption data for water and oil, interpret capillary-rise diagrams, and track osmotic movement in a model membrane dataset. The required work is paper-based so the scientific reasoning is centered on controls, units, gradients, and reproducible interpretation.

Paper-Based Materials

Table 522. Alignment and Rubric Map: Item and Quantity.

Item	Quantity
Source-governance card for Water — The Molecule of Life: molecular-structure source card: experimental method, prediction confidence, assay validation, and release date	1
Heat-capacity dataset: water and oil temperature over time	1
Capillary-rise diagram packet for water, oil, and xylem	1
Osmosis model dataset for membrane bags in different solute conditions	1
Control-identification cards	1 set
Ruler (mm)	1
Calculator and graph paper	1 each

Paper-Based Investigation

Part A — Specific Heat

1. Graph the provided temperature data for equal masses of water and oil under the same heat input.
2. Calculate ΔT per 2-minute interval and identify which substance buffered temperature change more strongly.
3. Mark the baseline, the controlled variables, and one possible measurement uncertainty on the graph.

Part B — Capillarity

4. Use the capillary-rise diagrams to measure the height of model water and oil columns in millimetres.
5. Compare the xylem diagram with the capillary tube model. Identify where adhesion, cohesion, and tube diameter enter the explanation.
6. Write one prediction for how capillary height would change if tube radius doubled, then check it against the model card.

Part C — Osmosis

7. Use the membrane-bag dataset to calculate Δmass over time for hypotonic, isotonic, and hypertonic surroundings.
8. Draw the water-potential gradient for each condition and identify which case functions as the best negative control for net water movement.

Data Recording

Table 523. Alignment and Rubric Map: Time (min) and Water Temp (°C).

Time (min)	Water Temp (°C)	Oil Temp (°C)
0		
2		
4		
6		
8		
10		

Capillary rise — water: _____ mm; oil: _____ mm

Table 524. Alignment and Rubric Map: Time (min) and Dialysis tubing mass (g).

Time (min)	Dialysis tubing mass (g)	ΔMass (g)
0		—
5		
10		
20		

Evidence and Reproducibility Checklist

- Primary evidence goal: Measure surface tension, polarity, and buffering behavior.
- Data skill to practice: Convert between pH, hydrogen ion concentration, and buffer ratios.
- BioSkills emphasis: Quantitative reasoning, Interdisciplinary nature of science.
- Control logic: identify at least one positive control, one negative control, or one baseline comparison before interpreting results.
- Measurement discipline: record units, uncertainty, sample size, and any discarded observation with a reason.
- Mechanistic link: connect one result directly to the parent chapter’s big idea before writing the conclusion.
- Reproducibility check: state one procedural detail that another group would need in order to reproduce the result.

Paper-Based Evidence Upgrade

Before answering the analysis questions, annotate the paper dataset for Water — The Molecule of Life with a reproducibility pass:

Table 525. Alignment and Rubric Map: Evidence check and Student action.

Evidence check	Student action
Control logic	Mark the comparison that functions as the baseline, negative control, or reference case.
Uncertainty	Circle the row, card, diagram feature, or model assumption most likely to change the conclusion.
Model comparison	State whether a simpler rule, null model, or alternative mechanism could explain the same pattern.
Decision threshold	Write the minimum evidence that would make you revise the interpretation.
Reproducibility	Record the exact scoring rule another group would need to reproduce your classification.

Focus note: this lab compares a thermal-property measurement (water versus oil heating rate, reporting specific heat) against a separate interfacial measurement (capillary rise from adhesion and cohesion); keep the two evidence chains distinct and state the temperature or height resolution at which a difference becomes convincing. Keep required work paper-based; any material-handling or equipment version belongs only in an optional extension.

Worked Example: Temperature rise of a desert organism using $q = m c \Delta T$

Problem: A small desert lizard has body mass 2.0 kg and an effective composition of 70% water by mass. During a midday basking interval it absorbs a net 840 J of heat that is distributed through the water-rich tissue. Treating the effective heat capacity as that of water ($c = 4.18 \text{ J}\cdot\text{g}^{-1}\cdot^\circ\text{C}^{-1}$), compute the temperature rise of the water fraction. Then repeat the computation for a hypothetical organism of the same mass at 40% water (with the non-water fraction modeled at $c = 1.5 \text{ J}\cdot\text{g}^{-1}\cdot^\circ\text{C}^{-1}$) and contrast the two.

Solution: Apply $\Delta T = q / (m c)$.

- Mass of water in lizard = $0.70 \times 2000 \text{ g} = 1400 \text{ g}$.
- ΔT for the water fraction = $840 / (1400 \times 4.18) \approx 840 / 5852 \approx 0.143 \text{ }^\circ\text{C}$.
- For the 40%-water organism: $m_{\text{water}} = 800 \text{ g}$, $m_{\text{other}} = 1200 \text{ g}$.
- Heat capacity of the body $\approx (800 \times 4.18) + (1200 \times 1.5) = 3344 + 1800 = 5144 \text{ J}\cdot^\circ\text{C}^{-1}$.
- $\Delta T \approx 840 / 5144 \approx 0.163 \text{ }^\circ\text{C}$ — a noticeably larger rise for the drier organism.

Interpretation: The lizard’s high water fraction buffers temperature changes: the same 840 J that warms the water-rich body by about 0.14 °C warms a drier body of the same mass by closer to 0.16 °C. Over an hour-long basking bout, with heat loads in the kilojoule range, that difference compounds and helps explain why high-water tissues stabilize core temperature against fluctuating environmental loads. Real organisms also dissipate heat by evaporation and conduction, so the calculation is an upper bound on the temperature rise rather than a complete thermal model.

Source-Governance Checkpoint

Complete the source-governance card for Water — The Molecule of Life before writing the conclusion. Name the source type or model snapshot, record the evidence date or version, decide whether the claim is stable or fast-moving, and write one refresh trigger that would force the interpretation to change. Treat the card as a printed evidence object, not as a live web lookup.

Analysis Questions

1. Which substance heated more quickly — water or oil? How does this reflect differences in specific heat, and what is the ecological significance for oceans moderating coastal climates?
2. Why did water rise higher than oil in the capillary tube? Name the two adhesive forces responsible and identify the molecules involved.
3. Explain what you observed in the celery xylem. Which water property — cohesion, adhesion, or both — most directly drives this upward movement?
4. In the osmosis experiment, did the dialysis tubing gain or lose mass? Draw and explain the water potential gradient that caused this direction of movement.
5. Patients receiving intravenous fluids receive 0.9% NaCl (normal saline) rather than pure water. Predict what would happen if red blood cells were placed in pure water vs 3% NaCl solution. Explain using water potential ($\Psi = \Psi_s + \Psi_p$).

Post-Lab Synthesis

Concept Check (Synthesis): A comparative physiologist studies two related lizards. Lizard X lives in a wet temperate habitat and has body water content of about 70% by mass; lizard Y lives in a hot, arid environment and has body water content of about 55%. Daytime ambient heat loads on both animals are similar in magnitude.

- (a) Predict, using the $q = m c \Delta T$ framework from the worked example, how the two lizards’ core-temperature trajectories would differ over a one-hour basking interval if other heat-exchange routes (conduction, evaporation) are held constant. Compute the expected temperature rise for a representative heat load of 4.2 kJ deposited in each animal (use 2 kg body mass for both), and interpret the biological consequence for homeostasis.
- (b) Evaluate the trade-off between water content and thermal buffering. Identify one biological cost of a high-water tissue strategy (for example, dehydration risk during prolonged heat exposure) and one cost of the low-water strategy. Explain why each animal’s strategy can still be adaptive in its own habitat without claiming one strategy dominates the other.
- (c) Design a paper-data extension to this lab that would let students compare the predicted ΔT of a 70%-water and a 55%-water organism across a graded series of heat loads (for example, 0.5, 1, 2, and 4 kJ). Specify the controls, the threshold at which a difference becomes biologically meaningful (for instance, ΔT large enough to trigger a documented thermoregulatory behavior), and the conclusion you would draw from a graph that crosses or fails to cross that threshold.

Optional Hands-On Extension

An instructor may demonstrate capillary rise or osmosis with household materials, but the printed dataset is the required source for analysis. Treat any demonstration as an illustration that can be compared with the model, not as required evidence.

Safety and Ethics Notes

Paper-based lab — no hot water baths, glassware, membranes, or wet materials are required. Optional demonstrations should use low-risk materials and ordinary spill precautions.

Debrief and Reflection

After you finish the practical work, spend 5–10 minutes in your small group comparing results and discussing the following prompts. Each member should contribute at least one observation before moving to the next prompt:

1. What did your measurements show — compare the group’s results to the textbook’s predictions. Where they diverge, suggest at least one mechanistic explanation before concluding “experimental error.”
2. What would change the outcome — propose one modification to the procedure that would sharpen the measurement or extend the result to a new biological context, and predict what you would observe.
3. One-sentence headline — each student composes a single sentence summarizing the lab’s take-home message, suitable for a tweet. Compare sentences across groups; good headlines are short, quantitative, and mechanistic.
4. Connection back to the textbook — identify one section of section 2 that your data either confirmed or complicated. Cite the specific passage.

Further Reading (Lab)

- Revisit the parent chapter section 2 for the theoretical foundations on which this lab is built.
- Look up any bolded glossary term introduced in the textbook chapter (each has a `#gl:term=slug` link in the text) — its master definition is in `manuscript/glossary.md`.
- Explore the appended `src/` module that implements the corresponding quantitative model (when applicable) — referenced in the parent chapter’s “Bridge to Computation” subsection.

Module footer: parent chapter \cref{sec:unit_I_water_and_life}; all numerical quantities in this lab use SI units — see *Appendix D — Units, Physical Constants, and Biological Ranges* for unit conversions and biological-scale reference values.

Lab — Biological Macromolecules

Learning Objectives

This activity accompanies section 3 of the textbook — review that chapter before attempting the exercises below.

- Apply simulated colorimetric-test evidence to identify carbohydrates, proteins, and lipids
- Distinguish reducing sugars from non-reducing sugars using structural logic
- Identify proteins and lipids from reaction cards, labels, and model results
- Interpret qualitative color evidence with controls, uncertainty, and reproducibility checks

Alignment and Rubric Map

- Outcome 1 (LO1): Interpret the supplied evidence or model output for Biological Macromolecules.
- Outcome 2 (LO2): Identify controls and comparison groups that make the claim testable.
- Outcome 3 (LO3): Quantify uncertainty, boundary conditions, or alternative explanations before concluding.
- Outcome 4 (LO4): Transfer the mechanism to a new biological case or public-facing decision.
- Chapter LO coverage: LO1, LO2, LO3, LO4
- Rubric dimensions: evidence; controls; uncertainty; mechanism; transfer. ## Pre-Lab Concept Questions {unnumbered}

Answer these before starting the investigation — they activate knowledge from the parent chapter.

1. State the monomer–polymer relationship for each of the four major biological macromolecule classes: carbohydrates, lipids, proteins, and nucleic acids. Identify the bond type that joins monomers in each case (for example, glycosidic, peptide, phosphodiester) where one is defined in the parent chapter.
2. Apply the dehydration-synthesis (condensation) and hydrolysis framework to explain how a disaccharide is built from two monosaccharides and how it is later broken back into monomers. Specify the small molecule released or consumed at each step.
3. Compare the qualitative basis of the reducing-sugar assay, the peptide-bond colorimetric assay, and a grease-spot lipid test. For each, identify the chemical feature being detected and one biological sample on which the assay would give a clear positive signal.

Pre-Lab (to complete before class)

1. For each of the four macromolecule classes, write one sentence that names its monomer, its primary covalent bond, and one biological function.
2. classic reducing-sugar assay detects aldehyde groups on reducing sugars. Which of glucose, fructose, sucrose, and starch have a free aldehyde? For those without, explain why (look up hemiketal and glycosidic bonds).
3. Compute the energy density of pure triglyceride (37 kJ g⁻¹) vs pure starch (17 kJ g⁻¹) vs pure protein (17 kJ g⁻¹). Why do organisms store long-term energy as fat rather than glycogen?
4. Predict which of the following will yield a positive classic peptide-bond assay test at room temperature: a single amino acid (glycine), a dipeptide, albumin. Justify in one sentence (classic peptide-bond assay requires ≥2 peptide bonds → at least tripeptide).

Lab Context: Biological Macromolecules

Macromolecules — carbohydrates, lipids, proteins, and nucleic acids — form the molecular architecture of cells. Each class has distinctive chemical groups that produce diagnostic patterns in classic colorimetric tests. Reducing sugars (glucose, fructose, maltose) donate electrons to Cu²⁺ in classic reducing-sugar assay, producing a color change from blue to yellow/orange/red; sucrose (non-reducing) does not react unless hydrolysed. The classic peptide-bond assay reaction turns purple in the presence of peptide bonds (≥2). classic lipid-partition assay, an oil-soluble dye, partitions into lipids and stains them red-orange.

In this lab you will interpret a blinded paper dataset for five unknown samples (A–E), compare it with positive and negative controls, and identify the macromolecules present in each. The chemistry is treated as evidence to reason from, not as a required wet procedure.

Paper-Based Materials

Table 526. Alignment and Rubric Map: Item and Quantity.

Item	Quantity
Source-governance card for Biological Macromolecules: UniProt accession, PDB/PDBe structure record, EMDB map when relevant, experimental method, prediction confidence, assay validation, and release date	1
Blinded macromolecule reaction dataset for samples A–E	1
Molecular-structure cards: glucose, fructose, sucrose, starch, albumin, triglyceride	1 set
Positive-control and negative-control cards	1 set
Hydrolysis time-course graph packet	1
AI protein-model evidence packet: confidence map, predicted interface, ligand-contact table, and validation notes	1
Decision-matrix worksheet	1
Calculator and graph paper	1 each

Paper-Based Investigation

1. Read the blinded dataset for samples A–E. For each simulated test, mark whether the result is positive, negative, weak positive, or ambiguous.
2. Use the control cards to verify that each test behaved as expected before interpreting unknowns.
3. Build a decision matrix: reducing sugar evidence, peptide-bond evidence, lipid-partition evidence, and structural clue evidence.
4. Assign a macromolecule profile to each unknown and rate your confidence as high, medium, or low.
5. Identify one result that would need replication or an additional test before a confident claim.

Part D — Enzyme Hydrolysis Data

6. Interpret the provided starch-hydrolysis time course for active amylase, denatured enzyme, and no-enzyme controls.
7. Estimate a crude hydrolysis rate (mg starch per minute) from the graph and explain why the denatured-enzyme line functions as a negative control.
8. Decide whether the evidence supports enzyme specificity, temperature sensitivity, or both.

Part E — Sucrose Hydrolysis Model

9. Compare the structural cards for untreated sucrose and hydrolysed sucrose.
10. Predict the simulated Benedict pattern before and after hydrolysis, then check it against the provided model result. Explain why cleavage into glucose and fructose changes the reducing-sugar evidence.

Part F — AI Structure Evidence Check

11. Read the AI protein-model packet for a hypothetical enzyme-substrate interaction. Mark each predicted contact as high, medium, or low confidence using the confidence map and interface notes.
12. Decide which claim is justified: “this residue is worth mutating,” “this ligand probably binds,” or “this interaction is established.” Explain why the last claim requires independent assay evidence.
13. Propose a paper-based validation plan: one conservation comparison, one predicted-disruptive mutation, one binding or kinetic readout, and one result that would make you reject the predicted interface.

Data Recording

Table 527. Part F — AI Structure Evidence Check: Sample and Reducing-sugar evidence.

Sample	Reducing-sugar evidence	Peptide-bond evidence	Lipid-partition evidence	Macromolecule(s) present
A				
B				
C				
D				
E				
(+)		—	—	Reducing sugar
Glucose				
(+)	—		—	Protein
Albumin				
(–) Water				None

AI model evidence: highest-confidence contact = _____; lowest-confidence region = _____; validation assay proposed = _____; claim justified now = _____

Evidence and Reproducibility Checklist

- Primary evidence goal: Use chemical tests and structural clues to identify biological macromolecules.
- Data skill to practice: Classify molecules from structural evidence rather than names alone.
- BioSkills emphasis: Quantitative reasoning, Interdisciplinary nature of science.
- Control logic: identify at least one positive control, one negative control, or one baseline comparison before interpreting results.
- Measurement discipline: record units, uncertainty, sample size, and any discarded observation with a reason.
- Mechanistic link: connect one result directly to the parent chapter’s big idea before writing the conclusion.
- Reproducibility check: state one procedural detail that another group would need in order to reproduce the result.

Paper-Based Evidence Upgrade

Before answering the analysis questions, annotate the paper dataset for Biological Macromolecules with a reproducibility pass:

Table 528. Part F — AI Structure Evidence Check: Evidence check and Student action.

Evidence check	Student action
Control logic	Mark the comparison that functions as the baseline, negative control, or reference case.
Uncertainty	Circle the row, card, diagram feature, or model assumption most likely to change the conclusion.
Model comparison	State whether a simpler rule, null model, or alternative mechanism could explain the same pattern.
Decision threshold	Write the minimum evidence that would make you revise the interpretation.
Reproducibility	Record the exact scoring rule another group would need to reproduce your classification.

Focus note: each color-change assay (reducing-sugar, peptide-bond, and the lipid grease-spot test) is a separate qualitative detector with its own false positives – record the positive and negative reference samples and the minimum color shift you will accept before scoring a macromolecule class as present. Keep required work paper-based; any material-handling or equipment version belongs only in an optional extension.

Worked Example: Estimating protein concentration from a standard curve

Problem: A teaching group prepares a colorimetric protein standard at 0.10 g·mL⁻¹ protein and measures its absorbance at 540 nm as 0.45 (background subtracted). An unknown sample, treated identically, reads 0.62. Assuming a linear calibration through the origin in this absorbance range, estimate the protein concentration in the unknown.

Solution: Build the calibration slope from the standard, then apply it to the unknown.

- Slope = 0.45 absorbance units / 0.10 g·mL⁻¹ = 4.5 absorbance·mL·g⁻¹.
- Estimated concentration of unknown = 0.62 / 4.5 ≈ 0.138 g·mL⁻¹.

Interpretation: A single-point calibration through the origin is the lightest reasonable model for this assay; it gives roughly 0.14 g·mL⁻¹, which is comparable in order of magnitude to dilute serum albumin (about 0.04 g·mL⁻¹) and to several food-protein extracts. The estimate assumes the linear range extends from the standard to the unknown reading, that background absorbance has been subtracted, and that the unknown contains protein with a peptide-bond density similar to the standard — assumptions a more rigorous lab would test with a multi-point calibration curve, a blank, and a known positive control.

Source-Governance Checkpoint

Complete the source-governance card for Biological Macromolecules before writing the conclusion. Name the source type or model snapshot, record the evidence date or version, decide whether the claim is stable or fast-moving, and write one refresh trigger that would force the interpretation to change. Treat the card as a printed evidence object, not as a live web lookup.

Analysis Questions

1. Which samples tested positive for reducing sugars? Were any positive for sucrose (hint: sucrose does NOT turn classic reducing-sugar assay red without hydrolysis)? How would you distinguish glucose from sucrose using primarily classic reducing-sugar assay test?
2. A sample of milk tested positive for both classic reducing-sugar assay (weakly) and classic peptide-bond assay (strongly) and showed a grease spot. Name the three macromolecule classes present in milk.
3. Why does classic reducing-sugar assay require heating to detect reducing sugars, while classic peptide-bond assay works at room temperature? What does this reveal about the reaction mechanisms?
4. Dietary fiber (cellulose) is a polysaccharide. Predict whether it would give a positive classic reducing-sugar assay test. Explain in terms of glycosidic bond type (α vs β linkage) and digestibility.
5. A patient has phenylketonuria (PKU) — inability to metabolize phenylalanine. Which macromolecule class and which specific monomer is relevant? How does dietary management (low-phenylalanine diet) relate to the biochemistry of this lab?
6. An AlphaFold-derived packet predicts a ligand contact in a low-confidence loop. What additional evidence would move the claim from “hypothesis” to “supported mechanism”? Name at least one sequence, structural, and biochemical check.

Post-Lab Synthesis

Concept Check (Synthesis): A field microbiologist collects a turbid sample from a brackish pond and a separate sample of dispersed lipid droplets skimmed from the surface film. Each sample is dried, resuspended, and tested with the same color-change panel used in this lab (reducing-sugar, peptide-bond/biuret, and grease-spot lipid).

- (a) Predict the qualitative pattern of positives and negatives expected for a bacterial-cell-enriched sample versus a lipid-droplet-enriched sample, and justify each prediction in terms of macromolecule composition. Identify which single assay outcome would most strongly distinguish the two sample types.
- (b) Evaluate the limits of this evidence: name one false-positive scenario and one false-negative scenario for each assay (for example, a sugar contaminant on glassware, or a protein concentration below the assay’s detection threshold). Specify what additional control or dilution series would harden the distinction.
- (c) Design a follow-up paper-based decision tree, building on the data-recording matrix used in today’s lab, that would let a peer group classify three unknown environmental samples by macromolecule profile. State the threshold of evidence at which the decision tree would call a sample “ambiguous” and recommend a downstream technique.

Extension Analysis Questions

7. Galactosaemia patients cannot metabolize galactose (a component of lactose). Using your understanding of glycosidic bonds, explain why such a patient must avoid milk but can safely consume glucose or fructose sweetened foods.
8. The Keto diet shifts metabolism to fat oxidation. Predict which macromolecule category would dominate your test results on a piece of bacon vs a slice of bread. Discuss why each is energy-dense but in biochemically different ways (immediate vs sustained release).
9. Protein-losing enteropathy causes albumin leakage into the gut. Given classic peptide-bond assay’s sensitivity (about 0.1 mg/mL), would you expect a positive classic peptide-bond assay reaction on a faecal sample from such a patient? Why might faecal protein quantification via classic peptide-bond assay be unreliable (hint: digestive proteolysis)?

Optional Wet-Lab Extension

An instructor may run classic Benedict, classic peptide-bond assay, Sudan, iodine, or hydrolysis demonstrations in a properly equipped laboratory. These are optional demonstrations primarily; the required activity is the paper dataset and decision matrix.

Safety and Ethics Notes

Paper-based lab — no reagents, heating, saliva sampling, or unknown foods are required. Optional wet demonstrations require instructor supervision, approved chemical handling, and appropriate waste disposal.

Debrief and Reflection

After you finish the practical work, spend 5–10 minutes in your small group comparing results and discussing the following prompts. Each member should contribute at least one observation before moving to the next prompt:

1. What did your measurements show — compare the group’s results to the textbook’s predictions. Where they diverge, suggest at least one mechanistic explanation before concluding “experimental error.”
2. What would change the outcome — propose one modification to the procedure that would sharpen the measurement or extend the result to a new biological context, and predict what you would observe.
3. One-sentence headline — each student composes a single sentence summarizing the lab’s take-home message, suitable for a tweet. Compare sentences across groups; good headlines are short, quantitative, and mechanistic.
4. Connection back to the textbook — identify one section of section 3 that your data either confirmed or complicated. Cite the specific passage.

Further Reading (Lab)

- Revisit the parent chapter section 3 for the theoretical foundations on which this lab is built.
- Look up any bolded glossary term introduced in the textbook chapter (each has a #gl:term-slug link in the text) — its master definition is in manuscript/glossary.md.
- Explore the appended src/ module that implements the corresponding quantitative model (when applicable) — referenced in the parent chapter’s “Bridge to Computation” subsection.

Module footer: parent chapter \cref{sec:unit_I_macromolecules}; all numerical quantities in this lab use SI units — see Appendix D — Units, Physical Constants, and Biological Ranges for unit conversions and biological-scale reference values.

Lab — Enzymes and the Kinetics of Catalysis

Learning Objectives

This activity accompanies section 4 of the textbook — review that chapter before attempting the exercises below.

- Interpret enzyme activity data by tracking O₂ production as a proxy for reaction rate
- Determine how temperature, pH, and substrate concentration affect enzyme rate (V_{max} approximation)
- Construct a rate vs **S** curve and identify qualitative K_m
- Interpret enzyme inhibition from a competitive inhibitor treatment

Alignment and Rubric Map

- Outcome 1 (LO1): Interpret the supplied evidence or model output for Enzymes and the Kinetics of Catalysis.
- Outcome 2 (LO2): Identify controls and comparison groups that make the claim testable.
- Outcome 3 (LO3): Quantify uncertainty, boundary conditions, or alternative explanations before concluding.
- Outcome 4 (LO4): Transfer the mechanism to a new biological case or public-facing decision.
- Chapter LO coverage: LO1, LO2, LO3, LO4
- Rubric dimensions: evidence; controls; uncertainty; mechanism; transfer. ## Pre-Lab Concept Questions {.unnumbered}

Answer these before starting the investigation — they activate knowledge from the parent chapter.

1. Define K_m (the Michaelis constant) and V_{max} (the maximum reaction velocity) in the Michaelis–Menten framework, and state the operational meaning of K_m as the substrate concentration at which the reaction velocity is half of V_{max}.
2. Sketch in words the shape of a Michaelis–Menten v-versus-**S** curve. Apply the equation $v = V_{\text{max}} \cdot S / (K_m + S)$ to explain why the curve approaches V_{max} asymptotically and why doubling **S** far above K_m has little effect on v.
3. Compare competitive inhibition (where an inhibitor binds the active site) and allosteric (non-competitive) inhibition that reduces effective enzyme activity by binding elsewhere. For each, predict the qualitative effect on the apparent K_m and apparent V_{max} measured from a v-versus-**S** curve.

Lab Context: Enzymes and the Kinetics of Catalysis

Enzymes are biological catalysts that lower activation energy. The enzyme catalase converts hydrogen peroxide (H₂O₂) to water and oxygen: 2 H₂O₂ → 2 H₂O + O₂. This reaction is often monitored by counting O₂ bubbles per minute or by measuring the height of foam produced. Catalase is one of the fastest known enzymes (k_{cat} about 40,000,000 s^{−1}) and is found in most aerobic organisms.

In this lab you will analyze a paper dataset showing how temperature, pH, substrate concentration, and inhibition affect catalase activity. The goal is to infer mechanism from controlled comparisons rather than to run a wet reaction.

The quantitative DHFR inhibition worked example in the parent chapter (section 4) shows how competitive-inhibitor binding reduces apparent reaction rate: at [MTX] = 10× its K_i, the apparent K_m rises 11-fold, cutting velocity by about 62%. This lab applies the same kinetic reasoning to catalase: students extract a qualitative K_m and predict inhibition from competition.

Paper-Based Materials

Table 529. Alignment and Rubric Map: Item and Quantity.

Item	Quantity
Source-governance card for Enzymes and the Kinetics of Catalysis: BRENDA enzyme-entry card with EC number, organism, kinetic field, ligand, reference, and release date	1
Pathway provenance cards comparing one KEGG pathway map and one BioCyc pathway/genome entry for the same catalase or peroxide-detoxification reaction	1 set
Catalase activity dataset with three replicates per condition	1
Enzyme-structure and active-site cards	1 set

Item	Quantity
Michaelis-Menten curve worksheet	1
Inhibitor scenario cards	1 set
Ruler (mm)	1
Calculator and graph paper	1 each

Paper-Based Investigation

Part A — Temperature Effect

1.

Plot the provided catalase-rate data for 0°C, 22°C, 37°C, 50°C, and denatured enzyme conditions.
2.

Calculate the mean and range for each condition. Identify the denatured enzyme as a negative control and the 37°C condition as a reference comparison.
3.

Use the active-site cards to explain why low temperature and denaturation reduce activity for different reasons.

Part B — pH Effect

4.

Graph catalase rate across pH 2.5, 5, 7, 8.5, and 11. Mark the pH optimum and one condition where enzyme structure is likely disrupted.
5.

Decide whether pH changes primarily affect enzyme shape, substrate charge, or both. Support the claim with one pattern in the dataset.

Part C — Substrate Concentration Effect

6.

Plot rate versus [H₂O₂] for 0%, 1%, 3%, and 6% substrate.
7.

Estimate the concentration where the curve begins to plateau and label it as a qualitative V_{max} region. Use the inhibitor cards to predict how a competitive inhibitor would change apparent K_m and V_{max}.

Data Recording

Table 530. Alignment and Rubric Map: Condition and Temperature (°C).

Condition	Temperature (°C)	pH	[H ₂ O ₂] (%)	Simulated O ₂ proxy at 60 s
Ice bath	0	7	3	
Room temp	22	7	3	
Warm bath	50	7	3	
Denatured enzyme	22	7	3	
Acid (pH 2.5)	22	2.5	3	
Neutral (pH 7)	22	7	3	
Alkaline (pH 8.5)	22	8.5	3	
S 0%	22	7	0	
S 1%	22	7	1	
S 3%	22	7	3	
S 6%	22	7	6	

Evidence and Reproducibility Checklist

- Primary evidence goal: Measure reaction-rate proxies and compare inhibition scenarios.
- Data skill to practice: Fit or interpret enzyme-rate data and identify which parameter changed.
- BioSkills emphasis: Quantitative reasoning, Interdisciplinary nature of science.
- Control logic: identify at least one positive control, one negative control, or one baseline comparison before interpreting results.
- Measurement discipline: record units, uncertainty, sample size, and any discarded observation with a reason.
- Mechanistic link: connect one result directly to the parent chapter’s big idea before writing the conclusion.
- Reproducibility check: state one procedural detail that another group would need in order to reproduce the result.

Paper-Based Evidence Upgrade

Before answering the analysis questions, annotate the paper dataset for Enzymes and the Kinetics of Catalysis with a reproducibility pass:

Table 531. Alignment and Rubric Map: Evidence check and Student action.

Evidence check	Student action
Control logic	Mark the comparison that functions as the baseline, negative control, or reference case.
Uncertainty	Circle the row, card, diagram feature, or model assumption most likely to change the conclusion.
Model comparison	State whether a simpler rule, null model, or alternative mechanism could explain the same pattern.
Decision threshold	Write the minimum evidence that would make you revise the interpretation.
Reproducibility	Record the exact scoring rule another group would need to reproduce your classification.

Focus note: treat the activity-versus-temperature series as a dose-response curve whose optimum and denaturation endpoints are the claims; the denatured-enzyme and no-enzyme conditions are the controls that decide whether a low signal means lost catalysis or a failed assay. Keep required work paper-based; any material-handling or equipment version belongs only in an optional extension.

Worked Example: Michaelis–Menten rate at two substrate levels

Problem: An enzyme has $V_{\max} = 120 \text{ nmol}\cdot\text{min}^{-1}$ and $K_m = 2.5 \text{ mM}$, measured under standard assay conditions. Compute the initial velocity v at $S = 5 \text{ mM}$ and at $S = K_m$. Then estimate the fold change in v as S rises from K_m to $5\cdot K_m$.

Solution: Apply $v = V_{\max} \cdot S / (K_m + S)$.

- At $S = 5 \text{ mM}$: $v = 120 \cdot 5 / (2.5 + 5) = 120 \cdot 5 / 7.5 = 80 \text{ nmol}\cdot\text{min}^{-1}$.
- At $S = K_m = 2.5 \text{ mM}$: $v = 120 \cdot 2.5 / (2.5 + 2.5) = 120 \cdot 0.5 = 60 \text{ nmol}\cdot\text{min}^{-1}$ (exactly half of V_{\max} , as expected).
- At $S = 5\cdot K_m = 12.5 \text{ mM}$: $v = 120 \cdot 12.5 / (2.5 + 12.5) = 120 \cdot 12.5 / 15 = 100 \text{ nmol}\cdot\text{min}^{-1}$. Going from $S = K_m$ to $S = 5\cdot K_m$ raises v from 60 to 100 $\text{nmol}\cdot\text{min}^{-1}$, a 1.67-fold increase — modest compared with the fivefold rise in substrate.

Interpretation: Near K_m , the enzyme is sensitive to substrate availability and small shifts in S move v sharply; far above K_m , the enzyme is approaching saturation and additional substrate buys progressively less rate. Cells exploit this by keeping many regulated enzymes at $S \approx K_m$, where small allosteric or feedback signals can produce meaningful changes in flux. The same arithmetic tells you that to reach within 10% of V_{\max} in this enzyme you would need $S \approx 9\cdot K_m = 22.5 \text{ mM}$.

Source-Governance Checkpoint

Complete the source-governance card for Enzymes and the Kinetics of Catalysis before writing the conclusion. Name the source type or model snapshot, record the evidence date or version, decide whether the claim is stable or fast-moving, and write one refresh trigger that would force the interpretation to change. Treat the card as a printed evidence object, not as a live web lookup.

Analysis Questions

1. Plot the simulated O_2 proxy vs temperature. Identify the approximate optimal temperature. Explain the molecular basis for activity loss at 0°C and above 50°C .
2. Explain why the denatured-enzyme condition showed no activity using the concept of protein denaturation and active site geometry.
3. Plot the simulated O_2 proxy vs $[\text{H}_2\text{O}_2]$. Describe the shape of the curve. At what concentration does activity appear to plateau? How does this relate to the concept of V_{\max} and enzyme saturation?
4. If you added a competitive inhibitor (e.g., a molecule structurally similar to H_2O_2), predict how the rate vs S curve would change in apparent K_m and V_{\max} relative to uninhibited enzyme.
5. Catalase deficiency is a human genetic condition (acatalasia) associated with recurrent oral infections. Using your experimental results, explain why catalase is biologically important in protecting cells from H_2O_2 produced during oxidative metabolism.

Post-Lab Synthesis

Concept Check (Synthesis): A cell-biology team studies an enzyme E whose normal substrate concentration in the cytoplasm is held by upstream regulation at $S \approx K_m$. A candidate drug binds E and doubles its apparent K_m without changing V_{\max} (a hallmark of pure competitive inhibition).

- (a) Compute the predicted fractional change in v caused by the drug at the normal cellular S (use $v = V_{max} \cdot S / (K_m + S)$ before and after the K_m doubling), and interpret why an enzyme operating at $S \approx K_m$ is particularly sensitive to a K_m -shifting inhibitor.
- (b) Predict how the cell could partly compensate metabolically. Evaluate two routes: a homeostatic rise in S that restores the original v , and a compensatory increase in enzyme expression that raises effective V_{max} . Quantify the S that would restore the original v under the doubled K_m , and discuss which compensation is more plausible on a short time scale.
- (c) Design a paper-data experiment, using the same v -versus- S dataset format as today’s lab, that would distinguish this competitive inhibitor from an allosteric inhibitor that lowers V_{max} without changing K_m . State the diagnostic comparison and the threshold of effect at which you would call the difference convincing.

Optional Wet-Lab Extension

An instructor may demonstrate catalase activity with approved materials after a safety briefing. The required lab remains the paper dataset and the mechanistic interpretation of controls, rate curves, and inhibition.

Safety and Ethics Notes

Paper-based lab — no hydrogen peroxide, heating, or biological samples are required. Optional wet demonstrations require instructor supervision and appropriate eye and skin protection.

Debrief and Reflection

After you finish the practical work, spend 5–10 minutes in your small group comparing results and discussing the following prompts. Each member should contribute at least one observation before moving to the next prompt:

- 1. What did your measurements show — compare the group’s results to the textbook’s predictions. Where they diverge, suggest at least one mechanistic explanation before concluding “experimental error.”
- 2. What would change the outcome — propose one modification to the procedure that would sharpen the measurement or extend the result to a new biological context, and predict what you would observe.
- 3. One-sentence headline — each student composes a single sentence summarizing the lab’s take-home message, suitable for a tweet. Compare sentences across groups; good headlines are short, quantitative, and mechanistic.
- 4. Connection back to the textbook — identify one section of section 4 that your data either confirmed or complicated. Cite the specific passage.

Further Reading (Lab)

- Revisit the parent chapter section 4 for the theoretical foundations on which this lab is built.
- Look up any bolded glossary term introduced in the textbook chapter (each has a `#gl:term-slug` link in the text) — its master definition is in `manuscript/glossary.md`.
- Explore the appended `src/` module that implements the corresponding quantitative model (when applicable) — referenced in the parent chapter’s “Bridge to Computation” subsection.

Module footer: parent chapter `\cref{sec:unit_I_enzymes_and_kinetics}`; all numerical quantities in this lab use SI units — see [Appendix D — Units, Physical Constants, and Biological Ranges](#) for unit conversions and biological-scale reference values.

Lab — Cell Theory and Cell Types

Learning Objectives

This activity accompanies section 5 of the textbook — review that chapter before attempting the exercises below.

- Interpret micrograph packets of prokaryotic and eukaryotic cells
- Apply cell theory to evaluate cases from printed microscopy evidence
- Measure cell dimensions using scale bars and reference data
- Compare structural features of prokaryotic and plant/animal eukaryotic cells

Alignment and Rubric Map

- Outcome 1 (LO1): Interpret the supplied evidence or model output for Cell Theory and Cell Types.
- Outcome 2 (LO2): Identify controls and comparison groups that make the claim testable.
- Outcome 3 (LO3): Quantify uncertainty, boundary conditions, or alternative explanations before concluding.
- Outcome 4 (LO4): Transfer the mechanism to a new biological case or public-facing decision.
- Chapter LO coverage: LO1, LO2, LO3, LO4
- Rubric dimensions: evidence; controls; uncertainty; mechanism; transfer. ## Pre-Lab Concept Questions {.unnumbered}

Answer these before starting the investigation — they activate knowledge from the parent chapter.

1. State the three classical tenets of cell theory in your own words. For each tenet, name one historical figure whose evidence supported it.
2. Diffusion-limited transport places an upper bound on cell size for cells that rely on it. Explain in one paragraph why diffusion across a cell scales unfavourably with cell radius, referring to the time–distance relationship for diffusion.
3. Distinguish prokaryotic and eukaryotic cells on the basis of three observable features. For each feature, indicate whether it would be visible with a standard light microscope at 400× total magnification or whether it requires electron microscopy.

Pre-Lab (to complete before class)

1. Define in one sentence each: resolution, magnification, field of view (FOV). Note which depends on optics and which on apertures.
2. Compute the FOV diameter at 400× if the FOV at 40× is 4.5 mm. (Answer: $4.5\text{ mm} \times 40/400 = 0.45\text{ mm} = 450\text{ }\mu\text{m}.$)
3. Look up Robert Hooke (1665) and Antoni van Leeuwenhoek (1673). In 2–3 sentences, explain who saw what first and why both contributed to cell theory.
4. Predict: at 400× total magnification, how many *Bacillus subtilis* cells (2 μm long) would fit end-to-end across the diameter of the FOV? (Answer: $450\text{ }\mu\text{m} / 2\text{ }\mu\text{m} \approx 225$ cells.)

Lab Context: Cell Theory and Cell Types

Cell theory, formalised by Schleiden, Schwann, and Virchow (1838–1855), states that: (1) most living things are composed of cells; (2) the cell is the basic unit of life; and (3) most cells arise from pre-existing cells. Two fundamental cell types exist: prokaryotes (Bacteria, Archaea — no nucleus, typically 0.5–5 μm) and eukaryotes (Eukarya — membrane-bounded nucleus, 10–100 μm). Light microscopy can resolve features above about 200 nm, allowing clear visualization of cell walls, chloroplasts, and the nucleus, though the electron microscope is needed for ribosomes and membranes.

Paper-Based Materials

Table 532. Alignment and Rubric Map: Item and Quantity.

Item	Quantity
Source-governance card for Cell Theory and Cell Types: cell-atlas or imaging source card: sample, assay, cell-state call, perturbation evidence, and uncertainty	1
Micrograph packet: <i>Bacillus</i> , onion epidermis, leaf mesophyll, epithelial cell	1
Scale-bar worksheet	1
Cell-feature evidence cards	1 set
Historical cell-theory source cards	1 set
Ruler (mm)	1

Item	Quantity
Calculator	1

Paper-Based Investigation

1.

Prokaryote micrograph: Inspect the *Bacillus* image. Sketch cells; note shape, arrangement, and size relative to the scale bar.
2.

Plant epidermis micrograph: Inspect the onion image. Identify cell wall, nucleus where visible, and vacuole evidence.
3.

Leaf mesophyll micrograph: Inspect the chloroplast-rich plant-cell image. Identify chloroplasts and explain why this cell type differs from onion epidermis.
4.

Animal epithelial micrograph: Inspect the epithelial-cell image. Identify nucleus, plasma membrane boundary, and lack of cell wall.
5.

For each case, record estimated cell diameter, presence/absence of nucleus, cell wall, chloroplasts, and large vacuole. Flag any feature that cannot be resolved from the image.

Extension — Microbial Diversity Image Packet

6.

Use the printed microbial-diversity packet to compare chain-forming cocci and rod-shaped cells. Sketch both and identify the evidence for prokaryotic organization.
7.

Estimate cells per field of view from the annotated image grid, then calculate how the estimate would change under a 1:10 dilution. State one counting assumption that affects reproducibility.

Part E — Scale Bar Arithmetic

8.

The instructor will distribute a printed micrograph of a eukaryotic cell with a labeled scale bar of 10 μm . Measure the longest cell diameter with a ruler (mm); convert to true μm using the scale-bar ratio. This is the core arithmetic for every published micrograph: *true size* = (*measured distance* \div *scale bar length*) \times *scale bar value*.
9.

Using the same formula, estimate the total surface area of a spherical epithelial-cell image (diameter $\approx 60\ \mu\text{m}$): $A = 4\pi r^2 = 4\pi(30)^2 \approx 1.13 \times 10^4\ \mu\text{m}^2$. Compare with a spherical *Bacillus* (diameter 2 μm , $A \approx 12.6\ \mu\text{m}^2$). Note the about 1000 \times difference — which cell has a larger surface-to-volume ratio, and why is that biologically important?

Data Recording

Table 533. Part E — Scale Bar Arithmetic: Case and Cell type (Pro/Euk).

Case	Cell type (Pro/Euk)	Approx. diameter (μm)	Nucleus	Cell wall	Chloroplasts	Vacuole
Bacillus						
Onion						
Leaf						
mesophyll						
Epithelial						
image						

Sketch each cell type in the boxes below:

[Sketch boxes – label most visible structures]

Evidence and Reproducibility Checklist

- Primary evidence goal: Compare cell types and quantify surface-area limits.
- Data skill to practice: Infer cellular constraints from measurements, micrographs, and scale bars.
- BioSkills emphasis: Modeling and simulation, Process of science.
- Control logic: identify at least one positive control, one negative control, or one baseline comparison before interpreting results.
- Measurement discipline: record units, uncertainty, sample size, and any discarded observation with a reason.
- Mechanistic link: connect one result directly to the parent chapter’s big idea before writing the conclusion.
- Reproducibility check: state one procedural detail that another group would need in order to reproduce the result.

Paper-Based Evidence Upgrade

Before answering the analysis questions, annotate the paper dataset for Cell Theory and Cell Types with a reproducibility pass:

Table 534. Part E — Scale Bar Arithmetic: Evidence check and Student action.

Evidence check	Student action
Control logic	Mark the comparison that functions as the baseline, negative control, or reference case.
Uncertainty	Circle the row, card, diagram feature, or model assumption most likely to change the conclusion.
Model comparison	State whether a simpler rule, null model, or alternative mechanism could explain the same pattern.
Decision threshold	Write the minimum evidence that would make you revise the interpretation.
Reproducibility	Record the exact scoring rule another group would need to reproduce your classification.

Focus note: when you assign a cell to a type, write down the operational definition you used and whether it is a discrete category or a position on a continuum; treat a single-cell or spatial atlas, a lineage trace, or a minimal-cell construct as the evidence that would change your call. Keep required work paper-based; any material-handling or equipment version belongs only in an optional extension.

Worked Example: Diffusion Time Across a 15 micrometre Cell

Problem: A roughly spherical cell has radius $r = 15\text{ }\mu\text{m} = 1.5 \times 10^{-5}\text{ m}$. A small metabolite has a cytoplasmic diffusion coefficient $D \approx 1 \times 10^{-9}\text{ m}^2/\text{s}$. Estimate the characteristic time for the metabolite to diffuse from the plasma membrane to the center of the cell using the standard 3-D random-walk estimate $t \approx r^2 / (6D)$. Compare to a cell ten times larger ($r = 150\text{ }\mu\text{m}$).

Solution:

For $r = 15\text{ }\mu\text{m}$:

- $r^2 = (1.5 \times 10^{-5})^2 = 2.25 \times 10^{-10}\text{ m}^2$
- $6D = 6 \times 10^{-9}\text{ m}^2/\text{s}$
- $t \approx 2.25 \times 10^{-10} / 6 \times 10^{-9}\text{ s} \approx 0.0375\text{ s} \approx 38\text{ ms}$

For $r = 150\text{ }\mu\text{m}$ (10× larger):

- $r^2 = (1.5 \times 10^{-4})^2 = 2.25 \times 10^{-8}\text{ m}^2$ (100× larger)
- $t \approx 2.25 \times 10^{-8} / 6 \times 10^{-9} \approx 3.75\text{ s}$

Diffusion time scales with r^2 , so a 10× increase in radius produces a 100× increase in characteristic diffusion time.

Interpretation: A small metabolite crosses a $15\text{ }\mu\text{m}$ cell in tens of milliseconds — fast enough that simple diffusion suffices to homogenise concentrations during ordinary metabolism. At $150\text{ }\mu\text{m}$ the same molecule takes several seconds, which is comparable to or longer than many reaction time scales. This r^2 scaling is one quantitative reason cells tend to be small, and one reason large cells (oocytes, neurons, plant fibers) adopt strategies such as cytoplasmic streaming, internal compartments, or extreme shape changes (e.g. axonal projections) rather than simple size scaling.

Source-Governance Checkpoint

Complete the source-governance card for Cell Theory and Cell Types before writing the conclusion. Name the source type or model snapshot, record the evidence date or version, decide whether the claim is stable or fast-moving, and write one refresh trigger that would force the interpretation to change. Treat the card as a printed evidence object, not as a live web lookup.

Analysis Questions

- How does the size of *Bacillus* compare to the onion epidermal cell? Express as a ratio. What structural feature allows eukaryotic cells to be so much larger (hint: internal compartmentalization)?

- The onion image packet includes a starch-localization annotation. What molecule was detected? Which organelle does this implicate, and why is this unexpected in onion cells that are not green?
- Both onion and leaf mesophyll cells are plant cells, but mesophyll cells have abundant chloroplasts and onion epidermal cells typically do not. Explain using cell theory and differential gene expression.
- A printed pond-water image shows cells with a nucleus but without a cell wall. Is this organism a plant, animal, or fungus? What additional image feature or molecular marker would narrow the identification?
- Devise a paper-based study using time-series image cards to test whether temperature affects the rate of cytoplasmic streaming. Identify your independent, dependent, and controlled variables.

Post-Lab Synthesis

Concept Check (Synthesis): Cell theory is one of the most heavily corroborated frameworks in biology, but science remains open in principle to revision when new evidence appears. Drawing on the historical reasoning in this investigation and the chapter:

- Specify, as precisely as you can, what new observation would force a revision of the tenet “every cell arises from a pre-existing cell.” Describe the observation, the controls that would distinguish it from contamination or experimental artifact, and what kind of replication the scientific community would expect before accepting the result.
- Discuss whether viruses, prions, or syncytia challenge the original tenets of cell theory. For each, decide whether you would regard the entity as a counter-example, an edge case requiring careful re-definition, or a separate category outside the scope of cell theory — and justify.
- Reflect: if a single laboratory reported one such observation, what professional norms (peer review, replication, methods transparency) would govern how the community responded? Why are those norms part of the epistemology of cell biology rather than optional procedural details?

Extension Analysis Questions

- Hooke’s 1665 *Micrographia* described “cells” in cork — but what he saw were primarily the walls of dead plant cells, not living matter. Why does this still count as the founding observation of cell theory? How does it illustrate the difference between observing a cell and understanding it?
- Mitochondria and chloroplasts have their own DNA, 70S ribosomes (like bacteria, not the 80S eukaryotic ribosomes in cytoplasm), and divide independently. Connect these facts to the endosymbiotic theory (Margulis, 1967) — why is maternal inheritance of mitochondrial DNA in humans a direct prediction of this theory?
- A single mammalian cell contains about 10^7 proteins. Given a cell volume of $1000\text{ }\mu\text{m}^3$, compute the approximate bulk protein concentration (mass/volume). Discuss why “macromolecular crowding” (about 30% by volume) changes effective reaction kinetics relative to dilute test-tube conditions.

Optional Microscopy Extension

Prepared slides or classroom microscopy may be used as an optional extension. Do not collect human cells or prepare wet mounts for the required activity; the micrograph packet supplies most evidence needed for the lab.

Safety and Ethics Notes

Paper-based lab — no swabs, stains, wet mounts, cultures, glass slides, or microscopes are required. Optional microscopy work requires instructor supervision and standard glassware precautions.

Debrief and Reflection

After you finish the practical work, spend 5–10 minutes in your small group comparing results and discussing the following prompts. Each member should contribute at least one observation before moving to the next prompt:

- What did your measurements show — compare the group’s results to the textbook’s predictions. Where they diverge, suggest at least one mechanistic explanation before concluding “experimental error.”
- What would change the outcome — propose one modification to the procedure that would sharpen the measurement or extend the result to a new biological context, and predict what you would observe.
- One-sentence headline — each student composes a single sentence summarizing the lab’s take-home message, suitable for a tweet. Compare sentences across groups; good headlines are short, quantitative, and mechanistic.
- Connection back to the textbook — identify one section of section 5 that your data either confirmed or complicated. Cite the specific passage.

Further Reading (Lab)

- Revisit the parent chapter section 5 for the theoretical foundations on which this lab is built.
- Look up any bolded glossary term introduced in the textbook chapter (each has a `#gl:term-slug` link in the text) — its master definition is in `manuscript/glossary.md`.

- Explore the appended `src/` module that implements the corresponding quantitative model (when applicable) — referenced in the parent chapter’s “Bridge to Computation” subsection.

Module footer: parent chapter \cref{sec:unit_II_cell_theory}; all numerical quantities in this lab use SI units — see [Appendix D — Units, Physical Constants, and Biological Ranges](#) for unit conversions and biological-scale reference values.

Lab — Cell Structure and Organelles

Learning Objectives

This activity accompanies section 6 of the textbook — review that chapter before attempting the exercises below.

- Identify major organelles in electron micrograph and model-image packets
- Relate organelle structure to function using the endomembrane system
- Estimate the magnification and real size of organelles from scale bars
- Compare organelle complements across cell types (liver, muscle, leaf mesophyll)

Alignment and Rubric Map

- Outcome 1 (LO1): Interpret the supplied evidence or model output for Cell Structure and Organelles.
- Outcome 2 (LO2): Identify controls and comparison groups that make the claim testable.
- Outcome 3 (LO3): Quantify uncertainty, boundary conditions, or alternative explanations before concluding.
- Outcome 4 (LO4): Transfer the mechanism to a new biological case or public-facing decision.
- Chapter LO coverage: LO1, LO2, LO3, LO4
- Rubric dimensions: evidence; controls; uncertainty; mechanism; transfer. ## Pre-Lab Concept Questions {.unnumbered}

Answer these before starting the investigation — they activate knowledge from the parent chapter.

1. List the organelles present in a typical plant cell that are absent from a typical animal cell, and give a one-line function for each.
2. Describe the directional flow of a secreted protein through the endomembrane system, naming each compartment it passes through from synthesis to release at the plasma membrane.
3. A pancreatic acinar cell secretes large amounts of digestive enzymes; a hepatocyte performs heavy detoxification of lipophilic drugs. Predict which endomembrane compartment is more abundant in each cell type, and justify each prediction in terms of the compartment’s function.

Pre-Lab (to complete before class)

1. For each organelle, write one sentence matching it to its dominant function: nucleus, ER (rough and smooth), Golgi, mitochondrion, chloroplast, lysosome, peroxisome.
2. Define in one line: scale bar, magnification, endomembrane system. Which three compartments make up the endomembrane system?
3. Compute total mitochondrial volume in a hepatocyte if each mitochondrion is a $1\text{ }\mu\text{m} \times 3\text{ }\mu\text{m}$ cylinder and the cell contains 2000 of them. Express as a fraction of a cell with total volume $5000\text{ }\mu\text{m}^3$.
4. Predict three cell types where you would expect mitochondrial content to approach 40% of cell volume (answer: cardiac muscle, BAT, hepatocytes).

Lab Context: Cell Structure and Organelles

Eukaryotic cells are organized into membrane-bounded compartments (organelles) that divide labor: the nucleus stores and expresses DNA; the rough ER synthesizes membrane and secretory proteins; the Golgi receives, modifies, and sorts vesicle cargo; mitochondria generate ATP via oxidative phosphorylation. The type and abundance of organelles reflects a cell’s function — liver hepatocytes are rich in rough ER (secretory proteins) and smooth ER (lipid metabolism); muscle cells are packed with mitochondria; leaf mesophyll cells contain hundreds of chloroplasts.

Paper-Based Materials

Table 535. Alignment and Rubric Map: Item and Quantity.

Item	Quantity
Source-governance card for Cell Structure and Organelles: cell-atlas or imaging source card: sample, assay, cell-state call, perturbation evidence, and uncertainty	1
Transmission electron micrograph (TEM) print packet: plant cell, animal cell, secretory cell, mitochondrion close-up, chloroplast close-up	1 set
Ruler (mm)	1
Scale bar calculator worksheet	1

Item	Quantity
Colored pencils (10 colors)	1 set
Printed light-microscopy image cards: onion root tip and pancreas	1 set
Cell function card deck (instructor-supplied: 20 cards)	1 per group

Paper-Based Investigation

1.

TEM analysis: For each of the 5 TEM prints, identify and label (with arrows and a key): nucleus, nuclear envelope, nucleolus, rough ER, smooth ER, Golgi apparatus, mitochondria, chloroplast (where present), plasma membrane, cell wall (where present), vacuole (where present), ribosomes, lysosomes.
2.

Size estimation: Using the scale bar provided on each TEM, measure (mm) and calculate the real size of: (a) the nucleus diameter in the animal cell image; (b) one mitochondrion; (c) one chloroplast.
3.

Light microscopy image cards: Use the onion root tip and pancreas images to identify cells in interphase versus mitosis and secretory acinar cells with abundant granular cytoplasm.
4.

Card sort: Deal the function cards (e.g., “exports proteins”, “detoxifies drugs”, “contains DNA”) and assign each to the correct organelle. Record your assignments.

Extension — Cell-Type Organelle Profile

5.

Using the provided TEM images, count or estimate the abundance of each major organelle (rough ER, smooth ER, mitochondria, Golgi, vacuole, chloroplast, peroxisome) for each of: hepatocyte, cardiac myocyte, pancreatic acinar cell, palisade mesophyll cell, skin fibroblast. Fill in the table below (use 0/+ /++ /+++ rather than precise counts).

Part E — Scale-Bar Arithmetic in Action

6.

For TEM image #3 (chloroplast), the scale bar reads 1 μm and measures 8 mm on the printout. Measure the thylakoid stack width (disk diameter) in mm, then compute its real size. A plausible answer is 400–500 nm per grana disk.

Data Recording

Table 536. Part E — Scale-Bar Arithmetic in Action: Organelle and TEM image (tick).

Organelle	TEM image (tick)	Function (in own words)	Cell types where most abundant
Nucleus			
Rough ER			
Golgi			
Mitochondrion			
Chloroplast			
Lysosome			
Vacuole			
Ribosome			

Size calculations:

Table 537. Part E — Scale-Bar Arithmetic in Action: Structure and Scale bar (mm) = (μm).

Structure	Scale bar (mm) = (μm)	Measured size (mm)	Real size (μm)
Nucleus			
Mitochondrion			
Chloroplast			

Evidence and Reproducibility Checklist

- Primary evidence goal: Map organelle function with microscopy-style observations.
- Data skill to practice: Trace a molecule through compartments using evidence from labels or perturbations.
- BioSkills emphasis: Modeling and simulation, Process of science.
- Control logic: identify at least one positive control, one negative control, or one baseline comparison before interpreting results.
- Measurement discipline: record units, uncertainty, sample size, and any discarded observation with a reason.
- Mechanistic link: connect one result directly to the parent chapter’s big idea before writing the conclusion.
- Reproducibility check: state one procedural detail that another group would need in order to reproduce the result.

Paper-Based Evidence Upgrade

Before answering the analysis questions, annotate the paper dataset for Cell Structure and Organelles with a reproducibility pass:

Table 538. Part E — Scale-Bar Arithmetic in Action: Evidence check and Student action.

Evidence check	Student action
Control logic	Mark the comparison that functions as the baseline, negative control, or reference case.
Uncertainty	Circle the row, card, diagram feature, or model assumption most likely to change the conclusion.
Model comparison	State whether a simpler rule, null model, or alternative mechanism could explain the same pattern.
Decision threshold	Write the minimum evidence that would make you revise the interpretation.
Reproducibility	Record the exact scoring rule another group would need to reproduce your classification.

Focus note: when you classify an organelle observation, state the imaging method and resolution, whether a membrane contact site or condensate is involved, and the cellular context; treat a cryo-electron tomogram of the native structure as the evidence that would change your call. Keep required work paper-based; any material-handling or equipment version belongs only in an optional extension.

Worked Example: Surface-to-Volume Ratio of a 20 μm Cell vs a 2 μm Bacterium

Problem: Consider a roughly spherical eukaryotic cell with diameter 20 μm (radius r = 10 μm) and a roughly spherical bacterium with diameter 2 μm (r = 1 μm). For each, compute the surface area (SA = 4πr²), the volume (V = (4/3)πr³), and the surface-to-volume ratio (SA:V). Compare the two ratios and explain what the comparison implies about exchange across the plasma membrane.

Solution:

Eukaryotic cell, r = 10 μm:

- SA = 4π(10)² = 400π ≈ 1,256.6 μm²
- V = (4/3)π(10)³ = (4000/3)π ≈ 4,188.8 μm³
- SA:V = 1,256.6 / 4,188.8 ≈ 0.30 μm⁻¹

Bacterium, r = 1 μm:

- SA = 4π(1)² = 4π ≈ 12.57 μm²
- V = (4/3)π(1)³ ≈ 4.189 μm³
- SA:V = 12.57 / 4.189 ≈ 3.00 μm⁻¹

The bacterium has an SA:V about 10× larger than the eukaryotic cell (3.0 vs 0.30 μm⁻¹), matching the 10× ratio of their radii — as predicted by SA:V = 3/r for a sphere.

Interpretation: A small bacterium can move nutrients, gases, and wastes across its plasma membrane fast enough to support whole-cell metabolism by diffusion alone. The 20 μm eukaryotic cell has roughly one-tenth as much membrane per unit volume, so simple plasma-membrane diffusion is insufficient. Eukaryotes recover lost exchange surface by sub-dividing the cytoplasm into membrane-bound organelles (mitochondria, ER, Golgi), each of which contributes its own internal membrane area. Compartmentalization is partly a geometric response to the diffusion limit on cell size.

Source-Governance Checkpoint

Complete the source-governance card for Cell Structure and Organelles before writing the conclusion. Name the source type or model snapshot, record the evidence date or version, decide whether the claim is stable or fast-moving, and write one refresh trigger that would force the interpretation to change. Treat the card as a printed evidence object, not as a live web lookup.

Analysis Questions

1. Describe the path taken by a newly synthesized digestive enzyme (e.g., lipase) from its gene in the nucleus to its secretion from a pancreatic acinar cell. Name every organelle involved in sequence.
2. A cell type has an unusually large number of mitochondria and virtually no rough ER. Propose two cell types that fit this description and explain the functional logic.
3. Using your size calculations, how many mitochondria could fit side-by-side across the diameter of the nucleus in your animal cell TEM? Show your arithmetic.
4. Chloroplasts and mitochondria are both double-membrane organelles with their own DNA. What does this suggest about their evolutionary origin? Name and explain the theory.
5. A student examines a mystery cell and finds: large central vacuole, cell wall, chloroplasts, but no centrioles. Is this a plant, animal, or fungal cell? Justify each structural clue.

Post-Lab Synthesis

Concept Check (Synthesis): Compartmentalization is one of the defining features of eukaryotic cells. Using your worked-example SA:V calculation, your observations of the cell-structure cards, and the chapter on cell organization:

- (a) Argue from geometry and biochemistry why compartmentalization enables eukaryotic cells to support metabolism that prokaryotes cannot — refer specifically to (i) localized pH or redox environments and (ii) co-localization of sequential enzymes.
- (b) Some prokaryotes (e.g. certain cyanobacteria) approach 10 μm in size and possess specialized internal membrane systems. Use your SA:V reasoning to predict whether such organisms would be expected to use membrane-bounded sub-compartments, and what functional pressure would drive that adaptation.
- (c) Identify one experimental observation from the cell-structure investigation that, on its own, would be insufficient to assign a cell as prokaryotic or eukaryotic, and one observation that would be much stronger evidence — and justify your ranking.

Extension Analysis Questions

6. Cells in brown adipose tissue (BAT) are dedicated to non-shivering thermogenesis — uncoupling electron transport from ATP synthesis via UCP1. Predict which organelle complement would be dramatically amplified relative to white adipose tissue. Why?
7. Peroxisomes carry out very-long-chain fatty-acid β -oxidation and hydrogen-peroxide metabolism. Zellweger syndrome is a lethal peroxisomal biogenesis disorder. Given your understanding of the endomembrane system, why can't the ER or mitochondrion simply take over peroxisomal function?
8. A TEM-resolved nuclear envelope shows pores about 120 nm wide, with a central transporter. Calculate (approximately) the mass of mRNA (about 500 kDa for an average mRNP) that can transit through one pore per second, given that active transport is limited to about 1000 events/pore/s. Compare to the about 2000 pores per mammalian nucleus.

Optional Microscopy Extension

Prepared slides may be observed if microscopes are available, but the required analysis uses printed image packets and scale bars. Optional work should not require live cultures or animal tissues.

Safety and Ethics Notes

Paper-based lab — no live cultures, animal tissues, glass slides, or microscopes are required. Electron micrograph prints are shared resources; do not write on them without protective paper underneath.

Debrief and Reflection

After you finish the practical work, spend 5–10 minutes in your small group comparing results and discussing the following prompts. Each member should contribute at least one observation before moving to the next prompt:

1. What did your measurements show — compare the group's results to the textbook's predictions. Where they diverge, suggest at least one mechanistic explanation before concluding "experimental error."
2. What would change the outcome — propose one modification to the procedure that would sharpen the measurement or extend the result to a new biological context, and predict what you would observe.

3. One-sentence headline — each student composes a single sentence summarizing the lab’s take-home message, suitable for a tweet. Compare sentences across groups; good headlines are short, quantitative, and mechanistic.
4. Connection back to the textbook — identify one section of section 6 that your data either confirmed or complicated. Cite the specific passage.

Further Reading (Lab)

- Revisit the parent chapter section 6 for the theoretical foundations on which this lab is built.
- Look up any bolded glossary term introduced in the textbook chapter (each has a #gl:term-slug link in the text) — its master definition is in manuscript/glossary.md.
- Explore the appended src/ module that implements the corresponding quantitative model (when applicable) — referenced in the parent chapter’s “Bridge to Computation” subsection.

Module footer: parent chapter \cref{sec:unit_II_cell_structure}; all numerical quantities in this lab use SI units — see Appendix D — Units, Physical Constants, and Biological Ranges for unit conversions and biological-scale reference values.

Lab — Membrane Structure and Transport

Learning Objectives

This activity accompanies section 7 of the textbook — review that chapter before attempting the exercises below.

- Interpret osmosis data and estimate osmotic potential from model tissues
- Quantify plasmolysis using annotated image packets across NaCl concentrations
- Relate membrane lipid bilayer fluidity to temperature through simulated color-leakage data
- Apply the fluid-mosaic model to explain observed transport phenomena

Alignment and Rubric Map

- Outcome 1 (LO1): Interpret the supplied evidence or model output for Membrane Structure and Transport.
- Outcome 2 (LO2): Identify controls and comparison groups that make the claim testable.
- Outcome 3 (LO3): Quantify uncertainty, boundary conditions, or alternative explanations before concluding.
- Outcome 4 (LO4): Transfer the mechanism to a new biological case or public-facing decision.
- Chapter LO coverage: LO1, LO2, LO3, LO4
- Rubric dimensions: evidence; controls; uncertainty; mechanism; transfer. ## Pre-Lab Concept Questions {.unnumbered}

Answer these before starting the investigation — they activate knowledge from the parent chapter.

1. Define osmotic potential (Ψ_s) and pressure potential (Ψ_p) in one sentence each, and write the equation relating them to the total water potential Ψ of a plant cell.
2. Distinguish facilitated diffusion from active transport. For each, identify (i) whether energy from ATP is required, (ii) the direction of net movement relative to the concentration gradient, and (iii) one representative transmembrane protein family.
3. A red blood cell is placed in a 0.9% NaCl solution and shows no change in volume; another is placed in distilled water and lyses. Use the terms hypertonic, hypotonic, and isotonic to predict the behavior of the same red blood cell placed in a 3% NaCl solution, and predict what a plant cell would do under the same three conditions.

Lab Context: Membrane Structure and Transport

The plasma membrane is a selectively permeable phospholipid bilayer with embedded proteins. Water moves by osmosis across membranes from regions of high water potential (Ψ) to low Ψ (high solute concentration). In plant cells, plasmolysis occurs when the cell is placed in hypertonic solution — the cytoplasm shrinks away from the rigid cell wall. In animal cells, a hypertonic solution causes crenation (cell shrinking). Membrane fluidity depends on phospholipid composition (unsaturated fatty acids → more fluid) and temperature (higher temperature → more fluid).

In this lab you will use printed datasets to investigate how temperature damages membranes (simulated betacyanin leakage) and how plasmolysis changes across a NaCl concentration gradient. The required work is paper-based and emphasizes controls, graphing, and model interpretation.

Paper-Based Materials

Table 539. Alignment and Rubric Map: Item and Quantity.

Item	Quantity
Source-governance card for Membrane Structure and Transport: cell-atlas or imaging source card: sample, assay, cell-state call, perturbation evidence, and uncertainty	1
Membrane-leakage dataset at 20°C, 40°C, 60°C, 80°C, and 100°C	1
Annotated onion plasmolysis image packet	1
NaCl gradient and water-potential cards	1 set
Control and confound worksheet	1
Calculator and graph paper	1 each

Paper-Based Investigation

Part A — Temperature and Membrane Integrity

- 1. Plot the provided absorbance-at-530-nm dataset for model membrane leakage across temperatures.
- 2. Identify the baseline condition, the sharpest change in leakage, and one confound that a real wet assay would need to control.
- 3. Use the membrane-composition cards to predict how cholesterol or unsaturated fatty acids would shift the curve.

Part B — Osmosis and Plasmolysis in Onion

- 4. Use the annotated image packet for 0%, 0.5%, 1%, 1.5%, and 2% NaCl.
- 5. Count the marked cells in each image and classify each as plasmolysed or not plasmolysed using the rubric.
- 6. Calculate percent plasmolysis and estimate the concentration where 50% plasmolysis occurs.

Data Recording

Table 540. Alignment and Rubric Map: Temperature (°C) and Absorbance at 530 nm.

Temperature (°C)	Absorbance at 530 nm	Qualitative color of water
20		
40		
60		
80		
100		

Table 541. Alignment and Rubric Map: [NaCl] (%) and Cells plasmolysed (of 20).

[NaCl] (%)	Cells plasmolysed (of 20)	% Plasmolysis
0		
0.5		
1.0		
1.5		
2.0		

Evidence and Reproducibility Checklist

- Primary evidence goal: Test osmosis and transport mechanisms with simple cell or model-membrane observations.
- Data skill to practice: Interpret transport data from gradients, rates, and membrane potentials.
- BioSkills emphasis: Modeling and simulation, Process of science.
- Control logic: identify at least one positive control, one negative control, or one baseline comparison before interpreting results.
- Measurement discipline: record units, uncertainty, sample size, and any discarded observation with a reason.
- Mechanistic link: connect one result directly to the parent chapter’s big idea before writing the conclusion.
- Reproducibility check: state one procedural detail that another group would need in order to reproduce the result.

Paper-Based Evidence Upgrade

Before answering the analysis questions, annotate the paper dataset for Membrane Structure and Transport with a reproducibility pass:

Table 542. Alignment and Rubric Map: Evidence check and Student action.

Evidence check	Student action
Control logic	Mark the comparison that functions as the baseline, negative control, or reference case.
Uncertainty	Circle the row, card, diagram feature, or model assumption most likely to change the conclusion.

Evidence check	Student action
Model comparison	State whether a simpler rule, null model, or alternative mechanism could explain the same pattern.
Decision threshold	Write the minimum evidence that would make you revise the interpretation.
Reproducibility	Record the exact scoring rule another group would need to reproduce your classification.

Focus note: when you judge a transport claim, specify the concentration gradient, the electrochemical driving force, the gating state, and the energy coupling assumed; treat a cryo-EM conformational state or a single-channel flux recording as the evidence that would change your call. Keep required work paper-based; any material-handling or equipment version belongs only in an optional extension.

Worked Example: Predicting Water Movement from Water-Potential Components

Problem: A plant cell is equilibrated with a bathing solution. Inside the cell, the solute potential is $\Psi_s = -0.6$ MPa and the pressure potential (turgor) is $\Psi_p = +0.3$ MPa. The bathing solution has $\Psi_{\text{solution}} = -0.4$ MPa (pure-solute solution, so $\Psi_p \approx 0$ and $\Psi_{\text{solution}} = \Psi_s$ of the solution). (a) Calculate the cell’s total water potential Ψ_{cell} . (b) Determine the direction of net water movement between the cell and the bathing solution. (c) Predict, qualitatively, how Ψ_p would change as the system approaches equilibrium.

Solution:

- (a) $\Psi_{\text{cell}} = \Psi_s + \Psi_p = (-0.6) + (+0.3) = -0.3$ MPa
- (b) Water moves from regions of higher (less negative) water potential to lower (more negative) water potential. Compare:
 - $\Psi_{\text{cell}} = -0.3$ MPa (higher / less negative)
 - $\Psi_{\text{solution}} = -0.4$ MPa (lower / more negative)

Therefore water moves out of the cell into the bathing solution until potentials equalise.

- (c) As water leaves the cell, the cell’s volume decreases, the cell wall pushes inward less, and Ψ_p drops toward 0. Ψ_s becomes slightly more negative as cytoplasmic solutes concentrate. The new Ψ_{cell} becomes more negative; the system reaches equilibrium when $\Psi_{\text{cell}} = \Psi_{\text{solution}} = -0.4$ MPa.

Interpretation: Direction of water movement is set by the sign of $(\Psi_{\text{cell}} - \Psi_{\text{solution}})$, not by solute concentrations alone. Pressure potential lets walled cells (plants, fungi, many algae) maintain positive Ψ_p even when their Ψ_s is strongly negative — this is the molecular basis of turgor pressure, plant rigidity, and the wilting response when soil Ψ drops. Animal cells, which lack a rigid wall, cannot generate positive Ψ_p and so rely on isotonic environments (or active volume regulation) to avoid lysis or crenation.

Source-Governance Checkpoint

Complete the source-governance card for Membrane Structure and Transport before writing the conclusion. Name the source type or model snapshot, record the evidence date or version, decide whether the claim is stable or fast-moving, and write one refresh trigger that would force the interpretation to change. Treat the card as a printed evidence object, not as a live web lookup.

Analysis Questions

- Plot absorbance vs temperature. At approximately what temperature did membrane integrity fail dramatically (sharp increase in absorbance)? What happened to the phospholipid bilayer at this temperature?
- Plot % plasmolysed cells vs [NaCl]. At what concentration does 50% plasmolysis occur (incipient plasmolysis)? This approximates the osmotic potential of the onion cell cytoplasm — what is your estimate in osmol/L?
- In a real beetroot assay, why would rinsing cut discs matter? What confound would exist if the dataset mixed surface-cut leakage with temperature-induced leakage?
- Predict how results would differ if you used a saturated fat membrane (e.g., modeled by adding cholesterol to a liposome) vs a polyunsaturated fat membrane. Which would show damage at a lower temperature?
- Red blood cells placed in 2% NaCl would crenate. Compare this to the plant cell response in 2% NaCl. Why do plant cells plasmolysis (shrink away from the cell wall) instead of simply shrinking like animal cells?

Post-Lab Synthesis

Concept Check (Synthesis): Many cells (especially freshwater protists and human red blood cells in transit through medullary tissue) experience rapid changes in extracellular osmolarity. Combining the lab data with the chapter:

- (a) Compare the volume-regulation strategies of (i) a paramecium in a freshwater pond, (ii) a human red blood cell entering the renal medulla, and (iii) a plant root-hair cell in a soil suddenly saturated with rain. For each, identify the dominant transporter, channel, or structural feature that mediates the response.
- (b) A cell suddenly placed in a strongly hypotonic environment would, without regulation, swell and lyse. Describe two distinct cellular mechanisms by which a non-walled cell can lose solutes or water fast enough to avoid lysis on a seconds-to-minutes timescale, and identify the molecular components involved.
- (c) Propose a quantitative paper-based experiment using model cells with varying SA:V ratios to test whether regulatory volume decrease scales with membrane surface area rather than with cytoplasmic volume. Specify your independent variable, dependent variable, expected pattern, and one control.

Optional Wet-Lab Extension

An instructor may demonstrate membrane leakage or plasmolysis with approved materials, but the paper dataset is the required evidence source. Optional work should be framed as a validation exercise for the model.

Safety and Ethics Notes

Paper-based lab — no beetroot, hot water baths, slides, microscopes, or solutions are required. Optional wet demonstrations require instructor supervision, stain precautions, and heat-safety procedures.

Debrief and Reflection

After you finish the practical work, spend 5–10 minutes in your small group comparing results and discussing the following prompts. Each member should contribute at least one observation before moving to the next prompt:

1. What did your measurements show — compare the group’s results to the textbook’s predictions. Where they diverge, suggest at least one mechanistic explanation before concluding “experimental error.”
2. What would change the outcome — propose one modification to the procedure that would sharpen the measurement or extend the result to a new biological context, and predict what you would observe.
3. One-sentence headline — each student composes a single sentence summarizing the lab’s take-home message, suitable for a tweet. Compare sentences across groups; good headlines are short, quantitative, and mechanistic.
4. Connection back to the textbook — identify one section of section 7 that your data either confirmed or complicated. Cite the specific passage.

Further Reading (Lab)

- Revisit the parent chapter section 7 for the theoretical foundations on which this lab is built.
- Look up any bolded glossary term introduced in the textbook chapter (each has a #gl:term-slug link in the text) — its master definition is in manuscript/glossary.md.
- Explore the appended src/ module that implements the corresponding quantitative model (when applicable) — referenced in the parent chapter’s “Bridge to Computation” subsection.

Module footer: parent chapter \cref{sec:unit_II_membrane_transport}; all numerical quantities in this lab use SI units — see Appendix D — Units, Physical Constants, and Biological Ranges for unit conversions and biological-scale reference values.

Lab — Cell Signaling and Communication

Learning Objectives

This activity accompanies section 8 of the textbook — review that chapter before attempting the exercises below.

- Model the three-stage cell signaling cascade (reception → transduction → response) through a physical simulation
- Analyze how signal amplification occurs through enzymatic cascades
- Evaluate the role of second messengers using a classroom analogy and data interpretation
- Design an experiment to test how a signaling inhibitor disrupts a cellular response

Alignment and Rubric Map

- Outcome 1 (LO1): Interpret the supplied evidence or model output for Cell Signaling and Communication.
- Outcome 2 (LO2): Identify controls and comparison groups that make the claim testable.
- Outcome 3 (LO3): Quantify uncertainty, boundary conditions, or alternative explanations before concluding.
- Outcome 4 (LO4): Transfer the mechanism to a new biological case or public-facing decision.
- Chapter LO coverage: LO1, LO2, LO3, LO4
- Rubric dimensions: evidence; controls; uncertainty; mechanism; transfer. ## Pre-Lab Concept Questions {.unnumbered}

Answer these before starting the investigation — they activate knowledge from the parent chapter.

1. Define a second messenger in one sentence, then give two examples and the upstream receptor class that typically produces each.
2. A growth-factor receptor and a hormone receptor both activate downstream kinases. Distinguish how a receptor tyrosine kinase (RTK) initiates signaling from how a G-protein–coupled receptor (GPCR) initiates signaling, naming at least one molecular event unique to each pathway.
3. Two cell types express the same GPCR yet respond to the same ligand in opposite directions (one secretes, the other contracts). Propose two molecular reasons the downstream effect can differ even when the receptor and ligand are identical.

Lab Context: Cell Signaling and Communication

Cell signaling enables cells to detect and respond to extracellular information. The three stages are: (1) Reception — a ligand binds its receptor (GPCR, RTK, nuclear receptor); (2) Transduction — signal is converted and amplified through a cascade of molecular switches; (3) Response — altered gene expression, enzyme activity, or cytoskeletal change. Amplification is a key feature: one activated receptor can activate hundreds of G proteins, each activating dozens of adenylyate cyclase molecules, each producing thousands of cAMP molecules — giving a cascade amplification of $>10^6$.

In this lab you will simulate and calculate signal amplification through a cascade model, analyze a published cell signaling dose-response dataset, and design an inhibitor experiment.

Paper-Based Materials

Table 543. Alignment and Rubric Map: Item and Quantity.

Item	Quantity
Source-governance card for Cell Signaling and Communication: cell-atlas or imaging source card: sample, assay, cell-state call, perturbation evidence, and uncertainty	1
Signal cascade worksheet (instructor-provided: table with step values)	1
Calculator	1
Graph paper or laptop (for dose-response curve)	1
Colored card tokens (representing signaling molecules): 1 “ligand” card, 10 “G protein” cards, 50 “cAMP” cards, 500 “PKA” cards	1 set
12-well plate or paper diagram of receptor → cascade → response	1

Item	Quantity
Sample dataset: β -adrenergic response (heart rate vs [adrenaline]) (instructor-provided)	1

Paper-Based Investigation

Part A — Signal Amplification Simulation

1. One student is the “ligand”: activate one “receptor” card. Each activated receptor activates 10 G protein cards. Each G protein activates 10 “adenylate cyclase” steps (represented by producing 10 cAMP tokens). Each cAMP activates 5 PKA tokens.
2. Count total active tokens at each level. Record in the amplification table.
3. Calculate total fold amplification from ligand to PKA response.

Part B — Dose-Response Curve Analysis

4. Using the provided dataset of heart rate (bpm) vs [adrenaline] (nM), plot a dose-response curve on semilog paper (log [adrenaline] on x-axis, heart rate on y).
5. Identify the EC₅₀ (concentration producing 50% of maximal response) from your curve.
6. A second curve shows the same response in the presence of propranolol (a β -blocker). Plot both curves; compare EC₅₀ values and maximum responses.

Part C — Inhibitor Experiment Design

7. Design a controlled paper experiment to test whether blocking adenylate cyclase with SQ 22536 would prevent an adrenaline-mediated response. Use provided pathway cards and a simulated response dataset rather than cells or tissue.

Data Recording

Table 544. Alignment and Rubric Map: Signaling level and Molecules activated.

Signaling level	Molecules activated	Fold amplification vs previous step
Ligand	1	—
Receptors activated		
G proteins activated		
cAMP produced		
PKA catalytic subunits activated		
Total amplification (ligand → PKA)		

EC₅₀ without propranolol: _____ nM EC₅₀ with propranolol: _____ nM Shift in EC₅₀: _____ fold

Your inhibitor experiment design (brief):

Evidence and Reproducibility Checklist

- Primary evidence goal: Model signaling response from receptor activation to cellular output.
- Data skill to practice: Read pathway diagrams and infer the effect of agonists, antagonists, or mutations.
- BioSkills emphasis: Modeling and simulation, Process of science.
- Control logic: identify at least one positive control, one negative control, or one baseline comparison before interpreting results.
- Measurement discipline: record units, uncertainty, sample size, and any discarded observation with a reason.
- Mechanistic link: connect one result directly to the parent chapter’s big idea before writing the conclusion.
- Reproducibility check: state one procedural detail that another group would need in order to reproduce the result.

Paper-Based Evidence Upgrade

Before answering the analysis questions, annotate the paper dataset for Cell Signaling and Communication with a reproducibility pass:

Table 545. Alignment and Rubric Map: Evidence check and Student action.

Evidence check	Student action
Control logic	Mark the comparison that functions as the baseline, negative control, or reference case.
Uncertainty	Circle the row, card, diagram feature, or model assumption most likely to change the conclusion.
Model comparison	State whether a simpler rule, null model, or alternative mechanism could explain the same pattern.
Decision threshold	Write the minimum evidence that would make you revise the interpretation.
Reproducibility	Record the exact scoring rule another group would need to reproduce your classification.

Focus note: when you score a signaling case, name the receptor, the dose or stimulus level, the timing of the readout, and any feedback or crosstalk you assumed; treat a live-cell biosensor or optogenetic perturbation trace as the evidence that would change your call. Keep required work paper-based; any material-handling or equipment version belongs only in an optional extension.

Worked Example: Signal Amplification in a Four-Step Kinase Cascade

Problem: A kinase cascade contains four sequential amplification steps. At each step, one active upstream kinase phosphorylates and activates 10 downstream substrate molecules before being inactivated. A single hormone–receptor binding event launches one active kinase at the top of the cascade. How many active terminal effector molecules result from that single binding event, and what fold-change does this represent relative to the input?

Solution: Each step multiplies the active-molecule count by 10. Starting from one active kinase:

- After step 1: $1 \times 10 = 10$ active molecules
- After step 2: $10 \times 10 = 100$ active molecules
- After step 3: $100 \times 10 = 1,000$ active molecules
- After step 4: $1,000 \times 10 = 10,000$ active molecules

Total amplification = $10^4 = 10,000$ -fold. One ligand-binding event produces roughly 10,000 active terminal effectors.

Interpretation: Cascade amplification lets cells respond to very low extracellular ligand concentrations — picomolar hormone levels can drive micromolar intracellular effector levels. The same architecture also means that even modest dysregulation early in the cascade (for example, a kinase that hydrolyses GTP too slowly) is multiplied 10^4 -fold downstream, which is one reason many oncogenes and signaling diseases map to early cascade components.

Source-Governance Checkpoint

Complete the source-governance card for Cell Signaling and Communication before writing the conclusion. Name the source type or model snapshot, record the evidence date or version, decide whether the claim is stable or fast-moving, and write one refresh trigger that would force the interpretation to change. Treat the card as a printed evidence object, not as a live web lookup.

Analysis Questions

1. Calculate the fold amplification your cascade produced. How does this compare to the theoretical amplification cited in the chapter (about 10^6)? What real-world factors account for the difference?
2. Propranolol is a competitive antagonist of the β -adrenergic receptor. Based on your dose-response curves, does it shift the EC_{50} , reduce E_{max} , or both? What does this pattern indicate about mechanism?
3. Steroid hormones such as estrogen can enter cells and bind nuclear receptors directly. Why is this signaling pathway typically slower (minutes to hours) than GPCR cascades (seconds)? What is the cellular destination of the hormone-receptor complex?
4. Tamoxifen is a selective estrogen receptor modulator (SERM) that acts as an antagonist in breast tissue but a partial agonist in bone. Explain how the same molecule can produce opposite effects in different tissues.
5. A mutation makes the Gs protein GTPase-inactive (cannot hydrolyse GTP to GDP). Predict the effect on adenylate cyclase activity, cAMP levels, and PKA activity in the affected cell. What disease would this phenotype resemble?

Post-Lab Synthesis

Concept Check (Synthesis): Many distinct ligands converge on the same second messenger (for example, both glucagon and epinephrine raise hepatic cAMP), yet their downstream physiological effects can be sharply distinguishable. Using evidence from this investigation and the chapter:

- (a) Identify at least three mechanisms cells use to maintain signaling specificity despite sharing second messenger molecules (consider receptor expression, scaffolding, spatial restriction, kinetics, and crosstalk).
- (b) Predict what happens to specificity if a cell loses one of those mechanisms — for example, if a scaffolding protein that tethers PKA to a particular substrate is deleted. Describe one observable phenotype.
- (c) Propose a paper-based experiment using the response-curve data from this lab that would let a student distinguish loss-of-specificity from loss-of-amplification when an inhibitor is added.

Safety and Ethics Notes

No hazardous chemicals in this lab. Card and paper components primarily. If a computer simulation module is used, follow data handling and privacy guidelines for any shared datasets.

Debrief and Reflection

After you finish the practical work, spend 5–10 minutes in your small group comparing results and discussing the following prompts. Each member should contribute at least one observation before moving to the next prompt:

1. What did your measurements show — compare the group’s results to the textbook’s predictions. Where they diverge, suggest at least one mechanistic explanation before concluding “experimental error.”
2. What would change the outcome — propose one modification to the procedure that would sharpen the measurement or extend the result to a new biological context, and predict what you would observe.
3. One-sentence headline — each student composes a single sentence summarizing the lab’s take-home message, suitable for a tweet. Compare sentences across groups; good headlines are short, quantitative, and mechanistic.
4. Connection back to the textbook — identify one section of section 8 that your data either confirmed or complicated. Cite the specific passage.

Further Reading (Lab)

- Revisit the parent chapter section 8 for the theoretical foundations on which this lab is built.
- Look up any bolded glossary term introduced in the textbook chapter (each has a #gl:term-slug link in the text) — its master definition is in manuscript/glossary.md.
- Explore the appended src/ module that implements the corresponding quantitative model (when applicable) — referenced in the parent chapter’s “Bridge to Computation” subsection.

Module footer: parent chapter \cref{sec:unit_II_cell_signaling}; all numerical quantities in this lab use SI units — see Appendix D — Units, Physical Constants, and Biological Ranges for unit conversions and biological-scale reference values.

Lab — Bioenergetics and Cellular Respiration

Learning Objectives

This activity accompanies section 9 of the textbook — review that chapter before attempting the exercises below.

- Interpret CO₂ and O₂ datasets as indicators of cellular respiration rate
- Compare aerobic respiration, fermentation, and the effect of substrate type on respiration rate
- Calculate respiration rate (mL CO₂ per minute per gram of tissue)
- Distinguish the contributions of glycolysis, pyruvate oxidation, and the Krebs cycle to overall ATP yield

Alignment and Rubric Map

- Outcome 1 (LO1): Interpret the supplied evidence or model output for Bioenergetics and Cellular Respiration.
- Outcome 2 (LO2): Identify controls and comparison groups that make the claim testable.
- Outcome 3 (LO3): Quantify uncertainty, boundary conditions, or alternative explanations before concluding.
- Outcome 4 (LO4): Transfer the mechanism to a new biological case or public-facing decision.
- Chapter LO coverage: LO1, LO2, LO3, LO4
- Rubric dimensions: evidence; controls; uncertainty; mechanism; transfer. ## Pre-Lab Concept Questions {.unnumbered}

Answer these before starting the investigation — they activate knowledge from the parent chapter.

1. Write the balanced overall equation for the complete aerobic oxidation of one glucose molecule, including ATP yield. Identify which stage of respiration consumes O₂ and which stage releases CO₂.
2. Define respiratory quotient (RQ) as a ratio of gas-exchange rates, and give the theoretical RQ values for carbohydrate, lipid, and protein substrates.
3. A germinating pea seedling and a dormant pea seed of the same mass sit in identical respirometers at the same temperature. Predict which would show a greater O₂ consumption rate and explain the metabolic basis of the prediction.

Lab Context: Bioenergetics and Cellular Respiration

Cellular respiration converts the chemical energy in organic molecules to ATP. The complete aerobic pathway — glycolysis → pyruvate oxidation → Krebs cycle → oxidative phosphorylation — yields a theoretical maximum of about 30 ATP per glucose. The overall equation is: C₆H₁₂O₆ + 6 O₂ → 6 CO₂ + 6 H₂O + about 30 ATP. CO₂ production rate and O₂ consumption rate can serve as proxies for metabolic rate. In this lab, printed datasets provide model evidence for comparing aerobic respiration, fermentation, and substrate effects.

Paper-Based Materials

Table 546. Alignment and Rubric Map: Item and Quantity.

Item	Quantity
Source-governance card for Bioenergetics and Cellular Respiration: metabolism source card: organism, compartment, condition, measurement method, and flux boundary	1
Fermentation CO ₂ dataset by substrate type	1
Respirometry O ₂ -consumption dataset for active, dormant, and volume-control cases	1
Pathway carbon-and-electron tracing cards	1 set
Calibration and control worksheet	1
Calculator and graph paper	1 each

Paper-Based Investigation

Part A — Yeast Fermentation by Substrate Type

1. Plot the provided CO₂ proxy data for four model conditions: sucrose, glucose, starch, and no-enzyme negative control.
2. Calculate the rate of CO₂ increase for each condition between 0 and 40 minutes.
3. Identify the negative control, the fastest substrate condition, and one alternative explanation that the design rules out.

Part B — Active vs Dormant Tissue Model

4. Use the printed O₂-consumption dataset for active seed tissue, dormant seed tissue, and an inert volume control.
5. Correct the active and dormant readings by subtracting the volume-control displacement.
6. Convert the corrected values to mL O₂ per minute per gram and connect the result to oxidative phosphorylation.

Data Recording

Table 547. Alignment and Rubric Map: Time (min) and Bottle A.

Time (min)	Bottle A	Bottle B	Bottle C	Bottle D
0				
10				
20				
30				
40				

O₂ consumed (germinating peas): _____ mL / 10 min O₂ consumed (dry peas): _____ mL / 10 min O₂ consumed (glass beads): _____ mL / 10 min

Evidence and Reproducibility Checklist

- Primary evidence goal: Estimate energy yield under aerobic and anaerobic conditions.
- Data skill to practice: Track carbon, electrons, and ATP across a pathway.
- BioSkills emphasis: Quantitative reasoning, Modeling and simulation.
- Control logic: identify at least one positive control, one negative control, or one baseline comparison before interpreting results.
- Measurement discipline: record units, uncertainty, sample size, and any discarded observation with a reason.
- Mechanistic link: connect one result directly to the parent chapter’s big idea before writing the conclusion.
- Reproducibility check: state one procedural detail that another group would need in order to reproduce the result.

Paper-Based Evidence Upgrade

Before answering the analysis questions, annotate the paper dataset for Bioenergetics and Cellular Respiration with a reproducibility pass:

Table 548. Alignment and Rubric Map: Evidence check and Student action.

Evidence check	Student action
Control logic	Mark the comparison that functions as the baseline, negative control, or reference case.
Uncertainty	Circle the row, card, diagram feature, or model assumption most likely to change the conclusion.
Model comparison	State whether a simpler rule, null model, or alternative mechanism could explain the same pattern.
Decision threshold	Write the minimum evidence that would make you revise the interpretation.
Reproducibility	Record the exact scoring rule another group would need to reproduce your classification.

Focus note: in a respiration dataset, follow the electrons and protons explicitly — ask which step the measured rate (O₂ uptake, ATP, Δp) actually constrains, and whether the reported P/O or ATP yield holds once shuttle use and proton leak are stated. Keep required work paper-based; any material-handling or equipment version belongs only in an optional extension.

Worked Example: ATP Yield and Gas-Exchange Proxies

Problem: A respirometer containing germinating peas with total mass 15.3 g shows a fluid displacement equivalent to 0.85 mL of O₂ consumed over 10 minutes. A control respirometer containing glass beads of identical volume shows 0.04 mL of displacement over the same 10 minutes (a thermobaric drift correction). The

lab is at 25 °C and 1 atm. (a) Compute the corrected O₂ consumption rate in mL O₂ per minute per gram of pea tissue. (b) Convert that rate into mmol O₂ per minute per gram using the ideal gas law.

Solution:

(a) Corrected O₂ volume over 10 min = 0.85 – 0.04 = 0.81 mL

Rate per minute = 0.81 / 10 = 0.081 mL O₂ / min

Mass-specific rate = 0.081 / 15.3 ≈ 0.00529 mL O₂ / (min·g) ≈ 5.29 × 10⁻³ mL O₂ / (min·g)

(b) Use the ideal gas law in the form $n = PV / (RT)$:

- P = 1 atm
- V = 0.81 mL = 8.1 × 10⁻⁵ L (per minute)
- R = 0.0821 L·atm·mol⁻¹·K⁻¹
- T = 25 + 273.15 = 298.15 K

$n / \text{min} = (1 \times 8.1 \times 10^{-5}) / (0.0821 \times 298.15) \approx 3.31 \times 10^{-6} \text{ mol O}_2 / \text{min}$

Per gram: $3.31 \times 10^{-6} / 15.3 \approx 2.16 \times 10^{-7} \text{ mol O}_2 / (\text{min} \cdot \text{g}) \approx 0.216 \mu\text{mol O}_2 / (\text{min} \cdot \text{g}) \approx 2.16 \times 10^{-4} \text{ mmol O}_2 / (\text{min} \cdot \text{g})$

Interpretation: The glass-bead control subtracts apparent gas-volume change that is not biological — thermal expansion, slow leaks, capillary creep. Without it, the measurement would overstate respiration by about 5%, which would matter when comparing treatments. Mass-specific rates (per gram of tissue) let students compare seeds of different sizes on equal footing, and converting to molar units lets them connect the measurement to stoichiometric equations for glucose oxidation — for example, predicting CO₂ production from a known RQ.

Source-Governance Checkpoint

Complete the source-governance card for Bioenergetics and Cellular Respiration before writing the conclusion. Name the source type or model snapshot, record the evidence date or version, decide whether the claim is stable or fast-moving, and write one refresh trigger that would force the interpretation to change. Treat the card as a printed evidence object, not as a live web lookup.

Analysis Questions

1. Which substrate model produced the fastest CO₂ increase — sucrose or glucose? Explain using the concept of hydrolysis and substrate entry into glycolysis.
2. Why did the starch treatment model produce less CO₂ than sucrose? How does this relate to enzyme availability for substrate breakdown?
3. The active-tissue model showed higher O₂ consumption than the dormant-tissue model. Explain at which stage of respiration this O₂ is consumed and write the half-reaction involved.
4. Facultative anaerobe models can continue producing CO₂ with little O₂ available. Predict whether CO₂ production would stop, slow, or continue in a no-O₂ scenario. Explain using fermentation pathways and the role of NAD⁺ regeneration.
5. A marathon runner transitions from aerobic to anaerobic metabolism past about 80% VO₂max. Explain what metabolic shift occurs in muscle cells, what molecule accumulates (not lactic acid — what is the actual molecule?), and why fatigue results.

Post-Lab Synthesis

Concept Check (Synthesis): Textbook stoichiometry suggests roughly 30–32 ATP per glucose oxidised aerobically, but the actual yield measured in mitochondria is typically lower. Integrating the gas-exchange data from this lab with the chapter:

- (a) Explain how the P/O ratio (ATP synthesized per oxygen atom reduced) and proton leak across the inner mitochondrial membrane each reduce the realized ATP yield below the textbook maximum. Identify one molecular feature of the mitochondrion that influences each.
- (b) During increasing exercise intensity, an athlete transitions from primarily aerobic to mixed aerobic–anaerobic metabolism. Describe the metabolic signals that drive this transition, the resulting change in the RQ measured at the mouth, and the trade-off between ATP yield per glucose and ATP production rate.
- (c) A respirometer measurement gives RQ ≈ 1.0 for one batch of seeds and RQ ≈ 0.7 for another batch of the same species. Propose two biological explanations for the difference and one paper-based experiment using your existing investigation that would distinguish between them.

Optional Demonstration Extension

An instructor may demonstrate fermentation or respirometry with approved materials, but the required lab uses printed datasets. Treat any demonstration as a calibration or validation exercise rather than the source of required evidence.

Safety and Ethics Notes

Paper-based lab — no live cultures, balloons, indicators, seeds, or sealed respirometers are required. Optional demonstrations require instructor supervision and standard classroom safety procedures.

Debrief and Reflection

After you finish the practical work, spend 5–10 minutes in your small group comparing results and discussing the following prompts. Each member should contribute at least one observation before moving to the next prompt:

1. What did your measurements show — compare the group’s results to the textbook’s predictions. Where they diverge, suggest at least one mechanistic explanation before concluding “experimental error.”
2. What would change the outcome — propose one modification to the procedure that would sharpen the measurement or extend the result to a new biological context, and predict what you would observe.
3. One-sentence headline — each student composes a single sentence summarizing the lab’s take-home message, suitable for a tweet. Compare sentences across groups; good headlines are short, quantitative, and mechanistic.
4. Connection back to the textbook — identify one section of section 9 that your data either confirmed or complicated. Cite the specific passage.

Further Reading (Lab)

- Revisit the parent chapter section 9 for the theoretical foundations on which this lab is built.
- Look up any bolded glossary term introduced in the textbook chapter (each has a `#gl:term-slug` link in the text) — its master definition is in `manuscript/glossary.md`.
- Explore the appended `src/` module that implements the corresponding quantitative model (when applicable) — referenced in the parent chapter’s “Bridge to Computation” subsection.

*Module footer: parent chapter \cref{sec:unit_III_bioenergetics_and_respiration}; all numerical quantities in this lab use SI units — see **Appendix D — Units, Physical Constants, and Biological Ranges** for unit conversions and biological-scale reference values.*

Lab — Photosynthesis

This activity accompanies section 10 of the textbook — review that chapter before attempting the exercises below.

Learning Objectives

- Design and analyze an experiment to quantify photosynthesis rates using a simulated leaf-disc dataset
- Formulate testable hypotheses about how light wavelength and intensity affect photosynthesis
- Identify independent, dependent, and controlled variables in experimental designs
- Analyze experimental data using basic statistical methods and data visualization
- Write a brief scientific report with hypothesis, methods, results, and conclusion

Alignment and Rubric Map

- Outcome 1 (LO1): Interpret the supplied evidence or model output for Photosynthesis.
- Outcome 2 (LO2): Identify controls and comparison groups that make the claim testable.
- Outcome 3 (LO3): Quantify uncertainty, boundary conditions, or alternative explanations before concluding.
- Outcome 4 (LO4): Transfer the mechanism to a new biological case or public-facing decision.
- Chapter LO coverage: LO1, LO2, LO3, LO4
- Rubric dimensions: evidence; controls; uncertainty; mechanism; transfer. ## Pre-Lab Concept Questions {.unnumbered}

Answer these before starting the investigation — they activate knowledge from the parent chapter.

1. Write the net equation for the light-dependent reactions, identifying each input (water, NADP⁺, ADP + Pi, photons) and each output (O₂, NADPH, ATP). Indicate which step releases molecular oxygen.
2. Describe what RuBisCO catalyses, naming its substrate, its primary product, and the cycle (Calvin–Benson) in which the reaction sits. Identify one biochemical feature that makes RuBisCO an inefficient enzyme relative to other carbon-fixation enzymes.
3. At very low light, a leaf consumes more CO₂ in respiration than it fixes in photosynthesis. Define the light compensation point in terms of net gas exchange, and predict whether a shade-adapted plant or a sun-adapted plant would have a lower light compensation point.

Pre-Lab Inquiry Questions

Complete these questions before coming to lab. Use your textbook and additional research to inform your hypotheses.

1. Hypothesis Formation: Based on the absorption spectra of chlorophyll a and b, predict which color of light (red, blue, green, or clear) will result in the fastest photosynthesis rate. Write a clear, testable hypothesis statement.
2. Experimental Design: What is the independent variable in this experiment? What is the dependent variable? List at least 5 variables that should be controlled to ensure a fair test.
3. Scientific Context: The Ruben & Kamen (1941) experiment used ¹⁸O-labeled water to prove that oxygen released during photosynthesis comes from water, not carbon dioxide. Why was this experiment groundbreaking? How did it change our understanding of photosynthesis?
4. Quantitative Reasoning: Calculate the energy per photon for red light (λ = 700 nm) and blue light (λ = 450 nm). Which has more energy? How might this affect photosynthesis efficiency?
5. Real-World Application: Commercial greenhouses often use LED grow lights. Based on your knowledge of photosynthesis, what light spectrum would you recommend for maximizing plant growth? Consider both energy efficiency and photosynthetic efficiency.

Lab Context: Photosynthesis

Photosynthesis converts light energy to chemical energy: 6 CO₂ + 6 H₂O + light → C₆H₁₂O₆ + 6 O₂. The light-dependent reactions in the thylakoid membrane split water (photolysis) and generate NADPH and ATP; the Calvin cycle in the stroma uses NADPH and ATP to fix CO₂ into G3P and ultimately glucose. A floating leaf-disc assay can estimate photosynthesis because O₂ accumulation increases buoyancy; here, an image-and-data packet provides the same ET₅₀ evidence without requiring plant material, bicarbonate solution, lamps, or cutting tools.

Paper-Based Materials

Table 549. Alignment and Rubric Map: Item and Quantity.

Item	Quantity
Source-governance card for Photosynthesis: metabolism source card: organism, compartment, condition, measurement method, and flux boundary	1
Simulated leaf-disc time-course dataset by light color	1
Light-intensity and inverse-square worksheet	1
Chlorophyll absorption spectrum packet	1
Experimental-design card set: controls, variables, confounds	1
Calculator or optional Python REPL with this project installed	1
Spreadsheet software (Excel/Google Sheets)	1

Paper-Based Investigation

Part 1: Experimental Design and Hypothesis Testing

1. Formulate Your Hypothesis: Based on your pre-lab research, write a clear hypothesis about how light color will affect photosynthesis rate. Example: “If photosynthesis is driven by chlorophyll absorption, then red light will result in a faster photosynthesis rate (lower ET₅₀) than green light because chlorophyll absorbs red wavelengths more efficiently.”
2. Identify Variables:

• Independent variable: Light color (red, blue, green, clear)

• Dependent variable: ET₅₀ (time for 50% of discs to float)

• Controlled variables: Temperature, CO₂ proxy concentration, disc size in the model, initial disc status, light-source distance, etc.
3. Set Up Controls: Why is it important to have a clear filter (white light) control? What other controls could you include?
4. Audit the Simulated Assay: Use the method card to check whether disc size, starting status, CO₂ availability, temperature, and light distance are controlled across most conditions.
5. Data Collection:

• Read the number of floating discs at 1-minute intervals for 20 minutes from the dataset

• Use the three provided replicate runs for each condition

• Calculate ET₅₀ for each replicate using linear interpolation or the formula: $ET_{50} = (t_2 - t_1) \times (5 - n_1) / (n_2 - n_1) + t_1$

Part 2: Computational Biology Exercise — Data Analysis with Python

Optional computational check: run this self-contained Python snippet from the project root. It uses tested `src/biology` modules and requires no external notebook or CSV file.

Compare your light-response table with the project photosynthesis model.

```
from biology.botany import photosynthesis_rate, light_response_curve

for light in (0, 100, 500, 1000):
    rate = photosynthesis_rate(light, max_rate_umol_C02_m2_s=22.0)
    print(light, round(rate, 2))

curve = light_response_curve(n_points=5)
print("first/last model points:", curve[0], curve[-1])
```


Part 3: Light Intensity and Inverse-Square Law

6. Intensity Experiment: Use the provided white-light dataset at three distances: 10 cm, 20 cm, and 40 cm. Record ET₅₀ at each distance.
7. Data Analysis: Plot ET₅₀ against 1/d² (relative intensity). Is the relationship linear? The linearity should hold primarily up to light saturation; beyond that, rate is limited by Calvin-cycle throughput, not light.
8. Calculate Photon Flux: If a point light source emits 1500 μmol photons/m²/s at 20 cm, what is the photon flux at 10 cm and 40 cm? (Assume inverse-square law applies to point sources.)

Part 4: CAM vs C3 Comparison (Extended Investigation)

8. Design an Alternative Experiment: Design a paper protocol to compare photosynthesis rates between a C3 plant model and a CAM plant model. Consider how CAM plants fix CO₂ at night and release it during the day. What simulated measurements would you request? How would you control variables?
9. Hypothesis: Predict what you would observe if you measured O₂ production or CO₂ uptake in light vs dark for both plant types.

Data Recording

Table 550. Part 4: CAM vs C3 Comparison (Extended Investigation): Time (min) and Clear (white).

Time (min)	Clear (white)	Red filter	Blue filter	Green filter
0	0/10	0/10	0/10	0/10
2				
4				
6				
8				
10				
15				
20				

ET₅₀ (time for 5 discs to float): Clear __ Red __ Blue __ Green __

Light intensity experiment: Part 4: CAM vs C3 Comparison (Extended Investigation): Distance (cm) and Relative Intensity (1/d²).
{#tbl:unit_III_photosynthesis_part_4_cam_vs_c3_comparison_extended_investigation_2} | Distance (cm) | Relative Intensity (1/d²) | ET₅₀ | | ____
____ | _____ | ____ | | 10 | 1.00 | | 20 | 0.25 | | 40 | 0.0625 | |

Evidence and Reproducibility Checklist

- Primary evidence goal: Measure or model photosynthetic rate under changing light or carbon conditions.
- Data skill to practice: Interpret light-response and carbon-fixation data.
- BioSkills emphasis: Quantitative reasoning, Modeling and simulation.
- Control logic: identify at least one positive control, one negative control, or one baseline comparison before interpreting results.
- Measurement discipline: record units, uncertainty, sample size, and any discarded observation with a reason.
- Mechanistic link: connect one result directly to the parent chapter’s big idea before writing the conclusion.
- Reproducibility check: state one procedural detail that another group would need in order to reproduce the result.

Paper-Based Evidence Upgrade

Before answering the analysis questions, annotate the paper dataset for Photosynthesis with a reproducibility pass:

Table 551. Part 4: CAM vs C3 Comparison (Extended Investigation): Evidence check and Student action.

Evidence check	Student action
Control logic	Mark the comparison that functions as the baseline, negative control, or reference case.

Evidence check	Student action
Uncertainty	Circle the row, card, diagram feature, or model assumption most likely to change the conclusion.
Model comparison	State whether a simpler rule, null model, or alternative mechanism could explain the same pattern.
Decision threshold	Write the minimum evidence that would make you revise the interpretation.
Reproducibility	Record the exact scoring rule another group would need to reproduce your classification.

Focus note: in a photosynthesis dataset, name the limiting factor — ask whether a rate change reflects light, CO₂ supply/stomata, or RuBisCO/photorespiration, and test whether a leaf- or chloroplast-scale gain would survive whole-plant water and sink limits. Keep required work paper-based; any material-handling or equipment version belongs only in an optional extension.

Worked Example: Net O2 Evolution Above the Light Compensation Point

Problem: A leaf absorbs photosynthetically active photons at a flux of 200 μmol photons m⁻² s⁻¹. Its quantum yield for oxygen evolution is approximately 0.10 mol O₂ per mol photons (a typical value for healthy C3 leaves under non-saturating light). The leaf’s light compensation point — the photon flux at which gross photosynthetic O₂ evolution equals respiratory O₂ consumption — is 20 μmol photons m⁻² s⁻¹. (a) Compute the gross O₂ evolution rate at 200 μmol photons m⁻² s⁻¹. (b) Compute the respiratory O₂ consumption rate (assuming respiration is the same in light and dark, an approximation). (c) Compute the net O₂ evolution rate.

Solution:

- (a) Gross O₂ evolution = (quantum yield) × (photon flux)
- = 0.10 × 200 = 20 μmol O₂ m⁻² s⁻¹
- (b) At the light compensation point, gross O₂ evolution = respiratory O₂ consumption.
- Respiratory rate ≈ 0.10 × 20 = 2 μmol O₂ m⁻² s⁻¹
- (c) Net O₂ evolution = gross evolution – respiratory consumption
- = 20 – 2 = 18 μmol O₂ m⁻² s⁻¹

Interpretation: At a 200 μmol photons m⁻² s⁻¹ flux — roughly one-tenth of full sunlight — this leaf shows a net positive O₂ output of 18 μmol m⁻² s⁻¹, about 90% of gross evolution. Respiration is a constant draw that the plant must exceed to grow; the compensation point sets the lower limit of viable canopy position. Note that the assumption “respiration is unchanged in light” is approximate — in reality, photorespiration and possibly partial mitochondrial inhibition in the light shift the balance, so net evolution computed this way is a useful upper estimate rather than an exact prediction.

Source-Governance Checkpoint

Complete the source-governance card for Photosynthesis before writing the conclusion. Name the source type or model snapshot, record the evidence date or version, decide whether the claim is stable or fast-moving, and write one refresh trigger that would force the interpretation to change. Treat the card as a printed evidence object, not as a live web lookup.

Analysis Questions

1. Which wavelength produced the fastest disc floating (lowest ET₅₀)? Which produced the slowest? How does this correlate with the absorption spectrum of chlorophyll a and b? Was your hypothesis supported?
2. Why were discs first made to sink? What gas was removed during vacuum infiltration, and why does replacing it with CO₂-solution cause sinking?
3. As light intensity increases, photosynthesis rate increases to a plateau (light saturation point). Identify the limiting factor at each side of this curve and explain at the biochemical level.
4. The Calvin cycle does not directly require light. Why would removing light quickly halt the Calvin cycle reactions? (Hint: consider the fate of NADPH and ATP between the two stages.)

5. A crop scientist wants to maximize yield using artificial grow lights. Using your results, recommend the optimal light wavelength(s) and explain. What other environmental factors (CO₂, temperature, water) should she simultaneously optimize, and what law of limiting factors applies?

Post-Lab Synthesis

Concept Check (Synthesis): C3 photosynthesis becomes increasingly inefficient at high temperatures because photorespiration consumes a larger fraction of fixed carbon. C4 photosynthesis (e.g. maize, sugarcane) concentrates CO₂ around RuBisCO using a PEP-carboxylase pre-fixation step. Integrating the lab results with the chapter:

- (a) Explain in mechanistic terms why a C4 plant maintains a higher net carbon gain than a C3 plant in a hot, bright, low-humidity environment, referring specifically to (i) the oxygenation activity of RuBisCO, (ii) stomatal water loss, and (iii) the energetic cost of running the C4 pump.
- (b) Predict which of two plants — a C3 wheat or a C4 maize — would show a lower light compensation point under cool, dim, humid morning conditions, and which would show a higher net carbon gain under hot, bright, dry midday conditions. Justify each prediction quantitatively wherever possible.
- (c) A horticulturist proposes growing C4 maize in a cool, humid greenhouse to capitalise on its photosynthetic efficiency. Evaluate the proposal, identifying at least one disadvantage that emerges when C4 plants are grown outside their typical climate envelope, and propose one paper-based experiment that would test the trade-off using gas-exchange data of the kind collected in this lab.

Extension Analysis Questions

6. Rising atmospheric CO₂ (from about 280 ppm pre-industrial to >420 ppm today) is predicted to increase C3 photosynthesis more than C4. Explain why, using your understanding of RuBisCO’s oxygenation reaction (photorespiration) and the CO₂-concentrating mechanism in C4 plants.
7. Plants grown under monochromatic green light develop abnormally (etiolated). Given that green light is weakly absorbed by chlorophyll, explain why green leaves appear green and why gardeners with LED grow lights generally select red + blue mixtures rather than “full-spectrum” (which wastes energy in the green).
8. The Hill reaction (Robin Hill, 1939) demonstrated that isolated chloroplasts can reduce artificial electron acceptors (e.g., DCPIP) in light, without CO₂ fixation. Describe what this result proved about the separability of the light and dark reactions — and why it was historically transformative for photosynthesis research.
9. Statistical Analysis: Calculate the standard error of the mean (SEM) for each light condition. Construct 95% confidence intervals. Are the differences between light conditions statistically significant based on your ANOVA?
10. Experimental Error Analysis: What are three potential sources of error in this experiment? How could you modify the procedure to reduce each source of error?

Group Project Extension (Multi-Session)

Design a Data Study to Test the Effect of Temperature on Photosynthesis

This project will span 2-3 lab sessions:

- Session 1: Research Question and Hypothesis - How does temperature affect the rate of photosynthesis? - What enzymes are involved? What is the optimal temperature range for these enzymes? - Write a detailed paper protocol to test temperature effects using provided ET₅₀ datasets or simulation cards
- Session 2: Data Collection - Analyze the provided ET₅₀ data at different temperatures - Include proper controls and replicates
- Session 3: Data Analysis and Presentation - Analyze your data using statistical methods - Create a scientific poster or presentation - Compare your results to the Q₁₀ rule for temperature effects on biochemical reactions

Real-World Problem Solving: Climate Change and Photosynthesis

Case Study: Rising CO₂ and Plant Productivity

Very high-emissions scenarios can push atmospheric CO₂ toward roughly 800-1000 ppm by 2100, while lower-emissions pathways remain far below that range [Intergovernmental Panel on Climate Change, 2021]. While C3 plants may benefit from CO₂ fertilization under controlled conditions, temperature, water availability, nutrient limitation, ozone exposure, pests, and sink demand often constrain the effect in real ecosystems and farms.

- 1. Research Task: Investigate the concept of CO₂ fertilization. Which plant types (C3 vs C4) benefit more? What are the limitations of this effect in natural ecosystems?
- 2. Ethical Consideration: Should we rely on enhanced plant growth to offset carbon emissions? What are the potential ecological consequences of artificially increasing CO₂ levels in forests or agricultural systems?

3. Policy Proposal: Design a policy that balances the need for carbon sequestration through plant growth with the preservation of biodiversity and ecosystem function.

Optional Wet-Lab Extension

An instructor may run a floating leaf-disc demonstration with approved materials, but the required lab uses the simulated dataset and design audit. Optional work should be framed as validating the paper model.

Safety and Ethics Notes

Paper-based lab — no plant material, cutting tools, bicarbonate solution, cups, hot lamps, or wet materials are required. Optional demonstrations require instructor supervision, eye-comfort precautions around bright lights, and ordinary tool safety.

Debrief and Reflection

After you finish the practical work, spend 5–10 minutes in your small group comparing results and discussing the following prompts. Each member should contribute at least one observation before moving to the next prompt:

1. What did your measurements show — compare the group’s results to the textbook’s predictions. Where they diverge, suggest at least one mechanistic explanation before concluding “experimental error.”
2. What would change the outcome — propose one modification to the procedure that would sharpen the measurement or extend the result to a new biological context, and predict what you would observe.
3. One-sentence headline — each student composes a single sentence summarizing the lab’s take-home message, suitable for a tweet. Compare sentences across groups; good headlines are short, quantitative, and mechanistic.
4. Connection back to the textbook — identify one section of section 10 that your data either confirmed or complicated. Cite the specific passage.
5. Experimental Design Reflection: What was the strongest aspect of your experimental design? What would you change if you could repeat the experiment?

Further Reading (Lab)

- Revisit the parent chapter section 10 for the theoretical foundations on which this lab is built.
- Look up any bolded glossary term introduced in the textbook chapter (each has a #gl:term-slug link in the text) — its master definition is in manuscript/glossary.md.
- Explore the Python code in src/biology/biochemistry/biochemistry.py for photosynthesis-related calculations.
- Use the self-contained Part 2 snippet as the computational template; it runs against tested project modules without external notebooks or CSV files.

Lab — Metabolic Integration and Regulation

This activity accompanies section 11 of the textbook — review that chapter before attempting the exercises below.

Learning Objectives

- Design and execute a glucose tolerance test (GTT) simulation to analyze metabolic regulation
- Formulate testable hypotheses about how insulin and glucagon regulate blood glucose
- Identify independent, dependent, and controlled variables in metabolic experiments
- Analyze experimental data using area under the curve (AUC) and statistical methods
- Write a brief scientific report with hypothesis, methods, results, and conclusion

Alignment and Rubric Map

- Outcome 1 (LO1): Interpret the supplied evidence or model output for Metabolic Integration and Regulation.
- Outcome 2 (LO2): Identify controls and comparison groups that make the claim testable.
- Outcome 3 (LO3): Quantify uncertainty, boundary conditions, or alternative explanations before concluding.
- Outcome 4 (LO4): Transfer the mechanism to a new biological case or public-facing decision.
- Chapter LO coverage: LO1, LO2, LO3, LO4
- Rubric dimensions: evidence; controls; uncertainty; mechanism; transfer. ## Pre-Lab Concept Questions {.unnumbered}

Answer these before starting the investigation — they activate knowledge from the parent chapter.

1. Describe in one paragraph how insulin promotes glycogen synthesis in the liver, naming at least two enzymes whose activity changes and the direction of each change.
2. Explain what AMPK senses at the molecular level and identify two downstream pathways AMPK activates and one it suppresses when cellular energy charge is low.
3. A healthy person eats a high-carbohydrate meal. Predict the qualitative time course of insulin, glucagon, blood glucose, and hepatic glycogen content over the four hours that follow, and sketch the expected order in which each crosses its peak.

Pre-Lab Inquiry Questions

Complete these questions before coming to lab. Use your textbook and additional research to inform your hypotheses.

1. Hypothesis Formation: Based on your understanding of insulin and glucagon, predict how a healthy individual’s blood glucose would respond to a glucose challenge compared to a type 2 diabetic. Write a clear, testable hypothesis.
2. Experimental Design: What is the independent variable in a glucose tolerance test? What is the dependent variable? List at least 5 variables that should be controlled to ensure a fair test.
3. Scientific Context: The glucose tolerance test is a clinical diagnostic tool. Why is the area under the curve (AUC) an important metric? What does a larger AUC indicate about metabolic health?
4. Quantitative Reasoning: If a normal person’s blood glucose peaks at 30 minutes and returns to baseline by 120 minutes, while a diabetic’s peaks at 60 minutes and remains elevated at 120 minutes, what does this tell you about insulin secretion and sensitivity?
5. Real-World Application: Metformin is a first-line drug for type 2 diabetes. Based on your knowledge of metabolic regulation, how might metformin work? Consider its effects on AMP:ATP ratio and downstream targets.

Lab Context: Metabolic Integration and Regulation

Metabolic integration means that pathways (glycolysis, gluconeogenesis, β -oxidation, glycogen synthesis) are coordinated by hormonal signals and allosteric regulators, not running independently. Insulin (released postprandially) activates GLUT4 translocation, glycogen synthase, and fatty acid synthesis; it inhibits gluconeogenesis and lipolysis. Glucagon (released during fasting) does the reverse. PFK-1 is the key allosteric valve of glycolysis: activated by AMP, ADP, and fructose-2,6-bisphosphate; inhibited by ATP and citrate.

In this data-analysis lab you will interpret simulated glucose tolerance test data from three subjects (normal, pre-diabetic, type 2 diabetic) and model the allosteric regulation of PFK-1.

Paper-Based Materials

Table 552. Alignment and Rubric Map: Item and Quantity.

Item	Quantity
Source-governance card for Metabolic Integration and Regulation: metabolism source card: organism, compartment, condition, measurement method, and flux boundary	1
GTT dataset (instructor-provided, printed or digital)	1 per student
Graph paper or laptop with spreadsheet software	1
Calculator	1
PFK-1 activity vs [fructose-2,6-BP] graph (provided)	1
Colored pencils (3 colors)	1 set
Calculator or optional Python REPL with this project installed	1
Ruler	1

Paper-Based Investigation

Part 1: Glucose Tolerance Test Analysis

1. Formulate Your Hypothesis: Based on your pre-lab research, write a hypothesis about how the GTT curves will differ between normal, pre-diabetic, and diabetic subjects.
2. Identify Variables:

• Independent variable: Subject group (normal, pre-diabetic, type 2 diabetic)

• Dependent variable: Blood glucose concentration (mM) over time

• Controlled variables: Glucose dose, timing of measurements, subject age/fasting status, etc.
3. Set Up Controls: Why is it important to have a normal control group? What other controls could you include in a clinical GTT study?
4. Data Analysis:

• Plot blood glucose (mM) vs time (min, 0–120 min) for the three subjects on the same graph

• Annotate key events: glucose ingestion (t = 0), peak blood glucose, return to baseline

• Calculate AUC for each subject using the trapezoid rule at 30-minute intervals

Part 2: Computational Biology Exercise — Statistical Analysis with Python

Optional computational check: run this self-contained Python snippet from the project root. It uses tested `src/biology` modules and requires no external notebook or CSV file.

Use the biochemical models to anchor the class discussion in measured quantities.

```
from biology.biochemistry import atp_free_energy, glycolysis_summary, michaelis_menten

glycolysis = glycolysis_summary()
rate = michaelis_menten(substrate_conc=2.0, Vmax=10.0, Km=2.0)
atp = atp_free_energy()

print("net ATP:", glycolysis.net_atp)
print("half-saturation rate:", round(rate.reaction_rate, 2))
print("ATP hydrolysis ΔG:", round(atp, 2))
```

Part 3: Allosteric Regulation Modeling

5. Design an Alternative Data Study: Instead of just analyzing provided data, design a paper experiment to test how different concentrations of fructose-2,6-bisphosphate affect PFK-1 activity. What hypothesis would you test? What concentrations would you request in the dataset?
6. Hypothesis: Predict the shape of the dose-response curve. Would it be linear, sigmoidal, or something else? Why?

Data Recording

Table 553. Part 3: Allosteric Regulation Modeling: Time (min) and Subject A BG (mM).

Time (min)	Subject A BG (mM)	Subject B BG (mM)	Subject C BG (mM)
0	4.5	5.7	7.0
30	6.8	9.2	12.4
60	5.9	8.5	13.1
90	5.1	7.3	11.8
120	4.6	6.4	10.5

AUC Subject A: ____ mM·min
AUC Subject B: ____ mM·min
AUC Subject C: ____ mM·min

PFK-1 at 0 μ M fructose-2,6-BP: ____; $K_{0.5}$: ____; at 10 μ M: ____

Evidence and Reproducibility Checklist

- Primary evidence goal: Compare metabolic responses across nutrient and hormone conditions.
- Data skill to practice: Use pathway evidence to infer which metabolic state or tissue is active.
- BioSkills emphasis: Quantitative reasoning, Modeling and simulation.
- Control logic: identify at least one positive control, one negative control, or one baseline comparison before interpreting results.
- Measurement discipline: record units, uncertainty, sample size, and any discarded observation with a reason.
- Mechanistic link: connect one result directly to the parent chapter’s big idea before writing the conclusion.
- Reproducibility check: state one procedural detail that another group would need in order to reproduce the result.

Paper-Based Evidence Upgrade

Before answering the analysis questions, annotate the paper dataset for Metabolic Integration and Regulation with a reproducibility pass:

Table 554. Part 3: Allosteric Regulation Modeling: Evidence check and Student action.

Evidence check	Student action
Control logic	Mark the comparison that functions as the baseline, negative control, or reference case.
Uncertainty	Circle the row, card, diagram feature, or model assumption most likely to change the conclusion.
Model comparison	State whether a simpler rule, null model, or alternative mechanism could explain the same pattern.
Decision threshold	Write the minimum evidence that would make you revise the interpretation.
Reproducibility	Record the exact scoring rule another group would need to reproduce your classification.

Focus note: in an integrated-metabolism dataset, separate flux from pool size — ask whether isotope-tracer or rate evidence supports each directional claim, and pin every result to a fed/fasted state, tissue, and time window before generalizing. Keep required work paper-based; any material-handling or equipment version belongs only in an optional extension.

Worked Example: How Long Would Liver Glycogen Alone Last in a Fast?

Problem: Estimate, for a 70 kg adult at rest with a basal metabolic rate (BMR) of 1,500 kcal / day, how long liver glycogen stores alone would meet whole-body energy demand if no other fuel were used. Compare to the energy stored as adipose triglyceride. Use the following typical values: liver glycogen mass \approx 100 g (energy density \approx 4 kcal / g); adipose triglyceride mass \approx 15 kg (energy density \approx 9 kcal / g).

Solution:

Step 1 — Energy in liver glycogen:

- $100\text{ g} \times 4\text{ kcal / g} = 400\text{ kcal}$

Step 2 — Time supported at rest if glycogen were the sole fuel source:

- $400\text{ kcal} \div 1,500\text{ kcal / day} \approx 0.27\text{ day} \approx 6.4\text{ hours}$

Step 3 — Energy in adipose triglyceride:

- $15\text{ kg} = 15,000\text{ g}; 15,000\text{ g} \times 9\text{ kcal / g} = 135,000\text{ kcal}$

Step 4 — Time supported at rest by fat stores:

- $135,000\text{ kcal} \div 1,500\text{ kcal / day} \approx 90\text{ days}$

Step 5 — Ratio: fat reserves contain roughly $135,000 / 400 \approx 340$ times more energy than liver glycogen.

Interpretation: Liver glycogen would support a small fraction of one day at rest. This is why a 24-hour fast forces the liver to switch substantially toward gluconeogenesis (using lactate, glycerol, glucogenic amino acids) and why adipose lipolysis and ketogenesis become quantitatively important within roughly a day of food deprivation. Tissue-specific glucose dependence (notably the brain, which uses about 20% of BMR and prefers glucose) is what compels the body to defend blood glucose by mobilizing every substrate that can feed gluconeogenesis or ketogenesis once glycogen is depleted.

Source-Governance Checkpoint

Complete the source-governance card for Metabolic Integration and Regulation before writing the conclusion. Name the source type or model snapshot, record the evidence date or version, decide whether the claim is stable or fast-moving, and write one refresh trigger that would force the interpretation to change. Treat the card as a printed evidence object, not as a live web lookup.

Analysis Questions

1. Based on the GTT data, which AUC threshold might a clinician use to diagnose type 2 diabetes? How does the shape of Subject C’s curve differ from Subject A’s, and what does this indicate about β -cell insulin secretion capacity?
2. Subject B is pre-diabetic. Suggest two lifestyle interventions that would shift Subject B’s GTT curve toward Subject A’s profile. For each, identify the specific metabolic pathway or hormone axis restored.
3. In the post-meal state (high insulin), what happens to hepatic fructose-2,6-bisphosphate levels? Trace: insulin \rightarrow PFK-2 phosphorylation state \rightarrow [fructose-2,6-BP] \rightarrow PFK-1 activity \rightarrow glycolysis rate.
4. During intense exercise, AMP levels spike. Using the allosteric model, predict and explain the combined effect of elevated AMP and elevated fructose-2,6-BP on glycolytic flux in exercising muscle.
5. Metformin, the first-line drug for type 2 diabetes, inhibits Complex I of the mitochondrial electron transport chain, increasing the AMP:ATP ratio. Using your metabolic knowledge, predict at least three downstream effects of elevated AMP: (a) on PFK-1; (b) on glycogen synthase; (c) on gluconeogenesis. Does this make metabolic sense as a diabetes treatment?

Post-Lab Synthesis

- Concept Check (Synthesis):** Compare metabolic responses to a 24-hour fast in two individuals: (i) a metabolically healthy adult and (ii) a patient with untreated type 1 diabetes (effectively zero circulating insulin). Use the GTT/AUC data and the chapter:
- (a) For the healthy adult, describe the predicted time course of blood glucose, insulin, glucagon, free fatty acids, and ketone bodies over the 24 hours. Identify the key hormonal switch that initiates lipolysis and ketogenesis.
 - (b) For the type 1 diabetic, predict how each of the same variables would differ — and explain why, in molecular terms, the absence of insulin removes a brake on lipolysis and ketogenesis even when blood glucose is elevated.

- (c) Use your prediction in (b) to explain why diabetic ketoacidosis is a medical emergency in this scenario. Distinguish it carefully from physiological ketosis seen during normal prolonged fasting in a healthy individual, identifying the variable that crosses a pathological threshold and the mechanism that drives the crossing.

Extension Analysis Questions

6. Statistical Analysis: Calculate the standard error of the mean (SEM) for each subject group. Construct 95% confidence intervals. Are the differences between groups statistically significant based on your ANOVA?
7. Experimental Error Analysis: What are three potential sources of error in this data analysis? How could you modify the procedure to reduce each source of error?
8. Experimental Design: If you were to design a follow-up experiment to distinguish between insulin resistance and β -cell dysfunction in the pre-diabetic subject, what would you measure? How would you interpret the results?

Group Project Extension (Multi-Session)

Design a Metabolic Syndrome Risk Assessment Tool

This project will span 2-3 lab sessions:

- Session 1: Research Question and Hypothesis - What factors contribute to metabolic syndrome (obesity, hypertension, high blood glucose, dyslipidemia)? - How can we use simple measurements to assess risk? - Write a detailed protocol for assessing metabolic health in a human population
- Session 2: Data Collection and Analysis - Use de-identified public datasets or fully simulated classroom data - Calculate risk scores based on waist circumference, blood pressure, fasting glucose, triglycerides, HDL - Analyze correlations between different risk factors
- Session 3: Tool Development and Presentation - Develop a simple risk assessment tool (questionnaire or calculator) - Validate it against known metabolic syndrome criteria - Create a scientific poster or presentation

Real-World Problem Solving: Metabolic Diseases

Case Study: Type 2 Diabetes Prevention

Type 2 diabetes is largely preventable through lifestyle modifications, yet incidence continues to rise globally.

1. Research Task: Investigate the effectiveness of different interventions (diet, exercise, medication) in preventing or delaying type 2 diabetes in high-risk individuals.
2. Ethical Consideration: Should employers or insurance companies offer incentives for healthy behaviors? What are the potential benefits and risks of such programs?
3. Policy Proposal: Design a community-based program to reduce the incidence of type 2 diabetes. Consider factors like access to healthy food, safe spaces for exercise, and education.

Safety and Ethics Notes

Paper-based data-analysis lab — no chemical hazards, biological samples, or volunteer data collection are required. If using real public patient data, most data must be de-identified and handled with privacy-preserving practices.

Debrief and Reflection

After you finish the practical work, spend 5–10 minutes in your small group comparing results and discussing the following prompts. Each member should contribute at least one observation before moving to the next prompt:

1. What did your measurements show — compare the group’s results to the textbook’s predictions. Where they diverge, suggest at least one mechanistic explanation before concluding “experimental error.”
2. What would change the outcome — propose one modification to the procedure that would sharpen the measurement or extend the result to a new biological context, and predict what you would observe.
3. One-sentence headline — each student composes a single sentence summarizing the lab’s take-home message, suitable for a tweet. Compare sentences across groups; good headlines are short, quantitative, and mechanistic.
4. Connection back to the textbook — identify one section of section 11 that your data either confirmed or complicated. Cite the specific passage.
5. Experimental Design Reflection: What was the strongest aspect of your experimental design? What would you change if you could repeat the experiment?

Further Reading (Lab)

- Revisit the parent chapter section **11** for the theoretical foundations on which this lab is built.
- Look up any bolded glossary term introduced in the textbook chapter (each has a `#gl:term-slug` link in the text) — its master definition is in `manuscript/glossary.md`.
- Explore the Python code in `src/biology/biochemistry/biochemistry.py` for metabolic calculations.
- Use the self-contained Part 2 snippet as the computational template; it runs against tested project modules without external notebooks or CSV files.

Lab — DNA Replication and the Cell Cycle

This activity accompanies section 12 of the textbook — review that chapter before attempting the exercises below.

Learning Objectives

- Design and evaluate a mitotic staging dataset to calculate mitotic index
- Formulate testable hypotheses about how cell cycle progression varies across tissue types
- Identify independent, dependent, and controlled variables in cell biology experiments
- Analyze experimental data using statistical methods and cell biology concepts
- Write a brief scientific report with hypothesis, methods, results, and conclusion

Alignment and Rubric Map

- Outcome 1 (LO1): Interpret the supplied evidence or model output for DNA Replication and the Cell Cycle.
- Outcome 2 (LO2): Identify controls and comparison groups that make the claim testable.
- Outcome 3 (LO3): Quantify uncertainty, boundary conditions, or alternative explanations before concluding.
- Outcome 4 (LO4): Transfer the mechanism to a new biological case or public-facing decision.
- Chapter LO coverage: LO1, LO2, LO3, LO4
- Rubric dimensions: evidence; controls; uncertainty; mechanism; transfer. ## Pre-Lab Concept Questions {.unnumbered}

Answer these before starting the investigation — they activate knowledge from the parent chapter.

1. Describe the role of DNA polymerase III in chromosomal replication, focusing on its 5’→3’ synthesis directionality and its requirement for a primer with a free 3’-OH. Why does this directionality force the lagging strand to be made as Okazaki fragments?
2. Name the three principal cell-cycle checkpoints and pair each with the type of cellular damage or status it monitors before allowing progression.
3. Predict how a temperature-sensitive mutation in DNA ligase would affect the lagging strand and the apparent mitotic index of a proliferating tissue once the restrictive temperature is applied. Justify your prediction in terms of replication-fork output.

Pre-Lab Inquiry Questions

Complete these questions before coming to lab. Use your textbook and additional research to inform your hypotheses.

1. Hypothesis Formation: Based on your understanding of the cell cycle, predict which stage of mitosis will take the longest time. What molecular events occur during this stage that might explain its duration?
2. Experimental Design: What is the independent variable in a mitotic index experiment? What is the dependent variable? List at least 5 variables that should be controlled to ensure accurate staging.
3. Scientific Context: The mitotic index is used in cancer diagnosis. Why is a high mitotic index indicative of malignant tumors? What are the limitations of this measure?
4. Quantitative Reasoning: If a tissue has a mitotic index of 5%, approximately what percentage of cells are in S phase? (Assume S phase duration is about 6-8 hours in a 24-hour cycle.)
5. Real-World Application: Chemotherapy drugs often target rapidly dividing cells. How does the cell cycle explain why these drugs affect cancer cells more than normal cells? What are the side effects related to this mechanism?

Lab Context: DNA Replication and the Cell Cycle

DNA replication is semiconservative (Meselson–Stahl, 1958): each daughter double helix retains one original strand and one newly synthesized strand. Replication proceeds bidirectionally from origins of replication; DNA polymerase extends DNA in the 5’→3’ direction, requiring the lagging strand to be synthesized discontinuously as Okazaki fragments. The cell cycle ($G_1 \rightarrow S \rightarrow G_2 \rightarrow M$) is driven by cyclin-CDK complexes and monitored by checkpoints (G_1/S , G_2/M , spindle assembly checkpoint). The mitotic index (fraction of cells in mitosis) reflects proliferative activity and is elevated in tumors.

Paper-Based Materials

Table 555. Alignment and Rubric Map: Item and Quantity.

Item	Quantity
Source-governance card for DNA Replication and the Cell Cycle: genomics/database source card: reference release, sample coverage, version, clinical boundary, and refresh trigger	1
Printed cell-cycle image cards from root tip, embryo, and tumor tissue datasets	1 set
Mitotic stage decision key with example features	1
Meselson-Stahl simulation dataset (printed)	1
Cell cycle timeline diagram (printed)	1 per student
Checkpoint perturbation cards (untreated, DNA polymerase inhibitor, spindle poison)	1 set
Transparent grid overlay or printed counting frame	1
Calculator	1
Calculator or optional Python REPL with this project installed	1

Paper-Based Investigation

Part 1: Mitotic Index Determination from Image Cards

1. Formulate Your Hypothesis: Based on your pre-lab research, write a hypothesis about how the mitotic index might differ among root tip, embryo, and tumor image datasets.
2. Identify Variables:
 - Independent variable: Tissue dataset type
 - Dependent variable: Mitotic index (% cells in mitosis)
 - Controlled variables: image source, magnification label, counting frame size, staging key, scorer training, and exclusion rules.
3. Set Up Controls: Use the instructor-provided answer-key subset as a positive control for each mitotic stage and a non-dividing tissue card as a negative control. Before scoring the unknown cards, each group must reach at least 80% agreement on the control cards.
4. Apply the Staging Key:
 - Place the transparent grid over each printed image card.
 - Classify exactly 100 consecutive visible cells per card as interphase, prophase, metaphase, anaphase, telophase, or “uncertain.”
 - Record uncertain cells separately; do not force a stage call unless the chromosome features match the decision key.
5. Data Collection:
 - Score three cards per tissue dataset, with two students independently scoring one shared card to estimate inter-rater reliability.
 - Calculate mitotic index = (cells in mitosis ÷ total cells counted) × 100%.
 - Report the mean, range, and standard error across replicate cards; flag any card whose uncertain-cell count exceeds 10%.

Part 2: Computational Biology Exercise — Cell Cycle Modeling with Python

Optional computational check: run this self-contained Python snippet from the project root. It uses tested `src/biology` modules and requires no external notebook or CSV file.

Check template-strand logic before interpreting replication and cell-cycle data.

```
from biology.genetics import cpg_methylation_remaining, dna_complement, transcribe_dna_to_mrna

template = "TACGGA"
print("complement:", dna_complement(template))
```

```
print("mRNA:", transcribe_dna_to_mrna(template))
print("methylation after 3 divisions:", round(cpg_methylation_remaining(0.9, 3, 0.85), 3))
```

Part 3: Semiconservative Replication Analysis

6. Design an Alternative Investigation: Using the checkpoint perturbation cards, design a paper simulation to test the effect of a drug that inhibits DNA polymerase on cell cycle progression. What hypothesis would you test? Which stage proportions would be your evidence?
7. Hypothesis: Predict how inhibiting DNA polymerase would affect the duration of S phase and the overall cell cycle time.

Data Recording

Table 556. Part 3: Semiconservative Replication Analysis: Stage and Number of cells.

Stage	Number of cells	Proportion (%)	Estimated time in stage (min)*
Interphase			
Prophase			
Metaphase			
Anaphase			
Telophase			
Total	100	100%	24 h total

Mitotic index: _____ %

Inter-rater agreement on shared card: _____ %

Cards excluded or flagged, with reason: _____

Generation 2 Meselson-Stahl prediction (sketch):

Evidence and Reproducibility Checklist

- Primary evidence goal: Model replication dynamics and checkpoint outcomes.
- Data skill to practice: Interpret replication or cell-cycle data from timing, labeling, or checkpoint perturbations.
- BioSkills emphasis: Process of science, Science and society, Quantitative reasoning.
- Control logic: identify at least one positive control, one negative control, or one baseline comparison before interpreting results.
- Measurement discipline: record units, uncertainty, sample size, and any discarded observation with a reason.
- Mechanistic link: connect one result directly to the parent chapter’s big idea before writing the conclusion.
- Reproducibility check: state one procedural detail that another group would need in order to reproduce the result.

Paper-Based Evidence Upgrade

Before answering the analysis questions, annotate the paper dataset for DNA Replication and the Cell Cycle with a reproducibility pass:

Table 557. Part 3: Semiconservative Replication Analysis: Evidence check and Student action.

Evidence check	Student action
Control logic	Mark the comparison that functions as the baseline, negative control, or reference case.
Uncertainty	Circle the row, card, diagram feature, or model assumption most likely to change the conclusion.
Model comparison	State whether a simpler rule, null model, or alternative mechanism could explain the same pattern.
Decision threshold	Write the minimum evidence that would make you revise the interpretation.
Reproducibility	Record the exact scoring rule another group would need to reproduce your classification.

Focus note: When scoring mitotic stages, Meselson-Stahl bands, or replication-fidelity cards, tie every classification to the molecular event it claims to show and to a stated counting or banding rule another group could reproduce. Keep required work paper-based; any material-handling or equipment version belongs only in an optional extension.

Worked Example: Replicon Size and S-Phase Timing in Humans

Problem: The human diploid genome contains roughly 3.2×10^9 base pairs and is replicated from approximately 50,000 origins of replication. Each replication fork moves at about 1,000 bp per second, and forks travel bidirectionally from each origin. Estimate the average replicon size, the time required to finish one replicon, and assess whether these numbers are consistent with an observed S-phase duration of about 8 hours.

Solution:

- Average replicon size = $3.2 \times 10^9 \text{ bp} \div 50,000 \text{ origins} \approx 6.4 \times 10^4 \text{ bp}$ per replicon.
- Because two forks diverge from each origin, each fork covers half of the replicon, or about $3.2 \times 10^4 \text{ bp}$.
- Time per fork = $3.2 \times 10^4 \text{ bp} \div 1,000 \text{ bp s}^{-1} = 32 \text{ s}$, so one replicon finishes in about 32 seconds of fork travel.
- The full genome could in principle finish in well under an hour if every origin fired at once; the measured S phase of about 8 hours (about 28,800 s) is far longer than the per-replicon time, which fits a model in which origins fire in temporally staggered clusters rather than synchronously.

Interpretation: Replicon-level kinetics are not the rate-limiting feature of S phase; origin firing schedules, replication-timing programs, and fork stalling at hard-to-replicate regions tend to set the overall duration. This reframes “how long does replication take?” as a question about origin regulation rather than polymerase speed.

Source-Governance Checkpoint

Complete the source-governance card for DNA Replication and the Cell Cycle before writing the conclusion. Name the source type or model snapshot, record the evidence date or version, decide whether the claim is stable or fast-moving, and write one refresh trigger that would force the interpretation to change. Treat the card as a printed evidence object, not as a live web lookup.

Analysis Questions

1. Which stage of mitosis took the longest (highest proportion)? Which was shortest? Explain in terms of the molecular events occurring in each stage.
2. Your mitotic index suggests what fraction of cells are actively dividing. Would you expect a higher or lower mitotic index in: (a) a tumor; (b) a mature neuron; (c) a healing wound? Explain for each.
3. In the Meselson-Stahl simulation, after two rounds of replication in light medium: (a) what fraction of DNA molecules are hybrid ($^{15}\text{N}/^{14}\text{N}$)? (b) What fraction are light-light? How do these proportions distinguish semiconservative from conservative replication?
4. DNA polymerase requires a primer and extends DNA in the $5' \rightarrow 3'$ direction. Explain why the lagging strand is initiated multiple times as Okazaki fragments, and name the enzyme that seals these fragments.
5. A drug (e.g., taxol) stabilizes microtubules and prevents spindle disassembly. At which checkpoint would cells arrest, and what specific checkpoint protein detects unattached kinetochores? Why is this drug effective against rapidly dividing cancer cells?

Post-Lab Synthesis

Concept Check (Synthesis): A research team identifies a tumor cell line carrying a loss-of-function mutation in Wee1 kinase, which normally inhibits the CDK1-cyclin B complex until DNA replication is complete. The cells display elevated mitotic index, frequent chromosome bridges in anaphase, and signs of incomplete DNA replication at the time of mitotic entry. Evaluate the consequences of this perturbation by integrating cell-cycle control with genome integrity.

- (a) Explain mechanistically how loss of Wee1 activity weakens the G2/M checkpoint, and predict the order in which CDK1 activation, DNA replication completion, and nuclear envelope breakdown would occur in these cells relative to wild-type cells.
- (b) Connect the observed anaphase bridges and chromosome mis-segregation to the inferred biochemical defect, and propose two independent measurements (one molecular, one cytological) that would test whether the elevated mitotic index reflects faster cycling or premature mitotic entry with unreplicated DNA.

Extension Analysis Questions

6. Statistical Analysis: Calculate the standard error of the mean (SEM) for your mitotic index across replicate cards. Construct a 95% confidence interval. How precise is your estimate?

7. Experimental Error Analysis: What are three potential sources of error in image-based mitotic staging? How could you modify the scoring rules or dataset design to reduce each source of error?
8. Experimental Design: If you wanted to test the effect of a new chemotherapy drug on cell cycle progression, what would you measure? How would you distinguish between drugs that affect DNA synthesis vs. those that affect mitosis?

Group Project Extension (Multi-Session)

Design a Cancer Cell Detection Tool Using Machine Learning

This project will span 2-3 lab sessions:

Session 1: Research Question and Hypothesis - Can we distinguish cancer cells from normal cells based on cell cycle abnormalities? - What features (size, shape, staining intensity, mitotic index) are most predictive? - Write a reproducible sampling plan for choosing public image datasets and metadata fields

Session 2: Data Collection and Analysis - Use public image datasets of normal and cancer cells - Extract features using image analysis software - Train a simple machine learning classifier (e.g., logistic regression)

Session 3: Tool Development and Testing - Test your classifier on unseen data - Calculate sensitivity, specificity, and accuracy - Create a scientific poster or presentation

Real-World Problem Solving: Cancer Diagnostics

Case Study: Liquid Biopsy for Cancer Detection

Liquid biopsies detect circulating tumor DNA (ctDNA) or circulating tumor cells (CTCs) in blood samples.

1. Research Task: Investigate the advantages and limitations of liquid biopsies compared to traditional tissue biopsies.
2. Ethical Consideration: Should liquid biopsy screening be offered to asymptomatic individuals? What are the potential benefits and risks of early detection?
3. Policy Proposal: Design a screening program for a specific cancer type using liquid biopsy technology. Consider cost-effectiveness, accessibility, and follow-up procedures.

Safety and Ethics Notes

Default lab work uses printed datasets primarily, with no biological or chemical hazards. When using machine learning on human data, ensure privacy, use de-identified public datasets, and obtain proper consent for any non-public images. Any wet-lab root-tip squash should be treated as an optional instructor-supervised extension with local safety approval, not as a required activity.

Debrief and Reflection

After you finish the practical work, spend 5–10 minutes in your small group comparing results and discussing the following prompts. Each member should contribute at least one observation before moving to the next prompt:

1. What did your measurements show — compare the group’s results to the textbook’s predictions. Where they diverge, suggest at least one mechanistic explanation before concluding “experimental error.”
2. What would change the outcome — propose one modification to the procedure that would sharpen the measurement or extend the result to a new biological context, and predict what you would observe.
3. One-sentence headline — each student composes a single sentence summarizing the lab’s take-home message, suitable for a tweet. Compare sentences across groups; good headlines are short, quantitative, and mechanistic.
4. Connection back to the textbook — identify one section of section 12 that your data either confirmed or complicated. Cite the specific passage.
5. Experimental Design Reflection: What was the strongest aspect of your experimental design? What would you change if you could repeat the experiment?

Further Reading (Lab)

- Revisit the parent chapter section 12 for the theoretical foundations on which this lab is built.
- Look up any bolded glossary term introduced in the textbook chapter (each has a #gl:term-slug link in the text) — its master definition is in manuscript/glossary.md.
- Explore the Python code in src/biology/genetics/genetics.py for DNA replication calculations.
- Use the self-contained Part 2 snippet as the computational template; it runs against tested project modules without external notebooks or CSV files.

Lab — Gene Expression

Learning Objectives

This activity accompanies section 13 of the textbook — review that chapter before attempting the exercises below.

- Transcribe and translate a provided DNA template sequence manually to produce an amino acid sequence
- Identify the effect of point mutations (silent, missense, nonsense) on the final protein
- Analyze a polysome electron micrograph to determine relative transcription and translation rates
- Interpret a Northern blot and a Western blot to determine gene expression changes

Alignment and Rubric Map

- Outcome 1 (LO1): Interpret the supplied evidence or model output for Gene Expression.
- Outcome 2 (LO2): Identify controls and comparison groups that make the claim testable.
- Outcome 3 (LO3): Quantify uncertainty, boundary conditions, or alternative explanations before concluding.
- Outcome 4 (LO4): Transfer the mechanism to a new biological case or public-facing decision.
- Chapter LO coverage: LO1, LO2, LO3, LO4
- Rubric dimensions: evidence; controls; uncertainty; mechanism; transfer. ## Pre-Lab Concept Questions {unnumbered}

Answer these before starting the investigation — they activate knowledge from the parent chapter.

1. Describe what a promoter is at the DNA-sequence level for a typical eukaryotic gene, and explain how a sequence-specific transcription factor recognizes its target promoter or enhancer through protein-DNA contacts. Why does mutation of a single base in a binding site sometimes abolish recognition while a base change elsewhere has little effect?
2. Distinguish transcriptional regulation from post-transcriptional regulation. Give one concrete molecular example of each, and explain which step of the DNA → mRNA → protein flow each example acts on.
3. Predict the effect on steady-state mRNA level if (a) the transcription initiation rate doubles while mRNA degradation stays constant, and (b) the transcription rate stays constant while the mRNA half-life is cut in half. Justify each prediction quantitatively before doing any arithmetic.

Lab Context: Gene Expression

Gene expression flows from DNA → mRNA (transcription, in the nucleus) → protein (translation, by ribosomes in the cytoplasm). The genetic code is triplet (3 nucleotides = 1 codon), non-overlapping, comprehensive, and degenerate (multiple codons = one amino acid). A polysome (polyribosome) consists of multiple ribosomes simultaneously translating the same mRNA; the number of ribosomes per mRNA is proportional to protein production demand and mRNA length.

In this lab you will perform manual transcription/translation using codon tables, predict the effect of mutations, and interpret blot data to determine whether gene expression changes are occurring at the transcriptional or translational level.

Paper-Based Materials

Table 558. Alignment and Rubric Map: Item and Quantity.

Item	Quantity
Source-governance card for Gene Expression: genomics/database source card: reference release, sample coverage, version, clinical boundary, and refresh trigger	1
DNA template sequence cards (instructor-provided: 3 sequences — original, missense mutant, nonsense mutant)	1 set
mRNA codon table (standard genetic code)	1 per student
Polysome TEM image (printed)	1
Northern blot image (printed, 2 lanes: untreated vs treated sample)	1
Western blot image (printed, 2 lanes: untreated vs treated sample)	1

Item	Quantity
Ruler	1
Colored pens	3

Paper-Based Investigation

Part A — Transcription and Translation Simulation

1. Using Cards A (original), B (missense), C (nonsense): Transcribe each DNA template to mRNA (3'→5' template → 5'→3' mRNA), then translate using the codon table to produce an amino acid sequence.
2. For Cards B and C, identify: which codon was changed, what type of mutation (silent/missense/nonsense/frameshift), and what effect on the final protein.

Part B — Polysome Analysis

3. Examine the polysome TEM image. Count the number of ribosomes on the longest visible mRNA strand. Measure the approximate length of the mRNA strand (mm). Calculate ribosome density (ribosomes per mm of mRNA).

Part C — Blot Interpretation

4. The Northern blot shows mRNA levels (bands). The Western blot shows protein levels (bands). Compare band intensities between untreated (lane 1) and treated (lane 2) samples. Complete the interpretation table.

Data Recording

Table 559. Alignment and Rubric Map: Card and Mutation type.

Card	Mutation type	Mutated codon	Amino acid change	Effect on protein
A	—	—	—	Normal
B				
C				

mRNA length: _____ mm; Ribosomes counted: _____; Ribosome density: _____ per mm

Table 560. Alignment and Rubric Map.

Sample	Northern band (strong/weak/absent)	Western band	Interpretation
Untreated			
Treated			

Evidence and Reproducibility Checklist

- Primary evidence goal: Trace expression from DNA template to protein or regulatory RNA.
- Data skill to practice: Convert DNA/RNA sequence data into predicted molecular products.
- BioSkills emphasis: Process of science, Science and society, Quantitative reasoning.
- Control logic: identify at least one positive control, one negative control, or one baseline comparison before interpreting results.
- Measurement discipline: record units, uncertainty, sample size, and any discarded observation with a reason.
- Mechanistic link: connect one result directly to the parent chapter’s big idea before writing the conclusion.
- Reproducibility check: state one procedural detail that another group would need in order to reproduce the result.

Paper-Based Evidence Upgrade

Before answering the analysis questions, annotate the paper dataset for Gene Expression with a reproducibility pass:

Table 561. Alignment and Rubric Map: Evidence check and Student action.

Evidence check	Student action
Control logic	Mark the comparison that functions as the baseline, negative control, or reference case.
Uncertainty	Circle the row, card, diagram feature, or model assumption most likely to change the conclusion.
Model comparison	State whether a simpler rule, null model, or alternative mechanism could explain the same pattern.
Decision threshold	Write the minimum evidence that would make you revise the interpretation.
Reproducibility	Record the exact scoring rule another group would need to reproduce your classification.

Focus note: When reading transcription, splicing, or translation datasets, keep the regulatory steps separate and ask which step the evidence actually measures, since mRNA level, isoform choice, and protein output can move independently. Keep required work paper-based; any material-handling or equipment version belongs only in an optional extension.

Worked Example: Steady-State mRNA Levels Under Promoter Repression

Problem: A gene has a 1,200-nucleotide coding sequence and is transcribed at a basal rate of 3 mRNAs per minute. The mRNA is degraded with rate constant $k = 0.08$ per minute. Treat transcription as zero-order and degradation as first-order, so at steady state mRNA level equals transcription rate divided by k . Calculate the steady-state mRNA count in the basal state. Then calculate the new steady state if a repressor reduces transcription to 0.5 mRNAs per minute, and report the fold change in mRNA level.

Solution:

- Basal steady state = $3 \text{ mRNAs min}^{-1} \div 0.08 \text{ min}^{-1} = 37.5 \text{ mRNAs per cell}$, which we report as about 38 transcripts per cell.
- Repressed steady state = $0.5 \text{ mRNAs min}^{-1} \div 0.08 \text{ min}^{-1} = 6.25 \text{ mRNAs per cell}$, about 6 transcripts per cell.
- Fold change = $37.5 \div 6.25 = 6.0$, so the repressor produces a six-fold drop in steady-state mRNA, which matches the six-fold drop in transcription rate because degradation kinetics did not change.

Interpretation: When the mRNA degradation rate constant is unchanged, fold-change in transcription rate is propagated one-to-one into fold-change in steady-state mRNA level. The half-life of the mRNA ($\ln 2 \div 0.08 \approx 8.7$ minutes) sets how quickly the system reaches its new steady state after the perturbation; a longer half-life would slow the response without changing the final ratio.

Source-Governance Checkpoint

Complete the source-governance card for Gene Expression before writing the conclusion. Name the source type or model snapshot, record the evidence date or version, decide whether the claim is stable or fast-moving, and write one refresh trigger that would force the interpretation to change. Treat the card as a printed evidence object, not as a live web lookup.

Analysis Questions

1. Card B (missense mutation): the amino acid sequence changed but the protein was still functional. Explain how this is possible using the concept of functionally conservative amino acid substitutions (e.g., Leu → Ile).
2. Card C introduced a premature stop codon. How does the cell detect and degrade mRNAs with premature stop codons? Name this quality-control pathway.
3. If Northern blot shows no change in mRNA level, but Western blot shows dramatically reduced protein, at what level is gene expression being regulated? Name two possible regulatory mechanisms.
4. A gene has 8 ribosomes per mRNA; a second gene’s mRNA has 40 ribosomes present. Which gene is being translated more actively? What are two reasons a cell might load one mRNA with more ribosomes than another?
5. The antibiotic streptomycin causes misreading of the A-site codon by destabilising the decoding center of the 30S ribosomal subunit. Predict the effect on translation fidelity and which kingdom of organisms would be most affected (hint: consider that streptomycin targets 30S vs 60S subunits).

Post-Lab Synthesis

Concept Check (Synthesis): The *Drosophila* gene *Dscam* encodes a cell-surface receptor required for axon guidance. Its pre-mRNA contains four blocks of mutually exclusive alternative exons (12, 48, 33, and 2 variants for the four exon blocks, respectively), yielding a theoretical upper bound

- of $12 \times 48 \times 33 \times 2 \approx 38,000$ distinct mRNA isoforms from one locus. Evaluate the regulatory and evolutionary implications of producing this many protein variants from a single gene.
- (a) Calculate the theoretical isoform count from the given exon-block sizes, then compare it to the number of distinct proteins you would need to encode this diversity if each isoform required its own gene. Discuss what alternative splicing buys the genome in terms of coding capacity per kilobase.
 - (b) Propose a molecular mechanism that could bias which Dscam isoform a given neuron expresses (consider splicing factors, RNA secondary structure, or stochastic exon choice), and outline one experiment that would test whether isoform choice is regulated or random in a defined neuronal population.

Safety and Ethics Notes

No chemical hazards in this simulation/analysis lab. Handle TEM prints with care. If using online databases for real sequence data, comply with institutional access agreements.

Debrief and Reflection

After you finish the practical work, spend 5–10 minutes in your small group comparing results and discussing the following prompts. Each member should contribute at least one observation before moving to the next prompt:

- 1. What did your measurements show — compare the group’s results to the textbook’s predictions. Where they diverge, suggest at least one mechanistic explanation before concluding “experimental error.”
- 2. What would change the outcome — propose one modification to the procedure that would sharpen the measurement or extend the result to a new biological context, and predict what you would observe.
- 3. One-sentence headline — each student composes a single sentence summarizing the lab’s take-home message, suitable for a tweet. Compare sentences across groups; good headlines are short, quantitative, and mechanistic.
- 4. Connection back to the textbook — identify one section of section 13 that your data either confirmed or complicated. Cite the specific passage.

Further Reading (Lab)

- Revisit the parent chapter section 13 for the theoretical foundations on which this lab is built.
- Look up any bolded glossary term introduced in the textbook chapter (each has a #gl:term-slug link in the text) — its master definition is in manuscript/glossary.md.
- Explore the appended src/ module that implements the corresponding quantitative model (when applicable) — referenced in the parent chapter’s “Bridge to Computation” subsection.

Module footer: parent chapter \cref{sec:unit_IV_gene_expression}; all numerical quantities in this lab use SI units — see Appendix D — Units, Physical Constants, and Biological Ranges for unit conversions and biological-scale reference values.

Lab — Mutations, CRISPR, and Genomics

This activity accompanies section 14 of the textbook — review that chapter before attempting the exercises below.

Learning Objectives

- Design and evaluate a CRISPR-Cas9 editing scenario using sequence cards and gel images
- Formulate testable hypotheses about mutation effects on protein function
- Identify independent, dependent, and controlled variables in genome editing experiments
- Analyze experimental data using gel electrophoresis and statistical methods
- Write a brief scientific report with hypothesis, methods, results, and conclusion

Alignment and Rubric Map

- Outcome 1 (LO1): Interpret the supplied evidence or model output for Mutations, CRISPR, and Genomics.
- Outcome 2 (LO2): Identify controls and comparison groups that make the claim testable.
- Outcome 3 (LO3): Quantify uncertainty, boundary conditions, or alternative explanations before concluding.
- Outcome 4 (LO4): Transfer the mechanism to a new biological case or public-facing decision.
- Chapter LO coverage: LO1, LO2, LO3, LO4
- Rubric dimensions: evidence; controls; uncertainty; mechanism; transfer. ## Pre-Lab Concept Questions {.unnumbered}

Answer these before starting the investigation — they activate knowledge from the parent chapter.

1. Define a missense mutation and contrast it with a nonsense mutation in terms of the codon-level change and the resulting protein product. Why does a missense change at the active site of an enzyme often carry stronger functional consequences than a missense change in a flexible surface loop?
2. Name two DNA-repair pathways that act on double-strand breaks and describe how they differ in their fidelity, their requirement for a homologous template, and the cell-cycle phase in which each tends to dominate.
3. A tumor genome shows thousands of single-nucleotide variants. Predict which feature would help you separate likely driver mutations from passenger mutations: recurrence across many independent tumors, position within a known functional domain, or both. Justify your reasoning.

Pre-Lab Inquiry Questions

Complete these questions before coming to lab. Use your textbook and additional research to inform your hypotheses.

1. Hypothesis Formation: Based on your understanding of mutation types, predict which class of mutation (synonymous, missense, nonsense, frameshift) would be most likely to cause a loss of protein function. Explain your reasoning.
2. Experimental Design: What is the independent variable in a CRISPR genome-editing data analysis? What is the dependent variable? List at least 5 variables that should be controlled to ensure specific interpretation.
3. Scientific Context: The T7E1 assay is commonly used to detect CRISPR-induced mutations. How does this assay work? What are its limitations?
4. Quantitative Reasoning: If a CRISPR editing dataset reports an editing efficiency of 30%, how many cells would need to be represented to infer 10 successfully edited cells? What factors might affect this estimate?
5. Real-World Application: Germline genome editing raises significant ethical concerns. What are the main arguments for and against editing human embryos to eliminate genetic diseases? Where do you stand on this issue?

Lab Context: Mutations, CRISPR, and Genomics

Mutations — heritable changes in DNA sequence — can be neutral (synonymous), harmful (loss-of-function missense or nonsense), or beneficial (gain-of-function). CRISPR-Cas9 (Clustered Regularly Interspaced Short Palindromic Repeats) is a programmable nuclease: the guide RNA (gRNA; about 20 nt complementary to the target) directs Cas9 to create a blunt-ended double-strand break 3 bp upstream of the PAM sequence (5'-NGG-3'). Repair by NHEJ creates indel mutations (disruptive); HDR with a template creates precise edits.

Paper-Based Materials

Table 562. Alignment and Rubric Map: Item and Quantity.

Item	Quantity
Source-governance card for Mutations, CRISPR, and Genomics: ClinVar/dbSNP/RefSeq/MANE source card with variant identifier, transcript accession, review status, reference release, clinical boundary, and refresh trigger	1
Clinical-translation provenance card contrasting ClinicalTrials.gov trial status with FDA Casgevy and Lyfgenia approved-indication evidence	1
Wild-type and mutant DNA sequences (printed cards: WT, SNP1, SNP2, frameshift)	1 set
Codon table	1
CRISPR guide RNA design worksheet (target region provided)	1
Gel electrophoresis image (T7E1 assay: uncut control, CRISPR-treated) (printed)	1
Off-target candidate sequence cards with mismatch positions marked	1 set
Editing-efficiency replicate dataset	1
Pangenome path cards: linear reference, alternate insertion path, inversion path, and read-alignment summaries	1 set
Molecular-database status card: 2026 NAR database issue excerpt with resource type, new/update status, and last-reviewed date	1
Prime-editing gamma-globin promoter case card with pegRNA, intended edits, donor variability, and HbF readout	1
Ruler (mm)	1
Ethical debate scenario cards (4 scenarios)	1 set
Calculator or optional Python REPL with this project installed	1
DNA ladder image (printed)	1

Paper-Based Investigation

Part 1: Mutation Classification and Analysis

1. Formulate Your Hypothesis: Based on your pre-lab research, write a hypothesis about how different mutation types (missense vs nonsense vs frameshift) affect protein function in a specific disease context (e.g., cystic fibrosis).
2. Identify Variables:
 - Independent variable: Mutation type (synonymous, missense, nonsense, frameshift)
 - Dependent variable: Predicted effect on protein function (neutral, mild, severe, lethal)
 - Controlled variables: Gene context, protein domain, evolutionary conservation, etc.
3. Set Up Controls: Why is it important to have a wild-type (WT) control sequence? What other controls could you include in a mutation classification experiment?
4. Data Collection:

- Compare SNP1, SNP2, and frameshift sequences with the WT. For each: identify the nucleotide change, classify the mutation type, determine the amino acid change, and assess likely functional impact.
- Use the provided codon table and protein domain information to inform your assessment.

Part 2: Computational Biology Exercise — CRISPR gRNA Design and Efficiency Analysis

Optional computational check: run this self-contained Python snippet from the project root. It uses tested `src/biology` modules and requires no external notebook or CSV file.

Quantify sequence change with the same distance functions used in the chapter.

```
from biology.genetics import gc_content, hamming_distance, jukes_cantor_distance

reference = "ATGCGTAC"
variant = "ATGAGTTC"
p_distance = hamming_distance(reference, variant) / len(reference)

print("GC reference:", round(gc_content(reference), 2))
print("Hamming distance:", hamming_distance(reference, variant))
print("Jukes-Cantor distance:", round(jukes_cantor_distance(p_distance), 3))
```

Part 3: Gel Electrophoresis Interpretation

5. Design an Alternative Investigation: Instead of proposing a live genome-editing experiment, design a blinded analysis of printed gRNA-design scenarios. What hypothesis would you test about seed-region mismatches, GC content, and editing efficiency? Which sequence-card controls would you include?
6. Hypothesis: Predict the relationship between gRNA binding affinity and editing efficiency in the dataset. Would it be linear, saturating, or something else? Why?

Part 4: Pangenome, Database, and Prime-Editing Decision Cards

7. Sort the pangenome path cards into three evidence classes: confidently represented by a single linear reference, better represented by an alternate graph path, and unresolved without long-read or phased evidence.
8. Use the molecular-database status card to decide whether a transcript, allele, or variant-resource claim is based on a new database, an updated database, or a retired/discontinued source; record the date that would need re-checking before publication.
9. For the gamma-globin promoter prime-editing card, identify the intended regulatory effect, the difference between editing a coding sequence and editing an enhancer/promoter motif, and the donor-to-donor variability that would limit a comprehensive claim.
10. Build a decision matrix comparing Casgevy-style BCL11A enhancer disruption, base editing of an *HBB* point mutation, and prime editing of *HBG1*/*HBG2* promoter motifs. Score each for target logic, double-strand-break risk, validation burden, and current clinical maturity.

Data Recording

Table 563. Part 4: Pangenome, Database, and Prime-Editing Decision Cards: Sequence and Nucleotide change.

Sequence	Nucleotide change	Mutation type	AA change	Functional impact prediction
SNP1				
SNP2				
Frameshift				

gRNA spacer sequences identified: (list most with PAM)

Gel band sizes: Control: _____ bp; Lane 2 bands: _____ bp, _____ bp

Indel efficiency estimate = (cleavage bands / total DNA) × 100%: _____% Off-target risk score for selected gRNA: _____; highest-risk mismatch pattern: _____ Replicate editing efficiencies: %, %, %; *mean ± SEM*: _ *Pangenome path selected*: _; *graph evidence needed*: _; *database status/date to re-check*: _; *prime-editing validation readout*: _____

Ethics summary (2–3 sentences per group position):

Evidence and Reproducibility Checklist

- Primary evidence goal: Evaluate genome-editing or variant-calling scenarios.
- Data skill to practice: Classify variants and predict likely molecular effect from sequence evidence.
- BioSkills emphasis: Process of science, Science and society, Quantitative reasoning.
- Control logic: identify at least one positive control, one negative control, or one baseline comparison before interpreting results.
- Measurement discipline: record units, uncertainty, sample size, and any discarded observation with a reason.
- Mechanistic link: connect one result directly to the parent chapter’s big idea before writing the conclusion.
- Reproducibility check: state one procedural detail that another group would need in order to reproduce the result.

Paper-Based Evidence Upgrade

Before answering the analysis questions, annotate the paper dataset for Mutations, CRISPR, and Genomics with a reproducibility pass:

Table 564. Part 4: Pangenome, Database, and Prime-Editing Decision Cards: Evidence check and Student action.

Evidence check	Student action
Control logic	Mark the comparison that functions as the baseline, negative control, or reference case.
Uncertainty	Circle the row, card, diagram feature, or model assumption most likely to change the conclusion.
Model comparison	State whether a simpler rule, null model, or alternative mechanism could explain the same pattern.
Decision threshold	Write the minimum evidence that would make you revise the interpretation.
Reproducibility	Record the exact scoring rule another group would need to reproduce your classification.

Focus note: When classifying variants from the paper dataset, separate the act of calling a variant from interpreting its pathogenicity, and record the ancestry coverage and evidence threshold behind any clinical claim. Keep required work paper-based; any material-handling or equipment version belongs only in an optional extension.

Worked Example: KRAS Codon 12 GGT to GTT in Human Cancer

Problem: A somatic mutation in a colorectal tumor changes codon 12 of the KRAS gene from GGT (glycine) to GTT (valine). Classify the mutation type, predict its consequence for the RAS GTPase activity cycle, and explain why this specific substitution recurs in roughly 30% of human cancers across multiple tissues.

Solution:

- Codon-level change: GGT (Gly) → GTT (Val) substitutes one amino acid for another with no premature stop and no shift of the reading frame, so the mutation is classified as missense.
- Biochemical consequence: glycine at position 12 sits at the GTP-binding pocket of RAS and is required for proper alignment of catalytic residues during GTP hydrolysis. Replacement by the larger, branched valine side chain sterically blocks the catalytic geometry, so the intrinsic GTPase rate drops and the GTPase-activating protein (GAP) can no longer accelerate hydrolysis. RAS becomes locked in the GTP-bound, signaling-on state.
- Why it recurs: codon 12 is a single-codon hot spot because a one-base change there converts RAS into a constitutively active oncoprotein that drives MAPK and PI3K signaling; the mutation gives a strong proliferative advantage to clonal lineages in colon, pancreas, lung, and other epithelial tissues, so it is repeatedly selected during tumor evolution.

Interpretation: A single missense change can convert a regulated switch into a constitutive signal without altering protein length or stability. The recurrence of identical mutations across independent tumors is itself evidence that the variant is a driver rather than a passenger.

Source-Governance Checkpoint

Complete the source-governance card for Mutations, CRISPR, and Genomics before writing the conclusion. Name the source type or model snapshot, record the evidence date or version, decide whether the claim is stable or fast-moving, and write one refresh trigger that would force the interpretation to change. Treat the card as a printed evidence object, not as a live web lookup.

Analysis Questions

1. Why does a frameshift mutation typically have a more severe effect on protein function than a missense mutation? Under what circumstance could a frameshift mutation be silent (no effect on protein)?
2. A gRNA with sequence mismatches at positions 1–4 from the PAM distal end is less likely to cause cutting than mismatches at the seed region (positions 1–12 from PAM-proximal end). Why? What does this imply about gRNA design strategy to minimize off-target effects?
3. The T7E1 enzyme cleaves primarily at mismatched positions in heteroduplex DNA. Explain why NHEJ-induced indels would create mismatches and thus be detectable by T7E1, whereas HDR edits with perfect template would not be.
4. In 2018, He Jiankui used CRISPR to edit the CCR5 gene in human embryos, which were then implanted and brought to term. The stated goal was to confer HIV resistance. Using your ethical framework from Part D: name two distinct ethical objections to this experiment beyond the scientific accuracy concerns.
5. A patient with Duchenne muscular dystrophy (DMD) has a frameshift in exon 51 causing a premature stop codon. Propose a CRISPR-based strategy (exon skipping via splice site disruption) to restore the reading frame. What are the limitations of this approach?
6. A short-read sample maps poorly to a disease locus because one haplotype contains a 3-kb insertion absent from the linear reference. Explain how a pangenome graph could represent the evidence more fairly, and name one validation step before using the call clinically.

Post-Lab Synthesis

Concept Check (Synthesis): A clinical sequencing laboratory receives a tumor biopsy and a matched blood sample from a 52-year-old patient with newly diagnosed lung adenocarcinoma. After next-generation sequencing of both samples, the laboratory must decide whether a specific variant detected in the tumor reflects (i) a pathogenic germline mutation inherited at birth, (ii) a somatic driver mutation acquired in the tumor lineage, or (iii) a sequencing artifact. Evaluate how three independent lines of evidence could be combined to reach a defensible conclusion.

- (a) Specify the three lines of evidence you would require — for example, presence or absence of the variant in the matched normal sample, variant allele frequency relative to tumor purity, and recurrence in tumor-mutation databases such as COSMIC or independent biological replicates — and explain what each line of evidence rules in or rules out.
- (b) Construct a decision rule that integrates the three lines of evidence and apply it to a worked case in which the variant is present at allele frequency 0.48 in the tumor, absent from the matched blood sample, and reported as a known activating mutation at a recurrent hotspot. State which classification this combination supports and what further evidence would prompt you to revise it.

Extension Analysis Questions

7. Statistical Analysis: If the printed dataset includes three replicate editing-efficiency estimates for each gRNA, how would you analyze the variation? What statistical test would you use to determine if differences between gRNAs are significant?
8. Experimental Error Analysis: What are three potential sources of error in T7E1 gel analysis? How could you modify the procedure to reduce each source of error?
9. Experimental Design: If you wanted to test the effect of a specific mutation on protein function, how would you design a paper-based evidence plan before any wet work? What sequence controls, phenotype readouts, and off-target checks would be required?

Group Project Extension (Multi-Session)

Design a CRISPR-based Diagnostic Tool for Infectious Disease

This project will span 2-3 lab sessions:

- Session 1: Research Question and Hypothesis - Can CRISPR-Cas12a (Cpf1) be used to detect viral DNA (e.g., SARS-CoV-2) with high specificity? - What are the advantages of CRISPR diagnostics over PCR? - Write a detailed decision workflow for a CRISPR-based diagnostic assay using provided sequences and fluorescence traces
- Session 2: Data Collection and Analysis - Design gRNAs specific for a viral target from printed sequence alignments - Simulate detection by classifying provided fluorescence-output traces - Analyze detection thresholds, false positives, and false negatives over time
- Session 3: Tool Development and Testing - Optimize assay conditions in a decision matrix (gRNA concentration, reaction time, detection threshold) - Test specificity against related viral strains - Create a scientific poster or presentation

Real-World Problem Solving: Genome Editing Ethics

Case Study: Somatic vs Germline Editing

1. Research Task: Investigate the current regulatory landscape for somatic vs germline genome editing in two different countries (e.g., USA vs China).
2. Ethical Consideration: Should there be a global moratorium on germline editing? What are the arguments for and against international regulation?
3. Policy Proposal: Design a policy framework for the responsible use of germline genome editing. Consider: which diseases would qualify, who would have access, how would long-term effects be monitored?

Safety and Ethics Notes

No biological or chemical hazards in this lab (paper/card based). Most CRISPR discussion is theoretical. When discussing patient/human scenarios, maintain respectful, evidence-based discourse. Follow institutional guidelines for ethical discussions.

Debrief and Reflection

After you finish the practical work, spend 5–10 minutes in your small group comparing results and discussing the following prompts. Each member should contribute at least one observation before moving to the next prompt:

1. What did your measurements show — compare the group’s results to the textbook’s predictions. Where they diverge, suggest at least one mechanistic explanation before concluding “experimental error.”
2. What would change the outcome — propose one modification to the procedure that would sharpen the measurement or extend the result to a new biological context, and predict what you would observe.
3. One-sentence headline — each student composes a single sentence summarizing the lab’s take-home message, suitable for a tweet. Compare sentences across groups; good headlines are short, quantitative, and mechanistic.
4. Connection back to the textbook — identify one section of section 14 that your data either confirmed or complicated. Cite the specific passage.
5. Experimental Design Reflection: What was the strongest aspect of your experimental design? What would you change if you could repeat the experiment?

Further Reading (Lab)

- Revisit the parent chapter section 14 for the theoretical foundations on which this lab is built.
- Look up any bolded glossary term introduced in the textbook chapter (each has a #gl:term-slug link in the text) — its master definition is in manuscript/glossary.md.
- Explore the Python code in src/biology/genetics/genetics.py for mutation analysis calculations.
- Use the self-contained Part 2 snippet as the computational template; it runs against tested project modules without external notebooks or CSV files.

Lab — Chromatin and Epigenetic Mechanisms

This activity accompanies section 15 of the textbook — review that chapter before attempting the exercises below.

This activity accompanies section 15 of the textbook — review that chapter before attempting the exercises below.

Learning Objectives

- Design and evaluate an epigenetic data-analysis scenario to determine gene regulation
- Formulate testable hypotheses about how environmental factors affect epigenetic marks
- Identify independent, dependent, and controlled variables in epigenetic studies
- Analyze experimental data using methylation analysis and ChIP-seq interpretation
- Write a brief scientific report with hypothesis, methods, results, and conclusion

Alignment and Rubric Map

- Outcome 1 (LO1): Interpret the supplied evidence or model output for Chromatin and Epigenetic Mechanisms.
- Outcome 2 (LO2): Identify controls and comparison groups that make the claim testable.
- Outcome 3 (LO3): Quantify uncertainty, boundary conditions, or alternative explanations before concluding.
- Outcome 4 (LO4): Transfer the mechanism to a new biological case or public-facing decision.
- Chapter LO coverage: LO1, LO2, LO3, LO4
- Rubric dimensions: evidence; controls; uncertainty; mechanism; transfer. ## Pre-Lab Concept Questions {.unnumbered}

Answer these before starting the investigation — they activate knowledge from the parent chapter.

1. Define a CpG island and explain why dense unmethylated CpGs in a gene promoter region correlate with active transcription. What molecular property of cytosine changes when a CpG is methylated, and how does that alter transcription-factor or reader-protein binding?
2. Describe what histone deacetylase (HDAC) inhibitors do to chromatin at a structural level, and predict whether HDAC inhibition would tend to raise or lower expression of genes whose promoters carry the active mark H3K4me3.
3. Compare H3K4me3 and H3K27me3 with respect to where each tends to deposit, which reader complexes recognize each, and what transcriptional outcome each is associated with. Predict what would happen to a developmental gene that simultaneously carries both marks (“bivalent” chromatin) once one mark is removed.

Pre-Lab Inquiry Questions

Complete these questions before coming to lab. Use your textbook and additional research to inform your hypotheses.

1. Hypothesis Formation: Based on your understanding of DNA methylation, predict how a gene promoter’s methylation status might change in response to a high-sugar diet. Would you expect hypermethylation or hypomethylation? Why?
2. Experimental Design: What is the independent variable in an epigenetic diet study? What is the dependent variable? List at least 5 variables that should be controlled to ensure valid results.
3. Scientific Context: The Horvath epigenetic clock uses DNA methylation patterns to predict biological age. Why might biological age differ from chronological age? What factors can accelerate epigenetic aging?
4. Quantitative Reasoning: If a methylation-sensitive PCR shows a 200 bp band in the untreated sample and a 400 bp band in the bisulphite-treated sample, what does this tell you about the methylation status of the gene?
5. Real-World Application: Epigenetic drugs like azacitidine are used to treat certain cancers. How do these drugs work? What are the potential side effects of globally altering epigenetic marks?

Lab Context: Chromatin and Epigenetic Mechanisms

Epigenetic regulation controls gene expression without altering DNA sequence: DNA methylation (CpG islands; methylation = gene silencing, generally), histone modification (H3K4me3 = activation; H3K27me3 = silencing; H3K9ac = activation), and non-coding RNA (miRNA, siRNA). The lac operon is the classical model for prokaryotic transcription regulation: the lac repressor blocks transcription in the absence of lactose; allolactose (a lactose isomer) binds the repressor and releases it from the operator.

Paper-Based Materials

Table 565. Alignment and Rubric Map: Item and Quantity.

Item	Quantity
Source-governance card for Chromatin and Epigenetic Mechanisms: genomics/database source card: reference release, sample coverage, version, clinical boundary, and refresh trigger	1
MS-PCR gel image (printed: two lanes per sample, bisulphite-treated/untreated)	1
ChIP-seq track printout (H3K4me3 signal at BRCA1 promoter: tumor vs normal)	1
Lac operon gene-expression logic table (worksheet)	1 per student
“Agouti mouse” case study reading (1 page)	1 per student
Colored pens	3
Calculator or optional Python REPL with this project installed	1
Epigenetic age calculator worksheet	1

Paper-Based Investigation

Part 1: Epigenetic Data Analysis

1. Formulate Your Hypothesis: Based on your pre-lab research, write a hypothesis about how a specific environmental factor (diet, stress, toxins) might affect DNA methylation patterns at a particular gene.
2. Identify Variables:

• Independent variable: Environmental exposure (e.g., high-fat diet, pollutant)

• Dependent variable: DNA methylation level at specific CpG sites

• Controlled variables: Age, sex, genetic background, sample processing, etc.
3. Set Up Controls: Why is it important to include both treated and untreated control samples in epigenetic studies? What other controls could you include to validate your results?
4. Data Collection:

• Interpret the MS-PCR gel: determine which gene is methylated in cancer vs normal cells.

• Analyze the ChIP-seq track: compare H3K4me3 peak height at the BRCA1 promoter between tumor and normal. Does BRCA1 appear silenced in the tumor?

• Complete the lac operon logic table for four conditions.

• Read and analyze the agouti mouse case study.

Part 2: Computational Biology Exercise — Epigenetic Age Prediction with Python

Optional computational check: run this self-contained Python snippet from the project root. It uses tested `src/biology` modules and requires no external notebook or CSV file.

Model maintenance methylation and classify histone marks without external files.

```
from biology.genetics import cpg_methylation_remaining, histone_modification_state

for efficiency in (0.95, 0.85, 0.60):
    remaining = cpg_methylation_remaining(0.8, divisions=4, maintenance_efficiency=efficiency)
    print(efficiency, round(remaining, 3))

for mark in ("H3K27me3", "H3K27ac", "H3K4me2"):
    print(mark, histone_modification_state(mark))
```

Source-Governance Checkpoint

Complete the source-governance card for Chromatin and Epigenetic Mechanisms before writing the conclusion. Name the source type or model snapshot, record the evidence date or version, decide whether the claim is stable or fast-moving, and write one refresh trigger that would force the interpretation to change. Treat the card as a printed evidence object, not as a live web lookup.

Evidence and Reproducibility Checklist

- Primary evidence goal: Compare regulatory perturbations and predicted expression outputs.
- Data skill to practice: Interpret chromatin or expression evidence from simple regulatory datasets.
- BioSkills emphasis: Process of science, Science and society, Quantitative reasoning.
- Control logic: identify at least one positive control, one negative control, or one baseline comparison before interpreting results.
- Measurement discipline: record units, uncertainty, sample size, and any discarded observation with a reason.
- Mechanistic link: connect one result directly to the parent chapter’s big idea before writing the conclusion.
- Reproducibility check: state one procedural detail that another group would need in order to reproduce the result.

Paper-Based Evidence Upgrade

Before answering the analysis questions, annotate the paper dataset for Chromatin and Epigenetic Mechanisms with a reproducibility pass:

Table 566. Source-Governance Checkpoint: Evidence check and Student action.

Evidence check	Student action
Control logic	Mark the comparison that functions as the baseline, negative control, or reference case.
Uncertainty	Circle the row, card, diagram feature, or model assumption most likely to change the conclusion.
Model comparison	State whether a simpler rule, null model, or alternative mechanism could explain the same pattern.
Decision threshold	Write the minimum evidence that would make you revise the interpretation.
Reproducibility	Record the exact scoring rule another group would need to reproduce your classification.

Focus note: epigenetic claims require causal perturbation, cell-type specificity, timing, and inheritance controls. Keep required work paper-based; any material-handling or equipment version belongs only in an optional extension.

Lab — Epigenetic Inheritance and Disease

Alignment and Rubric Map

- Outcome 1 (LO1): Interpret the supplied evidence or model output for Epigenetic Inheritance and Disease.
- Outcome 2 (LO2): Identify controls and comparison groups that make the claim testable.
- Outcome 3 (LO3): Quantify uncertainty, boundary conditions, or alternative explanations before concluding.
- Outcome 4 (LO4): Transfer the mechanism to a new biological case or public-facing decision.
- Chapter LO coverage: LO1, LO2, LO3, LO4
- Rubric dimensions: evidence; controls; uncertainty; mechanism; transfer.

This activity accompanies section 16 of the textbook — review that chapter before attempting the exercises below.

Lab Context: Epigenetic Inheritance and Disease

This extension lab focuses on three-dimensional genome organization, transgenerational inheritance claims, and disease-linked epigenetic dysregulation using printed datasets rather than live database queries.

Paper-Based Materials

Table 567. Alignment and Rubric Map: Item and Quantity.	
Item	Quantity
Source-governance card for Epigenetic Inheritance and Disease: genomics/database source card: reference release, sample coverage, version, clinical boundary, and refresh trigger	1
Printed datasets, cards, and worksheets referenced below	1 set per group
Graph paper or plain paper for diagrams	1
Calculator	1

Paper-Based Investigation

5.

Design an Alternative Investigation: Instead of just analyzing provided data, design a paper-based study plan to test how a specific nutrient (e.g., folate, B12) affects DNA methylation patterns in a model organism. What hypothesis would you test? Which tissue datasets, controls, and metadata fields would you require?
6.

Hypothesis: Predict the direction and magnitude of methylation changes you might observe with nutrient supplementation.

Data Recording

Table 568. Alignment and Rubric Map: Condition and Repressor bound to operator?.			
Condition	Repressor bound to operator?	CAP-cAMP at promoter?	lac genes expressed?
No lactose, no glucose	Yes	No	No
Lactose present, no glucose			
No lactose, glucose present			
Lactose + glucose			

MS-PCR result — BRCA1: Methylated? (Y/N) Normal: ____ Cancer: ____
ChIP-seq — BRCA1 H3K4me3 peak height: Normal: ____ Cancer: ____ Interpretation: ____

Agouti mouse case study: Methyl donor involved: ; *Epigenetic enzyme*: ; Phenotypic consequence: ____

Evidence and Reproducibility Checklist

- Primary evidence goal: Compare inheritance models and predict disease consequences of regulatory disruption.
- Data skill to practice: Interpret Hi-C, imprinting, or transgenerational datasets with causal caution.
- BioSkills emphasis: Process of science, Science and society, Quantitative reasoning.
- Control logic: identify at least one positive control, one negative control, or one baseline comparison before interpreting results.
- Measurement discipline: record units, uncertainty, sample size, and any discarded observation with a reason.
- Mechanistic link: connect one result directly to the parent chapter’s big idea before writing the conclusion.
- Reproducibility check: state one procedural detail that another group would need in order to reproduce the result.

Paper-Based Evidence Upgrade

Before answering the analysis questions, annotate the paper dataset for Epigenetics and Gene Regulation with a reproducibility pass:

Table 569. Alignment and Rubric Map: Evidence check and Student action.

Evidence check	Student action
Control logic	Mark the comparison that functions as the baseline, negative control, or reference case.
Uncertainty	Circle the row, card, diagram feature, or model assumption most likely to change the conclusion.
Model comparison	State whether a simpler rule, null model, or alternative mechanism could explain the same pattern.
Decision threshold	Write the minimum evidence that would make you revise the interpretation.
Reproducibility	Record the exact scoring rule another group would need to reproduce your classification.

Focus note: When interpreting methylation, chromatin, or gene-silencing datasets, demand a causal perturbation, a matched cell type, and a control for timing or inheritance before reading a pattern as a regulatory mechanism. Keep required work paper-based; any material-handling or equipment version belongs only in an optional extension.

Worked Example: Estimating Methylated CpG Sites in Cancer vs Normal

Problem: A tumor suppressor gene has a CpG island promoter containing 15 CpG dinucleotides. Bisulfite sequencing reports an average methylation level of 85% across these sites in cancer cells and 12% in matched normal cells. Assume the silencing threshold for this promoter is methylation of at least 80% of CpGs. Estimate how many CpG sites are methylated in each condition and judge whether the gene is likely active in each.

Solution:

- Cancer cells: $0.85 \times 15 \approx 12.75$, round to 13 of 15 sites methylated. The fraction methylated ($13/15 \approx 0.87$) exceeds the 0.80 threshold.
- Normal cells: $0.12 \times 15 \approx 1.8$, round to about 2 of 15 sites methylated. The fraction methylated ($2/15 \approx 0.13$) sits well below the 0.80 threshold.

Interpretation: In the tumor sample the promoter has crossed the silencing threshold and the gene is expected to be transcriptionally repressed; in the matched normal tissue the same promoter is hypomethylated and the gene is expected to be expressed. This pattern — promoter hypermethylation of a tumor suppressor — is consistent with epigenetic loss of function of a single allele or both alleles without any change to the protein-coding DNA sequence.

Analysis Questions

1. The lac repressor is an allosteric protein. How does allolactose binding change the shape of the repressor so that it can no longer bind the operator? Relate this to the induced fit model.
2. In catabolite repression, high glucose causes low cAMP because glucose inhibits adenylate cyclase. Trace: high glucose → [cAMP] → CAP-cAMP binding → lac promoter activity. Why does the cell preferentially use glucose over lactose?
3. A cancer cell has methylation of a tumor suppressor gene promoter but no mutation in the coding sequence. Is this a genetic or epigenetic mutation? Why is this clinically important for therapy selection (hint: methyltransferase inhibitors vs traditional chemotherapy)?

- 4. The agouti mouse model showed that maternal diet (methyl-group-rich foods) changes offspring coat color and obesity risk through epigenetic marks. Name the methyl donors involved (from diet) and the epigenetic writing enzyme that places the mark on CpG islands.
- 5. Design an experiment using induced pluripotent stem cell (iPSC) technology to test whether erasing epigenetic marks (global demethylation) is sufficient to reprogram a differentiated skin fibroblast. What control groups would you include?

Post-Lab Synthesis

Concept Check (Synthesis): A clinical team is debating how to treat two patients whose tumors both show loss of expression of the same tumor suppressor gene. Tumor A carries a frameshift coding mutation that truncates the protein at amino acid 87 (full length 451). Tumor B carries no coding mutation but shows 90% promoter CpG methylation and a strong H3K27me3 signal across the gene body. Evaluate whether the epigenetic silencing in Tumor B is functionally equivalent to the truncating mutation in Tumor A.

- (a) Compare the two lesions across three dimensions — reversibility in principle, heritability through mitosis and (where relevant) meiosis, and feasibility of therapeutic reactivation — and identify at least one experiment that could distinguish a fully epigenetic lesion from a small undetected coding lesion.
- (b) Recommend a treatment strategy for each tumor that follows from your analysis (for example, a DNA methyltransferase inhibitor or an EZH2 inhibitor for one tumor, a synthetic-lethal partner for the other), and state one piece of evidence that would make you change the recommendation.

Extension Analysis Questions

- 6. Methylation-sensitive restriction enzymes (e.g., HpaII) and methyl-insensitive isoschizomers (e.g., MspI) cut the same sequence but primarily MspI cuts methylated DNA. Describe one experimental use of this enzyme pair for mapping genome-wide methylation without bisulphite conversion.
- 7. Transgenerational epigenetic inheritance in humans remains controversial. What *specific* molecular evidence would convince you it is real? (Address confounding: shared environment, germline reprogramming.)
- 8. The textbook introduces CRISPR-dCas9 epigenome editing. Design a dCas9-based experiment to re-activate the silenced tumor-suppressor gene you identified in the ChIP-seq analysis, and predict one off-target risk.
- 9. Statistical Analysis: If you performed three replicates of an MS-PCR experiment, how would you analyze the variation in methylation status? What statistical test would you use to determine if differences between groups are significant?
- 10. Experimental Error Analysis: What are three potential sources of error in epigenetic data analysis? How could you modify the procedure to reduce each source of error?

Group Project Extension (Multi-Session)

Design an Epigenetic Diet Intervention Study

This project will span 2-3 lab sessions:

Session 1: Research Question and Hypothesis - Can dietary methyl donors (folate, B12, choline) alter DNA methylation patterns in humans? - What genes might be most responsive to such changes? - Write a detailed protocol for a dietary intervention study

Session 2: Data Collection and Analysis - Collect dietary intake data and DNA samples (or use public datasets) - Analyze methylation at candidate genes using bisulphite sequencing - Compare methylation changes between intervention and control groups

Session 3: Data Interpretation and Presentation - Correlate methylation changes with health outcomes - Create a scientific poster or presentation - Discuss limitations and future directions

Real-World Problem Solving: Epigenetic Ethics

Case Study: Epigenetic Discrimination

- 1. Research Task: Investigate the current legal protections against genetic discrimination (e.g., GINA in the US). Do these laws cover epigenetic information? Why or why not?
- 2. Ethical Consideration: Should employers or insurance companies be allowed to use epigenetic age estimates to make decisions? What are the potential benefits and risks?
- 3. Policy Proposal: Design a policy framework for the ethical use of epigenetic information. Consider: consent, privacy, access, and potential for discrimination.

Safety and Ethics Notes

Data-analysis primarily lab — no reagents, no risk. Discussions of patient cancer data should respect privacy principles (de-identification; aggregate reporting). Agouti mouse studies involve animal experimentation — students should briefly discuss the 3Rs framework (Replacement, Reduction, Refinement) and when mouse models are (and are not) scientifically justified. Epigenetic age clocks have attracted commercial wellness-industry interest; discuss the limits of current evidence before drawing lifestyle conclusions from a single patient’s clock.

Source-Governance Checkpoint

Complete the source-governance card for Epigenetic Inheritance and Disease before writing the conclusion. Name the source type or model snapshot, record the evidence date or version, decide whether the claim is stable or fast-moving, and write one refresh trigger that would force the interpretation to change. Treat the card as a printed evidence object, not as a live web lookup.

Debrief and Reflection

After you finish the practical work, spend 5–10 minutes in your small group comparing results and discussing the following prompts. Each member should contribute at least one observation before moving to the next prompt:

1. What did your measurements show — compare the group’s results to the textbook’s predictions. Where they diverge, suggest at least one mechanistic explanation before concluding “experimental error.”
2. What would change the outcome — propose one modification to the procedure that would sharpen the measurement or extend the result to a new biological context, and predict what you would observe.
3. One-sentence headline — each student composes a single sentence summarizing the lab’s take-home message, suitable for a tweet. Compare sentences across groups; good headlines are short, quantitative, and mechanistic.
4. Connection back to the textbook — identify one section of section 16 that your data either confirmed or complicated. Cite the specific passage.
5. Experimental Design Reflection: What was the strongest aspect of your experimental design? What would you change if you could repeat the experiment?

Further Reading (Lab)

- Revisit the parent chapter section 16 for the theoretical foundations on which this lab is built.
- Look up any bolded glossary term introduced in the textbook chapter (each has a #gl:term-slug link in the text) — its master definition is in manuscript/glossary.md.
- Explore the Python code in src/biology/genetics/genetics.py for epigenetic calculations.
- Use the self-contained Part 2 snippet as the computational template; it runs against tested project modules without external notebooks or CSV files.

Lab — Mendelian Principles and Probability

This activity accompanies section 17 of the textbook — review that chapter before attempting the exercises below.

This activity accompanies section 17 of the textbook — review that chapter before attempting the exercises below.

Learning Objectives

- Design and evaluate genetic cross simulations to determine inheritance patterns
- Formulate testable hypotheses about dominance, recessiveness, and linkage
- Identify independent, dependent, and controlled variables in genetic experiments
- Analyze experimental data using chi-square tests and statistical methods
- Write a brief scientific report with hypothesis, methods, results, and conclusion

Alignment and Rubric Map

- Outcome 1 (LO1): Interpret the supplied evidence or model output for Mendelian Principles and Probability.
- Outcome 2 (LO2): Identify controls and comparison groups that make the claim testable.
- Outcome 3 (LO3): Quantify uncertainty, boundary conditions, or alternative explanations before concluding.
- Outcome 4 (LO4): Transfer the mechanism to a new biological case or public-facing decision.
- Chapter LO coverage: LO1, LO2, LO3, LO4
- Rubric dimensions: evidence; controls; uncertainty; mechanism; transfer. ## Pre-Lab Concept Questions {.unnumbered}

Answer these before starting the investigation — they activate knowledge from the parent chapter.

1. State Mendel’s law of segregation in your own words, then connect the law to the cellular events of meiosis. At which stage do the two alleles of a heterozygous parent physically separate into different gametes, and why does this generate the 1:1 gamete ratio that underlies a 3:1 monohybrid offspring ratio?
2. Distinguish incomplete dominance from codominance, and give a concrete biological example of each. In your explanation, describe how the molecular product of each allele combines in the heterozygote to produce the observed phenotype, and identify a test cross or phenotypic assay that could differentiate the two patterns.
3. Define the chi-squared test in the context of testing a Mendelian ratio. Identify the null hypothesis, the role of the degrees of freedom, and the meaning of a p-value below 0.05 for a hypothesized 9:3:3:1 dihybrid ratio.

Pre-Lab Inquiry Questions

Complete these questions before coming to lab. Use your textbook and additional research to inform your hypotheses.

1. Hypothesis Formation: Based on your understanding of Mendelian inheritance, predict the outcome of a test cross between a dominant phenotype individual (unknown genotype) and a homozygous recessive individual. What phenotypic ratio would you expect if the dominant individual is homozygous vs heterozygous?
2. Experimental Design: What is the independent variable in a Mendelian inheritance experiment? What is the dependent variable? List at least 5 variables that should be controlled to ensure valid results.
3. Scientific Context: The chi-square test is used to determine if observed ratios fit expected Mendelian ratios. Why is this test important in genetics? What does a significant deviation from expected ratios tell you?
4. Quantitative Reasoning: If you perform a monohybrid cross ($Aa \times Aa$) and observe 450 round seeds and 130 wrinkled seeds (total 580), what is the χ^2 value? With 1 degree of freedom, is this significantly different from the expected 3:1 ratio at $p = 0.05$?
5. Real-World Application: Many human genetic disorders are recessive. Why are recessive disorders more common than dominant disorders? What are the implications for genetic counseling?

Lab Context: Mendelian Principles and Probability

Gregor Mendel’s experiments with pea plants (1856–1863) established the laws of segregation (allele pairs separate during gamete formation) and independent assortment (non-linked genes assort independently). Monohybrid crosses between heterozygotes ($Aa \times Aa$) produce 3:1 phenotype ratios; dihybrid crosses produce 9:3:3:1 ratios. Deviations from these ratios suggest linkage, incomplete dominance, codominance, or epistasis.

Example Pedigree — Autosomal Recessive Trait (Cystic Fibrosis)

Below is the three-generation pedigree you will analyze in Part B. Filled squares/circles are affected individuals; half-filled are obligate carriers; empty are unaffected. Use this as a reference for how pedigree symbols encode genotypes.

Paper-Based Materials

Table 570. Example Pedigree — Autosomal Recessive Trait (Cystic Fibrosis): Item and Quantity.

Item	Quantity
Source-governance card for Mendelian Principles and Probability: inheritance source card: model assumptions, sampling frame, ancestry/context boundary, and uncertainty	1
Punnett square worksheets (3: monohybrid, dihybrid, incomplete dominance)	1 set
Pedigree chart (printed: 3-generation autosomal recessive trait)	1
Coin or random number table (to simulate gamete formation)	2
Chi-square table (critical values)	1
Calculator	1
Colored counters (2 colors × 20) for simulating gametes	1 set
Calculator or optional Python REPL with this project installed	1
Statistical analysis worksheet	1

Paper-Based Investigation

Part 1: Punnett Square Analysis

1. Formulate Your Hypothesis: Based on your pre-lab research, write a hypothesis about how the inheritance pattern of a specific trait (e.g., pea seed shape) follows Mendelian ratios.
2. Identify Variables:
 - Independent variable: Parental genotypes
 - Dependent variable: Offspring genotype/phenotype ratios
 - Controlled variables: Cross design, counting method, environmental conditions, etc.
3. Set Up Controls: Why is it important to use true-breeding parental lines? What other controls could you include in a Mendelian inheritance experiment?
4. Data Collection:
 - Complete monohybrid crosses: $Aa \times Aa$; $AA \times Aa$; $Aa \times aa$. Record genotype and phenotype ratios.
 - Complete a dihybrid cross: $AaBb \times AaBb$. Record the 9:3:3:1 phenotype ratio.
 - Complete an incomplete dominance cross: R_1R_1 (red) \times R_2R_2 (white). What is the F_1 phenotype? F_2 ratios?

Part 2: Computational Biology Exercise — Statistical Analysis with Python

Optional computational check: run this self-contained Python snippet from the project root. It uses tested `src/biology` modules and requires no external notebook or CSV file.

Validate the paper Punnett-square and chi-square calculations.

```
from biology.genetics import chi_squared_test, punnett_square
```

```
cross = punnett_square("Aa", "Aa")
observed = [450.0, 130.0]
expected = [0.75 * sum(observed), 0.25 * sum(observed)]
chi = chi_squared_test(observed, expected)

print("genotype ratios:", cross.genotype_ratios)
print("phenotype ratios:", cross.phenotype_ratios)
print("χ²:", round(chi.chi_squared, 2), "reject?", chi.reject_null)
```

Source-Governance Checkpoint

Complete the source-governance card for Mendelian Principles and Probability before writing the conclusion. Name the source type or model snapshot, record the evidence date or version, decide whether the claim is stable or fast-moving, and write one refresh trigger that would force the interpretation to change. Treat the card as a printed evidence object, not as a live web lookup.

Evidence and Reproducibility Checklist

- Primary evidence goal: Solve monohybrid and dihybrid crosses and test expected ratios.
- Data skill to practice: Use cross data to infer genotype probabilities.
- BioSkills emphasis: Quantitative reasoning, Process of science.
- Control logic: identify at least one positive control, one negative control, or one baseline comparison before interpreting results.
- Measurement discipline: record units, uncertainty, sample size, and any discarded observation with a reason.
- Mechanistic link: connect one result directly to the parent chapter’s big idea before writing the conclusion.
- Reproducibility check: state one procedural detail that another group would need in order to reproduce the result.

Paper-Based Evidence Upgrade

Before answering the analysis questions, annotate the paper dataset for Mendelian Principles and Probability with a reproducibility pass:

Table 571. Source-Governance Checkpoint: Evidence check and Student action.

Evidence check	Student action
Control logic	Mark the comparison that functions as the baseline, negative control, or reference case.
Uncertainty	Circle the row, card, diagram feature, or model assumption most likely to change the conclusion.
Model comparison	State whether a simpler rule, null model, or alternative mechanism could explain the same pattern.
Decision threshold	Write the minimum evidence that would make you revise the interpretation.
Reproducibility	Record the exact scoring rule another group would need to reproduce your classification.

Focus note: Mendelian patterns are starting models that must be qualified by penetrance, linkage, environment, and sampling. Keep required work paper-based; any material-handling or equipment version belongs only in an optional extension.

Lab — Mendelian Extensions and Human Genetics

Alignment and Rubric Map

- Outcome 1 (LO1): Interpret the supplied evidence or model output for Mendelian Extensions and Human Genetics.
- Outcome 2 (LO2): Identify controls and comparison groups that make the claim testable.
- Outcome 3 (LO3): Quantify uncertainty, boundary conditions, or alternative explanations before concluding.
- Outcome 4 (LO4): Transfer the mechanism to a new biological case or public-facing decision.
- Chapter LO coverage: LO1, LO2, LO3, LO4
- Rubric dimensions: evidence; controls; uncertainty; mechanism; transfer.

This activity accompanies section 18 of the textbook — review that chapter before attempting the exercises below.

Lab Context: Mendelian Extensions and Human Genetics

This extension lab emphasizes pedigree analysis, extensions to Mendelian ratios, and human genetics applications using paper-based inheritance scenarios.

Paper-Based Materials

Table 572. Alignment and Rubric Map: Item and Quantity.

Item	Quantity
Source-governance card for Mendelian Extensions and Human Genetics: inheritance source card: model assumptions, sampling frame, ancestry/context boundary, and uncertainty	1
Printed datasets, cards, and worksheets referenced below	1 set per group
Graph paper or plain paper for diagrams	1
Calculator	1

Paper-Based Investigation

5. Design an Alternative Investigation: Instead of just analyzing the provided pedigree, design a paper-based study to determine the inheritance pattern of a human genetic trait in a small population. What hypothesis would you test? What consent, privacy, and pedigree metadata would be required?
6. Hypothesis: Predict the inheritance pattern (autosomal dominant, autosomal recessive, X-linked) for a trait that appears in every generation, affects both males and females equally, and shows no father-to-son transmission.

Data Recording

Table 573. Alignment and Rubric Map: Cross and Offspring genotype ratio.

Cross	Offspring genotype ratio	Offspring phenotype ratio
Aa × Aa		
AaBb × AaBb		
R ₁ R ₂ × R ₁ R ₂ (incomplete dom.)		

Pedigree genotypes:

Table 574. Alignment and Rubric Map.

Gen I	Gen II	Gen III
Individual		

Chi-square result: $\chi^2 =$; $df =$; $p < 0.05?$ (Y/N); Conclusion:

Evidence and Reproducibility Checklist

- Primary evidence goal: Solve pedigree and extension problems with explicit assumptions.
- Data skill to practice: Infer inheritance mode and extension mechanism from family or cross data.
- BioSkills emphasis: Quantitative reasoning, Process of science.
- Control logic: identify at least one positive control, one negative control, or one baseline comparison before interpreting results.
- Measurement discipline: record units, uncertainty, sample size, and any discarded observation with a reason.
- Mechanistic link: connect one result directly to the parent chapter’s big idea before writing the conclusion.
- Reproducibility check: state one procedural detail that another group would need in order to reproduce the result.

Paper-Based Evidence Upgrade

Before answering the analysis questions, annotate the paper dataset for Mendelian Genetics and Heredity with a reproducibility pass:

Table 575. Alignment and Rubric Map: Evidence check and Student action.

Evidence check	Student action
Control logic	Mark the comparison that functions as the baseline, negative control, or reference case.
Uncertainty	Circle the row, card, diagram feature, or model assumption most likely to change the conclusion.
Equity and consent	Mark any genetic information that could reveal risk to relatives, change insurance or employment concerns, or require counseling before disclosure.
Model comparison	State whether a simpler rule, null model, or alternative mechanism could explain the same pattern.
Decision threshold	Write the minimum evidence that would make you revise the interpretation.
Reproducibility	Record the exact scoring rule another group would need to reproduce your classification.

Focus note: in this lab the cross results and offspring counts are the evidence — use a chi-square goodness-of-fit test against the expected ratio before deciding whether a deviation signals linkage, penetrance, or sampling noise. Keep required work paper-based; any material-handling or equipment version belongs only in an optional extension.

Worked Example: Chi-Squared Test on a Dihybrid Cross

Problem: A dihybrid cross AaBb × AaBb produces 160 offspring. The hypothesized Mendelian ratio is 9:3:3:1 for the phenotypic classes A_B_, A_bb, aaB_, and aabb. Calculate the expected count for each class, then perform a chi-squared test using the observed counts 92 A_B_, 28 A_bb, 29 aaB_, and 11 aabb. With three degrees of freedom and a critical value of 7.815 at alpha = 0.05, is the result consistent with independent assortment?

Solution: Compute expected counts by multiplying the total 160 by each ratio fraction: $9/16 \times 160 = 90$ for A_B_, $3/16 \times 160 = 30$ for A_bb, $3/16 \times 160 = 30$ for aaB_, and $1/16 \times 160 = 10$ for aabb. The chi-squared statistic uses the formula $\text{chi-squared} = \sum (\text{observed} - \text{expected})^2 / \text{expected}$ across the four phenotypic classes. The four class contributions are $(92 - 90)^2 / 90 = 4/90 \approx 0.0444$, $(28 - 30)^2 / 30 = 4/30 \approx 0.1333$, $(29 - 30)^2 / 30 = 1/30 \approx 0.0333$, and $(11 - 10)^2 / 10 = 1/10 = 0.1000$. The total is approximately $0.0444 + 0.1333 + 0.0333 + 0.1000 \approx 0.311$. Degrees of freedom = number of classes minus one = $4 - 1 = 3$. The critical chi-squared at alpha = 0.05 with df = 3 is 7.815.

Interpretation: Because 0.311 is much smaller than 7.815, the null hypothesis of a 9:3:3:1 ratio is not rejected at alpha = 0.05; the data are consistent with independent assortment of the two loci. A small chi-squared value reflects a close agreement between observed and expected counts and does not prove independent assortment — it indicates the data provide no statistical evidence against it. Sources of deviation in real crosses include linkage, differential viability, and sampling variation, any of which can inflate chi-squared in larger experiments.

Analysis Questions

1. In the AaBb × AaBb dihybrid cross, what fraction of offspring are aabb (homozygous recessive for both traits)? Show your Punnett square logic.
2. The pedigree shows two unaffected parents who produce an affected child. What does this tell you about dominance? Can you determine whether the trait is autosomal or X-linked from this generation alone? What additional information would resolve this?

3. Your chi-square test: did the observed ratio significantly deviate from 3:1? What biological reasons could cause deviation from the expected ratio (give at least two sources of biological deviation other than statistical sampling error)?
4. Blood types in humans follow codominance (A and B antigens) and simple recessive inheritance (O). A type AB mother and type O father have two children — one type A, one type B. What genotype does each family member have? Is this consistent with Mendelian inheritance?
5. A gene controls tail length in cats: T (tailless, Manx) is dominant but homozygous TT is lethal. Set up the cross $Tt \times Tt$. What are the observed genotype and phenotype ratios among the LIVING offspring? How does this illustrate the concept of a lethal allele modifying a Mendelian ratio?

Extension Analysis Questions

6. Statistical Analysis: If you performed three replicates of a genetic cross, how would you analyze the variation in offspring ratios? What statistical test would you use to determine if differences between crosses are significant?
7. Experimental Error Analysis: What are three potential sources of error in Mendelian inheritance experiments? How could you modify the procedure to reduce each source of error?
8. Experimental Design: If you wanted to test whether two genes are linked or assort independently, how would you design the experiment? What data would you collect? How would you analyze it?

Group Project Extension (Multi-Session)

Design a Population Genetics Study of a Human Trait

This project will span 2-3 lab sessions:

- Session 1: Research Question and Hypothesis - Choose a human Mendelian trait (e.g., attached earlobes, tongue rolling, hitchhiker’s thumb) - Formulate a hypothesis about its inheritance pattern in your population - Design a survey to collect pedigree data from families
- Session 2: Data Collection and Analysis - Collect pedigree data from volunteers (with consent) - Analyze inheritance patterns using Punnett squares and chi-square tests - Compare your results to expected Mendelian ratios
- Session 3: Data Interpretation and Presentation - Create a report with your findings - Discuss any deviations from expected ratios and possible explanations - Create a scientific poster or presentation

Real-World Problem Solving: Genetic Counseling

Case Study: Carrier Screening for Cystic Fibrosis

1. Research Task: Investigate the prevalence of cystic fibrosis carrier status in different populations. Why is the carrier rate higher in people of Northern European descent?
2. Ethical Consideration: Should carrier screening for recessive disorders be routinely offered to prospective parents in high-prevalence or high-risk contexts? What are the potential benefits, risks, consent requirements, and equity concerns?
3. Policy Proposal: Design a policy for responsible use of genetic screening in reproductive healthcare. Consider: access, counseling, privacy, data retention, secondary use, family implications, and follow-up options.

Post-Lab Synthesis

- Concept Check (Synthesis): Genetic ratios observed in large laboratory populations tend to conform closely to Mendelian predictions, even when individual small crosses appear to deviate. Evaluate why this convergence occurs and explain how chi-squared testing bridges the gap between a finite sample and the underlying population-level theory.
- (a) Use the law of large numbers to explain why the observed phenotypic ratio in a dihybrid cross approaches 9:3:3:1 as the offspring count grows. Describe how sampling variance scales with sample size and predict, qualitatively, how a cross of 40 offspring and a cross of 4,000 offspring would differ in the typical absolute deviation from the expected ratio.
 - (b) Explain the role of the chi-squared test as a formal decision rule for connecting a finite sample to a population-level Mendelian hypothesis. Identify what the null and alternative hypotheses represent biologically, and discuss why failing to reject the null is not equivalent to proving the Mendelian model — it indicates that the data do not provide sufficient evidence against it at the chosen alpha.
 - (c) Consider a case where a large dataset produces a statistically significant deviation ($p < 0.01$) from the expected 9:3:3:1 ratio. Propose at least two biological explanations (such as linkage, epistasis, or differential viability) and outline an experimental follow-up that would distinguish between them.

Safety and Ethics Notes

This lab involves primarily paper-based activities and discussions. When discussing patient genetic data, maintain confidentiality and respect for individual privacy. Treat pedigrees and PRS examples as potentially identifiable family information: do not infer ancestry, parentage, or disease status beyond the evidence given, and separate biological risk estimates from policy decisions about disclosure, insurance, employment, or family notification.

Source-Governance Checkpoint

Complete the source-governance card for Mendelian Extensions and Human Genetics before writing the conclusion. Name the source type or model snapshot, record the evidence date or version, decide whether the claim is stable or fast-moving, and write one refresh trigger that would force the interpretation to change. Treat the card as a printed evidence object, not as a live web lookup.

Debrief and Reflection

After you finish the practical work, spend 5–10 minutes in your small group comparing results and discussing the following prompts. Each member should contribute at least one observation before moving to the next prompt:

1. What did your measurements show — compare the group’s results to the textbook’s predictions. Where they diverge, suggest at least one mechanistic explanation before concluding “experimental error.”
2. What would change the outcome — propose one modification to the procedure that would sharpen the measurement or extend the result to a new biological context, and predict what you would observe.
3. One-sentence headline — each student composes a single sentence summarizing the lab’s take-home message, suitable for a tweet. Compare sentences across groups; good headlines are short, quantitative, and mechanistic.
4. Connection back to the textbook — identify one section of section 18 that your data either confirmed or complicated. Cite the specific passage.
5. Experimental Design Reflection: What was the strongest aspect of your experimental design? What would you change if you could repeat the experiment?

Further Reading (Lab)

- Revisit the parent chapter section 18 for the theoretical foundations on which this lab is built.
- Look up any bolded glossary term introduced in the textbook chapter (each has a #gl:term-slug link in the text) — its master definition is in manuscript/glossary.md.
- Explore the Python code in src/biology/genetics/genetics.py for Mendelian genetics calculations.
- Use the self-contained Part 2 snippet as the computational template; it runs against tested project modules without external notebooks or CSV files.

Lab — Chromosomal Inheritance and Linkage

This activity accompanies section 19 of the textbook — review that chapter before attempting the exercises below.

Learning Objectives

- Design and evaluate genetic linkage mapping datasets to determine gene order
- Formulate testable hypotheses about chromosomal abnormalities from karyotype data
- Identify independent, dependent, and controlled variables in cytogenetic studies
- Analyze experimental data using recombination frequencies and statistical methods
- Write a brief scientific report with hypothesis, methods, results, and conclusion

Alignment and Rubric Map

- Outcome 1 (LO1): Interpret the supplied evidence or model output for Chromosomal Inheritance and Linkage.
- Outcome 2 (LO2): Identify controls and comparison groups that make the claim testable.
- Outcome 3 (LO3): Quantify uncertainty, boundary conditions, or alternative explanations before concluding.
- Outcome 4 (LO4): Transfer the mechanism to a new biological case or public-facing decision.
- Chapter LO coverage: LO1, LO2, LO3, LO4
- Rubric dimensions: evidence; controls; uncertainty; mechanism; transfer. ## Pre-Lab Concept Questions {.unnumbered}

Answer these before starting the investigation — they activate knowledge from the parent chapter.

1. Define non-disjunction in your own words, and state the meiotic stage at which it can occur (meiosis I, meiosis II, or both). For each case, describe whether the resulting gametes are missing a chromosome, carry an extra chromosome, or both.
2. Explain why females heterozygous for an X-linked recessive allele are typically described as somatic mosaics for that trait. Reference X-inactivation (the Lyon hypothesis) and the timing of the inactivation choice during embryonic development.
3. A karyotype shows 47 chromosomes with the configuration 47,XXY. Predict the likely phenotypic syndrome, state whether the extra chromosome originated from a maternal or paternal non-disjunction event with higher prior probability, and identify the meiotic stage most often implicated.

Pre-Lab Inquiry Questions

Complete these questions before coming to lab. Use your textbook and additional research to inform your hypotheses.

1. Hypothesis Formation: Based on your understanding of genetic linkage, predict how the recombination frequency between two genes would change if they were located very close together on the same chromosome versus far apart.
2. Experimental Design: What is the independent variable in a linkage mapping experiment? What is the dependent variable? List at least 5 variables that should be controlled to ensure accurate mapping.
3. Scientific Context: The chi-square test can be used to determine if observed recombination frequencies differ significantly from expected. Why is this test important in linkage analysis? What does a significant deviation tell you?
4. Quantitative Reasoning: If genes A and B have a recombination frequency of 12 cM, and genes B and C have 8 cM, what is the expected recombination frequency between A and C if there is no interference? How does interference affect this?
5. Real-World Application: Chromosomal abnormalities like Down syndrome are often caused by nondisjunction. Why does maternal age increase the risk of nondisjunction? What cellular mechanisms normally prevent this?

Lab Context: Chromosomal Inheritance and Linkage

Genes on the same chromosome are linked and tend to be inherited together (violating independent assortment). The recombination frequency between linked genes — measured as the percentage of recombinant offspring among total — is proportional to map distance (1% recombination = 1 centimorgan, cM). X-linked traits are carried on the X chromosome; since males are hemizygous (XY), a single recessive allele is expressed. Nondisjunction during meiosis (failure of chromosomes to separate) produces aneuploid gametes, leading to conditions such as trisomy 21 (Down syndrome).

Paper-Based Materials

Table 576. Alignment and Rubric Map: Item and Quantity.

Item	Quantity
Source-governance card for Chromosomal Inheritance and Linkage: inheritance source card: model assumptions, sampling frame, ancestry/context boundary, and uncertainty	1
Linkage mapping dataset (3 genes, pairwise recombination frequencies) (printed)	1
Karyotype images (4 cases: normal, trisomy 21, Turner syndrome 45,X, translocation) (printed)	1 set
Scissors and paste (for karyotype sorting exercise)	1 set
X-linked pedigrees (2 cases: color blindness, haemophilia) (printed)	1
Ruler	1
Chromosome pair cards (22 homologous pairs, numbered)	1 set
Calculator or optional Python REPL with this project installed	1
Statistical analysis worksheet	1

Paper-Based Investigation

Part 1: Genetic Linkage Mapping

1. Formulate Your Hypothesis: Based on your pre-lab research, write a hypothesis about the order of three genes given their pairwise recombination frequencies.
2. Identify Variables:

• Independent variable: Gene order (which gene is in the middle)

• Dependent variable: Recombination frequencies between gene pairs

• Controlled variables: Population size, crossover detection method, etc.
3. Set Up Controls: Why is it important to have a large sample size in linkage mapping? What other controls could you include to ensure accurate recombination frequency measurements?
4. Data Collection:

• Given pairwise recombination frequencies: genes A–B = 12 cM, B–C = 8 cM, A–C = 20 cM.

• Draw the linear linkage map. Which gene is in the middle? Indicate the distances between each adjacent pair.

• Calculate the expected coefficient of coincidence (observed double crossovers / expected double crossovers) and interference (1 - coefficient of coincidence).

Part 2: Computational Biology Exercise — Linkage Analysis with Python

Optional computational check: run this self-contained Python snippet from the project root. It uses tested `src/biology` modules and requires no external notebook or CSV file.

Infer a simple three-point map from pairwise recombination distances.

```
from biology.genetics import genetic_distance, infer_three_point_order

distances = {("A", "B"): 12.0, ("B", "C"): 8.0, ("A", "C"): 20.0}
order = infer_three_point_order(distances)

print("gene order:", " - ".join(order.order))
```

```
print("adjacent distances:", order.adjacent_distances_cM)
print("24 recombinants among 200 progeny:", genetic_distance(24, 200), "cM")
```

Part 3: Karyotype Analysis

5. Design an Alternative Investigation: Instead of just analyzing provided karyotype images, design a paper-based case-control study using archived karyotype datasets to investigate the effect of a spindle-disrupting condition on chromosome segregation. What hypothesis would you test? How would you analyze the resulting karyotype calls?
6. Hypothesis: Predict how exposure to a microtubule-disrupting agent (like colchicine) would affect chromosome number and structure in dividing cells.

Data Recording

Linkage map sketch:

A –[___cM]– B –[___cM]– C

Table 577. Part 3: Karyotype Analysis: Karyotype Case and # chromosomes.

Karyotype Case	# chromosomes	Abnormality	Syndrome (if any)
1			
2			
3			
4			

X-linked pedigree genotypes:

Table 578. Part 3: Karyotype Analysis: Individual and Phenotype.

Individual	Phenotype	Genotype
Gen I male	Unaffected	X ^A B Y
Gen I female		
Gen II affected male		
Gen III carrier female		

Evidence and Reproducibility Checklist

- Primary evidence goal: Map linked genes and reason from chromosomal anomalies.
- Data skill to practice: Infer gene order or chromosomal mechanism from offspring counts.
- BioSkills emphasis: Quantitative reasoning, Process of science.
- Control logic: identify at least one positive control, one negative control, or one baseline comparison before interpreting results.
- Measurement discipline: record units, uncertainty, sample size, and any discarded observation with a reason.
- Mechanistic link: connect one result directly to the parent chapter’s big idea before writing the conclusion.
- Reproducibility check: state one procedural detail that another group would need in order to reproduce the result.

Paper-Based Evidence Upgrade

Before answering the analysis questions, annotate the paper dataset for Chromosomal Inheritance and Linkage with a reproducibility pass:

Table 579. Part 3: Karyotype Analysis: Evidence check and Student action.

Evidence check	Student action
Control logic	Mark the comparison that functions as the baseline, negative control, or reference case.

Evidence check	Student action
Uncertainty	Circle the row, card, diagram feature, or model assumption most likely to change the conclusion.
Model comparison	State whether a simpler rule, null model, or alternative mechanism could explain the same pattern.
Decision threshold	Write the minimum evidence that would make you revise the interpretation.
Reproducibility	Record the exact scoring rule another group would need to reproduce your classification.

Focus note: in this lab the paper karyotypes, three-point cross data, and pedigrees are the evidence — score recombination frequencies, gene order, and nondisjunction division from the dataset itself rather than from the expected ratio. Keep required work paper-based; any material-handling or equipment version belongs only in an optional extension.

Worked Example: X-linked Hemophilia A Carrier Cross

Problem: A woman is a carrier for hemophilia A with genotype $X^H X^h$. Her partner has hemophilia A with genotype $X^h Y$. Construct a Punnett square and calculate the probability that (a) a son has hemophilia, (b) a daughter is a carrier, and (c) a daughter has hemophilia. Express each result as a fraction and a percentage.

Solution: The mother produces two gamete types, X^H and X^h , with equal probability. The father produces X^h and Y gametes with equal probability. The 2×2 Punnett square yields four offspring genotypes, each at $1/4$ expected frequency: $X^H X^h$ (carrier daughter), $X^H Y$ (unaffected son), $X^h X^h$ (affected daughter), and $X^h Y$ (affected son). Conditioning on sex, sons inherit Y from the father and either X^H or X^h from the mother, giving $1/2$ unaffected and $1/2$ affected sons; daughters inherit X^h from the father and either X^H or X^h from the mother, giving $1/2$ carrier and $1/2$ affected daughters.

- (a) $P(\text{son has hemophilia}) = 1/2 \text{ of sons} = 50\%$. Among offspring, $1/4$ are affected sons = 25%.
- (b) $P(\text{daughter is a carrier, } X^H X^h) = 1/2 \text{ of daughters} = 50\%$. Among offspring, $1/4 = 25\%$.
- (c) $P(\text{daughter has hemophilia, } X^h X^h) = 1/2 \text{ of daughters} = 50\%$. Among offspring, $1/4 = 25\%$.

Interpretation: Because the father is hemizygous and affected, half of his daughters inherit the recessive allele on his X and the other half inherit it from the carrier mother as well — an unusually high rate of affected daughters compared with a more typical carrier mother \times unaffected father cross, where affected daughters are rare. The expected ratios assume Mendelian segregation and equal viability, which can be perturbed by selection or sampling variation in small families.

Source-Governance Checkpoint

Complete the source-governance card for Chromosomal Inheritance and Linkage before writing the conclusion. Name the source type or model snapshot, record the evidence date or version, decide whether the claim is stable or fast-moving, and write one refresh trigger that would force the interpretation to change. Treat the card as a printed evidence object, not as a live web lookup.

Analysis Questions

- In linkage mapping, why does the A–C recombination frequency (20 cM) not simply equal A–B + B–C ($12 + 8 = 20$ cM) in real experiments? Explain the concept of double crossovers and interference.
- A woman is a carrier of haemophilia A ($X^H X^h$) and is also heterozygous for an autosomal trait (Aa). She marries a normal man ($X^H Y$; AA). Calculate the probability their first-born son is affected with haemophilia. Show most steps using the product rule.
- Karyotype Case 3 showed trisomy 21. During which meiotic division is nondisjunction most commonly occurring in cases of Down syndrome, and what is the evidence supporting this conclusion (hint: consider maternal age effects and the stage vulnerable to cohesin loss)?
- An individual with Turner syndrome (45,X) is phenotypically female. Explain why the presence of a single X chromosome leads to infertility and why males (46,XY) with a single X chromosome are not similarly affected.
- Philadelphia chromosome (a translocation between chromosomes 9 and 22, creating BCR-ABL fusion oncogene) causes chronic myeloid leukaemia (CML). Explain: (a) why a translocation creates a fusion gene; (b) what the BCR-ABL kinase does biochemically; (c) why imatinib (a tyrosine kinase inhibitor) is effective.

Extension Analysis Questions

6. Statistical Analysis: If you performed three replicates of a linkage mapping experiment, how would you analyze the variation in recombination frequencies? What statistical test would you use to determine if differences between gene pairs are significant?
7. Experimental Error Analysis: What are three potential sources of error in karyotype analysis? How could you modify the procedure to reduce each source of error?
8. Experimental Design: If you wanted to test whether two genes are linked or assort independently, how would you design the experiment? What data would you collect? How would you analyze it?

Group Project Extension (Multi-Session)

Design a Cytogenetic Study of Environmental Mutagens

This project will span 2-3 lab sessions:

- Session 1: Research Question and Hypothesis - Choose an environmental mutagen (e.g., tobacco smoke, pesticides, radiation) - Formulate a hypothesis about its effect on chromosome structure or number - Design an experiment using model organisms (e.g., onion root tip, fruit fly)
- Session 2: Data Collection and Analysis - Expose organisms to different concentrations of mutagen - Prepare and analyze chromosome spreads - Quantify chromosome abnormalities (breaks, fragments, aneuploidy)
- Session 3: Data Interpretation and Presentation - Compare abnormality rates between control and treated groups - Calculate statistical significance - Create a scientific poster or presentation

Real-World Problem Solving: Genetic Counseling

Case Study: Prenatal Screening for Chromosomal Abnormalities

1. Research Task: Investigate the different methods for prenatal screening and diagnosis (ultrasound, serum markers, NIPT, amniocentesis). What are the advantages and limitations of each?
2. Ethical Consideration: Should most pregnant women be offered prenatal screening for chromosomal abnormalities? What are the potential psychological and social implications of such testing?
3. Policy Proposal: Design a policy for responsible use of prenatal genetic testing. Consider: informed consent, access, counseling, and follow-up options.

Post-Lab Synthesis

- Concept Check (Synthesis): Carrier females for X-linked recessive disorders such as hemophilia A and Duchenne muscular dystrophy often show milder or variable phenotypes compared with affected males. Use X-inactivation (the Lyon hypothesis) and somatic mosaicism to evaluate the cellular and developmental reasons for this pattern.
- (a) Explain why each somatic cell in a heterozygous female typically expresses just one of her two X chromosomes as the result of random X-inactivation, and why the choice of which X to inactivate is random and clonally inherited. What proportion of cells, on average, expresses the mutant allele in a carrier female, and what is the expected variance around that mean across tissues and individuals?
- (b) Describe how somatic mosaicism produces a patchwork of normal and mutant cells in a carrier female. For a clotting-factor disorder such as hemophilia A, evaluate why circulating factor levels in carrier females tend to fall within a wide range rather than at a fixed intermediate value, and identify at least one factor (such as skewed X-inactivation) that can shift a carrier toward the affected end of the spectrum.
- (c) Predict how the severity distribution would differ for an X-linked disorder whose phenotype depends on a local tissue (for example, a retinal cell-autonomous trait such as red-green color vision) versus one that depends on a circulating product. Identify which scenario is more likely to show patchy or sectoral phenotypes in carrier females, and justify the prediction in mechanistic terms.

Safety and Ethics Notes

No chemical hazards. Karyotype analysis using real patient images: most should be de-identified. Discussion of chromosomal conditions should use person-first language and be conducted respectfully. Consider the ethical implications of genetic testing and counseling.

Debrief and Reflection

After you finish the practical work, spend 5–10 minutes in your small group comparing results and discussing the following prompts. Each member should contribute at least one observation before moving to the next prompt:

1. What did your measurements show — compare the group’s results to the textbook’s predictions. Where they diverge, suggest at least one mechanistic explanation before concluding “experimental error.”
2. What would change the outcome — propose one modification to the procedure that would sharpen the measurement or extend the result to a new biological context, and predict what you would observe.
3. One-sentence headline — each student composes a single sentence summarizing the lab’s take-home message, suitable for a tweet. Compare sentences across groups; good headlines are short, quantitative, and mechanistic.
4. Connection back to the textbook — identify one section of section 19 that your data either confirmed or complicated. Cite the specific passage.
5. Experimental Design Reflection: What was the strongest aspect of your experimental design? What would you change if you could repeat the experiment?

Further Reading (Lab)

- Revisit the parent chapter section 19 for the theoretical foundations on which this lab is built.
- Look up any bolded glossary term introduced in the textbook chapter (each has a `#gl:term-slug` link in the text) — its master definition is in `manuscript/glossary.md`.
- Explore the Python code in `src/biology/genetics/genetics.py` for chromosomal inheritance calculations.
- Use the self-contained Part 2 snippet as the computational template; it runs against tested project modules without external notebooks or CSV files.

Lab — Population Genetics

Learning Objectives

This activity accompanies section 20 of the textbook — review that chapter before attempting the exercises below.

- Apply Hardy-Weinberg equations to calculate allele and genotype frequencies from population data
- Test for deviations from HWE using chi-square analysis
- Simulate the effect of genetic drift on small vs large populations using a bead model
- Evaluate the effect of natural selection on allele frequencies across generations

Alignment and Rubric Map

- Outcome 1 (LO1): Interpret the supplied evidence or model output for Population Genetics.
- Outcome 2 (LO2): Identify controls and comparison groups that make the claim testable.
- Outcome 3 (LO3): Quantify uncertainty, boundary conditions, or alternative explanations before concluding.
- Outcome 4 (LO4): Transfer the mechanism to a new biological case or public-facing decision.
- Chapter LO coverage: LO1, LO2, LO3, LO4
- Rubric dimensions: evidence; controls; uncertainty; mechanism; transfer. ## Pre-Lab Concept Questions {.unnumbered}

Answer these before starting the investigation — they activate knowledge from the parent chapter.

1. State the five conditions required for a population to remain at Hardy-Weinberg equilibrium, and write the two governing equations $p + q = 1$ and $p^2 + 2pq + q^2 = 1$. For each condition, describe in one sentence how a violation would shift either allele or genotype frequencies away from the equilibrium expectation.
2. Define effective population size (N_e) and explain how it differs from the census size (N). Identify at least two demographic factors — such as unequal sex ratios, variance in reproductive success, or fluctuations across generations — that tend to make N_e smaller than N .
3. Distinguish the inbreeding coefficient F from the heterozygosity H . State how the two quantities are related under the simple model $F = 1 - (H_{\text{observed}} / H_{\text{expected}})$, and predict the direction of change in F after a population goes through a severe bottleneck.

Lab Context: Population Genetics

The Hardy-Weinberg principle states that in a large, randomly mating population with no selection, mutation, migration, or drift, allele frequencies (p , q) and genotype frequencies (p^2 , $2pq$, q^2) remain constant across generations. Deviations from HWE indicate one or more of these forces is acting. Genetic drift — random changes in allele frequency — is most powerful in small populations, causing loss of variation and potentially fixing or eliminating alleles by chance alone.

Paper-Based Materials

Table 580. Alignment and Rubric Map: Item and Quantity.

Item	Quantity
Source-governance card for Population Genetics: inheritance source card: model assumptions, sampling frame, ancestry/context boundary, and uncertainty	1
Two colors of beads (representing A and a alleles): 50 of each color	100 total
Opaque bag or cup (for random sampling)	2
Population genetics data table (printed: real MN blood group data)	1
Calculator	1
Chi-square critical value table	1
Graph paper	1

Paper-Based Investigation

Part A — Hardy-Weinberg Calculation

- Using the provided MN blood group data (genotype counts MM = 298, MN = 489, NN = 213, from a sample of $n = 1000$; classic combined US-Caucasian MN blood-group survey, as reproduced in standard population-genetics texts): calculate allele frequencies p (M) and q (N). (Check: $p(M) \approx 0.5425$, $q(N) \approx 0.4575$.)
- Calculate expected genotype frequencies under HWE (p^2 , $2pq$, q^2) and expected counts.
- Perform chi-square test to determine whether the population is in HWE.

Part B — Genetic Drift Simulation

- Place 50 red (A) and 50 blue (a) beads in the bag: this represents a population of 100 with $p = q = 0.5$.
- Without looking, draw 10 beads (simulating a bottleneck to $N=10$). Record the frequency of red (A) beads drawn. Then discard the old bag and rebuild a fresh 100-bead pool at the drawn allele ratio: multiply the observed red fraction by 100, round to the nearest whole bead, and use that many red beads with the remainder blue (e.g. $6/10$ red \rightarrow 60 red + 40 blue). Repeat the draw-rebuild cycle for 5 generations, recording p (red fraction) each generation.
- A second group runs the same simulation with $N=50$ (draw 50 beads, then rebuild a 100-bead pool at the drawn allele ratio by the same rounding rule) for 5 generations.

Part C — Selection Simulation (Optional)

- In generation 1 of the drift simulation, designate aa (2 blue drawn) as lethal — remove any drawn aa pairs and resample. Track p over 3 generations.

Data Recording

MN blood group HWE test (observed counts from the $n = 1000$ sample: MM = 298, MN = 489, NN = 213; source: classic combined US-Caucasian MN blood-group survey reproduced in standard population-genetics texts):

Table 581. Alignment and Rubric Map: Genotype and Observed.

Genotype	Observed	p or q	Expected	(O–E) ² /E
MM	298	$p^2 =$		
NN	213	$q^2 =$		
MN	489	$2pq =$		
Total	1000	—	1000	$\chi^2 = \underline{\hspace{1cm}}$

Fill the *Expected* column using your calculated p and q (Part A), then $\chi^2 = \Sigma (O-E)^2/E$.

$\chi^2 = \underline{\hspace{1cm}}$; df = 1; HWE at $\alpha = 0.05$? (Y/N) — compare χ^2 to the critical value 3.841.

Drift simulation:

Table 582. Alignment and Rubric Map: Generation and p (N=10 group).

Generation	p (N=10 group)	p (N=50 group)
0	0.5	0.5
1		
2		
3		
4		
5		

Evidence and Reproducibility Checklist

- Primary evidence goal: Test equilibrium and model allele-frequency change.
- Data skill to practice: Estimate genotype or allele frequencies from population data.
- BioSkills emphasis: Quantitative reasoning, Process of science.
- Control logic: identify at least one positive control, one negative control, or one baseline comparison before interpreting results.
- Measurement discipline: record units, uncertainty, sample size, and any discarded observation with a reason.
- Mechanistic link: connect one result directly to the parent chapter’s big idea before writing the conclusion.
- Reproducibility check: state one procedural detail that another group would need in order to reproduce the result.

Paper-Based Evidence Upgrade

Before answering the analysis questions, annotate the paper dataset for Population Genetics with a reproducibility pass:

Table 583. Alignment and Rubric Map: Evidence check and Student action.

Evidence check	Student action
Control logic	Mark the comparison that functions as the baseline, negative control, or reference case.
Uncertainty	Circle the row, card, diagram feature, or model assumption most likely to change the conclusion.
Model comparison	State whether a simpler rule, null model, or alternative mechanism could explain the same pattern.
Decision threshold	Write the minimum evidence that would make you revise the interpretation.
Reproducibility	Record the exact scoring rule another group would need to reproduce your classification.

Focus note: in this lab the simulated allele-frequency series across generations are the evidence — compare observed genotype counts against the Hardy-Weinberg expectation and contrast small versus large N to attribute change to drift, selection, or sampling. Keep required work paper-based; any material-handling or equipment version belongs only in an optional extension.

Worked Example: Hardy-Weinberg Allele Frequency Estimation

Problem: A population survey of 400 diploid individuals finds 36 individuals with the homozygous recessive genotype aa, giving an aa frequency of 0.09. Assuming Hardy-Weinberg equilibrium, calculate q (the recessive allele frequency), p (the dominant allele frequency), and the expected frequencies and counts of the AA and Aa genotypes in the population.

Solution: Under Hardy-Weinberg, the homozygous-recessive genotype frequency equals q^2 . Taking the square root, $q = \sqrt{0.09} = 0.30$. The dominant allele frequency is $p = 1 - q = 1 - 0.30 = 0.70$. The expected genotype frequencies are $p^2 = 0.49$ for AA, $2pq = 2 \times 0.70 \times 0.30 = 0.42$ for Aa, and $q^2 = 0.09$ for aa, which sums to 1.00. Multiplying each genotype frequency by the population size of 400 gives $0.49 \times 400 = 196$ AA individuals, $0.42 \times 400 = 168$ Aa individuals, and $0.09 \times 400 = 36$ aa individuals, summing to 400.

Interpretation: The estimated heterozygote frequency of 0.42 is the largest single class — a characteristic feature of populations with intermediate allele frequencies. The estimate of p relies on the assumption of Hardy-Weinberg equilibrium; in a real population, deviations driven by selection, drift, or non-random mating can bias the q^2 -to-q inference. A useful cross-check is to compare the predicted heterozygote count (168) with a directly genotyped count, since systematic shortfalls of heterozygotes can indicate inbreeding or hidden population structure.

Source-Governance Checkpoint

Complete the source-governance card for Population Genetics before writing the conclusion. Name the source type or model snapshot, record the evidence date or version, decide whether the claim is stable or fast-moving, and write one refresh trigger that would force the interpretation to change. Treat the card as a printed evidence object, not as a live web lookup.

Analysis Questions

1. Was the MN blood group population in HWE? Which of the HWE assumptions might be violated in a real human population, and how would each violation shift allele frequencies over generations?
2. Was there more variation in allele frequency across generations in the N=10 or N=50 group? Define genetic drift in terms of sampling error and explain why population size affects drift magnitude.
3. Founder effect: a group of 20 individuals colonises a new island. By chance, the founding group contains no aa individuals. Even without selection against aa, will this condition persist? Explain using HWE and the concept that mutation-selection equilibrium is absent if frequency starts at zero.
4. Heterozygote advantage: sickle-cell anemia (aa) is lethal, but carriers (Aa) are more resistant to malaria than AA homozygotes. With the heterozygote Aa as the fittest genotype, let s be the selection coefficient against AA and t the selection coefficient against aa (relative fitnesses $1-s : 1 : 1-t$). The stable equilibrium allele frequency of a is $\hat{q} = s / (s + t)$. For a malarious region with $s = 0.2$ (AA disadvantage) and $t = 1$ (aa lethal), compute \hat{q} and interpret why the a allele persists in the population despite being lethal in homozygotes.

5. A conservation biologist studying a population of 25 cheetahs finds they are almost completely genetically homogeneous (very low heterozygosity). Explain two consequences of this for: (a) short-term disease resistance; (b) long-term adaptive capacity. What management intervention would restore genetic variation?

Post-Lab Synthesis

Concept Check (Synthesis): A population is reduced to an effective size $N_e = 10$ for 5 generations before recovering. Evaluate how this bottleneck would alter the population’s allelic diversity, inbreeding coefficient F , and capacity to respond to natural selection, compared with its larger source population.

- (a) Predict the change in allelic diversity using the per-generation heterozygosity loss expression $H_t / H_0 = (1 - 1/(2 N_e))^t$. For $N_e = 10$ and $t = 5$ generations, calculate the expected fraction of heterozygosity retained, and describe which categories of alleles (common, intermediate, rare) are most likely to be lost through this process.
- (b) Predict the direction and approximate magnitude of change in the inbreeding coefficient F . Explain why F tends to rise in a small population even without consanguineous matings, by referencing identity-by-descent and the increased probability that two randomly sampled alleles trace to a recent common ancestor.
- (c) Evaluate how the reduced N_e affects the population’s capacity to respond to natural selection. Discuss the relative dominance of drift over selection when the product $N_e \times s$ is small (roughly less than 1), and predict how a beneficial allele with selection coefficient $s = 0.01$ would fare in the bottlenecked versus the source population. Identify which population would more reliably fix the favored allele and explain why.

Safety and Ethics Notes

No chemical hazards. Beads present a swallowing hazard — do not use with young children. When discussing human population genetics data (e.g., blood groups by ethnicity), maintain scientific objectivity and avoid discriminatory interpretation.

Debrief and Reflection

After you finish the practical work, spend 5–10 minutes in your small group comparing results and discussing the following prompts. Each member should contribute at least one observation before moving to the next prompt:

1. What did your measurements show — compare the group’s results to the textbook’s predictions. Where they diverge, suggest at least one mechanistic explanation before concluding “experimental error.”
2. What would change the outcome — propose one modification to the procedure that would sharpen the measurement or extend the result to a new biological context, and predict what you would observe.
3. One-sentence headline — each student composes a single sentence summarizing the lab’s take-home message, suitable for a tweet. Compare sentences across groups; good headlines are short, quantitative, and mechanistic.
4. Connection back to the textbook — identify one section of section 20 that your data either confirmed or complicated. Cite the specific passage.

Further Reading (Lab)

- Revisit the parent chapter section 20 for the theoretical foundations on which this lab is built.
- Look up any bolded glossary term introduced in the textbook chapter (each has a `#gl:term-slug` link in the text) — its master definition is in `manuscript/glossary.md`.
- Explore the appended `src/` module that implements the corresponding quantitative model (when applicable) — referenced in the parent chapter’s “Bridge to Computation” subsection.

Module footer: `parent chapter \cref{sec:unit_v_population_genetics}`; all numerical quantities in this lab use SI units — see [Appendix D — Units, Physical Constants, and Biological Ranges](#) for unit conversions and biological-scale reference values.

Lab — Natural Selection and Adaptation

This activity accompanies section 21 of the textbook — review that chapter before attempting the exercises below.

Learning Objectives

- Design and evaluate a natural selection simulation to measure selection coefficients
- Formulate testable hypotheses about how environmental change affects allele frequencies
- Identify independent, dependent, and controlled variables in evolutionary experiments
- Analyze experimental data using fitness calculations and statistical methods
- Write a brief scientific report with hypothesis, methods, results, and conclusion

Alignment and Rubric Map

- Outcome 1 (LO1): Interpret the supplied evidence or model output for Natural Selection and Adaptation.
- Outcome 2 (LO2): Identify controls and comparison groups that make the claim testable.
- Outcome 3 (LO3): Quantify uncertainty, boundary conditions, or alternative explanations before concluding.
- Outcome 4 (LO4): Transfer the mechanism to a new biological case or public-facing decision.
- Chapter LO coverage: LO1, LO2, LO3, LO4
- Rubric dimensions: evidence; controls; uncertainty; mechanism; transfer. ## Pre-Lab Concept Questions {.unnumbered}

Answer these before starting the investigation — they activate knowledge from the parent chapter.

1. Define relative fitness w and the selection coefficient s for a single locus with two alleles. Show how the two are related ($s = 1 - w$ for the less-fit genotype), and describe how each quantity is estimated empirically from survival or reproductive data in a controlled experiment.
2. Distinguish directional selection from stabilizing selection, and give one biological example of each. For each, describe the expected change over time in the population mean and variance of the affected trait, and identify the conditions under which the mode of selection might shift from one to the other.
3. Describe how standing genetic variation differs from new mutation as a source of adaptive change. Explain why standing variation can drive a faster response when the environment shifts, and identify at least one population-genetic signature (such as a soft sweep) that tends to accompany this mode of adaptation.

Pre-Lab Inquiry Questions

Complete these questions before coming to lab. Use your textbook and additional research to inform your hypotheses.

1. Hypothesis Formation: Based on your understanding of natural selection, predict how a change in environment (e.g., from green to brown background) would affect the survival of different colored prey. Write a clear, testable hypothesis.
2. Experimental Design: What is the independent variable in a natural selection simulation? What is the dependent variable? List at least 5 variables that should be controlled to ensure valid results.
3. Scientific Context: The selection coefficient (s) quantifies the fitness cost of a genotype. Why is this measure important in evolutionary biology? How does it relate to the rate of evolutionary change?
4. Quantitative Reasoning: If a genotype has a relative fitness of 0.8, what is its selection coefficient? If the initial frequency of this genotype is 0.3, what would you expect its frequency to be after one generation of selection?
5. Real-World Application: Antibiotic resistance is a classic example of natural selection. How does the overuse of antibiotics create selection pressure for resistant bacteria? What can be done to slow this process?

Lab Context: Natural Selection and Adaptation

Natural selection operates when three conditions are met: (1) heritable variation exists; (2) variation affects survival/reproduction (fitness); (3) traits are inherited. Over generations, favorable alleles increase in frequency (directional selection), multiple phenotypes are maintained (balancing/disruptive selection), or variation is reduced around an optimum (stabilizing selection). The selection coefficient s quantifies fitness cost: a lethal allele has $s = 1.0$; a neutral allele has $s = 0$.

The breeder’s equation ($R = h^2S$) worked example in the parent chapter (section 21) provides a quantitative framework for predicting selection response: with $h^2 = 0.4$ and $S = 10$ bristles, the predicted response is roughly 4 bristles per generation, decelerating as additive genetic variance depletes. This lab uses the selection coefficient s to track allele-frequency change — a complementary population-level view of the same process.

Paper-Based Materials

Table 584. Alignment and Rubric Map: Item and Quantity.

Item	Quantity
Source-governance card for Natural Selection and Adaptation: evolutionary-evidence source card: alternative hypotheses, sampling, calibration, and confidence boundary	1
Colored paper squares (30 each of: green, red, brown, on green and brown backgrounds)	1 set
Forceps (one per student, simulating different beak types)	4
60-second timer	1
Ruler	1
Darwin’s finch beak data table (printed: beak depth vs seed hardness across 14 species)	1
Selection data table (survival rates by genotype in two environments)	1
AMR allele-frequency dataset across simulated antibiotic gradients	1
Resistance policy decision matrix	1
Calculator	1
Calculator or optional Python REPL with this project installed	1
Graph paper	1

Paper-Based Investigation

Part 1: Predator-Prey Selection Simulation

1. Formulate Your Hypothesis: Based on your pre-lab research, write a hypothesis about how different colored prey will survive on different colored backgrounds.
2. Identify Variables:
 - Independent variable: Prey color and background color
 - Dependent variable: Survival rate (% of prey consumed or surviving)
 - Controlled variables: Foraging time, number of prey, predator type, etc.
3. Set Up Controls: Why is it important to have a control background (e.g., green prey on green background)? What other controls could you include in a predation simulation?
4. Data Collection:
 - Scatter 90 colored squares randomly across a green (grassy) background table.
 - Students “forage” for 30 seconds using forceps, prioritizing whatever they can pick up fastest (competitive foraging).
 - Count survivors in each color category. Calculate % survival per color on the green background.
 - Repeat on a brown paper background.
 - Perform at least 3 replicates for each background type.

Part 2: Computational Biology Exercise — Selection Coefficient Analysis with Python

Optional computational check: run this self-contained Python snippet from the project root. It uses tested `src/biology` modules and requires no external notebook or CSV file.

Compare a hand-calculated allele-frequency change with the selection simulator.

```
from biology.evolution import Population, simulate_selection

start = Population(name="demo", p=0.3, q=0.7, fitness_AA=1.0, fitness_Aa=0.9, fitness_aa=0.6)
history = simulate_selection(start, generations=10)

print("starting p:", start.p)
print("final p:", round(history[-1].p, 3))
print("generations recorded:", len(history))
```

Part 3: Finch Beak Analysis

5. Design an Alternative Experiment: Instead of just analyzing provided data, design an experiment to test how seed availability affects beak morphology in a bird population over multiple generations. What hypothesis would you test? How would you measure beak depth?
6. Hypothesis: Predict the relationship between seed hardness and average beak depth. Would you expect a linear relationship, or something else? Why?

Data Recording

Table 585. Part 3: Finch Beak Analysis: Color and Starting #.

Color	Starting #	# Surviving (green)	% Survival (green)	# Surviving (brown)	% Survival (brown)
Green	30				
Red	30				
Brown	30				

Selection coefficients:

Table 586. Part 3: Finch Beak Analysis: Genotype and Habitat A fitness (w).

Genotype	Habitat A fitness (w)	s (A)	Habitat B fitness (w)	s (B)
AA				
Aa				
aa				

Finch graph trend description:

Evidence and Reproducibility Checklist

- Primary evidence goal: Simulate selection across generations under alternative fitness assumptions.
- Data skill to practice: Interpret fitness data and distinguish selection from other forces.
- BioSkills emphasis: Modeling and simulation, Quantitative reasoning, Communication and collaboration.
- Control logic: identify at least one positive control, one negative control, or one baseline comparison before interpreting results.
- Measurement discipline: record units, uncertainty, sample size, and any discarded observation with a reason.
- Mechanistic link: connect one result directly to the parent chapter’s big idea before writing the conclusion.
- Reproducibility check: state one procedural detail that another group would need in order to reproduce the result.

Paper-Based Evidence Upgrade

Before answering the analysis questions, annotate the paper dataset for Natural Selection and Adaptation with a reproducibility pass:

Table 587. Part 3: Finch Beak Analysis: Evidence check and Student action.

Evidence check	Student action
Control logic	Mark the comparison that functions as the baseline, negative control, or reference case.
Uncertainty	Circle the row, card, diagram feature, or model assumption most likely to change the conclusion.
Model comparison	State whether a simpler rule, null model, or alternative mechanism could explain the same pattern.
Decision threshold	Write the minimum evidence that would make you revise the interpretation.
Reproducibility	Record the exact scoring rule another group would need to reproduce your classification.

Focus note: in this background-survival and finch-beak lab, treat each generation’s surviving color or beak counts as a measured fitness differential, and separate selection acting on heritable variation from within-generation plasticity before claiming adaptation. Keep required work paper-based; any material-handling or equipment version belongs only in an optional extension.

Worked Example: Allele Frequency Change Under Selection

Problem: A beneficial dominant allele starts at frequency $p_0 = 0.02$ in a large population. The recessive genotype has a selection coefficient $s = 0.08$ against it (relative fitnesses 1, 1, $1 - s$ for AA, Aa, aa). Using the approximation for a rare dominant beneficial allele, $\Delta p \approx s \times p \times (1 - p) \times (1 - p) \approx s \times p \times (1 - p)^2$, estimate the allele frequency after 20 generations of recursive selection.

Solution: At each generation, update $p_{t+1} = p_t + s \times p_t \times (1 - p_t)^2$ with $s = 0.08$. Starting at $p_0 = 0.02$, the per-generation increments are small while p is rare and grow as p increases. Iterating the recursion gives approximately $p_1 \approx 0.02154$, $p_5 \approx 0.02893$, $p_{10} \approx 0.04075$, $p_{15} \approx 0.05625$, and $p_{20} \approx 0.07585$. The trajectory is concave-up in the rare-allele regime and accelerates as the favored allele becomes more common.

Interpretation: Over 20 generations, the allele frequency rises from 0.02 to roughly 0.076 — a near-fourfold increase, but the allele remains far from fixation. Two features of the trajectory are characteristic of selection on a rare dominant: the initial increase is slow because $(1 - p)^2$ is near 1 and p is small, and the rate of change is governed by the product $s \times p$. As p grows past about 0.5, the $(1 - p)^2$ factor pulls Δp back down, producing the familiar sigmoid sweep. The approximation neglects drift, which becomes important when $N_e \times s \times p$ is below about 1 — in small populations this trajectory would show much greater stochastic variation.

Source-Governance Checkpoint

Complete the source-governance card for Natural Selection and Adaptation before writing the conclusion. Name the source type or model snapshot, record the evidence date or version, decide whether the claim is stable or fast-moving, and write one refresh trigger that would force the interpretation to change. Treat the card as a printed evidence object, not as a live web lookup.

Analysis Questions

1. On the green background, which color survived best? Explain in terms of camouflage and predator visual system. How does this simulate directional selection in a real habitat?
2. If the green background was then “burned” and replaced with brown substrate (environmental change), predict how allele frequencies for “green color” would change over generations. Which type of selection would now operate?
3. The finch beak data showed that species with deep beaks eat harder seeds. Explain how this pattern could arise through: (a) individual phenotypic plasticity within one generation; (b) natural selection across many generations. How would you distinguish these mechanisms with an experimental test?
4. Antibiotics are not “mutagens” — they do not create resistant mutants. They primarily *select for* pre-existing resistant mutants. Explain why this distinction matters for how we should use antibiotics clinically, and how the selection coefficient for resistance changes with antibiotic presence vs absence.
5. Compare the evidence supporting the gradual-change model of evolution (phyletic gradualism) vs the punctuated equilibrium model. What does the fossil record actually show, and what is the current consensus about the pace of evolutionary change?

Extension Analysis Questions

- 6. Statistical Analysis: If you performed three replicates of the selection simulation, how would you analyze the variation in survival rates? What statistical test would you use to determine if differences between prey colors are significant?
- 7. Experimental Error Analysis: What are three potential sources of error in the predator-prey simulation? How could you modify the procedure to reduce each source of error?
- 8. Experimental Design: If you wanted to test whether a particular trait is under directional, stabilizing, or disruptive selection, how would you design the experiment? What data would you collect? How would you analyze it?

Group Project Extension (Multi-Session)

Design an Evolutionary Study of Antibiotic Resistance

This project will span 2-3 lab sessions:

- Session 1: Research Question and Hypothesis - How does antibiotic concentration affect the rate of resistance evolution in bacteria? - Formulate a hypothesis about the relationship between selection pressure and resistance development - Design a simulation using provided allele-frequency and MIC datasets across different antibiotic concentrations
- Session 2: Data Collection and Analysis - Analyze printed time-series data showing resistant and sensitive genotypes over generations - Estimate resistance levels from provided minimum inhibitory concentration tables - Compare allele-frequency changes against a no-antibiotic baseline and a high-dose scenario
- Session 3: Data Interpretation and Presentation - Compare resistance evolution across different antibiotic concentrations - Calculate selection coefficients for resistant vs sensitive bacteria - Evaluate whether each scenario is reproducible by checking sample size, replicate count, and starting allele frequency - Create a scientific poster or presentation

Real-World Problem Solving: Evolution and Medicine

Case Study: Evolution of Virulence

- 1. Research Task: Investigate the trade-off hypothesis for the evolution of virulence. Under what conditions would a pathogen evolve to be more or less virulent?
- 2. Ethical Consideration: Should we use anti-evolution drugs (e.g., “anti-evolution” compounds that reduce mutation rates or horizontal gene transfer) to slow the evolution of resistance? What are the potential benefits and risks?
- 3. Policy Proposal: Design a policy for the responsible use of antibiotics in agriculture. Consider: growth promotion vs disease prevention, alternatives to antibiotics, and monitoring of resistance.

Post-Lab Synthesis

- Concept Check (Synthesis): Antibiotic resistance in bacterial pathogens illustrates natural selection acting on either standing genetic variation or new mutations. Evaluate how to distinguish the two modes empirically, then design a treatment protocol that would slow resistance evolution in a pathogen with a generation time near 30 minutes.
- (a) Compare the two modes of adaptation. Describe the population-genetic signatures expected for selection on standing variation (a soft sweep, with multiple resistant haplotypes rising together) versus selection on a new mutation (a hard sweep, with a single haplotype rising and reducing local diversity). Identify at least one sequencing or phylogenetic observation that could discriminate the two scenarios in a clinical or environmental sample.
 - (b) Estimate the within-host evolutionary potential of a pathogen with a 30-minute generation time. Calculate the number of generations per day (48), and describe how a population size of roughly 10^9 cells provides many opportunities for resistance mutations to arise. Discuss why monotherapy at a sub-therapeutic dose tends to favor stepwise resistance evolution.
 - (c) Design a treatment protocol intended to slow resistance evolution. Include at least three components, such as (i) combination therapy targeting multiple pathways to raise the effective number of independent mutations required for resistance, (ii) high-dose short-course dosing aimed at suppressing the pathogen population below the threshold where resistant variants can establish, and (iii) cycling or rotational use of antibiotics to lower the steady selective pressure on any single mechanism. Identify at least one trade-off (such as toxicity, cost, or compliance) for each component, and explain why the protocol would tend to reduce, rather than fully prevent, the emergence of resistance.

Safety and Ethics Notes

Forceps (plastic or blunt-tip) are low risk. Ensure fairness in simulation — most students forage simultaneously. Small colored squares: keep away from young children (swallowing hazard). Antibiotic-resistance work in this lab is paper-based primarily; do not culture bacteria or handle antibiotics. When discussing antibiotic resistance, emphasize following current prescriber instructions, avoiding unnecessary antibiotic starts, using diagnostics when available, and protecting access to effective treatment.

Debrief and Reflection

After you finish the practical work, spend 5–10 minutes in your small group comparing results and discussing the following prompts. Each member should contribute at least one observation before moving to the next prompt:

1. What did your measurements show — compare the group’s results to the textbook’s predictions. Where they diverge, suggest at least one mechanistic explanation before concluding “experimental error.”
2. What would change the outcome — propose one modification to the procedure that would sharpen the measurement or extend the result to a new biological context, and predict what you would observe.
3. One-sentence headline — each student composes a single sentence summarizing the lab’s take-home message, suitable for a tweet. Compare sentences across groups; good headlines are short, quantitative, and mechanistic.
4. Connection back to the textbook — identify one section of section 21 that your data either confirmed or complicated. Cite the specific passage.
5. Experimental Design Reflection: What was the strongest aspect of your experimental design? What would you change if you could repeat the experiment?

Further Reading (Lab)

- Revisit the parent chapter section 21 for the theoretical foundations on which this lab is built.
- Look up any bolded glossary term introduced in the textbook chapter (each has a #gl:term-slug link in the text) — its master definition is in manuscript/glossary.md.
- Explore the Python code in src/biology/evolution/evolution.py for evolutionary calculations.
- Use the self-contained Part 2 snippet as the computational template; it runs against tested project modules without external notebooks or CSV files.

Lab — Genetic Drift, Gene Flow, and Speciation

This activity accompanies section 22 of the textbook — review that chapter before attempting the exercises below.

Learning Objectives

- Design and evaluate a founder effect simulation to measure genetic drift
- Formulate testable hypotheses about how population size affects genetic diversity
- Identify independent, dependent, and controlled variables in population genetics experiments
- Analyze experimental data using allele frequency calculations and Fst statistics
- Write a brief scientific report with hypothesis, methods, results, and conclusion

Alignment and Rubric Map

- Outcome 1 (LO1): Interpret the supplied evidence or model output for Genetic Drift, Gene Flow, and Speciation.
- Outcome 2 (LO2): Identify controls and comparison groups that make the claim testable.
- Outcome 3 (LO3): Quantify uncertainty, boundary conditions, or alternative explanations before concluding.
- Outcome 4 (LO4): Transfer the mechanism to a new biological case or public-facing decision.
- Chapter LO coverage: LO1, LO2, LO3, LO4
- Rubric dimensions: evidence; controls; uncertainty; mechanism; transfer. ## Pre-Lab Concept Questions {.unnumbered}

Answer these before starting the investigation — they activate knowledge from the parent chapter.

1. Explain why random genetic drift has a larger per-generation effect in small populations than in large ones. Reference the variance of allele frequency change $\text{Var}(\Delta p) = p \times (1 - p) / (2 N_e)$ and describe how this sampling-variance scaling relates to the random outcome of allele transmission across generations.
2. State the biological species concept (BSC) in your own words, and identify one well-known limitation. Give a concrete example (such as asexual lineages, ring species, or extinct taxa) where the BSC is difficult to apply, and briefly describe an alternative species concept that handles the case more gracefully.
3. Distinguish pre-zygotic from post-zygotic reproductive isolation, and give two examples of each. For each example, describe whether the isolating mechanism would tend to be reinforced or weakened by ongoing gene flow between diverging populations.

Pre-Lab Inquiry Questions

Complete these questions before coming to lab. Use your textbook and additional research to inform your hypotheses.

1. Hypothesis Formation: Based on your understanding of genetic drift, predict how the allele frequency in a small founding population (e.g., 6 individuals) would compare to the source population (100 individuals). Write a clear, testable hypothesis.
2. Experimental Design: What is the independent variable in a genetic drift simulation? What is the dependent variable? List at least 5 variables that should be controlled to ensure valid results.
3. Scientific Context: The Fixation Index (Fst) quantifies genetic differentiation between populations. Why is this measure important in evolutionary biology? How does it relate to gene flow and speciation?
4. Quantitative Reasoning: If two populations have allele frequencies of 0.8 and 0.2 for the same gene, what would their Fst be? Show your calculation.
5. Real-World Application: The founder effect is thought to have played a role in the high prevalence of certain genetic disorders in isolated populations (e.g., Tay-Sachs in Ashkenazi Jews). How does the founder effect explain this pattern? What are the implications for genetic counseling?

Lab Context: Genetic Drift, Gene Flow, and Speciation

Even without natural selection, populations evolve through random genetic drift, gene flow, and mutation. The founder effect (a special case of bottleneck) occurs when a small number of individuals colonise a new area, carrying primarily a subset of the original gene pool’s variation. Speciation — the formation of new species — occurs when reproductive isolation evolves between populations, typically after geographic (allopatric) or ecological (sympatric) separation. The Fixation Index $F_{st} = (H_T - H_S) / H_T$ quantifies genetic differentiation between populations (0 = no differentiation; 1 = complete differentiation).

The effective-population-size worked example in the parent chapter (section 22) shows how sex-ratio skew reduces genetic drift from $N_e = N$ toward $N_e = 4N_mN_f/(N_m + N_f)$: a 10:90 male-to-female ratio with $N = 100$ gives $N_e = 36$. This lab simulates drift empirically using dice rolls across replicate populations and then compares the observed variance in allele frequency to the theoretical expectation under different N_e values.

Paper-Based Materials

Table 588. Alignment and Rubric Map: Item and Quantity.

Item	Quantity
Source-governance card for Genetic Drift, Gene Flow, and Speciation: evolutionary-evidence source card: alternative hypotheses, sampling, calibration, and confidence boundary	1
100 beads (50 red, 50 blue — representing two alleles) in a bag	1
Second bag for “new island”	1
Speciation case study cards (allopatric: Hawaiian honeycreepers; sympatric: cichlid fish in Lake Victoria)	1 set
Galapagos mockingbird morphological data (printed: beak length, body mass per island)	1
Calculator	1
Graph paper	1
Calculator or optional Python REPL with this project installed	1
Population genetics worksheet	1

Paper-Based Investigation

Part 1: Founder Effect Simulation

1. Formulate Your Hypothesis: Based on your pre-lab research, write a hypothesis about how the size of a founding population affects the rate of genetic drift.
2. Identify Variables:

• Independent variable: Founder population size (6 vs 20 individuals)

• Dependent variable: Change in allele frequency from source population

• Controlled variables: Source population allele frequency, number of generations, etc.
3. Set Up Controls: Why is it important to start with a known source population allele frequency? What other controls could you include in a genetic drift simulation?
4. Data Collection:

• Start: 100 beads at $p = 0.5$. Draw 6 beads randomly (founder population) — do not replace.

• Record allele frequencies in the founder group; use these to repopulate to 100 (multiply founder frequencies $\times 100$).

• Repeat sampling: draw 20 from the new population to simulate a moderate founding event.

• Compare p values: original, 6-founder, 20-founder.

• Perform at least 3 replicates for each founder size.

Part 2: Computational Biology Exercise — Population Genetics Analysis with Python

Optional computational check: run this self-contained Python snippet from the project root. It uses tested `src/biology` modules and requires no external notebook or CSV file.

Run deterministic drift simulations by fixing the random seed.

```
from biology.evolution import isolation_index, simulate_drift

small = simulate_drift(p=0.5, N=20, generations=10, rng_seed=7)
```

```
large = simulate_drift(p=0.5, N=500, generations=10, rng_seed=7)

print("small-population final p:", round(small[-1], 3))
print("large-population final p:", round(large[-1], 3))
print("isolation example:", round(isolation_index(gene_flow_rate=0.01, mutation_rate=0.001), 3))
```

Part 3: Morphological Divergence Analysis

5. Design an Alternative Investigation: Instead of just analyzing provided morphological data, design a paper-based comparison to test how geographic isolation affects trait divergence in a natural population. What hypothesis would you test? Which archived measurements, sample sizes, and map distances would you need?
6. Hypothesis: Predict the relationship between geographic distance and morphological divergence. Would you expect a linear relationship, or something else? Why?

Data Recording

Table 589. Part 3: Morphological Divergence Analysis: Founding event and Sample size.

Founding event	Sample size	p (red allele)	q (blue allele)
Original	100	0.5	0.5
6-founder	6		
20-founder	20		

Mockingbird data summary (fill from provided table):

Table 590. Part 3: Morphological Divergence Analysis: Island and Mean beak length (mm).

Island	Mean beak length (mm)	Mean body mass (g)	Distinct from others?
Santa Cruz			
Genovesa			
Española			
Fernandina			

Fst calculation: $H_T =$; $H_S =$; $F_{st} =$ ____; Interpretation:

Evidence and Reproducibility Checklist

- Primary evidence goal: Model drift and speciation scenarios with repeated trials.
- Data skill to practice: Distinguish stochastic from directional change in allele-frequency data.
- BioSkills emphasis: Modeling and simulation, Quantitative reasoning, Communication and collaboration.
- Control logic: identify at least one positive control, one negative control, or one baseline comparison before interpreting results.
- Measurement discipline: record units, uncertainty, sample size, and any discarded observation with a reason.
- Mechanistic link: connect one result directly to the parent chapter’s big idea before writing the conclusion.
- Reproducibility check: state one procedural detail that another group would need in order to reproduce the result.

Paper-Based Evidence Upgrade

Before answering the analysis questions, annotate the paper dataset for Genetic Drift, Gene Flow, and Speciation with a reproducibility pass:

Table 591. Part 3: Morphological Divergence Analysis: Evidence check and Student action.

Evidence check	Student action
Control logic	Mark the comparison that functions as the baseline, negative control, or reference case.
Uncertainty	Circle the row, card, diagram feature, or model assumption most likely to change the conclusion.
Model comparison	State whether a simpler rule, null model, or alternative mechanism could explain the same pattern.
Decision threshold	Write the minimum evidence that would make you revise the interpretation.
Reproducibility	Record the exact scoring rule another group would need to reproduce your classification.

Focus note: in this founder-event and F_{ST} lab, distinguish allele-frequency change caused by sampling in small colonising groups (drift) from differentiation maintained by restricted gene flow, and state which reproductive-isolation barrier each cichlid or mockingbird comparison would require before calling the populations distinct species. Keep required work paper-based; any material-handling or equipment version belongs only in an optional extension.

Worked Example: Effective Population Size with Unequal Sex Ratio

Problem: A population contains 100 individuals (50 male, 50 female), but breeding success is highly skewed — 10 males father about 90 percent of the offspring while the other 40 males contribute negligibly. Treating the breeding males as $N_m = 10$ and the breeding females as $N_f = 50$, calculate the effective population size using $N_e = 4 \times N_m \times N_f / (N_m + N_f)$, and compare it with a random-mating population of 100.

Solution: Substitute $N_m = 10$ and $N_f = 50$ into the formula. The numerator is $4 \times 10 \times 50 = 2000$. The denominator is $N_m + N_f = 10 + 50 = 60$. Dividing, $N_e \approx 2000 / 60 \approx 33.3$ — roughly one-third of the census size. For a random-mating population of the same census size 100 with equal breeding success, N_e would be much closer to 100, although seldom exactly equal because of generational and reproductive variance.

Interpretation: Reducing the breeding sex ratio from 50:50 to 10:50 cuts the effective population size from near 100 to about 33. The per-generation loss of heterozygosity is governed by $1 / (2 N_e)$, so this skew triples the rate of drift compared with the random-mating case. Two consequences follow: rare alleles are lost more readily, and the inbreeding coefficient F accumulates faster. In a conservation context, this is why a census count alone can give an overly optimistic view of a population’s genetic health — the relevant quantity for diversity loss is N_e , not N .

Source-Governance Checkpoint

Complete the source-governance card for Genetic Drift, Gene Flow, and Speciation before writing the conclusion. Name the source type or model snapshot, record the evidence date or version, decide whether the claim is stable or fast-moving, and write one refresh trigger that would force the interpretation to change. Treat the card as a printed evidence object, not as a live web lookup.

Analysis Questions

1. How would the allele frequencies in the 6-founder event compare to the original population? What does this demonstrate about why small colonising populations often show low genetic diversity compared to mainland populations?
2. The mockingbird populations on different Galapagos islands show morphological divergence. What mechanism prevented gene flow between islands, and what type of speciation does this represent? What reproductive isolation mechanisms would need to evolve for them to become separate species?
3. $F_{ST} = 0$ indicates populations are identical (freely exchanging genes). $F_{ST} = 1$ indicates complete isolation. How would you interpret $F_{ST} = 0.15$ — is there gene flow? Use your calculated F_{ST} to describe the degree of isolation between cichlid populations A, B, and C.
4. Lake Victoria cichlids underwent adaptive radiation in about 15,000 years, producing >500 species. What does this rapid speciation suggest about the speed at which reproductive isolation can evolve? What kind of speciation (allopatric, parapatric, or sympatric) is most consistent with this pattern?
5. Ring species (like *Larus* gulls circling the Arctic) demonstrate speciation in action: adjacent populations can interbreed, but the two ends of the ring cannot. Explain what this demonstrates about the continuity of the speciation process and why ring species challenge a strict definition of “species.”

Extension Analysis Questions

6. Statistical Analysis: If you performed three replicates of the founder effect simulation, how would you analyze the variation in allele frequency change? What statistical test would you use to determine if differences between founder sizes are significant?
7. Experimental Error Analysis: What are three potential sources of error in the bead simulation? How could you modify the procedure to reduce each source of error?
8. Experimental Design: If you wanted to test whether two populations are diverging due to genetic drift or natural selection, how would you design the experiment? What data would you collect? How would you analyze it?

Group Project Extension (Multi-Session)

Design a Study of Human Population Differentiation

This project will span 2-3 lab sessions:

- Session 1: Research Question and Hypothesis - How does geographic distance affect genetic differentiation in human populations? - Formulate a hypothesis about the relationship between distance and Fst - Design a study using publicly available genetic data (e.g., 1000 Genomes Project)
- Session 2: Data Collection and Analysis - Download genetic data for multiple populations - Calculate Fst between population pairs - Plot Fst against geographic distance
- Session 3: Data Interpretation and Presentation - Analyze the correlation between distance and genetic differentiation - Discuss the implications for understanding human migration history - Create a scientific poster or presentation

Real-World Problem Solving: Conservation Genetics

Case Study: Genetic Rescue of Endangered Populations

1. Research Task: Investigate the Florida panther bottleneck. How did genetic drift and inbreeding depression affect the population? What was the outcome of the genetic rescue program?
2. Ethical Consideration: Should we introduce individuals from other populations to increase genetic diversity in endangered species? What are the potential benefits and risks (e.g., outbreeding depression)?
3. Policy Proposal: Design a policy for managing genetic diversity in small, isolated populations. Consider: when to intervene, how to select individuals for translocation, and how to monitor success.

Post-Lab Synthesis

- Concept Check (Synthesis): A peripheral isolate of 40 individuals has split off from a large continental source population and become geographically isolated. Evaluate whether this isolate is more likely to undergo speciation predominantly via genetic drift or via natural selection, and predict the genomic signatures that would distinguish the two modes in a follow-up sequencing study.
- (a) Compare the expected per-generation magnitudes of drift and selection in the isolate. Estimate the drift scale as $1 / (2 N_e) \approx 1/80 \approx 0.0125$ per generation, and discuss when this exceeds the selection coefficient s on a candidate adaptive locus. Describe the conditions (low s , low N_e , novel environment) under which drift would tend to dominate the divergence, and the conditions (moderate s , distinct selective regime) under which selection would.
- (b) Predict the genomic signatures for each mode. Drift-dominated divergence tends to produce a broadly uniform increase in differentiation across the genome (elevated genome-wide F_{ST}), an excess of rare and lineage-private alleles, and few sharp peaks of divergence. Selection-driven divergence tends to produce localized peaks of high F_{ST} around loci tied to the new environment, reduced diversity in those windows, and extended haplotype homozygosity consistent with recent sweeps. Note that gene flow can blur both signatures.
- (c) Outline a sequencing study that would discriminate the two modes. Recommend whole-genome resequencing of about 20 individuals from each population, computation of windowed F_{ST} and nucleotide diversity, and a genome-wide scan for selective sweeps. Predict the expected outcome under each hypothesis and identify at least one confound (such as recent admixture, low-recombination regions, or background selection) that could mimic a drift or selection signature and complicate the interpretation.

Safety and Ethics Notes

Bead simulation: ensure beads are not ingested. Discussions of speciation based on genetic data should be careful not to conflate genetic population differences with outdated racial taxonomic thinking. Consider the ethical implications of conservation genetics.

Debrief and Reflection

After you finish the practical work, spend 5–10 minutes in your small group comparing results and discussing the following prompts. Each member should contribute at least one observation before moving to the next prompt:

1. What did your measurements show — compare the group’s results to the textbook’s predictions. Where they diverge, suggest at least one mechanistic explanation before concluding “experimental error.”
2. What would change the outcome — propose one modification to the procedure that would sharpen the measurement or extend the result to a new biological context, and predict what you would observe.
3. One-sentence headline — each student composes a single sentence summarizing the lab’s take-home message, suitable for a tweet. Compare sentences across groups; good headlines are short, quantitative, and mechanistic.
4. Connection back to the textbook — identify one section of section 22 that your data either confirmed or complicated. Cite the specific passage.
5. Experimental Design Reflection: What was the strongest aspect of your experimental design? What would you change if you could repeat the experiment?

Further Reading (Lab)

- Revisit the parent chapter section 22 for the theoretical foundations on which this lab is built.
- Look up any bolded glossary term introduced in the textbook chapter (each has a #gl:term-slug link in the text) — its master definition is in manuscript/glossary.md.
- Explore the Python code in src/biology/evolution/evolution.py for population genetics calculations.
- Use the self-contained Part 2 snippet as the computational template; it runs against tested project modules without external notebooks or CSV files.

Lab — Phylogenetics and the Tree of Life

Learning Objectives

This activity accompanies section 23 of the textbook — review that chapter before attempting the exercises below.

- Construct a cladogram from a morphological character matrix using parsimony
- Interpret a molecular phylogeny to determine divergence times and evolutionary relationships
- Identify synapomorphies and plesiomorphies from a character matrix
- Evaluate conflicting phylogenetic hypotheses using bootstrap support values

Alignment and Rubric Map

- Outcome 1 (LO1): Interpret the supplied evidence or model output for Phylogenetics and the Tree of Life.
- Outcome 2 (LO2): Identify controls and comparison groups that make the claim testable.
- Outcome 3 (LO3): Quantify uncertainty, boundary conditions, or alternative explanations before concluding.
- Outcome 4 (LO4): Transfer the mechanism to a new biological case or public-facing decision.
- Chapter LO coverage: LO1, LO2, LO3, LO4
- Rubric dimensions: evidence; controls; uncertainty; mechanism; transfer. ## Pre-Lab Concept Questions {.unnumbered}

Answer these before starting the investigation — they activate knowledge from the parent chapter.

1. Define a synapomorphy and explain why shared derived characters, rather than shared ancestral characters (symplesiomorphies), are used to recover phylogenetic relationships. Provide a concrete example, such as the amniotic egg uniting reptiles, birds, and mammals, and describe how the same character can be a synapomorphy at one level of the tree and a symplesiomorphy at a deeper level.
2. Describe what bootstrap support represents in a maximum-likelihood or parsimony phylogeny. Explain how the sites of a sequence alignment are re-sampled with replacement to build pseudo-replicate trees, and how a bootstrap value (for example, 95) on a branch is interpreted as the fraction of pseudo-replicates that recovered that clade.
3. Distinguish parsimony, maximum likelihood, and Bayesian inference as tree-building criteria. State the optimality criterion or objective function used by each, and identify one strength and one limitation per method (for example, parsimony is conceptually simple but susceptible to long-branch attraction).

Lab Context: Phylogenetics and the Tree of Life

Phylogenetics reconstructs evolutionary history by identifying shared derived characters (synapomorphies) that define clades. Maximum parsimony selects the tree requiring the fewest evolutionary changes. Molecular phylogenies use DNA/protein sequence differences, calibrated with fossil dates, to construct ultrametric trees with branch lengths proportional to substitution rate or time. Bootstrap values (percentage of resampled datasets recovering the same clade) indicate support for individual nodes.

Paper-Based Materials

Table 592. Alignment and Rubric Map: Item and Quantity.

Item	Quantity
Source-governance card for Phylogenetics and the Tree of Life: evolutionary-evidence source card: alternative hypotheses, sampling, calibration, and confidence boundary	1
Character matrix (12 taxa × 10 morphological characters; 0=absent, 1=present)	1 printed
Molecular phylogeny printout (5 taxa; with branch lengths and bootstrap values)	1
Cladogram construction guide	1
Scissors; paste; paper	1 set
Calculator	1

Paper-Based Investigation

Part A — Manual Cladogram Construction

1. Using the character matrix, identify which characters are shared among subsets of taxa (synapomorphies) vs ancestral (plesiomorphies shared by outgroup).
2. Use the principle of parsimony to construct the most parsimonious cladogram for 6 selected taxa (the other 6 are “outgroups” — use to root the tree).
3. Count the total number of character-state changes on your tree vs an alternative arrangement. Identify which tree requires fewer changes (most parsimonious).

Part B — Molecular Phylogeny Interpretation

4. On the provided molecular phylogeny: identify (a) the most recent common ancestor of taxa A and B; (b) which taxon diverged first from the others; (c) any polytomies (unresolved nodes); (d) the clade with the highest bootstrap support.

Data Recording

Character matrix (excerpt — 5 taxa):

Table 593. Alignment and Rubric Map: Taxon and Vertebrae.

Taxon	Vertebrae	Four limbs	Feathers	Mammary glands	Placenta
Lamprey	1	0	0	0	0
Salamander	1	1	0	0	0
Crocodile	1	1	0	0	0
Robin	1	1	1	0	0
Human	1	1	0	1	1

Your cladogram sketch:

Most parsimonious tree — total changes: *Alternative tree — total changes:*

Molecular phylogeny notes: - Taxon diverging first: - *Highest bootstrap node: (% support)* - *Any polytomies?*

Evidence and Reproducibility Checklist

- Primary evidence goal: Infer relationships from character or sequence evidence.
- Data skill to practice: Read trees correctly and map traits or sequences onto branches.
- BioSkills emphasis: Modeling and simulation, Quantitative reasoning, Communication and collaboration.
- Control logic: identify at least one positive control, one negative control, or one baseline comparison before interpreting results.
- Measurement discipline: record units, uncertainty, sample size, and any discarded observation with a reason.
- Mechanistic link: connect one result directly to the parent chapter’s big idea before writing the conclusion.
- Reproducibility check: state one procedural detail that another group would need in order to reproduce the result.

Paper-Based Evidence Upgrade

Before answering the analysis questions, annotate the paper dataset for Phylogenetics and the Tree of Life with a reproducibility pass:

Table 594. Alignment and Rubric Map: Evidence check and Student action.

Evidence check	Student action
Control logic	Mark the comparison that functions as the baseline, negative control, or reference case.
Uncertainty	Circle the row, card, diagram feature, or model assumption most likely to change the conclusion.
Model comparison	State whether a simpler rule, null model, or alternative mechanism could explain the same pattern.
Decision threshold	Write the minimum evidence that would make you revise the interpretation.
Reproducibility	Record the exact scoring rule another group would need to reproduce your classification.

Focus note: in this character-matrix and tree-building lab, justify each clade with a shared derived character (synapomorphy) rather than overall similarity, treat bootstrap percentages as resampling support rather than proof, and flag where horizontal gene transfer or hybridization would make a strictly bifurcating tree the wrong model. Keep required work paper-based; any material-handling or equipment version belongs only in an optional extension.

Worked Example: UPGMA Tree from a Pairwise Distance Matrix

Problem: Three species A, B, and C share a common ancestor. The pairwise distances are $d(A, B) = 0.05$, $d(A, C) = 0.12$, and $d(B, C) = 0.10$. Using the UPGMA algorithm, infer the tree topology, calculate node depths, draw the tree with branch lengths, and convert the depths to divergence times assuming a molecular clock of 2 percent per million years.

Solution: UPGMA joins the two closest lineages first. The smallest distance is $d(A, B) = 0.05$, so A and B cluster first. The node AB lies at depth $d(A, B) / 2 = 0.025$ (each tip is 0.025 from the node). The new distance from the AB cluster to C is the average of the original distances from C to each member: $d(AB, C) = (d(A, C) + d(B, C)) / 2 = (0.12 + 0.10) / 2 = 0.11$. The node ABC then lies at depth $d(AB, C) / 2 = 0.055$. The branch length from the AB node up to the ABC node is $0.055 - 0.025 = 0.030$, and the branch from C up to the ABC node is 0.055. Converting depths to divergence times with a clock of 2 percent per million years (i.e., 0.02 substitutions per site per million years), the A–B split occurred at $0.025 / 0.02 = 1.25$ million years ago, and the AB–C split occurred at $0.055 / 0.02 = 2.75$ million years ago.

Interpretation: UPGMA produces an ultrametric tree, in which every tip is equidistant from the root — an assumption equivalent to a strict molecular clock across lineages. The estimated split times here depend on that assumption; if the clock varies among lineages, neighbor-joining or a relaxed-clock model in a Bayesian framework would be more appropriate. The distances in this example are also small enough that no multiple-hit correction is applied; for larger distances, a Jukes-Cantor or more parameter-rich substitution model is typically used before tree construction.

Source-Governance Checkpoint

Complete the source-governance card for Phylogenetics and the Tree of Life before writing the conclusion. Name the source type or model snapshot, record the evidence date or version, decide whether the claim is stable or fast-moving, and write one refresh trigger that would force the interpretation to change. Treat the card as a printed evidence object, not as a live web lookup.

Analysis Questions

1. In your character matrix, which character (vertebrae, four limbs, feathers, etc.) defines the broadest clade (most inclusive group)? Which is the most restricted synapomorphy (smallest clade)? Explain the concept of nested hierarchy.
2. Crocodiles share a more recent common ancestor with birds than with lizards, despite looking more like lizards. What does this illustrate about the limits of morphological similarity as an indicator of evolutionary relationship?
3. A bootstrap value of 95% means that 95% of resampled datasets recover that node. How would you interpret a node with 42% bootstrap support? Should it be included in the published tree?
4. Horizontal gene transfer (HGT) in bacteria allows genes to jump between unrelated lineages — violating the vertical (parent-to-offspring) assumption of phylogenetics. Explain how HGT would appear as a misleading signal in a molecular phylogeny, and describe one method used to detect it.
5. The “Tree of Life” analogy implies a bifurcating, hierarchical structure. However, hybridization (interspecies mating, e.g., in plants) produces reticulate evolution — a network rather than a tree. Name two plant genera where reticulate evolution occurs and describe how allopolyploidy contributes to speciation.

Post-Lab Synthesis

Concept Check (Synthesis): A clade of recently diverged species presents a phylogenetic pattern that could either reflect a true adaptive radiation or be an artifact of incomplete lineage sorting (ILS). Evaluate the additional data — morphological, behavioral, and geographic — that would help discriminate between the two scenarios, and explain why ILS is especially problematic in rapidly diversifying groups.

- (a) Identify the genomic signature of incomplete lineage sorting: discordance among gene trees across loci, with each gene tree retaining a different sampling of ancestral polymorphism. Describe how a coalescent-based species-tree method (such as ASTRAL) or a tool detecting introgression (such as the D-statistic) can summarize this discordance, and note why ILS is more frequent in clades with short internal branches and large effective population sizes — precisely the regime expected during rapid radiation.
- (b) Describe the morphological, behavioral, and geographic data that would help resolve the ambiguity. Morphological synapomorphies (such as shared adaptive structures) and behavioral traits (such as courtship displays or feeding modes) that consistently track the molecular species tree support a true radiation; mosaic patterns that conflict with the gene-tree majority hint at ILS or introgression. Geographic data — current ranges, fossil localities, paleo-environmental reconstructions — can corroborate plausible isolation events that would have driven divergence.

- (c) Outline a verification plan. Sequence many independent loci from across the genome, build per-locus gene trees, summarize their concordance with a species-tree method, and overlay morphological and biogeographic evidence. Predict that a true radiation will show coherent signal across these data types, while a pattern dominated by ILS will show discordant gene trees with little morphological or geographic alignment. Identify at least one remaining ambiguity — such as ancient introgression between sister lineages — that this plan would not fully resolve and that would require additional approaches (for example, ancestral-state reconstruction or ancient-DNA sampling) to address.

Safety and Ethics Notes

No chemical hazards. When discussing evolutionary relationships involving humans and other primates, maintain scientific respect for most organisms and evolutionary histories.

Debrief and Reflection

After you finish the practical work, spend 5–10 minutes in your small group comparing results and discussing the following prompts. Each member should contribute at least one observation before moving to the next prompt:

1. What did your measurements show — compare the group’s results to the textbook’s predictions. Where they diverge, suggest at least one mechanistic explanation before concluding “experimental error.”
2. What would change the outcome — propose one modification to the procedure that would sharpen the measurement or extend the result to a new biological context, and predict what you would observe.
3. One-sentence headline — each student composes a single sentence summarizing the lab’s take-home message, suitable for a tweet. Compare sentences across groups; good headlines are short, quantitative, and mechanistic.
4. Connection back to the textbook — identify one section of section 23 that your data either confirmed or complicated. Cite the specific passage.

Further Reading (Lab)

- Revisit the parent chapter section 23 for the theoretical foundations on which this lab is built.
- Look up any bolded glossary term introduced in the textbook chapter (each has a #gl:term-slug link in the text) — its master definition is in manuscript/glossary.md.
- Explore the appended src/ module that implements the corresponding quantitative model (when applicable) — referenced in the parent chapter’s “Bridge to Computation” subsection.

Module footer: parent chapter \cref{sec:unit_VI_phylogenetics}; all numerical quantities in this lab use SI units — see Appendix D — Units, Physical Constants, and Biological Ranges for unit conversions and biological-scale reference values.

Lab — Bacteria, Archaea, and Viruses

This activity accompanies section 24 of the textbook — review that chapter before attempting the exercises below.

Learning Objectives

- Design and evaluate a bacterial identification case packet using Gram-stain images
- Formulate testable hypotheses about how environmental factors affect simulated bacterial growth
- Identify independent, dependent, and controlled variables in microbiology experiments
- Analyze experimental data using colony counting and statistical methods
- Write a brief scientific report with hypothesis, methods, results, and conclusion

Alignment and Rubric Map

- Outcome 1 (LO1): Interpret the supplied evidence or model output for Bacteria, Archaea, and Viruses.
- Outcome 2 (LO2): Identify controls and comparison groups that make the claim testable.
- Outcome 3 (LO3): Quantify uncertainty, boundary conditions, or alternative explanations before concluding.
- Outcome 4 (LO4): Transfer the mechanism to a new biological case or public-facing decision.
- Chapter LO coverage: LO1, LO2, LO3, LO4
- Rubric dimensions: evidence; controls; uncertainty; mechanism; transfer. ## Pre-Lab Concept Questions {.unnumbered}

Answer these before starting the investigation — they activate knowledge from the parent chapter on prokaryote and viral biology.

1. Explain how Gram staining differentiates between Gram-positive and Gram-negative bacteria. Reference the role of peptidoglycan thickness and the outer membrane, and describe what color each type appears after the full stain sequence (crystal violet, iodine, ethanol, safranin).
2. Describe the lytic and lysogenic cycles of a temperate bacteriophage. For each cycle, state where the phage genome resides and one molecular event that defines that phase.
3. Prokaryotes lack membrane-bound organelles. State one process (e.g., respiration, transcription) that occurs in a different cellular location in bacteria compared to eukaryotes, and explain the implication for antibiotic targeting.

Pre-Lab Inquiry Questions

Complete these questions before coming to lab. Use your textbook and additional research to inform your hypotheses.

1. Hypothesis Formation: Based on your understanding of Gram staining, predict which type of bacteria (Gram-positive or Gram-negative) would be more resistant to antibiotics that target cell wall synthesis. Explain your reasoning.
2. Experimental Design: What is the independent variable in a bacterial growth dataset? What is the dependent variable? List at least 5 variables that should be controlled to ensure valid conclusions.
3. Scientific Context: The Gram stain is a fundamental tool in microbiology. Why is it important to classify bacteria as Gram-positive or Gram-negative? How does this classification inform treatment decisions?
4. Quantitative Reasoning: A printed dilution dataset shows 150 colonies on a 10^{-5} dilution plate, with 0.1 mL plated. What is the concentration of bacteria in the original culture? Show your calculation.
5. Real-World Application: Antibiotic resistance is a growing problem. How does the misuse of antibiotics in agriculture contribute to the evolution of resistant bacteria? What policies could help address this issue?

Lab Context: Bacteria, Archaea, and Viruses

Prokaryotes — Bacteria and Archaea — are the most abundant life forms on Earth (about 10^{31} cells). Gram staining differentiates bacteria based on cell wall composition: Gram-positive (thick peptidoglycan layer retains crystal violet — purple) vs Gram-negative (thin peptidoglycan + outer membrane — loses crystal violet, appears pink after safranin counterstain). Viruses are acellular entities that replicate primarily inside host cells; bacteriophages infect bacteria and follow either lytic (immediate replication and lysis) or lysogenic (DNA integration, dormancy) cycles.

Paper-Based Materials

Table 595. Alignment and Rubric Map: Item and Quantity.

Item	Quantity
Source-governance card for Bacteria, Archaea, and Viruses: pathogen-surveillance source card: organism-resistance pair, official guidance date, setting, and intervention limit	1
Gram-stain image cards with metadata removed	1 set
Known Gram-positive and Gram-negative control image cards	1 set
Printed serial-dilution plate images (10^{-4} to 10^{-6} , three replicates)	1 set
Bacterial growth curve data under temperature, pH, and salt scenarios	1
Phage life-cycle decision cards	1 set
AMR treatment decision matrix	1
Horizontal-gene-transfer map cards: plasmid, transposon, integron, phage, transformation, wastewater, and hospital ward	1 set
<i>Candida auris</i> clinical triage card: colonization vs infection, identification method, surface persistence, susceptibility result	1
Calculator or optional Python REPL with this project installed	1
Ruler or transparent counting grid	1

Paper-Based Investigation

Part 1: Gram-Stain Image Classification

1. Formulate Your Hypothesis: Based on your pre-lab research, write a hypothesis about how the Gram stain results will differ between *E. coli* and *Bacillus* species.
2. Identify Variables:
 - Independent variable: Bacterial species
 - Dependent variable: Gram stain result (purple vs pink) and cell morphology
 - Controlled variables: image source, colorcalibration note, scale label, scoring key, scorer training, and blind-card order.
3. Set Up Controls: Score the known Gram-positive and Gram-negative control cards first. What other controls could you include to ensure accurate identification, such as a mixed-species image, a low-quality image, or a blinded duplicate?
4. Data Collection:
 - Classify each blinded image card as Gram-positive, Gram-negative, mixed, or uninterpretable.
 - Record: color (purple = Gram+, pink = Gram-), cell shape (coccus, bacillus, spirillum), arrangement (single, pairs, chains, clusters), and confidence score (1-5).
 - Compare independent scorers. Resolve disagreements primarily after recording the original calls.

Part 2: Computational Biology Exercise — Bacterial Growth Analysis with Python

Optional computational check: run this self-contained Python snippet from the project root. It uses tested `src/biology` modules and requires no external notebook or CSV file.

Use the microbiology module to check growth and MIC calculations.

```
from biology.microbiology import bacterial_growth_curve, doubling_time, mic_fold_dilution

growth = bacterial_growth_curve(N0=1_000, doubling_time_hr=0.5, t_end_hr=4.0)
print("final population:", int(growth.populations[-1]))
print("doubling time from counts:", round(doubling_time(1_000, 16_000, 2.0), 2))
print("MIC dilution series:", mic_fold_dilution(128.0, dilution_factor=2, n_tubes=5))
```

Part 3: Serial Dilution and Colony Counting from Plate Images

5. Design an Alternative Investigation: Instead of performing a standard dilution series, design a data-card investigation to test how different environmental conditions (temperature, pH, salt concentration) affect bacterial growth rates. What hypothesis would you test? Which printed curve or plate-image evidence would measure growth?
6. Hypothesis: Predict how increasing salt concentration would affect the growth of *E. coli*. Would you expect a linear decrease in growth rate, or a threshold effect? Why?

Part 4: AMR Network and Fungal Triage Cards

7. Build an AMR transfer map from the provided cards. For each arrow, label whether it represents selection, horizontal gene transfer, environmental persistence, or surveillance.
8. Use the *Candida auris* card to decide whether the scenario calls for treatment, infection-control action, both, or neither. Justify your answer using colonization status, clinical infection evidence, identification method, and susceptibility data.
9. Compare the bacterial AMR map with the fungal triage card. Identify one shared One Health principle and one difference between bacterial resistance-gene transfer and healthcare-associated fungal persistence.

Data Recording

Table 596. Sample data for Part 4: AMR Network and Fungal Triage Cards.

Species	Gram stain result	Cell shape	Cell arrangement
<i>E. coli</i>			
<i>Bacillus sp.</i>			

Table 597. Part 4: AMR Network and Fungal Triage Cards: Dilution and Colonies counted.

Dilution	Colonies counted	CFU/mL
10 ⁻⁴		
10 ⁻⁵		
10 ⁻⁶		

Best estimate of original concentration: _____ CFU/mL Blinded duplicate agreement: _____%; plate images excluded, with reason: _____ AMR transfer pathway most supported: _____; *Candida auris* action selected: _____; surveillance evidence needed: _____

Evidence and Reproducibility Checklist

- Primary evidence goal: Measure growth and compare microbial life strategies.
- Data skill to practice: Interpret microbial observations from growth, sequence, or structural evidence.
- BioSkills emphasis: Science and society, Process of science, Modeling and simulation.
- Control logic: identify at least one positive control, one negative control, or one baseline comparison before interpreting results.
- Measurement discipline: record units, uncertainty, sample size, and any discarded observation with a reason.
- Mechanistic link: connect one result directly to the parent chapter’s big idea before writing the conclusion.
- Reproducibility check: state one procedural detail that another group would need in order to reproduce the result.

Paper-Based Evidence Upgrade

Before answering the analysis questions, annotate the paper dataset for Bacteria, Archaea, and Viruses with a reproducibility pass:

Table 598. Part 4: AMR Network and Fungal Triage Cards: Evidence check and Student action.

Evidence check	Student action
Control logic	Mark the comparison that functions as the baseline, negative control, or reference case.
Uncertainty	Circle the row, card, diagram feature, or model assumption most likely to change the conclusion.
Model comparison	State whether a simpler rule, null model, or alternative mechanism could explain the same pattern.
Decision threshold	Write the minimum evidence that would make you revise the interpretation.
Reproducibility	Record the exact scoring rule another group would need to reproduce your classification.

Focus note: in this lab, treat each microbe as an evidence claim built from a Gram-stain phenotype, a colony or plaque count, and a wall-structure or phage-genetics inference, and state for every conclusion whether it rests on a cultured isolate or on a sequence/diagram on paper. Keep required work paper-based; any material-handling or equipment version belongs only in an optional extension.

Worked Example: Exponential growth of an E. coli culture

Problem: A flask of *E. coli* starts at $N_0 = 10^5$ cells/mL with a doubling time of $t_d = 20$ min. Using $N = N_0 \times 2^{(t/t_d)}$, estimate the cell density after $t = 2$ h, the number of doublings, and the final density in scientific notation.

Solution: First, convert time to a consistent unit: $t = 2\text{ h} = 120\text{ min}$. The number of doublings is $t / t_d = 120 / 20 = 6$. Apply the formula: $N = 10^5 \times 2^6 = 10^5 \times 64 = 6.4 \times 10^6$ cells/mL. Six doublings multiply the population by 64, producing a final density of about 6.4×10^6 cells/mL.

Interpretation: This estimate presumes exponential growth with nutrients and space not limiting; in a closed flask the culture tends to enter stationary phase before the simple model holds for many more doublings. A typical mid-log *E. coli* culture saturates near 10^9 cells/mL, so the 6.4×10^6 value is consistent with early-to-mid log phase rather than late-stationary phase.

Source-Governance Checkpoint

Complete the source-governance card for Bacteria, Archaea, and Viruses before writing the conclusion. Name the source type or model snapshot, record the evidence date or version, decide whether the claim is stable or fast-moving, and write one refresh trigger that would force the interpretation to change. Treat the card as a printed evidence object, not as a live web lookup.

Analysis Questions

1. Why does *E. coli* stain Gram-negative? Describe the structural difference between the cell walls of Gram-positive and Gram-negative bacteria, and explain why ethanol decolourises Gram-negative but not Gram-positive cells.
2. Calculate the CFU/mL from your best printed plate count. Assuming exponential growth at a doubling time of 20 minutes, estimate how many cells would be present after 4 hours if starting from 100 CFU/mL.
3. Penicillin inhibits transpeptidase (cross-links peptidoglycan). Based on cell wall structure, predict whether penicillin is more effective against *E. coli* or *Bacillus subtilis*, and why Gram-negative bacteria often require higher doses.
4. A bacteriophage follows a lysogenic cycle for 200 generations, then enters the lytic cycle. What molecular signal might trigger the switch from lysogeny to lysis? Name the specific protease involved and the CI repressor it degrades.
5. SARS-CoV-2 is a single-stranded, positive-sense RNA virus with an envelope. Compare its replication cycle to a lytic bacteriophage: identify two key differences in where replication occurs, the host enzyme used, and the method of exiting the host cell.
6. A carbapenemase gene appears in related *Klebsiella* isolates on two hospital wards and in a wastewater sample. Use plasmid, integron, and clonal-spread evidence to decide what additional data would distinguish horizontal transfer from one expanding clone.

Extension Analysis Questions

- 7. Statistical Analysis: If the dataset includes three replicate plate images, how would you analyze the variation in CFU/mL estimates? What statistical test would you use to determine if differences between species are significant?
- 8. Experimental Error Analysis: What are three potential sources of error in bacterial colony counting from images? How could you modify the scoring rules or image set to reduce each source of error?
- 9. Experimental Design: If you wanted to test the effectiveness of different antibiotics on bacterial growth without culturing, how would you design the dataset? What controls would you include? How would you measure the effect from growth curves, MIC tables, or inhibition-zone images?

Group Project Extension (Multi-Session)

Design a Study of Antibiotic Resistance Evolution

This project will span 2-3 lab sessions:

- Session 1: Research Question and Hypothesis - How does sub-lethal antibiotic concentration affect the rate of resistance evolution in bacteria? - Formulate a hypothesis about the relationship between antibiotic concentration and resistance development - Design a simulation using provided *E. coli* growth curves and different antibiotic concentrations
- Session 2: Data Collection and Analysis - Analyze printed growth curves collected under antibiotic gradients - Measure resistance levels from minimum inhibitory concentration tables - Analyze allele-frequency changes using provided PCR or sequencing summaries
- Session 3: Data Interpretation and Presentation - Compare resistance evolution across different antibiotic concentrations - Calculate selection coefficients for resistant vs sensitive bacteria - Create a scientific poster or presentation

Real-World Problem Solving: Microbial Ethics

Case Study: Antibiotic Use in Agriculture

- 1. Research Task: Investigate the use of antibiotics as growth promoters in livestock. What percentage of antibiotics sold in the US are used for this purpose? What are the most common antibiotics used?
- 2. Ethical Consideration: Should the routine use of antibiotics for growth promotion in agriculture be banned? What are the potential economic impacts on farmers vs the public health benefits?
- 3. Policy Proposal: Design a policy to reduce antibiotic use in agriculture while ensuring animal health and farmer livelihoods. Consider: alternatives to antibiotics, monitoring systems, and transition assistance for farmers.

Post-Lab Synthesis

- Concept Check (Synthesis): Antibiotics such as penicillin and vancomycin act on peptidoglycan biosynthesis, and they tend to be well tolerated by humans even at therapeutic doses.
- (a) Explain why a drug class that disrupts peptidoglycan cross-linking is selectively toxic to bacteria relative to eukaryotic cells, with reference to the structural component the drug targets and where it is found.
 - (b) *Mycoplasma* species lack a cell wall altogether. Predict whether a peptidoglycan-targeting antibiotic would be effective against *Mycoplasma* and propose an antibiotic class likely to be more useful, justifying your choice by referencing a target the bacterium does still possess (for example, a ribosomal subunit or a nucleic-acid enzyme).

Safety and Ethics Notes

Default lab work uses printed image cards, growth curves, and decision matrices primarily. No cultures, plates, antibiotic discs, or environmental samples are required. Optional wet microbiology demonstrations must use approved BSL-1 organisms under instructor supervision and local disposal rules. When discussing antibiotic resistance, emphasize following current prescriber instructions, avoiding unnecessary antibiotic starts, using diagnostics when available, and protecting access to effective treatment.

Debrief and Reflection

- After you finish the practical work, spend 5–10 minutes in your small group comparing results and discussing the following prompts. Each member should contribute at least one observation before moving to the next prompt:
- 1. What did your measurements show — compare the group’s results to the textbook’s predictions. Where they diverge, suggest at least one mechanistic explanation before concluding “experimental error.”

2. What would change the outcome — propose one modification to the procedure that would sharpen the measurement or extend the result to a new biological context, and predict what you would observe.
3. One-sentence headline — each student composes a single sentence summarizing the lab’s take-home message, suitable for a tweet. Compare sentences across groups; good headlines are short, quantitative, and mechanistic.
4. Connection back to the textbook — identify one section of section 24 that your data either confirmed or complicated. Cite the specific passage.
5. Experimental Design Reflection: What was the strongest aspect of your experimental design? What would you change if you could repeat the experiment?

Further Reading (Lab)

- Revisit the parent chapter section 24 for the theoretical foundations on which this lab is built.
- Look up any bolded glossary term introduced in the textbook chapter (each has a #gl:term-slug link in the text) — its master definition is in manuscript/glossary.md.
- Explore the Python code in src/biology/microbiology/microbiology.py for bacterial growth calculations.
- Use the self-contained Part 2 snippet as the computational template; it runs against tested project modules without external notebooks or CSV files.

Lab — Microbial Ecology and the Microbiome

This activity accompanies section 25 of the textbook — review that chapter before attempting the exercises below.

Learning Objectives

- Design and evaluate a microbial community analysis using printed culture-independent datasets
- Formulate testable hypotheses about how environmental factors affect microbial diversity
- Identify independent, dependent, and controlled variables in microbial ecology experiments
- Analyze experimental data using diversity indices and network analysis
- Write a brief scientific report with hypothesis, methods, results, and conclusion

Alignment and Rubric Map

- Outcome 1 (LO1): Interpret the supplied evidence or model output for Microbial Ecology and the Microbiome.
- Outcome 2 (LO2): Identify controls and comparison groups that make the claim testable.
- Outcome 3 (LO3): Quantify uncertainty, boundary conditions, or alternative explanations before concluding.
- Outcome 4 (LO4): Transfer the mechanism to a new biological case or public-facing decision.
- Chapter LO coverage: LO1, LO2, LO3, LO4
- Rubric dimensions: evidence; controls; uncertainty; mechanism; transfer. ## Pre-Lab Concept Questions {.unnumbered}

Answer these before starting the investigation — they activate knowledge from the parent chapter.

1. Why is the 16S rRNA gene used to identify and classify bacteria rather than a protein-coding gene?
2. Describe nitrogen fixation — what chemical transformation occurs, which type of organisms perform it, and why is this process ecologically important?
3. Define the Shannon diversity index H' and explain what a higher value indicates about a microbial community.

Pre-Lab Inquiry Questions

Complete these questions before coming to lab. Use your textbook and additional research to inform your hypotheses.

1. Hypothesis Formation: Based on your understanding of microbial ecology, predict which provided community dataset (soil, skin, tap water, or gut) will have the highest microbial diversity. Write a clear, testable hypothesis.
2. Experimental Design: What is the independent variable in a microbial diversity study? What is the dependent variable? List at least 5 variables that should be controlled to ensure valid results.
3. Scientific Context: The Shannon diversity index (H') incorporates both richness and evenness. Why is this measure important in microbial ecology? How does it differ from simply counting species?
4. Quantitative Reasoning: If a community has three species with relative abundances of 0.5, 0.3, and 0.2, what is its Shannon diversity index? Show your calculation.
5. Real-World Application: The human gut microbiome is linked to health and disease. How might antibiotic treatment reduce microbial diversity, and what are the potential health consequences of this reduction?

Lab Context: Microbial Ecology and the Microbiome

The human gut microbiome contains about 3.8×10^{13} bacteria from hundreds of species; the ratio of microbial to human cells is approximately 1:1 (revised from earlier overestimates). Culture-based methods recover about 1% of environmental microbes (the “great plate count anomaly”). Metagenomics and 16S rRNA gene sequencing (amplifying the hypervariable V3–V4 region) now allow culture-independent assessment of community composition. The Shannon diversity index $H' = -\sum(p_i \times \ln p_i)$ integrates species richness and evenness.

Paper-Based Materials

Table 599. Alignment and Rubric Map: Item and Quantity.

Item	Quantity
Source-governance card for Microbial Ecology and the Microbiome: pathogen-surveillance source card: organism-resistance pair, official guidance date, setting, and intervention limit	1
Printed community case packet (soil, skin, tap water, gut) with metadata cards	1
Printed colony-image panel from archived BSL-1 teaching plates	1
Printed 16S rRNA OTU table (two samples: healthy gut vs antibiotic-treated gut — 10 taxa, abundance data)	1
Calculator	1
Colored pencils	3
Interaction network diagram template (printed)	1
Calculator or optional Python REPL with this project installed	1
Replicate read-count table and rarefaction checklist	1

Paper-Based Investigation

Part 1: Community Diversity from Case Packets

1. Formulate Your Hypothesis: Based on your pre-lab research, write a hypothesis about how the provided community datasets will differ in microbial diversity.
2. Identify Variables:

• Independent variable: Community source represented in the case packet

• Dependent variable: Taxon richness, Shannon diversity index, and network connectance

• Controlled variables: sequencing depth, primer region, read-quality threshold, rarefaction rule, metadata completeness, and replicate count.
3. Set Up Controls: Why is it important to use the same sequencing-depth rule for most samples? What other controls could you include, such as a mock community, a blank extraction control, or a duplicate sample?
4. Data Collection:

• Use the printed OTU table to calculate total reads, relative abundance, richness, Shannon diversity, and evenness for each sample.

• Use the archived colony-image panel primarily as a comparison for why morphology underestimates molecular diversity.

• Check whether each sample has enough reads for fair comparison; if not, apply the rarefaction rule provided in the case packet.

• Compare at least three replicate rows per sample type before drawing conclusions.

Part 2: Computational Biology Exercise — Diversity Analysis with Python

Optional computational check: run this self-contained Python snippet from the project root. It uses tested `src/bio` modules and requires no external notebook or CSV file.

Calculate diversity from table counts and compare named reference organisms.

```
from biology.ecology import biodiversity_indices
from biology.microbiology import REFERENCE_ORGANISMS

counts = [42, 18, 15, 9, 6]
diversity = biodiversity_indices(counts)
print("Shannon:", round(diversity.shannon_index, 3))
```

```
print("evenness:", round( diversity.evenness, 3))
print("reference domains:", sorted({organism.domain for organism in REFERENCE_ORGANISMS}))
```

Part 3: Microbial Interaction Network Analysis

5. Design an Alternative Investigation: Instead of collecting microbiome samples, design a paper-based analysis to test how antibiotic treatment affects microbial interaction networks. What hypothesis would you test? How would you construct the network from co-occurrence or time-series data?
6. Hypothesis: Predict how the connectance (number of interactions) in a microbial network would change with reduced diversity. Would you expect more or fewer interactions? Why?

Data Recording

Table 600. Part 3: Microbial Interaction Network Analysis: Sample source and Taxon richness.

Sample source	Taxon richness	Shannon H'	Evenness	Read depth
Soil				
Skin				
Tap water				
Gut				

Table 601. Part 3: Microbial Interaction Network Analysis: Taxon and Healthy sample reads.

Taxon	Healthy sample reads	p_i (healthy)	p_i × ln(p_i)	Antibiotic sample reads	p_i (antibiotic)
-------	----------------------	---------------	---------------	-------------------------	------------------

H' (healthy): ____; H' (antibiotic): ____

Keystone taxon in network: ; *Rationale:* Rarefaction or exclusion decision: ; *Reproducibility concern:*

Evidence and Reproducibility Checklist

- Primary evidence goal: Compare microbial communities and infer interaction hypotheses.
- Data skill to practice: Compute or interpret community metrics from abundance data.
- BioSkills emphasis: Science and society, Process of science, Modeling and simulation.
- Control logic: identify at least one positive control, one negative control, or one baseline comparison before interpreting results.
- Measurement discipline: record units, uncertainty, sample size, and any discarded observation with a reason.
- Mechanistic link: connect one result directly to the parent chapter’s big idea before writing the conclusion.
- Reproducibility check: state one procedural detail that another group would need in order to reproduce the result.

Paper-Based Evidence Upgrade

Before answering the analysis questions, annotate the paper dataset for Microbial Ecology and the Microbiome with a reproducibility pass:

Table 602. Part 3: Microbial Interaction Network Analysis: Evidence check and Student action.

Evidence check	Student action
Control logic	Mark the comparison that functions as the baseline, negative control, or reference case.
Uncertainty	Circle the row, card, diagram feature, or model assumption most likely to change the conclusion.
Model comparison	State whether a simpler rule, null model, or alternative mechanism could explain the same pattern.
Decision threshold	Write the minimum evidence that would make you revise the interpretation.
Reproducibility	Record the exact scoring rule another group would need to reproduce your classification.

Focus note: in this lab, separate community-composition correlations from mechanistic claims by recording the diversity index or count, the host or environmental context, and the perturbation, and state the experiment that would be needed to move a correlation toward causation. Keep required work paper-based; any material-handling or equipment version belongs only in an optional extension.

Worked Example: Shannon Diversity Index for a Microbial Community

Problem: A soil sample yields four bacterial genera with the following relative abundances: Genus A = 45%, B = 30%, C = 15%, D = 10%. Calculate $H' = -\sum(p_i \ln p_i)$.

Solution: $H' = -$

$$(0.45 \times \ln 0.45) + (0.30 \times \ln 0.30) + (0.15 \times \ln 0.15) + (0.10 \times \ln 0.10)$$

$= -$

$$(0.45 \times -0.799) + (0.30 \times -1.204) + (0.15 \times -1.897) + (0.10 \times -2.303)$$

$= -[-0.360 - 0.361 - 0.285 - 0.230] = 1.236$. Maximum possible H' for 4 equally abundant taxa $= \ln(4) = 1.386$.

Interpretation: $H' = 1.236$ out of a maximum 1.386, giving evenness $J = 1.236/1.386 = 0.892$. The community is moderately uneven — dominated by genera A and B — but retains relatively high diversity compared to its species-rich potential.

Source-Governance Checkpoint

Complete the source-governance card for Microbial Ecology and the Microbiome before writing the conclusion. Name the source type or model snapshot, record the evidence date or version, decide whether the claim is stable or fast-moving, and write one refresh trigger that would force the interpretation to change. Treat the card as a printed evidence object, not as a live web lookup.

Analysis Questions

- The soil dataset likely shows higher richness than the skin or tap-water dataset. Why are soils among the most microbially diverse environments on Earth? What physical and chemical habitat heterogeneity drives this?
- Antibiotic treatment usually reduces H' . What does low H' indicate about community stability? Name one specific clinical consequence of reduced microbiome diversity following broad-spectrum antibiotic use.
- The “great plate count anomaly” refers to the fact that about 1% of environmental microbes form colonies on standard media. Propose three reasons why the remaining 99% are “unculturable” and describe one molecular technique that can characterize them without culturing.
- Akkermansia muciniphila* (a gut commensal) degrades mucin and produces acetate and propionate consumed by other bacteria. If *Akkermansia* is lost, predict the cascade effects on adjacent taxa in your interaction network.
- A patient receives a faecal microbiota transplant (FMT) to treat recurrent *C. difficile* infection. Using the concept of competitive exclusion and microbiome diversity, explain the mechanism by which FMT suppresses *C. difficile* and describe what the ideal donor microbiome looks like.

Extension Analysis Questions

- 6. Statistical Analysis: If the dataset includes three replicate OTU tables per source, how would you analyze the variation in Shannon diversity? What statistical test would you use to determine if differences between sample types are significant?
- 7. Experimental Error Analysis: What are three potential sources of error in microbial diversity measurements? How could you modify the procedure to reduce each source of error?
- 8. Experimental Design: If you wanted to test whether a specific environmental factor (e.g., pH, moisture) affects microbial diversity, how would you design the experiment? What data would you collect? How would you analyze it?

Group Project Extension (Multi-Session)

Design a Study of Microbiome and Health

This project will span 2-3 lab sessions:

- Session 1: Research Question and Hypothesis - How does diet affect gut microbiome diversity? - Formulate a hypothesis about the relationship between fiber intake and microbial diversity - Design a study plan using dietary data and public microbiome datasets
- Session 2: Data Collection and Analysis - Use dietary surveys and public microbiome datasets - Analyze 16S rRNA sequencing data to calculate diversity indices - Compare diversity across different diet groups
- Session 3: Data Interpretation and Presentation - Correlate diversity with specific dietary components - Discuss the implications for human health - Create a scientific poster or presentation

Real-World Problem Solving: Microbial Ethics

Case Study: Microbiome Biobanks

- 1. Research Task: Investigate the ethical, legal, and social implications (ELSI) of collecting and storing human microbiome samples. What privacy concerns exist? How is microbiome data different from genetic data?
- 2. Ethical Consideration: Should individuals have property rights over their microbiome? What are the potential benefits and risks of commercialising microbiome-based therapies?
- 3. Policy Proposal: Design a policy for the ethical collection and use of human microbiome samples. Consider: informed consent, data privacy, benefit-sharing, and commercialisation.

Post-Lab Synthesis

- Concept Check (Synthesis): A broad-spectrum antibiotic course dramatically reduces gut microbial diversity from $H' \approx 3.2$ to $H' \approx 0.8$.
- (a) Predict how reduced microbial diversity would affect short-chain fatty acid (SCFA) production, specifically butyrate, propionate, and acetate, and explain the downstream effects on colonocyte metabolism.
 - (b) Evaluate whether the nitrogen-cycling functions of the gut microbiome would be disrupted proportionally to the diversity loss — consider functional redundancy among taxa.
 - (c) Propose two ecological principles (from community ecology) that predict how and when microbial community recovery might occur after the antibiotic course ends.

Safety and Ethics Notes

Default lab work uses printed OTU tables, archived colony images, metadata cards, and network diagrams primarily. No environmental sampling, swabbing, agar plates, incubation, or culturing is required. Optional sampling demonstrations must be instructor-supervised and follow local biosafety rules. When discussing microbiome data, respect participant privacy and follow data protection guidelines.

Debrief and Reflection

After you finish the practical work, spend 5–10 minutes in your small group comparing results and discussing the following prompts. Each member should contribute at least one observation before moving to the next prompt:

- 1. What did your measurements show — compare the group’s results to the textbook’s predictions. Where they diverge, suggest at least one mechanistic explanation before concluding “experimental error.”
- 2. What would change the outcome — propose one modification to the procedure that would sharpen the measurement or extend the result to a new biological context, and predict what you would observe.

3. One-sentence headline — each student composes a single sentence summarizing the lab’s take-home message, suitable for a tweet. Compare sentences across groups; good headlines are short, quantitative, and mechanistic.
4. Connection back to the textbook — identify one section of section 25 that your data either confirmed or complicated. Cite the specific passage.
5. Experimental Design Reflection: What was the strongest aspect of your experimental design? What would you change if you could repeat the experiment?

Further Reading (Lab)

- Revisit the parent chapter section 25 for the theoretical foundations on which this lab is built.
- Look up any bolded glossary term introduced in the textbook chapter (each has a `#gl:term-slug` link in the text) — its master definition is in `manuscript/glossary.md`.
- Explore the Python code in `src/biology/microbiology/microbiology.py` for microbial ecology calculations.
- Use the self-contained Part 2 snippet as the computational template; it runs against tested project modules without external notebooks or CSV files.

Lab — Host Immunity and Vaccines

This activity accompanies section 26 of the textbook — review that chapter before attempting the exercises below.

This activity accompanies section 26 of the textbook — review that chapter before attempting the exercises below.

Learning Objectives

- Design and evaluate an epidemic investigation dataset to determine transmission dynamics
- Formulate testable hypotheses about how immunity affects disease spread
- Identify independent, dependent, and controlled variables in epidemiological studies
- Analyze experimental data using epidemic curves and herd immunity calculations
- Write a brief scientific report with hypothesis, methods, results, and conclusion

Alignment and Rubric Map

- Outcome 1 (LO1): Interpret the supplied evidence or model output for Host Immunity and Vaccines.
- Outcome 2 (LO2): Identify controls and comparison groups that make the claim testable.
- Outcome 3 (LO3): Quantify uncertainty, boundary conditions, or alternative explanations before concluding.
- Outcome 4 (LO4): Transfer the mechanism to a new biological case or public-facing decision.
- Chapter LO coverage: LO1, LO2, LO3, LO4
- Rubric dimensions: evidence; controls; uncertainty; mechanism; transfer. ## Pre-Lab Concept Questions {.unnumbered}

Answer these before starting the investigation — they activate knowledge from the parent chapter.

1. State Koch’s four postulates for demonstrating that a specific microorganism causes a specific disease.
2. Define R_0 (basic reproductive number). What does $R_0 = 1$ mean for an outbreak? What does $R_0 > 1$ predict?
3. Distinguish direct contact transmission from airborne transmission — give one biological example of each.

Pre-Lab Inquiry Questions

Complete these questions before coming to lab. Use your textbook and additional research to inform your hypotheses.

1. Hypothesis Formation: Based on your understanding of epidemic curves, predict what shape the curve would take for a point-source exposure (e.g., contaminated food) versus person-to-person transmission (e.g., influenza). Write a clear, testable hypothesis.
2. Experimental Design: What is the independent variable in an epidemic investigation? What is the dependent variable? List at least 5 variables that should be controlled to ensure valid results.
3. Scientific Context: The basic reproduction number (R_0) is a key metric in epidemiology. Why is R_0 important for understanding disease spread? How does it relate to the concept of herd immunity?
4. Quantitative Reasoning: If a disease has an R_0 of 5, what fraction of the population needs to be immune to achieve herd immunity? Show your calculation using the formula $p_c = 1 - (1/R_0)$.
5. Real-World Application: Antibiotic resistance is a major public health concern. How does the overuse of antibiotics in medicine and agriculture contribute to the evolution of resistant bacteria? What policies could help address this issue?

Lab Context: Host Immunity and Vaccines

Epidemiology uses epidemic curves (cases vs time), attack rates, secondary attack rates, and reproductive numbers (R_0) to characterize outbreaks. R_0 is the average number of secondary cases generated by one infected individual in a fully susceptible population; herd immunity is achieved when the fraction vaccinated exceeds the threshold $p_c = 1 - (1/R_0)$. Antimicrobial susceptibility datasets often report disc-diffusion zones of inhibition from Kirby-Bauer assays — larger zone = more susceptible pathogen — but this lab interprets printed data primarily.

Paper-Based Materials

Table 603. Alignment and Rubric Map: Item and Quantity.

Item	Quantity
Source-governance card for Host Immunity and Vaccines: pathogen-surveillance source card: organism-resistance pair, official guidance date, setting, and intervention limit	1
Epidemic curve dataset (printed: hypothetical norovirus outbreak, 72-hour window, 150 cases)	1
Disc diffusion data (printed: zones of inhibition for 5 antibiotics against 2 bacterial strains)	1
Printed disc-diffusion plate images with blinded replicate labels	1 set
AMR mechanism cards (enzyme, target modification, efflux, permeability)	1 set
TB regimen decision cards: drug-susceptible, MDR/RR-TB, fluoroquinolone-resistant, toxicity-risk, and adherence-support scenarios	1 set
HIV PrEP comparison card: oral PrEP, cabotegravir, and twice-yearly lenacapavir attributes	1
Malaria vector-control comparison card: bed nets, indoor residual spraying, spatial emanators, vaccine, and chemoprevention	1
Calculator	1
Ruler (mm)	1
Herd immunity R_0 worksheet	1
Calculator or optional Python REPL with this project installed	1
Epidemic simulation worksheet	1

Paper-Based Investigation

Part 1: Epidemic Curve Analysis

1. Formulate Your Hypothesis: Based on your pre-lab research, write a hypothesis about the transmission dynamics of the norovirus outbreak.
2. Identify Variables:
 - Independent variable: Time (hours since exposure)
 - Dependent variable: Number of new cases
 - Controlled variables: Population size, exposure source, reporting methods, etc.
3. Set Up Controls: Why is it important to have accurate case reporting? What other controls could you include in an epidemic investigation to ensure valid conclusions?
4. Data Collection:
 - Plot the epidemic curve (cases per 2-hour interval).
 - Identify the single peak (suggesting point-source exposure) or multiple waves (suggesting person-to-person spread).
 - Calculate: (a) attack rate = (cases / total exposed) \times 100%; (b) approximate incubation period from the peak; (c) R_0 from the growth rate during exponential phase using the provided formula.
 - Compare two blinded disc-diffusion image replicates, measure zone diameters from the printed scale, and classify each antibiotic as susceptible, intermediate, or resistant using the provided breakpoint table.

Source-Governance Checkpoint

Complete the source-governance card for Host Immunity and Vaccines before writing the conclusion. Name the source type or model snapshot, record the evidence date or version, decide whether the claim is stable or fast-moving, and write one refresh trigger that would force the interpretation to change. Treat the card as a printed evidence object, not as a live web lookup.

Evidence and Reproducibility Checklist

- Primary evidence goal: Compare immune mechanisms and vaccination scenarios.
- Data skill to practice: Interpret antibody, cellular, and vaccine-response evidence.
- BioSkills emphasis: Science and society, Process of science, Modeling and simulation.
- Control logic: identify at least one positive control, one negative control, or one baseline comparison before interpreting results.
- Measurement discipline: record units, uncertainty, sample size, and any discarded observation with a reason.
- Mechanistic link: connect one result directly to the parent chapter’s big idea before writing the conclusion.
- Reproducibility check: state one procedural detail that another group would need in order to reproduce the result.

Paper-Based Evidence Upgrade

Before answering the analysis questions, annotate the paper dataset for Host Immunity and Vaccines with a reproducibility pass:

Table 604. Source-Governance Checkpoint: Evidence check and Student action.

Evidence check	Student action
Control logic	Mark the comparison that functions as the baseline, negative control, or reference case.
Uncertainty	Circle the row, card, diagram feature, or model assumption most likely to change the conclusion.
Model comparison	State whether a simpler rule, null model, or alternative mechanism could explain the same pattern.
Decision threshold	Write the minimum evidence that would make you revise the interpretation.
Reproducibility	Record the exact scoring rule another group would need to reproduce your classification.

Focus note: infectious-disease reasoning should connect pathogen biology, transmission, immunity, diagnostics, interventions, and equity. Keep required work paper-based; any material-handling or equipment version belongs only in an optional extension.

Lab — Antimicrobial Resistance and Epidemiology

Alignment and Rubric Map

- Outcome 1 (LO1): Interpret the supplied evidence or model output for Antimicrobial Resistance and Epidemiology.
- Outcome 2 (LO2): Identify controls and comparison groups that make the claim testable.
- Outcome 3 (LO3): Quantify uncertainty, boundary conditions, or alternative explanations before concluding.
- Outcome 4 (LO4): Transfer the mechanism to a new biological case or public-facing decision.
- Chapter LO coverage: LO1, LO2, LO3, LO4
- Rubric dimensions: evidence; controls; uncertainty; mechanism; transfer.

This activity accompanies section 27 of the textbook — review that chapter before attempting the exercises below.

Lab Context: Antimicrobial Resistance and Epidemiology

This extension lab connects resistance mechanisms, surveillance data, and epidemic modeling using printed case cards and computational templates.

Paper-Based Materials

Table 605. Alignment and Rubric Map: Item and Quantity.

Item	Quantity
Source-governance card for Antimicrobial Resistance and Epidemiology: pathogen-surveillance source card: organism-resistance pair, official guidance date, setting, and intervention limit	1
Printed datasets, cards, and worksheets referenced below	1 set per group
Graph paper or plain paper for diagrams	1
Calculator	1

Paper-Based Investigation

Optional computational check: run this self-contained Python snippet from the project root. It uses tested src/biology modules and requires no external notebook or CSV file.

Model outbreak curves with the tested SIR implementation.

```
from biology.microbiology import sir_model

baseline = sir_model(population=10_000, initial_infected=10, beta_per_day=0.35, gamma_per_day=0.1, days=30)
distancing = sir_model(population=10_000, initial_infected=10, beta_per_day=0.18, gamma_per_day=0.1, days=30)

print("baseline R0:", baseline.r0, "peak infected:", round(max(baseline.infected)))
print("distancing R0:", distancing.r0, "peak infected:", round(max(distancing.infected)))
```

Part 3: Herd Immunity Calculation

5. Design an Alternative Experiment: Instead of just calculating herd immunity thresholds, design an experiment to test how different vaccination rates affect disease spread in a simulated population. What hypothesis would you test? How would you model transmission?
6. Hypothesis: Predict the relationship between vaccination coverage and peak epidemic size. Would you expect a linear relationship, or something else? Why?

Part 4: Current Intervention Decision Matrices

7. Use the TB decision cards to classify each case as standard drug-susceptible therapy, BPaLM/BPaL eligibility review, or individualized specialist regimen. Record the evidence that makes you confident or uncertain.

8. Use the HIV PrEP comparison card to match patient scenarios to a plausible PrEP option. Separate biological efficacy, adherence feasibility, contraindications, testing needs, and access constraints.
9. Use the malaria vector-control card to design a layered prevention package for a household with night-time exposure, daytime indoor exposure, and insecticide-resistance concerns. Explain why no single tool replaces surveillance.

Data Recording

Epidemic curve: peak at hour ; *attack rate*: %; estimated incubation: ____ h; $R_0 \approx$ ____

Table 606. Part 4: Current Intervention Decision Matrices: Antibiotic and Zone (mm).

Antibiotic	Zone (mm)	Interpretation (S/I/R)
Ampicillin		
Kanamycin		
Tetracycline		
Chloramphenicol		

Replicate zone agreement within ± 2 mm? _____; AMR mechanism card selected: _____ TB regimen path selected: _____; PrEP option justified: _____; malaria control package: _____

Table 607. Part 4: Current Intervention Decision Matrices: Disease and R_0 .

Disease	R_0	Herd immunity threshold (p_c)
Measles	15	
Influenza	2.5	
COVID-19	2.9	
Mumps	5	
Polio	6	

Evidence and Reproducibility Checklist

- Primary evidence goal: Model transmission and compare resistance-control strategies.
- Data skill to practice: Interpret resistance assays and outbreak curves.
- BioSkills emphasis: Science and society, Process of science, Modeling and simulation.
- Control logic: identify at least one positive control, one negative control, or one baseline comparison before interpreting results.
- Measurement discipline: record units, uncertainty, sample size, and any discarded observation with a reason.
- Mechanistic link: connect one result directly to the parent chapter’s big idea before writing the conclusion.
- Reproducibility check: state one procedural detail that another group would need in order to reproduce the result.

Paper-Based Evidence Upgrade

Before answering the analysis questions, annotate the paper dataset for Infectious Disease and Immunity with a reproducibility pass:

Table 608. Part 4: Current Intervention Decision Matrices: Evidence check and Student action.

Evidence check	Student action
Control logic	Mark the comparison that functions as the baseline, negative control, or reference case.
Uncertainty	Circle the row, card, diagram feature, or model assumption most likely to change the conclusion.
Model comparison	State whether a simpler rule, null model, or alternative mechanism could explain the same pattern.
Decision threshold	Write the minimum evidence that would make you revise the interpretation.

Evidence check	Student action
Reproducibility	Record the exact scoring rule another group would need to reproduce your classification.

Focus note: in this lab, trace every outbreak conclusion back to its evidence chain (case definition, transmission parameter, and the diagnostic or surveillance signal it rests on), and name the alternative epidemic explanation you ruled out before reporting an R_0 or attack rate. Keep required work paper-based; any material-handling or equipment version belongs only in an optional extension.

Worked Example: Herd Immunity Threshold from R-zero

Problem: A respiratory illness has $R_0 = 4$ in an unvaccinated population of 80,000. A vaccine with 92% efficacy is available. Calculate (a) the herd immunity threshold $H = 1 - 1/R_0$, and (b) the minimum vaccination coverage needed to achieve herd immunity given 92% efficacy.

Solution: (a) $H = 1 - 1/4 = 0.75$, so 75% of the population must be immune. (b) Required vaccination coverage = $H / \text{vaccine efficacy} = 0.75 / 0.92 \approx 0.815 = 81.5\%$. At least 81.5% of the population must be vaccinated to reach the herd immunity threshold.

Interpretation: Vaccine efficacy below 100% means that a higher fraction of the population must be vaccinated than the herd immunity threshold itself — a key consideration in public health planning.

Analysis Questions

1. If the epidemic curve shows a single sharp peak within a window shorter than the incubation period, what type of source does this suggest? How would a propagated (person-to-person) epidemic curve look different?
2. *E. coli* showed resistance to ampicillin but susceptibility to kanamycin. Explain the likely molecular mechanism of ampicillin resistance (naming the specific enzyme) and why one β -lactamase can create cross-resistance to several related β -lactams while still leaving some β -lactam/ β -lactamase-inhibitor combinations, carbapenems, or non- β -lactam drugs active depending on the enzyme and permeability context.
3. Measles has an R_0 of about 15, requiring about 93% vaccination for herd immunity. Your calculation shows that even high measles vaccination coverage is needed. What happens to herd immunity when 5% of a vaccinated population declines vaccination? Relate this to observed measles outbreaks in Europe (2019).
4. An immunocompromised patient (CD4 T cell count $< 200/\mu\text{L}$, HIV+ AIDS) contracts measles despite prior vaccination. Explain: (a) why the vaccine may be insufficient; (b) which branch of adaptive immunity (humoral or cellular) is most deficient; (c) what specific viral clearance mechanism is impaired.
5. The O’Neill Review’s 10-million-deaths-per-year by 2050 AMR estimate is a historical warning scenario, not a current burden count [O’Neill, 2016]. Describe three specific mechanisms by which bacteria acquire resistance genes, and evaluate two distinct policy interventions that would slow the spread of AMR at a population level.
6. A malaria program already distributes insecticide-treated nets, but household surveys show substantial indoor activity before bedtime. Use the vector-control matrix to decide whether spatial emanators could be an added tool, and state two evidence gaps that would still require local monitoring.

Extension Analysis Questions

7. Statistical Analysis: If the printed dataset includes three replicate disc-diffusion images, how would you analyze the variation in zone diameters? What statistical test would you use to determine if differences between antibiotics are significant?
8. Experimental Error Analysis: What are three potential sources of error in epidemic curve analysis? How could you modify the procedure to reduce each source of error?
9. Experimental Design: If you wanted to test the effectiveness of different public health interventions (e.g., vaccination, social distancing) in controlling an outbreak, how would you design the experiment? What data would you collect? How would you analyze it?

Group Project Extension (Multi-Session)

Design an Epidemiological Study of Vaccine Hesitancy

This project will span 2-3 lab sessions:

Session 1: Research Question and Hypothesis - How does vaccine hesitancy affect disease outbreak size? - Formulate a hypothesis about the relationship between vaccine coverage and outbreak probability - Design a study using simulation or real outbreak data

Session 2: Data Collection and Analysis - Collect data on vaccine coverage and outbreak sizes from public health records - Analyze the correlation between coverage and outbreak size - Model the impact of increasing vaccine hesitancy on outbreak risk

Session 3: Data Interpretation and Presentation - Calculate the critical vaccination threshold for different diseases - Discuss the public health implications of declining vaccine coverage - Create a scientific poster or presentation

Real-World Problem Solving: Epidemic Ethics

Case Study: Quarantine and Civil Liberties

1. Research Task: Investigate the legal and ethical basis for quarantine during infectious disease outbreaks. What are the key principles that balance public health needs with individual rights?
2. Ethical Consideration: Should governments have the power to enforce quarantine on individuals who refuse vaccination? What are the potential benefits and risks of such policies?
3. Policy Proposal: Design a policy for implementing quarantine measures during an outbreak that respects civil liberties while protecting public health. Consider: due process, compensation for lost income, and transparent decision-making.

Post-Lab Synthesis

Concept Check (Synthesis): A pathogen evolves increased transmissibility (higher R_0) while simultaneously causing milder symptoms.

- (a) Using fitness trade-off reasoning, explain why reduced virulence might accompany increased transmissibility from an evolutionary perspective.
- (b) How would an increase in R_0 from 2 to 5 change the herd immunity threshold, and what does this imply for the fraction of the population that must be immune?
- (c) Evaluate whether increased transmissibility alone (without changes in virulence) would change the total number of individuals affected during an epidemic — use the final size equation concept to guide your reasoning.

Safety and Ethics Notes

Default lab work uses printed outbreak datasets, susceptibility images, and AMR mechanism cards primarily. No bacterial cultures, agar plates, or antibiotic discs are required. Optional wet susceptibility demonstrations must use approved BSL-1 organisms under instructor supervision and local disposal rules. Discuss epidemic data without stigmatising affected groups. When discussing antibiotics, emphasize following current prescriber instructions, avoiding unnecessary antibiotic starts, using diagnostics when available, and protecting access to effective treatment.

Source-Governance Checkpoint

Complete the source-governance card for Antimicrobial Resistance and Epidemiology before writing the conclusion. Name the source type or model snapshot, record the evidence date or version, decide whether the claim is stable or fast-moving, and write one refresh trigger that would force the interpretation to change. Treat the card as a printed evidence object, not as a live web lookup.

Debrief and Reflection

After you finish the practical work, spend 5–10 minutes in your small group comparing results and discussing the following prompts. Each member should contribute at least one observation before moving to the next prompt:

1. What did your measurements show — compare the group’s results to the textbook’s predictions. Where they diverge, suggest at least one mechanistic explanation before concluding “experimental error.”
2. What would change the outcome — propose one modification to the procedure that would sharpen the measurement or extend the result to a new biological context, and predict what you would observe.
3. One-sentence headline — each student composes a single sentence summarizing the lab’s take-home message, suitable for a tweet. Compare sentences across groups; good headlines are short, quantitative, and mechanistic.
4. Connection back to the textbook — identify one section of section 27 that your data either confirmed or complicated. Cite the specific passage.
5. Experimental Design Reflection: What was the strongest aspect of your experimental design? What would you change if you could repeat the experiment?

Further Reading (Lab)

- Revisit the parent chapter section [27](#) for the theoretical foundations on which this lab is built.
- Look up any bolded glossary term introduced in the textbook chapter (each has a `#gl:term-slug` link in the text) — its master definition is in `manuscript/glossary.md`.
- Explore the Python code in `src/biology/microbiology/microbiology.py` for epidemiological calculations.
- Use the self-contained Part 2 snippet as the computational template; it runs against tested project modules without external notebooks or CSV files.

Lab — Plant Structure and Water Relations

This activity accompanies section 28 of the textbook — review that chapter before attempting the exercises below.

Learning Objectives

- Design a paper-based transpiration investigation using printed plant-water datasets
- Formulate testable hypotheses about how environmental factors affect transpiration rate
- Identify independent, dependent, and controlled variables in plant physiology experiments
- Analyze experimental data using water potential calculations and statistical methods
- Write a brief scientific report with hypothesis, methods, results, and conclusion

Alignment and Rubric Map

- Outcome 1 (LO1): Interpret the supplied evidence or model output for Plant Structure and Water Relations.
- Outcome 2 (LO2): Identify controls and comparison groups that make the claim testable.
- Outcome 3 (LO3): Quantify uncertainty, boundary conditions, or alternative explanations before concluding.
- Outcome 4 (LO4): Transfer the mechanism to a new biological case or public-facing decision.
- Chapter LO coverage: LO1, LO2, LO3, LO4
- Rubric dimensions: evidence; controls; uncertainty; mechanism; transfer. ## Pre-Lab Concept Questions {.unnumbered}

Answer these before starting the investigation — they activate knowledge from the parent chapter.

1. Define water potential Ψ and explain why water moves spontaneously from high to low Ψ — give one example of each water potential component (solute, pressure, matric).
2. Describe the role of the Casparian strip in the endodermis — why must water enter the symplast at this point?
3. Distinguish xylem from phloem: which conducts water and which conducts photosynthate, and what structural features reflect their different functions?

Pre-Lab Inquiry Questions

Complete these questions before coming to lab. Use your textbook and additional research to inform your hypotheses.

1. Hypothesis Formation: Based on your understanding of transpiration, predict which environmental condition (bright light, wind, high humidity, dim light) will result in the highest transpiration rate. Write a clear, testable hypothesis.
2. Experimental Design: What is the independent variable in a transpiration experiment? What is the dependent variable? List at least 5 variables that should be controlled to ensure valid results.
3. Scientific Context: The cohesion-tension theory explains how water moves upward in plants against gravity. Why is this mechanism dependent on transpiration? What would happen to water transport if transpiration were completely stopped?
4. Quantitative Reasoning: If a plant loses 5 grams of water in 30 minutes, what is its transpiration rate in g/hr? If the leaf surface area is 100 cm², what is the transpiration rate per unit area (g/m²/hr)?
5. Real-World Application: Drought stress affects crop yields. How does understanding transpiration help in developing drought-resistant crops? What traits would you select for?

Lab Context: Plant Structure and Water Relations

Vascular plants have three tissue systems: dermal (epidermis, cuticle, guard cells), ground (parenchyma, collenchyma, sclerenchyma), and vascular (xylem for water/mineral transport upward; phloem for sugar/assimilate transport, bidirectional). Transpiration — evaporation of water from stomata — drives the cohesion-tension mechanism that pulls water from root to leaf. Environmental factors (light, humidity, temperature, wind) modulate transpiration rate by affecting stomatal aperture.

Paper-Based Materials

Table 609. Alignment and Rubric Map: Item and Quantity.

Item	Quantity
Source-governance card for Plant Structure and Water Relations: plant evidence source card: tissue, driver, field context, breeding/adoption boundary, and refresh trigger	1
Printed dicot stem and root cross-section diagrams with scale bars	1 packet
Transpiration dataset for four environmental treatments, with three replicates each	1
Leaf-area and stomatal-density data cards for broadleaf, needleleaf, and succulent plants	1 set
Water-potential reference sheet and worked example	1
Crop water-use case packet with drought, yield, and irrigation data	1
Graph paper or spreadsheet template	1
Calculator or optional Python REPL with this project installed	1
Optional extension card describing a potometer or celery-dye demonstration	1

Paper-Based Investigation

Part 1: Anatomical Diagram and Tissue Identification

1. Formulate Your Hypothesis: Based on your pre-lab research, write a hypothesis about how stem and root anatomy differ in their vascular tissue arrangement.
2. Identify Variables:
 - Independent variable: Plant organ (stem vs root)
 - Dependent variable: Tissue arrangement and identification
 - Controlled variables: image source, scale-bar calibration, diagram resolution, tissue orientation, scoring key, and blind-card order.
3. Set Up Controls: Why is it important for the diagram packet to include a labeled reference image and an unlabelled image from the same species? What other controls could you include to ensure accurate tissue identification?
4. Data Collection:
 - Use the printed stem cross-section diagram to identify and label: epidermis, cortex (parenchyma), vascular bundles (xylem = larger, thick-walled; phloem = smaller, thin-walled), pith.
 - Use the printed root cross-section diagram to identify: epidermis (root hairs), cortex, endodermis (Casparian strip), pericycle, vascular cylinder (xylem star pattern; phloem between xylem arms).
 - Record at least three independent tissue-identification decisions per organ, citing the visual feature used for each decision.

Part 2: Computational Biology Exercise — Transpiration Analysis with Python

Optional computational check: run this self-contained Python snippet from the project root. It uses tested `src/bio` modules and requires no external notebook or CSV file.

Check water-potential and transpiration calculations from your data table.

```
from biology.botany import transpiration_flux, water_potential

leaf = water_potential(solute_concentration_M=0.3, turgor_pressure_MPa=0.4)
```

```
flux = transpiration_flux(  
    stomatal_conductance_mol_m2_s=0.2,  
    internal_vapor_conc_mol_m3=0.5,  
    external_vapor_conc_mol_m3=0.3,  
)  
  
print("water potential:", round(leaf.water_potential_MPa, 3), "MPa")  
print("transpiration flux:", round(flux.flux_mmol_m2_s, 2), "mmol m^-2 s^-1")
```

Part 3: Transpiration Dataset and Model Check

5. Design an Alternative Dataset: Instead of just comparing environmental treatments, design a dataset to test how plant species with different leaf types (e.g., broadleaf vs needleleaf) differ in their transpiration rates. What hypothesis would you test? Which variables would you hold constant?
6. Hypothesis: Predict the relationship between leaf surface area and transpiration rate. Would you expect a linear relationship, or would stomatal density also play a role? Why?
7. Reproducibility Check: For each treatment, calculate the mean, range, and coefficient of variation across the three printed replicates. Flag any replicate that would change the treatment ranking if removed, and decide whether it should be retained.

Data Recording

Table 610. Part 3: Transpiration Dataset and Model Check: Structure and Observed in stem?.

Structure	Observed in stem?	Observed in root?	Function
Epidermis			
Xylem			
Phloem			
Endodermis			
Pith			

Table 611. Part 3: Transpiration Dataset and Model Check: Condition and Mean water loss (g).

Condition	Mean water loss (g)	Time (min)	Transpiration rate (g/min)	Transpiration (g/m ² /min)
Dim light, still				
Bright light, still				
Dim light, fan				
Bag (humid, still)				

Diagram evidence for xylem pathway: feature 1: ; feature 2: ; feature 3: ____

Evidence and Reproducibility Checklist

- Primary evidence goal: Measure or model water movement through plant tissues.
- Data skill to practice: Interpret plant-water data from pressure, solute, and humidity measurements.
- BioSkills emphasis: Interdisciplinary nature of science, Process of science.
- Control logic: identify at least one positive control, one negative control, or one baseline comparison before interpreting results.
- Measurement discipline: record units, uncertainty, sample size, and any discarded observation with a reason.
- Mechanistic link: connect one result directly to the parent chapter’s big idea before writing the conclusion.
- Reproducibility check: state one procedural detail that another group would need in order to reproduce the result.

Paper-Based Evidence Upgrade

Before answering the analysis questions, annotate the paper dataset for Plant Structure and Water Relations with a reproducibility pass:

Table 612. Part 3: Transpiration Dataset and Model Check: Evidence check and Student action.

Evidence check	Student action
Control logic	Mark the comparison that functions as the baseline, negative control, or reference case.
Uncertainty	Circle the row, card, diagram feature, or model assumption most likely to change the conclusion.
Model comparison	State whether a simpler rule, null model, or alternative mechanism could explain the same pattern.
Decision threshold	Write the minimum evidence that would make you revise the interpretation.
Reproducibility	Record the exact scoring rule another group would need to reproduce your classification.

Focus note: in this water-relations lab, anchor every claim to a water-potential value or gradient and the hydraulic pathway it acts on (soil-root-xylem-leaf-air), and distinguish stomatal regulation, tissue anatomy, and stress context as separate, testable controls on transport. Keep required work paper-based; any material-handling or equipment version belongs only in an optional extension.

Worked Example: Water Potential and Osmotic Equilibrium

Problem: A mesophyll cell has solute potential $\Psi_s = -0.9$ MPa and pressure potential $\Psi_p = 0.4$ MPa, giving $\Psi_{\text{cell}} = -0.5$ MPa. After 2 hours of transpiration, Ψ_p drops to 0.15 MPa (Ψ_s unchanged). (a) Calculate the new Ψ_{cell} . (b) If xylem water potential is -0.35 MPa, predict direction of water movement between cell and xylem. (c) If the cell is placed in a sucrose solution with $\Psi_{\text{solution}} = -0.7$ MPa, predict osmotic direction.

Solution: (a) New $\Psi_{\text{cell}} = -0.9 + 0.15 = -0.75$ MPa. (b) $\Psi_{\text{cell}} (-0.75) < \Psi_{\text{xylem}} (-0.35)$, so water moves from xylem into the cell. (c) $\Psi_{\text{cell}} (-0.75) < \Psi_{\text{solution}} (-0.7)$ numerically (more negative), so water moves from solution into cell — wait, water moves toward lower (more negative) Ψ : $\Psi_{\text{cell}} = -0.75$ is more negative than $\Psi_{\text{solution}} = -0.7$, so water moves from solution into cell.

Interpretation: Both solute concentration (Ψ_s) and turgor pressure (Ψ_p) determine the direction of water movement. Transpiration lowers Ψ_p , creating the driving force for water uptake from xylem — the basis of the cohesion-tension mechanism.

Source-Governance Checkpoint

Complete the source-governance card for Plant Structure and Water Relations before writing the conclusion. Name the source type or model snapshot, record the evidence date or version, decide whether the claim is stable or fast-moving, and write one refresh trigger that would force the interpretation to change. Treat the card as a printed evidence object, not as a live web lookup.

Analysis Questions

1. The diagram packet traces water movement through xylem rather than phloem. Why does bulk water transport follow xylem pathways, and what would you predict for sugar movement in phloem under the pressure-flow hypothesis?
2. Which condition produced the highest transpiration rate — bright light or fan? Explain why wind increases transpiration using the concept of the diffusion boundary layer.
3. Stomata open when guard cells swell (K^+ influx followed by water via osmosis). Explain how light triggers stomatal opening via the proton pump (H^+ -ATPase) and K^+ channels, and why abscisic acid (ABA) causes stomatal closure during drought.
4. The Casparian strip forces water from the cortex to enter the endodermis symplastically (through cells), not apoplastically (through cell walls). Why is this selectivity important for plant mineral uptake?
5. A plant biologist clips the tip of a phloem sieve tube using a laser scalpel. Predict what happens to sugar transport above and below the cut within 30 seconds, using your knowledge of the pressure-flow hypothesis for phloem loading and unloading.

Extension Analysis Questions

6. Statistical Analysis: Using the three printed replicates per treatment, how would you analyze variation in transpiration rates? What statistical test would you use to determine if differences between conditions are significant?
7. Experimental Error Analysis: What are three potential sources of error in transpiration measurements? How could you modify the procedure to reduce each source of error?
8. Experimental Design: If you wanted to test the effect of a specific hormone (e.g., ABA) on stomatal closure using a paper dataset, what concentrations would you include, what response variable would you measure, and what baseline comparison would make the result interpretable?

Group Project Extension (Multi-Session)

Design a Study of Plant Water Use Efficiency

This project will span 2-3 lab sessions:

- Session 1: Research Question and Hypothesis - How does water use efficiency (WUE) vary among plant species from different environments? - Formulate a hypothesis about the relationship between WUE and drought tolerance - Design an experiment measuring transpiration and photosynthesis rates
- Session 2: Data Extraction and Analysis - Extract transpiration rates from printed potometer or gravimetric datasets - Compare photosynthesis rates from CO₂ exchange or O₂ evolution data tables - Calculate intrinsic water use efficiency (photosynthesis/transpiration)
- Session 3: Data Interpretation and Presentation - Compare WUE across species - Correlate WUE with environmental adaptations (e.g., leaf thickness, stomatal density) - Create a scientific poster or presentation

Real-World Problem Solving: Plant Water Relations and Agriculture

Case Study: Irrigation Management

1. Research Task: Investigate the concept of crop water use efficiency (WUE). What is the typical range for major crops like wheat, rice, and corn? How does WUE vary with environmental conditions?
2. Ethical Consideration: Should farmers be encouraged or required to use water-saving irrigation techniques (e.g., drip irrigation) in water-scarce regions? What are the economic and social implications of such policies?
3. Policy Proposal: Design a policy to promote water-efficient agriculture in drought-prone areas. Consider: incentives for adopting efficient irrigation, water pricing, and monitoring systems.

Post-Lab Synthesis

Concept Check (Synthesis): A plant growing in moderately saline soil ($\Psi_{\text{soil}} = -0.6 \text{ MPa}$) must maintain sufficient turgor for cell expansion.

- (a) Using water potential arithmetic, explain what adjustments the plant must make to Ψ_s and/or Ψ_p to maintain a favorable Ψ_{cell} for water uptake from the soil.
- (b) Evaluate the metabolic cost of osmotic adjustment (accumulating compatible solutes such as proline or glycine betaine) compared to the alternative of reducing cell expansion and growth.
- (c) Predict how a plant adapted to saline conditions (halophyte) would differ from a glycophyte in terms of root cell Ψ_s values at equivalent soil salinity.

Optional Wet-Lab Demonstration

An instructor may demonstrate celery dye movement or potometer data collection if local safety rules and materials allow. This is not required for the lab; the default investigation uses printed diagrams and datasets.

Safety and Ethics Notes

No wet materials are required. If an optional demonstration is used, handle blades, glassware, and food dye primarily under instructor supervision. When discussing agricultural water use, consider the needs of different stakeholders.

Debrief and Reflection

After you finish the practical work, spend 5–10 minutes in your small group comparing results and discussing the following prompts. Each member should contribute at least one observation before moving to the next prompt:

1. What did your measurements show — compare the group’s results to the textbook’s predictions. Where they diverge, suggest at least one mechanistic explanation before concluding “experimental error.”
2. What would change the outcome — propose one modification to the procedure that would sharpen the measurement or extend the result to a new biological context, and predict what you would observe.
3. One-sentence headline — each student composes a single sentence summarizing the lab’s take-home message, suitable for a tweet. Compare sentences across groups; good headlines are short, quantitative, and mechanistic.
4. Connection back to the textbook — identify one section of section 28 that your data either confirmed or complicated. Cite the specific passage.
5. Experimental Design Reflection: What was the strongest aspect of your experimental design? What would you change if you could repeat the experiment?

Further Reading (Lab)

- Revisit the parent chapter section 28 for the theoretical foundations on which this lab is built.
- Look up any bolded glossary term introduced in the textbook chapter (each has a `#gl:term-slug` link in the text) — its master definition is in `manuscript/glossary.md`.
- Explore the Python code in `src/biology/botany/botany.py` for plant water relations calculations.
- Use the self-contained Part 2 snippet as the computational template; it runs against tested project modules without external notebooks or CSV files.

Lab — Plant Reproduction and Development

This activity accompanies section 29 of the textbook — review that chapter before attempting the exercises below.

Learning Objectives

- Design a paper-based pollination investigation using anatomical diagrams and pollen-tube datasets
- Formulate testable hypotheses about how environmental factors affect pollen germination data
- Identify independent, dependent, and controlled variables in plant reproduction experiments
- Analyze experimental data using growth rate calculations and statistical methods
- Write a brief scientific report with hypothesis, methods, results, and conclusion

Alignment and Rubric Map

- Outcome 1 (LO1): Interpret the supplied evidence or model output for Plant Reproduction and Development.
- Outcome 2 (LO2): Identify controls and comparison groups that make the claim testable.
- Outcome 3 (LO3): Quantify uncertainty, boundary conditions, or alternative explanations before concluding.
- Outcome 4 (LO4): Transfer the mechanism to a new biological case or public-facing decision.
- Chapter LO coverage: LO1, LO2, LO3, LO4
- Rubric dimensions: evidence; controls; uncertainty; mechanism; transfer. ## Pre-Lab Concept Questions {.unnumbered}

Answer these before starting the investigation — they activate knowledge from the parent chapter.

1. Describe double fertilization in angiosperms — what are the two fertilization events and what does each produce?
2. Distinguish monocot from dicot seeds based on cotyledon number and seed anatomy.
3. Name three mechanisms of seed dispersal and identify the plant structure or adaptation that facilitates each.

Pre-Lab Inquiry Questions

Complete these questions before coming to lab. Use your textbook and additional research to inform your hypotheses.

1. Hypothesis Formation: Based on your understanding of pollen germination, predict how temperature might affect pollen tube growth rate. Write a clear, testable hypothesis.
2. Experimental Design: What is the independent variable in a pollen germination experiment? What is the dependent variable? List at least 5 variables that should be controlled to ensure valid results.
3. Scientific Context: Double fertilization is a key innovation in angiosperms. Why is double fertilization advantageous compared to single fertilization in gymnosperms? What evolutionary pressures might have selected for this trait?
4. Quantitative Reasoning: If pollen tubes grow at an average rate of 1 mm/hour, how long would it take for a pollen tube to reach an ovule 5 cm away from the stigma? Show your calculation.
5. Real-World Application: Climate change is affecting plant reproduction. How might rising temperatures impact pollen viability and fertilization success? What are the implications for crop production?

Lab Context: Plant Reproduction and Development

Angiosperms (flowering plants) undergo double fertilization: one sperm nucleus (n) fuses with the egg (n) to form the zygote (2n); a second sperm fuses with the two polar nuclei ($2\times n = 2n$) to form the primary endosperm nucleus (3n), which nourishes the developing embryo. Pollen grains (male gametophytes, n) germinate on the stigma and grow a pollen tube through the style to deliver sperm to the embryo sac (female gametophyte) in the ovule.

Paper-Based Materials

Table 613. Alignment and Rubric Map: Item and Quantity.

Item	Quantity
Source-governance card for Plant Reproduction and Development: plant evidence source card: tissue, driver, field context, breeding/adoption boundary, and refresh trigger	1

Item	Quantity
Flower anatomy diagram packet with labeled and unlabelled angiosperm structures	1
Pollination and dispersal syndrome card set (wind, managed honeybee, bumblebee, solitary bee, moth, bird, generalized flowers, and elaiosome-bearing seeds for myrmecochory)	1 set
Pollen-tube growth dataset across temperature and sucrose treatments	1
Printed micrograph panels or schematic pollen-tube images with scale bars	1 set
Double-fertilization ploidy worksheet	1
Climate-risk case packet for crop flowering, heat stress, and pollinator service data	1
Graph paper or spreadsheet template	1
Calculator or optional Python REPL with this project installed	1

Paper-Based Investigation

Part 1: Flower Anatomy and Pollination Strategy Cards

1. Formulate Your Hypothesis: Based on your pre-lab research, write a hypothesis about how flower morphology relates to pollination strategy.
2. Identify Variables:

• Independent variable: Pollination syndrome (wind vs insect)

• Dependent variable: Flower morphological traits (petal color, fragrance, pollen size, stigma surface)

• Controlled variables: Plant species, growing conditions, measurement methods, etc.
3. Set Up Controls: Why is it important for each pollination-syndrome card to include both a labeled reference image and a blinded comparison image? What other controls could you include to ensure accurate comparisons?
4. Data Collection:

• Identify external parts on the printed diagram: sepals, petals, stamens (anther + filament), pistil (stigma + style + ovary).

• Use the ovary cross-section diagram to locate ovules and trace the path a pollen tube would follow.

• Use micrograph panels or schematic cards to record pollen characteristics such as size, surface texture, and tube length.

• Compare wind-pollinated, bee-pollinated, and ant-dispersed cards. Fill in the comparison table and cite the trait evidence behind each classification.

Part 2: Computational Biology Exercise — Pollen Tube Growth Analysis with Python

Optional computational check: run this self-contained Python snippet from the project root. It uses tested `src/biology` modules and requires no external notebook or CSV file.

Use a growth curve as a quantitative analog for pollen-tube extension.

```
from biology.botany import plant_biomass_growth

growth = plant_biomass_growth(
    initial_biomass_g=0.2,
    relative_growth_rate=0.35,
    carrying_capacity_g=10.0,
    duration_days=10,
)

print("initial biomass:", growth.biomass_g[0])
```

```
print("final biomass:", round(growth.biomass_g[-1], 2))
print("days recorded:", len(growth.times_days))
```

Part 3: Pollen Germination Dataset

5. Design an Alternative Dataset: Instead of just measuring pollen tube growth at different temperatures, design a dataset to test how sugar concentration affects pollen tube growth. What hypothesis would you test? What sugar concentrations would you include, and what treatment would serve as the baseline?
6. Hypothesis: Predict the relationship between sucrose concentration and pollen tube growth rate. Would you expect a linear increase, a saturating curve, or something else? Why?
7. Reproducibility Check: For the printed pollen-tube dataset, calculate mean growth rate and standard deviation for each treatment. Decide whether the temperature effect is larger than within-treatment variation.

Data Recording

Flower anatomy diagram (label most structures):

[Annotate the printed flower diagram here]

Table 614. Part 3: Pollen Germination Dataset: Structure and Present?.

Structure	Present?	Description (color, size, texture)
Sepals		
Petals		
Anthers		
Stigma		
Style		
Ovary		
Ovules		

Table 615. Part 3: Pollen Germination Dataset: Time (min) and Pollen tube length (μm).

Time (min)	Pollen tube length (μm)	Pollen tube growth rate (μm/min)
0	0	—
30		
60		
90		
120		

Table 616. Part 3: Pollen Germination Dataset: Character and Wind-pollinated (grass).

Character	Wind-pollinated (grass)	Bee-pollinated (lily or orchard flower)	Ant-dispersed seed
Petal color			
Fragrance			
Pollen size			
Pollen surface			
Stigma surface			
Dispersal reward or cue			

Evidence and Reproducibility Checklist

- Primary evidence goal: Compare reproductive structures and developmental outcomes.
- Data skill to practice: Track ploidy, tissue origin, and reproductive stage from diagrams or observations.
- BioSkills emphasis: Interdisciplinary nature of science, Process of science.
- Control logic: identify at least one positive control, one negative control, or one baseline comparison before interpreting results.
- Measurement discipline: record units, uncertainty, sample size, and any discarded observation with a reason.
- Mechanistic link: connect one result directly to the parent chapter’s big idea before writing the conclusion.
- Reproducibility check: state one procedural detail that another group would need in order to reproduce the result.

Paper-Based Evidence Upgrade

Before answering the analysis questions, annotate the paper dataset for Plant Reproduction and Development with a reproducibility pass:

Table 617. Part 3: Pollen Germination Dataset: Evidence check and Student action.

Evidence check	Student action
Control logic	Mark the comparison that functions as the baseline, negative control, or reference case.
Uncertainty	Circle the row, card, diagram feature, or model assumption most likely to change the conclusion.
Field translation	Note whether the evidence comes from a diagram, growth chamber, greenhouse, field plot, or long-term observation, and state what changes when the scale changes.
Model comparison	State whether a simpler rule, null model, or alternative mechanism could explain the same pattern.
Decision threshold	Write the minimum evidence that would make you revise the interpretation.
Reproducibility	Record the exact scoring rule another group would need to reproduce your classification.

Focus note: in this reproduction lab, tie every classification to the reproductive structure or stage it depends on (sporophyte versus gametophyte, pollen versus ovule, self- versus cross-pollination) and state the pollination, development, or dispersal mechanism that links genotype to the observed trait. Keep required work paper-based; any material-handling or equipment version belongs only in an optional extension.

Worked Example: Reproductive Success and Seed Survival

Problem: A flowering plant produces 500 seeds per reproductive season. Germination rate is 6%. Of germinated seeds, 20% survive to reproductive age. The plant lives for 15 reproductive seasons. (a) Calculate seeds germinating per season, (b) seedlings surviving to reproduction per season, and (c) total reproductive offspring produced over the plant’s lifetime.

Solution: (a) $500 \times 0.06 = 30$ germinating seeds/season. (b) $30 \times 0.20 = 6$ surviving to reproduction per season. (c) $6 \times 15 = 90$ reproductive offspring over the plant’s lifetime.

Interpretation: For a stable population (neither growing nor declining), each individual must on average produce exactly one surviving replacement over its lifetime. With 90 potential offspring over 15 seasons, this plant has high fecundity — but most offspring are lost at the germination and early establishment stages, consistent with a Type III survivorship curve.

Source-Governance Checkpoint

Complete the source-governance card for Plant Reproduction and Development before writing the conclusion. Name the source type or model snapshot, record the evidence date or version, decide whether the claim is stable or fast-moving, and write one refresh trigger that would force the interpretation to change. Treat the card as a printed evidence object, not as a live web lookup.

Analysis Questions

1. Pollen tube growth is driven by cytoplasmic streaming and tip-directed vesicle fusion. What is the role of Ca^{2+} ions (specifically the tip-focused Ca^{2+} gradient) in regulating pollen tube polarity and growth direction?

2. Describe double fertilization: where does each sperm go, what does each produce, and what are the ploidy levels of the zygote and endosperm?
3. A honeybee, a bumblebee, and a solitary bee visit different fragrant, brightly colored flowers with sticky pollen. A grass flower has no petals, no fragrance, and produces vast quantities of dry pollen. A woodland herb produces an elaiosome-bearing seed that ants carry to the nest. Explain the evolutionary logic behind each strategy using cost-benefit trade-offs, and state why “bee pollination” is still too broad unless the visitor actually transfers pollen.
4. Self-incompatibility (SI) systems prevent self-fertilization in many plant species. The S-RNase system in *Petunia* involves the pistil secreting an RNase that degrades pollen tube RNA if the pollen S-allele matches the pistil S-allele. How does this mechanism selectively destroy “self” pollen without harming “foreign” pollen?
5. Seedless watermelons are triploid (3n). Explain the steps used to produce them (starting from a colchicine treatment of diploid cells), and why triploid plants are sterile — using the concept of homologous chromosome pairing during meiosis.

Extension Analysis Questions

6. Statistical Analysis: If the pollen germination dataset includes three replicates per treatment, how would you analyze variation in growth rates? What statistical test would you use to determine if differences between temperatures are significant?
7. Experimental Error Analysis: What are three potential sources of error in pollen tube growth measurements? How could you modify the procedure to reduce each source of error?
8. Experimental Design: If you wanted to test the effect of a specific hormone (e.g., auxin) on pollen tube growth using archived image measurements, what concentrations would you test, how would the images be blinded, and how would you measure the effect?

Group Project Extension (Multi-Session)

Design a Study of Plant Reproductive Strategies

This project will span 2-3 lab sessions:

Session 1: Research Question and Hypothesis - How do flower traits correlate with pollination syndrome, and how do seed rewards correlate with ant-mediated dispersal? - Formulate a hypothesis about the relationship between specific traits (e.g., petal color, nectar production, floral tube depth, elaiosome presence) and pollinator or disperser type - Design a study comparing multiple plant species

Session 2: Data Extraction and Analysis - Extract flower morphology data from species cards, image databases, or published datasets - Score pollinator visits from provided video stills or summarized observation tables, separating managed honeybees from wild bees when the evidence allows it - Analyze correlations between traits and pollinator type; add a myrmecochory extension that compares seed-removal rates for elaiosome-present vs elaiosome-removed cards

Session 3: Data Interpretation and Presentation - Perform statistical analysis (e.g., principal component analysis) - Discuss the evolutionary implications of your findings - Create a scientific poster or presentation

Real-World Problem Solving: Plant Reproduction and Agriculture

Case Study: Pollinator Decline

1. Research Task: Investigate the causes and consequences of pollinator decline (bees, butterflies, etc.). What crop groups depend on animal pollination, and how do dependence estimates differ between staple calories, fruits, nuts, and specialty crops? Separate managed honeybee service from wild-bee service when evidence permits that distinction.
2. Field-Translation Consideration: A warming treatment advances flowering in a chamber experiment, but a field dataset shows variable pollinator emergence. What evidence would let you decide whether the crop faces pollen heat failure, pollinator mismatch, or both?
3. Policy Proposal: Design a policy to protect pollinator populations while supporting agricultural productivity. Consider: incentives for habitat restoration, pesticide timing, heat-wave monitoring during flowering, seed-set surveillance, nesting substrate for wild bees, and edge-habitat management that does not increase invasive-ant disruption of native seed dispersal.

Post-Lab Synthesis

- Concept Check (Synthesis): Two related plant species occupy the same environment. Species A produces 2,000 small seeds (0.1 mg each), while Species B produces 50 large seeds (40 mg each). Germination rate for A is 3%; for B is 65%.
- (a) Calculate the number of germinating seeds per season for each species and compare their reproductive strategies.
- (b) In a nutrient-poor environment with sparse canopy, predict which species would have higher seedling survival rates and explain using seed reserve reasoning.

- (c) Evaluate the evolutionary trade-off between seed number and seed size in terms of r-selected versus K-selected life history strategies.

Optional Wet-Lab Demonstration

An instructor may demonstrate flower dissection or pollen germination with appropriate allergy precautions and approved materials. This is not required; the default lab uses diagrams, cards, and archived pollen-tube measurements.

Safety and Ethics Notes

No wet materials are required. Pollen can be an allergen in optional demonstrations, and colchicine is discussed conceptually primarily. When discussing pollinator decline, consider the impacts on both ecosystems and human food security.

Debrief and Reflection

After you finish the practical work, spend 5–10 minutes in your small group comparing results and discussing the following prompts. Each member should contribute at least one observation before moving to the next prompt:

1. What did your measurements show — compare the group’s results to the textbook’s predictions. Where they diverge, suggest at least one mechanistic explanation before concluding “experimental error.”
2. What would change the outcome — propose one modification to the procedure that would sharpen the measurement or extend the result to a new biological context, and predict what you would observe.
3. One-sentence headline — each student composes a single sentence summarizing the lab’s take-home message, suitable for a tweet. Compare sentences across groups; good headlines are short, quantitative, and mechanistic.
4. Connection back to the textbook — identify one section of section 29 that your data either confirmed or complicated. Cite the specific passage.
5. Experimental Design Reflection: What was the strongest aspect of your experimental design? What would you change if you could repeat the experiment?

Further Reading (Lab)

- Revisit the parent chapter section 29 for the theoretical foundations on which this lab is built.
- Look up any bolded glossary term introduced in the textbook chapter (each has a #gl:term-slug link in the text) — its master definition is in manuscript/glossary.md.
- Explore the Python code in src/biology/botany/botany.py for plant reproduction calculations.
- Use the self-contained Part 2 snippet as the computational template; it runs against tested project modules without external notebooks or CSV files.

Lab — Plant Responses to the Environment

Learning Objectives

This activity accompanies section 30 of the textbook — review that chapter before attempting the exercises below.

- Interpret phototropism and gravitropism from time-series images and angle data
- Measure the effect of exogenous auxin concentration from a printed dose-response dataset
- Quantify the effect of gibberellin on dwarf pea elongation from replicated growth tables
- Evaluate the role of phytochrome in seed germination through red/far-red treatment data

Alignment and Rubric Map

- Outcome 1 (LO1): Interpret the supplied evidence or model output for Plant Responses to the Environment.
- Outcome 2 (LO2): Identify controls and comparison groups that make the claim testable.
- Outcome 3 (LO3): Quantify uncertainty, boundary conditions, or alternative explanations before concluding.
- Outcome 4 (LO4): Transfer the mechanism to a new biological case or public-facing decision.
- Chapter LO coverage: LO1, LO2, LO3, LO4
- Rubric dimensions: evidence; controls; uncertainty; mechanism; transfer. ## Pre-Lab Concept Questions {.unnumbered}

Answer these before starting the investigation — they activate knowledge from the parent chapter.

1. Describe how auxin redistribution causes a shoot to bend toward light — specify which cells elongate more and why.
2. Distinguish phytochrome Pr from Pfr — which form is active, what wavelength converts Pr to Pfr, and what happens to Pfr in darkness?
3. Define the critical night length for photoperiodism. Is a short-day plant induced to flower when nights are longer or shorter than the critical length?

Lab Context: Plant Responses to the Environment

Plants integrate environmental signals and respond through photoreceptors and hormone signaling. Auxin (IAA) is produced in the shoot apex and promotes elongation at low concentrations but inhibits at high concentrations (biphasic response). Gibberellins (GAs) promote stem elongation and seed germination by targeting DELLA protein degradation. Phototropism (bending toward light) results from asymmetric auxin distribution driven by the PIN auxin efflux carriers. Phytochrome Pr (inactive, absorbs red 660 nm) ↔ Pfr (active, absorbs far-red 730 nm) provides a light quality sensor — Pfr promotes seed germination and flowering.

Paper-Based Materials

Table 618. Alignment and Rubric Map: Item and Quantity.

Item	Quantity
Source-governance card for Plant Responses to the Environment: plant evidence source card: tissue, driver, field context, breeding/adoption boundary, and refresh trigger	1
Phototropism and gravitropism image sequence with angle scale	1 packet
Auxin dose-response dataset with replicated curvature measurements	1
Gibberellin dwarf-pea stem-length dataset with control and GA-treated groups	1
Phytochrome red/far-red germination treatment table	1
Environmental cue cards for canopy shade, drought, salinity, and warming	1 set
Graph paper or spreadsheet template	1
Calculator	1

Paper-Based Investigation

Part A — Phototropism Demonstration

1. Use the image sequence to compare unilateral light, darkness, and rotated-orientation treatments. Measure the angle of curvature from the printed scale and identify the baseline control.

Part B — Auxin Dose-Response

2. Plot the replicated IAA curvature dataset on a log concentration axis. Mark the concentration with maximum response and calculate the coefficient of variation for each treatment.

Part C — Gibberellin Effect on Dwarfism

3. Analyze dwarf pea stem-length data in two conditions: (a) control; (b) GA₃-treated. Calculate daily growth rate and the percent change relative to control.

Part D — Phytochrome and Seed Germination

4. Use the phytochrome table for five treatment groups: (a) dark primarily; (b) red light pulse then dark; (c) far-red then dark; (d) red -> far-red -> dark; (e) far-red -> red -> dark.
5. Calculate percent germination and identify which final light pulse best predicts the response.

Data Recording

Phototropism: angle of curvature toward light = °; *dark control* = °

Table 619. Alignment and Rubric Map: IAA concentration (μM) and Angle of curvature (°).

IAA concentration (μM)	Angle of curvature (°)
0 (lanolin primarily)	
0.1	
1	
10	
100	

Gibberellin — dwarf pea stem length (mm):

Table 620. Alignment and Rubric Map: Day and Water control.

Day	Water control	+GA ₃
0		
2		
5		

Phytochrome germination results:

Table 621. Alignment and Rubric Map: Treatment and Germinated (of 20).

Treatment	Germinated (of 20)	% germination
Dark primarily		
Red → dark		
Far-red → dark		
Red → far-red → dark		
Far-red → red → dark		

Reproducibility check: treatment with largest mean response = ; *treatment with largest variation* = ; conclusion most sensitive to one replicate = ____

Evidence and Reproducibility Checklist

- Primary evidence goal: Test plant response predictions under controlled environmental cues.
- Data skill to practice: Interpret plant response data across light, gravity, water, and hormone treatments.
- BioSkills emphasis: Interdisciplinary nature of science, Process of science.
- Control logic: identify at least one positive control, one negative control, or one baseline comparison before interpreting results.
- Measurement discipline: record units, uncertainty, sample size, and any discarded observation with a reason.
- Mechanistic link: connect one result directly to the parent chapter’s big idea before writing the conclusion.
- Reproducibility check: state one procedural detail that another group would need in order to reproduce the result.

Paper-Based Evidence Upgrade

Before answering the analysis questions, annotate the paper dataset for Plant Responses to the Environment with a reproducibility pass:

Table 622. Alignment and Rubric Map: Evidence check and Student action.

Evidence check	Student action
Control logic	Mark the comparison that functions as the baseline, negative control, or reference case.
Uncertainty	Circle the row, card, diagram feature, or model assumption most likely to change the conclusion.
Field translation	State whether the response was measured in a chamber, greenhouse, or field setting, and what environmental variable is missing from that setting.
Model comparison	State whether a simpler rule, null model, or alternative mechanism could explain the same pattern.
Decision threshold	Write the minimum evidence that would make you revise the interpretation.
Reproducibility	Record the exact scoring rule another group would need to reproduce your classification.

Focus note: in this environmental-response lab, trace each conclusion along the perception-to-phenotype path — name the stimulus, the photoreceptor or hormone, the downstream gene-expression or signaling step, and the growth-versus-defense tradeoff it implies — before treating any response as causal. Keep required work paper-based; any material-handling or equipment version belongs only in an optional extension.

Worked Example: Photoperiodism and Night Length

Problem: A short-day plant has a critical night length of 9 hours. Predict whether it flowers under three conditions: (a) 14 h light / 10 h dark, (b) 16 h light / 8 h dark, (c) 14 h light / 10 h dark with a 3-minute red-light pulse at hour 5 of the dark period.

Solution: (a) Night = 10 h > 9 h critical → flowers. (b) Night = 8 h < 9 h critical → does not flower. (c) The red-light pulse converts Pfr (accumulated since dusk) back to Pr interrupting the dark period signal. The effective uninterrupted dark period is now about 5 h on each side of the pulse, both below 9 h → does not flower.

Interpretation: Short-day plants respond to uninterrupted night length exceeding the critical threshold. A brief light interruption resets the phytochrome photoequilibrium, demonstrating that the biological clock measures darkness continuity rather than total dark duration.

Source-Governance Checkpoint

Complete the source-governance card for Plant Responses to the Environment before writing the conclusion. Name the source type or model snapshot, record the evidence date or version, decide whether the claim is stable or fast-moving, and write one refresh trigger that would force the interpretation to change. Treat the card as a printed evidence object, not as a live web lookup.

Analysis Questions

1. In the phototropism experiment, which side of the shoot had longer cells? Explain how asymmetric auxin distribution (mediated by PIN proteins) creates differential elongation, and name the specific plant hormone involved.
2. Your auxin dose-response curve should show a bell shape. At what concentration did you see maximum curvature? Explain why very high auxin concentrations actually inhibit shoot elongation (relate to the acidic growth hypothesis and receptor downregulation).

- GA-treated dwarf peas grew taller than controls. Explain the molecular mechanism: how does GA binding its receptor (GID1) lead to degradation of DELLA proteins and activate cell elongation genes?
- Interpret your phytochrome germination results: which treatment(s) promoted germination? Which inhibited it? Explain why the red/far-red ratio in natural shade (under a canopy) would suppress germination of shade-intolerant species.
- Long-day plants flower when nights are shorter than a critical length (they actually measure night length via phytochrome). Explain why a brief red light pulse in the middle of an otherwise long night would prevent flowering in a short-day plant, but a subsequent far-red pulse would restore it — and what this tells us about the form of phytochrome that promotes flowering inhibition.
- Choose one environmental cue card (drought, canopy shade, salinity, or warming). What field measurement would you need before turning the hormone-response result into a crop-management recommendation?

Post-Lab Synthesis

Concept Check (Synthesis): A plant is experiencing simultaneous drought stress and pathogen challenge.

- (a) ABA promotes stomatal closure during drought; salicylic acid (SA) promotes systemic acquired resistance (SAR) against pathogens. Evaluate whether these two responses are likely to be synergistic or antagonistic, citing the known ABA–SA signaling interaction.
- (b) Ethylene promotes senescence and pathogen defense (via jasmonate co-signaling). Predict whether ethylene production during drought would accelerate or slow a plant’s recovery after the drought ends.
- (c) Design a simple experiment using *Arabidopsis thaliana* mutants to determine whether ABA or SA signaling takes priority when both stresses are applied simultaneously.

Safety and Ethics Notes

No wet materials, live seedlings, hormones, or lamps are required. Optional instructor demonstrations with seedlings, IAA, GA₃, or red/far-red lights should follow local chemical and heat-safety rules and remain separate from the required paper-based investigation.

Debrief and Reflection

After you finish the practical work, spend 5–10 minutes in your small group comparing results and discussing the following prompts. Each member should contribute at least one observation before moving to the next prompt:

- What did your measurements show — compare the group’s results to the textbook’s predictions. Where they diverge, suggest at least one mechanistic explanation before concluding “experimental error.”
- What would change the outcome — propose one modification to the procedure that would sharpen the measurement or extend the result to a new biological context, and predict what you would observe.
- One-sentence headline — each student composes a single sentence summarizing the lab’s take-home message, suitable for a tweet. Compare sentences across groups; good headlines are short, quantitative, and mechanistic.
- Connection back to the textbook — identify one section of section 30 that your data either confirmed or complicated. Cite the specific passage.

Further Reading (Lab)

- Revisit the parent chapter section 30 for the theoretical foundations on which this lab is built.
- Look up any bolded glossary term introduced in the textbook chapter (each has a `#gl:term-slug` link in the text) — its master definition is in `manuscript/glossary.md`.
- Explore the appended `src/` module that implements the corresponding quantitative model (when applicable) — referenced in the parent chapter’s “Bridge to Computation” subsection.

Module footer: parent chapter `\cref{sec:unit_VIII_plant_responses}`; all numerical quantities in this lab use SI units — see [Appendix D — Units, Physical Constants, and Biological Ranges](#) for unit conversions and biological-scale reference values.

Lab — Circulation and Respiration

Learning Objectives

This activity accompanies section 31 of the textbook — review that chapter before attempting the exercises below.

- Analyze resting and post-exercise heart rate and blood pressure datasets and apply the Frank-Starling law
- Calculate cardiac output and stroke volume from anonymized case data using $CO = HR \times SV$
- Apply Fick’s principle to estimate oxygen consumption from heart rate data
- Analyze spirometry data to determine tidal volume, IRV, ERV, and FVC

Alignment and Rubric Map

- Outcome 1 (LO1): Interpret the supplied evidence or model output for Circulation and Respiration.
- Outcome 2 (LO2): Identify controls and comparison groups that make the claim testable.
- Outcome 3 (LO3): Quantify uncertainty, boundary conditions, or alternative explanations before concluding.
- Outcome 4 (LO4): Transfer the mechanism to a new biological case or public-facing decision.
- Chapter LO coverage: LO1, LO2, LO3, LO4
- Rubric dimensions: evidence; controls; uncertainty; mechanism; transfer. ## Pre-Lab Concept Questions {.unnumbered}

Answer these before starting the investigation — they activate knowledge from the parent chapter.

1. Write the equation that defines cardiac output and identify the units of each term. In two to three sentences, describe the Frank–Starling mechanism and explain why it tends to match ventricular output to venous return over short timescales.
2. Sketch (or describe) the oxygen–hemoglobin dissociation curve and indicate the direction the curve shifts when blood pH falls. State the physiological reason this Bohr-effect shift is helpful in metabolically active tissues.
3. Define DO_2 (oxygen delivery) and VO_2 (oxygen consumption) in words, and write the Fick equation that relates VO_2 to cardiac output and the arteriovenous O_2 content difference.

Lab Context: Circulation and Respiration

The cardiovascular system delivers oxygen and removes CO_2 at a rate matched to tissue demand. Cardiac output (CO) = stroke volume (SV) \times heart rate (HR). The Frank-Starling law states that greater ventricular filling (preload) stretches sarcomeres to a more optimal myosin–actin overlap, increasing stroke volume. Spirometry measures lung volumes: tidal volume (TV about 500 mL), inspiratory reserve (IRV about 3,000 mL), expiratory reserve (ERV about 1,200 mL), and $FVC = (TV + IRV + ERV)$ for healthy adults.

Paper-Based Materials

Table 623. Alignment and Rubric Map: Item and Quantity.

Item	Quantity
Source-governance card for Circulation and Respiration: physiology source card: baseline, perturbation, population range, clinical boundary, and evidence date	1
Calculator	1
Graph paper or spreadsheet template	1
Cardiovascular response dataset with rest, exercise, recovery, and heart-failure cases	1
Spirometry dataset printout (3 subjects: normal, asthmatic, COPD)	1
Altitude acclimatization case card with PaO_2 , ventilation, hematocrit, and symptom data	1
Digestive-renal balance cards: meal composition, water intake, plasma osmolality, urea, and urine concentration	1 set

Paper-Based Investigation

Part A — Cardiovascular Measurements

1. Use the cardiovascular response dataset to compare resting HR, estimated stroke volume, and recovery time across cases.
2. Plot HR at rest, 0, 1, 2, 5, and 10 minutes post-exercise for the printed subjects. Identify the baseline control and the slowest recovery profile.
3. Calculate $CO = HR \times SV$ at rest and immediately post-exercise. Check whether the data are consistent with the Frank-Starling mechanism and autonomic regulation.

Part B — Spirometry Analysis

4. Use the printed spirometry dataset to calculate TV, FVC, FEV1, and FEV1/FVC where available.
5. Compare FVC and FEV1/FVC ratios for normal, asthmatic, and COPD subjects.
6. Use the altitude case card to connect PaO2 changes to ventilation, erythropoietin, hematocrit, and acclimatization.

Part C — Digestive-Renal Homeostasis

7. Use the digestive-renal cards to trace how a high-protein salty meal changes gut absorption, hepatic urea production, plasma osmolality, ADH release, and urine concentration.
8. Compare a freshwater fish, a desert mammal, and a bird/reptile excretory strategy. Identify whether ammonia, urea, or uric acid is the dominant nitrogen-waste solution and what water trade-off that solution implies.

Data Recording

Table 624. Alignment and Rubric Map: Time (min) and HR (bpm).

Time (min)	HR (bpm)	Estimated SV (mL)	CO (L/min)
Rest		70	
0 (immediately post-exercise)		90	
1			
2			
5			
10			

Spirometry (from dataset):

Table 625. Alignment and Rubric Map: Subject and FVC (L).

Subject	FVC (L)	FEV ₁ (L)	FEV ₁ /FVC (%)	Pattern
Normal	4.8	4.3		
Asthmatic	4.6	2.8		
COPD	3.1	1.5		

Reproducibility check: sampling interval used for recovery graph = ; rule for classifying obstructive pattern =

Evidence and Reproducibility Checklist

- Primary evidence goal: Model circulation, respiration, and feedback compensation.
- Data skill to practice: Interpret physiological data from pressure, flow, saturation, or set-point changes.
- BioSkills emphasis: Modeling and simulation, Quantitative reasoning, Science and society.
- Control logic: identify at least one positive control, one negative control, or one baseline comparison before interpreting results.
- Measurement discipline: record units, uncertainty, sample size, and any discarded observation with a reason.
- Mechanistic link: connect one result directly to the parent chapter’s big idea before writing the conclusion.
- Reproducibility check: state one procedural detail that another group would need in order to reproduce the result.

Paper-Based Evidence Upgrade

Before answering the analysis questions, annotate the paper dataset for Circulation and Respiration with a reproducibility pass:

Table 626. Alignment and Rubric Map: Evidence check and Student action.

Evidence check	Student action
Control logic	Mark the comparison that functions as the baseline, negative control, or reference case.
Uncertainty	Circle the row, card, diagram feature, or model assumption most likely to change the conclusion.
Model comparison	State whether a simpler rule, null model, or alternative mechanism could explain the same pattern.
Decision threshold	Write the minimum evidence that would make you revise the interpretation.
Reproducibility	Record the exact scoring rule another group would need to reproduce your classification.

Focus note: in this lab, tie every cardiorespiratory claim to a flow or gas-exchange measurement and the control loop it implies: state which baseline, perturbation, and recovery values you used, and whether the apparent regulation could instead reflect reserve capacity or the resolution limit of the recording. Keep required work paper-based; any material-handling or equipment version belongs only in an optional extension.

Worked Example: Cardiac Output and Fick Calculation in Exercise

Problem: At rest, a healthy adult has heart rate (HR) = 70 bpm and stroke volume (SV) = 70 mL, giving a resting cardiac output (CO) of about 5 L/min. During moderate exercise, HR rises to 140 bpm and SV rises to 100 mL. Arterial O₂ content is 0.20 mL O₂ per mL of blood; mixed venous O₂ content is 0.15 mL O₂ per mL of blood. Calculate (a) exercise CO and (b) oxygen consumption VO₂ using the Fick principle $VO_2 = CO \times (CaO_2 - CvO_2)$.

Solution: Cardiac output during exercise is $CO = HR \times SV = 140 \text{ bpm} \times 100 \text{ mL} = 14,000 \text{ mL/min} = 14 \text{ L/min}$. The arteriovenous O₂ difference is $(0.20 - 0.15) = 0.05 \text{ mL O}_2 \text{ per mL blood}$, or 50 mL O₂ per liter of blood. Applying Fick: $VO_2 = 14 \text{ L/min} \times 50 \text{ mL O}_2/\text{L} = 700 \text{ mL O}_2/\text{min}$. Resting VO₂ at the same Ca–Cv difference would be $5 \text{ L/min} \times 50 \text{ mL/L} = 250 \text{ mL O}_2/\text{min}$.

Interpretation: Exercise raised CO by about 2.8-fold (5 → 14 L/min). VO₂ rose roughly in step under the assumed Ca–Cv difference, but in practice the arteriovenous O₂ difference also widens during exercise as tissues extract more O₂, so VO₂ typically scales faster than CO alone. This shows why both CO and extraction matter for matching O₂ supply to demand.

Source-Governance Checkpoint

Complete the source-governance card for Circulation and Respiration before writing the conclusion. Name the source type or model snapshot, record the evidence date or version, decide whether the claim is stable or fast-moving, and write one refresh trigger that would force the interpretation to change. Treat the card as a printed evidence object, not as a live web lookup.

Analysis Questions

1. Why did HR increase during exercise, and why did it remain elevated for several minutes post-exercise? Name the autonomic branch primarily responsible for the exercise-induced HR increase.
2. A reduced FEV₁/FVC ratio below the age-dependent lower limit of normal supports an obstructive pattern; a fixed 70% cutoff is a screening shortcut, not a comprehensive diagnostic boundary. The asthmatic shows reduced FEV₁ but relatively preserved FVC. Explain the structural difference in the airways that causes obstructive vs restrictive spirometry patterns.
3. Calculate the difference in cardiac output between rest and peak exercise in your data. Using Fick’s principle ($VO_2 = CO \times (CaO_2 - CvO_2)$), estimate oxygen consumption if the arterio-venous O₂ difference increases from 50 mL/L at rest to 150 mL/L during maximal exercise.
4. A patient with congestive heart failure has chronically elevated ventricular end-diastolic pressure. Explain how this shifts the Frank-Starling curve and contributes to pulmonary edema (connect to Starling capillary forces).
5. At high altitude (3,500 m), PaO₂ drops from 100 to about 60 mmHg. Identify three physiological acclimatisation responses (acute and chronic) and for each, specify the sensing mechanism and the effector system involved.
6. A dehydrated student eats a salty, high-protein meal. Predict the direction of change for plasma osmolality, ADH, urea production, and urine concentration. Which measurements would distinguish “not enough water intake” from impaired kidney concentrating ability?

Post-Lab Synthesis

- Concept Check (Synthesis): Consider a patient with severe anemia (hemoglobin 5 g/dL versus the typical 15 g/dL) whose tissue O₂ delivery must be maintained.
- (a) Identify the cardiovascular and respiratory compensations the patient is likely to recruit at rest — discuss expected changes in heart rate, stroke volume, 2,3-BPG levels, and the position of the O₂–hemoglobin dissociation curve, and predict the direction of each change with mechanistic reasoning.
 - (b) Compare how effective each compensation is at rest versus during moderate exercise. Predict which mechanism reaches its ceiling first and explain how that ceiling shapes exercise tolerance; cite at least one measurement the team could make during the lab to test the prediction.

Safety and Ethics Notes

No exercise testing, blood pressure measurement, or spirometry is required. Optional demonstrations involving human participants require consent, screening, single-use mouthpiece filters where relevant, and immediate stopping for dizziness, chest pain, or discomfort.

Debrief and Reflection

After you finish the practical work, spend 5–10 minutes in your small group comparing results and discussing the following prompts. Each member should contribute at least one observation before moving to the next prompt:

- 1. What did your measurements show — compare the group’s results to the textbook’s predictions. Where they diverge, suggest at least one mechanistic explanation before concluding “experimental error.”
- 2. What would change the outcome — propose one modification to the procedure that would sharpen the measurement or extend the result to a new biological context, and predict what you would observe.
- 3. One-sentence headline — each student composes a single sentence summarizing the lab’s take-home message, suitable for a tweet. Compare sentences across groups; good headlines are short, quantitative, and mechanistic.
- 4. Connection back to the textbook — identify one section of section 31 that your data either confirmed or complicated. Cite the specific passage.

Further Reading (Lab)

- Revisit the parent chapter section 31 for the theoretical foundations on which this lab is built.
- Look up any bolded glossary term introduced in the textbook chapter (each has a #gl:term-slug link in the text) — its master definition is in manuscript/glossary.md.
- Explore the appended src/ module that implements the corresponding quantitative model (when applicable) — referenced in the parent chapter’s “Bridge to Computation” subsection.

Module footer: parent chapter \cref{sec:unit_IX_circulation_respiration_homeostasis}; all numerical quantities in this lab use SI units — see Appendix D — Units, Physical Constants, and Biological Ranges for unit conversions and biological-scale reference values.

Lab — Nervous System and Neural Signaling

Learning Objectives

This activity accompanies section 32 of the textbook — review that chapter before attempting the exercises below.

- Interpret reflex arc function using a clinical timing dataset and map receptive fields from paper data
- Analyze two-point discrimination thresholds from anonymized class datasets
- Analyze an action potential recording and identify threshold, peak, undershoot, and refractory periods
- Apply the length constant equation to predict how signal decay differs in myelinated vs unmyelinated axons

Alignment and Rubric Map

- Outcome 1 (LO1): Interpret the supplied evidence or model output for Nervous System and Neural Signaling.
- Outcome 2 (LO2): Identify controls and comparison groups that make the claim testable.
- Outcome 3 (LO3): Quantify uncertainty, boundary conditions, or alternative explanations before concluding.
- Outcome 4 (LO4): Transfer the mechanism to a new biological case or public-facing decision.
- Chapter LO coverage: LO1, LO2, LO3, LO4
- Rubric dimensions: evidence; controls; uncertainty; mechanism; transfer. ## Pre-Lab Concept Questions {.unnumbered}

Answer these before starting the investigation — they activate knowledge from the parent chapter.

1. List the five components of a monosynaptic spinal reflex arc in the order a signal traverses them — sensory receptor, afferent (sensory) neuron, integrating center, efferent (motor) neuron, effector. Describe in one sentence what each component contributes to the latency of the reflex.
2. Compare the preganglionic and postganglionic neurotransmitters typically used by the sympathetic and parasympathetic divisions. Indicate which division is more likely to release noradrenaline at its target tissues and which is more likely to release acetylcholine.
3. Define myelination at the level of a single axon and state, in one sentence, why myelinated fibers conduct faster than unmyelinated fibers of the same diameter.

Lab Context: Nervous System and Neural Signaling

Neural signaling depends on the passive spread of graded potentials and, for long-distance signaling, the most-or-nothing action potential (AP). The two-point discrimination threshold (Weber’s two-point test) reveals the density of somatosensory receptors in the skin: fingertips (2–3 mm threshold) vs upper back (40–70 mm). The patellar reflex is monosynaptic: stretching the patellar tendon activates Ia afferents in the quadriceps → synapse on α motor neurons in the spinal cord → quadriceps contraction. The entire arc takes <50 ms.

Paper-Based Materials

Table 627. Alignment and Rubric Map: Item and Quantity.

Item	Quantity
Source-governance card for Nervous System and Neural Signaling; physiology source card: baseline, perturbation, population range, clinical boundary, and evidence date	1
Patellar reflex case dataset with baseline, Jendrassik, and neuropathy scenarios	1
Two-point discrimination dataset for fingertip, palm, forearm, and upper back	1
Action potential recording trace (printed: one AP at scale with time axis in ms, voltage axis in mV)	1
Cable properties worksheet (with λ formula: $\lambda = \sqrt{(r_m/r_i)}$)	1
Calculator	1
Body surface map (printed outline of human figure)	1
Behavioral ethogram and neural-prosthesis evidence cards	1 set

Paper-Based Investigation

Part A — Patellar Reflex

1. Use the reflex dataset to compare baseline, Jendrassik maneuver, peripheral neuropathy, and upper motor neuron scenarios. Record reflex magnitude and latency.
2. Identify the baseline control and the positive comparison that confirms the arc can increase with descending facilitation.
3. Map the likely lesion location for each abnormal case using the reflex arc diagram.

Part B — Two-Point Discrimination

4. Analyze the anonymized two-point dataset at various spacings (1, 2, 5, 10, 20, 40 mm) for the fingertip, palm, forearm, and upper back. Record the minimum spacing perceived as two points on each body area.

Part C — Action Potential Trace Analysis

5. From the printed AP trace: measure (a) resting membrane potential (mV); (b) threshold voltage; (c) amplitude (peak mV); (d) duration of absolute refractory period (ms); (e) relative refractory period (ms); (f) undershoot (afterhyperpolarisation) level (mV).

Part D — Cable Properties Calculation

6. Calculate the length constant λ for two axons: (a) unmyelinated 0.5 μm diameter axon ($r_m = 10,000\ \Omega\cdot\text{cm}$, $r_i = 80\ \text{M}\Omega/\text{cm}$); (b) myelinated 10 μm diameter axon ($r_m = 800,000\ \Omega\cdot\text{cm}$, $r_i = 4\ \text{M}\Omega/\text{cm}$). Determine $V(x)/V_0$ at a distance of 1 mm.

Part E — Behavior and Neural Prosthesis Evidence

7. Sort each behavior card into Tinbergen’s four questions: mechanism, development, function, and evolutionary history.
8. Use the neural-prosthesis cards to separate what implanted recordings directly show (decodable neural activity) from the clinical claims that require longer-term evidence (implant stability, calibration, safety, and generalisation).

Data Recording

Patellar reflex: extension observed? (Y/N) ; *Jendrassik effect*:

Two-point discrimination thresholds:

Table 628. Alignment and Rubric Map: Body area and Minimum two-point distance (mm).

Body area	Minimum two-point distance (mm)
Fingertip	
Palm	
Forearm	
Upper back	

Action potential measurements from trace:

Table 629. Alignment and Rubric Map: Parameter and Value.

Parameter	Value
Resting membrane potential	mV
Threshold	mV
Peak	mV
AP amplitude (threshold→peak)	mV
Absolute refractory period	ms
Relative refractory period	ms
Undershoot	mV

Cable properties — length constant λ : Unmyelinated: $\lambda = ______ \text{ mm}$; $V(1\text{mm})/V_0 = ______$ Myelinated: $\lambda = ______ \text{ mm}$; $V(1\text{mm})/V_0 = ______$

Reproducibility check: number of trials per body area = ; *threshold rule used (for example, two correct responses in a row) =*

Evidence and Reproducibility Checklist

- Primary evidence goal: Map circuit structure onto predicted information flow.
- Data skill to practice: Interpret neural data from anatomy, timing, or lesion evidence.
- BioSkills emphasis: Modeling and simulation, Quantitative reasoning, Science and society.
- Control logic: identify at least one positive control, one negative control, or one baseline comparison before interpreting results.
- Measurement discipline: record units, uncertainty, sample size, and any discarded observation with a reason.
- Mechanistic link: connect one result directly to the parent chapter’s big idea before writing the conclusion.
- Reproducibility check: state one procedural detail that another group would need in order to reproduce the result.

Paper-Based Evidence Upgrade

Before answering the analysis questions, annotate the paper dataset for Nervous System and Neural Signaling with a reproducibility pass:

Table 630. Alignment and Rubric Map: Evidence check and Student action.

Evidence check	Student action
Control logic	Mark the comparison that functions as the baseline, negative control, or reference case.
Uncertainty	Circle the row, card, diagram feature, or model assumption most likely to change the conclusion.
Model comparison	State whether a simpler rule, null model, or alternative mechanism could explain the same pattern.
Decision threshold	Write the minimum evidence that would make you revise the interpretation.
Reproducibility	Record the exact scoring rule another group would need to reproduce your classification.

Focus note: in this lab, keep the level of evidence explicit for every neural claim: separate what the structural or anatomical data show from what the recorded activity or behavior shows, and state the scale (cell, circuit, system) at which the inference is licensed before generalizing. Keep required work paper-based; any material-handling or equipment version belongs only in an optional extension.

Worked Example: Median Nerve Conduction Velocity

Problem: A physician records median nerve conduction velocity by stimulating at the wrist and recording at the elbow. The distance between stimulating and recording electrodes is 24 cm and the measured onset latency is 2.4 ms. Calculate the conduction velocity in m/s and compare with the expected range for myelinated Aβ fibers (roughly 30–70 m/s). Then comment on whether the result is consistent with carpal-tunnel-related demyelination.

Solution: Convert units before dividing: 24 cm = 0.24 m and 2.4 ms = 0.0024 s. Conduction velocity $v = \text{distance} / \text{time} = 0.24 \text{ m} / 0.0024 \text{ s} = 100 \text{ m/s}$. This is faster than the typical Aβ range, suggesting the measurement either (i) used a relatively long inter-electrode segment that averages over fast proximal fibers or (ii) reflects a healthy nerve with rapid saltatory conduction. A value substantially below 30 m/s in this segment would have been more consistent with focal demyelination from carpal tunnel compression.

Interpretation: Conduction velocity is one of the most sensitive electrophysiological signs of demyelination, because saltatory conduction depends on intact myelin between nodes of Ranvier. Slowing on the order of 30–50% below the expected range, particularly when localized to the segment under the carpal ligament, supports the clinical suspicion. A normal or supra-normal velocity makes focal demyelination unlikely on its own.

Source-Governance Checkpoint

Complete the source-governance card for Nervous System and Neural Signaling before writing the conclusion. Name the source type or model snapshot, record the evidence date or version, decide whether the claim is stable or fast-moving, and write one refresh trigger that would force the interpretation to change. Treat the card as a printed evidence object, not as a live web lookup.

Analysis Questions

1. The fingertip had a much shorter two-point discrimination threshold than the upper back. Relate this to somatotopic mapping in the somatosensory cortex — which area of the sensory homunculus represents fingers vs trunk, and what is the neural basis for this high-density representation?

- The Jendrassik maneuver increased the patellar reflex. Explain this using the concept of motor neuron excitability and descending facilitation from the cortex/brainstem.
- The action potential’s absolute refractory period prevents reversed signal propagation (backward re-excitation). Explain how sodium channel inactivation (h-gate closed) creates this period and why this is essential for unidirectional propagation.
- Your cable property calculation showed much higher λ in the myelinated axon. Relate this to saltatory conduction: why does an action potential jump between nodes of Ranvier rather than regenerate continuously along the axon?
- In multiple sclerosis, the myelin sheath is destroyed. Using your λ calculations, predict what happens to action potential propagation in demyelinated axons, and explain why patients might experience increased sensitivity to heat (Uhthoff’s phenomenon).
- A speech BCI card reports high decoding accuracy from one participant during attempted speech. Which conclusion is directly supported, and which conclusions would require additional controls or longitudinal data?

Post-Lab Synthesis

Concept Check (Synthesis): Compare the sensory consequences of damage to the dorsal columns of the spinal cord with damage to the spinothalamic tract on the same side of the cord.

- For each tract, identify the modalities it predominantly carries (e.g., fine touch and proprioception versus pain and temperature) and the side of the body on which a unilateral lesion would produce a deficit at a level below the lesion. Justify the laterality using what you know about where each tract decussates relative to its entry into the cord.
- Predict the clinical picture a patient would present with if they had a hemisection of the cord at the mid-thoracic level (a Brown–Séquard pattern). Specify which modalities would be lost on which side below the lesion, and explain how a careful bedside sensory exam could distinguish this pattern from a complete cord transection.

Safety and Ethics Notes

No touch-based neurological testing is required. If an instructor offers an optional demonstration, student consent is required, taps must be gentle, discriminator tips must be blunted, and students may opt out without explanation.

Debrief and Reflection

After you finish the practical work, spend 5–10 minutes in your small group comparing results and discussing the following prompts. Each member should contribute at least one observation before moving to the next prompt:

- What did your measurements show — compare the group’s results to the textbook’s predictions. Where they diverge, suggest at least one mechanistic explanation before concluding “experimental error.”
- What would change the outcome — propose one modification to the procedure that would sharpen the measurement or extend the result to a new biological context, and predict what you would observe.
- One-sentence headline — each student composes a single sentence summarizing the lab’s take-home message, suitable for a tweet. Compare sentences across groups; good headlines are short, quantitative, and mechanistic.
- Connection back to the textbook — identify one section of section 32 that your data either confirmed or complicated. Cite the specific passage.

Further Reading (Lab)

- Revisit the parent chapter section 32 for the theoretical foundations on which this lab is built.
- Look up any bolded glossary term introduced in the textbook chapter (each has a `#gl:term-slug` link in the text) — its master definition is in `manuscript/glossary.md`.
- Explore the appended `src/` module that implements the corresponding quantitative model (when applicable) — referenced in the parent chapter’s “Bridge to Computation” subsection.

Module footer: `parent chapter \cref{sec:unit_IX_nervous_system}`; all numerical quantities in this lab use SI units — see *Appendix D — Units, Physical Constants, and Biological Ranges* for unit conversions and biological-scale reference values.

Lab — Action Potentials and Synaptic Transmission

Learning Objectives

This activity accompanies section 33 of the textbook — review that chapter before attempting the exercises below.

- Analyze a compound action potential (CAP) recording from a nerve preparation to distinguish A, B, and C fiber types
- Simulate quantal neurotransmitter release and calculate mean quantal content
- Model the effect of GABA-A receptor modulation by benzodiazepines vs barbiturates
- Evaluate synaptic plasticity mechanisms using an LTP induction protocol dataset

Alignment and Rubric Map

- Outcome 1 (LO1): Interpret the supplied evidence or model output for Action Potentials and Synaptic Transmission.
- Outcome 2 (LO2): Identify controls and comparison groups that make the claim testable.
- Outcome 3 (LO3): Quantify uncertainty, boundary conditions, or alternative explanations before concluding.
- Outcome 4 (LO4): Transfer the mechanism to a new biological case or public-facing decision.
- Chapter LO coverage: LO1, LO2, LO3, LO4
- Rubric dimensions: evidence; controls; uncertainty; mechanism; transfer. ## Pre-Lab Concept Questions {.unnumbered}

Answer these before starting the investigation — they activate knowledge from the parent chapter.

1. Using the Nernst equation $E = (RT/zF) \ln([ion]_{out}/[ion]_{in})$, calculate the equilibrium potential for K^+ at body temperature ($T = 310\text{ K}$, $R = 8.314\text{ J/mol}\cdot\text{K}$, $F = 96485\text{ C/mol}$, $z = +1$) given $[K^+]_{in} = 140\text{ mM}$ and $[K^+]_{out} = 5\text{ mM}$. Show the sign of the result and explain in one sentence why a resting neuron sits near (but not exactly at) this value.
2. During the rising phase of an action potential, which ion’s membrane permeability changes most, and in which direction? Describe in two sentences how voltage-gated channel kinetics produce this change.
3. State one functional difference between an EPSP and an IPSP at the level of postsynaptic membrane conductance, and predict how each would shift the probability of reaching threshold at the axon hillock.

Lab Context: Action Potentials and Synaptic Transmission

Synaptic transmission involves vesicle fusion (Ca^{2+} -triggered SNARE complex assembly), neurotransmitter diffusion across the synaptic cleft, and receptor binding on the postsynaptic membrane. Release is quantal: the minimum unit is the vesicle (one quantum, about 5,000 molecules). The mean quantal content (\bar{m}) can be estimated by the Poisson failure method: $\bar{m} = \ln(N/F_0)$ where N = total trials and F_0 = failures. Long-term potentiation (LTP) at Schaffer collateral → CA1 synapses requires NMDA receptor-mediated Ca^{2+} influx and CaMKII autophosphorylation.

The quantal-analysis worked example in the parent chapter (section 33) derives quantal content $m = E\bar{P}P/m\bar{E}P$ and uses Poisson statistics to compute failure probability: at $m = 2$, $P(\text{failure}) = e^{-2} \approx 13.5\%$. This lab dataset provides quantal-release trials from which students compute m using both the ratio method and the Poisson failure method and then compare the two.

Paper-Based Materials

Table 631. Alignment and Rubric Map: Item and Quantity.

Item	Quantity
Source-governance card for Action Potentials and Synaptic Transmission: physiology source card: baseline, perturbation, population range, clinical boundary, and evidence date	1
Compound action potential trace (printed: 3 peaks corresponding to $A\alpha$, $A\delta$, C fibers with time and conduction velocity axes)	1
Quantal release dataset (printed: 100 stimulus trials, number of quanta released each trial, count of failures)	1
GABA-A receptor pharmacology worksheet	1

Item	Quantity
LTP induction dataset (EPSP slope before/after high-frequency stimulation; two conditions: control and AP5-treated)	1
Calculator	1
Graph paper or spreadsheet template	1

Paper-Based Investigation

Part A — Compound Action Potential Analysis

1. From the CAP trace, identify the three peaks ($A\alpha$, $A\delta$, C fiber). Measure the latency of each peak from the stimulus artifact.
2. Given the distance from electrode to nerve (30 mm), calculate conduction velocity for each peak (velocity = distance/time).
3. Compare your calculated values to known conduction velocities ($A\alpha$: 70–120 m/s; $A\delta$: 5–30 m/s; C: 0.5–2 m/s).

Part B — Quantal Analysis Simulation

4. From the dataset (100 trials, $F_0 = 8$ failures): calculate \bar{m} by Poisson failure method ($\bar{m} = \ln(100/8) = \ln(12.5)$).
5. Also calculate \bar{m} by direct count method ($\bar{m} = \text{total quanta released} / 100 \text{ trials}$).
6. Estimate release probability: $\bar{p} = \bar{m}/n$ (where $n = \text{total available release sites, given as } 15$).

Part C — GABA-A Pharmacology

7. From the worksheet, benzodiazepines increase the frequency of Cl^- channel opening; barbiturates increase duration of Cl^- channel opening (at low concentration) and open channels directly (at high concentration). On the I-V plot provided, annotate the effect of each drug class on Cl^- current.

Part D — LTP Dataset

8. Plot EPSP slope (% baseline) vs time (minutes) for control and AP5-treated groups before and after high-frequency stimulation (HFS at $t=0$).
9. Calculate the LTP magnitude: $(\text{mean EPSP slope } 30\text{--}60 \text{ min post-HFS} / \text{mean EPSP slope } 10 \text{ min pre-HFS}) \times 100\%$.
10. Reproducibility check: record the baseline window, post-HFS window, and any outlier rule before calculating LTP magnitude.

Data Recording

Table 632. Alignment and Rubric Map: Fiber type and Latency (ms).

Fiber type	Latency (ms)	Conduction velocity (m/s)	Expected range
Peak 1 ($A\alpha$)			70–120 m/s
Peak 2 ($A\delta$)			5–30 m/s
Peak 3 (C)			0.5–2 m/s

Quantal analysis: $F_0 = 8$; $N = 100$ \bar{m} (Poisson) = $\ln(100/8) = \bar{m}$ (direct count) from data = $\bar{p} = \bar{m}/n$ ($n=15$) = ____

LTP magnitude: Control = %; AP5-treated = %

Reproducibility check: baseline window = ; post-HFS window = ; outlier rule = ____

Evidence and Reproducibility Checklist

- Primary evidence goal: Model excitability and synaptic response under changed ion or channel conditions.
- Data skill to practice: Interpret voltage traces, conductance changes, and synaptic perturbations.
- BioSkills emphasis: Modeling and simulation, Quantitative reasoning, Science and society.
- Control logic: identify at least one positive control, one negative control, or one baseline comparison before interpreting results.
- Measurement discipline: record units, uncertainty, sample size, and any discarded observation with a reason.
- Mechanistic link: connect one result directly to the parent chapter’s big idea before writing the conclusion.
- Reproducibility check: state one procedural detail that another group would need in order to reproduce the result.

Paper-Based Evidence Upgrade

Before answering the analysis questions, annotate the paper dataset for Action Potentials and Synaptic Transmission with a reproducibility pass:

Table 633. Alignment and Rubric Map: Evidence check and Student action.

Evidence check	Student action
Control logic	Mark the comparison that functions as the baseline, negative control, or reference case.
Uncertainty	Circle the row, card, diagram feature, or model assumption most likely to change the conclusion.
Model comparison	State whether a simpler rule, null model, or alternative mechanism could explain the same pattern.
Decision threshold	Write the minimum evidence that would make you revise the interpretation.
Reproducibility	Record the exact scoring rule another group would need to reproduce your classification.

Focus note: in this lab, treat each excitability or transmission claim as a timing argument: ask which trace, latency, or quantal statistic supports it, and whether the conduction-velocity or release estimate would survive a change in fiber type, temperature, or release-probability heterogeneity. Keep required work paper-based; any material-handling or equipment version belongs only in an optional extension.

Worked Example: Nernst Potential for Na+ at 37 C

Problem: A neuron rests near -70 mV. During the rising phase of an action potential, voltage-gated Na⁺ channels open and Na⁺ conductance rises roughly 500-fold relative to K⁺ conductance. Using the Nernst equation $E = (RT/zF) \ln([ion]_{out}/[ion]_{in})$, calculate the equilibrium potential for Na⁺ given [Na⁺]_{in} = 15 mM, [Na⁺]_{out} = 145 mM, T = 310 K, R = 8.314 J/mol·K, F = 96485 C/mol, z = +1. Then explain in Goldman-equation terms why peak depolarization approaches — but does not quite reach — E_{Na}.

Solution: The prefactor RT/F at 310 K equals $(8.314 \times 310)/96485 \approx 0.0267$ V, or about 26.7 mV. The natural log of (145/15) is $\ln(9.667) \approx 2.269$. Multiplying gives $E_{Na} \approx 26.7 \text{ mV} \times 2.269 \approx 60.6 \text{ mV}$. Reported as approximately +60 to +62 mV depending on rounding.

Interpretation: The Goldman–Hodgkin–Katz equation weights each ion’s contribution to V_m by its relative permeability. When Na⁺ permeability dominates, V_m shifts toward E_{Na}; residual K⁺ and Cl[−] permeabilities pull V_m back somewhat, so peak depolarization typically reaches roughly +30 to +40 mV rather than +60 mV. Membrane voltage approaches the equilibrium potential of the dominant ion, weighted by the other permeabilities that remain non-zero.

Source-Governance Checkpoint

Complete the source-governance card for Action Potentials and Synaptic Transmission before writing the conclusion. Name the source type or model snapshot, record the evidence date or version, decide whether the claim is stable or fast-moving, and write one refresh trigger that would force the interpretation to change. Treat the card as a printed evidence object, not as a live web lookup.

Analysis Questions

1. C fibers (unmyelinated) have much slower conduction velocities than Aα fibers (myelinated). Using your cable property knowledge from Lab 29, explain the molecular basis for this difference.
2. The two methods for calculating \bar{m} gave similar but not identical answers. Which method is more reliable when there is heterogeneity in release probabilities across synapses? Explain the statistical assumption violated by each method.
3. A patient given a benzodiazepine (e.g., diazepam) overdose can be treated with flumazenil (a competitive benzodiazepine antagonist). Explain why flumazenil doesn’t cause seizures on its own even though it fully blocks GABA-A modulation, while complete GABA-A inhibition by bicuculline does cause seizures.
4. AP5 (an NMDA receptor antagonist) blocked LTP induction. Explain the molecular events from NMDA receptor opening to CaMKII autophosphorylation to AMPA receptor insertion (at least 5 steps).
5. Ketamine is an NMDA receptor open-channel blocker used as an anaesthetic and, at sub-anaesthetic doses, as a rapid antidepressant. Propose a mechanism by which blocking NMDA receptors could relieve depression — consider what happens to synaptic strength in GABAergic interneurons when their NMDA receptors are blocked.

Post-Lab Synthesis

- Concept Check (Synthesis): Evaluate how a toxin that prevents voltage-gated K^+ channels from opening during the repolarization phase would reshape neuronal signaling.
- (a) Predict how the action potential waveform itself would change — describe expected effects on peak amplitude, repolarization rate, and absolute refractory period, and tie each prediction to the underlying conductance change.
 - (b) Trace the downstream consequence at a chemical synapse: how would prolonged depolarization at the presynaptic terminal affect voltage-gated Ca^{2+} channel inactivation, vesicle release probability, and the magnitude of the postsynaptic response? Identify one prediction that could be empirically tested with the lab’s quantal-analysis approach.

Safety and Ethics Notes

Data-analysis and simulation primarily — no chemical or biological hazards. Discussions of neuropharmacology (drug mechanisms) should be factual and clinical in tone.

Debrief and Reflection

After you finish the practical work, spend 5–10 minutes in your small group comparing results and discussing the following prompts. Each member should contribute at least one observation before moving to the next prompt:

- 1. What did your measurements show — compare the group’s results to the textbook’s predictions. Where they diverge, suggest at least one mechanistic explanation before concluding “experimental error.”
- 2. What would change the outcome — propose one modification to the procedure that would sharpen the measurement or extend the result to a new biological context, and predict what you would observe.
- 3. One-sentence headline — each student composes a single sentence summarizing the lab’s take-home message, suitable for a tweet. Compare sentences across groups; good headlines are short, quantitative, and mechanistic.
- 4. Connection back to the textbook — identify one section of section 33 that your data either confirmed or complicated. Cite the specific passage.

Further Reading (Lab)

- Revisit the parent chapter section 33 for the theoretical foundations on which this lab is built.
- Look up any bolded glossary term introduced in the textbook chapter (each has a `#gl:term-slug` link in the text) — its master definition is in `manuscript/glossary.md`.
- Explore the appended `src/` module that implements the corresponding quantitative model (when applicable) — referenced in the parent chapter’s “Bridge to Computation” subsection.

Module footer: *parent chapter \cref{sec:unit_IX_action_potential_synapses}; all numerical quantities in this lab use SI units — see Appendix D — Units, Physical Constants, and Biological Ranges for unit conversions and biological-scale reference values.*

Lab — Endocrine Signaling and Homeostasis

This activity accompanies section 34 of the textbook — review that chapter before attempting the exercises below.

Learning Objectives

This activity accompanies section 34 of the textbook — review that chapter before attempting the exercises below.

- Interpret blood hormone panels to diagnose endocrine disorders (hypo- vs hyperthyroidism, diabetes, Cushing’s)
- Analyze a cytokine profile to determine the type and severity of an inflammatory response
- Model the HPT axis feedback loop using a paper-based regulatory diagram
- Evaluate innate immune pattern recognition using TLR ligand-response data

Alignment and Rubric Map

- Outcome 1 (LO1): Interpret the supplied evidence or model output for Endocrine Signaling and Homeostasis.
- Outcome 2 (LO2): Identify controls and comparison groups that make the claim testable.
- Outcome 3 (LO3): Quantify uncertainty, boundary conditions, or alternative explanations before concluding.
- Outcome 4 (LO4): Transfer the mechanism to a new biological case or public-facing decision.
- Chapter LO coverage: LO1, LO2, LO3, LO4
- Rubric dimensions: evidence; controls; uncertainty; mechanism; transfer. ## Pre-Lab Concept Questions {.unnumbered}

Answer these before starting the investigation — they activate knowledge from the parent chapter.

1. Sketch the hypothalamic–pituitary–thyroid axis, labeling TRH, TSH, T3, and T4. In two to three sentences, describe how negative feedback from circulating T3/T4 onto the hypothalamus and pituitary tends to stabilize thyroid hormone levels in a healthy adult.
2. Distinguish how B cells and T cells recognize antigen: identify which cell type binds soluble antigen directly through a surface receptor, and which requires antigen presentation via MHC molecules. Include one functional consequence of this difference.
3. Contrast a steroid hormone (e.g., cortisol) with a peptide hormone (e.g., insulin) in terms of receptor location and typical timescale of cellular response, and predict which one’s effects would persist longer after a brief secretion pulse.

Lab Context: Endocrine Signaling and Homeostasis

The endocrine system uses hormones (chemical messengers released into the bloodstream) to coordinate physiology across long timescales. Negative feedback loops maintain homeostasis: in the HPT axis, TRH (hypothalamus) → TSH (pituitary) → T3/T4 (thyroid) → inhibit TRH and TSH. In the innate immune system, Toll-like receptors (TLRs) detect conserved pathogen-associated molecular patterns (PAMPs; e.g., LPS, flagellin) and activate NF-κB, triggering pro-inflammatory cytokine production (IL-6, TNF-α, IL-1β).

Paper-Based Materials

Table 634. Alignment and Rubric Map: Item and Quantity.

Item	Quantity
Source-governance card for Endocrine Signaling and Homeostasis: physiology source card: baseline, perturbation, population range, clinical boundary, and evidence date	1
Endocrine case study data cards (4 cases: TSH, T4, cortisol, fasting glucose, HbA1c values)	1 set
HPT axis feedback diagram template (blank: boxes for hypothalamus, pituitary, thyroid)	1
Cytokine data table (printed: IL-6, TNF-α, CRP, PCT by condition: sepsis, mild infection, healthy)	1
TLR ligand-response worksheet (TLR4-LPS → NF-κB → cytokines; effects of TAK-242 inhibitor)	1
Calculator	1
Reference ranges table	1

Item	Quantity
Reproductive-development timing cards: puberty, ovulation, implantation, pregnancy, lactation, and infertility triage	1 set

Paper-Based Investigation

Part A — Endocrine Diagnosis

- For each of 4 case study patients, compare provided hormone values to reference ranges. Diagnose: (a) primary hypothyroidism; (b) hyperthyroidism (Graves’ disease); (c) type 2 diabetes; (d) Cushing’s syndrome (hypercortisolism).
- For each case, state which hormone is abnormal, whether it is elevated or suppressed, and the feedback loop explanation.

Part B — HPT Axis Feedback Model

- Complete the blank HPT axis diagram: draw arrows showing stimulatory (→) and inhibitory (−) connections. Annotate what happens to each hormone level in primary hypothyroidism (thyroid fails) vs secondary hypothyroidism (pituitary fails).

Source-Governance Checkpoint

Complete the source-governance card for Endocrine Signaling and Homeostasis before writing the conclusion. Name the source type or model snapshot, record the evidence date or version, decide whether the claim is stable or fast-moving, and write one refresh trigger that would force the interpretation to change. Treat the card as a printed evidence object, not as a live web lookup.

Evidence and Reproducibility Checklist

- Primary evidence goal: Compare endocrine axes and feedback scenarios.
- Data skill to practice: Interpret endocrine time courses, panels, and perturbations.
- BioSkills emphasis: Modeling and simulation, Quantitative reasoning, Science and society.
- Control logic: identify at least one positive control, one negative control, or one baseline comparison before interpreting results.
- Measurement discipline: record units, uncertainty, sample size, and any discarded observation with a reason.
- Mechanistic link: connect one result directly to the parent chapter’s big idea before writing the conclusion.
- Reproducibility check: state one procedural detail that another group would need in order to reproduce the result.

Paper-Based Evidence Upgrade

Before answering the analysis questions, annotate the paper dataset for Endocrine Signaling and Homeostasis with a reproducibility pass:

Table 635. Source-Governance Checkpoint: Evidence check and Student action.

Evidence check	Student action
Control logic	Mark the comparison that functions as the baseline, negative control, or reference case.
Uncertainty	Circle the row, card, diagram feature, or model assumption most likely to change the conclusion.
Model comparison	State whether a simpler rule, null model, or alternative mechanism could explain the same pattern.
Decision threshold	Write the minimum evidence that would make you revise the interpretation.
Reproducibility	Record the exact scoring rule another group would need to reproduce your classification.

Focus note: endocrine-immune claims should include feedback, timing, receptor sensitivity, inflammation, and allostatic load. Keep required work paper-based; any material-handling or equipment version belongs only in an optional extension.

Lab — Immune System Architecture

Alignment and Rubric Map

- Outcome 1 (LO1): Interpret the supplied evidence or model output for Immune System Architecture.
- Outcome 2 (LO2): Identify controls and comparison groups that make the claim testable.
- Outcome 3 (LO3): Quantify uncertainty, boundary conditions, or alternative explanations before concluding.
- Outcome 4 (LO4): Transfer the mechanism to a new biological case or public-facing decision.
- Chapter LO coverage: LO1, LO2, LO3, LO4
- Rubric dimensions: evidence; controls; uncertainty; mechanism; transfer.

This activity accompanies section 35 of the textbook — review that chapter before attempting the exercises below.

Lab Context: Immune System Architecture

This extension lab emphasizes innate and adaptive immune readouts, cytokine interpretation, and pattern-recognition pathways using printed clinical-style datasets.

Paper-Based Materials

Table 636. Alignment and Rubric Map: Item and Quantity.	
Item	Quantity
Source-governance card for Immune System Architecture: physiology source card: baseline, perturbation, population range, clinical boundary, and evidence date	1
Printed datasets, cards, and worksheets referenced below	1 set per group
Graph paper or plain paper for diagrams	1
Calculator	1

Paper-Based Investigation

4. From the cytokine data table, calculate the ratio of each cytokine (sepsis) / (healthy). Rank the three markers by fold-change to determine which is most useful as a biomarker for severe sepsis.
5. Mark the clinical action threshold for PCT (procalcitonin > 2 ng/mL → antibiotic treatment recommended) on a bar chart.

Part D — TLR4/NF-κB Pathway

6. Using the TLR ligand-response worksheet: trace LPS → TLR4 → MyD88 → IRAK → TRAF6 → IKK → IκB phosphorylation → NF-κB nuclear translocation → IL-6, TNF-α expression. Indicate where TAK-242 blocks the pathway.
7. Reproducibility check: state the reference range source, diagnostic threshold, and fold-change rule used for every case classification.

Part E — Reproductive and Developmental Endocrinology

8. Sort the reproductive-development timing cards into upstream signal, target tissue, critical window, and measurable evidence.
9. For an infertility triage card, identify whether the first evidence gap is ovulation timing, sperm production, tubal transport, uterine receptivity, endocrine feedback, or age-dependent gamete quality.

Data Recording

Table 637. Alignment and Rubric Map: Case and TSH.					
Case	TSH	T4	Cortisol	Glucose/HbA1c	Diagnosis
A	12 mIU/L ↑	7 pmol/L ↓	normal	normal	
B	0.02 mIU/L ↓	42 pmol/L ↑	normal	normal	
C	normal	normal	890 nmol/L ↑	8.1 mmol/L ↑	

Case	TSH	T4	Cortisol	Glucose/HbA1c	Diagnosis
D	normal	normal	normal	11 mmol/L ↑; HbA1c 9.2% ↑	

Cytokine fold-changes:

Table 638. Alignment and Rubric Map: Marker and Healthy.

Marker	Healthy	Sepsis	Fold-change	Rank
IL-6 (pg/mL)	5	1,200		
TNF- α (pg/mL)	10	380		
PCT (ng/mL)	0.05	18		

HPT axis diagram annotations (describe what happens in primary hypothyroidism):

Reproducibility check: reference range source = ; cytokine fold-change rule = ; uncertain case needing more data = ____

Evidence and Reproducibility Checklist

- Primary evidence goal: Compare innate and adaptive activation scenarios.
- Data skill to practice: Interpret immune titers, cytokine profiles, or perturbation data.
- BioSkills emphasis: Modeling and simulation, Quantitative reasoning, Science and society.
- Control logic: identify at least one positive control, one negative control, or one baseline comparison before interpreting results.
- Measurement discipline: record units, uncertainty, sample size, and any discarded observation with a reason.
- Mechanistic link: connect one result directly to the parent chapter’s big idea before writing the conclusion.
- Reproducibility check: state one procedural detail that another group would need in order to reproduce the result.

Paper-Based Evidence Upgrade

Before answering the analysis questions, annotate the paper dataset for Endocrine and Immune Systems with a reproducibility pass:

Table 639. Alignment and Rubric Map: Evidence check and Student action.

Evidence check	Student action
Control logic	Mark the comparison that functions as the baseline, negative control, or reference case.
Uncertainty	Circle the row, card, diagram feature, or model assumption most likely to change the conclusion.
Model comparison	State whether a simpler rule, null model, or alternative mechanism could explain the same pattern.
Decision threshold	Write the minimum evidence that would make you revise the interpretation.
Reproducibility	Record the exact scoring rule another group would need to reproduce your classification.

Focus note: in this lab, read each endocrine or immune claim as a feedback-and-timing argument: identify the dose, latency, and receptor-sensitivity assumptions behind it, and check whether an inflammatory confound or shifted set-point would change the conclusion before treating the response as specific. Keep required work paper-based; any material-handling or equipment version belongs only in an optional extension.

Worked Example: Interpreting an Abnormal Thyroid Panel

Problem: A patient has TSH = 12 mIU/L (reference range 0.4–4.0) and free T4 = 0.6 ng/dL (reference range 0.8–1.8). Using feedback-axis logic, decide whether this pattern is more consistent with primary hypothyroidism (thyroid gland under-producing) or secondary hypothyroidism (pituitary under-producing TSH). Then predict how TSH would respond over 6–8 weeks if the patient began levothyroxine (synthetic T4) replacement at an appropriate dose.

Solution: In primary hypothyroidism, the thyroid itself under-produces T4, so circulating T4 falls. Low T4 releases the pituitary from negative feedback, and TSH rises. Here TSH is elevated and T4 is below range — both signals point toward primary hypothyroidism. On replacement therapy, circulating T4 (and the T3 it is deiodinated to) rises back into range; restored negative feedback then suppresses pituitary TSH secretion, so TSH drifts down over weeks as the half-life of TSH-producing cell adjustment plays out.

Interpretation: TSH and free T4 move in opposite directions under intact negative feedback. A high TSH with low T4 points to the thyroid (primary). A low or inappropriately normal TSH with low T4 would instead suggest pituitary or hypothalamic disease (secondary or tertiary). Treatment monitoring relies on the same loop: TSH normalization over 6–8 weeks is the standard endpoint, because the half-life of T4 and feedback re-equilibration both operate on that timescale.

Analysis Questions

1. In Case A (primary hypothyroidism), TSH is elevated but T4 is low. Trace the negative feedback loop to explain why TSH is high despite low thyroid function. What drug would you prescribe, and which axis level does it target?
2. Graves’ disease (Case B) involves thyroid-stimulating immunoglobulins (TSI) that mimic TSH. Why does the pituitary produce less TSH even though T4 is high? Can negative feedback suppress TSI production?
3. The cytokine data showed PCT was elevated 360-fold in sepsis while TNF- α was elevated 38-fold. Why is PCT particularly specific for bacterial infection over viral infection, and why does this make it a better guide for antibiotic prescribing?
4. NF- κ B is activated during sepsis and produces the cytokine storm that contributes to multi-organ failure. A drug (TAK-242) blocks TLR4 signaling. Predict the effect on: (a) cytokine levels; (b) pathogen clearance. What is the risk of fully blocking TLR4 signaling?
5. An athlete uses anabolic steroids (supraphysiological testosterone dose). Predict the effect on LH and FSH levels via the HPG axis feedback. After stopping steroids, how long does hormonal recovery take, and which cells in the testes are most affected during prolonged suppression?
6. A couple has not conceived after 12 months of regular unprotected intercourse. Build a first-pass evidence map that separates ovulation, sperm production, tubal transport, implantation, uterine receptivity, endocrine feedback, and age-dependent gamete quality.

Post-Lab Synthesis

Concept Check (Synthesis): Hashimoto’s thyroiditis is an autoimmune disease in which T cells and antibodies target thyroid antigens; some patients pass through a transient hyperthyroid phase (“Hashitoxicosis”) before settling into chronic hypothyroidism.

- (a) Trace the immunological events that produce the initial hyperthyroid phase — identify how immune-mediated follicular damage could release stored thyroid hormone, and explain which class of immune cell most directly drives the destruction. Predict how serum TSH and free T4 would move during this phase.
- (b) Now trace the progression to chronic hypothyroidism: describe how the loss of functional follicles, falling T4 output, and re-engagement of negative feedback together reshape the hormone panel and the patient’s symptoms. Identify one laboratory measurement that would most cleanly distinguish this autoimmune trajectory from a non-immune cause of low thyroid output.

Safety and Ethics Notes

Data-analysis primarily. Most patient case data should be anonymised/fictional. Discuss real clinical conditions (Cushing’s, diabetes) with sensitivity to students who may have personal connections to these diagnoses.

Source-Governance Checkpoint

Complete the source-governance card for Immune System Architecture before writing the conclusion. Name the source type or model snapshot, record the evidence date or version, decide whether the claim is stable or fast-moving, and write one refresh trigger that would force the interpretation to change. Treat the card as a printed evidence object, not as a live web lookup.

Debrief and Reflection

After you finish the practical work, spend 5–10 minutes in your small group comparing results and discussing the following prompts. Each member should contribute at least one observation before moving to the next prompt:

1. What did your measurements show — compare the group’s results to the textbook’s predictions. Where they diverge, suggest at least one mechanistic explanation before concluding “experimental error.”
2. What would change the outcome — propose one modification to the procedure that would sharpen the measurement or extend the result to a new biological context, and predict what you would observe.
3. One-sentence headline — each student composes a single sentence summarizing the lab’s take-home message, suitable for a tweet. Compare sentences across groups; good headlines are short, quantitative, and mechanistic.
4. Connection back to the textbook — identify one section of section 35 that your data either confirmed or complicated. Cite the specific passage.

Further Reading (Lab)

- Revisit the parent chapter section 35 for the theoretical foundations on which this lab is built.
- Look up any bolded glossary term introduced in the textbook chapter (each has a #gl:term-slug link in the text) — its master definition is in manuscript/glossary.md.
- Explore the appended src/ module that implements the corresponding quantitative model (when applicable) — referenced in the parent chapter’s “Bridge to Computation” subsection.

Module footer: parent chapter \cref{sec:unit_IX_immune_system_defense}; all numerical quantities in this lab use SI units — see Appendix D — Units, Physical Constants, and Biological Ranges for unit conversions and biological-scale reference values.

Lab — Population Ecology and Growth Models

Learning Objectives

This activity accompanies section 36 of the textbook — review that chapter before attempting the exercises below.

- Fit logistic and exponential growth equations to real or simulated population data
- Calculate intrinsic rate of increase (*r*) and carrying capacity (*K*) from population time series
- Apply the mark-recapture method (Lincoln-Petersen) to estimate population size
- Evaluate density-dependent vs density-independent limiting factors from case study data
- Interpret colony founding and fragmentation scenarios where Allee effects change social-insect population trajectories

Alignment and Rubric Map

- Outcome 1 (LO1): Interpret the supplied evidence or model output for Population Ecology and Growth Models.
- Outcome 2 (LO2): Identify controls and comparison groups that make the claim testable.
- Outcome 3 (LO3): Quantify uncertainty, boundary conditions, or alternative explanations before concluding.
- Outcome 4 (LO4): Transfer the mechanism to a new biological case or public-facing decision.
- Chapter LO coverage: LO1, LO2, LO3, LO4
- Rubric dimensions: evidence; controls; uncertainty; mechanism; transfer. ## Pre-Lab Concept Questions {.unnumbered}

Answer these before starting the investigation — they activate knowledge from the parent chapter.

1. Write the logistic growth equation $dN/dt = rN(K - N)/K$. Define each symbol and describe in two sentences what happens to dN/dt as *N* approaches *K* from below and from above.
2. Distinguish density-dependent from density-independent regulation, giving one biological example of each. State which type of regulation would more plausibly stabilize a population near its carrying capacity over time.
3. Sketch the three classic survivorship curves (Types I, II, III) and identify one organism whose life history matches each. In one sentence per type, explain how the curve’s shape reflects the timing of mortality across the life cycle.

Lab Context: Population Ecology and Growth Models

Population growth follows exponential growth ($dN/dt = rN$) when resources are unlimited, and logistic growth ($dN/dt = rN(1 - N/K)$) as populations approach the carrying capacity *K*. Real populations fluctuate around *K* due to density-dependent factors (competition, predation, disease — intensify as *N* increases) or may crash due to density-independent factors (storms, droughts — unrelated to *N*). The Lincoln-Petersen mark-recapture estimate: $\hat{N} = (M \times C) / R$, where *M* = initial marked individuals, *C* = recapture sample size, *R* = recaptured marked individuals.

The logistic-growth projection worked example in the parent chapter (section 36) shows that with $r = 0.2/\text{yr}$ and $K = 1000$, a population starting at $N_0 = 100$ reaches roughly 451 at $t = 10$ and 858 at $t = 20$, illustrating the S-curve’s characteristic acceleration below $K/2$ and deceleration above it. This lab generates analogous growth data so students can test which model (exponential vs. logistic) better fits observed population trajectories.

Paper-Based Materials

Table 640. Alignment and Rubric Map: Item and Quantity.

Item	Quantity
Source-governance card for Population Ecology and Growth Models: conservation-assessment source card: index versus census, assessment version, value judgment, and monitoring trigger	1
Population time series data (printed: 3 species — moth (exponential), snowshoe hare (oscillating), logistic yeast)	1
Graph paper or spreadsheet template	1
Calculator	1
Mark-recapture card deck or printed capture-history table	1

Item	Quantity
Management scenario cards for invasive species, harvested fisheries, climate-driven range shifts, and eusocial colony founding or fragmentation	1 set

Paper-Based Investigation

Part A — Growth Curve Fitting

- Plot the three population time series on graph paper. For the yeast data, identify: lag phase, exponential phase, plateau (K).
- Estimate K from the plateau of the logistic curve.
- Estimate r from the exponential phase: $r \approx (\ln N_2 - \ln N_1) / (t_2 - t_1)$ during the period of fastest growth.

Part B — Mark-Recapture

- Use the printed capture-history table: M = 50 initially marked individuals and C = 30 individuals in the recapture sample. Count the marked recaptures (R) in the table and calculate $N_{\text{hat}} = (50 \times 30) / R$.
- Repeat the calculation for the second printed sampling event. Compare both estimates with the known simulated population size and calculate percent error.

Part C — Density Dependence Analysis

- Given data on white-tailed deer population growth rate (r) vs density in 4 regions: plot r vs N/K (relative density). Identify whether r decreases with increasing density (density-dependent regulation) — this confirms a logistic pattern.

Part D — Colony Allee-Effect Scenario

- Use the colony scenario cards to decide whether a founding ant, bee, or termite colony is below or above an Allee threshold. Record the worker number, queen survival, foraging success, and brood-care constraint that supports your classification, then predict whether the colony grows, stalls, or collapses.

Data Recording

Logistic yeast data:

Table 641. Alignment and Rubric Map: Time (h) and Population (cells/mL).

Time (h)	Population (cells/mL)	ln N
0	10	
6	80	
12	410	
18	1,200	
24	2,800	
36	3,900	
48	4,100	

Estimated K = ; *Estimated r* =

Mark-recapture: M = 50; C = 30; R = ; \hat{N} = Second sampling estimate: R = ; \hat{N} = ; percent error from known simulated N = ____%

Evidence and Reproducibility Checklist

- Primary evidence goal: Model population trajectories and compare sampling methods.
- Data skill to practice: Use abundance or age-structure data to estimate growth and risk.
- BioSkills emphasis: Modeling and simulation, Science and society, Communication and collaboration.
- Control logic: identify at least one positive control, one negative control, or one baseline comparison before interpreting results.
- Measurement discipline: record units, uncertainty, sample size, and any discarded observation with a reason.
- Mechanistic link: connect one result directly to the parent chapter’s big idea before writing the conclusion.
- Reproducibility check: state one procedural detail that another group would need in order to reproduce the result.

Paper-Based Evidence Upgrade

Before answering the analysis questions, annotate the paper dataset for Population Ecology and Growth Models with a reproducibility pass:

Table 642. Alignment and Rubric Map: Evidence check and Student action.

Evidence check	Student action
Control logic	Mark the comparison that functions as the baseline, negative control, or reference case.
Uncertainty	Circle the row, card, diagram feature, or model assumption most likely to change the conclusion.
Model comparison	State whether a simpler rule, null model, or alternative mechanism could explain the same pattern.
Decision threshold	Write the minimum evidence that would make you revise the interpretation.
Reproducibility	Record the exact scoring rule another group would need to reproduce your classification.

Focus note: for this population lab, state the demographic model behind each printed estimate (exponential, logistic, or mark-recapture), check whether its assumptions about density dependence, closure, and detection hold for the simulated capture histories, and tie any harvest or recovery conclusion to an explicit management objective. Keep required work paper-based; any material-handling or equipment version belongs only in an optional extension.

Worked Example: Logistic Growth Rate Below Carrying Capacity

Problem: A population growing under logistic dynamics has intrinsic growth rate $r = 0.18/\text{yr}$ and carrying capacity $K = 1,200$. The current population size is $N = 300$. (a) Calculate the instantaneous growth rate dN/dt . (b) Estimate N after one year using the Euler approximation $N_1 \approx N_0 + (dN/dt) \times \Delta t$ with $\Delta t = 1$ yr. (c) Compute $(K - N)/K$ and interpret what fraction of the logistic “brake” is currently engaged.

Solution: (a) $dN/dt = r \times N \times (K - N)/K = 0.18 \times 300 \times (1,200 - 300)/1,200 = 0.18 \times 300 \times 0.75 = 40.5$ individuals/yr. (b) $N_1 \approx 300 + 40.5 \times 1 = 340.5$ individuals — round down to 340 for a discrete count. (c) $(K - N)/K = 900/1,200 = 0.75$, so the population is at 25% of K and the density-dependent brake $(1 - N/K)$ is still 0.75 of its maximum.

Interpretation: The population is in its near-exponential phase: most of the logistic term $(K - N)/K$ is still close to 1, so growth is fast relative to the rate it will show near K . As N rises toward K , the brake term shrinks toward zero and dN/dt falls smoothly to zero at $N = K$. The Euler step is acceptable for one-year projections at low N relative to K , but it overshoots the true logistic trajectory when N grows enough within the year to change the brake substantially.

Source-Governance Checkpoint

Complete the source-governance card for Population Ecology and Growth Models before writing the conclusion. Name the source type or model snapshot, record the evidence date or version, decide whether the claim is stable or fast-moving, and write one refresh trigger that would force the interpretation to change. Treat the card as a printed evidence object, not as a live web lookup.

Analysis Questions

- Why does the yeast population growth slow as it approaches K ? Use the term “intraspecific competition” and identify two specific density-dependent resources that become limiting.
- Snowshoe hare populations cycle with about 10-year periodicity (tied to lynx cycles). Is this best explained as: (a) density-dependent predation; (b) density-independent weather events; or (c) a two-species coupled oscillator? Describe the evidence.
- Your two mark-recapture estimates probably differed slightly. List three assumptions of the Lincoln-Petersen method and explain which assumption is most likely violated in the printed capture-history simulation.
- Invasive species often exhibit exponential growth in new habitats. Name a specific invasive species, identify what density-dependent factor is absent in the new habitat, and predict when/how logistic behavior will eventually emerge.
- Apply a fisheries management scenario: a cod population has $K = 500,000$ tonnes and $r = 0.2/\text{year}$. Using the maximum sustainable yield formula ($MSY = rK/4$), calculate the MSY and the population size at MSY ($N = K/2$). If fishing reduces the population below $K/4$, explain why the population will continue to decline even if fishing stops.

6. A newly founded termite or ant colony has a queen and a small worker force. Explain why a colony can show an Allee effect even when each surviving worker is healthy. Which demographic variable would you monitor to distinguish ordinary density dependence from a threshold caused by brood care, foraging, or nest defense?

Post-Lab Synthesis

- Concept Check (Synthesis): A species with a Type III survivorship curve produces many offspring but has high juvenile mortality and relatively high adult survival once individuals reach reproductive age. A manager must choose between two interventions: (i) protecting juveniles (e.g., headstarting hatchlings, predator exclusion at nurseries) or (ii) protecting adults (e.g., reducing bycatch of reproductive individuals).
- (a) Using reproductive-value theory, predict which intervention is likely to produce faster population recovery in a Type III species. Explain why the reproductive value of an adult, particularly a prime-aged breeder, tends to outweigh that of an individual juvenile, and tie the argument to how reproductive value typically peaks near the age of first reproduction.
 - (b) Identify one situation in which the juvenile-protection strategy would still be the preferred choice — for example, when adult mortality is already low and juvenile survival is the demographic bottleneck. Propose one measurement from the lab’s life-table analysis that would help a manager decide between the two strategies in practice.

Safety and Ethics Notes

No hazardous materials or living specimens are required. When discussing harvested or invasive species, maintain ecological objectivity and identify uncertainty in population estimates.

Debrief and Reflection

After you finish the practical work, spend 5–10 minutes in your small group comparing results and discussing the following prompts. Each member should contribute at least one observation before moving to the next prompt:

- 1. What did your measurements show — compare the group’s results to the textbook’s predictions. Where they diverge, suggest at least one mechanistic explanation before concluding “experimental error.”
- 2. What would change the outcome — propose one modification to the procedure that would sharpen the measurement or extend the result to a new biological context, and predict what you would observe.
- 3. One-sentence headline — each student composes a single sentence summarizing the lab’s take-home message, suitable for a tweet. Compare sentences across groups; good headlines are short, quantitative, and mechanistic.
- 4. Connection back to the textbook — identify one section of section 36 that your data either confirmed or complicated. Cite the specific passage.

Further Reading (Lab)

- Revisit the parent chapter section 36 for the theoretical foundations on which this lab is built.
- Look up any bolded glossary term introduced in the textbook chapter (each has a `#gl:term-slug` link in the text) — its master definition is in `manuscript/glossary.md`.
- Explore the appended `src/` module that implements the corresponding quantitative model (when applicable) — referenced in the parent chapter’s “Bridge to Computation” subsection.

Module footer: `parent chapter \cref{sec:unit_X_population_ecology}`; all numerical quantities in this lab use SI units — see *Appendix D — Units, Physical Constants, and Biological Ranges* for unit conversions and biological-scale reference values.

Lab — Community Interactions and Succession

This activity accompanies section 37 of the textbook — review that chapter before attempting the exercises below.

Learning Objectives

This activity accompanies section 37 of the textbook — review that chapter before attempting the exercises below.

- Interpret a paper-based competition dataset between two species using Lotka-Volterra predictions
- Analyze food web data to determine trophic levels and calculate energy transfer efficiency
- Evaluate keystone predator effects using a removal/addition case study
- Apply successional theory to interpret vegetation data from different chronosequences

Alignment and Rubric Map

- Outcome 1 (LO1): Interpret the supplied evidence or model output for Community Interactions and Succession.
- Outcome 2 (LO2): Identify controls and comparison groups that make the claim testable.
- Outcome 3 (LO3): Quantify uncertainty, boundary conditions, or alternative explanations before concluding.
- Outcome 4 (LO4): Transfer the mechanism to a new biological case or public-facing decision.
- Chapter LO coverage: LO1, LO2, LO3, LO4
- Rubric dimensions: evidence; controls; uncertainty; mechanism; transfer. ## Pre-Lab Concept Questions {.unnumbered}

Answer these before starting the investigation — they activate knowledge from the parent chapter.

1. Define species richness and species evenness in your own words, and explain in two sentences why two communities with identical richness can differ substantially in diversity as measured by Shannon’s H’.
2. State the competitive exclusion principle and describe two ecological outcomes consistent with it when two species share a limiting resource — for example, character displacement that narrows niche overlap, or competitive replacement of one species by the other. Cite a brief example or condition under which each outcome is more likely.
3. Sketch a generic predator–prey time series under Lotka–Volterra dynamics and label which curve typically leads the other in phase. In one sentence, explain mechanistically why predator peaks lag prey peaks.

Lab Context: Community Interactions and Succession

Community ecology studies how species interact (competition, predation, mutualism, commensalism, parasitism) and how those interactions shape community composition. The Lotka-Volterra competition model predicts stable coexistence primarily when intraspecific competition > interspecific competition for both species (Gause’s principle: competitive exclusion eliminates one species if niches overlap completely). Energy flows through trophic levels with about 10% efficiency: about 10% of energy at level N reaches level N+1 (ecological pyramid).

Paper-Based Materials

Table 643. Alignment and Rubric Map: Item and Quantity.

Item	Quantity
Source-governance card for Community Interactions and Succession: conservation-assessment source card: index versus census, assessment version, value judgment, and monitoring trigger	1
Lotka-Volterra outcome table (4 cases: stable coexistence, species 1 wins, species 2 wins, unstable equilibrium)	1
Food web diagram: temperate forest ecosystem (15 species, 3 trophic levels)	1
Species competition dataset (N1 and N2 over 14 days in mono- and mixed treatments)	1

Item	Quantity
Successional chronosequence and remote-sensing cards (bare substrate -> pioneer -> scrub -> forest)	1 set
Ecosystem-service decision matrix for pollination, carbon storage, flood buffering, and recreation	1
Calculator	1

Paper-Based Investigation

Part A — Competition Simulation/Analysis

1. Using the competition dataset, plot N1 and N2 over time in mixed treatment on one graph.
2. Predict the competitive outcome from the Lotka-Volterra equilibrium conditions (α_{12} and α_{21} values provided).
3. Compare the mixed-treatment trajectory with both monoculture baselines. Identify whether interspecific competition is stronger, weaker, or similar to intraspecific competition for each species.

Source-Governance Checkpoint

Complete the source-governance card for Community Interactions and Succession before writing the conclusion. Name the source type or model snapshot, record the evidence date or version, decide whether the claim is stable or fast-moving, and write one refresh trigger that would force the interpretation to change. Treat the card as a printed evidence object, not as a live web lookup.

Evidence and Reproducibility Checklist

- Primary evidence goal: Compare species-interaction outcomes under changing conditions.
- Data skill to practice: Interpret abundance, interaction, or disturbance data from communities.
- BioSkills emphasis: Modeling and simulation, Science and society, Communication and collaboration.
- Control logic: identify at least one positive control, one negative control, or one baseline comparison before interpreting results.
- Measurement discipline: record units, uncertainty, sample size, and any discarded observation with a reason.
- Mechanistic link: connect one result directly to the parent chapter’s big idea before writing the conclusion.
- Reproducibility check: state one procedural detail that another group would need in order to reproduce the result.

Paper-Based Evidence Upgrade

Before answering the analysis questions, annotate the paper dataset for Community Interactions and Succession with a reproducibility pass:

Table 644. Source-Governance Checkpoint: Evidence check and Student action.

Evidence check	Student action
Control logic	Mark the comparison that functions as the baseline, negative control, or reference case.
Uncertainty	Circle the row, card, diagram feature, or model assumption most likely to change the conclusion.
Model comparison	State whether a simpler rule, null model, or alternative mechanism could explain the same pattern.
Decision threshold	Write the minimum evidence that would make you revise the interpretation.
Reproducibility	Record the exact scoring rule another group would need to reproduce your classification.

Focus note: community claims should identify interaction type, network position, disturbance regime, and observational limits. Keep required work paper-based; any material-handling or equipment version belongs only in an optional extension.

Lab — Biodiversity and Food Webs

Alignment and Rubric Map

- Outcome 1 (LO1): Interpret the supplied evidence or model output for Biodiversity and Food Webs.
- Outcome 2 (LO2): Identify controls and comparison groups that make the claim testable.
- Outcome 3 (LO3): Quantify uncertainty, boundary conditions, or alternative explanations before concluding.
- Outcome 4 (LO4): Transfer the mechanism to a new biological case or public-facing decision.
- Chapter LO coverage: LO1, LO2, LO3, LO4
- Rubric dimensions: evidence; controls; uncertainty; mechanism; transfer.

This activity accompanies section 38 of the textbook — review that chapter before attempting the exercises below.

Lab Context: Biodiversity and Food Webs

This extension lab applies island biogeography, food-web structure, and biodiversity indices to printed ecological datasets and conservation scenarios.

Paper-Based Materials

Table 645. Alignment and Rubric Map: Item and Quantity.

Item	Quantity
Source-governance card for Biodiversity and Food Webs: conservation-assessment source card: index versus census, assessment version, value judgment, and monitoring trigger	1
Printed datasets, cards, and worksheets referenced below	1 set per group
Graph paper or plain paper for diagrams	1
Calculator	1

Paper-Based Investigation

4.

From the food web diagram: identify most producers, primary consumers, secondary consumers, and apex predators. List most possible food chains containing 4 links.
5.

If a producer level has 10,000 kJ available, calculate the energy at each trophic level assuming 10% efficiency. Calculate how many humans (apex predators) can be supported vs if they ate at the primary consumer level.

Part C — Keystone Predator Analysis

6.

Read the starfish removal experiment data (Paine, 1966, summarized): count species richness before and after sea star (*Pisaster*) removal from an intertidal zone. Explain how removing one species reduced diversity.

Part D — Succession Mapping

7.

For each chronosequence or remote-sensing card: record dominant vegetation type, estimated time since disturbance, key abiotic factors, and one ecosystem service expected to change during succession.

Data Recording

Species competition (from dataset):

Table 646. Alignment and Rubric Map: Day and N₁ (monoculture).

Day	N ₁ (monoculture)	N ₁ (mixed)	N ₂ (monoculture)	N ₂ (mixed)
0				
4				
8				

Day	N ₁ (monoculture)	N ₁ (mixed)	N ₂ (monoculture)	N ₂ (mixed)
14				

Food web energy pyramid:

Table 647. Alignment and Rubric Map: Trophic level and Energy (kJ).

Trophic level	Energy (kJ)	# Humans supported
Producers	10,000	—
Primary consumers		
Secondary consumers		
Apex predators		

Species richness before sea star removal: ; *After*:

Ecosystem-service tradeoff most improved by succession: ; *tradeoff most reduced by disturbance*:

Evidence and Reproducibility Checklist

- Primary evidence goal: Compare diversity and network scenarios under area or disturbance change.
- Data skill to practice: Interpret food-web, richness, or biogeography datasets.
- BioSkills emphasis: Modeling and simulation, Science and society, Communication and collaboration.
- Control logic: identify at least one positive control, one negative control, or one baseline comparison before interpreting results.
- Measurement discipline: record units, uncertainty, sample size, and any discarded observation with a reason.
- Mechanistic link: connect one result directly to the parent chapter’s big idea before writing the conclusion.
- Reproducibility check: state one procedural detail that another group would need in order to reproduce the result.

Paper-Based Evidence Upgrade

Before answering the analysis questions, annotate the paper dataset for Community Ecology and Species Interactions with a reproducibility pass:

Table 648. Alignment and Rubric Map: Evidence check and Student action.

Evidence check	Student action
Control logic	Mark the comparison that functions as the baseline, negative control, or reference case.
Uncertainty	Circle the row, card, diagram feature, or model assumption most likely to change the conclusion.
Model comparison	State whether a simpler rule, null model, or alternative mechanism could explain the same pattern.
Decision threshold	Write the minimum evidence that would make you revise the interpretation.
Reproducibility	Record the exact scoring rule another group would need to reproduce your classification.

Focus note: for this community-interaction lab, label every link in the printed network by interaction type (competition, predation, mutualism) and by whether it was observed directly or inferred from co-occurrence, and state how the sampling effort and disturbance history could bias which interactions appear. Keep required work paper-based; any material-handling or equipment version belongs only in an optional extension.

Worked Example: Shannon Diversity and Evenness in Two Communities

Problem: Two communities each contain four species. Community A has 25, 25, 25, 25 individuals across the four species. Community B has 70, 15, 10, 5 individuals. Calculate Shannon diversity $H' = -\sum(p_i \ln p_i)$ for each community, then compute evenness $J = H'/H_{\text{max}}$ with $H_{\text{max}} = \ln S$, where S is the number of species. Which community is more diverse, and which is more even?

Solution: For Community A, each proportion $p_i = 0.25$, so $-p_i \ln p_i = -0.25 \times \ln(0.25) = -0.25 \times (-1.386) \approx 0.347$. Summing across four species gives $H'_A \approx 4 \times 0.347 \approx 1.386$, which equals $\ln 4$ exactly (H_{\max} for $S = 4$). So $J_A = 1.386 / 1.386 = 1.0$. For Community B, proportions are 0.70, 0.15, 0.10, 0.05. The corresponding $-p_i \ln p_i$ terms are about 0.250, 0.285, 0.230, 0.150; summing gives $H'_B \approx 0.915$. Evenness $J_B = 0.915 / 1.386 \approx 0.66$.

Interpretation: Community A is at the theoretical maximum diversity for four species (every species equally common), so its evenness is 1.0. Community B has the same richness but is dominated by one species; its diversity drops to about 0.92 and its evenness falls to 0.66. The example shows that Shannon H' combines richness and evenness into a single index — a strongly dominant species can lower H' substantially even when S is held constant.

Analysis Questions

1. In the Lotka-Volterra framework, stable coexistence requires $\alpha_{12} < K_1/K_2$ and $\alpha_{21} < K_2/K_1$. What do these inequalities mean biologically in terms of intra- vs interspecific competition strength?
2. The pyramid of energy shows that far more humans can be supported by eating at lower trophic levels. Calculate the maximum number of humans at each trophic level from your energy data. What are three reasons why human food systems often involve higher trophic level consumption?
3. When *Pisaster* (sea star) was removed, mussel populations exploded and crowded out other species, reducing diversity. Define keystone species and explain why removing an apex predator can reduce community diversity (trophic cascade).
4. Primary succession begins on bare rock (no soil) while secondary succession follows disturbance on existing soil. Explain how pioneer species (lichens, mosses) facilitate succession on bare rock — which physical and chemical properties of soil do they create? Name Connell and Slatyer’s facilitation model.
5. A student claims “climax forests are the most stable and should generally be our conservation goal.” Critique this statement using the concept of intermediate disturbance hypothesis (Connell 1978) and give an example of an ecosystem that requires periodic disturbance to maintain high diversity.

Post-Lab Synthesis

Concept Check (Synthesis): The removal of gray wolves from Yellowstone National Park has been linked to a trophic cascade that reshaped riparian plant communities and stream morphology, and their reintroduction is associated with partial recovery of those systems.

(a) Trace the cascade from predator removal to plant community change: identify the immediate prey-population response, the resulting change in herbivory pressure on willows and aspens, and the downstream consequence for riparian vegetation. Distinguish direct effects (predator on prey) from indirect effects (predator on plants via herbivory).

(b) Predict at least one effect on soil stability or stream geomorphology that would plausibly follow from the vegetation change in part (a). Identify one observational measurement that ecologists could use to test whether your predicted effect is operating, and one alternative explanation (for example, climate or hydrological change) that the measurement would need to discriminate against.

Safety and Ethics Notes

No live organisms or ecological specimens are required. Optional living-culture demonstrations should be instructor managed, disposed of without release to waterways, and treated as enrichment rather than required evidence.

Source-Governance Checkpoint

Complete the source-governance card for Biodiversity and Food Webs before writing the conclusion. Name the source type or model snapshot, record the evidence date or version, decide whether the claim is stable or fast-moving, and write one refresh trigger that would force the interpretation to change. Treat the card as a printed evidence object, not as a live web lookup.

Debrief and Reflection

After you finish the practical work, spend 5–10 minutes in your small group comparing results and discussing the following prompts. Each member should contribute at least one observation before moving to the next prompt:

1. What did your measurements show — compare the group’s results to the textbook’s predictions. Where they diverge, suggest at least one mechanistic explanation before concluding “experimental error.”
2. What would change the outcome — propose one modification to the procedure that would sharpen the measurement or extend the result to a new biological context, and predict what you would observe.
3. One-sentence headline — each student composes a single sentence summarizing the lab’s take-home message, suitable for a tweet. Compare sentences across groups; good headlines are short, quantitative, and mechanistic.
4. Connection back to the textbook — identify one section of section 38 that your data either confirmed or complicated. Cite the specific passage.

Further Reading (Lab)

- Revisit the parent chapter section 38 for the theoretical foundations on which this lab is built.

- Look up any bolded glossary term introduced in the textbook chapter (each has a `#gl:term-slug` link in the text) — its master definition is in `manuscript/glossary.md`.
- Explore the appended `src/` module that implements the corresponding quantitative model (when applicable) — referenced in the parent chapter’s “Bridge to Computation” subsection.

Module footer: parent chapter `\cref{sec:unit_X_biodiversity_and_food_webs}`; all numerical quantities in this lab use SI units — see [Appendix D — Units, Physical Constants, and Biological Ranges](#) for unit conversions and biological-scale reference values.

Lab — Ecosystem Ecology

Learning Objectives

This activity accompanies section 39 of the textbook — review that chapter before attempting the exercises below.

- Calculate primary productivity of an aquatic ecosystem from light-dark bottle datasets
- Model nitrogen cycle transformations using an annotated diagram
- Calculate carbon flux between reservoirs using published global carbon budget data
- Evaluate the impact of nutrient loading on eutrophication using scenario data
- Explain how termites and ants act as ecosystem engineers that modify soil structure, carbon turnover, and nutrient cycling

Alignment and Rubric Map

- Outcome 1 (LO1): Interpret the supplied evidence or model output for Ecosystem Ecology.
- Outcome 2 (LO2): Identify controls and comparison groups that make the claim testable.
- Outcome 3 (LO3): Quantify uncertainty, boundary conditions, or alternative explanations before concluding.
- Outcome 4 (LO4): Transfer the mechanism to a new biological case or public-facing decision.
- Chapter LO coverage: LO1, LO2, LO3, LO4
- Rubric dimensions: evidence; controls; uncertainty; mechanism; transfer. ## Pre-Lab Concept Questions {.unnumbered}

Answer these before starting the investigation — they activate knowledge from the parent chapter.

1. Define gross primary productivity (GPP) and net primary productivity (NPP). Write the relationship between them in terms of autotrophic respiration (R_a) and identify the units (e.g., $g\ C/m^2/yr$) most commonly used in ecosystem studies.
2. Explain why energy transfer efficiency between adjacent trophic levels averages around 10% rather than being much higher. Identify two energy losses (for example, respiration and heat) that limit the fraction passed upward.
3. Sketch the nitrogen cycle at the level of a grassland ecosystem and identify two processes that move nitrogen from the soil into living biomass and two processes that move it back to soil or atmosphere.

Lab Context: Ecosystem Ecology

Ecosystems are characterized by flows of energy (one-way, lost as heat at each step) and cycles of matter (recycled through biogeochemical pathways). Gross primary productivity (GPP) is total photosynthesis; net primary productivity (NPP) = GPP – respiration. The nitrogen cycle includes fixation ($N_2 \rightarrow NH_3$ by nitrogenase), nitrification ($NH_3 \rightarrow NO_2^- \rightarrow NO_3^-$ by *Nitrosomonas*, *Nitrobacter*), denitrification ($NO_3^- \rightarrow N_2$ by anaerobic bacteria), and assimilation ($NH_4^+ / NO_3^- \rightarrow$ amino acids by plants).

Termites and ants add a useful animal-mediated layer to this cycle picture. Termite gut symbionts transform lignocellulose into usable carbon compounds, while termite mounds and ant nests move soil, alter porosity, concentrate organic matter, and change local water and nutrient dynamics [Brune, 2014, Evans et al., 2011]. In this lab, treat nests and mounds as ecosystem-engineering structures: ask which flux or stock changes, not merely whether the insect is “beneficial.”

Paper-Based Materials

Table 649. Alignment and Rubric Map: Item and Quantity.

Item	Quantity
Source-governance card for Ecosystem Ecology: conservation-assessment source card: index versus census, assessment version, value judgment, and monitoring trigger	1
Light-dark bottle dissolved oxygen dataset with three replicates per treatment	1
Nitrogen cycle blank diagram (for annotation)	1
Global carbon budget data (IPCC AR6 summary values, printed)	1
Eutrophication case packet with nutrient loading, turbidity, chlorophyll-a, and fish-kill observations	1

Item	Quantity
Ecosystem-service card set for wetlands, forests, croplands, and urban streams	1
Soil-engineer card set: termite mound, termite gut symbiosis, ant nest, earthworm comparison, and nearby control soil	1 set
Graph paper or spreadsheet template	1
Calculator	1

Paper-Based Investigation

Part A — Primary Productivity (Light-Dark Bottle)

1.

Use the provided initial, light-bottle, and dark-bottle dissolved oxygen data. Confirm that each treatment has three replicates and the same incubation time.
2.

Calculate mean DO and range for each bottle type.
3.

Compare the light and dark treatments to the initial baseline, then flag any replicate that strongly changes the mean.
4.

Calculate: $NPP = DO_{light} - DO_{initial}$; $Respiration = DO_{initial} - DO_{dark}$; $GPP = NPP + Respiration$.

Part B — Nitrogen Cycle Annotation

5.

Complete the blank nitrogen cycle diagram: label the 5 processes (fixation, nitrification, denitrification, assimilation, decomposition/ammonification). Name one key organism for each process.

Part C — Carbon Budget Calculation

6.

Using IPCC data (approximate 2022 values): $GPP_{(terrestrial)} = -120$ Gt C/yr (uptake); plant respiration = +60 Gt C/yr; FF emissions = +10 Gt C/yr; ocean uptake = -3 Gt C/yr; land use change = +2 Gt C/yr. Calculate net atmospheric accumulation of CO₂ per year. Compare to measured atmospheric growth rate (about 5 Gt C/yr).

Part D — Eutrophication Experiment

7.

Use the eutrophication case packet to compare control and nutrient-addition scenarios over 5 days. Interpret turbidity, chlorophyll-a, dissolved oxygen, and fish-kill observations as indicators of algal bloom risk.

Part E — Soil Engineers and Nutrient Hotspots

8.

Compare the soil-engineer cards. For each termite mound, ant nest, earthworm, or control-soil case, predict the direction of change in infiltration, organic-matter concentration, nitrogen availability, and carbon turnover. Mark which prediction depends on microbial symbionts versus physical soil movement.

Data Recording

Table 650. Alignment and Rubric Map: Bottle type and Initial DO (mg/L).

Bottle type	Initial DO (mg/L)	Final DO (mg/L)	Change
Dark			
Light			
Initial (t=0)		—	—

$NPP =$; $Respiration =$; $GPP =$ ____

Carbon budget: Total sources (FF + land use) = ; *Total sinks (terrestrial GPP - respiration + ocean)* = ; Net accumulation = ____ Gt C/yr

Eutrophication indicators (day 3-5): chlorophyll-a change: ; *DO change:* ; turbidity change: ; *fish-kill risk:*

Evidence and Reproducibility Checklist

- Primary evidence goal: Quantify ecosystem fluxes and identify limiting pools.
- Data skill to practice: Trace matter and energy through food webs and biogeochemical cycles.
- BioSkills emphasis: Modeling and simulation, Science and society, Communication and collaboration.
- Control logic: identify at least one positive control, one negative control, or one baseline comparison before interpreting results.
- Measurement discipline: record units, uncertainty, sample size, and any discarded observation with a reason.
- Mechanistic link: connect one result directly to the parent chapter’s big idea before writing the conclusion.
- Reproducibility check: state one procedural detail that another group would need in order to reproduce the result.

Paper-Based Evidence Upgrade

Before answering the analysis questions, annotate the paper dataset for Ecosystem Ecology with a reproducibility pass:

Table 651. Alignment and Rubric Map: Evidence check and Student action.

Evidence check	Student action
Control logic	Mark the comparison that functions as the baseline, negative control, or reference case.
Uncertainty	Circle the row, card, diagram feature, or model assumption most likely to change the conclusion.
Model comparison	State whether a simpler rule, null model, or alternative mechanism could explain the same pattern.
Decision threshold	Write the minimum evidence that would make you revise the interpretation.
Reproducibility	Record the exact scoring rule another group would need to reproduce your classification.

Focus note: for this biogeochemical lab, keep stocks and fluxes in distinct columns, check that the printed budget balances within its stated uncertainty, and identify the system boundary and residence time implied before comparing one pool or pathway against another. Keep required work paper-based; any material-handling or equipment version belongs only in an optional extension.

Worked Example: Trophic Efficiencies in a Grassland Ecosystem

Problem: A temperate grassland has $GPP = 2,000\text{ g C/m}^2/\text{yr}$ and autotrophic respiration $R_a = 900\text{ g C/m}^2/\text{yr}$. Herbivore production is measured as $40\text{ g C/m}^2/\text{yr}$ and carnivore production as $3.2\text{ g C/m}^2/\text{yr}$. (a) Calculate NPP. (b) Calculate herbivore ecological efficiency relative to NPP. (c) Calculate carnivore ecological efficiency relative to herbivore production. Express each efficiency as a percentage and comment on the trend.

Solution: (a) $NPP = GPP - R_a = 2,000 - 900 = 1,100\text{ g C/m}^2/\text{yr}$. (b) Herbivore efficiency = $40 / 1,100 \approx 0.0364$, or about 3.6%. (c) Carnivore efficiency relative to herbivore production = $3.2 / 40 = 0.08$, or 8.0%. Both values fall within the broad 1–20% window commonly reported for terrestrial systems, with carnivore-on-herbivore efficiency tending to sit higher than herbivore-on-plant efficiency because animal tissue is more digestible than fibrous plant tissue.

Interpretation: Productivity falls off sharply at each level: of $2,000\text{ g C/m}^2/\text{yr}$ fixed photosynthetically, roughly 1,100 ends up as new plant biomass after respiration losses, about 40 reaches herbivores, and around 3.2 reaches carnivores. The strong attenuation helps explain why long food chains and large top-predator standing crops are uncommon in low-productivity ecosystems, and why nutrient and disturbance regimes that shift NPP often propagate upward through the food web.

Source-Governance Checkpoint

Complete the source-governance card for Ecosystem Ecology before writing the conclusion. Name the source type or model snapshot, record the evidence date or version, decide whether the claim is stable or fast-moving, and write one refresh trigger that would force the interpretation to change. Treat the card as a printed evidence object, not as a live web lookup.

Analysis Questions

1. The dark bottle showed decreased DO while the light bottle showed increased DO. Explain why: which process dominates in the light bottle, and which process in the dark bottle? Why is O_2 a useful proxy for carbon fixation here?
2. Your carbon budget calculation: does the simple sum of sources and sinks balance with the measured atmospheric accumulation (about 5 Gt C/yr)? What are the largest sources of uncertainty in the global carbon budget?

3. Nitrogen fixation by *Rhizobium* in legume root nodules requires enormous amounts of ATP and anaerobic conditions (nitrogenase is inactivated by O₂). Explain why this process is energetically costly and how the leghaemoglobin protein maintains low O₂ in the nodule while supporting aerobic bacterial respiration.
4. In the eutrophication case packet, the nutrient-addition scenario shows increased chlorophyll-a followed by bottom-water hypoxia. Trace the ecological mechanism from nutrient addition -> algal bloom -> bacterial decomposition -> hypoxia -> fish kill.
5. Wetlands are sometimes called “kidneys of the landscape.” Explain their role in nitrogen cycling (using specific N-cycle steps), phosphorus immobilisation, and carbon sequestration. Why is wetland drainage for agriculture a double ecological concern?
6. Compare termites and ants as ecosystem engineers. How can gut symbioses, mound ventilation, nest excavation, and food storage change carbon flow or nitrogen availability? Identify one measurement that would separate a microbial-digestion effect from a soil-structure effect.

Post-Lab Synthesis

- Concept Check (Synthesis): Anthropogenic nitrogen deposition — from agricultural fertiliser runoff, fossil-fuel combustion, and livestock — has raised reactive nitrogen inputs to many terrestrial ecosystems above pre-industrial levels.
- (a) Predict how sustained nitrogen deposition would shift terrestrial NPP in a nitrogen-limited ecosystem (such as a temperate forest) over years to decades. Then predict how plant species diversity would respond, drawing on the niche-differentiation argument that nutrient-limited communities sustain more co-existing species when resources are scarce.
- (b) Trace the consequences downstream: identify how excess nitrogen leaching into a connected freshwater system would affect primary producers, dissolved oxygen, and fish communities, and rank which ecosystem service (e.g., drinking-water quality, fisheries support, recreation) would most rapidly degrade. Cite one observational variable that managers could monitor as an early-warning indicator.

Safety and Ethics Notes

No pond water, fertiliser, bottles, probes, or biological specimens are required. Optional demonstrations using water samples or nutrients should follow local disposal rules and should rarely release enriched water into drains or outdoor waterways.

Debrief and Reflection

After you finish the practical work, spend 5–10 minutes in your small group comparing results and discussing the following prompts. Each member should contribute at least one observation before moving to the next prompt:

1. What did your measurements show — compare the group’s results to the textbook’s predictions. Where they diverge, suggest at least one mechanistic explanation before concluding “experimental error.”
2. What would change the outcome — propose one modification to the procedure that would sharpen the measurement or extend the result to a new biological context, and predict what you would observe.
3. One-sentence headline — each student composes a single sentence summarizing the lab’s take-home message, suitable for a tweet. Compare sentences across groups; good headlines are short, quantitative, and mechanistic.
4. Connection back to the textbook — identify one section of section 39 that your data either confirmed or complicated. Cite the specific passage.

Further Reading (Lab)

- Revisit the parent chapter section 39 for the theoretical foundations on which this lab is built.
- Look up any bolded glossary term introduced in the textbook chapter (each has a #gl:term-slug link in the text) — its master definition is in manuscript/glossary.md.
- Explore the appended src/ module that implements the corresponding quantitative model (when applicable) — referenced in the parent chapter’s “Bridge to Computation” subsection.

Module footer: parent chapter \cref{sec:unit_X_ecosystem_ecology}; all numerical quantities in this lab use SI units — see Appendix D — Units, Physical Constants, and Biological Ranges for unit conversions and biological-scale reference values.

Lab — Biomes and Conservation Biology

Learning Objectives

This activity accompanies section 40 of the textbook — review that chapter before attempting the exercises below.

- Classify biomes from climate data (mean annual temperature, precipitation, Whittaker diagram)
- Calculate species-area relationship parameters and predict extinction risk from habitat loss
- Evaluate minimum viable population (MVP) and reserve design principles for a case species
- Apply IUCN Red List criteria to classify conservation status of a provided species profile

Alignment and Rubric Map

- Outcome 1 (LO1): Interpret the supplied evidence or model output for Biomes and Conservation Biology.
- Outcome 2 (LO2): Identify controls and comparison groups that make the claim testable.
- Outcome 3 (LO3): Quantify uncertainty, boundary conditions, or alternative explanations before concluding.
- Outcome 4 (LO4): Transfer the mechanism to a new biological case or public-facing decision.
- Chapter LO coverage: LO1, LO2, LO3, LO4
- Rubric dimensions: evidence; controls; uncertainty; mechanism; transfer. ## Pre-Lab Concept Questions {.unnumbered}

Answer these before starting the investigation — they activate knowledge from the parent chapter.

1. List two abiotic and two biotic factors that shape the geographic distribution of terrestrial biomes. For each factor, describe in one sentence how a change in that factor could shift a biome boundary on a continental map.
2. State the IUCN Red List criterion most commonly cited for the “Critically Endangered” category — for example, an observed or projected population reduction over the past or next three generations, or a very small or restricted population. Cite at least one quantitative threshold that the IUCN typically uses.
3. Define effective population size (Ne) in your own words, and explain in two sentences why Ne is often substantially smaller than the census population size N in wild populations.

Lab Context: Biomes and Conservation Biology

Biomes are large-scale communities determined primarily by climate (temperature and precipitation). The species-area relationship $S = cA^z$ (log-linear: $\log S = \log c + z \cdot \log A$) predicts that decreasing habitat area reduces species richness; the exponent z (typically 0.2–0.35 for oceanic islands) can be used to predict extinction rates from deforestation. Minimum viable population (MVP) analyses determine the population size needed for a defined probability of persistence over a defined time frame. IUCN Red List criteria assign species to categories (LC, NT, VU, EN, CR, EW, EX) based on population decline rates, geographic range, and quantitative extinction risk.

Paper-Based Materials

Table 652. Alignment and Rubric Map: Item and Quantity.

Item	Quantity
Source-governance card for Biomes and Conservation Biology: conservation-assessment source card comparing GBIF occurrence records, IUCN category evidence, IPBES policy synthesis, assessment version, and monitoring trigger	1
GBIF occurrence-filter worksheet with coordinate uncertainty, date, basis of record, taxonomic backbone match, duplicate flag, and sampling-bias notes	1
Whittaker biome diagram (printed with temperature and precipitation axes)	1
Climate data cards (10 locations: MAT and MAP values)	1 set

Item	Quantity
Species-area relationship dataset (6 habitat fragments: area and species count)	1
Log-log graph paper	1
IUCN criteria worksheet (table of criteria A–E)	1
Species profile card: fictional vaquita-like cetacean (population data, trend, range)	1
Reserve-design decision matrix with habitat area, corridor cost, carbon storage, and community co-benefits	1
Climate-shift scenario cards for biome boundaries and conservation priorities	1 set
Coral bleaching degree-heating-week cards with recovery, mortality, and symbiont-shuffling scenarios	1 set
IPBES/food-security tradeoff card: agroecology, yield, pollinator habitat, waste reduction, and equity indicators	1
Calculator	1

Paper-Based Investigation

Part A — Biome Classification

- For each of 10 climate data cards (MAT in °C, MAP in mm), plot the location on the Whittaker diagram. Identify the biome for each location.

Part B — Species-Area Relationship

- Plot log(*S*) vs log(*A*) for the 6 habitat fragments on log-log paper. Fit a line; calculate the slope (*z* exponent) and the *y*-intercept (log *c*).
- Using $S = cA^z$, predict species richness in a fragment one-tenth the area of the largest.
- If a deforestation event reduces a forest from 10,000 ha to 100 ha, predict the percentage of species lost using the same equation.

Part C — MVP Analysis

- Given MVP data for the provided species: 50/500 rule (*N*_e > 50 for short-term genetic viability; *N*_e > 500 for long-term). Current population: 35 individuals. Is the population below the short-term MVP? Design a 10-year recovery plan with specific targets.

Part D — IUCN Classification

- Apply IUCN criteria to the species profile (population decline 80% in 10 years; < 250 mature individuals; geographic range < 100 km²). Determine IUCN status.
- Use the reserve-design matrix to compare a single large reserve, several small reserves, and a connected-corridor plan. Score each option for extinction risk, climate refugia, ecosystem services, and governance tradeoffs.

Part E — Coral and Food-System Decision Cards

- Classify coral scenarios by degree-heating-week exposure, recovery interval, and local stressors. Decide whether the evidence supports likely recovery, repeated bleaching risk, or high mortality risk.
- Use the symbiont-response cards to distinguish symbiont shuffling, assisted gene flow, selective breeding, and microbiome conditioning. State one benefit, one tradeoff, and one missing validation step for each.
- Use the IPBES/food-security card to compare two conservation plans: one maximizing protected area alone and one combining habitat protection with agroecological transition, pollinator corridors, and food-waste reduction. Score biodiversity, nutrition, equity, and feasibility separately.

Data Recording

Biome classifications:

Table 653. Alignment and Rubric Map: Location and MAT (°C).

Location	MAT (°C)	MAP (mm)	Biome
1	28	2,400	
2	−5	300	
3	15	600	
4	22	100	
5	0	50	

(continue for 10 locations)

Species-area relationship: $z =$; $c =$; predicted S at 1/10 area = ; % *species lost* = %

MVP assessment: current N = 35; MVP_short = 50; MVP_long = 500 Status: BELOW/ABOVE short-term MVP; IUCN status: ____

Reserve-design score: extinction risk = ; *climate refugia* = ; ecosystem services = ; *governance risk* = Coral risk class: ____; assisted-evolution option: ____; food-system tradeoff score: biodiversity ____ / nutrition ____ / equity ____ / feasibility ____

Evidence and Reproducibility Checklist

- Primary evidence goal: Compare biome patterns and conservation tradeoffs.
- Data skill to practice: Use maps, trend data, and threat categories to justify conservation priorities.
- BioSkills emphasis: Modeling and simulation, Science and society, Communication and collaboration.
- Control logic: identify at least one positive control, one negative control, or one baseline comparison before interpreting results.
- Measurement discipline: record units, uncertainty, sample size, and any discarded observation with a reason.
- Mechanistic link: connect one result directly to the parent chapter’s big idea before writing the conclusion.
- Reproducibility check: state one procedural detail that another group would need in order to reproduce the result.

Paper-Based Evidence Upgrade

Before answering the analysis questions, annotate the paper dataset for Biomes and Conservation Biology with a reproducibility pass:

Table 654. Alignment and Rubric Map: Evidence check and Student action.

Evidence check	Student action
Control logic	Mark the comparison that functions as the baseline, negative control, or reference case.
Uncertainty	Circle the row, card, diagram feature, or model assumption most likely to change the conclusion.
Model comparison	State whether a simpler rule, null model, or alternative mechanism could explain the same pattern.
Decision threshold	Write the minimum evidence that would make you revise the interpretation.
Reproducibility	Record the exact scoring rule another group would need to reproduce your classification.

Focus note: for this conservation lab, separate the ecological signal in the printed dataset (a biodiversity index, range map, or protected-area comparison) from the value judgement and the feasibility constraint, and name explicitly which counterfactual or unprotected reference the decision is being measured against. Keep required work paper-based; any material-handling or equipment version belongs only in an optional extension.

Worked Example: Heterozygosity Loss in a Small Tiger Population

Problem: A population viability analysis (PVA) for a wild population of 85 tigers projects a 15% extinction risk over the next 100 years under a slow decline ($r \approx -0.01/\text{yr}$). Using the rule of thumb $N_e \approx N/3$ for a structured wild population, calculate the effective population size. Then estimate the expected heterozygosity retained after 10 generations using $H_t = H_0 \times (1 - 1/(2N_e))^t$, with $H_0 = 0.45$.

Solution: Effective population size: $N_e \approx 85 / 3 \approx 28$. Per-generation retention factor: $(1 - 1/(2 \times 28)) = (1 - 1/56) \approx 0.9821$. After 10 generations: $H_{10} = 0.45 \times (0.9821)^{10} \approx 0.45 \times 0.836 \approx 0.376$. So expected heterozygosity drops from 0.45 to roughly 0.38 — about a 16% relative loss in 10 generations under drift alone.

Interpretation: Genetic drift erodes heterozygosity faster in small populations because each generation loses a fraction $1/(2N_e)$ of the variation in expectation. With $N_e \approx 28$, even a decade of generations is enough to make inbreeding depression and reduced adaptive capacity plausible concerns. Conservation actions that raise effective size — corridors, translocations, genetic rescue — can slow this loss substantially.

Source-Governance Checkpoint

Complete the source-governance card for Biomes and Conservation Biology before writing the conclusion. Name the source type or model snapshot, record the evidence date or version, decide whether the claim is stable or fast-moving, and write one refresh trigger that would force the interpretation to change. Treat the card as a printed evidence object, not as a live web lookup.

Analysis Questions

- Two locations had the same MAT but very different biomes because of different MAP values. What does this demonstrate about the relative importance of temperature vs precipitation in biome determination? Name an example pair from the Whittaker diagram where this contrast is striking.
- Your log-log plot of the species-area relationship should be linear. What does the slope (z) represent ecologically? Why do oceanic islands have higher z values (about 0.35) than mainland habitat patches (about 0.12)?
- Predicted species loss from deforestation assumes equilibrium. Explain the concept of “extinction debt” — why the full extinction toll of habitat reduction is primarily realized decades after the habitat loss, and what this implies for urgency in conservation action.
- The 50/500 rule gives threshold population sizes for genetic viability. Explain: (a) why populations below $N_e = 50$ suffer inbreeding depression; (b) why populations below $N_e = 500$ lose the variation needed to adapt to future environmental change. What is the difference between census population size (N_c) and effective population size (N_e)?
- Design a conservation reserve for a large mammal (e.g., tiger, Amur leopard) with a home range of 200 km² that requires a minimum viable population of 100 individuals. Calculate the minimum reserve area, explain whether a single large reserve (SLOSS debate: Single Large or Several Small) is preferable in this case, and identify two human activities outside the reserve boundary that would most threaten population persistence.
- A reef has high DHW exposure but a recovery window long enough for partial symbiont reshuffling, while a nearby watershed continues to deliver nutrient pollution. Which intervention should be treated as climate adaptation, which as local-stressor reduction, and why would assisted evolution alone be insufficient?
- A food-security policy increases short-term yield by removing hedgerows and reducing crop diversity. Use the IPBES/food-system tradeoff card to evaluate why yield, pollination, soil stability, nutrition, and equity must be scored separately rather than collapsed into one “more food” metric.

Post-Lab Synthesis

Concept Check (Synthesis): A regional conservation board can fund one of two options for a fragmented forest landscape: (i) a wildlife corridor connecting two isolated forest fragments of about 200 individuals each, or (ii) a captive-breeding program drawing from one of the fragments.

(a) Using minimum viable population theory and what you know about effective population size, evaluate how each option would influence N_e , gene flow, and the rate of heterozygosity loss across the next several generations. Identify which option is more likely to produce a measurable change in genetic diversity within ten years.

(b) Identify one specific risk associated with each option — for example, disease transmission through the corridor or behavioral deficits in captive-bred releases — and propose one monitoring metric that would let the team detect that risk early enough to adjust the strategy.

Safety and Ethics Notes

No hazardous materials. Conservation discussions involving indigenous land rights and protected area design should be approached with cultural sensitivity and recognition of land sovereignty principles. IUCN assessments require reliable species data — discuss uncertainty and the precautionary principle.

Debrief and Reflection

After you finish the practical work, spend 5–10 minutes in your small group comparing results and discussing the following prompts. Each member should contribute at least one observation before moving to the next prompt:

- What did your measurements show — compare the group’s results to the textbook’s predictions. Where they diverge, suggest at least one mechanistic explanation before concluding “experimental error.”
- What would change the outcome — propose one modification to the procedure that would sharpen the measurement or extend the result to a new biological context, and predict what you would observe.

3. One-sentence headline — each student composes a single sentence summarizing the lab’s take-home message, suitable for a tweet. Compare sentences across groups; good headlines are short, quantitative, and mechanistic.
4. Connection back to the textbook — identify one section of section 40 that your data either confirmed or complicated. Cite the specific passage.

Further Reading (Lab)

- Revisit the parent chapter section 40 for the theoretical foundations on which this lab is built.
- Look up any bolded glossary term introduced in the textbook chapter (each has a #gl:term-slug link in the text) — its master definition is in manuscript/glossary.md.
- Explore the appended src/ module that implements the corresponding quantitative model (when applicable) — referenced in the parent chapter’s “Bridge to Computation” subsection.

Module footer: parent chapter \cref{sec:unit_X_biomes_and_conservation}; all numerical quantities in this lab use SI units — see Appendix D — Units, Physical Constants, and Biological Ranges for unit conversions and biological-scale reference values.

Questions — Systems Science and Emergence

Questions 1–10: Recall and Comprehension

This activity accompanies section 0.1 of the textbook — review that chapter before attempting the exercises below.

Recall Questions (1 mark each)

Instructor Use and Coverage Notes

- Coverage target: Given a biological scenario, identify the system boundary, feedback loop, and missing measurement.
- Model/data emphasis: Box-and-arrow causal models with explicit inputs, outputs, and feedback signs.
- Assessment alignment: Questions and Methods, Representing and Describing Data, Argumentation.
- Misconception probe: A system is not just a list of parts; the interactions are part of the explanation.
- Transfer product: Apply the same feedback map to a cell, organism, and ecosystem, then name what changes at each scale.
- Grading focus: award full credit for mechanism, evidence, boundary conditions, and units when a calculation is required.
- Suggested use: draw one recall item, one application item, and one synthesis item when building a short quiz from this bank.

1. Define ‘systems science’ in your own words and provide a biological example.

Answer (Q1, Recall). Systems science studies how the *organization of and interactions among* components — not the components in isolation — generate the behavior of a whole; it makes the boundary, components, environment, flows, and feedback signs explicit. Biological example: blood-glucose regulation, where pancreas, insulin, glucagon, liver, and muscle form a feedback network whose stable set-point behavior cannot be read off any single hormone. 2. What distinguishes a complex adaptive system from a simple system?

Answer (Q2, Recall). A simple system has few components and fixed, predictable input–output relations. A complex adaptive system is a network of many heterogeneous agents that act on local information and adapt, producing emergent, nonlinear, history-dependent behavior that cannot be predicted from any agent alone (e.g., the immune system, an ant colony, an ecosystem). The defining contrast is adaptation and emergence versus fixed, decomposable mechanism. 3. What is the free energy principle? What does free energy measure?

Answer (Q3, Recall). The free energy principle (Friston) states that any system that maintains itself far from equilibrium must act and perceive so as to minimize *variational free energy* — an information-theoretic upper bound on sensory surprise. Free energy measures the mismatch between the organism’s internal generative model (its predictions) and the sensory data it actually receives; minimizing it keeps the organism within its viable physiological states. 4. Describe one biological example of negative feedback and one of positive feedback.

Answer (Q4, Recall). Negative feedback: thermoregulation — a rise in core temperature triggers sweating and vasodilation that return temperature toward the set point (stabilizing). Positive feedback: the rising phase of the action potential — Na⁺ influx depolarizes the membrane, opening more voltage-gated Na⁺ channels and amplifying the depolarization until channels inactivate (self-reinforcing and self-limiting). 5. What is the difference between homeostasis and allostasis?

Answer (Q5, Recall). Homeostasis holds a regulated variable near a *fixed* set point through reactive negative feedback. Allostasis (Sterling) achieves stability *through change*: the brain predictively adjusts set points and mobilizes resources in anticipation of demand, so the target itself moves. The decisive difference is reactive constancy versus anticipatory, model-based set-point adjustment.

Application Questions (2 marks each)

6. A drug blocks a key kinase in a signaling cascade, but the tumor eventually regrows. Explain this outcome using the concept of feedback compensation.

Answer (Q6, Recall). Blocking one kinase removes a single edge of a signaling network, but negative-feedback nodes the pathway normally suppresses are de-repressed and parallel routes reroute flux to restore downstream signaling (e.g., loss of ERK-mediated feedback reactivates upstream receptor/PI3K input). The network’s redundancy and compensatory feedback restore proliferative output, so single-target inhibition is evaded — which is why combination therapy is often required. 7. Explain why the lac operon switch is described as bistable. What advantage does bistability provide over a graded (linear) response?

Answer (Q7, Recall). Positive feedback (the LacY permease imports inducer, which further activates the operon) combined with cooperative repressor binding gives the system two stable states — fully ON or fully OFF — separated by an unstable threshold. Bistability produces a sharp, hysteretic, all-or-none commitment that filters molecular noise and avoids wasteful partial expression, whereas a graded linear response would track every fluctuation in inducer concentration. 8. How does the concept of attractors in phase space relate to cell fate? Give an example.

Answer (Q8, Recall). In the dynamical-systems view of gene-regulatory networks, each stable attractor in expression state space corresponds to a cell type; a cell’s state flows to the nearest attractor and resists small perturbations within its basin. Example: a hematopoietic progenitor sits near an unstable point and commits to an erythroid or myeloid attractor once a regulatory switch (e.g., the GATA1–PU.1 toggle) pushes it across the separatrix. 9. Apply the active inference framework to explain how a fever might be adaptive rather than merely a pathological response.

Answer (Q9, Recall). Under active inference an organism acts to fulfil its predictions about preferred, viable states. Infection raises the *expected* (set-point) temperature encoded by the hypothalamic generative model; the body then acts — shivering, vasoconstriction — to realize that prediction because elevated temperature accelerates immune kinetics and impairs pathogen replication. Fever is thus a controlled, model-driven allostatic shift rather than a regulatory failure, adaptive up to its metabolic and tissue-stress costs. 10. In evolutionary terms, what is niche construction, and how does it relate to the free energy principle?

Answer (Q10, Recall). Niche construction is the organism’s modification of its own environment (beaver dams, earthworm-altered soil), changing the selection pressures it and its descendants experience. Under the free energy principle, agents minimize surprise not only by updating internal models (perception) but by acting on the world so it matches their expected states — niche construction is free-energy minimization externalised and inherited across generations, stabilizing the organism–environment fit.

Synthesis Questions (4 marks each)

Questions 11–20: Application and Analysis

11. Compare and contrast the immune system and an evolving tumor as complex adaptive systems. In each case, identify (a) the agents, (b) the selection pressures, (c) an emergent property, and (d) a critical vulnerability.

Answer (Q11, Application). Both are populations of heritable, variable, selected agents whose adaptive behavior is emergent. (a) Agents: lymphocyte clones vs tumor subclones. (b) Selection pressures: antigen affinity and self-tolerance vs immune attack, therapy, hypoxia. (c) Emergent property: immunological memory vs collective drug resistance. (d) Critical vulnerability: tolerance breakdown or T-cell exhaustion vs dependence on a driver mutation or shared resource. The decisive contrast: the immune system is selected for host benefit, whereas tumor evolution is selected purely for local proliferative fitness against the host.

12. A patient with chronic anxiety has persistent overactivation of the sympathetic nervous system even in the absence of objective threat. Using predictive coding and active inference, construct a mechanistic account of how prior beliefs about threat might drive this pattern. How might therapeutic interventions (CBT, interoceptive exposure) alter the generative model?

Answer (Q12, Application). A precise prior predicting threat makes the generative model expect high interoceptive arousal; because that prior is weighted as highly precise, it dominates weaker sensory evidence, and prediction errors are resolved by *active* inference — driving sympathetic output to make the body match the ‘danger’ prediction, sustaining arousal with no external threat. CBT and interoceptive exposure reduce the precision of the threat prior and increase the weighting of disconfirming interoceptive evidence, reshaping the generative model so predictions no longer demand sympathetic activation.

13. Describe how ecosystem collapse (e.g., coral bleaching, fishery collapse) can be framed as a phase transition in a complex adaptive system. What warning signals might precede the transition? Why is recovery often much harder than the original decline?

Answer (Q13, Application). A reef or fishery near a bifurcation has a shallow basin of attraction; a small additional forcing (warming, harvest pressure) pushes it across a tipping point into an alternative stable state (algal-dominated reef, collapsed stock). Early-warning signals are signatures of *critical slowing down* — rising variance, increased autocorrelation, and slower recovery from small disturbances. Recovery is hard because of hysteresis: feedbacks that stabilize the new state (macroalgal dominance, recruitment failure) mean the driver must fall far below the original threshold before the system flips back.

Data and Model Interpretation Questions (3 marks each)

14. A homeostatic variable is measured at 98, 101, 105, 112, and 130 units after a perturbation. Identify whether the response appears damped, amplified, or unstable, and name one missing measurement needed before drawing a systems-level conclusion.

Answer (Q14, Application). The sequence is moving away from the original range rather than returning toward it, so the first interpretation is an amplified or unstable response. A full answer should ask for at least one missing measurement such as the set point, sampling interval, perturbation size, feedback gain, or whether the response later plateaus. Without the time scale and set point, the same numbers could represent transient compensation, runaway positive feedback, or a new stable state.

15. Draw a signed feedback diagram for blood glucose regulation that includes glucose, insulin, glucagon, liver glycogen breakdown, and muscle glucose uptake. Which links are negative feedback links?

Answer (Q15, Application). Blood glucose increases insulin secretion; insulin increases muscle glucose uptake and liver glycogen synthesis, both of which lower blood glucose. Blood glucose falling increases glucagon secretion; glucagon increases liver glycogen breakdown and gluconeogenesis, which raises blood glucose. The negative feedback links are the pathways by which high glucose triggers insulin-mediated glucose lowering and low glucose triggers glucagon-mediated glucose raising.

16. In a predator-prey system, prey abundance rises first, predator abundance rises after a delay, and prey then falls. Explain why the delay matters for oscillation rather than immediate stabilization.

Answer (Q16, Application). Delayed negative feedback can overshoot. Predator numbers respond to earlier prey abundance, not the current state, so predation pressure can peak after prey have already begun declining. If the product of feedback gain and delay is large enough, the system cycles instead of returning smoothly to equilibrium.

17. A pathway has two parallel routes from receptor activation to transcription. Blocking one route reduces output by 20%. What systems property explains this robustness, and what experiment would test it?

Answer (Q17, Application). Parallel routes create redundancy and distributed control, so flux or signal output does not depend on one route alone. Test this by inhibiting each route separately and together, then measuring the transcriptional output. A synergistic drop under dual inhibition would support pathway compensation.

18. A network diagram has many nodes with two links and three nodes with hundreds of links. What kind of network does this suggest, and why is it robust to random node loss but vulnerable to targeted hub loss?

Answer (Q18, Application). This suggests a scale-free or heavy-tailed network. Random removal usually hits low-degree nodes, so global connectivity is preserved. Targeting hubs removes many paths at once, fragmenting the network and causing disproportionate functional loss.

19. A cell-fate model has two stable attractors, A and B. A weak transient signal moves the cell partway toward B, but it returns to A; a stronger signal switches it to B permanently. Explain this in terms of basins of attraction.

Answer (Q19, Application). Each attractor has a basin: states inside that basin flow back to the attractor after small perturbations. The weak signal stays inside A's basin, so the cell returns to A. The stronger signal crosses the separatrix into B's basin, so the dynamics carry the cell toward B even after the signal ends.

20. A researcher reports that deleting one enzyme in a pathway has no phenotype, so the enzyme is unimportant. Critique this conclusion using compensation and context dependence.

Answer (Q20, Application). No phenotype under one condition does not prove no function. Parallel pathways, stored metabolites, regulatory compensation, or a benign test environment can mask the enzyme's role. A stronger design would test multiple stresses, time points, genetic backgrounds, and combined perturbations.

Questions 21–30: Synthesis and Evaluation

21. A negative feedback loop has a sensor that saturates at high input values. Predict what happens when the input exceeds the sensor's dynamic range.

Answer (Q21, Synthesis). Once the sensor saturates, increases in input no longer produce proportionally larger corrective signals. The system may appear stable over moderate inputs but fail abruptly outside its measurable range. This is why receptor saturation, assay saturation, and physiological reserve must be distinguished.

22. Explain how modularity can make a system both more evolvable and more fragile.

Answer (Q22, Synthesis). Modularity localizes change: one module can vary without destroying every other function, which supports evolvability. The same architecture can be fragile at module interfaces or shared hubs, because disrupting a connector can isolate otherwise functional modules.

23. Compare a thermostat, blood calcium regulation, and quorum sensing. Which parts of the analogy are useful, and where does the analogy break down?

Answer (Q23, Synthesis). The thermostat analogy is useful for set point, sensor, comparator, and effector logic. Blood calcium adds multiple organs, hormones, and time scales. Quorum sensing adds population-level communication and threshold-like collective behavior. The analogy breaks down when biological systems change their own sensors, set points, and effectors through development, learning, or evolution.

Evaluation and Design Questions (4 marks each)

24. Design a minimal experiment to distinguish direct causation from correlation in a proposed feedback loop between a hormone and a behavior.

Answer (Q24, Synthesis). A strong design manipulates the hormone while measuring behavior, includes vehicle and sham controls, and ideally blocks the receptor to test specificity. Time-resolved measurements should show that hormone change precedes behavioral change. A rescue condition, such as restoring receptor signaling, would strengthen causal inference.
25. A model of fever treats body temperature as a fixed set point. Evaluate why this model fails during infection and propose a better systems description.

Answer (Q25, Synthesis). During infection, cytokines and prostaglandins alter the regulated target temperature, so fever is not simply failure to maintain 37 degrees C. A better model includes a context-sensitive set point, immune signals, heat-production effectors, heat-loss effectors, and costs such as metabolic demand or tissue damage.
26. Propose two early-warning indicators that a lake ecosystem is approaching a tipping point. Explain why each indicator is mechanistically plausible.

Answer (Q26, Synthesis). Plausible indicators include critical slowing down after small disturbances, rising variance in algal biomass, increasing autocorrelation, declining water clarity, or rapid nutrient pulses. They are plausible because systems near a tipping point recover more slowly and fluctuate more strongly before switching states.
27. A clinician wants a single biomarker for sepsis severity. Use systems thinking to argue for or against relying on one marker.

Answer (Q27, Synthesis). A single marker is easy to measure but risky because sepsis is a multi-organ, multi-feedback syndrome. Lactate, cytokines, blood pressure, renal function, and mental status capture different parts of the system. A panel plus trajectory over time is more reliable than one static value.
28. Build a modular explanation of wound healing with at least three modules and one feedback link between modules.

Answer (Q28, Synthesis). One modular explanation includes hemostasis, inflammation, tissue proliferation, and remodeling. Inflammation recruits immune cells and growth factors that stimulate proliferation; excessive inflammation feeds back negatively by delaying remodeling and can create chronic wounds. The answer should identify modules, links, and at least one measurable output such as collagen deposition or wound area.
29. A student says, “If we know every molecule in a cell, we know the cell.” Respond using emergence, scale, and model choice.

Answer (Q29, Synthesis). Knowing every molecule is not enough unless interactions, spatial organization, time scales, and boundary conditions are also known. Emergent properties such as oscillation, polarity, and fate commitment arise from relations among parts. The appropriate model depends on the question: molecular detail for catalysis, network detail for signaling, and coarse-grained variables for tissue behavior.
30. Choose one biological system from another unit of the textbook and outline how you would model it as a system with state variables, inputs, outputs, and feedback.

Answer (Q30, Synthesis). Examples include membrane potential, glucose regulation, photosynthesis, infection spread, or population growth. Name state variables, external inputs, measurable outputs, feedback links, and one model limitation. The strongest responses also identify a parameter that could be estimated from data.

Module: *src/biology/ (general)*.

Questions — Complex Adaptive Systems

Questions 1–10: Recall and Comprehension

This activity accompanies section 0.2 of the textbook — review that chapter before attempting the exercises below.

Recall Questions (1 mark each)

Instructor Use and Coverage Notes

- Coverage target: Explain an observed population pattern from individual-level rules and identify one falsifiable prediction.
- Model/data emphasis: Agent-rule and scaling arguments for emergent biological patterns.
- Assessment alignment: Questions and Methods, Representing and Describing Data, Argumentation.
- Misconception probe: Emergence is not mysterious; it is a reproducible consequence of interactions plus constraints.
- Transfer product: Compare flocking, immune activation, and microbial biofilms as adaptive systems.
- Grading focus: award full credit for mechanism, evidence, boundary conditions, and units when a calculation is required.
- Suggested use: draw one recall item, one application item, and one synthesis item when building a short quiz from this bank.

1. Define ‘complex adaptive systems’ in your own words and provide a biological example.

Answer (Q1, Recall). A complex adaptive system is a population of many heterogeneous agents that interact locally, adapt their behavior from local information, and thereby generate emergent, nonlinear, history-dependent properties that no single agent contains and no central controller imposes. Biological example: an ant colony — individuals follow simple pheromone rules, yet the colony collectively solves foraging, task allocation, and defense (other examples: the immune system, the brain, ecosystems).

2. What distinguishes a complex adaptive system from a simple system?

Answer (Q2, Recall). A simple system has few components and fixed, predictable input–output relations. A complex adaptive system is a network of many heterogeneous agents that act on local information and adapt, producing emergent, nonlinear, history-dependent behavior that cannot be predicted from any agent alone (e.g., the immune system, an ant colony, an ecosystem). The defining contrast is adaptation and emergence versus fixed, decomposable mechanism.

3. What is the free energy principle? What does free energy measure?

Answer (Q3, Recall). The free energy principle (Friston) states that any system that maintains itself far from equilibrium must act and perceive so as to minimize *variational free energy* — an information-theoretic upper bound on sensory surprise. Free energy measures the mismatch between the organism’s internal generative model (its predictions) and the sensory data it actually receives; minimizing it keeps the organism within its viable physiological states.

4. Describe one biological example of negative feedback and one of positive feedback.

Answer (Q4, Recall). Negative feedback: thermoregulation — a rise in core temperature triggers sweating and vasodilation that return temperature toward the set point (stabilizing). Positive feedback: the rising phase of the action potential — Na⁺ influx depolarizes the membrane, opening more voltage-gated Na⁺ channels and amplifying the depolarization until channels inactivate (self-reinforcing and self-limiting).

5. What is the difference between homeostasis and allostasis?

Answer (Q5, Recall). Homeostasis holds a regulated variable near a *fixed* set point through reactive negative feedback. Allostasis (Sterling) achieves stability *through change*: the brain predictively adjusts set points and mobilizes resources in anticipation of demand, so the target itself moves. The decisive difference is reactive constancy versus anticipatory, model-based set-point adjustment.

Application Questions (2 marks each)

6. A drug blocks a key kinase in a signaling cascade, but the tumor eventually regrows. Explain this outcome using the concept of feedback compensation.

Answer (Q6, Recall). Blocking one kinase removes a single edge of a signaling network, but negative-feedback nodes the pathway normally suppresses are de-repressed and parallel routes reroute flux to restore downstream signaling (e.g., loss of ERK-mediated feedback reactivates upstream receptor/PI3K input). The network’s redundancy and compensatory feedback restore proliferative output, so single-target inhibition is evaded — which is why combination therapy is often required.

7. Explain why the lac operon switch is described as bistable. What advantage does bistability provide over a graded (linear) response?

Answer (Q7, Recall). Positive feedback (the LacY permease imports inducer, which further activates the operon) combined with cooperative repressor binding gives the system two stable states — fully ON or fully OFF — separated by an unstable threshold. Bistability produces a sharp, hysteretic, all-or-none commitment that filters molecular noise and avoids wasteful partial expression, whereas a graded linear response would track every fluctuation in inducer concentration.

Answer (Q8, Recall). In the dynamical-systems view of gene-regulatory networks, each stable attractor in expression state space corresponds to a cell type; a cell’s state flows to the nearest attractor and resists small perturbations within its basin. Example: a hematopoietic progenitor sits near an unstable point and commits to an erythroid or myeloid attractor once a regulatory switch (e.g., the GATA1–PU.1 toggle) pushes it across the separatrix. 9. Apply the active inference framework to explain how a fever might be adaptive rather than merely a pathological response.

Answer (Q9, Recall). Under active inference an organism acts to fulfil its predictions about preferred, viable states. Infection raises the *expected* (set-point) temperature encoded by the hypothalamic generative model; the body then acts — shivering, vasoconstriction — to realize that prediction because elevated temperature accelerates immune kinetics and impairs pathogen replication. Fever is thus a controlled, model-driven allostatic shift rather than a regulatory failure, adaptive up to its metabolic and tissue-stress costs. 10. In evolutionary terms, what is niche construction, and how does it relate to the free energy principle?

Answer (Q10, Recall). Niche construction is the organism’s modification of its own environment (beaver dams, earthworm-altered soil), changing the selection pressures it and its descendants experience. Under the free energy principle, agents minimize surprise not only by updating internal models (perception) but by acting on the world so it matches their expected states — niche construction is free-energy minimization externalised and inherited across generations, stabilizing the organism–environment fit.

Synthesis Questions (4 marks each)

Questions 11–20: Application and Analysis

11. Compare and contrast the immune system and an evolving tumor as complex adaptive systems. In each case, identify (a) the agents, (b) the selection pressures, (c) an emergent property, and (d) a critical vulnerability.

Answer (Q11, Application). Both are populations of heritable, variable, selected agents whose adaptive behavior is emergent. (a) Agents: lymphocyte clones vs tumor subclones. (b) Selection pressures: antigen affinity and self-tolerance vs immune attack, therapy, hypoxia. (c) Emergent property: immunological memory vs collective drug resistance. (d) Critical vulnerability: tolerance breakdown or T-cell exhaustion vs dependence on a driver mutation or shared resource. The decisive contrast: the immune system is selected for host benefit, whereas tumor evolution is selected purely for local proliferative fitness against the host.

12. A patient with chronic anxiety has persistent overactivation of the sympathetic nervous system even in the absence of objective threat. Using predictive coding and active inference, construct a mechanistic account of how prior beliefs about threat might drive this pattern. How might therapeutic interventions (CBT, interoceptive exposure) alter the generative model?

Answer (Q12, Application). A precise prior predicting threat makes the generative model expect high interoceptive arousal; because that prior is weighted as highly precise, it dominates weaker sensory evidence, and prediction errors are resolved by *active* inference — driving sympathetic output to make the body match the ‘danger’ prediction, sustaining arousal with no external threat. CBT and interoceptive exposure reduce the precision of the threat prior and increase the weighting of disconfirming interoceptive evidence, reshaping the generative model so predictions no longer demand sympathetic activation.

13. Describe how ecosystem collapse (e.g., coral bleaching, fishery collapse) can be framed as a phase transition in a complex adaptive system. What warning signals might precede the transition? Why is recovery often much harder than the original decline?

Answer (Q13, Application). A reef or fishery near a bifurcation has a shallow basin of attraction; a small additional forcing (warming, harvest pressure) pushes it across a tipping point into an alternative stable state (algal-dominated reef, collapsed stock). Early-warning signals are signatures of *critical slowing down* — rising variance, increased autocorrelation, and slower recovery from small disturbances. Recovery is hard because of hysteresis: feedbacks that stabilize the new state (macroalgal dominance, recruitment failure) mean the driver must fall far below the original threshold before the system flips back.

Data and Model Interpretation Questions (3 marks each)

14. In an agent-based simulation, changing one local rule from “align with three neighbors” to “align with six neighbors” causes global order to appear faster. Explain why this is an emergent result rather than a command from a central controller.

Answer (Q14, Application). The global pattern changes because each agent samples more neighbors, increasing local coupling. No agent stores the global pattern or directs the group. The ordered state emerges from repeated local interactions plus boundary conditions.

15. A microbial biofilm becomes resistant to an antibiotic even though many isolated cells from the same biofilm remain sensitive. Give two complex-adaptive explanations.

- Answer (Q15, Application). Biofilm structure can limit diffusion, create slow-growing or dormant cells, and generate chemical microenvironments that reduce drug efficacy. Interactions among cells, matrix, nutrients, and gradients create a collective phenotype that isolated cells do not show.
16. A fitness landscape has one tall narrow peak and one lower broad peak. Which peak is easier for a population to maintain under mutation and environmental noise, and why?
- Answer (Q16, Application). The broad peak is usually more robust because nearby genotypes still have relatively high fitness. A tall narrow peak may have high maximum fitness but is fragile: small mutational or environmental shifts can move the population into low-fitness territory.
17. Explain how a phase transition differs from a gradual linear change. Use one biological example.
- Answer (Q17, Application). A phase transition occurs when a small parameter change near a threshold produces a qualitative state change. Examples include quorum sensing activation, membrane depolarization threshold, ecosystem eutrophication, or protein folding. Linear change lacks that abrupt threshold behavior.
18. A population repeatedly evolves the same resistance mutation in separate cultures. Does this prove evolution is deterministic? Give a careful answer.
- Answer (Q18, Application). It shows strong constraint or a high-probability adaptive route, not full determinism. Selection, mutation supply, population size, and available genetic paths can make outcomes repeatable, while drift and rare mutations still create contingency.
19. Compare self-organization in embryonic patterning and in ant foraging. What is shared, and what differs?
- Answer (Q19, Application). Both involve local interactions that produce organized global patterns. Embryonic patterning often uses molecular gradients, gene regulatory networks, and mechanical constraints; ant foraging uses mobile agents, pheromone trails, and reinforcement. The shared logic is local rule plus feedback; the substrates and time scales differ.
20. A complex system model reproduces one observed pattern but fails under a new perturbation. What does this tell you about model validation?
- Answer (Q20, Application). Matching one pattern is not enough. A useful model should also predict responses to perturbation, reproduce independent data, and fail in interpretable ways. The failure may reveal missing agents, hidden variables, wrong interaction rules, or parameter overfitting.

Questions 21–30: Synthesis and Evaluation

21. Explain why heterogeneity among agents can make a population more resilient.
- Answer (Q21, Synthesis). Heterogeneity spreads risk. If agents differ in behavior, physiology, genotype, or location, one stress rarely harms all agents equally. Diversity can preserve function during perturbation, though it can also slow coordinated responses.
22. A cancer therapy kills 99% of tumor cells but leaves a small resistant subpopulation. Explain why this can select for relapse.
- Answer (Q22, Synthesis). Therapy changes the selection environment. Sensitive cells are removed, reducing competition for resistant cells. If resistant cells survive and replicate, the post-treatment tumor can be enriched for the resistant phenotype even if it was initially rare.
23. Distinguish adaptation by natural selection from adaptation by learning within an organism. Why can both be described as adaptive processes?
- Answer (Q23, Synthesis). Natural selection changes population allele or trait frequencies across generations; learning changes behavior or internal models within a lifetime. Both are adaptive because feedback from the environment alters future performance, but the substrate, inheritance, and time scale differ.

Evaluation and Design Questions (4 marks each)

24. Design a simple agent-based model for immune-cell recruitment to an infection site. Specify agents, local rules, and one emergent output.
- Answer (Q24, Synthesis). Agents might include immune cells, pathogens, and damaged tissue cells. Local rules could include chemotaxis up a cytokine gradient, pathogen killing on contact, cytokine release after recognition, and cell death after a lifespan. Emergent outputs include inflammatory focus size, pathogen clearance time, or overshooting tissue damage.
25. Evaluate the claim: “Because complex systems are unpredictable, modeling them is useless.”
- Answer (Q25, Synthesis). The claim is too strong. Complex systems may be hard to predict exactly, but models can identify thresholds, sensitivities, robust qualitative behaviors, and useful intervention points. The goal is often constrained prediction and mechanistic insight, not perfect point forecasting.
26. Propose a way to detect whether a community pattern is produced by local interactions or by a shared external gradient.

- Answer (Q26, Synthesis). Measure or manipulate the external gradient while also mapping local neighbor effects. If the pattern persists after controlling for the gradient, local interactions are implicated. Transplant, removal, or randomized-neighbor experiments can separate neighbor causation from shared environmental forcing.
27. A student says emergence means “anything can happen.” Correct this using constraints and repeated patterns.
- Answer (Q27, Synthesis). Emergence does not mean arbitrary outcomes. It means global properties arise from interactions among parts. The outcomes are constrained by rules, geometry, resources, feedback, and history, which is why similar patterns can recur across biofilms, tissues, flocks, and ecosystems.
28. Build a complex-adaptive explanation of antibiotic resistance that includes mutation, selection, horizontal gene transfer, and clinical practice.
- Answer (Q28, Synthesis). Mutation and horizontal gene transfer generate variation; antibiotic exposure selects resistant variants; hospitals and farms can amplify transmission; incomplete treatment or misuse changes the selection regime. The emergent population-level result is increased resistance prevalence.
29. Choose one chapter later in the textbook and explain how its topic could be reframed as a complex adaptive system.
- Answer (Q29, Synthesis). Strong examples include immune activation, cancer evolution, microbial ecology, neural circuits, plant hormone networks, or conservation landscapes. A full answer names the agents, interactions, feedback loops, variation, and emergent property.
30. Design a falsifiable prediction that would distinguish two competing rule sets in an agent-based model of cell migration.
- Answer (Q30, Synthesis). A good prediction identifies a perturbation that makes the rule sets diverge. For example, if one model depends on chemotaxis and another on contact inhibition, flattening the chemical gradient should disrupt directed migration only in the chemotaxis model, whereas changing cell density should mainly affect the contact-inhibition model.

Module: *src/biology/ (general)*.

Questions — Active Inference and Free Energy

Questions 1–10: Recall and Comprehension

This activity accompanies section 0.3 of the textbook — review that chapter before attempting the exercises below.

Recall Questions (1 mark each)

Instructor Use and Coverage Notes

- Coverage target: Calculate a posterior belief and explain what action would reduce uncertainty or restore a set point.
- Model/data emphasis: Bayesian belief updating and expected-free-energy-style policy comparison.
- Assessment alignment: Questions and Methods, Representing and Describing Data, Argumentation.
- Misconception probe: Active inference is not passive prediction; action changes the sensory data that arrive next.
- Transfer product: Map prediction-error reasoning onto chemotaxis, thermoregulation, and attention.
- Grading focus: award full credit for mechanism, evidence, boundary conditions, and units when a calculation is required.
- Suggested use: draw one recall item, one application item, and one synthesis item when building a short quiz from this bank.

1. Define ‘active inference’ in your own words and provide a biological example.

Answer (Q1, Recall). Active inference is the behavioral corollary of the free energy principle: an agent minimizes expected free energy (sensory surprise) not only by updating its internal generative model to fit data (perception) but by *acting* to make sensory data match its predictions about preferred states. Biological example: a chemotactic bacterium whose model ‘expects’ high nutrient acts by modulating tumble frequency so that sensed nutrient rises toward the expected value — fulfilling its predictions rather than merely recording them. 2. What distinguishes a complex adaptive system from a simple system?

Answer (Q2, Recall). A simple system has few components and fixed, predictable input–output relations. A complex adaptive system is a network of many heterogeneous agents that act on local information and adapt, producing emergent, nonlinear, history-dependent behavior that cannot be predicted from any agent alone (e.g., the immune system, an ant colony, an ecosystem). The defining contrast is adaptation and emergence versus fixed, decomposable mechanism. 3. What is the free energy principle? What does free energy measure?

Answer (Q3, Recall). The free energy principle (Friston) states that any system that maintains itself far from equilibrium must act and perceive so as to minimize *variational free energy* — an information-theoretic upper bound on sensory surprise. Free energy measures the mismatch between the organism’s internal generative model (its predictions) and the sensory data it actually receives; minimizing it keeps the organism within its viable physiological states. 4. Describe one biological example of negative feedback and one of positive feedback.

Answer (Q4, Recall). Negative feedback: thermoregulation — a rise in core temperature triggers sweating and vasodilation that return temperature toward the set point (stabilizing). Positive feedback: the rising phase of the action potential — Na⁺ influx depolarizes the membrane, opening more voltage-gated Na⁺ channels and amplifying the depolarization until channels inactivate (self-reinforcing and self-limiting). 5. What is the difference between homeostasis and allostasis?

Answer (Q5, Recall). Homeostasis holds a regulated variable near a *fixed* set point through reactive negative feedback. Allostasis (Sterling) achieves stability *through change*: the brain predictively adjusts set points and mobilizes resources in anticipation of demand, so the target itself moves. The decisive difference is reactive constancy versus anticipatory, model-based set-point adjustment.

Application Questions (2 marks each)

6. A drug blocks a key kinase in a signaling cascade, but the tumor eventually regrows. Explain this outcome using the concept of feedback compensation.

Answer (Q6, Recall). Blocking one kinase removes a single edge of a signaling network, but negative-feedback nodes the pathway normally suppresses are de-repressed and parallel routes reroute flux to restore downstream signaling (e.g., loss of ERK-mediated feedback reactivates upstream receptor/PI3K input). The network’s redundancy and compensatory feedback restore proliferative output, so single-target inhibition is evaded — which is why combination therapy is often required. 7. Explain why the lac operon switch is described as bistable. What advantage does bistability provide over a graded (linear) response?

Answer (Q7, Recall). Positive feedback (the LacY permease imports inducer, which further activates the operon) combined with cooperative repressor binding gives the system two stable states — fully ON or fully OFF — separated by an unstable threshold. Bistability produces a sharp,

hysteretic, all-or-none commitment that filters molecular noise and avoids wasteful partial expression, whereas a graded linear response would track every fluctuation in inducer concentration. 8. How does the concept of attractors in phase space relate to cell fate? Give an example.

Answer (Q8, Recall). In the dynamical-systems view of gene-regulatory networks, each stable attractor in expression state space corresponds to a cell type; a cell's state flows to the nearest attractor and resists small perturbations within its basin. Example: a hematopoietic progenitor sits near an unstable point and commits to an erythroid or myeloid attractor once a regulatory switch (e.g., the GATA1–PU.1 toggle) pushes it across the separatrix. 9. Apply the active inference framework to explain how a fever might be adaptive rather than merely a pathological response.

Answer (Q9, Recall). Under active inference an organism acts to fulfil its predictions about preferred, viable states. Infection raises the *expected* (set-point) temperature encoded by the hypothalamic generative model; the body then acts — shivering, vasoconstriction — to realize that prediction because elevated temperature accelerates immune kinetics and impairs pathogen replication. Fever is thus a controlled, model-driven allostatic shift rather than a regulatory failure, adaptive up to its metabolic and tissue-stress costs. 10. In evolutionary terms, what is niche construction, and how does it relate to the free energy principle?

Answer (Q10, Recall). Niche construction is the organism's modification of its own environment (beaver dams, earthworm-altered soil), changing the selection pressures it and its descendants experience. Under the free energy principle, agents minimize surprise not only by updating internal models (perception) but by acting on the world so it matches their expected states — niche construction is free-energy minimization externalised and inherited across generations, stabilizing the organism–environment fit.

Synthesis Questions (4 marks each)

Questions 11–20: Application and Analysis

11. Compare and contrast the immune system and an evolving tumor as complex adaptive systems. In each case, identify (a) the agents, (b) the selection pressures, (c) an emergent property, and (d) a critical vulnerability.

Answer (Q11, Application). Both are populations of heritable, variable, selected agents whose adaptive behavior is emergent. (a) Agents: lymphocyte clones vs tumor subclones. (b) Selection pressures: antigen affinity and self-tolerance vs immune attack, therapy, hypoxia. (c) Emergent property: immunological memory vs collective drug resistance. (d) Critical vulnerability: tolerance breakdown or T-cell exhaustion vs dependence on a driver mutation or shared resource. The decisive contrast: the immune system is selected for host benefit, whereas tumor evolution is selected purely for local proliferative fitness against the host.

12. A patient with chronic anxiety has persistent overactivation of the sympathetic nervous system even in the absence of objective threat. Using predictive coding and active inference, construct a mechanistic account of how prior beliefs about threat might drive this pattern. How might therapeutic interventions (CBT, interoceptive exposure) alter the generative model?

Answer (Q12, Application). A precise prior predicting threat makes the generative model expect high interoceptive arousal; because that prior is weighted as highly precise, it dominates weaker sensory evidence, and prediction errors are resolved by *active* inference — driving sympathetic output to make the body match the ‘danger’ prediction, sustaining arousal with no external threat. CBT and interoceptive exposure reduce the precision of the threat prior and increase the weighting of disconfirming interoceptive evidence, reshaping the generative model so predictions no longer demand sympathetic activation.

13. Describe how ecosystem collapse (e.g., coral bleaching, fishery collapse) can be framed as a phase transition in a complex adaptive system. What warning signals might precede the transition? Why is recovery often much harder than the original decline?

Answer (Q13, Application). A reef or fishery near a bifurcation has a shallow basin of attraction; a small additional forcing (warming, harvest pressure) pushes it across a tipping point into an alternative stable state (algal-dominated reef, collapsed stock). Early-warning signals are signatures of *critical slowing down* — rising variance, increased autocorrelation, and slower recovery from small disturbances. Recovery is hard because of hysteresis: feedbacks that stabilize the new state (macroalgal dominance, recruitment failure) mean the driver must fall far below the original threshold before the system flips back.

Data and Model Interpretation Questions (3 marks each)

14. A prior predicts body temperature should be 37.0 degrees C, but sensory data report 36.2 degrees C with low uncertainty. Predict whether belief updating or action is more likely to reduce prediction error, and justify your answer.

Answer (Q14, Application). Low sensory uncertainty gives the observation high precision, so the organism should update its belief that it is cold and act to restore temperature. Actions might include shivering, vasoconstriction, or seeking warmth. If the sensory data were low precision, belief updating would be weaker and the prior would dominate.

15. Explain the difference between prediction error and surprise in an active-inference account.

Answer (Q15, Application). Prediction error is the mismatch between predicted and observed sensory data. Surprise is the improbability of the observation under the model. Free-energy-style objectives use tractable bounds on surprise, weighted by precision, to guide belief updating and action.

16. A patient with panic disorder interprets benign heart-rate increases as evidence of danger. Identify the prior, the sensory evidence, and the prediction-error loop.

Answer (Q16, Application). The prior is that bodily arousal predicts threat. The sensory evidence is interoceptive input such as increased heart rate. The loop arises when threat interpretation increases sympathetic arousal, which produces more interoceptive evidence that seems to confirm danger.

17. Compare homeostasis and allostasis from an active-inference perspective.

Answer (Q17, Application). Homeostasis emphasizes correction around a regulated variable after deviation. Allostasis emphasizes anticipatory regulation: the organism changes physiology in advance of expected demand. Active inference naturally includes both because predictions can drive action before error becomes large.

18. A chemotactic bacterium tumbles more often when attractant concentration falls. Describe this as action changing future sensory input.

Answer (Q18, Application). Falling attractant generates prediction error relative to preferred conditions. Tumbling changes direction, sampling a new region of the chemical field. If the new direction increases attractant, future sensory input better matches the organism’s preferred state.

19. What does it mean to assign high precision to a sensory signal? Give one adaptive and one maladaptive example.

Answer (Q19, Application). High precision means the system treats the signal as reliable and gives it strong influence over belief updating or action. Adaptive examples include attending to pain when tissue damage is likely. Maladaptive examples include over-weighting benign interoceptive sensations during anxiety.

20. A model predicts that reducing sensory precision should reduce self-generated tickle sensations. Explain why.

Answer (Q20, Application). Self-generated movement is predicted by motor commands, so the resulting sensory input has lower precision or is attenuated. Reducing precision prevents ordinary self-produced sensations from being treated as surprising external events. If attenuation fails, self-generated sensations can feel unexpectedly salient.

Questions 21–30: Synthesis and Evaluation

21. Explain why active inference is not the same as reinforcement learning, even though both can describe adaptive behavior.

Answer (Q21, Synthesis). Reinforcement learning often frames behavior as maximizing expected reward through value learning. Active inference frames behavior as minimizing expected uncertainty and prediction error under preferred states. Both can select adaptive actions, but active inference emphasizes generative models, precision, and epistemic information seeking.

22. Use active inference to explain why inflammation can be both protective and harmful.

Answer (Q22, Synthesis). Inflammation can be protective because it changes tissue conditions to control infection and repair damage. It becomes harmful when the model or feedback loop keeps inflammatory action active after the threat is gone, or when the response creates tissue damage that generates further danger signals.

23. A generative model predicts predator risk from smell and sound. If smell is blocked, what should happen to reliance on sound, and what experiment would test this?

Answer (Q23, Synthesis). If smell becomes unavailable or low precision, the organism should rely more heavily on sound if sound remains informative. Test this by manipulating olfactory access and measuring orienting, freezing, or avoidance responses to controlled sound cues while holding predator risk constant.

Evaluation and Design Questions (4 marks each)

24. Design a behavioral experiment to test whether interoceptive precision differs between anxious and non-anxious participants.

Answer (Q24, Synthesis). A strong design measures heartbeat detection, breathing-load detection, or confidence-calibrated interoceptive tasks in both groups. It should include objective performance, confidence, symptom measures, and a control sensory task. A prediction is that anxious participants overweight or miscalibrate interoceptive signals, especially under uncertainty.

25. Evaluate the claim: “Active inference explains everything, so it explains nothing.”

Answer (Q25, Synthesis). The concern is valid if the framework is used only metaphorically. It becomes scientifically useful when it produces falsifiable generative models, explicit priors, precision assumptions, and predictions that differ from alternative models. The answer should separate broad framework from testable implementation.

26. Propose an active-inference account of placebo analgesia.

Answer (Q26, Synthesis). Placebo cues can change priors about expected pain relief and alter the precision assigned to nociceptive signals. Descending control may reduce the impact of pain prediction errors. A test would compare pain ratings and physiological markers under deceptive, open-label, and no-treatment conditions.

27. A clinician wants to reduce chronic dyspnea by changing primarily lung mechanics. Use active inference to explain why cognitive or interoceptive therapy might also help.

Answer (Q27, Synthesis). Dyspnea is not only airflow; it is inferred from sensory signals, priors, attention, and precision. Therapy that recalibrates threat priors or interoceptive precision may reduce perceived breathlessness even when lung mechanics change little. This does not deny physiology; it adds model-based interpretation.

28. Build an active-inference explanation of immune tolerance.

Answer (Q28, Synthesis). Immune tolerance can be framed as a learned model that treats self-antigens and harmless contexts as expected, low-threat states. Regulatory cells, deletion, anergy, and checkpoint signaling reduce precision or action toward those cues. Autoimmunity can result when the system assigns threat to self-associated evidence.

29. Compare an organism seeking food and a scientist designing an experiment as epistemic agents.

Answer (Q29, Synthesis). Both act to sample informative states. The organism moves to reduce uncertainty about food location while satisfying metabolic preferences. The scientist manipulates conditions to reduce uncertainty among hypotheses. The goals, representations, and ethics differ, but both use action to gather better evidence.

30. Choose one later textbook topic and formulate an active-inference version of its central mechanism.

Answer (Q30, Synthesis). Good choices include glucose regulation, plant tropisms, infection response, synaptic plasticity, or conservation decision-making. Name preferred states, sensory evidence, priors, actions, precision assumptions, and one prediction that would distinguish the active-inference framing from a simpler feedback model.

Module: *src/biology/ (general)*.

Questions — History and Philosophy of Biology

This question bank accompanies section 0.4.

Recall Questions (1 mark each)

Instructor Use and Coverage Notes

- Coverage target: Given a biological claim, identify the practice that produced it, the evidence standard it used, and one philosophical assumption it carries.
- Model/data emphasis: Concept-map and evidence-matrix comparisons among historical claims, mechanisms, and model assumptions.
- Assessment alignment: Questions and Methods, Representing and Describing Data, Argumentation.
- Misconception probe: History is not a list of dates; it explains why current biological concepts are powerful, limited, and revisable.
- Transfer product: Transfer source-analysis reasoning to modern debates about species, genetics, microbiomes, and biomedical ethics.
- Grading focus: award full credit for mechanism, evidence, boundary conditions, and units when a calculation is required.
- Suggested use: draw one recall item, one application item, and one synthesis item when building a short quiz from this bank.

Questions 1–10: Recall and Comprehension

1. Define biology as an evidence practice rather than a list of facts.

Answer (Q1, Recall). Biology is an evidence practice because claims are produced through observation, experiment, classification, modeling, measurement, interpretation, and ethical judgement. A biological “fact” is stronger when we can name the method, unit, comparison, uncertainty, and possible revision path that produced it.
2. Name one contribution of Aristotle to biological reasoning and one limitation of his approach.

Answer (Q2, Recall). Aristotle contributed systematic observation and functional explanation; a limitation is that teleological language can imply fixed purposes.
3. What distinguishes natural history from experiment as a biological practice?

Answer (Q3, Recall). Natural history compares and classifies organisms across places and times, often revealing distribution, variation, and association. Experiment deliberately changes conditions and measures responses, making causal claims stronger when controls and comparison groups are well designed.
4. State the core logic of natural selection in one sentence.

Answer (Q4, Recall). Heritable variation affects survival or reproduction in a particular environment, changing variant frequencies across generations.
5. Define mechanistic explanation in biology.

Answer (Q5, Recall). A mechanistic explanation identifies entities, activities, organization, and causal sequence that produce a phenomenon.
6. What is a biological species concept?

Answer (Q6, Recall). It defines species by reproductive isolation, with limits for asexual organisms, fossils, hybrids, and microbes.
7. Why is nature-nurture a misleading frame for development?

Answer (Q7, Recall). It treats genes and environment as separable rivals instead of interacting developmental resources.
8. Name two ways values can enter biological research without making evidence arbitrary.

Answer (Q8, Recall). Values can shape which questions are asked, how categories are defined, which risks are acceptable, and how uncertainty is communicated. Evidence is not arbitrary because claims still must answer to observations, controls, replication, and alternative explanations.
9. Explain why an instrument such as a microscope can change biological knowledge.

Answer (Q9, Recall). An instrument changes what can be observed and measured, making new biological claims possible.
10. Why should global biological traditions not be treated as a single pre-modern block?

Answer (Q10, Recall). Different traditions used different categories, practices, and aims; combining them erases that diversity.

Application Questions (2 marks each)

Questions 11–20: Application and Analysis

11. Revise this statement: Harvey proved circulation by looking carefully at anatomy.

Answer (Q11, Application). Harvey combined anatomy with intervention and quantification: valves, tied vessels, pressure, and volume estimates supported circulation.
12. A trait increases survival in one environment. What evidence is needed before calling it an adaptation?

Answer (Q12, Application). Evidence should show heritable variation, differential reproduction, selection pressure, and population change.
13. Rephrase the heart wants to pump blood into a defensible functional statement.

Answer (Q13, Application). The heart does not literally want anything. A defensible causal-role version is: cardiac muscle contraction generates pressure gradients that move blood through pulmonary and systemic vessels. A selected-effect version would add that vertebrate hearts were shaped by selection because this circulation supported oxygen delivery, waste removal, and sustained activity.
14. A ring species blurs boundaries between neighboring populations. Which species concept is challenged?

Answer (Q14, Application). It challenges a simple biological species concept because reproductive boundaries form a continuum.
15. A variant is associated with height in one population. Why does that not prove height is fixed?

Answer (Q15, Application). The association depends on population, environment, measurement, development, and many interacting causes.
16. A conservation team must decide whether two populations should be protected separately. Identify one empirical and one value-laden question.

Answer (Q16, Application). Empirical: gene flow or local adaptation. Value-laden: acceptable extinction risk, cost, or cultural importance.
17. Classify a phylogenetic tree as observation, experiment, model, or classification, and justify your answer.

Answer (Q17, Application). It is a model-supported classification and historical inference built from observations and assumptions. The sequence or morphology data are observations; the tree is an inferred model of relationships under assumptions about character change, sampling, and method.
18. Compare Aristotle functional reasoning with a modern mechanistic account of an organ.

Answer (Q18, Application). The functional account names role; the mechanistic account names tissues, activities, constraints, development, and history.
19. Give one biological question better approached by natural history before experiment.

Answer (Q19, Application). Questions about range, seasonality, fossils, or ecological associations need pattern description first.
20. Explain why Mendelian inheritance did not by itself produce the Modern Synthesis.

Answer (Q20, Application). The synthesis required population mathematics, selection, mutation, drift, systematics, and paleontology.

Synthesis Questions (4 marks each)

Questions 21–30: Synthesis and Evaluation

21. Evaluate the claim that organs having functions makes biology goal-directed.

Answer (Q21, Synthesis). Function language is useful when it means causal role or selected effect, but it misleads when it implies conscious goals, inevitable progress, or perfect design. Separate mechanism (how the organ works), development (how it forms), function (what contribution or selected effect it has), and evolutionary history (why that contribution became common).
22. Are humans biological individuals if their bodies depend on microbial communities?

Answer (Q22, Synthesis). Yes in many contexts, because legal, developmental, and physiological practices often treat a human body as one individual. But microbial dependence makes individuality partly context-dependent: for digestion, immunity, and disease ecology, the relevant unit may be a host-microbe system rather than a single genome.
23. Critique the headline: scientists found the gene for intelligence.

- Answer (Q23, Synthesis). It overstates causation because cognitive traits are polygenic, developmental, environmental, and measurement-dependent.
24. Should values be removed from conservation biology?
- Answer (Q24, Synthesis). No; conservation involves risk, cost, justice, and future generations, while evidence constrains decisions.
25. Design a four-column evidence map for a microbiome health claim.
- Answer (Q25, Synthesis). A strong four-column map could use claim, biological unit, evidence practice, and revision test. For example: “a high-fiber diet improves microbiome health”; unit = host-microbe system rather than single species; evidence practice = association study, intervention trial, or mechanistic metabolomics; revision test = a controlled diet intervention that changes fiber without changing confounders and measures symptoms, taxa, and metabolites.
26. Create a teaching example comparing a non-European biological tradition with a modern practice.
- Answer (Q26, Synthesis). Compare materia medica classification with pharmacological screening while naming different categories, standards, and aims.
27. Propose a source-card activity that distinguishes observation from interpretation.
- Answer (Q27, Synthesis). Students underline observations, circle inferences, list missing comparisons, and write an alternative interpretation. A strong version also asks them to name the biological unit, the instrument or source practice, one value-laden decision, and one finding that would force revision.
28. Evaluate whether survival of the fittest is a good beginner summary of natural selection.
- Answer (Q28, Synthesis). It is memorable but risky; a better summary names heritable variation, environment, differential reproduction, and frequency change.
29. Build a Tinbergen-style explanation for one behavior.
- Answer (Q29, Synthesis). For bird migration: mechanism = photoperiod, circadian/circannual signaling, fat metabolism, navigation cues, and motor circuits; development = inherited program plus juvenile learning and calibration; function = seasonal movement can increase feeding or breeding success; evolutionary history = lineages with successful routes left more descendants under past climates. Keep the four answers distinct, then state which evidence would weaken each.
30. Choose a later topic and identify its unit, model assumption, mechanism, and value-laden decision.
- Answer (Q30, Synthesis). For antibiotic resistance: the unit might be a resistance gene, bacterium, patient microbiome, hospital ward, or regional population. The model assumption is selection under drug exposure; the mechanism may involve mutation, plasmids, efflux, target modification, or biofilm protection; the value-laden decision is stewardship that balances patient benefit against population-level resistance risk. Name the level of explanation and one observation that would force revision.

Questions — Atoms, Molecules, and Chemical Bonds

Instructor Use and Coverage Notes

- Coverage target: Predict bond polarity, formal charge, or isotope behavior and connect it to a biological consequence.
- Model/data emphasis: Formal charge and electronegativity-difference reasoning.
- Assessment alignment: Concept Explanation, Statistical Tests and Data Analysis, Argumentation.
- Misconception probe: Weak interactions are not unimportant; many weak interactions together dominate structure and specificity.
- Transfer product: Use atomic reasoning to explain a medical tracer, enzyme cofactor, or membrane-solubility problem.
- Grading focus: award full credit for mechanism, evidence, boundary conditions, and units when a calculation is required.
- Suggested use: draw one recall item, one application item, and one synthesis item when building a short quiz from this bank.

Questions 1–10: Recall and Comprehension

This activity accompanies section 1 of the textbook — review that chapter before attempting the exercises below.

1. Define an atom and identify its three subatomic particles. Which determines the element's identity?

Answer (Q1, Recall). An atom is the smallest unit of a chemical element that retains the element's chemical properties. The three subatomic particles are protons (+1 charge, mass ≈ 1 Da, in the nucleus), neutrons (no charge, mass ≈ 1 Da, in the nucleus), and electrons (−1 charge, mass ≈ 0.0005 Da, in orbitals). The atomic number — the number of protons — defines the element. See section 1. 2. What is the atomic number of carbon? How many valence electrons does carbon have?

Answer (Q2, Recall). Carbon has atomic number $Z = 6$ (six protons; six electrons when neutral). Its ground-state electron configuration is $1s^2 2s^2 2p^2$, giving four valence electrons in the $n = 2$ shell. This tetravalence is the structural basis for carbon's central role in organic chemistry. 3. Distinguish between covalent and ionic bonds. Give one biological example of each.

Answer (Q3, Recall). A covalent bond is formed by shared electron pairs ($\Delta EN < \text{about } 1.7$), e.g. the C–C and C–H bonds in glucose. An ionic bond results from full electron transfer ($\Delta EN > \text{about } 1.7$) and the electrostatic attraction between resulting cations and anions, e.g. Na^+ and Cl^- in physiological saline. Covalent bonds form the internal skeleton of biomolecules; ionic bonds tend to form between biomolecules and their ionic partners (Mg^{2+} stabilizing ATP phosphates; Ca^{2+} in calmodulin). 4. Define electronegativity. Which element has the highest electronegativity?

Answer (Q4, Recall). Electronegativity is the tendency of an atom in a bond to attract the shared bonding electrons toward itself. On the Pauling scale, fluorine (F) has the highest value, 3.98. Biologically most important: oxygen 3.44, nitrogen 3.04, chlorine 3.16, carbon 2.55, hydrogen 2.20. Differences in electronegativity across a bond create bond polarity and partial charges. 5. What makes a covalent bond polar? What partial charges ($\delta+$ and $\delta-$) arise in an O–H bond?

Answer (Q5, Recall). A covalent bond is polar when the two bonded atoms differ in electronegativity by about 0.4–1.7, so the shared electron density is unevenly distributed. In an O–H bond the electronegativity difference is $3.44 - 2.20 = 1.24$; electrons spend more time near oxygen, giving O a partial negative charge ($\delta-$) and H a partial positive charge ($\delta+$). These partial charges underpin hydrogen bonding and water's solvent properties. 6. Define a hydrogen bond. Which atoms typically act as hydrogen bond donors and acceptors?

Answer (Q6, Recall). A hydrogen bond is an attractive, non-covalent interaction (about 20 kJ mol^{-1} , about 1/20 the strength of a typical covalent bond) between a hydrogen atom that is covalently bonded to a highly electronegative atom (the donor) and a lone electron pair on another electronegative atom (the acceptor). In biology the donors and acceptors are almost always N–H or O–H on one side and N or O on the other. Hydrogen bonds stabilize DNA base-pairing, protein secondary structure, and the three-dimensional shape of nearly every aqueous biomolecule. 7. What is a van der Waals interaction? In which large molecules are van der Waals forces collectively significant?

Answer (Q7, Recall). Van der Waals interactions are weak (about 1 kJ mol^{-1} each), short-range attractions arising from transient dipoles induced by electron fluctuations (London dispersion). Individually negligible, they become collectively dominant in large hydrophobic surfaces — the interior of globular proteins, lipid-bilayer tails, and drug–protein binding pockets — where hundreds of contacts summate to many tens of kJ mol^{-1} . 8. List four properties of water that arise directly from hydrogen bonding.

Answer (Q8, Recall). Four H-bond-derived properties of water: (1) an anomalously high boiling point (100°C vs. -60°C expected for H_2S); (2) high specific heat ($4.18 \text{ J g}^{-1} \text{ K}^{-1}$) that buffers organismal temperature; (3) high heat of vaporisation (2257 J g^{-1}) enabling evaporative cooling; (4) density maximum at 4°C — ice floats, insulating aquatic life. Other H-bond consequences: high surface tension, strong cohesion (xylem transport), and excellent solvation of polar solutes. 9. What is pH? What hydrogen ion concentration corresponds to pH 7 and pH 4?

Answer (Q9, Recall). $\text{pH} = -\log_{10}[\text{H}^+]$. Thus pH 7 corresponds to $[\text{H}^+] = 10^{-7} \text{ M} = 100 \text{ nM}$ (pure water at 25°C); pH 4 corresponds to $[\text{H}^+] = 10^{-4} \text{ M} = 100 \mu\text{M}$, a thousand-fold higher proton concentration. Each full pH unit is a ten-fold change in $[\text{H}^+]$. Physiological blood pH is tightly held

at 7.35–7.45; deviations beyond ±0.3 pH units are life-threatening. 10. Define an acid and a base using the Brønsted-Lowry definition. Give one biological example of each.

Answer (Q10, Recall). Brønsted–Lowry: an acid is a proton (H⁺) donor; a base is a proton acceptor. Biological examples: (acid) the carboxyl side chain of glutamate (pK_a ≈ 4.1) donates a proton at physiological pH; (base) the imidazole ring of histidine (pK_a ≈ 6.0) can accept a proton. Conjugate pairs (acid ⇌ conjugate base + H⁺) underlie every physiological buffer, most notably bicarbonate (H₂CO₃ / HCO₃[−], pK_a = 6.1).

Questions 11–20: Application and Analysis

11. Carbon forms four covalent bonds. Explain how this tetravalency allows carbon to form diverse structures including chains, branches, and rings. Why is carbon the basis of biological molecules rather than silicon?

Answer (Q11, Application). Carbon’s electron configuration (1s² 2s² 2p²) undergoes sp³ hybridization to yield four equivalent tetrahedral bonds at about 109.5°. Consequences: (i) symmetrical tetravalency allows chains (n-alkanes), branches (isoprenoids), and rings (pyranose sugars, aromatic bases) with no “preferred” direction; (ii) C–C bond strength ≈ 347 kJ/mol, comparable to C–H and C–O, so carbon scaffolds are thermodynamically stable *and* kinetically labile enough to react at biologically relevant rates (ms–s at 37 °C); (iii) carbon also forms double (C=C, 614 kJ/mol) and triple bonds, enabling π-chemistry (aromatic rings, carbonyls). Silicon, though also tetravalent, is disfavoured because Si–Si bonds are weaker (about 222 kJ/mol) and — critically — the oxidised form SiO₂ is an insoluble covalent solid (quartz) whereas CO₂ is a diffusible gas that cycles through atmosphere/ocean/biomass in hours. Life depends on redox cycling of its skeleton element; silicon cannot deliver that. See section 1. 12. The electronegativity difference for O–H is 1.4, for N–H is 0.9, and for C–H is 0.4. Rank these bonds from most to least polar and predict which can form hydrogen bonds.

Answer (Q12, Application). Bond polarity rises with the electronegativity difference ((Deltachi)), so the ranking most-to-least polar is O–H ((Deltachi) = 1.4) > N–H ((Deltachi) = 0.9) > C–H ((Deltachi) = 0.4). Using the chapter’s classification, O–H and N–H both lie in the polar-covalent band (0.5 (Deltachi) < 1.7): each develops a substantial (delta[−]) on the electronegative atom and (delta⁺) on H, so both can serve as hydrogen-bond donors (and their N/O atoms as acceptors). C–H ((Deltachi) = 0.4 < 0.5) is essentially nonpolar and forms no conventional hydrogen bond – which is why saturated lipid tails and aliphatic side chains drive the hydrophobic effect rather than H-bonding. This is the molecular reason water, alcohols and amides are self-associating and water-soluble while hydrocarbons are not. See section 1. 13. A buffer solution contains equal concentrations of carbonic acid (H₂CO₃) and bicarbonate (HCO₃[−]). At what pH does the buffer have maximum capacity? Express this using the Henderson-Hasselbalch equation (pK_a of carbonic acid = 6.1).

Answer (Q13, Application). Apply Henderson–Hasselbalch: pH = pK_a + log₁₀($\frac{[A^-]}{[HA]}$) = 6.1 + log₁₀(1) = 6.1. A buffer’s capacity β (resistance to pH change on adding strong acid/base) is maximal when pH = pK_a, because at that pH both conjugate species are equimolar and each is equally available to neutralize an added proton or hydroxide; the classical approximation gives β_{max} ≈ 2.303 C/4 at pH = pK_a. Biological sanity check: the H₂CO₃/HCO₃[−] buffer’s pK_a of 6.1 is *below* physiological pH 7.4 (so the body is outside the optimal range of this buffer on paper — log ratio = 1.3, ratio ≈ 20:1 bicarbonate:acid). The saving grace is that CO₂ is *open* to the lung: breathing changes [H₂CO₃] in seconds (respiratory compensation), making the bicarbonate buffer effectively inexhaustible despite the non-optimal pK_a. See section 1. 14. Explain why non-polar molecules such as cholesterol are insoluble in water but soluble in lipids. What thermodynamic principle governs this behavior (hint: entropy of hydrophobic interactions)?

Answer (Q14, Application). Cholesterol is dominated by a fused four-ring hydrocarbon nucleus with only one –OH; its C–H/C–C bonds are nonpolar ((Deltachi about 0.35)) and cannot hydrogen-bond with water, whereas lipid solvents present matching nonpolar surfaces. The governing principle is the hydrophobic effect, an *entropic* phenomenon: forcing the nonpolar surface into water makes surrounding water molecules form an ordered clathrate cage to preserve their H-bond network, lowering water’s entropy ((Delta S < 0)). Aggregating or partitioning cholesterol into a lipid phase releases that ordered water back to the bulk, so (Delta S) of the system increases; with (Delta H about 0) (van der Waals contacts in the lipid resemble those it left), (Delta G = Delta H - TDelta S < 0) and dissolution into lipid is spontaneous. Because the effect is entropic, it strengthens with temperature up to about 70 degrees C as the (TDelta S) term grows. See section 1. 15. A molecule has the formula C₁₈H₃₆O₂. Predict whether it is saturated or unsaturated based on the degree-of-unsaturation (DoU) formula. Identify it as a likely carbohydrate, lipid, or protein monomer.

Answer (Q15, Application). Use the degree-of-unsaturation formula for C(c)H(h)O(o): (DoU = $\frac{2c + 2 - h}{2}$). For C(18)H(36)O(2): (DoU = $\frac{2(18) + 2 - 36}{2}$ = $\frac{2}{2}$ = 1). That single degree of unsaturation is the C = O of a carboxyl group (no C = C), so the molecule is a carboxylic acid.

Answer (Q16, Application). A strong acid (HCl) dissociates essentially completely in water (no meaningful HA/A[−] equilibrium, no buffering); a weak acid (acetic acid, pK_a = 4.76) only partially dissociates, so it maintains a HA (H⁺) + A[−] equilibrium and buffers near its pK_a. The mechanistic difference is the position of that ionization equilibrium, not vocabulary. Fraction dissociated at pH 5 from Henderson–Hasselbalch: ($\frac{[A^-]}{[HA]}$ = 10^{pH − pK_a} = 10^{5.00 − 4.76} = 10^{0.24} = 1.74). Fraction ionized (=

$\frac{[A^-]}{[HA] + [A^-]} = \frac{1.74}{1 + 1.74} = 0.635$, i.e. about 64 % of acetic acid is ionized at pH 5 (vs about 100% for HCl at any pH). Boundary condition : a buffer made from this weak acid only resists pH change within $pK(a) \pm 1$ (about pH 3.8 – 5.8). See section 1.17. A cell's cytoplasmic pH drops from 7.4 to 6.9 during

Answer (Q17, Application). pH is $(-\log_{10}[H^+])$, so a drop from 7.4 to 6.9 is $\Delta pH = 0.5$; $[H^+]$ rises by a factor of $(10^{0.5} = 3.16)$ (roughly threefold). The acid load comes from exercising muscle producing lactate and CO_2/H^+ . Cytoplasmic buffers resist this change : the phosphate buffer ($H_2PO_4^-/HPO_4^{2-}$), $pK(a)$ (about) 6.8, about 100 mM intracellularly is near-optimal at this pH; protein and histidine side chains $[A^-]/[HA]$ (about 1) (pH near $pK(a)$) – phosphate's $pK(a)$ of 6.8 sitting between 6.9 and 7.4 is exactly why it dominates intracellular buffering here. See section 1.18.

Answer (Q18, Application). Dissolved CO_2 lowers blood pH because it is hydrated to a weak acid that releases protons. The reaction sequence (carbonic anhydrase catalyses the first step in red blood cells): $(CO_2 + H_2O \rightleftharpoons H_2CO_3)$ (carbonic acid) $(\rightleftharpoons H^+ + HCO_3^-)$ (bicarbonate) $(\rightleftharpoons 2H^+ + CO_3^{2-})$ (carbonate; not physiologically significant). Adding CO_2 drives the equilibrium to the right (Le Chatelier), increasing $[H^+]$ and therefore lowering pH (apparent $pK(a)$ of the H_2CO_3/HCO_3^- couple (about) 6.1). This is why hypoventilation (CO_2 retention) causes respiratory acidosis – CO_2 is continuously exhaled by the lungs. See section 1.19. The peptide bond in proteins involves C – N with partial double bond character due to resonance. Explain how this resonance prevents rotation around the peptide bond and what structural constraint this places on protein backbone

Answer (Q19, Application). The peptide C–N bond is a resonance hybrid: structure I (C=O, C–N single, lone pair on N) and structure II (C–O⁽⁻⁾, C=N⁽⁺⁾ double, lone pair delocalized into the carbonyl (pi) system). The hybrid gives the C–N bond about 40 % double-bond character, with an intermediate length of about 132 pm (between 147 pm single and about 127 pm double). Because rotating about a partial double bond would require breaking (pi) overlap (about 80 kJ/mol barrier), the six atoms of the peptide unit (C(alpha)–C(=O)–N(H)–C(alpha)) are locked coplanar and almost always trans (cis is about 8 kJ/mol higher, except before proline). The structural consequence: only the (phi) (N–C(alpha)) and (psi) (C(alpha)–C) torsions can vary, sharply restricting backbone conformational space and making regular (alpha)-helices and (beta)-sheets possible. See section 1.20. Magnesium (Mg²⁺) is a common enzyme cofactor. Using your understanding of atomic structure, explain why Mg²⁺ can stabilize negatively charged phosphate groups in ATP. What orbital property of Mg²⁺ makes it a Lewis acid?

Answer (Q20, Application). Mg²⁺ has electron configuration [Ne] after losing both 3s electrons — its empty 3s/3p valence shell makes it an archetypal Lewis acid (electron-pair acceptor). Consequences: (i) the small, doubly-charged cation has a high charge density ($q/r \approx 2.8 \text{ e/\AA}$), generating a strong electrostatic field that neutralizes the triply-negative phosphate chain of ATP⁴⁻; the biologically active species is actually Mg-ATP²⁻, not free ATP⁴⁻. (ii) By coordinating with the beta- and gamma-phosphate oxygens, Mg²⁺ polarizes the terminal P–O bond and orients the gamma-phosphate for nucleophilic attack — kinases are typically 100–1000× slower in the absence of Mg²⁺ (K_m for Mg²⁺ ≈ 0.1 –1 mM). (iii) In ribosomes and ribozymes, Mg²⁺ similarly stabilizes RNA folding and activates the 2'-OH for phosphodiester attack. Physiological free $[Mg^{2+}] \approx 0.5 \text{ mM}$, total $\approx 20 \text{ mM}$ (mostly bound) — tight regulation, because even small shifts alter every ATP-dependent reaction. See section 1.

Questions 21–30: Synthesis and Evaluation

21. Evaluate the statement: “Life could have evolved using silicon instead of carbon as its molecular backbone.” Using comparative chemistry, identify at least two key chemical differences between the bonding properties of C and Si that make carbon uniquely suited for biological macromolecules.

Answer (Q21, Synthesis). The empirical chemistry argues against a silicon biosphere on at least two grounds. (1) Bond strength and catenation: carbon forms four strong, kinetically stable tetrahedral covalent bonds (C–C (about) 346 kJ/mol) and readily makes (pi)-bonds (C=C (about) 614 kJ/mol, C=O (about) 745 kJ/mol), enabling chains, branches, rings and reversible reactivity; Si–Si bonds are far weaker (about 222 kJ/mol) and silicon makes poor (pi)-bonds, so long stable Si backbones and silicon analogs of carbonyl/amide chemistry do not form. (2) Oxidised form: carbon's oxidised product CO_2 is a soluble, diffusible gas that cycles through air, water and biomass, whereas oxidised silicon (SiO_2) is an insoluble polymeric solid (quartz), so a silicon metabolism cannot cycle its skeleton element. The judgment that carbon is uniquely suited rests on these conditional facts; it would change only if a solvent/temperature regime existed where Si catenation and a volatile Si oxide were stable – not the case under biological conditions. See section 1.22. Design an experiment to test whether the hydrophobic effect is entropy-driven. Describe what measurements you would take, what temperature you would vary, and what thermodynamic parameters you would calculate. Predict the outcome.

Answer (Q22, Synthesis). Hypothesis: the hydrophobic effect (e.g. transfer of a nonpolar solute such as benzene from a nonpolar phase into water) is entropy-driven – ($\Delta G_{\text{transfer}}$) is dominated by an unfavorable ($-T\Delta S$) rather than (ΔH). Design: measure the partition/solubility equilibrium constant (K) for benzene between water and a reference nonpolar phase across a temperature series (e.g. 5, 15, 25, 35, 45 degrees C), with replicate samples and a temperature-controlled bath as the controlled variable. Calculate: ($\Delta G^\circ = -RT \ln K$); from a van't Hoff plot of ($\ln K$) vs ($1/T$) extract (ΔH°); then ($\Delta S^\circ = (\Delta H^\circ - \Delta G^\circ)/T$). Predicted outcome: near 25 degrees C, (ΔH° about 0) and (ΔS°) is large and negative for dissolving benzene in water ($-T\Delta S$) dominates

0)); the effect strengthens with temperature up to about 70 degrees C. Falsification: if (ΔH°) were large and positive while (ΔS°) were about 0, the effect would be enthalpic and the hypothesis rejected. See section 1.23. A drug molecule must cross the blood-brain barrier (which is composed of lipid bilayer membranes). Using the structure–activity relationship principle, explain what molecular properties (MW, logP, logD, logP_{o/w}, logP_{o/a}, logP_{o/s}, logP_{o/l}, logP_{o/g}, logP_{o/b}, logP_{o/t}, logP_{o/c}, logP_{o/d}, logP_{o/e}, logP_{o/f}, logP_{o/g}, logP_{o/h}, logP_{o/i}, logP_{o/j}, logP_{o/k}, logP_{o/l}, logP_{o/m}, logP_{o/n}, logP_{o/o}, logP_{o/p}, logP_{o/q}, logP_{o/r}, logP_{o/s}, logP_{o/t}, logP_{o/u}, logP_{o/v}, logP_{o/w}, logP_{o/x}, logP_{o/y}, logP_{o/z}) favor CNS penetration. How would you modify a highly polar drug to improve CNS penetration?

Answer (Q23, Synthesis). CNS penetration requires crossing a lipid bilayer, so the structure-activity rules favor molecules that partition into the nonpolar core: low molecular weight (\leq about 450 Da), moderate lipophilicity (logP (about) 2–4), few hydrogen-bond donors (\leq 3) and acceptors (\leq 7), and low polar surface area ($< 90 \text{ \AA}^2$). Each H-bond donor/acceptor must shed its ordered hydration shell to enter the hydrocarbon interior – an energetic penalty – so excess polarity blocks permeation, while C–H/C–C-rich nonpolar surface promotes it via the hydrophobic effect and van der Waals contacts with lipid tails. To improve a highly polar drug: mask H-bond donors (methylate or acylate –OH/–NH groups, e.g. a prodrug ester), reduce charged groups or raise their pK_a so the neutral form predominates at pH 7.4, lower molecular weight, and add nonpolar substituents to raise logP – the standard medicinal-chemistry route to CNS-active analogs. See section 1.24. Carbonic anhydrase catalyses $\text{CO}_2 + \text{H}_2\text{O} \rightleftharpoons \text{H}_2\text{CO}_3$ with a rate constant about $10^6 \times$ faster than the uncatalysed reaction. The active site uses a Zn^{2+} ion to polarize the O–H bond of a water molecule. Explain the mechanistic logic: why does metal coordination of water make it a better nucleophile in this context?

Answer (Q24, Synthesis). Water alone is a poor nucleophile toward CO_2 because its O–H pK_a ≈ 15.7 — almost no hydroxide is available at pH 7. Zn^{2+} coordination drops the pK_a of bound water to ≈ 7 , so at physiological pH roughly half of the Zn-OH_2 is deprotonated to Zn-OH^- — a potent nucleophile already positioned in the active site. The mechanism: (1) Zn-OH^- attacks the electrophilic carbon of CO_2 ; (2) carbonate product dissociates, regenerating Zn-OH_2 ; (3) a proton shuttle (His64 \rightarrow bulk water) re-ionizes the Zn-bound water. The result is $k_{\text{cat}} \approx 10^6 \text{ s}^{-1}$ and $k_{\text{cat}}/K_m \approx 10^8 \text{ M}^{-1}\text{s}^{-1}$ — carbonic anhydrase is diffusion-limited, one of the fastest enzymes known. Generalisation: metal-activated water is a universal strategy (alcohol dehydrogenase Zn^{2+} , metalloproteases, alkaline phosphatase). Proposed experimental intervention: replace Zn^{2+} with Cd^{2+} (weaker Lewis acid) \rightarrow predicted about $100 \times$ slower; validate by stopped-flow kinetics of CO_2 -induced pH drop. See section 1.25. Compare the evolutionary origins of the genetic code (DNA/RNA using N- and O-containing bases) with a hypothetical alternative code using entirely non-polar building blocks. What biochemical properties would be lost or gained? Evaluate why polarity and hydrogen bonding in nucleobases are essential for genetic fidelity.

Answer (Q25, Synthesis). Both real and hypothetical codes rely on the same shared principle: specific, reversible molecular recognition through complementary weak interactions. The difference that changes interpretation is *polarity*. Genetic fidelity depends on the N–H and C=O groups of the bases forming directional hydrogen bonds (A–T uses 2, G–C uses 3; Deltachi) of N–H = 0.84, O–H = 1.24 supplying the partial charges), so only correctly paired bases fit geometrically and energetically – mispairs cost several kJ/mol and are rejected, giving low error rates. A purely non-polar building set could still stack via van der Waals/(pi) interactions but could not form the specific, directional, distinguishable hydrogen-bond patterns that encode A pairs with T, not C. It would therefore lose base-pairing specificity (catastrophic for replication fidelity and template-directed information transfer) while gaining only nonspecific hydrophobic aggregation. Polarity and hydrogen bonding are essential precisely because they make recognition specific rather than merely sticky. See section 1.26. A newly discovered antibiotic (X) functions by chelating Mg^{2+} ions in bacterial ribosomes. Predict: (a) which step of protein synthesis would be disrupted; (b) whether X would be active vs gram-positive or gram-negative bacteria; (c) possible mechanisms of resistance the bacterium might evolve.

Answer (Q26, Synthesis). Mg^{2+} is essential to ribosome structure and function because its high charge density neutralizes and folds the polyanionic rRNA backbone and stabilizes the peptidyl-transferase center. (a) Chelating Mg^{2+} collapses rRNA tertiary structure and destabilises subunit association and the tRNA sites – translation fails broadly, but the most Mg^{2+} -sensitive step is peptidyl transfer/elongation (and assembly of the 70S/80S ribosome), so protein synthesis halts. (b) Activity vs Gram type depends on reaching the target: Gram-positive bacteria have a thick but porous peptidoglycan layer and no outer membrane, so a Mg^{2+} -chelating agent is more likely to be active against Gram-positives; Gram-negative bacteria have an LPS outer membrane that excludes many such compounds (and that membrane itself depends on divalent cations). (c) Resistance routes: altered Mg^{2+} import/efflux raising intracellular Mg^{2+} , reduced uptake of X (permeability/efflux pumps), enzymatic modification of X, or rRNA/r-protein mutations that lower Mg^{2+} dependence. See section 1.27. The Henderson-Hasselbalch equation assumes that pK_a is constant. However, the pK_a of His residues in proteins is strongly context-dependent (ranging from 4.0 to 8.0). Explain how protein microenvironment (electrostatics, hydrophobicity, hydrogen bonding) shifts the pK_a of an ionisable side chain, and why this is functionally important for enzyme catalysis.

Answer (Q27, Synthesis). A side chain's pK_a reflects the relative free energy of its protonated vs deprotonated forms — any perturbation to that energy shifts the pK_a. Three mechanisms: (i) Electrostatics — a nearby positive charge stabilizes the deprotonated anionic form \rightarrow lower pK_a (Asp in lysozyme's active site: solution pK_a 3.9, in-protein pK_a 2.0, $\Delta\text{pK}_a = -1.9$). A nearby negative charge does the opposite. (ii) Hydrophobic burial — removing a charge from bulk water into a non-polar pocket *destabilises* the charged state (loss of about 40–80 kJ/mol of solvation), *raising* pK_a for acids and *lowering* it for bases; a buried Lys can drop from pK_a 10.5 to about 6. (iii) Hydrogen bonding — an H-bond donor that specifically

stabilizes one protonation state shifts pKa accordingly. Functional importance: serine proteases require the catalytic His57 to be a general base at physiological pH — its pKa is tuned to about 7 by the Asp102-His57 H-bond. Validating measurement: NMR titration of the His57 C-H resonance ($\delta = 8.0 \rightarrow 7.5$ ppm across pKa) gives the in-protein pKa directly; combine with a D102N mutant (pKa shifts to about 5) to confirm the tuning mechanism. See section 1. 28. Bohr effect: CO₂ and H⁺ reduce hemoglobin's O₂ affinity by stabilizing the T-state (deoxy form). Using atomic-level reasoning: (a) which specific residues of hemoglobin are protonated at low pH; (b) how does protonation alter quaternary structure; (c) why is this physiologically beneficial in exercising tissues?

Answer (Q28, Synthesis). (a) At low pH the protonated groups are mainly the His146 (beta-chain C-terminus) imidazole (pK_a (about) 6) plus the alpha-amino N-termini and other His residues that contribute to the Bohr effect; protonation also promotes CO(2) binding as carbamino groups on N-termini. (b) Protonated His146 forms a salt bridge with Asp94 of the same beta-chain, an ionic interaction (5–20 kJ/mol) that stabilizes the low-affinity T (deoxy) quaternary state; stabilizing T shifts the allosteric T (T) R equilibrium toward T, lowering O(2) affinity (right-shifted O(2) dissociation curve). (c) Exercising tissue is acidic and CO(2)-rich (lactate, metabolic CO(2)), so the Bohr effect makes hemoglobin **release more O(2)** exactly where it is needed, while in the lungs (high pO(2), low CO(2), higher pH) the salt bridges break, R-state is favored and O(2) is loaded – a pH-coupled delivery switch built from a protonation-controlled salt bridge. See section 1. 29. A patient presents with severe metabolic acidosis (blood pH 7.1, HCO₃[–] = 12 mEq/L, pCO₂ = 30 mmHg). Using Henderson-Hasselbalch ($\text{pH} = 6.1 + \log[\text{HCO}_3^-]/[0.03 \times \text{pCO}_2]$), verify the expected pH vs measured. Is there respiratory compensation? What primary disorder is this (metabolic or respiratory) and how would you distinguish a primary from a compensatory change?

Answer (Q29, Synthesis). Verify: $\text{pH} = 6.1 + \log_{10}\left(\frac{[\text{HCO}_3^-]}{0.03 \times \text{pCO}_2}\right) = 6.1 + \log_{10}\left(\frac{12}{0.03 \times 30}\right) = 6.1 + \log_{10}(13.33) = 6.1 + 1.12 = 7.22$. Measured pH is 7.1 — slightly more acidic than predicted, but the calculation confirms the internal consistency of the arterial gas. Interpretation: (i) Low HCO₃[–] (normal ≈ 24 mEq/L) with low pH identifies the primary disorder as metabolic acidosis (e.g., lactic acidosis, diabetic ketoacidosis, renal tubular acidosis). (ii) Low pCO₂ (normal ≈ 40 mmHg) indicates respiratory compensation — the patient is hyperventilating to blow off CO₂ and raise pH back toward 7.4. (iii) Use Winters' formula to distinguish primary vs compensatory: expected pCO₂ = $(1.5 \times \text{HCO}_3^-) + 8 \pm 2 = (1.5 \times 12) + 8 = 26 \pm 2$ mmHg. Measured pCO₂ (30) is *slightly higher* than expected — indicating *incomplete* respiratory compensation. Rule of thumb: a respiratory *primary* disorder would show pCO₂ and HCO₃[–] moving in the *same* direction (both up or both down over days), whereas metabolic primary shows them in the *same* direction acutely (both down here). Validating measurement: serial arterial blood gases 2 h apart — if pCO₂ continues to fall while HCO₃[–] stabilizes, compensation is still active. See section 1. 30. Propose a molecular mechanism by which a histone deacetylase (HDAC) inhibitor (e.g., vorinostat) could be used to treat cancer. Trace from HDAC inhibition → altered histone acetylation state → chromatin opening → transcription of tumor suppressor genes → reduced tumor cell survival. Identify the specific bond type removed/restored at each step.

Answer (Q30, Synthesis). Hypothesis: inhibiting HDAC with vorinostat raises histone acetylation, opens chromatin, and re-expresses silenced tumor-suppressor genes, reducing tumor-cell survival. Step-by-step bond chemistry: (1) HDAC normally hydrolyses the amide (isopeptide) bond of acetyl-lysine, removing the acetyl group and regenerating a positively charged Lys –NH(3⁺); vorinostat's hydroxamate chelates the active-site Zn(2+), blocking this hydrolysis. (2) Histone acetyltransferases keep forming the amide bond between acetyl-CoA's thioester acetyl group and Lys –NH(2), so acetyl-lysine accumulates. (3) Neutralizing the Lys epsilon-amino charge weakens the ionic bond/salt bridge between histone tails and the phosphodiester DNA backbone, loosening nucleosome packing. (4) Open chromatin permits transcription of tumor-suppressor genes (e.g. CDKN1A/p21), driving cell-cycle arrest and apoptosis. Comparison/control: treat matched tumor vs normal cells +/- vorinostat, measure acetyl-H3/H4 (Western/ChIP), chromatin accessibility (ATAC-seq), p21 mRNA and viability, with a catalytically irrelevant analog as negative control. Falsifying result: if acetylation rises but tumor-suppressor transcription and killing do not track it, the causal chain is refuted. See section 1.

Questions — Water — The Molecule of Life

Instructor Use and Coverage Notes

- Coverage target: Calculate a pH or buffer ratio and interpret what it means for a biological system.
- Model/data emphasis: Henderson-Hasselbalch and pH-scale calculations.
- Assessment alignment: Concept Explanation, Statistical Tests and Data Analysis, Argumentation.
- Misconception probe: Water is not an inert background; it is an active participant in structure and reaction chemistry.
- Transfer product: Transfer water-property reasoning to blood buffering, plant transport, or protein folding.
- Grading focus: award full credit for mechanism, evidence, boundary conditions, and units when a calculation is required.
- Suggested use: draw one recall item, one application item, and one synthesis item when building a short quiz from this bank.

Questions 1–10: Recall and Comprehension

This activity accompanies section 2 of the textbook — review that chapter before attempting the exercises below.

1. Draw the water molecule; label the bond angle (104.5°), partial charges, and hydrogen bonds with adjacent molecules.

Answer (Q1, Recall). H₂O is a bent V-shaped molecule with the O at the vertex. The H–O–H angle is 104.5° — less than the ideal tetrahedral 109.5° because the two lone pairs on oxygen compress the bonding pairs (VSEPR). Oxygen pulls electron density away from the hydrogens, leaving O with a partial δ– charge and each H with a partial δ+ (bond dipole 1.85 D). Each H can donate to, and each lone pair accept, a hydrogen bond — so one water can engage in up to 4 hydrogen bonds at once, the basis of water’s tetrahedral network. See section 2. 2. Define specific heat capacity. Why does water have a high specific heat compared to most liquids?

Answer (Q2, Recall). Specific heat capacity is the energy required to raise 1 g of a substance by 1 K (or 1 °C). Water’s is 4.184 J g^{–1} K^{–1} — roughly 5× that of most metals and 2× most organic solvents. The unusually high value arises because much of the added energy is spent breaking hydrogen bonds rather than raising molecular kinetic energy. Biologically this means organisms (mostly water) resist temperature fluctuation, and oceans moderate global climate (coastal regions are buffered against extremes). See section 2. 3. What is the heat of vaporisation of water (cal/g) and what biological process exploits this?

Answer (Q3, Recall). The heat of vaporisation of water is 540 cal g^{–1} (2260 J g^{–1} at 100 °C; about 580 cal g^{–1} at body temperature). This enormous value reflects the energy needed to break essentially all remaining hydrogen bonds as liquid becomes vapor. Biologically it enables evaporative cooling: sweating (humans) or panting (dogs) dissipates heat because each gram of perspiration evaporated removes about 580 cal from the body surface. Plants transpire for the same reason — leaf cooling is a major function of stomatal water loss. See section 2. 4. Define cohesion and adhesion. Which property allows water to form a meniscus in a glass tube?

Answer (Q4, Recall). Cohesion is the attractive force between like molecules (water–water hydrogen bonding). Adhesion is the attractive force between unlike molecules (water–glass or water–cellulose). A meniscus forms when adhesion to the container wall exceeds cohesion at the liquid surface, pulling water up at the edges (concave meniscus). Together, cohesion + adhesion drive capillary action, which is the mechanism that moves water tens of meters up tree xylem against gravity. See section 2. 5. What is osmosis? In which direction does water move — toward higher or lower solute concentration?

Answer (Q5, Recall). Osmosis is the net diffusion of water across a semi-permeable membrane (one that passes water but not solute) from a region of lower solute concentration (higher water potential) to higher solute concentration (lower water potential). Equivalently: water moves down its own chemical potential gradient. In a cell, osmotic equilibrium is achieved when the membrane-spanning osmotic pressure difference is balanced by hydrostatic pressure (turgor in plants, or physical rigidity of animal-cell cytoskeleton). See section 2. 6. Define water potential (Ψ). Write the equation Ψ = Ψ_s + Ψ_p and define each term.

Answer (Q6, Recall). Water potential (Ψ) is the free energy of water per unit volume relative to pure water at atmospheric pressure (reference Ψ = 0 MPa). Pure water has the highest Ψ; water moves *down* its Ψ gradient. For a plant cell: Ψ = Ψ_s + Ψ_p, where Ψ_s (solute or osmotic potential, always ≤ 0) reflects solute concentration — computed from van ’t Hoff Ψ_s = –iCRT for an ideal solution — and Ψ_p (pressure potential) is the hydrostatic pressure exerted by the cell wall (turgor, typically +0.3 to +0.7 MPa in turgid plant cells; 0 in animal cells). Typical values: mesophyll cell Ψ ≈ –1 MPa; soil Ψ ≈ –0.3 MPa; atmosphere Ψ ≈ –100 MPa — the gradient that drives xylem transport. See section 2. 7. What is tonicity? Distinguish hypertonic, hypotonic, and isotonic solutions relative to a red blood cell.

Answer (Q7, Recall). Tonicity is the effective osmotic pressure gradient that determines the direction of net water movement across a cell membrane, judged by the concentration of non-penetrating solutes outside relative to inside. The shared principle is osmosis down the water-potential gradient; the difference that changes interpretation is the external solute concentration. Relative to a red blood cell: a hypertonic solution has higher external solute, so water leaves the cell and it shrinks (crenation); a hypotonic solution has lower external solute, so water enters and the cell swells and may

lyse (hemolysis); an isotonic solution (e.g. 0.9 % NaCl) has equal effective solute, so there is no net water movement and the cell keeps its normal biconcave shape. See section 2. 8. Define capillarity. Name two forces responsible for capillary rise in a tube.

Answer (Q8, Recall). Capillarity (capillary action) is the rise of a liquid in a narrow tube against gravity, driven by the liquid’s surface tension and its wetting of the tube wall. The two responsible forces are cohesion (water–water hydrogen bonding, which holds the liquid column together and creates surface tension) and adhesion (water–wall attraction, e.g. water hydrogen-bonding to the –OH groups of glass or cellulose, which pulls the meniscus up the wall). Both arise from water’s polar O–H bonds and hydrogen-bond network. Boundary condition: rise height scales as ($h = \frac{2\gamma \cos \theta}{\rho g r}$), so the narrower the tube the higher the rise – the basis of water movement in xylem and soil. See section 2. 9. What is the pH of pure water at 25°C? What is the Kw of water at this temperature?

Answer (Q9, Recall). Pure water autoionises: $(\text{H}_2\text{O} \rightleftharpoons \text{H}^+ + \text{OH}^-)$, with ion product ($K_w = [\text{H}^+][\text{OH}^-]$). At 25 degrees C, ($K_w = 1.0 \times 10^{-14}$). In pure water ($[\text{H}^+] = [\text{OH}^-] = \sqrt{K_w} = 1.0 \times 10^{-7}$ M), so ($\text{pH} = -\log_{10}\{10^{-7}\} = 7.0$) (neutral). Note this is temperature – dependent : at 37 degrees C (K_w about 2.4×10^{-14}), so neutral pH is about 6.8, a physiologically meaningful shift. See section 2.10. Describe what happens to a freshwater fish placed in seawater (hypertonic to the fish).

Answer (Q10, Recall). Seawater is hypertonic to a freshwater fish (external solute concentration far exceeds the fish’s body fluids). Across the gill and gut epithelia water therefore moves by osmosis from the dilute body fluids (high water potential) to the concentrated seawater (low water potential): the fish loses water and dehydrates, and salt diffuses inward. A freshwater-adapted fish lacks the salt-secreting machinery to compensate, so without osmoregulatory adaptation it cannot survive – cells shrink and plasma osmolarity rises. (Marine teleosts solve this by drinking seawater and actively excreting NaCl through chloride cells.) See section 2.

Questions 11–20: Application and Analysis

11. Calculate: if the osmotic potential of a plant cell is –0.8 MPa and pressure potential is +0.3 MPa, what is the water potential? Will water enter or leave the cell if it is placed in a solution with $\Psi = -0.4$ MPa?

Answer (Q11, Application). Apply $\Psi = \Psi_s + \Psi_p = (-0.8) + (+0.3) = -0.5$ MPa. Water moves down the Ψ gradient (highest → lowest), so compare cell and solution: $\Psi_{\text{cell}} = -0.5$ MPa, $\Psi_{\text{solution}} = -0.4$ MPa. Since the solution has higher Ψ (less negative), water moves from solution → cell: the cell takes up water, cell volume increases, and turgor pressure rises until Ψ_{cell} rises to match Ψ_{solution} . This exact logic — solving Ψ gradient sign-by-sign — is how plants regulate wilting / turgor / stomatal aperture. See section 2. 12. During sweating, 1 liter of sweat evaporated removes approximately 580 kcal of heat from the body. Calculate: if a marathon runner produces 2 L/h of sweat, how many watts of heat are removed? (1 watt = 1 J/s)

Answer (Q12, Application). Heat removed per liter = 580 kcal \times 4184 J/kcal $\approx 2.43 \times 10^6$ J/L. At 2 L/h: total heat = $2 \times 2.43 \times 10^6 = 4.86 \times 10^6$ J/h. Convert to watts: $4.86 \times 10^6 \text{ J} \div 3600 \text{ s} \approx 1350 \text{ W}$ (≈ 1.35 kW). Biological sanity check: a marathon runner’s metabolic rate is about 1000–1500 W — so evaporative cooling via sweat is the dominant heat-dissipation pathway and exactly matches metabolic heat production. The extraordinary magnitude of this flux (dwarfing radiative and convective loss at ambient \approx body temperature) is a direct consequence of water’s uniquely high heat of vaporization (≈ 40.7 kJ/mol, driven by hydrogen bonding). See section 2. 13. Sea ice insulates frigid arctic waters and protects aquatic organisms. Explain, at the molecular level, why ice is less dense than liquid water and why this unusual property has profound ecological consequences.

Answer (Q13, Application). In liquid water at 25 degrees C each molecule forms about 3.4 transient hydrogen bonds at any instant, leaving the network partially broken and the molecules able to pack closely. On freezing, every water molecule forms exactly 4 hydrogen bonds in a fixed tetrahedral geometry, producing an open hexagonal lattice with more empty space between molecules. The same number of molecules thus occupies a larger volume, so ice (0.917 g/cm³) is less dense than liquid water and floats; liquid water reaches maximum density at 4 degrees C. Ecological consequence: ice forms an insulating floating layer, lakes stratify with 4 degrees C water at the bottom, and aquatic ecosystems do not freeze solid in winter – if ice sank, water bodies would freeze from the bottom up and most aquatic life in temperate/polar regions would be impossible. See section 2. 14. An onion cell with osmotic potential –0.6 MPa is placed in a 0.3 M NaCl solution. The NaCl solution has $\Psi_s = -0.75$ MPa. Predict the direction of water movement and whether the cell will plasmolyse or swell.

Answer (Q14, Application). Compare water potentials. The onion-cell osmotic (solute) potential is ($\Psi_s = -0.6$) MPa; assuming the cell is initially flaccid (Ψ_{ip} about 0), (Ψ_{cell} about -0.6) MPa. The 0.3 M NaCl bathing solution has ($\Psi_s = -0.75$) MPa (open beaker, ($\Psi_{\text{ip}} = 0$)), so ($\Psi_{\text{solution}} = -0.75$) MPa. Water moves from higher (Ψ) to lower (Ψ): since (Ψ_{cell}) (-0.6) $>$ (Ψ_{solution}) (-0.75), water leaves the cell. The cell loses volume, the protoplast pulls away from the wall, and the cell plasmolyzes (the NaCl solution is hypertonic to the cell). It will not swell. See section 2. 15. Compare the water requirements of a plant using C₄ photosynthesis (e.g., maize) vs C₃ photosynthesis (e.g., wheat) in a hot, dry environment. Explain in terms of stomatal conductance and water-use efficiency.

Answer (Q15, Application). Both C₃ (wheat) and C₄ (maize) plants face the same shared constraint: stomata must open to admit CO₂, but open stomata lose water vapor by transpiration along the same diffusion gradient. The difference that changes interpretation is CO₂-concentrating efficiency. C₄ plants pre-fix CO₂ into a 4-carbon acid in mesophyll cells and pump it to a high concentration around RuBisCO in bundle-sheath cells, nearly abolishing photorespiration. Consequently a C₄ plant achieves the same carbon gain at lower stomatal conductance, so its water-use efficiency (carbon fixed per unit water lost) is roughly double that of a C₃ plant. In a hot, dry environment maize can keep stomata more closed (less transpirational water loss, less wilting) while still fixing carbon efficiently, whereas wheat must keep stomata open longer and loses more water and is more drought-stressed. See section 2. 16. Describe three specific properties of water that make it essential for the cohesion-tension mechanism of xylem transport. What evidence refutes the alternative “root pressure” hypothesis as the primary force driving water to the tops of tall trees?

Answer (Q16, Application). Three water properties underpin cohesion–tension transport. (1) Strong cohesion – extensive water–water hydrogen bonding lets a continuous water column sustain large negative pressure (tension) without breaking. (2) Adhesion – water hydrogen-bonds to the hydrophilic cellulose of xylem walls, helping anchor the column and supporting capillarity in narrow tracheids/vessels. (3) High tensile strength/surface tension – the same H-bonding gives water enough tensile strength to resist cavitation as transpiration at the leaf pulls water up. The transpiring leaf generates very negative water potential (atmosphere (about -100) MPa) that pulls the cohesive column upward. Evidence refuting root pressure as the primary driver: root pressure is small (a few hundred kPa), is absent or negligible in tall transpiring trees at midday, cannot account for the about 0.1–3 MPa needed to raise water tens of meters, and transpiration continues (sap under tension, not positive pressure) even when roots are removed or killed – water still rises in a cut, transpiring shoot. See section 2. 17. A student proposes using ethanol instead of water as a biological solvent. Identify three properties of water (not of ethanol) that would be lost, and predict the consequences for enzyme function, ion transport, and pH buffering.

Answer (Q17, Application). Three water-specific properties that ethanol lacks: (1) High dielectric constant ($\epsilon_{\text{water}} \approx 80$ vs $\epsilon_{\text{ethanol}} \approx 24$) — ethanol cannot effectively screen ionic interactions, so Na⁺/K⁺/Cl⁻ ion pairs and salt bridges in enzyme active sites would remain associated, collapsing ionic transport gradients and distorting active-site geometry → enzyme K_m shifts catastrophically, Na⁺/K⁺-ATPase cannot maintain the 10:1 Na⁺ gradient. (2) Tetrahedral H-bond network with strong amphiprotic behavior — water both donates and accepts H-bonds symmetrically, stabilizing α -helix/ β -sheet backbones via patterned hydration; ethanol’s single OH disrupts this pattern → protein denaturation (the classic 70% ethanol sterilisation mechanism). (3) Autoionization yielding the pH scale ($2 \text{ H}_2\text{O} \rightleftharpoons \text{H}_3\text{O}^+ + \text{OH}^-$, $K_w = 10^{-14}$) — ethanol has no analogous conjugate pair, so bicarbonate buffering ($\text{HCO}_3^-/\text{H}_2\text{CO}_3$, $\text{pK}_a \approx 6.35$) would not function and physiological pH regulation collapses. Life as we know it is therefore inseparable from liquid water, not merely “a polar solvent.” See section 2. 18. During hypothermia, core body temperature drops to 32°C. Using specific heat capacity principles, calculate the heat (kJ) that must be extracted from a 70 kg person (composed of about 60% water) to lower their temperature from 37°C to 32°C (specific heat of the body $\approx 3.47 \text{ kJ/kg}\cdot^\circ\text{C}$).

Answer (Q18, Application). Model: ($Q = m \cdot c \cdot \Delta T$) (sensible-heat equation). Substitute the stated values: mass ($m = 70$) kg, specific heat of the body ($c = 3.47$) kJ kg⁻¹ degrees C⁻¹, temperature change ($\Delta T = 37 - 32 = 5$) degrees C. ($Q = 70 \times 3.47 \times 5 = 1214.5 \text{ kJ}$) (about 1.21 MJ) that must be extracted. Biological-range check: at a basal metabolic rate of about 80 W (= 80 J/s (about) 288 kJ/h), passively losing about 1.2 MJ corresponds to several hours of net heat loss exceeding metabolic production – consistent with hypothermia developing over hours of cold exposure, and showing why water’s high specific heat (4.18 kJ kg⁻¹ degrees C⁻¹; the body is about 60 % water) buffers core temperature against rapid swings. See section 2. 19. Explain the role of aquaporins in transmembrane water movement. How does the selectivity filter exclude protons (H₃O⁺) despite water molecules sharing similar size? What disease results from aquaporin-2 deficiency?

Answer (Q19, Application). Aquaporins (AQPs) are homotetrameric integral membrane proteins; each subunit is an independent hourglass-shaped pore that conducts about 3×10^9 water molecules/s in single file while excluding ions. Selectivity comes from a about 2.8 Å constriction (size/aromatic-arginine filter) and, crucially, two central NPA (Asn-Pro-Ala) motifs: their fixed dipoles reorient the central water molecule so its O–H bonds point away from neighbors, breaking the hydrogen-bond “wire.” Because protons move not as particles but by Grotthuss hopping along a continuous H-bonded water chain, breaking that chain blocks H⁽⁺⁾/H₃O⁽⁺⁾ transport even though water itself (moving vehicularly) passes freely. Deficiency or loss-of-function mutation of aquaporin-2 (the ADH-regulated channel of the kidney collecting duct) causes nephrogenic diabetes insipidus – inability to concentrate urine, with output of up to about 20 L/day of dilute urine. See section 2. 20. The mangrove tree lives in salty seawater. Its roots must extract fresh water against an extremely negative osmotic potential. Explain what root structure adaptations mangroves have developed, and calculate the minimum root pressure required if external seawater has $\Psi_s = -2.5 \text{ MPa}$ and leaf water loss creates $\Psi_p = -1.0 \text{ MPa}$.

Answer (Q20, Application). Adaptation: mangroves use ultrafiltration at the roots (a Casparian-strip/suberised endodermis acting as a salt-excluding membrane that filters most NaCl from incoming water), supplemented by salt-secreting glands on leaves and salt sequestration/leaf shedding; aerial pneumatophores handle the separate problem of waterlogged anoxic soil. Calculation – minimum root (xylem) pressure needed:

to draw water in, the plant's xylem water potential must be more negative than the seawater. Treating the values as water potentials, the seawater has ($\Psi_s = -2.5$) MPa and the transpirational pull contributes ($\Psi_p = -1.0$) MPa, so the xylem must reach at least ($\Psi = -2.5 + (-1.0) = -3.5$ MPa). Equivalently the root system must overcome the 2.5 MPa osmotic barrier plus the 1.0 MPa transport demand, i.e. generate (≥ 3.5) MPa of tension – well within the cohesion–tension range but far beyond ordinary root pressure, which is why filtration plus large negative leaf (Ψ) is required. See section 2.

Questions 21–30: Synthesis and Evaluation

21. Water is simultaneously the product and reactant of countless biochemical reactions (hydrolysis, condensation, and hydration). Evaluate whether increasing intracellular water concentration would shift equilibrium toward condensation reactions (protein synthesis) or hydrolysis reactions. What does Le Chatelier's principle predict?

Answer (Q21, Synthesis). Hydrolysis consumes water (polymer + $H_2O \rightarrow$ monomers); condensation (e.g. peptide-bond formation in protein synthesis) releases water (monomers \rightarrow polymer + H_2O). By Le Chatelier's principle, increasing the activity/concentration of water shifts the equilibrium toward the side that consumes water – i.e. toward hydrolysis, away from condensation. Initiating condition: raise intracellular water (lower solute, higher water activity (a_w)). Intermediate mechanism: the mass-action term for water in the hydrolysis direction increases, so the reaction quotient favors bond cleavage; high (a_w) also speeds water-dependent reactions generally. Observable outcome: net macromolecule breakdown rather than synthesis. This is exactly why cells keep water activity high yet drive biosynthesis only by *coupling* condensation to exergonic NTP hydrolysis and by sequestering reactions on enzymes/ribosomes – the thermodynamics of bulk water alone favor hydrolysis. See section 2. 22. Propose an experiment to test whether the anomalous expansion of water upon freezing is due to hydrogen bond structure. What control conditions and measurements would you use? What would falsify the hydrogen bond hypothesis?

Answer (Q22, Synthesis). Hypothesis: the volume expansion of water on freezing is caused by the open tetrahedral hydrogen-bond lattice of ice (each molecule fixed at 4 H-bonds) rather than by some non-H-bond effect. Comparison/controls: measure density vs temperature through the freezing transition for (a) normal H_2O and (b) a non-hydrogen-bonding control liquid of similar molar mass (e.g. H_2S , or an aprotic solvent) which should contract on freezing; also test D_2O (stronger H-bonds, slightly different transition). Changed factor: presence/strength of the H-bond network. Measurements: dilatometry/X-ray or neutron diffraction to record lattice geometry (expect about 4 H-bonds, hexagonal lattice in ice) and the density step at 0 degrees C; replicate samples and freeze/thaw cycles. Predicted outcome: only the hydrogen-bonding liquid expands on freezing and shows the open tetrahedral lattice; the control contracts. Falsification: if a non-H-bonding liquid of comparable structure also expanded on freezing, or if diffraction showed no open tetrahedral lattice in ice, the H-bond explanation would be refuted. See section 2. 23. The blood-brain barrier restricts water flux into the CNS. Cerebral edema (excess water accumulation in brain tissue) can be fatal. Using water potential principles, explain: (a) why hyponatraemia (low blood $[Na^+]$) causes cerebral edema; (b) why mannitol infusion reduces edema; (c) how AQP4 water channels contribute to normal fluid homeostasis.

Answer (Q23, Synthesis). (a) Hyponatraemia causes cerebral edema: lowering blood $[Na^+]$ raises plasma water potential (makes plasma hypotonic relative to brain cells), so water moves down the (Ψ)/osmotic gradient into neurons and astrocytes; constrained inside the rigid skull, the swelling raises intracranial pressure. (b) Mannitol reduces edema: mannitol is an osmotically active solute that the blood-brain barrier excludes; infusing it lowers plasma water potential (makes blood hypertonic to brain tissue), reversing the gradient so water moves from brain into blood and is excreted (osmotic diuresis), shrinking the swollen tissue. (c) AQP4 in normal homeostasis: AQP4, concentrated at astrocyte end-feet around capillaries, provides a high-capacity, bidirectional water pathway that lets the brain rapidly equilibrate water with the vasculature – clearing excess extracellular water (vasogenic edema) but also facilitating water influx in cytotoxic states. Net: water always follows its potential gradient; Na^+ sets the gradient and AQP4 sets how fast water can follow it. See section 2. 24. Compare the water potential of: (a) pure water; (b) 0.1 M sucrose solution; (c) wilted plant cell (-1.2 MPa osmotic, $+0.1$ MPa pressure); (d) turgid plant cell (-1.2 MPa osmotic, $+0.9$ MPa pressure). Rank them from highest to lowest Ψ and predict the direction of water flux between each pair.

Answer (Q24, Synthesis). Apply ($\Psi = \Psi_s + \Psi_p$) (pure water reference ($\Psi = 0$)). (a) Pure water: ($\Psi = 0$) MPa. (b) 0.1 M sucrose: ($\Psi_s = -iCRT$). With ($i=1$), ($C=0.1$) mol/L, ($R = 8.314 \times 10^{-3}$) L(MPa mol⁻¹) K⁻¹), (T about 298) K: ($\Psi_s = -(1)(0.1)(8.314 \times 10^{-3})(298)$ about -0.25) MPa, ($\Psi_p = 0$), so (Ψ about -0.25) MPa. (c) Wilted cell: ($\Psi = -1.2 + 0.1 = -1.1$) MPa. (d) Turgid cell: ($\Psi = -1.2 + 0.9 = -0.3$) MPa. Ranking highest to lowest: (a) $0 > (c)?$ No – order is (a) 0 MPa $>$ (b) $-0.25 >$ (d) $-0.3 >$ (c) -1.1 MPa. Water flows from higher to lower (Ψ): from pure water into the sucrose solution; from the sucrose solution into the turgid cell; and from the turgid cell into the wilted cell (the wilted cell, lowest (Ψ), takes up water from every other compartment). The shared principle is the additive water-potential equation; the differing (Ψ_p) (turgor) is what separates the wilted from the turgid cell despite identical (Ψ_s). See section 2. 25. Desiccation-tolerant (resurrection) plants can survive to $< 5\%$ water content and revive when rehydrated. Propose two cellular mechanisms that allow membranes and proteins to remain functional in the nearly anhydrous state. Consider the role of trehalose as a vitrifying agent.

Answer (Q25, Synthesis). In the near-anhydrous state, removing water destroys the hydrogen-bond shell that normally stabilizes membranes and

proteins, so the cell must replace water's structural role. Mechanism 1 – the “water-replacement” hypothesis: the disaccharide trehalose hydrogen-bonds its hydroxyl groups directly to phospholipid head groups and protein surfaces, substituting for the lost hydration shell, keeping bilayer phospholipids spaced (preventing the gel-phase transition and leakage on rehydration) and preventing protein unfolding. Mechanism 2 – vitrification: at high concentration trehalose forms an amorphous glass of extremely high viscosity; this kinetically traps macromolecules and membranes, arresting the molecular motions, diffusion and aggregation/denaturation reactions that would otherwise damage structures during desiccation and storage. Together (water replacement + glass formation) these allow membranes and proteins to remain intact and refold/reseal correctly when water returns. Late-embryogenesis-abundant (LEA) proteins act as additional molecular shields. See section 2. 26. Reverse osmosis (RO) desalination uses high pressure to push seawater through semi-permeable membranes. Calculate: if seawater has an osmotic pressure of approximately 27 atm (2.7 MPa), what minimum external pressure must the RO system exert to produce fresh water? What energy (kJ) is required per liter, given 1 atm \approx 101.3 kPa and volume = 1 L?

Answer (Q26, Synthesis). Model: to push fresh water through the membrane, the applied pressure must *exceed* the solution's osmotic pressure; the thermodynamic minimum work per unit volume equals the osmotic pressure. Minimum pressure: seawater (π about 27) atm = 2.7 MPa, so the RO system must apply just over 27 atm (>2.7 MPa) (more in practice to give finite flux and overcome rising concentration at the membrane). Minimum energy per liter: ($W = \pi \times V$). Convert (π): (27 atm \times 101.3 kPa/atm = 2735 kPa = 2.735×10^6 Pa). With ($V = 1$) L = (1×10^{-3}) m³): ($W = 2.735 \times 10^6$ Pa \times 1×10^{-3} m³ = 2735 J about 2.7 kJ per liter) (thermodynamic minimum; real plants use about 3–4 times this). Interpretation: this is the same van 't Hoff osmotic pressure that a cell membrane must withstand – desalination simply pays that energy back to separate water from solute. See section 2. 27. During ischemia (reduced blood flow), intracellular Na⁺ rises due to Na/K-ATPase failure. Predict the effect of rising intracellular Na⁺ on: (a) intracellular osmotic potential; (b) water flux across the plasma membrane; (c) cell volume. How does this contribute to ischemic cell death?

Answer (Q27, Synthesis). Initiating condition: ischemia stops ATP supply, so the Na^{(+)/K⁽⁺⁾}-ATPase fails and Na⁽⁺⁾ leaks in without being pumped out. (a) Intracellular osmotic potential: rising intracellular Na⁽⁺⁾ (and accompanying anions) increases intracellular solute, making the cytosolic water potential more negative (lower Ψ), higher effective osmolarity). (b) Water flux: water moves down its potential gradient from the relatively higher- Ψ extracellular fluid into the cell by osmosis. (c) Cell volume: the cell swells (cytotoxic/oncotic edema); without a wall the membrane is stretched. Contribution to ischemic death: progressive swelling, membrane blebbing and eventual plasma-membrane rupture (oncosis), release of damaging contents, and – in brain – raised intracranial pressure. The root cause is loss of the ATP-dependent ion gradient that normally keeps intracellular solute (and thus water) in check. See section 2. 28. Antarctic ice fish have no hemoglobin and survive at –1.9°C seawater by relying on the unusual fluidity of water at low temperatures. Explain: (a) how antifreeze proteins (AFPs) prevent ice crystal formation at subzero temperatures (using the concepts of ice crystal growth inhibition); (b) how AFP ice binding differs from osmotic freezing protection (as in glycerol).

Answer (Q28, Synthesis). (a) AFP mechanism: antifreeze proteins do not depress the freezing point colligatively. They have a flat, relatively hydrophobic ice-binding surface that adsorbs onto specific faces of tiny ice crystals. Once bound, further ice growth can only occur in the gaps between adsorbed proteins, forcing the ice front into energetically unfavorable high-curvature bulges (the Gibbs–Thomson/Kelvin effect). This inhibits crystal growth, producing a gap between the melting and freezing points called thermal hysteresis (about 1–5 degrees C; enough for polar fish to stay liquid at -1.9 degrees C seawater). (b) Contrast with glycerol: glycerol (or any high-concentration solute) protects colligatively – it depresses the equilibrium freezing point in proportion to the number of dissolved particles ($(\Delta T_f = iK_f m)$), affecting bulk thermodynamics non-specifically, and requires molar concentrations. AFPs act non-colligatively and substoichiometrically, binding ice surfaces kinetically rather than lowering bulk freezing point – a structural (lock-onto-crystal) mechanism versus a bulk solute (number-of-particles) mechanism. See section 2. 29. Water's high surface tension (72 mN/m at 20°C) is biologically critical. Describe two specific biological examples of surface tension exploitation (one arthropod, one mammalian respiratory) and explain the molecular basis of surface tension in each, and what would happen if surface tension were reduced by half in each case.

Answer (Q29, Synthesis). Surface tension arises because surface water molecules have fewer neighbors to hydrogen-bond with, creating a net inward cohesive force; water's value (72 mN/m) is the highest of common liquids because of its extensive H-bond network. Example 1 – arthropod (water strider): the insect's hydrophobic, hair-covered legs distribute its weight over a large area so the pressure stays below the surface-tension threshold, letting it stand and walk on water without breaking the surface. If (γ) were halved, the surface could no longer support the load and the strider would sink. Example 2 – mammalian respiratory (alveolus): the air–water interface lining alveoli generates surface tension that, by Laplace's law ($(P = 2\gamma/r)$), tends to collapse small alveoli; pulmonary surfactant (DPPC) lowers (γ) to about 25 mN/m to keep alveoli open. If alveolar (γ) were instead only halved (still too high, as in surfactant deficiency), small alveoli would still tend to collapse on expiration (atelectasis), requiring large pressures to reinflate – the pathology of neonatal respiratory distress syndrome. See section 2. 30. Critique the role of water activity (a_w) vs water potential in determining microbial growth. Explain why halophilic bacteria can grow at $a_w = 0.75$ (equivalent to about 5 M NaCl), while most bacteria cannot survive below $a_w = 0.95$. How does reduced water activity inhibit cellular processes even when cells are fully hydrated? What field of food science exploits this principle and how?

Answer (Q30, Synthesis). Water activity vs water potential: (a_w) is the effective thermodynamic concentration of water ($a_w = p/p^0$), pure water = 1.0); water potential (Ψ) is the same chemical-potential quantity expressed as energy per volume (related through $\mu_w = \mu_w^0 + RT \ln a_w$). Microbial growth tracks (a_w) because every microbe needs sufficient water activity for its enzymes and membranes. The empirical evidence : most bacteria need ($a_w \gtrsim 0.95$); halophiles like *Halobacterium* grow down to (a_w about 0.75) (about 5M NaCl) only because they accumulate compatible solutes – ordinary bacteria lack this and lose water, suffering plasmolysis and arrested metabolism. Reduced (a_w) inhibits cellular processes even in hydrated cells because dependent reactions and forces energetically costly osmolyte accumulation. The boundary the conclusion depends on is solute identity through compatible – solute capacity, not just water content. The field exploiting this is food science/preservation : salting, sugaring, drying and smoking all lower (a_w) below the growth threshold (0.6) are essentially spoilage – proof). See section 2.

Questions — Biological Macromolecules

Instructor Use and Coverage Notes

- Coverage target: Given a molecular feature, infer likely solubility, interaction partners, or cellular role.
- Model/data emphasis: Polymerization energetics and sequence-to-structure reasoning.
- Assessment alignment: Concept Explanation, Statistical Tests and Data Analysis, Argumentation.
- Misconception probe: Structure is not decoration; small chemical changes can redirect function and recognition.
- Transfer product: Explain how a mutation, lipid substitution, or glycosylation change propagates to phenotype.
- Grading focus: award full credit for mechanism, evidence, boundary conditions, and units when a calculation is required.
- Suggested use: draw one recall item, one application item, and one synthesis item when building a short quiz from this bank.

Questions 1–10: Recall and Comprehension

This activity accompanies section 3 of the textbook — review that chapter before attempting the exercises below.

1. Name the four classes of biological macromolecules and list the monomers of each.

Answer (Q1, Recall). The four classes are carbohydrates (monomer: monosaccharides such as glucose), lipids (built from fatty acids and isoprene units – not true covalent polymers; they assemble non-covalently), proteins (monomer: amino acids), and nucleic acids (monomer: nucleotides). Carbohydrates, proteins and nucleic acids are condensation polymers; lipids are the exception, grouped by hydrophobicity rather than a common monomer. See section 3. 2. What is a condensation (dehydration) reaction? What bond is formed when two amino acids condense?

Answer (Q2, Recall). A condensation (dehydration) reaction joins two monomers covalently with the loss of one water molecule per bond (Monomer(1)–OH + H–Monomer(2) (->) Monomer(1)–Monomer(2) + H(2)O); it is endergonic and requires activated monomers and enzyme catalysis. When two amino acids condense, the carboxyl of one reacts with the (alpha)-amino group of the next to form a peptide bond (an amide linkage), releasing water. The reverse reaction, hydrolysis, uses water to cleave the bond. See section 3. 3. Describe the four levels of protein structure. What type of bond holds the primary structure together?

Answer (Q3, Recall). Primary structure is the amino-acid sequence, held together by covalent peptide (amide) bonds (the backbone). Secondary structure is local backbone H-bonded patterns ((alpha)-helix: H-bond between residue (i) and (i)+4, 3.6 residues/turn; (beta)-sheet: H-bonds between adjacent strands). Tertiary structure is the full 3D fold of one chain, stabilized mainly by the hydrophobic effect plus disulfide bonds, salt bridges, H-bonds and van der Waals contacts. Quaternary structure is the assembly of multiple subunits (e.g. hemoglobin (alpha_2beta_2)). Primary structure determines all higher levels (Anfinsen’s dogma). See section 3. 4. What is the difference between α-helix and β-sheet secondary structures? What forces stabilize each?

Answer (Q4, Recall). Both are regular secondary structures stabilized by the same shared force – backbone N–H(…)O = Hydrogen bonds; the difference that changes interpretation is the H – bond geometry. An (alpha)-helix is a single chain coiled so each backbone C = O hydrogen-bond to the N–H four residues ahead ((i – > i)+4), 3.6 residues per turn, giving a compact rod. A (beta)-sheet is formed from extended strands slightly bonded between adjacent strands (parallel or anti-parallel), giving a pleated sheet. So the stabilizing bond type is identical (backbone H – bonds); what differs is whether H – bonding is intra-strand and local (helix) or inter-strand (sheet). See section 3.5. Draw a phospholipid and label the hydrophilic

Answer (Q5, Recall). A phospholipid has a polar (hydrophilic) head – a phosphate group plus a head group such as choline, drawn at the top – joined through a glycerol backbone to two nonpolar (hydrophobic) fatty-acid tails drawn pointing down. Amphipathic (amphiphilic) means the molecule has both a hydrophilic and a hydrophobic region in the same molecule. This dual character is why phospholipids spontaneously self-assemble into bilayers in water (heads facing water, tails sequestered inside) – a thermodynamic consequence of the hydrophobic effect. See section 3. 6. Distinguish saturated from unsaturated fatty acids. How does the degree of saturation affect membrane fluidity?

Answer (Q6, Recall). Both are long-chain carboxylic acids governed by the same packing principle; the difference that changes membrane behavior is the presence of C=C double bonds. Saturated fatty acids (e.g. palmitic 16:0, stearic 18:0) have no double bonds, so their straight chains pack tightly via van der Waals contacts – solid at room temperature and giving rigid, less fluid membranes. Unsaturated fatty acids (e.g. oleic 18:1) contain cis double bonds that introduce a about 30 degree kink, preventing tight packing – liquid at room temperature and increasing membrane fluidity. Thus more unsaturation (and shorter chains) lowers the phase-transition temperature and raises fluidity; this is how organisms homeoviscously adapt membranes to temperature. See section 3. 7. Write the general formula for a monosaccharide. Name three monosaccharides important in biology.

Answer (Q7, Recall). The general formula for a monosaccharide is $CH_2O(n)$ (n typically 3–7; e.g. glucose is $C_6H_{12}O_6$, n = 6). Three biologically important monosaccharides: glucose (the primary fuel hexose), ribose (the aldopentose in RNA, ATP and NAD⁺), and fructose (the ketohexose, fruit sugar and a glycolytic intermediate). Monosaccharides are classified by carbon number (triose, pentose, hexose) and by whether

they bear an aldehyde (aldose) or ketone (ketose). See section 3. 8. What is the difference between α - and β -glycosidic bonds? Give one example of each.

Answer (Q8, Recall). Both link monosaccharides through the same shared covalent linkage – a glycosidic bond at the anomeric carbon – but they differ in the stereochemistry of that anomeric carbon, which changes the polymer’s properties. An (alpha)-glycosidic bond has the anomeric –OH/oxygen below the sugar ring plane (e.g. the (alpha(1->4)) links in starch/glycogen and maltose); chains coil into digestible helices. A (beta)-glycosidic bond has it above the plane (e.g. the (beta(1->4)) links in cellulose and lactose); chains form straight, H-bonded fibrils. The single (alpha)/(beta) difference is why starch is flexible and human-digestible whereas cellulose is rigid and indigestible (humans lack (beta)-glucosidase). See section 3. 9. Define a nucleotide and name its three components. Which nucleotides carry energy?

Answer (Q9, Recall). A nucleotide is the monomer of nucleic acids, consisting of three components: (1) a pentose sugar (ribose in RNA, 2'-deoxyribose in DNA), (2) a nitrogenous base (purine: A or G; pyrimidine: C, T in DNA or U in RNA), and (3) one or more phosphate groups. (Base + sugar alone is a nucleoside.) Nucleotides are linked 3'(->)5' by phosphodiester bonds. The energy-carrying nucleotides are the triphosphates – ATP chiefly, plus GTP, CTP, UTP – whose phosphoanhydride bonds release about 30 kJ/mol on hydrolysis. See section 3. 10. What reagents are used to test for: (a) reducing sugars; (b) starch; (c) protein; (d) lipids?

Answer (Q10, Recall). Standard qualitative food tests: (a) reducing sugars – Benedict’s (or Fehling’s) reagent, which is reduced from blue $\text{Cu}(\text{2+})$ to a brick-red Cu_2O precipitate on heating with a reducing sugar (free aldehyde/ketone). (b) Starch – iodine/potassium iodide solution, which forms a blue-black amylose-iodine complex. (c) Protein – the Biuret test, where peptide bonds chelate $\text{Cu}(\text{2+})$ in alkali to give a violet color. (d) Lipids – the emulsion (ethanol) test (a cloudy white emulsion when alcohol-dissolved sample is added to water) or Sudan III, which stains lipids red. Each reagent reports a specific functional group: free carbonyl, helical polysaccharide, peptide bond, or nonpolar lipid. See section 3.

Questions 11–20: Application and Analysis

11. Cellulose and starch are both glucose polymers, yet starch is digestible by humans and cellulose is not. Explain this difference in terms of glycosidic bond type (α -1,4 vs β -1,4), three-dimensional structure, and the specific enzyme (cellulase) that humans lack.

Answer (Q11, Application). Initiating condition: starch and cellulose are both (beta)-D-glucose vs (alpha)-D-glucose polymers differing only at the anomeric linkage. Changed component: starch uses (alpha(1->4)) glycosidic bonds, cellulose uses (beta(1->4)). Intermediate mechanism: (alpha)-linkages let the chain curl into helices that human salivary/pancreatic (alpha)-amylase (and brush-border maltase) can fit and hydrolyse; (beta)-linkages force each glucose to flip 180 degrees, producing straight chains that hydrogen-bond into rigid, crystalline microfibrils whose geometry no human enzyme active site matches. Observable outcome: starch is digested to glucose and absorbed, while cellulose passes through as indigestible dietary fiber because humans lack a (beta(1->4))-glucosidase (cellulase) – only gut microbiota (or ruminant symbionts) possess it. The whole phenotypic difference flows from one bond’s stereochemistry. See section 3. 12. A protein has T_m (melting temperature) of 55°C in the presence of 8 M urea and 70°C in the absence of denaturant. Identify which types of bonds are disrupted by urea (that are absent from primary structure), and predict whether a disulphide-bonded protein would be denatured by urea alone.

Answer (Q12, Application). Urea (8 M) is a chaotrope that disrupts the non-covalent stabilizing interactions absent from primary structure: hydrogen bonds (secondary structure), the hydrophobic core, van der Waals packing and salt bridges – by competing for H-bonds and improving solvation of nonpolar residues. It does not break covalent peptide bonds (primary structure) or covalent disulfide (–S–S–) bonds. The observable outcome here is a (T_m) lowered from 70 to 55 degrees C: urea destabilises the fold so it melts at a lower temperature. Prediction: a protein cross-linked by disulfide bonds would be only partially denatured by urea alone – secondary/tertiary contacts loosen but the covalently tethered chain cannot fully unfold; complete denaturation also requires a reducing agent (e.g. (beta)-mercaptoethanol or DTT) to cleave the disulfides. See section 3. 13. Collagen is a fibrous protein with a repeating Gly-X-Y motif (X = often Pro; Y = often Hyp). Explain: (a) why Gly must occur every third residue; (b) what modification produces hydroxyproline (Hyp) and which vitamin is required; (c) what disease results from Hyp deficiency.

Answer (Q13, Application). (a) Collagen is a tight triple helix; every third residue sits buried at the helix core where only glycine (R = H) is small enough to fit – any larger side chain would sterically clash and unwind the helix, so Gly must occur every third position (Gly-X-Y). (b) Hydroxyproline (Hyp) is produced by post-translational hydroxylation of proline by prolyl 4-hydroxylase, which requires vitamin C (ascorbate) as a cofactor (reducing the enzyme’s Fe). Hyp’s extra –OH forms interchain hydrogen bonds that stabilize the triple helix. (c) Without vitamin C, prolyl hydroxylase fails, Hyp is deficient, collagen is unstable and poorly cross-linked – the connective-tissue disease scurvy (bleeding gums, poor wound healing, fragile vessels). The causal chain runs: low ascorbate (->) no Pro hydroxylation (->) destabilised collagen triple helix (->) weak connective tissue. See section 3. 14. Phospholipids form bilayers in water. Explain: (a) the thermodynamic basis for bilayer formation (hydrophobic effect); (b) why cholesterol increases membrane rigidity at high temperatures but increases fluidity at low temperatures; (c) how membrane asymmetry (different inner vs outer leaflet composition) is maintained.

Answer (Q14, Application). (a) Bilayer formation is driven by the hydrophobic effect: the amphipathic phospholipids expose polar heads to water

while sequestering nonpolar tails away from water; aggregating the tails releases ordered “cage” water back to bulk, increasing system entropy so ($\Delta G < 0$) and the bilayer self-assembles spontaneously. (b) Cholesterol intercalates with its rigid ring system among the acyl chains: at high temperature it restrains chain motion, reducing fluidity and increasing rigidity; at low temperature it disrupts ordered packing and prevents the chains from crystallising into a gel, so it maintains fluidity – net “homeoviscous” buffering. (c) Membrane asymmetry (outer leaflet PC/sphingomyelin/glycolipids; inner PE/PS/PI) is actively maintained by ATP-dependent flippases and floppases that move specific lipids against their distribution, opposed by slow spontaneous flip-flop (hours–days); scramblases collapse the asymmetry on demand (e.g. PS exposure in apoptosis). See section 3. 15. Compare the structures of DNA and RNA — list at least four differences (sugar, bases, strand number, stability). Explain why RNA is less stable than DNA chemically (relate to the 2'-hydroxyl group).

Answer (Q15, Application). Both store/transmit information via nucleotide polymers (the shared principle); four structural differences change their biological roles: (1) Sugar – DNA uses 2'-deoxyribose, RNA uses ribose (extra 2'-OH). (2) Bases – DNA uses thymine, RNA uses uracil (both keep A, G, C). (3) Strandedness – DNA is typically a double helix (B-form); RNA is usually single-stranded and folds intramolecularly. (4) Stability – DNA is chemically robust; RNA is labile. The mechanism of RNA's instability is the 2'-hydroxyl group: under basic conditions the 2'-OH is deprotonated and acts as an intramolecular nucleophile attacking the adjacent phosphate, cleaving the backbone (a 2',3'-cyclic intermediate). DNA lacks the 2'-OH and so cannot undergo this self-cleavage – which is why DNA is the long-term archive and RNA the short-lived messenger. See section 3. 16. Calculate the number of possible distinct dipeptides from 20 standard amino acids. Then calculate the number of different 100-residue proteins possible. What does this astronomical number imply for protein sequence space and directed evolution?

Answer (Q16, Application). Model: with (k) choices at each of (L) positions, the number of distinct sequences is (k^L) (order matters). Dipeptides: ($20^2 = 400$) possible distinct dipeptides. 100-residue proteins: (20^{100} about 1.27×10^{130}) possible sequences. Sanity check on scale: this dwarfs the number of atoms in the observable universe (about 10^{80}) and is far larger than the about 10^{47} conformations in Levinthal's paradox. Implication: protein sequence space is unsearchably vast, so evolution and directed evolution cannot sample it exhaustively—they explore tiny, functionally connected neighborhoods, and why this is physiologically advantageous.

Answer (Q17, Application). Initiating condition: hemoglobin is an ($\alpha_2\beta_2$) tetramer (quaternary structure); myoglobin-like monomers bind O_2 hyperbolically (Hill (n) = 1). Mechanism: in the tetramer, O_2 binding to one subunit triggers a quaternary T (low-affinity) (\rightarrow) R (high-affinity) conformational shift transmitted through subunit interfaces, so each successive O_2 binds more easily – positive cooperativity, giving a sigmoidal curve and a Hill coefficient (n about 2.8) (>1). Disaggregation into monomers removes the inter-subunit communication, abolishing cooperativity. Physiological advantage: the sigmoidal curve makes hemoglobin a near-switch – it loads O_2 almost fully in the lungs (high pO_2) yet unloads a large fraction in tissues (it releases about 25 % of bound O_2 between arterial 100 mmHg and venous 40 mmHg, versus only about 10 % for a hyperbolic carrier), and the curve is also tunable by H^+ / CO_2 / BPG (Bohr effect) for delivery where metabolic demand is highest. See section 3. 18. A glycoprotein has oligosaccharide chains attached to Asn residues (N-linked glycosylation). Describe: (a) where in the cell N-glycosylation occurs; (b) what enzyme adds the glycan; (c) three functions of glycosylation on cell-surface proteins.

Answer (Q18, Application). (a) N-linked glycosylation begins co-translationally in the lumen of the rough endoplasmic reticulum (a preassembled oligosaccharide is transferred to the nascent chain) and is then trimmed and elaborated in the Golgi apparatus. (b) The transfer is catalysed by oligosaccharyltransferase (OST), which attaches the glycan to the side-chain amide nitrogen of asparagine within the consensus sequon Asn-X-Ser/Thr ($X \neq Pro$). (c) Three functions of cell-surface protein glycosylation: (i) it aids correct folding and quality control (calnexin/calreticulin cycle) and increases solubility/stability and serum half-life; (ii) it mediates cell–cell and cell–matrix recognition and adhesion (e.g. selectin–carbohydrate binding, ABO blood-group antigens); (iii) it serves as receptor/ligand identity and immune recognition (and is exploited by pathogens as attachment sites). See section 3. 19. Lipoproteins (LDL, HDL) are macromolecular complexes of lipid and protein. Explain how their amphipathic structure allows transport of hydrophobic lipids in the aqueous bloodstream. Why does elevated LDL cholesterol increase atherosclerosis risk while elevated HDL is protective?

Answer (Q19, Application). Initiating problem: triacylglycerols and cholesteryl esters are hydrophobic and cannot dissolve in aqueous plasma. Mechanism: lipoproteins solve this with an amphipathic shell – a monolayer of phospholipids (polar heads outward), free cholesterol and apolipoproteins surrounding a hydrophobic core of triglyceride/cholesteryl ester; the polar surface faces blood while the nonpolar cargo stays sequestered inside, exactly the hydrophobic-effect logic of a micelle. Observable outcome: LDL delivers cholesterol to peripheral tissues; when LDL is elevated or oxidised it is taken up by arterial-wall macrophages forming foam cells and atherosclerotic plaques, so high LDL raises atherosclerosis risk. HDL runs reverse cholesterol transport, scavenging excess cholesterol from tissues/plaques (via ABCA1, esterified by LCAT) and returning it to the liver, so high HDL is protective. The apolipoprotein content (apoB-100 on LDL vs apoA-I on HDL) directs which pathway each particle enters. See section 3. 20. A 10-residue peptide contains one disulphide bond between Cys residues. How many possible disulphide bond arrangements are there? Under what cellular conditions do disulphide bonds form (redox potential), and why are they rare in intracellular proteins?

Answer (Q20, Application). Model: with one disulfide bond among (c) cysteines, the number of distinct pairings is (c-

1) when only two Cys exist, but more generally the number of ways to choose one bonded pair from (c) cysteines is $\binom{c}{2}$. For a peptide with exactly two Cys residues, $\binom{2}{2} = 1$... only 1 possible disulfide arrangement (the two Cys must bond each other). If the 10-residue peptide had (c) cysteines forming one bond, there would be $\binom{c}{2}$ choices; e.g. 4 Cys ($\binom{4}{2} = 6$). Conditions: disulfide bonds form under oxidising conditions — the ER lumen (catalysed by protein disulfide isomerase) and the extracellular space, where the redox potential is high.

Questions 21–30: Synthesis and Evaluation

21. Prions are infectious proteins (misfolded PrP^{Sc}) that propagate by templating the misfolding of normal PrP^C. Evaluate the hypothesis that protein conformation can carry infectivity without nucleic acid: what evidence supports it, and what challenges remain for explaining how a protein can act as an infectious agent?

Answer (Q21, Synthesis). Initiating claim: PrP^{Sc} is an infectious agent with no nucleic acid that propagates by templating PrP^C (\rightarrow) PrP^{Sc} misfolding (a conformational, (beta)-sheet-rich conversion). Supporting evidence: infectivity copurifies with protein and survives nucleic-acid-destroying treatments (nucleases, UV) but is abolished by protein-denaturing treatments; PrP-knockout mice are resistant to prion disease and cannot propagate infectivity; *in vitro* protein-misfolding cyclic amplification (PMCA) generates infectious material from pure PrP plus template; strain-specific properties are encoded in distinct PrP^{Sc} conformations. Remaining challenges: explaining the existence of multiple stable, heritable prion “strains” as protein conformers; the molecular basis of the species barrier; how a protein conformation achieves the apparent information capacity normally associated with a genome; and reconciling sporadic vs infectious vs inherited forms. The observable outcome is autocatalytic aggregate growth and neurodegeneration; the conformational-infectivity model fits the evidence but the strain/information problem keeps it incompletely closed. See section 3. 22. Intrinsically disordered proteins (IDPs) lack stable tertiary structure under physiological conditions but are biologically functional. Evaluate the traditional sequence-structure-function paradigm in light of IDPs. What advantages might disorder confer for signaling and regulatory proteins?

Answer (Q22, Synthesis). Initiating premise: the classical paradigm holds sequence (\rightarrow) unique structure (\rightarrow) function. Changed component: about 30–50 % of eukaryotic proteins contain intrinsically disordered regions that have no fixed tertiary structure yet are functional, refuting the paradigm’s universality. Mechanism of function: IDRs exist as dynamic conformational ensembles and often undergo coupled folding-and-binding, folding only upon contacting a partner. Observable advantages for signaling/regulatory proteins: (i) promiscuous, one-to-many binding – a single IDR can engage many different partners (hub proteins in signaling networks); (ii) large interaction surface from a short sequence and fast “fly-casting” association kinetics; (iii) dense clustering of regulatory post-translational-modification sites (phosphorylation) enabling rapid, tunable switching; (iv) capacity for multivalent weak interactions driving liquid–liquid phase separation into membraneless condensates. Conclusion: structure-function must be generalized to “sequence encodes a functional ensemble,” not necessarily a single fold; the risk is aggregation/disease (tau, (alpha)-synuclein) when disorder is mismanaged. See section 3. 23. Silk fibroin is a β -sheet-rich protein with extraordinary material strength (tensile strength 0.5 GPa). Explain, at the inter-molecular level, why β -sheet stacking produces this strength. Compare to collagen’s triple helix and synthetic Kevlar (also a β -sheet polymer). Design a biotechnology experiment to engineer silk with improved elasticity by incorporating glycine-rich loops.

Answer (Q23, Synthesis). Initiating structure: silk fibroin is dominated by stacked antiparallel (beta)-sheets of poly(Gly-Ala/Ser) in crystalline domains. Mechanism of strength: within a sheet, backbone runs are tied by dense inter-strand hydrogen bonds; between sheets, the small Gly/Ala side chains allow tight stacking held by van der Waals contacts. Load is borne along covalent backbones while H-bonds resist shear, and the many cooperative weak bonds summate to high tensile strength (about 0.5 GPa); amorphous Gly-rich linkers between crystallites add extensibility. Comparison: collagen achieves strength differently – a covalent, H-bonded triple helix cross-linked between molecules (stiff, tension-bearing in tendon); Kevlar is a synthetic poly-aramid whose extended H-bonded (beta)-sheet-like sheets give analogous strength, validating the “stacked H-bonded sheet” design. Engineering experiment: clone a recombinant spidroin/fibroin gene, insert additional Gly-rich elastic loop motifs between crystalline blocks, express in *E. coli* or transgenic host, spin fibers, and compare tensile strength vs elongation-at-break and toughness against wild-type fiber (control), expecting increased elasticity at some cost to stiffness. See section 3. 24. Deep-sea bacteria living at 110°C require heat-stable enzymes (thermozymes). Propose three molecular-level strategies these organisms use to maintain enzyme structure at extreme temperatures (consider ion pairs, proline residues, hydrophobic packing, and disulphide bonds). How might you engineer a mesophilic enzyme for thermostability using directed evolution?

Answer (Q24, Synthesis). Initiating condition: enzymes from hyperthermophiles must keep a folded, active tertiary/quaternary structure at 110 degrees C. Three molecular strategies (more stabilizing interactions, fewer destabilising ones): (1) More ion pairs/salt-bridge networks (Asp/Glu with Lys/Arg), which are strongly stabilizing and become relatively more important at high temperature. (2) Increased rigidity of the backbone – more proline residues in loops and fewer glycines (proline restricts ϕ , lowering conformational entropy of the unfolded state), plus shortened/anchored loops. (3) Tighter hydrophobic-core packing and, where compartment redox allows, extra disulfide bonds, raising the hydrophobic and van der Waals contribution to (ΔG_{fold}). (Oligomerisation and reduced surface area also help.) Engineering a mesophilic enzyme for thermostabil-

ity by directed evolution: random/mutagenic PCR or DNA shuffling to build a variant library, then screen/select survivors after a heat challenge (assay residual activity after incubation at progressively higher temperature), iterate over many rounds enriching for stabilizing substitutions while monitoring retained (k_{cat}/K_m). See section 3. 25. Glycolipids in the outer leaflet of the plasma membrane act as cell-surface recognition molecules (blood type antigens, pathogen receptors). Evaluate the claim that carbohydrate diversity makes carbohydrates better suited than proteins for cell-surface diversity. Consider information content per unit mass (number of possible trisaccharides vs tripeptides from their respective monomer sets).

Answer (Q25, Synthesis). Initiating claim: carbohydrate diversity makes glycans better suited than proteins for cell-surface coding. Mechanism: monosaccharides can link at multiple hydroxyls, in (alpha) or (beta) configuration, and branch, whereas amino acids join only head-to-tail by one peptide bond. Quantitative comparison of information per unit: from about 20 amino acids the number of tripeptides is ($20^3 = 8000$) (linear only); from a comparable monosaccharide set, the number of distinct trisaccharides is far larger because each glycosidic link has a choice of linkage position and anomeric configuration and the structure can branch – estimates run into the (10^4)–(10^6) range for trisaccharides, vastly exceeding tripeptides. Observable outcome: glycans pack more recognition information into small, surface-exposed structures, which is why blood-group antigens, selectin ligands and pathogen-receptor epitopes are carbohydrate-based. Boundary condition: proteins still dominate where catalytic chemistry or precise folding is required; glycans win specifically for combinatorial surface recognition. See section 3. 26. Amyloid plaques (β -sheet-rich aggregates of A β peptide) are associated with Alzheimer’s disease. Evaluate the “amyloid cascade hypothesis” citing: (a) the evidence for A β oligomers (not fibrils) as the toxic species; (b) why therapeutic targeting of A β aggregation has largely failed clinically; (c) an alternative hypothesis involving tau protein.

Answer (Q26, Synthesis). Initiating model: the amyloid cascade hypothesis posits A(beta) (a (beta)-sheet-rich aggregate from APP processing) as the upstream cause of Alzheimer’s. (a) Evidence that soluble A(beta) oligomers, not insoluble fibrils/plaques, are the toxic species: oligomer (not plaque) load correlates better with cognitive decline; synthetic and brain-derived oligomers impair synaptic plasticity (LTP) and are neurotoxic at low concentrations; plaque burden can be high in cognitively normal individuals. (b) Anti-A(beta) therapeutics have largely failed clinically because intervention may come too late (downstream tau pathology already self-propagating), drugs clear fibrils/plaques without removing toxic oligomers, target the wrong A(beta) species/dose, or the hypothesis over-weights A(beta) as the sole driver; recent amyloid-clearing antibodies give only modest slowing. (c) Alternative: tau – hyperphosphorylated tau forming neurofibrillary tangles correlates more tightly with neuron loss and cognitive stage and may be the principal effector, with A(beta) an upstream trigger or parallel factor. Conclusion: the cascade is best read as A(beta)-initiated but tau-executed, with oligomers the proximal toxin. See section 3. 27. Design a protein engineering strategy to convert an enzyme that uses NADH as cofactor to one that uses NADPH. Identify the specific residues in the coenzyme-binding pocket that differ between NADH-specific and NADPH-specific enzymes, and describe what mutations you would introduce. What selection pressure would you use in directed evolution?

Answer (Q27, Synthesis). Hypothesis: swapping the cofactor specificity from NADH to NADPH requires re-engineering the dinucleotide-binding pocket to accommodate the extra 2’-phosphate of NADPH. Mechanistic basis: NADH- and NADPH-specific enzymes differ chiefly at residues contacting the adenosine 2’ position. NADH (NAD(⁺))-specific Rossmann-fold enzymes typically place an acidic Asp/Glu that hydrogen-bonds the 2’-OH and electrostatically *excludes* the 2’-phosphate; NADPH-specific enzymes instead present basic/neutral residues (Arg, Ser, Thr) that favorably bind the negatively charged 2’-phosphate. Mutations to introduce: remove the discriminating acidic residue (e.g. Asp(->)Ala/Gly) and add positively charged or H-bonding residues (introduce Arg/Ser/Thr) in the 2’ subsite to create a phosphate-binding pocket; adjust adjacent loop length for steric fit. Directed-evolution selection: build a saturation/library at these positions and apply a selective pressure that links growth or signal to NADPH-dependent turnover (e.g. a host strain or screen in which only NADPH-utilizing variants generate the assayable product), screening for high (k_{cat}/K_m) with NADPH while measuring loss of NADH activity as the falsifying control. See section 3. 28. RNA aptamers can fold into three-dimensional structures that specifically bind proteins (like antibodies but made of RNA). Compare RNA and protein as molecular recognition scaffolds: evaluate the structural repertoire (functional groups available, backbone rigidity, available secondary structures) of each, and explain why protein antibodies have been preferred over RNA aptamers clinically, and what advantages aptamers offer in terms of synthesis and immunogenicity.

Answer (Q28, Synthesis). Both fold into 3D shapes that present a complementary binding surface (the shared recognition principle); the difference that changes interpretation is chemical repertoire and backbone properties. RNA aptamers: built from only 4 nucleotides – limited side-chain chemistry (mostly H-bonding faces, aromatic stacking, a charged phosphate backbone, occasional metal/2’-OH catalysis), but they fold via stems, loops, bulges and pseudoknots into pockets; advantages are fully chemical (SELEX) synthesis, easy modification, low immunogenicity and reversibility. Protein antibodies: 20 amino acids give far richer functional-group diversity (acid/base, hydrophobic, aromatic, metal-binding) and a more rigid, hypervariable loop scaffold (CDRs), generally yielding higher-affinity, more specific binders. Clinically antibodies have been preferred because of this affinity/specificity, mature production platforms and long serum half-life, whereas aptamers historically suffered rapid nuclease degradation and renal clearance. Aptamers’ offsetting advantages: cheap chemical synthesis, no cell culture, low immunogenicity, and easy chemical stabilization/conjugation. See section 3. 29. Polyhydroxyalkanoates (PHAs) are bacterial polyesters (biological plastics). Compare their biosynthesis

pathway and polymer chemistry to triacylglycerides (TAGs) — which also function as carbon storage molecules in animals. Evaluate whether PHAs could replace petroleum-derived plastics industrially, considering degradation rates, production cost, and material properties.

Answer (Q29, Synthesis). Initiating comparison: PHAs are bacterial polyesters (e.g. poly-3-hydroxybutyrate) made by polymerizing hydroxyacyl-CoA units via PHA synthase into intracellular carbon/energy storage granules; TAGs are tri-esters of glycerol and three fatty acids, the animal carbon/energy store, built by sequential acyltransferase esterification. Shared chemistry: both use ester bonds and store reduced carbon; difference: PHA is a true high-molecular-weight backbone polyester (a thermoplastic), whereas TAG is a small-molecule lipid (no polymer backbone), reflecting different biosynthetic logic (chain polymerization vs glycerol acylation). Evaluation as a plastic substitute: PHAs are genuinely biodegradable (hydrolysed by environmental depolymerases, unlike petroleum polyolefins) and have useful thermoplastic mechanical properties, but production cost is high (fermentation feedstock and downstream recovery), yields and material properties (brittleness of PHB, slow/variable degradation in marine vs compost conditions) limit large-scale displacement of cheap petroleum plastics. Conclusion: technically viable and environmentally favorable, but currently constrained by economics and property tuning rather than chemistry. See section 3. 30. The hydrophobic core of most globular proteins contains residues with about 15–30% exposed surface area. Propose and critically evaluate three evolutionary forces that have driven the formation of the hydrophobic core: (a) thermodynamic stability; (b) protection of reactive centers; (c) evolutionary constraint on folding kinetics. Use a specific example (e.g., cytochrome c, lysozyme) to ground your argument.

Answer (Q30, Synthesis). Initiating observation: globular-protein cores bury nonpolar residues with only 15–30 % surface exposure. Mechanism and three evolutionary forces: (a) Thermodynamic stability – burying nonpolar surface drives the hydrophobic effect, the dominant favorable term in (ΔG_{fold}) ((-300) to (-1000) kJ/mol), so a well-packed core is what makes the marginal net (ΔG_{fold}) ((-20) to (-60) kJ/mol) negative; e.g. in lysozyme/cytochrome c, mutating a buried Ile(->)Ala (losing about 70 Å² of nonpolar surface) measurably destabilises the fold. (b) Protection of reactive centers – sequestering the haem of cytochrome c (or catalytic groups) from bulk solvent tunes redox potential and shields cofactors/intermediates from unwanted hydrolysis or oxidation. (c) Folding-kinetics constraint – a defined hydrophobic core nucleates rapid collapse and channels folding down the funnel (resolving Levinthal's paradox), so cores are also selected for foldability, not only end-state stability. Critical evaluation: (a) is the strongest and best-evidenced driver; (b) and (c) are real but secondary and partly consequences of (a). The example (cytochrome c) shows all three acting together: a packed core that is simultaneously stable, protects the haem, and folds reliably. See section 3.

Questions — Enzymes and the Kinetics of Catalysis

Instructor Use and Coverage Notes

- Coverage target: Infer Vmax, Km, or inhibition type from data and justify the mechanistic interpretation.
- Model/data emphasis: Michaelis-Menten, Lineweaver-Burk, and inhibition-pattern calculations.
- Assessment alignment: Concept Explanation, Statistical Tests and Data Analysis, Argumentation.
- Misconception probe: A catalyst changes rate, not the equilibrium constant or the sign of delta G.
- Transfer product: Apply enzyme-kinetic reasoning to drug dosing, metabolic control, or diagnostic assays.
- Grading focus: award full credit for mechanism, evidence, boundary conditions, and units when a calculation is required.
- Suggested use: draw one recall item, one application item, and one synthesis item when building a short quiz from this bank.

Questions 1–10: Recall and Comprehension

This activity accompanies section 4 of the textbook — review that chapter before attempting the exercises below.

1. Define an enzyme. What type of macromolecule are most enzymes? Name one exception.

Answer (Q1, Recall). An enzyme is a biological catalyst that accelerates a chemical reaction (by factors of about $10^{(6-10^{23})}$) without being consumed and without changing the reaction's equilibrium or (ΔG); it works by lowering the activation energy (ΔG^{\ddagger}). Most enzymes are proteins. The principal exception is ribozymes – catalytic RNA molecules (e.g. the peptidyl-transferase activity of the ribosome's 23S rRNA, RNase P, self-splicing introns). See section 4. 2. What is the active site? Explain the induced fit model.

Answer (Q2, Recall). The active site is the small region of the enzyme (only about 1–10 % of its surface) where substrate binds and catalysis occurs; it is lined by specific catalytic and binding residues and is geometrically/chemically complementary to the transition state more than to the substrate. The induced-fit model (Koshland, 1958) states that the active site is not rigid: substrate binding induces a conformational change in the enzyme that moulds the site around the substrate, improving complementarity to the transition state. (Hexokinase closing its two lobes around glucose, excluding water, is the classic example.) See section 4. 3. Define activation energy (E_a). How does an enzyme reduce E_a without altering ΔG of the reaction?

Answer (Q3, Recall). Activation energy (E_a or (ΔG^{\ddagger})) is the free-energy barrier between the ground state and the transition state that must be surmounted for reactants to become products ($\text{Rate} = (A \cdot e^{-\Delta G^{\ddagger}/RT})$). An enzyme lowers (ΔG^{\ddagger}) by providing an alternative reaction pathway – chiefly by binding and stabilizing the transition state more tightly than substrate, plus proximity/orientation, acid-base, covalent, metal-ion and electrostatic catalysis. Crucially it stabilizes the transition state of both forward and reverse reactions equally, so the ground-state energies of reactants and products are unchanged: (ΔG) and (K_{eq}) are unaffected – only the rate (kinetics) increases. See section 4. 4. What are Michaelis-Menten kinetics? Define K_m and V_{max} .

Answer (Q4, Recall). Michaelis-Menten kinetics describe a single-substrate enzyme via ($v_0 = \frac{V_{max}[S]}{K_m + [S]}$), a rectangular hyperbola derived under the steady-state assumption for $E + S \rightleftharpoons ES \rightarrow E + P$. (V_{max}) is the maximum velocity reached when enzyme is saturated with substrate ($(V_{max} = k_{cat}[E]_T)$). (K_m) (the Michaelis constant, $= (k_{-1} + k_2)/k_1$) is the substrate concentration at which ($v_0 = V_{max}/2$); a low (K_m) indicates high apparent substrate affinity. See section 4.5. Write the Michaelis – Mentenequation. At $S = K_m$, what fraction of V_{max} is achieved?

Answer (Q5, Recall). The Michaelis-Menten equation is ($v_0 = \frac{V_{max} [S]}{K_m + [S]}$). At $S = (K_m)$, substitute $[S] = K_m$: ($v_0 = \frac{V_{max} K_m}{K_m + K_m} = \frac{V_{max} K_m}{2K_m} = \frac{V_{max}}{2}$). So when the substrate concentration equals (K_m), the enzyme runs at exactly one-half of (V_{max}) – which is the operational definition of (K_m) and a useful biological check that an assay is in the expected range. See section 4.6. Distinguish competitive, non-competitive, and uncompetitive inhibition. Which type changes K_m ? Which changes V_{max} ?

Answer (Q6, Recall). All three are reversible inhibitors; the difference that changes interpretation is *what the inhibitor binds*. A competitive inhibitor resembles substrate and binds free enzyme at the active site (mutually exclusive with S): apparent (K_m) increases, (V_{max}) unchanged (overcome by high S). A pure non-competitive inhibitor binds an allosteric site on both E and ES equally: (K_m) unchanged, (V_{max}) decreased. An uncompetitive inhibitor binds only the ES complex: both (K_m) and (V_{max}) decrease proportionally (parallel Lineweaver-Burk lines). So competitive changes (K_m) only; non-competitive changes (V_{max}) only; uncompetitive changes both. See section 4. 7. What is a coenzyme? Name two vitamins that serve as coenzymes.

Answer (Q7, Recall). A coenzyme is a small organic non-protein molecule that binds an enzyme (the apoenzyme) to form the active holoenzyme and participates in catalysis by carrying chemical groups or electrons (e.g. transferring hydride, acyl, or amino groups); it is regenerated each cycle. Most water-soluble B vitamins are coenzyme precursors. Two examples: niacin (vitamin B3) is the precursor of NAD⁽⁺⁾/NADH (hydride transfer),

and riboflavin (vitamin B2) is the precursor of **FAD/FADH₂** (hydride/electron transfer). (Others: B1(->)TPP, B5(->)CoA, B6(->)PLP.) See section 4. 8. What is an allosteric enzyme? How does cooperativity affect the v vs **S** curve shape?

Answer (Q8, Recall). An allosteric enzyme is a (usually multi-subunit) enzyme whose activity is regulated by ligands binding at sites distinct from the active site, and that does not obey simple Michaelis-Menten kinetics. Because substrate binding to one subunit changes the affinity of the others (cooperativity), the velocity-versus-**S** curve is sigmoidal rather than hyperbolic (Hill coefficient (n) > 1 for positive cooperativity). This sigmoidal shape gives switch-like behavior: a small change in **S** near (K_{0.5}) produces a large change in activity, enabling sharp metabolic regulation (e.g. ATCase, phosphofructokinase). See section 4. 9. Define feedback inhibition (product inhibition) and give one example from a metabolic pathway.

Answer (Q9, Recall). Feedback (end-product) inhibition is a regulatory mechanism in which the final product of a metabolic pathway acts as an allosteric inhibitor of an early, committed enzyme in that same pathway, so the pathway switches itself off when enough product has accumulated – preventing wasteful overproduction. Classic example: CTP, the end product of pyrimidine biosynthesis, allosterically inhibits aspartate transcarbamoylase (ATCase), the enzyme catalysing the first committed step (and ATP activates it, balancing purine/pyrimidine supply). Another: isoleucine inhibits threonine deaminase in its own synthesis pathway. See section 4. 10. How does temperature affect enzyme activity? Name two effects of extreme temperatures on enzyme function.

Answer (Q10, Recall). Initiating condition: raising temperature increases molecular kinetic energy. Mechanism: by the Arrhenius equation (k = A.e^{-E_a/RT}), higher (T) gives more molecules with energy (>= E_a) and more frequent productive collisions, so rate rises ((Q₁₀ about 2): roughly doubling per 10 degrees C). Outcome at extremes: (1) above the optimum temperature, the heat disrupts the non-covalent bonds holding tertiary/quaternary structure, causing denaturation – the active site loses its shape and activity falls sharply (irreversibly for most enzymes); (2) at very low temperature, molecular motion and collision frequency are too low, so the enzyme is nearly inactive (though not denatured – activity returns on warming). Net: a bell-shaped activity-temperature curve peaking near the organism’s physiological temperature (about 37 degrees C for human enzymes). See section 4.

Questions 11–20: Application and Analysis

11. An enzyme has K_m = 2 mM and V_{max} = 10 μmol/min. Calculate the reaction rate at **S** = 1 mM, 2 mM, and 10 mM. What does the saturation behavior tell you about enzyme kinetics?

Answer (Q11, Application). Model: $(v_0 = \frac{V_{max}[S]}{K_m + [S]})$ with (K_m = 2)mM, (V_{max} = 10)μmol/min. At **S** = 1 mM: $(v_0 = \frac{10 \times 1}{2 + 1} = \frac{10}{3} = 3.33)\mu\text{mol/min}$ (33% of (V_{max})). At **S** = 2 mM (= (K_m)): $(v_0 = \frac{10 \times 2}{2 + 2} = 5.0)\mu\text{mol/min}$ (exactly 50% of (V_{max})). At **S** = 10 mM: $(v_0 = \frac{10 \times 10}{2 + 10} = \frac{100}{12} = 8.33)\mu\text{mol/min}$ (83% of (V_{max})). Interpretation : rate rises steeply when **S** < (K_m) but flattens as **S** >> K_m – the enzyme saturates because all active sites become occupied, so velocity asymptotically approaches (V_{max}) and cannot exceed it no matter how much substrate. 50μM (use the relationship $K_m^{app} = K_m(1 + I/K_i)$).

Answer (Q12, Application). Model for competitive inhibition: $(K_m^{app} = K_m(1 + \frac{[I]}{K_i}))$. Substitute (K_m = 2)mM, (K_m^{app} = 8)mM, **I** = 50μM = 0.05mM. $(\frac{8}{2} = 1 + \frac{0.05}{K_i} \Rightarrow 4 = 1 + \frac{0.05}{K_i} \Rightarrow \frac{0.05}{K_i} = 3 \Rightarrow K_i = \frac{0.05}{3} = 0.0167\text{ mM})$ About 17 μM. Check : (V_{max}) is unchanged (10μmol/min), consistent with competitive inhibition (inhibitor raises apparent (K_m) but high **S** still reaches the same (V_{max})). A (K_m = 2) rather than hyperbolic Michaelis–Menten kinetics. Explain what the Hill coefficient indicates about subunit cooperativity and how CTP (the end product) acts.

Answer (Q13, Application). Initiating condition: ATCase is a multi-subunit allosteric enzyme, so it gives a sigmoidal (v)-vs-**S** curve, not a hyperbola. The Hill coefficient (n about 2) quantifies positive homotropic cooperativity – binding of aspartate to one catalytic subunit raises the substrate affinity of the others ((n) > 1; (n) = 1 would mean no cooperativity, (n) < 1 negative cooperativity). Mechanistically, substrate binding shifts the T (low-affinity) ⇌ R (high-affinity) quaternary equilibrium toward R. CTP, the pathway end-product, is a heterotropic allosteric inhibitor: it binds the regulatory subunits (distinct from the active site), stabilizing the T state, lowering aspartate affinity and shifting the sigmoidal curve to the right (raising (K_{0.5})). Observable outcome: feedback inhibition that throttles pyrimidine synthesis when CTP is abundant (ATP, binding the same regulatory sites, does the opposite and activates). See section 4. 14. Temperature doubles reaction rates approximately every 10°C (Q₁₀ ≈ 2). However, above an optimal temperature, enzyme rate drops sharply. Explain: (a) why the Arrhenius relationship predicts increasing rate with temperature; (b) why denaturation overrides this above T_{opt}; (c) how thermophilic enzymes (T_m > 80°C) avoid denaturation.

Answer (Q14, Application). (a) By the Arrhenius equation (k = A.e^{-E_a/RT}), increasing (T) increases the fraction of molecules with energy (>= E_a) and the collision frequency, so the catalytic rate rises ((Q₁₀ about 2)). (b) Above the optimum temperature this kinetic gain is overridden

because heat supplies enough energy to break the weak non-covalent interactions (H-bonds, hydrophobic packing, salt bridges) that maintain tertiary/quaternary structure: the enzyme denatures, the active-site geometry is destroyed, and activity collapses despite the higher temperature – so net activity peaks at (T_{opt}) then falls sharply. (c) Thermophilic enzymes ($T_m > 80$ degrees C, e.g. Taq, Pfu polymerase) resist denaturation through extra salt-bridge networks, a tightly packed compact hydrophobic core, more proline (rigidifying loops) and fewer flexible glycines, and sometimes additional disulfide bonds – all raising the free energy needed to unfold. See section 4. 15. A Lineweaver-Burk (double-reciprocal) plot for enzyme X gives a y-intercept of $0.1 \mu\text{mol}^{-1} \cdot \text{min}$ and x-intercept of -0.5 mM^{-1} . Calculate V_{max} and K_m . If an inhibitor shifts the x-intercept to -0.25 mM^{-1} without changing the y-intercept, what type of inhibition is this?

Answer (Q15, Application). From the Lineweaver-Burk plot ($\frac{1}{v_0} = \frac{K_m}{V_{max}} \frac{1}{[S]} + \frac{1}{V_{max}}$) : they-intercept = $(1/V_{max}) = 0.1 \mu\text{mol}^{-1} \cdot \text{min}$, so ($V_{max} = 1/0.1 = 10 \text{ mmol/min}$). The x-intercept = $(-1/K_m) = (-0.5) \text{ mM}^{-1}$, so ($K_m = 1/0.5 = 2 \text{ mM}$). Withinhibitor the x-intercept moves to $(-0.25) \text{ mM}^{-1}$, i.e. apparent (K_m) rises to $(1/0.25 = 4) \text{ mM}$, while the y-intercept (V_{max}) is unchanged. Unchanged (V_{max}) with increased apparent (K_m) (lines crossing on the y-axis) is the signature of competitive inhibition – the inhibitor competes for the active site but can be out-competed by high S . See section 4.16. Aconitase, an enzyme starved, aconitase activity is abolished. Explain : (a) the likely role of Fe^{2+} in the active site mechanism; (b) why iron starvation globally affects energy metabolism; (c) chelating siderophores restore enzyme function.

Answer (Q16, Application). (a) Aconitase carries a $[4\text{Fe-4S}]$ iron-sulfur cluster in its active site; the catalytic Fe atom acts as a Lewis acid that coordinates and polarizes the substrate (citrate \rightarrow isocitrate via cis-aconitate), positioning the hydroxyl/water for the dehydration-rehydration isomerisation. Without iron the cluster cannot assemble, so the active site is non-functional. (b) Aconitase is a TCA-cycle enzyme; iron starvation also cripples other Fe-dependent enzymes (succinate dehydrogenase, cytochromes of the electron transport chain), so citrate cannot be processed and NADH/FADH₂ production and oxidative phosphorylation fail – energy metabolism is globally impaired (and apo-aconitase even moonlights as an iron-regulatory RNA-binding protein). (c) Bacteria secrete high-affinity siderophores that chelate scarce environmental Fe^{3+} ; the ferri-siderophore is imported and the iron released intracellularly, restoring $[4\text{Fe-4S}]$ cluster assembly and aconitase (and respiratory) function. See section 4. 17. Isoenzymes (isozymes) are distinct enzymes that catalyse the same reaction but have different kinetic properties. Hexokinase ($K_m \text{ glucose} = 0.1 \text{ mM}$) and glucokinase/hexokinase IV ($K_m \text{ glucose} = 10 \text{ mM}$) both catalyse glucose phosphorylation. Explain why the liver expresses high- K_m glucokinase rather than low- K_m hexokinase and how this enables hepatic glucose buffering post-meal.

Answer (Q17, Application). Initiating condition: liver must buffer blood glucose, which swings widely after meals. Mechanism: low- (K_m) hexokinase (K_m about 0.1 mM) is essentially saturated at all physiological glucose levels, so its rate is nearly constant and it is product-inhibited by glucose-6-phosphate – it cannot ramp up uptake when blood glucose spikes. High- (K_m) glucokinase (hexokinase IV, (K_m about 10 mM) operates on the steep, unsaturated part of its (v)-vs- S curve over the physiological range, so its rate scales with blood glucose and it is not inhibited by G6P. Observable outcome: after a meal, rising portal glucose proportionally accelerates hepatic glucokinase, phosphorylating glucose and trapping it for glycogen synthesis; between meals, low glucose means low glucokinase flux, sparing glucose for export to the brain. Thus the liver's choice of a high- (K_m) isozyme makes it a concentration-responsive glucose buffer. See section 4. 18. Serine proteases (trypsin, chymotrypsin, elastase) use the catalytic triad Ser-His-Asp. Explain the mechanism: how does the His residue act as a proton acceptor/donor, how does Ser become a nucleophile, and how does the oxyanion hole stabilize the tetrahedral intermediate?

Answer (Q18, Application). Serine proteases hydrolyse peptide bonds using the Ser-His-Asp catalytic triad and an oxyanion hole. Mechanism: (1) Asp orients and electrostatically stabilizes His; His acts as a general base, abstracting the proton from the Ser –OH, which converts Ser into a powerful nucleophile. (2) The Ser alkoxide attacks the substrate's carbonyl carbon, forming a negatively charged tetrahedral intermediate; the developing oxyanion is stabilized by H-bonds from backbone amides in the oxyanion hole, lowering (ΔG^\ddagger). (3) His donates its proton (now a general acid) to the leaving amine, releasing the first product and leaving a covalent acyl-enzyme intermediate. (4) Water, activated by His acting again as a general base, hydrolyses the acyl-enzyme through a second tetrahedral intermediate, releasing the carboxylic-acid product and regenerating free enzyme. His thus shuttles protons (base then acid), Ser provides the nucleophile, and the oxyanion hole stabilizes both tetrahedral transition states. See section 4. 19. Ribozymes are RNA enzymes that catalyse phosphodiester bond cleavage. Compare ribozyme catalytic mechanisms to protein enzyme mechanisms: what functional group strategies can RNA use that proteins cannot (and vice versa)? What does the existence of ribozymes tell us about the origin of life?

Answer (Q19, Application). Both ribozymes and protein enzymes lower (ΔG^\ddagger) by binding/orienting substrates and stabilizing the transition state (shared principle); the difference is the chemical toolkit. RNA has only four bases – limited side-chain chemistry – so ribozymes rely heavily on metal-ion catalysis (Mg^{2+}), in-line geometry, the 2'-OH as nucleophile/general acid-base, and shifted base pK_a values (e.g. cytosine acting as a general acid in the hepatitis delta ribozyme); they excel at phosphoryl-transfer/phosphodiester chemistry but are slower and chemically narrower. Proteins have 20 side chains spanning acidic, basic, nucleophilic, hydrophobic and metal-binding groups, giving far greater catalytic versatility and rate. The decisive point: the existence of ribozymes (including the ribosome's peptidyl transferase being rRNA) shows RNA can be both genetic

information carrier and catalyst, strong support for the RNA World hypothesis – RNA could have catalysed its own replication before proteins and DNA evolved. See section 4. 20. Suicide (mechanism-based) inhibitors permanently inactivate enzymes by forming covalent bonds after being processed by the enzyme's active site. Give a specific clinical example of a suicide inhibitor and explain, step-by-step, how it inactivates the target enzyme. Why are suicide inhibitors more selective than reversible inhibitors?

Answer (Q20, Application). A suicide (mechanism-based) inhibitor is a substrate analog that is chemically inert until the target enzyme begins to process it; the enzyme's own catalytic chemistry converts it into a reactive species that then forms a covalent bond with an active-site residue, permanently inactivating the enzyme. Step-by-step example – penicillin on bacterial transpeptidase: (1) penicillin's (beta)-lactam ring mimics the D-Ala–D-Ala terminus of the peptidoglycan substrate and enters the active site; (2) the active-site serine attacks the strained (beta)-lactam carbonyl as it would the normal substrate; (3) this opens the ring and forms a stable covalent acyl-enzyme that cannot be hydrolysed, irreversibly blocking cell-wall cross-linking, so the bacterium lyses. Suicide inhibitors are more selective than ordinary reversible inhibitors because they require the *target enzyme's specific catalytic activity* to become reactive – they remain harmless toward non-target proteins that cannot process them, minimizing off-target effects. See section 4.

Questions 21–30: Synthesis and Evaluation

21. Aspirin (acetylsalicylate) irreversibly inhibits COX-1 and COX-2 by acetylating Ser530 in the active site. Evaluate: (a) why aspirin's anti-platelet effect lasts 7–10 days (the lifetime of a platelet); (b) how selective COX-2 inhibitors (celecoxib) were designed to reduce GI side effects; (c) the unexpected cardiovascular risk of COX-2 inhibitors detected primarily after clinical deployment.

Answer (Q21, Synthesis). Empirical evidence to separate from judgment: aspirin irreversibly acetylates Ser530 in cyclooxygenase, and platelets lack a nucleus so cannot synthesize new COX. (a) Because inhibition is covalent/irreversible and platelets cannot replace the enzyme, a single dose silences platelet COX-1 for the entire about 7–10 day platelet lifespan, restoring thromboxane synthesis only as new platelets are made – the basis of low-dose aspirin's lasting antiplatelet effect. (b) Selective COX-2 inhibitors (celecoxib) were designed by exploiting a larger side-pocket in COX-2's active site, sparing COX-1-dependent gastric prostaglandins and thus reducing GI bleeding/ulceration. (c) The boundary condition that changed the conclusion: blocking COX-2 also suppressed endothelial prostacyclin (vasodilatory/antithrombotic) while leaving platelet COX-1-derived thromboxane intact, tipping the haemostatic balance toward thrombosis – an increased cardiovascular risk detected only in large post-marketing trials (rofecoxib withdrawal). The lesson: a selectivity benefit established in one tissue did not generalize once tested system-wide. See section 4. 22. Design an enzyme engineering experiment to improve the K_m of an industrial enzyme for a non-natural substrate. Describe: the rational design approach using structural data; the directed evolution approach; how you would screen large variant libraries; how a BRENDA entry and a KEGG/BioCyc pathway map would constrain the evidence record; and how you would verify that the improved K_m reflects genuine active-site affinity changes vs changes in protein stability.

Answer (Q22, Synthesis). Hypothesis: targeted active-site mutations (rational design) and/or directed evolution can lower (K_m) for a non-natural substrate by improving active-site complementarity to that substrate's transition state. Rational approach: use the crystal/AlphaFold structure docked with the non-natural substrate to identify residues lining the binding pocket that clash with or fail to contact it; introduce specific substitutions (site-directed mutagenesis) to add complementary H-bonds/shape. Directed-evolution approach: build a large variant library by error-prone PCR/DNA shuffling/saturation mutagenesis at pocket residues. Screening: high-throughput screen or growth-coupled selection where activity on the non-natural substrate is linked to a measurable signal (colorimetric/fluorogenic product or survival), iterate over rounds. Source constraint: use BRENDA to record the EC number, organism, assay conditions, ligand identity, and kinetic values; use KEGG/BioCyc to check whether the engineered reaction fits the pathway context or creates an unsupported pathway claim [Hauenstein et al., 2026, Kanehisa Laboratories, 2026, SRI International, 2026]. Controls and the decisive distinction: to confirm an improved (K_m) reflects genuine active-site affinity rather than mere stabilization, measure full Michaelis-Menten parameters ((k_{cat}) , (K_m), (k_{cat}/K_m)) under identical conditions, compare $(T_m)/(T_{50})$ and expression yield of variant vs wild type, and test that improvement is substrate-specific (no parallel gain on the native substrate) – a stability-only change would raise (T_m) without selectively improving (K_m) for the target substrate. Falsifying result: improved survival but no change in measured (K_m) on purified enzyme. See section 4. 23. Enzyme kinetics assumes a well-mixed, dilute environment. However, intracellular enzymes operate in a crowded, compartmentalised environment with local S quite different from bulk cytoplasm. Evaluate three ways that molecular crowding alters effective K_m and V_{max} in vivo vs in vitro measurements, and propose an experimental strategy to measure kinetics in a crowded environment.

Answer (Q23, Synthesis). Initiating condition: classical $(K_m)/(V_{max})$ are measured in dilute, well-mixed buffer, but the cytosol is about 200–400 g/L of macromolecules and spatially organized. Three ways crowding alters effective kinetics: (1) Excluded volume raises effective concentrations and shifts equilibria toward more compact states and toward ES complex formation, lowering apparent (K_m) (tighter apparent binding) and favoring oligomerisation/association of enzymes. (2) Restricted diffusion lowers encounter rates, reducing apparent (k_{cat}/K_m) for diffusion-limited enzymes – the rate becomes diffusion- rather than chemistry-limited *in vivo*. (3) Compartmentation/channelling and local S gradients mean

bulk **S** misrepresents the substrate the enzyme actually sees, so in-vivo “apparent (K_m)” can differ markedly from in-vitro values. Experimental strategy: assay the purified enzyme in the presence of inert crowding agents (Ficoll, PEG, dextran) at physiological volume fractions, and/or measure activity in cell extracts and by single-molecule/in-cell fluorescence kinetics, comparing (K_m) and (k_{cat}) against dilute controls to isolate the crowding contribution. See section 4. 24. Zymogen activation (e.g., pepsinogen \rightarrow pepsin) is a mechanism for controlling enzyme activity. Evaluate the physiological logic of synthesizing inactive proenzymes, using three specific examples from digestion and blood coagulation. What happens when zymogen activation goes wrong (e.g., pancreatitis)?

Answer (Q24, Synthesis). Initiating logic: many hydrolytic/peptolytic enzymes would damage the cell that makes them, so they are synthesized as inactive zymogens (proenzymes) and activated only at the right place and time by limited proteolytic cleavage. Three examples: (1) Pepsinogen (\rightarrow) pepsin – activated by stomach acid (autocatalytic at low pH), so the protease is inert until it reaches the acidic lumen, protecting the secretory cells. (2) Trypsinogen (\rightarrow) trypsin (by enteropeptidase in the duodenum), which then activates chymotrypsinogen, proelastase, etc. – digestion is confined to the gut lumen, not the pancreas. (3) Coagulation cascade – prothrombin (\rightarrow) thrombin and other clotting factors are circulating zymogens, allowing an explosive, amplified, localized clot only upon vascular injury. When activation goes wrong: premature intrapancreatic trypsinogen activation triggers a cascade of self-digestion – acute pancreatitis – and dysregulated coagulation zymogen activation causes thrombosis or DIC. The shared principle: spatial/temporal control of dangerous catalytic power via a covalent activation step. See section 4. 25. Methotrexate inhibits dihydrofolate reductase (DHFR) by competitive inhibition. In cancer chemotherapy, it exploits rapidly dividing cells’ high demand for folate-derived nucleotides. Evaluate: (a) why cancer cells cannot simply overcome competitive inhibition by upregulating substrate concentration; (b) why resistance to methotrexate often involves DHFR gene amplification; (c) the trade-off between therapeutic index and resistance evolution.

Answer (Q25, Synthesis). Initiating condition: methotrexate is a folate analog that competitively inhibits dihydrofolate reductase (DHFR) with very high affinity (K_i) far below the substrate (K_m). (a) In principle competitive inhibition is overcome by raising **S**, but methotrexate binds DHFR about 1000-fold more tightly than the natural substrate (dihydrofolate), so the substrate concentration required to out-compete it is biologically unattainable – effectively the enzyme stays blocked, halting thymidylate/purine synthesis and DNA replication in rapidly dividing cells. (b) Because the drug acts by mass action at the active site, the most direct resistance mechanism is to make more enzyme: tumor cells frequently undergo DHFR gene amplification, producing enough DHFR that residual uninhibited enzyme sustains folate metabolism (also point mutations lowering drug affinity, or reduced drug uptake). (c) Trade-off: pushing dose/affinity to overwhelm amplified DHFR also harms normal proliferating tissues (marrow, gut), narrowing the therapeutic index, while sub-lethal exposure selects for resistant amplified clones – so dosing must balance tumor kill against toxicity and resistance evolution (rescue with folinic acid mitigates host toxicity). See section 4. 26. PCSK9 (proprotein convertase subtilisin/kexin type 9) is a serine protease that degrades LDL receptors, raising LDL cholesterol. Monoclonal antibody inhibitors of PCSK9 dramatically lower LDL. Evaluate why an enzyme inhibitor (rather than a simple receptor agonist) is necessary here, and explain how the enzyme-substrate-inhibitor kinetics differ from conventional small-molecule competitive inhibitors targeting PCSK9’s active site.

Answer (Q26, Synthesis). Initiating condition: PCSK9 binds the LDL receptor and targets it for lysosomal degradation, so fewer LDL receptors recycle and plasma LDL rises. Why an inhibitor rather than a receptor agonist: the therapeutic goal is to preserve LDL receptors, which requires *blocking PCSK9’s action on the receptor*, not stimulating a receptor – there is no agonist that would increase LDL-receptor recycling, whereas removing PCSK9 lets receptors survive and clear LDL. Kinetic contrast: PCSK9 acts here largely through a non-catalytic protein-protein interaction (it chaperones the receptor to degradation; its protease activity is mostly autocatalytic maturation), so a classic small-molecule active-site competitive inhibitor (which would compete with substrate at the catalytic site, raising apparent (K_m)) is ineffective/irrelevant. Instead a monoclonal antibody binds the PCSK9-LDLR interaction surface, acting more like a tight stoichiometric/non-competitive blocker of the binding interface than a Michaelis-Menten active-site competitor – it neutralizes the functional surface rather than competing for catalysis. Outcome: LDL receptors are spared, LDL clearance rises, plasma LDL falls sharply. See section 4. 27. Enzymes that catalyse the same reaction in different organisms often have different optimal pH values (e.g., pepsin pH 2 vs trypsin pH 8). Propose three molecular reasons why the optimal pH of an enzyme is tuned to its cellular compartment, and describe how you would experimentally shift the pH optimum of pepsin toward neutral pH by rational mutation.

Answer (Q27, Synthesis). Initiating observation: pepsin works optimally at pH about 2 (stomach), trypsin at pH about 8 (intestine), because catalysis depends on the protonation state of active-site residues. Three molecular reasons pH optimum is tuned to compartment: **(1) Catalytic-residue pK_a :** the chemistry needs specific residues protonated or deprotonated (pepsin uses Asp residues that must be appropriately protonated at acidic pH; trypsin needs His57 deprotonated to act as a general base near pH 8) – the bell-shaped activity curve reflects these ionisations. **(2) Electrostatic/microenvironment tuning:** surrounding charged residues and the local dielectric shift a residue’s pK_a so it titrates near the working pH. **(3) Structural stability:** the fold (and substrate-binding cleft) is only stable/correctly shaped over the pH range of its compartment; outside it the enzyme denatures or the substrate’s own charges change. Experiment to shift pepsin’s optimum toward neutral: use rational site-directed mutagenesis to substitute the catalytic/surrounding acidic residues (e.g. change key Asp microenvironment residues, add stabilizing charges) to raise the relevant pK_a values and stabilize the fold at pH 7, then measure the activity-pH profile of mutants vs wild type to confirm the optimum has moved. See section 4. 28. Single-molecule enzyme kinetics (SMEK) experiments reveal that individual enzyme molecules show fluctuating activity

— some are momentarily fast, some slow — a phenomenon called “dynamic disorder.” Evaluate what SMEK data reveals about the assumptions underlying the traditional Michaelis-Menten model, and propose what these fluctuations imply for drug design targeting enzymes in disease.

Answer (Q28, Synthesis). Initiating observation: single-molecule enzyme kinetics show individual enzyme molecules fluctuating between faster and slower catalytic states over time (“dynamic disorder”), even though the bulk follows Michaelis-Menten. Mechanism: an enzyme samples an ensemble of conformations interconverting on timescales comparable to turnover, so (k_{cat}) is not a single fixed constant but a distribution – consistent with the conformational-selection picture and inconsistent with the classical assumption of a single, time-invariant rate constant for every identical molecule. Why bulk MM still holds: ensemble and time averaging over many molecules/cycles recovers the hyperbolic mean behavior, so MM is an emergent average, not a molecular truth. Implication for drug design: because target enzymes occupy multiple conformational substates, inhibitors that bind only one conformation may be evaded by population shifts; designing inhibitors against the dominant or functionally critical conformational state (or trapping a specific substate) and accounting for conformational heterogeneity can improve potency and reduce escape – a rationale for allosteric and conformation-selective drugs. See section 4. 29. Metabolic channelling occurs when the product of enzyme A is directly transferred to enzyme B without diffusing into the bulk solution (e.g., tryptophan synthase, CAD complex, purinosome). Evaluate the advantages of metabolic channelling over free diffusion for: (a) reaction efficiency; (b) protection of unstable intermediates; (c) prevention of inhibitory product accumulation. Describe one experimental test that distinguishes channelling from free diffusion.

Answer (Q29, Synthesis). Initiating condition: in metabolic channelling the product of enzyme A is handed directly to enzyme B (via a physical tunnel or co-localized complex) without equilibrating with bulk solvent (e.g. tryptophan synthase, the CAD complex, the purinosome). Advantages: (a) Reaction efficiency – the local intermediate concentration at enzyme B’s active site is far above bulk, so B operates near (V_{max}) without waiting for diffusion, and transit time between active sites is minimized. (b) Protection of unstable/reactive intermediates – labile or toxic intermediates (e.g. indole, carbamoyl phosphate) are sequestered from water and side reactions, preventing decomposition or escape. (c) Prevention of inhibitory/competing accumulation – the intermediate never builds up in the cytosol where it could feedback-inhibit other enzymes or be diverted into competing pathways. Experimental test distinguishing channelling from free diffusion: an isotope-dilution (or “transient time”) experiment – add excess unlabelled bulk intermediate while feeding labeled precursor; with free diffusion the labeled intermediate equilibrates with the unlabelled pool and product label is diluted, whereas true channelling shows the product retains the precursor label (no dilution), demonstrating the intermediate never enters the bulk pool. See section 4. 30. Criticise the following hypothesis: “The optimal enzyme evolves to have a K_m equal to the in vivo substrate concentration.” Using evolutionary arguments, real enzyme kinetic data, and the concept of “catalytic perfection” (k_{cat}/K_m approaching the diffusion limit about $10^8\text{--}10^9 \text{ M}^{-1}\text{s}^{-1}$), evaluate whether enzymes are actually at evolutionary optimum, or whether constraints (protein stability, pleiotropic effects) prevent optimization. Cite specific examples.

Answer (Q30, Synthesis). Initiating hypothesis to criticise: enzymes evolve so that (K_m) equals the in-vivo S . Mechanism behind the idea: when $(K_m \text{ about } S)$, the enzyme operates on the steep part of the MM curve, so flux responds sensitively to S changes – a plausible regulatory optimum. Evidence and limits: the gold standard for catalytic power is (k_{cat}/K_m) , and “catalytically perfect” enzymes (catalase, fumarase, acetylcholinesterase, triosephosphate isomerase) push (k_{cat}/K_m) toward the diffusion limit about $10^{(8)\text{--}10(9)} \text{ M}^{(-1)}\text{s}^{(-1)}$, showing strong selection on efficiency. But genome-wide kinetic surveys show most enzymes are well below the diffusion limit and median (k_{cat}) and (k_{cat}/K_m) are modest, with (K_m) only loosely matched to physiological S . Conclusion: enzymes are not uniformly at evolutionary optimum because constraints intervene – protein stability/foldability trade-offs, pleiotropy (the same residue serves folding and catalysis), historical/contingent active-site architecture, weak selection when the enzyme is not rate-limiting (metabolic control analysis: control is shared, so most enzymes feel little pressure), and multi-substrate/regulatory demands. So “ $(K_m) = S$ ” holds only for the subset of strongly selected, flux-controlling enzymes; the general claim overstates optimization by ignoring these constraints. See section 4.

Questions — Cell Theory and Cell Types

Instructor Use and Coverage Notes

- Coverage target: Use size or microscopy evidence to classify a cell and predict a constraint on exchange.
- Model/data emphasis: Surface-area-to-volume scaling.
- Assessment alignment: Visual Representations, Questions and Methods, Argumentation.
- Misconception probe: Cells are not just small bags of fluid; boundaries and internal organization create function.
- Transfer product: Transfer scale reasoning to eggs, neurons, root hairs, and microbial colonies.
- Grading focus: award full credit for mechanism, evidence, boundary conditions, and units when a calculation is required.
- Suggested use: draw one recall item, one application item, and one synthesis item when building a short quiz from this bank.

Questions 1–10: Recall and Comprehension

This activity accompanies section 5 of the textbook — review that chapter before attempting the exercises below.

1. State the three principles of cell theory and name the three scientists who established it.

Answer (Q1, Recall). The three principles are: (1) all living organisms are composed of one or more cells; (2) the cell is the basic structural and functional unit of life; (3) all cells arise from pre-existing cells (Virchow’s *omnis cellula e cellula*). Matthias Schleiden (1838, botanist — plants) and Theodor Schwann (1839, zoologist — animals) proposed the first two principles; Rudolf Virchow (1855) added the third, closing the loop against spontaneous generation. 2. List five structural differences between a prokaryote and a eukaryote.

Answer (Q2, Recall). (1) Nucleus — prokaryotes have none (DNA in a nucleoid); eukaryotes have a membrane-bound nucleus. (2) Membrane-bound organelles — absent in prokaryotes, abundant in eukaryotes (mitochondria, ER, Golgi, lysosomes). (3) Genome — prokaryotes have a single circular chromosome; eukaryotes have multiple linear chromosomes. (4) Cell size — prokaryotes 1–10 μm; eukaryotes 10–100 μm. (5) Cytoskeleton — rudimentary in prokaryotes (MreB, FtsZ); elaborate in eukaryotes (actin, microtubules, intermediate filaments). See section 5. 3. What is the smallest known living cell? What is the largest known single cell?

Answer (Q3, Recall). Smallest: *Mycoplasma genitalium* at about 200 nm diameter — an obligate parasite with only about 470 genes. It lacks a cell wall and is near the theoretical lower bound for free-living life (about 250–300 nm for essential molecular machinery). Largest single cell: the ostrich egg (yolk only; about 15 cm diameter, 1.5 kg), or in plants, the single-celled alga *Caulerpa* (up to 3 m long). Neuron axons (e.g., giraffe recurrent laryngeal, 2 m) are also “single cells” by some measures. 4. What is the endomembrane system? List most organelles that belong to it.

Answer (Q4, Recall). The endomembrane system is the network of interconnected membrane compartments in eukaryotic cells that synthesize, modify, sort, and traffic lipids and proteins. Members: nuclear envelope, rough ER (ribosomes → secretory/membrane proteins), smooth ER (lipid synthesis, Ca²⁺ storage, detoxification), Golgi apparatus (post-translational modification + sorting), lysosomes (hydrolytic digestion), endosomes (endocytic sorting), and the plasma membrane (via vesicle traffic). Mitochondria and chloroplasts are NOT part of it — their double membranes are of endosymbiotic origin. 5. Define resolution in microscopy. What is the resolution limit of a light microscope?

Answer (Q5, Recall). Resolution is the minimum distance between two points at which they can still be distinguished as separate rather than merging into one blur; it is not the same as magnification. For light microscopy it is set by the Abbe diffraction limit, $d = \lambda / (2 \cdot NA)$, where λ is the illumination wavelength and NA the numerical aperture of the objective. For visible light (λ about 550 nm) and a high-quality oil-immersion objective (NA = 1.4), $d \approx 550 / (2 \times 1.4) \approx 200$ nm. This about 200 nm ceiling is why structures like ribosomes (25 nm) or the membrane bilayer (7–8 nm) are invisible by conventional light microscopy and require electron microscopy (about 0.1 nm) or super-resolution methods (STED, STORM, PALM; about 20–50 nm). See section 5. 6. What is the cell theory exception posed by viruses? Are viruses “alive”?

Answer (Q6, Recall). Viruses are excluded from cell theory by definition because they are not cells: they have no membrane of their own metabolism, no ribosomes, no autonomous reproduction, and no independent energy generation. They consist only of a nucleic acid genome plus a protein capsid (sometimes a stolen lipid envelope) and replicate exclusively by hijacking a host cell’s ribosomes, nucleotides, and ATP. By the usual “alive” criteria they fall in a gray zone — they evolve and carry heritable information (lifelike) but cannot metabolize or reproduce outside a host (non-lifelike). Most cell biologists treat them as obligate intracellular parasites, not living cells, while acknowledging they blur the living/non-living boundary. See section 5. 7. Describe the inner membrane of a mitochondrion. What are cristae and why are they important?

Answer (Q7, Recall). A mitochondrion has two membranes; the inner membrane is the metabolically active one. It is highly impermeable (rich in cardiolipin, a bacterial-type lipid that is a signature of endosymbiotic origin) and houses the electron transport chain complexes and ATP synthase, so chemiosmotic ATP synthesis occurs across it. Cristae are deep folds of this inner membrane projecting into the matrix. They are important because they multiply the inner-membrane surface area severalfold, packing in far more electron transport chains and ATP synthase per unit cell volume — the structural solution to the cube-law constraint, where a hepatocyte’s inner mitochondrial membrane provides about $3 \times 10^4 \text{ } \mu\text{m}^2$ of

respiratory surface, roughly 6x its plasma-membrane area. Highly aerobic cells such as cardiac muscle have densely packed cristae. See section 5. 8. What is the nucleolus and what is assembled there?

Answer (Q8, Recall). The nucleolus is a non-membrane-bound, dense subcompartment within the nucleus formed by liquid-liquid phase separation around the nucleolus organiser regions (NORs) — the clustered rRNA gene repeats located in humans on chromosomes 13, 14, 15, 21, and 22. It is the site of ribosome biogenesis: RNA polymerase I transcribes the rRNA precursor, the rRNA is processed and chemically modified, and it is assembled with ribosomal proteins (imported from the cytoplasm) into the 40S and 60S ribosomal subunits before export. The nucleolus disassembles during mitosis and re-forms around the NORs in the next interphase. See section 5. 9. Distinguish cell walls of bacteria, plants, and fungi (composition).

Answer (Q9, Recall). All three are rigid extracellular polymers that resist osmotic lysis, but the chemistry differs and that difference is what makes wall-targeting drugs selective. Bacteria: peptidoglycan (murein) — chains of alternating N-acetylglucosamine and N-acetylmuramic acid (beta-1,4 linked) cross-linked by short peptide bridges; Gram-positive walls are thick (20-80 nm) with teichoic acids, Gram-negative thin (about 2-7 nm) plus an outer LPS membrane. Plants: cellulose microfibrils (beta-1,4 glucose) embedded in hemicellulose and pectin, with lignin in secondary walls. Fungi: chitin (beta-1,4 N-acetylglucosamine polymer) plus beta-glucans and mannoproteins. Because peptidoglycan and its D-Ala-D-Ala cross-links are unique to bacteria, beta-lactams (penicillin) and vancomycin kill bacteria but not plant, fungal, or archaeal cells. See section 5. 10. What is meant by “compartmentalization” and why is it advantageous for eukaryotes?

Answer (Q10, Recall). Compartmentalization is the segregation of biochemical processes into discrete membrane-bound organelles within the eukaryotic cell. It is advantageous for four reasons given in the chapter: (1) incompatible reactions run simultaneously in separate compartments — e.g., protein synthesis in the cytoplasm (pH 7.2) versus protein degradation in lysosomes (pH 4.5); (2) substrates and enzymes are concentrated locally (TCA enzymes in the mitochondrial matrix raise reaction rates); (3) gene expression is regulated by separating transcription (nucleus) from translation (cytoplasm), enabling splicing and mRNA export control; (4) internal membranes add enormous surface area for membrane-associated reactions. This last point is the topological solution to the cube-law problem: a HeLa cell has about 5-fold lower surface-to-volume than E. coli yet 10x higher metabolic flux, only possible because internal membranes supply the missing surface area. See section 5.

Questions 11–20: Application and Analysis

11. Calculate the surface area-to-volume ratio (SA:V) for spherical cells with radii of 1 μm, 5 μm, and 10 μm. Explain why SA:V limits the maximum size of cells.

Answer (Q11, Application). For a sphere, $A/V = 4\pi r^2 / (\frac{4}{3}\pi r^3) = 3/r$. Substituting with units: at $r = 1 \text{ μm}$, $A/V = 3/1 = 3.0 \text{ μm}^{-1}$; at $r = 5 \text{ μm}$, $A/V = 3/5 = 0.6 \text{ μm}^{-1}$; at $r = 10 \text{ μm}$, $A/V = 3/10 = 0.3 \text{ μm}^{-1}$. The ratio falls as $1/r$. This limits maximum cell size because metabolic demand (nutrient consumption, waste production) scales with volume ($\propto r^3$) while exchange with the environment scales with surface area ($\propto r^2$). As a cell enlarges, demand outgrows supply: the membrane can no longer import nutrients or expel waste fast enough for the interior volume, so a uniform respiring cell hits a hard ceiling (about 60 μm radius for typical mammalian parameters via $r_{\text{max}} = 3P_{O_2}\Delta[O_2]/q$) unless it amplifies surface area (microvilli), lowers metabolic demand (vacuoles), or accepts core anoxia. See section 5. 12. Colchicine destroys microtubules. Predict its effects on: (a) mitosis; (b) vesicle trafficking; (c) cilia; (d) cell shape.

Answer (Q12, Application). Colchicine binds tubulin dimers and blocks microtubule polymerization, depolymerising existing microtubules. (a) Mitosis: the mitotic spindle is microtubule-based, so chromosomes cannot attach to or be pulled to the poles — cells arrest in metaphase (the classic spindle-poison or metaphase-arrest effect, exploited in karyotyping). (b) Vesicle trafficking: long-range vesicle transport runs on microtubule tracks via kinesin and dynein motors; without microtubules, directed organelle and vesicle movement (e.g., ER-to-Golgi, axonal transport) collapses. (c) Cilia: the ciliary axoneme is a 9+2 microtubule array, so cilia and flagella lose their structure and beating stops. (d) Cell shape: microtubules provide compressive struts and polarity cues, so cells lose directional shape and asymmetry, tending to round up. See section 5. 13. *Thiomargarita namibiensis* is a bacterium >750 μm in diameter — larger than many eukaryotes. How does it solve the SA:V problem?

Answer (Q13, Application). At a diameter of about 750 μm (radius about 375 μm) its surface-to-volume ratio is only $A/V = 3/375 \approx 0.008 \text{ μm}^{-1}$ — far too low to supply a metabolically active cytoplasm of that volume by diffusion across the plasma membrane. It evades the cube-law constraint not by increasing surface area but by reducing metabolically active volume: more than 95% of the cell is a giant central vacuole that stores nitrate (an electron acceptor) and elemental sulfur. The living, respiring cytoplasm is confined to a thin shell just beneath the plasma membrane, so the effective diffusion distance and the metabolically demanding volume are tiny even though the whole cell is huge. This is the same trick plant cells use with their large central vacuole. See section 5. 14. Describe the experimental basis for the discovery that cells arise from pre-existing cells (Pasteur’s swan-neck flask experiment).

Answer (Q14, Application). Virchow’s principle *omnis cellula e cellula* (1855) asserted that cells arise only from pre-existing cells, but it was Louis Pasteur (1859) who experimentally killed spontaneous generation. He boiled nutrient broth (sterilising it) in flasks with long S-shaped swan-neck necks. The bend trapped airborne dust and microbes in the curve so air could still reach the broth but particles could not. Result: the broth stayed

sterile indefinitely as long as the neck was intact; if the neck was snapped off or the flask tilted so broth contacted the trapped dust, microbial growth appeared within days. The decisive control showing the broth itself could still support life rules out the alternative that boiling destroyed a vital force. This established that microbes come only from pre-existing microbes, completing the third tenet of cell theory and the unbroken-lineage corollary. See section 5. 15. Explain five lines of molecular evidence supporting the endosymbiotic origin of mitochondria.

Answer (Q15, Application). (1) Double membrane: mitochondria have two bilayers — an inner one resembling a bacterial plasma membrane and an outer one derived from the host phagocytic membrane. (2) Circular genome: mitochondria carry their own small circular DNA, like a bacterial chromosome rather than the host's linear nuclear chromosomes. (3) 70S bacterial-type ribosomes: organelle ribosomes are inhibited by anti-bacterial antibiotics (chloramphenicol, erythromycin) that do not touch cytoplasmic 80S ribosomes. (4) Binary fission: mitochondria divide independently of the nucleus using FtsZ-related proteins, exactly as bacteria do. (5) Phylogenetics: mitochondrial rRNA sequences are most closely related to alpha-proteobacteria (e.g., *Rickettsia*). Additional support: cardiolipin in the inner membrane and N-formylmethionine-initiated protein synthesis, both bacterial signatures. See section 5. 16. A secretory cell is treated with brefeldin A (disrupts the Golgi). Predict the consequences for enzyme secretion.

Answer (Q16, Application). Brefeldin A collapses the Golgi apparatus, causing Golgi membranes and cargo to redistribute back into the ER. The secretory pathway is ER, then Golgi, then secretory vesicle, then plasma membrane, so disrupting the Golgi breaks the route at the modification and sorting step. Consequences: (1) newly synthesized secretory enzymes accumulate in the ER and fused ER-Golgi remnant compartments instead of being exported, so extracellular enzyme levels drop sharply; (2) the enzymes that do remain are not properly modified (terminal glycosylation and proteolytic maturation that occur in the Golgi do not happen), so even mis-localized enzyme is often inactive; (3) lysosomal hydrolases, which acquire their mannose-6-phosphate sorting tag in the Golgi, are mis-sorted and tend to be secreted rather than delivered to lysosomes, impairing intracellular digestion. Net result: loss of regulated enzyme secretion plus ER stress from cargo backup. See section 5. 17. Explain why red blood cells lack a nucleus and mitochondria. What metabolic consequences does this create?

Answer (Q17, Application). Mammalian erythrocytes extrude their nucleus and degrade their mitochondria and other organelles during maturation. This is adaptive: it maximizes the volume available for hemoglobin (oxygen-carrying capacity), produces the flexible biconcave disc that can squeeze through capillaries, and removes oxygen-consuming organelles so the cell does not burn the oxygen it is supposed to deliver. The metabolic consequence is that the RBC cannot perform oxidative phosphorylation (no mitochondria) and cannot synthesize new proteins or repair itself (no nucleus). It is therefore wholly dependent on anaerobic glycolysis for ATP and on the pentose phosphate pathway for NADPH to keep hemoglobin reduced and counter oxidative damage. Because it cannot replace damaged components, it has a finite lifespan of about 120 days before removal by the spleen. See section 5. 18. A mutation eliminates the peroxisomal targeting signal (PTS1) from catalase. Where will catalase end up? What biochemical consequence results?

Answer (Q18, Application). Catalase is normally imported into peroxisomes post-translationally because of its C-terminal PTS1 tripeptide (the -SKL motif), which is recognized by the cytosolic receptor Pex5. If PTS1 is deleted, Pex5 cannot bind catalase, so the protein is never imported and instead remains in the cytosol (it is still translated on free ribosomes; only the targeting tag is lost). Biochemical consequence: peroxisomes generate H₂O₂ during fatty-acid beta-oxidation and other oxidase reactions, and catalase is the enzyme that detoxifies that H₂O₂ to water and O₂. With catalase mislocalized to the cytosol, peroxisomal H₂O₂ is no longer cleared inside the organelle, raising reactive-oxygen stress and oxidative damage to lipids, proteins, and DNA, while the cytosol gains catalase activity it does not normally have. This illustrates that targeting, not synthesis, dictates organelle function. See section 5. 19. Ribosome composition differs between prokaryotes (70S = 50S + 30S) and eukaryotes (80S = 60S + 40S). How are antibiotics exploited to target primarily bacterial ribosomes?

Answer (Q19, Application). Bacterial ribosomes are 70S (50S large plus 30S small subunits) whereas eukaryotic cytoplasmic ribosomes are 80S (60S plus 40S); the rRNA and protein structures differ enough that drugs can bind the bacterial machine without binding the human one. This structural dichotomy is the basis of selective toxicity: aminoglycosides and tetracyclines bind the 30S subunit (blocking decoding and tRNA binding), while chloramphenicol, macrolides (erythromycin), and oxazolidinones bind the 50S subunit (blocking peptide-bond formation or the exit tunnel). These inhibit bacterial protein synthesis while sparing the host's 80S ribosomes. The important caveat is that mitochondrial ribosomes are bacterial-type 70S (endosymbiotic origin), so 70S-targeting antibiotics can have mitochondrial side effects in human cells. See section 5. 20. A student uses STED super-resolution microscopy and finds that nuclear pore complexes are distributed non-randomly on the nuclear envelope, clustering near transcriptionally active chromatin. Interpret this finding in terms of mRNA export and nuclear architecture.

Answer (Q20, Application). STED beats the about 200 nm Abbe diffraction limit (resolution about 30-50 nm), so it can resolve individual nuclear pore complexes (NPCs) and map their spatial distribution — something impossible by conventional light microscopy. The key variable is NPC position relative to active chromatin. If NPCs cluster over transcriptionally active regions, the most parsimonious interpretation is that this minimizes the diffusion distance for newly transcribed, processed mRNA to reach an export channel: the nuclear envelope separates transcription from translation, and NPCs are the only conduits for mRNA export, so co-localizing pores with active genes accelerates and spatially organizes mRNA delivery to

the cytoplasm. It implies the nuclear envelope is not a uniform barrier but a spatially patterned interface coupled to genome organization. A control and alternative to test: compare NPC distribution after transcriptional inhibition (e.g., actinomycin D); if clustering disperses, it supports an activity-coupled, dynamic arrangement rather than a fixed structural one. See section 5.

Questions 21–30: Synthesis and Evaluation

21. Evaluate the claim: “Most life evolved from a single comprehensive common ancestor (LUCA).” What molecular evidence supports LUCA, and what evidence (e.g., horizontal gene transfer) complicates the simple tree-of-life narrative?

Answer (Q21, Synthesis). Supporting evidence (empirical): genes shared by both Bacteria and Archaea and not explained by horizontal transfer form a conserved set of about 355 gene families (the LUCA core; Weiss et al. 2016), implying LUCA already had a DNA-to-RNA-to-protein machinery, the genetic code, about 20 aminoacyl-tRNA synthetases, ATP synthase, and a chemiosmotic membrane; its metalloenzyme inventory points to an anaerobic alkaline hydrothermal habitat. The near-universality of the genetic code and ribosome is the strongest single argument for common ancestry. Complications (what would qualify the conclusion): extensive horizontal gene transfer, especially among prokaryotes, means a single bifurcating tree is an oversimplification — the deep tree is partly a network. The lack of homology between bacterial and archaeal DNA polymerases suggests DNA replication evolved twice after the bacteria-archaea split, so LUCA may have been a pre-cellular, RNA-genome metabolic consortium rather than a fully autonomous free-living cell. LUCA is therefore best read as the last common ancestor of surviving lineages — earlier lineages may have existed but left no descendants — not proof there was ever only one origin of life. See section 5. 22. Synthetic biology aims to build minimal artificial cells (protocells). Evaluate three fundamental hurdles: (a) stable lipid encapsulation; (b) genetic self-replication; (c) energy supply. At what stage are current (2024–2025) efforts?

Answer (Q22, Synthesis). (a) Stable lipid encapsulation: lipid vesicles can self-assemble but must grow, divide, and stay permeable to nutrients yet retain macromolecules; controlled vesicle growth and division coupled to internal metabolism remains only partially solved. (b) Genetic self-replication: a protocell needs a genome that replicates with the protein machinery the genome itself encodes (the chicken-and-egg of replication). Top-down work has already produced a near-minimal living cell — JCVI-syn3.0 (473 genes, 531 kb, doubling about 3 h), still containing 149 essential genes of unknown function — so genome-down self-replication exists but is not yet bottom-up designed from scratch. (c) Energy supply: an autonomous protocell must regenerate ATP and redox cofactors; current systems usually feed in externally supplied energy substrates rather than running a self-sustaining chemiosmotic or fermentative metabolism. Stage of the field: the top-down route (minimal genomes like syn3.0) is the furthest along; the bottom-up route (self-replicating, self-energising vesicles) has demonstrated individual modules but not an integrated, autonomously reproducing protocell. The evidence does not yet settle whether a fully de novo cell is achievable, only that no single hurdle is in principle impossible. See section 5. 23. Organelles proliferate or contract depending on cellular demand. Design an experiment to determine whether smooth ER proliferation in response to lipid overload is controlled by transcriptional upregulation of ER resident proteins or by a different mechanism (e.g., membrane lipid incorporation itself driving ER expansion).

Answer (Q23, Synthesis). Hypothesis: smooth-ER expansion under lipid overload is driven primarily by transcriptional upregulation of ER-resident proteins (H1) versus driven primarily by direct incorporation of excess lipid into ER membrane independent of new gene expression (H2). Design: treat a hepatocyte line with a defined lipid load and split into arms. Arm 1 (control): vehicle only. Arm 2: lipid overload. Arm 3: lipid overload plus a transcription inhibitor (actinomycin D) applied before the load. Arm 4: lipid overload plus a translation inhibitor (cycloheximide). Measured outcomes (with replication, n at least 4 biological replicates, fixed seed for any image-analysis pipeline): quantify smooth-ER membrane area by TEM morphometry and ER marker fluorescence, plus qPCR and Western for ER-resident enzymes (e.g., CYP450, lipid-synthesis enzymes), with a time course. Decision rule: if blocking transcription or translation abolishes ER expansion, H1 is supported; if ER membrane still expands proportionally to the lipid dose despite transcription and translation block (with no rise in ER protein levels), H1 is falsified and H2 (lipid-driven membrane growth) is supported. A dose-response relationship between lipid load and ER area independent of mRNA levels would be the decisive falsifying result for H1. See section 5. 24. Aging cells accumulate dysfunctional mitochondria. Evaluate the “mitochondrial theory of aging”: does mitochondrial dysfunction cause aging, or result from it? Cite evidence from caloric restriction and NAD+ supplementation studies.

Answer (Q24, Synthesis). The mitochondrial theory holds that accumulated mitochondrial DNA damage and reactive-oxygen production progressively degrade respiratory capacity, driving aging. Distinguishing cause from consequence is the central problem: dysfunctional mitochondria are reliably correlated with aging, but correlation does not establish direction. Evidence consistent with a causal contribution: caloric restriction lowers metabolic flux and oxidative load and extends lifespan in many model organisms, and NAD+ precursor supplementation (which restores the NAD+ pool that mitochondrial dehydrogenases and sirtuins depend on) improves mitochondrial function and some aging phenotypes in animal models. Evidence that qualifies the strong causal claim: some interventions that increase reactive-oxygen species can extend lifespan (mitohormesis), and mtDNA-mutator mice age fast but without the predicted ROS surge, suggesting mitochondrial decline is one node in a network (also involving genome maintenance, proteostasis, senescence) rather than the sole driver. Honest verdict: mitochondrial dysfunction is best treated as a contributing and partly self-reinforcing cause, not a proven prime mover; the conclusion would change if NAD+ and caloric-restriction benefits were shown

to act entirely through non-mitochondrial pathways. See section 5. 25. Some unicellular organisms (e.g., *Euglena*) contain both mitochondria and chloroplasts. Evaluate how a single cell coordinates two endosymbiotic organelles with conflicting demands on the cell's redox state.

Answer (Q25, Synthesis). Both organelles are former free-living bacteria (mitochondrion from an alpha-proteobacterium, chloroplast from a cyanobacterium; in *Euglena* the chloroplast arrived by secondary endosymbiosis, hence its three bounding membranes). The conflict: chloroplasts reduce NADP⁺ and pump electrons in the light, generating reducing power and O₂, while mitochondria consume reducing equivalents and O₂ to make ATP — opposing demands on the cytosolic redox poise. Coordination mechanisms: (1) light and dark partitioning — photosynthetic electron flow dominates in light, respiration at night, separating the two in time; (2) redox shuttles — malate/oxaloacetate and triose-phosphate shuttles move reducing equivalents between compartments so excess chloroplast NADPH can be exported and balanced; (3) retrograde signaling — both organelles send redox and metabolite signals to the nucleus, which controls the roughly 1,500 nuclear-encoded organelle proteins, allowing the cell to tune the abundance and activity of each organelle to demand; (4) shared metabolite pools (ATP/ADP, NAD(P)(H)) act as the buffering currency. The endosymbiotic theory predicts exactly this: gene transfer to the host nucleus gives the cell central control over two formerly autonomous metabolisms. See section 5. 26. Evaluate the role of the centrosome as a signaling hub beyond its microtubule-organizing function. What kinases localize to the centrosome, and how does centrosome duplication failure contribute to cancer?

Answer (Q26, Synthesis). Beyond being the principal microtubule-organizing center, the centrosome acts as a concentrating scaffold for cell-cycle and mitotic-control kinases — notably Polo-like kinase 1 (PLK1), Aurora-A, and CDK1-cyclin B — so it functions as a localized signaling hub that couples microtubule nucleation to mitotic entry, spindle assembly, and cytokinesis. Empirically, centrosome amplification (more than 2 centrosomes per cell) is common in tumors. The causal link to cancer: extra centrosomes can form multipolar or merotelic spindles, mis-segregating chromosomes and generating chromosomal instability and aneuploidy, which accelerates tumor evolution; mislocalized Aurora-A and PLK1 activity further perturbs checkpoint control. Boundary condition and what would change the conclusion: many cancer cells cluster supernumerary centrosomes into pseudo-bipolar spindles and survive, so centrosome amplification is better described as a driver of instability and tumor heterogeneity than a strict requirement for transformation; if amplification were shown to be a purely passive consequence of an already-unstable genome, the active-driver interpretation would weaken. See section 5. 27. Apicoplasts in malaria parasites (*Plasmodium*) are non-photosynthetic plastids derived from a secondary endosymbiosis. Evaluate them as drug targets — what essential biosynthetic pathways occur exclusively in the apicoplast, and why does targeting apicoplast translation (e.g., with doxycycline) kill the parasite but spare human cells?

Answer (Q27, Synthesis). The apicoplast is a relic plastid (secondary endosymbiosis of a red alga) that has lost photosynthesis but retained essential prokaryote-derived biosynthesis: the non-mevalonate (MEP/DOXP) isoprenoid precursor pathway, parts of type II fatty-acid synthesis (FAS-II), haem biosynthesis, and Fe-S cluster assembly. Humans use the unrelated mevalonate pathway for isoprenoids and FAS-I, so these apicoplast pathways have no human counterpart — an ideal selective-toxicity gap. Why doxycycline (and other 70S-ribosome antibiotics like clindamycin) works: the apicoplast retains a bacterial-type genome and 70S ribosomes for its own gene expression, just like mitochondria. Doxycycline blocks 70S translation, crippling apicoplast biogenesis; the parasite dies (often with a characteristic delayed death one cycle later because the disabled apicoplast cannot be inherited functionally). Human cytoplasmic ribosomes are 80S and unaffected. The boundary condition is the mitochondrial caveat: human mitochondria also have 70S ribosomes, so dosing must stay within the therapeutic window that affects the parasite's smaller, more drug-accessible apicoplast more than host mitochondria. See section 5. 28. Liquid-liquid phase separation (LLPS) creates membraneless organelles (stress granules, P-bodies). Evaluate the evidence that these condensates are functionally equivalent to membrane-bounded organelles in concentrating reaction components.

Answer (Q28, Synthesis). Membraneless organelles (nucleolus, stress granules, P-bodies) form by liquid-liquid phase separation of multivalent proteins and RNA into droplet-like condensates. Evidence they resemble membrane-bound organelles functionally: they selectively concentrate specific RNAs and enzymes far above bulk cytoplasmic levels (so they can accelerate or sequester reactions, e.g., ribosome assembly in the nucleolus), they have defined composition, and they can be experimentally disrupted (1,6-hexanediol) with predictable loss of the localized activity. The decisive difference from true organelles is the absence of a bilayer: condensates have no semipermeable barrier, so they exchange components with the surroundings on a second timescale, are thermodynamically tuned by concentration and temperature rather than gated by transport machinery, and cannot maintain a distinct chemical environment (pH, ion composition) the way a lysosome can. Verdict: condensates are functionally analogous in concentrating reaction components and creating local microenvironments, but they are not equivalent to membrane-bound organelles for processes that require chemical isolation or active import gating — calling them organelles is justified for compartmentalised chemistry but not for barrier-dependent functions. See section 5. 29. Compare the evolutionary trajectories of a symbiotic bacterium becoming a mitochondrion vs becoming a lysosome. What structural and genomic changes would you expect in each pathway?

Answer (Q29, Synthesis). The shared principle is reductive evolution of an engulfed cell under host control, but the endpoint differs because a mitochondrion is a retained endosymbiont while a lysosome is not endosymbiotic at all — so the comparison sharpens what makes endosymbiosis distinctive. Becoming a mitochondrion (endosymbiotic path): the bacterium keeps a double membrane (its own plus the host phagosomal mem-

brane), retains a residual circular genome and bacterial 70S ribosomes, divides by binary fission with FtsZ-related proteins, but undergoes massive gene transfer to the host nucleus (about 1,500 genes), keeping only a core needed for in-situ assembly of the respiratory chain; metabolite and protein import machinery (TOM/TIM) evolves to re-couple the now-dependent organelle to the host. Becoming a lysosome (non-endosymbiotic path): no retained genome, no 70S ribosomes, single membrane derived from the host endomembrane system; it would arise instead by host-encoded biogenesis — Golgi-derived hydrolases tagged with mannose-6-phosphate, a V-ATPase to acidify the lumen to pH 4.5 — with all components nuclear-encoded from the start. Expected signature: a mitochondrion shows genomic remnants and bacterial-lipid (cardiolipin) and fMet-translation hallmarks; a lysosome shows none of these and is purely a host-built compartment. See section 5. 30. Critically assess the hypothesis that cancer is a disease of cell identity — a reversion to a primordial unicellular state where individual cell fitness (unlimited proliferation, resistance to death) overrides multicellular cooperation. What evidence from cancer evolutionary biology supports or contradicts this view?

Answer (Q30, Synthesis). The atavism hypothesis frames cancer as a breakdown of the multicellular social contract: somatic mutations release a cell from cooperative constraints (controlled division, programmed death, niche restriction) so that single-cell fitness traits — unlimited proliferation, apoptosis resistance, metabolic autonomy — re-dominate, echoing Virchow’s *omnis cellula e cellula* applied to malignant clones arising from normal cells. Supporting evidence: tumors evolve by mutation and clonal selection within the body (a microevolutionary process), preferentially activate ancient, conserved unicellular-like genes while downregulating genes that arose with multicellularity, and exhibit metabolic shifts (aerobic glycolysis, the Warburg effect) reminiscent of a fermentative ancestral state. Contradicting and qualifying evidence: cancers do not become free-living unicells — they remain dependent on host vasculature, stroma, and growth factors, and they acquire new metabolic and signaling adaptations rather than simply reverting to an ancestral program; the genetic changes are largely loss and dysregulation of metazoan controls, not resurrection of a coherent ancestral genome. Honest assessment: the atavism model is a useful heuristic for why proliferation and death-resistance programs are mutationally accessible, but the data better support cancer as Darwinian somatic evolution of metazoan cells under relaxed multicellular constraint than as a literal reversion to a primordial unicellular organism; the conclusion would shift if reactivated unicellular gene modules were shown to be necessary and sufficient for transformation. See section 5.

Questions — Cell Structure and Organelles

Instructor Use and Coverage Notes

- Coverage target: Predict which organelle or cytoskeletal process is disrupted from a phenotype.
- Model/data emphasis: Compartment-flow and motor-transport calculations.
- Assessment alignment: Visual Representations, Questions and Methods, Argumentation.
- Misconception probe: Organelles are dynamic process hubs, not static textbook icons.
- Transfer product: Apply compartment logic to secretion, apoptosis, infection, or cell division.
- Grading focus: award full credit for mechanism, evidence, boundary conditions, and units when a calculation is required.
- Suggested use: draw one recall item, one application item, and one synthesis item when building a short quiz from this bank.

Questions 1–10: Recall and Comprehension

This activity accompanies section 6 of the textbook — review that chapter before attempting the exercises below.

1. Which organelle is responsible for: (a) protein synthesis; (b) lipid synthesis; (c) protein glycosylation; (d) intracellular digestion; (e) ATP synthesis?

Answer (Q1, Recall). (a) Protein synthesis: the ribosome — free cytosolic ribosomes for cytosolic proteins, ER-bound (rough ER) ribosomes for secretory and membrane proteins. (b) Lipid synthesis: the smooth ER (phospholipids, cholesterol, steroid hormones). (c) Protein glycosylation: begins in the rough ER (initial N-glycosylation) and is completed in the Golgi apparatus (O-glycosylation and N-glycan trimming). (d) Intracellular digestion: the lysosome, using about 60 acid hydrolases at pH 4.5-5.0. (e) ATP synthesis: the mitochondrion — oxidative phosphorylation by the electron transport chain and ATP synthase on the inner membrane (with a smaller cytosolic glycolytic contribution). See section 6. 2. What is the difference between rough ER and smooth ER in structure and function?

Answer (Q2, Recall). Both are continuous membrane networks of the same organelle, but ribosome decoration is the structural difference that changes their function. Rough ER (RER) is studded with ribosomes on its cytosolic face; it is the site of synthesis, folding, quality control, and initial N-glycosylation of secreted and membrane proteins (chaperones BiP, calnexin, calreticulin ensure folding; misfolded proteins go to ERAD). Smooth ER (SER) lacks ribosomes; it performs lipid and steroid-hormone synthesis, cytochrome P450 drug and toxin detoxification (abundant in liver), Ca2+ storage and release for signaling (the muscle sarcoplasmic reticulum is specialized SER), and glycogen metabolism. The presence or absence of bound ribosomes is therefore what assigns each region to protein-handling versus lipid and detox roles. See section 6. 3. Describe the cis-to-trans polarity of the Golgi apparatus and the direction of cargo flow.

Answer (Q3, Recall). The Golgi is a polarized stack: the cis face (cis-Golgi network) sits nearest the ER and receives newly synthesized cargo, the medial cisternae are in the middle, and the trans face (trans-Golgi network, TGN) faces the plasma membrane and acts as the sorting station. Cargo flow is directional: proteins enter at the cis face from the ER in COPII-coated vesicles, move cis to medial to trans (anterograde) while being progressively modified (O-glycosylation, N-glycan trimming, mannose-6-phosphate addition), and exit from the TGN sorted to lysosomes (M6P), the plasma membrane (constitutive secretion), or secretory granules (regulated exocytosis). Retrograde traffic in COPI-coated vesicles returns escaped ER-resident (KDEL) proteins from the Golgi back to the ER. See section 6. 4. What is the optimal pH inside a lysosome and why?

Answer (Q4, Recall). The lysosomal lumen is maintained at pH 4.5-5.0 by a V-type H+-ATPase that pumps protons in using ATP. This acidic optimum exists because the roughly 60 lysosomal acid hydrolases (proteases, lipases, nucleases, glycosidases) have peak catalytic activity near pH 4.5-5. The acidity is also a built-in safety mechanism: if these enzymes leak into the cytosol (pH about 7.2) they are largely inactive, protecting the cell from self-digestion. The same acidity drives ligand release from receptors in the endocytic pathway. See section 6. 5. Name the three components of the cytoskeleton and one function of each.

Answer (Q5, Recall). (1) Actin microfilaments (about 7 nm; polar ATP-driven polymers of G-actin) — cell shape, the cytokinesis contractile ring, muscle contraction, and crawling via lamellipodia and filopodia. (2) Microtubules (about 25 nm; hollow alpha/beta-tubulin tubes, GTP-driven dynamic instability) — chromosome segregation by the mitotic spindle, intracellular vesicle and organelle transport along kinesin and dynein tracks, and the 9+2 axoneme of cilia and flagella. (3) Intermediate filaments (about 10 nm; ropelike coiled-coil proteins, non-polar, no motors) — purely mechanical resilience, e.g., keratin in epithelia and lamins forming the nuclear lamina. See section 6. 6. What are cilia and flagella made of (protein and structure)? What drives their beating?

Answer (Q6, Recall). Eukaryotic motile cilia and flagella are built from the axoneme: nine outer doublet microtubules surrounding two central singlet microtubules (the 9+2 arrangement), with the doublets linked by nexin bridges and bearing inner and outer dynein arms. Beating is driven by ciliary (axonemal) dynein, an ATPase motor: dynein arms on one doublet walk along the adjacent doublet, but because nexin links resist sliding, the relative microtubule sliding is converted into rhythmic bending. ATP hydrolysis powers the stroke; coordinated activation of dynein arms

around the axoneme produces the propagating waveform. (Note that the bacterial flagellum is structurally unrelated: a flagellin filament rotated by a proton-motive-force-driven rotary motor.) See section 6. 7. Describe the nuclear envelope. How many membranes does it have?

Answer (Q7, Recall). The nuclear envelope is a double membrane: two concentric phospholipid bilayers, an inner and an outer nuclear membrane separated by a perinuclear space. The outer nuclear membrane is continuous with the rough ER. The two membranes are perforated by nuclear pore complexes (about 3,000-5,000 per nucleus, roughly 10-20 per μm^2 of envelope), each a roughly 120 MDa assembly of about 30 nucleoporin species with 8-fold symmetry that gates molecular traffic: small molecules (<40 kDa) diffuse through the about 9 nm channel, while larger cargo needs an NLS or NES and is moved by importins and exportins powered by the RanGTP/GDP gradient. Underlying the inner membrane is the nuclear lamina (lamin intermediate filaments) that gives the nucleus mechanical rigidity. See section 6. 8. What two reactions does the peroxisome catalyse involving hydrogen peroxide?

Answer (Q8, Recall). Peroxisomal oxidase enzymes catalyse the first reaction — substrate oxidation that produces hydrogen peroxide, for example during fatty-acid beta-oxidation, where an oxidase transfers electrons to O_2 generating H_2O_2 ($\text{RH}_2 + \text{O}_2 \rightarrow \text{R} + \text{H}_2\text{O}_2$). The second reaction is catalase-catalysed decomposition of that H_2O_2 : $2 \text{H}_2\text{O}_2 \rightarrow 2 \text{H}_2\text{O} + \text{O}_2$. So the peroxisome both generates H_2O_2 (as a controlled byproduct of oxidative metabolism) and immediately detoxifies it with catalase, keeping reactive oxygen species in check while shortening very-long-chain fatty acids. See section 6. 9. Distinguish the large central vacuole of plants from contractile vacuoles of protists.

Answer (Q9, Recall). Both are large membrane-bound storage compartments, but they solve different problems with different mechanisms. The plant large central vacuole is a single, near-permanent organelle occupying up to 80-90% of cell volume; bounded by the tonoplast, it stores water, ions, pigments, and waste, and generates turgor pressure that drives plant cell growth and rigidity — it is largely metabolically inert volume that helps cells get large without raising metabolic demand. The contractile vacuole of freshwater protists is a small, dynamic osmoregulatory organelle that cyclically fills with excess water entering by osmosis and then contracts to expel it across the plasma membrane, preventing osmotic lysis in a hypotonic environment. So the difference is static structural and storage role versus active, cyclic osmotic-pump role. See section 6. 10. What is the centrosome? What happens to centrosomes during mitosis?

Answer (Q10, Recall). The centrosome is the primary microtubule-organizing center (MTOC) of animal cells: two barrel-shaped centrioles (each nine triplet microtubules in a pinwheel) surrounded by pericentriolar material containing gamma-tubulin ring complexes that nucleate microtubules. During the cell cycle the centrosome duplicates (one new centriole per existing one) in S phase; at mitosis the two centrosomes separate and migrate to opposite poles, where each nucleates the microtubules of the bipolar mitotic spindle that captures and segregates chromosomes. Centrosome amplification (more than 2 per cell) causes multipolar spindles and chromosomal instability, a common feature of cancer. See section 6.

Questions 11–20: Application and Analysis

- Trace the complete path of a secretory protein from its gene to the extracellular space, naming every organelle and vesicle type it passes through.

Answer (Q11, Application). A secretory protein follows the SRP and endomembrane route. (1) The gene is transcribed in the nucleus; mRNA exits through a nuclear pore complex. (2) Translation begins on a free cytosolic ribosome; the emerging signal peptide is bound by the signal recognition particle (SRP), which pauses translation and docks the ribosome at the SRP receptor on the rough ER. (3) The polypeptide is co-translationally threaded through the Sec61 translocon into the ER lumen, the signal peptide is cleaved, and the protein folds and is N-glycosylated under chaperone (BiP, calnexin) quality control. (4) Correctly folded cargo buds in COPII-coated vesicles to the cis-Golgi (via the ERGIC). (5) It moves cis to medial to trans through the Golgi stack, where it is further glycosylated and processed. (6) At the trans-Golgi network it is sorted into a secretory vesicle. (7) The vesicle traffics to and fuses with the plasma membrane (constitutive or Ca^{2+} -triggered regulated exocytosis), releasing the protein to the extracellular space. See section 6. 12. A mutation disables the signal recognition particle (SRP). Predict the fate of a lysosomal enzyme without functional SRP.

Answer (Q12, Application). SRP normally recognizes the signal peptide of a secretory or lysosomal protein as it emerges from the ribosome, pauses translation, and delivers the ribosome-nascent-chain complex to the SRP receptor and Sec61 translocon on the rough ER. If SRP is disabled, this co-translational targeting step fails for the lysosomal enzyme. The chain is therefore not paused and not delivered to the ER; translation completes in the cytosol, so the protein is synthesized as a cytosolic polypeptide instead of entering the ER lumen. Consequently it never gets its signal peptide cleaved, is not N-glycosylated, never reaches the Golgi to acquire the mannose-6-phosphate lysosomal tag, and is not delivered to the lysosome. The mistargeted, unmodified protein typically misfolds in the cytosol and is degraded by the ubiquitin-proteasome system; lysosomal hydrolase activity is lost. See section 6. 13. Colchicine prevents microtubule polymerization. Would it disrupt: (a) chromosome segregation; (b) ER-Golgi trafficking; (c) cell migration; (d) axonal transport? Justify each.

Answer (Q13, Application). Colchicine binds free tubulin and prevents microtubule polymerization, so every microtubule-dependent process is disrupted. (a) Chromosome segregation: YES — the mitotic spindle is microtubule-based, so chromosomes cannot be captured or moved and cells arrest in metaphase. (b) ER-Golgi trafficking: YES — long-range vesicle transport between ER and Golgi runs on microtubule tracks via kinesin and

dynein; the Golgi also disperses without microtubules. (c) Cell migration: YES (partly) — directed migration needs microtubule-based polarity and trafficking even though the protrusive force is actin-driven, so persistent directional crawling is impaired. (d) Axonal transport: YES — fast axonal transport of vesicles and organelles is kinesin/dynein movement along axonal microtubules, which collapses without microtubules. See section 6. 14. Gaucher disease results from a deficiency of the lysosomal enzyme glucocerebrosidase. What accumulates, in which cells, and why does this cause splenomegaly and bone marrow infiltration?

Answer (Q14, Application). Glucocerebrosidase normally hydrolyses glucocerebroside (glucosylceramide), a sphingolipid generated mainly from the turnover of membranes of senescent blood cells. With the enzyme deficient, undigested glucocerebroside accumulates inside the lysosomes of macrophages, because macrophages phagocytose large numbers of aged erythrocytes and leukocytes and depend on lysosomal degradation to recycle their membranes. The engorged lipid-laden macrophages (Gaucher cells) accumulate in the spleen, liver, and bone marrow. Splenic infiltration by these cells causes massive splenomegaly (and hypersplenism, cytopenias); bone marrow infiltration displaces normal hematopoiesis and erodes bone, causing anemia, thrombocytopenia, and bone disease. It is a lysosomal storage disease treatable by enzyme replacement therapy targeted to lysosomes via the M6P receptor. See section 6. 15. If a cell's mitochondria were removed, which metabolic pathways would be abolished and which would remain functional? Calculate the maximum ATP yield from 1 glucose in a cell without mitochondria.

Answer (Q15, Application). Removing mitochondria abolishes every pathway housed in or on them: the pyruvate dehydrogenase reaction, the TCA cycle, fatty-acid beta-oxidation, and oxidative phosphorylation (electron transport chain plus ATP synthase). Pathways that remain functional are the cytosolic ones: glycolysis, the pentose phosphate pathway, glycogen metabolism, and lactate fermentation (needed to regenerate NAD⁺). Maximum ATP yield from one glucose without mitochondria: glycolysis yields a net 2 ATP per glucose by substrate-level phosphorylation (4 made, 2 invested = net 2 ATP) plus 2 NADH that must be reoxidised by lactate dehydrogenase to sustain glycolysis. So the answer is 2 ATP per glucose, versus about 30-32 ATP with full oxidative phosphorylation — a roughly 15-fold loss of energy efficiency, which is why mitochondria-free cells (e.g., red blood cells) depend wholly on glycolysis. See section 6. 16. Clathrin-coated vesicles mediate receptor-mediated endocytosis. Describe the sequence from receptor-ligand binding to delivery of cargo to endosomes. Name two other coat protein systems and their functions.

Answer (Q16, Application). Clathrin-mediated endocytosis sequence: (1) an extracellular ligand binds its transmembrane receptor at the plasma membrane; (2) the adaptor complex AP2 links the receptor cytoplasmic tails to clathrin triskelions, which polymerize into a lattice and curve the membrane into a coated pit; (3) the GTPase dynamin assembles at the neck and pinches off a clathrin-coated vesicle; (4) the clathrin coat is removed (uncoating by Hsc70 and auxilin) and the naked vesicle fuses with the early endosome (pH about 6.0); (5) the acidic endosome dissociates ligand from receptor — receptors recycle to the plasma membrane while cargo is sent to late endosomes and lysosomes (pH about 4.5). Two other coat systems: COPII (Sar1, Sec23/24, Sec13/31) buds vesicles anterograde from ER to cis-Golgi; COPI (coatamer, Arf1) mediates retrograde Golgi-to-ER retrieval of escaped KDEL ER-resident proteins. See section 6. 17. Motor proteins kinesin (moves to + end) and dynein (moves to – end) both use microtubule tracks. How does a cell ensure organelles are delivered to the correct destination — axon terminal vs cell body?

Answer (Q17, Application). Microtubules are polar, with minus ends anchored at the centrosome/MTOC (cell body) and plus ends toward the periphery; in an axon they are uniformly oriented plus-end-out. Directionality of delivery is set by motor identity plus cargo-specific adaptors. Kinesin-1 walks toward the plus end (anterograde, about 0.8 $\mu\text{m/s}$), carrying newly synthesized synaptic-vesicle precursors, mitochondria, and membrane proteins from the cell body to the axon terminal. Cytoplasmic dynein walks toward the minus end (retrograde, about 1.0 $\mu\text{m/s}$), returning endosomes, signaling endosomes, autophagosomes, and damaged components from the terminal to the cell body. The cell ensures correct destination by attaching the appropriate motor (and regulatory adaptors that activate one motor and inhibit the other) to each cargo, so cargo identity selects the motor and the motor selects the direction along the oriented track. See section 6. 18. The rough ER membrane is studded with ribosomes, while the smooth ER is ribosome-free. A mutation eliminates the ribosome-binding site on the ER translocon (Sec61). Predict the consequence for: (a) membrane protein insertion; (b) secretory protein signal peptide cleavage.

Answer (Q18, Application). Co-translational targeting to the rough ER requires the ribosome to dock onto the Sec61 translocon (handed off from SRP/SR) so the nascent chain is threaded into the ER as it is made. If the ribosome-binding site on Sec61 is destroyed, ribosomes cannot dock, so secretory and membrane proteins are no longer co-translationally translocated. (a) Membrane protein insertion: fails — without ribosome docking the nascent chain cannot be threaded into or laterally released into the ER membrane, so type-I/II/multipass membrane proteins are not inserted (they are mistranslated in the cytosol and degraded). (b) Secretory protein signal-peptide cleavage: fails — signal peptidase acts on the luminal side of the translocon during translocation; if the chain never enters the translocon it is never presented to signal peptidase, so the signal peptide is not cleaved. Net effect: collapse of the secretory pathway with cytosolic accumulation and proteasomal degradation of these proteins. See section 6. 19. Zellweger syndrome (peroxisome biogenesis disorder) causes progressive neurological deterioration. Identify two specific metabolic functions of peroxisomes in neurons that would be disrupted, and explain the mechanism of neural damage.

Answer (Q19, Application). Zellweger syndrome results from PEX-gene mutations that abolish functional peroxisomes, so peroxisomal metabolism collapses. Two neuron-relevant functions disrupted: (1) Very-long-chain fatty acid (VLCFA, >C22) beta-oxidation — peroxisomes are the only site

that shortens VLCFAs; without it, VLCFAs accumulate and are incorporated into and destabilise neuronal and myelin membranes. (2) Plasmalogen biosynthesis — the early steps of ether-phospholipid (plasmalogen) synthesis occur in peroxisomes, and plasmalogens are essential structural lipids of myelin; their deficiency prevents normal myelination. Mechanism of neural damage: failure to make myelin plus toxic VLCFA accumulation produces dysmyelination and demyelination, neuronal migration defects, and oxidative or membrane damage, manifesting as severe hypotonia, seizures, and progressive neurological deterioration. See section 6. 20. A researcher fuses a nuclear localization signal (NLS) to a cytoplasmic protein (GFP). Describe the molecular events leading to the protein's nuclear import, including the roles of importin- α , importin- β , RanGTP, and the nuclear pore complex.

Answer (Q20, Application). GFP-NLS is imported by the classical importin pathway powered by the Ran gradient. (1) In the cytoplasm, importin- α binds the basic NLS (the adaptor) and importin- β binds importin- α and provides the affinity for the nuclear pore complex. (2) Importin- β interacts with the FG-repeat nucleoporins lining the NPC central channel, allowing the cargo complex to translocate through the roughly 9 nm gated channel. (3) Inside the nucleus, RanGTP (kept high in the nucleus by chromatin-bound RanGEF/RCC1) binds importin- β , causing a conformational change that releases importin- α and the GFP-NLS cargo into the nucleoplasm. (4) The importins are recycled back to the cytoplasm bound to RanGTP; cytoplasmic RanGAP then hydrolyses RanGTP to RanGDP, releasing the importins for another round. The roughly 10^4 :1 nuclear:cytoplasmic RanGTP ratio makes import vectorial; it is GTP-hydrolysis-powered, not driven by a translocation ATPase. See section 6.

Questions 21–30: Synthesis and Evaluation

21. Primary cilia are now recognized as signaling organelles for Hedgehog, Wnt, and PDGFR pathways. Evaluate why concentrating receptors in a small ciliary compartment (0.1% of total cell surface) enhances signaling sensitivity compared to distributing receptors over the entire plasma membrane.

Answer (Q21, Synthesis). The primary cilium is a 9+0 microtubule-based antenna making up only about 0.1% of total cell surface, into which specific receptors (Smoothed/Patched for Hedgehog, Frizzled for Wnt, PDGFR- α) are actively concentrated by intraflagellar transport. Concentrating receptors and their downstream machinery in this tiny compartment enhances sensitivity for several causal reasons: (1) the small volume means even a few activated receptors and second messengers reach a high local concentration, raising the signal-to-noise ratio relative to the same molecules diluted over the whole $1,300\text{ }\mu\text{m}^2$ plasma membrane; (2) co-localizing receptor, transducer (e.g., GLI processing machinery for Hedgehog), and effectors in one diffusion-limited space speeds productive collisions and reduces off-target dilution; (3) the ciliary membrane has a distinct lipid and protein composition and a diffusion barrier at the base (the transition zone) that retains active components and excludes inhibitors. Boundary condition: this gain depends on regulated trafficking into and out of the cilium; if intraflagellar transport or the transition-zone gate fails (ciliopathies), the concentrating advantage is lost and signaling becomes both insensitive and dysregulated. See section 6. 22. Design an experiment to determine whether a newly discovered organelle in a marine protist is related to the peroxisome or the lysosome, using: (a) proteomic analysis; (b) membrane lipid analysis; (c) fluorescent marker trafficking; (d) inhibitor sensitivity.

Answer (Q22, Synthesis). Hypothesis: the unknown organelle is peroxisome-related (H1) versus lysosome-related (H2). The discriminating expectations: peroxisomes import folded matrix proteins post-translationally via PTS1/PTS2 (PEX5/PEX7), contain catalase and beta-oxidation oxidases, have a near-neutral lumen, and arise by growth/division or from ER; lysosomes contain acid hydrolases, maintain pH about 4.5 via a V-ATPase, receive cargo by M6P-receptor sorting from the trans-Golgi, and are degradative. Tests, each with the matched control: (a) Proteomics — isolate the organelle by density-gradient fractionation and identify proteins; PEX proteins, catalase, and acyl-CoA oxidase support H1, whereas cathepsins and other acid hydrolases support H2 (control: co-fractionate with known peroxisome and lysosome markers). (b) Membrane lipid analysis — assay for plasmalogen-synthesis intermediates (peroxisomal) versus lysosomal-membrane-specific lipids (control: known organelle lipidomes). (c) Fluorescent marker trafficking — express GFP-SKL (PTS1) versus an M6P-tagged hydrolase and see which is delivered (control: wild-type markers in normal cells). (d) Inhibitor sensitivity — treat with bafilomycin A1 (V-ATPase): loss of luminal acidification and hydrolase activity supports H2; insensitivity supports H1. Decision rule: assign to the lineage matching the majority of independent assays; a falsifying result for H1 is an acidic, M6P-targeted, bafilomycin-sensitive compartment lacking PEX import. Replicate each assay (n at least 3) with fixed seeds for any image quantification. See section 6. 23. Autophagy (macro, micro, chaperone-mediated) degrades cytosolic material. Evaluate the selective vs non-selective aspects of each type, and propose why cells might preferentially use CMA (chaperone-mediated autophagy) rather than macroautophagy for long-lived soluble proteins.

Answer (Q23, Synthesis). All three deliver cytosolic material to the lysosome but differ in selectivity. Macroautophagy: a double-membrane phagophore engulfs bulk cytoplasm or, when tagged by receptors (p62/SQSTM1, NBR1) reading ubiquitin, specific cargo (mitophagy, ER-phagy); it is non-selective by default but can be made selective by receptors. Microautophagy: the lysosomal/vacuolar membrane directly invaginates and engulfs small portions of cytosol; largely non-selective, good for steady-state turnover. Chaperone-mediated autophagy (CMA): highly selective — Hsc70 recognizes a KFERQ-like pentapeptide motif in soluble substrate proteins and delivers them one by one across the lysosomal membrane via the LAMP-2A translocation receptor; no vesicle is formed. Why a cell would prefer CMA for long-lived soluble proteins: CMA targets individual proteins by sequence motif without sequestering and destroying neighboring organelles or bulk cytosol, so it allows precise removal of damaged

or regulatory soluble proteins (and selective amino-acid mobilization in prolonged starvation) while sparing functional structures — a precision tool versus the bulk demolition of macroautophagy. See section 6. 24. Reticulophagy (selective ER autophagy) is triggered by ER stress. Trace the molecular pathway from misfolded protein accumulation → IRE1 α /PERK/ATF6 activation → reticulophagy receptor induction → ER-phagy. What would happen if reticulophagy were completely blocked?

Answer (Q24, Synthesis). Pathway: accumulation of misfolded proteins in the ER lumen titrates the chaperone BiP away from the three stress sensors, activating them. IRE1- α dimerises and its endoribonuclease splices XBP1 mRNA to XBP1s, a transcription factor driving ER-expansion, ERAD, and lipid-synthesis genes; PERK phosphorylates eIF2- α to attenuate global translation (reducing new client load) while selectively translating ATF4; ATF6 traffics to the Golgi, is cleaved by S1P/S2P, and its fragment transcribes ER chaperones (BiP, GRP94). These outputs induce reticulophagy receptors (e.g., FAM134B, RTN3, CCPG1, SEC62) that bind LC3 on the phagophore, so excess and damaged ER is selectively engulfed and delivered to the lysosome (ER-phagy), restoring ER size and quality. If reticulophagy were completely blocked: damaged and surplus ER cannot be cleared, so misfolded-protein and expanded-ER load persists, the UPR stays chronically activated, and the PERK-ATF4-CHOP arm (plus IRE1 RIDD) biases the cell toward apoptosis; secretory cells (e.g., pancreatic beta-cells) are especially vulnerable, paralleling ER-stress-driven beta-cell loss in type 2 diabetes. See section 6. 25. The Golgi apparatus disperses into ministacks during mitosis and reassembles in each daughter cell after division. Evaluate the mechanism of Golgi fragmentation (role of mitotic kinases) and reassembly (role of p97 ATPase), and explain why Golgi inheritance must be coordinated with chromosome segregation.

Answer (Q25, Synthesis). Golgi fragmentation: at mitotic entry, CDK1-cyclin B and Polo-like kinase phosphorylate Golgi structural proteins (GRASP65/55, golgins), severing the cisternal stacking and tethering links; ongoing membrane fission (and inhibited fusion) converts the ribbon into dispersed tubulovesicular ministacks/clusters that partition stochastically with the cytoplasm to both daughters. Reassembly: after anaphase, mitotic kinases are inactivated and their sites are dephosphorylated; the AAA+ ATPase p97/VCP (with cofactors p47 and the SNARE machinery) uses ATP hydrolysis to drive homotypic fusion of Golgi membranes, and GRASP/golgin-mediated tethering rebuilds the stacked ribbon in each daughter cell. Why coordination with chromosome segregation matters: the Golgi has no template and cannot be synthesized de novo quickly, so each daughter must inherit roughly half of it; fragmentation into many small units makes inheritance statistically even, and tying disassembly/reassembly to the same CDK1-driven mitotic clock that controls chromosome segregation ensures the Golgi is partitioned in step with the genome rather than being lost or unequally divided. See section 6. 26. Compare endocytosis mechanisms: clathrin-mediated endocytosis, caveolae-mediated endocytosis, macropinocytosis, and phagocytosis. For each: what cargo is internalised, what signaling events initiate it, and how is cargo processed after internalization?

Answer (Q26, Synthesis). The shared principle is internalization by membrane invagination and vesicle formation; the mechanism-defining differences (coat, cytoskeleton, trigger, cargo, fate) change the interpretation. Clathrin-mediated endocytosis: small (about 100 nm) clathrin/AP2-coated vesicles internalise specific receptor-ligand pairs (LDL, transferrin, EGF) after ligand binding clusters receptors; dynamin scission; cargo to early then late endosome/lysosome, receptors recycled. Caveolae-mediated: about 50-80 nm caveolin/cavin flask-shaped invaginations of cholesterol/sphingolipid rafts; internalise certain toxins (cholera toxin), some viruses (SV40), and GPI-anchored proteins; signaling-platform regulated; cargo to caveosomes/endosomes, often bypassing lysosomal degradation. Macropinocytosis: large (0.5-5 μ m) actin-driven ruffle-derived vacuoles internalising bulk extracellular fluid and solutes; triggered by growth-factor (PI3K/Rac) signaling; cargo to macropinosomes that mature into lysosomes. Phagocytosis: very large (>1 μ m) actin-dependent engulfment by professional phagocytes; triggered by opsonin receptors (Fc, complement) recognizing microbes/apoptotic cells; cargo enclosed in a phagosome that fuses with lysosomes (phagolysosome) for destruction. The decisive contrast is coat-and-cytoskeleton: clathrin/dynamin and small cargo versus caveolin-raft versus large actin-driven uptake, which sets cargo size and post-internalization fate. See section 6. 27. COPI-coated vesicles mediate retrograde transport from Golgi back to ER (retrieval of escaped ER-resident proteins). How do KDEL-bearing ER-resident proteins get retrieved? What is the KDEL receptor, and what happens to its affinity for KDEL at Golgi pH vs ER pH?

Answer (Q27, Synthesis). ER-resident luminal proteins (BiP, PDI, calreticulin) carry a C-terminal KDEL tetrapeptide. They escape the ER by bulk flow into COPII vesicles and reach the cis/medial Golgi. There the KDEL receptor (KDEL R , a multipass Golgi membrane protein) binds them and is packaged into COPI-coated vesicles for retrograde transport back to the ER, where the proteins are released. The pH-dependent affinity switch makes this a cycle: the slightly acidic Golgi lumen (about pH 6.2-6.7) protonates key histidine residues in KDEL R , giving it high affinity so it captures KDEL ligands in the Golgi; on return to the more neutral ER lumen (about pH 7.2) those residues deprotonate, lowering KDEL R affinity so it releases the cargo back into the ER and the empty receptor recycles forward again. Thus KDEL R has high KDEL affinity at Golgi pH and low affinity at ER pH, producing vectorial retrieval that keeps ER-resident enzymes from being secreted. See section 6. 28. The nuclear lamina (lamin intermediate filaments) underlies the inner nuclear membrane. Mutations in lamin A cause laminopathies including Hutchinson-Gilford progeria syndrome (HGPS) — a premature aging disease. Evaluate how nuclear structural failure leads to an accelerated-aging phenotype at the cellular level.

Answer (Q28, Synthesis). The nuclear lamina is a meshwork of lamin A/C and B intermediate filaments underlying the inner nuclear membrane that gives the nucleus mechanical rigidity, anchors heterochromatin, and organizes the genome. In HGPS a point mutation activates a cryptic splice site in LMNA, producing progerin, a permanently farnesylated lamin A lacking 50 residues that cannot be processed and incorporates into the lamina abnormally. Causal chain to accelerated aging at the cellular level: progerin stiffens and distorts the nuclear lamina, producing misshapen, mechanically fragile nuclei; this disrupts lamina-associated heterochromatin and gene-expression programs, impairs DNA-damage repair (persistent double-strand breaks), and increases sensitivity to mechanical stress in load-bearing tissues (vasculature). The accumulating genomic damage and chromatin disorganization drive premature replicative arrest and cellular senescence (and apoptosis) in vascular smooth muscle and other cells, manifesting organismally as accelerated atherosclerosis and the progeroid phenotype. The interpretation generalizes: a structural nuclear protein failure becomes a genome-maintenance and senescence problem. See section 6. 29. Cells in developing lungs must convert from secreting surfactant (lipid-rich, packaged in lamellar bodies — lysosome-related organelles) to absorbing alveolar fluid at birth. Evaluate the signaling mechanisms controlling this switch and what organelle remodeling is required.

Answer (Q29, Synthesis). Before birth, alveolar type II cells are secretory: they synthesize surfactant lipids and proteins, package them into lamellar bodies (lysosome-related organelles), and release them by regulated exocytosis to line the airspaces. At birth the lung must rapidly switch from secreting fluid and surfactant to absorbing the alveolar liquid so gas exchange can begin. Signaling control: the perinatal surge in glucocorticoids and thyroid hormone (and the labor-associated catecholamine/beta-adrenergic surge, plus rising oxygen tension) reprogrammes the epithelium — beta-adrenergic and steroid signaling switch on apical epithelial Na⁺ channels (ENaC) and basolateral Na⁺/K⁺-ATPase, so the cells now drive vectorial Na⁺ (and osmotically obligated water) absorption out of the airspace. Organelle remodeling required: the secretory machinery is down-regulated (fewer lamellar bodies and reduced regulated-exocytosis apparatus) while the cell up-regulates ion-transport membrane proteins and the supporting endomembrane/trafficking and mitochondrial (ATP for the Na⁺ pump) capacity, converting a secretion-specialized cell into an absorption-specialized one. See section 6. 30. Evaluate the concept of “organelle crosstalk”: mitochondria-ER contact sites (MAM — mitochondria-associated membranes) facilitate Ca²⁺ and lipid exchange. How does disruption of MAM contact alter: (a) mitochondrial Ca²⁺ buffering; (b) phosphatidylserine transfer; (c) mitochondrial morphology? Cite evidence from neurodegenerative disease models.

Answer (Q30, Synthesis). Organelle crosstalk means organelles communicate through membrane-contact sites rather than working in isolation. Mitochondria-ER contact sites (MAMs) are zones where the ER and outer mitochondrial membrane are tethered about 10-30 nm apart, enabling local Ca²⁺ and lipid exchange. Empirical predictions of disrupting MAM tethering: (a) Mitochondrial Ca²⁺ buffering — MAMs deliver IP₃-receptor-released ER Ca²⁺ directly to the mitochondrial VDAC/MCU uniporter; loss of contact lowers mitochondrial Ca²⁺ uptake, blunting Ca²⁺-stimulated TCA dehydrogenases (less ATP) yet, paradoxically, can also dysregulate apoptotic Ca²⁺ signaling. (b) Phosphatidylserine transfer — PS made in the ER is handed to mitochondria at MAMs for conversion to phosphatidylethanolamine; disruption impairs mitochondrial PE supply and membrane composition. (c) Mitochondrial morphology — MAMs mark DRP1-mediated fission sites (the ER pre-constricts mitochondria); losing contacts reduces proper fission, shifting the network toward aberrant elongation or fragmentation and impairing quality control. Disease evidence (what would strengthen or weaken the causal claim): MAM proteins are perturbed in neurodegeneration — mutant presenilins/APP processing enrich at MAMs in Alzheimer disease, alpha-synuclein and PINK1/Parkin link MAM dysfunction to Parkinson disease, and VAPB mutations (ALS) disrupt ER-mitochondria tethering. These are largely correlative model-system findings; the conclusion that MAM disruption is causal would be strengthened by showing that restoring physiological tethering rescues the cellular phenotype and weakened if the defects persisted independent of contact-site status. See section 6.

Questions — Membrane Structure and Transport

Instructor Use and Coverage Notes

- Coverage target: Calculate or predict ion movement and explain which force dominates.
- Model/data emphasis: Nernst, Goldman, osmotic, and facilitated-transport calculations.
- Assessment alignment: Visual Representations, Questions and Methods, Argumentation.
- Misconception probe: Equilibrium does not mean equal concentration; charge and permeability matter.
- Transfer product: Transfer gradient logic to neurons, kidneys, roots, and mitochondrial membranes.
- Grading focus: award full credit for mechanism, evidence, boundary conditions, and units when a calculation is required.
- Suggested use: draw one recall item, one application item, and one synthesis item when building a short quiz from this bank.

Questions 1–10: Recall and Comprehension

This activity accompanies section 7 of the textbook — review that chapter before attempting the exercises below.

1. Describe the fluid-mosaic model of the plasma membrane (Singer-Nicolson, 1972). What are the two major components?

Answer (Q1, Recall). The fluid mosaic model (Singer & Nicolson, *Science* 1972) describes biological membranes as a two-dimensional fluid of phospholipids in which proteins are embedded like mosaic tiles, both components free to diffuse laterally. Two major components: (1) phospholipid bilayer — amphipathic phosphoglycerolipids (phosphatidylcholine, phosphatidylethanolamine, sphingomyelin) spontaneously organizing into a ≈ 4–5 nm thick bilayer with hydrophobic tails inward and polar heads at the aqueous interfaces, providing the fluid matrix; and (2) membrane proteins (integral/transmembrane such as GLUT1, ion channels, Na⁺/K⁺-ATPase; peripheral proteins docked via electrostatics), which account for about 50% of membrane mass and carry out transport, signaling, and recognition. A lipid molecule diffuses laterally at about 10^{−8} cm²/s (about μm-scale in seconds) but “flip-flops” between leaflets extremely rarely (hours without flippases) — asymmetry is *biological*, not physical. Canonical example: red blood cell membrane, where Band 3 (anion exchanger) and spectrin cytoskeleton give the lipid mosaic its characteristic deformability. See section 7. 2. What is a phospholipid bilayer? Explain why it forms spontaneously in an aqueous environment.

Answer (Q2, Recall). A phospholipid bilayer is a two-layer sheet of amphipathic phospholipids with hydrophobic fatty-acid tails facing inward and polar phosphate head groups facing the aqueous solutions on both sides, about 4-5 nm thick. It forms spontaneously because the hydrophobic effect: nonpolar tails minimize unfavorable contact with water by self-associating, while polar heads remain hydrated, so the bilayer is the lowest-free-energy arrangement and even seals into closed vesicles. See section 7. 3. Define selective permeability. Which types of molecules cross membranes freely and which require assistance?

Answer (Q3, Recall). Selective permeability means the membrane allows some substances to cross readily while restricting others, controlled by the lipid bilayer and specific transport proteins. Small nonpolar molecules (O₂, CO₂, N₂) and small polar uncharged molecules (water, urea, glycerol) cross freely by simple diffusion; large polar molecules (glucose, amino acids) and all ions (Na⁺, K⁺, Ca²⁺, Cl[−]) cannot cross the hydrophobic core and require channel or carrier proteins. See section 7. 4. Distinguish simple diffusion, facilitated diffusion, and active transport.

Answer (Q4, Recall). All three move solutes across membranes but differ in energy and protein use. Simple diffusion: solute moves down its electrochemical gradient directly through the lipid bilayer, no protein, no energy. Facilitated diffusion: still down-gradient and energy-free, but through a channel or carrier protein (saturable). Active transport: moves solute against its electrochemical gradient and therefore requires energy (ATP hydrolysis or a coupled ion gradient). The decisive difference is the direction relative to the gradient and whether energy is consumed. See section 7. 5. What is the sodium-potassium ATPase (Na⁺/K⁺-ATPase)? How many ions does it move per ATP?

Answer (Q5, Recall). The Na⁺/K⁺-ATPase is a primary active transport pump (P-type ATPase) in the plasma membrane that uses ATP hydrolysis to move Na⁺ and K⁺ against their gradients. Per ATP hydrolysed it exports 3 Na⁺ and imports 2 K⁺, a net movement of +1 charge outward, making it electrogenic. It maintains high intracellular K⁺ (about 140 mM) and low Na⁺ (about 12 mM) and consumes about 25% of body ATP (up to 70% in neurons). See section 7. 6. Define osmosis. In which direction does water move — toward high or low solute concentration?

Answer (Q6, Recall). Osmosis is the net diffusion of water across a semi-permeable membrane in response to a difference in solute concentration. Water moves toward the side of higher solute concentration (lower water concentration/activity), because added solute lowers water activity, so water flows from the dilute (hypotonic) side toward the concentrated (hypertonic) side until water chemical potential is equalised. See section 7. 7. What is a membrane potential? What is the typical resting membrane potential of a mammalian cell?

Answer (Q7, Recall). Membrane potential is the voltage difference across the plasma membrane, arising because ions are unequally distributed and the membrane is selectively permeable to them (largely K⁺ at rest, read out by the Goldman equation). A typical mammalian resting membrane potential is about −70 mV (inside negative), lying close to E_K (about −89 mV) because the resting membrane is about 25× more permeable to K⁺ than Na⁺. See section 7. 8. Distinguish primary from secondary active transport. Give one example of each.

Answer (Q8, Recall). Both move solutes against their gradient (active), but differ in energy source. Primary active transport hydrolyses ATP directly (e.g., the Na^+/K^+ -ATPase moving 3 Na^+ out / 2 K^+ in per ATP; also SERCA, H^+/K^+ -ATPase). Secondary active transport uses the electrochemical gradient of one ion (usually the Na^+ gradient set up by the primary pump) to drive uphill movement of another solute (e.g., SGLT1 symport: 2 Na^+ + glucose into intestinal cells). The decisive difference is direct ATP use versus exploiting a previously stored ion gradient. See section 7. 9. What is endocytosis? Distinguish phagocytosis, pinocytosis, and receptor-mediated endocytosis.

Answer (Q9, Recall). Endocytosis is the uptake of extracellular material by invagination of the plasma membrane to form an internal vesicle. Phagocytosis: actin-driven pseudopod engulfment of large particles ($>0.5\ \mu\text{m}$ — bacteria, debris) by professional phagocytes. Pinocytosis (here macropinocytosis): non-specific bulk uptake of extracellular fluid in large ($0.2\text{--}5\ \mu\text{m}$) actin-ruffle vesicles. Receptor-mediated (clathrin-mediated) endocytosis: specific cargo receptors cluster in AP2/clathrin-coated pits and are internalised in small (about $60\text{--}120\ \text{nm}$) coated vesicles (e.g., LDL receptor). See section 7. 10. What is the role of cholesterol in membrane structure? How does it affect fluidity at high and low temperatures?

Answer (Q10, Recall). Cholesterol intercalates between phospholipids with its rigid steroid ring near the head groups and acts as a fluidity buffer. At high temperature it restrains phospholipid motion and reduces fluidity (condensing effect); at low temperature it disrupts tight crystalline packing and prevents the membrane from becoming a rigid gel (fluidising effect). The net result is that membrane fluidity is stabilized across a physiological temperature range. See section 7.

Questions 11–20: Application and Analysis

11. A cell is placed in a hypertonic solution. Describe, at the molecular level, what happens to: (a) the direction of water movement; (b) cell volume; (c) the cytoskeleton if shrinkage is severe; (d) membrane potential due to increased ion concentration.

Answer (Q11, Application). (a) The external solution is hypertonic (higher solute, lower water activity), so water moves out of the cell down its chemical-potential gradient. (b) Cell volume decreases (the cell shrinks/crenates). (c) Severe shrinkage causes the cytoskeleton (actin cortex/spectrin) to crumple and buckle as membrane area exceeds the reduced volume. (d) As water leaves, intracellular ion concentrations rise; this alters the Nernst potentials in the Goldman equation, but the membrane potential is buffered by the dominant K^+ permeability and active pumping rather than tracking concentration linearly. See section 7. 12. The Na^+/K^+ -ATPase pumps 3 Na^+ out and 2 K^+ in per ATP hydrolysed. Explain why this creates an electrogenic current. Calculate the charge moved per pump cycle and predict how ouabain (a pump inhibitor) would affect membrane potential.

Answer (Q12, Application). Per ATP: +3 Na^+ extruded – 2 K^+ imported = net +1 charge out, so each pump cycle moves +1 elementary charge ($+1.60 \times 10^{-19}\ \text{C}$) outward — the pump is electrogenic. Current: typical neuron density $\approx 1000\ \text{pumps}/\mu\text{m}^2$, cycling at about $100\ \text{s}^{-1} \rightarrow$ surface current density $\approx 16\ \mu\text{A}/\text{cm}^2$. This direct contribution accounts for roughly -5 to $-10\ \text{mV}$ of the resting potential ($\approx 10\text{--}15\%$ of the total); the remaining $-60\ \text{mV}$ comes from the K^+ gradient read out by the Goldman–Hodgkin–Katz equation. Ouabain prediction: inhibiting Na^+/K^+ -ATPase abolishes the electrogenic component — immediate depolarization of about $5\text{--}10\ \text{mV}$. Over seconds-to-minutes, intracellular $[\text{Na}^+]$ rises and $[\text{K}^+]$ falls, collapsing the Nernst gradients that set the resting potential \rightarrow further, profound depolarization and failure to repolarise after an action potential. Secondary consequence: the Na^+ -gradient-driven $\text{Na}^+/\text{Ca}^{2+}$ exchanger reverses, intracellular Ca^{2+} rises, boosting cardiac contractility — the basis of ouabain/digoxin’s positive inotropic effect on the failing heart. See section 7. 13. Glucose enters intestinal epithelial cells via SGLT1 (Na^+ -glucose co-transporter) on the apical membrane and exits via GLUT2 (passive facilitated diffusion) on the basolateral membrane. Explain: (a) which transport is primary active and which is secondary active; (b) why this arrangement allows glucose to be absorbed against its concentration gradient.

Answer (Q13, Application). (a) Neither transporter hydrolyses ATP directly, so neither is primary active here; SGLT1 is secondary active transport (it uses the inward Na^+ electrochemical gradient — itself maintained by the primary Na^+/K^+ -ATPase on the basolateral membrane — to co-transport glucose), while GLUT2 is passive facilitated diffusion. (b) SGLT1 couples glucose uptake to favorable Na^+ entry, so glucose is dragged into the cell even when intracellular glucose already exceeds luminal glucose (uphill); accumulated glucose then exits down its gradient through GLUT2 into blood. The Na^+/K^+ -ATPase keeps intracellular Na^+ low, sustaining the gradient that powers net transcellular glucose absorption against its own gradient. See section 7. 14. CFTR is a Cl^- channel mutated in cystic fibrosis. The ΔF508 deletion causes CFTR misfolding and ER retention. Explain how this affects: (a) epithelial Cl^- secretion; (b) mucus viscosity; (c) bacterial colonization of airways.

Answer (Q14, Application). ΔF508 CFTR misfolds and is retained/degraded in the ER, so functional CFTR Cl^- channels never reach the apical membrane. (a) Epithelial Cl^- secretion is lost, so accompanying water secretion onto the airway surface falls. (b) The airway surface liquid becomes dehydrated, so mucus becomes thick and viscous and cannot be cleared by cilia. (c) Stagnant viscous mucus impairs mucociliary clearance, allowing chronic bacterial colonization (e.g., *Pseudomonas aeruginosa*) and recurrent infection. See section 7. 15. A cell biologist measures the fluorescence recovery after photobleaching (FRAP) of a fluorescently labeled membrane protein. Recovery takes 30 seconds in normal cells but 5 minutes in cells with disrupted actin cortex. Interpret this result using the fluid-mosaic model and the concept of membrane protein diffusion constraints.

Answer (Q15, Application). FRAP measures lateral mobility of membrane proteins, a core prediction of the fluid mosaic model. Normal cells recover in 30 s because labeled proteins diffuse laterally in the fluid bilayer into the bleached spot. With a disrupted actin cortex recovery should reflect free diffusion, but here it slows to 5 minutes — indicating the actin cortex normally is not what slows diffusion; instead its disruption alters the picket-fence corrals or traps proteins, showing that membrane protein diffusion is not free but constrained by cytoskeletal fences (Kusumi corrals, about 40-300 nm). The result demonstrates the membrane is more mosaic and compartmentalised than the original 1972 ‘free diffusion’ picture. See section 7. 16. Explain how the membrane potential arises from differences in ion permeability (Goldman equation). If a cell becomes 10× more permeable to Na⁺ (e.g., during an action potential), predict the direction of change in membrane potential and apply the Nernst equation to estimate the equilibrium potential for Na⁺.

Answer (Q16, Application). The Goldman equation makes V_m a permeability-weighted log average of the ion Nernst potentials, so the most permeable ion dominates; at rest P_K is high and V_m sits near E_K (about −70 mV). If the cell becomes 10× more permeable to Na⁺, the Na⁺ term grows and V_m shifts toward E_{Na}, i.e., the membrane depolarizes (toward positive). Estimate E_{Na} from the Nernst equation at 37 °C with [Na⁺]_{out} = 145 mM, [Na⁺]_{in} = 12 mM, z = +1: $E_{Na} = 61.5 \text{ mV} \cdot \log_{10}(145/12) = 61.5 \cdot \log_{10}(12.08) = 61.5 \cdot 1.082 \text{ approx} + 67 \text{ mV}$. So increased Na⁺ permeability drives V_m up toward about +60 mV (the basis of the action potential upstroke). See section 7. 17. Vesicle fusion requires SNARE proteins. Explain the zipper model of SNARE complex assembly and how this drives membrane fusion. Why does botulinum toxin (which cleaves SNARE proteins) block neurotransmitter release?

Answer (Q17, Application). SNARE complexes form a four-helix bundle from a v-SNARE (VAMP/synaptobrevin) on the vesicle and t-SNAREs (syntaxin + SNAP-25) on the target membrane. In the zipper model the bundle zippers progressively from the membrane-distal N-terminus toward the membrane-proximal C-terminus; this releases about 35 kBT per complex, more than the about 25 kBT barrier to fusion, pulling the two membranes together until their bilayers merge. Botulinum toxin is a zinc protease that cleaves VAMP, SNAP-25, or syntaxin, so the SNARE bundle cannot assemble or zipper; without a functional SNARE complex synaptic vesicles cannot fuse, blocking acetylcholine release and causing flaccid paralysis. See section 7. 18. Aquaporin-1 (AQP1) is absent in red blood cells from certain individuals, yet these individuals are healthy. AQP1 knockout mice have impaired urinary concentrating ability. Explain this discrepancy — what does it reveal about the relative importance of aquaporin vs lipid bilayer water permeability in different tissues?

Answer (Q18, Application). Both reflect AQP1’s role in water transport, but the importance of aquaporins versus the lipid bilayer differs by tissue. Red blood cells without AQP1 stay healthy because the bilayer itself provides enough baseline water permeability for the modest osmotic challenges erythrocytes normally face. The kidney, however, must move very large water volumes rapidly to concentrate urine; here bilayer permeability is far too slow, so AQP1 (proximal tubule/descending limb) is essential and its loss impairs urinary concentrating ability. The discrepancy shows aquaporins are critical only where fast, high-throughput water flux is physiologically required, while elsewhere lipid bilayer permeability suffices. See section 7. 19. LDL receptor-mediated endocytosis concentrates LDL receptors in clathrin-coated pits. FH (familial hypercholesterolaemia) patients lack functional LDL receptors. Explain: (a) why plasma LDL rises dramatically; (b) why heterozygous FH is less severe than homozygous; (c) why statins partially compensate for LDL receptor deficiency.

Answer (Q19, Application). (a) LDL is normally cleared when LDL receptors concentrate in clathrin-coated pits and internalise LDL by receptor-mediated endocytosis; without functional receptors LDL is not removed from plasma, so circulating LDL cholesterol rises dramatically. (b) Heterozygous FH patients have one working LDL-receptor allele, so roughly half-normal receptor activity gives intermediate LDL elevation, whereas homozygotes have essentially no functional receptors and far more severe hypercholesterolaemia/early atherosclerosis. (c) Statins inhibit HMG-CoA reductase, lowering intracellular cholesterol; cells respond by upregulating any residual LDL receptors, so statins partially compensate only when some functional receptor remains (heterozygotes respond; receptor-negative homozygotes respond poorly). See section 7. 20. Membrane asymmetry: phosphatidylserine (PS) is normally on the inner leaflet but is exposed on the outer leaflet of apoptotic cells. Explain: (a) the enzyme (flippase) that normally maintains PS on the inner leaflet; (b) the enzyme (scramblase) that destroys asymmetry during apoptosis; (c) the physiological consequence of outer-leaflet PS exposure (phagocyte recognition).

Answer (Q20, Application). (a) Flippases (ATP-dependent P4-ATPases) normally translocate phosphatidylserine (and PE) from the outer to the inner leaflet, keeping PS confined to the cytoplasmic face. (b) During apoptosis, Ca²⁺-activated scramblases (TMEM16F) bidirectionally and non-selectively randomize lipids across the bilayer (and flippases are inactivated), so PS moves to the outer leaflet. (c) Externalised PS is an ‘eat me’ signal recognized by phagocyte receptors (TIM-4, BAI-1, Stabilin-2), so the apoptotic cell is engulfed and cleared without releasing inflammatory contents. See section 7.

Questions 21–30: Synthesis and Evaluation

21. Evaluate the thermodynamic basis of lipid raft formation. What causes certain lipids (sphingomyelin, cholesterol, saturated phospholipids) to phase-separate into liquid-ordered domains? Evaluate the evidence that lipid rafts are real functional domains vs artifacts of cold detergent extraction.

Answer (Q21, Synthesis). Liquid-ordered raft domains form because cholesterol packs tightly against the long, saturated acyl chains of sphingomyelin/saturated phospholipids, maximizing favorable van der Waals contacts and lowering free energy, so these lipids preferentially segregate from the disordered, unsaturated bulk bilayer — a lipid-driven phase separation. The evidence that rafts are real functional domains rather than cold-detergent artifacts is the key judgement: detergent-resistant membrane fractions alone are weak evidence because cold detergent can itself induce domains, but live-cell single-molecule and STED super-resolution imaging (Eggeling et al. 2009) shows transient nanoscale (about 10-20 nm, about 10-20 ms) confinement of sphingolipids/GPI-anchored proteins, supporting a dynamic raft model. What would change the conclusion: if super-resolution/live-cell methods showed no preferential confinement and domains appeared only after detergent extraction, rafts would be artefactual. See section 7. 22. The membrane potential (typically -70 mV, inside negative) represents stored electrochemical energy. Calculate the energy available per mole of Na^+ flowing inward across a neuron membrane using $\Delta G = zF\Delta\Psi + RT \ln([\text{Na}^+]_{\text{in}}/[\text{Na}^+]_{\text{out}})$. How does this compare to the energy of ATP hydrolysis (about -57 kJ/mol at physiological concentrations)?

Answer (Q22, Synthesis). Model: electrochemical free energy for an ion crossing the membrane, $\Delta G = zF\Delta\Psi + RT \ln([\text{Na}^+]_{\text{in}}/[\text{Na}^+]_{\text{out}})$. Substitute for Na^+ entering a neuron ($z = +1$; $\Delta\Psi = -0.070$ V; $[\text{Na}^+]_{\text{in}} = 12$ mM, $[\text{Na}^+]_{\text{out}} = 145$ mM; $F = 96\,485$ C/mol; $R = 8.314$ J/mol·K; $T = 310$ K): electrical term = $(1)(96485)(-0.070) = -6754$ J/mol *approx* -6.8 kJ/mol; chemical term = $(8.314)(310) \ln(12/145) = 2577 \cdot \ln(0.0828) = 2577 \cdot (-2.49) = -6418$ J/mol *approx* -6.4 kJ/mol. Total ΔG *approx* $-6.8 + (-6.4) = -13.2$ kJ/mol (energy released as Na^+ flows in). Compared with ATP hydrolysis (about -57 kJ/mol at cellular concentrations), one inward Na^+ releases only about 23% as much energy, so the cell needs to couple several Na^+ entries (secondary active transport) to do work equivalent to one ATP, and about 4 Na^+ worth of gradient is recharged per ATP by the Na^+/K^+ -ATPase — consistent with the pump's 3 Na^+/ATP stoichiometry plus voltage cost. See section 7. 23. Ionophores are small molecules that carry specific ions across lipid bilayers. Valinomycin is a K^+ -selective ionophore; gramicidin is a non-selective cation channel. Compare their effects on: (a) membrane potential; (b) mitochondrial function; (c) cell viability at therapeutic vs toxic concentrations. How are they used experimentally as tools?

Answer (Q23, Synthesis). Valinomycin selectively shuttles K^+ , gramicidin forms a non-selective monovalent-cation channel. (a) Membrane potential: valinomycin clamps V_m toward E_K (can hyperpolarise or, by collapsing the K^+ gradient, depolarize depending on gradients); gramicidin lets Na^+ and K^+ flow freely and collapses V_m toward about 0. (b) Mitochondrial function: both dissipate the inner-membrane electrochemical gradient — valinomycin collapses the membrane potential component (K^+ uniport), gramicidin collapses both, so the proton-motive force needed for ATP synthase is lost and oxidative phosphorylation uncouples. (c) Cell viability: at low/therapeutic doses gramicidin is a useful topical antibiotic (kills bacteria by ion leak) while host cells tolerate brief exposure; at higher concentrations both are cytotoxic because gradient collapse halts ATP synthesis. Experimentally they are used as tools to clamp membrane potential, set defined K^+ diffusion potentials, and deliberately uncouple mitochondria. See section 7. 24. Membrane curvature is actively generated during endocytosis, vesicle budding, and tubule formation. Evaluate the mechanisms: (a) BAR domain protein scaffolding; (b) asymmetric lipid composition; (c) protein insertion into the cytoplasmic leaflet. Which mechanism is most critical for clathrin-mediated endocytosis at the cell's flat plasma membrane?

Answer (Q24, Synthesis). (a) BAR-domain proteins are banana-shaped dimers whose curved concave face binds the membrane and imposes its curvature as a rigid scaffold (and tubulates membranes). (b) Asymmetric lipid composition bends the bilayer when one leaflet has bulkier head groups or more area than the other, creating spontaneous curvature. (c) Amphipathic helix/protein insertion into the cytoplasmic leaflet acts as a wedge, expanding that leaflet locally and driving the membrane to curve away. For clathrin-mediated endocytosis starting from the flat plasma membrane, the dominant curvature generator is the clathrin coat itself (triskelions assembling into a curved polyhedral lattice via AP2 adaptors), with BAR proteins (e.g., at the neck) and dynamin assisting; coat-driven scaffolding is most critical for initiating the invagination from a flat membrane. See section 7. 25. Osmotic stress responses in bacteria involve membrane sensors (e.g., EnvZ osmosensor) that activate two-component signaling systems. Compare bacterial osmosensing to mammalian cell osmosensing via volume-sensitive ion channels (VSOR). Which system responds faster and why?

Answer (Q25, Synthesis). Bacterial osmosensing uses the membrane histidine kinase EnvZ, which detects osmotic change and autophosphorylates, then transfers phosphate to the response regulator OmpR, which alters gene transcription (porin expression) — a two-component signaling cascade requiring new gene expression and protein synthesis (minutes). Mammalian osmosensing via volume-sensitive outwardly rectifying anion channels (VSOR) is a direct mechanical/volume response: cell swelling opens the channels in seconds, allowing regulatory ion (and osmolyte) efflux for volume recovery without any transcription. The mammalian channel system responds faster because it is a direct conformational gating of pre-existing channels, whereas the bacterial response depends on the slower transcription-translation loop. See section 7. 26. Fatty acid composition of membrane phospholipids changes with temperature (homeoviscous adaptation). Design an experiment to determine whether *E. coli* adjusts membrane fluidity in response to temperature via: (a) transcriptional regulation of fatty acid desaturases; (b) selective incorporation of exogenous fatty acids; or (c) lipid flip-flop remodeling. What lipid analysis technique would you use?

Answer (Q26, Synthesis). Hypothesis: *E. coli* maintains membrane fluidity at low temperature mainly by transcriptionally upregulating fatty-

acid desaturase to add double bonds (vs. exogenous-fatty-acid incorporation or flip-flop remodeling). Experiment: shift cultures from 37 °C to a low temperature; controls are constant-37 °C cultures and a desaturase-deletion (or inhibitor) strain. Manipulate one variable at a time — (a) measure desaturase mRNA/activity and test the desaturase mutant; (b) supply isotopically labeled exogenous unsaturated fatty acids and test their incorporation; (c) test a flippase-deficient strain for impaired remodeling. Measured outcome: phospholipid acyl-chain unsaturation and membrane fluidity (fluorescence anisotropy / DPH probe), with replicates. If only desaturase induction tracks the fluidity change and the desaturase mutant fails to adapt, that mechanism is supported; if adaptation persists without desaturase or only with exogenous fatty acids, the hypothesis is falsified. Lipid analysis technique: gas chromatography-mass spectrometry of fatty-acid methyl esters (and/or LC-MS lipidomics). See section 7. 27. P-glycoprotein (MDR1) is an ABC transporter that pumps hydrophobic drugs out of cancer cells, causing multidrug resistance. Evaluate: (a) why hydrophobic drugs are its substrates; (b) why inhibiting MDR1 has largely failed clinically; (c) an alternative strategy (e.g., prodrug activation inside the cell) that bypasses MDR1.

Answer (Q27, Synthesis). (a) MDR1/P-glycoprotein has a large hydrophobic substrate cavity and extracts substrates from within the lipid bilayer, so lipophilic, membrane-partitioning drugs (taxol, doxorubicin, vincristine) are exactly the molecules it can grab and pump out using ATP hydrolysis. (b) Clinical MDR1 inhibition has largely failed because broad pump inhibitors are non-specific (P-gp also protects normal tissues like the blood-brain barrier and gut), causing toxicity and altered pharmacokinetics of co-administered drugs, and resistance is often multifactorial — so blocking one efflux pump rarely restores sensitivity at tolerable doses; what would change this judgement is a truly tumor-selective, potent inhibitor. (c) An alternative strategy is an inactive prodrug that freely enters cells and is converted to the active cytotoxic drug only intracellularly (or a non-substrate drug/nanocarrier delivery), so the toxic species is generated past the pump and is not a P-gp substrate, bypassing efflux. See section 7. 28. The mitochondrial inner membrane maintains a proton gradient ($\Delta\mu_{H^+} = -200$ mV, $\Delta pH = 1$ unit = -59 mV, electrical = -141 mV). Using the chemiosmotic equation $\Delta G = nF\Delta\Psi + 2.303RT\Delta pH$, calculate the total proton-motive force. How does this compare to the energy needed to synthesize ATP from ADP + Pi (about +37 kJ/mol at physiological [ATP]/[ADP])? Assume 3 H⁺ per ATP (c-ring H⁺/ATP coupling ratio).

Answer (Q28, Synthesis). Chemiosmotic equation (per mol H⁺): $\Delta G_{H^+} = F\Delta\Psi + 2.303RT\Delta pH$. At 37 °C, $F = 96.5$ kJ/(V·mol); $2.303RT = 5.92$ kJ/mol per pH unit. Substitute: $\Delta G_{H^+} = (96.5)(-0.141\text{ V}) + (5.92)(-1) = -13.60 - 5.92 = -19.5$ kJ/mol H⁺. Equivalent PMF in volts: $\Delta G/F = -19.5/96.5 = -0.202\text{ V} \approx -200$ mV (matches stated $\Delta\mu_{H^+}$). For 3 H⁺ transported per ATP synthesized: $\Delta G_{3H^+} = 3 \times (-19.5) = -58.5$ kJ. Energy needed per ATP at cellular [ATP]/[ADP]·[Pi] $\approx +50$ to $+57$ kJ/mol (higher than standard +30.5 because cells hold [ATP]/[ADP] $\approx 500:1$). Verdict: $58.5 > 50 \rightarrow$ thermodynamically favorable, but with about 6–8 kJ/mol margin only. This is why mitochondrial ATP synthesis is tightly coupled (F_0F_1 operates near equilibrium, c-ring stoichiometry 8–10 H⁺ per rotation \times 3 ATP per rotation = about 2.7–3.3 H⁺/ATP) and why small uncoupler doses (2,4-DNP, thermogenin in brown fat) convert PMF directly to heat rather than ATP. Intervention: DNP (protonophore) at 50 μ M; assay: oxygen-consumption rate + ATP:O₂ ratio (Seahorse XF) — predicts respiration \uparrow , ATP output \downarrow . See section 7. 29. Nanoparticle drug delivery systems exploit endocytosis for intracellular drug delivery. Evaluate the barriers nanoparticles face: (a) being taken up via endocytosis rather than direct membrane fusion; (b) endosomal escape before lysosomal degradation; (c) targeting specificity via surface ligands. What design features address each barrier?

Answer (Q29, Synthesis). (a) Nanoparticles are too large to cross the bilayer by fusion, so they enter via endocytosis and become trapped inside membrane-bound endosomes — the cargo is internalised but not yet in the cytosol where it must act. (b) Endosomes mature and fuse with lysosomes; without timely endosomal escape the drug/nucleic acid is degraded by acidic hydrolases. (c) Without targeting, uptake is non-specific, so off-target cells take up the particle. Design features: PEGylation and about 50-150 nm size to favor productive endocytic uptake and circulation; ionisable/cationic lipids or pH-buffering ('proton sponge') or fusogenic peptides to rupture/escape the endosome before lysosomal fusion; and surface ligands/antibodies (e.g., transferrin, folate, anti-receptor) to drive receptor-mediated uptake selectively into target cells. See section 7. 30. Stretch-activated ion channels (SACs) open when the plasma membrane is mechanically deformed. Design a complete research program to: (a) identify the molecular identity of a SAC in cardiac myocytes; (b) determine its role in cardiac arrhythmia during myocardial stretch; (c) develop a selective SAC inhibitor and evaluate its anti-arrhythmic potential in a relevant animal model.

Answer (Q30, Synthesis). (a) Identify the molecular SAC: patch-clamp isolated cardiac myocytes under membrane stretch to characterize the current, then use candidate mechanosensitive channels (e.g., Piezo1, TREK-1) — knock down/out each and test loss of the stretch current, and reconstitute the candidate in a heterologous system to confirm it is sufficient (controls: non-stretched cells, scrambled siRNA). (b) Role in arrhythmia: in a stretched-myocyte or isolated-heart preparation, apply controlled mechanical stretch and record stretch-induced depolarisations/ectopic beats with and without the channel present, establishing whether SAC activity causes mechanically induced arrhythmia (mechanism: stretch \rightarrow SAC opens \rightarrow depolarization \rightarrow triggered activity). (c) Develop and evaluate a selective inhibitor: screen for compounds that block the identified SAC without affecting other cardiac channels, confirm selectivity by patch-clamp, then test anti-arrhythmic efficacy in a relevant animal model (e.g., volume-overload or stretch-induced arrhythmia) versus vehicle controls, with replication and a predefined falsifying result (no reduction in arrhythmia despite target engagement disproves the SAC hypothesis). See section 7.

Questions — Cell Signaling and Communication

Instructor Use and Coverage Notes

- Coverage target: Predict the outcome of perturbing one pathway component and justify the causal chain.
- Model/data emphasis: Ligand-receptor occupancy and dose-response reasoning.
- Assessment alignment: Visual Representations, Questions and Methods, Argumentation.
- Misconception probe: A pathway diagram is a causal model, not a memorization chart.
- Transfer product: Apply signaling logic to hormones, neurotransmitters, immune receptors, or cancer mutations.
- Grading focus: award full credit for mechanism, evidence, boundary conditions, and units when a calculation is required.
- Suggested use: draw one recall item, one application item, and one synthesis item when building a short quiz from this bank.

Questions 1–10: Recall and Comprehension

This activity accompanies section 8 of the textbook — review that chapter before attempting the exercises below.

1. List the three stages of cell signaling. Give a brief description of each stage.

Answer (Q1, Recall). Cell signaling has three stages. Reception: a signaling molecule (ligand) binds a specific receptor, which detects the signal. Transduction: the receptor triggers an intracellular cascade (e.g., G-protein activation, kinase phosphorylation, second-messenger production) that amplifies and relays the signal. Response: effectors produce the cellular outcome — altered enzyme activity, gene transcription, or ion flux — followed by termination. See section 8. 2. Name four chemical classes of signaling molecules. Give one biological example of each.

Answer (Q2, Recall). Four classes are: proteins/peptides (e.g., insulin, growth factors), steroids/lipophilic hormones (e.g., cortisol, estrogen), amino-acid derivatives/amines (e.g., epinephrine, thyroid hormone), and gases/small molecules (e.g., nitric oxide). Peptide and amine signals are usually hydrophilic and bind cell-surface receptors, whereas steroids cross the membrane to bind intracellular receptors. See section 8. 3. Distinguish autocrine, paracrine, endocrine, and contact-dependent signaling.

Answer (Q3, Recall). The four modes differ by the distance between sending and receiving cell. Autocrine: a cell secretes a signal that acts on itself (e.g., IL-2 in T cells). Paracrine: local diffusion to nearby cells (<1 mm; growth factors, prostaglandins). Endocrine: hormones travel meters through the bloodstream (insulin, cortisol). Contact-dependent (juxtacrine): membrane-bound ligand binds a receptor on a touching cell (Notch-Delta, ephrin-Eph). See section 8. 4. What is a G protein-coupled receptor (GPCR)? Name the three subunits of the heterotrimeric G protein.

Answer (Q4, Recall). A GPCR is a cell-surface receptor with seven transmembrane alpha-helices, an extracellular N-terminus and intracellular C-terminus; it is the largest receptor superfamily (about 800 in humans). Ligand binding changes its conformation so it acts as a GEF for an associated heterotrimeric G protein. The three subunits are G-alpha, G-beta, and G-gamma (Gβγ acting as a functional unit). See section 8. 5. Describe the second messengers cAMP and IP₃/DAG and name the enzymes that produce each.

Answer (Q5, Recall). cAMP is produced from ATP by adenylyl cyclase, activated downstream of Gs; it activates protein kinase A (PKA). IP₃ and DAG are produced together when phospholipase C-beta (Gq pathway) cleaves PIP₂: IP₃ releases Ca²⁺ from the ER via IP₃ receptors, while DAG stays in the membrane and activates protein kinase C (PKC). See section 8. 6. What is a receptor tyrosine kinase (RTK)? Name two growth factor receptors of this type.

Answer (Q6, Recall). An RTK is a single-pass transmembrane receptor with an extracellular ligand-binding domain and a cytoplasmic tyrosine kinase domain; ligand binding causes dimerization and trans-autophosphorylation that recruits SH2/PTB adaptors. Two growth-factor receptors of this type are EGFR (HER1) and HER2 (also the insulin receptor, VEGFR2, FGFR are RTKs). See section 8. 7. Define signal amplification. Give a numerical example from a GPCR cascade.

Answer (Q7, Recall). Signal amplification is the production of many active downstream molecules per single activated upstream molecule; total gain is the product of per-step gains, $G_{\text{total}} = \prod_{i=1}^n A_i$. In the epinephrine→glycogenolysis GPCR cascade there are 4 enzymatic steps each with $A_i \approx 10^{1.5}$, giving $G_{\text{total}} \approx (10^{1.5})^4 = 10^6$, so one epinephrine molecule releases about 10⁸ glucose molecules. See section 8. 8. What is a MAP kinase cascade? List the three kinases in the Ras-MAPK pathway.

Answer (Q8, Recall). A MAP kinase cascade is a three-tier kinase relay in which each kinase phosphorylates and activates the next, providing amplification and ultrasensitivity. In the classical Ras-MAPK (ERK) pathway the three kinases are RAF (MAPKKK), MEK1/2 (MAPKK), and ERK1/2 (MAPK); ERK requires dual Thr/Tyr phosphorylation for activity. See section 8. 9. Define receptor downregulation. What cellular mechanism drives it?

Answer (Q9, Recall). Receptor downregulation is a sustained reduction in the number of surface receptors that lowers cell sensitivity during prolonged stimulation. It is driven by GRK phosphorylation of the active receptor, β-arrestin recruitment, and clathrin-mediated internalization;

receptors sorted to lysosomes are degraded, so restoring response requires hours-to-days of new receptor synthesis. See section 8. 10. What is the role of protein phosphatases in signal termination?

Answer (Q10, Recall). Protein phosphatases terminate signaling by removing the phosphate groups that kinases add, reversing activation of pathway components. Examples include PP1 and PP2A (dephosphorylate PKA substrates), calcineurin/PP2B (Ca^{2+} -dependent), MKPs/DUSPs (dephosphorylate MAPKs), and PTEN (removes the 3-phosphate from PIP_3 , opposing PI3K). See section 8.

Questions 11–20: Application and Analysis

11. Adrenaline binds β -adrenergic receptors (Gs-coupled). Trace the complete signaling cascade from ligand binding to glycogen phosphorylase activation, naming every molecule. How many molecules of glycogen phosphorylase are activated per initial adrenaline molecule?

Answer (Q11, Application). Adrenaline binds the β_2 -adrenergic receptor → receptor activates Gs → $\text{G}\alpha\text{s}$ -GTP dissociates and activates adenylyl cyclase → adenylyl cyclase converts ATP to cAMP → cAMP binds PKA regulatory subunits, releasing active PKA catalytic subunits → PKA phosphorylates and activates phosphorylase kinase → phosphorylase kinase activates glycogen phosphorylase. The 4-step enzymatic cascade has gain $\approx 10^6$ ($\prod A_i$, each $A_i \approx 10^{1.5}$), so one adrenaline molecule activates on the order of 10^6 glycogen phosphorylase molecules (releasing about 10^8 glucose). See section 8. 12. Steroid hormones (e.g., cortisol) exert their effects via intracellular receptors that act as transcription factors. Compare the timescale, reversibility, and specificity of steroid signaling vs adrenaline signaling via GPCR. Which is more suitable for rapid physiological responses, and why?

Answer (Q12, Application). Cortisol is lipophilic, diffuses through the membrane, binds the cytoplasmic glucocorticoid receptor, and acts as a ligand-activated transcription factor: slow (minutes-to-hours, requires transcription/translation), long-lasting, and highly gene-specific. Adrenaline via a GPCR acts in seconds through pre-existing enzymes and second messengers, is rapidly reversible upon termination. The GPCR pathway is more suitable for rapid physiological responses because it modifies existing proteins instead of waiting for new gene expression. See section 8. 13. Explain how Ca^{2+} acts as a second messenger. What keeps resting cytoplasmic $[\text{Ca}^{2+}]$ so low (about 100 nM)? What is the role of calmodulin as a Ca^{2+} sensor, and which kinase does Ca^{2+} -calmodulin activate?

Answer (Q13, Application). Ca^{2+} acts as a second messenger because resting cytoplasmic $[\text{Ca}^{2+}]$ is held about 100 nM by SERCA pumps (into the ER), plasma-membrane Ca^{2+} -ATPases/ Na^+ - Ca^{2+} exchangers, and cytoplasmic buffering (about 99% bound by calbindin/calretinin), so a small influx produces a large fractional rise. Calmodulin binds 4 Ca^{2+} ions and the Ca^{2+} -calmodulin complex changes conformation to act as a sensor; it activates CaMKII (Ca^{2+} /calmodulin-dependent protein kinase II), important in synaptic plasticity. See section 8. 14. Trastuzumab (Herceptin) is a monoclonal antibody that targets HER2 (an RTK overexpressed in about 25% of breast cancers). Explain its mechanism of action: how does receptor blockade inhibit downstream MAPK and PI3K-Akt signaling, and why does HER2 dimerization (with HER3) make it particularly potent?

Answer (Q14, Application). Trastuzumab binds the extracellular subdomain IV of HER2; in HER2-amplified cells it sterically blocks HER2 self-dimerization, so the receptors cannot trans-autophosphorylate, which shuts off recruitment of Grb2/SOS→RAS→MAPK and PI3K→Akt signaling. It also accelerates HER2 internalization/degradation and triggers antibody-dependent cellular cytotoxicity via NK cells. HER2-HER3 heterodimers are the strongest mitogenic pair, so blocking HER2 dimerization is particularly potent at silencing the dominant proliferative/survival drive. See section 8. 15. An inhibitor blocks PLC- β (phospholipase C- β). Predict the effects on: (a) IP_3 production; (b) DAG levels; (c) PKC activation; (d) intracellular Ca^{2+} release from the ER; (e) smooth muscle contraction downstream of M3 muscarinic receptor activation.

Answer (Q15, Application). PLC- β cleaves PIP_2 into IP_3 and DAG, so blocking it cuts both messengers. (a) IP_3 production falls; (b) DAG levels fall; (c) PKC activation falls (no DAG, and no IP_3 -driven Ca^{2+}); (d) IP_3 -receptor-mediated Ca^{2+} release from the ER is lost, so cytoplasmic Ca^{2+} does not rise; (e) M3 muscarinic (Gq-coupled) smooth muscle contraction is blocked because contraction depends on the $\text{IP}_3/\text{Ca}^{2+}$ signal. See section 8. 16. Cross-talk between signal pathways allows integration of multiple inputs. Describe two specific examples where activation of one signaling pathway inhibits or potentiates the response of another pathway. How might this cross-talk produce distinct cellular outcomes depending on context?

Answer (Q16, Application). Example 1: PKA (cAMP pathway) phosphorylates and inhibits RAF, so a Gs/cAMP signal dampens RTK-MAPK proliferative signaling — context determines whether a cell proliferates. Example 2: PI3K-Akt survival signaling phosphorylates and inactivates the pro-apoptotic protein BAD, so a growth-factor survival input potentiates resistance to a death signal. The same death or growth ligand therefore produces opposite outcomes (survival vs apoptosis) depending on which other pathways are concurrently active, because the cell responds to the integrated sum of all pathways. See section 8. 17. Wnt signaling inhibits the destruction complex (APC/Axin/CK1/GSK3 β), allowing β -catenin to accumulate and enter the nucleus. Explain how mutations in APC (found in >80% of colorectal cancers) constitutively activate Wnt signaling and promote cell proliferation.

Answer (Q17, Application). Normally the destruction complex (APC/Axin/CK1/GSK3 β) phosphorylates β -catenin, marking it for β -TrCP ubiquitination and proteasomal degradation, keeping target genes off. APC mutations (in >80% of colorectal cancers) disable the destruction complex, so

β -catenin is no longer degraded; it accumulates, enters the nucleus, binds TCF/LEF, and constitutively activates proliferative target genes (c-Myc, cyclin D1) — mimicking a permanent Wnt signal and driving uncontrolled proliferation. See section 8. 18. Nitric oxide (NO) is produced by nitric oxide synthase (NOS) and diffuses freely across membranes to activate soluble guanylate cyclase (sGC) in smooth muscle cells, producing cGMP. Explain: (a) why NO is unusual as a paracrine signal; (b) how sildenafil (Viagra) potentiates the NO-cGMP pathway; (c) what happens to cGMP without PDE5 inhibition.

Answer (Q18, Application). (a) NO is unusual because it is a small, membrane-permeant gas synthesized on demand by NOS; it diffuses directly into neighboring cells without a receptor or transporter and has a very short half-life, so its range is set by diffusion and decay. (b) NO activates soluble guanylate cyclase \rightarrow cGMP \rightarrow PKG \rightarrow smooth muscle relaxation; sildenafil inhibits PDE5, which normally degrades cGMP, so cGMP accumulates only where NO is being made, potentiating relaxation. (c) Without PDE5 inhibition, PDE5 rapidly hydrolyses cGMP to 5'-GMP, terminating the signal and ending relaxation. See section 8. 19. Notch signaling requires direct cell-cell contact (juxtacrine). When Notch receptor (on receiving cell) binds Delta ligand (on sending cell), γ -secretase cleaves the Notch intracellular domain (NICD), which enters the nucleus. Explain: (a) why this signaling cannot be mediated by a diffusible messenger; (b) the role of Notch in lateral inhibition during development.

Answer (Q19, Application). (a) Notch signaling cannot use a diffusible messenger because the ligand (Delta/Jagged) is membrane-bound on the sending cell and signaling depends on mechanical force from ligand endocytosis, which exposes Notch to ADAM and γ -secretase cleavage — this only occurs when the two cells are in direct contact. (b) In lateral inhibition, a cell expressing more Delta activates Notch in its neighbors; Notch signaling suppresses Delta in those neighbors, so one cell adopts the primary fate while adjacent cells are forced to the alternative fate, generating fine-grained 'salt-and-pepper' patterning during development. See section 8. 20. TGF- β receptors (type I and type II serine/threonine kinase receptors) signal via SMAD proteins. Explain: (a) how receptor dimerization activates SMAD2/3 phosphorylation; (b) how SMAD4 forms a complex with phospho-SMAD2/3; (c) how this complex regulates target gene transcription in the context of tumor suppression vs EMT (epithelial-mesenchymal transition).

Answer (Q20, Application). (a) Ligand binding brings type II and type I TGF- β receptors together; the constitutively active type II receptor transphosphorylates and activates the type I receptor, which then phosphorylates receptor-SMADs (SMAD2/3). (b) Phospho-SMAD2/3 binds the co-SMAD SMAD4, forming a heteromeric complex that translocates to the nucleus. (c) The SMAD complex binds DNA with cofactors to regulate transcription; in normal epithelium it acts as a tumor suppressor (induces p21, cytostasis), but with cooperating oncogenic signals the same complex drives an EMT program (Snail/Slug), promoting invasion — outcome is context-dependent. See section 8.

Questions 21–30: Synthesis and Evaluation

21. Evaluate the concept of “signal integration”: a cell simultaneously receives growth factor (MAPK activation), anchorage signals (integrin-FAK signaling), and survival signals (insulin \rightarrow PI3K-Akt). How does the cell integrate these three pathways to make a proliferation vs death decision? Name at least one molecular node where the three signals converge.

Answer (Q21, Synthesis). The cell integrates the three inputs at convergent nodes rather than treating them independently. Growth factor \rightarrow MAPK drives cyclin D1; survival (insulin \rightarrow PI3K-Akt) inactivates pro-apoptotic BAD and activates mTORC1; anchorage (integrin-FAK) is also required for full PI3K/mTORC1 activation. A key convergence node is mTORC1, which requires both growth-factor (PI3K/Akt) and integrin signals, providing an anchorage checkpoint: a cell receiving the combined growth, survival, and anchorage inputs proliferates, while loss of anchorage or survival input tips the balance toward apoptosis (anoikis). The decision reflects the integrated balance, and removing the integrin input would change the conclusion. See section 8. 22. Design a CRISPR screen to identify novel negative regulators of the EGFR-MAPK pathway in non-small-cell lung cancer cells. Describe the library design, the cellular readout, and how you would validate the top hits as therapeutically relevant targets.

Answer (Q22, Synthesis). Hypothesis: knocking out a true negative regulator increases EGFR-MAPK output and growth. Design a genome-wide CRISPR knockout library (e.g., about 4 sgRNAs/gene) transduced at low MOI into NSCLC cells; controls are non-targeting sgRNAs and known regulators (NF1, DUSP6, Sprouty). Readout: an ERK-activity transcriptional reporter (FACS sort high-ERK cells) or proliferation/dropout under EGFR-inhibitor selection, comparing sgRNA abundance vs the unsorted population. Replicate the screen; validate top hits with individual knockouts measuring phospho-ERK by Western blot, and test therapeutic relevance by checking whether re-expressing the gene or pairing its loss with a MEK inhibitor restores drug sensitivity. A hit whose loss does not raise phospho-ERK falsifies it as a negative regulator. See section 8. 23. Receptor endocytosis and downregulation reduce cell sensitivity to a signal. However, some endosomal signaling (e.g., from endosome-localized EGFR) is qualitatively different from plasma membrane signaling. Evaluate the concept of “spatial encoding” of signal quality by receptor location. What specific downstream effectors are activated preferentially from endosomal vs surface receptors?

Answer (Q23, Synthesis). Spatial encoding means a receptor’s signaling output depends on its location, not just its ligand. Surface EGFR strongly engages RAS-MAPK and PLC- γ for proliferative/immediate responses, whereas EGFR that has been internalised into endosomes preferentially sustains PI3K-Akt survival signaling and continues ERK signaling from the endosome via β -arrestin scaffolds, producing a qualitatively different,

prolonged output. Thus endocytosis is not merely ‘off’: it relocates the receptor to a compartment with different available effectors, so the same ligand produces compartment-specific signaling and downregulation simultaneously. See section 8. 24. Intracellular Ca^{2+} oscillations are widely used for signal encoding. Evaluate how the frequency and amplitude of Ca^{2+} oscillations can encode different cellular responses (NF- κ B vs NFAT activation). What molecular mechanism (IP_3 R sensitivity to Ca^{2+} and inhibition by Ca^{2+}) generates oscillations?

Answer (Q24, Synthesis). Ca^{2+} oscillations encode information in frequency and amplitude rather than a static level: low-frequency/transient spikes preferentially activate NF- κ B, whereas sustained or high-frequency oscillations are needed to keep the Ca^{2+} -dependent phosphatase calcineurin active long enough to dephosphorylate NFAT and drive its nuclear retention. The oscillations themselves arise because the IP_3 receptor is biphasically regulated by Ca^{2+} — modest cytosolic Ca^{2+} increases its open probability (Ca^{2+} -induced Ca^{2+} release) but high local Ca^{2+} inhibits it; this positive-then-negative feedback, plus SERCA re-uptake, produces repetitive spikes. Whether this ‘decoding’ interpretation holds can be tested by clamping Ca^{2+} at fixed frequencies and measuring NF- κ B vs NFAT activation. See section 8. 25. Synaptic signaling relies on glutamate receptor subtypes (AMPA, NMDA, mGluR) with vastly different ion conductances, Ca^{2+} permeabilities, and kinetics. Evaluate how the combination of fast ionotropic (AMPA) and slow modulatory (NMDA, mGluR) signaling enables both rapid synaptic transmission and long-term plasticity at the same synapse.

Answer (Q25, Synthesis). AMPA receptors are fast ionotropic channels (sub-millisecond Na^+/K^+ flux) that mediate rapid, moment-to-moment excitatory transmission. NMDA receptors are slower coincidence detectors: they conduct Ca^{2+} only when glutamate binds AND the membrane is already depolarized (removing the Mg^{2+} block), so Ca^{2+} entry occurs only with paired pre/post activity, triggering CaMKII and LTP. mGluRs are slow modulatory GPCRs that adjust synaptic gain over seconds. Co-locating fast (AMPA) and slow (NMDA/mGluR) systems lets one synapse both transmit signals instantly and use the Ca^{2+} -gated NMDA pathway to write long-term, activity-dependent plasticity. See section 8. 26. Drug resistance in targeted therapy often results from mutations that reactivate downstream signaling. In BRAF^{V600E} melanoma treated with vemurafenib (BRAF inhibitor), resistance arises via: (a) RAS mutation bypassing BRAF; (b) MEK1 mutation making it insensitive; (c) RAF1 dimerization activating MEK. Evaluate why combination therapy (BRAF + MEK inhibition) reduces resistance emergence.

Answer (Q26, Synthesis). Vemurafenib inhibits the BRAF V600E kinase, shutting MEK→ERK. Resistance reactivates ERK by routes that bypass drug-bound BRAF: (a) a RAS mutation drives signaling through CRAF independent of BRAF; (b) a MEK1 mutation makes MEK constitutively active downstream of BRAF; (c) RAF1(CRAF) dimerization can paradoxically transactivate and phosphorylate MEK. Each restores ERK output despite BRAF blockade. Combining a BRAF inhibitor with a MEK inhibitor (trametinib) blocks the pathway at two sequential nodes, so a single bypass mutation no longer reactivates ERK; the cell needs two coincident resistance events, which is far less probable, yielding more durable responses. See section 8. 27. The PI3K-Akt-mTOR pathway is a master regulator of cell growth and metabolism. Evaluate the consequences of complete mTOR inhibition in cancer vs healthy cells: why do rapalogs (mTORC1 inhibitors) produce cytostatic rather than cytotoxic effects in most cancers, and what feedback mechanisms restore Akt activity?

Answer (Q27, Synthesis). mTORC1 inhibitors (rapalogs) block protein synthesis and cell growth but do not directly trigger death, so most cancer cells arrest (cytostatic) rather than die (cytotoxic) — surviving cells can resume growth when the drug is withdrawn. Moreover mTORC1 normally drives a negative feedback (via S6K) that suppresses IRS-1/PI3K; relieving this feedback with rapalogs paradoxically reactivates PI3K→Akt, restoring survival signaling and blunting efficacy. This is why rapalogs are often combined with PI3K/Akt or upstream RTK inhibitors to prevent feedback-driven Akt rescue. See section 8. 28. Feedback loops in signaling networks can generate bistability (switch-like most-or-none responses) or oscillations (e.g., NF- κ B oscillations). Evaluate the mathematical conditions (using a two-state model) under which positive feedback creates bistability vs oscillations. Give one biological example of each.

Answer (Q28, Synthesis). In a two-state activation model, pure positive feedback with sufficient cooperativity (nonlinearity) creates two stable steady states — bistability — giving an all-or-none switch with hysteresis; the ERK→SOS positive-feedback loop produces such switch-like, irreversible ERK activation (and the p53→PUMA ‘point of no return’ in apoptosis). Oscillations require positive feedback combined with delayed negative feedback: NF- κ B activation induces I κ B, which re-inhibits NF- κ B after a time delay, producing repetitive nuclear NF- κ B pulses. So bistability needs strong fast positive feedback alone; oscillation needs that positive feedback plus a slower opposing negative loop. See section 8. 29. Exosomes (30–150 nm extracellular vesicles) carry signaling molecules (proteins, miRNAs, lipids) between cells over long distances. Evaluate the evidence that exosomes constitute a bona fide signaling mechanism distinct from classical paracrine signaling, and propose experimental criteria to distinguish “exosomal” from conventional secreted-protein-mediated communication.

Answer (Q29, Synthesis). Exosomes can transfer proteins, miRNAs, and lipids that change recipient-cell behavior, which argues they are a bona fide signaling mechanism distinct from soluble paracrine factors because the cargo is membrane-encapsulated, can be delivered over long distances, and includes nucleic acids that classical secreted proteins cannot carry. To distinguish exosomal from conventional secreted-protein communication: deplete or block exosome biogenesis/release (e.g., Rab27a or nMase2 knockdown) and test loss of effect; purify exosomes by density/size and show the isolated vesicles reproduce the response; and demonstrate cargo transfer (labeled miRNA/protein appearing in recipients). A bona fide

exosomal mechanism is supported if the response survives in the vesicle fraction but is lost when vesicle release is blocked. See section 8. 30. Critically evaluate the “oncogene addiction” hypothesis: cancer cells become “addicted” to a single dominant oncogene signal (e.g., BCR-ABL in CML), making targeted inhibition highly effective. Under what conditions does addiction arise, and why do multiple oncogenic mutations (e.g., in pancreatic cancer) prevent effective single-agent targeted therapy?

Answer (Q30, Synthesis). Oncogene addiction is the observation that some tumors depend on one dominant oncogenic signal (e.g., BCR-ABL in CML), so inhibiting that node (imatinib) collapses the survival/proliferation network and is highly effective. Addiction arises when a single driver mutation rewires the cell so that downstream survival and growth signaling are funnelled through that one node, making the cell acutely sensitive to its loss (synthetic dependence). When a tumor carries multiple independent oncogenic mutations (e.g., KRAS plus others in pancreatic cancer), redundant parallel inputs sustain signaling even if one node is blocked, so single-agent targeted therapy fails; the evidence for addiction is strongest in genetically simple, single-driver cancers and weakest in multi-mutation tumors. See section 8.

Questions — Bioenergetics and Cellular Respiration

Instructor Use and Coverage Notes

- Coverage target: Calculate an energy yield or redox consequence and connect it to cellular work.
- Model/data emphasis: Delta G, ATP yield, and electron-carrier accounting.
- Assessment alignment: Representing and Describing Data, Statistical Tests and Data Analysis.
- Misconception probe: ATP is not stored energy in a vague sense; it is a coupling currency with defined reaction chemistry.
- Transfer product: Transfer energy accounting to exercise, fermentation, hypoxia, and mitochondrial disease.
- Grading focus: award full credit for mechanism, evidence, boundary conditions, and units when a calculation is required.
- Suggested use: draw one recall item, one application item, and one synthesis item when building a short quiz from this bank.

Questions 1–10: Recall and Comprehension

This activity accompanies section 9 of the textbook — review that chapter before attempting the exercises below.

1. Define free energy (G). What does a negative ΔG indicate about a reaction?

Answer (Q1, Recall). Free energy (G) is the Gibbs free energy, the portion of a system’s energy available to do useful work at constant temperature and pressure. A negative ΔG (exergonic) indicates a spontaneous reaction that releases free energy; a positive ΔG (endergonic) requires an energy input. Cells couple endergonic reactions (e.g. biosynthesis) to highly exergonic ones such as ATP hydrolysis to drive them forward. See section 9. 2. Write the overall equation for aerobic cellular respiration.

Answer (Q2, Recall). Aerobic respiration: $C_6H_{12}O_6 + 6 O_2 \rightarrow 6 CO_2 + 6 H_2O$, with $\Delta G^{\circ} \approx -2,870 \text{ kJ/mol}$. Glucose is fully oxidised to CO₂, O₂ is the terminal electron acceptor reduced to water, and the released free energy is captured as about 30–32 ATP per glucose. See section 9. 3. What is ATP? What bonds are broken during ATP hydrolysis, and why is this energy release large?

Answer (Q3, Recall). ATP (adenosine triphosphate) is the cell’s energy-coupling currency: an adenosine linked to three phosphates by two phosphoanhydride bonds. Hydrolysis of the terminal phosphoanhydride bond ($ATP \rightarrow ADP + P_i$) has a large negative ΔG ($\approx -30 \text{ kJ/mol}$ standard, ≈ -50 to -54 kJ/mol in the cell). The release is large because the products are stabilized by relief of charge repulsion, resonance stabilization, and favorable solvation, not because the bond itself is unusually strong. See section 9. 4. Name the four stages of aerobic respiration and state where each occurs in the eukaryotic cell.

Answer (Q4, Recall). The four stages are: (1) glycolysis — cytoplasm; (2) pyruvate decarboxylation (PDC) — mitochondrial matrix; (3) the citric acid (Krebs/TCA) cycle — mitochondrial matrix; (4) the electron transport chain and oxidative phosphorylation — inner mitochondrial membrane. See section 9. 5. How many ATP are produced by substrate-level phosphorylation in glycolysis?

Answer (Q5, Recall). Glycolysis produces 4 ATP by substrate-level phosphorylation but consumes 2 ATP in the investment phase, for a net of 2 ATP per glucose by substrate-level phosphorylation (steps 7 and 10, phosphoglycerate kinase and pyruvate kinase). It also yields 2 net NADH. See section 9. 6. What is the purpose of the preparatory steps (pyruvate decarboxylation) before the Krebs cycle?

Answer (Q6, Recall). Pyruvate decarboxylation links glycolysis to the TCA cycle. The pyruvate dehydrogenase complex oxidatively decarboxylates each pyruvate (3C), releasing one CO₂, reducing one NAD⁺ to NADH, and attaching the remaining 2-carbon acetyl group to coenzyme A to form acetyl-CoA. This produces 2 NADH and 2 CO₂ per glucose and feeds acetyl-CoA into the cycle. See section 9. 7. What is the electron transport chain? Name the four major protein complexes.

Answer (Q7, Recall). The electron transport chain is a series of redox carriers in the inner mitochondrial membrane that pass electrons from NADH and FADH₂ to O₂, using the released energy to pump protons and build the proton-motive force. The four major complexes are Complex I (NADH dehydrogenase), Complex II (succinate dehydrogenase), Complex III (cytochrome bc₁, the Q cycle), and Complex IV (cytochrome c oxidase). See section 9. 8. What is the chemiosmotic theory? Who proposed it and when?

Answer (Q8, Recall). The chemiosmotic theory states that electron transport pumps protons across the inner mitochondrial membrane, creating an electrochemical proton gradient (proton-motive force) whose energy drives ATP synthesis by ATP synthase. It was proposed by Peter Mitchell in 1961 and earned him the 1978 Nobel Prize in Chemistry. See section 9. 9. What is fermentation? Name two types and the products of each.

Answer (Q9, Recall). Fermentation regenerates NAD⁺ from NADH so that glycolysis can continue without O₂; it does not itself make ATP. Lactic acid fermentation (muscle, erythrocytes) converts pyruvate to lactate; alcoholic fermentation (yeast) converts pyruvate to ethanol + CO₂. Both yield only 2 ATP per glucose, from glycolysis alone. See section 9. 10. What is the difference between substrate-level phosphorylation and oxidative phosphorylation?

Answer (Q10, Recall). In substrate-level phosphorylation a high-energy phosphate is transferred directly from a substrate to ADP by an enzyme (glycolysis steps 7 and 10, and the TCA GTP step); it is fast, O₂-independent, and yields little ATP. In oxidative phosphorylation, ATP synthase uses the proton-motive force generated by the electron transport chain; it requires O₂ and supplies about 28 of the about 32 ATP per glucose. See section 9.

Questions 11–20: Application and Analysis

11. Calculate the theoretical maximum ATP yield from one glucose molecule in aerobic respiration. How does the actual yield (about 30 ATP) differ from the textbook maximum (about 38), and why?

Answer (Q11, Application). Theoretical yield: 2 (glycolysis SLP) + 2 (TCA GTP) + 10 NADH × 2.5 + 2 FADH₂ × 1.5 ≈ 32 ATP using modern P/O ratios (the classic ‘38’ assumed 3 ATP/NADH and 2 ATP/FADH₂). The actual about 30 is lower because the malate-aspartate shuttle vs glycerol-3-phosphate shuttle changes the value of cytosolic NADH (2.5 vs 1.5 ATP each), and because proton leak and the cost of importing Pi/ADP siphon off part of the proton-motive force. See section 9. 12. In anaerobic fermentation, yeast converts pyruvate to ethanol + CO₂. Explain why this regeneration of NAD⁺ is essential for continued glycolysis, even though no ATP is produced in the process.

Answer (Q12, Application). Glycolysis nets 2 ATP but reduces 2 NAD⁺ to NADH at the GAPDH step. Cytosolic NAD⁺ is present in only catalytic amounts, so if NADH is not reoxidised, GAPDH stalls and glycolysis (and its 2 ATP) halts. Converting pyruvate to ethanol + CO₂ reoxidises NADH back to NAD⁺, sustaining flux through glycolysis even though the fermentation step itself makes no ATP. See section 9. 13. Cyanide (CN⁻) blocks Complex IV (cytochrome c oxidase). Predict the consequences for: (a) proton gradient; (b) NADH/NAD⁺ ratio; (c) ATP production; (d) O₂ consumption; (e) lactic acid production.

Answer (Q13, Application). Cyanide blocks Complex IV, so electrons cannot reach O₂. (a) Proton pumping stops, so the proton gradient collapses; (b) carriers stay reduced, so NADH/NAD⁺ rises sharply; (c) oxidative phosphorylation ATP production stops; (d) O₂ consumption falls to near zero; (e) cells switch to fermentation to regenerate NAD⁺, so lactic acid production rises. The result is a lethal histotoxic hypoxia. See section 9. 14. Uncoupling proteins (UCPs) such as thermogenin in brown adipose tissue dissipate the proton gradient as heat rather than driving ATP synthesis. Explain the physiological role of this process and calculate: if 50% of the proton gradient is uncoupled, what happens to O₂ consumption vs ATP output?

Answer (Q14, Application). Uncoupling proteins (e.g. thermogenin/UCP1 in brown adipose tissue) let protons re-enter the matrix bypassing ATP synthase, so the gradient’s energy is released as heat — important for non-shivering thermogenesis in neonates and cold-adapted mammals. Because the gradient is continually dissipated, electron transport speeds up: O₂ consumption rises while ATP output falls. With 50% of the gradient uncoupled, roughly half the proton flux makes heat instead of ATP, so ATP yield per O₂ drops by about half while total O₂ consumption increases. See section 9. 15. Glycolysis includes an irreversible phosphofructokinase-1 (PFK-1) step. PFK-1 is allosterically activated by AMP, ADP, and F-2,6-BP, and inhibited by ATP and citrate. Explain how this regulation matches glycolytic rate to cellular energy status.

Answer (Q15, Application). PFK-1 catalyses the committed, irreversible step of glycolysis. When energy is low, AMP and ADP rise and F-2,6-BP increases, allosterically activating PFK-1 so glycolysis speeds up to make ATP. When energy is plentiful, ATP and citrate accumulate and inhibit PFK-1, slowing glycolysis. This makes glycolytic flux track cellular energy charge moment to moment. See section 9. 16. Brown adipose tissue (BAT) is thermogenic. Compare the metabolic activity of BAT vs white adipose tissue (WAT): what substrate do they preferentially oxidise, how do they regulate UCP1 expression (adrenergic → cAMP → PKA → lipolysis → FA activation of UCP1), and what clinical interest does BAT activation generate?

Answer (Q16, Application). Brown adipose tissue oxidises fatty acids primarily to drive UCP1-mediated heat production; white adipose tissue stores triacylglycerol and oxidises little itself. In BAT, cold/adrenergic signaling → β-adrenergic receptor → cAMP → PKA → lipolysis → free fatty acids that both fuel and directly activate UCP1, uncoupling respiration to make heat. Clinically, activating or recruiting BAT is of interest for combating obesity and type 2 diabetes by increasing energy expenditure. See section 9. 17. The proton-motive force (pmf) has two components: electrical (ΔΨ ≈ −140 mV) and chemical (ΔpH ≈ 1 unit = −59 mV at 37°C; note sign convention for force driving H⁺ into the matrix). Calculate the total pmf in mV and the Gibbs energy per mole of protons entering the matrix (ΔG = FΔΨ + 2.303RT·ΔpH).

Answer (Q17, Application). Total pmf = ΔΨ + (−59 mV per ΔpH unit at 37°C) ≈ −140 mV + (−59 mV) ≈ −200 mV in magnitude. The Gibbs energy per mole of protons is ΔG = FΔΨ + 2.303 RT ΔpH ≈ 96,485 C/mol × 0.200 V ≈ 19–20 kJ/mol of protons entering the matrix — the per-proton energy budget that funds ATP synthesis. See section 9. 18. The malate-aspartate shuttle transfers NADH electrons from the cytoplasm into the mitochondrial matrix. Why is this shuttle needed, and why does a cell using the glycerol-3-phosphate shuttle instead produce slightly less ATP? (Hint: which NADH-equivalent is delivered to which complex?)

Answer (Q18, Application). Cytosolic NADH cannot cross the inner mitochondrial membrane, so its electrons must be shuttled in. The malate-

aspartate shuttle (liver, heart, kidney) regenerates matrix NADH, which enters at Complex I and yields about 2.5 ATP per electron pair. The glycerol-3-phosphate shuttle (skeletal muscle, brain) delivers electrons to ubiquinone via an FAD-linked enzyme, bypassing Complex I, so it yields only about 1.5 ATP per pair — hence about 30 ATP/glucose instead of about 32. See section 9. 19. Cancer cells preferentially use aerobic glycolysis (Warburg effect) even when oxygen is available. Propose three mechanistic explanations for why rapidly proliferating cells would benefit from this apparently inefficient strategy.

Answer (Q19, Application). Three rationales: (1) speed — glycolytic ATP is produced far faster than by oxidative phosphorylation, matching the high demand of proliferation; (2) biosynthesis — diverting glucose carbon supplies precursors (G6P → ribose for nucleotides via the pentose phosphate pathway, 3-PG → serine, pyruvate → amino acids); (3) redox/NADPH and microenvironment — supports antioxidant defense and adapts to hypoxic, poorly vascularised tumor regions, while secreted lactate acidifies the milieu and favors invasion. See section 9. 20. Chloramphenicol inhibits bacterial 50S ribosomes and mitochondrial ribosomes. Explain why chloramphenicol can cause myelosuppression (bone marrow failure) after prolonged use, and why it is still used clinically when other antibiotics fail.

Answer (Q20, Application). Mitochondria descend from bacteria and use bacteria-like 70S ribosomes, so chloramphenicol — which inhibits the 50S subunit of bacterial and mitochondrial ribosomes — also blocks mitochondrial protein synthesis. In rapidly dividing bone marrow this impairs synthesis of ETC subunits, causing dose-dependent reversible myelosuppression (and rarely idiosyncratic aplasia). It is still reserved for severe infections (e.g. typhoid, meningitis, rickettsiae) when safer antibiotics fail, because its broad efficacy can be life-saving. See section 9.

Questions 21–30: Synthesis and Evaluation

21. Evaluate the ATP synthase as a molecular motor. Describe the rotary mechanism (F_0 rotation driven by H^+ flux → F_1 conformational change → alternating binding-change mechanism). Calculate the torque generated if F_0 rotates at 100 rpm with a step size of 120° per ATP.

Answer (Q21, Synthesis). ATP synthase is a rotary motor: proton flux through the membrane-embedded F_0 c-ring drives rotation of the central γ stalk, which cycles the three F_1 β catalytic sites through loose, tight, and open states (Boyer's binding-change mechanism), synthesizing and releasing ATP. With about 3.67 H^+ per ATP and a 120° rotation per ATP, three ATP are made per full 360° turn; at 100 rpm that is about 5 ATP/s per enzyme. The torque equals the work per ATP ($\Delta G \approx 50\text{--}60\text{ kJ/mol} \approx \text{about } 80\text{--}100\text{ pN}\cdot\text{nm}$) divided by the $2\pi/3$ rad step, giving roughly 40–50 pN·nm. See section 9. 22. Evaluate the efficiency of oxidative phosphorylation: how close is the actual ATP/O ratio to the theoretical maximum, and what factors cause inefficiency (proton leak, incomplete coupling)? What impact does membrane composition (cardiolipin content) have on coupling efficiency?

Answer (Q22, Synthesis). The measured P/O ratios (about 2.5 ATP/NADH, about 1.5 ATP/FADH₂) fall short of idealised maxima because of intrinsic proton leak, pump slip, and the H^+ cost of importing P_i and ADP and exporting ATP. Cardiolipin, the inner-membrane signature phospholipid, binds and stabilizes the respiratory supercomplexes and ATP synthase and limits proton leak, so adequate cardiolipin content (and its remodeling, e.g. tafazzin in Barth syndrome) raises coupling efficiency; depletion lowers the effective ATP/O ratio. See section 9. 23. Design an experiment to test whether a newly discovered mitochondrially targeted compound acts as an uncoupler, a chain blocker, or an ATP synthase inhibitor. What measurements (O_2 consumption rate, membrane potential, ATP levels, pH) would you take, and in what order?

Answer (Q23, Synthesis). Hypothesis: the compound is an uncoupler, a chain blocker, or an ATP synthase inhibitor. Using isolated mitochondria, measure O_2 consumption rate, membrane potential, and ATP. Add substrate then ADP (State 3); add the compound. An uncoupler raises O_2 consumption while collapsing membrane potential and ATP. A chain blocker lowers O_2 consumption and membrane potential. An ATP synthase inhibitor lowers O_2 consumption and ATP but maintains or raises membrane potential, and adding an uncoupler afterward restores respiration — the decisive control distinguishing it from a chain blocker. Replicate across independent preparations. See section 9. 24. Cells can switch between aerobic respiration, fermentation, and fatty acid oxidation. Design a metabolic flux experiment using ^{13}C -labeled glucose and isotope mass spectrometry (metabolomics) to map which pathways are active under normoxia, hypoxia, and caloric restriction. What isotopomer patterns would distinguish glycolytic from TCA-derived carbon?

Answer (Q24, Synthesis). Feed cells uniformly ^{13}C -glucose and measure metabolite isotopomers by mass spectrometry under normoxia, hypoxia, and caloric restriction. Lactate/alanine carrying the full glycolytic ^{13}C label with little label in TCA intermediates indicates fermentative/Warburg flux (favored in hypoxia); progressive ^{13}C enrichment of citrate, α -ketoglutarate, succinate, and malate indicates pyruvate → TCA oxidation. Dilution of TCA labeling by unlabelled acetyl-CoA reveals fatty acid oxidation, prominent under caloric restriction. Distinct mass-isotopomer distributions thus separate glycolytic from TCA-derived carbon. See section 9. 25. The pentose phosphate pathway (PPP) branches from glycolysis at G6P and produces NADPH and ribose-5-phosphate. Evaluate the relative importance of PPP in: (a) red blood cells (where NADPH protects against oxidative damage via glutathione); (b) rapidly proliferating cancer cells (where ribose is needed for nucleotide synthesis). Design a therapeutic strategy targeting the PPP specifically in cancer cells.

Answer (Q25, Synthesis). The PPP oxidative branch converts G6P to ribulose-5-phosphate, generating NADPH and ribose-5-phosphate. (a) In red

blood cells NADPH keeps glutathione reduced to detoxify peroxides; without it (e.g. G6PD deficiency) oxidative hemolysis occurs. (b) In proliferating cancer cells the PPP supplies ribose-5-phosphate for nucleotide synthesis and NADPH for lipid synthesis and redox balance. A cancer-selective strategy is to inhibit G6PD or transketolase (or block NADPH regeneration), raising oxidative stress and limiting nucleotide supply in tumor cells, which are more PPP-dependent than most normal tissue. See section 9. 26. Mitochondria-derived reactive oxygen species (ROS) cause oxidative stress. Evaluate the paradox that low ROS function in redox signaling (activating NF- κ B, Nrf2, and HIF-1 α) while high ROS cause macromolecular damage. What antioxidant systems exist in mitochondria (SOD2, thioredoxin, peroxiredoxin), and how might targeted mitochondrial antioxidants (MitoQ, SS-31) prevent disease?

Answer (Q26, Synthesis). ROS arise mainly from electron leak at Complexes I and III. At low levels they act as second messengers, reversibly oxidising thiols to activate redox-sensitive pathways (NF- κ B, Nrf2, HIF-1 α); at high levels they oxidise lipids, proteins, and mtDNA — a dose-dependent, hormetic relationship rather than a contradiction. Mitochondrial defenses include MnSOD (SOD2), the thioredoxin/peroxiredoxin system, and glutathione peroxidase. Matrix-targeted antioxidants such as MitoQ and SS-31 (elamipretide) concentrate where ROS are generated and may limit oxidative damage in ischemia-reperfusion and neurodegeneration without blunting physiological signaling. See section 9. 27. Metabolic reprogramming in hypoxia (HIF-1 α pathway) switches cells from oxidative phosphorylation to anaerobic glycolysis. Evaluate the molecular logic: why would a cell transcriptionally upregulate glycolytic enzymes AND simultaneously downregulate Complex IV (via COX4-2 subunit switch) AND activate BNIP3-mediated mitophagy (selective mitochondrial degradation) in response to O₂ lack?

Answer (Q27, Synthesis). Low O₂ stabilizes HIF-1 α , which coordinately reprograms metabolism away from O₂-dependent ATP. It upregulates glycolytic enzymes and lactate dehydrogenase to sustain ATP without O₂; it switches Complex IV to the COX4-2 isoform that operates more efficiently at low O₂; and it induces BNIP3, triggering mitophagy to prune mitochondria, lowering O₂ demand and ROS output. Together these shift the cell to glycolytic ATP while protecting it from ROS damage during hypoxia. See section 9. 28. The ketone bodies (β -hydroxybutyrate, acetoacetate) produced during fasting and ketogenic diets are increasingly recognized as signaling molecules (not just fuel). Evaluate the evidence that β -hydroxybutyrate inhibits histone deacetylases (HDACs), thereby acting as an epigenetic regulator. What genes are induced, and how might this explain the neuroprotective and anti-inflammatory properties attributed to ketogenic diets?

Answer (Q28, Synthesis). During fasting and ketogenic diets the liver converts surplus fatty-acid-derived acetyl-CoA into β -hydroxybutyrate and acetoacetate, exported as fuel for brain, heart, and muscle. β -hydroxybutyrate is also an endogenous class-I HDAC inhibitor: inhibiting HDACs raises histone acetylation and induces genes such as FOXO3 and MT2 that strengthen antioxidant defenses. That antioxidant program plus suppression of inflammation (e.g. the NLRP3 inflammasome) are proposed mechanisms for the neuroprotective and anti-inflammatory effects of ketogenic states; the evidence is suggestive but still partly correlative. See section 9. 29. Thermodynamic coupling in oxidative phosphorylation can be described by non-equilibrium thermodynamics. Evaluate: when the ATP/ADP ratio is very high, does flow of H⁺ through ATP synthase reverse (ATP \rightarrow ADP + Pi, using pmf to rotate in reverse)? Under what physiological conditions does this reverse mode actually occur, and what is its role in maintaining mitochondrial membrane potential when Complex I/III activity is inhibited?

Answer (Q29, Synthesis). ATP synthase is reversible. When the proton-motive force falls but ATP/ADP stays high, the enzyme can run backward, hydrolysing ATP and pumping protons outward to defend the membrane potential. This reverse mode occurs physiologically in ischemia/hypoxia or when Complex I or III is inhibited, preserving $\Delta\Psi$ for protein/ion import and apoptotic gatekeeping at the cost of consuming ATP — a protective but expensive state usually limited by the inhibitor protein IF1. See section 9. 30. Critically evaluate the “two-hit” model of mitochondrial disease: patients with heteroplasmic mtDNA mutations are often asymptomatic until a critical threshold (often about 80% mutated mtDNA) is exceeded. What cellular mechanisms (quality control, complementation in fused networks) maintain function below the threshold? At what threshold does bioenergetic failure occur, and how does tissue-specific metabolism (brain vs muscle vs liver) determine which tissue is most sensitive?

Answer (Q30, Synthesis). Heteroplasmic cells tolerate mutant mtDNA because wild-type mitochondria and mtDNA-encoded subunits complement defective ones within the fused network, and quality-control fission/mitophagy removes the worst organelles — keeping bioenergetics adequate until mutant load passes a tissue-specific threshold (often about 70–90%, classically about 80%). Above threshold, oxidative phosphorylation fails and symptoms emerge. High-demand oxidative tissues (brain, then heart and skeletal muscle) cross the bioenergetic failure point first, whereas glycolytically flexible liver tolerates higher mutant loads, explaining the encephalo-myopathic presentation of many mtDNA diseases. See section 9.

Questions — Photosynthesis

Instructor Use and Coverage Notes

- Coverage target: Compute carbon-fixation requirements and explain a limiting factor.
- Model/data emphasis: Photon, ATP/NADPH, and Calvin-cycle stoichiometry.
- Assessment alignment: Representing and Describing Data, Statistical Tests and Data Analysis.
- Misconception probe: Plants do not eat sunlight; they use light energy to reduce carbon using electrons and enzymes.
- Transfer product: Transfer photosynthetic constraints to crops, algae, climate, or ecosystem productivity.
- Grading focus: award full credit for mechanism, evidence, boundary conditions, and units when a calculation is required.
- Suggested use: draw one recall item, one application item, and one synthesis item when building a short quiz from this bank.

Questions 1–10: Recall and Comprehension

This activity accompanies section 10 of the textbook — review that chapter before attempting the exercises below.

1. Write the overall equation for photosynthesis. Which reactant provides O₂?

Answer (Q1, Recall). Overall: 6 CO₂ + 6 H₂O + light → C₆H₁₂O₆ + 6 O₂ (ΔG ≈ +2,870 kJ/mol, an endergonic, light-driven reaction). The evolved O₂ comes entirely from water, not CO₂ — water is split by the oxygen-evolving complex of Photosystem II to supply electrons, protons, and O₂. See section 10. 2. Locate photosynthesis: in which organelle and in which specific membrane compartment do the light reactions occur?

Answer (Q2, Recall). Photosynthesis occurs in the chloroplast (in plants and algae). The light reactions occur in the thylakoid membrane (with proton accumulation in the thylakoid lumen), while the Calvin cycle takes place in the surrounding stroma. See section 10. 3. What are photosystems I and II? What is the primary electron donor in each?

Answer (Q3, Recall). Photosystems are pigment–protein reaction-center complexes in the thylakoid membrane. Photosystem II (P680) uses water as its primary electron donor (oxidising it via the oxygen-evolving complex to release O₂). Photosystem I (P700) receives electrons from the cytochrome b6f chain via plastocyanin, and its excited reaction center donates electrons ultimately to NADP⁺. See section 10. 4. Define the Z-scheme. Trace the path of electrons from water to NADP⁺.

Answer (Q4, Recall). The Z-scheme is the energetic ‘zig-zag’ diagram of non-cyclic electron flow through two photosystems in series. Path: H₂O → (oxygen-evolving complex of PSII) → P680* → pheophytin → plastoquinone (QA, QB) → cytochrome b6f → plastocyanin → P700* (PSI) → ferredoxin → ferredoxin-NADP⁺ reductase → NADP⁺ + H⁺ → NADPH. Two photons (one per photosystem) are absorbed per electron. See section 10. 5. What are the products of the light reactions passed to the Calvin cycle?

Answer (Q5, Recall). The light reactions supply ATP and NADPH (plus reduced ferredoxin transiently) to the Calvin cycle in the stroma; O₂ is released as a by-product and is not used by the cycle. ATP provides chemical energy and NADPH provides reducing power for CO₂ fixation. See section 10. 6. Name the three stages of the Calvin cycle (also called the C₃ cycle or light-independent reactions).

Answer (Q6, Recall). The three stages of the Calvin cycle are: (1) carboxylation — RuBisCO fixes CO₂ onto ribulose-1,5-bisphosphate (RuBP) to form two 3-phosphoglycerate; (2) reduction — 3-PGA is phosphorylated (ATP) and reduced (NADPH) to glyceraldehyde-3-phosphate (G3P); (3) regeneration — most G3P is used (with ATP) to regenerate RuBP. See section 10. 7. What is RuBisCO? What reaction does it catalyse and what is its substrate?

Answer (Q7, Recall). RuBisCO (ribulose-1,5-bisphosphate carboxylase/oxygenase) is the Calvin-cycle enzyme that catalyses carboxylation: it adds CO₂ to its substrate ribulose-1,5-bisphosphate (RuBP), producing two molecules of 3-phosphoglycerate. It also has an oxygenase side-activity (using O₂ instead of CO₂) that initiates photorespiration. See section 10. 8. Distinguish C₃, C₄, and CAM plants. Give one example species of each.

Answer (Q8, Recall). C₃ plants fix CO₂ directly via RuBisCO to 3-PGA (e.g. wheat/rice). C₄ plants first fix CO₂ with PEP carboxylase in mesophyll cells to a 4-carbon acid, then release CO₂ around RuBisCO in bundle-sheath cells (e.g. maize). CAM plants fix CO₂ at night into malate and release it to RuBisCO by day (e.g. pineapple or a cactus) — C₄ and CAM are CO₂-concentrating mechanisms that suppress photorespiration, with CAM giving the highest water-use efficiency. See section 10. 9. What is photorespiration? Under what conditions is it maximized?

Answer (Q9, Recall). Photorespiration begins when RuBisCO’s oxygenase activity adds O₂ (instead of CO₂) to RuBP, making 2-phosphoglycolate that must be salvaged through the C₂ pathway across chloroplast, peroxisome, and mitochondrion, releasing CO₂ and consuming ATP with no sugar gain. It is maximized under high temperature, high light, and low CO₂/high O₂ (e.g. closed stomata in hot, dry conditions), where the oxygenase reaction is favored. See section 10. 10. What is the wavelength absorbed by chlorophyll a and chlorophyll b?

Answer (Q10, Recall). Chlorophyll a absorbs maximally at roughly 430 nm (blue) and 662–680 nm (red). Chlorophyll b absorbs maximally at roughly 453 nm (blue) and 642 nm (red); it is an accessory pigment that broadens the harvested spectrum and funnels energy to chlorophyll a. Both reflect green light, giving plants their color. See section 10.

Questions 11–20: Application and Analysis

11. DCMU (herbicide, kills plants) blocks the electron acceptor site of Photosystem II. Predict its effects on: (a) O₂ evolution; (b) NADPH production; (c) ATP (photophosphorylation); (d) the Calvin cycle.

Answer (Q11, Application). DCMU blocks the QB plastoquinone-binding site of PSII, stopping electron flow out of PSII. (a) O₂ evolution stops (water splitting halts without electron acceptor turnover). (b) NADPH production stops (no electrons reach PSI/NADP⁺ via linear flow). (c) Linear photophosphorylation collapses because the proton gradient from PSII/b₆f is lost (only limited cyclic ATP around PSI may persist). (d) The Calvin cycle stops once ATP and NADPH are exhausted — the plant cannot fix carbon and dies. See section 10. 12. Non-cyclic photophosphorylation produces both ATP and NADPH. Cyclic photophosphorylation produces primarily ATP. Explain the mechanism of cyclic flow (electron recirculates through Fd → PQ → Cyt b₆f → PSI) and when a cell uses cyclic vs non-cyclic flow.

Answer (Q12, Application). In cyclic flow, PSI-excited electrons pass from ferredoxin back to the plastoquinone pool/cytochrome b₆f complex and return to P700, pumping protons and making ATP but no NADPH and no O₂. Cells use cyclic flow when ATP demand exceeds NADPH demand — the linear Z-scheme yields an ATP:NADPH ratio (about 9 ATP : 6 NADPH per 3 CO₂) below the about 3:2 the Calvin cycle requires, so cyclic flow tops up ATP, and it is also up-regulated under stress (high light, low CO₂) to balance the energy budget and support photoprotection. See section 10. 13. A student growing *Arabidopsis thaliana* increases light intensity 10-fold. Initially photosynthetic rate rises, then plateaus. Explain the two-phase response: which reaction limits at low light (light reactions) and which limits at high light (Calvin cycle enzyme capacity)?

Answer (Q13, Application). At low light the rate is light-limited: the light reactions cannot supply ATP/NADPH fast enough, so photosynthesis rises roughly linearly with intensity. As intensity increases the system becomes light-saturated: the rate plateaus because the Calvin cycle's enzymatic capacity (RuBisCO turnover, RuBP regeneration) and CO₂ supply become limiting, not photon capture. Adding CO₂ or more RuBisCO would raise the plateau; adding light would not — the predicted, testable signature of a Calvin-cycle (carbon/enzyme) limitation. See section 10. 14. C₄ plants (e.g., maize) separate initial CO₂ fixation (HCO₃⁻ → oxaloacetate, in mesophyll) from RuBisCO (in bundle sheath). Explain: (a) how this concentrates CO₂ around RuBisCO; (b) why it reduces photorespiration; (c) why C₄ plants outcompete C₃ plants in hot, sunny conditions.

Answer (Q14, Application). (a) In C₄ plants PEP carboxylase fixes HCO₃⁻ to oxaloacetate → malate in mesophyll cells; malate moves to bundle-sheath cells and is decarboxylated, releasing CO₂ right at RuBisCO (about 10× above ambient). (b) High local CO₂ outcompetes O₂ at RuBisCO's active site, so the oxygenase reaction and photorespiration are nearly eliminated. (c) In hot, sunny, dry conditions C₃ plants lose CO₂ to high photorespiration and must keep stomata more open; C₄ plants maintain high carboxylation with smaller stomatal opening, so they have higher water-use efficiency and outcompete C₃ plants there. See section 10. 15. The quantum yield of O₂ production is about 1 O₂ per 8 photons absorbed (theoretical: 1 O₂ per 8 photons absorbed). Why is this the minimum, and how does the Z-scheme energetically justify why 4 photons per PSII and 4 per PSI are needed to produce 1 O₂ and 2 NADPH?

Answer (Q15, Application). Producing one O₂ requires removing 4 electrons from 2 H₂O. In the Z-scheme each electron must be excited twice — once at PSII and once at PSI — so 4 photons at PSII + 4 photons at PSI = 8 photons minimum per O₂ (and per 2 NADPH). This is the theoretical minimum because each photosystem performs one charge separation per photon, and the energy of a single photon is insufficient to span the full about 1.1 V from water to NADP⁺; the two-photon (two-step) boost is energetically required. Real quantum yields are slightly worse (about 9–10 photons per O₂). See section 10. 16. Photorespiration occurs when RuBisCO oxygenates RuBP (instead of carboxylating it), producing phosphoglycolate, which must be recycled through the glycolate pathway. Calculate: if 25% of RuBisCO reactions are oxygenation rather than carboxylation, what fraction of carbon fixed is immediately lost? How does this affect net carbon gain?

Answer (Q16, Application). RuBisCO oxygenation makes one 2-phosphoglycolate (2C); salvage through the C₂ pathway recovers carbon but releases about 1 CO₂ per 2 glycolate processed, so roughly one quarter of the carbon entering photorespiration is lost. If 25% of RuBisCO turnovers are oxygenations, net carbon gain falls substantially — on the order of a about 20–30% reduction in net C₃ photosynthesis at 25°C — because fixed carbon is re-released as CO₂ and ATP/NADPH are consumed without sugar production. See section 10. 17. Antenna complexes (LHCI, LHCII) harvest photons and funnel excitation energy to reaction centers by resonance energy transfer (Förster transfer). Explain: (a) why antenna complexes increase efficiency; (b) why there is a risk of photodamage (singlet O₂ production) at high light; (c) what non-photochemical quenching (NPQ) does to protect the reaction centers.

Answer (Q17, Application). (a) Antenna complexes (LHCI/LHCII) hold many pigments that absorb photons over a broad spectrum and funnel the excitation by Förster resonance/exciton transfer to the reaction center at about 95% efficiency, so each reaction center is fed far faster than it could collect light alone. (b) At high light, excitation arrives faster than photochemistry can use it; long-lived triplet chlorophyll forms and transfers energy

to O₂, generating damaging singlet oxygen. (c) Non-photochemical quenching (NPQ) — driven by lumen acidification, the xanthophyll/zeaxanthin cycle and PsbS — safely dissipates excess excitation as heat, protecting the reaction centers from photodamage. See section 10. 18. Rubisco activase unfolds the tight inhibitory conformation of RuBisCO when CO₂ is absent. Explain: (a) why RuBisCO requires activation before catalysis; (b) how activase uses ATP hydrolysis to open the active site; (c) why rubisco activase is itself heat-sensitive and limits photosynthesis at high temperatures.

Answer (Q18, Application). (a) RuBisCO requires activation because a non-substrate CO₂ carbamylates an active-site lysine and recruits Mg²⁺ to form the catalytically competent site; tight-binding inhibitory sugar phosphates (e.g. RuBP, CA1P) also block uncarbamylated enzyme. (b) RuBisCO activase, an AAA+ ATPase, uses ATP hydrolysis to remodel RuBisCO and physically remove the inhibitory sugar phosphates, allowing carbamylation and catalysis. (c) Activase is thermolabile and denatures/aggregates at elevated temperature, so at high temperatures RuBisCO stays inhibited — making activase a key limit on photosynthesis under heat stress. See section 10. 19. CAM (Crassulacean acid metabolism) plants open stomata primarily at night. Trace: (a) nocturnal CO₂ fixation into malate (by PEPC); (b) daytime malate decarboxylation to CO₂; (c) CO₂ fixation by RuBisCO; (d) the advantage in arid environments. Compare water-use efficiency (WUE) of CAM vs C₃ plants.

Answer (Q19, Application). (a) At night, stomata open in the cool, humid dark; PEP carboxylase fixes CO₂ into oxaloacetate → malate, stored as malic acid in the vacuole (lumen pH drops about 7→4). (b) By day stomata close and malate is decarboxylated, releasing CO₂ internally. (c) RuBisCO fixes that concentrated CO₂ via the normal Calvin cycle behind closed stomata. (d) Opening stomata only at night drastically cuts transpirational water loss, so CAM plants achieve very high water-use efficiency (roughly 3–5× that of C₃ plants), an advantage in arid environments. See section 10. 20. The chloroplast ATP synthase (CF₁F₀) is structurally similar to the mitochondrial ATP synthase. Compare: the direction of proton gradient (lumen to stroma vs IMS to matrix); whether CF₁F₀ can run in reverse (hydrolyse ATP to pump H⁺); and the regulatory role of the thiol-regulated γ-subunit in the dark vs light.

Answer (Q20, Application). Chloroplast CF₁F₀ and mitochondrial F₁F₀ share the rotary catalytic mechanism. Proton-gradient direction differs: in chloroplasts protons accumulate in the thylakoid lumen and flow out to the stroma to make ATP, whereas in mitochondria protons flow from the intermembrane space into the matrix. CF₁F₀ can in principle run in reverse (ATP hydrolysis pumping H⁺), but the chloroplast enzyme is held off in the dark by a thiol-regulated γ-subunit: in the light, reduced thioredoxin (and the proton gradient) activates it for ATP synthesis; in the dark the oxidised γ-subunit inhibits it to prevent wasteful ATP hydrolysis. See section 10.

Questions 21–30: Synthesis and Evaluation

- Evaluate the artificial leaf as a technology for solar fuel production: splitting water to produce H₂ photochemically. What catalysts mimic the Mn cluster of the oxygen-evolving complex (OEC)? What are the current efficiency limits, and how do they compare to photosynthetic efficiency (about 3% vs photovoltaic about 25%)?

Answer (Q21, Synthesis). An ‘artificial leaf’ uses light-driven catalysts to split water into O₂ and H₂ (or reduce CO₂). The oxygen-evolving Mn₄CaO₅ cluster of PSII is mimicked by earth-abundant water-oxidation catalysts such as cobalt-phosphate (Co-Pi) and manganese/nickel oxides, as well as IrO₂; H₂ is generated at coupled photocathodes. Current integrated solar-to-fuel efficiencies are typically a few to about 10%, exceeding the about 1–3% net efficiency of crop photosynthesis but below about 25% silicon photovoltaics. The judgment that artificial leaves can scale depends on contestable evidence — catalyst durability, cost, and system-level efficiency — and would change if cheap, stable catalysts achieved high efficiency at scale. See section 10. 22. Rising CO₂ atmospheric concentrations (currently about 420 ppm) should theoretically increase C₃ photosynthesis (CO₂ fertilization effect) but FACE (Free Air CO₂ Enrichment) experiments show attenuated responses. Evaluate three mechanisms of “photosynthetic downregulation” under elevated CO₂ and assess the net impact on crop yields.

Answer (Q22, Synthesis). FACE experiments show smaller-than-predicted C₃ gains under elevated CO₂ because of photosynthetic downregulation: (1) acclimation — sustained sugar accumulation represses RuBisCO/photosynthetic gene expression and lowers RuBisCO content; (2) sink limitation — if growth/storage capacity does not increase, end-product feedback (Pi limitation) caps the rate; (3) co-limitation by nitrogen and water — extra CO₂ cannot be used without proportional N for RuBisCO and adequate water/nutrients. Net crop-yield effects are real but modest (often well below the theoretical CO₂-fertilization expectation) and are further offset by heat and drought, so the simple fertilization prediction should not be treated as settled. See section 10. 23. RuBisCO is notoriously inefficient (k_{cat} about 3 s⁻¹, compared to >1,000 s⁻¹ for most enzymes). Evaluate why evolution has not improved RuBisCO, and assess recent synthetic biology approaches to engineer an improved RuBisCO (e.g., Form II RuBisCO from bacteria, directed evolution) for crop improvement.

Answer (Q23, Synthesis). RuBisCO is slow (k_{cat} about 3 s⁻¹) and confuses CO₂ with O₂ because there is an intrinsic trade-off in its two-step carboxylation mechanism: variants with higher CO₂ specificity tend to be even slower, so evolution has reached a near-optimal compromise tuned to each organism’s CO₂ environment rather than a globally ‘better’ enzyme. Synthetic-biology strategies include installing faster bacterial Form II RuBisCO (high k_{cat} but poor specificity, useful with a CO₂-concentrating mechanism), engineering carboxysome/pyrenoid CO₂-concentrating systems around RuBisCO, and directed evolution that has roughly doubled the specificity factor in lab variants. These are promising but face the

speed–specificity trade-off and the difficulty of assembling functional plant RuBisCO in crops. See section 10. 24. Shade-adapted plants have higher LHCII content and lower PSII/PSI ratios than sun plants. Evaluate the molecular mechanisms of this acclimation: how does excess excitation pressure in low light signal LHCII assembly vs LHCII disassembly in high light? What role does STN7 kinase (LHCII phosphorylation) play in state transitions?

Answer (Q24, Synthesis). Acclimation is driven by the redox state of the plastoquinone pool sensing excitation balance. In low light/shade, cells build more LHCII and lower the PSII:PSI ratio to maximize capture. Imbalanced excitation that over-reduces the PQ pool activates the STN7 kinase, which phosphorylates LHCII so it migrates from PSII to PSI (state transition, redistributing energy); when PSI is over-excited and the PQ pool is oxidised, STN7 is inactive and the PPH1/TAP38 phosphatase dephosphorylates LHCII, returning it to PSII. Longer-term, this redox signaling also adjusts photosystem stoichiometry and antenna size between sun and shade plants. See section 10. 25. Oxygenic photosynthesis evolved about 2.7 billion years ago and fundamentally transformed Earth’s atmosphere. Evaluate the geochemical evidence (banded iron formations, the Great Oxidation Event) for the timing of oxygenic photosynthesis. What was the ecological impact on anaerobic life, and how did some lineages evolve oxygen tolerance?

Answer (Q25, Synthesis). Oxygenic photosynthesis arose in cyanobacteria, with the Great Oxidation Event about 2.4 Ga. Geochemical evidence: banded iron formations record episodic O₂ oxidising dissolved Fe²⁺ to insoluble Fe³⁺ before free O₂ accumulated; the disappearance of detrital pyrite/uraninite, the rise of red beds, and the loss of mass-independent sulfur isotope fractionation mark the GOE. Ecologically, O₂ was toxic to obligate anaerobes, driving them to anoxic refugia (a mass extinction for some lineages) while others evolved oxygen tolerance — antioxidant enzymes (superoxide dismutase, catalase) and ultimately aerobic respiration, which exploited O₂ as a high-yield electron acceptor. See section 10. 26. Synthetic biology has produced a “photosynthetic organism” where an entire C₄ photosynthetic apparatus is introduced into a C₃ plant (C₄ rice project). Evaluate what genetic modifications are required, which modifications have been achieved, and what the bottlenecks are for realizing this in a crop plant.

Answer (Q26, Synthesis). Engineering C₄ photosynthesis into C₃ rice requires installing the C₄ biochemical cycle (PEP carboxylase, NADP-malate dehydrogenase/malic enzyme, PEP carboxykinase, regulated RuBisCO localization) and, critically, Kranz-type leaf anatomy with distinct mesophyll and bundle-sheath cells plus appropriate plasmodesmatal connectivity and cell-specific gene expression. Individual C₄ enzymes have been expressed in rice, but the developmental programming of Kranz anatomy and proper inter-cellular metabolite partitioning remain the major unsolved bottlenecks, so a fully functional C₄ crop has not yet been achieved — judgement here is provisional pending demonstrated anatomical reprogramming. See section 10. 27. Photoinhibition occurs when PSII is irreversibly damaged by excess light. The D1 protein of PSII is a site of photodamage and must be replaced every about 30 minutes under high light. Evaluate the molecular mechanism of D1 turnover (degradation by FtsH protease, ribosomal de novo synthesis, PSII reassembly in thylakoid membrane) and explain why this turnover rate limits maximal photosynthetic productivity.

Answer (Q27, Synthesis). High light over-excites PSII; reactive oxygen species (notably singlet O₂) damage the D1 reaction-center protein, which must be replaced every about 30 minutes — the fastest protein turnover known. The PSII-repair cycle: damaged PSII is partly disassembled and moved from grana to stroma lamellae, D1 is selectively degraded by the FtsH (and Deg) proteases, a new D1 is synthesized by thylakoid-bound ribosomes and co-translationally inserted, then PSII is reassembled and the Mn₄CaO₅ cluster photoactivated. Because repair has a finite maximal rate, when photodamage outpaces it net photosynthesis declines (chronic photoinhibition), capping maximal productivity under intense light. See section 10. 28. Horizontal gene transfer of photosynthesis genes between cyanobacteria and early eukaryotes (primary endosymbiosis) versus between non-photosynthetic organisms and photosynthetic ones (secondary endosymbiosis) produced the diverse eukaryotic algal groups. Evaluate the complexity of gene transfer that was required to set up a functional chloroplast, focusing on the challenge of targeting nuclear-encoded proteins to the chloroplast (TIC/TOC translocon import).

Answer (Q28, Synthesis). Establishing a functional chloroplast required far more than transferring photosynthesis genes. After primary endosymbiosis of a cyanobacterium, the bulk of the endosymbiont genome was lost or transferred to the host nucleus (endosymbiotic gene transfer), so about 95% of chloroplast proteins are now nuclear-encoded and must be re-imported. This demanded evolution of N-terminal transit peptides and the TOC/TIC translocon machinery to target and translocate proteins across the double envelope, plus regulatory integration of two genomes. In secondary endosymbiosis (a eukaryotic alga engulfed by another eukaryote) the problem compounds: extra membranes require additional targeting signals and a more complex import route, making the assembly of a working plastid a remarkable multi-step evolutionary achievement. See section 10. 29. Phytoplankton (mainly diatoms, dinoflagellates, cyanobacteria) account for about 50% of global CO₂ fixation despite having about 1% of terrestrial plant biomass. Evaluate what properties of aquatic photosynthesis explain this high per-mass productivity, and assess the feasibility of enhancing ocean photosynthesis (e.g., iron fertilization) as a climate change mitigation strategy.

Answer (Q29, Synthesis). Phytoplankton fix about 50% of global CO₂ with about 1% of photosynthetic biomass because of extremely high turnover, not standing stock: short cell-cycle times, no investment in non-photosynthetic structural tissue (roots, wood), efficient nutrient and light capture

in the mixed layer, and many have CO₂-concentrating mechanisms (carboxysomes/pyrenoids) that suppress photorespiration. Iron fertilization can transiently bloom phytoplankton in iron-limited (HNLC) oceans, but its value as durable carbon sequestration is doubtful: most fixed carbon is rapidly respired and recycled, export to the deep ocean is low and hard to verify, and ecological side-effects (toxic blooms, deoxygenation, nutrient robbing) are significant — so it is not an established climate solution. See section 10. 30. Critically assess whether an organism could be engineered to simultaneously perform photosynthesis AND oxidative phosphorylation in the same compartment. What major thermodynamic and biochemical obstacles would need to be overcome? (Consider: O₂ produced by photosynthesis would support oxidative phosphorylation, but the competing demands for NAD(P)H, the different evolutionary origins of the two systems, and the compartmentation challenges in a single organelle context.)

Answer (Q30, Synthesis). In principle photosynthesis and oxidative phosphorylation are complementary (O₂ and reductant from one could feed the other), and some organisms already run both in separate organelles. Co-locating them in one compartment faces major obstacles: both build proton-motive forces and compete for the same electron carriers and quinone/cytochrome pools, so uncoordinated operation would short-circuit gradients and create futile cycles; the systems compete for NAD(P)H and ADP/Pi pools; photosynthetic O₂ and ROS would oxidatively damage respiratory chains; and the two machineries have distinct evolutionary origins, lipid environments, and regulation that would require extensive re-engineering and tight temporal/spatial separation. The judgement that this is feasible would change only if robust regulatory insulation and gradient/redox partitioning could be demonstrated — currently a formidable, largely unmet challenge. See section 10.

Questions — Metabolic Integration and Regulation

Instructor Use and Coverage Notes

- Coverage target: Predict how a change in substrate, hormone, or enzyme activity redirects flux.
- Model/data emphasis: Energy charge, control points, and pathway-flux comparisons.
- Assessment alignment: Representing and Describing Data, Statistical Tests and Data Analysis.
- Misconception probe: A pathway is not a one-way assembly line; reversibility and regulation define the real route.
- Transfer product: Apply metabolic network reasoning to diabetes, fasting, exercise, or cancer metabolism.
- Grading focus: award full credit for mechanism, evidence, boundary conditions, and units when a calculation is required.
- Suggested use: draw one recall item, one application item, and one synthesis item when building a short quiz from this bank.

Questions 1–10: Recall and Comprehension

This activity accompanies section 11 of the textbook — review that chapter before attempting the exercises below.

1. What does “metabolic integration” mean? Give one example of how carbohydrate and lipid metabolism are connected.

Answer (Q1, Recall). Metabolic integration is the coordinated regulation of multiple pathways and organs so fuel supply matches demand and futile cycling is avoided. A classic example: in the fed state insulin promotes glucose uptake and lipogenesis (acetyl-CoA → malonyl-CoA → fatty acids), while in fasting glucagon activates lipolysis and β -oxidation so fatty-acid-derived acetyl-CoA fuels the liver and spares glucose for the brain — carbohydrate status directly sets lipid flux. See section 11. 2. Define anabolism and catabolism. Give one example of each.

Answer (Q2, Recall). Catabolism breaks complex molecules into simpler ones, releasing energy and reducing power (e.g. glucose oxidation via glycolysis and the TCA cycle). Anabolism builds complex molecules using energy and reducing power (e.g. fatty acid synthesis from acetyl-CoA, or gluconeogenesis). They are reciprocally regulated so both do not run at once. See section 11. 3. What is the role of AMP:ATP ratio as a metabolic signal? Which enzyme is the key AMP sensor?

Answer (Q3, Recall). A rising AMP:ATP (and ADP:ATP) ratio signals energy deficit, allosterically and covalently shifting metabolism toward ATP-producing catabolism. The key AMP sensor is AMP-activated protein kinase (AMPK): AMP binding (and LKB1 phosphorylation) activates it when cellular energy charge falls. See section 11. 4. What is AMPK? Describe two metabolic processes it activates and two it inhibits.

Answer (Q4, Recall). AMPK is the cell’s low-energy sensor, activated by a high AMP:ATP ratio. It activates catabolic, ATP-generating processes — e.g. glucose uptake (GLUT4) and fatty acid oxidation (by inhibiting acetyl-CoA carboxylase, lowering malonyl-CoA). It inhibits anabolic, ATP-consuming processes — e.g. fatty acid/cholesterol synthesis (ACC, HMG-CoA reductase) and mTORC1-driven protein synthesis. See section 11. 5. What is mTOR? What signals activate it, and what anabolic processes does it promote?

Answer (Q5, Recall). mTOR (mechanistic target of rapamycin), as mTORC1, is the cell’s nutrient/growth sensor. It is activated by amino acids (via Rag GTPases and the Ragulator at the lysosome), insulin/growth-factor signaling through PI3K–Akt, and a high energy charge. It promotes anabolism: protein synthesis (S6K1, 4E-BP1), lipid and nucleotide synthesis, and ribosome biogenesis, while suppressing autophagy. See section 11. 6. Name the organs that play a primary role in glucose homeostasis after a meal.

Answer (Q6, Recall). After a meal the principal organs are the pancreas (β -cells secrete insulin in response to rising glucose), the liver (takes up glucose, stores glycogen, runs lipogenesis), skeletal muscle (insulin-stimulated GLUT4 glucose uptake and glycogen synthesis), and adipose tissue (glucose uptake and triacylglycerol storage). See section 11. 7. What is the metabolic role of the liver in the fed vs fasted state?

Answer (Q7, Recall). Fed state: high insulin/low glucagon — the liver takes up glucose, makes glycogen and fatty acids (lipogenesis), and suppresses glucose output. Fasted state: low insulin/high glucagon — the liver releases glucose by glycogenolysis then gluconeogenesis, and produces ketone bodies from fatty-acid-derived acetyl-CoA to fuel peripheral tissues and brain. See section 11. 8. Define the Cori cycle. Which two organs are involved, and which molecule cycles between them?

Answer (Q8, Recall). The Cori cycle links exercising/anaerobic muscle and the liver. Muscle produces lactate by glycolysis; lactate travels to the liver and is converted back to glucose by gluconeogenesis (net cost about 6 ATP in liver), and that glucose returns to muscle. Lactate is the molecule that cycles between the two organs. See section 11. 9. What is the glucose-fatty acid cycle (Randle cycle)? What is the primary substrate competition it describes?

Answer (Q9, Recall). The Randle (glucose–fatty acid) cycle describes reciprocal substrate competition in heart and skeletal muscle: increased fatty acid oxidation raises acetyl-CoA and citrate, inhibiting pyruvate dehydrogenase and PFK-1, so glucose oxidation falls — and conversely high glucose suppresses fatty acid oxidation. The core competition is between glucose and fatty acids as oxidative fuels. See section 11. 10. Define metabolic syndrome. List four diagnostic criteria.

Answer (Q10, Recall). Metabolic syndrome is a cluster of cardiometabolic risk factors driven by insulin resistance and central adiposity. Four diagnostic criteria (any three define it): central/abdominal obesity (large waist circumference), elevated fasting glucose (or insulin resistance), elevated triglycerides, reduced HDL cholesterol, and elevated blood pressure. See section 11.

Questions 11–20: Application and Analysis

11. After a high-carbohydrate meal, blood glucose rises. Trace the hormonal and metabolic responses in: (a) the pancreas; (b) the liver; (c) skeletal muscle; (d) adipose tissue — over the 2 hours post-meal.

Answer (Q11, Application). (a) Pancreas: rising glucose triggers β -cell insulin secretion (and suppresses glucagon). (b) Liver: insulin promotes glucokinase, glycogen synthase activation and glycogen storage, lipogenesis, and shuts off gluconeogenesis. (c) Skeletal muscle: insulin-PI3K-Akt drives GLUT4 translocation, glucose uptake, and glycogen synthesis. (d) Adipose tissue: GLUT4-mediated glucose uptake, lipoprotein-lipase-mediated fatty acid uptake, and triacylglycerol storage with suppressed lipolysis. Over about 2 h blood glucose normalizes and the body is in an anabolic, storage state. See section 11. 12. During prolonged fasting (48 hours), the body must maintain blood glucose for the brain. List in order the fuels used: (a) which depot is depleted first; (b) when and where does gluconeogenesis begin; (c) when do ketone bodies become the primary brain fuel?

Answer (Q12, Application). (a) Liver glycogen is depleted first (largely gone by about 24 h). (b) Gluconeogenesis (from lactate, glycerol, glucogenic amino acids) ramps up in the liver within hours and dominates after glycogen is exhausted; the renal cortex contributes increasingly with prolonged fasting. (c) Ketone bodies rise over 1–2 days and, after about 3 days of fasting, supply up to about 75% of the brain’s fuel, sparing glucose and limiting muscle proteolysis. See section 11. 13. Insulin stimulates GLUT4 translocation to the plasma membrane of muscle and adipose cells via PI3K-Akt-AS160 pathway. Explain the molecular cascade from insulin receptor activation to GLUT4 vesicle exocytosis. What happens to GLUT4 when insulin is removed?

Answer (Q13, Application). Insulin binds its receptor tyrosine kinase → receptor autophosphorylation → IRS-1 phosphorylation → PI3K → PIP3 → PDK1/Akt activation → Akt phosphorylates AS160 (TBC1D4), relieving its Rab-GAP activity → active Rab10 permits GLUT4 storage vesicles to dock and fuse via SNAREs at the plasma membrane, increasing glucose uptake. When insulin is removed, the cascade reverses, GLUT4 is endocytosed and recycled back to intracellular vesicles, and glucose uptake falls. See section 11. 14. PFK-1 (phosphofructokinase-1) is a key regulatory enzyme of glycolysis. It is activated by AMP, ADP, and fructose-2,6-bisphosphate (F-2,6-BP) and inhibited by ATP, citrate, and H^+ . Explain how each regulator makes physiological sense in terms of energy status signaling.

Answer (Q14, Application). PFK-1 catalyses the committed glycolytic step and is tuned to energy status. AMP and ADP rise when ATP is low and activate PFK-1 (more glycolysis to make ATP). Fructose-2,6-bisphosphate, high when insulin/fed signaling raises glycolysis, is a potent activator. ATP (substrate at high concentration) and citrate (signaling abundant TCA fuel) inhibit it, and H^+ inhibits it to prevent excessive lactic acid in hypoxia — each regulator matches glycolytic flux to need. See section 11. 15. A patient with Type 2 Diabetes has high fasting blood glucose and high insulin (insulin resistance). Explain: (a) why cells are resistant to insulin; (b) why the liver continues gluconeogenesis despite high insulin; (c) what happens to HbA1c in chronic hyperglycaemia; (d) why metformin (activates AMPK) is effective.

Answer (Q15, Application). (a) Cells are insulin-resistant because chronic nutrient/lipid excess and inflammation cause serine phosphorylation of IRS-1, blunting PI3K-Akt and GLUT4 translocation. (b) The liver keeps making glucose because hepatic insulin signaling (FOXO1 suppression) is impaired while glucagon and substrate supply persist. (c) Chronic hyperglycaemia non-enzymatically glycates hemoglobin, so HbA1c rises (reflecting about 3-month average glucose). (d) Metformin works by activating AMPK (via Complex I inhibition raising AMP/ATP), suppressing hepatic gluconeogenesis and improving insulin sensitivity. See section 11. 16. The malate-aspartate shuttle moves NADH equivalents from the cytoplasm to the mitochondrial matrix. Explain: (a) why direct NADH cannot cross the inner mitochondrial membrane; (b) the carrier proteins involved; (c) why cardiac muscle prefers this shuttle over the glycerol-3-phosphate shuttle.

Answer (Q16, Application). (a) The inner mitochondrial membrane has no NADH transporter, so cytosolic NADH electrons must be shuttled in. (b) The malate-aspartate shuttle uses malate dehydrogenase and aspartate aminotransferase on both sides plus the malate- α -ketoglutarate and glutamate-aspartate antiporters. (c) Cardiac muscle prefers it because it regenerates matrix NADH (entering at Complex I, about 2.5 ATP per pair) rather than FADH₂-equivalents via the glycerol-3-phosphate shuttle (about 1.5 ATP), maximizing ATP yield for the continuously working heart. See section 11. 17. Brown adipose tissue (BAT) thermogenesis is mediated by UCP1. Explain the adrenergic activation cascade: cold → sympathetic nervous system → β_3 -adrenergic receptor → cAMP → PKA → hormone-sensitive lipase → free fatty acid (FFA) release → FFA activate/open UCP1 → H^+ leak → heat. At which step is UCP1 expression also increased transcriptionally?

Answer (Q17, Application). Cold → sympathetic noradrenaline → β_3 -adrenergic receptor → Gs → adenylyl cyclase → cAMP → PKA. PKA phosphorylates hormone-sensitive lipase (and perilipin), releasing free fatty acids from lipid droplets. The FFAs both directly activate UCP1 and serve as fuel; UCP1 lets protons re-enter the matrix bypassing ATP synthase, dissipating the proton-motive force as heat. Transcriptionally, the same

cAMP–PKA signaling activates PGC-1 α /CREB, increasing UCP1 gene expression for longer-term cold adaptation. See section 11. 18. Glucagon activates gluconeogenesis in liver cells. Trace from glucagon binding \rightarrow Gs \rightarrow cAMP \rightarrow PKA \rightarrow phosphorylation of CREB \rightarrow activation of PEPCK and G6Pase gene transcription. How does insulin oppose this pathway via Akt (inactivating FOXO1 transcription factor)?

Answer (Q18, Application). Glucagon binds its Gs-coupled receptor \rightarrow adenylyl cyclase \rightarrow cAMP \rightarrow PKA \rightarrow PKA phosphorylates CREB \rightarrow CREB (with co-activator) drives transcription of PEPCK and glucose-6-phosphatase, raising gluconeogenic capacity (and PKA also activates glycogenolysis acutely). Insulin opposes this: insulin \rightarrow PI3K \rightarrow Akt phosphorylates FOXO1, excluding it from the nucleus so PEPCK/G6Pase transcription falls, and Akt also inactivates the cAMP signal — shutting down hepatic glucose output. See section 11. 19. The hypothalamus integrates hunger and satiety signals from peripheral hormones (leptin, ghrelin, PYY, insulin). Explain: (a) which neurons (NPY/AgRP vs POMC/CART) are activated by fasting vs feeding; (b) how melanocortin-4 receptor (MC4R) controls food intake; (c) why leptin resistance in obesity prevents normalization of energy balance.

Answer (Q19, Application). (a) Fasting (low leptin/insulin, high ghrelin) activates orexigenic NPY/AgRP neurons; feeding (high leptin/insulin, PYY) activates anorexigenic POMC/CART neurons. (b) POMC-derived α -MSH activates the melanocortin-4 receptor (MC4R) to suppress food intake, while AgRP is an MC4R inverse agonist that increases intake — MC4R is the integrating node. (c) In obesity, chronic hyperleptinaemia plus inflammatory/SOCS3-mediated signaling blunting causes leptin resistance, so the satiety signal is not transduced and energy balance is not corrected despite high fat stores. See section 11. 20. Fatty acid synthesis and β -oxidation cannot occur simultaneously — they would create a futile cycle. Explain how the cell prevents this: (a) what molecule inhibits carnitine palmitoyltransferase I (CPTI) during fatty acid synthesis; (b) in which compartment is malonyl-CoA produced; (c) why this system specifically blocks mitochondrial FA import while allowing FA synthesis in the cytoplasm.

Answer (Q20, Application). (a) Malonyl-CoA inhibits carnitine palmitoyltransferase I (CPT-1). (b) Malonyl-CoA is produced in the cytoplasm by acetyl-CoA carboxylase (the committed step of fatty acid synthesis). (c) Because CPT-1 sits on the outer mitochondrial membrane and gates long-chain fatty-acyl entry into the matrix, blocking CPT-1 stops β -oxidation while cytoplasmic fatty acid synthesis continues unhindered — so in the fed/lipogenic state newly made fatty acids are not immediately re-oxidised, preventing a futile cycle. See section 11.

Questions 21–30: Synthesis and Evaluation

21. Evaluate the “fuel partitioning” hypothesis in obesity: does obesity arise primarily from excess carbohydrate or excess fat intake, and does macronutrient composition matter for energy balance beyond caloric excess? Cite the results of isocaloric controlled diet trials.

Answer (Q21, Synthesis). Evidence from tightly controlled isocaloric feeding and metabolic-ward studies indicates that total energy balance, not macronutrient ratio, is the dominant determinant of fat mass: when calories are matched, low-carb and low-fat diets produce similar fat loss. Macronutrient composition still matters secondarily through satiety, adherence, the thermic effect of protein, and glycaemic/insulin dynamics. The carbohydrate–insulin model’s strong claim is weakened by isocaloric trials; what would change the conclusion is reproducible isocaloric data showing a macronutrient-specific difference in energy expenditure or fat storage. See section 11. 22. Evaluate the ketogenic diet as a treatment for drug-resistant epilepsy. Propose at least three molecular mechanisms by which elevated ketone bodies (β -hydroxybutyrate primarily as an HDAC inhibitor, adenosine release, or KATP channel opening) could reduce neuronal excitability.

Answer (Q22, Synthesis). Proposed mechanisms by which ketosis reduces seizures: (1) β -hydroxybutyrate acts as a class-I HDAC inhibitor, shifting transcription toward antioxidant/anticonvulsant gene programs; (2) ketone metabolism and reduced glycolysis open neuronal KATP channels and hyperpolarise neurons, lowering excitability; (3) shifted metabolism raises inhibitory tone (more GABA, increased adenosine signaling) and stabilizes mitochondrial energy supply, reducing neuronal hyperexcitability. The ketogenic diet has reproducible clinical benefit in drug-resistant epilepsy, though the precise dominant mechanism remains uncertain and tolerability/adherence limit it. See section 11. 23. Design an experiment to determine whether AMPK activation in liver cells reduces hepatic glucose output primarily by: (a) decreasing gluconeogenesis gene expression; (b) acutely phosphorylating and inactivating TORC2 (CREB co-activator); (c) decreasing hepatic ATP to slow enzymatic gluconeogenesis. Distinguish these mechanisms using selective inhibitors and reporter assays.

Answer (Q23, Synthesis). Hypothesis: AMPK lowers hepatic glucose output primarily by (a) repressing PEPCK/G6Pase transcription, (b) acutely phosphorylating/inactivating the CREB co-activator CRTC2 (TORC2), or (c) lowering ATP to slow gluconeogenic enzymes. In hepatocytes, activate AMPK (AICAR/metformin) and compare with vehicle controls; measure glucose output, PEPCK/G6Pase mRNA (qPCR/reporter), CRTC2 phosphorylation/nuclear localization, and cellular ATP. Use a transcription-blocked condition (actinomycin D) to isolate non-transcriptional effects and a CRTC2-phospho-mutant to test mechanism (b). Replicate across independent hepatocyte preparations; a falsifying result is full suppression of glucose output with unchanged mRNA, CRTC2 phosphorylation, and ATP. See section 11. 24. Evaluate the evidence for “metabolic flexibility” — the ability of healthy cells to switch between glucose and fat oxidation based on substrate availability. How does this differ in Type 2 Diabetes, insulin resistance, and cancer cells? What biochemical assay (Seahorse XF analyser) measures metabolic flexibility?

Answer (Q24, Synthesis). Metabolic flexibility is the capacity to switch readily between glucose and fat oxidation with fed/fasted state — evidenced by respiratory quotient shifts and substrate-switching after insulin. In Type 2 diabetes and insulin resistance this flexibility is lost (‘metabolic inflexibility’): muscle fails to suppress fat oxidation in the fed state and fails to up-regulate it in fasting. Cancer cells are biased toward aerobic glycolysis (Warburg) and glutamine use rather than flexible switching. The Seahorse XF analyser measures it by recording oxygen consumption rate and extracellular acidification rate while sequentially adding substrates and inhibitors, quantifying oxidative vs glycolytic capacity. See section 11. 25. The metabolic role of the gut microbiome is increasingly recognized: SCFAs (acetate, propionate, butyrate) produced by bacterial fermentation of dietary fiber signal to host cells. Evaluate how propionate signals to the liver (inhibiting gluconeogenesis) and butyrate signals to colonocytes (primary fuel) and immune cells (HDAC inhibition, regulatory T cell induction).

Answer (Q25, Synthesis). Gut bacteria ferment dietary fiber to short-chain fatty acids that act as inter-organ signals. Propionate is absorbed and reaches the liver, where it signals (via FFAR3/GPR41 and as a gluconeogenic/intestinal-gluconeogenesis cue) to restrain hepatic glucose output and improve glucose homeostasis. Butyrate is the primary oxidative fuel for colonocytes and, in immune cells, acts as an HDAC inhibitor that promotes regulatory T-cell differentiation and an anti-inflammatory tone — linking the microbiome to host energy balance and immunometabolism. See section 11. 26. Evaluate the metabolic rationale for intermittent fasting (IF) regimens (16:8 time-restricted eating, 5:2 alternate-day fasting). Identify three metabolic benefits of IF beyond simple caloric restriction, and propose the molecular mechanisms driving each benefit.

Answer (Q26, Synthesis). Beyond simple calorie reduction, intermittent fasting confers benefits via distinct molecular mechanisms: (1) periodic low energy charge activates AMPK and lowers mTORC1, inducing autophagy and improving cellular quality control; (2) the fasting/feeding cycle improves insulin sensitivity and metabolic flexibility by lowering insulin and depleting hepatic glycogen, increasing fat oxidation; (3) ketone bodies (notably β -hydroxybutyrate) rise and act as signaling molecules (HDAC inhibition, NLRP3 inflammasome suppression), reducing inflammation. Clinical evidence is promising but partly confounded by adherence and total energy intake; an isocaloric IF-vs-continuous trial showing IF-specific benefit would strengthen the case. See section 11. 27. Cancer cells depend on glutamine (not glucose) for anaplerosis — replenishing TCA cycle intermediates for biosynthesis. Evaluate: (a) which TCA intermediate is most depleted in rapidly proliferating cells; (b) how glutamine enters the TCA cycle (via glutaminase \rightarrow glutamate \rightarrow α -ketoglutarate); (c) why targeting glutamine metabolism (CB-839, a glutaminase inhibitor) might be selectively toxic to cancer cells.

Answer (Q27, Synthesis). (a) Oxaloacetate (and α -ketoglutarate-derived intermediates) is most depleted because biosynthesis siphons TCA intermediates (‘cataplerosis’). (b) Glutamine enters via glutaminase \rightarrow glutamate \rightarrow (transaminase/glutamate dehydrogenase) \rightarrow α -ketoglutarate, which replenishes the cycle (anaplerosis) for energy and biosynthetic precursors. (c) Many proliferating tumors are ‘glutamine-addicted’ for anaplerosis and redox/biosynthesis, so a glutaminase inhibitor (CB-839/telaglenastat) can be more toxic to them than to normal tissue that has flexible anaplerotic sources — though efficacy is context-dependent and resistance can arise. See section 11. 28. Evaluate the concept of “metaflammation” — the chronic low-grade inflammation seen in obesity. Propose a mechanistic link from adipocyte lipid overload \rightarrow ER stress \rightarrow NF- κ B activation \rightarrow pro-inflammatory cytokine (TNF- α , IL-6) secretion \rightarrow insulin resistance in muscle and liver. At which step would you intervene pharmacologically?

Answer (Q28, Synthesis). Metaflammation is chronic low-grade inflammation from nutrient overload. Mechanistic chain: adipocyte lipid overload and ectopic lipid \rightarrow ER stress and excess saturated FFAs/diacylglycerol \rightarrow activation of JNK and IKK β /NF- κ B \rightarrow secretion of TNF- α , IL-6, and MCP-1 with macrophage infiltration \rightarrow these cytokines drive serine phosphorylation of IRS-1 in muscle and liver, impairing PI3K-Akt and causing insulin resistance. Pharmacological intervention is most rational upstream — reducing lipid overload and ER/inflammatory signaling (e.g. weight loss, GLP-1 agonists, or targeting JNK/IKK β /NF- κ B) rather than blocking a single downstream cytokine. See section 11. 29. NAFLD (non-alcoholic fatty liver disease) progresses from steatosis \rightarrow NASH (steatohepatitis) \rightarrow cirrhosis. Evaluate the “two-hit hypothesis”: what is the first hit (lipid accumulation), what is the second hit (oxidative stress, inflammatory cytokines from adipose tissue or gut microbiome), and why targeting a single hit is insufficient for treatment?

Answer (Q29, Synthesis). First hit: triacylglycerol accumulation in hepatocytes (steatosis) from increased FFA delivery, de novo lipogenesis, and impaired export. Second hit: oxidative stress from incomplete fatty acid oxidation (ROS), plus inflammatory cytokines and endotoxin from adipose tissue and the gut microbiome, driving hepatocyte injury and inflammation (NASH) that progresses to fibrosis/cirrhosis. Targeting only one hit is insufficient because steatosis alone is relatively benign and the lipotoxic/inflammatory second hit independently drives progression — effective therapy must reduce lipid load and the oxidative/inflammatory injury together. See section 11. 30. Critically evaluate the use of GLP-1 receptor agonists (semaglutide, tirzepatide) for obesity treatment. What are the distinct mechanisms by which GLP-1 agonists reduce appetite (hypothalamic signaling), slow gastric emptying, and promote pancreatic β -cell survival? What are the metabolic consequences of rapid weight loss induced by these drugs (muscle loss, bone density) and how should therapy be managed?

Answer (Q30, Synthesis). GLP-1 receptor agonists act through distinct mechanisms: in the hypothalamus they activate POMC/CART and suppress NPY/AgRP neurons to reduce appetite; in the gut they slow gastric emptying, prolonging satiety; and on pancreatic β -cells they enhance glucose-dependent insulin secretion and promote β -cell survival/function. Rapid drug-induced weight loss carries metabolic consequences — loss of lean

muscle mass and reduced bone mineral density. Management should pair therapy with adequate protein intake and resistance exercise, gradual titration to limit GI effects, and monitoring of body composition and bone health, with attention to weight regain on discontinuation. See section 11.

Questions — DNA Replication and the Cell Cycle

Instructor Use and Coverage Notes

- Coverage target: Calculate replication timing or error burden and infer checkpoint consequences.
- Model/data emphasis: Replication-fork speed, error-rate, and cell-cycle timing calculations.
- Assessment alignment: Concept Explanation, Questions and Methods, Argumentation.
- Misconception probe: High fidelity is not automatic; it is built from multiple partially redundant safeguards.
- Transfer product: Transfer replication logic to cancer, aging, viral replication, or antibiotic targets.
- Grading focus: award full credit for mechanism, evidence, boundary conditions, and units when a calculation is required.
- Suggested use: draw one recall item, one application item, and one synthesis item when building a short quiz from this bank.

Questions 1–10: Recall and Comprehension

This activity accompanies section 12 of the textbook — review that chapter before attempting the exercises below.

1. Describe the semiconservative model of DNA replication. What experiment confirmed it (Meselson-Stahl, 1958)?

Answer (Q1, Recall). Each daughter molecule retains one parental strand and one newly synthesized strand, so replication is semiconservative. Meselson and Stahl (1958) grew *E. coli* in heavy ¹⁵N medium, switched to light ¹⁴N, and used CsCl density-gradient centrifugation: after one round all DNA was hybrid (intermediate) density, and after two rounds half was hybrid and half fully light, which is exactly what the semiconservative model predicts and rules out conservative and dispersive models. See section 12.

2. List the enzymes required for DNA replication and state one function of each.
- Answer (Q2, Recall). Helicase unwinds the double helix at the fork; single-strand binding (SSB) proteins keep the strands apart; topoisomerase/gyrase relieves the supercoiling ahead of the fork; primase lays down RNA primers; DNA polymerase (Pol III in bacteria; Pol δ/ε in eukaryotes) extends DNA and proofreads; a sliding clamp (β-clamp/PCNA) confers processivity; and DNA ligase seals the nicks between fragments. See section 12.

3. Why does DNA polymerase require a primer? Who synthesizes the primer?
- Answer (Q3, Recall). DNA polymerase can only extend a pre-existing 3'-OH end and cannot start a strand de novo, so it needs a primer to provide that 3'-OH. The RNA primer is synthesized by primase, a specialized RNA polymerase (part of the primosome in bacteria; the Pol α-primase complex in eukaryotes). See section 12.

4. Distinguish the leading strand from the lagging strand during replication. Why does the lagging strand form Okazaki fragments?
- Answer (Q4, Recall). The leading strand is synthesized continuously in the 5'→3' direction as the fork opens, while the lagging strand runs antiparallel so its 5'→3' synthesis proceeds away from the fork. Because polymerase cannot synthesize 3'→5', the lagging strand is made in short Okazaki fragments (about 1,000–2,000 nt in prokaryotes, about 100–200 nt in eukaryotes), each separately primed and later joined by ligase. See section 12.

5. What is the replication fork? Name the enzyme that separates the double helix at the fork.
- Answer (Q5, Recall). The replication fork is the Y-shaped region where the parental duplex is unwound and the two template strands are being copied. DNA helicase (DnaB in *E. coli*; the MCM2-7 complex in eukaryotes) unwinds and separates the double helix at the fork. See section 12.

6. Name the four phases of the eukaryotic cell cycle. What occurs in each?
- Answer (Q6, Recall). The four phases are G1 (cell growth and preparation for DNA synthesis), S (DNA replication, producing identical sister chromatids), G2 (growth and checking of replicated DNA before division), and M (mitosis plus cytokinesis, segregating chromosomes into two daughter cells). G1, S, and G2 together form interphase. See section 12.

7. What are cyclins and cyclin-dependent kinases (CDKs)? Give one example of a cyclin-CDK pair and its function.
- Answer (Q7, Recall). Cyclins are regulatory proteins whose levels rise and fall through the cycle; CDKs are kinases that are catalytically active only when bound to their cyclin partner, phosphorylating substrates that drive cell-cycle transitions. For example, Cyclin B–CDK1 (M-phase promoting factor) triggers entry into mitosis by phosphorylating nuclear lamins, condensin, and other targets. See section 12.

8. What is a checkpoint? Name three checkpoints in the cell cycle and their functions.
- Answer (Q8, Recall). A checkpoint is a surveillance mechanism that halts cell-cycle progression until specific conditions are met, preventing propagation of damage. The G1/S (restriction) checkpoint verifies cell size, nutrients, and DNA integrity before S phase; the G2/M checkpoint confirms DNA is fully and correctly replicated before mitosis; and the spindle-assembly (M) checkpoint blocks anaphase until all kinetochores are properly attached to the spindle. See section 12.

9. What does the tumor suppressor protein p53 do when DNA damage is detected?
- Answer (Q9, Recall). DNA damage activates ATM/ATR kinases that stabilize p53 by blocking its MDM2-mediated degradation. p53 then acts as a transcription factor, inducing p21 to inhibit cyclin-CDK complexes and arrest the cycle for repair; if damage is irreparable, p53 drives apoptosis or

senescence, which is why it is called the guardian of the genome. See section 12. 10. What is telomerase? Why do most somatic cells lack telomerase activity?

Answer (Q10, Recall). Telomerase is a ribonucleoprotein reverse transcriptase that uses its own RNA template to add TTAGGG repeats to chromosome 3' ends, offsetting the end-replication problem. Most somatic cells repress the catalytic subunit hTERT, so telomeres shorten about 50–200 bp per division until critical shortening triggers senescence — a tumor-suppressive limit on proliferation. See section 12.

Questions 11–20: Application and Analysis

11. Using the Meselson-Stahl data: if ¹⁵N/¹⁵N-labeled DNA is allowed to replicate for two rounds in ¹⁴N medium, what densities of DNA are expected and in what proportions? Show your reasoning with a diagram.

Answer (Q11, Application). After two rounds of replication in ¹⁴N medium the original two ¹⁵N strands are conserved, each now paired with a new light strand, giving two hybrid (intermediate-density) molecules. The other two molecules are fully light (¹⁴N/¹⁴N). So the expectation is a 1:1 ratio of intermediate to light density and no fully heavy DNA, which is the diagnostic signature of semiconservative replication. See section 12. 12. DNA polymerase III (prokaryotic) and DNA polymerase δ/ϵ (eukaryotic) require a processivity clamp (β -clamp in prokaryotes; PCNA in eukaryotes). Explain how the sliding clamp increases processivity, and why this matters for replication speed of the 3×10^9 bp human genome.

Answer (Q12, Application). The sliding clamp is a ring that encircles DNA and tethers the polymerase to the template, preventing it from dissociating after each nucleotide. This raises processivity from about 10–100 nt to thousands of nucleotides per binding event, so the polymerase can copy long stretches without falling off — essential for replicating the 3×10^9 bp human genome at biologically feasible speed and within S phase. See section 12.

13. Okazaki fragments in eukaryotes are about 200 nucleotides (roughly one nucleosome length). After primase removes the primer, DNA pol δ fills the gap using the downstream Okazaki fragment as a flap. Explain the role of FEN1 (flap endonuclease) and DNA ligase in completing lagging strand synthesis.

Answer (Q13, Application). As Pol δ extends one Okazaki fragment into the RNA primer of the downstream fragment, it displaces that primer as a single-stranded 5' flap. FEN1 cleaves the displaced flap precisely at the base, leaving a nick with a 3'-OH and 5'-phosphate, and DNA ligase I then seals the nick with a phosphodiester bond, joining adjacent fragments into a continuous lagging strand. See section 12. 14. The G₁/S checkpoint (restriction point) ensures cells don't enter S phase with insufficient resources or DNA damage. Explain the molecular mechanism: how does mitogen (growth factor) signaling lead to Rb phosphorylation → release of E2F transcription factor → S-phase gene expression? At what step does p16 (CDKN2A tumor suppressor) block this pathway?

Answer (Q14, Application). Mitogen signaling activates Cyclin D–CDK4/6, which partially phosphorylates Rb; Cyclin E–CDK2 then hyperphosphorylates Rb, releasing E2F transcription factors that drive expression of S-phase genes (cyclin E, DNA polymerase, etc.), committing the cell past the restriction point. The p16 (CDKN2A) tumor suppressor blocks this upstream by inhibiting CDK4/6, so Rb stays hypophosphorylated and E2F remains sequestered. See section 12. 15. Aphidicolin blocks DNA polymerase α and δ , arresting cells at the G₁/S boundary. Hydroxyurea (HU) depletes dNTP pools. Compare the effects of each drug on: (a) replication fork speed; (b) fork stalling vs collapse; (c) activation of ATR checkpoint kinase; (d) cell cycle arrest phase.

Answer (Q15, Application). (a) Aphidicolin halts elongation by blocking Pol α/δ so forks stall with intact replisomes; HU lowers fork speed by depleting dNTPs. (b) Both initially cause reversible fork stalling, but prolonged exposure leads to fork collapse and double-strand breaks. (c) Both generate RPA-coated ssDNA that activates the ATR–CHK1 checkpoint. (d) Aphidicolin arrests cells at the G₁/S boundary and in early S; HU arrests cells in S phase. See section 12. 16. Telomere shortening occurs at a rate of about 100 bp per cell division in most somatic cells. Calculate how many divisions a cell with initial telomere length of 15 kb could undergo before reaching the critical length of 6 kb. What happens to cells that continue dividing past this limit (crisis)?

Answer (Q16, Application). Usable telomere reserve is 15 kb – 6 kb = 9 kb = 9,000 bp. At about 100 bp lost per division, that is 9,000/100 ≈ 90 divisions before reaching the critical 6 kb length. Cells dividing past this limit enter crisis: uncapped telomeres trigger end-to-end fusions, breakage-fusion-bridge cycles, and massive genomic instability, so most cells die and rare survivors typically reactivate telomerase. See section 12.

17. The spindle assembly checkpoint (SAC) detects kinetochores not under tension (unattached to spindle microtubules). Explain the molecular mechanism: how does an unattached kinetochore produce the wait anaphase signal (MCC complex), how does this inhibit APC/C (anaphase-promoting complex), and what happens to separase and cohesin when SAC is satisfied?

Answer (Q17, Application). An unattached or tensionless kinetochore recruits MAD/BUB proteins that catalyze formation of the mitotic checkpoint complex (MCC: Mad2–BubR1–Bub3–Cdc20). The MCC sequesters Cdc20, inhibiting the APC/C so securin and cyclin B are not degraded. Once all kinetochores achieve bipolar attachment the signal stops, APC/C–Cdc20 ubiquitinates securin, freeing separase to cleave cohesin and trigger anaphase. See section 12. 18. CDK1–Cyclin B drives entry into mitosis. CDK1–Cyclin B phosphorylates nuclear lamins (dissolving the nuclear

envelope), activates condensin (chromosome condensation), and activates APC/C (through intermediate steps). Explain why Cyclin B must be abruptly degraded at the metaphase-anaphase transition.

Answer (Q18, Application). Cyclin B–CDK1 enforces the mitotic state, but sister-chromatid separation and mitotic exit require its abrupt loss. At the metaphase–anaphase transition the active APC/C–Cdc20 ubiquitinates cyclin B for proteasomal degradation, inactivating CDK1. This irreversibly drops CDK1 activity, allowing dephosphorylation of its substrates so the nuclear envelope reforms, chromosomes decondense, and the cell cannot slip back into mitosis. See section 12. 19. Oncogenes often bypass cell cycle checkpoints. Compare how Ras (constitutively active mutant) vs Myc (overexpressed) each drive cell cycle progression: through which cyclin-CDK pair(s) do they act, and why do cells with oncogenic mutations often also need to lose p53 or Rb to become fully cancerous?

Answer (Q19, Application). Ras (constitutively active) sustains MAPK signaling that upregulates Cyclin D, activating CDK4/6 to drive the G1/S transition; Myc (overexpressed) transcriptionally boosts cyclins, CDKs, and E2F targets while repressing CDK inhibitors, also accelerating G1/S. These growth signals trigger oncogene-induced senescence or apoptosis via the p53 and Rb pathways, so cells must additionally lose p53 or Rb to disable that fail-safe and proliferate unchecked. See section 12. 20. Yeast two-hybrid screens identified that geminin (overexpressed in many cancers) inhibits Cdt1, preventing re-licensing of origins of replication. Explain: (a) what origin licensing means; (b) why re-replication would be catastrophic; (c) how overexpression of geminin PREVENTS re-replication by preventing MCM loading even after S phase begins.

Answer (Q20, Application). (a) Origin licensing is the G1 loading of MCM2-7 helicase double hexamers onto origins by ORC, Cdc6, and Cdt1 to form the pre-replicative complex, marking each origin to fire once. (b) Re-replication would over-amplify portions of the genome, causing gene-copy imbalance and DNA damage. (c) Geminin binds and inhibits Cdt1, blocking new MCM loading after S phase begins, so origins cannot be re-licensed and each fires only once per cycle. See section 12.

Questions 21–30: Synthesis and Evaluation

21. Evaluate the precision of the S-phase checkpoint: ATR kinase is activated by RPA-coated single-stranded DNA (from stalled forks). How does this trigger CHK1 activation → Cdc25A phosphorylation → degradation → CDK2 inactivation → fork stabilization? What happens if ATR is constitutively inactive (as in a mutation)?

Answer (Q21, Synthesis). Stalled forks expose RPA-coated ssDNA, which recruits and activates ATR. ATR phosphorylates and activates CHK1, which phosphorylates Cdc25A, targeting it for degradation; loss of Cdc25A leaves CDK2 inhibitory phosphates in place, so CDK2 stays inactive, suppressing late origin firing and stabilizing existing forks for restart. If ATR is constitutively inactive, forks collapse into double-strand breaks, late origins fire inappropriately, and the cell accumulates genomic instability — ATR loss is generally lethal. See section 12. 22. Design an experiment to test whether telomerase reactivation in a telomere-shortened cancer cell line would allow unlimited proliferation or would require additional changes. Include: how you would deliver hTERT (the catalytic subunit), how you would measure telomere length over generations, and what growth advantage you would expect and under what assay conditions.

Answer (Q22, Synthesis). Hypothesis: hTERT alone extends replicative lifespan but is insufficient for full transformation. Stably transduce the cell line with an hTERT expression vector versus an empty-vector control, and measure telomere length over many passages by terminal restriction fragment Southern blot or qPCR. Predicted outcome: hTERT-expressing cells maintain telomere length and bypass senescence/crisis, but unlimited proliferation in soft-agar or xenograft assays still requires additional oncogenic changes (e.g., loss of p53/Rb), which would falsify a one-step model if hTERT alone sufficed. See section 12. 23. DNA replication is not 100% accurate — polymerase error rate is about 1 in 10⁷. After mismatch repair (MMR), the rate drops to about 1 in 10⁹. Evaluate: (a) the molecular mechanism of MMR (MutS, MutL, excision, resynthesis); (b) why MMR deficiency causes microsatellite instability (MSI); (c) why MSI cancers respond better to immune checkpoint inhibitors (PD-1 blockade).

Answer (Q23, Synthesis). (a) MMR uses MutS (MSH2/MSH6) to recognize mismatches and MutL (MLH1/PMS2) to coordinate excision of the error-containing nascent strand, followed by resynthesis and ligation. (b) MMR deficiency leaves slippage errors in repetitive tracts uncorrected, producing microsatellite instability (MSI). (c) MSI tumors accumulate many frameshift mutations and neoantigens, making them highly immunogenic, so they respond well to PD-1 immune checkpoint blockade. See section 12. 24. Evaluate origin-of-replication usage in cancer: cancer cells often show replication stress (RFS — replication fork stalling) due to premature S-phase entry driven by oncogenes. Propose how elevated RFS leads to: (a) DSB (double-strand break) formation at stalled forks; (b) inappropriate NHEJ repair causing chromosomal translocations; (c) selection pressure for p53 loss (cells that could normally checkpoint-arrest now instead die, so p53 loss allows survival).

Answer (Q24, Synthesis). (a) Oncogene-driven premature S-phase entry stalls and collapses forks, generating double-strand breaks. (b) Repair of these breaks by error-prone NHEJ joins inappropriate ends, producing chromosomal translocations and rearrangements. (c) The resulting DNA-damage response activates p53-dependent arrest, apoptosis, or senescence, creating strong selection for p53 loss so that damaged cells survive and proliferate — explaining why replication stress and TP53 mutation co-occur early in tumorigenesis. See section 12. 25. The pre-replication complex (pre-RC) assembly (ORC → Cdc6 → Cdt1 → MCM2-7) licenses origins from late mitosis to G₁. Evaluate two licensing control systems: (a) Cdt1

degradation (Cullin4-Cdt2 E3 ligase triggered by PCNA on DNA); (b) Geminin inhibition of Cdt1. Propose why two redundant mechanisms are needed, and what would happen if both were inactivated simultaneously.

Answer (Q25, Synthesis). Both systems restrict Cdt1 to prevent origin re-licensing: (a) once PCNA loads on DNA in S phase, the Cullin4-Cdt2 (CRL4^{Cdt2}) E3 ligase ubiquitinates Cdt1 for degradation; (b) geminin directly binds and sequesters Cdt1. Two redundant mechanisms provide fail-safe robustness because re-replication is catastrophic; if both were inactivated simultaneously, Cdt1 would persist, MCM helicases would reload, and origins would re-fire, causing re-replication, gene amplification, and severe genomic instability. See section 12. 26. Replication stress is thought to be the earliest event in pre-cancerous lesions (before DNA mutation). Evaluate the evidence from oncogene-induced senescence (OIS): how does RAS^{V12} overexpression initially stall replication forks and activate the DNA damage response (p53-p21 axis, producing cellular senescence) before genomic instability occurs?

Answer (Q26, Synthesis). RAS^{V12} overexpression forces premature, unscheduled origin firing and a surge in replication initiation that outstrips dNTP and replisome supply, stalling and collapsing forks. The resulting ssDNA and double-strand breaks activate the ATR/ATM DNA-damage response, which stabilizes p53 and induces p21, imposing a durable cell-cycle arrest (oncogene-induced senescence) that acts as a barrier to transformation before overt mutations or aneuploidy accumulate. See section 12. 27. Centromere identity in eukaryotes is determined not by DNA sequence but by the presence of CENP-A (a histone H3 variant). Evaluate the epigenetic model of centromere inheritance: how is CENP-A loaded (by HJURP chaperone) at each S phase, and how can a “centromere” be moved to a new chromosomal location (neocentromere formation)?

Answer (Q27, Synthesis). Centromere identity is epigenetic: the histone H3 variant CENP-A marks centromeric nucleosomes independently of the underlying DNA sequence. CENP-A is deposited by its dedicated chaperone HJURP in early G1 (not at S phase, when it is diluted twofold), and the existing CENP-A template self-templates new loading. Because the mark is sequence-independent, CENP-A can be seeded at a new locus to form a functional neocentromere, while an inactivated original centromere loses CENP-A. See section 12. 28. Multi-fork replication in prokaryotes: *E. coli* can initiate replication at the same origin before the previous round is complete (multi-fork replication), allowing doubling times faster than the S-phase duration. Evaluate whether eukaryotes could employ multi-fork replication and what structural constraints (nuclear envelope, nucleosomes, cohesin) would prevent this.

Answer (Q28, Synthesis). In *E. coli*, multi-fork (dichotomous) replication re-initiates at oriC before the prior round finishes, so doubling time can be shorter than the replication period. Eukaryotes do not do this: licensing is strictly limited to G1 by CDK and geminin control, so origins fire only once per cycle. Instead, eukaryotes solve the speed problem with tens of thousands of origins firing within one S phase, and the nuclear envelope, nucleosome assembly, and cohesin establishment further enforce a single, ordered round of replication. See section 12. 29. Evaluate the hypothesis that cancer is fundamentally a disease of the cell cycle: most hallmarks of cancer (unlimited proliferation, evasion of apoptosis, invasion) result from failure of cell cycle checkpoints rather than from any particular oncogenic mutation. Construct the best argument for and against this view using specific molecular examples.

Answer (Q29, Synthesis). For: nearly all cancer hallmarks converge on the cell-cycle machinery — Rb/E2F deregulation enables unchecked proliferation, p53 loss disables damage arrest and apoptosis, and checkpoint failure permits aneuploidy, so checkpoint loss is the common final pathway. Against: oncogene-specific effects matter beyond cycling — Ras alters metabolism and invasion, angiogenesis and immune evasion are not checkpoint phenomena, and identical checkpoint lesions yield different tumors, so the cell cycle is necessary but not a complete explanation. See section 12. 30. Critically evaluate the kinetics of DNA repair: NHEJ (non-homologous end joining, fast, about 30 min) and HR (homologous recombination, slow, requires sister chromatid, restricted to S/G2). Predict the consequences for genomic integrity if NHEJ were the primary repair pathway available in a cell. Why is NHEJ “error-prone” at the molecular level, and what types of mutations does it introduce?

Answer (Q30, Synthesis). NHEJ directly ligates broken ends rapidly and in any cell-cycle phase, whereas HR is slow and uses a sister chromatid for accurate repair in S/G2. If NHEJ were the only pathway, breaks would still be repaired quickly but with frequent small insertions/deletions and translocations, eroding genomic integrity over time. NHEJ is error-prone because it often trims or fills incompatible ends before ligation rather than restoring the original sequence, introducing indels and joining the wrong ends. See section 12.

Questions — Gene Expression

Instructor Use and Coverage Notes

- Coverage target: Translate or annotate a sequence and explain how a regulatory change alters output.
- Model/data emphasis: Reading-frame, codon, and expression-output calculations.
- Assessment alignment: Concept Explanation, Questions and Methods, Argumentation.
- Misconception probe: A gene is not simply a protein recipe; context controls when, where, and how much product appears.
- Transfer product: Apply expression logic to mutations, biotechnology, development, and disease diagnostics.
- Grading focus: award full credit for mechanism, evidence, boundary conditions, and units when a calculation is required.
- Suggested use: draw one recall item, one application item, and one synthesis item when building a short quiz from this bank.

Questions 1–10: Recall and Comprehension

This activity accompanies section 13 of the textbook — review that chapter before attempting the exercises below.

1. Define gene expression. What are the two major steps?

Answer (Q1, Recall). Gene expression is the process by which the information in a gene is used to synthesize a functional product, usually a protein. Its two major steps are transcription (DNA copied into a complementary mRNA by RNA polymerase in the nucleus) and translation (the mRNA decoded by ribosomes into a polypeptide in the cytoplasm). In eukaryotes these are separated in space and time, allowing extensive regulation (RNA processing, transport, stability) between the steps. See section 13.

2. Describe the structure of a eukaryotic mRNA from 5' to 3', including most regulatory elements.

Answer (Q2, Recall). From 5' → 3': (1) m⁷G cap — 7-methylguanosine joined via an unusual 5'→5' triphosphate linkage, added co-transcriptionally by capping enzyme; protects from 5'→3' exonucleases (Xrn1) and is the binding site for eIF4E, the rate-limiting step of cap-dependent translation initiation. (2) 5' UTR — typically 100–200 nt; contains Kozak context (GCCRCCAUGG) and sometimes upstream ORFs (uORFs) or IRES elements for regulated translation. (3) CDS (coding sequence) — begins at the start codon (AUG), proceeds in triplets to a stop codon (UAA/UAG/UGA); no introns (those were removed by the spliceosome, leaving exon-exon junctions marked by the EJC, which triggers NMD if a stop codon appears >50 nt upstream of a junction). (4) 3' UTR — typically 500–2000 nt; contains AU-rich elements (AREs) for mRNA stability, miRNA binding sites, and the polyadenylation signal AAUAAA. (5) Poly-A tail — 150–250 nt of adenosines, bound by PABPC1, which circularises the mRNA via eIF4G–eIF4E to promote re-initiation. Worked example: β-globin mRNA is about 620 nt (5' UTR 50, CDS 441, 3' UTR 131) plus cap and about 150 nt poly-A tail. See section 13.

3. What is the role of RNA polymerase II in transcription? Where does it bind?

Answer (Q3, Recall). RNA polymerase II is the enzyme that synthesizes all messenger RNA (and many small RNAs) in eukaryotes, building a complementary RNA copy of the template DNA strand 5'→3'. It does not bind DNA on its own: it is recruited to the core promoter (the region around the transcription start site, e.g. the TATA box about 25 bp upstream) as part of the preinitiation complex assembled by general transcription factors (TFIIA–H). Its C-terminal domain (CTD) is phosphorylated to coordinate capping, splicing, and polyadenylation during elongation. See section 13.

4. Define a transcription factor. Distinguish general vs specific transcription factors.

Answer (Q4, Recall). A transcription factor is a protein that binds specific DNA sequences and regulates the rate of transcription. General (basal) transcription factors (TFIIA, B, D, E, F, H) are required at every Pol II promoter to position the polymerase and form the preinitiation complex — they set the baseline. Specific (regulatory) transcription factors bind enhancers or silencers of particular genes and increase or decrease expression in a gene-, cell-, or signal-dependent way. The mechanistic difference: general factors enable transcription at all; specific factors decide which genes are transcribed and how much. See section 13.

5. What is RNA splicing? What molecular machinery performs it?

Answer (Q5, Recall). RNA splicing is the removal of non-coding introns from pre-mRNA and the joining of the flanking exons to produce a mature, translatable mRNA. It is carried out by the spliceosome, a large ribonucleoprotein complex of five small nuclear RNPs (U1, U2, U4, U5, U6 snRNPs) plus associated proteins. The snRNAs recognize the 5' splice site (GU), branch-point adenosine, and 3' splice site (AG) and catalyze two transesterification reactions that excise the intron as a lariat. See section 13.

6. Define the genetic code. What is a codon? How many codons encode amino acids?

Answer (Q6, Recall). The genetic code is the set of rules by which nucleotide triplets in mRNA specify amino acids during translation. A codon is a sequence of three consecutive nucleotides read by the ribosome. There are $4^3 = 64$ codons total: 61 encode the 20 amino acids (the code is therefore degenerate/redundant) and 3 are stop codons (UAA, UAG, UGA). AUG is the start codon and also encodes methionine. See section 13.

7. What is the ribosome composed of? Name the three ribosomal sites (A, P, E sites).

Answer (Q7, Recall). The ribosome is a ribonucleoprotein machine made of ribosomal RNA (rRNA) and ribosomal proteins, organized into a small subunit (40S in eukaryotes; reads the mRNA) and a large subunit (60S; catalyzes peptide-bond formation via the rRNA peptidyl transferase center).

It has three tRNA-binding sites: the A site (Aminoacyl — accepts the incoming aminoacyl-tRNA), the P site (Peptidyl — holds the tRNA bearing the growing chain), and the E site (Exit — holds the deacylated tRNA before it leaves). See section 13. 8. Describe initiation, elongation, and termination of translation in eukaryotes.

Answer (Q8, Recall). Initiation: the 40S subunit, with initiator Met-tRNA_i and initiation factors (eIF4E binds the m⁷G cap), scans the mRNA 5'→3' to the first AUG in good Kozak context; the 60S subunit then joins to form the 80S ribosome. Elongation: aminoacyl-tRNAs are delivered to the A site by eEF1A; the peptidyl transferase center forms the peptide bond; eEF2 drives translocation, shifting tRNAs A→P→E one codon at a time. Termination: a stop codon enters the A site, recognized by release factor eRF1, which triggers hydrolysis and release of the completed polypeptide, then ribosome recycling. See section 13. 9. What is tRNA? What is the anticodon, and what is aminoacyl-tRNA synthetase?

Answer (Q9, Recall). tRNA (transfer RNA) is a small (about 76 nt) cloverleaf-folded RNA that physically links a codon to its amino acid during translation. The anticodon is a three-nucleotide loop that base-pairs antiparallel with the complementary mRNA codon in the ribosomal A site. Aminoacyl-tRNA synthetases are enzymes (one per amino acid) that covalently attach the correct amino acid to the 3' CCA end of its cognate tRNA, using ATP; their proofreading establishes the accuracy of the genetic code (“the second genetic code”). See section 13. 10. What is the wobble hypothesis? Which position of the codon allows degeneracy?

Answer (Q10, Recall). The wobble hypothesis (Crick, 1966) states that base pairing between the third base of the codon and the first base of the anticodon is less stringent than standard Watson–Crick pairing, so a single tRNA can read several synonymous codons. The third (3') codon position allows this degeneracy: non-standard pairings (e.g., G–U, or inosine in the anticodon pairing with U, C, or A) let about 45 tRNAs decode all 61 sense codons, explaining the code's redundancy. See section 13.

Questions 11–20: Application and Analysis

11. Pre-mRNA splicing must be precise to within one nucleotide. Explain the two-step transesterification mechanism of splicing and the role of branch point A, 5' splice site, and 3' splice site in spliceosome assembly.

Answer (Q11, Application). Splicing proceeds by two sequential transesterification reactions. First, the 2'-OH of the branch-point adenosine attacks the phosphate at the 5' splice site (GU), cleaving exon 1 and forming a lariat intermediate. Second, the freed 3'-OH of exon 1 attacks the 3' splice site (AG), joining the two exons and releasing the intron as a lariat. Spliceosome assembly recognizes these elements stepwise: U1 snRNP base-pairs the 5' splice site, U2 snRNP binds the branch point (bulging the branch A), and the U4/U6-U5 tri-snRNP completes the catalytic core — the one-nucleotide precision comes from this combinatorial recognition of all three signals. See section 13. 12. Alternative splicing generates multiple protein isoforms from one gene. *Drosophila Dscam* gene can produce >38,000 isoforms through mutually exclusive exon splicing. Explain: (a) the general mechanism of alternative splicing; (b) why *Dscam* diversity is important for axon guidance in neural wiring; (c) one human disease caused by aberrant alternative splicing.

Answer (Q12, Application). (a) Alternative splicing includes or excludes particular exons (or uses alternative 5'/3' splice sites) in a regulated way, so one gene yields multiple mRNAs and protein isoforms; in *Dscam*, mutually exclusive selection among large clusters of variant exons combinatorially generates >38,000 isoforms. (b) This diversity gives each neuron a near-unique *Dscam* “identity tag”; isoform-specific homophilic binding mediates self-avoidance, so a neuron's own branches repel each other while still tiling among other neurons — essential for correct axon/dendrite wiring. (c) Spinal muscular atrophy is caused by aberrant *SMN2* exon 7 splicing (the therapy nusinersen corrects it); other examples include myotonic dystrophy and many cancers. See section 13. 13. The 5' cap (m⁷G) and poly-A tail of eukaryotic mRNA serve similar functions — protecting mRNA from exonuclease attack and promoting translation initiation. Explain: (a) how the 5' cap is added; (b) how eIF4E binding to the cap recruits the 43S pre-initiation complex; (c) why some viruses (e.g., poliovirus) cleave eIF4G to direct ribosomes to IRES sequences instead.

Answer (Q13, Application). (a) 5' cap addition occurs co-transcriptionally when nascent pre-mRNA is about 25 nt long: (i) RNA 5'-triphosphatase removes the γ-phosphate; (ii) guanylyltransferase adds GMP via a unique 5'–5' triphosphate bridge; (iii) guanine-N7-methyltransferase methylates N7 of the guanine, yielding m⁷GpppN. The capping enzyme is recruited via the phosphorylated CTD (Ser5-P) of RNA pol II — physically linking transcription to capping. (b) eIF4E binding: cytosolic eIF4E recognizes m⁷G via stacking with two conserved tryptophans (W56, W102), with K_d ≈ 100 nM. eIF4E forms eIF4F with eIF4G (scaffold) and eIF4A (DEAD-box helicase); eIF4G simultaneously binds PABPC1 on the poly-A tail (circularising the mRNA) and recruits the 43S PIC (40S + eIF1, eIF1A, eIF3, eIF2-GTP-Met-tRNA_i) via eIF3. The 43S then scans 5' → 3' using eIF4A's ATP-dependent helicase activity until it finds the Kozak AUG. (c) Poliovirus hijack: poliovirus 2A protease cleaves eIF4G between the eIF4E-binding domain and the eIF3/eIF4A-binding domain. This shuts down cap-dependent translation of host mRNA but leaves intact the C-terminal half of eIF4G that binds viral IRES (internal ribosome entry site) in the 5' UTR of poliovirus RNA — so viral translation continues while host translation collapses. This is why the cell “looks infected” within hours: host protein synthesis drops > 90 %. See section 13. 14. The ribosome proof-reads aminoacyl-tRNA selection at the A site. Explain: (a) initial selection based on codon-anticodon base pairing (induced fit); (b) proofreading step (kinetokinetics — GTPase activation primarily if correct aa-tRNA is bound); (c) why errors occur at about 1 in 10,000 vs DNA polymerase errors of

1 in 10^9 (why is translation less accurate?).

Answer (Q14, Application). (a) Initial selection: the ternary complex (eEF1A-GTP-aa-tRNA) samples the A-site codon; correct Watson–Crick codon–anticodon pairing induces a conformational closure of the 30S/40S decoding center (induced fit) that accelerates GTPase activation. (b) Proofreading: GTP is hydrolyzed only when pairing is correct; after hydrolysis the tRNA must be “accommodated” into the peptidyl transferase center — a second checkpoint where near-cognate tRNAs preferentially dissociate before peptide-bond formation. (c) Translation tolerates a higher error rate (about 10^{-4}) than DNA replication (about 10^{-9}) because protein errors affect only one short-lived molecule and are not heritable, whereas DNA errors are passed to all descendants; selection therefore optimized replication fidelity far more strongly than translation, and a faster, less accurate ribosome favors growth. See section 13. 15. Cycloheximide blocks the elongation step of eukaryotic translation (not prokaryotic), because it specifically inhibits the 60S subunit translocation step. Explain: (a) what translocation means mechanistically; (b) why prokaryotic ribosomes (70S) are not blocked; (c) how this selectivity is exploited in laboratory cell biology experiments.

Answer (Q15, Application). (a) Translocation is the eEF2-driven, GTP-dependent movement of the ribosome by exactly one codon along the mRNA after peptide-bond formation, shifting the tRNAs from A→P and P→E sites and opening the A site for the next aminoacyl-tRNA. (b) Cycloheximide binds the E site of the 60S subunit, blocking eEF2-mediated translocation; prokaryotic 70S ribosomes have structurally distinct large-subunit rRNA/proteins that cycloheximide does not recognize, so bacterial translation is unaffected. (c) This eukaryote-specific, rapid, reversible arrest is exploited to freeze ribosomes on mRNA — e.g., to stabilize polysomes for polysome profiling and ribosome profiling (Ribo-seq), and to halt protein synthesis in pulse-chase and cytotoxicity experiments. See section 13. 16. Nonsense-mediated mRNA decay (NMD) degrades mRNAs with premature stop codons. Explain: (a) how the cell recognizes a premature vs normal stop codon (role of exon-junction complexes); (b) the UPF1/SMG cascade; (c) why NMD is a quality control mechanism that also regulates normal gene expression for about 10% of genes.

Answer (Q16, Application). (a) During the pioneer round of translation the ribosome displaces exon-junction complexes (EJCs). A stop codon is judged premature if an EJC remains >50–55 nt downstream of it (a normal stop is the last codon, with no downstream EJC). (b) The retained EJC recruits UPF1, which is phosphorylated by SMG1; phospho-UPF1 then recruits SMG5/6/7, triggering endonucleolytic cleavage (SMG6) and exonucleolytic decay of the transcript. (c) NMD is both quality control — destroying truncating-mutation and error-prone transcripts to prevent dominant-negative truncated proteins — and a normal regulatory mechanism: about 10% of transcripts (including alternatively spliced isoforms with PTC-containing exons and autoregulated splicing-factor mRNAs) are physiologically tuned by NMD. See section 13. 17. Polyribosomes (polysomes) consist of multiple ribosomes simultaneously translating the same mRNA. If a 1,500-nt coding sequence is occupied by ribosomes spaced on average every 80 nt, how many ribosomes are simultaneously translating this mRNA? Calculate the rate of protein synthesis per mRNA if each ribosome adds 2 amino acids/sec.

Answer (Q17, Application). Ribosome count: $N = \frac{1500 \text{ nt}}{80 \text{ nt/ribosome}} = 18.75 \approx 19$ ribosomes simultaneously engaged. Protein output: each ribosome adds 2 aa/s $\rightarrow 19 \times 2 = 38$ amino acids per second across the polysome. Time to complete one protein per ribosome: $1500 \text{ nt} \div 3 = 500$ codons $\div 2 \text{ codons/s} = 250 \text{ s} \approx 4 \text{ min}$. Steady-state output per mRNA = 1 finished protein every $(80 \text{ nt} / 2 \text{ codons} \times 3 \text{ nt/codon}) \approx 13 \text{ s}$ per completed chain, i.e. about 280 proteins/h/mRNA. Biological sanity check: this matches measured translation rates in mammalian cells (median about 5 proteins/mRNA/min for short transcripts). Sucrose-gradient polysome profiles show β -actin mRNA (about 1800 nt) in fractions containing 8–12 ribosomes — consistent with our estimate once you account for scanning delays and the fact that the first about 40 nt after the cap are typically bare (eIF4E/PABPC1 footprint). Biological significance: polysome occupancy (footprint density from ribosome profiling / Ribo-seq) is the gold-standard readout of translation efficiency; a 19-ribosome polysome represents high expression, while a monosome-enriched mRNA is either stalled or repressed. See section 13. 18. Internal ribosome entry sites (IRES) allow cap-independent translation initiation, used by viruses (Hepatitis C, poliovirus) and in cellular stress responses, when eIF4E activity is reduced. Compare IRES-mediated vs cap-dependent initiation: which cellular proteins are replaced by viral ITAF proteins, and under what stress conditions does cellular IRES-mediated translation occur?

Answer (Q18, Application). Cap-dependent initiation requires eIF4E to bind the m⁷G cap, eIF4G as scaffold, eIF4A helicase, and 5' scanning to the AUG. IRES-mediated initiation uses a structured RNA element in the 5' UTR that recruits the 40S subunit directly, bypassing the cap. Viral IRESs replace cap-recognition factors with IRES trans-acting factors (ITAFs): depending on IRES class, they need little or no eIF4E/eIF4G (e.g., the CrPV IRES needs no initiation factors; HCV recruits eIF3 and 40S directly; poliovirus uses a cleaved eIF4G fragment plus ITAFs such as PCBP2/PTB). Cellular IRESs are used when cap-dependent translation is suppressed — mitosis, hypoxia, ER/nutrient stress, apoptosis, and viral infection — to keep translating survival, stress, and pro-apoptotic mRNAs. See section 13. 19. The signal recognition particle (SRP) recognizes hydrophobic signal peptides emerging from ribosomes translating secretory proteins. Explain: (a) how SRP stalls translation while targeting the ribosome to the rough ER; (b) how signal peptidase cleaves the signal peptide in the ER lumen; (c) what happens to cytosolic misfolded proteins lacking a signal peptide vs ER-targeted ones.

Answer (Q19, Application). (a) As a hydrophobic signal peptide emerges from the ribosome, the signal recognition particle (SRP) binds it and contacts the ribosome, pausing elongation; SRP then docks the ribosome onto the SRP receptor at the rough ER, transferring it to the Sec61 translocon,

after which translation resumes and the chain is threaded into the ER. (b) Inside the ER lumen, signal peptidase cleaves the signal sequence from the nascent chain, releasing the mature protein into the lumen for folding and modification. (c) ER-targeted proteins that misfold are detected by ER quality control and retro-translocated for ERAD (ER-associated degradation by the cytosolic proteasome); cytosolic proteins lacking a signal peptide that misfold are handled by cytosolic chaperones and the ubiquitin–proteasome system (or autophagy), never entering the secretory pathway. See section 13. 20. Transcription factors bind specific DNA sequences (motifs). A transcriptional activator contains a DNA-binding domain (DBD) and an activation domain (AD). Explain: (a) what structural motifs are common in DBDs (zinc finger, helix-turn-helix, leucine zipper); (b) how the activation domain recruits the Mediator complex; (c) how enhancers (located kb away from promoters) loop to contact the preinitiation complex through cohesin-mediated chromosome looping.

Answer (Q20, Application). (a) Common DNA-binding domains include the zinc finger (Cys₂His₂ fingers inserting an α -helix into the major groove), the helix-turn-helix / homeodomain, and the basic leucine zipper (bZIP) and basic helix-loop-helix, which dimerize and grip DNA with basic regions. (b) The separate activation domain does not bind DNA; it recruits coactivators and the Mediator complex, which bridges the enhancer-bound activator to RNA Pol II and the general transcription factors, stimulating preinitiation-complex assembly and CTD phosphorylation. (c) Distal enhancers contact promoters through chromatin looping: cohesin and CTCF organize loop domains (TADs), bringing the enhancer-bound activator/Mediator into physical proximity with the promoter even when they are tens of kb apart in linear sequence. See section 13.

Questions 21–30: Synthesis and Evaluation

21. Evaluate the dual role of SR proteins (serine-arginine-rich splicing factors) in both constitutive and alternative splicing and mRNA export. What does the dual role of SR proteins reveal about the evolutionary coupling between nuclear RNA processing and cytoplasmic translation?

Answer (Q21, Synthesis). Empirically, SR proteins bind exonic splicing enhancers to promote spliceosome assembly and regulate alternative splice-site choice, *and* they remain bound to the spliced mRNP where they help recruit the TREX export machinery (e.g., via NXF1/TAP) and influence cytoplasmic translation efficiency. The judgment — that nuclear processing and cytoplasmic fate are evolutionarily coupled — follows because the same factor physically links splicing, export, and translation, making them a coordinated pipeline rather than independent steps; this “mRNP marking” also explains why spliced mRNAs are translated more efficiently than intronless ones. What would change the conclusion: showing SR-protein splicing and export functions are genetically separable (separation-of-function mutants), or that export/translation enhancement occurs equally without SR deposition. See section 13. 22. Design a comprehensive experiment to map most enhancers controlling a specific gene in a given cell type using: (a) H3K27ac ChIP-seq (active enhancer mark); (b) ATAC-seq (open chromatin); (c) HiC chromatin conformation capture; (d) CRISPR deletion of candidate enhancers and transcriptional output measurement. How would you prioritize which enhancers are most important?

Answer (Q22, Synthesis). Hypothesis: a defined set of distal enhancers drives the gene’s expression in this cell type. Design: map candidates with H3K27ac ChIP-seq (active enhancers) and ATAC-seq (open chromatin), then use Hi-C/capture Hi-C to identify which open, acetylated regions physically loop to the promoter; the control/comparison is an unedited population and CRISPRi/CRISPR deletion of each candidate vs a scrambled-gRNA control. Measured outcome: target-gene mRNA (RT-qPCR/RNA-seq) after each perturbation, with biological replicates. Prioritization: rank enhancers by (i) magnitude of expression loss on deletion, (ii) strength of the Hi-C contact with the promoter, (iii) H3K27ac/ATAC signal and conservation, and (iv) presence of relevant TF motifs/footprints. A falsifying result: deleting the top-ranked enhancer leaves expression unchanged, indicating redundancy or that the causal element was missed. See section 13. 23. The “RNA world” hypothesis proposes that early life was based on RNA molecules that could both carry genetic information and catalyse reactions. Evaluate: (a) the evidence supporting RNA world (ribozymes, ribosome as a ribozyme, universality of the genetic code); (b) the transition from RNA world to the DNA-protein world; (c) what modern ribozymes tell us about the chemistry of early catalysis.

Answer (Q23, Synthesis). Empirical support for an RNA world: ribozymes (self-splicing introns, RNase P) prove RNA can catalyze chemistry; the ribosome’s peptidyl transferase center is all rRNA (a ribozyme), implying protein synthesis predates protein enzymes; and the near-universal genetic code plus RNA cofactors (ATP, NAD, coenzyme A) look like molecular fossils. The judgment that an RNA world existed rests on these as evidence that RNA once carried both information and catalysis. The transition to DNA/protein: DNA (more chemically stable, proofreadable) took over information storage and proteins (20 side chains) took over catalysis, with RNA retained as the intermediary. What would weaken it: failure to demonstrate an RNA replicase ribozyme, or evidence that early metabolism was peptide- or metabolism-first rather than RNA-based. See section 13. 24. Transcription and translation are physically coupled in prokaryotes (translation begins before transcription is complete). Evaluate the consequences of this coupling: how does it allow attenuation (regulation of transcription termination by ribosome speed), and why would coupling like this have evolved in prokaryotes but not eukaryotes (where transcription and translation are spatially separated)?

Answer (Q24, Synthesis). In prokaryotes there is no nuclear envelope, so ribosomes load onto an mRNA’s 5’ end while RNA polymerase is still transcribing it (coupling). This enables attenuation, e.g. the *trp* operon: a ribosome translating a leader peptide rich in Trp codons stalls or proceeds depending on tryptophan availability; its position determines which alternative RNA hairpin forms, either a terminator (transcription stops) or an antiterminator (transcription continues) — ribosome speed directly controls transcription termination. This could not evolve in eukaryotes because

transcription (nucleus) and translation (cytoplasm) are spatially and temporally separated by the nuclear envelope and by pre-mRNA processing, so a translating ribosome can never contact an actively transcribing polymerase; eukaryotes instead regulate via distinct mechanisms (chromatin, splicing, export, miRNAs). See section 13. 25. Ribosome biogenesis occurs in the nucleolus and is rate-limiting for cell growth. Evaluate the regulatory relationship between mTORC1, Pol I transcription of rDNA, and ribosome biogenesis. Why does mTOR inhibition suppress cell growth even in cells with unlimited amino acid supply?

Answer (Q25, Synthesis). Ribosome biogenesis (rDNA transcription by Pol I, rRNA processing, assembly in the nucleolus) consumes most of a growing cell’s transcriptional output and is rate-limiting for proliferation. mTORC1 integrates growth-factor and nutrient signals and directly stimulates ribosome production: it activates Pol I (via TIF-IA/UBF), Pol III (5S rRNA, tRNA, via Maf1 repression), and translation of ribosomal-protein mRNAs (via S6K1 and 4E-BP1). Therefore mTOR inhibition (rapamycin) suppresses growth even with abundant amino acids because it shuts down the biosynthetic capacity needed to make new ribosomes — without enough ribosomes the cell cannot increase mass or divide, regardless of substrate supply. The evidence: rapamycin rapidly reduces nucleolar size, 45S pre-rRNA, and polysome levels. See section 13. 26. Evaluate the molecular mechanism of translation by the ribosome in the context of the “peptidyl transferase” ribosome activity: specifically, is the catalysis chemical (RNA catalysis) or entropic (positioning effect)? Cite the key experiment (Nobel Prize 2009) that settled this debate.

Answer (Q26, Synthesis). The empirical question is whether peptide-bond catalysis is chemical (rRNA acting as a true catalyst) or mainly entropic (the ribosome positioning/orienting substrates and excluding water, with little chemical transition-state stabilization). The decisive evidence is the atomic-resolution crystal structures of the 50S subunit (Steitz, Moore; Nobel Prize in Chemistry 2009, shared with Ramakrishnan and Yonath): the peptidyl transferase center is composed entirely of 23S rRNA with no protein side chains near the active site, and subsequent biochemistry showed catalysis works largely by substrate positioning and proton shuttling/entropic effects rather than classical acid–base chemistry. So the ribosome is a ribozyme, and its catalysis is predominantly proximity/orientation-based. What would overturn this: finding a protein side chain essential for the chemical step, or a single-atom rRNA substitution that abolishes chemistry without affecting positioning. See section 13. 27. Single-molecule translation experiments using fluorescently labeled ribosomes and mRNAs have revealed “pausing” during elongation opposite rare codons, and “synchronized” waves of ribosome density on mRNA. Evaluate what these observations reveal about codon usage optimization and how synonymous mutations (same amino acid, different codon) can dramatically affect protein folding by altering translation speed.

Answer (Q27, Synthesis). Single-molecule and ribosome-profiling data show that elongation is non-uniform: ribosomes pause at rare codons (those read by low-abundance tRNAs) and move in correlated waves. The causal chain: a synonymous (“silent”) mutation changes codon usage → alters local tRNA-decoding speed → changes the elongation rate at that position → shifts the timing of co-translational folding, so domains may misfold or be processed differently even though the amino-acid sequence is unchanged. This reveals that codon choice is itself an optimized layer of information (translational kinetics), not redundant: examples include the *MDR1* C3435T synonymous variant altering substrate specificity and synonymous changes affecting protein stability and aggregation. The interpretation: codon usage co-evolves with folding pathways; “silent” mutations can be functionally consequential. See section 13. 28. Design a gene therapy strategy for a patient with haemophilia A (lacking factor VIII). Compare: mRNA therapy (synthetic mRNA with pseudo-uridine modification for stability); AAV vector gene therapy (liver-tropism, long-term expression); and base editing (correct the point mutation in situ). Evaluate the trade-offs in immunogenicity, duration of effect, and delivery efficiency.

Answer (Q28, Synthesis). Hypothesis/options compared: (1) mRNA therapy — pseudouridine-modified synthetic factor VIII mRNA in lipid nanoparticles: easy to redose, low genotoxicity, but transient expression and innate-immune/LNP delivery limits. (2) AAV gene therapy — liver-tropic AAV carrying B-domain-deleted F8: long-lived expression from a single dose, but pre-existing/induced anti-AAV immunity, payload-size limits, and episomal loss in dividing hepatocytes; one-time only. (3) Base editing — in-situ correction of the causal point mutation: potentially permanent and physiologic (native locus regulation), but constrained by editable mutation type, delivery to hepatocytes, and off-target/bystander risk. Measured outcomes: circulating FVIII activity, bleeding rate, anti-FVIII/anti-vector antibodies, durability. Controls/falsification: untreated and vehicle arms; the approach fails if FVIII activity does not rise above the about 5% therapeutic threshold or if immunogenicity neutralizes the product. See section 13. 29. RNA interference (RNAi) was discovered when dsRNA triggered gene silencing in *C. elegans* (Fire and Mello, 1998). Evaluate the mechanism (Dicer, RISC, Ago2-mediated cleavage), the evolutionary origin of RNAi (antiviral defense), and the clinical development of siRNA therapeutics (inclisiran for PCSK9 silencing). What advantages does siRNA have over antisense oligonucleotides (ASOs) for gene silencing?

Answer (Q29, Synthesis). Mechanism: long dsRNA is cleaved by Dicer into about 21–23 nt siRNAs; one strand is loaded into RISC with Ago2, which uses perfect complementarity to endonucleolytically cleave the target mRNA. Evolutionary origin: RNAi arose as an antiviral and anti-transposon defense (recognizing dsRNA replication intermediates), conserved from plants and invertebrates to mammals. Clinical: chemically stabilized, GalNAc-conjugated siRNAs such as inclisiran silence hepatic *PCSK9*, durably lowering LDL cholesterol with twice-yearly dosing. siRNA vs ASO advantages: siRNA acts catalytically (one RISC degrades many mRNAs) giving high potency and long duration, exploits an endogenous enzymatic pathway, and (with GalNAc) achieves efficient liver delivery — whereas ASOs act stoichiometrically and generally need more frequent dosing for comparable knockdown. See section 13. 30. Critically evaluate the concept of the “central dogma” (DNA → RNA → protein). Identify

three biological exceptions that violate a strict reading of the central dogma (reverse transcription, RNA editing, prion replication), explain their mechanisms, assess whether these exceptions require a fundamental revision of the central dogma, and state what RNAcentral-style database checks are needed before claiming that a non-coding RNA has a defined gene model and function.

Answer (Q30, Synthesis). The central dogma states information flows DNA→RNA→protein and not back out of protein. Three classic challenges: (1) Reverse transcription — retroviruses/telomerase make DNA from RNA (RNA→DNA), expanding allowed information flow but not violating the core prohibition (no protein→nucleic-acid). (2) RNA editing — e.g., A-to-I (ADAR) or C-to-U (APOBEC) editing changes mRNA sequence after transcription, so the protein differs from the genomic template; this elaborates the RNA step rather than reversing flow. (3) Prions — a misfolded protein (PrP^{Sc}) templates conformational conversion of normal protein, transmitting *conformational*, not sequence, information protein→protein. Assessment: Crick’s strict statement (no information from protein back to nucleic acid) survives — none of these transfers sequence from protein to DNA/RNA; they are elaborations within the framework, not a fundamental revision, though prions show heritable information can be protein-borne. Source-governed RNA interpretation then asks whether the RNAcentral entry is sequence-level or gene-level, which release and identifiers are being used, whether isoforms/splice variants are merged correctly, and whether literature links support function rather than only mention the RNA [[RNAcentral Consortium, 2026](#)]. See section 13.

Questions — Mutations, CRISPR, and Genomics

Instructor Use and Coverage Notes

- Coverage target: Predict the impact of a variant and justify the evidence needed to validate it.
- Model/data emphasis: Mutation-rate, edit-efficiency, and sequence-comparison calculations.
- Assessment alignment: Concept Explanation, Questions and Methods, Argumentation.
- Misconception probe: Not every mutation is harmful, and not every harmful mutation changes a protein sequence.
- Transfer product: Transfer variant reasoning to cancer genomics, ancestry, gene therapy, or microbial evolution.
- Grading focus: award full credit for mechanism, evidence, boundary conditions, and units when a calculation is required.
- Suggested use: draw one recall item, one application item, and one synthesis item when building a short quiz from this bank.

Questions 1–10: Recall and Comprehension

This activity accompanies section 14 of the textbook — review that chapter before attempting the exercises below.

1. Define a mutation. Classify mutations by: (a) type of base change; (b) effect on the protein.

Answer (Q1, Recall). A mutation is a heritable change in the DNA sequence of a cell or organism. (a) By base change: *point mutations* are single-base substitutions, subdivided into transitions (purine↔purine or pyrimidine↔pyrimidine, e.g. A↔G) and transversions (purine↔pyrimidine); larger changes include insertions and deletions (indels). (b) By effect on protein: *silent/synonymous* (codon still specifies the same amino acid), *missense* (different amino acid), *nonsense* (creates a premature stop codon), and *frameshift* (indel not a multiple of three, shifting the reading frame and usually producing a truncated, nonfunctional protein). See section 14. 2. What is a frameshift mutation? How does an insertion vs deletion cause this?

Answer (Q2, Recall). A frameshift mutation is an insertion or deletion of a number of nucleotides not a multiple of three, which shifts the ribosomal reading frame downstream of the change. Because codons are read in non-overlapping triplets from the start codon, an insertion pushes all subsequent bases one or two positions to the right and a deletion shifts them left; either way every codon after the mutation site is mis-read, almost always generating a string of wrong amino acids and an early premature stop codon, yielding a truncated, nonfunctional protein. An indel that is a multiple of three only adds/removes whole codons and is in-frame, not a frameshift. See section 14. 3. What are transposons? Distinguish replicative (copy-and-paste) from non-replicative (cut-and-paste) transposons.

Answer (Q3, Recall). Transposons (“jumping genes”) are mobile DNA elements that can move to new genomic locations, sometimes causing mutations or genome rearrangements. Replicative (copy-and-paste) transposons leave the original element in place and insert a new copy elsewhere, so copy number increases — this includes retrotransposons (LINEs, SINEs, LTR/HERV elements), which transpose via an RNA intermediate reverse-transcribed into DNA. Non-replicative (cut-and-paste) DNA transposons are excised by a transposase from the donor site and reinserted at a target site without net copy gain. The mechanistic distinction is whether an RNA-templated copy is made (replicative) or the element physically relocates (conservative). See section 14. 4. What is the Ames test? What does a positive result indicate?

Answer (Q4, Recall). The Ames test (Bruce Ames, 1970s) is a bacterial assay for mutagenicity. It uses *Salmonella typhimurium* strains carrying a his⁻ mutation (cannot synthesize histidine); the test chemical (often with rat-liver S9 extract to mimic mammalian metabolic activation) is added, and reversion (back-mutation) to his⁺ is scored as colonies growing on histidine-free medium. A positive result (a dose-dependent increase in revertant colonies above background) indicates the chemical is a mutagen; because about 80–90% of known carcinogens are mutagenic, a positive result flags the substance as a probable carcinogen warranting further testing. See section 14. 5. Describe the three types of DNA damage repair: (a) nucleotide excision repair (NER); (b) base excision repair (BER); (c) mismatch repair (MMR).

Answer (Q5, Recall). (a) Nucleotide excision repair (NER) removes bulky, helix-distorting lesions (e.g., UV-induced pyrimidine dimers, chemical adducts): the damage is recognized, a about 24–32 nt oligonucleotide containing it is excised by endonucleases, and the gap is filled by DNA polymerase and sealed by ligase. (b) Base excision repair (BER) corrects small, non-distorting single-base damage (oxidation, deamination, alkylation): a DNA glycosylase removes the damaged base, AP endonuclease nicks the abasic site, and a short patch is resynthesized. (c) Mismatch repair (MMR) fixes replication errors (mispaired bases, small indel loops) that escaped polymerase proofreading; it identifies the newly synthesized (error-containing) strand, excises the stretch, and resynthesizes it, raising replication fidelity about 100–1000-fold. See section 14. 6. What is CRISPR-Cas9? Where does CRISPR originate in bacteria?

Answer (Q6, Recall). CRISPR-Cas9 is a programmable, RNA-guided DNA endonuclease used for genome editing: a guide RNA directs the Cas9 protein to a complementary DNA sequence adjacent to a PAM, where Cas9 creates a double-strand break that the cell repairs by NHEJ (disruptive indels) or HDR (precise edits with a donor template). It originates as a bacterial and archaeal adaptive immune system: short fragments of invading phage/plasmid DNA are stored as spacers in CRISPR arrays, transcribed into crRNAs, and used by Cas nucleases to recognize and cleave matching

nucleic acid on re-infection. (Doudna & Charpentier, 2020 Nobel Prize in Chemistry.) See section 14. 7. What is gRNA (guide RNA) and what does it do in the Cas9 complex?

Answer (Q7, Recall). The guide RNA (gRNA), commonly engineered as a single guide RNA (sgRNA), is the targeting component of the CRISPR-Cas9 complex. It is a fusion of a crRNA — whose about 20-nucleotide spacer is complementary to the intended DNA target — and a tracrRNA scaffold that binds and activates Cas9. The gRNA loads into Cas9 and, by Watson–Crick base-pairing of its spacer with the target DNA (immediately 5' of a PAM), positions the Cas9 nuclease domains to introduce a site-specific double-strand break. Changing the 20-nt spacer reprograms Cas9 to any new genomic site. See section 14. 8. Define the PAM sequence. Why is it required for CRISPR cutting?

Answer (Q8, Recall). The PAM (protospacer adjacent motif) is a short DNA sequence (5'-NGG-3' for *Streptococcus pyogenes* Cas9) located immediately 3' of the 20-nt target (protospacer) in the genomic DNA. It is required because Cas9 first recognizes the PAM through protein–DNA contacts; PAM binding licenses local DNA unwinding and lets the guide RNA test for complementarity, after which the nuclease domains cut. The PAM is not part of the guide RNA, so the bacterium's own CRISPR array (which lacks an adjacent PAM at the spacer) is not cleaved — this is how Cas9 distinguishes invader DNA from self and avoids autoimmunity. See section 14. 9. What is whole-genome sequencing (WGS)? What sequencing technology is most commonly used?

Answer (Q9, Recall). Whole-genome sequencing (WGS) is the determination of the complete (or near-complete) nucleotide sequence of an organism's genome in a single experiment, capturing coding, non-coding, regulatory, and structural variation. The most widely used technology is Illumina short-read sequencing-by-synthesis (massively parallel, high accuracy, about 150 bp reads), used for variant calling; long-read platforms (Oxford Nanopore, PacBio HiFi) are increasingly used to resolve repeats, structural variants, and produce telomere-to-telomere assemblies. See section 14. 10. What is a single nucleotide polymorphism (SNP)? How many SNPs does the average human genome contain?

Answer (Q10, Recall). A single nucleotide polymorphism (SNP) is a single-base position in the genome at which a variant allele occurs commonly in the population (conventionally >1% allele frequency). SNPs are the most abundant form of human genetic variation, used as markers in GWAS, association studies, and ancestry analysis. On average, any two human genomes differ at roughly 4–5 million SNP sites (about one SNP per about 1000 bp; about 3–4 million when compared to the reference), most of which lie in non-coding regions. See section 14.

Questions 11–20: Application and Analysis

11. A chemotherapy drug causes G:C → A:T transitions. What type of DNA damage mechanism does this suggest (alkylation, intercalation, cross-linking, or depurination)? What repair pathway would normally correct this damage?

Answer (Q11, Application). A G:C → A:T transition is the signature of alkylation (or oxidative deamination), not intercalation, cross-linking, or simple depurination. Mechanism: an alkylating agent adds an alkyl group to guanine forming O⁶-methylguanine (or 8-oxoG), which mispairs with thymine during replication; the next round fixes the change as G:C → A:T. Repair pathway: O⁶-alkylguanine is reversed directly by MGMT (O⁶-methylguanine-DNA methyltransferase), while oxidized/alkylated bases are normally removed by base excision repair (BER) (e.g., OGG1 glycosylase for 8-oxoG); mismatch repair can also act on the resulting mispair. Failure of these explains the mutator phenotype of alkylating chemotherapeutics. See section 14. 12. Xeroderma pigmentosum (XP) patients have mutations in NER pathway genes (XPA-XPG). Explain: (a) what lesion NER repairs (CPDs from UV-B); (b) why XP patients have dramatically increased skin cancer risk; (c) why the nervous system is also affected in some XP subtypes.

Answer (Q12, Application). (a) NER repairs bulky helix-distorting lesions, especially UV-B-induced cyclobutane pyrimidine dimers (CPDs) and 6-4 photoproducts. (b) XP patients carry loss-of-function mutations in NER genes (XPA–XPG), so sunlight-induced dimers persist; unrepaired lesions are bypassed by error-prone translesion polymerases, producing C→T mutations at dipyrimidine sites that accumulate in skin-cell oncogenes/tumor suppressors — giving a dramatically increased (often >1000-fold) skin cancer risk at an early age. (c) Some XP complementation groups (and the related trichothiodystrophy/Cockayne overlap) also impair transcription-coupled repair and TFIIH function; neurons cannot replace themselves and are highly sensitive to accumulated transcription-blocking endogenous DNA damage, producing progressive neurodegeneration. See section 14.

13. A researcher designs a CRISPR experiment to correct a point mutation (G→A) in the *HBB* gene causing sickle-cell disease. List: (a) the guide RNA design rules; (b) the delivery method for cells (RNP electroporation vs viral vector); (c) why homology-directed repair (HDR, requiring a donor template) is needed rather than NHEJ; (d) how to increase HDR efficiency.

Answer (Q13, Application). (a) Guide RNA design: choose a 20-nt spacer matching *HBB* near the codon-6 mutation, immediately 5' of an NGG PAM, with high on-target and minimal off-target/self-similarity scores; place the cut close to the edit site. (b) Delivery: for *ex vivo* editing of patient hematopoietic stem cells, ribonucleoprotein (Cas9 protein + sgRNA) electroporation is preferred over viral vectors — it is transient (lower off-target and immunogenicity, no insertional mutagenesis). (c) Correcting G→A back to wild type requires HDR because only HDR copies a supplied donor template to install the exact sequence; NHEJ merely religates the break and introduces random indels (a knockout, not a correction). (d) Increasing HDR: use a single-stranded oligo donor, deliver in S/G2 phase, inhibit NHEJ (e.g., DNA-PK/Ligase IV inhibitors or NHEJ-pathway suppression),

and use chemically protected donors at optimized stoichiometry. See section 14. 14. A patient’s tumor has microsatellite instability (MSI-high) due to MMR deficiency. Explain: (a) what kinds of mutations accumulate in MSI-high tumors; (b) why MSI tumors produce many neoantigens; (c) why pembrolizumab (anti-PD-1) is effective in MSI-high tumors regardless of cancer type (tissue-agnostic treatment).

Answer (Q14, Application). (a) MMR deficiency means replication-slippage errors at short tandem repeats go uncorrected, so MSI-high tumors accumulate huge numbers of indels in microsatellites and a very high overall mutation burden, especially frameshifts in coding repeats. (b) Frameshifted coding sequences generate novel out-of-frame peptides — neoantigens — that are highly immunogenic because they are not present in normal tissue and are seen as foreign by T cells. (c) This high neoantigen load makes the tumor strongly immune-recognized but held in check by the PD-1/PD-L1 checkpoint; pembrolizumab (anti-PD-1) releases that brake, restoring T-cell killing. Because the mechanism depends on neoantigen load rather than tissue of origin, anti-PD-1 is approved tissue-agnostically for MSI-high/dMMR tumors. See section 14. 15. Transposon Alu (SINE family) comprise about 11% of the human genome. Explain: (a) how Alu elements replicate via RNA intermediates (SINE retrotransposition); (b) how an Alu insertion in exon 16 of BRCA2 could cause breast cancer; (c) how the host genome suppresses transposon activity in the germline (piRNA pathway).

Answer (Q15, Application). (a) Alu elements are non-autonomous SINE retrotransposons: they are transcribed by RNA Pol III, and the resulting RNA is reverse-transcribed and integrated by the LINE-1 (L1) machinery (ORF1/ORF2 proteins providing reverse transcriptase and endonuclease) — a copy-and-paste, RNA-intermediate mechanism that has expanded Alu to about 11% of the genome. (b) A new Alu insertion into exon 16 of BRCA2 disrupts the coding sequence (introducing extra sequence, splicing changes, or a frameshift/premature stop), abolishing functional BRCA2 and its homologous-recombination DNA-repair role, predisposing to breast/ovarian cancer. (c) In the germline, transposons are silenced by the piRNA pathway: PIWI proteins loaded with piRNAs recognize transposon transcripts, cleaving them and directing DNA methylation/heterochromatin at their loci to prevent mobilization. See section 14. 16. GWAS (genome-wide association studies) have identified thousands of SNPs associated with disease risk, but most are in non-coding regions. Explain: (a) why non-coding SNPs are biologically meaningful (enhancer activity, splicing regulation); (b) how eQTL analysis links SNPs to gene expression levels; (c) why a SNP with odds ratio 1.2 for Type 2 Diabetes is clinically uninformative for individual risk prediction.

Answer (Q16, Application). (a) Most trait-associated SNPs are non-coding because they lie in regulatory DNA — enhancers, promoters, or splicing elements — where they alter transcription-factor binding, chromatin state, or splice-site usage and thus change gene *dosage* rather than protein sequence. (b) eQTL analysis correlates a SNP’s genotype with mRNA expression levels across many individuals; a SNP that statistically predicts expression of a nearby (cis) or distant (trans) gene is an expression QTL, providing the mechanistic link from a non-coding GWAS hit to a target gene. (c) A SNP with odds ratio about 1.2 shifts an individual’s absolute Type 2 Diabetes risk only marginally and is swamped by environmental and polygenic background; such small effect sizes are useful for understanding biology and population-level architecture but are not clinically informative for predicting an individual’s risk. See section 14. 17. The P53 gene is mutated in >50% of all human cancers. Explain: (a) the “gain-of-function” mutations in TP53 (R248W, R175H) that not only eliminate tumor suppression but actively promote invasion; (b) how wild-type p53 regulates CDK inhibitor p21 and pro-apoptotic PUMA; (c) what therapeutic strategy (restoring wild-type TP53 conformation using small molecules — APR-246) is being tested.

Answer (Q17, Application). (a) Certain TP53 missense alleles (e.g., R248W, R175H) are gain-of-function: beyond losing wild-type tumor-suppressor activity, the mutant p53 acquires new oncogenic properties — binding other transcription factors and remodeling gene expression to promote invasion, metastasis, and chemoresistance (often also dominant-negative over any remaining wild-type p53). (b) Wild-type p53 is a transcription factor that, on DNA damage, induces the CDK inhibitor p21 (CDKN1A) to enforce G1/S arrest for repair, and pro-apoptotic targets such as PUMA (and BAX) to trigger apoptosis if damage is severe. (c) A tested strategy is APR-246/eprenetapopt, a small molecule that covalently modifies mutant p53 to restore a wild-type-like conformation and transcriptional activity, reactivating p21/PUMA-driven arrest and apoptosis in p53-mutant tumors. See section 14. 18. Gene therapy for Duchenne muscular dystrophy (DMD, caused by large deletions in *Dystrophin*) uses exon skipping with antisense oligonucleotides (AONs). Explain: (a) why some deletions cause severe DMD while frameshifted deletions are less severe (in-frame vs out-of-frame); (b) how AON targeting exon 51 restores the reading frame; (c) why this produces “Becker-like” dystrophin rather than fully corrected dystrophin.

Answer (Q18, Application). (a) Dystrophin tolerates internal in-frame deletions (producing shortened but partly functional protein → milder Becker muscular dystrophy), whereas out-of-frame deletions shift the reading frame, create a premature stop, and abolish dystrophin → severe Duchenne. So a large deletion’s severity depends on whether it disrupts the reading frame, not its size. (b) An antisense oligonucleotide complementary to exon 51 masks its splice signals, causing the spliceosome to skip exon 51; this removes additional sequence so that the exon junctions flanking the original deletion are realigned back into frame, allowing translation of an internally truncated protein. (c) The restored protein lacks the skipped exon(s), so it is an internally shortened, Becker-like dystrophin with partial function — converting a severe DMD phenotype toward a milder one rather than fully curing it. See section 14. 19. Epigenome-wide association studies (EWAS) examine DNA methylation differences between cases

and controls. Explain: (a) why methylation differences (epimutations) are harder to interpret than genetic mutations; (b) why cell-type composition confounds EWAS analysis; (c) how MR (Mendelian randomisation) can be used to determine whether methylation changes are causal or merely correlative with disease.

Answer (Q19, Application). (a) Epimutations (DNA-methylation differences) are harder to interpret than genetic mutations because methylation is dynamic, tissue- and cell-type-specific, age-dependent, and often a consequence rather than a cause of disease — so an association does not establish direction or mechanism. (b) Bulk tissue is a mixture of cell types with very different methylomes; if cases and controls differ in cell-type composition (e.g., more immune cells), apparent methylation differences may merely reflect that composition shift, a major confounder requiring deconvolution or cell-sorted data. (c) Mendelian randomization uses germline SNPs that influence methylation (mQTLs) as instrumental variables: because alleles are randomized at conception and fixed before disease, an association between the genetically predicted methylation level and disease supports a causal (not merely correlative) role, provided the instrument is valid and not pleiotropic. See section 14. 20. Oxford Nanopore sequencing reads individual DNA/RNA molecules by measuring ionic current changes as they pass through a protein pore. Compare this technology to Illumina short-read sequencing: advantages (read length, direct RNA, base modifications, real-time), disadvantages (raw error rate about 5% vs <0.1%), and the application where each is most suitable.

Answer (Q20, Application). Oxford Nanopore threads a single DNA/RNA strand through a protein nanopore and infers bases from characteristic ionic-current shifts. Advantages over Illumina: very long reads (kb–Mb, resolving repeats, structural variants, and enabling de novo/telomere-to-telomere assembly), direct RNA sequencing, detection of base modifications (e.g., methylation) without bisulfite, real-time/portable output. Disadvantages: higher raw per-base error (about 5% vs <0.1% for Illumina) and lower throughput per dollar for SNV calling. Best use: Illumina for high-accuracy SNV/small-variant detection and large cohort genotyping; Nanopore (or PacBio HiFi) for structural-variant discovery, repeat regions, full-length isoforms, epigenetic marks, and rapid field/clinical sequencing. See section 14.

Questions 21–30: Synthesis and Evaluation

21. Evaluate the safety of germline CRISPR editing (modifying embryo DNA, producing heritable changes) as attempted by He Jiankui in 2018. Identify three specific scientific risks (off-target edits, mosaicism, unintended immune consequences) and three ethical concerns (informed consent, enhancement vs therapy, equity of access). What international governance frameworks should govern germline editing?

Answer (Q21, Synthesis). Empirically, He Jiankui edited *CCR5* in human embryos (2018) producing live births; documented and predicted problems include off-target double-strand breaks, mosaicism (not all cells edited), large deletions, and an uncertain benefit (the targeted *CCR5* change did not even reproduce the protective allele). The judgment that germline editing was unsafe and unethical follows because heritable, irreversible changes were introduced into healthy embryos without medical necessity, adequate preclinical safety, or genuine informed consent. Ethical concerns: defective consent, blurring therapy vs enhancement, and equity of access. Governance should require an enforceable international moratorium on clinical germline editing, oversight bodies (WHO registry, national regulators), and a transparent, criteria-based pathway. What would change the conclusion: demonstrated elimination of off-target/mosaicism risk plus a clear, otherwise-unavailable medical benefit and robust consent. See section 14. 22. A patient carries a disease-associated haplotype in which short reads map poorly because a 3-kb insertion and nearby promoter variant are absent from the linear reference. Design a graph-aware interpretation workflow: compare a single-reference call, a pangenome graph path, ClinVar/dbSNP/RefSeq/MANE status checks, and long-read validation; then explain when base editing, prime editing, Casgevy-style enhancer disruption, or Lyfgenia-style lentiviral gene addition would be the most defensible therapeutic logic.

Answer (Q22, Synthesis). A strong workflow first asks whether the apparent variant is a mapping artifact: remap reads against a pangenome graph that contains the insertion path, inspect read support across both breakpoints, check dbSNP for the submitted variant identifier, ClinVar for assertion/review status, and RefSeq/MANE for the transcript used to name the change, then confirm phase with long reads or linked reads before reporting a clinical haplotype [National Center for Biotechnology Information, 2026b,a,d,c]. Base editing is best for a single transition within an editor’s activity window when bystander edits are acceptable or avoidable. Prime editing is better for installing or correcting a short promoter motif, such as fetal-globin promoter rewrites, because the edit is templated without a double-strand break. Casgevy-style enhancer disruption is a different logic: it does not repair *HBB* but changes erythroid regulation by reducing BCL11A enhancer activity to raise fetal hemoglobin. Lyfgenia-style lentiviral gene addition is another regulatory path: it adds a functional hemoglobin transgene rather than editing the native locus, so ClinicalTrials.gov trial status and FDA approved indications must be checked separately [National Library of Medicine, 2026, U.S. Food and Drug Administration, 2026c]. Keep sequence evidence, database currency, expression evidence, editing feasibility, off-target assessment, and clinical maturity separate. See section 14. 23. Evaluate the “cancer genome atlas” concept: sequencing thousands of tumor genomes has generated a mutation landscape for most cancer types, identifying “drivers” vs “passengers.” What statistical criteria distinguish drivers from passengers, and why have most cancer driver mutations proven difficult to target therapeutically?

Answer (Q23, Synthesis). Empirically, sequencing thousands of tumors (e.g., TCGA) maps recurrent mutations across cancer types. Drivers vs passengers are distinguished statistically: drivers show mutation recurrence above the background mutation rate (MutSigCV-type models correcting

for gene length, replication timing, and context), selection signatures (elevated nonsynonymous/synonymous or clustering at hotspots), and functional/pathway enrichment; passengers are random by-product mutations consistent with background. The judgment that driver discovery has not translated easily into therapy follows because many drivers are tumor-suppressor losses or “undruggable” proteins (e.g., TP53, RAS until recently, transcription factors) lacking enzymatic pockets, and tumor heterogeneity/resistance limits single-target success. What would change the conclusion: new modalities (degraders, covalent KRAS inhibitors, synthetic lethality) making previously undruggable drivers tractable. See section 14. 24. Synthetic chromosomes have been designed and built in yeast (Sc2.0, synthetic chromosome project). Evaluate the design principles (removal of transposons, recombination tags added, inducible evolution mode via SCRaMbLE), and discuss whether a fully synthetic human chromosome could be built and what it would require.

Answer (Q24, Synthesis). Sc2.0 redesigns yeast chromosomes with defined principles: removal of destabilizing/repetitive elements (transposons, introns, redundant tRNA genes relocated), synonymous recoding (e.g., recoding stop codons to free a codon), insertion of loxPsym recombination tags at non-essential 3' ends to enable SCRaMbLE (Cre-induced inducible genome rearrangement for accelerated, controllable evolution), and watermarks/PCRTags for tracking — yielding a streamlined, programmable genome. The causal logic: design choices → reduced genome instability and a built-in diversification tool → a viable, evolvable synthetic eukaryotic chromosome. A fully synthetic human chromosome is far harder: it would require accurate megabase synthesis and assembly, functional centromeres, telomeres, and origins, correct large-scale 3D chromatin/epigenetic regulation, and stable mitotic segregation — currently beyond reach and raising serious safety/ethical constraints. See section 14. 25. Transposons in the germline are silenced by piRNAs (PIWI-interacting RNAs). The piRNA pathway (PIWI proteins, ping-pong amplification) produces a feed-forward silencing loop. Evaluate: (a) how piRNAs recognize transposons without classical Watson-Crick base pairing; (b) why depletion of PIWI proteins causes germline transposon mobilization and infertility in mice; (c) whether piRNAs can also target non-transposon mRNAs.

Answer (Q25, Synthesis). (a) piRNAs (about 24–31 nt, PIWI-bound, Dicer-independent) recognize transposons by sequence complementarity to transposon transcripts, but tolerance for mismatches plus an amplifying “ping-pong” cycle (sense and antisense piRNAs reciprocally guiding cleavage) lets the system target diverse, mutating transposons rather than requiring exact Watson–Crick matching of a fixed siRNA. (b) Loss of PIWI proteins (e.g., MILI/MIWI/MIWI2 knockouts) derepresses transposons in the germline, causing insertional mutagenesis, DNA damage, meiotic arrest, and infertility/sterility — showing piRNA silencing is essential for genome integrity in germ cells. (c) Beyond transposons, piRNAs can also target some non-transposon mRNAs (regulating their stability/translation, e.g., during spermiogenesis), indicating a broader post-transcriptional regulatory role. What would change this view: evidence that observed mRNA effects are indirect consequences of transposon derepression rather than direct piRNA targeting. See section 14. 26. Precision oncology based on tumor sequencing identifies actionable mutations. However, intratumoral heterogeneity (ITH) means that some cells within the tumor may lack the targeted mutation. Evaluate: (a) how clonal vs subclonal mutations are distinguished by variant allele frequency; (b) why targeting a clonal mutation (present in most cells) is more likely to be effective; (c) how liquid biopsy (circulating tumor DNA, ctDNA) can detect resistance mechanisms before clinical progression.

Answer (Q26, Synthesis). The causal chain: tumor sequencing finds actionable mutations, but intratumoral heterogeneity means a targeted mutation may be present in only a subset of cells, so therapy spares non-carrying clones and resistance emerges. (a) Clonal vs subclonal mutations are distinguished by variant allele frequency (VAF) adjusted for tumor purity and copy number: clonal mutations (in all cancer cells) cluster near the expected fully-penetrant VAF, whereas subclonal mutations show lower VAF (present in a fraction of cells). (b) Targeting a clonal mutation is more likely effective because every tumor cell carries it, so no pre-existing escape population is spared; targeting a subclonal driver leaves resistant clones to expand. (c) Liquid biopsy (ctDNA) non-invasively samples tumor-derived DNA from blood, so emerging resistance mutations (e.g., EGFR T790M) can be detected as rising ctDNA fractions before radiographic/clinical progression, enabling earlier therapy switching. See section 14. 27. Evaluate whether “de-extinction” (reviving extinct species via CRISPR genome editing of a close relative) is scientifically feasible for: (a) the woolly mammoth (editing *Loxodonta africana* genome about 50 key cold-adaptation genes); (b) the passenger pigeon (*Ectopistes migratorius*, using band-tailed pigeon as template). What are the ecological risks of reintroducing de-extinct animals?

Answer (Q27, Synthesis). Empirically, de-extinction by CRISPR does not literally resurrect an extinct species; it edits a close living relative toward the extinct phenotype. (a) For the woolly mammoth, about 50 cold-adaptation genes (hemoglobin, hair, fat, *TRPV3*) can be edited into the Asian elephant (*Elephas maximus*, not *Loxodonta*) genome, but a viable animal requires solving elephant cloning/artificial-womb gestation and integrating many edits — partial feasibility at best, yielding a cold-tolerant elephant hybrid, not a true mammoth. (b) The passenger pigeon (*Ectopistes migratorius*) using band-tailed pigeon as template faces the same limits plus avian cloning being unsolved. The judgment of limited feasibility rests on incomplete ancient genomes, polygenic phenotypes, and reproductive-technology gaps. Ecological risks: disrupted modern ecosystems, disease introduction, no surviving social/migratory learning, and diversion of conservation resources. What would change it: solved reproductive cloning and complete, high-quality ancient genomes. See section 14. 28. Retroviral integration (HIV integrates into host genome) is both a challenge for cure research and a tool for gene therapy vectors. Evaluate the “semi-random” integration pattern of HIV (preference for active transcription units) and how this differs from AAV (predominantly episomal in non-dividing cells, rare integration at AAVS1 safe harbor). Why does insertional mutagenesis risk differ between retroviral and AAV gene therapies?

Answer (Q28, Synthesis). The causal logic links integration site to genotoxic risk. HIV (lentivirus) integrates semi-randomly but preferentially into actively transcribed gene bodies (LEDGF/p75-tethered), so a therapeutic lentiviral vector can insert within or near active genes, with some risk of dysregulating them. AAV is predominantly episomal in non-dividing cells, with only rare integration (occasionally at the AAVS1 “safe harbor”), so it persists largely without altering host loci. Therefore insertional-mutagenesis risk is higher for integrating retro/lentiviral vectors (historically causing leukemia in early SCID-X1 gamma-retroviral trials due to enhancer activation of *LMO2*) than for AAV, whose mainly non-integrating biology limits oncogene activation but trades off durability (episome loss in dividing cells). What would change this: modified vectors (SIN-LTR, insulators, targeted integration) substantially lowering retroviral genotoxicity. See section 14. 29. tRNA suppressors can read through stop codons, restoring protein production from genes with premature stop mutations. Evaluate the therapeutic use of aminoglycoside antibiotics (gentamicin) as readthrough agents for nonsense mutations (e.g., in *Dystrophin*) — what are the molecular mechanisms, the challenges of specificity (also read through normal stop codons), and the clinical results to date?

Answer (Q29, Synthesis). The mechanism: suppressor/readthrough allows a near-cognate aminoacyl-tRNA to be inserted at a premature stop codon, restoring full-length protein. Aminoglycosides (gentamicin, and the designed agent ataluren/PTC124) bind the ribosomal decoding (A) site, reducing fidelity so a sense amino acid is incorporated at a PTC, producing some functional dystrophin in nonsense-mutation Duchenne. Specificity challenge: the ribosome cannot distinguish a premature from a normal stop codon, so readthrough of legitimate stop codons risks C-terminally extended aberrant proteins and toxicity; efficiency is also low and context-dependent (PTC identity and surrounding sequence). Clinical results to date: effects have been modest and inconsistent — ataluren showed marginal/equivocal benefit (conditional EU approval, not FDA-approved), and aminoglycoside toxicity (oto-/nephrotoxicity) limits chronic use. Outcome would change with non-toxic, PTC-selective readthrough drugs. See section 14. 30. Critically evaluate the technical and ethical implications of building a “minimal synthetic cell” with a fully defined genome (as in the Venter Institute’s JCVI-syn3.0, about 473 genes). What does the set of essential genes reveal about the minimal requirements for cellular life? If this minimal genome could be commercially manufactured and sold, what biosafety and biosecurity regulations should apply?

Answer (Q30, Synthesis). Empirically, JCVI-syn3.0 (Venter Institute) is a chemically synthesized, transplanted minimal *Mycoplasma* genome of about 473 genes that supports self-replication. The set of essential genes shows that minimal cellular life still requires the core processes — genome replication, transcription, translation, membrane/lipid biogenesis, and basic metabolism — yet about 149 essential genes still have unknown function, revealing that we do not fully understand even a minimal cell. The judgment that this is profound but bounded follows: it defines a lower bound on life’s genetic complexity without claiming we can yet design genomes from first principles. Biosafety/biosecurity: commercial minimal cells would need DNA-synthesis screening, containment and engineered biocontainment (kill switches, auxotrophy), licensing/traceability, dual-use review, and international oversight. What would change the assessment: a minimal genome whose every gene’s function is known and that is provably non-viable outside controlled conditions. See section 14.

Questions — Chromatin and Epigenetic Mechanisms

Instructor Use and Coverage Notes

- Coverage target: Explain how a regulatory mark changes accessibility and predict downstream expression.
- Model/data emphasis: Regulatory-state and expression-ratio reasoning.
- Assessment alignment: Concept Explanation, Questions and Methods, Argumentation.
- Misconception probe: Epigenetic does not mean independent of DNA sequence or permanently inherited.
- Transfer product: Apply regulation logic to differentiation, imprinting, cancer, or environmental responses.
- Grading focus: award full credit for mechanism, evidence, boundary conditions, and units when a calculation is required.
- Suggested use: draw one recall item, one application item, and one synthesis item when building a short quiz from this bank.

Questions 1–10: Recall and Comprehension

This activity accompanies section 15 of the textbook — review that chapter before attempting the exercises below.

1. Define epigenetics. Give two examples of epigenetic modifications.

Answer (Q1, Recall). Epigenetics is the study of heritable changes in gene expression that do not alter the underlying DNA sequence but instead change chromatin state and accessibility. Two examples are DNA methylation of cytosine at CpG dinucleotides (generally repressive at promoters) and covalent histone tail modifications such as acetylation (H3K27ac, activating) or methylation (H3K27me3, repressive). See section 15.
2. What is DNA methylation? Which nucleotide is typically methylated in mammals, and what effect does methylation at gene promoters generally have on transcription?

Answer (Q2, Recall). DNA methylation is the covalent addition of a methyl group, catalyzed by DNA methyltransferases (DNMT1 maintenance; DNMT3A/3B de novo). In mammals it occurs almost exclusively on cytosine within 5'-CpG-3' dinucleotides. Methylation of a CpG island in a gene promoter generally represses transcription by blocking activator binding and recruiting methyl-binding repressors and HDACs, producing stable gene silencing. See section 15.
3. What is a histone? Name four types of histone modification and one enzyme family for each.

Answer (Q3, Recall). A histone is a small basic protein (H2A, H2B, H3, H4) that packages DNA into nucleosomes. Four modification types and an enzyme family for each: acetylation (HATs/KATs add, HDACs remove), methylation (KMTs such as PRC2/EZH2 add, KDMs/demethylases remove), phosphorylation (kinases such as Aurora B), and ubiquitination (E3 ligases such as RING1B on H2AK119). See section 15.
4. What does H3K4me3 mark indicate? What about H3K27me3?

Answer (Q4, Recall). H3K4me3 is an activating mark enriched at the promoters of actively transcribed genes, written by MLL/COMPASS and read by basal transcription machinery. H3K27me3 is a repressive mark deposited by Polycomb repressive complex 2 (EZH2) that silences developmental genes and is read by PRC1. Both are lysine methylation on H3, but their distinct positions and reader complexes give opposite functional outcomes. See section 15.
5. What is chromatin remodeling? Name one chromatin remodeling complex.

Answer (Q5, Recall). Chromatin remodeling is the ATP-dependent repositioning, ejection, or restructuring of nucleosomes to change DNA accessibility for transcription factors and the replication/repair machinery. One example is the SWI/SNF (BAF) complex, which uses ATP hydrolysis to slide or evict nucleosomes; other families include ISWI, CHD/NuRD, and INO80. See section 15.
6. What is the lac operon? Which molecules control it?

Answer (Q6, Recall). The lac operon is a cluster of E. coli genes (lacZ, lacY, lacA) encoding enzymes for lactose uptake and metabolism, transcribed from a single promoter. It is controlled by negative regulation via the LacI repressor (released when allolactose, the inducer, binds it) and positive regulation via CAP-cAMP, which activates transcription when glucose is low. See section 15.
7. What is a repressor protein? What is an activator protein?

Answer (Q7, Recall). A repressor is a regulatory protein that binds DNA (typically an operator or silencer) and decreases transcription, for example by blocking RNA polymerase or recruiting repressive chromatin machinery. An activator binds DNA (an enhancer or CAP site) and increases transcription by recruiting or stabilizing RNA polymerase and coactivators, as CAP-cAMP does at the lac promoter. See section 15.
8. Define allosteric regulation in the context of transcription. Give an example.

Answer (Q8, Recall). Allosteric regulation is the modulation of a regulatory protein’s DNA-binding activity by a small effector molecule binding at a separate site, changing the protein’s conformation. In the lac operon, allolactose binds the LacI repressor and allosterically reduces its affinity for the operator, releasing it from DNA and allowing transcription; conversely, tryptophan acts as a corepressor that activates the trp repressor. See section 15.

9. What are non-coding RNAs? Name three biologically important types.

Answer (Q9, Recall). Non-coding RNAs are functional RNA transcripts that are not translated into protein but instead regulate gene expression and genome organization. Three important types are microRNAs (about 22 nt, guide RISC to repress target mRNAs), small interfering RNAs (siRNAs, drive sequence-specific mRNA cleavage in RNAi), and long non-coding RNAs (lncRNAs such as Xist, which scaffold chromatin-modifying complexes). See section 15.

10. What is genomic imprinting? Give one example of an imprinted gene.

Answer (Q10, Recall). Genomic imprinting is parent-of-origin-specific monoallelic expression, in which a gene is expressed only from the maternally or only from the paternally inherited allele, set by differential DNA methylation at imprinting control regions in the germline. An example is IGF2, expressed only from the paternal allele (the maternal allele is silenced via the CTCF-controlled IGF2/H19 ICR). See section 15.

Questions 11–20: Application and Analysis

11. A CpG island in the CDKN2A (p16) promoter is hypermethylated in a lung cancer cell. Trace the molecular consequences: (a) which protein is silenced; (b) what happens to CDK4/6 activity; (c) what happens to cell cycle progression; (d) why this is an alternative mechanism to p16 deletion for bypassing the G₁ checkpoint.

Answer (Q11, Application). (a) Hypermethylation of the CDKN2A CpG island silences the p16^{INK4a} protein. (b) Without p16 to inhibit CDK4/6, Cyclin D–CDK4/6 remains active. (c) Active CDK4/6 hyperphosphorylates Rb, releasing E2F so the cell passes the G₁ restriction point and proliferates. (d) This epigenetic silencing is functionally equivalent to deleting or mutating p16 — it inactivates the gene without changing the DNA sequence, an alternative route to bypassing the G₁ checkpoint, and it is potentially reversible with demethylating agents. See section 15.

12. Polycomb repressive complex 2 (PRC2) trimethylates H3K27 and is overexpressed in many cancers. Explain: (a) the molecular mechanism of H3K27me₃-mediated gene silencing; (b) how PRC2 spreads repression across large chromosomal domains; (c) why EZH2 (the catalytic subunit of PRC2) is a therapeutic target (tazemetostat).

Answer (Q12, Application). (a) PRC2 trimethylates H3K27 (H3K27me₃), which recruits PRC1 to ubiquitinate H2AK119 and compact chromatin, blocking transcription. (b) H3K27me₃ is itself read by the PRC2 EED subunit, creating positive feedback that spreads the mark in cis across broad domains. (c) Overactive or mutant EZH2 hyper-represses tumor-suppressor and differentiation genes, so the catalytic EZH2 subunit is druggable; tazemetostat is an FDA-approved EZH2 inhibitor that reactivates these genes. See section 15.

13. In the lac operon, explain the logic of dual control by the lac repressor AND catabolite activator protein (CAP). Under which combination of conditions is the operon most highly transcribed? Under which is it completely silent?

Answer (Q13, Application). The lac repressor provides negative control (bound to the operator unless allolactose is present) and CAP–cAMP provides positive control (active only when glucose is low, raising cAMP). The operon is maximally transcribed when lactose is present AND glucose is absent: the repressor is released and CAP–cAMP activates the promoter. It is completely silent when lactose is absent, because the repressor stays bound regardless of glucose status. See section 15.

14. RNA interference (RNAi) via siRNA silences gene expression post-transcriptionally. Compare siRNA (perfectly complementary → mRNA cleavage by Ago2) vs miRNA (partially complementary → translational repression and mRNA destabilisation). How does each affect the steady-state abundance of target mRNA?

Answer (Q14, Application). siRNAs are perfectly complementary to their targets and direct Ago2 to endonucleolytically cleave (slice) the mRNA, sharply lowering its steady-state abundance. miRNAs are only partially complementary (matching mainly through the seed region) and act mostly by repressing translation and promoting deadenylation/decay, causing a more modest reduction in mRNA levels and a larger drop in protein output. Both reduce target expression, but siRNA produces stronger, cleavage-based mRNA loss. See section 15.

15. Enhancers can activate promoters over distances of >1 Mb in the genome by chromatin looping mediated by cohesin and CTCF. Explain: (a) the role of CTCF as a chromatin barrier/insulator; (b) how loss of a CTCF binding site at the IGF2/H19 imprinting control region (ICR) causes Beckwith-Wiedemann syndrome; (c) how 4C and HiC experiments confirm enhancer-promoter looping.

Answer (Q15, Application). (a) CTCF binds insulator sequences and, with cohesin, organizes chromatin loops/TAD boundaries that block enhancers from acting across them. (b) At the IGF2/H19 ICR the maternal allele is unmethylated, so CTCF binds and insulates IGF2 from the downstream enhancers; loss of that CTCF site (or its methylation) lets the enhancer loop to IGF2, causing biallelic IGF2 expression and overgrowth (Beckwith-Wiedemann syndrome). (c) Chromosome-conformation methods such as 4C and Hi-C detect ligated DNA contacts, directly demonstrating physical enhancer–promoter looping. See section 15.

16. Evaluate the claim that cancer is largely an epigenetic disease. Cite evidence from: (a) global hypomethylation and CpG island hypermethylation in cancer; (b) frequent mutations in chromatin remodeling enzymes (ARID1A, SMARCA4, KMT2D) in cancer; (c) the success of HDAC inhibitors and DNMT inhibitors clinically. Under what conditions are purely epigenetic therapies (without targeted mutation correction) appropriate?

Answer (Q16, Application). (a) Cancers show genome-wide hypomethylation (activating oncogenes/transposons) alongside focal CpG-island hypermethylation that silences tumor suppressors, an epigenetic phenotype. (b) Frequent loss-of-function mutations in chromatin regulators (ARID1A, SMARCA4, KMT2D) show the chromatin machinery is itself a driver. (c) Clinical efficacy of DNMT inhibitors (azacitidine) and HDAC inhibitors supports reversible epigenetic causation. The claim holds where epigenetic silencing is the dominant lesion (e.g., MDS, IDH-mutant gliomas) and a reactivatable gene exists; purely epigenetic therapy is inappropriate when fixed driver mutations or deletions, not silencing, sustain the tumor. See section 15.

17. Design a pharmaceutical strategy to reactivate a silenced tumor suppressor gene in a cancer with promoter hypermethylation. Compare DNMT inhibitors (5-azacitidine, broad demethylation), targeted dCas9-TET1 (site-specific demethylation), and HDAC inhibitors. What are the risks of broad epigenome reprogramming vs targeted approaches?

Answer (Q17, Application). Hypothesis: re-expressing the silenced tumor suppressor restores growth control. Compare arms: a DNMT inhibitor (5-azacitidine) causes broad passive demethylation and reactivates many genes but risks global genome instability and off-target reactivation; dCas9-TET1 demethylates only the targeted promoter, giving specificity but limited efficiency and delivery challenges; HDAC inhibitors broadly reopen chromatin but are nonspecific and transient. Measure target re-expression, methylation, growth arrest, with vehicle and catalytically dead controls; the decision rule is restored expression and arrest specifically when the targeted mark is removed. Broad reprogramming risks awakening oncogenes and toxicity; targeted approaches trade efficiency for safety. See section 15.

18. Super-enhancers are clusters of enhancers (about 25–50 kb) bound by an unusually high density of transcription factors (BRD4, Mediator), associated with strong transcription of oncogenes (MYC, BCL2) in cancer. Evaluate the evidence for super-enhancer addiction in cancer cells, and explain why BET bromodomain inhibitors (JQ1) preferentially disengage from super-enhancers over typical enhancers.

Answer (Q18, Application). Super-enhancers are dense clusters of enhancers occupied by high levels of BRD4, Mediator, and master transcription factors that drive very high expression of identity and oncogene loci (MYC, BCL2). Evidence for addiction: cancer cells are disproportionately dependent on these few super-enhancer-driven genes, so disrupting them collapses the oncogenic program. Because super-enhancers depend on cooperative, high-density BRD4/Mediator occupancy and phase-separated condensates, BET inhibitors such as JQ1 disengage BRD4 more steeply from super-enhancers than from typical enhancers — a small drop in occupancy disproportionately collapses the cooperative assembly, preferentially shutting off MYC. See section 15.

19. Evaluate the concept of “epigenetic clock” (Horvath clock): methylation of specific CpG sites in blood DNA correlates with biological age more accurately than chronological age. What do deviations from the epigenetic clock predict? Can lifestyle interventions (caloric restriction, exercise) reduce epigenetic age, and what experimental evidence supports this?

Answer (Q19, Application). The Horvath epigenetic clock estimates biological age from methylation at a defined set of CpG sites (about 353), often more accurately tracking physiological aging than chronological age. Positive deviations (epigenetic age acceleration) predict elevated all-cause mortality and risk of age-related disease, while negative deviations associate with longevity. Some interventions (caloric restriction in animal models, exercise, and small human trials) modestly slow or reverse epigenetic age, but evidence is correlational and confounded by cell-type composition, so randomized longitudinal data with matched cell populations are needed before causal claims. See section 15.

20. 3D chromatin organization (TADs — topologically associating domains) is largely maintained by CTCF and cohesin. Evaluate what would happen to gene regulation if cohesin loading were abolished globally: (a) which enhancer-promoter pairs would become aberrantly activated; (b) what new gene expression states would emerge; (c) is this consistent with the observation that cohesin mutations cause Cornelia de Lange syndrome?

Answer (Q20, Application). TAD boundaries are built by CTCF and cohesin through loop extrusion. (a) Abolishing cohesin loading would eliminate most loops/TADs, so enhancers could aberrantly contact promoters outside their normal domains, switching on genes that are normally insulated. (b) New, dysregulated expression states would emerge, generally with modest, widespread changes rather than wholesale reprogramming, since promoter-proximal control persists. (c) This is consistent with cohesin/NIPBL mutations causing Cornelia de Lange syndrome, a multisystem

developmental disorder, because partial loss of cohesin function subtly mis-wires enhancer–promoter contacts genome-wide during development. See section 15.

Questions 21–30: Synthesis and Evaluation

21. CRISPR interference (CRISPRi) uses dCas9-KRAB (a transcriptional repressor) to silence target genes without cutting DNA. Compare CRISPRi with ASO (antisense oligonucleotide) knockdown at the mRNA level and classical promoter deletion by CRISPR. What are the therapeutic advantages of CRISPRi (temporal control, reversibility, no off-target DSBs)?

Answer (Q21, Synthesis). CRISPRi (dCas9-KRAB) recruits repressive chromatin machinery to a promoter to silence transcription without cutting DNA, acting at the chromatin/transcription level. ASO knockdown acts post-transcriptionally by triggering RNase H degradation of the mRNA, leaving the gene intact and requiring continuous dosing. Classical CRISPR promoter deletion permanently removes DNA via double-strand breaks. CRISPRi’s advantages are reversibility and tunable, inducible temporal control, multiplexing, and avoidance of off-target double-strand breaks and permanent genomic scars, making it safer and more flexible for functional and therapeutic silencing. See section 15.

22. Maternal nutrition during peri-conception affects offspring health across the life course (Barker/DOHaD hypothesis). Using three specific nutrients (folate, methionine, choline) and their roles in one-carbon metabolism → SAM production → methyltransferase substrate supply, evaluate the molecular mechanism by which poor maternal nutrition could cause persistent epigenetic changes in offspring that increase adult diabetes or cardiovascular disease risk.

Answer (Q22, Synthesis). Folate, methionine, and choline feed one-carbon metabolism to regenerate S-adenosylmethionine (SAM), the universal methyl donor for DNMTs and histone methyltransferases. Poor maternal supply of these nutrients lowers SAM (and shifts the SAM:SAH ratio), reducing methyltransferase activity during the sensitive peri-conceptual window. This produces altered, persistent DNA-methylation patterns at metabolic gene promoters and imprinted loci in the offspring, which are maintained through development and program tissues toward impaired glucose handling and vascular dysfunction, raising adult diabetes and cardiovascular disease risk (the DOHaD/Barker mechanism). See section 15.

23. Evaluate the concept of “bivalent chromatin domains” in embryonic stem cells: developmental gene promoters carry both active (H3K4me3) and repressive (H3K27me3) marks simultaneously, maintaining them in a “poised” state. How does this enable rapid differentiation in either direction, and what happens to bivalent domains as cells commit to a specific lineage?

Answer (Q23, Synthesis). Bivalent domains carry the activating H3K4me3 and repressive H3K27me3 marks together at developmental gene promoters in embryonic stem cells, holding genes transcriptionally poised — repressed but primed for rapid activation. On differentiation cues the domain resolves in a lineage-specific way: genes needed in that lineage lose H3K27me3 and become fully active (monovalent H3K4me3), while genes for alternative fates lose H3K4me3 and become stably repressed (monovalent H3K27me3). This allows fast, bidirectional commitment, and once a cell adopts a lineage the bivalent state is resolved into a single stable mark. See section 15.

24. Fragile X syndrome is caused by CGG repeat expansion (>200 repeats) in the *FMR1* gene’s 5’ UTR, leading to hypermethylation and gene silencing. Evaluate the molecular relationship between repeat expansion and hypermethylation: which comes first, what protein (MBNL1/DNMT3A) reads the repeat expansion, and why does the “premutation” (55–200 repeats) have a partially different phenotype (FXTAS) compared to full mutation?

Answer (Q24, Synthesis). In Fragile X, the CGG repeat expansion comes first: when the *FMR1* 5’ UTR repeat exceeds about 200 (full mutation), the expanded CGG tract is recognized and triggers de novo DNA methylation (via DNMT3A and silencing RNA/heterochromatin pathways) of the *FMR1* promoter CpG island, shutting off FMRP. The premutation (55–200 repeats) is not methylated and *FMR1* is still transcribed — even overexpressed — so the toxic phenotype (FXTAS, premature ovarian insufficiency) is an RNA gain-of-function from excess CGG-containing mRNA, distinct from the loss-of-function silencing in the full mutation. See section 15.

25. Critically evaluate the potential of epigenetic editing as a permanent therapeutic intervention. Specifically: if dCas9-DNMT3A is used to methylate and silence an oncogene, will the silencing persist through cell division (via DNMT1 maintenance methylation), and what are the risks of epigenetic drift or passenger methylation at off-target sites? Propose experimental criteria to determine whether a therapeutic epigenetic edit is “safe and durable.”

Answer (Q25, Synthesis). dCas9-DNMT3A-induced promoter methylation can persist through division because the symmetric CpG mark is copied each S phase by DNMT1/UHRF1 maintenance methylation, so silencing is heritable even after the editor is removed. Risks include epigenetic drift (gradual loss or spreading of methylation), reactivation, and passenger/off-target methylation at unintended loci with their own phenotypic consequences. Criteria for a safe, durable edit: stable target silencing and methylation over many passages and in vivo, genome-wide methylation profiling showing minimal off-target marks, no oncogene reactivation or growth advantage, and reversibility/controllability if adverse effects appear. See section 15.

26. The X-inactivation center (Xic) on the inactive X chromosome produces Xist lncRNA, which coats the inactive X in cis. Explain: (a) how Xist RNA spreads along the chromosome; (b) how it recruits PRC2 (H3K27me3) and PRC1 (H2AK119ub1) to compact the Xi; (c) why a small region (pseudo-autosomal

region, PAR) escapes X-inactivation.

Answer (Q26, Synthesis). (a) Xist is transcribed only from the future inactive X and spreads in cis along that chromosome by exploiting its 3D proximity, nucleating from the X-inactivation center. (b) Xist recruits SPEN/HDAC3 and Polycomb complexes so PRC2 deposits H3K27me3 and PRC1 deposits H2AK119ub1, with later DNA methylation, compacting the Xi into a heterochromatic Barr body. (c) Genes in the pseudoautosomal region escape inactivation because they have homologous active partners on the Y chromosome, so dosage must be maintained from both sex chromosomes. See section 15.

27. A researcher uses Cas9 fused to a DNMT3A (DNA methyltransferase) domain (dCas9-DNMT3A) to specifically methylate a target promoter. Predict: (a) the epigenetic effect at the target gene; (b) whether the silencing will be maintained through DNA replication (yes, DNMT1 maintenance methyltransferase copies the pattern); (c) how you would verify that methylation, not dCas9 binding alone, is responsible for silencing.

Answer (Q27, Synthesis). (a) dCas9-DNMT3A targeted to the promoter deposits CpG methylation, repressing the gene by blocking activators and recruiting methyl-readers. (b) Yes — once the symmetric CpG pattern is established, DNMT1 (with UHRF1) recognizes hemimethylated CpGs after replication and restores full methylation, so silencing is heritably maintained through cell division. (c) Verify methylation is causal by using a catalytically dead DNMT3A fusion as a control (binding without methylation should not silence) and by treating with a DNMT inhibitor or bisulfite-sequencing the locus to confirm methylation tracks with silencing. See section 15.

28. Transgenerational epigenetic inheritance refers to the transmission of epigenetic marks across generations without DNA sequence change. The agouti mouse model showed that maternal methyl-donor diet changes offspring coat color and obesity risk via CpG methylation of the Avy allele. What does this imply about the erasure of epigenetic marks between generations (which normally occurs in primordial germ cells)?

Answer (Q28, Synthesis). If diet-induced methylation of the Avy allele in one generation alters offspring coat color and metabolism, then the genome-wide epigenetic reprogramming that normally erases methylation in primordial germ cells (and again after fertilization) is incomplete at certain loci. Some sequences — including metastable epialleles and certain repeat/transposon-associated regions like Avy — escape full erasure, allowing parental environmental information to be transmitted, although such transgenerational inheritance is locus-specific and the magnitude of true germline transmission requires careful controls. See section 15.

29. Long non-coding RNAs (lncRNAs) number >100,000 in the human transcriptome but most have unknown functions. Evaluate the challenges of studying lncRNA function: (a) conservation is low across species (cannot use model organisms easily); (b) knockdown may affect the genomic region itself (enhancer function of the locus); (c) lncRNAs have complex secondary structure but no ORFs. Propose a systematic approach to determine function.

Answer (Q29, Synthesis). (a) Because lncRNA sequences evolve rapidly, simple cross-species conservation cannot identify functional ones and model organisms may lack orthologues. (b) Knockdown or deletion can perturb the act of transcription or an underlying enhancer/DNA element rather than the RNA product itself, confounding interpretation. (c) Lacking ORFs and conserved domains, function must be inferred from structure and interactions. A systematic approach: combine RNA-targeting knockdown (ASOs/CRISPRi versus locus deletion controls), rescue with exogenous transcript, map RNA–chromatin/protein interactions (CHART/ChIRP, RAP), and test specific structural motifs by targeted mutation. See section 15.

30. Chromatin accessibility (measured by ATAC-seq) is strongly correlated with gene expression. Explain: (a) how nucleosome positioning regulates transcription factor accessibility; (b) the role of pioneer transcription factors (e.g., FOXA1) in opening closed chromatin; (c) how ATAC-seq works mechanistically (Tn5 transposase cuts accessible DNA and adds sequencing adapters).

Answer (Q30, Synthesis). (a) Nucleosomes occlude DNA, so where they are positioned determines whether transcription-factor binding sites and promoters are accessible; nucleosome-depleted regions correlate with active regulatory elements. (b) Pioneer factors such as FOXA1 can engage their motifs within closed, nucleosomal chromatin and recruit remodellers to open it, licensing other factors to bind. (c) ATAC-seq uses hyperactive Tn5 transposase that preferentially inserts into open chromatin, simultaneously cutting accessible DNA and adding sequencing adapters, so read density reports genome-wide accessibility. See section 15.

Questions — Epigenetic Inheritance and Disease

Instructor Use and Coverage Notes

- Coverage target: Explain how 3D organization or inherited marks alter expression and disease risk.
- Model/data emphasis: Chromatin-loop, inheritance, and disease-risk reasoning.
- Assessment alignment: Concept Explanation, Questions and Methods, Argumentation.
- Misconception probe: A chromatin contact map is not proof of function without perturbation.
- Transfer product: Apply inheritance logic to cancer, developmental disorders, and environmental exposure.
- Grading focus: award full credit for mechanism, evidence, boundary conditions, and units when a calculation is required.
- Suggested use: draw one recall item, one application item, and one synthesis item when building a short quiz from this bank.

Questions 1–10: Recall and Comprehension

This activity accompanies section 16 of the textbook — review that chapter before attempting the exercises below.

1. The X-inactivation center (Xic) on the inactive X chromosome produces Xist lncRNA, which coats the inactive X in cis. Explain: (a) how Xist RNA spreads along the chromosome; (b) how it recruits PRC2 (H3K27me3) and PRC1 (H2AK119ub1) to compact the Xi; (c) why a small region (pseudo-autosomal region, PAR) escapes X-inactivation.

Answer (Q1, Recall). (a) Xist is transcribed only from the future inactive X and spreads in cis along that chromosome by exploiting its 3D proximity, nucleating from the X-inactivation center. (b) Xist recruits SPEN/HDAC3 and Polycomb complexes so PRC2 deposits H3K27me3 and PRC1 deposits H2AK119ub1, with later DNA methylation, compacting the Xi into a heterochromatic Barr body. (c) Genes in the pseudoautosomal region escape inactivation because they have homologous active partners on the Y chromosome, so dosage must be maintained from both sex chromosomes. See section 16.

2. A researcher uses Cas9 fused to a DNMT3A (DNA methyltransferase) domain (dCas9-DNMT3A) to specifically methylate a target promoter. Predict: (a) the epigenetic effect at the target gene; (b) whether the silencing will be maintained through DNA replication (yes, DNMT1 maintenance methyltransferase copies the pattern); (c) how you would verify that methylation, not dCas9 binding alone, is responsible for silencing.

Answer (Q2, Recall). (a) dCas9-DNMT3A targeted to the promoter deposits CpG methylation, repressing the gene by blocking activators and recruiting methyl-readers. (b) Yes — once the symmetric CpG pattern is established, DNMT1 (with UHRF1) recognizes hemimethylated CpGs after replication and restores full methylation, so silencing is heritably maintained through cell division. (c) Verify methylation is causal by using a catalytically dead DNMT3A fusion as a control (binding without methylation should not silence) and by treating with a DNMT inhibitor or bisulfite-sequencing the locus to confirm methylation tracks with silencing. See section 16.

3. Transgenerational epigenetic inheritance refers to the transmission of epigenetic marks across generations without DNA sequence change. The agouti mouse model showed that maternal methyl-donor diet changes offspring coat color and obesity risk via CpG methylation of the Avy allele. What does this imply about the erasure of epigenetic marks between generations (which normally occurs in primordial germ cells)?

Answer (Q3, Recall). If diet-induced methylation of the Avy allele in one generation alters offspring coat color and metabolism, then the genome-wide epigenetic reprogramming that normally erases methylation in primordial germ cells (and again after fertilization) is incomplete at certain loci. Some sequences — including metastable epialleles and certain repeat/transposon-associated regions like Avy — escape full erasure, allowing parental environmental information to be transmitted, although such transgenerational inheritance is locus-specific and the magnitude of true germline transmission requires careful controls. See section 16.

4. Long non-coding RNAs (lncRNAs) number >100,000 in the human transcriptome but most have unknown functions. Evaluate the challenges of studying lncRNA function: (a) conservation is low across species (cannot use model organisms easily); (b) knockdown may affect the genomic region itself (enhancer function of the locus); (c) lncRNAs have complex secondary structure but no ORFs. Propose a systematic approach to determine function.

Answer (Q4, Recall). (a) Because lncRNA sequences evolve rapidly, simple cross-species conservation cannot identify functional ones and model organisms may lack orthologues. (b) Knockdown or deletion can perturb the act of transcription or an underlying enhancer/DNA element rather than the RNA product itself, confounding interpretation. (c) Lacking ORFs and conserved domains, function must be inferred from structure and interactions. A systematic approach: combine RNA-targeting knockdown (ASOs/CRISPRi versus locus deletion controls), rescue with exogenous transcript, map RNA–chromatin/protein interactions (CHART/ChIRP, RAP), and test specific structural motifs by targeted mutation. See section 16.

5. Chromatin accessibility (measured by ATAC-seq) is strongly correlated with gene expression. Explain: (a) how nucleosome positioning regulates transcription factor accessibility; (b) the role of pioneer transcription factors (e.g., FOXA1) in opening closed chromatin; (c) how ATAC-seq works mechanistically (Tn5 transposase cuts accessible DNA and adds sequencing adapters).

Answer (Q5, Recall). (a) Nucleosomes occlude DNA, so where they are positioned determines whether transcription-factor binding sites and promoters are accessible; nucleosome-depleted regions correlate with active regulatory elements. (b) Pioneer factors such as FOXA1 can engage their motifs within closed, nucleosomal chromatin and recruit remodellers to open it, licensing other factors to bind. (c) ATAC-seq uses hyperactive Tn5 transposase that preferentially inserts into open chromatin, simultaneously cutting accessible DNA and adding sequencing adapters, so read density reports genome-wide accessibility. See section 16.

6. Evaluate the claim that cancer is largely an epigenetic disease. Cite evidence from: (a) global hypomethylation and CpG island hypermethylation in cancer; (b) frequent mutations in chromatin remodeling enzymes (ARID1A, SMARCA4, KMT2D) in cancer; (c) the success of HDAC inhibitors and DNMT inhibitors clinically. Under what conditions are purely epigenetic therapies (without targeted mutation correction) appropriate?

Answer (Q6, Recall). (a) Cancers show genome-wide hypomethylation (activating oncogenes/transposons) alongside focal CpG-island hypermethylation that silences tumor suppressors, an epigenetic phenotype. (b) Frequent loss-of-function mutations in chromatin regulators (ARID1A, SMARCA4, KMT2D) show the chromatin machinery is itself a driver. (c) Clinical efficacy of DNMT inhibitors (azacitidine) and HDAC inhibitors supports reversible epigenetic causation. The claim holds where epigenetic silencing is the dominant lesion (e.g., MDS, IDH-mutant gliomas) and a reactivatable gene exists; purely epigenetic therapy is inappropriate when fixed driver mutations or deletions, not silencing, sustain the tumor. See section 16.

7. Design a pharmaceutical strategy to reactivate a silenced tumor suppressor gene in a cancer with promoter hypermethylation. Compare DNMT inhibitors (5-azacitidine, broad demethylation), targeted dCas9-TET1 (site-specific demethylation), and HDAC inhibitors. What are the risks of broad epigenome reprogramming vs targeted approaches?

Answer (Q7, Recall). Hypothesis: re-expressing the silenced tumor suppressor restores growth control. Compare arms: a DNMT inhibitor (5-azacitidine) causes broad passive demethylation and reactivates many genes but risks global genome instability and off-target reactivation; dCas9-TET1 demethylates only the targeted promoter, giving specificity but limited efficiency and delivery challenges; HDAC inhibitors broadly reopen chromatin but are nonspecific and transient. Measure target re-expression, methylation, growth arrest, with vehicle and catalytically dead controls; the decision rule is restored expression and arrest specifically when the targeted mark is removed. Broad reprogramming risks awakening oncogenes and toxicity; targeted approaches trade efficiency for safety. See section 16.

8. Super-enhancers are clusters of enhancers (about 25–50 kb) bound by an unusually high density of transcription factors (BRD4, Mediator), associated with strong transcription of oncogenes (MYC, BCL2) in cancer. Evaluate the evidence for super-enhancer addiction in cancer cells, and explain why BET bromodomain inhibitors (JQ1) preferentially disengage from super-enhancers over typical enhancers.

Answer (Q8, Recall). Super-enhancers are dense clusters of enhancers occupied by high levels of BRD4, Mediator, and master transcription factors that drive very high expression of identity and oncogene loci (MYC, BCL2). Evidence for addiction: cancer cells are disproportionately dependent on these few super-enhancer-driven genes, so disrupting them collapses the oncogenic program. Because super-enhancers depend on cooperative, high-density BRD4/Mediator occupancy and phase-separated condensates, BET inhibitors such as JQ1 disengage BRD4 more steeply from super-enhancers than from typical enhancers — a small drop in occupancy disproportionately collapses the cooperative assembly, preferentially shutting off MYC. See section 16.

9. Evaluate the concept of “epigenetic clock” (Horvath clock): methylation of specific CpG sites in blood DNA correlates with biological age more accurately than chronological age. What do deviations from the epigenetic clock predict? Can lifestyle interventions (caloric restriction, exercise) reduce epigenetic age, and what experimental evidence supports this?

Answer (Q9, Recall). The Horvath epigenetic clock estimates biological age from methylation at a defined set of CpG sites (about 353), often more accurately tracking physiological aging than chronological age. Positive deviations (epigenetic age acceleration) predict elevated all-cause mortality and risk of age-related disease, while negative deviations associate with longevity. Some interventions (caloric restriction in animal models, exercise, and small human trials) modestly slow or reverse epigenetic age, but evidence is correlational and confounded by cell-type composition, so randomized longitudinal data with matched cell populations are needed before causal claims. See section 16.

10. 3D chromatin organization (TADs — topologically associating domains) is largely maintained by CTCF and cohesin. Evaluate what would happen to gene regulation if cohesin loading were abolished globally: (a) which enhancer-promoter pairs would become aberrantly activated; (b) what new gene expression states would emerge; (c) is this consistent with the observation that cohesin mutations cause Cornelia de Lange syndrome?

Answer (Q10, Recall). TAD boundaries are built by CTCF and cohesin through loop extrusion. (a) Abolishing cohesin loading would eliminate most loops/TADs, so enhancers could aberrantly contact promoters outside their normal domains, switching on genes that are normally insulated. (b) New, dysregulated expression states would emerge, generally with modest, widespread changes rather than wholesale reprogramming, since promoter-proximal control persists. (c) This is consistent with cohesin/NIPBL mutations causing Cornelia de Lange syndrome, a multisystem

developmental disorder, because partial loss of cohesin function subtly mis-wires enhancer–promoter contacts genome-wide during development. See section 16.

Questions 11–20: Application and Analysis

11. CRISPR interference (CRISPRi) uses dCas9-KRAB (a transcriptional repressor) to silence target genes without cutting DNA. Compare CRISPRi with ASO (antisense oligonucleotide) knockdown at the mRNA level and classical promoter deletion by CRISPR. What are the therapeutic advantages of CRISPRi (temporal control, reversibility, no off-target DSBs)?

Answer (Q11, Application). CRISPRi (dCas9-KRAB) recruits repressive chromatin machinery to a promoter to silence transcription without cutting DNA, acting at the chromatin/transcription level. ASO knockdown acts post-transcriptionally by triggering RNase H degradation of the mRNA, leaving the gene intact and requiring continuous dosing. Classical CRISPR promoter deletion permanently removes DNA via double-strand breaks. CRISPRi’s advantages are reversibility and tunable, inducible temporal control, multiplexing, and avoidance of off-target double-strand breaks and permanent genomic scars, making it safer and more flexible for functional and therapeutic silencing. See section 16.

12. Maternal nutrition during peri-conception affects offspring health across the life course (Barker/DOHaD hypothesis). Using three specific nutrients (folate, methionine, choline) and their roles in one-carbon metabolism → SAM production → methyltransferase substrate supply, evaluate the molecular mechanism by which poor maternal nutrition could cause persistent epigenetic changes in offspring that increase adult diabetes or cardiovascular disease risk.

Answer (Q12, Application). Folate, methionine, and choline feed one-carbon metabolism to regenerate S-adenosylmethionine (SAM), the universal methyl donor for DNMTs and histone methyltransferases. Poor maternal supply of these nutrients lowers SAM (and shifts the SAM:SAH ratio), reducing methyltransferase activity during the sensitive peri-conceptual window. This produces altered, persistent DNA-methylation patterns at metabolic gene promoters and imprinted loci in the offspring, which are maintained through development and program tissues toward impaired glucose handling and vascular dysfunction, raising adult diabetes and cardiovascular disease risk (the DOHaD/Barker mechanism). See section 16.

13. Evaluate the concept of “bivalent chromatin domains” in embryonic stem cells: developmental gene promoters carry both active (H3K4me3) and repressive (H3K27me3) marks simultaneously, maintaining them in a “poised” state. How does this enable rapid differentiation in either direction, and what happens to bivalent domains as cells commit to a specific lineage?

Answer (Q13, Application). Bivalent domains carry the activating H3K4me3 and repressive H3K27me3 marks together at developmental gene promoters in embryonic stem cells, holding genes transcriptionally poised — repressed but primed for rapid activation. On differentiation cues the domain resolves in a lineage-specific way: genes needed in that lineage lose H3K27me3 and become fully active (monovalent H3K4me3), while genes for alternative fates lose H3K4me3 and become stably repressed (monovalent H3K27me3). This allows fast, bidirectional commitment, and once a cell adopts a lineage the bivalent state is resolved into a single stable mark. See section 16.

14. Fragile X syndrome is caused by CGG repeat expansion (>200 repeats) in the *FMR1* gene’s 5’ UTR, leading to hypermethylation and gene silencing. Evaluate the molecular relationship between repeat expansion and hypermethylation: which comes first, what protein (MBNL1/DNMT3A) reads the repeat expansion, and why does the “premutation” (55–200 repeats) have a partially different phenotype (FXTAS) compared to full mutation?

Answer (Q14, Application). In Fragile X, the CGG repeat expansion comes first: when the *FMR1* 5’ UTR repeat exceeds about 200 (full mutation), the expanded CGG tract is recognized and triggers de novo DNA methylation (via DNMT3A and silencing RNA/heterochromatin pathways) of the *FMR1* promoter CpG island, shutting off FMRP. The premutation (55–200 repeats) is not methylated and *FMR1* is still transcribed — even overexpressed — so the toxic phenotype (FXTAS, premature ovarian insufficiency) is an RNA gain-of-function from excess CGG-containing mRNA, distinct from the loss-of-function silencing in the full mutation. See section 16.

15. Critically evaluate the potential of epigenetic editing as a permanent therapeutic intervention. Specifically: if dCas9-DNMT3A is used to methylate and silence an oncogene, will the silencing persist through cell division (via DNMT1 maintenance methylation), and what are the risks of epigenetic drift or passenger methylation at off-target sites? Propose experimental criteria to determine whether a therapeutic epigenetic edit is “safe and durable.”

Answer (Q15, Application). dCas9-DNMT3A-induced promoter methylation can persist through division because the symmetric CpG mark is copied each S phase by DNMT1/UHRF1 maintenance methylation, so silencing is heritable even after the editor is removed. Risks include epigenetic drift (gradual loss or spreading of methylation), reactivation, and passenger/off-target methylation at unintended loci with their own phenotypic consequences. Criteria for a safe, durable edit: stable target silencing and methylation over many passages and in vivo, genome-wide methylation profiling showing minimal off-target marks, no oncogene reactivation or growth advantage, and reversibility/controllability if adverse effects appear. See section 16.

16. Define epigenetics. Give two examples of epigenetic modifications.

- Answer (Q16, Application). Epigenetics is the study of heritable changes in gene expression that do not alter the underlying DNA sequence but instead change chromatin state and accessibility. Two examples are DNA methylation of cytosine at CpG dinucleotides (generally repressive at promoters) and covalent histone tail modifications such as acetylation (H3K27ac, activating) or methylation (H3K27me3, repressive). See section 16.
17. What is DNA methylation? Which nucleotide is typically methylated in mammals, and what effect does methylation at gene promoters generally have on transcription?

Answer (Q17, Application). DNA methylation is the covalent addition of a methyl group, catalyzed by DNA methyltransferases (DNMT1 maintenance; DNMT3A/3B de novo). In mammals it occurs almost exclusively on cytosine within 5'-CpG-3' dinucleotides. Methylation of a CpG island in a gene promoter generally represses transcription by blocking activator binding and recruiting methyl-binding repressors and HDACs, producing stable gene silencing. See section 16.

18. What is a histone? Name four types of histone modification and one enzyme family for each.

Answer (Q18, Application). A histone is a small basic protein (H2A, H2B, H3, H4) that packages DNA into nucleosomes. Four modification types and an enzyme family for each: acetylation (HATs/KATs add, HDACs remove), methylation (KMTs such as PRC2/EZH2 add, KDMs/demethylases remove), phosphorylation (kinases such as Aurora B), and ubiquitination (E3 ligases such as RING1B on H2AK119). See section 16.

19. What does H3K4me3 mark indicate? What about H3K27me3?

Answer (Q19, Application). H3K4me3 is an activating mark enriched at the promoters of actively transcribed genes, written by MLL/COMPASS and read by basal transcription machinery. H3K27me3 is a repressive mark deposited by Polycomb repressive complex 2 (EZH2) that silences developmental genes and is read by PRC1. Both are lysine methylation on H3, but their distinct positions and reader complexes give opposite functional outcomes. See section 16.

20. What is chromatin remodeling? Name one chromatin remodeling complex.

Answer (Q20, Application). Chromatin remodeling is the ATP-dependent repositioning, ejection, or restructuring of nucleosomes to change DNA accessibility for transcription factors and the replication/repair machinery. One example is the SWI/SNF (BAF) complex, which uses ATP hydrolysis to slide or evict nucleosomes; other families include ISWI, CHD/NuRD, and INO80. See section 16.

Questions 21–30: Synthesis and Evaluation

21. What is the lac operon? Which molecules control it?

Answer (Q21, Synthesis). The lac operon is a cluster of *E. coli* genes (*lacZ*, *lacY*, *lacA*) encoding enzymes for lactose uptake and metabolism, transcribed from a single promoter. It is controlled by negative regulation via the LacI repressor (released when allolactose, the inducer, binds it) and positive regulation via CAP–cAMP, which activates transcription when glucose is low. See section 16.

22. What is a repressor protein? What is an activator protein?

Answer (Q22, Synthesis). A repressor is a regulatory protein that binds DNA (typically an operator or silencer) and decreases transcription, for example by blocking RNA polymerase or recruiting repressive chromatin machinery. An activator binds DNA (an enhancer or CAP site) and increases transcription by recruiting or stabilizing RNA polymerase and coactivators, as CAP–cAMP does at the lac promoter. See section 16.

23. Define allosteric regulation in the context of transcription. Give an example.

Answer (Q23, Synthesis). Allosteric regulation is the modulation of a regulatory protein's DNA-binding activity by a small effector molecule binding at a separate site, changing the protein's conformation. In the lac operon, allolactose binds the LacI repressor and allosterically reduces its affinity for the operator, releasing it from DNA and allowing transcription; conversely, tryptophan acts as a corepressor that activates the trp repressor. See section 16.

24. What are non-coding RNAs? Name three biologically important types.

Answer (Q24, Synthesis). Non-coding RNAs are functional RNA transcripts that are not translated into protein but instead regulate gene expression and genome organization. Three important types are microRNAs (about 22 nt, guide RISC to repress target mRNAs), small interfering RNAs (siRNAs, drive sequence-specific mRNA cleavage in RNAi), and long non-coding RNAs (lncRNAs such as Xist, which scaffold chromatin-modifying complexes). See section 16.

25. What is genomic imprinting? Give one example of an imprinted gene.

Answer (Q25, Synthesis). Genomic imprinting is parent-of-origin-specific monoallelic expression, in which a gene is expressed only from the maternally or only from the paternally inherited allele, set by differential DNA methylation at imprinting control regions in the germline. An example is IGF2, expressed only from the paternal allele (the maternal allele is silenced via the CTCF-controlled IGF2/H19 ICR). See section 16.

26. A CpG island in the CDKN2A (p16) promoter is hypermethylated in a lung cancer cell. Trace the molecular consequences: (a) which protein is silenced; (b) what happens to CDK4/6 activity; (c) what happens to cell cycle progression; (d) why this is an alternative mechanism to p16 deletion for bypassing the G₁ checkpoint.

Answer (Q26, Synthesis). (a) Hypermethylation of the CDKN2A CpG island silences the p16^{INK4a} protein. (b) Without p16 to inhibit CDK4/6, Cyclin D–CDK4/6 remains active. (c) Active CDK4/6 hyperphosphorylates Rb, releasing E2F so the cell passes the G₁ restriction point and proliferates. (d) This epigenetic silencing is functionally equivalent to deleting or mutating p16 — it inactivates the gene without changing the DNA sequence, an alternative route to bypassing the G₁ checkpoint, and it is potentially reversible with demethylating agents. See section 16.

27. Polycomb repressive complex 2 (PRC2) trimethylates H3K27 and is overexpressed in many cancers. Explain: (a) the molecular mechanism of H3K27me₃-mediated gene silencing; (b) how PRC2 spreads repression across large chromosomal domains; (c) why EZH2 (the catalytic subunit of PRC2) is a therapeutic target (tazemetostat).

Answer (Q27, Synthesis). (a) PRC2 trimethylates H3K27 (H3K27me₃), which recruits PRC1 to ubiquitinate H2AK119 and compact chromatin, blocking transcription. (b) H3K27me₃ is itself read by the PRC2 EED subunit, creating positive feedback that spreads the mark in cis across broad domains. (c) Overactive or mutant EZH2 hyper-represses tumor-suppressor and differentiation genes, so the catalytic EZH2 subunit is druggable; tazemetostat is an FDA-approved EZH2 inhibitor that reactivates these genes. See section 16.

28. In the lac operon, explain the logic of dual control by the lac repressor AND catabolite activator protein (CAP). Under which combination of conditions is the operon most highly transcribed? Under which is it completely silent?

Answer (Q28, Synthesis). The lac repressor provides negative control (bound to the operator unless allolactose is present) and CAP–cAMP provides positive control (active only when glucose is low, raising cAMP). The operon is maximally transcribed when lactose is present AND glucose is absent: the repressor is released and CAP–cAMP activates the promoter. It is completely silent when lactose is absent, because the repressor stays bound regardless of glucose status. See section 16.

29. RNA interference (RNAi) via siRNA silences gene expression post-transcriptionally. Compare siRNA (perfectly complementary → mRNA cleavage by Ago2) vs miRNA (partially complementary → translational repression and mRNA destabilisation). How does each affect the steady-state abundance of target mRNA?

Answer (Q29, Synthesis). siRNAs are perfectly complementary to their targets and direct Ago2 to endonucleolytically cleave (slice) the mRNA, sharply lowering its steady-state abundance. miRNAs are only partially complementary (matching mainly through the seed region) and act mostly by repressing translation and promoting deadenylation/decay, causing a more modest reduction in mRNA levels and a larger drop in protein output. Both reduce target expression, but siRNA produces stronger, cleavage-based mRNA loss. See section 16.

30. Enhancers can activate promoters over distances of >1 Mb in the genome by chromatin looping mediated by cohesin and CTCF. Explain: (a) the role of CTCF as a chromatin barrier/insulator; (b) how loss of a CTCF binding site at the IGF2/H19 imprinting control region (ICR) causes Beckwith-Wiedemann syndrome; (c) how 4C and HiC experiments confirm enhancer-promoter looping.

Answer (Q30, Synthesis). (a) CTCF binds insulator sequences and, with cohesin, organizes chromatin loops/TAD boundaries that block enhancers from acting across them. (b) At the IGF2/H19 ICR the maternal allele is unmethylated, so CTCF binds and insulates IGF2 from the downstream enhancers; loss of that CTCF site (or its methylation) lets the enhancer loop to IGF2, causing biallelic IGF2 expression and overgrowth (Beckwith-Wiedemann syndrome). (c) Chromosome-conformation methods such as 4C and Hi-C detect ligated DNA contacts, directly demonstrating physical enhancer–promoter looping. See section 16.

Questions — Mendelian Principles and Probability

Instructor Use and Coverage Notes

- Coverage target: Compute a genetic probability or chi-square result and explain the biological assumption.
- Model/data emphasis: Punnett, binomial, and chi-square calculations.
- Assessment alignment: Statistical Tests and Data Analysis, Representing and Describing Data.
- Misconception probe: Dominant does not mean common, stronger, or better.
- Transfer product: Transfer Mendelian probability to model organisms and introductory human genetics.
- Grading focus: award full credit for mechanism, evidence, boundary conditions, and units when a calculation is required.
- Suggested use: draw one recall item, one application item, and one synthesis item when building a short quiz from this bank.

Questions 1–10: Recall and Comprehension

This activity accompanies section 17 of the textbook — review that chapter before attempting the exercises below.

1. State Mendel’s two laws. Give the biological basis for each in terms of meiosis.

Answer (Q1, Recall). Law of segregation: the two alleles of a gene separate during gamete formation so each gamete carries only one allele; mechanistically this is the separation of homologous chromosomes (and their alleles) at meiosis I anaphase. Law of independent assortment: alleles of different genes segregate independently, because non-homologous chromosome pairs orient randomly at the metaphase I plate. Independent assortment holds only for genes on different chromosomes (or far apart on the same one). See section 17.

2. Define allele, locus, genotype, and phenotype.

Answer (Q2, Recall). An allele is one of the alternative DNA sequence variants of a gene. A locus is the fixed physical position of that gene on a chromosome. A genotype is the pair of alleles an individual carries at a locus (e.g. Aa), while the phenotype is the observable trait that genotype produces in a given environment. See section 17.

3. What is a Punnett square? Draw and solve: $Aa \times Aa$.

Answer (Q3, Recall). A Punnett square is a table that lists the possible gametes from each parent and combines them to predict offspring genotypes under Mendelian segregation. For $Aa \times Aa$, each parent produces gametes A and a . The four equally likely cells are AA , Aa , Aa , and aa , giving a genotype ratio of $1\ AA : 2\ Aa : 1\ aa$. With complete dominance, the phenotype ratio is 3 dominant : 1 recessive. This prediction assumes independent gamete formation, equal fertilization probability, and no viability difference among the genotypes; see section 17.

4. What are the expected phenotype ratios for a monohybrid cross between two heterozygotes?

Answer (Q4, Recall). A monohybrid cross between two heterozygotes ($Aa \times Aa$) yields a 3:1 phenotype ratio (3 dominant : 1 recessive) and a 1:2:1 genotype ratio ($1\ AA : 2\ Aa : 1\ aa$). This assumes complete dominance and that every genotype reliably expresses its expected phenotype. See section 17.

5. What are the expected phenotype ratios for a dihybrid cross between two double heterozygotes?

Answer (Q5, Recall). A dihybrid cross between two double heterozygotes ($AaBb \times AaBb$) yields the classic 9:3:3:1 phenotype ratio — $9\ A_B_ : 3\ A_bb : 3\ aaB_ : 1\ aabb$. This is the product of two independent 3:1 monohybrid ratios and requires the two genes to assort independently and act independently on the phenotype. See section 17.

6. Define codominance. Give the human blood type system as an example.

Answer (Q6, Recall). Codominance is an allelic relationship in which both alleles in a heterozygote are fully and simultaneously expressed, so neither masks the other. The human ABO system illustrates this: an $I^A I^B$ individual is blood type AB, expressing both the A and B surface antigens, rather than an intermediate or single antigen. See section 17.

7. What is incomplete dominance? Give one example and show the F_1 and F_2 ratios.

Answer (Q7, Recall). Incomplete dominance occurs when the heterozygote shows an intermediate phenotype because one functional allele produces insufficient product for the full dominant effect. In snapdragons, red ($C^R C^R$) \times white ($C^W C^W$) gives an all-pink F_1 ($C^R C^W$); selfing the F_1 gives an F_2 of 1 red : 2 pink : 1 white — the genotype ratio is visible directly because each genotype has its own phenotype. See section 17.

8. What is a testcross? For what is it used?

Answer (Q8, Recall). A testcross mates an individual showing the dominant phenotype to a homozygous recessive individual ($A? \times aa$). It reveals the unknown genotype: an all-dominant offspring set indicates AA , whereas a roughly 1:1 dominant:recessive split indicates Aa . See section 17.

9. What is epistasis? Give one example where two loci interact to modify phenotype.

Answer (Q9, Recall). Epistasis is a gene interaction in which the genotype at one locus masks or modifies the phenotypic expression of a second, independent locus. In Labrador retrievers, ee at the extension locus is recessive epistatic to the B (black/chocolate) locus: any ee dog is yellow regardless of its B genotype, collapsing the dihybrid F_2 to 9 black : 3 chocolate : 4 yellow. See section 17.

10. What is pleiotropy? Give one example of a single gene that affects multiple traits.

Answer (Q10, Recall). Pleiotropy is the phenomenon in which a single gene affects multiple, seemingly unrelated phenotypic traits. Sick-cell disease (a single β -globin mutation) is a classic example: it causes anemia, pain crises, organ damage, splenic dysfunction, and stroke risk, while also conferring malaria resistance in heterozygotes. See section 17.

Questions 11–20: Application and Analysis

11. A black cat (BB) is crossed with a white cat (bb). What is the F_1 phenotype? What is the F_2 ratio if F_1 cats are interbred? If black is incompletely dominant, what is the F_1 phenotype?

Answer (Q11, Application). With complete dominance, $BB \times bb$ gives an all-black F_1 (Bb). Interbreeding the F_1 ($Bb \times Bb$) gives an F_2 of 3 black : 1 white. If black is instead *incompletely* dominant, the F_1 heterozygotes (Bb) show an intermediate (gray) phenotype, and the F_2 would be 1 black : 2 gray : 1 white. See section 17.

12. A chi-square analysis of 580 pea seeds (450 round:130 wrinkled) gives $\chi^2 = 2.6$ (critical value 3.84, $p = 0.05$). Should the null hypothesis of 3:1 ratio be rejected? What does this conclusion mean biologically?

Answer (Q12, Application). $\chi^2_{\text{calc}} = 2.6 < \chi^2_{\text{crit}} = 3.84$ ($df = 1$, $\alpha = 0.05$), so we fail to reject the null hypothesis: the observed 450:130 split is statistically consistent with the expected 3:1 ratio (expected 435 round : 145 wrinkled). Biologically, this supports single-gene Mendelian inheritance with complete dominance; the deviation is attributable to chance sampling, not a different genetic mechanism. The test never *proves* 3:1 — it only fails to reject it. See section 17.

13. Two true-breeding strains of wheat produce red and white kernels. The cross produces medium-red F_1 , and F_2 shows a continuous range of colors with frequencies approximately 1:4:6:4:1. This is consistent with two genes each contributing an additive unit of color. What mode of inheritance does this illustrate?

Answer (Q13, Application). This is polygenic (quantitative) inheritance with additive alleles. Two genes each contributing one additive unit of pigment produce 5 phenotypic classes in F_2 with frequencies 1:4:6:4:1 (the binomial expansion of dose 0–4 across 4 alleles), with the medium-red F_1 intermediate between the parental extremes. Environmental variation further blurs the classes into a continuous distribution. See section 17.

14. A woman is phenotypically normal but her father had phenylketonuria (PKU, autosomal recessive). What is the probability that she is a carrier? If she marries a known carrier, what is the probability their first child will have PKU?

Answer (Q14, Application). Her father is aa , so the woman necessarily inherited one a allele; being unaffected she is Aa — she is a carrier with probability 1 (= 100%). Crossed with a known carrier ($Aa \times Aa$), each child has a $\frac{1}{4}$ probability of PKU (aa). Combined chance the first child is affected = $1 \times \frac{1}{4} = \frac{1}{4}$. See section 17.

15. In coat color genetics of Labrador retrievers: B is dominant for black pigment; b is recessive (brown/chocolate). E is dominant for coat expression; ee gives yellow regardless of B/b. Set up the dihybrid cross $BbEe \times BbEe$ and calculate the expected ratio of black:chocolate:yellow.

Answer (Q15, Application). $BbEe \times BbEe$ gives the standard 9 $B_E_$: 3 B_ee : 3 $bbE_$: 1 $bbee$. Because ee is epistatic (yellow regardless of B), the two ee classes merge: 9 $B_E_$ = black, 3 $bbE_$ = chocolate, and 3 B_ee + 1 $bbee$ = 4 yellow. Expected ratio = 9 black : 3 chocolate : 4 yellow. See section 17.

16. Evaluate the concept of “genetic heterogeneity”: the same phenotype (e.g., congenital deafness) can result from mutations in any of >100 different genes, each segregating in different families. How does genetic heterogeneity complicate: (a) pedigree analysis; (b) population frequency estimates; (c) the development of a comprehensive gene therapy?

Answer (Q16, Application). Genetic heterogeneity means one phenotype maps to many independent loci. (a) Pedigree analysis: different families may show different inheritance modes (AD, AR, X-linked, mitochondrial), so pooling pedigrees obscures the pattern and a single family’s mode

cannot generalize. (b) Population frequency: the overall trait frequency is the sum over many rare loci, so a single allele-frequency or Hardy–Weinberg estimate is invalid; per-locus data are required. (c) Gene therapy: no single corrective construct works for all patients — therapy must be allele/gene-specific, raising cost and complexity. The decisive test is locus mapping/sequencing per family. See section 17.

17. Design a genetic screen in *C. elegans* to identify most genes involved in a specific pathway (e.g., vulva development). Describe the EMS (ethyl methanesulfonate) mutagenesis strategy, the phenotypic screen, and how you would determine whether two mutations affect the same gene (complementation test) or the same pathway (epistasis test).

Answer (Q17, Application). Hypothesis: specific genes are required for vulval development. Mutagenesis: treat worms with EMS to induce random point mutations; screen F_2 for the vulvaless or multivulva phenotype (with isogenic untreated controls). Same gene vs. same pathway: a complementation test crosses two recessive mutants — mutant F_1 = allelic (same gene), wild-type F_1 = different genes. An epistasis test then orders genes in a pathway: in a double mutant, the phenotype of the downstream/epistatic gene prevails, revealing pathway order. Replication across independent alleles and a defined scoring rule guard against false positives. See section 17.

18. Quantitative traits (height, intelligence, blood pressure) are determined by many genes plus environment. Evaluate the methodology of heritability estimation from twin studies: what does $h^2 = 0.8$ actually mean, and why does high heritability NOT mean that environmental interventions are ineffective? Use PKU as a concrete counter-example.

Answer (Q18, Application). $h^2 = 0.8$ means 80% of the *phenotypic variance in that population, in its current environments* is attributable to genetic variance — it is a population-and-environment-specific variance ratio, not a statement about any individual or about modifiability. High heritability does not imply environmental interventions fail, because heritability only partitions the variance present, not the trait’s response to a *new* environment. PKU is the counter-example: it is highly heritable (single-gene), yet a low-phenylalanine diet — an environmental change outside the studied range — almost entirely prevents the intellectual disability. See section 17.

19. Evaluate Mendel’s choice of pea traits: several of the seven traits happened to be either not linked or on different chromosomes. If two of Mendel’s traits had been tightly linked (say, flower color and pod color on the same chromosome), how would the F_2 data have deviated from the 9:3:3:1 ratio, and would Mendel still have discovered independent assortment?

Answer (Q19, Application). If two traits were tightly linked, their alleles would not assort independently: parental allele combinations would be over-represented and recombinant types rare, so the F_2 would deviate sharply from 9:3:3:1 toward an excess of parental phenotypes (the deviation scaling with map distance / recombination frequency). Mendel could still have discovered segregation and independent assortment from his *other* unlinked traits, but the linked pair alone would have masked independent assortment — historically fortunate that his seven analyzed traits behaved independently. See section 17.

20. Inbreeding increases homozygosity and can reveal recessive deleterious alleles. Calculate the inbreeding coefficient (F) for offspring of a first-cousin mating, and predict the increase in: (a) homozygosity for a rare allele ($q = 0.01$); (b) probability of autosomal recessive disease compared to random mating. Why do many societies have legal or cultural prohibitions against close-relative marriages?

Answer (Q20, Application). For first cousins, the inbreeding coefficient is $F = 1/16 = 0.0625$. (a) The probability of homozygosity for a rare allele rises to approximately $q^2 + F \cdot q(1-q)$; for $q = 0.01$ this is $\approx 0.0001 + 0.0625 \cdot (0.0099) \approx 0.00072$, roughly 7× the random-mating value of $q^2 = 0.0001$. (b) Autosomal-recessive disease risk is likewise inflated by the $F \cdot q(1-q)$ term, the relative increase being largest for the rarest alleles. Societies restrict close-kin marriage chiefly because this elevated homozygosity sharply raises the burden of recessive disease in offspring. See section 17.

Questions 21–30: Synthesis and Evaluation

21. Anticipation (increasing severity across generations) occurs in trinucleotide repeat disorders (Huntington’s disease, myotonic dystrophy). Explain the molecular mechanism by which repeats expand between generations (slippage during DNA replication) and why larger repeats cause earlier onset and greater severity. Why is repeat expansion more common through the paternal germline in HD but the maternal germline in DM1?

Answer (Q21, Synthesis). Trinucleotide repeats (e.g. CAG in *HTT*, CTG in *DMPK*) expand through replication/repair slippage: the nascent strand mispairs on the repetitive template, forming hairpin loops that add repeat units, and longer tracts are more unstable, so they tend to grow each generation (anticipation). Larger repeats produce more toxic gene product (or RNA) earlier, giving earlier onset and greater severity. Expansion bias is germline-specific: large CAG expansions are favored in spermatogenesis (paternal bias in Huntington’s), whereas the CTG repeat expands preferentially in the maternal germline in myotonic dystrophy type 1, reflecting differences in replication/repair dynamics in the two gametogenic lineages. See section 17.

22. Evaluate the concept of “genomic imprinting conflict” (kinship theory): paternally imprinted genes (expressed primarily from paternal allele) are generally growth-promoting (*IGF2*), while maternally imprinted genes (expressed primarily from maternal allele) are generally growth-restraining (*H19*). Evaluate

the evolutionary logic that predicts this based on parent-offspring conflict theory. What happens when this balance is disrupted (Silver-Russell syndrome vs Beckwith-Wiedemann syndrome)?

Answer (Q22, Synthesis). Kinship (parent-of-origin conflict) theory predicts that paternally expressed genes favor extracting more maternal resources for the offspring (growth-promoting, e.g. *IGF2*), while maternally expressed genes restrain offspring demand to conserve resources for the mother's other (possibly different-father) offspring (growth-restraining, e.g. *H19*) — the asymmetry arises only when females mate with multiple males. Disrupting the balance shifts growth: loss of paternal *IGF2* expression underlies the growth-restricted Silver–Russell syndrome, whereas excess *IGF2* / loss of maternal restraint underlies the overgrowth Beckwith–Wiedemann syndrome. The theory is testable via the predicted directionality of imprinted-gene effects on growth. See section 17.

23. Multifactorial diseases (Type 1 Diabetes, schizophrenia) have both genetic and environmental contributions. Evaluate the strengths and limitations of GWAS and polygenic risk scores: (a) minimum detectable effect size at genome-wide significance ($p < 5 \times 10^{-8}$); (b) the “missing heritability” problem; (c) why PRS transferability across ancestries is a scientific and equity concern; (d) what consent and privacy information belongs in a clinical PRS report.

Answer (Q23, Synthesis). (a) GWAS detects variants whose effect is large enough that, given allele frequency and sample size, association reaches $p < 5 \times 10^{-8}$; common variants of small effect need very large cohorts and rare large-effect variants are missed. (b) The missing heritability problem: significant common variants typically explain a modest fraction of trait heritability, far below twin-study estimates, due to many sub-threshold variants, rare variants, gene–gene/gene–environment effects, and inflated twin estimates. (c) A PRS trained mainly in one ancestry can lose calibration and discrimination in another because linkage disequilibrium, allele frequency, environment, and health-system context differ; deployment without validation can therefore worsen health disparities. (d) A clinical report should state the discovery cohort, target population, calibration method, confidence interval, action threshold, data-retention plan, secondary-use policy, reidentification risk, and family implications. See section 17.

24. Phenocopies are environmentally caused conditions that resemble genetic conditions. Thalidomide-induced limb malformations in 1950s–60s phenocopied the autosomal recessive condition phocomelia. Evaluate: (a) how phenocopies complicate pedigree analysis; (b) how you would distinguish a phenocopy from a genetic condition in a clinical or research context; (c) the ethical implications of confusing genetic and environmental causation for public health policy.

Answer (Q24, Synthesis). A phenocopy is an environmentally induced phenotype mimicking a genetic disorder. (a) It complicates pedigrees by appearing as sporadic or non-Mendelian cases (no consistent transmission, possible shared environmental exposure rather than shared genotype). (b) Distinguish it by molecular testing (absence of the causative mutation), a documented environmental exposure (e.g. thalidomide timing), discordance in monozygotic twins, and lack of recurrence risk consistent with Mendelian ratios. (c) Misattributing an environmental cause to genetics — or vice versa — misdirects public-health policy: it can stigmatize families, divert resources from removing a preventable exposure, and delay protective regulation. See section 17.

25. Critically evaluate Mendel’s pea experiments, considering: (a) sample sizes (he used thousands of plants, giving high statistical power); (b) evidence that Mendel may have “improved” his data (Weldon’s 1902 re-analysis and Ronald Fisher’s 1936 statistical critique suggesting perfect ratios are too good to be true); (c) whether Mendel’s results are reproducible, and what this debate reveals about the role of confirmation bias in science.

Answer (Q25, Synthesis). (a) Mendel’s large samples (thousands of plants) gave high statistical power, making his ratios reliable estimates. (b) Fisher’s 1936 analysis (anticipated by Weldon, 1902) showed the aggregate fit to expected ratios is *too good* — the pooled χ^2 is improbably small — suggesting unconscious bias in classification or selective reporting, though no fraud is established. (c) Mendel’s core conclusions are robustly reproducible in modern crosses, so the laws stand; the debate illustrates that even correct conclusions can be reached via data that show confirmation bias, underscoring the need for pre-specified analysis and blinded scoring rather than discarding the findings. See section 17.

26. ABO blood type shows codominance (A and B antigens) and simple recessive (O, no antigen). A man of unknown blood type has a type O child with a type A woman (confirmed genotype $I^A i$). What is the man’s blood type? What are most possible blood types of this union’s children?

Answer (Q26, Synthesis). The type O child is ii , so it received an i from each parent. The type A mother is $I^A i$, contributing i ; the father must therefore also carry an i allele and be capable of producing a type O child — his blood type can be A ($I^A i$), B ($I^B i$), or O (ii), but not AB. For an $I^A i \times i i$ (e.g. type O father) union, children are $\frac{1}{2}$ type A ($I^A i$) : $\frac{1}{2}$ type O (ii); the full set across his possible genotypes is type A, B, AB, or O depending on his second allele. See section 17.

27. Maternal effect genes in *Drosophila* (e.g., *bicoid*) determine the embryo’s polarity based on the maternal genotype, not the embryo’s genotype. Explain how this violates the simple Mendelian expectation that offspring phenotype reflects offspring genotype. What does this tell us about developmental genetics?

Answer (Q27, Synthesis). With maternal-effect genes such as *bicoid*, the mother’s genotype, acting through mRNA/protein she deposits in the oocyte, fixes the embryo’s phenotype regardless of the embryo’s own genotype — so a genotypically mutant embryo from a heterozygous mother develops normally, and phenotypes lag one generation behind genotypes. This violates the Mendelian expectation that an offspring’s phenotype reflects its

- own genotype, and shows that early development is governed by maternally supplied cytoplasmic determinants, not just zygotic transcription. See section 17.
28. Haemophilia A is X-linked recessive. A carrier woman ($X^H X^h$) has children with a normal man ($X^H Y$). What are the expected phenotype ratios for daughters? For sons? What is the probability that the first four children include at least two affected sons (use binomial distribution)?
- Answer (Q28, Synthesis). Punnett square for $X^H X^h \times X^H Y$: gametes from mother $\{X^H, X^h\}$, from father $\{X^H, Y\}$. Offspring: $X^H X^H$, $X^H X^h$, $X^H Y$, $X^h Y$ — each with prob $1/4$. Daughters (inherit paternal X^H): $1/2$ homozygous unaffected ($X^H X^H$), $1/2$ carrier ($X^H X^h$); phenotype ratio $1:0$ (all phenotypically normal, since daughters always receive X^H from father). Sons (inherit paternal Y , maternal X): $1/2$ unaffected ($X^H Y$), $1/2$ affected ($X^h Y$); phenotype ratio $1:1$. Binomial probability of ≥ 2 affected sons among first 4 children: this conflates two coin flips per child — $P(\text{son}) = 1/2$ and $P(\text{affected} \mid \text{son}) = 1/2$, so $P(\text{affected son per child}) = p = 1/4$. With $n = 4$, $k \geq 2$: $P(k = 0) = \binom{4}{0}(0.25)^0(0.75)^4 = 0.3164$; $P(k = 1) = \binom{4}{1}(0.25)^1(0.75)^3 = 0.4219$; therefore $P(k \geq 2) = 1 - 0.3164 - 0.4219 = 0.2617 \approx 26\%$. Genetic counselling implication: about 1 in 4 such pedigrees will present with 2+ affected boys in the first 4 children — a common source of “unlucky” kindreds in pedigree analysis and a reason recurrence-risk counselling uses binomials, not single-child probabilities. See section 17.
29. Set up and interpret the F_2 results of a dihybrid cross ($AaBb \times AaBb$) if the two genes show complementary epistasis ($A-B-$ = one phenotype; $A-bb$, $aaB-$, $aabb$ = albino). What is the expected ratio? What does this imply about the biochemical pathway?
- Answer (Q29, Synthesis). $AaBb \times AaBb$ gives $9 A_B_ : 3 A_bb : 3 aaB_ : 1 aabb$. With complementary (duplicate-recessive) epistasis, only $A_B_$ shows the pigmented phenotype; the other three classes are albino, giving a $9:7$ ratio (9 colored : 7 albino). This implies both gene products are required, non-redundant enzymes in the same linear biosynthetic pathway — a block at either step (aa or bb) halts product formation. See section 17.
30. Three pea plants of unknown genotype most produce round seeds. Two plants crossed to a wrinkled plant (rr) produce: plant A = most round; plant B = 50% round:50% wrinkled; plant C = 75% round:25% wrinkled. Determine the genotype of each plant and explain the crosses.
- Answer (Q30, Synthesis). Each plant is testcrossed to rr . Plant A = all round \rightarrow no wrinkled offspring \rightarrow homozygous RR . Plant B = 1:1 round:wrinkled \rightarrow segregation expected from $Rr \times rr \rightarrow Rr$. Plant C = 3:1 (75% round) \rightarrow this ratio cannot come from a single testcross to rr unless C is Rr selfed/crossed to another Rr ; given a true testcross the 3:1 indicates additional round parents — most parsimoniously C is Rr with the 3:1 reflecting an $Rr \times Rr$ component. The informative testcross diagnostics are A = RR (no recessives) and B = Rr (1:1). See section 17.

Questions — Mendelian Extensions and Human Genetics

Instructor Use and Coverage Notes

- Coverage target: Use pedigree or extension evidence to justify an inheritance diagnosis.
- Model/data emphasis: Pedigree, epistasis, and multi-locus probability calculations.
- Assessment alignment: Statistical Tests and Data Analysis, Representing and Describing Data.
- Misconception probe: A single-gene model is a starting hypothesis, not the default for every trait.
- Transfer product: Transfer extension reasoning to counseling, GWAS interpretation, and breeding.
- Grading focus: award full credit for mechanism, evidence, boundary conditions, and units when a calculation is required.
- Suggested use: draw one recall item, one application item, and one synthesis item when building a short quiz from this bank.

Questions 1–10: Recall and Comprehension

This activity accompanies section 18 of the textbook — review that chapter before attempting the exercises below.

1. ABO blood type shows codominance (A and B antigens) and simple recessive (O, no antigen). A man of unknown blood type has a type O child with a type A woman (confirmed genotype IA*i*). What is the man’s blood type? What are most possible blood types of this union’s children?

Answer (Q1, Recall). The type O child is *ii*, so it received an *i* from each parent. The type A mother is I^A*i*, contributing *i*; the father must therefore also carry an *i* allele and be capable of producing a type O child — his blood type can be A (I^A*i*), B (I^B*i*), or O (*ii*), but not AB. For an I^A*i* × *i* *i* (e.g. type O father) union, children are ½ type A (I^A*i*) : ½ type O (*ii*); the full set across his possible genotypes is type A, B, AB, or O depending on his second allele. See section 18.

2. Maternal effect genes in *Drosophila* (e.g., *bicoid*) determine the embryo’s polarity based on the maternal genotype, not the embryo’s genotype. Explain how this violates the simple Mendelian expectation that offspring phenotype reflects offspring genotype. What does this tell us about developmental genetics?

Answer (Q2, Recall). With maternal-effect genes such as *bicoid*, the mother’s genotype, acting through mRNA/protein she deposits in the oocyte, fixes the embryo’s phenotype regardless of the embryo’s own genotype — so a genotypically mutant embryo from a heterozygous mother develops normally, and phenotypes lag one generation behind genotypes. This violates the Mendelian expectation that an offspring’s phenotype reflects its own genotype, and shows that early development is governed by maternally supplied cytoplasmic determinants, not just zygotic transcription. See section 18.

3. Haemophilia A is X-linked recessive. A carrier woman (X^HX^h) has children with a normal man (X^HY). What are the expected phenotype ratios for daughters? For sons? What is the probability that the first four children include at least two affected sons (use binomial distribution)?

Answer (Q3, Recall). Punnett square for X^HX^h × X^HY: gametes from mother {X^H, X^h}, from father {X^H, Y}. Offspring: X^HX^H, X^HX^h, X^HY, X^hY — each with prob 1/4. Daughters (inherit paternal X^H): 1/2 homozygous unaffected (X^HX^H), 1/2 carrier (X^HX^h); phenotype ratio 1:0 (all phenotypically normal, since daughters always receive X^H from father). Sons (inherit paternal Y, maternal X): 1/2 unaffected (X^HY), 1/2 affected (X^hY); phenotype ratio 1:1. Binomial probability of ≥ 2 affected sons among first 4 children: this conflates two coin flips per child — P(son) = 1/2 and P(affected | son) = 1/2, so P(affected son per child) = *p* = 1/4. With *n* = 4, *k* ≥ 2: $P(k = 0) = \binom{4}{0}(0.25)^0(0.75)^4 = 0.3164$; $P(k = 1) = \binom{4}{1}(0.25)^1(0.75)^3 = 0.4219$; therefore $P(k \geq 2) = 1 - 0.3164 - 0.4219 = 0.2617 \approx 26\%$. Genetic counselling implication: about 1 in 4 such pedigrees will present with 2+ affected boys in the first 4 children — a common source of “unlucky” kindreds in pedigree analysis and a reason recurrence-risk counselling uses binomials, not single-child probabilities. See section 18.

4. Set up and interpret the F₂ results of a dihybrid cross (AaBb × AaBb) if the two genes show complementary epistasis (A-B- = one phenotype; A-bb, aaB-, aabb = albino). What is the expected ratio? What does this imply about the biochemical pathway?

Answer (Q4, Recall). *AaBb* × *AaBb* gives 9 A_B_ : 3 A_bb : 3 aaB_ : 1 aabb. With complementary (duplicate-recessive) epistasis, only A_B_ shows the pigmented phenotype; the other three classes are albino, giving a 9:7 ratio (9 colored : 7 albino). This implies both gene products are required, non-redundant enzymes in the same linear biosynthetic pathway — a block at either step (*aa* or *bb*) halts product formation. See section 18.

5. Three pea plants of unknown genotype most produce round seeds. Two plants crossed to a wrinkled plant (*rr*) produce: plant A = most round; plant B = 50% round:50% wrinkled; plant C = 75% round:25% wrinkled. Determine the genotype of each plant and explain the crosses.

Answer (Q5, Recall). Each plant is testcrossed to *rr*. Plant A = all round → no wrinkled offspring → homozygous RR. Plant B = 1:1 round:wrinkled → segregation expected from R*r* × *rr* → R*r*. Plant C = 3:1 (75% round) → this ratio cannot come from a single testcross to *rr* unless C is R*r* selfed/crossed to another R*r*; given a true testcross the 3:1 indicates additional round parents — most parsimoniously C is R*r* with the 3:1 reflecting an R*r* × R*r* component. The informative testcross diagnostics are A = RR (no recessives) and B = R*r* (1:1). See section 18.

- Evaluate the concept of “genetic heterogeneity”: the same phenotype (e.g., congenital deafness) can result from mutations in any of >100 different genes, each segregating in different families. How does genetic heterogeneity complicate: (a) pedigree analysis; (b) population frequency estimates; (c) the development of a comprehensive gene therapy?

Answer (Q6, Recall). Genetic heterogeneity means one phenotype maps to many independent loci. (a) Pedigree analysis: different families may show different inheritance modes (AD, AR, X-linked, mitochondrial), so pooling pedigrees obscures the pattern and a single family’s mode cannot generalize. (b) Population frequency: the overall trait frequency is the sum over many rare loci, so a single allele-frequency or Hardy–Weinberg estimate is invalid; per-locus data are required. (c) Gene therapy: no single corrective construct works for all patients — therapy must be allele/gene-specific, raising cost and complexity. The decisive test is locus mapping/sequencing per family. See section 18.

- Design a genetic screen in *C. elegans* to identify most genes involved in a specific pathway (e.g., vulva development). Describe the EMS (ethyl methanesulfonate) mutagenesis strategy, the phenotypic screen, and how you would determine whether two mutations affect the same gene (complementation test) or the same pathway (epistasis test).

Answer (Q7, Recall). Hypothesis: specific genes are required for vulval development. Mutagenesis: treat worms with EMS to induce random point mutations; screen F₂ for the vulvaless or multivulva phenotype (with isogenic untreated controls). Same gene vs. same pathway: a complementation test crosses two recessive mutants — mutant F₁ = allelic (same gene), wild-type F₁ = different genes. An epistasis test then orders genes in a pathway: in a double mutant, the phenotype of the downstream/epistatic gene prevails, revealing pathway order. Replication across independent alleles and a defined scoring rule guard against false positives. See section 18.

- Quantitative traits (height, intelligence, blood pressure) are determined by many genes plus environment. Evaluate the methodology of heritability estimation from twin studies: what does $h^2 = 0.8$ actually mean, and why does high heritability NOT mean that environmental interventions are ineffective? Use PKU as a concrete counter-example.

Answer (Q8, Recall). $h^2 = 0.8$ means 80% of the *phenotypic variance in that population, in its current environments* is attributable to genetic variance — it is a population-and-environment-specific variance ratio, not a statement about any individual or about modifiability. High heritability does not imply environmental interventions fail, because heritability only partitions the variance present, not the trait’s response to a *new* environment. PKU is the counter-example: it is highly heritable (single-gene), yet a low-phenylalanine diet — an environmental change outside the studied range — almost entirely prevents the intellectual disability. See section 18.

- Evaluate Mendel’s choice of pea traits: several of the seven traits happened to be either not linked or on different chromosomes. If two of Mendel’s traits had been tightly linked (say, flower color and pod color on the same chromosome), how would the F₂ data have deviated from the 9:3:3:1 ratio, and would Mendel still have discovered independent assortment?

Answer (Q9, Recall). If two traits were tightly linked, their alleles would not assort independently: parental allele combinations would be over-represented and recombinant types rare, so the F₂ would deviate sharply from 9:3:3:1 toward an excess of parental phenotypes (the deviation scaling with map distance / recombination frequency). Mendel could still have discovered segregation and independent assortment from his *other* unlinked traits, but the linked pair alone would have masked independent assortment — historically fortunate that his seven analyzed traits behaved independently. See section 18.

- Inbreeding increases homozygosity and can reveal recessive deleterious alleles. Calculate the inbreeding coefficient (F) for offspring of a first-cousin mating, and predict the increase in: (a) homozygosity for a rare allele ($q = 0.01$); (b) probability of autosomal recessive disease compared to random mating. Why do many societies have legal or cultural prohibitions against close-relative marriages?

Answer (Q10, Recall). For first cousins, the inbreeding coefficient is $F = 1/16 = 0.0625$. (a) The probability of homozygosity for a rare allele rises to approximately $q^2 + F \cdot q(1-q)$; for $q = 0.01$ this is $\approx 0.0001 + 0.0625 \cdot (0.0099) \approx 0.00072$, roughly 7× the random-mating value of $q^2 = 0.0001$. (b) Autosomal-recessive disease risk is likewise inflated by the $F \cdot q(1-q)$ term, the relative increase being largest for the rarest alleles. Societies restrict close-kin marriage chiefly because this elevated homozygosity sharply raises the burden of recessive disease in offspring. See section 18.

Questions 11–20: Application and Analysis

- Anticipation (increasing severity across generations) occurs in trinucleotide repeat disorders (Huntington’s disease, myotonic dystrophy). Explain the molecular mechanism by which repeats expand between generations (slippage during DNA replication) and why larger repeats cause earlier onset and greater severity. Why is repeat expansion more common through the paternal germline in HD but the maternal germline in DM1?

Answer (Q11, Application). Trinucleotide repeats (e.g. CAG in *HTT*, CTG in *DMPK*) expand through replication/repair slippage: the nascent strand mispairs on the repetitive template, forming hairpin loops that add repeat units, and longer tracts are more unstable, so they tend to grow each generation (anticipation). Larger repeats produce more toxic gene product (or RNA) earlier, giving earlier onset and greater severity. Expansion bias is germline-specific: large CAG expansions are favored in spermatogenesis (paternal bias in Huntington’s), whereas the CTG repeat expands

- preferentially in the maternal germline in myotonic dystrophy type 1, reflecting differences in replication/repair dynamics in the two gametogenic lineages. See section 18.
12. Evaluate the concept of “genomic imprinting conflict” (kinship theory): paternally imprinted genes (expressed primarily from paternal allele) are generally growth-promoting (*IGF2*), while maternally imprinted genes (expressed primarily from maternal allele) are generally growth-restraining (*H19*). Evaluate the evolutionary logic that predicts this based on parent-offspring conflict theory. What happens when this balance is disrupted (Silver-Russell syndrome vs Beckwith-Wiedemann syndrome)?
- Answer (Q12, Application). Kinship (parent-of-origin conflict) theory predicts that paternally expressed genes favor extracting more maternal resources for the offspring (growth-promoting, e.g. *IGF2*), while maternally expressed genes restrain offspring demand to conserve resources for the mother’s other (possibly different-father) offspring (growth-restraining, e.g. *H19*) — the asymmetry arises only when females mate with multiple males. Disrupting the balance shifts growth: loss of paternal *IGF2* expression underlies the growth-restricted Silver–Russell syndrome, whereas excess *IGF2* / loss of maternal restraint underlies the overgrowth Beckwith–Wiedemann syndrome. The theory is testable via the predicted directionality of imprinted-gene effects on growth. See section 18.
13. Multifactorial diseases (Type 1 Diabetes, schizophrenia) have both genetic and environmental contributions. Evaluate the strengths and limitations of GWAS and polygenic risk scores: (a) minimum detectable effect size at genome-wide significance ($p < 5 \times 10^{-8}$); (b) the “missing heritability” problem; (c) why PRS transferability across ancestries is a scientific and equity concern; (d) what consent and privacy information belongs in a clinical PRS report.
- Answer (Q13, Application). (a) GWAS detects variants whose effect is large enough that, given allele frequency and sample size, association reaches $p < 5 \times 10^{-8}$; common variants of small effect need very large cohorts and rare large-effect variants are missed. (b) The missing heritability problem: significant common variants typically explain a modest fraction of trait heritability, far below twin-study estimates, due to many sub-threshold variants, rare variants, gene–gene/gene–environment effects, and inflated twin estimates. (c) A PRS trained mainly in one ancestry can lose calibration and discrimination in another because linkage disequilibrium, allele frequency, environment, and health-system context differ; deployment without validation can therefore worsen health disparities. (d) A clinical report should state the discovery cohort, target population, calibration method, confidence interval, action threshold, data-retention plan, secondary-use policy, reidentification risk, and family implications. See section 18.
14. Phenocopies are environmentally caused conditions that resemble genetic conditions. Thalidomide-induced limb malformations in 1950s–60s phenocopied the autosomal recessive condition phocomelia. Evaluate: (a) how phenocopies complicate pedigree analysis; (b) how you would distinguish a phenocopy from a genetic condition in a clinical or research context; (c) the ethical implications of confusing genetic and environmental causation for public health policy.
- Answer (Q14, Application). A phenocopy is an environmentally induced phenotype mimicking a genetic disorder. (a) It complicates pedigrees by appearing as sporadic or non-Mendelian cases (no consistent transmission, possible shared environmental exposure rather than shared genotype). (b) Distinguish it by molecular testing (absence of the causative mutation), a documented environmental exposure (e.g. thalidomide timing), discordance in monozygotic twins, and lack of recurrence risk consistent with Mendelian ratios. (c) Misattributing an environmental cause to genetics — or vice versa — misdirects public-health policy: it can stigmatize families, divert resources from removing a preventable exposure, and delay protective regulation. See section 18.
15. Critically evaluate Mendel’s pea experiments, considering: (a) sample sizes (he used thousands of plants, giving high statistical power); (b) evidence that Mendel may have “improved” his data (Weldon’s 1902 re-analysis and Ronald Fisher’s 1936 statistical critique suggesting perfect ratios are too good to be true); (c) whether Mendel’s results are reproducible, and what this debate reveals about the role of confirmation bias in science.
- Answer (Q15, Application). (a) Mendel’s large samples (thousands of plants) gave high statistical power, making his ratios reliable estimates. (b) Fisher’s 1936 analysis (anticipated by Weldon, 1902) showed the aggregate fit to expected ratios is *too good* — the pooled χ^2 is improbably small — suggesting unconscious bias in classification or selective reporting, though no fraud is established. (c) Mendel’s core conclusions are robustly reproducible in modern crosses, so the laws stand; the debate illustrates that even correct conclusions can be reached via data that show confirmation bias, underscoring the need for pre-specified analysis and blinded scoring rather than discarding the findings. See section 18.
16. State Mendel’s two laws. Give the biological basis for each in terms of meiosis.
- Answer (Q16, Application). Law of segregation: the two alleles of a gene separate during gamete formation so each gamete carries only one allele; mechanistically this is the separation of homologous chromosomes (and their alleles) at meiosis I anaphase. Law of independent assortment: alleles of different genes segregate independently, because non-homologous chromosome pairs orient randomly at the metaphase I plate. Independent assortment holds only for genes on different chromosomes (or far apart on the same one). See section 18.
17. Define allele, locus, genotype, and phenotype.

Answer (Q17, Application). An allele is one of the alternative DNA sequence variants of a gene. A locus is the fixed physical position of that gene on a chromosome. A genotype is the pair of alleles an individual carries at a locus (e.g. Aa), while the phenotype is the observable trait that genotype produces in a given environment. See section 18.

18. What is a Punnett square? Draw and solve: $Aa \times Aa$.

Answer (Q18, Application). A Punnett square is a table that lists the possible gametes from each parent and combines them to predict offspring genotypes under Mendelian segregation. For $Aa \times Aa$, each parent produces gametes A and a . The four equally likely cells are AA , Aa , Aa , and aa , giving a genotype ratio of $1 AA : 2 Aa : 1 aa$. With complete dominance, the phenotype ratio is 3 dominant : 1 recessive. This prediction assumes independent gamete formation, equal fertilization probability, and no viability difference among the genotypes; see section 18.

19. What are the expected phenotype ratios for a monohybrid cross between two heterozygotes?

Answer (Q19, Application). A monohybrid cross between two heterozygotes ($Aa \times Aa$) yields a 3:1 phenotype ratio (3 dominant : 1 recessive) and a 1:2:1 genotype ratio ($1 AA : 2 Aa : 1 aa$). This assumes complete dominance and that every genotype reliably expresses its expected phenotype. See section 18.

20. What are the expected phenotype ratios for a dihybrid cross between two double heterozygotes?

Answer (Q20, Application). A dihybrid cross between two double heterozygotes ($AaBb \times AaBb$) yields the classic 9:3:3:1 phenotype ratio — $9 A_B_ : 3 A_bb : 3 aaB_ : 1 aabb$. This is the product of two independent 3:1 monohybrid ratios and requires the two genes to assort independently and act independently on the phenotype. See section 18.

Questions 21–30: Synthesis and Evaluation

21. Define codominance. Give the human blood type system as an example.

Answer (Q21, Synthesis). Codominance is an allelic relationship in which both alleles in a heterozygote are fully and simultaneously expressed, so neither masks the other. The human ABO system illustrates this: an $I^A I^B$ individual is blood type AB, expressing both the A and B surface antigens, rather than an intermediate or single antigen. See section 18.

22. What is incomplete dominance? Give one example and show the F_1 and F_2 ratios.

Answer (Q22, Synthesis). Incomplete dominance occurs when the heterozygote shows an intermediate phenotype because one functional allele produces insufficient product for the full dominant effect. In snapdragons, red ($C^R C^R$) \times white ($C^W C^W$) gives an all-pink F_1 ($C^R C^W$); selfing the F_1 gives an F_2 of 1 red : 2 pink : 1 white — the genotype ratio is visible directly because each genotype has its own phenotype. See section 18.

23. What is a testcross? For what is it used?

Answer (Q23, Synthesis). A testcross mates an individual showing the dominant phenotype to a homozygous recessive individual ($A? \times aa$). It reveals the unknown genotype: an all-dominant offspring set indicates AA , whereas a roughly 1:1 dominant:recessive split indicates Aa . See section 18.

24. What is epistasis? Give one example where two loci interact to modify phenotype.

Answer (Q24, Synthesis). Epistasis is a gene interaction in which the genotype at one locus masks or modifies the phenotypic expression of a second, independent locus. In Labrador retrievers, ee at the extension locus is recessive epistatic to the B (black/chocolate) locus: any ee dog is yellow regardless of its B genotype, collapsing the dihybrid F_2 to 9 black : 3 chocolate : 4 yellow. See section 18.

25. What is pleiotropy? Give one example of a single gene that affects multiple traits.

Answer (Q25, Synthesis). Pleiotropy is the phenomenon in which a single gene affects multiple, seemingly unrelated phenotypic traits. Sick-cell disease (a single β -globin mutation) is a classic example: it causes anemia, pain crises, organ damage, splenic dysfunction, and stroke risk, while also conferring malaria resistance in heterozygotes. See section 18.

26. A black cat (BB) is crossed with a white cat (bb). What is the F_1 phenotype? What is the F_2 ratio if F_1 cats are interbred? If black is incompletely dominant, what is the F_1 phenotype?

Answer (Q26, Synthesis). With complete dominance, $BB \times bb$ gives an all-black F_1 (Bb). Interbreeding the F_1 ($Bb \times Bb$) gives an F_2 of 3 black : 1 white. If black is instead *incompletely* dominant, the F_1 heterozygotes (Bb) show an intermediate (gray) phenotype, and the F_2 would be 1 black : 2 gray : 1 white. See section 18.

27. A chi-square analysis of 580 pea seeds (450 round:130 wrinkled) gives $\chi^2 = 2.6$ (critical value 3.84, $p = 0.05$). Should the null hypothesis of 3:1 ratio be rejected? What does this conclusion mean biologically?

Answer (Q27, Synthesis). $\chi^2_{\text{calc}} = 2.6 < \chi^2_{\text{crit}} = 3.84$ ($df = 1$, $\alpha = 0.05$), so we fail to reject the null hypothesis: the observed 450:130 split is statistically consistent with the expected 3:1 ratio (expected 435 round : 145 wrinkled). Biologically, this supports single-gene Mendelian inheritance with complete dominance; the deviation is attributable to chance sampling, not a different genetic mechanism. The test never *proves* 3:1 — it only fails to reject it. See section 18.

28. Two true-breeding strains of wheat produce red and white kernels. The cross produces medium-red F_1 , and F_2 shows a continuous range of colors with frequencies approximately 1:4:6:4:1. This is consistent with two genes each contributing an additive unit of color. What mode of inheritance does this illustrate?

Answer (Q28, Synthesis). This is polygenic (quantitative) inheritance with additive alleles. Two genes each contributing one additive unit of pigment produce 5 phenotypic classes in F_2 with frequencies 1:4:6:4:1 (the binomial expansion of dose 0–4 across 4 alleles), with the medium-red F_1 intermediate between the parental extremes. Environmental variation further blurs the classes into a continuous distribution. See section 18.

29. A woman is phenotypically normal but her father had phenylketonuria (PKU, autosomal recessive). What is the probability that she is a carrier? If she marries a known carrier, what is the probability their first child will have PKU?

Answer (Q29, Synthesis). Her father is aa , so the woman necessarily inherited one a allele; being unaffected she is Aa — she is a carrier with probability 1 (= 100%). Crossed with a known carrier ($Aa \times Aa$), each child has a $\frac{1}{4}$ probability of PKU (aa). Combined chance the first child is affected = $1 \times \frac{1}{4} = 1/4$. See section 18.

30. In coat color genetics of Labrador retrievers: B is dominant for black pigment; b is recessive (brown/chocolate). E is dominant for coat expression; ee gives yellow regardless of B/b. Set up the dihybrid cross $BbEe \times BbEe$ and calculate the expected ratio of black:chocolate:yellow.

Answer (Q30, Synthesis). $BbEe \times BbEe$ gives the standard 9 B_E_ : 3 B_ee : 3 bbE_ : 1 bbee. Because ee is epistatic (yellow regardless of B), the two ee classes merge: 9 B_E_ = black, 3 bbE_ = chocolate, and 3 B_ee + 1 bbee = 4 yellow. Expected ratio = 9 black : 3 chocolate : 4 yellow. See section 18.

Questions — Chromosomal Inheritance and Linkage

Instructor Use and Coverage Notes

- Coverage target: Use progeny classes to calculate map distances and infer the most likely gene order.
- Model/data emphasis: Recombination frequency and three-point mapping.
- Assessment alignment: Statistical Tests and Data Analysis, Representing and Describing Data.
- Misconception probe: Independent assortment applies to unlinked loci, not to every pair of genes.
- Transfer product: Transfer linkage reasoning to disease mapping, breeding, and genome assemblies.
- Grading focus: award full credit for mechanism, evidence, boundary conditions, and units when a calculation is required.
- Suggested use: draw one recall item, one application item, and one synthesis item when building a short quiz from this bank.

Questions 1–10: Recall and Comprehension

This activity accompanies section 19 of the textbook — review that chapter before attempting the exercises below.

1. What is a chromosome? How many chromosomes does a normal human somatic cell contain?

Answer (Q1, Recall). A chromosome is a single, organized DNA–protein structure carrying many genes in linear order, condensed by histones into chromatin. A normal human somatic cell is diploid (2n) with 46 chromosomes — 22 autosomal pairs plus one pair of sex chromosomes (XX or XY). See section 19. 2. Define linkage. Why do linked genes violate Mendel’s law of independent assortment?

Answer (Q2, Recall). Linkage is the tendency of genes located close together on the *same* chromosome to be inherited together. They violate independent assortment because that law applies only to genes on *different* chromosomes (which assort with random metaphase-I orientation); linked alleles travel together on one chromosome unless separated by crossing over, so parental allele combinations are over-represented in the offspring. See section 19. 3. What is a centimorgan (cM)? What recombination frequency corresponds to 1 cM?

Answer (Q3, Recall). A centimorgan (cM) is the unit of genetic map distance. By definition, 1 cM corresponds to a 1% recombination frequency — i.e. a 1% chance that a crossover separates two loci per meiosis. The relation is approximately linear only for short distances ($RF \lesssim 50\%$). See section 19. 4. Describe the process of crossing over. At what stage of meiosis does it occur?

Answer (Q4, Recall). Crossing over is the reciprocal physical exchange of homologous DNA segments between non-sister chromatids of paired homologous chromosomes, producing recombinant chromosomes. It occurs during prophase I of meiosis (pachytene), when homologs are synapsed, and is visible cytologically as chiasmata. See section 19. 5. What is a genetic map? How is it constructed from recombination frequency data?

Answer (Q5, Recall). A genetic (linkage) map orders genes along a chromosome and spaces them by genetic distance. It is built by crossing strains differing at multiple loci, counting recombinant vs parental offspring, and converting recombination frequency to map distance (1% RF = 1 cM); distances between adjacent intervals are summed (with double-crossover correction) to assemble the full map. See section 19. 6. What is X-linked inheritance? Give two examples of X-linked recessive disorders.

Answer (Q6, Recall). X-linked inheritance describes genes on the X chromosome; for X-linked recessive traits, hemizygous males (one X) are affected if they carry the allele, while females must be homozygous to be affected, producing the characteristic male-biased, carrier-mother pedigree. Two classic X-linked recessive disorders are hemophilia A and red–green color blindness (also Duchenne muscular dystrophy). See section 19. 7. Define nondisjunction. What aneuploid conditions result from nondisjunction at meiosis I vs meiosis II?

Answer (Q7, Recall). Nondisjunction is the failure of homologous chromosomes or sister chromatids to separate properly during cell division, producing aneuploid gametes. Meiosis-I nondisjunction (homologs fail to separate) yields gametes with both homologs (one maternal + one paternal), giving trisomies such as Down syndrome (trisomy 21); meiosis-II nondisjunction (sister chromatids fail) yields gametes with two identical copies. Both can produce trisomy or monosomy after fertilization. See section 19. 8. What is trisomy 21? What maternal-age-related risk factor is associated with it?

Answer (Q8, Recall). Trisomy 21 (Down syndrome) is the presence of three copies of chromosome 21, usually from maternal meiosis-I nondisjunction. Its incidence rises sharply with maternal age, because oocytes are arrested in prophase I for decades and age-related loss of sister-chromatid cohesion increases nondisjunction; paternal age has little effect. See section 19. 9. What is a chromosomal translocation? How does the Philadelphia chromosome arise?

Answer (Q9, Recall). A chromosomal translocation is the transfer of a chromosomal segment to a non-homologous chromosome. The Philadelphia chromosome arises from a reciprocal translocation $t(9;22)$ that fuses *BCR* (chr 22) to *ABL1* (chr 9), creating the constitutively active *BCR-ABL1* tyrosine-kinase fusion oncogene that drives chronic myeloid leukemia. See section 19. 10. Compare XX/XY, ZW/ZZ, XO, and haplodiploid sex determination. Why should haplodiploidy be treated as a chromosome mechanism rather than a complete explanation for eusociality?

Answer (Q10, Recall). In XX/XY systems, typical mammalian females are XX and males are XY, with SRY initiating testis development. In ZW/ZZ systems, common in birds and butterflies, females are ZW and males are ZZ. In XO systems, males have one X and no second sex chromosome. In haplodiploidy, common in Hymenoptera, unfertilised haploid eggs develop as males and fertilized diploid eggs develop as females. Haplodiploidy changes relatedness patterns among relatives, so it matters for kin-selection models, but it is not a complete explanation for eusociality because ecology, mating system, colony demography, and phylogenetic history also matter; diploid termites are the key contrast. See section 19.

Questions 11–20: Application and Analysis

11. Three linked genes A, B, C have pairwise recombination frequencies: A–B = 12%, B–C = 7%, A–C = 19%. Does map distance A–C equal A–B + B–C? If not, why, and what genetic phenomenon accounts for the discrepancy?

Answer (Q11, Application). No — A–C (19%) does not equal A–B + B–C (12% + 7% = 19% here, which actually matches closely). When the sum exceeds the directly measured A–C distance, the discrepancy is due to double crossovers between A and C: a double crossover restores the parental arrangement of the outer markers, so those events are not counted as A–C recombinants and the apparent A–C distance is underestimated. Gene order is A–B–C, and additive map distances from short intervals are more accurate than a single long-interval measurement. See section 19. 12. Morgan’s experiments showed that white eye and miniature wing in *Drosophila* are X-linked and linked to each other (recombination frequency about 36%). Explain how these results violate both Mendel’s laws simultaneously, and how recombination still produces some parental and recombinant gamete classes.

Answer (Q12, Application). White eye and miniature wing are both on the X chromosome and physically linked. They violate independent assortment because, being on the same chromosome, their alleles do not assort independently — parental combinations predominate. They also depart from simple autosomal segregation expectations because X-linkage ties inheritance to sex (males hemizygous). Crossing over in the female’s meiosis recombines the two loci about 36% of the time, yielding about 64% parental and about 36% recombinant gametes — recombinants exist but are the minority, the signature of linkage. See section 19. 13. A man with color blindness (X-linked recessive) who has normal vision has a sister who is a confirmed carrier. What is the probability that his daughter will: (a) be a carrier; (b) be color blind; (c) have normal vision? What is the probability any son of his will be color blind?

Answer (Q13, Application). The man is X^cY (color blind), but offspring genotypes depend on the *mother*. His daughters each receive his X^c plus one maternal X; without information on the mother’s genotype, assume she is X^CX^C (non-carrier): then every daughter is X^CX^c — (a) carrier probability = 1, (b) color blind = 0, (c) normal vision = 1. The sister’s carrier status informs the man’s family but not his children. Probability any son is color blind = 0 with a non-carrier mother (sons get the father’s Y and the mother’s X), since sons inherit no X from their father. See section 19. 14. Barr bodies (condensed inactive X chromosomes) are present in cells with >1 X chromosome: 1 Barr body per n+1 X chromosomes. How many Barr bodies would be present in cells from: (a) 46,XX female; (b) 47,XXX female (triple X); (c) 47,XXY male (Klinefelter); (d) 45,X female (Turner)?

Answer (Q14, Application). Barr bodies = (number of X chromosomes) – 1. (a) 46,XX → 1 Barr body (2 X’s). (b) 47,XXX → 2 Barr bodies (3 X’s). (c) 47,XXY (Klinefelter) → 1 Barr body (2 X’s). (d) 45,X (Turner) → 0 Barr bodies (1 X). All X’s beyond one are inactivated to equalize X-linked gene dosage. See section 19. 15. Down syndrome (trisomy 21) risk rises with maternal age. Propose a mechanistic explanation: which proteins hold meiosis I arrested in the human oocyte, how does cohesin decline with age, and how does premature chromatid separation → nondisjunction → trisomy? Name the specific cohesin subunit implicated.

Answer (Q15, Application). Human oocytes arrest in prophase I from fetal life until ovulation, held by sister-chromatid cohesin complexes containing the meiosis-specific kleisin REC8 that keep chiasmata in place. Over decades, cohesin (and the shugoshin-protected centromeric cohesin) is not replenished and gradually degrades; weakened cohesion permits premature separation of homologs or sister chromatids, leading to meiosis-I nondisjunction and aneuploid (trisomy-21) eggs. The implicated subunit is REC8 (meiotic cohesin), explaining the maternal-age effect. See section 19. 16. Robertsonian translocation Down syndrome: a chromosome 21 fuses to chromosome 14. A carrier parent (45 chromosomes, with 14;21 translocation) produces offspring via meiosis. Using a diagram, show the three viable gamete types and predict the proportion of offspring who have translocation Down syndrome, normal karyotype, and carrier status.

Answer (Q16, Application). A balanced rob(14;21) carrier (45 chromosomes) produces six gamete types from 2:2 segregation, but only three give viable conceptuses: (1) normal (*separate* 14 + 21), (2) balanced carrier (the 14;21 fusion only — phenotypically normal), and (3) translocation Down syndrome (the 14;21 fusion *plus* a free 21 → effective trisomy 21). The other classes (monosomy 21, trisomy 14, monosomy 14) are non-viable. Among liveborns the three classes occur in roughly 1 normal : 1 carrier : 1 translocation Down syndrome, though the *observed* recurrence risk (about 10–15% for a female carrier, lower for male) is below the theoretical 1/3 due to selective loss of unbalanced conceptuses. See section 19. 17. The F_{st} (fixation index) of a particular autosomal gene between two human populations is 0.08. Interpret this value: how much of total human genetic variation lies between populations vs within populations? Compare this to the claim that “race explains most human genetic variation.”

Answer (Q17, Application). F_{ST} = 0.08 means only about 8% of the total genetic variation at this locus lies *between* the two populations, while

about 92% lies *within* them — individuals within a population differ from each other far more than the populations differ on average. This is consistent with the canonical human $F_{ST} \approx 0.10\text{--}0.15$ (Lewontin 1972; Rosenberg 2002) and directly refutes the claim that ‘race explains most human genetic variation’: the overwhelming majority of human genetic diversity is shared within all populations. See section 19. 18. Huntington’s disease is autosomal dominant. The causative allele (HTT with >36 CAG repeats) shows near-100% penetrance. If an affected parent (heterozygous, Hh) has five children, what fraction are expected to be affected? Why does penetrance differ from simple Mendelian dominant inheritance in this context?

Answer (Q18, Application). Each child of an Hh (heterozygous) affected parent and an unaffected (hh) partner has a ½ probability of inheriting the dominant disease allele, so on average 2–3 of the 5 children (expected 2.5) are affected. Penetrance for HD with >36 CAG repeats is near-100%, so genotype essentially equals phenotype — but onset is age-dependent and delayed, so carriers are unaffected for decades; this ‘reduced apparent penetrance at a given age’ and anticipation (repeat expansion) distinguish HD from textbook fully-penetrant Mendelian dominance. See section 19. 19. Genomic imprinting: if the paternal allele of IGF2 is expressed and the maternal allele is silenced, predict the phenotype of: (a) a child who inherits a deletion on the paternal chromosome 11 (Beckwith-Wiedemann: overgrowth); (b) a child inheriting a deletion on the maternal chromosome 11 (Silver-Russell: growth restriction). Use the concept of parent-of-origin-specific expression to explain both.

Answer (Q19, Application). Because IGF2 is expressed only from the paternal allele (maternal copy silenced by imprinting): (a) a child with a *paternal* chromosome-11 deletion (or instead double-dose maternal/paternal IGF2 dysregulation) — in Beckwith–Wiedemann, gain of paternal IGF2 expression — has excess IGF2 and overgrowth. (b) a child inheriting the deletion such that the active *paternal* IGF2 is lost (Silver–Russell, e.g. paternal hypomethylation or maternal UPD11) has little/no IGF2 and growth restriction. The asymmetry arises solely because only the paternal allele is transcriptionally active — the parent of origin of the lesion determines the phenotype. See section 19. 20. Inversion heterozygosity in *Drosophila* suppresses recombination in the inverted region because crossing over within an inversion produces unbalanced chromosomes (duplications and deletions), which are lethal. Explain the mechanism and why evolution often preserves inversions if they capture coadapted gene complexes.

Answer (Q20, Application). In an inversion heterozygote, the inverted and normal homologs can only synapse by forming an inversion loop. A crossover *within* the loop produces chromatids with duplications and deletions (paracentric inversions also yield acentric/dicentric chromatids), which are typically inviable, so only non-recombinant gametes survive — recombination in the region is effectively suppressed. Selection therefore favors inversions when they capture a set of co-adapted (epistatically beneficial) alleles, because the inversion locks the favorable haplotype together and shields it from being broken up by recombination (a ‘supergene’). See section 19.

Questions 21–30: Synthesis and Evaluation

21. Evaluate the role of the synaptonemal complex (SC) in meiotic recombination: how does the SC align homologous chromosomes, what components does it consist of, and how does SC disassembly correlate with chiasma formation? What happens when SC formation fails?

Answer (Q21, Synthesis). The synaptonemal complex (SC) is a tripartite proteinaceous zipper — two lateral elements (SYCP2/SYCP3, on each homolog axis) joined by transverse filaments (SYCP1) and a central element — that mediates full synapsis, holding homologs in close, stable register along their lengths during pachytene. SC assembly stabilizes early recombination intermediates and promotes crossover maturation; SC disassembly at diplotene leaves chiasmata (the cytological manifestation of completed crossovers) holding homologs together until anaphase I. When SC formation fails, homolog pairing/crossing over is defective, crossovers drop, and nondisjunction and aneuploidy or meiotic arrest/sterility result — showing recombination is an actively regulated process, not passive. The conclusion would change if crossovers proceeded normally without an SC. See section 19. 22. Comparative genomic hybridization (CGH) and SNP arrays detect copy number variation (CNVs) across the genome. Evaluate the clinical utility of chromosomal microarray (CMA) analysis in: (a) prenatal diagnosis (replacing karyotyping?); (b) diagnosing children with unexplained intellectual disability; (c) identifying germline vs somatic CNVs in cancer. What is the main limitation of CMA vs long-read sequencing for CNV detection?

Answer (Q22, Synthesis). Chromosomal microarray detects sub-microscopic copy-number gains/losses genome-wide. (a) Prenatal: CMA detects clinically relevant CNVs missed by karyotyping and is first-line for fetal anomalies, but it cannot detect balanced rearrangements or low-level mosaicism, so karyotyping/NIPT remain complementary. (b) Unexplained intellectual disability: CMA is the recommended first-tier test, yielding a diagnosis in about 15–20% of cases via pathogenic CNVs. (c) Cancer: comparing tumor vs matched normal DNA distinguishes somatic (tumor-only) from germline CNVs. The main limitation vs long-read sequencing is that CMA detects copy-number imbalance but is blind to balanced/copy-neutral rearrangements, breakpoints, and structural context that long reads resolve directly. See section 19. 23. Design an experiment to map the XIC (X-inactivation center) on the human X chromosome using: (a) X-autosome translocation cell lines; (b) CRISPR deletion of candidate regions; (c) Xist RNA FISH in human iPSC differentiation. What molecular result would confirm the XIC has been correctly identified?

Answer (Q23, Synthesis). Hypothesis: a defined cis-acting region (the XIC) is necessary and sufficient to initiate X inactivation. (a) In X-autosome translocation lines, test whether the autosomal segment becomes inactivated only when physically joined to the candidate region (spreading from

the XIC). (b) Use CRISPR to delete candidate sub-regions and ask which deletion abolishes initiation of silencing (loss-of-function mapping), with control deletions of neighboring DNA. (c) Perform Xist RNA FISH during iPSC differentiation to watch where the silencing ‘cloud’ nucleates. Confirmation: the minimal region whose deletion blocks Xist up-regulation/coating *and* whose presence is sufficient to silence an attached autosome — reproducibly across clones — is the XIC; failure to silence despite an intact candidate region would falsify the call. See section 19. 24. Evaluate the genomic consequences of chromosomal rearrangements that bring proto-oncogenes near active enhancers (“enhancer hijacking”). Give two specific examples (BCL2 and IGH in follicular lymphoma; MYC and IGH in Burkitt lymphoma) and explain why the same translocation in different individuals produces the same cancer phenotype.

Answer (Q24, Synthesis). ‘Enhancer hijacking’ juxtaposes a proto-oncogene with a strong, constitutively active enhancer, driving its overexpression. Follicular lymphoma: t(14;18) places *BCL2* under the immunoglobulin heavy-chain (*IGH*) enhancer → anti-apoptotic BCL2 overexpression. Burkitt lymphoma: t(8;14) places *MYC* under the *IGH* enhancer → constitutive MYC-driven proliferation. The same translocation produces the same cancer phenotype across individuals because the recurrent breakpoint reproducibly creates the same deregulated oncogene–enhancer configuration; the deterministic molecular consequence is what makes these translocations diagnostic. The interpretation would change if the same rearrangement failed to deregulate the oncogene (e.g. inactive enhancer in that lineage). See section 19. 25. The genetic and epigenetic mechanisms of centromere identity are distinct from those of euchromatin. Evaluate: (a) why centromeres require CENP-A (not canonical H3) for proper kinetochore assembly; (b) why centromere sequences are highly repetitive (α -satellite) despite being functionally defined by CENP-A deposition; (c) what would happen to chromosome segregation if CENP-A deposition were globally abolished.

Answer (Q25, Synthesis). (a) Centromere identity is epigenetic, defined by the histone-H3 variant CENP-A, which marks centromeric chromatin and is the assembly platform for the kinetochore (CCAN/KMN network); canonical H3 cannot template kinetochore formation. (b) Centromeric DNA is highly repetitive α -satellite, but sequence alone is neither necessary nor sufficient — neocentromeres can form on non-satellite DNA — so the repeats are a permissive substrate while CENP-A deposition is the actual determinant (sequence persists because it is recombinationally inert, not because it specifies the centromere). (c) Globally abolishing CENP-A deposition would prevent kinetochore assembly, causing failure of spindle attachment, massive missegregation/aneuploidy, mitotic-checkpoint arrest, and cell death. The interpretation would change if a CENP-A-null cell still segregated chromosomes faithfully. See section 19. 26. Position effects in *Drosophila* (position effect variegation, PEV) occur when a gene is relocated near heterochromatin via chromosomal inversion, causing mosaic silencing. Evaluate the molecular basis of heterochromatic silencing spreading (HP1-H3K9me3 loop), what suppresses PEV (loss of heterochromatin factors), and how this relates to genes at the chromosome 16p11.2 deletion locus in autism.

Answer (Q26, Synthesis). In PEV, an inversion places a euchromatic gene next to constitutive heterochromatin, and heterochromatin spreads via a self-propagating loop: H3K9 methyltransferase (Su(var)3-9) deposits H3K9me3, which recruits HP1, which recruits more methyltransferase, extending silencing variably from cell to cell (mosaic expression). Su(var) (suppressor of variegation) mutations that reduce HP1 or H3K9 methylation suppress PEV (more expression), while *E(var)* enhance it — directly demonstrating dose-dependent heterochromatic silencing. By analogy, position and chromatin context modulate the dosage-sensitive genes within the 16p11.2 CNV, helping explain the variable expressivity of its autism/neurodevelopmental phenotypes. See section 19. 27. Evaluate the selective sweep as an evolutionary force producing chromosomal linkage disequilibrium (LD). When a beneficial mutation sweeps to fixation, flanking variants are dragged along (“genetic hitchhiking”), producing extended LD. How is extended LD detected (iHS statistic), and what gene regions in the human genome show evidence of recent selective sweeps?

Answer (Q27, Synthesis). A selective sweep occurs when a beneficial mutation rises rapidly to high frequency; because there is little time for recombination, physically linked neutral variants ‘hitchhike’ to high frequency too, creating a region of extended haplotype homozygosity and strong linkage disequilibrium with reduced diversity around the selected site. It is detected by haplotype-based statistics such as the integrated haplotype score (iHS) (and EHH/XP-EHH), which flag unusually long, common haplotypes. Classic human examples include LCT (lactase persistence), the Duffy/*DARC* locus, *EDAR*, *SLC24A5* pigmentation, and HBB region malaria-resistance variants. The signal would be reattributed if the long haplotype were better explained by demography (a bottleneck) than selection. See section 19. 28. Chromosome conformation capture (3C/4C/HiC) reveals that chromosomes occupy specific territories in the nucleus and that A (active) and B (inactive) compartments are spatially separated. Evaluate how compartment identity is maintained through cell division (given that nuclear organization must be re-established after mitosis), and what proteins mark the A vs B compartment boundaries.

Answer (Q28, Synthesis). Hi-C shows chromosomes occupy distinct territories and partition into active A and inactive B compartments. Compartment identity is largely encoded in the chromatin/epigenetic state of the DNA itself (histone modifications, DNA methylation), so after mitosis it is re-established de novo as marks and architectural factors re-bind rather than being physically inherited — a robust attractor set by the underlying epigenome. A compartments are marked by active chromatin (H3K4me3/H3K27ac, RNA Pol II, open chromatin), and loop/domain boundaries are defined by CTCF and the cohesin complex (loop extrusion); B compartments carry repressive marks (H3K9me3/H3K27me3, HP1, lamina-associated domains anchored by lamin B). Compartmentalization would not be heritable if it could not be reconstructed from the chromatin state

after each division. See section 19. 29. Meiotic drive (non-Mendelian segregation) is a selfish genetic element that biases its own transmission into gametes at >50% frequency. Evaluate the molecular mechanisms of drive (*t*-allele in mice, SD system in *Drosophila*) and the population genetic consequences: under what conditions does a driving allele reach fixation vs form a stable polymorphism? What restricts drive from eliminating the drive-suppressor population?

Answer (Q29, Synthesis). Meiotic drive is a selfish element that biases its own transmission above 50%. In the mouse *t*-haplotype, a complex of distorters poisons all sperm via the *Tcd* loci while the linked responder *Tcr* rescues only *t*-bearing sperm; in *Drosophila* Segregation Distorter (SD), the *Sd* product disrupts chromatin condensation in *Rsp*-sensitive (non-SD) spermatids, so SD sperm preferentially survive. A driving allele tends toward fixation when its transmission advantage outweighs its fitness cost, but reaches a stable polymorphism when homozygotes suffer strong viability/fertility costs (balancing the drive advantage against homozygote lethality/sterility). Drive is restrained from sweeping the suppressor population by deleterious homozygous effects, recombination breaking up the drive complex, and rapid spread of unlinked drive-suppressor (modifier) alleles favored to restore fair segregation. See section 19. 30. Critically evaluate the concept of “chromosomal instability” (CIN) in cancer, where cells gain and lose whole chromosomes or large chromosome arms with each division. Is CIN a cause or consequence of cancer? Evaluate the evidence that CIN generates the aneuploidy needed for tumor evolution vs the evidence that CIN is incompatible with cell viability and is therefore tolerated primarily within a narrow window of “just right” instability.

Answer (Q30, Synthesis). Chromosomal instability (CIN) is an elevated *rate* of whole-chromosome/arm gain and loss per division (distinct from a static aneuploid state). The evidence is two-sided. *Cause-supporting*: CIN generates the ongoing karyotypic diversity (loss of tumor suppressors, gain of oncogene-bearing arms) that fuels Darwinian tumor evolution and drug resistance, and mutations in mitotic-checkpoint/cohesion genes can be early events. *Constraint-supporting*: gross aneuploidy imposes a strong proteostatic and growth burden and excessive missegregation is lethal, so cells tolerate only an intermediate (‘just-right’) instability — too little gives no adaptive variation, too much causes mitotic catastrophe. The reconciling view is that CIN is both consequence and driver, selected within a narrow viable window. The conclusion would change if engineered high-CIN cells reproducibly enhanced tumor fitness without a viability ceiling. See section 19.

Questions — Population Genetics

Instructor Use and Coverage Notes

- Coverage target: Calculate expected frequencies and identify which evolutionary force could explain deviations.
- Model/data emphasis: Hardy-Weinberg and allele-frequency recurrence calculations.
- Assessment alignment: Statistical Tests and Data Analysis, Representing and Describing Data.
- Misconception probe: Hardy-Weinberg is a null model, not a claim that populations do not evolve.
- Transfer product: Apply population-genetic reasoning to screening, conservation, and pathogen evolution.
- Grading focus: award full credit for mechanism, evidence, boundary conditions, and units when a calculation is required.
- Suggested use: draw one recall item, one application item, and one synthesis item when building a short quiz from this bank.

Questions 1–10: Recall and Comprehension

This activity accompanies section 20 of the textbook — review that chapter before attempting the exercises below.

1. State the Hardy-Weinberg principle and list the five conditions required for equilibrium.

Answer (Q1, Recall). The Hardy–Weinberg principle states that in a large, randomly mating population free of evolutionary forces, allele and genotype frequencies remain constant from generation to generation, with genotype frequencies given by $p^2 + 2pq + q^2 = 1$. The five conditions are: (1) no natural selection, (2) no mutation, (3) no gene flow (migration), (4) random mating, and (5) infinitely large population (no genetic drift). See section 20. 2. Write the Hardy-Weinberg equations for a two-allele system. What do p , q , p^2 , $2pq$, and q^2 represent?

Answer (Q2, Recall). For two alleles with frequencies p (dominant A) and q (recessive a), the allele equation is $p + q = 1$ and the genotype equation is $p^2 + 2pq + q^2 = 1$. Here p^2 is the frequency of homozygous dominant (AA), $2pq$ the frequency of heterozygotes (Aa), and q^2 the frequency of homozygous recessive (aa) individuals. See section 20. 3. What is allele frequency? What is genotype frequency? How do they relate?

Answer (Q3, Recall). Allele frequency is the proportion of a particular allele among all copies of that gene in a population (ranges 0–1). Genotype frequency is the proportion of individuals having a particular genotype. They relate through Hardy–Weinberg: allele frequencies can be computed from genotype counts (e.g. $p = \text{freq}(AA) + \frac{1}{2}\text{freq}(Aa)$), and under HWE genotype frequencies are predicted as p^2 , $2pq$, q^2 . See section 20. 4. Define genetic drift. Why is it more pronounced in small populations?

Answer (Q4, Recall). Genetic drift is the random change in allele frequencies across generations caused by sampling error in which gametes happen to form the next generation. It is more pronounced in small populations because the variance of allele-frequency change is proportional to $1/(2N_e)$ — with few individuals, chance sampling causes large frequency swings and rapid loss or fixation, whereas large populations average out sampling noise. See section 20. 5. What is the founder effect? Give one human example.

Answer (Q5, Recall). The founder effect is the loss and non-representative sampling of genetic variation that occurs when a new population is established by a small number of founding individuals, so the new gene pool reflects the founders’ alleles, not the source population’s. A classic human example is the Amish (Ellis–van Creveld syndrome) or Afrikaner / French-Canadian populations, where specific rare disease alleles reach unusually high frequency. See section 20. 6. Define gene flow (migration). How does it affect allele frequencies in two populations?

Answer (Q6, Recall). Gene flow (migration) is the transfer of alleles between populations when individuals or gametes move and reproduce. It homogenizes allele frequencies between populations — reducing differentiation (F_{ST}) — so that each generation the recipient population’s frequency moves toward the donor’s by $\Delta p_1 = m(p_2 - p_1)$, where m is the migration rate. See section 20. 7. What is mutation rate? What is the typical per-base-pair mutation rate in humans per generation?

Answer (Q7, Recall). Mutation rate is the probability that a new heritable change arises at a given site per generation. In humans the typical point-mutation rate is approximately 10^{-8} per base pair per generation (giving roughly 70–100 de novo mutations per diploid genome per generation). Mutation is the ultimate source of new alleles but, by itself, changes allele frequencies very slowly. See section 20. 8. Define natural selection. What is the selection coefficient (s)?

Answer (Q8, Recall). Natural selection is the differential survival and reproduction of genotypes due to heritable differences in fitness, systematically changing allele frequencies. The selection coefficient (s) quantifies the relative fitness disadvantage of a genotype: if the favored genotype has fitness $w = 1$, a genotype with fitness $1 - s$ is selected against; s ranges from 0 (no selection) to 1 (lethal/sterile). See section 20. 9. What is heterozygote advantage (overdominance)? Give the sickle-cell anemia example.

Answer (Q9, Recall). Heterozygote advantage (overdominance) occurs when the heterozygote has higher fitness than either homozygote, which maintains both alleles as a stable balanced polymorphism. In sickle-cell anemia, HbA/HbS heterozygotes are protected against severe *Plasmodium*

falciparum malaria while avoiding sickle-cell disease; *HbA/HbA* are malaria-susceptible and *HbS/HbS* have lethal anemia, so the *HbS* allele persists at elevated frequency in malarial regions. See section 20. 10. What is the neutral theory of molecular evolution? Who proposed it?

Answer (Q10, Recall). The neutral theory of molecular evolution holds that the great majority of molecular variation within and between species is selectively neutral and evolves by random genetic drift rather than positive selection, with deleterious mutations removed by purifying selection. It was proposed by Motoo Kimura (1968), with related work by King and Jukes and the nearly-neutral extension by Tomoko Ohta. See section 20.

Questions 11–20: Application and Analysis

11. A population has 500 individuals: 200 AA, 240 Aa, 60 aa. Calculate allele frequencies p and q. Calculate expected HWE genotype frequencies. Use chi-square to test if the population is in HWE.

Answer (Q11, Application). Allele counts: total alleles = $2 \times 500 = 1000$. $A = 2(200) + 240 = 640 \rightarrow p = 0.64$; $a = 2(60) + 240 = 360 \rightarrow q = 0.36$. Expected HWE counts: $AA = p^2 \cdot 500 = 0.4096 \cdot 500 \approx 204.8$, $Aa = 2pq \cdot 500 = 0.4608 \cdot 500 \approx 230.4$, $aa = q^2 \cdot 500 = 0.1296 \cdot 500 \approx 64.8$. $\chi^2 = \sum (O - E)^2 / E = (200 - 204.8)^2 / 204.8 + (240 - 230.4)^2 / 230.4 + (60 - 64.8)^2 / 64.8 \approx 0.112 + 0.400 + 0.356 = 0.87$. With $df = 1$ (3 genotypes – 1 allele estimated – 1), $\chi^2_{crit} = 3.84$ at $\alpha = 0.05$; since $0.87 < 3.84$ we fail to reject HWE — the population is consistent with Hardy–Weinberg equilibrium. See section 20. 12. After a natural disaster reduces a population from 10,000 to 100 individuals, what are the genetic consequences? Calculate how much genetic variation is expected to be lost (as measured by heterozygosity) in one generation: $H_t = H_0(1 - 1/(2N_e))$.

Answer (Q12, Application). Crashing from 10,000 to 100 is a bottleneck: it causes loss of rare alleles, reduced heterozygosity, increased drift and inbreeding, and a non-representative gene pool. Using $H_t = H_0(1 - 1/(2N_e))$ with $N_e = 100$ for one generation: the fraction of heterozygosity retained = $1 - 1/(2 \cdot 100) = 1 - 0.005 = 0.995$, i.e. only about 0.5% of heterozygosity is lost in that single generation. The deeper consequence is the durable loss of allelic diversity and elevated future drift, not the small one-generation H drop. See section 20. 13. In a population of $N_e = 50$ individuals, an allele at frequency $q = 0.2$ is selectively neutral. Calculate the probability it is lost by drift in the first generation (approximate using $1 - q = 0.8$). Over many generations, what is the probability it eventually reaches fixation ($= q_0$)?

Answer (Q13, Application). Under pure drift, a neutral allele’s probability of *eventual fixation equals its current frequency*: $P(\text{fixation}) = q_0 = 0.2$ (and $P(\text{loss}) = 0.8$), independent of N_e . The one-generation probability of immediate loss is small — every one of the $2N_e = 100$ sampled gametes must be the alternative allele, $\approx (1 - q)^{(2N_e)} = 0.8^{100} \approx 2 \times 10^{-10}$ (effectively zero). So loss in a single generation is essentially impossible, but over the long run the allele is fixed with probability 0.2 and lost with probability 0.8. See section 20. 14. Selection against a recessive allele ($s = 1$, lethal; aa dies before reproduction): starting from $q_0 = 0.5$, calculate the allele frequency after 1, 5, and 10 generations using $q_t = q_0 / (1 + t \cdot s \cdot q_0)$. How many generations to reduce q from 0.5 to 0.01?

Answer (Q14, Application). Using $q_t = q_0 / (1 + t \cdot s \cdot q_0)$ with $q_0 = 0.5$, $s = 1$: $t = 1$: $q = 0.5 / (1 + 0.5) = 0.333$; $t = 5$: $q = 0.5 / (1 + 2.5) = 0.143$; $t = 10$: $q = 0.5 / (1 + 5) = 0.0833$. To reach $q = 0.01$: solve $0.01 = 0.5 / (1 + t \cdot 0.5) \rightarrow 1 + 0.5t = 50 \rightarrow t = 98$, so about 98 generations. Note the hallmark of selection against a recessive: progress slows dramatically as q falls, because recessive alleles are increasingly hidden in heterozygotes and shielded from selection. See section 20. 15. Cystic fibrosis has a frequency of 1/2,500 in European populations. Calculate: (a) q (frequency of CF allele); (b) the carrier frequency (2pq); (c) what Hardy–Weinberg assumption must hold for this calculation to be valid; (d) why the CF allele is maintained at relatively high frequency (propose two hypotheses).

Answer (Q15, Application). (a) In Hardy–Weinberg, affected homozygotes occur at frequency $q^2 = 1/2500 = 4 \times 10^{-4}$, so $q = \sqrt{4 \times 10^{-4}} = 0.02$. (b) Carrier (heterozygote) frequency = $2pq$ where $p = 1 - q = 0.98$: $2 \times 0.98 \times 0.02 = 0.0392 \approx 1$ in 25. This is the striking clinical fact about autosomal recessive disease: rare disease (1/2500) \leftrightarrow common carriers (1/25). (c) Valid assumptions: random mating with respect to CF genotype, no selection currently depleting q (acceptable over one generation; see d), no mutation–selection–drift disequilibrium, and a large panmictic population. In pre-treatment populations selection against homozygotes was strong ($s \approx 1$), so q would be declining if the population started away from mutation–selection balance. (d) Two hypotheses for persistence: (i) Heterozygote advantage — CFTR $\Delta F508$ carriers may have reduced chloride secretion into the gut lumen, conferring resistance to cholera / typhoid / tuberculosis diarrhea during historic European epidemics (parallel to sickle-cell/malaria, though less firmly established). (ii) Mutation–selection balance — recurrent CFTR mutation ($\mu \approx 7 \times 10^{-7}$ per allele per generation) with $s \approx 1$ predicts $\hat{q} = \sqrt{\mu/s} \approx 8 \times 10^{-4}$ — much lower than observed, so mutation–selection balance alone cannot account for the 0.02 allele frequency; heterozygote advantage (or historical drift/founder events) must contribute. See section 20. 16. F_{ST} between two populations is 0.15 for an autosomal locus. Interpret this: what fraction of total variation is between vs within populations? Calculate the estimated gene flow (Nm) using the approximation $F_{ST} \approx 1/(1 + 4Nm)$.

Answer (Q16, Application). $F_{ST} = 0.15$ means about 15% of total genetic variation lies *between* the two populations and about 85% lies *within* them — populations are modestly differentiated, with most diversity shared. Using $F_{ST} \approx 1/(1 + 4Nm)$: $0.15 = 1/(1 + 4Nm) \rightarrow 1 + 4Nm = 1/0.15 = 6.667 \rightarrow 4Nm = 5.667 \rightarrow Nm \approx 1.4$ migrants per generation. This illustrates the classic result that even about 1 effective migrant per generation substantially limits differentiation by drift. See section 20. 17. A bottleneck reduces a population to 10 individuals for one generation, then expands.

If initial heterozygosity was 0.6, calculate expected heterozygosity after the bottleneck ($H = H_0(1 - 1/(2N_{\text{bottleneck}}))$). After 10 generations of recovery with large N , how does heterozygosity change?

Answer (Q17, Application). Using $H = H_0(1 - 1/(2N_{\text{bottleneck}}))$ with $H_0 = 0.6$ and $N = 10$: $H = 0.6 \times (1 - 1/20) = 0.6 \times 0.95 = 0.57$ — about a 5% loss of heterozygosity in the single bottleneck generation. After expansion, heterozygosity is not restored quickly: H stays near the reduced level and recovers only slowly (at rate about μ via new mutation, over many thousands of generations with large N), because expansion preserves but does not regenerate the lost allelic diversity. The bottleneck’s genetic signature (reduced heterozygosity, lost rare alleles, elevated LD) is therefore long-lasting. See section 20. 18. The neutral theory predicts that the rate of neutral molecular evolution equals the mutation rate (μ), independent of population size. Explain the logic: if advantageous mutations are rare and deleterious mutations are removed by selection, then substitutions in the fossil record should primarily reflect neutral changes. What types of sequences evolve fastest (synonymous sites) and slowest (amino acid-changing in essential proteins)?

Answer (Q18, Application). If new mutations are mostly neutral, the rate at which they enter the population is $2N \cdot \mu_n$ and each has fixation probability $1/(2N)$, so the substitution rate $= 2N \mu_n \times 1/(2N) = \mu_n$, independent of population size — advantageous mutations are too rare to dominate and deleterious ones are purged by purifying selection, so most fixed substitutions are neutral. Fastest-evolving sequences are those under least constraint: synonymous (silent) sites, pseudogenes, and non-coding spacer DNA; slowest-evolving are functionally critical sites — non-synonymous (amino-acid-changing) positions in essential, conserved proteins (e.g. histones), where most changes are deleterious and removed. See section 20. 19. Balancing selection maintains two or more alleles at a locus above neutral expectations. Name three types of balancing selection and one example of each: (a) heterozygote advantage; (b) frequency-dependent selection; (c) fluctuating selection (spatially or temporally varying). Which type is operative at MHC loci?

Answer (Q19, Application). Three types of balancing selection: (a) Heterozygote advantage (overdominance) — heterozygotes fittest, e.g. *HbS* sickle-cell/malaria. (b) Negative frequency-dependent selection — rare genotypes have higher fitness, e.g. self-incompatibility alleles in plants, or rare-prey/host advantage. (c) Fluctuating (spatially or temporally varying) selection — different alleles favored in different patches or seasons, e.g. *Drosophila* allozymes or banding morphs varying with climate. MHC (HLA) loci are the textbook case, maintained chiefly by heterozygote advantage (broader pathogen recognition) together with negative frequency-dependent selection. See section 20. 20. Sexual selection is a form of natural selection acting on mating success rather than survival. Distinguish intrasexual selection (competition between same-sex individuals) from intersexual selection (mate choice). Give one example of each in animals. How might sexual selection drive the rapid evolution of secondary sexual characteristics even if they reduce survival (Zahavian handicap model)?

Answer (Q20, Application). Sexual selection favors traits that increase mating success even at a survival cost. Intrasexual selection is competition among same-sex individuals for mates — e.g. male red deer (stag) antler combat for harem access. Intersexual selection is mate choice by the other sex — e.g. peahens choosing peacocks with the largest, most symmetric trains. Under the Zahavian handicap principle, a costly ornament can spread because only high-quality individuals can bear the cost and survive, so the handicap is an honest signal of genetic quality; choosy females gain fitter offspring, driving runaway elaboration of the trait despite its survival penalty. See section 20.

Questions 21–30: Synthesis and Evaluation

21. Evaluate the molecular clock hypothesis: if the neutral substitution rate equals μ (the mutation rate), then the number of differences between sequences accumulates linearly with time. What calibrates the molecular clock (fossil dates), how has the clock been used to date the human-chimpanzee split, and what are the sources of rate variation (generation time, effective population size, repair efficiency) that make the clock “sloppy”?

Answer (Q21, Synthesis). The molecular clock follows from neutral theory: since the neutral substitution rate equals μ (independent of N), neutral differences between two lineages accumulate roughly linearly with divergence time. It is calibrated with independently dated fossils (or known biogeographic/geological splits) to convert substitutions into absolute time, and has been used to estimate the human–chimpanzee split at roughly 5–7 million years ago (consistent with the hominin fossil record). The clock is ‘sloppy’ because the rate is not strictly constant: it varies with generation time (per-year rate higher in short-generation species), effective population size and slightly deleterious mutations (Ohta’s nearly-neutral effects), DNA-repair efficiency, metabolic rate, and lineage-specific mutation processes — so calibrated, lineage-specific (relaxed) clocks are required. The conclusion would change if substitution rates were demonstrably constant across all lineages and sequence classes. See section 20. 22. The 1000 Genomes Project revealed that most human genetic variants are rare (minor allele frequency < 1%). Evaluate what the site frequency spectrum (SFS) of human variants tells us about recent population expansion (bottleneck → colonization of new territories → rapid expansion), and how deviations from neutral SFS predictions (Tajima’s D) detect selection.

Answer (Q22, Synthesis). The site frequency spectrum (SFS) — the distribution of variant allele frequencies — is dominated by rare variants (MAF < 1%) in humans. This excess of rare alleles is the genomic signature of recent, rapid population expansion after out-of-Africa bottlenecks: many new mutations have arisen but have had too little time to drift to higher frequency, skewing the SFS toward rare variants relative to a constant-size

neutral expectation. Tajima's D compares two diversity estimators (π vs Watterson's θ): under neutral equilibrium $D \approx 0$; negative D (excess rare variants) indicates a recent sweep *or* population expansion, positive D (excess intermediate-frequency variants) indicates balancing selection *or* a bottleneck. Because demography affects the whole genome while selection acts locally, genome-wide vs locus-specific patterns distinguish selection from demography — that contrast is what would change a selection inference. See section 20. 23. Evaluate the evidence that human populations show significantly different allele frequencies at loci controlling pigmentation (MC1R, SLC24A5, HERC2/OCA2) and that these differences reflect recent local adaptation (UV radiation, vitamin D synthesis) rather than random drift. What evolutionary mechanism drove rapid adaptation at these loci in the past 10,000–20,000 years?

Answer (Q23, Synthesis). Pigmentation loci (*SLC24A5*, *MC1R*, *HERC2/OCA2*, *SLC45A2*) show far higher locus-specific F_{ST} (0.4–0.9) than the genome-wide average (about 0.12) and sit on long, high-frequency haplotypes (extended haplotype homozygosity) — patterns expected from positive directional selection (selective sweeps), not neutral drift, since drift would not single out functionally relevant pigmentation variants for extreme differentiation. The driving mechanism is local adaptation to the UV/latitude gradient: lighter skin at high latitudes improves cutaneous vitamin D synthesis under low UV, while darker skin near the equator protects folate and against UV damage, acting strongly over the last about 10–20 ka as humans colonized higher latitudes. The selection interpretation would be overturned if these loci's differentiation were no greater than neutral genome-wide F_{ST} or lacked sweep haplotype signatures. See section 20. 24. Design an analysis to identify signatures of selection in a genome-wide SNP dataset from 1,000 individuals in two populations. Describe the following statistical tests you would use: Fst outlier analysis, XP-EHH (cross-population extended haplotype homozygosity), and Tajima's D, stating what each detects. What results would indicate recent selective sweeps, and how would you validate a candidate gene using functional data?

Answer (Q24, Synthesis). Hypothesis: specific loci have experienced recent positive selection differing between the two populations. Tests: (1) F_{ST} outlier analysis — loci with F_{ST} far above the genome-wide neutral distribution flag local adaptation/differentiation; (2) XP-EHH — detects a sweep that is near-complete in one population but not the other via cross-population extended haplotype homozygosity; (3) Tajima's D — within-population skew of the SFS (strongly negative near a recent sweep). Recent sweep signature: an extreme F_{ST} outlier *plus* long high-frequency haplotype (XP-EHH) *plus* negative Tajima's D, all converging on the same region (the controls being the genome-wide neutral distributions and the comparison population). Validation: replicate the signal in independent cohorts and provide functional evidence — eQTL/allele-specific expression, reporter assays, CRISPR editing of the candidate variant, and a plausible phenotype/selective agent — to show the variant is causal rather than a hitchhiker or demographic artifact. See section 20. 25. Evaluate “negative frequency-dependent selection” at the ABO blood group locus. Propose why O (producing no antigen) remains at >60% frequency in many human populations despite the disadvantage of lacking most antigens (O individuals cannot receive A, B, or AB blood). What pathogens preferentially target specific blood group antigens, and how does this drive balancing selection?

Answer (Q25, Synthesis). At ABO, negative frequency-dependent selection by pathogens helps maintain the polymorphism: many pathogens mimic or bind specific ABO antigens, so individuals lacking a common antigen (or carrying a rarer type) gain a transient advantage as pathogens adapt to the most common antigens — keeping multiple alleles in the population. The high frequency of O (>60% in many populations) is consistent with O individuals having natural anti-A and anti-B antibodies that confer broad resistance to A/B-mimicking pathogens, offsetting the transfusion limitation (a modern, non-selective constraint). Documented antigen-pathogen links include cholera and norovirus (more severe in type O), severe malaria (worse in type A), and *Helicobacter pylori* / *E. coli* binding blood-group antigens — differing pathogen pressures across environments sustain balancing/frequency-dependent selection. The balancing-selection claim would weaken if ABO frequencies tracked neutral drift/demography rather than pathogen regimes. See section 20. 26. Effective population size (N_e) in humans is estimated at about 10,000–20,000 (from genetic diversity), far smaller than the current census population (about 8 billion). Evaluate three reasons why $N_e \ll N_c$: (a) highly unequal reproductive success; (b) past bottlenecks; (c) sex ratio inequality. How does a small historical N_e affect our genome (e.g., low heterozygosity, linkage disequilibrium)?

Answer (Q26, Synthesis). Effective population size N_e is the size of an idealized population that would lose genetic diversity at the observed rate; human N_e (about 10,000–20,000) is far below census size because N_e is reduced by: (a) highly unequal reproductive success (variance in offspring number lowers N_e below the count of adults), (b) past bottlenecks (a single small generation dominates the long-term harmonic-mean N_e — ‘one bad generation undoes a century’), and (c) unequal sex ratio of breeders ($N_e \approx 4N_mN_f/(N_m+N_f)$), so a skewed breeding sex ratio depresses N_e . A small historical N_e leaves enduring genomic signatures: low overall heterozygosity/nucleotide diversity, extensive long-range linkage disequilibrium and large LD blocks (haplotype structure exploited by GWAS/tag SNPs), and a relatively recent coalescence of human lineages. The interpretation would change if diversity-based N_e matched census size. See section 20. 27. Genetic load is the reduction in population fitness due to deleterious alleles. Evaluate the “mutation load paradox” in humans: each human carries about 70–100 de novo mutations per generation, yet the population continues to grow. How is deleterious load purged by selection (purifying selection), and what analytical framework (fitness decline per mutation, calculated from GWAS) resolves the paradox?

Answer (Q27, Synthesis). Genetic load is the fitness reduction caused by deleterious alleles segregating in a population. The apparent paradox — about 70–100 de novo mutations per person per generation yet a growing population — is resolved because most new mutations are neutral or only weakly deleterious, and purifying (negative) selection continuously removes the harmful ones, often efficiently when their effects combine (synergistic epistasis lets one ‘selective death’ purge several mildly deleterious variants). Quantitatively, equilibrium load depends on the genomic deleterious mutation rate U (load $\approx 1 - e^{-U}$ under multiplicative selection); GWAS/sequencing estimates of the per-mutation fitness decrement and the deleterious mutation rate show the realized mutational load is tolerable given truncation/soft selection and large population growth. The framework would be challenged if observed per-mutation fitness costs implied an unsustainable load. See section 20. 28. Evaluate the role of sexual reproduction vs asexual reproduction in maintaining genetic variation under selection. The Red Queen hypothesis proposes that sexual reproduction is advantageous because it generates novel combinations to keep pace with rapidly evolving parasites. Evaluate: (a) the ecological evidence (host-parasite coevolution in snails, *Potamopyrgus antipodarum*); (b) the genetic evidence (rate of Muller’s ratchet in asexual vs sexual populations); (c) the cost of sex (only about 50% of offspring bear offspring themselves).

Answer (Q28, Synthesis). Sex shuffles alleles into new combinations each generation, generating variation that selection can act on, whereas asexual clones can only spread existing genotypes. (a) Ecological evidence: in the New Zealand snail *Potamopyrgus antipodarum*, sexual lineages persist where parasite (trematode) pressure is high while asexual clones dominate parasite-free habitats — supporting the Red Queen prediction that sex tracks coevolving parasites. (b) Genetic evidence: asexual lineages accumulate deleterious mutations irreversibly via Muller’s ratchet (no recombination to recreate mutation-free genotypes), giving them faster fitness decay and higher extinction rates than recombining sexual lineages. (c) Cost of sex: an asexual female transmits her whole genome to all offspring, whereas a sexual female ‘wastes’ half her output on males (the two-fold cost / cost of males), so the benefits of recombination must exceed this cost to favor sex. The Red Queen interpretation weakens if sexual lineages persisted independently of parasite pressure. See section 20. 29. Population stratification in GWAS occurs when ancestry-related allele frequency differences confound disease-association signals. Evaluate how principal component analysis (PCA) corrects for stratification in GWAS, why failing to correct can generate spurious associations, and why the same caution applies to forensic or outbreak population-inference claims.

Answer (Q29, Synthesis). Population stratification confounds GWAS when cases and controls differ in ancestry: any allele whose frequency varies with ancestry can appear associated with disease even with no causal effect (the classic ‘chopstick gene’ fallacy — a marker tracking East-Asian ancestry spuriously ‘predicting’ chopstick use). Principal component analysis (PCA) on genome-wide genotypes extracts axes that capture ancestry/population structure; including the top PCs as covariates, or using mixed models, adjusts the association test for ancestry and removes systematic frequency differences. Without correction, the genomic inflation factor rises and false-positive associations appear because the test statistic is inflated by structure rather than biology. The same boundary applies outside GWAS: a forensic or outbreak phylogeny can support relatedness, but direction, responsibility, and identity require sampling density, timing, chain-of-custody, and explicit alternative histories. See section 20. 30. Critically evaluate the “mutation-selection-drift” balance framework as a complete explanation for the maintenance of genetic variation in natural populations. Where does this framework work well (e.g., for clearly deleterious alleles), and where does it break down (complex traits with many loci of small effect, phenotypic plasticity, developmental canalization, environmental gene \times environment interactions)? Propose how the modern extended synthesis incorporates concepts beyond classical population genetics.

Answer (Q30, Synthesis). The mutation–selection–drift balance framework works well for clearly deleterious or strongly selected single-locus alleles (e.g. recessive lethals at $q = \sqrt{\mu/s}$, classic balanced polymorphisms like sickle cell) and as a quantitative null for allele-frequency dynamics. It breaks down for highly polygenic complex traits built from thousands of small-effect loci (where per-locus selection is too weak relative to drift and most variation is effectively neutral or under stabilizing selection on the trait, not individual alleles), and it does not naturally accommodate phenotypic plasticity, developmental canalization (cryptic variation buffered until released), gene-by-environment interaction, linked selection/background selection, and epistasis. The extended evolutionary synthesis supplements it with quantitative-genetic and genomic models (infinitesimal/omnigenic architecture, stabilizing selection on traits), developmental bias and plasticity, niche construction, epigenetic inheritance, and explicit linked-selection/demography modeling. The classical framework’s adequacy would be vindicated if complex-trait variation were fully predicted by independent per-locus mutation–selection–drift parameters. See section 20.

Questions — Natural Selection and Adaptation

Instructor Use and Coverage Notes

- Coverage target: Estimate selection strength from data and explain why the result is context dependent.
- Model/data emphasis: Selection coefficient and allele-frequency trajectory calculations.
- Assessment alignment: Visual Representations, Statistical Tests and Data Analysis, Argumentation.
- Misconception probe: Evolution is not goal-directed progress; it is local change in populations under constraints.
- Transfer product: Transfer selection reasoning to antibiotics, pesticide resistance, cancer, or climate adaptation.
- Grading focus: award full credit for mechanism, evidence, boundary conditions, and units when a calculation is required.
- Suggested use: draw one recall item, one application item, and one synthesis item when building a short quiz from this bank.

Questions 1–10: Recall and Comprehension

This activity accompanies section 21 of the textbook — review that chapter before attempting the exercises below.

1. State Darwin’s mechanism of natural selection in four steps.

Answer (Q1, Recall). Darwin’s mechanism has four steps: (1) individuals vary in heritable traits; (2) more offspring are produced than can survive (overproduction); (3) variants whose traits raise survival and reproduction in the current environment leave more offspring (differential reproductive success); (4) over generations the population’s trait distribution shifts toward the favored variants (descent with modification). See section 21. 2. What is fitness in evolutionary biology? Does it relate to physical strength?

Answer (Q2, Recall). Fitness is an individual’s relative contribution of surviving, reproducing offspring to the next generation — not physical strength. A sterile but long-lived organism has zero fitness; a short-lived prolific one has high fitness. Fitness is always relative to the local environment and the rest of the population. See section 21. 3. Define adaptation. Give one structural, one physiological, and one behavioral example.

Answer (Q3, Recall). An adaptation is a heritable trait shaped by natural selection because it improves fitness in a given environment. Structural: the mammalian eye. Physiological: countercurrent heat exchange in extremities. Behavioral: honeybee waggle-dance recruitment. See section 21. 4. What is directional selection? What is stabilizing selection? Give one example of each.

Answer (Q4, Recall). Directional selection shifts the mean by favoring one extreme (e.g., larger beaks during drought in Galápagos finches). Stabilizing selection favors the intermediate and removes extremes, reducing variance (e.g., human birth weight, where very small and very large neonates have lower survival). See section 21. 5. What is the difference between microevolution and macroevolution?

Answer (Q5, Recall). Microevolution is change in allele frequencies within a population over a few generations (e.g., pesticide resistance). Macroevolution is large-scale change at or above the species level over long timescales (speciation, origin of major clades). They are the same process viewed over different timescales. See section 21. 6. Name four lines of evidence for evolution by natural selection.

Answer (Q6, Recall). Four lines: (1) the fossil record with transitional forms and temporal succession; (2) comparative anatomy (homologous and vestigial structures); (3) molecular/genetic homology (shared genetic code, conserved genes, pseudogenes); (4) biogeography and directly observed selection (e.g., antibiotic resistance). See section 21. 7. What is the fossil record? What is a transitional fossil? Give one example.

Answer (Q7, Recall). The fossil record is the preserved chronological sequence of past organisms in dated strata. A transitional fossil shows a mosaic of ancestral and derived traits linking groups — e.g., *Tiktaalik* (fish-to-tetrapod) or *Archaeopteryx* (dinosaur-to-bird). See section 21. 8. What is homology? Distinguish structural homology from molecular homology.

Answer (Q8, Recall). Homology is similarity due to shared ancestry. Structural homology is corresponding anatomical organization despite different function (the tetrapod forelimb). Molecular homology is shared sequence/gene identity (cytochrome c across eukaryotes), which is harder to mimic by convergence and so gives strong phylogenetic signal. See section 21. 9. What are vestigial structures? Give two examples in humans.

Answer (Q9, Recall). Vestigial structures are reduced, function-diminished remnants of ancestrally functional traits. In humans: the coccyx (reduced tail) and the vermiform appendix (reduced caecum); the palmaris longus muscle and goosebumps are further examples. See section 21. 10. What is convergent evolution? Give one example.

Answer (Q10, Recall). Convergent evolution is the independent evolution of similar traits in unrelated lineages under similar selection (analogy, not homology). Example: the streamlined body and fins of sharks (fish), ichthyosaurs (reptiles), and dolphins (mammals). See section 21.

Questions 11–20: Application and Analysis

11. Rock pocket mice in New Mexico exist on both dark lava and light soil habitats. Mice with dark coats survive better on lava; light mice survive better on soil. Explain: (a) the type of selection (disruptive); (b) the molecular basis of dark coat color (MC1R mutations); (c) what the independent evolution of

dark coats in different geographic populations tells us about convergent evolution.

Answer (Q11, Application). (a) Disruptive selection: two distinct phenotypes (dark and light) have higher fitness than the intermediate, because each matches one microhabitat's substrate. Quantitative measurements (Hoekstra et al. 2004) show a about 40 % survival advantage for matching morphs against raptor predation, translating to selection coefficients $s \approx 0.4$ per generation — extraordinarily strong by evolutionary standards. If dark-coat allele frequency is q in a lava population, the homozygous-dominant-dark genotype has relative fitness 1, homozygous light $1-s$, giving $\Delta q = \frac{sq(1-q)}{1-sq(2-q)}$ — a single adaptive locus can rise from 0.01 to > 0.5 in about 15 generations under $s = 0.4$. (b) Molecular basis: four non-synonymous substitutions in the MC1R (melanocortin-1 receptor) gene produce a constitutively active receptor in dark mice; high cAMP signaling shifts melanocyte output from red/yellow pheomelanin to black eumelanin, darkening the coat without altering pigment biochemistry elsewhere. (c) Convergent evolution: independent populations on Pinacate and Armendaris lava flows evolved dark coats via different molecular paths — at Pinacate the D84E + R109W allele sweeps, at Armendaris a distinct set of MC1R mutations. Parallel phenotypic convergence from non-identical molecular changes is the hallmark of convergent (as opposed to parallel) evolution: natural selection channels diverse mutational inputs toward the same adaptive solution when the selective landscape strongly favors it. See section 21. 12. The industrial melanism of the peppered moth (*Biston betularia*) is a textbook example of directional selection. Calculate: if initial light morph frequency = 0.99 and dark morph = 0.01, and selection coefficient against light morph = 0.33 (on industrial trees), after 50 years (50 generations), predict the approximate frequency of the dark morph using the directional selection equation.

Answer (Q12, Application). Treat the dark morph as favored with selection against light $s = 0.33$. Per generation $p_{\text{dark}}' = p_{\text{dark}} / (p_{\text{dark}} + (1-p_{\text{dark}})(1-s))$. Starting $p_{\text{dark}} = 0.01$ and iterating 50 generations with $s = 0.33$, the dark morph rises essentially to fixation ($\approx 0.98-0.99$) — matching the historical rise of melanic *Biston betularia* near industrial Manchester within about 50 years. See section 21. 13. Sexual selection can drive traits to fixation even when they reduce survival (peacock tail). Use the Zahavian handicap principle to explain: (a) why primarily males with good “condition” can afford to develop large ornaments; (b) how female preference for ornaments evolves (Fisherian runaway vs good genes models); (c) evidence distinguishing the two models.

Answer (Q13, Application). (a) Large ornaments are costly, so only individuals in good condition can grow them without dying — the handicap guarantees signal honesty. (b) Female preference can evolve by Fisherian runaway (preference and ornament alleles become genetically correlated and self-reinforce) or good-genes (ornaments index heritable viability). (c) The models are distinguished by testing whether ornament size predicts offspring viability (good genes) versus only attractiveness (runaway). See section 21. 14. Kin selection allows altruistic behavior to evolve when altruism benefits genetic relatives. Apply Hamilton's rule: altruism evolves when $rB > C$ (r = relatedness, B = benefit, C = cost). A worker honey bee ($r = 0.75$ to full sisters in a simplified haplodiploid case) helps raise 10 additional sisters ($B = 10$) at an opportunity cost of 3 own offspring ($C = 3$). Is helping favored? Then explain why haplodiploidy by itself cannot explain eusociality, using termites as the contrast case.

Answer (Q14, Application). Hamilton's rule is satisfied because $rB = 0.75 \times 10 = 7.5$, and $7.5 > 3$, so helping is favored under the stated assumptions. The threshold benefit is $B > C/r = 3/0.75 = 4$, so raising more than four equivalent full sisters would exceed the cost. The caveat is biological: haplodiploidy raises relatedness in many ants, bees, and wasps, but many haplodiploids are solitary and termites are diploid eusocial insects. Eusociality therefore needs kin structure plus ecology, mating system, nest defense, brood provisioning, and phylogenetic history. See section 21. 15. Selection on quantitative traits can be modeled by the breeder's equation: $R = h^2S$ (R = response to selection, h^2 = heritability, S = selection differential). If height heritability is 0.80 and we select parents who are 5 cm taller than the population mean, predict R . How many generations of selection would be needed to shift mean height by 10 cm?

Answer (Q15, Application). Apply breeder's equation: $R = h^2S$. Given $h^2 = 0.80$, $S = 5 \text{ cm} \rightarrow R = 0.80 \times 5 = 4.0 \text{ cm}$ per generation. To shift the mean by 10 cm: $N = 10/4 = 2.5$ generations (rounded up, 3 generations) under constant selection differential. Key conceptual point: only the additive genetic component of variance ($V_A / V_P = h^2$) responds; the remaining 20 % of variance (dominance, epistasis, environment) cannot be captured by selection. Biological sanity check: human height is about 80 % heritable; a selection differential of 5 cm is achievable in large populations (top about 5 % of the height distribution averages about +5 cm above the mean). Three generations of such directional selection would move the population mean by about 12 cm — which matches the order-of-magnitude of observed secular trends in human stature over a century (modern Dutch males about +20 cm vs 19th-century ancestors), most of which is environmental (nutrition, disease), not genetic — demonstrating why you must separate G from E before invoking the breeder's equation. Long-term cautions: as allele frequencies move toward fixation, V_A collapses and R decays (the “Bulmer effect”) — which is why artificial selection plateaus after 20–50 generations in classical experiments (e.g., Illinois corn protein selection, 100 generations). See section 21. 16. Gould and Lewontin's “spandrel” argument suggests that not most traits are adaptations — some are architectural by-products of other adaptations (spandrels in the context of evolutionary biology). Give two specific biological examples of putative spandrels and evaluate the methodological criteria needed to distinguish a spandrel from an adaptation.

Answer (Q16, Application). Spandrels are non-adaptive by-products of other adaptations. Putative examples: the human chin (a by-product of jaw remodeling) and male nipples (developmental by-product of a shared body plan). Distinguishing a spandrel from an adaptation requires evidence

of current fitness benefit, a history of selection on the trait itself, and a functional design match — not merely a plausible use story. See section 21. 17. Antibiotic resistance evolution offers real-time evidence of natural selection. Describe the Lenski long-term evolution experiment with *E. coli* (>75,000 generations). What phenotypic innovations have evolved, and how does the experiment distinguish “chance” events from adaptive improvement?

Answer (Q17, Application). The Lenski LTEE propagates 12 *E. coli* lineages by daily transfer for >75,000 generations. Adaptive improvement appears as steadily rising relative fitness and cell size; the key innovation is aerobic citrate utilization (Cit⁺) in one lineage. Replaying frozen ancestors shows Cit⁺ required specific potentiating mutations, distinguishing contingent ‘chance’ history from repeatable adaptive gains. See section 21. 18. Coevolution occurs when two species reciprocally affect each other’s evolution. Describe the Red Queen model of host-parasite coevolution: (a) why does the host need to evolve continuously; (b) what does the snail (*Potamopyrgus antipodarum*) – trematode parasite system teach us; (c) what arms race dynamics emerge between plant alkaloids and insect detoxification enzymes?

Answer (Q18, Application). (a) Hosts must evolve continuously because parasites adapt to common host genotypes, so rare host types are favored (negative frequency-dependent selection). (b) The *Potamopyrgus*–trematode system shows sexual lineages persist where parasite pressure is high, supporting the Red Queen explanation for sex. (c) Plant alkaloid diversification and insect detoxification (e.g., cytochrome P450) escalate reciprocally in a coevolutionary arms race. See section 21. 19. Punctuated equilibrium (Gould and Eldredge, 1972) argues that most evolutionary change is concentrated in rapid bursts associated with speciation, not in gradual anagenesis. Evaluate the fossil evidence for and against punctuated equilibrium using the *Cerion* land snail data from the Bahamas and the evolution of horse lineages.

Answer (Q19, Application). Punctuated equilibrium predicts long stasis punctuated by rapid change at speciation. *Cerion* land snails show long morphological stasis with abrupt shifts, supporting it; horse lineages show substantial gradual, branching change, supporting phyletic gradualism in places. The fossil record contains both patterns, so the debate is about relative frequency, not an either/or. See section 21. 20. Biogeography provides evidence for evolution: organisms on islands often resemble those on the nearest mainland but have evolved unique adaptations. Apply the concept of adaptive radiation to Hawaiian honeycreepers (about 50 species from one ancestral finch-like coloniser): which resources were exploited by different lineages, and what ecological opportunity allowed such rapid diversification?

Answer (Q20, Application). Hawaiian honeycreepers radiated from one finch-like coloniser into about 50 species exploiting nectar, seeds, insects, and snails, with bills specialized per resource. Ecological opportunity — vacant niches on isolated young islands with few competitors — plus repeated island formation drove rapid adaptive radiation. See section 21.

Questions 21–30: Synthesis and Evaluation

21. Evaluate the extended evolutionary synthesis (EES) relative to the modern synthesis. Which additional mechanisms does EES incorporate (developmental plasticity, epigenetic inheritance, niche construction, evolvability)? Choose one mechanism and evaluate the evidence that it plays a role comparable in importance to natural selection in at least one biological system.

Answer (Q21, Synthesis). The Extended Evolutionary Synthesis adds developmental plasticity, epigenetic inheritance, niche construction, and evolvability to the gene-frequency core of the Modern Synthesis. Niche construction has strong evidence (e.g., earthworm soil modification altering selection on themselves and descendants), but whether it rivals natural selection in importance is system-dependent and still debated; it modifies the selective environment rather than replacing selection. See section 21. 22. Design an experiment to test the “good genes” hypothesis for female preference in peacocks (*Pavo cristatus*). Describe: the relevant measurements (eyespot count, parasite load, extra-pair offspring survival), statistical analyses needed, and a falsification criterion. What result would confirm vs reject the hypothesis?

Answer (Q22, Synthesis). Measure male eyespot number, parasite/immune load, and survival of (cross-fostered) offspring; analyze with correlation/GLMs relating preference and ornament to offspring viability, controlling for maternal effects. Good-genes is confirmed if offspring of preferred, low-parasite males show higher survival; it is rejected if ornament predicts attractiveness but not offspring viability. See section 21. 23. Evaluate the evolutionary arms race between cuckoos and their hosts (*Cuculus canorus* vs reed warblers). Describe: (a) forgery (egg mimicry); (b) host counter-adaptations (pattern recognition, egg ejection); (c) what would have to happen for the host to “win” and cuckoos to go extinct. What does the coevolutionary balance tell us about the role of Red Queen dynamics in parasite-host coevolution?

Answer (Q23, Synthesis). (a) Cuckoos forge host-egg color/pattern (gens-specific egg mimicry). (b) Hosts counter-adapt by fine pattern discrimination and ejecting odd eggs. (c) For hosts to ‘win’ and cuckoos to go locally extinct, host rejection must approach 100% faster than cuckoos can improve mimicry or switch hosts. The persistent oscillating balance exemplifies Red Queen coevolution — neither side reaches a permanent advantage. See section 21. 24. Molecular convergence (independent evolution of the same molecular change in different lineages) provides the strongest evidence for adaptation at the sequence level. Evaluate three examples: (a) same amino acid substitution in hemoglobin for high-altitude adaptation in birds; (b) convergent microbial drug resistance mutations; (c) convergent VLDLR mutations for flight in birds. What does molecular convergence tell us about the size of genotypic variation space accessible by natural selection?

Answer (Q24, Synthesis). (a) Identical hemoglobin substitutions for high-altitude O₂ affinity in unrelated bird lineages; (b) recurrent *rpoB*/target-site resistance mutations across microbes; (c) convergent VLDLR-pathway changes associated with flight. Repeated independent fixation of the same change shows the accessible adaptive genotype space is small and selection is highly repeatable at the sequence level. See section 21. 25. The “fitness landscape” model represents most possible genotypes as a surface where height corresponds to fitness. Evaluate the limitations of this model for understanding: (a) epistasis (non-additive interactions between loci); (b) adaptive valleys (can evolution cross fitness valleys?); (c) frequency-dependent fitness (landscape changes with allele frequency). Propose an alternative model that addresses these limitations.

Answer (Q25, Synthesis). (a) Additive landscapes ignore epistasis, where a locus’s fitness depends on genotype at others, making the surface rugged. (b) Adaptive valleys require crossing low-fitness genotypes, hard under selection alone (drift, recombination, or environmental change help). (c) Frequency-dependent fitness means the surface is not static. A better model is a dynamic, high-dimensional genotype network (holey/ Gavrilets landscape) where neutral ridges connect peaks. See section 21. 26. Group selection (selection acting on groups rather than individuals) was largely dismissed after Williams (1966), but has been revived as multilevel selection (MLS) theory. Evaluate: (a) the conditions under which group selection overrides individual selection; (b) the evidence from slime mould (*Dictyostelium*) cooperation; (c) whether human cooperation can be explained by MLS or requires cultural group selection.

Answer (Q26, Synthesis). (a) Group selection overrides individual selection when between-group variance and differential group productivity are large relative to within-group selfish advantage and migration is low. (b) *Dictyostelium* fruiting-body cooperation (with cheater conflict) shows multilevel dynamics. (c) Human cooperation is better explained by kin selection, reciprocity, and cultural group selection (norms, punishment) than by simple genetic group selection. See section 21. 27. Evaluate the claim that evolutionary theory is a scientific fact while specific evolutionary narratives (the origin of feathers, the evolution of eukaryotes) are provisional hypotheses. What does “theory” mean in science compared to colloquial usage? How does the misunderstanding of “theory” fuel creationist objections, and what is the appropriate scientific response?

Answer (Q27, Synthesis). In science a ‘theory’ is a well-substantiated explanatory framework (evolution, like gravitation), not a guess. Evolution as a process is a fact and a theory; specific historical narratives (feather origin, eukaryogenesis) are provisional hypotheses tested against evidence. Creationist objections exploit the colloquial ‘just a theory’; the appropriate response is to clarify the scientific meaning and the strength of convergent evidence. See section 21. 28. Evolvability — the capacity to evolve — may itself be a product of natural selection. Evaluate: (a) the evidence that the modular architecture of proteins (protein domains) evolved to enhance evolvability; (b) whether mutation rate itself can be subject to natural selection; (c) the concept of robustness (canalization) and its relationship to evolvability.

Answer (Q28, Synthesis). (a) Modular protein-domain architecture lets domains recombine, plausibly enhancing evolvability, though it may be a by-product of structural constraints. (b) Mutation rate is heritable and selectable — mutator alleles rise in novel/stressful environments and fall once adapted. (c) Robustness (canalization) buffers phenotypes against mutation, accumulating cryptic variation that can fuel future evolvability when released. See section 21. 29. The “major evolutionary transitions” (Szathmáry and Maynard Smith, 1995) describe eight key events in the history of life (e.g., origin of the eukaryotic cell, origin of multicellularity). Evaluate what distinguishes each transition from ordinary speciation, and propose what the next major evolutionary transition might be (e.g., a digital information-based evolving system?).

Answer (Q29, Synthesis). The major transitions (e.g., origin of chromosomes, the eukaryotic cell, multicellularity, eusociality) each change the unit of selection and how information is stored/transmitted — formerly independent replicators become interdependent and reproduce as a whole, unlike ordinary speciation which does not create a new higher-level individual. A plausible next transition is a tightly integrated human–digital information system. See section 21. 30. Critically evaluate whether evolutionary theory can be directly applied to artificial systems (machine learning algorithms, memes, cultural evolution). What structural features must any system have to undergo Darwinian evolution (heritable variation, differential reproduction, competition)? Does cultural evolution satisfy these criteria, and how does it differ from biological evolution in terms of inheritance mechanisms and selection units?

Answer (Q30, Synthesis). Any Darwinian system needs heritable variation, differential reproduction/retention, and competition for limited resources. Cultural evolution satisfies these (ideas vary, are copied with error, and spread differentially) but differs from biology: inheritance can be horizontal and Lamarckian (acquired changes transmitted), selection units are memes/practices, and transmission is high-fidelity-optional and intentional. See section 21.

Questions — Genetic Drift, Gene Flow, and Speciation

Instructor Use and Coverage Notes

- Coverage target: Predict how population size or isolation changes divergence and fixation risk.
- Model/data emphasis: Fixation probability, effective population size, and migration-selection balance.
- Assessment alignment: Visual Representations, Statistical Tests and Data Analysis, Argumentation.
- Misconception probe: Random does not mean patternless; stochastic processes have predictable distributions.
- Transfer product: Apply drift reasoning to endangered populations, founder effects, and island radiations.
- Grading focus: award full credit for mechanism, evidence, boundary conditions, and units when a calculation is required.
- Suggested use: draw one recall item, one application item, and one synthesis item when building a short quiz from this bank.

Questions 1–10: Recall and Comprehension

This activity accompanies section 22 of the textbook — review that chapter before attempting the exercises below.

1. Define genetic drift. How does it differ from natural selection?

Answer (Q1, Recall). Genetic drift is random change in allele frequencies from sampling error between generations; natural selection is non-random change driven by fitness differences. Drift is strongest in small populations and can fix neutral or even mildly deleterious alleles, whereas selection consistently favors higher-fitness variants regardless of population size. See section 22. 2. What is the founder effect? What is the bottleneck effect? How do they differ?

Answer (Q2, Recall). The founder effect is the loss/skew of variation when a few individuals start a new population; the bottleneck effect is the loss when a population is drastically reduced then recovers. Both are drift, but the founder effect involves colonization by a non-random small sample, while a bottleneck reduces an existing population — both leave reduced heterozygosity. See section 22. 3. Define gene flow. What effect does gene flow have on genetic differentiation between populations?

Answer (Q3, Recall). Gene flow is the movement of alleles between populations via migration/interbreeding. It homogenises allele frequencies, reducing genetic differentiation (lower F_{ST}) and opposing divergence by drift or local selection. See section 22. 4. Define biological species concept (BSC). What is a reproductive isolation barrier?

Answer (Q4, Recall). The Biological Species Concept defines a species as groups of actually or potentially interbreeding natural populations reproductively isolated from other such groups. A reproductive isolation barrier is any heritable trait preventing successful interbreeding or fertile offspring between populations. See section 22. 5. Distinguish pre-zygotic from post-zygotic reproductive isolation barriers. Give two examples of each.

Answer (Q5, Recall). Pre-zygotic barriers act before fertilization: temporal isolation (different breeding seasons) and behavioral isolation (different mating signals). Post-zygotic barriers act after: hybrid inviability (zygote fails to develop) and hybrid sterility (e.g., the mule). They differ in whether they prevent zygote formation or hybrid success. See section 22. 6. What is allopatric speciation? What is sympatric speciation? Give one natural example of each.

Answer (Q6, Recall). Allopatric speciation occurs when a geographic barrier splits populations that then diverge (e.g., Isthmus of Panama snapping shrimp). Sympatric speciation occurs without geographic separation, often via host shift or polyploidy (e.g., apple maggot fly *Rhagoletis*, or polyploid *Tragopogon*). See section 22. 7. What is parapatric speciation? Give one example from plant populations.

Answer (Q7, Recall). Parapatric speciation occurs across a continuous range with a steep environmental gradient and limited gene flow, so divergence proceeds despite contact. Example: grasses (*Anthoxanthum/Agrostis*) diverging on mine-tailing boundaries through soil-metal tolerance and assortative flowering. See section 22. 8. Define peripatric speciation. How does it relate to the founder effect?

Answer (Q8, Recall). Peripatric speciation is allopatric speciation in a small peripheral isolate. It relates to the founder effect because the small founding population carries a non-random allele sample and experiences strong drift, accelerating divergence from the parent population. See section 22. 9. Define F_{ST} (fixation index). What does $F_{ST} = 0$ mean? What does $F_{ST} = 1$ mean?

Answer (Q9, Recall). F_{ST} (fixation index) measures the proportion of total genetic variance due to differences among populations. $F_{ST} = 0$ means populations are genetically identical (panmixia/high gene flow); $F_{ST} = 1$ means populations are completely differentiated (fixed for different alleles, no shared variation). See section 22. 10. What is adaptive radiation? Give one famous example.

Answer (Q10, Recall). Adaptive radiation is rapid diversification of one lineage into many species occupying different ecological niches. Classic example: Darwin’s finches on the Galápagos, diversified in beak form by diet. See section 22.

Questions 11–20: Application and Analysis

11. A population of 1,000 individuals is reduced to 5 for three generations, then recovers to 1,000. Calculate the harmonic mean of the effective population size over the three-generation bottleneck, and use $H_t = H_0(1 - 1/(2N_e))^t$ to estimate the heterozygosity remaining after recovery.

Answer (Q11, Application). Effective size over the bottleneck is the harmonic mean: $N_e = 3 / (1/5 + 1/5 + 1/5) = 5$. Heterozygosity retained $\approx H_0(1 - 1/(2N_e))^t = H_0(1 - 1/10)^3 = H_0(0.9)^3 \approx 0.729 H_0$ — about 27% of heterozygosity is lost over the three-generation bottleneck despite later recovery to 1,000. See section 22. 12. The Amish population (descended from 200 founders in the 1700s) has a 1,000-fold higher frequency of Ellis-van Creveld syndrome (short-limb dwarfism) than the general population. Explain: (a) which mechanism is responsible; (b) whether natural selection for or against the condition is required to explain its frequency; (c) what this implies for genetic counselling in this community.

Answer (Q12, Application). (a) The founder effect (drift), not selection. (b) No selection is required: the high frequency results from a founder carrying the recessive *EVC* allele plus subsequent isolation/endogamy. (c) Genetic counselling should account for the elevated recessive-carrier frequency and offer targeted carrier screening within the community. See section 22. 13. Two sister populations of fish separated 10,000 years ago are now parapatrically distributed along a river system. They differ in color pattern and mating call. When brought together in the lab, they hybridize successfully but hybrids show reduced fertility. Classify: (a) what type of speciation occurred; (b) what type of reproductive isolation is demonstrated; (c) whether they are currently separate species under the BSC.

Answer (Q13, Application). (a) Allopatric/parapatric divergence over 10,000 years. (b) Post-zygotic isolation (reduced hybrid fertility) plus incipient pre-zygotic (call/color) isolation. (c) Under the BSC they are incipient/partial species — reproductive isolation is incomplete (hybrids form but are sub-fertile), so they sit on the speciation continuum rather than being fully separate. See section 22. 14. Calculate the estimated gene flow (Nm = number of migrants per generation) between two populations with $F_{ST} = 0.08$, using $F_{ST} \approx 1/(1 + 4Nm)$. Is this a high or low level of gene flow? What migration rate ($Nm > 1$) is needed to prevent significant divergence?

Answer (Q14, Application). From $F_{ST} \approx 1/(1+4Nm)$: $0.08 = 1/(1+4Nm) \rightarrow 1+4Nm = 12.5 \rightarrow Nm \approx 2.9$ migrants per generation. This is relatively high gene flow; $Nm > 1$ (about one effective migrant per generation) is the classic threshold sufficient to prevent strong divergence by drift, so these populations are only weakly differentiated. See section 22. 15. In cichlid fish adaptive radiation in Lake Victoria, > 500 species evolved in < 15,000 years — an extremely rapid speciation event. Propose: (a) what ecological opportunity promoted rapid radiation; (b) what role mate choice based on color pattern played in sympatric speciation; (c) how light transmission in different lake depths may have driven divergence.

Answer (Q15, Application). (a) Vacant niches and habitat heterogeneity in a young, large lake offered ecological opportunity. (b) Divergent female preference for male nuptial color drove assortative mating and sympatric divergence. (c) Depth-dependent light spectra shifted optimal signaling color, coupling sensory drive to mate choice and accelerating speciation; turbidity collapse reverses it, showing the mechanism’s fragility. See section 22. 16. Ring species provide a spatial illustration of the speciation continuum. The *Larus* gull chain circles the Arctic: populations A interbreed with B, B with C, C with D, D with E, but A and E do not interbreed. Explain: (a) why A and E are or are not separate species under BSC; (b) what this shows about speciation as a gradual, continuous process; (c) how climate change and habitat connectivity changes could affect this ring.

Answer (Q16, Application). (a) Under the BSC A and E are not a single species where they fail to interbreed, yet a continuous chain connects them. (b) This shows speciation is gradual and continuous — reproductive isolation accumulates with genetic distance along the ring. (c) Breaking habitat connectivity (climate change, habitat loss) collapses the chain into discrete isolated species. See section 22. 17. Hybridization between species can produce evolutionary novelty. Allopolyploidy (hybrid + chromosome doubling) has produced many crop species: bread wheat (AABBDD, from three diploid ancestors). Explain: (a) how polyploidy immediately produces reproductive isolation from both ancestors; (b) why polyploid plants are often phenotypically superior (hybrid vigour/heterosis); (c) what the estimated contribution of allopolyploidy to flowering plant diversity is.

Answer (Q17, Application). (a) Allopolyploidy doubles chromosomes so backcrosses to either diploid ancestor yield sterile odd-ploidy hybrids — instantaneous reproductive isolation. (b) Fixed heterozygosity and gene/dosage redundancy give heterosis and buffering. (c) A large fraction of angiosperm diversity (most species have polyploidy in their ancestry; about 15% of speciation events are polyploid) traces to allopolyploidy. See section 22. 18. “Magic traits” are traits that simultaneously cause both ecological divergence (adaptation to different niches) and assortative mating (non-random mating based on the same trait). Give one example of a magic trait and explain why this simplifies the theory of sympatric speciation.

Answer (Q18, Application). A magic trait simultaneously causes ecological divergence and assortative mating. Example: beak size in Darwin’s finches, which determines both diet (natural selection) and song/mate recognition (assortative mating). One trait under divergent selection automatically generates non-random mating, removing the need for separate loci and recombination to align — greatly easing sympatric speciation. See section 22. 19. The biological species concept has been criticised as inapplicable to: (a) asexual organisms; (b) freely hybridizing plant species. Evaluate two alternative species concepts (phylogenetic species concept, ecological species concept) and explain which is most useful for biodiversity conservation.

Answer (Q19, Application). The BSC fails for asexual and freely hybridizing taxa. The Phylogenetic Species Concept (smallest diagnosable monophyletic unit) applies to asexuals and fossils but can oversplit; the Ecological Species Concept (lineage adapted to a distinct niche) captures adaptive divergence. For conservation, the PSC/ESU framework is most useful because it identifies diagnosable, independently evolving units for legal protection. See section 22. 20. Hybrid zones are regions where two distinct populations interbreed. Using the tension zone model: (a) explain why a hybrid zone maintains a stable width; (b) what happens to hybrid fitness at the center of the zone; (c) how hybrid zone data can estimate the selection against hybrids and the rate of gene flow.

Answer (Q20, Application). (a) A tension zone is maintained by a balance between dispersal of parental types into the zone and selection against hybrids, giving a stable cline width independent of the environment. (b) Hybrid fitness is lowest at the zone center. (c) Cline width and shape estimate the selection coefficient against hybrids and dispersal distance, hence effective gene flow across the boundary. See section 22.

Questions 21–30: Synthesis and Evaluation

21. Evaluate the evidence that speciation can occur without geographic separation (sympatric speciation) using the apple maggot fly (*Rhagoletis pomonella*) host-race formation as a case study. What conditions (assortative mating by habitat, additive gene effects, limited gene flow) are required, and what genetic evidence suggests incipient sympatric speciation is occurring?

Answer (Q21, Synthesis). *Rhagoletis* host-race formation supports sympatric speciation: apple vs hawthorn races show habitat-based assortative mating (host fidelity), allochronic isolation (different fruiting times), and additive genetic differences in diapause timing with reduced gene flow. Allele-frequency and diapause clines indicate incipient — not yet complete — sympatric divergence, the strongest empirical case for the process. See section 22. 22. Design a population genomics study to determine whether two morphologically distinct bird populations on isolated islands should be classified as separate species. Describe: the genomic data you would collect (RAD-seq or whole-genome resequencing), the analyses you would perform (F_{ST} , phylogeny, ABBA-BABA test for gene flow), and the threshold values you would use to make the classification decision.

Answer (Q22, Synthesis). Collect whole-genome resequencing (or RAD-seq) from both island populations; compute genome-wide F_{ST} , build a phylogeny, and run ABBA-BABA/D-statistics for gene flow; estimate divergence time and migration. Classify as separate species if F_{ST} is high and uniform, the populations are reciprocally monophyletic, and gene-flow tests show little/no admixture; treat low F_{ST} with ongoing gene flow as one species. See section 22. 23. Evaluate the “glacial refugia” hypothesis for European biodiversity: during Pleistocene glaciations, populations were isolated in southern refugia (Iberia, Italy, Balkans), underwent allopatric evolution, then expanded northward after glaciers retreated. What phylogeographic data would test this hypothesis, and what consequences does secondary contact of previously isolated populations have for hybrid zone formation?

Answer (Q23, Synthesis). Test phylogeographic predictions: southern refugial populations should show higher diversity and older, divergent lineages, with northern populations a subset (signature of post-glacial expansion). mtDNA/genomic phylogeography and demographic modeling test it. Secondary contact of refugial lineages produces hybrid zones whose width and clines reveal the strength of post-contact selection and gene flow. See section 22. 24. Gene drive technology (e.g., CRISPR-based homing drives) can spread a gene (e.g., infertility) through a wild population at rates faster than Mendelian inheritance. Evaluate the ecological risks of releasing a gene drive into a wild mosquito population to suppress malaria transmission: (a) off-target spread to non-target species; (b) irreversibility; (c) international governance challenges (the drive does not respect national borders).

Answer (Q24, Synthesis). (a) Off-target homing or hybridization could spread the drive into related non-target species. (b) Self-propagating drives are effectively irreversible once released. (c) Because organisms cross borders, a unilateral release imposes risk on other nations, demanding international governance, containment (split or daisy-chain drives), and reversal/immunising-drive contingencies before any field release. See section 22. 25. Inbreeding depression (reduced fitness in highly homozygous individuals) limits the viability of small, isolated populations. Evaluate: (a) the mechanisms of inbreeding depression (overdominance vs partial dominance of deleterious recessives); (b) the threshold F_{cr} (critical inbreeding coefficient) below which genetic rescue is needed; (c) policy implications for reintroduction of individuals from genetically distinct populations.

Answer (Q25, Synthesis). (a) Inbreeding depression arises from increased homozygosity exposing deleterious recessives (partial dominance) and loss of overdominant heterozygote advantage. (b) Below a critical inbreeding coefficient (rising F , shrinking N_e), fitness collapses and genetic rescue is warranted. (c) Policy: introduce a few migrants from genetically distinct populations to restore heterozygosity, weighing rescue against outbreeding depression and local adaptation loss. See section 22. 26. The concept of “reproductive character displacement” predicts that the signal used for mate recognition must diverge faster between sympatric sister species than between allopatric ones, to prevent costly hybridization. Evaluate the evidence for reproductive character displacement in: (a) *Ficedula* flycatchers in Scandinavia; (b) cricket frog calling frequencies; (c) *Phlox drummondii* flower color contrast.

Answer (Q26, Synthesis). Reproductive character displacement predicts faster signal divergence in sympatry than allopatry. (a) *Ficedula* flycatcher plumage/song diverges more where sympatric, reducing hybridization. (b) Cricker-frog call frequency shifts in sympatry. (c) *Phlox* flower color

diverges where congeners co-occur. Consistent sympatric exaggeration of the mate-recognition signal supports selection against costly hybridization. See section 22. 27. Evaluate the genomics of speciation: “genomic islands of divergence” are regions of elevated F_{ST} interspersed with regions of low F_{ST} in partially reproductively isolated populations. Interpret these patterns: do islands represent targets of selection, or artifacts of reduced recombination around centromeres? What sequencing/analysis strategy would distinguish selective sweeps from reduced recombination as drivers of F_{ST} peaks?

Answer (Q27, Synthesis). Genomic islands of divergence (high- F_{ST} regions in a low- F_{ST} background) can reflect selection/reproductive-isolation loci OR reduced recombination near centromeres inflating F_{ST} . Distinguish them by mapping recombination rate and absolute divergence (d_{XY}): true selective sweeps/barrier loci show elevated d_{XY} and recent coalescence, whereas low-recombination artifacts show high F_{ST} without elevated d_{XY} . See section 22. 28. Evaluate the concept of the “speciation continuum”: from partially isolated populations (e.g., $F_{ST} = 0.1$) through incipient species (partial reproductive isolation, fertile hybrids) to full species (complete reproductive isolation). At what point on this continuum should conservation efforts classify distinct evolutionary significant units (ESUs) for legal protection?

Answer (Q28, Synthesis). On the speciation continuum, conservation should designate Evolutionarily Significant Units where populations are reciprocally monophyletic at neutral markers and show adaptive/ecological divergence and restricted gene flow — i.e., independently evolving lineages — even before full reproductive isolation, so distinct evolutionary potential is protected without over-splitting clinal variation. See section 22. 29. Mass extinction events (e.g., end-Cretaceous, 66 Mya) dramatically restructured biodiversity. Evaluate: (a) what evolutionary patterns characterize the burst of diversification after mass extinction (adaptive radiation); (b) whether the sixth mass extinction (current human-driven biodiversity crisis) is comparable in rate to previous ones; (c) whether survivors of previous extinctions provide models for predicting which present-day species will persist.

Answer (Q29, Synthesis). (a) Post-extinction recovery shows adaptive radiation as survivors fill emptied niches (e.g., mammalian radiation after the K-Pg). (b) Current background-corrected extinction rates are 100–1000× the fossil baseline, comparable in rate to past mass extinctions though earlier in cumulative magnitude. (c) Previous survivors (generalists, wide ranges, small body size, broad tolerance) predict which present-day taxa are likeliest to persist. See section 22. 30. Critically evaluate the “two-speed genome” concept in fungi (*Zymoseptoria tritici*, wheat pathogen): the genome is divided into “core” (gene-rich, slowly evolving) and “accessory” (transposon-rich, rapidly evolving) chromosomes. How does this architecture accelerate host-pathogen coevolution, and how might it apply to our understanding of evolutionary rate variation in other organisms, including humans (conserved regions vs rapidly evolving regions)?

Answer (Q30, Synthesis). The two-speed genome separates a conserved core (housekeeping, slow) from a transposon-rich accessory compartment (effectors, fast) — compartmentalising rapid host-adaptation while preserving essential function, accelerating coevolution. The same conserved-vs-rapidly-evolving partitioning (e.g., constrained genes vs immune/recognition loci) generalizes to evolutionary-rate heterogeneity across genomes, including humans. See section 22.

Questions — Phylogenetics and the Tree of Life

Instructor Use and Coverage Notes

- Coverage target: Use a tree to infer shared ancestry, character transitions, or divergence time.
- Model/data emphasis: Tree-distance, parsimony, and molecular-clock calculations.
- Assessment alignment: Visual Representations, Statistical Tests and Data Analysis, Argumentation.
- Misconception probe: Living species are cousins, not ancestors of one another.
- Transfer product: Transfer tree thinking to pathogens, conservation units, gene families, and development.
- Grading focus: award full credit for mechanism, evidence, boundary conditions, and units when a calculation is required.
- Suggested use: draw one recall item, one application item, and one synthesis item when building a short quiz from this bank.

Questions 1–10: Recall and Comprehension

This activity accompanies section 23 of the textbook — review that chapter before attempting the exercises below.

1. What is a phylogenetic tree? What does each node, branch, and tip represent?

Answer (Q1, Recall). A phylogenetic tree depicts evolutionary relationships: tips (terminal taxa) are sampled species/sequences, internal nodes are inferred common ancestors (speciation/divergence events), and branches represent lineages through time (length may encode time or amount of change). See section 23. 2. What is a clade (monophyletic group)? Distinguish monophyletic, paraphyletic, and polyphyletic groups.

Answer (Q2, Recall). A clade (monophyletic group) is an ancestor and all its descendants. Paraphyletic groups include an ancestor and some but not all descendants (e.g., ‘reptiles’ excluding birds); polyphyletic groups unite taxa without their common ancestor (grouping by convergence). See section 23. 3. Define synapomorphy. How does it differ from a plesiomorphy?

Answer (Q3, Recall). A synapomorphy is a shared derived character inherited from the most recent common ancestor of a clade and used to diagnose it. A plesiomorphy is an ancestral character shared more broadly; only synapomorphies (not shared ancestral traits) define clades. See section 23.

4. What is parsimony in phylogenetics? What does the most parsimonious tree minimize?

Answer (Q4, Recall). Parsimony selects the tree requiring the fewest evolutionary changes (character-state transitions) to explain the data, invoking the minimum of independent origins/reversals (homoplasy). See section 23. 5. What is a molecular phylogeny? What type of data is used to construct one?

Answer (Q5, Recall). A molecular phylogeny infers relationships from molecular sequence data — DNA, RNA, or protein sequences (e.g., rRNA genes, mitochondrial genes, or genome-wide markers) — rather than morphology. See section 23. 6. What is a bootstrap value? What does a bootstrap of 90% indicate?

Answer (Q6, Recall). A bootstrap value is the percentage of pseudo-replicate datasets (resampled sites) that recover a given clade. A bootstrap of 90% means the clade is supported in 90% of replicates — strong but not absolute support for that grouping. See section 23. 7. What is an outgroup? How is it used to root a phylogenetic tree?

Answer (Q7, Recall). An outgroup is a taxon known to lie outside the clade of interest. It polarizes characters and roots the tree: the point where the ingroup attaches to the outgroup is the root, defining ancestral vs derived states. See section 23. 8. What is horizontal gene transfer (HGT)? In which domains of life is it most common?

Answer (Q8, Recall). Horizontal (lateral) gene transfer is the transfer of genetic material between organisms other than parent-to-offspring. It is most common among Bacteria and Archaea (and between them), and can make single-gene trees conflict with the organismal tree. See section 23.

9. Define convergent evolution. How can it mislead phylogenetic analysis?

Answer (Q9, Recall). Convergent evolution produces similar character states independently in unrelated lineages (homoplasy). It misleads phylogenetics by making distantly related taxa appear closely related if those convergent characters are scored as homologous. See section 23. 10. What are molecular clocks? How are they calibrated?

Answer (Q10, Recall). Molecular clocks use the roughly constant accumulation of substitutions over time to date divergences. They are calibrated with independent evidence — dated fossils at nodes or known biogeographic/geological events — to convert genetic distance into absolute time. See section 23.

Questions 11–20: Application and Analysis

11. Given the character matrix below (1=present, 0=absent): determine the synapomorphies that define the clade (birds + crocodiles) relative to lizards and snakes, using the parsimony principle.

Taxon	Archosaur skull	Feathers	4-chambered heart	Endothermy
Lizard	0	0	0	0
Crocodile	1	0	1	0
Bird	1	1	1	1

- Answer (Q11, Application). Map each character onto the tree and apply parsimony. Archosaur skull and a four-chambered heart are each present in crocodile and bird but absent in lizard (and snakes), so each is a shared derived character (synapomorphy) uniting birds + crocodiles as the clade Archosauria — one origin is more parsimonious than independent gains in two lineages. Feathers and endothermy are present only in birds, so they are bird-specific (autapomorphies) and do not diagnose the birds + crocodile clade. See section 23.
12. Two competing phylogenies are proposed for the Paleocene mammals: (A) requires 12 evolutionary changes; (B) requires 15 changes. By parsimony, which tree is preferred? Explain what assumption is made when choosing the more parsimonious tree.

Answer (Q12, Application). Tree A requires 12 changes, tree B requires 15; by parsimony tree A is preferred (fewer steps). The assumption is that evolutionary change is relatively rare, so the hypothesis invoking the fewest independent changes (least homoplasy) is the best estimate — an assumption that weakens when rates are high or branches are long. See section 23.

13. Dolphins and ichthyosaurs (extinct reptiles) both have streamlined bodies and fin-like forelimbs. Explain: (a) why a morphological phylogeny based solely on body shape would incorrectly group them; (b) what more reliable character would avoid this error; (c) what type of evolution produced the similarity.

Answer (Q13, Application). (a) Body shape is convergent for aquatic locomotion, so a shape-based tree wrongly groups dolphins with ichthyosaurs. (b) Reliable characters are independent homologies — DNA sequence and skeletal/developmental synapomorphies (mammalian middle-ear ossicles, mammary structures) place dolphins with mammals. (c) The similarity is convergent (analogous) evolution. See section 23.

14. A molecular phylogeny based on 16S rRNA sequences places Archaea as a sister clade to Eukaryotes, while Bacteria branch more basely. Explain what this means for the “three-domain of life” vs “two-domain of life” (Eocyte hypothesis) debate.

Answer (Q14, Application). 16S rRNA placing Archaea as sister to Eukaryotes with Bacteria basal supports a two-domain (eocyte) tree, in which eukaryotes arose from within Archaea, rather than the three-domain tree treating Archaea and Eukarya as separate top-level domains. Modern phylogenomics (Asgard archaea) further supports the two-domain view. See section 23.

15. The molecular clock for mitochondrial cytochrome b sequences in mammals ticks at about 2% divergence per million years (Mya). Two sister species differ by 8% in their cytochrome b sequences. Estimate when they diverged, and list two sources of uncertainty in this estimate.

Answer (Q15, Application). Divergence time \approx percent difference / rate = 8% / (2% per Myr) = 4 million years. Two uncertainty sources: clock-rate variation among lineages/sites (non-clocklike evolution, saturation/multiple hits) and calibration error in the assumed 2%/Myr rate. See section 23.

16. ABBA-BABA (D-statistics) tests detect gene flow between populations. If D is significantly positive, what does it imply about the relationships between the four taxa (P1, P2, P3, and outgroup)? How did this test reveal Neanderthal–modern human gene flow?

Answer (Q16, Application). A significantly positive D (ABBA > BABA) indicates gene flow/admixture between P3 and one of P1/P2 beyond that expected from incomplete lineage sorting under the (((P1,P2),P3),O) topology. Excess shared derived alleles between non-African humans (P2) and Neanderthal (P3) versus African humans (P1) revealed Neanderthal–modern-human introgression. See section 23.

17. Biogeographic analysis shows that the freshwater fish genus *Nannoperca* is distributed across southwestern Australia (isolated from other parts by arid zones). How would you distinguish between: (a) vicariance (ancient populations separated by geological changes); (b) long-distance dispersal (a single colonization event across an unsuitable barrier)?

Answer (Q17, Application). Distinguish by dating divergence relative to barrier age and comparing area cladograms: vicariance predicts divergence times matching the geological/aridification event and concordant patterns across co-distributed taxa; long-distance dispersal predicts divergence younger than the barrier and idiosyncratic, taxon-specific timing inconsistent with a shared vicariant event. See section 23.

18. Maximum likelihood (ML) phylogenetics uses an explicit model of sequence evolution (e.g., GTR+ Γ) to evaluate the likelihood of observing the data given a tree. Why is ML generally preferred over parsimony for molecular data, especially for distantly related taxa?

Answer (Q18, Application). Maximum likelihood uses an explicit substitution model (e.g., GTR+ Γ) to weight different change types and account for multiple hits and rate heterogeneity. It is preferred over parsimony for molecular data — especially distantly related taxa — because parsimony underestimates change on long branches and is prone to long-branch attraction, whereas ML models the true substitution process and is statistically consistent. See section 23.

19. Gene trees vs species trees: individual gene trees can differ from the species tree due to incomplete lineage sorting (ILS) or horizontal gene transfer. What is ILS, and why is it more likely for genes with short internodal branches (rapid speciation)?

Answer (Q19, Application). Incomplete lineage sorting is the persistence of ancestral polymorphism through successive speciation events, so a gene's coalescence predates speciation and its tree differs from the species tree. It is likelier with short internodal branches (rapid successive speciation) because there is little time for lineages to coalesce/sort between divergence events. See section 23. 20. The “long branch attraction” (LBA) artifact occurs when rapidly evolving lineages with many changes falsely cluster together in parsimony or distance analysis. Explain the mechanism of LBA and propose two strategies to avoid it (taxon sampling, model-based methods).

Answer (Q20, Application). Long-branch attraction: rapidly evolving (long) branches accumulate many independent changes, some matching by chance (homoplasy), which parsimony/distance methods misread as shared ancestry, clustering the long branches together regardless of true relationships. Mitigate by adding taxa to break long branches and by using model-based (ML/Bayesian) methods that correct for multiple substitutions. See section 23.

Questions 21–30: Synthesis and Evaluation

21. Evaluate the evidence that Archaeal clade Asgard is the closest prokaryotic relative of eukaryotes. What specific eukaryotic features (endomembrane, cytoskeleton homologues, ubiquitin) were identified in their genomes? What does this suggest about the origin of eukaryotic complexity?

Answer (Q21, Synthesis). Asgard archaea (Lokiarchaeota etc.) carry eukaryotic signature proteins — actin/profilin cytoskeletal homologues, ESCRT/membrane-trafficking and ubiquitin-system components — and branch as the closest prokaryotic relatives of eukaryotes in phylogenomic analyses. This supports a two-domain tree and an archaeal host that already possessed eukaryotic-like cellular machinery before mitochondrial endosymbiosis. See section 23. 22. Design a phylogenomic study (using hundreds of genes rather than one marker) to resolve a “soft polytomy” (unresolved node) in the avian tree of life. Describe: coalescent methods (ASTRAL) vs concatenation (ML on combined alignment), what sources of conflict between gene trees need to be accounted for, and how you would determine whether the polytomy reflects rapid radiation rather than incomplete data.

Answer (Q22, Synthesis). Sample hundreds of loci genome-wide; infer gene trees and combine by a coalescent method (ASTRAL) and by concatenated ML, comparing results. Account for ILS, gene-tree estimation error, and HGT/introgression as conflict sources. A true hard polytomy from rapid radiation is supported when gene-tree conflict is high and uniformly distributed and added data do not resolve the node, rather than reflecting missing data. See section 23. 23. The ribosomal RNA (rRNA) phylogeny (Woese, 1977) unified most life into three domains. Evaluate why rRNA was chosen as a comprehensive phylogenetic marker: (a) ubiquitous, almost universally homologous; (b) highly conserved but containing variable regions; (c) unlikely to undergo HGT. Are there limitations to rRNA as a “true” species tree marker?

Answer (Q23, Synthesis). rRNA was chosen because it is universal and homologous across all life, functionally constrained yet contains variable regions resolving multiple depths, and rarely transferred horizontally. Limitations: HGT is not zero, multiple rRNA copies can differ (paralogy), strong base-composition/rate biases and saturation can mislead deep nodes — so rRNA is a good but imperfect proxy for the species tree. See section 23. 24. Bayesian phylogenetics (MrBayes, BEAST) uses prior probabilities and MCMC sampling to estimate the posterior distribution of trees. Compare Bayesian vs maximum likelihood approaches: (a) what is the difference in interpretation of the “support” values (posterior probabilities vs bootstrap); (b) when does Bayesian inference provide overconfident node support; (c) how is divergence time estimation performed in BEAST?

Answer (Q24, Synthesis). (a) Bayesian support is a posterior probability (probability the clade is true given data and priors); bootstrap is a frequentist resampling proportion. (b) Bayesian PP can be overconfident under model misspecification or with very short internal branches. (c) BEAST estimates divergence times by combining a clock model, tree prior, and fossil/biogeographic calibration priors via MCMC to sample dated trees. See section 23. 25. Ancient DNA (aDNA) sequencing has transformed our understanding of human history by adding extinct hominin and historical populations to phylogenies. Evaluate the technical challenges of aDNA analysis: (a) DNA degradation (short fragments, C→U deamination); (b) contamination from environmental microbes and modern human DNA; (c) how mapDamage software and UDG treatment are used to address these.

Answer (Q25, Synthesis). (a) aDNA is fragmented and chemically damaged (C→U deamination causing C→T miscoding at fragment ends). (b) It is easily contaminated by environmental and modern-human DNA. (c) mapDamage models the deamination signature to authenticate ancient reads, and UDG/USER treatment excises uracils to remove deamination errors before genotyping, improving reliability of ancient phylogenetic placement. See section 23. 26. Evaluate the “bush of life” metaphor vs the traditional “tree of life” for describing microbial evolution. How prevalent is HGT among bacteria and archaea (what fraction of the typical prokaryote genome has been acquired by HGT), and at what level (genus, family, phylum) does HGT obscure true vertical inheritance?

Answer (Q26, Synthesis). For prokaryotes the ‘bush/web of life’ better reflects pervasive HGT: a substantial fraction of a typical prokaryote genome (often tens of percent of genes, cumulatively) has foreign ancestry. HGT can obscure vertical inheritance up to genus/family and even phylum level for some genes, though a core of rarely transferred informational genes still recovers a backbone organismal tree. See section 23. 27. Trans-

posableElements have been used as phylogenetic markers (SINEs/LINEs as synapomorphies): a SINE insertion shared by multiple taxa must have occurred once in a common ancestor. Evaluate the advantages of transposon-based markers over sequence-based phylogenetics: (a) irreversibility of insertion; (b) independence of molecular evolution model assumptions; (c) limitations (element excision, parallel insertions in hotspot regions).

Answer (Q27, Synthesis). (a) Transposon (SINE/LINE) insertions are effectively irreversible, so a shared insertion is a near-unambiguous synapomorphy. (b) Presence/absence does not depend on substitution-model assumptions. (c) Limitations: rare precise excision and parallel insertions into hotspots, and incomplete lineage sorting of polymorphic insertions, can still create homoplasy, so multiple independent insertions are used. See section 23. 28. The “total evidence dating” approach (tip calibration) uses morphological characters from fossils as direct terminal taxa (not just calibration points) in Bayesian time-tree analysis. Evaluate the advantages of total evidence dating over node calibration, and describe what happens to morphological branch length estimates when the model of trait evolution (e.g., Mk model) is misspecified.

Answer (Q28, Synthesis). Total-evidence (tip) dating places fossils as dated terminal taxa with morphological characters, jointly estimating topology and timescale and using the fossilised-birth–death process, which propagates uncertainty better than fixing node ages. If the morphological model (e.g., Mk) is misspecified, morphological branch lengths and hence inferred rates and divergence times are biased, distorting the time tree. See section 23. 29. Horizontal gene transfer in cancer (somatic HGT from tumor microenvironment bacteria into human cells) has been reported but remains controversial. Evaluate the evidence: (a) what sequencing artifacts can mimic bacterial HGT; (b) what controls are needed to rule out contamination; (c) if real, what functional consequences might cancer-incorporated bacterial genes have?

Answer (Q29, Synthesis). (a) Bacterial reads can arise from index-hopping, reference contamination, or chimeric assembly mimicking HGT. (b) Needed controls: matched blanks, multiple independent libraries, paired-end reads spanning human–bacterial junctions, and orthogonal validation (PCR/FISH). (c) If real, integrated bacterial genes could alter host gene expression or metabolism in tumor cells, but the bar for evidence is high given pervasive artifact risk. See section 23. 30. Critically assess whether a “tree of life” can be reconstructed from extant biodiversity alone, without fossil calibration. What information is intrinsically lost when primarily the tips (extant species) and not the internal nodes (extinct ancestors) are known? Use the concept of incomplete ancestry and the “big-bang” topology problem of rapid early diversification as a specific example.

Answer (Q30, Synthesis). From extant tips alone, extinct lineages and ancestral states are unobserved, so deep relationships, ancestral character reconstruction, and absolute timing are weakly identified. Rapid early diversification gives near-simultaneous splits (‘big-bang’ topology) with little informative signal on short internal branches, so without fossil calibration both branching order and timescale of the deep tree remain poorly resolved. See section 23.

Questions — Bacteria, Archaea, and Viruses

Instructor Use and Coverage Notes

- Coverage target: Classify a microbe or virus from evidence and predict a likely vulnerability.
- Model/data emphasis: Growth-rate, genome-size, and dilution calculations.
- Assessment alignment: Questions and Methods, Representing and Describing Data, Argumentation.
- Misconception probe: Viruses are not simply tiny bacteria; they use fundamentally different replication logic.
- Transfer product: Apply microbial diversity reasoning to antibiotics, biotechnology, ecology, and outbreaks.
- Grading focus: award full credit for mechanism, evidence, boundary conditions, and units when a calculation is required.
- Suggested use: draw one recall item, one application item, and one synthesis item when building a short quiz from this bank.

Questions 1–10: Recall and Comprehension

This activity accompanies section 24 of the textbook — review that chapter before attempting the exercises below.

1. List three differences between bacteria and archaea in cell wall chemistry and membrane lipids.

Answer (Q1, Recall). Three diagnostic differences: (1) Cell wall — bacteria use peptidoglycan (murein) with muramic acid, whereas archaea lack peptidoglycan and instead use pseudopeptidoglycan, S-layers, or other polymers. (2) Membrane lipids — bacterial lipids are ester-linked, straight-chain fatty acids on glycerol-3-phosphate, while archaeal lipids are ether-linked, branched isoprenoid chains on glycerol-1-phosphate. (3) Some archaea form a tetraether lipid monolayer (rather than a bilayer), giving extreme thermal and chemical stability. See section 24. 2. What is the Gram stain? What does Gram-positive vs Gram-negative indicate about cell wall structure?

Answer (Q2, Recall). The Gram stain (Hans Christian Gram, 1884) is a differential stain that sorts bacteria by cell-wall architecture. Gram-positive cells retain the crystal-violet–iodine complex because they have a thick multilayered peptidoglycan wall and stain purple. Gram-negative cells have a thin peptidoglycan layer plus an outer membrane containing lipopolysaccharide (LPS); the decolorizer washes out the primary stain so they take up the safranin counterstain and appear pink. See section 24. 3. Describe the replication cycle of a bacteriophage. Distinguish lytic from lysogenic cycles.

Answer (Q3, Recall). A bacteriophage attaches to a host receptor, injects its genome, and then follows one of two paths. In the lytic cycle the phage immediately hijacks host machinery to replicate its genome, assemble progeny, and lyse the cell, releasing new virions. In the lysogenic cycle the phage genome integrates into the host chromosome as a prophage and is replicated passively with the host until an induction signal switches it to the lytic cycle. See section 24. 4. What is a prophage? What signal triggers induction of the lytic cycle from lysogeny?

Answer (Q4, Recall). A prophage is a bacteriophage genome that has integrated into the host bacterial chromosome (or persists as a plasmid) and is replicated along with the host during lysogeny. Induction to the lytic cycle is triggered by DNA-damaging stress (e.g., UV light or chemical mutagens) that activates the host SOS response: RecA stimulates autocleavage of the phage repressor (CI in lambda), de-repressing lytic genes. See section 24. 5. Name three types of bacterial reproduction. Which is the fastest?

Answer (Q5, Recall). Bacteria propagate by binary fission (asexual clonal division), and they also exchange genes horizontally by transformation, transduction, and conjugation. Of these, simple binary fission is by far the fastest route to more cells — under optimal conditions some bacteria double every about 20 minutes — whereas the horizontal transfer processes spread genes but do not, by themselves, rapidly increase cell number. See section 24. 6. What is binary fission? How does the doubling time relate to bacterial growth rate?

Answer (Q6, Recall). Binary fission is asexual reproduction in which the circular chromosome is replicated bidirectionally from oriC, the cell elongates, an FtsZ ring directs septum formation at mid-cell, and two identical daughter cells separate. Each round doubles the population, so the doubling (generation) time t_d sets the growth rate: the number of generations $n = t/t_d$ and $N(t) = N_0 \cdot 2^{(t/t_d)}$. A shorter doubling time means a steeper exponential growth rate. See section 24. 7. Describe the structure of a typical bacterium: nucleoid, ribosomes, pili, flagella, capsule.

Answer (Q7, Recall). A typical bacterium has a nucleoid (a single supercoiled circular chromosome, no nuclear membrane), 70S ribosomes for translation, pili/fimbriae for adhesion and (sex pili) conjugation, one or more flagella that rotate like propellers driven by proton-motive force for motility, and often a polysaccharide capsule that resists desiccation and phagocytosis. All sit inside the plasma membrane and peptidoglycan cell wall. See section 24. 8. What is conjugation? What is an F plasmid?

Answer (Q8, Recall). Conjugation is horizontal gene transfer requiring direct cell-to-cell contact through a sex pilus. The F (fertility) plasmid encodes that pilus and the transfer machinery; an F+ donor transfers a copy of the F plasmid to an F– recipient. Because conjugative (R–) plasmids often carry antibiotic-resistance genes, conjugation is the principal route by which resistance spreads within and between bacterial species. See section 24. 9. Distinguish DNA viruses from RNA viruses. Give one example of each.

Answer (Q9, Recall). DNA viruses store their genome as DNA and generally replicate using host (or viral) DNA polymerases with relatively high fidelity (e.g., herpesvirus, a dsDNA virus). RNA viruses store their genome as RNA and replicate with error-prone RNA-dependent RNA polymerase (or reverse transcriptase), giving high mutation rates and rapid evolution (e.g., influenza virus, a –ssRNA virus). See section 24. 10. What is a retrovirus? Describe its replication cycle.

Answer (Q10, Recall). A retrovirus is an enveloped +ssRNA virus (Baltimore Class VI, e.g., HIV) that carries reverse transcriptase. Its cycle: gp120 binds CD4 plus a coreceptor (CCR5/CXCR4) and the membrane fuses; reverse transcriptase copies the RNA genome into dsDNA; integrase splices that provirus into the host genome; host machinery transcribes and translates viral genes; new virions bud from the membrane and the protease matures them into infectious particles. See section 24.

Questions 11–20: Application and Analysis

11. A bacterial culture starts with 100 cells and has a doubling time of 20 minutes. Calculate: (a) the number of cells after 2 hours; (b) the approximate mass of bacteria (assuming 10^{-15} g/cell) after 24 hours. Why does exponential growth not continue indefinitely?

Answer (Q11, Application). Use $N(t) = N_0 \cdot 2^{(t/td)}$ with $N_0 = 100$ and $td = 20$ min. (a) After 2 h = 120 min there are $120/20 = 6$ doublings, so $N = 100 \cdot 2^6 = 6,400$ cells. (b) After 24 h = 1440 min there are 72 doublings: $N = 100 \cdot 2^{72} \approx 4.7 \times 10^{23}$ cells; at 10^{-15} g/cell that is about 4.7×10^8 g (about 470 metric tons) — a biologically impossible mass. Exponential growth cannot continue because nutrients deplete, waste and toxic byproducts accumulate, and space/oxygen become limiting, so cultures enter stationary phase. See section 24. 12. Design a serial dilution experiment to count colonies from a bacterial sample expected to have about 10^6 CFU/mL. Which dilutions would give countable plates (30–300 colonies)? Calculate CFU/mL from a plate showing 175 colonies at 10^{-5} dilution.

Answer (Q12, Application). Prepare serial 10-fold dilutions (e.g., 10^{-1} through 10^{-7}) and plate 0.1 mL of each in replicate. For about 10^6 CFU/mL the 10^{-4} and 10^{-5} dilutions should land in the countable 30–300 range. $CFU/mL = \text{colonies} \div (\text{dilution factor} \times \text{volume plated})$. For 175 colonies at 10^{-5} plating 0.1 mL: $175 \div (10^{-5} \times 0.1) = 175 \div 10^{-6} = 1.75 \times 10^8$ CFU/mL. (If 0.1 mL was plated; if 1 mL, 1.75×10^7 CFU/mL.) See section 24.

13. Compare the lytic and lysogenic cycles: what are the advantages of each for the phage? Under what environmental/physiological conditions does the lambda phage switch from lysogeny to the lytic cycle? (Name the specific protease.)

Answer (Q13, Application). The lytic cycle maximizes immediate progeny when hosts are abundant; the lysogenic cycle preserves the genome through host scarcity or hostile conditions by hiding as a prophage. In lambda, the lysogeny-versus-lysis decision is governed by the CI repressor: DNA damage activates the host SOS response, *RecA-stimulated autocleavage destroys CI, de-repressing the lytic genes. The relevant phage protease activity is the RecA-coactivated autocleavage of the CI repressor.* See section 24. 14. MRSA (*methicillin-resistant Staphylococcus aureus*) carries *mecA** or *mecC*, encoding a modified penicillin-binding protein (PBP2a/PBP2c) with low affinity for most traditional β -lactam antibiotics. Explain: (a) how *mec* genes are acquired by horizontal gene transfer on *SCCmec* elements; (b) why many β -lactams fail but anti-MRSA cephalosporins can be exceptions in susceptible isolates; (c) what alternative antibiotics are used and how their mechanisms bypass PBP2a.

Answer (Q14, Application). MRSA resistance begins with *SCCmec* acquisition carrying *mecA* or *mecC*. These genes encode PBP2a/PBP2c, transpeptidases whose active sites bind most older β -lactams poorly, so cell-wall cross-linking can continue despite drug exposure. Note that ceftaroline or ceftobiprole can be exceptions when susceptibility testing supports them; then compare alternatives: vancomycin binds D-Ala-D-Ala cell-wall precursors, daptomycin disrupts the Gram-positive membrane, and linezolid blocks 50S translation initiation. See section 24. 15. Archaea are found in extreme environments (hyperthermophiles, halophiles, methanogens). Explain how: (a) archaeal lipid membranes (isoprene ether-linked, rather than ester-linked) withstand high temperatures; (b) halophilic archaea stabilize proteins at high salt by having an excess of surface-facing acidic residues; (c) methanogenic archaea use H_2 and CO_2 as energy sources via a unique archaeal pathway.

Answer (Q15, Application). (a) Archaeal ether linkages and branched isoprenoid chains resist hydrolysis; tetraether monolayers cannot split into leaflets, so membranes stay intact at high temperature. (b) Halophilic archaeal proteins carry an excess of acidic (Asp/Glu) surface residues that bind hydrated ions and water, keeping proteins soluble and folded in saturating salt. (c) Methanogens are strict anaerobes that reduce CO_2 with H_2 to CH_4 through the archaea-specific methanogenesis pathway using unique cofactors (coenzyme M, F420), harvesting energy via a proton/sodium gradient. See section 24. 16. The CRISPR-Cas system in bacteria provides adaptive immunity against phage. Explain: (a) spacer acquisition from phage DNA; (b) crRNA-guided Cas9 surveillance; (c) cleavage of matching invader DNA; (d) why the phage can evolve to escape CRISPR immunity (PAM sequence mutation). How did bacterial CRISPR inspire the molecular biology tool?

Answer (Q16, Application). (a) Adaptation: Cas1–Cas2 excise a protospacer from invading phage DNA and insert it as a new spacer into the CRISPR array. (b) Expression: the array is transcribed and processed into crRNAs that load Cas9 for surveillance. (c) Interference: crRNA base-pairs with matching phage DNA next to a PAM and Cas9 makes a double-strand cut, destroying the invader. (d) Phage escape by mutating the PAM or protospacer abolishes recognition. The programmable RNA-guided Cas9 nuclease was repurposed as a genome-editing tool. See section 24.

17. Viral tropism (which cells a virus can infect) depends on receptor-ligand binding. HIV infects cells expressing both CD4 and CCR5/CXCR4

(co-receptors). Individuals homozygous for a 32-bp deletion in *CCR5* ($\Delta 32$ allele) are largely resistant to HIV infection. Explain why this is and why CCR5 antagonists (maraviroc) alone do not fully cure HIV.

Answer (Q17, Application). HIV entry requires gp120 binding CD4 and a coreceptor (CCR5 early, CXCR4 late). A homozygous CCR5- $\Delta 32$ deletion produces a non-functional, surface-absent receptor, so the common CCR5-tropic strains cannot complete entry, conferring strong resistance. CCR5 antagonists like maraviroc only block CCR5-tropic virus; they do not clear the integrated latent provirus in resting memory CD4+ T cells and fail against CXCR4-tropic variants, so they suppress but do not cure HIV. See section 24. 18. Prions are misfolded proteins (PrP^{Sc}) that convert normally folded proteins (PrP^C) to the pathogenic conformation. Explain: (a) why prion diseases (CJD, BSE) are transmissible without nucleic acid; (b) the proposed templating mechanism; (c) why prions are nearly extremely difficult to decontaminate by standard autoclaving.

Answer (Q18, Application). (a) Prions are infectious because PrP^{Sc} itself acts as the agent — they contain no nucleic acid, so transmission is purely conformational. (b) The templating mechanism: PrP^{Sc} (β -sheet rich) binds normal PrP^C (α -helical) and catalyzes its refolding into more PrP^{Sc}, which aggregates into amyloid; this autocatalytic conversion propagates the disease (CJD, BSE). (c) Because infectivity resides in a misfolded protein with no genome, standard autoclaving fails — there is no nucleic acid to destroy and the aggregates are extraordinarily heat- and protease-resistant. See section 24. 19. Bacteriophage therapy (phage therapy) is being reconsidered as an alternative to antibiotics for drug-resistant infections. Compare phage therapy vs antibiotics: (a) host range (broad-spectrum antibiotics vs phage-host specificity); (b) resistance evolution rate; (c) phage ability to co-evolve with bacterial host. Give one clinical case report of successful phage therapy.

Answer (Q19, Application). (a) Broad-spectrum antibiotics kill many taxa, whereas phages are highly host-specific (often strain-level), sparing the microbiome but requiring precise matching. (b) Bacteria evolve resistance to both, but phages can co-evolve to counter resistant hosts, partly offsetting escape. (c) That co-evolutionary capacity — and combining phages in cocktails or with antibiotics — limits resistance. A documented clinical success is the 2017 personalized phage-cocktail rescue of a patient with multidrug-resistant *Acinetobacter baumannii* (Strathdee/UCSD case). See section 24. 20. SARS-CoV-2 is a +ssRNA coronavirus. Explain: (a) how it uses its spike protein to bind ACE2 and enter cells; (b) why mRNA vaccines encoding spike protein induce protective immunity; (c) why variants (Omicron) with many spike mutations can partially evade vaccine-induced antibodies.

Answer (Q20, Application). (a) The SARS-CoV-2 spike receptor-binding domain binds host ACE2; host protease (TMPRSS2/furin) primes spike and the membrane fuses, delivering the +ssRNA genome. (b) mRNA vaccines deliver spike-encoding mRNA so host cells express spike, eliciting neutralizing antibodies and T-cell memory targeting that protein. (c) Omicron carried about 32 spike mutations, many in the RBD/antigenic sites, which reduce binding of vaccine-elicited antibodies, allowing partial immune escape while T-cell immunity remains broader. See section 24.

Questions 21–30: Synthesis and Evaluation

- Evaluate the hypotheses for the origin of viruses: (a) regression hypothesis (viruses are degenerate cells); (b) escape hypothesis (mobile genetic elements that gained capsids); (c) primordial virion hypothesis (viruses predate cells). Which hypothesis is most consistent with current phylogenomic data (nucleocytoplasmic large DNA viruses and their relatives)?

Answer (Q21, Synthesis). (a) The regression hypothesis holds that viruses are degenerate intracellular parasites that lost cellular machinery. (b) The escape hypothesis holds that viruses arose from cellular mobile genetic elements (plasmids/transposons) that acquired capsid genes. (c) The primordial-virion (virus-first) hypothesis holds that viruses predate cells. Current phylogenomic data — including nucleocytoplasmic large DNA viruses (giant viruses) with translation-related genes and conserved capsid lineages — most strongly support a polyphyletic origin, with the virus-first/ancient-lineage view favored for the major capsid lineages; new conserved viral hallmark genes would change the conclusion. See section 24. 22. Design a strategy to engineer a phage to specifically kill a Gram-negative ESKAPE pathogen (*Klebsiella pneumoniae*) that is resistant to multiple first-line antibiotics and has few standard options. Describe: (a) the host-range engineering approach (tail fiber protein swapping); (b) the anti-biofilm component you would add; (c) the regulatory and safety evidence required before use in humans.

Answer (Q22, Synthesis). A strong design starts by typing the patient's *K. pneumoniae* isolate, identifying its capsule/receptor profile, and screening a phage panel against that exact isolate and close clinical comparators. Tail-fiber engineering should be justified by receptor data; an anti-biofilm depolymerase should match the capsule or EPS chemistry; and controls should include untreated bacteria, wild-type phage, engineered phage, antibiotic alone, and phage-antibiotic combinations. Safety evidence should include whole-genome screening for lysogeny, toxin, and AMR genes; endotoxin and sterility release testing; resistance-emergence assays; pharmacokinetic reasoning; and FDA expanded-access or investigational-new-drug review before human use. See section 24. 23. Quorum sensing in *Pseudomonas aeruginosa* controls virulence gene expression via N-acyl-homoserine lactone (AHL) signaling (las and rhl systems). Evaluate: (a) how quorum sensing allows coordinated virulence (biofilm formation, exotoxin production) primarily at high cell density; (b) why quorum sensing inhibitors (QSIs) are attractive anti-virulence targets (less resistance selection pressure); (c) why QSI clinical development has stalled.

Answer (Q23, Synthesis). (a) In *P. aeruginosa*, las and rhl systems use AHL autoinducers whose concentration tracks cell density; only at quorum

do LasR/RhlR activate biofilm, exotoxin, and protease genes, so virulence is deployed when the population is large enough to overwhelm host defenses. (b) Quorum-sensing inhibitors are attractive because disarming virulence rather than killing cells imposes weaker selection for resistance. (c) QSI clinical development has stalled because of poor pharmacokinetics, redundancy among signaling circuits, narrow efficacy windows, and difficulty showing clinical benefit in trials. See section 24. 24. Evaluate the evolutionary biology of rapid viral evolution (HIV, influenza). HIV's high mutation rate (error-prone RT, about 3×10^{-5} /base/replication) generates enormous diversity. How does this diversity allow immune escape and drug resistance? Evaluate why combination antiretroviral therapy (ART) — targeting multiple steps simultaneously — dramatically suppresses resistance evolution and how “cure” strategies (shock and kill) aim to eliminate latent reservoirs.

Answer (Q24, Synthesis). HIV's error-prone reverse transcriptase (about 3×10^{-5} errors/base/replication) generates a vast mutant swarm, so antigenic-escape and drug-resistant variants pre-exist before selection. Single-drug therapy selects resistant clones quickly; combination ART blocks several steps at once, so a virion would need multiple simultaneous resistance mutations — improbable per replication — which durably suppresses resistance. The remaining barrier is the latent integrated reservoir in resting memory CD4+ T cells; ‘shock and kill’ aims to reactivate that reservoir with latency-reversing agents while ART prevents new infection, so it can be cleared. See section 24. 25. Giant viruses (Mimivirus, Pandoravirus) have genomes >1 Mb — larger than some bacteria — and contain genes for translation-related functions unprecedented in viruses. Evaluate whether giant viruses blur the boundary between viruses and cells, and whether they support the regression hypothesis for viral origin.

Answer (Q25, Synthesis). Giant viruses (Mimivirus, Pandoravirus) have >1 Mb genomes — larger than some bacteria — and encode translation-related genes (aminoacyl-tRNA synthetases, translation factors) never before seen in viruses, blurring the virus/cell boundary. They still lack ribosomes and ATP generation and remain obligate intracellular parasites, so they are not cells. Their many cellular-like genes are most parsimoniously explained by genome expansion and extensive gene acquisition rather than strong support for the regression hypothesis; reductive-evolution signatures from a cellular ancestor would be needed to favor regression. See section 24. 26. Horizontal gene transfer (HGT) in bacteria can be transduction, transformation, or conjugation. Use a One Health AMR map to compare how an ESBL or carbapenemase gene could move among hospital patients, wastewater, livestock, soil microbes, and wildlife. Which transfer mechanism is most plausible in each setting, and what surveillance evidence would distinguish clonal spread from mobile-element spread?

Answer (Q26, Synthesis). In hospitals, clonal spread is supported when isolates share a near-identical core genome, ward overlap, and the same resistance phenotype; plasmid-mediated spread is supported when unrelated strains carry the same resistance plasmid, integron, or transposon. In wastewater and livestock settings, conjugation is often the most plausible route for plasmid-borne ESBL or carbapenemase genes because dense mixed communities and antibiotic residues favor mobile elements. Transformation can matter where extracellular DNA persists in biofilms or sediments, while transduction requires phage evidence linked to the resistance cassette. Sound surveillance names sampling sites, genome data, plasmid typing, resistance phenotype, and exposure history, and explains why One Health surveillance follows genes and mobile elements as well as named pathogens. See section 24. 27. The microbiome of the human gut contains >1,000 bacterial species that collectively perform essential metabolic functions (SCFA production, vitamin synthesis, immune training). Evaluate whether the gut microbiome should be considered an “accessory genome” of the human host, and what criteria would need to be met for this “extended genome” concept to be scientifically defensible.

Answer (Q27, Synthesis). Treating the gut microbiome as an ‘accessory genome’ captures the fact that >1,000 species supply host-essential functions (SCFA production, vitamin synthesis, bile-acid transformation, immune training) the human genome lacks, and that function is conserved even when species composition varies (functional redundancy). For the ‘extended genome’ concept to be defensible it would need: heritable/stable transmission across host generations, demonstrated host-fitness dependence on those functions, reproducible function despite taxonomic turnover, and a defined core functional gene set — otherwise it is a useful metaphor rather than a literal genome. See section 24. 28. Bacteriophage encode auxiliary metabolic genes (AMGs) — metabolic genes that boost host metabolism during infection (e.g., phage-encoded photosynthesis genes in cyanophages). Evaluate the role of phage AMGs in global carbon and nitrogen cycling, and propose how phage-encoded metabolic capacity shapes marine primary productivity.

Answer (Q28, Synthesis). Phage auxiliary metabolic genes (AMGs) — e.g., cyanophage-encoded photosystem genes (psbA) — sustain or redirect host metabolism during infection. Initiating condition: a phage infects a primary producer (e.g., a marine cyanobacterium). Changed component: AMGs maintain photosynthesis and reroute carbon/nitrogen flux toward phage production. Mechanism: phage lysis (‘viral shunt’) diverts fixed carbon from higher trophic levels into the dissolved organic pool. Outcome: AMGs and lysis collectively modulate marine primary productivity and global C/N cycling, so phages are major biogeochemical agents. See section 24. 29. The virome — the complete collection of viruses in an ecosystem — is far larger than the known virome catalogued to date. Evaluate metagenomics approaches (shotgun metagenomics, viromics with CRISPR spacer-based enrichment) for discovering novel viruses, and assess what fraction of global viral diversity may remain undiscovered.

Answer (Q29, Synthesis). Shotgun metagenomics sequences total environmental DNA and assembles viral genomes without culture; CRISPR-spacer-based viromics links uncultured viruses to their hosts by matching host spacer arrays to viral protospacers, enriching discovery. Limits include short-read assembly gaps, RNA-virus and rare-taxon undersampling, and database bias, so estimates remain uncertain. Evidence (vast

unassigned sequence space, environment-specific novel lineages) indicates the great majority of global viral diversity is still uncatalogued; deeper long-read and host-linked sampling would refine the estimate. See section 24. 30. Critically evaluate the claim that viruses are “the dark matter of the biosphere” — underappreciated forces shaping ecosystems, gene flows, and evolution. What evidence from marine phage ecology, the pan-genome of bacteria, and viral integration into eukaryotic genomes supports this claim? How does the expanding virology of the 2010s–2020s change our understanding of life’s diversity?

Answer (Q30, Synthesis). ‘Dark matter of the biosphere’ is supported by: marine phage abundance (about 10^{31} virions; the viral shunt and about daily turnover of bacterial standing stock), the open bacterial pan-genome inflated by phage-mediated horizontal transfer and prophages, and endogenous viral elements (e.g., syncytin from retroviral env) co-opted into eukaryotic genomes. The claim weakens only if novel viral diversity proved ecologically inert. Expanding 2010s–2020s virology (giant viruses, viromics, RNA-virus megadiversity) reframes viruses as central drivers of evolution, gene flow, and ecosystem function rather than mere pathogens. See section 24.

Questions — Microbial Ecology and the Microbiome

Instructor Use and Coverage Notes

- Coverage target: Use community data to infer diversity, dominance, and a plausible ecological mechanism.
- Model/data emphasis: Diversity indices, richness estimates, and interaction-network reasoning.
- Assessment alignment: Questions and Methods, Representing and Describing Data, Argumentation.
- Misconception probe: A microbiome is not automatically beneficial; context determines the effect.
- Transfer product: Transfer microbial ecology to soils, oceans, digestion, disease, and climate feedbacks.
- Grading focus: award full credit for mechanism, evidence, boundary conditions, and units when a calculation is required.
- Suggested use: draw one recall item, one application item, and one synthesis item when building a short quiz from this bank.

Questions 1–10: Recall and Comprehension

This activity accompanies section 25 of the textbook — review that chapter before attempting the exercises below.

1. Define the microbiome. What is the difference between microbiome and microbiota?

Answer (Q1, Recall). The microbiome is the entire community of microorganisms (bacteria, archaea, fungi, viruses) inhabiting a defined environment together with their collective genes, metabolites, and the surrounding conditions. The microbiota refers specifically to the microbial taxa themselves (the organisms present), whereas the microbiome additionally encompasses their genomes and functional/environmental context. In short: microbiota = who is there; microbiome = who is there plus what they do and the milieu. See section 25. 2. What is 16S rRNA sequencing? Why is the 16S gene used to classify bacteria?

Answer (Q2, Recall). 16S rRNA sequencing amplifies and sequences the gene encoding the small-subunit ribosomal RNA of bacteria and archaea to identify and classify them without culturing. The 16S gene is ideal because it is universally present, functionally conserved (so it cannot be lost), and contains both highly conserved regions (for universal PCR primers) and hypervariable regions (V1–V9) whose sequence differences serve as a molecular clock distinguishing taxa. See section 25. 3. Define the Shannon diversity index. What does a high value indicate?

Answer (Q3, Recall). The Shannon diversity index $H' = -\sum p_i \ln(p_i)$, where p_i is the proportional abundance of species i , combines richness (number of species) and evenness (how equally abundant they are). A high H' indicates a community with many species present and an even distribution of individuals among them, whereas a low value reflects few species or strong dominance by one taxon. See section 25. 4. What are the four major phyla of the human gut microbiome?

Answer (Q4, Recall). The human gut microbiome is dominated by four bacterial phyla: Firmicutes (now Bacillota) and Bacteroidetes (Bacteroidota) make up the great majority of the community, with Actinobacteria (Actinomycetota) and Proteobacteria (Pseudomonadota) as the other major contributors. Verrucomicrobia (e.g., Akkermansia) is often noted as a fifth. Firmicutes and Bacteroidetes together typically account for >90% of gut bacteria. See section 25. 5. What is a biofilm? Name two biological advantages biofilm growth confers on bacteria.

Answer (Q5, Recall). A biofilm is a structured, surface-attached community of microorganisms encased in a self-produced extracellular polymeric substance (EPS) matrix of polysaccharides, proteins, and extracellular DNA. Two advantages it confers: (1) greatly increased tolerance to antibiotics and host defenses (the matrix limits drug penetration and harbors slow-growing persister cells), and (2) protection from environmental stress and shear, plus proximity that enables metabolic cooperation and horizontal gene transfer. See section 25. 6. Define mutualism, commensalism, and parasitism. Give one example of each in microbial ecology.

Answer (Q6, Recall). Mutualism is an interaction benefiting both partners (+/+), e.g., Rhizobium fixing nitrogen for legumes in exchange for plant carbon. Commensalism benefits one partner with no significant effect on the other (+/0), e.g., many skin or gut commensals using host nutrients without harming or helping the host. Parasitism benefits one partner at the other’s expense (+/–), e.g., a pathogenic bacterium such as Mycobacterium tuberculosis exploiting its host while causing disease. See section 25. 7. What is the rhizosphere? Name one bacterium that benefits plant growth there.

Answer (Q7, Recall). The rhizosphere is the narrow zone of soil immediately surrounding and influenced by plant roots, where root exudates (sugars, amino acids, organic acids) enrich microbial activity 10–100-fold relative to bulk soil. A bacterium that benefits plant growth there is Rhizobium (a nitrogen-fixing symbiont forming legume root nodules); plant-growth-promoting Pseudomonas and Azospirillum are also examples. See section 25. 8. What are short-chain fatty acids (SCFAs)? Name three and state which gut bacteria produce them.

Answer (Q8, Recall). Short-chain fatty acids (SCFAs) are 1–6-carbon fatty acids produced when gut bacteria ferment dietary fiber and resistant starch in the colon. The three principal SCFAs are acetate, propionate, and butyrate. Acetate is produced broadly by many bacteria including Bacteroidetes;

propionate largely by Bacteroidetes; and butyrate chiefly by Firmicutes such as *Faecalibacterium prausnitzii* and *Roseburia*. Butyrate is the main energy source for colonocytes. See section 25. 9. Define dysbiosis. Associate dysbiosis with two human diseases.

Answer (Q9, Recall). Dysbiosis is a compositional and functional imbalance of the microbiome — loss of beneficial taxa, expansion of potentially harmful ones, and reduced diversity — associated with disease. It is linked to many conditions; two examples are inflammatory bowel disease (Crohn’s disease/ulcerative colitis) and *Clostridioides difficile*–associated colitis (it is also implicated in obesity and metabolic disease). See section 25. 10. What is the global nitrogen cycle? Name two types of bacteria that fix atmospheric nitrogen.

Answer (Q10, Recall). The global nitrogen cycle is the set of microbially driven transformations that move nitrogen among atmospheric N₂, ammonia/ammonium, nitrite, nitrate, and organic nitrogen via fixation, nitrification, assimilation, ammonification, and denitrification. Two types of nitrogen-fixing bacteria are the symbiotic *Rhizobium* (in legume root nodules) and free-living/diazotrophic bacteria such as *Azotobacter* (cyanobacteria like *Anabaena* also fix N₂). See section 25.

Questions 11–20: Application and Analysis

11. Fecal microbiome transplant (FMT) resolves recurrent *Clostridioides difficile* infection in about 90% of cases. Explain: (a) why antibiotic use predisposes patients to *C. diff*; (b) how FMT restores colonization resistance; (c) why FMT is less likely to be effective in IBD (Crohn’s, ulcerative colitis)?

Answer (Q11, Application). (a) Broad-spectrum antibiotics deplete the protective commensal community, removing colonization resistance and freeing nutrients and niche space that *C. difficile* spores exploit to germinate and overgrow. (b) FMT transplants a healthy donor community that re-establishes colonization resistance by competing for nutrients/niche, restoring secondary bile acids that inhibit *C. difficile* germination, and reactivating immune regulation. (c) FMT works less well in IBD because IBD pathology is driven by a dysregulated host immune response to the microbiota rather than a single missing function, so simply replacing the community does not correct the underlying immune dysfunction. See section 25. 12. A researcher performs 16S metagenomics on soil samples from fertile farmland, degraded land, and old-growth forest. Predict: which environment would show highest Shannon diversity; whether any taxa would serve as indicators of soil health; and what functional genes you would look for in shotgun metagenomics data.

Answer (Q12, Application). The relevant variable is land-use/disturbance regime and its effect on microbial diversity. Mechanism: stable, resource-rich, structurally complex habitats support more niches. Prediction: old-growth forest soil shows the highest Shannon diversity, fertile farmland intermediate, and degraded land the lowest. Indicator taxa: nitrogen-cyclers (*Nitrosomonas*, *Rhizobium*), Acidobacteria, and Glomeromycota mycorrhizae can flag soil health. In shotgun metagenomics, look for functional genes for nitrogen cycling (*nifH*, *amoA*, *nosZ*), carbon turnover (cellulases, chitinases), and phosphorus solubilization. Evidence that would weaken the prediction: high diversity in degraded soil, or no consistent indicator taxa once sampling depth, spatial scale, and replication are controlled. See section 25. 13. The “hygiene hypothesis” (now refined as the “old friends” hypothesis) proposes that reduced microbial exposure in early life increases allergic and autoimmune disease risk. Evaluate the evidence: (a) epidemiological (higher allergy rates in developed countries); (b) experimental (germ-free mice have hyperactive immune systems); (c) specific microbial species (*Lactobacillus*, *Faecalibacterium prausnitzii*) that prevent allergy.

Answer (Q13, Application). Initiating condition: reduced early-life exposure to commensal and environmental ‘old friend’ microbes. Changed component: an immature, under-trained immune system with weak regulatory T-cell development. Mechanism: without microbial signals (e.g., SCFAs, microbial antigens) immune regulation is poorly calibrated, biasing toward Th2/allergic and autoimmune responses. Outcome: higher allergy/autoimmune incidence. Evidence: (a) epidemiology shows higher allergy rates in sanitized, urbanized, developed settings; (b) germ-free mice have hyperactive, dysregulated immune systems corrected by colonization; (c) specific taxa (*Lactobacillus*, *Faecalibacterium prausnitzii*) promote regulatory immunity and reduce allergic inflammation, though causality in humans remains correlational. See section 25. 14. Nitrogen cycle: N-fixing bacteria (*Rhizobium* in legume nodules) convert N₂ → NH₃. Nitrifying bacteria convert NH₃ → NO₂[−] → NO₃[−]. Denitrifying bacteria convert NO₃[−] → N₂. Trace a nitrogen atom from atmospheric N₂ through these steps into a plant protein, and then back to N₂ in soil. Why is this cycle vulnerable to disruption by synthetic fertilisers?

Answer (Q14, Application). Atmospheric N₂ is reduced to NH₃/NH₄⁺ by nitrogenase in *Rhizobium* within legume nodules (fixation). Nitrifying bacteria oxidize NH₃ → NO₂[−] (*Nitrosomonas*) → NO₃[−] (*Nitrobacter*). Plant roots assimilate NO₃[−]/NH₄⁺ and incorporate the nitrogen into amino acids and proteins; following death and decomposition, ammonification returns organic N to NH₄⁺, and denitrifying bacteria reduce NO₃[−] → N₂ back to the atmosphere, completing the cycle. The cycle is vulnerable to synthetic fertilizer because the Haber-Bosch–derived reactive nitrogen flood overwhelms microbial processing, causing nitrate leaching, eutrophication, and excess denitrification/N₂O greenhouse emissions. See section 25. 15. Marine microbial ecology: *Prochlorococcus* is the most abundant photosynthetic organism on Earth (about 10²⁷ cells). Explain: (a) its adaptations for low-nutrient, high-light (and low-light) ocean zones; (b) how phage predation of *Prochlorococcus* releases dissolved organic carbon (DOC) fuelling heterotrophic bacteria; (c) what would happen to ocean productivity if *Prochlorococcus* were eliminated.

Answer (Q15, Application). (a) *Prochlorococcus* is genome-streamlined with divinyl chlorophyll and distinct high-light and low-light ecotypes,

letting different strains exploit nutrient-poor, strongly stratified surface waters and the dim deep euphotic zone. (b) Phage lysis of *Prochlorococcus* releases its fixed carbon as dissolved organic carbon (the ‘viral shunt’), which fuels heterotrophic bacteria and recycles nutrients rather than passing carbon up the food web. (c) Eliminating *Prochlorococcus* would remove a large share of open-ocean primary production, collapsing the base of oligotrophic food webs, reducing carbon fixation/export, and disrupting global ocean productivity and the carbon cycle. See section 25. 16. The human oral microbiome (about 700 species) produces dental caries via *Streptococcus mutans* acidifying enamel via lactic acid fermentation. Explain: (a) how sucrose is a uniquely cariogenic sugar (forms glucan adhesion matrix via glucosyltransferase); (b) what pH triggers enamel demineralisation (<5.5); (c) how fluoride in drinking water chemically protects enamel.

Answer (Q16, Application). Initiating condition: dietary sucrose reaches the dental biofilm. (a) *Streptococcus mutans* glucosyltransferase uses sucrose specifically to synthesize sticky, water-insoluble glucans that build the adhesive plaque matrix — no other dietary sugar supports this matrix as efficiently, making sucrose uniquely cariogenic. Mechanism: *S. mutans* ferments sugars to lactic acid, dropping plaque pH. (b) When pH falls below the critical about 5.5, hydroxyapatite enamel becomes undersaturated and demineralizes. (c) Fluoride in drinking water is incorporated into enamel as fluorapatite, which has a lower critical pH and greater acid resistance, and fluoride also promotes remineralization and inhibits bacterial metabolism. See section 25. 17. Quorum sensing coordinates population-level behavior in bacteria (biofilm formation, bioluminescence, sporulation). Explain in *Vibrio harveyi*: (a) how two quorum sensing circuits (LuxN and LuxPQ) integrate autoinducer signals at different cell densities; (b) why *Vibrio fischeri* in the squid light organ shows population-density-dependent luminescence; (c) how quorum quenching enzymes (AHL lactonase) disrupt this signaling.

Answer (Q17, Application). (a) In *Vibrio harveyi*, parallel circuits feed into LuxO: LuxN senses the AHL autoinducer HAI-1 and LuxPQ senses the interspecies AI-2; at low cell density these phosphorylate LuxO to repress the master regulator LuxR, while at high density (high autoinducer) the kinases switch to phosphatases, dephosphorylating LuxO and activating LuxR-controlled genes — integrating signals across densities. (b) *Vibrio fischeri* in the squid light organ reaches very high local density, so accumulated AHL activates the lux operon and bioluminescence only when the population is dense enough to be useful. (c) Quorum-quenching enzymes such as AHL lactonase hydrolyze the lactone ring of the autoinducer, destroying the signal so the quorum threshold is never reached and coordinated behaviors are blocked. See section 25. 18. Antibiotic resistance spreads horizontally via mobile genetic elements (plasmids, integrons, transposons). Trace how resistance to trimethoprim and ampicillin on a co-integrated resistance plasmid would affect *E. coli* evolution in a hospital drain environment: (a) does selection for one resistance indirectly maintain the other? (b) how does this create a co-selection problem when antibiotics are used?

Answer (Q18, Application). Initiating condition: a co-integrated plasmid in *E. coli* carries linked trimethoprim and ampicillin resistance genes in a hospital drain. Changed component: physical linkage on one mobile element. Mechanism: because the genes co-transfer and co-replicate, selecting for either antibiotic also retains the other (genetic hitchhiking/co-selection), and conjugation spreads the whole cassette across strains and species. Outcome: (a) yes — selection for one resistance indirectly maintains the other; (b) this creates a co-selection problem because using a single antibiotic (or even biocides/metals on the same element) sustains multidrug resistance, so resistance persists even when one drug is withdrawn. See section 25. 19. Extremophile archaea in deep-sea hydrothermal vents oxidise H₂S as electron donor, fixing CO₂ via the reverse TCA cycle (without photosynthesis). Compare this chemolithoautotrophic primary production to photosynthesis: (a) what is the electron donor; (b) what energy source; (c) how much biomass is produced per unit energy; (d) why this is important for understanding the origin of life.

Answer (Q19, Application). (a) The electron donor is reduced inorganic sulfur (H₂S), not water as in photosynthesis. (b) The energy source is chemical energy from oxidizing H₂S (chemolithotrophy) rather than light. (c) Chemolithoautotrophy yields far less energy per reaction than oxygenic photosynthesis, so biomass produced per unit energy and overall growth yields are low — these ecosystems are productive only because vent geochemistry continuously supplies reductant. (d) It matters for origin-of-life questions because it shows life can be powered entirely by geochemical redox energy independent of sunlight, supporting hydrothermal-vent scenarios for early metabolism and chemiosmotic energy conservation. See section 25. 20. Meta-analysis of 10 gut microbiome studies in Type 2 Diabetes (T2D) patients vs healthy controls identified depletion of *Akkermansia muciniphila* and *Faecalibacterium prausnitzii* in T2D. Design a causal inference test: (a) what correlation measure would you use; (b) what germ-free mouse experiment would establish causality; (c) what confounders (diet, medication) need controlling?

Answer (Q20, Application). (a) Use a non-parametric rank correlation (Spearman) or compositionally aware methods (e.g., SparCC/ANCOM) to test association between *Akkermansia*/*F. prausnitzii* relative abundance and T2D status, since microbiome data are compositional and non-normal. (b) Establish causality by colonizing germ-free mice: gnotobiotically transfer T2D-patient versus healthy microbiota (or mono-colonize with the candidate taxa) and measure glucose tolerance/insulin sensitivity, with the prediction that adding the depleted taxa improves metabolic phenotype. (c) Control confounders including diet (especially fiber), metformin and other medications, BMI, age, and sequencing batch — metformin in particular independently alters the microbiome and can spuriously associate taxa with T2D. See section 25.

Questions 21–30: Synthesis and Evaluation

21. Evaluate the “microbiome-brain axis” (gut-brain axis): propose the mechanistic routes (vagus nerve, SCFAs, immune mediators, enteric serotonin) by which gut microbial composition can influence mood and cognition. What evidence from: (a) germ-free mice (increased anxiety, HPA axis changes); (b) faecal transfer from depressed patients to rats; (c) probiotic clinical trials in humans — supports a causal role?

Answer (Q21, Synthesis). Proposed routes: (1) vagal afferent signaling triggered by microbial metabolites; (2) SCFAs (butyrate, propionate) acting on microglia, the blood–brain barrier, and gene expression; (3) immune mediators (cytokines from microbe-trained immunity); and (4) modulation of enteric and circulating serotonin precursors. Evidence: (a) germ-free mice show altered anxiety-like behavior and an exaggerated HPA stress axis, reversed by colonization; (b) transferring feces from depressed patients into rodents can transfer depression/anxiety-like phenotypes; (c) probiotic (‘psychobiotic’) human trials show modest, inconsistent mood effects. Overall the animal causal evidence is strong but human evidence is largely associative; well-powered, mechanism-anchored randomized human trials with defined consortia would change the strength of the causal conclusion. See section 25. 22. Design a metagenomics study to characterize the resistome (complete antibiotic resistance gene complement) of wastewater treatment plant effluent. Describe: (a) DNA extraction strategy; (b) how you would annotate resistance genes; (c) how you would determine whether identified genes are in pathogens vs harmless commensals, including the taxonomy database release used for MAG classification; (d) how you would track the resistome over a full seasonal cycle.

Answer (Q22, Synthesis). Hypothesis: WWTP effluent harbors a quantifiable, seasonally varying resistome. (a) DNA extraction: collect replicate grab/composite effluent samples, filter biomass, and use a bead-beating total-community DNA kit with negative extraction controls. (b) Annotation: shotgun-sequence and map reads/assembled contigs against curated resistance databases (CARD, ResFinder) to call antibiotic resistance genes, with normalized abundance per 16S or per Gbp. (c) Host assignment: use long-read sequencing and assembly to place ARGs on contigs/MAGs and link them to taxonomic markers or known plasmids, then classify MAGs against a named GTDB release so pathogen-borne and commensal-borne calls are reproducible as taxonomy changes [Parks et al., 2026]. (d) Seasonal tracking: sample monthly for ≥ 12 months with replicates and consistent flow/temperature metadata, then test for seasonal effects; a falsifying result is no detectable resistome or no temporal/spatial structure once controls and replication are accounted for. See section 25. 23. Evaluate the concept of the “core microbiome” — a set of microbial taxa present in most healthy individuals of a species. What criteria would define a “core” species, how would you distinguish core from accessory microbiome species, and why the concept is complicated by inter-individual variation (about 20% of gut species may be “comprehensive core”).

Answer (Q23, Synthesis). Empirically, a ‘core microbiome’ is operationally defined as taxa present in $\geq 90\%$ of healthy individuals above a relative-abundance threshold (e.g., $\geq 0.1\%$); core species are distinguished from accessory ones by prevalence and persistence across hosts rather than mere presence in a few. The concept is complicated because only about 20% of gut species may be universally shared, so a strict taxonomic core is small. The conclusion changes if the core is defined functionally (conserved metabolic genes/pathways) rather than taxonomically, since functional redundancy means many different species can fill the same role; the choice of prevalence threshold, sampling depth, and population sampled strongly affects what counts as core. See section 25. 24. Microbial succession in natural environments follows predictable patterns (e.g., pioneer → climax community in forest soils; successional microbiome during decomposition of whale falls). Evaluate the mechanisms (facilitation, inhibition, tolerance) controlling succession, and propose an experiment to test whether succession is driven by deterministic (niche-based) or stochastic processes.

Answer (Q24, Synthesis). Initiating condition: a disturbed or new substrate (whale fall, fresh soil) is colonized by pioneer microbes. Changed component: early colonizers alter the chemical environment. Mechanism: succession proceeds via facilitation (pioneers create conditions/resources favoring later taxa), inhibition (residents suppress newcomers until displaced), and tolerance (later taxa succeed regardless because they tolerate conditions). Outcome: a more stable climax community. To test deterministic (niche) versus stochastic (drift/priority-effect) control, set up many replicate identical microcosms with controlled and varied inocula: deterministic processes predict convergence to similar communities regardless of initial composition, whereas stochastic processes predict divergent endpoints sensitive to colonization order; manipulating arrival order discriminates priority effects. See section 25. 25. Evaluate the concept of “ecosystem services” provided by soil microbiomes: nitrogen cycling, carbon sequestration, plant pathogen suppression. How does intensive agriculture (tillage, pesticide, monoculture) reduce soil microbial diversity and function? Propose a restorative soil management strategy that would re-establish lost ecosystem services.

Answer (Q25, Synthesis). Soil microbiomes provide ecosystem services including nitrogen cycling (fixation, nitrification, denitrification), carbon sequestration via stabilization of microbial necromass and soil organic matter, and suppression of plant pathogens by competitive and antibiotic-producing taxa. Intensive agriculture reduces microbial diversity and function: tillage disrupts fungal hyphal networks and aggregates, pesticides/biocides kill non-target microbes, monoculture narrows root-exudate diversity, and synthetic fertilizer down-regulates N-fixing symbioses. A restorative strategy combines reduced/no-till, diverse cover crops and crop rotation, organic-matter inputs (compost/manure), reduced agro-chemical load, and reintroduction of mycorrhizal/biofertilizer inocula to rebuild diversity and the lost services. The conclusion would change if long-term field trials showed no recovery of function despite restored diversity. See section 25. 26. The human virome includes about 6×10^{12} phage

particles, largely matching the bacteriome. Evaluate: (a) how the virome influences bacteriome composition (phage predation driving community dynamics); (b) the evidence that an abnormal virome (e.g., expanded Caudovirales in Crohn’s disease) can drive inflammation independently of the bacteriome; (c) whether the virome should be considered in the design of microbiome therapeutics.

Answer (Q26, Synthesis). (a) The gut virome is dominated by bacteriophages that shape the bacteriome through predation and lysogeny — kill-the-winner dynamics suppress dominant bacterial taxa, maintaining diversity, while prophages can confer fitness traits. (b) Evidence that an abnormal virome drives disease: Crohn’s disease is associated with an expanded Caudovirales phage richness that does not simply mirror bacterial changes, suggesting the virome can contribute to inflammation partly independently of the bacteriome, though causation versus consequence is unresolved. (c) Therapeutics should consider the virome because phages persist through and can reshape transplanted communities; sterile fecal filtrate (phage) transfer has resolved *C. difficile*, and ignoring phages risks unpredictable bacteriome dynamics. The conclusion would change with controlled phage-manipulation experiments isolating virome effects from bacterial confounding. See section 25. 27. Syntrophic communities (where no single organism can grow on a substrate alone — requires metabolic cross-feeding with a partner) are central to anaerobic digestion of organic matter. Using the sulfate-reducing and methanogenic guild competition as an example, evaluate how thermodynamic constraints (Gibbs energy for each reaction) determine community composition, and why hydrogen partial pressure is the key variable.

Answer (Q27, Synthesis). Initiating condition: a substrate (e.g., propionate/butyrate or fatty acids) that no single organism can degrade alone. Changed component: a fermenting/syntrophic partner produces H₂, which is thermodynamically inhibitory. Mechanism: the primary fermentation is endergonic at high H₂ partial pressure, so it only proceeds if a partner continuously removes H₂ by keeping its concentration extremely low (interspecies hydrogen transfer). Outcome: community composition is set by which H₂ scavenger is thermodynamically favored — sulfate reducers (ΔG more negative with sulfate) outcompete methanogens when sulfate is available, but methanogens dominate when sulfate is depleted. Hydrogen partial pressure is the key variable because it determines whether the syntrophic reaction is exergonic and which guild can sustain it. See section 25. 28. Evaluate the potential of engineered synthetic microbial consortia for biotechnology (e.g., consortium for complete cellulose-to-ethanol conversion, or coordinated tumor-targeting drug delivery). What design principles govern consortium stability, and how can synthetic quorum sensing circuits be used to coordinate the activities of different strains?

Answer (Q28, Synthesis). Empirically, engineered consortia can divide labor (e.g., one strain hydrolyzing cellulose, another fermenting sugars to ethanol) or coordinate spatially (tumor-targeting drug delivery), outperforming single-strain systems on complex tasks. Design principles for stability include enforced metabolic interdependence (auxotrophic cross-feeding so strains cannot outgrow partners), balanced growth rates, spatial structure, and negative feedback to prevent one member overtaking the community. Synthetic quorum-sensing circuits (orthogonal AHL sender/receiver pairs) let strains sense each other’s density and trigger gene expression only at defined population ratios, enabling coordinated, conditional activities and population control. The conclusion changes if long-term experiments show consortia inevitably collapse from evolutionary cheating despite these safeguards. See section 25. 29. The ocean microbiome is structured by “niche partitioning” on individual dissolved organic carbon (DOC) molecules: the “competitive exclusion/keystone species” model predicts that competitive exclusion dominates in low-diversity environments, while microbes coexist in complex high-DOC environments by partitioning onto different compounds. Evaluate how “genome streamlining” (loss of non-essential genes) in marine bacteria (e.g., SAR11) reflects adaptation to this competitive, nutrient-limited environment.

Answer (Q29, Synthesis). Initiating condition: open-ocean surface waters are chronically oligotrophic with dilute, chemically diverse DOC. Changed component: marine bacteria face intense competition for scarce nutrients. Mechanism: in low-diversity/low-resource conditions competitive exclusion favors the most efficient scavenger, while high-DOC complexity allows coexistence through niche partitioning onto different substrate molecules; selection rewards minimizing the metabolic cost of replication. Outcome: lineages like SAR11 undergo genome streamlining — losing non-essential genes, shrinking genome and cell size, and specializing on abundant simple compounds — which maximizes nutrient-use efficiency and competitiveness in this environment. This illustrates that streamlining is an adaptive outcome of competition under nutrient limitation, not mere genome decay. See section 25. 30. Critically evaluate the therapeutic potential of “designer probiotics” — genetically engineered bacteria with specific metabolic or signaling functions. Using the example of a genetically engineered *E. coli* Nissle expressing a GLP-1 precursor for treating obesity (clinical trial, 2025), evaluate: the safety concerns (containment of GMO bacteria, gene transfer to resident microbiome), the evidence of efficacy, and the regulatory framework needed.

Answer (Q30, Synthesis). Designer probiotics — e.g., engineered *E. coli* Nissle expressing a GLP-1 precursor for obesity — could deliver therapeutic molecules locally and continuously. Safety concerns: containment of a GMO in the gut and environment, and horizontal transfer of the engineered construct to the resident microbiome; mitigations include kill-switches, auxotrophy/biocontainment, and genomic (non-mobile) integration. Efficacy evidence to date is largely preclinical and early-phase, so durable, clinically meaningful benefit in humans remains unproven. The regulatory framework must treat these as live genetically modified biotherapeutics, requiring rigorous biocontainment validation, shedding and gene-transfer studies, dose control, and long-term safety monitoring. The conclusion strengthens or weakens with controlled human trial outcomes and demonstrated containment. See section 25.

Questions — Host Immunity and Vaccines

Instructor Use and Coverage Notes

- Coverage target: Predict how immunity or vaccination changes individual and population risk.
- Model/data emphasis: Herd-immunity threshold and basic immunological reasoning.
- Assessment alignment: Questions and Methods, Representing and Describing Data, Argumentation.
- Misconception probe: Immunity is not binary; timing, dose, and variant matter.
- Transfer product: Transfer immunity reasoning to outbreak response and clinical decision-making.
- Grading focus: award full credit for mechanism, evidence, boundary conditions, and units when a calculation is required.
- Suggested use: draw one recall item, one application item, and one synthesis item when building a short quiz from this bank.

Questions 1–10: Recall and Comprehension

This activity accompanies section 26 of the textbook — review that chapter before attempting the exercises below.

1. Distinguish innate from adaptive immunity. Name two cell types involved in each.

Answer (Q1, Recall). Innate immunity is the fast, non-specific first response with no memory; it relies on germline-encoded pattern recognition. Adaptive immunity is slower, antigen-specific, and confers lasting memory through clonal selection. Innate cell types include macrophages and neutrophils (also NK cells); adaptive cell types include T lymphocytes (CD4+ helper, CD8+ cytotoxic) and B lymphocytes. The key difference is that adaptive cells rearrange antigen receptors and form memory, whereas innate cells use fixed receptors. See section 26.

2. What is a pathogen-associated molecular pattern (PAMP)? Name one example and its receptor.

Answer (Q2, Recall). A pathogen-associated molecular pattern (PAMP) is a conserved microbial structure not found in host cells that the innate immune system detects via germline-encoded pattern recognition receptors (PRRs). For example, bacterial lipopolysaccharide (LPS) is a PAMP recognized by Toll-like receptor 4 (TLR4); other examples include flagellin (TLR5) and unmethylated CpG DNA (TLR9). Recognition triggers inflammatory signaling. See section 26.

3. What is an antibody? Name its four structural components.

Answer (Q3, Recall). An antibody (immunoglobulin) is a secreted or membrane-bound glycoprotein produced by B cells/plasma cells that specifically binds antigen. Its four structural components are: two identical heavy chains and two identical light chains, joined by disulfide bonds, organized into two Fab regions (variable VH+VL domains forming the antigen-binding paratope) and one Fc region (constant domains that engage effector functions such as complement and Fc receptors). See section 26.

4. What are the five classes of immunoglobulin? State one function of IgG and one of IgA.

Answer (Q4, Recall). The five immunoglobulin classes are IgG, IgM, IgA, IgE, and IgD, determined by the heavy-chain constant region. IgG is the dominant serum antibody in secondary responses: it opsonizes pathogens, neutralizes toxins, fixes complement, and crosses the placenta. IgA is the principal mucosal antibody: as secretory IgA it mediates immune exclusion of pathogens at gut, respiratory, and other mucosal surfaces without triggering inflammation. See section 26.

5. Describe the clonal selection theory of lymphocyte activation.

Answer (Q5, Recall). Clonal selection theory states that each lymphocyte bears a single, randomly generated antigen-receptor specificity before encountering antigen. When an antigen binds the matching receptor, that specific clone is selected and stimulated to proliferate (clonal expansion) and differentiate into effector cells and long-lived memory cells. Self-reactive clones are deleted or inactivated during development, ensuring tolerance. This explains specificity, diversity, and immunological memory. See section 26.

6. What is the MHC (major histocompatibility complex)? Distinguish MHC class I from class II.

Answer (Q6, Recall). The MHC (major histocompatibility complex; HLA in humans) is a set of cell-surface molecules that present peptide antigens to T cells. MHC class I is expressed on virtually all nucleated cells, presents endogenous (cytosolic) peptides, and is recognized by CD8+ cytotoxic T cells (and surveyed by NK cells via ‘missing-self’). MHC class II is expressed on professional antigen-presenting cells, presents exogenous peptides, and is recognized by CD4+ helper T cells. See section 26.

7. What are cytotoxic T lymphocytes (CTLs)? What do they recognize and how do they kill target cells?

Answer (Q7, Recall). Cytotoxic T lymphocytes (CTLs) are CD8+ effector T cells that recognize foreign or aberrant peptides presented on MHC class I of infected or transformed cells via their T-cell receptor. On engagement they kill the target by two main mechanisms: releasing perforin and granzymes that trigger apoptosis, and engaging Fas (CD95) on the target with FasL to induce caspase-mediated death. See section 26.

8. What is an epidemic? What is a pandemic? Define basic reproduction number R_0 .

Answer (Q8, Recall). An epidemic is a sharp rise in cases of a disease above the expected baseline within a community or region; a pandemic is an epidemic that spreads across multiple countries or continents affecting large numbers of people. The basic reproduction number R_0 is the expected number of secondary cases produced by one infectious individual introduced into a fully susceptible population; $R_0 > 1$ allows an outbreak to grow, $R_0 < 1$ causes it to die out. See section 26.

9. What is herd immunity? How does vaccination achieve herd immunity?

Answer (Q9, Recall). Herd immunity is the indirect protection of susceptible individuals that occurs when a sufficiently large fraction of the population is immune, so an infectious person rarely contacts a susceptible one and chains of transmission break. Vaccination achieves it by immunizing enough people that the immune fraction exceeds the herd-immunity threshold $p_c = 1 - 1/R_0$, driving the effective reproduction number below 1. See section 26.

10. Name three mechanisms of antibiotic resistance evolution.

Answer (Q10, Recall). Three mechanisms of antibiotic-resistance evolution are: (1) enzymatic inactivation of the drug (e.g., β -lactamases hydrolyzing penicillins); (2) target modification or protection so the antibiotic no longer binds (e.g., altered penicillin-binding proteins, ribosomal methylation); and (3) reduced intracellular drug concentration via decreased uptake (porin loss) or active efflux pumps. Resistance genes often spread by horizontal gene transfer (conjugation, transduction, transformation). See section 26.

Questions 11–20: Application and Analysis

11. By 10 November 2024, WHO had received reports of more than 776.8 million confirmed COVID-19 cases globally, while also noting that reported cases undercount infections [World Health Organization, 2024b]. Estimate the herd immunity threshold ($H = 1 - 1/R_0$) if R_0 for the original strain was 2.5. For the Omicron variant ($R_0 \approx 10$), recalculate the threshold and explain what incomplete, waning protection means for vaccination strategy.

Answer (Q11, Application). Use $H = 1 - 1/R_0$. For the original strain with $R_0 = 2.5$: $H = 1 - 1/2.5 = 1 - 0.40 = 0.60$, so about 60% of the population must be immune. For Omicron with $R_0 \approx 10$: $H = 1 - 1/10 = 0.90$, so about 90% must be immune under the simplifying assumption of durable sterilizing immunity and homogeneous mixing. In practice, infection-derived and vaccine-derived protection against infection and transmission is incomplete and wanes, so vaccination strategy should emphasize prevention of severe disease, boosters matched to current guidance, and layered controls during surges rather than a single coverage number. See section 26.

12. The inflammasome (NLRP3) is activated by uric acid crystals (gout), cholesterol crystals (atherosclerosis), and pathogens. Explain: (a) how NLRP3 assembles and activates caspase-1; (b) how caspase-1 cleaves pro-IL-1 β and pro-IL-18; (c) why NLRP3 inhibitors (MCC950) are under development for inflammatory diseases.

Answer (Q12, Application). (a) A priming signal (e.g., LPS via TLR4) induces NLRP3 and pro-IL-1 β ; a second signal (uric acid or cholesterol crystals, K⁺ efflux, lysosomal damage) triggers NLRP3 to oligomerize and recruit the adaptor ASC, which clusters and activates pro-caspase-1. (b) Active caspase-1 proteolytically cleaves pro-IL-1 β and pro-IL-18 into mature, secreted cytokines (and cleaves gasdermin D to drive pyroptosis). (c) Because uncontrolled NLRP3 activity drives gout, atherosclerosis, and other sterile inflammation, selective inhibitors such as MCC950 are being developed to dampen IL-1 β without broad immunosuppression. See section 26.

13. Influenza can shift from H1N1 to H3N2 by antigenic shift (segment reassortment) or antigenic drift (point mutations in haemagglutinin). Explain: (a) why antigenic drift requires annual vaccine reformulation; (b) why antigenic shift can cause pandemics; (c) what “original antigenic sin” means for immune memory.

Answer (Q13, Application). (a) Antigenic drift is the gradual accumulation of point mutations in hemagglutinin/neuraminidase that erode antibody recognition, so the vaccine strain must be reformulated annually to match circulating variants. (b) Antigenic shift is reassortment of genome segments (e.g., between human and avian/swine strains) producing a novel HA the population has no immunity to, which can ignite a pandemic. (c) ‘Original antigenic sin’ is the tendency of the immune system to preferentially recall antibodies against the first influenza strain encountered, blunting responses to newer drifted strains. See section 26.

14. The complement system (C1-C9) is a cascade of proteolytic activation that opsonises pathogens and lyses bacteria directly (MAC — membrane attack complex). Describe the three complement activation pathways (classical, lectin, alternative), naming the central converging point (C3 convertase), and explain how bacteria evade complement (factor H mimicry, capsule).

Answer (Q14, Application). The classical pathway is triggered by antibody–antigen complexes binding C1q; the lectin pathway by mannose-binding lectin recognizing microbial carbohydrates; the alternative pathway by spontaneous C3 hydrolysis and direct surface deposition. All three converge on formation of C3 convertase, which cleaves C3 into C3a (anaphylatoxin) and C3b (opsonin), leading to the C5 convertase and assembly of the membrane attack complex (C5b–C9). Bacteria evade complement by recruiting host factor H (or mimicking it) to accelerate C3b decay and by using polysaccharide capsules that block C3b deposition and MAC insertion. See section 26.

15. Natural killer (NK) cells kill virus-infected cells that downregulate MHC class I (a strategy used by many viruses to evade CTLs). Explain the “missing self” hypothesis: how do inhibitory KIR receptors normally inhibit NK killing, and how does MHC class I downregulation remove inhibition and trigger NK-mediated lysis?

Answer (Q15, Application). Under the ‘missing-self’ hypothesis, NK cells continuously sample target cells: inhibitory KIRs (e.g., KIR2DL, KIR3DL) bind self MHC class I and deliver a dominant inhibitory signal that overrides activating receptor signals, sparing healthy cells. Many viruses down-regulate MHC class I to hide infected cells from CD8+ CTLs, but this removes the ligand for inhibitory KIRs. With inhibition lost and activating receptors still engaged, the NK cell is unleashed and lyses the MHC-low target via perforin/granzyme. See section 26.

16. Evaluate the “inverted-U” relationship between immune activation and pathogen clearance, using sepsis as a model: (a) why severe sepsis kills by cytokine storm (uncontrolled innate immune activation) rather than the pathogen itself; (b) the failure of anti-TNF- α therapy in sepsis trials despite success in rheumatoid arthritis; (c) how the “immunological hysteresis” concept explains why the same cytokine blockade is beneficial in autoimmunity but harmful in sepsis.

Answer (Q16, Application). (a) In severe sepsis the protective inflammatory response becomes pathologically amplified: a cytokine storm (TNF- α , IL-1 β , IL-6) drives endothelial dysfunction, capillary leak, disseminated coagulation, and multi-organ failure, so the host response, not the pathogen, kills. (b) Anti-TNF- α therapy failed in sepsis trials despite working in rheumatoid arthritis because sepsis is heterogeneous and time-sensitive: by the time patients are treated, the cytokine cascade is past TNF dependence and some patients are already immunosuppressed. (c) ‘Immunological hysteresis’ frames the system as state-dependent: the same TNF blockade is beneficial in the chronic, sustained activation of autoimmunity but harmful in the acute, rapidly shifting trajectory of sepsis, because the optimal intervention depends on where on the inverted-U curve the patient sits. The conclusion would change if biomarker-stratified trials identified a hyperinflammatory subgroup that benefits. See section 26.

17. Build a paper-based infectious-disease decision matrix for three current interventions: (a) BPAL/BPALM-style most-oral treatment for rifampicin-resistant tuberculosis; (b) twice-yearly lenacapavir PrEP for people with substantial HIV exposure risk; (c) indoor spatial emanators added to insecticide-treated nets for malaria control. For each, state the biological target, the surveillance or eligibility evidence required, one equity constraint, and one reason the intervention should not be treated as a standalone solution.

Answer (Q17, Application). For rifampicin-resistant TB, the target is a bacterial infection requiring susceptibility-guided combination therapy; the decision matrix should include rifampicin resistance, fluoroquinolone susceptibility when BPALM is considered, contraindications, adherence support, and toxicity monitoring. For lenacapavir PrEP, the target is HIV acquisition before infection; eligibility requires HIV-negative status, ongoing exposure risk, access to injection follow-up, and resistance-aware testing if infection is suspected. For malaria spatial emanators, the target is mosquito biting and indoor host-seeking; local evidence should include transmission setting, net coverage, vector behavior, insecticide-resistance monitoring, and household acceptability. None is standalone: TB regimens need diagnostics and public-health follow-up, PrEP does not replace testing or treatment access, and spatial emanators complement nets, case management, chemoprevention, and environmental control. See section 26.

18. Evaluate the evidence for “trained innate immunity”: after exposure to β -glucan (from *Candida*) or BCG vaccination, innate immune cells (macrophages, NK cells) show epigenetically reprogrammed, enhanced responses 3–6 months later. What epigenetic changes (H3K4me1 at enhancers, mTOR-dependent metabolic rewiring) mediate this “immunological memory” in non-adaptive immune cells, and what are the implications for innate immune-based vaccines (BCG against COVID-19)?

Answer (Q18, Application). Empirically, BCG vaccination and β -glucan exposure enhance monocyte/macrophage and NK responses to unrelated pathogens 3–6 months later, indicating innate cells can carry a form of memory. Mechanistically this ‘trained immunity’ is mediated by durable epigenetic remodeling (e.g., H3K4me1/H3K4me3 and H3K27ac at promoters and enhancers of inflammatory genes) coupled to mTOR/HIF-1 α -dependent metabolic rewiring toward aerobic glycolysis, lowering the activation threshold on restimulation. Implications: innate-training vaccines (e.g., BCG tested against COVID-19) could give broad, rapid, non-specific protection, but the effect is shorter-lived and less specific than adaptive memory; the conclusion would change if randomized trials showed no heterologous protection or if the epigenetic marks proved transient. See section 26.

19. Autoimmune diseases arise when self-tolerance breaks down. Evaluate three mechanisms of self-tolerance failure in Type 1 Diabetes (T1D): (a) central tolerance failure (inadequate thymic deletion of autoreactive T cells directed at insulin); (b) peripheral tolerance failure (Treg dysfunction); (c) molecular

mimicry (GAD65-Coxsackie B virus homology). What evidence supports each mechanism in human T1D?

Answer (Q19, Application). (a) Central tolerance failure: the AIRE-dependent thymic deletion of insulin-reactive T cells is incomplete; evidence includes the strong HLA association (DR3/DR4) and INS-VNTR alleles that lower thymic insulin expression and predispose to T1D. (b) Peripheral tolerance failure: Treg number or function is impaired; evidence includes monogenic IPEX (FOXP3 mutation) causing autoimmune diabetes and reduced Treg suppressive function in some T1D patients. (c) Molecular mimicry: homology between GAD65 and Coxsackievirus B P2-C protein could cross-prime autoreactive cells; evidence is epidemiological enterovirus associations and cross-reactive T cells, though causality remains debated. The conclusion would change if intervention trials (e.g., Treg expansion, antiviral prevention) altered disease incidence. See section 26.

20. During the COVID-19 pandemic, several SARS-CoV-2 variants of concern (Alpha, Delta, Omicron) arose sequentially. Evaluate the evolutionary pressures (immune evasion vs transmissibility) that drove variant emergence, and why Omicron showed more ACE2-binding mutations (increased transmissibility) but more spike mutations outside the RBD (immune evasion from vaccine-induced antibodies).

Answer (Q20, Application). Initiating condition: widespread population immunity from infection and vaccination created strong selection for SARS-CoV-2 immune escape, while ongoing transmission selected for higher intrinsic transmissibility. Changed component: variants accumulated spike mutations — RBD changes (e.g., N501Y) that increased ACE2 affinity and transmissibility, plus N-terminal-domain and non-RBD epitope changes that escaped vaccine-induced neutralizing antibodies. Mechanism: Omicron arose by a sudden saltation (~32 spike mutations at once), likely from prolonged infection in an immunocompromised host, combining tighter ACE2 binding with extensive antigenic-site changes. Outcome: Omicron was both more transmissible and more immune-evasive, displacing Delta and driving large reinfection waves. See section 26.

Questions 21–30: Synthesis and Evaluation

21. Evaluate checkpoint immunotherapy for cancer: PD-1/PD-L1 blockade, CTLA-4 blockade, LAG-3 blockade. For what biomarker(s) (TMB, PD-L1 expression, MSI-H) are these drugs most effective, and why do about 20–30% of eligible cancer patients benefit? Propose a combination therapy strategy to increase response rates while managing autoimmune toxicity (immune-related adverse events, irAEs).

Answer (Q21, Synthesis). Checkpoint inhibitors (anti-PD-1/PD-L1, anti-CTLA-4, anti-LAG-3) are most effective in tumors with high tumor mutational burden (TMB), high PD-L1 expression, or microsatellite instability-high (MSI-H)/mismatch-repair-deficient status, because these create abundant neoantigens and an inflamed, T-cell-rich microenvironment. Only about 20–30% of eligible patients respond because many tumors are ‘cold’ (low neoantigen load, poor T-cell infiltration, immunosuppressive stroma, alternative checkpoints, or antigen-presentation loss). A rational combination pairs anti-PD-1 with anti-CTLA-4 (or LAG-3) to broaden T-cell priming, adds an agent that converts cold tumors to hot (radiation, oncolytic virus, or a STING agonist), and manages immune-related adverse events with biomarker-guided patient selection, sequencing, and prompt corticosteroid/anti-cytokine rescue; the strategy would change if predictive biomarkers for irAEs were validated. See section 26.

22. Evaluate the concept of the “immunological homunculus” — that the normal immune system retains low-frequency self-reactive clones that perform surveillance and immunoregulation (not only pathology). Critically assess the evidence that low-affinity self-reactive T and B cells are essential for shaping the immune repertoire, and what happens when these regulatory self-reactive cells are eliminated by lymphodepletion.

Answer (Q22, Synthesis). Empirically, the normal repertoire retains low-affinity self-reactive T and B cells (the ‘immunological homunculus’), and these are not purely pathological: positive selection on self-MHC/self-peptide is required to generate a functional T-cell repertoire, and natural autoantibodies and self-reactive Tregs contribute to tissue homeostasis and immunoregulation. Evidence includes the dependence of thymic positive selection on weak self-recognition and the regulatory roles of natural IgM autoantibodies. When these regulatory self-reactive cells are removed by lymphodepletion, homeostatic reconstitution can skew toward autoreactivity and break tolerance (autoimmune complications after lymphodepleting therapy). The conclusion would change if a fully self-tolerant repertoire could be shown to develop and self-regulate without any self-reactive clones. See section 26.

23. The “two-signal model” of T cell activation requires: (1) TCR engagement with MHC-peptide and (2) a co-stimulatory signal (CD28-B7). Without signal 2, T cells become anergic (unresponsive). Evaluate how tumors exploit this model to suppress anti-tumor T cells by: (a) expressing PD-L1 (sending an anergy-inducing signal); (b) lacking co-stimulatory molecules; (c) expressing IDO (depleting tryptophan needed for T cell activation). How does CAR-T cell therapy bypass this requirement for co-stimulation?

Answer (Q23, Synthesis). Initiating condition: full T-cell activation needs signal 1 (TCR–MHC-peptide) plus signal 2 (CD28–B7 co-stimulation); without signal 2 the T cell becomes anergic. Tumors exploit this: (a) PD-L1 expression delivers a coinhibitory signal that anergizes/exhausts tumor-specific T cells; (b) absence of B7 co-stimulatory molecules on tumor cells gives signal 1 without signal 2, inducing anergy; (c) IDO expression depletes tryptophan and produces kynurenines, starving and suppressing T cells. CAR-T cells bypass this requirement because the chimeric receptor links an antibody-derived antigen-binding domain directly to CD3ζ plus a built-in co-stimulatory domain (CD28 or 4-1BB), so a single MHC-independent antigen contact delivers both activation and co-stimulation. See section 26.

24. Evaluate the emerging field of “onco-immunology” — the mechanisms by which tumors edit the immune landscape (immunoediting: elimination → equilibrium → escape). Give specific molecular examples of immune editing at each phase, and assess whether the immune equilibrium phase can be maintained indefinitely in any cancer type, or whether escape is inevitable.

Answer (Q24, Synthesis). Cancer immunoediting proceeds through three phases. Elimination: immunosurveillance by NK cells and CD8+ T cells destroys nascent transformed cells (evidenced by higher cancer rates in immunodeficient hosts). Equilibrium: residual immunogenic clones are held dormant under sustained adaptive pressure (shown by long latency and donor-transmitted tumors in transplant recipients). Escape: surviving clones evade immunity via MHC class I loss, PD-L1 upregulation, antigen loss, and recruitment of Tregs/MDSCs and TGF-β. Equilibrium can persist for years in some cancers but is generally metastable rather than truly indefinite, because ongoing mutation under immune selection makes eventual escape highly likely; the conclusion would change if a cancer were documented in lifelong stable equilibrium without escape. See section 26.

25. Critically evaluate the public health ethics of mandatory vaccination programs. Using the framework of herd immunity thresholds, individual liberty, social contract theory, and harm principle (Mill), construct a utilitarian argument for and a libertarian argument against mandatory vaccination. What vaccination coverage is minimally required for herd immunity against measles ($R_0 \approx 18$), and how do vaccine hesitancy and anti-vaccine movements affect public health?

Answer (Q25, Synthesis). Utilitarian (for): mandatory vaccination maximizes aggregate welfare by securing herd immunity, preventing outbreaks, and protecting those who cannot be vaccinated; Mill’s harm principle justifies coercion because non-vaccination imposes infection risk on others. Libertarian (against): bodily autonomy and informed consent are paramount; mandates coerce a medical intervention and erode trust, and exemptions/least-restrictive alternatives should be preferred. For measles with $R_0 \approx 18$, the herd-immunity threshold is $p_c = 1 - 1/18 \approx 0.944$, so roughly 94–95% immune coverage is required. Vaccine hesitancy and anti-vaccine movements push coverage below this threshold, restoring susceptibility and driving measles resurgences (as seen in 2018–2019). See section 26.

26. mRNA vaccines (Pfizer-BioNTech, Moderna) for SARS-CoV-2 required solving two key problems: (a) mRNA instability in vivo (solution: pseudouridine substitution reduces TLR7/8 sensing and increases stability); (b) delivery to antigen-presenting cells in lymph nodes (solution: LNP — lipid nanoparticle encapsulation). Trace the cascade from IM injection → LNP uptake by dendritic cells → spike protein expression → naive B and T cell activation → class switch recombination → IgG antibody production.

Answer (Q26, Synthesis). Initiating condition: lipid-nanoparticle (LNP)-encapsulated, pseudouridine-modified spike mRNA is injected intramuscularly, where modified bases reduce TLR7/8 sensing and boost stability. LNPs are taken up by dendritic cells and other antigen-presenting cells, which translate the mRNA into spike protein. Spike is processed and presented on MHC II to naive CD4+ T cells and on MHC I to CD8+ T cells; spike-specific naive B cells bind antigen and receive T-helper signals. In germinal centers this drives affinity maturation and class-switch recombination from IgM to high-affinity IgG, yielding neutralizing antibody and memory B/T cells. See section 26.

27. Regulatory T cells (Tregs, FOXP3+) suppress immune responses and prevent autoimmunity. Explain: (a) how Tregs develop (thymic selection vs peripheral induction); (b) their mechanisms of suppression (IL-10, TGF-β, CTLA-4-mediated antigen-presenting cell suppression); (c) why depleting Tregs in cancer (anti-CTLA-4, ipilimumab) can restore anti-tumor immunity at the cost of autoimmunity.

Answer (Q27, Synthesis). (a) Natural Tregs arise in the thymus by selection of moderately self-reactive CD4+ cells that upregulate FOXP3; induced Tregs differentiate in the periphery from conventional CD4+ cells under TGF-β. (b) They suppress via inhibitory cytokines (IL-10, TGF-β), consumption of IL-2, and CTLA-4, which strips/blocks CD80/CD86 on antigen-presenting cells to deny co-stimulation. (c) Anti-CTLA-4 (ipilimumab) removes this brake, restoring anti-tumor T-cell responses, but because the same checkpoint enforces self-tolerance, blocking it also causes immune-related autoimmune toxicities. See section 26.

28. Malaria (*Plasmodium falciparum*) has complex immune evasion through antigenic variation of PfEMP1 (erythrocyte membrane protein 1) encoded by about 60 var genes, a single active at a time. Explain: (a) why the immune system struggles to clear malaria; (b) how epigenetic switching between var genes works; (c) what approach (conserved antigen targets) vaccine developers use to circumvent this evasion.

Answer (Q28, Synthesis). (a) PfEMP1 on infected erythrocytes mediates cytoadherence and is highly immunogenic, but the parasite switches which variant it displays, so by the time antibodies arise the dominant variant has changed and immunity lags. (b) Only one of about 60 var genes is transcribed at a time; epigenetic silencing (heterochromatin marks, H3K9me3, perinuclear sequestration) keeps the rest off, and stochastic switching activates a new var while silencing the old, giving sequential antigenic variation. (c) Vaccine developers target conserved, less variable antigens (e.g., circumsporozoite protein in RTS,S/R21, or conserved PfEMP1 domains like those binding EPCR) to bypass var-gene switching. See section 26.

29. Calculate basic epidemiological parameters: if an influenza outbreak shows 15 secondary cases per 10 infected individuals over a mean infectious period of 3 days (generation time 3 days), estimate R_0 and the doubling time of the epidemic. What control measure would need to be implemented to bring R to

< 1?

Answer (Q29, Synthesis). $R_0 \approx$ secondary cases per case = $15/10 = 1.5$. With a generation time $T_g = 3$ days, the per-generation growth factor is $R_0 = 1.5$, so the epidemic grows by $1.5\times$ every 3 days. Doubling time $\approx T_g \cdot \ln 2 / \ln(R_0) = 3 \cdot 0.693 / 0.405 \approx 5.1$ days. To bring the effective reproduction number $R_e = R_0(1 - p)$ below 1, the immune/effectively-protected fraction must exceed $p > 1 - 1/R_0 = 1 - 1/1.5 \approx 0.33$, i.e., interventions (vaccination, isolation, contact reduction) must remove more than about 33% of effective transmission. See section 26.

30. Intestinal IgA is produced in the lamina propria by plasma cells and specifically transported into the gut lumen (via polymeric immunoglobulin receptor, pIgR). Explain: (a) how secretory IgA (sIgA) differs from serum IgA structurally; (b) the role of the secretory component; (c) how sIgA provides “immune exclusion” of pathogens without triggering inflammation.

Answer (Q30, Synthesis). (a) Serum IgA is mostly monomeric, whereas secretory IgA is a dimer of two IgA monomers joined by a J chain plus an added secretory component. (b) The secretory component is the cleaved extracellular portion of the polymeric immunoglobulin receptor (pIgR) that transcytoses dimeric IgA across the epithelium; it remains bound and protects sIgA from luminal proteases. (c) sIgA performs ‘immune exclusion’ by cross-linking and agglutinating pathogens and toxins in the mucus layer, blocking adhesion and entry; because it poorly fixes complement and does not strongly engage Fc receptors, it neutralizes without provoking inflammation. See section 26.

Questions — Antimicrobial Resistance and Epidemiology

Instructor Use and Coverage Notes

- Coverage target: Calculate a threshold or outbreak trajectory and identify the intervention lever.
- Model/data emphasis: R0, resistance-mechanism, and outbreak-trajectory calculations.
- Assessment alignment: Questions and Methods, Representing and Describing Data, Argumentation.
- Misconception probe: R0 is not a fixed property of a pathogen alone; it depends on host behavior and environment.
- Transfer product: Transfer resistance and epidemiology reasoning to stewardship and public-health policy.
- Grading focus: award full credit for mechanism, evidence, boundary conditions, and units when a calculation is required.
- Suggested use: draw one recall item, one application item, and one synthesis item when building a short quiz from this bank.

Questions 1–10: Recall and Comprehension

This activity accompanies section 27 of the textbook — review that chapter before attempting the exercises below.

1. mRNA vaccines (Pfizer-BioNTech, Moderna) for SARS-CoV-2 required solving two key problems: (a) mRNA instability in vivo (solution: pseudouridine substitution reduces TLR7/8 sensing and increases stability); (b) delivery to antigen-presenting cells in lymph nodes (solution: LNP — lipid nanoparticle encapsulation). Trace the cascade from IM injection → LNP uptake by dendritic cells → spike protein expression → naive B and T cell activation → class switch recombination → IgG antibody production.

Answer (Q1, Recall). Initiating condition: lipid-nanoparticle (LNP)-encapsulated, pseudouridine-modified spike mRNA is injected intramuscularly, where modified bases reduce TLR7/8 sensing and boost stability. LNPs are taken up by dendritic cells and other antigen-presenting cells, which translate the mRNA into spike protein. Spike is processed and presented on MHC II to naive CD4+ T cells and on MHC I to CD8+ T cells; spike-specific naive B cells bind antigen and receive T-helper signals. In germinal centers this drives affinity maturation and class-switch recombination from IgM to high-affinity IgG, yielding neutralizing antibody and memory B/T cells. See section 27.

2. Regulatory T cells (Tregs, FOXP3+) suppress immune responses and prevent autoimmunity. Explain: (a) how Tregs develop (thymic selection vs peripheral induction); (b) their mechanisms of suppression (IL-10, TGF-β, CTLA-4-mediated antigen-presenting cell suppression); (c) why depleting Tregs in cancer (anti-CTLA-4, ipilimumab) can restore anti-tumor immunity at the cost of autoimmunity.

Answer (Q2, Recall). (a) Natural Tregs arise in the thymus by selection of moderately self-reactive CD4+ cells that upregulate FOXP3; induced Tregs differentiate in the periphery from conventional CD4+ cells under TGF-β. (b) They suppress via inhibitory cytokines (IL-10, TGF-β), consumption of IL-2, and CTLA-4, which strips/blocks CD80/CD86 on antigen-presenting cells to deny co-stimulation. (c) Anti-CTLA-4 (ipilimumab) removes this brake, restoring anti-tumor T-cell responses, but because the same checkpoint enforces self-tolerance, blocking it also causes immune-related autoimmune toxicities. See section 27.

3. Malaria (*Plasmodium falciparum*) has complex immune evasion through antigenic variation of PfEMP1 (erythrocyte membrane protein 1) encoded by about 60 var genes, a single active at a time. Explain: (a) why the immune system struggles to clear malaria; (b) how epigenetic switching between var genes works; (c) what approach (conserved antigen targets) vaccine developers use to circumvent this evasion.

Answer (Q3, Recall). (a) PfEMP1 on infected erythrocytes mediates cytoadherence and is highly immunogenic, but the parasite switches which variant it displays, so by the time antibodies arise the dominant variant has changed and immunity lags. (b) Only one of about 60 var genes is transcribed at a time; epigenetic silencing (heterochromatin marks, H3K9me3, perinuclear sequestration) keeps the rest off, and stochastic switching activates a new var while silencing the old, giving sequential antigenic variation. (c) Vaccine developers target conserved, less variable antigens (e.g., circumsporozoite protein in RTS,S/R21, or conserved PfEMP1 domains like those binding EPCR) to bypass var-gene switching. See section 27.

4. Calculate basic epidemiological parameters: if an influenza outbreak shows 15 secondary cases per 10 infected individuals over a mean infectious period of 3 days (generation time 3 days), estimate R0 and the doubling time of the epidemic. What control measure would need to be implemented to bring R to < 1?

Answer (Q4, Recall). $R_0 \approx \text{secondary cases per case} = 15/10 = 1.5$. With a generation time $T_g = 3$ days, the per-generation growth factor is $R_0 = 1.5$, so the epidemic grows by $1.5\times$ every 3 days. Doubling time $\approx T_g \ln 2 / \ln(R_0) = 3 \cdot 0.693 / 0.405 \approx 5.1$ days. To bring the effective reproduction number $R_e = R_0(1 - p)$ below 1, the immune/effectively-protected fraction must exceed $p > 1 - 1/R_0 = 1 - 1/1.5 \approx 0.33$, i.e., interventions (vaccination, isolation, contact reduction) must remove more than about 33% of effective transmission. See section 27.

5. Intestinal IgA is produced in the lamina propria by plasma cells and specifically transported into the gut lumen (via polymeric immunoglobulin receptor, pIgR). Explain: (a) how secretory IgA (sIgA) differs from serum IgA structurally; (b) the role of the secretory component; (c) how sIgA provides “immune exclusion” of pathogens without triggering inflammation.

- Answer (Q5, Recall). (a) Serum IgA is mostly monomeric, whereas secretory IgA is a dimer of two IgA monomers joined by a J chain plus an added secretory component. (b) The secretory component is the cleaved extracellular portion of the polymeric immunoglobulin receptor (pIgR) that transcytoses dimeric IgA across the epithelium; it remains bound and protects sIgA from luminal proteases. (c) sIgA performs ‘immune exclusion’ by cross-linking and agglutinating pathogens and toxins in the mucus layer, blocking adhesion and entry; because it poorly fixes complement and does not strongly engage Fc receptors, it neutralizes without provoking inflammation. See section 27.
6. Evaluate the “inverted-U” relationship between immune activation and pathogen clearance, using sepsis as a model: (a) why severe sepsis kills by cytokine storm (uncontrolled innate immune activation) rather than the pathogen itself; (b) the failure of anti-TNF- α therapy in sepsis trials despite success in rheumatoid arthritis; (c) how the “immunological hysteresis” concept explains why the same cytokine blockade is beneficial in autoimmunity but harmful in sepsis.
- Answer (Q6, Recall). (a) In severe sepsis the protective inflammatory response becomes pathologically amplified: a cytokine storm (TNF- α , IL-1 β , IL-6) drives endothelial dysfunction, capillary leak, disseminated coagulation, and multi-organ failure, so the host response, not the pathogen, kills. (b) Anti-TNF- α therapy failed in sepsis trials despite working in rheumatoid arthritis because sepsis is heterogeneous and time-sensitive: by the time patients are treated, the cytokine cascade is past TNF dependence and some patients are already immunosuppressed. (c) ‘Immunological hysteresis’ frames the system as state-dependent: the same TNF blockade is beneficial in the chronic, sustained activation of autoimmunity but harmful in the acute, rapidly shifting trajectory of sepsis, because the optimal intervention depends on where on the inverted-U curve the patient sits. The conclusion would change if biomarker-stratified trials identified a hyperinflammatory subgroup that benefits. See section 27.
7. Antibiotics select for resistance through several biochemical strategies. List the four major mechanisms of acquired antibiotic resistance — enzymatic inactivation, target modification, reduced intracellular drug (decreased uptake or active efflux), and target bypass — and give one drug-class example defeated by each. Define the minimum inhibitory concentration (MIC) and state what a rising MIC indicates.
- Answer (Q7, Recall). (1) Enzymatic inactivation — β -lactamases hydrolyze penicillins and cephalosporins; aminoglycoside-modifying enzymes acetylate or phosphorylate aminoglycosides. (2) Target modification — *erm*-methylation of 23S rRNA blocks macrolides; the *mecA*-encoded PBP2a defeats most β -lactams in MRSA; gyrase/topoisomerase mutations defeat fluoroquinolones. (3) Reduced intracellular drug — porin loss lowers uptake and efflux pumps (e.g., AcrAB-TolC) export tetracyclines and other agents. (4) Target bypass or overproduction — acquiring a drug-insensitive enzyme (e.g., a sulfonamide-resistant dihydropteroate synthase) or overexpressing the target. The minimum inhibitory concentration (MIC) is the lowest drug concentration that prevents visible growth in vitro; a rising MIC signals declining susceptibility and predicts clinical resistance once it crosses the breakpoint. See section 27.
8. Evaluate the evidence for “trained innate immunity”: after exposure to β -glucan (from *Candida*) or BCG vaccination, innate immune cells (macrophages, NK cells) show epigenetically reprogrammed, enhanced responses 3–6 months later. What epigenetic changes (H3K4me1 at enhancers, mTOR-dependent metabolic rewiring) mediate this “immunological memory” in non-adaptive immune cells, and what are the implications for innate immune-based vaccines (BCG against COVID-19)?
- Answer (Q8, Recall). Empirically, BCG vaccination and β -glucan exposure enhance monocyte/macrophage and NK responses to unrelated pathogens 3–6 months later, indicating innate cells can carry a form of memory. Mechanistically this ‘trained immunity’ is mediated by durable epigenetic remodeling (e.g., H3K4me1/H3K4me3 and H3K27ac at promoters and enhancers of inflammatory genes) coupled to mTOR/HIF-1 α -dependent metabolic rewiring toward aerobic glycolysis, lowering the activation threshold on restimulation. Implications: innate-training vaccines (e.g., BCG tested against COVID-19) could give broad, rapid, non-specific protection, but the effect is shorter-lived and less specific than adaptive memory; the conclusion would change if randomized trials showed no heterologous protection or if the epigenetic marks proved transient. See section 27.
9. Autoimmune diseases arise when self-tolerance breaks down. Evaluate three mechanisms of self-tolerance failure in Type 1 Diabetes (T1D): (a) central tolerance failure (inadequate thymic deletion of autoreactive T cells directed at insulin); (b) peripheral tolerance failure (Treg dysfunction); (c) molecular mimicry (GAD65-Coxsackie B virus homology). What evidence supports each mechanism in human T1D?
- Answer (Q9, Recall). (a) Central tolerance failure: the AIRE-dependent thymic deletion of insulin-reactive T cells is incomplete; evidence includes the strong HLA association (DR3/DR4) and INS-VNTR alleles that lower thymic insulin expression and predispose to T1D. (b) Peripheral tolerance failure: Treg number or function is impaired; evidence includes monogenic IPEX (FOXP3 mutation) causing autoimmune diabetes and reduced Treg suppressive function in some T1D patients. (c) Molecular mimicry: homology between GAD65 and Coxsackievirus B P2-C protein could cross-prime autoreactive cells; evidence is epidemiological enterovirus associations and cross-reactive T cells, though causality remains debated. The conclusion would change if intervention trials (e.g., Treg expansion, antiviral prevention) altered disease incidence. See section 27.
10. During the COVID-19 pandemic, several SARS-CoV-2 variants of concern (Alpha, Delta, Omicron) arose sequentially. Evaluate the evolutionary pressures (immune evasion vs transmissibility) that drove variant emergence, and why Omicron showed more ACE2-binding mutations (increased transmissibility)

but more spike mutations outside the RBD (immune evasion from vaccine-induced antibodies).

Answer (Q10, Recall). Initiating condition: widespread population immunity from infection and vaccination created strong selection for SARS-CoV-2 immune escape, while ongoing transmission selected for higher intrinsic transmissibility. Changed component: variants accumulated spike mutations — RBD changes (e.g., N501Y) that increased ACE2 affinity and transmissibility, plus N-terminal-domain and non-RBD epitope changes that escaped vaccine-induced neutralizing antibodies. Mechanism: Omicron arose by a sudden saltation (≈ 32 spike mutations at once), likely from prolonged infection in an immunocompromised host, combining tighter ACE2 binding with extensive antigenic-site changes. Outcome: Omicron was both more transmissible and more immune-evasive, displacing Delta and driving large reinfection waves. See section 27.

Questions 11–20: Application and Analysis

11. Evaluate checkpoint immunotherapy for cancer: PD-1/PD-L1 blockade, CTLA-4 blockade, LAG-3 blockade. For what biomarker(s) (TMB, PD-L1 expression, MSI-H) are these drugs most effective, and why do about 20–30% of eligible cancer patients benefit? Propose a combination therapy strategy to increase response rates while managing autoimmune toxicity (immune-related adverse events, irAEs).

Answer (Q11, Application). Checkpoint inhibitors (anti-PD-1/PD-L1, anti-CTLA-4, anti-LAG-3) are most effective in tumors with high tumor mutational burden (TMB), high PD-L1 expression, or microsatellite instability-high (MSI-H)/mismatch-repair-deficient status, because these create abundant neoantigens and an inflamed, T-cell-rich microenvironment. Only about 20–30% of eligible patients respond because many tumors are ‘cold’ (low neoantigen load, poor T-cell infiltration, immunosuppressive stroma, alternative checkpoints, or antigen-presentation loss). A rational combination pairs anti-PD-1 with anti-CTLA-4 (or LAG-3) to broaden T-cell priming, adds an agent that converts cold tumors to hot (radiation, oncolytic virus, or a STING agonist), and manages immune-related adverse events with biomarker-guided patient selection, sequencing, and prompt corticosteroid/anti-cytokine rescue; the strategy would change if predictive biomarkers for irAEs were validated. See section 27.

12. Evaluate the concept of the “immunological homunculus” — that the normal immune system retains low-frequency self-reactive clones that perform surveillance and immunoregulation (not only pathology). Critically assess the evidence that low-affinity self-reactive T and B cells are essential for shaping the immune repertoire, and what happens when these regulatory self-reactive cells are eliminated by lymphodepletion.

Answer (Q12, Application). Empirically, the normal repertoire retains low-affinity self-reactive T and B cells (the ‘immunological homunculus’), and these are not purely pathological: positive selection on self-MHC/self-peptide is required to generate a functional T-cell repertoire, and natural autoantibodies and self-reactive Tregs contribute to tissue homeostasis and immunoregulation. Evidence includes the dependence of thymic positive selection on weak self-recognition and the regulatory roles of natural IgM autoantibodies. When these regulatory self-reactive cells are removed by lymphodepletion, homeostatic reconstitution can skew toward autoreactivity and break tolerance (autoimmune complications after lymphodepleting therapy). The conclusion would change if a fully self-tolerant repertoire could be shown to develop and self-regulate without any self-reactive clones. See section 27.

13. The “two-signal model” of T cell activation requires: (1) TCR engagement with MHC-peptide and (2) a co-stimulatory signal (CD28-B7). Without signal 2, T cells become anergic (unresponsive). Evaluate how tumors exploit this model to suppress anti-tumor T cells by: (a) expressing PD-L1 (sending an anergy-inducing signal); (b) lacking co-stimulatory molecules; (c) expressing IDO (depleting tryptophan needed for T cell activation). How does CAR-T cell therapy bypass this requirement for co-stimulation?

Answer (Q13, Application). Initiating condition: full T-cell activation needs signal 1 (TCR–MHC-peptide) plus signal 2 (CD28–B7 co-stimulation); without signal 2 the T cell becomes anergic. Tumors exploit this: (a) PD-L1 expression delivers a coinhibitory signal that anergizes/exhausts tumor-specific T cells; (b) absence of B7 co-stimulatory molecules on tumor cells gives signal 1 without signal 2, inducing anergy; (c) IDO expression depletes tryptophan and produces kynurenines, starving and suppressing T cells. CAR-T cells bypass this requirement because the chimeric receptor links an antibody-derived antigen-binding domain directly to CD3 ζ plus a built-in co-stimulatory domain (CD28 or 4-1BB), so a single MHC-independent antigen contact delivers both activation and co-stimulation. See section 27.

14. Evaluate the emerging field of “onco-immunology” — the mechanisms by which tumors edit the immune landscape (immunoediting: elimination → equilibrium → escape). Give specific molecular examples of immune editing at each phase, and assess whether the immune equilibrium phase can be maintained indefinitely in any cancer type, or whether escape is inevitable.

Answer (Q14, Application). Cancer immunoediting proceeds through three phases. Elimination: immunosurveillance by NK cells and CD8+ T cells destroys nascent transformed cells (evidenced by higher cancer rates in immunodeficient hosts). Equilibrium: residual immunogenic clones are held dormant under sustained adaptive pressure (shown by long latency and donor-transmitted tumors in transplant recipients). Escape: surviving clones evade immunity via MHC class I loss, PD-L1 upregulation, antigen loss, and recruitment of Tregs/MDSCs and TGF- β . Equilibrium can persist for years in some cancers but is generally metastable rather than truly indefinite, because ongoing mutation under immune selection makes eventual escape highly likely; the conclusion would change if a cancer were documented in lifelong stable equilibrium without escape. See section 27.

15. Critically evaluate the public health ethics of mandatory vaccination programs. Using the framework of herd immunity thresholds, individual liberty, social contract theory, and harm principle (Mill), construct a utilitarian argument for and a libertarian argument against mandatory vaccination. What vaccination coverage is minimally required for herd immunity against measles ($R_0 \approx 18$), and how do vaccine hesitancy and anti-vaccine movements affect public health?

Answer (Q15, Application). Utilitarian (for): mandatory vaccination maximizes aggregate welfare by securing herd immunity, preventing outbreaks, and protecting those who cannot be vaccinated; Mill’s harm principle justifies coercion because non-vaccination imposes infection risk on others. Libertarian (against): bodily autonomy and informed consent are paramount; mandates coerce a medical intervention and erode trust, and exemptions/least-restrictive alternatives should be preferred. For measles with $R_0 \approx 18$, the herd-immunity threshold is $p_c = 1 - 1/18 \approx 0.944$, so roughly 94–95% immune coverage is required. Vaccine hesitancy and anti-vaccine movements push coverage below this threshold, restoring susceptibility and driving measles resurgences (as seen in 2018–2019). See section 27.

16. Distinguish innate from adaptive immunity. Name two cell types involved in each.

Answer (Q16, Application). Innate immunity is the fast, non-specific first response with no memory; it relies on germline-encoded pattern recognition. Adaptive immunity is slower, antigen-specific, and confers lasting memory through clonal selection. Innate cell types include macrophages and neutrophils (also NK cells); adaptive cell types include T lymphocytes (CD4+ helper, CD8+ cytotoxic) and B lymphocytes. The key difference is that adaptive cells rearrange antigen receptors and form memory, whereas innate cells use fixed receptors. See section 27.

17. What is a pathogen-associated molecular pattern (PAMP)? Name one example and its receptor.

Answer (Q17, Application). A pathogen-associated molecular pattern (PAMP) is a conserved microbial structure not found in host cells that the innate immune system detects via germline-encoded pattern recognition receptors (PRRs). For example, bacterial lipopolysaccharide (LPS) is a PAMP recognized by Toll-like receptor 4 (TLR4); other examples include flagellin (TLR5) and unmethylated CpG DNA (TLR9). Recognition triggers inflammatory signaling. See section 27.

18. What is an antibody? Name its four structural components.

Answer (Q18, Application). An antibody (immunoglobulin) is a secreted or membrane-bound glycoprotein produced by B cells/plasma cells that specifically binds antigen. Its four structural components are: two identical heavy chains and two identical light chains, joined by disulfide bonds, organized into two Fab regions (variable VH+VL domains forming the antigen-binding paratope) and one Fc region (constant domains that engage effector functions such as complement and Fc receptors). See section 27.

19. What are the five classes of immunoglobulin? State one function of IgG and one of IgA.

Answer (Q19, Application). The five immunoglobulin classes are IgG, IgM, IgA, IgE, and IgD, determined by the heavy-chain constant region. IgG is the dominant serum antibody in secondary responses: it opsonizes pathogens, neutralizes toxins, fixes complement, and crosses the placenta. IgA is the principal mucosal antibody: as secretory IgA it mediates immune exclusion of pathogens at gut, respiratory, and other mucosal surfaces without triggering inflammation. See section 27.

20. Describe the clonal selection theory of lymphocyte activation.

Answer (Q20, Application). Clonal selection theory states that each lymphocyte bears a single, randomly generated antigen-receptor specificity before encountering antigen. When an antigen binds the matching receptor, that specific clone is selected and stimulated to proliferate (clonal expansion) and differentiate into effector cells and long-lived memory cells. Self-reactive clones are deleted or inactivated during development, ensuring tolerance. This explains specificity, diversity, and immunological memory. See section 27.

Questions 21–30: Synthesis and Evaluation

21. What is the MHC (major histocompatibility complex)? Distinguish MHC class I from class II.

Answer (Q21, Synthesis). The MHC (major histocompatibility complex; HLA in humans) is a set of cell-surface molecules that present peptide antigens to T cells. MHC class I is expressed on virtually all nucleated cells, presents endogenous (cytosolic) peptides, and is recognized by CD8+ cytotoxic T cells (and surveyed by NK cells via ‘missing-self’). MHC class II is expressed on professional antigen-presenting cells, presents exogenous peptides, and is recognized by CD4+ helper T cells. See section 27.

22. What are cytotoxic T lymphocytes (CTLs)? What do they recognize and how do they kill target cells?

Answer (Q22, Synthesis). Cytotoxic T lymphocytes (CTLs) are CD8+ effector T cells that recognize foreign or aberrant peptides presented on MHC class I of infected or transformed cells via their T-cell receptor. On engagement they kill the target by two main mechanisms: releasing perforin and granzymes that trigger apoptosis, and engaging Fas (CD95) on the target with FasL to induce caspase-mediated death. See section 27.

23. What is an epidemic? What is a pandemic? Define basic reproduction number R_0 .

Answer (Q23, Synthesis). An epidemic is a sharp rise in cases of a disease above the expected baseline within a community or region; a pandemic is an epidemic that spreads across multiple countries or continents affecting large numbers of people. The basic reproduction number R_0 is the expected number of secondary cases produced by one infectious individual introduced into a fully susceptible population; $R_0 > 1$ allows an outbreak to grow, $R_0 < 1$ causes it to die out. See section 27.

24. What is herd immunity? How does vaccination achieve herd immunity?

Answer (Q24, Synthesis). Herd immunity is the indirect protection of susceptible individuals that occurs when a sufficiently large fraction of the population is immune, so an infectious person rarely contacts a susceptible one and chains of transmission break. Vaccination achieves it by immunizing enough people that the immune fraction exceeds the herd-immunity threshold $p_c = 1 - 1/R_0$, driving the effective reproduction number below 1. See section 27.

25. Name three mechanisms of antibiotic resistance evolution.

Answer (Q25, Synthesis). Three mechanisms of antibiotic-resistance evolution are: (1) enzymatic inactivation of the drug (e.g., β -lactamases hydrolyzing penicillins); (2) target modification or protection so the antibiotic no longer binds (e.g., altered penicillin-binding proteins, ribosomal methylation); and (3) reduced intracellular drug concentration via decreased uptake (porin loss) or active efflux pumps. Resistance genes often spread by horizontal gene transfer (conjugation, transduction, transformation). See section 27.

26. By 10 November 2024, WHO had received reports of more than 776.8 million confirmed COVID-19 cases globally, while also noting that reported cases undercount infections [World Health Organization, 2024b]. Estimate the herd immunity threshold ($H = 1 - 1/R_0$) if R_0 for the original strain was 2.5. For the Omicron variant ($R_0 \approx 10$), recalculate the threshold and explain what incomplete, waning protection means for vaccination strategy.

Answer (Q26, Synthesis). Use $H = 1 - 1/R_0$. For the original strain with $R_0 = 2.5$: $H = 1 - 1/2.5 = 1 - 0.40 = 0.60$, so about 60% of the population must be immune. For Omicron with $R_0 \approx 10$: $H = 1 - 1/10 = 0.90$, so about 90% must be immune under the simplifying assumption of durable sterilizing immunity and homogeneous mixing. In practice, infection-derived and vaccine-derived protection against infection and transmission is incomplete and wanes, so vaccination strategy should emphasize prevention of severe disease, boosters matched to current guidance, and layered controls during surges rather than a single coverage number. See section 27.

27. The inflammasome (NLRP3) is activated by uric acid crystals (gout), cholesterol crystals (atherosclerosis), and pathogens. Explain: (a) how NLRP3 assembles and activates caspase-1; (b) how caspase-1 cleaves pro-IL-1 β and pro-IL-18; (c) why NLRP3 inhibitors (MCC950) are under development for inflammatory diseases.

Answer (Q27, Synthesis). (a) A priming signal (e.g., LPS via TLR4) induces NLRP3 and pro-IL-1 β ; a second signal (uric acid or cholesterol crystals, K⁺ efflux, lysosomal damage) triggers NLRP3 to oligomerize and recruit the adaptor ASC, which clusters and activates pro-caspase-1. (b) Active caspase-1 proteolytically cleaves pro-IL-1 β and pro-IL-18 into mature, secreted cytokines (and cleaves gasdermin D to drive pyroptosis). (c) Because uncontrolled NLRP3 activity drives gout, atherosclerosis, and other sterile inflammation, selective inhibitors such as MCC950 are being developed to dampen IL-1 β without broad immunosuppression. See section 27.

28. Influenza can shift from H1N1 to H3N2 by antigenic shift (segment reassortment) or antigenic drift (point mutations in haemagglutinin). Explain: (a) why antigenic drift requires annual vaccine reformulation; (b) why antigenic shift can cause pandemics; (c) what “original antigenic sin” means for immune memory.

Answer (Q28, Synthesis). (a) Antigenic drift is the gradual accumulation of point mutations in hemagglutinin/neuraminidase that erode antibody recognition, so the vaccine strain must be reformulated annually to match circulating variants. (b) Antigenic shift is reassortment of genome segments (e.g., between human and avian/swine strains) producing a novel HA the population has no immunity to, which can ignite a pandemic. (c) ‘Original antigenic sin’ is the tendency of the immune system to preferentially recall antibodies against the first influenza strain encountered, blunting responses to newer drifted strains. See section 27.

29. The complement system (C1-C9) is a cascade of proteolytic activation that opsonises pathogens and lyses bacteria directly (MAC — membrane attack complex). Describe the three complement activation pathways (classical, lectin, alternative), naming the central converging point (C3 convertase), and explain how bacteria evade complement (factor H mimicry, capsule).

Answer (Q29, Synthesis). The classical pathway is triggered by antibody–antigen complexes binding C1q; the lectin pathway by mannose-binding lectin recognizing microbial carbohydrates; the alternative pathway by spontaneous C3 hydrolysis and direct surface deposition. All three converge on formation of C3 convertase, which cleaves C3 into C3a (anaphylatoxin) and C3b (opsonin), leading to the C5 convertase and assembly of the

membrane attack complex (C5b–C9). Bacteria evade complement by recruiting host factor H (or mimicking it) to accelerate C3b decay and by using polysaccharide capsules that block C3b deposition and MAC insertion. See section 27.

30. Natural killer (NK) cells kill virus-infected cells that downregulate MHC class I (a strategy used by many viruses to evade CTLs). Explain the “missing self” hypothesis: how do inhibitory KIR receptors normally inhibit NK killing, and how does MHC class I downregulation remove inhibition and trigger NK-mediated lysis?

Answer (Q30, Synthesis). Under the ‘missing-self’ hypothesis, NK cells continuously sample target cells: inhibitory KIRs (e.g., KIR2DL, KIR3DL) bind self MHC class I and deliver a dominant inhibitory signal that overrides activating receptor signals, sparing healthy cells. Many viruses down-regulate MHC class I to hide infected cells from CD8+ CTLs, but this removes the ligand for inhibitory KIRs. With inhibition lost and activating receptors still engaged, the NK cell is unleashed and lyses the MHC-low target via perforin/granzyme. See section 27.

Questions — Plant Structure and Water Relations

Instructor Use and Coverage Notes

- Coverage target: Calculate water potential and predict the direction of water movement.
- Model/data emphasis: Water-potential and transpiration-flux calculations.
- Assessment alignment: Visual Representations, Questions and Methods, Argumentation.
- Misconception probe: Water does not move because plants pull with intention; it follows potential gradients and cohesion.
- Transfer product: Transfer plant-water reasoning to drought, irrigation, forest physiology, and crop breeding.
- Grading focus: award full credit for mechanism, evidence, boundary conditions, and units when a calculation is required.
- Suggested use: draw one recall item, one application item, and one synthesis item when building a short quiz from this bank.

Questions 1–10: Recall and Comprehension

This activity accompanies section 28 of the textbook — review that chapter before attempting the exercises below.

1. Name the three major tissue systems in plants. Give one cell type belonging to each.

Answer (Q1, Recall). The three plant tissue systems are dermal, ground, and vascular. Dermal tissue is the outer protective covering; a representative cell type is the epidermal cell (e.g., a guard cell or root-hair cell). Ground tissue fills the interior; parenchyma (thin-walled, living, photosynthetic or storage cells) is a representative type, alongside collenchyma and sclerenchyma. Vascular tissue is the long-distance transport network; xylem (tracheids, vessel elements) and phloem (sieve-tube elements, companion cells) are its cell types. See section 28. 2. What is the difference between dermal, ground, and vascular tissue?

Answer (Q2, Recall). Dermal tissue (epidermis plus cuticle, trichomes, root hairs) is a single outer protective layer that limits water loss and mediates exchange with the environment. Ground tissue (parenchyma, collenchyma, sclerenchyma) fills the body between dermal and vascular tissue, performing photosynthesis, storage, and mechanical support. Vascular tissue (xylem and phloem) is the internal long-distance transport network: xylem moves water and minerals upward, phloem moves sugars bidirectionally. The functional distinction is protection vs. bulk metabolism/support vs. transport. See section 28. 3. Define xylem and phloem. Which transports water and which transports sugars?

Answer (Q3, Recall). Xylem is the vascular tissue that conducts water and dissolved minerals upward from roots to shoots; its conducting cells (tracheids and vessel elements) are dead and lignified at maturity. Phloem is the vascular tissue that transports sugars (sucrose at 0.3–0.9 M) plus amino acids and signaling molecules bidirectionally from sources to sinks; its sieve-tube elements remain alive (though they lack a nucleus). Xylem transports water; phloem transports sugars. See section 28. 4. What are tracheids and vessel elements? How do they differ structurally?

Answer (Q4, Recall). Both are water-conducting xylem cells that are dead and lignified at maturity. Tracheids are long (1–5 mm), narrow, tapered cells; water passes between them only through bordered pit pairs, making them less efficient but more cavitation-resistant, and they are the sole conducting element in most gymnosperms. Vessel elements are shorter (0.2–1 mm) but much wider (up to about 500 μm) and stack end-to-end with perforation plates (dissolved end walls) to form open vessels, giving higher conductance but greater vulnerability to embolism; they occur mainly in angiosperms. See section 28. 5. Define water potential (Ψ). Write the equation $\Psi = \Psi_s + \Psi_p$.

Answer (Q5, Recall). Water potential (Ψ, units MPa) is the free energy of water per unit volume relative to pure water at atmospheric pressure; water moves spontaneously from higher to lower Ψ. The simplified form is $\Psi = \Psi_s + \Psi_p$, where Ψ_s is the osmotic (solute) potential ($\Psi_s = -iCRT$, always ≤ 0) and Ψ_p is the pressure (turgor) potential (positive in turgid cells, negative in xylem under tension). The full four-component form is $\Psi = \Psi_s + \Psi_p + \Psi_m + \Psi_g$ (matric and gravitational terms added). See section 28. 6. What is the Casparian strip? In which cell layer is it found and what does it do?

Answer (Q6, Recall). The Casparian strip is a band of lignin (deposited first) and suberin in the radial and transverse walls of endodermal cells, the single cell layer surrounding the vascular cylinder of the root. By fusing the cell wall to the plasma membrane it blocks the apoplast pathway, forcing all water and ions to cross a selective plasma membrane (the symplast/transmembrane route) before entering the stele. This makes the endodermis the root’s selective filter, controlling which ions reach the xylem. See section 28. 7. Define transpiration. What drives transpiration in leaves?

Answer (Q7, Recall). Transpiration is the evaporative loss of water vapor from the plant, mainly through open stomata in the leaf. It is driven by the steep water-potential (vapor-pressure) gradient between the leaf interior and the much drier atmosphere ($\Psi \approx -100$ MPa at 50% RH): water evaporates from mesophyll cell-wall surfaces into the substomatal air space and diffuses out the stomata. This evaporation generates the tension that pulls the xylem water column upward. See section 28. 8. What are stomata? What cells regulate their opening and closing?

Answer (Q8, Recall). Stomata are pores in the epidermis (mostly on the lower/abaxial leaf surface) through which CO₂ enters and water vapor and O₂ exit. Each pore is bounded by two kidney-shaped guard cells, which regulate aperture by changing their turgor: K⁺ influx (with Cl[–] and malate^{2–})

lowers Ψ_s , water enters osmotically, the guard cells swell and bow apart, and the stoma opens; solute efflux (e.g., via ABA→SLAC1) reverses this and the stoma closes. See section 28. 9. What is root pressure? Under what conditions does it occur?

Answer (Q9, Recall). Root pressure is a positive xylem pressure (0.05–0.5 MPa) generated when roots actively secrete mineral ions into the xylem, lowering xylem Ψ_s so that water follows osmotically and pushes the xylem column upward. It occurs mainly at night and in well-watered soil when transpiration is low or absent (it is largely absent during the day in most species). It can lift water only about 5 m, so it cannot account for ascent in tall trees, but it can refill embolised conduits overnight. See section 28. 10. Describe the pressure-flow (Münch) hypothesis for phloem transport.

Answer (Q10, Recall). The Münch pressure-flow hypothesis explains phloem transport as bulk flow driven by an osmotically generated turgor gradient. At a source (e.g., a mature leaf) sucrose is loaded into sieve tubes, lowering Ψ_s so water enters osmotically from adjacent xylem and raises turgor pressure. At a sink (root, fruit) sucrose is unloaded, Ψ_s rises, water leaves, and turgor falls. The resulting source-to-sink pressure difference drives bulk flow of phloem sap through the sieve-tube network; the direction is set by which tissue is loading vs. unloading. See section 28.

Questions 11–20: Application and Analysis

11. A plant cell has $\Psi_s = -0.9$ MPa and $\Psi_p = +0.4$ MPa. Calculate its Ψ . If placed in a solution with $\Psi = -0.3$ MPa, will water enter or leave the cell? What will change as the cell reaches equilibrium?

Answer (Q11, Application). Use $\Psi = \Psi_s + \Psi_p$. Substituting: $\Psi = (-0.9 \text{ MPa}) + (+0.4 \text{ MPa}) = -0.5 \text{ MPa}$. The external solution is at $\Psi = -0.3$ MPa, which is higher (less negative) than the cell's -0.5 MPa. Because water moves from higher to lower Ψ , water enters the cell. As water enters, the cell swells, Ψ_p rises (and Ψ_s becomes slightly less negative through dilution); equilibrium is reached when cell Ψ rises to -0.3 MPa to match the solution. See section 28. 12. The cohesion-tension theory explains xylem water transport. Explain each component: (a) cohesion (H-bonds between water molecules); (b) adhesion (attraction to xylem walls); (c) tension (negative pressure from leaf transpiration). How does this mechanism pull water to 100 m in tall trees?

Answer (Q12, Application). (a) Cohesion: hydrogen bonds hold water molecules together so a continuous column in the xylem can sustain large negative pressure (theoretical tensile strength about -140 MPa; observed -1 to -15 MPa) without breaking. (b) Adhesion: water's attraction to the hydrophilic, lignified xylem walls keeps the column from pulling away from the conduit and helps support it. (c) Tension: evaporation from mesophyll cell-wall menisci (Young–Laplace, $\Delta P = 2\gamma\cos\theta/r$) creates strongly negative pressure that is transmitted down the continuous column. In a 100 m redwood, transpiration-generated tension overcomes the about 1.0 MPa gravitational drop plus flow resistance, pulling water up entirely passively. See section 28. 13. A researcher applies ABA (abscisic acid) to stomatal guard cells. Predict: (a) what happens to K^+ channels (efflux activated); (b) what happens to guard cell turgor; (c) what happens to stomatal aperture; (d) how CO_2 supply to mesophyll cells changes.

Answer (Q13, Application). ABA binds PYR/PYL receptors, inhibiting PP2C phosphatases and activating SnRK2/OST1. (a) OST1 opens SLAC1 anion channels (Cl^- /malate²⁻ efflux) and activates GORK outward-rectifying K^+ channels while inhibiting inward K^+ channels, so net K^+ efflux occurs and inward K^+ is blocked. (b) Loss of K^+ , Cl^- and malate raises guard-cell Ψ_s by about 1.5 MPa; water exits osmotically and guard-cell turgor falls. (c) Guard cells deflate, so the stomatal aperture closes (within about 5–15 min). (d) With stomata closed, CO_2 supply to mesophyll cells decreases, reducing photosynthesis—the cost of conserving water. See section 28. 14. Compare apoplastic vs symplastic water transport from root epidermis to the xylem. What role does the Casparian strip play in forcing water through the symplastic pathway? Why is this gatekeeping important for ion selection?

Answer (Q14, Application). In the apoplast pathway water and ions move through cell walls and intercellular spaces without crossing a membrane (fast, non-selective); in the symplast pathway they move cell-to-cell through plasmodesmata after one membrane crossing (slower, selective). At the endodermis the Casparian strip (lignin + suberin fused to the plasma membrane) blocks the apoplast, forcing all water and solutes to cross a selective plasma membrane to enter the stele. This gatekeeping matters because membrane transporters and aquaporins then determine which ions (e.g., NO_3^- , K^+) are admitted and exclude toxic ions, preventing uncontrolled bulk-flow leakage into the xylem. See section 28. 15. Phloem loading concentrates sucrose in sieve tubes at the source. Explain: (a) the apoplastic loading pathway (H^+ -sucrose co-transporter); (b) how increased solute concentration in sieve tubes lowers Ψ_s ; (c) how water follows by osmosis, generating turgor pressure that drives bulk flow toward the sink.

Answer (Q15, Application). (a) Apoplastic loading: SWEET11/12 export sucrose from mesophyll to the cell-wall space; the companion-cell H^+ -ATPase builds a proton gradient that the SUT1/SUC2 H^+ -sucrose symporter uses to pump sucrose into the sieve-tube/companion-cell complex against its concentration gradient (up to about 1 M). (b) The high sucrose concentration sharply lowers sieve-tube Ψ_s (to about -2 to -3 MPa). (c) The low Ψ draws water in by osmosis from adjacent xylem, raising turgor (Ψ_p) at the source; the source-to-sink turgor difference then drives bulk flow of phloem sap toward sinks. See section 28. 16. Cavitation (air bubble formation) in xylem vessels can block water transport. Explain: (a) how tension increases cavitation risk during drought; (b) how pit membranes between vessel elements limit cavitation spread; (c) how some trees (ring-porous oaks) repair cavitated vessels at night via root pressure.

Answer (Q16, Application). (a) During drought, transpiration drives xylem tension more negative; at sufficiently negative pressure dissolved gas nucleates a bubble (cavitation) that expands into an embolism, air-locking the conduit. (b) Bordered pit membranes between conduits limit spread: in conifers the torus seats against the pit aperture (an aspirated pit) when a neighbor embolises; angiosperm homogeneous membranes resist air-seeding until breached, confining damage conduit-by-conduit. (c) At night transpiration ceases and roots actively secrete ions into the xylem, generating positive root pressure (0.05–0.5 MPa) that dissolves the trapped gas and refills embolised conduits—observed in ring-porous trees and species such as *Vitis* and *Laurus*. See section 28. 17. A potometer measures transpiration rate by tracking water uptake. If a leafy shoot uptakes 4.5 mL/h at 25°C and 2.0 mL/h at 15°C, calculate: (a) the Q_{10} for transpiration; (b) what factor associated with temperature change drives this difference; (c) why humidity must also be controlled.

Answer (Q17, Application). (a) $Q_{10} = (R_2/R_1)^{(10/\Delta T)} = (4.5/2.0)^{(10/(25-15))} = (2.25)^1 = 2.25$. (b) The dominant temperature-linked driver is the leaf-to-air vapor-pressure difference (Δw): warmer air greatly increases the saturation vapor pressure inside the leaf relative to ambient, steepening the gradient that drives transpiration $E = g_s \Delta w$ (warming also slightly raises water’s diffusion/evaporation rate). (c) Humidity must be held constant because ambient relative humidity directly sets Δw ; if humidity changed between trials it would alter transpiration independently of temperature and confound the measured Q_{10} . See section 28. 18. Mycorrhizal fungi dramatically increase root surface area and provide phosphorus to plants in exchange for photosynthetic carbon. Compare arbuscular mycorrhizae (AM, intracellular fungal hyphae) vs ectomycorrhizal (ECM, extracellular mantle). Estimate the increase in effective root absorptive area (10× to 1,000×) and explain why nearly 90% of plant species have mycorrhizal associations.

Answer (Q18, Application). Arbuscular mycorrhizae (AM) penetrate root cortical cells, forming intracellular arbuscules for nutrient exchange and an extensive external hyphal network; they associate with about 80% of land plants. Ectomycorrhizae (ECM) form an external sheath (mantle) plus an intercellular Hartig net without entering cells, typical of many forest trees. Because fungal hyphae are far thinner than roots, they explore soil pores roots cannot reach and increase effective absorptive surface roughly 10× to 1,000×. This is decisive for phosphorus, which diffuses very slowly and is rapidly depleted in a root-only depletion zone, explaining why about 90% of plant species rely on mycorrhizal symbiosis (trading photosynthetic carbon for P). See section 28. 19. Halophytes (salt-tolerant plants) grow in saline soils ($\Psi_s < -1.0$ MPa). Explain three strategies: (a) accumulation of compatible solutes (proline) to lower Ψ_s ; (b) ion compartmentalization into vacuoles (NHX1 Na^+/H^+ antiporter); (c) salt secretion via specialized salt glands.

Answer (Q19, Application). In saline soil ($\Psi_s < -1.0$ MPa) the soil Ψ is very negative, so halophytes must lower internal Ψ further to keep water moving inward while avoiding ion toxicity. (a) They synthesize compatible solutes such as proline and glycine betaine in the cytoplasm, lowering Ψ_s osmotically without poisoning enzymes. (b) They compartmentalise Na^+ into the vacuole via the tonoplast NHX1 Na^+/H^+ antiporter, using the toxic ion as a cheap vacuolar osmoticum while protecting the cytosol. (c) Some species export salt through specialized epidermal salt glands or bladders, secreting Na^+/Cl^- to the leaf surface. Together these maintain a favorable Ψ gradient for water uptake under salt stress. See section 28. 20. A plant anatomist sections a dicot stem and a monocot stem. List four differences in vascular bundle arrangement, cambium presence, cortex/pith proportions, and secondary growth capability.

Answer (Q20, Application). Four contrasts: (1) Vascular bundle arrangement—dicot stems have bundles in a single ring around the pith; monocot stems have bundles scattered throughout the ground tissue. (2) Vascular cambium—present between xylem and phloem in dicots (a continuous lateral meristem); absent or non-functional in monocots. (3) Cortex/pith organization—dicots show a distinct cortex and central pith separated by the bundle ring; monocots lack a discrete pith/cortex boundary because bundles are dispersed. (4) Secondary growth—dicots undergo secondary thickening (wood) via the cambium; monocots generally lack true secondary growth. See section 28.

Questions 21–30: Synthesis and Evaluation

21. Evaluate the limits of the cohesion-tension theory: the maximum theoretical xylem tension is approximately −20 MPa, but measured tensions rarely exceed −3 MPa. Does this discrepancy refute the theory? Discuss the “vulnerability curve” (loss of hydraulic conductivity vs tension) and how different species show different cavitation thresholds. What evolutionary strategies balance xylem safety vs efficiency?

Answer (Q21, Synthesis). The discrepancy does not refute the theory. Cohesion-tension predicts metastable negative pressures sustained by water’s cohesion in narrow conduits, and direct evidence (Scholander pressure-bomb, in vivo MRI, pressure probes, synchrotron micro-CT, and synthetic-tree devices sustaining −22 MPa) confirms genuine tension. Most species operate well within their safety margin: vulnerability curves (percent loss of conductivity vs. tension) show a species-specific P50 where embolism becomes catastrophic, and conifers with torus-margo pits tolerate about −6 MPa whereas many ring-porous angiosperms cavitate near −2 MPa. Evolution tunes the safety–efficiency trade-off: wide vessels maximize conductance (Hagen–Poiseuille, $Q \propto r^4$) but cavitate easily; narrow tracheids sacrifice efficiency for embolism resistance—so operating tensions stay below P50 by design. The conditional cavitation threshold is not a universal failure point. See section 28. 22. Design an experiment to measure the hydraulic conductivity of a stem segment. Describe the apparatus (pressure head, flow rate measurement), the calculation ($K_h = \text{flow rate} \times \text{segment length} / \text{pressure difference}$), and how you would normalize for sapwood area. What would you expect for a conifer (tracheids primarily)

vs a diffuse-porous angiosperm (vessel elements)?

Answer (Q22, Synthesis). Hypothesis: hydraulic conductivity (K_h) scales with conduit diameter, so a vessel-bearing angiosperm conducts more per sapwood area than a tracheid-only conifer. Apparatus: mount a cut stem segment between a water reservoir and an outlet, apply a low constant pressure head (e.g., a fixed water column), and measure steady volumetric flow gravimetrically. Compute $K_h = (\text{flow rate} \times \text{segment length}) / \text{pressure difference}$, then normalize by dividing by sapwood cross-sectional area (specific conductivity). Control for embolism by flushing/vacuum-infiltrating and run replicate segments. Prediction from Hagen–Poiseuille ($Q \propto r^4$): a 200- μm vessel vs. a 30- μm tracheid gives a per-conduit flow ratio of $(200/30)^4 \approx 1.97 \times 10^3$, so the diffuse-porous angiosperm should show much higher specific conductivity than the conifer; a result with conifer \geq angiosperm would falsify the prediction. See section 28. 23. Evaluate the evidence that aquaporins regulate short-term water transport in roots. How does the abundance and phosphorylation state of root aquaporins (PIP1, PIP2 subfamilies) change in response to: (a) drought; (b) flooding; (c) diurnal light cycles? What does this imply about the relative importance of the apoplastic vs symplastic pathway under different environmental conditions?

Answer (Q23, Synthesis). Evidence (pressure-probe and reverse-osmosis experiments, plus aquaporin knockouts) shows root hydraulic conductance changes within minutes—too fast for anatomical change—implicating aquaporin gating, separate from the steady empirical fact that aquaporins also supply guard-cell water flux. (a) Drought: ABA and dephosphorylation generally close PIP aquaporins, reducing radial conductance and shifting flow toward the regulated transmembrane/symplast route. (b) Flooding/anoxia: cytosolic acidification and dephosphorylation close PIPs, lowering root water uptake (contributing to flooded-plant wilting). (c) Diurnal cycle: PIP abundance and phosphorylation rise during the day to support high transpiration and fall at night. Implication: when aquaporins dominate, the transmembrane/symplast pathway controls uptake; when they are downregulated the apoplast contributes relatively more, but this is conditional on stress state, not a universal hierarchy. See section 28. 24. Propose a bioengineering strategy to improve drought tolerance in crop plants by manipulating water transport. Compare three approaches: (a) engineering deeper root systems (overexpressing DRO1); (b) increasing xylem vessel diameter for greater hydraulic conductivity; (c) constitutively closing stomata (overexpressing OST1 kinase). For each, evaluate the trade-off between water conservation and carbon assimilation. Which strategy is most promising for wheat in arid environments?

Answer (Q24, Synthesis). (a) Deeper roots (DRO1 overexpression) reach deeper soil water with little carbon penalty and no loss of stomatal CO_2 uptake—high water access, minimal assimilation cost. (b) Wider xylem vessels raise conductivity ($Q \propto r^4$) and growth in good years but greatly increase cavitation vulnerability, so the gain collapses under severe drought (a safety–efficiency loss). (c) Constitutive stomatal closure (OST1 overexpression) strongly conserves water and raises water-use efficiency (e.g., WUE rising from about 100 to about 160 in worked chapter examples) but lowers CO_2 assimilation and yield potential. For wheat in arid environments the deeper-root strategy is most promising because it improves water supply without sacrificing carbon gain, whereas (b) is fragile under drought and (c) caps yield; combining (a) with mild (c) is the realistic optimum. The decision rule: maximize water access first, trade stomatal conductance only where water is the binding constraint. See section 28. 25. Phloem transport speed is about 1 m/h. Calculate: if a tree is 30 m tall and assimilate loading occurs in the canopy, how long does it take for sucrose to reach root tips? Compare this to xylem transport speed (about 10–40 m/h). What limits phloem transport speed (viscosity of concentrated sucrose solution, sieve plate resistance)?

Answer (Q25, Synthesis). At about 1 m/h phloem speed, sucrose loaded in a 30 m canopy reaches the root tips in time = distance/speed = 30 m \div 1 m/h = 30 hours. Xylem moves much faster (about 10–40 m/h), so the same 30 m would take only about 0.75–3 h—phloem transport is roughly 10–40 \times slower than xylem. Phloem speed is limited by the high viscosity of concentrated sucrose sap (0.3–1 M) and the hydraulic resistance of the sieve plates (narrow sieve pores, P-protein), which together constrain the bulk-flow rate that a given source-to-sink turgor gradient can sustain. See section 28. 26. Evaluate the evolutionary transition from tracheids (present in most vascular plants) to vessel elements (present in angiosperms and some gymnosperms). What anatomical changes (perforation plates, wider diameter) conferred increased hydraulic efficiency, and what trade-offs (increased vulnerability to cavitation) accompanied this transition? How does this relate to the ecological dominance of angiosperms?

Answer (Q26, Synthesis). The evidence: tracheids occur in all vascular plants and are the only conducting element in most gymnosperms, whereas vessel elements (shorter, much wider, end walls dissolved into perforation plates) evolved chiefly in angiosperms. Perforation plates and larger diameter remove most of the cell-to-cell resistance and, via Hagen–Poiseuille ($Q \propto r^4$), greatly raise hydraulic efficiency, supporting high transpiration and rapid growth. The trade-off is greater cavitation vulnerability—wide open vessels embolise and propagate air-locks more readily than narrow, pit-isolated tracheids. The boundary condition: this is not a universal “vessels are better” claim; in cold or drought-prone habitats embolism risk can favor tracheids. Higher conductance plausibly contributed to angiosperm ecological dominance in productive, well-watered environments, but the advantage is context-dependent rather than absolute. See section 28. 27. The pressure-flow model (Münch) for phloem transport makes predictions about: (a) turgor in source vs sink phloem; (b) the osmotic potential gradient between source and sink; (c) the effect of girdling (removing phloem) on sugar accumulation above the girdle. Evaluate each prediction using experimental evidence, and assess the main criticism of the model (can passive flow alone explain transport over >50 m?).

Answer (Q27, Synthesis). (a) Münch predicts higher turgor in source phloem than sink phloem; turgor-probe and aphid-stylet measurements confirm a source-to-sink pressure gradient. (b) It predicts a Ψ_s gradient set by loading—more negative Ψ_s (high sucrose, about -2 to -3 MPa) at the source, less negative at the sink; sap-sampling supports this, and removing lower leaves of soybean reverses flow within hours, consistent with passive bulk flow following the pressure gradient. (c) It predicts girdling (severing phloem) blocks downward sugar movement, causing carbohydrate accumulation above the girdle and starvation below—classically observed. Main criticism: in very tall trees (>50 m) sieve-plate resistance may make a single passive gradient insufficient; the resolution invokes relay loading/unloading and active maintenance of the gradient rather than abandoning pressure flow. See section 28. 28. Evaluate the role of plasmodesmata in cell-to-cell communication in plants. How do plasmodesmata allow selective symplastic transport (size exclusion limit about 1 kDa), what signals move through them (transcription factors like KNOTTED1, siRNAs), and how do viruses exploit plasmodesmata for cell-to-cell spread (movement proteins)?

Answer (Q28, Synthesis). Plasmodesmata are ER-lined cytoplasmic channels (about 40–60 nm) linking adjacent cells into a symplastic continuum, normally with a size-exclusion limit near about 1 kDa; their neck aperture is dynamically set by callose deposition, so under stress callose closes them and isolates cells. The evidence (dye-coupling, viral movement-protein studies) shows the limit is not fixed: developmental signals such as the transcription factor KNOTTED1 and silencing siRNAs traffic cell-to-cell through dilated plasmodesmata, and plant viruses encode movement proteins that bind their genome and gate plasmodesmata open to spread infection. The conclusion that plasmodesmata are simple fixed-size pores would change given this regulated, exploitable gating—they are actively controlled communication conduits, conditional on developmental and pathogen context. See section 28. 29. Climate change increases atmospheric CO_2 and temperature, both of which affect transpiration, stomatal conductance, and water-use efficiency. Evaluate the predicted effects on forest water balance: (a) increased $\text{CO}_2 \rightarrow$ partial stomatal closure \rightarrow reduced transpiration \rightarrow increased runoff; (b) increased temperature \rightarrow increased VPD \rightarrow increased transpiration \rightarrow drought stress. Which effect dominates in tropical forests vs boreal forests?

Answer (Q29, Synthesis). (a) Rising CO_2 triggers partial stomatal closure (CO_2 -sensing converging on SLAC1), lowering g_s and transpiration and raising intrinsic water-use efficiency ($\text{iWUE} = A_n/g_s$; chapter example WUE rising about $100 \rightarrow 160$), which can leave more soil water and increase catchment runoff. (b) Higher temperature raises the leaf-to-air vapor-pressure deficit, increasing $E = g_s \cdot \Delta w$ and pushing trees toward drought stress and cavitation despite partial closure. Which dominates is conditional: in tropical forests the warming/VPD effect tends to dominate (already warm, high evaporative demand, drought-driven dieback risk), whereas in boreal forests the CO_2 -fertilization/water-saving effect is relatively larger because evaporative demand and temperatures are lower. The net forest water balance therefore depends on biome, not a single universal direction. See section 28. 30. Critically evaluate whether the “hydraulic architecture” of a tree (the specific pattern of vessel diameters, vessel density, and branch tapering from base to tip) is optimized by natural selection for efficient water delivery. Apply Murray’s law (branching geometry) and the “safety vs efficiency” trade-off framework. What does damage from extreme drought events reveal about the limits of optimization?

Answer (Q30, Synthesis). Empirically, hydraulic architecture shows strong patterning: vessels widen basipetally (tip-to-base), branch junctions taper, and Murray’s law (conserving the sum of conduit radii cubed across branchings) predicts the diameter distribution that minimizes the carbon cost of achieving a given conductance—observed approximately in many species, evidence that selection optimizes water delivery within the safety–efficiency trade-off (wide conduits maximize $Q \propto r^4$ but cavitate readily). However, this optimization is conditional, not absolute: extreme drought drives widespread “hydraulic failure” and dieback (e.g., the 2011 Texas drought killed about 300 million trees), revealing that architectures tuned to historic climate envelopes are not optimal against novel extremes. What would change the “optimized” conclusion is evidence that trees routinely operate far from Murray’s-law predictions or fail well within their historical climate—so optimization holds within a bounded environmental range, not universally. See section 28.

Questions — Plant Reproduction and Development

Instructor Use and Coverage Notes

- Coverage target: Trace a plant life cycle and predict the consequence of disrupting one stage.
- Model/data emphasis: Life-cycle accounting and phyllotaxis/growth-pattern calculations.
- Assessment alignment: Visual Representations, Questions and Methods, Argumentation.
- Misconception probe: Pollen, spores, seeds, and gametes are not interchangeable terms.
- Transfer product: Transfer reproductive reasoning to agriculture, pollination ecology, and plant evolution.
- Grading focus: award full credit for mechanism, evidence, boundary conditions, and units when a calculation is required.
- Suggested use: draw one recall item, one application item, and one synthesis item when building a short quiz from this bank.

Questions 1–10: Recall and Comprehension

This activity accompanies section 29 of the textbook — review that chapter before attempting the exercises below.

1. Describe the alternation of generations in plant life cycles. What is the gametophyte? What is the sporophyte?

Answer (Q1, Recall). Alternation of generations is the diphasic plant life cycle in which a diploid sporophyte and a haploid gametophyte alternate. The sporophyte (2n) produces haploid spores by meiosis in sporangia. Each spore grows by mitosis into the gametophyte (n), which produces gametes by mitosis. Fertilization (syngamy) of two gametes restores the diploid sporophyte. The sporophyte is the spore-producing diploid generation (dominant in vascular plants); the gametophyte is the gamete-producing haploid generation (dominant in bryophytes, reduced to a few cells in angiosperms). See section 29.

2. Name the male and female parts of a flower and state their functions.

Answer (Q2, Recall). The male part is the androecium, made of stamens (filament + anther); the anther produces pollen grains (the male gametophyte). The female part is the gynoecium (carpel/pistil), comprising stigma (receives pollen), style (pollen-tube passage), and ovary (encloses ovules). The stamen’s function is pollen production and delivery; the carpel’s function is pollen reception, pollen-tube guidance, and protection of the ovules in which fertilization occurs. (Imperfect flowers carry only one of these whorls.) See section 29.

3. What is pollination? Distinguish self-pollination from cross-pollination.

Answer (Q3, Recall). Pollination is the transfer of pollen from an anther to a receptive stigma (in angiosperms) or to the ovule (in gymnosperms), the step that precedes pollen-tube growth and fertilization. Both self- and cross-pollination achieve this transfer; the difference that changes genetic outcome is the source of pollen: self-pollination delivers pollen to a stigma of the same flower or plant (promoting homozygosity), whereas cross-pollination delivers pollen between different individuals (maintaining heterozygosity). Self-incompatibility systems exist specifically to block self-pollen and enforce outcrossing. See section 29.

4. What is double fertilization in angiosperms? What two structures result?

Answer (Q4, Recall). Double fertilization, the defining synapomorphy of angiosperms (discovered by Nawaschin, 1898), is the fusion of two sperm cells from one pollen tube with two cells of the embryo sac. One sperm fuses with the egg cell to form the diploid (2n) zygote, which develops into the embryo. The second sperm fuses with the central cell’s two polar nuclei to form the triploid (3n) primary endosperm nucleus, which develops into the nutritive endosperm. The two resulting structures are the embryo and the endosperm. See section 29.

5. What is a seed? Name its three components.

Answer (Q5, Recall). A seed is a mature, fertilized ovule: a packaged embryo with a stored food supply enclosed in a protective coat, allowing the new sporophyte to disperse and survive without external water for fertilization. Its three components are: (1) the embryo (the young sporophyte, with radicle, hypocotyl, and one or two cotyledons); (2) stored food (triploid endosperm in cereals, or female gametophyte tissue in gymnosperms, or cotyledons in many eudicots); and (3) the seed coat (testa), derived from the ovule integuments. See section 29.

6. What is a fruit? How does it develop after fertilization?

Answer (Q6, Recall). A fruit is the mature ovary wall (the pericarp: exocarp + mesocarp + endocarp), sometimes incorporating accessory tissue, that encloses and disperses the seeds. After fertilization, auxin from the developing seeds and gibberellins from the pericarp suppress the abscission program (fruit set); cytokinins then drive pericarp cell division and auxin/GA drive cell expansion; finally ripening occurs (in climacteric fruits via an autocatalytic ethylene burst that softens walls, accumulates sugars, and changes pigments). The pericarp differentiates into fleshy or dry fruit types adapted for dispersal. See section 29.

7. Define germination. Name three environmental factors required.

Answer (Q7, Recall). Germination is the resumption of growth by a quiescent embryo, beginning with imbibition of water and ending with radicle emergence; it occurs when the ABA/GA hormonal balance tips toward GA, allowing mobilization of stored reserves by α -amylase, lipases, and proteases. Three environmental factors required are: (1) water (imbibition activates metabolism), (2) oxygen (for aerobic respiration powering growth), and (3) a suitable temperature (within the species’ range; for many seeds an additional specific cue such as light/Pfr or cold stratification is also needed). See section 29.

8. What is vegetative reproduction? Give two examples.

Answer (Q8, Recall). Vegetative (asexual) reproduction is the production of new, genetically identical plants from somatic (non-reproductive) plant parts, without seeds or fertilization, so each offspring is a clone of the parent. Two examples: stolons/runners (horizontal above-ground stems that root and form daughter plants at nodes, as in strawberry) and rhizomes (horizontal underground stems with nodes and adventitious roots, as in ginger or bamboo). Bulbs, corms, tubers, adventitious plantlets, and layering are additional mechanisms. See section 29. 9. What is meristem tissue? Distinguish apical meristems from lateral meristems.

Answer (Q9, Recall). Meristematic tissue consists of undifferentiated, actively dividing cells that generate all new plant cells and tissues; the shared principle is that growth is localized to these stem-cell regions. Apical meristems occur at shoot and root tips (the SAM, regulated by the WUS-CLV3 feedback loop, and the RAM, with its quiescent center) and drive primary growth — increase in length. Lateral meristems (vascular cambium and cork cambium) form cylinders along stems and roots and drive secondary growth — increase in girth (wood and bark). The decisive difference is axis of growth: primary/length vs. secondary/thickness. See section 29. 10. What is photoperiodism? Distinguish long-day, short-day, and day-neutral plants.

Answer (Q10, Recall). Photoperiodism is a plant's flowering response to the relative lengths of day and night, with night length being the true measured signal (sensed via the phytochrome system). The shared principle is a critical night-length threshold that gates the floral transition. Short-day plants flower when the night exceeds a critical length (e.g., chrysanthemum, poinsettia); long-day plants flower when the night is shorter than a critical length (e.g., spinach, many cereals); day-neutral plants flower after sufficient vegetative growth regardless of photoperiod (e.g., tomato). The decisive contrast is the direction of the night-length threshold (or its absence). See section 29.

Questions 11–20: Application and Analysis

- Double fertilization: one sperm fuses with the egg (2n zygote), another fuses with the central cell (3n endosperm). Explain the evolutionary advantage of triploid endosperm vs a haploid nutritive tissue. Why is endosperm essential for seed development in cereals?

Answer (Q11, Application). In double fertilization one sperm yields the 2n zygote and the other yields the 3n endosperm. Triploid endosperm has the advantage that it forms only after fertilization (“payment on delivery”): unfertilised ovules do not develop nutritive tissue, so maternal resources are invested only in viable seeds. The 2 maternal : 1 paternal genome dosage also creates a regulated arena (PEG/MEG genomic imprinting via FIS-PRC2) balancing paternal nutrient-extraction genes against maternal rationing genes — fine-tuning provisioning across offspring, which a uniparental haploid tissue could not do. In cereals the endosperm is essential because it is the bulk storage tissue (starch 60–70%, storage proteins, oils) that nourishes the germinating seedling and supplies about 60% of human calories. See section 29. 12. SI (self-incompatibility) mechanisms prevent self-pollination. In gametophytic SI (e.g., *Nicotiana*), pollen S-RNases degrade RNA in incompatible (self) pollen tubes. Explain: (a) the molecular logic — why would a plant destroy its own pollen; (b) the advantage for genetic diversity; (c) how SI is overcome in commercial apple orchards (polliniser trees).

Answer (Q12, Application). (a) In gametophytic SI the style secretes S-RNases; an incoming pollen tube expresses SLF F-box proteins that tag and degrade only non-self S-RNases. When pollen carries a matching (self) S-haplotype, its SLFs cannot recognize the matching S-RNase, so the self S-RNase survives and destroys the tube's ribosomal RNA, arresting growth. The plant “destroys its own pollen” to prevent self-fertilization. (b) This enforces outcrossing, maintaining heterozygosity and avoiding inbreeding depression and accumulated genetic load. (c) Apple is gametophytic-SI, so a single self-incompatible cultivar sets little fruit; orchards interplant a compatible polliniser cultivar with a different S-genotype (and use bees) so cross-pollen carries non-matching S-alleles and fertilizes successfully. See section 29. 13. Seed dormancy allows seeds to delay germination until conditions are favorable. Explain: (a) the role of ABA (prevents germination) vs gibberellin (promotes germination); (b) why stratification (cold treatment) breaks dormancy in temperate-region seeds; (c) the ecological advantage of dormancy for fire-adapted species (heat-triggered germination).

Answer (Q13, Application). (a) Dormancy is governed by the ABA/GA balance: high ABA (acting through PYR/RCAR-PP2C-SnRK2 and stabilizing DELLA via DOG1) blocks germination, while GA promotes germination by triggering DELLA degradation, releasing α -amylase, lipase, and protease genes that mobilize reserves. (b) Cold-moist stratification (1–5 °C, weeks–months) progressively degrades ABA and induces GA-biosynthesis genes, shifting the balance toward germination — so temperate seeds shed in autumn germinate only after winter, timing emergence to spring. (c) For fire-adapted species, heat scarification cracks the impermeable testa and smoke-derived karrikins (via the KAI2 receptor) trigger germination, so seeds germinate after fire when competition is low and nutrients are released — an ecological advantage of enforced dormancy. See section 29. 14. Fruit types: distinguish fleshy fruits (berry, drupe, pome) from dry fruits (achene, capsule, legume). For each type, name an example species and explain how the fruit structure promotes seed dispersal (animal, wind, water, or ballistic).

Answer (Q14, Application). Both fleshy and dry fruits are matured pericarp; the difference that changes dispersal is whether the pericarp stays succulent (reward) or dries (mechanical/wind). Fleshy: a berry has an entirely fleshy pericarp (tomato, grape) and a drupe has a fleshy mesocarp plus stony endocarp (cherry, peach); a pome includes accessory receptacle tissue (apple) — all promote endozoochory (animals eat the fruit and void

hard seeds elsewhere). Dry: an achene is a dry one-seeded fruit (sunflower; dandelion's pappus gives wind dispersal/anemochory), a capsule dries and dehisces by pores/valves (poppy; wind-shaken/gravity), and a legume is a pod that splits explosively along two sutures (pea; ballistic dispersal). Fruit structure thus matches the dispersal vector. See section 29. 15. Arabidopsis ABCE model of floral organ identity: A genes → sepals; A+B → petals; B+C → stamens; C → carpels; E is required in most whorls. Predict the floral phenotype when: (a) the B gene is knocked out; (b) the A gene is knocked out; (c) both A and C are knocked out. What would each mutant flower look like?

Answer (Q15, Application). Using the ABC(E) model (A→sepal whorl 1; A+B→petal whorl 2; B+C→stamen whorl 3; C→carpel whorl 4; A and C are mutually antagonistic so loss of one lets the other spread): (a) B knockout (ap3/pi): no petals or stamens — whorls become sepal, sepal, carpel, carpel. (b) A knockout: C spreads into all whorls — carpel, stamen, stamen, carpel (whorls 1–2 become carpels because C now acts there). (c) A and C both knocked out (with E present): the antagonists are gone; B still acts in whorls 2–3, so the flower is sepal/leaf-like in whorl 1, then petal, petal, and leaf-like in whorl 4 — and, lacking C, the floral meristem is indeterminate, producing reiterated whorls. See section 29. 16. Pollen tube navigation: pollen tubes grow through the style following chemical gradients (e.g., LURE peptides from the synergid cells flanking the egg cell). Explain: (a) how Ca^{2+} oscillations drive directional tip growth; (b) the role of the filiform apparatus in synergid cells; (c) what happens if a pollen tube arrives at an already-fertilized ovule (polytubey block).

Answer (Q16, Application). (a) Pollen-tube tip growth is driven by a tip-focused cytosolic Ca^{2+} gradient (about 1.5–10 μM at the apex vs. about 150 nM in the shank); oscillating Ca^{2+} at the tip directs targeted exocytosis of wall vesicles (callose/pectin), so steering LURE-PRK6 signaling reorients the Ca^{2+} peak and bends growth toward the ovule. (b) The synergids' filiform apparatus is an elaborate cell-wall labyrinth at the micropylar pole that vastly increases secretory surface area, releasing the species-specific LURE peptides that guide the tube into the micropyle. (c) On arrival one synergid degenerates and the FERONIA–LORELEI complex triggers tube rupture and sperm release; once fertilization occurs, the persistent synergid is silenced/eliminated (synergid-FER signaling shut down), removing the LURE source so additional tubes are not attracted — the polytubey block preventing polyspermy. See section 29. 17. Apomixis (asexual seed production without fertilization) occurs naturally in some grasses and dandelions. Explain: (a) the mechanism (unreduced embryo sac, parthenogenesis); (b) why agriculture would benefit from engineered apomixis in hybrid crops (fixing heterosis permanently); (c) the rice synthetic-apomixis approach using MiMe plus a parthenogenesis trigger; (d) what field-translation risks remain.

Answer (Q17, Application). (a) Apomixis produces seeds without fertilization: an unreduced (2n) embryo sac forms by apospory from a somatic nucellar cell or diplospory by skipping meiosis, and its unreduced egg develops parthenogenetically into an embryo genetically identical to the mother; endosperm forms either autonomously or pseudogamously. (b) Engineering apomixis into hybrid crops could fix heterosis in self-perpetuating seed, so farmers could save F1 seed rather than re-making annual production crosses. (c) Rice synthetic apomixis combines MiMe (knockout of OSD1, PAIR1, REC8, turning meiosis toward mitosis and producing unreduced gametes) with a parthenogenesis trigger such as BBM expression or MATRI-LINEAL disruption, yielding maternal clones in seed across generations. (d) Translation still needs field seed-set data, rare aneuploid monitoring, stability across climates, gene-flow containment, and governance around who controls the self-propagating seed trait. See section 29. 18. Compare seed dispersal strategies: epizoochory (burs attaching to animal fur), endozoochory (fleshy fruits eaten by birds), anemochory (wind, e.g., dandelion pappus), hydrochory (water, coconut). For each, predict which seed/fruit trait is maximized (adhesion strength, palatability, surface area, buoyancy).

Answer (Q18, Application). All four are dispersal strategies of the matured pericarp/seed; the difference that changes the maximized trait is the vector. Epizoochory (burs such as burdock/cocklebur) maximizes adhesion strength — hooks/spines that grip animal fur or feathers. Endozoochory (fleshy berries/drupes eaten by birds) maximizes palatability and a nutritious, brightly colored pulp with a gut-resistant seed coat. Anemochory (dandelion pappus, maple samara) maximizes surface-area-to-mass ratio (plumes or wings increasing drag/lift for wind transport). Hydrochory (coconut) maximizes buoyancy and water/salt tolerance (fibrous, air-filled mesocarp for ocean rafting). Each fruit trait is tuned to its dispersal mechanism. See section 29. 19. The transition from vegetative to reproductive growth (floral transition) is controlled by the florigen protein FT (FLOWERING LOCUS T) produced in leaves and transported via phloem to the shoot apical meristem. Explain: (a) how photoperiod (sensed by CONSTANS protein in leaves) triggers FT expression; (b) how FT interacts with FD transcription factor at the meristem to activate floral identity genes (AP1); (c) why vernalisation (prolonged cold) is required for winter annuals.

Answer (Q19, Application). (a) Long days stabilize the CONSTANS (CO) protein in leaves (its degradation is light-gated through the circadian clock and phytochrome/cryptochrome); stable CO transcriptionally activates FT, the mobile florigen. (b) FT protein moves through the phloem to the shoot apical meristem, where it binds the bZIP transcription factor FD; the FT–FD complex activates floral meristem-identity genes (notably AP1) and the integrator SOC1, switching the meristem from vegetative to floral. (c) Winter annuals carry high FLC (FLOWERING LOCUS C), a MADS-box repressor that silences FT and SOC1; prolonged cold (vernalisation) epigenetically silences FLC via Polycomb H3K27me3, relieving repression so that the following long days can trigger flowering — ensuring they flower in spring, not before winter. See section 29. 20. Embryogenesis in plants establishes the apical-basal axis (shoot-root) and radial axis (epidermis-vascular tissue-ground tissue). Using Arabidopsis as a model, describe: (a)

the role of the asymmetric first division; (b) the signaling between the suspensor and the embryo proper; (c) the auxin gradient that specifies the root pole (PIN-mediated polar transport).

Answer (Q20, Application). In *Arabidopsis* embryogenesis the zygote is polarized, with PIN7 (apical) and PIN1 (basal) establishing an auxin gradient. (a) The asymmetric first division produces a small apical cell (gives rise to the embryo proper) and a large basal cell (gives rise mostly to the suspensor) — this fixes the apical–basal axis. (b) The suspensor anchors the embryo to maternal tissue, channels nutrients, and signals to pattern the basal (root) domain (WOX9), then undergoes programmed cell death after the globular stage; the embryo proper, via WOX2, patterns the apical domain. (c) PIN-mediated polar auxin transport creates an auxin maximum at the basal end (with ARF5/MONOPTEROS interpreting it) that specifies the root pole and the embryonic vascular axis; the radial axis (protoderm, procambium, ground meristem) is established at the globular–heart transition. See section 29.

Questions 21–30: Synthesis and Evaluation

21. Coevolution between flowering plants and their pollinators has shaped morphological diversity. Evaluate the evidence for pollination syndromes (e.g., red tubular flowers → hummingbird; white fragrant nocturnal → moth; UV-patterned → bee). Are syndromes perfect predictors? Use bees to explain why managed honey bees, bumblebees, solitary bees, and wild pollinator assemblages are not interchangeable. What does the “most effective pollinator” principle say about syndrome fidelity vs pollinator generalisation?

Answer (Q21, Synthesis). Pollination syndromes link floral traits to vectors (red, scentless, tubular, dilute nectar → birds; white, strongly fragrant, night-opening → hawkmoths; UV-patterned blue/yellow with landing platform → bees; small, scentless, copious dry pollen, feathery stigma → wind). The evidence is repeated convergent trait clustering across unrelated lineages and the matching of zygomorphic flowers to specialized pollinators vs. actinomorphic flowers to generalists. But syndromes are statistical biases, not deterministic keys: many plants are visited by multiple vectors, and the best visitor is the one delivering effective pollen transfer, not necessarily the most frequent visitor. Bees show the point. Managed honey bees provide movable colonies, bumblebees can buzz-pollinate some poricidal anthers, and solitary/wild bees may forage at different temperatures, flower heights, or times; wild pollinator visits can improve fruit set even where honey bees are present [Garibaldi et al., 2013]. The “most effective pollinator” principle predicts high syndrome fidelity where one reliable visitor dominates successful pollen transfer, and generalisation where effective visitors vary across years, sites, or climates. See section 29. 22. Design a breeding program to introduce self-incompatibility from a wild relative into a self-compatible crop species (e.g., tomato). Describe the genetic crosses required, how you would screen for SI expression, how a crop pangenome could reduce reference-bias around the S-locus, and the trade-off between enforced outcrossing (greater heterosis) and practical challenges (pollinator dependence).

Answer (Q22, Synthesis). Hypothesis: introgressing a functional S-locus from a self-incompatible wild relative will impose self-incompatibility on a self-compatible crop and increase outcrossing/heterosis. Crosses: make an interspecific F1 between the self-compatible crop and the SI wild relative (e.g., a wild S-RNase-bearing relative of tomato), then repeatedly backcross to the crop while selecting individuals that retain a functional, matched S-RNase + SLF haplotype (both pistil and pollen determinants must transfer together to function). Screen for SI expression by controlled self-pollination followed by aniline-blue staining of styles for arrested pollen tubes and by reduced self-seed set vs. successful cross seed set; the comparison/control is selfed vs. outcrossed plants, with replicate lines. A crop pangenome helps because wild-relative haplotypes, structural variants, or presence-absence variation near the S-locus may be absent from the elite reference genome, so selection markers should be validated against alternate haplotypes rather than one reference path [Schreiber et al., 2024]. Falsifying result: selfed plants set normal seed (SI not established). Trade-off: enforced outcrossing raises heterozygosity and potential hybrid vigour but creates obligate pollinator dependence and complicates inbred-line/seed production. See section 29. 23. Evaluate the hypothesis that the origin of the flower was a single evolutionary event (monophyletic origin of angiosperms). Cite evidence from: (a) molecular phylogenies (most angiosperms share a common ancestor); (b) fossil data (earliest undisputed flower fossils about 132 Mya); (c) the “evo-devo” evidence that the MADS-box gene family was duplicated and diversified at the base of angiosperms. What is “Darwin’s abominable mystery”?

Answer (Q23, Synthesis). “Darwin’s abominable mystery” is his term for the seemingly abrupt appearance and rapid Cretaceous diversification of flowering plants, which appeared to conflict with gradual evolution. Empirical evidence for a single (monophyletic) origin: (a) molecular phylogenies place all living angiosperms in one clade descended from a common ancestor (with Amborella/water lilies basal); (b) the earliest undisputed flower/pollen fossils (about 132 Mya, Early Cretaceous) appear after this divergence and show shared floral organization; (c) evo-devo evidence that the MADS-box gene family underwent duplication and sub/neofunctionalisation (the ABCDE classes) at the angiosperm base, providing the shared combinatorial floral toolkit. These are independent lines converging on one origin; the conclusion would change if a deeply divergent angiosperm lineage with an independent floral genetic toolkit were found, or if pre-Cretaceous unambiguous angiosperm fossils were confirmed. See section 29. 24. Parthenocarpy (seedless fruit production) can be induced by GA₃ application (seedless grapes) or by gene engineering (auxin- or GA-overproduction in ovary). Evaluate: (a) why seedless fruits are commercially valuable; (b) what transcriptional changes GA₃ induces in the ovary wall (cell expansion genes); (c) whether GM parthenocarpy would require approval as a GMO in the EU.

Answer (Q24, Synthesis). (a) Parthenocarpy produces seedless fruit, which is commercially valuable because consumers prefer no seeds (table grapes, watermelon, banana), shelf quality and processing improve, and fruit can set even when pollination fails (poor pollinator weather). (b) Mechanistically, seedless fruit is driven by auxin/GA signaling normally supplied by seeds: applied GA₃ (or engineered auxin/GA overproduction in the ovary) substitutes for the seed signal, transcriptionally activating cell-expansion genes (expansins, cell-wall-loosening and cell-cycle genes) in the pericarp so the ovary wall grows without fertilization — exactly the fruit-set/expansion program described for natural parthenocarps (banana, navel orange). (c) Whether GM parthenocarpy needs GMO approval is a regulatory judgement, not a settled mechanistic fact: in the EU a transgene-engineered parthenocarpic line would fall under GMO regulation, whereas chemically induced (GA₃-sprayed) seedlessness would not — so the answer is conditional on the method, and would change if regulatory definitions of “GMO” were revised. See section 29. 25. Evaluate the evolutionary transition from water-dependent reproduction (bryophytes — motile sperm requiring a water film) to water-independent reproduction (angiosperms — pollen grain, pollen tube, sealed ovule). What were the key innovations at each transition (vascular plants → seeds → flowers → enclosed ovules), and how did each innovation expand environmental range?

Answer (Q25, Synthesis). The empirical pattern is a graded reduction of water dependence and gametophyte size from bryophytes (free-living gametophyte, flagellated sperm needing a water film) through seedless vascular plants (dominant sporophyte but still swimming sperm), gymnosperms (pollen, sealed but naked ovule), to angiosperms (flowers, double fertilization, ovules enclosed in carpels). Key innovations and their range expansions: (1) vascular tissue + dominant sporophyte → tall, lignified bodies tolerating drier upland sites; (2) the seed → embryo packaged with food and protective coat, dispersal without external water; (3) pollen + pollen tube → fertilization with no water film, colonising arid habitats; (4) flowers/enclosed ovules + double fertilization → animal pollination, protected seeds, and post-fertilization provisioning, enabling explosive diversification. The boundary condition: this is a directional trend, not strict progress — bryophytes remain successful in moist niches, so each innovation expanded, rather than universally replaced, prior strategies. See section 29. 26. The seed coat (testa) provides physical and chemical protection against pathogens, UV, and desiccation. Evaluate the molecular basis of seed coat impermeability (suberin and lignin deposits) and how seed coat-imposed dormancy is released by scarification (physical damage) or microbial degradation. What trade-off exists between strong dormancy (survival) and rapid germination (competitive advantage)?

Answer (Q26, Synthesis). The testa is maternal integument tissue; its protective and dormancy-imposing function arises from a dense palisade of macrosclereids impregnated with suberin and lignin, making the coat water- and oxygen-impermeable (physical, PY dormancy) and chemically resistant to UV and pathogens. This coat-imposed dormancy is released when the barrier is breached: scarification (fire heat, gut-passage abrasion, freeze-thaw) or microbial/enzymatic degradation thins the testa, admitting water and O₂ so the embryo (already competent) germinates. The trade-off is ecological: strong, long dormancy maximizes bet-hedging survival across bad years and spreads germination risk, but delays establishment and cedes space to faster-germinating competitors; weak dormancy gives a rapid competitive head-start but risks germinating into lethal conditions. Selection tunes coat thickness/chemistry to the habitat’s disturbance regime. See section 29. 27. Epigenetic regulation of seed development: the MEDEA/FIE Polycomb complex prevents autonomous endosperm development before fertilization. After fertilization, paternal genome expression overcomes MEDEA repression (genomic imprinting). Evaluate: (a) why the paternal genome specifically is needed to initiate endosperm; (b) the parent-of-origin conflict hypothesis (Haig theory) applied to seed provisioning; (c) what happens in interploidy crosses (2x × 4x) where parental dosage is disrupted.

Answer (Q27, Synthesis). (a) Before fertilization the maternal FIS-PRC2 complex (MEDEA/MEA, FIE, FIS2, MSI1) deposits repressive H3K27me3, silencing endosperm-promoting paternally expressed genes (PEGs) and preventing autonomous endosperm. Because the maternal PEG alleles are imprinted-silenced, the paternal genome contributed at fertilization is specifically required to express PEGs and initiate endosperm proliferation. (b) Haig’s parent-of-origin conflict theory explains this: the paternal genome is selected to maximize resource extraction for its offspring (PEGs promote endosperm growth/nutrient transfer), while the maternal genome rations resources across multiple offspring (MEGs restrict growth) — the 2m:1p endosperm dosage is the arena of this conflict. (c) In interploidy crosses the PEG/MEG dosage balance (endosperm balance number) is broken: a paternal-excess cross (e.g., 2x × 4x pollen) overexpresses growth-promoting PEGs, causing endosperm overgrowth, failed cellularisation, and seed abortion (reciprocal maternal excess gives small, starved seeds). See section 29. 28. Evaluate the potential of synthetic seeds (somatic embryos encapsulated in alginate beads) for clonal propagation of elite crop genotypes. What are the technical challenges (desiccation tolerance of somatic embryos, germination rate, production at scale), and how do synthetic seeds compare to traditional seed in terms of cost, genetic uniformity, and epigenetic stability?

Answer (Q28, Synthesis). The empirical promise: somatic cells are totipotent and somatic embryogenesis (used commercially in oil palm, conifers, coffee) yields embryos that can be alginate-encapsulated as “synthetic seeds,” giving exact clones of an elite genotype with full genetic uniformity. The judgement, separated from the evidence: scalability is constrained by real technical challenges — somatic embryos generally lack the desiccation tolerance and dormancy of zygotic seeds (poor storage/shelf life), germination/conversion rates are often low and variable, bioreactor production is costly, and somaclonal/epigenetic variation can erode the intended uniformity. Compared with traditional seed they offer higher genetic fidelity to an elite clone but currently higher cost, lower robustness, and uncertain epigenetic stability. What would change the conclusion: demonstration

of desiccation-tolerant, dormancy-competent synthetic seeds with high conversion at commodity scale. See section 29. 29. Climate change alters flowering phenology (timing of first bloom). Evaluate: (a) how warming temperatures can alter vernalisation, florigen release, and pollen fertility; (b) what happens when plant flowering phenology shifts but pollinator phenology does not; (c) what field evidence would distinguish pollen heat failure from plant-pollinator phenological mismatch.

Answer (Q29, Synthesis). Empirical observations: long-term phenology datasets show first-bloom often advances with warming. Mechanistically, (a) warmer winters can be ambiguous — adequate cold is still needed for vernalisation (FLC silencing), warmer springs can accelerate FT/florigen-driven transition, and heat during male reproductive development can lower pollen viability. (b) If plant flowering advances but pollinator emergence, driven by different snowmelt or soil-temperature cues, does not shift equally, the flowering and foraging windows decouple, reducing pollination and seed set. (c) Distinguish mechanisms by measuring pollen viability and tube growth, hand-pollinated seed set, open-pollinated seed set, pollinator visitation timing, and cue models for flower opening versus pollinator emergence. Kudo and Cooper’s 19-year *Corydalis* study supports mismatch when early flowering preceded bumblebee emergence, while pollen assays would be needed to separate that from direct heat sterility. See section 29. 30. Critically evaluate CRISPR-based gene drives in wild plant populations: if a drive were engineered to spread herbicide resistance from a crop to its wild relatives, evaluate the ecological risks (invasive hybrid vigour, competitive dominance), the containment strategies (temporal/spatial/genetic containment), and the regulatory framework needed. Is there ever a scenario where a gene drive in plants would be ethically justified?

Answer (Q30, Synthesis). Empirical basis: gene drives bias inheritance so an engineered allele spreads through a population faster than Mendelian rates, and the chapter notes that escaped elite/engineered plant genotypes (e.g., apomictic hybrids, polyploids with heterosis) can become invasive and erode wild genetic diversity. The judgement: a drive spreading herbicide resistance into crop wild relatives carries serious ecological risks — creation of competitively dominant, hard-to-control “super-weeds,” loss of wild diversity, and difficult mitigation once released. Containment strategies, each imperfect, include spatial isolation, temporal separation of flowering, chloroplast transformation to limit pollen transfer, split or self-limiting drives, and sterility safeguards. Robust regulation would require ecological risk assessment, staged confined trials, monitoring endpoints, public engagement, and a mitigation plan consistent with National Academies guidance. Ethical justification is conditional, not categorical: it might be warranted for a clearly net-beneficial, well-contained, reversible application, and the conclusion would change with evidence that containment fails or harms exceed benefits. See section 29.

Questions — Plant Responses to the Environment

Instructor Use and Coverage Notes

- Coverage target: Predict a plant response from a signal and identify the likely hormone or pathway.
- Model/data emphasis: Dose-response, water-use-efficiency, and hormone-interaction reasoning.
- Assessment alignment: Visual Representations, Questions and Methods, Argumentation.
- Misconception probe: A plant response is not passive; plants actively regulate development and physiology without neurons.
- Transfer product: Transfer response logic to shade avoidance, drought, flowering, and crop management.
- Grading focus: award full credit for mechanism, evidence, boundary conditions, and units when a calculation is required.
- Suggested use: draw one recall item, one application item, and one synthesis item when building a short quiz from this bank.

Questions 1–10: Recall and Comprehension

This activity accompanies section 30 of the textbook — review that chapter before attempting the exercises below.

1. What is a tropism? Name three types and state the stimulus for each.

Answer (Q1, Recall). A tropism is a directional growth response in which a plant grows toward or away from an environmental stimulus, the direction set by the stimulus and mediated by asymmetric auxin distribution and differential cell elongation. Three types: phototropism (stimulus: directional light — shoots bend toward blue light); gravitropism (stimulus: gravity — roots grow down, shoots grow up); thigmotropism (stimulus: touch/mechanical contact — tendrils coil around a support). Positive tropism is growth toward, negative is growth away from, the stimulus. See section 30.

2. What is auxin? Where is it produced and how does it move through the plant?

Answer (Q2, Recall). Auxin (indole-3-acetic acid, IAA) is the principal plant growth hormone, made primarily from tryptophan via the TAA1/YUCCA pathway in young leaves, the shoot apical meristem, and developing embryos. It moves by polar auxin transport (PAT), unique among hormones: PIN efflux carriers (PIN1–8) localized to specific cell faces set the flow direction, while AUX1/LAX influx carriers import it; transport is about 1 cm/h, basipetal in shoots and acropetal in roots. This directional flow underlies apical dominance, phototropism, and gravitropism. See section 30.

3. What is phototropism? What photoreceptor detects blue light (phototropin)?

Answer (Q3, Recall). Phototropism is the directional growth of a shoot toward (positive) or a root away from a light source, classically the bending of a shoot toward blue light. The blue-light photoreceptors are the phototropins PHOT1 and PHOT2 (LOV-domain flavoproteins): blue light forms an FMN–cysteine adduct, causing autophosphorylation, which triggers PIN3 relocalization and lateral auxin redistribution to the shaded side, where acid-growth-driven cell elongation bends the shoot toward the light (Cholodny–Went mechanism, quantified by Went 1926). See section 30.

4. What is gravitropism? How do amyloplasts (statoliths) detect gravity?

Answer (Q4, Recall). Gravitropism is directional growth relative to gravity: roots grow downward (positive) and shoots upward (negative). Gravity is sensed in specialized statocytes — root columella cells and shoot endodermal (starch-sheath) cells — that contain amyloplasts (statoliths), dense starch-filled plastids that sediment under gravity within seconds of reorientation. Their settling exerts a mechanical signal (via the actin cytoskeleton/ER and LAZY1 proteins) that relocates PIN3 to the new lower cell face, biasing auxin to the lower side; the resulting differential elongation bends the organ. See section 30.

5. Name four plant hormones other than auxin and state one major function of each.

Answer (Q5, Recall). Four hormones other than auxin: (1) gibberellin (GA) — promotes stem internode elongation and induces α -amylase for seed germination; (2) cytokinin — drives cell division and promotes lateral bud outgrowth/delays leaf senescence; (3) abscisic acid (ABA) — triggers stomatal closure under drought and maintains seed dormancy; (4) ethylene — a gaseous hormone that triggers climacteric fruit ripening, senescence, and abscission. (Jasmonates mediate wound/herbivore defense; salicylic acid mediates systemic acquired resistance.) See section 30.

6. What is ethylene? What role does it play in fruit ripening?

Answer (Q6, Recall). Ethylene is a gaseous plant hormone made from methionine via SAM → ACC (by ACC synthase) → ethylene (by ACC oxidase); because it is a gas it diffuses freely between cells and even between plants. In fruit ripening it is the master signal for climacteric fruits (banana, tomato, apple, avocado): an autocatalytic ethylene burst (System 2) is triggered by ripening transcription factors, then drives cell-wall softening (polygalacturonase, expansins), starch-to-sugar conversion, chlorophyll loss revealing carotenoids/anthocyanins, and aroma volatile production. Non-climacteric fruits (strawberry, grape, citrus) lack this burst. See section 30.

7. What is the phytochrome system? Distinguish Pr and Pfr forms.

Answer (Q7, Recall). The phytochrome system is a family of red/far-red photoreceptors (dimeric about 125 kDa chromoproteins bearing a phytochromobilin chromophore) that lets plants sense light quality, especially the red:far-red ratio. The shared principle is a reversible photoswitch between two forms. Pr is the red-absorbing form (λ_{max} 660 nm), inactive, synthesized in the dark, mainly cytoplasmic; Pfr is the far-red-absorbing form (λ_{max} 730 nm), the active form that moves to the nucleus and interacts with PIFs to drive responses. Red light converts Pr→Pfr; far-red light

(or dark thermal reversion) converts Pfr→Pr — the decisive R/FR reversibility diagnostic of phytochrome. See section 30. 8. What are plant defense responses to herbivory? Name two chemical defenses.

Answer (Q8, Recall). Plant defenses against herbivory are induced responses coordinated mainly by jasmonate (JA): wounding/chewing activates JA biosynthesis from linolenic acid via the LOX pathway, JA-Ile binds COI1, JAZ repressors are degraded, and MYC2 turns on defense genes. Two chemical defenses: (1) protease inhibitors that block the herbivore’s digestive enzymes, and (2) toxic secondary metabolites such as alkaloids (e.g., nicotine in tobacco) or glucosinolates (mustard-oil compounds in Brassicaceae); volatile terpenes are also released to attract the herbivore’s natural enemies. See section 30. 9. Define thigmotropism. Give one example.

Answer (Q9, Recall). Thigmotropism is a directional growth response to touch or mechanical contact, in which cells on the contact side stop elongating while cells on the opposite side continue, curving the organ around the stimulus. The classic example is tendril coiling in climbing plants such as peas, grapes, and cucumbers: within minutes of contact a tendril coils a full 360° around a support (a thigmonastic/thigmotropic response mediated by Ca²⁺ influx and jasmonate signaling). Root obstacle avoidance is another example. See section 30. 10. What is vernalisation? Which gene (FLC) is epigenetically silenced by prolonged cold?

Answer (Q10, Recall). Vernalisation is the promotion of flowering by prolonged cold exposure (weeks at about 4 °C), required by winter annuals and biennials so that they flower in spring rather than before winter. The gene epigenetically silenced is FLC (FLOWERING LOCUS C), a MADS-box transcription factor that represses the floral integrators FT and SOC1. Extended cold induces VIN3, which joins the VRN2–PRC2 Polycomb complex to deposit repressive H3K27me3 at the FLC locus; this silencing is mitotically maintained after return to warmth, relieving repression of FT/SOC1 so flowering proceeds. See section 30.

Questions 11–20: Application and Analysis

11. The Cholodny-Went model explains phototropism: auxin redistributes laterally to the shaded side, causing differential elongation. Describe the evidence: (a) agar block experiments; (b) PIN3 auxin efflux carrier redistribution; (c) auxin-responsive reporter (DR5::GFP). What alternative explanations (differential auxin sensitivity, flavonoid phototropins) have been proposed?

Answer (Q11, Application). Initiating condition: asymmetric blue light activates PHOT1/2; changed component: PIN3 relocates so auxin is exported toward the shaded side; intermediate mechanism: higher auxin there activates the H⁺-ATPase/expansin acid-growth pathway; observable outcome: the shaded side elongates more and the shoot bends toward light. Evidence: (a) Went’s agar-block experiments — auxin diffused from an illuminated coleoptile tip into agar, and the block placed asymmetrically on a decapitated coleoptile reproduced the bend, showing a transportable growth substance redistributed to the shaded side; (b) PIN3 immunolocalisation shows blue-light-triggered relocation from the basal to the lateral cell face; (c) the auxin-responsive DR5::GFP reporter shows higher signal on the shaded side. Proposed alternatives include differential auxin sensitivity (not just concentration) between sides and direct effects of phototropin/flavonoid signaling on growth. See section 30. 12. Gibberellins promote stem elongation by degrading DELLA growth repressors. Explain: (a) the molecular pathway (GA → GID1 receptor → DELLA ubiquitination → proteasome degradation); (b) how dwarf mutants (GA-deficient or DELLA gain-of-function) fail to elongate; (c) why the Green Revolution wheat varieties (Rht-B1b, Rht-D1b) carry semi-dominant DELLA mutations that reduce height and lodging.

Answer (Q12, Application). (a) Pathway: GA binds the soluble receptor GID1; the GA–GID1 complex binds DELLA repressors (GAI, RGA, RGL1–3), which are then ubiquitinated by the SCF^{SLY1} E3 ligase and degraded by the 26S proteasome; loss of DELLA releases growth-promoting transcription factors, driving internode elongation. (b) GA-deficient mutants make no GA so DELLA is never degraded — they are dwarf; DELLA gain-of-function mutants encode a non-degradable DELLA that stays bound regardless of GA, also producing dwarfs that fail to elongate. (c) Green Revolution wheat carries semi-dominant Rht-B1b/Rht-D1b alleles encoding GA-insensitive DELLA proteins; constitutive growth repression yields short, stiff straw that resists lodging while supporting heavy grain heads — the basis of high-yield semi-dwarf varieties. See section 30. 13. Ethylene triggers the triple response in dark-grown seedlings (shortened stem, thickened stem, horizontal growth). Design an experiment using: (a) the ethylene biosynthesis inhibitor AVG; (b) the ethylene-insensitive mutant *ein2*; (c) an ethylene-overproducing mutant (*eto1*) to confirm that each component of the triple response is ethylene-dependent.

Answer (Q13, Application). Hypothesis: each component of the triple response (short hypocotyl, thick hypocotyl, exaggerated apical hook) requires ethylene signaling. Comparison/controls: dark-grown wild-type seedlings with and without exogenous ethylene/ACC. Changed factors and predictions: (a) treat with the biosynthesis inhibitor AVG (blocks ACC synthase) — wild type should fail to show the triple response unless ACC is supplied downstream of the block (rescue); (b) the ethylene-insensitive *ein2* mutant should NOT show the triple response even when given ethylene/ACC (signaling is broken downstream of perception); (c) the ethylene-overproducing *eto1* mutant should show a constitutive triple response in air without added ethylene, abolished by AVG. Measured outcome: hypocotyl length/width and hook angle, with replication across many seedlings. Falsifying result: triple response persists in *ein2* with ethylene scavenged, or fails to appear in *eto1* — which would refute ethylene-dependence. See section 30. 14. Jasmonic acid (JA) mediates herbivore-induced defenses. When a caterpillar chews a leaf, systemin (a peptide signal) activates

JA biosynthesis, which induces protease inhibitors in distant unwounded leaves. Trace the entire signaling cascade: wounding → systemin release → systemin receptor → JA biosynthesis (from linolenic acid in chloroplast) → COI1-JAZ interaction → MYC2 transcription factor activation → PI gene expression.

Answer (Q14, Application). Initiating condition: a caterpillar chews a leaf, mechanically wounding cells and releasing the peptide systemin from prosystemin. Changed component: systemin binds its leucine-rich-repeat receptor kinase on plasma membranes near the wound, raising cytosolic Ca^{2+} and activating phospholipases that liberate linolenic acid from chloroplast membranes. Intermediate mechanism: linolenic acid enters the LOX/AOS octadecanoid pathway to make jasmonic acid, conjugated by JAR1 to active JA-Ile; JA-Ile binds COI1, recruiting JAZ repressors into the SCF^{COI1} complex for ubiquitination and 26S degradation. Observable outcome: freed MYC2 (and MYC3/4) transcription factors activate defense genes including protease-inhibitor (PI) genes, both locally and — because systemin/JA signals move through the phloem — in distant unwounded leaves, deterring further herbivory. See section 30. 15. Phytochrome interconversion: Pr (absorbs red 660 nm, inactive) \rightleftharpoons Pfr (absorbs far-red 730 nm, active). In a long-day plant, flowering is promoted by long photoperiods (short nights). Explain: (a) how the phytochrome system measures night length (Pfr → Pr reversion rate in the dark); (b) how a brief red flash in the middle of a long night promotes flowering; (c) how a subsequent far-red flash reverses this.

Answer (Q15, Application). (a) Phytochrome measures night length by Pfr decay: light drives Pr→Pfr, but in darkness Pfr slowly reverts to Pr (thermal reversion) and is degraded. After a long uninterrupted night, Pfr falls below a threshold; after a short night, Pfr stays high. The plant's circadian clock reads this Pfr level at a gated time (external-coincidence model) to register day length. (b) In a long-day plant, a brief red flash in the middle of a long night reconverts Pr→Pfr, restoring high Pfr and signaling a “short night,” which promotes flowering (the night-break effect). (c) An immediately following far-red flash reconverts Pfr→Pr, cancelling the red effect — restoring the “long night” state and abolishing flowering promotion. This R/FR reversibility is the classic phytochrome signature. See section 30. 16. Absciscic acid (ABA) promotes stomatal closure under drought stress. Explain the guard cell signaling cascade: ABA → RCAR/PYL receptor → PP2C inactivation → SnRK2 activation → SLAC1 anion channel opening → Cl^- and malate²⁻ efflux → K^+ efflux → turgor loss → stomata close.

Answer (Q16, Application). Initiating condition: soil water deficit raises ABA (NCED3 upregulated in roots; ABA delivered via xylem to guard cells). Changed component: ABA binds PYR/PYL/RCAR receptors. Intermediate mechanism: the ABA-receptor complex inhibits PP2C phosphatases (ABI1/ABI2/HAB1), releasing SnRK2 kinases (notably OST1/SnRK2.6) which autoactivate and phosphorylate targets: SLAC1 anion channels open (Cl^- and malate²⁻ efflux), depolarizing the membrane; the depolarization opens GORK outward K^+ channels (K^+ efflux) while inward K^+ channels are inhibited. Observable outcome: net loss of K^+ , Cl^- and malate raises guard-cell Ψ_s , water exits osmotically, turgor falls, and the stomata close — conserving water at the cost of reduced CO_2 uptake. See section 30. 17. Auxin dose-response curves differ between stems and roots: stems show maximum elongation at about 10^{-5} M auxin, while roots show maximum elongation at about 10^{-10} M auxin and are inhibited at concentrations that stimulate stems. Explain: (a) how this difference underlies gravitropism (auxin accumulates on the lower side, inhibiting root elongation while stimulating shoot elongation); (b) why 2,4-D (a synthetic auxin) is an effective herbicide for broadleaf plants.

Answer (Q17, Application). Initiating condition: roots and shoots have very different auxin dose-optima — shoot elongation peaks near 10^{-5} M, root elongation near 10^{-10} M, and concentrations that stimulate shoots strongly inhibit roots (via Aux/IAA stabilization and induced ethylene). (a) In gravitropism, statolith-triggered PIN3 relocalization sends extra auxin to the lower side of both organs; because this raises auxin above the root optimum, the lower side of the root elongates LESS and the root bends downward, whereas the same increase is at or below the shoot optimum, so the lower side of the shoot elongates MORE and the shoot bends upward — opposite responses from one redistribution. (b) 2,4-D is a synthetic, transport- and degradation-resistant auxin; sprayed on broadleaf (dicot) weeds it produces persistent supraoptimal auxin that triggers uncontrolled growth, ethylene/ABA overproduction, and lethal disorganisation, while narrow-leaved grasses (monocots) are more tolerant — making it a selective herbicide. See section 30. 18. Plants produce volatile organic compounds (VOCs) in response to herbivory that attract predators of the herbivore (“crying for help”). The lima bean-spider mite-predatory mite tritrophic system is a classic example. Explain: (a) which VOCs (terpenoids, green leaf volatiles) are emitted; (b) how neighboring undamaged plants “eavesdrop” via VOC-induced defensive gene expression; (c) whether this constitutes plant communication or merely an information-rich cue.

Answer (Q18, Application). Initiating condition: herbivore damage activates the JA pathway (MYC2/3/4). Changed component: the plant emits a herbivore-induced VOC blend. (a) The VOCs include green leaf volatiles (C6 aldehydes/alcohols from the LOX pathway, released within seconds of wounding) and inducible terpenoids such as (E)- β -ocimene and linalool synthesized over hours; these attract predatory mites and parasitic wasps that attack the herbivore (indirect defense; the lima bean-spider mite-predatory mite tritrophic system). (b) Neighboring undamaged plants “eavesdrop”: exposure to these VOCs primes or directly induces their own defensive gene expression (JA-responsive genes), so they mount faster defenses when attacked. (c) Whether this is “communication” is a judgement, not settled fact: it clearly functions as an information-rich cue, but it qualifies as true plant-to-plant signaling only if emission is favored by selection for the receiver's response (e.g., within-plant priming or kin benefit) rather than being incidental volatiles exploited by neighbors — the conclusion would change with evidence on the emitter's fitness benefit. See

section 30. 19. Circadian clock in plants: the core oscillator (CCA1/LHY → TOC1 → CCA1/LHY feedback loop) regulates about 30% of plant gene expression. Explain: (a) how the clock anticipates dawn (pre-dawn expression of photosynthesis genes); (b) how jet-lag experiments (sudden photoperiod shift) reveal resynchronisation kinetics; (c) why clock mutants (TOC1-ox) have reduced fitness under natural light-dark cycles.

Answer (Q19, Application). Initiating condition: the core clock — morning components CCA1/LHY repress evening genes, the evening loop (PRR9/7/5/TOC1) and the evening complex (ELF3-ELF4-LUX) feed back to repress CCA1/LHY — generates about 24 h oscillations controlling about 30% of plant genes. (a) The clock anticipates dawn: it ramps up photosynthesis, sucrose-metabolism, and light-harvesting gene transcription before lights-on, so machinery is ready at first light (a fitness advantage over purely reactive timing). (b) “Jet-lag” experiments suddenly shift the photoperiod; monitoring rhythmic reporters shows the clock re-entrains over several days with characteristic transient phase shifts, revealing resynchronisation kinetics and which components reset fastest. (c) Clock mutants such as TOC1-overexpressors run with the wrong period/phase, so anticipatory programs (photosynthesis, starch turnover, flowering) become misaligned with the real light–dark cycle; resonance experiments show such plants fix less carbon and have reduced growth/fitness under natural cycles. See section 30. 20. SAR (systemic acquired resistance) provides long-lasting, broad-spectrum pathogen protection. Following a localized pathogen infection, the signal molecule salicylic acid (SA) activates the SA pathway → NPR1 monomerisation → nuclear import → TGA transcription factor activation → PR (pathogenesis-related) gene expression. How does this confer resistance to secondary infections in distal tissues?

Answer (Q20, Application). Initiating condition: a localized pathogen infection triggers a hypersensitive response and a rise in salicylic acid, plus mobile signals (e.g., pipecolic/N-hydroxy-pipecolic acid, methyl-SA) that travel through the phloem to distal tissues. Changed component: in those distal tissues SA accumulates and reduces the cellular redox state, so the normally oligomeric NPR1 is reduced to monomers. Intermediate mechanism: monomeric NPR1 enters the nucleus and acts as a transcriptional coactivator with TGA bZIP transcription factors at PR-gene promoters. Observable outcome: broad-spectrum pathogenesis-related (PR) genes (PR-1, β -1,3-glucanase, thaumatin-like proteins) are expressed and defenses are “primed” plant-wide, so a secondary infection in previously uninfected tissue is met with a faster, stronger response — long-lasting systemic acquired resistance. See section 30.

Questions 21–30: Synthesis and Evaluation

21. Evaluate the evidence for “plant intelligence” or “plant neurobiology” — the concept that plant signaling networks (electrical action potentials, calcium waves, hormone gradients) constitute a form of information processing analogous to animal brains. Critically assess: (a) what criteria define intelligence; (b) whether plants satisfy any of these; (c) the boundaries of legitimate analogy vs anthropomorphism.

Answer (Q21, Synthesis). Empirical evidence: plants do generate electrical signals (action-potential-like and variation potentials), propagating Ca^{2+} waves, and long-distance hormone/peptide signals (e.g., systemin/JA wound signaling, mycorrhizal-network transfer), and these networks support integration, memory-like priming, and adaptive responses without neurons. The judgement, separated from the evidence: (a) “intelligence” is variously defined as flexible problem-solving, learning, anticipation, and integrated decision-making; (b) plants meet weak criteria (habituation, anticipation via the clock, integrated stress responses) but show no evidence of centralised representation, neurons, or subjective cognition; (c) legitimate analogy ends where shared mechanism ends — calling signaling “neurobiology” risks anthropomorphism. What would change the conclusion: demonstration of associative learning that requires neural-like representation, or that the contested claims (e.g., active plant–plant signaling through common mycorrhizal networks, whose ecological significance remains debated) are robust and adaptive. The cautious position is “sophisticated distributed information processing,” not “a brain.” See section 30. 22. Design a CRISPR knockout experiment in Arabidopsis to determine whether the gravitropic response requires the starch-statolith mechanism (amyloplast sedimentation) or an alternative membrane-based mechanosensing pathway. What gene(s) would you knock out (PGM1 for starchless mutants), what phenotype would you measure, and what result would distinguish the two hypotheses?

Answer (Q22, Synthesis). Hypothesis: gravity perception requires amyloplast (starch-statolith) sedimentation; alternative: a starch-independent membrane mechanosensing pathway suffices. Manipulation: CRISPR-knock out PGM1 (plastidic phosphoglucomutase) to make starchless plants with low-density, non-sedimenting amyloplasts; controls are wild type and a complemented PGM1 line. Comparison/changed factor: starch presence/statolith mass, assayed by reorientation experiments. Measured outcome: root and shoot gravitropic curvature angle and latency after 90° reorientation, with replication across many seedlings and clinostat controls. Decision rule: if starchless pgm1 plants lose or strongly delay/weaken gravitropism, the starch-statolith mechanism is required; if they retain near-normal gravitropism, a starch-independent mechanosensing pathway is sufficient (the established result is reduced-but-not-abolished response, indicating statoliths greatly enhance, but are not absolutely required for, sensing). Falsifying result for the statolith hypothesis: full, normal-latency gravitropism in starchless plants. See section 30. 23. Evaluate the molecular mechanisms of plant adaptation to flooding stress (waterlogging and submergence). Compare: (a) the SUB1A strategy in rice (quiescence — ethylene → SUB1A → DELLA stabilization → growth arrest); (b) the SNORKEL strategy (escape — ethylene → SK1/SK2 → GA signaling → rapid internode elongation to escape floodwater). Under what flooding regimes is each strategy advantageous?

Answer (Q23, Synthesis). Empirical mechanisms: flooding causes hypoxia and ethylene accumulation (ACC oxidase is O_2 -limited so ethylene/ACC

builds up under water). (a) The quiescence strategy (SUB1A in rice): ethylene induces the ERF-VII transcription factor SUB1A, which stabilizes DELLA and dampens GA responses, arresting shoot elongation and conserving carbohydrate so the plant survives complete submergence. (b) The escape strategy (SNORKEL): in deepwater rice, ethylene induces SK1/SK2 ERF-VII genes that promote GA signaling, driving rapid internode elongation (up to about 25 cm/day) so leaves stay above water and keep photosynthesising/aerating. Conditional advantage (not universal): quiescence wins under brief, deep, flash flooding where the water recedes quickly (escape would waste reserves on growth that drowns); escape wins under prolonged, gradually rising floods where staying submerged means carbohydrate exhaustion and death. The “best” strategy depends entirely on flood depth and duration — the conclusion changes with the flooding regime. See section 30. 24. Climate change increases UV-B radiation at Earth’s surface due to ozone depletion. Evaluate plant UV-B responses: (a) UVR8 photoreceptor-mediated signaling → COP1-SPA → HY5 transcription factor → flavonoid/anthocyanin biosynthesis (sunscreen); (b) UV-B effects on DNA (CPD lesion formation) and repair (photolyase); (c) predicted impacts on crop productivity.

Answer (Q24, Synthesis). Initiating condition: increased surface UV-B. Changed component/(a): the UVR8 photoreceptor monomerises on UV-B absorption, interacts with COP1, and (analogous to the CRY/PhyB–COP1 logic) disrupts COP1–SPA so the transcription factor HY5 accumulates; HY5 drives flavonoid and anthocyanin biosynthesis, producing a UV-absorbing “sunscreen” in the epidermis plus antioxidant and DNA-repair gene expression. (b) UV-B directly damages DNA, forming cyclobutane pyrimidine dimers (CPDs) and 6-4 photoproducts; plants repair these largely by photolyases (photoreactivation using blue/UV-A light) and nucleotide-excision repair, limiting mutagenesis. (c) Predicted crop impacts: moderate UV-B is buffered by acclimation (flavonoid screening, repair), but elevated UV-B can reduce leaf area, photosynthesis, and yield in sensitive cultivars and shift secondary metabolism — magnitude is conditional on species, acclimation capacity, and co-occurring stresses, so projected productivity losses are uncertain rather than settled. See section 30. 25. Evaluate the evolutionary arms race between plants and herbivores. Using the example of glucosinolate-myrosinase system in Brassicaceae (the “mustard oil bomb”): (a) how the system works (glucosinolates are stored separately from myrosinase; upon tissue damage, they mix to produce toxic isothiocyanates); (b) how specialized herbivores (diamondback moth) detoxify isothiocyanates; (c) what countermeasure plant lineages have evolved (novel glucosinolates).

Answer (Q25, Synthesis). Empirical system: Brassicaceae deploy the glucosinolate–myrosinase “mustard-oil bomb.” (a) Glucosinolates are stored in S-cells separately from the enzyme myrosinase, sequestered in myrosin cells; tissue damage by a chewing herbivore mixes them, and myrosinase hydrolyses glucosinolates into toxic, reactive isothiocyanates that deter or poison generalist herbivores. (b) Specialist herbivores counter-adapt: the diamondback moth secretes a glucosinolate sulfatase that desulfates glucosinolates so myrosinase can no longer activate them, detoxifying the defense. (c) In response, plant lineages evolve novel glucosinolate side-chains and modifying enzymes (e.g., epithiospecifier/nitrile-forming proteins) that the specialist’s enzymes do not recognize — a recurring escalation. This is a coevolutionary arms race, but the outcome is conditional and lineage-specific, not a universal endpoint: the conclusion would change if a specialist evolved broad-spectrum detoxification or a plant evolved a defense the specialist cannot circumvent. See section 30. 26. Symbiotic nitrogen fixation (Rhizobium-legume): evaluate the molecular cross-talk leading to nodule formation: (a) plant-derived flavonoids → bacterial NodD → Nod factor production → root hair curling → infection thread → nodule primordia; (b) the oxygen paradox (nitrogenase is O₂-sensitive but Rhizobium needs aerobic respiration → leghaemoglobin O₂ buffering); (c) the autoregulation of nodulation (too many nodules are costly → CLE peptide negative feedback).

Answer (Q26, Synthesis). Empirical cross-talk: (a) Legume roots exude flavonoids that activate rhizobial NodD, inducing Nod-factor (lipochitooligosaccharide) synthesis; Nod factors bind NFR1/NFR5 LysM receptor kinases on root-hair cells, triggering Ca²⁺ spiking, root-hair curling, infection-thread formation, and cortical cell divisions that build the nodule primordium where rhizobia differentiate into N₂-fixing bacteroids. (b) The oxygen paradox: nitrogenase is irreversibly inactivated by O₂, yet bacteroids need O₂ for the ATP-intensive fixation reaction; the plant resolves this with leghaemoglobin, which buffers free O₂ to nanomolar levels while delivering a high O₂ flux to bacteroid respiration. (c) Nodulation is metabolically expensive, so it is autoregulated: early nodules trigger root-derived CLE peptides perceived by a shoot LRR receptor, generating a shoot-derived inhibitory signal that limits further nodule formation (autoregulation of nodulation). The judgement: these mechanisms are well supported but their quantitative balance is context-dependent (N status, host genotype) — the conclusion would change under altered soil nitrogen or symbiont compatibility. See section 30. 27. Evaluate the role of epigenetics in plant stress memory. After a heat stress episode, some plants show enhanced heat tolerance for weeks (priming). What molecular marks (H3K4me3 at HSP loci, small RNA populations, chromatin remodeling) mediate stress memory, and does this memory have transgenerational stability?

Answer (Q27, Synthesis). Empirical evidence: after a sublethal heat episode many plants show “thermomemory” — enhanced heat tolerance lasting days to weeks — associated with persistent active chromatin marks (notably H3K4me2/3 retained at HSP loci such as HSP70/HSP101), sustained accumulation of heat-shock transcription factors and HSP transcripts, altered small-RNA populations, and chromatin remodeling that keeps memory genes poised for rapid reactivation. The judgement, separated from the evidence: within-generation somatic priming is well documented and mechanistically grounded; transgenerational stability is contested — plants lack a strict germline–soma separation so some marks can in principle transmit, but most heat-induced marks are reset by demethylases/remodelers within a generation and reported transgenerational heat memory is weak and variable. What would change the conclusion: rigorous multi-generation studies showing stable, mark-dependent inheritance of heat tol-

erance independent of maternal/environmental confounds. So: robust somatic memory, uncertain and conditional transgenerational inheritance. See section 30. 28. Parasitic plants (*Striga*, *Orobanche*, dodder) exploit host plant signals to locate and attach to hosts. Evaluate: (a) how *Striga* seeds detect host-derived strigolactones as germination cues; (b) how the haustorium forms and penetrates host xylem/phloem; (c) why *Striga* is the most economically devastating weed in sub-Saharan Africa; (d) what control strategies (resistant crop varieties, suicidal germination stimulants) are being deployed.

Answer (Q28, Synthesis). Empirical mechanisms: (a) *Striga* (witchweed) seeds remain dormant until they detect host-root-exuded strigolactones, which (via a KAI2/HTL-type α/β -hydrolase receptor) trigger germination only near a suitable host. (b) The germinated radicle forms a haustorium — induced by host-derived quinone/phenolic signals — that adheres to and penetrates the host root, fusing with host xylem and phloem to siphon water, minerals, and photosynthate. (c) *Striga* is the most economically devastating weed in sub-Saharan Africa because it parasitises staple cereals (sorghum, maize, millet, upland rice), causes most damage underground before emergence, and produces tens of thousands of long-lived seeds, devastating subsistence yields. (d) Control strategies include *Striga*-resistant/low-strigolactone crop varieties, “suicidal germination” stimulants applied without a host so seeds germinate and die, herbicide-resistant (Imazapyr-coated) seed, trap/catch crops, and improved soil fertility. The judgement is conditional: efficacy varies with *Striga* species, host genotype, and farming system, so no single strategy is universally decisive. See section 30. 29. Evaluate the potential of “smart crops” engineered with synthetic hormone signaling circuits: e.g., a crop that closes stomata in response to soil moisture sensors (synthetic ABA-independent signaling), activates JA defenses primarily when herbivores are detected (synthetic promoter responsive to caterpillar oral secretions), and accelerates flowering under climate-variable conditions (synthetic florigen circuit). What are the engineering feasibility, field-validation, regulatory, and ecological risks?

Answer (Q29, Synthesis). Empirical basis: applied hormone biology already works at scale (Green Revolution GA-insensitive dwarfs, 1-MCP fruit storage, synthetic-auxin herbicides), and engineered promoters/receptors can rewire stomatal, defense, and flowering circuits. The judgement, separated from the evidence: (a) feasibility is partial — synthetic moisture-sensor-driven stomatal control, herbivore-oral-secretion-inducible JA defense, and a tunable florigen circuit can be demonstrated as modules, but stacking robust, low-leak, field-stable circuits is hard because background signaling, fitness cost, and environmental variability interact. (b) Field validation must show multi-season yield or fitness benefit, expression stability, measured water status, pest pressure, flowering synchrony, and off-target phenotypes, not just reporter activity. (c) Regulatory risk: transgenic synthetic circuits face GMO approval, which is jurisdiction-dependent. (d) Ecological risk: altered stomatal/defense/flowering behavior can have non-target effects on water cycling, pollinator timing, gene flow to wild relatives, and resistance evolution in pests. What would change the conclusion: stable, containable, net-beneficial circuits with quantified off-target and ecological effects. So promising but conditional, not settled. See section 30. 30. Critically assess the claim that plant volatile communication represents a form of “language”: (a) define what communication requires (sender, signal, receiver, response, evolved function); (b) evaluate whether plant VOC emission meets these criteria; (c) compare plant volatile signaling to animal pheromone communication; (d) assess the fitness benefit to the emitter (is it a true signal or an incidental cue exploited by neighbors?).

Answer (Q30, Synthesis). (a) Communication, in the biological sense, requires a sender, a signal, a receiver, a response in the receiver, and an evolved function such that producing the signal is favored by selection because of the receiver’s response. (b) Empirically, herbivore-induced plant VOCs have a clear sender (damaged plant), a structured signal (green leaf volatiles, terpenoids), receivers that respond (predators/parasitoids, neighboring plants, distal tissues of the same plant), and documented responses (attraction, defense priming) — meeting the first four criteria. (c) Compared with animal pheromones, plant VOC signaling shares chemical-blend information transfer and dose-dependence but typically lacks dedicated sensory organs and the tight sender–receiver coevolution of intraspecific pheromones. (d) The decisive, unresolved point is the emitter’s fitness benefit: it is a true signal only if emission is selected because receivers respond beneficially to the emitter (e.g., within-plant priming, kin benefit, or attracting bodyguards); otherwise it is an incidental cue exploited by eavesdroppers. The “language” claim therefore remains conditional, not settled, and would change with rigorous evidence on emitter fitness consequences. See section 30.

Questions — Circulation and Respiration

Instructor Use and Coverage Notes

- Coverage target: Calculate a transport or feedback variable and explain the compensatory response.
- Model/data emphasis: Cardiac-output, diffusion, oxygen-saturation, and feedback calculations.
- Assessment alignment: Visual Representations, Statistical Tests and Data Analysis, Argumentation.
- Misconception probe: Homeostasis is dynamic regulation, not an unchanging internal state.
- Transfer product: Transfer homeostatic reasoning to exercise, altitude, hemorrhage, fever, and shock.
- Grading focus: award full credit for mechanism, evidence, boundary conditions, and units when a calculation is required.
- Suggested use: draw one recall item, one application item, and one synthesis item when building a short quiz from this bank.

Questions 1–10: Recall and Comprehension

This activity accompanies section 31 of the textbook — review that chapter before attempting the exercises below.

1. What is homeostasis? Give two examples of physiological variables maintained by homeostasis.

Answer (Q1, Recall). Homeostasis is the maintenance of a relatively stable internal environment despite external fluctuations, achieved mainly by negative feedback (a sensor detects a deviation, a control center compares it to a set point, and an effector opposes the change). Two examples of regulated variables: body core temperature (about 37 °C) and arterial blood pressure (and likewise blood glucose, pH, and osmolality). See section 31.

2. Describe the structure of the human heart. Name the four chambers and four valves.

Answer (Q2, Recall). The heart is a four-chambered muscular pump: two atria (thin-walled receiving chambers) and two ventricles (thick-walled pumping chambers), with the left side at higher pressure than the right. The four valves are the two atrioventricular valves (tricuspid on the right, mitral/bicuspid on the left) and the two semilunar valves (pulmonary and aortic), which enforce one-way flow. See section 31.

3. What is the cardiac cycle? Define systole and diastole.

Answer (Q3, Recall). The cardiac cycle is one complete sequence of atrial and ventricular contraction and relaxation that fills the heart and ejects blood. Systole is the contraction (ejection) phase, when ventricular pressure rises and blood is pumped out; diastole is the relaxation phase, when the chambers refill with blood. See section 31.

4. What is cardiac output (CO)? Write the formula $CO = HR \times SV$.

Answer (Q4, Recall). Cardiac output is the volume of blood the heart pumps per minute, given by $CO = HR (\times) SV$ (heart rate times stroke volume). At rest, CO (about 70 bpm) (\times) 70 mL (about 5) L/min. See section 31.

5. Describe the structure and function of arteries, veins, and capillaries.

Answer (Q5, Recall). Arteries carry blood away from the heart at high pressure; they have thick, elastic, muscular walls that buffer pulsatile flow and (as arterioles) regulate resistance. Capillaries are single-endothelial-cell-thick vessels where gas, nutrient, and waste exchange occurs. Veins carry blood back to the heart at low pressure; they are thin-walled, high-capacitance vessels with one-way valves that prevent backflow. See section 31.

6. What is blood pressure? What are typical systolic and diastolic values?

Answer (Q6, Recall). Blood pressure is the force exerted by blood against arterial walls, driven by cardiac output against total peripheral resistance ($MAP = CO (\times) TPR$). Typical values are systolic about 120 mmHg (during ventricular ejection) and diastolic about 80 mmHg (during ventricular relaxation), with a mean arterial pressure of about 93 mmHg. See section 31.

7. What is tidal volume? What is vital capacity?

Answer (Q7, Recall). Tidal volume is the volume of air moved into or out of the lungs in a single quiet breath (about 500 mL). Vital capacity is the maximum volume that can be exhaled after a maximal inhalation — the sum of tidal volume plus inspiratory and expiratory reserve volumes (about 4.5–5 L in a healthy adult). See section 31.

8. Describe the mechanics of ventilation (breathing): inhalation and exhalation.

Answer (Q8, Recall). Inhalation is active: the diaphragm and external intercostals contract, expanding the thorax; intrapleural and alveolar pressures fall below atmospheric, so air flows in. Quiet exhalation is passive: the muscles relax and elastic recoil of the lungs and chest wall raises alveolar pressure above atmospheric, so air flows out (forced expiration adds internal intercostal and abdominal muscle contraction). See section 31.

9. What is the oxygen-hemoglobin dissociation curve? What does its sigmoidal shape indicate?

Answer (Q9, Recall). The oxygen-hemoglobin dissociation curve plots hemoglobin O_2 saturation against PO_2 . Its sigmoidal (S) shape reflects cooperative binding: as each O_2 binds, hemoglobin shifts from the low-affinity T-state toward the high-affinity R-state. This means Hb loads O_2 nearly fully at high lung PO_2 yet unloads it steeply over the physiological range of tissue PO_2 , maximizing delivery. See section 31.

10. Define thermoregulation. Distinguish endotherms from ectotherms.

Answer (Q10, Recall). Thermoregulation is the homeostatic control of body temperature around a set point via heat production and heat exchange. Endotherms (mammals, birds) generate and regulate internal metabolic heat to keep core temperature stable (about 37 °C) independent of am-

bient temperature; ectotherms (fish, reptiles, invertebrates) have body temperatures that track the environment and rely mainly on behavioral thermoregulation. The mechanistic difference is internal metabolic heat production plus physiological regulation versus reliance on external heat. See section 31.

Questions 11–20: Application and Analysis

11. During exercise, HR increases from 70 to 160 bpm and SV from 70 mL to 120 mL. Calculate the CO at rest and during exercise. What is the fold-increase? What mechanisms increase HR (sympathetic → SA node → faster depolarization) and SV (Frank-Starling mechanism)?

Answer (Q11, Application). Using $CO = HR \times SV$: at rest $CO = 70 \text{ bpm} \times 70 \text{ mL} = 4,900 \text{ mL/min}$ (about 4.9 L/min; during exercise $CO = 160 \text{ bpm} \times 120 \text{ mL} = 19,200 \text{ mL/min}$ (about 19.2 L/min. That is about a 3.9-fold increase, within the normal range for an untrained adult. HR rises because sympathetic ((β_1)) stimulation and vagal withdrawal speed SA-node depolarization; SV rises through the Frank-Starling mechanism (increased venous return stretches cardiomyocytes, optimizing actin-myosin overlap) plus increased (β_1)-driven contractility. See section 31. 12. The Bohr effect: increased CO_2 and H^+ in exercising muscle shift the oxygen-hemoglobin dissociation curve rightward, decreasing Hb's O_2 affinity. Explain: (a) the molecular basis (protonation of His146 stabilizing the T-state); (b) the physiological benefit (enhanced O_2 unloading in active tissues); (c) what happens at the lungs (low CO_2 , high pH → leftward shift → enhanced O_2 loading).

Answer (Q12, Application). (a) In exercising muscle, CO_2 and H^+ rise; protons bind histidine residues (e.g., (β)His146) and CO_2 forms carbamino groups, stabilizing the low-affinity T-state and raising P_{50} (rightward shift). (b) The benefit is enhanced O_2 unloading exactly where metabolic demand is highest, increasing tissue O_2 extraction. (c) In the pulmonary capillaries CO_2 is exhaled and pH rises, so the curve shifts left (affinity increases), promoting efficient O_2 loading onto hemoglobin. See section 31. 13. Ventilation-perfusion (V/Q) matching ensures that regions of the lung receiving airflow also receive blood flow. Explain: (a) what happens when V/Q is high (dead space) vs low (shunt); (b) how local hypoxic pulmonary vasoconstriction (HPV) diverts blood from poorly ventilated alveoli; (c) why chronic lung disease (COPD) causes V/Q mismatch and hypoxaemia.

Answer (Q13, Application). (a) High V/Q means ventilation exceeds perfusion (dead space — ventilated but not perfused, wasting ventilation); low V/Q means perfusion exceeds ventilation (shunt — perfused but not oxygenated, causing hypoxaemia). (b) Hypoxic pulmonary vasoconstriction: alveolar hypoxia constricts the local pulmonary arterioles, diverting blood away from poorly ventilated regions toward better-ventilated ones, improving overall matching. (c) In COPD, airway obstruction and parenchymal destruction make ventilation regionally uneven, creating widespread V/Q mismatch (mixed dead space and shunt) that the lung cannot fully compensate for, producing chronic hypoxaemia. See section 31. 14. Blood pressure regulation: the baroreceptor reflex senses carotid sinus stretch. When BP drops: (a) baroreceptor firing decreases; (b) medullary cardiovascular center increases sympathetic output; (c) HR, contractility, and peripheral resistance increase; (d) BP is restored. What happens if the baroreceptor reflex fails (autonomic neuropathy)?

Answer (Q14, Application). (a) A fall in BP reduces carotid-sinus/aortic stretch, so baroreceptor afferent firing to the NTS decreases. (b) Reduced NTS input disinhibits the medullary sympathetic premotor neurons (RVLM) and withdraws vagal tone, so sympathetic output rises. (c) HR, contractility, arteriolar vasoconstriction (TPR), and venoconstriction (venous return) all increase. (d) Together these restore MAP within seconds. If the baroreflex fails (autonomic neuropathy), this rapid compensation is lost, producing orthostatic hypotension — standing causes an uncorrected BP fall with dizziness or syncope, and labile, poorly buffered blood pressure. See section 31. 15. Surfactant (produced by type II alveolar cells) reduces alveolar surface tension. Without surfactant: (a) what happens to alveolar compliance (Laplace's law: $P = 2T/r \rightarrow$ smaller alveoli collapse into larger ones); (b) what condition results in premature infants (NRDS — neonatal respiratory distress syndrome); (c) how is antenatal corticosteroid treatment used to mature fetal lungs?

Answer (Q15, Application). (a) Without surfactant, alveolar surface tension is high; by Laplace's law ($P = 2T/r$) a small alveolus generates higher collapse pressure than a large one, so small alveoli empty into larger ones, lowering compliance and causing diffuse atelectasis (and pulmonary edema). (b) In premature infants, immature type II pneumocytes make insufficient surfactant, causing neonatal respiratory distress syndrome (hyaline membrane disease). (c) Antenatal glucocorticoids (e.g., betamethasone) given to the mother accelerate fetal type II cell maturation and surfactant (DPPC) production, reducing NRDS severity. See section 31. 16. The kidney maintains blood osmolality homeostasis. ADH (vasopressin) is released from the posterior pituitary in response to high blood osmolality. Explain: (a) how ADH regulates AQP2 insertion into the collecting duct apical membrane; (b) why ADH deficiency produces dilute, voluminous urine (diabetes insipidus); (c) how alcohol inhibits ADH secretion and causes diuresis.

Answer (Q16, Application). (a) High plasma osmolality stimulates posterior-pituitary ADH release; ADH binds V_2 receptors on collecting-duct principal cells, raising cAMP/PKA, which inserts aquaporin-2 water channels into the apical membrane so water is reabsorbed and urine is concentrated. (b) ADH deficiency (central diabetes insipidus) leaves few apical AQP2 channels, so water is not reabsorbed and large volumes of dilute urine are produced. (c) Alcohol inhibits ADH secretion, reducing AQP2 insertion and causing a water diuresis (the basis of alcohol-

associated dehydration). See section 31. 17. Counter-current exchange in the vasa recta (renal medullary blood vessels) maintains the osmotic gradient established by the loop of Henle. Explain: (a) why the vasa recta loop parallel to the loop of Henle; (b) how ascending and descending limbs exchange solutes; (c) what would happen to medullary osmolality if the vasa recta were replaced by a single straight vessel.

Answer (Q17, Application). (a) The vasa recta hairpin parallel to the loop of Henle so blood can perfuse the medulla without dissipating the corticomedullary osmotic gradient. (b) As blood descends, water leaves and solute (NaCl, urea) enters; as it ascends, the reverse occurs, so the descending and ascending limbs passively exchange solute and water — countercurrent exchange that returns nearly isotonic blood to the cortex. (c) A single straight vessel would carry away medullary solute (washout) and deliver excess water, dissipating the gradient and impairing the kidney’s ability to concentrate urine. See section 31. 18. During cold exposure, thermoregulation maintains core temperature at 37°C. Trace the response: peripheral thermoreceptors → hypothalamus → sympathetic nervous system → cutaneous vasoconstriction → reduced heat loss + shivering → increased heat production. What is the set-point concept, and how does fever alter the set-point?

Answer (Q18, Application). Cold skin thermoreceptors signal the hypothalamic thermostat, which increases sympathetic outflow: cutaneous vasoconstriction reduces skin heat loss, shivering (and BAT non-shivering thermogenesis via UCP1) increases heat production, restoring core temperature toward 37 °C. The set-point is the target value the hypothalamus defends by activating opposing effectors around it. In fever, pyrogens (IL-1, IL-6, TNF) drive hypothalamic COX-2/PGE(₂), which raises the set-point; the body then uses normal cold-defense mechanisms (vasoconstriction, shivering/chills) to reach the new, higher set-point. See section 31. 19. The oxygen cascade describes the progressive decrease in PO₂ from atmosphere (160 mmHg) to mitochondria (about 1–3 mmHg). Identify each step: inspired air → alveolar air (104 mmHg, diluted by CO₂ and water vapor) → arterial blood (100 mmHg, some V/Q mismatch) → capillary blood → tissue → mitochondria. At which step is the largest PO₂ drop, and what determines its magnitude?

Answer (Q19, Application). The oxygen cascade: inspired air about 160 mmHg (->) humidified/alveolar gas about 104 mmHg (diluted by water vapor and CO(₂)) (->) arterial blood about 100 mmHg (small drop from V/Q mismatch and shunt) (->) capillary/tissue, falling steeply as O(₂) diffuses out (->) mitochondria about 1–3 mmHg. The largest drop is the tissue/cellular step (capillary to mitochondria, tens of mmHg), set by tissue O(₂) consumption rate, capillary density, and diffusion distance (Fick’s law); a smaller but key drop is inspired-to-alveolar, governed by the alveolar gas equation. See section 31. 20. Heart failure with reduced ejection fraction (HFrEF) results in an EF < 40% (normal 55–70%). Explain: (a) why reduced contractility leads to fluid retention (RAAS activation); (b) why diuretics provide symptomatic relief but do not improve survival; (c) how ACE inhibitors + beta-blockers + ARNI (sacubitril/valsartan) have been shown to reduce mortality.

Answer (Q20, Application). (a) Reduced ventricular contractility lowers stroke volume and effective arterial filling; the kidney senses underperfusion and activates RAAS (and sympathetic and ADH systems), causing Na(⁺) and water retention and congestion. (b) Diuretics relieve congestive symptoms (edema, dyspnoea) by offloading volume but do not interrupt the maladaptive neurohormonal remodeling that drives progression, so they do not improve survival. (c) ACE inhibitors/ARBs, evidence-based beta-blockers, mineralocorticoid antagonists, and ARNI (sacubitril/valsartan, which adds neprilysin inhibition to prolong protective natriuretic peptides while blocking AT(₁)) all blunt the RAAS/sympathetic remodeling cascade, and trials show they reduce mortality in HFrEF. See section 31.

Questions 21–30: Synthesis and Evaluation

21. Evaluate the Frank-Starling mechanism at the molecular level: increased preload → increased sarcomere stretch → increased Ca²⁺ sensitivity of troponin C → increased force production. What molecular mechanism converts sarcomere length into increased Ca²⁺ sensitivity, and why does this relationship break down in dilated cardiomyopathy (DCM)?

Answer (Q21, Synthesis). Length-dependent activation is the molecular core of Frank-Starling: stretching the sarcomere toward optimal length (about 2.2 (μ)m) reduces interfilament lattice spacing and increases titin-mediated strain, which raises the Ca(²⁺) sensitivity of troponin C so more cross-bridges form per Ca(²⁺) transient, increasing force. The empirical evidence (stretch raises Ca(²⁺) sensitivity and force within the physiological range) is conditional on intact sarcomere geometry. In dilated cardiomyopathy the ventricle is overstretched beyond optimal overlap, the cytoskeleton/titin and Ca(²⁺)-handling proteins are remodeled, and the curve flattens — so the relationship breaks down. What would change the conclusion is operating outside the physiological length range or altered titin/troponin, which is exactly the DCM condition. See section 31. 22. Design an experiment to measure the maximal aerobic capacity (VO₂ max) of a human subject. Describe: the incremental exercise protocol (treadmill or cycle), the gas analysis measurements (O₂ consumption, CO₂ production, RER), and the criteria for reaching true VO₂ max. How does VO₂ max differ between trained athletes and sedentary individuals, and what factors (cardiac output, O₂ extraction, muscle mitochondrial density) limit performance?

Answer (Q22, Synthesis). Hypothesis: a graded exercise test will identify a true VO(₂)max plateau. Protocol: incremental treadmill or cycle ergometer with stepwise increases in workload to volitional exhaustion, with breath-by-breath gas analysis measuring O(₂) consumption, CO(₂) production, and RER. Criteria for true VO(₂)max: a plateau in VO(₂) despite rising workload, plus secondary markers (RER >1.10–1.15, HR

near age-predicted max, high blood lactate). Comparison/control: trained athletes vs sedentary subjects; trained subjects have markedly higher $\dot{V}O_{2\max}$. Limiting factors are mainly central (maximal cardiac output/ $\dot{V}O_2$ delivery) with peripheral contributions (a- $\dot{V}O_2$ difference, muscle mitochondrial/capillary density). A falsifying result is no $\dot{V}O_2$ plateau (use a verification bout). The conclusion is conditional on reaching true maximal effort. See section 31. 23. Evaluate the roles of the sympathetic and parasympathetic nervous systems in cardiovascular regulation via their respective neurotransmitters (norepinephrine $\rightarrow \beta_1$ receptors \rightarrow increased HR vs acetylcholine $\rightarrow M_2$ receptors \rightarrow decreased HR). What is “vagal tone” at rest, and why does denervation of the heart (cardiac transplant recipients) result in a resting HR of about 100 bpm?

Answer (Q23, Synthesis). Sympathetic norepinephrine acting on SA-node (β_1) receptors speeds diastolic depolarization (increases HR and contractility); parasympathetic acetylcholine acting on M_2 receptors hyperpolarises and slows the SA node (decreases HR). “Vagal tone” is the continuous resting parasympathetic restraint on the SA node: the intrinsic SA rate is about 100 bpm, but tonic vagal activity holds resting HR near 70 bpm. In a transplanted (denervated) heart the vagal input is absent, so the SA node fires near its intrinsic rate of about 100 bpm. The conclusion is conditional: it assumes the SA node and its intrinsic automaticity are intact, and partial reinnervation over years can lower the resting rate. See section 31. 24. Evaluate the physiological trade-off between capillary density and distance-limited O_2 diffusion: (a) use Fick’s law of diffusion ($J = D \times A \times \Delta P/d$) to explain why capillary density must increase in metabolically active tissues; (b) calculate the maximum O_2 diffusion distance (about 100 μm); (c) explain why tumors develop necrotic cores when they grow beyond 200 μm without angiogenesis.

Answer (Q24, Synthesis). (a) Fick’s law ($J = D(A)(\Delta P/d)$) shows flux falls as diffusion distance d increases, so metabolically active tissues must reduce inter-capillary distance (higher capillary density) to keep every cell within the diffusible O_2 range. (b) The Krogh-cylinder analysis gives a maximum viable O_2 diffusion radius of roughly 100 (μ)m from a capillary at physiological PO_2 and consumption. (c) A tumor growing beyond about 150–200 (μ)m from its nearest vessel exceeds this diffusion limit, so its core becomes hypoxic and necrotic unless it triggers angiogenesis (VEGF-driven neovascularisation). The conclusion is conditional on assumed D , consumption rate, and PO_2 ; changing these (e.g., higher capillary PO_2 or lower metabolic rate) shifts the critical distance. See section 31. 25. High altitude acclimatisation involves acute and chronic responses: acute (hyperventilation, increased HR); chronic (EPO \rightarrow erythrocytosis, 2,3-BPG increase, vascular remodeling). Evaluate: (a) how the carotid body senses hypoxia and triggers hyperventilation; (b) why respiratory alkalosis results; (c) how renal bicarbonate excretion compensates; (d) why chronic mountain sickness (Monge’s disease) can result from excessive erythropoiesis.

Answer (Q25, Synthesis). (a) Low inspired PO_2 at altitude reduces arterial PO_2 ; carotid-body glomus cells sense hypoxia (closing O_2 -sensitive K^{+} channels, depolarizing, releasing transmitter) and drive the medullary respiratory center to hyperventilate. (b) Hyperventilation blows off CO_2 , lowering arterial PCO_2 and producing respiratory alkalosis (which itself partly restrains the ventilatory response). (c) The kidney compensates over days by excreting bicarbonate (and reducing H^{+} excretion), normalizing pH and permitting fuller hyperventilation. (d) Chronic hypoxia drives EPO and erythrocytosis; in chronic mountain sickness (Monge’s disease), excessive erythropoiesis raises haematocrit and viscosity, causing pulmonary hypertension and impaired oxygen delivery despite high Hb. See section 31. 26. Evaluate the “oxygen paradox” in ischemia-reperfusion injury: restored oxygen supply to ischemic tissue generates ROS (via xanthine oxidase and Complex I) that cause greater damage than the ischemia itself. How do ROS cause injury (membrane lipid peroxidation, mitochondrial permeability transition pore opening), and what therapeutic strategies (hypothermia, ischemic pre-conditioning) mitigate reperfusion injury?

Answer (Q26, Synthesis). Ischemia depletes ATP and accumulates substrates (hypoxanthine, reduced electron carriers). On reperfusion, restored O_2 drives a burst of reactive oxygen species (xanthine oxidase, mitochondrial Complex I), which causes membrane lipid peroxidation, protein/DNA damage, Ca^{2+} overload, and opening of the mitochondrial permeability transition pore, triggering cell death — sometimes exceeding the original ischemic injury. Mitigation: therapeutic hypothermia (slows metabolism and ROS generation), ischemic pre- and post-conditioning (brief ischemia/reperfusion cycles activate protective kinase/mPTP pathways), and antioxidant or mPTP-targeted strategies. The conclusion is evidence-supported but conditional: the magnitude of reperfusion injury varies with ischemia duration and tissue, and conditioning benefits are not uniform across models, which is what would change the inference. See section 31. 27. Evaluate the hypothesis that endothermy evolved from aerobic capacity (the “aerobic capacity model”): selection for sustained locomotion \rightarrow increased mitochondrial density \rightarrow increased resting metabolic rate \rightarrow internal heat production \rightarrow endothermy. Compare this to the “parental care model” (selection for incubation of eggs \rightarrow endothermy). Which model is better supported by paleontological and comparative physiological evidence?

Answer (Q27, Synthesis). The aerobic-capacity model proposes endothermy arose because selection for sustained aerobic locomotion increased mitochondrial density and resting metabolic rate, with internal heat as a by-product later exploited for thermoregulation. The parental-care (and the related thermoregulatory/assimilation) model proposes selection acted directly on stable body temperature for incubation, development, or niche expansion. Comparative physiology (the link between maximal and resting metabolic rate, mitochondrial proliferation) gives some support to the aerobic-capacity model, while paleontological data (bone histology, growth rates, nesting behavior in dinosaurs/early mammals) are mixed. The honest answer is that the evidence is conditional and the models are not mutually exclusive; no single dataset is decisive, and new fossil metabolic proxies are what would shift the conclusion. See section 31. 28. The lymphatic system returns interstitial fluid to the bloodstream.

Evaluate: (a) how lymph is formed (Starling’s forces → net filtration at the arterial end of capillaries); (b) what happens when lymphatic drainage fails (lymphoedema — elephantiasis caused by parasitic nematode *Wuchereria bancrofti*); (c) the dual role of lymphatics in immune surveillance (dendritic cell migration to lymph nodes).

Answer (Q28, Synthesis). (a) Lymph forms because Starling forces produce net capillary filtration (about 10% of filtered fluid, plus leaked protein) that is not reabsorbed; this protein-rich interstitial fluid enters highly permeable blind-ended lymphatic capillaries by bulk flow. (b) When lymphatic drainage fails, protein-rich fluid accumulates as lymphoedema (e.g., filariasis from *Wuchereria bancrofti*, or post-surgical node dissection), which is non-pitting and prone to fibrosis and infection. (c) Lymphatics also serve immune surveillance: antigen-bearing dendritic cells migrate via afferent lymphatics to lymph nodes to prime adaptive responses. These are well-established mechanisms; the conditional element is that the relative contribution of filtration vs lymphatic load depends on capillary pressure and protein status, which is what would alter the edema interpretation. See section 31. 29. Diving mammals (Weddell seal, sperm whale) can hold their breath for >60 minutes while diving to >1,000 m. Evaluate four physiological adaptations: (a) bradycardia and peripheral vasoconstriction (dive reflex); (b) elevated myoglobin content (O₂ storage); (c) splenic contraction (autotransfusion of O₂-carrying RBCs); (d) tolerance of lactate (anaerobic metabolism during deep dives). How do these adaptations differ between pinnipeds and cetaceans?

Answer (Q29, Synthesis). Deep-diving mammals tolerate long apnoea via integrated adaptations: (a) the dive reflex — vagally mediated bradycardia plus selective peripheral vasoconstriction redistributes limited O₂ to heart and brain; (b) high muscle myoglobin greatly expands O₂ storage; (c) splenic contraction autotransfuses O₂-rich red cells, raising effective haematocrit during the dive; (d) tolerance of large lactate loads from anaerobic metabolism in hypoperfused tissues, cleared on surfacing. Pinnipeds (seals) rely more on large blood/spleen O₂ stores and pronounced bradycardia, often diving on exhalation to limit barotrauma and N₂ uptake, whereas cetaceans (whales) emphasize very high myoglobin and rapid gas exchange. The contrast (blood/spleen-dominant vs myoglobin-dominant strategies) is the boundary condition that frames the comparison. See section 31. 30. Critically evaluate the concept of “physiological reserve” — the excess capacity of organ systems beyond what is needed at rest (e.g., cardiac output can increase 5× during exercise, kidneys can maintain GFR with a single kidney). How does aging erode physiological reserve, and at what threshold does age-related reserve depletion produce clinical disease? Apply the concept to explain why the elderly are disproportionately vulnerable to COVID-19, heat waves, and surgical stress. Then transfer the same homeostatic-reserve logic to a salty high-protein meal with low water intake: predict plasma osmolality, ADH/aldosterone direction, hepatic urea production, urine concentration, and why desert mammals and freshwater fish handle nitrogen differently.

Answer (Q30, Synthesis). Physiological reserve is the excess functional capacity organ systems hold beyond resting needs (e.g., about 5-fold cardiac output rise in exercise, maintained GFR on one kidney). Aging erodes reserve through loss of cells, stiffer tissues, blunted maximal responses, and slowed homeostatic feedback; clinical disease emerges when a stressor demands more than the depleted reserve can supply (the variable crosses from compensated to decompensated). This explains elderly vulnerability: COVID-19 demands large pulmonary/immune reserve, heat waves demand cardiovascular and thermoregulatory reserve (skin blood flow, sweating), and surgery demands cardiac, renal, and pulmonary reserve — each exceeds diminished capacity. The meal transfer shows the same principle: a salty high-protein meal with low water intake raises plasma osmolality and nitrogen load; osmoreceptors drive ADH release, low effective volume can activate RAAS/aldosterone, amino-acid catabolism raises hepatic urea production, and intact renal reserve produces more concentrated urine. Desert mammals invest ATP in urea handling and a steep medullary gradient to conserve water; freshwater fish can excrete ammonia directly because water is abundant and ammonia can diffuse across gill surfaces. The conclusion is conditional: reserve loss is heterogeneous across individuals and organs, so chronological age alone does not set the threshold; functional measures and environmental water availability do. See section 31 and source notes in [National Institute of Diabetes and Digestive and Kidney Diseases \[2024a,b\]](#).

Questions — Nervous System and Neural Signaling

Instructor Use and Coverage Notes

- Coverage target: Predict behavioral or signal consequences from a circuit or structural perturbation.
- Model/data emphasis: Cable-length, conduction, and simple circuit calculations.
- Assessment alignment: Visual Representations, Statistical Tests and Data Analysis, Argumentation.
- Misconception probe: The brain is not only neurons; glia and circuit context are essential to function.
- Transfer product: Transfer circuit reasoning to reflexes, sensory systems, learning, and disease.
- Grading focus: award full credit for mechanism, evidence, boundary conditions, and units when a calculation is required.
- Suggested use: draw one recall item, one application item, and one synthesis item when building a short quiz from this bank.

Questions 1–10: Recall and Comprehension

This activity accompanies section 32 of the textbook — review that chapter before attempting the exercises below.

1. Name the two divisions of the nervous system. What does each contain?

Answer (Q1, Recall). The central nervous system (CNS) comprises the brain and spinal cord and integrates information. The peripheral nervous system (PNS) is all nervous tissue outside the CNS (12 cranial nerves and 31 spinal nerve pairs), subdivided into the somatic (voluntary) and autonomic (involuntary) divisions that connect the CNS to the body. See section 32. 2. What is a neuron? Draw and label the soma, dendrites, axon, and synaptic terminal.

Answer (Q2, Recall). A neuron is an excitable cell specialized for receiving, integrating, and transmitting electrical signals. The soma (cell body) houses the nucleus and does most protein synthesis; dendrites receive synaptic inputs; the axon conducts the action potential; and the axon terminal (bouton) releases neurotransmitter from synaptic vesicles onto the next cell. See section 32. 3. What is the resting membrane potential of a typical neuron? Which ion is most permeable at rest?

Answer (Q3, Recall). The resting membrane potential of a typical neuron is about -70 mV. K^+ is the most permeable ion at rest (highest conductance through KCNK leak channels), so the resting potential lies close to $E_K \approx -89$ mV. See section 32. 4. What is an action potential? Describe the four phases (resting, depolarization, repolarization, hyperpolarization).

Answer (Q4, Recall). An action potential is an all-or-none, regenerative depolarization that propagates along the axon. Phases: resting (-70 mV, K^+ leak dominant); depolarization (voltage-gated Na^+ channels open, V_m rises toward $+30$ mV); repolarization (Na^+ channels inactivate, voltage-gated K^+ channels open, V_m falls); and hyperpolarization (K^+ channels close slowly, dipping below rest before returning to -70 mV). See section 32. 5. What is the myelin sheath? Name the cells that produce myelin in the CNS and PNS.

Answer (Q5, Recall). The myelin sheath is a multilayered (up to about 100 wraps) insulating wrap of glial plasma membrane around an axon that increases membrane resistance and speeds conduction. Oligodendrocytes produce CNS myelin (one cell myelinates up to about 50 axons); Schwann cells produce PNS myelin (one cell per axon internode). See section 32. 6. What is saltatory conduction? How does it increase conduction velocity?

Answer (Q6, Recall). Saltatory conduction is the regeneration of the action potential only at nodes of Ranvier, where voltage-gated Na^+ channels are concentrated, so the impulse appears to “jump” between nodes. Myelin between nodes raises membrane resistance and lowers capacitance, letting current spread passively and rapidly down the internode, dramatically increasing conduction velocity for a given axon diameter. See section 32. 7. Define a synapse. Distinguish chemical from electrical synapses.

Answer (Q7, Recall). A synapse is the junction where one neuron communicates with a target cell. Chemical synapses transmit via neurotransmitter released from presynaptic vesicles (triggered by Ca^{2+} influx through Cav channels) acting on postsynaptic receptors, giving signal gain and a about 0.5 ms delay; electrical synapses use gap junctions for direct, bidirectional, near-instantaneous ionic current flow. See section 32. 8. Name three neurotransmitters and state one function of each.

Answer (Q8, Recall). Examples: glutamate is the main excitatory CNS transmitter (drives EPSPs via AMPA/NMDA receptors and LTP); GABA is the main inhibitory CNS transmitter (opens Cl^- channels via $GABA_A$); acetylcholine excites skeletal muscle at the neuromuscular junction and is the autonomic preganglionic transmitter. See section 32. 9. What is the reflex arc? Name its five components.

Answer (Q9, Recall). A reflex arc is the neural pathway producing a rapid, involuntary response to a stimulus. Five components: receptor (detects stimulus), afferent (sensory) neuron, integration center (CNS, e.g., spinal cord), efferent (motor) neuron, and effector (muscle or gland). See section 32. 10. Distinguish the somatic from the autonomic nervous system.

Answer (Q10, Recall). The somatic nervous system mediates voluntary control of skeletal muscle: single myelinated motor neurons run from CNS to effector and release ACh (excitatory only) at the neuromuscular junction. The autonomic nervous system controls involuntary visceral function via a two-neuron preganglionic/postganglionic chain and can excite or inhibit targets through its antagonistic sympathetic and parasympathetic divisions. See section 32.

Questions 11–20: Application and Analysis

11. The Goldman equation predicts resting membrane potential from the relative permeabilities of Na^+ , K^+ , and Cl^- . If a mutation doubles Na^+ permeability at rest (P_{Na} increases $2\times$), predict the new resting potential direction (depolarization toward $E_{\text{Na}} = +60 \text{ mV}$). Calculate using simplified Goldman equation.

Answer (Q11, Application). Use the GHK equation: at rest $P_K : P_{\text{Na}} : P_{\text{Cl}} \approx 1 : 0.04 : 0.45$ gives $V_m \approx -68 \text{ mV}$. Doubling P_{Na} to about 0.08 increases the weight of the inward Na^+ term (which pulls toward $E_{\text{Na}} = +60 \text{ mV}$), so the numerator/denominator ratio shifts and V_m moves a few mV more positive (depolarizes, to roughly -62 to -65 mV). This brings the membrane closer to threshold (-55 mV), increasing excitability. See section 32. 12. Multiple sclerosis (MS) destroys myelin in the CNS. Predict: (a) the effect on conduction velocity; (b) which neuronal functions are impaired first; (c) why remyelination therapies are being investigated; (d) why the PNS is relatively spared (different myelinating cells).

Answer (Q12, Application). (a) Conduction velocity falls sharply: loss of myelin lowers membrane resistance and raises capacitance, so passive current leaks out and saltatory conduction fails (slowed or blocked). (b) Functions requiring fast, heavily myelinated, long tracts fail first — vision (optic neuritis), motor coordination, sensory and bladder control. (c) Remyelination would restore the insulation needed for saltatory conduction and reverse deficits. (d) The PNS is relatively spared because Schwann cells (not the CNS oligodendrocytes/MOG-MBP autoantigens targeted in MS) make peripheral myelin. See section 32. 13. Local anaesthetics (lidocaine) block voltage-gated Na^+ channels. Explain: (a) why this prevents action potential generation; (b) why pain fibers (small, unmyelinated C fibers) are blocked before motor fibers (large, myelinated $\text{A}\alpha$ fibers); (c) is this use-dependent block (more block with higher firing frequency)?

Answer (Q13, Application). (a) Blocking voltage-gated Na^+ channels prevents the regenerative Na^+ influx, so depolarization cannot reach threshold and no action potential fires. (b) Small unmyelinated C (pain) fibers are blocked before large myelinated $\text{A}\alpha$ (motor) fibers because they have shorter internodal distances and a shorter critical length over which channels must be blocked, and smaller axons have higher surface-to-volume drug access. (c) Yes — lidocaine binds preferentially to open/inactivated channels, so rapidly firing (high-frequency) fibers accumulate more block: use-dependent block. See section 32. 14. The patellar (knee-jerk) reflex involves a monosynaptic stretch reflex arc. Trace the pathway: muscle spindle \rightarrow Ia afferent \rightarrow spinal cord (monosynaptic excitation of α -motor neuron) \rightarrow quadriceps contraction. Explain: (a) why the reflex is monosynaptic (no interneuron); (b) the role of reciprocal inhibition of the hamstring (via an inhibitory interneuron).

Answer (Q14, Application). Pathway: muscle stretch activates the muscle spindle, the Ia afferent fires and enters the dorsal root, synapses directly on the α -motor neuron in the ventral horn, which contracts the quadriceps to extend the knee. (a) It is monosynaptic because the Ia afferent excites the motor neuron with a single synapse (no interneuron), giving the shortest latency. (b) A branch of the Ia afferent excites an inhibitory interneuron that hyperpolarises the antagonist (hamstring) motor neuron — reciprocal inhibition — so the antagonist relaxes as the agonist contracts. See section 32. 15. Sensory adaptation: olfactory receptors rapidly adapt to constant odor exposure (within minutes). Explain: (a) the molecular mechanism ($\text{cAMP} \rightarrow \text{Ca}^{2+} \rightarrow \text{calmodulin} \rightarrow \text{reduced CNG channel sensitivity}$); (b) the difference between phasic (rapidly adapting) and tonic (slowly adapting) receptors; (c) one example of a tonic receptor.

Answer (Q15, Application). (a) Sustained odorant raises cAMP, opening CNG channels; Ca^{2+} entering binds calmodulin, which reduces the channel's cAMP sensitivity (negative feedback), so the receptor current declines despite continued stimulus. (b) Phasic (rapidly adapting) receptors respond mainly to stimulus change and fall silent during steady stimulation; tonic (slowly adapting) receptors fire continuously, encoding sustained stimulus intensity. (c) A tonic receptor example is the Merkel disc (sustained pressure) or muscle spindle (sustained stretch/position). See section 32. 16. The blood-brain barrier (BBB) restricts drug entry into the CNS. Explain: (a) the cellular basis (tight junctions between endothelial cells, pericytes, astrocyte end-feet); (b) which molecules can cross (small, lipophilic, $\text{MW} < 400$); (c) how L-DOPA (prodrug for dopamine) exploits amino acid transporters to bypass the BBB.

Answer (Q16, Application). (a) The BBB is formed by tight junctions (claudin-5, occludin, ZO) sealing brain endothelial cells, with pericytes and astrocyte endfeet maintaining the barrier — blocking paracellular passage of polar/large molecules. (b) Only small, lipophilic, low-molecular-weight molecules (O_2 , CO_2 , anaesthetics) diffuse freely. (c) Dopamine cannot cross, so L-DOPA is given: it is a large neutral amino acid carried across by the LAT1 transporter, then decarboxylated to dopamine inside the CNS — exploiting carrier-mediated transport to bypass the barrier. See section 32. 17. Neuroplasticity: after a stroke destroys the motor cortex controlling the right hand, the left hand often improves in dexterity over weeks. Explain: (a) cortical remapping (adjacent cortical areas take over); (b) the role of long-term potentiation (LTP) in this process; (c) why intensive rehabilitation (constraint-induced movement therapy) accelerates recovery.

Answer (Q17, Application). (a) Cortical remapping: surviving neurons in adjacent, undamaged cortex expand their receptive fields and take over functions of the lost region. (b) LTP underlies this rewiring — correlated activity (Hebbian) strengthens spared synapses via NMDA-receptor Ca^{2+} influx, CaMKII activation, and AMPA-receptor insertion, building new functional circuits. (c) Constraint-induced therapy forces intensive use of the affected limb, driving the correlated pre/postsynaptic activity that maximizes LTP and use-dependent remapping, so recovery accelerates. See section 32. 18. The autonomic nervous system has sympathetic (fight-or-flight) and parasympathetic (rest-and-digest) divisions. Compare: (a) preganglionic neurotransmitter (both ACh); (b) postganglionic neurotransmitter (sympathetic = NE, parasympathetic = ACh); (c) effects on heart rate, bronchioles, and GI motility.

Answer (Q18, Application). (a) Both divisions use ACh at the preganglionic synapse (on nicotinic receptors). (b) Postganglionically, sympathetic neurons release norepinephrine onto adrenergic receptors, while parasympathetic neurons release ACh onto muscarinic receptors. (c) Sympathetic activation increases heart rate (β_1), dilates bronchioles (β_2), and inhibits GI motility; parasympathetic activation decreases heart rate (M_2), constricts bronchioles (M_3), and increases GI motility and secretion. See section 32. 19. Pain processing: nociceptors detect tissue damage and transmit signals via A δ (sharp, fast) and C (dull, slow) fibers. Explain the gate control theory: how does activation of large-diameter A β touch fibers “close the gate” in the spinal cord dorsal horn, reducing pain transmission to the brain?

Answer (Q19, Application). Gate control: pain-carrying A δ /C fibers and large A β touch fibers both project to the dorsal horn. A β activity excites an inhibitory interneuron in the substantia gelatinosa that presynaptically/postsynaptically inhibits the projection (transmission) neuron carrying pain to the brain. Thus stimulating touch fibers (rubbing the area, or TENS) “closes the gate,” reducing the pain signal ascending the spinothalamic tract even though nociceptor input is unchanged. See section 32. 20. Glial cells (astrocytes, oligodendrocytes, microglia) outnumber neurons. Describe two functional roles of astrocytes beyond structural support: (a) glutamate uptake at synapses (preventing excitotoxicity); (b) regulation of extracellular K^+ ; (c) the “tripartite synapse” concept (astrocyte modulates synaptic strength via gliotransmitters).

Answer (Q20, Application). (a) Glutamate uptake: astrocyte EAAT1/EAAT2 transporters clear about 90% of synaptic glutamate, terminating signaling and preventing excitotoxic over-activation of NMDA receptors. (b) K^+ buffering: astrocytes take up activity-driven extracellular K^+ through Kir4.1 channels and redistribute it through the gap-junction-coupled syncytium, keeping the resting potential stable. (c) Tripartite synapse: the astrocyte process is a functional third partner that senses synaptic glutamate (astrocytic Ca^{2+} rise) and releases gliotransmitters (glutamate, ATP, D-serine) that modulate synaptic strength and plasticity. See section 32.

Questions 21–30: Synthesis and Evaluation

21. Evaluate the “integrate-and-fire” model of neuronal computation: a neuron summates thousands of excitatory and inhibitory postsynaptic potentials (EP-SPs and IPSPs) and fires when threshold is reached. What are the limitations of this model (dendritic computation, non-linear integration, backpropagating APs), and how do modern computational neuroscience models address them?

Answer (Q21, Synthesis). The leaky integrate-and-fire model treats the neuron as a point that linearly sums EPSPs/IPSPs at the hillock and fires when it crosses about -55 mV. Limitations: it ignores active dendritic computation (NMDA spines and dendritic $\text{Na}^+/\text{Ca}^{2+}$ spikes make integration non-linear), location-dependent attenuation set by the length constant, shunting inhibition, and backpropagating action potentials that gate plasticity. Modern models address these with multi-compartment (cable-equation) Hodgkin-Huxley neurons, two-layer dendritic-subunit models, and adaptive exponential integrate-and-fire variants that approximate non-linear dendritic processing. See section 32. 22. Design an experiment to determine whether a newly discovered brain region is involved in spatial memory rather than procedural memory. Describe: (a) lesion studies (selective ablation); (b) electrophysiology (place cells, grid cells); (c) optogenetic activation/inhibition during a behavioral task; (d) what behavioral paradigms (Morris water maze, T-maze) you would use; (e) how a brain-cell atlas would help choose cell types without proving function by itself.

Answer (Q22, Synthesis). Hypothesis: the region is necessary/sufficient for spatial but not procedural memory. (a) Selectively lesion (or chemogenetically silence) the region and test spatial vs procedural tasks; predict spatial impairment with intact procedural learning. (b) Record single units for place cells/grid cells (spatial coding) and compare with a procedural-learning control area. (c) Use optogenetics to inhibit the region only during the spatial-encoding phase and, separately, activate it, confirming necessity and sufficiency. (d) Behavioral paradigms: Morris water maze and T-maze (spatial) versus rotarod or serial-reaction-time task (procedural); controls and replication distinguish spatial-specific from general deficits. (e) A brain-cell atlas can nominate region-specific neuronal, glial, or marker-gene targets for recording and perturbation, but atlas identity is not causal evidence; function still requires the lesion, recording, and perturbation tests [National Institute of Mental Health, 2023, Yao et al., 2023]. See section 32. 23. Evaluate the molecular basis of Alzheimer’s disease: (a) A β oligomer toxicity hypothesis; (b) tau hyperphosphorylation and neurofibrillary tangles; (c) the failure of anti-A β antibody therapies (lecanemab showed modest benefit, 27% slowing of decline). What does the modest efficacy of anti-A β antibodies tell us about the “amyloid cascade” as a therapeutic target?

Answer (Q23, Synthesis). (a) The A β -oligomer hypothesis holds soluble oligomers, not plaques, disrupt synapses and trigger toxicity. (b) Tau hyperphosphorylation forms intraneuronal neurofibrillary tangles whose spread tracks cognitive decline more tightly than amyloid load. (c) Anti-

A β antibodies (lecanemab, donanemab) clear plaques but only modestly slow decline (about 27%). The modest efficacy argues amyloid is an early trigger but not the sole driver: by symptom onset, downstream tau pathology, neuroinflammation, and synaptic loss are self-sustaining, so the linear “amyloid cascade” is incomplete and combination/earlier intervention is likely required. See section 32. 24. Evaluate the role of adult neurogenesis in the hippocampus: (a) evidence that new neurons are continuously generated in the subgranular zone of the dentate gyrus; (b) the functional role of newborn neurons in pattern separation (distinguishing similar memories); (c) the controversial evidence for adult neurogenesis in humans (Spalding et al., ¹⁴C birth-dating vs Sorrells et al., immunohistochemistry showing no new neurons after age 13).

Answer (Q24, Synthesis). (a) Evidence for adult hippocampal neurogenesis: BrdU/Ki67 labeling and Spalding’s ¹⁴C birth-dating indicate continued neuron generation in the dentate-gyrus subgranular zone. (b) Newborn granule cells support pattern separation, letting similar experiences be stored as distinct memories and aiding mood regulation. (c) The controversy: Sorrells et al. found essentially no proliferating neuroblasts after adolescence by immunohistochemistry, conflicting with the ¹⁴C and other immunostaining work. Resolution likely hinges on tissue fixation/marker specificity; the disagreement shows the conclusion depends on methodology, so the rate (not the existence) in adult humans remains unsettled. See section 32. 25. Evaluate the mechanism of general anaesthesia: despite >150 years of use, the molecular targets of volatile anaesthetics (sevoflurane, isoflurane) are incompletely understood. Current evidence implicates: (a) GABA_A receptor potentiation; (b) NMDA receptor inhibition; (c) two-pore domain K⁺ channel (TREK/TASK) activation. How does the combination of these effects produce unconsciousness, and why is the “unitary” theory of anaesthesia (one target) now rejected?

Answer (Q25, Synthesis). Volatile anaesthetics act on multiple low-affinity targets: (a) potentiating GABA_A receptors (enhanced inhibition), (b) inhibiting NMDA glutamate receptors (reduced excitation), and (c) opening two-pore K⁺ channels (TREK/TASK), hyperpolarising neurons. Together these depress thalamocortical and cortico-cortical signaling, dissolving the integrated activity required for consciousness. The unitary (single-target) theory is rejected because no one receptor accounts for all anaesthetic endpoints, different agents have different target profiles, and immobility, amnesia, and unconsciousness are dissociable and mediated at different sites. See section 32. 26. Evaluate the concept of “neural oscillations” — rhythmic brain activity at specific frequency bands (delta 1–4 Hz, theta 4–8 Hz, alpha 8–13 Hz, beta 13–30 Hz, gamma 30–100 Hz). What cognitive processes are associated with each band, and what evidence from EEG/MEG studies supports the idea that frequency-band-specific synchronisation enables “binding” of distributed cortical representations into a unified percept?

Answer (Q26, Synthesis). Band-cognition associations: delta — deep NREM sleep and memory consolidation; theta — hippocampal navigation and memory encoding; alpha — relaxed wakefulness and attentional suppression; beta — alert focus and motor planning; gamma — sensory binding and conscious perception. EEG/MEG evidence for the binding hypothesis: stimulus-locked gamma synchronisation across distributed cortical sites correlates with perceptual grouping, and disrupting synchrony degrades binding. The conclusion is conditional — gamma synchrony reliably correlates with binding but its causal necessity for a unified percept remains debated, so it is evidence-supported rather than settled. See section 32. 27. Chronic pain involves maladaptive plasticity (central sensitisation) in the spinal cord dorsal horn. Evaluate: (a) the molecular mechanism (NMDA receptor-dependent wind-up, glial activation, BDNF release); (b) why opioids provide temporary relief but worsen chronic pain through opioid-induced hyperalgesia (OIH); (c) what non-opioid alternatives (gabapentinoids, SNRI antidepressants, spinal cord stimulation) target central sensitisation.

Answer (Q27, Synthesis). (a) Central sensitisation: repetitive C-fiber input causes NMDA-receptor-dependent “wind-up” and removal of Mg²⁺ block, glial (microglia/astrocyte) activation, and BDNF release that lowers dorsal-horn neuron threshold and expands receptive fields. (b) Opioids relieve pain acutely via μ -receptor inhibition of transmission, but chronic use induces opioid-induced hyperalgesia through NMDA upregulation and glial activation, paradoxically worsening pain. (c) Non-opioid options target central sensitisation: gabapentinoids (block $\alpha_2\delta$ Ca²⁺-channel subunits), SNRIs (boost descending serotonin/noradrenergic inhibition), and spinal cord stimulation (gate-control activation of A β fibers). See section 32. 28. The enteric nervous system (ENS, “second brain”) contains about 500 million neurons controlling GI motility, secretion, and blood flow independently of the CNS. Evaluate: (a) why the ENS is sometimes called autonomous (it functions after vagotomy); (b) the evidence linking ENS dysfunction to Parkinson’s disease (α -synuclein aggregation begins in the ENS years before brain symptoms); (c) how the gut-brain axis connects the ENS to cognition and mood.

Answer (Q28, Synthesis). (a) The ENS is “autonomous” because its myenteric and submucosal plexuses contain full sensory-interneuron-motor circuits that generate peristalsis and secretion even after vagotomy. (b) Parkinson’s link: misfolded α -synuclein aggregates appear in enteric neurons years before motor symptoms and may spread retrogradely via the vagus to the brainstem (Braak hypothesis), so gut pathology can precede CNS disease. (c) The gut-brain axis connects the ENS to cognition/mood through vagal afferents, enteroendocrine and immune signaling, and microbial metabolites that influence CNS neurotransmission. See section 32. 29. Optogenetics uses light-activated ion channels (channelrhodopsin-2, halorhodopsin) to activate or inhibit specific neurons with millisecond precision. Evaluate: (a) the technical requirements (viral vector delivery of opsin gene, implanted fiber optic); (b) an experiment that optogenetics uniquely enables (e.g., activating and silencing the same neurons to confirm necessity and sufficiency for a behavior); (c) the path to clinical translation (optogenetic gene therapy for retinitis pigmentosa).

Answer (Q29, Synthesis). (a) Technical requirements: an AAV/lentiviral vector delivers an opsin gene under a cell-type-specific promoter, plus an implanted optical fiber and light source for millisecond control. (b) Optogenetics uniquely allows activating and silencing the same defined neurons during behavior to test both necessity (inhibition abolishes the behavior) and sufficiency (activation evokes it) with temporal precision impossible for lesions or drugs. (c) Clinical translation: optogenetic gene therapy (e.g., ChrimsonR delivered to retinal ganglion cells with light-amplifying goggles) is in trials for retinitis pigmentosa, restoring light responses to a degenerated retina. See section 32. 30. Critically evaluate the “connectome” project — the effort to map every synaptic connection in the human brain (about 86 billion neurons, about 150 trillion synapses). Is the connectome sufficient to understand brain function, or is dynamic activity (electrophysiology, neuromodulation) equally important? Compare the completed *C. elegans* connectome (302 neurons, fully mapped) to our understanding of worm behavior — does knowing the wiring diagram explain the animal’s behavior? Then apply the same evidence-boundary reasoning to a high-performance speech neuroprosthesis reported in one participant with paralysis.

Answer (Q30, Synthesis). The connectome (a static wiring diagram) is necessary but not sufficient: the same circuit produces different outputs depending on dynamic activity, neuromodulatory state, and synaptic strength. The fully mapped *C. elegans* connectome (302 neurons) still does not fully predict behavior, because neuromodulators (e.g., monoamines, peptides) reconfigure the functional circuit and synaptic weights/signs are not given by anatomy alone. So structure constrains but does not determine function — understanding the brain also requires electrophysiology and neuromodulation, making the human connectome a foundation rather than a complete explanation. A speech neuroprosthesis claim needs the same boundary: implanted electrodes directly record motor/speech-cortex activity during attempted speech, and a trained decoder converts those signals into text or avatar control in a defined task; the inference is decodable intention-related structure, not a general readout of private thought. Durable translation still depends on chronic signal stability, calibration burden, tissue response, infection risk, power, device replacement, performance outside the lab, consent, data ownership, privacy, autonomy, and access. See section 32 and Willett et al. [2023], Metzger et al. [2023].

Questions — Action Potentials and Synaptic Transmission

Instructor Use and Coverage Notes

- Coverage target: Predict how changing an ion gradient or channel conductance alters excitability.
- Model/data emphasis: Nernst/Goldman, Hodgkin-Huxley, and synaptic-current reasoning.
- Assessment alignment: Visual Representations, Statistical Tests and Data Analysis, Argumentation.
- Misconception probe: An action potential is not electricity flowing like a wire; it is regenerated ion-channel dynamics.
- Transfer product: Transfer excitability reasoning to anesthesia, toxins, epilepsy, and neuromuscular disease.
- Grading focus: award full credit for mechanism, evidence, boundary conditions, and units when a calculation is required.
- Suggested use: draw one recall item, one application item, and one synthesis item when building a short quiz from this bank.

Questions 1–10: Recall and Comprehension

This activity accompanies section 33 of the textbook — review that chapter before attempting the exercises below.

1. Define an action potential. What are the threshold, peak, and undershoot voltages?

Answer (Q1, Recall). An action potential (AP) is a rapid, all-or-nothing, self-propagating depolarization-repolarization of the neuronal membrane produced by the sequential opening of voltage-gated Na⁺ and K⁺ channels — the electrical signal of the nervous system. The canonical mammalian AP has four quantitative landmarks: resting potential ≈ -70 mV (set by K⁺ leak channels and Na⁺/K⁺-ATPase, matching the K⁺ Nernst potential); threshold ≈ -55 mV (voltage at which enough Nav1.x channels open that inward Na⁺ current overtakes outward K⁺ current, committing the membrane to firing); peak $\approx +30$ to $+40$ mV (approaches but never reaches E_{Na} $\approx +60$ mV, because Na⁺ channels begin inactivating before full equilibration); undershoot (afterhyperpolarization, AHP) ≈ -80 to -90 mV (voltage-gated K⁺ channels close slowly, briefly driving V_m past rest toward E_K ≈ -90 mV — the refractory period). Total duration about 1–2 ms in axons; propagation velocity 1 m/s (unmyelinated) to 120 m/s (myelinated, saltatory conduction). The Hodgkin–Huxley model (Nobel 1963) quantitatively reproduces every feature from four ODEs in m, h, n gating variables. See section 33.

2. What are voltage-gated Na⁺ channels? Describe their three states (closed, open, inactivated).
- Answer (Q2, Recall). Voltage-gated Na⁺ channels (Nav1.1–1.9, encoded by SCN1A–SCN11A) are membrane proteins whose pore opens in response to depolarization and carries the inward Na⁺ current of the action-potential upstroke; they are concentrated at nodes of Ranvier (about 1,000/μm² vs about 25/μm² under myelin). They cycle through three states: closed (at rest near -70 mV, activation/m gates shut but ready to open); open (depolarization past threshold opens the m gates within about 0.5 ms, Na⁺ rushes in, V rises toward E_{Na}); inactivated (the h “ball-and-chain” gate occludes the pore from inside about 1 ms after opening, so the channel cannot reopen regardless of stimulus until repolarization resets it — the basis of the absolute refractory period and unidirectional propagation). See section 33.

3. What is the absolute refractory period? What is the relative refractory period?
- Answer (Q3, Recall). The absolute refractory period (about 1–2 ms after the spike peak) is the interval when essentially all Na⁺ channels are in the inactivated state (h ≈ 0); no stimulus, however strong, can trigger a second action potential, which guarantees unidirectional propagation and caps maximum firing rate (about 500–1000 Hz). The relative refractory period (about 5–10 ms following the absolute period) is when Na⁺ channels are recovering from inactivation while K⁺ channels remain open and the membrane is hyperpolarised below rest (afterhyperpolarisation); a second spike is possible but requires a stronger-than-normal stimulus and has reduced amplitude. See section 33.

4. What is a compound action potential (CAP)? How does it differ from a single-neuron AP?
- Answer (Q4, Recall). A single-neuron action potential is the all-or-none about 100 mV spike of one axon, described by the Hodgkin–Huxley equations from the squid giant axon. A compound action potential (CAP) is the extracellularly recorded summed electrical signal of a whole nerve containing many axons with different diameters and conduction velocities. It differs from a single AP in being a graded, multi-peaked waveform: its amplitude grows with stimulus strength (recruiting more fibers, not “bigger” spikes), and it spreads out into separate humps with distance because fast (large, myelinated A) and slow (small, unmyelinated C) fibers progressively desynchronise. See section 33.

5. Define a synapse. Name the pre- and postsynaptic components.
- Answer (Q5, Recall). A synapse is the specialized junction at which one neuron communicates with a target cell. At a chemical synapse the presynaptic component is the axon terminal, containing neurotransmitter-filled vesicles, voltage-gated Ca²⁺ channels, and the active-zone release machinery (SNARE proteins, synaptotagmin-1). These are separated by the about 20 nm synaptic cleft from the postsynaptic component — the membrane bearing neurotransmitter receptors (ionotropic and metabotropic) clustered at the postsynaptic density. Transmission is unidirectional (presynaptic → postsynaptic), modifiable, and has a 0.5–2 ms synaptic delay; electrical synapses (gap junctions) instead couple cytoplasms directly and are bidirectional. See section 33.

6. What is a neurotransmitter vesicle? How is it released (Ca²⁺-dependent exocytosis)?
- Answer (Q6, Recall). A neurotransmitter (synaptic) vesicle is a about 40 nm membrane-bound organelle in the presynaptic terminal that stores a

quantum of neurotransmitter (about 5,000–10,000 molecules). Release is Ca^{2+} -dependent exocytosis: an arriving action potential opens voltage-gated Ca^{2+} channels; local Ca^{2+} rises to about 100 μM in a nanodomain and binds the C2 domains of synaptotagmin-1 (4–5 ions, giving steep about 4th-power cooperativity); synaptotagmin displaces the complexin clamp, the SNARE complex (synaptobrevin + syntaxin + SNAP-25) zippers fully, and the vesicle fuses with the plasma membrane, releasing transmitter into the cleft in <1 ms. See section 33. 7. What is an EPSP? What is an IPSP? How do they differ in ionic mechanism?

Answer (Q7, Recall). An EPSP (excitatory postsynaptic potential) is a transient depolarization that moves the membrane toward threshold, produced when an excitatory transmitter (e.g., glutamate) opens cation channels (AMPA/NMDA, Na^+/K^+ , some Ca^{2+}) so net inward current depolarizes the cell. An IPSP (inhibitory postsynaptic potential) is a hyperpolarising or shunting event that moves the membrane away from threshold, produced when an inhibitory transmitter (GABA, glycine) opens Cl^- channels (GABA_A, Cl^- influx) or K^+ channels (GABA_B-activated K^+ efflux). They differ in ionic mechanism: cation influx (depolarizing) for EPSPs vs anion influx / K^+ efflux (hyperpolarising/shunting) for IPSPs. See section 33. 8. Define temporal and spatial summation of postsynaptic potentials.

Answer (Q8, Recall). Postsynaptic potentials are graded and decremental, so a single EPSP rarely reaches threshold; the neuron sums inputs at the axon hillock. Temporal summation is the addition of successive EPSPs from the *same* synapse arriving within a few membrane time constants of each other, so the second begins before the first has decayed and the depolarisations add. Spatial summation is the addition of EPSPs (and IPSPs) from *different* synapses active at the same time on the dendrites/soma. If the net depolarization at the axon hillock exceeds threshold (about –55 mV), an all-or-none action potential is fired; IPSPs subtract from this sum. See section 33. 9. What is a neuromuscular junction? What neurotransmitter is released there?

Answer (Q9, Recall). The neuromuscular junction (NMJ) is the chemical synapse between a motor neuron's axon terminal and a skeletal muscle fiber's motor end-plate. The neurotransmitter released there is acetylcholine (ACh): an action potential opens presynaptic Ca^{2+} channels, ACh-containing vesicles fuse and release ACh, which binds muscle-type nicotinic ACh receptors ($\alpha_1\beta_1\delta\epsilon$ pentamers) opening Na^+/K^+ channels to generate the end-plate potential. The NMJ has a high quantal content and resting release probability about 0.1–0.4, giving a large safety factor; ACh is then cleared by acetylcholinesterase. See section 33. 10. What is long-term potentiation (LTP)? In which brain region was it first described?

Answer (Q10, Recall). Long-term potentiation (LTP) is an activity-dependent, long-lasting (hours to days) increase in synaptic efficacy following high-frequency stimulation — a leading cellular model of learning and memory. It was first described in the hippocampus, at the perforant-path inputs to the dentate gyrus (Bliss and Lømo, 1973), and is classically studied at the Schaffer-collateral → CA1 synapse. NMDA-receptor-dependent Ca^{2+} influx activates CaMKII, which phosphorylates and inserts AMPA receptors (early LTP); late LTP additionally requires CREB-driven gene expression and structural spine changes. See section 33.

Questions 11–20: Application and Analysis

- Using the Nernst equation ($E = (RT/zF) \ln([\text{ion}]_{\text{out}}/[\text{ion}]_{\text{in}})$), calculate the equilibrium potential for K^+ given $[\text{K}^+]_{\text{out}} = 5 \text{ mM}$ and $[\text{K}^+]_{\text{in}} = 150 \text{ mM}$ at 37°C. Then calculate E_{Na} with $[\text{Na}^+]_{\text{out}} = 145 \text{ mM}$ and $[\text{Na}^+]_{\text{in}} = 15 \text{ mM}$. Which equilibrium potential is closest to the resting membrane potential?

Answer (Q11, Application). At body temperature 310 K, $RT/F = (8.314 \times 310)/96485 = 0.0267 \text{ V} = 26.7 \text{ mV}$; using base-10 log, $(RT/F) \ln 10 = 26.7 \times 2.303 = 61.5 \text{ mV}$. For a monovalent cation ($z = +1$): $E = 61.5 \log_{10}([\text{X}]_{\text{out}}/[\text{X}]_{\text{in}}) \text{ mV}$. $E_{\text{K}}: 61.5 \times \log_{10}(5/150) = 61.5 \times \log_{10}(0.0333) = 61.5 \times (-1.477) = -90.8 \text{ mV}$. $E_{\text{Na}}: 61.5 \times \log_{10}(145/15) = 61.5 \times \log_{10}(9.667) = 61.5 \times 0.985 = +60.6 \text{ mV}$. Resting membrane potential $\approx -70 \text{ mV}$ — much closer to E_{K} (–91 mV) than E_{Na} (+61 mV), indicating that K^+ permeability dominates at rest ($P_{\text{K}} : P_{\text{Na}} : P_{\text{Cl}} \approx 1 : 0.04 : 0.45$). Why not exactly E_{K} ? Because of small but non-zero Na^+ leak, and the electrogenic Na^+/K^+ pump (see Goldman-Hodgkin-Katz). Clinical significance: hyperkalaemia (e.g., $[\text{K}^+]_{\text{out}} = 8 \text{ mM}$ raises E_{K} to –80 mV) *depolarizes* the resting potential — at rest the membrane is closer to threshold, but sustained depolarization inactivates Nav channels → muscle weakness, cardiac conduction block, asystole (EKG peaked T waves → widened QRS → sine wave → flatline). This is why hyperkalaemia is a medical emergency. See section 33. 12. Tetrodotoxin (TTX, from pufferfish) blocks voltage-gated Na^+ channels. Tetraethylammonium (TEA) blocks voltage-gated K^+ channels. Predict the effects on the action potential waveform when: (a) TTX alone is applied; (b) TEA alone; (c) both together.

Answer (Q12, Application). Initiating condition: a depolarizing stimulus normally triggers the Na^+ -driven upstroke and K^+ -driven repolarization. (a) TTX alone blocks voltage-gated Na^+ channels, removing the inward Na^+ current: the action potential is abolished entirely (no upstroke, no spike) — only passive subthreshold depolarization remains. (b) TEA alone blocks voltage-gated K^+ channels, removing the delayed-rectifier outward current: the upstroke is normal but repolarization is markedly slowed and incomplete, so the AP is greatly prolonged/broadened with a reduced or absent afterhyperpolarisation (and enhanced transmitter release). (c) Both together: with Na^+ entry blocked there is still no regenerative upstroke, so no action potential occurs; TEA's effect on repolarization is moot — the membrane only shows a slow passive response, demonstrating the AP requires the regenerative Na^+ conductance. See section 33. 13. Quantal analysis of neurotransmitter release: at the neuromuscular junction, each

synaptic vesicle contains about 10,000 ACh molecules (one “quantum”). The miniature end-plate potential (mEPP) = 0.4 mV. A normal EPSP = 40 mV. Estimate the quantal content ($m = \text{EPSP}/\text{mEPP}$). What parameter does the quantal content depend on (n = number of release sites, p = release probability)?

Answer (Q13, Application). Quantal model: $\text{EPP} = n \cdot p \cdot q$, where q (quantal size) is the postsynaptic response to one vesicle (the mEPP) and quantal content $m = \text{number of quanta released per stimulus} \approx \text{EPP}/\text{mEPP}$. Substituting the stated values: $m = 40 \text{ mV} \div 0.4 \text{ mV} = 100$ quanta per stimulus. (This linear estimate assumes responses sum approximately linearly and is reasonable when the EPP is not strongly attenuated by nonlinear summation.) Quantal content depends on $m = n \times p$, where n is the number of release-ready vesicles/release sites and p is the per-vesicle release probability (each about 0.1–0.4 at physiological Ca^{2+} at the NMJ). Thus m can fall if either n drops (Lambert–Eaton, vesicle depletion) or p drops (low extracellular Ca^{2+} , high Mg^{2+}) — a quantitatively interpretable, biologically plausible result. See section 33. 14. NMDA receptors are both ligand-gated (glutamate) AND voltage-gated (Mg^{2+} block removed at depolarized potentials). Explain: (a) why NMDA receptors function as “coincidence detectors” (both presynaptic glutamate and postsynaptic depolarization are required); (b) why this property is considered the molecular basis for Hebbian learning (“neurons that fire together, wire together”); (c) the Ca^{2+} signal that enters via NMDA receptors and triggers LTP.

Answer (Q14, Application). Initiating condition: glutamate is released and binds NMDA receptors, but at resting potential the pore is blocked by extracellular Mg^{2+} . (a) Coincidence detection: the channel conducts only when glutamate is bound (presynaptic activity) AND the postsynaptic cell is sufficiently depolarized to expel the voltage-dependent Mg^{2+} block — so both pre- and postsynaptic activity must occur together. (b) This implements Hebb’s postulate (“neurons that fire together wire together”): the synapse is strengthened precisely when presynaptic firing coincides with postsynaptic depolarization, the molecular basis of associative/Hebbian learning. (c) When both conditions are met the relieved NMDA channel admits a large Ca^{2+} influx into the spine; this Ca^{2+} activates CaMKII (autophosphorylated at T286), which phosphorylates and inserts AMPA receptors, inducing LTP. See section 33. 15. Myasthenia gravis (MG) is an autoimmune disease where antibodies target nicotinic ACh receptors at the NMJ. Predict: (a) whether the EPSP amplitude at the NMJ is increased or decreased; (b) the clinical manifestation (fatigable muscle weakness); (c) why acetylcholinesterase inhibitors (pyridostigmine) temporarily improve symptoms.

Answer (Q15, Application). Initiating condition: autoantibodies bind and crosslink/internalise muscle nicotinic ACh receptors at the NMJ, reducing functional receptor number. (a) With fewer receptors, the same quantal ACh release produces a smaller end-plate potential — EPSP/end-plate-potential amplitude is decreased, sometimes failing to reach the muscle fiber’s threshold so transmission fails at some junctions. (b) Clinically this gives fatigable muscle weakness: with repetitive activity presynaptic ACh release normally declines (rundown), and because the safety factor is already eroded, more junctions fail as activity continues — weakness worsens with use and improves with rest (ocular, bulbar, limb muscles). (c) Acetylcholinesterase inhibitors (pyridostigmine) block ACh breakdown in the cleft, so each released quantum acts longer and on more of the remaining receptors, raising the end-plate potential above threshold and temporarily improving strength. See section 33. 16. GABAergic inhibition: GABA_A receptors are Cl^- channels. In adult neurons $E_{\text{Cl}} \approx -70 \text{ mV}$ (inhibitory). In neonatal neurons $E_{\text{Cl}} \approx -40 \text{ mV}$ (excitatory because resting potential is about -55 mV). Explain: (a) why GABA is excitatory in neonatal neurons; (b) the developmental switch (upregulation of KCC2 Cl^- transporter); (c) why this has implications for neonatal seizure treatment.

Answer (Q16, Application). Initiating condition: GABA_A receptors are Cl^- channels, so their effect depends on E_{Cl} relative to resting potential and threshold. (a) In neonatal neurons intracellular $[\text{Cl}^-]$ is high ($E_{\text{Cl}} \approx -40 \text{ mV}$), which is *above* the resting potential (about -55 mV); opening GABA_A channels lets Cl^- flow *out*, depolarizing the cell toward -40 mV — so GABA is excitatory early in development. (b) The developmental switch is driven by upregulation of the neuronal K^+/Cl^- cotransporter KCC2, which extrudes Cl^- and lowers intracellular $[\text{Cl}^-]$, shifting E_{Cl} to $\approx -70 \text{ mV}$; now GABA_A opening hyperpolarises/shunts the cell — GABA becomes inhibitory in adults (with the early NKCC1 importer dominating before the switch). (c) Clinically this means classic GABA_A potentiators (benzodiazepines, phenobarbital) can be ineffective or paradoxically excitatory for neonatal seizures; strategies that lower intracellular Cl^- (e.g., NKCC1 inhibition with bumetanide as an adjunct) are being explored. See section 33. 17. Short-term plasticity: paired-pulse facilitation (PPF) occurs when the second of two closely-spaced stimuli evokes a larger EPSP. Explain the residual calcium hypothesis: Ca^{2+} from the first stimulus remains and adds to Ca^{2+} from the second stimulus, producing greater vesicle release. Predict: would PPF be increased or decreased by a Ca^{2+} chelator (BAPTA)?

Answer (Q17, Application). Initiating condition: paired-pulse facilitation occurs when two stimuli arrive within tens–hundreds of ms and the second EPSP is larger. Changed component: Ca^{2+} entering on the first action potential is not fully cleared (pumped/buffered) before the second spike. Intermediate mechanism: this residual Ca^{2+} sums with the Ca^{2+} influx from the second action potential; because release probability rises super-linearly (about 4th power) with presynaptic Ca^{2+} , the elevated total Ca^{2+} raises p and more vesicles fuse. Observable outcome: the second EPSP is larger (facilitation), most prominent at low- p synapses (e.g., parallel-fiber → Purkinje, $p \approx 0.05$). Prediction: a fast Ca^{2+} chelator such as BAPTA mops up the residual Ca^{2+} before the second spike, so PPF is decreased/abolished — directly testing and supporting the residual-calcium hypothesis. See section 33. 18. Excitotoxicity: excessive glutamate release (e.g., during stroke) causes neuronal death via NMDA receptor overactivation → excessive Ca^{2+} influx → mitochondrial dysfunction → ROS production → cell death. Explain: (a) why NMDA-blocking drugs (memantine, at low

doses) are neuroprotective in clinical trials; (b) why high-dose NMDA block causes psychotic symptoms (dissociative anaesthetics — ketamine); (c) what the narrow therapeutic window implies for stroke intervention.

Answer (Q18, Application). Initiating condition: excess synaptic glutamate (stroke/ischemia) overactivates NMDA receptors, causing pathological Ca^{2+} overload, mitochondrial failure, ROS, and neuronal death. (a) Memantine at low (therapeutic) doses is a low-affinity, fast-off, voltage-dependent open-channel blocker: it preferentially blocks the tonically over-activated NMDA channels in pathological conditions while leaving brief, phasic, physiological NMDA signaling largely intact — so it dampens excitotoxic Ca^{2+} entry without abolishing normal synaptic transmission, giving modest neuroprotection. (b) High-dose, high-affinity NMDA block (ketamine, PCP) also blocks physiological NMDA signaling needed for normal cortical/thalamic processing, producing dissociative anaesthesia and psychotomimetic (psychotic-like) symptoms. (c) The narrow therapeutic window — enough block to stop excitotoxicity but not so much as to impair normal NMDA function — plus a short post-stroke time window, explains why broad NMDA antagonists have largely failed as acute stroke neuroprotectants; the conclusion would change only with agents that selectively target the excitotoxic (extrasynaptic) pool. See section 33. 19. Synaptic vesicle recycling occurs via three modes: kiss-and-run (transient fusion pore, rapid), full collapse/clathrin-mediated endocytosis (5–20 s), and bulk endocytosis (during intense stimulation). Explain: (a) how each mode is suited to different firing rates; (b) what happens when recycling capacity is exceeded (synaptic depression); (c) the role of dynamin GTPase in clathrin-mediated endocytosis.

Answer (Q19, Application). Initiating condition: vesicle fusion adds membrane and depletes the releasable pool, so terminals must retrieve membrane and refill vesicles. (a) Kiss-and-run (transient fusion pore, then resealing) is fast and conserves the vesicle, suited to low/moderate firing where rapid local reuse keeps up with demand; full-collapse / clathrin-mediated endocytosis (about 5–20 s) cleanly recovers vesicle components at moderate sustained rates; bulk endocytosis internalises large membrane infoldings during intense, high-frequency activity when single-vesicle retrieval cannot match the membrane added. (b) When firing outpaces recycling, the readily releasable pool is not replenished and the synapse shows short-term depression (declining EPSP amplitude) until activity slows and pools refill. (c) Dynamin is a GTPase that assembles a collar around the neck of the budding clathrin-coated pit and, on GTP hydrolysis, mediates fission to pinch off the recycled vesicle; without dynamin function endocytosis stalls and vesicles cannot be retrieved. See section 33. 20. Long-term depression (LTD) at cerebellar parallel fiber-Purkinje cell synapses is triggered by climbing fiber co-activation $\rightarrow \text{Ca}^{2+} + \text{PKC} \rightarrow \text{AMPA}$ internalization. Explain: (a) how LTD differs from LTP mechanistically (removal vs insertion of receptors); (b) the role of LTD in motor learning (error correction signals from climbing fibers); (c) how cerebellar LTD produces adaptation in the vestibulo-ocular reflex.

Answer (Q20, Application). Initiating condition: at cerebellar parallel-fiber \rightarrow Purkinje-cell synapses, coincident parallel-fiber input with climbing-fiber activation produces a large Ca^{2+} signal plus PKC activation. (a) LTD vs LTP mechanism: low/specific Ca^{2+} patterns here drive AMPA-receptor *internalization* (phosphatase- and PKC-dependent endocytosis), weakening the synapse — the mirror image of LTP, where larger NMDA-mediated Ca^{2+} drives CaMKII-dependent AMPA-receptor *insertion* and strengthening; the direction is set by the amplitude/pattern of postsynaptic Ca^{2+} (BCM-style sliding threshold). (b) In motor learning, the climbing fiber carries an “error” or teaching signal; pairing it with the parallel-fiber inputs active during a faulty movement depresses exactly those synapses, so the Purkinje cell’s output is corrected on subsequent attempts. (c) For the vestibulo-ocular reflex, retinal-slip errors relayed by climbing fibers induce parallel-fiber LTD in the flocculus, re-tuning the gain so eye movements again precisely cancel head movements — cerebellar LTD as the substrate of VOR adaptation. See section 33.

Questions 21–30: Synthesis and Evaluation

21. Evaluate the Hodgkin-Huxley (HH) model of the action potential (1952, Nobel Prize): using voltage-clamp data, they described Na^+ and K^+ conductances as m^3h and n^4 gating variables. Assess: (a) the key insight (ion-specific conductances with distinct kinetics); (b) the predictive power of the model (propagation velocity, frequency coding); (c) the limitations (no molecular detail, does not account for ion channel diversity, subthreshold oscillations).

Answer (Q21, Synthesis). Empirical evidence: Hodgkin and Huxley used voltage-clamp recordings from the squid giant axon to measure time- and voltage-dependent Na^+ and K^+ conductances and fit them with empirical gating variables (Na^+ as m^3h , K^+ as n^4). Separating evidence from judgement: (a) the key insight, strongly supported, is that excitability arises from independent, ion-specific, voltage- and time-dependent conductances with distinct kinetics — not a mysterious “membrane breakdown.” (b) Its predictive power is remarkable and well validated: from the fitted equations the model correctly predicts AP shape, threshold, refractory period, propagation velocity, and frequency coding without further tuning. (c) Limitations/boundary conditions: the m^3h/n^4 exponents are phenomenological, not molecular (no explicit channel structure), and the original model omits the diversity of channel subtypes, Ca^{2+} currents, subthreshold oscillations, and dendritic nonlinearities. What would change the evaluation: evidence that the gating formalism fails to capture a class of excitable behavior without ad hoc extension. So: a triumphantly predictive but admittedly empirical, extensible framework — not the final molecular word. See section 33. 22. Design an experiment to determine whether a specific synapse exhibits Hebbian LTP, anti-Hebbian LTP, or homeostatic plasticity. Describe: the stimulation protocols (high-frequency \rightarrow Hebbian, low-frequency \rightarrow homeostatic), the electrophysiological measurements (field EPSP slope), and the pharmacological tools (NMDA antagonist, AMPAR antagonist) needed to distinguish these forms.

Answer (Q22, Synthesis). Hypothesis: a given synapse expresses Hebbian LTP (input- and NMDA-dependent strengthening), anti-Hebbian/LTD (weakening), or homeostatic scaling (activity-set global gain), distinguishable by induction pattern and pharmacology. Design: record field EPSP slope (or whole-cell EPSC) at the test pathway with a separate independent control pathway. Changed factor = stimulation protocol: high-frequency/tetanic or theta-burst pairing to probe Hebbian LTP; low-frequency (1 Hz) stimulation to probe LTD; chronic activity blockade (TTX) or elevation to probe homeostatic scaling (measured as a multiplicative change in mEPSC amplitude across all synapses, not input-specific). Controls/replication: unstimulated control pathway must be unchanged (input-specificity), multiple slices/animals, interleaved conditions. Pharmacology to distinguish forms: an NMDA antagonist (APV) should block Hebbian LTP and NMDA-dependent LTD but not homeostatic scaling; an AMPA antagonist (CNQX) abolishes the synaptic response itself (a measurement control); homeostatic scaling persists under activity blockade. Decision rule: input-specific, NMDA-dependent potentiation = Hebbian LTP; input-specific NMDA-dependent depression = LTD; global, NMDA-independent, multiplicative change = homeostatic. Falsifying result: a “Hebbian LTP” that survives complete NMDA blockade and is not input-specific. See section 33. 23. Evaluate the “synaptic tagging and capture” hypothesis (Frey and Morris, 1997): early LTP is protein synthesis-independent (lasts about 1–2 h), while late LTP requires new protein synthesis. A weak stimulus sets a “tag” at activated synapses; the tag captures plasticity-related proteins (PRPs) synthesized in response to a strong stimulus at another input. Evaluate: (a) the evidence for this model; (b) how it explains input-specificity of LTP; (c) implications for memory consolidation.

Answer (Q23, Synthesis). Empirical claim: early LTP is protein-synthesis-independent (about 1–2 h) whereas late LTP requires new protein synthesis (CREB-dependent gene expression and structural change). (a) Evidence for synaptic tagging and capture (Frey & Morris, 1997): a weak tetanus that alone gives only decaying early LTP can be converted to persistent late LTP if a strong tetanus is delivered to a *separate* input on the same neuron shortly before/after — the strong input supplies diffusible plasticity-related proteins (PRPs) that are “captured” by a transient local tag set at the weakly stimulated synapse; protein-synthesis inhibitors block this rescue. (b) It explains input-specificity with shared resources: the tag is local and short-lived, so only recently activated synapses capture the cell-wide PRP pool, keeping potentiation specific to active inputs while allowing associative interactions across inputs. (c) Implications for memory consolidation: behavioral tagging predicts that a weak experience can be consolidated into long-term memory if a salient (PRP-inducing) event occurs nearby in time — a cellular basis for how arousal/novelty stabilizes otherwise transient memories. The judgement is well supported but conditional: it depends on tag identity (still incompletely defined) and on the temporal window — evidence that capture occurs without any local tag would weaken the model. See section 33. 24. Evaluate the role of astrocytic gliotransmission (release of glutamate, D-serine, ATP from astrocytes) in modulating synaptic plasticity. What evidence supports the “tripartite synapse” model, and what criticisms have been raised about the specificity of astrocytic Ca^{2+} signals and the difficulty of distinguishing neuronal from glial glutamate release?

Answer (Q24, Synthesis). Empirical evidence for the tripartite synapse: astrocytes ensheath synapses, show synaptically evoked Ca^{2+} elevations, supply the NMDA co-agonist D-serine, and can release glutamate/ATP that modulate transmission and plasticity; astrocytic Ca^{2+} also drives neurovascular coupling (synaptic glutamate → astrocyte Ca^{2+} → vasoactive arachidonic-acid metabolites onto arterioles), tying glial signaling to the BOLD signal. Separating evidence from judgement: the data establish that astrocytes can influence synapses, but the *physiological significance and specificity* are contested — IP3R2-knockout mice that lack astrocytic Ca^{2+} transients show largely normal synaptic plasticity in several studies, astrocytic Ca^{2+} signals are slow and spatially broad rather than synapse-specific, and it is technically hard to prove that detected glutamate is glial rather than neuronal. What would change the conclusion: cell-type-specific tools that selectively and reversibly silence only astrocytic release and reproducibly abolish a defined form of plasticity. So: gliotransmission is real and modulatory in some contexts but not established as a universal, synapse-specific controller of plasticity. See section 33. 25. Channelopathies: mutations in ion channels cause neurological diseases. Evaluate three examples: (a) SCN1A (Nav1.1) mutations → Dravet syndrome (severe childhood epilepsy); (b) KCNQ2/3 mutations → benign familial neonatal seizures; (c) CACNA1A mutations → familial hemiplegic migraine. For each, describe the channel, the mutation’s effect on neuronal excitability, and the therapeutic approach.

Answer (Q25, Synthesis). Channelopathies alter neuronal excitability through specific channel defects. (a) SCN1A (Nav1.1) — Dravet syndrome: loss-of-function in Nav1.1, which is enriched in inhibitory GABAergic interneurons, reduces interneuron firing → net disinhibition and severe early-childhood epilepsy; Na^+ -channel blockers (lamotrigine, carbamazepine) can paradoxically worsen it, so valproate/clobazam, stiripentol, and fenfluramine are used. (b) KCNQ2/3 — benign familial neonatal seizures: loss-of-function in the Kv7 (M-current) channels that normally restrain repetitive firing → hyperexcitability and neonatal seizures that usually remit; M-current openers (e.g., retigabine/ezogabine concept) and standard antiepileptics are options. (c) CACNA1A — familial hemiplegic migraine: gain-of-function in the Cav2.1 (P/Q-type) Ca^{2+} channel enhances glutamate release, lowering the threshold for cortical spreading depression → migraine with hemiplegic aura; prophylaxis (e.g., verapamil, acetazolamide, standard migraine preventives) is used. Causal chain in each: mutated channel → altered ionic current → shifted excitatory/inhibitory balance → the observed clinical syndrome, guiding mechanism-specific therapy. See section 33. 26. Evaluate the dopamine hypothesis of schizophrenia: (a) traditional version (excess D_2 receptor signaling in mesolimbic pathway); (b) revised version (hypo-dopaminergia in prefrontal cortex, hyper-dopaminergia in striatum); (c) the glutamate hypothesis (NMDA receptor hypofunction). How do these hypotheses explain the positive symptoms

(hallucinations, delusions) and negative symptoms (flat affect, cognitive deficits) of schizophrenia?

Answer (Q26, Synthesis). Empirical evidence: D2-antagonist antipsychotic potency correlates with D2 affinity, amphetamine (dopamine-releasing) exacerbates psychosis, and PET shows elevated striatal dopamine synthesis in schizophrenia; NMDA antagonists (ketamine, PCP) reproduce positive and negative/cognitive symptoms. Separating evidence from judgement: (a) the traditional hypothesis (excess mesolimbic D2 signaling) explains positive symptoms (hallucinations, delusions) and the efficacy of D2 blockers, but not negative/cognitive symptoms. (b) The revised hypothesis (striatal hyper-dopaminergia plus prefrontal hypo-dopaminergia) accounts for positive symptoms (striatal excess) and negative/cognitive deficits (cortical D1 hypofunction impairing working memory). (c) The glutamate hypothesis (NMDA-receptor hypofunction, especially on inhibitory interneurons) provides an upstream cause that can produce downstream dopamine dysregulation and explains the full symptom spectrum including cognitive deficits. The conclusion is conditional, not settled: no single transmitter abnormality is necessary and sufficient, and what would change it is mechanistically targeted treatments (e.g., effective non-D2 agents) demonstrating which node is causal. See section 33. 27. Spike-timing-dependent plasticity (STDP): if the presynaptic neuron fires before the postsynaptic neuron (within about 20 ms), the synapse is strengthened (LTP). If after, the synapse is weakened (LTD). Evaluate: (a) the molecular mechanism (STDP timing depends on NMDA receptor/ Ca^{2+} dynamics); (b) the computational significance (STDP allows precise temporal learning of sequences); (c) how STDP differs in inhibitory vs excitatory synapses.

Answer (Q27, Synthesis). Initiating condition: STDP makes synaptic change depend on the millisecond order of pre- and postsynaptic spikes. (a) Mechanism: if the presynaptic spike precedes the postsynaptic spike (within about 20 ms), glutamate is bound when the back-propagating action potential depolarizes the spine and relieves NMDA Mg^{2+} block, producing a large coincident Ca^{2+} transient that activates $\text{CaMKII} \rightarrow \text{LTP}$; if the order is reversed, only a small/delayed Ca^{2+} signal occurs, preferentially activating phosphatases ($\text{PP1/calcineurin} \rightarrow \text{LTD}$ — the sign is set by NMDA-receptor-controlled Ca^{2+} amplitude/timing (BCM-like). (b) Computational significance: because potentiation requires “cause before effect,” STDP lets networks learn temporal order and predictive sequences, sharpen input timing, and self-stabilize — a biologically grounded learning rule for sequence and causal learning. (c) Excitatory vs inhibitory: excitatory synapses follow the classic asymmetric pre-before-post $\rightarrow \text{LTP}$ window; many inhibitory (GABAergic) synapses show different, often symmetric or sign-inverted timing rules and rely on Ca^{2+} sources/signaling distinct from postsynaptic NMDA receptors, so inhibitory STDP tunes E/I balance rather than feedforward drive. See section 33. 28. Evaluate the molecular mechanism of presynaptic neurotransmitter release: Ca^{2+} entry \rightarrow synaptotagmin-1 (Ca^{2+} sensor) \rightarrow conformational change \rightarrow interaction with SNARE complex \rightarrow fusion pore opening \rightarrow transmitter release. Specifically: why is synaptotagmin-1 the timing sensor (low Ca^{2+} affinity, fast kinetics, about 200 μs from Ca^{2+} binding to fusion), and what does the about 4th power Ca^{2+} dependence of release tell us about the number of Ca^{2+} ions needed to trigger a single vesicle fusion event?

Answer (Q28, Synthesis). Empirical mechanism: Ca^{2+} entering through nearby voltage-gated channels binds synaptotagmin-1's C2A/C2B domains, which then displaces the complexin clamp and drives full SNARE-complex (synaptobrevin–syntaxin–SNAP-25) zippering, opening the fusion pore and releasing transmitter; NSF/ α -SNAP later disassemble SNAREs for reuse. Separating evidence from judgement: synaptotagmin-1 is identified as the *fast timing* sensor because it has relatively low Ca^{2+} affinity (so it responds only to the brief, high Ca^{2+} nanodomain right at the channel mouth, not to bulk Ca^{2+}) and fast binding/unbinding kinetics (release follows Ca^{2+} entry in about 200 μs), which is exactly what is needed to lock release to the action potential. The steep, approximately 4th-power dependence of release rate on $[\text{Ca}^{2+}]$ indicates that roughly four (cooperatively bound) Ca^{2+} ions must bind synaptotagmin to trigger a single vesicle fusion event — explaining why small Ca^{2+} changes produce large, switch-like changes in release. The conclusion is well supported but conditional on synaptotagmin-1 as the dominant sensor; some synapses use other synaptotagmin isoforms with different Ca^{2+} affinities, which would shift the quantitative relationship. See section 33. 29. Evaluate the clinical utility of transcranial magnetic stimulation (TMS) for modulating neural circuits non-invasively. How does TMS induce action potentials in cortical neurons, what stimulation patterns produce LTP-like (theta-burst) vs LTD-like (continuous low-frequency) effects, and what is the evidence for therapeutic efficacy in treatment-resistant depression?

Answer (Q29, Synthesis). Empirical basis: TMS uses a rapidly changing magnetic field to induce an electric field in cortex strong enough to depolarize axons/neurons and evoke action potentials non-invasively (measurable as motor-evoked potentials when over motor cortex). Separating evidence from judgement: stimulation pattern shapes the after-effect — intermittent theta-burst and high-frequency ($\geq 5\text{--}10\text{ Hz}$) repetitive TMS produce LTP-like lasting increases in cortical excitability, whereas continuous theta-burst and low-frequency (about 1 Hz) rTMS produce LTD-like decreases, plausibly engaging NMDA/ Ca^{2+} -dependent plasticity analogous to LTP/LTD. Therapeutic efficacy is supported but conditional: randomized trials and meta-analyses show prefrontal rTMS produces a real but moderate antidepressant effect in treatment-resistant depression (FDA-cleared, with newer accelerated/theta-burst protocols), yet response is heterogeneous, effect sizes are modest, and durability/optimal targeting are unsettled. What would change the conclusion: large rigorously sham-controlled trials showing the benefit is non-specific or not durable. So: a mechanistically grounded, clinically useful but not universally curative intervention. See section 33. 30. Critically evaluate the concept of the “synaptome” — the catalog of synapse types and their molecular composition across the brain. Using proteomics of isolated synaptosomes, researchers have identified >1,000 proteins at excitatory synapses. Evaluate: (a) what the molecular diversity of synapses implies for circuit function; (b) whether the synaptome concept is more informative than the connectome for understanding brain computation; (c) how synaptome-level mutations (SHANK3,

PSD-95) cause neurodevelopmental disorders.

Answer (Q30, Synthesis). Empirical basis: synaptosome proteomics identifies >1,000 proteins at excitatory postsynaptic densities (e.g., PSD-95, SHANK, glutamate receptors, scaffolds), and synaptome mapping shows that synapse molecular composition varies systematically across brain regions and cell types. Separating evidence from judgement: (a) this molecular diversity implies that “a synapse” is not uniform — different molecular types confer different plasticity rules, kinetics, and Ca^{2+} handling, so circuit computation depends on *which* synapse types connect which neurons, not merely on wiring. (b) Whether the synaptome is “more informative than the connectome” is a conditional claim, not settled: the connectome specifies the wiring graph while the synaptome specifies the weights/plasticity at each edge — they are complementary, and computation arguably requires both; claiming superiority overstates current evidence. (c) Synaptome-level mutations cause neurodevelopmental disorders by disrupting postsynaptic organization: SHANK3 (a master PSD scaffold) loss causes Phelan–McDermid syndrome/autism, and PSD-95 (DLG4) disruption impairs receptor anchoring and plasticity, linking single scaffold proteins to circuit-level dysfunction. The conclusion would change if synaptome diversity proved not to map onto functional/behavioral differences. See section 33.

Questions — Endocrine Signaling and Homeostasis

Instructor Use and Coverage Notes

- Coverage target: Predict the consequence of changing a hormone, receptor, or axis set-point.
- Model/data emphasis: Hormone feedback and dose-response reasoning.
- Assessment alignment: Visual Representations, Statistical Tests and Data Analysis, Argumentation.
- Misconception probe: A hormone surge is not always pathological; context and set-point matter.
- Transfer product: Transfer endocrine reasoning to metabolism, stress, and development.
- Grading focus: award full credit for mechanism, evidence, boundary conditions, and units when a calculation is required.
- Suggested use: draw one recall item, one application item, and one synthesis item when building a short quiz from this bank.

Questions 1–10: Recall and Comprehension

This activity accompanies section 34 of the textbook — review that chapter before attempting the exercises below.

1. What is the endocrine system? How does it differ from the nervous system in signaling speed and duration?

Answer (Q1, Recall). The endocrine system is the network of glands that secrete hormones into the blood to regulate physiology body-wide. Compared with the nervous system, endocrine signaling is slower (seconds to hours rather than milliseconds) and longer-lasting (minutes to days rather than brief), because it relies on chemical hormones travelling via the circulation to all cells bearing the receptor rather than fast electrical transmission across a narrow synapse. See section 34.

2. Name the major endocrine glands and one hormone secreted by each.

Answer (Q2, Recall). Major glands and a representative hormone each: hypothalamus (releasing hormones, e.g., CRH); anterior pituitary (ACTH, GH); thyroid (T4/T3); parathyroid (PTH); adrenal cortex (cortisol); adrenal medulla (epinephrine); endocrine pancreas (insulin from (beta)-cells); gonads (testosterone or oestradiol); pineal (melatonin). See section 34.

3. Distinguish peptide hormones from steroid hormones in terms of synthesis, transport, and receptor location.

Answer (Q3, Recall). Peptide hormones are made on ribosomes as preprohormones, stored in secretory granules, travel free in plasma, and act fast on plasma-membrane receptors (RTKs/GPCRs). Steroid hormones are synthesized on demand from cholesterol (not stored), carried bound to plasma proteins (e.g., CBG, SHBG), and act slowly via intracellular nuclear receptors that alter gene transcription. The receptor location (membrane vs nuclear) is the mechanistic difference that makes peptide signaling rapid/transient and steroid signaling slow/persistent. See section 34.

4. What is the hypothalamic-pituitary axis? Name one releasing hormone and one tropic hormone.

Answer (Q4, Recall). The hypothalamic-pituitary axis is the hierarchical control loop in which the hypothalamus secretes releasing hormones that drive anterior-pituitary tropic hormones, which in turn stimulate a peripheral target gland, with negative feedback at each level. Example: hypothalamic CRH (releasing hormone) stimulates pituitary ACTH (tropic hormone), which stimulates adrenal cortisol. See section 34.

5. What is negative feedback? Give an example involving the thyroid gland.

Answer (Q5, Recall). Negative feedback is regulation in which a system’s output inhibits the steps that produced it, stabilizing the variable around a set point. Thyroid example: rising free T3/T4 inhibits hypothalamic TRH and pituitary TSH secretion, reducing further thyroid hormone output; if T3/T4 fall, TRH and TSH rise again, restoring levels. See section 34.

6. What is cortisol? Name its target tissues and three physiological effects.

Answer (Q6, Recall). Cortisol is a glucocorticoid steroid made in the adrenal cortex (zona fasciculata) under ACTH control. Target tissues include liver, muscle, adipose, and immune cells (acting via the nuclear glucocorticoid receptor). Three effects: stimulates hepatic gluconeogenesis (mobilizing amino acids from muscle), is immunosuppressive/anti-inflammatory (inhibits NF-(kappa)B and cytokine production), and promotes lipolysis. See section 34.

7. What are the components of innate immunity? Name four.

Answer (Q7, Recall). Innate immunity is the rapid, non-specific, germline-encoded first line of defense. Four components: physical/chemical barriers (skin, mucus, lysozyme); phagocytes (neutrophils, macrophages, dendritic cells); the complement system; and NK cells (plus inflammation and interferons). See section 34.

8. What is a Toll-like receptor (TLR)? Name a ligand for TLR4.

Answer (Q8, Recall). A Toll-like receptor is a germline-encoded pattern-recognition receptor on the plasma membrane or endosomes that detects conserved pathogen molecules (PAMPs) and triggers inflammatory or antiviral signaling. The ligand for TLR4 is bacterial lipopolysaccharide (LPS), characteristic of Gram-negative bacteria. See section 34.

9. What is the complement system? What are its three outcomes (opsonisation, MAC, inflammation)?

Answer (Q9, Recall). The complement system is a cascade of about 30 plasma proteins that, once triggered (classical, lectin, or alternative pathway), generate C3/C5 convertases. Its three outcomes are opsonisation (C3b coats pathogens for phagocytosis), the membrane attack complex (C5b-9 lyses target cells), and inflammation (anaphylatoxins C3a/C5a recruit and activate leukocytes). See section 34.

10. Define phagocytosis. Name two professional phagocytes.

Answer (Q10, Recall). Phagocytosis is the receptor-mediated engulfment of particles or microbes into a phagosome that fuses with lysosomes to destroy the cargo. Two professional phagocytes: neutrophils and macrophages (dendritic cells also phagocytose). See section 34.

Questions 11–20: Application and Analysis

11. The HPA axis: CRH (hypothalamus) → ACTH (anterior pituitary) → cortisol (adrenal cortex). Cortisol feeds back negatively on CRH and ACTH secretion. If a patient has an adrenal tumor autonomously producing cortisol, predict: (a) ACTH levels; (b) CRH levels; (c) contralateral adrenal gland size; (d) response to the dexamethasone suppression test.

Answer (Q11, Application). An autonomous cortisol-secreting adrenal tumor produces high cortisol independent of ACTH. (a) ACTH is low (suppressed by negative feedback). (b) CRH is low (also feedback-suppressed). (c) The contralateral adrenal atrophies because, without ACTH trophic support, the normal cortex shrinks. (d) On the dexamethasone suppression test cortisol fails to suppress (it is autonomous and not under pituitary control), confirming an ACTH-independent adrenal source. See section 34.

12. Insulin (from pancreatic β -cells) and glucagon (from α -cells) have opposing metabolic effects. Compare: (a) the stimulus for secretion of each; (b) the target tissue responses (liver, muscle, adipose); (c) the blood glucose level at which each dominates. What happens in Type 1 Diabetes (complete β -cell destruction)?

Answer (Q12, Application). (a) Insulin is secreted when blood glucose rises (after a meal); glucagon is secreted when glucose falls (fasting). (b) Insulin drives hepatic/muscle glycogen synthesis, muscle/adipose GLUT4 glucose uptake, and adipose lipogenesis; glucagon drives hepatic glycogenolysis and gluconeogenesis. (c) Insulin dominates at high glucose (5.5 mmol/L postprandial), glucagon at low glucose (fasting). In Type 1 diabetes, autoimmune (beta)-cell destruction abolishes insulin, so glucose stays high, cells starve, unopposed glucagon drives hyperglycaemia and ketoacidosis. See section 34.

13. Thyroid hormones (T_3/T_4) are unusual peptide-derived hormones that act like steroids (entering cells, binding nuclear receptors). Explain: (a) why T_3/T_4 can cross membranes (lipophilic due to iodination); (b) how T_3 binds thyroid hormone receptors ($TR\alpha/TR\beta$) to regulate gene transcription; (c) why hypothyroidism causes bradycardia, fatigue, and weight gain.

Answer (Q13, Application). (a) T_3/T_4 are lipophilic because heavy iodination of the tyrosine-derived rings lets them cross the lipid bilayer (entering cells via MCT8/MCT10). (b) T_3 binds nuclear $TR(\alpha)/TR(\beta)$, which heterodimerise with RXR on thyroid response elements; without T_3 the receptor recruits corepressors and represses genes, while T_3 binding swaps in coactivators and activates transcription. (c) Hypothyroidism slows metabolism: reduced Na^{+}/K^{+} -ATPase and BMR cause fatigue and weight gain, and loss of (β_1) -receptor upregulation plus reduced cardiac drive causes bradycardia. See section 34.

14. The inflammasome (NLRP3) is activated by diverse danger signals (K^{+} efflux, ROS, crystal particles). Trace: (a) NLRP3 oligomerisation; (b) ASC adaptor recruitment; (c) caspase-1 activation; (d) IL-1 β and IL-18 maturation and release; (e) pyroptosis (inflammatory cell death). Name two diseases where NLRP3 is inappropriately activated.

Answer (Q14, Application). (a) A priming signal (TLR/NF-(κ)B) upregulates NLRP3 and pro-IL-1(β); a second signal (K^{+} efflux, ROS, crystals) triggers NLRP3 oligomerisation. (b) NLRP3 recruits the ASC adaptor, which polymerizes into a speck. (c) ASC clusters pro-caspase-1, enabling autocatalytic caspase-1 activation. (d) Active caspase-1 cleaves pro-IL-1(β) and pro-IL-18 to their mature secreted forms. (e) Caspase-1 also cleaves gasdermin D, whose N-terminal pores cause pyroptosis (lytic inflammatory death). Inappropriate NLRP3 activation occurs in gout (urate crystals) and cryopyrin-associated periodic syndromes (CAPS). See section 34.

15. Neutrophils are the first responders to bacterial infection. Describe their killing mechanisms: (a) phagocytosis and phagolysosome fusion; (b) respiratory burst (NADPH oxidase → superoxide → HOCl via myeloperoxidase); (c) NETosis (neutrophil extracellular trap formation). What disease results from NADPH oxidase deficiency (CGD)?

Answer (Q15, Application). (a) Neutrophils recognize and engulf opsonised bacteria into a phagosome that fuses with granules to form a phagolysosome. (b) The respiratory burst: assembled NADPH oxidase generates superoxide, dismutated to H_2O_2 ; myeloperoxidase converts $H_2O_2 + Cl^-$ to bactericidal hypochlorous acid (HOCl). (c) NETosis: the neutrophil extrudes decondensed chromatin studded with antimicrobial proteins (NETs) that trap and kill extracellular bacteria. NADPH oxidase deficiency causes chronic granulomatous disease (CGD), with recurrent catalase-positive infections. See section 34.

16. Evaluate the integration of endocrine and immune systems: cortisol (a glucocorticoid) suppresses inflammation by: (a) inhibiting NF- κ B transcription factor; (b) reducing prostaglandin synthesis (inhibiting PLA₂ and COX-2); (c) inducing lymphocyte apoptosis. Why do critically ill ICU patients sometimes develop adrenal insufficiency, and why does physiological stress-dose hydrocortisone improve sepsis survival?

Answer (Q16, Application). Cortisol restrains inflammation through several converging mechanisms: (a) ligand-bound GR tethers and inhibits NF-(kappa)B (transrepression), shutting off cytokine genes; (b) it induces annexin A1 and suppresses PLA₂ and COX-2, cutting prostaglandin synthesis; (c) it drives apoptosis of lymphocytes and shifts cytokines toward IL-10. Critically ill patients can develop “critical-illness-related corticosteroid insufficiency” (relative adrenal insufficiency plus tissue glucocorticoid resistance), so HPA output is inadequate for the inflammatory load. Stress-dose hydrocortisone restores vascular catecholamine responsiveness and dampens excessive inflammation, which improves shock reversal; however, the survival benefit is condition-dependent (clearest in vasopressor-refractory septic shock) — that conditionality is what would change the conclusion. See section 34.

17. Evaluate the molecular mechanisms of endocrine disruptors (BPA, phthalates, pesticides): how do these chemicals interfere with hormone signaling (estrogenic, anti-androgenic, thyroid-disrupting), at what environmental concentrations are effects seen (non-monotonic dose-response), and what evidence from wildlife populations (feminisation of male fish, reproductive abnormalities in alligators) supports endocrine disruption in the environment?

Answer (Q17, Application). Endocrine disruptors interfere with hormone signaling by mimicking or blocking receptors (BPA is weakly oestrogenic; phthalates are anti-androgenic) and by perturbing hormone synthesis, transport, or thyroid signaling. The evidence includes non-monotonic dose-response curves, where low developmental doses can produce effects absent or different at high doses, complicating classical toxicology thresholds. Wildlife data (feminisation/intersex in male fish below sewage outfalls, reduced phallus size and altered sex ratios in alligators at contaminated lakes) support real environmental endocrine disruption. The conclusion is evidence-supported but conditional: non-monotonic dosing and species/timing differences mean strength of inference depends on exposure window and endpoint, which is what would change it. See section 34.

18. Design an experiment to determine whether a newly discovered peptide is a hormone: (a) demonstrate that it is secreted into the bloodstream in response to a physiological stimulus; (b) show that it has a target tissue with specific receptors; (c) prove that removing the source gland eliminates the response and that hormone replacement restores it; (d) show that the response is dose-dependent.

Answer (Q18, Application). Hypothesis: peptide X is a hormone. Design: (a) show it is released into blood and rises in response to a defined physiological stimulus (measure plasma X before/after, with stimulus vs sham control); (b) demonstrate a distant target tissue expressing specific high-affinity receptors (radioligand binding/displacement); (c) perform a classic ablation-replacement experiment — surgically/genetically remove the source gland, show the response disappears, then restore it by exogenous X (necessity and sufficiency, with vehicle controls and replication); (d) establish a dose-response relationship (graded effect with graded X). A falsifying result is loss of effect despite receptor occupancy or no response on replacement, indicating it is not the causal hormone. See section 34.

19. Evaluate the concept of “trained immunity” — epigenetic reprogramming of innate immune cells (monocytes/macrophages) by prior pathogen exposure, resulting in enhanced responses to subsequent unrelated infections. How does BCG vaccination induce trained immunity (H3K4me3 at inflammatory gene promoters, mTOR-dependent metabolic shift from OXPHOS to glycolysis), and what are the implications for broad-spectrum vaccine development?

Answer (Q19, Application). Trained immunity is the epigenetic and metabolic reprogramming of innate cells (monocytes/macrophages) so that a prior exposure heightens responses to later, unrelated infections. BCG induces it by depositing activating histone marks (H3K4me3, H3K27ac) at inflammatory gene promoters and by an mTOR/HIF-1(alpha)-driven metabolic shift from oxidative phosphorylation toward aerobic glycolysis, priming faster cytokine output. The implication is the prospect of broad-spectrum vaccines that confer non-specific protection. The conclusion is conditional: effect size varies with host, timing, and pathogen, and durability is finite — heterogeneous clinical-trial outcomes are what would change the inference. See section 34.

20. Evaluate the evolutionary conservation and divergence of the HPA axis: fish have an HPI axis (hypothalamic-pituitary-interrenal), amphibians have an HPA axis with cortisol, and birds have corticosterone. What does this conservation tell us about the fundamental biological requirement for glucocorticoid stress response across vertebrates?

Answer (Q20, Application). Across vertebrates the stress axis is conserved in architecture but divergent in the terminal steroid: fish use the hypothalamic-pituitary-interrenal (HPI) axis, amphibians and mammals an HPA axis with cortisol, and birds and rodents use corticosterone. This

deep conservation of a CRH-ACTH-glucocorticoid loop indicates a fundamental, selectively maintained requirement for a rapid, glucocorticoid-mediated stress response (energy mobilization and immune modulation) in vertebrate survival. The inference is strong but comparative: it rests on homology arguments, and discovery of a vertebrate lineage lacking the axis or using an unrelated mediator would weaken the universality claim. See section 34.

Questions 21–30: Synthesis and Evaluation

21. Evaluate the therapeutic potential of checkpoint immunotherapy combined with endocrine modulation: tumor-associated macrophages (TAMs) are often immunosuppressive (M2-polarized). Propose a strategy combining: (a) CSF1R inhibitor to repolarise TAMs; (b) anti-PD-1 to release T cell checkpoint brakes; (c) low-dose dexamethasone to reduce treatment-related inflammation without suppressing anti-tumor immunity. What preclinical evidence supports this combination?

Answer (Q21, Synthesis). Proposed combination: (a) a CSF1R inhibitor depletes/repolarises immunosuppressive M2 tumor-associated macrophages toward an antitumour phenotype; (b) anti-PD-1 releases the checkpoint brake on tumor-infiltrating T cells, restoring cytotoxicity; (c) low-dose dexamethasone limits treatment-related cytokine toxicity while, at low doses, sparing effector T-cell function. Preclinical support: CSF1R blockade plus checkpoint inhibition shows synergistic tumor control in mouse models by remodeling the myeloid compartment and increasing CD8(+) infiltration. The conclusion is conditional — glucocorticoids can blunt antitumour immunity if dosed too high, so the net benefit depends on dose and timing, which is what would change it. See section 34.

22. The pineal gland produces melatonin in response to darkness (via the suprachiasmatic nucleus → sympathetic → pinealocyte). Evaluate: (a) the circadian rhythm of melatonin secretion; (b) the evidence for melatonin’s role in sleep-wake regulation vs a “darkness signal”; (c) the efficacy of exogenous melatonin for jet lag and shift work disorder; (d) the immunomodulatory effects of melatonin (anti-inflammatory, antioxidant, NK cell activation).

Answer (Q22, Synthesis). (a) Melatonin secretion is circadian: the SCN drives a sympathetic signal to the pineal so melatonin rises in darkness (night) and is suppressed by light. (b) Evidence favors melatonin acting primarily as a “darkness/timing signal” entraining circadian phase rather than a direct hypnotic, since it shifts sleep timing more than it sedates. (c) Exogenous melatonin is modestly effective for jet lag and circadian (shift-work/delayed-phase) disorders, mainly via phase-shifting when timed correctly. (d) Melatonin also has immunomodulatory effects (antioxidant, anti-inflammatory, NK-cell enhancing). These conclusions are evidence-supported but conditional on dose and timing; mistimed dosing can shift rhythms the wrong way, which is what would change the inference. See section 34.

23. Evaluate autoinflammatory diseases (distinct from autoimmune): conditions caused by inappropriate innate immune activation without autoantibodies. Using familial Mediterranean fever (FMF, pyrin mutations) as a case study: (a) how does mutant pyrin activate the inflammasome; (b) why does colchicine (inhibiting neutrophil migration) work as treatment; (c) how does IL-1 blockade (anakinra, canakinumab) provide definitive treatment?

Answer (Q23, Synthesis). Familial Mediterranean fever is autoinflammatory: it arises from dysregulated innate immunity (excess IL-1) without autoantibodies or autoreactive T cells. (a) Mutant pyrin escapes normal inhibitory phosphorylation and assembles an ASC-dependent pyrin inflammasome, activating caspase-1 and driving IL-1(β)/pyroptosis. (b) Colchicine works by disrupting microtubules, impairing neutrophil migration and inflammasome assembly, preventing attacks. (c) IL-1 blockade (anakinra, canakinumab) neutralizes the pathway’s effector cytokine, providing definitive control in colchicine-resistant disease. The framework is well supported; its limitation is that this is an evidence-based model of a specific monogenic syndrome, and atypical genotypes/phenotypes are what would qualify the conclusion. See section 34.

24. The gut-brain-immune axis: enteroendocrine cells in the gut produce >30 hormones (GLP-1, PYY, CCK, serotonin) that signal to the brain and immune system. Evaluate: (a) how gut serotonin (>90% of body’s serotonin) modulates gut motility and immune cell function; (b) the evidence linking gut endocrine dysfunction to IBS (irritable bowel syndrome); (c) how GLP-1 receptor agonists (semaglutide) affect not just glucose metabolism but also neuroinflammation.

Answer (Q24, Synthesis). (a) Gut enterochromaffin cells make >90% of body serotonin, which regulates gut motility/secretion and also modulates immune cells (mucosal mast cells, T cells) and signals to the brain via vagal afferents. (b) Evidence links altered enteroendocrine/serotonin signaling and low-grade immune activation to IBS, where dysregulated motility and visceral hypersensitivity track with these changes. (c) GLP-1 receptor agonists (semaglutide) act beyond glucose/appetite: GLP-1R on CNS and immune cells mediates anti-neuroinflammatory effects in preclinical models. These links are conditional and largely associative/preclinical; causal human data are limited, which is what would change the conclusion. See section 34.

25. Critically evaluate the concept of “immunometabolism” — the idea that metabolic reprogramming of immune cells determines their functional polarization. Using the M1 (pro-inflammatory, glycolytic) vs M2 (anti-inflammatory, OXPHOS) macrophage paradigm: (a) how does TCA cycle disruption in M1 macrophages lead to itaconate and succinate accumulation; (b) how does succinate stabilize HIF-1α and promote IL-1β production; (c) why targeting immunometabolism (e.g., dimethyl fumarate activating Nrf2) is a therapeutic frontier? Then apply the chapter’s evidence-map habit to reproductive

physiology: what evidence separates ovulation timing, sperm production, tubal transport, uterine receptivity, endocrine feedback, implantation, and age-dependent gamete quality after 12 months without conception?

Answer (Q25, Synthesis). Immunometabolism holds that the metabolic state of an immune cell determines its function. (a) In M1 macrophages the TCA cycle is “broken” at two points (after citrate and after succinate), so citrate is diverted to itaconate and succinate accumulates. (b) Accumulated succinate inhibits prolyl hydroxylases, stabilizing HIF-1(α), which transactivates pro-IL-1(β), reinforcing the inflammatory glycolytic program; M2 cells instead rely on oxidative phosphorylation and fatty-acid oxidation. (c) Targeting this metabolism (e.g., dimethyl fumarate activating Nrf2 and altering succinate/GAPDH) is a therapeutic frontier for inflammatory disease. The reproductive transfer starts with time-bounded criteria and then separates mechanisms: menstrual history and ovulation testing for ovulatory timing; semen analysis for count, motility, and morphology; tubal patency testing for transport; uterine imaging and endometrial history for receptivity; TSH/prolactin/FSH/LH/estradiol or indicated endocrine tests for feedback disruptions; pregnancy-loss or implantation history for early developmental failure; and age plus ovarian-reserve markers as context rather than destiny. The conclusion is a differential diagnosis, not a label: infertility can arise from one dominant bottleneck or from several modest constraints interacting. See section 34 and [Centers for Disease Control and Prevention \[2024b\]](#).

26. Adrenal medulla catecholamines (epinephrine, norepinephrine) are released in response to sympathetic stimulation. Compare: (a) the receptor subtypes activated by each (α_1 , α_2 , β_1 , β_2); (b) the effects on heart rate, blood vessels, and bronchioles; (c) why pheochromocytoma (adrenal medullary tumor) causes paroxysmal hypertension.

Answer (Q26, Synthesis). (a) Epinephrine activates (α_1), (β_1), and (β_2) receptors; norepinephrine acts mainly on (α_1)/(α_2) and (β_1) with little (β_2) effect. (b) Both raise heart rate/contractility ((β_1)); epinephrine causes net vasodilation in skeletal muscle and bronchodilation ((β_2)), whereas norepinephrine predominantly vasoconstricts ((α_1)), raising peripheral resistance. (c) A pheochromocytoma is a chromaffin-cell tumor that releases catecholamine surges, producing paroxysmal hypertension, palpitations, and sweating. See section 34.

27. Growth hormone (GH) from the anterior pituitary has both direct and indirect (via IGF-1 from the liver) effects. Explain: (a) the GH pulse pattern (nocturnal secretion regulated by GHRH and somatostatin); (b) the metabolic effects of GH (lipolysis, anti-insulin, protein synthesis); (c) why acromegaly (GH excess in adults) causes the symptoms it does.

Answer (Q27, Synthesis). (a) GH is secreted in pulses, largest during slow-wave sleep, under stimulatory GHRH and inhibitory somatostatin from the hypothalamus. (b) Directly, GH is lipolytic and anti-insulin (“diabetogenic”); indirectly, via hepatic IGF-1, it promotes protein synthesis and tissue/linear growth. (c) In adults the epiphyses are fused, so GH excess (acromegaly) cannot increase height; instead IGF-1-driven soft-tissue and bone growth enlarges hands, feet, and jaw, while the anti-insulin effect causes glucose intolerance. See section 34.

28. Dendritic cells (DCs) bridge innate and adaptive immunity. Explain: (a) how immature DCs in tissues sample antigens via macropinocytosis and TLR activation; (b) how DC maturation involves upregulation of MHC class II and co-stimulatory molecules (CD80/86); (c) how mature DCs migrate to lymph nodes to activate naïve T cells (antigen presentation). Why are DCs the most potent professional antigen-presenting cells?

Answer (Q28, Synthesis). (a) Immature tissue DCs are highly endocytic, sampling antigen by macropinocytosis/phagocytosis while TLR engagement signals infection. (b) PRR signals mature the DC: it upregulates MHC II loaded with processed peptide and co-stimulatory CD80/CD86, and reduces further uptake. (c) Maturation induces CCR7, guiding the DC up CCL19/21 gradients to the lymph node T-cell zone, where it presents peptide-MHC to naïve T cells. DCs are the most potent APCs because they uniquely provide all three signals (peptide-MHC, co-stimulation, and polarizing cytokines) needed to prime naïve T cells, including by cross-presentation. See section 34.

29. Parathyroid hormone (PTH) and calcitonin regulate blood calcium. PTH increases Ca^{2+} by: (a) stimulating osteoclasts (bone resorption); (b) increasing renal Ca^{2+} reabsorption; (c) activating 1α -hydroxylase (vitamin D activation \rightarrow intestinal Ca^{2+} absorption). Calcitonin decreases Ca^{2+} by inhibiting osteoclasts. What disease results from PTH excess (hyperparathyroidism)?

Answer (Q29, Synthesis). PTH raises blood Ca^{2+} : (a) it stimulates osteoclastic bone resorption (indirectly, via RANKL on osteoblasts); (b) it increases distal-tubule renal Ca^{2+} reabsorption (and phosphate excretion); (c) it activates renal $1(\alpha)$ -hydroxylase to make calcitriol, boosting intestinal Ca^{2+} absorption. Calcitonin opposes this by inhibiting osteoclasts. PTH excess (primary hyperparathyroidism) causes hypercalcaemia with bone demineralisation, kidney stones, and the classic “bones, stones, groans, psychiatric moans.” See section 34.

30. Natural killer (NK) cells use the “missing self” mechanism: inhibitory KIR receptors bind MHC class I on normal cells and suppress killing. Virus-infected cells and tumor cells often downregulate MHC I, releasing the NK cell from inhibition. Explain: (a) the activating receptors (NKG2D, recognizing stress ligands MICA/MICB); (b) how the balance of activating vs inhibiting signals determines the NK cell response; (c) how cancer immunotherapy exploits NK cells (bispecific engagers).

Answer (Q30, Synthesis). (a) NK activating receptors such as NKG2D recognize stress-induced ligands (MICA/MICB, ULBPs) upregulated on infected or transformed cells. (b) The response is set by the integration of activating versus inhibitory (KIR-MHC I) signals: when activating signals

exceed inhibition (e.g., MHC I downregulated but stress ligands present), the NK cell kills via perforin/granzyme and secretes IFN-(gamma). (c) Immunotherapy exploits this by bispecific NK-cell engagers (e.g., BiKEs/TriKEs) that bridge an NK activating receptor (CD16) to a tumor antigen, forcing targeted lysis. See section 34.

Questions — Immune System Architecture

Instructor Use and Coverage Notes

- Coverage target: Predict the consequence of changing an antigen, cell population, or checkpoint.
- Model/data emphasis: Immune-memory, cytokine, and recognition reasoning.
- Assessment alignment: Visual Representations, Statistical Tests and Data Analysis, Argumentation.
- Misconception probe: Immunity is not just attack; recognition, tolerance, memory, and regulation are equally central.
- Transfer product: Transfer immunity reasoning to vaccination, autoimmunity, infection, and cancer therapy.
- Grading focus: award full credit for mechanism, evidence, boundary conditions, and units when a calculation is required.
- Suggested use: draw one recall item, one application item, and one synthesis item when building a short quiz from this bank.

Questions 1–10: Recall and Comprehension

This activity accompanies section 35 of the textbook — review that chapter before attempting the exercises below.

1. Adrenal medulla catecholamines (epinephrine, norepinephrine) are released in response to sympathetic stimulation. Compare: (a) the receptor subtypes activated by each (α_1 , α_2 , β_1 , β_2); (b) the effects on heart rate, blood vessels, and bronchioles; (c) why pheochromocytoma (adrenal medullary tumor) causes paroxysmal hypertension.

Answer (Q1, Recall). (a) Epinephrine activates (α_1), (β_1), and (β_2) receptors; norepinephrine acts mainly on (α_1)/(α_2) and (β_1) with little (β_2) effect. (b) Both raise heart rate/contractility ((β_1)); epinephrine causes net vasodilation in skeletal muscle and bronchodilation ((β_2)), whereas norepinephrine predominantly vasoconstricts ((α_1)), raising peripheral resistance. (c) A pheochromocytoma is a chromaffin-cell tumor that releases catecholamine surges, producing paroxysmal hypertension, palpitations, and sweating. See section 35.
2. Growth hormone (GH) from the anterior pituitary has both direct and indirect (via IGF-1 from the liver) effects. Explain: (a) the GH pulse pattern (nocturnal secretion regulated by GHRH and somatostatin); (b) the metabolic effects of GH (lipolysis, anti-insulin, protein synthesis); (c) why acromegaly (GH excess in adults) causes the symptoms it does.

Answer (Q2, Recall). (a) GH is secreted in pulses, largest during slow-wave sleep, under stimulatory GHRH and inhibitory somatostatin from the hypothalamus. (b) Directly, GH is lipolytic and anti-insulin (“diabetogenic”); indirectly, via hepatic IGF-1, it promotes protein synthesis and tissue/linear growth. (c) In adults the epiphyses are fused, so GH excess (acromegaly) cannot increase height; instead IGF-1-driven soft-tissue and bone growth enlarges hands, feet, and jaw, while the anti-insulin effect causes glucose intolerance. See section 35.
3. Dendritic cells (DCs) bridge innate and adaptive immunity. Explain: (a) how immature DCs in tissues sample antigens via macropinocytosis and TLR activation; (b) how DC maturation involves upregulation of MHC class II and co-stimulatory molecules (CD80/86); (c) how mature DCs migrate to lymph nodes to activate naïve T cells (antigen presentation). Why are DCs the most potent professional antigen-presenting cells?

Answer (Q3, Recall). (a) Immature tissue DCs are highly endocytic, sampling antigen by macropinocytosis/phagocytosis while TLR engagement signals infection. (b) PRR signals mature the DC: it upregulates MHC II loaded with processed peptide and co-stimulatory CD80/CD86, and reduces further uptake. (c) Maturation induces CCR7, guiding the DC up CCL19/21 gradients to the lymph node T-cell zone, where it presents peptide-MHC to naive T cells. DCs are the most potent APCs because they uniquely provide all three signals (peptide-MHC, co-stimulation, and polarizing cytokines) needed to prime naive T cells, including by cross-presentation. See section 35.
4. Parathyroid hormone (PTH) and calcitonin regulate blood calcium. PTH increases Ca^{2+} by: (a) stimulating osteoclasts (bone resorption); (b) increasing renal Ca^{2+} reabsorption; (c) activating 1α -hydroxylase (vitamin D activation → intestinal Ca^{2+} absorption). Calcitonin decreases Ca^{2+} by inhibiting osteoclasts. What disease results from PTH excess (hyperparathyroidism)?

Answer (Q4, Recall). PTH raises blood Ca^{2+} : (a) it stimulates osteoclastic bone resorption (indirectly, via RANKL on osteoblasts); (b) it increases distal-tubule renal Ca^{2+} reabsorption (and phosphate excretion); (c) it activates renal $1(\alpha)$ -hydroxylase to make calcitriol, boosting intestinal Ca^{2+} absorption. Calcitonin opposes this by inhibiting osteoclasts. PTH excess (primary hyperparathyroidism) causes hypercalcaemia with bone demineralisation, kidney stones, and the classic “bones, stones, groans, psychiatric moans.” See section 35.
5. Natural killer (NK) cells use the “missing self” mechanism: inhibitory KIR receptors bind MHC class I on normal cells and suppress killing. Virus-infected cells and tumor cells often downregulate MHC I, releasing the NK cell from inhibition. Explain: (a) the activating receptors (NKG2D, recognizing stress ligands MICA/MICB); (b) how the balance of activating vs inhibiting signals determines the NK cell response; (c) how cancer immunotherapy exploits NK cells (bispecific engagers).

Answer (Q5, Recall). (a) NK activating receptors such as NKG2D recognize stress-induced ligands (MICA/MICB, ULBPs) upregulated on infected or transformed cells. (b) The response is set by the integration of activating versus inhibitory (KIR-MHC I) signals: when activating signals ex-

ceed inhibition (e.g., MHC I downregulated but stress ligands present), the NK cell kills via perforin/granzyme and secretes IFN-(gamma). (c) Immunotherapy exploits this by bispecific NK-cell engagers (e.g., BiKEs/TriKEs) that bridge an NK activating receptor (CD16) to a tumor antigen, forcing targeted lysis. See section 35.

6. Evaluate the integration of endocrine and immune systems: cortisol (a glucocorticoid) suppresses inflammation by: (a) inhibiting NF-κB transcription factor; (b) reducing prostaglandin synthesis (inhibiting PLA₂ and COX-2); (c) inducing lymphocyte apoptosis. Why do critically ill ICU patients sometimes develop adrenal insufficiency, and why does physiological stress-dose hydrocortisone improve sepsis survival?

Answer (Q6, Recall). Cortisol restrains inflammation through several converging mechanisms: (a) ligand-bound GR tethers and inhibits NF-(kappa)B (transrepression), shutting off cytokine genes; (b) it induces annexin A1 and suppresses PLA₂ and COX-2, cutting prostaglandin synthesis; (c) it drives apoptosis of lymphocytes and shifts cytokines toward IL-10. Critically ill patients can develop “critical-illness-related corticosteroid insufficiency” (relative adrenal insufficiency plus tissue glucocorticoid resistance), so HPA output is inadequate for the inflammatory load. Stress-dose hydrocortisone restores vascular catecholamine responsiveness and dampens excessive inflammation, which improves shock reversal; however, the survival benefit is condition-dependent (clearest in vasopressor-refractory septic shock) — that conditionality is what would change the conclusion. See section 35.

7. Evaluate the molecular mechanisms of endocrine disruptors (BPA, phthalates, pesticides): how do these chemicals interfere with hormone signaling (estrogenic, anti-androgenic, thyroid-disrupting), at what environmental concentrations are effects seen (non-monotonic dose-response), and what evidence from wildlife populations (feminisation of male fish, reproductive abnormalities in alligators) supports endocrine disruption in the environment?

Answer (Q7, Recall). Endocrine disruptors interfere with hormone signaling by mimicking or blocking receptors (BPA is weakly oestrogenic; phthalates are anti-androgenic) and by perturbing hormone synthesis, transport, or thyroid signaling. The evidence includes non-monotonic dose-response curves, where low developmental doses can produce effects absent or different at high doses, complicating classical toxicology thresholds. Wildlife data (feminisation/intersex in male fish below sewage outfalls, reduced phallus size and altered sex ratios in alligators at contaminated lakes) support real environmental endocrine disruption. The conclusion is evidence-supported but conditional: non-monotonic dosing and species/timing differences mean strength of inference depends on exposure window and endpoint, which is what would change it. See section 35.

8. Design an experiment to determine whether a newly discovered peptide is a hormone: (a) demonstrate that it is secreted into the bloodstream in response to a physiological stimulus; (b) show that it has a target tissue with specific receptors; (c) prove that removing the source gland eliminates the response and that hormone replacement restores it; (d) show that the response is dose-dependent.

Answer (Q8, Recall). Hypothesis: peptide X is a hormone. Design: (a) show it is released into blood and rises in response to a defined physiological stimulus (measure plasma X before/after, with stimulus vs sham control); (b) demonstrate a distant target tissue expressing specific high-affinity receptors (radioligand binding/displacement); (c) perform a classic ablation-replacement experiment — surgically/genetically remove the source gland, show the response disappears, then restore it by exogenous X (necessity and sufficiency, with vehicle controls and replication); (d) establish a dose-response relationship (graded effect with graded X). A falsifying result is loss of effect despite receptor occupancy or no response on replacement, indicating it is not the causal hormone. See section 35.

9. Evaluate the concept of “trained immunity” — epigenetic reprogramming of innate immune cells (monocytes/macrophages) by prior pathogen exposure, resulting in enhanced responses to subsequent unrelated infections. How does BCG vaccination induce trained immunity (H3K4me3 at inflammatory gene promoters, mTOR-dependent metabolic shift from OXPHOS to glycolysis), and what are the implications for broad-spectrum vaccine development?

Answer (Q9, Recall). Trained immunity is the epigenetic and metabolic reprogramming of innate cells (monocytes/macrophages) so that a prior exposure heightens responses to later, unrelated infections. BCG induces it by depositing activating histone marks (H3K4me3, H3K27ac) at inflammatory gene promoters and by an mTOR/HIF-1(alpha)-driven metabolic shift from oxidative phosphorylation toward aerobic glycolysis, priming faster cytokine output. The implication is the prospect of broad-spectrum vaccines that confer non-specific protection. The conclusion is conditional: effect size varies with host, timing, and pathogen, and durability is finite — heterogeneous clinical-trial outcomes are what would change the inference. See section 35.

10. Evaluate the evolutionary conservation and divergence of the HPA axis: fish have an HPI axis (hypothalamic-pituitary-interrenal), amphibians have an HPA axis with cortisol, and birds have corticosterone. What does this conservation tell us about the fundamental biological requirement for glucocorticoid stress response across vertebrates?

Answer (Q10, Recall). Across vertebrates the stress axis is conserved in architecture but divergent in the terminal steroid: fish use the hypothalamic-pituitary-interrenal (HPI) axis, amphibians and mammals an HPA axis with cortisol, and birds and rodents use corticosterone. This deep conservation of a CRH-ACTH-glucocorticoid loop indicates a fundamental, selectively maintained requirement for a rapid, glucocorticoid-mediated stress response (energy mobilization and immune modulation) in vertebrate survival. The inference is strong but comparative: it rests on homol-

ogy arguments, and discovery of a vertebrate lineage lacking the axis or using an unrelated mediator would weaken the universality claim. See section 35.

Questions 11–20: Application and Analysis

11. Evaluate the therapeutic potential of checkpoint immunotherapy combined with endocrine modulation: tumor-associated macrophages (TAMs) are often immunosuppressive (M2-polarized). Propose a strategy combining: (a) CSF1R inhibitor to repolarise TAMs; (b) anti-PD-1 to release T cell checkpoint brakes; (c) low-dose dexamethasone to reduce treatment-related inflammation without suppressing anti-tumor immunity. What preclinical evidence supports this combination?

Answer (Q11, Application). Proposed combination: (a) a CSF1R inhibitor depletes/repolarises immunosuppressive M2 tumor-associated macrophages toward an antitumour phenotype; (b) anti-PD-1 releases the checkpoint brake on tumor-infiltrating T cells, restoring cytotoxicity; (c) low-dose dexamethasone limits treatment-related cytokine toxicity while, at low doses, sparing effector T-cell function. Preclinical support: CSF1R blockade plus checkpoint inhibition shows synergistic tumor control in mouse models by remodeling the myeloid compartment and increasing CD8(+) infiltration. The conclusion is conditional — glucocorticoids can blunt antitumour immunity if dosed too high, so the net benefit depends on dose and timing, which is what would change it. See section 35.

12. The pineal gland produces melatonin in response to darkness (via the suprachiasmatic nucleus → sympathetic → pinealocyte). Evaluate: (a) the circadian rhythm of melatonin secretion; (b) the evidence for melatonin’s role in sleep-wake regulation vs a “darkness signal”; (c) the efficacy of exogenous melatonin for jet lag and shift work disorder; (d) the immunomodulatory effects of melatonin (anti-inflammatory, antioxidant, NK cell activation).

Answer (Q12, Application). (a) Melatonin secretion is circadian: the SCN drives a sympathetic signal to the pineal so melatonin rises in darkness (night) and is suppressed by light. (b) Evidence favors melatonin acting primarily as a “darkness/timing signal” entraining circadian phase rather than a direct hypnotic, since it shifts sleep timing more than it sedates. (c) Exogenous melatonin is modestly effective for jet lag and circadian (shift-work/delayed-phase) disorders, mainly via phase-shifting when timed correctly. (d) Melatonin also has immunomodulatory effects (antioxidant, anti-inflammatory, NK-cell enhancing). These conclusions are evidence-supported but conditional on dose and timing; mistimed dosing can shift rhythms the wrong way, which is what would change the inference. See section 35.

13. Evaluate autoinflammatory diseases (distinct from autoimmune): conditions caused by inappropriate innate immune activation without autoantibodies. Using familial Mediterranean fever (FMF, pyrin mutations) as a case study: (a) how does mutant pyrin activate the inflammasome; (b) why does colchicine (inhibiting neutrophil migration) work as treatment; (c) how does IL-1 blockade (anakinra, canakinumab) provide definitive treatment?

Answer (Q13, Application). Familial Mediterranean fever is autoinflammatory: it arises from dysregulated innate immunity (excess IL-1) without autoantibodies or autoreactive T cells. (a) Mutant pyrin escapes normal inhibitory phosphorylation and assembles an ASC-dependent pyrin inflammasome, activating caspase-1 and driving IL-1(beta)/pyroptosis. (b) Colchicine works by disrupting microtubules, impairing neutrophil migration and inflammasome assembly, preventing attacks. (c) IL-1 blockade (anakinra, canakinumab) neutralizes the pathway’s effector cytokine, providing definitive control in colchicine-resistant disease. The framework is well supported; its limitation is that this is an evidence-based model of a specific monogenic syndrome, and atypical genotypes/phenotypes are what would qualify the conclusion. See section 35.

14. The gut-brain-immune axis: enteroendocrine cells in the gut produce >30 hormones (GLP-1, PYY, CCK, serotonin) that signal to the brain and immune system. Evaluate: (a) how gut serotonin (>90% of body’s serotonin) modulates gut motility and immune cell function; (b) the evidence linking gut endocrine dysfunction to IBS (irritable bowel syndrome); (c) how GLP-1 receptor agonists (semaglutide) affect not just glucose metabolism but also neuroinflammation.

Answer (Q14, Application). (a) Gut enterochromaffin cells make >90% of body serotonin, which regulates gut motility/secretion and also modulates immune cells (mucosal mast cells, T cells) and signals to the brain via vagal afferents. (b) Evidence links altered enteroendocrine/serotonin signaling and low-grade immune activation to IBS, where dysregulated motility and visceral hypersensitivity track with these changes. (c) GLP-1 receptor agonists (semaglutide) act beyond glucose/appetite: GLP-1R on CNS and immune cells mediates anti-neuroinflammatory effects in preclinical models. These links are conditional and largely associative/preclinical; causal human data are limited, which is what would change the conclusion. See section 35.

15. Critically evaluate the concept of “immunometabolism” — the idea that metabolic reprogramming of immune cells determines their functional polarization. Using the M1 (pro-inflammatory, glycolytic) vs M2 (anti-inflammatory, OXPHOS) macrophage paradigm: (a) how does TCA cycle disruption in M1 macrophages lead to itaconate and succinate accumulation; (b) how does succinate stabilize HIF-1α and promote IL-1β production; (c) why targeting immunometabolism (e.g., dimethyl fumarate activating Nrf2) is a therapeutic frontier? Then apply the chapter’s evidence-map habit to reproductive physiology: what evidence separates ovulation timing, sperm production, tubal transport, uterine receptivity, endocrine feedback, implantation, and age-dependent gamete quality after 12 months without conception?

Answer (Q15, Application). Immunometabolism holds that the metabolic state of an immune cell determines its function. (a) In M1 macrophages the TCA cycle is “broken” at two points (after citrate and after succinate), so citrate is diverted to itaconate and succinate accumulates. (b) Accumulated succinate inhibits prolyl hydroxylases, stabilizing HIF-1(alpha), which transactivates pro-IL-1(beta), reinforcing the inflammatory glycolytic program; M2 cells instead rely on oxidative phosphorylation and fatty-acid oxidation. (c) Targeting this metabolism (e.g., dimethyl fumarate activating Nrf2 and altering succinate/GAPDH) is a therapeutic frontier for inflammatory disease. The reproductive transfer starts with time-bounded criteria and then separates mechanisms: menstrual history and ovulation testing for ovulatory timing; semen analysis for count, motility, and morphology; tubal patency testing for transport; uterine imaging and endometrial history for receptivity; TSH/prolactin/FSH/LH/estradiol or indicated endocrine tests for feedback disruptions; pregnancy-loss or implantation history for early developmental failure; and age plus ovarian-reserve markers as context rather than destiny. The conclusion is a differential diagnosis, not a label: infertility can arise from one dominant bottleneck or from several modest constraints interacting. See section 35 and [Centers for Disease Control and Prevention \[2024b\]](#).

16. What is the endocrine system? How does it differ from the nervous system in signaling speed and duration?

Answer (Q16, Application). The endocrine system is the network of glands that secrete hormones into the blood to regulate physiology body-wide. Compared with the nervous system, endocrine signaling is slower (seconds to hours rather than milliseconds) and longer-lasting (minutes to days rather than brief), because it relies on chemical hormones travelling via the circulation to all cells bearing the receptor rather than fast electrical transmission across a narrow synapse. See section 35.

17. Name the major endocrine glands and one hormone secreted by each.

Answer (Q17, Application). Major glands and a representative hormone each: hypothalamus (releasing hormones, e.g., CRH); anterior pituitary (ACTH, GH); thyroid (T4/T3); parathyroid (PTH); adrenal cortex (cortisol); adrenal medulla (epinephrine); endocrine pancreas (insulin from (beta)-cells); gonads (testosterone or oestradiol); pineal (melatonin). See section 35.

18. Distinguish peptide hormones from steroid hormones in terms of synthesis, transport, and receptor location.

Answer (Q18, Application). Peptide hormones are made on ribosomes as preprohormones, stored in secretory granules, travel free in plasma, and act fast on plasma-membrane receptors (RTKs/GPCRs). Steroid hormones are synthesized on demand from cholesterol (not stored), carried bound to plasma proteins (e.g., CBG, SHBG), and act slowly via intracellular nuclear receptors that alter gene transcription. The receptor location (membrane vs nuclear) is the mechanistic difference that makes peptide signaling rapid/transient and steroid signaling slow/persistent. See section 35.

19. What is the hypothalamic-pituitary axis? Name one releasing hormone and one tropic hormone.

Answer (Q19, Application). The hypothalamic-pituitary axis is the hierarchical control loop in which the hypothalamus secretes releasing hormones that drive anterior-pituitary tropic hormones, which in turn stimulate a peripheral target gland, with negative feedback at each level. Example: hypothalamic CRH (releasing hormone) stimulates pituitary ACTH (tropic hormone), which stimulates adrenal cortisol. See section 35.

20. What is negative feedback? Give an example involving the thyroid gland.

Answer (Q20, Application). Negative feedback is regulation in which a system’s output inhibits the steps that produced it, stabilizing the variable around a set point. Thyroid example: rising free T3/T4 inhibits hypothalamic TRH and pituitary TSH secretion, reducing further thyroid hormone output; if T3/T4 fall, TRH and TSH rise again, restoring levels. See section 35.

Questions 21–30: Synthesis and Evaluation

21. What is cortisol? Name its target tissues and three physiological effects.

Answer (Q21, Synthesis). Cortisol is a glucocorticoid steroid made in the adrenal cortex (zona fasciculata) under ACTH control. Target tissues include liver, muscle, adipose, and immune cells (acting via the nuclear glucocorticoid receptor). Three effects: stimulates hepatic gluconeogenesis (mobilizing amino acids from muscle), is immunosuppressive/anti-inflammatory (inhibits NF-(kappa)B and cytokine production), and promotes lipolysis. See section 35.

22. What are the components of innate immunity? Name four.

Answer (Q22, Synthesis). Innate immunity is the rapid, non-specific, germline-encoded first line of defense. Four components: physical/chemical barriers (skin, mucus, lysozyme); phagocytes (neutrophils, macrophages, dendritic cells); the complement system; and NK cells (plus inflammation and interferons). See section 35.

23. What is a Toll-like receptor (TLR)? Name a ligand for TLR4.

- Answer (Q23, Synthesis). A Toll-like receptor is a germline-encoded pattern-recognition receptor on the plasma membrane or endosomes that detects conserved pathogen molecules (PAMPs) and triggers inflammatory or antiviral signaling. The ligand for TLR4 is bacterial lipopolysaccharide (LPS), characteristic of Gram-negative bacteria. See section 35.
24. What is the complement system? What are its three outcomes (opsonisation, MAC, inflammation)?
- Answer (Q24, Synthesis). The complement system is a cascade of about 30 plasma proteins that, once triggered (classical, lectin, or alternative pathway), generate C3/C5 convertases. Its three outcomes are opsonisation (C3b coats pathogens for phagocytosis), the membrane attack complex (C5b-9 lyses target cells), and inflammation (anaphylatoxins C3a/C5a recruit and activate leukocytes). See section 35.
25. Define phagocytosis. Name two professional phagocytes.
- Answer (Q25, Synthesis). Phagocytosis is the receptor-mediated engulfment of particles or microbes into a phagosome that fuses with lysosomes to destroy the cargo. Two professional phagocytes: neutrophils and macrophages (dendritic cells also phagocytose). See section 35.
26. The HPA axis: CRH (hypothalamus) → ACTH (anterior pituitary) → cortisol (adrenal cortex). Cortisol feeds back negatively on CRH and ACTH secretion. If a patient has an adrenal tumor autonomously producing cortisol, predict: (a) ACTH levels; (b) CRH levels; (c) contralateral adrenal gland size; (d) response to the dexamethasone suppression test.
- Answer (Q26, Synthesis). An autonomous cortisol-secreting adrenal tumor produces high cortisol independent of ACTH. (a) ACTH is low (suppressed by negative feedback). (b) CRH is low (also feedback-suppressed). (c) The contralateral adrenal atrophies because, without ACTH trophic support, the normal cortex shrinks. (d) On the dexamethasone suppression test cortisol fails to suppress (it is autonomous and not under pituitary control), confirming an ACTH-independent adrenal source. See section 35.
27. Insulin (from pancreatic β -cells) and glucagon (from α -cells) have opposing metabolic effects. Compare: (a) the stimulus for secretion of each; (b) the target tissue responses (liver, muscle, adipose); (c) the blood glucose level at which each dominates. What happens in Type 1 Diabetes (complete β -cell destruction)?
- Answer (Q27, Synthesis). (a) Insulin is secreted when blood glucose rises (after a meal); glucagon is secreted when glucose falls (fasting). (b) Insulin drives hepatic/muscle glycogen synthesis, muscle/adipose GLUT4 glucose uptake, and adipose lipogenesis; glucagon drives hepatic glycogenolysis and gluconeogenesis. (c) Insulin dominates at high glucose (5.5 mmol/L postprandial), glucagon at low glucose (fasting). In Type 1 diabetes, autoimmune (beta)-cell destruction abolishes insulin, so glucose stays high, cells starve, unopposed glucagon drives hyperglycaemia and ketoacidosis. See section 35.
28. Thyroid hormones (T_3/T_4) are unusual peptide-derived hormones that act like steroids (entering cells, binding nuclear receptors). Explain: (a) why T_3/T_4 can cross membranes (lipophilic due to iodination); (b) how T_3 binds thyroid hormone receptors ($TR\alpha/TR\beta$) to regulate gene transcription; (c) why hypothyroidism causes bradycardia, fatigue, and weight gain.
- Answer (Q28, Synthesis). (a) T_3/T_4 are lipophilic because heavy iodination of the tyrosine-derived rings lets them cross the lipid bilayer (entering cells via MCT8/MCT10). (b) T_3 binds nuclear $TR(\alpha)/TR(\beta)$, which heterodimerise with RXR on thyroid response elements; without T_3 the receptor recruits corepressors and represses genes, while T_3 binding swaps in coactivators and activates transcription. (c) Hypothyroidism slows metabolism: reduced Na^{+}/K^{+} -ATPase and BMR cause fatigue and weight gain, and loss of (β_1)-receptor upregulation plus reduced cardiac drive causes bradycardia. See section 35.
29. The inflammasome (NLRP3) is activated by diverse danger signals (K^{+} efflux, ROS, crystal particles). Trace: (a) NLRP3 oligomerisation; (b) ASC adaptor recruitment; (c) caspase-1 activation; (d) IL-1 β and IL-18 maturation and release; (e) pyroptosis (inflammatory cell death). Name two diseases where NLRP3 is inappropriately activated.
- Answer (Q29, Synthesis). (a) A priming signal (TLR/NF-(κ))B upregulates NLRP3 and pro-IL-1(β); a second signal (K^{+} efflux, ROS, crystals) triggers NLRP3 oligomerisation. (b) NLRP3 recruits the ASC adaptor, which polymerizes into a speck. (c) ASC clusters pro-caspase-1, enabling autocatalytic caspase-1 activation. (d) Active caspase-1 cleaves pro-IL-1(β) and pro-IL-18 to their mature secreted forms. (e) Caspase-1 also cleaves gasdermin D, whose N-terminal pores cause pyroptosis (lytic inflammatory death). Inappropriate NLRP3 activation occurs in gout (urate crystals) and cryopyrin-associated periodic syndromes (CAPS). See section 35.
30. Neutrophils are the first responders to bacterial infection. Describe their killing mechanisms: (a) phagocytosis and phagolysosome fusion; (b) respiratory burst (NADPH oxidase → superoxide → HOCl via myeloperoxidase); (c) NETosis (neutrophil extracellular trap formation). What disease results from NADPH oxidase deficiency (CGD)?
- Answer (Q30, Synthesis). (a) Neutrophils recognize and engulf opsonised bacteria into a phagosome that fuses with granules to form a phagolysosome. (b) The respiratory burst: assembled NADPH oxidase generates superoxide, dismutated to H_2O_2 ; myeloperoxidase converts H_2O_2

+ Cl^- to bactericidal hypochlorous acid (HOCl). (c) NETosis: the neutrophil extrudes decondensed chromatin studded with antimicrobial proteins (NETs) that trap and kill extracellular bacteria. NADPH oxidase deficiency causes chronic granulomatous disease (CGD), with recurrent catalase-positive infections. See section 35.

Questions — Population Ecology and Growth Models

Instructor Use and Coverage Notes

- Coverage target: Calculate a growth or sampling parameter and interpret its conservation meaning.
- Model/data emphasis: Exponential/logistic growth, mark-recapture, and matrix projection.
- Assessment alignment: Representing and Describing Data, Statistical Tests and Data Analysis, Argumentation.
- Misconception probe: Carrying capacity is not a fixed magic number; it changes with resources, interactions, and disturbance.
- Transfer product: Transfer population models to fisheries, invasive species, epidemiology, and endangered species.
- Grading focus: award full credit for mechanism, evidence, boundary conditions, and units when a calculation is required.
- Suggested use: draw one recall item, one application item, and one synthesis item when building a short quiz from this bank.

Questions 1–10: Recall and Comprehension

This activity accompanies section 36 of the textbook — review that chapter before attempting the exercises below.

1. Define population ecology. What are the four demographic parameters that influence population size?

Answer (Q1, Recall). Population ecology is the study of the factors that determine the size, density, distribution, age structure, and growth of populations over time. The four demographic parameters that change population size are natality (births), mortality (deaths), immigration (entry), and emigration (exit): $\Delta N = (B + I) - (D + E)$. Births and immigration add individuals; deaths and emigration remove them. See section 36. 2. What is the exponential growth model? Write its equation.

Answer (Q2, Recall). The exponential growth model describes population dynamics when per-capita birth and death rates are constant and resources are effectively unlimited — every individual reproduces at the same rate regardless of population density. Differential form: $\frac{dN}{dt} = rN$, where N is population size and r = intrinsic rate of increase = (birth rate – death rate) with units time^{-1} . Integrated form: $N_t = N_0 e^{rt}$. Doubling time $T_2 = \ln 2/r \approx 0.693/r$. Key numerical benchmarks: bacteria (*E. coli* in rich medium) $r \approx 1.4 \text{ h}^{-1}$ (doubling every about 30 min); humans globally today $r \approx 0.01 \text{ yr}^{-1}$ (doubling every about 70 years); historic humans up to 1960 doubled every about 35 years. Classical biological example: the re-introduction of ring-necked pheasants to Protection Island (1937) — 8 birds → 1898 in 5 years, almost exactly exponential before running into food limits. Because pure exponential growth is biologically unsustainable, this model is an idealisation valid only for the initial “colonization” or “bloom” phase — crucial for biosecurity (invasive species) and public health (epidemic R_0) calculations. See section 36. 3. What is the logistic growth model? Write its equation and define K (carrying capacity).

Answer (Q3, Recall). The logistic growth model (Verhulst 1838; rediscovered Pearl & Reed 1920) extends exponential growth by adding density-dependent self-limitation: $\frac{dN}{dt} = rN\left(1 - \frac{N}{K}\right)$, where K is the carrying capacity — the equilibrium population size supported by resources in a given environment. When $N \ll K$, the $(1 - N/K)$ term ≈ 1 and growth is near-exponential; as $N \rightarrow K$, growth slows; at $N = K$, $dN/dt = 0$. Integrated form: $N(t) = \frac{K}{1 + \left(\frac{K - N_0}{N_0}\right)e^{-rt}}$, a sigmoid (S-shaped) curve with inflection at $N = K/2$ (point of maximum growth rate $dN/dt_{\text{max}} = rK/4$). K is not a physical constant: it reflects the resource ceiling — food, water, nesting sites, disease pressure — and can shift with environmental change. Classical biological example: yeast in batch culture (Gause 1934) fit the logistic almost exactly with $K \approx 665 \text{ cells/mL}$ and $r \approx 0.22 \text{ h}^{-1}$. Modern fisheries management uses the logistic to define maximum sustainable yield (MSY) at $N = K/2$; harvesting above MSY drives fisheries to collapse (North Atlantic cod, 1992). See section 36. 4. What are r-selected and K-selected species? Give one example of each.

Answer (Q4, Recall). r-selected species maximize the intrinsic rate of increase r : many small offspring, little parental care, early reproduction, short lifespan, Type III survivorship — favored in unstable or unpredictable environments (e.g., dandelions, mosquitoes, weedy annual plants). K-selected species are adapted to live near carrying capacity K : few large offspring, heavy parental investment, late reproduction, long lifespan, Type I survivorship — favored in stable, crowded environments (e.g., elephants, oak trees). See section 36. 5. Define survivorship curve. Describe Types I, II, and III.

Answer (Q5, Recall). A survivorship curve plots the proportion of an original cohort still alive (l_x , log scale) against age. Type I (late loss): low juvenile mortality, most deaths in old age (humans, large mammals) — convex curve. Type II (constant loss): death probability roughly constant at all ages (many songbirds, rodents, hydra) — straight line. Type III (early loss): very high juvenile mortality, survivors are long-lived (oysters, oak trees, sea turtles) — concave curve. See section 36. 6. What is the mark-recapture method? Write the Lincoln-Petersen equation.

Answer (Q6, Recall). Mark-recapture estimates the size of a mobile population: capture a sample, mark and release them, then later take a second sample and count the marked recaptures. The Lincoln–Petersen estimator is $\hat{N} = \frac{M \cdot C}{R}$, where M = number marked in the first sample, C = total caught in the second sample, and R = marked individuals recaptured. It assumes a closed population, no mark loss, and equal catchability. See section 36. 7. What is population density? Distinguish crude density from ecological density.

Answer (Q7, Recall). Population density is the number of individuals per unit area or volume ($D = N/\text{area}$). Crude density uses total habitat area as the denominator, including space the species cannot use. Ecological (specific) density uses only the area actually occupied or usable by the species, so it more accurately reflects the local intensity of intraspecific interaction and resource demand. See section 36. 8. Define natality, mortality, immigration, and emigration.

Answer (Q8, Recall). Natality is the per-capita birth rate (new individuals produced by reproduction). Mortality is the per-capita death rate. Immigration is the movement of individuals *into* the population from elsewhere. Emigration is the movement of individuals *out* of the population. Natality and immigration increase N ; mortality and emigration decrease it: $\Delta N = (B + I) - (D + E)$. See section 36. 9. What is a life table? What parameters does it include?

Answer (Q9, Recall). A life table is an age-specific summary of survival and reproduction in a cohort. It records, for each age class x : n_x (number alive), l_x (survivorship, proportion surviving from birth), d_x (deaths in the interval), q_x (age-specific mortality rate), and m_x (age-specific fecundity). From it one computes net reproductive rate $R_0 = \sum l_x m_x$, generation time T , and $r \approx \ln(R_0)/T$. See section 36. 10. What is the difference between density-dependent and density-independent limiting factors?

Answer (Q10, Recall). Density-dependent factors change in per-capita effect as population density changes — they intensify as N rises and provide regulatory feedback (competition for food, predation, disease, parasitism, accumulation of wastes). Density-independent factors affect the same *fraction* of individuals regardless of density (weather, fire, flood, drought, habitat destruction). Density-dependent factors stabilize populations near K ; density-independent ones cause fluctuations not tied to abundance. See section 36.

Questions 11–20: Application and Analysis

11. An *E. coli* population starts with $N_0 = 100$ cells. The intrinsic rate of increase $r = 0.693 \text{ h}^{-1}$ (doubling time = 1 hour). Calculate N_t at $t = 5$ hours using $N_t = N_0 e^{rt}$. At what time would the population reach 10^6 cells?

Answer (Q11, Application). Exponential model $N_t = N_0 e^{rt}$ with $N_0 = 100$, $r = 0.693 \text{ h}^{-1}$. At $t = 5 \text{ h}$: $N_5 = 100 e^{0.693 \times 5} = 100 e^{3.465} \approx 100 \times 31.96 \approx 3200$ cells (equivalently $100 \times 2^5 = 3200$, since r gives a 1-hour doubling time). Time to reach 10^6 : $t = \frac{\ln(10^6/100)}{0.693} = \frac{\ln(10^4)}{0.693} = \frac{9.21}{0.693} \approx 13.3$ hours (≈ 13.3 doublings). See section 36. 12. A deer population ($K = 1,000$) starts at $N = 50$ and grows logistically with $r = 0.3/\text{year}$. Calculate dN/dt at $N = 50$, $N = 500$, and $N = 900$. At which population size is growth rate highest? What happens to growth rate as N approaches K ?

Answer (Q12, Application). Logistic model $\frac{dN}{dt} = rN\left(1 - \frac{N}{K}\right)$, $r = 0.3 \text{ yr}^{-1}$, $K = 1000$. At $N = 50$: $0.3(50)(1 - 0.05) = 15 \times 0.95 \approx 14.3 \text{ ind/yr}$. At $N = 500$: $0.3(500)(1 - 0.5) = 150 \times 0.5 = 75 \text{ ind/yr}$. At $N = 900$: $0.3(900)(1 - 0.9) = 270 \times 0.1 = 27 \text{ ind/yr}$. Absolute growth rate is highest at $N = K/2 = 500$ ($dN/dt_{\max} = rK/4 = 75$). As $N \rightarrow K$, the $(1 - N/K)$ term $\rightarrow 0$, so $dN/dt \rightarrow 0$ and the population levels off. See section 36. 13. In a mark-recapture study: 200 butterflies are captured, marked, and released. A week later, 250 butterflies are captured, of which 40 are marked. Estimate population size using the Lincoln-Petersen formula. What assumptions must hold for this estimate to be valid?

Answer (Q13, Application). Lincoln-Petersen estimator: $\hat{N} = \frac{M \cdot C}{R}$, where M = first-capture marked (200), C = second-capture total (250), R = recaptured marked (40). Substitute: $\hat{N} = \frac{200 \times 250}{40} = \frac{50\,000}{40} = 1250$ butterflies. More bias-corrected Chapman estimator (for small samples): $\hat{N} = \frac{(M+1)(C+1)}{R+1} - 1 = \frac{201 \times 251}{41} - 1 = 1230 - 1 = 1229$ — about 2 % smaller; use this when $R < 20$ or when sample sizes are uneven.

Approximate 95 % confidence interval via $SE(\hat{N}) \approx \sqrt{\frac{M^2 C (C - R)}{R^3}} \approx \sqrt{\frac{200^2 \cdot 250 \cdot 210}{40^3}} \approx 181$; $CI \approx 1250 \pm 355 \rightarrow$ about [895, 1605] butterflies. Assumptions that must hold: (i) Closed population (no births, deaths, immigration, emigration between capture occasions — “closed” to N change); (ii) marks are not lost or overlooked; (iii) marking does not affect recapture probability (no trap-shyness, mark-induced predation, or reduced fitness); (iv) every individual has equal capture probability on both occasions (no sex-, age-, or site-heterogeneity); (v) sufficient mixing so that recaptured marked fraction is representative of the marked-to-total ratio in the full population. Violations bias the estimate — typically *upward* with trap-shyness, *downward* with heterogeneity. See section 36. 14. A population crash occurs when a population overshoots K (exceeds carrying capacity) and resources are depleted, causing K to decline. Using the logistic model, explain: (a) why the population exceeds K (time lag in density-dependent response); (b) the population trajectory after overshooting (damped oscillations vs extinction); (c) a real-world example (reindeer on St. Matthew Island).

Answer (Q14, Application). (a) Density-dependent regulation acts with a time lag: by the time food shortage depresses births and raises deaths, N has already shot past K because the prior reproduction was committed. (b) With a modest lag the population shows damped oscillations converging on K ; with a long lag or severe resource destruction K itself collapses and the population may crash toward extinction rather than oscillate. (c) St. Matthew Island reindeer: 29 introduced in 1944 grew to about 6,000 by 1963, overgrazed the slow-growing lichen, then crashed to about 42 by 1966 — overshoot followed by resource destruction and near-extinction, not damped oscillation. See section 36. 15. Compare r -selected (small, many offspring, high mortality, short lifespan) and K -selected (large, few offspring, low mortality, long lifespan) strategies. Place the following

organisms on the r-K continuum: elephant, dandelion, oak tree, mosquito, whale, annual grass. Explain why the r/K model is now considered an oversimplification.

Answer (Q15, Application). r-selected = small body, many offspring, high mortality, short life (fast end); K-selected = large body, few offspring, low mortality, long life (slow end). Ordering from r toward K: annual grass \approx dandelion \approx mosquito (r-end) \rightarrow oak tree \rightarrow elephant \approx whale (K-end). The r/K dichotomy is an oversimplification because life-history traits vary continuously and somewhat independently, environments are rarely cleanly stable or unstable, and modern demographic (life-history) theory predicts strategies from age-specific mortality and reproductive value rather than a single r-K axis. See section 36. 16. A Type I survivorship curve (e.g., humans) shows high survival until old age. A Type III curve (e.g., sea turtles) shows high juvenile mortality with high adult survival. Calculate: if a sea turtle lays 100 eggs per year and 2% survive to adulthood, what is the expected number of adult recruits per year? How many years of reproduction are needed to replace a dying adult (assume one-for-one replacement)?

Answer (Q16, Application). Adult recruits = $100 \times 0.02 = 2$ adults per year. Under strict one-for-one replacement, each turtle must produce one surviving adult to replace itself; at 2 recruits per reproductive year that requires only about 0.5 year of reproduction per adult replaced, but because each turtle replaces *itself* plus a mate's contribution, sustaining the population requires each female to survive and reproduce long enough to yield about 1 surviving daughter — so high adult survival across many reproductive years is essential. The Type III pattern means conservation gains come mainly from protecting adults and subadults (highest reproductive value), not eggs. See section 36. 17. The Allee effect describes a positive relationship between population density and per capita growth rate at low densities (below a threshold, the population cannot recover). Explain: (a) three mechanisms (mate finding difficulty, loss of cooperative defense, genetic problems from inbreeding); (b) how the Allee effect creates an extinction vortex for small populations; (c) what conservation strategies address the Allee effect.

Answer (Q17, Application). (a) Mate-finding failure (too few encounters at low density), loss of cooperative behaviors (group defense, cooperative foraging/hunting, predator dilution), and inbreeding/genetic decline (loss of heterozygosity, fixation of deleterious alleles). (b) Below the Allee threshold per-capita growth becomes negative, so small size lowers fitness, which lowers size further — a self-reinforcing extinction vortex coupling demographic and genetic decay. (c) Conservation responses raise effective density: translocation/augmentation to push N above threshold, captive breeding and head-starting, habitat consolidation, genetic rescue (introducing unrelated individuals), and protecting aggregation/breeding sites. See section 36. 18. Age-structured population models (Leslie matrix): a population with two age classes (juvenile and adult) has the following transition rates: juvenile survival = 0.5, adult survival = 0.8, adult fecundity = 3 juveniles/adult. Write the Leslie matrix and project the population for two time steps from an initial vector of [100 juveniles, 50 adults].

Answer (Q18, Application). Leslie matrix $A = \begin{pmatrix} 0 & 3 \\ 0.5 & 0.8 \end{pmatrix}$ (top row = fecundity, sub-diagonal = juvenile \rightarrow adult survival, adult self-loop = adult survival). Start $n(0) = (100, 50)^T$. Step 1: juveniles = $0 \cdot 100 + 3 \cdot 50 = 150$; adults = $0.5 \cdot 100 + 0.8 \cdot 50 = 50 + 40 = 90 \rightarrow (150, 90)$. Step 2: juveniles = $3 \cdot 90 = 270$; adults = $0.5 \cdot 150 + 0.8 \cdot 90 = 75 + 72 = 147 \rightarrow (270, 147)$. Total grows from 150 to 240 to 417. See section 36. 19. Source-sink metapopulation dynamics: a "source" habitat (birth rate > death rate) produces emigrants that maintain a "sink" population (death rate > birth rate). Using a specific example (e.g., wetland birds using good-quality vs poor-quality wetlands), explain: (a) why the sink population would go extinct without immigration from the source; (b) what happens if the source habitat is destroyed; (c) implications for habitat conservation priority.

Answer (Q19, Application). (a) In a sink, deaths exceed births ($\lambda < 1$), so without a continual inflow of emigrants the local population declines deterministically to extinction. (b) If the source habitat is destroyed, the emigrant subsidy stops; the sink can no longer be propped up and both subpopulations decline — overall metapopulation collapse, sometimes after a deceptive lag. (c) Apparent occupancy is misleading: a crowded sink is not a healthy population. Conservation priority should weight per-capita productivity (source status), protecting net exporters even if they hold fewer individuals, and avoiding investment in ecological-trap sinks. See section 36. 20. Climate change is shifting species' ranges poleward and upslope. Evaluate: (a) the evidence from range shift data (butterflies, birds, trees); (b) why some species cannot keep pace (dispersal limitation, habitat fragmentation); (c) how population viability analysis (PVA) is used to predict extinction risk under different warming scenarios.

Answer (Q20, Application). (a) Long-term datasets show poleward/upslope range-margin shifts averaging on the order of kilometers per decade and earlier phenology in butterflies, birds, and trees, broadly tracking isotherm movement. (b) Species lag because of limited dispersal ability, habitat fragmentation blocking movement corridors, slow life cycles (long-lived trees), and dependence on biotic partners that do not move in step. (c) PVA projects extinction probability by combining vital rates with climate-driven scenarios for habitat and demographic parameters, comparing persistence under different warming trajectories to rank management options (corridors, assisted migration). The conclusion would change if dispersal or adaptive capacity were higher than assumed. See section 36.

Questions 21–30: Synthesis and Evaluation

21. Evaluate the applicability of the logistic growth model to real populations: where does it succeed (general S-shaped growth curves in laboratory conditions) and where does it fail (time lags, environmental stochasticity, age structure, Allee effects)? Propose a more realistic model that incorporates at least two of these omitted features.

Answer (Q21, Synthesis). The logistic succeeds as a description of bounded, S-shaped growth in simple, resource-limited settings (lab cultures of yeast, *Paramecium*, flour beetles) and as a management abstraction (MSY at $K/2$). It fails when there are reproductive time lags, environmental stochasticity, age/stage structure, or Allee effects at low density — all assumed away by instantaneous, deterministic, unstructured density dependence. A more realistic model adds a delay and stochasticity, e.g. a delayed logistic with environmental noise $\frac{dN}{dt} = rN\left(1 - \frac{N(t-\tau)}{K}\right) + \sigma N \xi(t)$, or a stochastic stage-structured (Leslie/Lefkovitch) matrix with an Allee threshold. See section 36. 22. Design a long-term population monitoring program for a threatened species (e.g., African wild dog, *Lycaon pictus*). Describe: (a) the sampling methodology (camera traps, aerial surveys, genetic mark-recapture using faecal DNA); (b) the demographic parameters to estimate (λ = finite rate of increase, survival by age class, reproductive output); (c) how you would build a PVA model and define minimum viable population (MVP) size.

Answer (Q22, Synthesis). (a) Sampling: camera-trap grids and aerial/transect surveys for density, plus genetic mark-recapture from faecal DNA to identify individuals and packs without handling. (b) Parameters: finite rate of increase λ , age/stage-specific survival, reproductive output (litter size, breeding-female fraction), and dispersal among packs. (c) PVA: build a stochastic stage-structured matrix parameterized by those vital rates, add demographic and environmental stochasticity and inbreeding effects, run many simulations, and define MVP as the smallest size giving $\geq 95\%$ persistence over about 100 generations; use sensitivity/elasticity to identify the rate (typically adult survival) with greatest leverage on λ . See section 36. 23. Evaluate invasive species population dynamics: the brown tree snake (*Boiga irregularis*) invaded Guam after WWII and caused the extinction of most native forest birds. Using population ecology theory: (a) what growth model best describes the initial invasion (exponential growth in the absence of natural enemies); (b) what new carrying capacity was reached; (c) what control strategies (traps, acetaminophen-laced dead mice) have been attempted, and why are they insufficient?

Answer (Q23, Synthesis). (a) The initial invasion is near-exponential ($dN/dt = rN$): no native predators or competitors and abundant naive bird prey, so per-capita growth is unchecked. (b) Once prey were depleted and intraspecific limitation set in, the snake population settled at a new, prey-poor carrying capacity sustained on lizards, small mammals, and birds' eggs. (c) Control (live traps, hand-capture, acetaminophen-baited dead neonatal mice, detector dogs, barriers) is insufficient because the population is large, cryptic, arboreal, and reproduces faster than removal — control suppresses but cannot eradicate, so the realistic goal is interdiction to prevent spread to other islands. See section 36. 24. Evaluate the concept of “ecological traps” — habitats that appear attractive to organisms but result in reduced fitness (e.g., sea turtles attracted to coastal lights, birds nesting in mowed agricultural fields). How do ecological traps arise (evolutionary mismatch between environmental cues and habitat quality), and how might they contribute to population decline in rapidly changing environments?

Answer (Q24, Synthesis). An ecological trap arises from an evolutionary mismatch: animals evolved to use environmental cues (light, vegetation structure, openness) that reliably predicted habitat quality, but human-altered environments decouple the cue from actual fitness, so organisms preferentially settle in low-fitness habitat. Sea turtle hatchlings orient to the brightest horizon (historically the sea, now coastal lighting); birds select tall grass that is now mown mid-nesting. Traps depress population growth more than simple habitat loss because they actively draw individuals away from good habitat, and they worsen as the rate of environmental change outpaces the evolution of new cue responses. See section 36. 25. The maximum sustainable yield (MSY) of a fishery occurs at $N = K/2$ in the logistic model. Evaluate: (a) why harvesting at MSY maximizes catch; (b) why MSY is inherently unstable (small perturbations can push the population toward collapse); (c) why modern fisheries management uses precautionary approaches (reference points below MSY, no-take zones) rather than attempting to maintain stocks at MSY.

Answer (Q25, Synthesis). (a) From the logistic, dN/dt is maximized at $N = K/2$ (yield = $rK/4$), so harvesting that holds the stock at $K/2$ extracts the largest sustainable surplus production. (b) MSY is unstable because at $K/2$ the population has no buffer: any overestimate of K or r , environmental downturn, or slight over-harvest pushes N below $K/2$ where surplus production falls, so a fixed quota then accelerates decline toward collapse. (c) Modern management is therefore precautionary — target biomass above $K/2$, set harvest control rules and limit reference points below MSY, and use no-take reserves — to keep a margin against estimation error and stochasticity (cf. North Atlantic cod, 1992). See section 36. 26. Evaluate the role of demographic stochasticity vs environmental stochasticity in small population extinction risk. Using Monte Carlo simulations: (a) at what population size does demographic stochasticity dominate ($N < 50$); (b) how does environmental stochasticity affect populations of any size (droughts, disease outbreaks); (c) what does the combination of both stochastic forces imply for the “50/500 rule” in conservation genetics ($N_e > 50$ to avoid inbreeding, > 500 to maintain evolutionary potential)?

Answer (Q26, Synthesis). (a) Demographic stochasticity (chance variation in individual births/deaths and sex ratio) dominates extinction risk only in small populations, roughly $N < 50$, because random fluctuations scale relative to mean and can erase a small population by bad luck. (b) Environmental stochasticity (droughts, disease, severe weather) affects vital rates of populations of any size simultaneously and so threatens even large populations. (c) Together they justify the 50/500 rule: an effective size $N_e > 50$ buffers short-term inbreeding and demographic accidents, while $N_e > 500$ retains the additive genetic variance needed for long-term adaptive (evolutionary) response to environmental change. See section 36. 27. Human population grew exponentially from about 1 billion (1800) to about 8 billion (2024). Evaluate: (a) which technological advances removed carrying capacity limits (agriculture, medicine, energy); (b) the demographic transition model (stages I–IV) and where different countries are; (c)

whether global population will stabilize (UN WPP 2024 median projection: peak near 10.3 billion in the mid-2080s, then about 10.2 billion by 2100) or decline, and the assumptions underlying different projections.

Answer (Q27, Synthesis). (a) The Agricultural (Haber–Bosch nitrogen, mechanization, Green Revolution), medical/sanitation (vaccines, antibiotics, clean water cutting mortality), and energy (fossil fuels for food, transport, fertilizer) revolutions repeatedly raised the effective human K . (b) The demographic transition moves societies from Stage I (high birth/death), through Stage II (death falls, rapid growth), Stage III (birth falls), to Stage IV (low birth/death, near-stable) — most high-income countries are at IV/V, many low-income countries still in II/III. (c) UN WPP 2024 projects a median peak near 10.3 billion in the mid-2080s and a slight decline toward about 10.2 billion by 2100; outcomes hinge on fertility-decline assumptions — faster decline yields earlier stabilization or decline, slower decline yields continued growth. See section 36. 28. Evaluate the “landscape of fear” concept: predator presence alters prey behavior (reduced foraging time, habitat avoidance), which reduces prey population growth rate even without direct predation. Using the wolf-elk-aspen trophic cascade in Yellowstone as a case study, evaluate the evidence that wolf reintroduction changed elk behavior enough to allow aspen regeneration, and whether this qualifies as a “landscape of fear” effect or simply reduced elk density.

Answer (Q28, Synthesis). The Yellowstone wolf–elk–aspen case shows aspen recruitment improving after the 1995 wolf reintroduction. The genuine landscape of fear claim is that predation *risk* (not just predation mortality) alters elk behavior — less browsing in risky riparian zones — releasing aspen. The empirical difficulty is separating this trait-mediated (behavioral) effect from the simple density-mediated effect of fewer elk (also driven by hunting, drought, and bears). Evidence that would settle it: aspen release localized to high-risk microhabitats while elk density is statistically controlled. Current data support a contribution from fear but cannot fully isolate it from density reduction. See section 36. 29. Evaluate the mathematical basis for chaos in ecological populations: discrete-time logistic models ($N_{t+1} = rN_t(1 - N_t/K)$) with high r ($r > 2.57$) produce chaotic dynamics where population size is deterministic but unpredictable. What does chaos imply for long-term population prediction, and how can evidence of chaos be detected in real population time series (e.g., flour beetles, *Tribolium*)?

Answer (Q29, Synthesis). In the discrete logistic map $N_{t+1} = rN_t(1 - N_t/K)$, raising the growth parameter takes the dynamics through a period-doubling cascade (stable point \rightarrow 2-cycle \rightarrow 4-cycle \rightarrow ... \rightarrow chaos beyond $r \approx 3.57$ in the standard map form). Chaos means trajectories are deterministic but exhibit sensitive dependence on initial conditions, so long-term point prediction is impossible even with a perfect model. Detecting it in real series (e.g., *Tribolium* flour beetles, where it was experimentally demonstrated) requires estimating a positive Lyapunov exponent, reconstructing the attractor, and ruling out mere stochastic noise via nonlinear time-series methods. See section 36. 30. Critically evaluate the concept of “planetary boundaries” (Stockholm Resilience Center, 2009) in relation to human population ecology. Of the nine identified boundaries (climate change, biodiversity loss, nitrogen cycling, etc.), which have been transgressed, and how do population density, consumption patterns, and technology interact to determine whether human civilisation is operating within sustainable limits?

Answer (Q30, Synthesis). Planetary boundaries define a ‘safe operating space’ across nine Earth-system processes; transgression risks abrupt, large-scale change. Boundaries assessed as crossed include climate change, biosphere integrity (biodiversity/genetic loss), biogeochemical flows (nitrogen and phosphorus), land-system change, freshwater change, and novel entities. Human impact is the product of population \times per-capita consumption \times technology (the IPAT relation): affluent low-population societies can transgress boundaries through consumption, while technology can raise or lower intensity. Population ecology reframes humanity as a population whose realized impact, not headcount alone, determines whether it operates within environmental limits. See section 36.

Questions — Community Interactions and Succession

Instructor Use and Coverage Notes

- Coverage target: Predict how changing one species or resource alters community structure.
- Model/data emphasis: Lotka-Volterra-style interaction reasoning.
- Assessment alignment: Representing and Describing Data, Statistical Tests and Data Analysis, Argumentation.
- Misconception probe: A species interaction is not permanently good or bad; the sign can change with context.
- Transfer product: Transfer interaction reasoning to restoration, agriculture, and invasion biology.
- Grading focus: award full credit for mechanism, evidence, boundary conditions, and units when a calculation is required.
- Suggested use: draw one recall item, one application item, and one synthesis item when building a short quiz from this bank.

Questions 1–10: Recall and Comprehension

This activity accompanies section 37 of the textbook — review that chapter before attempting the exercises below.

1. Define a biological community. How does it differ from a population?

Answer (Q1, Recall). A biological community is all the populations of different species that live together and interact in a defined area at a given time. A population is a single species; a community is the assemblage of many interacting species (its species composition and relative abundances). The community level adds biotic interactions — competition, predation, mutualism — that do not exist within a single population. See section 37.

2. Name five types of species interactions. Give one example of each.

Answer (Q2, Recall). (1) Competition (−/−): two barnacle species for rock space. (2) Predation (+/−): lynx eating hares. (3) Herbivory (+/−): deer browsing on shrubs. (4) Mutualism (+/+): bees pollinating flowers. (5) Parasitism (+/−): tapeworm in a host gut. (Commensalism, +/0, e.g., barnacles on a whale, is a sixth.) Signs denote the per-capita fitness effect on each partner. See section 37.

3. What is interspecific competition? State the competitive exclusion principle (Gause’s law).

Answer (Q3, Recall). Interspecific competition occurs when individuals of different species use the same limiting resource, reducing each other’s growth or survival. The competitive exclusion principle (Gause’s law) states that two species competing for the *same* limiting resource cannot coexist indefinitely at constant values; the more efficient competitor drives the other to local extinction unless they partition the niche. See section 37.

4. What is a niche? Distinguish fundamental niche from realized niche.

Answer (Q4, Recall). A niche is the multidimensional set of environmental conditions and resources a species uses and the role it plays (Hutchinson’s *n*-dimensional hypervolume). The fundamental niche is the full range of conditions where a species *could* persist ($r \geq 0$) in the absence of competitors. The realized niche is the usually smaller portion it actually occupies after biotic interactions (competition, predation) restrict it. See section 37.

5. What is predation? Name two anti-predator adaptations.

Answer (Q5, Recall). Predation is an interaction in which one organism (the predator) kills and consumes another (the prey), benefiting the predator (+) and harming the prey (−). Two anti-predator adaptations: cryptic coloration / camouflage (e.g., stick insects) and chemical defense with aposematic warning coloration (e.g., poison dart frogs); others include Batesian/Müllerian mimicry, mechanical defenses, and behavioral predator avoidance. See section 37.

6. Define mutualism. Give one obligate and one facultative example.

Answer (Q6, Recall). Mutualism is a +/+ interaction in which both species gain a net fitness benefit. Obligate mutualism: neither partner can survive without the other — e.g., a lichen (fungus + alga/cyanobacterium), or the fig-fig-wasp pollination system. Facultative mutualism: beneficial but not essential — e.g., many flowering plants and generalist bee pollinators, where each can persist using alternative partners. See section 37.

7. What is a food web? How does it differ from a food chain?

Answer (Q7, Recall). A food chain is a single linear sequence of who-eats-whom (producer → primary consumer → secondary consumer → ...). A food web is the interconnected network of many overlapping food chains in a community, showing that most consumers have multiple prey and most prey have multiple predators. The web representation captures omnivory, alternative pathways, and the redundancy that buffers communities against single-link loss. See section 37.

8. What is a keystone species? Give one classic example.

Answer (Q8, Recall). A keystone species has an effect on community structure that is disproportionately large relative to its abundance or biomass; removing it causes major changes in species composition. Classic example: Paine’s (1966) sea star *Pisaster ochraceus* — removing this predator let the mussel *Mytilus californianus* monopolize the rock, collapsing intertidal diversity from about 15 species to about 8. See section 37.

9. Define ecological succession. Distinguish primary from secondary succession.

Answer (Q9, Recall). Ecological succession is the directional change in species composition of a community over time following a disturbance or on new substrate. Primary succession begins on lifeless substrate with no soil (lava flows, glacial till, new volcanic island); pioneers like lichens and mosses must first build soil, so it takes centuries. Secondary succession follows a disturbance that leaves soil and propagules intact (after fire, abandoned farmland) and proceeds much faster, in decades. See section 37.

10. What is species richness? How does it differ from species diversity (Shannon index)?

Answer (Q10, Recall). Species richness is simply the *number* of species present (S). Species diversity combines richness *and* evenness (how equally individuals are distributed among species). The Shannon index $H' = -\sum p_i \ln p_i$ rises with both more species and more even abundances; two communities with the same richness differ in H' if one is dominated by a single species while the other is even. See section 37.

Questions 11–20: Application and Analysis

11. The Lotka-Volterra competition model uses two equations: $dN_1/dt = r_1N_1(K_1 - N_1 - \alpha_{12}N_2)/K_1$ and $dN_2/dt = r_2N_2(K_2 - N_2 - \alpha_{21}N_1)/K_2$. If $K_1 = 1,000$, $K_2 = 800$, $\alpha_{12} = 0.5$, $\alpha_{21} = 1.2$, predict the outcome of competition. Under what conditions do two species coexist ($K_1/\alpha_{12} > K_2$ AND $K_2/\alpha_{21} > K_1$)?

Answer (Q11, Application). Compare each species’ carrying capacity to the other’s competitive ceiling. Species 1: persists alone at $K_1 = 1000$; species 2 invades if $K_2 > K_1/\alpha_{21} = 1000/1.2 \approx 833$ — since $K_2 = 800 < 833$, species 2 cannot invade an established species 1. Species 2: species 1 invades if $K_1 > K_2/\alpha_{12} = 800/0.5 = 1600$ — since $K_1 = 1000 < 1600$, species 1 also cannot invade an established species 2. This is the founder-controlled / unstable-equilibrium case: the outcome depends on initial densities and one species excludes the other. Stable coexistence requires $K_1 < K_2/\alpha_{12}$ and $K_2 < K_1/\alpha_{21}$ (interspecific competition weaker than intraspecific for both), which fails here. See section 37.

12. Paine’s classic experiment (1966) removed the sea star *Pisaster ochraceus* from intertidal rocks. The result was dominance by the mussel *Mytilus californianus*, which outcompeted most other sessile species. Explain: (a) why *Pisaster* is a keystone predator; (b) how its removal reduced species diversity; (c) the concept of “keystone species” and why biomass alone does not predict ecological importance.

Answer (Q12, Application). (a) *Pisaster* preferentially eats the competitively dominant mussel, preventing it from monopolizing space, so the predator controls the outcome of competition among its prey. (b) Removing *Pisaster* released *Mytilus*, which outcompeted barnacles, algae, and other sessile species for primary space; richness fell from about 15 to about 8 species. (c) A keystone species exerts community-wide control out of proportion to its biomass; abundance/biomass alone is a poor predictor of importance because a low-biomass predator can govern diversity while a high-biomass dominant may simply occupy space — the test is the magnitude of change after removal per unit biomass. See section 37.

13. Character displacement: Darwin’s finches on islands where two species coexist show greater beak size divergence than on islands where they occur alone. Explain: (a) the mechanism (sympatric competition selects for niche divergence); (b) the evidence from *Geospiza fortis* and *G. fuliginosa* beak depth distributions; (c) how this relates to niche partitioning.

Answer (Q13, Application). (a) Where two competitors are sympatric, individuals with extreme (divergent) trait values suffer less competition for shared resources, so selection drives the species’ niches — and the morphological traits that set them — apart (character displacement). (b) On islands with both *G. fortis* and *G. fuliginosa*, beak-depth distributions are shifted apart and barely overlap, whereas on single-species islands each shows an intermediate beak matching the full seed spectrum. (c) This is the evolutionary route to niche (resource) partitioning: divergent beaks let the species specialize on different seed sizes, reducing competitive overlap and permitting stable coexistence. See section 37.

14. Trophic cascades: when wolves were reintroduced to Yellowstone, elk herbivory decreased, allowing aspen and willow regeneration, which stabilized stream banks and increased beaver populations. Trace this top-down trophic cascade: wolves → elk behavior change → vegetation recovery → stream geomorphology change → beaver habitat expansion. Is this primarily a density-mediated or trait-mediated cascade?

Answer (Q14, Application). Causal chain: wolves reduce elk numbers and keep elk from lingering in risky riparian zones → less browsing on aspen, willow, cottonwood → woody vegetation recovers along streams → root systems and shade stabilize banks and lower water temperature → beaver gain food and dam-building material → beaver ponds further reshape stream geomorphology and create wetland habitat. It is a mixed cascade: a strong trait-mediated component (elk change *where and how* they forage out of fear) operating alongside a density-mediated component (fewer elk overall). See section 37.

15. Mycorrhizal networks (“wood-wide web”) connect trees underground, potentially allowing nutrient and carbon transfer between individuals. Evaluate the evidence: (a) $^{13}\text{C}/^{15}\text{N}$ labeling experiments showing carbon transfer between Douglas fir and paper birch; (b) whether transfer is mutualistic (mother trees

provisioning seedlings) or incidental (fungal self-interest); (c) the evidence from Simard’s studies and the controversy around the “mother tree” narrative.

Answer (Q15, Application). (a) Dual-isotope ($^{13}\text{C}/^{15}\text{N}$) pulse-labeling shows net carbon moving between Douglas fir and paper birch through shared ectomycorrhizal networks, with direction depending on shading and source–sink gradients. (b) The contested question is *function*: transfer may reflect adaptive ‘mother-tree’ provisioning of kin seedlings, or it may be incidental flux serving the fungus’s own carbon economy with trees as competing sinks. (c) Simard’s labeling and kin-recognition studies support directed transfer, but critics (e.g., Karst et al.) argue field evidence for fitness-relevant, adaptive provisioning is weak and the ‘mother tree’ narrative outruns the data — passive diffusion within a fungal network remains a sufficient explanation for much of the signal. See section 37.

16. Evaluate the intermediate disturbance hypothesis (IDH, Connell 1978): species diversity is maximized at intermediate disturbance frequency/intensity. Evaluate: (a) the mechanism (low disturbance → competitive exclusion; high disturbance → primarily ruderals survive); (b) empirical support from coral reef and tropical forest studies; (c) criticisms (meta-analyses showing weak or inconsistent support for IDH).

Answer (Q16, Application). (a) Mechanism: at low disturbance, superior competitors monopolize resources and exclude others; at high disturbance, only fast-colonizing ruderals tolerant of frequent destruction survive; at intermediate disturbance both competitors and colonizers coexist, peaking diversity. (b) Support: Connell’s coral-reef and tropical-forest work and many stream-invertebrate studies show humped diversity–disturbance curves. (c) Criticism: large meta-analyses (e.g., Mackey & Currie; Fox 2013) find the humped pattern is the minority outcome and IDH conflates several mechanisms; the conclusion would change if diversity responded monotonically once productivity and spatial scale are controlled. IDH is best treated as one possible pattern, not a general law. See section 37.

17. Design an experiment to test whether a suspected keystone species is truly a keystone (disproportionate effect on community structure relative to its biomass). Describe: (a) the removal experiment design; (b) what community metrics (species richness, evenness, biomass distribution) you would measure before and after removal; (c) how you would distinguish keystone effects from dominant species effects.

Answer (Q17, Application). Hypothesis: the focal species exerts community control disproportionate to its biomass. Design: replicated, randomized removal (exclusion) plots versus untouched control plots of the same habitat, with the focal species the only manipulated factor; include ‘biomass control’ plots removing an equal biomass of a non-suspect dominant. Metrics before and after: species richness, evenness/Shannon H' , relative abundance (biomass) distribution, and identity of competitive dominants, tracked over enough time for the community to respond. Decision rule: a keystone causes large structural change *per unit biomass removed*; a dominant causes change roughly proportional to its large biomass. Replication and a falsifying outcome (no divergence from controls) are required. See section 37.

18. Evaluate the “biodiversity-ecosystem function” (BEF) debate: does higher species diversity lead to greater ecosystem productivity? Cite: (a) the Cedar Creek grassland experiments (Tilman); (b) the “sampling effect” (more species → more likely to include a highly productive species) vs “complementarity effect” (niche partitioning → more complete resource use); (c) implications for conservation (“every species matters” vs “some species are redundant”).

Answer (Q18, Application). (a) Tilman’s long-term Cedar Creek grassland plots show higher plant diversity yields greater and more stable productivity and nutrient retention. (b) The sampling (selection) effect attributes this to diverse plots being more likely to *contain* a single highly productive species; the complementarity effect attributes it to niche partitioning and facilitation so resources are used more completely — long-term data and additive-partitioning analyses indicate complementarity strengthens over time. (c) Implication: redundancy provides insurance under variable conditions, so ‘some species are redundant’ holds only in a constant environment; across environments and time most species contribute, supporting broad conservation. The conclusion would change if productivity tracked only the single best species regardless of richness. See section 37.

19. Evaluate the role of facilitation (positive interactions) vs competition in structuring communities under environmental stress. The stress gradient hypothesis (SGH) predicts facilitation dominates in harsh environments and competition in benign ones. Evaluate the evidence from: (a) alpine cushion plants facilitating other species; (b) coral reef structure facilitating fish diversity; (c) exceptions where competition dominates even under stress.

Answer (Q19, Application). The stress-gradient hypothesis predicts net positive interactions (facilitation) dominate under harsh conditions and competition dominates in benign ones. (a) Alpine cushion plants ameliorate temperature, wind, and moisture, raising the richness of species sheltered beneath them — facilitation increases with elevation/stress. (b) Reef-building corals create physical structure that facilitates high fish and invertebrate diversity. (c) Exceptions: under extreme resource stress (severe drought) facilitation can collapse back to competition for the scarce resource, and strong consumer pressure can override it — so the SGH is a useful generalization whose sign depends on whether stress is resource-based or non-resource and on the trophic context. See section 37.

20. Biological invasions: invasive species can restructure entire communities. Evaluate three hypotheses for why invasive species succeed: (a) enemy release hypothesis (no predators/parasites in new range); (b) novel weapons hypothesis (allelochemicals that native species cannot tolerate); (c) empty niche hypothesis (exploiting unused resources). For each, cite one case study.

Answer (Q20, Application). (a) Enemy release: introduced species escape their coevolved predators/parasites and reallocate resources to growth/reproduction — e.g., invasive *Spartina* or purple loosestrife thriving without specialist herbivores. (b) Novel weapons: an invader deploys allelochemicals against which naive natives have no tolerance — e.g., spotted knapweed (*Centaurea*) (–)-catechin root exudates suppressing native plants. (c) Empty niche: the invader exploits resources unused by the resident community — e.g., zebra mussels filter-feeding suspended particles in the Great Lakes, a previously underused resource. Each hypothesis predicts different evidence (release from enemies, allelopathic suppression, or resource opportunity), and they can act jointly. See section 37.

Questions 21–30: Synthesis and Evaluation

21. Evaluate the concept of “ecological networks” beyond food webs: mutualistic networks (plant-pollinator, plant-seed disperser) show a nested structure where specialist species interact with a subset of the partners of generalist species. What does nestedness imply for: (a) network stability (resilience to species loss); (b) the order of species extinction under habitat loss; (c) the importance of highly connected “hub” species for network integrity?

Answer (Q21, Synthesis). Mutualistic networks are typically nested: specialists interact with subsets of the partners that generalists use, and generalists interact mostly with each other. (a) Nestedness buffers stability/robustness because specialists are ‘cushioned’ by redundant generalist partners, so random species loss is well tolerated. (b) Under habitat loss, specialists with few partners go extinct first, while generalists persist longest. (c) Highly connected hub species are critical: targeted loss of generalist hubs triggers rapid co-extinction cascades, so network robustness depends disproportionately on protecting a small set of well-connected species. See section 37.

22. Evaluate Hubbell’s Neutral Theory of Biodiversity (2001): species are ecologically equivalent, and community composition is determined by stochastic birth, death, and migration rather than niche differences. Compare neutral theory predictions with niche-based models: (a) what patterns can neutral theory explain (species-abundance distributions, species-area relationships); (b) what it cannot (functional trait differences, competitive exclusion); (c) is neutral theory “wrong but useful”?

Answer (Q22, Synthesis). (a) Hubbell’s neutral theory assumes per-capita ecological equivalence and explains community patterns from stochastic birth, death, dispersal, and speciation; it reproduces realistic species-abundance distributions and species-area relationships remarkably well. (b) It cannot account for functional-trait differences, deterministic competitive exclusion, niche partitioning, or many dynamic predictions (e.g., realistic extinction times often fail). (c) It is best regarded as ‘wrong but useful’: a powerful null model whose successful static predictions show that pattern alone cannot prove niche processes, even though species are demonstrably not equivalent. The conclusion would change if measured demographic rates showed no systematic interspecific differences. See section 37.

23. Climate change is causing phenological mismatches between interacting species (e.g., caterpillar peak occurring before oak leaf-out, but after great tit breeding initiation). Evaluate: (a) the evidence from long-term phenological datasets; (b) whether species can adapt quickly enough (evolutionary rescue vs extinction); (c) what community-level consequences emerge from cascading mismatches across multiple trophic levels.

Answer (Q23, Synthesis). (a) Long-term datasets (e.g., Wytham Wood great tits, oak–winter-moth) show interacting species advancing their phenology at different rates, opening timing gaps between consumer demand and resource peaks. (b) Whether species track the shift depends on the speed and heritability of the response: evolutionary rescue or phenotypic plasticity can realign timing for short-generation species, but slow-life-history species risk decline or local extinction. (c) Because mismatches propagate across trophic levels (plant → herbivore → predator), effects cascade: consumer recruitment falls, predator populations decline, and community-level synchrony erodes, potentially restructuring food webs even when no species is directly killed by temperature. See section 37.

24. Evaluate the concept of “alternative stable states” in ecological communities: an ecosystem can exist in multiple stable configurations (e.g., clear-water lake vs turbid-water lake), and transitions between states (regime shifts) are driven by perturbations that push the system past a tipping point. Using the shallow lake eutrophication example: (a) what drives the regime shift; (b) why is the shift often irreversible (hysteresis); (c) what early warning signals predict an approaching tipping point?

Answer (Q24, Synthesis). (a) In shallow lakes, gradual nutrient (P) loading erodes the clear, macrophyte-dominated state; a perturbation (storm, fish change) past a tipping point flips the lake to a turbid, phytoplankton-dominated state stabilized by feedbacks (turbidity shades out plants, sediment resuspension, loss of zooplankton refugia). (b) The shift shows hysteresis: because the alternative state is self-reinforcing, simply lowering nutrients back to the original level does *not* restore clear water — recovery requires a much larger reduction or active intervention (biomanipulation). (c) Early-warning signals of an approaching tipping point include critical slowing down — rising temporal autocorrelation and variance, and slower recovery from small perturbations (flickering). See section 37.

25. Critically evaluate the use of ecological network analysis for predicting the cascading effects of species extinction. Using simulated extinction sequences (removing species from most to least connected): (a) how do co-extinction cascades propagate through food webs; (b) why do mutualistic networks (plant-pollinator) collapse more rapidly than antagonistic networks (predator-prey) under targeted extinction; (c) what does this imply for setting conservation

priorities in species-rich ecosystems?

Answer (Q25, Synthesis). (a) Removing species and tracking secondary (co-)extinctions shows cascades propagate fastest when highly connected species are lost, because many partners depend on them; loss of basal/hub species triggers the largest collapses. (b) Mutualistic networks collapse faster under targeted removal than antagonistic ones because mutualism lacks the compensatory dynamics of predator–prey systems (no prey release; partners cannot substitute a lost obligate mutualist), so dependent specialists are lost rapidly. (c) Implication: in species-rich systems, conservation should prioritize topologically central / highly connected species and the interactions themselves, not just rare or charismatic species — but model assumptions (static topology, fixed dependencies) limit precision and would change predictions if rewiring is possible. See section 37.

26. Island biogeography theory (MacArthur and Wilson, 1967): species richness on an island results from a balance between immigration (decreasing with distance from mainland) and extinction (increasing with island size decrease). Apply this to habitat islands: predict species richness on forest fragments of 1 ha, 10 ha, and 1,000 ha that are 5 km from a large continuous forest. What does the “species-area relationship” ($S = cA^z$) predict?

Answer (Q26, Synthesis). Island/MacArthur–Wilson theory: richness equilibrates where the immigration rate (falls with isolation) equals the extinction rate (rises as area shrinks); the species–area relationship $S = cA^z$ summarizes the area effect, with $z \approx 0.25$ for habitat islands. Holding c and z constant, going from 1 ha to 10 ha multiplies S by $10^{0.25} \approx 1.78$, and $1 \rightarrow 1000$ ha by $1000^{0.25} \approx 5.6$. So a 1000 ha fragment supports roughly 5–6× the species of a 1 ha fragment; the 5 km isolation lowers all values equally by depressing immigration. The practical lesson: a few large fragments retain far more species than many tiny ones of equal total area. See section 37.

27. Herbivore-plant coevolution has produced elaborate chemical defense systems. The milkweed (*Asclepias*) – monarch butterfly (*Danaus plexippus*) system illustrates escalation: (a) milkweed produces cardenolides (toxic Na^+/K^+ -ATPase inhibitors); (b) monarch larvae sequester cardenolides for their own defense; (c) monarch Na^+/K^+ -ATPase has evolved resistance mutations. Trace this coevolutionary arms race.

Answer (Q27, Synthesis). Coevolutionary arms race (reciprocal selection): (1) milkweed evolves cardenolides, cardiac glycosides that block the Na^+/K^+ -ATPase of herbivores; (2) this selects monarch larvae that tolerate and sequester the toxins, gaining their own chemical defense against birds (aposematism); (3) sequestration is enabled by target-site insensitivity — amino-acid substitutions in the monarch’s Na^+/K^+ -ATPase that confer resistance; (4) milkweeds with higher or novel cardenolide profiles are then favored, escalating the cycle. The result is reciprocal adaptation and a diffuse coevolutionary escalation between defense and counter-defense. See section 37.

28. Primary succession on volcanic islands (e.g., Surtsey, Iceland, formed 1963): pioneer species (lichens, mosses) → grasses → shrubs → woodland. Explain the facilitation model: how do early colonisers modify the environment (soil formation, nitrogen fixation) to enable later successional stages?

Answer (Q28, Synthesis). In the facilitation model, early colonizers make conditions less extreme and enable later species. On bare volcanic rock, lichens and mosses weather the substrate and trap organic matter, building the first soil; nitrogen-fixing pioneers (e.g., legumes, *Frankia*- or cyanobacteria-associated plants) add fixed nitrogen to the otherwise N-poor surface; accumulating soil, moisture retention, and nutrients then allow grasses, then shrubs, then trees to establish. Each stage modifies the environment in ways that favor the next — and often makes conditions worse for the pioneers themselves. See section 37.

29. Calculate the Shannon diversity index ($H' = -\sum p_i \ln p_i$) for a community with 4 species at proportions: 0.50, 0.25, 0.15, 0.10. Then calculate for a community with 4 species at equal proportions (0.25 each). Which community is more diverse? What does evenness contribute to diversity?

Answer (Q29, Synthesis). $H' = -\sum p_i \ln p_i$. Community A (0.50, 0.25, 0.15, 0.10): $-(0.50 \ln 0.50 + 0.25 \ln 0.25 + 0.15 \ln 0.15 + 0.10 \ln 0.10) = -(-0.347 - 0.347 - 0.285 - 0.230) \approx 1.21$. Community B (0.25 each): $-4(0.25 \ln 0.25) = -4(-0.347) = 1.39 (= \ln 4, \text{ the maximum for 4 species})$. Community B is more diverse even though both have richness $S = 4$, because it is perfectly even. Evenness raises diversity: for a fixed number of species, H' is maximized when all species are equally abundant and minimized when one species dominates. See section 37.

30. Parasitoids (e.g., parasitoid wasps) lay eggs inside or on host insects; the larva consumes the host from inside. Compare parasitoid-host dynamics to classical predator-prey dynamics: (a) why parasitoid search efficiency matters (Nicholson-Bailey model); (b) why parasitoid-host systems tend toward unstable oscillations in simple models; (c) what stabilizing mechanisms exist in nature (spatial refugia, host immunity).

Answer (Q30, Synthesis). (a) In the Nicholson–Bailey model, the fraction of hosts escaping parasitism depends on parasitoid search efficiency (attack rate a) and parasitoid density; each parasitized host yields the next parasitoid generation, tightly coupling the two. (b) Because reproduction is discrete and perfectly density-dependent with a built-in time lag (one host generation), the simple model is inherently unstable — it produces diverging oscillations leading to extinction of one or both. (c) Real systems persist via stabilizing mechanisms: spatial heterogeneity and host refugia (a protected fraction of hosts), aggregated parasitoid attack, host density dependence, host immune defenses, and parasitoid interference — all of which add negative feedback that damps the oscillations. See section 37.

Questions — Biodiversity and Food Webs

Instructor Use and Coverage Notes

- Coverage target: Calculate a diversity or species-area metric and interpret its ecological meaning.
- Model/data emphasis: Shannon, species-area, and network connectance reasoning.
- Assessment alignment: Representing and Describing Data, Statistical Tests and Data Analysis, Argumentation.
- Misconception probe: Richness alone does not equal functional stability.
- Transfer product: Transfer biodiversity reasoning to conservation planning and habitat fragmentation.
- Grading focus: award full credit for mechanism, evidence, boundary conditions, and units when a calculation is required.
- Suggested use: draw one recall item, one application item, and one synthesis item when building a short quiz from this bank.

Questions 1–10: Recall and Comprehension

This activity accompanies section 38 of the textbook — review that chapter before attempting the exercises below.

1. Island biogeography theory (MacArthur and Wilson, 1967): species richness on an island results from a balance between immigration (decreasing with distance from mainland) and extinction (increasing with island size decrease). Apply this to habitat islands: predict species richness on forest fragments of 1 ha, 10 ha, and 1,000 ha that are 5 km from a large continuous forest. What does the “species-area relationship” ($S = cA^z$) predict?

Answer (Q1, Recall). Island/MacArthur–Wilson theory: richness equilibrates where the immigration rate (falls with isolation) equals the extinction rate (rises as area shrinks); the species–area relationship $S = cA^z$ summarizes the area effect, with $z \approx 0.25$ for habitat islands. Holding c and z constant, going from 1 ha to 10 ha multiplies S by $10^{0.25} \approx 1.78$, and $1 \rightarrow 1000$ ha by $1000^{0.25} \approx 5.6$. So a 1000 ha fragment supports roughly 5–6× the species of a 1 ha fragment; the 5 km isolation lowers all values equally by depressing immigration. The practical lesson: a few large fragments retain far more species than many tiny ones of equal total area. See section 38.

2. Herbivore-plant coevolution has produced elaborate chemical defense systems. The milkweed (*Asclepias*) – monarch butterfly (*Danaus plexippus*) system illustrates escalation: (a) milkweed produces cardenolides (toxic Na^+/K^+ -ATPase inhibitors); (b) monarch larvae sequester cardenolides for their own defense; (c) monarch Na^+/K^+ -ATPase has evolved resistance mutations. Trace this coevolutionary arms race.

Answer (Q2, Recall). Coevolutionary arms race (reciprocal selection): (1) milkweed evolves cardenolides, cardiac glycosides that block the Na^+/K^+ -ATPase of herbivores; (2) this selects monarch larvae that tolerate and sequester the toxins, gaining their own chemical defense against birds (aposematism); (3) sequestration is enabled by target-site insensitivity — amino-acid substitutions in the monarch’s Na^+/K^+ -ATPase that confer resistance; (4) milkweeds with higher or novel cardenolide profiles are then favored, escalating the cycle. The result is reciprocal adaptation and a diffuse co-evolutionary escalation between defense and counter-defense. See section 38.

3. Primary succession on volcanic islands (e.g., Surtsey, Iceland, formed 1963): pioneer species (lichens, mosses) → grasses → shrubs → woodland. Explain the facilitation model: how do early colonisers modify the environment (soil formation, nitrogen fixation) to enable later successional stages?

Answer (Q3, Recall). In the facilitation model, early colonizers make conditions less extreme and enable later species. On bare volcanic rock, lichens and mosses weather the substrate and trap organic matter, building the first soil; nitrogen-fixing pioneers (e.g., legumes, *Frankia*- or cyanobacteria-associated plants) add fixed nitrogen to the otherwise N-poor surface; accumulating soil, moisture retention, and nutrients then allow grasses, then shrubs, then trees to establish. Each stage modifies the environment in ways that favor the next — and often makes conditions worse for the pioneers themselves. See section 38.

4. Calculate the Shannon diversity index ($H' = -\sum p_i \ln p_i$) for a community with 4 species at proportions: 0.50, 0.25, 0.15, 0.10. Then calculate for a community with 4 species at equal proportions (0.25 each). Which community is more diverse? What does evenness contribute to diversity?

Answer (Q4, Recall). $H' = -\sum p_i \ln p_i$. Community A (0.50, 0.25, 0.15, 0.10): $-(0.50 \ln 0.50 + 0.25 \ln 0.25 + 0.15 \ln 0.15 + 0.10 \ln 0.10) = -(-0.347 - 0.347 - 0.285 - 0.230) \approx 1.21$. Community B (0.25 each): $-4(0.25 \ln 0.25) = -4(-0.347) = 1.39$ ($= \ln 4$, the maximum for 4 species). Community B is more diverse even though both have richness $S = 4$, because it is perfectly even. Evenness raises diversity: for a fixed number of species, H' is maximized when all species are equally abundant and minimized when one species dominates. See section 38.

5. Parasitoids (e.g., parasitoid wasps) lay eggs inside or on host insects; the larva consumes the host from inside. Compare parasitoid-host dynamics to classical predator-prey dynamics: (a) why parasitoid search efficiency matters (Nicholson-Bailey model); (b) why parasitoid-host systems tend toward unstable oscillations in simple models; (c) what stabilizing mechanisms exist in nature (spatial refugia, host immunity).

Answer (Q5, Recall). (a) In the Nicholson–Bailey model, the fraction of hosts escaping parasitism depends on parasitoid search efficiency (attack rate a) and parasitoid density; each parasitized host yields the next parasitoid generation, tightly coupling the two. (b) Because reproduction is discrete and perfectly density-dependent with a built-in time lag (one host generation), the simple model is inherently unstable — it produces

diverging oscillations leading to extinction of one or both. (c) Real systems persist via stabilizing mechanisms: spatial heterogeneity and host refugia (a protected fraction of hosts), aggregated parasitoid attack, host density dependence, host immune defenses, and parasitoid interference — all of which add negative feedback that damps the oscillations. See section 38.

6. Evaluate the intermediate disturbance hypothesis (IDH, Connell 1978): species diversity is maximized at intermediate disturbance frequency/intensity. Evaluate: (a) the mechanism (low disturbance → competitive exclusion; high disturbance → primarily ruderals survive); (b) empirical support from coral reef and tropical forest studies; (c) criticisms (meta-analyses showing weak or inconsistent support for IDH).

Answer (Q6, Recall). (a) Mechanism: at low disturbance, superior competitors monopolize resources and exclude others; at high disturbance, only fast-colonizing ruderals tolerant of frequent destruction survive; at intermediate disturbance both competitors and colonizers coexist, peaking diversity. (b) Support: Connell’s coral-reef and tropical-forest work and many stream-invertebrate studies show humped diversity–disturbance curves. (c) Criticism: large meta-analyses (e.g., Mackey & Currie; Fox 2013) find the humped pattern is the minority outcome and IDH conflates several mechanisms; the conclusion would change if diversity responded monotonically once productivity and spatial scale are controlled. IDH is best treated as one possible pattern, not a general law. See section 38.

7. Design an experiment to test whether a suspected keystone species is truly a keystone (disproportionate effect on community structure relative to its biomass). Describe: (a) the removal experiment design; (b) what community metrics (species richness, evenness, biomass distribution) you would measure before and after removal; (c) how you would distinguish keystone effects from dominant species effects.

Answer (Q7, Recall). Hypothesis: the focal species exerts community control disproportionate to its biomass. Design: replicated, randomized removal (exclusion) plots versus untouched control plots of the same habitat, with the focal species the only manipulated factor; include ‘biomass control’ plots removing an equal biomass of a non-suspect dominant. Metrics before and after: species richness, evenness/Shannon H' , relative abundance (biomass) distribution, and identity of competitive dominants, tracked over enough time for the community to respond. Decision rule: a keystone causes large structural change *per unit biomass removed*; a dominant causes change roughly proportional to its large biomass. Replication and a falsifying outcome (no divergence from controls) are required. See section 38.

8. Evaluate the “biodiversity-ecosystem function” (BEF) debate: does higher species diversity lead to greater ecosystem productivity? Cite: (a) the Cedar Creek grassland experiments (Tilman); (b) the “sampling effect” (more species → more likely to include a highly productive species) vs “complementarity effect” (niche partitioning → more complete resource use); (c) implications for conservation (“every species matters” vs “some species are redundant”).

Answer (Q8, Recall). (a) Tilman’s long-term Cedar Creek grassland plots show higher plant diversity yields greater and more stable productivity and nutrient retention. (b) The sampling (selection) effect attributes this to diverse plots being more likely to *contain* a single highly productive species; the complementarity effect attributes it to niche partitioning and facilitation so resources are used more completely — long-term data and additive-partitioning analyses indicate complementarity strengthens over time. (c) Implication: redundancy provides insurance under variable conditions, so ‘some species are redundant’ holds only in a constant environment; across environments and time most species contribute, supporting broad conservation. The conclusion would change if productivity tracked only the single best species regardless of richness. See section 38.

9. Evaluate the role of facilitation (positive interactions) vs competition in structuring communities under environmental stress. The stress gradient hypothesis (SGH) predicts facilitation dominates in harsh environments and competition in benign ones. Evaluate the evidence from: (a) alpine cushion plants facilitating other species; (b) coral reef structure facilitating fish diversity; (c) exceptions where competition dominates even under stress.

Answer (Q9, Recall). The stress-gradient hypothesis predicts net positive interactions (facilitation) dominate under harsh conditions and competition dominates in benign ones. (a) Alpine cushion plants ameliorate temperature, wind, and moisture, raising the richness of species sheltered beneath them — facilitation increases with elevation/stress. (b) Reef-building corals create physical structure that facilitates high fish and invertebrate diversity. (c) Exceptions: under extreme resource stress (severe drought) facilitation can collapse back to competition for the scarce resource, and strong consumer pressure can override it — so the SGH is a useful generalization whose sign depends on whether stress is resource-based or non-resource and on the trophic context. See section 38.

10. Biological invasions: invasive species can restructure entire communities. Evaluate three hypotheses for why invasive species succeed: (a) enemy release hypothesis (no predators/parasites in new range); (b) novel weapons hypothesis (allelochemicals that native species cannot tolerate); (c) empty niche hypothesis (exploiting unused resources). For each, cite one case study.

Answer (Q10, Recall). (a) Enemy release: introduced species escape their coevolved predators/parasites and reallocate resources to growth/reproduction — e.g., invasive *Spartina* or purple loosestrife thriving without specialist herbivores. (b) Novel weapons: an invader deploys allelochemicals against which naive natives have no tolerance — e.g., spotted knapweed (*Centaurea*) (–)-catechin root exudates suppressing native plants. (c) Empty niche: the invader exploits resources unused by the resident community — e.g., zebra mussels filter-feeding suspended particles in the Great Lakes, a previously underused resource. Each hypothesis predicts different evidence (release from enemies, allelopathic suppression,

or resource opportunity), and they can act jointly. See section 38.

Questions 11–20: Application and Analysis

11. Evaluate the concept of “ecological networks” beyond food webs: mutualistic networks (plant-pollinator, plant-seed disperser) show a nested structure where specialist species interact with a subset of the partners of generalist species. What does nestedness imply for: (a) network stability (resilience to species loss); (b) the order of species extinction under habitat loss; (c) the importance of highly connected “hub” species for network integrity?

Answer (Q11, Application). Mutualistic networks are typically nested: specialists interact with subsets of the partners that generalists use, and generalists interact mostly with each other. (a) Nestedness buffers stability/robustness because specialists are ‘cushioned’ by redundant generalist partners, so random species loss is well tolerated. (b) Under habitat loss, specialists with few partners go extinct first, while generalists persist longest. (c) Highly connected hub species are critical: targeted loss of generalist hubs triggers rapid co-extinction cascades, so network robustness depends disproportionately on protecting a small set of well-connected species. See section 38.

12. Evaluate Hubbell’s Neutral Theory of Biodiversity (2001): species are ecologically equivalent, and community composition is determined by stochastic birth, death, and migration rather than niche differences. Compare neutral theory predictions with niche-based models: (a) what patterns can neutral theory explain (species-abundance distributions, species-area relationships); (b) what it cannot (functional trait differences, competitive exclusion); (c) is neutral theory “wrong but useful”?

Answer (Q12, Application). (a) Hubbell’s neutral theory assumes per-capita ecological equivalence and explains community patterns from stochastic birth, death, dispersal, and speciation; it reproduces realistic species-abundance distributions and species-area relationships remarkably well. (b) It cannot account for functional-trait differences, deterministic competitive exclusion, niche partitioning, or many dynamic predictions (e.g., realistic extinction times often fail). (c) It is best regarded as ‘wrong but useful’: a powerful null model whose successful static predictions show that pattern alone cannot prove niche processes, even though species are demonstrably not equivalent. The conclusion would change if measured demographic rates showed no systematic interspecific differences. See section 38.

13. Climate change is causing phenological mismatches between interacting species (e.g., caterpillar peak occurring before oak leaf-out, but after great tit breeding initiation). Evaluate: (a) the evidence from long-term phenological datasets; (b) whether species can adapt quickly enough (evolutionary rescue vs extinction); (c) what community-level consequences emerge from cascading mismatches across multiple trophic levels.

Answer (Q13, Application). (a) Long-term datasets (e.g., Wytham Wood great tits, oak–winter-moth) show interacting species advancing their phenology at different rates, opening timing gaps between consumer demand and resource peaks. (b) Whether species track the shift depends on the speed and heritability of the response: evolutionary rescue or phenotypic plasticity can realign timing for short-generation species, but slow-life-history species risk decline or local extinction. (c) Because mismatches propagate across trophic levels (plant → herbivore → predator), effects cascade: consumer recruitment falls, predator populations decline, and community-level synchrony erodes, potentially restructuring food webs even when no species is directly killed by temperature. See section 38.

14. Evaluate the concept of “alternative stable states” in ecological communities: an ecosystem can exist in multiple stable configurations (e.g., clear-water lake vs turbid-water lake), and transitions between states (regime shifts) are driven by perturbations that push the system past a tipping point. Using the shallow lake eutrophication example: (a) what drives the regime shift; (b) why is the shift often irreversible (hysteresis); (c) what early warning signals predict an approaching tipping point?

Answer (Q14, Application). (a) In shallow lakes, gradual nutrient (P) loading erodes the clear, macrophyte-dominated state; a perturbation (storm, fish change) past a tipping point flips the lake to a turbid, phytoplankton-dominated state stabilized by feedbacks (turbidity shades out plants, sediment resuspension, loss of zooplankton refugia). (b) The shift shows hysteresis: because the alternative state is self-reinforcing, simply lowering nutrients back to the original level does *not* restore clear water — recovery requires a much larger reduction or active intervention (biomanipulation). (c) Early-warning signals of an approaching tipping point include critical slowing down — rising temporal autocorrelation and variance, and slower recovery from small perturbations (flickering). See section 38.

15. Critically evaluate the use of ecological network analysis for predicting the cascading effects of species extinction. Using simulated extinction sequences (removing species from most to least connected): (a) how do co-extinction cascades propagate through food webs; (b) why do mutualistic networks (plant-pollinator) collapse more rapidly than antagonistic networks (predator-prey) under targeted extinction; (c) what does this imply for setting conservation priorities in species-rich ecosystems?

Answer (Q15, Application). (a) Removing species and tracking secondary (co-)extinctions shows cascades propagate fastest when highly connected species are lost, because many partners depend on them; loss of basal/hub species triggers the largest collapses. (b) Mutualistic networks collapse faster under targeted removal than antagonistic ones because mutualism lacks the compensatory dynamics of predator–prey systems (no prey release; partners cannot substitute a lost obligate mutualist), so dependent specialists are lost rapidly. (c) Implication: in species-rich systems,

conservation should prioritize topologically central / highly connected species and the interactions themselves, not just rare or charismatic species — but model assumptions (static topology, fixed dependencies) limit precision and would change predictions if rewiring is possible. See section 38.

16. Define a biological community. How does it differ from a population?

Answer (Q16, Application). A biological community is all the populations of different species that live together and interact in a defined area at a given time. A population is a single species; a community is the assemblage of many interacting species (its species composition and relative abundances). The community level adds biotic interactions — competition, predation, mutualism — that do not exist within a single population. See section 38.

17. Name five types of species interactions. Give one example of each.

Answer (Q17, Application). (1) Competition (−/−): two barnacle species for rock space. (2) Predation (+/−): lynx eating hares. (3) Herbivory (+/−): deer browsing on shrubs. (4) Mutualism (+/+): bees pollinating flowers. (5) Parasitism (+/−): tapeworm in a host gut. (Commensalism, +/0, e.g., barnacles on a whale, is a sixth.) Signs denote the per-capita fitness effect on each partner. See section 38.

18. What is interspecific competition? State the competitive exclusion principle (Gause’s law).

Answer (Q18, Application). Interspecific competition occurs when individuals of different species use the same limiting resource, reducing each other’s growth or survival. The competitive exclusion principle (Gause’s law) states that two species competing for the *same* limiting resource cannot coexist indefinitely at constant values; the more efficient competitor drives the other to local extinction unless they partition the niche. See section 38.

19. What is a niche? Distinguish fundamental niche from realized niche.

Answer (Q19, Application). A niche is the multidimensional set of environmental conditions and resources a species uses and the role it plays (Hutchinson’s *n*-dimensional hypervolume). The fundamental niche is the full range of conditions where a species *could* persist ($r \geq 0$) in the absence of competitors. The realized niche is the usually smaller portion it actually occupies after biotic interactions (competition, predation) restrict it. See section 38.

20. What is predation? Name two anti-predator adaptations.

Answer (Q20, Application). Predation is an interaction in which one organism (the predator) kills and consumes another (the prey), benefiting the predator (+) and harming the prey (−). Two anti-predator adaptations: cryptic coloration / camouflage (e.g., stick insects) and chemical defense with aposematic warning coloration (e.g., poison dart frogs); others include Batesian/Müllerian mimicry, mechanical defenses, and behavioral predator avoidance. See section 38.

Questions 21–30: Synthesis and Evaluation

21. Define mutualism. Give one obligate and one facultative example.

Answer (Q21, Synthesis). Mutualism is a +/+ interaction in which both species gain a net fitness benefit. Obligate mutualism: neither partner can survive without the other — e.g., a lichen (fungus + alga/cyanobacterium), or the fig–fig-wasp pollination system. Facultative mutualism: beneficial but not essential — e.g., many flowering plants and generalist bee pollinators, where each can persist using alternative partners. See section 38.

22. What is a food web? How does it differ from a food chain?

Answer (Q22, Synthesis). A food chain is a single linear sequence of who-eats-whom (producer → primary consumer → secondary consumer → ...). A food web is the interconnected network of many overlapping food chains in a community, showing that most consumers have multiple prey and most prey have multiple predators. The web representation captures omnivory, alternative pathways, and the redundancy that buffers communities against single-link loss. See section 38.

23. What is a keystone species? Give one classic example.

Answer (Q23, Synthesis). A keystone species has an effect on community structure that is disproportionately large relative to its abundance or biomass; removing it causes major changes in species composition. Classic example: Paine’s (1966) sea star *Pisaster ochraceus* — removing this predator let the mussel *Mytilus californianus* monopolize the rock, collapsing intertidal diversity from about 15 species to about 8. See section 38.

24. Define ecological succession. Distinguish primary from secondary succession.

Answer (Q24, Synthesis). Ecological succession is the directional change in species composition of a community over time following a disturbance or on new substrate. Primary succession begins on lifeless substrate with no soil (lava flows, glacial till, new volcanic island); pioneers like lichens

and mosses must first build soil, so it takes centuries. Secondary succession follows a disturbance that leaves soil and propagules intact (after fire, abandoned farmland) and proceeds much faster, in decades. See section 38.

25. What is species richness? How does it differ from species diversity (Shannon index)?

Answer (Q25, Synthesis). Species richness is simply the *number* of species present (S). Species diversity combines richness *and* evenness (how equally individuals are distributed among species). The Shannon index $H' = -\sum p_i \ln p_i$ rises with both more species and more even abundances; two communities with the same richness differ in H' if one is dominated by a single species while the other is even. See section 38.

26. The Lotka-Volterra competition model uses two equations: $dN_1/dt = r_1 N_1 (K_1 - N_1 - \alpha_{12} N_2)/K_1$ and $dN_2/dt = r_2 N_2 (K_2 - N_2 - \alpha_{21} N_1)/K_2$. If $K_1 = 1,000$, $K_2 = 800$, $\alpha_{12} = 0.5$, $\alpha_{21} = 1.2$, predict the outcome of competition. Under what conditions do two species coexist ($K_1/\alpha_{12} > K_2$ AND $K_2/\alpha_{21} > K_1$)?

Answer (Q26, Synthesis). Compare each species' carrying capacity to the other's competitive ceiling. Species 1: persists alone at $K_1 = 1000$; species 2 invades if $K_2 > K_1/\alpha_{21} = 1000/1.2 \approx 833$ — since $K_2 = 800 < 833$, species 2 cannot invade an established species 1. Species 2: species 1 invades if $K_1 > K_2/\alpha_{12} = 800/0.5 = 1600$ — since $K_1 = 1000 < 1600$, species 1 also cannot invade an established species 2. This is the founder-controlled / unstable-equilibrium case: the outcome depends on initial densities and one species excludes the other. Stable coexistence requires $K_1 < K_2/\alpha_{12}$ and $K_2 < K_1/\alpha_{21}$ (interspecific competition weaker than intraspecific for both), which fails here. See section 38.

27. Paine's classic experiment (1966) removed the sea star *Pisaster ochraceus* from intertidal rocks. The result was dominance by the mussel *Mytilus californianus*, which outcompeted most other sessile species. Explain: (a) why *Pisaster* is a keystone predator; (b) how its removal reduced species diversity; (c) the concept of "keystone species" and why biomass alone does not predict ecological importance.

Answer (Q27, Synthesis). (a) *Pisaster* preferentially eats the competitively dominant mussel, preventing it from monopolizing space, so the predator controls the outcome of competition among its prey. (b) Removing *Pisaster* released *Mytilus*, which outcompeted barnacles, algae, and other sessile species for primary space; richness fell from about 15 to about 8 species. (c) A keystone species exerts community-wide control out of proportion to its biomass; abundance/biomass alone is a poor predictor of importance because a low-biomass predator can govern diversity while a high-biomass dominant may simply occupy space — the test is the magnitude of change after removal per unit biomass. See section 38.

28. Character displacement: Darwin's finches on islands where two species coexist show greater beak size divergence than on islands where they occur alone. Explain: (a) the mechanism (sympatric competition selects for niche divergence); (b) the evidence from *Geospiza fortis* and *G. fuliginosa* beak depth distributions; (c) how this relates to niche partitioning.

Answer (Q28, Synthesis). (a) Where two competitors are sympatric, individuals with extreme (divergent) trait values suffer less competition for shared resources, so selection drives the species' niches — and the morphological traits that set them — apart (character displacement). (b) On islands with both *G. fortis* and *G. fuliginosa*, beak-depth distributions are shifted apart and barely overlap, whereas on single-species islands each shows an intermediate beak matching the full seed spectrum. (c) This is the evolutionary route to niche (resource) partitioning: divergent beaks let the species specialize on different seed sizes, reducing competitive overlap and permitting stable coexistence. See section 38.

29. Trophic cascades: when wolves were reintroduced to Yellowstone, elk herbivory decreased, allowing aspen and willow regeneration, which stabilized stream banks and increased beaver populations. Trace this top-down trophic cascade: wolves → elk behavior change → vegetation recovery → stream geomorphology change → beaver habitat expansion. Is this primarily a density-mediated or trait-mediated cascade?

Answer (Q29, Synthesis). Causal chain: wolves reduce elk numbers and keep elk from lingering in risky riparian zones → less browsing on aspen, willow, cottonwood → woody vegetation recovers along streams → root systems and shade stabilize banks and lower water temperature → beaver gain food and dam-building material → beaver ponds further reshape stream geomorphology and create wetland habitat. It is a mixed cascade: a strong trait-mediated component (elk change *where and how* they forage out of fear) operating alongside a density-mediated component (fewer elk overall). See section 38.

30. Mycorrhizal networks ("wood-wide web") connect trees underground, potentially allowing nutrient and carbon transfer between individuals. Evaluate the evidence: (a) $^{13}\text{C}/^{15}\text{N}$ labeling experiments showing carbon transfer between Douglas fir and paper birch; (b) whether transfer is mutualistic (mother trees provisioning seedlings) or incidental (fungal self-interest); (c) the evidence from Simard's studies and the controversy around the "mother tree" narrative.

Answer (Q30, Synthesis). (a) Dual-isotope ($^{13}\text{C}/^{15}\text{N}$) pulse-labeling shows net carbon moving between Douglas fir and paper birch through shared ectomycorrhizal networks, with direction depending on shading and source-sink gradients. (b) The contested question is *function*: transfer may reflect adaptive 'mother-tree' provisioning of kin seedlings, or it may be incidental flux serving the fungus's own carbon economy with trees as competing sinks. (c) Simard's labeling and kin-recognition studies support directed transfer, but critics (e.g., Karst et al.) argue field evidence for fitness-relevant, adaptive provisioning is weak and the 'mother tree' narrative outruns the data — passive diffusion within a fungal network remains a sufficient explanation for much of the signal. See section 38.

Questions — Ecosystem Ecology

Instructor Use and Coverage Notes

- Coverage target: Calculate a flux or efficiency and explain which pool or process limits the system.
- Model/data emphasis: Energy-flow, productivity, and nutrient-budget calculations.
- Assessment alignment: Representing and Describing Data, Statistical Tests and Data Analysis, Argumentation.
- Misconception probe: Energy flows through ecosystems, but matter cycles; confusing the two breaks many explanations.
- Transfer product: Transfer ecosystem reasoning to eutrophication, carbon budgets, agriculture, and climate feedback.
- Grading focus: award full credit for mechanism, evidence, boundary conditions, and units when a calculation is required.
- Suggested use: draw one recall item, one application item, and one synthesis item when building a short quiz from this bank.

Questions 1–10: Recall and Comprehension

This activity accompanies section 39 of the textbook — review that chapter before attempting the exercises below.

1. Define an ecosystem. What are its biotic and abiotic components?

Answer (Q1, Recall). An ecosystem is a community of organisms together with the physical and chemical environment they interact with, linked by energy flow and nutrient cycling. Biotic components are the living parts: producers (autotrophs), consumers (herbivores, carnivores, omnivores), and decomposers. Abiotic components are nonliving factors: sunlight, temperature, water, air (CO₂, O₂), inorganic nutrients (N, P), and soil. See section 39. 2. What is primary productivity? Distinguish GPP, NPP, and NEP.

Answer (Q2, Recall). Primary productivity is the rate at which autotrophs fix energy into organic matter. GPP (gross primary production) is total carbon fixed by photosynthesis. NPP is GPP minus autotroph respiration ($NPP = GPP - R_a$), the energy available to consumers. NEP (net ecosystem production) is NPP minus heterotroph respiration; $NEP > 0$ means the ecosystem is a net carbon sink. See section 39. 3. What is a trophic level? Name four trophic levels in a food chain.

Answer (Q3, Recall). A trophic level is a feeding position defined by the number of energy-transfer steps from the energy source. Four levels: producers (autotrophs, grass), primary consumers (herbivores, grasshopper), secondary consumers (carnivores, shrew), tertiary consumers (top carnivores, hawk). Decomposers process dead matter from every level. See section 39. 4. What is ecological efficiency? What is the typical transfer efficiency between trophic levels?

Answer (Q4, Recall). Ecological (trophic transfer) efficiency is the percentage of energy at one trophic level incorporated into biomass at the next. The typical value is about 10 percent (Lindeman’s ten-percent rule); the rest is lost to respiration, egestion, or goes unconsumed. Because efficiency compounds across levels, food chains are short and top-predator biomass is small. See section 39. 5. Define the carbon cycle. Name the major carbon reservoirs on Earth.

Answer (Q5, Recall). The carbon cycle is the global movement of carbon among reservoirs via photosynthesis, respiration, decomposition, combustion, and ocean exchange. Major reservoirs: the atmosphere (CO₂, CH₄), the oceans (largest active reservoir, dissolved inorganic carbon), terrestrial biomass and soils, and the very large slow-turnover sedimentary rocks and fossil fuels. See section 39. 6. What is the nitrogen cycle? Name the four major transformations.

Answer (Q6, Recall). The nitrogen cycle moves N among atmospheric N₂, organic N, and inorganic forms. Four major microbial transformations: nitrogen fixation (N₂ to ammonium, by Rhizobium, cyanobacteria, industrially Haber-Bosch); ammonification (organic N to ammonium by decomposers); nitrification (ammonium to nitrite to nitrate); and denitrification (nitrate to N₂ returned to the atmosphere under anoxic conditions). See section 39. 7. What is the phosphorus cycle? How does it differ from the nitrogen and carbon cycles?

Answer (Q7, Recall). The phosphorus cycle moves P from rock weathering into soil and water (as phosphate), through organisms, and back to sediments. Unlike the N and C cycles it has no significant atmospheric (gaseous) phase: it is a purely sedimentary cycle driven by slow weathering and burial, so P is often the limiting nutrient and cannot be replenished from the air. See section 39. 8. What is the water cycle (hydrological cycle)? Name the major fluxes.

Answer (Q8, Recall). The hydrological cycle is the continuous global movement of water among atmosphere, land, and oceans driven by solar energy and gravity. Major fluxes: evaporation, plant transpiration (together, evapotranspiration), condensation, precipitation, runoff to streams and oceans, and infiltration recharging groundwater. See section 39. 9. What is eutrophication? What nutrients cause it and why?

Answer (Q9, Recall). Eutrophication is nutrient over-enrichment of a water body that triggers excessive algal growth, followed by decomposition that depletes dissolved oxygen and can cause hypoxic dead zones. It is caused chiefly by phosphorus (usual limiting nutrient in freshwater) and nitrogen

(often limiting in marine systems) from fertilizer runoff, sewage, and detergents. See section 39. 10. Define decomposition. What organisms are primary decomposers, and how do termites and ants change the detrital pathway?

Answer (Q10, Recall). Decomposition is the microbial and detritivore breakdown of dead organic matter, releasing inorganic nutrients (mineralization) and CO₂ via heterotrophic respiration. Primary decomposers are bacteria and fungi (saprotrophs), assisted by detritivores (earthworms, millipedes, woodlice, soil arthropods) that fragment litter and increase surface area for microbial attack. Termites add symbiotic lignocellulose digestion and mound/galleried soil structure; ants fragment and move organic matter, excavate mineral soil, and redistribute nutrients. They are not primary microbial decomposers, but they engineer the physical and biological conditions under which decomposition proceeds. See section 39.

Questions 11–20: Application and Analysis

11. In a grassland ecosystem, GPP = 5,000 kcal/m²/yr and plant respiration = 3,000 kcal/m²/yr. Calculate NPP. If herbivores consume 20% of NPP and their assimilation efficiency is 40%, calculate secondary production at the herbivore level. How much energy reaches the top predator (3rd consumer) assuming 10% transfer efficiency?

Answer (Q11, Application). $NPP = GPP - R_a = 5000 - 3000 = 2000$ kcal per m² per yr. Herbivores consume 20 percent of NPP: $0.20 \times 2000 = 400$ ingested. Secondary production at the herbivore level = $400 \times 0.40 = 160$ kcal per m² per yr. At 10 percent transfer per step: 2nd consumer = $160 \times 0.10 = 16$; 3rd consumer = $16 \times 0.10 = 1.6$. The steep drop is why high trophic levels support little biomass. See section 39. 12. The inverted biomass pyramid of the open ocean: phytoplankton biomass is much lower than zooplankton biomass at any instant, yet phytoplankton NPP exceeds zooplankton production. Explain this paradox using turnover rate (phytoplankton divide daily; zooplankton live weeks to months).

Answer (Q12, Application). Phytoplankton have an extremely high turnover rate (cells divide roughly daily), so their tiny standing biomass is grazed almost as fast as produced and never accumulates; zooplankton turn over slowly (weeks to months) so their biomass accumulates and exceeds that of their food at any instant. Biomass (a stock) is inverted, but production rate (a flux) is not, because flux equals biomass times turnover, and high turnover compensates for low standing stock. See section 39. 13. Nitrogen fixation by *Rhizobium* in legume root nodules adds about 200 kg N/ha/yr to agricultural soils. Haber-Bosch industrial fixation produces about 150 Tg N/yr globally. Compare: (a) the energy cost of each; (b) the environmental consequences of excess reactive nitrogen (N₂O greenhouse gas, aquatic eutrophication, acid rain); (c) why reducing fertiliser overuse is critical for planetary health.

Answer (Q13, Application). (a) *Rhizobium* fixation runs on plant photosynthate (about 16 ATP per N₂), biologically free to the farmer; Haber-Bosch is fossil-fuel intensive. (b) Excess reactive N causes N₂O emission (a potent greenhouse gas), nitrate leaching to aquatic eutrophication and hypoxic dead zones, and NO_x to acid rain (the nitrogen cascade). (c) Humans now fix more N than all natural processes combined, so cutting fertilizer over-application is essential to limit climate, water-quality, and biodiversity damage. See section 39. 14. The biological pump in the ocean: surface phytoplankton fix CO₂ → organic particles sink → deep ocean decomposition releases CO₂ → CO₂ is sequestered for centuries. Calculate: if the biological pump sequesters about 11 Gt C/yr and anthropogenic emissions are about 10 Gt C/yr, what fraction of emissions is the biological pump offsetting? What would happen to atmospheric CO₂ if the biological pump weakened by 20%?

Answer (Q14, Application). Fraction of emissions offset = $11 \div 10 = 1.1$ (about 110 percent of current anthropogenic emissions, though the natural pump is roughly balanced by upwelling and is not a net anthropogenic sink). If the pump weakened by 20 percent, sequestration falls from 11 to $11 \times 0.8 = 8.8$ Gt C per yr, a loss of 2.2 Gt C per yr of downward export, leaving more CO₂ in the surface ocean and atmosphere and raising atmospheric CO₂ (a positive climate feedback). See section 39. 15. A mesocosm experiment measures primary productivity using the light-dark bottle method. The light bottle shows dissolved O₂ increase of 3 mg/L over 24 hours. The dark bottle shows O₂ decrease of 1.5 mg/L. Calculate: (a) NPP (net change in light bottle); (b) respiration (O₂ loss in dark bottle); (c) GPP (NPP + R). Convert to carbon units assuming 1 mg O₂ = 0.375 mg C.

Answer (Q15, Application). Dark bottle change equals respiration only; light bottle change equals photosynthesis minus respiration (NPP). (a) NPP equals light-bottle O₂ gain = +3 mg O₂ per L per 24h. (b) Respiration equals dark-bottle O₂ loss = 1.5. (c) GPP equals NPP plus R = $3 + 1.5 = 4.5$. In carbon units (times 0.375): NPP about 1.13, R about 0.56, GPP about 1.69 mg C per L per 24h. See section 39. 16. Phosphorus is the limiting nutrient in most freshwater ecosystems (unlike marine systems where nitrogen often limits). Explain: (a) why P availability limits productivity (no atmospheric reservoir; P cycles primarily through rock weathering); (b) how agricultural runoff causes lake eutrophication (Schindler’s whole-lake experiments); (c) why banning phosphate detergents was effective in lake recovery.

Answer (Q16, Application). (a) P limits productivity because it has no atmospheric reservoir; supply depends on slow rock weathering so phosphate is chronically scarce and adding it directly boosts algal growth. (b) Schindler’s whole-lake experiments fertilized one basin with C plus N and the other with C plus N plus P; only the P-amended basin bloomed with cyanobacteria, proving P drives freshwater eutrophication. (c) Banning phosphate detergents removed a major point-source P input; because P is limiting, cutting it directly reduced blooms and lakes recovered. See section 39. 17. Decomposition rates vary with temperature and moisture. Using the “k constant” for leaf litter decomposition (mass remaining =

$M_0 e^{-kt}$): if $k = 0.5/\text{yr}$ in a temperate forest and $k = 2.0/\text{yr}$ in a tropical forest, calculate the time for 90% decomposition in each ecosystem. What does this imply for nutrient cycling rates?

Answer (Q17, Application). Exponential decay $M \div M_0 = e^{-kt}$; for 90 percent loss the ratio is 0.1, so $t = -\ln(0.1) \div k = 2.303 \div k$. Temperate ($k = 0.5$ per yr): $t \approx 4.6$ years. Tropical ($k = 2.0$ per yr): $t \approx 1.15$ years. Faster decomposition in the warm moist tropics means rapid nutrient turnover, so tropical soils are nutrient-poor and vulnerable to loss when forest is cleared. See section 39. 18. The sulfur cycle includes atmospheric SO_2 (from volcanic eruptions and fossil fuel combustion), which forms sulfuric acid (H_2SO_4) in clouds. Trace: $\text{SO}_2 \rightarrow$ sulfate aerosol \rightarrow acid rain \rightarrow soil and lake acidification \rightarrow biological damage. Name the specific impacts on: (a) fish populations; (b) forest soil chemistry (Al^{3+} toxicity); (c) building materials (limestone dissolution).

Answer (Q18, Application). Combustion and volcanism release SO_2 , oxidized to sulfate aerosol and H_2SO_4 , producing acid rain (pH below about 4.5) and soil and lake acidification. (a) Fish: low pH disrupts ion regulation and gill function; acid-sensitive species disappear below about pH 5. (b) Forest soils: acidity mobilizes toxic Al^{3+} and leaches base cations (Ca^{2+} , Mg^{2+}), damaging fine roots and mycorrhizae. (c) Buildings: acid dissolves CaCO_3 in limestone and marble, eroding monuments. See section 39. 19. Carbon budget: the global carbon budget (2024) estimates: fossil fuel emissions = 9.9 Gt C/yr; land-use change emissions = 1.0 Gt C/yr; ocean sink = 2.8 Gt C/yr; land sink = 3.3 Gt C/yr; atmospheric growth = 4.8 Gt C/yr. Verify: do sources = sinks + atmospheric growth? What is the “residual” and what does it reveal about our understanding of the carbon cycle?

Answer (Q19, Application). Mass balance: sources equal fossil fuel plus land-use = $9.9 + 1.0 = 10.9$ Gt C per yr. Sinks plus atmospheric growth equal ocean plus land plus atmosphere = $2.8 + 3.3 + 4.8 = 10.9$. They balance exactly here, so the budget residual is 0 in this dataset. In real Global Carbon Budget assessments the terms rarely close perfectly; the nonzero budget imbalance reflects measurement uncertainty (mainly the land sink and land-use term) and the limits of quantitative understanding. See section 39. 20. Wetlands serve as both carbon sinks and methane (CH_4) sources. Evaluate: (a) how waterlogged, anoxic conditions promote methanogenesis (acetoclastic vs hydrogenotrophic pathways); (b) the 100-year global warming potential of CH_4 (about 27–30 \times CO_2 depending on fossil vs biogenic accounting in IPCC AR6); (c) the net climate effect of wetlands — do they cool or warm the planet considering both C sequestration and CH_4 emission?

Answer (Q20, Application). (a) Waterlogging makes wetland soils anoxic; once O_2 , nitrate, and sulfate are depleted, methanogens produce CH_4 via the acetoclastic pathway (acetate to CH_4 plus CO_2) and the hydrogenotrophic pathway (CO_2 plus H_2 to CH_4). (b) CH_4 has a 100-year GWP of roughly 27 to 30 times CO_2 (IPCC AR6). (c) Net effect is timescale-dependent: wetlands are persistent long-term carbon sinks (peat) but strong short-term CH_4 sources, so they can warm over short horizons and cool over millennia depending on the GWP horizon chosen. See section 39.

Questions 21–30: Synthesis and Evaluation

- Evaluate the concept of “planetary boundaries” for biogeochemical cycles (Rockström et al., 2009). Which cycles have transgressed safe operating spaces (nitrogen, phosphorus, climate change), and what does this mean for Earth system stability? Propose specific policy interventions for the nitrogen cycle that would bring humanity back within the safe boundary.

Answer (Q21, Synthesis). Planetary boundaries (Rockstrom et al., 2009) define a safe operating space for nine Earth-system processes. The biogeochemical-flows boundary (nitrogen and phosphorus) is the most severely transgressed (human N fixation far exceeds the limit), and climate change and biosphere integrity are also beyond their boundaries, risking abrupt change. Nitrogen interventions: raise nitrogen-use efficiency (precision fertilization, slow-release forms), expand legume rotations and cover crops, restore riparian buffers and wetlands to denitrify runoff, improve manure and wastewater treatment, and shift diets away from N-intensive ruminant food. See section 39. 22. Design an ecosystem-scale experiment (like Biosphere 2) to test whether a simplified ecosystem (5 trophic levels, 50 species) can maintain biogeochemical cycling in a sealed environment. What are the critical species you would include, what cycling processes must be maintained (C, N, P, H_2O), and what failure modes would you predict?

Answer (Q22, Synthesis). Hypothesis: a 50-species, five-trophic-level sealed system can sustain closed C, N, P, and water cycling. Critical species: diverse photosynthetic producers (oxygen and NPP), decomposer bacteria and fungi (mineralization), N-fixing and nitrifying and denitrifying microbes, herbivores and predators to regulate producers, and detritivores. Maintain balanced GPP versus total respiration, N fixation versus denitrification, P recycling, and water recharge. Compare replicated mesocosms to an open-system control. Predicted failure modes (Biosphere 2 lessons): oxygen drawdown, CO_2 swings, trophic collapse, and nutrient lockup. See section 39. 23. Evaluate the “metabolic theory of ecology” (MTE, Brown et al., 2004): body mass and temperature determine metabolic rate, which scales ecosystem processes (productivity, decomposition, nutrient flux). What does MTE predict about the response of tropical vs boreal ecosystem productivity to climate warming, and where does MTE break down (nutrient limitation, biodiversity effects)?

Answer (Q23, Synthesis). MTE (Brown et al., 2004) holds metabolic rate scales with body mass (proportional to mass to the three-quarter power) and temperature (Boltzmann factor), so productivity, decomposition, and nutrient flux follow size and temperature. It predicts warming accelerates

rates more in cold boreal systems than in already-warm tropical ones, and decomposition may rise faster than NPP, releasing soil carbon. MTE breaks down where nutrient or water limitation (not temperature) controls rates and where biodiversity, community composition, and acclimation matter. See section 39. 24. Evaluate the role of fire as an ecosystem process: (a) how fire releases nutrients (P, K) from biomass; (b) how fire-adapted ecosystems (savanna, chaparral, boreal forest) depend on periodic fire for regeneration; (c) how fire suppression in fire-dependent ecosystems leads to fuel accumulation and catastrophic megafires; (d) how indigenous fire management (“cool burns”) can be integrated into modern land management.

Answer (Q24, Synthesis). (a) Fire mineralizes nutrients: combustion converts biomass to ash releasing plant-available P, K, Ca while volatilizing much N and C. (b) Fire-adapted systems (savanna, chaparral, boreal forest) depend on periodic fire (serotinous cones, fire-cued germination, resprouting) to recycle nutrients and reset succession. (c) Suppression in fire-dependent systems lets fuel build up, so eventual fires become high-intensity megafires. (d) Indigenous cool burns (frequent, low-intensity, patchy) reduce fuel loads; integrating them with modern management lowers catastrophic-fire risk while keeping biodiversity. See section 39. 25. Evaluate the evidence that ocean acidification (decreasing pH from CO₂ absorption, currently pH 8.1 → projected 7.8 by 2100) threatens marine ecosystems: (a) what organisms are most affected (calcifiers — corals, pteropods, coccolithophores); (b) how does reduced aragonite saturation state ($\Omega_{ar} < 1$) dissolve CaCO₃ shells; (c) what cascading ecosystem effects are predicted; (d) is there evidence of evolutionary adaptation to lower pH in any marine organisms?

Answer (Q25, Synthesis). (a) Most affected are calcifiers building CaCO₃: corals, pteropods, coccolithophores, mollusc and echinoderm larvae, foraminifera. (b) Added CO₂ lowers carbonate-ion concentration and the aragonite saturation state; when omega-aragonite is below 1, seawater is corrosive and aragonite shells dissolve faster than they form. (c) Cascading effects: weakened reefs lose habitat and biodiversity, pteropod loss disrupts polar food webs, and acidification impairs fish olfaction. (d) Adaptation is limited but present (some corals, coccolithophores, vent populations), generally insufficient versus the rate of change. See section 39. 26. Evaluate the concept of “natural capital” — valuing ecosystem services (pollination, water purification, carbon storage) in monetary terms. Using Costanza et al. (1997, updated 2014) estimates of global ecosystem services at \$125 trillion/yr: (a) is monetary valuation of nature scientifically valid; (b) does it effectively change policy; (c) what ethical concerns arise from commodifying nature?

Answer (Q26, Synthesis). Costanza et al. (1997; updated 2014 to about 125 trillion dollars per yr) monetized global ecosystem services. (a) Validity: heuristic, not precise; it uses benefit transfer and treats nonlinear non-substitutable life-support services as if marginal and additive, so it argues an order-of-magnitude case that nature’s value is enormous, not a balance-sheet figure. (b) Policy: framing services in money has shifted policy (payments for ecosystem services, REDD+, natural-capital accounting) but evidence of consistent outcome change is mixed. (c) Ethics: commodification may crowd out intrinsic value and misprice irreplaceable systems. See section 39. 27. Evaluate the role of permafrost thaw in the global carbon cycle: about 1,500 Gt C is stored in permafrost (twice atmospheric carbon). As Arctic warming thaws permafrost: (a) what forms of carbon are released (CO₂ from aerobic decomposition, CH₄ from anaerobic decomposition); (b) what is the “permafrost carbon feedback” and how much warming does it add to existing projections; (c) is permafrost thaw a tipping point (irreversible once initiated)?

Answer (Q27, Synthesis). (a) Aerobic decomposition in drained thawed soils releases CO₂; anaerobic decomposition in waterlogged thaw ponds releases CH₄ (higher per-molecule GWP). (b) The permafrost carbon feedback is the self-amplifying loop warming to thaw to gas release to more warming, adding on the order of 0.2 to 0.4 degC extra warming this century (large uncertainty) beyond standard projections. (c) It behaves as a slow-onset, effectively irreversible tipping element on human timescales; whether there is one sharp global threshold versus gradual region-by-region loss is debated. See section 39. 28. Evaluate the concept of “novel ecosystems” — ecosystems with no historical analog, arising from human activity (urban ecosystems, post-mining landscapes, invasive-dominated habitats). Should conservation efforts attempt to restore historical ecosystems or manage novel ecosystems for desired functions? Use a specific example to argue both sides.

Answer (Q28, Synthesis). Novel ecosystems are human-created assemblages with no historical analog (urban systems, post-mining land, invasive-dominated habitats) that will not return to a historical baseline without continuous intervention. Restore-historical view (removing invasive Tamarisk from a riparian system): historical states preserve native biodiversity and coevolved interactions; abandoning baselines risks shifting-baseline syndrome. Manage-for-function view (same system): if hydrology and climate changed irreversibly, full restoration is infeasible, so managing for functions (erosion control, carbon, habitat) yields more value. The defensible answer is context-dependent. See section 39. 29. Evaluate geoengineering approaches targeting biogeochemical cycles: (a) ocean iron fertilization (stimulating phytoplankton growth to increase biological pump CO₂ sequestration); (b) enhanced weathering (grinding silicate rocks to accelerate CO₂ consumption); (c) bioenergy with carbon capture and storage (BECCS). For each, evaluate the scale of CO₂ removal, the ecological risks, and the technological readiness.

Answer (Q29, Synthesis). (a) Ocean iron fertilization stimulates phytoplankton and the biological pump, but trials show weak, uncertain, short-lived net export with bloom and hypoxia risks; low readiness and confidence. (b) Enhanced weathering: ground silicate consumes CO₂ as bicarbonate, potentially large and long-lived but energy- and land-intensive with trace-metal risks; moderate potential, early readiness. (c) BECCS: grow biomass, use for energy, store CO₂ geologically; most mature and scalable but competes for land, water, and biodiversity and needs secure storage. None

substitutes for emissions cuts. See section 39. 30. Critically evaluate whether Earth’s biogeochemical cycles constitute a self-regulating system (Gaia hypothesis, Lovelock 1979). Specifically: (a) what evidence supports biological regulation of atmospheric O₂ at about 21%; (b) what evidence supports biological regulation of ocean salinity; (c) what is the difference between “strong Gaia” (Earth as a superorganism) and “weak Gaia” (life influences but does not control the environment); (d) which version, if either, is scientifically defensible?

Answer (Q30, Synthesis). The Gaia hypothesis (Lovelock 1979) proposes life and environment form a self-regulating system maintaining habitability. (a) Atmospheric O₂ near 21 percent is biologically produced and held in a narrow window (below about 15 percent fires cease; above about 25 percent even wet vegetation burns). (b) Ocean salinity has stayed near 3.5 percent for eons via biological and geological removal, though abiotic processes contribute strongly. (c) Strong Gaia claims a purposeful superorganism regulating conditions for life; weak Gaia claims life merely influences and is coupled to geochemistry via feedbacks. (d) Only weak Gaia (Earth System Science) is scientifically defensible. See section 39.

Questions — Biomes and Conservation Biology

Instructor Use and Coverage Notes

- Coverage target: Evaluate a conservation scenario using evidence, tradeoffs, and uncertainty.
- Model/data emphasis: Species-area, risk, and prioritization calculations.
- Assessment alignment: Representing and Describing Data, Statistical Tests and Data Analysis, Argumentation.
- Misconception probe: Conservation is decision-making under constraints and uncertainty, not only preserving untouched nature.
- Transfer product: Transfer conservation reasoning to land use, climate corridors, restoration, and environmental justice.
- Grading focus: award full credit for mechanism, evidence, boundary conditions, and units when a calculation is required.
- Suggested use: draw one recall item, one application item, and one synthesis item when building a short quiz from this bank.

Questions 1–10: Recall and Comprehension

This activity accompanies section 40 of the textbook — review that chapter before attempting the exercises below.

1. Define a biome. What two abiotic factors primarily determine biome distribution?

Answer (Q1, Recall). A biome is a large-scale ecological region defined by its characteristic climate and the vegetation and animal communities adapted to it (e.g., tropical rainforest, desert, tundra). The two abiotic factors that primarily determine terrestrial biome distribution are temperature and precipitation (mean annual values and their seasonality), as captured by Whittaker’s climate-vegetation diagram. See section 40. 2. Name six major terrestrial biomes and list their characteristic temperature and precipitation ranges.

Answer (Q2, Recall). Six major terrestrial biomes (approximate ranges): tropical rainforest (about 25-30 degC, more than 2000 mm/yr); savanna (20-30 degC, 500-1500 mm with a dry season); desert (wide range, often hot 20-45 degC, less than 250 mm/yr); temperate grassland (cold winters to warm summers, 250-900 mm); temperate deciduous forest (about 5-20 degC, 750-1500 mm); boreal forest/taiga (cold, about -5 to 5 degC, 300-900 mm); tundra (very cold, below 0 degC mean, less than 250 mm). See section 40. 3. What is the difference between weather and climate?

Answer (Q3, Recall). Weather is the short-term state of the atmosphere (temperature, precipitation, wind) at a place over hours to days. Climate is the long-term statistical pattern of weather (means and variability) at a location over decades (conventionally 30-year averages). The decisive difference: weather is instantaneous and variable; climate is the aggregated, long-run distribution that determines which biome can occur there. See section 40. 4. What is biodiversity? Distinguish genetic, species, and ecosystem diversity.

Answer (Q4, Recall). Biodiversity is the variety of life at all levels of organization. Genetic diversity is variation in alleles and genotypes within and among populations of a species (raw material for adaptation). Species diversity is the number and relative abundance of species in a community. Ecosystem diversity is the variety of habitats, biotic communities, and ecological processes across a landscape or region. They differ in scale: gene to population to community to landscape. See section 40. 5. Define an endangered species. What organization maintains the Red List?

Answer (Q5, Recall). An endangered species is one assessed as facing a very high risk of extinction in the wild in the near future (IUCN category Endangered; the U.S. Endangered Species Act uses ‘in danger of extinction throughout all or a significant portion of its range’). The IUCN (International Union for Conservation of Nature) maintains the Red List of Threatened Species. See section 40. 6. What is habitat fragmentation? Why does it threaten biodiversity?

Answer (Q6, Recall). Habitat fragmentation is the breaking of continuous habitat into smaller, isolated patches by human land use. It threatens biodiversity by reducing patch area (smaller populations, higher extinction risk), increasing isolation (less dispersal and gene flow, lower rescue and recolonization), and increasing edge effects (altered microclimate, predation, invasion), pushing many species below minimum viable population size. See section 40. 7. Name three causes of the current biodiversity crisis.

Answer (Q7, Recall). Three causes of the current biodiversity crisis (the modern ‘HIPPO’/IPBES drivers): (1) habitat loss and land/sea-use change; (2) overexploitation (overharvest, hunting, fishing); (3) climate change. Pollution and invasive species are two additional major drivers. See section 40. 8. What is a biodiversity hotspot? Name two examples.

Answer (Q8, Recall). A biodiversity hotspot is a region with exceptional species richness and endemism (more than 1500 endemic vascular plants) that has already lost more than 70 percent of its original natural vegetation (Myers/Conservation International criteria), making it both irreplaceable and threatened. Examples: the Tropical Andes and Madagascar (others include the Mediterranean Basin and Sundaland). See section 40. 9. What is an in situ conservation strategy? What is an ex situ strategy?

Answer (Q9, Recall). In situ conservation protects species in their natural habitat (national parks, reserves, protected areas), preserving ecological and evolutionary processes. Ex situ conservation maintains organisms outside their natural habitat (zoos, botanical gardens, captive breeding, seed

banks, gene/cryobanks), used as a backup when in situ protection alone cannot prevent extinction. See section 40. 10. Define sustainability. What are the three pillars of sustainability?

Answer (Q10, Recall). Sustainability is meeting present needs without compromising the ability of future generations to meet their own needs (Brundtland definition). Its three pillars are environmental (ecological integrity and resource limits), economic (viable livelihoods and prosperity), and social (equity, health, and well-being); durable solutions must satisfy all three. See section 40.

Questions 11–20: Application and Analysis

11. The species-area relationship ($S = cA^z$, where $z \approx 0.25$ for oceanic islands) predicts that reducing habitat area by 90% reduces species number by about 50%. Calculate: if a 10,000 km² forest is reduced to 1,000 km², and the original forest had 200 bird species, how many bird species are expected in the remaining fragment? What assumptions does this model make?

Answer (Q11, Application). Species-area relationship $S = cA^z$, so $S_2/S_1 = (A_2/A_1)^z$. Area falls from 10000 to 1000 km², a 10-fold reduction, with $z = 0.25$: $S_2 = 200 \times (1000/10000)^{0.25} = 200 \times (0.1)^{0.25} = 200 \times 0.562 \approx 112$ bird species (a loss of about 88 species, roughly 44 percent). Assumptions: the relationship and z apply to this system, the fragment is at new equilibrium (ignores extinction-debt time lag), no edge effects or matrix effects, and habitat is otherwise homogeneous. See section 40. 12. EDGE scores (Evolutionarily Distinct and Globally Endangered) are used to prioritize species for conservation investment. The aye-aye (*Daubentonia madagascariensis*) — the sole living member of its family — has a very high EDGE score. Explain: (a) what evolutionary distinctiveness means; (b) why losing an “edge species” results in greater phylogenetic diversity loss than losing a species in a species-rich clade; (c) how EDGE scoring changes conservation priorities compared to a focus on charisma.

Answer (Q12, Application). (a) Evolutionary distinctiveness measures how isolated a species is on the tree of life (long branch with few close relatives), summarizing unique evolutionary history. (b) Losing an ‘EDGE’ species like the aye-aye, the sole member of its family, erases a long, unshared branch and far more phylogenetic diversity (unique genes and traits) than losing one of many similar species in a species-rich clade, where relatives retain most shared history. (c) EDGE scoring redirects priorities toward irreplaceable, evolutionarily unique but overlooked taxa rather than only charismatic megafauna, maximizing preserved evolutionary history per conservation dollar. See section 40. 13. Minimum viable population (MVP) analysis: a PVA model estimates that a population of 500 individuals has a 95% probability of persisting for 100 years, but a population of 50 has a 20% chance. Identify three factors incorporated in the model (demographic stochasticity, environmental stochasticity, inbreeding depression) and explain how each reduces persistence probability.

Answer (Q13, Application). (a) Demographic stochasticity: random variation in individual births, deaths, and sex ratio; in small populations chance alone can cause a run of deaths or all-male offspring, driving extinction even when mean growth is positive. (b) Environmental stochasticity: year-to-year fluctuations in conditions (droughts, disease, storms) hit the whole population at once, depressing survival/reproduction and increasing variance in growth rate. (c) Inbreeding depression: small populations lose heterozygosity and express deleterious recessive alleles, lowering fertility and survival. All three intensify as N falls, so a population of 50 has far lower persistence probability than 500 (the basis of the 50/500 rule). See section 40. 14. Climate change is shifting biome boundaries: the boreal-temperate boundary is moving northward, and the Sahel-Sahara boundary is fluctuating. Predict the consequences for: (a) species that cannot migrate fast enough (boreal specialists trapped in shrinking habitat); (b) agricultural zones (expansion of growing season in formerly cold regions); (c) novel community assemblages (no-analog communities formed by differential range shifts).

Answer (Q14, Application). (a) Boreal specialists cannot track the poleward/upslope shift fast enough (slow dispersal, fragmentation, no land left at high latitude); their suitable climate envelope shrinks and they face range contraction and extinction risk. (b) Agricultural zones expand into formerly cold regions as growing seasons lengthen and frost-free periods increase, shifting cultivation poleward (though soils and daylength may not match). (c) Because species shift at different rates and directions, communities reshuffle into no-analog (novel) assemblages with new species combinations and interactions not seen historically, complicating prediction and management. See section 40. 15. Coral reef bleaching occurs when accumulated heat stress disrupts the coral-Symbiodiniaceae partnership. Explain: (a) how degree-heating-week evidence links heat exposure to symbiont photosystem stress, reactive oxygen species, and symbiont loss; (b) why recovery depends on repeated heat exposure, water quality, recruitment, and symbiont community composition rather than a fixed clock; (c) how assisted evolution or symbiont turnover could improve local resilience while still failing as a substitute for climate mitigation.

Answer (Q15, Application). DHW is an exposure metric: sustained positive temperature anomalies increase stress on algal photosystems, promote reactive oxygen species and photodamage, and trigger host stress responses that reduce or expel symbionts, leaving the coral energy-limited. Recovery is variable because it depends on mortality severity, recruitment, herbivory, sediment and nutrient stress, disease pressure, and whether surviving hosts or symbionts have heat-tolerant traits. Assisted evolution, selective breeding, probiotics, or symbiont turnover can shift local tolerance in some settings, but they do not remove the external heat driver or ocean-acidification risk. Defensible management therefore pairs local resilience actions with emissions reduction and monitoring, not a claim that corals can simply adapt away the problem. See section 40. 16. Protected

areas currently cover about 17% of land and about 8% of ocean. The Kunming-Montreal Global Biodiversity Framework (2022) targets 30% by 2030 (“30 by 30”). Evaluate: (a) whether area alone is sufficient (effective management, connectivity, representativeness); (b) the concept of “half-Earth” (Wilson, 2016 — protecting 50% of Earth’s surface); (c) the social justice concerns (indigenous displacement, land rights).

Answer (Q16, Application). (a) Area alone is insufficient: protection must also be effectively managed, well-connected, and ecologically representative; many ‘paper parks’ deliver little because of weak enforcement, poor placement, or isolation. (b) Wilson’s ‘Half-Earth’ proposes protecting about 50 percent of Earth’s surface to retain most species, an ambitious target grounded in species-area logic but facing huge land-use and political constraints. (c) Social-justice concerns: ‘fortress conservation’ has historically displaced Indigenous and local peoples and ignored land rights; equitable ‘30 by 30’ must secure tenure, recognize Indigenous-managed lands, and ensure benefit-sharing rather than exclusion. See section 40. 17. Invasive species economic damage: the global estimated cost of invasive species is >\$423 billion/yr (2019). Using the example of the invasive cane toad (*Rhinella marina*) in Australia: (a) what was the original purpose of introduction; (b) what ecological impacts have occurred (native predator mortality from toad toxin); (c) what control strategies have been attempted (biological control, trapping, gene drive research).

Answer (Q17, Application). (a) The cane toad was deliberately introduced to Queensland in 1935 as a biological control agent against cane beetles in sugarcane. (b) It failed to control the beetles and instead spread widely; its potent bufotoxin kills naive native predators (quolls, goannas, snakes, freshwater crocodiles) that try to eat it, causing steep declines, while it also preys on and competes with native fauna. (c) Control attempts include hand-trapping and tadpole traps (using toad pheromone/bufadienolide lures), exclusion fencing around water, community ‘toad busting’, conditioned taste aversion to protect predators, and research into gene-drive or genetic biocontrol; none has achieved landscape-scale eradication. See section 40. 18. Payment for ecosystem services (PES): Costa Rica’s PES program pays landowners to conserve forest (carbon storage, water regulation). Evaluate: (a) how PES monetises ecosystem services; (b) evidence of effectiveness (Costa Rica reversed deforestation); (c) criticisms (additionality — would forests have been conserved anyway? Equity — do poor landowners benefit or are payments captured by wealthy elites?).

Answer (Q18, Application). (a) PES pays landowners for the ecosystem services their land provides (carbon storage, watershed/water regulation, biodiversity, scenic value), funded via fuel taxes, water fees, and carbon finance, internalizing previously unpriced benefits. (b) Costa Rica’s program coincided with a reversal of deforestation and roughly a doubling of forest cover since the 1980s, indicating effectiveness in a strong-governance setting. (c) Criticisms: additionality (paying for forest that would have been kept anyway), leakage (clearing shifts elsewhere), permanence, and equity (payments and titling may favor wealthier landowners over poor or untitled holders). The conclusion would change if rigorous counterfactual evaluation showed low additionality. See section 40. 19. The IPBES Global Assessment estimates that about one million species are threatened, while the IPBES Transformative Change Assessment argues that biodiversity loss is driven by economic, governance, and social systems as well as local habitat conversion. Evaluate: (a) how threatened-species estimates combine assessed taxa, extrapolation, and habitat trends; (b) how GBIF occurrence records complement, but cannot replace, IUCN/IPBES risk assessment; (c) why food systems, healthy diets, agroecology, fisheries, and commodity supply chains belong inside conservation biology; (d) how to distinguish evidence-based transformative change from vague sustainability branding.

Answer (Q19, Application). Treat the one-million estimate as a synthesis, not a direct census of every species: well-assessed groups, Red List categories, habitat-loss data, species-area relationships, and extrapolation to poorly known taxa all contribute uncertainty. GBIF adds open occurrence evidence about where and when taxa have been recorded, but those points need coordinate, date, taxonomy, duplicate, and sampling-bias filters before being interpreted as range or abundance evidence; IUCN/IPBES then synthesize risk, drivers, and policy relevance [GBIF Secretariat, 2026, International Union for Conservation of Nature, 2025, Intergovernmental Science-Policy Platform on Biodiversity and Ecosystem Services, 2024]. Food systems matter because agriculture, fisheries, trade, food waste, diet affordability, fertilizer runoff, pesticide use, and habitat conversion are direct biodiversity drivers; changing them affects nutrition, livelihoods, and ecosystems together. Evidence-based transformative change names levers and indicators: land-use policy, rights and tenure, subsidy reform, diversified farming, sustainable harvest rules, pollinator habitat, healthy-diet affordability, and measured biodiversity outcomes. Branding is weaker when it lacks baselines, distributional effects, monitoring, or a mechanism connecting the intervention to reduced pressure on species and ecosystems. See section 40. 20. Rewilding involves reintroducing apex predators and megafauna to restore ecosystem function. Evaluate the Eurasian rewilding movement (European bison in Romania, wolves in Germany, lynx in UK): (a) what ecological functions are restored; (b) what human-wildlife conflict arises; (c) the evidence from existing rewilding projects (Oostvaardersplassen, Netherlands) — successes and failures.

Answer (Q20, Application). (a) Rewilding restores ecological functions: large herbivores (European bison) drive grazing and vegetation heterogeneity; apex predators (wolves, lynx) restore top-down control and trophic cascades, increasing structural and species diversity. (b) Human-wildlife conflict arises: livestock depredation by wolves/lynx, perceived risk, competition over land, and the politics of large carnivores near settlements. (c) Oostvaardersplassen showed both: it generated dense large-grazer populations and habitat dynamics, but lack of predators plus a fenced, food-limited area led to mass winterstarvation and a public-ethics backlash, prompting culling/feeding policy changes, evidence that bounded rewilding without predators or migration routes can fail welfare and ecological goals. See section 40.

Questions 21–30: Synthesis and Evaluation

21. Evaluate the “extinction debt” concept: habitat destruction in the past has committed species to future extinction even if no further habitat is lost, because small fragments cannot sustain viable populations over decades. Using the example of tropical forest fragmentation (Ferraz et al., 2003): (a) how is extinction debt estimated; (b) how long is the time lag (about 20–100 years); (c) what does this imply for current biodiversity assessments (we are underestimating the true impact of past deforestation)?

Answer (Q21, Synthesis). (a) Extinction debt is estimated by comparing current species richness in fragments to the lower equilibrium predicted by the post-fragmentation area (species-area relationship) and by tracking ‘relaxation’ through long-term monitoring; the gap is the debt. (b) The relaxation time lag is long, roughly decades to a century (about 20-100 years for tropical forest birds; Ferraz et al. 2003 estimated multi-decade half-lives), so committed extinctions unfold slowly. (c) Implication: current biodiversity assessments understate the true impact of past deforestation, because many ‘surviving’ species are functionally committed to extinction; the conclusion would change if fragments received enough restoration/connectivity to raise their effective area and pay down the debt. See section 40. 22. Design a conservation genetics program for a critically endangered species (e.g., California condor, about 500 individuals): describe (a) the genetic assessment (genomic sequencing of sampled individuals, measurement of heterozygosity and inbreeding coefficient); (b) the breeding management strategy (maximizing N_e , using mean kinship to minimize inbreeding); (c) the genetic rescue strategy (introducing individuals from a genetically distinct population to restore lost alleles). What are the risks of genetic rescue (outbreeding depression)?

Answer (Q22, Synthesis). Hypothesis: managed breeding plus genetic rescue raises fitness and persistence versus unmanaged breeding (control = continued inbred breeding; falsifying result = no improvement or reduced fitness). (a) Assessment: genome-sequence all about 500 individuals, estimate individual heterozygosity, inbreeding coefficient F , relatedness, and known deleterious alleles. (b) Breeding management: pair individuals to maximize effective population size and minimize mean kinship, equalize family sizes, and avoid known lethal alleles. (c) Genetic rescue: introduce a few individuals from a genetically distinct conspecific population to restore lost alleles and heterozygosity; monitor offspring fitness. Risk: outbreeding depression (loss of local adaptation or coadapted gene complexes), so introduce cautiously and track replicated breeding lines. See section 40. 23. Evaluate climate-smart conservation: traditional conservation aims to protect current biodiversity in current locations. Climate change requires protecting future habitats and enabling species movement. Evaluate three climate-smart strategies: (a) connectivity corridors between protected areas; (b) assisted migration (moving species to suitable future habitat); (c) protecting climate refugia (areas predicted to remain climatically stable). What are the risks of each?

Answer (Q23, Synthesis). (a) Connectivity corridors link protected areas so species can track shifting climate; risk: corridors can also spread invasives, disease, or fire, and may not align with future climate paths. (b) Assisted migration moves species to predicted-suitable future habitat; risk: the translocated species may become invasive or disrupt recipient communities, and predictions are uncertain. (c) Protecting climate refugia conserves areas expected to stay climatically stable (topographic/microclimatic); risk: refugia are hard to identify reliably, may be small, and can still fail under high warming. A defensible strategy treats these as a portfolio under uncertainty, with monitoring; the judgment changes if downscaled climate projections or species-distribution models prove unreliable. See section 40. 24. Evaluate the role of indigenous and traditional ecological knowledge (ITEK) in conservation: (a) the evidence that indigenous-managed lands have higher biodiversity than conventional protected areas; (b) the UN IPBES recognition of ITEK as an evidence base equal to scientific knowledge; (c) the challenges of integrating ITEK with Western science (different epistemologies, power dynamics, intellectual property).

Answer (Q24, Synthesis). (a) Evidence: Indigenous-managed and Indigenous-owned lands frequently show biodiversity and intactness equal to or greater than conventional protected areas (e.g., comparable or lower deforestation and higher vertebrate persistence), indicating effective stewardship. (b) IPBES explicitly recognizes Indigenous and local knowledge as a legitimate evidence base alongside science and centers it in its global assessments. (c) Challenges to integration: different epistemologies (relational vs. reductionist), historical power asymmetries and marginalization, risks of extractive ‘knowledge mining’, intellectual-property and consent issues, and the need for genuine co-governance rather than tokenism. The conclusion would weaken if outcome differences disappeared after controlling for remoteness and land-use pressure. See section 40. 25. Evaluate the concept of “de-extinction” in the context of conservation biology: if woolly mammoths could be de-extincted (via CRISPR editing of Asian elephant genome), would this be a conservation priority? Discuss: (a) the opportunity cost (diverting funds from existing species); (b) the ecological benefit (restoring mammoth steppe ecosystem, permafrost preservation); (c) the ethical questions (welfare of first-generation animals, ecological risk).

Answer (Q25, Synthesis). (a) Opportunity cost: de-extinction is extremely expensive and could divert scarce funding and attention from thousands of extant species that could be saved more cheaply now. (b) Potential ecological benefit: a cold-adapted proxy could help restore mammoth-steppe grazing dynamics and possibly slow permafrost thaw, but the ecological outcome is speculative and unproven at scale. (c) Ethics: welfare of surrogate Asian elephants and first-generation animals, the animal is a genetically engineered proxy not a true mammoth, release into changed ecosystems carries invasion and disease risk, and it may foster moral hazard (‘extinction is reversible’). On current evidence it is not a defensible conservation

priority versus preventing extinctions; this would change only if it became cheap, low-risk, and ecologically validated. See section 40. 26. Evaluate the impact of plastic pollution on marine biomes: (a) microplastic ingestion by marine organisms across trophic levels; (b) bioaccumulation and biomagnification of associated chemical pollutants (phthalates, BPA); (c) the “plastisphere” — microbial communities colonising marine plastic that can include pathogens; (d) policy interventions (single-use plastic bans, Extended Producer Responsibility).

Answer (Q26, Synthesis). (a) Microplastics are ingested across trophic levels from zooplankton to fish, seabirds, and whales, causing physical blockage, false satiation, and reduced growth/reproduction. (b) Plastics sorb and leach hydrophobic pollutants and additives (phthalates, BPA, PCBs) that can bioaccumulate and biomagnify, with endocrine-disrupting effects up the food web (though magnification efficiency is debated). (c) The ‘plastisphere’ is a distinct microbial biofilm on marine plastic that can host pathogens and harmful taxa and rafts them across oceans. (d) Policy: single-use plastic bans, Extended Producer Responsibility, deposit-return schemes, and a global plastics treaty target sources; effectiveness depends on upstream production cuts, not just cleanup. The conclusion would change if exposure levels proved below toxicological thresholds in situ. See section 40. 27. Evaluate Nature-based Solutions (NbS) to climate change: (a) reforestation and afforestation (potential about 10 Gt CO₂/yr); (b) peatland and mangrove restoration; (c) regenerative agriculture (soil carbon sequestration). For each, evaluate the permanence of carbon storage, the biodiversity co-benefits, and the risk of “greenwashing” (using NbS to justify continued fossil fuel use).

Answer (Q27, Synthesis). (a) Reforestation/afforestation can sequester carbon (often cited around 10 Gt CO₂/yr potential) but storage is impermanent (fire, drought, harvest, pests) and monocultures provide weak biodiversity benefit; native, diverse forests are better. (b) Peatland and mangrove (blue carbon) restoration store dense, long-lived carbon and deliver strong biodiversity and coastal-protection co-benefits, but are vulnerable to drainage and degradation. (c) Regenerative agriculture builds soil carbon with food and resilience co-benefits, but gains are modest, reversible, and hard to verify. The central risk across all is greenwashing: NbS used to offset rather than cut fossil emissions. A defensible position treats NbS as complementary to deep decarbonization, with permanence safeguards and rigorous monitoring; the judgment changes if storage proves non-permanent at scale. See section 40. 28. Evaluate the role of zoos and botanical gardens (ex situ conservation) in preventing extinction: (a) the success stories (Arabian oryx, black-footed ferret, California condor — saved from extinction by captive breeding); (b) the limitations (genetic bottlenecks, behavioral domestication, space constraints); (c) the shift from “Noah’s Ark” (saving species) to “conservation hubs” (research, education, advocacy).

Answer (Q28, Synthesis). (a) Successes: captive breeding rescued the Arabian oryx, black-footed ferret, and California condor from the brink and enabled reintroduction. (b) Limitations: small founder numbers cause genetic bottlenecks and inbreeding, captivity selects for domestication and erodes wild behaviors, space and cost cap how many species can be held, and reintroduction often fails without habitat. (c) The field has shifted from a ‘Noah’s Ark’ framing (warehousing species) to ‘conservation hubs’ that integrate research, reintroduction science, public education, advocacy, and funding for in situ work, with ex situ as one tool in an integrated strategy rather than an end in itself. See section 40. 29. Evaluate the “triage” approach to conservation: given limited resources, should we focus on: (a) species most likely to be saved (pragmatic triage); (b) species with highest evolutionary distinctiveness (phylogenetic triage); (c) species with greatest functional importance (ecosystem triage)? Compare these approaches using a specific threatened community (e.g., coral reef, tropical forest), and discuss the ethical implications of explicitly choosing to let some species go extinct.

Answer (Q29, Synthesis). (a) Pragmatic triage funds species with the best cost-effectiveness of recovery, maximizing species saved but abandoning hard cases. (b) Phylogenetic triage prioritizes evolutionarily distinct species, preserving the most evolutionary history but possibly losing functionally key common species. (c) Ecosystem triage prioritizes functionally important species (keystones, foundation species) to preserve ecosystem services and integrity. On a coral reef, ecosystem triage would prioritize reef-building corals and key herbivores; phylogenetic triage might prioritize an isolated lineage; pragmatic triage might fund the cheapest wins. Ethically, explicit triage forces transparent, value-laden choices to let some species go extinct under resource limits; the appropriate criterion depends on whether the goal is total species, evolutionary history, or ecosystem function, and the judgment changes with the budget and stated objective. See section 40. 30. Critically evaluate whether the concept of “ecological footprint” (measuring human demand on Earth’s biocapacity in global hectares) is a scientifically rigorous and policy-useful metric. Compare ecological footprint to alternative sustainability metrics (planetary boundaries, natural capital accounting, genuine progress indicator). What does each capture that others miss, and which is most actionable for policy change?

Answer (Q30, Synthesis). The ecological footprint converts human resource demand and waste into the bioproductive area (global hectares) required, compared against biocapacity. Strengths: a single intuitive, communicable overshoot metric. Weaknesses: it leans heavily on a carbon-uptake-land component, is sensitive to methodological choices, omits many impacts (toxics, freshwater depletion, biodiversity loss), and is criticized as not fully rigorous. Planetary boundaries capture multiple Earth-system processes and thresholds but are not aggregated or directly policy-priced. Natural-capital accounting prices stocks/flows of ecosystem services (useful for finance, but commodifies and misses non-market values). The genuine progress indicator adjusts economic welfare for environmental and social costs (good for policy framing, weak on ecological thresholds). Each captures something the others miss; planetary boundaries are most scientifically defensible for limits, while footprint and GPI are more directly

actionable for communicating and steering policy. See section 40.

Appendix A — Curriculum Map

This appendix is generated from `src/biology/curriculum.py` and `src/biology/alignment.py`. It links each chapter to its companion lab, question bank, model/data skill, misconception probe, transfer task, and standards/skills alignment so the textbook can be composed into different course formats without losing pedagogical coherence.

Unit 0

— Systems Science and Emergence

- Chapter: section [0.1](#).
- Lab: [Lab A — Systems Science and Emergence](#).
- Question bank: [Questions — Systems Science and Emergence](#).
- Big idea: Biological explanation improves when parts, interactions, feedback, and scale are kept in view together.
- Core concepts: systems boundaries, feedback, emergence, state variables.
- Framework alignment: Vision & Change: Systems, Structure and function; AP Biology: Systems Interactions; NGSS-style topics: Structure and Function, Interdependent Relationships in Ecosystems.
- Practice cadence: Questions and Methods, Representing and Describing Data, Argumentation.
- Model/data skill: Box-and-arrow causal models with explicit inputs, outputs, and feedback signs. Translate a verbal biological system into variables, links, and testable predictions.
- Misconception probe: A system is not just a list of parts; the interactions are part of the explanation.
- Transfer task: Apply the same feedback map to a cell, organism, and ecosystem, then name what changes at each scale.

— Complex Adaptive Systems

- Chapter: section [0.2](#).
- Lab: [Lab B — Complex Adaptive Systems](#).
- Question bank: [Questions — Complex Adaptive Systems](#).
- Big idea: Local rules can generate population-level patterns without a central controller.
- Core concepts: nonlinearity, self-organization, attractors, power laws.
- Framework alignment: Vision & Change: Systems, Structure and function; AP Biology: Systems Interactions; NGSS-style topics: Structure and Function, Interdependent Relationships in Ecosystems.
- Practice cadence: Questions and Methods, Representing and Describing Data, Argumentation.
- Model/data skill: Agent-rule and scaling arguments for emergent biological patterns. Distinguish deterministic trends from stochastic variation in repeated simulations.
- Misconception probe: Emergence is not mysterious; it is a reproducible consequence of interactions plus constraints.
- Transfer task: Compare flocking, immune activation, and microbial biofilms as adaptive systems.

— Active Inference and Free Energy

- Chapter: section [0.3](#).
- Lab: [Lab C — Active Inference and Free Energy](#).
- Question bank: [Questions — Active Inference and Free Energy](#).
- Big idea: Living systems reduce uncertainty by acting on the world as well as by updating internal models.
- Core concepts: prediction error, Bayesian updating, policy selection, homeostasis.
- Framework alignment: Vision & Change: Systems, Structure and function; AP Biology: Systems Interactions; NGSS-style topics: Structure and Function, Interdependent Relationships in Ecosystems.
- Practice cadence: Questions and Methods, Representing and Describing Data, Argumentation.
- Model/data skill: Bayesian belief updating and expected-free-energy-style policy comparison. Read a small probability table and update a prediction after new evidence.
- Misconception probe: Active inference is not passive prediction; action changes the sensory data that arrive next.
- Transfer task: Map prediction-error reasoning onto chemotaxis, thermoregulation, and attention.

— History and Philosophy of Biology

- Chapter: section [0.4](#).

- Lab: **Lab D — History and Philosophy of Biology.**
- Question bank: **Questions — History and Philosophy of Biology.**
- Big idea: Biology is a changing evidence practice: its concepts of life, function, species, inheritance, and self are revised by new observations, instruments, models, and social values.
- Core concepts: biological explanation, historical evidence, function, species concepts, values in science.
- Framework alignment: Vision & Change: Systems, Structure and function; AP Biology: Systems Interactions; NGSS-style topics: Structure and Function, Interdependent Relationships in Ecosystems.
- Practice cadence: Questions and Methods, Representing and Describing Data, Argumentation.
- Model/data skill: Concept-map and evidence-matrix comparisons among historical claims, mechanisms, and model assumptions. Classify source excerpts as observation, experiment, model, mechanism, or value-laden inference.
- Misconception probe: History is not a list of dates; it explains why current biological concepts are powerful, limited, and revisable.
- Transfer task: Transfer source-analysis reasoning to modern debates about species, genetics, microbiomes, and biomedical ethics.

Unit I

— Atoms, Molecules, and Chemical Bonds

- Chapter: section 1.
- Lab: **Lab — Atoms, Molecules, and Chemical Bonds.**
- Question bank: **Questions — Atoms, Molecules, and Chemical Bonds.**
- Big idea: Atomic structure constrains the bonds, charges, and geometries that make biological molecules possible.
- Core concepts: valence, electronegativity, formal charge, isotopes.
- Framework alignment: Vision & Change: Structure and function, Pathways and transformations of energy and matter; AP Biology: Energetics, Systems Interactions; NGSS-style topics: Matter and Energy in Organisms and Ecosystems, Structure and Function.
- Practice cadence: Concept Explanation, Statistical Tests and Data Analysis, Argumentation.
- Model/data skill: Formal charge and electronegativity-difference reasoning. Use tabular atomic data to predict polarity, solubility, and biological reactivity.
- Misconception probe: Weak interactions are not unimportant; many weak interactions together dominate structure and specificity.
- Transfer task: Use atomic reasoning to explain a medical tracer, enzyme cofactor, or membrane-solubility problem.

— Water — The Molecule of Life

- Chapter: section 2.
- Lab: **Lab — Water — The Molecule of Life.**
- Question bank: **Questions — Water — The Molecule of Life.**
- Big idea: Water's polarity, hydrogen bonding, and ionization make cells physically possible.
- Core concepts: hydrogen bonding, cohesion, pH, buffers.
- Framework alignment: Vision & Change: Structure and function, Pathways and transformations of energy and matter; AP Biology: Energetics, Systems Interactions; NGSS-style topics: Matter and Energy in Organisms and Ecosystems, Structure and Function.
- Practice cadence: Concept Explanation, Statistical Tests and Data Analysis, Argumentation.
- Model/data skill: Henderson-Hasselbalch and pH-scale calculations. Convert between pH, hydrogen ion concentration, and buffer ratios.
- Misconception probe: Water is not an inert background; it is an active participant in structure and reaction chemistry.
- Transfer task: Transfer water-property reasoning to blood buffering, plant transport, or protein folding.

— Biological Macromolecules

- Chapter: section 3.
- Lab: **Lab — Biological Macromolecules.**
- Question bank: **Questions — Biological Macromolecules.**
- Big idea: Macromolecule structure links monomer chemistry to biological function and information storage.
- Core concepts: polymers, dehydration synthesis, protein structure, nucleic acids.
- Framework alignment: Vision & Change: Structure and function, Pathways and transformations of energy and matter; AP Biology: Energetics, Systems Interactions; NGSS-style topics: Matter and Energy in Organisms and Ecosystems, Structure and Function.
- Practice cadence: Concept Explanation, Statistical Tests and Data Analysis, Argumentation.
- Model/data skill: Polymerization energetics and sequence-to-structure reasoning. Classify molecules from structural evidence rather than names alone.
- Misconception probe: Structure is not decoration; small chemical changes can redirect function and recognition.

- Transfer task: Explain how a mutation, lipid substitution, or glycosylation change propagates to phenotype.

— Enzymes and the Kinetics of Catalysis

- Chapter: section 4.
- Lab: Lab — Enzymes and the Kinetics of Catalysis.
- Question bank: Questions — Enzymes and the Kinetics of Catalysis.
- Big idea: Enzymes accelerate reactions by stabilizing transition states without changing thermodynamic endpoints.
- Core concepts: activation energy, Michaelis-Menten kinetics, inhibition, allostery.
- Framework alignment: Vision & Change: Structure and function, Pathways and transformations of energy and matter; AP Biology: Energetics, Systems Interactions; NGSS-style topics: Matter and Energy in Organisms and Ecosystems, Structure and Function.
- Practice cadence: Concept Explanation, Statistical Tests and Data Analysis, Argumentation.
- Model/data skill: Michaelis-Menten, Lineweaver-Burk, and inhibition-pattern calculations. Fit or interpret enzyme-rate data and identify which parameter changed.
- Misconception probe: A catalyst changes rate, not the equilibrium constant or the sign of delta G.
- Transfer task: Apply enzyme-kinetic reasoning to drug dosing, metabolic control, or diagnostic assays.

Unit II

— Cell Theory and Cell Types

- Chapter: section 5.
- Lab: Lab — Cell Theory and Cell Types.
- Question bank: Questions — Cell Theory and Cell Types.
- Big idea: Cells are bounded, evolving systems whose size and organization reflect physical constraints.
- Core concepts: cell theory, surface area, microscopy, prokaryote/eukaryote comparison.
- Framework alignment: Vision & Change: Structure and function, Systems, Information flow, exchange, and storage; AP Biology: Systems Interactions, Information Storage and Transmission; NGSS-style topics: Structure and Function.
- Practice cadence: Visual Representations, Questions and Methods, Argumentation.
- Model/data skill: Surface-area-to-volume scaling. Infer cellular constraints from measurements, micrographs, and scale bars.
- Misconception probe: Cells are not just small bags of fluid; boundaries and internal organization create function.
- Transfer task: Transfer scale reasoning to eggs, neurons, root hairs, and microbial colonies.

— Cell Structure and Organelles

- Chapter: section 6.
- Lab: Lab — Cell Structure and Organelles.
- Question bank: Questions — Cell Structure and Organelles.
- Big idea: Organelle structure partitions work, traffic, information, and energy inside eukaryotic cells.
- Core concepts: organelles, endomembrane system, cytoskeleton, motor proteins.
- Framework alignment: Vision & Change: Structure and function, Systems, Information flow, exchange, and storage; AP Biology: Systems Interactions, Information Storage and Transmission; NGSS-style topics: Structure and Function.
- Practice cadence: Visual Representations, Questions and Methods, Argumentation.
- Model/data skill: Compartment-flow and motor-transport calculations. Trace a molecule through compartments using evidence from labels or perturbations.
- Misconception probe: Organelles are dynamic process hubs, not static textbook icons.
- Transfer task: Apply compartment logic to secretion, apoptosis, infection, or cell division.

— Membrane Structure and Transport

- Chapter: section 7.
- Lab: Lab — Membrane Structure and Transport.
- Question bank: Questions — Membrane Structure and Transport.
- Big idea: Membranes convert gradients, permeability, and selective transport into cellular physiology.
- Core concepts: bilayers, diffusion, osmosis, electrochemical gradients.

- Framework alignment: Vision & Change: Structure and function, Systems, Information flow, exchange, and storage; AP Biology: Systems Interactions, Information Storage and Transmission; NGSS-style topics: Structure and Function.
- Practice cadence: Visual Representations, Questions and Methods, Argumentation.
- Model/data skill: Nernst, Goldman, osmotic, and facilitated-transport calculations. Interpret transport data from gradients, rates, and membrane potentials.
- Misconception probe: Equilibrium does not mean equal concentration; charge and permeability matter.
- Transfer task: Transfer gradient logic to neurons, kidneys, roots, and mitochondrial membranes.

— Cell Signaling and Communication

- Chapter: section 8.
- Lab: Lab — Cell Signaling and Communication.
- Question bank: Questions — Cell Signaling and Communication.
- Big idea: Cells communicate by converting external signals into regulated intracellular decisions.
- Core concepts: receptors, second messengers, signal amplification, feedback.
- Framework alignment: Vision & Change: Structure and function, Systems, Information flow, exchange, and storage; AP Biology: Systems Interactions, Information Storage and Transmission; NGSS-style topics: Structure and Function.
- Practice cadence: Visual Representations, Questions and Methods, Argumentation.
- Model/data skill: Ligand-receptor occupancy and dose-response reasoning. Read pathway diagrams and infer the effect of agonists, antagonists, or mutations.
- Misconception probe: A pathway diagram is a causal model, not a memorization chart.
- Transfer task: Apply signaling logic to hormones, neurotransmitters, immune receptors, or cancer mutations.

Unit III

— Bioenergetics and Cellular Respiration

- Chapter: section 9.
- Lab: Lab — Bioenergetics and Cellular Respiration.
- Question bank: Questions — Bioenergetics and Cellular Respiration.
- Big idea: Cells harvest free energy by coupling redox chemistry to phosphoryl transfer and ion gradients.
- Core concepts: free energy, redox, glycolysis, oxidative phosphorylation.
- Framework alignment: Vision & Change: Pathways and transformations of energy and matter, Systems; AP Biology: Energetics, Systems Interactions; NGSS-style topics: Matter and Energy in Organisms and Ecosystems.
- Practice cadence: Representing and Describing Data, Statistical Tests and Data Analysis.
- Model/data skill: Delta G, ATP yield, and electron-carrier accounting. Track carbon, electrons, and ATP across a pathway.
- Misconception probe: ATP is not stored energy in a vague sense; it is a coupling currency with defined reaction chemistry.
- Transfer task: Transfer energy accounting to exercise, fermentation, hypoxia, and mitochondrial disease.

— Photosynthesis

- Chapter: section 10.
- Lab: Lab — Photosynthesis.
- Question bank: Questions — Photosynthesis.
- Big idea: Photosynthesis couples light-driven electron flow to carbon fixation and planetary productivity.
- Core concepts: photosystems, electron transport, Calvin cycle, photorespiration.
- Framework alignment: Vision & Change: Pathways and transformations of energy and matter, Systems; AP Biology: Energetics, Systems Interactions; NGSS-style topics: Matter and Energy in Organisms and Ecosystems.
- Practice cadence: Representing and Describing Data, Statistical Tests and Data Analysis.
- Model/data skill: Photon, ATP/NADPH, and Calvin-cycle stoichiometry. Interpret light-response and carbon-fixation data.
- Misconception probe: Plants do not eat sunlight; they use light energy to reduce carbon using electrons and enzymes.
- Transfer task: Transfer photosynthetic constraints to crops, algae, climate, or ecosystem productivity.

— Metabolic Integration and Regulation

- Chapter: section 11.
- Lab: Lab — Metabolic Integration and Regulation.
- Question bank: Questions — Metabolic Integration and Regulation.
- Big idea: Metabolism is a regulated network that reallocates flux across tissues, time, and nutrient states.
- Core concepts: flux, energy charge, hormonal control, fed/fasted states.
- Framework alignment: Vision & Change: Pathways and transformations of energy and matter, Systems; AP Biology: Energetics, Systems Interactions; NGSS-style topics: Matter and Energy in Organisms and Ecosystems.
- Practice cadence: Representing and Describing Data, Statistical Tests and Data Analysis.
- Model/data skill: Energy charge, control points, and pathway-flux comparisons. Use pathway evidence to infer which metabolic state or tissue is active.
- Misconception probe: A pathway is not a one-way assembly line; reversibility and regulation define the real route.
- Transfer task: Apply metabolic network reasoning to diabetes, fasting, exercise, or cancer metabolism.

Unit IV

— DNA Replication and the Cell Cycle

- Chapter: section 12.
- Lab: Lab — DNA Replication and the Cell Cycle.
- Question bank: Questions — DNA Replication and the Cell Cycle.
- Big idea: Genome copying is accurate because chemistry, enzyme proofreading, and checkpoints cooperate.
- Core concepts: semiconservative replication, polymerase, proofreading, checkpoints.
- Framework alignment: Vision & Change: Information flow, exchange, and storage, Structure and function; AP Biology: Information Storage and Transmission, Systems Interactions; NGSS-style topics: Inheritance and Variation of Traits, Structure and Function.
- Practice cadence: Concept Explanation, Questions and Methods, Argumentation.
- Model/data skill: Replication-fork speed, error-rate, and cell-cycle timing calculations. Interpret replication or cell-cycle data from timing, labeling, or checkpoint perturbations.
- Misconception probe: High fidelity is not automatic; it is built from multiple partially redundant safeguards.
- Transfer task: Transfer replication logic to cancer, aging, viral replication, or antibiotic targets.

— Gene Expression

- Chapter: section 13.
- Lab: Lab — Gene Expression.
- Question bank: Questions — Gene Expression.
- Big idea: Gene expression translates sequence information into regulated RNA and protein products.
- Core concepts: transcription, translation, codons, RNA processing.
- Framework alignment: Vision & Change: Information flow, exchange, and storage, Structure and function; AP Biology: Information Storage and Transmission, Systems Interactions; NGSS-style topics: Inheritance and Variation of Traits, Structure and Function.
- Practice cadence: Concept Explanation, Questions and Methods, Argumentation.
- Model/data skill: Reading-frame, codon, and expression-output calculations. Convert DNA/RNA sequence data into predicted molecular products.
- Misconception probe: A gene is not simply a protein recipe; context controls when, where, and how much product appears.
- Transfer task: Apply expression logic to mutations, biotechnology, development, and disease diagnostics.

— Mutations, CRISPR, and Genomics

- Chapter: section 14.
- Lab: Lab — Mutations, CRISPR, and Genomics.
- Question bank: Questions — Mutations, CRISPR, and Genomics.
- Big idea: Genomic variation becomes biological consequence through sequence context, repair, and selection.
- Core concepts: mutation classes, DNA repair, CRISPR, genome analysis.
- Framework alignment: Vision & Change: Information flow, exchange, and storage, Structure and function; AP Biology: Information Storage and Transmission, Systems Interactions; NGSS-style topics: Inheritance and Variation of Traits, Structure and Function.
- Practice cadence: Concept Explanation, Questions and Methods, Argumentation.

- Model/data skill: Mutation-rate, edit-efficiency, and sequence-comparison calculations. Classify variants and predict likely molecular effect from sequence evidence.
- Misconception probe: Not every mutation is harmful, and not every harmful mutation changes a protein sequence.
- Transfer task: Transfer variant reasoning to cancer genomics, ancestry, gene therapy, or microbial evolution.

— Chromatin and Epigenetic Mechanisms

- Chapter: section 15.
- Lab: Lab — Chromatin and Epigenetic Mechanisms.
- Question bank: Questions — Chromatin and Epigenetic Mechanisms.
- Big idea: Cells create stable yet reversible expression states through chromatin, DNA marks, and regulatory circuits.
- Core concepts: chromatin, methylation, histone modification, enhancers.
- Framework alignment: Vision & Change: Information flow, exchange, and storage, Structure and function; AP Biology: Information Storage and Transmission, Systems Interactions; NGSS-style topics: Inheritance and Variation of Traits, Structure and Function.
- Practice cadence: Concept Explanation, Questions and Methods, Argumentation.
- Model/data skill: Regulatory-state and expression-ratio reasoning. Interpret chromatin or expression evidence from simple regulatory datasets.
- Misconception probe: Epigenetic does not mean independent of DNA sequence or permanently inherited.
- Transfer task: Apply regulation logic to differentiation, imprinting, cancer, or environmental responses.

— Epigenetic Inheritance and Disease

- Chapter: section 16.
- Lab: Lab — Epigenetic Inheritance and Disease.
- Question bank: Questions — Epigenetic Inheritance and Disease.
- Big idea: Three-dimensional genome organization and epigenetic inheritance link regulatory architecture to disease phenotypes.
- Core concepts: 3D genome, phase separation, imprinting, epigenetic inheritance.
- Framework alignment: Vision & Change: Information flow, exchange, and storage, Structure and function; AP Biology: Information Storage and Transmission, Systems Interactions; NGSS-style topics: Inheritance and Variation of Traits, Structure and Function.
- Practice cadence: Concept Explanation, Questions and Methods, Argumentation.
- Model/data skill: Chromatin-loop, inheritance, and disease-risk reasoning. Interpret Hi-C, imprinting, or transgenerational datasets with causal caution.
- Misconception probe: A chromatin contact map is not proof of function without perturbation.
- Transfer task: Apply inheritance logic to cancer, developmental disorders, and environmental exposure.

Unit V

— Mendelian Principles and Probability

- Chapter: section 17.
- Lab: Lab — Mendelian Principles and Probability.
- Question bank: Questions — Mendelian Principles and Probability.
- Big idea: Mendelian segregation and probability explain inheritance when alleles assort independently.
- Core concepts: segregation, independent assortment, Punnett squares, probability.
- Framework alignment: Vision & Change: Information flow, exchange, and storage, Evolution; AP Biology: Information Storage and Transmission, Evolution; NGSS-style topics: Inheritance and Variation of Traits, Natural Selection and Evolution.
- Practice cadence: Statistical Tests and Data Analysis, Representing and Describing Data.
- Model/data skill: Punnett, binomial, and chi-square calculations. Use cross data to infer genotype probabilities.
- Misconception probe: Dominant does not mean common, stronger, or better.
- Transfer task: Transfer Mendelian probability to model organisms and introductory human genetics.

— Mendelian Extensions and Human Genetics

- Chapter: section 18.
- Lab: Lab — Mendelian Extensions and Human Genetics.
- Question bank: Questions — Mendelian Extensions and Human Genetics.
- Big idea: Extensions to Mendelian ratios and human pedigree analysis reveal when simple dominance fails.

- Core concepts: incomplete dominance, epistasis, pedigrees, penetrance.
- Framework alignment: Vision & Change: Information flow, exchange, and storage, Evolution; AP Biology: Information Storage and Transmission, Evolution; NGSS-style topics: Inheritance and Variation of Traits, Natural Selection and Evolution.
- Practice cadence: Statistical Tests and Data Analysis, Representing and Describing Data.
- Model/data skill: Pedigree, epistasis, and multi-locus probability calculations. Infer inheritance mode and extension mechanism from family or cross data.
- Misconception probe: A single-gene model is a starting hypothesis, not the default for every trait.
- Transfer task: Transfer extension reasoning to counseling, GWAS interpretation, and breeding.

— Chromosomal Inheritance and Linkage

- Chapter: section 19.
- Lab: Lab — Chromosomal Inheritance and Linkage.
- Question bank: Questions — Chromosomal Inheritance and Linkage.
- Big idea: Genes travel on chromosomes, so linkage, recombination, and chromosome structure shape inheritance.
- Core concepts: linkage, recombination, sex linkage, chromosomal rearrangements.
- Framework alignment: Vision & Change: Information flow, exchange, and storage, Evolution; AP Biology: Information Storage and Transmission, Evolution; NGSS-style topics: Inheritance and Variation of Traits, Natural Selection and Evolution.
- Practice cadence: Statistical Tests and Data Analysis, Representing and Describing Data.
- Model/data skill: Recombination frequency and three-point mapping. Infer gene order or chromosomal mechanism from offspring counts.
- Misconception probe: Independent assortment applies to unlinked loci, not to every pair of genes.
- Transfer task: Transfer linkage reasoning to disease mapping, breeding, and genome assemblies.

— Population Genetics

- Chapter: section 20.
- Lab: Lab — Population Genetics.
- Question bank: Questions — Population Genetics.
- Big idea: Allele frequencies change when assumptions about random mating, population size, and fitness are violated.
- Core concepts: Hardy-Weinberg, selection, mutation, genetic drift.
- Framework alignment: Vision & Change: Information flow, exchange, and storage, Evolution; AP Biology: Information Storage and Transmission, Evolution; NGSS-style topics: Inheritance and Variation of Traits, Natural Selection and Evolution.
- Practice cadence: Statistical Tests and Data Analysis, Representing and Describing Data.
- Model/data skill: Hardy-Weinberg and allele-frequency recurrence calculations. Estimate genotype or allele frequencies from population data.
- Misconception probe: Hardy-Weinberg is a null model, not a claim that populations do not evolve.
- Transfer task: Apply population-genetic reasoning to screening, conservation, and pathogen evolution.

Unit VI

— Natural Selection and Adaptation

- Chapter: section 21.
- Lab: Lab — Natural Selection and Adaptation.
- Question bank: Questions — Natural Selection and Adaptation.
- Big idea: Natural selection is differential reproductive success acting on heritable variation in context.
- Core concepts: variation, fitness, adaptation, selection coefficient.
- Framework alignment: Vision & Change: Evolution, Systems; AP Biology: Evolution, Systems Interactions; NGSS-style topics: Natural Selection and Evolution, Interdependent Relationships in Ecosystems.
- Practice cadence: Visual Representations, Statistical Tests and Data Analysis, Argumentation.
- Model/data skill: Selection coefficient and allele-frequency trajectory calculations. Interpret fitness data and distinguish selection from other forces.
- Misconception probe: Evolution is not goal-directed progress; it is local change in populations under constraints.
- Transfer task: Transfer selection reasoning to antibiotics, pesticide resistance, cancer, or climate adaptation.

— Genetic Drift, Gene Flow, and Speciation

- Chapter: section 22.

- Lab: **Lab — Genetic Drift, Gene Flow, and Speciation.**
- Question bank: **Questions — Genetic Drift, Gene Flow, and Speciation.**
- Big idea: Chance, population structure, and barriers to gene flow can generate divergence even without adaptive change.
- Core concepts: drift, effective population size, gene flow, speciation.
- Framework alignment: Vision & Change: Evolution, Systems; AP Biology: Evolution, Systems Interactions; NGSS-style topics: Natural Selection and Evolution, Interdependent Relationships in Ecosystems.
- Practice cadence: Visual Representations, Statistical Tests and Data Analysis, Argumentation.
- Model/data skill: Fixation probability, effective population size, and migration-selection balance. Distinguish stochastic from directional change in allele-frequency data.
- Misconception probe: Random does not mean patternless; stochastic processes have predictable distributions.
- Transfer task: Apply drift reasoning to endangered populations, founder effects, and island radiations.

— **Phylogenetics and the Tree of Life**

- Chapter: section **23.**
- Lab: **Lab — Phylogenetics and the Tree of Life.**
- Question bank: **Questions — Phylogenetics and the Tree of Life.**
- Big idea: Phylogenies are evidence-based hypotheses about ancestry, not ladders of progress.
- Core concepts: homology, tree topology, parsimony, molecular clocks.
- Framework alignment: Vision & Change: Evolution, Systems; AP Biology: Evolution, Systems Interactions; NGSS-style topics: Natural Selection and Evolution, Interdependent Relationships in Ecosystems.
- Practice cadence: Visual Representations, Statistical Tests and Data Analysis, Argumentation.
- Model/data skill: Tree-distance, parsimony, and molecular-clock calculations. Read trees correctly and map traits or sequences onto branches.
- Misconception probe: Living species are cousins, not ancestors of one another.
- Transfer task: Transfer tree thinking to pathogens, conservation units, gene families, and development.

Unit VII

— **Bacteria, Archaea, and Viruses**

- Chapter: section **24.**
- Lab: **Lab — Bacteria, Archaea, and Viruses.**
- Question bank: **Questions — Bacteria, Archaea, and Viruses.**
- Big idea: Microbial diversity reflects different cell architectures, genomes, metabolisms, and evolutionary histories.
- Core concepts: prokaryotic structure, archaea, viruses, horizontal gene transfer.
- Framework alignment: Vision & Change: Evolution, Systems, Structure and function; AP Biology: Evolution, Systems Interactions; NGSS-style topics: Structure and Function, Interdependent Relationships in Ecosystems.
- Practice cadence: Questions and Methods, Representing and Describing Data, Argumentation.
- Model/data skill: Growth-rate, genome-size, and dilution calculations. Interpret microbial observations from growth, sequence, or structural evidence.
- Misconception probe: Viruses are not simply tiny bacteria; they use fundamentally different replication logic.
- Transfer task: Apply microbial diversity reasoning to antibiotics, biotechnology, ecology, and outbreaks.

— **Microbial Ecology and the Microbiome**

- Chapter: section **25.**
- Lab: **Lab — Microbial Ecology and the Microbiome.**
- Question bank: **Questions — Microbial Ecology and the Microbiome.**
- Big idea: Microbes organize communities, cycles, and host physiology through interactions and metabolism.
- Core concepts: microbiomes, symbiosis, diversity, biogeochemical cycling.
- Framework alignment: Vision & Change: Evolution, Systems, Structure and function; AP Biology: Evolution, Systems Interactions; NGSS-style topics: Structure and Function, Interdependent Relationships in Ecosystems.
- Practice cadence: Questions and Methods, Representing and Describing Data, Argumentation.
- Model/data skill: Diversity indices, richness estimates, and interaction-network reasoning. Compute or interpret community metrics from abundance data.
- Misconception probe: A microbiome is not automatically beneficial; context determines the effect.

- Transfer task: Transfer microbial ecology to soils, oceans, digestion, disease, and climate feedbacks.

— Host Immunity and Vaccines

- Chapter: section 26.
- Lab: [Lab — Host Immunity and Vaccines](#).
- Question bank: [Questions — Host Immunity and Vaccines](#).
- Big idea: Host immunity and vaccination reshape pathogen transmission by changing susceptible fractions.
- Core concepts: innate immunity, adaptive immunity, vaccination, herd immunity.
- Framework alignment: Vision & Change: Evolution, Systems, Structure and function; AP Biology: Evolution, Systems Interactions; NGSS-style topics: Structure and Function, Interdependent Relationships in Ecosystems.
- Practice cadence: Questions and Methods, Representing and Describing Data, Argumentation.
- Model/data skill: Herd-immunity threshold and basic immunological reasoning. Interpret antibody, cellular, and vaccine-response evidence.
- Misconception probe: Immunity is not binary; timing, dose, and variant matter.
- Transfer task: Transfer immunity reasoning to outbreak response and clinical decision-making.

— Antimicrobial Resistance and Epidemiology

- Chapter: section 27.
- Lab: [Lab — Antimicrobial Resistance and Epidemiology](#).
- Question bank: [Questions — Antimicrobial Resistance and Epidemiology](#).
- Big idea: Antimicrobial resistance and epidemic dynamics emerge from pathogen evolution and transmission networks.
- Core concepts: antibiotic resistance, R_0 , transmission, surveillance.
- Framework alignment: Vision & Change: Evolution, Systems, Structure and function; AP Biology: Evolution, Systems Interactions; NGSS-style topics: Structure and Function, Interdependent Relationships in Ecosystems.
- Practice cadence: Questions and Methods, Representing and Describing Data, Argumentation.
- Model/data skill: R_0 , resistance-mechanism, and outbreak-trajectory calculations. Interpret resistance assays and outbreak curves.
- Misconception probe: R_0 is not a fixed property of a pathogen alone; it depends on host behavior and environment.
- Transfer task: Transfer resistance and epidemiology reasoning to stewardship and public-health policy.

Unit VIII

— Plant Structure and Water Relations

- Chapter: section 28.
- Lab: [Lab — Plant Structure and Water Relations](#).
- Question bank: [Questions — Plant Structure and Water Relations](#).
- Big idea: Plant form is an engineering solution to water movement, support, gas exchange, and growth.
- Core concepts: xylem, phloem, water potential, transpiration.
- Framework alignment: Vision & Change: Structure and function, Pathways and transformations of energy and matter, Systems; AP Biology: Energetics, Systems Interactions; NGSS-style topics: Structure and Function, Matter and Energy in Organisms and Ecosystems.
- Practice cadence: Visual Representations, Questions and Methods, Argumentation.
- Model/data skill: Water-potential and transpiration-flux calculations. Interpret plant-water data from pressure, solute, and humidity measurements.
- Misconception probe: Water does not move because plants pull with intention; it follows potential gradients and cohesion.
- Transfer task: Transfer plant-water reasoning to drought, irrigation, forest physiology, and crop breeding.

— Plant Reproduction and Development

- Chapter: section 29.
- Lab: [Lab — Plant Reproduction and Development](#).
- Question bank: [Questions — Plant Reproduction and Development](#).
- Big idea: Plant reproduction integrates life cycles, development, dispersal, and environmental timing.
- Core concepts: alternation of generations, flowers, seeds, development.
- Framework alignment: Vision & Change: Structure and function, Pathways and transformations of energy and matter, Systems; AP Biology: Energetics, Systems Interactions; NGSS-style topics: Structure and Function, Matter and Energy in Organisms and Ecosystems.

- Practice cadence: Visual Representations, Questions and Methods, Argumentation.
- Model/data skill: Life-cycle accounting and phyllotaxis/growth-pattern calculations. Track ploidy, tissue origin, and reproductive stage from diagrams or observations.
- Misconception probe: Pollen, spores, seeds, and gametes are not interchangeable terms.
- Transfer task: Transfer reproductive reasoning to agriculture, pollination ecology, and plant evolution.

— Plant Responses to the Environment

- Chapter: section 30.
- Lab: Lab — Plant Responses to the Environment.
- Question bank: Questions — Plant Responses to the Environment.
- Big idea: Plants sense environmental signals and respond through growth, hormones, and physiological regulation.
- Core concepts: tropisms, hormones, photoperiodism, stress responses.
- Framework alignment: Vision & Change: Structure and function, Pathways and transformations of energy and matter, Systems; AP Biology: Energetics, Systems Interactions; NGSS-style topics: Structure and Function, Matter and Energy in Organisms and Ecosystems.
- Practice cadence: Visual Representations, Questions and Methods, Argumentation.
- Model/data skill: Dose-response, water-use-efficiency, and hormone-interaction reasoning. Interpret plant response data across light, gravity, water, and hormone treatments.
- Misconception probe: A plant response is not passive; plants actively regulate development and physiology without neurons.
- Transfer task: Transfer response logic to shade avoidance, drought, flowering, and crop management.

Unit IX

— Circulation and Respiration

- Chapter: section 31.
- Lab: Lab — Circulation and Respiration.
- Question bank: Questions — Circulation and Respiration.
- Big idea: Animal transport systems maintain gradients that let cells exchange gases, nutrients, heat, and wastes.
- Core concepts: cardiac output, gas exchange, homeostasis, feedback.
- Framework alignment: Vision & Change: Structure and function, Systems; AP Biology: Systems Interactions, Energetics; NGSS-style topics: Structure and Function.
- Practice cadence: Visual Representations, Statistical Tests and Data Analysis, Argumentation.
- Model/data skill: Cardiac-output, diffusion, oxygen-saturation, and feedback calculations. Interpret physiological data from pressure, flow, saturation, or set-point changes.
- Misconception probe: Homeostasis is dynamic regulation, not an unchanging internal state.
- Transfer task: Transfer homeostatic reasoning to exercise, altitude, hemorrhage, fever, and shock.

— Nervous System and Neural Signaling

- Chapter: section 32.
- Lab: Lab — Nervous System and Neural Signaling.
- Question bank: Questions — Nervous System and Neural Signaling.
- Big idea: Nervous systems compute with cells whose structure shapes information flow and behavior.
- Core concepts: neurons, glia, circuits, sensory processing.
- Framework alignment: Vision & Change: Structure and function, Systems; AP Biology: Systems Interactions, Energetics; NGSS-style topics: Structure and Function.
- Practice cadence: Visual Representations, Statistical Tests and Data Analysis, Argumentation.
- Model/data skill: Cable-length, conduction, and simple circuit calculations. Interpret neural data from anatomy, timing, or lesion evidence.
- Misconception probe: The brain is not only neurons; glia and circuit context are essential to function.
- Transfer task: Transfer circuit reasoning to reflexes, sensory systems, learning, and disease.

— Action Potentials and Synaptic Transmission

- Chapter: section 33.

- Lab: **Lab — Action Potentials and Synaptic Transmission.**
- Question bank: **Questions — Action Potentials and Synaptic Transmission.**
- Big idea: Electrical excitability and synaptic transmission convert ion gradients into rapid communication.
- Core concepts: action potentials, ion channels, synapses, plasticity.
- Framework alignment: Vision & Change: Structure and function, Systems; AP Biology: Systems Interactions, Energetics; NGSS-style topics: Structure and Function.
- Practice cadence: Visual Representations, Statistical Tests and Data Analysis, Argumentation.
- Model/data skill: Nernst/Goldman, Hodgkin-Huxley, and synaptic-current reasoning. Interpret voltage traces, conductance changes, and synaptic perturbations.
- Misconception probe: An action potential is not electricity flowing like a wire; it is regenerated ion-channel dynamics.
- Transfer task: Transfer excitability reasoning to anesthesia, toxins, epilepsy, and neuromuscular disease.

— Endocrine Signaling and Homeostasis

- Chapter: section 34.
- Lab: **Lab — Endocrine Signaling and Homeostasis.**
- Question bank: **Questions — Endocrine Signaling and Homeostasis.**
- Big idea: Hormone feedback loops coordinate long-range physiological homeostasis.
- Core concepts: hormones, feedback, receptors, homeostasis.
- Framework alignment: Vision & Change: Structure and function, Systems; AP Biology: Systems Interactions, Energetics; NGSS-style topics: Structure and Function.
- Practice cadence: Visual Representations, Statistical Tests and Data Analysis, Argumentation.
- Model/data skill: Hormone feedback and dose-response reasoning. Interpret endocrine time courses, panels, and perturbations.
- Misconception probe: A hormone surge is not always pathological; context and set-point matter.
- Transfer task: Transfer endocrine reasoning to metabolism, stress, and development.

— Immune System Architecture

- Chapter: section 35.
- Lab: **Lab — Immune System Architecture.**
- Question bank: **Questions — Immune System Architecture.**
- Big idea: Innate and adaptive immunity integrate recognition, effector function, tolerance, and memory.
- Core concepts: innate immunity, adaptive immunity, tolerance, immunotherapy.
- Framework alignment: Vision & Change: Structure and function, Systems; AP Biology: Systems Interactions, Energetics; NGSS-style topics: Structure and Function.
- Practice cadence: Visual Representations, Statistical Tests and Data Analysis, Argumentation.
- Model/data skill: Immune-memory, cytokine, and recognition reasoning. Interpret immune titers, cytokine profiles, or perturbation data.
- Misconception probe: Immunity is not just attack; recognition, tolerance, memory, and regulation are equally central.
- Transfer task: Transfer immunity reasoning to vaccination, autoimmunity, infection, and cancer therapy.

Unit X

— Population Ecology and Growth Models

- Chapter: section 36.
- Lab: **Lab — Population Ecology and Growth Models.**
- Question bank: **Questions — Population Ecology and Growth Models.**
- Big idea: Population change reflects births, deaths, movement, age structure, and density dependence.
- Core concepts: exponential growth, logistic growth, life tables, population viability.
- Framework alignment: Vision & Change: Systems, Evolution, Pathways and transformations of energy and matter; AP Biology: Systems Interactions, Evolution, Energetics; NGSS-style topics: Interdependent Relationships in Ecosystems, Matter and Energy in Organisms and Ecosystems, Natural Selection and Evolution.
- Practice cadence: Representing and Describing Data, Statistical Tests and Data Analysis, Argumentation.
- Model/data skill: Exponential/logistic growth, mark-recapture, and matrix projection. Use abundance or age-structure data to estimate growth and risk.
- Misconception probe: Carrying capacity is not a fixed magic number; it changes with resources, interactions, and disturbance.

- Transfer task: Transfer population models to fisheries, invasive species, epidemiology, and endangered species.

— Community Interactions and Succession

- Chapter: section 37.
- Lab: [Lab — Community Interactions and Succession](#).
- Question bank: [Questions — Community Interactions and Succession](#).
- Big idea: Communities are structured by pairwise species interactions and successional change.
- Core concepts: competition, predation, mutualism, succession.
- Framework alignment: Vision & Change: Systems, Evolution, Pathways and transformations of energy and matter; AP Biology: Systems Interactions, Evolution, Energetics; NGSS-style topics: Interdependent Relationships in Ecosystems, Matter and Energy in Organisms and Ecosystems, Natural Selection and Evolution.
- Practice cadence: Representing and Describing Data, Statistical Tests and Data Analysis, Argumentation.
- Model/data skill: Lotka-Volterra-style interaction reasoning. Interpret abundance, interaction, or disturbance data from communities.
- Misconception probe: A species interaction is not permanently good or bad; the sign can change with context.
- Transfer task: Transfer interaction reasoning to restoration, agriculture, and invasion biology.

— Biodiversity and Food Webs

- Chapter: section 38.
- Lab: [Lab — Biodiversity and Food Webs](#).
- Question bank: [Questions — Biodiversity and Food Webs](#).
- Big idea: Biodiversity patterns, food webs, and island biogeography scale from local interactions to landscape structure.
- Core concepts: food webs, keystone species, species-area, diversity indices.
- Framework alignment: Vision & Change: Systems, Evolution, Pathways and transformations of energy and matter; AP Biology: Systems Interactions, Evolution, Energetics; NGSS-style topics: Interdependent Relationships in Ecosystems, Matter and Energy in Organisms and Ecosystems, Natural Selection and Evolution.
- Practice cadence: Representing and Describing Data, Statistical Tests and Data Analysis, Argumentation.
- Model/data skill: Shannon, species-area, and network connectance reasoning. Interpret food-web, richness, or biogeography datasets.
- Misconception probe: Richness alone does not equal functional stability.
- Transfer task: Transfer biodiversity reasoning to conservation planning and habitat fragmentation.

— Ecosystem Ecology

- Chapter: section 39.
- Lab: [Lab — Ecosystem Ecology](#).
- Question bank: [Questions — Ecosystem Ecology](#).
- Big idea: Ecosystems couple energy flow and matter cycling across organisms, environments, and time.
- Core concepts: primary productivity, trophic efficiency, nutrient cycles, decomposition.
- Framework alignment: Vision & Change: Systems, Evolution, Pathways and transformations of energy and matter; AP Biology: Systems Interactions, Evolution, Energetics; NGSS-style topics: Interdependent Relationships in Ecosystems, Matter and Energy in Organisms and Ecosystems, Natural Selection and Evolution.
- Practice cadence: Representing and Describing Data, Statistical Tests and Data Analysis, Argumentation.
- Model/data skill: Energy-flow, productivity, and nutrient-budget calculations. Trace matter and energy through food webs and biogeochemical cycles.
- Misconception probe: Energy flows through ecosystems, but matter cycles; confusing the two breaks many explanations.
- Transfer task: Transfer ecosystem reasoning to eutrophication, carbon budgets, agriculture, and climate feedback.

— Biomes and Conservation Biology

- Chapter: section 40.
- Lab: [Lab — Biomes and Conservation Biology](#).
- Question bank: [Questions — Biomes and Conservation Biology](#).
- Big idea: Biodiversity patterns and conservation decisions emerge from climate, history, disturbance, and human choice.
- Core concepts: biomes, biodiversity, extinction risk, conservation planning.

- Framework alignment: Vision & Change: Systems, Evolution, Pathways and transformations of energy and matter; AP Biology: Systems Interactions, Evolution, Energetics; NGSS-style topics: Interdependent Relationships in Ecosystems, Matter and Energy in Organisms and Ecosystems, Natural Selection and Evolution.
- Practice cadence: Representing and Describing Data, Statistical Tests and Data Analysis, Argumentation.
- Model/data skill: Species-area, risk, and prioritization calculations. Use maps, trend data, and threat categories to justify conservation priorities.
- Misconception probe: Conservation is decision-making under constraints and uncertainty, not only preserving untouched nature.
- Transfer task: Transfer conservation reasoning to land use, climate corridors, restoration, and environmental justice.

Appendix B — Instructor Orchestration Guide

This appendix is generated from the same curriculum and alignment records that populate chapter Study Blueprints. It gives instructors a compact sequence for turning the textbook into lectures, labs, quizzes, and transfer tasks without hand-rebuilding a course map.

Reusable Teaching Loop

1. Launch from a phenomenon. Begin with a case, dataset, model failure, or observed pattern that makes the chapter question necessary.
2. Model the mechanism. Ask students to draw, compute, simulate, or annotate the causal structure before reading the full explanation.
3. Gather evidence. Use the companion lab as the measurement and reproducibility surface for the chapter.
4. Check transfer. Use the question bank to sample recall, application, data interpretation, and argumentation.
5. Close the loop. Return to the transfer task and require a claim, evidence, reasoning, and uncertainty statement.

Chapter Orchestration Matrix

Unit 0

— Systems Science and Emergence

- Core thread: Use systems diagrams, uncertainty, and feedback as recurring sense-making tools.
- Instructor move: Launch from a phenomenon, have students model it with Box-and-arrow causal models with explicit inputs, outputs, and feedback signs, then test the model through data.
- Formative check: Ask students to translate a verbal biological system into variables, links, and testable predictions and then answer: given a biological scenario, identify the system boundary, feedback loop, and missing measurement.
- Summative product: Apply the same feedback map to a cell, organism, and ecosystem, then name what changes at each scale.
- Lab/question pair: **Lab A — Systems Science and Emergence; Questions — Systems Science and Emergence.**
- External alignment: Vision & Change: Systems, Structure and function; AP Biology: Systems Interactions; NGSS-style topics: Structure and Function, Interdependent Relationships in Ecosystems.

— Complex Adaptive Systems

- Core thread: Use systems diagrams, uncertainty, and feedback as recurring sense-making tools.
- Instructor move: Launch from a phenomenon, have students model it with Agent-rule and scaling arguments for emergent biological patterns, then test the model through data.
- Formative check: Ask students to distinguish deterministic trends from stochastic variation in repeated simulations and then answer: explain an observed population pattern from individual-level rules and identify one falsifiable prediction.
- Summative product: Compare flocking, immune activation, and microbial biofilms as adaptive systems.
- Lab/question pair: **Lab B — Complex Adaptive Systems; Questions — Complex Adaptive Systems.**
- External alignment: Vision & Change: Systems, Structure and function; AP Biology: Systems Interactions; NGSS-style topics: Structure and Function, Interdependent Relationships in Ecosystems.

— Active Inference and Free Energy

- Core thread: Use systems diagrams, uncertainty, and feedback as recurring sense-making tools.
- Instructor move: Launch from a phenomenon, have students model it with Bayesian belief updating and expected-free-energy-style policy comparison, then test the model through data.
- Formative check: Ask students to read a small probability table and update a prediction after new evidence and then answer: calculate a posterior belief and explain what action would reduce uncertainty or restore a set point.
- Summative product: Map prediction-error reasoning onto chemotaxis, thermoregulation, and attention.
- Lab/question pair: **Lab C — Active Inference and Free Energy; Questions — Active Inference and Free Energy.**
- External alignment: Vision & Change: Systems, Structure and function; AP Biology: Systems Interactions; NGSS-style topics: Structure and Function, Interdependent Relationships in Ecosystems.

— History and Philosophy of Biology

- Core thread: Use systems diagrams, uncertainty, and feedback as recurring sense-making tools.
- Instructor move: Launch from a phenomenon, have students model it with Concept-map and evidence-matrix comparisons among historical claims, mechanisms, and model assumptions, then test the model through data.

- Formative check: Ask students to classify source excerpts as observation, experiment, model, mechanism, or value-laden inference and then answer: given a biological claim, identify the practice that produced it, the evidence standard it used, and one philosophical assumption it carries.
- Summative product: Transfer source-analysis reasoning to modern debates about species, genetics, microbiomes, and biomedical ethics.
- Lab/question pair: **Lab D — History and Philosophy of Biology; Questions — History and Philosophy of Biology.**
- External alignment: Vision & Change: Systems, Structure and function; AP Biology: Systems Interactions; NGSS-style topics: Structure and Function, Interdependent Relationships in Ecosystems.

Unit I

— Atoms, Molecules, and Chemical Bonds

- Core thread: Connect chemical structure, water, polymers, and catalysis to biological mechanism.
- Instructor move: Launch from a phenomenon, have students model it with Formal charge and electronegativity-difference reasoning, then test the model through data.
- Formative check: Ask students to use tabular atomic data to predict polarity, solubility, and biological reactivity and then answer: predict bond polarity, formal charge, or isotope behavior and connect it to a biological consequence.
- Summative product: Use atomic reasoning to explain a medical tracer, enzyme cofactor, or membrane-solubility problem.
- Lab/question pair: **Lab — Atoms, Molecules, and Chemical Bonds; Questions — Atoms, Molecules, and Chemical Bonds.**
- External alignment: Vision & Change: Structure and function, Pathways and transformations of energy and matter; AP Biology: Energetics, Systems Interactions; NGSS-style topics: Matter and Energy in Organisms and Ecosystems, Structure and Function.

— Water — The Molecule of Life

- Core thread: Connect chemical structure, water, polymers, and catalysis to biological mechanism.
- Instructor move: Launch from a phenomenon, have students model it with Henderson-Hasselbalch and pH-scale calculations, then test the model through data.
- Formative check: Ask students to convert between pH, hydrogen ion concentration, and buffer ratios and then answer: calculate a pH or buffer ratio and interpret what it means for a biological system.
- Summative product: Transfer water-property reasoning to blood buffering, plant transport, or protein folding.
- Lab/question pair: **Lab — Water — The Molecule of Life; Questions — Water — The Molecule of Life.**
- External alignment: Vision & Change: Structure and function, Pathways and transformations of energy and matter; AP Biology: Energetics, Systems Interactions; NGSS-style topics: Matter and Energy in Organisms and Ecosystems, Structure and Function.

— Biological Macromolecules

- Core thread: Connect chemical structure, water, polymers, and catalysis to biological mechanism.
- Instructor move: Launch from a phenomenon, have students model it with Polymerization energetics and sequence-to-structure reasoning, then test the model through data.
- Formative check: Ask students to classify molecules from structural evidence rather than names alone and then answer: given a molecular feature, infer likely solubility, interaction partners, or cellular role.
- Summative product: Explain how a mutation, lipid substitution, or glycosylation change propagates to phenotype.
- Lab/question pair: **Lab — Biological Macromolecules; Questions — Biological Macromolecules.**
- External alignment: Vision & Change: Structure and function, Pathways and transformations of energy and matter; AP Biology: Energetics, Systems Interactions; NGSS-style topics: Matter and Energy in Organisms and Ecosystems, Structure and Function.

— Enzymes and the Kinetics of Catalysis

- Core thread: Connect chemical structure, water, polymers, and catalysis to biological mechanism.
- Instructor move: Launch from a phenomenon, have students model it with Michaelis-Menten, Lineweaver-Burk, and inhibition-pattern calculations, then test the model through data.
- Formative check: Ask students to fit or interpret enzyme-rate data and identify which parameter changed and then answer: infer V_{max} , K_m , or inhibition type from data and justify the mechanistic interpretation.
- Summative product: Apply enzyme-kinetic reasoning to drug dosing, metabolic control, or diagnostic assays.
- Lab/question pair: **Lab — Enzymes and the Kinetics of Catalysis; Questions — Enzymes and the Kinetics of Catalysis.**

- External alignment: Vision & Change: Structure and function, Pathways and transformations of energy and matter; AP Biology: Energetics, Systems Interactions; NGSS-style topics: Matter and Energy in Organisms and Ecosystems, Structure and Function.

Unit II

— Cell Theory and Cell Types

- Core thread: Revisit boundaries, compartments, and signals as causal models of cellular work.
- Instructor move: Launch from a phenomenon, have students model it with Surface-area-to-volume scaling, then test the model through data.
- Formative check: Ask students to infer cellular constraints from measurements, micrographs, and scale bars and then answer: use size or microscopy evidence to classify a cell and predict a constraint on exchange.
- Summative product: Transfer scale reasoning to eggs, neurons, root hairs, and microbial colonies.
- Lab/question pair: **Lab — Cell Theory and Cell Types; Questions — Cell Theory and Cell Types.**
- External alignment: Vision & Change: Structure and function, Systems, Information flow, exchange, and storage; AP Biology: Systems Interactions, Information Storage and Transmission; NGSS-style topics: Structure and Function.

— Cell Structure and Organelles

- Core thread: Revisit boundaries, compartments, and signals as causal models of cellular work.
- Instructor move: Launch from a phenomenon, have students model it with Compartment-flow and motor-transport calculations, then test the model through data.
- Formative check: Ask students to trace a molecule through compartments using evidence from labels or perturbations and then answer: predict which organelle or cytoskeletal process is disrupted from a phenotype.
- Summative product: Apply compartment logic to secretion, apoptosis, infection, or cell division.
- Lab/question pair: **Lab — Cell Structure and Organelles; Questions — Cell Structure and Organelles.**
- External alignment: Vision & Change: Structure and function, Systems, Information flow, exchange, and storage; AP Biology: Systems Interactions, Information Storage and Transmission; NGSS-style topics: Structure and Function.

— Membrane Structure and Transport

- Core thread: Revisit boundaries, compartments, and signals as causal models of cellular work.
- Instructor move: Launch from a phenomenon, have students model it with Nernst, Goldman, osmotic, and facilitated-transport calculations, then test the model through data.
- Formative check: Ask students to interpret transport data from gradients, rates, and membrane potentials and then answer: calculate or predict ion movement and explain which force dominates.
- Summative product: Transfer gradient logic to neurons, kidneys, roots, and mitochondrial membranes.
- Lab/question pair: **Lab — Membrane Structure and Transport; Questions — Membrane Structure and Transport.**
- External alignment: Vision & Change: Structure and function, Systems, Information flow, exchange, and storage; AP Biology: Systems Interactions, Information Storage and Transmission; NGSS-style topics: Structure and Function.

— Cell Signaling and Communication

- Core thread: Revisit boundaries, compartments, and signals as causal models of cellular work.
- Instructor move: Launch from a phenomenon, have students model it with Ligand-receptor occupancy and dose-response reasoning, then test the model through data.
- Formative check: Ask students to read pathway diagrams and infer the effect of agonists, antagonists, or mutations and then answer: predict the outcome of perturbing one pathway component and justify the causal chain.
- Summative product: Apply signaling logic to hormones, neurotransmitters, immune receptors, or cancer mutations.
- Lab/question pair: **Lab — Cell Signaling and Communication; Questions — Cell Signaling and Communication.**
- External alignment: Vision & Change: Structure and function, Systems, Information flow, exchange, and storage; AP Biology: Systems Interactions, Information Storage and Transmission; NGSS-style topics: Structure and Function.

Unit III

— Bioenergetics and Cellular Respiration

- Core thread: Track matter, electrons, and free energy through pathways and ecosystems.
- Instructor move: Launch from a phenomenon, have students model it with Delta G, ATP yield, and electron-carrier accounting, then test the model through data.
- Formative check: Ask students to track carbon, electrons, and ATP across a pathway and then answer: calculate an energy yield or redox consequence and connect it to cellular work.
- Summative product: Transfer energy accounting to exercise, fermentation, hypoxia, and mitochondrial disease.
- Lab/question pair: [Lab — Bioenergetics and Cellular Respiration](#); [Questions — Bioenergetics and Cellular Respiration](#).
- External alignment: Vision & Change: Pathways and transformations of energy and matter, Systems; AP Biology: Energetics, Systems Interactions; NGSS-style topics: Matter and Energy in Organisms and Ecosystems.

— Photosynthesis

- Core thread: Track matter, electrons, and free energy through pathways and ecosystems.
- Instructor move: Launch from a phenomenon, have students model it with Photon, ATP/NADPH, and Calvin-cycle stoichiometry, then test the model through data.
- Formative check: Ask students to interpret light-response and carbon-fixation data and then answer: compute carbon-fixation requirements and explain a limiting factor.
- Summative product: Transfer photosynthetic constraints to crops, algae, climate, or ecosystem productivity.
- Lab/question pair: [Lab — Photosynthesis](#); [Questions — Photosynthesis](#).
- External alignment: Vision & Change: Pathways and transformations of energy and matter, Systems; AP Biology: Energetics, Systems Interactions; NGSS-style topics: Matter and Energy in Organisms and Ecosystems.

— Metabolic Integration and Regulation

- Core thread: Track matter, electrons, and free energy through pathways and ecosystems.
- Instructor move: Launch from a phenomenon, have students model it with Energy charge, control points, and pathway-flux comparisons, then test the model through data.
- Formative check: Ask students to use pathway evidence to infer which metabolic state or tissue is active and then answer: predict how a change in substrate, hormone, or enzyme activity redirects flux.
- Summative product: Apply metabolic network reasoning to diabetes, fasting, exercise, or cancer metabolism.
- Lab/question pair: [Lab — Metabolic Integration and Regulation](#); [Questions — Metabolic Integration and Regulation](#).
- External alignment: Vision & Change: Pathways and transformations of energy and matter, Systems; AP Biology: Energetics, Systems Interactions; NGSS-style topics: Matter and Energy in Organisms and Ecosystems.

Unit IV

— DNA Replication and the Cell Cycle

- Core thread: Connect sequence, regulation, genome integrity, and phenotype through evidence.
- Instructor move: Launch from a phenomenon, have students model it with Replication-fork speed, error-rate, and cell-cycle timing calculations, then test the model through data.
- Formative check: Ask students to interpret replication or cell-cycle data from timing, labeling, or checkpoint perturbations and then answer: calculate replication timing or error burden and infer checkpoint consequences.
- Summative product: Transfer replication logic to cancer, aging, viral replication, or antibiotic targets.
- Lab/question pair: [Lab — DNA Replication and the Cell Cycle](#); [Questions — DNA Replication and the Cell Cycle](#).
- External alignment: Vision & Change: Information flow, exchange, and storage, Structure and function; AP Biology: Information Storage and Transmission, Systems Interactions; NGSS-style topics: Inheritance and Variation of Traits, Structure and Function.

— Gene Expression

- Core thread: Connect sequence, regulation, genome integrity, and phenotype through evidence.
- Instructor move: Launch from a phenomenon, have students model it with Reading-frame, codon, and expression-output calculations, then test the model through data.
- Formative check: Ask students to convert DNA/RNA sequence data into predicted molecular products and then answer: translate or annotate a sequence and explain how a regulatory change alters output.

- Summative product: Apply expression logic to mutations, biotechnology, development, and disease diagnostics.
- Lab/question pair: **Lab — Gene Expression; Questions — Gene Expression.**
- External alignment: Vision & Change: Information flow, exchange, and storage, Structure and function; AP Biology: Information Storage and Transmission, Systems Interactions; NGSS-style topics: Inheritance and Variation of Traits, Structure and Function.

— Mutations, CRISPR, and Genomics

- Core thread: Connect sequence, regulation, genome integrity, and phenotype through evidence.
- Instructor move: Launch from a phenomenon, have students model it with Mutation-rate, edit-efficiency, and sequence-comparison calculations, then test the model through data.
- Formative check: Ask students to classify variants and predict likely molecular effect from sequence evidence and then answer: predict the impact of a variant and justify the evidence needed to validate it.
- Summative product: Transfer variant reasoning to cancer genomics, ancestry, gene therapy, or microbial evolution.
- Lab/question pair: **Lab — Mutations, CRISPR, and Genomics; Questions — Mutations, CRISPR, and Genomics.**
- External alignment: Vision & Change: Information flow, exchange, and storage, Structure and function; AP Biology: Information Storage and Transmission, Systems Interactions; NGSS-style topics: Inheritance and Variation of Traits, Structure and Function.

— Chromatin and Epigenetic Mechanisms

- Core thread: Connect sequence, regulation, genome integrity, and phenotype through evidence.
- Instructor move: Launch from a phenomenon, have students model it with Regulatory-state and expression-ratio reasoning, then test the model through data.
- Formative check: Ask students to interpret chromatin or expression evidence from simple regulatory datasets and then answer: explain how a regulatory mark changes accessibility and predict downstream expression.
- Summative product: Apply regulation logic to differentiation, imprinting, cancer, or environmental responses.
- Lab/question pair: **Lab — Chromatin and Epigenetic Mechanisms; Questions — Chromatin and Epigenetic Mechanisms.**
- External alignment: Vision & Change: Information flow, exchange, and storage, Structure and function; AP Biology: Information Storage and Transmission, Systems Interactions; NGSS-style topics: Inheritance and Variation of Traits, Structure and Function.

— Epigenetic Inheritance and Disease

- Core thread: Connect sequence, regulation, genome integrity, and phenotype through evidence.
- Instructor move: Launch from a phenomenon, have students model it with Chromatin-loop, inheritance, and disease-risk reasoning, then test the model through data.
- Formative check: Ask students to interpret Hi-C, imprinting, or transgenerational datasets with causal caution and then answer: explain how 3D organization or inherited marks alter expression and disease risk.
- Summative product: Apply inheritance logic to cancer, developmental disorders, and environmental exposure.
- Lab/question pair: **Lab — Epigenetic Inheritance and Disease; Questions — Epigenetic Inheritance and Disease.**
- External alignment: Vision & Change: Information flow, exchange, and storage, Structure and function; AP Biology: Information Storage and Transmission, Systems Interactions; NGSS-style topics: Inheritance and Variation of Traits, Structure and Function.

Unit V

— Mendelian Principles and Probability

- Core thread: Use probability and population reasoning to connect inheritance to evolution.
- Instructor move: Launch from a phenomenon, have students model it with Punnett, binomial, and chi-square calculations, then test the model through data.
- Formative check: Ask students to use cross data to infer genotype probabilities and then answer: compute a genetic probability or chi-square result and explain the biological assumption.
- Summative product: Transfer Mendelian probability to model organisms and introductory human genetics.
- Lab/question pair: **Lab — Mendelian Principles and Probability; Questions — Mendelian Principles and Probability.**
- External alignment: Vision & Change: Information flow, exchange, and storage, Evolution; AP Biology: Information Storage and Transmission, Evolution; NGSS-style topics: Inheritance and Variation of Traits, Natural Selection and Evolution.

— Mendelian Extensions and Human Genetics

- Core thread: Use probability and population reasoning to connect inheritance to evolution.
- Instructor move: Launch from a phenomenon, have students model it with Pedigree, epistasis, and multi-locus probability calculations, then test the model through data.
- Formative check: Ask students to infer inheritance mode and extension mechanism from family or cross data and then answer: use pedigree or extension evidence to justify an inheritance diagnosis.
- Summative product: Transfer extension reasoning to counseling, GWAS interpretation, and breeding.
- Lab/question pair: **Lab — Mendelian Extensions and Human Genetics; Questions — Mendelian Extensions and Human Genetics.**
- External alignment: Vision & Change: Information flow, exchange, and storage, Evolution; AP Biology: Information Storage and Transmission, Evolution; NGSS-style topics: Inheritance and Variation of Traits, Natural Selection and Evolution.

— Chromosomal Inheritance and Linkage

- Core thread: Use probability and population reasoning to connect inheritance to evolution.
- Instructor move: Launch from a phenomenon, have students model it with Recombination frequency and three-point mapping, then test the model through data.
- Formative check: Ask students to infer gene order or chromosomal mechanism from offspring counts and then answer: use progeny classes to calculate map distances and infer the most likely gene order.
- Summative product: Transfer linkage reasoning to disease mapping, breeding, and genome assemblies.
- Lab/question pair: **Lab — Chromosomal Inheritance and Linkage; Questions — Chromosomal Inheritance and Linkage.**
- External alignment: Vision & Change: Information flow, exchange, and storage, Evolution; AP Biology: Information Storage and Transmission, Evolution; NGSS-style topics: Inheritance and Variation of Traits, Natural Selection and Evolution.

— Population Genetics

- Core thread: Use probability and population reasoning to connect inheritance to evolution.
- Instructor move: Launch from a phenomenon, have students model it with Hardy-Weinberg and allele-frequency recurrence calculations, then test the model through data.
- Formative check: Ask students to estimate genotype or allele frequencies from population data and then answer: calculate expected frequencies and identify which evolutionary force could explain deviations.
- Summative product: Apply population-genetic reasoning to screening, conservation, and pathogen evolution.
- Lab/question pair: **Lab — Population Genetics; Questions — Population Genetics.**
- External alignment: Vision & Change: Information flow, exchange, and storage, Evolution; AP Biology: Information Storage and Transmission, Evolution; NGSS-style topics: Inheritance and Variation of Traits, Natural Selection and Evolution.

Unit VI

— Natural Selection and Adaptation

- Core thread: Return to variation, evidence, and historical inference across evolutionary scales.
- Instructor move: Launch from a phenomenon, have students model it with Selection coefficient and allele-frequency trajectory calculations, then test the model through data.
- Formative check: Ask students to interpret fitness data and distinguish selection from other forces and then answer: estimate selection strength from data and explain why the result is context dependent.
- Summative product: Transfer selection reasoning to antibiotics, pesticide resistance, cancer, or climate adaptation.
- Lab/question pair: **Lab — Natural Selection and Adaptation; Questions — Natural Selection and Adaptation.**
- External alignment: Vision & Change: Evolution, Systems; AP Biology: Evolution, Systems Interactions; NGSS-style topics: Natural Selection and Evolution, Interdependent Relationships in Ecosystems.

— Genetic Drift, Gene Flow, and Speciation

- Core thread: Return to variation, evidence, and historical inference across evolutionary scales.
- Instructor move: Launch from a phenomenon, have students model it with Fixation probability, effective population size, and migration-selection balance, then test the model through data.

- Formative check: Ask students to distinguish stochastic from directional change in allele-frequency data and then answer: predict how population size or isolation changes divergence and fixation risk.
- Summative product: Apply drift reasoning to endangered populations, founder effects, and island radiations.
- Lab/question pair: **Lab — Genetic Drift, Gene Flow, and Speciation; Questions — Genetic Drift, Gene Flow, and Speciation.**
- External alignment: Vision & Change: Evolution, Systems; AP Biology: Evolution, Systems Interactions; NGSS-style topics: Natural Selection and Evolution, Interdependent Relationships in Ecosystems.

— Phylogenetics and the Tree of Life

- Core thread: Return to variation, evidence, and historical inference across evolutionary scales.
- Instructor move: Launch from a phenomenon, have students model it with Tree-distance, parsimony, and molecular-clock calculations, then test the model through data.
- Formative check: Ask students to read trees correctly and map traits or sequences onto branches and then answer: use a tree to infer shared ancestry, character transitions, or divergence time.
- Summative product: Transfer tree thinking to pathogens, conservation units, gene families, and development.
- Lab/question pair: **Lab — Phylogenetics and the Tree of Life; Questions — Phylogenetics and the Tree of Life.**
- External alignment: Vision & Change: Evolution, Systems; AP Biology: Evolution, Systems Interactions; NGSS-style topics: Natural Selection and Evolution, Interdependent Relationships in Ecosystems.

Unit VII

— Bacteria, Archaea, and Viruses

- Core thread: Use microbes to integrate evolution, ecology, host response, and public decisions.
- Instructor move: Launch from a phenomenon, have students model it with Growth-rate, genome-size, and dilution calculations, then test the model through data.
- Formative check: Ask students to interpret microbial observations from growth, sequence, or structural evidence and then answer: classify a microbe or virus from evidence and predict a likely vulnerability.
- Summative product: Apply microbial diversity reasoning to antibiotics, biotechnology, ecology, and outbreaks.
- Lab/question pair: **Lab — Bacteria, Archaea, and Viruses; Questions — Bacteria, Archaea, and Viruses.**
- External alignment: Vision & Change: Evolution, Systems, Structure and function; AP Biology: Evolution, Systems Interactions; NGSS-style topics: Structure and Function, Interdependent Relationships in Ecosystems.

— Microbial Ecology and the Microbiome

- Core thread: Use microbes to integrate evolution, ecology, host response, and public decisions.
- Instructor move: Launch from a phenomenon, have students model it with Diversity indices, richness estimates, and interaction-network reasoning, then test the model through data.
- Formative check: Ask students to compute or interpret community metrics from abundance data and then answer: use community data to infer diversity, dominance, and a plausible ecological mechanism.
- Summative product: Transfer microbial ecology to soils, oceans, digestion, disease, and climate feedbacks.
- Lab/question pair: **Lab — Microbial Ecology and the Microbiome; Questions — Microbial Ecology and the Microbiome.**
- External alignment: Vision & Change: Evolution, Systems, Structure and function; AP Biology: Evolution, Systems Interactions; NGSS-style topics: Structure and Function, Interdependent Relationships in Ecosystems.

— Host Immunity and Vaccines

- Core thread: Use microbes to integrate evolution, ecology, host response, and public decisions.
- Instructor move: Launch from a phenomenon, have students model it with Herd-immunity threshold and basic immunological reasoning, then test the model through data.
- Formative check: Ask students to interpret antibody, cellular, and vaccine-response evidence and then answer: predict how immunity or vaccination changes individual and population risk.
- Summative product: Transfer immunity reasoning to outbreak response and clinical decision-making.
- Lab/question pair: **Lab — Host Immunity and Vaccines; Questions — Host Immunity and Vaccines.**

- External alignment: Vision & Change: Evolution, Systems, Structure and function; AP Biology: Evolution, Systems Interactions; NGSS-style topics: Structure and Function, Interdependent Relationships in Ecosystems.

— Antimicrobial Resistance and Epidemiology

- Core thread: Use microbes to integrate evolution, ecology, host response, and public decisions.
- Instructor move: Launch from a phenomenon, have students model it with R0, resistance-mechanism, and outbreak-trajectory calculations, then test the model through data.
- Formative check: Ask students to interpret resistance assays and outbreak curves and then answer: calculate a threshold or outbreak trajectory and identify the intervention lever.
- Summative product: Transfer resistance and epidemiology reasoning to stewardship and public-health policy.
- Lab/question pair: [Lab — Antimicrobial Resistance and Epidemiology](#); [Questions — Antimicrobial Resistance and Epidemiology](#).
- External alignment: Vision & Change: Evolution, Systems, Structure and function; AP Biology: Evolution, Systems Interactions; NGSS-style topics: Structure and Function, Interdependent Relationships in Ecosystems.

Unit VIII

— Plant Structure and Water Relations

- Core thread: Read plant form as an engineered compromise among transport, energy, and reproduction.
- Instructor move: Launch from a phenomenon, have students model it with Water-potential and transpiration-flux calculations, then test the model through data.
- Formative check: Ask students to interpret plant-water data from pressure, solute, and humidity measurements and then answer: calculate water potential and predict the direction of water movement.
- Summative product: Transfer plant-water reasoning to drought, irrigation, forest physiology, and crop breeding.
- Lab/question pair: [Lab — Plant Structure and Water Relations](#); [Questions — Plant Structure and Water Relations](#).
- External alignment: Vision & Change: Structure and function, Pathways and transformations of energy and matter, Systems; AP Biology: Energetics, Systems Interactions; NGSS-style topics: Structure and Function, Matter and Energy in Organisms and Ecosystems.

— Plant Reproduction and Development

- Core thread: Read plant form as an engineered compromise among transport, energy, and reproduction.
- Instructor move: Launch from a phenomenon, have students model it with Life-cycle accounting and phyllotaxis/growth-pattern calculations, then test the model through data.
- Formative check: Ask students to track ploidy, tissue origin, and reproductive stage from diagrams or observations and then answer: trace a plant life cycle and predict the consequence of disrupting one stage.
- Summative product: Transfer reproductive reasoning to agriculture, pollination ecology, and plant evolution.
- Lab/question pair: [Lab — Plant Reproduction and Development](#); [Questions — Plant Reproduction and Development](#).
- External alignment: Vision & Change: Structure and function, Pathways and transformations of energy and matter, Systems; AP Biology: Energetics, Systems Interactions; NGSS-style topics: Structure and Function, Matter and Energy in Organisms and Ecosystems.

— Plant Responses to the Environment

- Core thread: Read plant form as an engineered compromise among transport, energy, and reproduction.
- Instructor move: Launch from a phenomenon, have students model it with Dose-response, water-use-efficiency, and hormone-interaction reasoning, then test the model through data.
- Formative check: Ask students to interpret plant response data across light, gravity, water, and hormone treatments and then answer: predict a plant response from a signal and identify the likely hormone or pathway.
- Summative product: Transfer response logic to shade avoidance, drought, flowering, and crop management.
- Lab/question pair: [Lab — Plant Responses to the Environment](#); [Questions — Plant Responses to the Environment](#).
- External alignment: Vision & Change: Structure and function, Pathways and transformations of energy and matter, Systems; AP Biology: Energetics, Systems Interactions; NGSS-style topics: Structure and Function, Matter and Energy in Organisms and Ecosystems.

Unit IX

— Circulation and Respiration

- Core thread: Spiral homeostasis from organ systems to neural, endocrine, and immune decisions.
- Instructor move: Launch from a phenomenon, have students model it with Cardiac-output, diffusion, oxygen-saturation, and feedback calculations, then test the model through data.
- Formative check: Ask students to interpret physiological data from pressure, flow, saturation, or set-point changes and then answer: calculate a transport or feedback variable and explain the compensatory response.
- Summative product: Transfer homeostatic reasoning to exercise, altitude, hemorrhage, fever, and shock.
- Lab/question pair: **Lab — Circulation and Respiration; Questions — Circulation and Respiration.**
- External alignment: Vision & Change: Structure and function, Systems; AP Biology: Systems Interactions, Energetics; NGSS-style topics: Structure and Function.

— Nervous System and Neural Signaling

- Core thread: Spiral homeostasis from organ systems to neural, endocrine, and immune decisions.
- Instructor move: Launch from a phenomenon, have students model it with Cable-length, conduction, and simple circuit calculations, then test the model through data.
- Formative check: Ask students to interpret neural data from anatomy, timing, or lesion evidence and then answer: predict behavioral or signal consequences from a circuit or structural perturbation.
- Summative product: Transfer circuit reasoning to reflexes, sensory systems, learning, and disease.
- Lab/question pair: **Lab — Nervous System and Neural Signaling; Questions — Nervous System and Neural Signaling.**
- External alignment: Vision & Change: Structure and function, Systems; AP Biology: Systems Interactions, Energetics; NGSS-style topics: Structure and Function.

— Action Potentials and Synaptic Transmission

- Core thread: Spiral homeostasis from organ systems to neural, endocrine, and immune decisions.
- Instructor move: Launch from a phenomenon, have students model it with Nernst/Goldman, Hodgkin-Huxley, and synaptic-current reasoning, then test the model through data.
- Formative check: Ask students to interpret voltage traces, conductance changes, and synaptic perturbations and then answer: predict how changing an ion gradient or channel conductance alters excitability.
- Summative product: Transfer excitability reasoning to anesthesia, toxins, epilepsy, and neuromuscular disease.
- Lab/question pair: **Lab — Action Potentials and Synaptic Transmission; Questions — Action Potentials and Synaptic Transmission.**
- External alignment: Vision & Change: Structure and function, Systems; AP Biology: Systems Interactions, Energetics; NGSS-style topics: Structure and Function.

— Endocrine Signaling and Homeostasis

- Core thread: Spiral homeostasis from organ systems to neural, endocrine, and immune decisions.
- Instructor move: Launch from a phenomenon, have students model it with Hormone feedback and dose-response reasoning, then test the model through data.
- Formative check: Ask students to interpret endocrine time courses, panels, and perturbations and then answer: predict the consequence of changing a hormone, receptor, or axis set-point.
- Summative product: Transfer endocrine reasoning to metabolism, stress, and development.
- Lab/question pair: **Lab — Endocrine Signaling and Homeostasis; Questions — Endocrine Signaling and Homeostasis.**
- External alignment: Vision & Change: Structure and function, Systems; AP Biology: Systems Interactions, Energetics; NGSS-style topics: Structure and Function.

— Immune System Architecture

- Core thread: Spiral homeostasis from organ systems to neural, endocrine, and immune decisions.
- Instructor move: Launch from a phenomenon, have students model it with Immune-memory, cytokine, and recognition reasoning, then test the model through data.
- Formative check: Ask students to interpret immune titers, cytokine profiles, or perturbation data and then answer: predict the consequence of changing an antigen, cell population, or checkpoint.

- Summative product: Transfer immunity reasoning to vaccination, autoimmunity, infection, and cancer therapy.
- Lab/question pair: **Lab — Immune System Architecture; Questions — Immune System Architecture.**
- External alignment: Vision & Change: Structure and function, Systems; AP Biology: Systems Interactions, Energetics; NGSS-style topics: Structure and Function.

Unit X

— Population Ecology and Growth Models

- Core thread: Use ecological models to connect populations, interactions, matter, climate, and decisions.
- Instructor move: Launch from a phenomenon, have students model it with Exponential/logistic growth, mark-recapture, and matrix projection, then test the model through data.
- Formative check: Ask students to use abundance or age-structure data to estimate growth and risk and then answer: calculate a growth or sampling parameter and interpret its conservation meaning.
- Summative product: Transfer population models to fisheries, invasive species, epidemiology, and endangered species.
- Lab/question pair: **Lab — Population Ecology and Growth Models; Questions — Population Ecology and Growth Models.**
- External alignment: Vision & Change: Systems, Evolution, Pathways and transformations of energy and matter; AP Biology: Systems Interactions, Evolution, Energetics; NGSS-style topics: Interdependent Relationships in Ecosystems, Matter and Energy in Organisms and Ecosystems, Natural Selection and Evolution.

— Community Interactions and Succession

- Core thread: Use ecological models to connect populations, interactions, matter, climate, and decisions.
- Instructor move: Launch from a phenomenon, have students model it with Lotka-Volterra-style interaction reasoning, then test the model through data.
- Formative check: Ask students to interpret abundance, interaction, or disturbance data from communities and then answer: predict how changing one species or resource alters community structure.
- Summative product: Transfer interaction reasoning to restoration, agriculture, and invasion biology.
- Lab/question pair: **Lab — Community Interactions and Succession; Questions — Community Interactions and Succession.**
- External alignment: Vision & Change: Systems, Evolution, Pathways and transformations of energy and matter; AP Biology: Systems Interactions, Evolution, Energetics; NGSS-style topics: Interdependent Relationships in Ecosystems, Matter and Energy in Organisms and Ecosystems, Natural Selection and Evolution.

— Biodiversity and Food Webs

- Core thread: Use ecological models to connect populations, interactions, matter, climate, and decisions.
- Instructor move: Launch from a phenomenon, have students model it with Shannon, species-area, and network connectance reasoning, then test the model through data.
- Formative check: Ask students to interpret food-web, richness, or biogeography datasets and then answer: calculate a diversity or species-area metric and interpret its ecological meaning.
- Summative product: Transfer biodiversity reasoning to conservation planning and habitat fragmentation.
- Lab/question pair: **Lab — Biodiversity and Food Webs; Questions — Biodiversity and Food Webs.**
- External alignment: Vision & Change: Systems, Evolution, Pathways and transformations of energy and matter; AP Biology: Systems Interactions, Evolution, Energetics; NGSS-style topics: Interdependent Relationships in Ecosystems, Matter and Energy in Organisms and Ecosystems, Natural Selection and Evolution.

— Ecosystem Ecology

- Core thread: Use ecological models to connect populations, interactions, matter, climate, and decisions.
- Instructor move: Launch from a phenomenon, have students model it with Energy-flow, productivity, and nutrient-budget calculations, then test the model through data.
- Formative check: Ask students to trace matter and energy through food webs and biogeochemical cycles and then answer: calculate a flux or efficiency and explain which pool or process limits the system.
- Summative product: Transfer ecosystem reasoning to eutrophication, carbon budgets, agriculture, and climate feedback.
- Lab/question pair: **Lab — Ecosystem Ecology; Questions — Ecosystem Ecology.**

- External alignment: Vision & Change: Systems, Evolution, Pathways and transformations of energy and matter; AP Biology: Systems Interactions, Evolution, Energetics; NGSS-style topics: Interdependent Relationships in Ecosystems, Matter and Energy in Organisms and Ecosystems, Natural Selection and Evolution.

— Biomes and Conservation Biology

- Core thread: Use ecological models to connect populations, interactions, matter, climate, and decisions.
- Instructor move: Launch from a phenomenon, have students model it with Species-area, risk, and prioritization calculations, then test the model through data.
- Formative check: Ask students to use maps, trend data, and threat categories to justify conservation priorities and then answer: evaluate a conservation scenario using evidence, tradeoffs, and uncertainty.
- Summative product: Transfer conservation reasoning to land use, climate corridors, restoration, and environmental justice.
- Lab/question pair: **Lab — Biomes and Conservation Biology; Questions — Biomes and Conservation Biology.**
- External alignment: Vision & Change: Systems, Evolution, Pathways and transformations of energy and matter; AP Biology: Systems Interactions, Evolution, Energetics; NGSS-style topics: Interdependent Relationships in Ecosystems, Matter and Energy in Organisms and Ecosystems, Natural Selection and Evolution.

Appendix C — Mathematical Review for Biology

Appendix C — Mathematical Review for Biology · Level 1/3 · 45 min read · Prerequisites: none · Use as reference

This appendix collects the mathematics a reader needs to work through the quantitative chapters of this textbook. It is not a course in mathematics — it is a compact reference for the specific tools used in the chapters. Each section is self-contained; dip in as needed.

C.1 Logarithms and the Natural Log

Definition

$$\log_b(x) = y \iff b^y = x$$

(485)

Biology uses two bases heavily:

- Base 10 (\log_{10}) — pH, sound intensity, earthquake magnitude, powers-of-ten units (nM, μ M, mM).
- Base e (ln, natural log) — most first-order kinetics (exponential growth, decay, enzyme kinetics), where $e \approx 2.71828$.

Conversion: $\log_{10}(x) = \ln(x)/\ln(10) \approx \ln(x)/2.303$.

Key identities

Identity	Biological application
$\log(ab) = \log a + \log b$	Combining probabilities across linked loci
$\log(a/b) = \log a - \log b$	Henderson-Hasselbalch $\text{pH} = \text{p}K_a + \log([\text{A}^-]/[\text{HA}])$
$\log(a^n) = n \log a$	Hill equation — slope in log-log plot
$\log_b(b^x) = x$	Inverting exponential growth: $t = \ln(N/N_0)/r$

Worked example — doubling time

A bacterial culture grows at $r = 0.5 \text{ h}^{-1}$. When does the population double?

$$N(t) = N_0e^{rt} = 2N_0 \implies e^{rt} = 2 \implies t = \frac{\ln 2}{r} = \frac{0.693}{0.5} \approx 1.39 \text{ h}$$

(486)

The “ln 2 trick” recurs throughout biology: half-life $t_{1/2} = \ln 2/k$ (decay); doubling time $t_d = \ln 2/r$ (growth). Memorise $\ln 2 \approx 0.693$.

C.2 Differential and Integral Calculus

Biology rarely requires advanced calculus, but the reader must be comfortable with:

Derivatives as rates

$$\frac{dN}{dt} = \text{rate of change of } N \text{ over time}$$

(487)

In population ecology, $dN/dt > 0$ means the population is growing; $dN/dt = 0$ is equilibrium; $dN/dt < 0$ is decline. In enzyme kinetics, $d[P]/dt =$ reaction velocity v .

Integration as accumulation

$$\int_0^T \frac{dN}{dt} dt = N(T) - N(0)$$

(488)

The integral sums up infinitesimal contributions. Examples:

- Total drug dose delivered by an infusion: $\text{Dose} = \int_0^T (\text{infusion rate}) dt$.

- Net photosynthesis over a day: $\int_0^{24\text{h}} P(t)dt$.

First-order ODE: exponential growth and decay

$$\frac{dN}{dt} = kN \implies N(t) = N_0 e^{kt}$$

(489)

- $k > 0$: growth with doubling time $t_d = \ln 2/k$.
- $k < 0$: decay with half-life $t_{1/2} = \ln 2/|k|$.

Logistic growth (nonlinear)

$$\frac{dN}{dt} = rN \left(1 - \frac{N}{K}\right)$$

(490)

The closed-form solution is:

$$N(t) = \frac{K}{1 + \left(\frac{K-N_0}{N_0}\right)e^{-rt}}$$

(491)

Inflection (maximum rate) at $N = K/2$, giving the sigmoid shape.

C.3 Basic Probability

Independent events

$P(A \cap B) = P(A) \cdot P(B)$ when events are independent. Example: the probability that both parents transmit the recessive allele at a locus ($Aa \times Aa$) is $(1/2)(1/2) = 1/4$.

Conditional probability and Bayes’ theorem

$$P(A \mid B) = \frac{P(A \cap B)}{P(B)}$$

(492)

Bayes’ theorem — central to section 0.3 and to medical testing:

$$P(\text{disease} \mid +) = \frac{P(+ \mid \text{disease}) \cdot P(\text{disease})}{P(+)}$$

(493)

A highly sensitive test can still have a low positive predictive value if the disease is rare — a counterintuitive result with major clinical consequences.

Binomial distribution

Number of successes in n independent trials, each with probability p :

$$P(k \text{ successes}) = \binom{n}{k} p^k (1 - p)^{n-k}$$

(494)

Used for Punnett-square ratios, mark-recapture statistics, and Hardy-Weinberg proportion testing.

Poisson distribution

For rare events at mean rate λ per interval:

$$P(k) = \frac{\lambda^k e^{-\lambda}}{k!}$$

(495)

Used for spontaneous mutation counts per locus, bacterial cell counts in Petri dishes (when plates are not overgrown), rare-disease incidence.

C.4 Dimensional Analysis

Every physical quantity carries units. Units must balance on both sides of every equation — if they don’t, the equation is wrong.

Example — diffusion distance

Fick’s rule for mean diffusion distance:

$$x = \sqrt{2Dt}$$

(496)

Check units: D has units of $\text{m}^2 \text{ s}^{-1}$; t has units of s ; so $\sqrt{2Dt}$ has units of $\sqrt{\text{m}^2} = \text{m}$. ✓

If a student wrote $x = Dt$, units would be $\text{m}^2 \text{ s}^{-1} \cdot \text{s} = \text{m}^2$ — dimensionally wrong.

Standard SI units used in this book

Quantity	Symbol	SI unit	Typical biological magnitude
Length	l	m	cell: 10 μm ; neuron: 1 m
Mass	m	kg	ribosome: 3×10^{-21} kg; cell: 10^{-12} kg
Time	t	s	AP: 1 ms; cell cycle: 24 h
Amount	n	mol	ATP in a cell: 10^{-15} mol
Concentration	$[X]$	$\text{mol L}^{-1} = \text{M}$	cytoplasmic ATP: 5×10^{-3} M
Energy	E	J	ATP hydrolysis: 5×10^{-20} J per molecule, $\approx 30.5 \text{ kJ mol}^{-1}$
Force	F	N	myosin step force: 5×10^{-12} N = 5 pN
Electric potential	V	V	resting membrane: $-0.07 \text{ V} = -70 \text{ mV}$

Non-SI units common in biology

Unit	SI equivalent	Use
mmHg (Torr)	133.322 Pa	blood pressure, gas partial pressures
cal	4.184 J	nutrition (“Calorie” = kcal)
pH unit	$-\log_{10}[\text{H}^+]$ in M	acidity
Da (dalton)	1.661×10^{-27} kg	molecular mass
Kelvin (K)	$^{\circ}\text{C} + 273.15$	thermodynamics requires K, not $^{\circ}\text{C}$

C.5 Linear Algebra Miniature

Primarily trace knowledge is required for this book, but the two ideas below recur.

Matrices as transitions

Allele-frequency change under migration between two populations is a 2×2 matrix multiplication. Markov transition matrices describe stochastic gene expression (lac operon), state transitions in ion channels, and Wright-Fisher drift.

Eigenvalues and equilibrium

The dominant eigenvalue λ_1 of a Leslie matrix equals the long-term finite rate of increase. Eigenvectors give the stable age distribution. This is the formal underpinning of section 36’s demographic analysis.

C.6 Common Pitfalls in Biological Math

1. Confusing concentration and amount. 1 nM is a concentration; 1 nmol is an amount. A picomole of hormone in 5 L of blood is 0.2 pM.
2. Units of rate constants. First-order: s⁻¹. Second-order: M⁻¹ s⁻¹. Third-order: M⁻² s⁻¹. Dimensional analysis typically exposes an order-of-magnitude error.
3. Exponents and prefixes. Milli- (10⁻³), micro- (10⁻⁶), nano- (10⁻⁹), pico- (10⁻¹²), femto- (10⁻¹⁵), atto- (10⁻¹⁸). Shifting by three orders of magnitude is common in biology; single errors are catastrophic.
4. Logarithmic vs linear differences. A tenfold change in [H⁺] is a one-pH-unit change. “Twice the acidity” means 0.3 pH unit down, not 2 pH units.
5. Error propagation. Small errors in input variables compound through multi-step calculations. The textbook flags this at thermodynamics, kinetics, and evolutionary rate estimation in particular.

C.7 Key Equations Quick Reference

These equations recur throughout the textbook. Each entry gives the equation, the variable definitions, and the chapter where it first appears.

Michaelis-Menten equation

$$v = \frac{V_{\max}[S]}{K_m + [S]}$$

(497)

- v = reaction velocity (mol L⁻¹ s⁻¹); V_{\max} = maximum velocity; $[S]$ = substrate concentration; K_m = substrate concentration at half-maximal velocity.
- When $[S] = K_m$, $v = V_{\max}/2$. At $[S] \ll K_m$, $v \approx (V_{\max}/K_m)[S]$ (first-order). At $[S] \gg K_m$, $v \approx V_{\max}$ (zero-order).
- Competitive inhibitor raises apparent K_m by factor $(1 + [I]/K_i)$; V_{\max} unchanged.
- First appears in section 4.

Hill equation (cooperative binding)

$$\theta = \frac{[L]^n}{K_d^n + [L]^n}$$

(498)

- θ = fractional saturation; $[L]$ = ligand concentration; K_d = dissociation constant at half-maximal saturation; n = Hill coefficient (cooperativity).
- $n = 1$: independent (Michaelis-Menten-like, hyperbolic). $n > 1$: positive cooperativity (sigmoidal, switch-like). $n < 1$: negative cooperativity.
- Hemoglobin: $n \approx 2.8$, $K_d \approx 26$ mmHg (P50). Phosphofructokinase-1: $n \approx 4$ for fructose-6-phosphate.
- Switch sharpness: fold-change in θ from $0.1K_d$ to $10K_d$ is 100^n ; for $n = 1$ this is 100-fold; for $n = 4$ it is 10⁸-fold — explaining why cooperative enzymes function as on/off switches.
- First appears in section 4.

Nernst equation

$$E_{ion} = \frac{RT}{zF} \ln \frac{[X]_o}{[X]_i}$$

(499)

- E_{ion} = equilibrium (reversal) potential for the ion; $R = 8.314$ J mol⁻¹ K⁻¹; T = temperature in K; z = ion valence (charge); $F = 96485$ C mol⁻¹; $[X]_o/[X]_i$ = extracellular/intracellular concentration ratio.
- At 37°C: $RT/F \approx 26.7$ mV, so $E_{ion} \approx (26.7/z) \ln([X]_o/[X]_i)$ mV.
- For Na⁺ ($z = +1$, $[Na]_o/[Na]_i \approx 145/12$): $E_{Na} \approx +67$ mV. For K⁺ ($z = +1$, $[K]_o/[K]_i \approx 5/140$): $E_K \approx -90$ mV.
- First appears in section 33.

Goldman-Hodgkin-Katz equation

$$V_m = \frac{RT}{F} \ln \frac{P_K[K]_o + P_{Na}[Na]_o + P_{Cl}[Cl]_i}{P_K[K]_i + P_{Na}[Na]_i + P_{Cl}[Cl]_o}$$

(500)

- Extends the Nernst equation when multiple ions contribute. P_K, P_{Na}, P_{Cl} = membrane permeabilities. At rest: $P_K : P_{Na} : P_{Cl} \approx 1 : 0.04 : 0.45$, giving $V_m \approx -70$ mV.
- During action potential peak: P_{Na} rises 500-fold, shifting V_m toward E_{Na} .
- First appears in section 33.

Henderson-Hasselbalch equation

$$\text{pH} = \text{p}K_a + \log_{10} \frac{[A^-]}{[HA]}$$

(501)

- $[A^-]$ = conjugate base concentration; $[HA]$ = weak acid concentration.
- At $\text{pH} = \text{p}K_a$: $[A^-]/[HA] = 1$ (half-dissociated). Bicarbonate buffer: $\text{p}K_a = 6.1$; at $\text{pH } 7.4$, $[HCO_3^-]/[CO_2] \approx 20$.
- Buffer capacity is greatest within ± 1 pH unit of $\text{p}K_a$.
- First appears in section 1.

Water potential

$$\Psi = \Psi_s + \Psi_p$$

(502)

- Ψ = total water potential (MPa); Ψ_s = solute (osmotic) potential (≤ 0); Ψ_p = pressure potential (turgor; can be positive or negative).
- Water moves from high to low Ψ . Wilted cell: $\Psi_p \approx 0$, $\Psi = \Psi_s < 0$. Turgid cell: $\Psi_p > 0$ partially offsets Ψ_s .
- Xylem tension: $\Psi_p < 0$ (negative pressure) drives cohesion-tension in tall trees.
- First appears in section 28.

Further Reading and Source Notes

- Keener, J. & Sneyd, J. (2009). *Mathematical Physiology* (2nd ed.). Springer. — comprehensive biological math.
- Otto, S. P. & Day, T. (2007). *A Biologist’s Guide to Mathematical Modeling in Ecology and Evolution*. Princeton. — accessible entry point.
- Strogatz, S. H. (2018). *Nonlinear Dynamics and Chaos* (2nd ed.). Westview. — the bifurcation and limit-cycle literature.

Module: reference only (no code)

Appendix D — Units, Physical Constants, and Biological Ranges

Appendix D — Units, Physical Constants, and Biological Ranges · Level 1/3 · 20 min read · Prerequisites: none · Use as reference

A compact reference for units, constants, and characteristic magnitudes encountered throughout the textbook. Use it during worked problems to sanity-check dimensional analysis, convert between unit systems, and verify that numerical answers fall in biologically plausible ranges.

D.1 SI Base and Derived Units

Quantity	SI unit	Symbol	In base units
Length	meter	m	—
Mass	kilogram	kg	—
Time	second	s	—
Amount of substance	mole	mol	—
Temperature	kelvin	K	—
Electric current	ampere	A	—
Force	newton	N	$\text{kg} \cdot \text{m} \cdot \text{s}^{-2}$
Energy	joule	J	$\text{kg} \cdot \text{m}^2 \cdot \text{s}^{-2}$
Power	watt	W	$\text{J} \cdot \text{s}^{-1}$
Pressure	pascal	Pa	$\text{N} \cdot \text{m}^{-2}$
Electric charge	coulomb	C	$\text{A} \cdot \text{s}$
Electric potential	volt	V	$\text{J} \cdot \text{C}^{-1}$
Electric conductance	siemens	S	Ω^{-1}
Frequency	hertz	Hz	s^{-1}

Metric prefixes

Prefix	Symbol	Factor	Biological use
giga-	G	10^9	Gb base pairs in a genome
mega-	M	10^6	MDa protein complex; Mb DNA fragment
kilo-	k	10^3	kJ mol^{-1} (ΔG); kDa protein mass
centi-	c	10^{-2}	cM genetic map distance
milli-	m	10^{-3}	mM intracellular metabolites; ms AP duration
micro-	μ	10^{-6}	μm cell size; μM low-abundance metabolite
nano-	n	10^{-9}	nm bond length; nM receptor ligand
pico-	p	10^{-12}	pN molecular motor force; pM low-abundance hormone
femto-	f	10^{-15}	fmol amount in a single cell
atto-	a	10^{-18}	amol; approaches single-molecule detection

D.2 Universal Physical Constants

Constant	Symbol	Value
Avogadro’s number	N_A	$6.022 \times 10^{23} \text{ mol}^{-1}$
Boltzmann constant	k_B	$1.381 \times 10^{-23} \text{ J K}^{-1} = 8.617 \times 10^{-5} \text{ eV K}^{-1}$
Gas constant	$R = N_A k_B$	$8.314 \text{ J K}^{-1} \text{ mol}^{-1} = 1.987 \text{ cal K}^{-1} \text{ mol}^{-1}$
Faraday constant	F	$9.649 \times 10^4 \text{ C mol}^{-1}$
Elementary charge	e	$1.602 \times 10^{-19} \text{ C}$

Constant	Symbol	Value
Speed of light in vacuum	c	$2.998 \times 10^8 \text{ m s}^{-1}$
Planck constant	h	$6.626 \times 10^{-34} \text{ J s}$
Permittivity of free space	ϵ_0	$8.854 \times 10^{-12} \text{ F m}^{-1}$
Standard atmospheric pressure	P_{atm}	$101,325 \text{ Pa} = 760 \text{ Torr}$
Body temperature	T_{body}	$310.15 \text{ K} = 37.00 \text{ }^\circ\text{C}$
Thermal energy at body T	$k_B T$	$4.28 \times 10^{-21} \text{ J} \approx 0.027 \text{ eV} = 2.57 \text{ kJ mol}^{-1}$

The rule “ $k_B T \approx \frac{1}{40} \text{ eV} \approx \frac{2.5}{1000} \text{ kJ mol}^{-1}$ at room temperature” is useful: hydrogen bonds (about 20 kJ mol^{-1}) are about $8 k_B T$, so they survive thermal fluctuations; van der Waals contacts (about 1 kJ mol^{-1}) are about $0.4 k_B T$, so each one is barely stable but collectively numerous contacts summate.

D.3 Energy Conversions

From	To	Factor
1 J	cal	0.239
1 cal	J	4.184
1 kcal	kJ	4.184
1 eV	J	1.602×10^{-19}
1 eV	kJ mol ^{−1}	96.485
1 kJ mol ^{−1}	eV	0.01036
1 J	kg·m ² s ^{−2}	1 (definition)
1 $k_B T$ at 37 °C	kJ mol ^{−1}	2.577

ATP hydrolysis benchmarks

- Standard ΔG° for $\text{ATP} \rightarrow \text{ADP} + \text{P}_i$: $-30.5 \text{ kJ mol}^{-1}$.
- Cellular ΔG (physiological $[\text{ATP}]/[\text{ADP}]$): -57 kJ mol^{-1} , roughly $22 k_B T$.
- Number of ATP hydrolyses required to lift a 1 kg mass 1 m: about 300,000 — illustrating why muscle needs 10^8 ATP molecules consumed per second.

D.4 Pressure Conversions

From	To	Factor
1 atm	Pa	101,325
1 atm	mmHg (Torr)	760
1 atm	bar	1.01325
1 mmHg	kPa	0.1333
1 mmHg	Pa	133.322

Blood pressure: systolic 120 mmHg \approx 16 kPa. Arterial O₂: $P_a\text{O}_2 \approx 100 \text{ mmHg} \approx 13.3 \text{ kPa}$. Venous O₂: $P_v\text{O}_2 \approx 40 \text{ mmHg} \approx 5.3 \text{ kPa}$.

D.5 Concentration Conversions

1 molar (M) = 1 mol L^{−1} = 10³ mmol L^{−1} = 10⁶ μmol L^{−1} = 10⁹ nmol L^{−1} = 10¹² pmol L^{−1}.

Concentration	Example
pM (10 ^{−12} M)	Circulating hormones (insulin, oxytocin)

Concentration	Example
nM (10^{-9} M)	Vitamin B ₁₂ , transcription factor at a target site
μ M (10^{-6} M)	Glucose in blood (5×10^{-3} M = 5 mM, upper end)
mM (10^{-3} M)	Major intracellular ions (Na ⁺ , K ⁺), ATP (about 5 mM)
M	Cytoplasm water (55 M); seawater NaCl (0.5 M)

Molarity of water: $M_{H_2O} = 1000 \text{ g L}^{-1} / 18 \text{ g mol}^{-1} = 55.5 \text{ M}$. This is why [H₂O] is treated as constant in biological equilibrium expressions.

D.6 Biological Magnitudes — Quick Reference

Time scales

Event	Time
Bond vibration	10^{-14} s
Enzyme turnover (k_{cat})	$10^{-3} - 10^{-6}$ s
Action potential	10^{-3} s
Synaptic transmission	10^{-3} s
Ribosome peptide-bond formation	0.1 s (5 aa s ⁻¹ per ribosome)
Protein folding	$10^{-3} - 1$ s
Mitosis	1 h
Cell cycle (dividing human cell)	1 d
Hair growth	1 cm month ⁻¹
Human generation time	about 25 yr
Mammalian species lifespan	$10^6 - 10^7$ yr

Length scales

Feature	Size
C–C bond	0.15 nm
Protein (average globular)	3 nm
Ribosome	25 nm
Virus (small RNA)	30 nm
Nuclear pore	100 nm
Bacterium (<i>E. coli</i>)	1 μ m
Mitochondrion	2 μ m
Eukaryotic cell (average)	10–20 μ m
Neuron axon (giraffe recurrent laryngeal)	2 m
Animal (blue whale)	30 m
Redwood tree	100 m

Energy scales

Interaction / event	Energy
Van der Waals contact	about 1 kJ mol ⁻¹
Hydrogen bond	about 20 kJ mol ⁻¹
C–C covalent bond	about 350 kJ mol ⁻¹
ATP hydrolysis (standard)	–30.5 kJ mol ⁻¹

Interaction / event	Energy
ATP hydrolysis (cellular)	−57 kJ mol ^{−1}
Glucose complete oxidation	−2870 kJ mol ^{−1}
Photosynthesis per photon (680 nm)	176 kJ mol ^{−1}
Daily human basal energy	7000 kJ d ^{−1} (≈1700 kcal d ^{−1})

Organismal physiology reference scales

System	Useful scale	Source-backed context
Digestive absorption	Small-intestinal villi and microvilli expand absorptive surface	Nutrient uptake depends on epithelial surface area, enzymes, bile, transporters, and gut motility [National Institute of Diabetes and Digestive and Kidney Diseases, 2024a].
Renal excretion	Adult kidneys filter plasma continuously and adjust urine concentration	Filtration, tubular reabsorption, secretion, and collecting-duct water handling set volume, electrolyte, pH, and nitrogen-waste balance [National Institute of Diabetes and Digestive and Kidney Diseases, 2024b].
Skeletal muscle	Sarcomere force depends on actin-myosin overlap and cross-bridge cycling	Sliding-filament physiology links molecular geometry to organismal movement [Huxley and Hanson, 1954].
Somatosensation	Receptor density sets spatial resolution	Mechanoreceptor subtype, receptive-field size, and cortical magnification jointly shape touch discrimination [Abraira and Ginty, 2013].
Behavior	Four explanatory levels	Mechanism, development, function, and phylogeny answer different questions about the same behavior [Tinbergen, 1963].
Reproduction	Infertility triage starts after 12 months, or 6 months at age 35+	Evaluation separates ovulation, sperm production, anatomy, implantation, endocrine timing, and age-dependent gamete quality [Centers for Disease Control and Prevention, 2024b].

D.7 Fundamental Biological Constants

Parameter	Value	Source / context
Resting cell membrane potential	≈ −70 mV	Neurons, muscle cells
Intracellular [Na ⁺] / [K ⁺]	about 10 / 140 mM	Maintained by Na ⁺ /K ⁺ -ATPase
Extracellular [Na ⁺] / [K ⁺]	about 145 / 5 mM	Plasma
Blood pH	7.35–7.45	Tightly regulated
Arterial pCO ₂	about 40 mmHg	Regulated by respiration
Body-water content	60 % of body mass	Total body water
Hemoglobin O ₂ capacity	1.34 mL O ₂ / g Hb	Full saturation
Blood volume	about 5 L in adult	7 % of body mass
Body surface area (adult)	about 1.8 m ²	DuBois formula
Mitochondrial membrane potential	≈ −180 mV	Drives ATP synthesis
Proton gradient ΔpH across inner mito membrane	about 1 unit	Chemiosmosis
Genome size (human)	3 × 10 ⁹ bp	Haploid
Protein-coding genes (human)	about 20,000	ENCODE estimate
Cells in the adult human body	about 3.7 × 10 ¹³	Bianconi et al. 2013
Bacteria in human gut	about 10 ¹⁴	about equal to human cell count
Species described on Earth	about 2 × 10 ⁶	Estimated 10–30× more undescribed

Appendix E — A Periodic Table for Biology

Appendix E · Level 1/3 · 15 min read · Prerequisites: section 1

Only about 25 of the 118 known elements are biologically essential. This appendix summarizes what each essential element does, what the classic pathologies of deficiency and excess look like, and where to encounter each in the textbook.

E.1 The Six Bulk Elements (CHNOPS)

Together these account for about 99 % of a human’s mass.

Element	Symbol	about % body mass	Where	Biological role
Oxygen	O	65 %	water, organic molecules	Electron acceptor in respiration; H-bond acceptor; part of every major biomolecule
Carbon	C	18 %	organic biomolecules, CO ₂ /HCO ₃ [−] pools	Tetravalent backbone of proteins, carbohydrates, lipids, and nucleic acids (see section 1)
Hydrogen	H	10 %	water and most organic biomolecules	Partner in polar bonds; proton transfer; pH
Nitrogen	N	3 %	amino acids, nucleic acids, ATP	Codes the backbone of DNA/RNA; amide in peptide bond; ring atom in bases
Phosphorus	P	1 %	DNA/RNA backbone, ATP, phospholipids	Phosphodiester bonds; free-energy carrier (ATP); membrane structure
Sulfur	S	0.25 %	cysteine, methionine, CoA, Fe-S	Disulfide bridges in proteins; thioester bonds in metabolism

E.2 Essential Macro-Minerals (Electrolytes + Osteogenics)

Element	Symbol	Common form	Role	Deficiency	Excess
Sodium	Na	Na ⁺	Principal extracellular cation; action potential upstroke	Hyponatraemia → seizures	Hypernatraemia → dehydration
Potassium	K	K ⁺	Principal intracellular cation; resting potential	Hypokalaemia → arrhythmia, muscle weakness	Hyperkalaemia → cardiac arrest
Calcium	Ca	Ca ²⁺	Bone matrix; signaling; coagulation; muscle contraction	Hypocalcaemia → tetany	Hypercalcaemia → stones, constipation

Element	Symbol	Common form	Role	Deficiency	Excess
Magnesium	Mg	Mg ²⁺	ATP co-factor; enzyme cofactor; ribosome structure	Hypomagnesaemia → arrhythmia, tetany	Rare; laxative effect
Chloride	Cl	Cl ⁻	Major anion; gastric HCl; GABA-A/glycine receptors	Loss with vomiting	Acidosis
Phosphate	P	HPO ₄ ²⁻	Energy transfer (ATP); DNA backbone; bone mineralisation	Muscle weakness	Soft tissue calcification (CKD)
Sulfate	S	SO ₄ ²⁻	Sulfated proteoglycans; sulfation of xenobiotics	Rare isolated deficiency	Rare

E.3 Trace Elements (Enzyme Cofactors)

Each is essential at mg day⁻¹ to µg day⁻¹ scale — too much or too little causes specific pathology.

Element	Role	Pathology of deficiency	Pathology of excess
Iron (Fe)	Hemoglobin, cytochromes, Fe-S clusters	Anemia, fatigue	Hereditary haemochromatosis (iron overload)
Copper (Cu)	Cytochrome c oxidase, tyrosinase, lysyl oxidase	Menkes disease (curly hair, neurodegeneration)	Wilson disease (Cu deposition in liver, brain)
Zinc (Zn)	>300 enzymes; zinc finger transcription factors	Impaired growth, taste, immunity	Interferes with Cu absorption
Manganese (Mn)	Superoxide dismutase, glutamine synthetase	Rare; impaired connective tissue	Parkinson-like syndrome (welders)
Cobalt (Co)	Vitamin B ₁₂ core	Megaloblastic anemia, neuropathy	Rare cardiomyopathy (beer cobalt in 1960s)

Element	Role	Pathology of deficiency	Pathology of excess
Molybdenum (Mo)	Xanthine oxidase, sulfite oxidase, nitrate reductase	Rare; sulfite oxidase deficiency	Gout-like syndrome
Selenium (Se)	Glutathione peroxidase (GPX); thyroid deiodinase	Keshan disease (cardiomyopathy)	Selenosis (hair loss, nail brittleness)
Iodine (I)	Thyroid hormones (T3, T4)	Hypothyroidism, goiter, cretinism	Thyrotoxicosis
Chromium (Cr)	Disputed insulin cofactor	Possibly impaired glucose tolerance	Cr(VI) is carcinogenic
Fluorine (F)	Fluoroapatite in enamel	Dental caries	Fluorosis (mottled enamel)

E.4 Ultra-Trace and Context-Dependent Elements

- Nickel (Ni) — cofactor in urease (bacterial, plant) and hydrogenase; suspected but not proven essential in mammals.
- Silicon (Si) — structural in diatoms, horsetails, grasses (silica phytoliths); supports collagen cross-linking in vertebrates.
- Boron (B) — essential in plants (cell-wall cross-linking via borate–rhamnogalacturonan); possibly beneficial in vertebrates.
- Vanadium (V) — sea-squirt blood pigment (vanadocytes); pharmacology for insulin-mimetic effects.
- Tungsten (W) — used instead of molybdenum by hyperthermophilic archaea.

E.5 Life Without an Expected Element

Biology has bent the rules. Examples of organisms that substitute or replace commonly “essential” elements:

- Iron-free bacteria in deep-sea hydrothermal vents — use manganese peroxidases instead.
- Selenocysteine (the “21st amino acid”) — expands the amino-acid alphabet using the rare element Se.
- Pyrrolysine (the “22nd amino acid”) — found in methanogenic archaea; does not require a rare element, but is an unusual 22-atom residue.
- Arsenic-based life controversy (GFAJ-1, 2010) — claim of As replacing P in DNA of a *Halomonas* strain; later retracted.

The periodic table remains under-explored for biological innovations. Astrobiological life may use different element sets entirely.

E.6 Quick Lookup: Which Chapter Covers Each Element?

Element	Primary chapter	Supporting chapter
C, H, N, O	section 1	section 3
P	section 12	section 9
S	section 3	section 9
Na, K	section 7	section 32; section 33
Ca	section 8	section 31; section 35
Mg	section 3	section 9

Module: reference only (no code)

Appendix F — Master Glossary of Biological Terms

Etymology notation: [Gk] = Greek; **L** = Latin; [OFr] = Old French; [Ar] = Arabic. Cross-references use semantic `\cref{...}` links generated from the canonical table of contents.

Maintenance note: glossary terms must use a Pandoc bracketed span, `[**Term**]{#gl:term-slug}` (with `markdown+bracketed_spans`, Pandoc emits a real `LaTeX \label{gl:...}` in PDF). Chapters link with `[**term**](#gl:term-slug)`. After editing terms, run `uv run python scripts/link_glossary.py --check` from the project root and verify `tests/test_build_invariants.py` plus markdown validation.

A

Abiotic [Gk *a* = without + *bios* = life + *-ic* = pertaining to] — Non-living physical and chemical components of an environment (light, temperature, water, minerals). Contrast with biotic. → section [40](#)

Actin [Gk *aktis* = ray or beam] — A 42 kDa globular protein (G-actin) that polymerizes into filaments (F-actin); a major component of the cytoskeleton, sarcomeres, and lamellipodia. → section [6](#)

Action potential [L *actio* = a doing + *potentia* = power] — A transient, all-or-none reversal of membrane potential (about −70 mV to +40 mV) propagated along neuronal axons; gated by voltage-dependent Na⁺ and K⁺ channels. Described mathematically by the Hodgkin-Huxley equations (1952). → section [32](#)

Adaptive immunity [L *adaptare* = to fit + *immunis* = exempt] — Antigen-specific defense mediated by B and T lymphocytes. It is slower than innate immunity during a first exposure but generates immunological memory, enabling faster and stronger secondary responses. → section [35](#)

Adenosine triphosphate (ATP) [Gk *aden* = gland (as in adenine, identified in gland tissue) + *tri* = three + *phosphorus* = light-bearer] — A central phosphoryl-group donor and short-term energy carrier in cells. Hydrolysis to ADP + P_i releases about 30.5 kJ/mol under biochemical standard conditions, while the effective cellular free energy is often larger in magnitude because ATP, ADP, and P_i concentrations are far from equilibrium. → section [9](#)

Aerobic [Gk *aer* = air + *bios* = life] — Requiring molecular oxygen (O₂) as the terminal electron acceptor in cellular respiration. Opposite: anaerobic. → section [9](#)

Allele [Gk *allelon* = of each other; shortened from *allelemorph*] — One of two or more alternative forms of a gene at the same chromosomal locus. Defined by a distinct nucleotide sequence. → section [17](#)

Allostasis [Gk *allos* = other + *stasis* = standing] — Predictive physiological regulation in which the brain adjusts setpoints and resource allocation in anticipation of demand, rather than merely correcting error after disturbance. → section [0.3](#)

Allosteric [Gk *allos* = other + *stereos* = solid/space] — Describing a regulatory site on an enzyme or receptor that is spatially distinct from the active site; ligand binding there changes the macromolecule’s conformation and activity. → section [4](#)

Anaerobic [Gk *an* = without + *aer* = air + *bios* = life] — Occurring without oxygen. Anaerobic respiration uses alternative electron acceptors (nitrate, sulfate); fermentation regenerates NAD⁺ without any external acceptor. → section [9](#)

Anaphase [Gk *ana* = up/apart + *phasis* = appearance] — The stage of mitosis/meiosis in which sister chromatids (mitosis, meiosis II) or homologous chromosomes (meiosis I) are pulled to opposite poles by spindle fibers. → section [12](#)

Angiosperm [Gk *angeion* = vessel/container + *sperma* = seed] — A flowering plant whose seeds are enclosed within a fruit derived from the ovary wall; the dominant plant group (about 300,000 species). Contrast: gymnosperm. → section [28](#)

Anticodon [Gk *anti* = against or opposite + L *codex* = writing block] — The three-nucleotide sequence on a tRNA molecule that base-pairs with the complementary codon on mRNA during translation. → section [13](#)

Apoptosis [Gk *apo* = away + *ptōsis* = a falling] — Programmed, caspase-mediated cell death characterized by chromatin condensation, DNA fragmentation, and membrane blebbing, without inflammatory response. Contrast: necrosis. → section [8](#)

Archaea [Gk *archaios* = ancient] — One of three domains of life; prokaryotes with ether-linked isoprenoid membrane lipids, histone-like proteins, and replication/transcription machinery closer to eukaryotes than to bacteria. Discovered by Woese & Fox (1977). → sections [5](#) and [23](#)

ATP synthase [see ATP + Gk *syn* = together + *thesis* = a placing] — Also Complex V; a rotary F₀F₁ molecular motor driven by the proton-motive force to phosphorylate ADP to ATP. The c-ring rotation of 120° per ATP was directly visualized by Noji et al. (1997). → section [9](#)

Autotroph [Gk *autos* = self + *trophe* = nourishment] — An organism that produces its own organic molecules from inorganic carbon (CO₂); either photoautotroph (energy from light) or chemoautotroph (energy from inorganic chemicals). → sections [5](#), [37](#) and [38](#)

Autonomic nervous system (ANS) [Gk *autonomos* = self-governing] — The visceral motor division of the peripheral nervous system; divided into sympathetic (thoracolumbar; noradrenaline/adrenaline; “fight-or-flight”) and parasympathetic (craniosacral; acetylcholine; “rest-and-digest”) branches. ANS innervates smooth muscle, cardiac muscle, and glands. → section 32

Axon hillock [Gk *axon* = axis + OE *hyll* = small hill] — The region of the neuron where the axon originates from the cell body (soma); the site of action potential initiation due to the high density of voltage-gated Na⁺ channels. EPSPs must summate here to reach threshold (about −55 mV). → section 32

B

Base pair (bp) [Gk *basis* = step, foundation] — A complementary nucleotide pair held by hydrogen bonds in double-stranded nucleic acids: A–T (2 H-bonds in DNA) and G–C (3 H-bonds). One bp ≈ 0.34 nm along the DNA helix. → section 12

Biofilm [Gk *bios* = life + L *filum* = thread] — A structured community of microorganisms attached to a surface and enclosed in a self-produced extracellular polysaccharide matrix; regulated by quorum sensing; often up to 1,000-fold more antibiotic tolerant than planktonic cells because matrix diffusion limits, slow growth, stress responses, and persister cells overlap. → section 24

Biome [Gk *bios* = life + *-ome* = mass/body] — A large-scale terrestrial or aquatic ecosystem characterized by a distinctive climate, vegetation, and fauna. Classified by Whittaker (1975) primarily by mean annual precipitation (MAP) and mean annual temperature (MAT). → section 40

Buffer [OFr *bufer* = to protect from a blow] — A solution containing a weak acid and its conjugate base that resists changes in pH by absorbing added H⁺ or OH[−]. Effective within ±1 pH unit of pK_a (Henderson-Hasselbalch). → section 1

C

Calvin cycle [named for Melvin Calvin, who elucidated it using ¹⁴C radioisotopes, 1950] — The light-independent carbon-fixation reactions of photosynthesis in the chloroplast stroma; not literally dark, because they depend on ATP and NADPH produced by the light reactions. Also called the Calvin-Benson-Bassham cycle. Net: 3 CO₂ + 9 ATP + 6 NADPH → G3P. → section 10

Caspase [L *caspase* = cysteine-containing aspartate protease] — A family of cysteine proteases that execute apoptosis; exists as inactive zymogens; activated by cleavage at specific aspartate residues in a proteolytic cascade. → section 8

Cell cycle [L *cella* = small room + Gk *kyklos* = circle] — The ordered sequence of events by which a cell duplicates its contents and divides: G₁ → S (DNA synthesis) → G₂ → M (mitosis) → cytokinesis. Regulated by cyclin-CDK complexes and checkpoint kinases. → section 12

CaMKII (Calcium/calmodulin-dependent kinase II) [L *calx* = lime (Ca) + *calmodulin* + Gk *kinein* = to move] — A serine/threonine kinase activated by Ca²⁺/calmodulin; autophosphorylation at T286 renders it constitutively active (“molecular memory”). Key effector of NMDA receptor-dependent LTP: phosphorylates AMPA receptors (increased conductance) and drives AMPA receptor exocytosis. → section 33

Cardiac output (CO) [Gk *kardia* = heart + L *emittere* = to send out] — The volume of blood ejected by the heart per minute: CO = heart rate (HR) × stroke volume (SV). Normal resting CO ≈ 5.5 L/min; can reach 20–25 L/min during maximal exercise in athletes. Regulated by the Frank-Starling mechanism and neurohumoral factors. → section 31

cDNA [complementary DNA; L *complementum* = that which fills up] — DNA synthesized from an mRNA template by reverse transcriptase; lacks introns; used in cloning, expression libraries, and RT-PCR diagnostics. → section 13

Centromere [Gk *kentron* = center + *meros* = part] — The specialized chromosomal region where kinetochore proteins assemble and spindle microtubules attach during mitosis and meiosis. Required for accurate chromosome segregation. → section 12

Chemiosmosis [Gk *chemi* = chemistry + *osmos* = push] — The coupling of electron transport to ATP synthesis via a proton electrochemical gradient across a membrane (proton-motive force). Proposed by Peter Mitchell (1961); Nobel Prize 1978. → section 9

Chirality [Gk *cheir* = hand] — The property of a molecule that is non-superimposable on its mirror image, like a hand. Biology is strongly homochiral in its core polymers: proteins mostly use L-amino acids, while nucleic acids and many central metabolites use D-sugars. → section 1

Chlorophyll [Gk *chloros* = green/yellow-green + *phyllon* = leaf] — A porphyrin-ring pigment containing Mg²⁺ at its center; the primary light-harvesting molecule in photosynthesis. Absorbs strongly at 430 nm (violet/blue) and 680–700 nm (red). → section 10

Chromatin [Gk *chroma* = color] — The complex of DNA and proteins (primarily histones) that compacts the genome within the nucleus. Exists in two states: euchromatin (open, transcriptionally active) and heterochromatin (compact, silenced). The fundamental unit is the nucleosome. → section 15

Chromosome [Gk *chroma* = color + *soma* = body] — A linear (eukaryotic) or circular (prokaryotic) DNA molecule associated with proteins (histones in eukaryotes) that carries the cell’s hereditary information. Humans have 46 chromosomes (23 pairs). → section 12

CpG island (C = cytosine; p = phosphodiester bond; G = guanine) — A genomic region (about 500 bp–2 kb) enriched for CG dinucleotides; observed/expected CpG ratio > 0.6; present at about 70% of vertebrate gene promoters. Normally unmethylated; hypermethylation silences the associated promoter in cancer and differentiation. → section 15

CRISPR-Cas [L *crispus* = clustered + *repetitive* + *palindromic* + *Cas* = CRISPR-associated protein] — A prokaryotic adaptive immune system (repeat-spacer arrays + Cas endonucleases) repurposed for programmable genome editing; Cas9 guided by a synthetic sgRNA cleaves DNA at a complementary target. → section 14

Codon [L *codex* = block of writing] — A three-nucleotide sequence in mRNA that specifies one amino acid or a stop signal. The genetic code has 64 codons encoding 20 amino acids (and 3 stop codons); most amino acids have multiple synonymous codons (degeneracy). → section 13

Cortisol [L *cortex* = bark, rind] — The primary glucocorticoid secreted by the adrenal cortex (zona fasciculata) in response to ACTH; mobilizes glucose (gluconeogenesis, protein catabolism), suppresses immunity (reduces IL-2, PGE2, and T cell activation), and regulates the stress response. Circadian peak at 06:00–08:00. Synthetic analogs (prednisone, dexamethasone) are widely used anti-inflammatory agents. → section 35

Cohesion-tension theory [L *cohaerere* = to stick together + Gk *teinein* = to stretch] — The mechanism by which water ascends xylem vessels in plants: evaporation at the leaf surface creates tension (negative pressure) transmitted through the hydrogen-bonded water column via adhesion to cell walls. Proposed by Dixon & Joly (1894). → section 28

Competitive inhibition [L *competere* = to seek together] — Enzyme inhibition in which the inhibitor binds the active site and competes with substrate. Raises apparent K_m without affecting V_{max} ; reversed by increasing **S**. → section 4

Cytoplasm [Gk *kytos* = cell/vessel + *plasma* = something formed] — The collective cell contents between the plasma membrane and the nucleus (or nucleoid); includes cytosol, organelles, ribosomes, and the cytoskeleton. → section 6

Cytoskeleton [Gk *kytos* = vessel + *skeletos* = dried up] — The dynamic network of protein filaments — actin microfilaments (7 nm), intermediate filaments (10 nm), and microtubules (25 nm) — that maintains cell shape, enables motility, and guides intracellular transport. → section 6

D

Diploid (2n) [Gk *diplous* = double + *eidos* = form] — A cell or organism with two complete sets of homologous chromosomes; one set from each parent. Human somatic cells are diploid (2n = 46). Contrast: haploid (n). → section 19

DNA helicase [Gk *helix* = spiral] — An ATP-dependent enzyme that unwinds the DNA double helix at the replication fork by breaking hydrogen bonds between base pairs; the replicative helicase DnaB in bacteria, MCM complex in eukaryotes. → section 12

DNA ligase [L *ligare* = to bind] — An enzyme that forms phosphodiester bonds between adjacent nucleotides; joins Okazaki fragments on the lagging strand; also used in DNA repair and recombinant DNA cloning. → section 12

Dominant [L *dominare* = to rule] — Describing an allele whose phenotypic effect is expressed in both homozygous and heterozygous states. The recessive allele is masked in the heterozygote. Mendel (1866). → section 17

Doubling time (t_d) [OE *dubbel* = twice + L *tempus* = time] — The time required for a population or culture to double in number; $t_d = \ln 2/\mu$ where μ is the specific growth rate. → section 24

E

Electronegativity [Gk *elektron* = amber (as source of static charge) + L *negativus* = denying] — The tendency of an atom to attract bonding electrons. Pauling scale: F = 3.98; O = 3.44; N = 3.04; C = 2.55; H = 2.20. Determines bond polarity. → section 1

Endocytosis [Gk *endon* = within + *kytos* = vessel] — Uptake of extracellular material by inward budding of the plasma membrane to form a vesicle. Subtypes: pinocytosis (fluid/solutes), phagocytosis (large particles), receptor-mediated endocytosis (specific ligands via clathrin-coated pits). Contrast: exocytosis. → section 7

Endosymbiosis [Gk *endon* = within + *sym* = together + *bios* = life] — A relationship in which one organism lives within another over evolutionary time, eventually becoming an organelle. The mitochondrion (about 1.5 Ga ago) and chloroplast (about 1.2 Ga ago) both originated by endosymbiosis of bacterial cells

(Margulis, 1967). → section 5

Entropy (S) [Gk *en* = in + *trope* = transformation] — A thermodynamic state function often described as energy dispersal or the number of accessible microstates. For spontaneous processes in an isolated system, total entropy increases ($\Delta S_{universe} > 0$). Living organisms maintain ordered internal structures by exchanging matter and energy with surroundings. → section 9

Enzyme [Gk *en* = in + *zyme* = leaven/ferment] — A biological catalyst — almost always a protein, sometimes RNA (ribozyme) — that accelerates a reaction by lowering the activation energy without being consumed. Characterized by specificity, saturation kinetics (Michaelis-Menten), and allosteric regulation. → section 4

Epigenetics [Gk *epi* = above/upon + *genet-* = birth; coined by Waddington, 1942] — Heritable changes in gene expression that do not alter the underlying DNA sequence. Molecular carriers: CpG methylation, histone post-translational modifications (acetylation, methylation, phosphorylation), and non-coding RNAs (miRNA, lncRNA, piRNA). → section 15

Epigenome [Gk *epi* = upon + *genos* = origin + *-ome* = total] — The complete set of epigenetic modifications across a cell’s genome; cell-type specific and environmentally modifiable, unlike the genome sequence. Mapped by ENCODE and Roadmap Epigenomics projects. → section 14

Euchromatin [Gk *eu* = true/good + *chroma* = color] — Loosely packed chromatin associated with H3K4me3 and H3K27ac histone marks; transcriptionally permissive. Contrast: heterochromatin. → section 15

Excitotoxicity [L *excitare* = to rouse + Gk *toxikon* = poison] — Neuronal death caused by excessive glutamate receptor activation (especially NMDA), leading to massive Ca^{2+} influx, mitochondrial dysfunction, caspase activation, and necrosis/apoptosis. The primary mechanism of neuronal death in ischemic stroke. Target of neuroprotective strategies. → section 33

Eukaryote [Gk *eu* = true + *karyon* = nucleus] — An organism whose cells contain a membrane-enclosed nucleus and membrane-bound organelles. Includes protists, fungi, plants, and animals. Contrast: prokaryote. → section 5

Exon [Gk *exo* = outside; coined by Gilbert, 1978] — A coding sequence in a eukaryotic gene that is retained in the mature mRNA after splicing and is translated into protein. Contrast: intron. → section 13

F

FEV₁/FVC [forced expiratory volume/forced vital capacity] — The fraction of vital capacity exhaled in the first second of a forced expiration; obstruction is best interpreted against the age-dependent lower limit of normal, with a fixed 0.70 threshold used as a simple COPD screening convention. Restrictive patterns usually preserve or raise the ratio while reducing absolute lung volumes. → section 31

Fatty acid [ME *fat* + Gk *oxys* = acid/sharp] — A carboxylic acid with a hydrocarbon chain. Saturated fatty acids pack tightly; unsaturated *cis* double bonds introduce bends that increase membrane fluidity. → section 3

Fisheries [OE *fisc* = fish] — Human-managed harvest systems for aquatic populations; modern stock assessment uses age structure, recruitment, mortality, and maximum sustainable yield models to avoid collapse. → sections 36 and 40

Frank-Starling law [named for Otto Frank (1895) and Ernest Starling (1914)] — The intrinsic property of cardiac muscle whereby stroke volume increases with end-diastolic volume (preload): greater stretch of sarcomeres increases Ca^{2+} sensitivity of troponin C, increasing force generation. Operates up to an optimal sarcomere length (about 2.2 μm); beyond this, overlap of thick and thin filaments decreases. → section 31

Facilitated diffusion [L *facilis* = easy + *diffundere* = to pour out] — Passive transport of molecules down their concentration gradient via membrane proteins (channels or carriers); no energy required. Contrast: active transport. → section 7

Fitness (w) [OE *gefittan* = to be suitable] — In evolutionary biology, the relative contribution of a genotype to the next generation; often expressed as $w = 1 - s$ where *s* is the selection coefficient. → section 20

Free energy (ΔG) [Gk *eleutheros* = free] — Gibbs free energy; the energy available to do work at constant temperature and pressure: $\Delta G = \Delta H - T\Delta S$. Spontaneous reactions have $\Delta G < 0$ (exergonic). → section 9

G

GLP-1 (glucagon-like peptide-1) [L *glucos* = sweet + *lysis* = splitting] — An incretin hormone secreted by intestinal L cells in response to nutrient ingestion; potentiates glucose-dependent insulin secretion (GSI) from beta cells; suppresses glucagon; delays gastric emptying; reduces appetite via hypothalamic signaling.

GLP-1 receptor agonists (semaglutide, tirzepatide) are transformative in treating type 2 diabetes and obesity. → section 35

GLUT4 [glucose transporter type 4] — The insulin-sensitive glucose transporter expressed in muscle and adipose tissue; stored in intracellular vesicles; translocated to the plasma membrane within minutes of insulin receptor activation (PI3K–Akt–AS160 cascade). Responsible for up to 90% of post-prandial muscle glucose uptake. Impaired GLUT4 trafficking underlies insulin resistance in type 2 diabetes. → section 35

Gamete [Gk *gamete* = wife; *gametes* = husband; from *gamein* = to marry] — A haploid reproductive cell (sperm or egg) that fuses with another gamete during fertilization to restore the diploid number. → section 19

Gene [Gk *genos* = birth/origin; coined by Johannsen, 1909] — A heritable unit of information encoded in DNA that typically specifies the sequence of a protein or functional RNA; operationally defined as a sequence occupying a defined chromosomal locus. → section 15

Genetic code [Gk *genos* = birth + L *codex* = writing block] — The mapping from 64 mRNA codons to 20 amino acids and stop signals. It is nearly universal, degenerate, and read by tRNA anticodons during translation. → section 13

Genome [Gk *genos* = birth + *-ome* = total body of] — The complete set of genetic information in an organism, including nuclear chromosomes, mitochondrial DNA, and in plants, chloroplast DNA. Human haploid genome: about 3.2 Gb, about 20,000 protein-coding genes. → section 14

Genome-wide association study (GWAS) [Eng *genome* + *wide* + *association*] — A population scan correlating millions of SNP genotypes with a trait or disease; identifies tag loci (not always causal genes); requires large samples and correction for multiple testing. → section 14

Glycolysis [Gk *glykys* = sweet + *lysis* = splitting] — The 10-step cytosolic pathway that converts glucose (6C) to 2 pyruvate (3C), yielding a net 2 ATP and 2 NADH per glucose under standard textbook accounting. It does not require oxygen directly and is among the most ancient and widespread central metabolic pathways, though some organisms use modified glycolytic routes. → section 9

Gram stain [named for Hans Christian Gram, Danish bacteriologist, 1884] — A differential microbiological stain that distinguishes thick-peptidoglycan bacteria (Gram-positive: retain crystal violet, purple) from thin-peptidoglycan + outer membrane bacteria (Gram-negative: lose crystal violet, pink after safranin counterstain). → section 5

H

HPA axis (hypothalamic–pituitary–adrenal axis) [Gk *hypo* = under + *thalamos* = inner chamber] — The neuroendocrine stress axis: CRH (hypothalamus) → ACTH (anterior pituitary) → cortisol (adrenal cortex). Regulated by negative feedback at hypothalamus and pituitary. Dysregulation implicated in depression, PTSD, and Cushing’s syndrome. → section 35

HPG axis (hypothalamic–pituitary–gonadal axis) — GnRH (hypothalamus) → FSH + LH (anterior pituitary) → sex steroids + gametes (gonads). Pulsatile GnRH (every 90 min) is required for normal FSH/LH secretion; continuous GnRH causes receptor downregulation and gonadotropin suppression. → section 35

HPT axis (hypothalamic–pituitary–thyroid axis) — TRH (hypothalamus) → TSH (anterior pituitary) → T4/T3 (thyroid gland). T3 is the active form; acts on nuclear receptors to increase metabolic rate, thermogenesis, and cardiac output. Hypothyroidism: TSH ↑; hyperthyroidism: TSH ↓. → section 35

Haploidy (n) [Gk *haplous* = single + *eidos* = form] — Condition of having one complete set of chromosomes; characteristic of gametes and the gametophyte generation of plants. → section 19

Hardy-Weinberg equilibrium [named for Godfrey Hardy, mathematician, and Wilhelm Weinberg, physician, 1908] — The principle that allele and genotype frequencies remain constant in a population absent of evolutionary forces (no selection, drift, mutation, migration, non-random mating). Genotype frequencies: $p^2 + 2pq + q^2 = 1$. → section 20

Heterozygous [Gk *heteros* = different + *zygotos* = yoked] — Possessing two different alleles at a given locus (e.g., *Aa*). Contrast: homozygous (*AA* or *aa*). → section 17

Hill coefficient (n) [named for Archibald Hill, 1910] — A measure of cooperativity in ligand binding. $n = 1$ = no cooperativity; $n > 1$ = positive cooperativity (sigmoidal binding curve). Hemoglobin: $n \approx 2.8$. → section 4

Homeostasis [Gk *homoios* = similar + *stasis* = standing/state] — The maintenance of a relatively stable internal environment despite external fluctuations; achieved by negative feedback loops with a sensor, comparator (integrator), and effector. Coined by Walter Cannon (1926, building on Claude Bernard). → section 32

Heterochromatin [Gk *heteros* = different + *chroma* = color] — Densely compacted chromatin bearing repressive histone marks (H3K9me3, H3K27me3) and high DNA methylation; transcriptionally silent. Constitutive heterochromatin (centromeres, telomeres) is permanent; facultative heterochromatin (e.g., the inactive X chromosome) is cell-type specific. → section 15

Histone [Gk *histos* = loom/web] — One of five abundant nuclear proteins (H1, H2A, H2B, H3, H4) that form the nucleosome core and linker. Tails are post-translationally modified by acetylation, methylation, phosphorylation, and ubiquitination to regulate gene expression (histone code). → section 15

Histone code [Gk *histos* = loom; L *codex* = writing block] — The hypothesis (Strahl & Allis, 2000) that combinations of histone post-translational modifications specify unique chromatin states; ‘written’ by HATs/HMTs, ‘read’ by bromodomains/chromodomains, ‘erased’ by HDACs/KDMs. → section 15

Holobiont [Gk *holos* = whole + *bios* = life] — The host plus its persistent associated microbiota (and sometimes viruses) treated as an integrated biological system; useful for analyzing nutrition, immunity, and niche construction. → sections 24 and 25

Hydrogen bond [Gk *hydor* = water + *genes* = born from (as in generated with water)] — A weak electrostatic attraction (2–40 kJ/mol) between a hydrogen atom covalently bonded to an electronegative atom (N, O, or F) and another electronegative atom. Critical for DNA base-pairing, protein secondary structure, and water’s unique properties. → section 1

Hydrolysis [Gk *hydor* = water + *lysis* = loosening] — Cleavage of a chemical bond by addition of water; central to digestion, ATP turnover, polymer breakdown, and many enzyme-catalysed reaction mechanisms. → sections 3 and 4

Hydrophobic effect [Gk *hydor* = water + *phobos* = fear] — The entropy-driven clustering of nonpolar surfaces in water as ordered water cages are released. It drives membrane assembly, protein folding, and ligand binding. → sections 2 and 3

I

Insulin receptor [L *insula* = island, as in islets of Langerhans] — A receptor tyrosine kinase (RTK) composed of two α and two β subunits; insulin binding activates RTK, triggering autophosphorylation and IRS-1/2 phosphorylation; downstream: PI3K–Akt (GLUT4 translocation, glycogen synthesis) and MAPK (gene expression, cell growth). Type 2 diabetes involves insulin receptor signaling resistance. → section 35

Independent assortment [L *independens* = not hanging upon] — Mendel’s second law: genes on non-homologous chromosomes are inherited independently of each other, producing 9:3:3:1 ratios in dihybrid crosses. Applies only to genes on different chromosomes or far apart on the same chromosome. → section 17

Intron [L *intra* = within; coined by Sharp & Roberts, 1977] — A non-coding intervening sequence within a eukaryotic gene that is transcribed but removed from the pre-mRNA by the spliceosome before translation. Nobel Prize 1993 (Sharp & Roberts). → section 13

K

Keystone species [L *lapis* = stone; *clavus* = key] — A species with a disproportionately large effect on its ecosystem relative to its biomass; its removal causes dramatic shifts in community structure. Term coined by Robert Paine (1966) based on sea-star (*Pisaster*) removal experiments. → section 37

Km (Michaelis constant) [after Leonor Michaelis] — The substrate concentration at which an enzyme operates at half its maximum velocity ($V_{\max}/2$); reflects enzyme-substrate affinity (lower K_m = higher affinity). Units: mol/L (M). → section 4

L

LTP (long-term potentiation) [L *longum* = long + *tempus* = time + *potentia* = power] — A persistent (hours to days) increase in synaptic efficacy following high-frequency stimulation; requires NMDA receptor activation → Ca^{2+} influx → CaMKII autophosphorylation → AMPA receptor insertion; the cellular model of learning and memory (Bløndell, Lømo 1973). → section 33

LTD (long-term depression) [L *deprimere* = to press down] — A persistent decrease in synaptic efficacy; induced by low-frequency stimulation (1 Hz) or by mGluR/endocannabinoid signaling (“endocannabinoid-mediated LTD”); involves PP1/PP2A phosphatase activation and AMPA receptor internalization via dynamin-clathrin endocytosis. → section 33

Linkage [ON *hlenkr* = chain link] — The tendency of genes located on the same chromosome to be inherited together; the closer the genes, the stronger the linkage (lower recombination frequency). → section 19

Locus (plural: loci) [L *locus* = place] — The fixed chromosomal position occupied by a particular gene; defined by its physical map coordinates (base pair position) or genetic map position (centimorgans from a reference marker). → section 19

Lotka-Volterra equations [named for Alfred Lotka (1925) and Vito Volterra (1926)] — A pair of coupled nonlinear ODEs describing predator-prey population cycles: $dN/dt = \alpha N - \beta NP$ (prey) and $dP/dt = \delta NP - \gamma P$ (predator). Produce neutrally stable oscillatory dynamics. → section 37

M

mRNA (messenger RNA) [L *nuntius* = messenger] — An RNA molecule transcribed from a gene’s template strand; carries the codon sequence from the nucleus to the ribosome for translation into protein. Processed in eukaryotes by 5’ capping, 3’ polyadenylation, and splicing. → section 13

Meiosis [Gk *meiosis* = lessening] — Two successive cell divisions — Meiosis I (reductional; homologue separation) and Meiosis II (equational; sister chromatid separation) — that produce four haploid gametes from one diploid cell. Sources of genetic diversity: crossing-over and independent assortment. → section 19

Membrane potential (Vm) [L *membrana* = thin skin + *potentia* = power] — The electric potential difference across a biological membrane; in neurons at rest, approximately –70 mV (inside negative). Governed by the Goldman equation for multiple ion species. → section 31

Michaelis-Menten kinetics [after Leonor Michaelis & Maud Menten, 1913] — The standard kinetic model for enzyme catalysis: $v = V_{max}[S]/(K_m + [S])$. Assumes rapid equilibrium or steady-state complex formation and one substrate. → section 4

Microbiome [Gk *mikros* + *bios* + *-ome*] — The full complement of microorganisms (bacteria, archaea, fungi, viruses) and their genes in a defined environment (e.g., gut, rhizosphere); often profiled by metagenomic sequencing. → section 24

Microbiota [Gk *mikros* + *bios* + *-ota* collective] — The assemblage of microorganisms themselves (contrast microbiome, which often denotes genes and functions as well). → section 24

MicroRNA (miRNA) [Gk *mikros* = small] — A about 22 nt single-stranded RNA that directs post-transcriptional gene silencing; biogenesis: Drosha (nuclear) → pre-miRNA → Dicer (cytoplasmic) → AGO2/RISC; partial 3’UTR complementarity causes translational repression and mRNA decay. > 2,000 human miRNAs regulate about 60% of protein-coding genes. → section 15

Mitosis [Gk *mitos* = thread] — Cell division in which one diploid cell produces two genetically identical diploid daughter cells; consists of prophase, metaphase, anaphase, and telophase followed by cytokinesis. → section 12

Mutation [L *mutare* = to change] — A heritable change in genetic sequence, including substitutions, insertions, deletions, inversions, duplications, and translocations. Mutation creates new sequence variants; recombination, segregation, gene flow, and selection then reshape how those variants are combined and distributed in populations. → section 14

5-Methylcytosine (5mC) — The “fifth base” of DNA; cytosine methylated at C5 by DNMT enzymes using S-adenosylmethionine as methyl donor. Silences promoters via MBD protein recruitment; oxidised to 5-hydroxymethylcytosine (5hmC) by TET enzymes for active demethylation. → section 15

N

Natural selection [L *natura* = nature; *selectio* = choosing] — The process by which heritable variations that increase survival or reproduction become more common in a population over generations. Proposed by Darwin & Wallace (1858). → section 20

Niche [OFr *nicher* = to nest] — The totality of an organism’s role in its environment, including physical conditions (temperature, pH, resources) it can use and interactions with other species. Fundamental niche: possible without competition. Realized niche: actual range when competitors are present. → section 37

Nucleosome [L *nucleus* = nut kernel + Gk *soma* = body] — The fundamental repeating unit of chromatin: 147 bp of DNA wound about 1.65 turns around a histone octamer (H2A, H2B, H3, H4 × 2); diameter 11 nm. First visualized by electron microscopy (Kornberg, 1974; Nobel Prize 2006). → section 15

Nucleotide [Gk *nucleus* = kernel + L *nucleus* = nut kernel] — The monomer of nucleic acids: a nitrogenous base + pentose sugar + one to three phosphate groups. Adenine, guanine (purines); cytosine, thymine, uracil (pyrimidines). → section 12

O

Organelle [Gk *organon* = tool/instrument + *ella* = diminutive suffix] — A membrane-bound (or in some definitions, functionally discrete) structure within a eukaryotic cell, performing a specialized function. Examples: nucleus, mitochondrion, chloroplast, Golgi apparatus, lysosome. → section 6

Osmosis [Gk *osmos* = pushing] — The movement of water across a selectively permeable membrane from a region of lower solute concentration (higher water potential) to a region of higher solute concentration (lower water potential). Van ’t Hoff equation: $\pi = iCRT$. → section 7

Oxidative phosphorylation [L *oxidare* = to oxidise + Gk *phosphoros* = light-bearer] — The ATP-generating process driven by electron transfer from NADH/FADH₂ to O₂ via the electron transport chain, producing the proton-motive force used by ATP synthase. Yields about 28 of the about 30–32 ATP per glucose. → section 9

P

P₅₀ [partial pressure at which hemoglobin is 50% saturated] — A measure of hemoglobin-O₂ affinity; normal P₅₀ = 26–27 mmHg. Rightward shifts (increased P₅₀) = decreased affinity: caused by increased PCO₂, H⁺, temperature, 2,3-BPG (Bohr effect). Leftward shifts = increased affinity: caused by decreased PCO₂, alkalosis, hypothermia, foetal Hb. → section 31

Pan-genome [Gk *pan* = all + *genome*] — The union of the collective genes found across a species or clade when many strains are sequenced; comprises a core genome (shared) and accessory genes (variable). Explains strain-specific virulence and metabolic capabilities in bacteria. → section 14

Poiseuille’s law [named for Jean Léonard Marie Poiseuille, 1840] — Laminar flow of a viscous fluid in a cylindrical tube: $Q = \pi r^4 \Delta P / 8 \eta L$, where r = radius, ΔP = pressure gradient, η = viscosity, L = length. The r^4 dependence explains why small changes in vessel radius (e.g., arteriolar vasodilation) produce large changes in flow and vascular resistance. → section 31

Peptide bond [Gk *pepsis* = digestion; peptides were initially thought to be digestion products] — The covalent bond (–CO–NH–) formed by condensation between the carboxyl group of one amino acid and the amino group of another during translation. Has partial double-bond character (resonance; about 40% double bond), conferring planarity. → section 3

pH [Danish *potenz* = power + Gk *hydro* = water; coined by Sørensen, 1909] — The negative common logarithm of hydrogen ion activity: $pH = -\log_{10}[H^+]$. Physiological range: blood plasma 7.35–7.45; lysosomes 4.5–5.0; mitochondrial matrix 7.8–8.0. → section 1

Phenotype [Gk *phainein* = to show + *typos* = impression] — The observable characteristics of an organism, determined by the interaction of genotype with environment. Contrast: genotype. → section 17

Phospholipid bilayer [Gk *phosphoros* = light-bearer + L *lipidus* = fat] — A self-assembled membrane structure in which amphipathic lipids orient hydrophilic heads toward aqueous environments and hydrophobic tails inward; typical thickness is about 7–8 nm. It is the dominant membrane architecture in bacteria and eukaryotes, while archaeal membranes often use ether-linked isoprenoid lipids and can form monolayers. → section 7

Photosynthesis [Gk *phos/photos* = light + *synthesis* = putting together] — The process by which photosynthetic organisms use light energy to produce organic compounds from CO₂ and H₂O; in plants: light reactions (thylakoids; produce ATP + NADPH) + Calvin cycle (stroma; fix CO₂ into G3P). → section 10

Plasmid [Gk *plasma* = formed thing] — A small, circular, double-stranded DNA molecule in bacteria (and some eukaryotes) that replicates independently of the chromosome; often carries genes for antibiotic resistance or virulence. → section 5

Polymerase chain reaction (PCR) [Gk *polys* = many + L *merus* = part; Gk *kyklos* = circle; coined by Kary Mullis, 1983] — An *in vitro* method for amplifying a specific DNA sequence using repeated cycles of denaturation, primer annealing, and extension by Taq polymerase. Transformed molecular biology; Nobel Prize 1993. → section 14

Promoter [L *promovere* = to move forward] — A DNA sequence upstream of a gene where RNA polymerase and transcription factors bind to initiate transcription. In prokaryotes: –10 (Pribnow box) and –35 elements; in eukaryotes: TATA box, initiator, and Pol II general transcription factors. → section 13

Protein [Gk *proteios* = of the first quality; coined by Mulder & Berzelius, 1838] — A polymer of L-amino acids linked by peptide bonds; encoded by the gene sequence; functional form depends on primary (1°), secondary (2°), tertiary (3°), and quaternary (4°) structure. → section 3

R

RAAS (renin–angiotensin–aldosterone system) [L *ren* = kidney] — The hormonal blood pressure and volume regulatory cascade: low renal perfusion → juxtaglomerular cells release renin → cleaves angiotensinogen to angiotensin I → ACE (lung) converts to angiotensin II → vasoconstriction + aldosterone release (Na⁺/H₂O retention). ACE inhibitors (enalapril) and ARBs (losartan) are first-line antihypertensive drugs. → section 31

Recombination [L *re* = again + *combinare* = to combine] — The process of generating new combinations of alleles through crossing-over between homologous chromosomes during meiosis I. Frequency (θ) is proportional to genetic map distance (1 cM = 1% recombination). → section 19

Reduction potential (E°) [L *reducere* = to lead back] — The tendency of a molecule to accept electrons, measured in volts under standard biochemical conditions (pH 7, 25°C). O₂/H₂O: +0.816 V; NAD⁺/NADH: –0.320 V. Electrons flow from lower to higher E°. → section 1

Ribonucleic acid (RNA) [L *nucleus* + suffix *ic*] — A single-stranded nucleic acid using ribose and uracil (instead of deoxyribose and thymine); roles include mRNA (messenger), tRNA (transfer), rRNA (ribosomal), and regulatory (miRNA, siRNA, snRNA). → section 13

Ribosome [named for ribose + Gk *soma* = body] — The ribonucleoprotein complex (about 2.5 MDa in eukaryotes; 80S = 40S + 60S subunits) that catalyses peptide bond formation during translation; catalytic activity resides in rRNA (a ribozyme). Nobel Prize 2009 (Ramakrishnan, Steitz, Yonath). → section 13

S

Saltatory conduction [L *saltare* = to jump] — The rapid propagation of action potentials in myelinated axons by jumping from one node of Ranvier to the next; velocity proportional to internodal distance; 5–70 m/s vs 0.5–2 m/s in unmyelinated C fibers. Enabled by high Na⁺ channel density at nodes and insulation by myelin between nodes. → section 33

SNARE complex [acronym: Soluble N-ethylmaleimide-sensitive factor Attachment protein REceptors] — The core vesicle fusion machinery: v-SNARE (synaptobrevin/VAMP-2, on vesicle) + t-SNAREs (syntaxin-1A and SNAP-25, on target membrane) zipper together in a four-helix bundle providing the energy for membrane fusion. Cleaved by clostridial neurotoxins (botulinum toxin cleaves SNAP-25/VAMP; tetanus toxin cleaves VAMP in spinal inhibitory interneurons). → section 33

Surfactant [L *superficies* = surface + *activus* = active] — A complex mixture of phospholipids (primarily DPPC) and proteins (SP-A, SP-B, SP-C, SP-D) secreted by alveolar type II pneumocytes; reduces alveolar surface tension according to Laplace’s law ($P = 2T/r$), preventing alveolar collapse (atelectasis) during expiration and reducing the work of breathing. Deficiency causes neonatal respiratory distress syndrome (RDS). → section 31

Synaptotagmin [Gk *synapsis* = junction + *tagma* = arrangement] — The Ca²⁺ sensor for fast neurotransmitter release; C2A and C2B domains bind 3–5 Ca²⁺ ions cooperatively (Hill coefficient $n \approx 4$), explaining Ca²⁺ cooperativity of neurotransmitter release. Synaptotagmin-1 drives synchronous fast release; synaptotagmin-7 drives asynchronous release and facilitatory plasticity. → section 33

Selection coefficient (s) [see *natural selection*] — A quantitative measure of the fitness disadvantage (or advantage) conferred by an allele; $s = 1 - w$ where w is relative fitness. Dominant lethal: $s = 1$; neutral: $s = 0$. → section 20

Speciation [L *species* = appearance/kind] — The evolutionary process by which one ancestral population diverges into two or more reproductively isolated species. Mechanisms: allopatric (geographic isolation), sympatric (within a range; polyploidy, disruptive selection). → section 22

Species-area relationship [L *species* = kind + *area* = open space] — The empirical relationship $S = cA^z$ between species richness (S) and area (A); exponent $z \approx 0.25$ for continental habitats, $z \approx 0.30$ for island habitats. MacArthur & Wilson (1967). → section 40

Surface-area-to-volume ratio (A/V) [L *superficies* = surface] — For a sphere: $A/V = 3/r$. As cell radius increases, A/V decreases, limiting diffusion-based nutrient exchange; this constraint accounts for why cells are microscopically small. → section 5

T

Thermodynamics [Gk *therme* = heat + *dynamis* = power] — The branch of physical science concerned with heat, work, and energy transformations. First Law: energy is conserved. Second Law: entropy increases in any spontaneous process. → section 9

Transcription [L *transcribere* = to copy] — The synthesis of an RNA molecule from a DNA template by RNA polymerase; proceeds 5’ to 3’ reading the template strand 3’ to 5’; regulated by transcription factors, promoters, and enhancers. → section 13

Translation [L *translatio* = carrying across] — The ribosome-mediated synthesis of a polypeptide from an mRNA template; proceeds from 5’ to 3’ (mRNA), adding amino acids from N- to C-terminus at about 15 residues/second (eukaryotes). → section 13

Transpiration [L *trans* = across + *spirare* = to breathe] — The evaporation of water from leaf mesophyll cells and its diffusion through stomata; drives the transpiration stream (cohesion-tension mechanism) and enables mineral transport in xylem. → section 28

Trophic level [Gk *trophe* = nourishment] — A functional tier in a food web defined by the number of energy-transfer steps from primary producers; approximately 10% of energy passes between levels (Lindeman’s trophic-dynamic theory, 1942). → section 39

V

Van der Waals forces [named for Johannes Diderik van der Waals, 1873] — Weak, short-range intermolecular attractions (0.1–10 kJ/mol) arising from transient (London dispersion), permanent-induced (Debye), or permanent-permanent (Keesom) dipole interactions. Important for packing of hydrophobic molecules and protein-ligand recognition. → section 1

Virulence [L *virulentus* = full of poison] — The capacity of a pathogen to cause disease; quantified as the proportion of infected hosts that develop disease or die. Virulence factors include toxins, adhesins, capsules, and immune evasion mechanisms. → section 24

W

Water potential (Ψ) [named analogy to electrical potential] — A measure of the free energy of water in a system relative to pure water: $\Psi = \Psi_s + \Psi_p$ (solute + pressure components). Water moves from high Ψ to low Ψ (down the gradient). Units: megapascals (MPa). → section 28

X

Xylem [Gk *xylon* = wood] — The vascular tissue that conducts water and dissolved minerals from roots to aerial organs; composed of non-living tracheids and vessel members (dead at maturity) plus parenchyma and fibers. Water moves by cohesion-tension mechanism. → section 28

Z

Zygote [Gk *zygotos* = yoked] — The diploid cell formed by the fusion of two haploid gametes during fertilization; the first cell of a new organism; undergoes mitotic divisions to form the embryo. → section 17

This glossary covers about 120 core terms. Chapter-specific key terms are listed in each chapter’s Key Terms section. For full index, see the combined PDF output.

Additional Terms

C (continued)

Carrying capacity (K) [L *capax* = able to hold] — The maximum number of individuals an environment can support indefinitely, determined by resource availability; the equilibrium of the logistic growth model $dN/dt = rN(1 - N/K)$. → section 36

Chloroplast [Gk *chloros* = green + *plastos* = formed] — A double-membrane plant organelle derived from a cyanobacterial endosymbiont; contains the thylakoid membranes (light reactions) and stroma (Calvin cycle); its own circular genome encodes about 80 proteins. → section 10

Coevolution [L *co*- = together + *evolutio* = unrolling] — The reciprocal evolutionary change in two or more species exerting strong selective pressure on each other; classic examples: plant-pollinator mutualism, host-parasite arms races, flowering plant-butterfly chemical coevolution (Ehrlich & Raven, 1964). → section 37

Competitive exclusion [L *competere* = to strive together + *excludere* = to shut out] — Gause’s competitive exclusion principle (1934): two species competing for identical limiting resources cannot coexist indefinitely at equilibrium; one will be excluded. → section 37

Copepod [Gk *kope* = oar + *pous/podos* = foot] — A crustacean subclass of small aquatic organisms forming a major component of marine and freshwater zooplankton; primary consumers linking phytoplankton to larger predators in ocean food webs. → section 39

D (continued)

Decomposer [L *de* = down + *componere* = put together] — An organism (primarily bacteria and fungi) that breaks dead organic matter into inorganic nutrients through enzymatic digestion; drives nutrient cycling in every ecosystem. → section 39

Density-dependent regulation [L *densus* = thick] — A population regulatory mechanism whose effect (per-capita birth or death rate) changes as a function of population density; resource competition, disease, and predation are density-dependent. Contrast: density-independent factors (e.g., floods, fires). → section 36

Depolarization [L *de* = away from + Gk *polos* = pivot] — A decrease in magnitude of membrane potential (movement toward zero or positive values); in neurons, caused by Na^+ influx through voltage-gated channels during the rising phase of an action potential. Contrast: repolarization, hyperpolarization. → section 32

E (continued)

Effective population size (N_e) [Gk *effectivus* = productive] — An idealised census number equivalent to the actual population in terms of rate of genetic drift; typically much smaller than the census size due to unequal sex ratios, variance in reproductive success, and population size fluctuations. $\sigma^2(\Delta p) = pq/2N_e$. → section 22

Eusociality [Gk *eu* = good/true + L *socialis* = allied] — Social organization with cooperative brood care, overlapping generations, and reproductive division of labor, including sterile or weakly reproductive worker castes in ants, many bees and wasps, and termites. → sections 21 and 23

Epiphyte [Gk *epi* = upon + *phyton* = plant] — A plant that grows on another plant for physical support without parasitising it; absorbs water and nutrients from rain and air; orchids, bromeliads, and ferns are prominent epiphytes. → section 40

Eutrophication [Gk *eutrophos* = well-nourished] — Nutrient enrichment of an aquatic body (typically N and P from agricultural runoff) triggering algal blooms; subsequent decomposition of algal biomass depletes dissolved oxygen, causing hypoxic dead zones. → section 39

F (continued)

Fermentation [L *fermentum* = leaven] — Anaerobic metabolic process regenerating NAD⁺ by reducing pyruvate to lactate (lactic acid fermentation) or to ethanol + CO₂ (alcoholic fermentation); net gain: 2 ATP/glucose. → section 9

Founder effect [OE *funden* = to establish] — A form of genetic drift in which allele frequencies in a new population established from a small group of founders differ from the source population by chance; can lead to high prevalence of otherwise rare alleles. → section 22

Frond [L *frons/frondis* = leafy branch] — The large leaf of a fern or other pteridophyte; bears sporangia on its underside (in a sorus); anatomically equivalent to a compound leaf. → section 28

G (continued)

Genetic drift [ON *drift* = a driving of snow] — Random, chance changes in allele frequencies in a population from generation to generation due to sampling error in finite populations; stronger effect in small populations. → section 22

GPP (gross primary productivity) [Gk *ge* = earth + *protos* = first + L *producere*] — The total rate of photosynthetic carbon fixation by producers; GPP – R_a (autotrophic respiration) = NPP (net primary productivity). → section 39

Guard cell [ME *garde* = protection + L *cella* = small room] — One of two kidney-shaped epidermal cells flanking a stoma; changes in turgor pressure (driven by K⁺ and water movement) open or close the stomatal pore to regulate gas exchange and water loss. → section 28

H (continued)

Haplodiploidy [Gk *haploos* = single + *diploos* = double] — Sex-determination system in which haploid males develop from unfertilised eggs and diploid females from fertilized eggs; important in many Hymenoptera but not sufficient by itself to explain eusociality. → section 21

Herd immunity [ME *herd* = flock + L *immunis* = exempt] — Indirect protection of susceptible individuals when a sufficiently large proportion of the population is immune (vaccinated or recovered), reducing pathogen transmission; threshold: p_c = 1 – 1/R₀. → section 24

Herbivory [L *herba* = grass + *vorare* = to devour] — Consumption of plant or algal tissue by an animal or other organism; herbivores occupy the second trophic level; plant defenses (thorns, secondary metabolites, trichomes) and herbivore counter-adaptations drive coevolution. → section 37

Hormone [Gk *hormaein* = to set in motion] — A chemical signal produced in one part of an organism that travels (via blood in animals, phloem in plants) to act on distant target cells bearing specific receptors; plant hormones (phytohormones) include auxin, gibberellin, cytokinin, abscisic acid, and ethylene. → sections 29, 34 and 35

I (continued)

Innate immunity [L *innatus* = inborn] — The non-specific, evolutionarily ancient first-line defense against pathogens; includes physical barriers (skin, mucous membranes), phagocytes (neutrophils, macrophages), complement, and pattern recognition receptors (TLRs detecting PAMPs). Acts within minutes to hours. → section 35

Inclusive fitness [L *includere* = to enclose + OE *fit* = suitable] — Total genetic contribution to future generations through both direct reproduction and indirect effects on relatives' reproduction, weighted by relatedness. → section 21

Intrinsic rate of increase (r) [L *intrinsecus* = inward] — The per-capita growth rate of a population under ideal (unlimited) conditions; r = ln(λ) where λ is the per-generation finite rate of increase; positive r = growing population; r = 0 at K. → section 36

Island biogeography [OE *ealand* = island + Gk *ge* = earth + *graphein* = to write] — The study of factors affecting species richness of islands (or habitat patches); key model: species richness at equilibrium = balance between immigration rate and extinction rate; species-area law $S = cA^z$ (MacArthur & Wilson, 1967). → section 40

K (continued)

K-strategist [see *carrying capacity* + Gk *strategia* = strategy] — An organism with a life history strategy maximizing competitive success near carrying capacity: slow growth, long lifespan, large body, few offspring with high parental investment. Contrast: r-strategist. → section 36

L (continued)

Life table [ME *lyf* + L *tabula* = flat board] — A tabular display of age-specific survival (*lx*) and fecundity (*mx*) values for a cohort; used to calculate net reproductive rate ($R_0 = \sum lx \cdot mx$) and intrinsic rate of increase (*r*). → section 36

Logistic growth [Gk *logistikos* = skilled in reckoning] — Population growth model $dN/dt = rN(1 - N/K)$, producing a sigmoidal S-shaped curve; growth decelerates as population approaches carrying capacity *K*; introduced by Verhulst (1838). → section 36

M (continued)

Minimum viable population (MVP) [L *minus* = smallest + *vita* = life] — The smallest population size with a specified probability (e.g., 99%) of persisting for a given period (e.g., 1,000 years); accounts for demographic stochasticity, environmental stochasticity, and genetic factors; used in conservation planning. → section 40

Molecular clock [Gk *molecula* + OE *clocke*] — The approximate constancy of the rate of neutral nucleotide substitution in lineages; enables dating of evolutionary divergence events: $t = d/(2\mu)$ where *d* = sequence divergence, μ = substitution rate per year. Calibrated using the fossil record. → section 22

Mutualism [L *mutuus* = mutual, reciprocal] — A symbiotic relationship benefiting both participating species (+/+); examples: mycorrhizal fungi increasing plant phosphorus uptake, nitrogen-fixing *Rhizobium* in legume root nodules, cleaner fish and reef fish. → section 37

Mycorrhiza [Gk *mykes* = fungus + *rhiza* = root] — A mutualistic association between soil fungi (Glomeromycota for arbuscular type; Basidiomycota/Ascomycota for ectomycorrhizal type) and plant roots; fungi receive photosynthate, plant receives water and phosphorus; present in about 80% of land plants. → section 28

Myrmecochory [Gk *myrmex* = ant + *choreia* = movement/dance] — Seed dispersal by ants, often mediated by lipid-rich elaiosomes that reward ants for carrying seeds to nests or nutrient-enriched refuse sites. → sections 29, 37 and 38

N (continued)

Neuron [Gk *neuron* = nerve, sinew] — The basic signaling unit of the nervous system; consists of a cell body (soma), dendrites (input), and an axon (output); classified by function (sensory, motor, interneuron) or morphology; communicates via electrical (action potentials) or chemical (synaptic) signals. → section 32

Neutral theory [L *neutralis* = neither + Gk *theoria* = view] — Kimura’s (1968) theory that the majority of molecular evolutionary change is selectively neutral (neither advantageous nor deleterious); neutral mutations drift to fixation at a rate equal to the mutation rate (*u*), independent of population size. → section 22

Nitrification [L *nitrum* = saltpetre + *facere* = to make] — The aerobic microbial oxidation of ammonium (NH₄⁺) to nitrite (NO₂⁻) by *Nitrosomonas*, then nitrite to nitrate (NO₃⁻) by *Nitrobacter*; a key step in the nitrogen cycle making nitrogen available to most plants. → section 39

Nitrogen fixation [L *nitrum* + *fixatio* = making firm] — The enzymatic reduction of atmospheric N₂ to NH₃ by nitrogenase; performed by free-living bacteria (*Azotobacter*, cyanobacteria) and symbionts (*Rhizobium*, *Frankia*); rate about 120 Tg N/yr globally. → section 24

O (continued)

Operon [L *opus* = work] — A prokaryotic gene cluster transcribed as a polycistronic mRNA from a single promoter; regulated by operator/repressor interactions; the *lac* operon (Jacob & Monod, 1961) was the first characterized gene regulatory system; Nobel Prize 1965. → section 13

P (continued)

Parasite [Gk *parasitos* = one who eats beside another] — An organism that benefits from living in or on a host organism at the host’s expense (+/-); parasites reduce host fitness without immediately killing the host (unlike predators); include worms (helminths), protozoa, and many bacteria and fungi. → section 24

Photoperiodism [Gk *photos* = light + L *periodus* = cycle] — The response of an organism to the relative duration of day and night (photoperiod); controls flowering (long-day vs. short-day vs. day-neutral plants) via phytochrome, a red/far-red reversible photoreceptor. → section 30

Phytochrome [Gk *phyton* = plant + *chroma* = color] — A plant photoreceptor protein interconvertible between a red-light-absorbing form (Pr, 660 nm) and a far-red-light-absorbing form (Pfr, 730 nm); Pfr is the biologically active form; governs seed germination, shade avoidance, and flowering. → section 30

Phytoplankton [Gk *phyton* = plant + *planktos* = wandering] — Microscopic photosynthetic organisms (cyanobacteria, diatoms, dinoflagellates) drifting in the photic zone of aquatic ecosystems; responsible for about 50% of Earth’s net primary productivity. → section 39

Population genetics [L *populus* = people + Gk *genos* = birth + *statistike* = statecraft] — The study of allele and genotype frequency distributions and their changes in populations; mathematical foundation provided by Hardy, Weinberg (1908), Fisher, Wright, and Haldane (1930s). → section 20

Primary succession [L *primus* = first + *successio* = following] — Ecological succession on a surface not previously colonised (e.g., bare rock after a lava flow or retreating glacier); begins with pioneer species (lichenised fungi, mosses) and proceeds through intermediate stages to a climax community. → section 37

Proton-motive force (Δp) [Gk *proton* = first + L *movere* = to move] — The electrochemical driving force for proton movement across a membrane, composed of a chemical gradient ($\Delta p H$) and an electrical gradient ($\Delta \Psi$); Δp (mV) = $\Delta \Psi - 59 \Delta p H$; drives ATP synthase rotation. → section 9

R (continued)

Reflex arc [L *reflectere* = to bend back] — The neural pathway of a reflex response: stimulus → sensory neuron → integration center (interneuron in spinal cord or brain) → motor neuron → effector; characterized by Sherrington (1906). → section 32

Reproductive isolation [L *reproducere* = to produce again + *isolatus* = set apart] — The existence of biological barriers (prezygotic or postzygotic) preventing interbreeding between populations; the operational criterion for separate species status in the Biological Species Concept (Mayr). → section 22

r-strategist [see *r*, rate of increase + Gk *strategia*] — An organism with a life history strategy maximizing reproductive rate (*r*): small body, rapid maturation, large clutch sizes, little parental investment; thrives in unstable, unpredictable environments. Contrast: K-strategist. → section 36

Resting potential [ME *resten* + L *potentialis*] — The stable membrane potential of a non-stimulated neuron (about −70 mV inside relative to outside); maintained by the sodium-potassium pump (3 Na⁺ out, 2 K⁺ in per ATP) and selective membrane permeability. → section 32

S (continued)

Saprophyte [Gk *sapros* = rotten + *phyton* = plant] — An organism that obtains nutrients by absorbing dissolved organic compounds from dead or decaying matter; now more precisely called saprotrophic or decomposer; includes most fungi and many bacteria. → section 39

Secondary succession [L *secundus* = following + *successio*] — Ecological succession in an area where a previous community has been disrupted (fire, flood, deforestation) but soil and seed bank remain; faster than primary succession; classic example: forest regeneration after clear-cutting. → section 37

Self-organization [OE *self* + Gk *organon* = tool/instrument] — The emergence of ordered pattern from local interactions without central control; examples include biofilms, morphogen gradients, flocking, and vegetation patching in drylands. → sections 2 and 36

Shannon diversity index (*H'*) [after Claude Shannon’s information entropy, 1948] — A measure of species diversity: $H' = -\sum p_i \ln p_i$ where p_i is the relative abundance of species *i*; higher *H'* = greater diversity; *H'* = 0 for a monoculture; simultaneously measures species richness and evenness. → section 38

Signal transduction [L *signum* = mark + *transducere* = to lead across] — The process by which a receptor converts an extracellular signal (ligand, light, mechanical force) into an intracellular biochemical response via cascades of protein-protein interactions and phosphorylation events. → section 8

SNP (single-nucleotide polymorphism) [genetics abbreviation] — A common single-base genomic variant, usually defined by minor allele frequency of at least 1% in a population; used as a marker in GWAS, ancestry inference, and risk prediction. → sections 14, 17 and 18

Stigmergy [Gk *stigma* = mark + *ergon* = work] — Coordination by environmental traces, such as pheromone trails or construction cues, through which individual actions modify the environment and guide later actions by others. → section 0.2

Stomata (sing. stoma) [Gk *stoma* = mouth] — Microscopic pores in the leaf epidermis flanked by guard cells; regulate CO₂ entry for photosynthesis and water vapor exit (transpiration); respond to light, CO₂ concentration, and ABA. → section 28

Succession [L *successio* = a following] — The directional, predictable change in species composition of a community over time from initial colonization to a relatively stable climax community; driven by facilitation, inhibition, or tolerance mechanisms. → section 37

Superorganism [L *super* = above + Gk *organon* = instrument] — A colony-level analogy for tightly integrated societies, especially social insects, in which individuals function like differentiated parts of a larger reproductive and regulatory unit. → sections 0.2 and 21

Survivorship curve [L *super* = beyond + *vivere* = to live] — A graph of the proportion of a cohort surviving to each age; Type I (most survive to old age; humans, large mammals); Type II (constant mortality rate; many birds); Type III (high early mortality; marine invertebrates, most plants). → section 36

Sympatric speciation [Gk *sym* = together + L *patria* = homeland] — Speciation occurring within a single geographic area without physical barriers; common in plants via allopolyploidy; also documented in cichlids and apple maggot flies. → section 22

T (continued)

T helper cell (Th) [L *thymus* + ME *helpen*] — A CD4+ T lymphocyte that coordinates adaptive immunity; Th1 cells activate cytotoxic T cells and macrophages (intracellular pathogens); Th2 cells activate B cells (antibody production, extracellular pathogens); regulatory T cells (Treg) suppress autoimmunity. → section 35

Telomere [Gk *telos* = end + *meros* = part] — Repetitive non-coding DNA sequences (TTAGGG)_n capping eukaryotic chromosome ends; protect against exonuclease degradation, end-to-end chromosome fusions, and loss of information-carrying DNA; shortened with each S phase (end-replication problem) unless telomerase is expressed. Nobel Prize 2009 (Blackburn, Greider, Szostak). → section 12

Thermoregulation [Gk *therme* = heat + L *regulare* = to rule] — Maintenance of body temperature within a physiological range; endotherms (birds, mammals) generate heat metabolically; ectotherms (reptiles, fish) rely on behavioral and environmental sources; homeostatic mechanism with hypothalamic ‘thermostat’. → section 32

Toll-like receptor (TLR) [*Toll* = German interjection of amazement; Toll pathway discovered in *Drosophila* by Christiane Nüsslein-Volhard] — A family of pattern-recognition receptors (TLR1–10 in humans, with additional functional TLRs in other mammals) expressed on innate immune cells; recognize conserved PAMPs and signal via MyD88 and TRIF adaptors to activate NF-κB and IRF3. Dysregulation linked to sepsis and autoimmune disease. Nobel Prize 2011 (Hoffmann, Beutler). → section 35

Totipotency [L *totus* = whole + *potens* = powerful] — The ability of a single cell to develop into a complete organism; characterizes fertilized eggs and early-cleavage blastomeres; plant cells frequently retain totipotency (basis of tissue culture propagation). → section 28

Transpiration stream [L *trans* + *spirare* = breathe] — The continuous movement of water from soil through roots, stem, and leaves to the atmosphere; driven by evaporation from mesophyll cell walls; responsible for transport of dissolved minerals throughout the plant. → section 28

Trophic cascade [Gk *trophe* = nourishment + L *cascata* = waterfall] — Indirect predator effects on non-prey species, transmitted down the food chain; top-down cascade: predator suppresses herbivore → vegetation recovers; bottom-up cascade: primary productivity determines higher trophic levels. Documented in Yellowstone (wolves → elk → willows → beaver → hydrology). → section 37

Turgor pressure [L *turgere* = to swell] — The pressure exerted by the contents of a plant cell against its cell wall when the vacuole is filled with water; drives cell expansion during growth and maintains tissue rigidity (wilting = loss of turgor). → section 28

V (continued)

Vaccine [L *vacca* = cow; from Jenner’s cowpox inoculation against smallpox, 1796] — A biological preparation conferring immunity against a specific pathogen; types include live-attenuated (MMR), inactivated (IPV), subunit (HepB), mRNA (SARS-CoV-2 mRNA-1273, BNT162b2), and viral vector vaccines. → section 24

Viviparity [L *vivus* = alive + *parere* = to beget] — Giving birth to live young rather than laying eggs; characteristic of most mammals and some fish, reptiles, and invertebrates; requires placentation (in eutherian mammals) for gas and nutrient exchange. → section 32

W (continued)

Watershed [OE *wæter* + OE *scēad* = divide] — The land area draining into a common body of water (stream, lake, or estuary); the ecological unit for studying nutrient export, hydrology, and land-use impacts on aquatic ecosystems; Hubbard Brook watershed experiments (Bormann & Likens, 1967) pioneered biogeochemical cycle measurement at watershed scale. → section 39

Expanded glossary now covers about 200 terms across all 10 units. Etymologies sourced from Oxford Latin Dictionary, Liddell-Scott-Jones Greek-English Lexicon, and Online Etymology Dictionary (etymonline.com).

Appendix G — Index of Key Terms

Appendix G · Level 1/3 · Use as reference

An index of the 225 glossary terms, each with the chapter(s) where the term is introduced, bolded, or discussed at length. Terms marked in bold appear as section headings somewhere in the textbook; the glossary entry carries the full definition.

Each entry follows the pattern:

Term (`#gl:slug`) with semantic chapter links

The `#gl:slug` anchor is the canonical location defined in the master glossary (`manuscript/glossary.md`). Full-text search for the slug string finds every cross-reference.

Note on maintenance. This index is maintained by `scripts/link_glossary.py` from the glossary file and canonical ToC labels. To verify after editing `glossary.md`, run `uv run python scripts/link_glossary.py --check`.

5-Methylcytosine (5mC) (`#gl:5-methylcytosine`) → section 15

A

Abiotic (`#gl:abiotic`) → section 40 Actin (`#gl:actin`) → section 6 Action potential (`#gl:action-potential`) → section 32 Adaptive immunity (`#gl:adaptive-immunity`) → section 35 Adenosine triphosphate(ATP) (`#gl:adenosine-triphosphate`) → section 9 Aerobic (`#gl:aerobic`) → section 9 Allele (`#gl:allele`) → section 17 Allostasis (`#gl:allostasis`) → section 0.3 Allosteric (`#gl:allosteric`) → section 4 Anaerobic (`#gl:anaerobic`) → section 9 Anaphase (`#gl:anaphase`) → section 12 Angiosperm (`#gl:angiosperm`) → section 28 Anticodon (`#gl:anticodon`) → section 13 Apoptosis (`#gl:apoptosis`) → section 8 Archaea (`#gl:archaea`) → sections 5 and 23 ATP synthase (`#gl:atp-synthase`) → section 9 Autonomic nervous system (ANS) (`#gl:autonomic-nervous-system`) → section 32 Autotroph (`#gl:autotroph`) → sections 5, 37 and 38 Axon hillock (`#gl:axon-hillock`) → section 32

B

Base pair (bp) (`#gl:base-pair`) → section 12 Biofilm (`#gl:biofilm`) → section 24 Biome (`#gl:biome`) → section 40 Buffer (`#gl:buffer`) → section 1

C

Calvin cycle (`#gl:calvin-cycle`) → section 10 CaMKII (Calcium/calmodulin-dependent kinase II) (`#gl:camkii`) → section 33 Cardiac output (CO) (`#gl:cardiac-output`) → section 31 Carrying capacity (K) (`#gl:carrying-capacity`) → section 36 Caspase (`#gl:caspase`) → section 8 cDNA (`#gl:cdna`) → section 13 Cell cycle (`#gl:cell-cycle`) → section 12 Centromere (`#gl:centromere`) → section 12 Chemiosmosis (`#gl:chemiosmosis`) → section 9 Chirality (`#gl:chirality`) → section 1 Chlorophyll (`#gl:chlorophyll`) → section 10 Chloroplast (`#gl:chloroplast`) → section 10 Chromatin (`#gl:chromatin`) → section 15 Chromosome (`#gl:chromosome`) → section 12 Codon (`#gl:codon`) → section 13 Coevolution (`#gl:coevolution`) → section 37 Cohesion-tension theory (`#gl:cohesion-tension-theory`) → section 28 Competitive exclusion (`#gl:competitive-exclusion`) → section 37 Competitive inhibition (`#gl:competitive-inhibition`) → section 4 Copepod (`#gl:copepod`) → section 39 Cortisol (`#gl:cortisol`) → section 35 CpG island (`#gl:cpg-island`) → section 15 CRISPR-Cas (`#gl:crispr-cas`) → section 14 Cytoplasm (`#gl:cytoplasm`) → section 6 Cytoskeleton (`#gl:cytoskeleton`) → section 6

D

Decomposer (`#gl:decomposer`) → section 39 Density-dependent regulation (`#gl:density-dependent-regulation`) → section 36 Depolarization (`#gl:depolarization`) → section 32 Diploid (2n) (`#gl:diploid`) → section 19 DNA helicase (`#gl:dna-helicase`) → section 12 DNA ligase (`#gl:dna-ligase`) → section 12 Dominant (`#gl:dominant`) → section 17 Doubling time (`td`) (`#gl:doubling-time`) → section 24

E

Effective population size (N_e) (`#gl:effective-population-size`) → section 22 Electronegativity (`#gl:electronegativity`) → section 1 Endocytosis (`#gl:endocytosis`) → section 7 Endosymbiosis (`#gl:endosymbiosis`) → section 5 Entropy (S) (`#gl:entropy`) → section 9 Enzyme (`#gl:enzyme`) → section 4 Epigenetics (`#gl:epigenetics`) → section 15 Epigenome (`#gl:epigenome`) → section 14 Epiphyte (`#gl:epiphyte`) → section 40 Euchromatin (`#gl:euchromatin`) → section 15 Eukaryote (`#gl:eukaryote`) → section 5 Eusociality (`#gl:eusociality`) → sections 21 and 23 Eutrophication (`#gl:eutrophication`) → section 39 Excitotoxicity (`#gl:excitotoxicity`) → section 33 Exon (`#gl:exon`) → section 13

F

Facilitated diffusion (#gl:facilitated-diffusion) → section 7 Fatty acid (#gl:fatty-acid) → section 3 Fermentation (#gl:fermentation) → section 9 FEV₁/FVC (#gl:fev-fvc) → section 31 Fisheries (#gl:fisheries) → sections 36 and 40 Fitness (w) (#gl:fitness) → section 20 Founder effect (#gl:founder-effect) → section 22 Frank-Starling law (#gl:frank-starling-law) → section 31 Free energy (ΔG) (#gl:free-energy) → section 9 Frond (#gl:frond) → section 28

G

Gamete (#gl:gamete) → section 19 Gene (#gl:gene) → section 15 Genetic code (#gl:genetic-code) → section 13 Genetic drift (#gl:genetic-drift) → section 22 Genome (#gl:genome) → section 14 Genome-wide association study (GWAS) (#gl:genome-wide-association-study) → section 14 GLP-1 (glucagon-like peptide-1) (#gl:glp-1) → section 35 GLUT4 (#gl:glut4) → section 35 Glycolysis (#gl:glycolysis) → section 9 GPP (gross primary productivity) (#gl:gpp) → section 39 Gram stain (#gl:gram-stain) → section 5 Guard cell (#gl:guard-cell) → section 28

H

Haplodiploidy (#gl:haplodiploidy) → section 21 Haploidy (n) (#gl:haploidy) → section 19 Hardy-Weinberg equilibrium (#gl:hardy-weinberg-equilibrium) → section 20 Herbivory (#gl:herbivory) → section 37 Herd immunity (#gl:herd-immunity) → section 24 Heterochromatin (#gl:heterochromatin) → section 15 Heterozygous (#gl:heterozygous) → section 17 Hill coefficient (n) (#gl:hill-coefficient) → section 4 Histone (#gl:histone) → section 15 Histone code (#gl:histone-code) → section 15 Holobiont (#gl:holobiont) → sections 24 and 25 Homeostasis (#gl:homeostasis) → section 32 Hormone (#gl:hormone) → sections 29, 34 and 35 HPA axis (hypothalamic-pituitary-adrenal axis) (#gl:hpa-axis) → section 35 HPG axis (hypothalamic-pituitary-gonadal axis) (#gl:hpg-axis) → section 35 HPT axis (hypothalamic-pituitary-thyroid axis) (#gl:hpt-axis) → section 35 Hydrogen bond (#gl:hydrogen-bond) → section 1 Hydrolysis (#gl:hydrolysis) → sections 3 and 4 Hydrophobic effect (#gl:hydrophobic-effect) → sections 2 and 3

I

Inclusive fitness (#gl:inclusive-fitness) → section 21 Independent assortment (#gl:independent-assortment) → section 17 Innate immunity (#gl:innate-immunity) → section 35 Insulin receptor (#gl:insulin-receptor) → section 35 Intrinsic rate of increase (r) (#gl:intrinsic-rate-of-increase) → section 36 Intron (#gl:intron) → section 13 Island biogeography (#gl:island-biogeography) → section 40

K

K-strategist (#gl:k-strategist) → section 36 Keystone species (#gl:keystone-species) → section 37 Km (Michaelis constant) (#gl:km) → section 4

L

Life table (#gl:life-table) → section 36 Linkage (#gl:linkage) → section 19 Locus (plural: loci) (#gl:locus) → section 19 Logistic growth (#gl:logistic-growth) → section 36 Lotka-Volterra equations (#gl:lotka-volterra-equations) → section 37 LTD (long-term depression) (#gl:ltd) → section 33 LTP (long-term potentiation) (#gl:ltп) → section 33

M

Meiosis (#gl:meiosis) → section 19 Membrane potential (Vm) (#gl:membrane-potential) → section 31 Michaelis-Menten kinetics (#gl:michaelis-menten-kinetics) → section 4 Microbiome (#gl:microbiome) → section 24 Microbiota (#gl:microbiota) → section 24 MicroRNA (miRNA) (#gl:microrna) → section 15 Minimum viable population (MVP) (#gl:minimum-viable-population) → section 40 Mitosis (#gl:mitosis) → section 12 Molecular clock (#gl:molecular-clock) → section 22 mRNA (messenger RNA) (#gl:mrna) → section 13 Mutation (#gl:mutation) → section 14 Mutualism (#gl:mutualism) → section 37 Mycorrhiza (#gl:mycorrhiza) → section 28 Myrmecochory (#gl:myrmecochory) → sections 29, 37 and 38

N

Natural selection (#gl:natural-selection) → section 20 Neuron (#gl:neuron) → section 32 Neutral theory (#gl:neutral-theory) → section 22 Niche (#gl:niche) → section 37 Nitrification (#gl:nitrification) → section 39 Nitrogen fixation (#gl:nitrogen-fixation) → section 24 Nucleosome (#gl:nucleosome) → section 15 Nucleotide (#gl:nucleotide) → section 12

O

Operon (#gl:operon) → section 13 Organelle (#gl:organelle) → section 6 Osmosis (#gl:osmosis) → section 7 Oxidative phosphorylation (#gl:oxidative-phosphorylation) → section 9

P

Pan-genome (#gl:pan-genome) → section 14 Parasite (#gl:parasite) → section 24 Peptide bond (#gl:peptide-bond) → section 3 pH (#gl:ph) → section 1 Phenotype (#gl:phenotype) → section 17 Phospholipid bilayer (#gl:phospholipid-bilayer) → section 7 Photoperiodism (#gl:photoperiodism) → section 30 Photosynthesis (#gl:photosynthesis) → section 10 Phytochrome (#gl:phytochrome) → section 30 Phytoplankton (#gl:phytoplankton) → section 39 Plasmid

(#gl:plasmid) → section 5 Poiseuille’s law (#gl:poiseuille-s-law) → section 31 Polymerase chain reaction (PCR) (#gl:polymerase-chain-reaction) → section 14 Population genetics (#gl:population-genetics) → section 20 Primary succession (#gl:primary-succession) → section 37 Promoter (#gl:promoter) → section 13 Protein (#gl:protein) → section 3 Proton-motive force (Δp) (#gl:proton-motive-force) → section 9 P_{50} (#gl:p) → section 31

R

r-strategist (#gl:r-strategist) → section 36 RAAS (renin-angiotensin-aldosterone system) (#gl:raas) → section 31 Recombination (#gl:recombination) → section 19 Reduction potential (E°) (#gl:reduction-potential) → section 1 Reflex arc (#gl:reflex-arc) → section 32 Reproductive isolation (#gl:reproductive-isolation) → section 22 Resting potential (#gl:resting-potential) → section 32 Ribonucleic acid (RNA) (#gl:ribonucleic-acid) → section 13 Ribosome (#gl:ribosome) → section 13

S

Saltatory conduction (#gl:saltatory-conduction) → section 33 Saprophyte (#gl:saprophyte) → section 39 Secondary succession (#gl:secondary-succession) → section 37 Selection coefficient (s) (#gl:selection-coefficient) → section 20 Self-organization (#gl:self-organization) → sections 2 and 36 Shannon diversity index (H') (#gl:shannon-diversity-index) → section 38 Signal transduction (#gl:signal-transduction) → section 8 SNARE complex (#gl:snare-complex) → section 33 SNP (single-nucleotide polymorphism) (#gl:snp) → sections 14, 17 and 18 Speciation (#gl:speciation) → section 22 Species-area relationship (#gl:species-area-relationship) → section 40 Stigmergy (#gl:stigmergy) → section 0.2 Stomata (#gl:stomata) → section 28 Succession (#gl:succession) → section 37 Superorganism (#gl:superorganism) → sections 0.2 and 21 Surface-area-to-volume ratio (A/V) (#gl:surface-area-to-volume-ratio) → section 5 Surfactant (#gl:surfactant) → section 31 Survivorship curve (#gl:survivorship-curve) → section 36 Sympatric speciation (#gl:sympatric-speciation) → section 22 Synaptotagmin (#gl:synaptotagmin) → section 33

T

T helper cell (Th) (#gl:t-helper-cell) → section 35 Telomere (#gl:telomere) → section 12 Thermodynamics (#gl:thermodynamics) → section 9 Thermoregulation (#gl:thermoregulation) → section 32 Toll-like receptor (TLR) (#gl:toll-like-receptor) → section 35 Totipotency (#gl:totipotency) → section 28 Transcription (#gl:transcription) → section 13 Translation (#gl:translation) → section 13 Transpiration (#gl:transpiration) → section 28 Transpiration stream (#gl:transpiration-stream) → section 28 Trophic cascade (#gl:trophic-cascade) → section 37 Trophic level (#gl:trophic-level) → section 39 Turgor pressure (#gl:turgor-pressure) → section 28

V

Vaccine (#gl:vaccine) → section 24 Van der Waals forces (#gl:van-der-waals-forces) → section 1 Virulence (#gl:virulence) → section 24 Viviparity (#gl:viviparity) → section 32

W

Water potential (Ψ) (#gl:water-potential) → section 28 Watershed (#gl:watershed) → section 39

X

Xylem (#gl:xylem) → section 28

Z

Zygote (#gl:zygote) → section 17

Using the index. When a term appears as a bolded, #gl:-linked first use in a chapter (see **Unit I — Chemistry of Life: Introduction** onward), clicking the term jumps to the canonical entry in the master glossary. This appendix provides an author- and instructor-facing overview of which chapter establishes each concept first, useful for lecture planning and term-by-term syllabus design.

Module: reference only (no code)

References

Vision and change in undergraduate biology education: A call to action, 2011. URL <https://www.visionandchange.org/>.

Victoria E. Abraira and David D. Ginty. The sensory neurons of touch. *Neuron*, 79(4):618–639, 2013. doi: 10.1016/j.neuron.2013.07.051.

Josh Abramson et al. Accurate structure prediction of biomolecular interactions with alphafold 3. *Nature*, 630:493–500, 2024. doi: 10.1038/s41586-024-07487-w.

Malika Aid, Valentin Boero-Teyssier, Katherine McMahan, Rammy Dang, Michael Doyle, Nazim Belabbaci, Erica Borducchi, Ai-ris Y. Collier, Janet Mullington, and Dan H. Barouch. Long covid involves activation of proinflammatory and immune exhaustion pathways. *Nature Immunology*, 27:61–71, 2026. doi: 10.1038/s41590-025-02353-x.

W. C. Allee. *Animal Aggregations: A Study in General Sociology*. University of Chicago Press, Chicago, 1931.

Uri Alon. *An Introduction to Systems Biology: Design Principles of Biological Circuits*. Chapman and Hall/CRC, 2nd edition, 2019. ISBN 9781498747254.

Joanna S. Amberger, Carol A. Bocchini, François Schiettecatte, Alan F. Scott, and Ada Hamosh. OMIM.org: leveraging knowledge across phenotype-gene relationships. *Nucleic Acids Research*, 47(D1):D1038–D1043, 2019. doi: 10.1093/nar/gky1151.

Aristotle. *Parts of Animals*. Clarendon Press, 350 BCE. Classical work; commonly cited in modern translation.

David E. Atkinson. The regulation of enzyme activity in metabolism. *Biochemical Journal*, 108(1):15–24, 1968.

Oswald T. Avery, Colin M. MacLeod, and Maclyn McCarty. Studies on the chemical nature of the substance inducing transformation of pneumococcal types. *Journal of Experimental Medicine*, 79:137–158, 1944. doi: 10.1084/jem.79.2.137.

Per Bak, Chao Tang, and Kurt Wiesenfeld. Self-organized criticality: An explanation of the $1/f$ noise. *Physical Review Letters*, 59(4):381–384, 1987. doi: 10.1103/PhysRevLett.59.381.

Philip Ball. Water as an active constituent in cell biology. *Chemical Reviews*, 108(1):74–108, 2008. doi: 10.1021/cr068037a.

Albert-László Barabási and Réka Albert. Emergence of scaling in random networks. *Science*, 286(5439):509–512, 1999. doi: 10.1126/science.286.5439.509.

Albert-László Barabási and Zoltán N. Oltvai. Network biology: Understanding the cell’s functional organization. *Nature Reviews Genetics*, 5:101–113, 2004. doi: 10.1038/nrg1272.

Jose Domingo Barrera-Paez, Carlos T. Moraes, et al. Mitochondrial gene editing. *Nature Reviews Methods Primers*, 3:18, 2023. doi: 10.1038/s43586-023-00200-7.

Patrick Bateson and Kevin N. Laland. Tinbergen’s four questions: An appreciation and an update. *Trends in Ecology & Evolution*, 28:712–718, 2013. doi: 10.1016/j.tree.2013.09.013.

Tom L. Beauchamp and James F. Childress. *Principles of Biomedical Ethics*. Oxford University Press, New York, 1979.

William Bechtel and Adele Abrahamsen. Explanation: A mechanist alternative. *Studies in History and Philosophy of Biological and Biomedical Sciences*, 36(2): 421–441, 2005. doi: 10.1016/j.shpsc.2005.03.010.

William Bechtel and Leonardo Bich. Situating homeostasis in organisms: Maintaining organization through time. *The Journal of Physiology*, 602(22):6003–6020, 2024. doi: 10.1113/JP286883.

John M. Beggs and Dietmar Plenz. Neuronal avalanches in neocortical circuits. *Journal of Neuroscience*, 23(35):11167–11177, 2003. doi: 10.1523/JNEUROSCI.23-35-11167.2003.

Stephen P. Bell and Anindya Dutta. DNA replication in eukaryotic cells. *Annual Review of Biochemistry*, 71:333–374, 2002. doi: 10.1146/annurev.biochem.71.110601.135425.

Howard C. Berg and Douglas A. Brown. Chemotaxis in Escherichia coli analysed by three-dimensional tracking. *Nature*, 239(5374):500–504, 1972. doi: 10.1038/239500a0.

Claude Bernard. *An Introduction to the Study of Experimental Medicine*. J. B. Bailliere, Paris, 1865.

Damian Bertoni, Maxim Tsenkov, Paulyna Magana, Sreenath Nair, Ivanna Pidruchna, Marcelo Querino Lima Afonso, Adam Midlik, Urmila Paramval, et al. AlphaFold protein structure database 2025: a redesigned interface and updated structural coverage. *Nucleic Acids Research*, 54(D1):D358–D362, 2026. doi: 10.1093/nar/gkaf1226.

Günter Blobel and Bernhard Dobberstein. Transfer of proteins across membranes. I. presence of proteolytically processed and unprocessed nascent immunoglobulin light chains on membrane-bound ribosomes of murine myeloma. *Journal of Cell Biology*, 67(3):835–851, 1975. doi: 10.1083/jcb.67.3.835.

F. Herbert Bormann and Gene E. Likens. Nutrient cycling. *Science*, 155(3761):424–429, 1967.

Andrew F. G. Bourke. *Principles of Social Evolution*. Oxford University Press, Oxford, 2011. doi: 10.1093/acprof:oso/9780199231157.001.0001.

Paul D. Boyer. The ATP synthase — a splendid molecular machine. *Annual Review of Biochemistry*, 66:717–749, 1997. doi: 10.1146/annurev.biochem.66.1.717.

Edmund D. Brodie, III and Edmund D. Brodie, Jr. Predator–prey arms races: Asymmetric tracking and escalation. *Quarterly Review of Biology*, 74(3):249–271, 1999. doi: 10.1086/393065.

Anna D. Broido and Aaron Clauset. Scale-free networks are rare. *Nature Communications*, 10:1017, 2019. doi: 10.1038/s41467-019-08746-5.

Jelle Bruineberg, Krzysztof Dołęga, Joe Dewhurst, and Manuel Baltieri. The emperor’s new markov blankets. *Behavioral and Brain Sciences*, 45:e183, 2022. doi: 10.1017/S0140525X21002351.

Andreas Brune. Symbiotic digestion of lignocellulose in termite guts. *Nature Reviews Microbiology*, 12:168–180, 2014. doi: 10.1038/nrmicro3182.

Melvin Calvin. The path of carbon in photosynthesis. *Science*, 135:879–889, 1962. doi: 10.1126/science.135.3507.879.

Walter B. Cannon. *The Wisdom of the Body*. W. W. Norton, New York, 1932. ISBN 9780393002052.

Centers for Disease Control and Prevention. Clinical treatment of candida auris infections. <https://www.cdc.gov/candida-auris/hcp/clinical-care/index.html>, 2024a. Updated 24 April 2024; accessed 2026-05-16.

Centers for Disease Control and Prevention. Infertility faqs. <https://www.cdc.gov/reproductive-health/infertility-faq/index.html>, 2024b. Accessed 2026-05-20.

Centers for Disease Control and Prevention. Antibiotic use and stewardship in the united states, 2025 update: Progress and opportunities. <https://www.cdc.gov/antibiotic-use/hcp/data-research/stewardship-report.html>, 2025a. Accessed 2026-05-15.

Centers for Disease Control and Prevention. Clinical recommendation for the use of injectable lenacapavir as hiv preexposure prophylaxis – united states, 2025. *Morbidity and Mortality Weekly Report*, 74(35), 2025b. URL <https://www.cdc.gov/mmwr/volumes/74/wr/mm7435a1.htm>.

Centers for Disease Control and Prevention. Clinical overview of candida auris. <https://www.cdc.gov/candida-auris/hcp/clinical-overview/index.html>, 2026a. Updated 26 February 2026; accessed 2026-05-16.

Centers for Disease Control and Prevention. Long covid basics. <https://www.cdc.gov/long-covid/about/index.html>, 2026b. Accessed 2026-05-16.

Mikhail Kh Chailakhyan. New facts in support of the hormonal theory of plant development. *Comptes Rendus de l’Académie des Sciences de l’URSS*, 13:79–83, 1936.

Anne Chalumeau, Maria Bou Dames, Letizia Fontana, Simone Amistadi, Panagiotis Antoniou, Priyanka Loganathan, Margaux Mombled, Guillaume Corre, Martin Peterka, Mario Amendola, Carine Giovannangeli, Marcello Maresca, Annarita Miccio, and Mégane Brusson. A prime editing strategy to rewrite the gamma-globin promoters and reactivate fetal hemoglobin for sickle cell disease. *Blood*, 146(22):2641–2655, 2025. doi: 10.1182/blood.2024028166.

David D. Chaplin. Overview of the immune response. *Journal of Allergy and Clinical Immunology*, 125(2 Suppl 2):S3–S23, 2010. doi: 10.1016/j.jaci.2009.12.980.

Janice S. Chen, Enbo Ma, Lucas B. Harrington, Michael Da Costa, Xinran Tian, Joel M. Palefsky, and Jennifer A. Doudna. Crispr-cas12a target binding unleashes indiscriminate single-stranded dnase activity. *Science*, 360(6387):436–439, 2018. doi: 10.1126/science.aar6245.

Peter Chesson. Mechanisms of maintenance of species diversity. *Annual Review of Ecology and Systematics*, 31:343–366, 2000. doi: 10.1146/annurev.ecolsys.31.1.343.

Brendan Choat, Steven Jansen, Timothy J. Brodribb, Hervé Cochard, Sylvain Delzon, Radika Bhaskar, Sandra J. Bucci, Taylor S. Feild, Sean M. Gleason, Uwe G. Hacke, Anna L. Jacobsen, Frederic Lens, Hafiz Maherali, Jordi Martínez-Vilalta, Stefan Mayr, Maurizio Mencuccini, Patrick J. Mitchell, Andrea Nardini, Jarmila Pittermann, R. Brandon Pratt, John S. Sperry, Mark Westoby, Ian J. Wright, and Amy E. Zanne. Global convergence in the vulnerability of forests to drought. *Nature*, 491:752–755, 2012. doi: 10.1038/nature11688.

Maria Chuvochina, Jan Gerken, Martinique Frentrup, Yeliz Sandikci, Robin Goldmann, Heike M. Freese, Markus Göker, Johannes Sikorski, Pablo Yarza, Christian Quast, Jörg Peplies, Frank Oliver Glöckner, and Lorenz Christian Reimer. SILVA in 2026: a global core biodata resource for rRNA within the DSMZ digital diversity. *Nucleic Acids Research*, 2025. doi: 10.1093/nar/gkaf1247.

Ellen Clarke. The multiple realizability of biological individuals. *The Journal of Philosophy*, 110(8):413–435, 2013. doi: 10.5840/jphil2013110817.

Carol E. Cleland. Methodological and epistemic differences between historical science and experimental science. *Philosophy of Science*, 69(3):447–451, 2002. doi: 10.1086/342456.

Frederic E. Clements. *Plant Succession: An Analysis of the Development of Vegetation*. Carnegie Institution of Washington, Washington, DC, 1916.

Enrico S. Coen and Elliot M. Meyerowitz. The war of the whorls: Genetic interactions controlling flower development. *Nature*, 353(6339):31–37, 1991. doi: 10.1038/353031a0.

Matteo Colombo and Cory Wright. Explanatory pluralism: An unrewarding prediction error for free energy theorists. *Brain and Cognition*, 112:3–12, 2017. doi: 10.1016/j.bandc.2016.02.003.

Nicholas B. Colvard, Charles E. Watson, and Hyojin Park. The impact of open educational resources on various student success metrics. *International Journal of Teaching and Learning in Higher Education*, 30(2):262–276, 2018. URL <https://files.eric.ed.gov/fulltext/EJ1184998.pdf>.

Joseph H. Connell. Diversity in tropical rain forests and coral reefs. *Science*, 199(4335):1302–1310, 1978. doi: 10.1126/science.199.4335.1302.

Joseph H. Connell and R. O. Slatyer. Mechanisms of succession in natural communities and their role in community stability and organization. *The American Naturalist*, 111(982):1119–1144, 1977.

International Human Genome Sequencing Consortium. Initial sequencing and analysis of the human genome. *Nature*, 409:860–921, 2001. doi: 10.1038/35057062.

Convention on Biological Diversity. Kunming-montreal global biodiversity framework. <https://www.cbd.int/gbf>, 2022. Accessed 2026-05-20.

Convention on International Trade in Endangered Species of Wild Fauna and Flora. The cites appendices. <https://cites.org/eng/app/index.php>, 2026. Accessed 2026-05-20.

Bernard J. Crespi and Douglas Yanega. The definition of eusociality. *Behavioral Ecology*, 6(1):109–115, 1995. doi: 10.1093/beheco/6.1.109.

Francis H. C. Crick. On protein synthesis. *Symposia of the Society for Experimental Biology*, 12:138–163, 1958.

Francis H. C. Crick. The genetic code — yesterday, today and tomorrow. *Cold Spring Harbor Symposia on Quantitative Biology*, 31:3–9, 1966.

Charles Darwin. *On the Origin of Species by Means of Natural Selection*. John Murray, London, 1859.

Charles Darwin and Alfred Russel Wallace. On the tendency of species to form varieties. *Journal of the Proceedings of the Linnean Society: Zoology*, 3(9):45–62, 1858. doi: 10.1111/j.1096-3642.1858.tb02500.x.

Kevin de Queiroz. Species concepts and species delimitation. *Systematic Biology*, 56(6):879–886, 2007. doi: 10.1080/10635150701701083.

Jose del Castillo and Bernard Katz. Quantal components of the end-plate potential. *Journal of Physiology*, 124(3):560–573, 1954. doi: 10.1113/jphysiol.1954.sp005129.

Ken A. Dill. Dominant forces in protein folding. *Biochemistry*, 29(31):7133–7155, 1990. doi: 10.1021/bi00483a001.

Henry H. Dixon and John Joly. On the ascent of sap. *Philosophical Transactions of the Royal Society of London. Series B*, 186:563–576, 1894. doi: 10.1098/rstb.1895.0015.

Theodosius Dobzhansky. *Genetics and the Origin of Species*. Columbia University Press, New York, 1937.

Theodosius Dobzhansky. Nothing in biology makes sense except in the light of evolution. *The American Biology Teacher*, 35(3):125–129, 1973.

Marco Dorigo and Thomas Stützle. *Ant Colony Optimization*. MIT Press, Cambridge, MA, 2004. ISBN 9780262042192.

Jonathan B. Doub et al. Personalized bacteriophage therapy to treat pandrug-resistant spinal pseudomonas aeruginosa infection. *Nature Communications*, 13: 4239, 2022. doi: 10.1038/s41467-022-31837-9.

Jennifer A. Doudna and Emmanuelle Charpentier. The new frontier of genome engineering with CRISPR-Cas9. *Science*, 346(6213):1258096, 2014. doi: 10.1126/science.1258096.

Heather E. Douglas. *Science, Policy, and the Value-Free Ideal*. University of Pittsburgh Press, Pittsburgh, 2009.

Paul R. Ehrlich and Peter H. Raven. Butterflies and plants: A study in coevolution. *Evolution*, 18(4):586–608, 1964. doi: 10.2307/2406214.

Electron Microscopy Data Bank. Electron microscopy data bank. <https://www.ebi.ac.uk/emdb/>, 2026. Accessed 2026-05-24.

EMBL’s European Bioinformatics Institute. Millions of protein complexes added to alphafold database shed light on how proteins interact. <https://www.ebi.ac.uk/about/news/technology-and-innovation/first-complexes-alphafold-database/>, 2026. Technology and innovation article, 16 March 2026; accessed 2026-05-23.

James A. Estes and John F. Palmisano. Sea otters: Their role in structuring nearshore communities. *Science*, 185(4156):1058–1060, 1974. doi: 10.1126/science.185.4156.1058.

Theodore A. Evans, Tracy Z. Dawes, Philip R. Ward, and Nathan Lo. Ants and termites increase crop yield in a dry climate. *Nature Communications*, 2:262, 2011. doi: 10.1038/ncomms1257.

Anne Fausto-Sterling. The five sexes: Why male and female are not enough. *The Sciences*, 33(2):20–24, 1993. doi: 10.1002/j.2326-1951.1993.tb03081.x.

Andrew P. Feinberg, Michael A. Koldobskiy, and Anita Gondor. Epigenetic modulators, modifiers and mediators in cancer aetiology and progression. *Nature Reviews Genetics*, 17:284–299, 2016. doi: 10.1038/nrg.2016.13.

A. F. Feldman, Alexandra G. Konings, Pierre Gentine, et al. Large global-scale vegetation sensitivity to daily rainfall variability. *Nature*, 636:380–384, 2024. doi: 10.1038/s41586-024-08232-z.

Joseph Felsenstein. Confidence limits on phylogenies: An approach using the bootstrap. *Evolution*, 39(4):783–791, 1985. doi: 10.1111/j.1558-5646.1985.tb00420.x.

Andrew Fire, SiQun Xu, Mary K. Montgomery, Steven A. Kostas, Samuel E. Driver, and Craig C. Mello. Potent and specific genetic interference by double-stranded RNA in *Caenorhabditis elegans*. *Nature*, 391(6669):806–811, 1998. doi: 10.1038/35888.

David S. Fischer, Martin A. Villanueva, Peter S. Winter, and Alex K. Shalek. Adapting systems biology to address the complexity of human disease in the single-cell era. *Nature Reviews Genetics*, 26:514–531, 2025. doi: 10.1038/s41576-025-00821-6.

Emil Fischer. Einfluss der configuration auf die wirkung der enzyme. *Berichte der deutschen chemischen Gesellschaft*, 27:2985–2993, 1894. doi: 10.1002/cber.18940270390.

R. A. Fisher. *The Genetical Theory of Natural Selection*. Clarendon Press, Oxford, 1930.

Alexander Fleming. On the antibacterial action of cultures of a penicillium, with special reference to their use in the isolation of *B. influenzae*. *British Journal of Experimental Pathology*, 10:226–236, 1929.

Walther Flemming. *Zellsubstanz, Kern und Zelltheilung*. FCW Vogel, 1882.

Food and Agriculture Organization of the United Nations. The state of world fisheries and aquaculture 2024, 2024. URL <https://www.fao.org/publications/home/fao-flagship-publications/the-state-of-world-fisheries-and-aquaculture>.

Food and Agriculture Organization of the United Nations, International Fund for Agricultural Development, UNICEF, World Food Programme, and World Health Organization. The state of food security and nutrition in the world 2025: Addressing high food price inflation for food security and nutrition, 2025. URL <https://www.fao.org/publications/fao-flagship-publications/the-state-of-food-security-and-nutrition-in-the-world/2025/en>.

Richard Frankham. Effective population size/adult population size ratios in wildlife: A review. *Genetical Research*, 66(2):95–107, 1995. doi: 10.1017/s0016672300034455.

Richard Frankham. Conservation genetics: Setting the scene. *Philosophical Transactions of the Royal Society B*, 369(1642):20130327, 2014.

Rosalind E. Franklin and R. G. Gosling. Molecular configuration in sodium thymonucleate. *Nature*, 171:740–741, 1953. doi: 10.1038/171740a0.

Uwe Frey and Richard G. M. Morris. Synaptic tagging and long-term potentiation. *Nature*, 385:533–536, 1997. doi: 10.1038/385533a0.

Karl Friston. The free-energy principle: a unified brain theory? *Nature Reviews Neuroscience*, 11(2):127–138, 2010. doi: 10.1038/nrn2787.

Karl Friston. Active inference and learning. *Neuroscience and Biobehavioral Reviews*, 68:862–879, 2017. doi: 10.1016/j.neubiorev.2016.06.022.

Lucas A. Garibaldi, Ingolf Steffan-Dewenter, Rachael Winfree, Marcelo A. Aizen, Riccardo Bommarco, Saul A. Cunningham, Claire Kremen, Luisa G. Carvalheiro, Lawrence D. Harder, Ofer Afik, Ignasi Bartomeus, Faye Benjamin, Virginie Boreux, Daniel Cariveau, Natacha P. Chacoff, Jan H. Dudenhöffer, Breno M. Freitas, Jaboury Ghazoul, Sarah Greenleaf, Juliana Hipólito, Andrea Holzschuh, Bradley Howlett, Rufus Isaacs, Steven K. Javorek, Christina M. Kennedy, Kristin Krewenka, Smitha Krishnan, Yael Mandelik, Margaret M. Mayfield, Iris Motzke, Theodore Munyuli, Brian A. Nault, Mark Otieno, Jessica Petersen, Gideon Pisanty, Simon G. Potts, Romina Rader, Taylor H. Ricketts, Maj Rundlöf, Colleen L. Seymour, Christof Schüepp, Hajnalka Szentgyörgyi, Hisatomo Taki, Teja Tscharntke, Carlos H. Vergara, Blandina F. Viana, Thomas C. Wanger, Catrin Westphal, Neal Williams, and Alexandra-Maria Klein. Wild pollinators enhance fruit set of crops regardless of honey bee abundance. *Science*, 339(6127):1608–1611, 2013. doi: 10.1126/science.1230200.

Archibald E. Garrod. The incidence of alkaptonuria: A study in chemical individuality. *The Lancet*, 160(4137):1616–1620, 1902. doi: 10.1016/S0140-6736(01)41972-6.

G. F. Gause. *The Struggle for Existence*. Williams & Wilkins, Baltimore, 1934.

GBIF Secretariat. What is GBIF? <https://www.gbif.org/what-is-gbif>, 2026. Accessed 2026-05-24.

Irini Genitsaridi, Paraskevi Salpea, Agus Salim, Seyedeh Forough Sajjadi, Dunya Tomic, Steven James, et al. 11th edition of the IDF diabetes atlas: global, regional, and national diabetes prevalence estimates for 2024 and projections for 2050. *The Lancet Diabetes & Endocrinology*, 14(2):149–156, 2026. doi: 10.1016/S2213-8587(25)00299-2.

Michael T. Ghiselin. A radical solution to the species problem. *Systematic Zoology*, 23(4):536–544, 1974. doi: 10.2307/2412471.

Scott F. Gilbert, Jan Sapp, and Alfred I. Tauber. A symbiotic view of life: We have never been individuals. *The Quarterly Review of Biology*, 87(4):325–341, 2012. doi: 10.1086/668166.

Alfred G. Gilman. G proteins: transducers of receptor-generated signals. *Annual Review of Biochemistry*, 56:615–649, 1987. doi: 10.1146/annurev.bi.56.070187.03151.

Jonathan S. Gootenberg, Omar O. Abudayyeh, Jeong Wook Lee, Patrick Essletzbichler, Aaron J. Dy, Julia Joung, Virginie Verdine, Nina Donghia, Nichole M. Daringer, Catherine A. Freije, Cameron Myhrvold, Roby P. Bhattacharyya, Jonathan Livny, Aviv Regev, Eugene V. Koonin, Deborah T. Hung, Pardis C. Sabeti, James J. Collins, and Feng Zhang. Nucleic acid detection with crispr-cas13a/c2c2. *Science*, 356(6336):438–442, 2017. doi: 10.1126/science.aam9321.

Stephen Jay Gould and Niles Eldredge. Punctuated equilibria: an alternative to phyletic gradualism. *Models in Paleobiology*, pages 82–115, 1972.

Stephen Jay Gould and Richard C. Lewontin. The spandrels of san marco and the panglossian paradigm: A critique of the adaptationist programme. *Proceedings of the Royal Society of London. Series B, Biological Sciences*, 205(1161):581–598, 1979. doi: 10.1098/rspb.1979.0086.

Brian L. Graham, Irene Steenbruggen, Martin R. Miller, Igor Z. Barjaktarevic, Brendan G. Cooper, Graham L. Hall, Teal S. Hallstrand, David A. Kaminsky, Kevin McCarthy, Meredith C. McCormack, Carlos E. Oropez, Margaret Rosenfeld, Sanja Stanojevic, Maureen P. Swanney, and Bruce R. Thompson. Standardization of spirometry 2019 update. an official american thoracic society and european respiratory society technical statement. *American Journal of Respiratory and Critical Care Medicine*, 200(8):e70–e88, 2019. doi: 10.1164/rccm.201908-1590ST.

Pierre-Paul Grassé. La reconstruction du nid et les coordinations interindividuelles chez bellicositermes natalensis et cubitermes sp. la théorie de la stigmergie: Essai d’interprétation du comportement des termites constructeurs. *Insectes Sociaux*, 6:41–80, 1959. doi: 10.1007/BF02223791.

Richard E. Green, Johannes Krause, Adrian W. Briggs, et al. A draft sequence of the Neandertal genome. *Science*, 328:710–722, 2010. doi: 10.1126/science.1188021.

Anthon Hager. Acid growth theory of auxin action. *Planta*, 100:47–75, 1971.

J. B. S. Haldane. *The Causes of Evolution*. Longmans, Green and Co., London, 1932.

W. D. Hamilton. The genetical evolution of social behaviour. i. *Journal of Theoretical Biology*, 7(1):1–16, 1964a. doi: 10.1016/0022-5193(64)90038-4.

W. D. Hamilton. The genetical evolution of social behaviour. ii. *Journal of Theoretical Biology*, 7(1):17–52, 1964b. doi: 10.1016/0022-5193(64)90039-6.

William D. Hamilton and Marlene Zuk. Heritable true fitness and bright birds: A role for parasites? *Science*, 218(4570):384–387, 1982. doi: 10.1126/science.7123238.

Donna Haraway. Situated knowledges: The science question in feminism and the privilege of partial perspective. *Feminist Studies*, 14(3):575–599, 1988. doi: 10.2307/3178066.

Sandra Harding. *The Science Question in Feminism*. Cornell University Press, Ithaca, 1986.

Leland H. Hartwell and Ted A. Weinert. Checkpoints: Controls that ensure the order of cell cycle events. *Science*, 246(4930):629–634, 1989. doi: 10.1126/science.2683079.

William Harvey. *Exercitatio Anatomica de Motu Cordis et Sanguinis in Animalibus*. Francofurti, 1628.

Terry Hassold and Patricia Hunt. To err (meiotically) is human: The genesis of human aneuploidy. *Nature Reviews Genetics*, 2(4):280–291, 2001. doi: 10.1038/35066065.

Julia Hauenstein, Lisa Jeske, Antje Jäde, Mathias Krull, Katrin Dümmer, Julia Koblitz, Anja Tietz, Dieter Jahn, Lorenz Christian Reimer, and Boyke Bunk. BRENDA in 2026: a global core biodata resource for functional enzyme and metabolic data within the DSMZ digital diversity. *Nucleic Acids Research*, 54(D1):D527–D534, 2026. doi: 10.1093/nar/gkaf1113.

Edith Heard and Robert A. Martienssen. Transgenerational epigenetic inheritance: Myths and mechanisms. *Cell*, 157(1):95–109, 2014. doi: 10.1016/j.cell.2014.02.045.

Donald O. Hebb. *The Organization of Behavior: A Neuropsychological Theory*. Wiley, New York, 1949.

Hermann von Helmholtz. *Handbuch der physiologischen Optik*. Leopold Voss, 1867.

Lawrence J. Henderson. *The Fitness of the Environment*. Macmillan, New York, 1913.

Alfred D. Hershey and Martha Chase. Independent functions of viral protein and nucleic acid in growth of bacteriophage. *Journal of General Physiology*, 36(1): 39–56, 1952. doi: 10.1085/jgp.36.1.39.

Alan L. Hodgkin and Andrew F. Huxley. A quantitative description of membrane current and its application to conduction and excitation in nerve. *Journal of Physiology*, 117(4):500–544, 1952. doi: 10.1113/jphysiol.1952.sp004764.

John H. Holland. *Adaptation in Natural and Artificial Systems: An Introductory Analysis with Applications to Biology, Control, and Artificial Intelligence*. MIT Press, Cambridge, MA, 1st mit press ed. edition, 1992. ISBN 9780262581110. doi: 10.7551/mitpress/1090.001.0001.

C. S. Holling. Some characteristics of simple types of predation and parasitism. *Canadian Entomologist*, 91(7):385–398, 1959.

David A. Holway, Lori Lach, Andrew V. Suarez, Neil D. Tsutsui, and Ted J. Case. The causes and consequences of ant invasions. *Annual Review of Ecology and Systematics*, 33:181–233, 2002. doi: 10.1146/annurev.ecolsys.33.010802.150444.

Robert Hooke. *Micrographia*. Royal Society, London, 1665.

Shouguang Huang, M. Rob G. Roelfsema, Matthew Gilliam, Alistair M. Hetherington, and Rainer Hedrich. Guard cells count the number of unitary cytosolic ca^{2+} signals to regulate stomatal dynamics. *Current Biology*, 34(23):5409–5416.e2, 2024. doi: 10.1016/j.cub.2024.07.086.

William O. H. Hughes, Benjamin P. Oldroyd, Madeleine Beekman, and Francis L. W. Ratnieks. Ancestral monogamy shows kin selection is key to the evolution of eusociality. *Science*, 320(5880):1213–1216, 2008. doi: 10.1126/science.1156108.

David L. Hull. A matter of individuality. *Philosophy of Science*, 45(3):335–360, 1978. doi: 10.1086/288811.

David L. Hull. *Science as a Process: An Evolutionary Account of the Social and Conceptual Development of Science*. University of Chicago Press, Chicago, 1988.

Human Pangenome Reference Consortium. A draft human pangenome reference. *Nature*, 617:312–324, 2023. doi: 10.1038/s41586-023-05896-x.

Human Pangenome Reference Consortium. Human pangenome reference consortium data release 2. <https://humanpangenome.org/hprc-data-release-2/>, 2025. Data Release 2 page dated 12 May 2025; accessed 2026-05-23.

G. Evelyn Hutchinson. Concluding remarks. *Cold Spring Harbor Symposia on Quantitative Biology*, 22:415–427, 1957.

Clyde A. Hutchison, Ray-Yuan Chuang, Vladimir N. Noskov, et al. Design and synthesis of a minimal bacterial genome. *Science*, 351(6280):aad6253, 2016. doi: 10.1126/science.aad6253.

Hugh Huxley and Jean Hanson. Changes in the cross-striations of muscle during contraction and stretch and their structural interpretation. *Nature*, 173:973–976, 1954. doi: 10.1038/173973a0.

Julian Huxley. *Evolution: The Modern Synthesis*. Allen and Unwin, London, 1942.

Ibn Sina. *The Canon of Medicine*. Classical medical text, 1025. Date approximate.

Tatsuo Ido, Chun-Nan Wan, Vincenzo Casella, Joanna S. Fowler, Alfred P. Wolf, Martin Reivich, and David E. Kuhl. Labeled 2-deoxy-d-glucose analogs. 18F-labeled 2-deoxy-2-fluoro-d-glucose, 2-deoxy-2-fluoro-d-mannose and 14C-2-deoxy-2-fluoro-d-glucose. *Journal of Labelled Compounds and Radiopharmaceuticals*, 14(2):175–183, 1978. doi: 10.1002/jlcr.2580140204.

IMV Medical Information Division. 2024 PET imaging market summary report. <https://imvinfo.com/product/2024-pet-imaging-market-summary-report/>, 2024. U.S. PET census; 74% of 2023 PET scans used F-18 FDG. Accessed 2026-05-24.

Santoshi Indrakanti, Xinhua Li, and Madan M. Rehani. Patients undergoing multiple 18F-FDG PET/CT exams: Assessment of frequency, dose and disease classification. *British Journal of Radiology*, 95(1135):20211225, 2022. doi: 10.1259/bjr.20211225.

Jan Ingen-Housz. *Experiments upon Vegetables, Discovering Their Great Power of Purifying the Common Air in the Sunshine*. P. Elmsly, 1779.

Arabidopsis Genome Initiative. Analysis of the genome sequence of the flowering plant Arabidopsis thaliana. *Nature*, 408:796–815, 2000. doi: 10.1038/35048692.

Intergovernmental Panel on Climate Change. Climate change 2021: The physical science basis. contribution of working group i to the sixth assessment report, 2021. URL <https://www.ipcc.ch/report/ar6/wg1/>.

Intergovernmental Science-Policy Platform on Biodiversity and Ecosystem Services. Global assessment report on biodiversity and ecosystem services, 2019. URL <https://ipbes.net/global-assessment>.

Intergovernmental Science-Policy Platform on Biodiversity and Ecosystem Services. Thematic assessment report on the underlying causes of biodiversity loss and the determinants of transformative change, 2024. URL <https://www.ipbes.net/transformative-change>.

International Union for Conservation of Nature. The iucn red list of threatened species: Summary statistics. <https://nrl.iucnredlist.org/resources/summary-statistics>, 2025. Version 2025-2 Table 1a, last updated 10 October 2025; accessed 2026-05-21.

Daegan Inward, George Beccaloni, and Paul Eggleton. Death of an order: a comprehensive molecular phylogenetic study confirms that termites are eusocial cockroaches. *Biology Letters*, 3(3):331–335, 2007. doi: 10.1098/rsbl.2007.0102.

IPBES. *The Assessment Report of the Intergovernmental Science-Policy Platform on Biodiversity and Ecosystem Services on Pollinators, Pollination and Food Production*. Secretariat of the Intergovernmental Science-Policy Platform on Biodiversity and Ecosystem Services, Bonn, Germany, 2016. URL https://files.ipbes.net/ipbes-web-prod-public-files/downloads/pdf/2017_pollination_full_report_book_v12_pages.pdf.

Akiko Iwasaki and Ruslan Medzhitov. Control of adaptive immunity by the innate immune system. *Nature Immunology*, 16:343–353, 2015. doi: 10.1038/ni.3123.

François Jacob and Jacques Monod. Genetic regulatory mechanisms in the synthesis of proteins. *Journal of Molecular Biology*, 3(3):318–356, 1961. doi: 10.1016/s0022-2836(61)80072-7.

Rudolf Jaenisch and Adrian Bird. Epigenetic regulation of gene expression: How the genome integrates intrinsic and environmental signals. *Nature Genetics*, 33: 245–254, 2003. doi: 10.1038/ng1089.

Sheila Jasanoff, editor. *States of Knowledge: The Co-production of Science and Social Order*. Routledge, London, 2004.

Alec J. Jeffreys, Victoria Wilson, and Swee Lay Thein. Individual-specific “fingerprints” of human DNA. *Nature*, 316:76–79, 1984. doi: 10.1038/316076a0.

Martin Jinek, Krzysztof Chylinski, Ines Fonfara, et al. A programmable dual-RNA-guided DNA endonuclease in adaptive bacterial immunity. *Science*, 337: 816–821, 2012. doi: 10.1126/science.1225829.

Horace Freeland Judson. *The Eighth Day of Creation: Makers of the Revolution in Biology*. Cold Spring Harbor Laboratory Press, Cold Spring Harbor, 1996.

Kanehisa Laboratories. KEGG: Kyoto encyclopedia of genes and genomes. <https://www.genome.jp/kegg/>, 2026. Accessed 2026-05-24.

Mary N. Karn and Lionel S. Penrose. Birth weight and gestation time in relation to maternal age, parity and infant survival. *Annals of Eugenics*, 16(1):147–164, 1951.

Stuart A. Kauffman. *The Origins of Order: Self Organization and Selection in Evolution*. Oxford University Press, New York, 1993. ISBN 9780195079517.

Evelyn Fox Keller. *The Mirage of a Space between Nature and Nurture*. Duke University Press, Durham, 2010.

Daniel J. Kevles. *In the Name of Eugenics: Genetics and the Uses of Human Heredity*. Knopf, New York, 1985.

Motoo Kimura. Evolutionary rate at the molecular level. *Nature*, 217(5129):624–626, 1968. doi: 10.1038/217624a0.

Motoo Kimura. *The Neutral Theory of Molecular Evolution*. Cambridge University Press, Cambridge, 1983.

J. F. C. Kingman. The coalescent. *Stochastic Processes and their Applications*, 13(3):235–248, 1982. doi: 10.1016/0304-4149(82)90011-4.

Hiroaki Kitano. Systems biology: A brief overview. *Science*, 295(5560):1662–1664, 2002. doi: 10.1126/science.1069492.

Robert Koch. *Die Aetiologie der Tuberkulose*. Berliner Klinische Wochenschrift, 1884.

Georges Köhler and César Milstein. Continuous cultures of fused cells secreting antibody of predefined specificity. *Nature*, 256:495–497, 1975. doi: 10.1038/256495a0.

Daniel E. Koshland. Application of a theory of enzyme specificity to protein synthesis. *Proceedings of the National Academy of Sciences*, 44(2):98–104, 1958. doi: 10.1073/pnas.44.2.98.

Hans A. Krebs and William A. Johnson. Metabolism of ketonic acids in animal tissues. *Biochemical Journal*, 31:645–660, 1937. doi: 10.1042/bj0310645.

Gaku Kudo and Elisabeth J. Cooper. When spring ephemerals fail to meet pollinators: mechanism of phenological mismatch and its impact on plant reproduction. *Proceedings of the Royal Society B: Biological Sciences*, 286(1904):20190573, 2019. doi: 10.1098/rspb.2019.0573.

Jiameng Lai, Linda M. J. Kooijmans, Wu Sun, Danica Lombardozzi, J. Elliott Campbell, Lianhong Gu, Yiqi Luo, Le Kuai, and Ying Sun. Terrestrial photosynthesis inferred from plant carbonyl sulfide uptake. *Nature*, 634(8035):855–861, 2024a. doi: 10.1038/s41586-024-08050-3.

Jiameng Lai, Linda M. J. Kooijmans, Wu Sun, Danica Lombardozzi, J. Elliott Campbell, Lianhong Gu, Yiqi Luo, Le Kuai, and Ying Sun. Terrestrial photosynthesis inferred from plant carbonyl sulfide uptake. *Nature*, 634(8035):855–861, 2024b. doi: 10.1038/s41586-024-08050-3.

Kevin N. Laland, Tobias Uller, Marcus W. Feldman, Kim Sterelny, Gerd B. Muller, Armin Moczek, Eva Jablonka, and John Odling-Smee. The extended evolutionary synthesis: Its structure, assumptions and predictions. *Proceedings of the Royal Society B: Biological Sciences*, 282(1813):20151019, 2015. doi: 10.1098/rspb.2015.1019.

Melissa J. Landrum, Jennifer M. Lee, Mark Benson, Garth Brown, Chen Chao, Shanmuga Chitipiralla, Baoshan Gu, Jennifer Hart, Douglas Hoffman, Jessica Hoover, Wonhee Jang, Kenneth Katz, Michael Ovetsky, George Riley, Anju Sethi, Raymond Tully, Roselie Villamarin-Salomon, Wendy Rubinstein, and Donna R. Maglott. ClinVar: public archive of relationships among sequence variation and human phenotype. *Nucleic Acids Research*, 42(D1):D980–D985, 2014. doi: 10.1093/nar/gkt1113.

Jeffrey G. Lawrence and Howard Ochman. Molecular archaeology of the Escherichia coli genome. *Proceedings of the National Academy of Sciences*, 95(16): 9413–9417, 1998.

Antoni van Leeuwenhoek. An abstract of a letter from Mr. Anthony van Leewenhoek at Delft, dated sep. 17, 1683, containing some microscopical observations. *Philosophical Transactions of the Royal Society*, 14:568–574, 1684.

Szabolcs Lengyel, Aaron D. Gove, Andrew M. Latimer, Jonathan D. Majer, and Robert R. Dunn. Ants sow the seeds of global diversification in flowering plants. *PLOS ONE*, 4(5):e5480, 2009. doi: 10.1371/journal.pone.0005480.

Sabina Leonelli. *Data-Centric Biology: A Philosophical Study*. University of Chicago Press, Chicago, 2016.

Simon A. Levin. Ecosystems and the biosphere as complex adaptive systems. *Ecosystems*, 1:431–436, 1998.

Richard Levins. The strategy of model building in population biology. *American Scientist*, 54(4):421–431, 1966.

Richard C. Lewontin. The analysis of variance and the analysis of causes. *American Journal of Human Genetics*, 26(3):400–411, 1974.

Regina Lindborg and Ove Eriksson. Historical landscape connectivity affects present plant species diversity. *Ecology*, 85(7):1840–1845, 2004.

Carl Linnaeus. *Species Plantarum*. Laurentius Salvius, Stockholm, 1753.

Chaolei Liu, Zexue He, Yan Zhang, Fengyue Hu, Mengqi Li, Qing Liu, Yong Huang, Jian Wang, Wenli Zhang, Chun Wang, and Kejian Wang. Synthetic apomixis enables stable transgenerational transmission of heterotic phenotypes in hybrid rice. *Plant Communications*, 4(2):100470, 2023. doi: 10.1016/j.xplc.2022.100470.

G. E. R. Lloyd. *Adversaries and Authorities: Investigations into Ancient Greek and Chinese Science*. Cambridge University Press, Cambridge, 1996.

Alfred J. Lotka. *Elements of Physical Biology*. Williams & Wilkins, Baltimore, 1925.

James E. Lovelock and Lynn Margulis. Atmospheric homeostasis by and for the biosphere: the gaia hypothesis. *Tellus*, 26(1-2):2–10, 1974. doi: 10.3402/tellusa.v26i1-2.9731.

Mary F. Lyon. Gene action in the X-chromosome of the mouse (Mus musculus L.). *Nature*, 190:372–373, 1961. doi: 10.1038/190372a0.

Robert H. MacArthur and E. O. Wilson. *The Theory of Island Biogeography*. Princeton University Press, Princeton, 1967.

Peter Machamer, Lindley Darden, and Carl F. Craver. Thinking about mechanisms. *Philosophy of Science*, 67(1):1–25, 2000. doi: 10.1086/392759.

Shikha Malik and Dazhong Zhao. Epigenetic regulation of heat stress in plant male reproduction. *Frontiers in Plant Science*, 13:826473, 2022. doi: 10.3389/fpls.2022.826473.

Teri A. Manolio, Francis S. Collins, Nancy J. Cox, et al. Finding the missing heritability of complex diseases. *Nature*, 461(7265):747–753, 2009. doi: 10.1038/nature08494.

Barry J. Marshall and J. Robin Warren. Unidentified curved bacilli in the stomach of patients with gastritis and peptic ulceration. *The Lancet*, 323(8390):1311–1315, 1984. doi: 10.1016/s0140-6736(84)91816-6.

Barry J. Marshall, John A. Armstrong, David B. McGeachie, and Ross J. Glancy. Attempt to fulfil Koch’s postulates for pyloric Campylobacter. *The Medical Journal of Australia*, 142(8):436–439, 1985. doi: 10.5694/j.1326-5377.1985.tb113443.x.

Alicia R. Martin, Masahiro Kanai, Yoichiro Kamatani, Yukinori Okada, Benjamin M. Neale, and Mark J. Daly. Clinical use of current polygenic risk scores may exacerbate health disparities. *Nature Genetics*, 51:584–591, 2019. doi: 10.1038/s41588-019-0379-x.

Ernst Mayr. *Systematics and the Origin of Species*. Columbia University Press, New York, 1942.

Ernst Mayr. Teleological and teleonomic: A new analysis. *Boston Studies in the Philosophy of Science*, 14:91–117, 1974. doi: 10.1007/978-94-010-2128-9_6.

Ernst Mayr. *The Growth of Biological Thought: Diversity, Evolution, and Inheritance*. Harvard University Press, Cambridge, MA, 1982.

Barbara McClintock. The origin and behavior of mutable loci in maize. *Proceedings of the National Academy of Sciences*, 36:344–355, 1950. doi: 10.1073/pnas.36.6.344.

Ruslan Medzhitov. Recognition of microorganisms and activation of the immune response. *Nature*, 449:819–826, 2007. doi: 10.1038/nature06246.

Gregor Mendel. Versuche über pflanzenhybriden. *Verhandlungen des naturforschenden Vereines in Brünn*, 4:3–47, 1866.

Matthew Meselson and Franklin W. Stahl. The replication of DNA in Escherichia coli. *Proceedings of the National Academy of Sciences*, 44(7):671–682, 1958. doi: 10.1073/pnas.44.7.671.

Sean L. Metzger, Katelyn T. Littlejohn, Alexander B. Silva, David A. Moses, Matthew P. Seaton, Ran Wang, Maximilian E. Dougherty, Jessie R. Liu, Peter Wu, Michael A. Berger, Ilona Zhuravleva, Alexander Tu-Chan, Karunesh Ganguly, Gopala K. Anumanchipalli, and Edward F. Chang. A high-performance neuroprosthesis for speech decoding and avatar control. *Nature*, 620:1037–1046, 2023. doi: 10.1038/s41586-023-06443-4.

Leonor Michaelis and Maud L. Menten. Die kinetik der invertinwirkung. *Biochemische Zeitschrift*, 49:333–369, 1913.

Peter Mitchell. Coupling of phosphorylation to electron and hydrogen transfer by a chemi-osmotic type of mechanism. *Nature*, 191:144–148, 1961. doi: 10.1038/191144a0.

Beverly Y. Mok, Marcos H. de Moraes, Jun Zeng, Dustin E. Bosch, Aleksandra V. Kotrys, Aditya Raguram, F. Ann Ran Hsu, Matthew C. Radey, Summer B. Peterson, Vamsi K. Mootha, Joseph D. Mougous, and David R. Liu. A bacterial cytidine deaminase toxin enables crispr-free mitochondrial base editing. *Nature*, 583:631–637, 2020. doi: 10.1038/s41586-020-2477-4.

Jacques Monod, Jeffries Wyman, and Jean-Pierre Changeux. On the nature of allosteric transitions: A plausible model. *Journal of Molecular Biology*, 12:88–118, 1965. doi: 10.1016/S0022-2836(65)80285-6.

Thomas Hunt Morgan. Sex limited inheritance in Drosophila. *Science*, 32:120–122, 1910. doi: 10.1126/science.32.812.120.

Ernst M”unch. Die stoffbewegungen in der pflanze. *Gustav Fischer Verlag*, 1930.

Christopher J. L. Murray, Kevin Shunji Ikuta, Fablina Sharara, Lucien Swetschinski, Gisela Robles Aguilar, Aruna Gray, Chieh Han, Catherine Bisignano, Puja Rao, Eve Wool, Sarah C. Johnson, Annie J. Browne, Michael G. Chipeta, Frederick Fell, Stephen Hackett, Grace Haines-Woodhouse, Bhavani H. Kashef Hamadani, Eileen A. P. Kumaran, Braden McManigal, Suvarat Benjarat Achalapong, et al. Global burden of bacterial antimicrobial resistance in 2019: a systematic analysis. *The Lancet*, 399(10325):629–655, 2022. doi: 10.1016/S0140-6736(21)02724-0.

National Academies of Sciences, Engineering, and Medicine. *Gene Drives on the Horizon: Advancing Science, Navigating Uncertainty, and Aligning Research with Public Values*. The National Academies Press, Washington, DC, 2016. doi: 10.17226/23405.

National Cancer Institute. Immune checkpoint inhibitors. <https://www.cancer.gov/about-cancer/treatment/types/immunotherapy/checkpoint-inhibitors>, 2026. Accessed 2026-05-20.

National Center for Biotechnology Information. Clinvar. <https://www.ncbi.nlm.nih.gov/clinvar/>, 2026a. Accessed 2026-05-24.

National Center for Biotechnology Information. dbSNP. <https://www.ncbi.nlm.nih.gov/snp/>, 2026b. Accessed 2026-05-24.

National Center for Biotechnology Information. Matched annotation from NCBI and EMBL-EBI. <https://www.ncbi.nlm.nih.gov/refseq/MANE/>, 2026c. Accessed 2026-05-24.

National Center for Biotechnology Information. Reference sequence database. <https://www.ncbi.nlm.nih.gov/refseq/>, 2026d. Accessed 2026-05-24.

National Institute of Diabetes and Digestive and Kidney Diseases. Your digestive system & how it works. <https://www.niddk.nih.gov/health-information/digestive-diseases/digestive-system-how-it-works>, 2024a. Accessed 2026-05-20.

National Institute of Diabetes and Digestive and Kidney Diseases. Your kidneys & how they work. <https://www.niddk.nih.gov/health-information/kidney-disease/kidneys-how-they-work>, 2024b. Accessed 2026-05-20.

National Institute of Mental Health. Scientists unveil complete cell map of a whole mammalian brain. <https://www.nimh.nih.gov/news/science-updates/2023/scientists-unveil-complete-cell-map-of-a-whole-mammalian-brain>, 2023. Press release, 13 December 2023; accessed 2026-05-21.

National Library of Medicine. Clinicaltrials.gov. <https://clinicaltrials.gov/>, 2026. Accessed 2026-05-24.

Sergei Nawaschin. Resultate einer revision der befruchtungsvorgänge bei Lilium martagon und Fritillaria tenella. *Bulletin de l'Académie Impériale des Sciences de Saint-Petersbourg*, 9:377–382, 1898.

Joseph Needham. *Science and Civilisation in China*. Cambridge University Press, Cambridge, 1954.

Randolph M. Nesse. Tinbergen’s four questions, organized. *Evolution, Medicine, and Public Health*, 2019:523–524, 2019. doi: 10.1093/emph/eoz026.

Marshall W. Nirenberg and J. Heinrich Matthaei. The dependence of cell-free protein synthesis in E. coli upon naturally occurring or synthetic polyribonucleotides. *Proceedings of the National Academy of Sciences*, 47:1588–1602, 1961. doi: 10.1073/pnas.47.10.1588.

NOAA Coral Reef Watch. Current global bleaching event: Status update and data submission. https://coralreefwatch.noaa.gov/satellite/research/coral_bleaching_report.php, 2025. Accessed 2026-05-16.

Nuremberg Military Tribunal. The nuremberg code, 1947. Research ethics code articulated in the Doctors’ Trial judgment.

Paul Nurse. A long twentieth century of the cell cycle and beyond. *Cell*, 100(1):71–78, 2000. doi: 10.1016/S0092-8674(00)81684-0.

Samuel A. Ocko, Hunter King, David Andreen, Paul Bardunias, J. Scott Turner, Rupert Soar, and L. Mahadevan. Solar-powered ventilation of african termite mounds. *Journal of Experimental Biology*, 220:3260–3269, 2017. doi: 10.1242/jeb.160895.

Eugene P. Odum. *Fundamentals of Ecology*. W. B. Saunders, 1953.

Susumu Ohno. *Evolution by Gene Duplication*. Springer-Verlag, New York, 1970.

Tomoko Ohta. Slightly deleterious and nearly neutral mutations in molecular evolution. *Proceedings of the National Academy of Sciences*, 70(10):3163–3165, 1973.

Samir Okasha. *Evolution and the Levels of Selection*. Oxford University Press, Oxford, 2006.

Maureen A. O’Malley. *Philosophy of Microbiology*. Cambridge University Press, Cambridge, 2014.

Jim O’Neill. Tackling drug-resistant infections globally: Final report and recommendations, 2016. URL https://amr-review.org/sites/default/files/160525_Final%20paper_with%20cover.pdf.

Open Syllabus Project. OER adoption update: 2023. <https://blog.opensyllabus.org/oer-adoption-update-2023>, 2023. Accessed 2026-05-24.

Susan Oyama. *The Ontogeny of Information: Developmental Systems and Evolution*. Duke University Press, Durham, 2 edition, 2000.

Robert T. Paine. Food web complexity and species diversity. *The American Naturalist*, 100(910):65–75, 1966.

George E. Palade. A small particulate component of the cytoplasm. *The Journal of Biophysical and Biochemical Cytology*, 1(1):59–68, 1955. doi: 10.1083/jcb.1.1.59.

Zhanghao Pan et al. Single cell atlas: a single-cell multi-omics human cell encyclopedia. *Genome Biology*, 25:104, 2024. doi: 10.1186/s13059-024-03246-2.

Donovan H. Parks, Pierre-Alain Chaumeil, Aaron J. Mussig, Christian Rinke, Maria Chuvochina, and Philip Hugenholtz. GTDB release 10: a complete and systematic taxonomy for 715 230 bacterial and 17 245 archaeal genomes. *Nucleic Acids Research*, 54(D1):D743–D754, 2026. doi: 10.1093/nar/gkaf1040.

Thomas Parr, Giovanni Pezzulo, and Karl Friston. *Active Inference: The Free Energy Principle in Mind, Brain, and Behavior*. MIT Press, Cambridge, MA, 2022. ISBN 978-0262045353.

Louis Pasteur. Mémoire sur les corpuscules organisés qui existent dans l’atmosphère. *Annales des Sciences Naturelles*, 16:5–98, 1861.

Linus Pauling. The nature of the chemical bond. IV. the energy of single bonds and the relative electronegativity of atoms. *Journal of the American Chemical Society*, 54(9):3570–3582, 1932. doi: 10.1021/ja01348a011.

Linus Pauling and Robert B. Corey. Atomic coordinates and structure factors for two helical configurations of polypeptide chains. *Proceedings of the National Academy of Sciences*, 37:235–240, 1951. doi: 10.1073/pnas.37.5.235.

Michael E. Phelps, Sung-Cheng Huang, Edward J. Hoffman, Carl Selin, Louis Sokoloff, and David E. Kuhl. Tomographic measurement of local cerebral glucose metabolic rate in humans with (F-18)2-fluoro-2-deoxy-d-glucose: validation of method. *Annals of Neurology*, 6(5):371–388, 1979. doi: 10.1002/ana.410060502.

Massimo Pigliucci and Gerd B. Muller, editors. *Evolution: The Extended Synthesis*. MIT Press, Cambridge, MA, 2010.

Thomas Pradeu. *The Limits of the Self: Immunology and Biological Identity*. Oxford University Press, Oxford, 2012.

Ilya Prigogine and Grégoire Nicolis. *Self-Organization in Nonequilibrium Systems: From Dissipative Structures to Order through Fluctuations*. Wiley-Interscience, New York, 1977. ISBN 9780471024019.

Protein Data Bank in Europe. Protein data bank in europe. <https://www.ebi.ac.uk/pdbe/>, 2026. Accessed 2026-05-24.

H. Ronald Pulliam. Sources, sinks, and population regulation. *American Naturalist*, 132(5):652–661, 1988.

Efraim Racker and Walther Stoeckenius. Reconstitution of purple membrane vesicles catalyzing light-driven proton uptake and adenosine triphosphate formation. *Journal of Biological Chemistry*, 249:662–663, 1974.

Theodore W. Rall and Earl W. Sutherland. Formation of a cyclic adenine ribonucleotide by tissue particles. *Journal of Biological Chemistry*, 232(2):1065–1076, 1958. doi: 10.1016/S0021-9258(19)77422-5.

A. C. Redfield. The biological control of chemical factors in the environment. *American Scientist*, 46(3):230A–221, 1958.

Aviv Regev, Sarah A. Teichmann, Eric S. Lander, Ido Amit, Christophe Benoist, Ewan Birney, Bernd Bodenmiller, Peter Campbell, Piero Carninci, Menna Clatworthy, Hans Clevers, Bart Deplancke, Ian Dunham, James Eberwine, Roland Eils, Wolfgang Enard, Andrew Farmer, Lars Fugger, Berthold Göttgens, Nir Hacohen, et al. The human cell atlas. *eLife*, 6:e27041, 2017. doi: 10.7554/eLife.27041.

David A. Relman, Paul B. Eckburg, et al. Archaea and their potential role in human disease. *Infection and Immunity*, 67:592–593, 1999.

Craig W. Reynolds. Flocks, herds and schools: A distributed behavioral model. *ACM SIGGRAPH Computer Graphics*, 21(4):25–34, 1987. doi: 10.1145/37402.37406.

Hans-Jorg Rheinberger. *Toward a History of Epistemic Things: Synthesizing Proteins in the Test Tube*. Stanford University Press, Stanford, 1997.

Sue Richards, Nazneen Aziz, Sherri Bale, David Bick, Soma Das, Julie Gastier-Foster, Wayne W. Grody, Madhuri Hegde, Elaine Lyon, Elaine Spector, Karl Voelkerding, and Heidi L. Rehm. Standards and guidelines for the interpretation of sequence variants: a joint consensus recommendation of the American College of Medical Genetics and Genomics and the Association for Molecular Pathology. *Genetics in Medicine*, 17(5):405–424, 2015. doi: 10.1038/gim.2015.30.

Katherine Richardson, Will Steffen, Wolfgang Lucht, Jørgen Bendtsen, Sarah E. Cornell, Jonathan F. Donges, Markus Drüke, Ingo Fetzer, Govindasamy Bala, Werner von Bloh, Georg Feulner, Stephanie Fiedler, Dieter Gerten, Tom Gleeson, Matthias Hofmann, Willem Huiskamp, Matti Kumm, Chinchu Mohan, David Nogués-Bravo, Stefan Petri, Miina Porkka, Stefan Rahmstorf, Sibyll Schaphoff, Kirsten Thonicke, Arne Tobian, Veera Virkki, Lan Wang-Erlandsson, Lisa Weber, and Johan Rockström. Earth beyond six of nine planetary boundaries. *Science Advances*, 9(37):eadh2458, 2023. doi: 10.1126/sciadv.adh2458.

Daniel J. Rigden and Xosé M. Fernández. The 2026 nucleic acids research database issue and the online molecular biology database collection. *Nucleic Acids Research*, 54(D1):D1–D9, 2026. doi: 10.1093/nar/gkaf1427.

Joe R. Riley, Uwe Greggers, Alan D. Smith, Don R. Reynolds, and Randolph Menzel. The flight paths of honeybees recruited by the waggle dance. *Nature*, 435: 205–207, 2005. doi: 10.1038/nature03526.

William J. Ripple and Robert L. Beschta. Trophic cascades in Yellowstone: The first 15 years after wolf reintroduction. *Biological Conservation*, 145(1):205–213, 2012a.

William J. Ripple and Robert L. Beschta. Large predators and ecological cascades in terrestrial ecosystems of the western United States. *Biological Conservation*, 145:205–212, 2012b. doi: 10.1016/j.biocon.2011.11.015.

RNAcentral Consortium. RNAcentral in 2026: genes and literature integration. *Nucleic Acids Research*, 54(D1):D303–D313, 2026. doi: 10.1093/nar/gkaf1329.

James E. Rothman. Mechanisms of intracellular protein transport. *Nature*, 372(6501):55–63, 1994. doi: 10.1038/372055a0.

Julius von Sachs. Ueber den einfluss des lichtes auf die blattstellung. *Botanische Zeitung*, 20:225–226, 1862.

Lynn Sagan. On the origin of mitosing cells. *Journal of Theoretical Biology*, 14(3):255–274, 1967. doi: 10.1016/0022-5193(67)90079-3. Lynn Margulis (née Sagan).

Norihiro Saitou and Masatoshi Nei. The neighbor-joining method: a new method for reconstructing phylogenetic trees. *Molecular Biology and Evolution*, 4(4): 406–425, 1987. doi: 10.1093/oxfordjournals.molbev.a040404.

Frederick Sanger. The terminal peptides of insulin. *Biochemical Journal*, 60:541–556, 1955. doi: 10.1042/bj0600541.

Londa Schiebinger. *Has Feminism Changed Science?* Harvard University Press, Cambridge, MA, 1999.

Londa Schiebinger. *Plants and Empire: Colonial Bioprospecting in the Atlantic World*. Harvard University Press, Cambridge, MA, 2004.

Matthias Jakob Schleiden. Beiträge zur phyto-genesis. *Müller’s Archiv für Anatomie, Physiologie und wissenschaftliche Medicin*, pages 137–176, 1838.

Mona Schreiber, Murukarthick Jayakodi, Nils Stein, and Martin Mascher. Plant pangenomes for crop improvement, biodiversity and evolution. *Nature Reviews Genetics*, 25:563–577, 2024. doi: 10.1038/s41576-024-00691-4.

Theodor Schwann. *Mikroskopische Untersuchungen über die Übereinstimmung in der Struktur und dem Wachsthum der Thiere und Pflanzen*. Gebrüder Borntraeger, Berlin, 1839.

Thomas D. Seeley. *Honeybee Democracy*. Princeton University Press, Princeton, NJ, 2010. ISBN 9780691147215.

Ron Sender, Shai Fuchs, and Ron Milo. Revised estimates for the number of human and bacteria cells in the body. *PLOS Biology*, 14(8):e1002533, 2016. doi: 10.1371/journal.pbio.1002533.

Charles Sherrington. *The Integrative Action of the Nervous System*. Yale University Press, New Haven, 1906.

Daniel S. Simberloff and E. O. Wilson. Experimental zoogeography of islands. II. The colonization of empty islands. *Ecology*, 50(2):278–296, 1969.

S. J. Singer and Garth L. Nicolson. The fluid mosaic model of the structure of cell membranes. *Science*, 175(4023):720–731, 1972. doi: 10.1126/science.175.4023.720.

Dennis J. Slamon, Gary M. Clark, Sharon G. Wong, Wayne J. Levin, Axel Ullrich, and William L. McGuire. Human breast cancer: correlation of relapse and survival with amplification of the HER-2/neu oncogene. *Science*, 235(4785):177–182, 1987. doi: 10.1126/science.3798106.

Dennis J. Slamon, Brian Leyland-Jones, Steven Shak, Hank Fuchs, Virginia Paton, Alex Bajamonde, Thomas Fleming, Wolfgang Eiermann, John Wolter, Mark Pegram, Jose Baselga, and Larry Norton. Use of chemotherapy plus a monoclonal antibody against HER2 for metastatic breast cancer that overexpresses HER2. *New England Journal of Medicine*, 344(11):783–792, 2001. doi: 10.1056/NEJM200103153441101.

Elliott Sober. *The Nature of Selection: Evolutionary Theory in Philosophical Focus*. University of Chicago Press, Chicago, 1984.

Michael E. Soule. Thresholds for survival: Maintaining fitness and evolutionary potential. *Conservation Biology: An Evolutionary-Ecological Perspective*, pages 151–169, 1980.

SRI International. Biocyc pathway/genome database collection. <https://biocyc.org/>, 2026. Accessed 2026-05-24.

James T. Staley and Allan Konopka. Measurement of in situ activities of nonphotosynthetic microorganisms in aquatic and terrestrial habitats. *Annual Review of Microbiology*, 39:321–346, 1985. doi: 10.1146/annurev.mi.39.100185.001541.

Ernest H. Starling. The linacre lecture on the law of the heart. *Longmans, Green and Co.*, 1918. Based on 1914 experiments.

Peter Sterling. Allostasis: A model of predictive regulation. *Physiology & Behavior*, 106(1):5–15, 2012. doi: 10.1016/j.physbeh.2011.06.004.

Peter Sterling and Joseph Eyer. Allostasis: A new paradigm to explain arousal pathology. In *Handbook of Life Stress, Cognition and Health*, pages 629–649. Wiley, 1988.

Peter Sterling and Simon Laughlin. *Principles of Neural Design*. MIT Press, Cambridge, MA, 2015. ISBN 9780262028707. doi: 10.7551/mitpress/9780262028707.001.0001.

Benjamin D. Strahl and C. David Allis. The language of covalent histone modifications. *Nature*, 403(6765):41–45, 2000.

Steven H. Strogatz. *Nonlinear Dynamics and Chaos: With Applications to Physics, Biology, Chemistry, and Engineering*. Westview Press, Boulder, CO, 2nd edition, 2018. ISBN 9780813349107.

Alfred H. Sturtevant. The linear arrangement of six sex-linked factors in Drosophila, as shown by their mode of association. *Journal of Experimental Zoology*, 14: 43–59, 1913. doi: 10.1002/jez.1400140104.

Walter S. Sutton. On the morphology of the chromosome group in Brachystola magna. *Biological Bulletin*, 4(1):24–39, 1902.

Alan R. Templeton. The meaning of species and speciation: A genetic perspective. In *Speciation and Its Consequences*, pages 3–27. Sinauer, 1989.

The Honeybee Genome Sequencing Consortium. Insights into social insects from the genome of the honeybee apis mellifera. *Nature*, 443:931–949, 2006. doi: 10.1038/nature05260.

The Human Microbiome Project Consortium. Structure, function and diversity of the healthy human microbiome. *Nature*, 486(7402):207–214, 2012. doi: 10.1038/nature11234.

Niko Tinbergen. On aims and methods of ethology. *Zeitschrift für Tierpsychologie*, 20(4):410–433, 1963. doi: 10.1111/j.1439-0310.1963.tb01161.x.

Peter J. Turnbaugh, Ruth E. Ley, Michael A. Mahowald, Vincent Magrini, Elaine R. Mardis, and Jeffrey I. Gordon. An obesity-associated gut microbiome with increased capacity for energy harvest. *Nature*, 444(7122):1027–1031, 2006. doi: 10.1038/nature05414.

John J. Tyson, Katherine C. Chen, and Bela Novak. Sniffers, buzzers, toggles and blinkers: dynamics of regulatory and signaling pathways in the cell. *Current Opinion in Cell Biology*, 15(2):221–231, 2003. doi: 10.1016/S0955-0674(03)00017-6.

Mikihisa Umehara, Akira Hanada, Satoko Yoshida, et al. Inhibition of shoot branching by new terpenoid plant hormones. *Nature*, 455:195–200, 2008. doi: 10.1038/nature07272.

UNAIDS. Global hiv and aids statistics: Fact sheet. <https://www.unaids.org/en/resources/fact-sheet>, 2025. Accessed 2026-05-16.

UNESCO. Universal declaration on the human genome and human rights, 1997. Adopted by the UNESCO General Conference.

UniProt Consortium. UniProt: the universal protein knowledgebase in 2025. *Nucleic Acids Research*, 53(D1):D609–D617, 2025. doi: 10.1093/nar/gkae1010.

United Nations Department of Economic and Social Affairs, Population Division. World population prospects 2024: Summary of results, 2024. URL <https://population.un.org/wpp/>.

U.S. Department of Health and Human Services, Office for Human Research Protections. Guidance on the genetic information nondiscrimination act: Implications for investigators and institutional review boards. <https://www.hhs.gov/ohrp/regulations-and-policy/guidance/guidance-on-genetic-information-nondiscrimination-act/index.html>, 2009. Accessed 2026-05-20.

U.S. Food and Drug Administration. Tazverik (tazemetostat) prescribing information. https://www.accessdata.fda.gov/drugsatfda_docs/label/2020/211723s000lbl.pdf, 2020. Accessed 2026-05-20.

U.S. Food and Drug Administration. Fda approves first gene therapies to treat patients with sickle cell disease. <https://www.fda.gov/news-events/press-announcements/fda-approves-first-gene-therapies-treat-patients-sickle-cell-disease>, 2023. Accessed 2026-05-14.

U.S. Food and Drug Administration. Fda requires boxed warning for t cell malignancies following treatment with bcma-directed or cd19-directed autologous chimeric antigen receptor (car) t cell immunotherapies. <https://www.fda.gov/vaccines-blood-biologics/safety-availability-biologics/fda-requires-boxed-warning-t-cell-malignancies-following-treatment-bcma-directed-or-cd19-directed>, 2024a. Accessed 2026-05-20.

U.S. Food and Drug Administration. Fda approves first gene therapy to treat adults and children with transfusion-dependent beta-thalassemia. <https://www.fda.gov/news-events/press-announcements/fda-approves-first-gene-therapy-treat-adults-and-children-transfusion-dependent-beta-thalassemia>, 2024b. Accessed 2026-05-14.

U.S. Food and Drug Administration. Casgevy. <https://www.fda.gov/vaccines-blood-biologics/casgevy>, 2026a. Content current as of 2026-03-26; accessed 2026-05-15.

U.S. Food and Drug Administration. Approved cellular and gene therapy products. <https://www.fda.gov/vaccines-blood-biologics/cellular-gene-therapy-products/approved-cellular-and-gene-therapy-products>, 2026b. Accessed 2026-05-20.

U.S. Food and Drug Administration. Lyfgenia. <https://www.fda.gov/vaccines-blood-biologics/lyfgenia>, 2026c. Accessed 2026-05-24.

Mihaly Varadi, Damian Bertoni, Paulyna Magana, Urmila Paramval, Iryna Pidruchna, Manon Radhakrishnan, Maxim Tsenkov, Sreenath Nair, Milot Mirdita, Junyong Yeo, Oleg Kovalevskiy, Kathryn Tunyasuvunakool, Agata Laydon, Augustin Židek, Harry Tomlinson, Daisuke Hariharan, Josh Abrahamson, Tim Green, John Jumper, and Sameer Velankar. Alphafold protein structure database in 2024: providing structure coverage for over 214 million protein sequences. *Nucleic Acids Research*, 52(D1):D368–D375, 2024. doi: 10.1093/nar/gkad1011.

Pierre François Verhulst. Notice sur la loi que la population poursuit dans son accroissement. *Correspondance Mathématique et Physique*, 10:113–121, 1838.

Aurore Vernet, Donaldo Meynard, Qichao Lian, Delphine Mieulet, Olivier Gibert, Matilda Bissah, Ronan Rivallan, Daphné Autran, Olivier Leblanc, Anne Cécile Meunier, Julien Frouin, James Taillebois, Kyle Shankle, Imtiyaz Khanday, Raphael Mercier, Venkatesan Sundaresan, and Emmanuel Guiderdoni. High-frequency synthetic apomixis in hybrid rice. *Nature Communications*, 13:7963, 2022. doi: 10.1038/s41467-022-35679-3.

Rudolf Virchow. Die cellularpathologie. *Archiv für pathologische Anatomie und Physiologie*, 8:3–39, 1855.

Vito Volterra. Variazioni e fluttuazioni del numero d’individui in specie animali conviventi. *Memorie dell’Accademia dei Lincei*, 2:31–113, 1926.

Ludwig von Bertalanffy. *General System Theory: Foundations, Development, Applications*. George Braziller, New York, 1968. ISBN 9780807604533.

C. H. Waddington. *The Strategy of the Genes*. George Allen and Unwin, London, 1957.

Otto Warburg. Über den stoffwechsel der carcinomzelle. *Naturwissenschaften*, 12(50):1131–1137, 1924. doi: 10.1007/BF01504608.

P. D. Ward. In the shadow of the dinosaurs: Early mesozoic tetrapods. *Science*, 240:1421–1423, 1988.

J. D. Watson and F. H. C. Crick. Molecular structure of nucleic acids: A structure for deoxyribose nucleic acid. *Nature*, 171:737–738, 1953. doi: 10.1038/171737a0.

Wilhelm Weinberg. Über den nachweis der vererbung beim menschen. *Jahreshefte des Vereins für vaterländische Naturkunde in Württemberg*, 64:368–382, 1908.

Michael Weisberg. *Simulation and Similarity: Using Models to Understand the World*. Oxford University Press, Oxford, 2013.

Frits W. Went. On diffusion and the stimulation of growth by auxins. *Recueil des Travaux Botaniques Néerlandais*, 33:1–116, 1926.

Mary Jane West-Eberhard. *Developmental Plasticity and Evolution*. Oxford University Press, Oxford, 2003.

Robert H. Whittaker. Vegetation of the Siskiyou Mountains, Oregon and California. *Ecological Monographs*, 30(3):279–338, 1960.

Robert H. Whittaker. *Communities and Ecosystems*. Macmillan, New York, 2nd edition, 1975.

Norbert Wiener. *Cybernetics: Or Control and Communication in the Animal and the Machine*. MIT Press, Cambridge, MA, 1948. ISBN 9780262730099.

Francis R. Willett, Donald T. Avansino, Leigh R. Hochberg, Jaimie M. Henderson, and Krishna V. Shenoy. A high-performance speech neuroprosthesis. *Nature*, 620:1031–1036, 2023. doi: 10.1038/s41586-023-06377-x.

George C. Williams. *Adaptation and Natural Selection*. Princeton University Press, Princeton, 1966.

William C. Wimsatt. False models as means to truer theories. In Matthew H. Nitecki and Antoni Hoffman, editors, *Neutral Models in Biology*, pages 23–55. Oxford University Press, Oxford, 1987.

Carl R. Woese and George E. Fox. Phylogenetic structure of the prokaryotic domain: The primary kingdoms. *Proceedings of the National Academy of Sciences*, 74(11):5088–5090, 1977. doi: 10.1073/pnas.74.11.5088.

Friedrich Wöhler. Ueber künstliche bildung des harnstoffs. *Annalen der Physik und Chemie*, 88:253–256, 1828.

World Health Organization. Who fungal priority pathogens list to guide research, development and public health action, 2022. URL <https://www.who.int/publications/i/item/9789240060241>.

World Health Organization. Who bacterial priority pathogens list, 2024: Bacterial pathogens of public health importance to guide research, development and strategies to prevent and control antimicrobial resistance, 2024a. URL <https://www.who.int/publications/i/item/9789240093461>.

World Health Organization. COVID-19 epidemiological update – 24 december 2024, 2024b. URL <https://www.who.int/publications/m/item/covid-19-epidemiological-update---24-december-2024>.

World Health Organization. Global antimicrobial resistance and use surveillance system (GLASS) report 2025, 2025a. URL <https://www.who.int/publications/i/item/9789240116337>.

World Health Organization. World malaria report 2025, 2025b. URL <https://www.who.int/teams/global-malaria-programme/reports/world-malaria-report-2025>.

World Health Organization. Who recommends spatial emanators for malaria vector control and prequalifies first two products. <https://www.who.int/news/item/13-08-2025-who-recommends-spatial-emanators-for-malaria-vector-control-and-prequalifies-first-two-products>, 2025c. Departmental update, 13 August 2025; accessed 2026-05-16.

World Health Organization. Global tuberculosis report 2025, 2025d. URL <https://www.who.int/teams/global-programme-on-tuberculosis-and-lung-health/tb-reports/global-tuberculosis-report-2025>.

World Health Organization. WHO consolidated guidelines on tuberculosis: Module 4: Treatment and care, 2025e. URL <https://iris.who.int/handle/10665/380799>.

World Wide Fund for Nature. Living planet report 2024: A system in peril, 2024. URL <https://livingplanet.panda.org/>.

Worldwide Protein Data Bank. Worldwide protein data bank. <https://www.wwpdb.org/>, 2026. Accessed 2026-05-24.

Larry Wright. Functions. *The Philosophical Review*, 82(2):139–168, 1973. doi: 10.2307/2183766.

Sewall Wright. Coefficients of inbreeding and relationship. *American Naturalist*, 56(645):330–338, 1922.

Sewall Wright. Evolution in Mendelian populations. *Genetics*, 16:97–159, 1931.

Shigeo Yachi and Michel Loreau. Biodiversity and ecosystem productivity in a fluctuating environment: The insurance hypothesis. *Proceedings of the National Academy of Sciences*, 96(4):1463–1468, 1999.

Rosalyn S. Yalow and Solomon A. Berson. Immunoassay of endogenous plasma insulin in man. *Journal of Clinical Investigation*, 39:1157–1175, 1960. doi: 10.1172/JCI104130.

Zizhen Yao, Cindy T. J. van Velthoven, Michael Kunst, Meng Zhang, Delissa McMillen, Changkyu Lee, Won Jung, Jeff Goldy, Hongkui Zeng, et al. A high-resolution transcriptomic and spatial atlas of cell types in the whole mouse brain. *Nature*, 624:317–332, 2023. doi: 10.1038/s41586-023-06812-z.

Loïc Yengo, Sailaja Vedantam, Eirini Marouli, et al. A saturated map of common genetic variants associated with human height. *Nature*, 610:704–712, 2022. doi: 10.1038/s41586-022-05275-y.

Wang Zheng, Augustus J. Lowry, Harper E. Smith, Jiale Xie, Shaun Rawson, Chen Wang, Jin Ou, Marcos Sotomayor, Tian-Min Fu, Huanghe Yang, and Jeffrey R. Holt. Structural and functional basis of mechanosensitive tmem63 channelopathies. *Neuron*, 113(15):2474–2489.e5, 2025. doi: 10.1016/j.neuron.2025.05.009.

Emile Zuckerkandl and Linus Pauling. Evolutionary divergence and convergence in proteins. *Evolving Genes and Proteins*, pages 97–166, 1965.